

2011 Optics + Photonics

NanoScience
+ Engineering



Technical Summaries

spie.org/op

Conference Dates: 21–25 August 2011

Exhibition Dates: 23–25 August 2011

San Diego Marriott Marquis and Marina, San Diego Convention Center
San Diego, California, USA

Connecting minds for global solutions

Contents

8093: Metamaterials: Fundamentals and Applications IV	2	8101: Carbon Nanotubes, Graphene, and Associated Devices IV	123
8094: Nanophotonic Materials VIII	22	8102: Nanoengineering: Fabrication, Properties, Optics, and Devices VIII	129
8095: Active Photonic Materials IV	29	8103: Nanobiosystems: Processing, Characterization, and Applications IV	140
8096: Plasmonics: Metallic Nanostructures and Their Optical Properties IX	43	8104: Nanostructured Thin Films IV	145
8097: Optical Trapping and Optical Micromanipulation VIII	76	8105: Instrumentation, Metrology, and Standards for Nanomanufacturing, Optics, and Semiconductors V	156
8098: Physical Chemistry of Interfaces and Nanomaterials X	93	8106: Nanoepitaxy: Materials and Devices III	161
8099: Biosensing and Nanomedicine	103	8107: Nano-Opto-Mechanical Systems (NOMS)	167
8100: Spintronics IV	110		

Conference 8093: Metamaterials: Fundamentals and Applications IV

Wednesday–Thursday 24–25 August 2011 • Part of Proceedings of SPIE Vol. 8093
Metamaterials: Fundamentals and Applications IV

8093-02, Session 1

Nonlinear waves in metamaterials: state of the art

A. D. Boardman, P. Egan, R. R. C. Mitchell-Thomas, Univ. of Salford (United Kingdom)

Nonlinear waves in optical structures offer the prospect of many applications but are limited for ordinary materials by power limitations and the availability of intrinsic or extrinsic nonlinearity. Many new options, in the context of guided waves, will lead to new forms of computing and light manipulation. A range of planar waveguides will be introduced, in which the nonlinearity originates within a metamaterial component or is supplied through special bounding media. The stopping of light by such structures will be investigated. This will be shown to be a beautiful feature that leads to even more dramatic outcomes as the complexity of the waveguides increases. The trapped rainbow will be taken into a nonlinear regime and overall control using magneto-optics will be developed into forms that could be the basis of many applications. The whole question of soliton formation and propagation will be addressed next and will include both spatial and temporal solitons, and their interactions. The advantages of using couplers will be stressed, and their natural characteristics, through the use of metamaterials, will be connected to the stopping of light. The role of symmetry will be introduced, and the possibility of second-harmonic generation will be admitted, and the extent of metamaterial influence will be quantified. Finally, nonlinear bulk material will be examined using vortices as suitable probes. Many new outcomes will be delivered on this topic, which will emphasize, once again, how a whole range of different metamaterials can be deployed to reveal the fascinating world of nonlinear waves.

8093-03, Session 1

Nonlinear meta-atoms for multi-functional metamaterials

J. F. O'Hara, Los Alamos National Lab. (United States) and Oklahoma State Univ. (United States); M. Reiten, L. M. Earley, D. Roy Chowdhury, J. Zhou, A. J. Taylor, Los Alamos National Lab. (United States)

Nonlinearity adds an unprecedented amount of design flexibility and functionality to technology and is becoming increasingly studied in the context of metamaterials. Nonlinearity is the key to gain, bistability, photon mixing, rectification, and myriad other phenomena. Nonlinear behavior in natural materials begins at the atomic structure. We present a brief survey of some of the fundamentals of nonlinearity in natural materials. Then we present some recent progress in studying analogous behavior in metamaterials and meta-atoms, the fundamental building block of metamaterials. Specifically, we show microwave frequency meta-atoms that support self-sustained oscillations, harmonic generation, chaotic broadband generation, and injection locking and pulling.

In this work, meta-atoms and metamaterials are created using either circuit board milling or microfabrication techniques. Nonlinearity is added through the incorporation of semiconductor inclusions in the meta-atoms, such as varactors and tunnel diodes. Simulations and experiments are performed to determine nonlinear behavior. Meta-atoms are found to respond nonlinearly to both free-space and directly connected electromagnetic stimulation. In addition, nonlinear activity is achieved through either electric or magnetic excitation of the meta-atom. Measured results indicate a strong propensity of nonlinear meta-atoms to achieve numerous and simultaneous nonlinear behaviors, with mixing being the most common. We present our measured or simulated results and discuss their implications in the broader metamaterial perspective.

We also discuss the demarcation between basic lumped circuits and effective media.

8093-04, Session 1

Nonlinearity in metatronics

N. Engheta, Univ. of Pennsylvania (United States)

In recent years we have introduced and been developing the concept of “metatronics”, i.e. metamaterial-inspired optical nanocircuitry, in which the three fields of “electronics”, “photonics” and “magnetic” can be brought together seamlessly under one umbrella - a paradigm which I call the “Unified Paradigm of Metatronics”. We have now expanded this paradigm by including and exploring the role of optical nonlinearity in such metatronic circuits. In the present work, we will discuss our theoretical results in combining nonlinearity with the lumped optical circuit elements when accompanied with the ENZ materials for the difference-frequency generation, and the role of optical nanoantennas in enhancing the nonlinearity in metatronics. The enhancement of difference-frequency signal generation using proper design of nanoantennas may lead to composites with unusually strong difference-frequency effects.

8093-05, Session 1

Nonlinear and active metamaterials

A. K. Popov, Univ. of Wisconsin-Stevens Point (United States); I. R. Gabitov, The Univ. of Arizona (United States); N. M. Litchinitser, Univ. at Buffalo (United States); A. V. Kildishev, V. M. Shalaev, Purdue Univ. (United States)

In this talk, recent progress in nonlinear and active metamaterials will be reviewed. The phenomenon of anomalous field enhancement in graded-index metamaterials in the vicinity of zero index transition will be described. Exotic properties of coherent nonlinear-optical energy exchange between the ordinary and backward electromagnetic waves in negative-index materials, such as harmonic generation, frequency-mixing and optical parametric amplification, will be reviewed. Optical properties of active metamaterials with embedded amplifying centers will be described. The possibilities of compensating strong losses inherent to plasmonic metamaterials and for design of optical sensor and unique photonic microdevices will be discussed and numerically simulated.

8093-06, Session 1

Nonlinear spectroscopy on photonic metamaterials

S. Linden, Univ. Bonn (Germany); F. Niesler, N. Feth, M. Wegener, Karlsruher Institut für Technologie (Germany)

So far, research on photonic metamaterials has mostly concentrated on linear optics. However, photonic metamaterials can offer also interesting nonlinear optical properties, e.g., strong second harmonic generation (SHG). Unfortunately, our understanding of the nonlinear properties of photonic metamaterials is not as developed as the corresponding linear theory. In particular, the nonlinear mechanism for SHG from metallic nanostructures is still under debate.

Here, we report on our recent experiments on nonlinear optical spectroscopy of second SHG from split ring resonator (SRR) arrays. In our experiments, the laser frequency is tuned over the fundamental resonance of the SRRs. We find that the SHG process is governed by

Conference 8093:
Metamaterials: Fundamentals and Applications IV

the fundamental resonance while the SRR resonance at roughly twice the frequency does not further amplify the SHG but rather leads to reabsorption.

8093-07, Session 2

Nonlinear metamaterials

D. R. Smith, Duke Univ. (United States)

Artificially structured metamaterials have shown enormous promise for their ability to realize unique electromagnetic response that can be used to enable such exotic constructs as negative index or transformation optical media. But, as interesting are the passive materials that have resulted from the metamaterials concept, potentially even more interesting are nonlinear metamaterials, in which the nonlinear susceptibilities of a medium can be designed with considerable freedom simply not available-or not as readily available-in conventional materials. The resulting "metacrystals," which can be thought of as the analog of conventional nonlinear crystals, can provide new opportunities for managing the propagation of harmonics, and can have the capability to enhance or suppress certain nonlinear processes. We will describe a host of recently developed techniques for the accurate design and characterization of nonlinear metacrystals, showing that artificially structured media can be accurately described in the language of conventional nonlinear optics. Using metamaterial elements containing diodes and other nonlinear inclusions, we show the feasibility of nonlinear metacrystals at microwave frequencies, and demonstrate such phenomena as harmonic generation, three- and four-wave mixing, intensity-dependent resonance tuning, and similar phenomena. In all cases, analytical results, numerical simulations and measurements are all in excellent agreement, and point the way to the development of much more complex and interesting media.

8093-08, Session 2

Powered and nonlinear RF metamaterials

S. A. Cummer, B. Popa, Duke Univ. (United States)

The electromagnetic properties of metamaterials can be engineered to achieve substantially more flexibility and variety than those available from conventional materials. Yet even metamaterials as commonly realized through passive self-resonant metallic inclusions have some limitations. Adding some degree of external control or power to metamaterials can remove some of these limitations and gives metamaterials another level of functionality. We describe our recent efforts to develop an approach for realizing powered and nonlinear metamaterials in which each unit cell contains embedded active or nonlinear elements. Using a directly powered cell architecture, we demonstrate experimentally the effective electromagnetic material properties and the overall behavior that can be achieved with this type of active RF metamaterials. Characteristics such as loss and reciprocity that are dramatically different from passive metamaterials can be realized, potentially increasing the suitability of electromagnetic metamaterials for a variety of applications. We also describe our recent experimental work with active nonlinear metamaterials to create a phase conjugating lens. Varactor diodes are embedded in each metamaterial element and, when parametrically pumped with an external signal, can be made to generate a phase conjugated version of an illuminating source at close to half the pump frequency. We then demonstrate experimentally that an array of these nonlinear metamaterial elements does indeed act as a phase conjugating, and thus time-reversing and negative refracting thin material slab.

8093-09, Session 2

Second harmonic generation in index near zero transmission lines

I. V. Shadrivov, W. R. C. Somerville, D. A. Powell, The Australian

National Univ. (Australia)

Nonlinear parametric effects are substantially suppressed in natural materials, because of the so-called phase mismatch. Various techniques, such as quasi phase matching, are used in order to overcome this limitation for achieving, e.g., efficient second harmonic generation. The essence of phase matching is that the indices of refraction for the interacting waves should be equal. This is why it is hard to find in natural materials - which should be dispersionless over the whole octave. In this work we pursue the idea of achieving phase matching between the waves with zero phase velocity. Such waves appear, e.g. in plasma near the plasma frequency, or in the so-called epsilon-near zero metamaterials. Here, using the composite right-left handed (CRLH) transmission line we design the structure which supports zero phase velocity waves at both the fundamental frequency and at the second harmonic. The transmission line has a unit cell structure made of a combination of two regular nonlinear CRLH transmission lines with different parameters in order to achieve the required properties. We analyze the dispersion properties of such a transmission line, and study nonlinear effects experimentally. We observe second harmonic generation, and demonstrate that it is enhanced near the frequency of zero phase velocity. We also measure experimentally the field distribution in the structure in order to experimentally determine its dispersion properties. We expect that similar regimes of the phase matching can be achieved in dual-band index-near-zero metamaterials.

8093-10, Session 2

Magnetoelastic nonlinear metamaterials

M. Lapine, I. V. Shadrivov, Y. S. Kivshar, The Australian National Univ. (Australia)

*(Invited for the Special Session on Nonlinear Metamaterials)

For more than ten years, metamaterials are in a super-lens focus of research attention in electrodynamics and materials science. Rapid progress drives increasing interest in applied fields ranging from microwave engineering to optics. In particular, the possibility of nonlinear phenomena in metamaterials was soon explored [1,2], having established a new research direction with numerous promising ideas on nonlinear, tunable and active metamaterials [3,4].

The initial way to provide strong nonlinearity to metamaterials was found in either employing a nonlinear host medium [1] or engineering the elements of a metamaterial to include a nonlinear component [2]. Both the approaches result in a nonlinear response on the level of single element, which is further enhanced in a metamaterial, offering tools for harmonic generation, parametric amplification, loss compensation, solitons, tunability, etc.

Notably, the very structure of metamaterials remained fixed in such studies. At the same time, we recently reported [5,6] that structural changes in metamaterials offer an excellent means to control their properties, remarkably affecting resonance position and thus providing enhanced tunability of transmission, reflection and absorption.

In this talk, we report a further step forward and analyse a novel type of nonlinearity in metamaterials, which is achieved through specific conformational changes of the structure, analogous to those we employed in structural tuning. This results in exceptionally efficient self-action mechanisms.

For a detailed illustration, we consider an artificial magnetic metamaterial and analyse the nonlinear phenomena resulting from the structural changes, which give rise to unusual patterns of nonlinearity and bistability, providing a road towards interesting nonlinear phenomena.

REFERENCES

- [1] A.A. Zharov, I.V. Shadrivov, and Yu.S. Kivshar, Phys. Rev. Lett. 91, 037401, (2003).
- [2] M. Lapine, M. Gorkunov, and K.H. Ringhofer, Phys. Rev. E 67, 065601 (2003).
- [3] A.D. Boardman, V.V. Grimalsky, Yu.S. Kivshar, S.V. Koshevaya, M. Lapine, N.M. Litchinitser, V.N. Malnev, M. Noginov, Yu.G. Rapoport, and V.M. Shalaev, Laser Photonics Rev., 1-21 (2010) / DOI10.1002/

Conference 8093:
Metamaterials: Fundamentals and Applications IV

Ipqr.201000012.

[4] E. Poutrina, D. Huang, and D.R. Smith, *New J. of Physics* 12, 093010 (2010).

[5] M. Lapine, D. A. Powell, M. V. Gorkunov, I. V. Shadrivov, R. Marques, and Yu. S. Kivshar, *Appl. Phys. Lett.* 95, 084105, 2009.

[6] D. Powell, M. Lapine, M. Gorkunov, I. Shadrivov, and Yu. Kivshar, *Phys. Rev. B* 82, 155128 (2010).

8093-11, Session 3

Guiding waves with nonlinear metamaterials

N. M. Litchinitser, E. A. Gibson, G. Venugopal, Univ. at Buffalo (United States); Z. Kudyshev, Al-Farabi Kazakh National Univ. (Kazakhstan); A. Pandey, Univ. at Buffalo (United States)

Nonlinear optical metamaterials are likely to enable new reconfigurable, ultra-compact opto-plasmonic devices that would bridge existing gaps in electronic-photonics integration. Some of the major important functionalities to be realized in future opto-electronics chips include: i) buffering of optical signals to allow to avoid congestion of information traffic, ii) bridging the gap between micro-scale photonic waveguides (e.g., optical fibers) and nano-scale optical and electronic devices, and iii) low input power nonlinear optical signal processing. Although several approaches to the realization of such functionalities have been proposed and demonstrated, many of them are not easily scalable to a chip-size footprint.

In this talk we discuss our recent results on linear and nonlinear optics in guided-wave optical metamaterials and their applications for novel nonlinear photonic devices. We present a comprehensive analytical model for light propagation in coupled nonlinear waveguides for the most general case of arbitrary phase mismatch between the waveguides and arbitrary values of nonlinear coefficients and demonstrate that such nonlinear optical guided-wave structures enable a number of new phenomena and degrees of design freedom as compared to conventional nonlinear directional couplers. These unusual properties of metamaterial-based couplers form a basis for the development of ultra-compact all-optical processing applications, including all-optical buffers, flip-flops, and mirrorless lasers. We also discuss nonlinear optical wave propagation and interactions in transition metamaterial structures with various engineered graded refractive index profiles and discuss their potential applications for nonlinear low-intensity optical signal processing and sensing. Practical designs for the proposed structures will also be discussed.

8093-12, Session 3

Nonlinear metamaterial design for enhanced wave mixing.

E. Poutrina, A. Rose, D. Huang, D. R. Smith, Duke Univ. (United States)

For practical applications, the design and optimization of nonlinear metamaterial-based devices requires a quantitative approach, one that relates the particular metamaterial geometry incorporating nonlinear elements to the nonlinear properties of the composite, effective medium. In recent work by Poutrina et. al, an analytical approach was developed allowing the description of a nonlinear metamaterial in terms of effective nonlinear susceptibilities, in analogy with the standard representation common in nonlinear optics. The analytical model employs a perturbative solution to the nonlinear oscillator model that describes a metamaterial inclusion in terms of an effective RLC circuit. In the present work, we use the developed approach to design a metamaterial with the predictably enhanced effective nonlinear characteristics and verify the theory predictions by simulating the three- and four- wave mixing processes in the designed geometries and by performing experiments on a varactor-loaded split ring resonator-based medium. We also demonstrate the capability of designing the symmetry properties of the effective medium for suppressing or enhancing the even-orders nonlinear response. Finally,

we illustrate the manner in which the developed nonlinear metamaterial medium could be used to demonstrate nonlinear imaging based on wave-front reversal with four wave mixing.

8093-14, Session 3

Parametric amplification in optical metamaterials

I. R. Gabitov, The Univ. of Arizona (United States) and Southern Methodist Univ. (United States); A. I. Maimistov, National Research Nuclear Univ. MEPhI (Russian Federation); Z. Kudushev, Al-Farabi Kazakh National Univ. (Kazakhstan)

Parametric amplification based on three wave interactions in optical metamaterials is considered. A mathematical model of this phenomenon taking into account both saturation of a pump wave and phase mismatch is derived. Theoretical analysis of parametric amplification in the continuous wave approximation demonstrates a significant difference between the processes of amplification taking place in conventional and negative index materials. We have analyzed the characteristics of amplification depending on system parameters and showed strong dependence on the value of phase mismatch.

8093-39, Session 3

Nonreciprocal transmission and one-way slow light in plasmonic metamaterials

A. B. Khanikaev, C. Wu, S. H. Mousavi, G. Shvets, The Univ. of Texas at Austin (United States)

Nonreciprocity is associated with a special class of systems for which forward and backward propagation behave differently. We propose plasmonic metamaterials endowed with extraordinary nonreciprocal optical properties. The structures considered represent (i) a subwavelength array of holes in an optically thin metal film and (ii) a low-symmetry metamaterial composed of periodically arranged meta-atoms made of plasmonic antennas embedded into magneto-optical medium. We show that both structures behave as one-way photonic mirrors, transmitting light only in one direction while stopping it in the opposite direction. It is found that in the case of the perforated metal the structure supports surface plasmon modes with nonreciprocal dispersion. Coupling of the incident radiation to these modes gives rise to the nonreciprocal response of the metamaterial. In the case of metamaterial made of plasmonic antennas, the nonreciprocal response is stemming from the resonances of individual meta-atoms. This approach allows for more flexibility in the design of the structure; very diverse nonreciprocal effects can be attained with the topologically similar meta-atoms but with slightly different geometrical parameters. As an example we designed the structure exhibiting one-way slow-light behavior, i.e. delaying light propagating in one direction but not in the opposite.

The main advantage of the proposed metamaterials as compared to their contemporary photonic counterparts stems from their plasmonic nature. Plasmonics, thanks to its capability to trap light to subwavelength scales and boost magneto-optical response of the materials, enables the whole one-way mirror or nonreciprocal delay element to be as thin as just one wavelength of the incident light.

8093-15, Session 4

Ultrafast nonlinearities of plasmonic metamaterials

M. Ren, A. Nikolaenko, E. Plum, N. I. Zheludev, Univ. of Southampton (United Kingdom)

We report on extraordinary strong nonlinear properties and ultrafast

Conference 8093:
Metamaterials: Fundamentals and Applications IV

transient dynamics of gold-based plasmonic metamaterials and metamaterial nanostructures aggregated with semiconductor nanotubes

8093-16, Session 4

Optical negative refraction by four-wave mixing in thin metallic nanostructures

X. Zhang, Univ. of California, Berkeley (United States)

While all natural materials exhibit refraction in the positive direction, artificially engineered negative index metamaterials (NIM) have been shown capable of bending EM waves negatively. We report the experimentally observed nonlinear negative refraction at optical frequencies using four wave mixing (4WM), wherein the incident and negatively refracted beams are at different frequencies. The nonlinear negative refraction could potentially impact many important applications such as superlens imaging without using actual NIMs which are typically lossy, narrow band, and require complicated fabrication processes.

8093-17, Session 4

Harmonic generation and energy transport in GaP At visible and UV wavelengths

M. Scalora, U.S. Army Aviation and Missile Command (United States); V. Roppo, Univ. Politècnica de Catalunya (Spain); M. A. A. Vincenti, D. de Ceglia, N. Akozbek, The AEGis Technologies Group, Inc. (United States)

We study inhibition of absorption, optical transparency, energy and momentum transport of phase locked harmonic pulses in semiconductors like GaP, at visible and UV wavelengths. In these spectral regions semiconductors are characterized by large absorption, metallic behavior, or a combination of both. This phenomenon is attributed to phase locking between the fundamental and its harmonics that occurs under phase mismatched conditions, irrespective of material parameters, as long as the material is somewhat transparent to the pump. As a result of phase locking the pump impresses its dispersive properties to the generated harmonics which in turn experience no absorption or other de-phasing effects such as group velocity walk-off. The harmonics co-propagate phase- and velocity-locked to the pump, and any energy exchange between the pump and its harmonics ceases away from interfaces. We show experimental and theoretical evidence that phase locking causes the generated harmonics to propagate through GaP at 223nm, where the material displays metallic response, without being absorbed, and that the transport of electromagnetic energy and momentum is quite peculiar and seemingly anomalous. We also show that it is possible to exploit cavity environments to generate and enhance harmonic generation below 200nm in semiconductors like Silicon. These results make it clear that there are new opportunities in ultrafast nonlinear optics and nano-plasmonics in new wavelength ranges.

8093-18, Session 4

Z-scan simulations on metallodielectric stacks with nonlinear absorption

N. C. Kotte, J. Haus, P. Powers, J. Gao, A. M. Sarangan, Univ. of Dayton (United States); M. Scalora, U.S. Army Aviation and Missile Command (United States); R. Jakubiak, Air Force Research Lab. (United States)

Experimental investigations reveal significant nonlinear responses from metallodielectric stacks (MDSs) with constituent metal films of silver (Ag), gold (Au) or copper (Cu). In particular, the Cu dielectric MDS exhibited large non-linear absorption. Nevertheless, there is a need to investigate these materials with more faithful numerical techniques

in order to account for the underlying physical processes observed in the experiments. We apply a Finite Element Method (FEM) with radial symmetry to numerically solve for the Z-scan experiment of a MDS using the corresponding nonlinear Maxwell equations. The amplitude and the phase of the electromagnetic field at the exit interface of the MDS are used for transforming to the far-field regime.

8093-19, Session 4

Suppression of plasmon losses in metamaterials by means of parametric bichromatic irradiation

A. Kussow, A. Akyurtlu, Univ. of Massachusetts Lowell (United States)

Novel mechanism of suppression losses in plasmonic subsystem in metals and semiconductors is suggested. If two parametrically coupled fields are applied to a metal plasma, a non-linearity of the transport equation affects the electric response, or the permittivity. If the coupling constant between the probe wave and the support wave is small, the permittivity, at the frequency of the probe wave, is still Drude-like, with the re-normalized plasmon frequency. In the case of a strong coupling, unusual response effects are possible (the induced transparency and the considerable suppression of the plasmon losses), with profoundly non-Drude permittivity function.

8093-20, Session 5

Darker than black: the theory of hyperbolic radiation-absorbing metamaterials

E. E. Narimanov, C. Motti, Purdue Univ. (United States)

The broadband super-singularity of the photonic density of states of hyperbolic media leads to a dramatic enhancement of the light scattering from the defects and surface corrugations at the interface of the hyperbolic metamaterial, with nearly all the incident light "sucked" into the propagating modes of the hyperbolic medium. Here, we present the theoretical description of such radiation-absorbing systems.

8093-21, Session 5

Spontaneous emission near hyperbolic metamaterials

Z. Jacob, Univ. of Alberta (Canada); I. I. Smolyaninov, Univ. of Maryland (United States); E. Narimanov, Purdue Univ. (United States)

Engineering the photonic density of states using microcavities or photonic crystals helps to control a plethora of phenomena associated with light. While the unique electromagnetic response of metamaterials and their capabilities have received widespread attention, the role of the PDOS in nanostructured metamaterials has been unexplored. Here, we unravel how a unique dielectric response can give rise to a divergence in the PDOS for bulk propagating waves within a medium and understand other intriguing properties and advantages of metamaterial based PDOS engineering especially in connection to the Purcell effect.

As opposed to conventional methods for enhanced and directional spontaneous emission based on closed cavity Purcell enhancement of spontaneous emission or open cavity approaches based on photonic crystal waveguides, our design relies on a completely new approach, namely the singularity in the density of states of a hyperbolic dispersion medium. The dielectric response of the medium surrounding the emitter is engineered to provide dramatically increased density of photonic states in a broad bandwidth as well as inherent directionality to the emitted photons. An increased density of photonic states immediately translates

Conference 8093:
Metamaterials: Fundamentals and Applications IV

to a larger number of radiative decay channels available for an excited atom ensuring enhanced spontaneous emission, a necessary quality for single photon sources.

We use a green's function approach to calculate the local density of states. In the limit of zero losses, under the effective medium approximation, the LDOS near a hyperbolic dispersion medium is infinite. We use the semiclassical theory of spontaneous emission to analyze the divergence of the decay rate of an emitter near a metamaterial due to the singularity in the density of states. For a medium which has the dielectric permittivities of opposite signs in perpendicular directions and no losses, the decay rate of a point dipole diverges. This divergent behavior of the decay rate is counterintuitive to the conventional response of materials where the decay rate and the LDOS goes to a constant value when losses are zero.

8093-22, Session 5

Transition metamaterials in materials with hyperbolic dispersion

A. Pandey, E. A. Gibson, N. M. Litchinitser, Univ. at Buffalo (United States)

Recently, we predicted new phenomena occurring due to the electromagnetic wave propagation in metamaterials with material parameters gradually changing from positive to negative values, transition metamaterials. At oblique incidence, we predicted the phenomenon of anomalous electromagnetic enhancement and resonant absorption in the vicinity of the point where the refractive index changes sign. In all previous studies, we considered an effective isotropic medium with assigned values for dielectric permittivity and magnetic permeability that give rise to an effective gradually changing refractive index. However, the particular mechanism of dissipation and the influence of the microscopic structure of metamaterials on the field enhancement phenomenon would be determined by a physical model of a metamaterial.

In this work, we design and investigate electromagnetic wave propagation in transition metamaterials based on two materials systems: metal/dielectric multilayered structures for optical frequency range and highly doped/undoped semiconductors for mid-infrared frequency range. In the latter case, the level of doping is carefully adjusted such that the effective refractive index gradually changes from positive to negative values. It was shown (Narimanov et al.) that strongly anisotropic materials that possess a negative permittivity component along the direction perpendicular to the interface and positive component along the interface, have hyperbolic dispersion relations. As a result, the component of the Poynting vector along the interface is opposite to the direction of the wavevector component along the interface, leading to the effective negative refractive index. We investigate how the dispersion relation changes when the refractive index gradually changes from positive to negative in these structures.

8093-23, Session 5

Multilayered metamaterials with hyperbolic dispersion

T. U. Tumkur, G. Zhu, P. J. Black, C. E. Bonner, M. A. Noginov, Norfolk State Univ. (United States)

We have developed and studied a family of hyperbolic metamaterials consisting of lamellar metal-dielectric structures which can be fabricated on flat, flexible and curvilinear substrates and functionalized by emitting dye molecules. Hyperbolic materials can accommodate waves with high wavevectors and hence possess broadband singularity in the density of photonic states [1]. Owing to this property, we demonstrate the reduction of radiative lifetimes of emitters. We have also shown that the spontaneous lifetime reduction is much stronger when emitters are placed inside a metamaterial rather than on its surface. Three different types of metal-dielectric lamellar structures, consisting of organic and inorganic dielectric components have been fabricated. The first type

consisted of 20 alternating layers of silver and IR-140 dye-doped PMMA, which, in agreement with theoretical predictions [1], showed a strong reduction of the fluorescence lifetime, down to 286 ps when the sample was illuminated from the front and 217 ps when it was illuminated from the rear. For comparison, the emission life-times of the same dye deposited onto a glass substrate and silver film were equal 716 ps and 607 ps, respectively. Expectedly, the fluorescence lifetime reduction in films deposited on the top of other undoped metamaterials (including Ag-LiF, Ag-MgF₂ and Ag-PMMA lamellar structures), was considerably smaller, as in the case of Ag-LiF which had a fluorescence lifetime equal to 499 ps. Our observation paves the road to many exciting applications including a single photon gun needed for quantum optics and information technology [1].

[1] Z. Jacob, I. Smolyaninov, E. Narimanov, arXiv:0910.3981v2 [physics/optics] (2009).

8093-24, Session 5

Transfer matrix approach to propagation of angular plane wave spectra through metamaterial multilayer structures

P. P. Banerjee, H. Li, R. Aylo, G. T. Nehmetallah, Univ. of Dayton (United States)

The development of electromagnetic (EM) metamaterials for perfect lensing and optical cloaking has given rise to novel multilayer bandgap structures using stacks of positive and negative index materials. Gaussian beam propagation through such structures have been analyzed using transfer matrix method (TMM) with paraxial approximation [1], and unidirectional and bidirectional beam propagation methods (BPMs) [2,3].

Since TMM is naturally a plane wave approach, we use this technique to analyze the non-paraxial propagation of a collection of TE or TM polarized plane waves having an initial Gaussian amplitude profile in 1 transverse dimension (x) through a stack containing layers of positive and negative index materials. The spatial variation of the electric field at any plane (z) during bidirectional propagation through the stack is found from the composite angular plane wave spectrum. Specifically for the TM case, the spatial variations of both the x and z polarization components are calculated. The numerical results from TMM are compared with numerical simulations using FEM and FDTD techniques. The TMM calculations are exact, less computationally demanding, and can be performed for arbitrary angular plane wave spectra. Finally, the TMM based angular plane wave spectrum approach can be readily applied to a wide variety of other cases, such as propagation through induced reflection gratings in nonlinear media.

[1] I. V. Shadrivov et al, Appl. Phys. Lett., 22 (2003).

[2] A.Ghosh et al, Proc. SPIE, 7754 (2010).

[3] J. Lu and S. He, Microwave and Optical Tech. Lett., 37, 292 (2003).

8093-25, Session 5

Fingerprinting metamaterial behavior in 2D periodic composites: Fundamentals and applications to THz optics.

S. Foteinopoulou, The Univ. of Exeter (United Kingdom); M. Kafesaki, E. N. Economou, Foundation for Research and Technology-Hellas (Greece); C. M. Soukoulis, Iowa State Univ. (United States)

2D periodic composites can behave as uniaxial effective media, with the possibility of extra-ordinary hyperbolic dispersion, not available in natural materials. Such hyperbolic type of dispersion typically occurs when constituents with negative permittivity are present. Accordingly, 2D composites incorporating polar materials can act as uniaxial hyperbolic effective metamaterial. Thus, they become highly attractive structures, since they can enable extra-ordinary beam manipulation in the THz

Conference 8093:
Metamaterials: Fundamentals and Applications IV

regime (0.1-10 THz) where traditional visible optics is not suitable. While often the metamaterial composites can be described by traditional effective medium theories, this is not always the case. A mere deviation between actual transmission/reflection and the values predicted by effective medium theory does not necessarily imply effective medium picture breakdown.

Here, we developed a new criterion that establishes an angular fingerprint of effective metamaterial behavior for two-dimensional (2D) periodic composites. We apply such criterion to characterize different candidate polar-polar and polar-dielectric 2D composite structures as effective metamaterials. We found polar-polar metamaterial structures that are highly transmissive in cases where transmission through an identical slab made of either of the constituents would be next to none. In addition, our results suggest that polar-material based metamaterials demonstrate interesting and unusual angular transmission maps for the different polarization channels. We analyze and discuss the underpinning physics of such curious angular polarization-dependent transmission, and how to utilize it for the design of efficient polarization filters and converters.

8093-77, Poster Session

Toward curvilinear metamaterials based on silver filled alumina template

Y. A. Barnakov, P. J. Black, Norfolk State Univ. (United States); N. Kiri, Cornell Univ. (United States); H. Li, A. V. Yakim, L. Gu, M. A. Noginov, Norfolk State Univ. (United States)

The advent of metamaterials and their continued development over the past decade has revolutionized the fields of electrodynamics and photonics, giving new perspective to the classical interaction of light with matter and enabling scores of unparalleled physical phenomena. Despite of recent tremendous progress in both theory and experiment, the research field is hindered by a lack of inexpensive large-size three-dimensional metamaterials. One way to overcome this problem is to utilize bulk dielectric templates, which nanoporous space can be filled with metals or other dielectrics. Recently, we have demonstrated that an array of silver nanowires embedded into a flat alumina membrane matrix with 35nm-diameter pores behaves as a metamaterial with hyperbolic dispersion, characterized by different signs of the electric permittivity tensor elements. It has been theoretically predicted that a metamaterial with hyperbolic dispersion realized in curvilinear coordinates (with radial or azimuthal anisotropy of metallic inclusions) has a property of a hyperlens - a device allowing for sub-diffraction imaging in the far field. The structure with a similar 'hair brush' morphology but different radial distribution of electric permittivity has been predicted to have a functionality of a non-magnetic optical cloak. In this work, we explore a family of novel curvilinear metamaterials fabricated via inexpensive non-lithographic means. This synthetic route opens a door to design and fabrication of large, three-dimensional bulk metamaterials for a number of practical applications ranging from optical cloaking to broad band sub-wavelength imaging.

8093-78, Poster Session

Microwave superlens with sloped faces

M. K. Khodzitskiy, A. P. Slobozhanuk, D. S. Filonov, National Research Univ. of Information Technologies, Mechanics and Optics (Russian Federation); P. A. Belov, Queen Mary, Univ. of London (Russian Federation)

Over the last ten years, the various designs of superlens have been developed [1-3]. Some of them are based on the concept of canalization of sub-wavelength images [4]. These developments are widely used in the near-field microscopy and magnetic resonance imaging (MRI) [5-6]. In this paper, based on the existing designs of wire medium superlenses, a superlens with sloped faces has been designed. The superlens was developed to increase the resolution and sensitivity of the NMR tomograph with a resonant frequency of 63.86 MHz and magnetic field

induction of 1.5 T. The lens has length of 250 cm, the slope of faces is 30 degrees and the size of the working aperture is 40*20 cm². It consists of a 20x20 array of brass wires with diameter of 2 mm and period of 10 mm. Due to sloped faces, the lens becomes more convenient device for NMR tomography of biological objects. Investigation of near-field transfer by the lens was carried out in the frequency range of 60-68 MHz. A wire antenna in the form of a flag was selected as the source. The flag was located on the distance of 2 mm from the surface of the lens. Numerical simulation in the CST Microwave Studio software package has shown the transmission of the image in the form of a flag with $\lambda/500$ resolution to $\lambda/2$ distance.

[1] Pendry J. Negative refraction index makes perfect lens // Phys. Rev. Lett. 2000. V. 85. P. 3966-3969.

[2] Ikonen P., Belov P.A., Simovski C.R., Maslovski S.I. Experimental demonstration of sub-wavelength image canalization using capacitively loaded wire medium // Phys. Rev. B. 2006. V. 73. P. 073102.

[3] Silveirinha M.G., Belov P.A., Simovski C.R. Sub-wavelength imaging at infrared frequencies using an array of metallic nanorods // Phys. Rev. B. 2007. V. 75. P. 035108.

[4] Belov P.A., Simovski C.R., Ikonen P. Canalization of sub-wavelength images by electromagnetic crystals // Phys. Rev. B. 2005. V. 71. P. 193105.

[5] M. J. Freire, R. Marques and L. Jelinek, Experimental demonstration of metamaterial lens for magnetic resonance imaging//Applied Physics Letters. 2008. V. 93. P. 231108 (1-3).

[6] X.Radu, D.Garray, C.Craeye. Toward a wire medium endoscope for MRI imaging// Metamaterials . 2009. V. 3. 90-99.

8093-79, Poster Session

Polarization-insensitive and omnidirectional near perfect broadband metamaterial absorber in the near infrared regime

S. Chen, H. Cheng, J. Tian, Nankai Univ. (China)

We present a near perfect broadband metamaterial absorber in the near infrared regime. The electromagnetic response of mixed-size cut wires combined with thick metal layer is theoretically studied. The broadband absorber is polarization insensitive and the absorption remains high even at large incident angle for both transverse electric (TE) and transverse magnetic (TM) polarizations. By simply adding more loops of the cut wires, the bandwidth of the strong absorption can be effectively enhanced due to the hybridization of surface plasmons in different loops.

8093-80, Poster Session

Liquid crystal-metal nanorods composites with spatially distorted optic axis for transformation optics

J. Xiang, O. D. Lavrentovich, Kent State Univ. (United States)

Transformation optics uses materials with spatially varying optical properties to control the trajectories of light propagation. The concept is familiar to liquid crystals, in which the optic axis can adopt various configurations in space. For example, a cylindrical nematic LC sample with the optic axis arranged radially would form the light trajectories in such a way that they diverge, leaving a cylindrical wedge behind the axis of the structure un-illuminated, with the angle that depends on the optical anisotropy of the liquid crystal. In this work, we consider a hybrid system, representing a liquid crystal with dispersed metal nanorods, in which the effective refractive index depends on the volume fraction of the metal component. In this hybrid material, one can control not only the orientation of the local optic axis, but also the values of the effective refractive indices. We simulate propagation of light in three basic geometries, filling the composite material in the space between two concentric cylinders, with the optic axis represented in the cylindrical

Conference 8093:
Metamaterials: Fundamentals and Applications IV

coordinates as (a) ; (b,c) where changes from 0 to when increases (b) or decreases (c) in the range . We demonstrate that the geometries (b) produce a non-magnetic optical cloaking effect, while (c) produces a condensing effect on light propagation. This work was supported by AFOSR FA9550-10-1-0527 grant.

8093-81, Poster Session

Modeling of nonlinear metamaterials

P. L. Colestock, M. Reiten, J. F. O'Hara, Los Alamos National Lab. (United States)

We report the results of a study to model the behavior of nonlinear metamaterials in the microwave frequency range composed of arrays of split-ring resonators combined with nonlinear circuit elements. The overall model consists of an array of coupled damped oscillators whose inter-element coupling is a function of signal amplitude, similar to that which exists in the Fermi-Pasta-Ulam system. [1] We note the potential occurrence of classical nonlinear effects including parametric coupling and FPU recurrence. These in turn lead to nonlinear waves on the array which are a type of soliton particular to the form of nonlinearity that has been incorporated. We have studied, in particular, the nonlinear effects that arise from tunnel diodes embedded in the resonant circuits. Whether or not the aforementioned nonlinear phenomena occur is a function of the details of the nonlinearity and the inherent circuit losses. We derive conditions for stable oscillations and carry out simulations of the resulting circuit frequency response. We shall present these modeling results along with preliminary experimental data from laboratory measurements of prototype nonlinear metamaterials.

[1] E. Fermi, J. Pasta and S. Ulam, LASL Report-1940, May 1955

* Current address: Oklahoma State University

8093-82, Poster Session

Plasmonic toroidal response at optical frequencies

Y. Huang, W. T. Chen, P. C. Wu, National Taiwan Univ. (Taiwan); Y. Chau, Ching Yun Univ. (Taiwan); D. P. Tsai, National Taiwan Univ. (Taiwan) and National Applied Research Labs. (Taiwan) and Academia Sinica (Taiwan); V. A. Fedotov, V. Savinov, N. I. Zheludev, Univ. of Southampton (United Kingdom)

Toroidal dipole is created by currents flowing on a surface of a doughnut-shaped structure along its meridians first considered by Zel'dovich in 1957 [1]. Toroidal metamaterials were first theoretically proposed in 2007 [2]. In 2010, the toroidal metamaterials consisted by four three-dimensional resonant split rings show toroidal response in microwave region [3].

In this paper, we study the optical responses by integrating four U-shaped split-ring resonators (SRRs) together. The resonances of the four U-shaped SRRs array with magnetic field of incident light passing through the resonant rings was numerically investigated by using commercial software COMSOL 3.5a based on finite-element method (FEM). The permittivity of gold was described by the Lorentz-Drude model [4]. The size of a single U-shaped SRR is 110 nm (arms) \times 90 nm (bottom) and 30 nm line width wire loop. Simulation results shows toroidal and magnetic dipole resonance at free space wavelength 660 nm and 952 nm respectively. Incident light induced magnetic dipoles point in the same direction produced magnetic resonance. In contrast, four magnetic dipoles form a head-to-tail configuration which concentrates toroidal resonance.

References:

[1] Ia. B. Zel'dovich, Sov. Phys. JETP 6, 1184 (1958).

[2] K. Marinov, A. D. Boardman, V. A. Fedotov, N. Zheludev, N. J. Phys. 9, 324 (2007).

[3] T. Kaelberer, V. A. Fedotov, N. Papasimakis, D. P. Tsai, N. I. Zheludev,

Science 330, 1510 (2010).

[4] W. T. Chen, P. C. Wu, C. J. Chen, H. Y. Chung, Y. F. Chau, C. H. Kuan, Optics Express 18, 19665 (2010).

8093-83, Poster Session

A simple theoretical analysis of the Einstein relation for the DMR (diffusivity-mobility ratio) in Nono compounds on the basis of k.p formalism

S. Singha Roy, JIS College of Engineering (India)

An attempt is made to study the Einstein relation for the diffusivity-mobility ratio (DMR) in nonlinear optical and Optoelectronic compounds on the basis of a newly formulated electron energy spectrum. The results for ternary, III-V and quaternary types of optoelectronic materials form a special case of our generalized investigation. I have also studied the DMR in II-VI, Bi, IV-VI and stressed materials on the basis of various band models as applicable for such focused materials. It has been found taking n-Cd₃As₂, n-CdGeAs₂, n-InAs, n-InSb, n-Hg_{1-x}Cd_xTe, n-In_{1-x}Ga_xAs_yP_{1-y} lattice matched to InP, CdS, Bi, PbS, PbTe, PbSe and stressed InSb as examples of the aforementioned compounds that the DMR increases with increasing electron concentration in various manners for different band constants of the said materials and the rates of variation are totally band structure dependent. Now the well-known results for non-degenerate wide gap optical and Optoelectronic materials have been obtained as special cases of our generalized theory under definite limiting background.

8093-84, Poster Session

Infrared absorptance of wavelength-selection trapezoid grating

J. Sze, Instrument Technology Research Ctr. (Taiwan); A. Wei, Foxsemicom Integrated Technology Inc. (Taiwan); F. Chen, Instrument Technology Research Ctr. (Taiwan); K. Lee, Chinese Culture Univ. (Taiwan)

A trapezoid grating which improve the contrast of the wavelength-selection infrared absorptance is demonstrated. The absorptance of wavelength-selection trapezoid grating is studied by using the rigorous coupled-wave analysis (RCWA) numerical scheme. The side wall slope of the trapezoid silicon grating plays an important role in the infrared absorptance enhancement. According to the calculated spectral absorptance curves of the trapezoid gratings, it is found that the peak is located at the wavelength of 7.0 micrometer, which is equal to the period of the trapezoid grating. The analyzed results show that the maximum contrast absorptance of the trapezoid grating is given at the side wall slope of 18. The modified shape of the grating side walls can be used for further tailoring thermal radiation properties which is useful for enhancing the performance of infrared detectors.

8093-85, Poster Session

Polarization effects in second harmonic generation from G-shaped nanostructures

E. A. Mamonov, I. A. Kolmychek, A. I. Maydykovskiy, T. V. Murzina, O. A. Aktsipetrov, Lomonosov Moscow State Univ. (Russian Federation); A. V. Silhanek, V. V. Moshchalkov, V. K. Valev, T. Verbiest, Katholieke Univ. Leuven (Belgium)

Planar chiral nanostructures are novel structures that attract attention first of all by their possibility to influence the polarization properties of the transmitted or reflected light by rotating its polarization plane or changing

Conference 8093:
Metamaterials: Fundamentals and Applications IV

its ellipticity. In case of the second harmonic generation (SHG) the changes can be more significant. The high sensitivity of the SHG process to the symmetry and shape of the structures can lead to the appearance of new effects such as anisotropy of the rotation of the polarization plane or depolarization of the SHG response. In case of spiral structures one can expect different strength of the nonlinear interaction under the excitation by the left and right circularly polarized pump radiation. In this work polarization properties of optical SHG from arrays of gold G-shaped nanostructures are studied.

Samples were formed as an array of 1x1 microns gold G-shaped nanostructures of 25 nm thickness on the silicon surface. The reflected SHG was studied using an output of the Ti:Sapphire laser at 780 nm. A strong anisotropy of the SHG intensity is observed, induced by the anisotropic amplification of the distribution of the SHG and fundamental fields under the excitation of the structure by linear or circular polarized fundamental beams. Stokes parameters and intensities of polarized and depolarized SHG components were estimated from the experimental data. The intensity of the depolarized SHG component is found to be comparable with the polarized one, both of them being anisotropic and has the symmetry though nor each nanostructure nor the whole array are symmetric. It was found, that one of SHG efficiency is strongly dependent of the type of the circularly polarization of the fundamental radiation.

8093-86, Poster Session

Second and third harmonic generation at UV and soft x-ray wavelengths from semiconductor gratings

M. A. A. Vincenti, D. de Ceglia, The AEgis Technologies Group, Inc. (United States); M. Scalora, U.S. Army Aviation and Missile Command (United States)

Extraordinary transmission properties are demonstrated in the UV range for GaAs gratings with sub-wavelength apertures under TM-polarization excitation. The metal-like response below 270nm, typical of several semiconductors such as GaAs or GaP, in fact may be used to excite surface waves that lead to enhanced transmission in the linear regime and to novel nonlinear optical phenomena in the UV and soft X-ray ranges. An investigation of the linear transmission as a function of geometrical parameters of the grating reveals the formation of surface waves and relatively high transmission values even in regimes where the nominal absorption is significant. Strong field localization in sub-wavelength cavities and on the surface of the grating can be achieved under proper excitation conditions leading to the enhancement of harmonic generation. Nonlinear contributions to harmonic generation arise from symmetry breaking and the nonlinear magnetic Lorentz force. Preliminary results show promising nonlinear conversion efficiencies at wavelengths below 100nm, and demonstrate cross-coupling of TE and TM polarizations for pump and harmonic signals. A down-conversion process that can re-generate pump photons of polarization orthogonal compared to the incident pump field is also demonstrated.

8093-87, Poster Session

Enhanced nonlinear optics in resonant GaAs gratings: harmonic generation and optical bistability

D. de Ceglia, G. D'Aguzzo, N. Mattiucci, M. A. A. Vincenti, The AEgis Technologies Group, Inc. (United States); M. Bloemer, M. Scalora, U.S. Army Aviation and Missile Command (United States)

We present a study on nonlinear optical processes in GaAs gratings, made by perforating a single layer of GaAs with subwavelength slits. Large enhancement of conversion efficiency, for both second and third harmonic generation, is predicted when a TE-polarized pump field

excites the guided mode resonances of the grating. When these modes are excited, the spectrum near the pump wavelength shows abrupt changes of linear transmission and reflection that follow a typical Fano-like shape. At the same time the grating provides dramatic enhancement of local fields and fosters favorable conditions for harmonic generation processes, even in regimes of strong linear absorption at the harmonic wavelengths. In particular, in a GaAs grating pumped at 1064nm, we predict second (532nm) and third (354nm) harmonic conversion efficiencies several orders of magnitude larger than conversion rates achievable in either bulk or etalon structures made of the same material. We demonstrate that these efficiencies are not influenced by linear absorption at the harmonic wavelengths, and they are unrelated to grating thickness or to the order of the guided mode excited. We also analyze the effects of self phase modulation on resonant gratings. In particular we will demonstrate the possibility of triggering optical bistability at relatively low switching intensities by exploiting the strong field localization provided by the grating at the guided mode resonances. Finally, we will discuss the influence of self-phase modulation on the harmonic generation conversion efficiencies.

8093-88, Poster Session

Nonlinear optical couplers based on strongly anisotropic metamaterial waveguides

G. Venugopal, N. M. Litchinitser, Univ. at Buffalo (United States)

Nonlinear waveguide couplers have attracted a lot of interests in the recent years. Combined with the unique properties of metamaterials, nonlinear directional couplers open fundamentally new opportunities for the development of ultra-compact signal processing functionalities for on-chip applications. Recently, we proposed a novel kind of nonlinear coupler with one channel filled with linear negative index material and another one filled with positive index material one or both of which could be nonlinear. The opposite directionality of phase and velocity in such systems lead to an effective feedback mechanism. We found exact analytical solutions and predicted that such systems can be bi- or multi-stable and support a family of gap solitons. However all previous studies were based on coupled-mode analysis assuming that effective medium parameters for dielectric permittivity and magnetic permeability of metamaterials.

In this work we discuss the design and simulation of nonlinear couplers based on strongly anisotropic metamaterial waveguides. Such waveguides were shown to support negative-index propagating modes (Podolskiy and Narimanov). For these modes, the wave propagation is in a direction opposite to the phase velocity. As a result, the waveguide behaves as a 2-dimensional counterpart of 3-dimensional negative index material. The waveguides in a coupler that we design consists of alternating metal and dielectric subwavelength layers with positive and negative permittivities, respectively. As a nonlinear optical material, we incorporate chalcogenide glass that was demonstrated to have relatively high nonlinear refractive index of $\sim 10^{-13}$ cm²/W. We will report numerical simulations demonstrating novel transmission properties of such couplers, including distributed feedback and bistability.

8093-89, Poster Session

Optical negative refraction by four-wave mixing in metallic nanostructures

S. Palomba, Univ. of California, Berkeley (United States); S. Zhang, The Univ. of Birmingham (United Kingdom); Y. Park, X. Yin, X. Zhang, Univ. of California, Berkeley (United States); G. Bartal, Technion-Israel Institute of Technology (Israel)

While all natural materials exhibit refraction in the positive direction, artificially engineered materials have been utilized in various ways to bend EM waves negatively. Bulk metamaterials and photonic crystals demonstrated negative refraction of the EM energy flux and wavevectors. A direct way to obtain negative refraction from very thin film has been

Conference 8093:
Metamaterials: Fundamentals and Applications IV

theoretically proposed by Tretyakov and Pendry.

Here, we demonstrate nonlinear negative refraction, by using degenerate four-wave mixing (4WM) process to show efficient frequency conversion by a 20nm thick gold film where the newly generated frequency is emerged at a negative angle comparing to the exciting wave. The ratio between the sines of the incident and nonlinearly refracted angles remains a negative constant and depends only on the wavelengths ratio hence rigorously fulfills Snell's law, expanding the phenomenon of negative refraction into the nonlinear regime. Showing the ability for negative refraction by very thin slab, such nanosystems could constitute the building blocks for the implementation of a super lens in the visible region and possible further investigations.

Our approach can operate for all frequencies and polarizations and has no nonlocal effects typically present in metamaterials and it constitutes the first demonstration of negative refraction in ultrathin films.

8093-90, Poster Session

second order optical susceptibilities of ZnO(0001) and NiO(001) surfaces

A. V. Gavrilenko, V. I. Gavrilenko, Norfolk State Univ. (United States)

Direct fabrication of complex nanostructures with controlled crystalline morphology, orientation and surface architectures remains a significant challenge. Nonlinear optical spectroscopy of the second harmonic generation (SHG) is a tool that is extremely sensitive to a very thin surface layer (up to few atomic monolayers). This technology is therefore a very powerful tool for contact-less monitoring of the nanocrystal growth, as well as surface, and interface structural quality. In this work we study SHG spectra of hexagonal zinc oxide (0001) and nickel oxide (001) surfaces as materials extensively studied for different applications in nanophotonics. Electron energy structure and second order nonlinear optical susceptibilities have been studied from the first principles within the Density Functional Theory (DFT) using ab initio pseudopotentials. Equilibrium geometries of (001) surfaces are obtained by total energy minimization method using the Local Density Approximation (LDA). Optical functions are calculated within the independent particles picture. Analysis of the results is focused on understanding of the physics behind the formation of the second order optical response from the transition metal oxide surfaces, namely contributions of oxygen and metallic d-electron related excitations. Strong contribution to the nonlinear optical susceptibility functions of the high-density d-electrons below the Fermi energy in transition metals is demonstrated. Theoretical predictions are compared with available experimental data.

8093-91, Poster Session

Experimental harmonic generation in the metallic regime of GaP

V. Roppo, Univ. Politècnica de Catalunya (Spain) and Charles M. Bowden Research Ctr. (United States); J. V. Foreman, N. Akozbek, Charles M. Bowden Research Ctr. (United States); M. A. A. Vincenti, AEGis Technologies Group (United States); M. Scalora, Charles M. Bowden Research Ctr. (United States)

When a pump signal traverses an interface into a nonlinear medium it generates SH and/or TH fields, depending on the type of nonlinearity involved. Each harmonic consists in a homogeneous portion that walk-off from the pump field and in an inhomogeneous component phase- and velocity-locked to the pump. The key observation here is that the inhomogeneous component always experiences the same complex index of refraction the pump pulse.

This idea has already been experimentally proved when a pump pulse tuned at 1300nm was launched into a slab of GaAs 500micron thick. Transmitted SH and TH signals were detected far below the material absorption band edge (~900nm). The homogeneous SH and TH signals

were quickly absorbed, while the inhomogeneous components continued on through the sample experiencing an effective complex index of refraction identical to the index of the pump, which is tuned in a region of transparency. A detailed investigation of the propagation characteristics of the inhomogeneous component in different circumstances can bring about new interesting scenarios. For example, it has been shown that in a high-Q GaAs cavity the inhomogeneous SH signal (at 612nm) can achieve conversion efficiencies of the order of $1e-3$ with pumping field intensities as low as 0.15MW/cm^2 inside the cavity.

Following the evolution of this topic, it now comes natural to ask the following question: does this phenomenon hold for harmonic fields tuned at frequencies in the metallic range? That is to say, if the pump field is tuned in the transparency region, will a harmonic field propagate if it happens to be tuned in a region where $\text{sign}(\epsilon) < 0$, where one expects no propagating solutions? The short answer to this question is yes and we provide experimental evidence that show how an electromagnetic field is generated and propagates in otherwise forbidden wavelength ranges.

8093-92, Poster Session

Wave propagation in lossy MTMs surrounded by linear and nonlinear media with arbitrary nonlinearity

Z. I. Al-Sahhar, Al-Aqsa Univ. (Palestinian Territory, Occupied); H. J. El-Khozondar, M. M. Shabat, Islamic Univ. of Gaza (Palestinian Territory, Occupied)

The dispersion relation in a system consists of a lossy metamaterials (MTMs) film surrounded by a linear substrate and a nonlinear cladding with an arbitrary nonlinearity is derived. The surface plasmonic (SP) wave at the interfaces between metamaterials (MTMs) and the nonlinear cover is recovered by taking certain limits. Lossy MTMs have simultaneously complex-negative permeability μ and complex-negative permittivity ϵ . Results are presented by plotting the SP frequency as a function of the nonlinearity at chosen damping factors. Both the real and imaginary parts are studied. Results also display the wave frequency as a function of plasma frequency. For comparison, the imaginary part is set to zero and curves are reproduced.

8093-93, Poster Session

Super Talbot effect in anisotropic metamaterial

W. Zhao, Z. Lu, Rochester Institute of Technology (United States)

Advances in metamaterial provide the possibilities to engineer the permittivity of a metamaterial to be almost any arbitrary value (positive, zero, or negative). In particular, if the real part of the permittivity component along the light propagation direction is negative, while the transverse ones positive, the dispersion curve is in hyperbolic form. The anisotropic metamaterial (or hyperbolic metamaterial) can convert the evanescent waves which would normally decay in the conventional materials into propagating waves. The anisotropic metamaterial can be realized by depositing thin, alternating metal-insulator layers.

In this paper, we re-visit the classical optical phenomenon, called Talbot effect and investigate this effect in such an anisotropic metamaterial. From 2D and 3D numerical simulation results, we show that the super Talbot effect can be observed in the metamaterial even the period of the object is much smaller than the incident wavelength. Deep subwavelength resolution of the super Talbot effect can be achieved as long as the attenuation of the metamaterial is small enough. As the incident wavelength is 630nm, the period of the input grating is 94nm and the duty cycle is 50%, for an Ag-SiO₂ layered structure (dAg:dSiO₂=5nm:5nm), the image size measured at the fourth Talbot imaging plane is about 55nm. The Talbot distance measured is around 152nm. The corresponding effective permittivity is calculated as: $-6.46+i0.51$ (along propagation direction) and $4.94+i0.05$ (along transverse directions).

Conference 8093:
Metamaterials: Fundamentals and Applications IV

The super Talbot effect may have the applications in the areas of nanolithography and optical storage.

8093-94, Poster Session

Numerical optimization for the plasmonic Raman sensor including periodic hole arrays and tapering directions

K. Yamaguchi, Toyohashi Univ. of Technology (Japan); M. Fujii, Toba National College of Maritime Technology (Japan); D. K. Gramotnev, Nanophotonics Pty Ltd. (Australia)

Metal nanostructures are interesting for achieving new types of biosensors because they can work as nanocavities that have high sensitivity when surface plasmons are used. This approach should let us detect the binding reactions of molecules in real time with high sensitivity. However, to achieve this, we must greatly enhance the electromagnetic field and Raman radiation.

Nanofocusing structures for surface plasmons could present a breakthrough in achieving both nanoscale confinement of electromagnetic energy and large, highly controlled local field enhancement required for efficient surface-enhanced Raman scattering.

We previously fabricated a nanofocusing (tapered) hole array in a metal film on a dielectric substrate by using focused ion beam (FIB) lithography and succeeded in observing localized surface plasmon resonances. The results of experiments using this array agreed with most of the calculation results for a tapered hole array obtained using the finite-difference time-domain (FDTD) method. Moreover we numerically determined structural design optimization at the dependences of the expected local field enhancements on Au film thickness, focusing hole diameter, and hole period by the FDTD method in order to take into consideration the plasmonic resonance effects and we concentrated our efforts on periodic nanofocusing hole arrays at the metal-substrate interface.

In this paper, we analysed further structural parameters such as differ from tapered direction and incident direction with the theoretical predictions.

8093-26, Session 6

Metamaterials and plasmonics: improved material building blocks

G. V. Naik, J. Kim, P. R. West, A. Boltasseva, Purdue Univ. (United States)

Conventional metals like silver and gold that are used as building blocks for optical metamaterials exhibit excessive losses at optical frequencies. This seriously threatens to restrict plasmonic and metamaterial devices in this frequency range to only the proof-of-concept stage. A recent approach that could unlock the technological potential of plasmonics and optical metamaterials is to look for better plasmonic materials (which must have a negative real part of dielectric permittivity). Here we provide an overview of two classes of alternative plasmonic materials - doped semiconductors and intermetallics - that could allow realization of novel transformation optics and metamaterial devices with greatly improved performance operating at near infrared and visible frequencies.

8093-27, Session 6

Understanding and reducing losses in metamaterials

C. M. Soukoulis, Iowa State Univ. (United States)

One of the most serious obstacles when increasing the frequency towards the visible regime is the problem of ohmic losses in the metallic elements and absorption losses in the substrate. By optimizing the

overlap of the electromagnetic field and the metal, the metamaterial losses can be reduced by design to some extent. We will present a detailed study of developing the self-consistent calculations of gain with metallic nanostructures in 2D and 3D. The need for self-consistent calculations stems from the fact that by increasing the gain in the metamaterial, the metamaterial properties change, which, in turn, increasing the coupling to the gain medium until a steady state is reached. We will present theoretical and numerical studies has been demonstrated by optical pumping the effective gain coefficient of the combined system can be much higher than its bulk counterpart due to the strong local-field enhancement inside the metamaterials designs. Although optical pumping can compensate losses, it will not materialize to real world applications. We will review how one can reduce the losses with realistic applications; one needs to use semiconductors with gain (quantum dots and quantum wells), which can be pumped by electrical injection. This is compatible with semiconductor industry.

8093-28, Session 6

Effect of losses on nonlocal effects in metal-dielectric multilayered metamaterials

A. A. Orlov, P. M. Voroshilov, National Research Univ. of Information Technologies, Mechanics and Optics (Russian Federation); P. A. Belov, National Research Univ. of Information Technologies, Mechanics and Optics (Russian Federation) and Queen Mary Univ. of London (United Kingdom); Y. S. Kivshar, The Australian National Univ. (Australia) and National Research Univ. of Information Technologies, Mechanics and Optics (Russian Federation)

We study the effect of losses on spatial dispersion in metal-dielectric multilayered metamaterials. Previously we discovered that under certain conditions two waves instead of one can be excited in metamaterial under consideration by incident TM-polarized light beam. As was demonstrated earlier, under certain conditions such periodic structures demonstrate strong nonlocal effects manifested, e.g., in the appearance of the second extraordinary wave which can be excited in the metamaterial by an incident TM-polarized light beam and observed through the beam splitting. The existence of an additional light wave is a clear manifestation of the presence of spatial dispersion in the metamaterial, and it validates our earlier observation of strong nonlocal nature of metal-dielectric multilayered metamaterials. Our analysis of such structures with realistic losses demonstrate that losses naturally cause damping of the waves inside of the metamaterial and also reduce the frequency range where birefringence without splitting by polarization is observed. When we employ realistic losses for silver (Ag) as metal, we reveal that the typical losses of silver in the visible range are too high for our purposes. Hence, we consider an active medium with a gain in order to compensate losses.

8093-29, Session 6

Scaling of loss in metamaterials

J. B. Khurgin, The Johns Hopkins Univ. (United States)

It is important to distinguish two separate mechanisms of metamaterial loss increase with frequency: intrinsic material-related loss and purely size-dependent mechanism associated with inability of storing energy outside the metal at high frequencies when electro-static limit is being approached. By highlighting the above we establish the fact that fundamentally losses in the metamaterials with true sub-wavelength features cannot be improved for frequencies higher than 100's of GHz and show that at optical frequencies roughly the same performance is obtained using magnetic (ie.g. split rings) and non-magnetic (e.g. spherical and elliptical nanoparticles) metamaterials.

Conference 8093:
Metamaterials: Fundamentals and Applications IV

8093-30, Session 6

Graphene in metamaterials: What makes a material a good conductor?

P. Tassin, T. Koschny, Iowa State Univ. (United States); M. Kafesaki, Foundation for Research and Technology-Hellas (Greece); C. M. Soukoulis, Iowa State Univ. (United States)

Recent developments in the field of metamaterials--or engineered materials with novel electromagnetic properties--have promised a number of exciting applications, in particular at optical frequencies. Most metamaterials consist of carefully designed metallic structures that replace atoms in their role as the basic units of interaction with electromagnetic radiation. Unfortunately, the noble metals are not particularly good conductors at optical frequencies, resulting in significant absorptive loss in photonic metamaterials. Recently, several materials have been proposed to replace metals as the current-carrying elements in metamaterials, such as graphene at optical frequencies and high-Tc superconductors at terahertz frequencies. In this communication, we first address the question of what is a good conductor for use in a metamaterial. We develop a model based on the quasistatic response of metamaterial constituents to an incident electromagnetic field in order to develop a figure of merit for conductors. The results lead to two conclusions: (1) In determining the merits of a certain conducting material, its material properties cannot be uncoupled from certain geometric aspects, such as the layer thickness that can be experimentally obtained. (2) It is the resistivity of the material, rather than the conductivity or permittivity, that gives direct information on the absorptive loss in the metamaterial and on the frequency saturation caused by kinetic inductance. These considerations lead to a figure of merit for conducting materials. Finally, we apply the figure of merit to a number of materials, such as graphene and high-Tc superconductors.

8093-31, Session 7

All kinds of cloaks, all kinds of transformations

M. W. McCall, A. Favaro, P. Kinsler, Imperial College London (United Kingdom); A. D. Boardman, Univ. of Salford (United Kingdom)

Electromagnetic cloaking was the first example of so-called transformation optics where the invariance properties of Maxwell's equations are used to determine how coordinate deformations can be actualized in an electromagnetic medium cite{Pendry2006}. The concept was experimentally realized cite{Schurig2006} and the improvement towards an ideal macroscopic wide-bandwidth cloak continues to be a major goal for the experimentalists. This has included carpet cloaking in 3D cite{Ergin2010}, and the use of polarization selectivity using calcite cite{Chen2011}. Most recently, a significant extension of the concept has been proposed in which the coordinate transformations embrace time as well as space cite{McCall2011}. The electromagnetic medium for realizing spacetime transformations must be dynamic as well as inhomogeneous, and by influencing the local speed of light we showed how it is possible for the light reaching a camera to record an edited version of the events it surveys. Regulating the local speed of light about an average value likely requires that the medium within which the coordinate transformation is carried out be one of uniform refractive index, rather than vacuum. Although this extends the original programme of transformation optics, by using quite abstract methods we have shown how such an extension can be embedded within a general theory of non-birefringent transformations cite{Favaro2011}. However, what if the initial medium is nonlinear or otherwise programmable? Influencing the initial medium will influence the functionality of the final medium in ways that have yet to be explored, with controllable cloaking an obvious goal.

Beyond electromagnetics, transformation theory has been applied now to acoustics to produce a variety of interesting and experimentally realizable schemes cite{Zhang2011,Torrent2007}. Although acoustics is not mathematically equivalent to electromagnetics cite{Cummer2007}, the

ideas of actualizing a coordinate transformation do carry over. Therefore, we ask what are the essential ingredients of any transformation theory, and to what other areas of physics can the scheme be applied? We explore the structure and relationship between propagation and constitutive equations towards a general theory.

8093-32, Session 7

3D invisibility cloaks at visible wavelengths

T. Ergin, J. Fischer, Karlsruher Institut für Technologie (Germany); J. C. Halimeh, Ludwig-Maximilians-Univ. München (Germany); N. Stenger, M. Wegener, Karlsruher Institut für Technologie (Germany)

In this contribution, we review our latest work on three-dimensional cloaking utilizing the "carpet cloak" (or "ground-plane cloak") scheme. Here, a bump in a metallic carpet is rendered invisible to an observer by adding a nanostructured metamaterial cloak on top. As a result, the observer again sees a flat metal mirror. In our case, the metamaterial consists of a polymeric woodpile photonic crystal that is used in the long-wave limit. The woodpile is fabricated via stimulated emission depletion-inspired direct laser writing, which allows for a drastic miniaturization of the feature sizes and thus pushes the woodpile's effective medium limit into the visible regime. The filling fraction of the woodpile is changed locally to give rise to a tailored refractive-index distribution. This distribution is derived in the framework of transformation optics using quasi-conformal mapping. We characterize the three-dimensional cloak by optical bright-field and dark-field microscopy using monochromatic circular polarized illumination. A cone of light with a full opening angle of 50 degrees in three dimensions is sampled. Furthermore, we provide numerical ray-tracing calculations which simulate the complete experimental setup within ray optics and the carpet cloak within the effective-medium limit. We find excellent qualitative agreement between experimental results and calculations.

8093-33, Session 7

A transforming device formed by metamaterials creating a visual result of a changed scattering cross section

C. Du, X. Dong, G. Yuan, Q. Deng, C. Liu, Institute of Optics and Electronics (China)

A device for transforming the scattering cross section's shape of perfect electrical conductor (PEC) objects to other arbitrary shapes is presented based on transformation optics. The designed functional device covers the original PEC object with its electromagnetic parameters determined by the transformation expressions. Then, the virtual PEC objects with their definite shape of the scattering cross section will be produced visually. The validation of the device was made by means of finite-element method. Though the designed transformer is anisotropic and inhomogeneous, the development of metamaterials makes it more closely to practice. This device can find applications in many aspects like camouflage some objects from the radar or other target recognition systems.

8093-34, Session 8

Spaser action, loss compensation, and stability in plasmonic systems with gain

M. I. Stockman, Georgia State Univ. (United States)

We demonstrate analytically that the conditions of spaser generation and the full loss compensation in a dense resonant plasmonic-gain medium (metamaterial) are identical. Consequently, attempting the full compensation or overcompensation of losses by gain in such a medium

Conference 8093:
Metamaterials: Fundamentals and Applications IV

will lead to an instability and a transition to a spaser state. This will limit (clamp) the inversion and lead to the limitation on the maximum loss compensation achievable. The criterion of the loss overcompensation, leading to the instability and spasing, is given in an analytical and universal (independent from system's geometry) form.

8093-35, Session 8

Design and analysis of metamaterials for the continuous wave terahertz laser

J. Luo, Huazhong Univ. of Science and Technology (China)

The artificially structured electromagnetic materials, which called metamaterials, has led to the realization of phenomena which cannot be obtained with natural materials. We have found many fundamental progress and applications of metamaterials in millimeter wave or microwave, and many usefully potential applications of terahertz as well, but still need considerable efforts to fill this "THz-gap" in future. Therefore, it is especially important to design the metamaterials device in the terahertz frequency regime. For the first, we analyze the split ring resonators (SRRs) model in theory, and many planar SRR arrays with different periodic structures have been designed for later testing, the planar SRR arrays are fabricated using conventional photolithography and electron-beam deposition of gold on n-GaAs substrate, the metal array and n-GaAs together form a Schottky contact. Then the influences of background substrate and the shapes of the SRRs on the terahertz resonance are experimentally investigated at several terahertz frequencies of continuous wave terahertz laser in turn, such as 1.4THz, 2.52THz, 4.25THz, etc., and all the transmission properties are recoded and analyzed, especially, some SRR arrays can obtain about 80 percent absorption of THz amplitude transmission. In addition, computer simulations of the spectral response of the chosen planar metamaterials are performed to analyze the resonance frequency, surface current density and local electric field, which agree well with measured results. These metamaterials may be useful for future applications in the construction of various THz filters, THz antenna, or THz grid structures ideal for constructing THz switching devices.

8093-36, Session 8

Interference enhancement of photoluminescence of ultrathin layer with silicon nanocrystals

S. A. Dyakov, Trinity College Dublin (Ireland); D. M. Zhigunov, Lomonosov Moscow State Univ. (Russian Federation); T. S. Perova, Trinity College Dublin (Ireland); V. Y. Timoshenko, Lomonosov Moscow State Univ. (Russian Federation); A. Hartel, D. Hiller, M. Zacharias, Albert-Ludwigs-Univ. Freiburg (Germany)

Most of prospective applications of silicon nanocrystals (Si-NCs), such as active media for optical waveguides, amplifiers and lasers, or absorbing ultrathin layer for the third generation photovoltaic devices, imply utilization of thin films containing Si-NCs. Therefore, the control of optical properties of such films is of current importance. However, small optical thicknesses of the films and complicated multilayered structure make certain difficulties for the ordinary estimations using standard formulas. We present a model, which enables one to prognosticate the photoluminescence (PL) intensity of multilayered structure. Using theoretical predictions we experimentally observed PL intensity enhancement of 4 nm thick film with Si-NCs for optimally chosen silicon dioxide (SiO₂) buffer layer thickness. Moreover, our model enables one to explain nonmonotonic dependence of PL intensity from Si-NCs layer on its thickness.

Alternating layers of stoichiometric SiO₂ and silicon rich silicon oxynitride (SRON) were deposited on Si substrates using PECVD system. Subsequently, all samples were annealed for 1 h in high purity N₂ atmosphere at 1100°C in order to form Si-NCs in SRON layers. Triple-

layered structures consisting of buffer SiO₂ layer, emitting SRON layer and capping SiO₂ layer were fabricated. For the first set of samples the thickness of buffer layer was varied from 0 to 125 nm, while the thicknesses of emitting and capping layers were fixed. The second set of samples is characterized by variable thickness of emitting SRON layer, the thicknesses of other layers were constant. The PL process is approximated by radiation of chaotically oriented oscillating dipoles.

8093-37, Session 8

Interactions in planar metamaterials: from strong coupling to active tuning

I. Brener, Sandia National Labs. (United States)

The issue of interactions between different types of engineered metamaterial resonances has received considerable attention since it was shown that electromagnetically induced transparency behavior can be mimicked using coupling between metamaterials and/or plasmonic resonators. In this talk I will present some of our recent results on strong coupling between metamaterial resonators and other excitations such as phonons, free carriers and intersubband transitions in semiconductor heterostructures, and ways to exploit these for active tuning of metamaterial properties.

8093-38, Session 8

Octave-wide photonic band gap in three-dimensional plasmonic Bragg metamaterials

H. W. Giessen, R. Taubert, Univ. of Stuttgart (Germany)

Coupling between individual particle plasmon resonances (PPRs) has been a field of extensive research over the past few years. Most of the work was dedicated to near-field coupling with close spacing between the resonant particles. In this limit, retardation is negligible, but also the interesting properties of radiating PPRs are mostly neglected. In contrast, when particles are positioned at distances on the order of their emission wavelength, coupling can be mediated by the radiation fields of the PPRs.

We investigate far-field coupling in three-dimensional stacked plasmonic nanostructures. We show that a superradiant mode forms when particles are stacked at Bragg distance. Increasing the number N of stacked layers leads to the formation of a very broad photonic band gap of about 1 eV.

Ivchenko et al. predicted that the radiative width of the superradiant mode in a structure of Bragg-stacked oscillators is proportional to the number of layers. This can be intuitively understood by the matching of the oscillator phase to their vertical distance, which leads to an increased, "collective" dipole moment of the coupled system.

To demonstrate this, we extracted the FWHM from calculated spectra of Bragg stacked nanowires for one to ten layers. The FWHM of the coupled system increases strongly for increasing number of layers. The dependence of the stop gap width on the plasmonic oscillator strength is investigated by considering different wire geometries: w and h are changed, keeping a constant aspect ratio, in order to compensate for the spectral shift. Therefore the spectral position for the different geometries is constant and only the oscillator strength changes.

For the small wires with low oscillator strength, the width of the mode increases slowly but linearly up to approximately 7 layers and start to saturate for more layers. In contrast, the large wires, which exhibit a big oscillator strength, show a strong increase for the first two layers and almost no further change for higher N. This issue can be understood by taking into account that interaction is only possible within the coherence length of the oscillators. As the large wires couple more efficiently to the radiation field, their decay is on the order of only a few cycles of the light field. Interaction with oscillators beyond this range is not possible. This interpretation is supported by extracting the radiative lifetime for a single oscillator from the linewidth at N=1 and deducing the coherence length of propagation subsequently.

Conference 8093:
Metamaterials: Fundamentals and Applications IV

8093-13, Session 9

Linear and nonlinear properties of low spatial symmetry metamaterials

G. Shvets, C. Wu, A. B. Khanikaev, N. Arju, The Univ. of Texas at Austin (United States)

Plasmonic Low Spatial Symmetry Metamaterials (LSPMs) is a novel and exciting recent development in the area of electromagnetic metamaterials because they truly represent building blocks unavailable in Nature. Specifically, while most molecules and atoms possess at least some degree of spatial symmetry (e.g., a finite number of inversion planes), LSPMs can be designed to have none. This opens us exciting opportunities for making new optical devices that are based on both single-layer and multi-layers. For example, LSPM can be used for efficient polarization manipulation.

Three-dimensional LSPM whose properties slowly vary along the direction of light propagation can be used for making slow-light devices.

LSPMs can be used for engineering the radiative lifetimes of metamaterials because they can be designed to support both “bright” (radiant) and “dark” (sub-radiant) resonances. The interference between the two results in the so-called Fano resonance. One attractive feature of LSPMs is that, depending on the light polarization, the same resonance can give rise a Fano-like or Lorentzian line shapes. We will describe the fundamental theory explaining these resonant shapes and present experimental results for the pi-shaped plasmonic antennas. Field enhancement predicted by the simulations will be used to evaluate the potential of LSPM-based devices for nonlinear applications.

8093-40, Session 9

Temporally shaping ultrafast light with metamaterials

D. P. Brown, UES, Inc. (United States); A. M. Urbas, Air Force Research Lab. (United States)

Coherent excitation in optical spectroscopy and control of photo-induced processes like second harmonic generation depend on the temporal properties of ultrafast pulses. In this work, we demonstrate that metamaterials can be fabricated to have very large spectral dispersion properties that can affect both the temporal envelope and phase of each spectral component of an ultrafast pulse in useful ways. Values for the group delay dispersion were found to be as large as plus or minus 4000 fs². We simulated the effect these materials would have on an ultrafast pulse with a full width half max (FWHM) time duration between 12 and 15fs, and then experimentally tested the pulse shape by transmitting or reflecting off of the metamaterials an ultrafast pulse from an oscillator capable of the same pulse as the simulations. The pulse envelope was determined using fringe resolved autocorrelation (FRAC). Finally, we explored the effects on second harmonic generation and two photon fluorescence both numerically and experimentally, and we examined how the structure orientation of the metamaterial changes these effects.

8093-41, Session 9

Robust optical delay lines via topological protection

M. Hafezi, Joint Quantum Institute (United States); E. A. Demler, M. D. Lukin, Harvard Univ. (United States); J. M. Talyor, Joint Quantum Institute (United States)

Optical signals might be a promising alternative to electronic signals in future circuits. One key requirement is the ability to filter and delay light on-chip over a large bandwidth (several Gbps) for various time-domain processing such as optical buffering and multiplexing. However, disorder in fabrication rapidly degrades performance, leading to effects such as

unwanted signal modulation in transmission. Here we show theoretically how exploiting topological properties of optical systems forms a basis for robust optical devices which are immune to disorder.

Our method for realization of topological protected photonic devices makes use of two dimensional arrays of coupled resonator optical waveguides (CROW) to simulate a 2D magnetic tight-binding Hamiltonian with degenerate clockwise and counter-clockwise modes. This approach does not require explicit time-reversal symmetry breaking, but the degenerate modes — time-reversed pairs — behave analogously to spins with spin-orbit coupling in the electronic quantum spin Hall effect (QSHE), and experience a spin-dependent magnetic field. When the clockwise and counter-clockwise modes are decoupled, we can selectively drive each mode and observe quantum Hall behaviors without breaking the time-reversal symmetry in the tight binding Hamiltonian. In a direct analogy to the electronic integer quantum Hall effect, we show that photonic edge states carry light at the perimeter of the system, while being insensitive to disorder, and thereby forms a basis for robust photonic devices. In particular, in comparison to state-of-the-art 1-D CROW systems, our approach can be dramatically more resistant to scattering disorders and fabrication errors.

8093-42, Session 10

Layer-by-layer metamaterials using membrane projection lithography

D. B. Burckel, J. R. Wendt, I. Brener, A. R. Ellis, M. B. Sinclair, Sandia National Labs. (United States)

The lack of a suitable fabrication technique of bulk-like metamaterials containing 3D isotropic unit cells for operation in the IR and optical wavelength ranges continues to present a significant barrier to exploration of potential metamaterial solutions and applications. Recently we have introduced membrane projection lithography (MPL) a fabrication technique capable of creating truly 3D micron-scale metamaterial unit cells. The basic premise behind MPL is creating a patterned membrane suspended over a cavity (the unit cell). Directional evaporation(s) through the patterned membrane results in deposition of a replica of the membrane pattern on the interior face(s) of the cavity.

In this talk we report our recent progress extending MPL to 3D bulk-like materials in a layer-by-layer process. We will present fabrication details addressing complications associated with multi-layer processing as well as optical characterization data showing the impact of moving from a single layer of 3 dimensionally oriented resonators dominated by surface effects to one with resonators embedded in a medium with bulk-like behavior. These micron-scale 3D metamaterials demonstrate that MPL enables exploration into the viability of metamaterial concepts to applications in the thermal IR wavelength range.

Supported by the Laboratory Directed Research and Development program at Sandia National Laboratories. This work was performed, in part, at the Center for Integrated Nanotechnologies, a U.S. Department of Energy, Office of Basic Energy Sciences user facility Sandia is a multiprogram laboratory operated by Sandia Corporation, a Lockheed Martin Company, for the United States Department of Energy's National Nuclear Security Administration under Contract DE-AC04-94AL85000.

8093-43, Session 10

Bottom-up manufacturing methods for application in metamaterials

D. A. Pawlak, K. Bienkowski, M. Gajc, A. Klos, P. Osewski, K. Sadecka, A. Stefanski, Institute of Electronic Materials Technology (Poland)

One of the future ways of obtaining metamaterials or materials with unusual electromagnetic properties most probably will be methods based on self-organization. Novel developments in the bottom-up manufacturing approach towards metamaterials will be discussed. The methods presented are based on eutectic directional solidification as

Conference 8093:
Metamaterials: Fundamentals and Applications IV

well as on doping dielectric materials with plasmonic nanoparticles. The investigated methods allow for manufacturing of bulk 2 and 3 D micro and nanostructured materials with various geometries (rodlike, lamellar, spiral) as well as various component materials (oxides, metals, semiconductors). Recently even split-ring resonator geometry has been achieved.

8093-44, Session 10

All dielectric infrared metamaterial

M. B. Sinclair, J. C. Ginn, J. R. Wendt, J. O. Stevens, D. W. Peters, L. I. Basilio, L. K. Warne, I. Brener, P. G. Clem, J. F. Ihlefeld, Sandia National Labs. (United States)

Metamaterials comprising metallic inclusions such as split ring resonators have been utilized for numerous device demonstrations at microwave frequencies. Unfortunately, the increased impact of ohmic losses renders metal-based metamaterials too lossy for devices at optical wavelengths (infrared and shorter). A possible strategy to overcome this fundamental limitation is to replace the metallic inclusions with high permittivity dielectric resonators, thereby replacing lossy conduction currents with displacement currents. A further advantage of the utilization of dielectric resonators is the isotropic metamaterial response that arises due to the high degree of symmetry exhibited by typical resonator shapes (i.e. spheres and cubes). In this presentation, we will describe the design, fabrication, and characterization of all dielectric metamaterials operating in the thermal infrared. The dielectric metamaterials are based on cubic dielectric resonators fabricated from Tellurium and arrayed on a Barium Fluoride substrate. As predicted by analytical and numerical simulation, the metamaterial exhibits a magnetic resonance near 10 μm wavelength, as well as an electric resonance at a slightly shorter wavelength. The retrieved effective parameters indicate a negative permeability (permittivity) in the vicinity of the magnetic (electric) resonance. This work represents a first step toward the development of low loss infrared metamaterials suitable for device applications. This work was supported by the Laboratory Directed Research and Development program at Sandia National Laboratories. Sandia National Laboratories is a multi-program laboratory managed and operated by Sandia Corporation, a wholly owned subsidiary of Lockheed Martin Corporation, for the U.S. Department of Energy's National Nuclear Security Administration under contract DE-AC04-94AL85000.

8093-45, Session 10

Nanorod metamaterials as a new plasmonic platform

A. V. Zayats, King's College London (United Kingdom)

Guiding and manipulating light on length scales below the diffraction limit requires structural elements with dimensions much smaller than the wavelength. Recently, novel plasmonic metamaterial has been developed based on arrays of aligned gold nanorods grown in self-assembled anodic aluminium oxide templates. This metamaterial provides a flexible platform with tuneable resonant optical properties across the visible spectral range, that can be specifically designed by changing the length, diameter and separation between the nanorods. Such metamaterials, with a controllable and engineered plasmonic response, can be used instead of conventional plasmonic metals for designing plasmonic waveguides, plasmonic crystals, label-free bio- and chemo-sensors and for development nonlinear plasmonic structures with the enhanced nonlinearities. The high electromagnetic field confinement and hence enhancement makes these systems ideally suited to the creation of active plasmonic devices by hybridization with nonlinear optical materials or sensing applications which benefit from the large effective surface area in such self-assembled, template based materials.

In this talk we will overview applications of plasmonic nanorod metamaterial for designing new types of nanoscale waveguides, biosensing platforms and nonlinear optical devices with improved properties.

8093-46, Session 10

Enhanced transmission from a 2-D complementary metallic square array decorated with gold nanoparticles

M. J. Birnkrant, Air Force Research Lab. (United States); D. P. Brown, UES, Inc. (United States) and Air Force Research Lab. (United States); V. P. Tondiglia, SAIC (United States) and Air Force Research Lab. (United States); T. J. Bunning, A. M. Urbas, Air Force Research Lab. (United States)

Enhanced transmission from metallic hole arrays show promise as filters and environmental sensors. Recently, a subset of structures known as Metallic Complementary Arrays (MCA) have been studied. MCA are sandwich type structures that have a metal-insulator-metal (MIM) morphology. The MIM feature of MCA has one metal layer with complementary features to the other metal layer. These materials achieve selective transmission by matching plasmonic modes in the top and bottom layers. Understanding what influences the coupling between the two metal layers is not well understood. In this presentation we explore through simulation and experimentation a method for coupling the two metal complementary layers using nanoparticles. The MCA was fabricated using a modified interference-lithography technique to construct the insulator layer out of photoresist. Subsequently the metal layers were deposited through evaporation of gold. Finally nanoparticles were deposited on top of the MCA. The transmission spectra from a complementary array with nanoparticles showed enhanced transmission of light at wavelengths below the diffraction limit. Enhanced transmission below the diffraction limit is mediated by surface plasmon resonances. In the present case, the nanoparticles may act to impede surface plasmons on the MCA allowing for a number of surface plasmon modes to interact between the two metal layers. The influence of the impedance on the coupling between the two metal layers is investigated via nanoparticle coverage and separation distance.

8093-47, Session 10

Planar gradient index photonic metamaterials

Z. Wu, Toyota Technical Ctr., USA (United States)

Metamaterials operating at optical frequencies, referred to as optical or photonic metamaterials, require features fabricated at a subwavelength scale from 50 nm to 1000nm. In this work a planar gradient index metamaterial is designed and demonstrated at optical frequencies by numerical simulation through a finite-difference time domain method in conjunction with an electromagnetic retrieval technique. We confirm the gradient by simulating the deflection of a light beam passing through a multilayer silver (Ag) and magnesium fluoride (MgF₂) slab featured with specially designed nano-rectangular holes. The planar gradient index photonic metamaterials we propose can be fabricated by available nano-fabrication technologies. Optical tests can be performed since the designs are also based on the consideration of the frequency range available for evaluation. In this paper, we combined the graded index concept with the fishnet structure for the purpose of extending gradient index metamaterials into optical frequencies. We designed the fishnet unit cell with optimum refractive index range by tuning the unit cell dimensions. A commercial finite-difference time domain software package (CST MICROWAVE STUDIO), was used to calculate transmission and reflection coefficients, also known as S-parameters. A standard material parameter retrieval algorithm was developed to determine effective refractive index from transmission and reflection coefficients. Refractive indices as a function of unit cell geometry were used to the map index profile to the variation of unit cells. The electric field mapping simulations were utilized to show the beam forming mechanism. The light beam deflection was demonstrated by introducing the light passing through planar gradient metamaterial consisting of a multilayer Ag-MgF₂-Ag sandwich slab featured with specially designed and arranged fishnet unit cells. Unlike most of previous metamaterial gradient index designs, first, this was designed to operate in positive

Conference 8093:
Metamaterials: Fundamentals and Applications IV

index regime away from resonance to minimize losses; second, all of the patterned elements were planar which did not require volumetric unit cell; third, it was for optical frequencies.

8093-48, Session 10

Three-dimensional resonant guided wave networks

S. P. Burgos, E. Feigenbaum, H. A. Atwater, California Institute of Technology (United States)

It has recently been shown that resonant guided wave networks (RGWNs) are an artificial material class where the wave dispersion is controlled through strong coupling of local resonances throughout the waveguide network. In this work, we implement the RGWN concept at $\lambda = 1100\text{--}1600$ nm in three dimensions with a Cartesian mesh of regularly-spaced cylindrical plasmonic waveguides in a metallic mesh.

The RGWN concept is based on two basic types of elements: isolated waveguides, where the waves accumulate phase, and power-splitting junctions at the waveguide intersections. Due to the simplicity of these two basic network operations, it is possible to comprehensively describe the full network dynamics with a reduced numerical code, which greatly reduces computation time in comparison to full wave simulations and allows for an insightful study of the network dynamics.

The conditions required for designing three-dimensional plasmonic cavities as well as their dependence on wavelength and network layout will be presented. Furthermore, using the Q-factor analysis, we map the eigenmodes of finite-size networks, and we categorize their symmetry and degeneracy based on the steady-state time evolution of the energy density within the network. Lastly, by implementing Bloch boundary conditions instead of PMLs, the numerical code is also used to calculate the bandstructure of infinite 3D network layouts. This method of analysis illustrates the design potential of 3D-RGWNs, which can ultimately be used to program complex network dynamics and functions.

8093-49, Session 11

Optical forces in metamaterials

P. Tassin, R. Zhao, T. Koschny, C. M. Soukoulis, Iowa State Univ. (United States)

Since a few years, it has been proposed to harness optical forces, i.e., the forces that arise when linear momentum is transferred from photons to matter, in micro- and nanophotonic systems. Most attention was focused on optical forces in waveguides, where resonant waveguide modes enable forces on the space scale of the wavelength of light. Recently, we have extended such research to subwavelength structures. We start this communication with a study of optical forces in a prototype of metamaterial constituents--the nanowire pair. We show how the electric and magnetic dipole resonances lead to repulsive and attractive forces, respectively. However, the stacking of nanowire pairs in an array as in metamaterials may dramatically change the nature of optical forces, e.g., changing the forces associated with the electric dipole resonance from repulsive to attractive. In the second part of this communication, we show how the optical force can be exploited for the creation of nonlinear metamaterials. By optimizing a split-ring resonator structure for the enhanced interaction between the elastic and the electromagnetic modes mediated by the optical force, we demonstrate metamaterials with a transmission spectrum that depends on the power of the incident electromagnetic wave. This metamaterial thus allows for the switching of its transmittance by simply changing the incident beam power.

8093-50, Session 11

Electromagnetic forces on parallel plates cavity

J. Ng, Hong Kong Univ. of Science and Technology (Hong Kong, China); H. Liu, Nanjing Univ. (China); Z. Lin, Fudan Univ. (China); Z. Hang, C. Chan, Hong Kong Univ. of Science and Technology (Hong Kong, China); S. Zhu, Nanjing Univ. (China)

Metamaterials are man-made materials which possess unusual optical properties. These materials are often made from sub-wavelength metallic resonators. Most of the studies on these materials are focused on their optical properties, and the effect of optical forces associated with the excitation of resonances in these materials are much less discussed. In this talk, we will study the electromagnetic forces acting on resonating units comprising a simple parallel plate resonator made from gold. This simple system may serve as a prototypical building block of metamaterials. We first understand the physics using a qualitative Lagrangian model, and then full wave numerical simulation (CST microwave studio) is performed.

In microwave scale, gold behaves as perfect electric conductors. The two plates experience a repulsive force due to the leakage of electric fields at the edges. Even with a conventional microwave source (power ~ 15 mW), it is shown that the microwave force is significantly enhanced at resonance and it can lead to experimentally measurable forces.

In near infrared scale, we need to consider gold as a plasmonic material as the field can penetrate the plates. The two plates attract each other owing to a novel mechanism - the plasmon-induced kinetic energy of the conduction electron reduces the Faraday magnetic energy which induces attraction. We show that the optical forces in near infrared can be enhanced by orders of magnitude write respect to the usual photon pressure and it can be deployed to the manipulation of the cavity itself.

8093-51, Session 11

Electromagnetic radiation pressure on left- and right-handed dissipative media

H. Lezec, A. K. Agrawal, M. Abashin, S. Rajauria, National Institute of Standards and Technology (United States); K. J. Chau, The Univ. of British Columbia (Canada)

We investigate both experimentally and theoretically the radiation pressure exerted by a plane wave of visible-frequency light on a flat slab of dissipative material which is either left handed [1] or right handed (i.e. having electric permittivity and magnetic permeability which are both negative or both positive, respectively). We characterize the radiation-pressure response of an optical-frequency, broadband, left-handed metamaterial based on stacked Ag/Si/Ag plasmonic waveguides, each designed to be left-handed over most of the visible spectrum. A fully-absorbing flat slab of this metamaterial integrated onto a low-stiffness cantilever is shown to experience a pull when illuminated at normal incidence by a plane-wave of free-space wavelength in the range 460 nm to 600 nm. Radiation-induced pull is further confirmed by observation of levitation of free-standing slabs of the metamaterial under illumination at 532nm. An analytic model is proposed which is consistent with the spectral dependence of the measured pressure response. In this model, the real part of the effective refractive index of the metamaterial contributes to a proportionately-large, negative absorption force, which, when it exceeds the positive Lorentz force, yields in a net negative pressure on the object. The origin of the implied momentum-transfer non-equivalence between Lorentz and dissipative forces, related respectively to the wave and particle nature of the photon, is investigated through finite-difference-time-domain simulations of optomechanical pulse-slab interactions, as well as via interferometric measurements of the radiation-pressure response of thin films of high-index, dissipative, right-handed materials on silicon-nitride membranes. [1] V. Veselago, Sov. Phys. Usp. 10, 509-514 (1968).

Conference 8093:
Metamaterials: Fundamentals and Applications IV

8093-52, Session 12

Grating-assisted subwavelength far field imaging

V. A. Podolskiy, Univ. of Massachusetts Lowell (United States); S. Thongrattanasiri, N. A. Kuhta, Oregon State Univ. (United States)

High-resolution imaging is of interest for a broad class of applications spanning all parts of the electromagnetic spectrum. Unfortunately, conventional far-field imaging is fundamentally limited by the free-space wavelength. The diffraction limit can be halved with structured illumination microscopy where the spectrum of the incident light is effectively doubled via interference. Alternatively, in the far-field superlens, part of the evanescent radiation emitted by an object is resonantly enhanced via surface plasmon polaritons, and is subsequently converted into propagating waves with a subwavelength diffraction grating, again doubling the resolution. Here we present an approach capable of non-resonant imaging with resolution on the order of $1/20$ of the wavelength with far-field measurements.

The spectrum of a subwavelength focal spot is dominated by high-wavenumber components that exponentially decay away from the focal spot. The grating, that plays the role of image-reconstructing structure, located at the image plane, and translates the spectrum of the source by the multiple of inverse grating periods. This way, the diffraction gratings can convert the originally evanescent information into propagating waves which can be measured in the far field. Provided that the far-field measurements of the same object are performed for different values of incident angle, the contributions of different diffraction orders to the final intensity distribution can be separated from each other, and the original field distribution can be calculated.

Here we present a class of algorithms capable of recovering the subwavelength details of the objects and analyze the effect of imaging grating on image recovery

8093-54, Session 12

Gradient index metalenses for extraordinary light focusing

C. Ma, M. A. Escobar, Z. Liu, Univ. of California, San Diego (United States)

The lens is the most commonly used element in optical systems, which however can achieve only diffraction limited resolution at the scale of $\sim\lambda/2$, with λ being the working wavelength. Because of the versatile and exceptional designability of metamaterials, various superlenses have been proposed and demonstrated with resolving power beyond the conventional diffraction limit in the past decade. However, such superlenses behave remarkably different from their conventional counterpart. For instance, they cannot focus a plane wave due to the lack of phase compensation mechanism. We have recently proposed two types of phase compensated metamaterial lenses, i.e., the metamaterial immersion lens (MIL) and the metalens, which have super resolving power and are able to focus a plane wave to a spot. In this work, we proposed another type of phase compensated metalenses based on planar gradient-index (GRIN) or inhomogeneous permittivity metamaterials, which we refer to as GRIN metalenses. Using a generalized discretization method to analyze both the elliptically and hyperbolically dispersive GRIN metalenses, we investigate all the conditions of anisotropic GRIN material profiles required for both internal and external focusing. Simulation results show that the GRIN metalenses can achieve super resolution focusing and have ordinary or extraordinary Fourier transform functions. The extraordinary focusing behavior may enable exotic imaging applications.

8093-56, Session 12

Studies of plasmonic hot-spot translation by a metal-dielectric layered superlens

M. D. Thoreson, Purdue Univ. (United States) and Erlangen Graduate School in Advanced Optical Technologies (Germany); R. B. Nielsen, Technical Univ. of Denmark (Denmark); P. R. West, Purdue Univ. (United States); A. Kriesch, Max-Planck-Institut für die Physik des Lichts (Germany) and Erlangen Graduate School of Advanced Optical Technologies (Germany) and Cluster of Excellence Engineering of Advanced Materials (Germany); Z. Liu, Institute of High Performance Computing (Singapore); J. Fang, Purdue Univ. (United States); U. Peschel, Erlangen Graduate School in Advanced Optical Technologies (Germany) and Cluster of Excellence Engineering of Advanced Materials (Germany); A. Boltasseva, Purdue Univ. (United States) and Erlangen Graduate School of Advanced Optical Technologies (Germany) and Technical Univ. of Denmark (Denmark); V. M. Shalaev, Purdue Univ. (United States)

Single-layer and multilayer superlenses have been studied by a number of researchers in recent years. Most experimental studies have focused on the plasmonic operational regime that is limited to the near-UV range. Numerical studies have also predicted the existence of a canalization regime where superlensing occurs in a layered metal-dielectric system at wavelengths away from the plasmon resonance and into the visible range. This canalization regime has been experimentally observed in the microwave range. In this work, we have experimentally and numerically investigated superlensing in the visible range. By using the resonant hot-spot enhancements from optical nanoantennas as sources, we investigated the translation of these sources to the far side of a layered silver-silica superlens operating in the canalization regime. Using near-field scanning optical microscopy (NSOM), we have observed evidence of superlens-enabled enhanced-field translation at a wavelength of about 680 nm. Specifically, we discuss our recent experimental and simulation results on the translation of hot spots using a silver-silica layered superlens design. In this presentation we will compare experimental results with respective numerical simulations and discuss the perspectives and limitations of our approach.

8093-57, Session 12

Sub-wavelength imaging using stacks of metallic meander structures with different periodicities

P. Schau, K. Frenner, W. Osten, L. Fu, H. C. Schweizer, H. W. Giessen, Univ. Stuttgart (Germany)

Recently it has been questioned if bulk negative index materials (NIM) are really necessary for sub-wavelength imaging since it might not be possible to reduce losses in these materials to an acceptable degree. We suggest an alternative approach, which replaces a bulk NIM with two identical resonant surfaces that allow surface plasmon polariton propagation. The metallic meander structure, which is a thin metal film, corrugated periodically on both sides, acts as such a resonant surface. A direct resonant tunneling transmission of plasmons / photons is observed when two or more meander structures are stacked onto each other [1]. Recently, we have also found that stacks of meander structures with different periodicities show the same resonant tunneling transmission behavior when proper geometry parameters are used for each layer [2]. With respect to physical mechanisms we will explain in detail how changing structural parameters influences the optical properties of resonantly coupled surfaces. Furthermore, we will report on how the variation of the meander periodicity from layer to layer enables sub-wavelength imaging.

[1] P. Schau, K. Frenner, L. Fu, H. Schweizer, and W. Osten, "Coupling

Conference 8093:
Metamaterials: Fundamentals and Applications IV

between surface plasmons and Fabry-Pérot modes in metallic double meander structures,” in Proc. SPIE, Vol. 7711 2010, p. 77111F.

[2] P. Schau, K. Frenner, L. Fu, H. Schweizer, H. Giessen, W. Osten, “Design of high-transmission metallic meander stacks with different grating periodicities for subwavelength-imaging applications”, assigned to: Optics Express, Vol. 19, No. 4, 2011

8093-58, Session 13

Metamaterial models of exotic spacetimes

I. I. Smolyaninov, BAE Systems (United States)

We demonstrate that optical space in metamaterials may be engineered to mimic physics of various exotic spacetimes.

8093-59, Session 13

Frequency conversion by the transformation-optical analogue of the cosmological redshift

V. Ginis, Vrije Univ. Brussel (Belgium); P. Tassin, Iowa State Univ. (United States) and Vrije Univ. Brussel (Belgium); B. Craps, I. Veretennicoff, Vrije Univ. Brussel (Belgium)

Recently, there has been a lot of interest in electromagnetic analogues of general relativistic effects. Using the techniques of transformation optics, the material parameters of table-top devices have been calculated such that they implement several effects that occur in outer space, e.g., the implementation of an artificial event horizon inside an optical fiber, an inhomogeneous refractive index profile to mimic celestial mechanics, or an omnidirectional absorber based on an equivalence with black holes. In this communication, we show how we have extended the framework of transformation optics to a time-dependent metric—the Robertson-Walker metric, a popular model for our universe describing the cosmological redshift. This redshift occurs due to the expansion of the universe, where a photon of frequency ω_{em} , emitted at instance t_{em} , will be measured at a different frequency ω_{obs} at time t_{obs} . The relation between these two frequencies is given by $\omega_{obs} a(t_{obs}) = \omega_{em} a(t_{em})$, where $a(t)$ is the time-dependent scale factor of the expanding universe. Our results show that the transformation-optical analogue of the Robertson-Walker metric is a medium with linear, isotropic, and homogeneous material parameters that evolve as a given function of time. The electromagnetic solutions inside such a medium are frequency shifted according to the cosmological redshift formula. Furthermore, we have demonstrated that a finite slab of such a material allows for the frequency conversion of an optical signal without the creation of unwanted sidebands. Because the medium is linear, the superposition principle remains applicable and arbitrary wavepackets can be converted.

8093-60, Session 13

Geometric-optical studies for metamaterial representations of curved spacetime

T. H. Anderson, T. G. Mackay, The Univ. of Edinburgh (United Kingdom); A. Lakhtakia, The Pennsylvania State Univ. (United States)

Metamaterials offer opportunities to explore curved-spacetime scenarios which would otherwise be impractical or impossible to study. These opportunities arise from the formal analogy that exists between light propagation in vacuum curved spacetime and in a certain nonhomogeneous bianisotropic medium, called a Tamm medium. As the science and technology of nanostructured metamaterials continues its rapid development, the practical realization of Tamm mediums is edging ever closer. We considered two particular curved spacetimes associated with: (a) spinning cosmic strings, and (b) the Alcubierre drive. For both examples, a Tamm medium formulation was developed which is

asymptotically identical to vacuum and is therefore amenable to physical realization. A study of ray trajectories for both Tamm mediums was undertaken, within the geometric optics regime. For the spinning cosmic string, it was observed that: (i) rays do not cross the string’s boundary; (ii) evanescent waves are supported in regions of phase space that correspond to those regions of the string’s spacetime wherein closed timelike curves may arise; and (iii) a non-spinning string is nearly invisible whereas a spinning string may be rather more visible. For the Alcubierre drive, it was observed that: (i) ray trajectories are highly sensitive to the magnitude and direction of the warp bubble’s velocity, but less sensitive to the thickness of the transition zone between the warp bubble and its background; and (ii) the warp bubble acts as a focusing lens for rays which travel in the same direction as the bubble, especially at high speeds.

8093-61, Session 14

Collinear meta-acousto-optics and its application to tunable filters

P. P. Banerjee, G. T. Nehmetallah, Univ. of Dayton (United States)

Acousto-optics (AO) or diffraction of light by ultrasound, is used in numerous applications in signal processing, filtering, and image processing. In conventional AO (CAO), the acoustic group velocity has the same direction as the phase velocity, and hence, the acoustic propagation vector. However, in an acoustic metamaterial, dispersion may allow for negative phase velocity but positive group velocity. Therefore, interaction between light and ultrasound wave-vectors is different for noncollinear meta-AO (MAO), implying a new interpretation for upshifted and downshifted interactions [Banerjee, SPIE 7754 (2010)]. In this work, we investigate nominally collinear AO interaction in an acoustic metamaterial. We show that phase matching between the undiffracted and diffracted orders, not normally achievable in collinear CAO, can be satisfied using the dispersive acoustic behavior in MAO. For example, with zero acoustic refractive index, phase-matching between incident and diffracted orders is achievable in optically isotropic materials. Also, using negative acoustic refractive index, phase matching can be achieved using co-propagating incident optical field (e-polarized), diffracted optical (o-polarized) field, and pulsed ultrasound in positive uniaxial media. We develop heuristic theory and detailed model for collinear MAO for CW and multi-frequency (pulsed) ultrasound. Application of collinear MAO to spectroscopy using AO tunable filters is also investigated.

8093-62, Session 14

Plasmonic Bloch-Zener oscillations in metal-dielectric waveguide arrays

Y. Lan, R. Shiu, National Cheng Kung Univ. (Taiwan)

Plasmonic Bloch oscillations, an analog of electron Bloch oscillations in lattice, are periodic oscillations of optical beams that propagate in metal-dielectric waveguide arrays (MDWAs), which is caused by the alternating total internal reflection and Bragg reflection between the two boundaries of the waveguide arrays. When the electric field imposed on the lattice is increased, electron Zener tunneling will occur at the Brillouin zone boundary. However, plasmonic Zener tunneling has been never observed in MDWAs. Neither has the possibility that the optical beam tunneling into the next band will experience another Bloch oscillation been investigated. In this study, plasmonic Zener tunneling and the succeeding plasmonic Bloch oscillation in MDWAs are explored by performing both FDTD simulations and theoretical analyses. The MDWAs consists of alternative silver layers and dielectric layers. The relative permittivities of the dielectric layers have a constant gradient across the waveguide arrays. The plasmonic Zener tunneling is observed at the position of total reflection (Bloch wavevector $k_x=0$), which is caused by that the gap between the first and second equal- k_z (longitudinal wavevector) bands is minimum at $k_x=0$, originated from the effectively (transverse) negative refraction index of the MDWAs. The relation between tunneling rate and

Conference 8093:
Metamaterials: Fundamentals and Applications IV

permittivity gradient is elucidated. The FDTD-simulated contours of magnetic field intensity correlate well with the predicted ray trajectory using Hamiltonian optics. Furthermore, the tunneling beam is also observed to undergo Bloch oscillation in the FDTD simulation. This Bloch oscillation leads to beam's curling due to change of the direction of the energy flow. Depending on the geometry parameter, the curling beam will move backward, move forward, or even remain unmoved.

8093-63, Session 14

The Goos-Hänchen effect at the non periodic surface of a negative index metamaterial

V. Grünhut, M. A. Cuevas, R. A. Depine, Univ. de Buenos Aires (Argentina)

We present a rigorous analysis about the excitation of surface polaritons at a non periodic, rough interface between a conventional dielectric and a metamaterial with a negative index of refraction. In particular, we study the reflection of a Gaussian beam from a corrugated surface of finite length. We analyze the strong impact that surface polaritons have in the field reflected from this type of metamaterial rough surface and find new features of the well known Goos-Hänchen effect due to the resonant excitation of these surface waves. The dependence of the Goos-Hänchen lateral shift on the incident beam parameters is examined in detail and discussed in different situations among which is the total reflection case. We compare these characteristics with the limiting case of reflection of a beam from an infinitely periodic grating.

8093-64, Session 14

Anderson localization in one-dimension: quasiperiodic photonic bandgap structures

G. J. Kissel, Univ. of Southern Indiana (United States)

Existing in the "gray area" between perfectly periodic photonic bandgap structures and purely randomized photonic bandgap structures are the so-called "quasiperiodic" structures whose layers are chosen according to some deterministic rule rendering them aperiodic. We consider here a one-dimensional photonic bandgap structure, a quarter-wave stack, with the layer thickness of one of the bilayers subject to being either thin or thick according to various deterministic sequence rules. To produce these "quasiperiodic" structures we examine the following sequences: Fibonacci, Thue-Morse, Double Period, Rudin-Shapiro, as well as the triadic Cantor sequence. To make the approach as rigorous as possible, we model these structures numerically with a long chain (5,000,000 or greater) of transfer matrices, and then use the reliable algorithm of Wolf to calculate the (upper) Lyapunov exponent for the long product of matrices. The Lyapunov exponent is the statistically well-behaved variable used to characterize the Anderson localization effect (exponential confinement) when the layers are randomized, and so should likewise be calculated to ensure a proper characterization of the effect for the "quasiperiodic" systems. This is in contrast to some of the literature which avoids calculation of the Lyapunov exponent, or which calculates the Lyapunov exponent incorrectly. Calculating the Lyapunov exponent allows us to more precisely compare the purely randomized structure with its "quasiperiodic" counterparts. It is found that the "quasiperiodic" photonic systems show much fine structure in their Lyapunov exponents as a function of frequency, and, in a number of cases, the exponents are quite obviously fractal.

8093-65, Session 14

Near-field energy density enhancement in planar metamaterials

J. H. Shi, Harbin Engineering Univ. (China); C. Guan, Harbin Institute of Technology (China)

We theoretically investigate the positive/negative metamaterials with/without substrate built by asymmetrically split rings (ASRs) or asymmetrically split ring apertures (ASRAs) based on a full three-dimensional Maxwell finite element method. The asymmetry provides an easy and practical way to tune the electromagnetic response of metamaterials. The positive metamaterials on quartz glass and freestanding real metallic metamaterials show the quality factor of about 1000 and 1500, respectively. The near-field energy density enhancement 0.1 mm above the ASR metamaterial on glass substrate reaches at the ultra-high value of 150000, 500 times stronger than that of fundamental dipole resonance. The energy density enhanced factor attenuates to be one tenth only increasing the distance above the meta-surface to 0.5mm. The ultrahigh-Q trapped-mode resonances excited by broken structures confine most energy to a very small region of the surface of metamaterials. The freestanding metallic metamaterial will be good candidate to practical applications in microwave and terahertz range while increasing the thickness of quartz and choosing appropriate fabrication may pave the way to the practical design of the metamaterials on glass substrate. The low-loss trapped-mode metamaterials will be expected further and this tunable trapping of electromagnetic energy is of interest for new non-linear and switchable metamaterials, ultrasensitive media for chemical or biosensing and new types of optical switches.

8093-66, Session 14

Waveguide characteristics for arbitrary permittivity and permeability including for metamaterials

B. R. Lavoie, P. M. Leung, B. C. Sanders, Univ. of Calgary (Canada)

We calculate dispersion, absorption, power flow, and effective width vs input-field frequency for 3-layer slab and circular waveguides wherein the dielectric permittivity and magnetic permeability can both be arbitrary response functions for each of the media. Either permittivity or permeability is also allowed to be identically zero. We study the electromagnetic field behaviour at interfaces between these media and consider, as examples, heterogeneous waveguides based on a dielectric medium enclosed by metal or a metamaterial (including a negative-index metamaterial), i.e. dielectric-metal or dielectric-metamaterial waveguide. Our analysis provides a seamless model that accounts for dielectric-dielectric, dielectric-metal, and dielectric-metamaterial waveguides, and our results highlight that dielectric-metamaterial waveguides show reduced attenuation.

We treat metallic media according to the Drude model and metamaterial media with a modified Drude model that effectively models the magnetic response of the metamaterial. The modified Drude model is appropriate because its predictions are compatible with existing empirical results on metamaterials. Using these models we are then able to model the expected surface modes for metal or metamaterial waveguides; this surface mode is absent in the dielectric-dielectric waveguide. We show that, unlike the lossy surface mode for the dielectric-metal waveguide, which allows only the transverse-electric polarization, the dielectric-metamaterial waveguide can sustain either transverse-electric or transverse-magnetic polarizations with reduced loss.

8093-67, Session 15

Exotic properties of spinning particles metamaterials

A. Asenjo-Garcia, A. Manjavacas, Consejo Superior de Investigaciones Científicas (Spain); J. García de Abajo, Consejo Superior de Investigaciones Científicas (Spain) and Univ. of Southampton (United Kingdom)

We will present exotic electromagnetic properties of assemblies of spinning particles, including light amplification and extreme optical properties.

8093-69, Session 15

density functional study of spin polarization on a carbon material induced by iron atoms

M. M. Rahman, Univ. Putra Malaysia (Malaysia)

We investigate the spin polarization of a non magnetic material, e.g., a carbon material made from ten C atoms forming a hexagonal structure with total spin $S=0$, induced by a ferromagnetic material, e.g., two Fe atoms with a total spin $S=4$. Based on the density functional theory, we calculate the total spin density of the system. Our preliminary results show that the total spin for the ten C atoms changes from $S=0$ to $S=2$, while the total spin of the two Fe atoms changes from $S=4$ to $S=0$. These results seem to indicate that there is a promising possibility to induce spin polarization on a carbon material by Fe atoms.

References:

- [1] M. F. Crommie, C.P. Lutz and D.M. Eigler, *Science* 262, 218 (1993).
- [2] F. Komori, and K. Nakatsuji, *J. Phys. Soc. Jpn.* 68, 3786 (1999).
- [3] H. Nakanishi, H. Kasai, and A. Okiji, *Surf. Sci.* 493, 757 (2001).

8093-70, Session 16

Applied metamaterials

A. M. Urbas, Air Force Research Lab. (United States)

Metamaterials redefine the fundamental properties of systems by creating artificial, meso-scale meta-atoms which dictate the system response to external fields. When assembled into complex, structured materials, these meta-atoms and their mutual interactions can yield effective property sets not found in conventional materials and response tailored to specific application needs. The concept of defining the material properties with structure extends beyond electromagnetics to mechanical and thermal characteristics as well. Significant interest lies in the development of novel metamaterials structures and designs for electromagnetic and mechanical systems that possess properties optimized for selected applications. Key challenges are to develop capabilities to fully analyze the properties of these systems computationally and experimentally, to extract truly representative effective properties, and to understand the effectiveness of materials in an applications context. In the midst of this rapidly evolving field, AFRL is conducting a program to determine the utility of metamaterials in applications, evaluate their technological relevance and identify areas where focused efforts can enable rapid technological insertion. An overview of current research and application potential will be presented.

8093-71, Session 16

Highly sensitive nanostructured SnO₂-based sensors for hydrogen sensing

L. A. Patil, Pratap College (India)

Nanostructured SnO₂ thin films were prepared by ultrasonic spray pyrolysis technique. Aqueous solution (0.05 M) of SnCl₄·5H₂O in double distilled water was chosen as the starting solution for the preparation of the films. The stock solution was delivered to nozzle with constant and uniform flow rate of 70 ml/h by Syringe pump SK5001. Sono-tek spray nozzle, driven by ultrasonic frequency of 120 kHz, converts the solution into fine spray. The aerosol produced by nozzle was sprayed on glass substrate heated at 150 oC. The sensing performance of the films was tested for various gases such as LPG, hydrogen, ethanol, carbon dioxide and ammonia. The sensor (30 min) showed high gas response ($S = 3040$ at 350 oC) on exposure of 1000 ppm of hydrogen and high selectivity against other gases. Its response time was short (2 s) and recovery was also fast (12 s). To understand reasons behind this uncommon gas sensing performance of the films, their structural, microstructural, and optical properties were studied using X-ray diffraction, electron microscopy (SEM and TEM) respectively. The results are interpreted.

8093-72, Session 16

Data transmission performance of CVD grown sub-20 nm indium antimonide nanowires

A. B. Guvenc, M. V. Penchev, J. Zhong, C. S. Ozkan, M. Ozkan, Univ. of California, Riverside (United States)

We investigated the data transmission performance of indium antimonide (InSb) nanowires (NWs) synthesized on InSb (100) substrate using chemical vapor deposition (CVD) having diameters below 20 nm. The data transmission measurements were accomplished on the NW field effect transistors (NWFETs) fabricated on Si/SiO₂ substrates. The mobility values of the NWs were calculated from the transconductance, $g = dI_{ds}/dV_{gs}$, in which I_{ds} and V_{gs} values are acquired from the back gate measurements. Digital data stream is randomly generated and then uploaded to a waveform generator which generates the stream and transmits it repeatedly with the desired frequency. The signal was applied on the sources of the NWFETs and collected from the drains of the same devices. During the data transmission measurements no back gate voltage was applied. Collected data was first filtered with a low pass filter (LPF), to clear the noise and the high frequency parasitic effects then the output of the filter was used to create the eye diagrams of the NWs and by using these eye diagrams, the bit error rates (BERs), attenuation values, quality factor (Q-factor) values and maximum data transmission values are calculated. The results indicate that the data transmission performance of NWs suffer from low mobility values on the order of 10- to-15 cm²V⁻¹s⁻¹ because of their small diameters, crystal defects and oxidation occur during growth and cooling. 20 nm NWs can sustain data rates up to 10 mega bits per second (Mbps) and the data rate is directly proportional to the diameter of the NWs.

8093-73, Session 16

Surface-enhanced infrared absorption and refractive index sensing with highly compliant metamaterials

I. M. Pryce, Y. A. Kelaita, K. Aydin, R. M. Briggs, H. A. Atwater, California Institute of Technology (United States)

Surface enhanced spectroscopic techniques are used widely for chemical detection, and the sensitivity of such sensors depends on the high electric field intensities of nanostructured surfaces. Typically, sensors are limited by their constituent materials at fabrication. Ideally, however, they would be tunable and operate over a broader bandwidth. We propose an approach to designing tunable sensors that exploits the compliance of PDMS. We use split-ring resonator (SRR) based metamaterials as resonantly enhanced sensors and exploit the elastic and plastic deformation properties of PDMS to design tunable metamaterials where greater than linewidth tunability can be achieved. This tunability is used to both enhance absorption from vibrational modes by aligning the resonant frequency of the metamaterial and detect small changes in refractive index.

We fabricate Au SRRs in 100 μm arrays on Si and transfer the patterns to PDMS using a hard/soft nanolithographic pattern transfer technique. The resonators are functionalized with p-mercaptoaniline (pMA). FTIR reflection spectra are measured between 1.5 and 8 μm and we report the change in reflection, ΔR , corresponding to the surface-enhanced absorption of particular vibrational modes. ΔR values of up to 5% are shown and the limit of detection of vibrational modes as a function of strain will be discussed. We also demonstrate the use of these metamaterials as refractive index sensors and measure refractive index sensitivity values as high as 2070 nm/RIU (150 meV/RIU). We will discuss how inducing strain in the PDMS changes the resonator shape and improves the figure of merit for sensitivity.

8093-74, Session 16

Design and fabrication of a chitosan based integrated optical device for humidity sensing

A. Mironenko, Institute of Chemistry (Russian Federation)

Recently, polymers and polymer/inorganic hybrids have become of great interest for development of optical waveguides with tailored optical properties. Due to high availability, relatively low cost and good film-forming properties of some of the natural polymers, their use can be considered as an alternative to molecular design of synthetic polymers for optoelectronic applications. Aminopolysaccharide chitosan is one of the most promising biopolymer-candidates for development of optical waveguides and sensor [1, 2]. Advantages of chitosan are not limited to its easy processability. Refractive index of chitosan film can be tailored via metal ions binding, in-situ reduction and stabilization of metal nanoparticles [3] or incorporation of optically active inorganic nanocrystals into the polymer thin film. Moreover, interactions of chitosan, as a hydrophilic polybase, with organic solvents, water vapor, mineral and organic acids change level of polymer hydration and/or protonation degree, and thus, optical properties of the film that is beneficial for sensing application.

Here we report on preparation of optical waveguides and humidity sensors based on chitosan in different salt forms, chitosan/gold nanoparticles and chitosan/gold nanoparticles/silica hybrids with layered structure. Chitosan-based optical waveguides were obtained on quartz, glass and MgF₂ substrates by spin-coating and dip-coating. For investigation of optical properties, the light (wavelength 632 or 532 nm) was coupled into the planar waveguide via the flint glass prism using goniometer. A number of modes, effective refractive index, waveguide propagation losses were determined for all samples in the range of relative humidity 10-99%. It was demonstrated that chitosan-based thin films could be used as humidity sensors with fast response time (0.3-1 s), and highest sensitivity was found for chitosan/gold nanoparticles/silica hybrids with layered structure.

References

1. Optical Waveguiding and Morphology of Chitosan Thin Films. Hao JIANG, W. SU, S. CARACCI, T. J. BUNNING, T. COOPER, and W. W. ADAMS// *Journal of Applied Polymer Science*, Vol 61, 1163-1171, 1996
2. Yoshiaki KURAUCHI, Tohru OGATA, Naoyoshi EGASHIRA and Kazuya OHGA. Fiber-Optic Sensor with aDye-Modified Chitosan/Poly(vinyl alcohol) Cladding for the Determination of Organic Acids//*ANALYTICAL SCIENCES FEBRUARY* Vol. 12, p.55-59, 1996
3. Huang HZ, Yang XR: Synthesis of polysaccharide-stabilized gold and silver nanoparticles: a green method *CARBOHYDRATE RESEARCH* Vol. 339(15), P. 2627-2631, 2004

8093-75, Session 16

Bridging fiber optics with metamagnetics

X. Wang, G. Venugopal, J. Zeng, D. Lee, N. M. Litchinitser, A. N. Cartwright, Univ. at Buffalo (United States)

A majority of naturally existing optical materials are non-magnetic. In the past few years, it was shown that metamaterials can fundamentally change light-matter interactions by bringing the magnetic component of the field into play. Magnetism at optical frequencies may lead to new fundamental physics and novel applications, including negative index of refraction, super-resolution, and unprecedented opportunities for manipulating light trajectories in space (e.g., cloaking). Recently, Cai et al. demonstrated that coupled nano-strips with varying dimensions enable optical magnetic responses across the whole visible frequency range.

To date, optical metamaterials were primarily demonstrated in a form of thin films with thicknesses on the order of or less than the optical wavelength on a substrate. In order to use them in applications such as photonic integrated circuits or on-chip sensing devices the light in- and out-coupling issue should be solved. Thus, waveguide-coupled metamaterials would be desirable. Fiber optics is a mature technology

that enables long-distance, low-loss light delivery. Therefore, merging this mature fiber optics technology with the emerging metamaterials technology would likely enable a plethora of novel applications.

In this talk, we propose and experimentally demonstrate for the first time a fiber-coupled magnetic metamaterial structure. As an example, we demonstrate coupled nano-strip structures developed directly on the face of optical fiber that can serve as building blocks for more complex components such as multi-modality sensors (capable of measuring several properties of the sample at once), sensor arrays, imaging devices, ultra-compact components for photonic integrated circuits, and more.

8093-76, Session 16

Resonant coupling of dielectric waveguides with plasmonic metaatoms

T. Kaiser, C. Helgert, T. Paul, S. B. Hasan, F. Lederer, C. Rockstuhl, T. Pertsch, Friedrich-Schiller-Univ. Jena (Germany)

Metamaterials promise the possibility to tailor the propagation properties of light at the nano-scale. With this contribution we explore the possibility to combine the concept of metamaterials with integrated optics.

We investigate a system consisting of a one-dimensional array of double cut-wires (two very thin gold sheets separated by a dielectric spacer) placed on top of a dielectric slab waveguide, which supports only the fundamental TE and TM mode in the near infrared spectral region around 1550 nm. Strong coupling of the waveguide modes to the plasmonic eigenmodes of the double cut-wire is achieved via the longitudinal component of the electric field, being relatively large for an asymmetric refractive index profile. By tuning the length of the double cut-wires, we can tune the spectral position of the occurring hybrid resonance. We will show by rigorous calculations, that the resonance is anti-symmetric and hence produces artificial magnetism at optical frequencies in this simple scheme.

To further explore the physics of the system, we investigate the dispersion relation of a periodic array of double cut-wires with varying lattice periods. The slab waveguide mode leads to a coupling of the individual plasmonic nanostructures. We find that for short lattice periods the dispersion closely resembles that of the slab waveguide. However when the Bragg frequency approaches the plasmonic resonance frequency, a strong interaction takes place and leads to a back-bending of the dispersion relation with regions of negative group velocity near to the band edge while an avoided crossing of both resonances takes place.

Conference 8094: Nanophotonic Materials VIII

Wednesday–Thursday 24–25 August 2011 • Part of Proceedings of SPIE Vol. 8094
Nanophotonic Materials VIII

8094-01, Session 1

Lu₂O₃:Eu³⁺ nanocrystalline powders for nanophotonics materials

D. A. Nadiia, O. M. Vovk, R. P. Yavetskiy, Institute for Single Crystals (Ukraine)

In recent years observed an increasing interest in the scientific community to nanophotonic materials, such as radiation detectors, display device, devices for medical diagnosis, waveguides, modulators. Unique optical properties of such materials can be artificially created and controlled by choice properties of source nanoparticles. Should take into account a number of general requirements to be met by powders, regardless of the application in nanophotonics is a single-phase, compliance stoichiometric composition and low degree of aggregation. The diameter and morphology of nanocrystalline powders are among main critical factors determining their surface activity and possibility to obtain new functional materials. The question of influence phase and chemical composition of precursor on properties of nanocrystalline oxide powders and hence the properties of nanophotonic materials has attracted insufficient attention, thus it became the object of our work.

Lu₂O₃:Eu³⁺ nanocrystalline powders are considered as a promising “structural units” for creation of nanophotonics materials, such as optical ceramic, X-ray screens [1,2]. Metastability of the phase composition of precursors, which manifests itself in the coexistence of amorphous and crystalline phases Lu(OH)(CO₃)·nH₂O, leads to the formation after calcination at T=800°C well dispersed Lu₂O₃:Eu³⁺ nanopowders (average size of 25 nm, specific surface 25 m²/g). This nanopowder show excellent sinterability and favorable morphological features for their use in optical ceramic technology for radiation detectors or devices for medical diagnosis.

[1]. Dulina N.A., Yermolayeva Yu.V., Tolmachev A.V., Journal of the European Ceramic Society // 30 (2010) 1717–1724.

[2] Dulina N.A., Deineka T.G., Yavetskiy R.P., Ceramics International // in press.

8094-02, Session 1

Silanization of PECVD-grown silicon quantum dots for optoelectronics applications

I. E. Anderson, R. Shircliff, B. N. Jariwala, S. Agarwal, Colorado School of Mines (United States); P. S. Stradins, National Renewable Energy Lab. (United States); R. T. Collins, Colorado School of Mines (United States)

Semiconductor quantum dots have been the subject of intense research interest due to novel experimentally observed properties, such as tunable bandgap, phonon bottleneck, and a variety of surface effects. The control of these properties makes quantum dots a candidate for revolutionizing a variety of fields, including photovoltaics, optoelectronics, and biological imaging, labeling and sensing. Silicon, a material that is well characterized in its bulk form, may be most relevant to the fields that quantum dot research has aimed to metamorphose. For example, Si is relatively inert and may be an excellent biological sensor; its indirect gap may become more direct as size decreases, allowing for a fine-tuning of the absorption characteristics for photovoltaics and the emission characteristics for light-emitting devices. We present a plasma-based method for Si quantum dot synthesis coupled with a silanization passivation method. Functionalization with silanes enables creation of a stable, colloidal solution of dots, as measured by photoluminescence peak shift, transmission electron microscopy, and light scattering. Silanization requires an oxide shell around the Si core, alleviating concerns about oxidation and processing in an inert atmosphere, and can be performed on free-standing dots created by any synthetic method.

Unpassivated Si quantum dots show vastly different behaviors in photoluminescence and electron paramagnetic resonance than wet-chemically oxidized, silane-functionalized particles. The relative stability, dangling bond density, and relationship to quantum yield for these two populations will be discussed, in addition to their viability as building blocks for solution-processed optoelectronics devices.

8094-03, Session 1

Development of precise tuning method of inter-dot spacing and resonant energy transfer between Au clusters

M. Inada, Y. Yoshihara, H. Kawasaki, Y. Iwasaki, T. Saitoh, Kansai Univ. (Japan); I. Umezumi, A. Sugimura, Konan Univ. (Japan)

Nanostructure materials have attracted much attention in recent years for their potential applications. In particular, nanomaterial electronic structures consisting of coupled quantum dots such as in nanocrystal arrays are of considerable interest both fundamentally and technologically, because such electronic structures can be described as Hubbard models due to the competing effects between quantum size and interdot coupling. In addition, ultra-small Au clusters have molecular-like discrete energy structure, which induces distinctive features such as strong photoluminescence (PL) and ferromagnetism, etc. Therefore it is interesting to study a correlation between inter-dot space and collective properties of Au clusters. However it is difficult to control the inter-dot spacing with sub-nanometer resolution. In this study, we report on a development of precise tuning method of quantum-dot spacing and investigate fluorescence resonant energy transfer in Au clusters.

The tuning device consists of a DC motor and capacitance-positioning sensor. After Au nano-clusters, which include Au₅, Au₈ and Au₁₃ clusters, were deposited on poly(dimethylsiloxane) film, the film was gently and continuously stretched by the DC motor. The degree of stretching was monitored by the capacitance-positioning sensor. We investigated the PL spectra of Au clusters and we found the blue shift of the PL peak with stretching the film. This peak shift caused by the emission enhancement and quenching from smaller clusters and the larger clusters, respectively. So the stretching the film means an increase the inter-dot spacing, the result can be explained as fluorescence resonant energy transfer from smaller cluster to larger one.

8094-04, Session 1

Si quantum dots and different aspects of applications.

T. V. Torchynska, Instituto Politécnico Nacional (Mexico)

This presentation will discuss the different aspects of the application of Si quantum dots in quantum electronics, such as: light emitting and photonic devices, solar cells and memory structures, one electron transistors and spintronics [1]. The special attention will be paid to the comparison of optical parameters of crystalline and amorphous Si quantum dots embedded in the hydrogenated amorphous silicon (a-Si:H). Nanocrystalline silicon films (nc-Si:H) that are silicon nanocrystals or quantum dots embedded in the hydrogenated amorphous silicon matrix that considered as a promising candidate for the low cost and high efficiency solar cells have been analyzed as well.

[1] “Nanocrystals and quantum dots of group IV semiconductors”, Editors: T. V. Torchynska and Yu. Vorobiev, American Scientific Publisher, 2010, 300p. ISBN: 1-58883-154-X.

8094-05, Session 2

Engineering aperiodic order for optical devices with photonic-plasmonic nanostructures

L. Dal Negro, Boston Univ. (United States)

Deterministic Aperiodic Structures (DAS) are generated by the mathematical rules of L-systems and number theory, manifest unique light localization and transport properties associated with a great structural complexity, and can be fabricated on-chips using conventional nano-lithographic techniques. When combined with metal-dielectric nanostructures, they give rise to large energy gaps like periodic media (i.e. photonic-plasmonic crystals) and highly localized, enhanced field states like disordered random media, including the formation of Anderson-localized modes, forbidden in periodic scattering media. Contrary to random media, DAS possess controllable transport properties from ballistic to anomalous diffusion (slower diffusion than classical random walks) and strongly localized field states with large fluctuations of the photonic mode density - essential attributes to achieve spatio-temporal energy localization and enhanced light-matter coupling, i.e. radiative rates of fluorescent molecules, absorption cross-sections, non-linear optical processes on the nanoscale. In particular, DAS fabricated using metal/dielectric nanoparticles are suitable to engineer efficient nanoplasmonic structures for Surface Enhanced Raman (SERS) sensing, optical detectors, and enhanced light-emitting and nonlinear components.

In this talk, by combining dark-field scattering characterization, micro-photoluminescence and Raman measurements with accurate electro-dynamics calculations based on semi-analytical multiple-scattering theories, I will discuss electromagnetic coupling^{1,2}, resonant scattering³, colorimetric biosensing⁴, light emission⁵ and surface enhanced Raman sensing^{6,7} in two-dimensional metal-dielectric photonic-plasmonic arrays based on deterministic aperiodic sequences. In particular, I will survey the optical properties, and assess the device performances, of different aperiodic systems ranging from quasi-periodic crystals to pseudo-random nanoparticle arrays⁸ fabricated by Electron-Beam Lithography (EBL) on transparent quartz substrates. Finally, I will present novel aperiodic optical nano-antennas structures that can provide strong field localization at multiple frequencies over a broad spectral range⁹.

References:

1. L. Dal Negro, N.N. Feng, A. Gopinath "Electromagnetic coupling and plasmon localization in deterministic aperiodic arrays", *J. Opt. A: Pure Appl. Opt.* 10, 064013 (2008)
2. C. Forestiere, G. Miano, G. Rubinacci, L. Dal Negro, "Analysis of localized modes and spectral gaps in Fibonacci arrays of metal nanoparticles", *Phys. Rev. B.*, 79, 085404 (2009)
3. A. Gopinath, S. Boriskina, N.N. Feng, B.M. Reinhard, L. Dal Negro, "Photonic-plasmonic scattering resonances in deterministic aperiodic structures", accepted for publication in *Nanoletters* 8, 2423 (2008)
4. S. Boriskina, L. Dal Negro "Sensitive label-free biosensing using critical modes in aperiodic photonic structures", *Optics Express*, 16, 12511 (2008)
5. A. Gopinath, S. Boriskina, S. Yerci, R. Li, L. Dal Negro, Enhancement of the 1.54 μ m Erbium emission from quasi-periodic plasmonic arrays, *Appl. Phys. Lett.*, 96, 071113 (2010)
6. A. Gopinath, S. Boriskina, B. Reinhard, L. Dal Negro, "Deterministic Aperiodic Arrays of Metal nanoparticles for surface-enhanced Raman scattering", *Optics Express*, 17, 3741 (2009).
7. A. Gopinath, S. Boriskina, W. Premasiri, L. Ziegler, B. Reinhard, L. Dal Negro, "Plasmonic Nanogalaxies: multi-scale aperiodic arrays for surface enhanced Raman sensing", *Nanoletters* 9, 3922 (2009)
8. C. Forestiere, G.F. Walsh, G. Miano, L. Dal Negro, "Nanoplasmonics of prime number arrays", *Optics Express* 17, 24289 (2009)
9. S. Boriskina, L. Dal Negro, "Multiple-wavelength plasmonic nano-antennas" *Optics Letters*, 35, 538, (2010).

8094-06, Session 2

Plasmonic light trapping in nanostructured metal surfaces

A. Polyakov, Lawrence Berkeley National Lab. (United States) and Univ. of California, Berkeley (United States); H. A. Padmore, S. Cabrini, S. D. Dhuey, B. D. Harteneck, X. Liang, P. J. Schuck, Lawrence Berkeley National Lab. (United States)

Metals are commonly used as ultra-fast photoemitters for Free Electron Lasers[1] and as field concentrators for generation of harmonics in a laser-driven plasma. In these applications high optical reflectivity is problematic[1]. This is especially true of gold, silver, and aluminum, which are all efficient reflectors due to their free-electron like behavior. However, by collective excitation of electrons in the form of a plasmon, free-electron metals can completely absorb light[2]. In this work, we demonstrate a practical realization of a new method recently proposed theoretically[2] where light is converted into plasmons, which are trapped in nano-grooves (NGs).

The typical dimensions for the NGs are 10-15nm in width and 30-40nm in depth spaced few hundred nanometers apart. The fabrication steps are: (a) the initial template is made by electron beam lithography from the HSQ resist on the Si substrate (b) gold is evaporated on the template, (c) the template is removed from the gold structure in the KOH bath. The cross section analysis of the resulting gold structure revealed the slanted walls of the NG, which contributed to the reduced sample absorption efficiency (measured absorption is 80% of the theoretical model with perfect NG geometry). Comparison of the experimental data to the Finite Difference Time Domain (FDTD) modeling-based on the profile measurements-is a good agreement.

[1] P. Musumeci et al., *Phys. Rev. Lett.* 104(8), 084801 (2010).[2] J. L. Perchec et al., *Phys. Rev. Lett.* 100(6), 066408-4 (2008).

8094-07, Session 2

All-inorganic quantum-dot light-emitting diodes with metal oxide as charge transport/injection layers

Y. Zheng, L. Qian, R. Zhou, P. H. Holloway, J. Xue, Univ. of Florida (United States)

Light-emitting diodes (LEDs) employing colloidal semiconductor quantum dots (QDs) as emitting layers (EML) have received significant scientific and technological interests. Currently, charge injection/transport layers comprised of conjugated polymers or thermal evaporated small organic molecules are widely used in QD-LEDs in order to achieve high efficiency emission. However, these organic charge transport/injection layers suffer from inferior thermal stability and low charge mobility compared to inorganic materials, and are more susceptible to degradation induced by oxygen and/or water. Here, we have demonstrated two different types of all-inorganic QD-LEDs using metal oxides as charge injection/transport layers. By using thermal evaporated MoO₃ as a hole transport layer and ZnO nanoparticles as an electron transport layer, we have demonstrated red, green, and blue light-emitting QD-LEDs with performance approaching those of conventional quantum-dot LEDs with organic charge transport layers. For example, the green QD-LEDs we fabricated show a maximum luminance of 9,000 cd/m², a peak luminance power efficiency of 1.74 lm/W, and an external quantum efficiency of 1.3. We also demonstrated a novel all-solution processable inorganic QD-LEDs in which the vacuum deposited oxide layer was replaced with a solution deposited oxide nanoparticle layer. Our data show that superior device performance can be achieved by improving hole injection from the oxide layer into the QD EML, which requires engineering of the heterojunction formed between the QDs and the hole transport oxide layer. All-inorganic QD-LEDs have the potential to serve as low-cost, efficient and stable light sources for display and solid-state lighting applications.

8094-08, Session 2

Stability of organic nanowires

F. Balzer, M. Schiek, Univ. of Southern Denmark (Denmark); I. Wallmann, A. Schäfer, A. Lützen, Rheinische Friedrich-Wilhelms- Univ. Bonn (Germany); H. Rubahn, Univ. of Southern Denmark (Denmark)

Organic nanowires from light-emitting conjugated oligomers might become the key ingredient for organics based optoelectronic devices. Different methods for nanowire growth have been pursued in the past such as filling of nanoporous templates, organic molecular beam deposition, and precipitation from solution. The morphological stability of such nanowires with time, in the presence of various gases, and under thermal load is of major importance for their use in any device. In this study the stability of organic nanowires from para-phenylenes, thiophenes, and from naphthyl end-capped thiophenes grown by organic molecular beam epitaxy is investigated via atomic force microscopy and optical spectroscopy. Simple aging experiments under ambient conditions already show substantial changes. Nanoscopic organic clusters, which initially coexist with the nanowires, vanish within hours, whereas wires develop facets and even break up into smaller ones within days. The influence of various gases such as water vapor, oxygen, and nitrogen is investigated to clarify the underlying mechanisms. Thermal annealing of nanowire samples leads to even more pronounced morphology changes, such as a strong decrease in nanowire number density, a strong increase in nanowire height, and the formation of new types of crystallites. This happens even before sublimation of organic material starts. These experiments also shine new light on the formation process of the nanowires.

8094-09, Session 3

Light collimation and resonance in composite negative/positive index photonic crystals

J. Zhang, S. Dhuey, B. D. Harteneck, Y. Wu, D. Olynick, X. Liang, S. Cabrini, Lawrence Berkeley National Lab. (United States)

The negative refraction in photonic crystals (PC) is due to the negatively sloped band folding effect of a strongly modulated PC. However, a negative index PC cannot fulfill some physical functions alone because light diverges after self-focusing. We report two structures composed of super lattice Bragg media of both negative and positive refraction index on SOI wafer for confining light in collimation or resonance. The first structure is composed of positive index air slab ($n=1$) and negative index PC slab ($r=180$ nm, $a=470$ nm, $n=-1$) periodically. Each PC strip has a length of isolated by an air slab with a length of λ . The structure shows the zero-average-index condition at the communication wavelength and allows light propagation in collimation. The two termination interfaces of each PC slab assist electromagnetic wave coupling into the waveguide with maximum transmission. Laser at $1.55\mu\text{m}$ propagates 2 mm long without diffraction as our measurements. The second structure is a periodical arrangement of negative index PC ($n=-1$) and positive index air ($n=1$) both in equal-lateral triangle shapes. By choosing of the symmetric equal-lateral triangle shape, light can fold back at the interface of opposite index media and resonant within this structure. The simulation of $1.55\mu\text{m}$ wavelength propagation in TM polarization has been done by Rsoft. In conclusion, we are going to report light manipulating by two photonic crystal structures composed of opposite index media. The latest fabrication, simulation and optical measurement results will be presented in the conference.

8094-10, Session 3

Photonic crystal patterning of luminescent sol-gel films for light extraction

A. Revaux, G. Dantelle, Ecole Polytechnique (France); D.

Decanini, Ctr. National de la Recherche Scientifique (France); F. Guillemot, Ecole Polytechnique (France); A. Haghiri-Gosnet, Ctr. National de la Recherche Scientifique (France); C. Weisbuch, J. Boilot, T. Gacoin, Ecole Polytechnique (France); H. Benisty, Institut d'Optique Graduate School (France)

For enhanced light extraction, the surface of sol-gel layers containing luminescent centers is patterned by nano-imprint lithography with a square photonic crystal (PhC). Light has to be guided in the slab rather than emitted toward the substrate to be efficiently extracted by the PhC. To increase the light fraction guided in the sol-gel layer, titania sol-gel films ($n\sim 1.7$) are chosen rather than usual silicones ($n\sim 1.5$) and a low-index layer of porous latex-templated silica is inserted between the substrate and the TiO₂ film (porous down to 1.16).

To study the effect of the structure of the film itself, we developed model sol-gel waveguides including europium chelates as emitters, which do not induce any microstructure effects (no light scattering). Furthermore, the large Stokes shift and the small absorption cross-section of the chelate at its emission peaks discard reabsorption losses and ensure long propagation distances.

Chelates are spectrally and spatially coupled to the resonant modes of the PhC and the guided light is extracted via leaky modes to free space. We investigate the interaction between the guided mode and the PhC and the role of the porous underlayer with angle-resolved luminescence measurement and complementary simple simulations. This study gives access to the structure and the extraction strength of the guided modes, as well as the cladding influence on them. The role of an underlying porous layer that avoids leakage to the glass substrate has notably been revealed, with critical porous fraction thresholds identified for allowing guided modes to be seen, notably TM modes.

8094-11, Session 3

Controlling polarization anisotropy of site-controlled InAs quantum dots on InP nanopyramids using selective-area epitaxy

J. Yuan, Technische Univ. Eindhoven (Netherlands)

We have studied the shape and polarization control of site-controlled $1.55\text{-}\mu\text{m}$ -region multiple and single InAs QDs on InP (100) pyramids grown by selective-area metalorganic vapor phase epitaxy (MOVPE). The QD size increases with the elevated growth temperature and the QDs strongly elongate which is attributed to increasing As/P exchange. The linear excitation power-dependent PL efficiency reveals negligible nonradiative carrier recombination in single QDs as well as in the InP pyramids. The QDs reveal a distinct degree of linear polarization of the PL in agreement with their shape elongation. Most important the degree of polarization reduces with reduced pyramid base/pyramid top area/QD number due to increasing influence of the symmetric pyramid top on the QD shape, reaching zero for single QDs grown at lower temperature. This is an important finding for the realization of single and entangled photon sources operating in the $1.55\text{-}\mu\text{m}$ telecom wavelength region.

8094-12, Session 3

Structural and vibrational properties of Mg doped ZnO alloy nanostructures

B. Karthikeyan, R. T. Pandiyarajan, National Institute of Technology, Tiruchirappalli (India)

ZnO is II-IV type semiconductor with wide direct band gap of 3.37eV and it has the exciton binding energy of 60meV, which makes high efficiency UV light emitters and exciton related optoelectronic devices. The physical and chemical properties of ZnO nanoparticles can be altered by introducing dopants. Among the dopants Mg²⁺ doping makes wide range of applications like hydrogen storage material, field effect transistor etc. Owing to the importance of doping in ZnO, we

have prepared Mg doped ZnO alloy nanostructures and studied the structural and vibrational properties. Structural studies are performed through X ray diffraction technique, confirms that the prepared particles are in hexagonal wurtzite structure and the lattice parameters change considerably due to doping. Vibrational properties are done with Fourier Transform Infrared red spectroscopy (FTIR).

All the samples show the IR active optical phonon modes of ZnO show a characteristic broad reststrahlen band in the spectral range of 300-600 cm^{-1} . Gaussian fitted band show each band is composition of three different one. These fitted bands are named as B1, B2 and B3. The band centered at 427 cm^{-1} corresponds to E1(TO) mode. It is observed that the intensity decreases with the increase of Mg concentration, apart from that the surface phonon modes are appeared at 460 and 521 cm^{-1} . Compare to the undoped sample all the normal modes show red shift. We completely analysed the structural and phonon properties of mg doped ZnO particles.

8094-13, Session 4

Structural fluorescence in the butterfly *Morpho sulkowskyi* (Nymphalidae)

E. Van Hooijdonk, Facultes Univ. Notre Dame de la Paix (Belgium) and Univ. Pierre et Marie Curie (France); C. Barthou, Univ. Pierre et Marie Curie (France); J. Vigneron, Facultes Univ. Notre Dame de la Paix (Belgium); S. Berthier, Univ. Pierre et Marie Curie (France)

Evolution and natural selection have generated complexity and efficiency in all living families. *Morpho sulkowskyi* - a butterfly from Neotropic ecozone (South America) and belonging to the Nymphalidae family - concentrates on its wings distinct but complementary features contributing to its exceptional visual attraction: i) the wings are predominantly white but ii) present a bright blue metallic flash due to a iridescence process; iii) the presence of fluorescent molecules producing a violet-blue coloration when irradiated by ultraviolet light and finally iv) the particular ultrastructure of the scales presenting a three-dimensions natural photonic crystal.

Due to the confinement of the fluorescent sources in a photonic crystal, the emission is preferentially directed in space and its efficiency is enhanced for particular detection angles. Furthermore, a clear correlation is observed between the reflection and the fluorescent processes that control the surface optical response. So, collecting and analyzing data over every emerging direction is shown to be crucial. To quantify these observations and characterize these optical effects, three types of measurements were carried out. First of all, the morphology of the butterfly was examined by means of scanning electron microscopes. In addition, the angular distribution of the reflected light was measured with a high performance viewing angle instrument, providing BRDF data (Bidirectional Reflectance Distribution Function). Finally, an automatic method coupling an ultraviolet source to a goni-spectrophotometer allows fluorescent emission characterization. This set-up, developed on purpose, is composed of various excitation and analysis modules and provides angular emission maps. Tentative explanation for the measured correlation is presented.

8094-14, Session 4

Photo-induced self-organized dynamic pattern formation in bio-synthesized nanomaterials

N. V. Kukhtarev, T. Kukhtareva, F. Okafor, A. Johnson, Alabama A&M Univ. (United States)

We have observed a dynamic self-organization of laser scattering from the biosynthesized nanofluids with silver and gold nanoparticles.

Various procedures for nanofluid synthesis suitable for different applications are under constant investigation. In our present research

the green biosynthesis process has been used for noble nanoparticles production. The aqueous solution of *Magnolia Grandiflora* leaves has been used as a reductant for silver and gold nanofluids. We have applied the UV-visible spectroscopy method to control reaction process, fluorescent spectroscopy and nonlinear interferometric imaging experiments for characterization of nanofluids. From the experiments with laser-induced photothermal scattering it is possible to estimate the value of nonlinear refractive index coefficient. The kinetics observed in the pump-probe experiments with blue and red CW laser allowed us to estimate a timescale (~ 1 s) of photothermal lens formation and dissipation.

Moreover, we have observed the phenomena of self-organization of the non-linear laser scattering reflected from the fluid's surface. The diverse regular diffraction patterns (hexagons, rolls, squares etc), resembling diffraction of X-rays on crystal structures, were observed in the solutions of biosynthesized nanoparticles.

From the angular size of the observed hexagonal diffraction patterns it was possible to estimate the diameter of diffracting nanoclusters as 18 microns for silver and gold nanofluids and 9 microns for the *Magnolia* broth. The kinetics of the hexagonal scattering shows a quasiperiodic patterns (resembling heart beats), with a period of about 12 seconds with the slow build-up and sharp disappearance of scattering.

8094-15, Session 4

Multi-color reflection from chiral thin-film stacks

D. J. Brink, Univ. of Pretoria (South Africa)

Iridescence from nano-structured biological materials is fairly well known. Usually the process is based on simple multi-layer interference effects from a thin-film stack typically found in butterfly wings, bird feathers, insects and sea shells. Recently a more interesting and sophisticated nano-structure was found in the exocuticle of scarab beetles, which interacts specifically with circularly polarized light and produces strong resonant reflections of narrow wavelength bands. These structures consist of many hundreds of ultra-thin (~ 5 nm) transparent birefringent layers sandwiched together in such a way that the fast- and slow axes form a (usually left handed) spiral as you look deeper into the material.

In the work presented here we studied the optical reflection from the outer parts of the scarab beetle *Proagoderus brucei*, which is unusual in the sense that it is one of a very small group of species exhibiting different colors on different parts of its body. The optics of this insect has not been studied before.

Scanning electron microscopy and reflection spectroscopy were used to analyze the structure and optical properties of the exocuticle of this insect. Measurements were compared with a computer model of the optics of the nano structure. In this way observations could be explained, some unknown parameters could be quantified and the properties of similar artificial structures with possible practical applications can be predicted.

8094-16, Session 4

Nanoarchitecture in the black wings of the *Troides magellanus*: a natural case of absorption enhancement in photonic materials

A. Herman, C. Vandenberg, O. Deparis, P. Simonis, J. Vigneron, Facultes Univ. Notre Dame de la Paix (Belgium)

The birdwings butterfly *Troides magellanus* possess interesting properties for photonics. The black wings of the male exhibit strong (95%) absorption of the visible light as well as two strong peaks in the infrared (3 μm and 6 μm) both due to melanin. The study of absorption enhancement in this butterfly could be helpful, for instance to realize highly absorbent biomimetic materials. Observations of the wings

using a scanning electron microscope (SEM) revealed that the scales covering them were deeply nanostructured. From these observations, a periodic three-dimensional (3D) model of the scale nanoarchitecture was established and used in numerical simulations in order to calculate the absorption spectrum by means of a 3D transfer matrix electromagnetic method. In order to study separately the effect of the structure on the absorption, the complex refractive index, $n+ik$, was first taken spectrally constant ($n=1.56$, $k=0.0358$). A broad absorption was observed in the visible range as well as two peaks in the infrared, which were not present for a homogeneous layer. This result clearly demonstrated a structural effect on the absorption. A Lorentz dispersion model was then used to account for the spectral dependence of the complex refractive index. The infrared absorption peaks were enhanced in this case. Therefore a combination of nanostructure and material resonances led to enhancement of the absorption. Finally, in order to quantify this enhancement, a comparison with a planar layer with identical refractive index and identical volume led us to conclude that the absorption was 30% higher with nanostructures.

8094-22, Poster Session

Tuning Surface plasmon absorption in Au-Ag alloy polymer nanocomposite free standing films

B. Karthikeyan, National Institute of Technology, Tiruchirappalli (India)

Nanocomposite polymers gains interest because of its enhanced physical and chemical properties are depends on the nanofillers like noble metallic clusters and semiconducting quantum dots. In situ synthesis is a good way of synthesis for the incorporation of nanofillers in to the polymer host. Noble metal nanoparticles show absorption due to surface plasmon resonance (SPR) in the visible region where the delocalized conduction band electrons oscillate with the frequency of applied optical field. The resonance bandwidth and peak maximum depends on parameters such as nanoparticle size, morphology, concentration and dielectric constant of the host where the nanoparticles are embedded. Alloying is also one of the potential parameter to tune the SPR band. In the present work we prepared Au-Ag bimetallic and alloy nanoparticles. Particles are synthesized through polyol method where Poly vinyl alcohol is employed as a reducing and capping agent as well. Optical absorption measurements show the strong band at 410 nm and 532 nm is due to SPR of Ag and Au nanoparticles respectively. When the bimetallic structure is formed, there are both the bands in the polymer. Thermal annealing induced the alloy nanostructures makes the absorption band becomes broad and it is between 410 to 532 nm. Increase in annealing time makes more broadened SPR band. Results are discussed based on Mie and Maxwell- Garnet theory.

8094-23, Poster Session

Optical, phonon and structural analysis of Na doped ZnO nanostructures

T. Pandiyarajan, B. Karthikeyan, National Institute of Technology, Tiruchirappalli (India)

Semiconductor nanoparticles gained much attention due to its novel physical and chemical properties, its potential applications in biology and medicine make scientific community to understand the insight of these particles. Doping metal ions in to it will alter its electronic structure and control its band gap. In the present work we report, synthesis, linear optical properties and x ray peak broadening analysis of the Na doped ZnO nanostructure. To prepare Na doped ZnO, simple room temperature wet chemical method was adopted. X ray pattern shows prepared particles are in hexagonal wurtzite structure The individual contributions of small crystallite sizes and lattice strain to the peak broadening in undoped and Na doped ZnO nanoparticles were studied using Williamson-Hall (W-H) analysis. Analysis shows decrease in stress and

strain value when sodium is doped in ZnO nanoparticles. Morphological studies were investigated through Scanning Electron Microscopic (SEM). Optical absorption measurements show an exciton absorption peak around ~ 360 nm. When doping concentration increases exciton peak maximum shift towards the higher wavelength. Photoluminescence measurements were done by exciting at 335 nm, when doping concentration increases the intensity of exciton peak maximum is decrease, reveal an exciton peak emission and oxygen vacancy band emissions. All the three bands depend on sodium concentration. Vibrational studies were done by Fourier Transform Infrared Spectroscopy (FTIR), it shows band at 433 cm^{-1} is attributed to Zn-O bond and in Na doped samples shows red shift. Apart from Zn-O bond surface phonon modes are observed

8094-24, Poster Session

Synthesis of tin oxide, indium oxide and tin-doped indium oxide nanowires by chemical vapor deposition

K. K. Wong, M. K. Fung, Y. C. Sun, X. Y. Chen, A. M. C. Ng, A. B. Djurić, W. K. Chan, The Univ. of Hong Kong (Hong Kong, China)

Nanostructures of tin oxide (SnO_2), indium oxide (In_2O_3) and tin-doped indium oxide (ITO) have attracted researchers' attention due to their unique properties for device applications such as gas sensors, photovoltaic devices and organic light-emitting diodes (OLED). Different forms of the nanostructure such as nanowires, nanobelts and nanoribbons can simply be fabricated by vapor deposition. These wide bandgap metal oxides in the nanostructure forms have the advantages of large surface to volume ratio that make them suitable for device application. For instance, ITO nanowires substrate is a good candidate as conducting electrode for improving the charge collection for photovoltaic devices while SnO_2 nanostructures are of interest for gas sensors.

In this study, nanowires of tin oxide, indium oxide and tin-doped indium oxide were fabricated by vapor deposition from a mixture of metal oxide nanoparticles and single-wall carbon nanotubes (SWCNT) placed in the heating zone at 1100 . Nanostructures of different morphologies were found on the Au coated single crystal Si substrates (100) placed at different temperatures downstream from the source. The morphology, growth direction and optical properties were characterized by field emission scanning electron microscopy, transmission electron microscopy and photoluminescence spectroscopy. The influence of source material composition and substrate temperature on morphology and photoluminescence was discussed.

8094-25, Poster Session

Optical and vibrational studies of surface modified ZnO nanostructures

T. Pandiyarajan, R. Nagalakshmi, B. Karthikeyan, National Institute of Technology, Tiruchirappalli (India)

Understanding the optical and electronic properties of semiconductor quantum dots is gaining much interest because of its greater versatility in application, improved performance and new functionalities of the future optoelectronic and bio-sensing devices. Among these semiconductors ZnO attracted much concentration due to their prospective performance in electronics, sensing and imaging related areas. In the present work, we report room temperature synthesis of ZnO nanoparticles. X-Ray diffraction studies confirm the prepared particles are in wurtzite structure. Scanning Electron Microscopy (SEM) studies depict the shape and morphology of the particles. Optical absorption measurements show the presence of exciton peak around ~375 nm. High-energy heavy ion irradiation is relatively a new curiosity in materials science and technology. The nature of modification depends on electrical, thermal and structural properties of target material, the mass of the projectile ion and irradiation parameters. The prepared particles were irradiated at room temperature with 150 MeV Ag^{3+} ions at the fluences varying

from 1010 to 1012 ions/cm³ using 15 UD Pelletron accelerator. The pristine as well as irradiated ZnO nanostructures were characterized by X-Ray diffraction, Photoluminescence, FTIR and UV-Vis reflectance to study the radiation induced defects on the local structure of materials. Irradiation with the fluence changes the color of the sample from white to orange. Measured phonon modes show variation with fluence. Photoluminescence measurements are done at the excitation wavelength of 335 nm. Measured spectrum show the variation in peak intensity due to irradiation. These results will be discussed in detail in the complete paper.

8094-26, Poster Session

Gd and S sensitizer effect on the upconversion emission of ZrO₂:Yb, Er nanocrystals prepared by precipitation method with a hydrothermal process

A. Urbina, E. De La Rosa Cruz, T. López, Ctr. de Investigaciones en Óptica, A.C. (Mexico); P. Salas, Univ. Nacional Autónoma de México (Mexico); C. Angeles, Instituto Mexicano del Petróleo (Mexico); A. Torres, Univ. Autonoma de Nuevo Leon (Mexico)

In this work, it is presented the synthesis of ZrO₂:Yb³⁺, Er³⁺ nanocrystal by precipitation method with a hydrothermal process and annealing at 1000 oC. All the samples were prepared with 2% mol of Yb³⁺ and 1% mol of Er³⁺ and sensitized with different concentration of Gd³⁺ and S²⁺. The ceramic powders were characterized with different techniques to determine their chemical composition, crystalline structure, crystalline size, morphology and upconversion emission. All samples present the tetragonal crystalline phase with crystallite size lower than 70 nm with cubic shape. Experimental results suggest the presence of SO₄ on the surface of nanocrystals reducing the OHs and then improving the signal emitted. The nanocrystals presented strong upconversion emission enhanced by the presence of both sensitizer, Gd³⁺ and S²⁺. A synergistic effect was observed with the combination of both sensitizers, improving the upconverted visible emission. The emission peak centered at 654nm dominates the red band and controlling the dopant composition and sensitizer it is possible to control the red/green intensity ratio.

8094-28, Poster Session

Temperature and frequency dependent admittance of InAs self-assembled quantum dots embedded in GaAs.

A. Sellai, Sultan Qaboos Univ. (Oman)

We have studied using frequency and temperature dependent admittance some electronic properties of InAs QDs embedded in a GaAs structure with emphasis on G-V data which is found to be more sensitive to some aspects of carriers exchange mechanisms. The presence of QDs in our structure is evidenced in the C-V characteristics at all temperatures and frequencies by a plateau-like structure in the bias range -3 V to -2 V that is related to charging and discharging of QDs. Concurrently, the G-V characteristics show a manifest peak in the same bias range at all considered frequencies but only for temperatures below 150K. The peak magnitudes in the concentration profiles, which are directly related to occupancy of charge states, increase as the temperature is decreased with a concomitant reduction of broadening of the profile. Below 40K a second peak, attributed to tunnelling, appears consistently at a slightly higher depletion width. The variations of conductance with both the temperature and applied bias show two regions of maximum G in the range -3V to -2V and for two temperature ranges 50K - 90K and below 40K. The T-dependence of the G_{peak}, reveal two different behaviours depending on the T-range. These observations concur for the fact that one of two different mechanisms of carrier escape from the QDs prevails over each temperature range. Moreover, the measured G at any given

temperature shows a very significant increase with increasing frequency suggesting that the emission rates are much higher than the frequency of the applied ac signal.

8094-17, Session 5

The photoluminescence of CuInS₂ nanocrystals: Effect of surface modification

Y. Kim, Y. Cho, K. Chung, C. Choi, Korea Institute of Materials Science (Korea, Republic of)

We have synthesized highly luminescent Cu-In-S(CIS) nanocrystals (NCs) by heating the mixture of metal carboxylates and alkylthiol under inert atmosphere. We modified the surface of CIS NCs with zinc carboxylate and subsequent injection of alkylthiol. As a result of the surface modification, highly luminescent CIS@ZnS core/shell nanocrystals were synthesized. The luminescence quantum yield (QY) of best CIS@ZnS NCs was above 50%, which is 10 times higher than the initial QY of CIS NCs before surface modification (QY=3%). Detailed study on the luminescence mechanism implies that etching of the surface of NCs by dissociated carboxylate group (CH₃COO⁻) and formation of epitaxial shell by Zn with sulfur from alkylthiol efficiently removed the surface defects which are known to be major non-radiative recombination sites in semiconductor nanocrystals. In this study, we developed a novel surface modification route for monodispersed highly luminescent Cu-In-S NCs with less toxic and highly stable precursors. Investigation with the time- and the temperature-dependent photoluminescence showed that the trap related emission was minimized by surface modification and the donor-acceptor pair recombination was enhanced by controlling copper stoichiometry.

8094-18, Session 5

Nearly-total optical extinction in arrays of non-resonant nanorods

P. V. Ghenuche, Ctr. National de la Recherche Scientifique (France) and ONERA (France); G. Vincent, ONERA (France); M. Laroche, Institut d'Optique Graduate School (France); N. Bardou, Ctr. National de la Recherche Scientifique (France); R. Haïdar, ONERA (France); J. Pelouard, S. S. Collin, Ctr. National de la Recherche Scientifique (France)

The interaction of light with non-resonant, dielectric nanostructures can be considerably enhanced by employing the diffraction effect resulting from the multiple scattering of a periodic arrangement of these particles.

In this work we experimentally demonstrate nearly-total optical extinction in arrays of transparent material together with extremely sharp resonances. This phenomenon originates from multiple-scattering in a monolayer of periodical non-resonant scatterers.

Freestanding Si₃N₄ membranes made of subwavelength square rods (width between $\lambda/5 - \lambda/10$) on large surface areas (2.6×2.6 mm²) were fabricated on a Si substrate and drilled by dry etching. Following this procedure, membranes with one-dimensional and two-dimensional patterns were fabricated, both having 500 nm square section bars and 3 μm pitch. High-resolution dispersion diagrams have been measured for the absolute transmission and reflection. Remarkably for a transparent material with a fill factor of only 15%, up to 96% extinction, independent of polarization, is found. The results are quantitatively described by a simple multiple-scattering model.

In addition, when the lossy material is used to fabricate the rods, a considerable absorption enhancement was observed, an indication of the electric field enhancement that occurs in the vicinity of the rods.

A key advantages of such dielectric gratings is the ease of tuning the resonance parameters (frequency, width) by changing the geometrical parameters (period and radius of the rod) without being restricted to the range of frequencies of plasmons. The employment of these geometrical

resonances in dielectric systems may provide new opportunities for applications like stop-band filters, selective mirrors and for applications where fluorescence quenching must be avoided.

ongoing work is dedicated to determining the microscopic mechanisms responsible for this nonradiative process.

8094-19, Session 5

White light emissions from ZnO quantum dots under 350 nm excitation

J. Oliva, E. De La Rosa Cruz, Ctr. de Investigaciones en Óptica, A.C. (Mexico); A. Torres, Univ. Autonoma de Nuevo Leon (Mexico); O. Meza Espinoza, Ctr. de Investigaciones en Óptica, A.C. (Mexico)

There are many efforts around the world to design new lighting sources, above all for general illumination. Since Zinc Oxide (ZnO) is an innocuous, abundant and inexpensive material which has demonstrated its capacity to produce visible emission by electroluminescence or ultraviolet excitation, it could be an excellent candidate to produce white light. In this work, we synthesized ZnO quantum dots with a wet chemical method. By changing the content of surfactant (Dodecylamine), we were able to control the ratio between the blue and yellow emission bands of ZnO. Luminescence measurements of ZnO nanoparticles dispersed in chloroform under 350 nm excitation and annealing treatments from 70°C to 800°C indicated that blue emission is produced by surface defects due to the interaction of amines and OH groups with the surface of ZnO quantum dots and yellow emission is originated from oxygen vacancies. FTIR Spectra of as-prepared samples showed that the amount of OH groups, CO₂ and bands associated with dodecylamine decreases if the content of this surfactant diminishes, that in turn promotes an increase in luminescence. Also, HRTEM images indicate that the size of spherical nanocrystals increases as the amount of surfactant increases, we obtained nanocrystal sizes ranging from 3 to 10 nm, as consequence, energy band gap values changed from 3.4 eV to 4.3 eV. CIE coordinates were (0.313,0.295), (0.332,0.321) and (0.401,0.406) for the samples which contained 0.17 ml., 0.34 ml., and 0.45 ml. of dodecylamine respectively. All these results point out that our nanoparticles can be used to tune white light emission from cool to warm white light as well as to use them like "seeds" to growth nanorods with hydrothermal procedures, which would be suitable to fabricate ZnO based LEDs.

8094-20, Session 5

How nanoscale structure determines photoluminescent quantum yield of CdSe/CdS core/shell nanorods

M. A. Pelton, C. She, A. Demortiere, E. Shevchenko, Argonne National Lab. (United States)

Heterostructure nanocrystals consisting of a nearly spherical CdSe core and a larger, rod-shaped CdS shell have attracted considerable attention for their novel optical and optoelectronic properties. They exhibit large absorption cross-sections, good photostability, and strong luminescence, making them attractive for devices such as optically pumped lasers and luminescent solar concentrators. Practical application of the nanocrystals will require optimization of their photoluminescent quantum yield, which in turn requires a fundamental understanding of the processes that limit the yield. We have investigated how optical properties depend on nanoscale structure by measuring quantum yield, time-resolved photoluminescence, and transient absorption on a series of CdSe/CdS core/shell nanorods with different core and shell sizes. We find that the radiative decay rate for all of the samples has a universal dependence on nanoparticle volume, consistent with the conduction-band electron being delocalized throughout the particle and the valence-band hole being confined within the CdSe core. Transient-absorption measurements provide further support for this quasi-type-II band alignment, and also show that trapping of hot carriers is not a significant factor determining luminescence quantum yield. Rather, quantum yields are limited by sample-dependent nonradiative recombination of band-edge carriers;

8094-21, Session 5

Photoluminescence from silicon nitride alloys

J. O. Kistner, M. B. Schubert, J. H. Werner, Univ. Stuttgart (Germany)

Silicon nitride alloys emit photoluminescence (PL) all over the visible spectral range. Recent studies (e.g. Ref.[1]) ascribed this luminescence to quantum-size effects within silicon nanocrystals (Si-NC). These quantum dots were either shown or assumed to form inside the matrix of the silicon alloy. Possible luminescence of the alloy itself wasn't taken into account. We fabricate silicon alloys using plasma enhanced chemical vapor deposition and carefully analyze their optical properties. Similar to the published data, our samples show visible PL, and the PL peak shifts all over the visible range if we tune the composition of the silicon nitride alloy. In contrast to the published data, however, HRTEM analyses prove that our samples don't contain silicon nanocrystals. Therefore, the Si-NC luminescence model is inadequate to explain the observed luminescence. We found the Band Tail Luminescence model introduced by D.J. Dunstan to be in good agreement with our experimental results. This model suggests that the observed luminescence originates from the alloys matrix itself. While the Si-NC luminescence model merely links a predefined crystalline grain size to a luminescence center, the band tail luminescence model explains all aspects of the luminescence. Not only the PL peak position, but also spectral width and relative intensities of the luminescence are described by the band tail luminescence model. We conclude that silicon nitride is an inappropriate matrix for investigating photoluminescence from Si-NC.

References:

- [1] L.V. Mercaldo et. al., Mat. Sci. and Eng. B 159-160, 77 (2009).
- [2] D.J. Dunstan, Sol. Stat. Comm. 43, 341 (1982).

Conference 8095: Active Photonic Materials IV

Sunday–Thursday 21–25 August 2011 • Part of Proceedings of SPIE Vol. 8095
Active Photonic Materials IV

8095-01, Session 1

Lasing in photonic nanostructures

C. M. Soukoulis, Iowa State Univ. (United States)

A self-consistent computational scheme is presented for photonic systems with gain incorporated into the nanostructures. The gain is described by a generic four-level system. The loss compensation and the lasing behavior of the photonic nanostructures with gain are studied. A critical pumping rate exists in compensating the losses of the metamaterial. There exists a wide range of input signals where the composite system behaves linearly. When the pumping rate increases, there is a critical pumping rate at which the photonic crystals and or metamaterials systems start lasing.

8095-02, Session 1

Advancing active nanoplasmonics

A. V. Kildishev, V. P. Drachev, S. Xiao, X. Ni, Purdue Univ. (United States); L. Prokopenko, Institute for Computational Technologies (Russian Federation) and Purdue Univ. (United States); J. Trieschmann, J. Fang, V. M. Shalaev, Purdue Univ. (United States)

Loss-free and active metamaterials and nanostructured plasmonic devices can enable new important applications ranging from advanced sensing and imaging devices to nanoscale lasers and optical waveguides. The interaction of light with optical gain materials is of great importance especially in metal-dielectric nanostructures, where the compensation of losses is essential for practical engineering.

In order to design active nanoplasmonic devices, accurate models of this light-matter interaction are required.

A loss-free and active metamaterial in the visible has been recently experimentally demonstrated at the Birk Nanotechnology Center at Purdue; this experiment was supported by FEM-based simulations in frequency domain and the appropriate retrieval of the effective bianisotropic properties.

Our recent progress in this field will be reviewed followed by a brief discussion of the experiment-fitted parameters for (i) gain media - the 4-level system of auxiliary differential equations (ADE), and (ii) noble metals - the general dispersive material (GDM) model, which are imperative for accurate time-domain simulations of active nanoplasmonic devices.

8095-03, Session 1

Dynamics of amplification and gain in nanoplasmonic metamaterials

S. Wuestner, A. Pusch, K. L. Tsakmakidis, J. Hamm, O. Hess, Imperial College London (United Kingdom)

Negative-refractive-index metamaterials can enable a multitude of exciting and useful applications, such as subwavelength focusing, invisibility cloaking, and ‘trapped rainbow’ stopping of light. The realization of these materials has recently advanced from the microwave to the optical regime. However, at optical wavelengths, metamaterials suffer from high dissipative losses owing to the metallic nature of their constituent meta-molecules. It is therefore not surprising that overcoming loss restrictions is currently one of the most important topics in metamaterials’ research [1].

Here we study, based numerical on pump/probe experiments, the nonlinear dynamics of active, negative-refractive-index, double-fishnet metamaterials. We demonstrate that the use of an active medium (laser dyes) embedded into the structure of a double-fishnet NRI metamaterial

can lead to complete compensation of optical losses, and even to light amplification [2,3]. Our analysis is based on a full-vectorial time-domain approach that manages to self-consistently couple the evolution of the occupation densities in the gain medium directly to Maxwell’s equations in three dimensions [2]. Nonlinearity, saturation of the gain medium and spatiotemporal variations of, both, absorption and emission are all inherent to our model [2,4], avoiding the need for external, pre-calculated inputs. We show that the highly nonlinear character of the pump process for times shorter than ~ 5 ps, as well as the non-instantaneous decay (on a timescale of approximately 100 fs) of, both, the upper absorption state and the lower emission state - both of which, cannot be captured by frequency-domain analyses. Further, we illustrate the importance of a judiciously chosen delay between the pump and the probe pulses in order to maximise the harnessed gain, and probe the system in its linear regime (where the standard effective-parameters retrieval methods apply). Finally we show that the pump-induced population inversion (gain) is found, when properly calculated, to be highly spatially-nonuniform. There are spatial regions where no population inversion occurs, with the probe-pulse being therein absorbed rather than amplified - therefore, particular care should be exercised to avoid using spatially-uniform population/gain distributions, as these could lead to unphysical or optimistic outputs.

References

- [1] N. I. Zheludev, Science 328, 582 (2010).
- [2] S. Wuestner, A. Pusch, K. L. Tsakmakidis, J. M. Hamm, and O. Hess, Phys. Rev. Lett. 105, 127401 (2010).
- [3] S. Xiao, V. P. Drachev, A. V. Kildishev, X. Ni, U. K. Chettiar, H.-K. Yuan, and V. M. Shalaev, Nature 466, 735 (2010).
- [4] E. Gehrigh and O. Hess, Spatio-Temporal Dynamics and Quantum Fluctuations in Semiconductor Lasers (Springer, Heidelberg, 2003).

8095-04, Session 2

Active infrared metamaterials

I. Brener, Sandia National Labs. (United States)

In this talk I will review the current status of electrically tunable metamaterials, both at Terahertz and shorter infrared frequencies. Scaling these active devices to mid and near infrared optical frequencies poses considerable challenges and requires new tuning mechanisms. Some examples include controlling coupling to other dipolar resonances such as phonons and engineered transitions in semiconductor heterostructures.

8095-05, Session 2

Infrared detectors with plasmonic cavities

S. Krishna, Ctr. for High Technology Materials (United States)

There is an increased emphasis on obtaining multicolor detectors as a part of the third generation detector development. We have been undertaking research on infrared detectors based on InAs/GaAs quantum dots in a well (DWELL) and InAs/GaSb superlattices. We will discuss approaches to realize multicolor detectors using near field enhancement using surface plasmons coupled to infrared detectors. We will describe our recent work on the development of a plasmonic quantum dot focal plane array.

Acknowledgements: Acknowledgements: I wish to acknowledge my collaborators (Profs. Brueck/Hayat group at UNM, Dr. Cardimona’s group at AFRL, Prof. Perera’s group at Georgia State University, Prof. Painter’s group at Caltech, Profs. Ghosh and Grein at UIC, Dr. Toni Taylor, Rohit Prasankumar, Aaron Gin at Center for Integrated Nanotechnology (CINT) and Dr. S.K. Noh and Dr. S.J. Lee from Korean Research Institute of Standards and Science (KRISS). This work would not have been possible without the hard working members of the research group (Dr. L.R.

Dawson, Dr. E. Plis, Dr. Y.D. Sharma, Dr. M. Naydenkov, Dr. S.J. Lee, J. Shao, D. Ramirez, A. Barve, S. Myers, J. Montoya, M. Kutty, E. Jang, R. Sheno, S. Myers, B. Klein, G. Fiorante, T. Sandy and F. Santiago). Work supported by AFRL, AFOSR, MDA, IC Postdoc, KOSEF-GRL, DARPA, and NSF

8095-06, Session 2

Manipulating light with photonic metamaterials

B. Ou, J. Zhang, T. S. Kao, K. F. Macdonald, E. Plum, N. I. Zheludev, Univ. of Southampton (United Kingdom)

[invited] We report on a number of new approaches to control the interaction of light with nanostructured photonic metamaterials and new types of metamaterials. This includes nano-mechanical reconfigurable metamaterials for the visible and near-infrared parts of the spectrum; bas-relief and intaglio “full-metal” metamaterials and “loaded plasmon” metamaterials as new types of frequency selective surfaces, perfect absorbers and magnetic walls. We also show how tailoring profile of the excitation optical field can be used to control localization of light in a certain class of plasmonic nanostructures with strongly interacting meta-molecules which has a potential for applications in data storage and imaging

8095-59, Session 2

Miniaturized gas sensors based macroporous silicon

R. B. Wehrspohn, B. Gesemann, D. Pergande, Martin-Luther Univ. Halle-Wittenberg (Germany); S. Schweizer, Martin-Luther-Univ. Halle-Wittenberg (Germany); A. Lambrecht, Fraunhofer-Institut für Physikalische Messtechnik (Germany)

In many fields such as technical, environmental, automotive, and medical applications, miniaturized and mobile gas sensors are indispensable. Moreover, the 9/11 events have led to an increase in the request for sensors and sensor systems that can detect rapidly, efficiently, and at moderate cost trace explosives and a whole range of toxic substances at diverse control points, e.g., at airports and inside air conditioning systems in aircraft and public buildings. Most of the current miniaturized sensing methods are applicable only to certain specific gases that influence the physical properties of the detector materials. We will present two concepts of miniaturized element-specific sensors based on electrochemically-prepared macroporous silicon. Firstly, we will show a miniaturized optical sensor using low-group velocities in a 2D photonic crystals and selective thermal emitters for compact gas sensing in the ppm range [1]. Secondly, a micro-ionization-mobility-spectrometer using needle-like macroporous silicon surfaces is presented that has the potential to measure in the ppt range [2]. The technological limits as well as the physical limits will be discussed.

8095-07, Session 3

On-chip stimulated Brillouin scattering

B. J. Eggleton, R. Pant, The Univ. of Sydney (Australia)

We report the first demonstration of on-chip stimulated Brillouin scattering (SBS) using chalcogenide planar waveguides.

8095-08, Session 3

Slotted nanobeam microcavities enabling hybrid photonic devices

J. Schilling, C. Schriever, C. Bohley, Martin-Luther-Univ. Halle-Wittenberg (Germany)

Silicon nanobeam cavities consisting of two lines of equally spaced pores (Bragg mirrors) which enclose a straight section in a silicon strip waveguide gained recently renewed interest when several designs were developed allowing high Q-factors and relatively low mode volume. With these properties the nanobeam cavities are of special interest for the enhancement of nonlinear optical processes e.g. optical bistability and opto-optical switching. However for efficient nonlinear processes in the near infrared the strong two photon absorption of silicon is a serious obstacle.

We therefore suggest a hybrid approach where a slot is introduced into the silicon nanobeam cavities. This slot can be infiltrated with other nonlinear optical materials (e.g. polymers or chalcogenide glasses) which experience the strong field enhancement within the slot, thus combining the efficient light confinement due to the high refractive index of silicon with the tailored nonlinear optical properties of the infiltrated material.

Here we present first a theoretical investigation of the mode profiles, mode volume and Q-factors of such infiltrated slot nanobeam cavities. General design principles are discussed and in particular the impact of a gradual adjustment of the pore distance and pore diameter of the pores closest to the cavity is investigated. Especially the tapering of the pore diameter leads to a smoother transition of the mode profiles from the cavity centre to the adjacent Bragg mirror region resulting in a considerable increase of the Q-factors. Furthermore the influence of the length of the taper is considered and surprisingly a maximum Q-factor of 100 000 can be obtained with a linear taper including only two pores.

Besides these theoretical studies first experimental results demonstrating the described hybrid nanobeam cavity resonances in the near IR will be presented.

8095-09, Session 3

Nanoscale photonics: nonlinear materials and processes

C. Sibilia, Univ. degli Studi di Roma La Sapienza (Italy)

An overview of different nonlinear optical phenomena occurring in nanopatterned materials is presented. In particular a discussion about second order nonlinear effects is reported, including also some nonclassical properties of the interaction with non homogeneous materials

8095-10, Session 3

Enhancement of nonlinear refraction and absorption using cascaded plasmon resonances

S. Toroghi, P. G. Kik, CREOL, The College of Optics and Photonics, Univ. of Central Florida (United States)

Metal-dielectric composites exhibit strongly modified linear and nonlinear optical properties due to the existence of localized surface plasmon resonances. We have previously shown that silver nanoparticle arrays can be used to strongly enhance the nonlinear optical refractive and absorptive properties of a composite, and that the spatial arrangement of the particles has a significant effect on the figure of merit for nonlinear absorption. In this talk we discuss an additional enhancement of the nonlinear optical response of such nonlinear metamaterials by making use of cascaded plasmon resonances on coupled silver nanoparticle arrays. The arrays consist of chains of particles with alternating sizes,

i.e. with a binary size distribution. Through numerical simulation, we study plasmon-induced changes in the linear and nonlinear optical properties of these nanoparticle composites as a function of dissimilarity in nanoparticle size within the structure. In successive simulations, the relative size of the particles is varied systematically while maintaining a fixed metal fill fraction. The relative particle volumes were chosen to be 1, 2.3, 4.8, 11 and 30, at a fill fraction of 1%. We find that the introduction of even a small size difference leads to the appearance of new plasmon resonance modes of the coupled nanoparticle chains, which are identified to be an anti-symmetric plasmon resonance (opposite field on neighboring particles), as well as several multipolar modes. It is found that the internal field enhancement in the small particles is four times larger than that found in arrays consisting of particles with a single size, demonstrating the presence of a cascaded resonance effect. We demonstrate that this seemingly moderate additional cascaded enhancement leads to a dramatically enhanced nonlinear optical response of the composites at specific frequencies. Methods for fabrication similar structures using existing nanofabrication tools will be discussed, and the viability of experimentally observing the predicted effects will be addressed.

8095-11, Session 3

Amplification of the nonlinear optical response of metals in induced transmission filters

C. Fuentes-Hernandez, J. Hsu, D. T. Owens, A. R. Ernst, J. M. Hales, J. W. Perry, B. Kippelen, Georgia Institute of Technology (United States)

Metallic nanostructures, such as metal-dielectric photonic bandgaps have been proposed as one class of materials where the large nonlinear optical (NLO) response of metals can be accessed in spectrally broadband passbands that show high transmittance in the visible range. Here, we propose another structure which has been somewhat overlooked in the literature in the context of NLO filters, namely the induced-transmission filter (ITF). In an ITF, a single metal layer, several times thicker than its skin depth, is surrounded by admittance matching layers that allow the opening up of spectrally narrow passbands with high transmittance in the visible range. We present the design and fabrication of Ag-based ITFs having a peak linear transmittance of 63% and we discuss the experimental demonstration of an enhancement in its NLO response by a factor of 30 over an isolated Ag film. We also present a physical model that describes the NLO properties of thin Ag films in the context of ultrafast electron heating and show that its predictions also allow modeling of the NLO response of ITFs. We use this model, to describe how variations in structure impact the strength of the response and demonstrate the possibility of a further enhancement in the nonlinearity by a factor of 2. Finally, we show that a stronger NLO response than Ag can be obtained with the use of Ag/Au bi-metal layers and that these bi-metal layers can be used to fabricate ITFs with more than 80% peak transmittance.

8095-12, Session 3

Second harmonic nanoparticles in imaging applications

I. Papadopoulos, C. Hsieh, Y. Pu, J. Choi, D. Psaltis, Ecole Polytechnique Fédérale de Lausanne (Switzerland)

Recent developments in nano-science have provided us with a diverse group of nanoparticles capable of second harmonic generation. We review the applications of these particles in imaging. We will focus on how the shape and the size of the particles determine their imaging capabilities.

8095-13, Session 4

Ultrafast switching of semiconductor microcavities

G. Ctistis, W. L. Vos, E. Yüce, Univ. Twente (Netherlands); J. Claudon, J. Gérard, Commissariat à l'Énergie Atomique (France)

Switches are widely applied and necessary ingredients in modulation and computation. Recent progress on photonic integrated circuits [1] promises to overtake boundaries set by conventional switching. Therefore, ultrafast switching of photonic cavities is crucial as it allows the capture or release on demand of tunable photons [2], which is relevant to on-chip communication and to high-speed miniature lasers. Ultrafast switching would also permit the cavity quantum electrodynamical manipulation [3] in real-time.

Switching photonic nanostructures is achieved by changing the refractive index of the constituent materials. To date, the switching speed has been limited by material properties (see [4]), but not by optical considerations. We explore the ultimate fast switching of the cavity resonance in GaAs-AlAs in the telecom range. We exploit the instantaneously fast electronic Kerr effect by the judicious tuning of the pump and probe frequencies relative to the semiconductor bandgap, resulting in a shift of the cavity resonance by nearly one linewidth. The speed of the switching - both on and off - is only limited by the dynamics of the light in our cavity [5].

We explore the not-adiabatic regime of tuning of light in a single-resonance cavity. We observe that the frequency of probe light is changed to a value different from the cavity resonance. The light accumulates a phase shift while it is trapped in the cavity due to a fast change in the refractive index, induced by an earlier pump pulse. Consequently, all light trapped in the cavity obtains a frequency different from the cavity resonance. To our knowledge, such photonic not-adiabatic tuning has not been observed before [6].

References:

- [1] K. J. Vahala, *Nature* 424, 839 (2003)
- [2] P. M. Johnson, A. F. Koenderink, and W. L. Vos, *Phys. Rev. B* 66, 081102 (2002); S. F. Preble, Q. Xu, and M. Lipson, *Nature Photon.* 1, 293 (2007); T. Tanabe, M. Notomi, H. Taniyama, and E. Kuramochi, *Phys. Rev. Lett.* 102, 043907 (2009)
- [3] G. Khitrova, H. M. Gibbs, M. Kira, S. W. Koch, and A. Scherer, *Nature Phys.* 2, 81 (2006)
- [4] V. R. Almeida, C. A. Barrios, R. R. Panepucci, and M. Lipson, *Nature* 431, 1081 (2004)
- [5] G. Ctistis, E. Yüce, A. Hartsuiker, J. Claudon, M. Bazin, J.-M. Gérard, and W. L. Vos, <http://arxiv.org/abs/1102.3351>
- [6] P.J. Harding, H.J. Bakker, A. Hartsuiker, J. Claudon, A.P. Mosk, J.-M. Gérard, and W.L. Vos, <http://arxiv.org/abs/0910.5000>

8095-14, Session 4

Dynamic optical media: ultrafast bandgap photonics application

M. K. Rafailov, RCI Inc. (United States)

It is known that ultra-fast laser is able to change the physical state of solids: to melt, to evaporate, to ionize. It is less known that ultra-fast laser is able to change the optical state of some solids: to bleach it. The effect is most pronounced in semiconductors where the bandgap amplifies the effect in highly non-linear manner. Change in optical state is on the scale of recombination time. Such short time changes in semiconductor optical characteristics depend on the bandgap structure, therefore we are introducing the term - Ultrafast Bandgap Photonics. Phenomena of Ultrafast bandgap photonics are time-dependent and bandgap-dependent optical effects are reversible: ultra-fast laser "bleaches" semiconductor and temporally changes spectral reflectivity, absorptivity, and transmittance as well as polarization characteristics. Applications of Ultra-fast bandgap photonics are remote control of semiconductor characteristics and material properties. Ultrafast Bandgap Photonics

effects may temporally alter photodetector's fundamental characteristics - responsivity and detectivity as well as its response time and spectral bandwidth - all of these may happen with or without changes in photodetector electrical response. While Ultrafast Bandgap Photonics applications are directly depend on pulse dwell time and pulse repetition rate; it is important to say that laser energy per pulse should be carefully managed. In this paper we discuss some foundations of ultra-fast bandgap

photonics - specifically for low pulse energy

8095-15, Session 4

Optical response of a slab with time-periodic dielectric function $\epsilon(t)$: Towards a dynamic metamaterial

P. Halevi, J. R. Zurita-Sánchez, U. Algreto-Badillo, Instituto Nacional de Astrofísica, Óptica y Electrónica (Mexico)

A dielectric medium with time-periodic permittivity $\epsilon(t)$ gives rise to a band structure that is periodic in the frequency ω and exhibits wave vector gaps Δk . Light reflected from and transmitted by such a dynamic slab contains harmonics $\omega - n\Omega$ ($n = 0, \pm 1, \dots$) where Ω is the modulation frequency. Also, giant resonances are obtained in the response for $\omega = n\Omega/2$ with odd n , provided that a certain condition is satisfied for the slab thickness. Further, we show that a dynamic medium can be realized by means of a low-pass transmission line with varactors whose capacitance is $C(t) = d\epsilon(t)$ and inductances $L = d\mu(t)$, d being the period.

8095-16, Session 4

Theoretical modeling of the ultrafast recovery times and low saturation intensities of the intersubband absorption in the InGaAs/AlAs/AlAsSb coupled double quantum wells

P. Ma, Y. Fedoryshyn, H. Jäckel, ETH Zurich (Switzerland)

Nonlinear optical devices, which are capable of performing ultrafast all-optical switching at reasonably low power levels, are required to fulfill the demands of the coming generation of all-optical communication networks. The InGaAs/AlAsSb material system is very promising in this respect due to a number of its specific properties, such as the large optical nonlinearities of the intersubband transitions in quantum wells, the ultra-short relaxation times, and the large conduction band off-set [1].

The all-optical switching mechanism is based on the saturable intersubband absorption in the four-level quantum well system. Our recent pump-probe and absorption saturation experiments revealed ultrafast absorption recovery times with low material absorption saturation intensities in the strained InGaAs/AlAs/AlAsSb symmetric coupled double quantum wells. This article addresses a systematic study of the dynamic nonlinear processes in our quantum well structures by performing theoretical simulations in order to interpret the pump-probe and absorption saturation experimental results. First, the quantum well system is modeled by solving self-consistently the Schrödinger-Poisson equations. Then, modified optical Bloch equations in combination with the density matrix method are employed to simulate the time evolution of the optical nonlinearities under the pulsed excitation. Impact factors related to the dynamic and saturation characteristics of the material, such as the dephasing time, the doping concentration, and the pump pulse duration, are discussed theoretically. Furthermore, a novel switch operation mechanism, where the pump and signal light are resonant to two different intersubband transitions in the four-level quantum well system, are investigated theoretically. Our further experimental and theoretical studies, which are in progress, will provide a deeper understanding of the nonlinear phenomena and the dynamic processes in the coupled double quantum wells embedded into a waveguiding structure for all-optical switches [2].

Reference

- 1 T. Simoyama et al., IEEE Photon. Technol. Lett. 19, 604-606 (2007).
- 2 Y. Fedoryshyn et al., Opt.Lett. 32, 2680-2682 (2007)

8095-17, Session 5

Electromagnetic unidirectionality in the presence of absorption or gain

A. Figotin, Univ. of California, Irvine (United States); I. Vitebskiy, Air Force Research Lab. (United States)

Magnetic photonic crystals are spatially periodic structures composed of transparent materials, some of which being magnetically polarized. Magnetization, either spontaneous or induced, is always associated with nonreciprocal circular birefringence (magnetic Faraday rotation). It can qualitatively change electrostatics of the composite medium. In particular, magnetic photonic crystals of certain configuration can display strong spectral asymmetry, implying that electromagnetic waves propagate in one direction much faster or slower than in the opposite direction. This phenomenon is essentially nonreciprocal and unique to magnetic photonic crystals. It can only exist if both time reversal and space inversion symmetries of the composite structure are broken. The spectral asymmetry can result in electromagnetic unidirectionality [1, 2]. In a unidirectional medium, the electromagnetic wave of certain frequency propagating in the forward direction has zero group velocity and greatly enhanced amplitude. Such a wave is referred to as the frozen mode [2, 3]. The wave of the same frequency propagating in the backward direction can have group velocity comparable to speed of light in vacuum.

Consider now forward and backward transmittance of a plane-parallel unidirectional photonic slab. At first sight, the transmittance in the direction of zero group velocity (the forward transmission) should be suppressed, as compared to the backward transmittance, where the light group velocity is large. Our rigorous analysis, though, shows that in the absence of absorption, the forward transmittance averaged over incident light polarization is exactly equal to that of the backward transmittance. But, if we introduce even a modest absorption, the forward transmission reduces dramatically, while the backward transmittance remains almost unchanged. Such a behavior is reminiscent of a nonreciprocal linear isolator. Even more intriguing behavior is expected if a unidirectional photonic crystal includes a gain component. In the latter case, the forward propagating wave can experience a dramatic amplification, while the backward propagating wave is not enhanced at all, or even suppressed. Either effect can be very attractive for practical applications.

- [1] A. Figotin and I. Vitebskiy. Phys. Rev. E 63 (2001).
- [2] A. Figotin and I. Vitebskiy. Phys. Rev. B 67 (2003).
- [3] A. Figotin and I. Vitebskiy. Laser & Photonic Reviews 5, 201 (2011)

8095-18, Session 5

PT-synthetic optical materials

T. Kottos, Wesleyan Univ. (United States); D. Christodoulides, CREOL, The College of Optics and Photonics, Univ. of Central Florida (United States)

Transport properties of synthetic optical media, with Parity (P) and Time (T) symmetries imposed by a balanced arrangement of gain and loss, are investigated. We find that the temporal behavior of the total power of a propagating beam in linear PT media is insensitive to microscopic details of the system and follows three distinct universal laws which depends only on the magnitude of the gain/loss parameter.

We further show that PT-symmetric Bragg grating structures, at the spontaneous PT-symmetry breaking (exceptional) point, can act as unidirectional invisible media. In this regime the reflection from one end is diminished while it is enhanced from the other. At the same time the transmission coefficient and phase, are indistinguishable from those expected in the absence of a grating. The phenomenon is robust even in

the presence of Kerr non-linearities, and it can also effectively suppress optical bistabilities.

Away from the exceptional point, the interplay of optical nonlinearities with PT-symmetries, allow for diode action. Such PT-synthetic unidirectional optical valves may find promising applications in integrated photonic systems.

8095-19, Session 5

Retooling electromagnetic scattering: one-way photonic chiral edge states and optical manipulation

Z. Wang, Massachusetts Institute of Technology (United States); P. T. Rakich, Sandia National Labs. (United States); J. D. Joannopoulos, M. Soljacic, Massachusetts Institute of Technology (United States)

In ordinary waveguides, photons travel both ways, allowing discontinuities to readily scatter light and induce losses. Photonic chiral edge states, on the other hand, permit electromagnetic waves to propagate only in a single direction. Obstacles and disorder can no longer reflect waves, which exhibit 100% transmission in numerical simulations even across seemingly-impassible perfectly-conducting barriers introduced into the waveguide. I will explain how such phenomena, analogous to quantum-Hall edge states, can arise from magneto-optical photonic crystals. Generalizing earlier predictions by Raghu and Haldane, I show that the key requirement is related to a topological invariant of the bulk bands known as Chern number. I also present our experimental results verifying the existence of these novel phenomena. I will discuss the implications of these novel photonic states in altering the basic physics of momentum transfer. I will also discuss prospects of applying these novel photonic states in optical lattices and optical manipulation.

8095-20, Session 5

Time-reversal and nonlocal effects in PT-symmetric nonlinear lattices with balanced gain and loss

A. A. Sukhorukov, The Australian National Univ. (Australia)

Photonic structures composed of coupled waveguides with loss and gain regions offer new possibilities for shaping optical beams and pulses compared to conservative structures. Such structures can be designed as optical analogues of complex parity-time (or PT) symmetric potentials, which can have a real spectrum corresponding to the conservation of power for optical eigenmodes, for the magnitude of gain/loss below a certain threshold.

PT-symmetric potentials appear in many physical contexts, and one feature actively investigated in the context of quantum theories is the property of nonlocality. We reveal that effective nonlocality of PT-symmetric structures with gain and loss elements can lead to pronounced differences for optical beam dynamics in arrays of coupled waveguides with the same characteristics but different topology.

We also reveal a generic connection between the effect of time-reversals and nonlinear wave dynamics in systems with parity-time (PT) symmetry, considering a symmetric optical coupler with balanced gain and loss where these effects can be readily observed experimentally. We show that for intensities below a threshold level, the amplitudes oscillate between the waveguides, and the effects of gain and loss are exactly compensated after each period due to periodic time-reversals. For intensities above a threshold level, nonlinearity suppresses periodic time-reversals leading to the symmetry breaking and a sharp beam switching to the waveguide with gain. Another nontrivial consequence of linear PT-symmetry is that the threshold intensity remains the same when the input intensities at waveguides with loss and gain are exchanged.

8095-21, Session 6

Spatial coherence of random laser emission

B. Redding, Yale Univ. (United States); M. A. Choma, Yale School of Medicine (United States); H. Cao, Yale Univ. (United States)

Lasing action in disordered media has been studied extensively in recent years and many of its properties are well understood. However, few studies have considered the spatial coherence in these systems, despite initial observations indicating that random lasers exhibit much lower spatial coherence than conventional lasers. We performed a systematic investigation of the spatial coherence of random laser emission as a function of the scattering mean free path and the excitation volume. Our experiments were performed on a series of Rhodamine 640 doped diethylene glycol solutions with varying concentrations of 240 nm diameter polystyrene spheres. Lasing was achieved under optical excitation and spatial coherence was characterized by imaging the emission spot onto a Young's double slit and collecting the interference fringes in the far field. The visibility of these fringes provided a measure of the coherence between two points in the lasing spot separated by the distance of the two slits. We observed dramatic differences in the spatial coherence within our parameter space. Specifically, we found that samples with a shorter mean free path relative to the excitation volume exhibited reduced spatial coherence. We also found that the spatial coherence is strongest across a plane perpendicular to the longest dimension of the excitation volume. A qualitative explanation of the experimental results will be presented. This work provides a means to realize intense, spatially incoherent laser emission for applications in which speckle or spatial cross talk limits performance.

8095-22, Session 6

Classification of light sources and their interaction with active and passive environments

R. El-Dardiry, S. Faez, A. Lagendijk, FOM Institute for Atomic and Molecular Physics (Netherlands)

Emission from a molecular light source depends on its optical and chemical environment. This dependence is different for various sources. We present a general classification in terms of Constant Amplitude and Constant Power Sources. Using this classification, we have described the response to both changes in the LDOS and stimulated emission. To find the correct wave function from a single source or collection of sources becomes much more involved than previously assumed since it requires knowledge of the Green function for both the propagation and the generation of light.

The unforeseen consequences of this classification are illustrated for photonic studies by random laser experiments and are in good agreement with our correspondingly developed theory. In contrast to conventional lasers, random lasers have a statistically isotropic mode selectivity. Their mode selection is solely determined by the spectral shape of the gain curve. In a random laser therefore, measuring the emitted energy into a large enough solid angle corresponds to measuring the total emitted intensity: diffusion mimics an integrating sphere. In our experiments, we utilize this much neglected property of random lasers to study the influence of light source typology on the generation of light in complex media. Our results require a revision of studies on sources in complex media.

8095-23, Session 6

Random lasing in disordered arrays of ZnO nanorods

R. Frank, Karlsruher Institut für Technologie (Germany); A. Lubatsch, Rheinische Friedrich-Wilhelms-Univ. Bonn (Germany);

K. Busch, Karlsruher Institut für Technologie (Germany)

A random laser is in general a strongly disordered, laser-active optical medium. Despite substantial investigations, the physics of homogeneously disordered random lasers bears intriguing, open problems. The conditions for transport and localization and, in particular, the origin of confined spatial regions from which laser radiation is emitted (observed “lasing spots”) as well as the dependence of their size on for instance the pump rate, have remained poorly understood. Here, we consider spatially disordered ZnO nanorod arrays with uniform rod size, as also considered in experiments. These pillars have average diameter of 200 nm and a length of 4.7 μm , with an average rod-to-rod spacing of 500 nm. For such samples, we develop a semianalytical transport theory for random, laser-active systems, including light diffusion, localization, i.e. self-interference effects, and coupling to the semiclassical laser rate equations to account for (coherent) stimulated and (incoherent) spontaneous emission. We solve this laser transport theory with appropriate boundary conditions to obtain the average spatial distributions of the light intensity and of the occupation inversion. The full spatial intensity profile of the lasing spots is obtained numerically in dependence of the pump rate and other parameters such as the average number of nanorods per unitcell (filling fraction), system size and losses, caused by photons escaping out of the disordered array.

8095-24, Session 6

Ultrafast active control of optical eigenmodes in a multiple scattering nanowire layer

O. L. Muskens, M. Abb, Univ. of Southampton (United Kingdom);
E. P. A. M. Bakkers, Technische Univ. Eindhoven (United Kingdom)

The appearance of an interference pattern after transport of coherent waves through a random medium is the result of coherent summation of thousands of multiple scattering paths with random phases. Although the lack of many-body interactions makes phase coherence generally more robust for optical waves than for electrons, several dephasing processes can influence the transport of light, such as magnetic fields and inelastic scattering from colloids.

Here, we demonstrate a new regime of dephasing in photonic random media on ultrafast time scales. The random medium under study is a layer of strongly scattering nanowires, one of the most strongly scattering materials available today [1]. The nonlinear response of individual pseudomodes is found to be governed by dephasing of multiple scattering light paths on a picosecond time scale. By comparing our results with numerical simulations, we identify absorption and strain deformation as possible mechanisms responsible for the dephasing effects. The new dephasing nonlinearity results in large intensity modulations of around 50%, holding promise for ultrafast control of eigenmodes in nanophotonic switches, random lasers, and cavity quantum electrodynamics [2].

Of considerable importance is also the possibility of achieving nonadiabatic switching, i.e. dephasing of multiple scattering paths during the diffusion time of the light. We will discuss the possibility of controlling phase coherence of correlated paths in mesoscopic transport and, ultimately, the time-reversed light paths involved in photon localization.

[1] O. L. Muskens et al., Nano Lett. 9, 930 (2009)

[2] M. Abb, E. P. A. M. Bakkers, O. L. Muskens, submitted (2011)

8095-25, Session 7

Photonic band gap materials: light trapping crystals

S. John, Univ. of Toronto (Canada)

Photonic band gap (PBG) materials [1,2] are artificial periodic dielectric microstructures capable of trapping light in 3D [3] on sub-wavelength

scales. This offers new opportunities for efficient solar energy trapping and harvesting in suitably microstructured thin films [4]. It also enables virtually complete control of the flow of light on microscopic scales in a 3D optical chip [5-7] as well as very strong coupling of light to matter where desired. By further engineering the electromagnetic density of states [8-10] within the chip it is possible to realize unprecedented coherent optical control of the quantum state of resonant atoms or quantum dots [11, 12]. This defines a fundamentally new strong-coupling regime for quantum optics. It enables multiple-wavelength channel optical logic to be performed on a chip on picosecond time scales at micro-watt power levels.

I discuss further consequences of light trapping in classical and quantum electrodynamics. I also discuss the challenges and requirements for materials fabrication to realize these remarkable effects.

1. S. John, Physical Review Letters 58, 2486 (1987)
2. E. Yablonovitch, Physical Review Letters 58, 2059 (1987)
3. S. John, Physical Review Letters 53, 2169 (1984)
4. A. Chutinan and S. John, Physical Review A 78, 023825 (2008)
5. A. Chutinan, S. John, O. Toader, Phys. Rev. Lett. 90, 123901 (2003)
6. A. Chutinan and S. John, Physical Review B 72, 16, 161316 (2005)
7. A. Chutinan and S. John, Optics Express 14 (3), 1266 (2006)
8. D. Vujic and S. John, Physical Review A 76, 063814 (2007)
9. R.Z. Wang and S. John, Physical Review A 70, 043805 (2004)
10. R.Z. Wang, S. John, J. Photonics and Nanostructures 2, 137 (2004)
11. Xun Ma and Sajeev John, Physical Review Letters 103, 233601 (2009)
12. Xun Ma and Sajeev John, Physical Review A 80, 063810 (2009)

8095-26, Session 7

Strong coupling of plasmons in non-linear waveguides

D. Felbacq, A. Castanie, B. Guizal, Univ. Montpellier 2 (France)

Wave propagation in a planar metal plasmon waveguide is studied. More specifically, the dispersion curve of a metal-insulator-metal waveguide is investigated. Such structures have been investigated in the past in the situation of a thin insulator film. In this work, the situation when the insulator layer supports guided modes is considered. It is shown that, in that case, it is possible to realize the strong coupling of photon modes with plasmons. By means of complex plane analysis, the influence of this coupling on the losses is studied and, for the hybrid plasmon/waveguide photon mode, spatial Rabi oscillations are observed. Finally the introduction of gain is considered as well as some more complicated geometries in view of the practical realization of devices.

8095-27, Session 7

Quantum electrodynamics in photonic crystals

P. Lodahl, Technical Univ. of Denmark (Denmark)

2D photonic crystal membranes fabricated in GaAs containing InGaAs quantum dots have in recent years proven to be a very successful platform for all-solid-state quantum optics experiments [1-4]. In a photonic crystal, the light-matter interaction strength can be tailored, i.e. either enhanced or suppressed by controlling the lattice constant of the structure. We will present experimental results on how highly efficient single-photon sources can be constructed by coupling single quantum dots to a photonic crystal waveguide exploring slow light [3]. The role of disorder in the form of fabrication imperfections is explored and found to lead to Anderson localization of light enabling cavity quantum electrodynamics by exploiting disorder as a way to enhance light-matter interactions [4]. The fundamental limits of using Anderson localization to enhance light-matter interactions are discussed, and the results are compared to the performance of state-of-the-art engineered

nanocavities.

- [1] K. Hennessy et al., *Nature* 445, 896 (2007).
- [2] I. Fushman et al., *Science* 320, 769 (2008).
- [3] T. Lund-Hansen et al., *Phys. Rev. Lett.* 101, 113903 (2008).
- [4] L. Sapienza et al., *Science* 327, 1352 (2010).

8095-28, Session 7

Selective addressing of the resonant modes of a micropillar cavity with white light

G. Ctistis, A. Hartsuiker, E. van der Pol, Univ. Twente (Netherlands); J. Claudon, J. Gérard, Commissariat à l'Énergie Atomique (France); W. L. Vos, Univ. Twente (Netherlands)

There is a tremendous interest in high-quality micropillar resonators because of their potential in cavity-QED experiments such as the demonstration of the Purcell effect [1] or vacuum Rabi splitting [2, 3]. Most experiments are performed with quantum dots as internal light sources. Reflectivity experiments are rare because of symmetry constraints [4].

Here, we present broadband white-light reflectivity experiments on micropillar resonators with diameters ranging between 1 μm and 20 μm . The micropillars consist of a GaAs λ -layer, sandwiched between two Bragg-stacks made of $\lambda/4$ GaAs/AlAs layers, and were fabricated by molecular-beam epitaxy. We are able to spectrally resolve distinct transverse modes in the reflectivity experiments and to selectively address single modes by scanning the probe beam along the top facet of the micropillar. The positioning of the focused laser beam turns out to be crucial for pillar diameters exceeding the beam diameter, since at every position the coupling efficiency to different modes changes [5]. By decreasing the pillar diameter, we are able to resolve single modes, since the spacing between the modes increases.

References:

- [1] J.-M. Gérard, *Top. Appl. Phys.* 90, 269 (2003)
- [2] J. P. Reithmaier, G. S c, A. Löffler, C. Hofmann, S. Kuhn, S. Reitzenstein, L. V. Keldysh, V. D. Kulakovskii, T. L. Reinecke, and A. Forchel, *Nature* 432, 197 (2004)
- [3] G. Khitrova, H. M. Gibbs, M. Kira, S. W. Koch, and A. Scherer, *Nature Phys.* 2, 81 (2006)
- [4] J. L. Jewell, S. L. McCall, A. Scherer, H. H. Houh, N. A. Whitaker, A. C. Gossard, and J. H. English, *Appl. Phys. Lett.* 55, 22 (1989); T. Rivera, J.-P. Debray, and J.-M. Gérard, *Appl. Phys. Lett.* 74, 911 (1999).
- [5] G. Ctistis, A. Hartsuiker, E. van der Pol, J. Claudon, W. L. Vos, and J.-M. Gérard, *Phys Rev B* 82, 195330 (2010).

8095-29, Session 7

Diamond photonics and quantum optics

M. Loncar, Harvard Univ. (United States)

Individual color centers in diamond have recently emerged as a promising solid-state platform for quantum communication and quantum information processing systems, as well as sensitive nanoscale magnetometry with optical read-out. Performance of these systems can be significantly improved by engineering optical properties of color centers using nanophotonic approaches. In this work we describe a high-flux, room temperature, source of single photons based on an individual Nitrogen-Vacancy (NV) center embedded in a top-down nanofabricated, single crystal diamond nanowires. Using the nanowire geometry, an order of magnitude brighter single photon source is realized, with an order of magnitude lower pump power, compared to an NV center in a bulk diamond. We also describe fabrication process that combines ion implantation of nitrogen with nanowires fabricated in high-purity diamond crystals. This approach significantly improves single-photon properties of our devices. By embedding nanowires in metals, it is possible to

further increase photon production rate (via Purcell effect), as well as improve collection efficiency of emitted photons. Finally, we will describe optical cavities realized in diamond and materials transparent at visible wavelengths (Si₃N₄ and TiO₂) that can enable strong coupling between photons and NV centers.

8095-30, Session 8

Photonic crystal nanolasers with nanoslot structure for sensing applications

T. Baba, S. Kita, H. Abe, S. Hachuda, M. Narimatsu, S. Otsuka, K. Nozaki, Yokohama National Univ. (Japan)

Photonic crystals have achieved ultimately small nanolasers. For example, H₀-type devices in GaInAsP semiconductors operate under room temperature cw condition by photopumping with a modal volume of less than 0.2 times the cubic wavelength. The volume is further reduced beyond the diffraction limit by introducing a nanoslot in the cavity. A very narrow nanoslot of 30 nm width is formed by using inductively coupled plasma etching with HI gas. In such a nanoslot, strong mode localization occurs due to large discontinuity of electric field at high-index contrast boundaries. It enhances light-matter interaction in cavity QED and sensitivity of laser wavelength against environmental medium. The nanoslot nanolaser is particularly attractive as a sensor, because the device and optical I/O are much simpler and its performance is, in most cases, much better than passive cavity sensors'. As a sensor of liquid index, it exhibits a high sensitivity of 410 nm/RIU. In addition, it shows low temperature dependence in water, which is attributed to the negative TO effect of water compensating positive one in semiconductors. It suppresses the thermal chirping in laser spectrum to 10 pm order even with the small modal volume, ensuring high resolution sensing. Moreover, remarkable performance is observed when sensing protein; it detects an extremely low concentration of BSA protein in water, i.e. 17 pg/ml. This value implies 200 times higher sensitivity than that of surface plasmon resonance sensors.

8095-31, Session 8

Active semiconductor nanophotonics based on deterministic quantum wire and dot systems

E. Kapon, Ecole Polytechnique Fédérale de Lausanne (Switzerland)

Incorporating semiconductor quantum nanostructures such as quantum wires (QWRs) and quantum dots (QDs) into nano-photonics structures provides means for exploring both fundamental quantum photonics phenomena and applications in new photonic devices and systems. Examples include solid-state cavity quantum electrodynamics and quantum information processing and communications [1]. Most work in this field has been done using self-assembled quantum nanostructures, which, however, do not offer the necessary control in terms of optical spectra and positioning of the QWRs/QDs on the photonic chip.

Here, we review recent progress in quantum nano-photonics based on ordered QWR and QD structures grown on patterned substrates [2]. In particular, we discuss V-groove QWRs and pyramidal QDs formed due to growth rate anisotropy and nano-capillarity during metalorganic vapor phase epitaxy on nonplanar, patterned GaAs substrates [3]. This approach yields high quality, site-controlled (In)GaAs/(Al)GaAs QWR and QD systems, e.g., regular arrays of pyramidal QDs with ~1meV inhomogeneous broadening [4]. The confining potential of these wires/dots can be shaped by thickness and/or composition adjustment, producing structures of elaborated potential distributions, e.g., QD molecules and superlattices [5]. The intrinsically high symmetry of the pyramidal QDs yields unique excitonic features such as vanishing fine structure splitting, permitting efficient generation of polarization-entangled photons [6].

Based on these ordered QWR/QD systems, several nano-photonics

devices have been conceived and studied. These include coupled photonic crystal (PhC) cavities showing coupled-mode loss splitting [7], optically pumped, $\sim 1\mu\text{m}$ long PhC-QWR lasers with sub- μW threshold and coupled-cavity PhC-QWR lasers [8], and single-QDs integrated with PhC membrane cavities [9]. More recently, deterministic coupling of single pyramidal QDs in PhC membrane cavities has allowed the identification of phonon-mediated coupling of the QD exciton and the cavity mode, which persists only for limited (few meV) cavity detuning [10]. This paves the way to the deterministic coupling of several QD-excitons via cavity photons, interesting for exploring many-body quantum photonics phenomena [11]. Implications on the feasibility of realizing “true” QD lasers will also be discussed.

References:

1. See, e.g, J.L. O'Brien, A. Furusawa and J. Vuckovic, Nature Photonics 3, 687 (2009).
2. E. Kapon et al., Appl. Phys. Lett. 50, 347 (1987).
3. G. Biasiol and E. Kapon, Phys. Rev. Lett. 81, 2962 (1998).
4. A. Mohan et al., Small 6, 1268 (2010).
5. Q. Zhou et al., Small 5, 329 (2009).
6. A. Mohan et al., Nature Photonics, 4, 302 (2010).
7. K. Atlasov et al., Optics Express 16, 16255 (2008).
8. K. Atlasov et al., Optics Express 17, 18178 (2009); K. Atlasov et al., Optics Express (2011).
9. P. Gallo et al., Appl. Phys. Lett. 92, 63101 (2008).
10. M. Calic et al., 30th International Conference on the Physics of Semiconductor (ICPS 2010), 25-30 July, 2010, Seoul, Korea; and submitted (2010).
11. M.J. Hartmann, F.G.S.L. Brandao and M.B. Plenio, Laser&Photon. Rev. 2, 527 (2008).

8095-32, Session 8

Optical antenna electrodes for modification of QW electroluminescence

K. C. Y. Huang, Stanford Univ. (United States); M. Seo, KAIST (Korea, Republic of); M. L. Brongersma, Stanford Univ. (United States)

We simulated, fabricated and characterized the electroluminescence from InGaAs/ GaAs QW with metal electrodes which function as plasmonic resonator antennas. By patterning the antenna electrodes in the vicinity of a single QW layer with deeply subwavelength lateral width, charge carriers are confined near the antenna and subsequently recombine with enhanced radiative decay rate depending on the electrode/ QW separation and electrode shape. We show that the emission can be efficiently coupled to the antenna resonance which is engineered to reradiate with a specific polarization and unidirectional far-field pattern. The simultaneous control of carriers and photons can be used to improve light extraction and detection from the semiconductor while enabling fast direct modulation of the spontaneous emission.

8095-33, Session 8

Quantum dot and high-Q 3D photonic crystal nanocavity coupled system for manipulating exciton-photon interaction

Y. Arakawa, A. Tandraechanurat, S. Iwamoto, The Univ. of Tokyo (Japan)

No abstract available

8095-34, Session 9

High aspect ratio nanoscale metallic structures: a platform for photonic devices

P. Kuang, J. Park, W. Y. Leung, K. P. Constant, S. Chaudhary, K. Ho, Iowa State Univ. (United States)

We will report our progress in using high aspect ratio nanoscale metallic patterned structures in a number of optical devices such as light-emitting diodes or solar cells. They have high visible light transmission comparable to indium-tin-oxide electrodes and superior electrical conductivities. They can also provide a platform for switchable optical devices.

8095-35, Session 9

Exceeding the classical light-trapping limit in solar cells

J. N. Munday, D. M. Callahan, H. A. Atwater, California Institute of Technology (United States)

We describe a methodology for designing solar cells that have intensity and absorption enhancements that exceed the ergodic light-trapping limit. From thermodynamic arguments, Yablonovitch determined the maximum absorption enhancement in the ray optics limit for a bulk material to be $4n^2$, where n is the index of refraction of the absorbing layer. We extend this treatment by considering the local density of optical states (LDOS), which shows that absorption enhancements can exceed $4n^2$ under specific design criteria. Using a combination of analytical and numerical methods, we show how structures can be designed to beat the ergodic limit over an arbitrarily large wavelength range using frequency sum rules. For thin film solar cells, incorporating a plasmonic back reflector can result in spatially averaged LDOS enhancements of 1 to 3, and a metal-insulator-metal (MIM) structure can result in enhancements of over 200 near the bandedge of Si. We also find that placing the active material within a localized metallic resonator can lead to a nearly spatially uniform LDOS with enhancements above 1000. Purely dielectric structures can also lead to intensity enhancements exceeding the ergodic limit. For a low index active layer ($n=1.5$) clad by a high index layer ($n=3$), the LDOS enhancement is greater than 10. Finally, we show that for thin film solar cells with dispersive dielectric structures such as photonic crystals the ergodic light-trapping limit can be exceeded with LDOS enhancements of 2 to 5 by placing a planar solar cell in close proximity to a photonic crystal.

8095-36, Session 9

Multiexciton effects in semiconductor nanocrystals from the perspective of lasing and solar energy conversion

V. I. Klimov, Los Alamos National Lab. (United States)

Using semiconductor nanocrystals one can produce extremely strong spatial confinement of electronic wave functions not accessible with other types of nanostructures. One consequence of this effect is a significant enhancement in carrier-carrier interactions that lead to a number of novel physical phenomena including ultrafast multiexciton decay due to Auger recombination and efficient generation of multiple electron-hole pairs by single photons via carrier multiplication. In this talk, I will discuss the implications of ultrafast Auger decay for lasing applications of nanocrystals and several recent approaches developed in our group for resolving this problem by engineering carrier-carrier interactions in various types of heterostructured nanocrystals. I will also review the current status of carrier-multiplication research including experimental challenges in studies of this phenomenon, the role of extraneous effects, the competing energy relaxation channels such as hot-electron transfer, and implications of carrier multiplication in solar photovoltaics.

8095-37, Session 10

Explorations of photonic nanostructures for thermal and quantum applications

S. Fan, Stanford Univ. (United States)

I will review some of our recent progresses in understanding photonic nanostructures. Examples including modified photon-photon interactions in one-dimensional nanophotonic systems, and new understandings of near-field thermal transfer.

8095-38, Session 10

Near-unity collection efficiency of single photons using a planar dielectric antenna

K. Lee, X. Chen, Max-Planck-Institut für die Physik des Lichts (Germany); H. Eghlidi, A. Renn, ETH Zurich (Switzerland); S. J. Goetzinger, V. Sandoghdar, Max-Planck-Institut für die Physik des Lichts (Germany)

Single-photon sources have been discussed as the building blocks of quantum cryptography, optical quantum computation, spectroscopy, and metrology. However, the feasibility of these proposals depends on the availability of single photons with a high fidelity. For sources based on single emitters, this implies near-unity collection efficiency into well-defined modes. Some of the current state-of-the-art efforts aimed at achieving these criteria have been demonstrated, but despite an impressive progress the results still fall short. Here we report on a broad-band room-temperature scheme, which uses a layered dielectric structure for tailoring the angular emission of a single oriented molecule such that more than 96% of the emitted photons are collected with a commercially available microscope objective, leading to recorded photon count rates of about 50 MHz. Furthermore by adjusting the antenna parameters we could make an output mode to be very close to the radially polarized doughnut mode which can be converted into other modes such as the fundamental mode of an optical fibre with high fidelity. Our approach is wavelength insensitive and also compatible with cryogenic experiments. We will discuss various details of the design, fabrication and characterization of our dielectric planar antenna and its various applications to other types of single emitters - semiconductor quantum dots, diamond color centers, or solid-state ions.

8095-39, Session 10

Integrated quantum photonics

K. Aungkunsiri, D. Bonneau, E. Engin, D. Fry, J. P. Hadden, P. Kalasuwan, J. Kennard, T. Lawson, L. Marseglia, E. Martin-Lopez, J. C. F. Matthews, J. Meinecke, A. Peruzzo, K. Poullos, P. Shadbolt, A. Stanley-Clarke, M. Halder, J. Harrison, D. Ho, P. Jiang, A. Laing, M. Lobino, A. Politi, B. R. Patton, M. Rodas Verde, X. Zhou, M. J. Cryan, J. G. Rarity, M. G. Thompson, S. Yu, J. L. O'Brien, Univ. of Bristol (United Kingdom)

Quantum information science aims to harness uniquely quantum mechanical properties to enhance measurement and information technologies, and to explore fundamental aspects of quantum physics. Of the various approaches to quantum computing [1], photons are particularly appealing for their low-noise properties and ease of manipulation at the single qubit level [2]. Encoding quantum information in photons is also an appealing approach to quantum communication, metrology (eg. [3]), measurement (eg. [4]) and other quantum technologies [5]. However, the implementation of optical quantum circuits with bulk optics has reached practical limits. We have developed an integrated waveguide approach to photonic quantum circuits for high performance, miniaturisation and scalability [6]. Here we report high-fidelity silica-on-silicon integrated optical realisations of key

quantum photonic circuits, including two-photon quantum interference and a controlled-NOT logic gate [7]. We have demonstrated controlled manipulation of up to four photons on-chip, including high-fidelity single qubit operations, using a lithographically patterned resistive phase shifter [8]. We have used this architecture to implement a small-scale compiled version of Shor's quantum factoring algorithm [9] and demonstrated heralded generation of tuneable four photon entangled states from a six photon input [10]. We have combined waveguide photonic circuits with superconducting single photon detectors [11]. We describe complex quantum interference behaviour in multi-mode interference devices with up to eight inputs and outputs [12], and quantum walks of correlated particles in arrays of coupled waveguides [13]. Finally, we give an overview of our recent work on fundamental aspects of quantum measurement [14,15] and single photon sources [16,17].

[1] T. D. Ladd, F. Jelezko, R. Laflamme, Y. Nakamura, C. Monroe, and J. L. O'Brien, *Nature* 464, 45 (2010).

[2] J. L. O'Brien, *Science* 318, 1567 (2007).

[3] T. Nagata, R. Okamoto, J. L. O'Brien, K. Sasaki, and S. Takeuchi, *Science* 316, 726 (2007).

[4] R. Okamoto, J. L. O'Brien, H. F. Hofmann, T. Nagata, K. Sasaki, and S. Takeuchi, *Science* 323, 483 (2009).

[5] J.L.O'Brien, A.Furusawa, and J.Vuckovic, *Nature Photon.* 3, 687 (2009).

[6] A. Politi, M. J. Cryan, J. G. Rarity, S. Yu, and J. L. O'Brien, *Science* 320, 646 (2008).

[7] A. Laing, A. Peruzzo, A. Politi, M. R. Verde, M. Halder, T. C. Ralph, M. G. Thompson, and J. L. O'Brien, *Appl. Phys. Lett.* 97, 211109 (2010)

[8] J. C. F. Matthews, A. Politi, A. Stefanov, and J. L. O'Brien, *Nature Photon.* 3, 346 (2009).

[9] A. Politi, J. C. F. Matthews, and J. L. O'Brien, *Science* 325, 1221 (2009).

[10] J. C. F. Matthews, A. Peruzzo, D. Bonneau, and J. L. O'Brien, arXiv:1005.5119

[11] C. M. Natarajan, A. Peruzzo, S. Miki, M. Sasaki, Z. Wang, B. Baek, S. Nam, R. H. Hadfield, and J. L. O'Brien, *Appl. Phys. Lett.* 96, 211101 (2010).

[12] A. Peruzzo, A. Laing, A. Politi, T. Rudolph, and J. L. O'Brien, *Nature Comm.* in press; arXiv:1005.5119

[13] A. Peruzzo, M. Lobino, J. C. F. Matthews, N. Matsuda, A. Politi, K. Poullos, X.-Q. Zhou, Y. Lahini, N. Ismail, K. Wörhoff, Y. Bromberg, Y. Silberberg, M. G. Thompson, and J. L. O'Brien, *Science* 329, 1500 (2009)

[14] A. Laing, T. Rudolph, and J. L. O'Brien, *Phys. Rev. Lett.* 102, 160502 (2009).

[15] X-Q Zhou, TC Ralph, P Kalasuwan, M Zhang, A Peruzzo, BP Lanyon, and JL OBrien arXiv:1006.2670

[16] J. P. Hadden, J. P. Harrison, A. C. Stanley-Clarke, L. Marseglia, Y.-L. D. Ho, B. R. Patton, J. L. O'Brien, and J. G. Rarity, *Appl. Phys. Lett.* 97, 241901 (2010)

[17] C. Xiong, G. D. Marshall, A. Peruzzo, M. Lobino, A. S. Clark, D.-Y. Choi, S. J. Madden, C. M. Natarajan, M. G. Tanner, R. H. Hadfield, S. N. Dorenbos, T. Zijlstra, V. Zwiller, M. G. Thompson, J. G. Rarity, M. J. Steel, B. Luther-Davies, B. J. Eggleton, J. L. O'Brien *Appl. Phys. Lett.* 98, 051101 (2011)

8095-40, Session 10

Nonlinear optics near the single photon level with quantum dots coupled to photonic crystals

E. Waks, D. Sridharan, R. Bose, H. Kim, T. Shen, Univ. of Maryland, College Park (United States); G. S. Solomon, National Institute of Standards and Technology (United States)

Quantum dots (QDs) are stable, bright, semiconductor based light emitters that exhibit a quantized energy spectrum. For these reasons

they are excellent candidates for development of lasers, nonlinear optoelectronic components, and basic building blocks for future quantum information technology. Such applications critically depend on the ability to create strong interactions between QDs and photon fields. One method to engineer these strong interactions is to use photonic crystal structures. Photonic crystals are materials with a periodic index of refraction that can guide and confine light on the size scale of an optical wavelength, resulting in extremely strong atom-photon interactions. In this talk we will discuss our work to engineer strong nonlinear optical effects near the single photon level using a single quantum dot coupled to a photonic crystal cavity. We show that these interactions can be used to create all-optical switching with 8 GHz switching speeds using as few as two photons for the switching pulse. This device is approaching the fundamental limit where a single control photon can nonlinearly interact with a single target photon via cavity reflectivity modification. We then describe our effort to extend the device to a planar geometry that enables large scale integration on a chip. In addition, we show that by exploiting QD spin under high magnetic field we can attain improved switching performance, and also engineer entanglement between a photon and a single quantum dot, providing the potential for compact quantum devices that can be integrated on a semiconductor chip for future quantum information applications.

8095-52, Poster Session

The importance of nonlinear reflectance and transmittance measurements on the characterization of the nonlinear optical properties of metallic nanomaterials

C. Fuentes-Hernandez, Georgia Institute of Technology (United States); H. Hu, CREOL, The College of Optics and Photonics, Univ. of Central Florida (United States); A. R. Ernst, Georgia Institute of Technology (United States); D. A. Fishman, CREOL, The College of Optics and Photonics, Univ. of Central Florida (United States); J. Hsu, Georgia Institute of Technology (United States); S. Webster, D. J. Hagan, E. W. Van Stryland, CREOL, The College of Optics and Photonics, Univ. of Central Florida (United States); B. Kippelen, Georgia Institute of Technology (United States)

Z-scan is one of the most commonly used techniques to characterize the nonlinear optical (NLO) properties of many optical materials, including metallic nanomaterials such as ultrathin metal layers, metal nanoparticle doped glasses, and many others. To date, Z-scan data has been analyzed using the original formalism proposed by Sheik-Bahae M., et.al. (IEEE Journal of Quantum Electronics, 26, 760, 1990). In this formalism, the NLO changes in the sample's reflectance, $\Delta R(I(z))$, are neglected. This implies that the NLO changes in transmittance, $\Delta T(I(z))$, measured in open-aperture Z-scan experiments can be directly correlated with the NLO changes in absorptance, $\Delta A(I(z))$, such that $\Delta A = -\Delta T$. However, this approximation of the original Z-scan formalism, valid for most dielectrics and semiconductors, both organic and inorganic, is no longer valid in metallic nanostructures where the NLO changes in reflectance (R) and transmittance (T) can be of the same order of magnitude, hence making $\Delta A = -\Delta T - \Delta R$. Here, we discuss the implications of having strong changes in the reflectance by characterizing the NLO properties of a 20 nm Au film using a combination of T and R pump-probe and Z-scan experiments implemented with 500 fs pulses at 560 nm. We use spectroscopic ellipsometry to measure the linear refractive index of Au and use a physical model of the metal's permittivity to describe the linear and NLO properties measured by pump-probe experiments. Furthermore, we show that Z-scan traces can be recovered from these experiments and how neglecting ΔR in the analysis of transmittance Z-scan data leads to misleading estimations of the magnitude, and even the sign, of the NLO changes observed.

8095-53, Poster Session

thermal tuning of a silicon photonic crystal cavity infilled with an elastomer

A. K. Erdamar, M. van Leest, S. J. Picken, J. Caro, Technische Univ. Delft (Netherlands)

Thermal tuning of the transmission of a cavity in silicon photonic crystal (PhC) slab globally infilled with an elastomer was investigated. In contrast to liquids used for infiltration, elastomers are more stable and durable. In addition, elastomers have a high coefficient of thermal expansion and as a result exhibit a relatively strong decrease of the refractive index upon heating. This appreciable thermo-optic property ($-3.5 \times 10^{-4}/K$) can counteract the positive thermo-optic coefficient of the host material silicon ($1.85 \times 10^{-4}/K$), and thus enables a measurable blue shift of the cavity transmission. Here, we use the elastomer Kraton SEBS G 1657 using global infilling and global heating of the PhC. The triangular hole-type PhCs are fabricated in silicon-on-insulator (SOI) material, using electron-beam lithography and cryogenic inductively coupled plasma etching in an SF₆-based plasma. Membrane PhC devices are obtained by underetching the silicon layer in buffered HF. The infilling is done by applying a drop of the elastomer dissolved in cyclohexane (2% by weight) to the PhC membrane. The cavity we use is a hole-type cavity with modified surrounding holes. Transmission measurements are performed with the end-fire technique, using a white light source and an optical spectrum analyzer. The infill effect on the band gap and on the cavity resonance is clearly observed, the shift in either case being about 135 nm. Temperature-dependent measurements of the cavity resonance at eight temperatures in the range 293-333 K show a linear blue shift of 2.64 nm, large enough for tuning the transmission of modest Q cavities.

8095-54, Poster Session

Mode of propagation of optical radiation with self-similar pulse shape in layered medium with nonlinear absorption

V. A. Trofimov, O. V. Matusevich, D. A. Smotrov, Lomonosov Moscow State Univ. (Russian Federation)

We investigate the possibility of propagation of laser pulse which has self-similar shape at its propagation in a medium with two-photon absorption. The consideration is based on the solution of problem as nonlinear eigenfunction problem for the Schrödinger equation with periodic nonlinear coefficients which describe the nonlinear absorption and dielectric permittivity. Under certain conditions this eigenfunction gives us the pulse shape with requiring properties. We investigate the realization of mode of the laser pulse propagation with self-similar its shape in layered medium with two-photon absorption. In the case of homogeneous absorption medium the shape of pulse is similar to the soliton shape taking place for a propagation of laser radiation in a medium with Kerr nonlinearity.

8095-55, Poster Session

Photopolymer films doped with zeolite nanocrystals

M. Moothanchery, I. Naydenova, Dublin Institute of Technology (Ireland); S. Mintova, Ecole Nationale Supérieure d'Ingenieurs de Caen et Ctr. de Recherche (France); V. Toal, Dublin Institute of Technology (Ireland)

The effect of zeolites nanocrystals (pure silicate, aluminosilicates and aluminophosphate) incorporated in acrylamide based photopolymer layers for holographic applications is investigated. The presence of the zeolite nanocrystals improved the refractive index modulation and also resulted in substantial suppression of polymerization shrinkage. The

higher refractive index modulation achieved is beneficial for applications such as holographic data storage as it provides higher storage capacities. Besides, the high refractive index modulation is advantageous for the fabrication of spectroscopic devices and holographic optical elements. The holograms recorded in the acrylamide photopolymer films doped with the zeolite nanoparticles are identified for further sensor application.

8095-56, Poster Session

Coherent optical imaging through opaque photonic media

G. Ctistis, E. G. van Putten, D. Akbulut, J. Bertolotti, Univ. Twente (Netherlands); A. Lagendijk, FOM Institute for Atomic and Molecular Physics (Netherlands); W. L. Vos, A. P. Mosk, Univ. Twente (Netherlands)

Scattering of light is usually seen as a nuisance in microscopy. Scattering limits the penetration depth and strongly deteriorates the achievable resolution. However, by gaining active spatial control over the optical wave front it is possible to manipulate the propagation of scattered light even far in the multiple scattering regime [1]. It was recently shown that in this way scattered light can even be exploited for perfect optical focusing [2]. These wave front shaping techniques pave the way for new microscopy methods based on strong light scattering [3-6].

We use fluorescent beads to demonstrate concentration of scattered light into a focus much smaller than the wavelength. Exploiting such a small focus, we demonstrate imaging of gold nanostructures through an opaque scattering layer. We obtained a very high resolution proving that scattering can significantly improve the image quality in microscopy.

References:

- [1] I. M. Vellekoop and A. P. Mosk, *Opt. Lett.* 32, 2309 (2007).
- [2] I. M. Vellekoop, A. Lagendijk, and A. P. Mosk, *Nature Photon.* 4, 320 (2010).
- [3] I. M. Vellekoop and C. M. Aegerter, *Opt. Lett.* 35, 1245 (2010).
- [4] C.-L. Hsieh, Y. Pu, R. Grange, G. Laporte, and D. Psaltis, *Opt. Express* 18, 20723 (2010).
- [5] S. M. Popoff, G. Lerosey, M. Fink, A. C. Boccarda, and S. Gigan, *Nature Com.* 1, 81 (2010).
- [6] T. i már, M. Mazilu, and K. Dholakia, *Nature Photon.* 4, 388 (2010).

8095-57, Poster Session

The effects similar to quantum teleportation and superluminality at propagating of laser pulse in medium with combined nonlinear response

V. A. Trofimov, O. V. Matushevich, Lomonosov Moscow State Univ. (Russian Federation)

The effect of laser pulse propagation with group velocity, which is faster than light velocity at given conditions, is widely investigated at present, in particular for photonic crystals. We have found out the similar effect under the interaction of two laser pulse in medium with combined nonlinear response for 2D or 3D cases and for propagation of femtosecond pulse in nonlinear medium under the condition of temporal dispersion of nonlinear response.

The physical reason of such laser pulse propagation concludes in self-induced optical grating due to nonlinear interaction of laser radiation with matter. The grating acts on laser pulse in similar way as photonic crystal acts on velocity of laser light passed through the one.

We predict and investigate the increasing of group velocity of some sub-pulses, which appear under the dual-waves interaction in nonlinear medium.

We shown the distortion, introduced in one of pulses, acts on the other pulse immediately despite on time interval between the pulses. In this case we can say about the effect that is like to teleportation effect in quantum mechanics

8095-58, Poster Session

Tunable subradiant lattice plasmons by out-of-plane dipolar interactions

W. Zhou, T. W. Odom, Northwestern Univ. (United States)

Plasmonic nanostructures can concentrate optical fields into nanoscale volumes, which is useful for plasmonic nanolasers, surface enhanced Raman spectroscopy, and white-light generation. However, the short lifetimes of the emissive plasmons correspond to a rapid depletion of the plasmon energy, preventing further enhancement of local optical fields. Dark (subradiant) plasmons have longer lifetimes, but their resonant wavelengths cannot be tuned over a broad wavelength range without changing the overall geometry of the nanostructures. Also, fabrication cannot be readily scaled because their complex shapes have subwavelength dimensions. Here we report a new type of subradiant plasmon with a narrow (~5 nm) resonant wavelength that can be easily tuned by changing either the height of large (> 100 nm) gold nanoparticles arranged in a two-dimensional array or the incident excitation angle. At resonance, strong coupling between out-of-plane nanoparticle dipolar moments suppresses radiative decay, trapping light in the plane of the array and strongly localizing the optical field onto each nanoparticle. This new mechanism can lead to new applications for subradiant plasmons because height-controlled nanoparticle arrays can be manufactured over wafer-scale areas on a variety of substrates.

8095-41, Session 11

High-performance Ge quantum well modulators for optical interconnects

S. A. Claussen, E. H. Edwards, S. Ren, R. K. Schaevitz, R. M. Audet, E. Tasyurek, E. Fei, T. I. Kamins, J. S. Harris, D. A. B. Miller, Stanford Univ. (United States)

Electrical interconnects are rapidly nearing fundamental limitations related to their density-scaling a wire down in size does not allow it to carry more information-and the environmentally-significant amount of power they consume. Optical interconnects provide a promising solution, but require CMOS-compatible, low-energy optical components in order to be a feasible alternative. Ge/SiGe quantum wells (QWs) exhibit the quantum-confined Stark effect, a strong electroabsorption mechanism that enables compact optical modulators for use in future optical interconnect systems.

To design and optimize high-performance modulators, we have experimentally investigated the ultrafast carrier dynamics and transport properties of Ge/SiGe QWs. We have also developed a simple model for the electroabsorption spectrum of this material, which allows us to account for both absorption from our QW design and the less-desirable background absorption that limits device performance.

We have demonstrated Ge/SiGe QW modulators in both a surface-normal, asymmetric Fabry-Perot geometry and a waveguide geometry. The asymmetric Fabry-Perot design allows for high contrast ratios with small changes in absolute absorption. We have recently achieved contrast ratios of 4.8 dB over a 1 V swing. Better understanding of the background absorption in the QWs and resonator cavity will enable future contrast ratios of more than 10 dB with a greatly reduced insertion loss. The waveguide modulators are enabled by selective-area epitaxial growth of the QWs and provide easy integration with other interconnect components. We have demonstrated a waveguide modulator with an active area of 5µm², an extinction ratio of 3.2 dB and a speed of 3.5 Gb/s.

8095-42, Session 11

Engineering aperiodic order for optical devices with photonic-plasmonic nanostructures

L. Dal Negro, Boston Univ. (United States)

Deterministic Aperiodic Structures (DAS) are generated by the mathematical rules of L-systems and number theory, manifest unique light localization and transport properties associated with a great structural complexity, and can be fabricated on-chips using conventional nano-lithographic techniques. When combined with metal-dielectric nanostructures, they give rise to large energy gaps like periodic media (i.e. photonic-plasmonic crystals) and highly localized, enhanced field states like disordered random media, including the formation of Anderson-localized modes, forbidden in periodic scattering media. Contrary to random media, DAS possess controllable transport properties from ballistic to anomalous diffusion (slower diffusion than classical random walks) and strongly localized field states with large fluctuations of the photonic mode density - essential attributes to achieve spatio-temporal energy localization and enhanced light-matter coupling, i.e. radiative rates of fluorescent molecules, absorption cross-sections, non-linear optical processes on the nanoscale. In particular, DAS fabricated using metal/dielectric nanoparticles are suitable to engineer efficient nanoplasmonic structures for Surface Enhanced Raman (SERS) sensing, optical detectors, and enhanced light-emitting and nonlinear components.

In this talk, by combining dark-field scattering characterization, micro-photoluminescence and Raman measurements with accurate electro-dynamics calculations based on semi-analytical multiple-scattering theories, I will discuss electromagnetic coupling^{1,2}, resonant scattering³, colorimetric biosensing⁴, light emission⁵ and surface enhanced Raman sensing^{6,7} in two-dimensional metal-dielectric photonic-plasmonic arrays based on deterministic aperiodic sequences. In particular, I will survey the optical properties, and assess the device performances, of different aperiodic systems ranging from quasi-periodic crystals to pseudo-random nanoparticle arrays⁸ fabricated by Electron-Beam Lithography (EBL) on transparent quartz substrates. Finally, I will present novel aperiodic optical nano-antennas structures that can provide strong field localization at multiple frequencies over a broad spectral range⁹.

References:

1. L. Dal Negro, N.N. Feng, A. Gopinath "Electromagnetic coupling and plasmon localization in deterministic aperiodic arrays", *J. Opt. A: Pure Appl. Opt.* 10, 064013 (2008)
2. C. Forestiere, G. Miano, G. Rubinacci, L. Dal Negro, "Analysis of localized modes and spectral gaps in Fibonacci arrays of metal nanoparticles", *Phys. Rev. B.*, 79, 085404 (2009)
3. A. Gopinath, S. Boriskina, N.N. Feng, B.M. Reinhard, L. Dal Negro, "Photonic-plasmonic scattering resonances in deterministic aperiodic structures", accepted for publication in *Nanoletters* 8, 2423 (2008)
4. S. Boriskina, L. Dal Negro "Sensitive label-free biosensing using critical modes in aperiodic photonic structures", *Optics Express*, 16, 12511 (2008)
5. A. Gopinath, S. Boriskina, S. Yerci, R. Li, L. Dal Negro, Enhancement of the 1.54 μ m Erbium emission from quasi-periodic plasmonic arrays, *Appl. Phys. Lett.*, 96, 071113 (2010)
6. A. Gopinath, S. Boriskina, B. Reinhard, L. Dal Negro, "Deterministic Aperiodic Arrays of Metal nanoparticles for surface-enhanced Raman scattering", *Optics Express*, 17, 3741 (2009).
7. A. Gopinath, S. Boriskina, W. Premasiri, L. Ziegler, B. Reinhard, L. Dal Negro, "Plasmonic Nanogalaxies: multi-scale aperiodic arrays for surface enhanced Raman sensing", *Nanoletters* 9, 3922 (2009)
8. C. Forestiere, G.F. Walsh, G. Miano, L. Dal Negro, "Nanoplasmonics of prime number arrays", *Optics Express* 17, 24289 (2009)
9. S. Boriskina, L. Dal Negro, "Multiple-wavelength plasmonic nano-antennas" *Optics Letters*, 35, 538, (2010).

8095-43, Session 11

fJ/bit photonic platform based on photonic crystals

M. Notomi, NTT Basic Research Labs. (Japan)

Currently, demands for low-power integratable nano-photonic components are increasing for next-generation chips where the introduction of a large number of photonic components is discussed in order to resolve the energy consumption and heat generation problems of present CMOS chips. However, this is challenging because conventional photonic components are too large, too energy-consuming, and hard to integrate. In this talk, we argue that a photonic crystal is one of the promising candidates for this purpose. For the last several years, a number of sophisticated designs for high Q nanocavities based on photonic crystals have been developed. Recently, we have applied these nanocavities for various photonic devices, and achieved ultra-low energy consumption operation. First example is an all-optical switch. We applied a so-called H0 cavity which is the smallest dielectric-core cavity, composed from composition-optimized InGaAsP. By this design, we achieved fast all-optical switching operation with an optical pulse of less than 1 fJ and 10-25 ps length. Second example is a laser. We adopted a novel buried-heterostructure photonic-crystal cavity design to realize strong photon/electron confinement and small thermal resistance. We achieved room-temperature optically-pumped CW lasing with the threshold power of 1.5 micro-watts. Furthermore, we achieved 20GHz direct modulation, corresponding to 8.76fJ/bit energy consumption. These energy/bit numbers are about two orders of magnitude lower than previous results. They indicate that it is now possible to realize nanophotonic devices with fJ/bit energy consumption. I will also discuss other low-power nanophotonic devices based on photonic crystals and possible impacts for future ICT.

8095-44, Session 11

Ultra-low threshold lasers and modulators based on optical nanocavities

J. Vuckovic, B. Ellis, G. Shambat, A. Majumdar, A. Faraon, Stanford Univ. (United States)

Achieving the operation of semiconductor optoelectronic devices (lasers and modulators) at sub-10fJ control with speeds exceeding 10GHz, as is required by the ITRS roadmap [1], remains a big challenge and requires radical approaches. Nanophotonic devices could operate at such a low-energy and high-speed limit. A strong localization of light inside of optical nanocavities (such as photonic crystals) increases the strength of light-matter interaction, which in turn reduces thresholds for various optical effects, including lasing and modulation. We have employed such a platform to demonstrate the lowest threshold electrically injected semiconductor laser, operating at only 150nA threshold current - an order of magnitude lower than any electrically injected semiconductor laser so far. In addition, we have demonstrated ultra-fast electro-optic modulation with only ~0.6fJ control energy per bit. In both of these cases, we have developed practical, scalable structures employing lateral current injection into a photonic crystal nanocavity [2]. In addition to being fast and energy efficient, the small size of these devices is also important for achieving high density of integration; moreover, such operation can be achieved with moderate values of the resonator quality factors, which also alleviates the energy consumption of thermal stabilization circuit.

We have also demonstrated a proof of concept electro-optic modulator based on a single quantum dot strongly coupled to a photonic crystal nanocavity that enables operation at the ultimate limit of control energy - sub-aJ per bit [3]. Finally, to make these devices silicon CMOS compatible, we are investigating a platform based on a combination of silicon and germanium [4].

Financial support was provided by IFC, AFOSR, Office of Naval research, and DARPA.

References

- [1] D. A. B. Miller, "Device Requirements for Optical Interconnects to

Silicon Chips," Proc. IEEE 97, 1166-1185 (2009)

[2] Bryan Ellis, Tomas Sarmiento, James Harris, Marie Mayer, Eugene Haller, Bingyang Zhang, Yoshihisa Yamamoto, and Jelena Vuckovic, "Electrically pumped photonic crystal nanocavities using a laterally doped p-i-n junction," Applied Physics Letters Vol 96, 181103 (2010).

[3] Andrei Faraon, Arka Majumdar, Hyochul Kim, Pierre Petroff and Jelena Vuckovic, "Fast electrical control of a quantum dot strongly coupled to a photonic crystal cavity," Physical Review Letters, vol. 104, 047402 (2010)

[4] Szu-Lin Cheng, Jesse Lu, Gary Shambat, Hyun-Yong Yu, Krishna Saraswat, Jelena Vuckovic, Yoshio Nishi, "Room temperature 1.6 um electroluminescence from Ge light emitting diode on Si substrate," Optics Express, Vol 17, pp 10019-10024 (2009)

8095-45, Session 12

Integrated metapotonics

A. D. Boardman, P. Egan, R. R. C. Mitchell-Thomas, Univ. of Salford (United Kingdom)

Building up a range of integrated metamaterial waveguide devices is not only attractive from a fundamental point of view, but it is going to be possible to create a number of beautiful down-stream applications. It is in this sense that the presentation is developed under the general integrated metapotonics heading. In the first instance, the propagation of waveguide modes in double negative material and materials characterised by other combinations of relative dielectric permittivity and relative permeability, together with some degree of geometrical complexity will be considered. The general properties of linear metamaterial guides will be exposed, and the extent to which nonlinearity and magneto-optic influence can be used as control agents will be investigated. The degree of control obtained by manipulating planar waveguide interfaces is shown to be another fascinating outcome from the use of special metamaterials and this will be highlighted for certain frequency windows. Certain systems lead to the possibility of not only slowing light down, but to the concept of actually stopping light, heralding new types of all-optical computer chips. Tapered, and discontinuous guides will be investigated, with this in mind, leading to new ideas about switches and X-junctions and the famous trapped rainbows. All of these will be shown to emerge from the use of modern metamaterials, and that there are certain novel features that always emerge from them. In addition to this and soliton propagation, transformation optics will be invoked by reaching out for a dramatic use of the spacetime cloak, or the history editor

8095-46, Session 12

Active plasmonic devices enhanced by waveguide dispersion engineering

C. Min, G. Veronis, Louisiana State Univ. (United States)

Plasmonic devices, based on surface plasmons propagating at metal-dielectric interfaces, have shown the potential to manipulate light at deep subwavelength scales. One of the main challenges in plasmonics is achieving active control of optical signals. In this paper, we introduce active plasmonic devices enhanced by waveguide dispersion engineering. We consider plasmonic waveguide systems consisting of a metal-dielectric-metal waveguide (MDM) side-coupled to arrays of MDM stub resonators. The MDM waveguide and stubs are filled with an active material whose absorption coefficient can be modified with an external control beam. Such plasmonic waveguide systems can be engineered to support slow-light modes. We find that, as the slowdown factor increases, the sensitivity of the effective index of the mode to variations of the refractive index of the active material increases. Such slow-light enhancements of the sensitivity to refractive index variations lead to enhanced performance of active plasmonic devices such as switches. To demonstrate this, we consider absorption switches based on Fabry-Perot cavity structures, consisting of slow-light plasmonic waveguide systems

sandwiched between two conventional MDM waveguides. We find that increased slowdown factor leads to increased induced change of the propagation length of the slow-light mode for a given refractive index variation, and therefore to increased modulation depth. Compared to conventional MDM absorption switches, slow-light enhanced switches achieve significantly higher modulation depth with moderate insertion loss. We use a scattering matrix theory to account for the behavior of the devices which is in excellent agreement with numerical results obtained with the finite-difference frequency-domain method.

8095-47, Session 12

Slow light using negative metamaterials

S. Sridhar, W. Lu, Y. Huang, D. Casse, S. Savo, Northeastern Univ. (United States)

Controlling the speed of light is a fundamental challenge that can lead to new physical phenomena and applications. We show that a nonresonant planar waveguide consisting of conventional dielectric cladded with single-negative materials supports degenerate propagating modes for which the group velocity and total energy flow can be zero if the media are lossless.

We have carried out the first experimental observation of slow light utilizing the mechanism of the degeneracy of forward and backward waves, in the GHz microwave regime in a planar waveguide consisting of a dielectric core cladded with single-negative metamaterial. The metamaterial cladding consisted of periodic arrays of metallic split-ring resonators (SRRs), exhibiting an effective negative permeability. Group delay dispersions obtained from pulsed measurements are in complete agreement with that obtained from a theory of slowing light.

Absorptive losses severely limit the velocity reduction, and will even destroy the zero-group velocity condition for real frequency/complex wave vector modes. We show that by incorporating gain G into the core dielectric, there exists a critical gain value G_c at which we can recover the condition of zero group velocity, so that light pulses can be stopped and stored. This structure is simpler to achieve than double-negative metamaterials, has small footprint, and can be incorporated into ultracompact on-chip optoelectronics.

These nanoscale metamaterial waveguides offer the prospect of on-chip slow light devices where light speeds are reduced by orders of magnitude, enabling ultra-compact optical delay lines and buffers.

8095-48, Session 13

Electrically active 3D photonic and plasmonic crystals

P. V. Braun, Univ. of Illinois at Urbana-Champaign (United States)

Photonic and plasmonic crystals provide unprecedented control over light emission, absorption and propagation, which has led to the proposal of a large variety of optoelectronic devices. Three-dimensional devices with electronic functionality have however remained elusive, as fabrication of three-dimensional, electrically active nanostructured materials remains complex. Numerous techniques have been demonstrated to fabricate 3D photonic and plasmonic crystals, including colloidal crystallization, phase mask and multibeam interference lithography, direct laser writing, photolithography, and wafer bonding, but, most of these techniques result in amorphous or polycrystalline material which does not possess the required electronic properties for application in optoelectronics. There are a number of elegant techniques which make use of single crystal semiconductor substrates, however they tend to require elaborate, slow processing, are limited in what photonic crystal structures may be created, and have not demonstrated electrical functionality. In this work we demonstrate a method of forming 3D photonic and plasmonic crystals from single crystal III-V semiconductors by metal-organic vapor phase epitaxy (MOVPE). We employ a template-based fabrication method and grow semiconductor material to fill the structure using a form of selective area epitaxy.

The epitaxial growth process (originating at the substrate, in contrast to conformal growth) is much the same as the growth of planar III-V devices in that light emitting layers (e.g. quantum wells), cladding layers, electrically doped layers, etc may all be grown in a single process. Thus the layers of an optoelectronic device may be defined by the MOVPE growth parameters while the photonic crystal structure is simultaneously imparted to the material using the 3D template. To demonstrate the potential of this technique we have fabricated vertically emitting LED's with embedded InGaAs QW's. The fundamental behaviors of this growth technique will be discussed, including prevention of polycrystalline nucleation, doping and fabrication of light-emitting heterostructures.

8095-49, Session 13

'Giant' nanocrystal quantum dots: a new class of active emitters for photonics applications

J. Hollingsworth, Y. Ghosh, A. M. Dennis, J. Kundu, B. N. Pal, Y. Park, S. Brovelli, Los Alamos National Lab. (United States); A. V. Malko, The Univ. of Texas at Dallas (United States); V. I. Klimov, H. Htoon, Los Alamos National Lab. (United States)

Nanocrystal quantum dots (NQDs) are nearly ideal candidates for light-emission applications due to high quantum efficiencies, and narrow-band and particle-size-tunable photoluminescence. However, they suffer from important deficiencies, including intermittency in fluorescence intensity, or "blinking", at the single-NQD level and chemical-environment-dependent photo-instability at the ensemble level. We recently reported the first demonstration of an inorganic shell approach to address these outstanding issues; namely, the suppression of blinking and ensemble-level instabilities.[1,2] Here, I will review these results, as well as key findings establishing the new "giant" NQDs (g-NQDs) as a functionally new class of colloidal quantum dot: significant suppression of nonradiative Auger recombination,[3] highly emissive multiexcitons [4] and near-unity biexciton emission, and a shell-thickness-dependent transition from NQDs characterized by a continuous distribution of emission states (thin-shell systems) to NQDs characterized by a single emission state (thick-shell systems). Beyond a summary of these fundamental studies, I will focus on the fabrication of new g-NQD compositional systems and the ability to tune g-NQD emission wavelength by control of the core/shell electronic structure. Lastly, I will describe the integration of g-NQDs into light emitting devices, as (1) robust, "passive" phosphors and (2) active layers in electrically pumped light emitting diodes, where the thick-shell NQDs provide significant advantages compared to their thin-shell counterparts in terms of device efficiencies, self-reabsorption, and/or stabilities.

1. Chen, Y. et al., J. Am. Chem. Soc., 2008, 130, 5026-5027.
2. Vela, J. et al., J. Biophotonics, 2010, 3, 706-717.
3. García-Santamaría, F. et al., Nano Lett., 2009, 9, 3482-3488.
4. Htoon, H. et al., Nano Lett., 2010, 10, 2401-07.

8095-50, Session 13

Tunable mesoporous Bragg reflectors based on block-copolymer self-assembly

S. Guldin, Univ. of Cambridge (United Kingdom); M. Kolle, Univ. of Cambridge (United Kingdom) and School of Engineering and Applied Sciences, Harvard University (United States); M. Stefik, Cornell Univ. (United States) and Ecole Polytechnique Federal de Lausanne (Switzerland); U. B. Wiesner, Cornell Univ. (United States); U. Steiner, Univ. of Cambridge (United Kingdom)

Mesoporous distributed Bragg reflectors (MDBRs) are an emerging class of photonic materials with unique properties due their porosity on the sub-optical length scale.[1] MDBRs have great potential as sensing materials, as adsorption and desorption of gas phase molecules lead to reversible changes in the refractive index of the stack. MDBR based "photonic noses" have been proposed that mimic the olfactory system. [2] In optoelectronic applications, MDBRs can be used to manipulate the flow of light. Examples include light harvesting elements in dye sensitised solar cells and resonance cavities for hybrid lasers.

We present a new route for the fabrication of MDBRs which relies on the self-assembling properties of the block copolymer PI-b-PEO in combination with sol-gel chemistry. This allows unprecedented control to finely tune porosity and pore size in the outcome inorganic material, which is exploited to manipulate the refractive index of the building blocks. Stacking-up multiple layers of alternating refractive index results in a fast and reliable assembly of a continuous network with well-defined interfaces. The outcome are MDBRs of high quality optical properties even when made of the same type of material. The effects of these unique characteristics on the photonic functioning will be discussed in detail.

References

- [1] S.Y. Choi et al., Nano Letters, vol. 6, no. 11, pp. 2456-2461, 2006; S. Colodrero et al., Langmuir, vol. 24, 4430-4434, 2008.
[2] L.D. Bonifacio et al., Advanced Materials, vol. 22, no. 12, pp. 1351-1354, 2010

8095-51, Session 13

Fabrication of three-dimensional gyroid photonic microstructures

M. Gu, M. Turner, Swinburne Univ. of Technology (Australia)

Three-dimensional (3D) photonic microstructures are an important platform for 3D photonic bandgap materials. If their feature size becomes smaller than the operating wavelength, they physically behave as metamaterials providing new properties that do not exist in nature. More importantly, the 3D photonic microstructures are necessary platforms to produce chiral geometries. It has been shown that chiral microstructures have important nanophotonic functionalities including their ability to enhance and control the chirality of light, which leads to applications such as negative index metamaterials, compact broadband circular polarisation filters, ultrasensitive biosensing and nanoscale plasmonic motors. However, the lack of symmetry and uniaxial chirality within typical chiral microstructures is not suitable for certain applications. In this talk, we will present our recent progress on fabrication, characterisation and metallisation of 3D microstructures based on the chiral, cubic networks found within the gyroid minimal surface inspired by a recent finding in butterfly wings.

Conference 8096: Plasmonics: Metallic Nanostructures and Their Optical Properties IX

Sunday–Thursday 21–25 August 2011 • Part of Proceedings of SPIE Vol. 8096
Plasmonics: Metallic Nanostructures and Their Optical Properties IX

8096-01, Session 1

Recent progress in plasmonics (Keynote Presentation)

X. Zhang, Univ. of California, Berkeley (United States)

Plasmonics takes advantage of the properties of surface plasmon polaritons in which photons are coupled to the quasi-free electron oscillations on metal surface. Recent advances of plasmonic applications include nano photonics, sub-diffraction-limit imaging, and plasmonic nano-laser etc.

Motivated by transformation optics - an approach to controlling the propagation of light by spatially varying material optical properties - various plasmonic lens designs will be demonstrated that can focus or bend surface plasmon polaritons with significantly reduced scattering loss in comparison to previously reported plasmonic elements. A technique that uses Brownian motion of single molecules for two-dimensional imaging of the enhancement profile of single hotspots on the surfaces of metallic thin films and nanoparticle clusters will also be introduced. Additionally I will show a nanoscale plasmonic motor directly driven by light and its rotation velocity and direction are controlled by tuning the wavelength of the incident wave to excite different plasmonic modes. I will also present the experimental demonstration of nanometer-scale plasmonic lasers, generating optical modes a hundred times smaller than the diffraction limit. Direct measurements of the emission lifetime reveal a broad-band enhancement of exciton spontaneous emission rate and the signature of apparently threshold-less lasing.

The abilities of advanced plasmonic techniques to transform surface plasmon polaritons, to image nanometer-sized hotspots, to generate significant optical torques at the nanoscale, and to create coherent light source at truly nano scale will benefit applications such as energy conversion, in vivo biological detection and manipulation, mechanical transducers and actuators, and active photonic circuits.

8096-02, Session 1

Plasmonics with gain (Keynote Presentation)

A. V. Zayats, King's College London (United Kingdom)

We will consider strategies for amplification of surface plasmon waves propagating on the interface of metal and gain dielectric. Various amplifying configurations including hybrid plasmonic crystals will be considered. The applications of gain-effects in all-optical nanophotonics will be discussed.

Resonant interaction of surface plasmon polaritons (SPP) with molecules, ions and semiconductor quantum dots near a metal interface attracts considerable attention since its understanding may lead to new nanophotonic technologies for sensing, optical data processing and quantum information. One of the most significant applications may be the amplification of the SPP waves or lasing into SPP modes.

In this talk we will discuss various experimental realisations of SPP amplification in dielectric-loaded plasmonic waveguides as well as plasmonic crystals hybridised with gain medium. We will report on the observation of amplified spontaneous emission of surface plasmon polaritons excited at the inter-face with a resonant amplifying medium. Generally, amplified spontaneous emission occurs during light propagation in the gain medium with inverse population and is sometimes called, travelling wave lasing or superfluorescence. Significant spectral narrowing of the SPP emission line is observed with the very low ASE threshold. We will also report on SPP Bloch mode amplification in plasmonic crystals where this effect leads to the increase in the enhanced transmission.

The amplification of SPPs and associated Ohmic loss compensation during their propagation on a metal-dielectric interface have profound

implications in design of plasmonic interconnects and all-optical signal processing devices based on plasmonic components.

8096-03, Session 2

Superconducting plasmonics

A. Tsiatmas, R. Buckingham, V. A. Fedotov, N. I. Zheludev, Univ. of Southampton (United Kingdom)

[Invited] Superconductors due to their vanishing ohmic resistance and dominant kinetic inductance have the ability to support propagating plasmonic excitations from low frequencies up to the THz regime. These modes can be confined on the scale of few tens of nanometres and propagate up to hundreds of times their wavelength. This reveals a significant potential for applications of superconducting plasmonic structures that originates from the easy incorporation of active control in these devices

8096-04, Session 2

Near-field imaging of terahertz plasmon waves with a subwavelength aperture probe

O. Mitrofanov, R. Mueckstein, Univ. College London (United Kingdom)

Visualization of Terahertz (THz) plasmons with THz local near-field probes allows studying ultra-fast plasmonic phenomena in the time domain, with access to the electric field of plasmonic waves rather than the intensity. We demonstrate that the integrated sub-wavelength aperture near-field probe can be used to map THz surface plasmon waves in space and time with high resolution. The precise knowledge of the probe structure, which incorporates a photoconductive detector in the near-field zone of the sub-wavelength aperture, allows to identify the coupling mechanism and to explain the nature of the observed phenomena. Using this probe, we mapped (in space and time) THz plasmon waves formed on a metallic surface by tightly focused 2.0THz pulses (Ref. 1) and the formation of standing plasmon waves in THz antennas. Using several experimental near-field observations we show that this probe detects the spatial derivative of the electric field of surface plasmons rather than the field itself. The coupling mechanism results in an apparent spatial phase shift of the detected surface plasmon wave.

The understanding of the coupling mechanism provides a framework for analysis and interpretation of THz near-field images, where surface plasmon effects may be present. We will discuss how this microscopy method can be applied to track surface plasmon propagation and formation of plasmonic resonances. The method can provide a vital insight into the role of THz surface plasmons in basic physical phenomena and in THz devices.

Reference 1: Optics Express, 19, 3212 (2011)

8096-05, Session 2

From vacuum Rabi splitting towards stimulated emission with surface plasmon polaritons.

R. J. Moerland, A. Väkeväinen, A. Eskelinen, G. Sharma, P. Törmä, Aalto Univ. School of Science and Technology (Finland)

Coherent phenomena in Surface Plasmon Polariton (SPP)/emitter systems, where strong coupling dominates, are an intensely studied

Conference 8096: Plasmonics: Metallic Nanostructures and Their Optical Properties IX

subject for lasing and coherent energy transfer applications. Also a coherent phenomenon is vacuum Rabi splitting; we have reported on strong coupling between SPP and Rhodamine 6G (R6G) molecules, showing double vacuum Rabi splitting energies up to 230 and 110 meV [1]. The system in Ref. 1 consisted of a 50 nm layer of silver on top of a SiO₂ substrate. A layer of R6G molecules, embedded in PMMA, is deposited on top by spincoating. The same system is also interesting for studying enhancements in spontaneous emission, and for obtaining stimulated emission. The R6G molecules in the system are pumped by a 532 nm laser, while the emission spectrum of the hybrid SPP/emitter system is recorded. As the laser pump intensity is increased, the recorded spectrum reflects the change from spontaneous emission towards stimulated emission. We will show our latest results in this area of research.

[1] Hakala, T.K., Toppari, J. J., Kuzyk, A., Pettersson, M., Tikkanen, H., Kunttu, H., and Törmä, P., Vacuum Rabi splitting and strong coupling dynamics for surface plasmon polaritons and Rhodamine 6G molecules, *Physical Review Letters* 103, 053602 (2009). <http://link.aps.org/doi/10.1103/PhysRevLett.103.053602>

8096-06, Session 2

Transformation plasmonics and gradient index plasmonics

Y. Liu, T. Zentgraf, M. H. Mikkelsen, Univ. of California, Berkeley (United States); J. G. Valentine, Vanderbilt Univ. (United States); X. Zhang, Univ. of California, Berkeley (United States)

Taking advantage of transformation optics, we demonstrate that the confinement as well as propagation of surface plasmon polaritons (SPPs) can be managed in a prescribed manner by carefully controlling the dielectric material properties adjacent to a metal. Since the metal properties are completely unchanged and the transformed dielectric materials can be isotropic and non-magnetic, it provides a straightforward way for practical realizations. We show that our approach can assist to tightly bound SPPs over a broad wavelength range at uneven and curved surfaces, where SPPs would normally suffer from significant scattering losses. In addition, a 180-degree plasmonic bend with almost perfect transmission is designed.

We further propose to slowly change the thickness of an isotropic dielectric cladding layer and hence the local effective index of SPPs, instead of directly modifying the permittivity of the dielectric medium. As the local effective index of SPPs is varied gradually in a truly continuous manner we term our approach gradient index (GRIN) plasmonics, in analogy to the well-known GRIN optics. Applying this method, we design and demonstrate two different devices: a plasmonic Luneburg lens to focus SPPs and a plasmonic Eaton lens to bend SPPs. In comparison with previously reported plasmonic elements, the scattering loss of SPPs in our designs can be significantly reduced since the optical properties are adiabatically changed. Fluorescence imaging and leakage radiation microscopy are applied to characterize the performance of the fabricated GRIN plasmonic devices based on gray scale lithography, showing a good agreement with the numerical simulation.

8096-07, Session 2

Controlling the motion of metallic nanoparticles with fast electron beams

J. Aizpurua, Centro de Fisica de Materiales (Spain) and Donostia International Physics Ctr. (Spain); A. Reyes Coronado, Univ. Nacional Autónoma de México (Mexico); P. E. Batson, Rutgers, The State Univ. of New Jersey (United States); R. G. Barrera, Univ. Nacional Autónoma de México (Mexico); A. Rivacoba, Univ. del País Vasco (Spain) and Donostia International Physics Ctr. (Spain); P. M. Echenique, Donostia International Physics Ctr. (Spain) and Univ. del País Vasco (Spain)

We analyze the total momentum transfer from fast electron beams, like those employed in scanning transmission electron microscopy (STEM), to plasmonic nanoparticles. The calculation of the momentum transfer is obtained by integrating the electromagnetic forces acting on the particles over time. Numerical results for single and dimer metallic nanoparticles are presented, for nanoparticle sizes ranging between 2 and 10 nm. Our calculations show that depending on the specific values of impact parameter and separation distance, the total momentum transfer yields a force that can be either attractive or repulsive. We corroborate these findings with experimental results that confirm the theoretical predictions. The time-average forces calculated for electron beams commonly employed in STEM are on the order of piconewtons, comparable in magnitude to optical forces and are thus capable of producing movement in the nanoparticles. This effect can be exploited in mechanical control of nanoparticle induced motion, as demonstrated experimentally.

8096-08, Session 3

Quantum plasmonics and plexcitonics

P. J. Nordlander, Rice Univ. (United States)

A recently developed fully quantum mechanical approach for the description of plasmonic and excitonic nanoparticles is discussed.[1] It is shown that quantum effects can have a pronounced influence on the electric field enhancements near the nanoparticle surfaces and on the optical properties strongly coupled nanoparticles. For closely spaced metallic nanoparticles, electron transfer and nonlocal screening can drastically reduce the electric field enhancements across the gap and result in a Charge Transfer Plasmon (CTP) where an oscillatory electric current is induced between the different particles.[2] The energy of the CTP is found to depend strongly on the electronic structure of the junction and the presence of molecules inside the gap.[3] For the coupled plasmonic-excitonic system where bonding and antibonding hybrid plexciton states are formed,[4] quantum effects can lead to a drastic enhancement of the excitation cross section of the excitons.

[1] J. Zuloaga et al., *Nano Lett.* 9(2009)887, *ACS Nano* 4(2010)5269

[2] O. Perez et al., *Nano Lett.* 10(2010)3090, L.S. Slaughter et al., *ACS Nano* 4(2010)4657

[3] P. Song et al., to appear in *J. Chem. Phys.* 2011

[4] N.T. Fofang et al., *Nano Lett.* 8(2008)3481, J. Zuloaga et al., to be published 2011

8096-09, Session 3

Theoretical modeling of relaxation dynamics in gold nanorod-dye assemblies for fluorescence enhancement

J. Vella, Jr., Air Force Research Lab. (United States) and General Dynamics Information Technology (United States); A. Urbas, Air Force Research Lab. (United States)

Using metal nanostructures to concentrate optical-frequency electric fields has garnered significant interest in the literature. For example, by combining an organic dye with a nanorod whose plasmon resonance frequency is similar to the absorption maximum of the dye, a significant enhancement in the fluorescence quantum yield can be observed. The prevalent theory for describing such an enhancement is kinetic and ascribed to an increase in the intrinsic rate of fluorescence, while the rate of non-radiative decay remains constant. Analysis of the literature will reveal that systems exhibiting fluorescence enhancement also show an alteration of the Stokes shift. The traditional kinetic description of plasmon-enhanced fluorescence cannot explain the origin of this shift. Using well-known theories developed by Onsager and Debye, it will be shown that it is possible to model plasmon-enhanced fluorescence not as an increase in the intrinsic rate of fluorescence, but by a perturbation of the equilibrium, photoexcited dipole moment of an emitter situated between two gold nanorods. This theory not only offers an explanation

Conference 8096: Plasmonics: Metallic Nanostructures and Their Optical Properties IX

of the altered Stokes shift in plasmon-enhanced fluorescence systems, but also offers the possibility of the direct and absolute calculation of the electric field that is concentrated between two gold nanorods.

8096-10, Session 3

Quantum plasmonics

V. Zwiller, R. Heeres, S. Dorenbos, Technische Univ. Delft (Netherlands)

Our work centers on the demonstration of quantum plasmonics, where single plasmons are created, propagated and detected.

A crucial part is played by Superconducting Single-Photon Detectors, which have some very useful properties such as short dead-time, low dark counts, wide operating wavelength range (UV - IR) and straight-forward operation. The sensitivity in the $>1\mu\text{m}$ range is Especially interesting to ensure low losses for plasmons and for telecom applications. We have recently demonstrated that these detectors are also suitable for integrated quantum optics experiments by showing on-chip detection of single plasmons. In this experiment, a single quantum dot was used as a single photon source and the stream of single photons was coupled through free-space to a plasmonic waveguide made of a narrow gold stripe making its way to the superconducting detector. This on-chip detection of single plasmons enables the development of complex optics circuits at a small length scales. In the future, a single emitter could also be integrated in the near-field, resulting in more efficient excitation of plasmons and a potential enhanced emission rate due to the Purcell effect.

We are currently building more advanced systems where plasmonic beam splitters and pairs of detectors are combined to form an interferometer. An experiment that is now within reach is the observation of Hong-Ou-Mandel interference with plasmons.

8096-11, Session 3

Room temperature semiconductor plasmon laser

R. Ma, R. F. Oulton, V. J. Sorger, G. Bartal, Ctr. for Scalable and Integrated Nanomanufacturing (SINAM) (United States); X. Zhang, Ctr. for Scalable and Integrated Nanomanufacturing (SINAM) (United States) and Lawrence Berkeley National Lab. (United States)

Plasmon lasers are a new class of coherent optical amplifiers that generate and sustain light well below its diffraction limit. Their intense, coherent and confined optical fields can enhance significantly light-matter interactions and bring fundamentally new capabilities to bio-sensing, data storage, photolithography and optical communications. However, metallic plasmon laser cavities generally exhibit both high metal and radiation losses, limiting the operation of plasmon lasers to cryogenic temperatures, where sufficient gain can be attained. Here, we present room temperature semiconductor sub-diffraction limited laser by adopting total internal reflection of surface plasmons to mitigate the radiation loss, while utilizing hybrid semiconductor-insulator-metal nano-squares for strong confinement with low metal loss. High cavity quality factors, approaching 100, along with strong $\lambda/20$ mode confinement lead to enhancements of spontaneous emission rate by up to 18 times. By controlling the structural geometry we reduce the number of cavity modes to achieve single mode lasing.

8096-12, Session 4

Using chiral metamaterials for the ultrasensitive characterisation of biomacromolecular structure

M. Kadodwala, Univ. of Glasgow (United Kingdom)

Spectroscopic techniques based on circular dichroism, the differential interaction of circularly polarised electromagnetic (EM) radiation with matter, are powerful tools for studying bio-materials, liquid crystals, polymers, and magnetic materials. The inherent weakness of the underlying dichroic phenomena require relatively large amounts of material for spectroscopic measurements, typically for biomaterials \geq microgram are necessary. We have created a new type of light, which is generated in the vicinity of plasmonic chiral metamaterials, that has a greater level of chirality than circularly polarised light, this new property is referred to as superchirality. Our discovery transforms circular dichroic measurements, because the superchiral light magnifies the asymmetries displayed in dichroic measurements by at least six orders of magnitudes. This new form of spectroscopy, could presage new powerful biosensing array technologies, which would allow for the first time both the ultrasensitive detection and structural characterisation of a biomaterial.

8096-13, Session 4

Importance of magnetic polarization in the absorption of metallic nanoparticles

A. Asenjo-Garcia, A. Manjavacas, V. Myroshnychenko, J. García de Abajo, Consejo Superior de Investigaciones Científicas (Spain)

We study the dipolar magnetic polarizability of common metallic nanoparticles. Remarkably, particles of size and morphology commonly encountered in colloidal synthesis can exhibit a strong imaginary part in the magnetic polarizability, which is comparable in magnitude to or even larger than the electric polarizability. This means that the absorption of a particle can be dominated by its magnetic response.

However, this contribution is routinely overlooked. Our results demonstrate that this is not correct in many situations. We study the magnetic polarization of common metallic nanoparticles of different materials, sizes, shapes, and show that the magnetic contribution will dominate the absorption in many cases.

Various particle shapes, such as spheres, rods, ellipsoids, or disks, are numerically analyzed and compared to analytical solutions when available. In the case of spheres, analytical solutions are provided based upon the Mie formalism [1]. For non-spherical particles, we produce numerical calculations using the boundary element method [2]. It is found that this behavior is highly dependent on the particle geometry. For instance, the contribution of magnetic polarization to light absorption is largely enhanced in disk-shaped particles of large aspect ratio. The opposite behavior is found for metallic rods.

Our work provides a clear demonstration of the unexpected large effect of magnetic polarization in the absorption properties of commonly encountered metal nanoparticles extensively used in plasmonics.

[1] C. F. Bohren, and D. R. Huffman, Absorption and scattering of light by small particles, Wiley&Sons (1998).

[2] F. J. Garcia de Abajo, and A. Howie, Phys. Rev. Lett. 80, 5180 (1998).

8096-14, Session 4

Dipole limit and resonance-domain effects in second-harmonic generation from arrays of metal nanoparticles

M. Kauranen, G. Genty, R. Czaplicki, H. Pietarinen, H. Husu, M. Zdanowicz, K. O. Koskinen, R. Siikanen, Tampere Univ. of

Conference 8096: Plasmonics: Metallic Nanostructures and Their Optical Properties IX

Technology (Finland); J. Lehtolahti, J. Laukkanen, M. Kuittinen, Univ. of Eastern Finland (Finland)

The optical properties of metal nanoparticles are dominated by their plasmon resonances, which depend on the particle size and shape. The resonances give rise to strong local fields near the particles, which can enhance nonlinear interactions. However, localized surface defects can also support their own plasmonic modes and thereby lead to highly local nonlinear responses.

We have earlier shown that localized nonlinear sources that are retarded with respect to each other can lead to effective quadrupole effects in second-harmonic generation (SHG) from arrays of metal nanoparticles. Such effects significantly complicate the analysis of the nonlinear response. In this paper, we show that such effects are suppressed essentially completely by the improved sample quality made possible by state-of-the-art lithographic techniques. This opens the possibility of designing nonlinear metamaterials with truly engineered properties.

To demonstrate tunable nonlinear responses, we order anisotropic, L-shaped nanoparticles in a lattice with sub-wavelength period for their resonant wavelengths. By varying the mutual orientation of the particles, we modify the symmetry and dichroic properties of the structures. More importantly, the SHG responses of two samples that have similar orientational particle distribution are found to vary by more than an order of magnitude depending on the detailed particle ordering. The results are explained by long-range coupling between the particles, which becomes possible because the changes in particle ordering double the structural period and thus open diffraction orders. Such resonance-domain effects provide new approaches for optimizing the optical responses of metamaterials.

8096-15, Session 4

Directional light scattering of Au nanoshells and nanocups at a dielectric interface

N. S. King, Y. Li, Y. Zhang, P. J. Nordlander, N. J. Halas, Rice Univ. (United States)

The fields of plasmonic solar cell enhancement and remote sensing require a strong understanding of the effects of an inhomogeneous medium on the plasmonic response and resulting scattering profile. In this presentation, we show how the refractive index of a supporting substrate modifies the far-field radiation pattern of symmetric and asymmetric nanoparticles. Asymmetric nanoparticles, such as nanocups, are of particular interest because the reduction in symmetry produces two orthogonal dipole modes that align with the structure of the nanoparticle and are independent of the direction of the incident illumination. Controlling the orientation of these particles requires a supporting substrate or encapsulating medium, but offers the ability to selectively excite a specific plasmonic mode, determining the scattering properties of the system. Angular radiometric measurements confirm the predicted $\cos^2(\theta)$ dipole scattering of nanoshells and the unique scattering properties of oriented nanocups on simple glass substrates. High refractive index substrates, such as silicon, lift the degeneracy of the dipole plasmon modes and allow for hybridization with higher order modes. The resulting scattering profile for both nanoshells and nanocups differ greatly in both intensity and localization of the scattered light. Finite element method (FEM) simulations of the nanoparticle system with substrates varying in refractive index from glass to silicon confirm experimental results and show the progressive change in scattering profile.

8096-16, Session 4

Multi-band scattering and enhancement in a reduced symmetry cross nanoantenna

R. Adato, A. A. Yanik, H. Altug, Boston Univ. (United States)

Metal nanoparticles function as optical frequency antennas, providing a

means with which to impedance match nanoscale emitters, absorbers or scattering objects to far-field radiation. This antenna functionality, however, results from the particles' structural resonances, and is typically narrowband. Single element antenna geometries that extend the bandwidth, or offer tunable resonances at multiple frequencies would open new opportunities in surface enhanced spectroscopies, ultra fast / small detector elements and nonlinear process enhancement. To this end we propose a cross shaped nanoparticle antenna which provides multiple resonances that are independently tunable over a wide range of frequencies. By adjusting the polarization of the incident light, the dimensions and symmetry of the structure we experimentally demonstrate the ability to tune several addressable resonant modes over a spectral range of greater than 4-5 μm in the mid-infrared. Numerical simulations indicate strong near-field enhancements similar to those of the dipolar resonances of rod shaped antennas. Finally, we show that the behavior of the nanoparticle can be predicted via classical antenna / circuit theory. The particle design can therefore be systematically engineered in an intuitive manner and easily fabricated in a repeatable manner that is suitable to high-throughput methods. This is essential for practical implementation and in contrast to geometries that rely on near-field coupling effects and therefore the presence of nanoscale, difficult to control gaps.

8096-17, Session 5

Nonlinear photothermal and photoacoustic plasmonics beyond the spectral limits (Keynote Presentation)

V. P. Zharov, Univ. of Arkansas for Medical Sciences (United States)

Advanced plasmonic nanostructures with enhanced absorption, fluorescence, and scattering properties enable progress in microscopy, spectroscopy, diagnostics, and cancer therapy. However, because of their relatively broad plasmonic bands of 100 to 200 nm, multicolor capacity of these structures is limited.

To resolve this fundamental problem of conventional spectral microscopy we introduce a platform which comprises three interrelated steps 1-2 : 1) the development of nanostructures with relatively narrow conventional plasmonic bands (e.g., multilayer nanotubes); 2) laser-induced nonlinear signal amplification accompanied by spectral narrowing phenomena due to synergy of nonlinear effects (e.g., optical, thermal, acoustic, or nanobubbles); and 3) spectral reading of narrow plasmon resonances without broadening effects. Using nonlinear photothermal and photoacoustic spectroscopy with advanced tunable pulse lasers, we demonstrated ultrasharp resonances up to a few nanometers wide in relatively broad plasmonic spectra of various nanostructures, including golden carbon nanotubes and multilayer gold nanorods.

The described approaches can use various detection schematics (e.g., thermal-lens, photoacoustic, radiometry, phase-contrast, and heterodyne methods) for study of laser-nanoparticle interactions with resolution beyond the spectral limits, measurements of tiny red and blue plasmon resonance shifts in nanoplasmonic sensors, and multispectral imaging and multicolor cytometry.

References:

1. Zharov VP. Ultrasharp nonlinear photothermal and photoacoustic resonances and holes beyond the spectral limit. *Nature Photonics*, 2011; 5: 110-116.
2. Kim J-W, Galanzha EI, Shashkov EV, Moon H-M, Zharov VP. Golden carbon nanotubes as multimodal photoacoustic and photothermal high-contrast molecular agents. *Nature of Nanotechnology*, 2009; 4: 688-694.

8096-19, Session 5

Antenna-assisted hydrogen sensing in a single plasmonic nanofocus

N. Liu, M. Tang, Univ. of California, Berkeley (United States);

Conference 8096: Plasmonics: Metallic Nanostructures and Their Optical Properties IX

M. Hentschel, H. W. Giessen, Univ. Stuttgart (Germany); A. P. Alivisatos, Univ. of California, Berkeley (United States)

We present a plasmonic hydrogen sensor which consists of a single Pd dot and a plasmonic gold nanoantenna. The Pd dot is brought into the nanofocus of the gold nanoantenna, which is resonantly excited by light. Upon exposure to hydrogen, the Pd dot changes its dielectric properties. Hence, the resonance of the gold nanoantenna is shifted and can be easily detected.

We record several series of experiments, using different amounts of hydrogen as well as different shapes of nanoantennas and different separations between the Pd dot and the antenna. It turns out that the triangular nanoantenna with a distance of 10 to 20 nm yield the best results, giving a spectral shift of around 5 nm for a hydrogen concentration of 1% in nitrogen.

Our work will open a pathway for extremely sensitive detection of molecules and atoms down to the single particle level.

8096-20, Session 5

Engineering light scattering and field concentration in nano-plasmonic necklaces for multi-parametric sensing

A. J. Pasquale, B. M. Reinhard, L. Dal Negro, Boston Univ. (United States)

Particle clusters with different degrees of rotational symmetry consisting of circular loops of gold nanoparticles, dubbed "Nano-Plasmonic Necklaces," are proposed as a novel, reproducible platform for elastic and inelastic (SERS) optical sensors with polarization insensitive behavior. The engineering of nano-plasmonic necklaces allows for full control of the plasmonic hot-spot locations and optimization of near-field strength by photonic cavity coupling with gap plasmons, making them a promising candidate for inelastic surface-enhanced molecular Raman sensing. The polarization insensitivity of plasmonic necklaces guarantees that the plasmonic hot-spots remain excited within the necklaces irrespective of the incident polarization of the excitation field, which is a significant advantage compared to hot-spots in the usual plasmonic dimer configurations. Moreover, the necklace configuration enables photonic-plasmonic coupling effects where the incident radiation gets resonantly trapped into circular resonator modes which strongly enhance the hot-spot intensity. Plasmonic necklaces of different rotational axes were fabricated using electron-beam lithography and electron-beam deposition of gold films. Engineering design rules are determined for hot-spot formation, polarization insensitivity, and intensity distribution in nano-plasmonic necklaces and the results are confirmed by experimental Surface Enhanced Raman Scattering (SERS) data obtained using a molecular monolayer of p-mercaptoaniline as the analyte.

8096-150, Session 5

Electrically controlled nonlinear generation of light with plasmonics

W. Cai, A. Vasudev, M. L. Brongersma, Stanford Univ. (United States)

Plasmonics enables a unique opportunity to develop ultra-compact optical devices at a subwavelength scale by utilizing two of its most important strengths: extreme concentration light intensity to far below the diffraction limit and an ability to support simultaneous electrical and optical functions. These features also make plasmonics an ideal candidate for electrically manipulating nonlinear optical interactions at the nanoscale, an area that has remained largely unexplored. Here we experimentally demonstrate electrically controlled harmonic generation of light from a plasmonic nanocavity filled with a nonlinear medium. The metals that define the nano-resonator also serve as electrodes that can facilitate high electric fields across the nonlinear material. We tune the

frequency-doubling of a 1.56 μm fundamental wave by applying a control voltage to the electrodes, yielding a nonlinear modulation of $\sim 7\%$ per volt and $\sim 140\%$ at a bias of 20 volts.

8096-21, Session 6

Interacting with light at the nanoscale (Keynote Presentation)

L. K. Kuipers, FOM Institute for Atomic and Molecular Physics (United States)

As we perfect our ability to engineer the optical properties of nanostructures, we obtain a handle on light-matter interactions. We can enhance them and even induce new ones, such as the effective light-matter interaction mediated by the magnetic component of light rather than the electric component. Here, we present our latest results on local investigations of light-matter interactions. We use the fact that our near-field nanoprobe is actually metallo-dielectric nanostructure to gain access to light-matter interactions on a sub-wavelength scale. The symmetry of the probe allows, on the one hand, different vector components of the light to be distinguished and, on the other hand, diamagnetic light-matter interactions to be induced.

8096-22, Session 6

Close interactions in gap nanoantennas

J. Aizpurua, R. Esteban Llorente, P. Albella, Centro de Fisica de Materiales (Spain); N. Large, Centro de Fisica de Materiales (Spain) and Ctr. d'Elaboration de Matériaux et d'Etudes Structurales (France); A. Garcia Etxarri, Centro de Fisica de Materiales (Spain) and Stanford Univ. (United States); M. Schnell, P. Alonso-Gonzalez, CIC nanoGUNE Consolider (Spain); R. Hillenbrand, CIC nanoGUNE Consolider (Spain) and IKERBASQUE, Basque Foundation for Science, Bilbao (Spain)

Many concepts from the electromagnetic response in radiowave technology can be transferred to the optical and infrared range of the spectrum. In particular, metallic gap antennas offer the possibility to tune the spectral response by simple modification of the material properties within the gap. Particularly interesting is a situation where the gap surfaces forming the gap are in close proximity. Under these conditions, aspects such as non-locality of the response or the dimension of the gap modify drastically the near-field properties of the antenna. Furthermore, the presence of free-carriers within the gap can modify the optical response of the antenna within a very short time, showing the potential to act as an ultrafast optical switcher. We study theoretically the spectral response of these antennas and identify the surface modes that interfere to produce distinct spectral features. These modes are experimentally identified with use of scanning-near-field optical microscopy both in amplitude and phase. The characterization and understanding of the amplitude and phase of the local fields in gap antennas is of utmost importance in sensing and for design of optical nanodevices.

8096-23, Session 6

Seeing magnetic light-matter interactions: quantifying and enhancing magnetic dipole emission

R. Zia, Brown Univ. (United States)

Although it is often assumed that light-matter interactions are dominated by electric dipole transitions, strong optical frequency magnetic dipoles do exist. In fact, we see magnetic dipole emission everyday from the Lanthanide ions that help to illuminate everything from fluorescent lighting to solid-state lasers. Nevertheless, most applications have

Conference 8096: Plasmonics: Metallic Nanostructures and Their Optical Properties IX

overlooked the device implications of these magnetic dipole transitions throughout the visible and near-infrared regime. Moreover, the magnetic dipole contributions of many important transitions (such as the 1550nm line of Erbium) have not been fully characterized. In this talk, we will illustrate how the naturally occurring magnetic dipole transitions of Lanthanide ions provide a new degree of design freedom for photonic and plasmonic devices. Specifically, we will demonstrate how the different symmetries of electric and magnetic dipoles can be exploited to identify, enhance, and control light emission.

8096-24, Session 6

Coupling mechanisms for nano-U-dimers

N. Gneiding, E. Krutkova, Erlangen Graduate School in Advanced Optical Technologies (Germany); E. Tatartschuk, Erlangen Graduate School in Advanced Optical Technologies (Germany) and Clemson Univ. (United States); E. Shamonina, Imperial College London (United Kingdom) and Erlangen Graduate School in Advanced Optical Technologies (Germany)

Properties of split-ring metamaterials are governed by inter-element interactions. These interactions lead to slow eigenmodes of coupling, which, due to their short wavelengths, are ideal candidates for the design of near-field manipulating devices. In this paper we explore the electric and magnetic coupling mechanisms in nano-U dimers comprising two identical nano-U elements per unit cell arranged axially and twisted relative to each other by an arbitrary angle. We study theoretically coupling in a periodic chain of nano-dimers in the frequency range 100-300 THz. In our analytical model, the electric and magnetic coupling can be expressed through the self and mutual terms for magnetic and electric field energy, considering the continuity equation between the current and charge distributions within each U-element. In addition, we incorporate the effect of kinetic inductance due to the inertia of the electrons (noticeable as element dimensions become as small as 100 nm). The resulting dependence of the electric, magnetic and the total coupling constant on the twist angle within the dimer obtained analytically is shown to agree with numerical simulations (CST Microwave Studio). Our approach should enable an effective design of metamaterial structures with desired properties and would be a useful tool in developing THz range manipulating devices based on propagation of slow waves propagating by virtue of coupling.

8096-25, Session 6

Plasmonic enhancement of ultrafast all-optical magnetization reversal

V. Kochergin, L. A. Neely, MicroXact Inc. (United States); I. N. Krivorotov, Univ. of California, Irvine (United States); E. V. Kochergin, Donetsk National Technical Univ. (Ukraine); K. L. Wang, Univ. of California, Los Angeles (United States)

Ultrafast all optical magnetization switching in GdFeCo layers on the basis of Inverse Faraday Effect (IFE) was demonstrated recently and suggested as a possible path toward next generation magnetic data storage medium with much faster writing time. However, to date, the demonstrations of ultrafast all-optical magnetization switching require powerful femtosecond lasers and are not yet compatible with the size, cost, and power consumption requirements of data storage and data processing applications. In this contribution we show that utilization of IFE enhancement in plasmonic nanostructures may provide the way to achieve fast all-optical magnetization switching with smaller/cheaper laser sources with longer pulse durations. Our modeling results predict that significant enhancement of IFE around all major types of plasmonic nanostructures for a circularly polarized incident light. Unlike the IFE in uniform bulk materials, nonzero value of IFE is predicted in plasmonic nanostructures even with a linearly polarized excitation, which is the highest for the intrinsically chiral (non-rotationally symmetric) plasmonic nanostructures. The DC magnetic fields around plasmonic

nanostructures in most cases are highly nonuniform even on the nanoscale. However, we will show the plasmonic geometries at which the uniform on the nanoscale ExE^* product is predicted to exceed $\sim 10^4$ IFE enhancement. Experimentally, all-optical remagnetization at 20 times lower laser fluence and roughly 100 times lower value of laser fluence/pulse duration ratio was achieved in plasmon-enhanced samples to verify the model predictions. The path to achieve higher levels of enhancement experimentally will be discussed.

8096-26, Session 7

Strongly driven electron emission from nanoparticles in few-cycle laser fields (Keynote Presentation)

S. Zhrebtsov, F. Süßmann, Max-Planck-Institut für Quantenoptik (Germany); J. Plenge, Freie Univ. Berlin (Germany); J. Passig, Univ. Rostock (Germany); C. Graf, V. Mondes, Freie Univ. Berlin (Germany); M. I. Stockman, Georgia State Univ. (United States); E. Rühl, Freie Univ. Berlin (Germany); T. Fennel, Univ. Rostock (Germany); M. F. Kling, Max-Planck-Institut für Quantenoptik (Germany)

The acceleration of electrons in local near-fields of nanoparticles driven by few-cycle laser pulses is studied and provides insight into the electron dynamics and surface charging of the particle. Liberated electrons are accelerated / decelerated in the local field at the surface and affected in their attosecond dynamics by the build-up of a surface trapping potential and electron-electron interactions. By using isolated nanoparticles we can explore the regime near, at and beyond the material damage threshold. The extremely short pulse duration of only a few cycles in our studies ensures that the electron dynamics responsible for the observed phenomena occurs before any nuclear dynamics. At high intensities, a higher effective dielectric constant is predicted for dielectric nanoparticles. Experiments to observe such non-linearities are currently underway. They may allow insight into non-linear effects in bulk materials, which cannot be easily studied at these intensities. The approach holds promise that the regime of non-linear plasmonics may be reached and examined for the first time. Experimental results and calculations on the strongly driven electron emission from isolated nanoparticles in few-cycle laser fields will be presented.

8096-27, Session 7

Plasmonic field enhancement for generating ultrafast extreme-ultraviolet light pulses

I. Park, S. Kim, J. Choi, S. Kim, KAIST (Korea, Republic of)

Ultrafast extreme-ultraviolet (EUV) light pulses are a key tool for time-resolved spectroscopy to investigate atomic motion in molecules and electronic motion inside and between atoms. High-harmonic generation by focusing near-infrared (NIR) pulses on noble gases is a well-known method of generating such ultrashort EUV pulses. In this report, we show a 3-dimensional metallic waveguide that enables plasmonic generation of ultrashort EUV pulses through field enhancement by means of surface-plasmon polaritons. Compared with bow-ties previously used for field enhancement by stationary resonance of localized surface plasmons, the net volume of more than 20 dB intensity enhancement turns out to be three orders of magnitude larger. The intensity of incident NIR pulses is enhanced by a factor of ~ 350 , being strong enough to produce EUV harmonics up to the 43rd order in interaction with Xe gas directly from a modest input of $\sim 10^{11} \text{ Wcm}^{-2}$. This plasmonic method maintains pulse repetition rate as high as 75 MHz in our experiment without use of extra cavities. No phase-matching is needed since EUV pulses are generated within a sub-wavelength spot near an exit aperture of 100 nm diameter whereby driving NIR pulses are mostly blocked. Furthermore, ultrafast DUV pulses with a center wavelength of 266 nm can also be produced by means of surface third-harmonic generation with deposition of a SiO₂

layer at the exit aperture. The plasmonic waveguide is fabricated on a cantilever nanostructure, with immunity to thermal damage and optical breakdown, to be suited for near-field spectroscopy with atomic-scale lateral selectivity.

8096-28, Session 7

Adiabatic and nonadiabatic metallization of dielectric nanofilms by strong optical fields

M. I. Stockman, M. Durach, A. Rusina, Georgia State Univ. (United States); M. F. Kling, Max-Planck-Institut für Quantenoptik (Germany)

We consider a 1-10 nm-thin nanofilm of an insulator subjected to a strong oscillating electric field normal to it. The frequency of this field may be in the range from microwave to optical, depending on the film thickness (in the near-ir to visible range for a ~1-2 nm thickness). The strength of this field is considered to be in the range ~1-10 V/nm. When this field is slow, adiabatic, it induces a reversible phase transition in the film to a state reminding metal. The electron population can be transferred from one surface of this nanofilm to another. For fast, nonadiabatic fields, using quantum-mechanical treatment we demonstrate that a femtosecond pulse causes nonlinear polarization and ultrafast formation of plasmonic band in the high-frequency response of a nanostructure. This ultrashort pulse creates a non-equilibrium excitation of the nanostructure, which can be controlled using adiabatic phase accumulation effect. The demonstrated possibility of ultrafast switching between insulator and plasmonic metal phases can be employed for creation of active plasmonic elements for ultrafast nanocircuits

8096-29, Session 7

Attosecond control of electrons emitted from a nanometric metal tip

P. Hommelhoff, Max-Planck-Institut für Quantenoptik (Germany)

It is well known that plasmonic effects can lead to greatly enhanced field strengths near surfaces. In this contribution we discuss the interaction of few-cycle femtosecond laser pulses with a sharp tungsten tip. We measure the electron emission current and record electron energy spectra. We observe above-threshold photoemission (ATP), i.e., electrons promoted in energy to states higher than needed to leave the metal. When we increase the laser intensity, the electronic spectral peaks start to shift, indicating the onset of strong-field effects [1].

Further, we show measurements with carrier-envelope-phase (CEP) stable pulses. We observe strong CEP effects (spectral interference). We show that electrons are detected originating from either one or two sub-cycle emission points in time. We observe that plateau electrons re-collide with the tip elastically and coherently, well known from high harmonic generation and above-threshold ionization in the gas phase. Because of field-enhancement, a simple laser oscillator suffices to reach the required peak field strengths.

With different tip materials, we believe that this work will enable probing of plasmonic near-fields on the (sub-)nanometer-attosecond scale.

[1] M. Schenk, M. Krüger, P. Hommelhoff, Phys. Rev. Lett. 105, 257601 (2010)

[2] M. Krüger, M. Schenk, P. Hommelhoff, manuscript in preparation

8096-30, Session 8

Plasmonic nanoantennas: new properties and functions (Keynote Presentation)

N. J. Halas, Rice Univ. (United States)

Nanostructures designed to harvest light can have many functions:

energy and/or charge transfer and storage, light scattering or refraction, for example. We will describe two families of nanoantennas with unique properties: nanoscale hemispheres, and nanoantenna-diodes. Nanoscale hemispheres possess both electric and magnetic plasmon modes, each with their own unique light-refractive properties. Nanoscale hemispheres can also give rise to strong nonlinear optical effects, dependent upon their orientation with respect to incident excitation. These properties will be discussed. The integration of nanoantennas into electronics, where an optical structure can simultaneously provide an electrical response, is a new functionality better known in electrochemical than in electronic device contexts. We will describe how an optical antenna can also function as a photodetector, with a device response that is a hybrid combination of these two distinct types of devices.

8096-31, Session 8

Resonant properties of transmitting and receiving plasmonic resonator antennas

E. S. Barnard, Geballe Lab. for Advanced Materials (GLAM) (United States); M. L. Brongersma, Stanford Univ. (United States)

A combined theoretical and experimental study of wavelength-scale plasmonic resonator antennas is presented. Using full-field electromagnetic simulations and analytical optical antenna models, we are able to derive simple and intuitive design rules to achieve antennas with a desired set of optical properties (field enhancement, scattering cross section, absorption cross section, and resonant frequency) based on their geometric properties. As part of these design rules we are able to quantify reflection phase and understand this quantity in terms of the end-face near-field. With these design rules, we have constructed resonance maps that allow a designer to choose an antenna structure that provides desired resonant properties for a specific application. We then apply these design rules to create antennas that resonantly enhance absorption on thin silicon detectors as well as enhance emission of cathodoluminescence (CL). Through spatial and spectral mapping of both photocurrent and CL we clearly show the fundamental and higher-order resonant modes of these antennas. With CL we are also able to map the spatial distribution of these resonant modes with 10 nm resolution. In addition to these specific demonstrated applications, the results of this study enable optical engineers to more easily design a myriad of plasmonic devices that employ optical antenna structures, including nanoscale photodetectors, light sources, sensors, and modulators. Additionally the understanding of phase may be critical to designing resonant elements for metamaterials.

8096-32, Session 8

High resolution structural and optical characterization of top-down and bottom-up engineered plasmonic nanostructures

D. T. Schoen, M. L. Brongersma, Stanford Univ. (United States)

The use of electron energy loss spectroscopy (EELs) in the scanning transmission electron microscope (STEM) has been recently demonstrated to be a powerful tool for the high resolution mapping of plasmonic mode density in small metallic structures. To date, the majority of these studies have focused on small particles or the inverse structure, holes in a thin metallic film, either singly or in small clusters. One area largely unexplored so far by these techniques is the influence of material processing and quality on more complicated engineered nanostructures like would be used in integrated nanoplasmonic circuitry. Results of STEM EELs plasmon mode mapping of a variety of engineered metallic nanostructures will be presented. A comparison will be made between structures fabricated with top-down techniques, including electron beam lithography and focused ion beam milling, with structures fabricated by bottom up techniques, including chemically synthesized silver nanowires. Results of structural characterization by atomic force microscopy and high resolution TEM will also be presented and correlated with the optical property measurements.

8096-33, Session 8

High resolution fluorescence microscopy using nanoplasmonic antennas

K. Kim, Y. Oh, W. Lee, D. Kim, Yonsei Univ. (Korea, Republic of)

High resolution imaging below the diffraction limit has been widely investigated since precise molecular tracking and nanoscaled scanning are needed to understand various phenomena in sub-cellular environments. STED microscopy, field optical superlens imaging, and photo-activated light microscopy have been notably come into the spotlight as new approaches for sub-diffraction imaging.

In this paper, we introduce a concept for high resolution imaging based on the excitation of surface plasmons. It is commonly known that electromagnetic fields are localized to small spots, which is called hot spots, by nanoplasmonic antenna structures. Hot spots that are smaller than the diffraction limit can in principle excite molecular fluorescence. If a hot spot is formed in an extremely small size on a molecular scale by an optimum design of nanoplasmonic antenna, fluorescence excitation can be post-processed to produce highly localized images.

The concept was experimentally confirmed by imaging nanosized fluorescent beads, tracking dynamics of rhodamine tagged microtubule, and visualizing endocytotic internalization of GFP-tagged adenoviruses in live cells. Various nanoplasmonic antennas were fabricated by electron beam lithography and chemical annealing method. The imaging results confirm the enhancement of resolution after appropriate post processing methods.

8096-34, Session 9

Metamaterials from plasmonic nanoantenna arrays

M. Orenstein, Technion-Israel Institute of Technology (Israel)

Nano antennas are an exciting new addition to the field of photonics. The nanoantenna element exhibits two desirable characteristics - first it collects light from much larger effective area than its actual size and the second - it can concentrate the collected energy in an effective light capacitor (stopped light) with dimensions in the nano regime - much smaller than the actual antenna size. Using these unique features we constructed arrays of such nanoantennas to generate metamaterials - the latter was employed for the enhancement of light-matter interactions. In the process of construction of these metamaterials we would discuss parameters such as the inter-antenna spacing to avoid cells interactions (especially because such nanoantenna may have effective cross-section dimension of 1 wavelength - which contradicts the subwavelength requirements of metamaterials), and the separate optimization of the antenna efficiency and light field enhancement. We'll discuss robust ways to fabricate the antenna with predetermined resonance(s) and discuss in details nanoantenna configurations yielding either spectral broad-band or multi-harmonic responses.

In the second part of the talk, several applications of nanoantenna based metamaterials - that we experimentally realized, will be discussed, including high efficiency organic solar cells, enhanced emission rate communications wavelength LEDs - breaking the bottle neck for faster data modulation of such devices, and finally manipulating nonlinearly the vacuum field.

8096-35, Session 9

Diode-coupled Ag nanoantennas for nanorectenna energy conversion

R. M. Osgood, S. Giardini, M. Kinnan, P. Stenhouse, M. Hoey, J. Carlson, U.S. Army Natick Soldier Research, Development and Engineering Ctr. (United States); G. Fernandes, J. H. Kim, J. Xu, Brown Univ. (United States); W. R. Buchwald, Air Force Research

Lab. (United States); M. Chin, B. Nichols, U.S. Army Research Lab. (United States)

Arrays of "nanorectennas" consist of diode-coupled nanoantennas with plasmonic resonances in the visible/near-infrared (vis/nir) regime, and are expected to convert vis/nir radiative power into useful direct current [1,2]. We study plasmonic resonances in large format (~ 1 mm² area) arrays, consisting of electron beam-patterned horizontal (e.g., parallel to the substrate) Ag lines patterned on, and Ag nanoparticles dispersed atop, ultrathin (< 20 nm) tunneling barriers (NiO, Al₂O₃, and other oxides) [3]. These tunneling barriers, located on a metallic ground plane, rectify the alternating current generated in the nanoantenna at resonance. We measure the plasmonic resonances in these Ag nanoantennas, and find good agreement with modeling, which also predicts that the electric field driving the electrons into the ground plane (and therefore the rectification efficiency) is considerably enhanced at resonance. Various metal-insulator-metal tunneling diodes, incorporating the aforementioned barrier layers and different metals for the ground plane, are experimentally characterized and compared to our conduction model. We present experimental data on and analysis of nanorectenna power generation vs. wavelength and power of incident vis/nir radiation. Our e-beam fabrication technique is scalable to large dimensions [4], and allows us to easily probe different antenna dimensions.

[1] R. M. Osgood III, et. al., Proc. SPIE 6652, 665203 (2007).

[2] S. D. Novack, et. al., Proc. 2nd Intntl. Conf. Energy Sustainability, Aug. 10-14, 2008, Jacksonville, FL, USA (2008).

[3] M. L. Hoey, et. al., Appl. Phys. Letts. 97 (2010) 153104.

[4] H. S. Lee, et. al., Adv. Mats. 19 (2007) 4189.

8096-36, Session 9

Addressing quantum emitters with optical antennas

A. G. Curto, G. Volpe, T. H. Taminiau, M. P. Kreuzer, R. Quidant, N. F. van Hulst, ICFO - Instituto de Ciencias Fotónicas (Spain)

Optical antennas offer the promise of complete electromagnetic control over single photon emission and absorption at the nanoscale. They can efficiently address quantum emitters by modifying their interaction with light in polarization, angular radiation pattern and transition rates. Here, we report unidirectional and multipolar emission of quantum dots by near-field coupling to nano-antennas. The emitters are locally deposited at the end of metal nanowires. Yagi-Uda antennas are shown to direct and polarize quantum dot luminescence. Nanowire linear antennas supporting resonances of increasing order convert an otherwise purely dipolar emission into multipolar radiation. Finally, we quantify emitter-antenna coupling.

8096-37, Session 10

Toward low-loss plasmonics without metals

M. A. Noginov, L. Gu, J. E. Livenere, G. Zhu, A. K. Pradhan, R. Munde, M. J. Bahl, Norfolk State Univ. (United States); A. Urbas, J. Vella, Jr., Air Force Research Lab. (United States); V. A. Podolskiy, Univ. of Massachusetts Lowell (United States); E. Narimanov, Purdue Univ. (United States)

In this presentation, we will review our recent efforts aimed at the development of low-loss plasmonics that does not use metallic components. In particular, we will focus on two types of systems (i) highly concentrated dyes, in which the negative value of electric permittivity is sought in the vicinity of a very strong absorption line, and (ii) transparent conductive oxides - heavily doped degenerate semiconductors - in which plasma frequency corresponds to a near infrared range.

8096-38, Session 10

Nanoplasmonics in direct band-gap semiconductors

N. Dietz, M. I. Stockman, Georgia State Univ. (United States)

We explore nanoplasmonics concepts on selected group of III-Nitride compound semiconductor nanostructures, e.g., indium-rich InGaN alloys, that can be tuned over a large transmission range and fabricated with almost metal-like free-carrier concentrations of up to $\sim 10^{21} \text{ cm}^{-3}$. We have experimentally shown that for the highly doped InN the permittivity is negative (metal-like) and plasmonic quality factor is $Q=5-6$ for ir frequency 0.4-0.7 eV, or wavelength 1.5-3 micron, which is in the same range as for gold in the visible region. Thus, the heavily doped InN is a very promising plasmonic material in the near-ir. Theoretically, we have shown that an adiabatic cone compressor built on InN is able to enhance the optical intensity by a factor of ~ 500 with a high throughput. We also develop theory of a spaser built on a highly-doped InN plasmonic core surrounded by moderately-doped GaN gain medium.

8096-39, Session 10

All-optical control of single plasmonic nanoantenna-ITO hybrids

O. L. Muskens, Univ. of Southampton (United Kingdom); M. Abb, Univ. of Southampton (United States); N. Large, J. Aizpurua, Centro de Física de Materiales (Spain) and Donostia International Physics Ctr. (Spain)

Nanoscale plasmonic components are of enormous interest for their capabilities of locally enhancing electromagnetic fields and controlling emission. Active control of such components will enable a new generation of tunable devices. We present theoretical and experimental work exploring different routes toward achieving all-solid state modulation of nanoantenna resonances.

A new approach to antenna switching has been introduced recently where we make use of a photoconductive bridge between the two arms of a dimer antenna [1]. In order to experimentally achieve nonlinear control of nanoantennas on ultrafast time scale in a solid-state configuration, we are exploring hybrid nonlinear antenna systems. As a first important candidate, we have investigated Indium Tin Oxide (ITO) as a nonlinear optical material for plasmonic applications.

We have investigated the nonlinear response of nanoantenna-ITO hybrids under picosecond pulsed laser excitation using a combination of linear and ultrafast single-antenna spectroscopy [2]. We find that the modulation of the nanoantenna-ITO hybrid is distinct from that of a pure gold nanoantenna in absence of ITO, and from ITO in absence of the antenna. We will discuss possible mechanisms of enhanced antenna-ITO nonlinearity. Our results hold promise for new types of nonlinear antenna devices which could enable active control of local optical fields for use in nanophotonic modulators, nonlinear optics, sensing, and emission control.

[1] N. Large, M. Abb, J. Aizpurua, O. L. Muskens, Nano Lett. 10, 1741 (2010).

[2] M. Abb, O. L. Muskens, submitted (2011).

8096-40, Session 10

Coupling of plasmon with semiconductor nanoresonators: from modeling to device design

P. Fan, J. Liu, R. Pala, L. Cao, M. L. Brongersma, Geballe Lab. for Advanced Materials (GLAM) (United States)

As both metallic and semiconductor nanostructures have the unique

abilities to control the flow of light within a deep subwavelength volume, they are promising candidates as building blocks for compact photonic and optoelectronic devices and circuitry. Hereby, we theoretically and experimentally studied the light coupling of a propagating surface plasmon wave supported by a metal surface to the optical resonances of a semiconductor nanowire. We examined the structure as a side-coupled-cavity system and demonstrated efficient excitation of optical resonances in the nanowire by a propagating surface plasmon. Strong light coupling leads to a sharp suppression of plasmon transmission as well as efficient absorption in nanowire. These optical properties provide guidelines for incorporating multiple optical components and engineering complex optoelectronic functionalities within compact device systems, such as nanowire plasmonic photodetection and surface plasmon modulation.

8096-41, Session 10

Plasmonically enhanced emission from an inverted III-nitride light emitting diode

M. A. Mastro, U.S. Naval Research Lab. (United States)

Silver thin film and nanoparticles deposited on the surface of InGaN quantum well structures have been shown by several groups to plasmonically enhance the optically pumped emission. The necessity of placing the active region of the device within approximately 30 nm of the plasmonic metal is a subtle dilemma for GaN-based LEDs. Hence, nearly all reports of exciton to surface plasmon coupling have been based on quantum well structures that are not designed for electroluminescence.

The final grown layer in a traditional GaN-based LED structure is a p-type GaN:Mg contact layer. The magnesium dopant has a high activation energy in GaN, which limits the conductivity of the p-type contact layer. This necessitates a thick (100 to 300 nm) current-spreading p-type layer in commercial LEDs, which places the active region beyond the plasmon fringing field thickness, making exterior plasmonic enhancements impractical.

A new inverted LED approach was developed with the key layer for enabling plasmonic enhancement being a thin n++ (Al)GaN top contact, which brings the quantum well into the fringing field of the silver nanoparticles. This proximity allowed the excitons induced within the quantum well to couple to the surface plasmons, thereby increasing the emission by approximately a factor of four in a functional LED. Furthermore, the inverted LED allows flexibility in the alloy composition of the top contact layer, which alters the dielectric environment and plasmonic response of the metal.

8096-42, Session 10

Silicon plasmonics

U. Levy, B. Desiatov, I. Goykhman, The Hebrew Univ. of Jerusalem (Israel)

In the past two decades we are witnessing a rapid progress in towards the realization of CMOS compatible, silicon nanophotonic devices for monolithic on-chip integration of optical devices and systems. In parallel, the field of plasmonic is blooming, offering substantial advantages in the confinement of electromagnetic energy at the nanoscale. Thus, the combination of silicon nanophotonics with plasmonics seems to be a natural choice. In this work we review our work in the field of silicon plasmonics. Specifically, we demonstrate nanoscale confinement of light by the use of silicon plasmonic nanotapers on a chip. In addition, we report on our silicon plasmonic hybrid waveguide showing sub 100 nm confinement together with a propagation length of ~ 100 microns. Finally, we demonstrate a silicon plasmonic Schottky detector that allows the detection of signals at telecom wavelengths. The device is based on a self aligned process and combined LOCOS waveguide interfaced with a metal strip.

8096-43, Session 11

Surpassing conventional light-trapping and efficiency limits for solar energy conversion with plasmonic structures (Keynote Presentation)

H. A. Atwater, California Institute of Technology (United States)

Light-trapping and enhanced absorption is an important avenue for improved photovoltaic efficiency and cost reduction. We describe plasmonic thin film photovoltaic designs for light absorption and conversion efficiency that exceed what is achievable in conventional solar cell designs, and we report on experiments illustrating enhanced light absorption and conversion efficiency in thin film Si and GaAs and polymeric photovoltaic structures[1].

Thermodynamic arguments predict the maximum absorption enhancement in the ray optics limit for bulk dielectric materials to be $4n^2$, where n is the index of refraction of the absorbing layer [2]] and a similar analysis for thin waveguide structures found a maximum absorption enhancement of $<4n^2$ [3]. Using a combination of analytical and numerical methods, we describe why these structures do not surpass the conventional light trapping limit, and show how to design structures that can. The conventional limit can be exceeded in waveguide-like structures with elevated local density of optical states (LDOS) compared to that of the bulk, homogeneous material. To achieve this, modes of the structure must also be populated via an appropriate incoupling mechanism. We find using full wave simulations that ultrathin solar cells incorporating a plasmonic back reflector can achieve spatially averaged LDOS enhancements of 1 to 3, and a metal-insulator-metal (MIM) structure can achieve enhancements over 50 at a wavelength of 1100 nm, the band edge of Si. We also report in detail on plasmon-enhanced light trapping in thin film amorphous silicon solar cells that achieve near-record photovoltaic conversion efficiency.

8096-44, Session 11

Nonlinear optical responses of aperiodic plasmonic arrays for on chip applications

G. F. Walsh, Boston Univ. (United States) and U.S. Army Natick Soldier Research, Development and Engineering Ctr. (United States); S. Minissale, Boston Univ. (United States); B. R. Kimball, U.S. Army Natick Soldier Research, Development and Engineering Ctr. (United States); L. Dal Negro, Boston Univ. (United States)

Symmetry breaking in deterministic aperiodic plasmonic nano structures produces significant spatial field localization distributed over broad frequency spectra. These characteristics are ideally suited to enhance second and third order nonlinear processes for on-chip nanoplasmonic device applications. In this paper, we experimentally investigate the nonlinear optical properties of non-centrosymmetric aperiodic arrays of gold nanoparticles, with a controlled degree of disorder, fabricated by electron beam lithography. Two nonlinear optical phenomena, second harmonic generation (SHG) and the optical Kerr effect are investigated. Arrays are pumped with femto-second optical pulses at near infrared wavelengths and surface SHG is measured by angularly resolved scattering measurements. Experimental results are also reported for additional arrays coated with thin polymer films exhibiting strong optical Kerr effects. Localized enhancements of the nonlinear index are characterized by z-scan measurements and by a novel Fourier space measurement technique that we have developed to investigate optical nonlinearities in aperiodic structures ranging from quasi-crystals to pseudo-random media. These studies are important to the engineering of the next generation of plasmonic switches with controlled nonlinear index and frequency generation on a single chip.

8096-46, Session 11

Applications of plasmonic oligomers, metamaterials, and nanoantennas (Keynote Presentation)

H. W. Giessen, Univ. Stuttgart (Germany)

We present an overview of 2D and 3D plasmonic oligomers [1], metamaterials, and nanoantennas which are utilized for different purposes. Stacked 3D metamaterials can be used as perfect absorbers, which give angle and polarization independent absorption beyond 90% in the visible and near-infrared region [2]. Utilizing transition metals as well as plasmonic induced transparency schemes [3], the application of sensors for liquids and gases becomes feasible [4]. Cavity enhancement allows for tailoring the spectral resonances of plasmonic systems and results in very high figures of merit for the sensor schemes [5,6]. Arranging plasmonic substructures in 3D geometries, chirality can result as optical property. Using this method allows for the construction of novel broadband circular polarizers with large angle acceptance angles. Nanoantennas can aid the sensing and nonlinear properties of plasmonic nanostructures as well. We are going to discuss applications in this area as well.

References

- [1] Transition from isolated to collective modes in plasmonic oligomers M. Hentschel, M. Saliba, R. Vogelgesang, H. Giessen, A. P. Alivisatos, and N. Liu, Nano Lett. 10, 2721 (2010).
- [2] Infrared perfect absorber and its application as plasmonic sensor, N. Liu, M. Mesch, T. Weiss, M. Hentschel, and H. Giessen, Nano Lett. 10, 2342 (2010).
- [3] Planar metamaterial analog of electromagnetically induced transparency for plasmonic sensing, N. Liu, T. Weiss, M. Mesch, L. Langguth, U. Eigenthaler, M. Hirscher, C. Sönnichsen, and H. Giessen, Nano Lett. 10, 1103 (2010).
- [4] Hydrogen sensor based on metallic photonic crystal slabs, D. Nau, A. Seidel, R.B. Orzekowsky, S.-H. Lee, S. Deb, and H. Giessen, Opt. Lett. 35, 3150 (2010).
- [5] Cavity plasmonics: Large normal mode splitting of electric and magnetic particle plasmons induced by a photonic microcavity, R. Ameling and H. Giessen, Nano Lett. 10, 4394 (2010).
- [6] Cavity-enhanced localized plasmon resonance sensing, R. Ameling, L. Langguth, M. Hentschel, M. Mesch, P. V. Braun, and H. Giessen, Appl. Phys. Lett. 97, 253116 (2010).

8096-47, Session 12

Nonlinear plasmonics with nanocavity gratings

F. Capasso, Harvard Univ. (United States); P. Genevet, Univ. de Nice Sophia Antipolis (France)

Here we report on a novel approach based on plasmonic nanocavity gratings to enhance surface nonlinear processes. We have designed plasmonic nanocavities, made of nanogrooves in a gold film and arranged them periodically. A single narrow groove (tens of nanometers wide) defined on a metal surface can be viewed as a portion of a metal-insulator-metal waveguide terminated by a metallic mirror on one side and a dielectric mirror (air) on the other. It therefore forms a cavity that sustains Fabry-Perot modes. Because the cavity mode is confined in a sub-wavelength volume, large fields are established both in the metal and in the dielectric under resonant excitation. In addition to these localized surface plasmons a grating of nanogrooves enables the coupling of free space light to surface waves propagating on the corrugated surface.

We apply this concept of coupled resonances to four-wave-mixing in gold and demonstrate an enhancement of the generated signal of up to 2000 compared with an un-patterned surface, two orders of magnitude higher than previously reported. This result shows that

Conference 8096: Plasmonics: Metallic Nanostructures and Their Optical Properties IX

plasmonic nanocavity gratings are a promising route to enhancing optical nonlinearities in the metal and also in any material filling the cavities, with potential applications to nanoscale frequency conversion and highly sensitive vibrational spectroscopy and microscopy.

P. Genevet, J. P. Tetienne, E. Gatzogiannis, R. Blanchard, M. A. Kats, M.O. Scully, F. Capasso, *Nano Letters* 10, 4880 (2010)

8096-48, Session 12

Attosecond measurement of petahertz plasmonic near-fields

F. Süßmann, S. Zherebtsov, Max-Planck-Institut für Quantenoptik (Germany); T. Fennel, Univ. Rostock (Germany); E. Rühl, Freie Univ. Berlin (Germany); M. F. Kling, Max-Planck-Institut für Quantenoptik (Germany)

As compared to conventional electronics, plasmonic systems can operate at lightwave (petahertz) frequencies and have enormous potential to push the frontiers in electronics in both size and speed. The development of lightwave electronics would mark a major breakthrough and enable among other applications up to 6 orders of magnitude faster computation and communication technology. Attosecond metrology enables access to petahertz optical phenomena. We aim to control and measure nanoplasmonic fields on attosecond timescales and extend the attosecond streaking spectroscopy technique to measurements of enhanced plasmonic near-fields of isolated metal spheres. Temporal resolution is achieved by limiting the emission of high energetic, direct photoelectrons to a sub-cycle time window using attosecond XUV pulses that are phase-locked to the driving NIR field. These direct photoelectrons integrate the force exerted by the optical fields on their way to the detector, leading to a change in their kinetic energy. TOF spectra recorded for different time delays between the NIR and XUV pulses will give insight into the evolution of the local electric field and surface charge dynamics. Unlike in traditional streaking experiments, both the temporal and the spatial decay of the near-field cause the energetic shift of the electrons. This has to be considered during the reconstruction of the local field.

First experimental results and simulations will be presented, showing the feasibility of such an approach and the influence of laser intensity, particle size and composition on the obtained waveforms.

8096-49, Session 12

Optical response and ultrafast spectroscopy of metal-based hybrid nanoobjects

F. Vallee, D. Mongin, A. Lombardi, P. Maioli, A. Crut, N. Del Fatti, Univ. Claude Bernard Lyon 1 (France)

The size, shape and structure dependencies of the properties of nanoobjects, and the concomitant possibilities opened to control them, lead to considerable activities in the academic and industrial domains. Confinement effects in nanoobjects formed by a single material, e.g., a metal or a semiconductor, have now been extensively studied. Less interest has been devoted to complex systems, combining multiple material components in the same nanoparticle, e.g., bimetallic or hybrid metal-semiconductor particles. However, combining the nanoscale response of their components offer wide ranges of possibilities for developing novel plasmonic systems, and also raise fundamental questions on plasmon-plasmon or plasmon-exciton coupling and on energy and charge transfer mechanisms between the forming materials.

We report on investigation of the linear optical response (extinction) of hybrid hammer-like shape nanoparticles formed by a metal (Au sphere) and a semiconductor (CdS or ZnO rod). The results on ensemble and a single particle are interpreted in terms of dielectric coupling of the two-materials, yielding a good reproduction of the experiments in the non-resonant exciton-plasmon regime. The ultrafast nonlinear response of these nanohybrids has also been investigated using a two-color

wavelength-tunable femtosecond pump-probe technique. When carriers are injected in the semiconductor part, a spectral shift of the gold surface plasmon resonance is observed yielding evidence for ultrafast electron transfer between the two-materials. Measurements performed in CdS-Au hybrids probing the carrier population in the semiconductor part with 50 fs pulses suggest an upper limit for the electron transfer time of about 10 fs.

8096-50, Session 12

Light-field control of electronic motion at nanoscaled condensed matter interfaces

A. Schiffrin, Max-Planck-Institut für Quantenoptik (Germany); T. Paasch-Colberg, Max-Planck-Institut für Quantenoptik (Germany) and Technische Univ. München (Germany); D. Gerster, Technische Univ. München (Germany); N. Karpowicz, Max-Planck-Institut für Quantenoptik (Germany); S. Mühlbrandt, Max-Planck-Institut für Quantenoptik (Germany) and Technische Univ. München (Germany); J. Reichert, J. V. Barth, Technische Univ. München (Germany) and Max-Planck-Institut für Quantenoptik (Germany); R. Ernstorfer, Fritz-Haber-Institut der Max-Planck-Gesellschaft (Germany) and Max-Planck-Institut für Quantenoptik (Germany) and Technische Univ. München (Germany); F. Krausz, Max-Planck-Institut für Quantenoptik (Germany) and Ludwig-Maximilians-Univ. München (Germany)

The advent of intense few-cycle near infrared (NIR) laser pulses with stable and tunable carrier envelope phase (CEP) has enabled the control of electromagnetic fields with attosecond time precision [1]. Here we aim at exploiting these few-cycle NIR optical fields with well-defined CEP to generate and control the motion of charge carriers within heterogeneous nanoscaled solid state interfaces. We demonstrate the generation of directly measurable photocurrents in unbiased gold-coated SiO₂ nanogaps, whose magnitude and directionality can be tuned with the laser CEP. This effect vanishes with the increase of the laser pulse duration. We claim that such phenomenon is the signature of optically induced electron tunneling at the metal-dielectric interface with subsequent acceleration of the charge carrier in the ultrashort laser field. This ultrafast current injection at a nanoscaled condensed matter system represents a first step towards femtosecond lightwave electronics.

1. Baltuska, A. et al. Attosecond control of electronic processes by intense light fields. *Nature* 421, 611-615 (2003).

8096-51, Session 13

Resonance energy transfer near metal nanostructures mediated by surface plasmons

T. V. Shahbazyan, Jackson State Univ. (United States); V. Pustovit, Ctr. de Recherche Paul-Pascal (France)

A theory of resonance energy transfer (RET) between donor and acceptor molecules (or quantum dots) situated near a plasmonic nanostructure is presented that incorporates nonradiative and radiative transfer channels while maintaining energy balance between transfer, dissipation and radiation. It is shown that plasmon-enhanced radiative transfer (PERT) is the dominant RET mechanism in a wide range of parameters. Numerical calculations performed for molecules near spherical Ag nanoparticle indicate that RET is determined by competition between plasmon enhancement and metal quenching and its magnitude is highly sensitive to molecules positions. There are regions in parameter space where plasmon-mediated RET can be either enhanced or reduced relative to Foerster transfer, consistent with experiment. A comparison between our theory and previous models is performed.

8096-52, Session 13

Theory of energy transfer interactions near sphere and nanoshell based plasmonic nanostructures

M. S. Shishodia, Tel Aviv Univ. (Israel) and Holon Institute of Technology (Israel); B. D. Fainberg, Holon Institute of Technology (Israel) and Tel Aviv Univ. (Israel); A. Nitzan, Tel Aviv Univ. (Israel); G. Li, Northwestern Univ. (United States)

Molecular exciton-metallic nanoparticle complexes are the subject of intensive study. Metallic nanostructure mediated electric-field enhancement, and the proximity of a metal interface can greatly alter dipole-dipole interactions in excitonic and energy transfer donor-acceptor systems. In addition, excitonic (energy transfer) interactions accompanied by plasmonic response of metallic contacts can have substantial effects on the electronic transport properties of molecular nanojunctions [1]. In this paper, we present a theoretical model for energy transfer near sphere and nanoshell particle/particle-pair based metal nanostructures. The model is based on multipole spectral expansion and uses the surface plasmon-dressed Coulomb interaction [2]. We study also the energy transfer in a molecular wire between two metallic contacts representing a nanoparticle dimer in the presence of plasmonic hybridization. It is worthy to note that nanoshell exhibits superior plasmonic properties by virtue of geometry controlled spectral tuning of resonances arising from the hybridization of cavity and sphere plasmons. Exploiting tunability feature of nanoshells, wavelength specific designs for optimal energy transfer, and the possible effects on molecular junctions will be presented.

1. G. Li, B.D. Fainberg, A. Nitzan, S. Kohler and P. Hanggi. Phys. Rev. B, 81, 165310 (2010)
2. M. Durach, A. Rusina, V.I. Klimov and M.I. Stockman. New J. Phys., 10, 105011 (2008)

8096-53, Session 13

Fluorescence lifetime measurements of single molecules in DNA templated gold nanoparticle dimers

M. Busson, L'Institut Langevin (France); B. Rolly, B. Stout, N. Bonod, Institut Fresnel (France); S. Bidault, L'Institut Langevin (France)

Gold nanoparticle groupings can act as optical antennas: they couple efficiently in the near field to photon emitters to enhance their interaction with the far field. A typical way to design nanoantennas is to couple the plasmonic modes of gold nanoparticles positioned a few nanometers apart. We demonstrate here how efficient optical antennas can be synthesized by the programmed assembly of DNA functionalized gold nanoparticles. This bottom up strategy allows us to tune particle sizes and spacings while fully controlling the chemical environment of the antenna.

In practice, a known number of thiolated DNA single strands are grafted on the surface of polyethylene glycol stabilized gold particles with diameters ranging from 5 to 40 nm. Hybridization of complementary DNA sequences drives the assembly of well defined nanoparticle groupings with spacings ranging between 6 and 30 nm.

The optical properties of single groupings are studied by confocal scattering spectroscopy. Shortening the DNA linker induces a clear red shift of the plasmon resonance wavelength. Experimental data from scattering spectroscopy are correlated with electron microscopy images and theoretical calculations.

The interaction of the antenna with a single chromophore added to the DNA scaffold is studied using fluorescence lifetime measurements. Experiments are performed on single molecules using time-correlated single photon counting in a confocal geometry. The increased local density of optical states in the antenna enhances the de-excitation rate of

the fluorescent molecule. The influence of the dimer interparticle spacing on single molecule fluorescence lifetime is being investigated.

8096-54, Session 14

Hybrid semiconductor/plasmonic devices for nanophotonics (Keynote Presentation)

M. L. Brongersma, Stanford Univ. (United States)

Metamaterials and nanophotonic devices are most commonly constructed from metallic (i.e. plasmonic) nanostructures. However, recent research has begun to also exploit the optical resonances of high-permittivity semiconductor and dielectric nanostructures to realize similar optical functionalities. In this talk, I will illustrate the use of plasmonic, semiconductor, and dielectric nanostructures in a variety of applications (nanoscale sources, high-speed modulators, and detectors) and discuss their relative strengths and weaknesses. I will also discuss several exciting new hybrid semiconductor/plasmonic devices that capitalize the relative strengths of each of the constituent materials to obtain new functionalities.

8096-55, Session 14

Controlling electroluminescence from QW using plasmonic resonator antenna electrodes

K. C. Y. Huang, Stanford Univ. (United States); M. Seo, KAIST (Korea, Republic of); M. L. Brongersma, Stanford Univ. (United States)

We simulated, fabricated and characterized the electroluminescence from InGaAs/ GaAs QW with metal electrodes which function as plasmonic resonator antennas. By patterning the antenna electrodes in the vicinity of a single QW layer with deeply subwavelength lateral width, charge carriers are confined near the antenna and subsequently recombine with enhanced radiative decay rate depending on the electrode/ QW separation and electrode shape. We show that the emission can be efficiently coupled to the antenna resonance which is engineered to reradiate in a specific polarization and unidirectional far-field pattern. The simultaneous control of carriers and photons can be used to improve light extraction and detection from the semiconductor while enabling fast direct modulation of the spontaneous emission.

8096-56, Session 14

Enhancing photonic-plasmonic interactions on active devices using circular scattering in aperiodic spirals

J. Trevino, S. Yerci, L. Dal Negro, Boston Univ. (United States)

Deterministic arrays of Au nanoparticles arranged in aperiodic spiral geometries (Vogel's spirals) have been engineered and fabricated onto planar optical devices in order to enhance photonic-plasmonic coupling and increase light-matter interactions over broad frequency spectra. Vogel's spirals lack both translational and orientational symmetry in real space, while displaying continuous circular symmetry (i.e., rotational symmetry of infinite order) in reciprocal Fourier space. We investigate the novel regime of "circular multiple light scattering" in finite-size deterministic structures and we experimentally and theoretically show that circular symmetry in diffused reciprocal space gives rise to polarization-insensitive planar diffraction over a large and controllable range of wavelengths. The multi-band/broadband polarization-insensitive planar diffraction observed in aperiodic spirals is a highly desirable property for the engineering of a variety of device applications that require enhancing photonic-plasmonic coupling over planar optical

chips. In this work, we will present fabrication and characterization of both plasmon-enhanced Schottky solar cells and plasmon-enhanced electroluminescence from Er-doped silicon-rich silicon nitride (Er:SiNx) LEDs coupled to deterministic aperiodic Au nanoparticle arrays were fabricated using electron beam lithography on Si wafers. Arrays with different morphologies and nanoparticles sizes were systematically investigated in a large range of geometrical parameters. Our results demonstrate reproducible absorption and extraction enhancement from lithographically defined deterministic aperiodic arrays with optimized broadband scattering suitable for the engineering of reproducible Si-based devices.

8096-57, Session 14

Coupling of nanoparticle plasmons with molecular linkers

N. Zabala, Univ. del País Vasco (Spain) and Centro de Fisica de Materiales (Spain) and Donostia International Physics Ctr. (Spain); O. Pérez-González, Univ. del País Vasco (Spain) and Donostia International Physics Ctr. (Spain); P. J. Nordlander, Rice Univ. (United States); J. Aizpurua, Centro de Fisica de Materiales (Spain) and Donostia International Physics Ctr. (Spain)

Following the emerging interest in connecting molecular electronics and plasmonics, we study the spectral signatures of molecular linkers in plasmonic cavities of gold nanoparticle dimers. Different dielectric models and sizes for the linker are considered to envisage the relation between the spectral changes observed in the extinction spectra and the electronic transport through the molecules.

For thin junctions a BDP (Bonding Dimer Plasmon) mode, arising from the coupling of dipolar modes of the individual particles, is excited and blue-shifted as the radius is increased. When wider junctions are involved another mode, which corresponds to a real charge transfer between the nanoparticles and is known as CTP (Charge Transfer Plasmon), emerges at longer wavelengths. The characteristics of these modes are observed with a simple pure conductor, but when an excitonic bridge is considered, more features appear in the extinction spectra as a consequence of the plasmon-exciton coupling, as revealed from the dispersion curves obtained for different sizes and characteristic resonant frequencies of the molecules.

The electromagnetic field is obtained by solving Maxwell's equations numerically with the Boundary Element Method (BEM).

We believe that the understanding of the spectral changes in plasmonic cavities with molecular linkers may help to the control the switch of different plasmon modes.

8096-58, Session 14

Tayloring the optical properties of LEDs by using surface plasmon polariton gratings

J. Moosburger, OSRAM Opto Semiconductors GmbH (Germany)

The enhancement of light extraction and tailoring the emission characteristics are two of the major challenges for state of the art LED chips. Beside conventional approaches like surface roughening, metal gratings and metal nano particles can be used as an alternative approach.

Looking at the extraction efficiency of LED chips, SPP gratings on one side can be used to avoid the limitations of total internal reflection (TIR) at planar surfaces, where light should be coupled out. At a flat surface, light beyond the critical angle is reflected back and hence the probability of absorption within the chip increases. With SPP gratings, light beyond TIR can couple into extraction modes via SPP states.

On the other side, SPP gratings can be used to make unavoidable absorbers 'translucent'. The main focus here are metal contacts at the emitting surface that normally contribute to internal losses.

In addition, the emission characteristic of a LED chip can be shaped by defining SPP gratings on top. Due to the periodicity of the grating, the SPP's can couple to discrete extraction modes. Hence by changing periodicity, filling factor and over all pattern of the grating, the extraction profile can be altered.

The presentation will summarize theoretical calculations, experimental results and fabrication issues of plasmonic structures on inorganic LEDs. Furthermore a benchmark with state of the art LEDs and an outlook for future potentials of SPP gratings for LEDs will be given. This work was done within the EU funded project PLEAS.

8096-59, Session 14

Thermo-induced electromagnetic coupling in gold/polymer hybrid plasmonic structures probed by surface enhanced Raman scattering

N. Félijd, L. Dos Santos, H. Gehan, G. Charron, J. Grand, J. Aubard, C. Mangeney, Univ. Paris 7-Denis Diderot (France)

Since its discovery four decades ago, surface enhanced Raman scattering (SERS) has been considered as one of the most sensitive tools for the chemical analysis of very few amount of molecules adsorbed onto metallic nano-particles (NPs), especially gold and silver.

One challenging aspect in SERS concentrates on the demonstration that a single molecule or very few molecules could be detected under specific conditions. It requires very huge electric field enhancements occurring within the gap between two NPs or between NPs and a gold film. Of particular interest is the possibility to control this latter interaction in order to optimize the Raman enhancement factor. In this work, we propose to address this issue by designing a stimuable device made of gold colloidal nanoparticles connected to a gold flat film through an active thermosensitive polymer brush layer, capable to externally modulate the distance between the NPs and the substrate. As a linker, we used Poly (N-isopropylacrylamide) that undergoes a reversible, inverse phase transition at a lower critical solution temperature (LCST) of about 32°C in pure water. Below the LCST, the polymer chains are in an extended conformational state. Above the LCST, it is in a hydrophobically collapsed conformational state. These conformational changes of the linker between the gold nanoparticle assemblies and the surface induce dramatic modifications of the optical properties of the substrate. In particular, above the LCST, the proximity of the colloidal particles to the gold film leads to a strong interaction regime with higher SERS spectra than below the LCST.

H. Gehan, L. Fillaud, M. Chehimi, J. Aubard, A. Hohenau, N. Félijd, C. Mangeney, ACS Nano, 4, 6491 (2010).

H. Gehan, C. Mangeney, J. Aubard, G. Lévi, A. Hohenau, J. R. Krenn, E. Lacaze et N. Félijd, J. Phys. Chem. Letters, 2, 226 (2011).

8096-74, Poster Session

Origin of localized surface plasmon resonances in thin silver film over nanosphere patterns

S. K. Cushing, L. A. Hornak, J. Lankford, Y. Liu, N. Wu, West Virginia Univ. (United States)

Film over nanosphere (FON) patterns are formed by depositing a silver film on top of a close-packed polystyrene (PS) sphere template. Multiple localized surface plasmon resonance (LSPR) peaks are experimentally measured by transmission UV-Vis spectroscopy in the three dimensional FON pattern for thin silver films. Increasing the sphere size in the close-packed template or increasing the deposited silver film thickness redshifts the LSPR peaks to varying degrees. A finite difference time domain (FDTD) analysis reveals that the main LSPR peaks originate from a quadrupole and a dipole coupling mode near the triangle gap

surrounded by three adjacent PS spheres. The physical location and the electromagnetic enhancement of the two resonant modes are determined for different thickness of deposited silver films. It is found that the resonance modes do not change with varying film thickness.

8096-75, Poster Session

Semi analytical numerical analysis of plasmonic structures in layered geometries

A. Alparslan, C. Hafner, ETH Zurich (Switzerland)

Following the advancements in the fabrication process of photonic structures, various nano devices became quite popular, including photonic crystals, chemical and bio sensors, optical antennas and waveguides. Usually, these devices are fabricated in a multilayered structure. In the numerical analysis of such structures, the multilayered geometry is often ignored for sake of simplicity, which can cause inaccuracies in the results. Especially for structures that support Surface Plasmon Polariton (SPP) or guided wave modes, the errors become so high that the computations become useless. In order to analyze such structures, it is crucial to use a numerical tool that deals with layered geometries in an efficient and robust way.

The Multiple Multipole Program (MMP) is one of the most accurate simulation tools for the analysis of plasmonic structures. It uses a superposition of analytical solutions of Maxwell's equations (point sources, plane waves, Bessel functions, etc., so called expansions), to fulfill the boundary conditions on the boundaries or interfaces of structures. In the case of structures involving layered geometries, the boundary matching procedure becomes expensive, if not impossible, since the number expansions and matching points increases dramatically. In order to tackle this problem, layered media Green's functions (LMGF), which are the analytical responses of the layered geometry in presence of a point source, are introduced as a new expansion set for MMP. By using the advantages of MMP and LMGF, a robust, efficient and user-friendly simulation tool is obtained. In this talk, the derivation of the method together with some results from OpenMaX, the open-source program that includes the latest MMP version, will be presented.

8096-76, Poster Session

Site selective surface enhanced Raman scattering on nanostructured cavity arrays

F. Lordan, J. H. Rice, Univ. College Dublin (Ireland); B. Jose, R. J. Forster, T. E. Keyes, Dublin City Univ. (Ireland)

Raman spectroscopy is an extremely powerful analytical tool. Surface enhanced Raman spectroscopy (SERS) enables sample sensitivity to extend down to the single molecule level. There is presently great interest in using uniform nanostructured surfaces to give reproducible and strong SERS signal. The nanocavities studied here have spherical cap architecture and are arranged uniformly in an Au array. These structures support both localised and delocalised plasmons. Localised surface plasmon polaritons exist inside the nanocavities (Mie plasmons) and delocalised or propagating surface plasmon polaritons exist on the flat surface of the sample (Bragg plasmons). The angle dependence property of surface enhanced Raman is used in the present work to enable comparison between SERS caused by localised plasmons and SERS caused by delocalised plasmons. The samples used here were modified to enable separate investigations of the two plasmon types. The externally modified array had dye placed only on the flat top surface of the array. The internally modified array had dye placed only on the internal walls of the cavities. Results show that the changes in Raman intensities with respect to the incident angle depend on the location of dye on the array.

8096-77, Poster Session

Enhanced polarization anisotropy of metal nanoparticles and their spectral characteristics in the surface plasmon resonance band

N. Ghosh, J. Soni, Indian Institute of Science Education and Research (India)

The spectral and angular polarization behavior of light scattered from metal nanoparticles were investigated using polar decomposition of the scattering matrices $S(\theta, \lambda)$, θ is the scattering angle, λ the wavelength] for both preferentially and randomly oriented spheroidal (prolate and oblate) silver nanoparticles were generated in their surface plasmon resonance spectral region (380 - 600 nm) using the T-matrix approach. $S(\theta, \lambda)$ were generated for silver nanoparticles having varying sizes and aspect ratios and for dielectric particles having identical size and shape. These were analyzed using the polar matrix decomposition approach, to derive quantitative individual polarization properties, namely, retardance, diattenuation and depolarization. The decomposition-derived linear retardance (δ , phase difference between orthogonal linear polarizations) from preferentially oriented silver nanoparticles showed distinct spectral features, the values for δ peaking around the spectral overlap region (400 - 450 nm) of the longitudinal and the transverse plasmons. Further, the magnitude of δ and its spectral behavior was observed to undergo systematic changes with varying aspect ratio and the size of the nanoparticles. In contrary, for similar dielectric nanoparticles, the scattering-induced δ was considerably weaker and did not show any appreciable spectral variation. The decomposition-derived value for diattenuation (d , differential attenuation of two orthogonal polarization states) for the silver nanoparticles also showed interesting spectral characteristics, which were again absent for the dielectric particles. The enhanced linear retardance (and its distinct spectral characteristics) for the metal nanoparticles was attributed to the additional phase differences between the longitudinal and the transverse plasmon polarizabilities, which was confirmed further by studying the angular variation of δ (θ) for these nanoparticles. The analysis also revealed that when averaged over all possible orientation of the particles (for randomly oriented spheroids), addition of the retardance and diattenuation matrices having random orientation of axes manifests as stronger depolarization (D) of light in spheroidal metal nanoparticles as compared to their dielectric counterparts. The details of the studied dependence of δ , d and D on size parameter and aspect ratio of the nanoparticles will be presented. Initial results of complementary experimental studies and their implications for spectral, polarimetric biomedical imaging will also be discussed.

8096-78, Poster Session

Manipulation of multi-dimensional plasmonic spectra for information storage

K. Yang, W. T. Chen, P. C. Wu, C. J. Chen, National Taiwan Univ. (Taiwan); C. Weng, Instrument Technology Research Ctr. (Taiwan); C. Kuan, National Taiwan Univ. (Taiwan); M. Mansuripur, College of Optical Sciences, The Univ. of Arizona (United States); D. P. Tsai, National Taiwan Univ. (Taiwan) and Instrument Technology Research Ctr. (Taiwan) and Research Ctr. for Applied Sciences (Taiwan)

We demonstrate a concept of optical data storage through plasmonic resonances of metallic nano-structures. Metallic nano-structures exhibit strong variations in their reflectance and/or transmittance spectra due to surface plasmon polariton resonances. We study the variations of spectra through $50 \times 50 \mu\text{m}^2$ arrays of repeated unit cells covering a total area of $\sim 50 \times 50 \mu\text{m}^2$. Each cell contains 10 different nano-features, such as an ellipse, a ring, a circle, a triangle, a square, etc. The size of each unit cell is $500 \times 500 \text{nm}^2$, and the periodicity is $1.0 \mu\text{m}$. The variations of spectra is

Conference 8096: Plasmonics: Metallic Nanostructures and Their Optical Properties IX

obvious enough to be distinguished, so that it should be possible to store and then retrieve data from different spectra. This paper presents the results of a study aimed at proving the feasibility of the concept.

8096-80, Poster Session

Controlling the fluorescence dynamics of a single emitter by coupled metallic nanostructures

C. Vandenberg, Facultes Univ. Notre Dame de la Paix (Belgium); L. S. Froufe-Pérez, Instituto de Ciencia de Materiales de Madrid (Spain); R. Carminati, Ecole Supérieure de Physique et de Chimie Industrielles (France)

A key issue in photonics is the controlled modification of spontaneous emission. Changes of the spontaneous decay rate are induced by changes in the local density of electromagnetic modes, and are quantitatively described by the classical electrodynamic response of the surface. In consequence, the development of nano-optics techniques has stimulated the use of metallic nanostructures to act on the spontaneous decay rate but also on the fluorescence intensity, and on the radiation pattern of isolated emitters, leading to the concept of optical nanoantenna.

In addition, control of plasmon-resonance frequencies can be achieved either by playing with the shape of metallic nanostructures either by coupling different plasmonic modes of nanostructures. The latter case has the advantage that these hybrid plasmonic modes can lead to either radiative or non-radiative coupling depending on their coupling to free space.

In the present work, we study theoretically and numerically the possibility of controlling the fluorescence features with systems involving coupled plasmon modes. Depending if the emitter is coupled to the radiative mode or the non-radiative mode (dark mode), the apparent quantum yield and the fluorescence lifetime exhibit different behaviors. The concept is general and can be illustrated on several geometries such as the dimer of two nanoparticles, a thin metallic film or a hybrid system coupling a metallic film and a single metallic nanoparticle.

8096-81, Poster Session

Optical properties of silver nanoparticle dispersed in polymer matrix

A. Ziaemehr, Imam Khomeini International Univ. (Iran, Islamic Republic of); R. Poursalehi, Shahed Univ. (Iran, Islamic Republic of)

We studied the effects of nanofiller size on the refractive index and optical transparency of nanoparticle polymer nanocomposite. The size of nanofillers has been considered from 3 up to 30 nm. In a precise calculation of absorption and scattering of polymer matrix, the modified size dependent refractive index is used. In addition, this quantity obtained with considering size dependent surface effects.

The calculated results indicated the particles refractive index depends strongly on the diameter of particles, especially for smaller particles at long wavelengths. Also it was found that optical extinction intensity increases for larger nanoparticle and the wavelength of maximum of optical exhibited a red shift. Inconsistency between refractive index of nanofiller and polymer matrix increases the scattering, and in some application, light scattering and any other type of wastage are extremely important.

The results of this study can be applied for optimization of size and loading fraction of nanoparticle filler for preparation of modified nanocomposites with lower light scattering and lower refractive index mismatch.

8096-82, Poster Session

hp-FEM applied to scattering problems in plasmonics

M. Wang, C. Engström, ETH Zurich (Switzerland); K. Schmidt, Technische Univ. Berlin (Germany); H. Brandsmeier, C. Hafner, ETH Zurich (Switzerland)

The simulation of plasmonic structures is numerically difficult mainly because of the rapid field variation at the metallic surface. Standard low-order finite element and finite difference methods are inefficient for this class of problems. Therefore, it is highly desirable to develop efficient finite element methods able to simulate plasmonic structures.

In this paper, we use high-order curvilinear finite elements for scattering problems with both Absorbing Boundary Conditions (ABCs) and radial Perfectly Matched Layers (PMLs). For ABCs, we develop adaptive strategies, which are implemented in the hp-finite element code CONCEPTS. CONCEPTS uses blending technique for high-order boundary approximation, which is mandatory for curved boundaries.

We study the plasmonic behavior of two nearby nano particles with smooth interfaces and use solutions obtained with the Multiple Multipole Program (MMP) as reference solutions. The hp-FEM simulations with ABC and PML show a very good agreement with MMP. Of central importance is the use of quadrilateral curvilinear finite elements, which accurately describe the geometry of the problem. Together with high-order basis functions and an adaptive strategy, these elements significantly enhance the performance of FEM.

8096-84, Poster Session

near-field mapping by laser ablation of PMMA coatings

J. Fiutowski, C. Maibohm, J. Kjelstrup-Hansen, H. Rubahn, Univ. of Southern Denmark (Denmark)

Near-Field optics has attracted much attention in various fields of science due to its prospect for spatially resolving optical fields at length scales far below the diffraction limit. Though several applications for local field enhancement have been successfully demonstrated, spatial mapping and direct measurement of the optical near-field surrounding nanostructures of noble metals is still important both for basic and applied studies of exploitation of localized surface plasmons (LSP). Spatial mapping and direct measurement of the optical near-field surrounding noble metal nanostructures are often done with optical scanning techniques such as scanning near-field optical microscopy (SNOM) or photon scanning tunneling microscopy (PSTM). Here we report sub-diffraction spatially resolved mapping of strong localized field intensity enhancement on gold nanostructures based on local laser ablation of an "imaging" polymer layer. We take advantage of the transparency and well known ablation threshold of poly (methyl methacrylate) PMMA thin films, spin coated onto regular arrays of elevated gold nanostructures on a gold substrate. Sub-ablation threshold illumination is obtained via Laser Scanning Microscope with a femtosecond laser system tuned to excited Localised Surface Plasmons (LSP) on the nanostructures. The accompanying field enhancement on the nanostructures together with sub-threshold excitation exceeds the PMMA ablation threshold creating arrays of local ablations and corresponding topographic modifications of the polymer film. Such modifications can be quantified straightforwardly via, e.g., scanning electron or atomic force microscopy.

8096-85, Poster Session

Study of the morphology and optical properties of nanoparticle-polymer conjugates

R. C. Wadams, L. Fabris, Rutgers, The State Univ. of New Jersey

Conference 8096: Plasmonics: Metallic Nanostructures and
Their Optical Properties IX

(United States)

Organic-based bulk heterojunction solar cells (BHJSCs) consist of phase-separated blends of conducting polymers and fullerene derivatives. The polymer active layer donates electrons to the n-type fullerene phase upon absorption of solar radiation. Ideally, electrons diffuse into the heterojunction before recombination, and are dissociated at the polymer-fullerene interface. BHJSC quantum efficiency is limited by the polymer and fullerene morphology, and by the polymer's narrow absorption spectrum.¹ It has been proposed that nanoparticle incorporation into the active layer can enhance light absorption.

Noble metal nanoparticles exhibit localized surface plasmon resonances (LSPRs) upon absorption of electromagnetic radiation. The absorption spectrum is size, shape, and material dependent. Spherical nanoparticles exhibit one LSPR. Once symmetry is broken, such as with rods, multiple absorption bands are possible. Additionally, pairing nanoparticles in dimers creates intense electromagnetic field enhancements within the intermetallic junction due to plasmonic coupling. The introduction of nanoparticles in BHJSCs can potentially increase the absorption spectrum of the active polymer layer.

Recently, nanoparticles have been covalently bonded to polymeric chains allowing investigation of polymer-nanoparticle interactions, and 1-dimensional nanoparticle assemblies.² Our expectation is that binding nanoparticle dimers onto polymer backbones will affect the morphology and optical properties of the conjugate. It is anticipated that ordering of the polymer-based active layer can be induced by the presence of anisotropic nanoparticles with elongated shape, such as nanorods.

Herein we describe our approach for the synthesis of covalent nanoparticle dimer-polymer conjugates. Gold and silver nanoparticles, of various morphology (e.g. spheres, rods, bones), and their dimers are synthesized, and conjugated to polymer chains. The effects on the morphology and optical properties induced by the coexistence of the nanoparticle dimers and polymers are analyzed, and the potential benefit brought about by these hybrid nanostructures is evaluated.

[1] S. Gunes, H. Neugebauer, N.S. Sariciftci, Chem. Rev.2007, 107, 1324.

[2] R.Sardar, J.S. Shumaker-Parry, Nano Lett., 2008, 731.

8096-86, Poster Session

Optical characterization of nanopillar black silicon for plasmonic and Solar cell application

M. R. Gartia, Y. Chen, Y. C. Bordain, Z. Xu, J. Eichorst, J. C. Mabon, J. A. N. d. T. Soares, R. M. Clegg, G. L. Liu, Univ. of Illinois at Urbana-Champaign (United States)

With the goal of improving photo-absorption of photovoltaic device and for plasmonic application we have fabricated nanopillar black silicon devices through etching-passivation technique which does not require any photomask and whole wafer scale uniformity is achieved at room temperature in a short time. We have also performed a thorough optical characterization of the device. We have carried out cathodoluminescence (CL) and current dependent CL spectroscopy study for our device. Further we present the photoluminescence characteristics of our device both at room temperature and at low temperature (77 K) with different excitation sources. The characterization done using Raman spectroscopy showed the possible phonon broadening effects. We performed a reflectance and absorption measurement using Varian Cary-5 instrument to measure the effect of nano structuring the silicon wafer. In order to render the device for plasmonic property, we have applied a thin layer of silver (80 nm) using e-beam evaporation. Then we performed a series of different optical characterization to probe the plasmonic effect of our device such as surface plasmon enhanced fluorescence, angle dependent reflectance measurements to show the different surface plasmon modes, high resolution cathodoluminescence (CL) experiment, surface enhanced Raman spectroscopy (SERS) measurement, Fluorescence Lifetime Imaging Microscopy (FLIM) experiment to show the lifetime modification on nanoplasmonic device. Finally, we have made both organic and inorganic solar cell using our device to demonstrate the

utility of the current device. The results for the I-V measurement for the devices is provided in the paper.

8096-87, Poster Session

Surface-plasmon-enhanced visible light emission of ZnO/Ag grating structures

M. Gwon, E. Lee, Ewha Womans Univ. (Korea, Republic of); K. Yee, Chungnam National Univ. (Korea, Republic of); D. Kim, Ewha Womans Univ. (Korea, Republic of)

Surface plasmon polaritons (SPP) are resonant interactions between the surface charge oscillations and the electromagnetic waves at the metal/dielectric interface. Periodic nanostructures can bridge the SPP-photon momentum gap and modify the optical properties of the dielectric layers. ZnO/Ag thin films can be used as back reflectors in silicon thin film solar cells. It is interesting to investigate how the grating structures can influence SPP-photon coupling and resulting optical properties of ZnO/Ag layers.

ZnO/Ag thin films were deposited on one-dimensional periodic structures, with the periodicity of 1000 and 1400 nm, fabricated by nanoimprint lithography. The ZnO/Ag grating structures exhibited multiple peak features in visible-range photoluminescence (PL). Whereas a ZnO/Ag planar thin film showed two major PL peaks in UV and visible region. Moreover the PL intensity of the periodic structures was 100 times larger than that of the planar counterpart. These results could be understood as a result of SPP-exciton interaction. The grating structures also exhibited quite distinctive features in reflectance from the planar samples. There were several reflectance dips, which were caused by photon-induced SPP excitation via the grating coupling. Thus, the PL peaks, well matched with the reflectance dips, represent the excited SPP energies, determined by the grating periodicity. Finite-difference time-domain simulations supported all the experimental results.

8096-88, Poster Session

Two dimensional standing wave surface plasmon fluorescence imaging by subwavelength slit arrays

W. Qian, Nanyang Technological Univ. (Singapore); J. Bu, Nankai Univ. (China); P. S. Tan, Sr., Nanyang Technological Univ. (Singapore); X. C. Yuan, Sr., Nankai Univ. (China)

Four counter-perpendicular sub-wavelength slit arrays embedded on the silver film are proposed to convert free-space light to surface plasmon (SP) waves. The excited counter-propagating SP waves interfere each other to form two dimensional standing wave patterns in the region of the structure center area. Since the SP wavelength is shorter than free space propagating electromagnetic waves, this constructive interference pattern contains an attenuation of the high spatial frequency $k_{SP}=4\pi/\lambda_{SP}$. This standing wave profile can served as the virtual probing mechanism to excite fluorescence near the metal surface. Then a linear inversion scheme is utilized to recover the fluorescence density from a serial of images obtained by conventional microscopy by using phase shifting method. The simulation results show that the resolution can reach to $\lambda_{SP}/4$ which is clearly beyond diffraction limit. The main advantages of these promising new paths are that they do not require any scanning of the sample and do not require one to mount an interference setup in the microscope. This designed sub-wavelength slit arrays structure is one of the potential methodologies to realize the real time, wide field, on-chip, and high-spatial resolution fluorescence imaging.

8096-89, Poster Session

Numerical study of optical and EELS response of coupled metallic nanoparticles

S. Guillaume, L. Henrard, Facultes Univ. Notre Dame de la Paix (Belgium)

Localized surface plasmon resonances (LSPR) govern the optical properties of metallic nanoparticles at the nanoscale level and depend strongly on their shape, size and environment. Furthermore, for particles close to one another, coupling occurs and gives rise to new plasmon modes that can be described in terms of hybridization of the plasmon modes of the individual nanoparticles. For given geometries, such as a dolmen-like structure made of 3 gold nanorods, a transmission window appears in the optical spectrum due to Fano resonances. Because, dark modes are invisible in optics, one has to probe locally the response of the nanoparticles to get insight on the origin of these Fano resonances. This is why we investigate numerically the energy electron loss (EELS) response of coupled metallic nanoparticles, together with their optical properties. To achieve this, calculations are performed in the frame of the discrete dipole approximation both for optical and EELS excitations.

In the case of a gold dolmen-like structure, the bright mode of the monomer and the dark mode of the dimer are found to have a similar energy. Moreover, the dark mode is narrow compared to the broad dipolar mode of the monomer. These observations explain the origin of the transmission window and the Fano resonances of the spectrum. However, it also appears that the "optical Fano mode" is unexpectedly very active in EELS at a lower energy than in the optical spectra. Influence of the system configuration on EELS excitability is then questioned for other geometries.

8096-90, Poster Session

Design and analysis of subwavelength plasmonic waveguide array

V. Dillu, S. Singh, R. K. Sinha, Delhi Technological Univ. (India)

We examine the propagation of plasmonic TM (Transverse Modes) modes generated in the designed periodic array of silicon (Si) and silver (Ag) on Si substrate. The properties of surface plasmons are tailored by altering the size of Ag nano rods and its periodicity. Conventional waveguides cannot guide electromagnetic energy below the diffraction limit of light, which can be overcome by texturing the metal or dielectric surface. In this design we have textured by placing metallic, Ag nanorods on Si substrate. This provides the missing momentum needed, since SPP modes always lay beyond the light line. Ag nanorods are structured at nano dimensions to control and manipulate Surface Plasmon Polariton (SPP) propagation and thus open new possibilities in light matter interaction.

Here, we report the design and analysis of subwavelength plasmonic photonic crystal structure for the purpose of generation and propagation of SPP. TM polarized SPP propagating through the linear defect created in the periodic array of Ag (Silver) and Si (Silicon) nano rods on Si substrate have been theoretically analyzed using Finite Difference Time Domain (FDTD) computational calculations. The band gap and transmission spectra for the full structure are studied and further the structure with linear defect is designed for propagating plasmonic radiations. The structure shows high confinement below the diffraction limit and helps in scaling down the size of the proposed device. These investigations validate the use of nano structures for SPP propagation and hence miniaturize the optical and electronic devices for specific applications.

8096-91, Poster Session

Plasmonic cavity made of defect in an array of asymmetric T-shaped structures

Y. Chang, M. N. Abbas, M. Shih, Academia Sinica (Taiwan)

Plasmonic cavities that strongly confine light are finding applications in many areas of physics and engineering, including coherent electron-photon interactions. Here, we introduce a defect in a 1D array of asymmetric T-shaped structures to form an optical cavity to confine the light in small area, and we obtained a relatively high quality factor (≈ 200) with very small effective mode area $[0.0375(\lambda/n)^2]$ which is far below the diffraction limit. Furthermore, we showed that abrupt change at defect edge will increase the radiation losses and will suppress the quality factor to 64.

8096-92, Poster Session

Properties of nano-ridge surface plasmon mode

J. Guo, The Univ. of Alabama in Huntsville (United States); R. A. Soref, W. R. Buchwald, Air Force Research Lab. (United States); G. Sun, Univ. of Massachusetts Boston (United States)

We investigate the surface plasmon-polariton mode guided by nanometer scale metal ridges embedded in dielectric materials. We calculate the mode confinement, attenuation, and figure-of-merit for a variety of metal ridge structures in the 1.5 to 4.5 μm infra-red wavelength range. We compare the properties of the surface plasmon nano-ridge mode and the nano-strip surface plasmon mode. Although the trade-off between the confinement and the propagation length always holds, we find the properties of the nano-ridge surface plasmon mode are quite different from the nano-strip mode. The nano-ridge surface plasmon waveguide can provide a more strongly confined mode within the surrounding dielectric. This mode property enables potentially a variety of integrated sensor applications in the infra-red wavelength regime.

8096-93, Poster Session

Mapping localized plasmon modes in metal nanoparticles via electron energy loss spectroscopy and cathodoluminescence

V. Myroshnychenko, J. García de Abajo, Consejo Superior de Investigaciones Científicas (Spain); G. Boudarham, J. Nelayah, O. Stéphan, M. Kociak, C. Colliex, Univ. Paris-Sud 11 (France); A. I. Denisyuk, G. Adamo, K. F. MacDonald, N. I. Zheludev, Univ. of Southampton (United Kingdom); J. Rodríguez-Fernandez, Univ. de Vigo (Spain) and Ludwig-Maximilians-Univ. München (Germany); E. Carbó-Argibay, L. M. Liz-Marzan, Univ. de Vigo (Spain)

Localized surface plasmon (SP) modes can be tailored by controlling the size and morphology of metal nanoparticles. This finds exciting applications in photonic devices and optical sensing. The development of these applications requires knowledge of the spatial variation of the near fields associated to SPs.

In this work, the rich structure of SP modes localized in individual noble-metal nanoparticles prepared via lithography or colloidal chemistry is explored by optical spectroscopy [1], spatially resolved electron energy-loss spectroscopy (EELS) performed in a scanning transmission electron microscope (STEM) [2,3], and by electron beam-induced radiation emission performed in a scanning electron microscope (SEM) [4]. Spectral features and spatially-resolved maps of SP modes collected for individual nanoparticles of different morphologies (rods, decahedra, prisms, and split-ring resonators) are shown to be in good agreement

with theoretical STEM-EELS and optical excitation calculations obtained using the boundary element method based upon rigorous solution of Maxwell's equations [5]. Our results show the unmatched capability of electron beams for spectrally and spatially probing SP modes in nanoparticles with a wide variety of morphologies.

- [1] J.Rodriguez-Fernandez et al, J. Phys. Chem. C. 113, 18623 (2009).
- [2] J. Nelayah et al., Nature Physics 3, 348 (2007).
- [3] G.Boudarham et al., Phys. Rev. Lett. 105, 255501 (2010).
- [4] A.I.Denisyuk et al., Nano Lett. 10, 3250 (2010).
- [5] F. J. García de Abajo, A. Howie, Phys. Rev. B 65, 115418 (2002).

8096-94, Poster Session

Role of silver nanoparticles in the laser-induced reversible colour-marking and controlled crystallization of mesoporous titania films

N. Crespo-Monteiro, Univ. Claude Bernard Lyon 1 (France) and Univ. Jean Monnet (France) and Lab. Hubert Curien (France); N. Destouches-Castagna, Univ. Claude Bernard Lyon 1 (France) and Lab. Hubert Curien (France) and Univ. Jean Monnet (France); L. Bois, F. Chassagneux, Univ. Claude Bernard Lyon 1 (France); E. Gamet, Lab. Hubert Curien (France)

Due to their surface plasmon resonance silver nanoparticles are known to absorb visible light and give glasses various colors. Grown in mesoporous titania films, they give the material a photochromic behaviour that can be used to produce rewritable data carriers. On the one hand, UV light forms silver nanoparticles thanks to the photo-induced generation of electrons by titania matrix. On the other hand, visible light oxidizes the silver nanoparticles via the photoexcitation of electrons on Ag and their stabilization by oxygen molecules. The well controlled porosity of the mesoporous films allows to tune the nanoparticles size and to obtain, under UV illumination, homogenous distributions of small nanoparticles embedded within the titania matrix, which color the films. As all nanoparticles absorb light similarly, the film can then be completely bleached under exposure to a visible laser beam whose wavelength falls in the SPR band of the particles. Therefore, CW UV and visible focused-laser radiations, respectively, can repeatedly print and completely erase colored micropatterns within TiO₂/Ag films. The paper shows patterns printed under different conditions, deals with the reproducibility of the process and the inscription stability, and explains the nanoscale mechanisms, including silver migration during exposures, leading to the reversible color changes on the basis of TEM, SEM, absorption spectroscopy and Raman micro-spectroscopy characterizations. The paper also evidences that CW laser illuminations at higher intensity locally crystallize the titania matrix and investigates the influence of the absorption-induced heating around nanoparticles.

1 N. Crespo-Monteiro et al., Adv. Mater. 22, 3166, 2010.

8096-95, Poster Session

Three-dimensionally arranged metal-nanoparticles based on phase separation of block-copolymers

H. Yabu, T. Higuchi, M. Shimomura, Tohoku Univ. (Japan)

Metal-dielectric hybrid nanostructures are received great interests due to their potentials for novel photonic materials including left-handed metamaterials. Recently, we found a simple method for preparing block-copolymer and polymer blend particles by evaporation of good solvent from their solution containing poor solvent (Self-Organized Precipitation (SORP) method). Moreover, lamellae and other phase-separation structures are formed in block-copolymer nanoparticles. In this paper, we show the preparation of nano-structured metal-polymer hybrid particles

by combination of the SORP method and electroless plating. Their optical properties will be discussed.

Metal-dielectric hybrid nanostructures are received great interests due to their potentials for novel photonic materials including left-handed metamaterials. However, few effort has been done for developing nanoparticles having well-controlled metal-dielectric hybrid nanostructures. Recently, we found a simple method for preparing block-copolymer and polymer blend particles by evaporation of good solvent from their solution containing poor solvent (Self-Organized Precipitation (SORP) method). Moreover, lamellae and other phase-separation structures are formed in block-copolymer nanoparticles.

In this paper, nanoparticles of metals stabilized with block-copolymer micelles are also embedded in the phase-separated block-copolymer nanoparticles. Au nanoparticles were prepared in the block-copolymer micelles of poly(styrene-block-2-vinylpyridine) (PS-b-P2VP). PS-b-P2VP micelles were formed in toluene, and then, Au ions are complexed with pyridine moieties of PS-b-P2VP. After reduction of Au ion to Au, Au nanoparticles embedded in PS-b-P2VP micelles (AuNP@PS-b-P2VP) were prepared. The tetrahydrofuran (THF) solution of AuNP@PS-b-P2VP was mixed with THF solution of poly(styrene-block-isoprene) (PS-b-PI), water was added into the mixed solution. After evaporation of the THF, the polymer-metal composite particles were prepared. Their internal structures were observed by using a transmission electron microscope (TEM), the particles with phase separation structures were formed. Furthermore, Au nanoparticles were included into the phase-separated particles. Their optical properties will be discussed.

8096-96, Poster Session

Experimental demonstration of long range surface plasmon devices based on metallic subwavelength gratings

Z. Wu, Q. Zhan, Univ. of Dayton (United States)

The electron density oscillations along metallic surfaces, or on metallic films can cause electromagnetic surface waves propagation, which is known as surface plasmon polaritons (SPPs). When the incident light couples into SPPs, a sharp decrease in reflectivity of the incident light will occur. This sharp decrease in reflectivity is known as surface plasmon resonance (SPR). Devices such as electro-optic (EO) modulators, spectral notch filters, and refractive index and biochemical sensors have been designed using attenuated total reflection type arrangement based on SPR. The performance of the SPR in these applications is largely determined by the width as well as the depth of the dip in the reflectance curve. Recently, long range surface plasmon (LRSP) device design that replaces the metallic thin film with a metallic subwavelength grating to support the propagation of LRSP and offer much narrower SPR has been proposed and studied. In this paper, we experimentally demonstrate the SPR of LRSP propagating along metallic gratings is indeed narrower than that propagating along metallic films. An ultra-high resolution rotational stage with a resolution of 5.5×10^{-5} rad is used to resolve the ultra-narrow SPR curves.

The experiment measurement of the SPR curves of LRSP devices with a gold film and a gold grating are shown, which clearly demonstrates that the device with a gold grating yields a much narrower SPR curve. The experiment result confirms our numerical prediction that LRSP devices with metal gratings give better device performance than those with metal films.

8096-97, Poster Session

A plasmonic phase plate using nanoslits

E. H. Khoo, A*STAR Institute of High Performance Computing (Singapore); K. Crozier, Harvard Univ. (United States)

Today's demand for sensing and imaging application are greatly satisfied by nano-plasmonics devices. One interesting property of plasmonics is their polarization sensitivity in nanoslits. Lightwave with polarization

Conference 8096: Plasmonics: Metallic Nanostructures and Their Optical Properties IX

perpendicular to the nanoslit is transmitted with amplitude greater than unity. This is termed as “extraordinary optical transmission” [1]. When the polarization is parallel to the nanoslits, no light is transmitted. The phase of lightwave transmitting through the nanoslits can be altered. It is done by altering the geometrical dimension and/or filling the nanoslits with high index materials.

We propose a phase plate using nanoslits. The nanoslits are placed in perpendicular on a gold film with thickness 200 nm. Incident lightwave with linear polarization 45 degree from x and y axis are transmitted through the corresponding nanoslits N_y and N_x . The nanoslit, N_x is altered to have phase delay for electric field polarization in y direction (E_y).

Nanoslit N_x is filled up with SiO_2 so as to create a 0.5 pi phase delay. It is observed that the transmitted amplitude of E_y through N_x is twice of E_x through N_y . Hence to equalize the amplitude, two N_y nanoslits are required.

The field distribution amplitude is obtained by using FDTD with Lorentz-Drude model of gold film. Hence a linear polarization lightwaves at 45 degree from x and y axis is converted to a right-hand circular (RHC) polarization. If RHC polarized light is incidence onto the phase plate, then linear polarized light at 45 degree from x and y axis is obtained.

8096-98, Poster Session

Distance-dependent fluorescence intensity on PMMA structures on a metallic film

Y. Hung, National Sun Yat-sen Univ. (Taiwan); J. Tai, National Sun Yat-Sen Univ. (Taiwan) and Academia Sinica (Taiwan); C. Yuan, M. Shih, J. Tang, Academia Sinica (Taiwan)

Fluorescence intensity on PMMA gratings and plain PMMA mesa on Au film was investigated. The intact Au film thickness is 50nm on a cover glass and PMMA thickness on top of Au ranges from 50nm to 320nm. A layer of fluorophore material was spun on top of PMMA grating structures which are patterned by using E-beam lithography system. It is found that the fluorescence intensity changes rapidly by varying the PMMA thickness. The fluorescence intensity performs quite the opposite on PMMA grating area and plain PMMA mesa. Both are on Au film. Detailed surface plasmon mode calculations on the different PMMA thickness will be performed and analyzed. The lifetime of fluorophore material on the PMMA mesa and PMMA grating structures has been measured. This is to distinguish how the optical mode distribution of the pumping light affects the fluorescence intensity and how the different dielectric environment (optical mode density) affects the emission cycles which result in the emission intensity difference. Spatially-precise lifetime measurement and fluorescence intensity on grating valley and hill are performed by using a confocal microscope. The fluorescence emission shows different intensity performance on grating valley and hill when different PMMA thickness is coated. The measurement and observation is quite different from what people think about the quenching effect on a direct metal film. The optical field distribution will be analyzed by simulations.

8096-99, Poster Session

Localized surface plasmon lithography for Nanopatterning fabrication

X. Dong, Y. Zhang, Institute of Optics and Electronics (China); J. Du, Sichuan Univ. (China); L. Shi, C. Du, Institute of Optics and Electronics (China); F. Gao, Sichuan Univ. (China)

A method is reported for manufacturing nanostructures by employing localized surface plasmon (LSP) lithography. At the first, the mechanism for realizing LSP lithography by using different kind of masks for exciting LSPs and accumulating a large amount of localized energy from the incident light field are described, where the masks can be selected with formal of nano-tip array, nano-pattern with the fine tapers and a structure formed by a soft mould on a thin metal film; then, the masks

as the important part for fulfilling the nanolithography are characterized in design and fabrication under the available lab environment; finally, the typical experiments by using the mask formed of a soft mould on a thin metal film are carried out for fabricating nanopatterns with the minimum feature size from 100 nm ~ 30 nm in both regular and arbitrary arrangement and the dependence of the resolution (pattern periodicity) and stability of lithography on the geometrical parameters of the soft mould, such as ridge width, mould periodicity, ridge depth and slope, have been systematically studied and analyzed by Finite-Difference Time-Domain. In conclusion, the optimal minimum feature size can reach 17 nm by the proposed method.

8096-100, Poster Session

Measurement of spontaneous emission enhancement in subwavelength metallo-dielectric lasers using phase-resolved spectroscopy

Q. Gu, M. Nezhad, B. Slutsky, O. Bondarenko, Y. Fainman, Univ. of California, San Diego (United States)

Subwavelength scale laser devices are of great interest as potential components for integrated photonic circuits. We previously reported room temperature lasing operation of subwavelength scale metallo-dielectric cavity lasers with InGaAsP MQW in the 1.5 μ m region [1]. In this paper, we investigate the Purcell effect, which describes the enhancement of spontaneous emission (SE) in a small volume and/or highly resonant cavity. Using phase-resolved spectroscopy, we measure carrier lifetimes of bulk InGaAsP MQW wafer as well as optically pumped metallo-dielectric lasers with cavity size ranging from 300nm to 1 μ m. After extracting the SE lifetime from carrier lifetime through numerical models, we are able to obtain the SE enhancement rate of various sizes of lasers with respect to their bulk counterpart. Through rate equation modeling and fitting to experimental light-light (LL) curves, we study the SE enhancement’s effect in lasing characteristics, especially in the sub-threshold region. In addition, by using cavity quantum electrodynamics (CQED) theory, we investigate SE enhancement’s dependence on various parameters including homogenous broadening linewidth of emitters, density of emitter states, quality factor Q and effective mode volume V_{eff} . With this knowledge, we can further optimize the design of our laser cavity structure. Due to shortened SE lifetime and potentially low lasing thresholds, these lasers can find applications in high-speed optical communications, information processing, and on-chip optical interconnects.

[1] Nezhad, M. P., Simic, A., Bondarenko, O., Slutsky, B., Mizrahi, A., Feng, L., Lomakin, V. and Fainman, Y. “Room-temperature subwavelength metallo-dielectric lasers,” Nature Photonics 4(6), 395-399, 2010

8096-101, Poster Session

Scattering readout at detuned surface plasmon resonance of gold nanorods for continuous-wave multi-dimensional optical storage

A. B. Taylor, J. W. M. Chon, Swinburne Univ. of Technology (Australia)

Exciting progress has been made in the field of gold-nanorod based five-dimensional optical storage, utilizing surface Plasmon resonance (SPR) mediated photothermal melting and two-photon luminescence (TPL) from gold nanorods as the recording and read-out mechanisms [1]. However the requirement of femtosecond pulses limits the applicability to consumer electronics. To address this, we propose the use of a continuous wave (CW) readout mechanism. CW readout is however hampered by exponential signal extinction in multi-layer setting.

For multilayered gold nanorod films, readout is achieved by strong scattering under SPR condition. Due to the magnitude of this scattering decreasing away from the peak SPR wavelength, detuning the readout wavelength can reduce the level of signal extinction through the layers, yielding more efficient readout at deeper layers in the sample matrix. Detuning from SPR however results in reduced scattering from the nanorods. We show that balancing these two factors results in an optimal readout wavelength that is specific to each layer.

Continuous wave laser operation provides a viable alternative to TPL based readout, and should be studied rigorously for its successful device application. We have already demonstrated that the continuous wave recording is possible [1]. Here, we demonstrate the viability CW readout in a 16-layer gold nanorod sample matrix.

[1] P. Zijlstra, J. W. M. Chon and M. Gu, Nature 459, 410 (2009).

8096-102, Poster Session

Hybrid photonic-plasmonic crystal nanocavities

X. Yang, Ctr. for Scalable and Integrated Nanomanufacturing (SINAM) (United States); A. Ishikawa, Univ. of California, Berkeley (United States); X. Yin, Ctr. for Scalable and Integrated Nanomanufacturing (SINAM) (United States); X. Zhang, Univ. of California, Berkeley (United States)

Optical cavities with both high quality factor Q and small modal volume V_m are of great importance in the enhancement of light-matter interaction. Although conventional dielectric cavities can be designed to have ultrahigh Q factors, such as microspheres, microtoroids and photonic crystal cavities, the physical sizes of these cavities cannot be smaller than the wavelength scale in order to confine photon effectively. Therefore, the mode volumes for these dielectric cavities are diffraction limited. Surface plasmon polaritons (SPPs) provide a new way to confine electromagnetic waves beyond the diffraction limit. The unique dispersion relation of SPPs supports high wave vectors with ultrashort wavelengths, resulting in different kinds of plasmonic nanocavities with subwavelength mode volumes and metal-loss-limited Q factors. Here, we propose a novel hybrid photonic-plasmonic crystal nanocavity consisting of photonic crystal structures coupled to a metal surface with a nanoscale air gap in between. Based on the periodic variation in the effective index of hybrid mode, a unique hybrid photonic-plasmonic crystal with a transverse magnetic (TM) band gap is formed at the wavelength of 1,550 nm. One-dimensional hybrid crystal nanocavities having parabolic variation of lattice constant are then designed with high quality factor Q_{tot} of 330 and deep subwavelength mode volume V_m of $0.0056 \lambda^3$. The calculated Purcell factor is as high as 4,560 with an extremely large Q_{tot}/V_m of 60,000 λ^{-3} . This new type of high- Q/V_m broadband nanocavity will be of great importance in the enhancement of light-matter interactions, such as cavity QED, nonlinear optics, low-threshold nanoscale lasers, and optomechanics.

8096-103, Poster Session

Optimizing of the surface plasmon induced strengthening of PV efficiency

W. A. Jacak, Wroclaw Univ. of Technology (Poland); J. Krasnyj, Odessa International Univ. (Ukraine); L. Jacak, Wroclaw Univ. of Technology (Poland)

The experimentally observed significant increase of photo-voltaic efficiency due to surface plasmons mediating the energy transfer in solar cells with metallic nanoparticles deposited on a photo-active layer of semiconductor (i.e. Si or III-V type and also of conjugated organic polymer semiconductor) is explained as the result of strengthening of inter-band transition probability induced by electrons coupling to plasmons in the near-field regime. We identify and analyze two competitive mechanisms which contribute to the overall PV efficiency

increase which can be optimized with respect to the dimension of metallic nano-components. The first effect resolves itself to strengthening of the dipole plasmon oscillation amplitude with the nanoparticle radius growth, which favors larger nanoparticles sizes in regard to PV efficiency increase. The second one, oppositely, favors lower radii of particles, as it is related to partial departure from the momentum conservation principle in a translation non-invariant nano-system with coupling in the near-field. The atomic scale limit of the latter effect gives pronounced enhancement of the interband transition probability due to allowing all indirect (with nonconserved momentum) transitions [1]. The effect is, however, strongly reduced with the growth of metallic nano-particle radius. Particularities of this dependence are analyzed, including various types of nanoparticles depositions on the photo-active layer. The other effect of plasmon radiation efficiency size dependence is analyzed also for larger metallic nanospheres (with radii beyond 50 nm for Au and Ag nanoparticles) when saturation of Lorentz friction is predicted and experimentally confirmed.

[1] J. Jacak et al, PRB 82, 035418 (2010)

8096-104, Poster Session

Au/TiO₂ and Ag/TiO₂ nanocomposites with high concentrated "hot spots" under near IR femtosecond pulsed excitation

A. Aiboushev, A. Astafiev, N.N. Semenov Institute of Chemical Physics (Russian Federation); Y. Lozovik, Institute of Spectroscopy (Russian Federation); O. M. Sarkisov, N.N. Semenov Institute of Chemical Physics (Russian Federation); V. Nadtochenko, N.N. Semenov Institute of Chemical Physics (Russian Federation) and Institute of Problems of Chemical Physics (Russian Federation)

Luminescence of gold and silver nanoparticles photodeposited on titanium dioxide mesoporous films was studied by multi-photon and near-field apertureless microscopy. Luminescence was registered under the multi-photon excitation by femtosecond pulses of Ti:sapphire laser. It was observed that Me/TiO₂ (Me=Au, Ag) nanocomposites have high concentration ($\sim 10^5$) of bright luminescence spots ("hot spots") which reveal stability to degradation under long illumination. Moreover the most intense "hot spots" have luminescence enhancement of order of 10^5 . Application of Me/TiO₂ mesoporous films for Raman scattering spectroscopy was demonstrated for Rhodamine B molecules. Me nanoparticles configuration of "hot spot" was established by polarized multi-photon experiments and FDTD analysis. "Hot spots" luminescence enhancement analyzed by FDTD in terms of Me nanoparticles near-field enhancement coefficient at wavelength of excitation. It was shown that the highest enhancement coefficients are in near IR wavelengths for Me/TiO₂ nanocomposites. Thus Me/TiO₂ nanocomposites can be effectively used for near IR single molecule spectroscopy and biological objects visualization. Additionally various Me/substrate (Me=Au, Ag; substrate permittivity range: from 1 to 10) systems were analysed by FDTD to get the "best" substrate in terms of near-field enhancement coefficient for each wavelength of excitation.

8096-106, Poster Session

Silver core-pectin shell nanoparticles on metal enhanced singlet oxygen generation

L. S. A. de Melo, A. S. L. Gomes, R. E. de Araujo, Univ. Federal de Pernambuco (Brazil)

The photosensitized production of singlet oxygen can induce cell death, and therefore be explored in several areas, such as Photodynamic Therapy (PDT). PDT is a photochemical process that has been used on cancer treatment, photorejuvenation, wrinkles, discoloration, fungal and bacterial infections. Photosensitizer molecules, as Riboflavin, can activate singlet oxygen generation by a triplet interaction with ground-state molecular oxygen. We demonstrate the potential application of

Conference 8096: Plasmonics: Metallic Nanostructures and Their Optical Properties IX

new monodisperse core-shell (Silver core-Pectin shell) nanoparticles on PDT. Here, localized Plasmon Resonance was explored improving PDT photosensitizer excitation process. Metal-enhanced singlet oxygen generation in Riboflavin-Silver colloid was observed. The developed Silver-Pectin nanoparticles consist of 13 nm Silver nanospheres involved by a 11 nm thicker monolayer of Pectin. Pectin, a complex carbohydrate found in plants primary cell walls, isolates the Silver nanosphere increasing the biocompatibility of the colloid. The nanoparticle-photosensitizer distance is an important parameter for the enhancement of singlet oxygen production. Therefore, the Riboflavin interaction with Silver nanospheres without Pectin shell was also analyzed. Both Riboflavin photosensitizer and Silver Localized Plasmon can be excited with a blue light. Blue LEDs were used to excite the colloid with Riboflavin. The singlet oxygen fluorescent sensor Green Reagent was used to monitor the singlet oxygen production in the colloid. We report a 1.8-fold increase in the Riboflavin emission and a 1.7-fold enhancement in singlet oxygen production.

8096-108, Poster Session

Complete three-dimensional optical characterization of single gold nanorods

F. Wackenhut, Eberhard Karls Univ. Tübingen (Germany); A. V. Failla, Max-Planck-Institut für Entwicklungsbiologie (Germany) and Eberhard Karls Univ. Tübingen (Germany); T. Züchner, A. J. Meixner, Eberhard Karls Univ. Tübingen (Germany)

We will show a powerful technique to fully characterize individual gold nanorods by using confocal microscopy in combination with higher order laser modes. We obtain topological information far beyond the optical diffraction limit. This achievement extends and completes what was previously shown using a 2D system. We demonstrate that it is possible to determine the orientation of gold nanorods by looking at their elastic and inelastic scattering patterns. This extends the results achieved already in [1] with high precision (i.e less than 1 degree for the in plane and about 5 degree for the out of plane angle) to a 3D system. On the other hand, we clearly show that this improved technique permits to detect local changes of the refractive index of the dielectric medium surrounding the particles. In order to extend the results already shown in [2] we applied this technique to a 3D system. More over the elastic scattering pattern is strongly dependent on the phase relation of the scattered and reflected light, while the inelastic scattering pattern does not depend on this phase relation. Thus, by measuring in-situ the elastic and inelastic scattering patterns, it is possible to gain additional information while measuring the 3D orientation. For example, when the distance of a particle to an interface changes, the phase relation changes and therefore the elastic scattering pattern is strongly influenced. This phase relationship can be also influenced by the aspect ratio of the particle. Thus by comparing elastic and inelastic scattering, one can determine either the distance from the interface or the aspect ratio of a single gold nanorod.

[1] A. V. Failla, H. Qian, H. Qian, A. Hartschuh and A. J. Meixner, (2006), Nano Letters, 6, 1374-1378

[2] T. Züchner, A. V. Failla, M. Steiner and A. J. Meixner, (2008), Opt. Express, 16, 14635-14644

8096-109, Poster Session

Controlling inter-nanoparticle coupling: Highly uniform SERS substrates of plasmonic colloids

N. Pazos-Perez, Univ. Bayreuth (Germany) and Univ. de Vigo (Spain); A. Schweikart, Univ. Bayreuth (Germany); R. A. Alvarez-Puebla, L. M. Liz-Marzan, Univ. de Vigo (Spain); A. Fery, Univ. Bayreuth (Germany)

Metallic nanoparticles and especially gold, are in the focus of interest

because of their highly depend electric and optical properties on the specific particle size, shape, and surrounding environment. Therefore, they are ideal candidates for their potential use in microelectronic, optical, and biomedical applications. Thus, a big effort has been put in developing new methods which allow a fine control over the particle shape and size. These achievements allow us to fine tune the materials properties in order to use them for a desired application. However, the lack of capability to form organized structures is still a very important challenge in order to use these materials in many applications. In this work we report a novel method to structure, in a macroscale range, arrays of organized gold colloids into 1 and 2D linear parallel arrays which are highly uniform substrates for Surface Enhanced Raman Scattering (SERS). These structures were fabricated through self-assembly of gold nanoparticles upon solution-drying in a periodic confining structure. The technique leads to uniform, parallel linear nanoparticle arrays with the precise arrangement defined through the dimensions of the particles and the grooves. Moreover, the good reproducibility of these structures among big areas, make them perfect candidates as ultrasensitive substrates for SERS due to the controlled formation of arrays of hot spots. Which provide high and uniform SERS enhancement over extended areas. Furthermore, this method, is completely lithography-free so, low cost processing and allows tuneability of the width and spacing of the channels and consequently of the particle patterns between fractions of a micron and many micrometers. Characterization was done by means of transmission electron microscopy (TEM), scanning electron microscopy (SEM), atomic force microscopy (AFM), UV-vis, dark field, and SERS spectroscopy.

8096-111, Poster Session

Selective plasmonic excitation of rotation-symmetric nanostructures

S. Jäger, M. Fleischer, K. Braun, D. P. Kern, A. J. Meixner, D. Zhang, Eberhard Karls Univ. Tübingen (Germany)

The plasmonic properties of nanostructures depend strongly on their size, shape and environment [1]. We investigated the plasmonic excitation of rotation-symmetric gold nano-post arrays fabricated on a Si wafer under different laser wavelengths and polarization conditions. Confocal optical microscopy and spectroscopy were performed by confocal optical microscopes using either parabolic mirror or an air-objective-lens for laser focusing and signal collection. Instead of using linearly polarized Gaussian beams, we used cylindrical vector beams to distinguish between different plasmonic modes. Our experiments demonstrated that radially polarized beam focusing by parabolic mirror excited the plasmonic modes along the z-direction of the nano-posts more effectively than by the objective-lens due to a dominant out-of-the-plane electric field. Azimuthally polarized beam focusing by either parabolic mirror or objective lens was effective to excite the circular plasmonic modes of the rotation-symmetric nanostructures. Spectroscopic investigations revealed that the two-photon photoluminescence intensity was an excellent indicator of the resonance excitation of the nano-structures [2]. In addition, a short excitation wavelength such as 514 nm was found to selectively excite the plasmonic modes along the circular rim of the posts, whilst the 633 nm excitation was more effective to excite the plasmonic modes along the z-direction of the posts. The capability of selective excitation of different plasmonic modes is important for optical sensor design based on metallic nanostructures.

[1] K. L. Kelly et al., J. Phy. Chem. B 107, 668 (2003).

[2] M. Steiner et al., J. Phy. Chem. C 112, 3103 (2008).

8096-113, Poster Session

Spectral dependence of the amplification factor in surface enhanced Raman scattering

A. Irrera, C. D'Andrea, B. Fazio, Istituto per i Processi Chimico-Fisici (Italy); P. Artoni, Univ. degli Studi di Catania (Italy); O. M. Maragò, M. A. Iati, G. Calogero, P. G. Gucciardi, Istituto per i

Processi Chimico-Fisici (Italy)

Surface Enhanced Raman Scattering (SERS) is characterized by a strong signal amplification (up to 10⁸-10¹⁰) when both the excitation and the Raman photons frequencies match the localized plasmon resonances (LSPR) of the nanoparticles (NPs). In order to understand if the effective LSPR profile refers to the bare NPs or to the resonance of NPs "dressed" with the probe molecules, we perform multiwavelength (514nm, 633nm and 785nm) SERS experiments using evaporate gold NPs as SERS-active substrate on which we deposited Methylene Blue molecules (MB) that yields a resonance energy red-shift and a broadening of LSPR profile.

The SERS spectra at the investigated excitation wavelengths display a different intensity ratio of the characteristic MB band (peaks at 450 cm⁻¹ and 1620 cm⁻¹) with respect to the Raman counterpart. While at 515nm the 1620 cm⁻¹ mode is more enhanced with respect to the peak at 450 cm⁻¹, at 785 nm the opposite is observed. At 633 nm the two modes experience the same enhancement factor. This behavior is compatible with the hypothesis that the re-radiation enhancement factor is proportional to the LSPR of "dressed" NPs.

The results are, also, compared with experiments carried out on Mercaptopyridine and L-Tyrosine molecules that not affect the LSPR profile.

8096-114, Poster Session

Laser induced photothermal aggregation of gold nanorods for SERS detection of biomolecules in liquid environment

A. Irrera, B. Fazio, C. D'andrea, V. Villari, N. Micali, O. M. Maragò, M. A. Iati, M. G. Donato, G. Calogero, P. G. Gucciardi, Istituto per i Processi Chimico-Fisici (Italy)

Surface-Enhanced Raman Scattering (SERS) from isolated metal nanoparticles is usually much weaker compared to what is observed on aggregates due to the strong field enhancement occurring in the gap regions (hot spots) between adjacent nanoparticles [1]. The controlled creation of highly efficient hot spots in liquid (the natural habitat of biomolecules) is a challenge in which optical forces can play an important role by promoting the aggregation of metal nanoparticles in the focus of a laser beam (optical trapping) or their accumulation on a surface (by radiation pressure). Here we show that laser induced aggregation of gold nanorods in a buffered solution of Bovine Serum Albumin (BSA) leads to the formation of SERS-active agglomerates. Indeed, due to the blue shifted excitation (632.8 nm line of a He-Ne laser) with respect to their localized surface plasmon resonance ($\lambda_{LSP} = 687$ nm [2]) the gold nanorods are pushed by the radiation forces. Approaching the laser focus towards the bottom of the glass cell containing the solution, the optical forces and the involved thermal effects, make to aggregate such rods into highly efficient "hot spots" regions. This occurrence enables us to observe a strong SERS signal of BSA molecules staying in their proximity, with an enhancement factor of 10⁵ allowing the detection of protein at concentrations as low as 10⁻⁷ M in its natural habitat.

References

1. Qin L. et al., (2006) Proc. Natl. Acad. Sci. 103:13300-13303
2. Jones P. H. et al., (2009) ACS Nano 3: 3077-3084

8096-115, Poster Session

Optical properties of metal coated nanoscrew Si

H. Jin, G. L. Liu, Univ. of Illinois at Urbana-Champaign (United States)

Optical properties of random nanoscale features provide applications such as light scattering in photovoltaics or surface enhanced

Raman scattering (SERS) substrates for biosensing. Randomized nanostructures reduces the specular reflectance and in turn increases diffusive reflectance. Nanowire growth, chemical etching or RIE based random etch has been demonstrated to form such surfaces. Previously demonstrated work have produced nanoscale features that resemble nanowhiskers, porous surface, cones or straight pillars.

In this paper, a unique nanoscrew Si structure is presented. The nanoscrew surface is made by anodized aluminum oxide (AAO) mask formation followed by extended deep reactive ionic etching (DRIE). Dense random zig-zag pillar structures that represent screw shapes are formed, with 1 μ m in height and the bottom base width ranging from 100 nm to 250 nm. The tip of the nanoscrews have radius of curvature even lower than 10 nm. The apparent naked-eye view of the nanoscrew surface, which only consists of nanopatterned N-type single crystalline Si is diffusively green. The optical properties of nanoscrew Si with and without metal deposition is presented as discussion in applications for SERS.

8096-117, Poster Session

Reshaping the fluorescence spectrum with random metal dielectric films

K. Seal, The Univ. of Tennessee (United States); X. Xu, Oak Ridge National Lab. (United States); Z. Zhang, Q. Li, The Univ. of Tennessee (United States); B. Gu, Y. Li, Oak Ridge National Lab. (United States); D. A. Genov, Louisiana Tech Univ. (United States)

The effects of metallic nanostructures on the emission of fluorophores result in a number of important effects, including increased photostability, fluorescence resonance energy transfer and directional emission. The complexity of fluorophore-metal interactions is influenced by the structure of the metal nanostructures, which governs their optical response. In disordered metallic nanostructures illuminated at visible and near-infrared frequencies, the optical response can involve localized and propagating surface plasmon modes which interact individually with the fluorophores. Specifically, semicontinuous metal films are characterized by broad absorption across the visible and near-infrared frequencies. This absorption spectrum can be controllably altered by effecting structural changes via a process called photomodification, wherein sufficiently intense coherent light at a specific frequency and polarization can be used to induce "holes" in the absorption spectrum. This tailoring of the optical response can in turn be used to alter the fluorescence spectrum in a controllable manner, with applications including bio-markers and sensing. In this study, semicontinuous films were photomodified to alter the absorption spectrum. Consequently, changes in the peak position and width were observed in the resulting emission from fluorophores placed in proximity to the metal films. The changes were sensitive to the polarization, incident angle and excitation frequency. Directionality was also observed in the fluorescent emission, indicative of surface plasmon coupled emission due to the effective dielectric response of the films. Theoretical calculations based on the finite difference frequency domain method show good correspondence with experimental data and provide a direction toward optimizing the photomodification process to effect sensitive changes to the fluorescence spectrum.

8096-118, Poster Session

Subwavelength directional SPP couplers

A. Kriesch, Max Planck Institute for the Science of Light (Germany) and Erlangen Graduate School in Advanced Optical Technologies (Germany) and Friedrich-Alexander-Univ. of Erlangen-Nuernberg (Germany); J. Wen, Max Planck Institute for the Science of Light (Germany) and Friedrich-Alexander-Univ. of Erlangen-Nuernberg (Germany); D. Ploss, Max Planck Institute for the Science of Light (Germany) and Erlangen Graduate School in Advanced Optical Technologies (Germany) and Friedrich-Alexander-Univ. of Erlangen-Nuernberg (Germany); P.

Conference 8096: Plasmonics: Metallic Nanostructures and Their Optical Properties IX

Banzer, Max Planck Institute for the Science of Light (Germany) and Friedrich-Alexander-Univ. of Erlangen-Nuernberg (Germany); U. Peschel, Friedrich-Alexander-Univ. of Erlangen-Nuernberg (Germany)

Plasmonic gap-waveguides open up new dimensions for the manipulation of light on a subwavelength scale. Based on recent progress in fabrication technologies, the interest in highly integrated SPP components has grown substantially. A lot of attention has been attracted by subwavelength directional SPP couplers and waveguide loaded optical antennas; the first of which allow for connecting individual SPP transmission lines, the latter of which are used for probing sub wavelength circuitry from the far field.

Here we report on experiments, in which we investigated directional coupling between highly integrated adjacent SPP gap waveguides (~80nm gap width, ~15µm long, ~130nm pitch), in a broad wavelength range. Gap-waveguides are well known to allow for a further miniaturization compared to SPP stripe waveguides, due to their higher field confinement. Waveguides and connected plasmonic antennas were etched into plane silver films (~100 nm thickness) on a silica substrate using focused ion beam milling (FIB). For exciting the SPP waveguide, we optimized a plasmonic antenna for the NIR wavelength range of 1400 nm λ \leq 1700 nm, where losses are expected to be small.

In the presentation, we compare experimentally measured wavelength dependent coupling parameters with those, obtained from rigorous finite element method (FEM) and finite difference time domain (FDTD) calculations. We demonstrate that the concept of directional couplers, known from integrated optics, can be transferred to the nanoscale, thus enabling future nanoplasmonic circuitry. At the same time control of plasmonic coupling is a first step towards subwavelength discrete diffraction in larger arrays.

8096-119, Poster Session

Cooperative infrared to visible upconversion and visible to near-infrared quantum cutting in Tb and Yb co-doped glass containing Ag nanoparticles

Z. Pan, G. Sekar, R. Akrobetu, R. Mu, S. H. Morgan, Fisk Univ. (United States)

Tb, Yb, and Ag co-doped glass nano-composites were synthesized in a glass matrix Li₂O-LaF₃-Al₂O₃-SiO₂ (LLAS) by a melt-quench technique. Ag nanoparticles (NPs) were formed in the glass matrix and confirmed by optical absorption. Plasmon enhanced luminescence was observed. Cooperative infrared to visible upconversion and visible to near-infrared quantum cutting were studied for glass samples with different thermal annealing times. Because the Yb³⁺ emission at 940 - 1020 nm is matched well with the band gap of crystalline Si, the phosphors studied may be potentially applied for silicon-based solar cells.

8096-120, Poster Session

Plasmon-based light enhancement from a hybrid copper-gold planar structure

M. S. Nawrocka, S. Shrestha, Adelphi Univ. (United States); R. R. Panepucci, Ctr. de Tecnologia da Informacao Renato Archer (Brazil)

For Raman and fluorescence spectroscopy, the ability to fabricate plasmonic nanostructures using readily available materials and processes offers remarkable advantage in the development of methods to characterize trace amounts of physical, chemical and biological substances. We report a novel configuration and an optical characterization of a copper-gold planar structure resulting in strong plasmonic enhancement of the electromagnetic field in the red region of

the spectrum. The structure consists of aggregates of gold nanospheres (20 +/- 2) nm in diameter and dried from a colloidal solution) on a thin continuous copper film (50 +/- 20) nm thick (deposited on a silicon substrate using sputter deposition). We observed enhanced plasmon resonances with a peak at 665 nm and FWHM of 150 nm, measured from a light scattered from the structure using a dark-field reflection-mode microspectroscope. We attribute the strong field enhancement to the coupling of interparticle plasmon resonances from gold nanospheres to the surface plasmons induced in the copper film. Additionally, the high reflectivity of the copper layer reflects the portion of light that would otherwise be transmitted, thus increasing the collection efficiency of the scattered light. We achieved the homogeneity and planarity of the copper-gold structure through the electrostatic attraction between the negative surface charge of gold nanospheres and a lattice of positive ions of copper oxide, formed by ionic bonds during the exposure of copper to air. Such homogeneity and planarity cannot be achieved using gold and silver films that do not possess the lattice of ions and where the deposited nanospheres move towards the edge of the drop. We foresee that when integrated with easily available lasers emitting red wavelengths, the proposed copper-based nanostructure is a cost-effective step towards the development of lab-on-chips with applicability in public safety, global health-care, homeland security and defense.

8096-121, Poster Session

Emission control with metallic hole arrays

R. J. Moerland, Aalto Univ. School of Science and Technology (Finland); L. K. Kuipers, FOM Institute for Atomic and Molecular Physics (Netherlands) and Univ. Twente (Netherlands); M. Kaivola, Aalto Univ. School of Science and Technology (Finland)

Adding holes in a periodic arrangement to metallic thin films greatly affects the optical properties of the metal film. The compound structure can exert a large influence on electromagnetic fields that interact with the hole array. Many parameters affect the actual response of the hole array, such as the periodicity, the size of the holes and their shape. We will show that, for a fixed periodicity and hole area, a change in aspect ratio of rectangular holes over a narrow range is sufficient to significantly alter the lifetime and far-field radiation patterns of a single emitter, e.g., a molecule, embedded in the central hole of a hole array. Due to the complexity of the geometry, analytical results are hard - if not impossible - to obtain. Therefore, an FDTD simulation scheme is used to obtain the evolution in time of the radiated fields by a single dipole, which models the emitter. By recording the electric field and current at the location of the dipole, the relative local density of states can be obtained after Fourier-transforming the fields. From the spatially Fourier-transformed time-harmonic near fields, far-field angular emission spectra are calculated, showing a strong dependence on the aspect ratio of the holes: the directionality of the emission is radically altered with increasing aspect ratio.

8096-122, Poster Session

Growth of ultra thin silver films monitored by in situ spectroscopic ellipsometry during high power impulse magnetron sputtering

L. Sun, N. R. Murphy, Air Force Research Lab. (United States) and General Dynamics Information Technology (United States); A. R. Waite, Air Force Research Lab. (United States) and Universal Technology Corp. (United States); J. G. Jones, R. Jakubiak, Air Force Research Lab. (United States)

High precision in both film thickness and optical constant of ultra thin Ag films is crucial for their application in optical coatings and plasmonic metamaterials. For such applications, very thin layers of Ag must be used to minimize optical losses; however, it is difficult to make continuous Ag films that are less than 20 nm thick. Deposition of noble metals on oxides follows the Volmer-Weber island growth process with island formation

Conference 8096: Plasmonics: Metallic Nanostructures and Their Optical Properties IX

occurring at the initial stages followed by nucleation and coalescence. Below the coalescence threshold the optical dispersion does not follow that of bulk Ag, with both the index of refraction and extinction coefficient deviated in the visible wavelength region. Since island formation results from an imbalance in cohesive energies between adatoms within the film and atoms with the substrate, one way to decrease the adatom-adatom interaction is to use highly energetic deposition techniques such as high power impulse magnetron sputtering (HiPIMS). Coalescence thresholds of thin Ag films grown by DC magnetron sputtering and HiPIMS were determined using in situ spectroscopic ellipsometry (SE) during growth. With SE, the coalescence threshold was reached when the optical dispersion of the film matched that of the bulk Ag. The high degree of ionization and low deposition rate offered by HiPIMS resulted in increased film densities, refractive indices, lower coalescence thresholds and smoother film surfaces compared to those grown with DC magnetron sputtering.

8096-123, Poster Session

Subradiant plasmonic fano resonances For ultrasensitive biomolecular detection

A. A. Yanik, A. E. Cetin, M. Huang, A. A. Artar, Boston Univ. (United States); S. H. Mousavi, A. B. Khanikaev, G. Shvets, The Univ. of Texas at Austin (United States); H. Altug, Boston Univ. (United States)

We introduce an ultrasensitive label free detection technique based on asymmetric Fano resonances in plasmonic band-gap devices with far reaching implications for real time biosensing and point-of-care diagnostics. By exploiting high quality factor ($Q_{\text{solution}} \sim 200$) sub-radiant dark modes, we experimentally demonstrate record high figures of merits (FOM ~ 162) for intrinsic detection limits. Our experimental record high sensitivities are attributed to the nearly complete suppression of the radiative losses that are made possible by the high structural quality of the fabricated devices as well as the sub-radiant nature of the resonances. To fabricate high optical quality sensors, we introduce a novel high-throughput nanofabrication technique with extremely uniform and precisely controlled nano-features. The demonstrated label free sensing platform offers unique opportunities for point-of-care diagnostics in resource poor settings by eliminating the need for labeling as well as mechanical and light isolation.

8096-124, Poster Session

High tunability of the optical response with a metal-multiferroic composite

X. Xu, K. Seal, X. Xu, I. Ivanov, Oak Ridge National Lab. (United States); C. Hsueh, National Taiwan Univ. (Taiwan); N. A. Hatab, Oak Ridge National Lab. (United States); L. Yin, Fudan Univ. (China); X. Zhang, Z. Cheng, Institute of Physics (United States); B. Gu, Oak Ridge National Lab. (United States); Z. Zhang, The Univ. of Tennessee (United States); J. Shen, Fudan Univ. (United States)

Plasmon resonances in metal nanostructures depend strongly on the size, shape, composition, orientation and dielectric environment of the metal nanostructure. However, most metal nanostructures have been restricted to passive templates, with little dynamic tunability in the optical response. In the current experiment study, we demonstrate active control of the plasmonic response from Au nanostructures by the use of a novel multiferroic substrate -LuFe₂O₄ (LFO) - to tune the surface enhanced Raman scattering (SERS) response in real time. From both experiments and numerical simulations based on the finite-difference time-domain method, a threshold field is observed, above which the optical response of the metal nanostructure can be strongly altered through changes in the dielectric properties of LFO. This offers the potential of optimizing the SERS detection sensitivity in real-time as well as the unique functionality

of detecting multiple species of Raman active molecules with the same template. We also observe evidence of interaction between the plasmon modes and polaron excitations that are inherent in multiferroic LFO. Our results indicate that the plasmons have a strong screening effect on the polarons which can be mediated by altering the dielectric response of LFO via external applied fields.

8096-125, Poster Session

Tunability of plasmonic fano resonances in nanoparticle clusters

H. Sobhani, P. J. Nordlander, Rice Univ. (United States)

Fano resonances in strongly coupled metallic nanostructures such as Heterodimers,[1] Ring/Disk cavities,[2] Fanoshells, [3] Heptamer and Octamer clusters [4] enable highly efficient LSPR sensing due to their narrow linewidths. They are also of significant importance in plasmonic waveguiding and light harvesting applications such as photodiodes. In this talk, we describe how plasmonic Fano resonances can be modeled using a combination of fully retarded electromagnetic simulation methods such as FDTD and FEM. We also discuss Fano resonance modeling using a simple intuitive harmonic oscillator model which expose the underlying physics, the interference between superradiant and subradiant collective plasmon modes.

[1] L.V. Brown, H. Sobhani, J.B. Lassiter, P. Nordlander, and N.J. Halas, ACS Nano 4(2010)819

[2] N. Verellen, Y. Sonnefraud, H. Sobhani, F. Hao, V.V. Moschalkov, P.V. Dorpe, P. Nordlander, and S.A. Maier, Nano Lett. 9(2009)1663; Y. Sonnefraud, N. Verellen, H. Sobhani, G.A.E. Vandenbosch, V.V. Moschalkov, P.V. Dorpe, P. Nordlander, and S.A. Maier, ACS Nano 4(2010)1664

[3] S. Mukherjee, H. Sobhani, J.B. Lassiter, R. Bardhan, P. Nordlander, and N.J. Halas, Nano Lett. 10(2010)2694

[4] J.B. Lassiter, H. Sobhani, J.A. Fan, J. Kundu, F. Capasso, P. Nordlander, and N.J. Halas, Nano Lett. 10(2010)3184; K. bao, H. Spobhani, and P. Nordlander, Chin. Sci. Bull. 55(2010)2629

8096-126, Poster Session

Enhanced and suppressed transmission through metal gratings at the plasmonic band edges

M. Bloemer, U.S. Army Aviation and Missile Command (United States); D. de Ceglia, M. A. A. Vincenti, The AEgis Technologies Group, Inc. (United States); M. Scalora, U.S. Army Aviation and Missile Command (United States); N. Akozbek, The AEgis Technologies Group, Inc. (United States)

Extraordinary optical transmission through metallic gratings is mediated by Fabry-Perot cavity modes inside the apertures and surface waves propagating along the grating. Anomalous features arise in the grating transmission spectrum when the optical period for the surface wave is equal to the grating pitch. The surface waves can be plasmonic in nature or due to diffracted orders propagating parallel to the surface. At optical frequencies, plasmonic effects are well separated from Wood-Rayleigh anomalies. The plasmonic band gap properties were determined with COMSOL by propagating a plasmon on a smooth Ag surface followed with a section containing a series of air gaps. The reflection spectrum for the plasmons shows a well defined frequency gap for plasmon propagation. The COMSOL simulations for light transmitted through the grating reveal anomalies in the vicinity of the plasmonic band gap. At the center frequency of the gap where surface waves are forbidden, the transmission through the grating is very low and the reflection is 98%. Standing waves are formed at the band edges and the fields become localized. At the high energy band edge the electric field localizes in the low index medium and the magnetic field in the high index medium. The

field localization reverses at the low energy band edge. As a result of the localization at the band edges, the surface plasmons couple strongly to the Fabry-Perot cavity modes at the high energy band edge leading to enhanced transmission through the grating with the opposite properties for the low energy band edge.

8096-127, Poster Session

Numerical investigation of the plasmonic properties of bare and cysteine-functionalized silver nanoparticles

M. Csete, A. Sipos, A. Szalai, E. Csapo, V. Hornok, I. Dekany, Univ. of Szeged (Hungary)

Theoretical and experimental studies were performed to develop silver nanoparticles (Ag NPs) based Localized Surface Plasmon Resonance sensor which can be used to determine the dependence of aggregation on pH and bio-molecule concentration, and to follow the aggregation kinetics based on spectral monitoring. The absorption spectra of different Ag NPs containing aqueous dispersions were numerically computed by Finite Element Method (FEM) applying the RF module of COMSOL software package, and compared to spectra determined by UV-Visible spectroscopy between 300 and 650 nm. This comparative study proved that the spectrum measured on citrate-stabilized bare Ag NPs aqueous dispersion with absorbance maximum at $\lambda_{meas} = 385$ nm corresponds to the characteristic surface plasmon band of spherical Ag NPs with 8.25 ± 1.5 nm diameter. The presence of aggregates in aqueous dispersions resulted in splitting on the spectrum, when the surface of the Ag NPs having a concentration of $c_{Ag} = 2 \times 10^{-4}$ M was functionalized with L-cysteine (Cys) having a concentration of $c_{Cys} = 5.7 \times 10^{-6}$ M. The FEM computation proved that the maximum at $\lambda_{meas_1} = 390$ nm corresponds to quadrupolar resonance, while the second maximum red-shifted to $\lambda_{meas_2} = 574$ nm and $\lambda_{meas_2'} = 625$ nm originates from coupled dipolar plasmon resonances on extended aggregates at pH=2.98 and pH=4.92, respectively. The most simple aggregate-type that exhibits resonance at the measured absorbance maxima was determined by varying the number of Ag NPs, the thickness of the Cys shell, and the inter-particle distance in linear chains aligned along the E-field oscillation direction.

8096-128, Poster Session

Resonance behaviour of gold nanoparticles: coupled plasmonic modes

A. Mahdavi, Erlangen Graduate School in Advanced Optical Technologies (Germany); E. Tatartschuk, Erlangen Graduate School in Advanced Optical Technologies (Germany) and Clemson Univ. (United States); E. Shamonina, Imperial College London (United Kingdom) and Erlangen Graduate School in Advanced Optical Technologies (SAOT) (Germany)

Metamaterials acquire their functionality from the structuring of the small building blocks, "artificial atoms". Understanding the nature of the resonance behaviour of unit cells is crucial for designing a structure with desired properties. In this paper we study the resonant behaviour of a variety of metallic nanoparticles in the region of hundreds of THz, including square-cross-section nanorods, nanoparticles of L, U and O shapes, and split rings with a variable gap size.

The split ring, the most prominent subwavelength resonator, can be described as an LC circuit. However, if it is miniaturized to be as small as several hundreds of nanometers, its resonant behavior does not just simply scale with the size. The resonance frequency saturates and the field modes change significantly. The effects that need to be incorporated here are those of kinetic inductance due to the inertia of the electrons and of plasmon-polaritons at the metal/dielectric interface noticeable as the surface plasma frequency is being approached.

For a better understanding of the resonant behavior of plasmonic

nanoparticles we investigated standing wave patterns of surface plasmon polaritons on nanoparticles of different shapes. Our numerical results (CST Microwave Studio) suggest that the resonant behavior of each of these particles is similar to that of periodic arrays of nanorods with specific lengths and periodicities. For the first time to our knowledge, the interaction of the gap edges of a split ring, previously described in terms of the self-capacitance, has been interpreted in terms of coupled plasmonic modes.

8096-129, Poster Session

Effective permittivity of concentrated random multiple component linear plasmonic composites

S. Wani, T. Cong, A. Sangani, R. Sureshkumar, Syracuse Univ. (United States)

Electromagnetic wave propagation in plasmonic media is of fundamental and practical interest. We present a new technique for calculating the effective medium properties of concentrated linear plasmonic composites containing multiple metallic (Ag, Au, Al and Cu) monodisperse spherical inclusions in a homogeneous absorbing matrix. The underlying physical motif was the separation of the space surrounding any inclusion into two regions, one immediately surrounding the particle with the properties of the matrix (the size of this region depends on the static structure factor) and an outer effective medium. Ensemble averaged Maxwell equations were derived for the system. Self consistent closure relations were found for the conditionally averaged fields by solving the vector Helmholtz equations for a layered sphere in an infinite matrix. In the quasi-static limit, predicted values of effective permittivity were in excellent agreement with those of Maxwell-Garnett theory. However, for large particle sizes and relatively high volumetric concentrations (~ 1%), the relationship between the concentration and the attenuation constant becomes nonlinear as evidenced by experimental measurements on Ag nanoparticle suspensions in ethylene glycol. Further, the resonance peak red shifted and broadened with increasing concentration.

8096-130, Poster Session

Broad band, tunable super-lenses in the visible region of electromagnetic spectrum with metallodielectric stacks (MDS)

N. C. Katte, J. Haus, A. M. Sarangan, J. Gao, Univ. of Dayton (United States); R. Jakubiak, Air Force Research Lab. (United States); M. Scalora, U.S. Army Aviation and Missile Command (United States)

We compare the two main designs based upon combinations of Ag/GaP and Au/GaP, and calculate the super-resolving band widths. The super-resolving bandwidth of the Ag/GaP design is (520nm-560nm), while that of the Au/GaP design is (630nm-660nm). We evaluate these two designs in their ability to resolve two 20nm wide apertures separated by a center-to-center distance of 80nm. We also compare two numerical techniques, used to study these systems, namely the transfer matrix method (TMM) and the finite element method (FEM). The TMM is simple and provides a first evaluation of the samples' expected performance. The FEM technique is numerically more demanding, but it is more robust for determining super-resolution. Finally we discuss the practical limitations of our super-resolving imaging devices in resolving objects that are much smaller than the incident wavelength.

8096-131, Poster Session

Tunable surface plasmon polaritons in Ag composite films by adding dielectrics or semiconductors

D. Lu, J. Kan, E. E. Fullerton, Z. Liu, Univ. of California, San Diego (United States)

Surface plasmon polaritons (SPPs) in metal films concentrate electromagnetic energy into subwavelength scale in the optical regime. Its unique properties enable light guiding and manipulation at the nanoscale, sub-diffraction-limited optical imaging, highly-sensitive biomolecular detection, highly efficient semiconductor light emissions, and enhanced solar energy utilization, etc. However, all these useful applications rely on the fixed SPP properties associated with existing materials, which on the other hand limit their capabilities to specific conditions. By adding a small percentage of SiO₂ or Si into pure Ag films, we recently demonstrate SPP properties of metal films can be well tuned. Those composite films are characterized by an oil-immersion optical microscope to obtain their angular resolved reflection spectra in the Fourier space for different wavelenghts. The resonance position and bandwidth of SPPs in the composite films can be well predicted by an adopted phenomenological model after taking into account both the volumetric average of the permittivities of the mixed components and the size and interface effects. Their dispersion relations deviate from those of pure Ag films and have advantages to provide a larger SPP wave vector at longer wavelenghts. This type of tunable composite films serves as a promising alternative to current metals for broader working frequencies.

8096-132, Poster Session

Metallic nanoshells with semiconductor cores: optical characteristics modified by core medium properties

N. K. Grady, Institute of Physics (China) and Rice Univ. (United States); R. Bardhan, Rice Univ. (United States); T. A. Ali, Institute of Physics (China); H. Xu, N. J. Halas, Rice Univ. (United States)

It is well-known that the geometry of a nanoshell controls the resonance frequencies of its plasmon modes; however, the properties of the core material also strongly influence its optical properties. Here we report the synthesis of Au nanoshells with semiconductor cores of cuprous oxide (Cu₂O) and examine their optical characteristics. This material system allows us to systematically examine the role of core material on nanoshell optical properties, comparing Cu₂O core nanoshells ($\epsilon_c = 7$) to lower core dielectric constant SiO₂ core nanoshells ($\epsilon_c = 2$) and higher dielectric constant mixed valency iron oxide nanoshells ($\epsilon_c = 12$). Increasing the core dielectric constant increases nanoparticle absorption efficiency, reduces plasmon line width, modifies plasmon energies and changes which mode is "bright." We show that these effects arise from realignment of the cavity and sphere plasmon energies, changing the composition of the hybridized nanoshell plasmons. Modifying the core medium provides an additional means of tailoring both the near- and far-field optical properties in this unique nanoparticle system.

8096-133, Poster Session

Engineering dispersion in omnidirectional single-layer plasmonic metamaterials at visible frequencies

S. P. Burgos, R. M. Briggs, H. A. Atwater, California Institute of Technology (United States)

It has recently been shown that an array of coupled coaxial metal-dielectric-metal plasmonic waveguides can serve as a wide-angle polarization insensitive metamaterial with a tunable effective index

response at visible frequencies. The metamaterial index is set by the antisymmetric mode index of the constituent plasmonic waveguides, which ranges from positive to negative values in the visible frequency spectrum as set by the surface plasmon resonance of the metal-dielectric material combination and the thickness of the dielectric channel slot.

Full-wave simulations and three-dimensional dispersion calculations are used to engineer the metamaterial dispersion. In-plane dispersion curves $\omega(k_x, k_y)$ show that the metamaterial has an isotropic response in the x-y plane as characterized by a hyperbolic band diagram. By matching this with the mode index dispersion of the coupled waveguide array $\omega(k_z)$, we show that it is possible to access omnidirectional refractive indices ranging from negative ($n_{\text{eff}} = -2$) to positive values ($n_{\text{eff}} = 1$) in the $\lambda = 400\text{--}600\text{nm}$ freespace wavelength range. Further simulations investigate the structure's imaging capabilities, and confirm the metamaterial omnidirectional response over the visible spectrum.

The metamaterial refractive index response is verified through Snell-Descartes refraction experiments conducted on a metamaterial slab composed of a close-packed hexagonal array of 25-nm thick Si annular apertures embedded in a 200-nm Ag film and cut at a 3° angle using focused ion-beam milling. The metamaterial effective index is measured for both s- and p-polarized waves at incident angles ranging from $\theta = 0\text{--}50^\circ$, and the results verify the functionality of the design as a wide-angle polarization insensitive metamaterial at visible frequencies.

8096-134, Poster Session

Plasmonic and photonic realizations of resonant guided wave networks

E. Feigenbaum, S. P. Burgos, R. M. Briggs, H. A. Atwater, California Institute of Technology (United States)

In the last two decades, plasmonics has become an important tool for designing the optical properties of complex media due to its ability to manipulate nanoscale light-matter interactions. Recently, we reported a new class of artificial photonic materials, called resonant guided wave networks (RGWNs), which define new directions in optical dispersion control. In a RGWN, localized waves resonate in closed paths throughout a network of waveguides connected by power splitting junctions, enabling wave dispersion that is dependent on the waveguide network layout. Control of the local wave interference allows for "programming" the network to achieve a desired photonic function.

Here we describe realizations of resonant guided wave networks: a two dimensional network of intersecting 200nm-wide plasmonic air channel waveguides in a Au matrix and a mesh of Si-based 500nm-wide photonic waveguides with careful designed power splitting elements introduced into their intersection junctions. In both cases, we couple $\lambda = 1500\text{nm}$ light using a grating into a Si-on-insulator ridge waveguide that is in turn end-coupled to the network inputs. We will present concept designs of waveguides profiles, power splitting elements, and waveguide terminations. We also compare and verify NSOM measurements of near-field interference patterns of various network designs with analytical network representations and FDTD numerical simulations. These results highlight the viability of the RGWN concept, and once again the powerful design capabilities facilitated by plasmonics.

8096-136, Poster Session

Multiple fano resonances with hybridized metamaterials

A. A. Artar, A. A. Yanik, H. Altug, Boston Univ. (United States)

We experimentally and theoretically demonstrate a physical phenomenon that is used to obtain Fano resonances at multiple spectral positions by constructing a scalable metamaterial medium. This metamaterial system is formed by multiple layers of coupled meta-atoms, where each layer possesses radiant and subradiant modes. A strong near field coupling between the layers results in hybridized modes of the total structure, which are pulled to different resonant frequencies. These hybridized

Conference 8096: Plasmonics: Metallic Nanostructures and Their Optical Properties IX

modes of different decay characters interact through the structural asymmetry, giving rise to multiple Fano resonances. An analogy to the atomic physics concept of electromagnetically induced transparency is drawn, where the eigenstates of the three-dimensional metamaterial system can be modeled as multiple three-level systems. A theoretical perturbative model taking into account both the plasmon hybridization and subradiant-radiant mode coupling is presented to provide further insight to the behavior of the multi-layered metamaterial. For experimental demonstration of this novel phenomenon, we propose a lift-off free fabrication technique, which utilizes dielectric membranes as the building blocks. This fabrication scheme allows simultaneous patterning of multi-layered structures that are automatically registered in the third-dimension. Excellent agreement between simulated and experimental results is observed. The proposed multi-layered metamaterial can be used to enhance non-linear processes at multiple frequency domains opening up new possibilities in optical information processing.

8096-137, Poster Session

PEDOT:PSS light sensor enhanced by localized surface plasmon of gold nanoparticles

S. Zeng, National Taiwan Univ. (Taiwan)

In this paper, we used PEDOT:PSS(Poly(3,4-ethylenedioxythiophene) poly(styrenesulfonate)) as light sensing material with enhanced sensitivity by localized surface Plasmon resonance generated by gold nanoparticles. PEDOT:PSS was spin coated on ITO glass substrate and 120 nm of Al were evaporated above the PEDOT:PSS. The electrical properties of PEDOT:PSS was then enhanced after adding the gold nanoparticles between the ITO glass substrate and the film of PEDOT:PSS. We observed that the sample with gold nanoparticles has lower resistance when the samples were lighted. Compared with no illumination, the sample resistance (with nanoparticles) decreased about 30%. This is not observed in the sample without gold nanoparticles. And when the density of the gold nanoparticles was increased, the total resistance of the sample was further decreased. When the sample with nanoparticles was illuminated at different wavelengths, the total resistance of the sample was distinct. We measured the current intensity at 0.5 voltage at various wavelengths, and we can obtain that the current intensity correlate with the surface Plasmon resonance frequency of gold nanoparticles.

8096-138, Poster Session

Size and periodicity effects of tuned extraordinary transmission through hole arrays in a Ag-Al₂O₃ metamaterial thin film

E. A. Ray, R. Lopez, The Univ. of North Carolina at Chapel Hill (United States)

We show the effects of hole shape, size, and periodicity variation on extraordinary transmission through a tuned metamaterial of 4 pairs of alternating layers of Ag-Al₂O₃ with 20 nm thicknesses. Transmission through cross or rectangular holes is shifted to the red by 200 nm from transmission through circular or square arrays with square arrays exhibiting a strong enhancement in the blue end of the spectrum. The advantage of a metamaterial over a Ag film of similar thickness is the tunability of the surface plasmons coupling k-vector. For the metamaterial, we are able to tune it to support surface plasmons from periodicities ranging from 130 nm to 215 nm, which effectively shifts the transmission peaks from the blue end of the spectrum in Ag films across the visible and into the red. With this adaptation, we can selectively tune the metamaterial or periodicity to exhibit enhanced transmission over a wide range of wavelengths in the visible. In a parallel vein, when the hole arrays are replaced by pillar arrays, we see the red shift more pronounced from the Ag film to the metamaterial in all shapes, and an asymmetric hole shape exhibits a 100 % increase in transmission from hole to

pillar. For all shaped pillars, transmission is highest in the red end of the spectrum and exhibits a relatively small shift in transmission despite a 20 % increase in periodicity.

8096-139, Poster Session

Mapping near-field coupling effects in infrared gap antennas

P. Alonso-Gonzalez, P. Albella, L. Arzubiaga, M. Schnell, J. Chen, F. Huth, F. Golmar, F. Casanova, L. Hueso, CIC nanoGUNE Consolider (Spain); J. Aizpuru, Centro de Fisica de Materiales (Spain); R. Hillenbrand, CIC nanoGUNE Consolider (Spain)

The vector near-field distribution of infrared gap antennas (linear dipole antennas coupled via a nanometric gap) is mapped by scattering-type scanning near-field microscopy (s-SNOM). The images provide direct experimental evidence of strong in-plane near-field localization inside a gap as small as 50 nm. By measuring the gap fields as a function of the total antenna length (near-field spectroscopy), we observe a clear resonance shift compared to uncoupled linear dipole antennas, thus verifying strong near-field coupling via the gap. We also find significant differences between near-field and far-field spectra of the antennas and discuss their implications.

Vector near-field imaging of the infrared antennas [1, 2] was carried out with s-SNOM where s-polarized laser light is used for antenna excitation. A dielectric Si tip scatters the local near fields of the antennas. Interferometric and polarization-resolved detection of the tip-scattered light yields amplitude E and phase ϕ of the in- (x) and out-of-plane (z) near-field components (E_x, ϕ_x) and (E_z, ϕ_z).

Fig. 1 shows the near-field patterns obtained for a single gap antenna with a gap width of about 50 nm. The out-of-plane near-field component (E_z, ϕ_z) shows large near-field amplitudes at both sides of the gap, while a phase jump of about 180° occurs at the gap center [3]. The in-plane near-field component (E_x, ϕ_x), in contrast, is strongly enhanced exactly inside the gap and directly verifies field concentration inside the gap.

To provide experimental evidence of near-field coupling in the infrared gap antennas, we perform near-field spectroscopy. We fabricate gap antennas of different total length (but constant gap size) and measure the in-plane gap field as a function of the antenna length. A comparison with near-field spectra of single dipole antennas (continuous nanorods) shows a pronounced resonance shift, which clearly verifies near-field coupling across the antenna gap.

Our results show that vector near-field mapping is a powerful tool for measuring spectral resonance shifts in the near field of infrared antennas, in both amplitude and phase. This enables detailed studies of near-field coupling signatures, including the mapping of strongly localized field enhancement (“hot spots”) and resonance shifts of near-field spectra, which are not accessible by far-field spectroscopy.

8096-140, Poster Session

Generalized surface plasmon modes partially coherent

J. C. Juarez-Morales, Instituto Nacional de Astrofísica, Óptica y Electrónica (Mexico)

Elementary long-range plasmon modes are described assuming an exponential dependence of the refractive index in the neighbourhood of a conductive thin film. The study is performed using coupling mode theory. The interference between long-range plasmon modes allows the synthesis of surface sinusoidal plasmon modes which can be considered as generalized plasmon modes completely coherent. These sinusoidal plasmon modes are used for the synthesis of new surface plasmon modes partially coherent, which are obtained by means of an incoherent superposition of sinusoidal plasmon modes where each period is considered as a random variable. The kinds of surface modes generated have a profile easily tuneable which is controlled by means of

the probability density function associated to the period. The numerical simulation for sinusoidal, Bessel, Gaussian and dark hollow plasmon modes are presented.

8096-141, Poster Session

Multipoles on crescent silver nanorod excited by light with different frequencies

S. Chen, C. Yue, W. Lin, Far East Univ. (Taiwan)

In this study, we numerically analyze the interaction of a crescent silver nanorod with polarized visible light, and some specific optical properties are demonstrated. Crescent nanorod is constructed from a cylinder by removing a smaller eccentric cylinder from it, thus, the thickness of the shell has a continuous variation. In comparison with a tube-like nanorod, crescent nanorod could provide a wider freedom to electromagnetic modes. For single frequency, the electric multipoles are different with frequency expectedly. And a strong intensity of surface plasmon polariton could stay inside the chamber of the nanorod only at the resonant frequencies. For continuous wave, the types of multipoles are important evidences in understanding the optical characteristics, though it is hard to be predicted. We are studying the possibility of Fano-like resonance in a crescent nanorod if the incident light includes two or more frequencies. Due to the gradual variation of the wall thickness, a Fano-like extinction spectrum might be obtained under some specific conditions.

8096-142, Poster Session

Nanogap-engineerable Raman-active nanodumbbells for single-molecule detection

Y. D. Suh, Korea Research Institute of Chemical Technology (Korea, Republic of)

Surface-enhanced Raman scattering (SERS)-based signal amplification and detection methods using plasmonic nanostructures have been widely investigated for imaging and sensing applications. However, SERS-based molecule detection strategies have not been practically useful because there is no straightforward method to synthesize and characterize highly sensitive SERS-active nanostructures with sufficiently high yield and efficiency, which results in an extremely low cross-section area in Raman sensing. Here, we report a high-yield synthetic method for SERS-active gold-silver core-shell nanodumbbells, where the gap between two nanoparticles and the Raman-dye position and environment can be engineered on the nanoscale.

Atomic-force-microscope-correlated nano-Raman measurements of individual dumbbell structures demonstrate that Raman signals can be repeatedly detected from single-DNA-tethered nanodumbbells. These programmed nanostructure fabrication and single-DNA detection strategies open avenues for the high-yield synthesis of optically active smart nanoparticles and structurally reproducible nanostructure-based single-molecule detection and bioassays.

8096-143, Poster Session

Optical and electrical characterization of carbon nanotubes by terahertz spectroscopy: comparison between modeling and experimental results

E. Dadrasnia, H. Lamela, Univ. Carlos III de Madrid (Spain)

Electromagnetic terahertz (THz) radiation in frequency range of 0.3 to 10 THz is the next border in science and technology. The first THz-wave time-domain spectroscopy (THZ-TDS) was shown in the late 1990s (Ugawa, et al., Physical Review B, 60, 1999, Kang, et al., Physical Review B, 75, 2007, Parrott, et al., Advanced Materials, 21, 2009). Following

then, carbon nanotubes have been widely investigated to find their unique properties and structure in electronic and mechanic fields. Their structures and properties have been applied for enormous applications in photonic emission, scanning, microscopy and tuning fields (Dresselhaus, et al., 2001). The study of the plasma frequency of carbon nanotube films in high frequency range of THz-TDS is increasingly interested topic since the THz-TDS uses coherent electromagnetic pulse and does need the complicated numerical solution compared to Fourier transformation infrared (FTIR) (Kim, et al., Journal of the Korean Physical Society, 50, 2007).

This paper studies about the optical and electrical properties of carbon nanotubes by utilizing THz electromagnetic wave spectroscopy. Absorption and dispersion of single-walled carbon nanotubes (SWNT) films are investigated by Terahertz time-domain spectroscopy (THZ-TDS) in order to recognize the electrical and optical characteristics of carbon nanotubes of pure and F-doped single-walled carbon nanotubes in the frequency range of 0.2-3 THz. To fit well results based on the Jeon et al. (Journal of Applied Physics, 98, 2005) experimental setup, this study combines the Maxwell-Garnett with Drude models. It allows us to better understand a sequence numerical modelling of carbon nanotubes for different devices based on the experimental data.

This work is supported by MITEPHO project (http://www.uc3m.es/portal/page/portal/grupos_investigacion/optoelectronics/european_projects/miteph) which is coordinated by GOTL research group in Carlos III de Madrid University with foundation grant agreement number 238393 (EU-FP7) in order to develop compact tunable dual-mode diode lasers and terahertz spectroscopy in sensing and biomedical applications.

8096-144, Poster Session

New laser optoacoustic spectroscopy (LOS) system to quantify gold nanoparticles in a liquid tissue phantom for biomedical applications

H. Lamela, V. Cunningham, D. C. Gallego, Univ. Carlos III de Madrid (Spain)

The increasing demand for new techniques to enhance the spectroscopic characterisation and optical contrast of in-vivo unhealthy tissue is at the forefront of new innovations in nanomedicine. Such novel optical based medical techniques can provide physiological definition, enhanced therapeutic efficiency and aid in early and effective diagnostic decisions. Targeted gold nanostructures are forming an integral part in solving current demands for biomedical applications, already providing numerous advances in fields of high sensitive diagnostic imaging (Eghtedari, et al., Nano Letters, 7, 2007, Eghtedari, et al., Nano Letters, 9, 2009), optical enhanced targeted drug delivery (Yih, et al., Journal of Cellular Biochemistry, 97, 2006, Han, et al., Angewandte Chemie-International Edition, 45, 2006) and localized cancer cell destruction by means of phototherapy (Rozanova, et al., Science in China Series B-Chemistry, 52, 2009, Huang, et al., Nanomedicine, 2, 2007). Knowledge of the optical properties of such nanostructures is vital for efficient medical procedures.

In this paper, a novel real-time Laser Optoacoustic Spectrometer (LOS) prototype which demonstrates the potential of the photon to ultrasound conversion, via optoacoustics, is presented and proven to be a valuable technique for characterisation of gold nanorod solutions within turbid media that mimics the optical properties of healthy soft tissue. This analysis has been motivated by the authors previous work in the field of nanoparticle concentration characterization at a single wavelength (532 nm) (Cunningham, et al., Optics and Laser Technology, 42, 2010) and spectroscopic characterisation of spherical nanoparticles within the visible range from 410 to 650 nm (Lamela, et al., Optics and Laser Technology, 2010). In this paper real-time results from the LOS on an embedded gold nanorod colloidal solution are presented for the complete wavelength range from 410 nm to 1000. The optical source used is a Q-switched Nd:YAG pumped Optical Parametric Oscillator (OPO) controlled by specifically designed software. A comparative analysis of results obtained from a parallel reference measurement scheme,

based on standard collimated optical transmission and standard UV-VIS spectrophotometry will be provided.

8096-145, Poster Session

Analyzing symmetry in photonic band structure of gyro-magnetic photonic crystals

S. Khorasani, A. Najafi, Sharif Univ. of Technology (Iran, Islamic Republic of)

In the band structure analysis of photonic crystals it is normally assumed that the full photonic gaps could be found by scanning high-symmetry paths along the edges of Irreducible Brillouin Zones (IBZ). We have recently shown [1] that this assumption is wrong in general for sufficiently symmetry breaking geometries, so that the IBZ is exactly half of the complete BZ. That minimal required symmetry arises from the requirement on time-reversal symmetry. In this paper we show that even that requirement might be broken by using gyro-magnetic materials in the composition of photonic structures, under which the time-reversal symmetry no longer holds. As a result, for sufficiently asymmetric structures we can observe that the IBZ extends fully to the boundaries of the complete BZ, that is IBZ must be taken to be as the same as the BZ.

[1] S. H. Moosavi Mehr and S. Khorasani, "Influence of asymmetry on the band structure of photonic crystals," Proceedings of SPIE, vol. 7609, 76091G (2010).

8096-146, Poster Session

Surface enhanced coherent anti-Stokes Raman scattering on nanostructured gold surfaces

C. Steuwe, J. J. Baumberg, S. Mahajan, Univ. of Cambridge (United Kingdom)

In this paper, we demonstrate a novel method for combining plasmonic surface enhancement with Coherent anti-Stokes Raman Scattering (CARS) on gold sphere segment void substrates. We show that Surface-Enhanced CARS (SECARS) allows for a 10^5 enhancement within our nanostructures, which is a key approach towards reliable single molecule Raman spectroscopy.

Plasmonic enhancement of Raman scattering and fluorescence on surfaces has been a topic of strong interest over the last three decades. However, so far only a few attempts of plasmonic-enhanced nonlinear Raman scattering have been reported, on colloidal spheres [1]. Here colloidal-crystal templated electrodeposition is used to fabricate sphere segment void (SSV) substrates that show large, reproducible enhancements in surface-enhanced Raman spectroscopy (SERS) [2]. Since the plasmonic properties of nanostructures are extremely sensitive to geometry, it is possible to optimize the substrates for SERS by fine tuning the structural architecture. With these substrates, enhancement factors exceeding 10^6 in SERS have been shown [3]. Since CARS is a third-order effect, it overcomes the weak scattering cross section of spontaneous Raman scattering by coherently converting three photons of two different frequencies into an anti-Stokes photon. Hence, combining plasmonic enhancement and CARS gives rise to strong Raman scattering in SECARS.

Here we demonstrate SECARS of a monolayer of benzenethiol molecules on a plasmonic SSV substrate using a single laser approach (in combination with nonlinear wavelength conversion). SECARS spectra in presence of Raman active bonds coincide with spontaneous Raman spectra of the same sample.

We compare the SECARS enhancement to SERS and CARS on a variety of structures and show that the enhancement is strongly dependent on the structural geometry of the sample.

[1]Tae-Woong Koo et al., OPTICS LETTERS, 9, 1024 (2005)

[2]Sumeet Mahajan et al., J. Phys. Chem. C, 21, 9284 (2009)

[3] Sumeet Mahajan et al., Phys. Chem. Chem. Phys., 9, 6016 (2007)

[4] C. Steuwe et al., submitted (2011)

8096-147, Poster Session

Broadband optical antenna with a disk structure

I. Wang, The Hong Kong Polytechnic Univ. (Hong Kong, China)

Broadband optical antennas are of interest as they can transmit more information like traditional microwave UWB antennas. This paper presents a design of broadband optical antennas with a concentric disk structure. An equivalent circuit for the optical antenna with a disk structure is introduced. The broadband radiation at optical frequencies was demonstrated via the computer simulation.

8096-149, Poster Session

Investigation of cross-dipole metallic infrared frequency selective surfaces

J. Zhou, L. Wang, W. Zeng, Y. Y. Wang, Wuhan Univ. of Technology (China)

In this paper, we investigate cross-dipole infrared frequency selective surfaces using the finite element method (FEM). The Lorentz-Drude model is used to model the metallic film plasmonic effect at near infrared frequencies (1 -5 μm). The transmission spectrum is obtained and compared to those without considering the plasmonic effect. The filter transmittivity and ohmic loss as a function of metallic film thickness are also studied. The results show that the plasmonic effect of metallic film reduces the filter transmittivity and shifts the resonant frequency to longer wavelength while the increased metal film thickness reduces both amplitude and bandwidth of the transmitted signal at infrared frequency.

Key words: cross-dipole, infrared frequency selective surfaces, finite element method, Lorentz-Drude model

*correspondent jianzhou@whut.edu.cn

8096-151, Poster Session

Surface plasmon propagation and coupling in silver nanowires

Y. Peng, K. Kempa, Boston College (United States)

Nanowire plasmonics have attracted a lot of research attention recently [Takahara et al, 1997; Liu et al, 2008; Ma et al, 2010]. In our study, we simulate surface plasmons in nanowires using the FDTD method. We investigate the details of the surface plasmon propagation, including the dispersion, field profiles, and the material and radiative damping. We also investigate the radiative emission from plasmons at nanowire ends, as well as the coupling of plasmons between nanowires. These results are compared with experiments, and are used to validate the idea of employing these nanowires as transmission lines in the discretely guided electromagnetic effective medium [Kempa et al, 2008]. These results could also be important to the nanocircuit design [Assefa et al, 2010], and in the field of the nanostructure fabrication [Nah et al, 2010].

8096-152, Poster Session

Fabrication and test of an optical magnetic mirror

J. G. Hagopian, P. A. Roman, S. Shiri, E. J. Wollack, NASA Goddard Space Flight Ctr. (United States); M. Roy, U.S. Army Research Lab. (United States)

Conference 8096: Plasmonics: Metallic Nanostructures and Their Optical Properties IX

Traditional mirrors at optical wavelengths use thin metallized or dielectric layers of uniform thickness to approximate a perfect electric field boundary condition. The electron gas in such a mirror configuration oscillates in response to the incident photons and subsequently re-emit fields where the propagation and electric field vectors have been inverted and the phase of the incident magnetic field is preserved. The author suggested fabrication of sub-wavelength-scale conductive structures that could be used to interact with light at a nano-scale and enable synthesis of the desired perfect magnetic-field boundary condition. In a magnetic mirror, the interaction of light with the nanowires, dielectric layer and ground plate, inverts the magnetic field vector resulting in a 0 degree phase shift upon reflection. Geometries such as split ring resonators and sinusoidal conductive strips were subsequently shown to demonstrate magnetic mirror behavior in the microwave [1] and then in the visible [2]. Work to design, fabricate and test a magnetic mirror began in 2007 at the NASA Goddard Space Flight Center under an Internal Research and Development (IRAD) award. Our initial nanowire geometry was sinusoidal but orthogonally asymmetric in spatial frequency, which allowed clear indications of its behavior by polarization. We report on the fabrication steps and testing of magnetic mirrors using a phase shifting interferometer and optical imaging techniques.

[1] V. A. Fedotov, A. V. Rogacheva, N. I. Zheludev, P. L. Mladyonov and S. L. Prosvirnin, "Mirror that does not change the phase of reflected waves", *APPLIED PHYSICS LETTERS* 88, 091119 2006.

[2] A. S. Schwanecke, V. A. Fedotov, V.V. Khardikov, S.L. Prosvirnin, Y. Chen and N.I. Zheludev, "Optical magnetic mirrors", *J. Opt. A: Pure Appl. Opt.* 9 (2007) L1-L2; doi:10.1088/1464-4258/9/1/L01

8096-60, Session 15

Plasmons in nanoscale, metal junctions: optical rectification and thermometry (Keynote Presentation)

D. Natelson, D. R. Ward, Rice Univ. (United States); F. Heuser, F. Pauly, Karlsruhe Institut für Technologie (Germany); J. C. Cuevas, Univ. Autónoma de Madrid (Spain); D. A. Corley, J. M. Tour, Rice Univ. (United States)

For more than 15 years, physicists (and chemists) have been able to perform experimental studies of electronic transport through single molecules in nanoscale junctions, looking at current as a function of voltage. These studies have revealed rich physics, including evidence for quantum entanglement (the Kondo effect) and inelastic processes involving vibrations. However, there are limits to how much one can learn from dc conduction. Fortunately, we have found that some of the same nanoscale metal structures used to perform the electronic measurements have tremendous utility in optical studies. Thanks to plasmons, the collective modes of the electronic fluid, these metal structures act like an optical antenna, channeling optical energy into and out of precisely the region of interest. We use simultaneous electronic transport and optical characterization measurements to reveal new information about electronic and optical processes in nanoscale junctions fabricated by electromigration. Comparing electronic tunneling and photocurrents allows us to infer the optical frequency potential difference produced by the plasmon response of the junction. Together with the measured tunneling conductance, we can then determine the locally enhanced electric field within the junction. In similar structures containing molecules, anti-Stokes and Stokes Raman emission allow us to infer the effective local vibrational and electronic temperatures as a function of DC current. This permits new fundamental studies of heating and dissipation at the nanometer scale.

8096-61, Session 15

Digital plasmonics

B. Gjonaj, J. Aulbach, P. M. Johnson, FOM Institute for Atomic and Molecular Physics (Netherlands); A. P. Mosk, Univ. Twente

(Netherlands); L. K. Kuipers, A. Lagendijk, FOM Institute for Atomic and Molecular Physics (Netherlands)

No abstract available

8096-62, Session 15

Magnetic and fano resonance engineering with nanoscale plasmonic clusters

J. Fan, Harvard School of Engineering and Applied Sciences (United States); K. Bao, Rice Univ. (United States); C. Wu, Univ. of Texas (United States); J. Bao, Univ. of Houston (United States); V. Manoharan, Harvard School of Engineering and Applied Sciences (United States); N. J. Halas, P. J. Nordlander, Rice Univ. (United States); G. Shvets, Univ. of Texas at Austin (United States); F. Capasso, Harvard School of Engineering and Applied Sciences (United States)

Subwavelength metallic structures enable the broad manipulation of electromagnetic fields at the nanoscale due to their ability to support surface plasmons, which are oscillations of free electrons in metal that couple with the electromagnetic field. We show that clusters of strongly interacting metallic particles support a hierarchy of tunable plasmonic structures that exhibit strong electric, magnetic and Fano-like resonances. Two materials systems are discussed: lithographically defined metallic disk clusters and the self-assembled metal-dielectric colloidal clusters.

Magnetic dipole resonances are the basis for many types of metamaterials. We show that they are supported in close-packed arrangements of three nanoparticles, which can be characterized as closed loops of nanoinductors and nanocapacitors. Furthermore, magnetic resonators that are isotropic in three dimensions can be constructed with tetrahedral clusters, which can be viewed as a cluster of four trimers with varying spatial orientations. We experimentally verify magnetic resonances in trimer clusters and propose routes to the assembly of tetrahedral clusters.

Fano-like resonances result from the coherent coupling between a superradiant and subradiant plasmon mode, and they are characterized by a narrow minimum in the scattering spectra. We show that clusters of four and seven spheres exhibit strong Fano resonances that are, respectively, anisotropic and isotropic in the plane of the nanostructure. We also show that the Fano resonance can be broadly tailored by fabricating clusters comprising disks of varying size. Finally, we demonstrate that these structures are the basis for highly sensitive nanoscale localized surface plasmon resonance (LSPR) detection.

8096-63, Session 15

Ab initio engineering of fano resonances

B. Gallinet, O. J. F. Martin, Ecole Polytechnique Fédérale de Lausanne (Switzerland)

Under certain conditions, the coupling between a bright (radiative) and a dark (non radiative) mode leads to the formation of asymmetric Fano resonances. Although Fano resonances are widely used in plasmonic nanostructures and metamaterials, how their shape is affected by the individual modes and their coupling is not yet well known. In this work, we pave the route towards the engineering of strong and spectrally sharp Fano resonances by building a link between the two classical oscillators' model, electrodynamics and the quantum theories of autoionization of Fano and Feshbach to describe the asymmetric resonance in terms of electromagnetic field configuration in plasmonic nanostructures. General conclusions for the determination of the resonance parameters are drawn, in particular on its width and asymmetry. Using a surface integral simulation technique for electromagnetic scattering on three-dimensional individual and periodic nanostructures, we investigate the resonance properties of each building block separately, in the near-field

Conference 8096: Plasmonics: Metallic Nanostructures and Their Optical Properties IX

and the far-field zones, to induce the properties of the coupled system. We numerically validate our model for structures that are currently under extensive investigation in the plasmonic and metamaterial communities. The insights into the physical comprehension of Fano resonances gained this way will be of great interest for the design of plasmonic sensing platforms and metamaterials.

8096-64, Session 15

Wide-angle spectrally selective plasmonic metamaterials for energy applications

G. Shvets, B. Neuner III, C. Wu, The Univ. of Texas at Austin (United States); S. Savoy, J. John, A. Milder, Nanohmics, Inc. (United States)

The infrared part of the spectrum is of particular interest for a broad range of applications, including thermal photovoltaics, thermal signature camouflage, and solar thermal applications. It is also a very appealing optical spectral range for plasmonic metamaterials because metallic losses are significantly lower in the infrared than in the visible part of the optical spectrum. I will describe the concept and the first experimental demonstration of a large-area spectrally-selective wide-angle infrared absorber based on a single-layer plasmonic metamaterial. This large-area structure is fabricated using the Nano Imprint Lithography (NIL) and tested using angle-resolved spectroscopy. By changing the dimensions and material composition of this metamaterial, we demonstrate the ability to control its spectral properties.

Angle-resolved spectroscopy of these structures reveals a wide-angle response, including complete absorption at the resonant frequency due to the excitation of the short-range plasmon. The short propagation length of the plasmon is used for engineering a more sophisticated (broadband) spectral response by designing sub-wavelength macro-cells consisting of several base unit cells.

We will also describe a simple design paradigm of engineering the spectral response of the macro-cell by analytically expressing its characteristic impedance in terms of the impedances of the base unit cells. Applications to thermal photovoltaics will be addressed by designing a plasmonic structure that compresses the broad solar spectrum into a spectrally-narrow infrared photons which are emitted with the peak emissivity approaching that of the black body.

8096-65, Session 16

Optical spin-Hall effects in plasmonics (Keynote Presentation)

E. Hasman, Technion-Israel Institute of Technology (Israel)

Spin-Hall effect is a basic phenomenon arising from the spin-orbit coupling of electrons. In particular, the spatial trajectory of the moving electrons is affected by their intrinsic angular momentum. The optical spin-Hall effect (OSHE) - beam deflection due to the optical spin (polarization helicity) - was recently presented. The effect was attributed to the optical spin-orbit interaction occurring when the light passes through an anisotropic and inhomogeneous medium. Here, we present and experimentally observe the OSHE in coupled localized plasmonic chains. The OSHE is due to the interaction between the optical spin and the path of the plasmonic chain with an isotropic plasmonic mode. In addition, OSHE was observed due to the interaction between the optical spin and the local anisotropy plasmonic mode, which is independent on the chain path. A spin-dependent orbital angular momentum was observed in a circular path. Moreover, a wavefront phase dislocation due to the scattering of surface plasmons from a topological defect is directly measured in the near-field by means of interference. The dislocation strength is shown to be equal to the incident optical spin and with analogy to the magnetic flux parameter in the Aharonov-Bohm effect. OSHE in spontaneous emission was also obtained in a structure consisting of a coupled thermal antenna array. The effect is due to a spin-orbit interaction resulting from the dynamics of the surface waves

propagating along the structure whose local anisotropy axis is rotated in space. The OSHE in the nanoscale provides an additional degree of freedom in spin-based optics.

8096-66, Session 16

Plasmon propagation in gold and silver nanowires

M. A. Pelton, Argonne National Lab. (United States); B. Wild, L. Cao, Univ. of Chicago (United States); B. Khanal, Los Alamos National Lab. (United States); Y. Sun, Argonne National Lab. (United States); E. Zubarev, Rice Univ. (United States); S. Gray, Argonne National Lab. (United States); N. F. Scherer, Univ. of Chicago (United States)

Noble-metal nanowires can serve as plasmonic waveguides, efficiently transporting optical energy along the wire while confining electromagnetic fields laterally on dimensions much smaller than the diffraction limit. Nanoplasmonic waveguides fabricated using top-down lithographic methods suffer from significant losses due to scattering from edge roughness and grain boundaries. Chemically synthesized silver nanowires have been demonstrated to overcome this limitation. However, these structures have limited chemical and physical stability: they degrade in ambient environments, and they are easily damaged by intense radiation. We therefore investigate plasmon propagation in individual chemically synthesized gold nanowires and compare to propagation in silver nanowires. Propagation length is measured as a function of wavelength using a fluorescence-imaging technique, and group-velocity dispersion is measured using an interferometric spectroscopic technique. By comparing measurement results to electromagnetic simulations based on the finite-difference time-domain method, we find that plasmon propagation is determined by the intrinsic properties of the metal for both gold and silver wires. Although inherent absorption means that propagation lengths in gold are shorter than in silver, the greater stability of the gold wires opens up new scientific and technical possibilities, including detailed structural characterization using x-ray diffraction and nonlinear-optical effects at high field strengths.

8096-67, Session 16

Reversed diffraction laws and anomalous scaling properties in plasmonic systems.

G. Bartal, Technion-Israel Institute of Technology (Israel)

Periodic nanostructures made of metals and dielectrics have shown the ability to guide and transmit optical information much smaller than the wavelength of the carrier wave, overriding the fundamentals limits of diffraction. Owing to the plasma-like nature of the metallic constituents, manifested as negative dielectric function, these nano-structures enable the formation of surface plasmons on the metal-dielectric interfaces and exhibit strong mode confinement and anomalous propagation characteristics, such as negative refraction, anomalous diffraction and enhanced transmission through hole arrays. The strong metal dispersion, along with the loss inherent in such systems, also results in unique scaling of the diffraction and resolution properties with the wavelength which can even be opposite to those found in conventional dielectrics. We study those anomalous scaling phenomena in both resonant and non-resonant plasmonic nano-structures. We show how the resolution and diffraction in periodic metal-dielectric systems scale anomalously with the wavelengths, where longer wavelengths exhibit better resolution power and weaker diffraction - opposite to those found in conventional dielectrics. Likewise, resonant plasmonic systems like silver superlens also show interesting scaling properties where the angular frequency spectrum of a thin silver slab sandwiched between dielectric layers scales in a super-linear manner with the refractive index of the dielectrics, comparing to linear scaling of the dielectric media alone.

8096-68, Session 16

Plasmonic logic gates and devices in silver nanowire networks (Keynote Presentation)

H. Xu, Institute of Physics (China)

Here we show that the local electric field distribution of propagating SPs along Ag NWs can be imaged by coating the NWs with a layer of quantum dots. In Ag NW networks of simple geometries, plasmons launched along a NW can be controllably routed to a specific NW output. The underlying physical mechanism, interference between SPs launched at different positions along a primary NW, is clearly observable, as is the detailed evolution of the plasmon field along the device. The addition of a second plasmon input makes it possible to turn on or off emission paths, resulting in combinations of optical signals that execute specific interferometric Boolean logic operations. This primary NW can thus be viewed as the plasmonic equivalent of a bus in a central processing unit. By loading the primary NW with plasmons launched with specific input properties at the secondary input NWs, the resulting plasmonic interference enables routing and out-coupling to specific output NWs. We believe this concept can be further generalized and expanded to more complex structures that can combine optical signals in various ways, and that a multiple-input, multiple-output plasmonic bus may serve as an efficient splitter, router, switcher and/or multiplexer in future complex plasmonic networks designed for computation and information processing functions. These findings shed new light onto both fundamental understanding of propagating plasmons in complex networks and may advance the development of integrated plasmonic devices for new generation information technologies.

8096-70, Session 16

Localized field enhancements in two-dimensional V-groove metal arrays

J. Beermann, S. M. Novikov, Univ. of Southern Denmark (Denmark); T. Søndergaard, J. Rafaelsen, K. Pedersen, Aalborg Univ. (Denmark); S. I. Bozhevolnyi, Univ. of Southern Denmark (Denmark)

We investigate field enhancements in two-dimensional 800-nm-periodic arrays of (108 - 121 nm deep) V-grooves (opening angles 38 -75 degrees) fabricated using focused ion beam milling in a 190 nm thick gold film on top of a fused silica substrate. Simulated and experimental reflection spectra, high-resolution two-photon luminescence (TPL) images, and microscopy of surface enhanced Raman scattering (SERS) obtained from the V-groove metal arrays are compared revealing good correspondence in the spectral dependences of reflection and local TPL as well as SERS measured at the groove bottom. We relate the obtained field intensity enhancements reaching 85 with nanofocusing and resonant interference of counter-propagating plasmons by the periodic closed tapered groove gaps. We discuss the complementarities of the TPL and SERS techniques used for estimating the relative field intensity enhancement in the nanostructures, i.e., TPL signals originating from inside the metal compared to SERS originating from Raman active molecules adsorbed at the metal surface. The achieved reflection spectra and enhancements depend on the geometry of the V-groove arrays and can actually be tuned in the wavelength range from visible to infrared, making this configuration promising for a wide range of practical applications, e.g., within surface-enhanced spectroscopies.

8096-71, Session 17

Biosensing based on plasmon resonance energy transfer (PRET)

S. Dutta Gupta, G. Suarez, C. Santschi, O. J. F. Martin, Ecole Polytechnique Fédérale de Lausanne (Switzerland)

In 2009, Choi et al. introduced the concept of plasmon resonance energy transfer (PRET, Nano Letters vol. 9, p. 85, 2009) to enhance the absorption of cytochrome c for measuring oxidative stress in living cells. In this contribution, we study in detail both theoretically and experimentally the conditions under which strong coupling can exist between cytochrome c and plasmon nanoparticles. By monitoring the optical absorption of cytochrome c, we introduce a non-invasive way of monitoring the release of oxidative stress, which plays a complex and multifaceted role in cell physiology. Such oxidative stress occurs for example when cells are exposed to toxic agents. The technique is extremely sensitive and enables measuring hydrogen peroxide released by micro-organisms with an unprecedented sensitivity. The versatility of this approach is illustrated by two series of experiments on aquatic micro-organisms and on cancerous cells. For aquatic micro-organism, the ability to monitor PRET over long periods provides insights into the relation between toxicity and photosynthesis. The proposed scheme is not limited to cytochrome c and detection of reactive oxygen species, but can also find a broad range of applications in strongly coupled bio-plasmonic system, such as for example oxygen sensing using hemoglobin.

8096-72, Session 17

Design of hybrid plasmonic materials for SERS direct and indirect sensing

R. A. Alvarez-Puebla, Univ. de Vigo (Spain)

Surface-enhanced Raman scattering (SERS) is gaining prominence as an ultrasensitive and ultrarapid detection technique. In the recent years many applications involving both direct and indirect sensing has been developed in biomedicine, biolabelling, medical imaging, multiplex high-throughput screening, pollutant monitoring or molecular and material characterization. Notwithstanding, several aspects such as colloidal stability, plasmon tunability, detection of molecular species with low affinity for gold or silver surfaces, low SERS cross-sections of aliphatic molecules or transition metals detection are still challenging. Here we demonstrate how the rational design in materials from controlling shape, size and composition of the initial colloidal nanoparticles, that will act as optical enhancers, to their integration into hybrid materials for advanced sensing, may resolve most of those SERS shortcomings. 1-5 Furthermore we disuse the advantages or disadvantages of the different SERS approaches (direct sensing with single particles, generation of hot spots and indirect sensing with biological interfaces and encoded nanoparticles) to the different analytical and bioanalytical problems.

References

- [1] L. Rodríguez-Lorenzo, R.A. Álvarez-Puebla, I. Pastoriza-Santos, S. Mazzucco, O. Stéphan, M. Kociak, L.M. Liz-Marzán, F.J. García de Abajo J. Am. Chem. Soc. 2009, 131, 4616-4618.
- [2] R.A. Alvarez-Puebla, R.F. Aroca Anal. Chem. 2009, 81, 2280-2285.
- [3] M. Sanles-Sobrido, W. Exner, L. Rodríguez-Lorenzo, B. Rodríguez-González, M.A. Correa-Duarte, R. Alvarez-Puebla, L.M. Liz-Marzán J. Am. Chem. Soc. 2009, 131, 2699-2705.
- [4] R.A. Álvarez-Puebla, R. Contreras-Cáceres, I. Pastoriza-Santos, J. Pérez-Juste, L.M. Liz-Marzán Angew. Chem. Int. Ed. 2009, 48, 138-143
- [5] H. Fenniri, R. Alvarez-Puebla Nature Chem. Biol. 2007, 3, 247-249

8096-73, Session 17

Experimental demonstration of $n=0$ in metal-insulator-metal waveguides at cutoff

E. J. R. Vesseur, T. Coenen, FOM Institute for Atomic and Molecular Physics (Netherlands); N. Engheta, Univ. of Pennsylvania (United States); A. Polman, FOM Institute for Atomic and Molecular Physics (Netherlands)

The spatial advance of the phase of light is controlled by the refractive index, essential to many if not all optical applications. Surface plasmons enable a strong modification of the dispersion of light, allowing to tailor effective refractive indices that are very large or even negative. A special case occurs when the refractive index reaches a value close to 0. This condition can be met in waveguides near cutoff, which was experimentally demonstrated in the microwave regime and was also predicted for plasmonic waveguides. So far, it was impossible to reach this condition at visible wavelengths due to limitations in nanofabrication and the difficulty of probing the $n = 0$ condition in a buried waveguide.

Here, we present a metal-insulator-metal plasmon waveguide that shows an effective $n = 0$ at cutoff. Waveguides with accurately controlled dimensions were fabricated using a sequence of steps including focused ion beam milling. Modes of the waveguides were excited using a 30 keV electron beam penetrating through the layer stack. By collecting the emitted radiation as a function of electron beam position we directly observe the spatial mode profiles and determine the dispersion relation of plasmon modes near cutoff. At cutoff, the enhanced density of optical states is directly observed from a peak in the electron-beam induced emission spectrum.

Conference 8097: Optical Trapping and Optical Micromanipulation VIII

Sunday–Thursday 21–25 August 2011 • Part of Proceedings of SPIE Vol. 8097
Optical Trapping and Optical Micromanipulation VIII

8097-01, Session 1

iTweezers: from toy to tool

R. W. Bowman, G. M. Gibson, Univ. of Glasgow (United Kingdom); D. M. Carberry, L. Picco, M. J. Miles, Univ. of Bristol (United Kingdom); M. J. Padgett, Univ. of Glasgow (United Kingdom)

Holographic optical tweezers are fast becoming an established tool in micro- and nano-science. We present developments in both the interface and the underlying technology as used in our lab, along with some of the uses we have put them to. Real time particle tracking from stereoscopic video images enables us to determine position to nanometre precision in 3D. This can be performed in real time at several kHz, allowing us to position-clamp trapped objects in 3D and measure positions and forces with optically controlled tools. Our multi-touch iPad interface gives interactive control over multiple traps at the same time, which opens new possibilities for controlling tools, structures and other dynamic processes.

8097-02, Session 1

Profile measurement using standing wave trapping

T. Washitani, M. Michihata, T. Hayashi, Y. Takaya, Osaka Univ. (Japan)

We proposed a new measurement technique for surface profile using the standing wave trapping in air condition. The high-accuracy scale and the high-sensitive sensor are required in the profile measurement. In our measurement system, the optical trapping particle is used as the sensor. The standing wave pattern is used as the measurement scale, which has wavelength-determined interference pitch ($\lambda/2$). Therefore, this measurement technique is expected to perform the high-accuracy measurement. It was experimentally found that the vertical measurement range is about 250 μm . The uncertainty of the sensor is $\pm\lambda/100$. Thus, this technique is capable of measuring large objects in height. When measuring the continuous surface, the sensor particle is scanned in the horizontal direction above the measured surface. The trapped sensor particle in the standing wave field axially moves to follow the measured surface topography. The particle jumps when the surface profile exceeds the pitch of the standing wave pattern. Therefore, the surface profile can be calculated based on the measurement of the particle motional variation. At first, we realized to measure the smooth surface profile such as micro-lens. As pre-measurement, the dependency of the scale pitch on measured surface angles was investigated. A micro-lens was measured with the angle dependency correction. This shows the improvement of the measurement accuracy. When measuring the discontinuous surface, the sensor particle is scanned in the vertical direction on the measured surface. Cross-correlation of sensor signals reveals the step height distance of the discontinuous surface.

8097-03, Session 1

Surface imaging of biological samples using holographic optical tweezers

D. B. Phillips, J. A. Grieve, S. Olof, S. Kocher, Univ. of Bristol (United Kingdom); R. W. Bowman, M. J. Padgett, Univ. of Glasgow (United Kingdom); M. J. Miles, D. M. Carberry, Univ. of Bristol (United Kingdom)

We present an imaging technique using an optically trapped cigar-

shaped probe controlled using holographic optical tweezers. The probe is raster scanned over a surface, allowing an image to be taken in a manner analogous to scanning probe microscopy (SPM), with automatic feedback control provided by analysis of the probe position recorded using a high speed CMOS camera. The probe is held using two optical traps centred at least 10 μm from the ends, minimising laser illumination of the tip, so lowering the chance of optical damage to delicate samples. The technique imparts less force on samples than contact SPM techniques, and allows highly curved and strongly scattering sample to be imaged, which present difficulties for imaging using photonic force microscopy. To calibrate our technique, we first image a known sample - the interface between two 8 μm diameter polystyrene beads. We then demonstrate the advantages of this technique by imaging the surface of the soft algae *Pseudopediatrum*. The scattering force of our laser applied directly onto this sample is enough to remove it from the surface, however we can use our technique to image the algae surface with minimal disruption while it is alive, un-adhered and in physiological conditions. The resolution is currently equivalent to confocal microscopy, but as our technique is not diffraction limited, there is scope for significant improvement by reducing the tip diameter and limiting the thermal motion of the probe.

8097-05, Session 1

Back-focal-plane interferometry: position or force detection?

A. Farré, M. Montes-Usategui, Univ. de Barcelona (Spain)

After an intense development of optical tweezers as a biophysical tool during the last decades, quantitative experiments in living cells have not found in this technique its best ally, mainly due to the lack of a reliable method to measure forces in complex environments. The detection of forces is usually carried out in an indirect manner, through the measurement of the sample position in the trap. However, this method depends critically on the experimental conditions. The attempts to overcome this problem either require complicated in situ calibrations, which make their use impossible in the study of dynamic processes, or they are inaccurate. Using a different approach, Smith et al. developed a method based on the direct measurement of the momentum change of the trapping beam, but its diffusion has been modest mainly because it requires a counter-propagating optical trapping system, which is difficult to implement and combine with other techniques. Although it has not been used for this purpose yet, it seems a more suitable method for in vivo experiments since the measurement depends only on some properties of the sensor apparatus but not on the experiment itself. Recently, we showed that this method can also be used in single-beam traps. Here, we provide further evidence of this and, more importantly, we show that this method is essentially equivalent to back-focal-plane interferometry with some specific restrictions on the force sensor system. An important implication is, as we will show with some examples, that the signal recorded with back-focal-plane interferometry can be used to directly track forces inside living cells.

8097-06, Session 1

Three dimensional force and torque transduction with holographic optical tweezers: calibration techniques and experimental realisation

J. A. Grieve, S. H. Simpson, D. B. Phillips, S. Hanna, Univ. of Bristol (United Kingdom); R. W. Bowman, G. M. Gibson, M. J. Padgett, Univ. of Glasgow (United Kingdom); M. J. Miles, D. M.

Conference 8097:
Optical Trapping and Optical Micromanipulation VIII

Carberry, Univ. of Bristol (United Kingdom)

Mechanical microtools that are actuated with holographic optical tweezers exhibit many differences to traditional microspheres. Calibration of these tools can prove to be a challenge, and the often used power spectral density technique cannot be fit accurately due to the presence of six corner frequencies. In this talk we explain the intricacies of calibrating any rigid 3D structure, demonstrate three dimensional control of them, and the measurement of all six degrees of freedom. This is achieved by utilising a stereoscopic imaging system to produce precise, three dimensional CCD tracking of the tools, leading to the calibration of the full 6x6 stiffness matrix. In an experimental setting we further demonstrate concurrent force and torque curves obtained by interacting samples with our microtools, along with discussion on the sensitivity and accuracy which may be obtained.

8097-07, Session 2

Hydrodynamic synchronization of light driven propellers

R. Di Leonardo, Univ. degli Studi di Roma La Sapienza (Italy); A. Buzas, L. Kelemen, G. Vizsnyiczai, L. Oroszi, P. Ormos, Biological Research Ctr. (Hungary)

Hydrodynamic interactions are believed to be responsible for the coordinated motion of cilia and flagella in motile microorganisms. Very recently numerical simulations and macroscopic experiments have begun to provide insights in this phenomenon of hydrodynamic synchronization. We investigate a simple microscopic system of independently light driven propellers coupled by hydrodynamic interactions. Microscopic propellers are fabricated by using two photon polymerization while holographic optical tweezers are used to trap and drive them by radiation pressure. Hydrodynamic synchronization is clearly observed when the applied optical torques are finely tuned and disappears progressively as the two propellers are brought far apart. Due to the unavoidable presence of noise in any micron sized system, we discuss hydrodynamic synchronization as a stochastic phenomenon.

8097-08, Session 2

A microsyringe controlled using a triple beam optical trap

W. T. Ramsay, M. Bechu, L. Paterson, Heriot-Watt Univ. (United Kingdom)

A limited range of instruments are available which allow the controlled injection of sub-picoliter volumes; cumbersome, commercially produced mechanical microinjection systems and microfluidic, lab-on-a-chip devices account for the majority. We present an optically controlled microsyringe capable of dispensing femtolitres of liquid. Triple beam optical tweezers are used to manipulate hollow glass microneedles and also polymer microspheres which were used as 'handles' to assist the manipulation of microneedles and 'plungers' to dispense liquid from the microneedle.

Standard optical tweezers were used with the addition of a Ronchi ruling (250 lines per inch) mounted in the image relay telescope. The diffraction pattern generated by the Ronchi ruling produced three optical traps in the sample chamber. Trap spacing was controlled by translating the ruling along the axis of beam propagation within the image relay telescope.

Utilizing the three-beam trap, it was possible to manipulate pulled, borosilicate capillaries (5-50µm in length, 1-5µm in diameter) both perpendicular and parallel to the axis of the capillary. Rolled SO/SO₂ microtubes (4µm diameter, 50µm long) were also manipulated, however in this case polymer microspheres were used as 'handles'. In both cases the microneedles did not align vertically along the propagation axis; an advantage over using a single beam optical trap. Tweezing a microsphere within a microneedle dispenses femtolitres of liquid from the needle. The force exerted on microneedles is calculated to be in the order of

picoNewtons so may have applications where femtolitre volumes must be controllably delivered beyond a barrier, such as single cell microinjection.

8097-09, Session 2

Fast optical force based cell sorter assisted with CUDA and computer vision techniques

G. Xu, W. Qin, N. L. Johnson, Z. Ma, Clemson Univ. (United States); X. Peng, Shenzhen Univ. (China); B. Z. Gao, Clemson Univ. (United States)

Optical force and microfluidics based cell sorting is a newly developed cell manipulation technique. It is non-invasive and easy to control comparing with conventional flow cytometry methods. We investigate a novel high speed, computer vision assisted cell sorting device that utilizes the optical force generated by a weakly focused laser beam to move individual cells and direct cell separation in a microfluidics system. This paper focus on the computer vision based detecting cell, tracking cell position, and estimating moving speed, which are the core of the cell sorting components. In order to distinguish cells by their size and moving speed that indicates cells' physiological characteristics, high speed computer-vision techniques are first introduced. We use sobel edge detector to find potential edges of moving objects (cells or other noises) in each video frame captured by a high speed camera first. Then Hough transform (HT) is used to calculate parameters (center and radius) of the real moving cell's contour. Finally particle filter (PF) is selected to realize cell tracking and its speed measurement. Because HT and PF are all time consuming, in our study we use CUDA compatible GPU-Tesla 1060 and Quadro FX 1800 and program on it to implement real-time processing. The experimental results show that this method can track five to nine cells at approximately 130 to 170 frames per second. The signals from the imaging system are used to trigger a laser beam to laterally move the cells in the microfluidic channel to achieve cell separation.

8097-10, Session 2

Active matter on asymmetric substrates

C. J. Olson Reichhardt, J. Drocco, T. Mai, C. M. Reichhardt, Los Alamos National Lab. (United States)

We investigate the dynamics of self-driven particles on symmetric and asymmetric substrates. This system could be realized using self-driven colloids on optical traps or swimming microorganisms such as bacteria in microstructures. In an asymmetric array of funnel-shaped barriers, particles that undergo only Brownian motion experience no net flow; however, if the particles are undergoing run and tumble type dynamics we find a net flow of particles or a ratchet effect. We investigate the effect of different particle dynamics on the ratchet effect. For example, if the particles reorient to follow the barrier walls they encounter, we observe a ratchet effect; however, if the particles reflect or scatter off the barrier walls, the rectification is reversed or destroyed. We also consider particle-particle interactions which can either promote or decrease the ratchet effect in accordance with different rules. In certain swarming modes the ratchet effect can even be reduced.

8097-11, Session 3

Direct force and ionic-current measurements on DNA in a nanocapillary

O. Otto, L. J. Steinbock, R. Skarstam, J. L. Gornall, U. F. Keyser, Univ. of Cambridge (United Kingdom)

We demonstrate for the first time combined optical tweezers and ionic-current measurements in which the nanopore is located perpendicular to the trapping laser. Traditionally, quadrant photo-detectors are used to measure the displacement of a trapped colloid while the attached DNA is

Conference 8097:
Optical Trapping and Optical Micromanipulation VIII

pulled into a silicon nitride nanopore [1,2]. High-speed video cameras in combination with glass nanocapillaries offer an alternative [3,4]. We apply novel optical fiber illumination for real-time tracking of optically trapped colloids on a microsecond time scale. Using a cross-correlation based algorithm after image acquisition from a CMOS camera we are able to measure the position of a colloid at rates up to 10,000 frames per second over hours [5].

A complete understanding of polyelectrolyte kinetics in strongly confined environments like nanopores or nanocapillaries is still elusive. In order to gain new insight we perform electrophoretic force and ionic-current measurements on single and multiple DNA molecules inside the orifice of a nanocapillary and attached to an optically trapped colloid [6]. We quantitatively model our findings with a combined Poisson-Boltzmann and Stokes-Equation approach and show that our results are in good agreement with data obtained for Si₃N₄ nanopores [2].

- [1] Keyser et al., Nature Phys. 2, 473 (2006).
[2] van Dorp et al., Nature Phys. 5, 347 (2009).
[3] Otto et al., Rev. Sci. Instrum. 79, 023710 (2008).
[4] Otto et al., J. Opt. A: Pure Appl. Opt. in press (2011).
[5] Otto et al., Opt. Express 18, 22722 (2010).
[6] L. J. Steinbock and O. Otto et al., Phys. Condens. Matter 22, 454113 (2010)

8097-12, Session 3

Sequence dependent effect on DNA elasticity

K. Raghunathan, J. Milstein, Univ. of Michigan (United States);
Y. Chen, Cornell Univ. (United States); J. D. Meiners, Univ. of Michigan (United States)

We have used constant force axial optical tweezers to understand the subtle effects of DNA sequence variations on its mechanical properties. Sequence variations in the DNA can affect two fundamental properties, namely the intrinsic curvature and the elasticity of the molecule. To delineate the effects of curvature from elasticity, we have designed sequences of DNA which have nearly identical curvatures but varied AT content and measured their elasticity. We have verified the similarity of curvatures of these sequences computationally and using polyacrylamide gels. Our experiments have shown that the persistence length is highly dependent on the elasticity of DNA; in fact it varied almost two fold between sequences containing 67% AT and 40% AT content region. Thus, the cost of bending a GC rich region of the DNA is energetically much costly compared to an AT rich sequence. The biological implications of this may be substantial, as the need to bend DNA is involved in a host of regulatory schemes, ranging from nucleosome positioning to the formation of protein-mediated repressor and enhancer loops.

8097-13, Session 3

Laser microbeam - kinetic studies combined with molecule - structures reveal mechanisms of DNA repair

B. Altenberg, European Molecular Biology Lab. (Germany);
P. Grigaravicius, Deutsches Krebsforschungszentrum DKFZ (Germany); K. O. Greulich, Fritz Lipmann Institute (Germany)

Kinetic studies on double strand DNA damages induced by a laser microbeam have allowed a precise definition of the temporal order of recruitment of repair molecules. The order is Ku70/80 - XRCC4 --- NBS1 --- Rad 51. Ku70/80 and XRCC4 molecules represent the inaccurate NHEJ pathway, NBS1 a switch and Rad51 the almost error free HRR pathway. These kinetic studies are now complemented by studies on molecular structures of the repair proteins, using the program YASARA which does not only give molecular structures but also physicochemical details on forces involved in binding processes. It turns out that the

earliest of these repair proteins, the Ku70/80 dimer, has a hole with high DNA affinity. The next molecule, XRCC4, has a body with two arms, the latter with extremely high DNA affinity at their ends and a binding site for Ligase 4. Together with the laser microbeam results this provides a detailed view on the early steps of DNA double strand break repair. The sequence of DNA repair events is presented as a movie.

Grigaravicius P, Greulich K.O, Monajembashi S Laser Microbeams and Optical Tweezers in Ageing Research. ChemPhysChem 2009 10 79-85

8097-14, Session 3

Ultrafast Imaging of Microbubble Cavitation using Integrated Optical Trapping for Spatial Control: Progress and Prospects

P. A. Campbell, Univ. of Dundee (United Kingdom)

Cavitation, which involves the formation and dynamic evolution of bubbles, is a ubiquitous phenomenon in fluids.

Recently, the area has received heightened interest in medical contexts due to the utility of [shelled] bubbles for exploitation both as contrast agents for clinical diagnostic ultrasound imaging, and increasingly, for their emerging potential as microscopic drug delivery systems. Micrometer-sized bubbles [microbubbles (μBs)] are most clinically relevant as their small size allows them to flow easily within even the smallest vessels of the vascular system. This size constraint results in bubble resonant frequencies lying in the MHz range, and in turn, requires [ultrasonic] driving frequencies in a comparable range. Accurate monitoring of μB response at sampling rates greater than the Nyquist limit thus requires the use of ultra-high speed microphotography. Moreover, in order to develop a fundamental understanding of bubble behavior over a range of clinically relevant scenarios, it is imperative that spatial control be exercised over their whereabouts relative to any proximal surfaces, and indeed, to other bubbles, so that the effects of any boundary constraints and acoustic cross-talk can be discriminated. Only one technique can be applied readily to this situation, that neither interferes with the incident ultrasound wave, nor perturbs any resultant hydrodynamical response in the surrounding fluid: that technique is optical trapping.

Interestingly, the first demonstration of such optical trapping for low-index μBs occurred in 1988 [1], however it was not until 2005, when the first fully integrated study incorporating high speed imaging sequences of optically trapped μBs activated by ultrasound was published [2]. This was followed in 2007 by an independent study, using an alternative architecture, and which demonstrated the explicit role of proximal walls on the dynamic of shelled μB for the first time [3]. Both of these latter studies underscored the flexibility and power of combining optical trapping and high speed imaging as an innovative new approach to cavitation studies. In this review paper, the lead authors and architects of those latter two studies [2,3] bring their collective experience together for the first time, assessing the process of how their respective integrative solutions converged, and moreover how emerging technologies such as the use of spatial light modulators can be exploited fully in this context. A full reference list, including all conference papers in this area, is included, so that this review represents a completely up-to-date snapshot of the state of the art, as well as a sober assessment of where the most fruitful future directions may lie, given the rapidly evolving CCD industry that underpins modern high speed imaging systems.

8097-15, Session 4

Characterization of oil-producing microalgae using Raman tweezers

O. Samek, P. Zemánek, Z. Pilát, M. ?er?, S. Bernatová, J. Je?ek, Institute of Scientific Instruments of the ASCR, v.v.i. (Czech Republic)

In order to utilize algae for efficient fuel production, the optimal cultivation

Conference 8097:
Optical Trapping and Optical Micromanipulation VIII

parameters have to be determined which, in turn lead to high production of oil in the selected cell line. Therefore, rapid techniques allowing for the characterisation/identification of algal species, and consequently for the determination of the unsaturation degree of the constituent fatty acids in the algal lipid bodies are required. Thus, Raman spectroscopy can offer an attractive alternative for lipid characterization that has not yet been sufficiently exploited in algae investigations.

We present that Raman spectroscopy can be combined with optical tweezers and with microfluidic chips so that this instrument is capable to measure algal nutrient dynamics and metabolism in vivo, in real-time, and label free, making it possible to detect population variability as a biosensor. Moreover, employing an active sorting switch, cells can be sorted depending on input parameters obtained from Raman spectra.

8097-16, Session 4

High speed tracking of intracellular structures: understanding the transport mechanisms in living plant cells

C. López-Quesada, Univ. de Barcelona (Spain); M. Joseph, Consejo Superior de Investigaciones Científicas (Spain); J. Selva, A. Farré, G. Egea, Univ. de Barcelona (Spain); M. D. Ludevid, Consejo Superior de Investigaciones Científicas (Spain); E. Martín-Badosa, M. Montes-Usategui, Univ. de Barcelona (Spain)

Intracellular transport in plant cells is governed by an internal flux, known as cytoplasmic streaming, which facilitates the exchange of materials between organelles and between the cell and its surroundings. Recent studies have shown that this directed flow of the cytosol is dependent on the actin filament integrity and requires the proper action of myosin XI molecular motors. However, the role that myosins play in the movement of particular intracellular organelles remains unclear. These may be directly pulled by myosin motors or carried away by the flux in the cytosol produced by the active movement of another organelle. In order to elucidate the underlying mechanism by which cytoplasmic streaming is generated, we analysed the motion both protein bodies, which are membranous structures that are artificially induced in transgenic tobacco leaves. In addition, these synthetic organelles can be used as a handle to exert large forces by means of optical tweezers, which may be important for the study of the mechanics of the cell transport system in living cells.

In vitro myosin XI motors move processively along actin filaments with a fixed step size of 35 nm. These transporters, which are the fastest known molecular motors, stride along the actin tracks at velocities up to 7 $\mu\text{m/s}$. In order to determine whether a particular transported cargo moves in a stepwise mode, a high-speed, highly accurate tracking method is required, such as FIONA. Large temporal resolution is guaranteed by using a fast back-illuminated EM-CCD camera (Ixon-860, Andor Technologies), which is characterized by its high frame rate and sensitivity. Our results reveal that cargos move in a stepwise mode, suggesting that myosin XI directly pulls these structures through cell's cytosol.

8097-17, Session 4

The viscoelastic properties of the vitreous humour measured using an optically trapped local probe

F. Watts, L. E. Tan, Univ. of Strathclyde (United Kingdom); M. Tassieri, Univ. of Glasgow (United Kingdom); C. G. Wilson, Univ. of Strathclyde (United Kingdom); J. M. Girkin, Durham Univ. (United Kingdom); A. J. Wright, Univ. of Strathclyde (United Kingdom)

We present results demonstrating for the first time that optical tweezers can be used as a local probe to measure the variation in the viscoelastic properties of the vitreous humour of a rabbit eye. The beads were

injected into a dissected vitreous and optically trapped using a 532nm wavelength laser beam and an inverted microscope. The quasi-Brownian motion of the optically trapped bead was monitored on a fast CCD camera on the millisecond timescale. Analysis of the bead trajectory provides local information about the viscoelastic properties of the medium surrounding the particle [1]. The linear viscoelastic properties of a material can be represented by the frequency-dependent dynamic complex modulus, where $G'(\omega)$ is the storage (elastic) modulus and $G''(\omega)$ the loss (viscous) modulus. Previous methods for measuring the viscoelastic properties of the vitreous destroy the sample and allow only a single averaged measurement to be taken per eye, whereas, with our approach, we were able to observe the variation in $G'(\omega)$ and $G''(\omega)$ across the sample and the inhomogeneous nature of the vitreous. The motivation behind these measurements is to gain a better understanding of the structure of the vitreous humour in order to design effective drug delivery techniques. In particular, we are interested in methods for delivering drug to the retina of the eye in order to treat sight threatening diseases such as age related macular degeneration.

1] M. Tassieri et. al, Phys. Rev. E, 81, 026308, (2010).

8097-18, Session 4

Investigating the interaction forces between T-cells and antigen-presenting cells using an optical trapping system

A. J. Wright, Univ. of Strathclyde (United Kingdom); R. Benson, R. W. Bowman, G. M. Gibson, M. J. Padgett, Univ. of Glasgow (United Kingdom); J. M. Girkin, Durham Univ. (United Kingdom); J. M. Brewer, P. Garside, Univ. of Glasgow (United Kingdom)

The interactions between T-cells and antigen-presenting cells (APCs) are crucial in triggering a successful antigen-specific, adaptive immune response leading to protection against a particular pathogen or disease. At present very little is known about the magnitudes of the forces involved in these interactions. We present results showing for the first time that optical tweezers can be used to measure these cell-cell interaction forces. We were able to see a clear difference in the interaction force depending on the presence or absence of specific antigen. The optical trapping system incorporated a fast camera to provide sensitive position detection and was developed to be stable and vibration free, allowing interaction forces to be measured on a time scale of several minutes. We combined two Laguerre-Gaussian beams, with equal but opposite handedness, to create a trapping beam with a 'petal pattern' intensity profile that had no net orbital angular momentum and therefore did not cause the trapped object to rotate. The T cell of interest was trapped directly with this beam and no exogenous beads were added to the sample. Interaction forces between T cells and APCs in the presence of specific antigen ranged from 0-6.5pN, whereas, when the specific antigen was absent the interaction forces ranged from 0-1.5pN. The accuracy of the system will be discussed in terms of how accurately we can track the position of the optically trapped cell and the methods we used for limiting cell roll.

8097-19, Session 4

Viability studies of optically trapped T-cells

N. McAlinden, D. Glass, O. Millington, A. J. Wright, Univ. of Strathclyde (United Kingdom)

We present a viability study of optically trapped live T cells and T cell hybridomas. T cells form an important part of the adaptive immune response system which is responsible for fighting particular pathogens or diseases. The cells of interest were directly trapped by a laser operating at a wavelength of 1064 nm and their viability was measured as a function of time. Cell death was monitored using an inverted fluorescent microscope to observe the uptake by the cell of the fluorescent dyes propidium iodide and trypan blue. Studies were undertaken at various laser powers and beam profiles and the data compared to results taken

Conference 8097:
Optical Trapping and Optical Micromanipulation VIII

using a laser beam with a wavelength of 532nm to optical trap the cells. There is a growing interest in optically trapping immune cells and this is the first study that investigates the viability of a T cell when trapped using a conventional optical trapping system. In such experiments it is crucial that the T cell remains viable and trapping the cell directly means that any artefacts due to a cell-bead interface are removed. Our motivation behind this experiment is to use optical tweezers to gain a greater understanding of the interaction forces between T cells and antigen presenting cells. Measuring these interactions has become important due to recent theories which indicate that the strength of this interaction may underlie the activation of the T-cell and subsequent immune response.

8097-20, Session 4

Elastic light scattering measurements from multiple red blood cells in line tweezers

A. Kauppila, M. Kinnunen, Univ. of Oulu (Finland); A. Karmenyan, National Yang-Ming Univ. (Taiwan); R. Myllylä, Univ. of Oulu (Finland)

Different theoretical models have been developed to understand light scattering processes in biological medium and for helping in analysis of experimental data, both at a cellular level and in bulk tissues. Experimental verification of the simulation models is difficult at a cellular level. Optical tweezers, combined with a light scattering measurement facility, has enabled the measurement of elastic light scattering distributions from single particles and cells. The aim of this paper is to present elastic light scattering measurement results from several red blood cells (RBC) and compare the results with the theoretical ones found in literature. Elliptical optical tweezers is used to keep one, two and three RBCs next to each other and stable in place during the measurements. Face-on and rim-on incidences of He-Ne laser light (vertical polarization) in relation to the RBCs are used. In the face-on case, light scattering intensity is larger from two RBCs than from one RBC, but no difference was found when using 3 RBCs instead of two RBCs. In the rim-on case, clear changes in the shape of scattering light intensity field were found when the number of RBCs was increased from one to two. Those results are in agreement with modelling, where it was found that scattering patterns are almost independent of the lateral distance of the RBCs in the face-on case, and, the multiple scattering effect needs to be taken into account when several RBCs are along the direction of the incident wave.

8097-21, Session 5

Plasmonic nanogels with robustly tunable optical properties

T. Cong, S. Wani, R. Sureshkumar, Syracuse Univ. (United States)

Metal nanoparticles (e.g. Ag and Au) are widely investigated as attractive candidates for inorganic-organic assemblies because of their unique optical and electronic properties. Fluids with metal nanoparticles can be used to manufacture thin films and interfaces for applications such as light trapping in photovoltaic devices, microelectric devices and biosensor technology. In this study, plasmonic nanogels were produced by self-assembly of wormlike surfactant micelle and metal nanoparticles in an aqueous solution at room temperature. The structure of the nanogel was studied by cryogenic transmission electron microscopy and rheological measurements. The optical absorbance of the gels could be robustly tuned by varying the nanoparticle type (Au or Ag), size, shape and/or concentration. Specifically, multicomponent nanogels capable of broadband absorption of the solar radiation were synthesized. These gels had relatively low viscosity (~ 1), long shelf-life (\sim weeks), thermal stability up to 80 degree C and are thermoreversible. Hence, they can be easily processed to make thin films and interfaces with tunable optical properties. Structure, rheology and optical properties of these plasmonic nanogels as well as their potential application to high efficiency photovoltaics design will be discussed.

8097-22, Session 5

Femtosecond laser structured surfaces for opto-fluidics and sensing

R. Buividas, D. J. Day, S. Juodkakis, Swinburne Univ. of Technology (Australia)

Surface patterning by ripples, the self-organized quasi-periodic sub-wavelength relief structures, is demonstrated on large areas with sub-millimeter cross section using femtosecond laser pulses. The period of ripples, L , is determined by the wavelength of irradiation, w , and the refractive index of materials, n , as $L = w/2n$ in (semi)transparent materials and is close to $L = w$ on the metallic and absorbing surfaces for normal incidence. We choose high refractive index materials such as Si, TiO₂, GaP, GaAs, Al₂O₃ ITO for creating patterns where the width of a groove/ridge is between 100 - 200 nm. Such patterns are prospective for surface enhanced Raman scattering (SERS) after coating them by plasmonic metals. The orientation of the ripples, their wavevector, is determined by the orientation of the linearly polarized light. In the case of elliptical and circular polarization, patterns of a more complex geometry but with similar feature sizes are obtained. SERS activity of samples has been confirmed. Such directly written SERS sensors do not require multi-processing lithographic fabrication steps which are not practical or expensive for the large sub-1mm regions. The complex sub-wavelength roughening of the surface by ripples is found to change wetting conditions as revealed by video monitoring water droplet put in touch with the rippled regions. Application potential of ripples in applications of electrowetting on ITO substrates is discussed.

8097-23, Session 5

Electrowetting-controlled bio-inspired artificial iridophores

S. Manakasettharn, J. A. Taylor, T. Krupenkin, Univ. of Wisconsin-Madison (United States)

Many marine organisms have evolved complex optical mechanisms of dynamic skin color control that allow them to drastically change their visual appearance. In particular, cephalopods have developed especially effective dynamic color control mechanism based on the mechanical actuation of the micro-scale optical structures, which produce either variable degrees of area coverage by a given color (chromatophores) or variations in spatial orientation of the reflective and diffractive surfaces (iridophores). In this work we describe the design, fabrication and characterization of electrowetting-controlled bio-inspired artificial iridophores. The developed iridophores geometrically resemble microflowers with the flexible reflective petals. The microflowers are fabricated on a silicon substrate using surface micromachining techniques. After fabrication a small droplet of conductive liquid is deposited at the center of each microflower. This causes the flower petals to partially wrap around the droplet forming a capillary origami structure. The dynamic control over the degree of wrapping is achieved by applying a voltage differential between the conductive core of the petals and the droplet. The applied voltage causes dynamic contact angle change between the droplet and each of the petals due to the electrowetting effect. We have characterized mechanical and optical properties of the microstructures and discuss their electrowetting-based actuation. These experimental results are in good agreement with a simple theoretical model based on electrocapillarity and elasticity theory. This work forms the basis for a broad range of novel optical devices.

8097-25, Session 5

Femtosecond laser structuring of waveguides for sensing applications

D. J. Day, R. Buividas, G. Gervinskas, S. Juodkakis, Swinburne Univ. of Technology (Australia); M. Mikutis, G. Sleky, ALTECHNA

Conference 8097:
Optical Trapping and Optical Micromanipulation VIII

Co. Ltd. (Lithuania)

Tightly focused femtosecond laser pulses were used to open cavities and drill-throughout holes in the optical single and multi-mode fibers. The cross section of the holes and cavities ranging from 10 to 50 micrometers. This direct laser writing approach makes it possible to minimize the amount of waveguide material which should be removed for uncompromised mechanical performance. The proof-of-the-principle demonstration of incorporating fibers into a microfluidic chip is demonstrated. We show that fabricated open cavities and holes in the waveguides can be used for direct monitoring of absorption changes. Simple design and integration possibility of laser-fabricated waveguide sensors is prospective for optofluidic applications.

8097-79, Session 5

A thiol-ene/methacrylate-based polymer for creating integrated optofluidic devices

M. Baylor, Carleton College (United States); R. R. McLeod, R. Boyne, N. Cramer, C. N. Bowman, Univ. of Colorado at Boulder (United States)

We present a new photopolymer that allows the creation of physical features (e.g. micro-fluidic channels) and optical index features (e.g. waveguides) as coplanar components in an optofluidic device using standard photolithography techniques. The polymer consists of two monomer species that polymerize at different rates. The methacrylate gels rapidly to create a scaffolding structure. The thiol-ene is a high-index polymer that cures more slowly. An initial exposure of the fluidic-structure mask brings the polymer to a rubbery gel point. Any unexposed monomer is a liquid and can be removed using a solvent wash leaving physical structures in the polymer. A second short exposure of the waveguide mask initiates the creation of index structures resulting from diffusion of high-index monomer into the exposed region. A final flood-cure permanently fixes the optical structures.

Using the above process we create an integrated refractometer that includes a polymer waveguide crossed by a micro-fluidic channel, a butt-coupled fiber source and a detector attached to a single base. Waveguide loss for a 12 mm x 60 micron x 60 micron waveguide-only sample was 0.28 dB which includes material absorption, scattering losses, and coupling losses. When the 160.5 micron fluid channel was introduced in a waveguide plus channel device, the total loss of the waveguide plus the channel was 4.2 dB decreasing to 1.8 dB when filled with water due to improved index-matching between the channel and the waveguide. Using direct-write and contact liquid photopolymerization techniques, we believe this work can be extended to make 3D optofluidic structures.

8097-26, Session 6

Hydrodynamic assisted barrier escape

A. Curran, M. Lee, Univ. of Glasgow (United Kingdom); R. Di Leonardo, Univ. degli Studi di Roma La Sapienza (Italy); M. J. Padgett, Univ. of Glasgow (United Kingdom)

We present experimental evidence of hydrodynamic assisted escape from a potential barrier. Holographic optical tweezers are used to landscape a bistable system composed of two optical traps, separated by 400nm as seen by a Si colloid of radius 400nm. We observe thermally activated transitions between the two metastable states in the system with transition rates that are in agreement with Kramers' theory. Introducing a second bistable system into our experiment allows us to study the behavior of thermally activated transitions in the presence of hydrodynamic interactions.

The two bistable systems are placed in a line separated by a few micrometers. Using camera tracking technologies we track each of the two beads as they hop back and forth within their respective system. The escape events are recorded and any correlation between the two

systems are then computed. We consistently find that the number of observed correlations are as expected and that the number of correlations having a positive coefficient are greater than the number of correlations having a negative coefficient. The hydrodynamic interactions assist in the escape from a metastable potential.

Our results are particularly relevant in the context of concentrated colloidal suspensions where hydrodynamic interactions could lead to the formation of higher mobility paths along which it is easier to overcome barriers to structural rearrangement.

8097-27, Session 6

Probability distribution of colloidal nanoparticles in an optical trap

Y. Hu, X. Cheng, D. H. Ou-Yang, Lehigh Univ. (United States)

In a colloidal suspension of nanoparticles, the presence of an optical trap can exponentially enhance the probability of finding the particles in the vicinity of the trap. Intriguing questions arise regarding whether the probably distribution of particle number in the trap follows Poisson approximation, and if so, what is the upper limit of the trapping energy at which Poisson is followed. To answer these questions, we conduct experiments to determine directly the variance and the mean particle number in the trap at different trapping energies and compare with the predictions of the probability theory.

8097-28, Session 6

Particle interactions in colloids are revealed in a nonlinear effect in light transmission

J. Song, D. H. Ou-Yang, Lehigh Univ. (United States)

Studies on interactions between particles in highly concentrated suspensions are rare because the solutions are opaque and the interpretations from methods such as diffusing wave spectroscopy are often complicated.

We propose a simple method of probing particle interactions in opaque solutions by measuring light transmission affected by optically induced particle concentration enhancement. The increase in the particle concentration with the input light intensity depends on the interactions between particles. We demonstrate how this method can be used to determine the single particle trapping energy and the virial coefficients in aqueous suspensions of 190 nm polystyrene spheres.

8097-29, Session 6

Experimental and theoretical study of optical binding forces between two colloidal particles

M. Wei, Lehigh Univ. (United States); J. Ng, C. Chan, Hong Kong Univ. of Science and Technology (Hong Kong, China); D. H. Ou-Yang, Lehigh Univ. (United States)

Optical binding has been proposed to be responsible for the cluster formation of micron size dielectric spheres in coherent light fields. However, the measurement of the forces involved in binding is challenging due to overcome thermal fluctuations. In order to measure these forces, we trap two particles in two highly focusing laser beams created from a coherent laser source. We track the displacement of a particle in the stationary trap when the other trapping beam is blinking. The stationary trapping laser served as a force sensor which is able to isolate non-blinking signals. We report an experimental and theoretical study of optical binding forces between two optically trapped dielectric spheres. Results for optical forces are presented as a function of inter particle separation and respective polarizations. The results are useful to understand various inter-particle effects in dual trapping beams system.

Conference 8097:
Optical Trapping and Optical Micromanipulation VIII

8097-30, Session 6

Tunable multidimensional optical binding of particles in laser beams.

P. Zemanek, O. Brzobohaty, V. Karasek, M. Siler, J. Trojek, Institute of Scientific Instruments of the ASCR, v.v.i. (Czech Republic)

We will present a method that provides flexible real-time modifications of the spatial positions of self-arranged particles in optically bound structures. Particularly we will focus on tuning of the inter-particle distances in one-dimensional array of particles in counter-propagating Gaussian or Bessel laser beams and we will also present the first examples of two-dimensional and three-dimensional self-arranged optically bound structures far from the surfaces.

8097-31, Session 6

Dynamics and Directional Locking of Colloids on Quasicrystalline Substrates

C. M. Reichhardt, Los Alamos National Lab. (United States)

Recent experiments on colloids interacting with a quasiperiodic Penrose lattice created by an optical substrates have found that although for strong substrates the colloids have a quasicrystalline ordering, at intermediate substrate strengths the colloids order into what is called an Archimedean tiling consisting of triangles and squares, while for weak substrates the colloids have a triangular ordering [1]. Here we examine particles such as colloids driven over a quasiperiodic Penrose substrate. For strong substrates and low external drives the colloids form a quasiperiodic pinned state, while at higher drives the moving system exhibits a dynamically induced Archimedean ordering which is aligned with the driving direction [2]. The dynamically induced Archimedean ordering only occurs for driving along the five orientationally ordered directions of the Penrose lattice. For driving along other directions, the particles form either a moving liquid or a moving triangular lattice. We also find that the driving angles at which the Archimedean ordering occurs are associated with a directional locking effect in which the colloids remain aligned with lattice substrate symmetry directions even when the driving force is rotated away from these directions. This directional locking is similar the locking steps observed for particles driven over periodic substrates [3], indicating that orientational ordering of the substrate is sufficient to induce directional locking effects and that translational ordering is not required. Our results have implications for various systems including colloids moving through optical lattices, vortices moving in nanostructured superconductors, and frictional studies of particles on substrates.

[1] Archimedean-like tiling on decagonal quasicrystalline surfaces, J. Mikhael, J. Roth, L. Helden, and C. Bechinger, *Nature (London)* 454, 501 (2008).

[2] Dynamical Ordering and Directional Locking for Particles Moving over Quasicrystalline Substrates, C. Reichhardt and C. J. Olson Reichhardt, *Phys. Rev. Lett.* 106, 060603 (2011).

[3] Microfluidic sorting in an optical lattice, M.P. MacDonald, G.C. Spalding, and K. Dholakia, *Nature (London)* 426, 421 (2003).

8097-32, Session 7

Using optical tweezers to investigate colloidal phenomena

I. Cohen, Cornell Univ. (United States)

Colloids are micron scale particles that are suspended in a fluid. The large size and relatively slow motions of the particles, make these suspensions convenient to image in 3D using confocal microscopy and manipulate at the single particle level using optical tweezers. These tools

are revolutionizing our ability to link the microscopic structure of the suspension with the large scale macroscopic material properties. In this talk, I will discuss how we are using these systems to study a vast array of phenomena ranging from statistical mechanics problems including crystallization, defect motion in crystals, and the mechanics of glasses.

8097-33, Session 7

Optical tweezers as a micromechanical tool for studying defects in 2D colloidal crystals

X. S. Ling, Brown Univ. (United States)

In this talk, I'll discuss our experiments on using optical tweezers to create and manipulate defects in 2D colloidal crystals. This work is supported by NSF-DMR.

8097-34, Session 7

Message in a bottle: the statistical behavior of nanoparticles in optical confinement

D. H. Ou-Yang, L. Zhou, J. Junio, Lehigh Univ. (United States)

In an aqueous medium, container surfaces can significantly alter the behavior of suspended nanoparticles. We propose a method to investigate nanoparticle behavior in a boundary-free environment by transiently trapping them with a focused laser beam. While optically confined, as in an optical bottle, these particles are affected by both particle-light and particle-particle interactions. Time-averaged fluorescence imaging produces results in 3D mapping of the nanoparticle concentration in the bottle. We report how we analyze the messages in the bottle, i.e. the statistical behavior of these particles and the optical field intensity distribution.

8097-35, Session 7

Rotational micro-rheology with rotational optical tweezers

G. Maucort, D. C. Preece, T. A. Nieminen, N. R. Heckenberg, H. H. Rubinsztein-Dunlop, The Univ. of Queensland (Australia)

Recently the measurement of the visco-elastic properties of materials at the micron scale has received much interest. However, for biological experiments where the properties of the materials change drastically from point to point a localized measurement is necessary. Such measurement is complicated however by the need to obtain a measurement of the viscoelastic response of the material over sufficient frequency range. Optical tweezers represent one way in which such measurements may be achieved. However, it has proved difficult to take measurements of the visco-elastic properties of biological systems due to often complicated biological structures which may lead to differing measurements of visco-elasticity in different parts of the system. We present a method for localized measurement of the complex visco-elastic moduli of fluids utilizing the optical torque created when a birefringent Vaterite particle is exposed to light with modulated polarization. We use this method to acquire the frequency dependent, visco-elastic moduli while minimizing the associated interaction volume. Though a number of studies have looked at the possibility of using optical tweezers for the measurement of visco-elasticity this is the first time to our knowledge that birefringent properties have been utilized to perform such a measurement.

References:

[1] M. Tassieri, G.M. Gibson, R.M.L. Evans, A.M. Yao, R. Warren, M.J. Padgett, and J.M. Cooper, "Measuring storage and loss moduli using optical tweezers: Broadband microrheology," *Physical Review E*, vol. 81, Feb. 2010.

[2] A. Bishop, T. Nieminen, N.R. Heckenberg, and H. Rubinsztein-Dunlop,

Conference 8097:
Optical Trapping and Optical Micromanipulation VIII

“Optical Microrheology Using Rotating Laser-Trapped Particles,” Physical Review Letters, vol. 92, 2004, pp. 14-17.

[3] M. Funk, S.J. Parkin, T.A. Nieminen, N.R. Heckenberg, and H. Rubinsztein-Dunlop, “Microrheology with AOM Controlled Optical Tweezers,” Proceedings of SPIE, the International Society for Optical Engineering, Society of Photo-Optical Instrumentation Engineers, 2009, pp. 1-9.

8097-36, Session 8

Optical manipulation of aerosol particle arrays

J. P. Reid, J. S. Walker, R. Power, A. E. Carruthers, Univ. of Bristol (United Kingdom)

Aerosols play a crucial role in many areas of science, ranging from atmospheric chemistry and physics, to drug delivery to the lungs, combustion science and spray drying. The development of new methods to characterise the properties and dynamics of aerosol particles is of crucial importance if the complex role that particles play is to be more fully understood. Optical tweezers provide a valuable new tool to address fundamental questions in aerosol science. Single or multiple particles 1-15 micrometres in diameter can be manipulated for indefinite timescales using optical tweezing. Linear and non-linear Raman and fluorescence spectroscopies can be used to probe particles composition and size. In this paper we will report on the latest developments in the use of holographic optical trapping (HOT) to study aerosols. Although widely used to trap and manipulate arrays of particles in the condensed phase, the application of HOT to aerosols is still in its infancy. We will explore the opportunities provided by the formation of complex optical landscapes for controlling aerosol flow, for comparing the properties of multiple particles, for performing the first ever digital microfluidic operations in the aerosol phase, and for examining interparticle interactions that can lead to coalescence/coagulation. Although aerosol coagulation is the primary process driving the evolution of particle size distributions, it remains very poorly understood. Resolving the time-dependent motion of trapped particles and the light scattering from particles during the coalescence process, we see how HOT can be used to study this fundamental process.

8097-37, Session 8

Optical manipulation of ‘drops on rails’ in two dimensional microfluidic devices

C. McDougall, Univ. of Dundee (United Kingdom); E. Fradet, C. Baroud, Ecole Polytechnique (France); D. McGloin, Univ. of Dundee (United Kingdom)

In the context of using microfluidic droplets as isolated biological or chemical micro-reactors, control over droplet placement is crucial to successful device implementation. Previously we have demonstrated that optically induced heating of droplets from a focused laser beam can be used to control the formation of aqueous droplets in oil, merge or sort them. We have also demonstrated that more complex operations such as buffering droplets and mixing their contents are made possible by use of holographic or mobile laser beams. The localised heating produced by the focussed laser beam causes localised variations of the interfacial tension of the droplet. Consequently Marangoni flows are generated and exert a force upon the droplet. It is this optically driven force that can be used to move the drop in a controlled manner.

Here we demonstrate a combined mechanical and optical approach to bring a water-in-oil droplet to any desired position on a two-dimensional plane and hold it stationary against a mean flow. This is achieved using far lower laser powers than those required for purely optical manipulation. The technique makes use of the “drops on rails” technique, which mechanically forces droplets to follow predetermined paths on “rails” or holds them stationary on “holes”. The laser induced optical forcing is employed for intelligent operations such as stopping, guiding or derailing

droplets as they pass through the chip. In this way a droplets under study can be selectively sorted and then held stationary against the flow for prolonged observation.

8097-38, Session 8

Optical torque on a single gold nanorod

P. V. Ruijgrok, N. R. Verhart, P. Zijlstra, A. L. Tchebotareva, M. Orrit, Leiden Univ. (Netherlands)

We report the first quantitative measurements of the optical torque that can be exerted on a single gold nanorod (25 nm diameter, 60 nm length) in a three dimensional, linearly polarized optical trap. The torque is quantified by both the time-averaged amplitude and the relaxation rate of Brownian orientational fluctuations, obtained from polarization dependent white light scattering spectra, and time dependent light scattering respectively. The measurements are in good agreement with calculations where the temperature profile around the hot nanorod is taken into account as an effective, reduced viscosity. We find laser induced heating rates of the trapped nanorod of about 1 degree per milliWatt of trapping power. The maximum optical torque that could be exerted on a single gold nanorod was 100 pN nm, large enough to probe single-molecule processes in soft matter.

8097-39, Session 8

Direct measurement of angular momentum in highly focused light beams

D. C. Preece, A. B. Stilgoe, T. A. Nieminen, N. R. Heckenberg, H. H. Rubinsztein-Dunlop, The Univ. of Queensland (Australia)

The angular momentum of light beams has been widely used in a number of optical tweezers applications. Such angular momentum is often separated into two distinct parts. Firstly spin angular momentum, which occurs when birefringent particles such as Vaterite are exposed to circularly polarized light. Secondly, orbital angular momentum, which occurs when light with an azimuthal phase gradient is incident on a small absorbing particle. Both types of momentum can be used to provoke the rotation of micron sized objects. However spin and orbital components of torque become hard to separate in highly focused beams. Though a number of methods have been tried to measure the exerted torque. Such as using photo detectors positioned to measure the fraction of light split through a polarizing beam splitter. There has been no definitive measure of the torque generated by highly focused laser beam. In this paper we evaluate the torques created in highly focused light beams and discuss the mechanisms by which such torques are created.

References:

- [1] S.J. Parkin, R. Vogel, M. Persson, M. Funk, V.L. Loke, T.A. Nieminen, N.R. Heckenberg, and H. Rubinsztein-Dunlop, “Highly birefringent vaterite microspheres: production, characterization and applications for optical micromanipulation,” Optics express, vol. 17, 2009, p. 21944-21955.
- [2] N. Simpson, K. Dholakia, L. Allen, and M.J. Padgett, “Mechanical equivalence of spin and orbital angular momentum of light: an optical spanner,” Optics Letters, vol. 22, Jan. 1997, p. 52-54.
- [3] J.H. Crichton and P.L. Marston, “The measurable distinction between the spin and orbital angular momenta of electromagnetic radiation,” Electronic Journal of Differential Equations, Conf., vol. 04, 2000, pp. 37-50.

8097-40, Session 8

Optically driven Archimedes micro-screws for micropump applications

P. L. Baldeck, Univ. Grenoble 1 (France); C. Lin, Central Taiwan

Conference 8097:
Optical Trapping and Optical Micromanipulation VIII

Univ. of Science and Technology (Taiwan); M. Bouriau, Univ. Grenoble 1 (France); G. Vitrant, Institut de Microélectronique Électromagnétisme et Photonique (France)

Archimedes micro-screws have been fabricated by three-dimensional two-photon polymerization using a Nd:YAG Q-switched microchip laser at 532nm. Due to their small sizes they can be easily manipulated, and made to rotate using low power optical tweezers. Rotation rates up to 2400 rpm are obtained with a laser power of 200 mW. A photo-driven micropump action in a microfluidic channel is demonstrated with a non-optimized flow rate of 6pL/min.

This light-induced rotation results from the conservation of momentum that occurs when laser photons are reflected on their helical surface. The optical torque increase with the incident laser power, and with the total reflectivity of the irradiated surface, that has a complex dependency with the micro-screw geometry. An analytical expression is derived to evaluate the angular speed in the steady-state regime. The predicted rotation speeds and its dependency with the screw-number N are in very good agreement with experimental measurements.

This work opens the way to the implementation in microfluidics of the most efficient pump design that have been used in the macroscopic world by mankind over centuries.

8097-41, Session 8

Biophotonics workstation: a university tech transfer challenge

J. Glückstad, Technical Univ. of Denmark (Denmark)

No abstract available

8097-42, Session 9

Light-assisted self assembly using photonic crystal templates

C. Mejia, The Univ. of Southern California (United States); A. Dutt, Indian Institute of Technology Kharagpur (India); M. Povinelli, The Univ. of Southern California (United States)

In this paper, we explore a technique we call light-assisted templated self-assembly. We calculate optical forces on colloidal particles over a photonic crystal slab with a square lattice. We perform full-vectorial electromagnetic simulations of Maxwell's equations by means of the finite-difference time-domain method. Forces are calculated using the Maxwell stress tensor. We show numerically that optical forces can be enhanced by exciting guided resonance modes of the photonic crystal slab. Some of these optically enhanced forces trap particles near the slab while others repel particles from it. The magnitude of the trapping forces is dependent on the Q of the mode. Moreover, the trapping lateral forces form a two-dimensional periodic pattern of trapping positions over the slab, which depend on the resonance wavelength and the polarization of the light. The system should allow the trapping and assembly of two-dimensionally periodic patterns of particles, and tuning the wavelength or polarization of the light source should lead to reconfiguration. We calculate the power required for stable trapping and discuss fabrication of the photonic crystal templates using standard microfabrication techniques.

8097-43, Session 9

Simulations of optical lift

S. H. Simpson, S. Hanna, Univ. of Bristol (United Kingdom); G. A. Swartzlander, Jr., Rochester Institute of Technology (United States)

It has been recently demonstrated that a dielectric semi-cylinder, exposed to plane wave radiation, will rotate into a stable orientation thereafter it will experience a force that is not, in general, parallel to the flow of the momentum carried by the incident light. By analogy with aeronautics, the transverse component of this force can be thought of as "optical lift", and the semi-cylinder itself, as a "light-foil". We present a comprehensive examination of this effect using finite difference time domain (FDTD) and discrete dipole approximation (DDA) calculations. The effect of variations in particle size, shape and refractive index on the conditions for stable optical lift are considered. It is found that the phenomenon is common to particles containing precisely two mutually perpendicular mirror planes. For a particular shape of particle in this class the optical size determines the strength of the effect and is associated with Mie type resonances apparent in the magnitude of the lift force. Conversely, the shape itself influences the angular behavior in terms of the stable orientation and the direction of the equilibrium force. Finally, we examine the motion of a light-foil in a viscous medium. The symmetry required to generate optical lift also gives rise to hydrodynamic coupling between translational and rotational motion. As a consequence the conditions for orientational equilibrium are modified and the object acquires a steady velocity. These issues are examined for a range of novel geometries and ways of optimizing the effect are described.

8097-44, Session 9

Pulling particles backward using a forward propagating beam

J. Ng, Hong Kong Univ. of Science and Technology (Hong Kong, China); J. Chen, Z. Lin, Fudan Univ. (China); C. Chan, Hong Kong Univ. of Science and Technology (Hong Kong, China)

Can the scattering force of a forward propagating beam pull a particle backward? A photon carries momentum, so one may expect light will push against any object standing in its path. However, light can indeed "attract" in some cases. For example, small particles will be attracted towards a strongly focused spot in optical tweezers due to the gradient force. But it is probably more appropriate to say that the gradient force "grabs" rather than "pulls", as the particle will remain stable in the optical trap after being drawn to the focus. Here, we discuss another possibility—a backward scattering force which is always opposite to the propagation direction of the beam so that the beam keeps on pulling an object towards the source without an equilibrium point.

In the absence of intensity gradient, using a light beam to pull a particle backwards is counter intuitive. Indeed, this is not possible with a plane wave. However, the situation is more subtle for certain optical beams. Here, we show that it is possible to realize a backward scattering force which pulls a particle all the way towards the source without an equilibrium point. The underlining physics is the maximization of forward scattering via interference of the radiation multipoles. We show explicitly that the necessary condition to realize a pulling force is the simultaneous excitation of multipoles in the particle and if the projection of the total photon momentum along the propagation direction is small, attractive optical force is possible.

8097-45, Session 9

Theoretical studies of nonlinear resonance radiation force exerted on nano-sized objects

T. Kudo, H. Ishihara, Osaka Prefecture Univ. (Japan)

Laser manipulation (LM) is a technique for the mechanical control of small objects using radiation force (RF)[1]. We have previously proposed the LM by using electronically resonant optical response of nanostructures to enhance the RF and to select particular kinds of nanoparticles via quantum confinement effect [2], which has been demonstrated experimentally [3]. This scheme is effective for travelling- and standing-waves, while it is not the case of the trapping by a single focused laser beam because the enhanced dissipative force strongly pushes objects

Conference 8097:
Optical Trapping and Optical Micromanipulation VIII

toward outside the focal point. However, recent relevant experiments report positive results for trapping, showing puzzling phenomena contradicting our conventional understanding of the trapping mechanism [4].

The key element to understand these results is the nonlinear optical response. The laser intensity for single molecular trapping is usually beyond the perturbative nonlinear regime. In this contribution, we elucidate the effective resonant trapping by calculating the radiation force based on the nonperturbative calculation method [5]. The results successfully explain the recent experimental results, and further, we demonstrate how utilizing nonlinear effect enhances the degrees of freedom to manipulate nano-objects, showing novel effects such as “Stimulated Recoil Force” to “pull” the nanoparticles by travelling-waves.

[1]A. Ashkin, Phys. Rev. Lett. 24, 156(1970). [2]T.Iida and H.Ishihara, Phys. Rev. Lett. 90,057403 (2003), Phys. Rev. Lett. 97, 117402 (2006). [3] K. Inaba, et al., phys. stat. solid. (b) 243, 3829 (2006). [4]For example, Y. Tsuboi, et al., Appl. Surf. Sci.255,9906 (2009). [5]T. Kudo and H. Ishihara, phys. stat. solid. (c) 8,66 (2011).

8097-80, Session 9

Spin and orbital angular momenta of light reflected from a cone

M. Mansuripur, College of Optical Sciences, The Univ. of Arizona (United States); A. R. Zakharian, Corning Incorporated (United States); E. M. Wright, College of Optical Sciences, The Univ. of Arizona (United States)

We have examined several retro-reflecting optical elements, each involving two reflections. In the case of a hollow metallic cone having an apex angle of 90°, a circularly-polarized incident beam acquires, upon reflection, the opposite spin angular momentum. However, no angular momentum is transferred to the cone, because the reflected beam picks up an additional angular momentum (this one orbital) that is twice as large but opposite in direction to that of its spin. A 90° cone made of a transparent material in which the incident light suffers two total internal reflections before returning, may be designed to endow the retro-reflected beam with different mixtures of orbital and spin angular momenta. Under no circumstances, however, does it seem possible to transfer any angular momentum from the light beam to the cone without either allowing absorption or breaking the circular symmetry of the system.

8097-46, Session 10

Optimized optical manipulation

M. Mazilu, J. Baumgartl, M. Ploschner, A. C. De Luca, S. Kosmeier, K. Dholakia, Univ. of St. Andrews (United Kingdom)

Special beams such as Bessel beams, Laguerre Gaussian beams or Airy beams are each interesting for various applications in micro-manipulation. But which beam shape, what polarization and back aperture fill-factor is the optimum for trapping, sorting, manipulating or focusing? Here, we present a general method based on optical eigenmodes, that allows the determination of the beam shape optimizing each of the cases considered. The method is applied to optimize trapping, plasmonic based sorting and enhanced whispering gallery mode coupling enabling the Doppler cooling of mesoscopic particles. More precisely, optical eigenmodes (OEI) are solutions of Maxwell's equation that are orthogonal with respect to a quadratic measure of the electromagnetic field. The intensity, the focal spot size, the linear/angular momentum of the light field are such quadratic measures. Each eigenmode is associated with an eigenvalue corresponding to its measure. Ordering these eigenvalues delivers the field with largest/smallest measure enabling the determination of the optimal beam shape for any specific case.

8097-47, Session 10

Theory of resonant radiation force exerted on single organic molecules near metallic nanogap

H. Ishihara, Y. Mizumoto, Osaka Prefecture Univ. (Japan)

The targets of the laser manipulation have been shifting to nanoscale objects including single molecules. For manipulating nano-objects, we have proposed to utilize an electronic resonance[1], and recently its feasibility has been experimentally demonstrated[2]. On the other hand, there has been growing attention to the nanoparticle trapping by using gap plasmons[3]. A localized electric field with a steep gradient strongly attracts nanoparticles. Since such light electric field has a spatial structure with a single molecular scale, the spatial interplay between the electric field and molecular wavefunctions plays an essential role for the molecular manipulation, and hence, the resonant manipulation by using nanogap is expected to become a powerful tool to control molecular alignment and orientation.

In this contribution, we theoretically calculate the radiation force exerted on molecules near metallic nanogap, where the molecular wavefunctions obtained by the molecular orbital method are incorporated into the discrete dipole approximation method. We can treat the nonlocal response due to the field distribution within a molecule by this method, which enables us to demonstrate the force distribution and torque on a molecule. The results show the possibility of selective control of molecular alignment and orientation near metallic nanogap by resonant laser manipulation.

[1]T.Iida and H.Ishihara, Phys. Rev. Lett. 90,057403 (2003), Phys. Rev. Lett. 97, 117402 (2006) [2] For example, K. Inaba, et al., phys. stat. solid. (b) 243, 3829 (2006), Y. Tsuboi, et al., Appl. Surf. Sci.255, 9906 (2009). [3] Y. Tsuboi, et al. J. of Phys. Chem. Lett. 1, 2327 (2010).

8097-48, Session 10

Enhanced optical forces in hybrid plasmonic waveguides

X. Yang, Y. Liu, R. F. Oulton, X. Yin, X. Zhang, Univ. of California, Berkeley (United States)

Gradient optical forces have been broadly exploited in dielectric waveguides and cavities for realizing many exciting applications in optomechanics. Metallic nanostructures, with subwavelength optical confinement arising from surface plasmon polaritons, bring new capabilities in optical forces enhancement. Here we numerically demonstrate that the optical force applied on the silicon dielectric waveguide by the silver substrate in hybrid plasmonic waveguide system can be enhanced by more than one order of magnitude compared to the optical force generated between the silicon waveguide and the glass substrate in conventional photonic waveguide system, at wavelength of 1,550 nm. This enhancement arises from the deep subwavelength optical energy confinement and the small mode propagation loss of the hybrid plasmonic mode. The structural dependence of the optical forces and the optimized waveguide design are analyzed with both Maxwell's stress tensor formalism and the coupled mode theory, in order to reveal the mechanism of this enhanced optical force. We also demonstrate that the optical trapping force applied on a single dielectric nanoparticle with size of 5 nm in water can be strongly enhanced utilizing the hybrid plasmonic mode. The optical trapping potential for the nanoparticle from the hybrid plasmonic mode is approximately 30 times stronger than the one in the photonic mode, due to its strong localization of the optical field in the gap region. Such an interesting result may be useful to design nanoscale optical tweezers to manipulate individual nanoscale objects such as single biomolecules or quantum dots.

Conference 8097:
Optical Trapping and Optical Micromanipulation VIII

8097-49, Session 10

**Optical binding with anisotropic particles:
Resolving the forces and torques**

M. M. Coles, S. N. A. Smith, D. L. Andrews, Univ. of East Anglia
Norwich (United Kingdom)

In the phenomenon known as optical binding, optical fields induce significant forces between microparticles of dielectric matter. Most experimental studies have centred on particles of spherical morphology, assumed to be isotropic and able to tumble freely in a fluid. However, when birefringent microcrystals and anisotropic nanoparticles such as carbon nanotubes are held in an optical trap, it is essential to account for their orientation. These particles are susceptible not only to optical forces but also torques, and there is considerable interest in their response to light that conveys angular momentum - especially optical vortices. Before the full effects of such interactions can be fully understood, however, it is necessary to cultivate a thorough understanding of the rotational effects that operate in optical binding with conventional laser radiation. Here, the orienting effect of the radiation on each individual particle, as well as the orienting influences they exert on each other, need robust theory to account for partial alignment with the throughput radiation. The aim of this paper is to develop, using quantum electrodynamics and perturbation theory, analytical expressions for the observables associated with pair-wise optical binding in anisotropic, non-polar particles. The intricacies of weighted rotational averaging and tensor analysis are tackled, deploying newly devised methods to resolve results into forms amenable to experimental application. Analysing the resulting equations allows the identification of terms corresponding to specific properties of the considered particles, including terms reflecting the degree of anisotropy. It is then straightforward to recognise criteria for the validity of commonly held approximations.

8097-50, Session 11

Biophotonics in turbid environments.

T. Cizmar, H. I. C. Dalgarno, K. Dholakia, Univ. of St. Andrews
(United Kingdom)

We review recent advancements in laser field optimization within turbid environments. Before laser light enters random, turbid and scattering media its wavefront can be pre-shaped to form latter high intensity focal spots after or within the turbid layers to be further exploited for biophotonics methods such as optical trapping or nano-surgery to name a few.

The method is based on the field decomposition into a series of orthogonal modes. One of them is selected as a phase reference whilst the remaining ones are interferometrically tested for particular phase giving the highest intensity signal when interfering with the reference mode at an intensity probe such as fluorescent particle. When applying the optimal phase for all the modes simultaneously the optimal focus is produced at the intensity probe as all the modes meet in phase.

The original concept where relatively slow spatial light modulators were used to measure and further implement the appropriate holographic encoding was recently enhanced by additional adoptive optical components, acousto-optic modulators and galvo-mirrors, leading to light optimization achievable within sub-second intervals, thus opening up the applicability for rapidly time-varying environments including cell layers and living tissues.

We present an alternative strategy where reducing the spatial coherence along one direction allows simultaneous measurement of number of modes where intervals for optimization scale with root square of number of modes. We show that this strategy is particularly suitable for selected plane illumination microscopy (or light sheet microscopy) within turbid environments.

8097-51, Session 11

Digital holography through multimode fibers

S. Bianchi, R. Di Leonardo, Univ. degli Studi di Roma La
Sapienza (Italy)

Optical fibers can guide a light beam across long distances or through turbid media like biological tissues. Multimode fibers can propagate a light beam carrying a large information encoded in the complex coefficients of its expansion in the propagating modes. The main obstacle in using such a set of degrees of freedom comes from the fact that one always ends up having a random speckle pattern at a multimode fiber output. It is natural then to ask whether such a structured noisy pattern could be shaped with a spatial resolution of a single speckle size. Spatial light modulators seem to be the ideal tool for achieving this. We recently demonstrated that phase only modulation can be used to shape a light beam in such a way that, after propagation along a multimode fiber, most of the outgoing light will flow through one or few target spots having the size of a single speckle and arbitrarily located in space. By directly extracting the fiber's end-to-end field propagator we can infer the optimal phase modulation for a desired output, which means that we can have few dynamically reconfigurable target spots. We show that such light spots can optically trap dielectric objects allowing holographic optical micromanipulation with a single multimode fiber. We will also discuss the possibility of imaging using a single multimode fiber endoscope.

8097-52, Session 11

**Comparison of design algorithms for fast
hologram generation in CUDA**

M. P. Persson, D. Engström, Göteborg Univ. (Sweden); J.
Bengtsson, Chalmers Univ. of Technology (Sweden); M. Goksör,
Göteborg Univ. (Sweden)

We have implemented different algorithms for fast hologram generation, aimed for holographic optical tweezers applications, using the parallel computing architecture CUDA. We compare the performance of different implementations of the Gerchberg-Saxton algorithm and provide guidelines for choosing the best suited version with respect to the application. Included in the comparison are three versions of the Gerchberg-Saxton algorithm, one using fast Fourier transforms for propagation and two different implementations using direct summations. The latter two are mathematically equivalent but show radically different dependence on the number of traps in terms of calculation time. Included is also a "lenses and prisms" algorithm for extremely fast hologram generation. It is found that optimized holograms producing hundreds of traps using an FFT based- or tens of traps using direct summation based Gerchberg-Saxton algorithms may be generated in less than 10 ms. This is well below the response time of most commercially available spatial light modulators and thus the use of non-optimizing algorithms such as the "lenses and prisms" algorithm is no longer motivated in many applications. Accompanying this work is a software package including the implementations used in the comparison. The software is made available free of charge under The GNU General Public License (GPL) along with a graphical user interface for interactive control of holographic optical traps.

8097-53, Session 11

**Optical trapping using conical refraction of
light**

J. F. Donegan, D. O'Dwyer, K. Ballantine, C. Phelan, Y. P.
Rakovich, J. G. Lunney, Trinity College Dublin (Ireland)

Conical diffraction of linearly polarised light in a biaxial crystal produces a beam with a crescent-shaped intensity profile. Rotation of the plane of

Conference 8097:
Optical Trapping and Optical Micromanipulation VIII

polarisation produces the unique effect of spatially moving the crescent-shaped beam around a ring. We use this effect to trap microspheres and white blood cells and to position them at any angular position on the ring. Continuous motion around the circle is also demonstrated simply by rotating the polariser continuously. This crescent beam does not require an interferometric arrangement to form it, nor does it carry optical angular momentum. The ability to spatially locate a beam and an associated trapped object simply by varying the polarisation of light suggests that this optical process should find application in the manipulation and actuation of micro- and nano-scale physical and biological objects. Using the process of cascade conical refraction in which light travels through two biaxial crystals in succession, we can produce a ring beam with a Gaussian spot at the centre of the ring. We show using this geometry that we can trap a particle in the Gaussian beam and in the ring trap simultaneously. We can control both the separation of the particles and also their relative angular position using the linearly polarized conical refraction case.

8097-54, Session 12

Reconfigurable 3-dimensional optical route formed by fiber-optic pseudo-Bessel beam arrays

J. Kim, S. Lee, Y. Jeong, J. Shin, K. Oh, Yonsei Univ. (Korea, Republic of)

Due to its unique non-diffracting and self-reconstructing nature, Bessel beam has been successfully adopted to expand the single optical trap into multiple traps along the longitudinal direction. Here we present a novel implementation of Fourier optics along a single strand of hybrid optical fiber in a monolithic manner that can generate a pseudo-Bessel beam. The incident fundamental mode of an optical fiber is adiabatically transformed to a ring mode by a hollow optical fiber, which serves as a micro annulus aperture in the Fourier transformation. Multiple trapping experiments for both polystyrene beads and living Jurkat cell were realized along the beam. Especially four living Jurkat cells were trapped in a row, which can be applied to cellular level spectroscopy. Furthermore, optical transport of the trapped particles along a 3-dimensional curvilinear optical route was demonstrated by spatially multiplexing pseudo-Bessel beams. The radius curvature of the optical route was smaller than the particle size, which has not been possible in prior micro-fluidic channel technologies. The novel concept to spatially multiplex the fibre optic arrays could form a new all-optical building block to realize reconfigurable transportation of particles in true 3-dimensional space overcoming the prior microfluidic routes. Detailed discussion of optical route formation using fiber optic couplers and fiber lasers will be discussed along with explanation on device fabrication.

8097-55, Session 12

Optical chaining of dielectric particles by two counter-propagating all-fiber Bessel-like beams

S. Lee, J. Kim, Y. Jeong, J. Park, K. Oh, Yonsei Univ. (Korea, Republic of)

Optical chaining of multiple dielectric beads was experimentally demonstrated using two counter-propagating Bessel-like beam generated by multimode interference in optical fibers embedded in polydimethylsiloxane (PDMS) channel. The Bessel-like beam generator was composed of a single mode fiber concatenated with a segment of coreless silica fiber of 1600 μm length and a fiberized focusing lens. A Bessel-like beam was achieved by multimode interference along the coreless silica fiber, and the beam maintained an average center beam diameter of 4.9 μm over an axial length of 300 μm , having a nearly uniform output power within a variation of $\pm 0.25\%$. The proposed device was designed to be compatible with a continuous wave Yb-doped fiber laser oscillating at the wavelength of 1084 nm in order to provide all-

fiber solution. A micro-fluidic system of cross-channel was fabricated using PDMS to embed two counter-propagating fiber probes, which provided an accurate beam alignment and stable delivery of dielectric beads. One dimensional optical potential well was formed along the counter propagating beams, where the dielectric beads were trapped. For the particles with the diameter in the range of 2 to 4.5 μm , which is smaller than the central beam diameter, unique chaining of multiple particles was observed, where particles were assembled in a form of chain. By adjusting the optical power we could transport the whole chain of particles along the optical beams. Detailed discussion of the optical chaining of particles is presented along with characterization the optical force.

8097-56, Session 12

Generation of high efficiency vector beams with synthetic phase holograms

G. Mendez, V. Arrizon, R. Ramos-Garcia, Instituto Nacional de Astrofísica, Óptica y Electrónica (Mexico)

Recently, vector beams (VB) have attracted significant interest due to its quite unique characteristics. In particular, the presence of a strong longitudinal component of the electric field and tighter focusing in comparison to homogeneously polarized beam when the VB have axial symmetry in amplitude and polarization. Several generation methods for obtaining VB have been reported. However, most of them are unstable, complicated and the output efficiency is small.

In 2007, Wang et al. proposed a method to produce arbitrary VB using an amplitude spatial light modulator (SLM) and a common path interferometric arrangement. They use an amplitude hologram to generate VB and they only encode VB with constant intensity distribution. Recently we published two novel phase synthetic holograms (Arrizón et al. 2007) that allow us to encode arbitrary complex scalar fields into phase-only function with high quality reconstruction and efficiency of the encoded field. In this work we present a novel method to generate reconfigurable vector beams with arbitrary polarization states employing these phase synthetic holograms. The method is based on the linear recombination of two orthogonally homogeneous polarized scalar modes, that allow the generation of vector fields with arbitrary spatial varying polarization. The two orthogonally polarized modes are superposed by using a common path interferometer which consists of a 4-f system and a phase SLM. We demonstrate the generation of high efficiency and quality Bessel and Laguerre-Gaussian vector beams of different orders with radial and azimuthal (or any other combination) polarization distributions.

8097-57, Session 12

Vector fields with hybrid states of polarization and their orbital angular momentum

X. Wang, B. Gu, J. Chen, Y. Li, Nankai Univ. (China); J. Ding, Nanjing Univ. (China); C. Guo, Shandong Normal Univ. (China); H. Wang, Nankai Univ. (China)

Vector fields with spatially inhomogeneous states of polarization (SoPs) have become a subject of rapidly growing interest, due to its unique features and novel applications in various realms, such as optical trapping and particle manipulation, micromechanics, and biology. However, the generation of arbitrary vector fields is still a challenge. We describe a convenient approach for generating arbitrary vector fields in a 4f system with a spatial light modulator (SLM) and a common path interferometric arrangement. A computer-generated hologram is introduced onto SLM for performing the field conversion. Realization of a variety of polarization configurations confirms the reliability and flexibility of our method. As examples, we experimentally demonstrate the typical radially and azimuthally polarized fields, high order cylindrical vector fields and vector fields with hybrid SoPs.

It is generally accepted that optically isotropic materials are not

Conference 8097:
Optical Trapping and Optical Micromanipulation VIII

influenced by polarization, whereas anisotropic materials can be. However, we validate that the polarization feature can also influence isotropic materials. We predict a new category of optical orbital angular momentum that is associated with the curl of polarization and a kind of vector field with radial-variant hybrid states of polarization that can carry such novel optical orbital angular momentum. We present a scheme for creating the desired vector fields. Optical trapping experiments validate that the vector fields, which have no additional phase vortex, exert torques to drive the orbital motion of the trapped isotropic microspheres.

8097-58, Session 12

The sonic screwdriver

G. C. Spalding, Illinois Wesleyan Univ. (United States); A. Volovick, Z. Yang, C. Demore, M. P. MacDonald, S. Cochran, Institute for Medical Science & Technology (United Kingdom)

When samples of interest are small enough, even the relatively weak forces and torques associated with light can be sufficient for mechanical manipulation, can offer extraordinary position control, and can measure interactions with three orders of magnitude better resolution than atomic force microscopy. However, as the components of interest grow to slightly larger length scales (which may yet be of interest for microfluidic, "lab-on-a-chip" technologies and for research involving biomedical imaging), other approaches gain strength. This talk includes discussion of the angular momentum carried by sonic beams that we have implemented both to levitate and controllably rotate disks as large as four inches (!) across. Discussion of such acoustic beams complements the discussion of the angular momentum carried by light. Also, these beams are useful for a variety of reasons (not least for aberration correction). Methods, including the use of holographically structured fields, will be discussed.

8097-72, Session 12

Flexible dual-beam optical trapping

P. Zemanek, O. Brzobohaty, Institute of Scientific Instruments of the ASCR, v.v.i. (Czech Republic); T. Cizmar, K. Dholakia, Univ. of St. Andrews (United Kingdom)

We present an advanced configuration for optical manipulation of micro- and nano-objects employing adaptive optical element to control properties of more counter-propagating beams overlapping in a sample chamber. This system can eliminate optical aberrations in both pathways, online re-align the system remotely from a computer interface, arbitrarily switch in real time between various beams types (vortex, Gauss, Bessel etc.) and their spatial intensity distributions (beam width, vorticity etc.). We demonstrate variety of applications of this setup ranging from formation of spatial solitons, longitudinal optical binding, precise particle delivery via optical conveyor belt, stable confinement of low-index particles, and controlled rotation or swing of heterogeneous objects.

8097-64, Poster Session

Optical manipulation of aerosols using Surface Acoustic Wave Nebulisation

S. Anand, J. Nylk, C. D. Dodds, Univ. of Dundee (United Kingdom); J. M. Cooper, S. L. Neale, Univ. of Glasgow (United Kingdom); D. McGloin, Univ. of Dundee (United Kingdom)

High density micron sized aerosols from liquid surfaces were generated using surface acoustic wave (SAW) nebulisation. The SAWs are made from a set of interdigitated electrodes (IDT) deposited on a lithium niobate (LiNbO₃) substrate and are designed to operate around 12MHz. RF powers of ~235mW are used to achieve nebulisation. Powers below this results in droplet motion across the substrate surface. The nebulisation

process generated aerosols of a narrow size distribution with diameter ranging from 0.5-2 μm . We consider ways in which these aerosols can be loaded into optical traps for further study. In particular we look at how SAW nebulisation can be used to load particles into a trap in a far more robust manner than a conventional nebuliser device. We demonstrate trapping of a range of particle types and sizes and analyse the size distribution of particles as a function of the applied frequency to the SAW device. We show that it is simpler to load, in particular, solid particles into optical traps using this technique compared to conventional nebulisation. We also consider the possibilities for loading nanoparticles into aerosol optical tweezers.

8097-65, Poster Session

Brownian movement rectification of microparticles using pulsating ratchets

J. Silva-Barranco, Instituto Nacional de Astrofísica, Óptica y Electrónica (Mexico); U. Ruiz-Corona, Univ. della Calabria (Italy); M. Arias-Estrada, V. Arrizon, R. Ramos-García, Instituto Nacional de Astrofísica, Óptica y Electrónica (Mexico)

In recent years, particle transport at microscopic level has become an important research topic which has led to the understanding of directed particle transport subjected to thermal fluctuations. Brownian motors (also called ratchet mechanism) are one of the most interesting phenomena of work generation in nonequilibrium systems under random external forces. In this work, we report Brownian movement rectification of 0.5 micron diameter latex particles using pulsating ratchets. In order to implement the asymmetric potential, a 2D asymmetrical saw tooth phase pattern is displayed on a spatial phase modulator and then transformed into an intensity pattern by using the phase contrast method. This pattern is focused down with a 100x microscope objective obtaining a pattern of ~40x40 square microns at the focal plane. The pattern's parameters can be dynamically controlled: periodicity, asymmetry, and on/off rate which allows optimization of directed transport. We found that there is an optimum value for the on/off rate and particle diameter/spatial period obtaining an average speed of 0.6 microns/s. The 2D pattern allow us to manipulate a large number of particles, in contrast to previous studies were only one particle has been studied, opening the opportunity to massive sorting of particles.

8097-66, Poster Session

Optically induced zinc nanoparticles selective deposition on single-mode fiber end

G. J. Ortega, F. Chávez, P. Zaca-Moran, Benemérita Univ. Autónoma de Puebla (Mexico); R. Ramos-García, Instituto Nacional de Astrofísica, Óptica y Electrónica (Mexico); C. F. Mendoza, Instituto Politécnico Nacional (Mexico); G. F. Pérez, Benemérita Univ. Autónoma de Puebla (Mexico); J. G. Gutiérrez, Univ. Autónoma Benito Juárez de Oaxaca (Mexico); O. Goiz Amaro, Ctr. de Investigación y de Estudios Avanzados del IPN (Mexico)

Metal particles manipulation with radiation pressure of laser light is possible, only if the diameters of these particles are much smaller those of the wavelength of the laser light (Rayleigh particles). In this case, the gradient force is larger than both the scattering and absorption forces. We have made a numerical study considering a Gaussian beam with a fundamental mode that interacts with zinc spherical nanoparticles with different diameters (< 44 μm), and submerged into isopropyl alcohol in order to examine the behavior of the radiation pressure (scattering, absorption and gradient force). The results of this study show that the gradient force is greater than other forces only by particles with a certain diameter. Moreover, by using the gradient force of the laser light, the zinc nanoparticles were deposited on a single-mode fiber end. The images obtained by optical microscope and atomic force microscope

Conference 8097:
Optical Trapping and Optical Micromanipulation VIII

show that the particles deposited on the optic fiber end exhibit a uniform distribution of nanoparticles in the core which can be used as optical mirrors, sensors, saturable absorbers, etc.

8097-67, Poster Session

Trapping of nanoparticles in water by evanescent wave near a NSOM probe

B. Liu, L. Yang, Y. Wang, Harbin Institute of Technology (China)

Applying Maxwell stress tensor and 3D FDTD methods, physical properties of nanoparticle trapping by evanescent wave near the NSOM probe, including trapping size, trapping position and role of other forces versus optical trapping force, are revealed. From the distribution of trapping force acted on a nanoparticle along three axis directions, it is found that the nanoparticle tends to be trapped to the aperture edge and center surface of the probe tip. In experiments 120 nm polystyrene particles are trapped in a multi-circular shape and two circles of polystyrene particles are arranged to different positions on the substrate. The results indicate that the NSOM probe is able to trap nanoparticles with lower laser intensity than that required by conventional optical manipulator.

8097-68, Poster Session

Optical trapping of semi-conducting nanowires

S. H. Simpson, S. Hanna, Univ. of Bristol (United Kingdom)

Semi-conducting nanowires lend themselves to a variety of applications. For example, they are ideal candidates for components in novel electronic and optical devices. Evidently, optical trapping has a part to play in the assembly of such structures and there is much experimental work directed toward this goal. Theoretical work, however, is relatively sparse. One reason for this is that the very high aspect ratios involved, prohibiting the use exact methods. Here we investigate the use of the discrete dipole approximation to calculate optical forces on nanowires. Where possible, results are compared with available analytical and semi-analytical techniques, the accuracy is assessed and possible modifications to the algorithm are suggested. Subsequently we investigate the optical forces on nanowires trapped in single and multiple Gaussian beams. The domain between trapping and non-trapping behavior is demarcated, and observed to be highly dependent on the optical environment. Thus, a nanowire which will trap in a single beam, may not trap horizontally in a dual beam system, and a nanowire which will trap in this way may cease to do so if the polarization states of the beam are altered. For single beam trapping, with the nanowire vertically oriented, it is shown that the vertical stiffness decreases exponentially with increasing length, whilst it remains tightly trapped in other respects. Such systems can therefore be used as highly sensitive force or mass sensors. Finally, we show simulations of the thermal motion of optically trapped nanowires and investigate its impact on trap stability.

8097-69, Poster Session

Optical trapping of single gold nanoparticles with higher order laser modes

A. Huss, R. Jäger, A. M. Chizhik, J. Mihaljevic, A. J. Meixner, Eberhard Karls Univ. Tübingen (Germany)

Optical trapping is one of the most promising tools for nanochemistry and nanoengineering. Since Arthur Ashkin [1] brought optical trapping to life, many steps forward have been made. To form a stable trap it is required to overcome the scattering and absorption forces, therefore metallic and magnetic nanoparticles cannot be trapped easily. Recently, trapping of single gold nanoparticles in aqueous solutions with a linearly polarized Gaussian beam and fixing them in controlled pattern

on the sample surface has been experimentally shown [2,3]. However, to increase the trapping force and stability of the trap the use of cylindrical vector beams (also known as doughnut-modes) has been suggested according to theoretical calculations [4]. Since a focused radially polarized laser mode has higher electric field component in the propagation direction with respect to the linearly polarized Gaussian beam, it provides an advantage for optical trapping. Moreover, the weak in-plane component of the radially polarized laser mode pushes passing nanoparticles into the focus of the beam.

In this work we present our recent experimental and theoretical results upon optical tweezers using a radially polarized light. A home-built confocal microscope setup has been used for focusing a radially polarized laser beam with a high numerical aperture immersion oil objective lens. This allowed us to use the advantages of high-resolution confocal microscopy and cylindrical vector beams for trapping nanometer-size gold spheres.

[1] A. Ashkin, Phys. Rev. Lett., 1970, 24, 156.

[2] A. S. Urban, A. A. Lutich, F. D. Stefani, J. Feldmann, Nano Lett., 2010, 10, 4794.

[3] M. J. Guffey, N. F. Scherer, Nano Lett., 2010, 10, 4302.

[4] Q. Zhan, Opt. Exp., 2004, 12, 3377.

8097-70, Poster Session

Micro- and Nanoparticle Optical Trapping Using Cylindrical Vector Beams

S. Skelton, M. Sergides, A. Pawlikowska, Univ. College London (United Kingdom); M. G. Donato, P. G. Gucciardi, A. Irrera, O. M. Maragò, Istituto per i Processi Chimico-Fisici (Italy); P. H. Jones, Univ. College London (United Kingdom)

The vast majority of optical tweezers use a trapping laser beam with a spatially homogeneous state of polarization, such as linear, elliptical and circular polarizations. However, spatial modulation of the polarization of the trapping beam has the potential to add a further degree of control to trapping parameters and allow further optimization of the trap for certain particle types.

Laser beams in which the polarization is directed radially outwards from the beam axis have received significant recent attention due to their interesting focusing properties. These beams contain a polarization singularity along the beam axis where the electric field amplitude is identically zero, and thus exhibit an annular intensity distribution in the far-field. The polarization configuration and 'donut' intensity profile result in tighter focusing of the radially polarized beam when compared to a linearly polarized Gaussian beam, producing a smaller transverse size of the focal spot. Furthermore, due to symmetries in the polarization components, the time-averaged axial component of the Poynting vector is zero, thus the scattering force vanishes, making the radially polarized tweezer an ideal candidate for trapping nano-particles.

We investigate the use of radially polarized laser beams for optical trapping of micro- and nano-particles. We present quantitative experimental measurements of the trap spring constants for a wide range of parameters and particle sizes and compare the results to those obtained using the more conventional linearly- and circularly- polarized trapping beams. Additionally, we investigate shaping of the trapping volume for trapping of elongated micro and nanostructures (nanotubes, nanowires).

8097-71, Poster Session

Discrete complex amplitude filter for ultra long optical tube

J. Wang, Nanjing Univ. of Aeronautics and Astronautics (China) and State Key Lab. of Transient Optics and Photonics (China); Q. Liu, Y. Liu, Nanjing Univ. of Aeronautics and Astronautics (China);

Conference 8097:
Optical Trapping and Optical Micromanipulation VIII

W. Chen, Q. Zhan, Univ. of Dayton (United States)

In this paper, a discrete complex amplitude filter is designed to obtain the focused hollow field with ultra long depth of focus (DOF). As for a high numerical aperture (NA=0.95) objective lens obeying the sine condition, the distribution of the focused field in the focal region can be engineered into a field like a long "tube" with flat wall through manipulating the transmitted amplitude and the phase delay of the field at the incident pupil plane. This complex amplitude of the pupil plane can be discretized into multiple zones with different radius, transmitted amplitude and phase delay. A focused tube field with 9λ depth of focus can be created as an example through separating and averaging of the projected pupil radiation field of dipole array in the focal region. Imperfections of the designed filter will influence the quality of the generated optical tube field. Deviation of the radius, transmitted amplitude and phase in each zone will influence the profiles of the tube field to some extent and these are discussed (Fig.1 (a) and (b)). For the optical trapping and manipulation, this created tube field can expand the manipulated distance and increase the trapped particles' numbers.

8097-73, Poster Session

Femtosecond laser pulses for chemical-free embryonic and mesenchymal stem cell differentiation

P. Mthunzi, Council for Scientific and Industrial Research (South Africa); K. Dholakia, F. Gunn-Moore, Univ. of St. Andrews (United Kingdom)

Owing to their self renewal and pluripotency properties, stem cells can efficiently advance current therapies in tissue regeneration and/or engineering. Under appropriate culture conditions in vitro, pluripotent stem cells can be primed to differentiate into any cell type some examples including neural, cardiac and blood cells. However, there still remains a pressing necessity to answer the biological questions concerning how stem cell renewal and how differentiation programs are operated and regulated at the genetic level. Indeed, Uchugonova et al, 2008 [1] reported on an urgent requirement in stem cell research on technologies for non-invasive, marker-free observation of growth, proliferation and stability of living stem cells under physiological conditions. In their studies, through the detection of second-harmonic generation signal, they investigated two-photon excited autofluorescence of human stem cells and the onset of collagen production of differentiated cells.

Femtosecond (fs) laser pulses have been reported to non-invasively deliver exogenous materials, including foreign genetic species into both multipotent and pluripotent stem cells successfully [2, 3]. Through this multi-photon facilitated technique, directly administering fs laser pulses onto the cell plasma membrane induces transient submicrometer holes, thereby promoting cytosolic uptake of the surrounding extracellular matter [4]. To display a chemical-free method of stem cell differentiation that utilises micro-litre scale volumes of reagents, we report on using a diffraction limited near infrared pulsed laser beam spot for embryonic and mesenchymal stem differentiation. The produced specialized cell types could thereafter be characterized and used for cell based therapies.

References:

1. Uchugonova, A. and K. König, Two-photon autofluorescence and second-harmonic imaging of adult stem cells. *J. Biomed. Opt.*, 2008. 13(5): p. 054068.
2. Uchugonova, A., et al., Targeted transfection of stem cells with sub-20 femtosecond laser pulses. *Opt. Express.*, 2008. 16(13): p. 9357-64.
3. Mthunzi, P., K. Dholakia, and F.Gunn-Moore, Phototransfection of mammalian cells using femtosecond laser pulses: optimization and applicability to stem cell differentiation *Journal Biomedical Optics.*, 2010. 15(4): p. 041507.
4. Vogel, A., et al., Mechanisms of femtosecond laser nanosurgery of cells and tissues. *Appl. Phys. B-Lasers O.*, 2005. 81(8): p. 1015-1047.

8097-74, Poster Session

Heating effects on NG108 cells induced by laser trapping

I. Verdeny, A. Fontaine, A. Farré, M. Montes-Usategui, E. Martín-Badosa, Univ. de Barcelona (Spain)

Optical tweezers (OT) are an innovative and powerful technique with a wide range of applications in the physical and biological sciences. This novel microtool uses a highly focused laser beam to trap and manipulate microscopic neutral objects. Typical traps in cell biology are generally based on lasers producing from 25 mW to 2 W in the specimen plane. Non-contact force for cell manipulation, force resolution as accurate as 0.1 pN and amiability to liquid medium environments are the main advantages of this technique.

Nevertheless, the response of living matter to the interaction with laser light still remains unclear. Previous studies evaluating the cell response to laser irradiation with OT have already been performed. Several parameters (laser power, irradiation time, wavelength...) have been tested in various types of cells and organisms and different cell functions (cloning efficiency, ability to grow, motility...) and reactions (viability, apoptosis and stress response) have been used to assess damage. However, conclusions do not seem to be unanimous yet.

Photon absorption is a major detrimental process when laser radiation interacts with cells, consequently, generating both photodamage and thermodamage.

Particularly, this work is focused on the damage induced by heating of the sample or thermodamage. The heat shock or stress response is the earliest defence mechanism of cells when subjected to physiologically relevant changes in the environment. This mechanism gives the stressed cell added protection, thus, allowing for continued cell survival. However, high levels of thermodamage can lead to other type of reactions in the cell such as apoptosis or necrosis.

This work aims at assessing the induced laser heating effects on NG108 cells by studying the induction of apoptosis and necrosis on these cells. Furthermore, quantification of the local temperature increase in the focus of the optical trap with the back-focal-plane interferometry technique is also one of the main goals.

8097-75, Poster Session

Optical tweezers used to assess the effects of viscosity on sperm motility

N. Hyun, C. Chandsawangbhuwana, Q. Zhu, L. Z. Shi, C. Yang-Wong, Univ. of California, San Diego (United States); M. W. Berns, Univ. of California, San Diego (United States) and Beckman Laser Institute and Medical Clinic (United States)

The purpose of this study was to analyze sperm motility in a range of viscous media. Viscous media solutions were made by using varying concentration of methylcellulose yielding 3, 6, 9, and 15 centipoises. Motility parameters were collected using customized tracking software that measures the curvilinear velocity (VCL) and the escape force (Pesc) of an individual sperm. The Pesc was measured by using a 1064 nm Nd:YVO4 continuous wave laser that optically traps motile sperm at a maximum power of 450 mW in the focused trap spot. The VCL was measured frame by frame before trapping. Multiple experiments were performed to collect motility parameters in increasing viscosity media. To complement our motility data, sperm were labeled with the fluorescent dyes DiOC6(3) and JC-1 to measure mitochondria membrane potential located in the sperm's midpiece. Fluorescence was measured before and during trapping in to provide insight to the sperm energetics under various viscous conditions.

The preliminary results showed that there was a correlation between swimming speed (VCL) vs. viscosity and escape force (Pesc) vs. viscosity. The relationship between VCL and viscosity showed that there was a decreased VCL with increasing viscosity; however there was an increase in Pesc with increasing viscosity. There was no change in

Conference 8097:
Optical Trapping and Optical Micromanipulation VIII

fluorescent intensity between viscous media indicating that there was no change in sperm energetics. The results show that viscosity physically affects the mechanical motility properties of sperm rather than the sperm energetics.

8097-76, Poster Session

Measuring stall forces in vivo with optical tweezers through light momentum changes

J. Mas, A. Farré, C. López-Quesada, E. Martín-Badosa, M. Montes-Usategui, Univ. de Barcelona (Spain)

The stall forces of processive molecular motors have been widely studied in vitro. Even so, in vivo experiments are required for determining the actual performance of each molecular motor in its natural environment. We report the direct measurement of light momentum changes in single beam optical tweezers as a suitable technique for measuring forces inside living cells, where few alternatives exist. The simplicity of this method makes it convenient for measuring the forces involved in fast dynamic biological processes. We present our measurements of stalling events showing the pulling force of processive molecular motors inside living cells.

8097-77, Poster Session

Temporal evolution of thermocavitation bubbles using high speed video camera

J. P. Padilla-Martinez, J. C. Ramirez-San-Juan, Instituto Nacional de Astrofísica, Óptica y Electrónica (Mexico); G. Aguilar, Univ. of California, Riverside (United States); R. Ramos-Garcia, Instituto Nacional de Astrofísica, Óptica y Electrónica (Mexico)

Thermocavitation induced by CW low laser powers in highly-absorbing solution is new field of research that may have useful applications in lithography, micropatterning of metallic thin films and sonoporation among others. Thermocavitation bubbles are always in contact with the substrate due to the high absorption coefficient of the solution. The temporal evolution of these bubbles is quite complex as it has been already demonstrated in short pulsed-laser cavitation. In a previous work, we reported its temporal evolution using indirect methods; however details information cannot be obtained. In this work, a precise description of the bubble dynamics is achieved using a high speed video camera (Phantom V7, Version: 9.1) running to 111,111 frames per second of 64 × 64 pixels resolution. These videos give valuable information on the dynamics like bubble lifetime, maximum radius and collapse time as a function of laser power (62 to 200 mW) and beam waist. For a power laser of 150 mW (at the exit of the microscope objective) the bubble grows regularly without any significant modification of its half-hemisphere shape, reach its maximum radius (~1037 microns) in 180 micronseconds and then collapses rapidly in 135 micronseconds. Near the collapse, the bubble departs from its semi-spherical shape taking a step-like shape. Bubble's rebound is weak and not always is observed. The bubble's radius can be controlled with the beam waist, obtaining larger bubbles for larger beam waist.

8097-78, Poster Session

An optical manometer-on-a-chip

Y. Jin, K. Crozier, Harvard Univ. (United States)

We present a novel pressure-based approach combining optical trapping with microfluidics to investigate the properties of complex fluids in microscopic environments. In our device, termed a "manometer-on-a-chip", a shield structure divides a microfluidic channel into two parallel parts. In the center of the narrower 'side channel', a polystyrene bead is trapped by a traditional optical tweezer, whereas the wider 'main

channel' conveys fluids whose behavior we are interested in studying. Because parallel channels always share the same pressure drop when a flow is applied, the displacement of the bead in the 'side channel', which we monitor using a video camera, reflects the pressure variation over both channels. The pressure-displacement relation is calibrated by measuring the extension of a bead trapped in a test chip containing a channel with the same cross section as the 'side channel' of the actual device. This test chip is connected to an external pressure source. To demonstrate the device, we send oil droplets in water, generated by a T junction structure treated to be hydrophilic, through the manometer, and record the position of the bead trapped in the side channel. Our results illustrate that the device can detect single droplets and differentiate them based on size. The droplets are detected by monitoring the bead position with time. Comparison with calibration show that our device is sensitive enough to resolve a pressure variation below 0.1 Pa. We anticipate that our device will be useful for understanding the behavior of emulsions and multiphase flows.

8097-59, Session 13

Plasmonic nanopillar arrays for optical trapping, biosensing, and spectroscopy

A. E. Cetin, A. A. Yanik, Boston Univ. (United States); C. Yilmaz, S. Somu, A. A. Busnaina, Northeastern Univ. (United States); H. Altug, Boston Univ. (United States)

In this work, we propose a plasmonic platform based on monopole antenna arrays that can enable high sensitive biosensing, vibrational spectroscopy and high precision optical trapping at the same time. Perpendicular incident light is coupled to Surface Plasmon (SP) modes through the system. This is one of the significant advantageous over other sensing/trapping platforms based on angled illumination source. The tight localization of plasmonic excitation in nanopillar structure leads to narrow resonances in the spectrum. Hence, we achieve high refractive index sensitivity, ~675 nm/RIU with high figure of merit (FOM), ~112.5. This FOM value is higher than the preceding plasmonic structures based on the localized SP modes. SPs are localized at specific hot spots on the top surface of the gold nanopillars which lead large near-field intensities with enhancement factors of ~9000 highly desirable for surface Raman spectroscopy. The hot spots with high near-field enhancement depend on the polarization of the incident source. We also achieve high optical force, ~350 pN/W/μm², from these hot spots which allows optical trapping of nanoparticles with excitation source of low power. Since the location of the hot spots highly depends on the direction of polarization, we can always get the strongest directional force we can achieve from the system. Our proposed structure serves for optical trapping of bioparticles, spectroscopy measurement and real-time biodetection at the same platform which could attract many attentions from wide range of researches and studies.

8097-60, Session 13

Controlling and utilizing optical forces at the nanoscale with plasmonic antennas

A. Lovera, O. J. F. Martin, Ecole Polytechnique Fédérale de Lausanne (Switzerland)

Plasmonic dipole antennas are powerful optical devices for many applications since they combine a high field enhancement with outstanding tunability of their resonance frequency. The field enhancement, which is mainly localized inside the nanogap between both arms, is strong enough to generate attractive forces for trapping extremely small objects flowing nearby. Furthermore it dramatically enhances their Raman scattering cross-section generating SERS emission. In this talk, we demonstrate how plasmonic antennas provide unique means for bringing analyte directly into hot-spots by merely controlling the optical force generated by the plasmon resonance. This technique is very suitable for immobilizing objects smaller than the

Conference 8097:
Optical Trapping and Optical Micromanipulation VIII

diffraction limit and requires a very little power density. In this work, 20nm gold nanoparticles functionalized with Brilliant Cresyl Blue are trapped in the gap of nanoantennas fabricated with e-beam lithography on glass substrate. The entire system is integrated into a microfluidic chip with valves and pumps for driving the analyte. The field enhancement is generated by a near-IR laser ($\lambda=808\text{nm}$) that provides the trapping energy. It is focused on the sample through a total internal reflection (TIRF) objective in dark field configuration with a white light source. The scattered light is collected through the same objective and the spectrum of one single antenna spectrum is recorded and analyzed every second. A trapping event is characterized by a sudden red-shift of the antenna resonance. This way, it is possible to detect the trapping of extremely small objects. The SERS signal produced by a trapped analyte can then be studied by switching from the white light source to a second laser for Raman spectroscopy, while keeping the trapping laser on. The trapping and detection limit of this approach will be discussed in detail.

array of 4 μm holes was etched into the microfluidic devices gold surface using an amplified femtosecond pulse laser (Spitfire, Spectra Physics, 800 nm 1 kHz) and direct multiphoton etching using a 0.70 N.A. NIR objective lens. 15, 10, and 4.3 μm sized microspheres were placed in a sample of phosphorus buffer solution and pumped into the microfluidic chamber using a gravity pump system. The incident light illuminated the patterned region with the power being varied between 20 and 70 mW, both on the SPR angle and when the incident angle is de-turned by 4° off the resonance position. We've observed that via the patterning of the gold surface layer the trapping efficiency can be increased compared to the unpatterned case. We have also demonstrated that the number of trapped microspheres can be controlled by either changing the power of the incident light or by changing the size of the microspheres being trapped.

8097-61, Session 13

Holographic tweezers: a platform for plasmonics

M. Dienerowitz, G. M. Gibson, R. W. Bowman, A. Curran, M. J. Padgett, Univ. of Glasgow (United Kingdom)

Optical manipulation of metal nanoparticles has attracted a lot of interest over the past years yet it is still considered challenging¹⁻⁴. The nanoscale size of the particles as well as their enhanced absorption and reflectivity render them hard to control with standard trapping techniques. A well-known phenomenon from plasmonics is the strong interaction between adjacent plasmon resonances when excited by laser light. In the case of freely floating particles this results in a complex force mechanism displacing metal nanoparticles. It is possible to exploit the resonance to induce attractive as well as repulsive forces expanding the manipulation toolkit for metal nanoparticles⁵.

We present a nanoparticle workstation incorporating holographic tweezers to manipulate several trapped metal nanoparticles simultaneously. The versatility of the holographic tweezers and the submicron control of our sample stage allow precise particle positioning. In addition we assess each trapped particle by monitoring its specific spectral properties. By changing the distance between two trapped particles we monitor the interaction of their particle plasmons when brought close enough. This in situ monitoring of the changing plasmon resonances has provided new insights into plasmon coupling⁶. We focus particularly on nanoparticle imaging in our experiments and present a new darkfield microscopy technique which does not limit the numerical aperture of the trapping objective.

Metal nanoparticles have become popular tools for biological applications and enhanced spectroscopy techniques because of their biocompatibility. Improving the manipulation skills available and facilitate measurement techniques helps to advance the controllability of metal nanoparticles employing them as nanometric sensors and antennas.

8097-62, Session 13

Optical trapping in a microfluidic device via surface plasmon resonance on patterned hole arrays

S. Weber, D. J. Day, M. Gu, Swinburne Univ. of Technology (Australia)

The manipulation of polystyrene microspheres via the application of Surface Plasmon Resonance (SPR) based optical effects inside patterned and non-patterned microfluidic device was investigated. Using the Kretschmann geometry, light from a Nd:YAG laser ($\lambda = 1064 \text{ nm}$) is coupled into a $40 \pm 2 \text{ nm}$ gold film coated onto a glass slide, resting on a glass prism ($n = 1.785$) via an index matching liquid ($n = 1.516$). The SPR angle is calculated to occur at $63 \pm 1^\circ$ for an incident wavelength $\lambda = 1064 \text{ nm}$, this is confirmed via experimental observation. A $200 \times 200 \mu\text{m}$

8097-63, Session 13

Opto-mechanical force measurement of deep sub-wavelength plasmonic modes

J. Kohoutek, D. Dey, A. Bonakdar, A. Sklar, O. G. Memis, R. Gelfand, H. Mohseni, Northwestern Univ. (United States)

We show that the radiation force of a plasmonic antenna can be confined to an extremely small volume. We produce very high field intensities using compression of optical modes by orders of magnitude below their diffraction-limited volume using said antennae, and show significant radiation forces produced by these plasmonic modes. As a source we use a room temperature operated quantum cascade laser (QCL) working in the mid-infrared region of the optical spectrum as well as a commercially available fiber coupled laser operating at 1550 nm. We have used a finite-difference time domain method to simulate the plasmonic antenna to find the optimal resonance conditions, as well as the radiation force map computed by stress tensor method. We have then used electron beam evaporation and focused ion beam milling to fabricate the plasmonic antenna on the facet of the lasers. In parallel, we have developed a method capable of mapping the force with high sensitivity and nanometer spatial resolution, over the device. We have also used a lock-in to get the phase signal from the AFM in non-contact mode. We show that an external force can cause a change in phase of the AFM tip. We will compare our measured data with our FDTD simulation results. The ultra-small mode volume can make it possible in the future to move small objects with a relatively large force. These results also demonstrate the feasibility of novel opto-mechanical devices, such as switches and modulators, at very high speed.

Conference 8098: Physical Chemistry of Interfaces and Nanomaterials X

Sunday–Tuesday 21–23 August 2011 • Part of Proceedings of SPIE Vol. 8098
Physical Chemistry of Interfaces and Nanomaterials X

8098-01, Session 1

Ultrafast single and multiple electron transfer from quantum dots

T. T. Lian, Emory Univ. (United States)

Charge transfer to and from quantum dots (QDs) is of intense interest because of its important roles in QD-based devices, such as solar cells and light emitting diodes. Recent reports of multiple exciton generation (MEG) by one absorbed photon in some QDs offer an exciting new approach to improve the efficiency of QD-based solar cells and to design novel multi-electron/hole photocatalysts. However, two main challenges remain. First, the efficiency of MEG process needs to be significantly improved for practical applications. Second, the utilization of the MEG process requires ultrafast exciton dissociation prior to the exciton-exciton annihilation process, which occurs on the 10s to 100s ps time scale. In this presentation we report a series of studies of exciton dissociation dynamics in quantum dots by electron transfer to adsorbed electron acceptors. We show that excitons in CdSe and PbS QDs can be dissociated on the picosecond timescale to various adsorbates. As a proof of principle, we demonstrate that multiple excitons per QD (generated by multiple photons) can be transferred to adsorbed acceptors (J. Am. Chem. Soc. 2010, 132, 4858-4864). We will discuss the dependence of the electron transfer rates on the size and the nature of the quantum dots and possible approaches to optimize the multiple exciton dissociation efficiency.

8098-02, Session 1

Interfacial electron transfer in colloidal nanocrystals.

M. Jones, D. Woodall, S. Johnson, E. Williams, A. K. Tobias, Jr., K. J. Major, D. Woolford, The Univ. of North Carolina at Charlotte (United States)

Quantum confinement of photo-generated electrons and holes in colloidal semiconductor nanoparticles is well understood and results in a wide array of potentially important properties. Application of nanocrystals in photovoltaics requires rapid and efficient generation of separated charges, which must be transported away from the chromophore to do useful work. These charge separation processes originate from highly delocalized exciton states and can be understood in terms of electron transfer reactions that can localize an electron or hole into a ligand orbital or a nanocrystal trap state.

Electronic coupling of nanocrystal exciton states with states in the surrounding environment strongly influences relaxation dynamics. Nanocrystal charge transfer states typically have low absorption cross-sections, so it is hard to directly probe their role and relative impact on the underlying dynamics. Time resolved fluorescence spectroscopy reflects both radiative exciton recombination rates and non-radiative transitions rates to extrinsic surface or ligand states; however, interpretation of fluorescence transients is not trivial and typical multi- or stretched exponential decay models yield little specific photophysical insight.

I will describe a quantitative analysis method for temperature-dependent time-resolved fluorescence data applied to a series of nanocrystal systems and demonstrate how these data can be used to understand electron transfer dynamics. In addition I will present data obtained using a pulse-rate modulation technique with which we are able to unravel the contribution to these electron transfer dynamics from multi-exciton states. General features of charge transfer reactions are emerging from these analyses, which will be discussed in the context of future photovoltaic materials.

8098-03, Session 1

Nonlinear infrared spectroscopy of interface

W. Xiong, Univ. of Wisconsin-Madison (United States)

In this talk, I am going to cover two topics. First I will discuss our discovery of multiple conformations of Re dyes on nanocrystalline TiO₂ film and the different charge transfer mechanisms we observed using 2D IR spectroscopy. Secondly, I will show some results of our recently developed heterodyned time domain SFG spectroscopy. It is a technique with higher sensitivity and better resolution and lineshape fidelity than the popular broadband frequency domain SFG technique. These improvements are critical for measuring spectra of non-compact, low surface coverage and disordered surfaces such as the dye-TiO₂ interface.

Charge transfer across interfaces is an important step in many solar energy capture devices, such as dye-sensitized solar cells. Since the charge transfer happens right at the interface, the conformation of the molecules on the surface play a key role on their charge transfer behavior. Using 2D IR spectroscopy we found that there are at least three conformations of the dye molecules on the TiO₂ nanoparticle surface. Further, using a transient 2D IR pulse sequence which can correlate the ground and excited electronic states of the dye, we showed that all three conformations participate in the charge transfer process but one of the conformations has a completely different charge transfer pathway. Further research will include monitoring the electron transfer dynamics of each conformation and determining the dye orientations using Sum Frequency Generation Spectroscopy (SFG), which is related to the second topic of my talk.

SFG is an interface specific second order infrared spectroscopy. One of its advantages is the ability to measure the dipole orientation relative to the surface. In the second half of my talk, I will discuss our newly developed heterodyned time domain SFG spectroscopy technique. It is a Fourier transform based technique that has better resolution and lineshape fidelity than the popular broadband frequency domain SFG spectroscopy. Moreover, heterodyned detection significantly improves the sensitivity and also allows a much more intuitive interpretation of the spectra by acquiring the real and imaginary part of it, which is not available using the homodyned detection method. Using heterodyned time domain SFG, we showed there is an inhomogenous binding distribution of a simple aryl diisocyanide molecule on the gold surface, and this result agrees well with recent theoretical work. The sensitivity, resolution, and lineshape improvements using the heterodyned time domain SFG spectroscopy are critical for applying SFG on a non-compact, low surface coverage, and disordered monolayer surface such as the dye-TiO₂ surface in our charge transfer study.

Reference:

1. W. Xiong, J. E. Laaser, P. Paoprasert, R. Franking, R. J. Hamers, P. Gopalan, and M. T. Zanni, "Transient 2D IR spectroscopy of charge injection in dye-sensitized nanocrystalline thin films," J. Am. Chem. Soc., 131, 18040 (2010).
2. J. E. Laaser, W. Xiong, and M. T. Zanni, "Time-Domain SFG Spectroscopy Using Mid-IR Pulse Shaping: Practical and Intrinsic Advantages," J.Phys.Chem,B, ASAP

8098-04, Session 1

AC conductivity of nanoporous metal-oxide photoanodes for solar energy conversion

S. J. Konezny, V. S. Batista, Yale Univ. (United States)

The temperature- and frequency-dependent ac conductivity of nanoporous metal-oxide semiconductors commonly used in technologies for solar photoconversion is analyzed using a model based on

fluctuation-induced tunneling conduction (FITC). The model takes into account the potential barriers at the regions of nanoparticle contact that limit electron transport. In contrast to previous models, quantitative agreement is found with the FITC model with a single set of parameters over the entire temperature range studied. Guidelines for the design of new materials for dye-sensitized solar cells and solar photocatalysis are discussed.

8098-05, Session 2

Calculations of interface states between two polymers: polythiophene and polyselenophene

M. Côté, Univ. de Montréal (Canada)

Organic photovoltaic devices are presently the subject of intense research since they could eventually propose solar energy solutions at a much reduced cost compared to inorganic devices. Presently, electron transport in organic photovoltaic devices is achieved with a fullerene derivative (PCBM) but this solution has some disadvantages. First, the ratio of PCBM to polymer has to be quite high to assume good electronic transport, and second, the relatively high cost of PCBM is not ideal with the goal to reduce the cost of the device. For these reasons, a replacement for PCBM is desirable and an all polymer device solution is viewed as the best avenue. Since polythiophene (P3HT) is ideal for hole transport, its isovalent polyselenophene (P3HS) where sulfur atoms are replaced with selenium atoms might offer an interesting alternative to PCBM. The physical processes in organic devices are quite different from those of inorganic devices. Charge separation in organic devices is achieved by forming an interface between two organic materials with type 2 level alignment. However, because of the large binding energies observed in organic compounds, there is often the presence of H-aggregate states at the junction between the two organic materials. In this presentation, we will report the results of interface states in a blend of polythiophene and polyselenophene. Photoluminescence spectra will be presented along with calculations of these states with the help of the time-dependent density-functional theory.

8098-06, Session 2

Use of nucleating agents for microstructure manipulation of organic photovoltaic blends

N. Stingelin-Stutzmann, Imperial College London (United Kingdom) and ETH Zurich (Switzerland) and Freiburg Institute for Advanced Studies (Germany); J. Nekuda-Malik, Imperial College London (United Kingdom); P. Smith, ETH Zurich (Switzerland)

Poly(3-hexylthiophene) (P3HT) / phenyl-C60-butyric acid methyl ester (PCBM) bulk heterojunction (BHJ) blends are a promising organic photovoltaic system. However, lack of understanding of relevant fundamental relationships between the nano- and microstructure of the blend and electronic processes is hampering further improvement in device performance, and renders straight-forward implementation of even the most simple fabrication protocols to other BHJ binaries challenging. The origin of this complexity is the fact that P3HT/PCBM active photovoltaic layers, as well as many other BHJ systems, consist of a multiphase architecture comprising: 1) phase-separated crystalline P3HT and crystalline PCBM phase regions, and 2) a highly intermixed P3HT/PCBM amorphous phase. While it is well known that charge separation in these structures occurs at the interface between the P3HT donor and PCBM acceptor material, to date, it is unclear at which boundaries (crystalline or amorphous) this process predominantly takes place. We present use of well known clarifiers for the bulk commodity polymer isotactic polypropylene (i-PP), including 1,3:2,4-bis(3,4-dimethyl benzylidene) sorbitol (DMDBS) and an alkyl-substituted 1,3,5-benzenetrisamide, to nucleate P3HT. This nucleation process allows us to modify and control the size of the crystalline regions in P3HT/PCBM blends in an attempt to elucidate the primary region

of charge separation. Details of the methods used to manipulate the P3HT/PCBM blend microstructure will be discussed and the correlation between microstructural changes and device characteristics will be presented.

8098-07, Session 2

Ultrafast kinetics in polycrystalline pentacene: Exciton fission

M. W. B. Wilson, A. Rao, Univ. of Cambridge (United Kingdom); R. S. S. Kumar, Istituto Italiano di Tecnologia (Italy); D. Brida, G. Cerullo, Politecnico di Milano (Italy); R. H. Friend, Univ. of Cambridge (United Kingdom)

We report the use of ultrafast transient absorption spectroscopy with sub-20 fs time resolution to directly probe the process of exciton fission in polycrystalline thin films of pentacene. We observe that the overwhelming majority of initially photogenerated singlet excitons evolve into triplet excitons on an ~80 fs timescale independent of the excitation wavelength. This implies that exciton fission occurs at a rate comparable to phonon-mediated exciton localization processes, and may proceed directly from an initial delocalized state. The singlet population is identified due to the brief presence of stimulated emission, which is emitted at wavelengths which vary with the photon energy of the excitation pulse, a violation of Kasha's Rule that confirms that the lowest-lying singlet state is extremely short-lived. This direct demonstration that triplet generation is both rapid and efficient establishes multiple exciton generation by exciton fission as an attractive route to increased efficiency in organic solar cells. However, these results bear significantly on the task of realizing such a solar cell, as it would appear necessary to ensure the formation of ordered molecular aggregates that can support delocalized excitations, as opposed to simply including pentacene moieties in a disordered system.

8098-08, Session 2

On the correlation between structure, morphology, and charge transport in organic molecular films: the tetracene case

G. Tarabella, Consiglio Nazionale delle Ricerche (Italy); L. Lutterotti, Univ. di Trento (Italy); S. Bertolazzi, J. Wuensche, Ecole Polytechnique de Montréal (Canada); N. Coppédé, S. Iannotta, F. Cicoira, Consiglio Nazionale delle Ricerche (Italy); C. Santato, Ecole Polytechnique de Montréal (Canada)

Dielectric surface engineering is a tool to control organic molecular semiconducting films' morphology and structure, which in turn play a pivotal role in establishing films' functional properties.

We report an extended correlation between films morphology, studied by Atomic Force Microscopy, structure, investigated by Grazing Incidence X-ray diffraction (GIXRD), and charge carrier transport in Field Effect Transistor configuration for tetracene films vacuum sublimed on six different dielectric substrates, namely bare SiO₂ (reference substrate), OTS, HMDS, parylene C, polystyrene and PMMA. Tetracene is a model molecule exhibiting good charge transport and electroluminescence, attractive for applications such as Light Emitting Transistors. Films on polystyrene showed a mobility of 2·10⁻¹ cm²V⁻¹s⁻¹, the highest reported up to now for tetracene. Films on polystyrene showed the earliest complete substrate surface coverage: at 10 nm of nominal thickness tetracene islands appeared tightly packed and well interconnected.

GIXRD patterns, collected at different grazing incident angles in reflection mode, were analyzed using the Maud software, based on the Rietveld method extended to gain an unprecedented insight on the texture, phases amount, crystallites sizes and r.m.s. microstrains. Two different tetracene phases were identified: the beta phase showed a longer c axis with respect to the alpha one. A strong fiber texture perpendicular to the

Conference 8098:
Physical Chemistry of Interfaces and Nanomaterials X

sample surface was observed for both phases. Tetracene films grown on polystyrene showed the highest amount of alpha phase and the strongest grain alignment, in agreement with the highest mobility measured.

Herz, and R. J. Nicholas, *Nano Lett.* 11, 66 (2011).
[2] P. Tiwana, P. Parkinson, M. B. Johnston, H. J. Snaith, and L. M. Herz, *J. Phys. Chem. C* 114, 1365-1371 (2010).

8098-10, Session 3

Charge transport and recombination in organic solar cells

R. A. Street, Palo Alto Research Center, Inc. (United States)

Organic solar cells have reached about 8% efficiency, but need to be more efficient to compete with other materials. An understanding of the losses of organic bulk heterojunction solar cells requires knowledge of how the heterojunction interface influences the electronic transport and recombination mechanisms. We describe how transient photoconductivity measurements and the cell spectral response provide information about the carrier mobility, recombination mechanisms and the electronic structure. We find that geminate recombination is not a dominant recombination process in P3HT:PCBM or PCDTBT:PCBM cells. Instead, there is good evidence that recombination through interface traps is important. The measurements of the electronic structure show band tail effects attributed to the material disorder. The band tails contribute to suppressing geminate recombination and allowing trap recombination. The role of the interface on the electronic structure and the electronic properties will be discussed.

8098-11, Session 3

Charge generation dynamics at nano-scale interfaces in all-organic and hybrid materials

L. M. Herz, Univ. of Oxford (United Kingdom)

Conjugated polymers and molecules are increasingly used as cheap artificial light-harvesting materials in photovoltaic devices. The large exciton binding energy in these systems necessitates the use of blends comprising at least two materials at whose interface a type-II heterojunction is formed, thus making charge separation energetically favourable.

Examples of all-organic materials are blends of conjugated polymers with single-walled carbon nanotubes (SWNTs) with the latter promising large electron mobilities and percolation paths. We have investigated the charge photogeneration dynamics at the interface formed between SWNTs and poly(3-hexylthiophene) (P3HT) using a combination of femtosecond spectroscopic techniques [1]. We demonstrate that photoexcitation of P3HT forming a single molecular layer around a SWNT leads to an ultrafast (430 fs) charge transfer between the materials. The addition of excess P3HT leads to long-term charge separation in which free polarons remain separated at room temperature. Our results suggest that SWNT-P3HT blends incorporating only small fractions (1%) of SWNTs allow photon-to-charge conversion with efficiencies comparable to those for conventional (60:40) P3HT–fullerene blends, provided that small-diameter tubes are individually embedded in the P3HT matrix.

In addition, hybrid interfaces comprising organic dyes as sensitizer monolayers on metal-oxide mesostructures films have been highly successful when implemented in so-called dye-sensitized solar cells (DSSCs). We have used optical-pump terahertz-probe spectroscopy to explore the photoinduced conductivity dynamics in such mesoporous metal-oxide films [2]. We extract early-time mobility values and compare these to bulk values in order to determine factors limiting electron movement in these systems. In addition, we have utilized terahertz spectroscopy to investigate the influence of surface treatments for the metal oxide on early-time charge dynamics. For example, surface treatment of the mesoporous TiO₂ with TiCl₄ has been found to be critical to enable efficient operation of DSSCs. However, we find that neither early-time charge mobility nor charge injection rate or decay times are significantly affected by the treatment, which suggests that it may, instead, have an impact on phenomena occurring on longer time scales.

[1] S. D. Stranks, C. Weisspfenning, P. Parkinson, M. B. Johnston, L. M.

8098-30, Session 3

Giant pseudo-magnetic fields in graphene nanobubbles: locally probing graphene nanostructures with STM and STS

S. A. Burke, The Univ. of British Columbia (Canada); N. Levy, National Institute of Standards and Technology (United States); K. Meaker, M. Panlasigui, A. Zettl, Univ. of California, Berkeley (United States); F. Guinea, Instituto de Ciencia de Materiales de Madrid (Spain); A. H. Castro Neto, Boston Univ. (United States); M. Crommie, Univ. of California, Berkeley (United States)

Recent calculations have predicted that the relativistic charge carriers in strained graphene may behave as if under the influence of an applied magnetic field. This effect, dubbed a “pseudo-magnetic field” since no real magnetic field is present, arises from the special electronic structure of graphene as well as its honeycomb lattice. If the strain corresponds to a triangular geometry, then the strain-induced pseudo-magnetic field is nearly uniform, should give rise to a Quantum Hall Effect. This unusual effect requires the generation of large, non-uniform strains in a specific geometry, making its observation elusive.

The growth of graphene on Pt(111) generates nanoscale bubbles that incorporate strains of ~10% in a three-fold symmetric geometry. These “graphene nanobubbles” appear to arise from the differential thermal contraction between the graphene layer and the Pt(111) substrate when cooling from the growth temperature (1200K) to the measurement temperature (~7K). I will describe our recent low-temperature scanning tunnelling microscopy measurements of the graphene nanobubbles grown under strictly controlled ultrahigh vacuum conditions. Scanning tunnelling spectroscopy measurements, which can be used to locally probe the electronic structure at surfaces, exhibited sequences of peaks that can be attributed to Landau levels arising from strain-induced pseudo-magnetic fields of over 300 Tesla. The observation of such enormous strain-induced pseudo-magnetic fields opens the door for “strain-tronics” or “strain engineering” of the graphene band structure even at room temperature energy scales, as well as the study of charge carriers in extreme magnetic field regimes.

8098-12, Session 4

Modifying the fluorescence properties and determining the quantum yield of a single molecule with a tunable optical subwavelength microcavity

A. I. Chizhik, A. M. Chizhik, D. Khoptyar, S. Bär, Eberhard Karls Univ. Tübingen (Germany); J. Enderlein, Georg-August- Univ. Göttingen (Germany); A. J. Meixner, Eberhard Karls Univ. Tübingen (Germany)

We present experimental and theoretical results on changing the fluorescence emission spectrum of a single molecule by embedding it within a tunable planar microcavity with subwavelength spacing [1]. The cavity length is changed with nanometer precision by using a piezoelectric actuator. By varying its length, the local mode structure of the electromagnetic field is changed together with the radiative coupling of the emitting molecule to the field. Because mode structure and coupling are both frequency dependent, this leads to a renormalization of the emission spectrum of the molecule. We develop a theoretical model for these spectral changes and find excellent agreement between theoretical prediction and experimental results.

We also demonstrate controlled modulation of the radiative transition rate

Conference 8098:
Physical Chemistry of Interfaces and Nanomaterials X

of a single molecule, which is measured by monitoring its fluorescence lifetime [2]. By comparing the experimental data with a theoretical model, we extract both the pure radiative transition rate as well as the quantum yield of individual molecules. We observe a broad scattering of quantum yield values from molecule to molecule, which reflects the strong variation of the local interaction of the observed molecules with their host environment.

Our technique can be applied to any single quantum emitter of interest, such as dye molecules, semiconductor nanoparticles, carbon nanotubes, etc. Thus, the tunable cavity method makes it a versatile tool for single molecule spectroscopy and quantum yield measurements of individual quantum emitters.

[1] Chizhik, A. I.; Schleifenbaum, F.; Gutbrod, R.; Chizhik, A. M.; Khoptyar, D.; Meixner, A. J.; Enderlein, J. *Phys. Rev. Lett.* 2009, 102, 073002-1.

[2] Chizhik, A. I.; Chizhik, A. M.; Khoptyar, D.; Bär, S.; Meixner, A. J.; Enderlein, J. *Nano Lett.* 2011, accepted.

8098-13, Session 4

Electric-field dependent spectroscopy of single nanocrystal systems

S. Johnson, A. K. Tobias, Jr., E. Williams, M. Jones, P. Moyer, The Univ. of North Carolina at Charlotte (United States)

The most common explanation of spectral diffusion and fluorescence intermittency in nanocrystals (NCs) is biexciton annihilation via an Auger ionization process. In this charge-separated state, one electron or hole carrier is trapped on or near the surface while the other remains in the core. The effect of the electric field generated by this charge-separated state has been implicated in a number of studies as the cause of observed dynamics, but remains scarcely explored. The spectra of single CdSe/ZnS nanocrystals at low temperature have shown random spectral diffusion up to tens of meV. Similar shifts were induced under the presence of an applied electric field. This relation suggests that local electric fields could be responsible for spectral phenomena. More recent work shows an electric field effect on blinking and the photoluminescence quantum yield, which suggests modulation of surface trap sites with applied field.

We have designed experiments to explore the complex role of surface states in carrier dynamics. CdSe nanocrystals, with a variety of shells and surface ligands, were patterned onto a glass-mounted interdigitated gold electrode using electron beam evaporation. A modulated electric field was applied using a function generator. Using our homebuilt confocal microscope, we were able to locate individual nanocrystals, and simultaneously collect fluorescence trajectories, lifetimes, and spectra. I will discuss the analysis of these data from which we obtained field-dependent dynamic information about a range of nanocrystal systems. These experimental results and modeling of the charge transfer and relaxation dynamics of confined excitons will advance nanostructure applications.

8098-14, Session 4

Conformation and interactions in single polythiophene polymer chains

D. A. Vanden Bout, T. Adachi, J. Brazard, R. J. Ono, G. Lakhwani, M. C. Traub, J. C. Bolinger, P. F. Barbara, C. W. Bielawski, The Univ. of Texas at Austin (United States)

Morphology of conjugated polymer films is one of the most important parameters determining physical, electrical and optical properties that are crucial for many types of device application including organic solar cells. Although major obstacle for morphological research of these materials is their complexity and heterogeneity, single molecule spectroscopy enables us to simplify the system and make it tractable. Various experiments examined the conformation of polythiophene (P3HT) chains utilizing polarization modulation spectroscopy. Both the

excitation and emission anisotropy are examined to directly probe energy transfer to emitting sites along the chains. The measurements show that regioregularity of the polymer side chains has a profound effect on the ordering of the polymer chain even at the single molecule level. Studies will also be presented that examine interchain interactions utilizing model tri-block copolymer which consist of two P3HT chains connected by either a flexible or rigid linker

8098-15, Session 4

Imaging of photoinduced tautomerism in single porphyrin molecules

R. Jäger, A. M. Chizhik, A. I. Chizhik, S. Bär, H. Mack, A. Lyubimtsev, M. Hanack, A. J. Meixner, Eberhard Karls Univ. Tübingen (Germany)

Porphyrins play an important role in nature, e.g. as chlorophyll in photosynthesis. To understand how these processes work and could be imitated, first the basic structures and properties of the porphyrin-molecules have to be understood. Metal-free porphyrins serve as a very important model system in theoretical chemistry to improve computational methods and help to develop such efficient energetic processes as they occur in nature. Although tautomerization has been studied for decades, it is still difficult to say what happens within one single molecule undergoing this basic process. When the tautomers are chemically equivalent, such as is the case for porphyrins and similar symmetric molecules, few experimental methods can be employed for studying ground-state and especially photoinduced tautomerism.

Using the technique of optical imaging combined with cylindrical vector beams, we can determine the 3D-orientation of the excitation transition dipole moment (TDM) of single molecules. [1] As the TDM-orientation changes when the molecule converts from one trans-tautomer into another, we can distinguish between both of them. Recently we were able to visualize the conversion of one single molecule between its trans-forms. [2] Our method allows us to get a closer insight into the photoinduced tautomerism and the difference to the ground-state-process. By varying the substituents of the molecules, its environment and the excitation-wavelength, we are able to reveal new fundamental details of the excited-state tautomerization in single molecules.

[1] S. Bär et al., *Anal. Bioanal. Chem.*, 2010, 396, 3-14.

[2] A. M. Chizhik et al., *Phys. Chem. Chem. Phys.*, 2011, 13, 1722-1733.

8098-16, Session 4

Imaging the transition dipole moment for single CdSe/ZnS quantum dots and SiO₂ nanoparticles

A. M. Chizhik, A. I. Chizhik, Eberhard Karls Univ. Tübingen (Germany); T. Schmidt, F. Huisken, Friedrich-Schiller-Univ. Jena (Germany); A. J. Meixner, Eberhard Karls Univ. Tübingen (Germany)

We study the dimensionality, orientation and dynamical effects of the excitation-transition dipole moment for single CdSe/ZnS core-shell nanocrystals [1] and SiO₂ nanoparticles [2]. Using an argon ion laser at 488 nm with higher-order laser modes (azimuthally and radially polarized laser modes) for excitation, the three-dimensional orientation of the nanoparticles' transition dipole moment was investigated in a confocal microscope. The comparison of measured and simulated single nanocrystal excitation patterns shows that single CdSe/ZnS quantum dots possess a spherically degenerated excitation-transition dipole. We show that the dimensionality of the excitation-transition dipole moment distribution is the same for all individual CdSe/ZnS nanocrystals, disregarding the difference in core size and irrespective of variations in the local environment. In contrast to the emission-transition dipole moment, which is oriented in one plane, the excitation-transition dipole moment of a single CdSe/ZnS quantum dots possesses an isotropy in

Conference 8098:
Physical Chemistry of Interfaces and Nanomaterials X

three dimensions.

SiO₂ nanoparticles exhibiting strong red-orange photoluminescence were obtained by full oxidation in water of the silicon nanopowder synthesized by CO₂ laser pyrolysis of SiH₄. Samples of SiO₂ NPs embedded in low concentration in a thin polymer layer were prepared by spin-coating a dedicated solution on glass cover slides. The linear transition dipole moment was found to be rather stable and randomly oriented. However, dynamical effects such as fluorescence intermittency and transition dipole moment flipping could also be observed.

[1] Chizhik, A. I.; Chizhik, A. M.; Khoptyar, D.; Bär, S.; Meixner, A. J. *Nano Lett.* 2011, DOI: 10.1021/nl1040385.

[2] Chizhik, A. M.; Chizhik, A. I.; Gutbrod, R.; Meixner, A. J.; Schmidt, T.; Sommerfeld, J.; Huisken, F. *Nano Lett.* 2009, 9, 3239.

8098-17, Session 5

The nature of bound charge pairs at donor-acceptor interfaces

G. D. Scholes, Univ. of Toronto (Canada); G. Rumbles, National Renewable Energy Lab. (United States)

The primary product of exciton photodissociation at a donor-acceptor interface is a bound charge pair, known by various names including bound radical pair, polaron pair, exciplex, etc. The microscopic nature and properties of these species will be discussed and defined. Organic and inorganic heterostructures will be compared. We will ask whether a deeper understanding of bound charge pairs suggests new designs for organic photovoltaics.

8098-18, Session 5

Charge transfer processes at intra- and intermolecular heterojunctions

E. Da Como, Ludwig-Maximilians-Univ. München (Germany)

Photoinduced charge transfer is the primary process in photovoltaics. Here we probe the first steps of charge separation in a series of low-bandgap donor-acceptor copolymers by femtosecond infrared pump-probe spectroscopy. The results are discussed considering the donor acceptor strength of the units within the chain and how this influences the yield of polaron generation. In the second part we will combine the pump-probe experiments with time resolved luminescence to study charge separation at polymer/fullerene intermolecular heterojunctions. Upon doping of the conjugated polymer we report reduced recombination via charge transfer excitons and enhanced polaron formation.

8098-19, Session 5

Beyond the adiabatic limit: charge separation in organic photovoltaic materials

J. B. Asbury, R. D. Pensack, The Pennsylvania State Univ. (United States)

The dynamics of charge separation in photovoltaic polymer blends following photoinduced electron transfer from the conjugated polymer, CN-MEH-PPV, to the electron accepting functionalized fullerene, PCBM, are observed with ultrafast vibrational spectroscopy. The investigators take advantage of a solvatochromic shift of the vibrational frequency of the carbonyl (C=O) stretch of PCBM to directly measure the rate of escape of electrons from their Coulombically bound charge transfer (CT) excitons at donor/acceptor interfaces on ultrafast time scales. The data reveal that the rate of dissociation of CT excitons is temperature independent from 200 to 350 K indicating that excess energy in hot CT excitons plays an important role in mediating charge separation. These

observations suggest that conceptual and theoretical descriptions properly taking into account the strong coupling of electronic and nuclear degrees of freedom in organic semiconductors are essential to understand the mechanism of charge separation in organic photovoltaic materials. From a practical stand-point, efforts to develop new low band-gap polymers for organic solar cells should target electron donor and acceptor pairs capable of advantageously redistributing excess energy in hot CT excitons to enable efficient charge separation with minimal donor-acceptor energy level offsets.

8098-20, Session 5

Charge-transfer excitons at semiconductor polymer heterojunctions in efficient organic photovoltaic diodes

F. Provencher, C. Silva, Univ. de Montréal (Canada)

In organic photovoltaic (OPV) diodes based on blends of semiconductor polymers and fullerene derivatives, singlet intrachain excitons on the polymer created by the absorption of light dissociate into geminate polaron pairs (GPP) at the heterojunction. These are bound by a Coulomb potential, so they must then dissociate endothermally to form photocarriers. Alternatively, GPP can relax to form charge transfer excitons (CTX), where the electron and the hole sit on different molecules but are coulombically bound to form excitonic states across the interface. Since CTX can limit the internal quantum efficiency as well as the open-circuit voltage of OPV cells, our focus is to unravel the dynamics of branching from GPP to CTX, and subsequent recombination processes to re-generate intrachain singlet excitons in an efficient OPV blend.

A careful temperature-dependent study of combined spectroscopic methods of time-resolved photoluminescence, transient absorption and quasi-steady-state photoinduced absorption unravels the dynamics of those species on timescales ranging from picoseconds to milliseconds in films of polycarbazole/fullerene derivative blend (PCDTBT/PC70BM).

We find that GPP are precursors to photocarriers and act as a dark reservoir that feeds the CTX. At low temperature, the GPP are easily trapped and they feed the CTX via tunneling, but not the free photocarriers (polarons). At room temperature, the GPP overcome the Coulomb barrier and dissociate more easily into free polarons.

8098-21, Session 6

Excitonic charge separation at organic semiconductor interfaces

X. Zhu, The Univ. of Texas at Austin (United States)

Solar photovoltaics based on organic semiconductors commonly involve excitons. This results from strong Coulomb attraction between an electron and a hole due to the low dielectric constants of molecular materials. In this lecture, I will address the question of how excitons form, relax, multiple, and dissociate in organic semiconductor materials and at their interfaces. My group uses two experimental techniques to probe interfacial exciton dynamics: time-resolved two-photon photoemission spectroscopy (TR-2PPE) and time-resolved electric field induced second harmonic generation (TR-EFISH). The TR-2PPE technique tracks the electron in time and energy domains at it is initially excited, and as it relaxes, multiplies, and transfers. The complementary TR-EFISH technique monitors the transient electric field formed from exciton dissociation and charge separation at the interface. A particularly exciting aspect is the possibility of harvesting these excitons in dynamic time windows that may allow us to design solar cells with efficiency exceeding the so-called Shockley-Queisser limit, which is the thermodynamic limit of conventional solar cells.

8098-22, Session 6

Photogenerated charges in neat poly(3-hexylthiophene) films

G. Rumbles, National Renewable Energy Lab. (United States) and Univ. of Colorado, Boulder (United States); O. Reid, N. Kopidakis, National Renewable Energy Lab. (United States); N. Stingelin-Stutzmann, Imperial College London (United Kingdom); J. Nekuda-Malik, London Ctr. for Nanotechnology (United Kingdom); G. Latini, Consiglio Nazionale delle Ricerche (Italy); C. Silva, Univ. de Montréal (Canada)

The nature of the primary photoexcitation in conjugated polymers has been a subject of interest for a number of years, and two models have emerged: neutral excitons and free charge carriers. While excitons are recognized as the dominant of the two species, there are a small fraction of carriers that appear directly upon photoexcitation that have been detected experimentally either spectroscopically or through conductivity measurements. The fraction of near-instantaneous free charge carriers produced depends both on the chemical structure of the polymer and on the time-scale on which the study is performed. For example, poly(3-hexylthiophene) (P3HT) thin films have been reported to have free carrier yields as high as 15% , when measured on a fast time scale, but as low as 3% when measured on a slow time scale. It is unclear why these numbers are so different, and from where these carriers originate.

This presentation will report studies using flash photolysis, time-resolved microwave conductivity (fp-TRMC) to probe carriers produced in a number of thin films of P3HT of differing molecular weights. By correlating the free carrier yield with the solid-state microstructure of the polymer, and the corresponding electronic absorption spectra, we will propose a model that explains the origins of these carriers.

8098-23, Session 6

The mechanism of ultrafast exciton dissociation in neat regioregular poly(3-hexylthiophene)

G. Latini, Istituto Italiano di Tecnologia (Italy); F. Paquin, P. Karsenti, M. Sakowicz, Univ. de Montréal (Canada); N. Stingelin-Stutzmann, Imperial College London (United Kingdom); C. Silva, Univ. de Montréal (Canada)

Semiconductor polymer films with high molecular order display high apparent intrinsic charge photogeneration yields by a mechanism that has not been unravelled by contemporary literature. We address charge photogeneration dynamics in neat regioregular poly(3-hexylthiophene) by means of transient photoluminescence (PL) and absorption spectroscopies at 10 K. Charges are generated over ultrafast timescales, but furthermore over timescales that compete with the exciton lifetime (~1 ns) by a mechanism that excludes diffusion-limited exciton dissociation. They recombine with distributed rates that lead to delayed PL over microsecond timescales, accounting for >12% of the time-integrated emission intensity in the studied 1m microstructure. By analyzing the spectral bands of delayed PL, we conclude that charges recombine primarily at interfaces between photophysical aggregates comprised of lamellar polymer stacks and electronically uncoupled chains. This highlights the extrinsic role of boundaries between domains of contrasting microstructure in charge photogeneration processes in this important class of materials.

8098-24, Session 6

Ultrafast conformational readjustment through non-adiabatic state crossings in oligofluorenes

J. Clark, Univ. of Cambridge (United Kingdom); G. Lanzani, IIT@POLIMI, Milano (Italy) and Politecnico di Milano (Italy); S. Tretiak, Los Alamos National Lab. (United States)

A molecule's conformation in terms of whether it is twisted, planar or bent reflects a complex equilibrium resulting from thermodynamic, nuclear and electronic degrees of freedom. Changing electronic state (by absorption, for example) can dramatically alter the conformational minima of the multidimensional potential energy surface (PES). Readjustment to the new equilibrium position generally occurs on the 10-100 ps time scale, depending on the involved vibrational mode frequencies and the dissipation paths. This relaxation can be thought of in the classical picture as a damped oscillator.

Here, we apply an ultrafast pump-push-probe experiment and advanced computational techniques to investigate energy relaxation in oligofluorenes in solution. Results suggest direct observation in the time domain of ultrafast photoinduced planarization of oligofluorenes via internal conversion through non-adiabatic state crossings. By studying dynamic shifts in the stimulated emission band, we observe that conformational relaxation (planarization) in the first excited state (S1) takes place - as expected - on the 10s of picosecond time-scale. This conformational relaxation time is reduced by over two orders of magnitude when exciting a higher-lying (Ag) state as the wavepacket arrives at the S1 state within 100fs already planar. Calculations elucidate the path in configurational space taken by the wavefunction and highlight the role of non-adiabatic state crossings in dissipating the energy. We find a clear correlation between the ultrafast planarization and an intramolecular charge transfer state whose ultrashort lifetime is exploited in realizing all optical switching in plastic media.

8098-34, Poster Session

Nonlinear optical properties of two dimensional ferroelectric polymer film at the air/water interface

C. Jung, P. Jang, S. Kyu, K. H. Kim, Cheongju Univ. (Korea, Republic of)

Organic materials are generally attractive because of the possibility having exceptionally high nonlinear optic (NLO) coefficient. The most straightforward approach to increase the NLO coefficient is the development of new material through the systematic chemical design of the molecules. Even though the lack of amphiphilicity, the copolymer of vinylidene fluoride and trifluoroethylene, P(VDF-TrFE) makes its monomolecular (Langmuir layer) on the water surface. By stacking this layers onto a solid substrate with appropriate transfer technique, one can establish a well organized two dimensional films with a good non-centrosymmetric crystallinity. In this study, we focused our attention on the formation of polar monolayer on the air/ water interface by using nonlinear optical technique, such as second harmonic generation method. Up to now, many research group have reported the NLO properties of amphiphilic two dimensional films. However, the NLO study from this kind of poor amphiphilic film has not been reported yet.

In this work, a copolymer of vinylidene fluoride(70%) and trifluoroethylene (30%) were prepared on the water subphase and the time dependent NLO properties was studied by second harmonic generation method.

8098-35, Poster Session

Modeling interfacial charge transport of Quantum dots using Cyclic Voltammetry

A. K. Tobias, Jr., E. Williams, M. Jones, The Univ. of North Carolina at Charlotte (United States)

Quantum dot applications are numerous and range from photovoltaic devices and lasers, to bio labeling. Complexities in the electronic band structure of quantum dots create the necessity for analysis techniques that can accurately and reproducibly provide these band energies. Cyclic voltammetry (CV) has been used to estimate HOMO/LUMO levels in molecular species and, similarly, can also be used to estimate valence and conduction band levels in quantum dots. Energy and charge transfer between quantum dots and other electron/hole accepting materials can be tuned and optimized according to this data. CV has been utilized in recent research to study effects of electron and hole insertion on quantum dot ensembles and also investigate their band gap energies. These experiments can be done on quantum dots in solution, as thin films, or coated on metal electrodes. CV has potential to become a useful tool in engineering new nanocrystal technology, by providing information necessary for predicting and modeling interfacial charge transfer to and from quantum dots. Despite the potential use of CV analysis, limitations arise due to the physical nature of nanocrystals. Solubility and diffusion come into play in solution-state experiments, while sample degradation is an issue in thin films. Carbon paste electrodes have been used in electrochemical studies to eliminate these issues. I will present data obtained using a carbon paste electrode to investigate energy levels in core CdSe and core/shell CdSe/CdS quantum dots. Importantly, the results of this work allow us to determine HOMO-LUMO energy differences for candidate nanocrystal-molecule electron transfer systems.

8098-36, Poster Session

Modeling exciton dynamics of type II nanocrystals

D. Woodall, A. K. Tobias, Jr., E. Williams, P. Moyer, M. Jones, The Univ. of North Carolina at Charlotte (United States)

Semiconducting nanocrystals are becoming more important in light harvesting devices because of their tunable optical properties, stability, and ease of synthesis. In order to design high efficiency optoelectronic devices, the movement of charges within these nanocrystals needs to be fully understood. Electron transfer models such as Marcus theory exist for molecular systems, but critical parameters such as potential energy curves and electronic coupling strengths of Marcus theory have yet to be applied to nanocrystals. The development of such a model for nanocrystals is problematic because they are complex. Nanocrystals are complex because of inhomogeneities in size and shape, surface trap states, and ligand effects, all of which affect electron transfer rates in different ways. Nanocrystals consisting of type II core/shell CdSe/CdS with varying shell thicknesses were synthesized using a colloidal synthesis method. Each sample was characterized by various optical spectroscopies including UV-Vis absorption, steady state fluorescence, and time resolved photoluminescence. Lifetimes were measured at a range of temperatures and were directly analyzed using software previously shown to be effective in predicting carrier trapping and detrapping rates for CdSe/CdZnS core/shell nanocrystals. Computational modeling based on the premises of Marcus theory was performed to simulate experimental results. By combining lifetime measurements with simulations, we establish a kinetic model of nanocrystal exciton dynamics predicting electron transfer rates over a range of temperatures. The development of this model is critical for future design and fabrication of optoelectronic devices such as photovoltaics, photodectors, and chemical sensors.

8098-37, Poster Session

Effect of alloying on the photoluminescence of the CuInS₂ nanocrystals

Y. Kim, C. Choi, Korea Institute of Materials Science (Korea, Republic of)

We have developed a novel route to highly luminescent Cd-free core-shell nanocrystals. By simply refluxing as-synthesized CuInS₂ nanocrystals with zinc acetate and palmitic acid, highly luminescent CuInS₂/ZnS nanocrystals were synthesized. We modified the photoluminescence of the grown nanocrystal by alloying foreign atoms. Nanocrystals with alloyed cores were synthesized by adding selenium and nanocrystals with alloyed shell layers were synthesized by refluxing the as-synthesized CuInS₂ nanocrystals with mixture of cadmium acetate, zinc acetate and palmitic acid. It was found that the emission wavelength of the nanocrystals was shifted to longer wavelength side by alloying. The photoluminescence spectra showed clear red-shift without significant minimization of emission intensity. A Detailed study on the emission process of nanocrystals implies that the formation of shell layers with small lattice mismatch minimized mismatch strain generated from the shell layers in contrast to core alloyed nanocrystals.

8098-38, Poster Session

Noise and current-voltage characteristics of structures with porous silicon layer in different gas environments

Z. Mkhitarian, V. Aroutiounian, S. Geghamyan, Yerevan State Univ. (Armenia)

The experimental research of current-voltage characteristics and low-frequency noise in dry air, dry air+0.1% ammonia, dry air+0.1%(butane+propane), dry air+0.1% spirit (C₂H₅OH) were done. PS layers were formed using the electrochemical etching of heavily doped ($\rho=0.01 \Omega\text{cm}$) p+ type (100)-oriented silicon wafers. The thickness of the PS layer was 3 micro-meters; the porosity was equal to 80 %. The diameter of nanometrical filaments was equal to ~5nm; sizes of pores were equal up to 50nm approximately.

Measurements of noise characteristics were carried out by the method of direct filtration at room temperature in the range of frequencies 3 Hz - 500 Hz. Measuring setup for research of the noise in the semiconductor-gas system included the input chain, a gas cell, low noise preliminary amplifier SR 560 (SRS, USA), the analyzer of the spectrum realized by HANDYSCOPE 2 (Tie Pie Engineering).

Sensitivity diagrams for explored samples are shown after traditional (resistance) and noise measurement, correspondingly. We have shown that the noise sensitivity in the presence of target gas in air is much higher than the sensitivity of the sensor after the measurement of ohmic resistance. The largest change in the characteristics of our samples occurs in the environment of dry air+0.1% ammonia. The possible reason for this is the molecule size of target gas and its adsorption properties. The physical reasons of sensing properties of the investigated samples are detailed discussed in paper.

8098-40, Poster Session

Optical investigation of medicine solutions in micro-droplets form at interaction with laser radiation

V. V. Nastasa, M. Boni, I. Andrei, National Institute for Lasers, Plasma and Radiation Physics (Romania); L. Amaral, Instituto de Higiene e Medicina Tropical UNL (Portugal); M. L. Pascu, National Institute for Lasers, Plasma and Radiation Physics (Romania)

Conference 8098:
Physical Chemistry of Interfaces and Nanomaterials X

The multiple resistance to treatment, acquired by bacteria and malignant tumors requires finding alternatives to the existing medicines and treatment procedures. One of them is strengthening the effects of cytostatics by modifying their molecular structures through exposure to laser radiation. A method associated with this, is the generation of micro-droplets which contain medicines solutions; the droplets are utilized/produced as vectors to transport the medicines to targets.

In our studies we try to combine these two methods in order to obtain a new technique to deliver the efficient medicines to targets that can be applied for a relative large number of chemicals. For this purpose we have developed an experimental set-up containing a liquid droplets generator, a tunable laser source used to irradiate droplets, a subunit to measure the laser induced fluorescence signals and a real time recording system for droplet image analysis.

Measurements on different probes, like ultrapure water, commercial grade medicines, newly developed medicines and laser dyes were performed. For some of these samples, the wetting properties were also studied. All these measurements were performed on water-based solutions.

First we show the laser induced fluorescence measurements results on micro-droplets, that exhibit important modifications after the exposure at laser radiation. It was evidenced that the exposures to laser beams/coherent optical radiation of some medicines solutions in ultrapure water may produce molecular modifications in solutions. These slight modifications of the molecules made them more efficient against bacteria strains.

Secondly, we present results concerning the micro droplets behavior at laser beam interaction for different laser energies and impact geometries.

The laser beam incident on the droplet was emitted at 10 pulses per second or in single pulse regime at 540nm (green) with 6ns FTWHM. The beam focus diameter was 0.1mm and the irradiance in the focus was about 3kW/cm². The processes which might take place at the interaction of the laser beam with water microdroplets are: a. Droplet vibration; b. Generation/expulsion of micro/nano droplets at high speed by the initial droplet thorough loss of material; c. Microdroplet destruction by loosing the contact with the capillary used to generate it; d. Possible heating of the droplet's material although the laser beam wavelength was emitted in green, where the water absorption is negligible; e. Total sputtering in 4π of the droplet, when exposed to a single high power pulse. The effect of the mechanical pressure of light on the microdroplets is investigated in correlation with the superficial tension values for such droplets.

8098-41, Poster Session

Structure and optical properties of noble-metal and oxide nanoparticles dispersed in various polysaccharide biopolymers

V. Djoković^{#263}, D. K. Božanić, V. Vodnik, R. Kršmanović, Vinca Institute of Nuclear Sciences (Serbia); S. Dimitrijević-Branković, Univ. of Belgrade (Serbia); L. Trandafilović, Vinca Institute of Nuclear Sciences (Serbia)

The hybrids based on nanostructured noble-metal particles and polymers have been investigated for almost two decades but this subject is enjoying a constant resurgence of interest and activity as a result of the exceptional properties which can be realized from such nanocomposite materials. Since a polymer can be easily designed into almost any shape required by a particular application, the properties of the nanoparticles can be successfully utilized by incorporation of the nanoparticles into polymer matrices. Polymers can also influence the growth and spatial arrangement of the nanoparticles formed within the matrix that makes them convenient templates for the preparation of nanoparticles of different morphologies. Because of possible applications in biotechnology and environmental protection, biopolymers and particularly polysaccharides were recently employed as host materials for metal and semiconductor nanoparticles. The macromolecular chains of these biopolymers possess a large number of hydroxyl groups and they can complex well with metal ions, which in turn enables a good control of size, shape and dispersion of the nanoparticles formed. Here we present the results on the structure and the optical properties of

noble metal (Ag, Au), oxide (ZnO) and composite (Ag-Ag₂S) nanoparticles synthesized by various methods in different polysaccharide matrices such as chitosan, glycogen, alginate, and starch. The structure of the obtained nanoparticles was studied in detail with microscopic techniques (TEM, HRTEM, HAADF-STEM), while the XPS spectroscopy was used to investigate the effects at the nanoparticle biomolecule interfaces. The antimicrobial activity of the nanocomposite films with Ag and ZnO nanoparticles was tested against the *Staphylococcus aureus*, *Escherichia coli* and *Candida albicans* pathogens. In addition, we will present the results on the structure and optical properties of the tryptophan amino acid functionalized silver and gold nanoparticles dispersed in polyvinyl alcohol matrix.

8098-25, Session 7

Physical chemistry of acridine adsorption onto gold surface: The influence of nanostructure as revealed by near-infrared and tip-enhanced Raman spectroscopy (TERS)

R. M. Balabin, T. Schmid, ETH Zurich (Switzerland); R. Z. Syunyaev, Gubkin Russian State Univ. of Oil and Gas (Russian Federation); R. Zenobi, ETH Zurich (Switzerland)

The surface science of aromatic molecules has long been of interest, both on semiconductor and on metal surfaces, due to their high importance for industry. For example, catalytic purification of petroleum (crude oil) fractions is based on the adsorption/reaction behaviour of sulphur- and nitrogen-containing molecules. In this view, a systematic study of the adsorption and transformation of sulfur and nitrogen compounds on different solids (applicable as catalysts, catalyst components, or adsorbants) is needed. Here we report a detailed study of adsorption of acridine (C₁₃H₉N) and a number of its derivatives: benz[a]acridine, benz[c]acridine, etc. Thermodynamic and kinetic data, obtained by solution-phase near-infrared spectroscopy (NIRS), clearly show a great difference of adsorption behavior for flat and nanorough (~4 nm) gold surfaces. Gibbs free energies of -4.57±0.10 vs. -7.67±0.13 kcal mol⁻¹ and adsorption kinetic constants of 26±3 vs. 4160±220 min⁻¹ M⁻¹ were determined for flat and SERS-type surfaces, respectively. This result could be interpreted in terms of the type of adsorption model: adsorption by the conjugated pi-electron system or by the lone pair of the nitrogen atom in the former and latter cases, respectively. The characterization of the polyaromatic monolayer directly at the Au surface, as measured by tip-enhanced Raman spectroscopy in scanning tunneling microscope mode (STM-TERS), has confirmed the dependence of the adsorption parameters on the (nano)roughness of the metal surface. The shift of Raman active vibrations (by 2-8 cm⁻¹) of the molecules at the surface and the appearance of new bands were used as a direct indicator of the adsorption model type. Density functional theory calculations (DFT-B3LYP, DFT-M06) were used to confirm the assignment. A unique possibility of TERS to enhance the molecular Raman signal independent on the surface structure and type was fully realized. The importance of the findings for industry and nanotechnology are discussed.

8098-26, Session 7

Investigation of the influence of surface and heterogeneous radical stages on oscillation modes of methane oxidation

V. Malkhasyan, Yerevan State Univ. (Armenia)

The goal of our work is investigating the role of heterogeneous radical stages in the initiation oscillation modes of methane oxidation at flow conditions.

There is evidence of the existence of oscillations in the process of thermal oxidation of methane, which is accompanied by luminescence. However the mechanism of their appearance is little known. We

Conference 8098:
Physical Chemistry of Interfaces and Nanomaterials X

supposed and then proved, with the method of mathematical modeling, that one of its reasons could be the influence of nature of the state of the surface on character of dynamic regimes of process.

The short model of chain radical process was considered. The system of differential equations for changes of reagents concentration was solved in quasi-stationary approach for the concentration of some radicals at initial stage of the reaction, when the consumption of methane and oxygen can be neglected.

The luminescence during oxidation of organic compounds is routinely attributes to the recombination of radicals. In an oscillatory mode of methane oxidation of concentration oscillations of radicals will naturally cause oscillations of intensity of a luminescence. When we were varying the rate constants of heterogeneous stages of reaction process as a result we observed damping or swinging oscillations.

Summarizing results it is possible to conclude, that oscillatory regimes of thermal oxidation of methane is strictly connected with the heterogeneous factors that is with the nature of the surface and also revealed conditions, which they can be regulated.

8098-27, Session 7

Nanostructured silicon for surface passivation of solid-state photodetectors

M. E. Hoenk, Jet Propulsion Lab. (United States)

Surface-related instabilities, including especially quantum efficiency hysteresis, have plagued scientific solid-state imaging detectors since the 1970's, when NASA first invested in charge-coupled devices (CCDs) for astronomical instruments in space. Such instabilities are especially problematic in the deep ultraviolet, where photons carry sufficient energy to damage surface coatings, creating defects and traps associated with surface charging, carrier recombination, and dark current generation. Using molecular beam epitaxy to grow a 2 to 3 nm epitaxial layer of delta-doped silicon, we have created a highly stable surface passivation layer that uniquely enables reflection-limited quantum efficiency and completely eliminates quantum efficiency hysteresis in back-illuminated CCDs and CMOS imaging arrays. In this paper we study the physics of surface passivation in delta-doped, back-illuminated silicon imaging detectors. The silicon surface in these detectors is modified by epitaxial growth of silicon, within which a partial monolayer of boron is embedded in the silicon lattice, creating a delta-doped surface. In a delta-doped surface, the highly-localized sheet of dopant atoms creates a quantum well for majority carriers within a few nm of the surface. Here, the bandstructure of the delta-doped surface is calculated using self-consistent calculations of Poisson's equation and the Schrödinger equation, using an eight band $k \cdot p$ model of the valence band. Calculations affirm that the potential barrier formed by the delta-doped layer isolates the surface from the bulk. Thus a delta-doped silicon surface is virtually immune to environmentally induced changes in the surface charge that are known to degrade conventional silicon-based detectors. This immunity to surface charge is consistent with the absence of measurable quantum efficiency hysteresis in delta-doped imaging detectors.

8098-28, Session 7

Modulation of CdSe fluorescence using palladium nanoparticles

K. J. Major, M. Jones, The Univ. of North Carolina at Charlotte (United States)

The increasing demands for clean, efficient energy have strongly influenced the direction of nanoscale science. One of the most promising areas of solar energy research lies with cadmium selenide quantum dots (CdSe QDs). Metal nanoparticles have been examined as a means to improve the efficiency of solar energy conversion in QDs. It has been shown that in certain systems the presence of these metal nanoparticles increase electron - hole charge separation thus providing extended times

for electron harvesting. Most of the systems currently explored utilize gold nanoparticles, which is unsurprising due to the vast amount of synthetic methods for these particles and their plasmonic effects on the QDs. We seek to further examine metal nanoparticle - semiconductor quantum dot interactions through the study of CdSe - palladium nanoparticle systems. We employ both steady state and time resolved ensemble fluorescence spectroscopy to observe the effects of increasing palladium nanoparticle concentrations on both the fluorescence intensity and lifetime of various CdSe QDs. We find that decreasing separation distance between the particles, whether through increasing palladium concentration or QD shell thickness, leads to a stronger interaction between the particles. We find expected fluorescence quenching of the QDs at higher concentrations of palladium. At low palladium concentrations however we observe a unique fluorescence enhancement of the QDs. We use this data to explore the relative contributions of energy and electron transfer between the particles and determine the conditions under which the maximum effects of these interactions are observed.

8098-29, Session 7

Excited state dynamics in carbon nanotubes and graphene nanoribbons for electronics and biological applications

O. V. Prezhdo, Univ. of Rochester (United States)

No abstract available

8098-09, Session 8

Spectroscopic and modelling studies of charge generation in organic donor:acceptor heterojunctions

J. Nelson, Imperial College London (United Kingdom)

Photocurrent generation in organic photovoltaic devices follows from photoinduced charge pair generation at the interface between a donor (usually a conjugated polymer) and an acceptor (usually a fullerene). The efficiency of charge generation depends upon energy of the charge separated state relative to that of any neutral excited states such as triplets, but is also influenced by the specific chemical structure of the donor and acceptor species, the local molecular packing and the ease of energy transfer. We use spectroscopic, optoelectronic and modelling studies to probe these processes in a series of conjugated polymer:fullerene blend systems and relate the results to photocurrent generation in organic solar cells.

8098-31, Session 8

Environmental effects induced by the oxygen-water redox couple in carbon nanotube and graphene electronics

R. Martel, Univ. de Montréal (Canada)

Three terminal transport measurements using a back-gated FET geometry are facilitated by using a degenerately doped silicon wafer covered with a thin silicon oxide layer as the substrate. It has been widely assumed that measurements taken in air are dominated by the Schottky barrier at the contacts, which in turn is linked to the intrinsic properties of the material under study. Here we show that the redox active species present on the surface of the oxide substrate induced a drastic suppression of n-type behavior in FETs and provoke large threshold voltage shifts. By using carbon nanotubes and graphene FETs as testbeds, we investigated the impact of the chemical nature of the substrate and of ambient adsorbates on the field effect switching

Conference 8098:
Physical Chemistry of Interfaces and Nanomaterials X

behavior of different FETs. Our study revealed that the reduction of n-type conduction occurs when adsorbed water containing solvated oxygen is present on the SiO₂ surface. This finding demonstrates that an electrochemical charge transfer reaction is the underlying phenomenon governing the suppression of electron conduction in carbon nanotube and graphene devices.

8098-32, Session 8

Component identification with Raman spectroscopy colocalized with quantitative nano-mechanical mapping for complex polymer systems

S. Hu, N. Erina, C. Su, Bruker Nano Inc. (United States)

Most polymer materials are composed of multiple components. It is critical to be able to identify the chemical components and the concurring mechanical properties in the nanoscale. Raman spectroscopy has been historically used to probe structural characteristics of materials and investigate the chemical states of the bonds in the materials to identify the different chemical components with limited resolution. On the other hand, Atomic Force Microscope (AFM) has demonstrated nanometer resolution imaging with localized mechanical property measurements with the newly developed peak force tapping mode. The new technology enabled to quantitatively characterize materials at nanoscale with simultaneous topography and mechanical mapping such as modulus, adhesion and energy dissipation. In this paper we report systematic studies of complex polymer systems combining Raman spectroscopy mapping with quantitative nanomechanical mapping, yielding unprecedented capability to both chemically and mechanically characterize components in the complex polymer systems.

Blends based on thermoplastic Polypropylene (PP) and Ethylene-Propylene-Diene-Monomer (EPDM) rubber, so called thermoplastic vulcanizates (TPVs) in different component ratios have been investigated. TPVs are high-performance materials that combine the best attributes of the vulcanized rubber (flexibility and low compression set) with the processing ease of linear thermoplastics. That makes possible to design details with complex profiles with high precision, which has numerous benefits in appliance, electrical, construction, healthcare and packing applications. Raman spectroscopy microscopy can chemically identify the PP and EPDM domains with 1 μm resolution and give micro-scale distribution of components. Nano-mechanical mapping, performed in the same area, exhibits fine details of the component distribution concurrently, especially the details at the interface transition regions. Combination of the two technologies not only allows us to identify individual component unambiguously but also provides structural information at the interfaces.

8098-33, Session 8

Synthesis and electrochemical FTIR study of Pd-based nanostructured catalysts

A. Chen, R. M. Assumme, S. Chen, C. Asmussen, R. Laurin, Lakehead Univ. (Canada)

Driven by the increasing need for cleaner and more efficient engines in transportation applications, there has been growing interest in the study of the direct electrochemical oxidation of small organic molecules such as formic acid and methanol for the development of fuel cells. Palladium-based nanomaterials with high surface areas have been receiving great attention due to their unique properties, which enable a number of impressive applications in catalysis, fuel cells, hydrogen storage and chemical sensors. Recent studies have shown that the electrocatalytic performance of Pd-based nanomaterials is highly dependent on the composition, morphology and surface conditions of the synthesized materials. In this presentation, we report on the synthesis and electrochemical properties of different Pd-based nanostructured materials.

A variety of Pd-based nanostructured materials including nanoporous Pd networks and PdPt nanodendrites with different compositions have been synthesized using the hydrothermal method. The as-fabricated Pd-based nanostructured materials were characterized by scanning electron microscopy (SEM), energy dispersive X-ray spectroscopy (EDS), X-ray photoelectron spectroscopy (XPS) and X-ray diffraction (XRD). The electrochemical properties of these Pd-based nanomaterials were studied using cyclic voltammetry, chronoamperometry and in-situ electrochemical infrared spectroscopy. Our studies showed that the fabricated Pd-based nanostructures possess a very large surface area and high catalytic activity. The electrocatalytic activity of the different Pd-based nanostructured materials towards the electrochemical oxidation of formic acid will be compared, and the design of high-performance Pd-based electrocatalysts will be addressed in this talk.

8098-39, Session 8

Interaction between single walled carbon nanotubes and specific optically active molecules

H. Chaturvedi, N. O. Maheshwari, Indian Institute of Science Education and Research, Pune (India); J. C. Poler, The Univ. of North Carolina at Charlotte (United States)

Novel effects like photon enhanced aggregation are observed in solutions of functionalized SWNTs. SWNTs functionalized with optically sensitive molecules like MEH-PPV, ruthenium dyes exhibit enhanced rate of aggregation, due to charge dynamics and consequently its effect on electrical double layer in solutions. Rate of aggregation for functionalized SWNTs depends on the molecular absorption of the optically active molecule and increases linearly with power in the absorption window. We believe charges are transferred onto the nanotubes from the optically excited molecules, initiating rapid aggregation. DLVO theory has been extensively used to understand larger colloidal solutions. However with high specific surface area and enhanced reactivity DLVO theory needs to be well understood in relation to the nanoparticles. Critical coagulation concentration (CCC), the minimum concentration of ionic species to induce coagulation is experimentally ascertained using absorption spectroscopy and dynamic light scattering measurements on SWNT solutions. Schulze-Hardy rule which correlates CCC to the valence of counterions is theoretically based on DLVO theory thus inheriting various approximations. Modified Schulze-Hardy law is experimentally plotted for SWNT solutions using different inorganic salts. Effect of light, concentration, surface charges and ionic strength on CCC using various optically active coagulants are investigated for both semiconducting and metallic enriched solutions of SWNTs. Binding and molecular interaction between optically active supramolecules with semiconducting and metallic SWNTs are characterized using high resolution microscopic and spectroscopic techniques. Field effect transistor (FET) based on functionalized SWNT is fabricated using optical and e-beam lithography for electro-optical measurements. Optical effect on electronic transport through the functionalized SWNT devices is characterized. Optical doping of SWNTs is observed due to charge transfer onto the nanotubes from the optically active molecules bound to it. Optically controlled variation in electronic current through the FET device is discerned and scheme for realization of prospective optical switches and functional reliable devices will be presented.

Conference 8099: Biosensing and Nanomedicine

Sunday–Tuesday 21–23 August 2011 • Part of Proceedings of SPIE Vol. 8099
Biosensing and Nanomedicine IV

8099-01, Session 1

Carbon nanotube-mediated siRNA delivery for gene silencing in cancer cells

T. Hong, Vanderbilt Univ. (United States); J. Qiao, Vanderbilt Univ. Medical Ctr. (United States); H. Guo, Vanderbilt Univ. (United States); T. S. Triana, D. H. Chung, Vanderbilt Univ. Medical Ctr. (United States); Y. Xu, Vanderbilt Univ. (United States)

Carbon nanotubes (CNTs) have attracted much attention as a tool for transporting therapeutic molecules into cells; small interfering RNA (siRNA) is among the molecules which can be conjugated to CNTs for drug delivery. siRNA is potentially a promising tool in influencing gene expression with a high degree of target specificity. However, its poor intracellular uptake, instability *in vivo*, and non-specific immune stimulations have impeded its effect in clinical applications. In order to solve this problem, we have studied two types of CNT-mediated siRNA delivery systems for gene silencing in both neuroblastoma and breast cancer cells. In this study, carbon nanotubes functionalized with two types of phospholipid-polyethylene glycol (PL-PEG) have shown capabilities to stabilize siRNA in cell culture medium during the transfection and efficiently deliver siRNA into cells. Compared to Lipofectamine 2000-mediated siRNA delivery, CNT-mediated siRNA delivery systems yield equal or higher efficiency in silencing target gene expression. Our results have shown that CNT-mediated siRNA can efficiently silence various genes in both neuroblastoma and human breast cancer cells. Although both types of PL-PEGs stabilized siRNA molecules during transfection in cell culture media, PL-PEG 5000-Amine functionalized CNTs showed higher efficiency for gene silencing than CNTs functionalized by DSPE-mPEG 5000, the one without amine group. Based on these fundamental studies, we believe that CNTs hold great potential in mediating siRNA to silence specific genes in various human cancer cells, and will be a novel tool in further clinical applications.

8099-02, Session 1

Ebola virus detection using optofluidic-nanoplasmonic biosensors

A. A. Yanik, M. Huang, O. A. Kamohara, A. A. Artar, J. H. Connor, H. Altug, Boston Univ. (United States)

We demonstrate a label-free optofluidic-nanoplasmonic sensor that can directly detect live viruses from biological media at clinically relevant concentrations with little to no sample preparation. This work is the first demonstration of direct detection of intact viruses using extraordinary light transmission phenomena. So far, the questions remain for the possible limitations of this technique, as the penetration depths of the surface plasmon polaritons are comparable to dimensions of the pathogens. In this paper, we addressed this gap and showed that our nanoplasmonic sensors can reliably detect viruses down to 105 PFU/ml concentrations and operate over a wide dynamic range. Our sensing platform utilizes group specific antibodies for highly divergent strains of rapidly evolving viruses. We demonstrate direction detection and recognition of small enveloped RNA viruses, which make up almost all of the alarming new infectious diseases. Some of these viruses, e.g. the Ebola hemorrhagic fever virus are both emerging infectious and biological threat agent. Patients presenting with RNA virus infections often show symptoms that are not virus specific. Thus, there is great interest in developing sensitive, rapid diagnostics for these viruses to help direct proper treatment. We also tested our platform for the detection of enveloped DNA poxviruses, e.g. the Vaccinia virus, a poxvirus commonly used as a prototype for more pathogenic viruses such as smallpox. This platform, enabling fast and compact sensing of the intact viruses without any mechanical and light isolation, could open up biosensing applications for early and point of care diagnostics.

8099-03, Session 1

Novel, rapid DNA-based on-chip viable bacterial identification system combining dielectrophoresis and amplification-free fluorescent resonance energy transfer assisted in-situ hybridization (FRET-ISH)

M. M. Packard, E. Alcocija, Michigan State Univ. (United States)

Although real-time PCR (RT-PCR) has become a diagnostic standard for rapid identification of bacterial species in clinical and environmental samples, it remains time-intensive due to sample preparation and amplification cycle times and provides no insight into the viability of detected cells. The assay described in this work incorporates on-chip dielectrophoretic separation and concentration of live cells with fluorescence resonance energy transfer assisted in-situ hybridization (FRET-ISH) species identification. In addition, the assay includes a heating step which provides for simultaneous lysis, permeabilization and DNA denaturation via a Kapton® KHLV series (Polyimide Film and FEP adhesive) rectangular insulated heaters. Finally, signal amplification in the form of energy transfer from Syto 9, a non-specific DNA stain, to Hexachlorofluorescein (HEX) labeled Escherichia coli specific repetitive sequence probes allows confirmation of Escherichia species via FRET-ISH in real time. Identification of viable, and thus pathogenic cells, is achieved completely on chip in less than thirty minutes from receipt of sample compared to multiple hours required by RT-PCR and its requisite sample preparation. The simplicity, speed, and adaptability for detection of any DNA-based pathogen using this technique makes it an ideal candidate for field use, especially in cases of time-sensitive outbreak.

8099-04, Session 1

Localized drugs delivery hydroxyapatite microspheres for for osteoporosis therapy

J. H. Lee, I. H. Ko, Korea Institute of Ceramic Engineering and Technology (Korea, Republic of); S. Jeon, J. H. Chae, E. J. Lee, Hans Biomed Corp. (Korea, Republic of); J. H. Chang, Korea Institute of Ceramic Engineering and Technology (Korea, Republic of)

Hydroxyapatite [Ca₁₀(PO₄)₆(OH)₂, HAp] is the main mineral component of bones and hard tissues in mammals and well known for its high biocompatibility and osteoconductivity. In this study, we synthesized hydroxyapatite microspheres for localized drugs delivery, typically osteoporosis related medicines. The formation of calcium phosphate microspheres were initiated by enzymatic decomposition of urea and accomplished by emulsification process (water-in-oil). The microspheres obtained were sintered at 500 °C to remove organic compounds remained which potentially causes toxicity. The microspheres with a mean size range of 257 nm were in a spherical shape. Scanning electron microscope (SEM) indicated that the microspheres have various porous with random size, which maximizes the surface area. We performed load of alendronate and BMP-2 into HAp microspheres by adsorption process. The load of drugs was investigated by using FT-IR analysis. Releases of alendronate and BMP-2 were observed at 37 °C for 30 days and we found the release of both molecules showed sustained releasing profiles. Finally, animal trial showed the alendronate loaded HAp microspheres enhanced bone density in osteoporosis model rat after inject the drug loaded microspheres. Our study focused on development of non-toxic drug carrier, high drug loading, its sustained releasing and *in vivo* animal trial to verify the effectiveness. It was reported that oral dose is not adoptable to alendronate administration because oral administration of alendronate causes gastrointestinal disturbances. Hence, we believe that this material is suitable to locally deliver alendronate for osteoporosis therapy.

8099-05, Session 1

Highly efficient antibody immobilization with multimer protein G bound magnetic silica nanoparticles

J. H. Lee, H. K. Choi, J. H. Chang, Korea Institute of Ceramic Engineering and Technology (Korea, Republic of)

This work reports the immobilization of monomer, dimer and trimer (multimer) protein G onto silica magnetic nanoparticles for self-oriented antibody immobilization. To achieve this, we initially prepared the silica-coated magnetic nanoparticle having about 50 nm diameters. The surface of the silica coated magnetic nanoparticles was modified with 3-aminopropyl-trimethoxysilane (APTMS) to chemically link to multimer protein G. The conjugation of amino groups on the MNPs to cysteine tagged in multimer protein Gs was performed using a sulfo-SMCC coupling procedure. The binding efficiencies of mono-, di- and trimer were 78%, 62% and 54% respectively. However, the efficiencies of antibody immobilization were 71%, 81% and 90% for mono-, di- and trimer, respectively. To prove the enhancement of accessibility by using multimer protein G, FITC labeled goat anti-mouse IgG was treated to mouse IgG immobilized magnetic silica nanoparticles through multimer protein G. FITC labeled goat anti-mouse IgGs were more easily bound to mouse IgG immobilized by trimer protein G than others. Finally, multimer protein G bound silica magnetic nanoparticles were utilized to develop highly sensitive immunoassay to detect hepatitis B.

8099-06, Session 2

Recyclable optical microcavities for label-free sensing

H. K. Hunt, A. M. Armani, The Univ. of Southern California (United States)

Label-free biosensors with high sensitivity and high specificity have shown tremendous potential in medical diagnostics, environmental monitoring, and food safety evaluation. Optical microcavities have very low optical loss, and are therefore uniquely suited to sensing applications that require high sensitivity, particularly when paired with a biochemical recognition element that grants high specificity. The primary limitation of these biosensors, however, is that they are generally single-use systems, unless the recognition element is regenerated. Therefore, the ability to selectively functionalize the optical microcavity for a specific target molecule and then recycle the system, without degrading device performance, is extremely important. Here, we demonstrate a straightforward bioconjugation strategy that not only imparts specificity to optical microcavities, but also allows for biosensor recycling. In this approach, we selectively functionalize the surface of silica microtoroids with a biotin recognition element, using silane coupling agents and N-hydroxysuccinimide (NHS) ester chemistry to graft the biotin onto the surface. We then use a non-destructive O₂ plasma treatment to remove the surface chemistry, refresh the recognition element, and recycle the device. The surface chemistry of these devices is demonstrated using XPS, SEM, and fluorescent and optical microscopy. The optical performance of the functionalized and recycled devices is characterized by microcavity analysis. The resulting devices can be recycled several times without performance degradation, and show high density surface coverage of biologically active recognition elements. This work represents one of the first examples of a recyclable, bioconjugation strategy for optical microtoroid resonators, which can be used for label-free detection of biomolecules.

8099-07, Session 2

Surface enhanced Raman scattering (SERS)-based sensing schematics for detection and identification of biological samples

M. E. Hankus, P. M. Pellegrino, D. N. Stratis-Cullum, U.S. Army Research Lab. (United States)

There is a relevant Army need to detect, identify, quantify and differentiate hazardous from benign materials in theatre. These hazardous materials can be energetic, chemical or biological in nature. Raman-based techniques are becoming more commonly employed towards this end as they rely on specific vibrations within the molecule from which to produce a fingerprint spectrum, do not suffer from interferences from water, require little to no sample preparation, and can be used with several different excitation sources. Surface-enhanced Raman scattering (SERS) offers all the advantages of Raman, with the added advantage of increased analyte signal. SERS signal enhancements are achieved by irradiating a metalized surface with an analyte in close contact, and then measuring the signal from the chemical and electromagnetic enhancements that occur. In our research, we have characterized several different SERS substrate architectures and determined their applicability to Biological samples. Additionally, we have developed a molecular specific sensor schematic using a dual SERS fluorescence signal.

8099-08, Session 2

Bioconjugation strategies for improved optical sensor performance

C. E. Soteropoulos, H. K. Hunt, A. M. Armani, The Univ. of Southern California (United States)

The very low optical loss or high quality factors of silica optical microresonator sensors allow them to behave as very sensitive optical transducers. Therefore, they are a potential platform for real-time biosensing and diagnostics applications. However, their use is currently limited by the lack of high specificity and stable surface chemistries for the attachment of probe molecules. The main challenge when developing a method to functionalize optical devices is the need to maintain the optical performance of the device, while at the same time reliably attaching the probe. One extremely stable method of attaching biomolecules to silica surfaces is based on NHS-ester chemistry as the link between the inorganic surface and the biomolecule. This covalent attachment of the probe provides a robust interaction, and the method used is easily translated to a wide range of biomolecules, such as antibodies and antigens. In present work, we have applied this method to the surface of optical microsphere resonant cavities, and demonstrated quality factors above 1 million after probe attachment, thus verifying that the attachment strategy has minimal impact on the optical performance of the device. Through fluorescent imaging, we have confirmed the bioactivity of the binding site, as well as site stability even after long-term device storage (>30 days). Finally, we have performed resonant cavity detection experiments based on resonant frequency shift measurements using the functionalized devices, further confirming the applicability of this approach for imparting specificity while retaining optical performance.

8099-09, Session 2

Plasmonic biosensing with nanoimprint binary grating using ellipsometry

Y. Chang, R. S. Moirangthem, M. T. Yaseen, P. Wei, Academia Sinica (Taiwan)

An optical label free and high sensitivity plasmonic biosensor is presented based on the phase information of the ellipsometry signal. Plasmonic binary grating were prepared by using soft nano-imprinting

technique which significantly reduce the fabrication cost and can be realized for a transition from a laboratory-scale method to full-scale technology. The adsorption of bio-molecules on the nanostructure surface were investigated both in dynamic and spectroscopic mode by monitoring the change in polarization state or phase of reflected light as a sensing signal using ellipsometry. As a calibration, the bulk sensitivity obtained from our purposed plasmonic binary grating is about 9600 degrees/RIU by assuming a phase measurement accuracy of about 0.0010 as adopted in the literature. Furthermore, the experimental results were compared with an efficient theoretical simulation based on rigorous coupled wave analysis (RCWA).

8099-10, Session 3

CdSe/ZnS quantum dots with interface states as biosensors

T. V. Torchynska, G. Polupan, Instituto Politécnico Nacional (Mexico)

The paper presents the brief review of published results as well as the original study of photoluminescence (PL) and Raman scattering of core-shell CdSe/ZnS quantum dots (QDs) with radiative interface states. First commercially available CdSe/ZnS QDs with emission at 525 nm (2.36 eV), 565 nm (2.20 eV), 605 nm (2.05 eV) and 640 nm (1.96 eV) covered by PEG polymer have been compared in nonconjugated states. PL spectra of nonconjugated QDs are characterized by a superposition of PL bands related to exciton emission in CdSe cores and to hot electron-hole emission via high energy states (2.00, 2.37, 2.75 and 3.04 eV). The high energy states were studied using QDs of different sizes and at different temperatures. It is shown that these PL bands related to interface states. Then the CdSe/ZnS QDs have been conjugated with bio-molecules - anti IL-10 (Interleukin 10) and PSA (Prostate-Specific Antigen) antibodies. It is revealed that the PL spectrum of bioconjugated QDs has changed dramatically with essential decreasing of hot electron-hole recombination flow via interface states. The variation of PL spectra at the bioconjugation is explained on the base of electrostatic interaction and re-charging of QD interface states [1]. The Raman scattering study of nonconjugated and bioconjugated QDs has shown that mentioned antibodies are characterized by the dipole moment that provokes the surface enhance Raman scattering effect [2] in bioconjugated QD samples.

[1] T. Torchynska, Nanotechnology 20, 095401, 2009

[2] T. Torchynska et al., Nanotechnology 21, 134016, 2010

8099-11, Session 3

Characterization of a silicon photonic biosensor consisting of two cascaded ring resonators employing the Vernier-effect to improve sensitivity and interrogation.

T. Claes, W. Bogaerts, P. Bienstman, Univ. Gent (Belgium)

Many applications require label-free biosensors that consist of a transducer that directly responds to a selective affinity interaction between immobilized receptor molecules and analyte molecules.

Silicon-on-insulator ring resonators have already been proven to be excellent transducers that can be incorporated in a dense sensor array capable of multiplexed sensing and moreover can be manufactured with high quality using CMOS-compatible processes. However, ring resonators only have a limited sensitivity, of which an enhancement could not only further improve their detection limit, but it would also enable cheaper interrogation with a broadband light source and integrated wavelength filters.

We propose a sensor that employs the Vernier-effect to enhance the sensitivity of ring resonators with more than an order of magnitude. It consists of two cascaded silicon-on-insulator ring resonators of which only one is allowed to interact with biomolecules.

We designed and fabricated this sensor so that a periodic envelope signal is superposed on the sharp constituent resonance peaks, and experimentally prove that its sensitivity to a changing refractive index (2169nm/RIU) is thirty times larger than that of a single ring resonator. Its detection limit moreover benefits from the sharp transmission peaks that constitute the envelope. Analytical formulas describing the sensors transmission spectrum allow us to accurately track shifts of the envelope signal by data-fitting. Additionally, for the first time on-chip wavelength filtering of the sensor's signal with an integrated arrayed waveguide grating can be presented, making our sensor compatible with cheap interrogation with a broadband light source.

We think that these improvements make silicon-on-insulator ring resonator label-free biosensors even more attractive for many applications.

8099-12, Session 3

Block copolymer modified graphene field effect transistor robust biosensor

S. Guo, M. Ghazinejad, C. S. Ozkan, M. Ozkan, Univ. of California, Riverside (United States)

It is essential to control the electronic properties of graphene field effect transistors (GFETs). After spatially controlled CF₄ plasma doping, we succeed in controlling the Dirac point of a GFET covered with cylindrical-morphology polycrystalline block co-polymer (BCP) (Poly(styrene-*b*-4-vinylpyridine)). The BCP microdomain array assembled on graphene provides a new approach to tune both electron and hole conductivity of graphene simultaneously. The BCP-covered GFET could detect 1mM NaF solution under "dry" conditions in 60s. Time studies showed that the sensor lasted for over 3 months. It was also determined that the orientation and periodicity of the resulting BCP array of cylindrical microdomains facilitate the selective sensing property. These findings pave the way for developing more durable and sensitive graphene-based sensors for chemical or biological applications under ambient conditions.

8099-13, Session 3

Nanoplasmon coupled intracellular optical resonance excitation for ultrasensitive 3D fluorescence cell imaging

M. R. Gartia, A. Hsiao, S. Mayandi, Y. Chen, G. L. Liu, Univ. of Illinois at Urbana-Champaign (United States)

With the goal of creating a platform for enhanced 3D fluorescence cell imaging capability, we have fabricated a nanoplasmonic substrate on which three-dimensional confocal fluorescence cell imaging sensitivity is amplified for more than 100 folds especially for cell membrane and cytoplasm. The observed unprecedented three-dimensional fluorescence intensity enhancement on the entire cell microstructure including cell membrane 10 μm above the substrate surface is attributed to a novel far field enhancement mechanism, nanoplasmon coupled optical resonance excitation (CORE) mechanism which permits enhanced surface plasmon on the substrate being evanescently coupled to Whispering Gallery mode optical resonance inside the spheroidal cell membrane microcavity. This is distinctly different from metal enhanced fluorescence effects because of the fact that metal enhanced fluorescence is a near field effect and only available up to 100 nm above the metal surface. Evidenced by high-resolution vertical slices of cell fluorescence images, the strong intracellular optical resonance modes provide highly intensified laser excitation inside cells and then lead to the huge amplification of fluorescence imaging sensitivity. Further, we have established the theoretical model for coupling of surface Plasmon evanescent wave with whispering gallery mode using coupled mode theory. In addition, preliminary experiment has also been performed using our device to see the early stage of transfection in a cancer cell.

8099-15, Session 3

Kinetic analysis of biomolecular interactions by surface plasmon enhanced ellipsometry

H. M. Cho, W. Chegal, Y. J. Cho, J. M. Won, H. M. Lee, Korea Research Institute of Standards and Science (Korea, Republic of); J. H. Jo, Hannam Univ. (Korea, Republic of)

We present the application of ellipsometry to the phase measurement of surface plasmon resonance (SPR) in biomolecular detection. In this work, the experimental setup for the SPR sensor was based on a custom-built rotating analyzer ellipsometer, which was equipped with a SPR cell and a microfluidic system. We investigate the sensitivity of SPR sensor which is dependent on the thickness and roughness of metal film, alignment of optical system, and stability of microfluidics.

In the drug discovery process, to directly monitor the interaction of small molecule-protein, it is necessary to design a high-sensitivity SPR sensor with a sensitivity of greater than 1 pg/mm². Our sensor demonstrates a much better sensitivity in comparison to other SPR sensors based on reflectometry or phase measurements. The results of calibration indicate that the phase change, $\delta\Delta$, had an almost linear response to the concentration of ethanol in the double-distilled water solutions. A quantitative analysis of refractive index variation was possible using the results of the ellipsometric model fits for the multilayered thin film on the gold film. Thus, this method is applicable not only to sensor applications, such as affinity biosensors, but also to highly sensitive kinetics for drug discovery. In this paper, we demonstrate how a custom-built rotating analyzer ellipsometer in the SPR condition can be used to directly obtain the interactions and binding kinetics of low-molecular-weight analytes (biotins, peptides) with immobilized ligand (streptavidin, antibody). We achieved a detection limit of lower than 1.0×10^{-7} RIU, which is the equivalent of 0.1 pg/mm².

8099-16, Session 4

Nanobarcoding: a novel method of single nanoparticle detection in cells and tissues for nanomedical biodistribution studies

T. V. Eustaquio, J. F. Leary, Purdue Univ. (United States)

Determination of whether nanomedical devices accumulate in diseased (target) or normal (non-target) tissues, known as nanoparticle biodistribution, is absolutely critical in assessing the safety and efficacy of a given nanoparticle formulation for nanomedical purposes. However, current imaging-based methods of evaluating nanoparticle biodistribution are greatly limited. There is an overwhelming need for a more sensitive and more efficient imaging-based method that ideally can (1) detect small numbers of nanoparticles, even single nanoparticles, (2) associate preferential nanoparticle uptake with histological cell type, and (3) allow for relatively quick and accurate nanoparticle detection in the large, complex in vivo environment. One method that has the potential to fulfill the requirements of an improved nanoparticle detection strategy is in situ polymerase chain reaction (PCR). In situ PCR combines the extreme sensitivity of PCR and the cell-localizing ability of in situ hybridization. Since in situ PCR has had success in detecting viral DNA at a low-copy number inside single cells in a tissue section, which is analogous to the small numbers of nanoparticles that can be present, the in situ PCR technique can be adapted to the detection of single nanoparticles. We propose a novel method for nanoparticle detection that utilizes an oligonucleotide "nanobarcode" conjugated to the nanoparticle surface, which serves to amplify the optical signal from a single nanoparticle via in situ PCR for detection with standard microscopy. Nanobarcoding has the potential to fulfill the specifications of an ideal nanoparticle detection method. Herein, we describe the design process of the nanobarcoding method.

8099-17, Session 4

Surface enhanced Raman spectroscopy and fluorescence based on black silver

Z. Xu, J. Jiang, Y. Chen, M. R. Gartia, G. L. Liu, Univ. of Illinois at Urbana-Champaign (United States)

Surface plasmon-induced enhancements in spectroscopy and optical imaging are investigated on the mass producible black silver substrate (BSS) which is silver coated silicon with homogeneous and dense nanocones structure. On the contrary of highly reflective silver films or silver nanoparticles whose plasmon resonant modes are restricted within a few specific frequencies, the BSS of low reflectivity can efficiently trap and convert incident photons into localized plasmons within a broad frequency range. This unique physical property allows black silver to enhance optical absorption by 12 times from UV to NIR range, enhance surface fluorescence by 30 times and induce 7 more order of enhancement in the surface Raman scattering. Considerable potential of the BSS in high sensitive and broadband optical sensing and imaging is dominant with demonstrating enhanced fluorescence imaging and Raman spectroscopy of Rhodamine and oligo-peptide molecules.

8099-18, Session 4

Afterglow quantum dots for multispectral intraoperative fluorescence imaging

P. T. K. Chin, T. Buckle, Netherlands Cancer Institute (Netherlands); A. Aguirre de Miguel, S. C. J. Meskers, R. A. J. Janssen, Technische Univ. Eindhoven (Netherlands); F. W. B. van Leeuwen, Netherlands Cancer Institute (Netherlands)

Fluorescence molecular imaging is rapidly increasing its popularity in image guided surgery applications. To help develop its full surgical potential it remains a challenge to generate dual-emissive imaging agents that allow for combined visible assessment and sensitive camera based imaging. To this end, we now describe multispectral InP/ZnS quantum dots (QDs) that exhibit a bright visible green/yellow exciton emission combined with a long-lived far red defect emission. The intensity of the latter emission was enhanced by X-ray irradiation and allows for: 1) inverted QD density dependent defect emission intensity, showing improved efficacies at lower QD densities, and 2) detection without direct illumination and interference from autofluorescence.

8099-19, Session 4

Noble metal nanoparticles for LSPR-based optical sensing

W. Fritzsche, T. Schneider, O. Stranik, A. Csaki, Institut für Photonische Technologien e.V. (Germany)

The optical properties of noble metal nanoparticles depend on the excitation of localized surface plasmon resonance (LSPR) by electromagnetic irradiation. The position and intensity of the occurring plasmon band is influenced by particle specific features such as size, shape and material/composition. Important for biosensor applications are changes in the local refractive index of the surrounding medium, which can also cause a detectable plasmon band shift.

Micro spectroscopy to measure the scattering spectra of chosen particles undergoing biomolecular recognition process on the single particle level has been demonstrated successfully. In our experimental setup a spectrometer was coupled to a dark-field microscope by an optical fibre for collecting the emitted light. A small pinhole (150 μm) allows focusing on just one nanoparticle for collecting its optical information. Interparticle distances of larger than 5 μm excludes plasmon coupling effects of adjacent nanoparticles.

Herein, we investigate the sensing potential of different kinds of gold

nanoparticles for detecting DNA immobilization and hybridization. After immobilizing the gold nanoparticle on a glass substrate via silane chemistry, the single-stranded capture oligonucleotide was attached to the particle surface by thiol-gold interaction. Afterwards, single-stranded target DNA with a complementary sequence was hybridized to the capture oligonucleotide. Towards each step the scattering spectra of the particle was recorded. An example for 80 nm gold nanospheres is shown in figure 1. An obvious red shift of the plasmon band could be detected for both capture DNA attachment and target DNA hybridization.

8099-20, Session 4

Vertically emitting photonic bandgap cavity arrays for sensing applications

T. Moein, A. Pandey, Y. Yao, S. M. Durbin, Q. Gan, N. M. Litchinitser, A. N. Cartwright, Univ. at Buffalo (United States)

Highly selective sensing technologies continue to be of considerable interest because of their potential for applications in genetic screening, clinical diagnostics and single-molecule detection, among others. The reduction of the sensing element length scale and the formation of multiple patterned structures on a common substrate is essential for the development of arrayed biosensors. Thus, a patterned nano-structured material is an excellent candidate for such applications.

In this work, we demonstrate a simple and compact gas sensor array based on waveguide-coupled submicron multi-ring photonic bandgap ("bullseye") structures. The "bullseye" structures were patterned inside the SU-8 waveguide using focussed ion beam etching, which enables precise dimensional control in the submicron range. The center of each "bullseye" - the vertical cavity - was functionalized by incorporating analyte sensitive fluorescent molecules. The "bullseye" structures were designed to confine light at the fluorescence wavelength in the transverse direction by photonic bandgap effect. In this way, when excited by a broadband light source incident through the waveguide, the "bullseye" structure emits light in a cone pointing in the vertical direction. We discuss a methodology for translating this technology to biological sensing. In particular, this unique combination of transverse waveguide-based geometry for excitation and vertical detection will be beneficial for micro-fluidic based biological sensor systems.

8099-33, Session 4

A new glucose biosensor based on ECL technology and self-assembly GC electrode including GOx and silver nanoparticle

A. Shokuhi Rad, Islamic Azad Univ (Iran, Islamic Republic of); M. Ardjmand, Islamic Azad Univ. (Iran, Islamic Republic of); M. Jahanshahi, Babol Noshirvani Univ. of Technology (Iran, Islamic Republic of); A. Seyfordin, Sharif Univ. of Technology (Iran, Islamic Republic of)

Electrogenenerated Chemiluminescence (ECL) involves applying a certain electric potential to a chemical reaction, resulting in the oxidation or reduction of the substance which reacts to produce light. We determine the amount of glucose by its reaction to glucose oxidase (GOx) on the surface of proposed modified electrode which results hydrogen peroxide (H₂O₂) as side product. After that the reaction between luminol and H₂O₂ under oxidizing conditions generate dependent light which can be used to analysis. In the current article at first we proposed a convenient method to obtaining a self-assembly modified electrode. A nano based modified glassy carbon electrode (Glucose oxidase / Ag nanoparticles/ cysteamine/ p-aminobenzene sulfonic acid/ GC electrode) were prepared, and the ECL behavior of luminol in the presence of glucose was examined. Compared to the bare GC electrode, the modified electrode incorporating glucose oxidase significantly enhanced the response of the ECL biosensor to glucose due to the enhanced specificity of the modified surface to enzymatic reaction, and

the sensitivity of the luminal ECL reaction. Under optimal conditions, the electrode was found to respond linearly to glucose in the concentration range 5.0×10^{-7} to 8.0×10^{-3} mol/L, and the detection limit was established to be a glucose concentration of 4.0×10^{-8} mol/L.

8099-21, Poster Session

surface plasmon resonance imaging ellipsometry for quantitative analysis for cell-matrix adhesions

W. Chegal, S. Kim, H. M. Cho, Y. J. Cho, D. W. Moon, Korea Research Institute of Standards and Science (Korea, Republic of)

The interaction between live cell and extracellular matrix, termed as cell-matrix adhesion, extensively regulates human biology from tissue and organ developments to the fate of cells. Elucidating functional dynamics of cell-matrix adhesion provide critical clues for understanding cellular phenomena. We developed a novel surface plasmon resonance imaging ellipsometry (SPRIE) method for real-time visualization of cell-matrix adhesion in live cell. In the SPRIE, the null-type imaging ellipsometry technique was integrated with an attenuated total reflection (ATR) coupler to improve contrast and sensitivity of the cell-matrix adhesions and cell-free medium contact regions. In the ATR coupler 30 nm of gold film were grown on the bottom side of the prism and subsequent surface treatment process was followed to anchor live cells. The ATR coupler was installed in the custom-built incubation chamber and the culture fluid was circulated to maintain cells alive. The surface plasmon wave was resonantly coupled with measurement beam and its evanescent characteristic allowed contrast mechanism of cell-matrix adhesions. During experiments cell-free regions were nulled out by adjusting polarizing components in the null-type imaging ellipsometer. In the captured image cell-free region exhibited lowest intensity and cell-adhesions exhibited gray scale values. The distance between cell membrane and top surface of the ATR coupler was calculated by using multi layered thin film model and Jones calculus. SPRIE was applied to multifaceted biological systems, cell division, migration and cell-cell communication. We also investigated shear stress-induced adhesion dynamics in real time. Together these data, we expect SPRIE can be developed for a useful methodology to study the role of cell-matrix adhesion in biological phenomena.

8099-22, Poster Session

Mechanical properties of elastic honeycomb-patterned microporous substrate as cell scaffold

T. Kawano, Y. Nakamichi, M. Sato, H. Yabu, M. Shimomura, Tohoku Univ. (Japan)

Cell functions are regulated by various mechanical property of extracellular matrix. In particular, elasticity of substrate surface around the cells plays an important role in cellular proliferation, differentiation, migration and signaling.

The measurement of the mechanical property of the extracellular matrix is one of the critical basis of development of new functional biomaterials as scaffold for cell culture and tissue engineering. Previously, various measurements of mechanical properties of two-dimensional planar substrates were developed. However, it is clear discrepancies between cell behaviors in vivo and in artificial planar environments. Here, we reported the preparation of the elastic honeycomb-patterned microporous films (honeycomb films) as three-dimensional scaffold and measurement of surface elasticity and deformation of honeycomb films. The honeycomb films of poly(1,2-butadiene) with hexagonal micron sized pores could be tunable the surface elasticity by changing the photo-cross-linking degree, which are regulated by UV light irradiation. Surface elastic and deformational distributions on the prepared honeycomb films were determined using micro-indentation test using AFM. Analyzing the

cell morphology and focal adhesions of fibroblast on the honeycomb-patterned surface with high elasticity, the fibroblast were well spread and markedly organized large focal adhesions. In contrast, small focal adhesions of cells on surfaces with low elasticity were observed. These results suggested that cell shape and formation of focal adhesions responded to the elasticity of the honeycomb films.

8099-23, Poster Session

Nanoparticle-aided surface plasmon resonance: engineered nanoparticles for higher sensitivity with functionalities

S. Moon, D. Kim, J. Park, B. Kang, S. Haam, Yonsei Univ. (Korea, Republic of)

Simplicity along with relatively high sensitivity has been a great merit that surface plasmon resonance (SPR) based biosensors hold. As more demands towards molecular sensing emerged, abundant researches focused on enhancing the sensitivity even further appeared. Such include employing of surface nano to micro structures to alter the intrinsic surface sensitivity, switching the figure of merit to a more sensitive measure, and applying nanoparticles as signal enhancement agents. This study introduces use of multi-functional nanoparticles (MFNPs) for active selection of labeled biological samples with amplified optical signature. Particles are composed as gold nanoshell surrounding magnetic nanoclustered core and dielectric inner shell. $MnFe_2O_4$ has been reported as an outstanding magnetic resonance imaging contrast agent, which also possesses strong sorting capability in flow-based sorting labchips. Gold nanoshells are known for strong absorption characteristics, which implies that enhanced SPR sensor can replace giant magnetic resonance sensor which requires extreme accuracy in fabrication. As an empirical proof-of-concept, DNAs labeled with MFNPs are successfully sorted in a flow chamber and detected with enhanced sensitivity. Also, a range of structural availability is numerically analyzed to provide a guideline for optimized particle synthesis. The results are expected to open a wide application in terms of directed sensing.

8099-24, Poster Session

Gold @ silica core-shell nanoparticle for enhanced surface plasmon resonance detection of DNA hybridization in combination with gold nanowire gratings

S. Moon, Y. Oh, D. Kim, H. Lee, H. C. Kim, K. Lee, Yonsei Univ. (Korea, Republic of)

Metallic nanoparticles have drawn much interest due to their distinct plasmonic characteristics especially in imaging and sensing applications. Surface plasmon resonance (SPR) based biosensors have evolved in many ways, among which sensitivity enhancement towards molecular sensing capability came up with strategies to overcome the hard limit of the intrinsic sensitivity of gold thin film. Recently adoption of signal contrast materials has proven successful in biochemical sensing applications. This study employs gold-SiO₂ core-shell nanoparticles (CSNPs) as a strong SPR signal contrast agents. To reveal the underlying physics for the contrast mechanism, the particle characteristics were analytically evaluated in terms of light interaction coefficients. We experimentally demonstrate the effect of the CSNPs by applying them to acquire enhanced signal in DNA hybridization sensing scheme. We also applied gold nanowire grating structure on conventional gold thin film to further amplify the intrinsic sensitivity, where localized surface plasmon and locally amplified evanescent fields take parts. The results suggest that CSNPs and the grating structure cooperatively enhance the sensitivity and the role of nanowire gratings was analyzed with numerical methods to allow optimum sensitivity enhancement in terms of fill factor variations. The effects of field localization, amplification and enlarged signature of CSNPs are also discussed.

8099-27, Poster Session

Silver doped nanomaterials and their possible use for antibacterial photodynamic activity

K. Wysocka-Król, H. Podbielska, Wroclaw Univ. of Technology (Poland)

Bacteria, viruses and parasites elimination from human environment has been one of the most important problem, extensively studied by many researchers. The growing resistance to commonly used disinfection and/or sterilization methods and antibiotics, is one of the major problem in the health care sector. Nanomaterials with tailored antimicrobial features may find applications in this field. One of the promising application of nanomaterials is the antimicrobial photodynamic therapy (APDT), which combines a nontoxic photoactive dye - photosensitizer and nanomaterials properties. Titanium dioxide based material known due to its photocatalytic properties, will be examined. The paper focused on the examination of optical and antibacterial properties of silica- and titania-based nanopowders doped with silver and photosensitizer - Photolon. It is known that silver doped biomaterials inhibit microbial growth and have been examined against various bacteria. Silver may interact with cellular wall and disintegrate it. The main target of silver are structural and enzyme proteins. From the other hand, photosensitizers are able to generate singlet oxygen and free radicals after light exposure that kill microbial cells. Various concentration of Photolon and nanomaterials have been examined to check the fluorescence enhancement and increased antibacterial activity. It was proved that the fluorescence intensity of Photolon increased, depending on silver concentration. Antibacterial study showed that silver doped silica and titania nanoparticles revealed antibacterial activity, but in the presence of Photolon, the antibacterial activity of materials is more effective.

8099-28, Poster Session

Fluorescence enhancement by a dielectric Bragg resonant cavity

Y. Liu, S. Wang, Y. Park, X. Yin, X. Zhang, Univ. of California, Berkeley (United States)

The strong near-field enhancement of surface plasmon modes can significantly improve fluorescence emission. However, if fluorescent molecules are very close to the metal surface, the fluorescence can be quenched. On the other hand, it is found that purely dielectric structures, such as one-dimensional (1D) periodic gratings or two-dimensional (2D) photonic crystals, can also produce substantial local field enhancement thanks to the resonant photonic modes of the dielectric system. Such a platform based on mere dielectrics normally exhibits much less losses, in contrast to plasmonic structures. Consequently, fluorescence signals can be enhanced without suffering from pronounced quenching.

However, so far 1D or 2D periodic dielectric structures have not shown confined fluorescence emission. Under some conditions, we may want to selectively choose a certain area, sometimes a small one, to locally enhance fluorescence emission and use it for subcellular biosensing applications. Here we demonstrate that based on a 2D dielectric annular Bragg resonant cavity, electromagnetic waves can be focused to a diffraction-limited spot and significantly boost the fluorescence emission. Due to the constructive interference of the in-plane guided wave around the resonance wavelength, the electric field can be focused and amplified considerably. This leads to experimentally observed 20-fold fluorescence enhancement averaged over an area of 4 μm^2 , while theoretically the fluorescence emission can be increased by more than three orders of magnitude at the center of the cavity. Our findings may have broad applications including near-field optical trapping, ultrasensitive chemical and biological sensors and fluorescent microscopy at the single-molecule level.

8099-31, Poster Session

Nanotechnology in cancer treatment

M. Mironidou-Tzouveleki, K. Imprialos, A. Kintsakis, Aristotle Univ. of Thessaloniki (Greece)

Applications of nanotechnology, which include liposomes, nanoparticles, polymeric micelles, dendrimers, nanocantilever, carbon nanotubes and quantum dots, have significantly revolutionized cancer theragnostics . From a pharmaceutical viewpoint, it is critical that the biodistribution of active agents has to be controlled as much as possible. This aspect is vital in order to assure the proper efficiency and safety of the anticancer agents. These biocompatible nanocomposites show specific biochemical interactions with receptors expressed on the surface of cancer cells. With passive or active targeting strategies, an increased intracellular concentration of drugs can be achieved in cancer cells , while normal cells are being protected from the drug simultaneously. Thus, nanotechnology restricts the extent of the adverse affects of the anticancer therapy. Treatment for metastatic breast cancer, sarcoma in AIDS patients, ovarian and lung cancer is already on market or under final phases of many clinical trials, showing remarkable results. As nanotechnology is perfected, side effects due to normal cell damage will decrease, leading to better results and lengthened patient's survival.

8099-32, Poster Session

Optical immunosensor for endocrine disruptor nanolayer detection by surface plasmon resonance imaging

A. Karabchevsky, L. Tsapovsky, R. S. Marks, I. Abdulhalim, Ben-Gurion Univ. of the Negev (Israel)

The presence of chemicals, both natural and synthetic, in the environment with the potential to interfere with the endocrine system in both wildlife and humans has in the last decade become a major international concern. Endocrine disrupting compounds (EDCs) such as estrone are especially prevalent in surface and waste-waters [1] in nano-molar concentrations and therefore, there is a need for sensitive analytical device for its monitoring. We have designed a miniature, low cost and fast surface plasmon resonance (SPR) imaging liquid sensor based on the known Kretschman configuration [2]. Due to its stability to water environment and simple bio-immobilization protocol, gold is usually used as SPR biosensing metal nano-layer. However, poor attachment of gold to the glass substrate needs additional layer of few nm Cr or Ti which deform the SPR reflectivity vs. angle curve. Silver, unlike gold, adheres very well to the glass, has very sharp curve but it is oxidizing when introduced to water or air medium, therefore a thin protective layer (<15nm) is needed to prevent oxidation. We used dense and packed thiol (11-mercaptoundecanoic acid (MUA)) layer which protects the silver from oxidation and enable immobilization of Rabbit Anti-Estrone Polyclonal IgG antibody to the thiol layer through linker. 1-Ethyl-3-(3-dimethylaminopropyl)-carbodiimide and N-hydroxysuccinimide (NHS) were added to make the surface reactive. Shift in the SPR signal indicated the presence of the conjugated material-estrone and a detection limit of 5×10^{-6} RIU is demonstrated.

1. A. M. Sesay, and D. C. Cullen, "Detection of Hormone Mimics in Water using a Miniturised SPR Sensor," Environmental Monitoring and Assessment 70, 83-92 (2001).
2. A. Karabchevsky, S. Karabchevsky, and A. Abdulhalim, "Fast Surface Plasmon Resonance Imaging Sensor Using Radon Transform," In Press (2010).

Conference 8100: Spintronics IV

Sunday-Wednesday 21-24 August 2011 • Part of Proceedings of SPIE Vol. 8100 Spintronics IV

8100-01, Session 1

'Listening' to the spin noise of electrons and holes in semiconductor quantum structures

S. A. Crooker, Los Alamos National Lab. (United States)

The coherence and dynamical properties of spins in semiconductors are usually studied with powerful techniques based on optical pump-probe or spin resonance methods. Such methods are necessarily perturbative, in that one measures the (dissipative) response of the spins resulting from an external drive or excitation field (eg, free-induction decays). However, in accord with the fluctuation-dissipation theorem, the intrinsic fluctuations of the spin system - if experimentally measurable - can also reveal the same dynamical properties (such as g-factors and decoherence times) without ever perturbing the spin ensemble from thermal equilibrium.

This talk describes how we measure electron and hole spin dynamics in semiconductors by passively "listening" to these small spin noise signals [1]. We employ a spin noise spectrometer based on a sensitive optical Faraday rotation magnetometer that is coupled to a digitizer and field-programmable gate array (FPGA), to acquire noise spectra from 0-1 GHz in real time with picoradian/root-Hz sensitivity. In doped (In,Ga)As/GaAs quantum dots, both electron and hole spin fluctuations generate distinct noise peaks whose shift and broadening with magnetic field directly reveal their g-factors and dephasing rates. A large, energy-dependent anisotropy of in-plane hole g-factors is clearly exposed, reflecting systematic variations in the average confinement potential. In contrast with conventional pump-probe studies, noise signals increase as the probed volume shrinks, suggesting possible routes towards non-perturbative, sourceless magnetic resonance of few-spin systems. [1] PRL 104, 036601 (2010); PRB 79, 035208 (2009).

In collaboration with Yan Li, D. Smith, J. Brandt, C. Sandfort, A. Greilich, D. Reuter, A. Wieck, D. Yakovlev and M. Bayer; supported by LANL-LDRD programs.

8100-02, Session 1

Quantum spin Hall effect in topological insulators

E. B. Sonin, The Hebrew Univ. of Jerusalem (Israel)

The original motivation of great interest to topological insulators was the hope to observe the quantum spin Hall effect. Therefore if a material is in the topological insulator state they frequently call it the quantum spin Hall state. However, despite impressive experimental results confirming the existence of the quantum spin Hall STATE, the quantum spin Hall EFFECT has not yet been detected. After an introduction addressing topological insulators and the spin Hall effect, I shall discuss whether and how the quantum spin Hall effect could be observed.

8100-03, Session 1

Spin injection into silicon using Al₂O₃, SiO₂ and MgO tunnel barriers

O. M. J. van 't Erve, C. H. Li, A. T. Hanbicki, B. T. Jonker, U.S. Naval Research Lab. (United States)

We recently demonstrated injection of spin-polarized electrons from an Fe film into Si[1]. The tunnel barrier is the key component in achieving a large spin accumulation in the semiconductor. Here we will compare three different tunnel barriers, Al₂O₃, SiO₂ and MgO, on highly doped Si using three terminal Hanle measurements. Hanle measurements give insight in the spin-accumulation directly underneath the spin injecting contact. We demonstrate the electrical detection of spin accumulation in Si (doped n-type 3x10¹⁸ to 6x10¹⁹/cm³) up to 500K via injection

from a ferromagnetic contact through a SiO₂ tunnel barrier formed by plasma oxidation. Lorentzian fits to Hanle curves yield a spin lifetime of ~100 and 320ps for the 6e19 and 3e18 doped Si, respectively. The direct correlation between spin lifetime and carrier concentration in the Si, and that the magnitude of the Hanle signal agrees well with that expected from theory [2], providing clear evidence that the spin accumulation indeed occurs in the Si and not interface states. A spin lifetime of 120ps was obtained for 3e19 n-doped Silicon for both the Al₂O₃ and SiO₂ tunnel barrier. We will present the bias dependence and the temperature dependence of the spin lifetime for the different tunnel barriers. These results demonstrate that spin accumulation in Si can be a viable basis for spin-based devices. Supported by ONR.

[1] B. T. Jonker et al., Nature Phys. 3, 542 (2007), O.M.J. van 't Erve et al., App. Phys. Lett. 91, 212109, (2007)

[2] Fert et al., PRB 64, 184420 (2001), IEEE Elect. Dev. 54, 921 (2007).

8100-04, Session 2

Lateral spin injection in germanium nanowires

E. Tutuc, E. Liu, J. Nah, K. Varahramyan, The Univ. of Texas at Austin (United States)

Efficient spin injection from ferromagnetic metals (FM) into semiconductors (SC) is typically suppressed by the conductivity mismatch at the FM/SC contact. Spin injection can be achieved however if the contact resistivity at the FM/SC interface is appropriately engineered [1]. Here we examine the spin injection in n-type, phosphorus-doped germanium nanowires using cobalt as FM contacts, and MgO tunnel barriers for contact resistance engineering. The two-point magnetoresistance measurements reveal spin-valve effect, with a low (high) resistance for parallel (antiparallel) polarizations of the FM contacts. Non-local, four-point magnetoresistance measurements, which separate the spin diffusion path from the charge current path, demonstrate that the observed spin-valve effect stems from spin injection in the Ge nanowires. We map out the contact resistance window where lateral spin transport is observed, and manifestly show the conductivity matching required for spin injection. We discuss the implications of these results in the context of the spin diffusion theory.

[1] A. Fert and H. Jaffres, Phys. Rev. B. 64, 184420 (2001)

8100-05, Session 2

Hot-electron spin injection and detection in n-doped silicon

Y. Lu, Univ. Henri Poincaré Nancy (France); I. Appelbaum, J. Li, Univ. of Maryland, College Park (United States); M. Hehn, Univ. Henri Poincaré Nancy (France)

Silicon has been known for decades to have an extraordinarily long spin lifetime. Using unique spin-polarized hot-electron injection and detection techniques [1], we have observed unprecedented spin coherence, and extracted very long spin lifetimes of conduction electrons travelling over macroscopic distances [2]. It is necessary to investigate magnetic and electric field controls of electron spin in doped silicon for integration of spintronics into present-day silicon-based microelectronic technology, where impurity doping plays a critical role.

By reversing the Schottky barrier-height asymmetry in hot-electron semiconductor-metal-semiconductor ballistic spin filtering detectors [3], we have achieved the following: (1) demonstration of >50% spin polarization in silicon (Fig.1), resulting from elimination of the ferromagnet/silicon interface on the transport channel detector contact and (2) evidence of spin transport at temperatures as high as 260 K, enabled by an increase in detector Schottky barrier height.

Unlike previous studies with undoped Si, the presence of ionized

impurities in the depletion regions of these doped transport layers gives rise to conduction-band bending that (for sufficient biasing conditions) confines injected electrons for long dwell times. Recently, another unexpected source of non-equilibrium spin dephasing in n-type phosphorus-doped silicon is also observed when temperature and voltage conditions provide a confining electrostatic potential conduction band profile between injector and detector Schottky barriers [4]. In addition to Hanle spin precession features for magnetic fields in the kOe range, we also observe substantial (but incomplete) dephasing with much smaller characteristic widths of ~50-100 Oe (Fig.2). The possibility that this phenomenon originates from transit-time delays associated with capture/re-emission in shallow impurity traps is discussed in light of temperature, voltage, and electron density dependence measurements.

[1] Ian Appelbaum, B.Q. Huang, and D.J. Monsma, *Nature* 447, 295 (2007).

[2] B.Q. Huang, D.J. Monsma, and Ian Appelbaum, *Phys. Rev. Lett.* 99, 177209 (2007).

[3] Yuan Lu and Ian Appelbaum, *Appl. Phys. Lett.* 97, 162501 (2010).

[4] Yuan Lu, Jing Li, and Ian Appelbaum, arXiv:1101.1944v1

8100-06, Session 2

Optical spin orientation in SiGe heterostructures

G. Isella, F. Bottegoni, Politecnico di Milano (Italy); F. Pezzoli, Univ. degli Studi di Milano-Bicocca (Italy); S. Cecchi, Politecnico di Milano (Italy); E. Gatti, E. Grilli, M. Guzzi, Univ. degli Studi di Milano-Bicocca (Italy); F. Ciccacci, Politecnico di Milano (Italy)

Germanium lies between gallium and arsenide in the periodic table, therefore Ge and GaAs features many similarities. In particular, still being an indirect bandgap semiconductor, the absorption properties of Ge are dominated by direct-gap transitions coupling heavy holes (HH) and light holes (LH) states in the valence band with the local minimum of the conduction band (CB) at the Gamma point. As a result, selection rules valid for optical spin orientation in GaAs apply also to Ge. In Ge-based heterostructures strain and quantum confinement effects might be employed to remove the HH-LH degeneracy at Gamma, substantially increasing the polarization of excited carriers. Moreover Ge exhibits centre-of-inversion symmetry, a spin orbit interaction weaker than GaAs and a high compatibility with Si technology, all relevant features for spintronics applications.

We present spin polarized photo emission (SPPE) and photoluminescence (PL) measurements performed on bulk Ge, Ge/Si(100) epilayers and Ge/SiGe multiple quantum wells heterostructures.

SPPE data indicate that compressive bi-axial strain effectively lifts the HH LH degeneracy raising the polarization of injected electrons above the P=50% limit of bulk material.

PL measurements performed on bulk Ge crystal at different excitation energies give insights on the spin relaxation mechanism related to the thermalization of injected carrier at the Gamma point.

In Ge MQWs, direct-gap PL at excitonic resonances indicates that spin injection well above bulk values can be achieved. Part of the polarization is preserved during electron scattering from Gamma to the absolute CB minimum at L, as suggested by the polarization of light associated with indirect-gap transitions.

8100-07, Session 2

Spin injection in metal based lateral nanostructures

P. Laczowski, L. Vila, J. P. Attané, A. Marty, C. Beigné, L. Notin, Commissariat à l'Énergie Atomique (France)

The ability to control and manipulate spin currents, a flow in opposite directions of spin up and spin down without net electrical charge flux, is a

key point for the development of new spin based electronic devices in the field of spintronics. Admits the large variety of proposed spin structures [FER08], lateral spin valves (LSV) have recently attracted much attentions, giving the possibility of fabrication of multi-terminal nanostructures. The LSV structure quality can be quantified by its spin signal ΔR_s , which is related to the difference of non-local electrochemical potential between the anti-parallel and parallel magnetization states of the electrodes. The spin signal depends mainly on the geometry of the LSV, the quality of the interfaces, and the choice of the used materials.

We will review two basic methods for spin current generation in metal based lateral nanostructures, being current injection with the tunnel or transparent junctions through Ferromagnetic(F)/Nonmagnetic(NM) interfaces, or alternatively at the Ferromagnetic/Paramagnetic interface through the Spin Hall Effect (SHE). Recent experiments using the SHE [VAL09] opened new paths toward the generation and detection of spin current without requirements for magnetic materials neither magnetic fields. In this context, the insertion of materials with large spin-orbit coupling in LSV was demonstrated to be an efficient way to measure the Spin Hall angle [VIL07].

We will also present a technique used to optimize the spin signal of LSV using multi-angle deposition process, avoiding interface contamination and oxidation. Comparison of the spin signals obtained with NM material having either short or long spin diffusion length will be also carried out.

[FER08] A. Fert, *Rev. Mod. Phys.* 80,1517 (2008)

[VAL09] S. Valenzuela, *International Journal of Modern Physics B* 23, 2413 (2009)

[VIL07] L. Vila, T. Kimura, Y. Otani, *Phys. Rev. Lett.* 99, 226604 (2007)

8100-08, Session 3

Spin polarized electroluminescence and spin photocurrent in hybrid Semiconductor/Ferromagnetic heterostructures : an Asymmetric Problem

T. Amand, P. Renucci, V. G. Truong, Institut National des Sciences Appliquées de Toulouse (France); H. Jaffrès, Unité Mixte de Physique CNRS/Thales (France); L. Lombez, Institut National des Sciences Appliquées de Toulouse (France); P. H. Binh, Institute of Material Science (Viet Nam); J. George, Unité Mixte de Physique CNRS/Thales (France); X. Marie, Institut National des Sciences Appliquées de Toulouse (France)

The photocurrent obtained under polarized optical excitation and the polarized electroluminescence recorded under forward electric bias have been measured in the same hybrid Semiconductor/Ferromagnetic metal structures (Spin-Light Emitting Diode). The systematic investigations have been performed on devices with different ferromagnetic spin injectors: tunnel barrier of Al₂O₃ surmounted by a thin Co ferromagnetic layer or MgO tunnel barriers with a CoFeB FM layer. Though a very efficient electrical spin injection is demonstrated with a measured circular polarization of the electroluminescence up to 30% for an external field of 0.8 Tesla, very weak polarizations of the photocurrent are evidenced whatever the nature of the device is [1]. The maximum photocurrent polarization obtained under continuous resonant circularly polarized excitation of the quantum well excitons is about 3%. This demonstrates that the investigated devices do not act as an efficient spin filter for the electrons flowing from the semiconductor part to the ferromagnetic part of these structures though these systems are very efficient spin aligners for electrical spin injection. We interpret the weak measured polarization of the photocurrent as a consequence of the Zeeman splitting of the quantum well excitons which yields different absorption coefficients for the polarized excitation laser with different helicities. This leads to different intensities of photocurrent collected for the two different circularly polarized excitations. This interpretation is confirmed by an experiment exhibiting the same results for photocurrent measured on a device with a non ferromagnetic electrical contact.

[1] P. Renucci et al., *Phys Rev B* 82,195317 (2010)

8100-09, Session 3

Optically oriented electron spin transmission across ferromagnet/ semiconductor interfaces

T. Taniyama, Tokyo Institute of Technology (Japan)

An understanding of electron spin transmission across ferromagnet (FM)/ semiconductor (SC) interfaces is vital to the successful development of spintronic devices. Both electron transmission processes from the FM into the SC and from the SC into the FM are highly relevant to providing information about the surest route to achieving high efficiency of spin injection into SC. The aim of this work is to examine the electron spin transmission processes from a GaAs quantum well (QW) into a ferromagnetic metal layer using optical spin orientation method. The sample structure we used consists of an Fe layer or an Fe₃O₄ layer on a GaAs/AlGaAs QW. Once circularly polarized light irradiates the sample from the normal to the layer plane, spin polarized electrons are excited in the quantum well according to the optical transition selection rules, thereby photocurrent of the spin polarized electrons flows across the interface. Since the photocurrent varies depending on the excited electron spin orientation, measurement of the circular polarization dependence of the photocurrent, i.e., helicity dependent photocurrent, can provide information about the mechanism of electron spin transmission across the interface. One of the most significant results here we observe is a dip appears in the helicity dependent photocurrent at a particular bias voltage for the Fe/GaAs QW sample and even the sign reversal of the helicity dependent photocurrent occurs. The origin of the bias dependence of the helicity dependent photocurrent is discussed in detail using the Breit-Wigner type resonant tunneling process via interface resonant states.

8100-10, Session 3

Spin injection in silicon and germanium

M. Jamet, Commissariat à l'Énergie Atomique (France); A. Jain, L. Grenet, A. Barski, Commissariat à l'Énergie Atomique (France); P. Noé, Commissariat à l'Énergie Atomique (France); S. Auffret, P. Warin, J. Hartmann, A. P. Brenac, E. Augendre, V. Baltz, P. Gentile, L. Via, Commissariat à l'Énergie Atomique (France)

Spintronics aims at manipulating both charge and spins in semiconductors. It thus requires a robust scheme for injecting polarized current into these materials. Spin injection into GaAs has already been demonstrated optically and electrically. Recently an increasing number of works are performed on spin injection into silicon and germanium since they are the core materials for potential applications and promising candidates for spin polarized transport due to predicted long spin lifetimes. We present results obtained on spin injection from a ferromagnetic layer into silicon (optical detection) and germanium (electrical detection). SiGe quantum wells embedded in a Si-based pin diode are used to optically detect spin-polarized electrons injected into silicon whereas three-terminal and four-terminal geometries are used for electrical non-local detection of spin accumulation in germanium layers. The electron spins are aligned either in-plane using NiFe and Co electrodes or out-of-plane using a CoPt electrode with perpendicular magnetization. Spin injection through an alumina tunnel barrier is carried out to prevent depolarization due to conductance mismatch with silicon and germanium. For spin injection in silicon, the remanent configuration of the CoPt electrode magnetization allows to study spin injection without applying a magnetic field, avoiding spurious effects such as Faraday rotation in silicon. Light polarization of more than 3 percent has been measured and its temperature dependence will be discussed. Preliminary electrical detection of spin accumulation in germanium will also be presented after overcoming the issue of Fermi level pinning at the interface between germanium and the tunnel barrier.

8100-11, Session 4

Magnetization dynamics in the inertial regime: nutation predicted at short time scales

J. Wegrowe, H. Drouhin, Ecole Polytechnique (France)

The well-known Gilbert's equation describes the dissipative dynamics of the magnetic degrees of freedom coupled to a heat bath. We propose to discuss the derivation of the Gilbert's equation from both the point of view the Lagrangian approach [1] and the non-equilibrium thermodynamic (NET) approach.

The derivation based on the Lagrangian approach (used initially by Gilbert in 1955) [1] is performed in the phase space : the angular momentum (with the kinetic energy) is introduced as starting hypothesis. However, the Gilbert equation is a kinetic equation that does not contain any inertial terms for uniform magnetization. This paradoxical situation appeals at least two comments.

(1) On one hand, a full kinetic derivation of the Gilbert equation (with zero kinetic energy) would solve the paradox. Such a derivation is proposed within the NET approach [2]. This derivation is performed in the configuration space of the magnetic degrees of freedom, and not in the phase space (i.e. no need to introduce the angular momentum).

(2) On the other hand, the Gilbert's Lagrangian approach can be pushed to its logical consequences, i.e. a generalization of the equation with the introduction of inertial terms proportional to the second derivative of the uniform magnetization [3]. This derivation is obtained straightforwardly by enlarging the configuration space of the magnetization to the phase space, i.e. to the angular momentum. Beyond, the transient nature of this inertial regime is derived in the framework of the NET theory.

[1] Thomas L. Gilbert, IEEE Trans. Mag. 40 (2004) 3443, Phys. Rev. 100, 1243 (1955) (abstract only), and PhD Dissertation "Formulation, Foundations and Applications of the phenomenological theory of ferromagnetism" Illinois Institute of Technology, 1956.

[2] J.E. Wegrowe, Phys. Rev B 62, 1067 (2000), J.-E. Wegrowe et al. J. Phys. : Condens. Matter 19, 165213 (2007), Phys. Rev. B 77, 174408 (2008) and Sol. State Com. 150 (2010), 519

[3] C. Ciornei, M Rubi, and J.-E. Wegrowe, Phys. Rev. B 020410(R) (2011)

8100-12, Session 4

Ferromagnetic nanostructures for magnonic crystals and waveguides

D. Grundler, Technische Univ. München (Germany)

Collective spin excitations in ferromagnets have regained great interest in the course of spintronics research. Recent observations such as spin-wave quantization, localization and interference have stimulated the field of magnonics where spin waves (magnons) are explored in order to carry and process information.[1] We investigate nanopatterned ferromagnetic thin films which form magnonic waveguides [2,3] and magnonic crystals [4], i.e. the magnetic counterpart of photonic crystals. Allowed minibands and forbidden frequency gaps are created by coherent coupling of confined spin wave modes. The devices open intriguing perspectives for the manipulation of spin waves at the nanoscale and the realization of magnetic metamaterials.[5] We gratefully acknowledge collaborations and discussions with M. Becherer, B. Botters, G. Dürr, F. Giesen, G. Gubbiotti, D. Heitmann, M. Kostylev, M. Krawczyk, V. Kruglyak, S. Neusser, J. Podbielski, D. Schmidt-Landsiedel, M.L. Sokolovsky, S. Tacchi, and J. Topp. The research has received funding from the European Community's Seventh Framework Programme (FP7/2007-2013) under Grant Agreement no. 228673, from SFB 668 and the German Excellence Cluster 'Nanosystems Initiative Munich'.

References:

[1] S. Neusser and D. Grundler, Advanced Materials 21, 2927 (2009).

[2] J. Topp et al., Phys. Rev. B 78, 024431 (2008).

[3] S. Neusser et al., Phys. Rev. Lett. 105, 067208 (2010).

- [4] J. Topp et al., Phys. Rev. Lett. 104, 207205 (2010).
 [5] V.V. Kruglyak, S.O. Demokritov, and D. Grundler, J. Phys. D: Applied Physics 43, 264001 (2010); and references therein.
 [6] V. V. Kruglyak et al., Phys. Rev. Lett. 104, 027201 (2010).

8100-13, Session 4

Tailoring magnetic relaxation channels at the nanoscale

I. Barsukov, Univ. Duisburg-Essen (Germany)

Controlling spin relaxation is essential for spintronic and spin torque applications. Manipulating spin relaxation allows the adjustment of magnetization reversal speed at microwave frequencies. Moreover, the critical current in spin torque devices can be reduced and tuned. In the experiment it is possible to distinguish between the intrinsic and extrinsic relaxation channels. The latter can be tailored with respect to the intensity and anisotropic behaviour. In particular, methods for inducing elementary relaxation channels of uniaxial symmetry and their impact on the magnetization dynamics are discussed in this presentation.

Fe-based thin films have been studied by means of the ferromagnetic resonance technique, by which the intrinsic and extrinsic relaxation processes can be disentangled. While the former are rather isotropic and can be adjusted via spin-orbit interaction, the latter can be modified in an advanced way. It is shown, how crystalline defects, inhomogeneities of chemical composition, and interface modifications can induce the 2-magnon scattering. Control and systematic manipulation of these parameters allow tailoring the overall spin relaxation in a desired manner.

In cooperation with J. Lindner, R. Meckenstock, H. Wende, P. Landeros, K. Lenz, and M. Farle.

Financial support by the DFG, SFB 491 is acknowledged.

8100-14, Session 4

Emergent magnetic monopoles and associated Dirac strings in artificial kagome spin ice

L. J. Heyderman, Paul Scherrer Institut (Switzerland)

Artificial spin ice systems, consisting of two-dimensional arrangements of single-domain nanomagnets, have recently been in the focus of scientific interest since they provide an opportunity to directly study the effects of frustration [1, 2]. Our work has focused on artificial kagome spin ice, with elongated nanomagnets arranged on the kagome lattice forming an array of hexagonal rings. Synchrotron x-ray photoemission microscopy allows direct imaging of the magnetic state of each nanomagnet, having moments pointing in one of two orientations parallel to their long axis. Our recent observations demonstrate the existence of emergent magnetic monopoles and their associated Dirac strings at room temperature in a quasi-infinite nanomagnet array [3]. In an applied magnetic field, monopole-antimonopole pairs nucleate and then separate in an avalanche-type manner along one-dimensional Dirac strings, consisting of overturned dipoles. This behaviour is distinct from conventional domain growth in two-dimensional systems and results in the formation of a 'stripe phase' towards the end of magnetization reversal. The observed hysteresis, monopole densities and 1D Dirac-string avalanches are quantitatively explained by Monte Carlo simulations and the results open the way to a controlled manipulation of magnetic charges that may lead to new spintronic devices.

- [1] R.F. Wang et al., Nature 439, 303 (2006)
 [2] E. Mengotti et al., Phys. Rev. B 78, 144402 (2008)
 [3] E. Mengotti et al., Nature Physics (2010)

8100-15, Session 4

Indirect localization of a magnetic domain wall mediated by its quasi wall

D. Lacour, Univ. Nancy 2 (France) and Institut Jean Lamour (France) and CNRS (France); F. Montaigne, M. Hehn, Univ. Henri Poincaré Nancy (France); R. Belkhou, Synchrotron Soleil (France); N. Rougemaille, Institut Néel (France) and CNRS (France) and Univ. Joseph Fourier (France); J. Raabe, Paul Scherrer Institut (Switzerland)

The manipulation of a single magnetic domain wall in thin films and nanostructures opened up new insight and opportunities for fundamental and applied researches. Studies have all focused on the control of the pinning and the depinning processes of domain walls on centers localized in the magnetic layer in which the wall moves (active layer). Here we report an indirect localization process of 180° domain walls that occurs in commonly used multilayer nanostructures in which an active and a reference magnetic layer coexist. Combining Scanning Transmission X-Ray Microscopy with micromagnetic simulations, magnetic configurations in both layers have been resolved. The nucleation of a 180° domain wall in the active layer creates a quasi wall in the reference layer atop of the wall. Then the wall and the quasi propagate together. The quasi wall pinning in reference layer is shown to be responsible for this indirect localization process of the domain wall in the active layer.

8100-16, Session 5

Optical pumping of electron and nuclear spins in GaAs/AlGaAs droplet epitaxy quantum dots

T. Amand, G. Sallen, S. Kunz, D. Lagarde, X. Marie, B. Urbaszek, Institut National des Sciences Appliquées de Toulouse (France); T. Kuroda, M. Abbarchi, T. Mano, K. Sakoda, National Institute for Materials Science (Japan)

The spin properties of semiconductor quantum dots are extensively investigated, due to their potential applications in spintronics and quantum cryptography. Quantum dots elaborated by molecular droplet epitaxy are very attractive since they provide strong confinement for carriers as in Stransky-Krastanov grown dots, but in the absence of lattice strain. Here, we review the optical and spin properties of GaAs/AlGaAs droplet dots.

First, we investigate the impact of the dot anisotropy on the optical selection rules for samples grown on [100] and on novel [111] oriented substrates. The single dot emission spectra display exciton and biexcitons, as well charged exciton complexes. The linearly polarized emission dependence of each emission line reveals a departure from the standard optical selection rules. Using a 6-bands k.p model including the electron-hole exchange we show that the exciton fine structure as well as the polar emission diagrams are determined by heavy/light-hole state mixing. The physical origin of this mixing is a lowering of the quantum dot confinement potential symmetry.

Second, dynamic nuclear polarization is investigated, revealing that remarkably, even without external magnetic fields, the oriented electron spin can polarize the nuclear spin system. Dynamic polarization of the nuclear spins, up to about 50%, is also demonstrated in a longitudinal magnetic field. Using a time resolved spectroscopy technique, it is shown that the build-up of the dynamic nuclear polarization occurs within a few hundred milliseconds, and increases with the applied external magnetic field.

8100-17, Session 5

Single-electron spin ratchet

S. O. Valenzuela, Institució Catalana de Recerca i Estudis Avançats (Spain) and Catalan Institute of Nanotechnology (Spain) and Univ. Autònoma de Barcelona (Spain)

We describe a spin ratchet at the single-electron level that produces spin currents with no net bias or charge transport. Our device [1] is based on the ground-state energetics of a single-electron transistor (SET). The SET comprises a superconducting island connected to normal leads via tunnel barriers with different resistances that break spatial symmetry. We demonstrate spin transport and quantify the spin ratchet efficiency by using ferromagnetic leads with known spin polarization.

[1] M.V. Costache and S.O. Valenzuela, *Science* 330, 1645 (2010)

8100-18, Session 5

Single spins in quantum dots and impurities

C. E. Pryor, The Univ. of Iowa (United States)

There are a variety of methods available for confining and manipulating single spins in solid state systems. While heterostructures can be engineered to the requirements of the problem, their variability is a disadvantage compared to identical impurities. I will discuss theoretical calculations of single spins both in quantum dot heterostructures and bound to impurities. These include calculations of the spin state itself, the effective coupling to a magnetic field, the response to an electric field, and include both electrons and holes.

8100-19, Session 5

Nuclear spin dynamics in semiconductor nanostructures

I. Tifrea, California State Univ., Fullerton (United States)

I will discuss recent advances in understanding the nuclear spin dynamics in low dimensional systems. The focus will be on the hyperfine interaction between nuclear and electronic spins and the role this interaction plays on the dynamical nuclear polarization of semiconductor nanostructures. The natural confinement provided by low dimensional semiconductor nanostructures such as quantum wells and quantum dots is responsible for a position dependent nuclear spin dynamics in these physical systems. Consequently, the nuclear spin relaxation time and implicitly the nuclear spin polarization will be position dependent leading to important implications for optical NMR and Faraday rotation experiments. Additionally, numerical simulations prove that nuclear spin diffusion may be reduced in the same conditions. As an example I will discuss the case of a GaAs quantum well. I will present results for Overhauser shifts, measurable in Faraday rotation experiments, and Knight shifts, measurable in optical NMR experiments. In connection with these results I will present results for nuclear spin diffusion and prove its relatively small effect on the overall polarization of As nuclei.

This work was supported by Research Corporation.

8100-20, Session 6

Spin relaxation and spin transport in graphene and the interface of multiferroic oxides

M. Wu, Univ. of Science and Technology of China (China)

Invited talk for SPINTRONICS IV

8100-21, Session 6

Dopants and charge carriers in colloidal semiconductor quantum dots

D. R. Gamelin, Univ. of Washington (United States)

The generation, manipulation, and detection of electron spins in semiconductor nanostructures are all central themes in spintronics and spin-photonics. This talk will describe recent advances in the introduction, study, and manipulation of spins in colloidal semiconductor nanocrystals, focusing on properties of doped nanocrystals such as transition-metal-doped CdSe, ZnO, and ZnSe quantum dots. Topics will include unusual photoluminescence phenomena, magneto-optical spectroscopies, magnetic resonance spectroscopies, photoluminescence dynamics, spin relaxation dynamics, carrier-dopant magnetic exchange interactions, and photon-controlled magnetization. The properties to be discussed underlie many important spin-electronic and spin-photonics phenomena including carrier-mediated ferromagnetism, excitonic magnetic polaron nucleation, and proposed spin-based quantum information processing. Basic aspects of doped quantum dot electronic structures will be discussed in this context.

Related references:

“Colloidal Transition-Metal-Doped Quantum Dots.” Beaulac, R.; Ochsenein, S. T.; Gamelin, D. R., Chapter 7 in *Nanocrystal Quantum Dots*, 2nd edition (edited by V. I. Klimov), 2010, CRC Press, 397. (review)

“Quantum Oscillations in Magnetically Doped Colloidal Nanocrystals.” Ochsenein, S. T.; Gamelin, D. R., *Nature Nanotechnology*, 2011, 6, 112.

“Light-Induced Spontaneous Magnetization in Colloidal Doped Quantum Dots.” Beaulac, R.; Schneider, L.; Archer, P. I.; Bacher, G.; Gamelin, D. R., *Science*, 2009, 325, 973.

8100-22, Session 6

Inelastic light scattering of hole spin excitations in p-modulation-doped GaAs-AlGaAs single quantum wells

M. Hirmer, M. Hirmer, T. Korn, D. Schuh, Univ. Regensburg (Germany); W. Wegscheider, ETH Zürich (Switzerland); R. Winkler, Northern Illinois Univ. (United States); C. Schüller, Univ. Regensburg (Germany)

We have investigated spin-density excitations of holes in one-sided p-modulation-doped GaAs-AlGaAs single quantum wells by means of resonant inelastic light scattering. The experiments yield a direct measure of the Rashba spin splitting of holes in quantum wells with an asymmetric potential profile. The samples are highly-doped GaAs-AlGaAs single quantum wells with well widths of 15, 20 and 25 nm, and different doping densities. The experiments were performed at temperatures of about 4 K, using a tunable Ti:Sapphire laser and a triple Raman spectrometer with liquid-nitrogen cooled CCD detector. In the low-energy range of the inelastic light scattering spectra, we observe in all samples well-defined excitations with excitation energies between about 1 meV and 4 meV, which can be attributed to spin-density excitations of the two-dimensional hole systems due to polarization selection rules. We interpret the excitations as spin-density excitations, where holes are excited between the Rashba spin-split ground states, performing a spinflip. The strong resonance behavior of the inelastic light scattering process allows us to scan the k dependence of the hole spin splitting. Comparison to k² bandstructure calculations, performed with the NextNano3 program package, shows good agreement of the measured and calculated k-dependent spin splittings. Details of the spectra show a distinct dependence on the directions of light polarizations with respect to crystallographic axes. In particular, we have detected a doublet structure of the hole spin excitations, which may be attributed to the anisotropic hole spin splitting within the quantum-well plane.

8100-23, Session 6

New insights into nanomagnetism by spin-polarized scanning tunneling microscopy and spectroscopy

H. Oka, P. Ignatiev, S. Wedekind, G. Rodary, L. Niebergall, V. Stepanyuk, D. Sander, J. Kirschner, Max-Planck-Institut für Mikrostrukturphysik (Germany)

Spin-polarized scanning tunneling microscopy (SP-STM) allows imaging and spectroscopic characterization of nanostructures with unsurpassed spatial resolution. Its working principle exploits the dependence of the tunnel current on the relative magnetization orientation of a sample and the magnetic STM tip. We present results by SP-STM, where we investigate the correlation between structural, electronic, and magnetic properties of individual nm small Co islands with several hundred to thousands of atoms. We use external magnetic fields of up to 4 T to tune the magnetic state of both tip and sample, and we extract the corresponding change of the differential conductance of the tunnel junction.

A recent example is our measurement of magnetic hysteresis loops of individual nm small Co islands on Cu(111) at 8 K by SP-STM in external magnetic fields. We find switching fields of up to 2.5 T for islands with roughly 8,000 atoms. The quantitative analysis of these results provides novel insights into the magnetization reversal on the nanoscale, and deviations from the venerable Stoner-Wohlfarth model are discussed.

We also exploit the high spatial resolution of SP-STM in magnetic fields to measure maps of the differential conductance within a single nm-small Co island. In connection with density functional theory calculations we demonstrate for the first time that the spin polarization is not homogeneous but spatially modulated within the Co island. We ascribe the spatial modulation of the spin polarization to spin-dependent electron confinement effect within the Co island [1].

[1] Oka, Ignatiev, Wedekind, Rodary, Niebergall, Stepanyuk, Sander, Kirschner, *Science* 327, 843 (2010).

*Present address (G.R.): Laboratoire de Photonique et de Nanostructures, CNRS UPR20, Route de Nozay, 91460 Marcoussis, France.

8100-24, Session 6

Magneto-resistance in a lithography defined single constrained domain wall spin valve

C. H. de Groot, Y. Wang, Univ. of Southampton (United Kingdom); D. Claudio-González, Univ. de Guanajuato (Mexico); H. Fangohr, Univ. of Southampton (United Kingdom)

We have measured domain wall magnetoresistance in a single constrained domain wall [1]. In 1999, Bruno [2] proposed that in nanostructured devices the domain wall width can be constricted by geometric means. A sudden large expansion of the magnetic area will constrict the domain wall as the energy cost of increasing the area of the domain wall outweighs the exchange interaction. An H-shaped Ni nanobridge device based on this idea was fabricated by e-beam lithography with the two sides being single magnetic domains showing independent magnetic switching. The bridge connecting between the sides constrains the domain wall when the sides' magnetization line up antiparallel. The magnetoresistance curve clearly identifies the magnetic configurations that are expected from a spin-valvelike structure. The value of the magnetoresistance at room temperature is around 0.1% or 0.4 Ω . This value is shown to be in agreement with a theoretical formulation based on spin accumulation. This is the first inplane transport measurement of an individual nanomagnetic structure.

In this conference we are going to show the experimental realization of this proposed structure and magnetoresistance in a lithographically defined constrained domain wall structure in between two independently switching single magnetic domains. The e-beam lithography and metal lift-off procedures will be introduced as well, such as dose proximity effect correction (PEC), bi-layer lift-off structure.

8100-25, Session 7

Computational studies of model Hamiltonians for strongly correlated materials in the bulk and at interfaces

E. Dagotto, The Univ. of Tennessee (United States)

The current status of computer simulations of model Hamiltonians for transition metal oxides, such as the manganites with the colossal magnetoresistance (CMR) and the high- T_c superconducting cuprates, will be reviewed. It will be shown that state-of-the-art computer simulations involving Monte Carlo simulations of double-exchange models with Jahn-Teller phonons do display the CMR effect, while one-orbital Hubbard models for Cu-oxides (and multiorbital models suitable for the recently discovered superconducting pnictides) have tendencies to pairing in exotic channels. These materials, and others, also play an important role in the novel area of oxide superlattices. A brief review of this field will be presented followed by results of our group with an emphasis on the stabilization at interfaces of novel states that do not have an analog in the materials that form the superlattice when they are in bulk form. Time allowing, recent developments in manganite multiferroics will also be discussed. Here, computer simulations have recently predicted the existence of new phases with unusual arrangements of spin and charge when narrow bandwidth manganites are hole doped.

8100-26, Session 7

Oxide interfaces: spin transport at the nanoscale

T. Banerjee, Univ. of Groningen (Netherlands)

Oxide spintronics is an emerging research direction where the fundamental thrust is on understanding the physics of electron charge/spin/orbital interactions in perovskite oxide interfaces at the nanoscale. Epitaxial interfaces of half-metallic ferromagnets on oxide semiconductors are the building blocks of spintronic devices. Very little is known about spin transport across such interfaces, at the nanoscale, where intriguing phenomena are likely to emerge. In this talk, I will discuss our recent experiments on nanoscale (spin) electron transport across epitaxial interface of La_{0.67}Sr_{0.33}MnO₃(LSMO) on Nb:SrTiO₃, using the technique of Ballistic Electron Emission Microscopy (BEEM) and illustrate its importance in oxide electronics.

8100-27, Session 7

An antiferromagnetic insulator with voltage controlled surface polarization

P. A. Dowben, N. Wu, X. He, C. Binek, K. Belashchenko, T. Komesu, Univ. of Nebraska-Lincoln (United States)

For the prototypical magneto-electric Cr₂O₃(0001), we have observed a finite remanent polarization at the surface in spin-polarized photoemission [1], spin polarized inverse photoemission, and X-ray magnetic circular dichroism. This occurs when the antiferromagnetic single domain state is selected in a magneto-electric annealing process. In a magneto-electric material, an applied electric field induces a net magnetic moment. This becomes important to surface magnetism because there is also a finite remanent magnetization at the surface or boundary of magneto-electric antiferromagnets, predicted using symmetry arguments, and recently demonstrated [1]. In the single domain antiferromagnetic state of Cr₂O₃, the magnetic Cr₂O₃(0001) surface moment evolves and is robust against surface roughness, which may be useful for device fabrication. The surface polarization has now been measured to be as high as 70 to 80%, at binding energies corresponding to a strongly weighted surface density of states.

This surface magnetic order, combined with the magneto-electric behavior of Cr₂O₃(0001) enables the investigator to have electric control

of a net magnetic moment at the Cr₂O₃(0001) surface. The surface magnetic domain structure has also been imaged in X-ray circular dichroism combined with photoemission electron microscopy (PEEM) at the surface of Cr₂O₃(0001), under conditions of no electric field cooling and with electric field cooling. Consistent with the other measurements, profound differences are observed.

[1] Xi He, Yi Wang, Ning Wu, A.N. Caruso, E. Vescovo, Kirill D. Belashchenko, P.A. Dowben and C. Binck, *Nature Materials* 9 (2010) 579-585.

8100-61, Session 7

Spin injection and relaxation in graphene

W. Han, R. K. Kawakami, Univ. of California, Riverside (United States)

Graphene is a unique and promising candidate for spintronics due to its high mobility, gate tunable transport properties, and low intrinsic spin-orbit and hyperfine coupling. However, the spin injection efficiency has been low (< 10%) and spin lifetime is still much shorter (50-200 ps) than predicted theoretically (~ micro seconds). To fulfill the potential of graphene for spintronics, two major advances need to be accomplished; enhance the spin injection efficiency and extend the spin lifetime. In this talk I will focus on the following two results in graphene spintronics. First, tunneling spin injection into graphene is achieved using MgO tunnel barrier. The non-local spin signal is found to be as high as 130 ohms at 300 K, with a spin injection efficiency of 30%. Second, using tunneling contacts to suppress the contact-induced spin relaxation, we observed the spin lifetimes as long as 771 ps at 300 K, 1.0 ns at 4 K in SLG, and 6.2 ns at 20 K in Bilayer graphene. These advances are important for the development graphene for spintronic applications in logic and storage.

8100-28, Session 8

Chemically-driven nanoscopic magnetic phase separation at the SrTiO₃(001)/La_{1-x}Sr_xCoO₃ interface

C. Leighton, M. Sharma, M. Torija, Univ. of Minnesota, Twin Cities (United States); J. Gazquez, M. Varela, Oak Ridge National Lab. (United States) and Univ. Complutense de Madrid (Spain); J. Schmitt, C. He, Univ. of Minnesota, Twin Cities (United States); J. Borchers, M. Varela, National Institute of Standards and Technology (United States); S. El-Khatib, Univ. of Minnesota, Twin Cities (United States)

The remarkable functionality of complex oxides provides many opportunities for new physics and applications. The perovskite cobaltites are an excellent example, being of interest in gas sensing, catalysis, ferroelectric memory, and solid oxide fuel cells. From the magnetism perspective they have high conduction electron spin polarization, and a variety of functional ground states. However, the same delicate balance between phases that provides such impressive functionality also leads to a serious problem; it can be difficult to maintain desired properties close to the interface with a dissimilar oxide. In this work, using SrTiO₃(001)/La_{1-x}Sr_xCoO₃ as a model system, we have combined epitaxial growth with detailed structural characterization (including STEM/EELS imaging), conventional magnetometry, electronic transport, and small-angle neutron scattering (SANS). In the SrTiO₃(001)/La_{1-x}Sr_xCoO₃ case we observe the usual degradation in magnetization and conductivity in the very thin film limit. We demonstrate that this is due to nanoscopic magnetoelectronic phase separation in the interface region. Essentially, nanoscopic ferromagnetic (FM) clusters form in an insulating non-FM matrix near the interface, resulting in reduced magnetization and conductivity, even at compositions that display no such phase separation in the bulk. Depth profiling of the chemical composition reveals that this effect has a chemical origin, being due to subtle depth-wise variations in Sr and O content, resulting in reduced hole doping near the interface.

Simple thermodynamic and structural arguments for the origin of these variations are provided.

Work at UMN supported by NSF and DoE, at ORNL by DoE, and at UCM by the European Research Council.

8100-29, Session 8

Structural and magnetic properties of the Mn-based antiperovskites from first principles

P. Lukashev, Univ. of Nebraska-Lincoln (United States)

Magnetomechanical coupling in crystals has many practical applications, such as in sensors, magnetic recording devices, etc. Recent experimental and theoretical studies of the magnetoelectric (ME) effect in the nanocomposite structures and in laminates show an enhanced ME coefficient. These materials combine piezoelectric properties of the paramagnetic phase and magnetostrictive properties of the magnetic phase. In my talk I will present density functional theory (DFT) based results of the structural and magnetic properties of antiperovskite compounds, such as Mn₃GaN - a potential candidate for practical applications in ME devices. Due to interplay of magnetic and elastic properties these compounds exhibit variety of interesting features, such as invar effect (or even negative thermal expansion) and a near zero temperature coefficient of resistance. I will show that the magnetic structure of antiperovskite compounds (Mn₃GaN) can be controlled by a small applied biaxial strain. The lowering of symmetry with the strain causes the local magnetic moments of Mn atoms to rotate from the trigonal T_{5g} structure with symmetric curl of spin density in the (111) plane to a monoclinic symmetry structure. As a result, an appreciable net magnetization appears in the strained system. I will also discuss the appearance of the net magnetization in Mn-based antiperovskite compounds as a result of the external strain gradient (flexomagnetic effect). In particular, I will describe the mechanism of the magnetization induction in the Mn₃GaN at the atomic level in terms of the behavior of the local magnetic moments of the Mn atoms. I will show that the flexomagnetic effect is linear and results from the nonuniformity of the strain, i.e., it is absent not only in the ground state but also when the applied external strain is uniform. At the moderate values of the strain gradient (0.1%) the flexomagnetic contribution to the net induced magnetization is comparable with the nonlinear contribution, thus making it attractive for practical applications. Finally, I will discuss the possibility of combining Mn₃GaN with typical ferroelectric, such as PbTiO₃ to form a prototypical magnetoelectric device.

8100-30, Session 8

Spintronic nanoelectronics using graphene based magneto-logic gates

H. Dery, Univ. of Rochester (United States)

We present a novel design concept for a seamless integration of spin-based logic and memory circuits. The building blocks are universal and reconfigurable magneto-logic gates based on a hybrid graphene/oxide/ferromagnet material system. These nano-gates consist of five ferromagnetic electrodes using nonlocal spin-valve geometries. The logic operations rely on the generation of non-equilibrium spin accumulation when spin polarized electrons tunnel from a ferromagnetic contact into the graphene via a tunnel barrier. Readout of logic operations is triggered by perturbing the magnetization direction of one of the ferromagnetic terminals. This leads to a binary transient current response whose speed and amplitude depend on the RC of the system and on the spin accumulation profile in the graphene layer.

In our simulations we use extracted parameters from recent nonlocal spin-valve measurements in Co/MgO/graphene at room temperature. In addition, we employ spin-transfer torque magnetization writing techniques using all-metallic paths. These path allow significant energy savings compared to the standard spin-transfer torque pillar technique (i.e., if the writing current flows through the tunnel barriers and graphene).

Finally, we present circuit prototypes in which over 100 spin-based logic operations are carried out before any need for a spin-charge conversion. Consequently, supporting CMOS electronics requires little power consumption. Specifically, network search engines are used as a technology demonstration vehicle. We present a spin-based circuit design with smaller area, faster speed, and lower energy consumption than the state-of-the-art CMOS counterparts. This design can also be applied in applications such as data compression, coding, image recognition, and business analytic.

8100-31, Session 8

Spintronics using the graphene, fullerene and other group IV materials

E. Shikoh, M. Shiraishi, Osaka Univ. (Japan)

In the research field of spintronics, studies using group IV elements have recently attracted much attention. Our group has been focusing not only the graphene spintronics, but also the spintronics using other carbon materials and Si. The gigantic MR effect (1.4 million % at 2K) in C60(fullerene)-Co nanocomposites was observed. That MR effect was well explained with our original theory including the Coulomb Blockade regime. The spin transport properties in Si, such as the bias-current dependence of spin polarization in Si, were observed at room temperature. Those researches are also introduced in addition to our topics in graphene spintronics.

8100-32, Session 9

Direct growth of graphene on MgO for spin and charge device applications

J. Kelber, Univ. of North Texas (United States)

We have demonstrated the growth of single and few layer graphene on MgO(111). Graphene/MgO interactions induce a graphene band gap of ~ 0.5-1eV. The importance of graphene/MgO heterojunctions for both conventional transistor and spin transport applications will be discussed.

8100-33, Session 9

The influence of lattice relaxation on the electron-spin motion in ferromagnetic films: Experiment and theory

W. Weber, A. Hallal, T. Berdot, P. Dey, L. Tati-Bismaths, L. Joly, Institut de Physique et Chimie des Matériaux de Strasbourg (France); A. Bourzami, Univ. Ferhat Abbas de Sétif (Algeria); F. Scheurer, Institut de Physique et Chimie des Matériaux de Strasbourg (France); J. Henk, Max-Planck-Institut für Mikrostrukturphysik (Germany); M. Alouani, Institut de Physique et Chimie des Matériaux de Strasbourg (France)

By taking the example of Fe films on Ag(001), we report, first, the discovery of a 180 degrees electron-spin precession in spin-polarized electron reflection experiments, which marks the ultimate limit of spin manipulation in reflection. In fact, this is the largest possible precession angle which can be measured in a single electron reflection. Both experiments as a function of Fe film thickness and ab initio calculations show that the appearance of this giant spin precession depends with utmost sensitivity on the relaxation of the Fe lattice during growth.

Second, the effect of submonolayer MgO coverage on the Fe films is studied. We note that the interface system MgO/Fe(001) has attracted great interest in recent years for its large room temperature TMR, which has been predicted and observed in epitaxial Fe/MgO/Fe(001) tunnel junctions. Although many results have been published concerning the interfacial structure of MgO/Fe, little effort was devoted to elucidate the

spin-dependent electron reflection properties of MgO/Fe interfaces. It is thus an open question how MgO is modifying the spin-dependent electron reflection properties of the Fe(001) surface. It is shown in this contribution that the spin polarization direction of the reflected electrons on Fe(001) strongly changes with minute amounts of MgO. Our calculations reveal that the MgO-induced out-of-plane relaxation of the Fe surface layer is responsible for this behavior. Our study points towards the subtle feature that the major change of the spin-dependent electron reflection properties of the Fe(001) surface is already caused by the very first MgO coverage.

8100-34, Session 9

Development of low-RA perpendicular-MTJs for spin-RAM application

K. Yakushiji, T. Saruya, H. Kubota, A. Fukushima, S. Yuasa, K. Ando, National Institute of Advanced Industrial Science and Technology (Japan)

MgO-based magnetic tunnel junctions with perpendicularly magnetized electrodes (p-MgO-MTJs) have been attracting a great deal of attention as memory cells in ultra-high-density spin-transfer-torque random access memory (Spin-RAM or STT-RAM) because nanometer-sized perpendicular magnetic cells can have a thermal stability high enough for data retention over 10 years. A p-MgO-MTJ is required to have not only a magnetoresistance (MR) ratio higher than 100% at RT but also a low resistance-area (RA) product. A low RA product is required for matching the MTJ resistance to the resistance of pass transistors. Assuming a Spin-RAM over 1 gigabit (F = 65 nm), it requires the MTJ cells to have an RA product of about 30 $\Omega\mu\text{m}^2$. In this study, we have aimed to achieve high MR ratios of more than 100% in p-MgO-MTJs with ultra-low resistance-area (RA) products less than 5 $\Omega\mu\text{m}^2$. [1, 2]

We fabricated p-MgO-MTJs with a [Co/Pt]_n/CoFeB/CoFe bottom electrode (free layer) and a CoFe/CoFeB/TbFeCo top electrode (reference layer) using C-7100 (Canon Anelva), and successfully attained high MR ratios of 100% at room temperature and a low RA product of 2 $\Omega\mu\text{m}^2$, simultaneously. We have also fabricated various p-MgO-MTJs by changing the composition of the CoFeB insertion layers. The results suggested that the use of an Fe-rich CoFeB layer gave rise to a high MR ratio. Such a high MR ratio in low-RA p-MgO-MTJs is the key to developing ultra-high-density spin-transfer-torque MRAMs.

This work was supported by New Energy and Industrial Technology Development Organization (NEDO).

[1] K. Yakushiji et al., Appl. Phys. Exp. 3 (2010) 053003.

[2] K. Yakushiji et al., Appl. Phys. Lett., 97 (2010) 232508.

8100-35, Session 10

Utilization of Rashba spin orbit coupling in a semiconductor channel

J. Chang, Y. H. Park, H. C. Koo, H. C. Jang, S. H. Han, Korea Institute of Science & Technology (Korea, Republic of)

Spin orbit coupling (SOC) in semiconductors couples the spin of electron to its momentum and provides a new way for electrically initializing and manipulating electron spins for future spintronic devices and spin-based quantum information processing. The effective magnetic field induced by Rashba SOC, which is controllable by electric field, in a quantum channel produces spin splitting and population imbalance between spin-up and -down electrons even in the absence of applied magnetic field. It is widely used in the applications in spintronics such as spin field effect transistor and spin Hall effect. In the paper, we present a detection of Rashba SOC using rotational applied field in addition to the Shubnikov-de Haas oscillation, the channel resistance of InAs based quantum channel depending on the alignment between the applied field and the Rashba field and finally oscillatory channel conductance as a function of gate voltage.

8100-36, Session 10

Spin currents in solids: definition and application to semiconductors

F. Bottegoni, H. Drouhin, Ecole Polytechnique (France); G. Fishman, Institut d'Électronique Fondamentale (France); J. Wegrowe, Ecole Polytechnique (France)

The concept of current plays a key role in modern solid state physics. It allows a proper and physically meaningful definition of the transport and dynamical properties. In particular, the spin current (SC) is of crucial importance in spintronics, whose main purpose is the control and the subsequent handling of spin degrees of freedom. However, the concept of SC is still a debated point in medium where the spin-orbit interaction (SOI) cannot be neglected and indeed semiconductors are paradigmatic systems to verify the consistency of theoretical and experimental arguments about the SC. In 2D electron gases, where the Rashba Hamiltonian applies, the standard definition of SC (6 X 6 tensor J_{ij}) is commonly used; this is not the case for 3D systems without inversion symmetry, like bulk GaAs.

We developed a new definition of SC, based on an effective Hamiltonian of the system, given by a momentum operator expansion that is suitable to describe the SC not only in presence of Rashba term, but also when the D'yakonov-Perel (DP) Hamiltonian is included. We prove that a redefinition of the SC is mandatory when dealing with the DP field and we also show how to derive properly source terms, related to "spin transfer torque" complying with the continuity equation for the current. We illustrate our findings in the case of bulk GaAs along different crystallographic directions and in the case of electron tunneling through GaAs barriers with different orientations of the spin.

8100-37, Session 10

Nanomechanical modulation of (Ga,Mn)As

Y. D. Park, Seoul National Univ. (Korea, Republic of)

We present nanomechanical modulation of (Ga,Mn)As magnetic properties including the anomalous Hall effect (AHE) as well as magnetic anisotropy (MA) by realizing mechanically buckled micro-Hall bar structures. From multiple lateral probes along an asymmetrically buckled (Ga,Mn)As beam, we find the modulation of the AHE as function of lateral stress. The origins of the lateral compressive stress stem from lattice mismatch between the sacrificial (Al,Ga)As layer with the diluted magnetic semiconductor (Ga,Mn)As layer. By changing the orientation, from planar Hall effect measurement, we also see a large changes in the MA. From a simple Hall cross structure, we demonstrate a reversible nanomechanical element which mechanically buckled state can be robustly read electronically.

8100-38, Session 10

Electron-beam formation from spin-orbit interactions in zinc-blende semiconductor quantum wells

M. E. Flatté, D. H. Berman, The Univ. of Iowa (United States)

Spin transport in semiconductors can be dramatically modified by spin-orbit interactions, producing such effects as coherent precession without a magnetic field. These effects vanish, however, for transport of unpolarized electrons, as the features generated for an initial electron spin polarized up are complementary to those generated from an initial electron with spin down. An open question is whether the spin-averaged transport of unpolarized spins can be influenced by the spin-orbit interaction in a nontrivial fashion.

Here we describe a dramatic enhancement of electronic propagation along a narrow range of real-space angles which occurs in the presence of Rashba and Dresselhaus spin-orbit fields of specific,

different strengths. The angular width of this "electron beam" depends sensitively on the ratio of the strengths of the Rashba and Dresselhaus fields, and the direction of the beam changes by 90 degrees when the relative sign of the fields changes. This surprising spatial anisotropy, originating from the anisotropic dispersion relations of electrons in the two fields, is due to general features of the energy contour surface of the electrons. Furthermore, the electron-beam formation can be traced, using a stationary phase analysis of the real-space Green's function, to coalescing stationary points. Such beams should appear in two-contact transconductance as well as other transport and scattering phenomena.

8100-39, Session 10

Anisotropic spin dephasing in an (110)-grown high-mobility AlGaAs/GaAs quantum well measured by resonant spin amplification technique

M. Griesbeck, Univ. Regensburg (Germany); M. Glazov, Ioffe Physico-Technical Institute (Russian Federation); E. Sherman, Univ. del País Vasco (Spain); T. Korn, D. Schuh, Univ. Regensburg (Germany); W. Wegscheider, ETH Zurich (Switzerland); C. Schüller, Univ. Regensburg (Germany)

The spin dynamics in zincblende-based two-dimensional electron systems (2DESs) is usually dominated by the D'yakonov-Perel spin dephasing mechanism resulting from the underlying spin-orbit (SO) fields. Due to the symmetry of the SO fields an exception could be found in symmetrically grown and doped AlGaAs/GaAs quantum wells (QWs) grown along the [110] direction, where the Rashba contribution is negligible and the effective Dresselhaus SO field is perpendicular to the sample plane. In such a system the spin dephasing times (SDTs) for in- and out-of-plane crystallographic directions are expected to be strongly different. We observed this spin relaxation anisotropy in resonant spin amplification (RSA) measurements in a sample consisting of a 30 nm wide double-sided δ -doped single QW with a very high mobility of about $3 \cdot 10^6$ cm²/Vs. A comparison of the measured RSA traces with the developed theory taking into account the spin dephasing anisotropy yields the resulting SDTs. We found that the ratio of in-plane and out-of-plane SDTs is strongly influenced by the sample temperature, the excitation density, and the initial spin polarization of the 2DES. The observed out-of-plane SDTs in the investigated temperature interval from 4 to 50 K are on the tens of nanoseconds time scale and exceed the previously reported values for (110)-grown systems. We attribute this fact to the precise control of the band profile via MBE growth.

8100-40, Session 11

Synchronization of high power vortex oscillators at multiple of the fundamental frequency.

C. Baraduc, S. Martin, Commissariat à l'Énergie Atomique (France); C. Thirion, Institut NÉEL (France); Y. Liu, M. Dovek, Headway Technologies, Inc. (United States); B. Diény, Commissariat à l'Énergie Atomique (France)

RF vortex spin-transfer oscillators based on low RA magnetic tunnel junctions were investigated. A very high power of excitations has been obtained characterized by a power spectral density containing a very sharp peak at the fundamental frequency and a series of harmonics. The observed behaviour is attributed to the combined effect of Oersted-Ampère field generated by the large applied dc-current and of the spin transfer torque. We furthermore show the synchronization of a vortex oscillation by applying a RF bias current which frequency is twice the oscillator fundamental frequency.

8100-41, Session 11

Coupling of two vortices in spin-valve nanopillars for spin-transfer oscillators

N. Locatelli, Unité Mixte de Physique CNRS/Thales (France)

Spin transfer induced vortex dynamics and the radio-frequency signal thereof have recently focused many interest, in particular to address the issues of coherence and power for spin transfer oscillators. However the signal linewidth obtained for a single vortex gyration is still too large (about 1 MHz). In this work, we will focus on using coupled vortices oscillators. Besides the drastic improvement of the signal coherence, fundamental interests of this system lie in the identification of the excited coupled modes and their selection rules.

The samples are Py(15nm)/Cu(10nm)/Py(4nm) spin-valve nanopillars having a vortex nucleated in each of the magnetic layer. In such systems with interacting vortices, the influence of the various interactions on the dynamical properties is central. Besides the observation of highly coherent vortex oscillations, we demonstrate that the dynamic behaviour is highly dependent on the vortices parameters, notably relative chiralities and polarities. We will compare the results to analytical predictions and simulations, studying the importance of different sources of coupling between the vortices. This work will be extended further to conditions to synchronize arrays of interacting vortex oscillators.

References:

N. Locatelli et al., App. Phys. Lett., 98, 062501 (2011)

8100-42, Session 11

Spin-torque vortex oscillators in nanopillar geometry

D. E. Buegler, V. Sluka, A. Kakay, R. Hertel, C. M. Schneider, Forschungszentrum Jülich GmbH (Germany)

We present experiments on current-induced vortex dynamics in nanopillars fabricated by optical and e-beam lithography from epitaxially grown Fe/Ag/Fe(001) multilayers. The pillar diameters range from 150 to 230 nm, and the Fe layers with thicknesses between 2 and 30 nm are separated by a 6 nm Ag spacer. Both layer magnetizations and the external field are in-plane. We measure current-driven high-frequency (HF) excitations of spin-torque oscillators (STO) with the free layer in the vortex or uniform state. Our ability to switch between them in a given STO enables a direct comparison of STO properties yielding for the vortex state larger emitted HF power and a wider frequency tuning range. Injection locking of the gyrotropic mode to external HF signals reveals for our GMR-based nanopillars a gap of three orders of magnitude between the HF power emitted by one oscillator and the power needed for phase-locking. Finally we modify the sample geometry such that magnetic vortices can be formed in both Fe disks. We study the dynamics of the single and double vortex state and find for the latter a dependence of the excitation frequency on the current polarity that we relate to exchanged roles of free and fixed layer.

8100-43, Session 12

3-dimensional spintronics for ultrahigh density data storage

R. P. Cowburn, Univ. of Cambridge (United Kingdom)

Spintronics could have a revolutionary impact on microelectronics and data storage if it provides the enabling step for transforming today's planar 2-dimensional devices into volume-filling 3-dimensional devices, where the data storage and processing capacity are related to the minimum feature size of the fabrication process, F , by F^{-3} instead of F^{-2} . Although magnetic domain wall devices have been discussed as a possible approach to 3-dimensional architectures (e.g. 'racetrack'), no convincing demonstration has yet been realised. In this talk I describe a

new approach to 3-dimensional spintronics. I show that the domain wall is not the only possible topological object in nanostructured magnetic materials; topological kink solitons can also exist in multilayered magnetic materials if anisotropy and interlayer exchange coupling are carefully chosen in the correct proportion. Such solitons can be extremely stable at room temperature, highly compact, and easily injected, detected and synchronously propagated. They are therefore an ideal candidate for the manipulation and storage of digital information. Most importantly, their natural environment is a 3-dimensionally structured one, making them ideal for 3-dimensional architectures. I illustrate one of many potential applications of topological solitons by showing an outline design for an MRAM-like device that could store data at an equivalent areal density in excess of 10 Tbits/inch² using only 100nm lithography and common magnetic materials.

8100-44, Session 12

Nanoring or nano-elliptic-ring shaped magnetic tunneling junctions and their applications in developing MRAM devices

X. Han, Institute of Physics (China)

A series of nano-elliptic-ring (NER)-shaped magnetic tunnel junctions (MTJs) with the major axis of around 120 nm and minor axis of around 60 nm, and ring width of around 25 nm was fabricated successfully. Magnetic field and current-driven magnetization switching were observed in such NER-MTJs with key stack layers of both spin-valve-type antiferromagnetic (AFM)/ferromagnetic (FM)/insulator (I)/ferromagnetic (FM) and sandwich-type hard-FM/I/soft-FM structures. When the electric current density exceeds a critical value of the order of $7.8 \times 10^6 \text{ A/cm}^2$ (critical driven current is 0.40 mA), the magnetization of the free (soft-FM) and reference (hard-FM) layer nano-elliptic-rings can be switched back and forth between parallel and antiparallel onion states. Tunneling magneto-resistance (TMR) ratio between 10% and 40% with different thickness of thin Al-O barrier waere measured at room temperature as we apply a magnetic field or a pulsed current. The experiments and micromagnetic analysis show that the spin transfer torque (STT) plays a main switching role in the magnetization reversal and the pulse-current-induced elliptic magnetic field play an assisted-switching role in such NER-MTJs. Compared with our previous studies of nano-ring-shaped (NR) MTJs and Nanoring MRAM, the NER-MTJ has a relative symmetric current driven critical behavior, which is due to the shape anisotropy of elliptic-ring architecture. The NER-MTJs also show the comparative lower switching field or critical current value (or density) and can be as the memory bit cells. Therefore, the manipulation of anisotropy in NER-shaped MTJs open a new way to develop more reliable and easier operational NER-MRAM devices.

8100-45, Session 12

Vortex-gyration-mediated information-signal transfer in one-dimensional arrays of soft magnetic nanodisks

S. Kim, D. Han, Seoul National Univ. (Korea, Republic of)

Low-energy input signals and their transport with low-energy dissipation are the key technological factors in the design of information processing devices. Coupling between different oscillators allows for the possibility of mutual energy transfer between them and the information-signal propagation. Recently, it was found that stimulated vortex gyration is a robust new mechanism for energy transfer between spatially separated dipolar-coupled magnetic disks based on the concept of coupled vortex-core oscillators. The rate of energy transfer from one disk to the other is determined by the two normal modes' frequency splitting caused by dipolar interaction. Here, we present collective vortex gyration modes in one-dimensional arrays of dipolar coupled vortex-state nanodisks, as studied from micromagnetic simulations and analytical derivations of their characteristic band structures that vary with the relative polarization

states. The quantized mode can be referred to as “vortex gyration”. This mechanism provides the advantages of tunable energy transfer rate, low-power input signal, and low-energy dissipation for magnetic elements with negligible damping. Coupled vortex-state disks might be implemented in applications for information-signal processing.

8100-46, Session 12

Different geometries for spin-transfer oscillators

A. M. Deac, Ecole Polytechnique Fédérale de Lausanne (Switzerland)

Several geometries have recently been proposed for spin-transfer oscillators, with the purpose of optimizing the output power and frequency dependence on the applied current, as well as minimizing the external magnetic field required to stabilize the dynamics. The two structures most compatible with applications involve hybrid multilayers, including magnetic films magnetized in the plane, as well as perpendicular to the plane of the layers - acting either as polarizing layer for the current, or as excited/free layer, respectively. The feasibility of both types of devices has been experimentally demonstrated. Here, we present a quantitative numerical comparison between the two.

8100-47, Session 13

Organic spintronics: playing with spins and molecules

S. Sanvito, Trinity College Dublin (Ireland)

Weak spin-orbit and hyperfine interaction make the spin-lifetime in organic molecules and molecular solids reaching up to the second mark. However organic materials have also poor mobilities, so that their spin-diffusion lengths are rather short. These peculiar characteristics position organic molecules in a unique space within Spintronics and one should envision applications where the spins are manipulated close to where they are injected [1]. This is the realm of single molecule spintronics.

In this contribution I will review the current state of the art of the theory of spin-transport and manipulation in organic materials. In particular I will discuss how to manipulate and how to read the spin configuration of a magnetic molecule. I will start by discussing a range of mechanisms for manipulating the spin state of a molecule by means of a static electric field. These are based either on the Stark effect in super-exchanged coupled molecules with two magnetic centers [2] or on electric-field induced tautomeric interconversion [3].

Then I will move to discuss the consequences of such effects on the transport properties of the molecules, addressing both the temperature dependence of the electron transport and the description of the low-bias spin-flip inelastic spectra. Finally I will present results for spin-transport in Mn12 and demonstrate that the magnetic state of the molecule can be read electrically with a single I-V read-out obtained by using non-magnetic electrodes [4].

[1] G. Szulczewski, S. Sanvito and J.M.D. Coey, *Nature Materials* 8, 693 (2009).

[2] N. Baadjji, M. Piacenza, T. Tugsuz, F. Della Sala, G. Maruccio and S. Sanvito, *Nature Materials* 8, 813 (2009).

[3] A. Droghetti and S. Sanvito, arXiv:1101.4777

[4] C.D. Pemmaraju, I. Rungger and S. Sanvito, *Phys. Rev. B* 80, 104422 (2009).

8100-48, Session 13

Electrical spin injection in a hybrid organic/inorganic spin-polarized light emitting diode (spin-LED)

E. Johnston-Halperin, The Ohio State Univ. (United States)

The field of semiconductor spintronics promises the extension of spin-based electronics beyond memory and magnetic sensing into active electronic components with implications for next-generation computing and quantum information. The development of organic-based magnets with room temperature magnetic ordering and semiconducting functionality promises to further broaden this impact by providing a route to all-organic spintronic devices and hybrid organic/inorganic structures capable of exploiting both the multifunctionality of organic systems and the well established spintronic functionality of inorganic materials. Here we report the successful extraction of spin polarized current from a thin film of the organic-based room-temperature ferrimagnetic semiconductor V[TCNE]_x (x~2; TCNE: tetracyanoethylene) and its subsequent injection into a GaAs/AlGaAs light-emitting diode (LED). The orientation of this spin current is determined by polarization analysis of the electroluminescence from the LED and is found to be parallel to the magnetization of the V[TCNE]_{x~2} layer, in agreement with theoretical predictions. Detailed analysis of the optical selection rules in the LED, coupled with control measurements of magnetic circular dichroism in the V[TCNE]_{x~2} layer, reveals the magnitude of the electron spin polarization to be largely insensitive to both electrical bias and temperature. This successful demonstration of spin injection in a hybrid organic/inorganic structure opens the door to a new class of active, hybrid spintronic devices with the potential for multifunctional behaviour defined by the optical, electronic and chemical sensitivity of the organic layer.

8100-49, Session 14

Semiconductor spin-lasers

I. Zutic, J. Lee, R. Oszwaldowski, C. D. Gothgen, Univ. at Buffalo (United States)

Practical paths to spin-controlled devices are typically limited to magnetoresistive effects, successfully employed for magnetically storing and sensing information. However, spin-polarized carriers generated in semiconductors by circularly polarized light or electrical injection, can also enhance the performance of lasers, for communications and signal processing. While such spin-lasers already demonstrate a lower threshold current for the lasing operation [1-3] as compared to their conventional (spin-unpolarized) counterparts, many theoretical challenges remain. Even in the steady-state regime, several surprises have only recently been revealed. For example, we show that a very short spin relaxation time of holes can be advantageous [4], with the maximum threshold reduction larger than what was theoretically thought possible. We also analyze dynamical operation of spin-lasers and reveal that the spin modulation can improve their performance. Spin-polarized injection can lead to an enhanced bandwidth and desirable switching properties of spin-lasers [5]. Future advances in spin-lasers may depend on progress in magnetic memories and data storage related to the ultrafast magnetization dynamics and timescales for magnetization reversal. Experimental efforts to increase the temperature of electrically-injected spin-lasers have also used quantum dots as the active region [6] and we compare their operation to the lasers based on quantum wells[7]. Supported by NSF-CAREER, ONR, AFOSR-DCT, and DOE-BES.

[1] J. Rudolph et al., *APL* 82, 4516 (2003); 87, 241117 (2005).

[2] M. Holub et al, *PRL* 98, 146603 (2007).

[3] S. Hovel et al., *APL* 92, 041118 (2008).

[4] C. Gothgen, R. Oszwaldowski, A. Petrou, and I. Zutic, *APL* 93, 042513 (2008).

[5] J. Lee, W. Falls, R. Oszwaldowski, and I. Zutic, *APL* 97, 041116 (2010).

[6] D. Basu et al., *PRL* 102, 093904 (2009).

- [7] R. Oszwaldowski, C. Gothgen, and I. Zutic, PRB 82, 085316 (2010).
 [8] J. Lee, R. Oszwaldowski, C. Gothgen, and I. Zutic, preprint.

8100-50, Session 14

Ferromagnet/semiconductor spin-LEDs for optical communication of spin information

R. Farshchi, M. Ramsteiner, J. Herfort, A. Tahraoui, H. T. Grahn, Paul-Drude-Institut für Festkörperelektronik (Germany)

Exciting advances are being made in the field of semiconductor spintronics toward the realization of spin-based transistors and logic architectures [1, 2]. However, for the full implementation of circuits that exploit the spin degree of freedom of electrons, it is necessary to transport the spin information from one device to another. Electrons in semiconductors can carry spin information, but they often suffer from high spin relaxation rates that significantly limit the spin diffusion lengths [3], making electrical transport of spin information highly inefficient.

It is well-known that injection of spin-polarized electrons from a ferromagnetic layer into an underlying semiconductor quantum well structure in so-called spin light emitting diodes (spin-LEDs) leads to the emission of circularly polarized light [4-7]. According to the selection rules in the quantum well, injection of opposite spin polarizations (up or down spin) leads to the emission of opposite light helicities (right- or left-handed). Therefore, the spin information of electrons can be optically transported in the form of light helicity.

In this presentation, we will demonstrate that the spin information associated with electrons injected into the quantum well of a spin-LED structure can be transported optically and retrieved by a second spin-LED. Different ferromagnetic layers, namely Fe and Co₂FeSi, are used to inject opposite spins into the emitter LED structure and generate light with opposite helicity. The spin information can be remotely deciphered based on the magnetic field dependence of the photocurrent in the detector spin-LED. This work opens the door for employing light as a functional component in spintronic circuits.

References:

- [1] H. C. Koo et al., Science 325, 1515 (2009).
 [2] J. Wunderlich et al., Science 330, 1801 (2010).
 [3] H. Sanada et al., Appl. Phys. Lett. 81, 2788 (2002).
 [4] R. Fiederling et al., Nature 402, 787 (1999).
 [5] Y. Ohno et al., Nature 402, 790 (1999).
 [6] H. J. Zhu et al., Phys. Rev. Lett. 87, 016601 (2001).
 [7] M. Ramsteiner et al., Phys. Rev. B 78, R121303 (2008).

8100-52, Session 14

Spin-orbit interactions in optics

K. Y. Bliokh, National Univ. of Ireland, Galway (Ireland)

We re-examine the problem of the identification of the spin and orbital parts of the angular momentum (AM) of an electromagnetic wave, which has a long history and has posed fundamental difficulties both in quantum electrodynamics and classical optics. We give an exact self-consistent solution in terms of the fundamental photon operators and unify previously disjointed results:

- (i) non-canonical orbital AM and spin AM operators obtained for the second-quantized fields;
- (ii) non-commutative photon position operator and Berry monopole field in momentum space;
- (iii) separation of the spin and orbital parts of Poynting energy flows.

We show that the polarization-dependent non-paraxial part of the orbital AM arises from Berry-phase terms describing the spin-orbit interaction (SOI) of light. A similar effect occurs dynamically upon spin-to-orbital AM conversion in focusing and scattering of polarized light. Other

manifestations of the SOI are the spin and orbital Hall effects of light (i.e., transverse shifts of the field centre of gravity) which are described by our position operator and take place even in free space. We apply the general theory to Bessel-beam solutions where the fundamental operators manifest themselves in immediately observable orbital- and spin-dependent intensity distributions.

8100-62, Session 14

Electron and hole spin coherence in semiconductor quantum wells

D. R. Yakovlev, Technische Univ. Dortmund (Germany)

An overview of the effects related to generation, control, and relaxation of the electron and hole spin coherence in III-V and II-VI semiconductor quantum wells will be presented. Spin dynamics has been measured by pump-probe Faraday- and Kerr rotation techniques also with the use of the Resonant Spin Amplification regime. Structures based on GaAs, InGaAs, CdTe, and ZnSe containing resident carriers of low density have been investigated. For all of them a long-living spin coherence (up to 20-40 ns for electrons and few ns for holes) has been found under conditions providing carrier localization. We discuss spin relaxation and spin dephasing mechanisms and dependence of their efficiency on temperature and magnetic field. The role of the charged exciton states for the generation of the carrier spin coherence under resonant excitation is highlighted. The generated spin coherence can be controlled optically and additive and nonadditive contributions of the control pulses are discussed.

8100-53, Poster Session

Simulation and optimization of magnetoresistance in Schottky barrier spin MOSFETs

A. M. Roy, Stanford Univ. (United States); D. E. Nikonov, Intel Corp. (United States); K. C. Saraswat, Stanford Univ. (United States)

Schottky barrier spin MOSFETs have emerged as a strong contender for future logic and memory promising low power consumption and reconfigurable circuits. However the development of these devices has been stymied by low values of magnetoresistance (MR) measured in experiments. Simulation studies have largely focused on diffusion driven or ballistic transport in the semiconductor and a simplistic treatment of spin injecting contacts. Here we demonstrate a novel framework to simulate spin injection and spin transport in semiconductors in the drift-diffusion regime and a tunneling based model for spin injecting contacts thereby enabling simulation and optimization of experimental devices.

The main contributions of this work are

- [a] the development of an efficient transfer matrix formalism for spin transport in semiconductors including electric field effects
- [b] the prediction of spin saturation effects leading to high magnetoresistance at high electric fields in spite of large resistance area product of the contacts
- [c] the development of a Tsu-Esaki tunneling based model for spin injecting contacts accounting for spin accumulation in the semiconductor
- [d] the simulation of Schottky barrier spin MOSFETs through a self consistent solution of spin injecting contacts and spin transport in the semiconductor channel
- [e] the optimization of material and structure properties (tunnel barrier materials, tunnel barrier thickness, semiconductor doping density etc.) for magnetoresistance of Schottky barrier spin MOSFETs

Our approach and implementation are general and provide a useful tool for experimental research on spin injection and detection in semiconductors.

8100-54, Poster Session

Thickness and substrate dependence of ferromagnetism in Mn doped ZnO thin films

G. Nammalvar, B. Ananthan, B. Lakshmi Narayanan, J. Gurusamy, T. Balasubramanian, National Institute of Technology, Tiruchirappalli (India)

We report the effect of thickness and substrate on ferromagnetism in Mn doped ZnO thin films grown by RF magnetron sputtering. The films of various thicknesses (15, 35 & 105 nm) have been grown on Si (100) and Si (111) substrates. The films have been grown from the 5 mol% Mn doped ZnO target which is prepared by conventional solid state reaction route. The grown films have been characterized by X-ray diffraction (XRD), Photoluminescence (PL), Hall measurement and Vibrating sample magnetometer to study its structural, optical, electrical and magnetic properties, respectively. The XRD result shows that all the films are preferentially oriented along (002) plane and free from the formation of secondary phases. The PL spectroscopy shows that the concentration of defects varies with the film thickness comparatively in both the substrates. This has been well acknowledged by our Hall measurements. It has been found that the observed ferromagnetism is strongly influenced by film thickness as well substrate surfaces. The presence of dopants in the films has been confirmed by Energy dispersive spectroscopy. The important features have been discussed in detail.

8100-55, Poster Session

Defect induced Raman active modes in Mn doped ZnO thin films

A. Aravind, K. Hasna, M. K. Jayaraj, Cochin Univ. of Science & Technology (India)

Zinc oxide is a II-VI semiconductor with a wide direct band gap of about 3.37 eV at room temperature. Among the various growth techniques of 'Mn' doped ZnO thin films, pulsed laser deposition (PLD) offers the advantages such as deposition at relatively high oxygen pressure, high deposition rate and growth of highly oriented crystalline films at low substrate temperature. The substitution of 'Mn' in ZnO host lattice affects the lattice dynamical properties. Raman scattering provides a great deal of information in the optical modes of vibrations at the center of Brillouin zone. The parameters of Raman mode such as frequency, line width and lifetime provide the basic information of lattice dynamics. The PLD grown films were analysed using x-ray diffraction (XRD), scanning electron microscopy (SEM), UV-Vis-NIR spectroscopy and Raman spectroscopy. Good optical quality of the films was confirmed from the transmittance of the film greater than 80% in the visible region. The presence of non-polar E₂high and E₂low Raman modes in thin films indicates that 'Mn' doping didn't change the wurtzite structure of ZnO. The intensity of E₂high mode and the peak position shifted towards the lower frequency with increase of 'Mn' concentration. Apart from the normal modes of ZnO the Zn_{1-x}Mn_xO ceramic targets shows two additional modes at 332 cm⁻¹ (I₂) and 524 cm⁻¹ (I₄). The modes I₂ and I₄ are assigned as multi-phonon scattering considering the two phonon process in the disorder lattice due to Mn doping.

8100-60, Poster Session

Numerical study of spin diffusion effects on the spin transfer torque effect and the dynamics of domain walls

D. Claudio-González, Univ. de Guanajuato (Mexico); A. Thiaville, J. E. Miltat, Univ. Paris-Sud 11 (France)

We report the observation of an increase of DW velocity at steady-state that can be as high as 21.5% due to spin diffusion when implementing a method that couples micromagnetics with the semiclassical transport

model proposed by Zhang and Li [S. Zhang and Z. Li, Phys. Rev. Lett. 93, (2004) 127204]. Experimental measurements of two of the quantities that can be associated with the non adiabatic component, the so-called beta term [T. Taniguchi et al., IEEE Trans. Magn. 44, (2008) 2636] [J. Bass and W. P. P. Jr, Journal of Physics: Condensed Matter 19, 183201 (41pp)] used to model spin transfer torque (STT) effects in Ni80Fe20 nanowires [A. Thiaville et al., Europhys. Lett. 69, (2005) 990] makes relevant the use of spin diffusive models to analyze and study the dynamics of domain walls (DWs). The geometry considered in this study corresponds to a semi infinite Ni80Fe20 nanowire featuring a single domain wall. Unlike previous approaches, we explicitly take spin diffusion into account along with experimentally measured values to show that these parameters can truly define the non adiabatic spin torque and that spin diffusion causes an effective beta value which is responsible for velocity increase observed.

8100-63, Poster Session

Revealing the long spin lifetimes of holes in self-assembled (In,Ga)As quantum dots via spin noise spectroscopy

Y. Li, S. A. Crooker, D. L. Smith, N. A. Sinitsyn, Los Alamos National Lab. (United States); D. Reuter, A. D. Wieck, Ruhr-Univ. Bochum (Germany); D. R. Yakovlev, M. Bayer, Technische Univ. Dortmund (Germany)

"Spin noise spectroscopy" is a recently-developed technique that uses optical Faraday rotation to passively measure the intrinsic spin fluctuations of electrons and holes in semiconductor systems. As guaranteed by Fluctuation-Dissipation Theorem, the frequency spectra of the spin noise alone reveals dynamic spin properties such as spin lifetimes and Lande g-factors. Here we use spin noise spectroscopy to measure the spin relaxation of holes that are confined in self-assembled (In,Ga)As/GaAs quantum dots (QDs) grown by molecular beam epitaxy. Owing to their p-type wavefunctions, holes experience much less hyperfine interaction with nuclei as compared with confined electrons, leading (in principle) to long spin decoherence times which are favorable for potential qubit applications. In zero applied magnetic field, we observe a narrow spin noise peak centered at 0 Hz, indicating long hole spin relaxation times of a few hundred nanoseconds. In transverse magnetic fields, we observe that a portion of the 0 Hz peak still remains (in addition to the expected noise peak at the hole Larmor precession frequency), which we attribute to the presence of an effective hyperfine field arising from dipole-dipole interactions between the hole spin and the nuclear spins. We suppress these hyperfine fields using applied longitudinal magnetic fields, and observe hole spin lifetimes further enhanced by over one order of magnitude at low temperatures. Systematic studies as a function of temperature and applied field allow us to identify different regimes of spin relaxation.

Conference 8101: Carbon Nanotubes, Graphene, and Associated Devices IV

Tuesday-Wednesday 23-24 August 2011 • Part of Proceedings of SPIE Vol. 8101
Carbon Nanotubes, Graphene, and Associated Devices IV

8101-01, Session 1

Recent progresses in carbene functionalization of SWCNTs and graphene

Q. Zhang, C. Liu, Nanyang Technological Univ. (Singapore)

In this talk, we will focus on our recent progresses in carbene functionalization of single walled carbon nanotubes (SWCNTs). The influences of carbene-based covalent functionalization on the electrical properties of an isolated m-SWCNT, a semiconducting (s)-SWCNT, and a mixture network of both m- and s-SWCNTs are studied. We find that the functionalization does not reduce the conductance of m-SWCNTs significantly. It does deactivate the semiconducting feature of s-SWCNTs. Interestingly, the influences of the functionalization are reversible upon thermal annealing under ambient conditions.¹

1. Chao Liu, Qing Zhang, Francesco Stellacci, Nicola Marzari, Lianxi Zheng and Zhaoyao Zhan, "Carbene-Functionalized Single-Walled Carbon Nanotubes and Their Electrical Properties", *SMALL* 7(2011)1257.

8101-02, Session 1

structure reactivity of single-walled carbon nanotubes for various diazonium reagents and its application for separation by electronic types

W. Kim, Kyungwon Univ. (Korea, Republic of)

Diazonium salts are reported to selectively react with metallic Single-Walled Carbon Nanotube (SWNT) over semiconducting SWNT and we showed that covalently attached chemical groups can alter the densities of individual SWNT in a predictable and highly controllable manner, enabling SWNT separation by electronic types. In this study, we investigated the structure reactivity of SWNT with diazonium salts having different electron donating or withdrawing functional groups, analyzed their influence on the reaction selectivity using UV-Vis-NIR absorption spectroscopy, and developed structure-reactivity relations to understand and correlate the reactivity of a number of electron acceptors. Metallic SWNT react preferentially with diazonium salts over semiconducting SWNT in all diazonium studied, however the reactivity as well as the selectivity for metallic SWNT of this reaction strongly depends on the functional groups attached to the diazonium salts. Diazonium salts having electron withdrawing groups (Cl) have higher reactivity metallic for SWNT than those having electron donating groups (OH or COOH), thus lower selectivity for metallic SWNT, which would lower the separation efficiency in the following separation process. We also show that covalently attached functional groups can alter the densities of individual SWNT in a predictable and highly controllable manner, and the density increase of SWNT due to the attached functional groups varies. These results together with the structure reactivity of SWNT with different diazonium reagent are utilized for SWNT separation by electronic types and diameters.

8101-03, Session 1

Pillared graphene nanostructure: a new 3D carbon hybrid architectures

M. Ghazinejad, S. Guo, R. K. Paul, M. Ozkan, C. S. Ozkan, Univ. of California, Riverside (United States)

Using chemical vapor deposition technique a novel 3D carbon nano-architecture called a pillared graphene nanostructure (PGN) is

synthesized in situ. The fabricated novel carbon nanostructure consists of CNT pillars of variable length grown vertically from large-area graphene planes. A one-step CVD process for large-area PGN fabrication through combination of surface catalysis and in situ vapor-liquid- solid mechanisms is described. The dependence of the morphology of the large-area PGN on the synthesis process conditions was investigated by optical microscopy, SEM, TEM, HRTEM, and Raman Spectroscopy techniques. The highly crystalline interface between the CNT pillar and graphene floor confirmed the seamless contact between the two carbon allotropes. Moreover, to tune the PGN architecture, arrays of catalyst particles with controlled size and separation distance are fabricated using block copolymer films as template. This strategy yields tunable diameter and separation distance of pillar carbon nanotubes, and provides control over the amount of final carbon structure surface area. The successful transfer of the large area PGN onto arbitrary substrates, while keeping the 3D architecture intact, was also accomplished. The new synthesis methodology offers a promising pathway for fabricating novel 3D nanostructures with huge potential in hydrogen storage and supercapacitors, and provides a powerful means to fulfill Department of Energy's targets for energy storage.

8101-04, Session 1

Centimeter-scale metrology of CVD graphene on glass

J. Reiber Kyle, A. B. Guvenc, C. S. Ozkan, M. Ozkan, Univ. of California, Riverside (United States)

In this work, we demonstrate a high-throughput metrology method for measuring the thickness and uniformity of entire large-area chemical-vapor deposition (CVD) grown graphene sheets on arbitrary substrates. This method utilizes fluorescence quenching microscopy (FQM), a novel technique for visualizing graphene that is based on the discovery that graphene quenches fluorescence via resonant energy transfer. Fluorescence quenching is visualized by spin-coating a solution of polymer mixed with fluorescent dye onto the graphene then viewing the sample under a fluorescence microscope. Graphene regions are identified by dark regions in the fluorescence image of the sample. The contrast between graphene and the substrate can be customized by controlling the thickness of the dye layer. Currently, FQM has only been used to visualize graphene-oxide and exfoliated graphene samples and has been unable to achieve quantitative characterization of the graphene samples. In this work, we calibrate the fluorescent quenching by the graphene layers, measuring the contrast between graphene and the substrate for different graphene layer thicknesses and dye layer thicknesses. Using the results from our fluorescence quenching calibration, we quantify the thickness and uniformity of entire CVD-grown samples. This is achieved by creating a large-scale, high-resolution fluorescence montage image of the entire graphene sample using a microscope with a motorized stage. Next, we identify graphene layers by histogram-based segmentation of the image based on contrast relative to the substrate. This work introduces a new method for graphene quantification that can quickly and easily identify the graphene layer thickness throughout the entire graphene sample.

8101-05, Session 1

Hierarchical large-area graphene materials and functionalization

C. S. Ozkan, Univ. of California, Riverside (United States)

I will first describe the patterning of biomolecules on graphene layers to modulate their electronic properties. Single stranded Deoxyribonucleic Acids (ssDNA) are found to act as negative potential gating agents

Conference 8101: Carbon Nanotubes, Graphene, and
Associated Devices IV

that increase the hole density in single layer graphene. Current-voltage measurement of the hybrid ssDNA/graphene system indicates a shift in the Dirac point and intrinsic conductance after ssDNA was patterned. The effect of ssDNA was to increase the hole density in the graphene layer. Next I will describe block co-polymer patterning of large-area graphene layers grown by chemical vapor deposition which enables spatially controlled fluorine plasma doping to provide a tuning mechanism for the Dirac point. Poly(styrene-*b*-4-vinylpyridine) with cylindrical-morphology polycrystalline block co-polymer was employed in the patterning process. X-ray photoelectron spectroscopy (XPS) characterization revealed the existence of fluorine after doping graphene; high doping levels could be achieved just in 10s. The BCP-Graphene composite FET has been used for the detection of chemical agents including NaF. Finally, I will describe a new class of graphene material in the form of a three dimensional architecture called pillared graphene nanostructure (PGN), which is a combination of the two allotropes of carbon including graphene floors and carbon nanotube pillars. We developed a one step chemical vapor deposition process for large-area PGN fabrication via a combination of surface-catalysis and in-situ vapor-liquid-solid mechanism. We also developed a process by which PGN layers can be transferred onto arbitrary substrates. Single and multilayer stacked PGN are envisioned for future ultra-large and tunable surface area applications in hydrogen storage and super-capacitors.

8101-06, Session 2

Unique thermal properties of graphene: prospects of thermal management applications

A. A. Balandin, Univ. of California, Riverside (United States)

As the electronic industry moves towards few-nanometer-scale CMOS and 3D IC designs thermal management becomes crucially important for achieving high performance and reliability of advanced electronic chips [1]. One approach for mitigating the self-heating problems is finding materials with very high thermal conductivity, which can be integrated with Si ICs or used as fillers in the next generation of the thermal interface materials (TIMs). In 2008, we discovered that graphene reveals extremely high intrinsic thermal conductivity, which can exceed that of bulk graphite [2-3]. We explained this fact by the fundamental difference in the low-energy phonon transport in 2D graphene and 3D graphite [4-6]. Thermal conductivity of graphene layers depends strongly on their geometrical size, coupling to the adjacent substrate or capping layers, edges roughness and defect concentration. I will overview the experimental and theoretical results for the thermal conductivity evolution of the few-layer graphene (FLG) considering two limiting cases of the phonon transport limited by the intrinsic and extrinsic effects. The use of graphene as interconnects and heat spreaders in advanced 2D and 3D computer chips will also be discussed. The last section of the talk will have a description of the data for graphene TIM materials.

The work was supported by SRC-DARPA Functional Engineered Nano Architectonics (FENA) center and ONR project on Graphene Quilts for Thermal Management.

[1] A.A. Balandin, IEEE Spectrum, October 2009. [2] A.A. Balandin, et al., Nano Letters, 8, 902 (2008). [3] S. Ghosh, et al., Applied Physics Letters, 92, 151911 (2008). [4] D.L. Nika, et al., Applied Physics Letters, 94, 203103 (2009). [5] D.L. Nika, et al., Physical Review B, 79, 155413 (2009). [6] S. Ghosh, et al., Nature Materials, 9 555 (2010).

8101-07, Session 2

Investigating the nanoscale surface chemistry of graphene

K. F. Kelly, Rice Univ. (United States)

In this talk, I will review our recent success in applying probe microscopy to understanding the chemistry of graphene and graphitic nanoparticles. We have used STM to compare the morphology and defect density in

graphene grown on copper foils by liquid-phase epitaxy to that produced by other methods such as mechanical exfoliation and pyrolysis of silicon carbide. In addition, we have applied a similar analysis to the characterization of chemically suspended graphitic nanoparticles. Lastly we obtained an atomic-scale view of the fluorination and defluorination. Coupled with these studies, we performed chemical characterization of these systems using Raman microscopy.

8101-08, Session 2

Scanning Raman spectroscopy of nanostructured graphene: Doping due to presence of edges

S. Heydrich, M. Hirmer, T. Korn, J. Eroms, D. K. Weiss, C. Schüller, Univ. Regensburg (Germany)

We have investigated nanostructured graphene layers, which were prepared on exfoliated graphene single layers via electron-beam lithography and oxygen-based reactive ion etching, by means of scanning Raman spectroscopy. The peak positions, peak widths and intensities of the characteristic phonon modes of the carbon lattice have been studied systematically in a series of samples. In nanopatterned samples, where periodic arrays of holes (a so called antidot lattice) with typical hole diameters on the order of a few tens of nanometers and periods of a few hundreds of nanometers were prepared, we found a systematic stiffening of the G band mode, accompanied with a line narrowing, while the 2D mode energies are found to be linearly correlated with the G mode energies. We interpret this as evidence for p-type doping of the graphene antidot lattices [S. Heydrich et al., Appl. Phys. Lett. 97, 043113 (2010)]. Moreover, we have detected and analyzed a two-phonon mode at about 2450 wavenumbers in single layer plain graphene. Wavelength-dependent measurements show that it can be interpreted as a LO-LA mode from the K point of the Brillouin zone. A detailed analysis of the electron-phonon coupling strength of this mode shows that it is of the same order of magnitude as that of the G mode. This would have significant implications for the upper limit of carrier mobilities in intrinsic graphene layers.

8101-10, Session 3

Highly selective CNTFET based sensors using metal diversification methods

P. Bondavalli, L. Gorintin, G. Feugnet, Thales Research & Technology (France)

This contribution deals with Carbon Nanotubes Field Effect transistors (CNTFETs) based gas sensors fabricated using a completely new dynamic air-brush technique (patented) for SWCNTs deposition. The extreme novelty is that our technique is compatible with large surfaces, flexible substrates and allows to fabricate high performances transistors exploiting the percolation effect of the SWCNTs networks achieved with extremely reproducible characteristics. This technique is extremely interesting considering that it is suitable for industrial transfer. More precisely, we have developed a machine which allows us the dynamic deposition on heated substrates of SWCNT solutions, improving dramatically the uniformity of the SWCNTs mats. The CNTFETs have been developed for gas sensing applications. Indeed we have fabricated arrays of CNTFETs achieved using different metal electrodes (patented approach) to exploit the change of metal/SWCNTs junction characteristics as a function of the gas detected in order to identify a sort of electronic fingerprinting. This phenomenon is related to the change of the metal work function and so of the Schottky barrier and seems to be extremely selectivity. Results concerning exposure to NH₃, NO₂, DMMP, that will be extensively shown at the conference, at different concentration (from 100ppb to 10ppm) demonstrate that each gas interacts in a specific way with each CNTFET. For example, , for the same concentration, CNTFET fabricated using Pt are more sensitive than those fabricated using gold electrodes for DMMP. Inversely, CNTFET fabricated

using gold electrodes are more sensitive than those fabricated using Pt electrodes for NH₃.

8101-11, Session 3

Printed CNT transistors with high on-off ratio and linearity

G. Gu, R. Liu, Y. Ling, X. Lu, Univ. of Massachusetts Lowell (United States)

We report an all-printed flexible carbon nanotube (CNT) thin-film transistor (TFT). All the CNT TFT components, including the source and drain electrodes, the TFT transport channel, and the gate electrode, are printed on a flexible substrate at room temperature. A high ON/OFF ratio of over 1000 was achieved. The all printed CNT-TFT also exhibits bias-independent transconductance over a certain gate bias range. This all -printed process avoids the conventional procedures in lithography, vacuum, and metallization, and offers a promising technology for low-cost, high-throughput fabrication of large-area flexible electronics on a variety of substrates, including glass, Si, indium tin oxide and plastics.

8101-12, Session 3

Light-triggered conducting properties of a random Carbon Nanotubes network in a photochromic polymer matrix

R. Castagna, Istituto Italiano di Tecnologia (Italy) and Politecnico di Milano (Italy); C. Sciascia, Istituto Italiano di Tecnologia (Italy); A. R. S. Kandada, Politecnico di Milano (Italy); M. Meneghetti, Univ. degli Studi di Padova (Italy); G. Lanzani, Istituto Italiano di Tecnologia (Italy); C. Bertarelli, Politecnico di Milano (Italy) and Istituto Italiano di Tecnologia (Italy)

It is well known that photochromic materials reversibly change their colours due to a photochemical reaction that takes place when the material is irradiated with photons of suitable energy. This peculiar feature has been exploited to develop smart sunglasses, filters and inks. With a proper molecular design it is possible to enable modulation not only of colour but also of other properties such as refractive index, dipole moment, nonlinearity or conductivity by a photoswitching of the molecular structure. The approach herein followed consists in modifying, upon irradiation, the properties of another component the photochromic molecule is coupled to. In particular, the switching features of photochromic systems are matched with the intriguing peculiar properties of carbon nanotubes (CNTs). A photochromic polyester has been properly synthesised to be used as switching polymer matrix coupled with a network of CNTs. Irradiation of the polymer/CNTs blend results into a light-triggered conductance switching. Supported by electrical and spectroscopic evidences, we argue that the reversible electrocyclization, experienced by the polymer under UV-vis illumination, affects the inter-tube charge mobility resulting in a dramatic overall resistance variation. Differently from previous literature, based on single molecule approach,[1-3] we obtain blended films by simple solution techniques, with sheet-resistance modulation larger than 50%, FET characteristic, good thermal stability and remarkable fatigue resistance at room conditions.

1 X. Guo et al. Science , 311, 356 (2006);

2 J. M. Simmons et al. Phys. Rev. Lett. 98, 086802 (2007);

3 A. C. Whalley et al. J. Am. Chem. Soc. 129, 12590 (2007).

8101-13, Session 3

CdSe/ZnS coated single layer graphene photovoltaic devices

S. Guo, J. Reiber Kyle, W. Wang, M. Ozkan, C. S. Ozkan, Univ. of California, Riverside (United States)

Large-area flexible and transparent optoelectronic devices were fabricated through non-covalent interaction between CdSe/ZnS quantum dots and single layer graphene. Single layer graphene was synthesized via CVD method. Pyridine was utilized for capping the quantum dots and the pi-pi interaction between pyridine and graphene enable QD immobilized on the surface of graphene. The photo induced charge transfer was confirmed by photoconductivity measurements. Quantum dots decorated graphene device display good photo-switching property which could be utilized for long wavelength sensitive sensor. Further construction of layered solar cell was accomplished with graphene and QDs layer by layer assembly technique.

8101-14, Session 3

Optical and structural modifications and characterization of ion- irradiated glassy polymer carbon

M. A. Abunaemeh, Alabama A&M Univ. (United States) and Ctr. for Irradiation of Materials (United States); M. Seif, Alabama A&M Univ. (United States); A. Elsamadicy, The Univ. of Alabama in Huntsville (United States); D. Ila, Alabama A&M Univ. (United States) and Ctr. for Irradiation of Materials (United States)

The TRISO fuel that is planned to be used in the GenerationIV nuclear reactor consists of a fuel kernel of UO_x coated in several layers of materials with different functions. We are looking at the ion irradiation induced optical structural modifications of the glassy polymeric carbon (GPC) microstructure and their effect on the mechanical and physical properties. GPC is considered as a potential replacement for the pyrolytic carbon coatings, with a function of diffusion barrier for the fission products. We irradiated GPC samples with 1 MeV protons, 5 MeV Ag and Au ions. We chose protons to simulate the effects of neutrons. During the nuclear fission of ²³⁵U, the fission fragment mass distribution has two maxima around 98 and 137 that would best fit Rb and Cs. However, both ions are hard to produce from our SNICS source therefore we chose Ag (107 amu) and Au (197 amu) as best replacements

8101-15, Session 4

Radio-frequency transmission of graphene layer

H. S. Yoon, J. Y. Oh, W. Kim, J. Y. Kang, J. Lim, J. Kim, S. C. Jun, Yonsei Univ. (Korea, Republic of)

Graphene has shown high potential to be used as interconnects in the field of high frequency electrical devices. In this study, we demonstrate the effect of graphene geometry on the microwave properties using the measurements of S-parameter in range of 500 MHz - 40 GHz. Graphene used in this study was fabricated by mechanical cleavage of highly oriented pyrolytic graphite and CVD method. High frequency properties of graphene, such as impedance, insertion loss, R, L, G and C were extracted from S-parameters at room temperature condition. We confirm that impedance and resistance decrease with increasing the number of graphene layer and w/L ratio. This result shows proper geometry of graphene to be used as high frequency interconnects.

8101-16, Session 4

Carbon nanotube terahertz spectroscopy: study of absorption and dispersion properties of SWNT and MWNT

H. Lamela, E. Dadrassia, Univ. Carlos III de Madrid (Spain); J. Lampin, Institut d'Electronique, de Microélectronique et de Nanotechnologies (France); M. B. Kuppam, F. Garet, J. Coutaz, Univ. de Savoie (France)

Carbon nanotubes (CNT) have been widely investigated because of their unique properties in view of applications in electronics and mechanics (Dresselhaus, et al., Springer, 2000). Their structures and properties have been studied by several means such as photonic emission, scanning, microscopy and tuning fields. It appears that several physical parameters of CNT's are within the terahertz (THz) frequency range (Ugawa, et al., Phys. Rev. B 60, 1999, Hilt, et al., Phys. Rev. B 61, 2000) like the plasma frequency and the phonon frequency. In addition, GHz CNT transistors have been demonstrated and THz CNT transistors are predicted (Burke, Nanosensing: Materials and Devices, SPIE, 2004). Therefore, THz spectroscopy of CNT samples is nowadays subject to intense researches. THz time-domain spectroscopy (TDS) is certainly the best tool to perform these studies, as it leads to the simultaneous determination of both the refractive index and absorption coefficients of the material over a very large frequency band, extending from typically 0.1 THz up to several THz (Mittleman, Springer Series in Optical Sciences, 2003, Duvillaret et al., Topics in Quant. Electron., 739, 1996). First reports on THz spectra of CNT obtained by THz-TDS have been published in the late 90's (Ugawa, et al., Phys. Rev. B 60, 1999.), and more recent papers have permit to define precise physical models to describe the THz properties of CNT films (T.-I. Jeon, et al., J. Appl. Phys. 98, 2005, C. Kang, et al., Phys. Rev. B 75, 2007, Kim, et al., J. Korean Phys. Soc. 50, 2007, E. P. J. Parrott, et al., Adv. Mat.21, 2009).

In this paper, we report on the optical and electrical properties of single-walled CNT films (SWNT), pure or F-doped, investigated by THz-TDS. The SWNT electromagnetic properties are modeled with a Drude model to describe the free carrier contribution associated to a Maxwell-Garnett model that accounts for the composite tubular structure of the films. The calculated spectra of the absorption coefficient and index of refraction for pure SWNT and F-doped SWNT are demonstrated. At the conference, we will present corresponding experimental results as well as the effect of various ranges of filling factor and geometrical factor in these two SWNT samples and multi-walled carbon nanotubes (MWNT).

This work is supported by MITEPHO project (www.uc3m.es/portal/page/portal/grupos_investigacion/optoelectronics/european_projects/miteph0) which is coordinated by GOTL research group in Carlos III de Madrid University with foundation grant agreement number 238393 (EU-FP7) in order to develop compact tunable dual-mode diode lasers and terahertz spectroscopy in sensing and biomedical applications.

8101-18, Session 4

Electronic cooling in a single flake of bi-layer graphene studied by ultrafast spectroscopy

E. Da Como, T. Limmer, J. Feldmann, Ludwig-Maximilians-Univ. München (Germany)

Graphene and few-layer graphene have demonstrated unique electrical properties such as ballistic transport and gigahertz switching frequencies in field effect transistors. Recently, the applications of graphene have entered the optoelectronics arena, with devices such as ultrafast photodetectors. Here, not only the transport properties are of interest, but also the optical response in terms of light absorption, electron-hole generation and carrier relaxation. In order to understand the operation of such devices and expand the application of graphene in optoelectronics, it becomes crucial to understand photocarrier relaxation with very high time resolutions.

In this communication, we report the first experiments probing the

carrier relaxation on a single flake of bi-layer graphene with femtosecond resolution. Bi-layer graphene flakes have been obtained by mechanical exfoliation of natural graphite and do not show signatures of extrinsic carrier doping. We have probed carrier relaxation by ultrafast pump-probe spectroscopy in the femtosecond time scale, with a unique range of probe energies spanning between 1.2 to 0.25 eV. This allows us for obtaining snapshots of the carrier population distribution after the initial photoexcitation pulse at 1.55 eV. By modeling the carrier distributions as two separated Fermi-Dirac distributions for electrons and holes we extract carrier temperatures and cooling rates. Our analysis shows that carriers loose half of their energy within the first 500 femtoseconds by carrier-phonon scattering. The results are relevant for graphene optoelectronic devices and give valuable information for the understanding and modeling of hot carrier transport in ultrafast graphene devices.

8101-19, Session 4

Low-frequency 1/f noise in graphene field-effect transistors

A. A. Balandin, Univ. of California, Riverside (United States)

Unique properties of graphene, such as its extremely high electron mobility, saturation velocity and breakdown current density make this material promising for future high-frequency and mixed-signal electronics. We have recently discovered that graphene has superior intrinsic thermal conductivity [1], which improves its prospects for practical applications in nanometer scale devices. Most of the proposed applications require low levels of the electronic 1/f noise, which dominates the noise spectrum at low frequencies. The up-conversion of noise, unavoidable in electronic systems, results in increased phase noise of the systems. Thus, it is important to investigate the noise level in graphene field-effect transistors and identify its sources. In this talk, I will overview the results of our experimental study of graphene devices [2]. A special attention will be given to the noise sources in these devices and the effects of aging and environmental exposure on their characteristics. I will present an experimental proof that the measured noise originates in the graphene channel itself rather than in contacts. The obtained results can be used for graphene device optimization for electronic and communication applications.

The work at UCR was supported by the DARPA - SRC Focus Center Research Program (FCRP) through its Center on Functional Engineered Nano Architectonics (FENA).

[1] A. A. Balandin, et al., Nano Lett. 8, 902 (2008); S. Ghosh, et al., Nature Mat., 9, 555 (2010).

[2] G. Liu, et al., Appl. Phys. Lett., 95, 033103 (2009); Q. Shao, et al., Electron Device Lett., 30, 288 (2009); S. Romyantsev, et al., J. Cond. Mat. Phys., 22, 395302 (2010).

8101-21, Session 5

Highly conductive, printable, and stretchable hybrid silver-carbon nanotube composites

K. Chun, Y. Oh, J. H. Rho, J. Ahn, Y. Kim, H. R. Choi, S. Baik, Sungkyunkwan Univ. (Korea, Republic of)

Conductive films with stretchability have received considerable attention for emerging electronic devices where arbitrary transformation in shape is required. Here we report highly conductive, printable and stretchable hybrid silver(Ag)-multi-walled carbon nanotube(MWNT) composites developed by blending and hot rolling ionic liquid, polyvinylidene fluoride copolymer, Ag flakes and MWNTs decorated with Ag nanoparticles [1]. The one-dimensional, flexible and conductive nanotubes constructed effective electrical networks among the Ag flakes, and the contact interface was improved by the self-assembled Ag nanoparticles on nanotubes. The maximum conductivities of the hybrid Ag-MWNT composite were 5710 S/cm at 0 % strain and 20 S/cm at 140 % strain where the film was ruptured [1]. The printable hybrid composite

with remarkable stretchability and conductivity might find practical applications in future electronic devices. [1] Kyoung-Yong Chun, Youngseok Oh, Jonghyun Rho, Jong-Hyun Ahn, Young-Jin Kim, Hyouk Ryeol Choi, and Seunghyun Baik, "Highly conductive, printable and stretchable composite films of carbon nanotubes and silver", Nature Nanotechnology, 5(12), 853-857, December, 2010

8101-22, Session 5

Digital data transmission performance of CVD grown few-layer graphene ribbons

A. B. Guvenc, J. Lin, M. V. Penchev, C. S. Ozkan, M. Ozkan, Univ. of California, Riverside (United States)

We investigated the electrical characteristics and digital data transmission performance of few-layer graphene ribbons grown by chemical vapor deposition. Data transmission measurements were accomplished on graphene field effect transistors (FETs) fabricated on Si/SiO₂ substrates. The mobility values were calculated from the transconductance, $g = dI_{ds}/dV_{gs}$, in which I_{ds} and V_{gs} values are acquired from back gate measurements. Data stream is randomly generated and uploaded to a waveform generator which generates the stream and transmits it repeatedly with the desired frequency. The signal was applied on the sources of the FETs and collected from the drains of the same devices. During the data transmission measurements no back gate voltage was applied. Collected data was first filtered with a low pass filter, to clear the noise and the high frequency parasitic effects then the output of the filter was used to create the eye diagrams of the devices and by using these eye diagrams, the bit error rates, attenuation values, quality factor values and maximum data transmission values are calculated. Graphene ribbons having a mobility of 2,180 cm²V⁻¹s⁻¹ can sustain data rates up to 90 megabits per second at 100 nm length and behave as RLC lines, thus the bandwidth is inversely proportional to resistance caused by defects in the graphene layers and the inductance and capacitance of the ribbons. Improving the graphene mobility to highest measured values (~200,000 cm² V⁻¹s⁻¹) and using structures with multiple coplanar transmission lines in parallel could carry the bandwidth beyond the terabits per second level.

8101-23, Session 5

Ultra thin films of carbon nanotubes for sustainability monitoring in civil engineering: New insight on promising nanosensors

B. Lebental, E. Norman, Ecole Polytechnique (France); A. Ghis, Commissariat à l'Énergie Atomique (France); C. Cojocaru, Ecole Polytechnique (France)

In recent years, requirements in terms of service-life of civil engineering structures have become more and more stringent, so that the focus of designers and owners is now set on structural durability. Foreseeing structural failures and repairing damaged structures at an early stage has become a major stake. This is the incentive for the world-wide development of various in-situ monitoring techniques for structural materials.

However, to this day, no existing sensor features the resolution required to investigate in-situ structural materials at the micro- and nanoscale. This is a major lack, as micro and nanoscale features play a significant role in the durability of cementitious materials. From this perspective, IFSTTAR, CEA-LETI and LPICM have set themselves the long-term goal to devise together innovative nanoscale structural health monitoring solutions using single-walled carbon nanotubes based nanosensors.

We will present two promising devices, ultrasonic nanotransducers for microporosity assessment and field-effect transistors for humidity monitoring, which both rely on ultra-thin SWNT films for sensing, either by electromechanical or adsorption effect. Processing of ultra-thin films by techniques such as dielectrophoresis, spray or CVD growth, as

well as thickness assessment by AFM or MEB will be the focus of our contribution. We will emphasize the relationship between high quality of the films and final sensing features of the devices.

8101-24, Session 5

A review of carbon based supercapacitor

P. Bondavalli, Thales Research & Technology (France)

The contribution deals with the state of the art and the critical analysis of studies concerning the fabrication of electric double layer capacitor (EDLC) also called super or ultracapacitors fabricated using carbon nanotubes (CNTs). From the first work in 1997, it was clear that supercapacitors achieved using carbon nanotube as electrodes showed very interesting results and that they could outperform traditional technologies based on activated carbon. Different methods to fabricate CNT based EDLC have been proposed in order to improve the performances (meanly energy densities and power), for examples CNT mats achieved by filtration, direct growth on metal collector or deposition using air-brush technique. The advantages and drawbacks of all these techniques will be analyzed. Recently, after a pause of some years, there has been a peak in the scientific community interest surely connected with the new challenges related to the research of new systems for the smart management of energy and to very hot topics such as the electric vehicles. This has been translated in a lot of new studies in the domain. We will focus our attention on the more interesting ones. We can also point out, for example, an increasing interest for supercapacitors achieved on flexible substrates for new kind of applications. Finally, we will try to find the coherence for the different research works and their related potential to strike the market : specific capacitance, energy and power densities, cost, versatility.

8101-33, Session 5

Graphene-based broadband optical modulator

M. Liu, X. Yin, Univ. of California, Berkeley (United States); F. Wang, X. Zhang, Univ. of California, Berkeley (United States) and Lawrence Berkeley National Lab. (United States)

Data communications have been growing at a speed even faster than Moore's Law, with a 44-fold increase expected within the next 10 years. Data Transfer on such scale would have to recruit optical communication technology and inspire new designs of light sources, modulators, and photodetectors. An ideal optical modulator will require high modulation speed, small device footprint and large operating bandwidth. Silicon modulators based on free carrier plasma dispersion effect and compound semiconductors utilizing direct bandgap transition have seen rapid improvement over the past decade. One of the key limitations for using silicon as modulator material is its weak refractive index change, which limits the footprint of silicon Mach-Zehnder interferometer modulators to millimeters. Other approaches such as silicon microring modulators reduce the operation wavelength range to around 100 nm and are highly sensitive to typical fabrication tolerances and temperature fluctuations. Growing large, high quality wafers of compound semiconductors, and integrating them on silicon or other substrates is expensive, which also restricts their commercialization. In this work, we demonstrate that graphene can be used as the active media for electroabsorption modulators. By tuning the Fermi energy level of the graphene layer, we induced changes in the absorption coefficient of graphene at communication wavelength and achieve a modulation depth above 3 dB. This integrated device also has the potential of working at high speed.

8101-25, Poster Session

Fabrication of transparent and conductive chemically converted graphene films by dip-coating technique

F. Ait medjane, R. Wendelbo, Abalonyx AS (Norway); S. Karazhanov, Institutt for Energiteknikk (Norway)

Transparent conductive films (TCFs) are crucial components in modern electronics. They are generally produced from indium thin oxide (ITO) and due to globally diminishing stocks of indium, are becoming more expensive. In addition, for many future applications, electrodes will need to be flexible, a development that can not be accomplished by ITO. Graphene is widely considered to be an ideal material for the use as TCFs because of its unique two-dimensional structure, remarkable electrical conductivity, and optical transparency to visible and near-infrared light as well as excellent mechanical properties. Graphene based TCFs are cheaper, far more flexible than traditional ITO films. Currently, mechanical cleavage of graphite is able to make high quality graphene reaching a millimeter size but with a very low yield. Alternatively, chemical exfoliation starting from the oxidation of graphite is an efficient process to produce graphene on a large scale and at low cost, combined with post-reduction processes.

Here we have developed, a simple and low cost approach for preparing TCFs using CCG dispersions and polycations. Graphene films were deposited onto glass and silicon substrates at ambient temperature by the dip-coating technique. An automated high-throughput set-up was developed for the purpose, by using a commercial robotic arm to dip 24 substrates in parallel. The set up include in house made instrumentation for on-line measurement of conductivity and transmittance. The properties of the obtained films were characterized by SEM, TEM, XPS and Raman spectroscopy. The resulting CCG films show promising electrical and optical properties.

8101-29, Poster Session

The enhanced mechanism of the CNTs/TiO₂ core-shell nanotubes

J. Syu, C. Chen, J. He, National Taiwan Univ. (Taiwan)

After pre-patterned electrodes, we connected the nanotubes by e-beam lithography followed by Ti/Au (70 nm/30 nm) E-gun system. We connected the nanotubes which one side was carbon nanotubes (CNTs) and the other side was TiO₂. The IV characteristic is asymmetric due to asymmetric connection. The thickness of TiO₂ film is about 4 nm from transmission electron microscopy. Compared to the TiO₂ nanotubes from others' research, the gain was at the same order of magnitude with ours under illumination but our response time and reset time were faster than the TiO₂ nanotubes. Our multi-walled carbon nanotubes (MWCNT) are metallic and make no response for the light. Upon illumination, the e-h pairs are generated and the electrons reach to the conduction band of TiO₂ and transfer to the CNTs. And the unpaired holes were left behind in the TiO₂. Since MWCNT behave as conducting wire, there is no possibility of accumulation of the electrons on CNT side. That will prevent the electrodes and holes from recombination so they can increase the density of the carriers. This enhances the electron-hole separation and helps in the faster growth of the photocurrent. When illumination is turned off, the photo-generated e-h pairs will stop. And the excess electrons in the CNT side transfer to the TiO₂ side for recombination with the holes which is a very fast process.

8101-30, Poster Session

Computational study of negative differential resistance in graphene bilayer nanostructures

K. M. M. Habib, S. Ahsan, R. K. Lake, Univ. of California,

Riverside (United States)

Although graphene has fascinating electronic properties featuring the Dirac fermion with high mobility and a long coherence length, lack of a band-gap reduces its utility for conventional electronic device applications.

A tunable bandgap can be induced in bilayer graphene by application of a potential difference between the two layers. The simplest geometry for creating such a potential difference consists of two overlaying single layer graphene nanoribbons (GNRs) with one placed on top of the other.

Each GNR is independently contacted so that one GNR is held at ground while the other has a bias applied to it. Independently contacting the top and bottom GNR maximizes the voltage drop between them. Such a geometry and biasing scheme would occur, for example, in a cross-bar architecture. Numerical simulations, based on density functional theory and the non-equilibrium Green's function formalism, show that transmission through such a structure is a strong function of applied bias. The calculated current voltage characteristics mimic the characteristics of resonant tunneling diode featuring negative differential resistance.

Semi-empirical tight binding model predicts that these characteristics prevail in large structures as well.

8101-32, Poster Session

Hydrogen storage in single-walled carbon nanotubes purified by microwave digestion method

N. Yuca, N. Karatepe, Istanbul Teknik Üniv. (Turkey)

Hydrogen is considered to be a clean energy carrier. However, the most serious barrier to potential uses is the development of feasible hydrogen storage systems. The discovery of high hydrogen storage capacity of carbon nanotubes (CNTs) makes up alternatives for hydrogen storage systems. To reach the full potential of the CNTs, many problems still need to be solved, including the development of an easy and effective purification procedure, since synthesized CNTs contain impurities, such as amorphous carbon, carbon nanoparticles and metal particles. These impurities impede utilization of the unique properties of CNTs. Also, as-synthesized CNTs usually have both ends closed, which may hinder their adsorption and capillarity properties. Therefore, a purification procedure should involve both opening the tubes ends and the elimination of the impurities to increase hydrogen storage capacity of CNTs.

In this study, the hydrogen adsorption on single-walled carbon nanotubes (SWCNTs) was investigated. SWCNTs were firstly synthesized by chemical vapor deposition (CVD) of acetylene (C₂H₂) on a magnesium oxide (MgO) powder impregnated with an iron nitrate (Fe(NO₃)₃·9H₂O) solution. The synthesis parameters were selected as: the synthesis temperature of 800°C, the iron content in the precursor of 5% and the synthesis time of 30 min. The microwave digestion method was applied for the purification of the synthesized SWCNT materials. Nitric acid (HNO₃) was used in the removal of the metal catalysts. Purification experiments were carried out at three different temperatures (120, 150 and 200 °C), three different acid concentrations (0.5, 1 and 1.5 M) and for three different time intervals (15, 30 and 60 min). The hydrogen storage capacities of the purified materials were measured using volumetric method at the liquid nitrogen temperature and gas pressure up to 100 bar and the effects of the purification conditions such as temperature, time and acid concentration on hydrogen adsorption were investigated.

Conference 8102: Nanoengineering: Fabrication, Properties, Optics, and Devices VIII

Tuesday-Wednesday 23-24 August 2011 • Part of Proceedings of SPIE Vol. 8102
Nanoengineering: Fabrication, Properties, Optics, and Devices VIII

8102-01, Session 1

Leaky-mode resonance photonics: an applications platform

R. Magnusson, The Univ. of Texas at Arlington (United States)

Incident light induces resonant leaky modes on dielectric and semiconductor layers patterned in one or two dimensions. Properly designed resonance structures may support a collection of complex, interacting waveguide modes providing interesting, novel spectral expressions. Here we present applications that include bandpass and bandstop filters, laser mirrors, polarizers, wave plates, ultrasensitive biosensors, absorption-enhanced solar cells, security devices, tunable filters, nanoelectromechanical display pixels, and dispersion/slow-light elements. We summarize the physical basis for this technology and provide numerous designed and fabricated device examples. Key issues in design and fabrication will be discussed. In particular, we invented and implemented highly accurate, label-free, guided-mode resonance (GMR) biosensors that operate in narrow-line reflection or transmission. The sensor is based on the high parametric sensitivity inherent in the fundamental resonance effect. As this sensor technology has high-value applications in medical diagnostics, drug discovery and development, industrial process control, and environmental monitoring, it is being commercialized. Moreover, the arsenal of optical components can be extended by use of the resonance concept. We have designed and fabricated a variety of bandstop and bandpass filters at differing spectral bands. Similarly, wideband polarizers fashioned in a single resonant layer have been fabricated and characterized showing high-quality response. We have designed ultra-wideband reflectors as well as new types of wave plates using a multilevel architecture. In general, these devices exhibit a minimal layer count relative to their classical multilayer thin-film counterparts. Another interesting pursuit relates to wideband tuning of these filters that is achievable by perturbing the structural symmetry using nano/microelectromechanical (MEMS) methods. Mixed metallic/dielectric resonance elements exhibit simultaneous plasmonic and leaky-mode resonance effects. Thus, leaky-mode resonance photonics technology is an enabling applications platform with interesting prospects.

8102-02, Session 1

Ultraslow photon diffusion in aperiodic nanostructure arrays

T. Rich, N. Lawrence, Boston Univ. (United States); J. Zhang, S. Cabrini, Lawrence Berkeley National Lab. (United States); L. Dal Negro, Boston Univ. (United States)

Stochastic models of the transport of photons through disordered media suggest that it is possible to create photonic materials that support ultra-slow diffusion of light, known as Sinai sub-diffusion. In disordered lattices, these stochastic processes are non-Markovian due to the effect of long-range correlations, and photon diffusion is significantly slowed down, according to a mean squared displacement that varies as t^β , where $\beta < 1$. In this work, based on multiple scattering Monte Carlo calculations and electrodynamics computations (Finite Difference Time Domain), we present our design and demonstration of complex photonic media with ultraslow photonic sub-diffusion over broad frequency spectra. Nanofabrication and optical characterization results of anomalous photon diffusion in aperiodic waveguide structures and two-dimensional nano-pillar arrays will also be presented. Characterizing the relationship between disorder and anomalous transport will allow for the engineering of novel materials whose transport properties can be actively tuned. Such precise control of the photon transport characteristics has not yet been demonstrated and will offer profound advancements in the

ability to develop novel optical devices such as optical buffers for solar and on-chip energy harvesting applications.

8102-03, Session 1

Experimental confirmation of fluorescence enhancement using one-dimensional GaP/SiO₂ photonic band gap structure

J. Gao, A. M. Sarangan, Q. Zhan, Univ. of Dayton (United States)

In this paper we report the experimental confirmation of the fluorescence enhancement effect using one-dimensional photonic band gap (1D PBG) structure. The 1D PBG structure consists of periodic multi layer thin films with gallium phosphide (GaP) and silicon dioxide (SiO₂) as the alternating high and low index materials. Strongly enhanced evanescent field can be generated at the last interface due to the combination of total internal reflection and photonic crystal resonance for the excitation wavelength. Meanwhile, the 1D PBG structure is designed as an omni-directional reflector for the red-shifted fluorescent signal emitted from the surface bounded molecules. Such an omni-directional reflection helps to improve the collection efficiency of the objective lens and further increase the detected fluorescent signal. Compared with the commonly used bare glass substrate, an average enhancement factor of 62 times has been confirmed experimentally with quantum dots as fluorescent markers. This fluorescence enhancer may find broad applications in single molecular optical sensing and imaging.

8102-04, Session 1

Aperiodic arrays of Er³⁺:SiN_x pillars for light emission enhancement at 1.55 μ m

N. Lawrence, L. Dal Negro, Boston Univ. (United States); S. Cabrini, J. Zhang, Lawrence Berkeley National Lab. (United States)

The engineering of optical devices in silicon (Si) has the potential to revolutionize the optoelectronics industry by providing a solution to interconnect bottleneck problems and enabling low-cost, high-performance applications ranging from inter and intra-chip interconnects and communication to integrated optical bio-sensing. The development of fully Si-based lasers can result in the mass production of high-performance optoelectronic components and systems through integration with CMOS technology, however, the progress limited by the lack of efficient light emission from Si. To overcome this, variation in the local density of photon states (LDOS) can be created by altering the surrounding environment to enhance material light emission. Unlike periodic photonic structures, Deterministic Aperiodic Structures (DAS) possess unique light localization and anomalous transport properties related to far richer spectral features, however, unlike random media, DAS are defined by the iteration of simple mathematical rules yielding repeatability. To exploit the unique light localization properties of these structures we have fabricated pillar arrays of Erbium (Er) doped Silicon-Rich Nitride (SRN) based on DAS using electron beam lithography and inductively coupled plasma (ICP) varied geometry to optimize the emission enhancement around 1.55 μ m. An over 30 fold increase in the volume normalized PL is measured along with angularly resolved emission profiles and emission time dynamics (TRPL). The experimental results have been interpreted using the null-field theory formulation (T-matrix) for systems of particles of arbitrary shape. These results suggest that light localization effects in engineered pillar arrays can lead to strong radiative enhancement for CMOS compatible on-chip integration.

8102-05, Session 1

Scattering optics resolves nanostructure (Keynote Presentation)

J. Bertolotti, E. G. van Putten, D. Akbulut, W. L. Vos, Univ. Twente (Netherlands); A. Lagendijk, FOM Institute for Atomic and Molecular Physics (Netherlands); A. P. Mosk, Univ. Twente (Netherlands)

Scattering of light is usually seen as a nuisance in microscopy. It limits the penetration depth and strongly deteriorates the achievable resolution. However, by gaining active spatial control over the optical wave front it is possible to manipulate the propagation of scattered light far in the multiple scattering regime. These wave front shaping techniques have given rise to new high-resolution microscopy methods based on strong light scattering. This is based on the realization that scattering by stationary particles performs a linear transformation on the incident light modes. By inverting this linear transformation, one can focus light through an opaque material and even inside it. An extremely high resolution focus can be obtained using scatterers embedded in a high-index medium, where the diffraction limit for focusing is reduced by a factor n . We have constructed a scattering lens made of the high-index material Gallium Phosphide (GaP) which is transparent over most of the visible spectrum and has the highest index of all nonabsorbing materials in the visible range. This yields a focal spot resolution of less than 100 nm, and it seems theoretically possible to create a focus of order 70 nm. We will discuss how the system resolution of a fluorescence microscope using this lens could be pushed even higher.

8102-06, Session 2

A photonic DNA processor: concept and implementation

T. Nishimura, Y. Ogura, K. Yamada, Osaka Univ. (Japan); H. Ymamoto, Univ. of Tokushima (Japan); J. Tanida, Osaka Univ. (Japan)

To deal with molecular information at a molecular level based on external signaling, a photonic DNA processor is a primal processing core of a nanoscale information system that works in molecular environment, for example, in situ. Use of photonic signals enables remote and spatio-temporal control of the processor. As an implementation example, we report a photonically-controlled DNA nanomachine which identifies and processes molecular information and implements physical processing as reporting the result using fluorescence signal. The nanomachine has two hairpin DNAs incorporating azobenzene and forms a tweezers-like structure. The hairpin structures are opened by ultraviolet-light irradiation, and a single-strand region is exposed to activate functionality in recognizing a target molecule. In contrast, visible-light irradiation makes the hairpin DNA close to inactivate the sensing function, and it releases the captured molecule. During activated term, the nanomachine changes its tweezers-like structure depending on existence or absence of the target molecule: the nanomachine transmutes into the closed state from the open state (initial state) by binding to the target molecule. Depending on the state, the nanomachine generates a fluorescence signal owing to fluorescence resonance energy transfer. In experiments, we demonstrated that the fluorescence intensities changed depending on existence and absence of the target molecule under photonic activation and inactivation. The result indicates that the nanomachine obtained information on the target molecule, changed the state, and reported the information to the outside world. In addition, we confirmed experimentally the functionality in measuring the concentration of the target molecule.

8102-07, Session 2

Threshold current calculations and optical cavity optimization for PbSe/PbSrSe MQW structures

M. Khodr, Hariri Canadian Univ. (Lebanon)

Threshold current is a key parameter in the design and proper operation of quantum well lasers. In this publication, threshold current analysis and calculations are done on four PbSe/Pb_{0.934}Sr_{0.066}Se quantum well laser structures: SQW, SCH-SQW, MQW, and MMQW. The current work is a continuation to previous publications where energy levels, modal gain, optical confinement, and total losses were published for these four structures assuming the energy bands are non-parabolic. The threshold current as a function of total losses, cavity length, and cavity end mirror reflectivity was obtained for these structures. It is shown that the threshold current decreases with a decrease in the cavity length and then increases at a critical cavity length. The effects of non-parabolicity on the threshold current values are more obvious for short cavities and decreases with an increase in cavity. Whether the SQW or the MQW is the better structure depends on the loss level. At low loss, the SQW laser is always better because of its lower current density where only one QW has to be inverted. At high loss, the MQW is always better because the phenomena of gain saturation can be avoided by increasing the number of QW's although the injected current to achieve this maximum gain also increases. Owing to this gain saturation effect, there exists an optimum number of QW's for minimizing the threshold current for a given total loss. At this typical value, the effects of non-parabolicity on the threshold current values can be neglected without loss of accuracy. However, there is a 20% shift in the output lasing energy that cannot be neglected.

8102-08, Session 2

Sub-micron channels for optofluidic bacterial analysis

A. E. Vasdekis, D. Psaltis, Ecole Polytechnique Fédérale de Lausanne (Switzerland)

Isolated cell analyses have attracted substantial attention in recent years due to their unique capability to reveal single target dynamics, commonly masked in population level studies. To this end, the most common techniques used are hydrodynamic trapping in microfluidics, due to the possibility of performing highly multiplexed measurements, but also due to their capacity to control the cells' growth conditions [1].

Similar efforts in bacteria however, have not reached yet such sophistication levels, primarily due to the absence of microfluidic architectures capable of microbial handling [2]. Such methodologies would potentially revolutionise drug research, especially within the field of antibiotic persisters [3].

To address this, we have developed a hybrid fabrication method based on electron-beam and cast-moulding lithography for PDMS microfluidics with sub-micron resolution. We will discuss the performance and limitations of this method, and our recent results in handling few and single bacteria. Integrated methods for high-throughput size determination will be also discussed.

1. Bennett, M.R. and J. Hasty, Microfluidic devices for measuring gene network dynamics in single cells *Nature Reviews Genetics*, 10, 628-638 (2009).
2. Weibel, D.B., W.R. DiLuzio, and G.M. Whitesides, Microfabrication meets microbiology *Nature Reviews Microbiology*, 5, 209-218 (2007).
3. Balaban, N.Q., J. Merrin, R. Chait, L. Kowalik, and S. Leibler, Bacterial persistence as a phenotypic switch *Science*, 305, 1622-1625 (2004).

Conference 8102: Nanoengineering:
Fabrication, Properties, Optics, and Devices VIII

8102-09, Session 2

Nano-imprint of photonic-plasmonic nanostructures on bio-polymers

D. Lin, Boston Univ. (United States); H. Tao, Tufts Univ. (United States); S. Y. Lee, Boston Univ. (United States); F. Omenetto, Tufts Univ. (United States); L. Dal Negro, Boston Univ. (United States)

Nanostructures have been extensively exploited to construct photonics and plasmonics device for light emission (lasers, LEDs) and optical biosensing. Current optical platforms are based on widely used substrates such as quartz, silicon, and other semi-conductor materials. Novel polymers, such as silk biopolymer, which are biocompatible and biodegradable, have emerged to expand the functionality of current photonics devices for biomedical applications. However, the nanofabrication of photonic-plasmonic nanostructures on top of these solvent-sensitive bio-polymers poses unique challenges. Here, we demonstrate a rapid nanoimprint method capable to fabricate at room temperature both nano-hole patterns and gold nanoparticle arrays on protein-based biopolymer (silk) substrates. Nano-hole structures are imprinted with mold of Si pillars, while gold nanoparticle patterns are predefined on a donor mold, and then transfer-imprinted onto the surface of a silk film. By this approach, various patterns with feature sizes down to 25nm scale can be reliably fabricated and scaled over cm² areas. The SEM images of imprinted nanostructures on silk and actively doped (luminescent) polymer layers demonstrate that a mold can be completely replicated onto a silk substrate with high fidelity. This technique provides an attractive approach to fabricate large-area nanostructures on the surface of solvent sensitive polymers with nanoscale resolution and at low cost. Since the imprint procedure relies on mechanical deformation, it preserves the biological, chemical and physical properties of biopolymers, and therefore it is applicable for implantable devices and environmental monitors.

8102-10, Session 3

Nanotechnologies for efficient solar energy conversion and storage

L. A. Eldada, SunEdison (United States)

The immense gap between solar energy's tremendous potential and our utilization of it to produce electricity can be overcome over time by increasing the efficiency of the conversion and storage processes, which are today well below their theoretical limits. We present nanotechnologies that improve the conversion efficiency of solar energy into electricity, and enhance the round-trip efficiency of energy storage systems. We describe nanostructures that enhance light concentration, light trapping, photon absorption, charge generation, carrier multiplication, hot electron extraction, charge transport, and current collection in photovoltaic systems, as well as nanomaterials that enhance the efficiency of electrochemical processes, boost gravimetric and volumetric energy densities, reduce the rate of self-discharge, increase the peak power rating, and extend the cycle life of secondary batteries and ultracapacitors.

8102-11, Session 3

Analytical approach to 3D device modeling of nanoarchitectures for solar energy conversion

A. Wangperawong, S. F. Bent, Stanford Univ. (United States)

Recently there have been many new experimental device architectures utilizing vertical nanojunctions to decouple light absorption from charge carrier collection. Despite great experimental work in the field, theoretical studies have been limited. We have developed models that for the first

time describe the device performance of nanostructured solar cells in three dimensions, distinguishing between isolated and interdigitated nanojunctions. Our analytical approach is a powerful tool for designing nanostructured solar cells of various architectures and materials that can be both efficient and cheap. Beyond photovoltaics, other applications include photoelectrochemical cells and photocatalytic devices.

8102-13, Session 3

Optimization of the spray parameters for ZnO based hybrid solar cells

A. Vasudevan, S. Jung, T. Ji, Univ. of Arkansas (United States)

Global energy demand has been increasing drastically and major share of this demand is met from fossil fuels. Fossil fuels being non-renewable, efforts are being made to tap energy efficiently from renewable energy sources. Among renewable energy sources, solar energy is a major energy source and solar cells are used to convert it into electrical energy. Solar cells currently used are silicon based because they have higher efficiency than cells from other materials but the manufacturing cost is high. Though cheaper cells can be fabricated using organic materials because it solution processable, the efficiency is very low. The low efficiency of organic solar cells is due to the low mobility of the carriers, the efficiency can be improved if inorganic materials are incorporated. The incorporated inorganic material provides better transport to the carriers generated by organic material. Hybrid solar cells with ZnO nanorods as the inorganic and P3HT and PCBM as the active layer reported in literature is usually prepared by spin coating. The major drawback of using spin coating technique is that large area fabrication is not possible. Large scale production is feasible if these cells can be prepared by spray coating. We will discuss the fabrication of these cells by spray coating technique. The dependence of efficiency of the cell on the active layer thickness, substrate temperature and spray parameters like pressure of the carrier gas will be studied. By comparing the efficiency of the cells prepared under different conditions the optimum condition for preparing efficient hybrid solar cells will be determined.

8102-14, Session 4

An active matrix arrayed microphone with acoustic bandwidth response

Y. Hsu, I. Kymissis, Columbia Univ. (United States)

We have demonstrated a monolithically integrated two dimensional (8X8) active matrix microphone fabricated on a flexible polymer piezoelectric sheet (polyvinylidene difluoride) which uses thin film organic field effect transistors to both locally amplify the piezoelectric charge signal and switch individual elements, allowing for sensing site localization. The integrated design of the sensor and amplifier eliminates a previously dominant parasitic capacitance, allowing an acoustic bandwidth response, and the flexible, thin film form factor allows maximum versatility in applications. Each sensor element is controlled by an organic thin film transistor. The switch transistor is sized significantly smaller than the amplifying/sensing transistor to optimize the cell isolation, on/off characteristic, and parasitic load. The sensor element converts the charge response of the polyvinylidene difluoride (PVDF) sheet into a current signal, overcoming downstream parasitic charge sharing from both switch transistors and interconnects. The device is tested using both turbulent air current and far field acoustic excitation in this work. Our design extends the bandwidth of a locally amplified piezoelectric sheet sensor to the acoustic range, and demonstrates a monolithically integrated active matrix sensing architecture capable of sensing in the acoustic range and mapping both boundary layer and far field acoustic excitation for a variety of applications.

8102-15, Session 4

Low temperature zinc oxide nanorod synthesis for gas detection applications

M. Roddy, S. Jung, T. Ji, Univ. of Arkansas (United States)

Devices fabricated on silicon substrates can have limited applications due to material costs and non-biocompatibility. Glass and flexible polymer substrates are inexpensive and biocompatible making them an excellent choice of substrate for sensor design due to their broad range of potential applications; however require low processing temperatures unlike conventional silicon based devices. To address this low temperature processing requirement of substrates, Zinc Oxide (ZnO) nanorods have been grown on glass and polymer substrates using a low temperature wet chemical synthesis process. Substrates were seeded with ZnO nanoparticles synthesized in methanol and then annealed at 125°C. The substrates were then inverted and placed in a sealed container of nanorod growth solution in a sealed container for 6 - 8 hours at 90°C. The resulting nanorods ranged from 1 - 2 μm in length and 50 - 150 nm in diameter. Samples were characterized with Scanning Electron Microscopy and X-ray Diffraction. The synthesis process was optimized to create vertically aligned single crystal nanorods suitable for gas detection with a proprietary interdigitated electrode design. The mechanism for gas detection is an upward shift in the conduction band structure of ZnO nanorods as gas is absorbed on its surface which results in a measurable increase in conductance. A gas sensor was fabricated with the optimized ZnO synthesis process and its response characterized using CO in N₂ at standard temperature and pressure at concentrations from 150 ppm to 10,000 ppm.

8102-16, Session 4

UV detector from ZnO nanorods with electrodes resembling a wheatstone bridge pattern

A. Vasudevan, S. Jung, T. Ji, Univ. of Arkansas (United States)

Detectors currently used for UV detection are Si based and photomultiplier tubes. These detectors being bulky and less sensitive, we need to find an alternative material that could improve the sensitivity and to build portable detector. Past work by different authors show that ZnO based photo detectors have better sensitivity even at room temperature, also have characteristics like radiation hardness, chemical stability and high temperature stability. The structure of the ZnO detectors can be of the following types (1) p-n junction diode (2) Schottky barrier type (3) Metal-semiconductor-metal type, of these metal-semiconductor-metal type detector is simple and cheaper for fabricating. Usually metal-semiconductor-metal structure detectors use simple interdigitated electrode but the sensitivity of these detector can be improved if better electrode design is chosen. We will use electrodes that are designed in square pattern which almost resembles a wheatstone bridge and this new improved design enhances the collection of carriers and also miniaturization of the detector. The nanorods for the detector will be grown by solution growth technique and rods of different length will be grown to know how it affects the response of the detector. To study how the response of the detector depends on the length of the interdigitated fingers and spacing between the interdigitated fingers, electrodes of different dimension will be fabricated. The response of the detector will be determined from I-V measurements made with and without UV light of wavelength 365nm for different bias voltage.

8102-17, Session 4

Polyaniline nanofilms as a base for novel optical sensor structures

V. Vařinek, J. Bocheza, S. Hejduk, K. Witas, J. Vitasek, Technical Univ. of Ostrava (Czech Republic)

Polyaniline hydrochloride was prepared by the oxidation of aniline hydrochloride with ammonium peroxodisulfate in dilute hydrochloric acid. The polyaniline films were produced during the polymerization on the microscope glass surfaces immersed in the reaction mixture. The thin film was created and its thickness has been about 100 nm. We have measured the spectral transmittance together with temperature changes. The polyaniline thin film is conductive and we observed changes in optical transmittance spectra and reflective spectra with electric current. Optical spectra have been measured in range from 380 nm to 1010 nm.

The electric conductivity has been changed with silicate substrate. This substrate influenced the free electrons distribution and therefore the optical properties of polyaniline. Due to electric current going through the nanofilm its sensitivity to temperature has been increased. We also observed two specific spectral windows. The first one was characterized by its insensitivity to temperature; the second one has been temperature sensitive. The central wavelength of insensitive window is about 500nm. This property can be the base for novel sensors structures.

We used Ocean Optics USB spectrometer for evaluation of spectral changes. Wideband white light halogen source from the same manufacturer has been applied as a light source. Small polarizing dependence of reflected light has been observed too.

8102-18, Session 4

Behavioral modeling of monolithically integrated tri-axis capacitive accelerometer based on metal MUMPs

M. S. Khan, COMSATS Institute of Information Technology (Pakistan); A. A. Iqbal, S. A. Bazaz, Ghulam Ishaq Khan Institute of Engineering Science and Technology (Pakistan)

This paper presents the behavioral modeling of monolithically integrated tri-axis capacitive accelerometer using standard MetalMUMPs process. The behavioral modeling is done to verify the design, structural, modal and electrostatic performance of the designed three axis capacitive accelerometer. The designed accelerometer is 3.2mm×3.5mm in size, designed for sensing the acceleration of 25g in three axis, has 0.291 $\mu\text{g}/\sqrt{\text{Hz}}$, 0.316 $\mu\text{g}/\sqrt{\text{Hz}}$, and 2.84 $\mu\text{g}/\sqrt{\text{Hz}}$ mechanical noise floor for in-plane(x & y) and out-of-plane(z) axes respectively. The total sense capacitance along x, y and z-axes is 68.5fF, 100fF and 6.19pF respectively. Sensitivity of 2.568fF/g, 4fF/g and 0.252pF/g is obtained for in-plane (x and y) and out-of-plane (z) axes respectively. The resonance frequency for the designed accelerometer is 800Hz and 2500 Hz for in-plane and out-of-plane axis. The results obtained by behavioral modeling are compared with the analytically calculated results using Matlab, which are approximately the same.

8102-19, Session 4

Optical and FTIR spectral studies on PZT multilayer thin films

G. N. Venkatesan, P. Jegatheesan, B. Karthikeyan, National Institute of Technology, Tiruchirappalli (India)

Dielectric resonance became an important theme in the physics of composites and fascinated by physicists for many decades due to its potential application in photonic crystals. Lead zirconate titanate $\text{Pb}(\text{Zr}_x\text{Ti}_{1-x})\text{O}_3$, PZT, which exhibits pyroelectric, piezoelectric and electro-optical properties. This material is promising candidate for practical applications like infrared detectors, ferroelectric non-volatile random access memories, optical modulators, optical waveguides, multilayer capacitors and for MEMs applications. One can tune its physical properties by varying 'x' in the composition as mentioned $\text{Pb}(\text{Zr}_x\text{Ti}_{1-x})\text{O}_3$. In the current work we report $\text{Pb}(\text{Zr}_x\text{Ti}_{1-x})\text{O}_3$ based multilayer thin films with different Zr/ Ti ratio where $x = 0.35, 0.40, 0.60$ and 0.65 . These films are prepared through sol-gel spin on technique. Films are coated onto Pt (111)/Ti/SiO₂/Si (100) substrate.

Conference 8102: Nanoengineering:
Fabrication, Properties, Optics, and Devices VIII

X-ray diffraction studies show that the films are switching its phase from rhombohedral to tetragonal phase when the Ti concentration increased. Optical absorption measurements are done on the reflective mode between the wavelength regime 200 to 1100 nm. Spectra show interference effects. To analyze the local structure variation Fourier Transform Infrared spectral measurements are done through KBr pellet technique. Variation in the IR band is expected due to phase change affecting the lattice parameters and it reflects in the IR frequency. The absorption band in FTIR is attributed to TiO₆ and ZrO₆ stretching and bending in the octahedral normal modes and the stretching vibration is the motion of Ti (Zr) and O. We analyzed the optical and structural properties.

8102-20, Session 4

Periodical microstructures induced by IR femtosecond laser pulses on silicon surface for color marking

S. Makarov, National Research Nuclear Univ. MEPhI (Russian Federation)

We investigate basic regimes for ripples formation by IR ($\lambda \approx 744$ nm) femtosecond laser pulses on silicon surfaces and topological evolution of quasi-periodic surface nanostructures with increasing laser irradiation dose (the product of the number of pulses and laser fluence). We demonstrate possibility of controllable and theoretically predictable surface color-marking, which is developing of the new method of surface colorizing by writing laser-induced periodical structures.

8102-21, Session 5

Fabry-Perot scanning probe for aperture-based near-field optical microscopy

A. A. Kuchmizhak, Y. N. Kulchin, O. B. Vitrik, Institute for Automation and Control Processes (Russian Federation)

In present paper we present a new type of interferometric aperture-based probe for near-field optical microscopy based on a fiber optic Fabry-Perot microresonator with a nanosized aperture milled in one of its mirrors. The dependence of resonant modes spectral shift $\delta\lambda$ in the Fabry-Perot microresonator on the distance between the output aperture and the test object was obtained by using finite-difference time-domain (FDTD) method. It was shown theoretically that minimal longitudinal resolution of the method is defined by the Q-factor of the resonator. In accordance with numerical data obtained, proposed method allow one to achieve the value of longitudinal and lateral resolutions more than $\lambda/15$ and $\lambda/40$ correspondently.

The spatial resolution not worse than 120 nm, which corresponds to $\sim \lambda/14$ at wavelength $\lambda = 1550$ nm was experimentally demonstrated using proposed probe based on the fiber optic Fabry-Perot interferometer (Q-factor $\sim 5 \cdot 10^4$) with the 100-nm-sized circular aperture milled in its output mirror with the focused ion beam. A further increase in spatial resolution of the proposed method can be achieved by using resonators with higher Q factor.

8102-22, Session 5

Nanoscale organic light-emitting transistors: NanoOLETs

J. Kjelstrup-Hansen, L. Tavares, R. M. de Oliveira Hansen, H. Rubahn, Univ. of Southern Denmark (Denmark)

Light-emitting organic crystalline nanofibers made from small molecules exhibit a wide range of extraordinary optical properties [1] such as intense, anisotropic luminescence, waveguiding, electroluminescence

and lasing. For lighting and display purposes, the defect free morphology of the nanofibers, the high quantum yield and the easy tunability of the color by changing the molecular building blocks are especially important.

The application of such nanostructures as electrically driven light-emitters requires integration with suitable metal electrodes for efficient carrier injection. Here, we implement two different methods for achieving such nanofiber integration. The first method is based on initially preparing the nanofibers by epitaxial growth on a special growth substrate (muscovite mica) and subsequently transferring them to a suitable device substrate by a recently developed roll-on transfer technique [2]. The second method relies on growing the nanofibers directly between the metal electrodes on a substrate that has been specially designed to guide the nanofiber growth [3]. We present results of both techniques in terms of morphological, optical and electrical characterization and demonstrate how appropriate biasing with an AC gate voltage enables electroluminescence from organic nanofibers. The electroluminescence occurs in the close vicinity of the electrodes (space charge region) and thus the characteristic dimension of the lighting transistor is on the nanoscale.

[1] F. Balzer and H.-G. Rubahn, Adv. Funct. Mater. 15, 17 (2005)

[2] L. Tavares, J. Kjelstrup-Hansen, and H.-G. Rubahn, in preparation

[3] R. M. de Oliveira Hansen, M. Madsen, J. Kjelstrup-Hansen, and H.-G. Rubahn, Nanoscale Res. Lett. 6, 11 (2011)

8102-23, Session 5

Deposition of sol-gel sensor spots by nanoimprint lithography and hemi-wicking

M. B. Mikkelsen, R. Marie, Technical Univ. of Denmark (Denmark); J. H. Hansen, H. O. Nielsen, DELTA (Denmark); A. Kristensen, Technical Univ. of Denmark (Denmark)

We present a method for homogeneous deposition of sol-gel sensor materials, which enables fabrication of sensor spots for optical pH and oxygen measurements inside plastic containers. Using the principle of hemiwicking [Quéré, Physica A (2002)], a deposited droplet is guided by posts imprinted in the surface and fills the imprinted structure automatically, not being sensitive to alignment as long as it is deposited inside the patterned area. A periodic pattern of posts is imprinted into a polycarbonate substrate, and a droplet of the sol-gel sensor material is deposited on the structured surface, where after it spreads, guided by the imprinted posts. The layer thickness of the deposited film is determined by the geometry of the posts and surface energy.

Hemiwicking is an effective method to immobilize a low viscosity liquid material in well-defined spots on a surface, when conventional methods such as screen- or stamp-printing do not work. On length scales of the order of the microstructure period, surface tension will govern the shape of the liquid-air interface, and the liquid will climb up the pillars to keep a fixed contact angle with the sidewalls. The surface to volume ratio is therefore constant all over the surface of the liquid spread by hemiwicking, when considering length scales larger than the microstructure period. Material redistribution caused by solvent evaporation, i.e., the "coffee ring effect" [Deegan et al., Nature (1997)], can therefore be avoided because the evaporation rate does not vary on length scales larger than the period of the pattern.

8102-24, Session 5

Design issue analysis for InAs nanowire tunnel FETs

S. S. Sylvia, M. A. Khayer, Univ. of California, Riverside (United States); K. Alam, East West Univ. (Bangladesh); R. K. Lake, Univ. of California, Riverside (United States)

InAs nanowire-tunnel-FETs (NW-TFETs) are being considered for future, beyond-Si electronics.

Conference 8102: Nanoengineering:
Fabrication, Properties, Optics, and Devices VIII

They offer the possibility of beating the ideal thermal limit to the inverse subthreshold slope of 60 mV/dec and thus promise reduced power operation.

However, whether the tunneling can provide sufficient ON-current for high-speed operation is an open question.

In this work, for a p-i-n device, we investigate the source doping level necessary to achieve a target ON-current (1 micro A) while maintaining a high I(ON)/I(OFF) ratio (1E6) for a range of NW diameters (2-8 nm). Our approach uses a fully-discretized 8 band k.p model combined with the non-equilibrium Green's function (NEGF) formalism.

The electrostatics is calculated using a finite difference solution of Poisson's equation. With a fixed drain bias voltage and a maximum gate overdrive, we compare the performance of the inverse subthreshold slope (SS) and I(ON)/I(OFF) ratio as a function of NW-diameter and source doping. Increasing the source doping level increases the current as a result of the reduced screening length and increased electric field at source which narrows the tunnel barrier.

However, since the degeneracy is also increasing, it reduces the effective energy window for tunneling which, in turn, tends to decrease the current for a given voltage.

This leads to an optimum choice of source doping considering the inverse SS and I(ON)/I(OFF) ratio for these TFETs.

8102-25, Session 5

Carrier leakage in Ge/Si core-shell nanocrystals for lasers: core size and strain effects

M. R. Neupane, R. K. Lake, Univ. of California, Riverside (United States); R. Rahman, Sandia National Labs. (United States)

Ge/Si core-shell nanocrystal lasers have been proposed because of their compatibility with existing Si based technology. They exhibit size dependent stimulated emission and reduced threshold current density. In such structures, lasing is obtained at lower current density because of large carrier confinement and a favorable density of states for population inversion. A recent experimental report suggested an increase in the light emission probability because of increased radiative lifetimes, however the performance is exponentially dependent on the temperature due to the current leakage mechanism. This hole current leakage mechanism is governed by the thermionic lifetime of the confined carrier which is determined by the height of the barrier over which the hole must be emitted. Higher thermionic lifetime indicates a minimal escape rate of the carriers from the core to the confining shell barrier. In this paper, we calculate the thermionic lifetimes as a function of the Ge-core size and strain. Our method also provides a novel and accurate barrier calculation that is required for the leakage current formulation by capturing the bound and extended eigenstates, well below the band edges, and corresponding eigenvalues using the atomistic tight binding method as implemented in NEMO3D. In addition, the effect of both core size variation and strain on the leakage current, and on other fundamental but important electronics and optical parameters will be presented.

8102-26, Session 6

3D tectons as functional nanostructures for self-assembled functional thin films towards nanophotonics

A. Attias, D. Bléger, D. Kreher, F. Mathevet, A. Bakhma, Univ. Pierre et Marie Curie (France); A. Bocheux, F. Charra, L. Douillard, C. Fiorini-Debuisschert, Commissariat à l'Énergie Atomique (France)

In order to achieve the nanometer-scale control over the positioning and organization of functional molecules into monolayers at surfaces, we developed an original approach allowing the exact positioning of

(photo)active organic molecules on the substrate (graphite) leading to the formation of nanostructured functional thin films. Here we present a strategy aimed at the decoupling of molecules from the surface, by lifting photoactive entities a few Å above the surface while maintaining the lateral organization of the array. This is achieved by using 2-level based building blocks. While the first level allows the precise organization of the building blocks on HOPG at the solid-liquid interface at room temperature, the second level is a photoactive compound, namely a chromophore. We will present a series of such building-block exhibiting tunable wavelength emission. This strategy results in the precise organization of chromophores arrays (subwavelength-sized photon sources) a few Å above the conducting surface, as determined by scanning tunneling microscopy (STM), opening interesting perspectives for applications in nanophotonics.

8102-28, Session 6

Boost nonlinearity by monolayer graphene

T. Gu, Columbia Univ. (United States)

Graphene exhibit interesting optical properties such as high Kerr nonlinearity, absorption saturation, Faraday rotation, but in all those experiments light has TM polarized component and thus hard distinguish the graphene effects from the substrate. Here we conformally place the CVD grown graphene on suspended silicon membrane, and send TE polarized light into the pattern defined on the suspended semiconductor membrane. It is observed that the refractive index of the media is sensitive to the light intensity, indicating the silicon's nonlinear effect is enhanced by the graphene cladding since the TE mode like does not direct interact with the one atom thick graphene sheet. Further discussions on the mechanism and fabrication are performed.

8102-29, Session 6

Exciton polariton coupling and enhanced emission in SiC nanocrystals

G. Polupan, T. V. Torchynska, Instituto Politécnico Nacional (Mexico)

The essential interest in last decade appears to different applications of SiC nano crystals (NCs) such as porous SiC (PSiC) or SiC NC composite layers. The large band gap of SiC NCs makes them the good candidates for blue and ultraviolet (UV) light emitter diodes and full-color displays. SiC-based homoepitaxial structures, new types of PSiC-based photodiodes and UV gallium nitride photodetectors grown on PSiC substrates have been reported recently [1].

The paper presents the results of SiC nanocrystal characterization using photoluminescence, its temperature dependence, scanning electronic microscopy (SEM) and X-ray diffraction techniques. Photoluminescence study of porous SiC layers with different SiC NC sizes reveals the intensity stimulation for high energy PL bands. The investigation of temperature dependences of high energy PL bands has shown that these PL bands related to different excitons in SiC NCs. The intensity enhancement of exciton-related PL bands in big size (50-250nm) SiC NCs is attributed to exciton recombination rate increasing due to the realization of exciton weak confinement and exciton-polariton coupling. The numerical simulation permits to estimate the optimal SiC NC size for exciton-polariton coupling. The comparison of experimental and numerically calculated results will be presented as well.

[1] "Nanocrystals and quantum dots of group IV semiconductors", Editors: T. V. Torchynska and Yu. Vorobiev, American Scientific Publisher, 2010, 300p. ISBN: 1-58883-154-X.

8102-30, Session 6

Advanced patterning for patterned magnetic media

E. A. Dobisz, R. Ruiz, G. Zeltzer, T. Hirano, K. Patel, D. Kercher, T. Wu, F. Rose, O. Hellwig, J. Lille, T. Albrecht, Hitachi Global Storage Technologies, Inc. (United States)

Patterned media is a solution to provide data bit thermal stability for future generation disk drives. Patterned bit media is not expected in the disk drive manufacturing until densities of 1 Tb/in² or greater. If the bits were to be placed on a square lattice, 1 Tb/in² would correspond to a dot period of 25 nm. The specifications for the patterned media geometry and accuracy are determined by the required magnetic switching field distribution of the magnetic bits and the recording head. One of the major contributors to a wider switching field distribution is a variation in island size. From configurations of today's write heads, the shape of the future bits may be rectangular rather than square or round. A bit aspect ratio of 2:1, corresponds to a track pitch of 36 nm and a downtrack bit pitch of 18 nm at 1 Tb/in².

Because of the tighter distribution of island sizes, e-beam lithographically guided self assembly of PS-b-PMMA is shown to narrow the island size distribution and the magnetic switching fields of patterned magnetic bits over bits patterned by e-beam lithography alone. Self assembly allows the multiplication of the density of the patterns to 1 Tb/in² or greater. In addition, we show e-beam writing strategies to minimize e-beam write time and exploit the pattern correction of directed self assembly. We also show techniques to address different shape bits. The application of e-beam directed self assembly to fabricating imprint templates and imprinted patterned media is demonstrated at densities up to 1 Tb/in².

8102-31, Session 6

Advanced holographic methods in EUV interference lithography

B. Terhalle, A. Langner, B. Päivänranta, C. David, Y. Ekinici, Paul Scherrer Institut (Switzerland)

Extreme ultraviolet interference lithography (EUV-IL) has recently been attracting growing interest as a fabrication tool for high-resolution periodic nanostructures due to its various fundamental features, e.g. high throughput, large depth of focus etc [1]. Consequently, the technique has been successfully applied to a variety of nanofabrication problems until now [2].

The most common experimental scheme in EUV-IL involves the illumination of a mask containing several diffraction gratings with a spatially coherent beam in order to overlap first-order diffracted beams at a certain distance from the mask and record the resulting interference pattern in a suitable photoresist. This way, the fabrication of high resolution one- and two-dimensional periodic nanostructures becomes possible. So far however, the existing experimental realizations are mostly limited to rather simple symmetries such as one dimensional line patterns or two-dimensional dot arrays [3].

In this contribution, we extend the above concept and study the generation of more complex pattern geometries using EUV-IL. In particular, we demonstrate the use of five or more interfering beams for the fabrication of sub-100nm quasiperiodic nanostructures. Furthermore, we investigate the generation of complex beam shapes such as EUV-vortices and Bessel beams and discuss potential applications for future use in EUV-IL.

[1] Solak, H. H., "Nanolithography with coherent extreme ultraviolet light," J. Phys. D: Appl. Phys. 39, R171 (2006).

[2] Auzelyte V. et al., "Extreme ultraviolet interference lithography at the Paul Scherrer Institut," J. Micro/Nanolith. MEMS MOEMS 8, 021204 (2009).

[3] Solak, H. H., "Space-invariant multiple-beam achromatic EUV interference lithography," Microelectron Eng. 78-79, 410 (2005).

8102-32, Session 6

Fabrication of complex structures with an array of nanopinhole cameras

H. S. Leipner, Martin-Luther-Univ. Halle-Wittenberg (Germany); N. Geyer, Max-Planck-Institut für Mikrostrukturphysik (Germany); F. Syrowatka, H. Cheng, B. Fuhrmann, Martin-Luther-Univ. Halle-Wittenberg (Germany)

There is a big demand of reliable lithographic techniques to produce a wide array of different nanostructures. Colloidal lithography has been proven to produce precise arrays of particles on a broad range of substrates. More complicated nanostructures are required for applications in real-time chemical and biological sensors, based e. g. on the effect of localised surface plasmon resonance. This powerful technique is sensitive to shape, size, interparticle distance, and composition of metallic nanoparticles and the dielectric surrounding. Metallic nanostructures are required for negative refractive index metamaterials as well. In this work, we present a method for the fabrication of ordered arrays of complex structures, which combines colloidal lithography with the principle of a pinhole camera well known in optics. By using atomic beams in high vacuum instead of light, it is possible to overcome the problem of the diffraction limit for small apertures with nanometer dimensions. There are no geometrical or chromatic aberrations, since no refracting elements exist. Limitations exist due to the finite size of the nanopinhole, which lead to a certain blurring of the replica deposited on the substrate. However, compared to focused ion beam technique or electron beam lithography, the method is rather simple and has a broad applicability.

8102-33, Session 6

Synthesis of surface patterned YAG:Ce/TiO₂ nanocomposite films as converter layer for white LEDs.

A. Revaux, G. Dantelle, Ecole Polytechnique (France); D. Decanini, A. Haghiri-Gosnet, Ctr. National de la Recherche Scientifique (France); C. Weisbuch, J. Boilot, T. Gacoin, Ecole Polytechnique (France)

Rare-earth doped oxides are well-known for their applications in light emitting devices. In the case of white LEDs, micron-sized YAG:Ce particles are commonly deposited on blue LED chips to produce an additional yellow component. To avoid losses due to backscattering effects, we propose to control separately the down-conversion and the extraction of light instead of using micron size luminescent particles acting simultaneously as both converters and scatterers. Very stable suspensions of luminescent YAG:Ce nanoparticles, with a crystallite size of 25 nm, were synthesized by a glycothermal method at relatively low temperature (300°C). A protected annealing process in a silica matrix, allowed further treatment of these nanoparticles at high temperature without any aggregation and growth and a significant improvement of their optical properties. The obtained colloidal nanoparticles were finally incorporated into a sol-gel matrix of TiO₂. Thanks to the relative matching of refractive indexes between TiO₂ and YAG, and to the sub-wavelength size of YAG particles, the resulting films are nearly transparent (i.e. non scattering). When used as light converters for white LEDs, these films could offer the opportunity to diminish the backscattered light absorption losses. We showed that the surface of these sol-gel TiO₂ films can be periodically patterned by soft nano-imprint lithography. The diffraction due to the obtained photonic crystal at the surface offers the opportunity to control the extraction the converted light. We investigate how the angular distribution of the emitted light depends on the chosen geometry.

8102-34, Session 7

Types, characterization, and applications of carbon nanotube grades

K. O. McElrath, Carbon Nanotechnologies, Inc. (United States)

Carbon Nanotubes are a quite complex class of materials. As such, there is no easy way to characterize the many grades available for purchase from scores of companies and distributors. The simplest classification that has found widespread use is single wall or multiwall, SWNT or MWNT. An alternate classification is either fullerene polymer molecules or nanoscale carbon fibers. This paper is concerned with the fullerene polymer sub-class of carbon nanotubes. Fullerene science and technology began in 1985 with the discovery of C₆₀, the molecule officially called buckminsterfullerene by the American Chemical Society, and “buckyballs” by the discoverers.

Fullerene nanotubes are a new class of electrically and thermally conducting polymers that are also useful for structural applications since they are strong, stiff, tough, resilient and durable. Similar to other polymers, they are polydisperse. We use a three level description of structure; primary, secondary and tertiary to describe this polydispersity. At the primary structure level, fullerene nanotubes have diameter, length and number of wall distributions. These three components contribute to the molecular weight distribution of the grade. These primary structural elements influence the character of the secondary structure called ropes or bundles. Similar to traditional semi-crystalline polymers, the fullerene polymers attract each other through van der Waal forces and bundle together. These bundles or ropes can be crystalline or non-crystalline. The arrangement of these bundles in macro dimensions creates the tertiary structure. This paper will illustrate this hierarchical characterization approach for a grade of fullerene nanotubes targeting high electrical conductivity applications.

8102-35, Session 7

The low-threshold nonlinear optical effects in suspensions of dielectric alpha Al₂O₃ nanoparticles, dispersed in dielectric organic immersion oil.

V. Dzyuba, V. Milichko, Y. N. Kulchin, Institute for Automation and Control Processes (Russian Federation)

This report presents the results of the study the low-threshold nonlinear optical effects in suspensions of dielectric alpha Al₂O₃ nanoparticles, which are dispersed in dielectric immersion oil. It was found that the refractive index of nanoparticles suspension changes in the weak laser radiation field of visible range (intensity did not exceed 0,2kW/cm²) and it is a function of intensity and frequency of the incident radiation. Nonmonotonic nonlinear additive to the refractive index (nonlinear refraction) was substantiated theoretically and confirmed experimentally as well as additive numerical values were calculated. Maximum absolute value of this nonlinear additive to refractive index was 10⁻⁴. The proposed theory of nonlinear optical properties formation in these suspensions of wide-dielectrics nanoparticles presented the results which consistent with experimental results.

We also investigated the transmission spectra of suspensions of nanoparticles in liquid matrices of different chemical composition and the theoretical assumption about the causes of the difference spectra and optical properties of nanoparticles in various matrices was given. The results of these studies could form the basis for a deeper investigation of suspensions of dielectric nanoparticles, both in liquid and in solid dielectric matrices as well as allow for creation of new types of nanostructured materials for electronics and laser optics.

8102-36, Session 7

Enhancement of optical nonlinearity in β-AgVO₃ nanobelts by incorporation of Ag nanoparticles

M. R. Parida, C. Vijayan, Indian Institute of Technology Madras (India)

The synthesis of Silver vanadium oxides (SVO) with well-controlled size, morphology, and chemical composition can offer great opportunities for exploring their novel optical properties and for the fabrication of nanodevices. These nanostructures of SVO are synthesized by a simple hydrothermal reaction and characterized by standard techniques. The XRD pattern of the as-prepared β-AgVO₃ can be indexed to the phase of β-AgVO₃ monoclinic structure. The HRSEM image shows the diameter of the nanobelts to be in the 100-300 nm range with length upto several micron which is also conformed from TEM. The optical nonlinearity is measured by the Z-scan technique using 5 ns pulse of Nd-Yag laser. The results indicate strong nonlinear absorption which is fitted theoretically two photon absorption process followed by saturable absorption process. The values of two photon absorption coefficient and saturation intensity are calculated. Ag nanoparticles are supported on β-AgVO₃ synthesis by the same hydrothermal technique by increasing the concentration of silver nitrate in synthesis reaction. The HRSEM and TEM images conform that there is no definitive interface relations between the particles, the branches and the stem. They are separated by grain boundaries. There is an enhancement of optically nonlinearity observed in this system compared to undoped SVO. The values of two photon absorption coefficient and saturation intensity are found to be enhanced that because of surface plasmon effect.

8102-37, Session 7

Effect of nano-particles on the dynamic and thermal characteristics of composite materials

M. Seif, M. A. Abunaemeh, Alabama A&M Univ. (United States)

The effect of the nano-silica fillers and dispersion parameters on the mechanical and thermal properties of graphite/epoxy composite materials have been investigated. The dispersion of nano-particles in epoxy resin is carried out using sonication method. The study summarizes the effect of different nano-silica concentrations on the tensile strength of the Epoxy. Modal analysis has been used to determine the vibration properties and damping parameters. The vibration characteristics of nano-composites have been compared with neat epoxy resin. Moreover, the effects of nano-silica fillers on the thermal conductivity and the glass transition temperature of the epoxy resin have been studied. The results show that nano particles have a direct effect on the thermal conductivity and glass transition temperature of the new composite materials. This will allow the possibility of developing new composite materials that will have certain thermal and dynamic properties for wide applications.

8102-38, Session 7

fabrication of quartz nanoneedles by using Cr thin films as wet etching masks

M. Hung, J. Liou, C. Chang, National Central Univ. (Taiwan)

Quartz crystals are widely used in many engineering fields due to their exceptional piezoelectric, optical, and many other properties. Micro/nano-structured quartz is crucial for miniaturization of quartz devices and many potential MEMS/NEMS applications. The manufacturability for quartz crystals, however, is very limited. Unlike the silicon wet etching that generally has simple etching patterns, the wet etching of quartz crystals results in complex and poor symmetric patterns. Thus,

**Conference 8102: Nanoengineering:
Fabrication, Properties, Optics, and Devices VIII**

to fabricate elaborate micro/nanoscale quartz structures is usually not straightforward and requires expensive dry etching processes.

In this manuscript, we present a study of the fabrication of quartz nanoneedles by wet etching. Chromium is evaporated on the Z-cut quartz surface and serves as the etching mask. The deposition process is tuned to certain conditions for Cr atoms to accumulate and form nanosized individual Cr islands. Ammonium bifluoride solutions are used as the etchant. Due to the particular etching anisotropy of quartz crystal orientation, nanoneedles can be formed. By controlling the Cr nanoparticle distributions and etching time, quartz nanoneedles of different sizes are produced. The lengths and shapes of the nanoneedles are observed using scanning electron microscope (SEM) to study the anisotropy of the quartz etching and the mechanism of the needle formation. We have successfully produced very sharp and high aspect ratio nanoneedles with lengths of few micrometers. The growth rate of nanoneedles is found to be increased with the etching time but have a maximum value. The experimental results fit well with our simulated predictions. This study may have potential impacts in quartz MEMS/NEMS.

8102-39, Session 7

An alternative approach to fabricate metal nanoring structures based on nanosphere lithography

Z. A. Lewicka, V. L. Colvin, Rice Univ. (United States)

In this work we present an improved, cost-effective fabrication method for metal ring-shaped nanostructure arrays based on nanosphere lithography. Periodic arrays of symmetric nanorings, non-symmetric nanorings, and nanocrescents with different sizes were fabricated using a simple method that includes self-assembled monolayer formation, plasma treatment and sputter deposition of metal. Lower cost and higher throughput were achieved due to the replacement of focused ion beam milling with reactive ion etching usually used in other methods. The dimensions of ring-like structures could be controlled by the size of the polystyrene spheres, the amount of deposited metal and the argon plasma etching time. These nanostructures may be made of essentially any metal and be used as elements in optoelectronic nanodevices.

8102-40, Session 7

fabrication and optical characterization of nanopore Si

H. Jin, G. L. Liu, Univ. of Illinois at Urbana-Champaign (United States)

Nanopore Si has been applied to demonstrate advantages in various fields such as photovoltaic, biosensing, DNA sequencing, and also particle sorting. The optical and mechanical properties provide enhanced solar conversion efficiency, surface enhanced Raman effects, elongation of DNA, and also blocking of vapor phase molecules. Typical fabrication of nanopores would utilize e-beam lithography followed by DRIE. Focused ion beam may also be utilized. The use of such methods are time consuming in formation of nanopores on a relatively larger area. Another approach would be the use of anodized aluminum oxide (AAO), by applying a voltage to high purity aluminum foil (99.999%) in oxalic acid. The non-lithographic fabrication method would enable cost effect approach of nanopore fabrication. However, the use of aluminum foil based AAO results in a film that is too thick to transfer the nanopore features to another substrate.

In this paper, the fabrication and the optical properties of nanopore Si is presented. Aluminum is evaporated on the surface of N-type Si by e-beam evaporation. Nanopore structure is formed by a two-step AAO formation in oxalic acid. Diameter size from 30 to 80 nm is achieved, depending on the condition of anodization and etch. Deep reactive ionic etch (DRIE) is done, with AAO as the mask layer. The nanopore AAO template allows etching depth of up to 700 nm. Parameters that affects

the fabrication are evaluated. Optical properties of various pore depth is discussed.

8102-41, Poster Session

Efficient approach for the calculation of transmission and reflection spectra of photonic crystal waveguide devices

R. Chen, Y. Lin, Lunghwa Univ. of Science and Technology (Taiwan)

Photonic crystal (PC) waveguide devices have inspired great interest because of their potential in realizing compact photonic integrated circuits. To design a PC waveguide device, it is important to know its transmission and reflection spectra. Among the various simulation techniques, the finite-difference time-domain (FDTD) method is popularly employed due to its versatility in dealing different structures. However, the traditional approach to calculate the transmission and reflection spectra by the FDTD method is a task of both time and memory demanding. A sizable computational cell must be used and several pulses covering different ranges of frequencies must be sent down the waveguide and the field amplitudes are monitored at two proper locations. The monitored field profiles are then Fourier transformed to obtain the transmission and reflection spectra. In this work, we propose a more efficient approach to obtain these spectra. First, the PC-based absorbing boundary condition proposed by Koshiba is employed instead of the popularly used perfectly matched layer boundary condition. Second, the reflected pulse is obtained by subtracting from a reference input waveform. To demonstrate the effectiveness of this approach, a T-junction in square lattice PC is simulated. A computational cell of only 40 x 36 lattice constants can be used for the proposed approach, compared to 150 x 80 lattice constants for the traditional approach. Accordingly, the simulation time is reduced to only one tenth of that using the traditional approach.

8102-42, Poster Session

Design of sharp waveguide bends with a wide high-transmission bandwidth in triangular photonic crystal slab

R. Chen, Y. Lin, Y. Lin, Lunghwa Univ. of Science and Technology (Taiwan)

Photonic crystal slabs (PCSs) have received considerable attention due to their potential in high-density photonic integrated circuits. Optical confinement is provided via the photonic bandgap in the plane of periodicity and via refractive index in the vertical direction. By removing one row of air holes, a single-line-defect waveguide can be obtained. Some sharp waveguide bends in PCSs have been proposed but their high-transmission bandwidths were limited. In this work, we design a 60-degree waveguide bend with a wide high-transmission bandwidth (~ 9.8% of the center frequency, or 150 nm at the wavelength of 1550 nm) in a triangular PCS. Within the high-transmission bandwidth, power reflection at the bend is found to be lower than 2% of the input power. Based on this 60-degree bend, a sharp 120-degree bend with a compact device area is proposed. A similar transmission efficiency is also found for this 120-degree bend.

The principle of the proposed sharp bends is as follows. First, the adjacent air holes along the two sides of the single-line-defect waveguide is enlarged such that the waveguide becomes single-mode. Second, a mirror plane is introduced at the bend region to improve the power transmission. This is done by further enlarging three air holes at the bend region and by moving inward one of them such that a photonic crystal mirror plane is formed. Numerical simulation is performed by employing the finite-difference time-domain method and power transmission and reflection spectra are calculated by launching pulses and by Fourier transformation.

8102-43, Poster Session

Nano and micro structures imaging based on asymmetric Bragg diffraction

A. V. Kuyumchyan, American NanoScience and Advanced Medical Equipment, Inc. (United States); D. A. Kuyumchyan, Riverside Community Colleges (United States); A. Snigirev, I. Snigireva, European Synchrotron Radiation Facility (France); M. V. Grigorev, E. V. Shulakov, Institute of Microelectronics Technology and High Purity Materials (Russian Federation)

We present results of focusing and imaging properties of lens-crystal system for hard x-ray radiation; consisting of such elements as parabolic refractive lens made from beryllium and asymmetric mono crystal from silicon. The beryllium refractive lens has advantages like small absorption, high efficiency and high spatial resolution.

This work demonstrates for the first time a phenomenon of image transmission using the Bragg diffraction of focused x-ray beam from asymmetric mono crystal. For recording the magnification X-ray phase contrast was used asymmetric mono crystal Si (220) with factor asymmetry $b=9$ at the x-ray energy 17 keV. The experimental investigations have been conducted on the station BM-5, ESRF, France.

The peculiarities of redistribution of intensity are investigated both experimentally and theoretically when the focus of refractive lens is moved across the optical axis. The intensity distribution along the optical axis is also investigated. We elaborate a computer program for theoretical study of image transmission based on lens - crystal system with asymmetric Bragg diffraction. The calculation is based on the use of Kirchhoff propagator in a paraxial approximation and fast Fourier procedure. The intensity map on the plane perpendicular across the optical axis is calculated for any parameters, including the phase shift of the test object.

8102-44, Poster Session

Fabrication of Multiple Si Nanohole Thin Films from Bulk Wafer by Controlling Metal-Assisted Etching Direction

S. Shiu, T. Lin, K. Pun, H. Syu, S. Hung, C. Lin, National Taiwan Univ. (Taiwan)

Crystalline Si photovoltaic modules still have high production cost due to significant consumption of the Si wafer. Reducing the large amount of Si material consumption is thus a critical issue. Here we develop a two-step metal-assisted etching technique for forming vertically-aligned Si nanohole thin films from bulk Si wafers. The formation of Si nanohole thin films includes a series of solution processes: deposition of Ag nanoparticles in an AgNO₃/ HF aqueous solution, formation of Si nanohole arrays at the first-step metal-assisted etching, and side etching of the roots of the nanohole structure at the second-step metal-assisted etching. All the processes can proceed at around room temperature. A Si nanohole thin film with an average hole size of 100 nm and a thickness of 5 μ m-20 μ m was hence formed at the top of the wafer. Afterwards, the Si nanohole thin film was transferred onto alien substrates. The Si nanohole thin film has the crystal quality similar to the bulk Si wafer. The above bulk Si substrate can be reused. With similar processes, other Si nanohole thin films can be formed from the above recycled Si wafer. The hole size and thickness are similar. The Si wafers recycled will significantly reduce the material consumption of Si. Thus, such technique is promising for lowering the cost of Si solar cells.

8102-45, Poster Session

Design and fabrication of 3D dielectrophoretic chip on separating 2-type of bacteria

C. W. Su, Tatung Univ. (Taiwan)

With the improvement of quality of life, people want to have better medical treatment. MEMS technology is applied by biotechnology such as PCR chip, detection chip, separated chip and etc. Biological, chemical, or medical processes involving complex fluids with embedded particles often require preparative separation of particles, cells, or even molecules that are needed for the subsequent procedures.

In this research, the MEMS technologies which is applied to make the 3D electrodes with the 3D electric field. The structure of biochip is consisted of PDMS flow channel, copper electrode and glass. In order to achieve DEP performance, we utilize CFD-ACE+(Computational Fluid Dynamics) to simulate the effect of the sharp electrodes, wide electrodes and narrow electrodes. We deposited 50 μ m of copper as electrodes on glass and 50 μ m of PDMS as flow channel. We use the 3D DEP chip to separate yeast cells and aspergillus niger. We succeeded in trapping yeast cells at 5Mhz, 10Vpp, and separating the different cells. Compared with typical planar DEP devices, the proposed 3D DEP chip, presents an increased DEP force in the vertical direction. The electric field will become wider than before. Fabrication 3D electrodes on glass can result in lower costs and less time-consumong. The chip we fabricated is demonstrated that the electrodes which is fabricated by MEMS technologies can manipulate the bioparticle. As the result, the trapping or levitation effect can be achieved at a lower voltage and with a reduced heating of the solution.

8102-46, Poster Session

A model of photoconductivity of porous silicon

L. S. Monastyrsky, B. Sokolovskii, Ivan Franko National Univ. of L'viv (Ukraine)

It is presented a model of the photoconductivity of porous silicon in the conditions of homogeneous generation of photocarriers. By the finite element method it is calculated the stationary photoconductivity and the time evolution of photoconductivity after instantaneous shutdown of light. Dependences of the stationary photoconductivity and relaxation time of photoconductivity on the velocity of surface recombination of nonequilibrium carriers at the surfaces of pores, radius of pores and average distance between them are analyzed. It is shown that increase of the surface recombination velocity leads to decreasing both the value of stationary photoconductivity and the time of photoconductivity relaxation, with at lower values of the distance between the pores these changes being more significant. Decrease of the relaxation time at the expense of changing the surface recombination velocity can reach almost one order of magnitude. The latter occurs in the materials with high level of porosity when the area of pore's surface per unit volume is large. The results of modeling show that peculiarities of the photoconductivity of porous silicon is of interest for manufacturing gas sensors.

8102-47, Poster Session

Investigation of 0-3 composites for novel capacitors and energy storage

A. Buchsteiner, H. S. Leipner, J. Glenneberg, C. Ehrhardt, M. Zenkner, T. Grossmann, S. Ebbinghaus, H. Beige, Martin-Luther-Univ. Halle-Wittenberg (Germany)

Up to now, rechargeable batteries are mostly used for energy storage purposes.

However, their electrochemical working principle limits the field of application.

Capacitors with very high energy densities are an alternative approach for energy storage. They can be very quickly charged/discharged and have long lifetimes.

We develop novel capacitors on the basis of 0-3 composites, where nanoparticles of perovskites are embedded in a matrix material. Specific organic surfactants of the nanoparticles force their uniform distribution in the matrix.

These new materials combine the electrical advantages of ceramics and glasses/polymers (high permittivities and breakdown voltages) and can easily be processed as thin films.

8102-49, Poster Session

Engineering of Photonic Crystal Waveguide Defects for Slow Light Applications

V. Janyani, Malaviya National Institute of Technology (India)

In recent years photonic crystal waveguides (PCWs) made of silica and air holes have provided a new approach for dispersion compensation and slow light generation, due to the design flexibility obtained by variation in the geometric parameters of the holes and corresponding tailoring of the effective refractive index. For slow light generation, a large value of group index is desirable to slow down the light. At the same time, however, the bandwidth of the range over which the slow light is achieved and the dispersion produced in the signal as a result of slow-down of the pulses of become much significant.

The signal propagates through the 'defect' in the PCW which is obtained by removing one linear row of air holes in the hexagonal-lattice photonic crystal. The effect of the rows nearest to this line defect have been found to have much influence on the propagation characteristics of the signal and on the slow light generation process. This paper proposes a new geometry of PCWs, which uses carefully designed elliptical holes in the two rows adjacent to the defect through which the signal propagation takes place. These elliptical holes are shifted along the longitudinal direction in such a way that the arrangement provides a delay-bandwidth product which is significantly higher than that previously reported in literature. The paper discusses the theory behind the design process and the principle of operation, and necessary numerical results are presented to verify the behavior claimed.

Conference 8103: Nanobiosystems: Processing, Characterization, and Applications IV

Sunday-Monday 21-22 August 2011 • Part of Proceedings of SPIE Vol. 8103
Nanobiosystems: Processing, Characterization, and Applications IV

8103-01, Session 1

Developments of high-sensitive DNA sensors (Keynote Presentation)

N. Ogata, Chitose Institute of Science and Technology (Japan)

Pure DNA which is isolated from Salmon roe has a huge high molecular weight of over billion and can form a strong and uniform film and the double helical structure of DNA has a characteristic feature of intercalation of various optical dyes among stacked layers of nucleic acid bases to enhance optical properties of dyes, so that applications of DNA as materials are now possible in such areas as photonics, separation process or biomedical materials. Recent research results on DNA-lipid complexes have shown various attractive applications such as E/O or O/E devices, optical memories, switches and sensors¹⁻⁴. It was reported² to study on possibility of basic optical characteristics, such as refractive indices, absorbance and fluorescence intensity, and photochromic properties, of spiropyran-doped DNA-cetyltrimethylammonium (CTMA) complex films, which were derived from DNA from Salmon, which showed potential applications to optical switches^{5, 6}. Although DNA-lipid complexes showed promising potentials for optical functional devices such as switching or signal processing devices, their response speeds were relatively slow to apply them to practical uses. It was shown^{5, 6} that much faster response speed (switching times) could be attained by increasing the excitation light intensity. Thus, applications of DNA photonic devices have been widely studied in the world⁷⁻¹⁰.

The large enhancements of optical properties of the dye-intercalated DNA lead us to apply the dye-intercalated DNA as various sensors with a high sensitivity to detect environmentally toxic gases such as dioxine, NOx or carbon monoxide. This paper reports on DNA sensors for the further applications of DNA as materials. Also, bio-medical applications of DNA sensors such as alcohol or glucose sensors will be reported.

References

- (1) L. Wang, J. Yoshida, N. Ogata, S. Sasaki and T. Kamiyama: "Self-assembled supramolecular films derived from marine deoxyribonucleic acid (DNA) - cationic lipid complexes: large-scale preparation and optical and thermal properties", *Chem. Mater.*, 13, 1273-1281, 2001.
- (2) J. Yoshida, L. Wang, S. Kobayashi, G. Zhang, H. Ikeda and N. Ogata: "Optical properties of photochromic-compound derived from dye-doped marine-biopolymer DNA-lipid complex films for switching applications", *Proc. SPIE*, 5351, 260-268, 2004.
- (3) W. M. Heckman, J. Grote, P. P. Yaney and F. K. Hopkins: "DNA-based nonlinear photonic materials", *Proc. SPIE*, 5516, 47-51, 2004.
- (4) P. P. Yaney, E. M. Heckman, D. E. Diggs, F. K. Hopkins and J. Grote: "Development of chemical sensors using polymer optical waveguides fabricated with DNA", *Proc. SPIE*, 5724, 224-233, 2005.
- (5) A. Watanuki, J. Yoshida, S. Kobayashi, H. Ikeda and N. Ogata: "Optical and photochromic properties of spiropyran-doped marine-biopolymer DNA-lipid complex films for switching applications", *Proc. SPIE*, 5724, 234-241, 2005.
- (6) J. Yoshida, A. Watanuki, S. Kobayashi, H. Ikeda and N. Ogata: "Potential switching application based on the photochromism of spiropyran-doped marine-biopolymer DNA-lipid complex films", *Tech. Digest, 10th Optoelectronics and Communication Conference (OECC2005)*, 342-343, 2005, Seoul, Korea.
- (7) K. Yamaoka and N. Ogata: "Effect of lipids on physical properties of DNA-lipid complexes", *Kobunshi Ronbunshu*, 61, 384-390, 2004.
- (8) C. M. Wu, W. Kiou, H. L. Chen, T. L. Lin, and U. S. Jeng, "Self-assembled structure of the binary complex of DNA and cationic lipid", *Macromol.*, 37, 4974-4980, 2004.
- (9) N. Ogata "Novel Applications of DNA Materials", *Proceeding of SPIE*, Vol. 7403, 740305-1(2009)

(10) T. T. Sada, M. Yoshikawa, and N. Ogata, "Oxygen Permeable Membranes from DNA-Lipid-Complexes", *Membrane*, 31, No. 5, 281-283(2006)

8103-02, Session 1

BiOTFT memory with DNA complex

N. Kobayashi, T. Yukimoto, K. Nakamura, Chiba Univ. (Japan); S. Uemura, H. Kamata, National Institute of Advanced Industrial Science and Technology (Japan)

No abstract available

8103-03, Session 1

Novel DNA-cationic lipid complexes and their application as gate dielectrics

L. Cui, Univ. of Connecticut (United States); X. Wei, Case Western Reserve Univ. (United States); L. Zhu, Univ. of Connecticut (United States)

In this study, we report molecular shape and size effects of lipid tails on the mesophase self-assembly of various cationic lipids complexed with double-stranded DNA. The molecular shape of the cationic lipids changes from rod-like (a cyanobiphenyl imidazolium salt) to discotic (a triphenylene imidazolium salt), and finally to cubic [a polyhedral oligomeric silsesquioxane (POSS) imidazolium salt]. An increase in the cross-sectional area of the hydrophobic tails with respect to the hydrophilic imidazolium head induces a negative spontaneous curvature of the cationic lipids. As a result, a morphological change from lamello-columnar phase for the DNA-cyanobiphenyl imidazolium salt (DNA-rod) and DNA-triphenylene imidazolium salt (DNA-disk) complexes to an inverted hexagonal phase for the DNA-POSS imidazolium salt (DNA-cube) complex is observed. The DNA-rod complex has a typical smectic A (SmA) lamellar morphology, while the DNA-disk complex has a double lamello-columnar phase. However, when the lipid tail changes to POSS, an inverted hexagonal morphology is achieved. Their application as the gate dielectrics in transistors will be briefly introduced.

8103-04, Session 1

Biopolymers-based gate insulators for BioFETs

F. Ouchen, Air Force Research Lab. (United States); P. P. Yaney, Univ. of Dayton (United States); C. M. Bartsch, E. M. Heckman, M. B. Dickerson, J. G. Grote, Air Force Research Lab. (United States)

No abstract available

8103-05, Session 2

Photophysical properties of lanthanide(III) chelates-doped DNA-CTMA complex

K. Nakamura, A. Sagara, N. Kobayashi, Chiba Univ. (Japan)

No abstract available

Conference 8103: Nanobiosystems:
Processing, Characterization, and Applications IV

8103-06, Session 2

Metal incorporated M-DNA: structure, magnetism, optical absorption

K. Mizoguchi, Tokyo Metropolitan Univ. (Japan)

No abstract available

8103-07, Session 2

Optical and electrical properties of DNA-CTMA biopolymers in Metal-Biopolymer-Metal photodetectors

B. Zhou, Univ. at Buffalo (United States); S. J. Kim, Univ. of Miami (United States); C. M. Bartsch, E. M. Heckman, F. Ouchen, Air Force Research Lab. (United States); A. N. Cartwright, Univ. at Buffalo (United States)

The application of a DNA biopolymer into an electro-optic device is investigated. Specifically, a complex of DNA with cationic surfactant hexadecyltrimethylammonium chloride (CTMA) is used to obtain organic-soluble DNA material. In order to increase the electrical conductivity of the DNA biopolymer, PEDOT:PSS is added to DNA-CTMA. Optical and electrical conductivity properties of the DNA-CTMA and DNA-CTMA-PEDOT are investigated. CW absorbance and time-resolved photoluminescence of the resulting DNA samples were studied experimentally. Both DNA samples demonstrated absorbance peaks at ~260 nm and photoluminescence at ~470nm. The PEDOT doped DNA polymer shows shorter lifetime (260ps) than the undoped DNA biopolymer; which may be indicative of charge transfer from the DNA-CTMA to the PEDOT in the composite biopolymer. Interestingly, the PL lifetime was observed to decrease in both cases with increasing excitation in an air ambient. Specifically, after excitation with a high power ultrafast (~150fs) UV (266nm) pulse in air, the lifetime decreases dramatically after a few minutes of exposure. This is most likely due to photo-oxidation that results in trap creation on the polymer surface and an increase in the non-radiative recombination. In order to investigate the photoconductivity, metal-biopolymer-metal (MBM) ultraviolet photodetectors with interdigitated electrodes were fabricated. The optical responsivity of these MBM UV photodetectors increased as the electron transport length (the space between the MBM fingers) were decreased to the nano-scale. Prospects for the use of these materials in optical devices will be discussed.

8103-13, Session 2

Modeling of stochastic kinetics for process of photochromic dye semi-intercalation into DNA-based polymeric matrix

A. C. Mitus, G. Pawlik, J. Mysliwiec, A. Miniewicz, Wroclaw Univ. of Technology (Poland); J. G. Grote, Air Force Research Lab. (United States)

The semi-intercalation of an azo-dye Disperse Red 1 (DR1) molecule into a biopolymeric material made of deoxyribonucleic acid (DNA) complexed with the cationic surfactant hexadecyltrimethyl-ammonium chloride (CTMA) formulated recently [1,2] has successfully explained the main experimental results [3] of laser dynamic inscription of diffraction gratings: short response time, low diffraction efficiency, single-exponential kinetics and flat wavelength dependence [4]. In this paper we generalize the analytic model of Ref. [1] to account for a more realistic dynamics of DNA-CTMA matrix. To this end we use Monte Carlo method to study the spatial distribution of local voids and calculate void - void correlation functions, which play the central role for the kinetics of photoinduced trans - cis - trans cycles of DR1 dye under the polarized laser light illumination. We formulate a stochastic master equation which

generalizes the simple model of Ref. [1]. We also address the topic of non - exponential grating inscription in modeling and in recent experiments. [1] A.C. Mitus, G. Pawlik, F. Kajzar, and J.G. Grote, Proc. SPIE, Vol. 7040 (2008) 70400A. [2] H. Sou, H. Spaeth, V.N.L. Linhard, and A.J.Steckl, Langmuir 25 (2009) 11698. [3] A. Miniewicz, A. Kochalska, J. Mysliwiec, A. Samoc, M. Samoc, and J.G. Grote, Appl.

Phys. Lett. 91, 04118 (2007). [4] G. Pawlik, A.C. Mitus, J. Mysliwiec, A. Miniewicz, and J.G. Grote, Chem. Phys. Lett., 484 (2010) 321.

8103-09, Session 3

Invited Presentation

J. G. Grote, Air Force Research Lab. (United States)

No abstract available

8103-10, Session 3

DNA architectures for templated material growth

A. S. Finch, J. Sumner, U.S. Army Research Lab. (United States)

We will present a methodology that allows for the coupling of biology and electronic materials, where double stranded DNA serves as a template for electronic material growth. Self-assembled DNA structures allow for a variety of patterns to be achieved on the nanometer size scale that are difficult to achieve using conventional patterning techniques. Herein, we describe the procedures for the creation of self-assembled DNA nanostructures in aqueous and non-aqueous media, and their subsequent deposition onto substrates of interest. DNA self assembly under non-aqueous conditions has yet to be presented in literature, and is necessary if unwanted oxidation of certain electronic substrates is to be avoided. Solubilization of the DNA in non-aqueous solvents is achieved by replacing charge stabilizing salts with surfactants. Retention of DNA hierarchical structure under both conditions will be presented by observing the structures using AFM imaging, gel electrophoresis, and circular dichroism spectroscopic studies.

8103-11, Session 3

Morphological and physical properties of graphene/DNA layered bio-nanocomposites

Z. Bai, Univ. of Dayton Research Institute (United States); T. D. Dang, S. N. Kim, R. R. Naik, Air Force Research Lab. (United States)

No abstract available

8103-08, Session 4

Evanescence field excitation of Cy5-conjugated lipid bilayers using optical microcavities

L. M. Freeman, The Univ. of Southern California (United States) and Univ. of California, San Diego (United States); Y. Dayani, S. Li, H. Choi, N. Malmstadt, A. M. Armani, The Univ. of Southern California (United States)

Whispering gallery mode optical microresonators are devices used for performing ultra-sensitive optical detection. Although the majority of the sensor research has been focused on label-free detection strategies for diagnostics, a whispering gallery mode device is ideally suited to perform fluorescent label-based biodetection as well. However, previous research using optical microcavities to excite fluorescent molecules has focused

Conference 8103: Nanobiosystems:
Processing, Characterization, and Applications IV

on cavity quantum electrodynamics applications and fundamental studies of the interactions of large fluorescent nanoparticles with the resonant cavity.

In the present work, a method for forming self-assembled lipid bilayers, a mimic for cell membranes, on a spherical microresonator is developed. Solid-supported lipid bilayers, which are approximately 5nm thick, have been shown to accurately model cell membranes, and researchers use lipid bilayers in combination with fluorescent microscopy when developing theoretical models for the transport of molecules across the cell membrane. The bilayer-nature is verified using both fluorescent resonance energy transfer and fluorescence recovery after photobleaching. The evanescent tail of the microresonator is used to excite a Cy5-conjugated lipid located within the bilayer while the underlying optical device behavior is characterized at 633nm and 980nm. The emission wavelength of the Cy5 dye and the optical performance (Q factor) of the microcavity agree with theoretical predictions.

8103-12, Session 4

Influence of DNA on J-aggregate formation of cyanine dyes

Y. Kawabe, S. Kato, Chitose Institute of Science and Technology (Japan)

DNA plays an important role for the enhancement of luminescence from some organic dyes. On the other hand, interaction of dyes with DNA sometimes stimulates the formation of dye aggregates in solutions and solid films.

Studying the absorption and circular dichroic (CD) spectra for the solutions of PIC coexisting with DNA and polyvinylalcohol in aqueous solutions, we found that J-aggregates of pseudo-isocyanine (PIC) were formed with lower dye concentration than ever. The details of the effects from the dye concentration, the ratio to DNA, and the type of counter ions were investigated and optimized. One example is that J-aggregate peak has the largest magnitude when the molar ratio of DNA base pair/PIC was 1/4. The J-aggregate characteristics were reproduced after fabricating films from the solution, the fact would be important for development of devices.

More than 20 types of water soluble cyanine dyes were studied by the same methods. Most of dyes show aggregates (not always J-aggregates) by interacting with small amount of DNA, and these aggregates dissociated with the addition of excess DNA. Concentration dependences of photoluminescence intensity and CD spectra suggest that the optical characteristics are strongly influenced by molecular size. Mechanism of dye-DNA interactions will be discussed.

8103-14, Session 4

Photodegradation of melanin thin films by UV lithography

C. W. Farley III, A. Kassu, A. Sharma, Alabama A&M Univ. (United States)

Effect of ambient humidity on the photodegradation of melanin is investigated using an interferometric technique to fabricate gratings on thin films. A low power 355 nm diode laser is used to fabricate gratings on melanin thin films, while a 1 mW He-Ne laser is used to probe grating formation. Effects at several different UV intensities, ranging from 1 mW to 30 mW, and ambient humidities, ranging from 15% to 98%, are investigated on melanin thin films of two different thicknesses; 22 nm and 40nm. It is found that humidity has a significant effect on the rate of photodegradation of melanin. It is also found that existing gratings on melanin thin films can be enhanced by raising ambient humidity. These results have implications in the biological evolution of many mammals; as well as implications in fabrication and effective lifetime of organic electronics. The interferometric technique used shows great promise for fabricating grating to analyze photodegradation of different biomolecules under varying conditions. A simple mathematical model is also developed

to help explain the contribution of light intensity and ambient humidity to the photodegradation of melanin.

8103-15, Session 4

Fluorescence study on DNA based thin films with synthetic and natural chromophores

I. Rau, A. Tane, Polytechnical Univ. of Bucharest (Romania); C. Andraud, Ecole Normale Supérieure de Lyon (France); A. Meghea, Polytechnical Univ. of Bucharest (Romania)

No abstract available

8103-16, Session 5

Studies of charge transport in DNA films using the time-of-flight (TOF) technique (Keynote Presentation)

P. P. Yaney, T. Gorman, Univ. of Dayton (United States); F. Ouchen, J. G. Grote, Air Force Research Lab. (United States)

Measurements were carried out on a variety of DNA-based films, including as-received DNA (molecular weight, MW>1000 kDa), DNA with MW<1000 kDa and DNA doped with conductive additives. The test specimens were spin-coated or drop-cast films on ITO-coated quartz slides with a gold charge-collecting electrode. To protect the films from atmospheric influences, the TOF devices were coated with a ~200 nm polyurethane passivation layer. A quadrupled 10 ns, pulsed Nd:YAG laser with output at 266 nm was used for charge injection. The photoconductive responses ranged from mildly to strongly dispersive with hole mobilities in DNA materials films ranging between 7E-6 to 7E-5 cm²/V-s.

8103-17, Session 5

DNA-assisted fabrication of luminescent and Raman active silver nanoparticles for dual-modal bioimaging

K. Ijiri, G. Wang, T. Nishio, K. Nambara, Y. Matsuo, K. Niikura, Hokkaido Univ. (Japan)

No abstract available

8103-18, Session 5

Keynote Presentation

R. Zamboni, Consiglio Nazionale delle Ricerche (Italy)

No abstract available

8103-19, Session 5

Bio-dielectrics based on DNA-Ceramic hybrid films for potential energy storage applications

N. Venkat, Univ. of Dayton Research Institute (United States); D. Joyce, F. Ouchen, Air Force Research Lab. (United States); P. P. Yaney, Univ. of Dayton (United States); K. M. Singh, Air Force Research Lab. (United States); T. Miller, UES, Inc. (United States); S. R. Smith, Univ. of Dayton Research Institute (United States); J.

Conference 8103: Nanobiosystems:
Processing, Characterization, and Applications IV

G. Grote, R. R. Naik, Air Force Research Lab. (United States)

The potential of DNA-based dielectrics for energy storage applications was explored via the incorporation of high dielectric constant (ϵ) ceramics such as TiO₂ and BaTiO₃ in the DNA bio-polymer. The DNA-Ceramic hybrid films were fabricated from stable suspensions of the nanoparticles in aqueous DNA solutions. Dielectric characterization revealed that the incorporation of TiO₂ (rutile) in DNA resulted in enhanced dielectric constant and decreased dielectric loss factor ($\tan \delta$) relative to DNA in the entire frequency range of 1 kHz-1 MHz. Variable temperature dielectric measurements, in the 20-80°C range, of both DNA-TiO₂ and DNA-BaTiO₃ films revealed that the ceramic additive stabilizes DNA against large temperature-dependent variations in both ϵ and $\tan \delta$. The bulk resistivity of the DNA-Ceramic hybrid films in the case of both TiO₂ and BaTiO₃ additives was measured to be two to three orders of magnitude higher than that of the control DNA films, indicating their potential for utilization as insulating dielectrics in capacitor applications. Results based on a comparison of the temperature-dependent dielectric behavior of DNA and DNA-CTMA complex films as well as their frequency-dependent polarization behavior are also discussed.

8103-20, Session 6

Origin of dielectric tunability in DNA-CTMA film at microwave frequencies

R. S. Aga, Jr., General Dynamics Information Technology (United States); C. M. Bartsch, Air Force Research Lab. (United States); B. Telek, G. Subramanyam, Univ. of Dayton (United States); E. M. Heckman, J. G. Grote, Air Force Research Lab. (United States)

No abstract available

8103-21, Session 6

Effective bio-imaging using two-photon absorbing nanoparticles

K. Lee, Hannam Univ. (Korea, Republic of)

This presentation discusses the synthesis and use of nanoparticles with two-photon absorption for bioimaging. We present the synthesis of two-photon chromophores capable of forming fluorescent nanoparticle in the aggregated state. These chromophores are further complexed with materials like polysiloxane and phospholipids to aid their transport to and penetration of tumor cells. Derivatives of 4-bis(cyanostyryl)benzene (CSB)-based quadrupolar isomeric molecules (a- and b-CSB-TPs) were designed to produce enhancement in fluorescence quantum yield and two-photon absorption cross-sections for the nanoaggregate form. This and other two-photon absorbing materials were successfully incorporated in hyperbranched polysiloxysilane (HBPS) materials containing terminal carboxylic acid and quaternary ammonium groups. These polymers exhibited desirable characteristics, including amphiphilicity for nanoparticle formation, and contained various terminal groups for surface-charge control on the nanoparticles or for further bioconjugation for targeted imaging. Aggregation induced fluorescence was further observed in polymeric nanomicelles. The fluorescent nanomicelles have two unique features: (1) It gives much brighter fluorescence emission than mono-fluorophore. (2) The biocompatible nanomicelles with amphiphilic copolymers [e.g., phospholipids-PEG (polyethylene glycol)] make the encapsulated fluorophores more stable in various bio-environments and easier for further conjugation with bio-molecules. After chemical and optical characterizations, these fluorescent nanomicelles are utilized as efficient optical probes for in vivo sentinel lymph node (SLN) mapping of mice.

8103-22, Session 6

Two-photon absorbing chromophores for photodynamic therapy: molecular engineering and in vivo applications

C. Monnereau, Univ. de Nantes (France); P. Lanoë, Univ. de Rennes 1 (France); T. Gallavardin, O. Maury, C. Andraud, Ecole Normale Supérieure de Lyon (France)

Photodynamic therapy (PDT) is a therapeutic approach based on the light induced production of cytotoxic molecular singlet oxygen, through irradiation of a photosensitizer near a tumoral tissue. In recent years, it has been used with success in the treatment of certain cancers and gliomas at their early stages ; however, it suffers from one major limitation that hinders a more widespread use in cancer therapy : due to biological absorption and scattering of the incident light, it is impossible to efficiently activate a conventional photosensitizer through more than few millimeters of tissue, making non-invasive deep tissue and organ therapy practically impossible.

Two-photon activation of the sensitizers, using lasers with wavelengths around 800-900 nm could be a very advantageous strategy to overcome these limitations. This range of wavelengths corresponds to the domain of transparency of human tissues, which would allow deeper penetration of the light. Another advantage is the highly confocal character of two-photon excitation, leading to very localized sensitizer activation, which is ideal to avoid undesirable damages of healthy tissues in the tumor's surroundings.

In spite of all its promises, two-photons PDT is still in its infancy, and practical issues now have to be addressed:

1/ Relatively few two-photon chromophoric structures that can efficiently sensitize singlet oxygen have been reported so far. Thus, we believe that molecular engineering has to be performed, with an accent put on the establishment of structure/ properties relationships

2/ Two photons chromophores require a large conjugated carbon backbone, which makes them very hydrophobic compounds : chemical modification have therefore to be carried out, in order to allow their dispatching within the physiological medium, and cellular up-take.

These two aspects will be discussed in our presentation. The first part will deal with recent results in our group concerning the structural optimization of chromophores for two-photon induced dynamic therapy. The second part will focus on new "cargo" systems that we have recently developed, owe to a general strategy recently established in the group.1

1/T. Gallavardin, M. Maurin, T. Simon, A.-M. Gabudean, Y. Bretonnière, O. Maury, P. L. Baldeck, O. Stéphan, Y. Leverrier, S. Marotte, J. Marvel, M. Lindgren, F. Lerouge, S. Parola, C. Andraud ; Photochem.Photobiol.Sci., accepted

8103-23, Session 6

All optical switching in a photochromic dye-doped biopolymeric matrix

J. Mysliwiec, A. Malak, J. Sikora, A. Miniewicz, Wroclaw Univ. of Technology (Poland); I. Rau, Polytechnical Univ. of Bucharest (Romania); F. Kajzar, Polytechnical Univ. of Bucharest (Romania) and Univ. of Angers (France)

All optical switching has been studied using the Optical Kerr Effect (OKE) configuration in a biopolymer matrix containing a photochromic molecule. The biopolymer system consisted of a deoxyribonucleic acid blended with cationic surfactant molecule cetyltrimethyl-ammonium chloride suitable for optical quality thin film fabrication. The excitation beams inducing birefringence were delivered from a continuous wave lasers at 473 and 532 nm and chopped using a variable frequency chopper. Additionally auxiliary nanosecond pulses coming from Nd:YAG laser were used. The birefringence was instantaneously monitored by a weak non-absorbed light from a cw He-Ne laser working at 632.8 nm under crossed polarizer system. An excellent switching times in the range

of microseconds and full reversibility of the studied processes have been observed.

8103-24, Session 6

Tunable dye lasers based on DNA-surfactant-dye complexes

T. Chida, Y. Kawabe, Chitose Institute of Science and Technology (Japan)

There have been several studies of laser action from dyes incorporated into deoxyribonucleic acid (DNA) complexes, because fluorescence was strongly enhanced by molecular isolation due to the intercalation or binding to the double helix structure of DNA. We have already demonstrated the amplified spontaneous emission (ASE) and laser action from several dyes, such as a hemicyanine, (4-[4-(dimethylamino)styryl]-1-dococylpyridinium bromide) or several types of cyanines doped in DNA-surfactant films.

In this presentation, we will show recent achievements on DNA dye lasers. First, we succeeded to generate tunable laser emissions from solutions including the hemicyanine and DNA- cetyltrimethylammonium (CTMA) complex in a Littrow type cavity. The concentration of the dye and DNA-CTMA, and also the ratio of both were optimized (about 1.0×10^{-3} mol/l for the dye and DNA-CTMA 20 times concentrated), obtaining the laser emission in the range about 600 ~ 630 nm under the pumping by a green nano-second pulsed laser. The conversion efficiency was 3 % and their beam divergence was 0.016 rad.

We also succeeded to prepare DNA laser medium by using another method, by which dye complex was prepared by immersing the DNA-CTMA into aqueous solution of the dye, resulting in dyed DNA polymers. We employed eosin Y which is a water soluble xanthene compound, and observed ASE emission from fabricated films.

8103-25, Poster Session

An Investigation on films used for chemical and biological sensors

M. J. Curley, A. K. Chilvery, T. V. Kukhtareva, C. W. Farley, Alabama A&M Univ. (United States)

Bioterrorism as well as the use of explosive devices have been a key threat not only in Iraq and Afghanistan but also on the southern border of the United States. Biosensors as well as chemical sensors are mandatory in the field of sensing the existence of detrimental gases like methyl isocyanides, sensing the presence of bacteria's like anthrax and detecting the presence of explosives like RDX, TNT's etc. These biosensors combined with a low power lasers for remote sensing should be able to be used for biological and chemical detection. In this paper we also mentioned the importance of study of micro-organisms in the synthesis of nanomaterials is a possible viable alternative to the more popular physical and chemical methods currently in use. We shall discuss the development of green and energy saving technologies in materials synthesis, environmentally caring nanoparticle synthesis processes that do not use toxic chemicals. Optimizing the characteristics and fabrication of biosensors with different nanoparticles for selective and sensitive detection will be performed. Testing using the method of Stimulated Emission Raman Scattering (SERS), FTIR, SEM and AFM measurements in our laboratories shall be disclosed. We have also investigated the presence of two photon compounds and Rhodamine B to determine if the prototype sensor will amplify the signals of biological agents as well as explosives. The results in this paper are promising in developing a Chemical and Biological sensors for the use in the Department of Defense, USDA and commercial applications.

8103-26, Poster Session

Synthesized nanomaterials based on extracellular soluble fungal poliketide

N. Radu, Institutul National de Cercetare (Romania); M. Ferdes, Polytechnical Univ. of Bucharest (Romania); C. Corobea, D. Donescu, Institutul National de Cercetare (Romania); I. Rau, Polytechnical Univ. of Bucharest (Romania)

Monascorubrin obtained in submerged media of different fungal strain from Monascaceae family can be used as biomaterials, in order to obtain nanoproducs with therapeutic properties. In this respect, using soluble monascorubrin obtained in submerged media and isopropylmiristate as conditioning agent, nanodispersions was obtained, with dimensions under 100 nm (determined by dynamic light scattering). The first preclinical tests performed on the main raw materials revealed that these nanodispersions could be used as adjuvant in skin disorders having an important role in tissular reparation in case of derma lesions.

8103-27, Poster Session

Characterization of some nanamaterials based on insoluble fungal poliketide

N. Radu, Institutul National de Cercetare (Romania); M. Ferdes, Polytechnical Univ. of Bucharest (Romania); C. Corobea, D. Donescu, Institutul National de Cercetare (Romania); I. Rau, Polytechnical Univ. of Bucharest (Romania)

Biopigments obtained in solid state biosynthesis was used as raw materials in order to obtain bioproducts used in the dermatology treatment. The main formulation was nanomaterials with dimensions under 60 nm according to dynamic light scattering measurements. The new nanoproducs which contain three biopigments biosynthesized on rice were characterised by fluorescence diffraction, FT-IR and mass spectrum, and the results indicate the presence in the nanoproducs of main poliketide based on monascorubrin and monascorubramin.

In this paper the main results concerning characterisation and possible applications of these new nanoproducs will be presented and discussed.

Conference 8104: Nanostructured Thin Films IV

Tuesday-Thursday 23-25 August 2011 • Part of Proceedings of SPIE Vol. 8104
Nanostructured Thin Films IV

8104-01, Session

Green nanotechnology (Keynote Presentation)

G. B. Smith, Univ. of Technology, Sydney (Australia)

Nanotechnology, in particular nanophotonics, is proving essential to achieving green outcomes of sustainability and renewable energy supply at the scales needed. Coatings, composites and polymeric structures used in windows, roof and wall coatings, energy storage, insulation and other components in energy efficient buildings will increasingly involve nanostructure, as will solar cells. Nanostructures have the potential to revolutionize thermoelectric power and hence solar thermal power, and may one day provide efficient refrigerant free cooling.

Nanomaterials enable us to optimize optical, opto-electrical and thermal responses to this urgent task. Optically harmonization of material responses to environmental energy flows involves two aspects, large changes in spectral response over limited wavelength bands and tailoring responses to environmental dynamics. The latter includes engineering angle of incidence dependencies and switchable (i.e chromogenic) responses. Nanomaterials can be made at sufficient scale and low enough cost to be both economic and to have a high impact on a short time scale. Issues that must be addressed however include human safety, plus property changes induced during manufacture, handling and use outdoors. Some unexpected multiple bonus' have arisen in this work, for example the savings and environmental benefits of cool roofs are manifold and extend beyond the more obvious benefit of substantial reduced heat flows from the roof into the building.

8104-02, Session 1

Surface multiplasmonics

A. Lakhtakia, The Pennsylvania State Univ. (United States)

Surface plasmon-polariton waves are guided by planar interfaces of metals and homogeneous dielectric materials. At a give frequency, only one SPP wave is possible. If the dielectric material is periodically nonhomogeneous in the thickness direction, multiple SPP waves are possible, leading to exciting possibilities for optical sensing and solar cells.

8104-03, Session 1

Broad band plasmonic superabsorption and anti-reflection

K. Kempa, Boston College (United States)

Collective resonances, plasmons, of conducting electrons in structured metals can dramatically enhance light transmission and trapping. The effective medium, metamaterial approach is a convenient framework for guiding studies of such systems. We have demonstrated earlier how the plasmonics of the Escheric and Babinet series of metallic, planar structures, can benefit from this approach. The talk will briefly review the relevant background, but will focus on the superabsorber action of such structures. In particular, we demonstrate that ultra-thin semiconducting layers, sandwiched between thin structured metallic layers nearly perfectly absorb, in a wide frequency band, when one of the metallic layers is a checkerboard. We show, that while microscopically this effect is a result of a resonant coupling between surface plasmons of the various interfaces, the exceptionally broad-band response is a result of the metamaterial action of this self-Babinet structure. We also show, how a broad-band anti-reflection action can be achieved by employing ITO coated, Escheric structures near the percolation threshold.

8104-04, Session 1

High-throughput nanofabrication of plasmonic structures and metamaterials with high resolution nanostencil lithography

S. Aksu, A. A. Yanik, R. Adato, A. A. Artar, M. Huang, H. Altug, Boston Univ. (United States)

In this talk, we will demonstrate a novel fabrication approach for high-throughput fabrication of engineered infrared plasmonic antenna arrays and metamaterials with high resolution nanostencil lithography (NSL)¹. NSL technique, relying on deposition of materials through a shadow mask, offers the flexibility and the resolution to fabricate radiatively engineered nanoantenna arrays for excitation of collective plasmonic resonances. Spectral measurements and electron microscopy images faithfully confirm the feasibility of NSL technique for large area patterning of nanorod antenna arrays, plasmonic dimers (such as bowties) and metamaterials with high resolution that is achievable by electron-beam lithography. Furthermore, we show nanostencils can be reused multiple times to fabricate same structures with identical optical responses repeatedly and reliability. This capability is particularly useful when high-throughput replication of the optimized nanoparticle arrays is desired. In addition to its high-throughput capability, NSL permits fabrication of devices on surfaces that are difficult to work with electron/ion beam techniques. Nanostencil lithography is a resist free process thus allows the transfer of the nanopatterns to any planar substrate whether it is conductive, insulating or magnetic. As proof of the versatility of the NSL technique, we show fabrication of plasmonic structures and metamaterials in a variety of designs on traditional and unconventional substrates. High-resolution Nanostencil Lithography enables plasmonic substrates and metamaterials supporting spectrally narrow far-field resonances with enhanced near-field intensities. Overlapping these collective plasmonic resonances with molecular specific absorption bands can enable ultrasensitive vibrational spectroscopy². We will also present our recent results on spectroscopic identification of proteins with antenna arrays fabricated by nanostencil lithography.

1 S. Aksu, A. A. Yanik, R. Adato, A. Artar, M. Huang and H. Altug "High-throughput Nanofabrication of Plasmonic Infrared NanoAntenna Arrays for Vibrational Nanospectroscopy" Nano Lett., 10 (7), 2511-2518 (2010).

2 R. Adato, A. A. Yanik, J. J. Amsden, D. L. Kaplan, F. G. Omenetto, M. K. Hong, S. Erramilli and H. Altug, "Ultra-sensitive Vibrational Spectroscopy of Protein Monolayers with Plasmonic Nanoantenna Arrays", Proc. Natl. Acad. Sci. U.S.A. 106, 19227 (2009).

8104-05, Session 1

Spatiotemporal-photothermal and photoacoustic conversions with local plasmon resonators

K. Namura, M. Suzuki, K. Nakajima, K. Kimura, Kyoto Univ. (Japan)

Recently, we demonstrated the self-assembly of Au nanoparticles/ structured dielectric layer/ Ag mirror sandwiches, namely, the local plasmon resonator, by using a dynamic oblique deposition technique¹. Due to strong interference, their optical absorption can be controlled between 0.1% and 100% by changing the thickness of the dielectric layer. Now we notice that photothermal conversion efficiency can be spatiotemporally tuned by using the local plasmon resonators. This work is the feasibility study of their application to the spatiotemporally controlled nanoheaters.

We prepared local plasmon resonator chips on a single substrate by oblique deposition and measured the absorption spectrum on each element. In order to evaluate the heat generation from the chips, we measured the temperature of the water, with which a small cell created

on a chip was filled, irradiating the laser of the wavelength of 785 nm. Photoacoustic measurement was also done on the chip, irradiated with the laser, of which intensity was modulated sinusoidally.

The local plasmon resonator with high absorption heats up the water on itself higher and generates stronger photoacoustic signal than that with low absorption. Furthermore, the photoacoustic signal from the local plasmon resonators with high absorption is stronger than that from an Ag thin film by two orders of magnitude between 50 kHz and 100 kHz. These results suggest that heat generation from the Au nanoparticle layer can be spatiotemporally controlled by the interference and incident light intensity.

1. M. Suzuki, et al., Journal of Nanophotonics, 3, 031502 (2009).

8104-06, Session 1

Monitoring the reactivity of Ag nanoparticles for different atmospheres by using in situ and real time optical spectroscopy

V. V. Antad, L. Simonot, D. Babonneau, S. Camelio, F. Pailloux, P. Guérin, Univ. de Poitiers (France)

Surface differential reflectance spectroscopy (SDRS), an optical characterization technique, is sensitive enough to observe the minute changes in surface plasmon resonance (SPR) of noble metal nanoparticles (NPs), which is a collective oscillation of the electrons owing to their interactions with electromagnetic radiations, causing sharp absorption of light in the visible range. This SPR is extremely sensitive not only to the morphology and organization of the noble metal NPs but also to the chemical atmosphere surrounding them.

Hence, taking SPR as a signature phenomenon in the Ag NPs, we have studied their reactivity for different gases and their ions using an optical mean. For this purpose, a dedicated in-situ SDRS set-up has been mounted on a magnetron sputtering machine, with which real time optical characterizations were possible not only during the deposition of Ag NPs but also during their exposure to gases such as O₂, N₂, Ar, either non-ionized or partially ionized.

This optical study reveals the reactivity of Ag NPs with non-ionized O₂ in the form of changes in the SPR characteristics (width, amplitude and position of the absorption band) in contrast to N₂ and Ar. Moreover, this study also elaborates the increased reactivity of Ag NPs due to the partially ionized gases where, on one hand, complete disappearance of the SPR can be seen in case of O₂(+) and on the other hand, increased reactivity in Ag NPs can be seen for the N₂(+) gas, whereas Ar remains non-reactive in both forms.

8104-07, Session 1

Surface plasmon resonance of super-periodic metal nano-slits structures

H. Leong, J. Guo, R. G. Lindquist, The Univ. of Alabama in Huntsville (United States)

We investigate surface plasmon resonance in super-periodic metal nano-slits arrays. A super-periodic metal nano-slits array consists of periodic metal nano-slits and periodic defects in the nano-slits array. Our simulation and experimental results show that spectral peaks measured in the zeroth order transmission and the first order diffraction reveal the surface plasmon resonances in the super-periodic metal nano-slits structure. The resonance wavelength can be tuned accordingly by adjusting the nano-slits period or the super-period of the device. The new metal nanostructure device functions as a resonant optical diffraction grating and can be used for integrated nano-fluidic surface plasmon sensors.

8104-08, Session 2

Nanostructure effects and the performance of optical interference coatings

O. Stenzel, U. Schulz, N. Kaiser, Fraunhofer-Institut für Angewandte Optik und Feinmechanik (Germany)

The theory of "classical" optical interference coatings is based on assumptions like ideal homogeneity and isotropy of the materials, as well as absolutely smooth and infinitesimally thin interfaces between the individual coating materials. Within the framework of these assumptions, there exists an elaborated theoretical apparatus for solving design and characterization tasks for optical coatings. At the same time, coating deposition techniques have been perfected in order to match with the requirements of homogeneity and smoothness of these coatings in practice.

Remaining discrepancies between the theoretically predicted and practically achieved coating performance can - at least partially - be attributed to the violation of the above-mentioned ideal assumptions. But a closer look on this matter reveals a more differentiated picture: Nanostructure effects can be tackled as additional degrees of freedom for coating design, and can lead to useful property combinations that are inaccessible to "classical" coatings prepared on the basis of the traditionally available coating materials.

This presentation deals with practical examples, where explicit violations of the usually assumed perfect homogeneity and smoothness of the coatings have resulted in novel and innovative coating material properties or coating designs. Examples include:

- Effects of noble metal islands embedded in semiconductor films: applications in photovoltaics
- Antireflection effects of nanostructured surfaces: moth-eye-structures
- Effects of nanoporosity in oxide films on refractive index, thermal shift and mechanical stress: balanced coating properties

The examples demonstrate the possible benefits of the exploitation of nanostructure-caused effects in interference coating science and technology.

8104-09, Session 2

Using a single anisotropic thin film as a phase retarder for oblique incident wave

Y. Jen, S. Wang, C. Lin, M. Lin, National Taipei Univ. of Technology (Taiwan)

This work presents a wide angle phase retarder by using a single anisotropic Ta₂O₅ columnar thin film. The single anisotropic Ta₂O₅ columnar thin film can provide phase retardation between p-polarization and s-polarization to modulate the polarization state of light reflected from the prism-coupling system (BK7 prism/anisotropic thin film/air). In experiment, glancing angle deposition technique is used to prepare single layer film of Ta₂O₅ tilted nanorod array with thickness 270nm. In this analysis, we use wave tracing based on the Berreman calculus to calculate the variations of reflection coefficient, transmission coefficient on the interface and the variations of phases of ordinary and extraordinary waves in the anisotropic thin film when the electromagnetic wave is incident to the prism-coupling system. The phase retardation is observed about $\delta=100^\circ(\pm 5^\circ)$ over the angle ranged from 61° to 75° and the wavelength ranged from 630nm to 680nm. A linearly polarized incident ray can be reflected as a specific elliptical polarized ray uniformly over the region. In addition, the phase retardation is varied smoothly over the designated range when the deposition plate is rotated from 90° to 45° with respect to the plane of incidence.

8104-10, Session 2

Quenched transmission of light through ultrathin metal films

N. A. Mortensen, S. Xiao, Technical Univ. of Denmark (Denmark)

It is well known that the transmission of light is prominent for an ultrathin metal film with the thickness comparable to its optical penetration depth. When the film is periodically modulated by subwavelength apertures, intuitively one expects that the ultrathin film could transmit even more light since less material is blocking the light. To much surprise, it was recently predicted by means of analytical and numerical calculations that the transmission can nevertheless be totally suppressed. This nontrivial phenomenon is opposite to the widely known extraordinary optical transmission of light through periodically modulated optical thick metal films, which was first reported by Ebbesen et al. Subsequently, the quenched transmission of light through ultrathin films pierced with periodic arrays of subwavelength apertures was experimentally demonstrated. In this paper, we experimentally demonstrate quenched transmission of light through ultrathin films when the films are periodically structured. We used E-beam lithography technology to fabricate the devices and free-space measurement setup to characterize them. The measured results show the transmission is significantly suppressed, which is an opposite phenomenon as compared with the extraordinary optical transmission of the light through the film when perforated by the subwavelength holes. We emphasize that the measurement demonstrates less light transmitted through the gold disks array. The physics behind it is also discussed and it turns out that this abnormal phenomenon is ascribed to the surface plasmon resonance effect.

8104-11, Session 2

Optical properties of UT-shaped plasmonic nanoaperture antennas

M. Turkmen, S. Aksu, A. E. Cetin, A. A. Yanik, H. Altug, Boston Univ. (United States)

The subject of light transmission through optically thin metal films perforated with arrays of subwavelength nanoholes has recently attracted significant attention [1]. In this talk, we will present numerical and experimental results on optical properties of a multi-resonant UT-shaped plasmonic nanoaperture antenna for enhanced optical transmission and near-field resolution. We will propose different structure designs in order to prove the effect of geometry on resonance spectrum and near-field enhancement. Theoretical calculations of transmission spectra and field distributions of UT-shaped nano-apertures are performed by using three-dimensional finite-difference time-domain method [2]. The results of these numerical calculations show that transmission through the apertures is indeed concentrated in the gap region. In addition to theoretical calculations, we also performed a lift-off free plasmonic device fabrication technique based on positive resist electron beam lithography (EBL) and reactive ion etching in order to fabricate UT-shaped nanostructures. For further confirmation of the multi-resonant behavior, we checked the individual U- and T-shaped nano-aperture antenna responses. We also studied the parameter dependence of the structure to determine the control mechanism of the spectral response. Theoretical calculations are supported with experimental results to prove the enhanced field distribution and multi-resonant behavior which can be suitable for infrared detection of biomolecules, wavelength-tunable filters, optical modulators, and ultrafast switching devices.

[1]. T. W. Ebbesen, H. J. Lezec, H. F. Ghaemi, T. Thio, and P. A. Wolff, "Extraordinary optical transmission through subwavelength hole arrays," *Nature* 391, 667 (1998).

[2]. Lumerical Solutions, Inc., www.lumerical.com, 2011.

8104-12, Session 2

Optical birefringence in a bideposited nanorod array with symmetric and periodic structure

Y. Jen, C. Yu, M. Lin, C. Lin, National Taipei Univ. of Technology (Taiwan)

A new kind of nanorod array grown with two orthogonal bideposited directions is fabricated and measured its birefringence optical property. The Ta₂O₅ nanorod arrays composed of several subdeposits are fabricated by serial bideposition (SBD) technique. Each nanorod consists of several identical units and each unit consists of symmetrical sections ABA. The deposition planes for section A and section B are perpendicular to each other. The bideposited symmetric nanorod arrays can be equivalent to a homogeneous layer of the equivalent refractive index and phase thickness. For normal incident ray, the polarization-dependent refractive indices and phase thicknesses of the film are presented as functions of wavelength and optical constants of each layer. The transmittance spectra of symmetrical sections have a pass band property as the equivalent refractive indices are real. With each subdeposition thickness of 5 nm, samples bideposited at flux angles 65°, 70°, 75° and 80° are prepared. The principal indices associated with the two orthogonal polarizations are measured by ellipsometer. According to principal indices database, a phase retardation between the two orthogonal polarization directions can be designed for a specific wavelength. In order to apply the multilayered structure in changing the polarization state, a match layer is designed and arranged in the layered system to reduce the difference between the two orthogonal polarization transmissions.

8104-13, Session 3

Effective properties of metamaterials

C. Rockstuhl, C. Menzel, T. Paul, E. Pshenay-Severin, M. Falkner, C. Helgert, A. Chipouline, T. Pertsch, Friedrich-Schiller-Univ. Jena (Germany); W. Smigaj, J. Yang, P. Lalanne, Univ. Bordeaux 1 (France); F. Lederer, Friedrich-Schiller-Univ. Jena (Germany)

Optical properties of nanostructured thin films, i.e. metamaterials, are usually linked to the assignment of an effective permittivity and permeability and, if polarization conversion occurs, chirality. To consider the underlying constitutive relations as valid, it is required that only weak spatial dispersion occurs. At operational frequencies of optical metamaterials close to resonance this assumption ceases to be valid. In consequence, a description using effective material properties tends to be inadequate and new approaches are required. We outline here our latest achievements along this direction and discuss two approaches.

The first assumes that if effective properties are pointless since they explicitly depend on the frequency and the incidence angle, a more primary source of information is sufficient to quantify metamaterials, i.e. the polarization resolved complex transmission and reflection; leading to a characterization of metamaterials in terms of Jones matrices. We discuss the implications of such description and show that all metamaterials can be categorized into five classes only, each supporting distinguishing properties which we disclose. Experimental results of measured complex Jones matrices of three-dimensional metamaterials underline the applicability of this approach.

The second approach resorts to an effective description but restricts its consideration entirely on a dispersion relation, characterizing the propagation of light in bulk metamaterials, and an impedance, characterizing the coupling of light into and from metamaterials to their surroundings. Feasible definitions of both properties linked to a single Bloch mode are discussed and metamaterials are introduced which can be homogenized while considering only the properties of this single mode.

8104-14, Session 3

On dipole emission from an infiltrated chiral sculptured thin film

S. S. Jamaian, T. G. Mackay, The Univ. of Edinburgh (United Kingdom)

This study was motivated by the prospect of harnessing chiral sculptured thin films (CSTFs) as optical sensors based on chemiluminescent emission. A dipole source positioned inside a CSTF was considered. The void regions of the CSTF were filled with a fluid of refractive index greater than unity. The theory describing the emitted field far from the dipole source was developed, using a spectral Green function formalism. A combination of inverse and forward homogenization techniques were used to estimate the relative permittivity parameters of the infiltrated CSTF. This involved the extended Bruggeman homogenization formalism, which accommodates constituent particles that are small compared to wavelength but not vanishingly small. Our numerical studies, based upon a titanium oxide CSTF, revealed that left circularly polarized (LCP) light was preferentially emitted through one face of the CSTF while right circularly polarized (RCP) light was preferentially emitted through the opposite face, at wavelengths within the Bragg regime. A red shift in the centre wavelength for the preferential emission of LCP/RCP light took place as the refractive index of the infiltrating fluid increased from unity. Furthermore, this red shift was accentuated when the size of the constituent particles in the homogenization model was increased. In addition, as the refractive index of the infiltrating fluid increased from unity, the bandwidth of the preferential LCP/RCP emission regime was observed to decrease.

8104-15, Session 3

Homogenization of metallic metamaterials and electrostatic resonances

D. Felbacq, Univ. Montpellier 2 (France); F. Zolla, Institut Fresnel (France); B. Guizal, Univ. Montpellier 2 (France)

It has been noted that the usual approaches for homogenization (e.g. Bruggeman) could lead to singularities when considering composites comprising materials with positive and negative permittivities. This situation is specifically encountered in the field of metamaterials, in particular in the visible range. The question then arises to understand if these resonances are just artifacts or possess, on the contrary, a clear physical meaning.

In this work, we study the homogeneous properties of a bidimensional structure that is made of a periodic set of metallic wires embedded in a dielectric host medium. The structure is considered in a region of wavelengths that are much larger than the period of the structure. The work comprises a theoretical part where we develop a two-scale approach to the homogenization of the structure. As it is the case for the common physical approach, it leads to an effective permittivity with strong (electrostatic) resonances as well. The theoretical results, and the presence of resonances, are confirmed by numerical computations based on a rigorous modal approach. In the numerical results we consider specifically the case of silver and gold nanowires, described by a dispersive negative permittivity. We show that the main parameters for the onset of resonances is the optical filling ratio of the structure. Keeping in mind the possibility of performing experiments, it is far easier to keep the geometrical filling ratio constant and to consider strongly dispersive materials in the range of wavelengths considered. Here, besides the crucial fact that they are widely used in nanotechnology, silver and gold nanowires comply with our needs in the visible region of the spectrum.

8104-16, Session 4

Engineering the optical response of hybrid plasmonic systems: fano resonances and applications for sensing

A. Farhang, B. Gallinet, O. J. F. Martin, Ecole Polytechnique Fédérale de Lausanne (Switzerland)

We study the optical response of hybrid plasmonic systems composed of nanoparticles in strong interaction with a thin film. While the latter supports propagating surface plasmon-polaritons, the former supports localized plasmon resonances. Engineering the coupling between these two families of modes produces extremely sharp optical resonances - so-called Fano resonances - characterized by narrow spectral features and a very strong near-field enhancement. Furthermore, these features can be easily tuned by changing the geometry of the system: materials, film thickness, spacing between particles and film, or the shape of the particles. We show that it is possible to a large extent to determine a priori the spectral response of the coupled system, by analyzing the spectral responses of its individual components (i.e. the infinite film and the localized particles), in particular their modal overlap in the optical density of states space. With this approach, we design specific structures where individual particles, dipole antennas, or more complex arrangements of metallic nanoparticles are coupled to a metallic thin film. A conventional e-beam lithography followed by lift-off is used for their fabrication. Hybrid plasmonic systems prove extremely efficient for sensing: the strongly localized near-field associated with Fano resonances makes them very responsive to their environment and significantly enhances the figure of merit for sensing, when compared to individual structures such as isolated thin films or isolated nanoparticles.

8104-17, Session 4

Metamaterial and nanoplasmonic toolkit for spectroscopy and biosensing

H. Altug, Boston Univ. (United States)

No abstract available.

8104-18, Session 4

3D characterization of a TiO₂-based photoanode for solar cells

G. Divitini, Univ. of Cambridge (United Kingdom); A. Li Bassi, Politecnico di Milano (Italy); F. Di Fonzo, Istituto Italiano di Tecnologia (Italy); C. S. Casari, V. Russo, Politecnico di Milano (Italy); X. Peng, C. Ducati, Univ. of Cambridge (United Kingdom)

The performance of dye-sensitized (DSSC) and hybrid solar cells crucially depends on the structure of the photoanodes on the micro- and nano-scale. Transmission electron microscopy (TEM) is a good candidate for investigating such length scales, but the limitation of conventional TEM to extract only bi-dimensional information hinders our ability to have a full understanding of the three-dimensional structure and properties. We instead apply advanced TEM techniques to characterize a photoanode prototype, combining high resolution crystallographic studies with three-dimensional information obtained from dark field electron tomography. In this work we present the study of a TiO₂-based photoanode where the titania layer has been produced via pulsed laser deposition. We employed a dual beam FIB (FEI Helios Nanolab) to prepare a cross-section of a polymer heterojunction solar cell based on said photoanode and acquired a tilt series in a FEI Tecnai F20 (200 kV acceleration voltage). The photoanode TiO₂ layer is composed by small (10-20 nm) crystalline particles assembled in columnar aggregates, which constitute a forest-like film with high porosity. Such a hierarchical structure combines a large surface area with good electrical transport properties, leading to promising performance. The characterization provided information on

surfaces and interfaces of the nanocrystalline titania, as well as a view of the fine scale cell architecture after the infiltration of the polymer hole transporter.

8104-19, Session 4

Antireflective Nanostructured Thin Films and Their Applications in Solar Cells

J. He, National Taiwan Univ. (Taiwan)

It is of current interest to develop the antireflection (AR) coatings with nanowire arrays (NWAs) since the ability to suppress the reflection over a broad range of wavelengths and incident angles plays an important role in the performance of optoelectronic devices, such as photodetectors, light-emitting diodes, optical components, or photovoltaic systems. Superior AR characteristics of NWAs, including polarization-insensitivity, omnidirectionality, and broadband working ranges are demonstrated in this study. These advantages are mainly attributed to the subwavelength dimensions of the NWAs, which make the nanostructures behave like an effective homogeneous medium with continuous gradient of refraction index, significantly reducing the reflection through destructive interferences. The relation between the geometrical configurations of NWAs and the AR characteristics is discussed. We also demonstrated their applications in solar cells. This report paves the way to optimize the nanostructured optoelectronic devices with efficient light management by controlling structure profile of nanostructures.

8104-20, Session 4

Microspot surface enhanced fluorescence biosensing from sculptured thin films

A. Karabchevsky, Ben-Gurion Univ. of the Negev (Israel); C. Khare, B. Rauschenbach, Leibniz-Institut für Oberflächenmodifizierung e.V. (Germany); I. Abdulhalim, Ben-Gurion Univ. of the Negev (Israel)

Nano-sculptured thin films (STF) are prepared by the glancing angle deposition technique and take different forms of nano columnar structures. Varieties of STFs are investigated to find the optimum structure for biosensing based on the surface enhanced fluorescence (SEF). Comparative study is presented from STFs containing variety of nano structures different in their shape, height (h), tilt angle with respect to the surface (θ), thickness (d), arrangement, etc. The highest enhancement factor of the fluorescent signal is found for Ag based STFs on Si(100) giving an enhancement factor of $\times 71$, where $h=400\text{nm}$, $d=75\text{nm}$, $\theta=23^\circ$ relative to Ag closed film using fluorescent dye Rhodamine 123. Based on this a demonstration of an E-coli bacteria sensor and fluorescent antibody sensors are presented. Bound antibody to the thiol self assembly monolayer on sample surface is then quantified by means of the fluorescent signal. Upon excitation of the fluorophore by Hg source light, a CCD camera with a controlled exposure time detects the pattern of fluorescent antibody/E-coli bacteria colonies on the STF surface. A fiber optic holder attached to the microscope allowed quantitative measurement of the fluorescence spectrum on a microspot.

8104-21, Session 5

Intimate effects of surface functionalization on biosensing performances with porous silicon microcavities

C. Gergely, L. Massif, M. Martin, E. Estephan, M. Saab, Univ. Montpellier 2 (France); C. Larroque, Univ. Montpellier 1 (France); V. Agarwal, Univ. Autónoma del Estado de Morelos (Mexico); F. Cuisinier, Univ. Montpellier 1 (France)

We study the effect of different surface functionalization methods on the sensing performances of porous silicon (PSi) microcavities when used for detection of various biomolecules. Previous research on porous silicon demonstrated versatility of these devices for sensor applications based on their photonic responses. The interface between biological molecules and the Si semiconductor surface is a key issue for improving biomolecular recognition in these devices.

PSi microcavities were fabricated to reveal reflectivity pass-band spectra in the visible and near-infrared domain. To assure uniform infiltration of proteins the number of layers of Bragg mirrors was limited to five, the first layer being of high porosity. In one approach the devices were thermally oxidized and functionalized to assure covalent binding of molecules. Secondly, the as etched PSi surface was modified with adhesion peptides isolated via phage display technology and presenting high binding capacity for Si. Functionalization and molecular binding events were monitored via reflectometric interference spectra as shifts in the resonance peaks of the cavity structure due to changes in the refractive index when a biomolecule is attached to the large internal surface of PSi. Improved sensitivity is obtained due to the peptide interface linkers between the PSi and biological molecules compared to the silanized devices. We investigate the formation of peptide-Si interface layer via vibrational FTIR spectroscopy, X-ray photoelectron spectroscopy and atomic force microscopy. When monitored via fluorescence and biphoton microscopy we observe that PSi microcavity structures strongly confine and localize light emission resulting in enhanced photoluminescence of the infiltrated molecules.

8104-22, Session 5

Infiltration of Fe₃O₄-nanoparticles into porous silicon with respect to magnetic interactions

P. Granitzer, K. Rumpf, Karl-Franzens-Univ. Graz (Austria); K. Ali, M. Reissner, G. Hilscher, Technische Univ. Wien (Austria); L. Cabrera, P. Morales, Consejo Superior de Investigaciones Científicas (Spain); P. Poelt, T. Uusimäki, M. Sezen, M. Albu, Technische Univ. Graz (Austria)

Mesoporous silicon (PS) is used as matrix for infiltration of Fe₃O₄ nanoparticles (5 and 8 nm). The structure and magnetic behaviour of such composites are investigated and a correlation between the morphology of the nanocomposite (structure of the matrices, size and distribution of Fe₃O₄ particles) and the magnetic properties of the system is figured out. Magnetic exchange interaction is excluded due to capping of the particles. This system shows a superparamagnetic (SPM) behaviour at room temperature and becomes ferromagnetic (FM) at lower temperatures. The transition temperature between SPM and a blocked state depends on the particle size, their coating and on their magnetic interactions. Dipolar coupling between the particles can be influenced by varying the PS morphology as well as by the filling factor. The blocking temperature (TB) of the composite is tunable and changes due to the variation of dipolar coupling of the Fe₃O₄-particles (distance between particles). To gain deeper information about the stoichiometric homogeneity and spatial distribution, dual electron energy loss spectroscopy is employed. This method provides areal and volumetric densities of each element over the investigated area. Electron tomography, a method to get full 3D characterization in the nanometer scale, is utilized whereas from reconstructions various parameters of the composite morphology can be obtained (size and spatial distribution of the particles and dependence of the local curvature of the pore walls with respect to the preferred docking site). These results together with the magnetic data lead to a more detailed knowledge of the Fe₃O₄/silicon nanocomposite system.

8104-23, Session 5

Controlled skeletal progenitor cell migration on nanostructured porous silicon/silicon micropatterns

V. Torres-Costa, V. Sánchez-Vaquero, Á. Muñoz-Noval, M. J. Pérez-Roldán, E. Punzón-Quijorna, D. Gallach, L. González-Méndez, Univ. Autónoma de Madrid (Spain); A. Valsesia, G. Ceccone, European Commission Joint Research Ctr. (Italy); M. Manso-Silván, G. Martínez-Muñoz, Univ. Autónoma de Madrid (Spain); F. Rossi, European Commission Joint Research Ctr (Italy); A. Climent-Font, J. P. García-Ruiz, R. J. Martín-Palma, Univ. Autónoma de Madrid (Spain)

Nanostructured porous silicon (nanoPS) shows photoluminescence and wide-scale adaptable wettability as a result of its particular surface morphology and chemistry. These properties can be simultaneously exploited for the preparation of surface micropatterns to mimic cellular function. Surface patterns of nanoPS and Si can be engineered through high-energy ion-beam irradiation and subsequent anodization. Human skeletal progenitor cells are sensitive to one- and two-dimensional patterns and focal adhesion is inhibited on nanoPS areas. In spite of this anti-fouling characteristics, studies on patterns with reduced Si areas show that cells conform to nanoPS pathways favoring migration through cell protrusion, body translocation and tail retraction from two parallel Si traction rails. Moreover, migration can be blocked and cells tend to arrange when grid patterns with the appropriate dimensions are fabricated. The experimental results confirm that progenitor cells are able to exploit nanoPS anti-fouling designs by adapting to it for migration purposes.

8104-24, Session 5

Nanostructured porous silicon dioxide films as substrate for on-chip visible light photonic devices

C. W. Gladden, M. Gharghi, Univ. of California, Berkeley (United States); J. G. Valentine, Vanderbilt Univ. (United States); X. Zhang, Univ. of California, Berkeley (United States)

A variety of photonic devices are available at telecom wavelengths, implemented using on-chip silicon ($n=3.5$) waveguides where silicon oxide ($n=1.5$) can serve as a lower index substrate with sufficient contrast. However, waveguides made of materials suitable for visible light (e.g. silicon nitride $n=1.9$) can become lossy on top of oxide especially when the mode index is reduced by confinement. A Si-photonics compatible low index substrate can enable realization of on-chip photonic devices in the visible range.

We have developed a porous silicon dioxide substrate with exceptionally small pore sizes and low solid filling fraction. The index can be less than 1.2 while maintaining less than 2nm RMS surface roughness over thicknesses up to 10 micron. The films are generated by electrochemical etching of silicon in acid/organic solution. Thickness, porosity, and pore size can be controlled by adjusting voltage, time, and solvent concentration. To obtain filling fractions as low as 15% we repeatedly oxidize and chemically remove the surface layer of silicon inside the porous network. Finally, the substrates are fully oxidized at high temperature to convert the remaining silicon network into silicon dioxide.

The smoothness and small pore size enables subsequent fabrication of devices on the substrate with very little interface scattering. While other low index geometries (such as aerogel and nanowire) have limited functionality due to surface roughness and processing, our easy to fabricate, fully Si-photonics and bio compatible substrates allow implementation of chip level visible wavelength devices such as single mode waveguides or transformation optics.

8104-25, Session 5

Investigation of the interfaces of a metal/porous silicon nanocomposite and its influence on the physical properties

K. Rumpf, P. Granitzer, Karl-Franzens-Univ. Graz (Austria); K. Ali, M. Reissner, G. Hilscher, Technische Univ. Wien (Austria); P. Poelt, M. Albu, Technische Univ. Graz (Austria)

Metal-nanostructures are electrochemically deposited within the pores of porous silicon to achieve a hybrid material with specific magnetic properties. The metal structures can be precipitated with various geometries and different spatial distributions depending on an accurate control of the deposition conditions. This method allows to deposit structures as spheres, ellipsoids or wires with a size up to a few micrometers whereas the diameter corresponds to the pore-diameter. Furthermore small Ni-particles between 3 and 6 nm can be deposited in a densely packed arrangement on the pore walls forming a quasi metal tube. Analysis of this tube-like arrangement by transmission electron microscopy shows that the distribution of the Ni-particles is quite narrow, which means that the distance between the particles is smaller than 10 nm. Such a close arrangement of the Ni-particles assures magnetic interactions between them. Due to their size these small Ni-particles are superparamagnetic but dipolar coupling between them results in a ferromagnetic behaviour of the whole system. Moreover, to investigate the interface in more detail electron energy loss spectroscopy is employed, whereas in using multiple linear least square fitting procedure, EELS fine structure and absolute edge energy information can be added to map the oxygen bounded in different phases (SiO_x, metal-oxide). Magnetic measurements show an anisotropy between easy axis and hard axis magnetization which corresponds to the behaviour of a metal tube. This composite is an interesting candidate for integrable magnetic and magneto-optic devices and also for spin-injection from a ferromagnetic metal into silicon.

8104-40, Poster Session

Nanostructured Lu₂O₃:Eu³⁺ phosphor thin film

N. V. Babayevskaya, A. S. Bezkrivnyi, P. V. Mateychenko, O. M. Vovk, R. P. Yavetskiy, Institute for Single Crystals (Ukraine)

Nowadays oxide scintillating films are considered as promising materials for digital medical imaging. Lu₂O₃:Eu³⁺ is an inorganic scintillator which was introduced as one of the most perspective material for X-ray detectors due to excellent scintillation properties, chemical stability as well as high light conversion efficiency (approximately 80 % of CsI:Tl). To obtain thin films of high optical quality possessing spatial resolution in the submicron range the uniform, smooth phosphor layers free from pores and cracks are necessary. Different methods are known to produce close-packed thin films [1]. Sol-gel technology is one of the most promising approaches to obtain nanostructured, transparent films with controlled thickness and homogeneous distribution of activator in the phosphor lattice [2,3]. The aim of this study is to obtain and characterize nanostructured Lu₂O₃:Eu³⁺ films with submicron thickness.

Simple sol-gel method has been used to fabricate homogeneous, transparent Lu₂O₃:Eu³⁺ (Eu³⁺=5 at. %) films with thickness in the 200-1200 nm range (1 - 6 layers) on sapphire substrates. The film morphology and structure has been studied by atomic force microscopy, scanning and transmission electron microscopy. The formation conditions of homogeneous films with average crystallite size of 10-50 nm have been determined. The luminescent properties of Lu₂O₃:Eu³⁺ films depending on annealing temperature and their thickness have been studied.

[1]. N.V.Babayevskaya, T.G.Deyneka, P.V.Mateychenko et al. / J. of Alloys and Comp., 507, 26 (2010).

[2]. N.V. Babayevskaya, A.S. Bezkrivnyi, P.V. Mateychenko et al. // Functional Materials, 17, 537 (2010).

[3]. H.Guo, M.Yin, N.Dong et al., App. Surf. Sci., 243, 245 (2005).

8104-41, Poster Session

A double positive thin film comprising silver-pillar arrays at visible wavelengths

C. Yu, Y. Jen, J. Zhou, W. Wang, National Taipei Univ. of Technology (Taiwan)

A thin film comprising silver-pillar arrays is deposited on a glass substrate by continuously rotating the substrate about its normal via glancing angle deposition. During deposition the rotation speed and the deposition rate are kept at 10 rpm and 1 nm/s, respectively. The deposition angle of 89 degree with respect to the substrate normal is chosen due to the fact that the larger deposition angle results in the higher porosity of the film. Here we use the effective-medium theory to investigate the magnetic responses in a pair of silver pillars. The simulated result shows that the conduct and displacement currents are induced as the applied electric field is perpendicular to the major axis of the pillar at normal incidence. A larger overlapping of the length of the pillars causes a stronger magnetic field, leading to the larger positive real part of the equivalent permeability of the film. Walk-off and polarization interferometers are employed in measuring the transmission and reflection coefficients of a 230nm-thick silver-pillar arrays film with a diameter of 175 nm in the visible regime. Experiment result shows its real parts of the equivalent permeability and permittivity are 2.441 and 0.846 at a wavelength of 639 nm, respectively. Together with our previous study, it is possible to grow metamaterials covering the whole quadrant in the permittivity-permeability diagram at visible wavelengths.

8104-42, Poster Session

Tungsten nanostructured thin films obtained via HFCVD

O. Goiz Amaro, Ctr. de Investigacion y de Estudios Avanzados del IPN (Mexico); F. Chávez, P. Zaca-Moran, G. J. Ortega, G. F. Pérez, N. Morales, Benemérita Univ. Autónoma de Puebla (Mexico); C. F. Mendoza, Instituto Politécnico Nacional (Mexico); R. Peña, Ctr. de Investigacion y de Estudios Avanzados del IPN (Mexico)

By using the Hot Filament Chemical Vapor Deposition (HFCVD) technique tungsten thin films were deposited on both amorphous quartz and silicon substrates. To achieve this, a tungsten filament was heated at 1500 oC during one hour maintaining a constant pressure of 460 mTorr. The whole process was carried out into a quartz tube. Besides the filament temperature, and substrate temperature were determinant in the deposition of the tungsten. The latter was established at 750 oC in order to cover the substrate by a 200 nm tungsten thin film. The thin films were characterized by means of Scanning Electron Microscope, Atomic Force Microscope and X-Ray Diffraction. SEM micrographs revealed that the films have no more than 200 nm in thickness while XRD show evidence of the films crystallize in the (alfa)-tungsten modification. On the other hand, AFM shows a uniform surface composed with semi-spherical shapes whose diameters are below than 200 nm. To the naked eye, the as-deposited films exhibit a highly mirror-like appearance.

8104-43, Poster Session

Study on magnetic metamaterials of aluminum nanostructures in the visible range

Y. Jen, W. Wang, C. Yu, National Taipei Univ. of Technology (Taiwan)

In this work, the optical properties of pillar arrays of metal-dielectric-metal nanostructures are investigated. Based on the finite-difference time-domain (FDTD) simulation, the magnetic field reversal is observed due to the fact that the phases of the electric fields oscillating in the top

and the bottom pillars are in the opposite directions. The anti-phase electric fields are coupled in the dielectric layer and the equivalent permeability of the film is negative. Compared with the dielectric pillar sandwiched by the Ag pillars, the aluminum(Al)-dielectric-aluminum(Al) film has a good transmission property because of its low absorption and large real part of dielectric constant at the short wavelengths. Whereas Ag pillar exhibits transverse plasmon mode around the wavelength of 350 nm, Al has the dipolar plasmon resonance at the wavelength of 250 nm. Moreover, the simulation result shows the strong magnetic field reversal in Al-SiO₂-Al nanostructures of diameters 175 nm is induced at the wavelengths from 400 nm to 600 nm. The thicknesses about the structure are 100 nm for Al and 70 nm for SiO₂ of the film is 270 nm. The blue-shift of the inverse magnetic intensity occurs as the diameters of the pillars decrease from 175 nm to 150 nm. Such the films provide a good candidate for achieving optical magnetic metamaterials in the visible regime.

8104-44, Poster Session

Anisotropic optical property of an asymmetric bideposition TiO₂ film: fabrication and measurement

Y. Jen, C. Lin, T. Yu, C. Lai, National Taipei Univ. of Technology (Taiwan)

To develop diverse anisotropic thin films, asymmetric bideposition technique is introduced to fabricate tilt columnar TiO₂ films with biaxial optical property. The asymmetric bideposition is achieved using two different opposite deposition angles (α_+ , α_-) at the same pitch thickness or two different pitch thicknesses (d_+ , d_-) at the same two opposite deposition angles. The two sets of TiO₂ columnar thin films associated with deposited subdeposits (d_+ , d_-)=(20,10) and (30,10) are prepared at the opposite deposition angles (α_+ , α_-)=(70,-40), (70,-50), (80,-40), and (80,-50). Columnar thin films with various column angle and biaxial properties are measured their planar birefringence and three principal indexes. The larger column angle leads to lower planar birefringence and principal indices. Experimental result indicates that an anisotropic thin film deposited at (α_+ , α_-)=(80,-50) with deposited subdeposits (d_+ , d_-)=(30,10) could be applied in a prism coupling system (BK7 prism/ TiO₂ anisotropic thin film/air) to have enhanced polarization conversion reflectance (PCR). As the film thickness is 887 nm, there is over 60% of PCR detected at the incident angle ranged from 55 degree to 75 degree.

8104-45, Poster Session

The nanostructure and morphology of biodegradable PLLA films with DBS nanofibrils

W. Lai, Tamkang Univ. (Taiwan)

The morphologies and nanostructures of neat 1,3:2,4-dibenzylidene-D-sorbitol (DBS) and DBS/poly(L-lactic acid) (PLLA) films have been investigated by polarizing optical microscopy (POM) and scanning electron microscopy (SEM). The morphology of neat DBS samples prepared from solution had unspecific structures, and no fibrils formed. In comparison, DBS molecules self-assembled into fibrils with diameters ranging from 100 nm to 1 μ m when samples were prepared from the melt. The DBS fibrils were also found in DBS/PLLA systems, but the average diameter was only around 20 nm. The DBS architectures could be well tuned by varying the DBS contents and PLLA crystallization temperatures. Micron-sized fibrillar rings or disks due to the aggregation of DBS nanofibrils were found using SEM in samples with DBS contents more than 3 wt% and crystallized above 120 oC. Meanwhile, "concentric-circled" PLLA spherulites were observed by POM. The DBS nanofibrils largely formed at the circles, but some nanofibrils formed beyond the circles and were dispersed in the PLLA spherulites. These dispersed nanofibrils affected the orientation of PLLA lamellae and caused a change in birefringence, yet the growth rate of PLLA was not

significantly influenced by the formation of DBS nanofibrils. In addition, porous PLLA structures could be obtained by solvent extraction of the DBS nanofibrils.

8104-46, Poster Session

Effect of solar radiation on photovoltaic characteristics of Si-P3HT core-shell nanowire solar cells

S. Tsai, Ntionalai Taiwan Univ. (Taiwan); H. Chang, C. Lin, H. Wang, J. He, National Taiwan Univ. (Taiwan)

We report an hybrid inorganic-organic solar cells (HSCs) fabricated by regioregular poly(3-hexylthiophene) (P3HT) on the n-type silicon (n-Si) nanowire arrays (NWAs). P3HT tends to order at n-Si NWAs under simulated sunlight, leading to a remarkable enhancement of power conversion efficiency (η) from 0.96% to 2.31% and broadband external quantum efficiency (EQE) values under AM 1.5G illumination for 90 minutes because of the core-shell structure (shown in fig. 1). The efficiency enhancement under simulated sunlight results from the increase in open-circuit voltage (V_{oc}), short-circuit current density (J_{sc}) and fill factor (FF) due to the improved crystallinity of P3HT further characterized by absorption, external quantum efficiency (EQE), and Raman measurements.

8104-47, Poster Session

Nanowire arrays with controlled structure profiles for maximizing optical collection efficiency

H. Chang, K. Lai, Y. Dai, H. Wang, C. Lin, J. He, National Taiwan Univ. (Taiwan)

The Nanowire array (NWA) layers with controlled structure profiles fabricated by maskless galvanic wet etching on Si substrates are found to exhibit extremely low specular reflectance ($< 0.1\%$) in the wavelengths of 200-850 nm. The significantly suppressed reflection is accompanied with other favorable antireflection (AR) properties, including omnidirectionality and polarization-insensitivity. The NWA layers are also effective in suppressing the undesired diffuse reflection. These excellent AR performances benefit from the rough interfaces between air/NWA layers and NWA layers/substrate and the decreased nanowire densities, providing the gradient of effective refractive indices. The Raman intensities of Si NWAs were enhanced by up to 400 times as compared with the signal of the polished Si, confirming that the NWA layers enhance both insertion and extraction efficiencies of light. This study provides an insight into the interaction between light and nanostructures, and should contribute to the structural optimization of various optoelectronic devices.

8104-48, Poster Session

Three methods of fabricating controlled Si nanowire arrays by self-assembling templates and etching for broadband and omnidirectional antireflection

H. Wang, K. Tsai, K. Lai, Y. Lin, Y. Wang, J. He, National Taiwan Univ. (Taiwan)

Ordered arrays of silicon nanowires have attracted great attentions because their unique properties and many potential applications in renewable energy technologies. However, it remains a challenge to fabricate such an ordered array with large scale, well-controlled and periodicity less than 100 nm (diameters less than 60 nm). Here, we

demonstrate three methods for the fabrication of large scale ordered silicon nanowires arrays using reactive ion etching (RIE) or metal-assisted chemical etching through colloidal lithography or anodic aluminum oxide (AAO) templates. Si NWAs with desirable diameters could be obtained by shrinking the sizes of colloidal lithography or the pore sizes of AAO templates. The porous anodic alumina membrane with self-organized ordering is employed as the mask for the high-throughput patterning formation of hexagonal-close-packed hole array. Ordered arrays of silicon nanowires with 100 nm in periodicity (50 nm in diameter) can be cost-effectively fabricated. The reflection can be eliminated effectively over broadband regions by controlled NWAs; i.e., the wavelength-averaged total reflectance is decreased to 10.0 % at the wavelengths of 200-850 nm. The resulting nanostructures might have great potential applications in photovoltaics.

8104-49, Poster Session

Polarization anisotropy of oblique-aligned ZnO nanowire arrays

C. Chen, National Taiwan Univ. (Taiwan); J. Huang, National Cheng Kung Univ. (Taiwan); K. Lai, National Taiwan Univ. (Taiwan); Y. Jen, National Taipei Univ. of Technology (Taiwan); C. Liu, National Cheng Kung Univ. (Taiwan); J. He, National Taiwan Univ. (Taiwan)

We demonstrated that a combined method of modified oblique-angle deposition and hydrothermal growth to grow a novel photonic metamaterial based on single crystalline ZnO nanowire arrays (NWAs) with highly oblique angles (75° - 85°), exhibiting large artificial in-plane birefringence and optical polarization degree in emission. The giant in-plane birefringence (0.11), exceeding by a factor of 10 that of natural quartz. The strong optical anisotropic in emission due to the optical confinement was observed. Unlike the conventional oblique-angle-deposited thin films, the NWAs also showed light emitting ability, leading us to conclude that the oblique-aligned NWAs not only could be applied in passive photonic components, such as optical waveplates and optical isolators, but also can open up important technological applications in polarized light sensing and emission devices.

8104-50, Poster Session

Antireflective nanostructured thin films and their applications in solar cells

J. He, National Taiwan Univ. (Taiwan)

It is of current interest to develop the antireflection (AR) coatings with nanowire arrays (NWAs) since the ability to suppress the reflection over a broad range of wavelengths and incident angles plays an important role in the performance of optoelectronic devices, such as photodetectors, light-emitting diodes, optical components, or photovoltaic systems. Superior AR characteristics of NWAs, including polarization-insensitivity, omnidirectionality, and broadband working ranges are demonstrated in this study. These advantages are mainly attributed to the subwavelength dimensions of the NWAs, which make the nanostructures behave like an effective homogeneous medium with continuous gradient of refraction index, significantly reducing the reflection through destructive interferences. The relation between the geometrical configurations of NWAs and the AR characteristics is discussed. We also demonstrated their applications in solar cells. This report paves the way to optimize the nanostructured optoelectronic devices with efficient light management by controlling structure profile of nanostructures.

8104-51, Poster Session

Properties of RF sputtered ZnO thin films under different oxygen flux

Z. Guo, Shanghai Univ. (China)

The microstructures, optical, and mechanical properties of zinc oxide (ZnO) thin films deposited on glass substrates by rf magnetron sputtering were studied. Microstructures were examined using atomic force microscopy (AFM) and X-ray diffraction (XRD), respectively. Optical property was measured by photoluminescence spectrum. The mechanical properties were measured by nanoindentation. The crystalline structures of ZnO thin films are well ordered with high c-axis (002) orientations and the crystallinity is strongly affected by O₂ flux. Surface morphologies of ZnO thin films are smooth and grains grow and distribute uniformly. The hardness and Young's modulus of ZnO thin films are ranged from 8.2 to 10.4 GPa and 105 to 120 GPa, respectively.

8104-26, Session 6

The stability of carbon nanostructures in silicon oxycarbide materials

J. V. Ryan, Pacific Northwest National Lab. (United States); P. Kroll, The Univ. of Texas at Arlington (United States); C. G. Pantano, The Pennsylvania State Univ. (United States); V. Shutthanandan, Pacific Northwest National Lab. (United States)

Silicon oxycarbide (SiOC) is a metastable material that has generated interest because of the great flexibility in properties that is attainable with a change in carbon-to-oxygen ratio. These materials have exhibited a strong propensity to include carbon-carbon - "free carbon" - bonding within the structure regardless of synthesis method, although the relative amounts can be controlled to some degree. Despite strong experimental evidence for the presence of this phase as nanostructures, models of the composite system have had difficulty producing a stable structure bonded to the matrix. Characterization techniques sensitive to ordered bonding in the length scale of roughly 0.5 to 5nm such as fluctuation electron microscopy (FEM), Raman spectroscopy, and nuclear magnetic resonance along with compositional studies by x-ray photoelectron spectroscopy and nuclear reaction analysis were used to produce a new view of the structural role of carbon in SiOC materials. Through coupling of these experimental approaches with molecular dynamics modeling, a new theory on the stability of these nanostructures is presented here.

8104-27, Session 6

Tunable Stoichiometry of BC_xN_y Thin-Films through Multi-Target PLD with In situ Ellipsometry

J. G. Jones, R. Jakubiak, A. R. Waite, L. Sun, Air Force Research Lab. (United States); M. Lange, Air Force Institute of Technology (United States); N. R. Murphy, Air Force Research Lab. (United States)

Much interest has been shown in Boron Carbon Nitride, BC_xN_y, with B₄C, C, and BN each individually having unique properties: B₄C - high hardness and stability, C - high thermal conductivity and electrical semi-conductivity, and BN - insulating with high band gap. Using these bulk materials in conjunction with pulsed laser deposition (PLD) provides stoichiometric material transfer from each laser target material to substrate surface, which when combined with multiple targets and a programmable mirror system provides tunability of the stoichiometry of the resulting thin-film. Initial laser pulses onto a target material create island growth that coalesces into a uniform film above a thickness threshold of a few nanometers. In situ ellipsometry allows determination of optical properties of a thin-film during growth including the real

component of the index of refraction (n) and the extinction coefficient (k), which when coupled with a model provides for a real-time virtual measurement of thickness during deposition. Ellipsometry can be used to detect the transition of island growth to uniform film growth, but after the film becomes opaque no more optical variations can be detected. Two 5cm diameter targets, one graphite and one boron-nitride, were rotated inside a UHV deposition chamber evacuated to a base pressure below 0.1 mPa, while a Lambda Physik 248nm excimer laser was triggered in a synchronized fashion with a high speed galvanometer mirror system thereby delivering a programmable number of 250mJ 20nsec duration pulses on each target. Results presented will include stoichiometry of the thin-films measured with XPS.

8104-28, Session 6

Study on the structure and optical properties of plasma-polymerized Zr_{Nx}CyOz thin films

H. Jiang, L. Sun, General Dynamics Information Technology (United States); J. T. Grant, Univ. of Dayton Research Institute (United States); A. Reed, Air Force Research Lab. (United States); W. Su, General Dynamics Information Technology (United States); R. Jakubiak, Air Force Research Lab. (United States)

A modified room temperature PECVD process was used to prepare plasma-polymerized (PP-)ZrNCO thin films, using tetrakis(diethylamido) Zr (IV) (TEDAZ) as a precursor. The structure and optical properties of the films were characterized by XPS, FT-IR, Raman, AFM, SEM, UV-Vis and spectroscopic ellipsometry. The preliminary results show that although there is no oxygen components in the monomer or carrier gases (N₂ and Ar), due to the residual moisture and oxygen in reaction areas, the resulting PP-ZrNxCyOz films contained a certain amount of oxygen, from 15 to 30 atm%, depending upon the processing conditions. Additionally, the refractive index of the films does not scale proportionately with metal atom concentration as has been observed for PP - ferrocene, titanium isopropoxide and tetraphenyl lead. This suggests that morphological features that affect the film density such as microvoids have significant influence on the optical properties of the films. Further studies include a systemic investigation of the titanium analogue of TEDAZ to elucidate structure-property relationships that will have import when both organo-metallic precursors undergo co-polymerization to form broadband, UV protective coatings.

8104-29, Session 6

An investigation on magnetic responses in Ag-SiO₂-Ag nanosandwich structures

Y. Jen, J. Jhou, C. Yu, National Taipei Univ. of Technology (Taiwan)

In this work, we investigate magnetic responses in various Ag-SiO₂-Ag nanosandwich structures at visible wavelengths. The two electric resonant modes corresponding to the in-phase (symmetric) and anti-phase (asymmetric) electric dipole on the top and the bottom nanopillars are observed by the finite difference time domain (FDTD) simulation. In the asymmetric resonant mode, the phases of electric fields oscillating in the top and bottom pillars have opposite directions, leading to a virtual current loop that induces the magnetic field reversal. The nanosandwich structure produces a large enhancement of the magnetic field as the thickness of SiO₂ nanopillar decreases. By increasing the diameter of nanopillars from 125 nm to 160 nm, the inverse magnetic response wavelength shifts from 550 nm to 650 nm. On account of the magnetic field reversal caused by the anti-phase electric dipole coupling, the real part of the equivalent permeability of the film is negative. Therefore, the wavelength range associated with the intensity of inverse magnetic response is tunable by varying the size of Ag-SiO₂-Ag nanosandwich structure. The analysis can be applied to interpret extraordinary optical properties such as negative index of refraction from an Ag-SiO₂-Ag sandwich array prepared by glancing angle deposition.

8104-30, Session 7

Sculptured thin films: nanorods, nanopipes, nanosmiles

D. Gall, Rensselaer Polytechnic Institute (United States)

Atomic shadowing during physical vapor deposition causes exacerbated growth of surface protrusions and leads to a chaotic 3D layer growth, which can result in the development of well-separated nanorods, nanosprings, or nanopipes, which are surprisingly regular and have potential applications ranging from fuel cell electrodes and pressure sensors to self-lubricating coatings and nanoactuation. Glancing angle deposition (GLAD) causes particularly strong atomic shadowing and can be used to systematically investigate the effect of shadowing on the morphological evolution. These extremely rough layers cannot be described as a chaotic perturbation from a flat surface. However, using a model which describes them as a nanorod array with an average rod width that follows power law scaling results in experimental curves where all metals converge on a single master curve which exhibits a discontinuity at 20% of the melting point, associated with a transition from a 2D to a 3D island growth mode, and a single homologous activation energy of 2.46 for surface diffusion on curved nanorod growth fronts, which is applicable to all metals at all temperatures. Also, under extreme shadowing conditions, the conventional structure zone model is simplified as there is a direct transition from an underdense (zone I) to a dense (zone III) structure at ~50% of the melting point.

8104-31, Session 7

Electrophoretic deposition of Cu-In composite nanoparticle thin films for fabrication of CuInSe₂ solar cells

B. Liu, W. Guo, K. Hagedorn, IMRA America, Inc. (United States)

Electrophoretic deposition (EPD) is traditionally used in ceramic industry for coating micron-sized ceramic particles. In this work, we applied EPD to metal nanoparticles in liquid solvents and successfully produced thin films of Cu-In composite nanoparticles. The nanoparticles were produced with pulsed laser ablation in the same liquid solvents. Pulsed laser ablation has recently been recognized as a promising method for producing high purity nanoparticles. We first demonstrated femtosecond pulsed laser ablation production of nanoparticles of various metals including elemental Cu, In, Ga, Se and their binary alloys and compounds. We found that the overall composition was preserved during laser ablation, which provided means of compositional control for thin film applications. The colloids were stable against agglomeration without stabilizing chemicals, and the mechanisms were explained based on charging of nanoparticle surfaces via electrochemical interaction with ambient solvents. We also found that the surface charge density was sufficient to enable migration of the nanoparticles in solvents under an electric field. The success of EPD of metal nanoparticles was explained based on charge transfer between the nanoparticle surfaces and the electrode. With atmospheric pressure annealing in selenium vapor, we have produced polycrystalline CuInSe₂ films, and effective solar cell structures have also been made. The whole process was performed in non-vacuum ambient conditions, and can also be applied to flexible substrates such as metal foils. These results open up a new route of non-vacuum fabrication of thin film CuInGaSe₂ solar cells.

8104-32, Session 7

X-ray absorption fine-structure and optical studies of AlZnO nano-thin films grown on sapphire by pulsed laser deposition

Y. Lan, Z. Wei, M. H. Wang, Z. R. Jiang, National Taiwan Univ. (Taiwan); S. P. Liu, National Chung Hsing Univ. (Taiwan); J.

Chen, National Synchrotron Radiation Research Ctr. (Taiwan); R. Horng, D. Wu, National Chung Hsing Univ. (Taiwan); Z. C. Feng, National Taiwan Univ. (Taiwan)

Al-doped ZnO can replace tin-doped indium oxide (ITO) as a transparent conductive oxide (TCO) for optoelectronic applications. We investigated nanometer scale AlZnO thin films on sapphire from pulsed laser deposition (PLD) in 350-650°C. Synchrotron radiation X-ray absorption fine-structure spectroscopy at O K-edge showed that Al-doped ZnO can't form alloy at 350°C without Al-O bonding feature, Al-O transition of AZO550 is stronger than AZO650, and crystalline qualities of AZO550 and AZO650 are much better than AZO350. Raman scattering and 266nm excitation micro-PL measurements further confirm these results. Al-doped ZnO at 350°C has weak and broad Raman and PL signals. Comparing Raman spectra between AZO550 and AZO650, the peak of E₂ (high) mode is observed in AZO550 but not in AZO650. The E₂ (high) mode is strong and narrow in AZO550. PLD grown AlZnO film on sapphire could get a better crystalline quality at 550°C than 350°C and 650°C.

8104-33, Session 7

Janus-like 3D tectons as functional nanostructures for self-assembled functional thin films towards nanophotonics

A. Attias, D. Bléger, D. Kreher, F. Mathevet, Univ. Pierre et Marie Curie (France); A. Bocheux, F. Charra, L. Douillard, C. Fiorini-Debuisschert, Commissariat à l'Énergie Atomique (France)

In order to achieve the nanometer-scale control over the positioning and organization of functional molecules into monolayers at surfaces, we developed an original approach allowing the exact positioning of (photo)active organic molecules on the substrate (graphite) leading to the formation of nanostructured functional thin films.. Here we present a strategy aimed at the decoupling of molecules from the surface, by lifting photoactive entities a few Å above the surface while maintaining the lateral organization of the array. This is achieved by using 2-level based building blocks. While the first level allows the precise organization of the building blocks on HOPG at the solid-liquid interface at room temperature, the second level is a photoactive compound, namely a chromophore. We will present a series of such building-block exhibiting tunable wavelength emission. This strategy results in the precise organization of chromophores arrays (subwavelength-sized photon sources) a few Å above the conducting surface, as determined by scanning tunneling microscopy (STM), opening interesting perspectives for applications in nanophotonics.

8104-34, Session 8

Multifunctional organic-inorganic hybrids based on bacterial cellulose membranes

S. J. L. Ribeiro, Univ. Estadual Paulista (Brazil)

Bacterial cellulose (BC) is produced by *Gluconacetobacter xylinus* strains in the form of highly hydrated (98% water) membranes. The chemical structure is the same of the one found for plants cellulose but BC presents a pure cellulose network, free of lignin and hemicellulose, composed of a random assembly of ribbon shaped fibers less than 100 nm wide. The unique properties provided by the nanometric structure have lead to a number of commercial products including dietetic fibers, headphone membranes, special papers, and textiles, medical applications including temporary skin substitution, contact lenses, optoelectronic devices (e-paper, OLEDs). We have been exploring this multifunctional character studying luminescence properties, photochromism and different application of BC as biomaterials. -Photochromism is been explored by preparing BC membranes containing polyoxometalates and metal colloids. Light induced redox process (W₆+ W₅+) and tuning of the plasmon resonance energy

of metal (Au-Ag) colloids lead to different colors and photochromic materials; -Luminescence is being explored by obtaining lanthanide containing luminescent species in the BC structure. Emission efficiency is observed to strongly depend on the specific interactions between the BC host and the lanthanide compounds. BC membranes are also being used as substrates for flexible organic light emitting diodes and emission efficiencies are found to be of the same order of glass OLED's. -Finally biomedical applications is being addressed. BC is being for decades used as substitutes for the skin in the treatment of difficult wounds. In our work antibacterial activity is being added to BC membranes by using Ag colloids and propolis.

8104-36, Session 8

Chromogenic behaviours of silver containing mesoporous titania films

L. Nadar, N. Destouches-Castagna, N. Crespo-Monteiro, F. Vocanson, Y. Lefkir, S. Reynaud, Univ. Jean Monnet Saint-Etienne (France)

Multicolour photochromism was reported few years ago on nanoporous titania films loaded with silver nanoparticles (NP). The formation of heterogeneous silver nanoparticles under UV light gives the films a brown color, whereas illuminations under a colored visible light change the film color to almost the same color as that of the incident light. This photochromic behaviour was interpreted as resulting from a selective oxidation of nanoparticles whose size corresponds to a surface plasmon resonance band centered on the illumination wavelength.

The use of mesoporous titania films as host matrix for the growth of silver nanoparticles is likely to lead to homogeneous NP size distributions and to changes in the photochromic behaviour. We firstly investigate the effects of three reduction processes on the formation of silver nanoparticles in mesoporous titania films. The later are impregnated with silver salt and then either exposed to UV laser light, chemically treated or annealed. Depending on the reduction process the in situ grown NP can be confined inside the mesopores or not, leading to different NP size distributions and to various film colors. These three TiO₂/Ag nanocomposite films also exhibit different photochromic behaviours when exposed to visible laser radiations. We characterize the color changes as well as the NP deformation and oxidation under visible illuminations and we propose new mesoscopic mechanisms to interpret our results.

8104-37, Session 8

Electron microscopy characterization of some carbon based nanostructures with application in divertors coatings from fusion reactor

V. Ciupina, Univ. Ovidius Constanta (Romania); I. G. Morjan, C. Lungu, National Institute for Lasers, Plasma and Radiation Physics (Romania); R. Vladioiu, G. Prodan, M. Prodan, Univ. Ovidius Constanta (Romania); V. Zarovschi, National Institute for Lasers, Plasma and Radiation Physics (Romania); I. Stanescu, M. Contulov, A. Mandes, V. Dinca, Univ. Ovidius Constanta (Romania)

Nanostructured carbon materials have increasingly attracted the interest of the scientific community, because of their fascinating physical properties and potential applications in high-tech devices. In order to prepare nanostructured carbon-tungsten nanocomposite for the divertor part in fusion applications, the original method thermionic vacuum arc (TVA) was used in two electronic guns configuration. One of the main advantages of this technology is the bombardment of the growing thin film just by the ions of the depositing film. Moreover, the energy of ions can be controlled. Thermo-electrons emitted by an externally heated

cathode and focused by a Wehnelt focusing cylinder are strongly accelerated towards the anode whose material is evaporated and bright plasma is ignited by a high voltage DC supply.

The nanostructured C-W films were characterized by Scanning Electron Microscopy (SEM), Transmission Electron Microscopy (TEM) and Atomic Force Microscopy (AFM). Tribological properties in dry sliding were evaluated using a CSM ball-on-disc tribometer. The C-W films were identified as a nanocrystals complex (5 nm average diameter) surrounded by amorphous structures with a strong graphitization tendency, allowing the creating of adherent and wear resistant films. The friction coefficients (0.15 - 0.35) of the C-W coatings was decreased more than 3-5 times in comparison with the uncoated substrates proving excellent tribological properties. C-W nanocomposites coatings were designed to have excellent tribological properties while the structure is composed by nanocrystals complex surrounded by amorphous structures with a strong graphitization tendency, allowing the creating of adherent and wear resistant films.

8104-38, Session 8

Optical investigation on plasmonic effect of the nanostructured Surface Plasmon Resonance sensor chips fabricated by Langmuir-Blodgett technique

C. Yeon, S. Sung, H. Kim, J. Kim, Ajou Univ. (Korea, Republic of)

The surface plasmon resonance (SPR) has been widely employed for biosensor applications because of the capability for label-free detection of biomolecular interactions. However, the sensitivity of SPR sensor is lower than the conventional labeling immuno-sensing methods. The metal nanostructure-amplified surface plasmon resonance analysis has been investigated to enhance the sensitivity. We used trigonal pyramid Au nanostructured SPR chips for SPR sensitivity enhancement and took a theoretical approach by evaluating optical properties of the Au-nanostructures and nanostructured SPR chips in the point of localized surface plasmon (LSP)- surface plasmon polariton (SPP) conjugation.

We used the Langmuir-Blodgett (LB) method for preparation of defect-free and large-area silica-nanoparticles-monolayer as a template for the fabrication of nano-scaled Au patterns on an Au substrate for surface plasmon resonance. Well organized, trigonal pyramid shaped Au nanostructures were able to construct on 34 separate chips in one fabrication process. The dimensions of trigonal pyramid nano-structures were precisely controlled by changing the particle diameter of the silica LB template as follows: 150, 300, 500, and 700 nm.

The nano-structure patterned substrate fabricated with 300 nm-sized silica nanoparticles demonstrated a sensitivity enhancement up to 120 % compared to a conventional SPR chip when 20% aqueous ethanol solution was used as an analyte. To improve the optical basis of the enhancement in the sensitivity, we measured the SPR curves to wavelength. Also we tried to measure UV-visible spectra of the Au nanostructured pattern in the attenuated total reflectance (ATR) mode to observe the LSP mode of each Au nanostructure.

Conference 8105: Instrumentation, Metrology, and Standards for Nanomanufacturing, Optics, and Semiconductors V

Wednesday–Thursday 24–25 August 2011 • Part of Proceedings of SPIE Vol. 8105 Instrumentation, Metrology, and Standards for Nanomanufacturing, Optics, and Semiconductors V

8105-04, Session 2

Strategies for Nanoscale Contour Metrology using Critical Dimension Atomic Force Microscope

N. G. Orji, R. G. Dixson, A. E. Vladar, M. T. Postek, National Institute of Standards and Technology (United States)

Contour metrology is one of the techniques used to verify optical proximity correction (OPC) in lithography models. The use of these methods, which are known as resolution enhancement techniques (RET), are necessitated by the continued decrease in feature sizes. Broadly speaking, RET are used to compensate for lithography errors such as corner rounding caused during image transfer from the mask to the wafer and subsequence processing. Contours extracted from the printed features are used to verify the OPC models. Currently, the scanning electron microscope (SEM) is used to generate and verify the contours. The critical dimension atomic force microscope, a reference instrument in lithography metrology, has been proposed as a supplemental instrument for contour verification. This is mostly due to the relative insensitivity of the CD-AFM to material properties, the three dimension data, and the ability to make the instrument traceable to the SI unit of length.

However, although the data from the CD-AFM is inherently three dimensional, the planar two dimensional data required for contour metrology is not easily compared with the top-down AFM data. This is mostly due to the effect of the CD-AFM tip and the scanning strategy. In this paper we outline some of the methods for acquiring contour data using the CD-AFM. Specifically, we look at different scanning strategies, the effect of tip types, contour extraction methods, and imaging modes. We compare contours extracted using our method to those acquired using the SEM and helium ion microscope.

8105-05, Session 2

Sidewall slope sensitivity of CD-AFM metrology

A. M. Cordes, SEMATECH North (United States)

CD-AFM is a metrology technique used as a reference measurement system to support accurate control of critical dimensions in precision high volume manufacturing. To test the process range of the AFM, we use a controlled variation in the sidewall across a range of samples to test measurement sensitivity over a critical range of probe types and scan parameters. We find sharp cutoff points in the ability of particular probes and modes to accurately track sidewall variation. We further use cross-section SEM and HR-TEM data as a reference check on the accuracy of CD-AFM sidewall measurements under varying scan conditions.

8105-06, Session 2

High precision surface-profile metrology by scanning the repetition rate of femtosecond pulses

W. Joo, Y. Kim, Y. Kim, J. Park, S. Kim, KAIST (Korea, Republic of)

We report high precision surface-profile metrology using femtosecond pulse lasers as a low-coherence Interferometric light source. Unequal-path non-symmetric Twyman-Green interferometer is configured to test

large-sized optics with small-sized reference surfaces, which is only feasible with ultrafast mode-locked pulses of the repeated temporal coherence and high spatial coherence. The time delay between the pulses from the reference and target optics is precisely scanned by tuning the repetition rate of femtosecond pulses referenced to the Rb clock of a time standard. This enables us to perform traceable high precision surface metrology following the SI definition of the meter and remove all the moving parts from the interferometer.

8105-07, Session 2

Progress in the development of the metrological Scanning Probe Microscope at NMIA

J. Herrmann, B. Babic, C. Freund, M. B. Gray, M. T. L. Hsu, M. Lawn, J. Miles, National Measurement Institute of Australia (Australia)

The design, manufacture and assembly of a metrological Scanning Probe Microscope (mSPM) is well underway at the National Measurement Institute Australia (NMIA). The mSPM is the key instrument in NMIA's SPM metrology facility, traceably linking dimensional measurements at the nanoscale with the realization at NMIA of the SI definition of the metre.

Here, we give an overview of recent progress in the establishment of the mSPM facility at NMIA and present first results of its operational and metrological characteristics.

The mSPM incorporates a quartz tuning fork oscillator-mounted tip operating in non-contact mode, a flexure-hinged, piezo-actuated three-axis translation stage providing a measurement volume of $100\ \mu\text{m} \times 100\ \mu\text{m} \times 25\ \mu\text{m}$, and a plane mirror differential heterodyne interferometry system for traceable measurement of the displacements between the scanned sample and the fixed probe. To achieve the target combined uncertainty of 1 nm for the position measurement, the mSPM body is designed to minimize uncertainties caused, in particular, by thermal expansion and distortion, alignment errors (particularly Abbé errors) and environmental vibrations. The interferometry system is designed to achieve high resolution and bandwidth to facilitate its use for closed-loop position control. The selection of materials with low thermal expansion coefficient for the manufacture of the mSPM body and the low power dissipation of the SPM probe detection system contribute to the excellent temperature stability of the instrument.

8105-10, Poster Session

ZnO nanorod arrays as antireflection layers for III-V solar cells

L. K. Yeh, National Taiwan Univ. (Taiwan)

Single-junction GaAs solar cells were grown by metal organic chemical vapor deposition with Veeco turboDisc E450 As/P system. The solar cells were fabricated with standard processes, including the top contact (Ti/Au) formed by photo-lithography and e-beam evaporation, followed by the mesa definition with the area of $2 \times 2\ \text{mm}^2$, and the deposition of the bottom contact (Ge/Au). The syringe-like ZnO NRAs were synthesized using the one-step hydrothermal process. Before the synthesis, a 200-nm SiO₂ passivation layer was deposited on the device by e-beam evaporation to prevent the potential shortage caused by the conductive ZnO. Subsequently, a ZnO seed layer was deposited by e-beam evaporation on SiO₂ for the following growth of ZnO NRAs. The samples

with ZnO seed layers were then placed downward, positioned at the bottom of the beaker, and heated to 95 °C for 3.5 hours in the aqueous solution containing zinc nitrate hexahydrate (10 mM) and ammonia. Finally the obtained syringe-like NRAs were cleaned with ethanol and dried in air ambience.

8105-23, Poster Session

Development of multichannel rotating-polarizer ellipsometers based on generic data acquisition method

Y. J. Cho, W. Chegal, H. M. Cho, Korea Research Institute of Standards and Science (Korea, Republic of)

A data acquisition method based on a novel Fourier analysis of irradiance waveform was introduced to capture Fourier coefficients for multichannel rotating-element ellipsometers [1]. Most of detector line arrays used for common rotating-element ellipsometers are integrating photometric detectors because their output signals are proportional to not only the light intensity but also the integration time. For earlier studies [2], the photodiode arrays did not respond when the light amount accumulated in each pixel during an integration time was read out and the status was initialized. To reflect this effect, measured exposure is corrected by the primary approximation of the non-response time [3]. To obtain accurate Fourier coefficients without the approximation, we adopt a discrete Fourier transform on the exposures measured with a detector-dependent non-response time and an arbitrary integration time. This analysis gives a generic function that encompasses the Hadamard transform [3] or the discrete Fourier transform, depending on the specific conditions. Thus, the novel Fourier analysis is applicable to various line arrays with either non-overlap or overlap readout-mode timing. To assess the effects of the generic Fourier analysis, we built a multichannel rotating-polarizer ellipsometer composed of a white light source, a fixed polarizer, a rotating polarizer, a sample, a fixed analyzer, and a spectrometer in which the fixed polarizer is introduced to remove source polarization. The ellipsometric data for SiO₂ thin films on c-Si were measured with the custom-built ellipsometer, using the novel Fourier analysis with various numbers of scans, integration times, and rotational speeds of the polarizer.

References

- [1] Y. J. Cho, W. Chegal, and H. M. Cho, *Opt. Lett.* 36, 118 (2011).
- [2] R. W. Collins, I. An, J. Lee, and J. A. Zapien, "Multichannel ellipsometry," in *Handbook of Ellipsometry*, H. G. Tompkins and E. A. Irene, eds. (William Andrew, 2005), pp. 481-566.
- [3] I. An and R. W. Collins, *Rev. Sci. Instrum.* 62, 1904-1911 (1991).

8105-26, Poster Session

Vector modulation method for north finder capability gyroscope

O. Celikel, F. Sametoglu, H. Sozeri, TÜBITAK National Metrology Institute (Turkey)

This paper deals with the implementation of Vector Modulation Method (VMM) to an open-loop North Finder Capability Gyroscope (NFCG), designed in TUBITAK UME (National Metrology Institute of TURKEY). The method proposes a use of a secondary modulation/demodulation with AD630 to derive voltage information, depending on the periodic variation of the orientation of the sensing coil sensitive surface vector with respect to geographic north at laboratory latitude in time domain. The resultant DC voltage of the secondary modulation/demodulation circuit, proportional to 1st kind Bessel function based on Sagnac Phase Shift for 1st order, is obtained as a throughput vector modulation together with Earth rotation.

8105-09, Session 3

Verification of scatterometer design and data processing

W. Zhao, Helmut-Schmidt-Univ. (Germany); C. F. Hahlweg, Helmut-Schmidt Univ. (Germany)

Scatterometric applications demand strategies for the selection from the various basic scatterometer principles as well as detailed design rules to fit the final optical instrument, the data processing and user interface into the requirements of the application in scope. In recent years we proposed methods based on the optical properties of various basic measurement structures to support the synthesis process for scatterometers, including the decision for the structure itself.

In continuation of last years paper on design rules for catadioptric scatterometers the present paper is dedicated to the metrological verification of the proposed design methods for devices with elliptical mirrors in off-axis alignment. Further questions of data processing and analysis, especially the necessary coordinate transformations and calibration procedures will be discussed, practical examples included.

8105-11, Session 3

IR nanoscopy and nanoimaging

J. H. Rice, Univ. College Dublin (Ireland)

Infrared (IR) spectroscopy is a well developed method for characterizing chemical composition. Imaging materials using IR spectroscopy is extremely valuable where sample heterogeneity presents challenges to analysis using topographical imaging alone, such as in pharmaceuticals or cell biology. Optical imaging using far-field methods is limited by diffraction to length scales at approximately equal to $\lambda/2$. We present a technique for infrared nanoimaging and nanospectroscopy based on an induced resonant motion phenomena to enable IR imaging with a resolution beyond the diffraction limit. Our method enables the surface features of a sample to be chemical characterized via inspection of the resulting local IR spectra and images. This was achieved by combining a phase matched optical parametric oscillator laser as the IR source and an atomic force microscope as the detection mechanism. The technique applies a diffraction limited tuneable excitation source and the resulting light-matter interaction is probed by the AFM tip resulting in IR imaging with nanoscale resolution. We apply this method to image protein bio-systems with a spatial resolution $< \lambda/100$.

8105-12, Session 3

Quantification of the systematic and random measurement uncertainty of a polarimetric scatterometry system designed for enhanced E-field device characterization

T. M. Fitzgerald, Univ. of Dayton Research Institute (United States); M. Marciniak, S. Nauyoks, Air Force Institute of Technology (United States)

Enhanced E-field metamaterials feature the careful selection of restricted nanoparticle or nanofeature geometries and complementary materials to develop nanoscale-level extremely high local electric field strengths when the metamaterial is illuminated by appropriate electro-magnetic energy. Enhanced E-field metamaterials improve sensitivity and spectral location of remote sensing techniques such as Localized Surface Plasmon Resonance (LSPR) and facilitate extremely low concentration detection of compounds or biological factors of interest. Early detection at low concentration levels can allow for the medical treatment of life-threatening conditions such as Alzheimers and the rapid detection of hazardous airborne biological agents. A unique model-based Dual-Rotating-Retarder (DRR) polarimetric scatterometry system has been

Conference 8105: Instrumentation, Metrology, and Standards for
Nanomanufacturing, Optics, and Semiconductors V

developed to characterize enhanced E-field metamaterials by measuring their effective medium full Mueller-matrix (Mm) scatter characteristics at wavelengths of 544 and 633 nm and 3.39 and 10.6 μ m. The system has been enhanced by automation, addition of multiple light sources, an improved sample positioning and orientation interface, and enhanced data-analysis software. The system features multiple systematic and random uncertainty sources. Systematic measurement errors are reduced by generation of eigen-polarizations and measurement of their angularly dependent scatter response due to position dependent surface scatter from optical components. Random measurement errors are reduced by careful application of system condition number and a rigorously model based measurement analysis. Several measurement examples for canonical Fresnel targets and enhanced E-field geometries are presented. The goals are to improve understanding of application of effective medium theory to Metamaterials and to improve instrument sensitivity to allow polarimetric probing of enhanced E-field “meta-atoms.”

8105-13, Session 4

Experimental investigation of non steady state photo-EMF effect induced by 1-D light pattern and its application for Talbot self images localization

I. Guizar-Iturbide, Instituto Nacional de Astrofísica, Óptica y Electrónica (Mexico); L. G. de la Fraga, Ctr. de Investigación y de Estudios Avanzados del IPN (Mexico); P. Rodríguez-Montero, S. Mansurova, Instituto Nacional de Astrofísica, Óptica y Electrónica (Mexico)

Recently, the analytical expression for non-steady-state photoelectromotive force (photo-EMF effect) current density in a case of light distribution containing only odd harmonics had been derived, and the results demonstrated, that the photo-EMF current was proportional to the sum of the squares of the spatial harmonics visibilities. Furthermore, an adaptive photodetector based on the photo-EMF effect, have been proposed for efficient localization of the Talbot patterns or self-images (planes with minimal and maximal visibility) generated by periodical object in real time, high spatial resolution and without any image processing. Here, we present the experimental analysis of the photo-EMF effect induced by an arbitrary 1-D periodical light pattern and the possibility for localization of the Talbot self-images was also investigated.

8105-14, Session 4

Linear variable filter based oil condition monitoring systems for offshore windturbines

B. R. Wiesent, D. G. Dorigo, A. W. Koch, Technische Univ. München (Germany)

A major part of future renewable energy will be generated in offshore wind farms. The used turbines of the 5 MW class and beyond often feature a planetary gear with 1000 liters lubricating oil or even more. Monitoring the oil aging process gives early indication of necessary maintenance and oil change. Thus maintenance is no longer time-scheduled but becomes wear dependent thus providing ecological and economical benefits. This paper describes two approaches based on a linear variable filter (LVF) as dispersive element in a setup of a cost effective infrared miniature spectrometer for oil condition monitoring purposes. Spectra and design criteria of a static multi element detector and a scanning single element detector system are compared and rated. Both LVF miniature spectrometers are appropriately designed for the suggested measurements but have certain restrictions. LVF multi-channel sensors combined with sophisticated multivariate data processing offer the possibility to use the sensor for a broad range of lubricants just by a software update of the calibration set. An all-purpose oil sensor may be obtained.

8105-16, Session 4

Two-photon fluorescence near-field pH measurement for mitochondria activity

Y. Kanazashi, Y. Li, T. Onojima, K. Iwami, Y. Ohta, N. Umeda, Tokyo Univ. of Agriculture and Technology (Japan)

A proton distribution in the vicinity of mitochondria attracts interest due to its influence to a necrotic cell death. Mitochondria produce by ATP using proton concentration gradient generated across the membrane. Accordingly, pH distribution in the vicinity of mitochondria changes from time to time. However, if mitochondria are exerted by physical and/or chemical stresses, proton concentration gradient disappears and ATP couldn't be produced. As a result, the necrotic cell death happens. This process is considered as a part of the reason of the necrotic cell death. Therefore, it is expected that measuring pH distribution in the vicinity of mitochondria leads to clarification of a mechanism of the necrotic cell death. However, it is very difficult to measure pH in vicinity of mitochondria accurately, because a spatial resolution of the conventional microscope is limited.

In this study, we propose pH measurement method based on two-photon fluorescence excitation of dual wavelength pH sensitive dye and scanning near-field optical microscopy (SNOM) to improve spatial resolution. This method utilizes a femtosecond pulse laser to generate two-photon absorption and excites the dye locally. Then the fluorescent signal is collected by a near-field probe. The fluorescent signals for each wavelength are detected separately by cooled photomultiplier tubes, and their intensity ratio is calculated as a figure of pH. The calibration of the pH using proposed method is achieved, and temporal variation of the pH by dropping acid is successfully observed.

8105-17, Session 4

Real-time monitoring of indium bump reflow and oxide removal enabling optimization of indium bump morphology

F. Greer, M. R. Dickie, T. J. Jones, M. E. Hoenk, S. Nikzad, Jet Propulsion Lab. (United States)

Flip chip hybridization, also known as bump bonding, is a packaging technique for microelectronic devices which directly connects an active element or detector to a substrate readout face down, eliminating the need for wirebonding. Indium bump technology has been a part of hybridization for many years and has been extensively employed in the infrared imager industry. However, obtaining a reliable, high yield process for high density patterns of bumps can be quite difficult in part due to the tendency of the indium bumps to oxidize during exposure to air. In this study, plasma, thermal, and wet chemical methods were screened to determine their ability to remove indium oxide from indium bumps and reflow them. Plasma processes using methane, argon, and/or hydrogen were developed to remove indium oxide from indium bumps after prolonged air exposure. A novel hardware configuration was developed to optically monitor indium bump morphology in real time during reflow to optimize and control the process and therefore, the indium bump contact angle, to obtain unique, highly wetted bump morphologies. These methods were tested by fabricating fully hybridized visible CMOS detectors and imaging a standard test pattern. The results of these tests, and a discussion of the mechanisms and merits of the different plasma chemistries and approaches will be discussed.

8105-18, Session 4

Light confinement by structured metal tips for antenna-based scanning near-field optical microscopy

J. D. Jambrech, Fraunhofer-Institut für Integrierte System und

Conference 8105: Instrumentation, Metrology, and Standards for
Nanomanufacturing, Optics, and Semiconductors V

Bauelementetechnologie (Germany); M. Böhmler, Ludwig-Maximilians-Univ. München (Germany); M. Rommel, Fraunhofer-Institut für Integrierte System und Bauelementetechnologie (Germany); A. Hartschuh, Ludwig-Maximilians-Univ. München (Germany); A. J. Bauer, Fraunhofer-Institut für Integrierte System und Bauelementetechnologie (Germany); L. Frey, Fraunhofer-Institut für Integrierte System und Bauelementetechnologie (Germany) and Chair of Electron Devices, Friedrich-Alexander-University Erlangen-Nuremberg (Germany) and Erlangen Graduate School in Advanced Optical Technologies (SAOT) (Germany)

Scanning near-field optical microscopy (SNOM) aims at imaging nanostructured samples with sub-wavelength resolution. For antenna-based SNOM, a large ratio of the near-field signal to the background signal resulting from far-field excitation and detection is highly desirable. In this work, we improve this ratio in the case of sharp conical metal tips by optimizing the local field enhancement, the origin of the near-field signal, using focused ion beam (FIB) structuring. Electrochemically etched conical metal tips are widely used for antenna-based SNOM. Compared to these quasi-infinite structures, finite length antennas and particle-like probes are expected to provide stronger field enhancement. To limit the effective size of our probes, we fabricated surface plasmon Bragg reflectors in suitable distance to the tip apex. These reflectors are realized by appropriate multiple FIB structuring all around the tip.

The design of the structures and the fabrication strategies are discussed. Scanning electron microscopy images, optical raster scans at the targeted wavelength, and optical spectra at different positions of the tips before and after FIB modification are analyzed. An increase of the light confinement of 60 % is observed after structuring the tips as determined from the apex-to-shaft contrast in confocal PL images. The results show that optimized design, FIB patterns, FIB parameters, and structures are crucial to achieve increased signal-to-background-ratios.

8105-19, Session 4

See-through-silicon inspection applications study based on traditional silicon imager

W. Zhou, D. Hart, N. Bock, R. Shervey, Rudolph Technologies, Inc. (United States)

See-through-silicon inspection is becoming an essential quality control method for semiconductor manufacturing in three-dimensional integrated circuit (3DIC) and chip-stacking and related industries such as crack inspection in solar panel manufacturing. Due to silicon's band-gap structure silicon wafers are transparent to light beyond 1.2 micron wavelength range, so silicon-based detectors have very low sensitivity to this wavelength range. InGaAs detectors are typically favored for such applications, even with much higher cost, larger pixel size and smaller detector resolution.

This paper discusses a series of studies to improve silicon-based imagers' detection signal-to-noise ratio for this see-through-silicon inspection application. Silicon based detector sensitivity increases when light wavelength shifts shorter from 1.2 micron. But both photon penetration depth and percentage of penetrated photons drop accordingly. Non-through-penetrated photons are scattered in all directions both at the wafer top surface and inside of the silicon material. A portion of scattered photons will be collected by inspection optics and reach the imager eventually, to cause a white noise background in images out of silicon based detectors. This essentially results in low image contrast.

Effectively removing this background noise is the key to fundamentally improve the signal-to-noise ratio of silicon based detectors for this application. We studied a series of methods, including simple image processing methods, advanced frequency domain analysis and reference subtraction, and compared each method's pros and cons for industrial inspection applications.

8105-20, Session 4

Whole field curvature and residual stress determination of silicon wafers by reflectometry

C. S. Ng, A. K. Asundi, Nanyang Technological Univ. (Singapore)

Reflectometry, a simple whole-field curvature measurement system using a novel computer aided phase shift reflection grating method has been improved to certain extend. The similar system was developed from our earlier works on Computer Aided Moiré Methods and Novel Techniques in Reflection Moiré, Experimental Mechanics (1994) in which novel structured light approach was shown for surface slope and curvature measurement. This method uses similar technology but coupled with a novel phase shift system to accurately measure surface profile, slope and curvature.

In our previous paper, "Stress Measurement of thin wafer using Reflection Grating Method", the surface curvature and residual stresses were evaluated using the versatility of the proposed system. The curvature of wafers due to the deposition of backside metallization was evaluated and compared with a commercially stress measurement system from KLA-Tencor.

In this paper, some aspects of the work is extended. Our proposed system is calibrated using a reference flat mirror and spherical mirror certified by Zygo Coporation. The mirrors together with the camera calibration toolbox allow the system to acquire measurement accuracy that is demanded by semiconductor industry. Finally, the results obtained from Reflectometry are compared and contrast with results from KLA Tencor System.

8105-21, Session 5

Common-path laser encoder system for nanopositioning

C. Wu, C. Cheng, Tamkang Univ. (Taiwan)

Scanning probe microscopy and nanoimprint are powerful and promising techniques for nanotechnology. In order to get precise dimensions of microstructures, the displacement sensor is required for precise displacement feedbacks. Out of all displacement sensors, the laser encoder has been an important subsystem and widely adopted for advanced manufactures such as semiconductor industry. However, the used laser encoders inevitably suffer from environmental disturbances or noises, which mainly result from atmospheric influences, background vibration, thermal drift, and electronic high frequency noises. In this paper, a common-path laser encoder for nanopositioning is proposed. Based on the common-path optical configuration, our system can offer high stability and high resolution displacement measurements. An expanded laser source is focused on the grating scale. The grating then diffracts the focus beam. The zero order diffraction beam overlaps partially with the first one. This interference beam is divided into two parts by the polarization beam splitter (PBS). When the grating scale moves $\Delta(x)$, the Doppler effect will induce the phase variation $\phi = 2\pi \Delta(x)/d$ in first order diffracted beam. Here d is the grating pitch. According to the Jones calculation, the light intensities on the detectors D1 and D2 can be written as: I_1 proportional to $1 + \cos(\phi)$ and I_2 proportional to $1 + \cos(-\phi)$, respectively. As the phase difference $\phi = 2\pi \Delta(x)/d$ between I_1 and I_2 , the displacement $\Delta(x)$ of the grating scale can be obtained by the following equations: $\Delta(x) = \phi d / (2\pi)$. The principle of the displacement measurement and the method of the positioning method will be detailed and the system performance will be provided.

8105-22, Session 5

Quasi static short range lidar for volume scatterometry

C. F. Hahlweg, Helmut-Schmidt Univ. (Germany)

In continuation of previous publications the use of short range Lidar techniques for measuring volume scatter behaviour of semi-transparent materials is investigated with focus on budget designs power modulated FMCW devices in GHz range. Standard components as supplied for telecom transmission lines are used. A main topic is the definition of the scatter geometry for goniometric measurements. Further the use of short range Lidar in imaging scatterometers is discussed. Theoretical and practical investigations are presented.

8105-24, Session 5

Rapid defects detection of bonded wafer using near infrared polariscope

C. S. Ng, A. K. Asundi, Nanyang Technological Univ. (Singapore)

Wafer bonding has emerged as an important processing step in wide range of MEMS manufacturing applications. During the manufacturing process, even in the modern clean room, small defects result from trapped particles and gas exist at bonded interface. Defects and trapped particles may exist on the top and bottom of the wafers, or at the interface of bonded wafer pair. These inclusions will generate high stress around debond region at the wafers bonded interface. In this paper, inspection at the bonded interface will be the area of investigation.

Since silicon wafer is opaque to visible light, defect detection at the bonded interface of silicon wafer is not possible. Due to the fact that silicon wafer is transparent to wavelength greater than 1150nm, an Near Infrared Polariscope which has showed some promises on residual stress measurement on silicon devices has been adapted and developed. This method is based on the well known photoelastic principles, where the stress variations are measured based on the changes of light propagation velocity in birefringence material. The results are compared and contrast with conventional Infrared Transmission Imaging tool (IRT) which is widely used to inspect the bonded silicon wafer.

In this research, the trapped particles that are not visible via conventional infrared transmission method are identified via the generated residual stress pattern. The magnitude of the residual stress fields associated with each defect are examined qualitatively and quantitatively. The stress field generated at the wafers bonded interface will look like a 'bow tie' pattern.

8105-25, Session 5

Circular Si waveguides from bulk Si by using laser reformation technique

S. Hung, S. Shiu, J. Chao, C. Lin, National Taiwan Univ. (Taiwan)

Silicon is on the verge of the choice for the photonics industry. Sub-wavelength optical wires fabricated using CMOS (Complementary Metal-Oxide-Semiconductor) materials and techniques promise economic integration of optics and electronics. On the CMOS transistor layer, which necessitates thermal conduction through the silicon substrate, the SiO₂ layer typically has a thickness of below 100nm. However, such thin SiO₂ underneath the Si waveguide creates excessive optical loss into Si substrate. It makes an incompatibility for the integration of optics and electronics. Here, we present a novel method to fabricate Si/SiO₂ waveguides from regular Si wafers using laser reformation technique. Deep silicon ridges were firstly created using typical lithography and dry-etching processes. Then, high-power excimer laser was used to illuminate the Si ridges. Under proper illuminating condition, the top portion of Si ridges would be melted and reshaped to circular-profile structure. The principle of laser reformation is to melt the Si ridges by a high-power laser pulse. During the period of liquid-phase Si, the surface

tension forces the surface area to be the minimum, so the Si ridges are transformed to a circular-profile structure. Finally, high-temperature oxidation process was used to oxidize the unmelted portion below the top reformed structure. The circular cross section has a maximum diameter of about 600nm. The final oxidation of the unmelted neck, still over 1 um long, prevents optical loss due to negligible light coupling from the waveguide to the substrate. This technique allows great flexibility in design and fully compatible with the CMOS circuitry.

8105-27, Session 5

Development of cavity ring-down ellipsometry with spectral and submicrosecond time resolution

V. M. Papadakis, Foundation for Research and Technology-Hellas (Greece); M. A. Everest, Foundation for Research and Technology-Hellas (Greece) and George Fox Univ. (United States); K. Stamataki, Foundation for Research and Technology-Hellas (Greece) and Univ. of Crete (Greece); S. Tzortzakis, B. Loppinet, P. Rakitzis, Foundation for Research and Technology-Hellas (Greece)

Cavity-enhanced ellipsometry, using nanosecond pulsed lasers and without moving parts, is demonstrated to have submicrosecond time resolution. The ellipsometric phase angles are measured from the Fourier transform of the cavity ring-down experimental signals, with a sensitivity 0.01 degrees. The technique is applied to highly reflective surfaces, including total internal reflection, where the samples are placed within the evanescent wave. The technique can be generalized to broadband sources, such as from supercontinuum generation, allowing spectral resolution of thin films and monolayer samples.

Conference 8106: Nanoepitaxy: Materials and Devices III

Wednesday–Thursday 24–25 August 2011 • Part of Proceedings of SPIE Vol. 8106
Nanoepitaxy: Materials and Devices III

8106-01, Session 1

Development and performance of zinc selenide nanowire based photodetectors

M. King, S. McLaughlin, D. Kahler, A. Berghmans, D. Knuteson, M. Aziz, N. B. Singh, Northrop Grumman Electronic Systems (United States)

This work will showcase recent developments in the growth and performance of zinc selenide (ZnSe) nanowire (NW) based photodetectors. Specifically the ability to transition from single NW devices to arrays of detectors will be discussed. We have demonstrated the growth of semiconducting nanowires (NWs) using the physical vapor transport (PVT) method and have found that the growth orientation can be controlled to generate NW arrays. These arrays show promising optical properties, including high transparency and for photoluminescence a high ratio of band edge/deep level defect emission. Such properties are critical for producing high quality photodetectors.

As-grown material was also used for fabrication of photodetectors. Metal-semiconductor-metal (MSM) structures were fabricated from an array of ZnSe NWs and Ti/Au contacts. The array of devices was tested using a 150W tungsten halogen lamp and an automated probe station. Current-voltage plots from -20 to 20V show generally symmetric behavior, with Schottky barriers from the Ti/Au contacts. Upon illumination through a microscope objective lens, the nanowire devices showed orders of magnitude increases in photocurrent. These results will provide the foundation for developing nano-avalanche photodiodes (nanoAPDs), in which p-type and n-type NWs will be utilized to create high efficiency, low noise junctions.

8106-03, Session 1

Nanowire based heterostructures: fundamental properties and applications

A. Fontcuberta i Morral, M. Heiss, Ecole Polytechnique Fédérale de Lausanne (Switzerland)

Nanowires are filamentary crystals with a diameter of few to a hundred of nanometers. Thanks to their dimensions they are the perfect playground for fundamental studies and for improving devices such as solar cells. Nanowires are typically obtained by the vapor-liquid-solid method in which a metal catalyst is used for the gathering of the precursor species and nanowire growth. In most of the cases gold is used, though it has been shown to affect negatively the electronic and optical properties of semiconductors.

We fabricate ultra-high purity GaAs nanowires by avoiding the use of gold and by the use of molecular beam epitaxy (MBE) [1]. MBE offers also the unique possibility of growing with epitaxial quality on the nanowire facets [2]. Prismatic quantum wells and Stranski-Krastanov quantum dots are obtained with a very high quality, as demonstrated by the optical spectroscopy measurements [3,4]. Finally, we show how these nanowires are excellent candidates for the fabrication of solar cells [5] and high mobility transistors by using a modulation doped structure.

References:

- [1] C. Colombo et al., Phys. Rev. B, 77, 155326 (2008)
- [2] A. Fontcuberta i Morral et al., Small 4, 899 (2008)
- [3] M. Heigoldt et al., J. Mater. Chemistry 19, 840 (2009)
- [4] E. Uccelli et al., ACS Nano 4, 5985 (2010)
- [5] C. Colombo et al., Appl. Phys. Lett. 94, 173108 (2009)

8106-04, Session 1

Poole-Frenkel effect and phonon-assisted tunneling in GaAs nanowires

F. Leonard, Sandia National Labs., California (United States)

We present electronic transport measurements of GaAs nanowires grown by catalyst-free metal-organic chemical vapor deposition. Despite the nanowires being doped with a relatively high concentration of substitutional impurities, we find them inordinately resistive. By measuring sufficiently high aspect ratio nanowires individually in situ, we decouple the role of the contacts and show that this semi-insulating electrical behavior is the result of trap-mediated carrier transport. We observe Poole-Frenkel transport that crosses over to phonon-assisted tunneling at higher fields, with a tunneling time found to depend predominantly on fundamental physical constants as predicted by theory. By using in situ electron beam irradiation of individual nanowires, we probe the nanowire electronic transport when free carriers are made available, thus revealing the nature of the contacts.

8106-05, Session 1

Intentional doping and epitaxial regrowth of radial p-n silicon nanowires grown with alternative catalysts

J. M. Redwing, The Pennsylvania State Univ. (United States)

No abstract available

8106-06, Session 1

TBD

D. L. Huffaker, Univ. of California, Los Angeles (United States)

No abstract available

8106-07, Session 2

Epitaxy: an atomistic and kinetic view for all length scales (Keynote Presentation)

A. Madhukar, The Univ. of Southern California (United States)

No abstract available

8106-08, Session 2

CuO thin-film and nanowire for e-textile applications

J. Han, NASA Ames Research Ctr. (United States); A. J. Lohn, N. P. Kobayashi, Univ. of California, Santa Cruz (United States); M. Meyyappan, NASA Ames Research Ctr. (United States)

Device fabricated from materials in low dimensional structures can provide performance enhancement as well as open a new application. Integration of electronics into textile, referred as e-textile, offers an opportunity of future electronics. Here, copper (Cu) and copper oxide (CuO) based nanostructures are embedded for e-textile. Metallic Cu wire is utilized for a growth substrate, which is simultaneously used as a fiber

Conference 8106:
Nanoepitaxy: Materials and Devices III

of mesh textile. Among various metals, Cu is promising as it is non-toxic and relatively abundant on earth. The motivating factor in Cu is ease of growth of nanostructure; the nanowire and thin-film are synthesized by self-catalytic vapor-solid growth. Simply heating Cu with oxygen gas can form CuO nanowire and thin-film according to the growth conditions. As key building blocks in e-textile, memory, transistor, and interconnect are presented. The resistive memory is comprised of CuO thin-film sandwiched within two orthogonal Cu fibers. For a metal semiconductor field effect transistor (MESFET), Schottky junction is used for gate to channel barrier. The Cu fiber and CuO thin-film are devoted for the gate and channel, respectively. For an interconnection, the neighboring fibers are electrically connected by transforming CuO nanowire into Cu nanowire. The thermal reduction of CuO is proved to be effective to make conductive nanowires.

8106-09, Session 2

Growth of Group III nitrides: from films to nanowires to hybrid structures

A. Davydov, D. Tsvetkov, A. Motayed, I. Levin, K. A. Bertness, N. A. Sanford, J. B. Schlager, A. Sanders, P. Blanchard, J. E. Maslar, National Institute of Standards and Technology (United States)

In addition to traditional thin film structures, Group III nitride nanowires (NWs) have attracted considerable attention due to their high structural quality and unique physical properties enabling their use in nanoelectronics. To realize new applications, the controlled fabrication of NWs with defined geometries and electronic properties as well as their integration with planar device structures are required. Thus, it would be beneficial to develop a combination of 2D (films) and 3D (NWs) growth processes in a single reactor using traditional nitride technology to enable fabrication of novel hybrid structures.

In this paper the enhanced capabilities of horizontal Halide Vapor Phase Epitaxy (HVPE) reactor are demonstrated by growth of: (a) GaN NWs and nanotubes (NTs), (b) GaN NW core/shell n/p epitaxial heterostructures (p-type shell over n-type core), (c) AlN NWs, and (d) GaN films on top of AlN NWs. Examples from (a) include the first demonstrations of vapor-liquid-growth growth of GaN NWs and vapor-solid growth of GaN NTs by HVPE. The [0001]-oriented GaN NWs were grown on Al₂O₃ (0001) substrate from catalytic gold particles and were 1 μm to 5 μm in length and 50±10 nm in diameter. The [0001]-oriented GaN NTs were grown by casting GaN shells over InN NWs with subsequent removal of InN core material by thermal decomposition and/or chemical etching. GaN NTs were 1 μm in length with typical wall thickness of 40±10 nm.

The growth models, nanostructures/films/substrates epitaxial relationships, and correlation of growth conditions to the morphological/structural/electronic properties of NWs, NTs and hybrid structures will be presented in details.

8106-10, Session 2

InGaN/GaN nanostructures grown by selective area growth for solid-state lighting

T. Yeh, Y. Lin, L. Stewart, P. D. Dapkus, B. Ahn, S. Nutt, The Univ. of Southern California (United States)

Ordered GaN nanorod and nanosheet arrays were successfully grown by selective area growth using metalorganic vapor phase deposition (MOCVD). Hexagonal GaN nanorods with six non-polar planes and vertical nanosheets with parallel continuous non-polar sidewalls were grown on the patterned c-plane GaN bulk material using a pulsed MOCVD growth mode. A wurtzite crystal structure in the rods was confirmed by high-resolution transmission electron microscope (HRTEM) analysis. Unlike the general III-V nanowires, no stacking faults were found in the GaN nanorods eliminating the possible influence of the stacking faults on the electrical conductivity along the nanorods. InGaN/GaN multiple quantum wells (MQWs) were grown on GaN nanostructure arrays. Cross-section TEM images reveal a core-shell heterostructures on

GaN nanorods and nanosheets. Photoluminescence measurements were performed to confirm the light emission from the MQWs. Strong emission peaks were observed from the nanostructures. We believe the dominant emission peak results from the large exposed surface area of the nonpolar {1-100} sidewalls of GaN nanostructures. Active regions formed on nonpolar planes have reduced piezoelectric fields and potentially increase the radiative recombination efficiency for the LED applications.

This work was supported in part by NSF through Award ECS-0507270 and by the Center for Energy Nanoscience, an Energy Frontier Research Center funded by the U.S. Department of Energy, Office of Basic Energy Sciences under Award Number DE-SC0001013.

8106-12, Session 3

Towards epitaxial integration of metallic nanostructures into photonic devices

S. R. Bank, A. M. Crook, H. P. Nair, V. D. Dasika, The Univ. of Texas at Austin (United States)

The epitaxial integration of metals and semiconductors offers tantalizing possibilities to realize new functionality from (nano)photonic devices. Unfortunately, metals are typically relegated to the periphery of semiconductor devices, due to practical challenges associated with their integration, including interfacial instability and epitaxial incompatibility. ErAs and the other semimetallic rare-earth monpnictides provide a potential pathway to integration, because they may be epitaxially integrated with high-quality III-V semiconductors as both nanostructures and films, with thermodynamically stable interfaces. Such materials could greatly benefit the field of plasmonics where progress towards active devices, such as light-emitting diodes that make use of the Purcell enhancement, is hampered by the design constraint that metallic (nano) structures must remain at the device periphery. Indeed, this limitation renders even structures as simple as a quantum well/dot surrounded by parallel metal plates exceedingly challenging to fabricate. We show how this and other similarly tantalizing structures can now be grown directly in a single epitaxial growth run, using ErAs and III-V semiconductors.

We review our on-going efforts to epitaxially integrate semimetallic hetero- and nano-structures into the heart of III-V devices, highlight some important device applications, and discuss key challenges. In particular, we examine the optical quality of III-V material surrounding the ErAs nanostructures and demonstrate that high-quality III-V emitters may be brought into very close proximity to ErAs nanostructures, ~10 nm, without degrading their emission characteristics.

This finding is very promising for harnessing Purcell enhancements in light-emitting diodes.

The authors acknowledge ARO, AFOSR, and NSF for support.

8106-13, Session 3

Integrated amplifying nanowire FET for surface and bulk sensing

C. O. Chui, K. Shin, Univ. of California, Los Angeles (United States)

Quasi-one-dimensional semiconductor nanowires are uniquely suitable for very high sensitivity detection applications. Their large surface area-to-volume ratio and tiny volume are respectively attractive for surface sensing, e.g. biochemical molecules, and bulk detection, e.g. radiation. Commonly configured as the substrate-gated field-effect transistor (FET) channel, the exposed semiconductor nanowires atop an insulator layer have exhibited very high detection sensitivity on immunoglobulins and nucleic acid molecules. For charged biomolecule sensing in particular, the charge-to-current signal transduction occurs at the nanowire FET front-end which thereby minimizes parasitics and thus noise. This scheme additionally requires no imaging equipments and the sensors themselves are readily interfaced and integrated with readout electronics. The detection sensitivity, and especially the limit of detection (LOD) and limit of quantification (LOQ) that takes into account the blank and signal

Conference 8106:
Nanoepitaxy: Materials and Devices III

noise, however, needs to be further improved before its deployment in portable diagnostic and detection platforms.

In this talk, a transformative nanowire FET structure will be disclosed that significantly boosts the sensitivity through a built-in amplification mechanism with lowest possible parasitics. This is accomplished through the seamless integration of a sensing nanowire with an amplifying nanowire FET. The development of the novel amplifying nanowire FET sensor prototypes as well as their surface and bulk sensing characterizations will be discussed. Preliminary experimental data will also be presented revealing around 1 order of magnitude sensitivity improvement in solution pH and cancer protein detection. Finally, an appreciable improvement in photodetection sensitivity will be illustrated over the generic nanowire FET sensors.

8106-14, Session 3

Fabrication and in situ testing of solid-state all nanowire Li ion batteries

A. A. Talin, D. Ruzmetov, H. Lezec, V. Oleshko, A. V. Davydov, S. Krylyuk, National Institute of Standards and Technology (United States)

The ability to measure the morphological, chemical, and transport characteristics with nanoscale resolution in electrochemical energy storage devices is critical for understanding the complex interfacial reactions and phase transformation that accompany cycling of secondary batteries. In this paper we will describe the use of an all-nanowire Li ion battery for in situ characterization of charge and discharge reactions. The nanobatteries consist of a metalized core, a LiCoO₂ cathode, LiPON solid electrolyte, and a thin film Si anode. Measuring several micrometers in length and several hundred nanometers in diameter, the nanobatteries can be readily imaged in a transmission electron microscope. We test the nanobatteries using a piezo actuated electrical nanoprobe. In addition to being well suited for in situ electrochemical testing, nanowire batteries may also have other advantages, such as superior strain accommodation. To investigate this hypothesis, we also characterize in situ thin film batteries fabricated using similar methods.

8106-15, Session 4

Thin film semiconductor strain engineering for optoelectronic devices

M. S. Leite, E. Warmann, H. A. Atwater, California Institute of Technology (United States)

Historically in materials science, the limited number of substrates available in bulk form significantly limits epitaxial growth versatility. We suggest an approach to elastically relax the strain of single crystalline layers and, therefore, engineer its band gap energy. By transferring coherently-strained ultrathin III-V semiconductor films from their original substrates to a handling support, full strain relaxation occurs and the material unit cell assumes its bulk value a_x . For the successful fabrication of this new template, 40 nm thick dislocation-free films are grown on a substrate, e. g. In_xGa_{1-x}As on InP or GaAs. A viscoelastic wax support is used to coat the epitaxial film, which allows for film relaxation and mechanical support. Once the film is relieved from the substrate by a selective chemical etch it fully relaxes. The crystalline film, independent of the alloy composition, is always compressed with respect to the wax because of the difference between the shear modulus of the two materials. Thus, it is stable against crack formation. The film is then bonded to a handle cheap substrate, e. g. SiO₂/Si. X-ray diffraction and transmission electron microscopy measurements were used to quantify the template relaxation and reconstruct its unit cell, in very good agreement with Vegard's Law. Photoluminescence measurements showed the dependence of band gap offset and strain relief. The creation of a dislocation-free template with arbitrary lattice parameter has the potential for new crystalline material designs for technologies such as solar cells, which will be discussed.

8106-16, Session 4

Recent advances toward III-V based micro/nano pillar solar cells

L. Tsakalakos, J. E. Balch, A. T. Byun, A. Elasser, J. Fronheiser, T. C. Kreutz, O. V. Sulima, GE Global Research (United States); S. P. Rawal, Lockheed Martin Space Systems Co. (United States); J. J. Likar, Lockheed Martin Commercial Space Systems (United States)

No abstract available

8106-17, Session 4

Metal oxide nanowire growth for nanotechnology-enhanced device applications

M. Oye, NASA Ames Research Ctr. (United States)

No abstract available

8106-18, Session 4

Synthesis of crystalline ZnO nanostructures on arbitrary substrates at ambient conditions

P. Nayyar, K. Vabbina, N. Pala, Florida International Univ. (United States); A. P. Nayak, M. S. Islam, Univ. of California, Davis (United States)

No abstract available

8106-19, Session 5

Transport in fused InP nanowire device in dark and under illumination: Coulomb staircase scenario

T. Yamada, Santa Clara Univ. (United States) and Univ. of California, Santa Cruz (United States); H. Yamada, Univ. of California, San Diego (United States); A. J. Lohn, N. P. Kobayashi, Univ. of California, Santa Cruz (United States)

Detailed DC electron transport analysis is performed for a device consisting of fused conical indium phosphide nanowires (InP NWs) bridging two hydrogenated n+-silicon electrodes. These NWs are a few microns long and 100 nm wide. The current-voltage (I-V) plot at room temperature exhibits an unusual staircase shape with a period of ~1 V in dark, but under increasing light illumination, the device conductance gradually increases and the staircase gradually disappears. We explain this observation in terms of the Coulomb staircase scenario - a tiny Coulomb island is created between two tunneling barriers (possibly around the fused portion) and transport is dominated with tunneling. Electrons tunnel in and out of the Coulomb island in a correlated manner, resulting in the staircase I-V in dark. Light illumination raises the electron quasi-Fermi level and the relevant tunneling barriers are buried, causing the staircase I-V to disappear. Although multiple NW pairs bridge electrodes, one pair practically dominates transport. This is because tunneling depends exponentially on the barrier width with the sensitivity as small as Angstroms (hence this is the principle of STM), and unavoidable scattering in physical dimension around the tunneling barriers will result in a significant conductance difference from one NW pair to another. Based on the Coulomb island dimension deduced from the voltage period, NWs are shown unintentionally n-doped with $10^{15-16} \text{ cm}^{-3}$. The quasi-Fermi level difference in dark and under light

Conference 8106:
Nanoepitaxy: Materials and Devices III

illumination is about 25-85 meV, and this is interpreted as a tunneling barrier height.

No abstract available

8106-21, Session 5

Local carrier dynamics in InGaN quantum wells studied by scanning near-field optical microscopy

A. Kaneta, M. Funato, Y. Kawakami, Kyoto Univ. (Japan)

The progress of growth technology has led to the achievement of highly efficient InGaN-based light-emitting diodes (LEDs) in the violet to blue spectral region. However, further improvement of emission efficiency is required, overcoming the problem of the efficiency droop. Many research groups have studied emission mechanism in InGaN quantum wells (QWs). However, most of them were based on macroscopic spectroscopy. The emission mechanism is unclear because nanometer scale potential fluctuation is strongly correlated with recombination dynamics in InGaN QWs. Therefore, nanoscopic spectroscopy is necessary to clarify the correlation between local structures and recombination mechanisms of InGaN QWs. To date, we have developed temporally and spatially resolved photoluminescence (PL) spectroscopy using a scanning near-field optical microscope (SNOM) to investigate the recombination dynamics in InGaN single QWs (SQWs). As an example, we have succeeded in clarifying the correlation between the radiative/nonradiative recombination processes and threading dislocations as well as carrier diffusion/localization processes by comparing SNOM-PL mapping and atomic force microscope taken at the same scanning area. However, a conventional SNOM based on one fiber probe cannot detect the detailed carrier motion diffused out of an aperture. Therefore, we have developed a dual-probe SNOM, where a photoexcitation probe is fixed at specific position while a light collection probe is scanned around the photoexcitation probe, and succeeded in visualizing the anisotropic carrier diffusion in an InGaN SQW. Thus, it is worth emphasizing that this technique can be a versatile tool for assessing photonic phenomena such as transport and recombination processes of various elemental excitations.

8106-25, Session 6

Growth of ZnO-based nanorod heterostructures and their photonic device applications

J. Yoo, S. T. Picraux, Los Alamos National Lab. (United States); G. Yi, Seoul National Univ. (Korea, Republic of)

Position-controlled and vertically-aligned semiconductor nanoscale heterostructures can serve as ideal components for photonic devices because the structures provide not only integratable building blocks but also give unique properties such as enhanced light absorption, waveguiding, and large active volumes compared to thin films and bulk materials. This good versatility and performance of photonic devices based on nanomaterials can be accomplished by fabrication of nanorod heterostructures with compositional modulation along either the axial or the radial direction. Semiconductor nanorods are particularly promising since high-quality semiconducting building blocks can be easily obtained. Additionally, growth of semiconductor nanorods can give insight into the nanoepitaxial growth on various substrates. Such novel nanoepitaxy techniques make it possible to fabricate monolithic integrated circuits and sophisticated quantum devices on otherwise incompatible substrates.

Here, we present research results on ZnO nanorod heterostructures and their photonic device applications from the viewpoint of using position-controlled growth for integration and fabrication of quantum structures for controlling physical properties. In this research, we used a combination of catalyst-free metal-organic vapor phase epitaxy and lithographic techniques to prepare position-controlled vertically aligned ZnO nanorod heterostructures. Using the combined approach, ZnO/MgZnO and ZnO/InxGa1-xN nanomaterial heterostructures were prepared successfully. The position-controlled ZnO-based nanomaterial heterostructures exhibited quantum confinement indicating the formation of well-defined heterostructures. Based on these structures three-dimensional nanoarchitecture photonic devices such as light-emitting diode arrays and embedding quantum structures are demonstrated.

8106-22, Session 5

Scanning photocurrent microscopy in single nanowire devices

D. Yu, Univ. of California, Davis (United States)

No abstract available

8106-26, Session 6

Metal-organic frameworks: charting a course to device integration

M. D. Allendorf, Sandia National Labs., California (United States)

Among the new classes of nanomaterials created during the past decade, metal-organic frameworks (MOFs) are possibly the most versatile. MOFs represent the "inside out" of nano: these supramolecular, crystalline materials are nanoporous and display record-setting surface areas. Unlike many other nanoporous materials, MOFs are inorganic-organic hybrids composed of an organic "linker" group connected to a metal ion such as Zn(II). This feature creates unprecedented synthetic flexibility, combining the vast organic reaction chemistry with rational structural design enabled by metal-linker coordination bonds. As a result, both pore geometry and chemical features can be tailored for specific applications, which to date include gas storage, separations, drug delivery, and chemical sensing. However, integration of MOFs with electronic devices is still in its infancy, even though their highly ordered structure suggests the potential for defect-free electronics in the single-digit nm scale. This presentation will provide an introduction to MOFs and their properties that are attractive for use in electronic devices. Specific examples developed will then be presented, including growth of thin films on micro-electromechanical systems (MEMS) for chemical sensing, nanolithography to create nanoparticles and nanowires from silver-infiltrated frameworks, and luminescent MOFs in which manipulation of nanoscale structure enables the spectrum, intensity, and timing of light output to be tuned. Finally, we will introduce a roadmap to MOF device integration intended to stimulate new research efforts and interdisciplinary collaboration.

8106-23, Session 5

Epitaxial growth of ZnO nanowires on retroreflector microspheres and the resulting light channeling and plasmonic properties

S. M. Prokes, U.S. Naval Research Lab. (United States)

No abstract available

8106-24, Session 6

Nanoepitaxy of regularly arranged GaN-based nanocolumns and related nano-devices (Keynote Presentation)

K. Kishino, S. Ishizawa, K. Yamano, J. Kamimura, A. Kikuchi, T. Kouno, Sophia Univ. (Japan)

8106-27, Session 6

Enhanced conductivity of ErAs nanoparticle containing tunnel junctions via bandgap engineering

R. Salas, E. M. Krivoy, A. M. Crook, H. P. Nair, S. R. Bank, The Univ. of Texas at Austin (United States)

Low-loss tunnel junctions are essential components of a number of optoelectronic devices and are particularly important for serially connecting the junctions in multijunction solar cells. Placing semimetallic ErAs nanoparticles at the pn junction greatly enhances tunneling currents by breaking the band-to-band tunneling process into two smaller back-to-back Schottky barriers. Modifying the size and density of the embedded ErAs nanoparticles provides a route to enhance the conductivity of the junctions. In addition, tuning of the Schottky barrier height through compositional grading of the III-V material can further improve the conductivity by lowering the bandgap of the material at the interface of the barrier. We investigate the combined benefits of both techniques in this work by refining the growth parameters of the nanoparticles and digitally grading the GaAs to $\text{In}(x)\text{Ga}(1-x)\text{As}$ on the n-type side. Samples were grown on a Varian Gen II molecular beam epitaxy system on n-type GaAs (100) substrates. Abrupt junctions and compositionally graded junctions of varying thicknesses and strains were grown with and without nanoparticles at the interface. Graded regions were kept thin to avoid increased optical absorption and performance degradation. Preliminary results show a 7x improvement in the forward bias current over abrupt nanoparticle junctions. Further enhancements are anticipated with the use of lattice matched dilute-nitrides for the n-type side and mixed arsenide-antimonide-nitrides for the p-type side. These improvements in conductivity have the potential to advance the performance of many optoelectronic devices, especially concentrator multijunction solar cells.

8106-28, Session 7

Nanocomposites for thermoelectric power generation: rare-earth metal monoantimonide nanostructures embedded in InGaSb and InSbAs ternary alloys

N. P. Kobayashi, T. Onishi, Univ. of California, Santa Cruz (United States); E. Coleman, G. S. Tompa, Structured Materials Industries Inc. (United States)

Technologies that can harvest untapped waste heat energy by utilizing thermoelectrics are gaining strong attention. Thermoelectrics that convert heat directly into electric power are solid-state heat engines in which energy conversion efficiency is limited by the second law of thermodynamics. Thermoelectric figure of merit (ZT) depends on three material properties; electrical conductivity, thermal conductivity, and Seebeck coefficient. ZT of a thermoelectric material needs to be at least 1.0 to envision practical implementations. Despite extensive investigation on both material and device aspects of thermoelectrics to improve energy conversion efficiency, traditional bulk semiconductors have been suffering from ZT \sim 1.0 or below for many years. Maximizing ZT simply requires that electrical conductivity and Seebeck coefficient be high to reduce Joule heating and to increase energy conversion efficiency while thermal conductivity needs to be low to maintain temperature gradient across a thermoelectric material. Unfortunately these three material properties are closely correlated each other in homogeneous bulk semiconductors. Recent demonstrations that employ various semiconductor materials tuned at the nanometer-scale (nanomaterials) have shown great promise in advancing thermoelectrics. Among a wide range of nanomaterials, we focus on "nanocomposites" in which semimetallic nanostructures are epitaxially embedded in a ternary compound semiconductor host to tune the three material properties independently. We demonstrate co-deposition of erbium monoantimonide (ErSb) and $\text{In}_{1-x}\text{Ga}_x\text{Sb}$ or $\text{InAs}_y\text{Sb}_{1-y}$ ternary alloy to

form nanometer-scale ErSb structures within the ternary alloys using low-pressure metal organic chemical vapor deposition (LP-MOCVD). The grown nanocomposites are structurally and thermoelectrically analyzed to assess their potential for advanced thermoelectric power generation.

8106-29, Session 7

Growth of semimetallic ErAs films epitaxially embedded in GaAs

A. M. Crook, H. P. Nair, D. A. Ferrer, S. R. Bank, The Univ. of Texas at Austin (United States)

We investigate the critical growth parameters for epitaxially embedding ErAs films in GaAs, with application to electronic and photonic devices. Traditionally, growth of GaAs on ErAs films resulted in antiphase domain formation, due to the additional rotational symmetry of the rocksalt crystal structure of ErAs, compared with the zincblende GaAs. We leverage the recent discovery that, below a critical areal density during growth, surface erbium adatoms will preferentially incorporate into subsurface ErAs nanoparticles. As compared to traditional layered heterostructure growth, this method offers the advantage that a thin layer of GaAs floats on the surface and remains registered to the substrate, preventing antiphase domain formation during subsequent III-V growth. Samples were grown on a Varian Gen II solid-source molecular beam epitaxy system to investigate the role of ErAs growth rate and GaAs cap thickness on the formation of a surface ErAs nanoparticle layer - one of the experimentally observed failure mechanisms for the embedded growth mode. High resolution transmission electron microscopy (HR-TEM) was used to characterize the integrity of the film as well as to observe the formation of antiphase domains in the GaAs overgrowth. By keeping the GaAs cap sufficiently thin and the ErAs growth rate sufficiently low, we show full ErAs films can be embedded in GaAs without exceeding the critical areal density of surface erbium for formation of a surface ErAs nanoparticle layer. This approach provides a path towards the realization of plasmonic devices based on the epitaxially integration of a semimetal/semiconductor system.

8106-30, Session 7

Epitaxial rare-earth nanostructures in III-V semiconductors

B. Schultz, Univ. of California, Santa Barbara (United States)

No abstract available

8106-31, Session 7

Broadband photodetection in Si:Ge alloy nanocrystals

M. Jo, Pohang Univ. of Science and Technology (Korea, Republic of)

No abstract available

8106-32, Session 8

III-V nanowires and nanowire heterostructures: controlling the growth and nanoscale properties

S. Gradecak, S. K. Lim, S. Crawford, M. Tambe, Massachusetts Institute of Technology (United States)

No abstract available

8106-33, Session 8

Dopant and heterostructure profiles in semiconducting nanowire

D. E. Perea, S. T. Picraux, Los Alamos National Lab. (United States)

The fundamental operation of many silicon and germanium nanowire devices relies on the ability to controllably modulate the composition to create both heterostructures as well as and modulation-doped nanowires with compositionally-abrupt junctions. The vapor-liquid-solid (VLS) growth process is an approach to bottom-up nanowire synthesis that provides an apparently straightforward route to axial heterostructure formation and dopant incorporation. However, the formation of abrupt heterojunctions remains a challenge utilizing VLS growth from the conventional gold catalyst. Moreover, controlled doping with electronic impurities also remains an important challenge in large part due to a lack of a technique or tool sensitive enough to directly quantify the distribution and dopant concentration in individual nanowires. In this talk, I will discuss use of atom probe tomography (APT) as a tool to directly map the 3D dopant distribution and axial heterojunction profiles between Si and Ge nanowires. Dopant depletion studies along the nanowire growth axis reveal a long depletion profile of hundreds of nanometers which is much longer compared to the Si-Ge heterojunction width which is on the order of the nanowire diameter. A dopant incorporation model suggests that the interfacial width depends on the solute solubility in the liquid catalyst. I will further discuss a new approach of using a liquid AuGa alloy catalyst to create a sharper axial heterojunction in Ge-Si, relative to that obtained using pure Au. Finally, I will conclude with some results of increasing the pn-junction sharpness in Si and Ge nanowires using an alloy catalyst.

8106-34, Session 8

Ultralow-voltage and efficient electrostatic precipitation using metal catalyzed silicon nanowhiskers

J. Oh, A. P. Nayak, Univ. of California, Davis (United States); S. Kaya, Ohio Univ. (United States); M. S. Islam, Univ. of California, Davis (United States)

This paper presents our experimental results on gas ionization at atmospheric pressure at very low bias voltages (less than 100 Volts) using gold-catalyzed silicon nanowhiskers. An advantageous combination of field enhancement on nanoscale silicon tips, surface states introduced by defects, metal impurities and bandgap widening through quantum confinement contributes to such lowering of ionization voltage. Usual range of ionization voltage is 5,000 - 15,000 Volts in standard electrostatic precipitators used for pollution control in oil and coal-fired industrial power plants or in the removal of toxic and harmful solid particulate from the gas exhaust stream. Our results show that VLS processes offer distinctive benefits by synthesizing nanostructures with unrivaled dimensions along with high density of surface states contributed by the impurities and immobilized free radicals on the whisker-surface.

8106-35, Session 8

Indium phosphide nanowires integrated directly on carbon fiber

A. J. Lohn, T. J. Longson, N. P. Kobayashi, Univ. of California, Santa Cruz (United States)

Much attention has been given to integration of group III-V semiconductors onto silicon platforms to combine superior optical and electrical properties of group III-V semiconductors with mature processing capabilities of silicon. Less effort however, has been directed

towards integration on other group IV elements such as carbon. Carbon fiber is generally utilized as a structural material in a wide variety of products because of its light weight and large stiffness and tensile strength. Carbon fiber can also offer additional advantages of large electrical and thermal conductivities when integrated with group III-V semiconductors. We have demonstrated the growth of a group III-V semiconductor binary alloy, indium phosphide (InP), directly on carbon fibers thereby enabling a union of semiconductor and structural materials. Carbon fibers with diameter approximately 500 nm were prepared by electrospinning solutions of polyacrylonitrile (PAN) and dimethylformamide (DMF) followed by carbonization at 750 C in inert atmosphere. Gold nanoparticles were dispersed on the fibers to catalyze metal organic chemical vapor deposition (MOCVD) growth of InP nanowires. X-ray diffraction indicates that despite the graphite surface, InP nanowires adopt primarily zinc blende crystal structures. Geometrical parameters have been determined by scanning electron microscopy and elemental analysis has been carried out using energy dispersive spectroscopy. Optical properties of InP nanowires integrated on carbon fibers are also investigated. Our demonstration is a first step towards direct integration of semiconductors onto one of the important structural materials with the view toward a new class of material platform for solid-state devices.

8106-36, Session 8

Comparative study on nucleation and growth of InP nanowires on micro-crystalline- and single-crystalline-Si surfaces

C. W. Greene, A. J. Lohn, N. P. Kobayashi, Univ. of California, Santa Cruz (United States)

Increased capacity for strain relaxation in semiconductor nanowires allowing for heteroepitaxy on large-mismatch single-crystalline substrates has enabled unprecedented combinations of dissimilar crystalline materials. Through the use of a thin microcrystalline silicon ($\mu\text{-Si}$) template layer, we have demonstrated that the concept of heteroepitaxy can be further extended to low-cost non-single crystalline substrates such as stainless steel or glass. Details of nucleation and growth of nanowires on the $\mu\text{-Si}$ surfaces, in contrast to those on single-crystalline surfaces, are still far from complete understanding. In this study, effects of the $\mu\text{-Si}$ layer on nucleation and growth of indium phosphide (InP) nanowires are investigated. Metal organic chemical vapor deposition was used to grow InP nanowires with diameter approximately 50 nm on $\mu\text{-Si}$ and single-crystalline Si surfaces. Growth time was varied between 1 and 20 minutes, resulting in samples quenched at various nucleation and growth stages. No nanowires were found on either substrate after 1 minute. Dense nanowires were observed on the single crystalline Si surface but only sparse growth was observed for the $\mu\text{-Si}$ surface after 5 minutes. Samples grown for 10 minutes and 20 minutes both showed dense nanowire growth. Nucleation and growth between crystalline (100) and $\mu\text{-Si}$ surfaces is further compared through x-ray diffraction and x-ray reflection. X-ray diffraction is also used to assess crystallographic changes in the $\mu\text{-Si}$ template layer occurring during the growth of nanowires. This study is a critical step towards understanding various stages of nanowire growth on non-single crystalline surfaces.

Conference 8107: Nano-Opto-Mechanical Systems (NOMS)

Sunday 21 August 2011 • Part of Proceedings of SPIE Vol. 8107 Nano-Opto-Mechanical Systems (NOMS)

8107-01, Session 1

Light-induced disorder in liquid-crystalline elastomers for actuation

A. Sanchez-Ferrer, ETH Zurich (Switzerland)

Liquid-Crystalline Elastomers (LCEs) are materials which combine the entropic properties of a crosslinked polymer melt with the enthalpic properties of a liquid-crystalline state of order. LCEs show unique characteristics: visco-elasticity and order at the same time in one system. The elastic and the viscosity properties come from the crosslinking and friction of the polymer chains, respectively, while the orientation comes from the mesophase which keeps the polymer backbone aligned.

LCEs behave as normal polymer networks or rubbers when no energy-storing mesophase is present. This state of disorder can be induced by means of temperature or light.

Thermally, the change in shape of LCEs can easily reach 300% when all the enthalpy stored by the mesophase is released and the crosslinked polymer chains are free to move and adopt a random coil conformation.

The light-induced local disorder can be achieved when shape-changing molecules are incorporated in the LCE matrix. These compounds are able to absorb light, rearrange themselves in a new shape and thus disturb the mesophase. This results in the molecules that are keeping the order no longer being able to sustain the retractive force from the polymer backbone, and the material contracts exerting an actuating force.

But, how does a light sensitive side-chain LCE elastomer behave? And a main-chain LCE? What about nematics or smectics? Is a different kind of actuation, besides the common retractive force possible? To answer this questions, new chemistry needs to be developed, together with new physics to understand the systems, and new applications need to be created.

8107-02, Session 1

In-situ control of shape and molecular order in liquid crystalline polymeric nanoparticles

S. Tsoi, J. Zhou, U.S. Naval Research Lab. (United States); S. Wu, Agilent Technologies, Inc. (United States); C. Spillmann, J. Naciri, N. Hashemi, U.S. Naval Research Lab. (United States); T. Ikeda, Tokyo Institute of Technology (Japan); B. Ratna, U.S. Naval Research Lab. (United States)

Two types of stable 100-nm liquid crystalline polymeric nanoparticles were synthesized and when immobilized on solid substrates, actuation of their shape and internal molecular order, respectively, experimentally demonstrated. The first type contains azo-benzene-based liquid crystals fused into an elastomeric network. The shape of the nanoparticles can be reversibly altered by illumination with light. AFM measurements reveal that exposure of the immobilized nanoparticles to UV radiation results in reduction of their height and concomitant increase of the lateral size. Conversely, exposure to visible light increases the height of the nanoparticles and decreases their lateral size. The amount of the strain achieved is controlled by the exposure dosage and can reach values as high as 20%. The second type of nanoparticles studied is gel-like and contains cyano-biphenyl liquid crystals 5CB and 8CB. The nanoparticles are immobilized on a metallic substrate and Scanning Kelvin Probe Microscopy is employed to probe effect of electrostatic field on them. Experimental data and finite element modeling suggest that exposure to the field induces collective mesogen re-orientation inside the nanoparticles without noticeable change in their shape.

8107-03, Session 1

Opto-mechanical parameters of liquid crystal elastomers with carbon nanotubes

N. Torras, K. E. Zinoviev, H. Campanella, C. J. Camargo, J. Esteve, Ctr. Nacional de Microelectrónica (Spain); E. M. Campo, Univ. of Pennsylvania (United States); J. E. Marshall, E. M. Terentjev, Univ. of Cambridge (United Kingdom)

Nematic liquid-crystal elastomers (LCE) have demonstrated great potential as actuators. Due to unidirectional orientation order of the mesogenic groups the material suffers uniaxial contraction when heated. The heat might be supplied from outside or generated inside the material and the latter gives additional functional capabilities for a range of applications. Energy generation inside the material can be provided by illumination of the material if the elastomer contains light absorption component. Liquid crystal elastomers enriched with the carbon nanotubes combine thermoelastic properties of nematic LCEs and the capability of carbon nanotubes (CNT) to absorb infrared and visible light and transform it into thermal energy.

The studies of photo induced actuation of LCE-CNTs present lack of phenomenological step despite intuitive simplicity and the existing theory of contraction mechanism. This work was aimed at experimental characterization of the material with the purpose of general understanding the macro properties of it and of behavior of the elastomer when illuminated by light and with the final objective to facilitate the design of optical actuators on the basis of LCE-CNTs. The parameters like absorption spectra and absorption coefficients of the material as a function of CNTs concentration have been studied. Temperature induced three dimensional deformations were compared with the photo-induced deformations monitored using SEM and conventional optical microscopy techniques combined with thermal imaging done with the IR camera. The basic test structures, cantilever beams and circular plates, have been applied for studies of thermal and mechanical properties of the material.

The work was done within the EU FP7 project (NMP 228916).

8107-04, Session 1

Light-responsive actuation materials based on the photodeformable liquid crystal polymers

Y. Yu, Fudan Univ. (China)

In recent years, photodeformable polymer materials have experienced a vigorous development due to their potential applications such as artificial muscles, photomobile actuators, Micro Opto Mechanical System (MOMS) and so on. On the other hand, as a combination of polymer networks and liquid crystals (LC), crosslinked LC polymers (CLCPs) exhibit such unique properties as elasticity, anisotropy, stimuli-responsiveness and molecular cooperation effect. In this work, a good method was developed to incorporate widely-used photodeformable trigger molecules, azobenzenes, into side chains of polymer networks, in which the azobenzene units are able to act as mesogens. Then the cooperative motion of liquid crystals was utilized to magnify the microscopic structural change of azobenzene units to a significant macroscopic deformation of the whole material upon irradiation of UV light. For example, photoinduced bending was successfully achieved by inducing an asymmetry contraction in the azobenzene CLCP films. Recently, such interesting motions as a motor rotation, an inchworm walk, and a robotic arm motion fully controlled by light have also been demonstrated with the use of CLCP/polyethylene laminated films. Most lately, azotolane-containing liquid crystal polymer networks have been developed whose deformations can be induced by visible light and even directly by sunlight. Furthermore, full-light-driven microrobots,

Conference 8107:
Nano-Opto-Mechanical Systems (NOMS)

microvalves and micropumps have also been fabricated. With these modes of deformations and all plastic actuators, one can convert the light energy directly to mechanical energy, which leads to such applications as micro-or nano-mechanical machines.

8107-05, Session 1

Light-activated shape memory of glassy, azobenzene liquid crystalline polymer networks

K. Lee, H. Koerner, R. Vaia, T. J. Bunning, T. White, Air Force Research Lab. (United States)

We present a distinctive approach to generating reconfigurable light-activated shape memory behavior of glassy azobenzene liquid crystalline polymer network (azo-LCN). Linearly polarized, eye-safe 442 nm light is used to photo-fix temporary shapes in both cantilever and free-standing geometries. The original permanent shape is all-optically recovered with exposure to circularly polarized light. All-optical, isothermal shape memory cycles (photo-fixing and photo-recovery) will be discussed. Due to the glassy nature of the azo-LCN materials utilized here, the all-optical shape memory can be combined with thermal-shape fixing that is independent of the photo-fixing of the material, yielding substantial functionality in a single adaptive material.

8107-06, Session 1

Photoactuators on the base of polymeric elastomers and carbon nanotubes

I. Krupa, M. Omastová, J. Mosnáček, M. Micu?ík, K. Czaníková, M. Ilčíková, P. Kasák, Polymer Institute (Slovakia)

Carbon nanotubes (CNT) represent attractive and challenging structures for formation various, especially electro-conductive polymeric nanocomposites. Other interesting feature of polymer/CNT nanocomposites is their photoactuating behaviour. The main problem is that CNT do not spontaneously suspend in polymers, thus the chemistry and physics of filler dispersion is a major issue in actual research. One way to achieve a homogenous CNT dispersion is to decrease the surface energy of this filler via surface modification.

This work is focused on the non-covalent modification of CNT by various surfactants and their characterization.

Modified CNT were used for preparation of nanocomposites with an elastomeric matrix from solution. The orientation of CNT within a matrix was ensured by cross-linking

Acknowledgements.

Project NOMS which is funded by the European Commission under contract no. 228916

8107-07, Session 2

Nanotube micro- and nano-opto-mechanical systems

B. Panchapakesan, P. Xu, Univ. of Louisville (United States)

Ever since the discovery of carbon nanotubes, its electro-mechanical actuation has been well studied. However no such investigation has happened in the area of photomechanical actuation of nanotubes. When light is irradiated on nanotubes, they undergo stretching, relaxation, bending and actuation. Several attempts have been made in the past to combine nanotubes with polymeric materials to create photomechanical actuators that release the stored energy on infra-red trigger. However these polymers are neither compatible with MEMS process nor the actuation was reversible.

In this paper we discuss our efforts in the development of micro/nano-optomechanical actuators. Using a combination of SU8 patterning process and carbon nanotube films, we demonstrated micro-optomechanical actuators that exhibited a displacement of 24 microns for 400 micron long cantilever at 170 mW of laser power. Since then several new devices has been created using the same process. In one such study micro-grippers were shown to manipulate polystyrene microspheres and cells at about 240 micro-watts of laser power. In another study, we were able to demonstrate photomechanically actuated micro-mirrors about 500 microns in diameter with large rotational angles of 19 degrees at only 170 mW. Finally, we integrated optical filters on the rotational micro-mirrors to demonstrate 10:1 and 20:1 wavelength selectivity of the mirror using red and green filters and their corresponding wavelengths. All these studies show the potential for new area of optomechanical systems that can rival silicon based electrically driven MEMS technologies. Currently we are working on integrating our process with all silicon technologies. Further, integration of 50 nm nano-needles with both SU8 as well as silicon grippers creating the first opto-mechanically actuated nano-grippers for nano-positioning and manipulation. Such grippers have the potential for nano-manipulation of particles, nano-assembly and nano-lithography. We will discuss our efforts in all these new area of nano-opto-mechanical systems.

8107-08, Session 2

Microstamped opto-mechanical actuator for tactile displays

C. J. Camargo, N. Torras, H. Campanella, Ctr. Nacional de Microelectrónica (Spain); J. E. Marshall, Univ. of Cambridge (United Kingdom); K. E. Zinoviev, Ctr. Nacional de Microelectrónica (Spain); E. M. Campo, Univ. of Pennsylvania (United States); E. M. Terentjev, Univ. of Cambridge (United Kingdom); J. Esteve, Ctr. Nacional de Microelectrónica (Spain)

Over the last few years, several technologies have been adapted for use in tactile displays, such as thermo-pneumatic actuators, piezoelectric polymers and dielectric elastomers. None of these approaches offers high-performance for refreshable Braille display system (RBDS), due to considerations of weight, power efficiency and response speed. Optical actuation offers an attractive alternative to solve limitations of current-art technologies, allowing electromechanical decoupling, elimination of actuation circuits and remote controllability. Creating these optically-driven devices requires liquid crystal - carbon nanotube (LC-CNT) composites that show a reversible shape change in response to an applied light. This work thus reports on novel opto-actuated Braille dots based on LC-CNT composite and silicon mold microstamping.

The manufacturing approach succeeds on producing blisters according to the Braille standard for the visually impaired, by taking shear-aligned LC-CNT films and silicon stamps. For this application, we need to define specifically-shaped structures. Some technologies have succeeded on elastomer microstructuring. Nevertheless, they are not applicable for LC-CNT molding because they do not consider the stretching of the polymer which is required for LC-CNT fabrication. Our process demonstrates that composites micro-molding and their 3-D structuring is feasible by silicon-based stamping. Its work principle involves the mechanical stretching, allowing the CNTs alignment, which is an important aspect to act the LC-CNT due to the alignment-dependence of its actuation.

Our European Union FP7 NOMS (Nano Optical Mechanical Systems) Consortium aims at building a tactile tablet for the visually-impaired. This will be the main application of the microstamped optomechanical actuator concept presented in this work.

8107-09, Session 2

Opto-thermal actuation in double layer polymer microcantilevers

C. Martin-Olmos, L. G. Villaneva, A. Llobera, Ctr. Nacional de

Conference 8107:
Nano-Opto-Mechanical Systems (NOMS)

Microelectrónica (Spain) and Instituto de Microelectrónica de Barcelona (Spain) and Consejo Superior de Investigaciones Científicas (Spain); A. Voigt, G. Gruetzner, Microresist Technology (Germany); M. Arroyo, M. Calleja, Ctr. Nacional de Microelectrónica (Spain) and Instituto de Microelectrónica de Madrid (Spain) and Consejo Superior de Investigaciones Científicas (Spain); F. Perez-Murano, Ctr. Nacional de Microelectrónica (Spain)

Actuation at the micro scale and nanoscale without direct contact is of high interest in different areas, as for example the manipulation of small objects for cell manipulation. We present a simple fabrication process of photo-thermal actuators using low-cost modified photosensitive materials.

The fabrication of these photo-thermal actuators was performed using two layers of polymers: one layer is epoxy-based resist with high optical transparency that allows the realization of high aspect ratio patterns for micromachining applications with high resolution. The second polymeric layer is obtained using the same resist but doped with polyaniline. Polyaniline is an organic dye that changes the absorbance spectrum of the bare epoxy based resist, providing the polymer with absorbance bands in the visible-infrared range. Absorbed photons undergo a phononic transition, resulting in localized thermal effects.

Cantilevers with dimensions in the following ranges have been fabricated: length: 200-450 µm; width: 50 µm and thickness: 4-6 µm. According to this, the elastic constant of these cantilevers range from 0.4 N/m to 0.05 N/m (assuming a Young's modulus value of 4,02 GPa).

Two sets of experiments have been performed, one at a constant temperature and measuring deflection (only thermal actuation) and the other locally applying a constant incident power by means of laser focused in the actuator, and measuring the deflection (opto-thermal actuation).

Using the theoretical calculations to analyze the experimental data, it has been possible to determine the coefficient of thermal expansion (CTE) and the thermal conductivity of the doped resist. These measurements show that systems fabricated with such technology will be valid as actuators, with a very low fabrication cost and high displacement.

8107-10, Session 2

In-situ TEM studies of thin film nanobatteries prepared by focused ion beam

T. McGilvray, S. Meng, Univ. of California, San Diego (United States)

Lithium ion battery electrodes are continuously improving, and it is becoming increasingly important to understand the complex dynamic processes that occur during electrochemical cycling. Li de-intercalation often proceeds as a two-phase process in complex oxides such as lithium nickel manganese spinel. Ex-situ methods fall short in describing the actual processes occurring during electrochemical cycling, such as, how does the lithiation front move within an electrode as a function of state of charge and charging rate? This study aims to observe these processes in-situ in a high resolution transmission electron microscope (TEM). In-situ capabilities exist in other analytical techniques such as XRD, XPS, and other beamline methods, but so far no group has observed a thin film battery in-situ in a TEM. equipped with chemical analytical tools such as energy dispersive X-ray spectroscopy (EDXS).

We prepare nanoscale batteries suitable for in situ TEM study by using a "DualBeam" Focused Ion Beam (FIB) paired with a Scanning Electron Microscope (SEM) to mill a cross section out of a thin-film microbattery. We then mount the nanoscale cross section to a custom grid capable of biasing in the TEM. Finally, we thin the sample to a thickness suitable for EELS characterization. We present the main challenges and corresponding solutions, since cross section milling requires high energy ions and the deposition of a protective layer on the battery surface. It is our goal that this work produces a standardized method of studying electrochemical thin film nanodevices in the TEM for applications beyond battery research.

8107-11, Session 3

Materials science: the key to revolutionary breakthroughs in micro-fluidic devices

M. Czugala, B. Ziolkowski, R. Byrne, D. Diamond, F. Benito-Lopez, Dublin City Univ. (Ireland)

Nowadays, precise flow control, provision of exact reagent amounts, contamination prevention between reagents, autonomy, disposability and low-cost manufacture are factors that can not be found together for micro-fluidic valves.

Valves made using photo-responsive materials are of great interest as functional materials within micro-fluidic systems since actuation can be controlled by simple light irradiation, without physical contact, offering improvements in versatility during manifold fabrication, and control of actuation. Nevertheless, their poor versatility, slow response times and limited robustness render them currently as scientific curiosities rather than ideally functioning devices.[1]

The incorporation of photo-responsive gels with ionic liquids (ILs) produces hybrid ionogels with many advantages over conventional materials. For example, through the tailoring of chemical and physical properties of ILs, robustness, acid/ base character, viscosity and other critical operational characteristics can be finely adjusted. Therefore, the characteristics of the ionogels can be tuned by simply changing the IL and so the actuation behaviour of micro-valves made from these novel materials can be more closely controlled.[2]

We have investigated the potential use of spiropyran-modified ionogels for controlling fluid within micro-fluidic channels. This remote ability could greatly simplify specific device design and cost. We have effectively incorporated ionic liquids into hydrogels to attain specific material contraction performance.[3] An advantage of using ionic liquids is the plethora of synthetic and material design options that can be used to design devices optimized for certain performance parameters or behaviours.

[1]F. Benito-Lopez, et al., Mater.Today, 13, 7-8, 2010, 26-33

[2]R. Byrne, et al., Biosens. Bioelectron. 26, 2010, 1392-1398

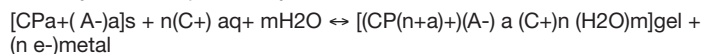
[3]F. Benito-Lopez, et al., LabChip, 10, 2, 2009, 195-201

8107-12, Session 3

Polypyrrole/DBSA actuators sense working conditions and surrounding variables.

T. Fernández Otero, L. Valero, Y. A. Ismail, J. G. Martínez-Gil, Univ. Politécnica de Cartagena (Spain)

The electrochemical reactions of oxidation-reduction in a film of any conducting polymer (CP) with prevailing cation (C+) exchange with solution during reaction can be written in presence of an aqueous electrolyte in a simplified way as:



This reaction supports both, electrochemical properties and the electrochemical applications of those non-stoichiometric [1], reactive and biomimicking materials. Driven by a constant current the electric potential of the film, followed versus a reference electrode, gives increasing anodic, or increasing cathode potentials along oxidation, or reduction processes, respectively. The reaction is influenced by ambient conditions: electrolyte concentration, temperature, mechanical conditions (when the reaction promotes a change of volume). Those influences follow the Ohms law applied to electrochemical reactions: $E = IR$. Driven by constant current (I) decreasing electrical energies ($\int E dt$) will be consumed at increasing values of the variables favouring the reaction rate. Both, the potential evolution and the consumed electrical energy are sensors of the ambient variable during the reaction. Sensing abilities from oxidation and reduction reactions from films of different polypyrrole/DBS films and bimorph actuators will be presented Polypyrrole/DBS films and devices were characterized for different variables: electrolyte

Conference 8107:
Nano-Opto-Mechanical Systems (NOMS)

concentrations, temperature, weight of objects attached to the bottom of the muscle, or current flowing through the device will be presented. Lineal evolutions are obtained for the electrical energy consumed by the artificial muscles to move across a constant distance as a function of the studied experimental variable. Both signals, the actuating current and the sensing potential response, are included by the same two connecting wires, opening a new paradigm for those devices including chemical reactions.

8107-13, Session 3

Self-powered system for structural vibration sensing

P. Gaudenzi, F. Capece, S. Gabriele, Univ. degli Studi di Roma La Sapienza (Italy)

The problem of investigating the structural integrity is a critical aspect for a great number of complex system; an airplane, for instance, needs scheduled revisions to check the perfect status of each component. Many problems arose when a component to be inspected lies in a position requiring the disassembly and successive reassembly of many structural elements, and the consequent time during which the vehicle, or every other equipment which status needed to be checked, is not available due to maintenance, imply additional costs. Therefore, a system that can remotely monitor the components, without the need to physically inspect them, should constitute an advantageous mean for reducing costs and time.

Such a system could be a network of sensors, which sense the vibration stressing the structure, integrated with a system able to remotely transmit the data collected: this kind of system, known as WSNs (Wireless Sensor Networks) have drawn significant attention in monitoring plants, resources, and infrastructures. For the supply of energy needed to this system to work we propose to develop some energy harvesting form vibration sources, the same to be monitored. In fact the use of traditional source of stored energy, like electrochemical batteries, is not practical for small scales. Smart materials can come to the aid of solving this issue: integrating piezoelectric patches on the vibrating structures could be not only the way to monitor vibration but also to generate electric current capable to produce energy to charge a rechargeable battery, or to be stored in a supercapacitor, according to the energy needs.

A critical issue of the system is the evaluation of the level of power needed by the sensing system.

Furthermore, differently from some application, in which the inspections can be carried out only post-operation, i.e. with the vehicle or resources not working, such a system can continuously and on-line test and sense the structural behaviour of the under-investigation components.

8107-14, Session 3

Some electrical transport properties of PLA/MWCNT composites

S. Kumar, E. Marwah, R. Cardona, J. J. Santiago-Aviles, Univ. of Pennsylvania (United States)

Super-capacitors are becoming commonplace, which makes its environmental friendliness an important attribute. For high capacitance, we need suitable materials, formulations and electrodes. Super-capacitors can store energy as part of double layer capacitance (a purely physical effect) or through the charge and discharge of an electro-active polymer (Faradaic, or electro-chemical contribution). Of course, both schemes need a compliant and flexible packaging material with particular electrical and thermal properties. In this abstract we would like to briefly describe how the authors addressed some issues in these types of materials. For this work, we utilize commercially available biodegradable electrospun polymer fibers. In this case, Poly Lactic Acid (PLA) which is a popular corn derived material. It is synthesized by corn fermentation, which generates Lactic Acid. As received, PLA is a solid resin in pellet form. It is dissolved in dichloroethane as to achieve the

proper electrospinning kinematic viscosity. Once in the liquid phase, the material is mixed with commercially available dispersed multiwall CNT at concentrations varying from 2 to 5 w/o. This mixture is then spun at room temperature using a home built electrospinning apparatus capable of depositing randomly oriented fiber mats or oriented fibers onto different substrates, ranging from oxidized Si wafers, Alumina squares or glass microscope slides. The fibers diameters and lengths are statistically distributed following a log-normal distribution and the mean and dispersion are controlled by spinning parameters. One of the challenges achieved in this work lies in obtaining fibers with a small as possible mean diameter, ideally, in the nano-scale range.

Once the fibers are obtained, they are compositionally, morphologically and structurally characterized using thermal analysis, EDX (Energy dispersive X-rays), SEM images, Raman scattering and XRD. The electronic transport properties as function of temperature were measured from 2K to room temperature on a computer controlled superconducting cryostat. Results point to the formation of a PLA / CNT composite with a conductive filler and insulating binder, and where the electronic transport properties strongly correlate with the filler to binder ratio. The room temperature photoconductivity using a visible / near IR monochromator points to a charge carriers photo-transport dominated by the CNT filler as expected.

8107-15, Session 3

The continuing quest for the 'Holy Braille' of tactile displays

D. B. Blazie, N. H. Runyan, National Braille Press, Inc. (United States)

The Boston-based National Braille Press has established a Center for Braille Innovation (CBI), whose mission is to research and develop affordable braille literacy products. The primary focus has been to facilitate the development of dramatically lower cost electronic braille display devices, and the much-sought-after "Holy Braille" of a full-page braille display.

The NBP specs include braille dot dimensions, spacing, displacement, lifting force, and response time requirements. In addition to summarizing the technical requirements and specifications for braille and other tactile displays. We discuss human factors issues, such as why multiplexing with only a single braille character display is not acceptable for most applications. Several of the common and repeated pitfalls and assumptions that have led many previous tactile display developments astray are reviewed. We briefly summarize past efforts to use optical actuation in tactile displays. Finally, we list what appear to be the remaining challenges to developing practical tactile displays employing Electro Active Polymer actuator materials.

8107-16, Session 3

Nano opto-mechanical systems (NOMS) as a proposal for tactile displays

B. Mamojka, Slovak Blind and Partially Sighted Union (Slovakia); J. Roig, Univ. Autònoma de Barcelona (Spain); B. Roeder, Univ. Hamburg (Germany); F. Cromptoets, Philips Research Nederland B.V. (Netherlands); N. Walker, Microsharp Corp. Ltd. (United Kingdom); D. Wenn, iXscient Ltd. (United Kingdom); E. M. Campo, Univ. of Pennsylvania (United States); M. Omastová, Polymer Institute (Slovakia); E. M. Terentjev, Univ. of Cambridge (United Kingdom); J. Esteve, Ctr. Nacional de Microelectrónica (Spain)

Nano-opto mechanical Systems (NOMS) based on the photoactuation of photoactive polymer actuators and devices is a much sought-after technology. In this scheme, light sources promote mechanical actuation producing a variety of nano-opto mechanical systems such as nano-

Conference 8107:
Nano-Opto-Mechanical Systems (NOMS)

grippers. The European Union NOMS consortium is a multidisciplinary team assembled to build a tactile tablet for the visually-impaired. The consortium is formed by experts in materials, optics, microsystems, neuropsychology, as well as end users, and commercial partners. In this paper, we will provide a series of specifications that the NOMS team is targeting in the development of a tactile display using optically-activated smart materials. Indeed, tactile displays remain mainly mechanical, compromising reload speeds and resolution which inhibit 3D tactile representation of web interfaces, much needed by the visually impaired. We will also discuss how advantageous NOMS tactile displays could be for the general public. Tactile processing based on stimulation delivered through the NOMS tablet will be tested using psychophysics and neuroscience methods, in particular event-related brain potentials. Additionally, the NOMS tablet will be instrumental to complete basic neuroscience research.

8107-17, Session 4

A nonlinear model an actuator

P. V. Negron-Marrero, Univ. de Puerto Rico en Humacao (United States); E. M. Campo, Univ. of Pennsylvania (United States)

We consider a mixture of carbon nanotubes (CNT's) with a polymer matrix. Laboratory experiments have shown that this composite reacts mechanically to infrared irradiation (IR). Ahir and Terentjev (2005) proposed a model based on linear elasticity in which the mechanical behavior of the CNT is assumed to be that of an incompressible material. The mechanical properties of the polymer do not enter into their model. A stress vs strain test of an actual specimen of this composite shows that at approximately 10% applied pre-strain, there is a crossing of the corresponding stress responses with and without IR stimuli. Ahir and Terentjev's model predicts this crossing at a 20% compression or reduction of the CNT's while actual experimental data shows the crossing at a 1--2% compression. We propose to improve on this by including the mechanical response of the polymer into the model and by using more general models of material response. The actuator process is incorporated into the model as a constitutive equation for the CNT's which changes its behavior in response to an external stimuli. We use a variational model in which the potential energy function corresponds to one for a mixture of two phases. To compute approximate minimizers we use a finite element method which incorporates the requirement that the stresses within the composite are continuous, yet it allows for jump discontinuities in the deformation gradient across interfaces. We perform calculations both in two and three dimensions and compare our numerical results with previous experimental data.

8107-18, Session 4

Mechanical modeling of thermally actuated LC-CNT composite

C. J. Camargo, H. Campanella, K. E. Zinoviev, N. Torras, Instituto de Microelectrónica de Barcelona (Spain); E. M. Campo, Univ. of Pennsylvania (United States); J. E. Comrie, E. M. Terentjev, Univ. of Cambridge (United Kingdom); J. Esteve, Instituto de Microelectrónica de Barcelona (Spain)

Optoactive polymer actuators and devices (OAPAD) are, undoubtedly, promising technologies. Analytical and finite element models describing dynamics of photo-induced deformation in OAPADs have already been developed, particularly for liquid crystal elastomers (LCE). Advanced materials like LCE - Carbon Nanotube (CNT) composites, require a more complex physical analysis involving different coupled phenomena like photochemistry, photophysics and chemomechanical coupling. The need for rigorous modeling of such complex physics as well as the imminent implantation and development of ground-breaking practical OAPADs like tactile tablets, demand a fast way to model the light-induced deformation of the material.

Our European Union FP7 NOMS (Nano Optical Mechanical Systems)

Consortium aims at building a tactile tablet for the visually-impaired. Hence, modeling of optoactive polymer blister - Braille dot - geometries is the basis of further tactile tablet design.

The purpose of this work is to build a finite element model serving as a bridge between basic elastomer physics and device engineering and design. We take advantage of experimental actuation data to build an empirical model describing the material deformation. The concept that sets the basis of the model is explained: the light irradiation provokes the heating of the material mainly thanks to the absorption properties of the CNTs. Thus, we can consider that CNTs behave as internal heat generators. Consequently, an opto-mechanical system based on LCE-CNT can be evaluated and the mechanical response optimized.

8107-19, Session 5

Education and dissemination strategies in photoactuation

E. M. Campo, Univ. of Pennsylvania (United States); D. Wenn, iXscient Ltd. (United Kingdom); I. Ramos, Univ. de Puerto Rico en Humacao (United States); J. Esteve, Ctr. Nacional de Microelectrónica (Spain); E. M. Terentjev, Univ. of Cambridge (United Kingdom)

Photoactuation is a novel property where a material system actuates upon light irradiation. Few material systems have shown this effect; such as carbon nanotubes (CNTs) and CNT-polymer composites. Recent efforts aim at promoting photoactuation to mainstream research and development. Indeed, these efforts span from developing a basic understanding of mechanisms behind photoactuation, to creating methods within microsystem technologies to integrate these smart materials into practical devices. Ultimately, we envision optical actuation in multiple environments such as intracellular motors, artificial muscles, and tactile displays for the general public.

In the current information age, scientists and educators are urged to disseminate scientific findings in a prompt manner for increased public acceptance later on in the market place. Customer acceptance of highly novel technologies is an education-driven effort that requires attention early-on during the stage of technology development, particularly where nanoparticles are employed. Another driving force to disseminate photoactuation is to generate interest and curiosity amongst the K-12 population that could eventually lead to increased enrollment of graduate students in the physical sciences.

In this paper, we present a work plan for the dissemination of photoactuation to society at large; from K-12 to the general public. The work plan will be designed in accordance to the logic model and will include a thorough assessment plan to gauge the effectiveness of deploying these education programs. We also discuss the prompt integration of photoactuation on the academic curriculum, striving to emphasize the similarities amongst other smart systems such as electro and thermal actuators.

8107-20, Session 5

CNT dispersion and precursor synthesis for electrospinning of polymer-CNT composites

J. P. Crespo, S. Rosa, Univ. de Puerto Rico en Humacao (United States); L. Rotkina, J. J. Santiago-Aviles, Univ. of Pennsylvania (United States); I. Ramos, Univ. de Puerto Rico en Humacao (United States); E. M. Campo, Univ. of Pennsylvania (United States)

In electrospinning, the reported ease of use combined with the spatially controlled deposition of fibers in adequately patterned substrates, could open unexplored avenues in micro and nano-systems technology manufacturing. In the context of nanocomposites, electrospun fibres appear to yield well-aligned CNTs; critical to the advent of these

**Conference 8107:
Nano-Opto-Mechanical Systems (NOMS)**

nanocomposites in practical applications. In fact, great effort is being dedicated to develop effective methods for dispersion and alignment of CNTs; for which some researchers have proposed electrospinning and pyrolysis. Following this trend, and combining the advantages of electrospinning with the promise of actuating nanocomposites, we study the suitability of electrospinning to synthesize photoactuators.

Dispersed MWCNTs were dissolved in a Poly(dimethylsiloxane)/Poly(methylmethacrylate) precursor solution which was then fed into a homemade electrospinning apparatus. Electrospun nanofibers were collected on a (25 x 25) cm cardboard with two strips of aluminum foil to improve alignment. The nanofibers were irradiated with a visible light source of 40W and a deformation of approximately 1mm was observed as discussed elsewhere. In this work, we study the effects of different filler concentrations on dispersion and in-matrix distribution, as well as the subsequent response of the composite to light.

8107-21, Session 5

Electrospun polymer-CNT actuators

S. Rosa, J. P. Crespo, D. M. Yates, J. J. Santiago-Aviles, I. Ramos, E. Campo, Univ. de Puerto Rico en Humacao (United States)

Electrospinning of technology-relevant compounds could offer a simple bottom-up solution to integrate one-dimensional nanostructures in practical devices. Electrospun nanocomposites present well-aligned CNTs; presumably a critical factor in actuation. Electrospun polymer-CNT fibers discussed here, exhibited faceted morphologies of 1 μ m width. In the physical properties space, polymer-CNT composites are known to have increased thermal, electrical, and mechanical properties. Contrary to their thin-film counterparts; little effort has been dedicated to examine the active behavior of electrospun polymer-CNT composites. In this work, we report evidence of photoactuation in electrospun PDMS/PMMA-CNT composites. In this scheme, micron-width fibers were collected in a mesh pattern and then weaved onto threads. When irradiated with a visible light source, the threads bent by 1mm. However, no deformation was observed when the composites were irradiated with a heat source; suggesting the actuation mechanism is of optical nature.

2011 Optics + Photonics

Solar Energy
+ Technology 

Technical Summaries

spie.org/op

Conference Dates: 21–25 August 2011

Exhibition Dates: 23–25 August 2011

San Diego Marriott Marquis and Marina, San Diego Convention Center
San Diego, California, USA

Connecting minds for global solutions

Contents

8108: High and Low Concentrator Systems for Solar Electric Applications VI.	2
8109: Solar Hydrogen and Nanotechnology VI	8
8110: Thin Film Solar Technology III	16
8111: Next Generation (Nano) Photonic and Cell Technologies for Solar Energy Conversion II	25
8112: Reliability of Photovoltaic Cells, Modules, Components, and Systems IV	38

Conference 8108: High and Low Concentrator Systems for Solar Electric Applications VI

Monday-Wednesday 22-24 August 2011 • Part of Proceedings of SPIE Vol. 8108
High and Low Concentrator Systems for Solar Electric Applications VI

8108-15, Poster Session

Compact solar concentrator designed by minilens and slab waveguide

S. Wan-Chieh, National Taiwan Univ. (Taiwan)

Solar power is a supplying inexhaustibly, causes no pollution, and requires slightly maintenance economic energy source. Currently, very high efficiency solar cells based on III-V semiconductors are available on the market. Since these solar cells are more expensive than silicon or thin film ones, they need to be used at high concentration ratio to reduce III-V multi-junction solar cell area. Concentrated photovoltaic (CPV) system is to collect light by using low-cost optical elements so that the total cost can be reduced. A common design uses Fresnel lens as a concentrator is bulky and the acceptance angle is very small that requires a high accurate stepper motor for tracking system.

This paper presents a new solar concentrator for III-V concentrated photovoltaic. Minilens array focus sunlight to triangular prisms causing traveling wave by total internal refraction in a waveguide. High efficiency solar cell is placed on the sidewall of the waveguide. The light and thin optical system can be fabricated by low-cost process and have the linear property for the tilt of the sun light. As the result, the sun tracker rotates nine times a day accompanying by linear-moving waveguide. It also reduces the cost by decreasing the electricity demand for tracking system. At 200X and 400X concentration ratio, the design system reached 92.35% and 90.02% optical efficiency, respectively. The accepting is +/- 10 degree at each rotate.

8108-16, Poster Session

Recent progress in high-concentration Photovoltaic Cavity Converter (PVCC) development for extreme high efficiencies

U. Ortabasi, United Innovations, Inc. (United States); J. Waszczak, S. Allen, Raytheon Missile Systems (United States)

A collaboration team supported by United Innovations, Raytheon, California Energy Commission, Science Foundation Arizona and the University of Arizona has designed, fabricated and tested a Photovoltaic Cavity Converter (PVCC)/Parabolic Dish system that efficiently converts the sun's energy into electricity. The down scaled (1/36) kaleidoscopic PVCC receiver (module) developed under this demonstration project uses EMCORE's CTJ cells optimized for the "Photon Re-cycling" process.

The re-cycling of photons benefits the performance of the PVCC particularly at high concentrations (e.g. 500 suns and above). The improvement of conversion efficiency occurs due to the following effects.

1. The reflected photons from cells (metal grid fingers and active cell areas) are reutilized
2. The contact grid fingers can be denser with no significant increase in shadowing losses (minimized series resistance losses)
3. The inevitable areas between the cells can be made reflective, thus the absorption losses are minimized
4. The photon-recycling allows the spectral splitting of the trapped solar spectrum inside the cavity by using Rugate filters. This allows to create a 6- bandgap system by using two types of available 3-j cells, each responding two half of the full solar spectrum.

The demonstration tests with photon re-cycling showed significant relative improvements of the electric output (53%) when compared to "one hit" mode of operation. Further tests gave the first indication of module efficiencies better than 35% with Photon Recycling. This result compares well when compared to the existing "one hit" HCPV systems that use advanced 3-j cells and operate at 500 suns.

8108-17, Poster Session

The package structure of solar photovoltaic module and method of manufacturing texture interface

C. Peng, C. Huang, Industrial Technology Research Institute (Taiwan)

A package structure of solar photovoltaic module and method of manufacturing the same are provided. The package structure of solar photovoltaic module includes a transparent substrate, a backsheet disposed opposite to the transparent substrate, a plurality of solar cells between the transparent substrate and the backsheet, and several encapsulants sandwiched in between the transparent substrate and the textured backsheet, wherein the encapsulants encapsulate the solar cells. There is at least one embossing interface (texture) between the encapsulants, and the encapsulant having the embossing interface is a thermosetting material.

The package structure is manufactured according to the texture interface with an embossing glass, which has a bottom width of about 0.1mm, a period of about 1mm, and a height of about 0.1mm. Then, a first fabrication process is performed to laminate a structure of the glass/ the EVA adhesive (the EVA adhesive having the embossing interface between the solar cells). Then, a second fabrication process is performed to complete laminating the module package, and fabrication parameters thereof are the same to that of the first lamination process. The EVA adhesive and the EVA adhesive have the same material, and according to the IEC61215 standard test conditions, the output power is tested according to the same method as that of the comparison example. By comparing the voltage-current output characteristics of the comparison example and the first experiment, it is discovered that the module power can be enhanced by 0.77%.

8108-18, Poster Session

The electricity enhancement of solar module through the optical sheet interlayer

C. Peng, F. Lin, Industrial Technology Research Institute (Taiwan)

One optical sheet is added between the glass plate and the solar cell of the general type package structure. The new laminate structure is designed as: (glass plate/encapsulant /optical sheet/encapsulant/ solar cell/encapsulant/highly reflective back sheet) (from the front to the back). According to the present pressing processes, the above laminate structure is placed into the laminator at 165.0 and a vacuum in 10-2 torr is drawn from the upper and lower chambers for 8 minutes in total. Next, the vacuum of the upper chamber is broken for 8 minutes and the solar module package structure is pressed and sealed. The above laminate structure can be fabricated by employing the pressing processes compatible with the currently used laminator machinery.

Under STC conditions, A-class flash simulator is used to test the power output of the above laminate structure, when compared with the control group (without the optical sheet), the power output of the above laminate structure is increased. When the surface textures of the optical sheet are serration structures, the cell maximum power of the above solar module package structure is increased about 0.25%. When the surface textures of the optical sheet are waved structures, the cell maximum power of the above solar module package structure is increased about 1.12%.

Conference 8108: High and Low Concentrator
Systems for Solar Electric Applications VI

8108-19, Poster Session

Reflectance optimization using thin film coating on concentrating photovoltaic optics

G. Butel, B. M. Coughenour, College of Optical Sciences, The Univ. of Arizona (United States); R. Angel, The Univ. of Arizona (United States)

High concentration photovoltaic systems require several reflections to achieve a concentration level of approximately 1000 suns in order to make triple junction cells cost efficient. In the system we develop, we use two cascaded concentration stages that reflect the sunlight onto triple junction cells. Optimization of the reflectance of those surfaces is critical to increase the efficiency of the whole system. In this paper we report the research being carried out in order to maximize the overall reflectance of the optical surfaces of the high concentration system. More specifically it presents the different results we obtained, using different thin films coatings on the first and second concentration stages, to optimize the global efficiency for the specific cells we are using. The primary mirror is a back-silvered glass which has a high reflectance over the range of useful wavelength, 350 nm to 1600 nm. In the region below 400 nm, silver reflectance requires a boost in order to collect a broader spectrum of the sun radiation. With this new thin film design, the mirror reflectance increases by 1 to 2 % from 350 nm to 550 nm. The secondary funnels were first made with nickel over coated with silver. This specific coating not has only the role of increasing the reflectance of silver at steep incident angles (70°) in the short wavelengths by about 1 %, but also to protect silver against tarnishing since it is the layer exposed to air.

8108-20, Poster Session

Closed-loop control for solar thermal heliostats

M. R. Convery, SLAC National Accelerator Lab. (United States)

In a large-scale solar thermal power plant, alignment and control of the heliostats constitutes one of the largest costs of both time and money. This is especially the case in systems where individual heliostats are small (~1m²). Widely used techniques for performing alignment and control are “open-loop” in which heliostat alignment constants are obtained offline and applied over time with little feedback. While some closed-loop techniques have been previously been proposed, they have not been widely adopted.

In this paper, I describe a system that generates the required feedback by inducing small mechanical vibrations in the heliostat reflector surface using piezoelectric actuators. These vibrations induce time-dependent changes in the reflected wavefront that can be detected by photosensors surrounding the thermal receiver target. Time and frequency encoding of the vibrations allows identification of a misaligned heliostat from among the thousands in the system. Corrections can then be applied to bring the reflected beam onto the receiver target.

Outdoor testing of a small-scale model of this system has confirmed that such a system is effective and can achieve milliradian tracking accuracy. Furthermore, the time series of required corrections can be used to calculate precise alignment constants that can be subsequently used in open loop tracking.

This work has been supported by a grant from the California Energy Commission EISG 56084A/08-20.

8108-01, Session 1

A profile of the Amonix 7700 CPV solar power system

A. P. Plesniak, Amonix Inc. (United States)

The Amonix 7700 CPV power system is a massive pedestal mounted,

dual axis tracking photovoltaic generator and truly a sight to see. The fit, form and function of the system is one of a kind when compared to other products in the PV marketplace, but the features of the system are no accident. Discussed is the reasoning behind the profile of the Amonix 7700 CPV power system and why the Amonix 7700 product is the lowest cost CPV solution of today and the lowest cost energy solution of tomorrow.

8108-02, Session 1

>41% efficient lattice matched solar cells

M. Wiemer, V. Sabnis, H. Yuen, Solar Junction (United States)

The most common triple-junction solar cell design which has been commercially available to date utilizes a germanium bottom cell with an InGaAs and InGaP middle and top cell. This type of device has a well known efficiency limitation somewhere around 40% at 500 suns. Higher efficiencies can be obtained by changing the effective bandgaps of the three junctions, but the choice of materials and approaches to do so is very limited. Solar Junction has adopted the dilute nitride material system to obtain these new bandgaps, and break through the 40% efficiency barrier.

The unique advantage of the dilute nitrides is that the bandgap and lattice constant can be tuned independently, allowing Solar Junction to make bulk material lattice matched to Germanium or GaAs over a range of bandgaps. Our dilute nitride technology in our first commercial product has enabled us to maximize the efficiency of a triple junction solar cell by using the optimal set of bandgaps (including one around 1eV). Solar Junction concentrator cells with efficiencies in excess of 41.4% have been independently verified by NREL, and represent typical cells on a wafer. These higher efficiencies are generally the result of higher output voltage, not higher current, which keeps system-level resistive wiring losses in check.

8108-03, Session 1

Optics development for micro-cell based CPV modules

W. Wagner, E. Menard, M. Meitl, M. Samarskiy, K. Ghosal, Semprius, Inc. (United States)

Semprius’ two-stage pupil imaging CPV design incorporates optically imperfect but extremely cost-effective glass ball secondary lenses, in addition to standard primary lens arrays. Our secondary lens design process involves modeling the illumination uniformity of the primary aperture (the ‘pupil’) on the transfer-printed, multi-junction solar cell in response to the secondary lens index, diameter, surface quality, location, and tolerance offsets. We reconcile our theoretical model with experimental results from a single fully adjustable ‘concentrating unit’, and we thereby create a robust model for design updates, for tolerance and sensitivity modeling, and for prediction of full module and on-sun tracker performance based on receiver placement relative to our primary lens array.

In this presentation, we discuss the rationale behind our optics approach, our criteria for optimizing our optics, and our tolerancing approach. Then we discuss our experimental approach, including our universally adjustable ‘concentrating unit’ fixture, our light source, and our primary and secondary optics. We show sensitivity curves of our ‘concentrating unit’ towards receiver placement, receiver tilt, and ball lens size. We reconcile these with our ray-traced model, and, finally, we show predicted module performance based on receiver tolerance data and receiver wiring in the module. Finally, we compare data from our trackers with predicted module performance.

8108-21, Session 1

Boeing ultrahigh performance, low-cost CPV system

J. C. Hall, G. Martins, M. Cameron, T. Crooks, The Boeing Co.
(United States)

No abstract available

8108-01, Session 2

Optical properties and solar radiation durability of PV materials and solar mirrors

R. H. French, W. Lin, M. Murray, Case Western Reserve Univ.
(United States); S. A. Brown, K. A. Shell, M. Schuetz, Replex
Plastics (United States)

Solar and environmental durability of materials and components used in photovoltaic (PV) systems is a critically important issue, so as to ensure the reliability and ultimate bankability of PV systems. We have been developing quantitative optical properties and solar radiation durability methods and metrics for materials used in flat panel, and in low concentration PV (LCPV) systems. We'll discuss solar radiation durability of PV and LCPV materials such as frontsheet, encapsulant and back sheet materials, and of acrylic solar mirrors. Solar mirror durability is important for both mirror augmentation of flat panel PV, and other LCPV type systems.

A useful solar radiation durability metric is the induced absorbance rate (Incremental Δ Abs/cm per GJ/m²), which quantitates the wavelength dependent change in the absorbance/cm for a material exposed to a full spectrum AM1.5 solar radiation dose, in units of GJ/m². The induced absorbance to dose, allows one to identify wavelengths and rates of photodarkening and photobleaching processes in materials. Since it is normalized to full spectrum dose, comparisons of rates at different irradiances (e.g. 1, 3.8, and 48.2 kW/m²) allow serve to check linearity and reciprocity of the observed photochemical degradation processes. We will discuss results from EVA, PMMA, PET and silicones.

8108-02, Session 2

Direct comparison of PMMA and silicone-on-glass

H. P. Annen, L. Fu, R. Leutz, L. González, Concentrator Optics GmbH (Germany)

The CPV community is still undecided on one critical issue: what material to use best for Fresnel lens parquets. Reliability and longevity are the most important, but all other properties play roles as well.

We have developed and manufactured Fresnel lenses with the two commonly used materials: PMMA and silicone on glass (SOG). Both lenses are designed for the same optical train for best comparability.

This allows for better understanding the pros and cons of the materials and making an informed choice for a specific CPV module.

Theory predicts a slight optical performance benefit for PMMA lenses due to the higher refractive index and only two instead of three optical transitions. This can be directly tested and compared under laboratory and outdoor conditions. While PMMA lenses are embossed from pre-fab sheets in a hot-cold process, the silicone lenses are cast from a heat-curing silicone rubber at moderate temperatures, reducing the energy consumption. PMMA allows for the inclusion of custom low-profile 3D (2.5D) structures for module assembly and mechanical alignment, a feature not possible in silicone due to its low rigidity.

SOG lenses are prone to delamination of the silicone film. The adhesive strength of the film to the glass can be measured using a modified blister test that we developed. The results show large difference with different

materials and confirm the necessity of controlling this issue closely. While the small thermal expansion of the glass sheets allows for larger parquet sizes, the deformation of the prisms with temperature may cause a performance hit.

Failure modes for PMMA lenses include cracking and yellowing. Cracking is accelerated by internal stress, material and geometry. Also, PMMA lenses tend to global deformations and the thermal expansion limits the maximum usable parquet size.

Acknowledgment: This study is part of the Triple Primaries project, initiated as research project for various primary and secondary optics in combination with cells, by Concentrator Optics, Azur Space Solar and Isuzu Glass.

8108-04, Session 2

Field performance of concentrix CPV systems

A. Gombert, C. Crawford, T. Gerstmaier, S. van Riesen, M. Röttger, J. Wüllner, Concentrix Solar GmbH (Germany)

Concentrix Solar GmbH - a division of the Soitec Group - is manufacturing and installing concentrating photovoltaic (CPV) systems. Concentrix modules are based on III-V triple junction cells, a Fresnel lens array with a relatively small single lens aperture of 5 square inch, and a cover and bottom plate made out of glass. In case of this small primary lens, a simple heat spreader made out of a metal with a satisfying thermal conductance is sufficient for the thermal management. The first installations were conducted in 2008 in Europe, later installations followed in the US, in East Asia, in the Arabian Peninsula, and in Africa. This paper gives an overview of the performance of Concentrix Solar's CPV systems with special focus on the different climatic conditions and their impact on the system performance. The seasonal distribution of the direct normal irradiation at the mentioned locations was found to be very different which enabled us to perform studies on the system performance depending on irradiation and ambient temperature. The first generation modules which were installed in 2008 had an average efficiency of 25%, resulting in a peak solar-to-grid system efficiency of 23% and an average AC system energy efficiency of > 20%. The system peak efficiencies of the second and third module generations reach maximum values of > 25% and average AC system efficiencies of > 22%. A detailed analysis of the performance of the different system generations will be presented.

8108-05, Session 2

Techniques, regression, and applications of glass strength measurements for concentrator photovoltaic (CPV) mirrors

D. Krevor, M. Milbourne, SolFocus, Inc. (United States)

A primary failure mode for glass failure in reflective CPV systems is the mechanical stress caused by a thermal gradient. To establish the necessary reflector specifications, it is essential to have both economic techniques to measure glass strength and an insight into the failure mechanisms. Due to the highly stochastic nature of glass fracture, large data sets are necessary for statistical validity and to provide meaningful estimates of field failure rates. This paper discusses experimental measurement techniques for both value-added reflectors and for non-value surrogate substrates which are generated as waste during the manufacturing process. Specialized tooling enables measurement by commercially available stress-strain equipment (e.g., "Instron" testers). The glass strength is calculated from the force-to-break data, sample thickness and a substrate shape dependence. These strength data are regressed using a two-parameter Weibull model, which enables calculation of the Weibull modulus, which is a measure of the distribution of flaws of a brittle material. Using a finite element analysis model of the thermal-mechanical stress to determine the critical stress, the Weibull analysis enables extrapolation of the data to predict field failure rates. The test and regression now comprise an On-going Reliability Test (ORT) that is inherently low-cost and appropriate for high-volume manufacture.

For fracture, the initiating flaws are the result of glass cutting and trimming operations. There can be low-strength outliers which result from bulk glass defects, though such flawed product should be culled during the manufacturing and inspection processes. As expected and commonly known, the as-cut glass strength is very sensitive to the cutting method and resulting quality.

8108-06, Session 2

Concentrating PV survey: an unbiased overview

J. Handy, Objective Analysis (United States)

Concentrating photovoltaics (CPV) technology is well positioned to contribute in an important way to utility-scale power generation. All CPV systems share certain attributes and certain shortcomings. This presentation is intended to help attendees understand the commonalities of all CPV systems and the differences between the leading technologies, and to present criteria to help understand which technologies are likely to succeed and which are less likely to survive.

The analysis is based upon the CPV technologies themselves along with arguments involving economics, insolation, and policy. It encompasses all aspects of CPV combined with its strengths and weaknesses to illustrate the likelihood that some of these technologies will participate in the power grid of tomorrow.

The author has reviewed all leading CPV technologies and has interviewed key CPV suppliers and important test sites to better understand the reasons that some CPV systems are more likely to succeed than are others.

8108-07, Session 3

A CPV thesis

S. Ghosh, D. S. Schultz, Banyan Energy Inc. (United States)

This decade is different for CPV because of optic innovations capable of delivering low to mid levels of concentration within a compact form factor, increases in mono-silicon cell efficiencies (complimentary increases in capacity) and the maturation of vertically integrated solar companies more focused on delivering system oriented solutions that minimize the levelized cost of energy. Monosilicon cells are well-suited for concentration because of their high cost structure and robust efficiency. This category of receiver achieves the greatest system capital efficiency benefit when paired with an appropriate module-integrated concentrator technology. The viability of a concentrator technology is determined by five interrelated factors: economic benefit, cell efficiency under concentration, thermal management, optical performance and manufacturability. These factors impose tradeoffs that dictate that the 5-10x concentration range is ideal for silicon-based receivers. This range of concentration provides substantial improvement in capital efficiency while mitigating technical risk. Below the 5x concentration level, the cost to integrate optics with receiver approximately equalizes with economic benefit. Above 10x, the vast majority of the capital efficiency benefit is achieved, but substantial threats to reliability arise. The combination of thermal management costs, reduced manufacturing yields (for cell and module) and increased degradation rate serve to erode any marginal economic benefit from increasing concentration significantly beyond 10x.

8108-08, Session 3

Design and performance of a low-cost, low-concentration PV module

K. A. Shell, S. A. Brown, M. Schuetz, Replex Plastics (United States); B. Davis, The Ohio State Univ. (United States); R. H. French, Case Western Reserve Univ. (United States)

Replex Plastics is developing a low-cost, low-concentration PV (LC2PV) module using Replex acrylic solar mirror. The module is designed for use in northern climates, where lower insolation and higher levels of atmospheric scattering result in system designs with wide acceptance angles and reduced tracking accuracy requirements. The first generation prototype uses silicon cells and a reflective compound parabolic concentrator (CPC) designed specifically for relatively low-accuracy (~1°) single axis tracking systems. The asymmetric CPC has a nominal geometric concentration factor of 10x, and acceptance angles of 12.1° in the tracking direction and 23.5° in the non-tracking direction to allow for seasonal variation of the sun.

The challenge of a low-concentration system is to minimize the additional cost from the reflector, heat dissipation, and additional electrical bus material so that it does not negate the benefits from using 1/10th the silicon content. Accordingly, three critical performance parameters are being addressed in the LC2PV design: (1) Maximizing the optical efficiency of the mirrored reflector, (2) Designing a low-cost, light-weight passive heat sink suitable for low-concentration heat dissipation, and (3) Minimizing electrical losses in the PV ribbon due to increased current.

The first LC2PV module prototype was installed on a tracker in Athens, OH in October 2010, and achieved a 7.1x concentration over a receiver with no concentration. The power output of the module is being monitored continuously, and has exhibited a peak output of 140W. Environmental monitoring is currently being installed at the test site so that module performance can accurately be compared to irradiance, temperature and wind-speed conditions. The next generation prototype is currently under development with an expected installation Summer 2011.

8108-09, Session 3

Significant cost reduction through new optical, thermal, and structural design for a medium-CPV system

M. A. Finot, B. MacDonald, Skyline Solar, Inc. (United States)

The design of cost-efficient medium-concentration CPV (MCPV) systems requires the analysis of dozens of engineering, manufacturing and financial trade-offs. In 2007, Skyline Solar designed its first system, HGS1000, based on a 7x concentration factor and 0.5 m aperture width. Due to the modular aspect of the Skyline Solar architecture, the system has been re-optimized for the current cost/performance roadmap of the critical components using a combination of field data and advanced performance modeling for lowest levelized cost of energy (LCOE). The key area is to design a system using high-volume, high quality commodity components. Use of efficient high volume Si cells, standard mirrors and tracking structure minimizes supply chain and reliability risk and ensures a fast ramp-up of a new architecture.

All CPV designs substitute optical and structural materials with lower area cost than the PV cells they are replacing. Design choices span many engineering disciplines including optical, thermal, structural, electrical, packaging - each of which has many parameters. Optimization requires deep understanding of system cost and performance under a variety of conditions. We used field performance data from multiple installations of the HGS1000 system and comprehensive design modeling tools to re-optimize our CPV design. The analysis led to a new design with cost reductions exceeding 40% with major changes in several design parameters - most notably 14x concentration and 1 meter aperture width. We will discuss optimization of thermal and structural designs in the context of peak power cost and energy cost. Early field performance data will be presented along with correlation to predicted results.

8108-10, Session 3

Bringing new technology to the solar market: low concentrating solar and trackers for maximum generation for PV installations

K. Gibson, Solaria Corp. (United States)

Solaria's photovoltaic silicon modules offer industry-leading costs with the reliability and performance of traditional crystalline solar modules. Solaria modules are manufactured with an efficient use of silicon that leads to the smallest carbon footprint and fastest energy payback of any silicon-based panel; the company is a leader in the solar industry in reducing the environmental impact of PV manufacturing.

Solaria delivers more energy and lower LCOE. The patented technology combines silicon solar cells with proprietary glass optics to reduce module costs without compromising performance. Solaria's proprietary flat-plate optical concentrator delivers maximum output.

The company uses only proven, UL-listed materials that are standard in the PV industry, thereby eliminating risks associated with new materials.

The modules are specifically designed and optimized for tracking systems, which yield additional cost savings in installation and balance of system costs, providing a low-cost, high-performance solution for developers of large-scale solar tracking systems. The form factor, mounting system and installation processes are also optimized for efficiency and reliability. Solaria provides large integrators and system developers with the most cost-effective and reliable module for large- and utility scale solar electric installations.

8108-11, Session 4

Comparison of tracking and non-tracking holographic planar concentrator systems

R. K. Kostuk, D. Zhang, J. M. Castro, J. M. Russo, S. D. Vorndran, The Univ. of Arizona (United States)

In this paper we review the properties of holographic planar concentrators (HPCs) with tracking as a design consideration. Static holographic concentrators have been shown to collect approximately 50% of the available solar illumination illuminating the hologram area and deliver it to the photovoltaic (PV) surface. Another feature of the static concentrator is that the composition of the spectrum varies as the sun moves in its daily and seasonal trajectory. This results in a variation in the PV cell output due to changes in the responsivity and the spectrum of the solar illumination. In addition the uniformity of the illumination can vary considerably as the sun moves resulting in effective shading effects which diminish the PV system output.

A variety of tracking systems have been developed to increase efficiency and energy yield of different photovoltaic systems. Tracking has primarily been developed for high concentration systems that use expensive multi junction cells and require high pointing accuracy. However tracking has also been shown to be near cost competitive by improving energy yield of one-sun systems with more expensive PV cells. For holographic planar concentrators tracking can be used to control the spectrum of the diffracted solar illumination directed to the photovoltaic cell surface and has important consequences on the performance of the overall solar concentrator system. In this presentation we examine the use of single axis tracking systems as a design parameter to optimize the energy yield of holographic planar concentrators. A levelized cost of energy analysis is also performed to determine the point at which tracking HPC systems become cost effective.

8108-12, Session 4

New luminescent materials and filters for luminescent solar concentrators

D. K. de Boer, C. R. Ronda, W. K. Keur, Philips Research Nederland B.V. (Netherlands); A. Meijerink, Utrecht Univ. (Netherlands)

In a Luminescent Solar Concentrator (LSC), short-wavelength light is converted by a luminescent material into long-wavelength light, which is light guided towards a photovoltaic cell. In principle, an LSC allows for high concentration, since the heat generated by the conversion process can be used to lower the entropy of light. In practice, however, this is prevented by less controlled loss mechanisms, like limited sunlight absorption, limited quantum efficiency and high self absorption. To tackle these problems, a suitable luminescent material is needed. Another important loss mechanism is the escape of luminescent radiation into directions that do not stay inside the light guide. To reduce this amount, wavelength-selective filters can be applied that reflect the luminescent radiation back into the light guide while transmitting the incident sunlight. In a previous paper [1], we used simulations to clarify the optimal luminescent and filter properties. In this paper, we discuss experiments and simulations of new luminescent and filter materials. We will introduce a phosphor with close-to-optimal luminescent properties. A problem for use in an LSC is the large scattering of this material; we will discuss possible solutions for this. Furthermore, we will discuss the use of broad-band cholesteric filters [2] in combination with this phosphor.

[1] D.K.G. de Boer, Proc. of SPIE Vol. 7725, 77250Q (2010).

[2] D.K.G. de Boer, C.-W. Lin, M.P. Giesbers, H.J. Cornelissen, M.G. Debije, P.P.C. Verbunt, and D.J. Broer, Appl. Phys. Lett. 98, 021111 (2011).

8108-13, Session 4

Efficient hybrid electric and thermal energy generation

X. Xia, A. Parfenov, T. Aye, M. Shih, T. Jansson, Physical Optics Corp. (United States)

Ideally, solar Photovoltaic (PV) panels should be efficient, lightweight, and more affordable to manufacture than they are today. Recently, power generation systems using Concentrated Solar Thermal (CST) energy have demonstrated conversion efficiency levels over 30% under optimal conditions. Multi-junction Concentrated Solar Photovoltaics (CSP) have demonstrated conversion efficiencies over 40%. In this paper, we demonstrate a novel hybrid electrical and thermal energy cogeneration system for combined solar photovoltaic electricity and heat conversion with much higher efficiency (reaching over 50%), at reduced overall weight and size compared with current solar power systems. The new system is based on highly efficient photovoltaic solar panels and tubular water thermal receivers, incorporating POC's proprietary holographic spectral beam light guide concentrators resulting in a more cost-effective solution. The holographic concentrator consists of a dual-film broadband holographic optical element device, so that the first hologram collects energy in the visible part of the spectrum (400-680 nm) for electricity generation via thin strips PV, and the second hologram collects infrared (680-2000 nm) radiation to cogenerate heat using tubular thermal receivers. The holographic structure is angularly, spectrally, and spatially multiplexed to accept incoming light from a range of incidence angles so that it can be mounted at an optimized angle tilted to south at latitude-15 degrees in a nontracking configuration, collecting both direct and diffuse light. Details of fabrication and experimental testing results will be presented.

8108-14, Session 4

Novel luminescent solar concentrators (LSCs) enabled by large-area microoptical sheets

P. H. Schmaelzle, Palo Alto Research Center, Inc. (United States)

Luminescent Solar Concentrators have not yet found broad commercial adoption despite their unique ability to concentrate direct and (!) diffuse light without any tracking.

A major impediment --besides fading lifetime and efficiency challenges-- originates from the dimensional coupling between the lightguide slab's thickness and the width of the receiving photovoltaic (PV) cells. While embodied energy and materials cost considerations mandate to minimize slab thickness, we explain how a thin slab requires the outcouplers to be small (in at least one dimension). If the consequently large number of outcouplers are conventionally realized as PV cells directly attached to the lightguide, then assembly cost, yield and efficiency issues of small cells become limiting. This leads to severe design compromises and prevents ultra-lowcost LSCs.

Instead, we propose a novel architecture using microoptical outcouplers as an intermediary between the lightguide and the receiving PV cells. The microoptical elements we have designed are on the 100um scale, finely spaced in arrays and partially collimate the light which they tap out. Film replicated sheets comprising large arrays of elements are simply laminated onto a luminescent slab and direct light to a few external, conveniently large PV cells.

We will discuss our designs based on raytracing studies and use Markov-chain models to predict efficiency. We will review the constraints which were observed to ensure processability with existing industrial roll-to-roll equipment for fabless manufacturability on a square-kilometer (photonic GW) scale.

Conference 8109: Solar Hydrogen and Nanotechnology VI

Tuesday-Thursday 23-25 August 2011 • Part of Proceedings of SPIE Vol. 8109 Solar Hydrogen and Nanotechnology VI

8109-01, Session 1

Charge photogeneration in nanostructured photoelectrodes for water oxidation

J. R. Durrant, Imperial College London (United Kingdom)

My lecture will focus upon the charge separation and recombination in photoelectrodes for solar water photolysis. I will focus upon dynamics in nanocrystalline TiO₂ (1) and Fe₂O₃ (2) electrodes - but also consider dye sensitized and catalyst functionalised electrodes. My talk will discuss address in particular the role of recombination dynamics in limiting photoelectrode performance, and how these dynamics can be modulated both by electrical bias and surface functionalisation.

(1) Tang J, Durrant JR, Klug DR, Mechanism of photocatalytic water splitting in TiO₂. Reaction of water with photoholes, importance of charge carrier dynamics, and evidence for four-hole chemistry., J Am Chem Soc, 2008, Vol:130, 13885-13891.

(2) Pendlebury SR, Barroso M, Cowan AJ, Sivula K, Tang J, Grätzel M, Klug D, Durrant JR Dynamics of photogenerated holes in nanocrystalline -Fe₂O₃ electrodes for water oxidation probed by transient absorption spectroscopy., Chem Commun, 2011, Vol:47, 716-718.

8109-02, Session 1

Interfacial charge separation and recombination dynamics in photocatalytic systems consisted of alpha-Fe₂O₃ and carbon-free water oxidation catalysts

T. T. Lian, Emory Univ. (United States)

Solar-driven photocatalytic water splitting ($\text{H}_2\text{O} + \text{h}\nu \rightarrow \text{H}_2 + \frac{1}{2} \text{O}_2$) is an attractive general approach to sustainable and environment-friendly energy. We have demonstrated that the carbon-free, stable and soluble polyoxometalate (POM) complexes, $[\{\text{Ru}_4\text{O}_4(\text{OH})_2(\text{H}_2\text{O})_4\}(\text{SiW}_{10}\text{O}_{36})_2]^{10-}$ (Ru₄-POM) and $[\text{Co}_4(\text{H}_2\text{O})_2(\text{PW}_9\text{O}_{34})_2]^{10-}$ (Co₄-POM), are highly effective homogeneous catalysts for light-driven water oxidation. To ultimately realize stable light-driven water splitting systems, we have successfully synthesized economic and robust photocatalytic anodes by grafting these POM catalysts onto nanoporous colored (narrow bandgap) iron oxide (hematite, -Fe₂O₃) films. The performance of these photocatalytic anodes was tested in a photoelectrochemical cell of water splitting. Co₄-POM significantly enhanced the photocurrent of the Fe₂O₃ photoanode. The catalyst was shown to be stable under water oxidation conditions as confirmed by ATR-FTIR spectroscopy. We have also carried out transient absorption studies of interfacial charge separation and recombination dynamics in these materials in an effort to determine factors limiting the efficiency of photo-driven water oxidation in this system. In this talk, we will report recent progress in the characterization and optimization of this hybrid photocatalytic water oxidation system.

8109-03, Session 1

Transient absorption study on photogenerated carrier dynamics in visible light responsive photocatalysts GaN:ZnO

A. Furube, National Institute of Advanced Industrial Science and Technology (Japan); K. Maeda, K. Domen, The Univ. of Tokyo (Japan)

Transient absorption of visible light responsive powder photocatalysts,

solid solution of GaN and ZnO (denoted as GaN:ZnO), and other related materials were measured by using femtosecond diffuse reflectance spectroscopy in order to evaluate the nature of photogenerated electrons and holes through spectral information in visible and near-infrared and kinetics from 100 fs to 1 ns. The GaN:ZnO is known to be one of successful photocatalysts which are able to split water into oxygen and hydrogen molecules under visible-light irradiation. Since photoexcitation generates electrons and holes in the conduction and valence bands, respectively, it is important to understand their trapping and recombination processes in details. Generally efficient and quick trapping and slow recombination of them are required to increase the chance of charge transfer of them to protons and water molecules. We have elucidated that the charge trapping was within time resolution (~200 fs) and recombination time was about 100 ps for 30% of carriers and much longer for 70%, clearly indicating that most of photogenerated carriers have long lifetime as we have previously reported for TiO₂, where no recombination was observed until 1 ns. Other photocatalysts with lower photocatalytic activity showed much shorter lifetimes. These results indicated that the long carrier lifetime in GaN:ZnO is one of the reasons for the efficient reactivity.

8109-04, Session 1

Solar hydrogen generation pathways investigated by static and transient x-ray absorption spectroscopy

L. X. Chen, Argonne National Lab. (United States) and Northwestern Univ. (United States)

Solar hydrogen generation, a process of splitting water, involves multiple step reactions using frequently multiple metal centered complexes. In spite of progress made in recent years, some reaction pathways are still unclear. The ambiguity arises from the identities of the catalyst intermediates along the reaction pathways. Using in-situ and pump-probe X-ray spectroscopy, we investigated different intermediate structures of photocatalysts used for solar hydrogen generation. In a di-iron complex mimicking the hydrogenase function, we carried out in-situ electrolysis combine with x-ray absorption spectroscopy where we identified two different intermediates with significant structural change from the starting materials. The intermediate structure provides an explanation about proton binding and then hydrogen generation. In a solar energy storage material of a di-ruthenium complex, the structural analysis from the results of pump-probe x-ray transient absorption (XTA) spectroscopy identified an intermediate that has severe distortion from what was perceived, suggesting new reaction pathways. These results suggest that static and pump-probe x-ray absorption spectroscopy is one of the ideal methods to clearly identify the structural details of the photocatalysts during the reactions. These studies will significantly help in catalyst design and reaction control.

This research is supported by the ANSER Center, an Energy Frontier Research Center funded by the U.S. Department of Energy, Office of Science, Office of Basic Energy Sciences, under Award Number DE-SC0001059, and the Division of Chemical Sciences, Office of Basic Energy Sciences, the U. S. Department of Energy under contract DE-AC02-06CH11357. Work at the Advanced Photon Source was supported by the U. S. Department of Energy, Office of Science, Office of Basic Energy Sciences, under Contract No. DE-AC02-06CH11357.

8109-05, Session 2

Excited state dynamics in nanoscale materials for solar energy harvesting

O. V. Prezhdo, Univ. of Rochester (United States)

Conference 8109:
Solar Hydrogen and Nanotechnology VI

Solar energy applications require understanding of dynamical response of novel materials on nanometer scale. Our state-of-the-art non-adiabatic molecular dynamics techniques, implemented within time-dependent density functional theory, allow us to model such response at the atomistic level and in real time. The talk will focus on exciton generation, relaxation and fission in semiconductor quantum dots (QDs) and photoinitiated charge transfer at molecule/bulk interfaces.

QDs are quasi-zero dimensional structures with a unique combination of molecular and bulk properties. They exhibit new physical phenomena, including phonon bottleneck and multiple exciton generation, with the potential to increase solar cell efficiency. Photoinduced charge separation across molecular/bulk interfaces drives dye-sensitized semiconductor solar cells. It creates many challenges due to stark differences between molecular and periodic systems.

Our simulations provide a unifying description of quantum dynamics on nanometer scale, resolve highly debated issues, and generate theoretical guidelines for development of novel systems for energy harvesting and storage.

1. O. V. Prezhdo "Photoinduced dynamics in semiconductor quantum-dots: insights from time-domain ab initio studies", *Acc. Chem. Res.*, 42, 2005 (2009).
2. O. V. Prezhdo, W. R. Duncan, V. V. Prezhdo, "Dynamics of the photoexcited electron at the chromophore-semiconductor interface", *Acc. Chem. Res.*, 41, 339 (2008).

8109-06, Session 2

First principle calculation of the effects of doping on Sulfur-doped TiO₂

S. Arab, R. Lake, Univ. of California, Riverside (United States)

TiO₂ has proven to be one of the most stable photocatalytic materials for solar-hydrogen cells, but it has a wide band gap, absorbing in the UV and limiting its performance in the visible spectrum. We aim to design doped material that will enable highly-efficient production of hydrogen via electrolysis of water using the visible solar spectrum. In order to have an efficient solar-hydrogen cell, the electrode should have a band gap that falls within the visible solar spectrum while maintaining the potential for redox couples of water (1.23 eV). In pursuit of a reduced band gap material we focused on S-doped TiO₂ in both the anatase and rutile phases. This study is based on Density Functional Theory (DFT) using Perdew Burke Ernzerhof (PBE) pseudopotentials which were implemented in Vienna ab initio simulator (VASP). Optoelectronic and molecular dynamic properties of doped supercells consisting of 24 and 48 atoms in rutile and anatase phases were calculated, and analyzed. The band gap reduction effect of sulfur doping as a function of dopant concentration is investigated, most stable substitution sites for sulfur are predicted based on theoretical calculation and electronic transport properties of the S-doped TiO₂ are analyzed. Based on the previous experimental results and the theoretical calculations in this presentation we claim that S-doping is a promising and experimentally feasible approach for photocatalytic improvements of TiO₂.

8109-07, Session 2

Derivative coupling constants and their relation to excited state dynamics in dye-sensitized solar cell applications

K. Yamashita, The Univ. of Tokyo (Japan)

Recombination in dye-sensitized solar cells with direct injection is cast as internal conversion in the dye-Ti(OH)₂ complex. For catechol-thiophene dyes with 1, 2, or 3 thiophene units, the complex reproduces the previously observed dye-to-semiconductor bands. Based on ab initio calculations, we compare the decomposition of the internal conversion rate by vibrational mode and predict a trend in recombination with the extension of conjugation, which offers an explanation for the trend in

DSSC efficiency. We employ a simple model for the vibrational factors and show that they are only important in the presence of vibrational modes with low frequencies ($\leq kT$) and strong electronic factors. We also analyze derivative coupling constants in dyes NK1 (2E,4E-2-cyano-5-(4-dimethylaminophenyl) penta-2,4-dienoic acid) and NK7 (2E,4E-2-cyano-5-(4-diphenylaminophenyl) penta-2,4-dienoic acid) and relate them to the different dynamics that was observed for these dyes on TiO₂. We compute vibronic coupling constants in the excited and cationic states obtained by the ionization of the excited state as well as the electronic part of the internal conversion rate. We discuss that derivative coupling analysis connects molecular structure to excited state dynamics and explains the slower injection from NK7 into TiO₂. The analysis suggests this is not due to low-frequency motions of the benzene moieties in NK7.

8109-08, Session 2

Electronic structure study of nanostructured Co₃O₄ in artificial photosynthesis

J. Guo, Lawrence Berkeley National Lab. (United States); J. Chen, Lawrence Berkeley National Lab. (United States) and Tamkang Univ. (Taiwan); P. Glans, Lawrence Berkeley National Lab. (United States); W. Wang, Lawrence Berkeley National Lab. (United States) and Tamkang Univ. (Taiwan); F. Jiao, Lawrence Berkeley National Lab. (United States); C. Chang, Tamkang Univ. (Taiwan); H. M. Frei, Lawrence Berkeley National Lab. (United States)

Solar energy can be converted to chemical fuels for energy use and storage. However, the cost and conversion efficiency have been the biggest challenge for potential use of solar energy. There are the emerging technologies of using semiconductors for light harvesting assemblies. The ability to control the particle size, morphology of nanoparticles and the arrangement of atoms along the surface of nanostructured material will determine most of its physical properties.

In general, electronic structure ultimately determines the properties of matter. Soft x-ray absorption spectroscopy (XAS) and emission spectroscopy (XES) have some basic features that are important to consider. X-ray is originating from an electronic transition between a localized core state and a valence state. As a core state is involved, elemental selectivity is obtained because the core levels of different elements are well separated in energy, meaning that the involvement of the inner level makes this probe localized to one specific atomic site around which the electronic structure is reflected as a partial density-of-states contribution. The participation of valence electrons gives the method chemical state sensitivity and further, the dipole nature of the transitions gives particular symmetry information.

The high-resolution selectively excitation has opened a new field of study by disclosing many new possibilities of soft x-ray resonant inelastic scattering (RIXS). In this presentation, we show recent findings regarding XAS, XES, and RIXS studies of shows the charge transfer peak in Co₃O₄ nanoclusters grown in silica nanopores that act as efficient and robust catalysts for water oxidation.

8109-09, Session 3

Immobilization of stable, tunable, fast catalysts for solar-driven water oxidation

C. L. Hill, Emory Univ. (United States)

In both natural and artificial photosynthesis, dioxygen is the unavoidable by-product. The oxygen evolving center (OEC) in photosynthesis and technologically useful water oxidation catalysts (WOCs) alike must be fast and selective, but unlike the OEC, technologically viable WOCs must also be extremely stable.

Our team has developed oxidatively, hydrolytically and thermally stable WOCs based on polyoxometalate (POM) ligands. This new class of WOCs combine the stability and cost advantages of heterogeneous

Conference 8109:
Solar Hydrogen and Nanotechnology VI

catalysts with the many advantages of homogeneous catalysts. Thus far, we have developed 6 POM WOCs, including $[\{\text{Ru}4\text{O}_4(\text{OH})_2(\text{H}_2\text{O})_4\}(\gamma\text{-SiW}_{10}\text{O}_{36})_2]_{10-}$ (Ru4) and $[\text{Co}_4(\text{H}_2\text{O})_2(\text{PW}_9\text{O}_{34})_2]_{10-}$ (Co4) and characterized their structural, spectroscopic and redox properties using a range of physical methods. They are the fastest soluble WOCs to date for water oxidation in both the dark ($[\text{Ru}(\text{bpy})_3]^{3+}$ oxidant) and light (S2O8²⁻ oxidant with $[\text{Ru}(\text{bpy})_3]^{2+}$ as photosensitizer).

These WOCs can be immobilized on photoanodes and other surfaces by several approaches. The immobilized POM WOCs, like those in solution, exhibit encouraging O₂ yields (or photocurrents) and quantum yields.

Acknowledgment: We thank the DOE BES for support.

8109-10, Session 3

A two-step photoexcitation system for photocatalytic water splitting into hydrogen and oxygen under visible light irradiation

R. Abe, Hokkaido Univ. (Japan)

Photocatalytic water splitting into H₂ and O₂ using a semiconductor photocatalyst has received much attention recently due to the potential of this method for the clean production of H₂ from water utilizing solar energy. Although a number of metal oxides have been reported to be active photocatalysts for the water-splitting reaction, most only function under ultraviolet (UV) light owing to the large band gap energy of the materials. Because almost half of all incident solar energy at the Earth's surface falls in the visible region, the efficient utilization of visible light remains indispensable for realizing practical H₂ production based on photocatalytic water splitting. We have recently developed a new type of photocatalytic water splitting system, mimicking the mechanism of photosynthesis in green plants. This system reduces the energy required to drive each photocatalysis process, allowing visible light to be utilized more efficiently than in conventional water splitting system. We have achieved overall water splitting using various visible light responsive photocatalysts, such as SrTiO₃ doped with Cr, tantum oxynitrides (TaON or BaTaO₂N), and organic dyes, which work as a H₂ evolution photocatalyst, combined with tungsten oxide (WO₃) for O₂ evolution in the presence of a shuttle redox mediator such as iodate/iodide (IO₃⁻/I⁻). The use of BaTaO₂N or coumarin organic dye was demonstrating to be photoactive at wavelength up to ca. 700 nm. These results demonstrate the potential of a two-step water-splitting system for utilizing a broader band of visible spectrum.

8109-12, Session 4

Nanonet-based heteronanostructures for solar water splitting

D. Wang, Boston College (United States)

We present our recent results on using a heteronanostructure design to solve a key challenge in semiconductor-based solar water splitting - the charge diffusion distances within oxide semiconductors (e.g., Fe₂O₃) are generally too short. A key enabling factor of our design is the TiSi₂ nanonet, a unique two-dimensional nanomaterials that possess high conductivities and suitably high surface areas. By introducing TiSi₂ nanonets to the semiconductors, we obtain a dedicated charge transport pathway that also works as a structural support. The semiconductor absorbs light to generate photoelectrons and photoholes; the holes are scavenged by the solution to oxidize H₂O and to produce O₂ while the electrons are transported away by the nanonets to be used for H₂O reduction at the counter electrode. We found that the ability to effectively remove photoelectrons leads to improved charge separation and hence higher solar water splitting efficiencies. This design principle is significant because it makes it possible to alleviate the reliance on a material's intrinsic properties and allows for the measurement of high performance on materials with undesired electronic properties.

We demonstrate the nanonet-based design principle within the context of three transition metal oxides: TiO₂, WO₃ and Fe₂O₃. The results we

obtained on Fe₂O₃ is particularly significant because the short charge diffusion within Fe₂O₃ represents a challenge that has prevented the widespread usage of this otherwise appealing material. By having a material component dedicated to charge transport, we measured the highest external quantum efficiencies on intrinsic Fe₂O₃. Further improvement should be possible when doping of Fe₂O₃ and co-catalysts are applied.

8109-13, Session 4

Polyoxometalate-based solar cells for water splitting

L. Cronin, Univ. of Glasgow (United Kingdom)

Metal oxide based materials are all-pervasive in the modern world. Utilized in microchips, hard disks, displays, glass coatings, sun screen, chemical catalysts and superconductors it is hard to think of a modern technology that does not require metal oxides of one form or another. In almost all instances the metal oxide based materials are comprised of 'solid-state' infinite materials which require high temperature processing and can be difficult to modify systematically or to dope with 'molecular' additives.

In this talk I will describe routes to 'programmed' or designed assembly of complex metal-oxides under non-equilibrium conditions using molecular precursors. The use of non-equilibrium conditions will allow us to trap new types of catalytically and electronically active materials with radically new structures and morphologies via a Universal Building Block (UBB) approach. The UBB approach offers a rational methodology for the isolation of transient intermediate molecular metal oxide cluster anions and allows unprecedented design in the self-assembly processes from atoms to nano- and meso-scale materials.

Thus, I will describe how this research allows the development of radical new material design and assembly paradigms using non-equilibrium approaches, and the applications will be placed in context by describing two possible technology areas (1) Metal oxide coatings for photochromic and electrochromic devices including solar cells and (2) Heterogeneous metal oxide integrated devices for photo and electro-catalytic processes including water splitting.

8109-35, Session 4

Advantages of nanoporous 'black silicon' for photoelectrochemical water splitting

J. Oh, T. G. Deutsch, H. Yuan, H. M. Branz, National Renewable Energy Lab. (United States)

We report that a nanoporous 'black silicon' hydrogen-evolving photocathode provides a significant improvement in the rate of hydrogen production and reduces the overpotential required for the water-splitting half-reaction, compared to a planar Si photocathode.

Photoelectrochemical production of H₂ at a semiconductor/water interface has potential to convert solar energy directly to a clean and storable fuel. Together with an appropriate photoanode for O₂ evolution and/or an external bias, a p-type Si photocathode can produce H₂ from water. However, about 25% of incident solar photons reflect from the silicon-water interface and would not contribute to H₂ production. Anti-reflection (AR) coatings, such as quarter-wavelength films of SiN_x and indium tin oxide (ITO), are used to reduce the reflectance from solid-state photovoltaic devices. For H₂ production by water splitting, however, an interference-based AR coating can impede charge transfer from Si to the electrolyte interface and/or corrode in the electrolyte.

Our nanoporous Si forms a density-graded surface layer that suppresses reflectance in air to below 2 % over the entire solar spectrum, without any AR coating layer and has been used in 16.8%-efficient PV devices. [Yuan et al., Appl. Phys. Lett., vol. 94, 123501, 2009] The p-type nanoporous Si photocathode is fabricated in less than 3 minutes by a one-step metal-assisted liquid etch technique. Our photoelectrochemical water splitting measurement under simulated 1-sun, AM1.5G, illumination

Conference 8109:
Solar Hydrogen and Nanotechnology VI

shows that the light-limited photoreduction current density under reverse bias at the nanoporous Si photocathode increased about 20%, from 30 mA/cm² to 36 mA/cm², due primarily to enhanced photon absorption in the silicon. In addition, the overpotential to create H₂ was reduced by 70 to 200 mV, due to the large surface area for the reduction reaction. Finally, H₂ gas bubbles released efficiently from the nanoporous Si electrode surface, even without the surfactant required on planar Si.

This work was supported by the SISGR program of the U.S. Department of Energy, Office of Basic Energy Sciences, Division of Chemical Sciences, Biosciences, and Geosciences, under DOE Contract No. DE-AC36-08-GO28308.

8109-14, Session 5

Bio-inspired approaches to solar hydrogen production

D. Gust, T. A. Moore, A. L. Moore, Arizona State Univ. (United States)

Fossil fuels represent solar energy captured and stored in fuel by photosynthetic organisms. Thus, photosynthesis can serve as inspiration for the design of artificial photosynthetic systems for production of hydrogen or other fuels. Photosynthetic antennas collect sunlight, transport excitation energy to reaction centers, and perform regulatory and photoprotective functions. Reaction centers are molecular-scale photovoltaics that convert excitation energy into electrochemical energy in the form of redox potential. Biological catalysts use the oxidation potential of reaction centers to oxidize water. The reduction potential of the reaction centers is used by other catalysts to produce fuels. Living organisms have developed catalysts for production of carbohydrate fuels, precursors of biodiesel, hydrogen gas, and other fuels.

Following the photosynthetic paradigm, it is possible to design and construct artificial antennas that efficiently harvest light throughout the visible spectral region, transfer the excitation to artificial reaction centers, and regulate the artificial photosynthetic process. Artificial reaction centers use excitation energy from the antennas to carry out photoinduced electron transfer reactions that store a large fraction of the photon energy as redox potential. Catalysts based on natural proteins that use earth-abundant elements to oxidize water and to produce hydrogen are being developed and functionally interfaced to reaction centers. Several examples of progress towards hydrogen production by artificial photosynthesis will be discussed.

8109-15, Session 5

How nature harnesses quantum mechanics for light harvesting in photosynthesis: what we can learn from it

J. Koehler, Univ. of Bayreuth (Germany)

Currently there is an enormous interest to develop new strategies for light-harvesting and solar energy conversion based on organic matter. Important issues that have to be considered in order to optimise the energy- and charge transfer properties of the supramolecular building blocks without loss in efficiency concern the character of the donor-acceptor materials, their chemical nature, their mutual arrangement (distance and orientation), their electronic couplings, their reorganisation energies, the influence of the surrounding matrix and the hierarchical organisation of individual components. By the evolution of photosynthesis, nature has proven that organic matter can be successfully exploited for this purpose on large scales. In this regard, the nanomachinery of photosynthetic purple bacteria has served as a cornerstone to elucidate the key principles of biophysics, biochemistry, and molecular biology that are at the basis of photosynthesis. This presentation provides an overview of the basic quantum mechanical principles that are exploited in the light-harvesting apparatus found in purple bacteria and discusses possible implications for novel manmade devices.

8109-16, Session 5

Light-induced charge accumulation in molecular systems

A. Harriman, A. C. Benniston, Newcastle Univ. (United Kingdom); F. Odobel, Univ. de Nantes (France)

The design of effective molecular systems capable of the sustained generation of solar fuels is a non-trivial operation and has yet to be realized at any level. The most promising systems have been built around a finely balanced cocktail of reagents, usually involving an enzyme-based catalyst, that quickly moves from the optimised position. In seeking to overcome this challenge, two critical problems can be identified. First, photo-induced electron transfer is an inherently one-electron process, unlike multi-electron fuel production, and second the excited state is quenched very effectively by radical species. This latter feature, whereby an excited reacts with an electron stored momentarily on the catalytic site before discharge, can be used to drive unusual electron-transfer reactions but not in a cyclic manner. The most logical solution, based on bio-inspired molecular chemistry, demands the synthesis of novel arrays of tailored co-factors able to form a one-directional electronic conduit. This approach uses several chromophores to push electrons along a short molecular wire under visible light illumination until trapped at the catalyst. Discharge of the catalyst via fuel generation has to be faster than reverse electron transfer along the wire but not so fast that charge accumulation is by-passed. The key feature becomes the arrangement and selection of the co-factors.

Several molecular arrays have been built that offer promise along the above lines. Each system is capable of directing electrons along a pathway in a one-directional manner. The mechanism, and rates of individual steps, can be probed by laser flash photolysis and used to optimise the system.

8109-17, Session 6

All-inorganic polynuclear assemblies for artificial photosynthesis

H. M. Frei, Lawrence Berkeley National Lab. (United States)

An artificial photosynthetic system for the conversion of carbon dioxide and water to liquid transportation fuel requires the arrangement and coupling of light absorption, charge separation and catalytic units in a nanostructured membrane. The function of the membrane is to provide a physical barrier for separating evolving fuel and oxygen molecules, thereby minimizing back reaction. With the goal of combining the advantages of molecular components with the robustness of inorganic matter, we have developed well defined inorganic polynuclear units for visible light water oxidation and carbon dioxide reduction in inert nanoporous silica scaffolds. The chromophore is an all-inorganic oxo-bridged binuclear unit such as ZrOMn(II) or TiOCr(III) covalently anchored on the silica nanopore surface. These chromophores, which have unusually long excited state lifetimes of microseconds under ambient conditions, act as photon-driven electron pumps. When coupled to oxygen evolving catalysts such as iridium oxide nanoclusters inside the nanopores, efficient oxidation of water is achieved under visible light in neutral aqueous solution. Structural characterization of the units is based on vibrational, EPR, and X-ray spectroscopic analysis, while transient Fourier-transform-infrared and time resolved optical spectroscopy provide dynamic and mechanistic insights into the functioning of the photocatalysts. The molecular nature of the chromophore allows for the precise tuning of the redox properties of the donor and acceptor center by selecting appropriate metals and oxidation states. Such control is the key for optimizing thermodynamic efficiency and directional charge flow within the artificial photosynthetic system. Focusing on Earth abundant materials for reasons of scalability, we have developed cobalt oxide and manganese oxide nanostructured catalysts on mesoporous silica supports that evolve oxygen from water at high rates. The clusters have sufficiently high catalytic activity for developing integrated systems that are able to keep up with the photon flux at high solar intensity. Coupling of the photocatalytic units across nanoscale silica walls with embedded

Conference 8109:
Solar Hydrogen and Nanotechnology VI

rectifying molecular wires for assuring directional charge flow and separation of evolving oxygen from the reductive catalysis is in progress.

8109-18, Session 6

Supramolecular photocatalysts for CO₂ reduction and hydrogen evolution

O. Ishitani, Tokyo Institute of Technology (Japan)

Both the problems of the global warming and shortage of the fossil fuels have brought about great interest in both photochemical utilization of CO₂ and hydrogen evolution with solar energy. Efficient and visible-light driven photocatalysts must be necessary for development of such an important technology. We have synthesized supramolecular photocatalysts constructed by connecting [Ru(diimine)₃]²⁺ type photosensitizer and catalyst, which is a Re(I) or Ru(II) complex for CO₂ reduction and a Rh(II) complex for hydrogen evolution, with an alkyl chain. These new photocatalytic systems are driven by visible-light irradiation with high efficiency, high durability, and high turnover frequency. The architecture of such photocatalytic systems will be discussed in the presentation.

[References] Takeda, H.; Ishitani, O., *Coord. Chem. Rev.* 2010, 254, 346-354.

8109-19, Session 6

Hydrogen production from ethanol: surface science and catalysis study

H. Idriss, Univ. of Aberdeen (United Kingdom)

Solar hydrogen production from renewables such ethanol and water is one of the promising methods for fuel generation either for direct combustion or to power fuel cells. The presentation will focus on the photoreactions of ethanol over rutile TiO₂ single crystal and Au/TiO₂ anatase and rutile catalysts. On rutile TiO₂ (110) single crystal we focus on the first step of the reaction: ethanol dehydrogenation to acetaldehyde while on Au/TiO₂ the focus is on the effect of both particle size of the support (TiO₂) and Au on the production of hydrogen from ethanol. In addition the possible synergetic effect between the two main phases of TiO₂ (anatase and rutile) on the production of ethanol is also studied.

8109-20, Session 6

A light-assisted biomass fuel cell for renewable electricity generation

F. E. Osterloh, R. L. Chamousis, Univ. of California, Davis (United States)

Approximately \$25 Billion are spent annually in the US for the treatment of municipal waste water (sewage). This talk describes a photoelectrochemical device that converts organic waste components into H₂O and CO₂ while generating electrical energy. The device consists of a two-compartment cell that is separated by a proton conducting membrane. In one half cell compartment, a platinum-air electrode catalyzes the reduction of oxygen into water, while the other half cell contains a TiO₂ photoelectrode in contact with the waste water. To demonstrate the function of the device, electrochemical and photoelectrochemical measurements on aqueous solutions of glucose were conducted at variable pH. The onset potentials for glucose oxidation and IPCE values recorded at various wavelengths provide an estimate of the efficiency of the device.

8109-21, Session 7

Ultrafast studies of charge carrier dynamics in nanomaterials and relevance to solar energy conversion

J. Z. Zhang, Univ. of California, Santa Cruz (United States)

Nanomaterials possess novel optical and electronic properties promising for solar energy conversion into electricity or chemical fuels such as hydrogen. In particular, metal oxide (MO) nanomaterials are attractive due to their high stability and low cost. Their typically large bandgap requires sensitization for visible light absorption. Strategies include dye or quantum dot sensitization, doping, or bandgap off-setting using composite structures. Charge carrier dynamics in these nanostructures play a critical role in their performance for light energy conversion. A better fundamental understanding of processes such as charge generation, separation, recombination, trapping, transfer, and transport will significantly aid the design of new nanostructures for various applications including solar energy conversion. In this presentation, we will review our recent efforts on using ultrafast laser techniques to probe charge carrier dynamics in a number of MO systems, including TiO₂, WO₃, and Fe₂O₃ nanoparticles and nanorods, to demonstrate the important correlation between charge carrier properties and structural characteristics of the nanomaterials.

8109-22, Session 7

Photo-induced electron transfer reactions at semiconductor quantum dot interfaces

Y. Tachibana, RMIT Univ. (Australia)

Solar fuel has recently received significant interests as an alternative to fossil fuel. Solar water splitting is an ultimate system to generate hydrogen and oxygen from water using sun light. Photoelectrochemical process is believed to be one of the most attractive systems for the water splitting reaction, and such reactions at TiO₂ surface were first reported by Fujishima and Honda in 1972. However, unfortunately, the efficiency in this system has remained low.

Photoelectrochemical water splitting occurs through electron transfer reactions at material interfaces and catalytic reactions at material surface, following light absorption. Interfacial nanomaterial structural design in addition to material selection is vital to enhance both electron transfer and catalytic efficiency. Semiconductor quantum dot (QD) is an attractive nanomaterial to architect this type of system. By employing the most characteristic property known as "quantum size effect", the potential energy levels of QD conduction and valence bands can be adjusted with the QD size. Thus, the light absorption onset can be tuned by adjusting the QD size. In contrast, fundamental understanding for the factors controlling the electron transfer reactions at the QD interfaces is still limited. In this presentation, we attempt to elucidate relationship of the QD nanostructures with the interfacial electron transfer rates and efficiency.

This work was financially supported by JST PRESTO program, Japan, and TEPCO Research Foundation, Japan. The Venture Business Laboratory, Osaka University is also acknowledged for the financial support.

8109-23, Session 7

Charge separation and recombination processes in bare and dye-sensitized nanocrystalline TiO₂ films

R. Katoh, National Institute of Advanced Industrial Science and Technology (Japan)

TiO₂ have been attracting much interest because they can be applied

Conference 8109:
Solar Hydrogen and Nanotechnology VI

to water splitting, degradation of environmental pollutants, solar energy conversion and so on. We have so far studied primary process in bare and dye-sensitized TiO₂ by using wide-wavelength-range (400-2500 nm), highly sensitive transient absorption (TA) spectroscopy and time-resolved microwave conductivity (TRMC) technique. Following subjects will be presented.

Assignment of active species in bare-TiO₂

We have studied optical absorption spectra of nanocrystalline TiO₂ films through TA spectroscopy. Three active species, trapped hole and electron, and conducting electron in the spectra can be identified in the spectra. This assignment is very useful to study charge recombination and primary reactions.

Temperature dependence of recombination rate

We observed slow recombination kinetics in nanocrystalline TiO₂ films, which occurred within microsecond time region. Recently, we have measured temperature dependence of TA and TRMC signals in bare and dye-sensitized nanocrystalline TiO₂ films. Small temperature dependence was observed for bare-films, suggesting that tunneling-type recombination occurs effectively.

Sub-ns dynamics of electron injection from excited dyes into TiO₂ nanoparticles

From absorbance of TA signal of both dye-cation and injected electron, efficiency of electron injection can be evaluated. TRMC is also useful technique because only conducting electrons can be detected. Using these techniques, we have studied the efficiency of electron injection under various conditions. Recently, we developed new TA spectrometer with sub-ns time resolution to observe slow injection dynamics from triplet state. The results suggest that the efficiency is controlled by ultrafast charge recombination.

8109-24, Session 8

Solar hydrogen production with disorder-engineered titanium dioxide nanocrystals

S. S. Mao, Lawrence Berkeley National Lab. (United States)

This presentation will provide an overview of recent progress in the development of disorder-engineered titanium dioxide nanocrystals as applied to solar-driven hydrogen production from water. Starting with a brief introduction of the literature on titanium dioxide modification aimed to increase solar absorption, the concept of disorder engineering will be introduced along with the electronic band structure resulted from disorder incorporation. Synthesis of disorder-engineered titanium dioxide nanocrystals will be presented, as well as measurements of their structural, electronic, and optical properties. Photocatalysis experiments based on solar-driven degradation of organic compounds in water will be discussed, followed by detailed measurements of hydrogen production using disorder-engineered titanium dioxide nanocrystals that can absorb solar energy in both visible and infrared wavelength regions. The talk will end with a brief discussion of the perspective of solar hydrogen production based on disorder-engineered nanocrystal photocatalysts.

8109-25, Session 8

Bio-inspired co-catalysts bonded to a silicon photocathode for solar hydrogen evolution

I. Chorkendorff, Technical Univ. of Denmark (Denmark)

A selection of incomplete cubane-like clusters (Mo₃S₄) and complete cubanes like (Mo₃X₃S₄) where X is a transition metal have been shown capable of efficiently catalyze the evolution of hydrogen as a cathode. It has been tested both on planar hydrogen-terminated p-type Si semiconductor and on Si pillars with high aspect ratios using a photolithographic method in order to further improve the photo-electrochemical by orthogonalize the light capture and charge-carrier collection in the photoelectrode. The samples have been illuminated with a simulated red part of the solar spectrum i.e. long wavelength (> 620 nm) part

of simulated AM 1.5G radiation. The current densities at the reversible potential match the requirement of a photo-electrochemical hydrogen production system with a solar-to-hydrogen efficiency in excess of 10%. Assuming that the coverage of Mo₃S₄ clusters present on the pillar surface during operation is similar to that measured on the planar surface (the accurate working coverage on the pillared structure could not be measured by XPS), the calculated TOF of hydrogen evolution is 65 sec⁻¹ for the Mo₃S₄ modified Si pillars. Of course, the TOF is quite dependent on the light intensity. With an increase in light intensity, the photocurrent increases. The system is known to be susceptible to oxygen and the stability of the system will be discussed. The experimental observations are supported by DFT calculations of the Mo₃S₄ cluster adsorbed on the hydrogen-terminated Si(100) surface providing insights into the nature of the active site.

8109-26, Session 8

New layered semiconductors for efficient photoelectrochemical hydrogen generation

L. Wang, The Univ. of Queensland (Australia)

The increasing concerns over climate change and exhausting fossil fuels have seen great efforts being directed toward the development of new energy generation /conversion systems. Innovative materials for energy conversion hold the key for renewable energy production. The ability to design these nanomaterials with tailored structures and functionalised properties is an important challenge that researchers strive to meet. Aimed at developing new nanostructures for efficient photocatalytic and electrochemical energy conversion, we have recently advanced the design, band-gap and structural modifications of several types of transition metal oxides including layered titanate, clays, tantalates and niobate-based perovskites.¹⁻³ The exfoliation of these layered structures led to the formation of colloidal suspensions containing exfoliated nanosheets. These unique nanosheets can be structural modified into ideal two-dimensional building blocks for new nano-architecture fabrication. The self-assembly and flocculation of nanosheets led to multilayer ultrathin films and restacked nanoporous structures, which exhibited excellent visible light photocatalytic and electrochemical performances.

References:

1. Reviews in a) G. Liu, LZ Wang, HG Yang, HM Cheng, GQ Lu, J. Mater. Chem., 2010, 20,831. b) W. Zhang, L. Zou, L.Z Wang, Applied Catalysis A: General, 371 (2009) 1-9.

8109-27, Session 9

Low cost quantum-confined metal oxide heteronanostructures for direct solar water splitting

L. Vayssieres, National Institute for Materials Science (Japan)

Changing the fundamental physics and chemistry of materials to overcome their theoretical bulk limitations has become a crucial challenge for scientists to improve the efficiency and capability of existing materials to create a new generation of multifunctional and more efficient devices. R&D exploiting chemical nanoscience and nanotechnology has the greatest potential to efficiently contribute to such challenging goals. Indeed, the creation of new materials with higher performance and improved stability achieved by atomic and molecular design and control using unique nanoscale phenomena such as quantum confinements is the key to succeed.

Our strategy to contribute to these drastic requirements is the ability to design clean metal oxide semiconductor based on vertically oriented anisotropic (hetero)nanostructures with quantized band structure such as quantum rods and dots to enable high absorption in the visible range as well as bandgap and band edges engineering by size dependent confinement effects. Such unique characteristics, combined with in-depth investigation and modeling of their electronic structure and large

Conference 8109:
Solar Hydrogen and Nanotechnology VI

scale and low cost fabrication methods provide a substantial advance and (r)evolutionary prospect in the field of materials for sustainable development.

Such ideas will be illustrated and demonstrated on the modeling, design and low cost fabrication of metal oxide quantum dots and quantum rods-based large band semiconductor structures, arrays and devices, the in-depth characterization of their size dependent electronic structure performed at synchrotron radiation facilities and their applications for visible light-active semiconductors for direct solar hydrogen generation.

8109-28, Session 9

Titania-based nano-photocatalysts with solar energy applications

S. E. Hnyadi Murph, Savannah River National Lab. (United States)

Energy is the vital force powering every aspect of our society from business, manufacturing, transportation of products, and services to serve the people and worlds economies. Nanotechnology has introduced new concepts for innovative technology applications in energy research, such as solar energy harvesting, storage and conversion, hydrogen production and storage, conversion and use of energy.

Titania has been considered the most appropriate candidate for photocatalytic processes due to its powerful oxidation capability, superior charge transport, and corrosion resistance. Despite these attributes, the efficiency of TiO₂ for photovoltaic and photocatalytic applications is severely limited by its large bandgap (~3.2 eV) and rapid charge carrier recombination dynamics which means that anatase titania can use less than 1% of the solar spectrum. However, Au, Ag and Pt nanoparticles and CdS quantum dots can be utilized to sensitize TiO₂ and extend its photo-response to the visible region of the solar spectrum. Gold and silver strongly absorb and scatter light in the visible region of the electromagnetic (EM) spectrum and are tunable as a function of nanoparticle size, shape, and local environment. Additionally, by coupling TiO₂ with other oxides new nano-composite with enhanced photo-catalytic activity can be produced.

In this presentation we bring to light recent advances in our laboratory on synthesis, characterization, optical and physico-chemical properties of titania-based nano-materials with solar energy production applications. Nano-photocatalysts with various designs, geometries and compositions prepared by wet chemical synthesis approaches and electron-beam lithography will be described. We'll highlight work from the author's laboratory on photo-catalytic applications, using noble metallic nanoparticles (Au, Ag, Pt) and titania-based nanoparticles, including TiO₂ and TiO₂ coupled with various other oxides such as SiO₂, MnO_x, WO₃. The catalytic activity of these nano-photocatalysts under visible and UV-light demonstrates their potential use for solar energy applications.

8109-29, Session 9

Laser ablation to fabricate high-efficiency photo anodes

R. Ghosh, M. K. Brennaman, R. Lopez, The Univ. of North Carolina at Chapel Hill (United States)

A significant challenge for dye-sensitized photo-electrochemical synthesis cells (DS-PECs) is to either oxidize H₂O for H₂ production or to simultaneously split H₂O and reduce CO₂ with visible light without application of an external voltage bias. Our efforts are focused on the metal oxide semiconductor material of the photoanode: TiO₂ for reference, and Nb₂O₅ or Sr₂TiO₃ due to their suitable conduction band energies for both H₂ production and artificial photosynthesis. We have used pulsed laser deposition (PLD) to coat the surface of an optically transparent electrode (Fluorine-doped Tin Oxide glass) with a mesoporous network of vertically aligned metal oxide (TiO₂, Nb₂O₅ or Sr₂TiO₃) bundles which are formed only by controlling oxygen background pressure during deposition, film thickness, and annealing

conditions. As a first step in characterizing the overall performance of these nanostructured metal oxides, dye-coated electrodes were used as photoanodes in a DSSC configuration. PLD-TiO₂ DSSC IPCE values are comparable to 3x thicker sol-gel films and nearly 92% APCE values have been observed using optimized PLD-TiO₂ structures. UV-Vis studies show that there is a factor of 1.4 enhancement of surface area for PLD-TiO₂ photoanodes compared to the best sol-gel films. Taken together, these data show that our PLD-synthesized metal oxide nanostructure simultaneously optimizes both charge transport properties and surface area for facile dye loading. The chemical states, crystallinity, film structure, and optical constants of these films have been characterized using X-ray photo-electron spectroscopy (XPS), Raman spectroscopy, scanning electron microscopy (SEM) and ellipsometry.

8109-30, Session 10

Efficient synthesis of complex oxide-metal particle electrodes

G. Westin, Uppsala Univ. (Sweden)

Utilisation of photo-catalysts for solar energy harvesting, weather through production of fuels or electricity requires versatile and cost efficient synthesis routes capable of producing complex functional nano-materials. The wide spectrum of solution based processes probably provide the most important routes for this purpose, but the complexity and diversity of the reactions taking the precursor molecules in solution to gels or nano-particles and their further processing into ceramic purpose designed structures require much understanding. Therefore knowledge about the entire route from precursor to target oxide is needed to produce well controlled high quality materials and make choices of suitable techniques. The synthesis of complex materials systems will be described with an emphasis on the addition of metal nano-particle co-catalysts to doped and non doped oxide semi-conductors such as; TiO₂, ZnO and WO₃. The processes were studied by a wide array of techniques including; TGA, DSC/DTA, SEM, TEM, XRD, XAS, IR-, Raman and UV-Vis-NIR spectroscopy. The photo-catalytic properties of the prepared materials will be described.

8109-31, Session 10

Synthesis and characterization of titanium doped iron oxide for photoelectrochemical water splitting

H. W. Tang, National Renewable Energy Lab. (United States) and Univ. of Denver (United States); M. A. Matin, Univ. of Denver (United States); Y. Yan, M. M. Al-Jassim, J. A. Turner, National Renewable Energy Lab. (United States)

Iron Oxide is a potential candidate for hydrogen production by photoelectrochemical decomposition of water due to its good band gap and excellent chemical stability. However, its poor conductivity limits its PEC performance. 3d transition metals are predicted to be a good choice of dopants to improve the conductivity. In this paper, we report our synthesis of titanium doped iron oxide thin films by RF magnetron co-sputtering of iron oxide and titanium targets at various conditions. Our work shows that the structure and morphology of iron oxide can be modified by controlling the doping concentration of titanium. Moreover, our results show that the PEC performance of titanium doped iron oxide is better than the undoped films.

8109-32, Session 10

Surface nitridation of p-GaN/P2 for durable photoelectrochemical water splitting

H. Wang, T. G. Deutsch, J. A. Turner, National Renewable Energy

Conference 8109:
Solar Hydrogen and Nanotechnology VI

Lab. (United States)

High efficient III-V semiconductor materials have been successfully applied for photoelectrochemical (PEC) water splitting systems. Monolithic p-GaInP₂/n/p-GaAs PEC-PV tandem cell device demonstrated a 12.4% solar-to-hydrogen (STH) conversion efficiency [1], however the lifetime of the device was limited due to the stability issue in aqueous solution.

To extend the lifetime of the device, thin films of p-GaInP₂ were tested in different solutions (including 3M H₂SO₄ for comparison) at 1 sun for 24h, and different techniques were used to analyze the surfaces and the tested solutions. Samples tested in sulfuric acid experienced extensive corrosion and surface Ga was selectively dissolved. The surfaces and XPS depth profiles of samples tested in ammonium-bearing solutions were kept almost identical to that of an as-received one. SEM and EDX investigation also confirmed the significant reduced corrosion with samples tested in ammonium-bearing solutions. In other words, ammonium showed inhibitive effect for p-GaInP₂, which is very promising to meet US DOE's 2013 goal of 8% STH efficiency for 1000h duration.

efficiency by two times whereas Ru and Co decreased the efficiency as compared to undoped iron oxide. Detailed surface analyses (XPS, XRD, SEM, etc) were performed to investigate the role of dopants in affecting the PEC efficiencies.

8109-33, Session 10

Nanostructured phosphides as photoelectrode materials for artificial photosynthesis

S. Maldonado, Univ. of Michigan (United States)

In this presentation I describe our recent efforts to enhance and augment the photoresponse of gallium phosphide (GaP) for the purposes of designing a fuel-forming photoelectrochemical system. GaP is a potentially useful material in artificial photosynthetic systems but is hampered by short minority carrier diffusion lengths relative to visible light penetration depths. In this work, I will show data on several types of nanostructured n-type and p-type GaP photoelectrodes with thicknesses ranging from 0 - 45 microns. Solar-to-electrical energy conversion properties in regenerative and photosynthetic photoelectrochemical cells are reported. Larger short-circuit photocurrents, increased internal quantum yields at long wavelengths, and decreased open-circuit photovoltages were observed for photoelectrodes with optimal doping-morphology combinations. For these materials, the short-circuit photocurrents, open circuit photovoltages, and fill factors collectively resulted in more than an order of magnitude improvement in the photoelectrode efficiency as compared to single-crystalline planar GaP photoelectrodes. Additional data are shown on that explore alloying GaP, in conjunction with high aspect ratio nanostructured morphologies, as a means to produce more active solar energy conversion materials. The data thus comprehensively detail strategies for overcoming the carrier-collection limitation of GaP and related phosphides in solar energy conversion applications.

8109-34, Session 10

Metal-doped hematite nanocrystalline films for photoelectrochemical water oxidation

A. Bak, S. K. Choi, T. H. Jeon, H. Park, Kyungpook National Univ. (Korea, Republic of)

Solar-light driven water splitting has attracted great attention over the past decades yet the solar-to-fuel conversion efficiencies are still very low. The water oxidation has been studied in a photoelectrochemical (PEC) cell with various metal-doped iron oxide films synthesized by electrodeposition. Despite its proper energetics for water oxidation, the iron oxide has showed disappointingly low PEC efficiency due to small optical absorption coefficients in the visible light region, short carrier diffusion lengths, and rapid charge pair recombination. Attempt have been made to improve the PEC efficiency by synthesizing iron oxide films doped with more than 10 elements (Cr, Co, Ni, Ru, Pd, Ag, Cd, Ir, Pt, Au, Sn, etc). Experimental results indicated that Pt improved the PEC

Conference 8110: Thin Film Solar Technology III

Sunday-Monday 21-22 August 2011 • Part of Proceedings of SPIE Vol. 8110 Thin Film Solar Technology III

8110-01, Session 1

Progress and challenges in low-temperature, high-rate epitaxy for film silicon photovoltaics

C. W. Teplin, National Renewable Energy Lab. (United States)

Progress and challenges in low-temperature, high-rate epitaxy for film silicon photovoltaics

8110-02, Session 1

Microluminescence mapping of intragrain and grain boundary recombination in silicon film solar cells

M. J. Romero, National Renewable Energy Lab. (United States)

The expansion of the silicon production capacity will drive down the price of the feedstock but the costs associated to the fabrication of the wafers will continue at current levels at about half the cost of the final module. A wafer replacement approach, where crystalline silicon films are grown on inexpensive substrates, can provide high solar conversion efficiency and eliminate the expensive and energy-intensive wafer fabrication process.

There are numerous strategies for the fabrication of silicon film solar cells depending on the temperature compatibility of the supporting substrate. Hot-wire chemical vapor deposition (HWCVD) and electron- or ion-assisted deposition are compatible with inexpensive borosilicate glass substrates (requiring temperatures < 650 °C), which is a more attractive approach to the production of solar cells.

The best projected efficiency of a silicon film solar cell is primarily determined by the collective effects of intragrain and grain boundary recombination. The diagnostics of the recombination (whether associated with grain boundaries, extended defects, or dissolved metallic impurities) is therefore critical to the progress of silicon film solar cells. In this contribution, we introduce the application of cathodoluminescence to the mapping of intragrain and grain boundary recombination in silicon films. The mutual contributions of these recombination processes can be differentiated by their effects on the local emission spectrum. Using this microluminescence mapping, the factors limiting the performance of silicon film solar cells are further discussed and guidelines to further improve efficiency are suggested.

8110-03, Session 1

Advanced light management for thin-film crystalline-silicon solar cells

I. Gordon, O. El Daif, F. Dross, IMEC (Belgium)

In order to decrease the cost of Silicon solar cells, presently the dominating technology on the market, there is a need to go towards cheaper fabrication techniques. A promising bottom-up approach is the fabrication of crystalline silicon (Si) on inexpensive substrates. Aluminium induced crystallisation (AIC) allows to obtain polycrystalline Si with grains in the order of 10µm in diameter and a thickness of around 3 µm, 2 orders of magnitude lower than Si wafers used in photovoltaics. Efficiencies of 8.5% were obtained with such structures fabricated on alumina substrates. These thin film cells still suffer from important optical losses which decrease dramatically their short-circuit current (now 20mA/cm²), whereas their open-circuit voltage (530mV) has a value comparable to the state-of-the-art. Although plasma texturing of the front surface of the cells allows for a good light-in coupling, the low thickness and the absorption coefficient of silicon (low for wavelengths higher than 500nm) yield important losses.

We will show both experimental measurements and numerical simulations of the optical losses in thin Si solar cells on various substrates. We will then compare innovative light trapping techniques,

showing that it is possible to strongly enhance absorption and therefore efficiency. We will compare various back reflecting schemes: a simple metallic layer, a pigmented dielectric layer, a patterned dielectric, and metallic nanoparticles using plasmons modes. Experimental optical characterisation of these various features will be shown. We then performed optical simulations, showing that there is a great room for optimisation depending on topographical parameters. Optimal parameters and how to implement them in a solar cell fabrication chain from the material preparation through AIC until the light trapping features and the contacting will be presented. We show that thin film crystalline-silicon solar cells are a promising path to decreasing the cost of crystalline-Si solar cells. Beyond the absorption increase experimentally shown, modelling shows that efficiencies up to 14% can be reached through an increase of the short-circuit current.

8110-04, Session 2

Fabrication of copper zinc tin sulfide (C2ZTS4) solar cells using spray chemical vapor deposition

D. Lee, J. Seo, A. N. Cartwright, P. N. Prasad, Univ. at Buffalo (United States)

We investigated fabrication of Cu₂ZnSnS₄ (C2ZTS4) thin film solar cells using a spray chemical vapor deposition (CVD) technique. The devices studied are fabricated using the inverse stacking sequence of conventional CuInGaSe₂ (CIGS₂) solar cell structure (Glass/Mo/CIGS₂/CdS/ZnO/Metal). The absorber layer of the device was deposited after the buffer layer deposition. This order of fabrication was necessary because the surface characteristic of the C2ZTS4 absorber layer is too rough to deposit further layers. Unlike other processes, these devices do not need the high temperature annealing above 400°C. All layers are sprayed on the fluorine doped tin oxide (FTO) substrate at distinct temperatures. The spraying temperature for the In₂S₃ buffer layer and the C2ZTS4 absorber layer were systematically investigated. Devices fabricated under different spraying temperatures were investigated and characterized. The optimum temperature for In₂S₃ the buffer layer and the C2ZTS4 absorber layer were 360°C and 380°C, respectively. The C2ZTS4 layer sprayed at low temperature (340°C) has a lower quality of crystallinity with secondary phases (ZnS and Cu_xS) and poor adhesion. The absorber layer sprayed at high temperature showed higher crystalline quality but the entire device performance was degraded due to poor fill factor (<25%). Moreover, the sheet resistance of the C2ZTS4 layer was drastically increased at high temperature spraying. The best cell shows power conversion efficiency (PCE) of 4.4%, open circuit voltage (VOC) of 410mV, short circuit current density (JSC) of 30.4mA/cm² and fill factor (FF) of 35.3% under simulated AM 1.5G illumination condition.

8110-05, Session 2

Probing the defect physics of Cu₂ZnSnS₄ by luminescence spectrum imaging

M. J. Romero, H. Du, G. Teeter, Y. Yan, M. M. Al-Jassim, National Renewable Energy Lab. (United States)

Cu₂ZnSnS₄ (CZTS) is attracting considerable interest because it contains abundant elements Cu, Zn, Sn, and S and the reported bandgap is near the optimum for solar cells. First principle calculations predict that our understanding of the electronic structure and defect formation in CZTS can be partly extrapolated from CIGS, which will benefit the development of CZTS. CZTS shows a very limited region of stability in the Cu-Zn-Sn-S phase diagram and minor deviations from stoichiometry leads to the formation of secondary phases (ZnS, CuS, Cu₂S, SnS).

The success of CIGS is based primarily on the exceptionality of its electronic structure which, in the regime of Cu deficiency, is dominated by the formation of Cu vacancies and their stabilization in defect

complexes. Under such conditions, the evidence suggests that (i) grain boundaries are non detrimental to efficiency, (ii) the surface electronics promotes the formation of the junction, and (iii) nanoscale fluctuations of the stoichiometry assist the transport of electrons and holes. These beneficial effects can be measured by luminescence spectrum imaging, which provides a direct correlation between the microstructure of the CIGS (or CZTS) and the electronic properties as revealed on the emission spectrum at cryogenic temperatures.

In this contribution, we apply this luminescence microscopy to the investigation of the defect physics, the electronic structure of grain boundaries, and the surface electronics of CZTS. When comparing these results to those obtained from CIGS, a strategy for the future development of CZTS solar cells will be presented.

8110-06, Session 3

Solution-based precursors in conjunction with rapid thermal processing for high-quality hybrid CIGS

P. A. Hersh, HelioVolt Corp. (United States); L. A. Eldada, SunEdison (United States); B. J. Stanbery, C. R. Martinez, HelioVolt Corp. (United States)

The use of liquid precursors offers potential benefits over traditional physical vapor deposition (PVD) methods, including better material utilization, higher throughput, and improved scalability. Rapid thermal processing (RTP) offers the potential to selectively heat the precursor films, allowing the substrate to remain relatively cool. This study shows that we are able to make high quality CIGS at ultra-high speeds, while keeping the substrate temperature below 350°C, reducing the risk of glass softening, warpage, and breakage, and enabling the potential use of alternative substrate materials.

In this study, we deposit metal-organic precursor inks on heated substrates using ultrasonic spray deposition to make precursor films that are subsequently rapid thermal processed into CIGS. To complete the devices, the CIGS film is covered with a chemical bath deposited CdS layer, which facilitates junction formation, and acts as a buffer to the transparent conducting oxide (TCO) based contact. The TCO consists of a bi-layer of insulating ZnO (100 nm) and conductive Al:ZnO (120 nm and 60 Ω/square). Device performance from liquid precursors and RTP has been on par with devices deposited via PVD methods and processed using the field assisted simultaneous synthesis and transfer (FASST®) method.

8110-07, Session 3

Characteristics of CIGS thin films prepared by RF sputtering employing CIGS single target

T. Kim, Y. Kim, S. Song, J. Lee, Korea Institute of Industrial Technology (Korea, Republic of)

Copper indium diselenide based materials including copper indium gallium diselenide (CIGS) have attracted much attention as a promising absorber layer for high conversion efficiency thin film solar cell due to their high absorption coefficient. Co-evaporation and selenization of metallic precursor film, which is so-called two-stage method, have been adopted as a conventional process to prepare CIGSe films. However, two-stage method is more promising from a commercialization perspective because the method is more favorable to produce high-quality CIGS film with good uniformity in large scale. Although the two-stage method possesses previous advantage, it is true that there are several problems such as agglomeration of Ga on the interface of CIGSe/Mo and formation of harmful gas phases during the process have been not still solved.

In this study, CIGS films were prepared by a RF sputtering system using a CIGS single target having a composition of CuIn_{0.75}Ga_{0.25}Se₂. X-ray diffraction measurement confirmed that CIGS films grown on

Mo-coated soda-lime glass at 350 °C exhibited polycrystalline structure with no compositional deviation. For the CIGS film treated at 550 °C by RTP the intensity of (112) diffraction increases 3 times more than that of the films grown at 350 °C, revealing crystal-quality of the film improved. Furthermore, SIMS analysis for the interface of CIGS/Mo revealed that heat treatment for Mo layer prior to CIGS film deposition suppresses the inter-diffusion of Cu, Ga, and Mo at the interface. These results demonstrate that RF sputtering of CIGS single target can be a promising method of high quality CIGS film and heat treatment of Mo layer is indispensable to control the interface of CIGS/Mo. In the presentation, we will give more details of our experimental results including the effects of heat treatment for Mo layer prior to CIGS film deposition and surface morphologies and optical properties of the CIGS films.

8110-08, Session 3

Synthesis and electrophoretic deposition of composite metal nanoparticles and non-vacuum fabrication of CuInSe₂ solar cells

B. Liu, K. Hagedorn, W. Guo, IMRA America, Inc. (United States)

A method of non-vacuum synthesis of thin film solar absorbers is presented. The method is based on electrophoretic deposition (EPD) of elemental and composite nanoparticles onto conductive substrates (metal foils) in solvents. EPD is a traditional method for coating ceramic thin films with micron-sized particles. In this work, using Cu-In composite nanoparticles as an example, we demonstrate the feasibility of EPD as a low-cost route of producing thin film metal precursors for synthesis of CuInSe₂ (CIS). Colloidal suspensions of Cu-In composite nanoparticles are prepared with pulsed laser ablation in solvents. Pulsed laser ablation is a fast way of producing high purity nanoparticles of various forms of materials, including elemental, alloy, and compound. We show that the nanoparticles acquire surface charges through electrochemical interaction with solvents, and the surface charge density is sufficient to enable migration of the metal nanoparticles in liquids under a moderate electric field. The success of deposition of nanoparticles on the electrode surfaces is also explained based on electrochemical charge transfer between the particles and the electrode. However, compared with the electroplating method of coating thin metal film, the EPD process has several advantages, including one-step deposition of multiple elements, compositional control through nanoparticle precursors, and high coating speed. After EPD coating, the thin films of metal nanoparticles are selenized in selenium vapor under atmospheric pressure. Solar cell devices have also been finished. This method provides a new choice of low-cost synthesis of thin film solar absorber materials on flexible substrates.

8110-09, Session 3

Characterization of intrinsic ZnO thin film deposited by sputtering and its effect on CuIn_{1-x}Ga_xSe₂ solar cells

M. Jiang, South Dakota State Univ. (United States) and Optron Co. Ltd. (Japan); X. Yan, South Dakota State Univ. (United States); K. Tang, Optron Co., Ltd. (Japan)

Intrinsic ZnO (i-ZnO) thin film is commonly used as a buffer layer between CdS layer and TCO layer for CuIn_{1-x}Ga_xSe₂ (CIGS) thin film solar cells. This film prevents the leakage current between the absorber layer and TCO layer due to its high resistivity. In general, i-ZnO thin film is deposited by RF sputtering. The electrical and optical properties of RF-sputtered i-ZnO thin films vary with the working gas pressure, the ratio of O₂ to Ar partial pressure, sputtering power, substrate temperature, and thickness. However, most of these parameters were rarely reported in literatures concerning deposition of i-ZnO thin films for CIGS TFSCs except a thickness ranging from 50 to 100 nm was mentioned. Furthermore, the optimization of deposition of i-ZnO thin films has seldom been performed for the fabrication of CIGS TFSCs.

In this work, the correlation of the cell performance of CIGS TFSCs with i-ZnO thin films deposited under different conditions was studied. The substrates were heated to 250 °C or kept at 25 °C. The deposition was carried out either using pure Ar as sputtering gas or under partial pressure of O₂. It was found that the average conversion efficiency was significantly improved by 16% from 10.59% to 12.30% when i-ZnO thin film was coated at 25 °C without addition of O₂ instead of 200 °C with addition of O₂. This improvement was mainly attributed to the increase of fill factor and slight enhancement of short-circuit current density.

8110-10, Session 4

Nanophotonic light management in solar cells

S. Fan, Z. Yu, A. P. Raman, Stanford Univ. (United States)

We review some of the theoretical developments in understanding nanophotonic light trapping in solar cells, as well as in developing strategies for absorption enhancement over the entire solar spectrum.

8110-11, Session 4

Effects of metallic nanoparticle arrays in Si solar cell structures

T. Benkenstein, M. Flämmich, T. Harzendorf, Fraunhofer-Institut für Angewandte Optik und Feinmechanik (Germany); T. Käsebier, Friedrich-Schiller-Univ. Jena (Germany); D. Michaelis, M. Oliva, C. A. Wächter, U. D. Zeitner, Fraunhofer-Institut für Angewandte Optik und Feinmechanik (Germany)

Metallic inclusions in layered structures can have noticeable effects onto scattering and absorption due to the coupling of the external electromagnetic field and local charge oscillations. These effects are strongly related to both the geometry of the individual particle as well as to the array structure. Thus, sophisticated implementations of numerical methods like Rigorous Coupled Wave Analysis and Finite Element Methods are required in order to model the effects with adequate accuracy. To achieve a deeper understanding of peculiar scattering effects within the complete geometry it is helpful to consider the interplay of occurring individual plasmonic resonances, waveguide modes and Bloch modes, which depend on optical frequency, particle shape and array geometry, eventually. Based on that, and having in mind the efficiency improvement of silicon solar cells due to plasmonic effects, we report on the modeling, the fabrication and the characterization of periodic arrays of metallic nanoparticles on planar substrates. Special emphasis is placed on detailed parameter retrieval for non-ideal particle geometries. Since the very details of the individual particle at the one hand critically depend on the fabrication process and at the other hand reflection and transmission of the complete structure depend critically on the particle shape, corresponding optical measurements data contain precise information about processing induced geometry deviations. In combination with AFM characterization numerical modeling techniques are used to clarify corresponding implications which are due to non-perfect material removal as well as to material re-deposition during the etch-process.

8110-12, Session 4

Plasmonic effects and light-trapping in thin-film photovoltaics

E. A. Schiff, H. Zhao, B. Ozturk, Syracuse Univ. (United States); L. Sivec, J. Yang, S. Guha, United Solar Ovonic, LLC (United States)

Surface plasmons at metal-dielectric interfaces affect any solar cell that incorporates textured silver or other metallic reflectors. The effects can be deleterious, but recent research has explored possible

plasmonic improvements in thin-film cells. In this paper we present our findings on three plasmonic effects. We show that optical phase shifts associated with surface plasmons substantially affect quantum efficiency measurements for silicon thin films; these results lead us to re-assess the early work indicating large plasmonic enhancements in photocurrents in silicon-on-insulator films. On the other hand, we show that plasmonic effects do contribute positively to the performance of some well-optimized back reflectors, essentially by enhancing the diffraction of light by the textured reflector. The experiments involve reflectance measurements of backreflectors with varying dielectric overlayers, and comparisons of silver and aluminum back reflectors with similar textures. Finally, we show that plasmonic effects can, in principle, lead to “supraclassical” light trapping beyond these diffraction effects. For cells based on crystalline silicon, 0.5 micron absorbers in plasmonically-enhanced cells should outperform 1.0 micron absorbers in fully optimized, conventional cells. We describe the experimental efforts to realize this improvement.

This research has been supported by the U.S. Department of Energy, by United Solar Ovonic LLC, and by the Empire State Development Corporation.

8110-13, Session 4

Enhanced absorbance of light due to multiple surface-plasmon-polariton waves

M. Faryad, A. Lakhtakia, The Pennsylvania State Univ. (United States)

Rigorous coupled wave analysis was used to compute the absorbance of a metal grating coated with a dielectric layer. The grating is formed by periodic bumps on an otherwise planar layer of a suitable metal. When the period of the grating is appropriate, the incident light excites a p-polarized surface-plasmon-polariton (SPP) wave at a certain incidence angle if the dielectric layer is homogeneous. However, if the dielectric layer is periodically non-homogeneous normal to the mean metal/dielectric interface, more than one p-polarized SPP waves with different phase speeds and attenuation rates are excited. In addition to p-polarized SPP waves, s-polarized SPP waves may be excited if the periodic non-homogeneity of the dielectric layer is sufficiently pronounced. The capability of periodically non-homogeneous dielectric layer to excite multiple SPP waves with different polarization states, phase speeds, and attenuation rates can help enhance light absorbance in thin-film solar cells.

8110-14, Session 5

Measurement and analysis of non-uniformities in CdTe solar cells

J. R. Sites, Colorado State Univ. (United States)

CdTe and other thin-film polycrystalline solar cells have potential spatial non-uniformities in their photovoltaic response that can both lower their performance and complicate the analysis of their current-voltage curves. Polycrystalline cells have inherent non-uniformities associated with their grain structure, but there are a variety of other possibilities including thickness variations, local shunts, and weak-diode areas. Additionally, there are possible issues associated with the fabrication process due to cleaning residues, scratches, thermal variations, and particulate inclusions.

The primary measurements used to map the non-uniformities of CdTe cells are light-beam-induced current (LBIC), which gives a direct measure of the local PV response, and electroluminescence (EL), which is the inverse of the PV effect. The former is attractive, because it can be used to deduce the local current-voltage curve, but data collection is time consuming. The latter though the use of modern CCD cameras takes only a few seconds and is compatible with production-line screening.

The presentation will show examples of several types of non-uniformity seen in LBIC and EL measurements, it will compare the current-voltage

curves of the cells with and without specific non-uniformities, and it will give the basic analysis strategies for connecting the uniformity measurements with cell performance.

8110-15, Session 5

Raman spectroscopy metrology for in-line quality control supporting high-throughput polycrystalline thin-film PV manufacturing

V. Bermudez, NEXCIS (France); V. Izquierdo, Univ. de Barcelona (Spain); E. Saucedo, A. Perez-Rodriguez, J. Morante, Institut de Recerca en Energia de Catalunya (Spain)

Raman scattering is an optical non destructive technique well suited for quality control and process monitoring in advanced chalcogenide PV thin film technologies. This includes state-of-the-art chalcopyrite absorber alloys as well as new emerging technologies based on kesterite absorbers. The Raman spectra from these compounds are strongly sensitive to defects, strain, chemical composition and secondary phases, being all these features determining for the performance of the cells. However, development of Raman scattering based process monitoring techniques is conditioned by the low efficiency of inelastic scattering processes in these materials which implies the need for high throughput optics in combination with very high sensitivity detectors, as well as the relative limited size of the measured surface in the layers and the integration time required for collection of spectra with good signal-to-noise ratio.

These experimental limitations can be solved by the use of resonant or pre-resonant excitation conditions. This allows for a significant decrease of the measuring time to levels compatible with on-line process monitoring requirements. There is also the possibility for in-situ implementation which means that quasi-real time measurements can be achieved simultaneously to the process. Combination with suitable excitation and light collection optics allows for the analysis of phase, structure or composition inhomogeneities at both macroscopic and microscopic scales for the non destructive assessment of these complex absorbers at early process stages during the fabrication of the cells and modules.

8110-16, Session 5

Hall measurements on low-mobility, high-resistivity materials

J. R. Lindemuth, Lake Shore Cryotronics, Inc. (United States); S. Mizuta, Toyo Corp. (Japan)

Making Hall measurements of amorphous materials, organic materials or other low mobility materials is known to be very difficult¹⁻³. There are two intertwined problems for Hall measurements on these materials. The first is an instrument problem. Experience has shown that instruments do not provide reliable results when making Hall measurements of materials with high resistivity and low mobility materials. In these materials, the true Hall voltage is often overwhelmed with large offset voltages.

To overcome these problems, first it is necessary to explicate and demonstrate a method that produces reliable, consistent results for Hall measurements of low mobility materials. With this knowledge, the researcher can then begin to confidently attribute "strange" results to the material, rather than to the instrument.

We propose a method using AC magnetic fields for measuring the Hall effect in low mobility materials. The Hall voltage is measured using phase sensitive detection. We have calculated the limits of the measurement method including sample shape effects and show measurements of amorphous and microcrystalline silicon which confirm these limits. AC field Hall can expand the limits of mobility that can be reliably measured by a factor of 100 or more.

1. Electronic Processes in Organic Crystal and Polymers, Martin Pope and Charles E. Swenberg, 2nd edition (1999).

2. Hydrogenated amorphous Silicon, R. A. Street, (1991).

3. Semiconductors and Semimetals Vol. 21 Hydrogenated Amorphous Silicon part C Electronic and transport properties, J. Dresner, (1984) .

8110-17, Session 5

First outdoor measurements on amorphous thin film photovoltaic panels performance embedded on curvilinear surfaces

A. Spina, G. D'Angiolini, C. Strati, S. Bartocci, Univ. degli Studi di Roma Tor Vergata (Italy)

The flexible thin film photovoltaic devices are finding a growing popularity as they offer very interesting prospects for building integrated together with a satisfactory electrical conversion efficiency especially in adverse weather conditions. The development of these technologies opens a new work range combining availability of energetic and environmental systems with the opportunity of original design shape going to realize embedded systems. The photovoltaic plant assumes the function of electricity producer and building element: curvilinear roof cover, cladding, architectural accessories (i.e. shelters, parapets,...).

One of problems related to this photovoltaic system is the lack of data on energy producibility and photovoltaic components behavior when are embedded on surfaces unable to maximize solar radiation reception. Our research propose to analyze outdoor performances of thin film components on special surfaces, such as curvilinear. In this way it will be possible to have a more complete scenario of realistic performances to reach the best balance between architectural needs and energetic performances. For this purpose a test section of thin film photovoltaic panels is been built going to integrate with existing appliances for outdoor monitoring of photovoltaic panels of Technical and Physics for Environment laboratories of University of Rome, Tor Vergata. The building, facing south, is composed of two pair of centering with radii of curvatures as 1.2 and 2.5 meters and of a pair of horizontal tubular enable to monitor panels also on horizontal plan. Measurements, data capture and transfer system is constituted of MPPT modules tracking maximum power point, of electronic compass, 3 RTD for each pair of centering to measure the temperature.

8110-18, Session 5

Correction methods and stabilisation of outdoor measurements of thin film modules

K. Weiss, K. Scharmach, J. Wirth, M. Koehl, Fraunhofer-Institut für Solare Energiesysteme (Germany)

Stabilised performance data are necessary to compare different types of modules in the emerging thin film PV market and as basic information for energy yield calculations. The test standard IEC 61646 ed. 2 describes demanding light soaking and repeated STC measurements to ensure stabilized values for thin-film modules.

Various types of CdTe, Cl(G)S and a-Si modules were installed on a outdoor test facility in Freiburg, Germany, facing south in 45° inclination. IV-Curves of all these modules are measured every ten minutes. Between the measurements of IV-curves the modules are held in MPP conditions by electronic loads. Isc, Voc, efficiency and filling factor are determined automatically.

Measured irradiation, module temperature and air mass are used for analysis and comparison of the IV curves. The influence of the respective air mass was higher than expected and therefore regarded more intensely. Measured data were corrected to 1000 W/m² irradiation and 25°C module temperature according to IEC 60891 to make them comparable.

Different procedures of filtering and correction have been compared. The results show that the best results are achieved when the data are selected in a small range of air mass and module temperature and corrected to the same irradiation.

Modules of the same types like the outdoor exposed modules were stored without irradiation for some years. Afterwards, they were exposed at the test site with the other modules. Comparison of the module data of the same type allows the investigation of the stabilisation behaviour of the modules directly.

8110-21, Session 6

Application of nanostructured silicon for solar cells manufacturing

A. I. Luchenko, V. Lashkaryov Institute of Semiconductor Physics (Ukraine); T. Bilyk, M. M. Melnichenko, National Taras Shevchenko Univ. of Kyiv (Ukraine); O. Shmyryeva, National Technical Univ. of Ukraine (Ukraine); K. Svezhentsova, V. Lashkaryov Institute of Semiconductor Physics (Ukraine)

It is known, that a thin layer of nanostructured silicon on a textured substrate of single-crystal silicon considerably reduces reflection of light in comparison with usual textured substrates. However methods and mechanisms of formation of nanostructured silicon are ambiguous and are not yet completely investigated.

Therefore, detailed studying of mechanisms of formation and properties of the thin layers of nanostructured silicon is necessary for increasing efficiency of transformation of solar cells.

We studied the process of formation of nanostructured silicon, the influence of the formation technique type on its structural, photoluminescent and antireflecting properties. The layers of nanostructured silicon have been formed on the textured surface of solar cells. The layer of the nanostructured silicon was created by chemical etching in a mix of acids HF and HNO₃. The thickness of a layer of the nanostructured silicon (3 - 60 nm) during chemical modification of textured surface of single-crystal silicon was supervised by preset parameters of technological process and was determined by a method of Auger electron spectroscopy.

It is shown, that the formation of contact systems on the nanostructured silicon on the textured substrate results in decrease of consecutive resistance, increase of a short circuit current, increase of shunting resistance, and increase of efficiency.

8110-22, Session 6

Conductive conformal thin film coatings for textured PV: ALD versus sputtering

T. Gennett, A. Dameron, S. Christensen, J. Perkins, J. Berry, D. T. Gillaspie, D. S. Ginley, National Renewable Energy Lab. (United States)

Physical vapor deposition techniques have been widely used for thin-film deposition in many photovoltaic applications. However, the conformal nature of films from conventional line of sight deposition processes are limited due to self-shadowing that can lead to poor step coverage on sidewalls and bottoms of trenches. These effects can lead to void formation when attempting to fill or coat a surface feature, which is especially important as one starts to apply TCO's to the up-and-coming realm of 3-D interdigitated solar devices. This preliminary work has taken a three-pronged approach to develop methods to deposit conductive materials conformally onto three-dimensional and textured supports.

While many materials with countless chemical compositions have been developed effectively for the sputter depositions for planar applications, this line-of-sight process struggles to deposit these same materials with uniform-reproducible coverage over textured or shadowed surfaces. On the other hand, the self-limiting surface-gas phase reactions of atomic layer deposition (ALD) provide a means to generate extremely conformal thin films that are much improved compared to any other methodologies (both chemical vapor deposition and PVD). However, currently the materials reported for ALD coatings on PV relevant materials are limited because these ALD materials currently do not have the well-

established physio-chemical properties of analogous sputtered films. Potential conformal materials developed by both these techniques can be further improved by development of a surface that promotes uniform growth.

This work will report on the preliminary findings associated with conformal metal oxides on structured substrates including: 1) Discovery of sputtering process conditions that can be made semi-conformal combined with in-situ techniques such as ion-beam milling for honing surface structures; 2) Development of relevant ALD chemistries that are materials-properties competitive with sputtered materials; 3) Evaluation of chemically-functionalized surface structures that maximize surface area but are structurally tailored for efficient gas flow and to minimize line-of sight shadowing.

The initial experiments have centered on combinations of amorphous and crystalline indium oxide, zinc oxide, aluminum zinc oxide, indium tin oxide, fluorinated tin oxide and indium zinc oxide. This presentation will describe these initial experiments and elucidate key physiochemical nature of the deposited thin films.

8110-23, Session 7

Colloidal quantum dot photovoltaics

S. M. Thon, E. H. Sargent, Univ. of Toronto (Canada)

Colloidal quantum dot solar cells offer to combine low-cost roll-to-roll solution-processing with efficient infrared as well as visible spectral harvesting. Their quantum size effect tunability offers a path to tandem and triple-junction cells. The first solution-processed infrared solar cells were reported in 2005; the latest devices offer greater than 5% AM1.5 PCE and many paths remain for further improvement to 10% and beyond. We will review the field and its prospects.

8110-24, Session 7

Low-cost fabrication of improved n-Si/p-AgGaSe₂ heterojunction solar cells

K. C. Mandal, S. Das, Univ. of South Carolina (United States)

The fabrication of low-cost n-Si/p-AgGaSe₂ heterojunction solar cells by controlled thermal evaporation method is reported. It is observed that in the case of p-AgGaSe₂ films deposited on H-terminated n-Si (H-Si) substrates at higher temperature of 550K, the photovoltaic properties of the n-Si/p-AgGaSe₂ junctions are considerably improved. The improved junction, under solar simulator AM1 illumination, demonstrated an efficiency of ~5.2% on an active area of 0.18 cm² without any antireflection coating whereas the AgGaSe₂ films thermally evaporated at lower substrate temperature of 400K on H-Si substrates showed the efficiency ~2.7%.

8110-25, Session 7

Minority carrier transport length in electrodeposited Cu₂O for heterojunction solar cells

Y. Liu, H. Turley, J. R. Tumbleston, R. Lopez, The Univ. of North Carolina at Chapel Hill (United States)

The minority carrier transport length (L) is a critical parameter limiting the performance of inexpensive Cu₂O-ZnO photovoltaic devices. In this work, this length is determined for electrochemically deposited Cu₂O by linking the optical carrier generation profile from back and front and incident photon conversion efficiency (IPCE) measurements to a one dimensional carrier transport model. A diffusion length of ~400 nm is estimated. This critical length explains the losses typically presented by these devices. The consequences of this L on device design with the aim of improving solar cell performance are described.

8110-26, Session 8

Application of electrochemical deposition techniques to thin film solar cell processing

B. Basol, EncoreSolar, Inc. (United States)

During the last eight years the manufacturing volume of thin film modules has grown at a compounded annualized rate of over 90%. Today the share of thin film products in the global PV market is in the range of 10-15%. Considering the fact that the wafer Si technologies have achieved impressive cost reductions during the last few years, any increase in thin film market share during the next decade will require these technologies to aggressively drive for cost reductions through device efficiency improvements and utilization of lower cost manufacturing techniques. Electrodeposition is an attractive low cost approach for the deposition of thin film coatings. Such coatings have already found large scale applications in circuit board fabrication and integrated circuit manufacturing. In these applications, the electroplated layers are mainly used as passive components that carry electrical current. Application of electrodeposition techniques to thin film solar cell fabrication involves formation of semiconductor absorber layers that actively participate in power generation. This requirement brings along certain challenges that need to be overcome. In this paper we will present a review of work carried out for the application of electrodeposition techniques to the fabrication of CdTe and CIGS based solar cells and modules.

8110-27, Session 8

CdTe, CIGS and a-Si thin film PV technologies: factors impacting LCOE

L. A. Eldada, SunEdison (United States)

We describe some of the most promising thin film photovoltaic (PV) technologies and contrast their attributes and how they impact the levelized cost of electricity (LCOE). The thin film PV technologies reviewed include cadmium telluride (CdTe), copper indium gallium selenide (CIGS), and amorphous silicon (a-Si), produced by a variety of methods. The factors studied include conversion efficiency and efficiency improvement potential, module lifetime, module cost and cost reduction potential, installation cost, operation cost, maintenance cost, and various factors affecting the internal rate of return (IRR), such as early-life annual degradation rate and energy yield under different lighting and environmental conditions. These thin film PV technologies are compared with crystalline silicon, the most widely deployed PV technology.

8110-28, Session 8

Novel concepts for low-cost and high-efficient thin film solar cells

D. Gomez, A. Menéndez, P. Sanchez, A. Martinez, L. Andrés, M. F. Menéndez, Fundación ITMA (Spain)

Although the development of different thin film solar technologies has represented an important advance along last years, further progresses are still required in order to reduce their manufacturing costs (below grid parity) and to increase their efficiency (closer to crystalline silicon cells). Among different approaches focused on overcoming these difficulties, the present work gives a short description of different concepts developed at ITMA Materials Technology in the framework of different industrial projects.

These novel concepts can be grouped in three categories:

- (i) The development of surface treatment technology (low cost inorganic coatings by sol gel and tape casting) for the deposition of thin film solar cells on non transparent substrates (steel, ceramics, polymers)
- (ii) The embedment of metal nanoparticles for light trapping following two different strategies: the increase of quantum efficiency width by electronic plasmon resonance of nanoparticles in the 10nm-range and

the increase of light path by means of light scattering (in the 100-nm range)

- (iii) The use of novel laser scribing and encapsulation methods in substrate configuration

It is important to point out that these advances are not directly related to any specific thin film solar technology and seem to be suitable for silicon based, CIGS and CdTe solar cells.

As an example, these progresses have been successfully demonstrated in single junction amorphous silicon solar cells in substrate configuration (n-i-p sequence) on different substrates. The work shows the individual improvements in cell efficiency according to the concepts previously described. As a second step, they have been joined together in a innovative cell structure with an increase of efficiency up to 2% (absolute). Moreover, the possibility to apply this cell concept on different rigid and flexible substrates opens their use on building materials for BIPV, as it will be shown for steel and ceramics.

All these facts represent a clear success. In addition, a detailed cost analysis is carried out and the decrease of the ΔW is estimated. An extrapolation of these results to other thin film technologies has also been evaluated.

8110-29, Session 9

Laser-induced localized strain and ultrafast absorption in the ablation of thin film solar cells

S. Buratin, E. Favero, P. Villaresi, Univ. degli Studi di Padova (Italy)

The selective removals of areas as well as the realization of narrow channels in the multilayer structure are central issues in thin film solar cell technology. The difference in optical absorption and the different mechanical parameters, including density, thermal conductivity, surface adhesion energy and stress-strain curve, allow for the exploitation of laser driven non contact removal processes based on different principles.

In this work we will address on the layer removal along channels for the serial connections of the cell by comparing two novel approaches. The two opposing cases of the ultrafast absorption and of the controlled thermal stress in microsecond timescale are investigated for their potentials in reaching a clean layer separation with sharp edges. The rationale for the investigation of the two processes in parallel is the different optimal removal required in the cell layer stack.

By using low energy and high repetition rate femtosecond laser pulses the ablation rate may be precisely controlled. The thermal effects are limited due to the short pulse duration and the threshold for the material ablation is beyond the Bloembergen square root law. We model and experimental observe the processing for different wavelengths and pulse parameters.

On a longer time scale, the exploitation of the temporal control of the laser pulse irradiance allows for the induction of mechanical strain of suitable amplitude and extension. We model the tridimensional distribution of the strains and its time evolutions as well as the experimental investigations of the induction of layer removal in a series of relevant cases for the thin film solar cells technology.

Our aim is to point out the optimal laser process for the different cell layers. We are convinced that these novel techniques are potentially superior with standard approaches.

8110-30, Session 9

Novel adhesion methods for solar cell assemblies using pressure sensitive adhesives

R. Thomaier, NuSil Technology LLC (United States)

Traditionally engineers and solar cell assemblers have used liquid silicone adhesives to bond solar cells to panel substrates and silicones with high light transmittance to bond cover glasses to cells. As advances are made in solar cell assemblies, innovative next generation silicone technology is used. Low outgassing silicone pressure sensitive adhesives (PSA) and thin film sheeting can serve the same purpose as liquid adhesives but eliminate the need to wait for a long room temperature cure or additional equipment such as ovens to heat accelerate the cure process. While both methods for manufacturing solar cell assemblies are viable they present different options for customers who are looking for flexibility in their application processes.

Solar cell assembly is made easier by using films and PSAs by controlling the bond line thickness between the cell and the cover glass through the PSA or film thickness. Design engineers have the ability to rework panels where PSAs are applied - cutting cost for components and time. The low outgassing PSAs and film adhesives have similar performance as liquid silicone adhesives without the need of mixing and deairing. Performance characteristics include: broad operating temperature ranges, maintain chemical stability, and offer stress release during thermal cycling. With dimethyl backbone chemistries, similar to traditional adhesives, the clear PSAs and thin films are resistant to yellowing and have light transmittance greater than 97% at 400 nm. This paper will demonstrate how the film adhesives and PSAs will perform similar to the liquid silicone adhesives in solar environments through optical transmission, optical transmission after heat and UV exposure, and adhesion at elevated temperatures.

8110-31, Session 9

Multilayer front-sheet with tuned color appearance

H. Rooms, TNO Science and Industry (Netherlands)

The acceptance of solar cells in the built environment is partly dependent on the appearance of the modules. One aspect is color. In most cases a solar cell itself reflects either blue or no color and will appear blackish. For the blue solar cells it is possible to tune the antireflection layer in such a way that a different color is reflected. We propose a front-sheet consisting of a multilayer stack of thin layers deposited from sol-gel onto PET foil such that only a particular wavelength range is reflected. We show through modeling that by alternating layers consisting of silicon dioxide (SiO₂) and SiO₂:TiO₂ on PET foil such color reflection can be achieved. In modeling exercises the influence of the number of layers, thickness variations and angle of incidence on the reflected color are predicted. We will show that with a four layer stack we can reach chroma values of 60 for green and 40 for red color in the CIELCH system. In experimental results we achieve a peak reflection at a desired wavelength of 40% with a band width of 100 nm while transmission is more than 90% for the other parts of the spectrum.

8110-19, Poster Session

Fabrication and properties of mechanically grooved silicon solar cells with buried contact Cu electrode

P. Jang, C. Jung, S. Kyu, K. H. Kim, Cheongju Univ. (Korea, Republic of)

Due to larger shadowing area, higher contact resistivity and high intrinsic resistivity of screen printed Ag electrode, there is a limitation in the conversion efficiency of the cell. In order to solve the problem, buried contact solar cells have been developed. P-type Si wafer was successfully scribed by a home-made mechanical scriber which was composed of HDD 3 phase synchronous motor, 3-axis LM guide, phase shifter, audio amplifier, Labview, signal generator and etc. SiN_x insulating films with a refraction index of 2.02 and an etching rate of 0.8 nm/min were successfully sputtered in an optimized sputtering condition, which is used to have Cu electrode selectively deposited in the scribed

grooves. Uniform Ni films were successfully deposited in the scribed grooves with a conventional Ni electroless plating solution. After Cu plating, the buried contact solar cell was fabricated with a published condition and, however, the conversion efficiency was as small as 0.42 %. The reason was analyzed so that the contact resistance between Si wafer and electrodes was revealed to be much higher. With an optimized Ni annealing time of 30 min at 350°C the conversion efficiency was enhanced to 12.2 %. And when the electric potential difference was reduced to a voltage lower than 10 V, the conversion efficiency was further enhanced. Detail optimized conditions of the individual process will be reviewed in the conference site.

8110-32, Poster Session

Physical properties of Al-doped MgZnO film grown by RF magnetron sputtering using ZnO/MgO/Al₂O₃ target

K. Hsueh, Y. Cheng, W. Lin, Vanung Univ. (Taiwan); H. Chiu, Chang Gung Univ. (Taiwan); Y. Huang, G. Chi, National Central Univ. (Taiwan); W. Liu, Yuan Ze Univ. (Taiwan)

In this work, we report on an investigation of the characteristics of Al-doped MgZnO (AMZO) films which were deposited on top of the sapphire by RF magnetron sputtering system using the ZnO/MgO/Al₂O₃ (76/19/5 wt%) 4 inch target. All AMZO films used in this study were grown by RF sputtering method (HELIX) on c-face sapphire substrates.

The XPS was performed by a Thermo VG-Scientific/ Sigma Probe instrument. The XPS results by varying the etching time were shown. The contents of AMZO were also estimated by varying the etching depth.

The transmittance spectrum of AMZO film is obtained. In this study, the AMZO film show high transparency with transmittances over 89.8 % in the visible region (400 ~ 700nm) and the sharp absorption edge is visible in UV region due to the Mg content. The absorption edges of AMZO shift toward the short wavelength compared with the previous report of ZnO, implying that band gaps can be tuned by changing the Mg content of AMZO layer.

We summarized the Hall measurement on the AMZO samples which were deposited at RF power of 150W and 200W, respectively. The results show that the Hall measurement of AMZO films which were deposited at lower RF power obtained the lower resistivity and higher mobility, but the doping concentration is not a strong function of the RF power and annealing temperatures.

8110-33, Poster Session

Production of highly conductive copper doped ZnS thin films by dip-coating for solar energy technology

F. Ait medjane, R. Wendelbo, Abalonyx AS (Norway)

Thin copper doped ZnS film is promising materials for the use in various application devices such as a photocatalyst or light-emitting diode in the blue to UV spectral region due to its wide band gap at room temperature.

Here we report a simple, low cost and very effective technique to prepare highly conductive copper doped ZnS thin films. The films were deposited on glass substrates by the dip-coating technique adopting the SILAR method. An automated high-throughput set-up was developed for the purpose, by using a commercial robotic arm to dip 24 substrates in parallel. The set-up includes in house made instrumentation for on-line measurement of conductivity and transmittance. X-ray diffraction (XRD), SEM, AFM and XPS techniques have been employed to investigate the structure and surface morphology of as-deposited films. It was found that, in narrow compositional range around Zn/Cu=100, semi-transparent films with sheet resistivity lower than 100 Ohms/sq were obtained. This is about 100 time higher conductivity than for materials previously reported. SEM-analysis indicated that the films were not uniform in early stages

of process. Elongated “islands” could be observed, which grows with increasing number of dipping cycles. However, after 90 dipping the SEM analysis shows continuous and homogeneous films.

8110-34, Poster Session

The influence of active cell design on a monolithic organic photovoltaic module: fabrication and simulation

H. Lyu, Daegu Gyeongbuk Institute of Science & Technology (Korea, Republic of) and Kyungpook National Univ. (Korea, Republic of); J. H. Sim, S. Jeong, S. Woo, Daegu Gyeongbuk Institute of Science & Technology (Korea, Republic of); J. Shin, Kyungpook National Univ. (Korea, Republic of); Y. S. Han, Daegu Gyeongbuk Institute of Science & Technology (Korea, Republic of)

In this study, the influence of active cell design on the power conversion efficiency (PCE) of a monolithic organic photovoltaic (PV) module was investigated using experimental methods and circuit simulation. For computer simulation-based study, the organic PV cell was described by a circuit-based two-diode model and the modules were simulated under several conditions including shading effect, diode model parameters, series resistance and shunt resistance, etc. A unit organic PV cell as a reference device and four types of monolithic organic PV modules with different active cell length were fabricated together on a same glass substrate. The characteristics of the fabricated unit organic PV cell were measured and the electrical parameters were extracted to use it for simulation of the four types of monolithic organic PV modules. To analyze the influence of organic PV cell design on the PCE of monolithic organic PV modules, the I-V characteristic curves and the PCEs of the four type monolithic OPV modules with different active cell length were obtained and compared with the simulated results. The simulated I-V curves were matched well with the measured I-V curves for four types of monolithic organic PV modules with different active cell length. The highest PCE of the monolithic organic PV module was 2.86% with the active cell length of 11.6mm. This work is meaningful to enhance the performance of a monolithic organic PV module to a certain extent and offers a method to design a high-efficiency large-area monolithic organic PV module.

8110-35, Poster Session

Effect of nanostructured FTO surface on photovoltaic characteristics of thin film solar cells

H. Chang, H. Wang, K. Lai, National Taiwan Univ. (Taiwan); P. Yang, AU Optronics Corp. (Taiwan); J. He, National Taiwan Univ. (Taiwan)

Nowadays, how to increase the optical paths of infrared light in uc-Si layer is the severe challenge in tandem thin film (TF) solar cells. In this study, we utilize nanostructured FTO electrodes to enhance both the transmittance and haze in broadband wavelengths. The enhancement of optical transmittance in nanostructured FTO films with the surface roughness could lower the reflectance between the FTO/a-Si interfaces. Furthermore, the high haze benefits from nanostructures could allow much incident light strongly scattering to increase not only optical paths but light absorption especially in the infrared region.

Upon the application of the nanostructured FTO surfaces, the current density of TF solar cell was increased from 10.01 to 11.05 mA/cm², and the conversion efficiency could be improved from 8.82% to 9.74%. The concept and technique presented in this study should benefit the development of next generation of TF solar cells.

8110-36, Poster Session

Preparation and properties of CdS film used in CIGS-based solar cell with CBD method and thermal treatments

T. Hsieh, W. Wu, C. Chuang, M. Chang, C. Liu, Yuan Ze Univ. (Taiwan)

Since CdS material has a direct and wide band-gap, it is very potential for fabricating photovoltaic devices. Due to its wide band-gap, CdS film can be acted as a window material to combine with Cu(In, Ga)Se₂ film. Therefore, CdS film grown on ITO substrate is usually used to fabricate a high efficiency solar cell. To obtain a quite uniform, easily scaling-up, and inexpensive sample, the CdS thin film with a thickness of 50 nm was deposited by using chemical bath deposition (CBD) method. Through varying annealing temperatures and annealing times, the electrical and optical properties of CdS film could be obviously improved. From measurements, the transmittance of CdS sample annealed at 100°C with 5 min was increased from 80 to 90% in the wavelength range of 510-600 nm. The photoluminescence peak of CdS sample annealed at 150°C with 20 min is the maximum and its sheet resistance is the minimum. By using those data obtained at various annealing temperatures and times, we can find an optimum condition for growing CdS film application on Cu(In, Ga) Se₂-based solar cell.

8110-37, Poster Session

Effects of substrate temperature on the properties of MgF₂ thin films and their applications on CuInGaSe₂ solar cells

J. Chang, T. Hsieh, M. Yang, J. Guo, C. Chuang, Industrial Technology Research Institute (Taiwan)

Chalcopyrite CuInGaSe₂ (CIGS) based thin-film solar cells are regarded as most promising candidates for film power modules due to high efficiencies and low cost. In order to increase cell efficiencies, anti-reflective (AR) coatings have been designed and applied to solar cells. MgF₂ are usually utilized as an AR coating on CIGS solar cells and deposited on the surface of transparent-conductive oxides. In this study, MgF₂ thin films were respectively formed on the 2 2 cm² soda-lime glass (SLG) and SLG/ZnO/AZO substrates via e-beam evaporation at different substrate temperature. X-ray diffraction (XRD), scanning electron microscopy (SEM), transmittance and reflectance investigated characteristics of the films. Further, the AR coatings were also deposited on the CIGS cells at different substrate temperature.

Fig. 1 shows the XRD patterns of MgF₂ thin films deposited on SLG substrate at different substrate temperature. The (110) peak intensity of MgF₂ films clearly increases as the substrate temperature increases. High substrate temperature enhances the crystal growth. Fig. 2 shows the transmittance and reflectance of blank SLG and SLG/MgF₂. The transmittance and reflectance of blank SLG are about 89.1% and 8.9%. Depositing MgF₂ films on SLG substrates could increase the transmittance and decrease the reflectance. XRD patterns of MgF₂ thin films deposited on SLG/ZnO/AZO substrate at different substrate temperature are shown in Fig. 3. The intensity of MgF₂ peak at 2θ increases with the substrate temperature. The peak appeared obviously at 200 oC. Fig. 4 shows the transmittance and reflectance of blank SLG/ZnO/AZO substrates and SLG/ZnO/AZO/MgF₂. MgF₂ AR-coatings sufficiently increase the transmittance and decrease the reflectance. SEM images of MgF₂ thin films deposited on SLG/ZnO/AZO substrate are shown in Fig. 5. We have deposited 50 nm ZnO and 450 nm AZO films on SLG substrates. All of the MgF₂ film thickness are ~100 nm. The surface looks much smooth. Fig. 6 shows the current-voltage characteristic of CuInGaSe₂ solar cell without and with 100 nm MgF₂ thin films. It could be find that the short-circuit current density of solar cell characteristics has been increased with adding AR coatings.

8110-38, Poster Session

Laser scribing performance in thin-film silicon photovoltaic micromorph tandem modules using short pulse lasers

J. Cashmore, V. Cervetto, H. Chabane-Amat, S. Gardin, M. Lindic, S. Ristau, Oerlikon Mechatronics AG (Switzerland)

In thin-film silicon photovoltaic modules it is important to optimise the laser scribing processes to achieve low-loss performance of the segment interconnections and thereby obtain the highest module power outputs. The characterisation of the component scribes and the contribution of the complete interconnect structure to the module behaviour enable the optimisation of the laser scribing processes. Current laser patterning processes based on nanosecond (ns) pulse duration lasers are irradiated from the substrate side to enable high speed scribing. These through-the-glass processes require more than one laser wavelength for targeted removal of the different layers in the photovoltaic cell structure. Development of processes using lasers with picosecond (ps) pulse durations allow scribing from the deposition layer side of the module for all scribe processes using a single wavelength and at scribe speeds of up to 120 m/min. This approach has the advantage that the glass surface and bulk properties can be chosen to enhance the module performance unrestricted by the need for the laser to pass without absorption or scattering through the substrate (e.g. using an optimised glass transmission spectrum, an anti-reflection coating, or a scattering surface structure). In addition a single tool can efficiently process the complete interconnect structure. This allows improved flexibility of tool-routing and minimises the number of tools required within a fab. A comparison of ps-laser and ns-laser patterning results for Oerlikon Solar's Micromorph modules, together with process characterisation and optimisation methods will be presented.

8110-39, Poster Session

Pulse-electrodeposition of lead sulfide thin films for PV applications

N. R. Mathews, E. F. E. Carrillo, Ctr. de Investigación en Energia (Mexico)

In this work we report the pulse electrodeposition of lead sulfide thin films on metallic and Tec 7 (Pilkington) glass substrates. For electrodeposition, the potential was fixed by the cyclic voltammetry studies. The deposition bath contained an aqueous solution of $PbCl_2$ and $Na_2S_2O_3$, the pH of which was adjusted to 2.5 by adding diluted HCl. It was observed that the deposition potential has an influence on the crystalline size. The films were deposited with potentials in the range of -0.9V to -0.5 V and was observed that the film deposited at 0.5V had the smallest crystalline size. The potential pulses applied was $V_{on} = -0.5V$ and $V_{off} = +.1V$. The obtained PbS thin films were characterized by XRD, Raman, AFM, and optical transmittance. The films were crystallized in cubic structure, with an average crystalline size of 10 nm. The band gap of the films was estimated at 0.7 eV and was found to vary with the crystalline size. The AFM analysis showed a uniform surface. The films exhibited photoresponse, and the resistivity in the dark was $4 \times 10^4 \text{ Ohm-cm}$.

8110-41, Poster Session

Effects of plasma enhancement on the Al:ZnO MOCVD

S. Kyu, Cheongju Univ. (Korea, Republic of)

Undoped ZnO and Al doped ZnO thin films were deposited on Si(100) and 7059 glass substrates by metal organic chemical vapor deposition (MOCVD) using diethyl zinc (DEZ) and N-methylpyrrolidine alane (MPA) precursors. Effects of substrate temperature, reaction pressure, feed ratio of Zn/O and Zn/Al on the growth rate, preferred orientation, resistivity and transparency were investigated. The growth rate showed a maximum value of 750 nm/min at the substrate temperature 350oC, reaction pressure 1.5 torr. From the Arrhenius plot of deposition rate vs. substrate temperature, it was found that the activation energy of surface reaction was 41.7 kJ/mole. Below 300oC, amorphous films were obtained, while (002) plane preferred oriented ZnO films were deposited above 300 oC. Optical transparency of the films deposited at various experimental conditions showed good quality above 80%, and band gap of the films decreased with the substrate temperature in the range of 3.93~4.14 eV. Especially, effects of plasma enhancement on the properties of film such as optimum substrate temperature, film quality were investigated. Surface morphology have been changed into faceting crystalline with plasma enhancement, especially in the direct plasma condition. XRD analyses show the positive effect of plasma enhancement. But at a high power conditions, diffraction intensity of the films decreased rapidly. Similar tendencies are observed in the growth rate and electrical resistivity of deposited films. It is assumed that mild energetic reactive radicals in the indirect plasma region are more effective for MOCVD process rather than highly energetic, aggressive ionic particles in the direct plasma region.

Conference 8111: Next Generation (Nano) Photonic and Cell Technologies for Solar Energy Conversion II

Sunday–Tuesday 21–23 August 2011 • Part of Proceedings of SPIE Vol. 8111
Next Generation (Nano) Photonic and Cell Technologies for Solar Energy Conversion II

8111-01, Session 1

Advances in spectral conversion for photovoltaics

J. Marques Hueso, S. Ciorba, S. K. W. MacDougall, Heriot-Watt Univ. (United Kingdom); Y. Wang, D. Chen, Fujian Institute of Research on the Structure of Matter (China); B. S. Richards, Heriot-Watt Univ. (United Kingdom)

Up- and down-conversion constitutes two singular routes to achieve improved energy harvesting along the whole solar spectrum by changing the shape of this one rather than to change the absorption properties of the semiconductor layer. One of the materials more extensively studied for these propose have been lanthanides glasses, due to their stability and feasibility as real components of out-door solar panels. To obtain a significant conversion rate two main premises have to be accomplished. First, the excited ions have to emit efficiency, target that has been already achieved with efficiencies near 200%. Secondly, the absorption by the ions has to be significant, with large quantum yields to assure the harvesting at the wavelength to convert, thing that still constitutes a challenge, especially in up-conversion where the transformation has a non-linear dependence on the power.

In this paper we are going to review the materials used as spectral converters for PV, paying special attention to the up- and down-conversion processes in lanthanide glasses in fluoride matrices. We will discuss some strategies pursued to increase their quantum yield, and therefore their overall conversion efficiency. Finally, some methodologies form nanooptics are going to be discussed as possible candidates to overcome the low absorbance of the lanthanide ions.

8111-03, Session 1

Embedded metallic nanopattern for enhanced optical absorbance and photovoltaics

F. Ye, M. J. Burns, M. J. Naughton, Boston College (United States)

Novel metallic nanopatterns integrated with semiconductor films form optical metamaterials that can enable enhanced absorption. When employed in photovoltaics, such integrated nanostructures may facilitate a significant increase in power conversion efficiency. 3-D electromagnetic computer simulations in both time and frequency domains show that the absorbance of amorphous silicon can be enhanced by more than 3,000% for 1 to 30 nm-thick metal nanopatterns integrated with 30 to 100 nm thick a-Si films. Compared even to conventional thickness a-Si cells (e.g. 400 nm), a several 100% enhancement is observed in simulations. We show these calculated enhancements to be nanopattern shape- and material-dependent, with empirical dispersion relations for a-Si and the metals (Ag, Al, Au, Cu, In, Mg and Pt) employed. The role of plasmonics is investigated with respect to metal choice. Progress on experimental investigations into these effects will be discussed. Such metallic nanopattern integration represents a potential route to high efficiency solar power with ultrathin absorbers enhanced by optical metamedia.

8111-04, Session 1

Visible to infrared down conversion in rare-earth doped fluorides for luminescent solar converters

D. Serrano, A. Braud, Ecole Nationale Supérieure d'Ingenieurs de Caen et Ctr. de Recherche (France)

One of the well-known loss mechanisms in Si solar cells is the thermalization of charge carriers generated by the absorption of high-energy photons. These losses could be reduced by using a rare-earth based luminescent converter to realize multiple electron-hole pairs per incident photon. We present here results obtained in (Pr³⁺, Yb³⁺) codoped CaF₂ and KY₃F₁₀ crystals showing absorption of blue light by Pr³⁺ ions, followed by an efficient energy transfer towards Yb³⁺ ions which subsequently emit around 1.2eV (1030 nm). Ytterbium ions are excellent candidates for the enhancement of Si solar cell efficiency since the Yb³⁺ emission around 1µm is adapted to the Silicon cell absorption.

Experimental results show an increase of the energy transfer efficiency from Pr³⁺ to Yb³⁺ when increasing the Yb³⁺ concentration. For the first Pr³⁺ to Yb³⁺ energy transfer, an efficiency of 97% is achieved in KY₃F₁₀: 0.5%Pr³⁺- 20%Yb³⁺. However, this promising result faces challenging issues since a high Yb³⁺ concentration induces energy migration between Yb³⁺ ions which impairs the Yb³⁺ luminescence. CaF₂ appears then to be particularly interesting. A low Yb³⁺ concentration, only 2%, is sufficient to obtain a 97% energy transfer efficiency because of the creation of Pr³⁺/Yb³⁺ clusters. This clustering effect limits the need for a high Yb³⁺ concentration and therefore reduces the Yb³⁺ concentration quenching in CaF₂. However, a detailed study of the CaF₂ clustering process is required for a better understanding of the experimental results so as to asses precisely the potential of CaF₂: Pr³⁺,Yb³⁺ as an effective luminescent converter.

8111-05, Session 1

Solar energy harvesting by 3D thin-slab photonic crystals

G. Demésy, S. John, Univ. of Toronto (Canada)

While silicon is a promising photovoltaic material, its limited absorption spectrum has rendered first generation photovoltaic devices with poor quantum efficiency in the near infrared spectral region. A light-trapping mechanism is required to harvest solar energy in thin films in this spectral range.

Earlier theoretical work showed that photonic crystals enable light harvesting in weakly absorbing semiconductors due to a broad band, wide angle, Parallel Interface Refraction (PIR) effect. Here light is trapped in slow group velocity modes in a region of enhanced electromagnetic density of states. We demonstrate that three-dimensional sculpting of silicon into cubic photonic crystals (e.g. cubic woodpiles, modulated nanoholes and nanowires) enables PIR based light trapping and strong absorption in the near-infrared with structured slabs of micron thickness.

We determine the optimum set of radii and lattice constants for 2D photonic crystals based on silicon nanowires at constant equivalent homogeneous slab thickness. A simple sinusoidal modulation of the rod radii along the propagation direction, resulting in a 3D cubic lattice is shown to offer an enhancement of 15% in absorption over the best 2D nano-rod array. These structures exhibit comparable performance to the most efficient silicon-based nanostructures proposed so far and offer more opportunities for optimization.

We describe mechanisms to further reduce reflection and transmission losses of light not captured by PIR resonances through anti-reflective surfaces, such as graded index layers and nano-cones. Back-reflectors made of different 3D photonic crystal architectures with targeted stop gaps are shown to be more effective than metallic mirror plates.

8111-06, Session 2

Plasmonic enhancement of thin-film solar cells using gold-black coatings

C. J. Fredricksen, LRC Engineering Inc. (United States); D. R. Panjwani, F. Khalilzadeh-Rezaie, R. E. Peale, K. Baillie, J. Colwell, Univ. of Central Florida (United States); S. Peppernick, A. G. Joly, K. M. Beck, Pacific Northwest National Lab. (United States)

Coatings of conducting gold-black nano-structures on commercial thin-film amorphous-silicon solar cells enhance the short-circuit current by 20% over a broad spectrum from 400 to 800 nm wavelength. The efficiency, i.e. the ratio of the maximum electrical output power to the incident solar power, is found to increase 7% for initial un-optimized coatings. Metal blacks are produced cheaply and quickly in a low-vacuum process requiring no lithographic patterning. The inherently broad particle-size distribution is responsible for the broad spectrum enhancement in comparison to what has been reported for mono-disperse lithographically deposited or self-assembled metal nanoparticles. Photoemission electron microscopy reveals the spatial-spectral distribution of hot-spots for plasmon resonances, where scattering of normally-incident solar flux into the plane increases the effective optical path in the thin film to enhance light harvesting. Efficiency enhancement is correlated with percent coverage and particle size distribution, which are determined from histogram and wavelet analysis of scanning electron microscopy images. Electrodynamic simulations reveal how the gold-black particles scatter the radiation and locally enhance the field strength.

8111-07, Session 2

Plasmonic back contacts for light trapping in thin-film silicon solar cells

U. W. Paetzold, E. Moulin, B. E. Pieters, R. Carius, U. Rau, Forschungszentrum Jülich GmbH (Germany)

Light-trapping concepts are essential for high performance thin-film silicon solar cells made of amorphous (a-Si:H) or microcrystalline silicon ($\mu\text{c-Si:H}$). Conventional devices apply randomly textured TCO (e.g. ZnO) substrates serving as front contacts and reflective metal back contacts (e.g. Ag). In this contribution, a novel light-trapping concept based on Ag nanostructures at the back contact of a thin-film silicon solar cell is introduced. Plasmonic modes in the Ag nanostructures enable scattering of incident light to very large angles at low optical losses. This way, Ag nanostructures can serve as efficient sub-wavelength scattering components of solar cells which couple incident light into thin a-Si:H or $\mu\text{c-Si:H}$ absorber layers. In addition, specific arrangements of Ag nanostructures offer ways to control the scattering angle distribution via diffraction orders.

Both, three-dimensional simulations and experimental results of thin-film silicon solar cells with Ag nanostructures at the Ag back contact will be shown. The interaction of electromagnetic waves and nanostructures on flat silver layers as well as complete solar cells is simulated with a numerical solver of Maxwell's equations. Spatial absorption profiles and photocurrents of solar cells as well as scattering profiles of Ag nanostructures are calculated from three-dimensional electromagnetic field distributions. To demonstrate the plasmon induced light-trapping effect of Ag nanostructures, state-of-the-art n-i-p substrate-type thin film silicon solar cells are fabricated on patterned substrates by conventional plasma-enhanced chemical vapour deposition (PECVD) and compared to those solar cells fabricated with the conventional light-management concept.

8111-08, Session 2

Self-assembly as a design tool for the integration of photonic structures into excitonic solar cells

S. Guldin, Univ. of Cambridge (United Kingdom); P. Docampo, Univ. of Oxford (United Kingdom); S. Hüttner, N. Yufa, P. Kohn, Univ. of Cambridge (United Kingdom); M. Stefik, Cornell Univ. (United States) and Ecole Polytechnique Federal de Lausanne (Switzerland); H. J. Snaith, Univ. of Oxford (United Kingdom); U. B. Wiesner, Cornell Univ. (United States); U. Steiner, Univ. of Cambridge (United Kingdom)

One way to successfully enhance light harvesting of excitonic solar cells is the integration of optical elements that increase the photon path length in the light absorbing layer. Device architectures which incorporate structural order in form of one- or three-dimensional refractive lattices can lead to the localisation of light in specific parts of the spectrum, while retaining the cell transparency.

In our work, we employ the self-assembly of soft matter to design inorganic material with photonic properties. We have previously shown the integration of a three dimensional photonic crystal into a dye-sensitized solar cell. [1] Recent efforts have now led to the incorporation of one dimensional photonic crystals - so called mesoporous Bragg reflectors (MDBR) - into the device architecture. Our new route relies on the use of the block copolymer PI-b-PEO in combination with sol-gel chemistry [2]. This allows unprecedented control to finely tune porosity and pore size in the resulting titania network, which is exploited to manipulate the refractive index within the photoanode. Deposition in a layer-by-layer fashion enables the stacking of alternating high and low refractive index layers. The result are bicontinuous, electron-conductive MDBRs made of TiO₂ with an action spectrum which can be tuned over wide range of wavelengths.

References

[1] S. Guldin et al., Dye-sensitized solar cell based on a three-dimensional photonic crystal, Nano Letters, vol. 10, pp. 2303-2309, 2010.

[2] S. Guldin et al., Tunable mesoporous Bragg reflectors based on block-copolymer self-assembly, submitted

8111-53, Session 2

Femtosecond laser doped silicon for photovoltaic applications

M. Sher, Y. Lin, Harvard Univ. (United States); M. T. Winkler, Massachusetts Institute of Technology (United States); E. Mazur, Harvard Univ. (United States)

Doping silicon to concentrations above the metal-insulator transition threshold yields a novel material that has potential for photovoltaic applications. By focusing femtosecond laser pulses on the surface of a silicon wafer in a sulfur hexafluoride (SF₆) environment, silicon is doped with 1% atomic sulfur. This material exhibits near-unity, broadband absorption from the visible to the near infrared (< 0.5 eV, deep below the silicon bandgap), and metallic-like conduction. These unusual optical and electronic properties suggest the formation of an intermediate band. We report on the femtosecond laser doping techniques and material properties.

By changing the laser parameters and ambient environment we can control the dopant profiles, crystallinity, and surface morphology. We investigate mid-infrared absorption of femtosecond laser doped silicon.

In addition, we use temperature-dependent Hall measurements to investigate electron transport and to identify the energy states of the sulfur donors. These two techniques could shed light on energy levels of dopant states or bands. We will also discuss potential applications for intermediate-band photovoltaics.

8111-09, Session 3

Metamaterial-based photonic black-hole device for solar light energy harvesting

M. Gharghi, C. W. Gladden, Univ. of California, Berkeley (United States); J. G. Valentine, Vanderbilt Univ. (United States); X. Yin, X. Zhang, Univ. of California, Berkeley (United States)

One of the challenges in harvesting solar light is to control the flow of the optical energy inside the device. Ideally, a solar energy device would guide the optical energy in the desired direction to optimize the conversion process. Traditionally this was accomplished by simple light trapping in the optical ray regime. Recent advances in the understanding of sub-wavelength optical phenomena and in nanofabrication technology open new avenues to control and harvest light through stronger light matter interactions.

We have designed a photonic black-hole that is capable of attracting the propagating optical waves to a central spot. The device is based on a metamaterial structure with a radially increasing index of refraction toward the center, and a sudden steep decrease in the proximity of the center. The designed device is implemented in a two dimensional silicon-on-insulator (SOI) slab structure. The index modulation is achieved by a variable density of silicon pillars formed through electron beam lithography and reactive ion etching. The structure is designed to absorb to the center the infrared light propagating in arbitrary direction.

The strong concentration of the light by the photonic black-hole is useful for solar energy harvesting in several different schemes. The designed device is in principal spectrally wideband, the currently employed platform (SOI slab) is useful for frequencies below the silicon bandgap. A potential application is to enhance the density of the infrared light through concentrating at the center for up-conversion to visible light using rare-earth elements deposited at the center of the black-hole.

8111-10, Session 3

Light absorption enhancement in a high-efficiency Gallium Arsenide solar cell using a whispering gallery mode dielectric nanosphere array

J. Grandidier, D. M. Callahan, J. N. Munday, H. A. Atwater, California Institute of Technology (United States)

Light trapping is a critical requirement in thin film photovoltaics, and dielectric texturing is a viable method to induce light trapping, but thin film device quality often suffers upon direct texturing of the semiconductor active material. Thus it is desirable to develop a design method in which textured dielectric layers provide for light trapping on smooth planar thin film cells. We propose here an approach for coupling light into smooth untextured thin film solar cells of uniform thickness using periodic arrangements of resonant dielectric nanospheres deposited as a continuous film on top of a thin cell. Freely propagating sunlight can be diffractively coupled and transformed into several guided modes within the array of wavelength scale dielectric spheres. Incident optical power is then transferred to the thin film cell by leaky mode coupling into the cell thin absorber layer. It is shown that guided whispering gallery modes in the spheres can be coupled into particular modes of the solar cell and significantly enhance its efficiency by increasing the fraction of incident light absorbed. We numerically demonstrate this enhancement using full field finite difference time domain (FDTD) simulations of a SiO₂ nanosphere array above a 1 μm thick Gallium arsenide (GaAs) solar cell structure featuring back reflector and double anti-reflection coating. In the case of a flat cell, the calculated current density is 27.6 mA/cm². The incoupling element in this design has advantages over other schemes as it is a lossless dielectric material and its spherical symmetry naturally accepts a wide range of incidence angles. Moreover, analytical models show that for SiO₂ nanospheres of a given dielectric material, a large number of resonant modes can be supported which can give rise to a 2.3% absorption enhancement

in the GaAs absorber layer at several wavelength between 280nm and 900nm. Also, the SiO₂ nanosphere array can be fabricated using simple, well developed self assembly methods and is easily scalable without the need for lithography or patterning. This concept can be easily extended to other thin film solar cell materials, such as silicon or copper indium gallium diselenide (CIGS), which are also considered.

8111-11, Session 3

Non-periodic plasmonic elements for broadband absorption in thin-film solar cells

R. Pala, J. Liu, E. S. Barnard, D. Askarov, M. L. Brongersma, Stanford Univ. (United States)

Choosing the optimum size and spatial arrangement of light trapping structures is essential for optically thin solar cells made of a semiconductor with a broadband absorption spectrum. Here we develop a simple model that describes the light trapping via waveguide coupling resonances in terms of the coupling response of individual scattering particles and the optical properties of the waveguide mode. We define a "Spectral Region of Interest" (SRI) where scattering will maximally contribute to the total absorption. An optimum distribution of particles with a coupling response matching with the spectral region of interest can easily be identified using this model. To test our model we analyze the increase in absorption induced by uniform periodic and non-periodic metallic nanostructures in an ultra-thin Si film. A simple system consisting of a 2-dimensional array of Ag strips with periodic, quasi-periodic, quasi-random and random patterns on a silica-coated Si film supported by a silica substrate is used in calculations. We find that non-periodic structures can offer a better performance with the tunability of coupling over the SRI as compared to uniform periodic structures in agreement with full-field simulations. We experimentally test our predictions on an ultra-thin (50nm) Si Schottky-Barrier photodetector platform and report a good agreement in between experimental and theoretical results. The model described here can serve as a useful tool in future ultra-thin solar cell designs incorporating 3-dimensional dielectric and metallic light trapping structures approaching the fundamental limit of light trapping.

8111-12, Session 3

Fundamental investigations of singlet fission and its potential in solar photoconversion

J. C. Johnson, National Renewable Energy Lab. (United States); J. Michl, A. Akdag, Univ. of Colorado at Boulder (United States); A. J. Nozik, National Renewable Energy Lab. (United States)

Singlet fission is a process by which a single photoexcited singlet exciton becomes two triplet excitons. If the process is efficient, there are a variety of situations in which singlet fission could result in greatly enhanced photovoltaic or photoelectrochemical yields. The fundamental photophysics that leads to the multiplication of excitons is poorly understood, and there are only a few cases in which singlet fission was found to be reasonably efficient. Our recent focus is to understand the molecular design criteria and the intermolecular interactions that give rise to a fast singlet fission rate. The regimes of weak, intermediate, and strong interchromophore coupling are considered in a class of model compounds that have appropriate singlet-triplet splitting. The interchromophore geometry is also explored and particular configurations discovered in polycrystalline solids yield extremely high efficiency (approaching 200%). Covalently bound dimers that mimic this geometry have been investigated spectroscopically and have the ability to inject multiple electrons per absorbed photon into nanocrystalline supports. The ultrafast photophysics of more commonly studied crystalline organic semiconductors (e.g., pentacene, tetracene) are also being explored and provide information about the mechanisms by which singlet fission occurs.

8111-13, Session 4

Highly efficient quantum dot sensitized solar cell

N. Park, J. Im, S. Park, C. Lee, Sungkyunkwan Univ. (Korea, Republic of)

Highly efficient quantum dot sensitized (QDS) solar cell is presented. Lead iodide based quantum dot was synthesized from methyl ammonium iodide and lead iodide and deposited on nanocrystalline TiO₂ film. The synthesized organic-inorganic hybrid QD showed perovskite structure and was stable upto 300 oC in air. High resolution TEM confirmed that semi spherical QD with about 2 nm in diameter was covered on TiO₂ surface. Surface and cross-sectional EDXS analysis also confirmed that QD sensitizer was homogeneously distributed in 3-dimensional TiO₂ layer. From the detailed investigations on parameters affecting photovoltaic property of QD sensitized solar cell, we achieved the conversion efficiency of 5.7% at AM 1.5G full sun light intensity (100 mW/cm²). For the given thin TiO₂ film (thickness is less than 4 μm), the photocurrent density observed from external quantum efficiency (EQE) spectrum was 16.6 mA/cm² that was two times higher than the conventional N719 dye. In addition, very high EQE of 61.3% was obtained even at long wavelength light of 700 nm, while N719 showed only 8.15% at the 700 nm. Moreover, QD sensitized TiO₂ film exhibited charge collection efficiency being close to 100%. As far as we are concerned, the demonstrated conversion efficiency is the highest one among the reported QD sensitized solar cells.

8111-14, Session 4

Multiple chemical treatments for improved PbSe quantum dot solar cells

O. E. Semonin, Univ. of Colorado at Boulder (United States) and National Renewable Energy Lab. (United States); J. Gao, J. M. Luther, A. J. Nozik, M. C. Beard, National Renewable Energy Lab. (United States)

An essential component of third generation solar cells is the combination of a high-efficiency device with low cost materials and highly scalable manufacturing processes. This is generally considered essential for achieving the “dollar-a-watt” cost target for installed photovoltaic energy generation. Multiple exciton generation (MEG), where absorbed high energy photons generate more than one excitation at the band gap, has been proposed to be more efficient in quantum dots (QDs) than bulk materials, which would increase their theoretical solar cell efficiency. However, MEG has not been observed in a solar cell, leading to some debate about its effectiveness. Regardless, lead chalcogenide QD solar cells, with their relative precursor abundance, solutions-processing, and potential for increased theoretical device efficiencies, have seen significant research as a means to accelerate the cost of solar energy beyond the experience curve. In this work, we present progress with an improved ZnO/PbSe QD heterojunction solar cell that uses a second treatment layer to produce robust, stable, high current devices which nearly double the 1-sun efficiency from our previous work. Optical modeling, impedance analysis and additional progress towards measuring MEG in this solar cell will also be presented.

8111-15, Session 4

TiO₂/PbS colloidal nanoparticle heterojunction solar cells and limiting factors on the performance

G. Zhai, Univ. of California, Santa Cruz (United States); A. J. Breeze, Solexant Corp. (United States); G. B. Alers, S. A. Carter, Univ. of California, Santa Cruz (United States)

In this work, we report on the fabrication and characterization of TiO₂/PbS colloidal quantum dot (QD) solar cells, showing power conversion efficiencies above 4% under AM 1.5 illumination and peak external quantum efficiency over 80%. While our devices show record for short circuit current density of about 21 mA/cm² for PbS- based QD devices, low fill factor (~25%--40%) impedes achievement of record power conversion efficiency. To understand the working mechanism and limiting factors of our solar cells, we studied the relationship between photocurrent and effective voltage applied on the devices as well as the light intensity dependence of the photocurrent and open circuit voltage, respectively. According to the physical model developed by Goodman and Rose for photoconductive layers, the results indicate that the mobility-lifetime product is responsible for the low fill factor of our devices. Moreover, trap-assisted recombination exists in our solar cells. These results give some insight into a potential limiting mechanism in QD solar cells and are valuable for the optimization and further improvement of QD solar cell performance.

8111-16, Session 4

High-efficiency quantum dot solar cells due to inter-dot n-doping

K. A. Sablon, U.S. Army Research Lab. (United States)

Similar to midgap impurities, quantum dots allow for harvesting the IR energy but at the same time increase the recombination losses. The tradeoff between harvesting and recombination processes in quantum dot solar cells is an ongoing problem studied in a number of theoretical and experimental investigations. Compared with the midgap impurities, the quantum dots offer substantially more flexibility for nano-engineering of electron processes via dot size, correlation of dot positions, and selective doping. We investigated effects of doping on the photovoltaic efficiency in GaAs reference cell, undoped, n-doped, and p-doped InAs/GaAs quantum dot solar cells (QDoSCs). We found that photovoltaic efficiency of the undoped QDoSC is almost the same as that of the reference cell. However, the efficiency improves monotonically with increasing inter-dot n-doping, while p-doping deteriorates the photovoltaic conversion. We observed a 50% increase in photovoltaic efficiency in the device n-doped to provide approximately six electrons per dot. In this QDoSC, the short circuit current density increases to 24.30 mA/cm² compared with 15.07 mA/cm² in undoped QDoSC without deterioration of the open circuit voltage. To identify the physical mechanisms that provide this improvement, we investigated the spectral characteristics of the photovoltaic response and photoluminescence of our QDoSCs. We found that the electron capture into QDs is substantially faster than the hole capture, which leads to an accumulation of electrons in QDs. The electrons trapped in dots enhance IR transitions. The built-in-dot electron charge together with charged dopants outside the dots creates the potential barriers, which suppress the fast electron capture processes and at the larger scale form the potential profile which precludes degradation of the open circuit voltage. All of these factors lead to the enhanced harvesting of IR energy and a radical improvement of the QDoSC efficiency. Higher efficiencies are anticipated with the further increase of doping levels and at higher radiation intensities. This makes the QDoSCs promising candidates for use with concentrators of solar radiation.

8111-17, Session 4

High-voltage quantum well waveguide solar cells

A. K. Sood, R. E. Welser, A. W. Sood, Magnolia Solar, Inc. (United States); E. F. Schubert, Rensselaer Polytechnic Institute (United States)

Quantum structured solar cells seek to harness a wide spectrum of photons at high voltages by embedding low energy-gap wells within a high energy-gap matrix in a single-junction device. Quantum well solar cells have the potential to deliver ultra-high power conversion efficiencies

in single junction devices, efficiencies that in theory can approach 45% in un-concentrated sunlight over a wide range of environmental conditions. In this paper, we review and summarize our recent experimental efforts to enhance the open circuit voltage of InGaAs quantum well waveguide solar cell structures.

Photon absorption, and thus current generation, is hindered in conventional thin film solar cell designs, including quantum well structures, by the limited path length of incident light passing vertically through the device structure. Optical scattering into lateral waveguide structures provides a physical mechanism to dramatically increase photocurrent generation through in-plane light trapping. However, the insertion of wells of high refractive index material with lower energy gap into the device structure often results in lower voltage operation, and hence lower photovoltaic power conversion efficiency. In this work, we demonstrate that the voltage output of an InGaAs quantum well waveguide photovoltaic device can be increased to over 1.05 V @ 25 mA/cm² by employing a novel III-V material structure with an extended wide band gap emitter heterojunction. Analysis of the light IV characteristics from small area test devices reveals that both non-radiative and radiative recombination components of the underlying dark diode current have been suppressed.

8111-19, Session 5

Plasmon-enhanced photoelectrochemical cells

I. Thomann, B. Pinaud, R. Pala, Z. Chen, T. Jaramillo, M. L. Brongersma, Stanford Univ. (United States)

We will present progress towards the use of plasmonic metal nanostructures to enhance the efficiency of solar fuel generation. In the past, solar-to-fuel-efficiencies have been limited because of a large mismatch in the length scales for optical absorption and carrier extraction. Future generations of photoelectrodes must employ cheap, earth-abundant absorber materials in order to provide a large-scale source of clean energy. These materials will likely have relatively poor electrical properties requiring them to be thin to ensure efficient carrier extraction.

The central idea of this work is to employ plasmonic metal nanostructures to efficiently concentrate sunlight near the surface of such thin-film semiconductor electrodes. In this way, optical absorption close to the electrode surface is enhanced, precisely where the relevant chemical reactions are taking place.

We will present various device concepts under study. Full-field electromagnetic simulations were employed to identify suitable geometries for enhancing absorption close to the semiconductor-liquid interface. Thin-film electrodes made from cheap, earth-abundant semiconductors, such as iron oxide, were grown and their materials properties were characterized. Metal nanostructures were fabricated via e-beam lithography, as well as nanoparticle deposition methods. Photoelectrochemical characterization results clearly demonstrate that plasmonic effects are present, and I will discuss our progress towards a more systematic investigation of plasmonic enhancements, catalytic effects and charge recombination.

This project opens up an exciting new avenue for the use of plasmonic structures, exploiting the unique optical properties of metal nanostructures to direct electromagnetic energy precisely where it is needed to drive photoelectrochemical reactions.

8111-20, Session 5

Toward photonic fluorescent solar concentrators

J. Gutmann, M. Peters, B. Bläsi, M. Hermle, Fraunhofer-Institut für Solare Energiesysteme (Germany); H. Zappe, Albert-Ludwigs- Univ. Freiburg (Germany); J. C. Goldschmidt, Fraunhofer-Institut für Solare Energiesysteme (Germany)

Fluorescent concentrators concentrate both diffuse and direct solar radiation with no need for tracking. They consist of transparent plates doped with fluorescent materials such as organic dyes. These fluorescent materials absorb incident light and emit at longer wavelengths. Most of the emitted light is trapped inside the plate by total internal reflection and guided to the edges where solar cells convert the concentrated light.

We present a new concept for these concentrators that mitigates the two major loss mechanisms, namely the escape cone of total internal reflection and reabsorption of emitted light. Embedding the fluorescent material in a photonic structure enables highly efficient light guiding. The modification of both emission direction and spectrum by the surrounding structure can reduce path length dependant losses as well as reabsorption, thus enhancing system efficiency.

In 2D wave optical FDTD simulations we obtained a spectral light guiding efficiency of up to 97.7% for a multilayer system. That means that the loss is over 20 times smaller than in conventional fluorescent concentrators. We present how the photonic structure modifies the emission spectrum as the local density of states for photons inside the structure is different from the one in homogeneous media. In order to design suitable photonic structures, the angular characteristic has to be considered: We show for a Bragg filter, that optimum light guiding is obtained for wavelengths smaller than the design wavelength.

We further report on progress in device fabrication for experimental verification pursuing both a multilayer and a 3D photonic crystal design.

8111-21, Session 5

Many body effects in intervalence band thermophotovoltaic structures

M. Fernandes Pereira, Jr., Sheffield Hallam Univ. (United Kingdom)

In conventional single-energy-gap photovoltaic devices, only photons with energy close to the semiconductor bandgap are effectively absorbed and converted into current [1]. In contrast, intersubband - based Thermophotovoltaic (TPV) devices [2] are not limited by the bandgap. This study demonstrates that inter-valence band absorption structures may lead to devices that can potentially convert thermal photons to current efficiently in the far infrared, which is a range that remains to be further exploited. Absorption due to valence band transitions [3] allows simple perpendicular incidence in the TE mode without the need of prisms or other couplers that increase the complexity, cost, practicality and also the losses in a conduction-band-based TPV. Furthermore, the analysis demonstrates the relevance of many body effects, which are now routinely considered in laser and optoelectronic device simulators, but have been essentially overlooked for photo and thermophotovoltaic simulation and design considerations.

References

- [1] S. Tomi, Phys. Rev. {bf B82} 195321 (2010).
- [2] J. Yin and R. Paiella, Optics Express 18, 1618 (2010).
- [3] M.F. Pereira Jr. and H. Wenzel, Phys. Rev. {bf B70}, 205331 (2004).

8111-22, Session 5

Theoretical analysis of nanostructured solar cells: opportunities, practical limitations, and results from bulkheterojunction inorganic devices

H. W. Hillhouse, Purdue Univ. (United States)

A basic feature of nanostructured solar cells is presence of increased interfacial area. Here, we define a simple model and several dimensionless groups that show how geometric factors and surface recombination interplay with bulk recombination (predominantly Shockley-Read-Hall recombination) to set practical efficiency limits and also illustrate opportunities for nanostructured photovoltaics. The model

**Conference 8111: Next Generation (Nano) Photonic
and Cell Technologies for Solar Energy Conversion II**

is also extended to quantify the potential benefits of multiple exciton generation (MEG). We will also present recent experimental results on bulk heterojunction inorganic solar cells based on highly ordered “double-gyroid” arrays of PbS quantum wires. The wire segments that compose the ordered array are 4 nm in diameter and intersect at y-junctions every 12 nm. These unique nanomaterials are fabricated using self-assembled double-gyroid nanoporous films as the nanowire template. 2D grazing incidence small-angle x-ray scattering (GISAXS) patterns exhibit 96 diffraction peaks from the nanoscale order. The patterns are indexed with a (211) oriented cubic unit cell with Ia-3d symmetry and lattice constant equal to 18 nm. Thus, the PbS wire segments are interconnected with crystallographic periodicity. All-inorganic Schottky junction and interpenetrated p-n junction photovoltaic devices have been fabricated with a variety of contacts and device architectures.

8111-23, Session 6

Exceeding the limit in solar energy conversion

X. Zhu, The Univ. of Texas at Austin (United States)

The Shockley-Queisser (SQ) limit, i.e., the maximum power conversion efficiency of a conventional solar cell, results mainly from the loss of excess photon energy above a semiconductor band gap to the heat bath. The first approach to exceed this fundamental limit is to convert part of the excess photon energy to multiple electron-hole pairs in a process called exciton fission or multiple exciton generation (MEG). I will illustrate the harvesting of MEG via direct multi-electron transfer from the illusive “dark” multiexciton state. The second approach is to harvest the hot electrons/holes before they lose their excess energy. This must be a dynamic process occurring on ultrafast time scales to compete with hot carrier cooling. I will discuss challenges in implementing both approaches in solar cells with efficiency exceeding the SQ limit.

8111-24, Session 6

**Plasmon-induced current rectification
and power conversion through hot carrier
tunneling**

F. Wang, N. Melosh, Stanford Univ. (United States)

In spite of their high power conversion efficiency in the microwave regime, rectennas are facing fabrication challenges and parasitic capacitance at optical and infrared frequencies. We propose a new architecture of metal-insulator-metal (MIM) devices for solar energy harvesting at visible and infrared frequencies based on insulating barrier asymmetrical alignment relative to Fermi level and spatial confinement of hot electrons excited through plasmon absorption. As plasmons excited in the upper metal are absorbed, they create a high concentration of hot electrons, which can tunnel through the thin insulating barrier, producing current. The theoretical efficiency enhancement by using surface plasmons can be greater than 75 times than direct illumination, and is effective for visible to IR wavelengths. Here we present both theoretical estimates of the power conversion efficiency and the first device measurements, which show clear rectification and power conversion behavior. Photocurrent enhanced by surface plasmons excited through high-index prism and grating structures will be discussed.

8111-25, Session 6

**Ultrafast photocurrent in the nanotube PN
junction: probing the interplay between
electron-hole pair creation and annihilation**

N. M. Gabor, Massachusetts Institute of Technology (United States); Z. Zhong, Univ. of Michigan (United States); K. Bosnick, National Research Council of Canada, Univ. of Edmonton

(Canada); P. McEuen, Cornell Univ. (United States)

Understanding the efficient generation (creation) and recombination (annihilation) of electron-hole pairs in low-dimensional devices, as well as developing new optoelectronic nanotechnologies that incorporate efficient generation of multiple electron-hole pairs [1], will require the ability to measure individual device behavior at time scales comparable to electron motion. In individual carbon nanotubes (NTs), purely optical [2-6] and purely electronic [7] measurements have probed carrier dynamics at ultrafast (sub-picosecond) time scales by exploiting intrinsic nonlinear processes. In nanoscale optoelectronic devices, the microscopic details and characteristic time scales of nonlinear processes determine device performance limits for applications in ultrafast photodetectors, light emitting diodes (LEDs), lasers, and energy harvesting devices. Therefore, understanding the physical mechanisms that lead to nonlinear behavior is of paramount importance, yet no measurements have combined ultrafast optical and electronic techniques to probe the fundamental nonlinear processes in individual NTs at subpicosecond time scales.

Here, we present the first ultrafast photocurrent measurements of an individual NT optoelectronic device that explore the interplay between efficient creation and annihilation of electron-hole pairs. By using ultrafast lasers to excite photocurrent in a nanotube PN junction, we are able to probe optoelectronic device behavior at sub-picosecond time scales. Using this technique, we directly probe the transit of electrons and holes across the device in the time domain, finding that charge carriers escape the junction and travel to the device contacts within ~1 picosecond. The carrier escape time is found to result from an electric field-dependent velocity, in which carriers in the first subband (of effective mass $m1^*$) escape the device in half the time as carriers in the second subband ($m2^* = 2m1^*$). Additionally, we observe strong photocurrent saturation at high optical powers that occurs more dramatically for carriers excited into the second subband $\epsilon 2$. We attribute this strong saturation to the annihilation of electron-hole pairs by high-energy free carriers, a process that is more efficient for $\epsilon 2$ carriers due to energy and momentum constraints.

8111-33, Poster Session

**Efficiency enhancement of InGaN-based
multiple quantum well solar cells via
antireflective ZnO nanorod arrays**

K. Lai, National Taiwan Univ. (Taiwan)

ZnO nanorod arrays (NRAs) were applied as the antireflection coating for InGaN-based multiple quantum well solar cells. The NRAs were obtained by a low-temperature (95 °C) hydrothermal method with two different process times: 105 minutes and 135 minutes, giving the average lengths of 1.0 μm and 2.4 μm , respectively. It was found that the 1- μm NRAs results in the enhanced external quantum efficiencies (EQE), fill factor (FF) and conversion efficiency (η) of the solar cell due to the suppressed surface reflections. However, the 2.4- μm NRAs, though exhibiting even lower reflections, led to decreased EQE, FF, and η . The deteriorated device performances were attributed to the absorption of ZnO at the wavelengths below 450 nm. This study indicates that the trade-off between optical transmission and absorption of wide-bandgap nanostructural ARCs should be considered when optimizing the morphology of nanostructures for solar applications.

8111-34, Poster Session

**Embedded nanoparticles for absorption
enhancement in Si-based photovoltaics**

N. Kadakia, H. Bakhru, M. Huang, Univ. at Albany (United States)

Due to the low absorption of silicon, the majority of silicon-based photovoltaic cells are several hundred micrometers thick, limiting their economic feasibility. To achieve cost parity with conventional sources of energy, silicon-based photovoltaics have begun to move towards thinner substrates; such thinner cells necessitate the use of light-trapping

Conference 8111: Next Generation (Nano) Photonic and Cell Technologies for Solar Energy Conversion II

methods to increase the optical path length. We are investigating the use of metallic nanoparticles, which can increase the carrier transition rates, and therefore the absorbance, in the surrounding silicon by orders of magnitude. The enhancement however decreases exponentially with the radial distance from the particle and is virtually diminished by 10 nanometers from its surface. To exploit this phenomenon, therefore, such particles would need to be embedded into the silicon itself. To that end, we have developed a method to create subsurface silver nanospheres using a combination of implantation, thermal deposition, and thermal annealing. By adjusting the implantation parameters, we can localize the layer of nanospheres at specified depths. Through Rutherford backscattering characterization and secondary ion mass spectroscopy, we have found that the silver has indeed agglomerated into the desired location at high concentrations. Furthermore, through transmission electron microscopy bright field imaging and selected area diffraction patterns, we have ensured that the silver has formed bulk-phase nanoparticles, on the order of 30-50 nanometers in diameter. With further work, this method can help realize more efficient surface plasmon-enhanced silicon-based photovoltaics.

8111-36, Poster Session

Optical and electrical properties of crystalline silicon wire arrays

Y. Pai, B. J. Simonds, J. Fields, R. T. Collins, C. Taylor, Colorado School of Mines (United States)

Silicon wire arrays have been synthesized through two step Ag-assisted electrode-less etching from an n-type silicon wafer with (100) orientation. FESEM(Field Emission Scanning Electron Microscopy), UV-VIS-NIR(Ultra Violet-Visible-Near Infrared) spectrophotometer and RCPCD(Resonant-coupled photoconductivity decay) have been used to characterize the morphology, optical, and electrical properties of silicon wires at varying etching times. The reflectivity of the wire arrays decreased with increasing etching time because of light scattering from micro-roughness of the silicon wire surfaces. The effective carrier lifetime decreased with increasing wire length due to the increased surface area. We also created smoother wire surfaces by thermal oxidation followed by HF dipping. From FESEM cross sectional images and reflectivity results, this treatment remove the micro-roughness, but effective minority carrier lifetime is lower than the as-grown wire arrays. A photoluminescence peak observed only in the smoother wires suggests that the lower effective carrier lifetime is due to the diffusion of the residual Ag atoms from the wire surfaces into the bulk during the thermal oxidation process.

8111-37, Poster Session

Optical absorption in vertical silicon nanowires for solar cell applications

M. Foldyna, L. Yu, B. O'Donnell, P. Roca Cabarocas, Ecole Polytechnique (France)

Photovoltaic research has moved from popular solar cells, based on crystalline silicon substrates with thicknesses of around 250 μm , to the thin film structures saving large amount of the active material. The next generation of solar cells requires substantial increase of the energy conversion efficiency, which can be achieved by enhancing of the optical trapping inside the cell. Light trapping can be improved either by texturing, using materials of different gap in multi-junction solar cells or by structuring the active materials and/or reflectors inside the solar cell.

In this work we study efficiency of the light trapping inside the silicon nanowire solar cells produced using cost-efficient PECVD plasma assisted growth process. The main focus is on the optical trapping inside the single vertical nanowires, which can enhance optical absorption far beyond capabilities of a thin film. A spectral optical absorption modelling together with an electro-magnetic field distribution analysis give insight into the light trapping inside the nanowires. The results provide a guide for the optimization of nanowires diameters, spectral absorbance as a

function of nanowire length and optimal density maximizing absorption with minimal material demands. The effect of the regular (periodic) organization is also studied and compared with dense and sparse random structures.

8111-38, Poster Session

Improvement of solar cell efficiency using nano-scale top and bottom grating

X. Jin, A. Ellaboudy, G. Chavoor, California Polytechnic State Univ., San Luis Obispo (United States)

Solar cells are very critical for the energy conversion and they are irreplaceable energy sources. How to increase the efficiency of a solar cell is always an important research topic. We study solar-cell designs using nano-grating on both top (transmission) and bottom (reflection) of solar cells. First, we perform simulations based on rigorous coupled wave analysis (RCWA) to evaluate the diffraction top gratings. In the RCWA method, we calculate up to 20 harmonics, and sweep the launch angle of incident light from 0 to 90 degree. The incident light wavelength varies from 100nm to 1200nm weighted. The total efficiency is the summation of transmission powers of each harmonics, each incident angle, and each wavelength. Triangular gratings can achieve higher light absorption compared to rectangular gratings. The best top grating is around 200nm grating period, 100nm grating height, and 50% filling factor, which corresponds to 37% improvement for triangular grating and 23% for rectangular grating compared to the non-grating case. Then, we use Finite-Difference Time-Domain (FDTD) to simulate transmission/reflection double grating cases. Here the light source is placed on the top of solar cell. The time monitor is at the center of the cell to collect transmission power. We simulated triangular-triangular (top-bottom) grating cases and triangular-rectangular (top-bottom) grating cases. By varying the bottom reflection grating period from 100nm to 900nm and keep the top grating fixed as 200nm-period triangular grating, The solar cell efficiency improvement can reach about 42%. For the triangular-rectangular (top-bottom) grating case, the 20% efficiency improvement can be achieved.

8111-39, Poster Session

Undamped collective surface plasmon oscillations in metallic nano-chains

W. A. Jacak, Wroclaw Univ. of Technology (Poland); J. Krasnyj, Odessa International Univ. (Ukraine); L. Jacak, Wroclaw Univ. of Technology (Poland)

We investigate utilization of nano-spheres organized in chain structures within the photo-voltaic setup to employ collective modes of surface plasmons, in order to aid plasmonic energy transport and enhance coupling to semiconductor medium for increased solar cells efficiency. The previously described [1] instability of collective surface plasmon oscillations in chains of metallic nanospheres with appropriately selected spheres radii and separation of particles is now discussed and analyzed within a nonlinear approach enabling description of undamped collective mode with appropriately adjusted amplitude, without instabilities. The nonlinear terms arise due to nonlinear contributions to Lorentz friction and effectively quench amplitude instability, thus resulting in stable undamped mode with strictly determined amplitude. This effect is helpful in theoretical interpretation of long range signals in metallic nano-chains observed experimentally by the group of Atwater [2], in terms of the near-field coupling with inclusion of retardation effects and beyond the extremely weak positive interference of the far-field radiation, as was already analyzed within the semi-numerical methods [3]. Considered nano-chain structures (possibly vertically oriented within the semiconductor layered solar cell setup) due to plasmonic undamped collective oscillation mode would enhance internal distribution of energy, providing a novel plasmon subsystem arrangement in layered cell setup, holding a potential for applications towards more efficient solar cells designs. With respect to the undamped collective modes, it is important

Conference 8111: Next Generation (Nano) Photonic
and Cell Technologies for Solar Energy Conversion II

to consider nonlinear propagation model in order to remove instabilities and to determine optimal amplitude of the signal and geometry/size system parameters, and such nonlinear model for plasmon propagation is analyzed.

- [1] W. Jacak et al., JAP 108, 084304 (2010)
[2] M. Brongersma et al., PRB 62, 16356 (2000)
[3] V. Markel, A. Sarichev, PRB 75, 085426 (2007)

8111-40, Poster Session

CNTs electric field enhancement of CIGS solar

S. Han, Hanyang Univ. (Korea, Republic of)

Compound semiconductor/CNTs composites have shown considerably improved efficiency improvement in photovoltaic devices, which is often attributed to two different factors. One is the formation of efficient electronic energy cascade structures. The other effect of CNTs on the performance of photovoltaic devices is the decrement of interfacial resistance. The interfacial resistances at n-type/p-type materials and/or n-type materials/TCO electrode are reduced by an outstanding electrical property of CNTs.

In addition to the effects of CNTs, we report the third reason for increment of efficiency in photovoltaic devices by CNT's well-known electrical field enhancement effects. The improved β values in reverse-FE currents of CIGS electrode with SWNTs layers indicate the enhancement of electrical field in photovoltaic devices, which implies the acceleration of the electron transfer rate in the cell. Due to the formation of an efficient electronic energy cascade structure and the decrease of the interfacial resistance as well as the improvement of the electrical field in the photovoltaic devices, the power conversion efficiency of electrochemically deposited superstrate-type CIGS solar cells was increased 24.3% in the presence of SWNTs and showed 10.40% conversion efficiency.

8111-41, Poster Session

TiO₂-nanotube-based dye-sensitized solar cells containing fluorescent material

W. Kim, Gangneung-Wonju National Univ. (Korea, Republic of);
H. Park, KAIST (Korea, Republic of); W. Choi, Gangneung-Wonju National Univ. (Korea, Republic of)

Highly ordered TiO₂ nanotube arrays were prepared by anodic oxidation of Ti foil in an application to dye-sensitized solar cells (DSCs). Vertical structure of TiO₂ nanotube arrays is very attractive due to a high electron transfer from dye to electrode. To improve the power conversion efficiency, fluorescent material was inserted in a liquid electrolyte to use a light spectrum efficiently. Fluorescent material to emit the absorbed light energy provided an additional light for dye in DSCs and additional electrons was created. Thickness of TiO₂ nanotube arrays grown by anodic oxidation was 15 μ m. N719 dye and I³-/I⁻ electrolyte were used to fabricate the DSCs. DSCs containing fluorescent material show a higher short circuit current densities (J_{sc}) than DSCs without fluorescent material. Therefore the power conversion efficiency of DSCs was improved by fluorescent material. Electrochemical impedance spectroscopy (EIS) was observed to understand an electron transfer and life time.

8111-43, Poster Session

A freestanding silicon nanowire array solar cell using plasmonic back reflection for broadband optical absorption

J. Jung, S. Jee, Z. Guo, K. Zhou, H. Um, K. Park, J. Lee, Hanyang Univ. (Korea, Republic of)

Si nanowire (SiNW) has been known to be one of the nanomaterials promising for future solar cell applications. Representative attractive features are low material consumption enabling the flexible design, and strong broadband optical absorption by multiple scattering [1]. Freestanding SiNW arrays without Si substrate show the superior absorption characteristics compared to a thin film at short wavelengths of incident light [2], in contrast to a poor light absorbance due to the insufficient thickness of absorbing material at long wavelengths. This paper demonstrates the additional light-trapping techniques for effective optical concentration of incident photon at a long wavelength region. Plasmonic nanostructures are focused as a promising technique for light trapping in high-efficiency solar cells [3].

A SiNW array is embedded in a PDMS matrix to make a flexible thin film in which the Ag plasmonic nanograting is formed at backside for solar cell applications. This metallic nanograting structure shows the plasmonic potential to enhance the absorption of incident light above the bandgap energy through the broadband and polarization insensitive absorption enhancements. This method yielded the light absorption of ~92.6% with only ~5% of silicon consumption in a conventional crystalline solar cell. Three major routes for light trapping such as back reflection, Surface Plasmon Polaritons (SPP), and SPP scattering have been introduced for absorption enhancement at a long wavelength range.

- 1.M. D. Kelzenberg, S. W. Boettcher, J. A. Petykiewicz, D. B. Turner-Evans, M. C. Putnam, E. L. Warren, J. M. Spurgeon, R. M. Briggs, N. S. Lewis and H. A. Atwater, Nat. Nanotech. 9, 239 (2010).
2.L. Hu and G. Chen, Nano Lett. 7, 3249 (2007).
3.W. Wang, S. Wu, K. Reinhardt, Y. Lu, and S. Chen, Nano Lett. 10, 2012 (2010).

8111-44, Poster Session

Fine-tuning the structure of unsymmetrical squaraine dyes towards the development of efficient dye-sensitized solar cells

S. S. Pandey, R. Watanabe, N. Fujikawa, Y. Ogomi, Kyushu Institute of Technology (Japan); Y. Yamaguchi, Nippon Steel Chemical Co., Ltd. (Japan); S. Hayase, Kyushu Institute of Technology (Japan)

In the recent past of development of sensitizer having effective light absorption and photon harvesting in NIR wavelength region has attracted a great deal of attention towards the fabrication of efficient dye-sensitized solar cells. Squaraine dyes exhibit strong and sharp absorption having very high molar extinction coefficient whose wavelength can be tailored from visible to IR wavelength region has a great potential toward the development of novel NIR sensitizers. Fabrication of dye-double layer dye sensitized solar cells (reported by our group recently) with efficient visible dye and novel NIR dyes are expected to open a window for the development of high efficiency dye sensitized solar cells. Recently it has been reported that unsymmetrical squaraine dyes possess enhanced photon harvesting leading to increased photoconversion efficiency but no further insight has been proposed for the fine tuning of molecular structure of unsymmetrical dyes. We have synthesized a number of unsymmetrical indole bases squaraine dyes where carboxyl anchoring group was directly introduced in the indole ring. It has been found that relative length of alkyl groups and their positioning in the unsymmetrical dye molecular structure affects their photon harvesting behavior. Best efficiency 4.4 % (J_{sc} 10.86 mA/cm², V_{oc} 9.64 V and ff 0.61) was obtained when a long alkyl group was substituted in the ring bearing

carboxyl anchoring group while it was short chain length in the counter indole ring. The photovoltaic performances for different sensitizers will be discussed in detail in the light of structure property correlation.

8111-45, Poster Session

Aluminum nanoparticles for improved OPV devices

V. Kochergin, L. A. Neely, MicroXact, Inc. (United States); H. D. Robinson, Virginia Polytechnic Institute and State Univ. (United States)

At present, the energy conversion efficiencies achievable with organic photovoltaic (OPV) technology are significantly below those in inorganic PV devices. The conversion efficiency of OPV devices is limited by the material properties: the high energy and narrow spectral range of the absorption band result in inefficient harvesting of solar radiation, while low charge carrier mobilities limits the possible active layer thickness. Utilization of plasmonic structures in or around the OPV active layer has been suggested as a way to improve the conversion efficiency of thin film photovoltaic devices. However, this promise remains unfulfilled, and the experimental results are often contradictory to theoretical predictions. We will present theoretical and experimental results indicating that the aluminum-based plasmonic nanostructures hold significant promise for conversion efficiency enhancement in OPV devices. The high plasma frequency of aluminum permits the use of particle concentrations close to the percolation threshold, which results in a wider band of enhanced absorbance and correspondingly better overlap between the plasmon resonance band and the intrinsic absorption bands of OPV materials than what is achievable with gold or silver plasmonic structures. While aluminum nanoparticles are prone to oxidation, the path toward stabilization of aluminum nanoparticles via proper surface functionalization is demonstrated, and we will present data demonstrating a significantly enhanced absorption across a broad frequency range in P3HT:PCBM layer with embedded functionalized aluminum nanoparticles.

8111-46, Poster Session

Device properties of nanopore PN junction Si for photovoltaic application

H. R. Jin, G. L. Liu, Univ. of Illinois at Urbana-Champaign (United States)

Improvement of energy conversion efficiency of solar cells has led to innovative approaches, in particular the introduction of nanopillar photovoltaics. Previous work on nanopillar Si photovoltaic has shown broadband reduction in optical reflection and enhancement of absorption. Radial or axial PN junctions have been of high interest for improved photovoltaic devices. However, with the PN junction incorporated as part of the pillar, the discreteness of individual pillar requires additional conductive layer that would electrically short the top of each pillar for efficient carrier extraction. The fragile structure of the surface pillars would also require a protection layer for possible mechanical scratch to prevent pillars from breaking. Any additional layer that is applied, either for electrical contact or for mechanical properties may introduce additional recombination sites and also reduce the actual light absorption by the photovoltaic material.

In this paper, nanopore Si photovoltaics that not only provides the advantages but also addresses the challenges of nanopillars is demonstrated. PN junction substrate of 250 nm thick N-type polycrystalline Si on P-type Si wafer is prepared. The nanopore structure is formed by using anodized aluminum oxide (AAO) as an etching mask against deep reactive ionic etching (DRIE). The device consists of semi-ordered pores of ~70 nm diameter. Pore depths are studied in 4 distinct conditions compared to the 250 nm PN junction: 140 nm, 250 nm, 320nm, and 400 nm. IV characteristics of each condition is presented, with discussion on photovoltaic efficiency.

8111-47, Poster Session

Nanoparticles for down-conversion: concept and theory

Z. R. Abrams, A. Niv, X. Zhang, Univ. of California, Berkeley (United States)

The Shockley-Queisser limit for solar cells assumes that each photon creates one electron, which is extracted at the band-gap of a semiconducting material. In this framework, all photons below the band-gap are lost to transparency, and higher energy photons lose their excess energy to the thermalization of electrons created above the band-gap. 3rd generation solar cells are aimed at surpassing these limitations and increasing efficiency.

From an energy conservation perspective, down-converting with energy larger than the band gap into two lower energy photons is one way to improve the overall efficiency. This is fundamentally different from a multi-exciton solar cell, where each high energy photon produces two electrons, despite the apparent similarities in their end result. However, currently no down-converting material system has been discovered with efficient quantum splitting characteristics.

We are inspecting the use of semiconducting nanoparticles as a possible material system that can be used to down-convert light. Since nanoparticles have large surface-to-volume ratios, the concentration of surface states per nanoparticle can reach a theoretical threshold beyond which they can become radiative with high quantum efficiencies. We analyze the efficiency gains for such a system, both with and without non-radiative losses, as well as describe the entropic processes of such a conversion system. Using direct band gap nano-materials, with high absorption properties, one can add a thin-film layer of nanoparticles and improve the overall efficiency of a cell by a few percentages, without the need to change the underlying solar cell.

8111-48, Poster Session

Using oblique angle scatter depolarization as a metric of absorption for front surface nanoparticle enhanced solar collectors

T. M. Fitzgerald, Univ. of Dayton Research Institute (United States); M. A. Marciniak, Air Force Institute of Technology (United States); J. Vella, Jr., General Dynamics Information Technology (United States); A. M. Urbas, Air Force Research Lab. (United States)

The study of nanophotonic structures for advanced nanostructured solar cell concepts featuring enhanced light-to-energy conversion mechanisms is of significant interest to the solar energy harvesting community. A technique to augment the traditional integrating sphere method and provide precise angular quantification of enhanced absorption due to placement, composition, concentration, and geometry of nanoparticles on a solar cell surface is presented. The technique is based on the measured angular dependent depolarization of scattered light reflected from the nanoparticle-enhanced solar cell surface. The amount of depolarization, or loss of degree of total polarization, of obliquely scattered light from known incident polarization states is dependent on the degree of interaction of the light with the surface nanoparticles. Proper selection of nanoparticles increases surface scatter, increases the absorption of incident light energy, and increases the depolarization of the scattered light. The technique is model-based through the DDSCAT direct dipole approximation tool. This technique allows for the comparison of measured to modeled depolarization and permits selection of nanoparticle geometry for optimal light-to-energy conversion. Comparisons are presented for the oblique angle scatter depolarization to traditional absorption measurements for gold prism enhanced solar cells. The technique is based upon the measurement capabilities of the Air Force Institute of Technology (AFIT) Dual-Rotating-Retarder (DRR) full-Mueller-matrix (Mm) Complete Angle Scatter Polarimeter at 544nm wavelength. The technique is enabled by enhancements such

as automation, addition of multiple light sources, an improved sample positioning and orientation interface, and enhanced data-analysis software to a Schmitt Measurement Systems (SMS) Complete Angle Scatter Instrument (CASI®).

8111-49, Poster Session

Fabrication and optical characterization of antireflective sub-lambda structures and nanotemplates of silicon nitride for photovoltaics

B. Sadeghimakki, M. Moradi, S. Sivoththaman, Univ. of Waterloo (Canada)

Antireflection coatings (ARCs) are keys to enhancing the photon collection in photovoltaic solar cells. One well-known and industrially applied but somewhat narrow-band ARC in silicon (Si) based solar cells is the silicon nitride (SixNy) thin film. However, if sub-wavelength structures of SixNy can be formed and deployed on Si, this will lead to much improved and broad-band antireflection properties. During the last decade, a great deal of work has been dedicated to show the potential of nanoscale structures on Si substrates in several application areas - from microelectronics to biological/chemical sensing. In this report, we demonstrate a simple and maskless process employing reactive ion etching (RIE) technique in a CF₄ chemistry for the top-down fabrication of SixNy nanostructures on SixNy thin films pre-formed by plasma enhanced chemical vapor deposition (PECVD). The formation mechanism of SixNy nanopillars, the process controllability, and the dependence of their shape and size on plasma process conditions are discussed in detail. It is also shown that the fabricated nanopillar array can be used as a template to form nanostructures on the underlying Si substrate surface this time using a less aggressive different plasma etch chemistry (SF₆). Spectroscopic measurements performed on the different types of nanostructure layers revealed a low reflectivity over a broad range of photon spectrum, as opposed to the thin film ARC. The spectral reflectance of the single/double layer with different nanostructure dimensions and pitches is compared to obtain the optimized ARC structure. Finally, we have analytically calculated the spectral reflectivity of the fabricated structures by assigning an effective refractive index to the sub-wavelength layer, as well as adopting experimentally obtained wavelength-dependent refractive indices for Si and SixNy. Excellent fits were obtained between the analytical calculations and experimental data. The simplicity, repeatability, and scalability of the developed process have strong potential for deployment on photovoltaic device architectures.

8111-50, Poster Session

Comparison of graphene film thickness to power conversion efficiency in a graphene-based solar cell

I. Ruiz, Univ. of California, Riverside (United States)

Since the experimental extraction of graphene in 2004, one focus for its application has been as a window electrode in solar cells. Not only is graphene more plentiful and low cost compared to other materials used as window electrodes but it is also expected to have the right characteristics to make it a viable window electrode alternative. One of the important characteristics is the transparency of the window electrode. The transparency is determined by the thickness of the graphene sample, which affects the resistance of the solar cell. The resistance of the graphene film affects the power conversion efficiency (PCE) of the solar cell and in the following set of experiments the PCE is measured as functions of resistance due to varying graphene film thicknesses. The results of the PCE of graphene are then compared to the PCE of common materials used as window electrodes.

8111-51, Poster Session

Properties of Si/SiOx quantum well structure for solar cells applications

K. H. Kim, Cheongju Univ. (Korea, Republic of)

By restricting the dimensions of silicon to less than Bohr radius of bulk crystalline silicon (~5 nm), quantum confinement cause its effective bandgap to increase. Therefore, silicon quantum wells (QWs) using these quantum phenomena could be a good candidate to achieve high performance silicon solar cells.

The SiO_x/Si QW structures were fabricated by using the successive deposition technique, as quantum confinement device to increase the effective energy bandgap and passivation effect in Si surface for the 3rd generation solar cell applications. In Si/SiO_x QWs, the thicknesses of Si layers and SiO_x layers were varied between 1 to 5 nm, respectively.

The roughness of sputter-deposited Si on SiO_x was less than 4 Å in the thickness of 2 nm.

By using the SiO_x/Si QW structures on Si surfaces, the lifetime measured by u-PCD technique increased as a result of passivated surface effects.

The discussion about the other properties such as electrical, structural and optical properties of the QWs will be presented at the conference.

8111-26, Session 7

Silicon nanowire solar cells with a-Si heterojunction showing 7% efficiency

F. Falk, G. Jia, G. Andrä, I. Sill, Institut für Photonische Technologien e.V. (Germany)

Core-shell TCO/a-Si/Si nanowire (SiNW) heterojunction solar cells were fabricated on SiNW arrays. The nanowire arrays were prepared by metal-assisted electroless etching of an n-type silicon wafer (1015 cm⁻³ P). As etchant a AgNO₃-HF mixture (HF 5 M:AgNO₃ 0.02 M = 1:1 by volume) was used in which Ag nanoparticles form acting as a catalyst for silicon etching. The silver catalyst was carefully removed after the etching by a three-step procedure. The nanowires are about 900 nm long with diameters in the 200 to 300 nm range. The distance between wires is in the range of several 10 nm to 500 nm. A stack of intrinsic and p-doped hydrogenated a-Si was deposited as a shell around the SiNWs by plasma enhanced chemical vapor deposition (PECVD). Finally, an about 200 nm thick TCO layer (aluminum doped zinc oxide) was deposited on top of the a-Si layer by atomic layer deposition (ALD) at 225°C substrate temperature. In a mesa-structured solar cell with contact area of 7 mm², an open circuit voltage of 476 mV, short circuit current density of 27.03 mA/cm², a fill factor of 0.562, and a power conversion efficiency of 7.29% were determined under AM 1.5 illumination. Electron beam induced current (EBIC) measurements show clear evidence that most of the current comes from the thin SiNW layer and not from the wafer beneath.

8111-27, Session 7

Comparison of novel 3D nanoarchitectures for solar cells

A. Wangperawong, S. F. Bent, Stanford Univ. (United States)

Several new solar cell device architectures utilizing vertical nanojunctions to decouple light absorption from charge carrier collection are presented. Using models we developed that for the first time describe the device performance of nanostructured solar cells in three dimensions, we have analyzed point-contact nanojunctions, extended nanojunctions, isolated radial nanopillars, and inverted grain boundaries. Our modeling shows that for CdTe solar cells using low quality materials, the power conversion efficiency of nanostructured solar cells is superior to the planar junction.

8111-28, Session 7

Modeling light trapping in silicon microwire arrays

E. D. Kosten, E. L. Warren, H. A. Atwater, California Institute of Technology (United States)

Silicon nanowire and microwire arrays have attracted significant interest as an alternative to traditional wafer-based technologies for solar cell applications. In addition to the device physics advantages of a radial junction, such arrays have been found to exhibit significant light trapping and absorption properties, and some recent experimental results suggest that these structures could exceed the ergodic light trapping limit.[1,2] In an attempt to understand this strong light trapping, we have developed a ray optics model of silicon microwire arrays. For an array on a Lambertian back reflector, this model shows asymptotic increase in the light trapping factor for low areal filling fractions. This asymptotic increase exceeds the ergodic limit for light trapping within the wires, as the back reflector acts like a concentrator with a large acceptance angle.[3] Comparing the ray optics model to experimental data, we find that it shows reasonable agreement with large (4 μm radius) wires, but underpredicts the absorption in smaller (1 μm radius) wires, suggesting wave optics effects are significant in the stronger absorption observed in wires on this scale.[3] Thus, in addition to the ray optics results, we will present a hybrid model that accounts for wave optics effects by combining a ray tracing multiple scattering model with cross sections derived from exact solutions to Maxwell's equations.

References

- [1] E. Garnett and P. Yang. Nano Lett., 10:1082-1087, 2010.
- [2] M. Kelzenberg et. al. Nat. Mater., 9:239-244, 2010.
- [3] E. Kosten, E. Warren, and H. Atwater. Opt. Exp., 19:3316-3331, 2011.

8111-29, Session 7

Spectroscopic studies of dopant incorporation in solution-grown Ga:ZnO nanostructures

R. J. Noriega-Manez, Stanford Univ. (United States); S. Misra, Stanford Synchrotron Radiation Lightsource (United States); S. Mehra, Stanford Univ. (United States); M. F. Toney, Stanford Synchrotron Radiation Lightsource (United States); A. Salleo, Stanford Univ. (United States)

ZnO nanostructures have the potential to become an alternative to ITO as transparent electrodes for photovoltaics by combining their light scattering properties with a suitable electrical performance, all in a low-cost solution-based approach. The observation of a dramatic decrease in the free charge density of gallium-doped ZnO nanostructures upon annealing in air at moderate temperatures (200-600 C) poses questions on the mechanisms that determine the defect chemistry in this material system. ZnO nanostructures of varying impurity concentrations, morphologies and sizes were synthesized in the presence of a high boiling point organic solvent and surfactant. Doping effectiveness depends on the incorporation of impurities into electrically active sites in the crystal lattice; in this case, Ga atoms in Zn substitutional sites. We probe the efficiency of solution-based doping using anomalous X-ray diffraction, monitoring the intensity of a set of diffraction peaks as the incoming radiation energy is scanned across the atomic absorption edge (Ga K-edge, 10370 eV). These types of experiments require the use of a synchrotron lightsource in order to tune the photon energy, achieve an excellent monochromaticity across a wide and continuous range of X-ray energies, and maintain a high brightness as well as the necessary angular resolution. The coordination power of the growth environment and the precursor/solvent molar ratio are critical variables in determining doping efficiency and nanostructure morphology. Complementary experiments are performed with photothermal deflection spectroscopy, studying the amplitude and shape of the free carrier absorption peak in the near

infrared to calculate the mobility and density of free charges in the nanostructures using the Drude model.

8111-30, Session 7

Engineering optical absorption in aperiodic silicon nanostructures for photovoltaic applications

C. Lin, M. Povinelli, The Univ. of Southern California (United States)

We maximize the solar absorption within an aperiodic, vertically-aligned silicon nanowire structure by manipulating the positions of nanowires. We use a random walk optimization algorithm integrated with a rigorous electromagnetic forward solver based on the transfer matrix method (TMM). We found the configuration of the optimal structure to be highly non-intuitive and symmetry-broken. For a wire diameter of 65nm and initial spacing of 100nm, the optimal aperiodic structure showed a dramatic 2.35 times enhancement in ultimate efficiency compared to its periodic counterpart. Moreover, with only one third the absorbing material volume, the optimal structure can outperform a silicon bulk film of equal thickness with an optimal single layer Si₃N₄ anti-reflection coating. The significant absorption enhancement can be explained by examining the absorbance spectrum of the optimal aperiodic structure, which mimics that of a periodic array with a larger lattice constant. Specifically, we observe a large overall red shift of the absorption spectrum and numerous absorption enhancement peaks in the low absorption range of crystalline silicon. The absorption profile within the optimal structure exhibits highly localized strong absorption "hot spots" at resonance. These local resonance modes introduce a unique and effective light trapping mechanism that gives rise to resonantly-enhanced absorption at multiple wavelengths, in a similar fashion to that of guided resonance modes in periodic systems with larger lattice constants. We further investigate whether aperiodicity in a silicon nanowire array is in general beneficial for enhancing optical absorption. Interestingly, we found that one thousand randomly picked aperiodic structures invariably have higher ultimate efficiency than that of the corresponding periodic system.

8111-09, Session 8

Broadband absorption enhancement in organic photovoltaics based on nanopatterned ultra-thin metal films

Q. Gan, Univ. at Buffalo (United States); W. Bai, Institute of Semiconductors (China); Z. H. Kafafi, National Science Foundation (United States) and Lehigh Univ. (United States); F. J. Bartoli, Lehigh Univ. (United States)

Three-dimensional finite-difference time domain calculations have shown that plasmonic structures can significantly enhance the optical absorption of active layers in polymer- or molecular-based organic photovoltaics (OPVs).* A polarization-independent nanopatterned ultra-thin metallic structure supporting short-range surface plasmon polariton (SRSP) modes is used to improve the performance of OPVs via broadband absorption resonances. The physical mechanism of the excited SRSP modes is delineated and their distributions are analyzed. In this talk, we will demonstrate that the SRSP-assisted broadband absorption enhancement could be spectroscopically tuned by carefully designing the OPV devices and tailoring the parameters of the nanopatterned metallic structure(s). These results are very promising for the development of OPVs with enhanced performance.

8111-10, Session 8

Towards fully printed organic solar cells: material aspects and process challenges

C. J. Brabec, Friedrich-Alexander-Univ. Erlangen-Nürnberg (Germany); M. Heyder, Bavarian Ctr. for Applied Energy Research E.V. (Germany); F. Jakubka, F. Machui, T. Stubhan, I. Litzow, J. Krantz, Friedrich-Alexander-Univ. Erlangen-Nürnberg (Germany)

Organic PV is rapidly gaining high attraction because of its simple production process and its potential for a true low cost solar technology. The compatibility with printing and coating requires a careful stack design - in the simplest scenario, functional solar modules consist of only three layers, while more advanced and efficient device concepts require the deposition of 5 layers. This is an outstanding simple production process compared to inorganic thin film PV technologies. However, the challenge is in the detail of the printing process and in the formulation of suitable inks.

In this contribution we introduce and discuss material aspects and process challenges towards fully printed solar cells, including the replacement of the ITO electrode. Various concepts were already discussed to develop a fully printed OPV stack, including lamination techniques, printing of CNT networks as well as deposition of highly conductive PEDOT. However, none of these material combinations and concepts currently does fulfill the specifications for highly performing solar modules.

In detail, we discuss the combination of printed metallic nanowire electrodes in combination with metal oxide interface layers as a viable process towards fully printed organic solar modules. Experimental data for fully printed cells will be combined with results from process simulation. The overall process will be evaluated by a cost estimations to give a realistic picture on the potential cost scenario for organic photovoltaics.

8111-11, Session 8

Transparent, non-TCO electrodes for organic photovoltaics

L. Müller-Meskamp, C. Sachse, Y. H. Kim, C. Häfner, A. Zakhidov, Technische Univ. Dresden (Germany); O. R. Hild, Fraunhofer-Institut für Photonische Mikrosysteme (Germany); K. Leo, Technische Univ. Dresden (Germany)

Transparent conducting oxides (TCO) are still the first choice for transparent electrode applications. However, for organic photovoltaics, strong demand for flexible and low-cost substrates led to several alternative technologies and ideas. Using our highly efficient OPV technology, based on the evaporation of small molecules, doped transport layers and bulk-heterojunction geometries, we have studied polymer electrodes (PEDOT:PSS), Ag-nanowire electrodes, and carbon nanotube based electrodes. For PEDOT:PSS, we could enhance the conductivity by optimized solvent treatment, resulting in a selective removal of PSS from the electrode film, as could be shown by XPS and optical spectroscopy. Using these materials, we could achieve the same cell performance than for ITO on small area. Nanowire based electrodes, using random networks of highly conductive material, such as silver or CNTs, are very promising candidates, with Ag-NWs achieving similar transmission and conductivity properties as ITO (ca. 85% Transmission, <10Ohm/sq.). We used different Ag-NWs (diameter, length) coated by dipping or spraying from solution, show the influence of different post-treatment methods, and examined the optical and electrical properties of the network layer. For integration into solar cells, these electrodes were combined with an additional polymer coating, to improve the surface roughness. Carbon nanotubes were used in form of free-standing membranes, as top electrodes in semitransparent solar cells. All systems are shown to yield decent solar cells, with every technology having certain benefits and specific issues, but certainly with huge potential to rival ITO in the future.

8111-12, Session 8

Efficient heterojunction photovoltaic cell utilizing nanocomposites of lead sulfide nanocrystals and a low-bandgap polymer

J. Seo, M. J. Cho, D. Lee, A. N. Cartwright, P. N. Prasad, Univ. at Buffalo (United States)

Hybrid polymer-inorganic nanocrystal (NC) solar cells consisting of a hole-conducting conjugated polymer and inorganic semiconducting quantum dots, like cadmium selenide (CdSe), lead sulfide (PbS) and lead selenide (PbSe), have attracted considerable research attention since the advantages of two classes of materials can be effectively combined. In this work, we demonstrate a facile approach to make an efficient hybrid bulk heterojunction photovoltaic device with PbS NCs and a polymer. Herein, we introduced a low band gap polymer as the electron donor host and fabricated a blended film of oleic acid (OA)-capped PbS NCs with a polymer. Direct post-deposition chemical treatment using a short length cross-linker molecule, 1,2-ethanedithiol, applied to the blend film on the PEDOT:PSS layer kept the bulk heterojunction intact by selectively solubilizing the OA ligand of the PbS NCs without affecting the polymer matrix during the process of ligand exchange. Subsequently, inspired by the use of a multifunctional buffer layer in organic polymer photovoltaic devices, we deposited a titanium dioxide (TiO₂) thin layer (through non-hydrolytic sol-gel method) on the blend film to facilitate efficient electron transfer and extraction from the blend toward the metal and to prevent holes from reaching the metal. In addition, the effect of the PbS NC size, and thus excitonic energy, on the power conversion efficiency was studied. Power conversion efficiencies of 2-3% were observed in the resulting devices.

8111-13, Session 8

Polymer nanocomposite solar cells based on in-situ formed CuInS₂

C. Fradler, T. Rath, M. Edler, A. Fischereder, S. Moscher, A. Pein, Technische Univ. Graz (Austria); R. Trattinig, E. J. W. List, JOANNEUM RESEARCH Forschungsgesellschaft mbH (Austria); W. Haas, F. Hofer, G. Trimmel, Technische Univ. Graz (Austria)

Inorganic-organic nanocomposite solar cells have become a research topic of great interest within the last decade as, by choosing a suitable inorganic compound as acceptor phase, e.g. CdSe, CuInS₂, the amount of absorbed light can be enlarged. Such inorganic semiconductors have a bandgap matching the maximum of the solar spectrum quite well, and therefore significantly contribute to the light absorption in a solar cell.

We developed a CuInS₂ in-situ formation process by using new metal xanthate precursor materials. We were able to prepare stable bulk solutions containing the mentioned metal xanthate precursor materials and photoactive polymers like PCDTBT (poly[[9-(1-octylnonyl)-9H-carbazole-2,7-diyl]-2,5-thiophenediyl-2,1,3-benzothiadiazole-4,7-diyl-2,5-thiophenediyl]) or PSiF-DBT (poly[2,1,3-benzothiadiazole-4,7-diyl-2,5-thiophenediyl(9,9-dioctyl-9H-9-silafluorene-2,7-diyl)-2,5-thiophenediyl]) from solvents like toluene or chlorobenzene. In order to prepare nanocomposite solar cells this precursor solution can be coated by spin coating or doctor blading on glass/ITO substrates that have been coated with a thin PEDOT:PSS layer first. The conversion of the precursor material to CuInS₂-nanostructures is performed by an annealing step and takes place at a temperature below 200°C. The annealing leads to a homogenous network of the organic and the inorganic phase. In a final step a photocathode was put about the photoactive layer. This solar cell assembly led to efficiencies above 2% up to now.

The solar cells were analyzed by their I-V curves as well as by transmission electron microscopy, optical spectroscopy and IPCE measurements

This work was funded by the Austrian Ministry of Economy, Family and Youth and Isovoltaic AG.

8111-31, Session 8

GaAs nanowire/PEDOT:PSS hybrid solar cells: the relationship between nanowire morphology and device performance

J. Chao, S. Shiu, C. Lin, National Taiwan Univ. (Taiwan)

In this study, we demonstrate a new type of hybrid solar cell based on a heterojunction between poly(3,4-ethylenedioxythiophene):poly(styrenesulfonate) (PEDOT:PSS) and vertically-aligned n-type GaAs nanowire. The GaAs nanowire arrays are fabricated by directly performing the nano-etching of GaAs wafer with spun-on SiO₂ nanoparticles as the etch mask through inductively coupled plasma reactive ion etching. The use of vertically-aligned GaAs nanowire makes the interpenetrating heterojunction interface possible. Thus a large heterojunction interface and short collection paths of photo-generated carriers can be achieved. Moreover, vertically-aligned GaAs nanowire arrays with high aspect ratio can provide much smaller optical reflectance. The hybrid cells are prepared by attaching the GaAs nanowire arrays onto ITO glass substrates coated with PEDOT:PSS films. The PEDOT:PSS adheres to the surface of GaAs nanowire arrays to form a p-n junction. Our study shows that the GaAs nanowire/PEDOT:PSS heterojunction clearly exhibits a solar cell behavior. The morphology of GaAs nanowire arrays strongly influences the characteristics of hybrid solar cells. The suppression of reflectance and the interpenetrating heterojunction interface of GaAs nanowire arrays will offer great improvements in device performance. The reduction of reflectance is in agreement with the increase in J_{sc} of hybrid cells. On the other hand, a larger heterojunction interface between PEDOT:PSS and GaAs nanowire arrays results in a high J_{sc}. A good PEDOT:PSS coverage also provides improved Voc due to the reduction in shunts. The power conversion efficiency of GaAs nanowire/PEDOT:PSS cells under AM 1.5 global one sun illumination can achieve 5.8 %.

8111-32, Session 8

Silicon/silicon nanowire/poly(3,4-ethylenedioxythiophene):poly(styrenesulfonate) heterojunction solar cells

H. Syu, S. Shiu, C. Lin, National Taiwan Univ. (Taiwan)

Conventional manufacturing processes of solar cells, including epitaxy, diffusion, deposition and dry etching, are high cost and high power consumption. To save energy and reduce expenses, we use organic material, silicon nanostructure and solution process. The device structure is n-type bulk Si (n-Si)/n-type silicon nanowires (n-SiNWs)/poly(3,4-ethylenedioxythiophene):poly(styrenesulfonate) (PEDOT:PSS) heterostructure. The active region includes n-Si and n-SiNW arrays, promising the property of ultra low reflection for high light absorption. In this work, SiNWs of only a few hundred nanometers could lower the reflectance to below 5%. In addition, an organic material - PEDOT:PSS, instead of p-type doping, is introduced to form a p-n junction with n-Si/n-SiNWs for separating the electron-hole pairs. The use of PEDOT:PSS can also passivate the surface defects of n-SiNWs.

N-type SiNW arrays are made by aqueous etching process. The etchant contains Ag ions and HF etching vertically to the 1-10 Ω-cm Si (100) wafers. After etching and removing residual Ag and SiO₂ by nitric acid and diluted HF successively, n-SiNW arrays existed on either surfaces of n-Si with very dark color; then Ti and Ag were evaporated on n-Si to be a cathode. Finally, nanowires of n-Si/n-SiNWs were stuck on the PEDOT:PSS that were spin-coated on the ITO coated glass to form a core-sheath heterojunction.

The performance and quantum efficiencies (QE) were measured. The short circuit current density and power conversion efficiency are 27.46 mA/cm² and 8.05%, respectively, which are higher than other solar cells containing SiNWs. The external and internal QE are beyond 50% and 60% in visible range, respectively.

Conference 8112: Reliability of Photovoltaic Cells, Modules, Components, and Systems IV

Monday-Thursday 22-25 August 2011 • Part of Proceedings of SPIE Vol. 8112
Reliability of Photovoltaic Cells, Modules, Components, and Systems IV

8112-32, Poster Session

An LED-based solar simulator

L. L. Tobin, Univ. College Dublin (Ireland) and Science Foundation Ireland (Ireland); L. McManus, D. Zerulla, Univ. College Dublin (Ireland); J. T. Sheridan, Univ. College Dublin (Ireland) and Science Foundation Ireland (Ireland)

Solar simulators are used as an integral part of the standard testing conditions (STC) for solar cells. They provide a close spectral match to the solar spectrum without the natural variability of outdoor conditions. Typically xenon or sulphur lamps are used to produce this artificial light. However, the output differs considerably from the natural AM 1.5 global spectrum and consequently, filters and sophisticated spectral matching principles are necessary. These solar simulators are less than ideal as their lamps have short lifetimes (~1000 hours) that are expensive to replace and they produce a considerable amount of heat. One relatively inexpensive alternative to xenon and sulphur solar simulators is to replace the lamp with light emitting diodes (LEDs). The advantages of using LEDs are that they are cool, economical and highly energy efficient with extended lifetimes (~10,000 hours). By strategically placing LEDs with various appropriate wavelengths in difference planes and geometries and using suitable controls optical modulation, it is anticipated that the collective spectral output from the LEDs can be matched to the AM 1.5 global spectrum.

8112-33, Poster Session

Automatic recognition of defects in solar cells and modules

A. Vesely, J. Vanek, R. Stojan, J. Dolensky, Brno Univ. of Technology (Czech Republic)

This paper deals with automatic computer analyze of LBIC images. The output data of defect detection method like LBIC or electroluminescence image contains lots of information about contacts structure and about the defects in the area of solar cell. This data can be analyzed by operator in image form or can be analyzed by computer system in row form.

Presumption of automatic computer analyze of LBIC image is knowledge of defects of silicon solar cells. Next necessary step is choosing right image processing method which convert raster image to the numeric values.

Whole processing of LBIC image has a following four steps:

- Scanning and digitalizing
- Pre-processing
- Segmentation
- Classification

Scanning and digitalizing which means conversion of the solar cell image to the digital matrix. Pre-processing is responsible for preparation of the images for highlighting of the defects. We use several different, filters that help us to separate defect from the rest of the solar cell. Segmentation then make themselves separated defect from the rest of the solar cell. And the last step of analysis is classification. It compares the image obtained with a database of defects and determine that the defect is.

We are present in this paper what kind of defects we are able to analyze and how correctly the defects is specified.

8112-34, Poster Session

Reverse bias test of c-Si single-cell PV modules

Y. Jin, K. Ikeda, T. Doi, National Institute of Advanced Industrial Science and Technology (Japan)

As a new method for the deterioration test, we have been trying reverse bias constant current test (RBCC test) and IV duty cycle test (IDC test). We have conducted the both kinds of tests to single-cell modules under different loading levels, input power to the cell. We observed finger electrodes discoloration, inflated back sheet, burnt back sheet in the modules, these are often observed in the field PV modules. We found the change ratio of series resistance R_s in the cell increased exponentially with loading level, and shunt resistance R_{sh} in RBCC test decayed exponentially with time, and than approached constant values. We also found that around 70 to 80 watt is a certain threshold level for whether the breakdown breakage occurs or not in our cells. Our results showed the possibility for applying the reverse bias test to deterioration test.

8112-36, Poster Session

The influence of different metal ions on light scattering properties of pattern microbial fuel cells' bacteria *Desulfuromonas acetoxidans*

O. M. Vasylyv, O. I. Bilyy, V. B. Getman, Y. P. Ferensovich, R. Y. Yaremyk, S. O. Hnatysh, Ivan Franko National Univ. of L'viv (Ukraine)

Desulfuromonas acetoxidans are uncoloured gram-negative obligatory anaerobic sulfurreducing bacteria that are considered to be used as microbial-anode fuel cells with high electron recovery (>80%) from acetate oxidation to electric current. Microbial fuel cell (MFC) technologies represent the newest approach for generating electricity - bioelectricity generation from biomass using bacteria. The power generation by a pure culture of *D. acetoxidans* in MFC is approximately 15 mW/m². The development of processes that can use bacteria to produce electricity represents a highly effective method for bioenergy production as the bacteria are self-replicating, and thus the catalysts for organic matter oxidation are self-sustaining. The influence of cooper sulfate, cadmium sulfate, lead nitrate and zinc sulfate on bacteria *Desulfuromonas acetoxidans* on the base of their cells' light scattering properties changes according to it's size distribution and relative content have been investigated by the new method of measurement. The most crucial changes of the cells' concentration dependences, comparable with other investigated metals, have been observed under the influence of copper ions. The distribution curve is in the range of 0,4 - 1,4 μm and with increase of the copper ions' concentration from 0.5 to 2.5 mM the size of the cells decreased. Distribution curves of the cell sizes under the influence of cadmium, zinc and lead are in the range 0,4 - 1,8 μm and have high similarity. Their maximum is 0,58 μm . The ability of sulfurreducing bacteria *D. acetoxidans* to produce electric current under the influence of investigated metal ions has been shown.

8112-37, Poster Session

Design and implementation of a power management module for a UAV

H. H. Torres-Ortega, G. Garcia-Torales, J. L. Flores-Nuñez, R. Estrada-Marmolejo, Univ. de Guadalajara (Mexico)

**Conference 8112: Reliability of Photovoltaic Cells,
Modules, Components, and Systems IV**

The function of rotor-wing UAVs is to perform complex tasks for longer periods of time. The flight time is usually short and is limited by the battery, but for most cases is not enough, so the use of renewable energy sources is considered necessary. In this work, the results of the implementation of an array of solar cells and a module that manages the energy supplied by the cells are explained. The module provides a substantial improvement in the flight time and energetic autonomy of the UAV. This module consists of an electronic circuit which tracks the maximum power point of the cell; it offers a PWM controller with a high accuracy current and voltage regulation to charge a Lithium-ion battery. To make an efficient adjustment between electronics and the array of cells it is necessary the characterization and modeling of solar cells under different conditions of temperature and solar irradiance. It is also important to conduct a computer simulation to estimate several parameters such as the speed the battery charges and flight duration of the UAV. The increase in the energetic autonomy of the UAV is reflected in a more robust system which can perform tasks for longer periods of time.

8112-01, Session 1

Optical properties and solar radiation durability of PV materials and solar mirrors

R. H. French, W. Lin, M. Murray, Case Western Reserve Univ. (United States); S. A. Brown, K. A. Shell, M. Schuetz, Replex Plastics (United States)

Solar and environmental durability of materials and components used in photovoltaic (PV) systems is a critically important issue, so as to ensure the reliability and ultimate bankability of PV systems. We have been developing quantitative optical properties and solar radiation durability methods and metrics for materials used in flat panel, and in low concentration PV (LCPV) systems. We'll discuss solar radiation durability of PV and LCPV materials such as frontsheet, encapsulant and back sheet materials, and of acrylic solar mirrors. Solar mirror durability is important for both mirror augmentation of flat panel PV, and other LCPV type systems.

A useful solar radiation durability metric is the induced absorbance rate (Incremental $\Delta Abs/cm$ per GJ/m^2), which quantitates the wavelength dependent change in the absorbance/cm for a material exposed to a full spectrum AM1.5 solar radiation dose, in units of GJ/m^2 . The induced absorbance to dose, allows one to identify wavelengths and rates of photodarkening and photobleaching processes in materials. Since it is normalized to full spectrum dose, comparisons of rates at different irradiances (e.g. 1, 3.8, and 48.2 kW/m^2) allow serve to check linearity and reciprocity of the observed photochemical degradation processes. We will discuss results from EVA, PMMA, PET and silicones.

8112-02, Session 1

Direct comparison of PMMA and silicone-on-glass

H. P. Annen, L. Fu, R. Leutz, L. González, Concentrator Optics GmbH (Germany)

The CPV community is still undecided on one critical issue: what material to use best for Fresnel lens parquets. Reliability and longevity are the most important, but all other properties play roles as well.

We have developed and manufactured Fresnel lenses with the two commonly used materials: PMMA and silicone on glass (SOG). Both lenses are designed for the same optical train for best comparability.

This allows for better understanding the pros and cons of the materials and making an informed choice for a specific CPV module.

Theory predicts a slight optical performance benefit for PMMA lenses due to the higher refractive index and only two instead of three optical transitions. This can be directly tested and compared under laboratory and outdoor conditions. While PMMA lenses are embossed from pre-fab

sheets in a hot-cold process, the silicone lenses are cast from a heat-curing silicone rubber at moderate temperatures, reducing the energy consumption. PMMA allows for the inclusion of custom low-profile 3D (2.5D) structures for module assembly and mechanical alignment, a feature not possible in silicone due to its low rigidity.

SOG lenses are prone to delamination of the silicone film. The adhesive strength of the film to the glass can be measured using a modified blister test that we developed. The results show large difference with different materials and confirm the necessity of controlling this issue closely. While the small thermal expansion of the glass sheets allows for larger parquet sizes, the deformation of the prisms with temperature may cause a performance hit.

Failure modes for PMMA lenses include cracking and yellowing. Cracking is accelerated by internal stress, material and geometry. Also, PMMA lenses tend to global deformations and the thermal expansion limits the maximum usable parquet size.

Acknowledgment: This study is part of the Triple Primaries project, initiated as research project for various primary and secondary optics in combination with cells, by Concentrator Optics, Azur Space Solar and Isuzu Glass.

8112-04, Session 1

Field performance of concentrator CPV systems

A. Gombert, C. Crawford, T. Gerstmaier, S. van Riesen, M. Röttger, J. Wüllner, Concentrix Solar GmbH (Germany)

Concentrix Solar GmbH - a division of the Soitec Group - is manufacturing and installing concentrating photovoltaic (CPV) systems. Concentrix modules are based on III-V triple junction cells, a Fresnel lens array with a relatively small single lens aperture of 5 square inch, and a cover and bottom plate made out of glass. In case of this small primary lens, a simple heat spreader made out of a metal with a satisfying thermal conductance is sufficient for the thermal management. The first installations were conducted in 2008 in Europe, later installations followed in the US, in East Asia, in the Arabian Peninsula, and in Africa. This paper gives an overview of the performance of Concentrix Solar's CPV systems with special focus on the different climatic conditions and their impact on the system performance. The seasonal distribution of the direct normal irradiation at the mentioned locations was found to be very different which enabled us to perform studies on the system performance depending on irradiation and ambient temperature. The first generation modules which were installed in 2008 had an average efficiency of 25%, resulting in a peak solar-to-grid system efficiency of 23% and an average AC system energy efficiency of > 20%. The system peak efficiencies of the second and third module generations reach maximum values of > 25% and average AC system efficiencies of > 22%. A detailed analysis of the performance of the different system generations will be presented.

8112-05, Session 1

Techniques, regression, and applications of glass strength measurements for concentrator photovoltaic (CPV) mirrors

D. Krevor, M. Milbourne, SolFocus, Inc. (United States)

A primary failure mode for glass failure in reflective CPV systems is the mechanical stress caused by a thermal gradient. To establish the necessary reflector specifications, it is essential to have both economic techniques to measure glass strength and an insight into the failure mechanisms. Due to the highly stochastic nature of glass fracture, large data sets are necessary for statistical validity and to provide meaningful estimates of field failure rates. This paper discusses experimental measurement techniques for both value-added reflectors and for non-value surrogate substrates which are generated as waste during the manufacturing process. Specialized tooling enables measurement by commercially available stress-strain equipment (e.g., "Instron" testers). The glass strength is calculated from the force-to-break data, sample

**Conference 8112: Reliability of Photovoltaic Cells,
Modules, Components, and Systems IV**

thickness and a substrate shape dependence. These strength data are regressed using a two-parameter Weibull model, which enables calculation of the Weibull modulus, which is a measure of the distribution of flaws of a brittle material. Using a finite element analysis model of the thermal-mechanical stress to determine the critical stress, the Weibull analysis enables extrapolation of the data to predict field failure rates. The test and regression now comprise an On-going Reliability Test (ORT) that is inherently low-cost and appropriate for high-volume manufacture. For fracture, the initiating flaws are the result of glass cutting and trimming operations. There can be low-strength outliers which result from bulk glass defects, though such flawed product should be culled during the manufacturing and inspection processes. As expected and commonly known, the as-cut glass strength is very sensitive to the cutting method and resulting quality.

8112-06, Session 1

Concentrating PV survey: an unbiased overview

J. Handy, Objective Analysis (United States)

Concentrating photovoltaics (CPV) technology is well positioned to contribute in an important way to utility-scale power generation. All CPV systems share certain attributes and certain shortcomings. This presentation is intended to help attendees understand the commonalities of all CPV systems and the differences between the leading technologies, and to present criteria to help understand which technologies are likely to succeed and which are less likely to survive.

The analysis is based upon the CPV technologies themselves along with arguments involving economics, insolation, and policy. It encompasses all aspects of CPV combined with its strengths and weaknesses to illustrate the likelihood that some of these technologies will participate in the power grid of tomorrow.

The author has reviewed all leading CPV technologies and has interviewed key CPV suppliers and important test sites to better understand the reasons that some CPV systems are more likely to succeed than are others.

8112-14, Session 2

Toward bulk-heterojunction solar cells with stable morphology

S. Bertho, B. Conings, F. Piersimoni, D. F. Spoltore, J. D'Haen, L. J. Lutsen, H. Boyen, Univ. Hasselt (Belgium); B. Van Mele, G. Van Assche, Vrije Univ. Brussel (Belgium); D. J. Vanderzande, J. V. Manca, Univ. Hasselt (Belgium)

The nanomorphology of interpenetrating donor:acceptor networks is of crucial importance for state-of-the-art bulk heterojunction (BHJ) solar cells. For each combination of donor:acceptor materials, specific preparation procedures are developed and optimised in order to obtain the required 'ideal' morphology, which results in the highest photovoltaic energy conversion efficiency for the given material system. However, when these optimised solar cells with 'ideal' morphology are submitted to a prolonged storage or to a prolonged operation at elevated temperatures (e.g. solar cells in outdoor applications), a temperature induced disruption of this ideal morphology can occur and therefore also the corresponding photovoltaic performance will deteriorate. In this contribution the effect of temperature on morphology and photovoltaic properties is investigated for different sets of donor:acceptor materials by using a variety of analytical techniques (e.g. Transmission Electron Microscopy - TEM, Thermal Analysis Techniques,...) and electro-optical techniques (e.g. Fourier Transform Photocurrent Spectroscopy - FTPS). This approach provides a better insight in the underlying mechanisms causing the temperature induced morphology changes. Complementary to this analytical and electro-optical characterisation, an accelerated ageing system is used to study in-situ the degradation kinetics of the BHJ solar cells at various temperatures in order to obtain an accelerated

ageing model to predict lifetime. Solutions and concepts are proposed and investigated towards thermally stable morphologies and therefore towards next generation BHJ solar cells with an increased intrinsic thermal stability.

8112-15, Session 2

Understanding degradation in unencapsulated organic photovoltaics

M. T. Lloyd, A. Garcia, J. J. Berry, N. Kopidakis, M. O. Reese, D. S. Ginley, D. C. Olson, National Renewable Energy Lab. (United States)

We employed an automated combinatorial testing system to monitor the degradation rates for inverted geometry poly(3-hexylthiophene):fullerene bulk heterojunction solar cells in air. These devices utilize ZnO and Ag for electron and hole contacts, respectively, the relative stability of which enables meaningful studies of unencapsulated device lifetimes. For inverted devices under constant illumination, we find oxygen and moisture ingress to be the primary cause for decay in power conversion efficiency (PCE) via decreased short-circuit current (while the fill factor and open-circuit voltage are unchanged). Consequently, we find that the contacts serve as a de facto encapsulation layer and the detailed method for contact preparation becomes the first order, rate-limiting factor in determining device lifetime. In an ex-situ experiment, we evaluate the water vapor transmission rate (WVTR) of commonly used electrode materials to show that the permeability of the metal electrode is determined by its thickness and composition (in multi-layer configurations). Parallel findings confirm the observed transmission rates in devices monitored under constant illumination, where electrodes of the lowest WVTR yield devices with lifetimes extending beyond 5000 hrs. End-of-life behavior consistently results in a catastrophic loss of photocurrent. We use high-resolution photocurrent mapping to reveal circular regions of zero photocurrent in the active area indicative of pinhole ingress and lateral diffusion of oxygen and water vapor. Using a modified form of the Avrami equation, which describes nucleation and island growth in two-dimensional systems, we are able to mathematically model photocurrent vs. time as the device experiences catastrophic failure.

8112-16, Session 2

Reliability of organic materials using photothermal deflection spectroscopy

A. Bezryadina, Univ. of California, Santa Cruz (United States) and NASA Ames Research Ctr, Advance Study Labs. (United States); J. Olson, APV Research (United States); C. France, S. Carter, G. Alers, Univ. of California, Santa Cruz (United States)

Degradation of organic materials used for solar energy collection was measured with photothermal deflection spectroscopy (PDS). PDS has the ability to measure absorption over a range of 5 decades and can detect the first signs of degradation in organic films. From the tail of the optical absorption trap states and defects are deduced to quantify light induced and temperature induced degradation due to photo-oxidation and polymer/dye decomposition. In this work we look at degradation of common solar energy polymer materials like P3HT and MEH-PPV and commercial dyes that are used for photon downconversion and luminescent solar concentrators.

Most polymers have inherently weak optical absorption in the visible-IR region and might exhibit scattering due to surface roughness. PDS measurements are independent of scattering and can detect slight changes in band-edge absorption after temperature or light soaking treatments. At the tail region non-radiative absorption processes for the material are present with no detectable photoluminescence emission. A commercial red luminescent material was tested and had strong degradation after 50 hours of light soaking at 35C under 100mW/cm² illumination from a metal-halide lamp. Absorption increased by a factor

**Conference 8112: Reliability of Photovoltaic Cells,
Modules, Components, and Systems IV**

of 4 in the tail and the band-edge region. Another commercial material showed no changes in absorption after ~100 hours of light soaking. Highly sensitive PDS measurements can test optical absorption of organic films after long exposure under the sun, high humidity and/or high temperatures. Small changes in absorption can be extrapolated to quantify degradation behavior from 1000 hour measurements to predict 20-year lifetime and the long term efficiency of photovoltaic devices.

8112-17, Session 2

High-efficiency polymer-based OPV with lifetimes approaching 7 years

C. H. Peters, I. T. Sachs-Quintana, J. P. Kastrop, M. D. McGehee, Stanford Univ. (United States)

As efficiencies increase, the questions of lifetime and reliability of OPV gain importance. Current polymer-based OPV devices typically show lifetimes of 2-4 years when encapsulated. In this study we performed accelerated lifetime testing on poly(-heptadecanyl-2,7-carbazole-alt-5,5-(di-2-thienyl--benzothiadiazole) (PCDTBT). From the testing, we estimate a lifetime approaching 7 years which, to the best of our knowledge, is a record for reported polymer OPV devices.

PCDTBT has been used with PC(70)BM to achieve device efficiencies over 6.1%, making it one of the most efficient polymer-based OPV materials. 16 high-efficiency devices were encapsulated using state-of-the-art encapsulation techniques. The devices were held at the maximum power point, closely mimicking the actual conditions under which they would be operated in the field. The lamp intensity and temperature of each device were monitored in real-time. 16 P3HT:PCBM devices, encapsulated in an identical manner, were testing along with the 16 PCDTBT devices for comparison.

Results show an initial burn-in where the PCDTBT devices experience an exponential decay in efficiency, which lasts 500 hours. After this period the devices are incredibly stable, showing a linear decay for the remaining 4,000 hours of the test. Taking the initial value from the start of the linear decay period at 500 hours and extrapolating to where 20% of this initial value has been lost leads to a lifetime approaching 7 years.

The P3HT:PCBM devices show a more gradual burn-in lasting close to 1,300 hours which is also followed by a linear decay period but with a more severe slope. Performing the same lifetime analysis on these devices leads to an estimated lifetime of 3.3 years.

We will also introduce results of advanced optical and electrical characterization techniques that were used to understand degradation. This will provide the scientific community with greater insight into approaches to make more stable devices.

8112-18, Session 2

Luminescence imaging as characterization tool for polymer solar cells and modules

H. Hoppe, M. Seeland, R. Rösch, B. Muhsin, M. Bärenklau, G. Gobsch, Technische Univ. Ilmenau (Germany)

We demonstrate luminescence imaging to be a powerful tool for characterizing organic solar cells and modules with respect to deficiencies in the production process, local defects and degradation processes. As an example, the complementary use of photoluminescence and electroluminescence imaging has been employed to identify the cause and nature of polymer solar cell degradation stressed under different storage conditions. In this study we directly relate imaging results with solar cell parameters.

Furthermore we have developed a quantitative analysis for electroluminescence images obtained on organic solar cells. This approach is based on a complex device modeling employing a network of interconnected micro-diodes. The equivalent circuit network model takes interface and bulk resistances as well as the sheet resistance of the transparent electrode into account. The application of this model allows

direct calculation of the lateral current and voltage distribution as well as determination of internal resistances and the sheet resistance of the higher resistive electrode. Furthermore, we have extended the micro-diode-model to also describe and predict current-voltage characteristics for devices under illumination. The local nature of this description enables important conclusions concerning the geometry dependent performance of thin film solar cells.

Finally the beneficial use of luminescence imaging as tool for quality control is shown for single devices and monolithically connected polymer solar cell modules.

8112-19, Session 2

Degradation of PCBM-P3HT organic photovoltaic cells and structure changes as determined by defect investigations

F. Reisdorffer, Univ. de Nantes (France); L. Wang, National Taiwan Univ. (Taiwan); T. Nguyen, Univ. de Nantes (France)

We present an investigation of the intrinsic degradation of organic photovoltaic cells using poly(3-hexylthiophene) (P3HT) and phenyl-C61-butyric acid methyl ester (PCBM) composite as an active layer. The encapsulated devices of structure ITO/PEDOT:PSS/P3HT-PCBM/Ca/Al were investigated using the Charge based Deep Level Transient Spectroscopy (Q-DLTS). An efficiency of ~ 4.0% and a fill factor of the IV characteristics of ~ 64% have been obtained in fresh devices. Trap density determined in these samples is ~ 10¹⁷ cm⁻³ and their levels are found in the range from 0.1 to 0.5 eV from the band edges. Comparing the defect spectra obtained in freshly fabricated devices and those degraded over 1000 hours under 1.5 AM conditions, we observed a strong increase in intensity of deep traps, which indicated an alteration of the blend structure. On the other hand, a noticeable decrease of the trap peak of relaxation time of ~ 1s after degradation has occurred. The corresponding traps have been identified as defects induced by the presence of PCBM in P3HT matrix, and their reduction suggests a modification of the PCBM structure organization. We discuss the possible modifications of the blend structure induced by degradation and we propose a mechanism involving the transformations of PCBM basing on the defect measurement results.

8112-03, Session 3

Which factors need to be improved for array models to correctly predict “real-world” performance?

B. von Roedern, National Renewable Energy Lab. (United States)

This paper poses the question how statistically varying data should be handled by models? It asks the question whether modeled data or real-world data are of greater importance, when the real-world data may also show significant variation. This question is asked in the context of what is more important, e.g., having a model that correctly predicts real-world energy generation of a PV array or the “typical” generation for such array. Sometimes, modeling can predict standard performance, but real-world performance can only be predicted within an uncertainty level. A good standard value is obtained when the standard predicts the real-world average as close as possible.

This realization has major impacts on the expectations. It is cumbersome that some variables (like solar cell efficiency) may depend on parameters that can be controlled and others that cannot be controlled. There is a tendency to either over-value factors that can be controlled, or by being of the (fatalistic) opinion that such control is entirely useless, because uncontrollable factors are also in control. In other words, if there is current knowledge that greater control will not always achieve greater precision, is there a point to improve the precision of a model's input when it does not always predict the outcome more accurately? In other words, one should be open to the possibility that while

greater precision helps with the accuracy of the output, at under some circumstances little or nothing is to be gained by further improving such control. Medical science has acknowledged such variation, by defining acceptable numerical ranges for certain parameters, rather than optimum values. There is some agreement in the medical community that once a parameter falls within the acceptable range, there is little value to find a further improved value for such parameter. There is also the realization that persons with parameters falling within the acceptable range may be sick from an associated or unassociated disease, while certain individuals with parameter values falling outside the acceptable range may be healthy. The process of solar cell optimization hence poses the following question: Are best solar cell parameters achievable by optimizing numerical values alone? (e.g., better dialing in the knobs for an established deposition process), or should one look for improved processes, which may or may not exist? It is argued that whenever there is more than one important factor determining the outcome, the observations (rather than expectations) would be correct. Solar cell performance depends on more than one optimization skill (e.g., materials skills and device fabrication skills) hence an argument for interactive optimization can be made, rather than trying to find “a single best” optimum. In other words, is there “an” optimum process to achieve the greatest solar cell efficiency, or are there multiple approaches leading to high solar cell efficiency.

It has recently been reported that multiple approaches can deliver very high solar cell efficiencies, e.g., for GaAs based (III-V) cells, metamorphic, inverted metamorphic, Ge substrated and the “Spire” processed cells have all led to similar high solar cell efficiencies [1]. Similarly, for wafer Si PV cells, various “selective emitter” approaches have all yielded a similar performance improvement (often, much smaller than advertised) [2]. I ask myself the question whether or not such observations are coincidental, or if there could be a mechanism for explaining such observations?

Ultimately, modeling also has to ask the following question: When is greater modeling precision “only” a value and when will greater modeling precision allow better control? This issue is of importance when “champion value” solar cell efficiency values are to be “further improved or optimized” by applying better control to an established process. Champion cells are cells made with a high-efficiency cell process, such that

$$\eta_{\text{champion}} = \eta_{\text{average}} + \eta_{\text{variation}} \quad (1)$$

Solar cell champions are obtained by selecting a large average value having a large positive variation. Some in the PV community believe that a reduction of variation could increase the average efficiency. It is argued that this may or may not be the case. Only if a unique mechanism linking variation and average performance could be established would the foregoing claim be uniquely acceptable. According to equation (1) above, a reduction of variation could in fact decrease champion efficiency values. Reduction of variation for an established process may or may not lead to greater average solar cell efficiency. The question is to determine (not assume!) when greater precision will be of value and when such greater precision will also provide a greater means of control. For example, a more accurate weather forecast is of value, but will not change the weather pattern. The assumption that more precise control would automatically allow fabrication of solar cells with greater efficiency is challenged.

Solar and other energy generators show a significant noise level in energy output. Such variation questions the value of rankings if the difference between ranks is less than the uncertainty of the prediction. For PV arrays, the largest variation in energy production arises from the fluctuating solar radiation resource. Such variation, if averaged properly, decreases. Other factors for energy generation of a solar PV array are: the quality of the installation, shading, soiling, component choice and matching, transients in module performance, component breakdown, and maintenance diligence. Energy data today are typically acquired with great accuracy. Typical data are averaged and an average line is plotted, for example in plots showing solar irradiation and energy generation. I advocate that good models have to model the output determined by such line, not the outlying best or worst (real-world!) points of such curves, which might be picked by advocates or foes of a specific technology to make their point. There are also differences as to the purpose of a procedure or modeling exercise. For example, for an acceptance test for a new PV array, one may measure its output on a cloudless cool day. Such acceptance test data is helpful in improving

the energy generation data for such PV array, but such test data will only reduce, not eliminate, variations observed in real-world system energy generation. For example, acceptance test data are only valid at the time of the observation, they do not allow to estimate the system’s long-term degradation. The group at Sandia National Laboratory has done a great job to “verify” different models predicting PV system energy generation and the actual system generation in a few locations [3]. The question to be asked is: Is the current modeling precision good enough or can greater accuracy result in greater insight and control?

This paper makes a point that individual PV system component behavior may be different from average system behavior. On the scale that different energy generators are compared (say in terms of cost of electricity) it has to be realized that even average electricity or energy prices have a different averaged “willingness” for spending such monies. Such “willingness” is not controlled alone by technical factors. Borders for bins can be set at levels of low or high impact. An example of setting borders at high level of impact are the commercial module tables presented by Photon International [4]. A T-coefficient bin limit (border) for power is set at 0.48%/C, which falls in the uncertainty range for standard wafer Si T-coefficients $-(0.46 \pm 0.05)\%/C$. It then depends on the accuracy of the data sheet and on currently unpredictable behavior into which T-coefficient bin a module really falls.

Often, it appears to me that the correct use of a less accurate but correct model would have to result in the same average prediction as a more accurate model, except for a greater variation being associated with a less accurate model. It remains to be seen when a more accurate model would result in greater control. Observations have shown that sometimes greater accuracy results in greater controllability, and sometimes not. When the real-world observations are variable, like the energy output of a PV array, judgment must be used when an acceptable modeling accuracy has been reached. The fact that greater precision leads to greater controllability has to be proved, it cannot be assumed as a given.

Acknowledgement

This work was supported by the U.S. Department of Energy under Contract No. DEAC36-99GO10337 with the National Renewable Energy Laboratory. I would like to thank many colleagues in the PV field for fruitful interactions.

References

- [1] S. Wojtczuk, final NREL PV Incubator Spire subcontract presentation (2010) and final report, to be published (2011).
- [2] NREL seminar and PV Incubator subcontracts final presentation and final reports, private communication (2010), also see E. M. Sachs, A. M. Gabor, P. Madden, S. Olibet, H. Gates, A. Ersen, V. Tarasov, D. Harris, K. Passino, and F. van Mierlo, Proc. of the EC PVSEC (2010, Valenzia), p. 1475.
- [3] C.P. Cameron, W.E. Boyson, and D.M. Riley, Proc 33rd IEEE PVSC (San Diego, 2008), p. , and J.S. Stein, C.P. Cameron, B. Bourne, A. Kimber, J. Posbic, and T. Jester, Proc35th IEEE PVSC (Hawaii, 2010), p. 255
- [4] Photon International, February issue, most recent issue is (02-20110, p. 174, tables beginning pages 184/185.

8112-05, Session 3

Correlation between mechanical properties and microstructure of copper-ribbons used for cell interconnection

R. Meier, Fraunhofer-Ctr. für Silizium-Photovoltaik (Germany); S. Klengel, Fraunhofer-Institut für Werkstoffmechanik (Germany); M. Pander, S. Dietrich, Fraunhofer-Ctr. für Silizium-Photovoltaik (Germany); J. Bagdahn, Fraunhofer-Ctr. für Silizium-Photovoltaik (Germany) and Anhalt Univ. of Applied Sciences (Germany)

Soldering of solar cell strings is a critical step in the production of photovoltaic modules. During the soldering process significant mechanical stresses are induced in the stringed cell assembly. Since silicon has a very small coefficient of thermal expansion it is compressed

**Conference 8112: Reliability of Photovoltaic Cells,
Modules, Components, and Systems IV**

by the copper-ribbon during the cooling phase. The resulting stresses generate micro-cracks in the silicon cell, which are responsible for a high amount of cell breakage within the production line and even may lead to a delayed failure of the solder interconnections or cell cracking in field. Therefore the manufacturer try to create very soft ribbon material, which tends to be rather plastically deformed than generating stresses such that the silicon is prevented from damage.

Nevertheless, the general tendency of using thinner and thinner cells - in order to save silicon stock - and the projected step towards the usage of lead-free solder increase the mechanical requirements on the cell interconnectors and make systematic scientific investigations inescapable.

The purpose of this work is to analyze the micro-structure of ribbon in detail and to correlate it with its mechanical material behavior. An electron backscatter diffraction method was used to evaluate grain sizes and orientations in various annealing steps of the ribbon. These results were compared to their mechanical properties, achieved by conventional mechanical testing. As a result of these investigations the annealing process of the ribbon was optimized on laboratory scale to achieve highly adjusted material properties. Finally the benefit was verified by numerically simulation of the soldering process.

8112-06, Session 3

Impact of heavy soiling on the power output of PV modules

K. Weiss, M. Koehl, M. Heck, S. Brachmann, C. Schill, Fraunhofer-Institut für Solare Energiesysteme (Germany)

Fraunhofer ISE is running a PV-module outdoor testing set-up at the Gran Canaria island. The performance of the modules is assessed by IV-curve monitoring every 10 minutes. The electronic set-up of the monitoring system consisting of individual electronic loads for each module, which goes into a MPP-tracking mode between the IV-measurements will be described in detail.

Soiling of the exposed modules happened because of building constructions nearby. We decided not to clean the modules, but the radiation sensors und recorded the decrease of the power output and the efficiency over time. The efficiency dropped to 20 % within 5 months before a heavy rain cleaned.

A smaller rain-fall in between washed the dust partly away and accumulated it at the lower part of the module, what could be concluded from the shape of the IV-curves, which were similar to partial shading by hot-spot-tests and by partial snow cover.

8112-07, Session 3

Antistatic effect of power-enhancement coating for photovoltaic modules

D. Narushima, Asahi Kasei Chemicals Corp. (Japan)

Photovoltaic (PV) modules are periodically cleaned, particularly in large grid-connect photovoltaic plants, in order to avoid losses caused by dust accumulation. However, this maintenance task is often expensive, especially in those areas with water shortage.

A hydrophilic coating on the surface of PV modules is one of typical methods to reduce the dust accumulation. But it is not commonly used yet, because the electrical performance of PV modules with conventional hydrophilic coating was slightly degraded by the decrease of transmittance.

We have already developed a new hydrophilic coating and reported its fundamental characters and results of several ISO/IEC standard tests in SPIE Solar Energy + Technology in 2010.

One of the important characters was antistatic effect. It was showed that the surface resistances of the coated glass and the uncoated glass were $1.3 \times 10^{10}\Omega$ and $5.3 \times 10^{14}\Omega$, respectively. It would be understood that low surface resistance of the coated glass resulted in antistatic

characteristics, which reduced dust attraction onto the coated glass. With this surface resistance result, it could be elucidated that the 3% additional energy production resulted from the antistatic effect of the coating on PV modules in the exposure test after several months without rain in Spain.

In this paper, the durability of antistatic effect performed under several ISO/IEC tests will be discussed.

8112-08, Session 3

Investigations on crack development and crack growth in embedded solar cells

M. Sander, Fraunhofer-Ctr. für Silizium-Photovoltaik (Germany) and Fraunhofer-Institut für Werkstoffmechanik (Germany); S. Dietrich, M. Pander, Fraunhofer-Ctr. für Silizium-Photovoltaik (Germany); S. Schweizer, Fraunhofer-Ctr. für Silizium-Photovoltaik (Germany) and Ctr for Innovation Competence SiLi-nano@ (Germany); M. Ebert, Fraunhofer-Ctr. für Silizium-Photovoltaik (Germany); J. Bagdahn, Fraunhofer-Ctr. für Silizium-Photovoltaik (Germany) and Anhalt Univ. of Applied Sciences (Germany)

Photovoltaic modules (PV modules) are supposed to have a lifetime of more than 20 years under various environmental conditions like temperature changes, mechanical loads, etc.

In recent investigations using various analysis methods it has been shown that loading of PV modules leads to mechanical stress in the module parts and especially in the solar cells. Cracks in crystalline solar cells are a characteristic defect and can lead to efficiency losses and lifetime reduction. They are mostly invisible for optical inspection but can be identified using electroluminescence. Thus they are often called "micro-cracks".

The mechanisms of crack initiation and crack growth under thermal and mechanical loading have been investigated systematically using electroluminescence imaging. For this purpose laminated test specimens on smaller scales were produced using different cell types and module layouts.

The test specimens were analyzed after the production steps (cell delivery state, soldering and lamination) and several times during loading (thermal cycling or mechanical load steps). The crack origin and the crack length were identified and assessed manually. A statistical evaluation of all test specimens allows conclusions about crack propagation over module lifetime. This results in a basis for reliability and lifetime concepts.

The contribution presents new experiments under thermal and mechanical loading using different test specimen types. The experimental results are compared to results from investigations on full scale PV modules and to results from numerical simulations.

8112-09, Session 4

Developing standards for PV packaging materials

J. H. Wohlgemuth, M. D. Kempe, D. C. Miller, S. R. Kurtz, National Renewable Energy Lab. (United States)

The existing PV standards were designed to help develop safe PV modules, capable of reasonably long lifetimes when deployed in the field. To accomplish this, TC-82 of the International Electro-Technical Commission (IEC), published module qualification standards (IEC 61215 for crystalline Si, IEC 61646 for thin films and IEC 62108 for concentrators) and module safety standards (IEC 61730 -1 and 2). As PV has grown and the technology has become better understood, the properties of packaging materials used in the module have become increasing critical to the safety and long term durability of PV modules. It is recognized that certain basic properties of the material are required for

the module to be safe and able to survive in the field.

Working Group 2 of IEC TC-82 has recently begun work on developing characterization standards specifically designed for PV packaging materials. Standards are being developed for four specific classes of polymeric materials:

- Encapsulants
- Back Sheets
- Edge Seals
- Adhesives and Pottants

These standards will utilize existing standards (when available), modified for use with PV materials and modified to incorporate environmental conditions specific to PV applications. The goal is to provide a uniform approach to characterizing packaging materials, providing the necessary information to those selecting materials for use in PV module products as well as to those assessing the quality and safety of the products made from these materials. By standardizing the testing of materials, module manufacturers can more accurately evaluate products from different suppliers.

8112-10, Session 4

Qualification of polymeric components for use in PV modules

G. Oreski, Polymer Competence Ctr. Leoben GmbH (Austria); K. Möller, SP Technical Research Institute of Sweden (Sweden)

The aim of these investigations was to develop, implement and evaluate an appropriate procedure in order to qualify new polymeric components for the use in PV modules and to predict the lifetime of materials and modules. A test program concerning six accelerated artificial aging tests (varying UV, temperature and humidity levels) was set up and the degradation behavior of six polymers was investigated. Two main degradation indicators for chemical aging of the polymers were identified and evaluated. Both indicators (solar transmittance, strain-at-break), which are sensitive indicators for chemical aging, are related to PV-module performance and failure and were used as input data for lifetime modelling.

A suitable material specific material degradation model was obtained, where changes of the material properties are accurately related to the applied environmental stresses. Reaction rates and activation energies for the degradation processes caused by temperature, humidity and UV were calculated. For the modelling of service life time the micro-climate, to which the encapsulation materials are exposed in a PV-module, was considered and reasonable end-of-life criteria were defined.

The results of the lifetime modelling showed that the standard Damp Heat Test (85°C, 85%RH) seems to be sufficient for the qualification of most polymers. If the material properties do not exceed a certain limit within an appropriate time period, the material is qualified for PV module encapsulation for the use in a defined climate. If a certain limit is exceeded, a second damp heat test at a lower temperature is to be done in order to predict the lifetime.

8112-11, Session 5

Impact of polymer stabilization compounds in EVA encapsulation foils on long-term module performance

I. Sinicco, F. Roth, M. Gossila, T. Schuhmacher, Oerlikon Solar Ltd. (Switzerland); K. Proost, NovoPloymers NV (Belgium)

It is known that one of the main functions of an encapsulation foil is to protect the module against external aging factors. But, what about the lamination foil itself? The polymer will need to be protected from external factors such as moisture, UV light and possibly oxygen diffusion in glass - glass modules. Next to this EVA polymer foils have a very low melting point and high flow characteristics, making it necessary to cross-link the

polymer to allow for long term durability. In this study we will focus on (standard) EVA based lamination foils and the impact of some chemicals contained in such foils on the module performance. Special attention will be devoted to impact of the degree of cross linking on long term module performance and on the effect of several standard HALS (hindered amine light stabilizer) components on reliability of thin film silicon modules. Due to the earlier mentioned environmental factors, free radicals can be formed that can induce degradation effects. The link between the ability to scavenge these radicals, cross-linking chemistry and reliability will be studied.

8112-12, Session 5

PV modules with optimized energy balance

J. Weixlberger, LiSEC Group of Companies (Austria); R. Bruckner, INOVA-LiSEC Technologiezentrum GmbH (Austria)

Lisec Group as global player in glass processing equipment focuses on innovation and new technologies for advanced applications. Glass tempering for enhanced impact resistivity (like hail resistivity) along with reduced thicknesses thus minimized weight and raw material consumption is the key for a new PV-module encapsulation. 2 mm TVG-glass on front and backside, based on innovative frameless sealing and solar cell embedding can reduce raw material consumption - thus energy consumption for its preparation - for more than 50 % compared to today's conventional module setup with single side glass and backside Tedlar laminate. Several additional advantages appear as a side effect of this approach like less weight, reduced mounting costs through frameless approach, optimized light transmission efficiency and enhanced coating possibilities for anti-reflection, de-icing etc. Its rigidity in terms of hail resistivity and even bending robustness without cell breakage can be convincingly demonstrated.

8112-13, Session 5

Novel edge sealing getter tape: ultra long breakthrough time and high mechanical properties at high temperature

A. Bonucci, M. Amiotti, P. Gallina, SAES Getters S.p.A. (Italy); R. van der Wel, SAES Getters USA, Inc. (United States)

Long operational lifetime, reliability and stability of PV modules are still crucial topics in the PV world since both performance as well as economics may strongly be affected by these parameters. Thin Film PV modules are especially subjected to many discussions about their stability over long outdoor periods, due to degradation for moisture permeation.

On the other hand, mechanical stability is an important requirement for different ageing and hard environmental conditions.

In particular, the mounted panels must resist to temperature of about 60°C in the daily sunny hot weather also at mid-latitudes and peaks of about 100°C cannot be excluded. Stressed areas near the clamps are subjected to irreversible deformation.

The regulation EIC 61646 can partially ensure these requirements.

In this work, we will show the relations between the regulation EIC 61646 and real outdoor requirements.

Moreover, we will present an edge sealant, the B-Dry® that has been developed to ensure long breakthrough time not only in the damp heat test conditions, but also for the real operative ones, as it has been demonstrated from characterization both in dummy panels and in real photovoltaic modules.

B-Dry® expresses a good mechanical resistance in elastic behavior also at higher temperature due to the nature of its bulk matrix and the lap shear adhesion is resistant after prolonged Miami test and damp heat conditions.

8112-14, Session 5

Next-generation ionomer encapsulants for thin film technology

A. Smith, E.I. du Pont de Nemours & Co., Inc. (United States); R. Czyzewicz, Dupont CR&D (United States)

The characteristic properties of newly developed ionomer-based encapsulants are highlighted along with an in-depth analysis of moisture ingress and electrical properties. The mechanical properties of these encapsulants with their high stiffness and strength have been found to allow the use of thinner glass and a possible shift from tempered to annealed glass.

These new materials have improved melt flow properties when compared to other encapsulant families such as EVA or PVB. This characteristic allows for faster processing which reduces production cost by shortening the lamination cycle. During the lamination process the sheets show excellent dimensional stability and low shrinkage behavior; and, as there is no need for curing, the energy costs are lower due to lower lamination temperature. The high melt flow index also allows module makers to minimize the caliper of the new encapsulants while still ensuring integration of features like busbars and edge delete areas.

The superior electrical and moisture properties may allow removal of edge seal and possibly reduced edge delete width when compared to modules made with PVB or EVA. Finally, these new thermoplastic grades are easy to handle. They have an extended shelf life versus traditional EVA encapsulants and need no refrigeration or interleaving during storage.

The combination of high surface resistivity and low moisture ingress provides the potential to remove edge tape and/or frames while retaining the edge integrity of the module. By optimization of encapsulant properties, the module manufacturer can significantly reduce costs by shortening cycle time and/or eliminating process steps.

8112-15, Session 6

Interlaboratory comparison of UV-light sources for accelerated durability testing of PV modules

M. Koehl, K. Weiss, D. Philipp, Fraunhofer-Institut für Solare Energiesysteme (Germany)

Accelerated testing of the durability of materials exposed to natural weathering requires testing of the UV stability, especially for polymeric materials. The type approval testing of PV-modules according to the standards IEC 61215 and IEC 61646 includes a so-called UV-preconditioning test with a total UV dose of 15 kWh/m². The testing according to the edition 1 and IEC 61215 ed. 2 needed a UV-B fraction of 5 kWh/m², while the IEC 61646 edition 2 reduced the requirements to 3-10%. There are no more specifications on the spectral distribution of the UV irradiation.

Fraunhofer ISE performed an Interlaboratory comparison of UV-light sources used for this durability testing of PV-modules in accredited test labs and in test centres of major PV module manufacturers. One topic was the spectral measurement of the used UV sources. Another main issue was the comparison of the integral measurements by the sensors used for control of the tests. Errors up to 180% were found.

The evaluation of the results include a consideration of the filtering of the spectral irradiation by the glazing of the modules resulting in a changed action spectra for the polymers inside the module and a comparison of the material degradation over testing time caused by different UV sources.

8112-16, Session 6

Reliability evaluation of a photovoltaic module using accelerated degradation models

R. Laronde, A. Charki, D. Bigaud, Univ. d'Angers (France); P. Excoffier, GINGER CEBTP (France)

Many photovoltaic modules are installed all around the world. However, the reliability of this product is not enough really known. The electrical power decreases in time due mainly to corrosion, encapsulation discoloration and solder bond failure. The failure of a photovoltaic module is obtained when the electrical power reaches a threshold value equal to 50% of the initial power. Accelerated life tests are used to estimate the reliability of the photovoltaic module. However, we have few values on the degradation of this product and the realisation of accelerated life testing is expensive. Thus, the degradation is simulated for each several condition of accelerated life testing using the accelerated degradation models, the Wiener process and the few values we have. The Wiener process permits to carry out many simulations and to determine the time distribution when the threshold value is reached. So, the lifetime distribution can be obtained for each several condition and parameter of the acceleration model can be determined. Thus, the proposal modal allows us evaluating the reliability of a photovoltaic module taking into account stochastic conditions.

8112-17, Session 6

UV-accelerated test based on analysis of field-exposed PV modules

T. Shioda, Mitsui Chemical Analysis & Consulting Service, Inc. (Japan)

We proposed the UV accelerated test with low UV irradiation, based on analysis of long term field exposed photovoltaic (PV) modules.

Transmittance spectra of the EVA encapsulant sheets with discoloration in over 20 years field exposed PV modules have been obtained.

We found that absorbance due to UV absorber formulated in EVA in the transmittance spectrum still remained for long term exposed one.

In addition, we have carried out UV accelerated test using xenon weather-o-meter (XWOM) for the EVA encapsulant with the same old grade as that for long term field exposed.

Absorbance for UV accelerated test with high irradiation was disappeared, even though that with low irradiation correspond to 1SUN still remained as same as that for field exposed one.

This indicates that strong UV irradiation into EVA encapsulant leads to the fast decomposition of UV absorber, which has never seen in the field exposed PV modules.

Furthermore we observed the strong temperature dependence of change in transmittance spectrum for UV accelerated test.

As a result, we confirmed that low UV irradiation intensity and high temperature were suitable as UV accelerated test condition from viewpoint of lifetime prediction of PV modules and encapsulant.

8112-18, Session 6

Optical and opto-electronic equipment for testing solar cells and modules

A. Feldman, Oriel® Instruments, a Newport Corp. Brand (United States)

Newport Corp, ORIEL products Div, developed new line of devices for testing Solar cells, encapsulants and modules. It includes Solar simulators, concentrators, and PV-IV measuring systems. Improvements include superior uniformity of illumination, higher energy concentration, variable irradiance and dose control and feedback for energy stability.

**Conference 8112: Reliability of Photovoltaic Cells,
Modules, Components, and Systems IV**

Also available are Quantum Efficiency measuring systems which allow testing spectral stability and aging of cells and modules.

Paper provides specifications and capabilities of instruments, such as power, field and uniformity of illumination, spectral range and stability of irradiance, PV-IV measuring capability.

8112-19, Session 7

“PVResQ!”: a research activity on reliability of PV systems from an user’s viewpoint in Japan

K. Kato, National Institute of Advanced Industrial Science and Technology (Japan)

Recent government policy successfully has brought about over 500 thousand residential PV systems in Japan. Because both the government and PV industries have not been interested in operation and maintenance of PV system, however, almost all the PV users never knows troubles and/or risks which may happen to their PV systems during long-term operation.

Since 2006, I have been carrying out nation-wide field survey of existing residential PV systems in order to find troubles/failures and develop practical techniques to detect these troubles/failures. I have been also doing statistical analysis on reliability of PV modules and power conditioners by collecting operation records from PV users. I call these activities “PVResQ! (PV - Reliable, Safe and Sustainable Quality!)”.

I visited 28 residential PV systems so far and found about 2/3 of them had PV modules failures. Though these PV modules must have been replaced according to 10-year warranty provided by PV manufacturers, nobody could not find them due to following reasons: 1)it is impossible for users to be aware of PV module failure, 2)PV manufacturers and installers have no legal obligation to check PV systems, and 3)the maintenance and inspection guideline for residential PV systems prepared by PV industries is not effective against detecting PV module failures. In addition, present statistical analysis showed that 69 PV users out of 483 have replaced PV modules within 10-year operation.

In this paper, I will introduce recent topics obtained from the PVResQ! activity and point out reliability issues to be solved.

8112-20, Session 7

Failure modes effects and criticality analysis (FMECA) approach to the crystalline silicon photovoltaic module reliability assessment

J. M. Kuitche, G. M. Tamizh-Mani, Arizona State Univ. (United States) and TUV Rheinland PTL (United States); R. M. Pan, Arizona State Univ. (United States)

Traditional degradation or reliability analysis of photovoltaic (PV) modules has historically consisted of some combination of accelerated stress and field testing, including field deployment and monitoring of modules over long time periods, and analyzing commercial warranty returns. This has been effective in identifying failure mechanisms and developing stress tests that accelerate those failures. For example, BP Solar assessed the long term reliability of modules deployed outdoor and modules returned from the field in 2003; and presented the types of failures observed. Out of about 2 million modules, the total number of returns over nine year period was only 0.13%. An analysis on these returns resulted that 86% of the field failures were due to corrosion and cell or interconnect break. These failures were eliminated through extended thermal cycling and damp heat tests. Considering that these failures are observed even on modules that have successfully gone through conventional qualification tests, it is possible that known failure modes and mechanisms are not well understood. Moreover, when a defect is not readily identifiable or for unknown failures, the existing accelerated tests might no longer be sufficient. Thus, a detailed study with more extensive statistical tools is

essential. In this paper, we combine the physics of failure analysis with traditional approach to develop a statistical FMECA model that allows a more conclusive identification of root cause. This technique examines the failure of individual components of fielded modules to statistically determine its critical impact on the module reliability.

8112-21, Session 7

PV system reliability: lessons learned from a fleet of 400 systems

A. Kaushik, MEMC India (India); T. Golnas, SunEdison (United States)

The levelized cost of energy (LCOE) from PV systems can be reduced by maximizing the energy production of existing/future PV plants through increased availability. This can be achieved by detailed study of root cause and failure analysis of component failures leading to a systematic progress towards improving the reliability of various sub-systems.

SunEdison owns/operates ~400 sites across the world and systematically collects field failure data in addition to power output and weather data. Analysis of this information allows following-up on corrective actions to eliminate/minimize the re-occurrence of failures and leads to continuous improvements. This paper will analyze some of the key findings from the system failures as follows:

- 1) Inverter failures not only cause most of the system outages, but also result in substantial energy losses. Component failures in PCBs and inverter software/firmware bugs are the most common root cause of system outages
- 2) From a systemic root cause perspective, lack of robust quality systems at multiple levels of the supply chain is quite evident, which points toward the need for collectively inculcating the quality culture at every stage of the supply chain
- 3) This paper will try to establish the need for “Continuous Improvement Process” (CIP) where systemic issues are confronted and solutions are internalized in the operating procedures as the only path to improving component reliability
- 4) For a given level of reliability, cost associated with servicing the plant becomes critical. This paper highlights the importance of using “cost of ownership” metrics for making procurement decisions

8112-22, Session 7

Normalization technique for two matching solar arrays of the same size

A. A. Dubhashi, J. Wood, Xandex, Inc. (United States)

The power output of two solar arrays with same configuration and same type of solar modules is not equal due to module mismatch and array wiring. In addition, differences in ambiance can create difficulty in side-by-side comparison tests.

Tests performed on solar arrays require a data normalization method to account for differences in array power output and ambiance. This is done by swapping the location of the Units Under Test on the two arrays in order to cancel the differences between the arrays.

This paper illustrates and describes two experiments performed at the Xandex Solar Lab and demonstrates how normalization was performed using two arrays of the same system size. It is to be noted that the normalization technique presented in this paper is valid if only the Units Under Test are swapped between the arrays.

It is critical that the array modules, wiring and inverter are not swapped during the experiments. The normalization technique presented in the two experiments is an effective way to eliminate the difference in array power. This makes it possible to compare the performance of DC Power Optimizers when they are placed on the two arrays over a span of multiple days.

8112-23, Session 7

Methods for high-voltage bias testing of PV modules in hot and humid climate

N. G. Dhere, A. Kaul, Univ. of Central Florida (United States)

High voltage bias testing of PV modules is a very useful testing technique to estimate the reliability of PV modules. This paper describes and compares the methods for carrying out the high voltage bias testing of PV modules and provides recommended procedures and guidelines. Currently there are two approaches to carry out such a study. In the first method, the individual modules are connected in an array string to build a maximum voltage based upon the location of up to ± 600 V in USA or higher e.g. 1000 V in Europe and elsewhere. This method although time intensive is desirable in a way that it duplicates the actual conditions the PV modules will be subjected to in the field. Over the years at the Florida Solar Energy Center many PV systems have been deployed and are being studied for over a dozen years.

The second method includes individually biasing the PV modules and measuring the leakage currents from the module frames to ground. A study of leakage currents in Photovoltaic (PV) modules has been shown to be effective in early detection of design, material, as well as process flaws. The modules have been biased to ± 150 V, ± 300 V, ± 600 V and even ± 1500 V and higher since higher voltage systems are being built across the world especially in Europe. The necessary high voltage test bed has been built complying with the NEC codes to test the modules up to ± 3000 V. Since the modules are biased even during night, it enables calculation of the acceleration factors while calculating the degradation rates.

8112-24, Session 7

Long-term performance degradation of grid-tied photovoltaic modules in a hot and dry climatic condition

A. Suleske, J. M. Kuitche, J. M. Singh, G. M. Tamizh-Mani, Arizona State Univ. (United States)

Individual crystalline silicon photovoltaic (PV) modules typically degrade at a rate of about 0.5% per year. However, it is suspected that the modules in an array level may degrade at higher rates because of higher string voltage and increasing module mismatch over the years of operation in the field. This paper compares and analyzes the degradation rates of grid-tied photovoltaic modules operating over 10-17 years in a desert climatic condition of Arizona. The nameplate open-circuit voltage of the strings ranged between 400 and 450 V. Six different types/models of crystalline silicon modules with glass/glass and glass/polymer constructions were evaluated. About 1900 modules were inspected using an extended visual inspection checklist and infrared (IR) scanning. The visual inspection checklist included encapsulant discoloration, cell/interconnect cracks, delamination and corrosion. Based on the visual inspection and IR studies, a large fraction of these modules were identified as allegedly healthy and unhealthy modules and they were electrically isolated from the system for current-voltage (I-V) measurements of individual modules. The annual degradation rate for each module type is determined based on the I-V measurements. Finally, the paper attempts to correlate the performance degradation with observed visual defects and IR test results.

8112-25, Session 7

Fire hazard and other safety concerns of PV systems

N. G. Dhere, Univ. of Central Florida (United States)

With the exponentially increase of PV installations, there are serious concerns regarding fire hazard and other safety issues. There are

several instances of solar systems on fire. Unfortunately, there is very little data from systematic studies of long-term liability and durability of PV modules, inverters and connectors, etc. In the absence of extensive systematic study on long-term exposure of PV systems, there is tendency to rely on accelerated testing. However, the essential acceleration factors have not been determined for the various failure modes and mechanisms. The problem is compounded by new and inexperienced manufacturers who are trying to cut corners and installers who have not received adequate hands-on training. This paper describes the instances of PV modules and inverters on fire; summarizes current practices of emergency response and provides recommendations for minimizing these concerns.

8112-26, Session 8

Long-term performance analysis of CIGS thin film PV modules

N. G. Dhere, S. V. Pethe, A. Kaul, Univ. of Central Florida (United States)

Current accelerated tests of photovoltaic (PV) modules mostly prevent infant mortality but cannot duplicate changes occurring in the field nor can predict useful lifetime. A clear correlation between indoor, accelerated testing and outdoor performance is still being sought. The long term outdoor testing of PV modules aids in determining the approximate degradation rate of PV modules, thus, providing means to approximately forecast the amount of degradation in PV modules under actual operating conditions. Moreover, it is helpful in detecting long term degradation, if any, and understanding the correlation of PV performance and the meteorological parameters. As a rule of thumb, each three-year study will increasingly assure approximately nine-year segments of useful life time. Hence to guarantee a US DOE goal of 30 years useful lifetime it is necessary to continue the outdoor testing of CIGS PV modules. Therefore, monitoring of field-deployed PV modules was undertaken at FSEC with goals to assess their performance in hot and humid climate under high voltage operation and to correlate the PV performance with the meteorological parameters. This paper presents performance analysis of commercially available CIGS PV modules. Statistical data analysis of PV parameters along with meteorological parameters, monitored continuously, is carried out on regular basis with PVUSA type regression analysis. Current-voltage (I-V) characteristic of module arrays that are obtained periodically complement the continuous data monitoring. One difficulty with the outdoor testing is that due to seasonal changes, several complete cycles are required in order to obtain reasonably accurate degradation rates.

8112-27, Session 8

Using PV module certification standards tests as evaluation tools for product development

M. Reinhout, T. Brehmer, S. Lim, A. Brown, T. Macrina, R. Adkar, K. Doering, C. Shetty, J. Jalbert, P. Mehra, T. Nguyen, A. Srivatsa, K. Ramanathan, S. Goyal, L. Dounas, K. Zak, R. G. Pethe, A. Tandon, B. Wieting, L. Rios, Stion Corp. (United States)

Standards used for certification testing of photovoltaic modules contain a comprehensive group of tests that, when successfully completed, attest to the safety and performance of a module. These tests can also be used as a guideline when developing internal reliability tests as a company moves from module design to evaluation, and eventually into production. Using the accepted certification standards as a guideline, some common photovoltaic module failures may be discovered during in-house testing that could later present themselves in the field. In this talk we will discuss the importance of reliability testing from the early stages of module design, material selection, and final product. Also, we will cover some key reliability testing methodologies, derived from the certification standards, which can be implemented as the module proceeds through these various stages. Some common photovoltaic module failures like

interconnect failures and material delamination can be identified in their infancy when widely accepted environmental testing is followed. Evaluating components by certain tests enable informed decisions on component selection for module design. The goal is to develop a product with all possible speed but also with sufficient preliminary knowledge of the module reliability so that the confidence level in the product lifetime is high.

8112-28, Session 8

Metastable behavior of the electrical characteristics of CIGS photovoltaic modules upon exposure and stabilization

C. A. Deline, D. S. Albin, S. R. Rummel, National Renewable Energy Lab. (United States)

We report on our studies to devise practical procedures to stabilize the measured performance of polycrystalline thin-film photovoltaic modules. We subjected 11 older and newer modules from three manufacturers through various steps and measured performance (current-voltage) and capacitance-voltage (C-V) characteristics as a function of a sequence of exposures: short outdoor preconditioning, 48-hour dark thermal (85°C) anneal, indoor light- and dark current-soaks at 65°C, final longer-term outdoor exposures.

For all modules, preconditioning shifts performance parameters to within a few percent of baseline values, carrier densities shift slightly. The dark thermal anneal diminishes performance by 5% to 12%, largely through losses in fill factor (FF) and open-circuit voltage (Voc), with declines in Voc or FF more prominent in the newer or older modules, respectively. Concurrently, carrier concentrations suffer large drops by factors of 5-10 while depletion widths double in size. Subsequent incremental chamber exposures-light-soaking and dark current-soaking in forward bias-restore performance and carrier profiles after 120-200 hours.

Long periods of dark storage following chamber exposures alter performance parameters more prominently for higher efficiency newer modules. The final outdoor exposure (300 kW-h/m²) recovers performance levels closer to those after indoor exposures thus validating our stabilization plan: dark current-soaking in forward bias and light soaking are equivalent stabilization procedures. Albeit, a conundrum appears in subsequent dark storage for the higher performing modules: Voc and carrier densities relax toward levels similar to those measured after dark thermal anneal, which are lower than at baseline. This suggests our procedures have altered some device properties.

8112-29, Session 8

Automated shading for cell-level failure detection in solar modules using differential IV analysis

G. B. Alers, Univ. of California, Santa Cruz (United States); J. Olson, N. Green, APV Research (United States)

Rigorous testing of photovoltaic modules is critical to maintaining high lifetime projections and thus a small number of dollars per watt. Although accelerated lifetime tests provide a useful method for quality assurance, there is no better test-bed for expected lifetime than already deployed modules. Unfortunately, monitoring the parameters of the individual cells in a module is challenging. Infrared and electroluminescence images are the dominate method for identifying degradation in a solar module.

Here we present a method by which critical parameters of each cell within a module can be measured quickly using an automated shading screen and differential IV analysis. By shading each cell individually with a flat-spectrum shading device, we can use differential I-V analysis to extract shunt resistance, power output, and short-circuit current of the shaded cell. Automated shading reduces both time for the measurement and opportunities for technician error. Problematic cells are pin-pointed within the module, and module statistics are improved by orders of

magnitude. This technique provides a quick method to monitor the parameters of individual cells in the field or determine the best and worst cells for hot-spot testing. The results from this test would help detect failures and guide R&D in the development of new procedures and materials.

8112-30, Session 8

Characterization of damp heat degradation of CuInGaSe₂ solar cell components and devices by (electrochemical) impedance spectroscopy

F. J. Pern, R. N. Noufi, National Renewable Energy Lab. (United States)

This work investigated the suitability of (electrochemical) impedance spectroscopy (ECIS) to monitor in early stage the damp heat (DH) susceptibility of CIGS solar cell contact materials, components and devices. A sample set was prepared with the conducting silver epoxy or Ag paste applied to different substrates and CIGS solar cells, with Au wires soldered at ~177°C onto the heat-dried paste spots. The sample set was exposed in an ESPEC environmental chamber, and characterized by ECIS, 4-probe, optical micro-imaging, I-V and QE measurements. The results show that, within first 50-100 h of DH exposure, ECIS was sensitive to detect notable changes on the contact resistance that allowed us to determine that (1) the conducting Ag paste was more stable and preferred over the Ag-epoxy, (2) the Al/Ni on glass and on BZO rapidly degraded (corroded) while Ni was very stable, (3) the Mo/SLG corrosion occurred with pinhole-like features, resulting in localized high resistance, and (4) the moisture-absorbed BZO showed a "transient" behavior of high resistance that was not detected by 4-probe. The ECIS results also showed the CIGS solar cells could be modeled essentially by a simple circuit of a series resistance with a parallel capacitor and resistor, while shorted or degraded devices, either initially or by short DH exposure, could be readily detected.

8112-31, Session 8

A novel approach for correlating capacitance data with performance during thin-film device stress studies

R. Graham, D. S. Albin, National Renewable Energy Lab. (United States)

A new data mining technique was applied to capacitance and performance measurement data to systematically identify the strongest correlations between these two sets of data during stress testing of CdS/CdTe solar cells. Instead of starting with a physical model (like the one-sided, abrupt junction model), this method scans the data for all possible correlations between 1st and 2nd level metrics (efficiency, Voc, Jsc, FF, resistance terms) and capacitance-derived data (carrier density, depletion width, conductance) collected during stress testing. The correlation coefficient, R₂, for all combinations of these parameters is then determined, thus identifying where the best correlations exist. In doing so, we commonly observe that the best correlations exist when using higher, positive voltages. At these voltages, the data appear to fit quite accurately, the one-sided abrupt junction model, which is useful for determining junction built-in voltage, V_{bi}. The ability to uncover these hidden correlations is important from a practical perspective since it allows more insight into why devices degrade from a mechanistic perspective than measuring 1st and 2nd level metrics alone. The results of this approach will be demonstrated for a recent case involving CdTe devices where V_{bi} was observed to increase with degradation.

2011 Optics + Photonics

Photonic Devices + Applications

Technical Summaries

spie.org/op

Conference Dates: 21–25 August 2011

Exhibition Dates: 23–25 August 2011

San Diego Marriott Marquis and Marina, San Diego Convention Center
San Diego, California, USA

Connecting minds for global solutions

Contents

8113: Linear and Nonlinear Optics of Organic Materials XI	2
8114: Liquid Crystals XV	13
8115: Organic Light Emitting Materials and Devices XV	23
8116: Organic Photovoltaics XII	44
8117: Organic Field-Effect Transistors X	69
8118: Organic Semiconductors in Sensors and Bioelectronics IV.	80
8119: Terahertz Emitters, Receivers, and Applications II	87
8120: Photonic Fiber and Crystal Devices: Advances in Materials and Innovations in Device Applications V.	92
8155B: Single-Photon Imaging II	105

Conference 8113: Linear and Nonlinear Optics of Organic Materials XI

Sunday-Monday 21-22 August 2011 • Part of Proceedings of SPIE Vol. 8113
Linear and Nonlinear Optics of Organic Materials XI

8113-01, Session 1

Recent advances in photorefractive polymers

J. Thomas, College of Optical Sciences, The Univ. of Arizona (United States) and UCF NanoScience Technology Ctr. (United States); C. Christenson, P. Blanche, R. Voorakaranam, College of Optical Sciences, The Univ. of Arizona (United States); M. Yamamoto, Nitto Denko Technical Corp. (United States); R. A. Norwood, N. N. Peyghambarian, College of Optical Sciences, The Univ. of Arizona (United States)

Photorefractive composites derived from conducting polymers offer the advantage of dynamically recording holograms without the need for processing of any kind. Thus, they are the material of choice for many cutting edge applications, such as updatable three-dimensional (3D) displays and 3D telepresence. Using photorefractive polymers, 3D images or holograms can be seen with the unassisted eye and are very similar to how humans see the actual environment surrounding them. Absence of a large-area and dynamically updatable holographic recording medium has prevented realization of the concept. We will discuss the development of a novel nonlinear optical chromophore doped photoconductive polymer composite as the recording medium for a refreshable holographic display which led to the development of a quasi-real time proof-of-principle 3D telepresence without the need for special eyewear. Further improvements in the polymer composites could bring applications in telemedicine, advertising, updatable 3D maps and entertainment.

8113-02, Session 1

Thermally stable hybrid organic/inorganic resonant cavities

H. S. Choi, A. M. Armani, The Univ. of Southern California (United States)

Whispering gallery mode (WGM) optical microresonators, such as microspheres, toroids, disks and rings, have been used in a wide range of applications including fundamental physics, bio/chem sensors, narrow linewidth lasers, and add/drop filters. The silica microtoroid resonator is an ideal platform because of its high quality factor (Q), small mode volume and straightforward on-chip fabrication. Also, it is easy to incorporate additional functionalities, such as frequency tuning and lasing, by adding gain material into the silica or coating the device. However, the resonant frequency position of these devices is very unstable because the large build-up intensities inside the cavity change the refractive index of the medium, also known as the thermo-optic effect. By balancing the thermo-optic coefficient of silica with that of a second material, it is possible to design a device which is thermally neutral. To demonstrate a thermally stable resonant cavity, we coat two distinctly different polymers, polydimethylmethacrylate (PMMA) and polystyrene (PS) on the surface of silica microtoroid resonant cavities, forming hybrid optical cavities. It is important to note that the thermo-optic coefficient of silica and the two polymeric materials have opposite signs. The hybrid microcavity's resonant wavelength is temperature stabilized, while maintaining a Q factor above 1 million. The distribution of the optical field in the polymer layers and in the silica was predicted through a series of finite element method simulations. The predicted optimal polymer film thickness agrees very well with the experimentally demonstrated one.

8113-03, Session 1

An electro-optic silicon-polymer hybrid modulator

R. Himmelhuber, College of Optical Sciences, The Univ. of Arizona (United States); L. Li, Tiptd, LLC (United States); A. M. Jones, O. Herrera, R. A. Norwood, N. N. Peyghambarian, College of Optical Sciences, The Univ. of Arizona (United States)

We present the concept and design of a silicon/polymer hybrid modulator that is suitable for integration with silicon photonic components, exhibiting high optical confinement in the electro-optic (EO) polymer, while providing a much simpler fabrication process than existing hybrid Si/polymer approaches. EO polymers have been shown to have very high Pockel's coefficients and low optical losses, as well as enabling modulators with sub-volt $V\pi$ and > 100 GHz operation. Because of their outstanding properties, it is desirable to integrate EO polymers with silicon photonic components and benefit from state-of-the-art CMOS fabrication technology. One major challenge is that because of the large refractive index contrast between silicon and the polymer, it is difficult to arrange for sufficient light to be in the low index EO polymer for effective interaction. One approach to address this issue has been the use of nano-slotted silicon waveguides, where part of the light is confined in the slot region into which the EO polymer is infiltrated. However, these slotted structures are very challenging to fabricate and, at the same time, suffer from high coupling and propagation losses. Here we present a novel approach to taper down a regular 500-nm-wide silicon waveguide to a width of 100 nm, resulting in more than 90% of the light being in the EO polymer overlaid; meanwhile, an inverse silicon taper facilitates the coupling of light from fiber, which dramatically reduces the loss. We show that this design will be extremely useful towards achieving realistic integrated EO modulators built on silicon platforms.

8113-04, Session 1

Microcavity polariton electroluminescence via radiative pumping from a weakly coupled organic semiconductor

G. H. Lodden, R. J. Holmes, Univ. of Minnesota, Twin Cities (United States)

The strongly coupled regime is defined by a reversible and periodic energy exchange between the excitonic resonance of a semiconductor and the resonant photon mode of an optical microcavity. The eigenfunctions of this system are referred to as microcavity polaritons. Organic semiconductors have garnered significant interest as the active medium in strongly coupled optical microcavities due to their large exciton oscillator strengths and binding energies that permit the study of strong coupling at room temperature under both optical and electrical excitation. In these systems, the population of microcavity polariton states typically occurs via an uncoupled exciton reservoir. This results in the inefficient excitation of the upper polariton branch, and a significant population of uncoupled excitons in the active material. Here, an alternate excitation approach is demonstrated that permits the direct population of microcavity polariton states in tetraphenylporphyrin under both optical and electrical excitation without first forming an exciton reservoir. This is realized by introducing a weakly coupled emitter into an optical microcavity that also contains an organic semiconductor suitable for strong exciton-photon coupling. In contrast to previous work on organic microcavity polariton luminescence, angle-resolved measurements of the photo- and electroluminescence show variations in upper and lower branch emission intensity consistent with the branch photon character. This observation confirms that the excitation of the microcavity polariton states is by radiative pumping from the weakly

Conference 8113: Linear and Nonlinear Optics of
Organic Materials XI

coupled emitter. This alternate approach for microcavity polariton excitation may ultimately permit the development of new architectures for the study of polariton luminescence.

8113-05, Session 2

Quantum dots, low bandgap polymers and C60 derivatives for photonic applications

K. Lee, Hannam Univ. (Korea, Republic of)

This presentation engrosses on the development of highly efficient organic and inorganic materials for photonic applications such as photodetectors, field effect transistors (FET), photovoltaic (PV) cells, light emitting diodes, and other display materials. Various issues addressed involves the development of new materials, study of device architecture and improving it to suit the materials by developing a fundamental understanding of transport mechanism in devices. Developing new materials including photopatternable quantum dots (QDs) to form patterned bulk heterojunctions (BHJ), synthesis of new low band-gap polymers for light harvesting and designing fullerene derivatives to act as electron acceptors during excitonic transport are the strategies adapted to achieve these goals.

Modified C60 derivatives were synthesized as acceptor materials to get improved open circuit voltage in bulk heterojunction solar cells and high mobility in field effect transistors. Different low band gap polymers were synthesized to utilize as efficient materials for organic FET and PV cells. Some polymers were found with interesting photovoltaic and ambipolar transfer characteristics. Effect of ligand in a QD-polymer solar cells using PbS and PDTPBDT polymer is summarized. Ligand exchange between oleic acid (OA) and 1,2-ethanedithiol (EDT) on the surface of the QD in a solar cell were found with increase in device efficiency. CdSe/ZnS QDs were functionalized with photoacid cleavable surface ligands as well as, polymerizable surface ligands. They were found to produce a large enhancement in photoluminescence. The effects of these modifications on the electronic and optical properties of devices employing these materials were studied extensively.

8113-06, Session 2

Investigation of highly nonlinear composite of Co3O4 nanoparticles and poly(vinylalcohol) in the nanosecond regime

X. Zhu, D. T. Nguyen, J. Thomas, R. A. Norwood, N. N. Peyghambarian, College of Optical Sciences, The Univ. of Arizona (United States)

Nonlinear properties of thin films made of a composite of Co₃O₄ nanoparticles and poly(vinylalcohol) (PVA) have been investigated using nanosecond lasers in the visible. Thin films with thicknesses of hundreds of nanometers were fabricated by spin coating. Extremely high nonlinearities have been found in these composites. Nonlinear refractive index (n₂) of ~ 10-10 cm²/W and nonlinear absorption () of ~ 10⁻³ cm/GW have been measured from 425 nm to 675 nm; the films also exhibit exceptional optical damage thresholds. The experimental results show that the Co₃O₄ nanoparticle/PVA composite is a promising material for nonlinear optical devices in the visible, since it takes advantages of the high optical nonlinearities of transition metal oxides and the superior mechanical properties and convenient fabrication properties of polymers.

8113-07, Session 2

Influence of aggregation on the optical properties of dye-doped porous, plasma polymerized titanium oxide films

R. Jakubiak, Air Force Research Lab. (United States); H. Jiang,

W. Su, L. Sun, General Dynamics Information Technology (United States)

Solid host materials with functional materials have potential use in a variety of optical and photonic applications. An ongoing challenge is to get the dopant loading as high as possible without causing aggregation or phase separation. In particular, aggregation of dye molecules within thin films can lead to changes in the optical absorption and performance degradation. For this study porphyrin and phthalocyanine dyes were doped within porous plasma polymerized (PP-) TiO_xCy films. By varying the processing conditions, including plasma reaction chamber pressure and carrier gas ratio (O₂/Ar), we were able to control the porosity of the PP-TiO_xCy films and, hence the degree of dye aggregation. Using UV-Vis, XPS, FTIR and Raman spectroscopy along with morphological studies including SEM, AFM and X-ray diffraction we were able to establish structure-property relationships to gain insight in how to decrease the deleterious effect of dye aggregation in titania derivatives that have potential use in photocatalysis.

8113-08, Session 3

Nonlinear photochemistry and 3D microfabrication by with Q-switched Nd:YAG microchip lasers

P. L. Baldeck, M. Bouriau, O. Stephan, Univ. Grenoble 1 (France) and Ctr. National de la Recherche Scientifique (France); G. Vitrant, IMEP-LAHC (France); V. Dewaele, O. Poizat, Univ. Lille 1 (France); J. Malval, Univ. Haute Alsace (France)

We review our recent advances in two-photon induced photochemistry to fabricate tri-dimensional micro-objects made in polymers, proteins and noble metals using Q-switched Nd:YAG microchip lasers. Such sub-nanosecond lasers have recently appeared to be more efficient than femtosecond lasers for such processes. Their longer pulse duration allows not only for the initiating two-photon absorption step but also for an additional energy deposition through excited-state absorption that is more favorable for photochemistry processes.

The 532-nm laser wavelength is particularly convenient to fabricate polymer 3D micro-objects that are transparent in the visible region. The two-photon resonance is at 266 nm. Thus, photoinitiators can be transparent at daylight wavelengths, that facilitates the sample preparation and fabrication process. Typical lasers parameters are 0.1 mW average powers and tens of millisecond exposure times to obtain sub- 200 nm lateral resolutions. We will report on recent results using new commercial resins including epoxyacrylate, PDMS, and electroactive hydrogels, that have been polymerized with new photoinitiators including photo-acid generators. The fabricated 3D micro-objects concern mainly new functionalities for microfluidic microchannels.

The 532-nm laser wavelength is also very suitable to fabricate micro-objects based on biomaterials. We will report on the cross-linking of collagen proteins to fabricate artificial extracellular matrix. We will also report on the fabrication of three-dimensional enzymatic microreactors within PDMS microfluidic channels, and demonstrate that the fabricated trypsin microstructures maintain their catalytic activity.

The 1064-nm wavelength is more adapted for metallic microfabrication. 3D gold and silver microstructures are obtained by the photo-precipitation that follows the two-photon induced reduction of soluble metallic cations at the laser focal point. We will particularly report on new plasmonic microlenses and Raman sensors that we have fabricated with different silver nanowire architectures.

8113-09, Session 3

New directions in nonlinear plasmonics

P. G. Kik, CREOL, The College of Optics and Photonics, Univ. of Central Florida (United States)

Conference 8113: Linear and Nonlinear Optics of
Organic Materials XI

The use of surface plasmons for the enhancement of nonlinear optical effects is gaining momentum due to the promise of enhanced performance in ever smaller nonlinear optical devices. By designing structured metal-dielectric composites, one can obtain nonlinear metamaterials (NLM) that exhibit vastly enhanced nonlinear susceptibilities at specific design frequencies. These enhancements follow from the resonantly enhanced electric fields associated with surface plasmon resonances of the structures, resulting in a composite nonlinear optical response that is radically different from that of the constituent materials. In order to use these NLMs in applications, the improvement in nonlinear optical response must be achieved at acceptable linear optical absorption levels. This leads to application specific requirements and figures of merit (FOM). Here we summarize recent work on nonlinear optical refraction and absorption in a variety of metal dielectric composites with a focus on the figure of merit for nonlinear absorption. Based on 3D electromagnetic simulations it is shown that the presence of plasmon resonances in these composites results in complex enhancement factors related to the frequency dependent phase of the plasmon response. It is demonstrated that geometry optimization using only particle placement at a fixed amount of metal in the composite can be used to improve the FOM for nonlinear absorption by over an order of magnitude. We show that the use of coupled plasmon resonances can lead to an additional enhancement by at least an order of magnitude. Methods to extend the presented approach, as well as suggested fabrication approaches will be discussed.

8113-10, Session 3

Realizing metal and quantum dot containing patterns by two-photon lithography

P. Prabhakaran, K. Lee, K. K. Jang, Hannam Univ. (Korea, Republic of); D. Yang, Y. Son, KAIST (Korea, Republic of)

In this presentation are results from the design of materials and processes suited for two-photon lithographic microfabrication of : metal coated polymeric structures, metal nanoparticle embedded polymeric structures, quantum dot (QD) embedded polymeric structures and direct writing of metal structures.

For silver coated structures we have developed a simple strategy to incorporate amino groups on polymeric microstructures. These amino groups are then used as templates for generation of gold seeds by reduction of gold solutions by amino groups. The gold seeds further aid reduction of silver onto them through electroless coating. For silver nanoparticle embedded systems we developed a combination of photocuring and thermal curing techniques for a resin containing a metal precursor. Using this curing scheme we could successfully fabricated nanoparticle embedded three-dimensional microstructures. For achieving QD embedded microstructures, we designed and synthesized QDs stabilized with photopatternable ligands. These QDs could easily be doped into photopatternable resins to fabricate quantum dot embedded microstructures. Silver patterns were directly reduced from silver salts dispersed in poly electrolytes or amphiphilic block-co-polymers.

1. Park, J.-J, Prabhakaran, P., Jang, K. K., Lee, Y. G., Lee, J., Lee, K.-H, Hur, J., Kim, J.-M., Cho, N., Son, Y., Yang, D.-Y., & Lee, K-S. Nano Lett. 10, 2310 (2010).
2. Park, J.-J, Bulliard, X., Lee, J. M., Hur, J., Im, K., Kim, J.-M., Prabhakaran, P., Cho, N., Lee, K-S., Lee, Min, S.-Y., Lee, T.-W, Son, Y., & Yang, D.-Y. Adv. Funct. Mater. 20, 1(2010).

8113-11, Session 3

Metal plasmon enhanced luminescence of organic dyes

F. Liu, S. Rao, G. Aldea, J. Nunzi, Queen's Univ. (Canada)

Plasmons are known as collective vibrations of the electron gas surrounding the atomic lattice sites of a metal. When plasmons couple with a photon, a polariton is generated, it propagates along the surface

of metal until it decays, either by absorption, whereupon the energy is converted into phonons, or by a far field radiative transition into a photon. As regard to surface plasmon (SP), it is referred to fluctuation in the electron density at the boundary of two materials, while when the surface plasmon is excited by light, a surface plasmon resonance (SPR) was generated, which usually occurs at the interface of a material with a positive dielectric constant with that of a negative dielectric constant (such as a metal). Now SPR is attracting increasing interest for their broad application in Surface Enhanced Raman Spectroscopy (SERS), Surface Plasmon Resonance Spectroscopy (SPRS) etc. [1-2]. In SERS, a rough metal surface can enhance the Raman scattering signals as high as 14 to 15 orders, which allows the technique to be sensitive enough to detect single molecules [3]. That's because when the light is incident on a rough metal surface, the SP was excited and the localized electronic field is enhanced by SP. As a results, the intensity of incident light was magnified, which therefore increases the signal of Raman scattering. For SPRS, one of its most common applications is the measurement of the adsorbed self-assembled molecule on metallic substrate [4], since the SPR frequency sensitively depends on the permittivity of both the metal and dielectric, thus, along the deposition of molecule on metallic surface, the SPR peak wavelength changes gradually.

Along with the surge of interests in micro-scale phenomena, the investigation of plasmon is also extended to nano-scale combined with nanotechnology. Due to the strong coupling between light and surface plasmons in nanostructures, there are novel phenomena emerging in plasmonics such as optical force enhancement, transport, storage, localization and guiding of light energy in nanoaggregates [5-9]. Besides, the investigation of Metal Enhanced Fluorescence (MEF) phenomenon in last decade breaks a new path to apply SP into the field of chromophore luminescence, and now more or less SP has found its application in the field of medical and biological imaging [10]. In this paper, we will focus on the application of surface plasmons to metal enhanced fluorescence; we discuss the interaction mechanism based on time resolved luminescence experiments and propose future developments.

References:

1. J.M. Baik, S.J. Lee, M. Moskovits. Nano Letters 9 (2009) 672
2. C. Cle, A.P. Gunning, K. Syson, L. Bowater, R.A. Field, S. Bornemann. J. Am. Chem. Soc. 130 (2008) 15234
3. S. Nie, S.R. Emory, Science 275 (1997) 1102
4. K. Fujiwara, H. Watarai, H. Itoh, E. Nakahama, N. Ogawa. Anal. Bioanal Chem 386 (2006) 639
5. H. Xu, M. Kall. Phys. Rev. Lett. 89 (2002) 2468021
6. E. Ozbay. Science 331 (2006) 189
7. S.A. Maier, P.G. Kik, H.A. Atwater, S. Meltzer, E. Harel, B.E. Koel, A.A.G. Requicha. Nat. Mater. 2 (2003) 229
8. S.A. Maier, H.A. Atwater. J.Appl. Phys. 98 (2005) 011101
9. Y. Zhang, C. Gu, A. Schwartzberg, S. Chen, J.Z. Zhang. Phys. Rev. B 73 (2006) 1654051
10. M. Hu, J. Chen, Z.Y. Li, L. Au, G.V. Hartland, X. Li, M. Marquez, Y. Xia. Chem. Soc. Rev. 35 (2006) 1084

8113-12, Session 4

Record-high intrinsic hyperpolarizabilities in conjugated polymers: a counterintuitive result

I. Asselberghs, K. Clays, T. Verbiest, G. Koeckelberghs, Katholieke Univ. Leuven (Belgium)

We present a new approach for attaining record-high intrinsic second-order nonlinear optical properties for a set of conjugated polymers, leaving the classical paradigms in second-order nonlinear optics unexplored. We will be focusing on the modulated conjugation present in a series of conjugated polymers. Moreover, we will demonstrated the influence of polaron formation on the second-order nonlinear optical response in the polythiophene derivatives.

8113-13, Session 4

Measurement of stress and strain applied to electrochemically aligned collagen fibres by second-harmonic generation microscopy

N. Goami, K. Yoshiki, T. Namazu, S. Inoue, Univ. of Hyogo (Japan)

Collagen fibres provide mechanical strength to biological tissues. When mechanical stress is applied, a cell enzymatically degrades and restructures the collagen fibres to relieve the stress in the extracellular matrix around the cell. For quantitative research of this mechanism, visualization of stress distribution in collagen fibres is essential. We demonstrated quantitative measurement of stress in collagen fibres by second-harmonic generation (SHG) microscopy and a tensile test. The collagen molecule is an ampholyte and forms bundles spontaneously under the conditions of pH 7. Based on this behaviour, electrochemically aligned collagen fibres were fabricated under a pH gradient generated between parallel electrodes after application of DC voltage in the collagen solution.

Both ends of the fibre were bonded to a tensile tester consisting of one pair of translation arms, and tensile stress was applied in the longitudinal direction of the fibre. Simultaneously, the intensity of SHG light emitted from the collagen fibre excited by a femtosecond pulsed laser was measured at the transmission and reflection sides. SHG intensities on both sides increased with the strain applied on the fibre. This result suggests that the alignment homogeneity of the collagen molecules in the fibre was improved by the strain. On the other hand, the transmission to reflection ratio of SHG intensity decreased with an increase in the strain because of an increase in reflectance due to a change in the degree of organization in the collagen fibrils.

The dependence of SHG intensity on stress and strain provides us with a non-contact probe to visualize stress and strain distribution in the extracellular matrix in the living body.

8113-14, Session 4

Spontaneous chirality in discotic liquid crystals: a linear and nonlinear optical spectroscopic investigation

S. J. Van Cleuvenbergen, K. Clays, T. Verbiest, Katholieke Univ. Leuven (Belgium); G. Hennrich, Univ. Autónoma de Madrid (Spain)

The unusual linear and nonlinear optical behaviour of a new family of discotic, octupolar 1,3,5-trisalkynylbenzenes is described. These molecules organize themselves in various crystalline and liquid crystalline (meso)phases that show great potential for nonlinear optical applications. Surprisingly, some of these phases consisting of clearly achiral molecules, exhibit strong circular dichroism in the linear and the second-order nonlinear regime. This seems to be indicative of a spontaneous chiral supramolecular ordering. A novel technique using polarized second harmonic generation microscopy was used as a tool to map this nonlinear circular dichroism effect and to study the symmetry properties of these materials, amongst other techniques such as X-ray diffraction and polarized optical microscopy.

8113-15, Session 4

Optimizing the second-order nonlinear optical response in some indoline-based chromophores at the molecular and macroscopic levels

A. Teshome, Katholieke Univ. Leuven (Belgium); D. Bhuiyan, M.

M. Ashraf, G. J. Gainsford, A. J. Kay, Industrial Research Ltd. (New Zealand); I. Asselberghs, K. Clays, Katholieke Univ. Leuven (Belgium)

The effect of extending the conjugation length, the deployment of various substituents and configurational locking of the polyene backbone on the second-order nonlinear optical (NLO) response of a series of indoline based compounds has been investigated by Hyper-Rayleigh scattering (HRS). All of the compounds were found to have high molecular hyperpolarizabilities with values up to $1485 \times 10E-30$ esu. At the macroscopic level - for poled polymer thin-films - a strong second-order NLO signal has been detected by using relative second-harmonic generation (SHG) techniques. A femtosecond operating system at 1300 nm fundamental wavelength was used for both the HRS and SHG experiments. X-ray crystallographic studies were performed on three of the compounds and bond length alternation (BLA) values obtained. These were then related back to the observed NLO responses.

8113-16, Session 4

Nonreciprocal silicon-organic nanophotonic structures

M. Eich, Technische Univ. Hamburg-Harburg (Germany)

No abstract available.

8113-17, Session 5

The origin of SRG formation: a cage breaking mechanism at the nanoscale

J. Nunzi, Queen's Univ. (Canada); V. Teboul, Univ. d'Angers (France) and MOLTECH GmbH (France); J. Accary, Univ. d'Angers (France)

Illuminating thin polymer films doped with azo-dyes Rochon et al. [1] and Kim et al. [2] observed the formation of surface relief gratings (SRG) corresponding to a massive photoinduced mass transport well below the glass transition temperature of the material. An increase of the local diffusion has been suggested as a possible cause for SRG formation. Indeed a local diffusion increase has been observed experimentally [3]. This result suggests that the isomerization-induced massive mass transport that leads to surface relief gratings formation in these materials, is induced by this huge increase of the matrix diffusion coefficient around the probe. In order to investigate the microscopic origin of this amazing controlled local modification of the dynamical properties of the matrix, we use molecular dynamics simulations of the photo-isomerization of probe DR1 molecules dispersed inside a glassy molecular matrix. The simulations confirm that the probe isomerization modifies locally the diffusion coefficient of the matrix leading to liquid like diffusion properties below the glass transition temperature. Results show that the increased diffusion is due to an isomerization-induced cage breaking process. A process that explains the induced cooperative motions recently observed in these photoactive materials [4].

[1] P.L. Rochon, E. Batalla, A.L. Natansohn, App. Phys. Lett. 66, 136 (1995)

[2] D.Y. Kim, S.K. Tripathy, L. Li, J. Kumar, App. Phys. Lett. 66, 1166 (1995)

[3] P. Karageorgiev, et al., Nature Materials 4, 699-703 (2005)

[4] V. Teboul, M. Saiddine, J.M. Nunzi, Phys. Rev. Lett. 103, 265701 (2009)

8113-18, Session 5

Optical nonlinearity and power limiting in organic molecules and nanocomposites

R. Philip, Raman Research Institute (India)

Nonlinear optical transmission in materials has several applications including laser mode-locking, pulse shaping, optical bistability, optical switching, and optical power limiting. Chemically stable organic molecules which are easily processable and suitable for functionalization have been extensively investigated for their third order nonlinearities employing different experimental methods. We have measured the optical nonlinearity of different novel organic and composite systems including nanocomposite polymer films of Au, Ag and Pt, Organic ionic crystals (pyridinium and quinolinium salts), Au-alkanethiol clusters, thiophene based polymers, and Schiff base complexes, using the z-scan and degenerate four wave mixing techniques, employing laser pulses of nanosecond and femtosecond durations respectively. It is found that most of these materials are efficient optical power limiters (except a few showing saturable absorption) under our excitation conditions. Their nonlinear extinction coefficients have been calculated. From degenerate four wave mixing experiments, the third order nonlinear susceptibility and figure of merit / also have been determined. A passive all-optical diode action of high contrast ratio, observed in a porphyrin-semiconductor nanocrystal device, is discussed. It is shown that enhancement in the optical nonlinearity can often be obtained even by simple actions like mechanical mixing of two organic media. The above experiments conducted in a large number of organic and composite materials unravel the potential of these media for diverse photonic applications.

8113-19, Session 5

Assessing limitations to the two-level approximation in nonlinear optics for organic chromophores by ab initio methods

M. M. Coles, J. N. Peck, V. S. Oganessian, D. L. Andrews, Univ. of East Anglia Norwich (United Kingdom)

The use of a two-level approximation to simply characterize the nonlinear optical properties of organic materials is well known. Usually only electronic ground states are significantly populated; higher levels are engaged only in the capacity of virtual states, and it is frequently assumed that just one such state dominates in determining the response. Calculating nonlinear optical susceptibilities on this basis, excluding all but the ground and one excited state in a sum-over-states formulation, is a technique widely deployed in the calculation and analysis of nonlinear optical properties. However, the necessity for such an approach is diminishing as, particularly within the last decade, the accuracy of ab initio calculations has reached unprecedented levels. This offers new opportunities for a vigorous test of existing models using real molecular structures. Here we report the results of our recent work on testing the general validity of two-level calculations in nonlinear optics. Firstly, through the extension of approximation to a three-level model we demonstrate that the neglect of additional excited states can lead to substantially erroneous results for the hyperpolarizability elements. Secondly, using high levels of theory and basis set we report the results of ab initio calculations for both ground and electronically excited states of the optimised structures, for selected merocyanine dyes. The results are used for the calculation of hyperpolarizabilities by a rigorous sum-over-states formulation. A systematic comparison with the two-level approach provides a means for identifying the limits of the model and the criteria for its validity.

8113-20, Session 5

Why do we need three levels to understand the molecular optical response?

J. Pérez-Moreno, K. Clays, Katholieke Univ. Leuven (Belgium); M. G. Kuzyk, Washington State Univ. (United States)

Traditionally, the nonlinear optical response at the molecular level has been modeled using the two-level approximation, under the assumption that the behavior of the exact sum-over-states (SOS) expressions for the molecular polarizabilities is well represented by the contribution of only two levels. However, a rigorous application of the Thomas-Kuhn sum-rules over the SOS expression for the diagonal component of the first-hyperpolarizability proves that the two-level approximation is unphysical. We show how the contributions of potentially infinite number of states to the SOS expressions for the first-hyperpolarizability are well represented by the contributions of a generic three-level system. This explains why the analysis of the three-level model in conjugation with the sum rules has led to successful paradigms for the optimization of organic chromophores.

8113-21, Session 5

The nonlinear optical response of quantum graphs

S. Shafei, M. G. Kuzyk, Washington State Univ. (United States)

The study of nonlinear optical properties of materials and their applications is a well-established area in science and technology. The nonlinear susceptibilities have found applications in 3-D nanophotolithography, telecommunications, and designing new materials for cancer therapies, to name a few. These activities have required tremendous experimental and theoretical efforts to discover and design materials with better nonlinear response as well as finding general characteristics of systems for which the nonlinear response is optimized.

A network of nanowires can form a quantum graph. Semiconductor nanowires are known for their potential as the building blocks of future optical devices. During their synthesis, key parameters such as the chemical composition, diameter and length, can be controlled enabling a wide range of devices and applications such as LED's, transistors and nano-scale lasers, the generation of single-cycle pulses and optical processing with sub-mW powers.

In the present work, we will show how the theory of fundamental limits of the first and second hyperpolarizabilities can be used to optimize the nonlinear optical properties of quantum graphs. The nonlinear response of three- and four-segment quantum graphs will be studied in detail. We discuss the geometries that provide the largest nonlinear response for each class of quantum graphs. The work extends our techniques to quantum wires, which will allow scientists and engineers to reduce to practice our theoretical work.

8113-22, Session 6

Single, two-, and multi-photon driven molecular motion and nanofabrication in azo-polymer films

Z. Sekkat, Moroccan Foundation for Advanced Science, Innovation and Research (Morocco)

Polymers containing azobenzene derivatives have been the subject of intensive research for two decades owing to their unique "smartness", i.e., the ability to tailor and/or control materials properties by photoisomerization. In particular, it was shown that photoisomerization creates optical anisotropy by nonpolar orientation, and poling by polar optical excitation (all optical poling), and it triggers molecular movement far below the glass transition temperature (T_g) of the polymer

(photo-assisted poling), and polymer mass movement proceeds in spatial gradients of the excitation light (surface relief gratings). In solid polymers, photoisomerization of azobenzene derivatives creates free volume and drives efficient chromophore and polymer segmental and chain motion far below the polymer's T_g ; an effect which is at the origin of photo-assisted and all optical poling and surface relief gratings. Most of the studies reported to date on azo-polymers used single photon isomerization, and it is of critical importance to investigate two- or multiphoton isomerization of azobenzene derivatives in polymers since it would trigger additional studies and applications of azobenzenes containing polymers at the interface of nonlinear optics and photochemistry, in that all of the effects that have been demonstrated in azo-polymers by one-photon isomerization may be reproduced by two- or multi-photon isomerization with potential applications in nanophotonics. In two-photon absorption, the photoreaction can be induced by tightly focused lasers into confined volumes - a resolution of 120 nm has been achieved for three dimensional nanofabrication in photopolymerizable resins. In this presentation, I will discuss our recent work on light induced molecular movement and induced plasticity in azo-polymers by one and two-photon isomerization. Nanoscale polymer movement is induced by a tightly focused laser beam in an azo-polymer film just at the diffraction limit of light both by one- and two-photon isomerization. The deformation pattern which is produced by photoisomerization of the azo dye is strongly dependent on the incident laser polarization and the longitudinal focus position of the laser beam along the optical axis. The anisotropic nanofluidity of the polymer film and the optical gradient force played important roles in the light induced polymer movement. The limits of the size of the photo-induced deformation were explored, and it was found that the deformation depends on the laser intensity and the exposure time. The smallest deformation size achieved was 200 nm in full width of half maximum; a value which is nearly equal to the size of the diffraction limited laser spot. Beyond the limit of light diffraction, a nano protrusion was optically induced on the surface of the films by metal tip enhanced near-field illumination. A silver coated tip was located inside the diffraction limited spot of a focused laser beam (460 nm), and an enhanced near-field, with 30 nm light spot, was generated in the vicinity of the tip due to localized surface plasmons. A nano protrusion with 47 nm full width of half maximum and 7 nm height was induced with a resolution beyond the diffraction limit of the light.

References:

Photoreactive Organic Thin Films, Z. Sekkat and W. Knoll, ed., (Academic Press, USA, 2002).

8113-23, Session 6

Useful nonlinear optical properties of multi-chromophore materials

T. G. Goodson III, Univ. of Michigan (United States)

Organic conjugated macromolecules have received great attention due to their use in optical and electronic applications. Certain molecular assemblies have shown enhanced nonlinear optical properties by virtue of strong excitonic coupling in the multi-chromophore system. Organic dendrimers, two-dimensional networks, and circular macromolecular aggregates have shown properties of strong intra-molecular interactions which have been utilized in light harvesting processes, photovoltaic (solar) devices, dielectric effects, as well as for enhanced nonlinear optical effects. This talk will discuss our basic results and conclusions over the past years utilizing these systems. The excitation mechanism in these systems depends on the nature of the branching center, the geometrical orientation of covalently attached chromophores, and the extent of delocalization. Through steady-state and time-resolved spectroscopy, we have characterized the mechanism of energy transport and the relative strength of intra-molecular interactions. In this presentation the photo-physical properties and applications in optical and electronic devices will be described. For particular assemblies the processes of efficient energy transfer, fast energy re-distribution, and enhanced two-photon absorption cross-sections will be discussed.

8113-24, Session 6

Linkage dependence of nonlinear optical properties of porphyrin-appended mixed (porphyrinato)(phthalocyaninato) yttrium(III) double-decker complexes

Y. Li, South Dakota State Univ. (United States); X. Zhang, Univ. of Science and Technology Beijing (China); M. Yan, X. Yan, South Dakota State Univ. (United States); J. Jiang, Univ. of Science and Technology Beijing (China)

Nonlinear optical (NLO) materials have drawn considerable attention worldwide in the last few decades due to their potential applications in the field of optoelectronics and photonics. These include passive optical power limiting, optical switching, and the design of logic gates. In this report, the nonlinear optical properties of three mixed (porphyrinato)(phthalocyaninato) yttrium double-decker complexes appended with one metal free porphyrin chromophore at the para, meta, and ortho position, respectively, of one meso-phenyl group of the porphyrin ligand in the double-decker unit through ester linkage, 2-4, have been comparatively investigated along with a model complex, mixed [1,4,8,11,15,18,22,25-oc ta(butyloxy)phthalocyaninato][tetra(4-butyl)-porphyrinato] yttrium double-decker complex YH(TBPP)[Pc(α -OC4H9)8] (1) by using the Z-scan technique with the fundamental (800 nm) laser emission from a Ti:sapphire femtosecond laser system. The nonlinear optical absorption and refraction have been measured with different incident laser power. Both the open-aperture and close-aperture results have shown significant dependence on the position of the porphyrin-substituent of the triads.

8113-25, Session 7

Monte Carlo simulations of the photomechanical effect in polymeric fibers

A. C. Mitus, P. Wrobel, G. Pawlik, Wroclaw Univ. of Technology (Poland); M. G. Kuzyk, Washington State Univ. (United States)

We formulate the kinetic Monte Carlo (MC) model for the study of physical phenomena underlying the photomechanical effect in polymeric fibers pumped with a linearly polarized laser beam, which propagates off-axis along the fiber, and causes its reversible bending [1,2]. The present model constitutes a generalization of the MC kinetic model used for the study of diffraction grating inscription [3]. The model fiber is a host - guest system consisting of the polymeric matrix (simulated using the bond fluctuating MC method [4]) and azodye chromophores, which undergo multiple trans - cis -trans cycles when illuminated by linearly polarized light. Special attention is focused on the characterization of the spatial distribution of local voids and on the calculation of void - void correlation functions, which play the central role in the hypothetical cooperative mechanism of stress relaxation in the photomechanical effect [1]. The model assumes that the translational movements of the monomers are stimulated in the vicinity of the voids as the result of laser light driven local kinetics of the chromophores. The Monte Carlo kinetic model correctly reproduces the elongation of the fiber along the direction of laser light propagation.

[1] S. Bian, D. Robinson, and M.G. Kuzyk, JOSAB 23, 697 (2006).

[2] Mark. G. Kuzyk, "Polymer Fiber Optics: Materials, Physics, and Applications," CRC Press, Taylor and Francis, Boca Raton (2007).

[3] G. Pawlik, A. C. Mitu, A. Miniewicz, and F. Kajzar, J. Nonl. Opt. Phys. Mat. 13, 481 (2004).

[4] H. P. Deutsch, and K. Binder, J. Chem. Phys. 94, 2294 (1991).

8113-26, Session 7

Photomolecular motions on azopolymer nano-objects: toward new applications for photonics and biology

R. Barillé, Univ. d'Angers (France)

Advance in the fabrication of nano-objects becomes more and more important. In this direction, assembly of nanometer-scaled building blocks into device configurations and functionalization is an intensively investigated research field in nanotechnology. Azopolymer has been emphasized in the past few years because of the ability to photoswitch. This ability comes from the trans-cis photoisomerization where molecules induce motions when they relax from cis to trans.

We show in this work how the structure properties of polymer nanofilms, nanotubes, nanospheres or nanowires containing azobenzene can be controlled by light for new photonics applications. Spatially confined excitation of unidirectional motions could make it possible the local control of mechanical properties of the material and its structuration.

In this goal the production of uniform-sized nano-objects is important. We review the possibilities given by these nano-size objects in view of future application in photonics and biology.

i) We show the possibility to inscribe a nanostructure on the surface of azopolymer nanotubes with laser illumination. These patterns on the surface of nanometer objects open new possibilities as a means of optical processing on a nanoscale. ii) Using a white light we photoinduce a deformation effect of azopolymer nanospheres. A modification of the diameter can reach 35 % of the initial diameter. This experiment allows modifying the curvature of a nano-object without a shape change. iii) We induced structuration with a laser beam of nanowires made by electrospinning. iv) we show the possibility of using patterned nanofilms for applications in the growth of neuronal cells.

8113-27, Session 7

Photochromic polymers as a versatile tool for devices based on switchable absorption and other optical properties

C. Bertarelli, Politecnico di Milano (Italy) and IIT@PoliMI (Italy);
R. Castagna, IIT@PoliMI (Italy) and Politecnico di Milano (Italy);
G. Pariani, Politecnico di Milano (Italy) and INAF - Osservatorio
Astronomico di Brera (Italy); A. Bianco, INAF - Osservatorio
Astronomico di Brera (Italy)

The ability to reversibly change colour upon irradiation with suitable wavelength is the peculiar property of photochromic materials. In organic photochromic switches, the chromic effect is a consequence of the reversible modification of the chemical structure (photoisomerization) and this feature finds application in smart sunglasses and inks. We exploited the light-triggered change in colour of suitably designed diarylethene-based photochromic polymers to develop multi-object focal plane masks for astronomical instrumentation (1) and holographic optical elements for interferometric optical testing (2). With a proper molecular approach it was also possible to enable a light-induced modulation of properties such as light emission, refractive index, dipole moment, nonlinear properties or conductivity, thus opening the way to many other applications into technology. Photochromic polyurethane with a high content of diarylethene units in the main chain has been designed to develop volume phase holographic gratings (3) and rewritable multistate optical memories with stored data to be read with a non-destructive method. Finally, a highly sensitive reversible quenching of amplified spontaneous emission (ASE) and photocurrent of a polyfluorene was achieved through an energy/charge transfer to the photochromic switching unit(4).

1. A. Bianco et al. *Astronomische Nachrichten* 2005, 326, 370.
2. G. Pariani et al. *Optics Express* 2011, in press.

3. A. Bianco et al. *SPIE Advanced Optical and Mechanical Technologies in Telescopes and Instrumentation 2010*, 77394P-1.

4. A. Bianco et al. *Lasers and Photonics Reviews*, accepted

8113-28, Session 7

Role of symmetry and planarization in one- and two-photon properties of conjugated compounds based on arylamine donors and arylborane acceptors

N. S. Makarov, J. W. Perry, Georgia Institute of Technology (United States); A. Pron, M. Kivala, K. Müllen, Max-Planck-Institut für Polymerforschung (Germany)

Triarylamino donors and triarylborane acceptors are playing an important role in organic photonics and electronics as chromophores, luminescent compounds and charge-transport materials. The triarylborane group acts as a relatively strong electron acceptor comparable to the nitro group. Even though the structure-property relations for two-photon absorption (2PA) of dipolar compounds are well studied, the 2PA properties of systems combining D-A groups in various geometries, such as bent dipolar or octupolar compounds, are not fully understood.

We have examined six triarylamino-triarylborane compounds with one, two or three arms to investigate the role of symmetry, as well as the effect of planarization. We performed studies of 2PA, excited-state absorption (ESA), linear spectroscopy, and fluorescence lifetimes of these systems. We find that the higher degree of symmetry and higher planarity yields larger peak 2PA cross sections. Experimentally determined permanent and transition dipole moments were used with essential states models (two- and three-levels), as well as an excitonic model, for description of 2PA for the low energy transitions.

We have compared the experimental 2PA cross sections with the results of the simple models listed above. Generally, we observe that exciton model explains reasonably the frequencies of the transitions in the multi-arm compounds, and the 2PA cross sections for the lowest-energy transition of three-arm compounds, but it fails in the case of the higher energy band, which may result from further electronic state interactions.

8113-29, Session 8

Optical nonlinearities of triphenylamine substituted tridentate pyridyl ruthenium complexes

X. Yan, M. Yan, P. Lu, South Dakota State Univ. (United States);
H. Zeng, East China Normal Univ. (China)

Nonlinear refractive index n_2 of four new polypyridyl ruthenium complexes (labeled as 1, 2, 3, and 4) was measured by using Z-scan techniques with femtosecond laser pulses. As a result, large nonlinear refractive indexes of $2.27 \times 10^{-4} \text{ cm}^2/\text{GW}$, $11.4 \times 10^{-4} \text{ cm}^2/\text{GW}$, $44.8 \times 10^{-4} \text{ cm}^2/\text{GW}$ and $199 \times 10^{-4} \text{ cm}^2/\text{GW}$ were measured for the ruthenium complexes 1, 2, 3 and 4, respectively at a wavelength of 800 nm. Time-resolved fluorescence spectroscopy provided interesting behavior which is related to their nonlinear optical response. It was found that the symmetry and coplanarity of ruthenium complex was quite important for obtaining high nonlinear optical refractivity. Meanwhile, no clear nonlinear absorption behavior was found for the four complexes at 800 nm, which indicated that the ruthenium complexes had a large real part of third-order susceptibilities but a very small imaginary part. This will highly extend their potential applications in nonlinear optical fields.

8113-30, Session 8

Hyperpolarizability dispersion in the wavelength domain: prediction using TKS-SOS and verification at long wavelengths using HRS

K. De Mey, Katholieke Univ. Leuven (Belgium)

The search for new non-linear optical (NLO) molecular materials has been one of the main focuses of the organic materials research field for the past decades. The screening of viable candidates for NLO applications has been a tedious work, much helped by the advent of the hyper-Rayleigh scattering (HRS) technique. The downside of this technique is the low efficiency, which usually means that measurements have to be performed at wavelengths that are close to the molecular resonances, in the visible area. This means generally that one has to extrapolate the results from HRS characterization to the longer wavelengths that are useful for applications. Such extrapolation is far from trivial and the 2-level model can only be used for the most straightforward single charge-transfer chromophores. An alternative is the TKS-SOS technique, which uses a few input-hyperpolarizabilities and UV-Vis absorption data to calculate the entire hyperpolarizability spectrum. We have applied this TKS-SOS technique on a set of porphyrines to calculate the hyperpolarizability dispersion. We have also build a tunable HRS set up, capable of determining hyperpolarizabilities in the near infrared (up to 1600 nm). This has allowed us to directly confirm the results predicted in the application region. Due to the very sharp transitions in the hyperpolarizability dispersion, the calculation is subjected to a very precise calibration with respect to the input-hyperpolarizabilities, resulting in very accurate predictions for long wavelength hyperpolarizabilities.

Our results not only underscribe the aforementioned technique, but also confirm the use of porphyrines as powerfull moieties in NLO applications.

8113-31, Session 8

Investigation of nonlinear optical properties of mixed (porphyrinato)(phthalocyaninato) rare-earth double-decker complexes by Z-scan technique

Y. Li, M. Yan, M. Jiang, X. Yan, South Dakota State Univ. (United States); J. Jiang, Univ. of Science and Technology Beijing (China)

Nonlinear optical (NLO) materials can provide efficient suppression or extinction of potentially damaging light to human eyes or other delicate elements under conditions of intense irradiation, while allow efficient transmission of low photonic energy under ambient conditions. Among the large number of organic materials, tetrapyrrole compounds, including phthalocyanines, porphyrins, and their analogues, are promising candidates for NLO applications, due to their extensively delocalized π -electron systems, extraordinary stability, tailor-ability, and processability. Due to the strong intramolecular π - π interactions and intrinsic nature of the metal centers, sandwich-type rare-earth tetrapyrrole complexes show extraordinary optical, electronic, thermodynamic and magnetic properties, which have enabled them to be versatile materials such as novel molecular conductors, molecular magnets, molecular electronics, and sensing materials. NLO studies on some sandwich-type rare-earth phthalocyaninato double-decker complexes have been carried out recently. They were found to exhibit reverse saturable absorption, which makes them to be optical limiting materials. However, the results reported thus far on the NLO properties of sandwich-type mixed (porphyrinato)(phthalocyaninato) rare-earth complexes still remain extremely rare.

In this paper, the nonlinear optical properties of a series of mixed (porphyrinato)(phthalocyaninato) rare-earth double-decker complexes MH(TCIPP)[Pc(α -OC4H9)8] (1-7; M = Sm, Eu, Tb, Dy, Y, Ho, Lu; TCIPP = meso-tetrakis(4-chlorophenyl)porphyrinate; Pc(α -OC4H9)8 = 1,4,8,11,15,18,22,25-octakis(1-butylxy)phthalocyaninate) in dichloromethane have firstly been investigated by using the Z-scan

technique with the fundamental (800 nm) laser emission from a Ti:sapphire femtosecond laser system. The nonlinear optical absorption and refraction have been measured with different incident laser power, both of which have shown significant dependence on the metal centers.

8113-32, Session 8

Multi-wavelength top-hat nanosecond Z scans to determine excited-state absorption cross sections of a platinum bipyridyl complex in the visible

W. M. Shensky III, T. Pritchett, U.S. Army Research Lab. (United States); R. Liu, Z. Li, W. Sun, North Dakota State Univ. (United States); M. J. Ferry, U.S. Army Research Lab. (United States)

We report the results of measurements performed on a particular platinum(II) 4,4'-bis[3-ethyl-1-(2-ethylhexyl)heptyl]-2,2'-bipyridyl complex bearing 2-(benzothiazol-2'-yl)-7-ethynyl-9,9-dihexadecyl-fluorenyl units. A similar complex, identical except for the presence of ethyl groups at the 9-position of the fluorenes and tert-butyl groups at the 4- and 4'-positions of the bipyridine, was recently reported to possess a very high ratio of triplet excited-state absorption to ground-state absorption, a quantity that has long been used as a figure of merit for reverse saturable absorbers; in addition, femtosecond transient difference absorption experiments and picosecond open-aperture Z scans have shown it to display broad nonlinear absorption throughout the visible spectrum. In this work, we measured the triplet excited-state absorption cross section at several representative wavelengths between 450 nanometers and 660 nanometers in an open-aperture top-hat Z-scan experiment employing a nanosecond-pulsed tunable optical parametric oscillator (OPO). The open-aperture Z scan is a highly sensitive single-beam experiment used to measure nonlinear absorption. Since the spatial profile of the OPO beam resembled a cross-pattern, we closed an adjustable iris on the beam to create a top-hat profile. A dynamic five-level model was used to fit the Z-scan data.

8113-33, Session 8

Nonreciprocal phase shift enabled by magnetite core-polymer shell nanoparticles embedded in SU-8 cladding on direct laser written polymer waveguide Mach-Zehnder interferometer

A. Lopez Santiago, P. Gangopadhyay, R. Voorakaranam, College of Optical Sciences, The Univ. of Arizona (United States); A. Bablumyan, Tiptd, LLC (United States); J. Thomas, R. A. Norwood, N. N. Peyghambarian, College of Optical Sciences, The Univ. of Arizona (United States)

Faraday rotation measurements of magnetite core-polymer shell nanoparticles embedded in SU-8 and their application in direct laser written polymer waveguide Mach-Zehnder interferometers (MZI) are presented. This type of nanocomposite material demonstrates enhanced Verdet constant values due to the long range magnetic coupling between neighboring nanoparticles and is strongly related to the size and concentration of nanoparticles in the polymer matrix host. This exceptional magneto-optic response can be exploited to fabricate integrated waveguide devices such as optical isolators and circulators, magnetic field modulators, and switches by using the magneto-optic nanocomposite as a cladding material and carefully controlling the film thickness to induce a low loss non-reciprocal phase shift via evanescent field effect when a DC magnetic field is applied in the vicinity of the nanocomposite. The losses introduced by the nanocomposite scattering are minimized by employing virtually symmetric and polarization independent polymer waveguides fabricated with a direct laser writing system thus confining the propagating mode in a polymer core with

intrinsic propagation losses of $\sim 0.3\text{dB/cm}$. A thin film of 120nm of the nanocomposite was deposited on the MZI devices showing a power transfer in the output ports of nearly 23%, while it was negligible in the absence of magnetic field, indicating that the interface refractive index change did not induce birefringence due to nanocomposite deposition.

8113-35, Poster Session

Synthesis and nonlinear optical properties of novel N,N-dihydroxyethyl based molecular organic glasses using triaryl substitutes as amorphous phase formation enhancers

K. Traskovskis, Riga Technical Univ. (Latvia); I. Mihailovs, A. Tokmakovs, Univ. of Latvia (Latvia); V. Kokars, V. Kampars, Riga Technical Univ. (Latvia); M. Rutkis, Univ. of Latvia (Latvia)

Organic materials exhibiting nonlinear optical (NLO) properties are increasing object of interest as an active media in designing of novel optoelectronic devices. Such material together with high NLO activity should meet several other standards. Among them is formation of stable amorphous phase, good optical quality, thermal and chemical resistance. Different material design architectures regarding placement of a NLO active chromophore have been applied to meet those standards: covalent bonding to polymer main chain, guest-host systems, dendrimeric compounds and amorphous small-molecular organic glasses. Compared to other approaches small-molecular compounds have several advantages as relatively easy synthesis, well-defined structure, higher purity and increased concentration of active chromophore. Nevertheless, by contrast these compounds have been less explored. To create NLO active material chromophores containing N,N-dihydroxyethyl building block are widely used as polymer precursors. We present series of novel small-molecular materials based on the same building block, with further introduction of triphenylmethyl and triphenylsilyl groups. Presence of bulky and non-polar substitutes ensures amorphous phase formation of given molecular organic glasses. As NLO chromophores, series of well-known azobenzenes with different electron accepting groups and benzylidene 1,3-indandione derivatives, were used. Results of quantum chemical calculations, synthesis, chemical characterization and experimentally obtained linear and nonlinear optical properties of materials will be presented.

8113-36, Poster Session

Time-resolved optical writing on a photosensitive and fluorescent polymer film

Z. Pan, R. Akrobetu, Fisk Univ. (United States); C. Ryan, A. Saini, J. Shan, Case Western Reserve Univ. (United States); R. Mu, S. H. Morgan, Fisk Univ. (United States)

We have performed time-resolved optical writing experiments on a melt-processed blend of polyethylene terephthalate glycol (PETG) and 1.1 % w/w of 1,4-bis(α -cyano-4-octadecyloxyethyl)-2,5-dimethoxybenzene (C18-RG) film. The C18-RG/PETG can be used for 3D optical data storage, which relies on the laser-induced switching of the aggregation state of an excimer-forming fluorescence dye in the inert host polymer. The optical writing here is realized by the localized excimer to monomer conversion and characterized by the fluorescence change. We obtained time-resolved writing results of excimer to monomer conversion. Our results indicate that the conversion time of excimer to monomer is in the order of 10 ms.

8113-37, Poster Session

Design and fabrication of a chitosan-based integrated optical device for humidity sensing

A. Mironenko, Institute of Chemistry (Russian Federation)

Recently, polymers and polymer/inorganic hybrids have become of great interest for development of optical waveguides with tailored optical properties. Due to high availability, relatively low cost and good film-forming properties of some of the natural polymers, their use can be considered as an alternative to molecular design of synthetic polymers for optoelectronic applications. Aminopolysaccharide chitosan is one of the most promising biopolymer-candidates for development of optical waveguides and sensor [1, 2]. Advantages of chitosan are not limited to its easy processability. Refractive index of chitosan film can be tailored via metal ions binding, in-situ reduction and stabilization of metal nanoparticles [3] or incorporation of optically active inorganic nanocrystals into the polymer thin film. Moreover, interactions of chitosan, as a hydrophilic polybase, with organic solvents, water vapor, mineral and organic acids change level of polymer hydration and/or protonation degree, and thus, optical properties of the film that is beneficial for sensing application.

Here we report on preparation of optical waveguides and humidity sensors based on chitosan in different salt forms, chitosan/gold nanoparticles and chitosan/gold nanoparticles/silica hybrids with layered structure. Chitosan-based optical waveguides were obtained on quartz, glass and MgF₂ substrates by spin-coating and dip-coating. For investigation of optical properties, the light (wavelength 632 or 532 nm) was coupled into the planar waveguide via the flint glass prism using goniometer. A number of modes, effective refractive index, waveguide propagation losses were determined for all samples in the range of relative humidity 10-99%. It was demonstrated that chitosan-based thin films could be used as humidity sensors with fast response time (0.3-1 s), and highest sensitivity was found for chitosan/gold nanoparticles/silica hybrids with layered structure.

References

1. Optical Waveguiding and Morphology of Chitosan Thin Films. Hao JIANG, W. SU, S. CARACCI, T. J. BUNNINC, T. COOPER, and W. W. ADAMS// Journal of Applied Polymer Science, Vol 61, 1163-1171, 1996
2. Yoshiaki KURAUCHI, Tohru OGATA, Naoyoshi EGASHIRA and Kazuya OHGA., Fiber-Optic Sensor with a Dye-Modified Chitosan/Poly(vinyl alcohol), Cladding for the Determination of Organic Acids//ANALYTICAL SCIENCES FEBRUARY Vol. 12, p.55-59, 1996
3. Huang HZ, Yang XR: Synthesis of polysaccharide-stabilized gold and silver nanoparticles: a green method CARBOHYDRATE RESEARCH Vol. 339(15), P. 2627-2631, 2004

8113-38, Poster Session

Stable frequency doubling by all-optical poling in dye-doped polymer optical fibres

R. Barille, Univ. d'Angers (France); J. Nunzi, Queen's Univ. (Canada); B. Luther-Davies, A. Samoc, The Australian National Univ. (Australia); M. Samoc, Wroclaw Univ. of Technology (Poland)

We present experimental studies of all-optical poling in large-core dye doped poly-methylmethacrylate plastic optical fibres. We show that the confinement of light within the fibre core permits to reach the upper limit of second harmonic generation achievable by all-optical poling using repeated trans-cis isomery. Quantification of the output power provides clear demonstration that self-seeding can counteract relaxation of the orientation during readout of the induced nonlinearity.

8113-39, Poster Session

Strong intramolecular coupling in organic cyclic aggregates

J. Donehue, O. Varnavski, T. G. Goodson III, Univ. of Michigan (United States)

A series of π -extended cyclic thiophene oligomers of 12, 18, 24, and 30 repeat units have been studied using methods of ultrafast time-resolved absorption, fluorescence up-conversion, and three-pulse photon echo. Previous study of these molecules showed evidence of cooperative enhancement in their nonlinear optical responses, and the ultrafast measurements were conducted in order to examine the structure-function relationships that may affect the coherence between chromophores within the organic macrocycles. Our results indicated an initial delocalized state can be seen upon excitation of the cyclic thiophenes. Anisotropy measurements show this delocalized state decays on an ultrafast timescale and is followed by the presence of incoherent hopping. Using theoretical models, we concluded our ultrafast anisotropy decay measurements suggest the system does not reside in the Förster regime and coherence within the system must be considered. Three-pulse photon echo peak shift experiments reveal a clear dependence of initial peak shift with ring size, indicating a weaker coupling to the bath (and stronger intramolecular interactions) as the ring size is increased. Our results suggest that the initial delocalized state increases with ring size to distances (and number of chromophores) comparable to the natural light harvesting system.

8113-40, Poster Session

Ultrafast energy transfer in Pt-containing macromolecules at low temperature

D. Flynn, T. G. Goodson III, Univ. of Michigan (United States)

Platinum containing macromolecular structures are important for the development of novel optical, electrical, and energy related applications. These materials are potentially promising for optical limiting and other nonlinear absorption applications. Previous experiments have detailed the nonlinear optical properties of these materials. And in this poster we present information regarding the fundamental excitations in these systems utilizing ultra-fast pulses. In these studies we utilize fluorescence upconversion to probe the relaxation process with very fast time resolution. We also investigate the materials in neat samples where the concentration is particularly high to offer investigation of the inter-molecular interactions as well. We have carried out low-temperature measurements to probe the fundamental excitations and dynamics of the energy transfer and molecular dynamics of these interesting materials. The ultrafast dynamics of aggregated platinum acetylide complex has been investigated by femtosecond fluorescence upconversion down to 4.2 Kelvin. The results of this study are used to describe the mechanism for the enhanced nonlinear properties of platinum acetylide.

8113-41, Poster Session

Synthesis of the novel beta-cyclodextrin-chromophore inclusion compound and research on the electro-optic activity of its systems

S. Bo, Z. Chen, Z. Zhen, X. Liu, Technical Institute of Physics and Chemistry (China)

Cyclodextrins (CDx's) have been the subject of many studies in the field of supramolecular chemistry due to their ability to bind a variety of organic compounds within their hydrophobic cavities via noncovalent interactions. In this work, we formed β -cyclodextrin-chromophore inclusion compounds by embedding dumb-bell shape chromophores in the β -cyclodextrin. β -cyclodextrin-chromophore inclusion compound

was calculated to have a binding energy of 16.1 kcal/mol, which meant the compound was steady. Since it is inconvenient to purify the inclusion and spin coat in polymers. A donor- β -cyclodextrin inclusion compound was formed firstly, and then bonded to the acceptor. The NLO chromophore and the inclusion compound were characterized by UV-Vis, FT-IR, MALDI-TOF, and ¹HNMR. Thermal properties of the inclusion compounds were characterized by DSC and TGA. The highest EO coefficient (r_{33}) of the β -cyclodextrin-chromophore inclusion compound in the polymer is about three or four times than the NLO chromophores in the polymer at 1310 nm. So, there results show this inclusion compound could reduce electrostatic interactions between the NLO chromophores and improve polarization efficiency because of the big distance between any chromophore in β -cyclodextrin inclusion compound. Highly stable NLO properties have been achieved through inclusion compound, and the EO coefficients values of the polymer films could keep 90% of the original ones even after 500 hours under 80 . We provides a convenient method to reduce the aggregation of chromophores and enhance the electro-optic activity in different polymer systems for technical bottleneck of the nonlinear optical materials.

8113-42, Poster Session

Synthesis and nonlinear optical properties of a novel crosslinkable system containing TCF-based chromophores

Z. Chen, S. Bo, Z. Zhen, X. Liu, Technical Institute of Physics and Chemistry (China)

In the crosslinkable system, poling process generally goes with crosslinking progress, and then the rigid polymer chains would limit the movement of the chromophores, thus the poling efficiency and the EO coefficient of the crosslinked polymer may be lower than the guest-host polymer system and uncrosslinked polymer system. For this reason, only a relatively small number of thermal crosslinking reactions have been reported in the field of organic second order nonlinear materials, just like Huisgen reaction and Diels-Alder cycloaddition. In this work, a novel crosslinkable polymer with side-chain system was investigated to increase the content of NLO chromophores and to improve the stability of oriented chromophores in second order nonlinear optical materials. A series of crosslinkable copolymers which bear different concentrations of strong push-pull type chromophores with the tricyanofurane (TCF) acceptor were successfully synthesized. The NLO monomer and the copolymers were characterized by ¹HNMR, MS and GPC. Thermal properties and EO coefficients (r_{33}) of the uncrosslinked and the crosslinked NLO copolymers were also characterized and discussed. For our synthesized copolymer system, the similar EO coefficients can be achieved in the uncrosslinked and crosslinked NLO copolymer films, since the crosslinking temperature (T_c) has to be above to the glass transition temperature (T_g) to ensure an efficient poling of the chromophores before the crosslinking reaction starts. Higher stable NLO properties occur in the crosslinked copolymer, such as the EO coefficient values of crosslinked NLO copolymer films could keep 83% of the original ones even after 500 hours at 80 degrees Celcius.

8113-43, Poster Session

Non-linear optical time-resolved studies on dendritic oligothiophene-perylene bisimide hybrids

J. Zhang, Univ. of Michigan (United States); M. K. R. Fischer, P. Bäuerle, Univ. Ulm (Germany); T. G. Goodson III, Univ. of Michigan (United States)

A series of novel dendritic oligothiophene-perylene bisimide hybrid (DOTPBI) system, as novel dendritic p-n heterojunction materials, up to the second generation (G0, G1, G2) was investigated using non-linear optical time-resolved measurements. Results of these measurements reveal the ability of these molecules to undergo intramolecular

**Conference 8113: Linear and Nonlinear Optics of
Organic Materials XI**

fluorescence resonance energy transfer (FRET) from the DOT to the PBI moiety. In addition, the existence of delocalization of the excited state in the DOTPBIs was discovered. The photoinduced electron transfer (PET) process is facilitated by increasing the DOT generation and donor strength, and increasing the distance between the donor and acceptor. Although both thiophene dendrons and PBIs have extremely rigid structures, in the higher generation, a high degree of structural conformational flexibility of the perylene exists. This distorted structure and the energy migration time scale explains the decreased lifetime of the fluorescence and the ultrafast excited state relaxation dynamics.

Conference 8114: Liquid Crystals XV

Sunday-Monday 21-22 August 2011 • Part of Proceedings of SPIE Vol. 8114 Liquid Crystals XV

8114-01, Session 1

A combined study of mesomorphism, optical, and electronic properties of donor-acceptor columnar liquid crystals

S. H. Eichhorn, M. Ahmida, H. Kayal, S. Chen, Univ. of Windsor (Canada); B. R. Kaafarani, American Univ. of Beirut (Lebanon)

Donor-acceptor structures are commonly found in polymeric semiconductors but have been little studied in columnar liquid crystals. [1] Presented here are two new types of donor-acceptor liquid crystals that both form columnar mesophases. All compounds show rich polymesomorphism (different columnar and nematic mesophases) that affect their alignment, optical and electronic properties. Charge carrier mobility of discotic compounds based on extended hexaazatrinaphthalene cores, for example, sharply increases at the transition from a Col(r) to a Col(h), which is reasoned with the associated change in charge transfer integrals of occupied and empty frontier orbitals. Interestingly, electron and hole mobility are not equally affected and derivatives that show electron but no hole mobility will be presented. Board-shaped liquid crystals based on a quinoxalino[2',3':9,10]phenanthro[4,5-abc]phenazine core form rectangular and hexagonal columnar mesophases despite their large aspect ratios of 1:5-6. All compounds are highly fluorescent in solution and in their mesophases but, more importantly, their fluorescence intensity reversibly decreases with increasing temperature within one mesophase. Computational studies confirm that these changes in fluorescence intensity correlate with changes in molecular mobility and intracolumnar packing.

8114-02, Session 1

Confined blue phases: trapping of colloidal particles in new disclination superstructures

S. Zumer, Univ. of Ljubljana (Slovenia); M. Ravnik, Univ. of Oxford (United Kingdom); J. Fukuda, National Institute of Advanced Industrial Science and Technology (Japan)

Following revival of interest in blue phases stimulated by the new broad temperature range materials [1] we have recently examined stable colloidal blue phases [2,3]. The Landau - de Gennes description and topological theory has proven to be extremely useful in dealing with nematic and blue phase colloids [4,2,3]. Here we use our experience with bulk blue phase colloids to focus on confined blue phases. Recently we have found that confinement to thin layers yields numerous disclination networks not present in bulk blue phases. In case of homeotropic anchoring at certain layer thickness we have found that double twist cylinders are accompanied by disclinations forming double helices [5]. In case of planar anchoring a 2D lattice of disclination rings have been found [6]. Such networks represent complex effective trapping potentials that mediate the attraction of particles to disclinations. This process allow for a self-assembling of superstructures in confined blue phases. Here we examine effects of particle properties and sizes. Such assemblies can lead to colloidal crystals that can be manipulated via affecting the liquid crystal matrix and/or colloidal particles by external stimuli. We expect that some of these assemblies will open new ways to photonic applications. [1] F. Castles et al. PRL 2010, [2] S. Zumer et al., Proc. SPIE 77750H 2010, [3] M. Ravnik et al. accepted for publication in PNAS 2011, [4] M. Ravnik & S. Zumer, Soft Matter 2009, [5] J. Fukuda & S. Zumer, PRL 2010, [6] J. Fukuda & S. Zumer accepted in PRL 2011.

8114-04, Session 1

Photomobile polymer materials: from nano to macro

T. Ikeda, Tokyo Institute of Technology (Japan)

An actuator is an energy transducer that can convert input energies of a variety of forms into mechanical work. Many actuators that respond to various external stimuli have been developed. Crosslinked liquid-crystalline (LC) polymers show a strong coupling between the alignment of mesogens and the conformation of polymer chain, which gives rise to the characteristic properties of the crosslinked LC polymers. If the crosslinked LC polymer is heated toward LC-isotropic phase transition temperature, the order of the mesogens decreases, and the mesogens become disordered when the temperature exceeds the phase transition temperature. With this phase transition, the crosslinked LC polymers in general show contraction along the alignment direction of mesogens. If photochromic molecules such as azobenzene are incorporated into crosslinked LC polymers, the LC-isotropic phase transition can be induced isothermally and reversibly by photoirradiation. Then a variety of three-dimensional movements of the polymers can be brought about just by photoirradiation. Light-driven polymer actuators are promising in a wide range of micro- and macroscale devices. We will show some recent examples of the three-dimensional movements of crosslinked LC polymers in response to light.

8114-17, Session 1

Nanoparticle-doped isotropic liquid crystal for sensor protection

A. V. Parfenov, X. Xia, A. Shapoury, E. A. DeHoog, F. Zhang, S. Pradhan, T. M. Aye, M. Shih, Physical Optics Corp. (United States)

Advances in protecting the eye or optical sensors and visual devices from laser radiation are particularly important with operations in intelligence, surveillance, and reconnaissance (ISR) becoming increasingly critical, not only in the military and law enforcement communities, but also in other commercial fields where imaging using intense light is required. Various nonlinear optical materials and devices have been investigated and developed to meet the challenge of protecting the sensing devices from laser radiation of wide spectral and temporal ranges. In most devices, the nonlinear absorption mechanism at a specific wavelength has been used for optical limiting; and the material has to be placed in the focal plane of the optical system in order to utilize the increased laser energy fluence to achieve the desired limiting performance characteristics. In this paper, we demonstrate a novel high-speed, multiple-notch broadband passive optical switching material to selectively discriminate bands of electromagnetic radiation in ISR systems. This new material is composed of isotropic liquid crystal (ILC) blended with semiconductor nanoparticles, and has demonstrated fast response (~1 ns), high nonlinear 3rd order optical Kerr coefficients (light-induced refractive index change, $n_2 = -4E-9$ esu) exceeding 200 300 times of classic nonlinear material CS2 with $n_2 = 1.2E-11$ esu. Unlike conventional absorptive notch switches, our device is based on passive "notched-out" reflection resulting in negligible heating that is in particular desired by the close-by near or short-wave IR imaging sensors when applied in day/night and all inclement weather conditions. Details of fabrication and experimental results will be presented.

8114-05, Session 2

Spatial optical soliton used as a spectral probe in colloids of liquids crystals and nanoparticles

J. Henninot, J. Blach, M. Warenghem, Univ. d'Artois (France)

Since 10 years, Spatial Optical Solitons (SOS) have been widely studied in Nematic Liquid Crystal (NLC) for their potential application in optical routing or switching devices. In this work, we describe another use of spatial optical solitons: the recovery of a spectral signal escaping from a soliton propagating into a nanoparticles/NLC colloid. As a dye is mixed

with the colloidal suspension, the induced fluorescence is trapped within the soliton, collected by a fiber and analysed in a spectrometer. To the best of our knowledge, this is the first time that a spectral analysis is performed through a spatial soliton. We demonstrate first the enhancement of the fluorescence intensity recovery by comparing the collected fluorescence signal of quinzarin in a NLC host (5CB), excited either by a spatial soliton or by a freely propagating beam induced between two optical fibers. The enhancement factor is in the order of 4. Next, we collected a set of spectra, for different inter-fiber distances d , from 125 to 500 microns, at constant input pump power. The main result is that the signal of fluorescence is quite constant whatever the d values. A model based on the waveguide properties of the soliton will be presented and confirms such a behavior. Finally we will give recent results concerning the localization of polystyrene particles inserted in NLC host by spectral analysis during the scanning of the sample by a soliton.

8114-06, Session 2

Spatial light modulators: a tool to image multiple-scattering media

S. Gigan, S. Popoff, P. Bondareff, N. Curry, S. Farahi, F. Ramaz, G. Lerosey, S. Grésillon, M. Fink, A. C. Boccara, Ecole Supérieure de Physique et de Chimie Industrielles (France)

Scattering of coherent light in heterogeneous biological media and tissues, leads to strong scattering and interferences phenomena which destroy both the spatial amplitude and phase information of any laser illumination. At the spatial level, it gives rise to the well-known "speckle" interference patterns. At the temporal (or spectral) level, a short pulse entering a scattering medium will be stretched due to the multiplicity of path lengths in the propagating medium. Consequently this greatly limits the imaging of an object through a scattering medium.

Multiple scattering is a highly complex but nonetheless deterministic process: it is therefore reversible, in the absence of absorption. Speckle can be coherently controlled. By « shaping » or « adapting » the incident wavefront, it is in principle possible to control the propagation and to overcome the scattering process.

Liquid crystal spatial light modulator (SLM) is a tool of choice to shape a laser beam over a very large number of modes, in order to match the high complexity of a multiple scattering medium. I will show how, using a SLM, one can measure the transmission matrix which links the input - output modes of the scattering medium. We present our original approach of solving the inverse problem for the reconstruction of an arbitrary image through the scattering media. I will detail our recent experiments with phase SLMs applied to, spatial -temporal focusing, imaging and phase conjugation through a thick opaque multiple scattering media. These experimental results confirm that phase-only SLMs are well suited to control laser light propagation in scattering media.

8114-08, Session 2

Graded-subdomain diffraction grating based on a nematic liquid crystal with semi-radial alignment

J. Kim, J. Na, S. Lee, Seoul National Univ. (Korea, Republic of)

Liquid crystals (LCs) are widely used for optical devices due to the large electro-optic modulation resulting from the high optical anisotropy, the electrically tuning capability at low voltages, and the design flexibility on various substrates. Among a number of the LC devices, the LC grating elements play an important role in many optical systems such as 3-dimensional displays and optical data storages through the modification of the phase or the polarization of light. In typical LC gratings, the uniform alignment of the LC molecules has been employed for obtaining the constant phase retardation from one domain to the other. Recently, for certain applications, graded types of the LC gratings

have been fabricated using a micro-rubbing method, a graded-electrode patterning method, and a photo-alignment method based on either multiple laser beams or the optical interference but they suffer from the continuity in the graded phase retardation within each domain. In this work, we demonstrate a new type of the LC grating device exhibiting the continuously graded phase retardation where the semi-radial alignment of a nematic LC is spontaneously produced on a microgrooved surface constructed by imprinting. Our graded LC grating device with the semi-radial LC alignment provides the high diffraction efficiency with the continuity in the phase retardation.

8114-45, Session 2

Liquid crystal-coil block copolymers: from hierarchical micelles to responsive monolayers

P. Pirogovsky, Z. Kurji, R. Hule, J. A. Kornfield, California Institute of Technology (United States)

The spontaneous anisotropy of side-group liquid-crystal polymers (SGLCPs) in a nematic solvent leads to ordering on multiple length scales when an SGLCP block is covalently linked to a random coil polymer. Micelles that form in a nematic solvent can have anisotropy at the level of the SGLCP chains in the corona that is orthogonal to the anisotropy of the micelle core that is, in turn, orthogonal to the anisotropy of the assembly as a whole. The orientational coupling between the SGLCP-block and the nematic liquid can be used to "transduce" changes in the conformation of the coil domain when it resides that the interface between an LC and an aqueous solution. Structural characterization by neutron scattering will be presented, along with examples of potential applications of LC-coil block copolymers.

8114-09, Session 3

Molecularly oriented surface relief formation and multi-directionally oriented crossed gratings in photoreactive liquid crystalline copolymer films

N. Kawatsuki, A. Tashima, Univ. of Hyogo (Japan); H. Ono, Nagaoka Univ. of Technology (Japan)

Photo-control of the molecular reorientation has received much attention in fabricating of polarization-sensitive and polarization-controllable optical devices. In this contribution, we demonstrate surface relief (SR) gratings and crossed SR gratings with molecularly oriented structure using photo-cross-linkable liquid crystalline copolymer films. For intensity holography, SR gratings were formed after annealing the exposed films, where the molecular migration to the higher-exposed region occurred. The reorientational direction and SR height were dependent on the degree of the photoreaction. When the exposure doses were low, molecular reorientation at the convex region was generated. In contrast, higher exposing doses resulted in the molecular reorientation at the concave area. Additionally, molecular reorientation was not generated for the much higher doses, although SR structure was formed. The generated SR height reached up to 300 nm for a 1 μ m-thin film, and the resulting gratings showed polarization sensitivity for diffraction efficiencies of the probe light beam according to the molecularly reorientation direction. Furthermore, combining the multi-holographic exposure and the unidirectional linearly polarized UV light exposing yield multi-directionally oriented film structure. Surface topology, molecular orientation and diffraction properties of the fabricated gratings were discussed.

8114-10, Session 3

Measuring Sagnac effect using liquid crystal adaptive holography

S. Residori, U. Bortolozzo, J. Rubin, Institut Non Linéaire de Nice Sophia Antipolis (France); J. Huignard, Jphopto (France)

Sagnac effect, due to different optical paths of counterpropagating waves in a rotating system, attracts a lot of attention both for its fundamental interest and its important applications in rotation sensing. For enhancing Sagnac detection different systems have been proposed, such as ring laser gyroscopes [1], fiber gyroscopes [2], nonlinear interferometers [3-5] and, recently, slow and fast light interferometers [6-7]. Here, we show the first realization of nonlinear Sagnac detection, which is made by inserting a liquid crystal light-valve, LCLV, in a Mach-Zehnder interferometer. The detection is based on slow-light effects [8] and adaptive holography [9] in the LCLV.

Two-wave mixing between the beams traveling clockwise, respectively, counterclockwise, in the interferometer is performed, while the whole experiment is mounted on a rotating platform. Before interfering in the LCLV the two beams acquire a differential phase shift due to the Sagnac effect. The refractive index grating induced in the liquid crystals is highly sensitive to instantaneous phase changes, therefore, by measuring the intensity of the diffracted orders we can obtain direct information on the Sagnac effect.

The liquid crystal response time [10] provides a frequency bandwidth determining two detection regimes: at low variation rate of the rotation speed, the LCLV operates in the slow-light regime providing a direct measurement of the angular acceleration [11]. For fast variation rate of the rotation speed, the interferometer detects, instead, the amplitude of the Sagnac phase shift. In both case, the adaptive character of the wave-mixing in the liquid crystals fixes automatically the optimum detection condition.

[1] E. J. Post, *Rev. Mod. Phys.* 39, 475 (1967).

[2] H. Lefèvre, *The Fiber-Optic Gyroscope*, (Artech House, Boston-London, 1993).

[3] A. E. Kaplan and P. Meystre, *Opt. Lett.* 6, 12 (1981).

[4] B. Fischer, and S. Sternklar, *Appl. Phys. Lett.* 47, 1 (1985).

[5] P. Yeh, I. McMichael, and M. Khoshnevisan, *Appl. Opt.* 25, 1029 (1986).

[6] G.T. Purves, C.S. Adams, and I.G. Hughes, *Phys. Rev. A* 74, 023805 (2006).

[7] M. Salit, G.S. Pati, K. Salit, and M.S. Shahriar, *J. Mod. Opt.* 54, 2425 (2007).

[8] S. Residori, U. Bortolozzo, and J.P. Huignard, *Phys. Rev. Lett.* 100, 203603 (2008).

[9] U. Bortolozzo, S. Residori, and J.P. Huignard, *Opt. Lett.* 34, 2006 (2009).

[10] I. C. Khoo, *Physics Reports* 471, 221 (2009).

[11] U. Bortolozzo, S. Residori, and J.P. Huignard, to appear in *Opt. Lett.* 2011.

8114-11, Session 3

Anchoring strength of o-, m-, and p-methyl red-dye-doped nematics on rubbed and unrubbed polyimide surfaces

D. Statman, Allegheny College (United States)

It is demonstrated that the photoinduced gliding of the easy axis for nematics doped with various azo dyes on rubbed polyimide involves the formation of a second easy axis on the polyimide surface. While some azo dyes, such as disperse orange 3, do not exhibit large surface induced nonlinear effects, other dyes, such as methyl red, do. The amount of gliding on rubbed polyimide is determined by the relative

anchoring strengths of the easy axis formed from adsorbed dye and that formed from rubbing. One question of interest is what is the source of the anchoring strength? In this presentation, I will discuss the formation of easy axes via the photo-induced adsorption of azo dye. Using the results of optical measurements, I compare the anchoring strengths between dyed nematic liquid crystals and the easy axes formed by photoinduced adsorption of three isomers of the methyl red azo dye, ortho, meta, and para. I will also discuss the impact of the carboxyl group position in the dye molecule on the anchoring strength.

8114-12, Session 3

Monitoring anchoring energy in LC-based sensors

R. G. Lindquist, Y. Zou, D. Ke, The Univ. of Alabama in Huntsville (United States)

Liquid crystal (LC) based sensors have been investigated over the past decades in an effort to develop low cost, portable, field-deployable, highly selective chemical and biological sensors. Due to the collective behavior and the highly anisotropic properties of liquid crystal molecules, detection of very low levels (ppbs) of chemical and biological agents is possible. However, present LC sensors rely on a threshold concentration of a targeted analyte to cause a surface driven molecular reorientation of the LC molecules. At a lower concentration, a molecular reorientation will not be induced and thus undetected by passive transduction. The surface anchoring energy maintaining the initial molecular alignment will, however, weaken. By forcing a reorientation of LC molecules near the surface with an applied electric field and then tracking the deformation via capacitive transduction, the anchoring energy can be monitored. In this paper, we present a technique to significantly improve the sensitivity of LC - based sensor by monitoring changes in anchoring energy via capacitive transduction.

Theoretical and experimental results indicated a minimum of 10-fold and potentially 1000-fold improvement can be achieved. Several electrode structures have been investigated with preliminary experimental results closely matching the simulations. By incorporating these techniques with microfluidic systems, portable, compact and highly sensitive chemical and biological sensors can be achieved for either gas or liquid environments. Preliminary experimental results with LC in microfluidics channels will be presented.

8114-03, Session 4

Metallic subentities embedded in micro-periodic composite structures for the realization of metamaterials

L. De Sio, R. Caputo, U. Cataldi, Univ. della Calabria (Italy); J. Dintinger, H. Sellame, T. Scharf, Ecole Polytechnique Fédérale de Lausanne (Switzerland); C. Umeton, Univ. della Calabria (Italy)

We report on the fabrication and characterization of a micro periodic structure realized in soft-composite materials containing metallic nanoparticles. These are used to infiltrate a passive polymer template realized by combining an optical holographic curing setup and a microfluidic etching process. In experiments, a small amount of nanoparticles are dissolved in the original mixture normally utilized for the realization of polymer-liquid-crystal-polymer-slices gratings (POLICRYPS) in order to fabricate POLICRYPS-like structures showing novel electromagnetic (metamaterial) properties. Obtained structures are characterized towards the impinging probe light polarization in the UV/visible range. Correlation between the optical response and external perturbations (electric field, temperature) is also reported. First attempts are oriented to the fabrication of devices with tuneable metamaterial properties.

8114-13, Session 4

Nanoparticle-dispersed cholesteric blue phase and its electro-optic and photonic applications

M. Ozaki, H. Yoshida, S. Yabu, Y. Tanaka, Y. Ogawa, A. Fujii, Osaka Univ. (Japan); N. Uehara, Santec Corp. (Japan); H. Kikuchi, Kyushu Univ. (Japan)

Cholesteric blue phases (BPs) appear in very narrow temperature range because of the inevitable existence of disclinations. We have proposed the BP stabilization by introducing nano-scale particles into BP LC. With doping spherical gold nanoparticles (NPs) with a mean diameter of 3 nm in a BP-exhibiting LC using a unique technique without having to chemically modify NPs' surfaces, the temperature range of the BPs expanded from 0.5 to 5 oC. We tentatively interpret that the NP localization in the lattice disclinations stabilizes the BP structure, which is similar to that of polymer-stabilized BPs. We also discuss about not only phase transition characteristics but also electro-optic and photonic behaviors in NP-doped BP LC. Using the stabilized BP LC, polarization independent refractive index modulation was demonstrated, which is expected to use in a telecommunication application. The light propagation and emission characteristics in BP and NP-doped BP LCs have also been investigated using both a numerical calculation and experimental approaches.

8114-14, Session 4

Novel photorefractive CdSe/CdS nanorods liquid crystal nanocomposites

L. L. Petti, M. Rippa, Consiglio Nazionale delle Ricerche (Italy); M. Zanella, L. Manna, Istituto Italiano di Tecnologia (Italy); P. Mormile, Consiglio Nazionale delle Ricerche (Italy)

Nematic liquid crystals (NLCs)-based photorefractive materials are very attractive for photonic applications such as dynamic hologram, optical information processing, phase conjugation and optical switching because of their large optical anisotropy, low driving voltage, and large electro optic effects.

Multimaterial nanocrystal heterostructures that contain two or more different functionalities are attractive candidates for enabling the bottom-up fabrication of unprecedented materials. CdSe/CdS nanorods present the appealing characteristics of strong and tunable light emission from green to red, are highly fluorescent and show linearly polarized emission.

These characteristics open the way to a new class of nanocomposite devices based on LCs and colloidal NRs in which the unique optical properties of the inorganic moiety are combined with the electro-optical and the large optical anisotropy of the host system to develop new high performing optical and photonic devices/systems. In the present contribution we designed and fabricated novel nanocomposites devices prepared by incorporating CdSe/CdS core/shell nanorods into a NLC to realize homeotropically aligned cells. We studied the photorefractive and the orientational responses of these samples by both asymmetric two-beam coupling to measure two beam coupling gain and diffraction efficiency under the influence of an applied electric field, and forced light scattering technique. Nanorods alignment with the orientation of the LC molecules has been also investigated. A refractive index grating was written in the device in a holographic tilted configuration by two p-polarized laser beams at 514 nm. Self-diffraction of the writing beams and diffraction of a probe beam at 633 nm were measured. A high TBC gain coefficient of 270 cm⁻¹ was achieved at a DC field applied of 3.4V/ μ m. First-order diffraction efficiencies were evaluated with a maximum efficiency of 7% in the dynamic grating with a nonlinear refractive index, n_2 , 4×10^{-2} cm²/W for $E_0 = 3$ V/ μ m.

8114-15, Session 4

Toward cloaking in nanosphere dispersed liquid crystal (NDLC) metamaterial: Monte Carlo studies

G. Pawlik, W. Salejda, K. Tarnowski, W. T. Walasik, A. C. Mitus, Wroclaw Univ. of Technology (Poland); I. C. Khoo, The Pennsylvania State Univ. (United States)

We discuss cloaking at infrared frequencies in NDLC metamaterial [1] using Monte Carlo and FEM methods. It requires a design of an inhomogeneous configuration of liquid crystal molecules which corresponds to the spatial inhomogeneity of effective permittivity and permeability resulting from optical transformation. Recently, we have shown that external electric field and anchoring forces [2,3] as well as filling factor and size of coated nanospheres [4] constitute relevant parameters for tuning of the magnitude and gradients of local optical properties of NDLC. We present first results for cloaking in NDLC at chosen infrared frequencies.

[1] I. C. Khoo, D. H. Werner, X. Liang, A. Diaz, B. Weiner, Opt. Lett. 31 (2006) 2592.

[2] W. Walasik, M. Jarema, G. Pawlik, A.C. Mitus, I.C. Khoo, submitted to Nonl. Opt. Quant. Opt.

[3] G. Pawlik, M. Jarema, W. Walasik, A. C. Mitus, I. C. Khoo, JOSA B 27 (2010) 567.

[4] G. Pawlik, W. Walasik, A.C. Mitus, I.C. Khoo, Opt. Mater., (2011) accepted.

8114-16, Session 4

Nanomaterials dispersed in liquid crystals: how they change LC-properties

W. Haase, Technische Univ. Darmstadt (Germany)

It is well known small amount of nanomaterials dispersed in Liquid Crystals can change their physical properties remarkably. This allows for practical application, although the so far reported properties are in part wide spreading.

Within this Invited Talk our recent results on Nanodispersions of Carbon Nanotubes, of metallic functionalized particles like gold and silver and of dipolar particles like Bariumtitanate in Nematic and Ferroelectric Liquid Crystals will be presented and discussed.

8114-18, Session 5

Photochemical on-off switching of structural color of a multi-bilayered film consisting of azobenzene-polymer liquid crystal and polyvinylalcohol

S. Kurihara, M. Moritsugu, Y. Kuwahara, T. Ogata, Kumamoto Univ. (Japan)

We have found that some side chain type polymer liquid crystals having an azobenzene group as a side chain group showed thermally spontaneous out-of-plane molecular orientation by annealing at a smectic phase. We prepared a multi-bilayered film consisting of PA6Az1, which is one of the azobenzene polymer liquid crystals, and polyvinylalcohol (PVA) on a glass substrate by spin coating of the polymer solutions alternately. The multi-bilayered film reflected light of a wavelength depending on the layer thickness as well as refractive index of the polymers. The reflectivity of the multi-bilayered film disappeared by annealing at 80 °C. The disappearance of the reflection by the annealing was related to the thermal out-of-plane molecular orientation of PA6Az1 in the multi-bilayered film, leading to very small difference in refractive

indices between PA6Az1 and PVA. The reflectance of the multi-bilayered film was increased again by UV irradiation because of the transformation from the out-of-plane orientation to the in-plane random orientation. The on-off switching of the reflection was achieved by the combination of the thermally spontaneous out-of-plane molecular orientation and following photoisomerization of PA6Az1.

8114-19, Session 5

Optofluidics based on liquid crystal microflows

A. E. Vasdekis, J. G. Cuennet, L. De Sio, D. Psaltis, Ecole Polytechnique Fédérale de Lausanne (Switzerland)

Optofluidics emerged in early 2000 as the fusion between integrated optics and microfluidics, focusing primarily on novel photonic devices and analytical methods [1, 2]. Typical examples involve light sources [3] and waveguides [4], but also miniaturized microscopes [5] and adaptive imaging components. Optofluidics has also significantly impacted the field of molecular manipulation and sensing, with the recent demonstration of sub-100 nm particle trapping [6], and the manipulation of fluids via laser radiation [7].

In this presentation, we will discuss our recent efforts in optofluidics based on anisotropic fluids. To this end, we replaced common microfluidic buffers with nematic liquid crystals in microfluidic channels and controlled the director orientation via flow. Rapid pulsatile flows were possible via micro-flow engineering and integrated micro-pumps. We will present the steady state analysis of liquid crystal molecules inside the channels and present the results of our recent efforts in developing optical modulators operating in the kHz regime [8].

1. Psaltis, D., S.R. Quake, and C.H. Yang, Developing optofluidic technology through the fusion of microfluidics and optics *Nature*, 442, 381-386 (2006).
2. Monat, C., P. Domachuk, and B.J. Eggleton, Integrated optofluidics: A new river of light *Nature Photon.*, 1, 106-114 (2007).
3. Song, W.Z., A.E. Vasdekis, Z.Y. Li, and D. Psaltis, Optofluidic evanescent dye laser based on a distributed feedback circular grating *Appl. Phys. Lett.*, 94, 161110 (2009).
4. Vezenov, D.V., B.T. Mayers, D.B. Wolfe, and G.M. Whitesides, Integrated fluorescent light source for optofluidic applications *Appl. Phys. Lett.*, 86, 041104 (2005).
5. Cui, X.Q., L.M. Lee, X. Heng, W.W. Zhong, P.W. Sternberg, D. Psaltis, and C.H. Yang, Lensless high-resolution on-chip optofluidic microscopes for *Caenorhabditis elegans* and cell imaging *P. Natl. Acad. Sci. USA*, 105, 10670-10675 (2008).
6. Yang, A.H.J., S.D. Moore, B.S. Schmidt, M. Klug, M. Lipson, and D. Erickson, Optical manipulation of nanoparticles and biomolecules in sub-wavelength slot waveguides *Nature*, 457, 71-75 (2009).
7. Liu, G.L., J. Kim, Y. Lu, and L.P. Lee, Optofluidic control using photothermal nanoparticles *Nature Mat.*, 5, 27-32 (2006).
8. Cuennet, J.G., A.E. Vasdekis, L. De Sio, and D. Psaltis, under revision, (2011).

8114-20, Session 5

Photodriven, multidimensional oscillation of glassy azobenzene liquid crystalline polymer networks

K. Lee, M. L. Smith, H. Koerner, Air Force Research Lab. (United States); N. Tabiryan, BEAM Engineering for Advanced Measurements Co. (United States); R. A. Vaia, T. J. Bunning, T. J. White, Air Force Research Lab. (United States)

Glassy, photoresponsive monodomain azobenzene liquid crystalline polymer networks (azo-LCN) are prepared by photo-polymerization,

and show large amplitude, high frequency in-plane oscillation (~ 50 Hz) when exposed with a 442 nm coherent-wave (CW) laser. In addition to the in-plane oscillation, multidimensional out-of-plane twisting behaviors are observed by adjusting the orientation of the nematic director to the long axis of the azo-LCN cantilever. The frequency of photodirected oscillations is strongly correlated to the length of the cantilever (width/length ratio), while the amplitude and threshold laser intensity for oscillation are strongly correlated to temperature. The effect of cantilever aspect ratio, laser intensity, and temperature on the photoresponsive bending, twisting and oscillation behaviors of azo-LCN will be discussed.

8114-21, Session 5

Simple and functional photonic devices from printable liquid crystal lasers

D. J. Gardiner, P. J. W. Hands, S. M. Morris, T. D. Wilkinson, H. J. Coles, Univ. of Cambridge (United Kingdom)

We report on printable laser sources formed by the emulsification of dye-doped chiral nematic liquid crystals within a polymeric binder. Such lasers can be easily formed on single substrates with no alignment layers. The system comprises the self-organizing periodic structure of chiral nematic liquid crystals with the simplicity of the emulsion procedure so as to produce a material that retains the emission characteristics of band-edge lasers yet can be readily coated. [1]

Under optical excitation, it is shown that it is possible to generate both single-mode photonic band edge [2] and random lasing [3] depending upon the droplet morphology. Specifically, the laser output is determined by the size and number density of the droplets. Band-edge lasing is observed for large droplets (tens of μm) and low number densities. On the other hand, small droplets ($< 10\mu\text{m}$) and high number densities, promotes random lasing via a diffuse scattering feedback mechanism. The preparation, characterization and optical output of both types of emulsion-based sources are discussed in detail. Finally, sequential and stacked layers demonstrate simultaneous multi-wavelength (white) laser output from glass, metallic and flexible substrates, permitting new application areas into mass manufacturable, flexible and conformable laser devices.

References:

- [1] D. J. Gardiner, S.M. Morris, P. J. W. Hands, C. Mowatt, R. Rutledge, T.D. Wilkinson, and H.J. Coles. *Opt. Express* 19, 2432 (2011)
- [2] H.J. Coles and S.M. Morris, *Nature Photonics* 4, 676 (2010).
- [3] D.S. Wiersma, *Nature Physics* 4, 359 (2008)

8114-22, Session 5

Broadband ultrafast all-optical processing with nematic liquid crystals

K. Hong, S. Zhao, I. C. Khoo, The Pennsylvania State Univ. (United States)

We present a critical review of the nonlinear optical responses of transparent as well as plasmonic- or dye-doped nematic liquid crystals. Experimental studies have demonstrated the feasibility of sub-microseconds - nanoseconds all-optical one-way switching of nanoseconds pulsed lasers spanning the entire visible - near infrared regime (488nm, 532 nm, 750 nm, 1060 nm, 1550 nm). These effects will be useful for developing tunable metamaterials and to realize faster-response version of many coherent optical image processing applications demonstrated previously with slower mechanisms.

8114-23, Session 6

Diffuse cone behavior and microscopic structure of the de Vries smectic-A and smectic-C phases

S. Kumar, Kent State Univ. (United States)

In the smectic-A (SmA) and smectic-C (SmC) liquid crystal phases, calamitic molecules are arranged in layers. In the uniaxial SmA phase, the director is parallel to the layer normal but tilted at a polar angle $\alpha(T)$ in the SmC phase. In conventional cases, the director tilt occurs in a well defined azimuthal direction and the corresponding layers shrinkage is can be as high as $\sim 11\%$. In 1979, deVries discovered materials in which the layer shrinkage was about an order or magnitude smaller, and yet the system transformed from uniaxial to biaxial smectic phase. He proposed that the local director is already tilted in the SmA phase, but without any coordination in the azimuthal direction. In the SmC phase, the aximuthal tilt becomes increasingly coordinated with decreasing temperature rendering the phase biaxial. This "diffuse cone model" has been investigated by various groups, but the evidence obtained has mostly been indirect. In our x-ray experiments, we directly measured the molecular tilt, director orientation, and find differetn values of the nematic order parameters for the siloxane and hydrocarbon parts of the molecules. Specifically, the results show that exponent of the tilt order parameter β agrees with tricritical behavior. Among other results, we also show that linear extrapolation of the thermal evolution of SmA layer spacing into the SmC region requires modification. These results provide a quantitative picture of the structure of the two deVries phases and the transition between them which changes from second order to first order for different homologs.

8114-24, Session 6

Liquid crystal beam shaping devices employing patterned photoalignment layers for high-peak-power laser applications

K. L. Marshall, S. K. H. Wei, K. Wegman, M. Vargas, C. Dorrer, P. Leung, J. Boule, Z. Zhao, S. Chen, Univ. of Rochester (United States)

Optical elements with spatially varying transmission are required for laser engineering and imaging systems. Although refractive systems can transform the Gaussian energy distribution of a laser beam into a "top-hat" distribution, they lack the versatility to produce the more complex and precise intensity distributions required for high-peak-power laser systems such as the OMEGA and OMEGA EP laser systems at the University of Rochester's Laboratory for Laser Energetics and the National Ignition Facility at Lawrence Livermore National Laboratory. Previously, distributions of opaque metal pixels on a transparent glass substrate have been used for such beam-shaping efforts, but the laser damage thresholds of the order of 0.2 J/cm^2 in the nanosecond regime limits their applicability. By applying the process of photolithographic patterning of either cinnamate-based or coumarin-based photoalignment layers using polarized UV light to generate spatially-varying molecular orientation in a nematic liquid crystal device, we have developed and demonstrated high-resolution beam shaper devices optimized for such high peak power laser applications in the near IR region. Operating at 1054 nm , these devices demonstrated a contrast ratio of 430:1, a pixel size of $10 \mu\text{m}$ with inter-pixel resolution of $1.7 \mu\text{m}$, and laser damage resistance ranging between $20\text{-}40 \text{ J/cm}^2$ at 1054 nm (1 ns pulse width) using a $10 \mu\text{m}$ layer of commercially available nematic LC materials. Coupled with the ability to generate almost an infinite variety of binary and grey-scale apodization and beam-shaping profiles by the photoalignment process, the high laser damage threshold of these devices makes them attractive and useful tools for a multitude of laser applications.

8114-25, Session 6

Liquid crystal lasers: from basics to practical holographic systems

H. J. Coles, Univ. of Cambridge (United Kingdom)

We briefly describe the background to Microscopic Liquid Crystal lasers and then consider the key properties of the liquid crystal host & cavity design that lead to high slope efficiency ($\sim 70\%$), low laser thresholds ($\sim 100 \text{ nJ/pulse}$), narrow line widths ($< 0.01 \text{ nm}$) and quasi-continuous working 53 kHz pulse rate) giving average powers of 5 mW per pixel or laser spot. The birefringence, the elastic constants and the orientational order parameters of the liquid crystals and the dye (as well as the spectral absorption coefficient and peak absorption wavelength), were the key parameters that influenced markedly the performance of such LC lasers. Further, through cavity design/construction and using 2-D lenslet arrays of up to 100 by 100 spots we can optimize the gain to give a quasi- continuous working wide color gamut RGB laser output with powers of Watts in the far field. We will show how the narrow band output from these microscopic cavity lasers may be continuously wavelength tuned through the application of in-plane electric and we will describe a multi-wavelength prototype, continuously tunable from the ultraviolet to near infrared, with an 8 inch by 5 inch footprint and 2 inches high used for projection through computer generated holograms and medical applications. We will consider new Blue Phase systems, stable over a 100°C temperature range, in which an electric field is used to switch the photonic band gap from red to green. Finally we will describe new paintable lasers, that have been coated on flexible plastic and foil substrates that have been used for holographic projection displays.

8114-26, Session 6

Polymer stabilization of phototunable cholesteric liquid crystals

L. V. Natarajan, SAIC (United States); T. J. White, Air Force Research Lab. (United States); Q. Li, Kent State Univ. (United States); T. J. Bunning, Air Force Research Lab. (United States)

We have recently demonstrated phototuning of more than 2000 nm in an azobenzene-based cholesteric liquid crystal (CLC) composed of a nematic liquid crystal and a high helical-twisting power chiral bis(azo) molecule. Phototuning range and rate were dependent on azo dopant concentration, light intensity, and cell thickness. The time for restoration of the original spectral properties in the absence of light source was long, lasting for several hours. Polymer stabilization of the CLC by LC monomers reduced the relaxation time to less than an hour. In this work, we present the results of a systematic study of the effect of polymer stabilization on the kinetics of phototuning and dark relaxation of the bis(azo) based CLC. The impact of varying LC monomer structure, polymer concentration, cross linker concentration, curing power, and cell thickness on the optical performance of these photoresponsive CLCs will be discussed.

8114-27, Session 7

Liquid crystal molecular orientation properties of microrubbing cells and its application to electrically tunable gratings

M. Honma, W. Toyoshima, T. Nose, Akita Prefectural Univ. (Japan)

Liquid crystal (LC) gratings consisting of twisted nematic orientation domains have been demonstrated. The LC grating cells were fabricated by the microrubbing, which is microscale rubbing technique using a tiny stylus. Fabricated LC cells exhibited multistable LC molecular orientation state, which could be divided into two types of twist orientation states; that is, ± 90 and ± 180 degrees twist orientation states. After the LC

grating cells were heated and cooled so that the nematic-isotropic phase transition was induced, the mixed orientation state of ± 90 and ± 180 degrees twist domains was observed. The entire microrubbing area was covered with the ± 90 degrees twist domains by inducing LC flow in an appropriate direction in the LC grating cells. Furthermore, the ± 180 degrees twist domain spreading over the entire microrubbing area could be obtained after a suitable voltage application. Diffraction properties of the LC grating cells under the voltage application were also investigated. The LC grating cells exhibited symmetric diffraction properties with the same light intensities of positive and negative order diffractions when the incident light was linearly polarized. However, for the circularly-polarized incident light, asymmetric diffraction properties were revealed. Namely, the diffraction efficiency of the positive order diffraction exceeded 70%, while that of the negative order diffraction was quite low (less than 10%).

8114-28, Session 7

Wavelength-tuneable liquid crystal lasers from the visible to the near-infrared

P. J. W. Hands, C. A. Dobson, S. M. Morris, Q. M. Malik, D. J. Gardiner, T. D. Wilkinson, H. J. Coles, Univ. of Cambridge (United Kingdom)

Photonic band-edge lasers made from dye-doped chiral nematic liquid crystals have been a subject of detailed academic interest in recent years [1]. Their periodic micro-molecular structure is self-organising, allowing mirror-free lasing with low thresholds and high slope efficiencies in simple device architectures. Thus far, liquid crystal lasing has been restricted to wavelengths within the ultra-violet and visible spectrum. Extending emission into the near-infrared offers the opportunity of developing a new range of low-cost optical sources, with applications including sub-dermal medical imaging, point-of-care medical diagnostics tools, telecommunications, and unique optical signatures for security coatings.

In this paper, a wide range of commercially available organic dyes are examined for their suitability within a liquid crystal host as light emitters in the near-infrared [2]. Problems such as poor dye solubility and reduced quantum efficiencies are overcome, and successful band-edge lasing is demonstrated up to 850 nm, using the dyes LD800, HITC-P and DOTC-P. Despite reduced quantum efficiencies, near-infrared lasing slope efficiencies are comparable to their visible counterparts. A discussion of the mechanisms behind these results and other important factors in their fabrication is presented.

By combining both visible and near-infrared lasing mixtures, array-based gradient-pitch systems can be produced [3], capable of outputting multiple simultaneous band-edge laser emissions that are arbitrarily selectable across the visible and near-infrared spectrum (460-850 nm). Forster transfer enables such polychromatic emission to be achieved whilst pumping the device with a single-wavelength optical source.

References:

1. H.J. Coles and S.M. Morris, *Nature Photonics* 4, 676 (2010).
2. P.J.W. Hands, C.A. Dobson, S.M. Morris, Q.M. Malik, T.D. Wilkinson, and H.J. Coles, *Appl. Phys. Lett.* (in submission) (2011).
3. S.M. Morris, P.J.W. Hands, S. Findeisen-Tandel, R.H. Cole, T.D. Wilkinson, and H.J. Coles, *Opt. Express* 16 (23), 18827 (2008).

8114-29, Session 7

Dynamic selective reflection properties in cholesteric liquid crystals

T. J. Bunning, M. E. McConney, J. Hurtubise, M. Duning, Air Force Research Lab. (United States); L. V. Natarajan, V. P. Tondiglia, SAIC (United States); T. J. White, Air Force Research Lab. (United States)

We discuss the development of spatially templated polymer networks formed from a templated cholesteric liquid crystal fluid. By controlling the

nuances of the anisotropic photopolymerization conditions employed and the nature of the monomer mixture used, liquid crystal films with a variety of dynamic electro-optic, photo-optic, and thermo-optic responses can be formed.

8114-30, Session 7

Waveguides with liquid crystals

K. Neyts, J. Beeckman, W. De Cort, P. Vanbrabant, Univ. Gent (Belgium)

The orientation of liquid crystal near an optical waveguide determines the propagation speed and the losses in that waveguide. This principle can be exploited for tuning the resonance frequency of a ring resonator or for sensing the presence of molecules at the interface between water and liquid crystal. In this work, experimental evidence and qualitative explanations are provided for the case of silicon-on-insulator high index-contrast waveguides with liquid crystal and for the case of liquid crystal in a section of a low index contrast doped glass waveguide.

8114-07, Session 8

Universal soft matter template: from photonic to metamaterial applications

C. Umeton, L. De Sio, R. Caputo, S. Ferjani, G. Strangi, R. Bartolino, Univ. della Calabria (Italy)

We report on the realization and characterization of a polymeric template sculptured in photosensitive material, on a chemical inert surface. The structure is devoted to micro/nano-confinement and stabilization of a wide range of organic and nano-particle components with self-arrangement properties at the nanoscale [1]. High quality morphology of a polymeric, micro-patterned, arrays is obtained by combining a nano-precision level optical holographic setup and a multi-step chemical-physical process. The "universal" template represents the basic platform to be filled with different organic materials, which can also include metallic nano-particles. The long range self-organization is induced without making use of any kind of surface chemistry. Due to their capability of exhibiting self organization, light responsive Liquid Crystals (LC) [2], short pitch cholesterics LC [3] and ferroelectrics LC have been exploited, and experimental studies have been carried out in order to investigate the photo-optical and electro-optical response of obtained composite structures for the realization of photonic devices. Finally, the possibility of including metallic nano-particles has been also investigated, with the aim of inducing a "metamaterial" behavior of the realized structure.

References

- 1) L. De Sio, S. Ferjani, G. Strangi, C. Umeton and R. Bartolino *Nature Photonics* (submitted)
- 2) L. De Sio, S. Serak, N. Tabiryani, S. Ferjani, A. Veltri, C. Umeton *Adv. Mater.*, 22, 2316-2319 (2010)
- 3) L. De Sio and C. Umeton, *Opt. Lett.* 35, 2759-2761 (2010)
- 4) Carbone G., Salter P., Elston S. J., Raynes P., De Sio L., Ferjani S., Strangi G., Umeton C. P., Bartolino R. *APL*, 2009, 95, 011102-1-011102-3 (2009)

8114-31, Session 8

Design of SmAPF mesogens

E. D. Korblova, D. M. Walba, T. Gong, Univ. of Colorado at Boulder (United States); A. Reddy, VVI Bright, Inc. (United States); C. Zhu, R. Shao, Y. Shen, J. E. MacLennan, M. A. Glaser, N. A. Clark, Univ. of Colorado at Boulder (United States)

Smectics with both tilted and/or untilted phases are quite commonly

found in mesogens with linear cores, but untilted (orthogonal) phases are very rare among known bent-core materials, these systems usually transition directly from the isotropic melt to SmCP phases, smectics with tilted molecules and polar layers.

SmAPF phases although rare are very desirable for applications due to an interesting set of unique features, including fast analog switching, phase-only modulation, and electro-optic latching. A disadvantage of existing SmAPF mesogens is relatively small maximum modulation depth (Δn).

One class of known SmAP mesogens possesses a bent molecular core with a single flexible tail, which stabilizes fluid smectic layers with untilted molecules and in-plane polar ordering. In single tail wedge systems SmAP phase may occur, but the antiferro arrangement is the only arrangement seen.

Our design approach uses the principle of nanosegregation of the layers. We used carbosilane units in conjunction with a single tail to get a prototypical SmAPF material W586. Modification of the core bite angle, ester unit reversal and other features will be presented and discussed in the context of controlling the spontaneous polarization, birefringence change (Δn) and other electro-optics properties.

B. K. Sadashiva, R. A. Reddy, R. Pratibha, N. V. Madhusudana, J. Mater. Chem. 12, 943-950 (2002).

8114-32, Session 8

Liquid crystal homo and alternating (co) polymers based on pi-conjugated backbone

F. Mathevet, I. Tahar-Djebbar, D. Zeng, Univ. Pierre et Marie Curie (France); B. Heinrich, B. Donnio, D. Guillon, Univ. de Strasbourg (France); D. Kreher, A. Attias, Univ. Pierre et Marie Curie (France)

The self-organization of pi-conjugated organic materials forming highly ordered supramolecular architectures has been extensively investigated in the last two decades in view of optoelectronic applications. Indeed, the control of both the mesoscopic and nanoscale organization within thin semiconducting films is the key issue for the improvement of charge transport properties and achievement of high charge carrier mobilities. These well-ordered materials are currently either self-organized semiconducting polymers or liquid crystals.

In this context, we endeavored to investigate the self-organization of a side-chain liquid crystal (SCLC) semiconducting polymer where (i) the backbone is a pi-conjugated polymer and (ii) the side groups are pi-conjugated discotic mesogens.

Here we describe the design and synthesis of columnar side-chain liquid crystal homo and alternating (co)polymers with triphenylene mesogens as side groups, and well-defined regioregular polythiophene as backbone.

These different kinds of architectures prepared following the Grignard methathesis (GRIM), allow the control of the triphenylene side group ratio along of the polymer chains, and lead to tunable electronic properties and nanostructures.

In this work, we will give the details on the synthesis and structural characterization studied by Polarized-light Optical Microscopy (POM), Differential Scanning Calorimetry (DSC) and Temperature-dependent, small-angle X-ray diffraction. Moreover, their photophysical properties and the preliminary charge transport results will also be depicted in view of applications for organic optoelectronics.

8114-33, Session 8

Polymer-stabilized isotropic liquid crystal and display

D. Yang, Kent State Univ. (United States)

We constructed a polymer-stabilized isotropic liquid crystal by polymerizing monomers in the isotropic phase of liquid crystal materials at elevated temperatures. The system exhibits an optically isotropic state under zero field at room temperature, and becomes optical birefringent

when externally applied electric fields are applied. We studied the field-induced birefringence as a function of applied field and temperature. We also developed a simple theory to explain the experimental results. We used the material to make flat panel display with in-plane-switch cell, which has large view angle and sub-million second response time.

8114-34, Session 8

Phototropic liquid crystals

B. Taheri, T. Kosa, L. Sukhomlinova, AlphaMicron, Inc. (United States); T. J. White, T. J. Bunning, Air Force Research Lab. (United States); A. Munoz, AlphaMicron, Inc. (United States)

Analogous to the melting of a crystalline solid into a liquid melt, heating liquid crystals transitions the mixture from crystalline solid, to liquid crystal, to isotropic liquid. In general, liquid crystals are classified into thermotropic, lyotropic, and polymeric liquid crystals based on the stimulus that is responsible for the phase transition. Within each liquid crystal regime, a number of well-known mesophases are observed including nematic, cholesteric, and many variations of smectic. Here, we present a new class of liquid crystal material wherein light induces the phase transition. In contrast to previous examinations of photoresponsive liquid crystal systems, this work presents a system in which light exposure increases the order parameter of the mixture, allowing for "phototropic" phase transitions. In particular, light illumination can increase the order of the mixture and induce phase transition from isotropic to nematic, isotropic to cholesteric, or nematic to smectic phases. This system is based on series of novel photodichroic dyes that are disruptive to liquid crystallinity in the ground state and favorable to liquid crystallinity in the open form. The increase in order with light exposure has profound implications in dynamic optics, photonics, lasing, and displays.

8114-35, Session 8

Plasmonics-enhanced optical fields and nonlinearities in liquid crystals

I. C. Khoo, J. Huang, Y. Ma, The Pennsylvania State Univ. (United States)

Optically induced localized plasmonic fields of Au- and Ag- nano-spheres and nano-strips embedded in liquid crystals are calculated. Results for uniform distribution of the nano-spheres show large resonant peaks shift with nematic index change. For paired nano-strips, we have quantitatively examined the dependence of these field enhancement effects on the separation distance, periodicity, aspect ratio and the size of the nanostrip. Complex third order ultrafast electronic nonlinearities due to the laser-induced plasmonic local fields are also 'observed', theoretically and experimentally using short-pulsed lasers. These effects will be useful for tunable optical sensor, all-optical switching, tunable filters and nonlinear transmission applications. References: I. C. Khoo, Physics Report 471, pp. 221-267 [2009]; I. C. Khoo et al, IEEE JSTQE 16, pp. 410-417 (2010); ibid Opt. Lett. 31, 2592 (2006); ibid, J. Mater. Chem. 19, 7525-7531 (2009)

8114-37, Poster Session

Tunable retarder made of pentaprisms and liquid crystal

M. Saito, K. Hayashi, Ryukoku Univ. (Japan)

Nematic LC ($n_o=1.53$, $n_e=1.82$) was sandwiched between two Si pentaprisms ($n=3.4$) with its director being oriented perpendicular to the Si surface (homeotropic alignment). When an angle of incidence was 28° (Brewster's angle), p-polarized light passed through the LC layer, while s-polarized light, which took the smaller index (n_o), suffered total internal reflection. Consequently, this LC layer acted as a polarization

beam splitter. The reflected light beam (s polarization) propagated in the Si prism and reached the opposite surface of the pentagon. A gold mirror was adhered to this surface for creating a gap (5-15 μm) between them. This gap was filled with the nematic LC, which was aligned parallel to the Si surface with its director being rotated by 45° from the direction of s polarization. Since this LC layer acted as a retarder, the beam that was reflected at this surface took different polarization state depending on wavelength. Consequently, when the beam returned to the beam splitter, it was reflected or transmitted at the Si-LC boundary depending on its polarization state. The transmitted beam (selected wavelength) passed through the LC layer and emerged from the other Si prism. The transmission wavelengths could be tuned by applying an electric voltage between the gold mirror and the Si prism. Since this device was symmetrical with respect to the beam-splitting LC layer, the similar phenomenon took place for p polarization in the opposite Si prism. This wavelength tuning function was confirmed by measuring infrared transmission spectrum of the device.

8114-38, Poster Session

Cost-efficient manufacturing process of switchable glazing based on twisted nematic LC cells

E. Kurz, L. Rau, N. Fruehauf, M. Prskalo, W. Haase, W. Sobek, Univ. Stuttgart (Germany)

Large-area glass facades are widely spread in contemporary architecture. They meet demands for natural light illumination of rooms and satisfy esthetic requirements of modern architecture. However, larger glass facades increase transfer of energy into the building. Since this has to be compensated by the intense use of air condition, modulation of the energy passing through the glazing is essential.

The authors have been developing a system for modulation of penetrating sunlight. It consists of a modified twisted nematic (TN) liquid crystal (LC) cell which is embedded in a double glazing. The materials used in the TN-LC cell must withstand certain environmental conditions, primarily UV radiation, moisture and heat. In particular, this applies to the polarizer. Since a conventional outside film polarizer is susceptible to heat, the authors substituted this component for an inside coatable polarizer. Long term outdoor weathering tests demonstrated that the concept is viable. Part of the current research is the integration of the TN-LC cell into double-glazing focusing on increased stability towards external loads and a reduction of energy transferred into the building.

A further demand for such a system is a cost-efficient manufacturing process. It has been investigated to use the coatable polarizer at the same time as an alignment layer for the liquid crystal. Aluminum zinc oxide (AZO) is to be used for the electrode material substituting conventionally used indium tin oxide (ITO) which is expensive.

Currently the authors are looking into the coating process for the inside polarizer. The polarizer consists of lyotropic liquid crystal and has to be aligned linearly during its application defining the polarizing direction.

8114-39, Poster Session

Waveguide display using polymer-dispersed liquid crystal

Y. Cheng, G. J. Su, National Taiwan Univ. (Taiwan)

In this paper, we demonstrate two promising novel displays: light waveguide display and arrayed waveguide display. In the light waveguide display, light emitted from commercial LEDs propagates in a glass planar waveguide with a polymer dispersed liquid crystal (PDLC) upper layer. When the voltage is off, light would be partially scattered via PDLC and that pixel becomes bright and opaque. When the voltage is on, PDLC is properly aligned so that light would not be scattered, showing a transparent pixel. By electrically controlling the PDLC, a counting seven-segment pattern is clearly displayed. Arrayed waveguide display has

been theoretically proposed to be a full color display with high light-use efficiency. Light of three primary colors from an emitter array is coupled into a waveguide array upon which is the PDLC switches. In our design, the core of the waveguide is made of SU-8 photoresist while the side and under cladding is polymethyl methacrylate (PMMA). The upper cladding PDLC is controlled pixel by pixel such that the light can be selectively scattered. Both displays are well patterned and packaged with their driving circuits so that finalized products can be shown. Furthermore, since most materials are transparent, the displays are applicable for head-mounted displays (HMD).

8114-40, Poster Session

Slope efficiency characteristics of mode-hop driven tunable single-mode cholesteric liquid crystal laser

Y. Inoue, H. Yoshida, K. Inoue, Y. Shiozaki, H. Kubo, A. Fujii, M. Ozaki, Osaka Univ. (Japan)

Cholesteric liquid crystals (ChLCs) are known to self-organize into helical structures with periodicities of a few hundred nanometers and thus possess a reflection band attributed to their periodicity p and birefringence dn . By introducing a gain medium (usually dyes) with appropriate fluorescence properties, lasing can be realized in these materials. Consequently, ChLCs lasers have attracted a large amount of interest as compact, low-threshold and tunable coherent light sources.

In this study, we report the improvement in the slope efficiency of tunable single-mode ChLC lasers with a three-layered structure. The device consists of one photo-polymerized ChLC layer with a wide reflection band, another ChLC layer with a notch reflection band and a Rhodamine6G doped ionic liquid layer acting as the gain medium. Single-mode lasing is obtained from this device structure because the ChLC layer with the notch reflection band strongly reflects only one of the Fabry-perot cavity modes, and mode-hop driven tuning of the lasing wavelength is possible because the reflection band of the notch ChLC can be tuned by external stimuli, such as heat. Our device showed a maximum slope efficiency of 16% (considering emission only in the forward direction), and was found to be approximately 1.5 times larger than ordinary DFB-type ChLC lasers doped with the Pyrromethene597 laser dye.

8114-41, Poster Session

Degradation of liquid crystals device performance due to ionic adsorptions: issues and solutions

L. Lu, Kent State Univ. (United States); A. Alagh, Okaya Electric America, Inc. (United States); P. J. Bos, Kent State Univ. (United States)

In this paper, we first investigated the degradation of the performance of liquid crystals display (LCD) units after driving by a DC bias. Missed segments were found in the test LCD units. By carefully investigating the alignment layer and ITO layer separately, an explanation of the ITO failure is proposed: voltages applied to the liquid crystal cell causes accumulation of charged impurities or ions, resulting in a decomposition reaction of ITO in regions where segment and common planes overlap and there are scratches on the PI layer. Consequent, missing segments in the corresponding regions is generated.

To prevent this kind of degradation, we studied the correlation between the alignment layer and ions adsorption. Both organic alignment layer (PI2555, SE1211, and FPI) and inorganic alignment layer (SiOx, SiO2, and Al2O3) are analyzed by residual DC and voltage holding ratio measurement. A correlation between ion adsorption and the dielectric constant of the alignment layer is demonstrated. Alignment layer with a smaller dielectric constant is good for reducing ion adsorption in the alignment layer. Alignment layer with a bigger dielectric constant is good

for reducing mobile ions in the LC device, and could be used in non-active areas of the liquid crystal device to remove ion from the active area.

8114-42, Poster Session

Polarization twisted nematic gratings: a study of the far-field diffraction patterns

D. Statman, R. Pettit, S. Bottini, A. Jockers, Allegheny College (United States)

When left and right circularly polarized beams of light from a pump laser interfere in a nematic liquid crystal doped with azo dye, a polarization twisted nematic (PTN) grating is formed in the sample. The same is true if two beams of light linearly polarized perpendicular to the rubbing direction of the sample interfere. In the first case the easy axis is rotated toward the polarization direction of interfering beams. In the latter case rotation toward the polarization only occurs at the bright regions. The absorption of the pump beam by the dye is strong enough so that there is no reorientation of the easy axis on the opposite side of the sample. However, photoinduced gliding measurements demonstrate that the reoriented easy axis is not parallel to the polarization of the interfering pump beams. The far-field diffraction pattern of a probe beam entering the sample from the opposite side consists of elliptically polarized spots. Fourier analysis of the far-field pattern determines how the easy axis of the nematic has been reoriented. In this presentation, we compare the PTN ratings formed by interfering circularly polarized light and linearly polarized light.

state. At the field-off state, the QD-dispersed LC cell presents highly scattering and the excitation photons (from 514 nm pumping laser) undergoes multiple scattering before the pumping laser getting out off the LC cell that the situation increases the possibility for pumping laser hitting and be absorbed by the dispersed QDs. At the field-on state (from 405 nm laser irradiation), the trans-to-cis photoisomerization of azobenzene makes the QD-dispersed LC cell presenting highly transparent, most pumping photons go straight through the LC cell, reducing the possibility for the QDs being excited. The PL intensity can be modulated by controlling the light intensity from laser irradiation. In view of the considerable interests in PL of QDs for photonic applications, our study on optically switchable PL from azobenzene doped LC-dispersed QDs introduces a new approach of controlling emission of QDs by means of light. This may open the door to new exploitation for applications of QD such as light switchable, emission based liquid-crystal display (LCD).

8114-43, Poster Session

Study of cholesteric liquid crystal: rhodamine 6G doped polymer thin film, cholesteric liquid crystal system

T. Dadalyan, R. Alaverdyan, N. Hayrapetyan, Yerevan State Univ. (Armenia)

The creation of compact, easy processible, low threshold and tunable optical components and laser sources is in great demand in science and industry. One of the strategies for solving this problem are multilayer structures consisting of laser dye-doped polymer thin films, as solid active element and Cholesteric Liquid Crystals (CLC)-s as resonators.

In this work we have experimentally investigated optical properties of multilayered structure, consisting of two right handed CLC with the same pitch and Rhodamine 6G doped polymethyl metacrilate (PMMA) 10nm micrometer thin film. The CLC was a compound of commercial NLC E7 and the chiral agent. The transmission and luminescence spectra and their temperature dependences for this system were measured, for visible wavelength light. About 10 nm temperature tunability of selective reflection band is observed. The experiments are in process, now we are working on achieving efficient lasing from this system.

8114-44, Poster Session

Optically switchable photoluminescence using liquid-crystal dispersed quantum dots

M. Cheng, W. Chang, V. K. S. Hsiao, National Chi Nan Univ. (Taiwan)

In the conference, we will show the suggested mechanism formatting liquid-crystal (LCs) dispersed quantum dot (QDs) and achieve the reversible optical switching of photoluminescence (PL) intensity of QDs. By mixing QDs into azobenzene-doped cholesteric LCs, it is possible to switch the PL of QDs into two different states, switching between high intensity at optical field-off state and low intensity at optical field-on

Conference 8115: Organic Light Emitting Materials and Devices XV

Sunday–Tuesday 21–23 August 2011 • Part of Proceedings of SPIE Vol. 8115
Organic Light Emitting Materials and Devices XV

8115-01, Session 1

Polymer hosts for efficient electrophosphorescence

H. Yang, SAMSUNG Electronics Co., Ltd. (Korea, Republic of)

New series of printable novel polymer host materials for electrophosphorescent organic light emitting devices (PhOLEDs) was developed, which exhibited starburstic core monomer connected by linker units. Moreover, the hole mobilities were controlled by the number of carbazole of linker units. Development of high efficient host materials for electrophosphorescent device could improve quantum efficiency of light output intrinsically, which is a real challenge. Our materials could be summarized following: i) The linkage mode of para position of polymer should be prohibited by synthetic modification. ii) By introducing the linker units, the HOMO levels are finely tuned and the contribution portion of HOMOs could be shifted to the linker units, which resulted in hole injection and transporting property could be controlled. iii) When looking at the results of current density vs voltage, it is tendency to be increased as increasing the number of carbazole units, which means that the hole mobility tends to increase. iv) These host materials shows wide bandgaps ($E_g > 3.0$ eV) and high triplet energies ($E_T > 2.4$ eV). The present work provides a new route for designing host materials with wide bandgap and high triplet energy, and for controlling hole transporting property simultaneously.

8115-02, Session 1

Recent advances in materials for efficient green and blue electrophosphorescent light emitting diodes

B. Kippelen, S. Kim, D. Cai, W. Haske, E. M. Najafabadi, C. Fuentes-Hernandez, J. Leroy, C. Zuniga, Y. Zhang, L. Zhu, J. S. Sears, S. Barlow, J. Brédas, S. R. Marder, Georgia Institute of Technology (United States)

(Invited talk)

In recent years, significant progress has been made towards the development of organic-based semiconductors for display and lighting applications. However, the search for new materials for blue organic light-emitting devices (OLEDs) remains of importance for the development of satisfactory full-color flat-panel displays and of efficient and stable white-light devices. Furthermore, materials should preferably be processed from solution to further lower the fabrication cost.

In the first part of this talk, we will discuss the use of a bis-sulfone small molecule, 4,4'-bis(phenylsulfonyl)biphenyl, as a host for the phosphor iridium(III) bis(2-(4,6-difluorophenyl)pyridinato-N,C2')picolinate in blue-green organic light-emitting devices. In addition, we will report on the use of a new poly(norbornene)-based polymer functionalized with a 3,6-bis(carbazol-9-yl)carbazole moiety as a side group as a solution-processible hole-transport layer. Comparison will be made to the widely-used hole-transport polymer poly(N-vinylcarbazole) (PVK). At 100 cd/m², the highest efficiency device incorporating the new polymer achieved an external quantum efficiency (EQE) of 6.9 % (12.9 cd/A) with a turn-on voltage of 4.3 V. In the second part of the talk we will report on high-efficiency organic light-emitting devices (OLEDs) fabricated with solution-processed blends of hole- and electron-transport side-chain polymer hosts doped with a green-emitting iridium complex. The ambipolar host blends consist of blends of bis-oxadiazole-functionalized poly(norbornene) electron-transport materials and poly(N-vinylcarbazole). For the best device examined, an external quantum efficiency of 13.6% and a maximum luminous efficiency of 44.6 cd/A at 1000 cd/m² with a turn-on voltage of 5.9 V were obtained.

8115-03, Session 1

Materials design concepts for efficient blue OLEDs: a joint theoretical and experimental study

A. B. Padmaperuma, L. Cosimbescu, J. S. Swensen, E. Polikarpov, P. K. Koech, L. Wang, D. J. Gaspar, Pacific Northwest National Lab. (United States)

Organic light emitting devices (OLEDs) have great potential for lighting, displays and TVs. One remaining technical challenge for very high efficiency OLEDs for solid-state lighting applications is the blue component. Optimization of not only blue emitters, but also host matrices and transport layers is necessary to achieve efficiency and lifetime targets. Charge balance and exciton confinement are key factors in achieving high quantum efficiency in OLED devices. It is a commonly held view that the host material for a phosphorescent emitter in an organic light emitting device (OLED) must have a triplet energy higher than that of the phosphorescent emitter in order to obtain high quantum efficiencies. We show that a combination of HTL, ETL and host with appropriate energy levels can provide high external quantum efficiency (EQE), even with a host triplet energy lower than that of the emitter. Specifically, we report results demonstrating improved OLED performance for a new host material, 4-(di-p-tolylamino)phenyl diphenylphosphine oxide, with a triplet energy lower than Flrpic. Our results suggest modified design rules for the development of new, high performance host materials. Molecular design strategies, device design and OLED data will be discussed.

8115-04, Session 1

Highly efficient new hole injection materials for OLEDs based on phenothiazine and phenoxazine derivatives

J. Park, Y. Park, B. Kim, The Catholic Univ. of Korea (Korea, Republic of)

New hole injection layer (HIL) materials for organic light-emitting diodes (OLEDs) based on phenothiazine and phenoxazine were synthesized, and the electro-optical properties of the synthesized materials were examined by UV-vis and photoluminescence (PL) spectroscopy, and by cyclic voltammetry (CV). 1-PNA-BPBPOX showed glass transition temperatures (T_g) of 161°C, which was higher than that (110°C) of Tris(N-(naphthalen-2-yl)-N-phenyl-amino) triphenylamine (2-TNATA), a commercial HIL material. The HOMO levels of the synthesized materials were 4.9–4.8 eV, indicating a good match between the HOMO of indium tin oxide (ITO) (4.8 eV) and the HOMO of N,N'-bis(naphthalen-1-yl)-N,N'-bis(phenyl)benzidine (NPB) (5.4 eV), a common hole transfer layer (HTL) material. Because the synthesized materials showed minimal absorption at wavelengths shorter than 450 nm, they have good potential for use as effective HIL materials. The synthesized materials were used as the HIL in OLED devices, yielding power efficiencies of 2.8 lm/W (1-PNA-BPBPOX) and 2.1 lm/W (2-TNATA). These results indicate that 1-PNA-BPBPOX yields a higher power efficiency, by a factor of 33%, than the 2-TNATA commercial HIL material. Also, 1-PNA-BPBPOX exhibited longer device life-time than 2-TNATA.

8115-05, Session 1

Novel hole transport materials for blue phosphorescent OLEDs: synthesis, properties, and performance

L. Cosimbescu, E. Polikarpov, J. S. Swensen, L. Wang, D. J. Gaspar, A. B. Padmaperuma, Pacific Northwest National Lab. (United States)

We report the development of novel hole transport (HTM) and host materials, to achieve a stable and efficient blue phosphorescent OLED system. Developing compatible HTMs for blue phosphorescent devices remains a challenge, due to the fact that their triplet energies have to be higher than the dopant for maximum efficiency as well as maintaining a good charge transport into the emissive layer analogous to state of the art HTMs. The new HTMs contain known moieties such as triphenyl amine or phenyl carbazole, but linked through bulky or inert spacers, and the design is based on the well known HTMs, TAPC and DTASi. A thorough computational analysis of all HTM structures was performed to determine the relative HOMO/LUMO energetic and excited state properties. Excited state calculations using TD-DFT-B3LYP/6-31G* as implemented in NWChem was conducted and was used to select the best set of candidates for synthesis and then further evaluation in blue OLEDs. The novel compounds have photophysical properties such as EHOMO, ELUMO and ET values, similar to their analogs, TAPC and DTASi. Based on the estimated values from CV and emission, the new molecules are perfectly suitable for use as high bandgap, hole transport materials. The new molecular design provided materials with good morphological properties, which is expected to add to the overall stability of the OLED system. The work presented herein will encompass the design and synthesis of a series of hole transport materials, their electronic and photophysical properties and their performance in an OLED device.

8115-06, Session 1

Exploration of highly luminescent exciplexes and their application to OLEDs

K. Yoshida, K. Goushi, K. Sato, C. Adachi, Kyushu Univ. (Japan)

The external electroluminescence (EL) quantum efficiency (η_{ext}) based on fluorescent materials as an emission center is limited to only 5%. Recently, without phosphorescent materials we proposed the novel EL mechanism to enable the η_{ext} of 5% by using up-conversion from triplet (T1) to singlet (S1) excited states. In this mechanism, in order to realize the high up-conversion efficiency, the energy gap between S1 and T1 (dEST) should be close to zero. dEST is determined by the exchange energy between the highest occupied molecular orbital (HOMO) and the lowest unoccupied molecular orbital (LUMO). Therefore, the separation of the HOMO from the LUMO can enhance the reverse intersystem crossing from T1 to S1 (RISC). More recently, we reported that organic donor and acceptor interfaces give rise to a small dEST; dEST for exciplexes is expected to be very small, due to the separation of the positive and negative charges located mainly in donor and acceptor molecules, respectively. Our observations showed that a high RISC efficiency can be realized using exciplexes, which lead to high efficiency for radiative-exciton production. By taking advantage of the highly efficient ISC, we demonstrated a pronounced enhancement of electroluminescence efficiency under electrical excitation. The observed EL efficiency is, however, still at a low level. In order to highly EL efficiency, high PL efficiency of exciplexes is a key factor. In this paper, we demonstrate the external EL quantum efficiency over 5% by using highly luminescent exciplexes as emitter layers.

8115-07, Session 1

Asymmetric molecular design for high-efficiency in blue phosphorescent organic light emitting diodes

J. Y. Lee, Dankook Univ. (Korea, Republic of)

Asymmetric organic materials were synthesized as the host materials for blue phosphorescent organic light emitting diodes. The design of asymmetric high triplet energy host material was effective to reduce the driving voltage and improve the quantum efficiency of blue phosphorescent organic light emitting diodes. A high quantum efficiency over 20% was achieved in the blue phosphorescent organic light emitting diodes using the asymmetric high triplet energy host materials.

8115-08, Session 1

High-efficient yellow-emitting materials based on thieno-pyridine framework for yellow and white OLEDs

H. Huang, T. Chao, Industrial Technology Research Institute (Taiwan); V. Van Elsbergen, Philips Technologie GmbH (Germany); M. Tseng, Industrial Technology Research Institute (Taiwan)

High efficient yellow light-emitting materials based on thieno-pyridine framework have been synthesized for organic-light emitting diodes (OLEDs). We investigated and synthesized different orientation and substituted group of the thieno-pyridine framework organo-iridium complexes (PO-01 series materials). These materials exhibited yellow light. Fabrication of these emissive phosphorescent dopants with conventional materials and the device configuration of ITO/HTL/CBP: yellow Ir-complex emitters (4-6%) /BCP/Alq3/LiF/Al showed the EL emitting peak of 560 nm. The electroluminescent efficiencies of the devices were from 35.1 lm/W (51.6 cd/A) to 37.1 lm/W (62.8 cd/A) under the brightness of 1000 cd/m² and external quantum efficiencies were all above 16.9% to 18.5%. With some advanced materials applied on the yellow devices, we also can obtain efficiencies of the devices were from 84.4 lm/W (76.7 cd/A) to 97.7 lm/W (88.9 cd/A) under the brightness of 1000 cd/m² and external quantum efficiencies were all above 19.3% to 20.4%. Besides, we also apply the PO-01 series materials on WOLED and obtain good power efficiency of 44 lm/W under 1000 cd/m². We demonstrated high-efficiency, high-brightness and saturated yellow Ir-complex phosphorescent materials for yellow and white OLEDs.

8115-09, Session 1

Theoretical design for carrier-transporting molecules in view of vibronic couplings

T. Sato, K. Shizu, K. Tanaka, H. Kaji, Kyoto Univ. (Japan)

Novel carrier-transporting materials are proposed in view of vibronic, or electron-phonon couplings.

To design for highly efficient organic-light-emitting diodes (OLED), it is necessary to develop a carrier-transporting molecule with a high carrier mobility and low power loss. The mobility of available electron-transporting molecules in OLED is smaller than that of hole-transporting molecules. This gives rise to carrier unbalance which result in low efficiency. Therefore an electron-transporting molecule with a high mobility is necessary.

Vibronic couplings cause a decrease of the carrier mobility and a energy dissipation.

Therefore a vibronic coupling is an important interaction in designing for such a molecule as well as frontier levels. We have recently proposed a concept of vibronic coupling density which enable us to control vibronic couplings in a molecule (Sato et al, "Vibronic coupling constant and vibronic coupling density", in "The Jahn-Teller Effect: Fundamentals and

Conference 8115:
Organic Light Emitting Materials and Devices XV

Implications for Physics and Chemistry” , Springer Series in Chemical Physics 97 (Springer-Verlag, Heidelberg and Berlin, 2009)). Based on the concept, we can design a novel carrier-transporting molecule with small vibronic couplings which can result in high mobility and low power consumption.

A vibronic coupling is small if the electron-density difference between the neutral and ionic state is localized not on bonds but on atoms. In addition, if the electron-density difference is equivalently delocalized over the molecule, the vibronic couplings are small due to the selection rule.

We design organoborane compounds as an electron-transporting molecule based on these guiding principles.

We also discuss the effect of asymmetric perturbations on the electronic-density difference.

8115-10, Session 1

Models of excited states of Ir(III) complexes for optoelectronic applications

B. J. Powell, A. R. G. Smith, M. J. Riley, S. Lo, P. L. Burn, I. R. Gentle, The Univ. of Queensland (Australia)

Realistic accurate predictions spectra of organometallic complexes have remained difficult, this has hampered the rational design of new complexes for optoelectronic applications. We show that relativistic effects cause important changes in the spectra of phosphorescent Ir(III) complexes. This is achieved by comparing high field magnetic circular dichroism (MCD), absorption and photoluminescence (PL) spectra with time-dependent density functional theory (TDDFT) calculations for a series of blue phosphorescent Ir(III) complexes. By gradually turning on the relativistic effects we identify several distinct relativistic effects in the spectra of these complexes. We show that both spin-free (scalar) relativistic and spin-orbit coupling must be included to accurately predict the observed spectra. Further, we use this combined theoretical and experimental methodology to investigate the changes in spectra as electron withdrawing groups are added to the organic ligand: tuning the emission towards a deeper blue, but also leading to a decrease in the observed photo luminescent quantum yield (PLQY). This leads to new insights into the low-lying excitations responsible for the observed phosphorescence, and suggests new avenues to improve the performance of organic light-emitting diodes (OLEDs).

8115-11, Session 2

Correlating hole injection layer film morphology and composition to the performance of single carrier and OLED devices

N. Chopra, S. B. Li, V. Seshadri, C. McGuinness, E. Scott, R. Mitchell, M. K. Mathai, Plextronics Inc. (United States); L. Scipioni, C. T. Huynh, Carl Zeiss SMT Inc. (United States)

In the space of organic light emitting diodes (both vapor and solution processed devices), most of the devices with low operating voltages and long lifetimes are obtained using doped charge injection layers. We focus our research on Plexcore® OC, a conducting polymer, aqueous based hole injection layer (HIL). The present study explores factors limiting the current state of the art HIL technology which will pave the way to realization of low power consumption OLEDs. We will present a detailed study outlining the effect of HIL composition, conductive polymer, resistivity and work function of hole injection layer on performance and stability of organic devices. The HILs were characterized using helium ion microscopy (HeIM), conductive AFM film conductivity uniformity, AFM for morphology and roughness, AC2 for work function measurements and ellipsometry for optical characterization. HeIM is emerging as one of most effective new microscopy technique for imaging nanostructured organic materials. Analysis of HeIM images reveal similar nanostructure to conducting AFM current map. Also, He ion beam

modified surface of our HIL was clearly able to reveal the morphology of underlying structure hidden below the conducting polymer network. Hence, a combination of HeIM images with conducting AFM can help us to understand how different composition and processing conditions affect the nanomorphology of the polymer composite film. Finally the understanding from film characterization is correlated with the device data to investigate the effect of modulating HIL properties on device performance and voltage stability under operation.

8115-12, Session 2

Water/alcohol-soluble conjugated polymers for interface engineering of optoelectronic devices

F. Huang, South China Univ. of Technology (China)

The applications of water/alcohol soluble conjugated polymers in optoelectronic devices have attracted more and more attentions due to their unique characteristics different from the traditional conjugated polymers as interfacial modification/active materials in devices. The polar pendant groups of them not only render the materials good solubility in water and other polar solvents, which can overcome the challenge interfacial mixing problems in multilayer optoelectronic devices fabrication, but also can dramatically improve charge injection from metallic electrodes into organic active layers to greatly improve the device performance. Different from the traditional electron transporting/injection materials, this kind of materials can effectively enhance electron injection from high work-function metals (such as Al, Ag, Au). As a result, high-efficiency printable polymer light-emitting diodes (PLEDs) with Ag-paste as cathode have been realized. Moreover, the newly developed materials and protocols has led to significant improvements on the performance of PLEDs. By using a doped water/alcohol soluble conjugated polymer as electron transporting/injection, the resulting solution-processed white-emitting PLEDs showed a maximum forward viewing luminance efficiency of 36.1 cd/A (61.4 cd/A for total viewing) and a power efficiency of 23.4 lm/W (39.8 lm/W for total viewing), which is comparable to those reported from the state-of-the-art vacuum deposited small molecule white-emitting OLEDs.

References

1. F. Huang, H. B. Wu, Y. Cao, Chem. Soc. Rev. 2010, 39, 2500.
2. F. Huang, H. B. Wu, J. B. Peng, W. Yang, Y. Cao, Curr. Org. Chem. 2007, 11, 1207.

8115-13, Session 2

Highly efficient and spectral stable blue light emitting polyfluorenes containing dibenzothiophene-S, S-dioxide unit

W. Yang, South China Univ. of Technology (China)

Polymer light-emitting diodes (PLEDs) have attracted great attention because of their potential applications in large-area, flat-panel displays. high-efficiency and stable blue light-emitting polymers with good color purity remain as a great challenge. Polyfluorene derivatives are a very attractive class of blue materials, however, a major drawback is their excimer and/or aggregate formation upon thermal annealing or the passage of current, leading to red-shifted emission. We present a detailed study on the 9,9-bis(2-ethylhexyl)fluorene-co-benzothiophene-S,S-dioxide copolymers (PF-FSO). The substantial improvements in PF-FSO device performances can be achieved by employing hole transport/electron block layer (HTL/EBL), as well as by performing an appropriate cathode buffer (CB). In particular, the simultaneously utilizing the aforementioned steps bring about a significant performance improvement.

References

- [1] J. Liu, J. H. Zou, H. B. Wu, W. Yang, C. Li, B. Zhang, Y. Y. Li, J. B. Peng, Y. Cao. Chem. Mater. 20 (2008) 4499.

Conference 8115:
Organic Light Emitting Materials and Devices XV

[2] Y. Li, H. Wu, J. Zou, L. Ying, W. Yang, Y. Cao, *Organic Electronics* 10 (2009) 901

[3] J. Liu, S. Hu, W. Zhao, Q. Zou, W. Luo, W. Yang, J. Peng, Y. Cao, *Macromol. Rapid Commun.* 31 (2010) 496.

8115-14, Session 3

Top-emitting OLED for mobile display: the comparison between inverted and normal top-emitting OLED

J. Lee, K. Lee, M. Kim, J. Kim, C. Yoo, J. Yoon, S. Yoon, C. Kim, LG Display (Korea, Republic of)

Top emitting OLEDs (TOLEDs) are implemented into mobile products with the great advantages of high filling factors and color gamut. The most commercialized AMOLEDs are consisted of TOLED using thin metal microcavity structure. However, thin metal TOLED has very little thickness tolerance in the manufacturing process. Due to the strong microcavity effects of thin metal TOLED, only 5nm thickness off of total organic layers alters CIE coordinate, which is one of crucial criteria in the display standard. This gives the big challenge on increasing productivity of OLED display panel. Therefore, inverted OLED are studied as one of options with less sensitive to thickness variation. The inverted configuration allows for integration of OLEDs with preferentially used n-channel TFTs for driver backplanes in active matrix OLED displays. Recently, Face Target Sputtering (FTS) system is introduced without sputtering damage to organic layers.

In this talk, thin metal TOLED and inverted structure TOLED are compared in electrical and optical performances. Capacitance-Voltage (CV) measurements as a powerful technique to analyze electric properties of Top emitting OLED (TOLED) devices are introduced. After comparing CV characteristics between inverted TOLED and conventional TOLED with thin metal, it is found that inverted OLED struggles charge injections, electron and hole injections both. Here Current-Voltage-Luminance (IVL) and CV characteristics are carefully analyzed for single carrier devices and dual carrier devices systematically. Thin metal TOLED shows more efficient electron injection and higher efficiency than that of inverted TOLED, which is attributed to the order of thermal deposition of organic/metal layers.

8115-15, Session 3

Effect of excited state interactions on the efficiency and lifetime in PLED

N. Akino, T. Yamada, Y. Tsubata, C. Sekine, Sumitomo Chemical Co., Ltd. (Japan)

Polymer light emitting diode (PLED) has been attracting considerable attention due to their potential for commercial applications such as flat panel displays and solid-state lighting. In the course of improving PLED performance, it has been realized that the interactions between singlet excitons, triplet excitons, and polarons play an important role in the efficiency and degradation in the devices, however their influences are not fully understood. Actually, part of singlet excitons is considered to be originated from the triplet-triplet annihilation process. Thus, a device with the use of triplet-triplet annihilation process would be able to have more fluorescent singlet excitons than a device without that process, thus leading to higher efficiency. On the other hand, the quenching of triplet excitons in the device degradation seems a major factor of the rapid initial decay in the device lifetime, suggesting the importance of the control of triplet excitons for better device stability.

In this presentation, we will present an efficiency and degradation analysis of PLED, and demonstrate that the triplet exciton transfer and triplet-triplet annihilation processes are of crucial importance in realizing the efficiencies and device stabilities required for commercialization of the technology.

8115-16, Session 3

Improvement of device efficiency in PIN-OLEDs by controlling the charge carrier balance and intrinsic outcoupling methods

F. Löser, T. Romainczyk, C. Rothe, D. Pavicic, A. Haldi, M. Hofmann, S. Murano, T. Canzler, J. Birnstock, Novaled AG (Germany)

For both display and lighting applications, OLEDs with high power efficiency are desirable. A prerequisite for high power efficiency is the achievement of a low driving voltage, which can be done via charge carrier doping of the transport layers in PIN OLEDs. However the reduction of the driving voltage may in some cases give rise to a reduction in current efficiency and device lifetime.

The reason for this is not the PIN structure and its material sets as such, but the change in charge carrier balance inside the device that is caused mainly by the greatly enhanced conductivity of the n-ETL.

We have looked for ways of how to combine low voltage with high current efficiency and long lifetime and have therefore investigated different ways of changing the charge carrier balance in PIN-OLEDs.

We demonstrated that good lifetime and efficiency in low-voltage OLEDs depend crucially on a well balanced charge carrier supply of electrons and holes to the emitting layer.

In further investigations we have developed highly efficient and stable white PIN top and bottom emission OLED devices using novel evaporation processable outcoupling enhancement materials inside the PIN OLED stack. In white bottom emission OLED structures the use of this outcoupling enhancement material in combination with a standard MLA outcoupling film can yield an efficiency enhancement of up to 1.8. A Power efficiency of 50.2 lm/W and color coordinates of 0.46/0.41 at a brightness of 1000 cd/m² has been demonstrated.

8115-17, Session 3

Low voltage, low power, organic light emitting transistors for AMOLED displays

M. A. McCarthy, B. Liu, E. P. Donoghue, I. Kravchenko, D. Y. Kim, F. So, A. G. Rinzler, Univ. of Florida (United States)

No abstract available

8115-18, Session 3

Efficient spin-coated small-molecule OLEDs

M. Cai, E. Hellerich, T. Xiao, R. Shinar, J. Shinar, Iowa State Univ. (United States)

Efficient fluorescent and phosphorescent spin-coated small molecule OLEDs are described. The structure of the fluorescent devices is ITO/PEDOT:PSS/spin-coated NPB:Alq3/thermally evaporated BPhen or BCP/CsF/Al. The structure of the phosphorescent devices is ITO/PEDOT:PSS/spin-coated Ir(ppy)₃:CBP/thermally evaporated BPhen or BCP/CsF/Al. The fluorescent devices exhibited a peak luminous efficiency exceeding 10 Cd/A at low current, which gradually decreased to 8 Cd/A at 400 mA/cm². The phosphorescent devices exhibited peak power efficiencies exceeding 60 lm/W or > 120 lm/W with outcoupling enhancement. The nature of the high efficiency and initial results on device stability will be discussed.

Conference 8115:
Organic Light Emitting Materials and Devices XV

8115-19, Session 3

Fluorescent OLEDs with unusually high external quantum efficiency around 8%

Y. Pu, G. Nakata, J. Hu, Y. Yamashita, K. Kobayashi, D. Yokoyama, H. Sasabe, J. Kido, Yamagata Univ. (Japan)

Upper limit of external quantum efficiency (EQE) in fluorescent OLEDs has been considered to be 5%, which is introduced as the product of the following factors: charge balance of holes and electrons (~100%), fraction of singlet and triplet excitons in recombination (25%), photoluminescent quantum efficiency (~100%), and optical outcoupling (20%). However, recently, there are some reports on highly efficient fluorescent OLEDs showing the EQE over 5%.[1] First of all, we focused on making the charge balance as high as possible because it is a prerequisite to achieve an high EQE. Coumalin C545T and DPAVBi were used as an emitting dopant for green and blue emission, respectively. 2-Methyl-9,10-di(2-naphthyl)anthracene (MADN) was used a host. Several types of hole-transporting and electron-transporting materials were used to control energy levels to improve injection of charges to the emitting layer. When TAPC and 3,5,3',5'-tetra-3-pyridyl-[1,1';3',1']terphenyl (B3PyPB)[2] were used in a hole-transporting layer and electron-transporting layer, respectively, 7.5% of EQE at 100 cd/m² and 7.2% at 1000 cd/m² were achieved in green emission, and 8.1% at 100 cd/m² and 7.7% at 1000 cd/m² were achieved in blue emission. Those efficiencies were estimated from front luminance and spectrum with Lambertian assumption, which was supported by angular dependence of radiance measurement. Microsecond order of delayed emission from the device after pulse voltage application was observed and indicated that these unusually high EQEs could be resulted from triplet-triplet annihilation process.

[1] D. Y. Kondakov et al., J. Appl. Phys., 106, 124510 (2009).

[2] H. Sasabe et al., Chem. Mater., 20, 5951 (2008).

8115-20, Session 3

Organic light emitting diodes with roll-up character

J. Jou, Y. Wang, C. Lin, P. Chen, M. Tang, National Tsing Hua Univ. (Taiwan); S. Chen, C. Chen, C. Wang, Industrial Technology Research Institute (Taiwan)

Highly efficient organic light-emitting diodes (OLEDs) are strongly demanded for both display and illumination applications. High efficiency would also help prolong the device lifespan. However, many OLEDs encounter significant roll-off problem, leading to undesired low device efficiency at high luminance, unfavorable to their commercial realization for lighting. OLED devices with mild or even little roll-off are hence highly expected. We have, nevertheless, observed some OLEDs to exhibit roll-up phenomenon; i.e. that their external quantum efficiency (EQE) or current efficiency increases as the applied voltage or brightness is increased. By taking such advantage in device architecture design, OLEDs with an approaching or even above the theoretical limit EQE are obtained at high luminance. We will present how this works for a monochromatic yellow OLED having a record-high power efficiency among reported fluorescent yellow OLEDs, and an OLED with very-low color temperature with a record-breaking efficacy based on the same color-temperature. The plausible mechanism regarding why roll-up occurs in some certain structure systems will also be reported.

8115-21, Session 3

Polymeric hole injection layers for highly efficient and stable organic light emitting diodes

M. Choi, T. Han, Pohang Univ. of Science and Technology (Korea, Republic of); D. H. Huh, Cheil Industries Inc. (Korea, Republic of);

T. Lee, Pohang Univ. of Science and Technology (Korea, Republic of); K. Shin, J. Jang, Seoul National Univ. (Korea, Republic of)

We introduced conducting polymer compositions based on water-dispersible polyaniline:poly(styrene sulfonate) (PANI:PSS) and water-soluble self-doped conducting polymer (PSS-g-PANI) as hole injection layers (HILs) in small molecule organic light-emitting diodes (SM-OLEDs). The luminous efficiencies of SM-OLEDs remarkably increased using our compositions, blended with perfluorinated ionomer (PFI) as HILs. Because the PFI was self-organized at the surface and, thereby, caused a high work function, we can tune work functions of HILs and make nearly ohmic hole-injection contact. Due to improved injection efficiency and electron blocking ability, we achieved very high luminous efficiencies (PANI:PSS/PFI : ~ 17 cd/A, PSS-g-PANI/PFI : ~20 cd/A), compared with a conventional small molecule HIL (2TNATA : ~12cd/A) and a commonly-used water-dispersed polymeric HIL (PEDOT:PSS : ~15 cd/A). Device half-lifetimes at 2000 cd/m² using our water-dispersible compositions were remarkably improved because of the diffusion blocking capability of the PFI surface layer. (PANI:PSS/PFI : ~ 95 hrs, PEDOT:PSS : ~ 7.6 hrs). In the case of self-doped conducting polymer compositions (PSS-g-PANI/PFI), the maximum lifetime of the device reached ~ 290 hrs, which can be attributed to high doping stability as well as the PFI surface layer effect. PANI-based conducting polymer compositions can be good candidates for reliable HILs in SM-OLEDs.

8115-22, Session 3

High-work-function indium tin oxide for simplified high-performance organic light emitting diodes

M. G. Helander, Z. Wang, J. Qiu, M. T. Greiner, Z. Lu, Univ. of Toronto (Canada)

Transparent conducting oxides (TCOs), such as tin-doped indium oxide (ITO), are the electrode materials of choice in state-of-the-art organic photovoltaics (OPVs), organic light emitting diodes (OLEDs) and flat-panel displays due to their unique combination of high electrical conductivity and high optical transparency across the visible spectrum. Controlling the interface properties between ITO and organic materials is of great importance for device engineering since the performance, stability and lifetime of organic devices are greatly influenced by the electrode/organic contacts. Organic electronic devices fabricated on bare ITO electrodes are problematic due to insufficient charge injection and poor operational stability caused by the large mismatch between the low work function of ITO (~ 4.7 eV) and the highest occupied molecular orbital (HOMO) of the organic. We report a simple method for tuning the work function of TCO thin films using a novel halogenation technique. Using this facile technique we achieve an unprecedented high work function of > 6.1 eV for ITO. The application of the high work function ITO in organic electronic devices allows efficient charge injection into organic materials without the need for additional injection layers, greatly simplifying device design and fabrication.

8115-23, Session 3

High-performance green fluorescent host materials with high-thermal stability

T. H. Kim, Doosan Corp. (Korea, Republic of)

We demonstrate high efficiency green fluorescent Indenoanthracene-host material for OLED. Many derivatives of Indenoanthracene show high efficiency, but they have an issue of thermal stability for mass production. Most of melting typed Indenoanthracene host materials showed the low thermal stability. To increase thermal stability of a lot of derivatives in mass production evaporation system, we searched the sublimation typed Indenoanthracene host materials. Two approaches to the goal were available for us. One was to make the structure of product simple for low evaporation temperature. Another was to introduce some

Conference 8115:
Organic Light Emitting Materials and Devices XV

bulky substituent in molecule for reducing the interaction between the molecules. Most of sublimation typed molecules kept their purity for quiet long time, compared to melting typed materials.

8115-24, Session 4

Solution-processed organic light emitting transistors

E. B. Namdas, The Univ. of Queensland (Australia)

Light emitting field effect transistors (LEFETs) are a new class of devices that combine the electrical properties of a transistor with light emitting capability in a single device architecture. One of the key problems with LEFET is their low brightness which limits their application. So far the gate dielectric has been viewed as a passive electronic component of the LEFET. Here we introduce a new strategy of an optoelectronic gate dielectric to improve, simultaneously, the brightness and efficiency of the LEFET. The optoelectronic gate dielectric (OEG) consists of three pairs of alternating high and low refractive index layers of quarter wave thickness and gives an LEFET with excellent electrical characteristics, very high brightness of 4500cd/m², and an efficiency at this brightness of 0.9 cd/A. This is the highest brightness obtained so far from the LEFET device architecture. The efficiency was improved by a factor of 4.5 compared to the control device on SiNx gate dielectric.

8115-25, Session 4

Self-organized polymeric anodes for high-performance organic light emitting diodes with simplified structures

S. Woo, T. Han, M. Choi, T. Lee, Pohang Univ. of Science and Technology (Korea, Republic of)

Most of research on flexible transparent electrode materials has been focused on the improvement of conductivity at a fixed transmittance. However, all the reported flexible transparent anode materials suffer from poor charge injection due to low work function and thus an additional organic layer is necessary to facilitate hole injection/extraction in organic electronics. Here, we report a new material concept of flexible polymeric anode (we call "AnoHIL") which has easy work-function tunability and thus makes ohmic-contact between the anode and organic layer even with high ionization potential up to 5.8 eV. In this manner, the device structure is simplified. We demonstrate highly efficient green organic light-emitting diodes (OLEDs) (~22 cd/A) and solution processed phosphorescent white OLEDs (~34 cd/A) using our AnoHILs without a hole-injection layer. This proves promising replacement of conventional brittle electrodes with even greatly improved performance toward flexible solid-state lighting sources and full-color displays.

8115-26, Session 4

Polarizer-free high-contrast organic light emitting diodes

S. Yoo, H. Cho, KAIST (Korea, Republic of)

We present our study on polarizer-free high-contrast organic light-emitting diodes (OLEDs) that are considered better positioned in terms of cost effectiveness and compatibility with highly flexible displays. A particular emphasis is placed on those compatible with inverted top-emitting (ITE) geometry in consideration of the growing importance of n-type thin-film transistors based on oxide semiconductors. As an introduction, the definition of contrast ratio (CR) and its practical implications are briefly discussed, and then the prior arts are reviewed and compared in an effort to find a strategy toward the best possible configuration for high-CR OLEDs. Promising high-CR OLED structures compatible with ITE geometry are then proposed that are based on (i)

partially reflecting bottom electrodes and (ii) damage-free top electrodes consisting of dielectric-metal-dielectric multilayer structure. A particular attention is paid first to the bottom electrode configuration from both electrical and optical perspectives and then to the top electrode configuration from optical perspectives that consider the overall cavity structure. An exemplary ITE-OLED under the proposed scheme is demonstrated to exhibit luminous reflectance of ~2% with the current efficacy comparable to or higher than that of conventional high-CR OLEDs relying on circular polarizing films. A choice of outer dielectric layers is shown to play an important role in reducing reflectance in the wide range of the visible spectrum for truly "black" appearance. General optimization strategies to realize ITE-OLEDs striking a good balance between CR and performance are discussed as a conclusion.

8115-27, Session 4

Channel-wide illumination and angular emission profile in tri-layer organic light emitting transistors

S. Toffanin, W. Koopman, G. Generali, R. Capelli, M. Muccini, Istituto per lo Studio dei Materiali Nanostrutturati (Italy)

Organic light-emitting field-effect transistors (OLETs) are emerging as an innovative class of multifunctional devices that integrates the electronic properties of a transistor, the light generation capability and the full potential of organic photonics. OLETs can provide both a novel device architecture to investigate fundamental optoelectronic properties and can be used in applications as diverse as optical communications system, simplified flat panel displays and solid-state lightening [1].

We recently reported [2] a trilayer heterostructure OLET with a device external quantum efficiency of 5% in which not only the electrode-induced photon losses and exciton-metal interaction, but also the charge-induced exciton absorption were simultaneously controlled.

Apart from the potential advantage of the OLETs related to the higher EQE and brightness [1], the limited width of the recombination zone in the device channel might be a limitation for a number of application such as OLET-based active matrix displays and lab-on-a chip photonic detection. Moreover, optical and photonic investigations on light extraction from OLETs are mandatory to locate resonators and waveguides into field-effect planar structure for the realization of highly integrated optoelectronic multifunctional devices.

Here, we implement high performance trilayer heterostructures for realizing for the first time an OLET in which the emission area extends over the entire channel length in ambipolar conditions.

Moreover, we measure directly the angular emission profiles on trilayer OLETs in different bias conditions. Indeed, we correlate the lateral extension of the emitting zone and the bias-invariant angular emission profiles in trilayer OLETs with the device characteristics of charge transport and exciton formation processes.

[1] M. Muccini Nat. Mater. 5, 605 (2006).

[2] R. Capelli, S. Toffanin, G. Generali, H. Usta, A. Facchetti, M. Muccini Nat. Mater. 9, 496 (2010).

8115-28, Session 4

Phosphorescent organic light emitting diode with >60% external quantum efficiency at >10,000 cd/m²

Z. Wang, M. G. Helander, J. Qiu, D. P. Puzzo, M. T. Greiner, Z. Lu, Univ. of Toronto (Canada)

Phosphorescent organic light emitting diodes (PHOLEDs) attracted considerable research interest due to their potential to reach 100% internal quantum efficiency. However, two major factors limit the external quantum efficiency (EQE) for PHOLEDs, i.e. the light out-coupling factor and the efficiency roll-off. In this work, a novel out-coupling enhancement

Conference 8115:
Organic Light Emitting Materials and Devices XV

method is presented. Using this new enhancement, a green PHOLED with up to 63 % EQE is realized. Moreover, the efficiency remains as high as 60% at 10,000 cd/m². The peak value of power efficiency reaches 290 lm/W without using electrical doping.

8115-29, Session 4

Photostability of the organic/metal cathode interface in organic light emitting devices

Q. Wang, H. Aziz, Univ. of Waterloo (Canada)

We have studied the photo-stability of two types of organic/metal contacts widely used in organic light-emitting devices (OLEDs), namely, organic/Mg:Ag and organic/LiF/Al interfaces. Irradiating OLEDs which contain these contacts by external illumination is found to result in a gradual increase in driving voltage (V_d) and decrease in electroluminescence (EL) efficiency. This photo-induced degradation in device performance is found to be caused by changes at the organic/metal interface, possibly due to photochemical processes, that lead to a deterioration in electron injection. Evidence of interface photo-degradation, inherently, by device own EL, during electrical driving is investigated by means of removing the cathode and re-depositing a new one. The correlation between the density of excited states in the organic material adjacent to the organic/metal interface and the rate of the photo-degradation in device performance is also investigated. The results uncover an important degradation mechanism in OLEDs and shed the light on a phenomenon that might limit the stability of other organic optoelectronic devices.

8115-30, Session 5

Color tunable light sources based on organic light emitting diodes

J. Lee, J. Han, J. Huh, J. Shin, D. Cho, H. Chu, Electronics and Telecommunications Research Institute (Korea, Republic of)

We have fabricated color tunable white light sources by combining a transparent and a bottom emission organic light emitting diodes (OLEDs). White spectra could be obtained by mixing up two different light emissions from two OLEDs. To improve light extractions in color tunable OLEDs, we have taken advantage of micro-cavity effect and a transparent anode containing thin metal layer (about 1 nm of Ag) was used in the bottom emission OLED. Optical lengths could be optimized by controlling the thickness of a hole transporting layer (HTL) and 40% of light extraction could be enhanced in a blue bottom emission OLED. Although the thickness of the HTL was thicker than conventional HTL thicknesses, similar operating voltages could be obtained due to the special layer structure and therefore luminous efficacy could be also improved according to the enhancement of light extraction. As for transparent OLEDs, yellow and red emitting OLED was fabricated. In this case, we have used conventional ITO transparent anodes and tried to improve transmittance and light extraction. The transmittance of the transparent OLED was strongly correlated with the transmittance of the cathode as well as the optical thicknesses of each layers in the OLED. Light extractions could be engineered by optimizing the structure and thickness of the capping layer on the transparent cathode. Optimized transparent OLEDs showed 70 % of transmittance at 550 nm with a common glass encapsulation and about 80-90 % of external efficiencies of the corresponding bottom emission OLEDs. Finally, color tunable OLEDs could be demonstrated by combining the two OLEDs and the detailed results will be revealed in this presentation.

8115-31, Session 5

Stretchable polymer LEDs fabricated on silver nanowire polymer composite electrodes

Z. Yu, L. Li, Q. Zhang, J. Liu, Q. Pei, Univ. of California, Los Angeles (United States)

Various new transparent electrodes have been investigated to replace indium tin oxide (ITO). We report a new transparent electrode based on silver nanowires (AgNW) using a simple fabrication process. The AgNW-polyacrylate composite electrodes have sheet resistances tunable in the range of 8-100 Ohm/sq with transmission of 80-95%. The surface roughness is <5 nm. Polymer LEDs fabricated on the new composite electrodes show similar performance as controls on ITO/glass. Some of the devices could be stretched by greater than 10%, repeatedly and reversibly.

8115-32, Session 5

Light emitting diodes based on quantum dot nanohybrid active layers

K. Char, Seoul National Univ. (Korea, Republic of)

Dispersion of colloidal quantum dots (QDs), which are considered quite useful for LEDs due to emitting visible light with narrow spectral bandwidth, within unconventional block copolymer (BCP) thin films was investigated and its effect on LED performance was studied. Unconventional BCP composed of either thiol (SH) anchoring groups or fluorinated (F) phenyl groups in the minor block (11 repeat units) and poly(triphenylamide) in the major block (60 repeat units) were synthesized through the Reversible Addition Fragmentation chain Transfer (RAFT) polymerization method. QDs (diameter ~ 8 nm) encapsulated with alkyl hydrocarbon (~ 1 nm) were mixed with both types of BCPs and deposited on substrates to create hybrid thin film (less than 100 nm). With combined techniques of TEM, AFM and Kelvin Probe Microscopy (KPM), we confirmed that QDs are evenly distributed within the BCP matrix with thiol (SH) anchor block as a result of enthalpic attraction between QD and BCP, while QDs are phase-separated from the BCP matrix with fluorinated phenyl block either to the top surface or bottom surface and laterally segregated to form QD clusters in order to minimize the interfacial energies between QD and BCPs during the deposition (solvent evaporation) steps. On the basis of this experiment, we realized electrically driven QD based light-emitting diodes with organic-inorganic hybrid active layers of evenly distributed QDs within conducting host thin films, demonstrating that QD hybrid active layers are quite useful in LED applications due to the combination of emission and hole/electron transport layers as well as the ease of film deposition.

8115-33, Session 5

Micro-optical beam-shaping concept for tailored light-emission patterns from OLEDs

C. A. Wächter, D. Michaelis, M. Flämmich, N. Danz, P. Dannberg, A. Bräuer, Fraunhofer-Institut für Angewandte Optik und Feinmechanik (Germany)

The OLED technology introduces thin, large area light sources. Any application that desires a shaped OLED emission pattern inevitably needs thin micro-optical systems in order to retain the OLEDs features of slimness and light-weight. In this contribution we will show that micro-optical arrays are well suited to fully open up the potential of OLED lights.

An OLED beam-shaping scheme utilizing thin micro-optical arrays will be demonstrated. Each array channel consists of a micro lens and a proper reflective/absorptive aperture. This approach combines two effects for OLED pattern shaping: (a) light recycling due to multiple reflections between the OLED and the beam-shaper, (b) distorted and arrayed Fourier imaging, where the aperture induced spatial light pattern

Conference 8115:
Organic Light Emitting Materials and Devices XV

is transformed into a distinct angular light distribution. It may be applied with OLEDs readily comprising substrate outcoupling structures or OLEDs with planar substrates. In either way the light emission pattern of large area OLEDs can be tailored efficiently.

By means of such a beam-shaping concept several different illumination patterns (e.g. circles, triangles or letters) with divergence angles up to $\pm 40^\circ$ will be demonstrated. Furthermore, a reduction of the divergence angle down to about $\pm 10^\circ$ accompanied by a stray-light level minimization to $<1\%$ at larger angles will be presented. In either case intensity enhancements by a factor of 2 can be realized with the thickness of the optics remaining below 2 mm.

8115-95, Session 5

Continuous-wave organic semiconductor lasing

Y. Zhang, S. R. Forrest, Univ. of Michigan (United States)

Optically pumped organic semiconductor lasers (OSLs) have, up until now, only operate in pulsed mode with a maximum duration of several tens of nanoseconds. This limitation is imposed by triplets generation along with radiative singlets. Triplet absorption typically overlaps the singlet emission spectrum, leading to losses at high triplet densities that accumulate over time during the pumping pulse, thereby prohibiting OSLs from achieving continuous-wave (CW) operation. In this work, we introduce "triplet manager" molecules into the emissive region of an OSL that prevent triplets from interacting with the singlet exciton or photon populations. Using this approach, we observe lasing time increase to 100 μs , limited only by device degradation. Theoretical analysis suggests that the devices have exceeded the CW lasing threshold that is higher than the pulse threshold. This result changes a fundamental understanding of OSL dynamics and opens a new route to electrically pumped organic lasers.

8115-34, Session 6

Organic semiconductor lasers: materials, photophysics, and fabrication

G. Tsiminis, Y. Wang, N. A. Montgomery, Univ. of St. Andrews (United Kingdom); S. Schumacher, J. Denis, I. Galbraith, Heriot-Watt Univ. (United Kingdom); A. Kanibolotsky, Univ. of Strathclyde (United Kingdom); I. Perepichka, Bangor Univ. (United Kingdom); P. J. Skabara, Univ. of Strathclyde (United Kingdom); I. D. W. Samuel, G. A. Turnbull, Univ. of St. Andrews (United Kingdom)

Organic semiconductors have considerable potential for compact, tunable, visible lasers. A particular advantage of these materials is their scope for simple fabrication. We show that nanoimprint lithography is a powerful technique for fabricating distributed feedback lasers and report the factors affecting the quality of replication and laser threshold. The choice of lasing material is also a key factor and we will report a systematic study of the photophysical and lasing properties of a family of star-shaped molecules consisting of a truxene core and fluorene oligomers arms. A combined experimental and theoretical study was performed, exploring the effect of the length of the arms on the transition dipole for absorption and emission. It is found that although the entire molecule absorbs, the excitation quickly localises on a single arm. Very good laser performance is obtained. For example the materials with 3 fluorene units in each arm gives an exceptionally broad tuning range for a deep blue material from 422 to 473 nm, high gain (38 cm^{-1}), loss loss (3.5 cm^{-1}) and a low threshold for lasing of 515 W/cm^2 .

8115-35, Session 6

Last advances in optimizing organic solid-state lasers based on photostable materials and high-quality resonators

M. A. Diaz-Garcia, E. M. Calzado, M. G. Ramirez, V. Navarro-Fuster, P. Boj, I. Vragovic, J. M. Villalvilla, J. A. Quintana, Univ. de Alicante (Spain); I. Alonso, A. Juarros, A. Retolaza, S. Merino, Tekniker (Spain)

In this presentation we will discuss the last advances achieved in our group in relation to the development of efficient and photostable organic solid-state lasers, including advances in improving both, the active material and the resonator.

From the material's point of view, we have focused our efforts on searching for photostable and low-threshold materials in waveguide configuration. For such purpose we have investigated small organic molecules doped into different types of inert polymers, searching for high index-contrast between the active film and the substrate. We have also studied organic single crystals, as model systems to advance understanding of the mechanisms involved in laser emission.

Concerning the resonator, we have designed, fabricated and characterized second-order distributed feedback (DFB) lasers by holographic lithography (HL) and by nanoimprint lithography (NIL). HL, a versatile method that allows the design to be easily changed and large samples to be prepared, has been used to test new designs. In these devices the photoresist has been used directly as the substrate, in order to simplify the fabrication process. NIL has been used to fabricate high-performing and low-cost DFB devices. Detail studies of the influence of several parameters, i.e. grating depth, film thickness, index contrast between film and substrate and location of the grating (over the substrate or over the active film), have allowed us to control the emission characteristics of the devices.

8115-36, Session 6

Electrically pumped organic laser device with a coupled microcavity structure

X. Liu, Y. Li, J. Lin, S. Qu, Changchun Institute of Optics, Fine Mechanics and Physics (China)

As laser gain media, organic materials are intrinsically quasi-four-level systems. They are materials that have high fluorescent quantum efficiencies, low absorption losses, and can be easily prepared in a film configuration. Although optically pumped laser action has been observed in a broad range of organic materials including polymers or small molecules with lasing wavelengths spanning the visible spectrum, the compact, low cost and practical organic laser devices (OLDs) should be electrically pumped. Obstacles are still in the way of realizing electrically pumped organic lasers in waveguide, distributed feedback (DFB), and light-emitting TFT structures. Recently, significant progress has been made in electrically pumped organic lasers with a microcavity structure. In this work, we will show some further results in this respect.

An electrically pumped OLD has been developed with a coupled microcavity (CMC) structure: Glass/bottom mirror/SiO₂/middle mirror/ITO/MoO₃/2T-NATA/NPB/NPB/DCM/Alq/DCM/Alq /LiF/Al/top mirror. The OLD shows a single longitudinal cavity mode at 618 nm with a threshold current density of about 600 mA/cm^2 under room temperature CW operation. The OLD has an active light emitting area of $1 \times 1 \text{ mm}^2$, and the output light beam shows apparent coherence. The design of device structure has been illustrated. Furthermore, we will show that the electrically pumped green light OLDs based on Alq:C545T gain layer has reached a maximum output power density of 1 mW/cm^2 .

Conference 8115:
Organic Light Emitting Materials and Devices XV

8115-37, Session 6

Transparent electrodes for plastic electronics

J. C. de Mello, Imperial College London (United Kingdom)

Organic semiconductors are attracting widespread interest due to their potential applications in lighting, displays and solar cells. A key obstacle to successful commercialisation, however, is the absence of high performance flexible electrodes that can be processed at plastic-compatible temperatures. For rigid applications, indium tin oxide (ITO) is the transparent conductor of choice, but its high cost, tendency to crack when flexed, and need for high temperature processing are problematic for large area applications. Here we investigate the use of conducting polymers, single wall carbon nanotubes, and silver nanowires as ambient processable transparent electrodes for organic light-emitting diodes and solar cells.

Key issues that will be discussed include: ITO-free OLEDs based on vapour phase polymerised PEDOT; organic field-effect transistors utilising PEDOT:PSS and graphene source and drain electrodes; and efficient organic solar cells using solution processed single wall carbon nanotubes and silver nanowires for the transparent electrode.

8115-38, Session 6

Resonant optical antenna effects in organic photonic devices

D. M. O'Carroll, Rutgers, The State Univ. of New Jersey (United States)

Nanoscale optical antennas can modify the direction, decay rate and luminescence quantum efficiency (QE) of excitonic emission from organic semiconductors by concentrating optical modes into nanometer-scale volumes. Here, the emission properties of heterostructured optical antennas (fabricated by template-directed sequential electrodeposition [1]) consisting of plasmonic (noble metal) nanowire antennas coupled to poly(3-hexylthiophene), P3HT, conjugated polymer disks (20 nm high; 60 nm diameter) are presented. The radiative decay rate (τ_r) of P3HT in the presence of a single gold nanoantenna is determined to be $440 \times 10^6 \text{ s}^{-1}$ from photoluminescence lifetime measurements - an increase by a factor of 31 over P3HT in the absence of antennas. Both τ_r and QE enhancements of up to 135 and 55 are shown to be possible in theory (full-field electromagnetic simulations), for plasmonic nanowire antennas with optimized length and diameter (180 and 40 nm, respectively) that resonate at the emission wavelength of P3HT. Work is underway to characterize arrays of plasmonic nanoantennas coupled to 20 nm-thick P3HT films to demonstrate large-area enhancements in τ_r and QE. Benefits to the absorption characteristics of P3HT thin films using silver nanoantennas with resonances tuned to the polymer absorption band will also be discussed. When incorporated onto the metallic electrode of bulk-heterojunction photovoltaic test devices the nanoantennas will be shown to render the electrode optically active resulting in improved red response in the photocurrent spectra.

[1] D. M. O'Carroll, C. E. Hofmann, H. A. Atwater, Conjugated Polymer/Metal Nanowire Heterostructure Plasmonic Antennas. *Adv. Mater.* 22 (2010) 1223.

8115-39, Session 7

Carrier-blocking nature of polarized organic-organic interfaces studied by DCM, UPS, and TOF methods

H. Ishii, Y. Miyazaki, N. Ogawa, T. Nishi, Y. Nakayama, Y. Noguchi, Chiba Univ. (Japan)

We have investigated the interface charge of Alq3-based OLED. The charge is due to orientation polarization of Alq3 layer, and is a key to understand carrier-blocking mechanism at organic-organic interfaces.

Recently we have found not only Alq3 but also other OLED materials such as BCP show similar effect. In this presentation, we will report on an effort to clarify the carrier-blocking nature of these materials by several methods.

Displacement current measurement (DCM) and Time-of-flight (TOF) measurement allow us to directly monitor how the carrier is accumulated and blocked. So far TOF measurement has been applied to single layer device to determine mobility. We applied it to a double-layered device, and successfully observed the carrier behavior in the operating state with light emission.

Kelvin probe (KP) measurement and ultraviolet photoemission spectroscopy (UPS) give us the information of the polarization and energy barrier at the interfaces. KP results confirmed that orientation polarization is formed in the exact device structure. This is necessary to estimate the blocking nature due to the interface charge. UPS determined the barrier heights at organic-organic interfaces. This information is necessary to discuss the blocking nature due to barrier height. From the obtained results, we will discuss on the blocking nature of OLED interfaces.

8115-40, Session 7

Electroabsorption spectroscopy of vacuum-sublimed organic light emitting diodes and solar cells

P. A. Lane, U.S. Naval Research Lab. (United States)

We studied the influence of interfaces on the electric field distribution in organic devices by electroabsorption spectroscopy. Incorporation of a polymer hole injection layer in bilayer organic LEDs profoundly alters the field distribution. In reverse bias, the electric field is suppressed within the hole transport layer and concentrated in the electron transport layer. Excited state absorption by field-modulated cations dominates the forward bias spectrum. We also studied multilayer films of C60 and zinc phthalocyanine, a model system for organic photovoltaics. Dipoles at the organic heterojunction oppose the external field, emphasizing the importance of drift diffusion for charge transport.

8115-41, Session 7

Probing light emitting films with neutrons

P. L. Burn, A. R. G. Smith, I. R. Gentle, The Univ. of Queensland (Australia)

Advances in light-emitting materials design and manufacturing have brought the first organic light-emitting diodes (OLEDs) to market. For all the materials used as light-emitting layers the morphology of the film plays an important role in controlling their opto-electronic and device properties. Neutron techniques such as neutron reflectometry (NR) and small angle neutron scattering are important methods for studying physical structures of (macro)molecules and their interactions in solution and/or the solid state. We have been using an in situ photoluminescence-NR measurement for elucidating the relationship between physical structure and emissive properties. In this presentation we discuss the structure of films comprised of phosphorescent iridium(III) complexes. OLEDs containing iridium(III) complexes are highly efficient but achieving this efficiency usually involves diluting the emissive complex in a host material such as 4,4'-bis(N-carbazolyl)biphenyl. We will report our study on blended films containing fac-tris(2-phenylpyridyl)iridium(III). We will show that not only is the concentration of complex in a blend important for the emissive properties of the film but also the morphological thermal stability. In addition, we will discuss the effect of thermal annealing on multilayer OLED structures.

8115-42, Session 7

Molecular orientation in OLEDs

D. Yokoyama, Yamagata Univ. (Japan); C. Adachi, Kyushu Univ. (Japan); J. Kido, Yamagata Univ. (Japan)

The molecular orientation in organic amorphous films has been disregarded for ~20 years in the research in OLEDs, and its effects on device characteristics have not sufficiently been discussed at the microscopic molecular level. Only recently, the intermolecular interaction and the subsequent horizontal molecular orientation in OLEDs have been investigated and reported. In this presentation, the overview of the recent studies on the molecular orientation in OLEDs will be presented.

First, the general properties of the molecular orientation in OLEDs will be discussed. By variable angle spectroscopic ellipsometry (VASE), it was demonstrated that molecules in amorphous organic semiconductor films are generally oriented on any underlying layer and even in doped films depending on the anisotropy of the molecular shape [1-3].

Then, the effects of the orientation on the optical and electrical performances of OLEDs will be discussed. The horizontal molecular orientation of emitting materials improves the outcoupling efficiency of OLEDs, and the horizontal orientation of charge transport materials improves the carrier mobilities in the films [4,5]. Furthermore, it was reported that the singular molecular orientation induced by intermolecular hydrogen bonds can contribute to the enhancement of mobility [6].

These results show the vital importance of the molecular orientation in OLEDs for the improvement of the device characteristics and the development of new materials.

[1] D. Yokoyama et al., *Org. Electron.* 10, 127 (2009). [2] D. Yokoyama et al., *Appl. Phys. Lett.* 93, 173302 (2008). [3] D. Yokoyama et al., *J. Appl. Phys.* 107, 123512 (2010). [4] D. Yokoyama et al., *Appl. Phys. Lett.* 95, 243303 (2009). [5] D. Yokoyama et al., *Adv. Funct. Mater.* 20, 381 (2010). [6] D. Yokoyama et al., *Adv. Funct. Mater.* (in press, DOI: 10.1002/adfm.201001919).

8115-43, Session 7

Thermal study of the photonic band-gap effect on a resonant energy transfer process

L. González-Urbina, K. Clays, Katholieke Univ. Leuven (Belgium)

Optical confinement can induce enhancement of the resonant energy transfer between fluorescent molecules by modifying the available energy levels. In this work we study the energy transfer between a pair of molecules, fac tris(2-phenylpyridine) iridium (Ir(ppy)₃) and bis(2-methyl-8-quinolino)-4-phenylphenolate aluminum (BALq) which are extensively used in OLED technology. These chelates have previously shown both Dexter and Förster energy transfer giving rise to phosphorescence emission at low temperatures. Here, we present the result of the dipolar coupling of these two molecules embedded in a polymer film and inserted in a colloidal photonic crystal and how the photonic crystal may improve the efficiency of the energy transfer. A thermal study of the emission under the effect of the photonic band gap is performed.

8115-44, Session 7

Nearly zero-gap formation between singlet- and triplet-excited states and application for organic light emitting diodes

K. Sato, K. Goushi, C. Adachi, Kyushu Univ. (Japan)

Recently, in order to improve the exciton production efficiency at a singlet excited level (S₁) in OLEDs, we employed the mechanism of thermally activated delayed fluorescence (TADF). To realize high TADF efficiency, we need materials that have a small energy gap between S₁ and a triplet excited (T₁) levels (EST). EST becomes smaller when

the exchange energy that is overlapping between the highest occupied molecular orbital (HOMO) and the lowest unoccupied molecular orbital (LUMO) is small. Therefore, the separation of the HOMO from the LUMO is crucial to enhance the up-conversion from T₁ to S₁ (RISC). More recently, based on this conception, we developed a triazin derivative (PIC-TRZ) that realizes a small EST of 0.1 eV and the OLED using PIC-TRZ for an emitting layer achieved a high external quantum efficiency of ext=5.3% that exceeds the theoretical limitation of ext in conventional fluorescence OLEDs. In this study, to achieve higher EL efficiency using TADF, we developed a novel triazin derivative (PIC-TRZ2) having a nearly zero energy gap between S₁ and T₁, which was confirmed by the fact that fluorescence and phosphorescence spectra of PIC-TRZ2 shows exactly same 0-0 transition peak (T=5 K). Furthermore, intense delayed fluorescence is confirmed in both the neat and a 6 wt%-PIC-TRZ2:1,3-bis(9-carbazolyl)benzene (m-CP) co-deposited film under photo-excitation at room temperature. In addition, the OLED using PIC-TRZ2 shows a high external quantum efficiency of ext=7.9% at 0.01 mA/cm² with delayed fluorescence.

8115-45, Session 7

Delayed electroluminescence measurements: a technique for investigating the emission mechanism in phosphorescent organic light emitting devices

H. Zamani Siboni, H. Aziz, Univ. of Waterloo (Canada)

Delayed electroluminescence (Delayed EL) measurements are used to investigate the emission mechanism in typical Phosphorescent Organic Light Emitting Devices (PHOLED). In this study, the emission layer is doped with various concentrations of the emitter guest. Delayed EL is used to understand whether the EL emission arises from charge recombination directly on guest sites or from recombination on host material followed by host to guest energy transfer. The results show that the emission mechanism changes with guest concentration. At low guest concentration, device shows strong host triplet-triplet annihilation (TTA), suggesting the presence of significant energy transfer from host to the guest. At high guest concentration, on the other hand, host triplet-triplet annihilation is insignificant suggesting that direct charge trapping on the guest is the main emission mechanism. Results also show no significant guest TTA in the latter, indicating guest TTA does not significantly influence emission. Observations related to the role of guest concentration on the operational stability of PHOLEDs are also reported.

8115-46, Session 7

Precise determination of OLED emitter properties

M. Flämmich, D. Michaelis, C. A. Wächter, N. Danz, Fraunhofer-Institut für Angewandte Optik und Feinmechanik (Germany)

The detailed properties of the internal dipolar emission (which are e.g. the internal electroluminescence spectrum, the profile of the emission zone, and the orientation of the transition dipole moments) strongly affect the device efficiency and the radiation pattern of OLEDs. In recent years, the characterization of OLED emitter properties by optical analysis of the far-field radiation patterns of OLEDs in electrical operation was established as a method to determine these data experimentally. Unfortunately, bottom emitting standard devices optimized for maximum emission in air are not suitable to measure all active emitter properties exactly.

In our contribution a simplified layered stack is discussed as an example of typical bottom emitting OLED structures. As known from rigorous optical modeling, the distance of the emissive sites to the metal cathode is the most crucial parameter to enhance or suppress certain emitter contributions to the far-field emission. Varying this emitter-cathode distance allows changing the different emitter contributions advantageously. In result, the emitter properties can be determined with highest precision from radiation pattern analyses when utilizing adapted

Conference 8115:
Organic Light Emitting Materials and Devices XV

OLED stacks. General rules for setting up adapted OLED systems for emitter characterization in electrically driven OLED devices are concluded. Furthermore, selected experimental results will accompany the theoretical discussion in order to illustrate and to demonstrate the applicability of this approach.

8115-47, Session 7

Carrier mobility and diffusion length measurements via impedance-voltage characteristics in organic light emitting diodes

I. Wu, J. Chang, C. Wu, National Taiwan Univ. (Taiwan)

The correlation between the impedance versus voltage (Z-V) characteristics and the carrier mobility and diffusion length of OLEDs was investigated. With the existence of the accumulation charges at the organic layers interfaces, the Z-V characteristics present a particular transition before the device turns on and the voltage at where the transition occurs is related to the film thickness and the density of the accumulation charges. Devices with systematically varied film structures, including various cathode structures and different thicknesses of the organic layers were investigated. For the devices with common structures, NPB as the hole transport layer (HTL) and Alq3 as the electron transport layer (ETL), the density of the accumulation charges is constant. However, the impedance transition happens at different voltage bias in the devices with an electron injection layer, which may result from the decrease of the effective thickness.

The devices with other combinations of HTLs and ETLs were also studied and the results showed that there is an extra impedance transition only in the devices with the hole mobility in the HTL much larger than the electron mobility in the ETL. It implies that the extremely different carrier mobilities somehow have a great influence on the existence of the accumulation charges. Thus the difference between the carrier mobilities in the HTL and the ETL can be surveyed through the Z-V characteristics of OLEDs, and this property makes the Z-V characteristics a potential tool to quickly estimate the carrier mobility in organic materials.

8115-91, Session 7

Organic light emitting diodes toward flexible displays

S. Kim, J. Lee, J. Kim, Seoul National Univ. (Korea, Republic of); P. Wang, C. Wu, National Taiwan Univ. (Taiwan)

No abstract available

8115-64, Poster Session

Study of charge injection in inverted organic unipolar devices using n-type hole injection layers

C. E. Small, J. Subbiah, K. R. Choudhury, F. So, Univ. of Florida (United States)

Improved hole injection efficiency was demonstrated by inverting the device architecture of small molecule unipolar devices with n-type hole injection layers. Current-voltage and dark-injection space-charge-limited current (DI-SCLC) techniques were used to characterize normal and inverted N,N'-diphenyl-N,N'-bis(1-naphthyl)(1,1'-biphenyl)-4,4'-diamine (NPB) unipolar devices consisting of molybdenum trioxide (MoO₃) or 1,4,5,8,9,11-hexaazatriphenylene hexacarbonitrile (HAT-CN) hole injection layers. Both normal and inverted devices with HAT-CN showed larger injection efficiencies compared to similar devices with MoO₃. The injection efficiency enhancement observed by inverting the device

architecture was attributed to improved charge transfer at the n-type layer/NPB interface due to improved interfacial doping. We validate this claim by fabricating NPB unipolar devices with MoO₃-doped NPB injection layers, in which further enhancement in injection efficiency is observed.

8115-65, Poster Session

Organic light up-conversion devices with hole-blocking layers

D. W. Song, D. Y. Kim, F. So, Univ. of Florida (United States)

The integration of organic photodetector and organic light-emitting diode (OLED) enables the fabrication of infrared-to-visible up-conversion devices. However, due to the proximity between the work function of indium-tin oxide (ITO) and the HOMO level of IR absorbing tin (II) phthalocyanine (SnPc), hole injection from ITO starts even at low voltages, and hence decreasing the sensitivity of the up-conversion performance. In this presentation, we report the enhancement in the up-conversion performance by controlling hole blocking properties.

We have fabricated control OLED devices, devices with an IR sensitizing mixed layer of SnPc:C60, and devices with hole blocking layer. The control devices had the following structure: ITO/SnPc:C60 (1:1 ratio, 20 nm)/1,1-bis[di-(4-tolylamino)phenyl]cyclohexane (TAPC) (45 nm)/7% fac-tris(2-phenylpyridinato)iridium(III) (Ir(ppy)₃):4,4-N,N-dicarbazole-biphenyl (CBP) (30 nm)/tris[3-(3-pyridyl)-mesityl]borane (3TPYMB) (45 nm)/LiF(1 nm)/Al (100 nm). We used p-bis(triphenylsilyl)benzene (UGH2) and bathocuproine (BCP) as hole blocker between ITO and the IR absorbing layer. The luminance-current-voltage (LIV) characteristics were measured with and without the 830 nm infrared light irradiation.

The comparison between the devices with different thickness of the IR sensitizing mixed layer and the devices with various hole blocking layers will be presented. Without infrared light irradiation, emission was not observed until 14.5 V in the up-conversion device with 10 nm thick BCP, compared with the control device was turned on at 6 V. It shows that hole injection from ITO was effectively limited by the hole blocking layer. On the contrary, when the device was irradiated with infrared light, photo-generated holes were injected to the light-emitting layer and the device turned on at around 3 V, without a significant change of current efficiency (80 cd/A). The maximum photo-conversion efficiency was measured as 2.5 %.

8115-66, Poster Session

Organic light emitting diodes with polyaniline/silver nanocomposites or aniline oligomers as a hole injection layer

J. Wu, J. Chiu, A. Wang, C. Chang, S. Tang, K. Chiu, Chung Yuan Christian Univ. (Taiwan)

Effects of hole injection layer (HIL) on the performance of organic light emitting diode (OLED) with a basic heterostructure of ITO/HIL/NPB/Alq₃/LiF/Al were studied; and polyaniline/silver nanocomposites or aniline oligomers were adopted as a HIL. At first, the surface morphology of HIL after spin-coating on top of ITO substrate was observed by SEM and AFM. Then, the characteristics of current density (J) and electro-luminance (L) versus bias voltage (V) of these as-fabricated OLEDs were measured. The experimental J-L-V curves were numerically analyzed by a model/equivalent circuit. From experimental J-L-V data, an enhancement of L by factor of around 11 at the same V was obtained for an OLED with polyaniline/silver nanocomposite of a specific ratio being used as a HIL, as compared with the one without a HIL. From numerical fitting results, the causes of this improvement were explored. Finally, the physical significance of polyaniline/silver nanocomposites or aniline oligomers used as a HIL on OLED was discussed.

8115-68, Poster Session

CMOS-compatible high-brightness and low-operating voltage green OLEDs

V. Gohri, J. Boizot, MicroOLED (France); H. Doyeux, Commissariat à l'Énergie Atomique (France); G. Haas, MicroOLED (France)

We report high brightness and low operating voltage efficient green organic light-emitting diodes (OLEDs) based on silicon CMOS backplane which can be used in applications such as microdisplays. The small molecule top-emitting OLEDs are based on a fluorescent green emitter accompanied by blocking, doped charge transport layers and an anode fabricated with standard CMOS processes of a 200 mm IC fab. The devices are designed to maximize the efficiency under low operative bias so as to fit the limited voltage budget of the IC. This was done by making optical simulations of the device structure to maximize light outcoupling within a 20° extraction cone, optimizing the organic layer thicknesses and charge injection in the n and p transport layers and utilizing a double emission layer stack. The resulting OLED has a current efficiency of 21 cd/A at a luminance of 20,000 cd/m². Furthermore, the device exhibits a voltage swing of just 2.2 V for a contrast ratio of 1000. The device has a lifetime of 6,000 hours at 5000 cd/m². Similar device performances were reproduced on an active matrix 5 megapixel microdisplay.

8115-69, Poster Session

Nanotransfer for light extraction in top-emitting organic light emitting devices

Z. Wang, J. Hauss, C. Vannahme, U. Bog, S. Klinkhammer, T. Mappes, U. Lemmer, Karlsruhe Institut für Technologie (Germany)

Organic light-emitting devices (OLEDs) have attractive and promising applications in next-generation lighting and displays. Even though the internal quantum efficiency of OLEDs with phosphorescent emitters could increase to nearly 100%, the external quantum efficiency of conventional OLEDs is as low as ~20%. And up to 50% of the generated light is trapped in waveguide modes and surface plasmon polariton modes. Therefore, aiming to extract those trapped modes for enhanced emission, we explored a rigiflex mold-assisted nanotransfer method for damage free integration of nanostructures into OLEDs. Compared to the conventional nanofabrication method, for example, interference lithography, this technique offers the possibility to optimize nanofabrication and OLED fabrication independently, and could avoid detriments on electrical properties of OLEDs from the nanofabrication process.

In this work, nanogratings were transferred under low pressure and low temperature on top of top-emitting OLEDs without damage by rigiflex cyclic olefin copolymer molds. Waveguide mode extraction was investigated by Photoluminescence and electroluminescence (EL) measurements. A transfer matrix method and rigorously coupled wave theory based numerical simulations were carried out to identify those extracted waveguided modes. Furthermore, the scanning electron microscopy image shows no damage on the top-emitting OLED structure by this nanotransfer process. EL properties of the EL devices with nanogratings exhibit that this nanotransfer process does not adversely affect the OLED performance. All the results indicate that top-emitting OLEDs and other organic optoelectronic devices could benefit from this one-step, solvent-free and etchless nanotransfer approach, which is compatible with roll-to-roll printing techniques suitable for industrial production schemes.

8115-70, Poster Session

Highly efficient fluorescent flexible green and white organic light emitting diodes with multilayered graphene anode

T. Han, Pohang Univ. of Science and Technology (Korea, Republic of); Y. Lee, Sungkyunkwan Univ. (Korea, Republic of); S. Woo, Pohang Univ. of Science and Technology (Korea, Republic of); B. H. Hong, J. Ahn, Sungkyunkwan Univ. (Korea, Republic of); T. Lee, Pohang Univ. of Science and Technology (Korea, Republic of)

We realized the highly efficient fluorescent green and white organic light-emitting diodes (OLEDs) with multilayered graphene anode which was modified with self-organized polymeric hole injection layers (HILs). Traditionally, conventional transparent anode, indium-tin-oxide (ITO), has been used as anode for OLEDs. However, the ITO anode has many weaknesses for application to organic electronic devices such as increasing cost of raw material, non-flexible substrate, and problems of diffusion of indium and tin atoms into overlying organic layers during the device operation. To overcome these problems of conventional ITO anodes, alternative anode which has appropriate optical and electrical properties is strongly required like graphene anode. Graphene has unique electrical and transparent properties as a promising transparent and flexible conductor, there is major drawback for application to electrodes for OLEDs. The relatively low workfunction of graphene (~ 4.4 eV) compared with that ITO anode (~4.8 eV) makes OLEDs difficult to inject holes overlying layers (e.g. EML). Our self-organized polymeric hole injection layer (HIL) has gradient work function toward overlying organic layers and thus makes holes be injected efficiently to the organic layer despite high injection barrier for holes at interface between graphene anode and organic layer. The good ohmic injection of holes between graphene anode and overlying organic layers with our workfunction tunable polymeric HIL is demonstrated by Dark Injection space charge limited current (DI SCLC) measurement. Furthermore, we found very high and much higher luminous efficiency of fluorescent green and white OLEDs with graphene anode than those with ITO anode by using our workfunction tunable polymeric HILs. This kind of strategy to molecularly modify the workfunction of graphene anode with self-organized polymeric hole injection layers make chances to very efficient replacement of ITO anode to flexible graphene anode without sacrificing luminous efficiency.

8115-71, Poster Session

Highly efficient simple-structure small-molecule organic light emitting diodes by using a molecularly controlled polymeric hole injection layer

T. Han, M. Choi, Pohang Univ. of Science and Technology (Korea, Republic of); C. Lee, Gwangju Institute of Science and Technology (Korea, Republic of); T. Lee, Pohang Univ. of Science and Technology (Korea, Republic of)

Since the standard fabrication method to make multilayered small-molecule organic light-emitting diodes (OLEDs) is thermal vacuum deposition with a series of shadow masks, which needs considerably high material and processing cost. Therefore, we have focused on the reduction of small molecule OLED layers to avoid the high cost issue caused by using many vacuum deposition steps. This paper presents very simplified small molecule OLEDs with a very high luminous efficiency which include only a single layer of small molecules on top of a spin-coated polymeric hole injection layer. We found that the simplification of the device structure using well-known small molecular and polymeric HIL such as 2-TNATA and PEDOT:PSS resulted in significant drop of the luminous efficiency comparing with multilayered structure each. However, when we applied our hole injecting conducting polymer compositions composed of PEDOT:PSS and a perfluorinated ionomer (PFI)

Conference 8115:
Organic Light Emitting Materials and Devices XV

(PEDOT:PSS/PFI) as a hole injecting conducting polymer buffer layer, the luminous efficiency of the simplified device (~ 20 cd/A) was dramatically enhanced compared with standard multilayered small molecule OLED devices (~ 12 cd/A). Furthermore, with comparing the device comprising multilayered structure with PEDOT:PSS:PFI (~ 18 cd/A), the very simplified device with same polymeric HIL compositions (PEDOT:PSS:PFI) showed a little higher luminous efficiency. Since PFI has a lower surface energy and a higher ionization potential than PEDOT:PSS respectively, this polymeric HIL has gradient work function by self-organization of the PFI. This gradient workfunction of HIL makes holes be injected very efficiently to THE overlying emitting layer (EML) and insulating properties of self-organized PFI layer shows great capability of preventing quenching of excitons at interface between HIL and EML, which was supported by relative photoluminescence intensity measurements and time-correlated single photon counting experiments. In this manner, the very simplified OLEDs can have highly efficient radiative recombinations of holes and electrons without quenching of excitons in recombination zone of these devices nearby the interface between the HIL and the EML.

8115-72, Poster Session

Device failure mode analysis of highly efficient and reliable small-molecule organic light emitting devices with a self-organized polymeric hole injection layer

T. Han, M. Choi, T. Lee, Pohang Univ. of Science and Technology (Korea, Republic of)

We realized the effect of a self-organized polymeric hole injection layers (HILs) with various composition of polymeric HILs, PEDOT:PSS:PFI, on the luminous efficiency and device lifetime in small-molecule organic light-emitting diodes (OLEDs). Our high performance polymeric HIL comprising PEDOT/PSS and a perfluorinated ionomer (PFI) has gradient work function toward overlying organic layers. Since the PFI has a lower surface energy and a higher ionization potential than the PEDOT:PSS, this polymeric HIL has gradient work function by self-organization of PFI. Therefore, this polymeric HIL makes holes be injected very efficiently to the emitting layer and blocking electrons at the interface between HIL and emitting layer. This good hole-injection capability makes good charge balance and reliable operation in small-molecule OLEDs. This good hole injection contact is demonstrated by Dark Injection Space Charge Limited Current (DI SCLC) measurement with various PFI compositions in PEDOT:PSS:PFI. OLEDs fabricated by using a hybrid process of solution process of HIL and vacuum deposition process showed a very high luminous efficiency (~18 cd/A), a much higher luminous efficiency compared with conventional small-molecule OLEDs comprising only vacuum deposited small molecules (~12 cd/A). To analyze the influences of our high performance HIL, PEDOT:PSS:PFI on the device, we performed various device characterizations with the varying PFI concentrations in the conducting polymer compositions with a function of luminance degradation percentage by measuring current-voltage characteristics, capacitance-voltage characteristics, photoluminescence and electroluminescence spectra, transient electroluminescence, and mechanical properties of degraded films by nanoindentation.

8115-73, Poster Session

Highly efficient solution-processed small-molecule organic light emitting devices with novel tetraphenylsilane blue phosphorescent host materials

T. Han, Pohang Univ. of Science and Technology (Korea, Republic of); D. Oh, S. Kwon, Y. Kim, Gyeongsang National Univ. (Korea, Republic of); T. Lee, Pohang Univ. of Science and Technology (Korea, Republic of)

We report highly efficient solution-processed blue electrophosphorescent small-molecule organic light emitting devices using novel small molecular blue phosphorescent host materials. We have commonly used commercially available phosphorescent blue guest, Iridium(III) bis(4,6-difluorophenylpyridinato)picolate (Flrpic) and poly N-vinylcarbazole (PVK) as an interlayer between a hole injection layer (HIL) and the emitting layer (EML) respectively. The EML consists of an electron and hole transporting co-host and a blue dopant (Flrpic). 4,4',4''-tris(N-carbazolyl)-triphenylamine (TCTA) and (1,3-bis(N-carbazolyl)benzene (mCP) were commonly used for the hole transporting host materials. We presents three kinds of new tetrasilane electron transporting hosts materials, diphenylbis(3-(pyridine-x-yl)phenyl)silane (x=2,3,4) (2, 3, and 4TPPS), for blue phosphorescent solution-processed small-molecule OLEDs which have the maximum luminous efficiency reached about 15 cd/A with a conventional PEDOT:PSS HIL. Comparing with 1,3,5-tris N-phenylbenzimidazol-2-yl benzene (TPBI) as a electron transporting host with PEDOT:PSS HIL (~9 cd/A), devices with our new blue phosphorescent co-host showed much higher efficiency than that with conventional host materials because of more efficient charge balance in the EML and efficient energy transfer to the guest molecules. Furthermore, the use of our self-organized polymeric hole injection layer, PEDOT : PSS : Perfluorinated ionomer (PFI) compositions resulted a in even higher luminous efficiency with 3TPPS (~20 cd/A) and TPBI (~12cd/A) in solution-processed small molecular OLEDs than those with the conventional PEDOT:PSS.

8115-74, Poster Session

Enhancement of current injection in organic light emitting diodes with sputter-treated molybdenum oxides as hole injection layers

P. Wang, I. Wu, W. Tseng, C. Wu, National Taiwan Univ. (Taiwan)

Molybdenum oxide (MoO₃) has been widely used in organic light emitting diodes (OLEDs) to provide superior hole injection efficiency. The origins of assistance in hole injection from MoO₃ hole injecting layers are the lowering of injection barrier and formation of gap states between valence band edge of MoO₃ and the Fermi level of electrodes when N,N'-di(naphthalene-1-yl)-N,N'-diphenyl-benzidine (NPB) molecules are deposited on MoO₃ layers. The chemical reaction between NPB and MoO₃ reduces the oxidation states of molybdenum atoms in MoO₃ and results in gap state formation. These gap states enhance the conductivity of MoO₃ and provide transition paths of carrier to assist the injection of hole from indium tin oxide (ITO) anodes to NPB layers. To enhance the metallic characteristics of MoO₃ and facilitate better hole injection directly, in-situ Argon ion sputter is incorporated with the fabrication process of OLEDs in this work. When treating the surface of MoO₃ with slight Argon sputtering, ion bombardment removes the bonding oxygen atoms in MoO₃ layers. As a result, the oxidation states of molybdenum atoms in MoO₃ are reduced. The enhancement of current density in OLEDs is effectively achieved by treating MoO₃ layers with slight argon sputtering. After sputter treatment for 10 seconds, the modified MoO₃ layers provide improved current injection efficiency, resulting in better current density which is about ten times higher than that of the reference devices. Ultraviolet and X-ray photoemission spectra provide evidences that molybdenum atoms are reduced to lower oxidation states after sputter treatment due to the removal of oxygen atoms.

8115-75, Poster Session

Highly efficient, ITO-free white organic light emitting diodes (WOLEDs) fabricated by solution processes

M. Choi, S. Woo, T. Han, T. Lee, Pohang Univ. of Science and Technology (Korea, Republic of)

White organic light-emitting diodes (WOLEDs) have aroused a great attention due to their potential as solid-state lighting sources and

Conference 8115:
 Organic Light Emitting Materials and Devices XV

application in full-color displays. Recently, solution processable WOLEDs have been received much interest to realize low-cost, large-area and printable displays. In this work, we demonstrate high-performance, solution-processed small molecule WOLEDs. A single white-emitting layer was composed of two complementary phosphorescent dopants of sky blue and orange red (Flrpic and Bt2Ir(acac)) doped into a co-host of hole-transporting and electron-transporting small molecules. We achieved a very high luminous efficiency (~ 25 cd/A) and external quantum efficiency (EQE) (~ 10 %). We also fabricated highly efficient simplified ITO-free solution-processed small-molecule WOLEDs by incorporating polymeric anodes with high hole injection efficiency (we call this anode as AnoHILs). The AnoHIL is a single spin-coated polymeric conductive layer functioning as both the anode and the HIL in the OLED device. Luminous efficiency (~ 32 cd/A) and EQE (~ 13 %) of ITO-free WOLEDs were much higher than those of ITO-based WOLEDs due to high work function and injection efficiency of AnoHILs. These results suggested the possibility of high-efficient flexible WOLEDs via a simple solution process for next generation lighting sources.

8115-77, Poster Session

Highly efficient top-emitting organic light emitting diodes with LiF/Yb bilayer as an electron injection layer

H. Ahn, W. Song, H. Lee, K. Char, S. Lee, C. Lee, Seoul National Univ. (Korea, Republic of)

We demonstrated the highly efficient top emitting organic light emitting diodes (TOLEDs) with lithium fluoride (LiF) and ytterbium (Yb) bilayer as an effective electron injection layer (EIL) from the silver (Ag) semitransparent cathode. Furthermore we employed 2,2',2''-(1,3,5-Benzinetriyl)-tris(1-phenyl-1-H-benzimidazole) [TPBi] for a capping layer to enhance the efficiency as well as an electron transporting layer. Depending on the results of the simulation, the transmittance of the top side has the highest value of 80.4% ($\lambda=530$ nm) at the thickness of TPBi cap layer of 45 nm. Using this, we fabricated the TOLEDs with structure of Al (80 nm)/MoO₃ (10 nm)/di-[4-(N,N-ditolyl-amino)-phenyl]cyclohexane [TAPC] (50 nm)/4,4'-Bis(carbazol-9-yl)biphenyl [CBP]:tris(2phenylpyridine) iridium(III) [Ir(ppy)₃] (8%, 30 nm)/TPBi (40 nm)/Yb (4 nm) or LiF (0.5 nm)/Yb (4 nm) and Ag (12 nm)/TPBi (45 nm). The device with an EIL of LiF/Yb bilayer shows drastically reduced driving voltage of 11.3 V at 100 mA/cm² and operating voltage of 7.2 V at 1000 cd/m² compared to 12.2 V and 7.9 V of the device with Yb as an EIL because of lower electron injection barrier and better balance of carriers. And the device with LiF/Yb bilayer exhibits peak efficiencies of 16.9%, 24.3 lm/W and 53.2 cd/A. These values are higher than that of 15.3%, 21.4 lm/W and 48.8 cd/A with Yb as an EIL. The highly efficient characteristics of the TOLEDs are attributed to efficient electron injection from Ag cathode by using LiF/Yb bilayer as well as capping layer effect.

8115-78, Poster Session

A study on the improved performances of OLED using horizontal oriented amorphous material

J. Kim, C. Adachi, Kyushu Univ. (Japan)

Recently, horizontally oriented amorphous thin films have been used in organic light-emitting diodes (OLEDs), making use of their high-performance electrical characteristics based on the enhancement of π - π interaction between adjacent molecules. Also, horizontally oriented amorphous materials have been developed for hole and electron injection in the organic layer/electrode interface. To determine the effects of the orientation of these films, we investigated optical anisotropy of the films by using variable angle spectroscopic ellipsometry (VASE). When the molecules have anisotropic orientation in the films, the ordinary refractive indices and extinction coefficient were different from the extraordinary ones. We found that BT-DDP and Bpy-OXD having disk-like and rod-

type shape clearly showed a horizontal orientation based on the VASE measurement. We fabricated multilayer OLEDs using horizontally oriented amorphous thin films of all components. The devices based on N1, N1, N4, N4-tetrakis(4-(benzo[b]thiophen-2-yl)phenyl)benzene-1,4-diamine (BT-DDP) as a hole-transport layer (HTL) and 1,3-bis[2-(2,2'-bipyridin-6-yl)-1,3,4-oxadiazol-5-yl] (Bpy-OXD) as an electron-transport layer (ETL) achieved low driving voltage of 3.7 V at 20 mA/cm². Also, Carrier balance condition is achieved due to the incorporation of horizontally oriented BTDDP and Bpy-OXD. We expect that, by combination of HTL, EML and ETL having horizontally oriented amorphous materials, very low driving voltage with highly efficiency can be surely achieved in OLEDs.

8115-79, Poster Session

Charge carrier generation efficiency in reverse biased organic p-n junctions

S. Lee, J. Lee, Seoul National Univ. (Korea, Republic of); C. Park, Samsung Mobile Display Co., Ltd. (Korea, Republic of); J. Kim, Seoul National Univ. (Korea, Republic of)

Charge carrier generation efficiency in organic semiconductor p-n junctions under reverse bias will be presented, which is important as a charge generation layer (CGL) in tandem organic light-emitting diodes (OLED). 1,4,5,8,9,11-hexaazatriphenylene hexacarbonitrile (HAT-CN) possessing deep lying lowest unoccupied molecular orbital (LUMO) energy level was used as the p-layer and various electron transporting materials doped with rubidium carbonate (Rb₂CO₃) as the n-layers in the CGL unit. Current density-voltage and capacitance-voltage characteristics of the CGL units showed that the voltage drop for charge carrier generation in CGL unit depends on the vacuum level shift, electron mobility, and free carrier density of ETL, rather than the LUMO energy level of ETL. Moreover, the voltage drop for charge generation in CGL unit can be further reduced by increasing the doping concentration of n-ETL. Consequently, the CGL unit with 30 mol% Rb₂CO₃ doped BPhen with HAT-CN have been demonstrated that the voltage drop at junction for the current density of 10 mA/cm² was around 0.17 V, which is infinitesimally small comparing with other literatures. The mechanism of charge generation and recombination is suggested by tunneling of electron through the thin depletion layer.

8115-80, Poster Session

On the way to efficient: bright and wafer-level Quantum dot light emitting diodes

H. Bourvon, S. Le Calvez, H. Kanaan, S. Meunier-Della-Gatta, Lab. d'Electronique de Technologie de l'Information (France); C. Philippot, P. Reiss, Commissariat à l'Énergie Atomique (France)

Solution-processed Quantum Dot Light Emitting Diodes (QDLEDs) have recently paid the way for low-cost and colour saturated displays. Indeed, Quantum dots (QDs) have the appealing property to emit at a tunable wavelength determined by their nature and diameter. According to materials, emission can be tuned from visible to near infrared range. Therefore, QDLED electroluminescent spectra exhibit a narrow bandwidth (FWHM ~30nm) and QDs-based displays offer high colour purity and saturation. Moreover, QDs deposit is compatible with methods such as spin coating, inkjet printing or stamping already implemented for Polymer Light Emitting Diodes at wafer-level. We present in this conference our optimization steps and our recently developed QDLEDs. We established a layer by layer strategy, from a whole evaporated small molecule based OLED to our first QDLED developed by wet deposition techniques for the first layers and by evaporation for the last ones. In an intermediary step, we managed to develop hybrid OLEDs where efficacies of 12cd/A at 4V were obtained, with 2.17 % of EQE, and a luminance of 4000 cd/m² at 4V. In QDLEDs cases, QDs were spin coated, inkjet printed or stamped with a PDMS stamp. The problematic was to find an economical method to form a continuous monolayer of QDs on our 200mm wafers. Trials were done as well by mixing QDs in a polymer matrix for carrier injection

Conference 8115:
Organic Light Emitting Materials and Devices XV

requirements. We present advantages and drawbacks relative to each method of QDs deposition. Finally, we report our first Near Infrared QDLEDs, emitting at around 1.5 micron based on PbS QDs.

8115-81, Poster Session

Inorganic/organic composite structures in OLEDs: new approaches for efficiency enhancement

B. Riedel, J. Hauss, Y. Shen, U. Lemmer, Karlsruher Institut für Technologie (Germany); M. Gerken, Christian-Albrechts-Univ. zu Kiel (Germany)

Organic light-emitting diodes (OLEDs) already being used in commercial display applications or general lighting lack a high efficiency. The high internal quantum efficiency, which is achieved by phosphorescent emitters, is lowered by a poor outcoupling efficiency. A large fraction of the generated light is trapped as waveguide modes inside the glass substrate, the anode and the organic layers as well as in surface plasmon polaritons at the metal/organic interface. The total internal reflection of substrate modes may be overcome by simple techniques such as applying microlenses or other microstructures on the substrate/air interface. The waveguide modes within the OLED stack demand for more sophisticated approaches. Bragg gratings or low-index-grids are two common structures being used to extract these trapped modes. In this work, we report on an approach for extracting waveguided modes in OLEDs by scattering in inorganic/organic composite layers. We fabricated OLEDs with thick (up to 1000 nm), transparent, nanocomposite hole transport layers consisting of the hole transporting polymer PEDOT:PSS and varying volume fractions of SiO₂-nanoparticles and TiO₂-nanoparticles. These layers reveal a dense packing of nanoparticles. Even for a volume fraction of more than 80% of SiO₂-nanoparticles and thus less than 20% PEDOT:PSS functioning OLEDs with enhanced efficiency are demonstrated. This is attributed to scattering effects, which occur in the nanocomposite layer. The TiO₂-particles are used to increase the index of refraction. By changing the nanoparticle concentration and the thickness, the optical properties of OLEDs may be optimized further.

8115-82, Poster Session

A carbazole-based compound capable of bipolar transport for application in green phosphorescent and fluorescent OLEDs

C. Chang, Yuan Ze Univ. (Taiwan); M. Kuo, National Taiwan Univ. (Taiwan); W. Lin, Yuan Ze Univ. (Taiwan); K. Wong, National Taiwan Univ. (Taiwan)

In general, charge transporting and balancing are two crucial factors for high-efficiency OLEDs. One promising strategy for carrier balancing is to incorporate an electron-donating moiety and an electron-withdrawing moiety into a single host material. However, host materials possessing the bipolar characteristics as well as a large triplet gap are scarce. In addition, the developments of true-blue phosphors so far were still immature and thus blue phosphors were not widely adopted in the industries. The commonly techniques were employing blue fluorophor combined with green and red phosphors to display full-color images. Here, a study of newly developed bipolar host material, 9-(4,6-diphenyl-1,3,5-triazin-2-yl)-9'-phenyl-3,3'-bicarbazole (CzX), is presented, including synthesis, characterization, and electroluminescent device applications. The molecular design was combining N-phenylcarbazole moiety as electron donor (D) and 1,3,5-triazine moiety as electron acceptor (A) for the bipolar transport purpose. The hole-transport and electron-transport abilities of CzX were superior to that of 4,4'-Bis(carbazol-9-yl)biphenyl (CBP). By using the CzX as emitting host, the maximum efficiencies of 20%, 75.7 cd/A and 71.3 lm/W were achieved in green Ir(tmp)2-doped OLEDs with a simplified architecture.

Particularly, the CzX can not only be used as host material for phosphorescent emitters, but also used as a green fluorescent emitter for non-doped fluorescent OLEDs. The maximum efficiencies of green fluorescent OLEDs were up to 7.0 %, 21.6 cd/A, and 22.5 lm/W. These results provided useful insights for the design of bipolar host materials and efficient electrofluorescent and electrophosphorescent devices.

8115-83, Poster Session

Modelization of the chaotic-like behavior of external quantum yield as a function of humidity during fabrication

S. Gauvin, Univ. de Moncton (Canada)

It is well known that organic light-emitting devices (OLEDs) and other organic electronic devices are generally sensitive to atmospheric water, especially when combined with oxygen. It is generally admitted that such gas are responsible to a great extent for a systematic and irreversible degradation of the organic devices performance. In this study, we have chosen absolute humidity as the (statistical) independent variable instead of relative humidity because the number of water molecules per unit of volume in the atmosphere surrounding an OLED is a more significant parameter than relative humidity. Our experimental data stand for a quantitative confirmation that the reproducibility of OLEDs performance is better when they are fabricated under dry atmospheric condition. Accordingly, at high humidity level (7 g/m³ to 13 g/m³) we observe an increase in the dispersion of external quantum yield. This strongly suggest that the occurrence of antagonist mechanisms and a devices sensitivity to initial structural conditions therefore lead to an unpredictable, chaotic-like, behavior of organic light-emitting external quantum yield after they are exposed to atmospheric water vapor. Even though the dispersion in performance data increases at high humidity level, surprisingly a significant amount of samples (~50 %) show better performance than those prepared at low humidity level. Thus high humidity level is not only detrimental to OLEDs. In some circumstances, oxidation processes accelerated by water vapor can be beneficial to performance. Through suitable theoretical modelization, based on interfacial insulating layers and electrode porosity we get a better understanding of the required conditions that lead to an increase of performance. Finally, we suggest a process (before encapsulation) to enhance the external quantum yield and obtain better reproducibility in performance of OLEDs.

8115-84, Poster Session

Organic interlayer for OLED passivation using vacuum thermal evaporable acrylic monomer

W. M. Yun, S. H. Kim, J. Jang, S. Nam, C. Park, Pohang Univ. of Science and Technology (Korea, Republic of)

In this paper, vacuum thermal evaporable acrylic monomer is investigated for simple fabrication of organic interlayer for OLED multi-layer passivation so that the steps for passivation can be compatible with other steps of conventional vacuum processed OLED fabrication process. Thermal evaporation of metallic acrylate monomer and consecutive UV crosslinking is performed for organic interlayer formation. FTIR and breakdown voltage measurement show formation of polymeric film. In addition, resulting film shows good surface morphology (roughness < 0.7nm), good photo-patternability and somewhat weak barrier characteristics (WVTR: 2.929 g/m²day). For OLED passivation application, plasma enhanced atomic layer deposited Al₂O₃ layer is used as an inorganic passivation layer. As a result, single interlayer insertion of 50nm acrylate film between two 50nm Al₂O₃ layers shows over 1,500 hr shelf lifetime without shrinkage of emission area under 60°C, 90% RH condition even though 100nm Al₂O₃ only passivated OLED device show 1,000 hr shelf lifetime.

8115-85, Poster Session

A high-performance inverted bottom-emission organic light emitting diode using an electron-transporting material with no-energy barrier for electron injection between the doped and undoped homojunctions

J. Lee, Seoul National Univ. (Korea, Republic of); P. Wang, National Taiwan Univ. (Taiwan); H. Park, Seoul National Univ. (Korea, Republic of); C. Wu, National Taiwan Univ. (Taiwan); J. Kim, Seoul National Univ. (Korea, Republic of)

We investigated the effect of the n-doped electron transporting layer (n-ETL)/electron transporting layer (ETL) interface in homojunctions on the performance of inverted bottom emission organic light emitting diode (OLED). Among three kinds of devices having different electron transporting materials (ETMs) like bis-4,6-(3,5-di-3-pyridylphenyl)-2-methylpyrimidine (B3PYMPM), 4,7-diphenyl-1,10-phenanthroline (Bphen), and 2,2',2''-(1,3,5-benzenetriyl)tris-[1-phenyl-1H-benzimidazole] (TPBi), the device with the B3PYMPM resulted in the lowest injection and turn-on voltages of 1.9 V, and 2.4 V, respectively, and the highest maximum external quantum efficiency (EQE) of 20% which is the highest efficiency reported up to now in the inverted bottom emission OLEDs to the best of our knowledge. Furthermore, the maximum power efficiency of the device with the B3PYMPM ETL is very high with the value of 80 lm/W, followed by 43 lm/W for TPBi ETL and 37 lm/W for Bphen ETL. The characteristics were interpreted based on the charge injection from ITO to the n-ETL and from n-ETL to ETL, and electron transport in the ETM by fabricating electron only devices. The electron only device with the B3PYMPM exhibited a large increase in current at a much lower voltage than the other two materials. Ultra-violet photoelectron (UPS) spectroscopy also showed that there is no energy barrier for electron injection between n-B3PYMPM and B3PYMPM, while Bphen and TPBi have energy barriers of 0.2 eV and 0.25 eV, respectively. As a result, we demonstrated that the interface between n-ETL and ETL even in homojunctions is one of the most important factors for high performance inverted OLEDs.

8115-86, Poster Session

Charge generation efficiencies of p-dopants in organic semiconductors

J. Lee, H. Kim, K. Kim, Seoul National Univ. (Korea, Republic of); R. Kabe, P. Anzenbacher, Jr., Bowling Green State Univ. (United States); J. Kim, Seoul National Univ. (Korea, Republic of)

We report that an organic p-dopant tri[1,2-bis(trifluoromethyl)ethane-1,2-dithiolene] [Mo(tfd)3] resulted in higher density of holes than inorganic metal oxide dopants of rhenium oxide (ReO3) or molybdenum oxide (MoO3) in 1,4-bis[N-(1-naphthyl)-N'-phenylamino]-4,4'-diamine (NPB) even though the metal oxide dopants possess deeper work functions compared to Mo(tfd)3. Higher charge generation efficiency which is defined as the ratio of generated carriers to dopant molecules, results largely from the homogeneous dispersion of Mo(tfd)3 in the host. In contradistinction, the transmission electron microscopy (TEM) analysis shows that an origin of the low charge generation efficiency of metal oxide dopants is revealed to be the formation of dopant nanoclusters. The number ratio of the nanoclusters to dopant molecules (dispersion efficiency) was measured to be 0.62-1.3% for the ReO3-doped NPB. The low dispersion efficiency is close to the charge generation efficiency of 0.7-1.1%, indicating that charge generation efficiency in the dopants is predominantly controlled by the dispersion of dopants in organic semiconductors. This highlights the importance of homogeneous dispersion for an efficient doping. It is expected that our findings will be valuable for identifying efficient dopants for various organic semiconductors.

8115-87, Poster Session

Polarizer-free high-contrast top-emitting organic light emitting diodes with high-intensity ratio

S. Kim, J. Lee, H. Park, J. Lee, J. Kim, Seoul National Univ. (Korea, Republic of)

Top emitting organic light emitting diodes (TOLEDs) are widely used in mobile display technology such as portable media player (PMPs), and smart phone etc. Unfortunately, in outdoor environment, ambient light significantly degrades the contrast ratio (CR) of TOLEDs due to strong reflection of ambient light by reflective metal electrode of TOLEDs. Therefore, suppressing reflection from surface of OLEDs is key parameter to fabricate TOLEDs with high contrast ratio. In commercial fields, circular polarizers (CPs) are most favorable technique to fabricate high CR TOLEDs. However, CP is generally thick, expensive and not flexible. First of all, CPs show a reduction of output power to half of conventional device, which is critical disadvantage to fabricate high performance OLEDs. In addition, CPs are difficult to integrate conventional OLEDs fabrication process because CP does not apply to fabrication of OLED by evaporation or solution process. In this presentation, we demonstrate a high CR and high performance TOLEDs using multilayer cathode structures, which is composed to metal and dielectric layer. From their asymmetric reflectance properties, our cathode structures have advantages, which is fully adoptable with any kind of TOLEDs regardless of using highly reflective metal (Al or Ag etc.) as top and bottom electrodes. Therefore, contrary to the results of other groups, enhancement of light emission is expectable due to maintaining strong microcavity effect. Through theoretical and experimental procedures, our polarizer free TOLEDs demonstrate low luminous reflectance and high intensity ratio comparing with TOLEDs with CR.

8115-88, Poster Session

Bipolar spirobifluorene: highly efficient electroluminescence based on thermally activated delayed fluorescence

T. Nakagawa, Kyushu Univ. (Japan); S. Ku, K. Wong, National Taiwan Univ. (Taiwan); C. Adachi, Kyushu Univ. (Japan)

A highly luminescent organic light emitting diode based on thermally activated delayed fluorescence (TADF) is achieved by using spirofluorene derivatives (Spiro-CN) as an emitting layer. The spirofluorene derivatives are composed of two di-p-tylamine and cyano units as electron donating and electron accepting units, respectively, which are connected in the central spirofluorene core. This specific structure provides the high efficient TADF. Spiro-CN emits yellow fluorescence with photoluminescence efficiency of 27 % in the thin films. Highly efficient yellow-light-emitting diodes were fabricated using the Spiro-CN as an emitting layer. The device structure used in this study is ITO/ α -NPD/6wt% Spiro-CN:mCP/Bphen/MgAg/Ag, where α -NPD and Bphen are used as a hole-transporting and a hole-blocking/electron-transporting layer. The Spiro-CN based devices displayed a low turn-on voltage of 3 V and a maximum luminance of 12000 cd/m² at voltage of 15 V. The maximum external quantum efficiency, maximum luminous efficiency and maximum power efficiency of the Spiro-CN based devices reached 4.4 %, 13.5 cd/A and 13.0 lm/W, respectively. The transient PL and EL clearly demonstrated the presence of TADF, contributing high EL efficiency. In this study, we also succeeded to obtain a relationship between the molecular design and small Δ ES-T, the energy difference between the S1 and T1 energy levels.

8115-89, Poster Session

Photonic crystal electrode for enhanced light extraction in OLED

L. L. Petti, M. Rippa, Consiglio Nazionale delle Ricerche (Italy);
G. Nenna, A. De Girolamo Del Mauro, V. La Ferrara, C. Minarini,
ENEA (Italy)

In this work we show how it is possible to realize a high index grid embedded in a relatively large-area photonic crystal (PC) structure to drastically reduce the light trapped in the OLED device. Thus, a 2D-PC pattern with a period of 392 nm and a depth of 350 nm has been uniformly modelled by Electron Beam Lithography (EBL) technique on a surface of 2x2 mm² removing partially a resist co-polymer (ZEP-520) deposited on a thin Indium Tin Oxide (ITO) grown itself on a glass substrate. The PC was realized taking into account the relationship between the guided light spectrum and Bragg's diffraction condition. Luminance measurements showed a peak emission at 592 nm with a full width half-maximum of 20 nm.

A Focused Ion beam (FIB) was then used for milling the large area PC structure realizing holes into the ITO layer using the structured ZEP-520 as a lithographic mask. FIB working conditions were optimized to control the ITO milling process until the glass-substrate. After removing the resist, highly conductive PEDOT:PSS was deposited filling the holes, realizing a continuous path for the current and obtaining a high refractive index jump for the PC structure. Finally, the OLED was grown on the PC to monitor the efficacy of the realized structure.

In conclusion, we demonstrated the possibility to realize a discontinuous refractive index path directly on the substrate surface combining EBL and FIB processes enhancing the performance of the PC structure and removing a further refractive index jump between the PC and the substrate.

8115-90, Poster Session

Top emission organic light emitting diodes with high reflective Ag alloy

M. Kim, J. Lee, K. Kim, K. Kim, K. Lee, J. Yoon, S. Yoon, C. Kim,
S. Lee, LG Display (Korea, Republic of)

Top emitting OLEDs (TOLEDs) need the efficient reflecting layer underneath anode to minimize absorption loss and to maximize the efficiency. Previously aluminum-Neodymium (AlNd) reflecting layer was commonly used in fabricating OLED display panel. Here, Ag alloy is used as reflecting layer to enhance the efficiency of TOLED rather than pure Ag layer due to its easy process and stable adhesion property. The efficiency enhancement of 30, 33, and 45% for each RGB TOLED devices with Ag alloy reflecting layer, although the difference of reflectance (R) between AlNd (RAINd = 88% @ 530 nm) and Ag alloy (RAg alloy = 99% @ 530 nm) is only 11%. Optical simulation analysis of AlNd and Ag alloy TOLED shows that reflective difference of 11% in reflective layer amplifies the efficiency gap due to strong resonant micro-cavity effect.

We fabricate TOLED with reflective anode/hole injection layer/hole transporting layer/emitting layer/electron transporting layer/ Mg:Ag cathode/capping layer on the top of glass substrate. Mg:Ag with the transmittance of 30%~70% in the visible regions is used as thin metal cathode. For reflective anode, Ag alloy/ITO and AlNd/ITO are sputtered on the glass substrate before thermal evaporation of organic and cathode layers. The comparison of TOLED performances with the Ag alloy/ITO and AlNd/ITO reflective anode will be shown here.

8115-92, Poster Session

High work function transparent electrodes by UV halogenation

M. G. Helander, Z. Wang, Z. Lu, Univ. of Toronto (Canada)

Transparent electrodes, such as indium tin oxide (ITO), are required in state-of-the-art organic photovoltaics (OPVs), organic light emitting diodes (OLEDs) and flat-panel displays. Controlling the interface properties between transparent electrodes and organic materials is of great importance for device engineering since the performance, stability and lifetime of organic devices are greatly influenced by the electrode/organic contacts. Unfortunately the work function of many transparent electrodes is too low to form a good electrical contact with many of the commonly used organic semiconductors and polymers. We report a simple method for tuning the work function of transparent electrodes using a novel UV assisted halogenation technique. We demonstrate that decomposition of halogenated solvents using UV treatment can be used to functionalize the surface of a variety of different transparent electrodes with halogen atoms. Using this facile technique we achieve unprecedented high work functions of ~6 eV for various transparent conducting oxides, transition metal oxides and metal thin films. Organic devices fabricated using these halogenated transparent electrodes show markedly improved performance in highly simplified device structures.

8115-93, Poster Session

Phosphorescent organic light emitting diode with >60% external quantum efficiency at >10,000 cd/m²

Z. Wang, M. G. Helander, Z. Lu, Univ. of Toronto (Canada)

Phosphorescent organic light emitting diodes (PHOLEDs) attracted considerable research interest due to their potential to reach 100% internal quantum efficiency. However, two major factors limit the external quantum efficiency (EQE) for PHOLEDs, i.e. the light out-coupling factor and the efficiency roll-off. In this work, a novel out-coupling enhancement method is presented. Using this new enhancement, a green PHOLED with up to 63 % EQE is realized. Moreover, the efficiency remains as high as 60% at 10,000 cd/m². The peak value of power efficiency reaches 290 lm/W without using electrical doping.

8115-94, Poster Session

Enhanced efficiency OLEDs with semitransparent anode

H. Zhang, W. C. H. Choy, The Univ. of Hong Kong (Hong Kong, China)

Through introducing dielectric distributed Bragg reflectors (DBRs) into the OLED structure, the light emitting properties can be enhanced by microcavity effects [1-4]. However, typical DBR structures are made from dielectric materials and not electrically conductive. In addition, semitransparent thin metals such as Ag and Au with relatively high work function [5,6] and good reflectance which can be used as the anode material and offering the Purcell effect [7,8]. Furthermore, no ITO is required in our OLEDs with semitransparent DBRs while the shortage of indium has become an alarming issue for the use of ITO. In addition, there are no clear study to combine DBRs and the metals together to offer both microcavity effect and electrical conduction.

In this article, we report enhanced light outcoupling and efficiency from the bottom-emitting microcavity OLEDs by using semitransparent thin Au layers integrated with DBR as an anode. Our results indicate that using metal Au combining with DBR instead of ITO, the electroluminescent (EL) efficiency of the microcavity OLEDs is significantly enhanced due to the strong microcavity caused by Au. For the OLEDs with DBR/Au anode, the maximum luminance efficiency (4.8 cd/A) is about 1.7 times higher as compared with that of the OLED (2.8 cd/A) with ITO/V₂O₅ anode. The OLEDs with DBR/Au anode have also about 1.2 times higher efficiency than that of the OLEDs (4.1 cd/A) with Au/V₂O₅ anode and with DBR/ITO anode. In addition, the EL saturated color has better purity, due to the effective modification of the spontaneous emission through microcavity effect.

1. V. Bulovic, V. B. Khalfin, G. Gu, P. E. Burrows, D. Z. Garbuzov, and S.

Conference 8115:
Organic Light Emitting Materials and Devices XV

1. R. Forrest, Phys. Rev. B 58 (1998) 3730.
2. N. Takada, T. Tsutsui, and S. Saito, Appl. Phys. Lett. 63 (1993) 2032.
3. T. Tsutsui, N. Takada, S. Saito and E. Ogino, Appl. Phys. Lett. 65 (1994) 1868.
4. R. H. Jordan, L. J. Rothberg, A. Dodabalapur, and R.E. Slusher, Appl. Phys. Lett. 69 (1996) 1997.
5. H. M. Zhang and W. C. H. Choy, J. Phys. D: Appl. Phys. 41 (2008) 062003.
6. H. Peng, X. Zhu, J. Sun, Z. Xie, S. Xie, M. Wong, and H. S. Kwok, Appl. Phys. Lett. 87 (2005) 173505.
7. E. M. Purcell, Phys. Rev., 69 (1946) 681.
8. X.W. Chen, W. C. H. Choy and S. He, IEEE/OSA J. Display Technol., 3, (2007) 110.

8115-12, Session 8

Photo-recycling effects in LED lighting

C. Sun, National Central Univ. (Taiwan)

No abstract available

8115-13, Session 8

From dark to bright: novel daylighting applications in solid state lighting

H. G. Adler, OSRAM SYLVANIA Inc. (United States)

The term "daylighting" is used in various ways, on one hand in a more architectural sense, i.e. using existing daylight to illuminate spaces, and on the other, more recently, for using light sources to replicate daylight. The emergence of solid state lighting (SSL) opens up a large number of new avenues for daylighting. SSL allows innovative controllability of intensity and color for artificial light sources that can be advantageously applied to daylighting. With the assistance of these new technologies the combination of natural and artificial lighting could lead to improvements in energy savings and comfort of living beings. Thus it is imperative to revisit or even improve daylighting research so that lighting and building networks of the future with their sensor, energy (e.g. HVAC) and lighting requirements can benefit from the new emerging capabilities. The current talk will review existing daylighting concepts and technology and discuss new ideas. An example of a tunable multi-color SSL system will be shown.

8115-48, Session 8

Intensity shaping and the application efficiency of indoor OLED lighting

P. Y. Ngai, J. Fisher, M. M. Lu, Acuity Brands Lighting, Inc. (United States)

Most indoor lighting is uniform, targeted for the most demanding visual tasks, a practice driven by limitations of conventional lighting systems, resulting in waste. It has been shown that discrete low-luminance tiles of OLED lighting can achieve a practical overhead lighting system that precisely tunes illumination for user requirements, resulting in energy savings, increased comfort, and enhanced flexibility. In this paper, the application efficiency of OLED lighting is further explored by evaluating how intensity shaping can vary photometric performance, create more targeted lighting effects, and increase the types of lighting applications for which OLED can be considered. Several non-Lambertian distributions are considered, along with multiple configurations of OLED panels.

8115-49, Session 8

Toward mass production of OLED lighting

C. Lee, C. Chen, C. Yang, C. Fang, T. Chang, AU Optronics Corp. (Taiwan)

Toward mass production of OLED lighting, differential application field, satisfying performance and competitive cost structure are all very important. In this article, from manufacture point of view, challenges and potential approaches to achieve such performance and cost structure will be discussed. Besides, comparison of OLED lighting with other light sources in some specific application field will be also described.

8115-50, Session 9

Transparent and reflective electrodes of organic light emitting diodes for solid state lighting

J. Lee, Pohang Univ. of Science and Technology (Korea, Republic of)

Specific developments in electrode materials of organic light emitting diodes (OLEDs) including transparent and reflective electrodes will be discussed. Because of its high transmittance (> 85%) and excellent electrical properties (RS < 20 ohm/sq), thin film of indium-tin-oxide (ITO) has been the most widely used transparent electrode in OLEDs for general lighting. To reduce the cost of processing ITO films, thermally deposited dielectric/metal/dielectric multilayer was proposed as an ITO alternative. Due to the multiple reflections and interferences, WO₃/Ag/WO₃ (WAW) multilayer showed high transmittance of ~90% and low sheet resistance (7.22 ohm/sq). The luminance and power efficiency of OLEDs in glass substrate could be increased about 22% and 36%, respectively, by employing the combination of nano-facet structured MgO and WAW electrode instead of ITO. Recent progress of dielectric constant (ε) matching technique will be described on the basis of our recent results. When Ag film deposited on metal oxide (MO) layer with large ε, surface plasmons at the MO/Ag interface could be suppressed and optical transmittance can be significantly enhanced from 41.1 to 78.1%.

From the requirement to possibility of highly rugged, enhancing design freedom, and low-cost roll-to-roll manufacturing for lighting source, flexible OLEDs with steel substrate have been proposed. Because the steel is an opaque substrate, highly reflective metal (Al, Ag) films have been employed as a bottom electrode. Metal/ITO bilayer showed not only high reflectivity but excellent charge injection efficiency and distributed Bragg reflector/ITO gave the most improved luminance and efficiency of OLEDs on steel substrate.

8115-51, Session 9

High efficiency white organic light emitting device using a single emitter

J. Li, Arizona State Univ. (United States)

The white organic light emitting diodes (WOLEDs) with high power efficiency (>100 lm/W) are considered as strong candidates for next generation illumination devices. Especially, WOLEDs use environmentally benign organic materials and their fabrication cost can be significantly reduced with potential roll-to-roll processing technology. To date, however, the white electroluminescent (EL) spectrum is generated using multiple emitters embedded in a comparably complex device structure. In this presentation, we will discuss some of our efforts towards the development of efficient WOLEDs using a single emitter, which include our progress on 1) excimer-based WOLEDs, 2) the development of halogen-free Pt-based blue phosphorescent emitters and 3) the design and the synthesis of broadband phosphorescent emitters.

8115-52, Session 9

Phosphorescent OLEDs for high-efficacy long-lifetime solid state lighting

P. A. Levermore, H. Pang, R. Ma, J. J. Brown, Universal Display Corp. (United States)

In this paper we report on the rapid development of high efficacy, large area phosphorescent OLED (PHOLED) lighting panels with excellent operational stability. In particular, we focus on device performance at high luminance levels typically required for mainstream commercial lighting applications. We report a 15 cm x 15 cm all-phosphorescent OLED lighting panel with lifetime to LT70 > 4,000 hrs and 49 lm/W power efficacy when operating at 3,000 cd/m² with CRI = 82, CCT = 3100 K and CIE 1931 (x, y) = (0.439, 0.422).

The OLED lighting panel uses a simple non-stacked 6 layer all-phosphorescent layer design that ensures excellent power efficacy. The all-phosphorescent device stack also enables extremely low operating temperature of < 30C at 3,000 cd/m², without any thermal management, because the phosphorescent emitters have close to 100% internal quantum efficiency (IQE), so minimal heat is generated from non-emissive excited states. The OLED lighting panel has also been carefully designed to minimize any Joule heating arising from the distribution of electronic charge from the electrode contacts to the emissive area. This marriage of high IQE and careful panel design enables extremely low panel temperature, even at high luminance, which in turn, allows for exceptional operational lifetime.

In this paper, we describe some simple techniques that may be used to design OLED lighting panels for low operating temperature and long lifetime, and describe a basic thermal characterization of a 15 cm x 15 cm panel.

8115-53, Session 9

White top-emitting OLEDs: from optical simulations to highly efficient devices

B. Lüssem, P. Freitag, M. Furno, S. Hofmann, M. Thomschke, K. Leo, Technische Univ. Dresden (Germany)

Organic light emitting diodes (OLEDs) are highly promising for lighting applications due to their advantageous properties such as high power efficiency, good color quality and new design possibilities. To reduce OLED production cost significantly, a roll-to-roll fabrication of top-emitting OLEDs onto low-cost, flexible but opaque metal foils is envisaged. However, the optimization of top-emitting OLEDs is still challenging as the strong optical micro-cavity formed between the metallic top and bottom electrodes leads to a narrowing of the emission spectrum and a strong dependence of the spectrum on the viewing angle.

In this presentation it is shown how the transmission of the top electrode can be optimized and the micro-cavity effect can be weakened. By detailed optical simulations, the different loss channels in top-emitting OLEDs (waveguided and plasmonic modes, absorption, electronic and non-radiative losses) are quantified and the effect of an additional outcoupling layer is clarified. By thoroughly optimizing the optical properties of the OLED, monochrome red OLEDs with external quantum efficiencies of 29% are obtained, which clearly demonstrates the potential of top-emitting devices.

Furthermore, it is shown how the knowledge obtained from optical simulations can be used to realize white top-emitting OLEDs. Using a hybrid fluorescent blue/phosphorescent red and green device setup, white top-emitting OLEDs with high power efficiency, good color quality and a spectrum almost insensitive to the viewing angle are obtained. These white OLEDs are highly promising for low-cost but high efficiency lighting applications.

8115-54, Session 9

White organic light emitting diodes with improved angular emission characteristics employing silver nanowire electrodes

S. Hofmann, Technische Univ. Dresden (Germany); W. Gaynor, G. Christoforo, Stanford Univ. (United States); C. Sachse, M. Thomschke, L. Müller-Meskamp, B. Lüssem, K. Leo, Technische Univ. Dresden (Germany)

We report on white bottom-emitting organic light-emitting diodes (OLEDs), where the commonly used indium tin oxide (ITO) electrode is replaced by a spray-deposited silver nanowire (NW) contact on the polymer Poly(methyl methacrylate) (PMMA).

By mechanical pressing, the surface of the NW electrode is smoothed and the roughness is considerably reduced. Hence, shorts in the OLEDs can be avoided, the leakage current is lowered, and the device performance is enhanced.

For the OLED, we use p- and n-doped charge transport layers, and a hybrid arrangement of red and green phosphorescent and blue fluorescent emitters, where the distribution of excitons is controlled by a thin interlayer. The placement of the red emitter into the second field maximum of the electromagnetic field, and at the same time the blue emitter into the third one, allows the employment of a thick (180nm) p-doped transport layer on top of the NW. This fills the cavities between the single NW and results in lower leakage currents for the devices. Furthermore, coupling to surface plasmons is reduced.

We achieve slightly increased efficiencies with the NW-OLEDs compared to control samples. At 1000cd/m², we reach 7% external quantum efficiency and 12 lm/W luminous efficacy for the ITO-OLED, respectively, for the NW-OLED we obtain 7.5% and 13 lm/W.

Additionally, the NW scattering causes Lambertian emission at viewing angles up to 70° with improved color stability. The CIE color coordinates shift from (0.453/0.376) at 0° to (0.458/0.386) at 70°, whereas for the ITO-OLED the CIE coordinates are (0.453/0.398) at 0° and (0.426/0.358) at 70°.

8115-55, Session 9

Highly efficient long-lived phosphorescent white-stacked OLEDs for solid state lighting

V. Adamovich, P. A. Levermore, A. Dyatkin, Z. Elshenawy, M. S. Weaver, J. J. Brown, Universal Display Corp. (United States)

Organic light emitting devices (OLEDs) are an attractive and energy saving form of solid-state lighting. Key requirements to their commercialization are high color rendering index (CRI), high power efficacy and long operational lifetime. Single unit structure (no internal junction) warm white phosphorescent OLEDs (WOLEDs) have been demonstrated with power efficacies over 100 lm/W. However, achieving commercial lifetime for single unit WOLEDs is challenging. For example for a WOLED with a correlated color temperature of 2,600K, a CRI of 85 and a power efficacy of 75lm/W at 1,000cd/m² the best lifetime to date is 30,000h LT70%. This is approximately an order of magnitude less than inorganic LED lighting sources.

Stacked OLEDs (SOLEDs) offer higher device efficiency (due to multiple stacks) and increased operational stability. We demonstrated a 5x5cm² white SOLED panel with an active area of 19.1cm² and achieved 55.7 lm/W at 1,000cd/m² with 2,900K CCT, CRI of 90, 11,000h LT70% at 3,000cd/m² with ~1.5x light outcoupling enhancement.

The combination of extremely high efficiency phosphorescent OLEDs and SOLEDs resulted in outstanding WOLED performance.

Conference 8115:
Organic Light Emitting Materials and Devices XV

8115-56, Session 10

Light management in OLED devices: from generation to extraction

D. S. Setz, B. C. Krummacher, T. Reusch, T. D. Dobbertin, OSRAM Opto Semiconductors GmbH (Germany); A. Winnacker, Friedrich-Alexander-Univ. Erlangen-Nürnberg (Germany)

Topic of the present talk is the Light Management of organic light-emitting diodes (OLEDs). We discuss the entire path of the light through the device. From the generation of light in the thin film stack to the formation of desired emission profiles. First the properties of the light emitting zone are discussed: The internal luminescence quantum efficiency, emitter orientation and shape of the emission zone have strong influence on the light extraction efficiency of OLED device. Furthermore the light losses by the different waveguides in the device are analyzed by optical simulation. It is shown, that the extraction of so-called ITO/Organic modes leads to significant efficiency enhancement. Finally, we demonstrate, how the formation of application tailored emission profiles increases the application efficiency of the device.

8115-57, Session 10

Light extraction from organic light emitting diodes by silica microsphere array pattern

W. Koo, W. Yun, Univ. of Florida (United States); X. Li, R. Song, N. Tansu, Lehigh Univ. (United States); F. So, Univ. of Florida (United States)

Organic light emitting diodes (OLEDs) consisting of organic layers, indium tin oxide (ITO), and a glass substrate with different refractive indices inevitably accompany the waveguide modes trapped in the ITO/organic layer and the glass substrate, which significantly limits the device efficiency. Although many grating structures with the short periodicity of 300 ~ 500 nm have been studied to extract the ITO/organic waveguide mode directly into the air mode by Bragg diffraction, there is no report about grating with a long periodicity around 1 μm in OLED because of its insufficient grating vector for countering the ITO organic mode. In this study, we report, for the first time, that a grating with the long periodicity of 1 μm also can effectively outcouple the ITO/organic mode as well as the substrate mode through appropriate device dimensions. Hexagonal closed-packed array of 1 μm -diameter-silica sphere embedded in a polystyrene layer was by rapid convection deposition and used as a template for grating. The hexagonal closed-packed pattern of the template was transferred to an epoxy layer by imprinting technique for device fabrication. With the 1 μm period grating, the power of the ITO/organic waveguide modes can be transferred to the substrate modes and the amplified substrate modes can be extracted through multiple reflection of the guiding light with the corrugated aluminum electrode in a 0.1-mm-thick glass substrate. The device with grating showed 50% enhancement in the current efficiency and the additional enhancement was obtained with a 3mm-diameter-hemisphere lens on the back of the substrate. Finally, we investigated the light extraction mechanism by the long period grating.

8115-58, Session 10

Periodic nanostructures for efficient waveguide mode extraction in OLEDs

J. Hauss, B. Riedel, T. Bocksrocker, C. Vannahme, S. Klinkhammer, M. Guttmann, U. Lemmer, Karlsruher Institut für Technologie (Germany); M. Gerken, Christian-Albrechts-Univ. zu Kiel (Germany)

Organic light emitting diodes (OLEDs) are found in a variety of commercial display and even lighting applications. OLEDs with

phosphorescent emitters, harvesting also triplet excitons, reach nearly 100% internal quantum efficiency. However, poor light extraction still limits the external quantum efficiency of common OLEDs. A typical thin film OLED has a planar waveguide structure, giving rise to guided modes in anode and organic layers, surface plasmons at the cathode/organic interface, and substrate modes in the glass substrate. The substrate mode extraction is widely studied and established. Waveguide mode extraction is more difficult to realize, because the extraction structures need to be located inside or close to the OLED thin film stack. Furthermore, highly efficient extraction structures are necessary to achieve extraction within the absorption length of the waveguide modes. OLEDs with periodic dielectric nanostructures (Bragg gratings, planar photonic crystals) as well as periodic metallic nanostructures for waveguide mode extraction were designed and fabricated. Photoluminescence and electroluminescence results are presented and analyzed. We investigate the influence of the nanostructure geometry and quality as well as the influence of waveguide mode absorption and OLED stack design on the extraction efficiency. The experimental results are compared to optical device simulations with a transfer matrix code and the software Setfos from Fluxim AG. Based on the experimental and theoretical results, design rules for efficient waveguide mode extraction structures in OLEDs are deduced.

8115-59, Session 11

How to make ITO a better anode

I. Irfan, S. Graber, Y. Gao, Univ. of Rochester (United States)

Indium tin oxide (ITO) is predominantly employed as a transparent conducting electrode in devices including organic photovoltaic (OPV) cells, and organic light-emitting diodes (OLED). As ITO is used as an anode, the higher the workfunction (WF) the better anode it will be. As received ITO surface WF is usually around 4.5 eV. We investigated changes introduced by oxygen plasma treatment of ITO with ultraviolet photoemission spectroscopy (UPS), inverse photoemission spectroscopy (IPES), and x-ray photoemission spectroscopy (XPS), and found that the workfunction can be increased up to 6.15 eV. We also investigated the evolution of the ITO surface WF as a function of oxygen and air exposure, and found that the WF was reduced to 4.8 eV by 1014 L of air exposure. We have also investigated the interface formation of the high WF ITO with organic materials, and found that it introduced barrier reduction and interface band bending, indicating that the high WF ITO should be a better anode.

*Graber also Grinnell College, Grinnell, Iowa 50112. Gao also Institute for Super Microstructure and Ultrafast Process, the Central South University, Changsha, Hunan 410083, The People's Republic of China

8115-60, Session 11

Laser patterned flexible organic light emitting diode

R. Mandamparambil, TNO Science and Industry (Netherlands); G. Van Steenberge, S. Van Put, Univ. Gent (Belgium); H. Fledderus, TNO Science and Industry (Netherlands); A. Gielen, J. Debaets, Univ. Gent (Belgium); A. Dietzel, TNO Science and Industry (Netherlands)

Techniques such as slot-die are highly suited for fast large area coating and can yield extremely uniform layers. Yet, no solution exists currently for patterning the resulting layers, casting them impossible to use for the roll to roll (R2R) processing for flexible OLEDs (Organic Light Emitting Diode) and flexible OPVs (Organic Photo Voltaics). Selective laser patterning enables post-patterning of large area coated OLED or OPV layers in a R2R manufacturing process such as opening the contacts and tiling to enable encapsulation. Most of the laser patterning work reported so far concentrates on patterning of inorganic TCO (transparent conductive oxides) layers on glass. In this paper we report the first TCO less FOLED (Flexible OLED) made by laser patterning utilizing

Conference 8115:
Organic Light Emitting Materials and Devices XV

a high conductive PEDOT: PSS (Poly (3,4-ethylenedioxythiophene) poly(styrenesulfonate)) and a white LEP (Light Emitting Polymer). The layers are uniformly coated on a multilayer barrier stack on PEN (Poly (ethylene naphthalate)) substrate. A 248nm excimer laser with a 10 ns pulse width operating at a pulse repetition frequency of 100 Hz is utilized for the experiments. The laser patterning is carried out to isolate the contacts and for device encapsulation. Laser processing steps include selectively removing PEDOT and LEP layers on top of the multilayer barrier stack (SiN-Organic-SiN) and from metal bus bars. Al cathode is deposited by shadow masking technique afterwards and is followed by thin film device encapsulation. The devices are then successfully tested under accelerated conditions for its robustness. Major findings will be discussed in the manuscript.

8115-61, Session 11

Digitally-controllable Jet-On-Demand Organic Vapor-Jet Printing (D-OVJP) for OLED displays

C. Yun, J. Choi, T. Koh, H. Cho, S. Yoo, KAIST (Korea, Republic of)

We present our study on a digitally-controllable organic vapor-jet printing (D-OVJP) system in which deposition of organic materials is controlled point by point in a digital manner by producing a jet of organic vapor in a pulsed mode only on demand. D-OVJP inherits all the benefits of a conventional OVJP such as solvent-free deposition, mask-less pattern formation, a good scalability, and, moreover, use of well-established, sublime-grade small molecules that can promises both performance and long-term reliability. In addition to such benefits, however, D-OVJP further provides the real analogue of modern inkjet printing such that (i) deposition can occur only on the desired pixels; and (ii) thickness can be modulated in a straightforward way by a input digital signal; To realize the enhanced OVJP system with such capabilities, the fast solenoid valves are incorporated at the inlets of the carrier gas in OVJP nozzle modules, thus enabling "jet-on-demand"-type deposition of organic materials in which the thickness of organic materials can be controlled by the number of the pulses and/or the duty ratio of the digital signal applied to the valve. With the careful configuration of the valve/ exhaust structure, the thickness control of organic thin films in a resolution of ~ nm/pulse is successfully demonstrated. After presenting the overall concept of the proposed D-OVJP system and its operation, we provide the results of case studies utilizing the enhanced capabilities of D-OVJP methods. Their potential applications are then discussed from the perspectives of OLED displays.

8115-62, Session 11

Multilayer blade coating and cathode printing for large-area efficient organic light emitting diodes

H. Meng, H. Zan, National Chiao Tung Univ. (Taiwan); S. Horng, National Tsing Hua Univ. (Taiwan)

Small-molecule and polymer semiconductors are deposited in large area by rapid blade coating followed by immediate solvent evaporation by heating. Multilayer structure can be made as dissolution is avoided. Uniform film over 10 cm is achieved without spinning. Small molecules even with low solubility can be coated. Blade coated phosphorescent and fluorescent OLED has efficiency about 60 percent of the best vacuum deposited devices for all colors. A three-layer structure including hole transport, emissive, and electron transport layers are used. Cathode is LiF/Al. For phosphorescence polymer is used for hole transport layer and host for the triplet emitter. For fluorescence small molecules are used for the entire device for all three colors. PEDOT:PSS can also be deposited by blade coating for the same device performance as spin coating. In addition to ITO glass this process is made on stainless steel substrate for top emission. The cathode deposition is further

simplified by vacuum-free transferring from a soft silicon rubber mold. Surface modification of Al is used to reduce the work function to 3-3.5 eV. A low-melting point sacrificial polymer layer is inserted between the cathode and the soft mold for easy transfer and subsequent mold removal. Current efficiency close to the device with evaporated cathode is achieved, with slightly higher voltage. Combination of multi-layer blade coating for organic films and printing for cathode makes high throughput production of efficient OLED possible. Such method is extended to polymer solar cell with efficiency close to that of spin coating.

8115-63, Session 11

OLED fabrication by means of OVPD®

D. Keiper, M. Gersdorff, M. Long, B. Beccard, C. Cremer, M. Kunat, J. Kreis, M. Schwambera, M. Heuken, AIXTRON SE (Germany)

Organic Light Emitting Diodes (OLEDs) are emerging as a promising technology for new, high efficient area light sources.

Today, OLED fabrication is dominated by evaporation techniques under vacuum conditions using small organic molecules. Here the Organic Vapor Phase Deposition (OVPD®) works in the fine vacuum utilizing the advantages of carrier-gas enhanced vapor phase deposition, where the materials are transported to the substrate by an inert carrier gas. AIXTRON combined its proprietary Close Coupled Showerhead® (CCS) with the OVPD® technology, enabling organic film deposition with high thickness uniformity and high material utilisation efficiency. We will present this deposition technique focusing on the options for sophisticated OLED stacks design concepts, namely mixing of more than 2 materials through gradual concentration changes. This enables new freedom for OLED stack optimization with respect to device performance, such as 100% efficacy increase. These new concepts of OLED fabrication will be discussed together with illustrating examples and latest results.

OVPD® technology has been exclusively licensed to AIXTRON from Universal Display Corporation (UDC), Ewing, N.J. USA for equipment manufacture. OVPD® technology is based on an invention by Professor Stephen R. Forrest et al. at Princeton University, USA, which was exclusively licensed to UDC. AIXTRON and UDC have jointly developed and qualified OVPD® pre-production equipment.

Part of this work was financially supported by the Federal Ministry of Education and Research in Germany (BMBF) within the Projects Solight, TOPAS, and OPAL.

Conference 8116: Organic Photovoltaics XII

Monday-Thursday 22-25 August 2011 • Part of Proceedings of SPIE Vol. 8116 Organic Photovoltaics XII

8116-54, Poster Session

Achieving high-performance polymer solar cells via incorporating alcohol/water-soluble conjugated polyelectrolytes as cathode interlayer

H. Wu, Z. He, C. Zhong, C. He, Y. Cao, South China Univ. of Technology (China)

Polymer solar cells (PSCs) based on a blend of semiconducting polymer and fullerene derivatives have attracted a lot of attention in recent years because they can produce inexpensive electricity directly from the sun due to their ease of fabrication and inherent low cost of solution processing.[1,2,3] The power conversion efficiency of PSCs is mainly determined by the quantum yield of the photoexcitation and the exciton dissociation and the charge collection. It has been previously shown that incorporating alcohol/water-soluble conjugated polyelectrolytes (CPE) as cathode interlayers can substantially enhance the open circuit voltage (Voc) of bulk heterojunction polymer solar cells. [4, 5] We present a detailed study on the influence of the alcohol/water-soluble conjugated polyelectrolytes interlayer on the exciton generation, dissociation and charge collection process by performing electroabsorption measurement, space-charge limited current characteristics analysis and surface potential measurement.

References

- [1] G. Yu, J. Gao, J. C. Hummelen, F. Wudl and A. J. Heeger, *Science* 270 (1995), 1789.
- [2] N.S. Sacriciftci, L. Smilowitz, A. J. Heeger, and F. Wudl, *Science* 258 (1992), 1474.
- [3] H. Y. Chen, J. H. Hou, S. Q. Zhang, Y. Y. Liang, G. W. Yang, Y. Yang, L. P. Yu, Y. Wu and G. Li, *Nature Photonics* 3 (2009), 649.
- [4] J. Luo, H. B. Wu, C. He, A. Y. Li, W. Yang and Y. Cao, *Appl. Phys. Lett.*, 95 (2009), 043301.
- [5]. C. He, C. M. Zhong, H. B. Wu, R. Q. Yang, G. C. Bazan and Y. Cao, *J. Mater. Chem.* 20 (2010) 2617.

8116-55, Poster Session

Optimization of transparent electrode processing conditions for bulk heterojunction solar cells

Y. Sun, A. Ng, M. K. Fung, The Univ. of Hong Kong (Hong Kong, China); A. M. C. Ng, The Univ. of Hong Kong (Hong Kong, China); A. B. Djurisic, W. K. Chan, The Univ. of Hong Kong (Hong Kong, China)

Among different device architectures of bulk heterojunction solar cells, semi-transparent bulk heterojunction solar cells are of interest due to their potential use in window applications and tandem cells. For such applications, it is necessary to achieve a compromise between transmission and the conductivity of the transparent electrode. While indium tin oxide is commonly used as a transparent bottom electrode, its deposition on top of the polymer layer is difficult due to the need for high substrate temperature and sputtering damage of the polymer. Therefore, other materials such as conductive polymers are of interest. The use of poly(3,4-ethylenedioxythiophene): poly(styrenesulfonate) (PEDOT:PSS) as a top electrode is promising due to its compatibility with large scale roll-to-roll fabrication process and its mechanical flexibility. The challenge in using PEDOT:PSS for top electrodes mainly concerns spin-coating of the hydrophilic PEDOT:PSS on top of the hydrophobic photoactive layer and the low conductivity of PEDOT:PSS.

In this work, semi-transparent inverted polymer solar cells with PEDOT:PSS top electrode were fabricated by spin-coating process. Poly(3-hexylthiophene) (P3HT):[6,6]-phenyl C61-butyric acid methyl

ester (PCBM) was used as a model material combination for a bulk heterojunction solar cell. For enhancing the wetting of P3HT:PCBM blend film, different plasma etching conditions were tried. In addition, different organic additives were tried to enhance the conductivity of PEDOT:PSS. The performance of solar cells with different fabrication conditions for the top electrode was compared. The best performance was obtained for Ar plasma etching to improve wetting of PEDOT:PSS and the addition of ethylene glycol to improve conductivity.

8116-56, Poster Session

Synthesis, characterization, and photovoltaic properties of donor-acceptor copolymer based on 2,1,3-benzoxadiazole with high open-circuit voltage

J. Jiang, K. Wei, National Chiao Tung Univ. (Taiwan)

We have used Suzuki polycondensation to prepare a series of low-bandgap copolymers, PFLUBO and PBDBTO by conjugating the electron-accepting benzo[c][1,2,5]oxadiazole (BO) moieties with the electron-rich fluorene (FLU) or benzo[1,2-b:3,4-b']dithiophene (BDT) units. All of these polymers exhibited excellent thermal stability and sufficient energy offsets for efficient charge transfer and dissociation, as determined through thermogravimetric analyses and cyclic voltammetry, respectively. The bandgaps of the polymers could be tuned in the range 1.8-2.0 eV by using the two different donors, which have different electron-donating abilities. Through these two structurally related polymers, we demonstrate that incorporating electron-withdrawing BO unit would lead to a lower HOMO energy level. This lower HOMO energy level translates into a higher open circuit voltage (Voc) of 1.04V in PFLUBO based BHJ devices. In contrast, the slightly higher HOMO energy level (- 5.4 eV) of PBDBTO limits the Voc to 0.9V. Since the LUMO levels of both polymers are similar, the higher HOMO energy level of PBDBTO leads to a smaller band gap of 1.8 eV. The BHJ devices based on PFLUBO as the donor polymer (with PC61BM as the acceptor and 1:1 weight ratio) exhibit overall efficiencies of 2.57% under the illumination of AM1.5, 100 mW/cm². Future research needs to focus on the employment of even lower electron donating ability donor and stronger electron withdrawing ability acceptors via innovative structural modification in order to achieve a deeper HOMO and a lower band gap to expect the high Voc, Jsc and the better efficiency.

8116-57, Poster Session

Effects of exciton-blocking layers on the performance of organic photovoltaic cells

C. Chang, R. Lin, J. Chiu, K. Lin, S. Tang, K. Chiu, Chung Yuan Christian Univ. (Taiwan)

Effects of exciton blocking layer (EBL) on the performance of organic photovoltaic cell (OPVC) with a basic heterostructure of ITO/CuPc/C60/EBL/Al were studied; and Alq₃, CuPc, and/or LiF thin layers of various thicknesses were adopted as an EBL. The characteristics of current density (J) versus bias voltage (V) of the as-fabricated OPVCs were measured in a dark room and under illumination, respectively. Then, these J-V curves were numerically analyzed by a model/equivalent circuit. From experimental J-V data, an enhancement of the overall efficiency by 20% was achieved for an OPVC with Alq₃ layer of 10 nm thick being adopted as an EBL, as compared with the one without an EBL. From numerical fitting results, this improvement can be identified dominantly by an increase of photo-current density (J_{ph}) and a decrease of series resistance (R_s). In addition, from a durability test, the OPVC with Alq₃ EBL can also have the best performance than that one without EBL. Finally, the physical significance of EBL on the improvements of OPVC was discussed.

8116-58, Poster Session

Solvent induced self-organization of crystalline conjugated polymer and fullerenes for heterojunction solar cells

M. Su, K. Wei, M. Chiu, M. Yuan, C. Kuo, National Chiao Tung Univ. (Taiwan); U. Jeng, National Synchrotron Radiation Research Ctr. (Taiwan)

The nature of the processing solvent critically affects the phase-separated morphologies and orientations of PBTPD crystallites in thin films of PBTPD/PCBM blends and, therefore, the performance of BHJ solar cells incorporating such PBTPD/PCBM blends as active layers. Specifically, highly crystalline fibrillar PBTPD structures and much smaller PCBM aggregates were present in PBTPD/PCBM thin films that had been processed with CF. Through optimization of the active layer's composition, a device incorporating a PBTPD/PCBM blend (1:1.5, w/w) that had been processed using CF displayed balanced carrier mobility transport in the BHJ thin film and, therefore, a solar power conversion efficiency of 6.15%.

Here, we report the effects of the processing solvent and the composition on the morphology and photovoltaic device performance of thin films comprising the highly crystalline polymer and PCBM. Using atomic force microscopy (AFM) and transmission electron microscopy (TEM), the relationship between the nano-morphology and the device performance is allowed to be elucidated. In addition, grazing incidence small-angle X-ray scattering (GISAXS) provided information relating to the dimensions and orientations of the PBTPD crystallites and the sizes of the PCBM aggregates in the PBTPD/PCBM films.

8116-59, Poster Session

Synthesis and characterization of indolocarbazole- and indenofluorene-based low-band-gap polymers for photovoltaic cells

W. Lee, L. T. Nguyen, E. Jeong, Pusan National Univ. (Korea, Republic of); G. Kim, J. Y. Kim, Ulsan National Institute of Science and Technology (Korea, Republic of); H. Y. Woo, Pusan National Univ. (Korea, Republic of)

Polymeric solar cells (PSCs) have emerged as a promising candidate for renewable energy sources due to its low cost, light weight, mechanical flexibility and portability, etc. A bulk-heterojunction structure realized an ideal morphology for efficient PSCs because it increases the interfacial area between a donor polymer and acceptor PCBM resulting in high yields of exciton dissociation. In order to realize the high efficiency of devices, the active layer must have broad absorption of sunlight and high carrier mobility. Here, Donor-acceptor type copolymers, poly[[5,11-di(9'-Heptadecanyl)indolo[3,2-b]carbazole]-alt-{2,5-di(thiophen-2-yl)thiazolo[5,4-d]thiazole-5,5'-diyl}] (PIC-TZ) and poly[[6,6',12,12'-tetraoctylindenof[1,2-b]fluorene]-alt-{2,5-di(thiophen-2-yl)thiazolo[5,4-d]thiazole-5,5'-diyl}] (PIF-TZ), were synthesized by Suzuki polymerization and examined for applications in polymeric photovoltaic solar cells (PSCs). The number-average molecular weights (M_n) of the synthesized polymers were determined to be 11,000 g/mol (PDI = 2.27) for PIC-TZ, and 17,000 g/mol (PDI = 1.77) for PIF-TZ by gel permeation chromatography (GPC) using a polystyrene standard. PIC-TZ and PIF-TZ showed good solubility in common organic solvents. These polymers exhibited good thermal stability, showing < 5% weight loss up to 410 ~ 430 °C. The optical band gap of PIC-TZ and PIF-TZ thin film was measured to be 2.14 V~2.21 eV. SCLC mobility measurements showed hole mobility of ~10-3 cm²·V⁻¹·s⁻¹ for the copolymers. When the polymers were blended with PCBM, PIC-TZ exhibited the best performance with an open circuit voltage of 0.86 V, short-circuit current of 4.16 mA/cm², and power conversion efficiency of 1.64% under air mass (AM) 1.5 global (1.5 G) illumination conditions (100 mW/cm²).

8116-60, Poster Session

Significant enhancement in conversion efficiency of inverted organic solar cells based on ZnO thin films via aluminum incorporation

S. Tsai, W. Lien, J. He, National Taiwan Univ. (Taiwan)

The power conversion efficiency (η) of hybrid solar cells (HSCs) based on ZnO/P3HT:PCBM was improved by incorporating Al into ZnO acting as an electron transport layer. The Al-doped ZnO (AZO) thin film was deposited via an aqueous solution method. The η can be enhanced by up to 2.2 times due to Al incorporation into ZnO layers. It was found that the short-circuit current density and open-circuit voltage were affected by transmission, surface roughness, electrical conductivity, and band-gap of AZO thin films. This study provides new insights into the design optimization of the electron transport layer for HSCs.

8116-61, Poster Session

Combination of titanium oxide-conjugated polyelectrolyte for high-performance inverted-type organic optoelectronic devices

H. Choi, Ulsan National Institute of Science and Technology (Korea, Republic of); J. S. Park, KAIST (Korea, Republic of); E. Jeong, Pusan National Univ. (Korea, Republic of); G. Kim, B. Lee, Ulsan National Institute of Science and Technology (Korea, Republic of); S. O. Kim, KAIST (Korea, Republic of); M. H. Song, Ulsan National Institute of Science and Technology (Korea, Republic of); H. Y. Woo, Pusan National Univ. (Korea, Republic of); J. Y. Kim, Ulsan National Institute of Science and Technology (Korea, Republic of)

We demonstrate the remarkable improvement in device performances of inverted polymer solar cells (iPSCs) and polymer light-emitting diodes (iPLEDs) by employing a combination of titanium oxide (TiO_x) and conjugated polyelectrolyte (CPE) as an electron injection/transporting layer. For iPSCs, the CPE layer increased the power conversion efficiency from 2.65 % to 3.55 % by enhancements of the short circuit current and fill factor. For iPLEDs, the device with CPE layer exhibits increased luminance efficiency from 4.3 cd/A to 18.0 cd/A and maximum luminance from 1850 cd/m² to 25800 cd/m², and reduced turn-on voltage from 4.4 V to 3.8 V. These high efficiencies of inverted-type organic optoelectronic devices are attributed to spontaneously oriented interfacial dipoles within the CPE layer, which lower the energy barrier for electron injection/transport and reduce the interfacial contact resistance and inherent incompatibility between the hydrophilic TiO_x and hydrophobic active layers.

8116-62, Poster Session

Open-circuit voltage in zinc phthalocyanine-C60 organic photovoltaic cells

J. P. Mudrick, J. D. Myers, Univ. of Florida (United States); T. B. Fleetham, N. Bakkan, J. Li, Arizona State Univ. (United States); J. Xue, Univ. of Florida (United States)

Organic photovoltaic (OPV) device performance has steadily approached that of inorganic photovoltaics while offering advantages including low temperature processing, mechanical flexibility, and high throughput manufacturing capability. Despite this progress there are aspects of OPV device physics that are not well understood, the most important of which being the origin of the open circuit voltage (V_{oc}). We have studied V_{oc} in

vacuum-deposited zinc phthalocyanine (ZnPc)/C60 OPV devices using different sources of ZnPc: one source was obtained from a commercial vendor and the other was synthesized in house from a heated reaction between zinc chloride and excess phthalonitrile. While elemental analysis revealed no detectable differences in the bulk chemical composition of the two ZnPc materials, capacitance-voltage measurements showed a ~50% reduction in the concentration of electrically active defects in home-synthesized ZnPc. Planar bilayer OPV devices using home-synthesized ZnPc had 0.1-0.2V (20-50%) greater Voc compared to those with commercial ZnPc while also exhibiting significantly lower dark current. The type of ZnPc at the donor/acceptor heterojunction was varied to show that the ZnPc species present at the interface is responsible for the difference in Voc. Synchronous photocurrent measurement showed a slower reduction in photocurrent with the increase of forward bias for devices with home-synthesized ZnPc. We attribute the higher VOC in devices with home-synthesized ZnPc to the reduced recombination of charges at the ZnPc/C60 interface, which leads to lower dark current.

8116-63, Poster Session

Photoelectrochemical energy conversion based on conducting polymers

T. Yohannes, Addis Ababa Univ. (Ethiopia)

The utilization of organic materials for photovoltaic devices has been investigated intensely during the last decades. Earlier studies concentrated on molecules that had high optical absorption in the visible region of the electromagnetic spectrum. Discovery of conjugated polymers having semiconductor-like behavior has started to stir excitement because such materials are not only able to function in a similar manner to the inorganic semiconductors but also have important advantages such as: low cost, light weight, ease of fabrication and the possibility of large area coatings.

In this presentation an overview of the studies carried in our research laboratory on photoelectrochemical solar energy conversion devices will be given. The photoelectrochemical cells contain a thin film of semiconducting conducting polymers as a light-harvesting unit, a redox couple and a counter electrode.

8116-65, Poster Session

Charge-pair and free-charge carrier photogeneration and recombination in polymer/fullerene bulk heterojunction films

G. Sliuzys, Vilnius Univ. (Lithuania); V. Gulbinas, Institute of Physics (Lithuania); K. Arlauskas, Vilnius Univ. (Lithuania)

Photogeneration and recombination of charge pairs and free charge carriers in poly-3 (hexylthiophene) (P3HT) and [6,6]-Phenyl C61 butyric acid methyl ester (PCBM) bulk heterojunction has been studied at different PCBM concentrations by means of fluorescence spectroscopy, time-of-flight (ToF) and extraction of photogenerated charge carriers by a linearly increasing voltage (photo CELIV) techniques. Quenching of P3HT fluorescence by PCBM, has been used for the evaluation of the exciton dissociation efficiency. The quantum efficiency of free carrier generation has been evaluated from ToF current transients at different electric fields. The free charge carrier recombination properties have been estimated from photo-CELIV current transients at different delay times between laser and voltage pulses. Obtained results shows better carrier photogeneration quantum efficiency, and lower geminate recombination rate in samples with higher PCBM concentration.

8116-66, Poster Session

Transparent, conductive oxide-less cylinder type dye-sensitized solar cells (TCO-less cylinder DSC): solar cells with optical pathway

J. Usagawa, T. Kogo, K. Sadamasu, S. S. Pandey, Y. S. Ogomi, S. Hayase, Kyushu Institute of Technology (Japan)

A flexible transparent conductive oxide-less dye-sensitized solar cells (flexible TCO-less DSC) was fabricated by assembling plastic sheet without TCO layer, self-standing porous titania film (TiO sheet), gel electrolyte sheet, and Ti sheet with Pt. The efficiency increased to 6.1 %, one of the highest efficiencies for TCO-less flexible DSCs, by using a specially designed unsymmetrical TiO sheet. A TCO-less cylinder type DSC was fabricated by inserting a ring shaped-TiO sheet into glass tube, followed by ring shaped gel electrolyte sheet and Ti rod with Pt catalyst layer. The efficiency was 3.9 % (Jsc 8.85 mA/cm², Voc 0.67 V, FF 0.65). Since this process does not need a TCO layer inside the glass tube, the fabrication process is simplified. Charge collection grids are not required, because the protected mesh does work for the charge collection grids. In addition, encapsulation is expected to be done easily because the encapsulation area is small, namely, only a portion of the end of the glass tube. The current distribution of the cylinder toward a diameter direction was measured by a LBIC method. The current distribution was flat from one edge to another edge, suggesting that reflection on a round shaped rod does not affect the efficiency seriously. This was explained by the optical simulation results that light introduced in a portion close to the edge was refracted into an inside of the cylinder. In addition, it was found by using an optical simulation that the glass cylinder wall acts as a light wave guide.

8116-67, Poster Session

Mechanism of the improvements in efficiency using calcium cathodes in P3HT:PCBM-based organic solar cells

W. Tseng, National Taiwan Univ. (Taiwan); M. Chen, National Dong Hwa Univ. (Taiwan); J. Wang, C. Tseng, C. Wu, National Taiwan Univ. (Taiwan)

Bulk heterojunction solar cells based on poly(3-hexylthiophene) (P3HT) mixed with [6,6]-phenyl C61-butyric acid methyl ester (PCBM) have attracted much attention because of the power conversion efficiency can exceed 4%-5%. It has been reported that calcium (Ca) incorporated in the cathode structures with the P3HT:PCBM active layer improve the efficiency since it forms an ohmic-contact at the active layer/cathode interface. On the other hand, in practical device fabrications, the vapor deposition of energetic alkaline earth metals like Ca on polymer surfaces might induce chemical reactions, which will also significantly affect the performance of devices. Therefore, the mechanisms of improvements due to Ca in the cathode of the P3HT:PCBM based devices may not be just due to the formation of ohmic contacts and have not been fully explored in the previous literatures.

In this work, we propose the mechanisms of the efficiency improvement in P3HT:PCBM based organic solar cells using Ca as cathodes. The electronic properties and chemical interactions between P3HT:PCBM blended active layer and Ca cathode were studied via ultraviolet and x-ray photoemission spectroscopy (UPS and XPS). UPS results show that the HOMO level of P3HT is pulled down by 0.8 eV with respect to the Fermi level after a few angstrom of Ca deposition, which implies that the electron exchange occurs at this interface. However, no such phenomenon is found between PCBM and Ca. In addition, the XPS investigations also indicate that electrons transfer from Ca to the sulfur atom in P3HT, which results in the increase of energy difference between the HOMO of P3HT and the LUMO of PCBM, and subsequently improves the Voc in solar cell devices.

8116-68, Poster Session

Effect of light intensity on Schottky barrier widths and I-V characteristics of polymer heterojunction photovoltaic devices

A. B. Guvenc, C. S. Ozkan, M. Ozkan, Univ. of California, Riverside (United States)

The Schottky barriers that forms on the interface between aluminum and organic semiconductor of polymer heterojunction photovoltaic devices based on poly(3-hexylthiophene): [6,6]-phenyl- C61-butyrac acid methylester blend, has been investigated according to Mott-Schottky curves. We focused on the effect of light intensity on the Schottky barrier widths and I-V characteristics of the devices. In order to investigate the effect of light intensity, power of light was increased from 0 mW/mm² to 1.34 mW/mm². As the light power increases, the slopes of the I-V curves in the reverse saturation region increase. When the tangents to the saturation region of these curves are extrapolated, all the tangent lines intersect the voltage-axis at the same voltage value. This shows that, the increase in the slopes of the curves has a certain order. This behavior looks similar to Early effect in n-p-n bipolar junction transistors, i.e. increasing barrier width causes and increase in the slopes of the I-V curves. We used this similarity to build a mathematical model for the I-V characteristics of the devices under reverse bias which involves the effect of light intensity on the Schottky barrier widths. Comparison of the mathematical model and experimental data measured under different light intensities indicate both the dependency of Schottky barrier to the light intensity and the accuracy of the mathematical model. Additionally, increasing barrier width causes the photodetection performance of the devices to increase; however, the devices turn into ohmic devices after a light intensity threshold, because, the barriers merge and the devices break-down.

8116-69, Poster Session

Fullerene multiadducts for higher open-circuit voltages in bulk heterojunction solar cells

M. A. Faist, T. Kirchartz, J. M. Frost, Imperial College London (United Kingdom); W. Gong, Beijing Jiaotong Univ. (China); S. Foster, N. J. Ekins-Daukes, J. R. Durrant, D. D. C. Bradley, J. Nelson, Imperial College London (United Kingdom)

Organic Photovoltaics are a promising technology because of their solution processability and potential for low-cost production. In spite of these advantages, low power conversion efficiency remains a major issue. While high external quantum efficiencies have been achieved, much energy is lost when comparing the photon energy with the final extracted voltage in the cell. Reducing this energetic loss by increasing the open circuit voltage (Voc) is a major route to achieve higher power conversion efficiency.

Fullerene multiadducts with smaller electron affinity have been shown to raise the Voc [1,2], and in combination with P3HT they have been shown to increase device performance significantly. Combinations of fullerenes multiadducts with other donor polymers, however, do not show the expected performance. In this work, we use spectroscopic [3,4] and voltammetric [5] methods as well as device measurements to investigate how the use of fullerene multiadducts influences charge pair generation, charge transport and voltage generation in polymer:fullerene heterojunction devices. We study a series of fullerenes with different LUMO levels with P3HT and other donor polymers, with the aim to understand the factors that limit device performance.

[1] Y. He, H. Chen, J. Hou, and Y. Li, Journal of the American Chemical Society, vol. 132, no. 4, pp. 1377-1382, Feb. 2010.

[2] M. Lenes, G. A. H. Wetzelaer, F. B. Kooistra, S. C. Veenstra, J. C. Hummelen, and P. W. M. Blom, Advanced Materials, vol. 20, no. 11, pp. 2116-2119, 2008.

[3] K. Tvingstedt, K. Vandewal, A. Gadisa, F. Zhang, J. Manca, and O. Inganäs, Journal of the American Chemical Society, vol. 131, no. 33, pp.

11819-11824, 2009.

[4] J. Nelson, Physical Review B, vol. 67, no. 15, p. 155209, Apr. 2003.

[5] J. M. Frost, M. A. Faist, and J. Nelson, Advanced Materials, vol. 22, no. 43, pp. 4881-4884, 2010.

8116-70, Poster Session

Aqueous dye-sensitized hole injection into p-GaP from organic chromophores: an alternative design for highly efficient dye-sensitized solar cells

M. J. Price, S. Maldonado, Univ. of Michigan (United States)

This poster presentation will identify and quantitatively characterize aspects of light-stimulated hole injection from a photoexcited organic chromophore into a p-type phosphide semiconductor relevant to the development of efficient, aqueous solar energy conversion systems. Data will be presented for dye sensitization of single-crystalline p-type gallium phosphide (GaP) electrodes. Such dye-sensitized photocathodes are well suited to drive reduction reactions relevant to solar-to-chemical energy conversion, and their resistance to deleterious surface oxide formation and natural compatibility with common organic chromophores make their development as 'inverse' analogs of traditional dye-sensitized solar cells (DSSCs) attractive. Measured external quantum efficiencies were approximately doubled for polar p-GaP(111)B versus non-polar p-GaP(100) photocathodes, suggesting that hole injection occurs from dye molecules that are only loosely physisorbed to the electrode surface via coulombic attraction. Hole injection was only observed for sensitizers with highest occupied molecular orbital (HOMO) energies more positive than the p-GaP valence band edge in acidic to neutral pH aqueous solutions, suggesting surface trap-state mediated injection pathways were not operative. Further analysis will be presented illustrating the advantages for dye sensitization of nanostructured phosphide photoelectrodes that feature (a) a mid-sized bandgap that eases the requirements for the panchromaticity of sensitizing dyes, (b) strong internal electric fields that simultaneously support the large emf values compatible with water photoelectrolysis and high internal quantum efficiencies for hole injection and (c) strong optical absorption dictated by selective light scattering. Collectively, this work will explore the plausibility of developing dye sensitized phosphide photoelectrodes that parallel the success of conventional n-type DSSCs.

8116-71, Poster Session

Charge transport and recombination in small molecule non-fullerene electron acceptors for organic solar cells

K. B. Krueger, P. E. Schwenn, K. Gui, A. Pandey, The Univ. of Queensland (Australia); A. Pivrikas, Johannes Kepler Univ. Linz (Austria); P. L. Burn, P. Meredith, The Univ. of Queensland (Australia)

Fullerenes and their derivatives are the most successful electron accepting materials in organic Bulk Heterojunction (BHJ) Solar Cells today. In this presentation we report on our studies on a family of solution processable non-fullerene electron acceptors, based on the small molecule 2-[[7-(9,9-di-n-propyl-9H-fluoren-2-yl)benzo[c][1,2,5]thiadiazol-4-yl]methylene]malononitrile (K12). Devices comprising of blends of poly(3- n -hexylthiophene-2,5-diy) P3HT as donor and K12 as acceptor have been shown to reach efficiencies of up to 0.73% under AM1.5G simulated sunlight.

To understand K12 and its application in BHJ Solar Cells, Photo Induced Charge-Extraction-in-Linearly-Increasing-Voltage (PhotoCELIIV) and Transient Photo Voltage measurements (TPV) were employed to investigate the charge transport properties and recombination of free charge carriers. It was found that in neat films of K12 the molecular order

in as-cast films can be dramatically improved by annealing at moderate temperatures (60 °C) leading to a greatly enhanced electron mobility to be as high as $10^{-4} \text{ cm}^2 \text{ V}^{-1} \text{ s}^{-1}$, comparable with some of the best non-fullerene acceptor materials reported to date. In the blend, similar high average carrier mobilities could be found but the overall carrier extraction was limited by carrier recombination. Furthermore, we found that the free carrier lifetime in the devices is strongly dependent on the carrier concentration. In our paper we will present our results and compare the findings with those obtained on state-of-the-art solar cell systems based on low-bandgap polymers.

8116-73, Poster Session

Impact of temperature and thickness of an active layer on charge transport of bulk-heterojunction cells

A. M. Syed, Hanyang Univ. (Korea, Republic of); C. W. Chul, Sungkyunkwan Univ. (Korea, Republic of); H. Um, S. Jee, M. Park, Y. Nam, K. Park, Hanyang Univ. (Korea, Republic of); J. Jung, Hanyang Univ. (Korea, Democratic Peoples Republic of); Z. Guo, Hanyang Univ. (Korea, Republic of); S. Kim, H. K. Cho, Sungkyunkwan Univ. (Korea, Republic of); J. Lee, Hanyang Univ. (Korea, Republic of)

Despite numerous advantages of poly[N-9'-heptadecanyl-2,7-carbazole-alt-5,5-(4',7'-di-2-thienyl-2',1',3'-benzothiadiazole)] (PCDTBT) in bulk heterojunction (BHJ) composited with a fullerene derivative [6,6]-phenyl C70-butyric acid methyl ester (PC70BM), the charge transport mechanism required for device optimization is still not clear. To address this challenge, systematic studies on carrier transport in pristine thin films of PCDTBT, PC70BM and PCDTBT:PC70BM sandwiched between indium-tin-oxide (ITO) and silver electrode were carried out using various PCDTBT:PC70BM blend ratios (from 1:1 to 1:5) as functions of temperature and a film thickness. Compared to a pristine PCDTBT, significant enhancement in mobility was observed for all room-temperature blended devices owing to intercalation of PC70BM molecules between the side chains of PCDTBT polymer for efficient carrier transport from donor to acceptor molecules. Since the excessive amount of PC70BM degrades the crystallinity of PCDTBT with mobility, an optimal blend ratio of PCDTBT:PC70BM was estimated to be 1:3 through the tradeoff relation in mobility of BHJ cells. While interpreting the temperature and electric field dependent experimental results of PCDTBT:PC70BM (1:3) correlated with the Gaussian disorder and correlated disorder models, the influence of active layer thickness on a charge carrier mobility is also investigated and discussed in term of energetic and spatial disorder in bulk heterojunction cells. Negative field dependence mobility was observed at low electric field for small thickness BHJ cells and vanished gradually when the cell sizes is increased. Such occurrence of negative field dependent mobility is attributed by the small energetic, but large spatial disorder.

8116-74, Poster Session

Synthesis and photovoltaic properties of quinoxaline-based alternating copolymers for high-efficiency bulk-heterojunction polymer solar cells

S. K. Lee, W. S. Shin, J. Lee, S. Moon, Korea Research Institute of Chemical Technology (Korea, Republic of)

Polymer solar cells (PSCs) have attracted considerable attention over previous decades because of their unique advantages, which include low cost, lightweight, solution processability, and flexibility. Despite considerable progress in this field, power conversion efficiencies (PCE) of PSCs must be further improved for commercialization. So far, poly(3-hexylthiophene) (P3HT) is typically used in construction of PSCs.

However, a bottleneck in conversion efficiency seems to be reached by using P3HT because it harvests a small absorption portion with respect to the solar spectrum. Recently, several classes of low-bandgap polymers by using internal charge transfer (ICT) from an electron-rich unit to an electron deficient moiety within the fundamental repeat unit have been developed to better harvest the terrestrial solar spectrum. Among them, relatively high-performance polymer solar cells made from a mixture of poly(2,7-carbazole) derivatives, PCDTBT, and [6,6]-phenyl C71 butyric acid methyl ester (PC70BM) have been reported, with maximum power conversion efficiency of 6.1%. In this poster, we report a series of quinoxaline-based copolymers. We systematically investigated the synthesis, thermal stability, as well as the optical and electrochemical properties of these polymers. Bulk heterojunction solar cells made from the result polymer produced a power conversion efficiency of 4.0% under AM 1.5 conditions. Detailed synthetic scheme, optical, electrochemical, and photovoltaic properties of the copolymers will be presented.

8116-75, Poster Session

Bulk-heterojunction solar cells utilizing solution-processable phthalocyanine derivative

T. Hori, Osaka Univ. (Japan); Y. Miyake, National Institute of Advanced Industrial Science and Technology (Japan) and Osaka Univ. (Japan); N. Fukuoka, T. Masuda, T. Hayashi, H. Yoshida, A. Fujii, Osaka Univ. (Japan); Y. Shimizu, National Institute of Advanced Industrial Science and Technology (Japan); M. Ozaki, Osaka Univ. (Japan)

Organic semiconductors are classified into two types, pi-conjugated polymers and low-weighted molecules. Organic thin-film solar cells based on a bulk heterojunction active layer utilizing pi-conjugated polymers fabricated by a wet process achieved high energy conversion efficiency. On the other hand, some low-weighted molecular semiconductors demonstrate a high crystallinity and charge mobility by strong intermolecular interactions, however, they are inappropriate for wet processes because of their poor solubility in typical organic solvents. Recently, we have demonstrated ambipolar high carrier drift mobility of $1.4 \text{ cm}^2/\text{Vs}$ of a soluble and mesogenic phthalocyanine derivative, 1,4,8,11,15,18,22, 25-octahexylphthalocyanine (C6PcH2) which was evaluated by means of time-of-flight measurement.

In this study, we demonstrate the photovoltaic properties of simple bulk heterojunction solar cells based on the blend film of phthalocyanine derivative C6PcH2 and a fullerene derivative (PCBM) as the active layer, which was fabricated by spin-coating.

As a results, two broad peaks exist in the external quantum efficiency (EQE) spectrum, which correspond to the absorbance spectrum. One of the peaks, which originates from the Q-band absorption of C6PcH2, exhibited an EQE higher than 70%. The energy conversion efficiency of the solar cell with the C6PcH2:PCBM composite layer at a weight ratio of 2:1 reached 3.1% with Voc of 0.84 V, Isc of 8.4 mA/cm², and FF of 0.44 under AM1.5G (100 mW/cm²) solar-illuminated condition. It is considered that C6PcH2 is a promising donor material for organic thin-film solar cells fabricated by a solution process.

8116-77, Poster Session

Functionalized cyclopentadithiophene-based low-bandgap copolymers for photovoltaic applications

S. Van Mierloo, Univ. Hasselt (Belgium); W. Maes, Univ. Hasselt (Belgium) and Katholieke Univ. Leuven (Belgium); L. J. Lutsen, D. J. Vanderzande, Univ. Hasselt (Belgium)

Third generation low bandgap copolymers such as poly[2,6-(4,4-bis-(2-ethylhexyl)-4H-cyclopenta[2,1-b;3,4-b']dithiophene)-alt-4,7-

(2,1,3-benzothiadiazole)] (PCPDTBT), which exceed 5% efficiency when blended with PC70BM in organic bulk heterojunction solar cells, have gained substantial interest in recent years. In this contribution we present the synthesis of novel low bandgap copolymers based on functionalized 4H-cyclopenta(2,1-b:3,4-b')dithiophenes (CPDT) alternating with 2,5-bis(3-alkylthiophene-2-yl)thiazolo[5,4-d]thiazoles (TzTz), and solar cell performances of films of these polymers blended with fullerene acceptors. Elaborated synthetic studies have resulted in the development of a convenient and efficient three-step route toward both symmetrically and asymmetrically functionalized CPDTs. Using this method a broad collection of functionalized bridged bithiophenes can smoothly be accessed. Starting from 3-bromo-2,2'-bithiophene, lithiation and subsequent reaction with dialkyl ketones afforded (a) symmetrically dialkylated tertiary alcohol derivatives. By means of a Friedel-Crafts dehydration cyclization in sulfuric acid medium, these derivatives were converted to 4,4'-dialkyl-4H-cyclopenta(2,1-b:3,4-b')dithiophenes. The developed three-step procedure also allows introduction of functional groups on the alkyl substituents starting from a versatile ester-functionalized CPDT scaffold. The ester function could further be converted into carboxylic acid and amide moieties. The variety of CPDT building blocks could be coupled to alkylated TzTz monomers via Suzuki polymerization generating a new series of low bandgap polymers. Incorporation of specific functional groups on the monomers offers the opportunity to control the morphology of the conjugated polymer:fullerene blend (toward optimization of the efficiency of the devices) and to explore its (thermal) stability in organic solar cells. Hence, this study represents a rational approach toward morphology control via modification of the chemical structure rather than via processing.

8116-78, Poster Session

Controlling of initial molecular arrangement of copper(II) phthalocyanine for interpenetrating networks in a mixed donor/acceptor layer

H. J. Kim, J. W. Kim, T. Kim, J. Jang, Seoul National Univ. (Korea, Republic of); H. H. Lee, Pohang Univ. of Science and Technology (Korea, Republic of)

We observed that thermally evaporated Copper(II) Phthalocyanine (CuPc) ultra thin layer (5 nm) was consisted in disc type CuPc nano grains on a hydrophilic Si surface, which was analytically confirmed by structure factors in GISAXS measurement. The disc type grains were consisted in crystalline part and non-crystalline part. On the other hand, the disc type grains disappeared in case of the evaporation on a octadecyltrichlorosilane (ODTS) treated hydrophobic Si surface, which showed lower crystallinity with random distribution. Interestingly, the mobility was lower in a FET device fabricated on a hydrophilic surface than on a ODTS Si surface due to the low average density of molecules relating porous molecular packing between nano grains on a hydrophilic surface. Despite of the low FET mobility, the disc type CuPc has a potential to be applied to fabricate bulk heterojunction (BHJ) donor/acceptor (D/A) mixed layer with C60 for organic photovoltaic devices, and the device showed improved current voltage characteristics. The initial molecular arrangement of CuPc was also affected by the adoption of thin CuI layer before evaporating CuPc. The nano structure of a mixed D/A layer on CuI was characterized in detail with AFM, GIWAXD, and GISAXS measurements. The device performance supported improved nano structure of a mixed D/A layer on CuI.

8116-79, Poster Session

Charge photogeneration in organic donor/acceptor blends

S. Shoaee, Imperial College London (United Kingdom)

Organic solar cells formed from conjugated polymers based on dialkylpyrrolopyrrolid, thiazolothiazole and dithienosilole moieties blended with small molecules are gaining interest for low cost, high

efficient (> 5%) solar energy conversion. The function of such devices is based on photoinduced charge separation (CS) at the donor /acceptor (D/A) interface. There is increasing evidence that the efficiency of this CS process can be determined by the presence of coulombically bound charge transfer (CT) states at the D/A interface.¹⁻³ In this work we focus upon the role of interfacial energetics in influencing the separation of these CT states into dissociated charge carriers. In particular, we undertake transient optical studies of D/A blend films. Transient absorption spectroscopy has proven useful in this regard and can monitor the formation and decay dynamics of the charged species present in the blends. In this work, this technique has been applied to a range of D-A and polythiophene-based materials in blends with series of perylene diimide derivatives and PCBM.³ The efficiency of charge photogeneration in organic D/A blend films has been reported to depend on a range of factors, including film nanomorphology, and the energy difference driving charge separation (GCS).^{2,3,4} The photoluminescence quenching has been used in conjunction with the transient dynamics data to create a model of charge generation and dissociation. For these film series, we observe a close correlation in the yields of charge separation with the GCS.

In this work we aim to address:

- 1) Charge generation
- 2) Carrier mobility
- 3) Free energy for charge separation

References

1. H. Ohkita; S. Cook; Y. Astuti; W. Duffy; S. Tierney; W. Zhang; M. Heeney; I. McCulloch; J. Nelson; D. D. C. Bradley; J. R. Durrant, JACS 2008, 130, 3030.
2. T. M. Clarke; J. R. Durrant, Chem Comm 2010, 110, 6736.
3. S. Shoaee, T. M. Clarke, C. Huang, S. Barlow, S. R. Marder, M. Heeney, I. McCulloch, J. R. Durrant, JACS 2010, 132, 12919.
4. S. Shoaee; Z. An; X. Zhang; S. Barlow; S. R. Marder; W. Duffy; M. Heeney; I. McCulloch; J. R. Durrant, Chemical Communications 2009, (36), 5445.

8116-80, Poster Session

CuInS₂-polymer nanocomposite solar cells

A. Pein, E. Strunz, W. Haas, F. Hofer, T. Rath, G. Trimmel, Technische Univ. Graz (Austria)

Inorganic-organic nanocomposite solar cells (NCSCs) have attracted considerable interest in recent years due to several advantages compared to organic solar cells. One of the main advantages is that the optical and electronic properties of the acceptor phase can be tuned by the size and shape of the nanoparticles. Moreover, also the acceptor phase contributes to the absorption of light and therefore higher current densities are expected. This contribution deals with the synthesis of CuInS₂ and its use in solar cells. The high absorption coefficient and the ideal bandgap of 1.5 eV provide promising properties in combination with polymers of suitable energy levels. Using the oleylamine route particles of different size and shapes were prepared by variation of the temperature profile, the heating mechanism and the used reagents. The size and crystal structure of the obtained nanoparticles was characterized by x-ray diffraction, dynamic light scattering and transmission electron microscopy. The optical properties were investigated by absorption and emission spectra. One crucial point in nanoparticle synthesis is the surface of the particles that have to be stabilized with long-chained organic molecules that prevent the agglomeration. However, while necessary during the synthesis and for the solubility that ensures mixing with polymers in common organic solvents, the performance of prepared solar cells is negatively influenced by this isolating, organic capping sphere. Therefore different strategies to minimize this effect will be discussed including acid treatment and capper exchange. The influence of the performance of solar cells will be argued in terms of current density-voltage plots and incident photon to current efficiency spectra.

8116-82, Poster Session

Low-bandgap thiophene-based heterophenoquinones for organic photosensitive films

E. V. Canesi, L. Colella, Istituto Italiano di Tecnologia (Italy); C. Bertarelli, Politecnico di Milano (Italy) and Istituto Italiano di Tecnologia (Italy); G. Lerario, P. E. Keivanidis, Istituto Italiano di Tecnologia (Italy)

Thiophene-based quinoidal molecules (QBTs) have found a renewed interest in the recent literature; their amphoteric redox character makes them suitable materials for ambipolar [1] and n-channel [2] organic transistor applications, while their intense absorption band in the red and near-infrared spectral region suggests the use in photodetecting and photovoltaic (PV) devices. Particularly for the case of a blend film of a QBT species, 5,5'-bis(3,5-di-tert-butyl-4-oxo-2,5-cyclohexadiene-1-ylidene)-5,5'-dihydro-2,2'-bithiophene, with poly[2-methoxy-5-(2'-ethyl-hexyloxy)-1,4-phenylene vinylene] (MEH-PPV), it was recently shown that photocurrent generation can be driven by a photo-induced hole transfer from QBT to MEH-PPV, which is enabled by the absorption of 700 nm photons.[3]

In this work we present a series of newly synthesized symmetric and asymmetric QBT derivatives, bearing side-chains of different length and diverse electron-active groups.

We focus our attention on the effect of structural variation on the tendency of the QBT species to aggregate when deposited as thin films. Our study employs time-integrated UV-Vis absorption and photoluminescence spectroscopy experiments combined with optical and atomic force microscopy imaging techniques. We investigate pure QBT thin films and blend films of QBT composites prepared by mixing QBTs either with poly(3-hexylthiophene) (P3HT) or with poly(styrene) host matrices.

Finally, the electrical characterization of photodiodes based on P3HT:QBT active layers will be presented.

[1] Ribierre, J. C. et al., *Adv. Mater.* 22, 4044-4048 (2010)

[2] Suzuki, Y. et al., *Chem. Mater.* DOI : 10.1021/cm102109p

[3] Agostinelli, T. et al., *J. Appl. Phys.* 104, 114508 (2008)

8116-83, Poster Session

Al₂O₃:ZnO nanolaminates as electron-collecting electrode in inverted polymer solar cells

H. Cheun, H. Li, Y. Zhou, Y. Fang, Y. Cai, J. W. Shim, C. Fuentes-Hernandez, K. H. Sandhage, J. Brédas, B. Kippelen, Georgia Institute of Technology (United States)

Recently, polymer solar cells with a transparent electron collecting electrode have been fabricated to improve stability in air. In such a structure, called an inverted structure, ITO is commonly used as transparent electrode. To serve as electron-collecting electrode, ITO must be modified in order to reduce its work function. An alternative is to replace ITO with another transparent conductive oxide that has a lower work function.

Here, we propose (Al₂O₃)_x:(ZnO)_y nanolaminates fabricated by atomic layer deposition (ALD) as electron-collecting electrodes in organic solar cells. In this work, we studied the structural, electrical, and optical properties of these nanolaminates as a function of the relative values of x and y. 300-nm-thick (Al₂O₃)₁:(ZnO)₂₀ nano-laminates on a glass substrate showed a high optical transmittance (> 80%) in the visible region with a high conductivity of 2500 S/cm and a low work function (4.2 eV). A 60 times increase of the electrical conductivity of these (Al₂O₃)₁:(ZnO)₂₀ nanolaminates compared with neat ZnO films fabricated by ALD is attributed to a combination of morphological changes, doping, and quantum confinement effects. We tested these

electrodes in P3HT:PCBM polymer-based inverted solar cells and obtained power conversion efficiency values of 3 % under simulated AM 1.5G, 100 mW/cm² illumination.

8116-84, Poster Session

Technological challenges and future prospects for improvement in the performance of organic solar cells

S. Baghel, R. Jha, Netaji Subhash Institute of Technology (India)

The field of organic solar cells is rapidly accelerating due to the need of new clean and cheap energy sources. A large fraction of the cost of Si based solar cells is attributed to sophisticated and energy intensive processing technologies. The organic solar cells offer a cost effective alternate and are promising as they can be manufactured on plastic substrates by various types of printing techniques. This technology offers several advantages over silicon solar cells or other inorganic counterparts: the polymers are soluble in common organic solvents allowing the deposition of ultra-thin semiconductor films.

This paper presents, an overview of basic operational principles and recent development of polymer solar cells paying particular attention to possible routes for improving stability, absorption, open circuit voltage, power conversion efficiency and development of new device design and materials that includes development of ITO free flexible solar cells, use of metal gratings as transparent electrodes. Future prospects and possible solutions to problems related to practical application of organic solar cell technology have been addressed.

This study on material requirements and current technical challenges in making more efficient solar cells will serve as a guide to new researchers in this field who plan to develop better materials and optimize devices for better conversion efficiency. This study on material requirements and current technical challenges in making more efficient solar cells will serve as a guide to new researchers in this field who plan to develop better materials and optimize devices for better conversion efficiency.

8116-85, Poster Session

Inverted organic solar cells using a water-soluble polymer-modified indium tin oxide as an electron-collecting electrode

Y. Zhou, J. W. Shim, H. Cheun, A. Dindar, C. Fuentes-Hernandez, Georgia Institute of Technology (United States); J. Meyer, A. Kahn, Princeton Univ. (United States); B. Kippelen, Georgia Institute of Technology (United States)

Organic solar cells are emerging as a potentially low-cost, flexible, and portable renewable energy source. Organic solar cells with an inverted structure typically have better air stability than non-inverted geometries because they do not use low-work function metals that are sensitive to air. Inverted solar cells can be fabricated by reducing the work function of indium tin oxide (ITO) in order to turn it into an electron-collecting electrode. Metal oxides such as ZnO, TiO_x, Al₂O₃, or Cs₂CO₃, are commonly used as interlayers to modify the work function of ITO. However, they typically require either vacuum deposition techniques or high processing temperatures when processed from solution. Water-soluble polymeric modifiers are highly desirable because they could be mass-produced at a low-cost onto large areas.

Here, we report on the properties of inverted organic solar cells with an ITO electrode modified with polyvinylpyrrolidone (PVP) prepared by spin-coating from a water solution. This modification reduced the work function of ITO from 4.6 eV to 4.2 eV, and allowed ITO to act as an electron collecting electrode. Changes in work function were measured independently by a Kelvin probe and by UV photoemission spectroscopy. Inverted solar cells based on Poly(3-hexylthiophene) (P3HT):[6,6]-phenyl C₆₁ butyric acid methyl ester (PC60BM) yielded a power conversion efficiency of 3.2% under 100 mW/cm² air mass 1.5G illumination, after

exposing them for 20 minutes to an ultraviolet (UV) lamp. The current density-voltage characteristics of the newly-fabricated devices showed an S-shape kink which was efficiently removed after UV treatment. The origin of this kink and its reversible control will be discussed.

8116-86, Poster Session

Performance prediction of dye-sensitized solar cells using innovative nanomaterials

R. Jha, S. Baghel, Netaji Subhash Institute of Technology (India)

Dye sensitized solar cells have attracted the attention of researchers as a cost effective alternative to the conventional solar cells. Till now solid state junction based photovoltaic devices dominated this field. The basic difference between dye sensitized solar cells and their conventional counterparts lie in the fact that, the process of both light absorption and charge transportation are carried out separately. Sensitizer molecules which are adsorbed on the semiconductor material absorb light and initiates the charge separation process. To enhance the photovoltaic performance of dye solar cells many new techniques and materials have been used, which includes electrode modifications using single walled carbon nanotubes that leads to low cost and minimal material use, fabrication of dye sensitized solar cells using graphene based carbon nanocomposite as counter electrode. Dye sensitized solar cells with liquid electrolyte have attained efficiency over 10%, but the possibility of evaporation of electrolyte and its leakage from the cell, pose as a threat to the stability of these cells. This led to the use of nanoparticle based gel electrolyte, replacement of electrolyte with solid p type semiconductor and development of solid state heterojunction dye solar cells.

To increase the photovoltaic efficiency, many alternatives have been explored including the use of metal oxide nanoparticles based light scattering structures, application of photonic crystals to enhance light path length, also development of sensitizing dyes using quantum dots to extend absorption range. The recent developments and current efforts that are being made in this field including the development of new hybrid tandem designs, application of nano-wires and analysis of the future prospects of the technology have been presented in this paper.

8116-87, Poster Session

A new approach for dye studies of dye-sensitised solar cells

L. L. Tobin, D. Zerulla, J. T. Sheridan, Univ. College Dublin (Ireland) and SFI-Strategic Research Cluster in Solar Energy Conversion (Ireland)

Dye-sensitised solar cells (DSSCs) are 3rd generation solar cells. DSSCs are biomimetic solar cells, they mimic the process of photosynthesis i.e. incoming light is absorbed by an organic dye and electrons are produced thereby producing both positive and negative charge carriers. The appeal of these cells is due to their low cost, flexibility and the ability to work in diffuse light. At present their efficiencies are far lower than that of the more common 1st generation single junction silicon solar cells. In order to improve DSSCs efficiencies, suitable dyes must be used. We present a new approach to dye studies for DSSCs involving dyes in-situ in polymer (organic) layers.

8116-88, Poster Session

Organic n-type interfacial layer for organic photovoltaic devices having inverted architecture

A. W. Hains, H. Chen, T. H. Reilly III, B. A. Gregg, National Renewable Energy Lab. (United States)

A crosslinking perylene derivative is synthesized, characterized, and employed as an n-type interfacial layer (IFL) situated between the tin-doped indium oxide (ITO) and the active layer in organic photovoltaic (OPV) devices having inverted geometry. The initial 1,6,7,12-tetrachloroperylene-3,4,9,10-tetracarboxylic acid (Cl4PTCDA) is synthetically fitted with two trimethoxysilylpropyl linkages to form Cl4PSi2. These silanated "tethers" function both to chemisorb the molecule to the hydroxylated ITO surface and to crosslink the film, rendering it insoluble and thereby enabling successive spin-coating steps in the device fabrication process without worry of problematic IFL dissolution. Smooth, thin films of Cl4PSi2 are deposited by substrate immersion into a dilute solution, followed by annealing in air to complete the crosslinking process. The thickness and surface morphology of these films are characterized by profilometry and atomic force microscopy, and the optoelectronic properties of the film are examined with cyclic voltammetry (CV) and UV-visible spectroscopy to determine the LUMO energy and the optical band gap. The LUMO energy of 4.0 eV properly aligns the IFL with LUMO energies of many common electron-accepting species in the OPV active layer such that electron transfer to the IFL should be energetically unhindered. Finally, OPV devices are fabricated having an n-type IFL consisting of either Cl4PSi2 or Cl4PSi2 blended with an n-type polymer, poly(9,9-dioctylfluorene-co-benzothiadiazole) (F8BT), to enhance film-forming properties, and device power conversion efficiencies of around 2% are observed. The effect on film and device properties of the addition of charges to Cl4PSi2 is also explored by adding N-trimethoxysilylpropyl-N,N,N-trimethylammonium chloride (APMS+) in various amounts.

8116-89, Poster Session

Electronic properties of polymer electrode materials for polymer photovoltaics

A. J. Moule, Univ. of California, Davis (United States); D. Huang, Univ. of Adelaide (Australia); S. Mauger, Univ. of California, Davis (United States); S. Friedrich, Lawrence Livermore National Lab. (United States); C. Rochester, Univ. of California, Davis (United States)

Polyethylenedioxythiophene Polystyrenesulphonate (PEDOT:PSS) is a highly conducting transparent polymer mixture that is used as a hole carrying electrode for nearly all organic optoelectronic devices, including OLED's and solar cells. Its ability to conduct exclusively holes is essential for high filling factors for OPV devices. We show that the hole selectivity of PEDOT:PSS comes partially from heat induced mixing with donor polymers and oxidization of the donor polymers at the PEDOT:PSS / BHJ layer interface. This mechanism is proven using x-ray absorption spectroscopy, neutron scattering, UV/vis absorption, and detection of H₂, a side product of the reaction, using GCMS. The electronic significance of a mixed polymer/PEDOT:PSS layer is shown by observing the change in the IV characteristics that comes about through the growth of a mixed layer with the polymers P3HT, OC1C10-PPV, APFO-3, and F8BT followed by deposition of a BHJ layer. We show that the dopant HPSS is only strong enough to oxidize donor polymers with work function values below -5.1 eV so that the nature of the mixed layer depends strongly on the mixed polymers.

The research is broadened by examination of the transparent electrode materials PTMESS and doping using both small molecule and polymeric dopants. We show that the interface layer formed is not unique to PEDOT:PSS and that the apparent work function of the electrode layer is not a strong indicator of the ability of the layer to preferentially conduct holes. Instead formation of doped surface layers and morphology of the transparent organic conductor is for more important.

8116-92, Poster Session

Novel concepts for light management in organic photovoltaics

E. J. Klem, RTI International (United States); M. Dickey, North

Carolina State Univ. (United States); J. Lewis, RTI International (United States); J. Maria, North Carolina State Univ. (United States)

We have explored novel concepts for light management suited for thin film photovoltaics by engineering surface topography in an effort to enhance the overall efficiency light absorption. The concepts utilized surface instabilities that produced hierarchically corrugated surfaces on the nanometer scale without lithographic patterning. These processes are applicable to many thin-film photovoltaic technologies and are particularly well-suited for mechanically flexible, low-cost systems. We developed techniques for generating corrugated surfaces on substrates suitable for photovoltaic device processing and then applied these substrates to the fabrication of thin film small molecule organic photovoltaic (OPV) devices as well as to quantum dot photovoltaics (QDPVs). These are appealing technologies for their low-cost and compatibility with flexible substrates and have a common feature; relatively short charge transport lengths requiring devices with thin active regions for efficient charge separation. Small molecule OPV devices fabricated using these high surface topography substrates have demonstrated a 30% increase in the short circuit current densities and a 20% increase in the power conversion efficiency as compared to their planar

8116-93, Poster Session

Flexible polymer solar cells with oxide/metal/oxide trilayer as transparent anode

W. Cao, Y. Zheng, E. Wrzesniewski, W. Hammond, J. Xue, Univ. of Florida (United States)

Organic solar cells (OSCs) have attracted much attention as a renewable energy conversion system, owing to the low-cost and easy-processing nature of organic materials. Transparent electrode is an essential component in OSCs and the material of choice so far has been indium tin oxide (ITO). However, the rising cost of indium, brittleness and the high temperature process make it not compatible for low-cost and large-area applications.

Here we use a semi-transparent oxide/metal/oxide (OMO) trilayer structure to replace ITO in OSCs. This trilayer structure has a similar conductivity and transparency to ITO and can be deposited through vacuum thermal evaporation to avoid the damage to the active layers. The ITO-free devices were fabricated by successively spin-coating ZnO nanoparticles and poly(3-hexylthiophene) (P3HT) and [6,6]-phenyl-C61-butyrac acid methyl ester (PCBM) blend onto glass with Al electrodes, finished by thermally evaporating MoO₃/Au/MoO₃ trilayer as the anode. Such ITO-free device on glass shows a power conversion efficiency (PCE) of ~2.5% under simulated 1 sun AM1.5 solar illumination. We also fabricated ITO-free devices on flexible PET substrates, which show almost the same performance (~2.4% PCE) as that on rigid glass substrates. Due to the high flexibility of the trilayer electrode, the efficiency of the flexible device is only reduced by ~6% from its original performance after 500 cycles of bending test with a bending radius of 0.5 inch. The performance of these ITO-free devices suggests that this oxide/metal/oxide trilayer electrode is a promising candidate to replace ITO in OSCs.

8116-94, Poster Session

Effect of processing additives on the structural and electrical properties of bulk heterojunction films for organic photovoltaics

N. Shin, X. Zhang, R. J. Kline, L. J. Richter, D. M. DeLongchamp, National Institute of Standards and Technology (United States)

Bulk heterojunction (BHJ) organic photovoltaic (OPV) cells based on polymer : fullerene blends have offered a promising solution for future energy need. Recently, it has been shown that the power conversion

efficiency of BHJ OPV devices can be increased by the addition of small amounts of processing additives with high boiling points, which are believed to affect the morphology of the BHJ active layer. In this work, we apply detailed microstructure measurements to BHJ films based on a poly(3-hexylthiophene) (P3HT):[6,6]-phenyl-C61-butyrac acid methyl ester (PCBM) blend and prepared with various processing additives (1,8 diiodooctane and 1,8 octanedithiol, and 1 chloronaphthalene) and different processing methods. Aspects of thin film microstructure such as degree of ordering, molecular orientation, and nanoscale morphology were systematically characterized by techniques including grazing incidence X-ray diffraction, near edge X-ray absorption fine structure spectroscopy, variable angle spectroscopic ellipsometry, and transmission electron microscopy. The results were correlated with device performance, illuminating the mechanism by which these additives improve the power conversion efficiency of BHJ OPV devices.

8116-95, Poster Session

The impact of squaraine functionalization on the efficiencies of NIR-active bulk-heterojunction photovoltaics

C. J. Collison, J. Cody, S. D. Spencer, A. Ioannidis, A. Monfette, H. Hu, B. Zhu, Rochester Institute of Technology (United States)

Organic photovoltaic (OPV) solar cells are inexpensive since their manufacture relies only upon spin-coating or spray coating technology. Yet organic solar cells suffer from lower efficiencies when compared to their more expensive silicon-based counterparts. Low efficiencies ultimately mean excessive investment costs, which prevent their widespread use.

We describe a series of squaraine dyes that will be targeted specifically for optimal application in more efficient NIR tandem cells, so as to broaden the range of spectral harvesting from the sun. Squaraines form a family that is among the very few successful solution processable molecular chromophores. Our current goal is to describe how 2,4-Bis-(4-diisobutylamino-2,6-dihydroxy-phenyl)-cyclobutane-1,3-dione can be substituted in order to achieve high power conversion efficiencies for our devices. We will systematically vary the functional groups on synthesized squaraines and we will measure the impact on isolated variables, in particular the aggregation/morphology, the exciton diffusion length and the mobilities of photogenerated charges in bulk heterojunction devices with PC[60]BM as the electron acceptor. We will present corresponding increases in power conversion efficiencies given a baseline efficiency of 0.5% for a single active-layer device as measured in our laboratory. The results of this work will allow us to prescribe improved device efficiency through chemical tuning and design.

8116-97, Poster Session

Enhanced efficiency of polymer and organic small-molecule-based solar cells by improved charge extraction

T. Xiao, W. Cui, J. Shinar, R. Shinar, Iowa State Univ. (United States)

Power conversion efficiency (PCE) of organic solar cells based on commercial materials remains low. We present approaches that improve the PCE by up to 27%. These include spin-coating ethylene glycol (EG) on PEDOT:PSS layer in devices of the structure ITO/PEDOT:PSS/EG/P3HT:PCBM/Ca/Al, and depositing a thin, plasma etched LiF layer in cells of the structure ITO/LiF/CuPc/C70/BPhen/Al. Via comprehensive measurements, including surface morphology and chemistry, in P3HT:PCBM cells we observed improved absorption with higher short-circuit current and fill factor, including a more favorable vertical phase segregation in the active layer, leading to improved charge extraction. Improved PCE in the small-molecule-based cells is possibly associated with a LiF-induced modified interface and consequently improved energy level alignment.

8116-98, Poster Session

Cathode modifications in organic photovoltaic cells

J. Chen, South China Univ. of Technology (China)

Recently, the special solubility of conjugated polymers in alcohol or water has drawn tremendous attention for the realization of optoelectronic devices consisting multilayer polymers as well as for the enhanced device performances in polymeric LEDs and FETs. Here, alcohol-soluble conjugated polymers (ASCPs) as cathode buffer layer in organic photovoltaic cells (PVCs) were evaluated. The ASCP/AI bilayer cathode showed obvious contributions to elevate the photovoltaic performances in comparison to the sole AI cathode. Not only the loss of open-circuit voltages could be recovered, but also short-circuit current and fill factor could be improved. The N-N interactions between a polymer donor and a ASCP may modify interfacial contact, resulting in enhancement of electron extraction and decreasing hole-electron recombination in the active layer. Consequently, significant increasing of power conversion efficiency (PCE) from a level of ~3% to ~6% could be realized for certain polymer donors, suggesting that the bilayer cathode would have great potential to elevate PCE of PVCs.

8116-99, Poster Session

Multilayer transparent cathode of organic-inorganic hybrid materials for solar cells

G. H. Jung, K. Hong, W. J. Dong, J. Lee, Pohang Univ. of Science and Technology (Korea, Republic of)

Thin-film solar cells based on organic and inorganic have various advantages of high efficiency, low-cost, and flexible solar cells. However, such cells using a glass substrate have the inherent disadvantages of high cost, low flexibility, and careful handle. Replacing the glass substrate with flexible opaque materials such as steel sheets or plastic films makes possible the fabrication of flexible, thin, and low-cost solar cell through roll-to-roll mass production. For the thin-film solar cells with these substrates, the direction of incoming light has to be from top to the bottom. Thus, formation of a high transparency top cathode which has high efficiency of electron collection is one of the most significant factors for high efficiency thin-film solar cells.

We investigated the optical properties of dielectric/metal/dielectric (DMD) structured bathocuproine (BCP)/silver (Ag)/MoO₃ transparent cathode. Different optical effects between BCP, Ag layer, and outer MoO₃ layer were identified in experimental measurement and theoretical calculation. From these studies, we optimized the suitable multilayer structure for transparent top cathode in OPVs. Thermally evaporated BCP (10 nm)/Ag (10 nm)/MoO₃ (25 nm) cathode showed high transmittance (81.2 %) and low sheet resistance (8.6 ohm/sq). Organic photovoltaics (OPVs) of poly(3-hexylthiophene):[6,6]-phenyl-C61 butyric acid methyl ester (P3HT:PCBM) with BCP/Ag/MoO₃ multilayer as a transparent top cathode exhibited the J_{sc} = 5.8 mA/cm², Voc = 0.573 V, and PCE = 1.8 %. Thus, we can expect this thermally evaporable BCP/Ag/MoO₃ with high transmittance and low sheet resistance multilayer can be applicable to general transparent cathode organic opto-electronic devices.

8116-100, Poster Session

Oxide/polymer interfaces for hybrid and organic solar cells: Anatase versus Rutile TiO₂

M. Lira-Cantu, CIN2 (Spain)

We report the effect of the crystalline structure of TiO₂ and the polymer applied in polymer/oxide solar cells interfaces. The presence of TiO₂ in its the Rutile phase increase solar cell stability under inert atmospheres than devices fabricated with the Anatase phase and devices based on

MEH-PPV show higher Voc (as high as 1 V), while the application of P3HT results in lower Voc, but higher J_{sc} and longer device stability. Our findings suggest that P3HT can be linked to the TiO₂ though the S-end atom, which results in devices with lower Voc. All these observations are also valid for devices, where the bare TiO₂ is replaced by an Nb-TiO₂ but the solar cells applying the doped oxide resulted in devices with photoresponse under inert atmosphere even after several hours under inert (or encapsulated) conditions. We conclude that the application of TiO₂ in its Rutile phase is beneficial for long-term stability devices. Moreover there is an interplay between low Voc and J_{sc} in devices applying P3HT, since power conversion efficiency can be partially canceled by their lower Voc in comparison with MEH-PPV. These findings are important for polymer/oxide solar cells, but also for organic solar cells, where a layer of semiconductor oxides are in direct contact with a polymer, like in inverted or tandem organic solar cells.

8116-101, Poster Session

Self-assembled indium-tin-oxide (ITO) nano-branches for high-efficient polymer solar cells

W. J. Dong, H. K. Yu, G. H. Jung, J. Lee, Pohang Univ. of Science and Technology (Korea, Republic of)

Developments in three-dimensional highly conductive and transparent electrode of organic photovoltaics (OPV) will be discussed. Thin-film solar cells based on organic materials have various advantages of easy fabrication, low-cost, and flexibility. However, OPVs have lower hole mobility in donor materials (2 10⁻⁴cm²V⁻¹s⁻¹) compare to electron mobility in acceptor (3 10⁻³cm²V⁻¹s⁻¹). Relatively low hole mobility induces unbalanced charge transport, leading to limited photocurrent generation of solar cell device. Since two-dimensional morphology of ITO film cannot efficiently extract holes in bulk region of active layer, three-dimensional nanostructure is proposed as efficient hole collecting electrode to balance the charge transport.

Self assembled and single crystalline ITO nano-branches were fabricated by vapor-liquid-solid process using electron beam evaporation process, which is free of any catalyst and carrier gas. The {100} family planes of bixbyite In₂O₃ have the termination of metallic indium; self In-Sn catalyst could be easily formed at those planes, resulting in ITO nano-branch structure with 90° rotation angle. The large surface to volume ratio in anode by ITO nano-branches increases not only the hole mobility by 3-dimensional pathway but also the light absorbance by light scattering at a time. Highly conductive (RS < 8 ohm/sq) and transparent (84.8%) single crystalline ITO nano-branches result in increase of 12% photocurrent (8.4 mA/cm² to 9.4 mA/cm²) and 20% photo conversion efficiency (3.03% to 3.67%) of polymer solar cells based on bulk hetero-junction of regioregular poly(3-hexylthiophene) and phenyl-C61-butyric acid methyl ester. In this study, we successfully fabricated nanostructured hole conducting electrode for high efficient bulk hetero-junction OPVs.

8116-102, Poster Session

An investigation on solution processed films for organic solar cells via multiple techniques

A. K. Chilvery, Alabama A&M Univ. (United States)

The demand for low cost and durable solar cells has paved the way for unprecedented advancement in usage of organic semiconductors. Organic solar cells (OSC) hold the potential of low-cost production and a high throughput as compared to inorganic solar cells besides the increase in efficiency. To realize these possibilities, objective should be to fabricate most of functional films in OSC structure via solution-process technologies: spin; spray; brush and other coating methods. We merged all the solution-processed techniques in order to fetch a better quality films. We discovered this is a high-rate, large-area deposition technique that ensures an ideal coating on a variety of surfaces with different morphologies and topographies. Systematic efforts are being made to

fabricate various films of important efficient OSC materials such as ZnO, TiO₂, P3HT, PCBM, and others by solution-processed techniques. The results obtained in regard to their microstructures, dark- and photo-electric transport and junction characteristics are promising and shall be presented. Also the complete process and electrical characterization results will be presented and discussed.

The 'process-property' relations shall be described in order to obtain best set of performance characteristics. The details of modified fabrication techniques along and facilities established for testing the films and organic solar cells will also be presented. * work supported by NSF-RISE grant: id 0927644.

8116-103, Poster Session

Schottky devices based on polyaniline doped with different metals chloride

H. A. Motaweh, A. H. Elsayed, M. M. Saad, A. H. A. Sakr, Alexandria Univ. (Egypt)

Polyaniline (PANI) doped with metal chloride with nanometer size were used to fabricate the Schottky device Al/PANI -Fe₃O₄ /Au. Current density -voltage (J-V) and capacitance-voltage(C-V) characteristics for this device resemble the typical characteristic for conventional Schottky diode. The characteristic parameters of the structure such as ideality factor, series resistance, barrier height, built-in potential at zero bias and depletion width (W) have been determined from J-V and C-V measurements.

8116-104, Poster Session

Synthesis of low bandgap polymers and their applications in photovoltaics and organic thin film transistors

D. Chandran, P. Kandoth Madathil, Y. Koh, T. Kim, K. Lee, Hannam Univ. (Korea, Republic of)

Organic low bandgap polymers were designed and synthesized for high performance bulk heterojunction (BHJ) photovoltaic (PV) cells and polymer based organic thin film transistors (OTFT). Simple organic units yielding high power conversion efficiencies (PCE) from both small molecules and polymers were adapted as design motifs for the synthesis of donor-acceptor-type materials well suited for use in OPVs. Monomer units were designed to extend the polymer coplanarity and promote a more delocalized HOMO distribution along the backbone. A series of polymers based on diketopyrrolopyrrole (DPP) derivatives and thienothiophene derivatives has been synthesized for this study. The substituents were optimized to get better solubility. Structural characterization of new monomer molecules and the polymers were done based on their ¹H NMR, ¹³C NMR and gel permeation chromatography (GPC). Their optical characteristics were studied with ultraviolet (UV) and photoluminescence (PL) spectroscopy. Cyclic voltametric analysis, small angle XRD and atomic force microscopy (AFM) were done to collect further information of the materials. Thermal properties of the polymers have been determined by thermo gravimetric analysis (TGA) and differential scanning calorimetry (DSC). Devices were optimized for the new materials to get high power conversion efficiency for PV cells and better mobility for the OTFT.

8116-109, Poster Session

Manipulating the morphology and ordering of polymer blends for improving performances of bulk-heterojunction polymer solar cells

F. Xie, W. C. H. Choy, The Univ. of Hong Kong (Hong Kong, China); X. Li, Z. Li, Shanghai Institute of Applied Physics (China)

Bulk-heterojunction polymer solar cells (PSCs) have attracted considerable attention for its remarkable advantages^{1, 2}. The solution based film-growth dynamics of polymer blends become one of the crucial processes to improve the efficiency from bulk-heterojunction structures^{3, 4}. However, the nanoscale network structure in this blend system may change for different solution parameters and spin-coating conditions^{3, 4}.

In the work, we will study driving force effects on the order and phase of crystallization of the blended polymer in solution based self-assembly, which is a key factor of self-assembly of soft materials⁵ but has been neglected in studying PSC morphology. We investigate driving force effects by flipping the substrate up-side-down after spin-coating the wet polymer blend. We introduce Brown's capillarity theory to explain the polymer film formation and study the effects of downward driving force. Our results of absorption spectrum, atomic force microscopy (AFM) and 2D grazing incidence X-ray diffraction (GIXRD) measured using synchrotron radiation show that better chain packing and local order of polymer is formed by the up-side-down method as compared to that by the conventional method. Therefore, the hole transport, carrier balance, short-circuit circuit (J_{sc}), and fill factor (FF) and power conversion efficiency (PCE) improve. For un-annealed devices, PCE improves from 1.68% (conventional device) to 2.64% (up-side-down). For annealed PSCs, PCE of up-side-down devices is also better than that of the conventional ones. When the thickness of active layer increases to 300nm, the PCE of the up-side-down device increases to 3.58% when that of conventional device drops to 2.55%.

[1] G. Dennler, et al., "Polymer-Fullerene Bulk-Heterojunction Solar Cells," *Advanced Materials*, vol. 21, pp. 1323-1338, 2009.

[2] B. C. Thompson and J. M. J. Fréchet, "Polymer-Fullerene Composite Solar Cells," *Angewandte Chemie International Edition*, vol. 47, pp. 58-77, 2008.

[3] G. Li, et al., "High-efficiency solution processable polymer photovoltaic cells by self-organization of polymer blends," *Nat Mater*, vol. 4, pp. 864-868, 2005.

[4] Y. Yao, et al., "Effects of Solvent Mixtures on the Nanoscale Phase Separation in Polymer Solar Cells," *Advanced Functional Materials*, vol. 18, pp. 1783-1789, 2008.

[5] C. J. Morris, et al., "Self-assembly for microscale and nanoscale packaging: steps toward self-packaging," *Advanced Packaging, IEEE Transactions on*, vol. 28, pp. 600-611, 2005.

8116-110, Poster Session

Dye sensitized solar cells using non-aggregated silicon phthalocyanines

L. Martín-Gomis, Univ. Miguel Hernández de Elche (Spain); E. M. Barea, Univ. Jaume I (Spain); F. Fernández-Lázaro, Univ. Miguel Hernández de Elche (Spain); J. Bisquert, Univ. Jaume I (Spain); Á. Sastre-Santos, Univ. Miguel Hernández de Elche (Spain)

Two new silicon phthalocyanines (SiPcs 1 and 2) axially substituted with carboxylic acid appends have been synthesized and chemically characterized. DSC devices using SiPcs as sensitizers have been prepared for the first time. Although similar HOMO-LUMO values are obtained for both SiPcs, the device prepared with the SiPc 2 gives both higher open circuit voltage (V_{oc}) and also higher injection (j_{sc}), so the overall conversion efficiency is longer than for the one where SiPc 1 is used as a dye. The results we obtained are fairly promising and should encourage further studies on DSCs using axially anchored SiPc derivatives substituted with withdrawing groups.

8116-01, Session 1

Advances in polymer and dye-sensitized solar cells

M. D. McGehee, Stanford Univ. (United States)

Using synchrotron x-ray diffraction and molecular mechanics simulations we have determined the unit cell of polymer-fullerene co-crystals that are found in bulk heterojunction solar cells. We will show how this detailed picture of molecular packing makes it possible to model and understand the electronic processes that occur in the solar cells.

Light harvesting in dye sensitized solar cells can be improved by introducing energy relay dyes that absorb light and transfer it to the sensitizing dyes that are attached to the titania. We will show recent progress towards increasing the amount of dye that can be incorporated into the cells. We will also show that light absorption can be improved by 5 to 20% by incorporating a plasmonic back reflector.

We have measured a seven-year lifetime in polymer solar cells and will discuss our efforts to determine the degradation mechanisms and extend this lifetime.

8116-02, Session 1

Small-molecule organic solar cells employing novel materials

M. K. Riede, Technische Univ. Dresden (Germany)

In contrast to polymer solar cells, which are investigated by a large number of researchers and where many materials have been tested, the activities in the field of small-molecule solar cells and the number of available materials classes are much more limited. However, small molecules can be synthesised and purified to high purity and deposited by vacuum sublimation, allowing e.g. for electrically doped organic layers, a high control of layer thicknesses, and simple access to multilayer structures. These advantages yield on the one hand the opportunity to systematically study the device physics using homologous series of materials, e.g. using different side chain lengths in oligothiophenes to study the exciton separation process with spectroscopy. On the other hand, tandem structures are easily accessible for harvesting a large part of the sun spectrum with complementary absorbers. Here, doping of transport layers can create an efficiency recombination contact as well as facilitates the optical optimisation of the stack with optical spacers based on numerical simulations. Both topics are currently under intense investigation and the current state of the art for vacuum deposited small-molecule solar cells will be presented.

8116-03, Session 1

Efficiency enhancement in narrow-bandgap-based polymer solar cells via introducing processing additives and titanium oxide optical spacer

K. Lee, Gwangju Institute of Science and Technology (Korea, Republic of)

We report the fabrication and measurement of bulk-heterojunction (BHJ) solar cells using a narrow-bandgap conjugated polymer, poly[(4,4-didodecyldithieno[3,2-b:2',3'-d]silole)-2,6-diyl-alt-(2,1,3-benzothiadiazole)-4,7-diyl] (P1) in composites with the fullerene derivative [6,6]-phenyl C70-butyric acid methyl ester (PC70BM). In particular, we focus on the enhancement in the device performance by introducing a processing additive and titanium sub-oxide (TiO_x) optical spacer simultaneously. When we introduced 4 % 1-chloronaphthalene (1-CN) as a processing additive to the P1/PC70BM BHJ composite, the morphology of the BHJ layers was improved dramatically, thereby resulting in ~70% increase in the short-circuit current (J_{sc}) with 4.5% power conversion efficiency (PCE). Moreover, the excellent surface smoothness of the BHJ layer with 1-CN enables to incorporate the TiO_x optical spacer to the devices, which has not been achieved previously in any BHJ cells using narrow bandgap polymers. The TiO_x optical spacer further increased J_{sc} with PCE~5%. The significance of our results is the fact that the TiO_x layer also acts as a lifetime enhancing layer as confirmed in our previous studies. The devices processed with the 1-CN

additive and also with the TiO_x optical spacer layer exhibited not only enhanced efficiency, but also prolonged device lifetime without sacrificing any device performance.

8116-04, Session 1

Novel p-type oxides as hole transport layers in organic photovoltaic cells

D. S. Ginley, J. J. Berry, M. T. Lloyd, A. Garcia, N. Kopidakis, X. Steires, A. Sigdel, N. Widjonarko, J. Perkins, A. Zukutayev, P. Ndione, D. C. Olson, National Renewable Energy Lab. (United States)

Organic Photovoltaics offer one key route for impacting the world's energy problems. However, in order to achieve both efficiency and lifetime requires robust contacts to complex organic materials achieving carrier transport, interfacial adhesion and band edge alignment simultaneously.

We have recently shown that the conventional PEDOT:PSS (Poly(3,4-ethylenedioxythiophene) poly(styrenesulfonate)) can be replaced effectively by a thin layer of p-type NiO. While this effect is not fully understood at present a clear question that arises is if this is a general effect or if NiO is unique. Also as the active polymer goes to increasingly deep HOMO materials such as the change from P3HT (poly 3 hexyl thiophene) to PCDTBT (Poly[[9-(1-octylonyl)-9H-carbazole-2,7-diyl]-2,5-thiophenediyl-2,1,3-benzothiadiazole-4,7-diyl-2,5-thiophenediyl]) the work function and transport properties of the contact layer will need to be adjusted.

We have been trying to develop new p-type TCO materials for a wide variety of applications from the general class of spinels and inverse spinels based on Co, Ni and Zn oxides. In particular we have investigated NiCo₂O₄ and a-ZnCoO as HTL layers using P3HT and PCDTBT respectively. We report on the efficiencies of devices based on these two HTL materials in comparison to PEDOT:PSS control devices. We will also report on recent results on the lifetime of devices with oxide HTLs.

We will discuss our efforts to use combinatorial approaches to develop new materials in the general class of p-type spinel based materials and their subsequent application as HTL layers. These results demonstrate that the NiO effect is not unique and can be generalized to a broader class of p-type oxides both crystalline and amorphous. These materials point the way to improving both efficiency and lifetime in high performance OPV devices. Many of these results may be applicable to contacts for OLEDs as well.

We gratefully acknowledge the support of the DOE PV program and the Center for Inverse Design EFRC at NREL and the Center for Interface Science for Hybrid Solar Electric Materials centered at the University of Arizona

8116-05, Session 2

High-efficiency solution-processed hybrid polymer: colloidal nanocrystal photovoltaic cells

R. Zhou, Y. Zheng, D. Xie, W. Cao, Y. Yang, R. Stalder, M. Plaisant, K. S. Schanze, P. H. Holloway, J. R. Reynolds, J. Xue, Univ. of Florida (United States)

Hybrid polymer:colloidal nanocrystal photovoltaic (PV) cells have attracted significant attention as an alternative for all-organic solar cells. However, so far the highest efficiencies for hybrid PV cells have been limited to 2-3%, significantly lower than that of all-organic PV cells. One main reason for the lower performance is attributed to the complex interfaces and surfaces involving the inorganic nanocrystals.

Here we demonstrate that power conversion efficiencies (η_P) of hybrid PV cells can be significantly enhanced by chemically treating the hybrid active layer, containing CdSe nanorods and either P3HT or the lower-gap

PCPDTBT, in an acetonitrile solution with 1% ethanedithiol (EDT) prior to the deposition of the metal cathode. The P3HT:CdSe devices showed a ~30% increase in η_P from 2.2% to 2.9% after the EDT treatment. The efficiency of the hybrid PV cells can be improved by using PCPDTBT to better harvest near-infrared photons, leading to $\eta_P = 3.4\%$ without the EDT treatment, and an efficiency of approximately 5.0% after the EDT treatment was obtained, which is the highest reported efficiency for hybrid PV cells. The efficiency enhancement upon EDT treatment is primarily due to an increase in the photocurrent, with a secondary contribution from the increased fill factor. Detailed characterizations of the hybrid active layers before and after the EDT treatment revealed no appreciable differences in their morphology and absorption spectra; however the phosphonic acid organic ligands on CdSe nanocrystals are more completely removed, and an improved electron mobility was obtained upon EDT treatment.

8116-06, Session 2

Developing oxide: organic hybrid photovoltaics

J. B. Franklin, J. Downing, R. Hewlett, S. Thomas, M. P. Ryan, N. Stingelin-Stutzmann, T. D. Anthopoulos, M. A. McLachlan, Imperial College London (United Kingdom)

The development of hybrid (oxide:organic) photovoltaic devices (h-PV) is an attractive prospect because of the suitability of such devices for low-cost solution processing. Despite this promise the development of such devices has been slow and the best reported efficiencies (< 0.5%) are significantly lower than even modest organic photovoltaics (OPVs). Our efforts to overcome current performance limitations have been focused on two complementary approaches, i) preparation of highly crystalline planar heterojunctions and ii) preparation of controlled interdigitated architectures.

i) Using pulsed laser deposition (PLD) we have been able to deposit highly crystalline ZnO on rigid and flexible substrates at temperatures as low as 50°C. The low temperature processing has allowed the preparation of normal and inverse device architectures based on ZnO and a range of polymers (P3HT, P3HS) and small molecules (pentacene). Additionally the planar devices have allowed charge transfer at the organic:oxide interface to be studied effectively for the different compositions, allowing correlation between device performance, composition and configuration to be made unambiguously.

ii) Using a modified hydrothermal growth method we have successfully formed a range of ZnO nanorods in which the aspect ratio has been controllably varied. We report the preparation of highly interpenetrating networks using these rods and P3HT infiltrated using both conventional solution and novel solid state processing techniques. The role of rod length/spacing in addition to infiltration method on measured device performance will be discussed in addition to limitations of the processing encountered during our studies.

For both families of structures we describe the changes in measured device performance observed as structure and composition are varied. We pay particular attention to the bulk and interfacial properties of the oxide:organic components. The measurements are supported by detailed structural (SEM, AFM, XRD) and electronic (mobility, resistivity) characterization of the individual layers and (where appropriate) the complete device structures

8116-07, Session 2

Improved energy conversion in confined, inverted bulk-heterojunction solar cells with radial electron contacts

J. E. Allen, C. T. Black, Brookhaven National Lab. (United States)

We demonstrate a new organic semiconductor solar cell device structure that improves energy conversion in the active material by over 50%.

Inverted devices are fabricated using nanoporous aluminum oxide templates to confine blended poly(3-hexylthiophene): [6,6]-phenyl-C61-butyric acid methyl ester to nanoscale volumes. Prior to organic blend infiltration, the porous template is coated with TiO₂ via atomic layer deposition to serve as a radial electron contact layer. The final structure is shown to dramatically improve the internal quantum efficiency compared to planar devices and those confined within uncoated templates. Both planar and coated confined devices achieve power conversion efficiencies of over 2% while the confined structure utilizes 60% less active material. Ultra-violet visible light spectroscopy confirms that the confined structure absorbs just 45% of the light of a planar device indicating an improvement in charge collection by over 50%. Improved performance is attributed to enhanced hole mobility in the poly(3-hexylthiophene) due to nano-confinement in addition to accelerated electron extraction by the radial electron contact. Organic semiconductor solar cells may enable large-scale integration of solar energy solutions through easily scalable and low-cost manufacturing. Much of the recent exciting scientific and technological progress in this vibrant field has largely come through the introduction of new polymer semiconductor materials. In this work, we demonstrate that nanostructuring the organic semiconductor solar cell active material can dramatically increase the performance in existing, well-established materials - an approach that may provide benefits for new organic semiconductors as well.

8116-08, Session 2

Effect of low-concentration donor doping in bulk-heterojunction fullerene photovoltaic cells

M. Zhang, H. Wang, C. W. Tang, Univ. of Rochester (United States)

The effect of doping MoOx/C60 bulk-heterojunction (BHJ) photovoltaic cells with a non-absorbing, hole-transport donor, 1,1-bis-(4-bis(4-methyl-phenyl)-amino-phenyl)-cyclohexane (TAPC), has been investigated. With very low TAPC concentration in C60 (~1%), the TAPC:C60 BHJ cells exhibit a high Voc (~ 1.0 V) along with low short-circuit current (Jsc) and fill factor (FF), a characteristic which is of typical MoOx/C60 Schottky-barrier cells. With high TAPC concentration (~50%), the photovoltaic characteristics are largely determined by the TAPC:C60 BHJ, showing improved Jsc and FF but reduced Voc (~0.7 V) due to HOMO-LUMO gap limitation. The BHJ cell performance is optimized at about 5% TAPC with Voc = 0.91 V, Jsc = 5.94 mA/cm², and FF = 0.52. At this low concentration range, the TAPC:C60 BHJ cells exhibit a high Voc derived from the MoOx contact. Also both Jsc and FF are relatively high, as they are enhanced by the improved charge generation and hole-transport in the BHJ. At higher TAPC concentration, the roll-off in efficiency can be attributed not only to a reduction in the built-in potential, but also to a reduction in absorption, dielectric constant, and electron mobility in the BHJ due to the dilution of C60. A power conversion efficiency of 3.2 % has been achieved for 5% TAPC:C60 BHJ cells based on a thicker BHJ (150 nm) deposited at an elevated temperature (75 °C).

8116-09, Session 3

Broadband absorption enhancement in organic photovoltaics based on nanopatterned ultra-thin metal films

Q. Gan, Univ. at Buffalo (United States); W. Bai, Institute of Semiconductors (China); Z. H. Kafafi, National Science Foundation (United States) and Lehigh Univ. (United States); F. J. Bartoli, Lehigh Univ. (United States)

Three-dimensional finite-difference time domain calculations have shown that plasmonic structures can significantly enhance the optical absorption of active layers in polymer- or molecular-based organic photovoltaics (OPVs).^{*} A polarization-independent nanopatterned

ultra-thin metallic structure supporting short-range surface plasmon polariton (SRSP) modes is used to improve the performance of OPVs via broadband absorption resonances. The physical mechanism of the excited SRSP modes is delineated and their distributions are analyzed. In this talk, we will demonstrate that the SRSP-assisted broadband absorption enhancement could be spectroscopically tuned by carefully designing the OPV devices and tailoring the parameters of the nanopatterned metallic structure(s). These results are very promising for the development of OPVs with enhanced performance.

* Wenli Bai, Qiaoqiang Gan, Guofeng Song, Lianghai Chen, Zakya Kafafi, and Filbert Bartoli, Optics Express 18 (104), A620 (2010).

8116-10, Session 3

Towards fully printed organic solar cells: material aspects and process challenges

C. J. Brabec, Friedrich-Alexander-Univ. Erlangen-Nürnberg (Germany); M. Heyder, Bavarian Ctr. for Applied Energy Research E.V. (Germany); F. Jakubka, F. Machui, T. Stubhan, I. Litzow, J. Krantz, Friedrich-Alexander-Univ. Erlangen-Nürnberg (Germany)

Organic PV is rapidly gaining high attraction because of its simple production process and its potential for a true low cost solar technology. The compatibility with printing and coating requires a careful stack design - in the simplest scenario, functional solar modules consist of only three layers, while more advanced and efficient device concepts require the deposition of 5 layers. This is an outstanding simple production process compared to inorganic thin film PV technologies. However, the challenge is in the detail of the printing process and in the formulation of suitable inks.

In this contribution we introduce and discuss material aspects and process challenges towards fully printed solar cells, including the replacement of the ITO electrode. Various concepts were already discussed to develop a fully printed OPV stack, including lamination techniques, printing of CNT networks as well as deposition of highly conductive PEDOT. However, none of these material combinations and concepts currently does fulfill the specifications for highly performing solar modules.

In detail, we discuss the combination of printed metallic nanowire electrodes in combination with metal oxide interface layers as a viable process towards fully printed organic solar modules. Experimental data for fully printed cells will be combined with results from process simulation. The overall process will be evaluated by a cost estimations to give a realistic picture on the potential cost scenario for organic photovoltaics.

8116-11, Session 3

Transparent, non-TCO electrodes for organic photovoltaics

L. Müller-Meskamp, C. Sachse, Y. H. Kim, C. Häfner, A. Zakhidov, Technische Univ. Dresden (Germany); O. R. Hild, Fraunhofer-Institut für Photonische Mikrosysteme (Germany); K. Leo, Technische Univ. Dresden (Germany)

Transparent conducting oxides (TCO) are still the first choice for transparent electrode applications. However, for organic photovoltaics, strong demand for flexible and low-cost substrates led to several alternative technologies and ideas. Using our highly efficient OPV technology, based on the evaporation of small molecules, doped transport layers and bulk-heterojunction geometries, we have studied polymer electrodes (PEDOT:PSS), Ag-nanowire electrodes, and carbon nanotube based electrodes. For PEDOT:PSS, we could enhance the conductivity by optimized solvent treatment, resulting in a selective removal of PSS from the electrode film, as could be shown by XPS and optical spectroscopy. Using these materials, we could achieve the same cell performance than for ITO on small area. Nanowire based electrodes,

using random networks of highly conductive material, such as silver or CNTs, are very promising candidates, with Ag-NWs achieving similar transmission and conductivity properties as ITO (ca. 85% Transmission, <100hm/sq.). We used different Ag-NWs (diameter, length) coated by dipping or spraying from solution, show the influence of different post-treatment methods, and examined the optical and electrical properties of the network layer. For integration into solar cells, these electrodes were combined with an additional polymer coating, to improve the surface roughness. Carbon nanotubes were used in form of free-standing membranes, as top electrodes in semitransparent solar cells. All systems are shown to yield decent solar cells, with every technology having certain benefits and specific issues, but certainly with huge potential to rival ITO in the future.

8116-12, Session 3

Efficient heterojunction photovoltaic cell utilizing nanocomposites of lead sulfide nanocrystals and a low-bandgap polymer

J. Seo, M. J. Cho, D. Lee, A. N. Cartwright, P. N. Prasad, Univ. at Buffalo (United States)

Hybrid polymer-inorganic nanocrystal (NC) solar cells consisting of a hole-conducting conjugated polymer and inorganic semiconducting quantum dots, like cadmium selenide (CdSe), lead sulfide (PbS) and lead selenide (PbSe), have attracted considerable research attention since the advantages of two classes of materials can be effectively combined. In this work, we demonstrate a facile approach to make an efficient hybrid bulk heterojunction photovoltaic device with PbS NCs and a polymer. Herein, we introduced a low band gap polymer as the electron donor host and fabricated a blended film of oleic acid (OA)-capped PbS NCs with a polymer. Direct post-deposition chemical treatment using a short length cross-linker molecule, 1,2-ethanedithiol, applied to the blend film on the PEDOT:PSS layer kept the bulk heterojunction intact by selectively solubilizing the OA ligand of the PbS NCs without affecting the polymer matrix during the process of ligand exchange. Subsequently, inspired by the use of a multifunctional buffer layer in organic polymer photovoltaic devices, we deposited a titanium dioxide (TiO₂) thin layer (through non-hydrolytic sol-gel method) on the blend film to facilitate efficient electron transfer and extraction from the blend toward the metal and to prevent holes from reaching the metal. In addition, the effect of the PbS NC size, and thus excitonic energy, on the power conversion efficiency was studied. Power conversion efficiencies of 2-3% were observed in the resulting devices.

8116-13, Session 3

Polymer nanocomposite solar cells based on in-situ formed CuInS₂

C. Fradler, T. Rath, M. Edler, A. Fischereeder, S. Moscher, A. Pein, Technische Univ. Graz (Austria); R. Trattnig, E. J. W. List, JOANNEUM RESEARCH Forschungsgesellschaft mbH (Austria); W. Haas, F. Hofer, G. Trimmel, Technische Univ. Graz (Austria)

Inorganic-organic nanocomposite solar cells have become a research topic of great interest within the last decade as, by choosing a suitable inorganic compound as acceptor phase, e.g. CdSe, CuInS₂, the amount of absorbed light can be enlarged. Such inorganic semiconductors have a bandgap matching the maximum of the solar spectrum quite well, and therefore significantly contribute to the light absorption in a solar cell.

We developed a CuInS₂ in-situ formation process by using new metal xanthate precursor materials. We were able to prepare stable bulk solutions containing the mentioned metal xanthate precursor materials and photoactive polymers like PCDTBT (poly[[9-(1-octylonyl)-9H-carbazole-2,7-diyl]-2,5-thiophenediyl-2,1,3-benzothiadiazole-4,7-diyl-2,5-thiophenediyl]) or PSiF-DBT (poly[2,1,3-benzothiadiazole-4,7-diyl-2,5-thiophenediyl(9,9-dioctyl-9H-9-silafluorene-2,7-diyl)-2,5-

thiophenediyl)) from solvents like toluene or chlorobenzene. In order to prepare nanocomposite solar cells this precursor solution can be coated by spin coating or doctor blading on glass/ITO substrates that have been coated with a thin PEDOT:PSS layer first. The conversion of the precursor material to CuInS₂-nanostructures is performed by an annealing step and takes place at a temperature below 200°C. The annealing leads to a homogenous network of the organic and the inorganic phase. In a final step a photocathode was put about the photoactive layer. This solar cell assembly led to efficiencies above 2% up to now.

The solar cells were analyzed by their I-V curves as well as by transmission electron microscopy, optical spectroscopy and IPCE measurements

This work was funded by the Austrian Ministry of Economy, Family and Youth and Isovoltaic AG.

8116-31, Session 3

GaAs nanowire/PEDOT:PSS hybrid solar cells: the relationship between nanowire morphology and device performance

J. Chao, S. Shiu, C. Lin, National Taiwan Univ. (Taiwan)

In this study, we demonstrate a new type of hybrid solar cell based on a heterojunction between poly(3,4-ethylenedioxythiophene):poly(styrenesulfonate) (PEDOT:PSS) and vertically-aligned n-type GaAs nanowire. The GaAs nanowire arrays are fabricated by directly performing the nano-etching of GaAs wafer with spun-on SiO₂ nanoparticles as the etch mask through inductively coupled plasma reactive ion etching. The use of vertically-aligned GaAs nanowire makes the interpenetrating heterojunction interface possible. Thus a large heterojunction interface and short collection paths of photo-generated carriers can be achieved. Moreover, vertically-aligned GaAs nanowire arrays with high aspect ratio can provide much smaller optical reflectance. The hybrid cells are prepared by attaching the GaAs nanowire arrays onto ITO glass substrates coated with PEDOT:PSS films. The PEDOT:PSS adheres to the surface of GaAs nanowire arrays to form a p-n junction. Our study shows that the GaAs nanowire/PEDOT:PSS heterojunction clearly exhibits a solar cell behavior. The morphology of GaAs nanowire arrays strongly influences the characteristics of hybrid solar cells. The suppression of reflectance and the interpenetrating heterojunction interface of GaAs nanowire arrays will offer great improvements in device performance. The reduction of reflectance is in agreement with the increase in J_{sc} of hybrid cells. On the other hand, a larger heterojunction interface between PEDOT:PSS and GaAs nanowire arrays results in a high J_{sc}. A good PEDOT:PSS coverage also provides improved Voc due to the reduction in shunts. The power conversion efficiency of GaAs nanowire/PEDOT:PSS cells under AM 1.5 global one sun illumination can achieve 5.8 %.

8116-32, Session 3

Silicon/silicon nanowire/poly(3,4-ethylenedioxythiophene):poly(styrenesulfonate) heterojunction solar cells

H. Syu, S. Shiu, C. Lin, National Taiwan Univ. (Taiwan)

Conventional manufacturing processes of solar cells, including epitaxy, diffusion, deposition and dry etching, are high cost and high power consumption. To save energy and reduce expenses, we use organic material, silicon nanostructure and solution process. The devices structure is n-type bulk Si (n-Si)/n-type silicon nanowires (n-SiNWs)/poly(3,4-ethylenedioxythiophene):poly(styrenesulfonate) (PEDOT:PSS) heterostructure. The active region includes n-Si and n-SiNW arrays, promising the property of ultra low reflection for high light absorption. In this work, SiNWs of only a few hundred nanometers could lower the reflectance to below 5%. In addition, an organic material - PEDOT:PSS, instead of p-type doping, is introduced to form a p-n junction with n-Si/n-SiNWs for separating the electron-hole pairs. The use of PEDOT:PSS can also passivate the surface defects of n-SiNWs.

N-type SiNW arrays are made by aqueous etching process. The etchant contains Ag ions and HF etching vertically to the 1-10 Ω-cm Si (100) wafers. After etching and removing residual Ag and SiO₂ by nitric acid and diluted HF successively, n-SiNW arrays existed on either surfaces of n-Si with very dark color; then Ti and Ag were evaporated on n-Si to be a cathode. Finally, nanowires of n-Si/n-SiNWs were stuck on the PEDOT:PSS that were spin-coated on the ITO coated glass to form a core-sheath heterojunction.

The performance and quantum efficiencies (QE) were measured. The short circuit current density and power conversion efficiency are 27.46 mA/cm² and 8.05%, respectively, which are higher than other solar cells containing SiNWs. The external and internal QE are beyond 50% and 60% in visible range, respectively.

8116-14, Session 4

Toward bulk-heterojunction solar cells with stable morphology

S. Bertho, B. Conings, F. Piersimoni, D. F. Spoltore, J. D'Haen, L. J. Lutsen, H. Boyen, Univ. Hasselt (Belgium); B. Van Mele, G. Van Assche, Vrije Univ. Brussel (Belgium); D. J. Vanderzande, J. V. Manca, Univ. Hasselt (Belgium)

The nanomorphology of interpenetrating donor:acceptor networks is of crucial importance for state-of-the-art bulk heterojunction (BHJ) solar cells. For each combination of donor:acceptor materials, specific preparation procedures are developed and optimised in order to obtain the required 'ideal' morphology, which results in the highest photovoltaic energy conversion efficiency for the given material system. However, when these optimised solar cells with 'ideal' morphology are submitted to a prolonged storage or to a prolonged operation at elevated temperatures (e.g. solar cells in outdoor applications), a temperature induced disruption of this ideal morphology can occur and therefore also the corresponding photovoltaic performance will deteriorate. In this contribution the effect of temperature on morphology and photovoltaic properties is investigated for different sets of donor:acceptor materials by using a variety of analytical techniques (e.g. Transmission Electron Microscopy - TEM, Thermal Analysis Techniques,...) and electro-optical techniques (e.g. Fourier Transform Photocurrent Spectroscopy - FTPS). This approach provides a better insight in the underlying mechanisms causing the temperature induced morphology changes. Complementary to this analytical and electro-optical characterisation, an accelerated ageing system is used to study in-situ the degradation kinetics of the BHJ solar cells at various temperatures in order to obtain an accelerated ageing model to predict lifetime. Solutions and concepts are proposed and investigated towards thermally stable morphologies and therefore towards next generation BHJ solar cells with an increased intrinsic thermal stability.

8116-15, Session 4

Understanding degradation in unencapsulated organic photovoltaics

M. T. Lloyd, A. Garcia, J. J. Berry, N. Kopidakis, M. O. Reese, D. S. Ginley, D. C. Olson, National Renewable Energy Lab. (United States)

We employed an automated combinatorial testing system to monitor the degradation rates for inverted geometry poly(3-hexylthiophene):fullerene bulk heterojunctions solar cells in air. These devices utilize ZnO and Ag for electron and hole contacts, respectively, the relative stability of which enables meaningful studies of unencapsulated device lifetimes. For inverted devices under constant illumination, we find oxygen and moisture ingress to be the primary cause for decay in power conversion efficiency (PCE) via decreased short-circuit current (while the fill factor and open-circuit voltage are unchanged). Consequently, we find that the contacts serve as a de facto encapsulation layer and the detailed method for contact preparation becomes the first order, rate-limiting

factor in determining device lifetime. In an ex-situ experiment, we evaluate the water vapor transmission rate (WVTR) of commonly used electrode materials to show that the permeability of the metal electrode is determined by its thickness and composition (in multi-layer configurations). Parallel findings confirm the observed transmission rates in devices monitored under constant illumination, where electrodes of the lowest WVTR yield devices with lifetimes extending beyond 5000 hrs. End-of-life behavior consistently results in a catastrophic loss of photocurrent. We use high-resolution photocurrent mapping to reveal circular regions of zero photocurrent in the active area indicative of pinhole ingress and lateral diffusion of oxygen and water vapor. Using a modified form of the Avrami equation, which describes nucleation and island growth in two-dimensional systems, we are able to mathematically model photocurrent vs. time as the device experiences catastrophic failure.

8116-16, Session 4

Reliability of organic materials using photothermal deflection spectroscopy

A. Bezryadina, Univ. of California, Santa Cruz (United States) and NASA Ames Research Ctr, Advance Study Labs. (United States); J. Olson, APV Research (United States); C. France, S. Carter, G. Alers, Univ. of California, Santa Cruz (United States)

Degradation of organic materials used for solar energy collection was measured with photothermal deflection spectroscopy (PDS). PDS has the ability to measure absorption over a range of 5 decades and can detect the first signs of degradation in organic films. From the tail of the optical absorption trap states and defects are deduced to quantify light induced and temperature induced degradation due to photo-oxidation and polymer/dye decomposition. In this work we look at degradation of common solar energy polymer materials like P3HT and MEH-PPV and commercial dyes that are used for photon downconversion and luminescent solar concentrators.

Most polymers have inherently weak optical absorption in the visible-IR region and might exhibit scattering due to surface roughness. PDS measurements are independent of scattering and can detect slight changes in band-edge absorption after temperature or light soaking treatments. At the tail region non-radiative absorption processes for the material are present with no detectable photoluminescence emission. A commercial red luminescent material was tested and had strong degradation after 50 hours of light soaking at 35C under 100mW/cm² illumination from a metal-halide lamp. Absorption increased by a factor of 4 in the tail and the band-edge region. Another commercial material showed no changes in absorption after ~100 hours of light soaking. Highly sensitive PDS measurements can test optical absorption of organic films after long exposure under the sun, high humidity and/or high temperatures. Small changes in absorption can be extrapolated to quantify degradation behavior from 1000 hour measurements to predict 20-year lifetime and the long term efficiency of photovoltaic devices.

8116-17, Session 4

High-efficiency polymer-based OPV with lifetimes approaching 7 years

C. H. Peters, I. T. Sachs-Quintana, J. P. Kastrop, M. D. McGehee, Stanford Univ. (United States)

As efficiencies increase, the questions of lifetime and reliability of OPV gain importance. Current polymer-based OPV devices typically show lifetimes of 2-4 years when encapsulated. In this study we performed accelerated lifetime testing on poly(-heptadecanyl-2,7-carbazole-alt-5,5-(di-2-thienyl--benzothiadiazole) (PCDTBT). From the testing, we estimate a lifetime approaching 7 years which, to the best of our knowledge, is a record for reported polymer OPV devices.

PCDTBT has been used with PC(70)BM to achieve device efficiencies over 6.1%, making it one of the most efficient polymer-based OPV

materials. 16 high-efficiency devices were encapsulated using state-of-the-art encapsulation techniques. The devices were held at the maximum power point, closely mimicking the actual conditions under which they would be operated in the field. The lamp intensity and temperature of each device were monitored in real-time. 16 P3HT:PCBM devices, encapsulated in an identical manner, were testing along with the 16 PCDTBT devices for comparison.

Results show an initial burn-in where the PCDTBT devices experience an exponential decay in efficiency, which lasts 500 hours. After this period the devices are incredibly stable, showing a linear decay for the remaining 4,000 hours of the test. Taking the initial value from the start of the linear decay period at 500 hours and extrapolating to where 20% of this initial value has been lost leads to a lifetime approaching 7 years.

The P3HT:PCBM devices show a more gradual burn-in lasting close to 1,300 hours which is also followed by a linear decay period but with a more severe slope. Performing the same lifetime analysis on these devices leads to an estimated lifetime of 3.3 years.

We will also introduce results of advanced optical and electrical characterization techniques that were used to understand degradation. This will provide the scientific community with greater insight into approaches to make more stable devices.

8116-18, Session 4

Luminescence imaging as characterization tool for polymer solar cells and modules

H. Hoppe, M. Seeland, R. Rösch, B. Muhsin, M. Bärenklau, G. Gobsch, Technische Univ. Ilmenau (Germany)

We demonstrate luminescence imaging to be a powerful tool for characterizing organic solar cells and modules with respect to deficiencies in the production process, local defects and degradation processes. As an example, the complementary use of photoluminescence and electroluminescence imaging has been employed to identify the cause and nature of polymer solar cell degradation stressed under different storage conditions. In this study we directly relate imaging results with solar cell parameters.

Furthermore we have developed a quantitative analysis for electroluminescence images obtained on organic solar cells. This approach is based on a complex device modeling employing a network of interconnected micro-diodes. The equivalent circuit network model takes interface and bulk resistances as well as the sheet resistance of the transparent electrode into account. The application of this model allows direct calculation of the lateral current and voltage distribution as well as determination of internal resistances and the sheet resistance of the higher resistive electrode. Furthermore, we have extended the micro-diode-model to also describe and predict current-voltage characteristics for devices under illumination. The local nature of this description enables important conclusions concerning the geometry dependent performance of thin film solar cells.

Finally the beneficial use of luminescence imaging as tool for quality control is shown for single devices and monolithically connected polymer solar cell modules.

8116-19, Session 4

Degradation of PCBM-P3HT organic photovoltaic cells and structure changes as determined by defect investigations

F. Reisdorffer, Univ. de Nantes (France); L. Wang, National Taiwan Univ. (Taiwan); T. Nguyen, Univ. de Nantes (France)

We present an investigation of the intrinsic degradation of organic photovoltaic cells using poly(3-hexylthiophene) (P3HT) and phenyl-C61-butyric acid methyl ester (PCBM) composite as an active layer. The encapsulated devices of structure ITO/PEDOT:PSS/P3HT-PCBM/Ca/Al were investigated using the Charge based Deep Level Transient

Spectroscopy (Q-DLTS). An efficiency of ~ 4.0% and a fill factor of the IV characteristics of ~ 64% have been obtained in fresh devices. Trap density determined in these samples is ~ 10^{17} cm⁻³ and their levels are found in the range from 0.1 to 0.5 eV from the band edges. Comparing the defect spectra obtained in freshly fabricated devices and those degraded over 1000 hours under 1.5 AM conditions, we observed a strong increase in intensity of deep traps, which indicated an alteration of the blend structure. On the other hand, a noticeable decrease of the trap peak of relaxation time of ~ 1s after degradation has occurred. The corresponding traps have been identified as defects induced by the presence of PCBM in P3HT matrix, and their reduction suggests a modification of the PCBM structure organization. We discuss the possible modifications of the blend structure induced by degradation and we propose a mechanism involving the transformations of PCBM basing on the defect measurement results.

8116-21, Session 6

Semi-random copolymers as a multichromophoric platform for bulk-heterojunction solar cells

B. C. Thompson, B. Burkhart, P. P. Khlyabich, The Univ. of Southern California (United States)

Even as the efficiency of bulk heterojunction polymer solar cells increases into the 7-8% range, it is clear that there is much room for improvement in efficiency, lifetime, and cost-effective synthetic and fabrication strategies. It has been proposed numerous times that efficiencies greater than 10% should be possible with this device platform. The main obstacle appears to be the development of ideal donor-acceptor pairs that are optimal for light harvesting, charge generation and collection, and form stable morphologies. Here, an avenue toward developing optimal donor-acceptor pairs is discussed, based on the development of optimized donor polymers that possess broad spectral absorption, high absorption coefficients, high charge carrier mobilities, and semi-crystalline structures effective for blending with fullerene acceptors. As an extension beyond the simple donor-acceptor approach to narrow band gap polymers, a route toward multichromophoric (broad spectral absorbing) polymers has been developed. A new family of semi-random hexyl-thiophene based donor-acceptor copolymers, which broadly absorb sunlight, due to their unique structure, has been synthesized. The restricted linkage pattern of monomers (due to a careful choice of functional groups) retains a high degree of structural order in polymers preserving attractive properties of regioregular poly(3-hexylthiophene) (P3HT), such as crystallinity and high hole mobility, while also taking advantage of the multichromophoric nature of random polymers, which allows broad spectral absorption of light. These donor-acceptor semi-random copolymers show broadened absorption and semicrystalline morphology, as evidenced by the high measured hole mobilities. Optimization of processing conditions has also demonstrated high solar cell efficiencies in several cases.

8116-22, Session 6

Solution-processable small molecules for highly efficient solar cells

Y. Chen, Nankai Univ. (China)

Due to the numerous advantages of small molecule compared with polymer, such as monodisperse, well defined structures and better batch-to-batch reproducibility for commercial applications, organic solar cells using solution-processable small molecules as donor materials have achieved a dramatic progress in very recent years. Here, we report a new class of solution processable small molecules with molar mass lower than 1700 g mol⁻¹. These molecules have good solubility and film quality. By introducing different soluble alkyl end group, the properties can be tune very effectively. Using the simple solution spinning process, BHJ solar cells based on these molecules have achieved a power conversion efficiency of 5.08%, with a fill factor of 55.0% and a high IPCE of 67%.

8116-23, Session 6

Molecular engineering of conjugated polymers for highly efficient bulk-heterojunction solar cells

W. You, H. Zhou, The Univ. of North Carolina at Chapel Hill (United States); S. C. Price, L. Yang, A. C. Stuart, University of North Carolina at Chapel Hill (United States)

The bulk heterojunction (BHJ) organic photovoltaic cells of regioregular poly(3-hexylthiophene) (RR-P3HT) and [6,6]-phenyl C61-butiric acid methyl ester (PCBM) represent one of the most successful systems with reproducible efficiencies approaching 5% after careful optimization. However, with a fixed band gap of 1.9 eV, P3HT can only harvest a small portion of the solar spectrum (maximum 22.4%). Therefore low band gap polymers for better light harvesting have been intensively pursued in recent years. Though impressive progresses have been made, the outstanding question remains: how to rationally design ideal polymers to approach 10% efficiency and beyond?

I will summarize the design criteria for "ideal" polymers to be used with PCBM to further improve the efficiency of BHJ photovoltaic devices. Specifically, I will focus on three main topics: (a) design of new conjugated backbone to control the band gap and energy levels; (b) the significant influence of "trivial" side chains; (c) the impact of substituents such as F. A number of new polymers will be discussed in detail to elaborate these topics. A design motif has been proposed, which successfully produced polymers that demonstrated over 7% efficiency in BHJ devices.

8116-24, Session 6

A small-molecule non-fullerene electron acceptor for organic solar cells

P. Meredith, P. E. Schwenn, K. Gui, K. B. Krueger, K. E. Lee, K. E. Mutkins, P. E. Shaw, The Univ. of Queensland (Australia); N. Kopidakis, A. Nardes, National Renewable Energy Lab. (United States); P. L. Burn, The Univ. of Queensland (Australia)

Solution processed organic BHJ solar cells predominantly use the fullerene derivatives [C60]PCBM and [C70]PCBM as the electron acceptor. These systems in combination with polymer donors have generated efficiencies in excess of 7%¹. Few examples of "non-fullerene" acceptors have been reported with maximum efficiencies in combination with poly(3-n-hexylthiophene-2,5-diyl) (P3HT) of 2%. Given this situation, one is led to ask: "what is so special about the fullerenes as acceptors"? To address this question we have embarked upon a program to design a new class of acceptors based upon fluorene benzothiadiazols whose properties can be systematically varied². In this paper, we present results on a successful candidate from this family: 2-[[7-(9,9-di-n-propyl-9H-fluoren-2-yl)benzo[c][1,2,5]thiadiazol-4-yl]methylene]malononitrile (K12). We show it can be processed by evaporation or from solution to give amorphous films and can be annealed at modest temperature to give films with greater order and enhanced charge transport. The molecule can efficiently quench the photoluminescence of P3HT and time resolved microwave conductivity measurements show that mobile charges are generated. We also find that conversion efficiencies of the resultant devices depend strongly on the acceptor packing. Optimized K12:P3HT BHJ devices have efficiencies of 0.73±0.01% which are limited by the level of crystallinity that is achievable in the blend. Building and studying such model systems will, we believe, lead to a more in-depth understanding of the requirements for high efficiency electron acceptors tailored to particular donor materials.

[1] Y. Liang, et al. *Adv. Mater.*, 2010, 22, E135.

[2] P. Schwenn, et al., *Adv. Ener. Mater.*, 2011, 1, 73.

8116-25, Session 6

The effect of regio-regularity on the optoelectronic properties of PTVs

E. Lafalce, X. Jiang, Univ. of South Florida (United States)

Poly(thienylene vinylene) (PTV) is a π -conjugated polymer with potential applications for use in photovoltaics owing to its low bandgap, good hole-mobility and low oxidation potential. It is generally considered a non-luminescent material and reports suggest its emissive properties are highly dependent upon excitation energy, conjugation length, alkyl side group and regio-regularity, complicating the interpretation of the non-radiative decay routes for photo-generated excitations. We have studied a class of PTV with controlled regioregularities, and our results are contrary to the normal understanding of the role regioregularity has played in π -conjugated polymers, for instance, in the case of poly (3-hexylthiophene) (P3HT), where it has been shown that increased regioregularity enhances interchain interaction, crystallinity of polymer films, and carrier mobility, as well as drastically reduced photoluminescence quantum yield. Through a thorough investigation of photoluminescence, photoinduced absorption, Raman Scattering and electroabsorption, we have deduced the physical mechanisms competing with radiative recombination process, and evaluated phonon coupling effect on the optoelectronic properties of these polymers. By varying the excitation energy, temperature, and modulation frequency, and also by controlling the morphology through the use of different solvents, concentrations, and film preparation techniques, we offer a detailed report on recombination dynamics of various long-lived photoexcitations in this class of polymers. Complimentary characterization of films through XRD and electro-absorption yield detailed information about the semi-crystalline structure and electronic levels, respectively. Our findings could help to improve the performance of solar cells based on this low bandgap polymers, as well as a guide for better material engineering.

8116-26, Session 6

A planar alkoxy-substituted benzothiadiazole-based low-band-gap copolymer for photovoltaic solar cells

H. Y. Woo, W. Lee, Pusan National Univ. (Korea, Republic of);
H. Choi, J. Y. Kim, National Institute of Science and Technology (Korea, Republic of)

Recently, bulk-heterojunction (BHJ) polymer solar cells (PSCs) have been extensively studied as one of the attractive renewable energy sources due to low cost, light weight, solution processibility and potential applications in flexible large-area devices. Their performances are affected by many factors: electronic properties of the polymers (as a donor) and fullerene derivatives (as an acceptor), morphology of the films, and interfacial properties, etc. Among them, structural planarity of the polymer is one key parameter since it mainly influences intermolecular ordering and carrier mobility. Here, we report a planar donor-acceptor type benzothiadiazole-containing copolymer, PTBT with a simple molecular structure and easy synthesis. The measured number-average molecular weight (M_n) was 30,000 g/mol (PDI=1.7) and optical band gap was determined to be ~ 1.72 eV with absorption spectrum covering the entire visible region in a range of 400 nm \sim 800 nm. The UV-vis absorption in film showed a fine-structure with a shoulder peak, which indicates a strong π - π intermolecular interaction. Differential scanning calorimetric (DSC) data also indicated clear melting and recrystallization points. PTBT blended with PC61BM shows high photovoltaic performance with open circuit voltage of 0.72 V, short-circuit current of 10.4 mA/cm², fill factor of 0.68, and the resulting power conversion efficiency of $\sim 5.0\%$ under air mass (AM) 1.5 global (1.5 G) illumination conditions (100 mW/cm²)

8116-27, Session 7

Influence of molecular acceptor design on the blend morphology of bulk-heterojunction organic solar cells

A. Amassian, King Abdullah Univ. of Science and Technology (Saudi Arabia)

The dominant solution-fabricated device configuration in organic photovoltaic (OPV) devices is the bulk heterojunction, where donor and acceptor are blended during device fabrication, and self-assembly processes yield the phase separation essential to photovoltaic performance. Traditionally, this phase separation is achieved through simple size or shape incompatibility between a ribbon like donor polymer and spherical acceptor fullerene. Further aided by the high dimensionality of electron transport of fullerene materials, these acceptors have become the standard for high performance OPVs. There are compelling reasons to investigate alternatives to fullerene-based acceptors for OPVs: In order to improve OPV performance, it is critical to understand why the fullerenes are currently superior OPV acceptors. Is it strictly their shape leading to improved phase segregation? Fortuitously appropriate energy levels? High electron mobility in all dimensions? By investigating several series of other molecular acceptors that exhibit only a few of these properties, we can determine which ones are critical to OPV performance and in what way they are influencing the BHJ OPV. Here, We focus on the role of acceptor molecular design in mediating phase separation, blend morphology and domain structure of the bulk heterojunction thin film, which we relate to the photocurrent. Our results reveal important and meaningful correlations between design of acceptor molecules and the resulting bulk heterojunction formation, which should provide helpful insight for future discovery of high performance acceptor molecules.

8116-28, Session 7

Characterization of bulk-heterojunction-inverted polymer solar cells probed by depth-profiling X-ray photoelectron spectroscopy

H. Cheun, J. D. Berrigan, Y. Zhou, M. Fenoll, J. W. Shim, C. Fuentes-Hernandez, K. H. Sandhage, B. Kippelen, Georgia Institute of Technology (United States)

Polymeric bulk heterojunction solar cells show promise as a versatile portable source of renewable energy. So far, extensive efforts have been devoted to increasing their power conversion efficiencies through the development of novel polymers, but controlling the active layer morphology remains a challenge. Phase separation and vertical segregation of the donor and acceptor materials in the blend were found to strongly influence device performance. Recently, polymer solar cells with a transparent electron collecting electrode have been fabricated to improve stability in air. In such a structure, called an inverted structure, ITO is modified with a thin metal oxide layer to reduce its work function. Vertical phase segregation in such inverted structures is expected to be influenced by the different substrates on which the bulk heterojunction film is formed.

In this work, we investigated vertical phase separation in photoactive layers of poly(3-hexylthiophene) (P3HT) and [6,6]-phenyl C61 butyric acid methyl ester (PCBM) blends on a ZnO layer using depth profiling X-ray photoelectron spectroscopy (XPS). Experiments were performed on films as a function of annealing times at an annealing temperature of 160°C. Results show that annealing leads to vertical phase segregation where P3HT-rich regions are adjacent to the bottom ZnO layer used as an electron-collecting electrode. These depth profiles were correlated with the photovoltaic performance of such films incorporated in solar cells with a structure ITO/ZnO/P3HT:PCBM/MoO₃/Ag. Best performance was obtained when the polymer blend was high in P3HT near the electron collecting electrode, against the conventional wisdom. These results shed new light on the role of vertical phase segregation on the performance of bulk heterojunction solar cells.

8116-29, Session 7

Effect of vertical phase segregation in polymer solar cells using a silole-containing low-bandgap donor-acceptor polymer

J. Subbiah, F. Steffy, C. M. Amb, J. R. Reynolds, F. So, Univ. of Florida (United States)

In bulk-heterojunction (BHJ) polymer solar cells, the vertical phase morphology of the active layer plays a crucial role in determining the exciton dissociation efficiency, charge extraction efficiency and thus the overall power conversion efficiency. In order to maximize the device efficiency, the donor and acceptor molecules should segregate toward the anode and cathode, respectively. However, several polymer-PCBM systems have exhibited phase segregation that could only be optimized if the device structure was inverted such that the cathode is at the bottom and the anode is on the top. To investigate the effect of this vertical phase segregation on device performance, we fabricated inverted solar cells that exploit the natural vertical phase separation of the bulk heterojunction layer. We realized the inverted architecture by modifying the bottom ITO electrode with a solution-processed ZnO layer, followed by the BHJ layer. A thin layer of MoOx was used as a hole-extraction layer on top for efficient charge extraction.

In this work, we have studied the performance of normal and inverted BHJ solar cells with an active layer composed of a blend of poly[[4,4'-bis(2-ethylhexyl)dithieno[3,2-b:2',3'-d]silole]-2,6-diyl-alt-(2,1,3-benzothiadiazole)-4,7-diyl] (DTS-BTD) as the donor and {6,6}-phenyl-C71 butyric acid methyl ester (PC70BM) as the acceptor. Here, the inverted devices exhibited an increase in short circuit current density (J_{sc}) by 32% over the conventional solar cells (16.77 mA/cm² in the inverted devices compared to 12.71 mA/cm² in the conventional devices). Overall, the inverted structure had a higher power conversion efficiency of 5.8% compared to 4.9% for the conventional device. The enhanced device performance for inverted device geometry attributed to the formation of favorable vertical phase segregation in the active layer where the top surface of the polymer blend is donor-rich and bottom surface is acceptor-rich resulting in a significant enhancement in the short-circuit current. With further optimization we were able to achieve a power conversion efficiency of 6.4% for the inverted device.

8116-30, Session 7

The effects of trace solvents on the morphology of P3HT:PCBM solar cells

A. J. Moule, L. Chang, Univ. of California, Davis (United States)

The efficiency of bulk-heterojunction solar cells is highly sensitive to changes in the nanostructure of the active layer. Despite exhaustive research into various processing (varying casting solvents) or post-processing (heat tempering or solvent soaking) techniques to "improve" the morphology of the active layer, the relationship between fabrication conditions and device performance is poorly understood. This work examines the role that excess solvent that remains in the active layer after coating has on the morphology and the diffusion rate of PCBM within the active layer. We examine how solvents with a range of boiling temperatures effect the stability of morphology after the device is completed and conclude that high boiling temperature solvents lead to increased PCBM agglomeration. Laser beam induced current (LBIC) mapping of the active layer suggested that PCBM agglomerations are unfavorable to device performance as low photocurrents were detected on regions where PCBM agglomerates are present.

Next we examine the role that solvent additives have on morphology, PCBM diffusion, and temperature stability of the morphology. We show that good solvents lead to poor morphological stability, an effect that can be traced to a reduction of the energy cost for melting or glass transition. Differential scanning calorimeter (DSC) results indicate that addition of a poor-solvent or non-solvent increases the onset of melting for polymer side chains and backbone. J-V (current density vs. voltage) characteristics show that a device fabricated using a nitrobenzene

additive has similar performance to an annealed device but that the morphology is more stable to heat cycling.

8116-31, Session 7

Evolution of surface, sub-surface, and bulk morphology and its effects on organic photovoltaic performance

B. Lyons, N. Clarke, C. Groves, Durham Univ. (United Kingdom)

In order to maximise the performance in an organic solar cell it is necessary to balance the competing needs of efficient charge generation with the requirement of an efficient percolating network to the electrodes. This has led to considerable efforts to optimise both the bulk and surface morphologies through many techniques such as solvent or vapour annealing, use of co-solvents, self-assembled monolayers and others. In particular, a variety of recent NEXAFS and XPS data have shown that improper preparation of the substrate-blend interface can give rise to charge-blocking barriers that are detrimental to device performance.

In this work we use Cahn-Hilliard-Cook theory to examine the evolution of a 3-dimensional blend morphology during drying, including the effects of surface energy. This method provides a realistic facsimile of bulk heterojunction blend evolution through solvent evaporation and/or thermal annealing. The solar cell performance associated with these blends is then examined using a Monte Carlo model.

It is shown that the coverage and thickness of surface layers formed due to surface energy effects increase as the blend evolves, as do sub-surface features that can also impede current flow. We show how this surface and sub-surface composition variation effects organic solar cell performance, and in turn offer guidance as to when surface layers are current blocking. Additionally, we show that the optimum degree of annealing/drying differs between films where surface effects are important and are absent.

8116-32, Session 7

Time-resolved characterization of the nanoscale structure and morphology of spin-cast bulk-heterojunction photoactive thin films

K. W. Chou, R. Li, D. Marques, E. Li, King Abdullah Univ. of Science and Technology (Saudi Arabia); O. Wodo, B. Ganapathysubramanian, Iowa State Univ. (United States); R. Gassaway, A. Biocca, A. Hexemer, Lawrence Berkeley National Lab. (United States); J. E. Anthony, Univ. of Kentucky (United States); S. Thoroddsen, A. Amassian, King Abdullah Univ. of Science and Technology (Saudi Arabia)

Despite significant improvements in organic photovoltaic (OPV) technology there still remain several issues that prevent the wide-spread use and profitable commercial production of OPVs. One major challenge is the weak control over the manufacturing processes to get tailored morphologies of the active thin films. Current state-of-the-art approaches to understand the morphological evolution and tailoring of the manufacturing processes for high efficiency organic solar cells are either limited to a combinatorial experimental investigation or single scale analysis, and provide only limited data for analysis. The main reasons for that are related to the difficulty of attaining high spatial resolution and to the requirement of good contrast between components. In situ analysis is further complicated by the incompatibility of many traditional characterization techniques with solution processes. These challenges hinder our ability to understand and subsequently control the interaction of multiple factors affecting the morphological evolution.

We report the in situ monitoring of the growth of thin films during solution processing. A compact spin coater and liquid dispensing system was

built and time-resolved grazing incidence x-ray scattering (small angle and wide angle) measurements were performed during the spin coating process with sub-second time resolution. The evolution of the liquid layer was monitored in situ using fast CCD camera imaging. The film growth was investigated for different donor and acceptor materials, as well as for blends thereof as a function of processing conditions. The results are compared to phase-field simulation model predictions of the 3D evolution of the morphology during solution-processing of the organic bulk heterojunction layer.

8116-108, Session 7

Structural measurements of polymer-fullerene blend films for organic photovoltaics

D. M. DeLongchamp, National Institute of Standards and Technology (United States)

Organic photovoltaic (OPV) technology has the potential to lower the cost of solar cell fabrication by ink-based coating techniques. In bulk heterojunction (BHJ) OPV devices, the power conversion efficiency critically depends on the distribution of the polymer absorber and the fullerene electron acceptor. I will describe measurement methods to probe the morphology of the BHJ layer.

The vertical distribution of absorber and electron acceptor in BHJ films follows segregation behavior similar to that of miscible polymer blends. The top (air) interface becomes rich in the polymer absorber, whereas the bottom interface composition depends on the substrate surface energy. I will discuss whether interfacial segregation can impact power conversion efficiency by comparing hole transport layers that have similar work functions but different surface energies. I will show that interfacial segregation strongly impacts aging-related morphology deterioration.

The nanometer-scale three-dimensional structure of the BHJ interior is critical to the efficiency of exciton harvesting. Solid-state nuclear magnetic resonance can be used to measure the size distribution of polymer and fullerene domains. The nanoscale morphology can also be directly imaged using chemical contrast tomographic transmission electron microscopy. Order and crystal orientation within domains can be probed with grazing-incidence X-ray diffraction. We consolidate this information to correlate fine structural details to performance for BHJs using poly(3-hexylthiophene) as well as small bandgap push-pull absorbers such as benzodithiophene-containing and silole-containing polymers that exhibit power conversion efficiencies in the range of 5% to 8%.

8116-33, Session 8

Charge photogeneration and recombination in organic solar cells

J. R. Durrant, Imperial College London (United Kingdom)

My lecture will focus on charge separation and recombination in polymer / fullerene solar cells and their impact upon device photovoltaic performance. The talk will be based around transient optical and optoelectronic studies of yields, lifetimes and densities of dissociated charges in blend films and solar cells. (1-3) Comparative studies will be presented of different materials systems, including over 20 different polymers, and perylene as well as fullerene acceptors. On the basis of these data, I will address the parameters which influencing charge photogeneration, including the roles of molecular structure, film nanostructure, interfacial energetics, and macroscopic electric fields

References

1. Shoaee, S.; Clarke, T.M.; Huang, C.; Barlow, S.; Marder, S.R.; Heeney, M.; McCulloch, I.; Durrant, J.R., Acceptor energy level control of charge photogeneration in organic donor/acceptor blends., *Journal of the American Chemical Society*, 2010, Vol:132, 12919-12926.
2. Clarke, T. M.; Durrant, J. R., Charge Photogeneration in Organic Solar Cells. *Chemical Reviews* 2010, 110, 6736-6767

3. Clarke, T.M.; Ballantyne, A.; Shoaee, S.; Soon, Y.W.; Duffy, W.; Heeney, M.; McCulloch, I.; Nelson, J.; Durrant, J.R., Analysis of charge photogeneration as a key determinant of photocurrent density in polymer: fullerene solar cells., *Advanced Materials*, 2010, Vol:22, 5287-5291

8116-34, Session 8

Photocarrier dynamics in nanostructured phthalocyanine: fullerene films

P. A. Lane, U.S. Naval Research Lab. (United States); E. J. Heilweil, National Institute of Standards and Technology (United States); J. S. Melinger, U.S. Naval Research Lab. (United States)

We have studied photocarrier generation and decay in zinc phthalocyanine and C60 on a wide range of time scales using transient and CW pump-probe spectroscopy. Photocarrier generation was studied by terahertz time domain spectroscopy (THz-TDS), an optical, non-contact technique which measures transient decay dynamics of photo-generated carriers on a picosecond to nanosecond time scale. We find a dependence of the THz absorption on concentration for composite films and on layer thickness for ZnPc/C60 superlattice films. Superlattices with layer thicknesses less than 10 nm show stronger THz absorption than an optimized composite and with slower decay dynamics.

The decay dynamics extend well out past the maximum pump-probe delay. In order to examine carrier yield and decay dynamics, we turned to photoinduced absorption (PA) spectroscopy. Combining THz-TDS and PA spectroscopy permits us to study carrier generation and decay on a range of time scales from picoseconds to milliseconds. We find stronger signals from the thinnest nanolayered samples, in agreement with the results of THz-TDS. This combined study reveals a simple way to improve film morphology for organic photovoltaics, free of electrical contacts or other device related characteristics.

8116-35, Session 8

Impact of trap-assisted recombination on the performance of polymer-fullerene bulk-heterojunction solar cells

C. Deibel, J. Lorrman, A. Baumann, J. Gorenflot, A. Wagenpfahl, V. Dyakonov, Julius-Maximilians-Univ. Würzburg (Germany)

Charge carrier recombination in organic solar cells limits the power conversion efficiency, and therefore deserves a closer look. We investigated devices made from P3HT or PCDTBT and their blends with fullerene derivatives by temperature dependent transient absorption and charge extraction by linearly increasing voltage measurements. The results clearly show that recombination in the blend is trap-limited with recombination orders beyond two for low temperatures, while the recombination in the pure material is mainly rendered by a recombination order of two. We present a multiple trapping model in which the traps are intrinsic, corresponding to the tail of the density of states distribution. With this model, we can describe the experimentally determined charge carrier dynamics quantitatively. We find that a trap-induced delay of the bimolecular recombination leads to the higher apparent recombination orders. This mechanism relies on the phase separation of donor and acceptor: charge carriers trapped within one of the material phases can only recombine with a mobile charge (or be extracted from the device) once they are re-emitted from the trap. The strong dependence of the recombination rate on the energetic disorder and temperature explains the experimentally observed deviations from Langevin theory predicting second order losses. Thus, counterintuitively, a higher concentration of traps leading to a higher recombination order is connected to a longer effective charge carrier lifetime of the mobile charges. By applying a macroscopic device simulation, we discuss the impact of trap-assisted bimolecular recombination on the solar cell characteristics.

8116-36, Session 8

Enhanced charge separation in polymer/fullerene heterojunctions by molecular doping

E. Da Como, F. Deschler, J. Feldmann, Ludwig-Maximilians-Univ. München (Germany)

Charge separation at polymer:fullerene interfaces is the primary process for organic bulk-heterojunction solar cells. Following the ultrafast photoinduced charge transfer, electrons and holes are still bound because of Coulomb interactions, resulting in the formation of charge transfer excitons (CTEs). Those are known to play a crucial role in solar cells being responsible for the open circuit voltage and the short circuit current.

In this contribution, we propose a novel strategy to overcome some of the recombination channels due to CTEs. This new approach considers the modification of the electronic properties of the conjugated polymer by doping with 2,3,5,6-Tetrafluoro-7,7,8,8-tetracyanoquinodimethane (F4TCNQ) molecules. The free holes induced by F4TCNQ on the low-bandgap polymer poly[2,6-(4,4-bis-(2-ethylhexyl)-4H-cyclopenta[2,1-b;3,4-b']dithiophene)-alt-4,7-(2,1,3-benzothiadiazole)] PCPDTBT fill the tail of states in the highest occupied molecular orbital (HOMO) and in addition are expected to screen Coulomb interactions of CTEs at the interface between PCPDTBT and the fullerene derivative PCBM. By the unique combination of time resolved photoluminescence and photoinduced absorption spectroscopy, we demonstrate how doping results in a decreased population of CTEs and enhanced formation of free carriers. The spectroscopy experiments are complemented by measurements on solar cells showing an overall increase of more than 30% in the power conversion efficiency.

8116-37, Session 8

On the maximum power conversion efficiency of organic photovoltaics

J. C. Hummelen, Univ. of Groningen (Netherlands); S. E. Shaheen, Univ. of Denver (United States); L. J. A. Koster, Univ. of Groningen (Netherlands)

General design rules for high efficiency OPV have been given by several groups, with a strong focus on optimization of the properties of the donor material and neglecting charge carrier generation as the result of light absorption by the acceptor. We report on our analysis of a single junction donor/acceptor OPV device. We take an approach in which there is no fundamental difference between the donor and acceptor other than the fact that the donor has frontier orbitals at energies higher than the corresponding ones of the acceptor. We argue that such a symmetrical version of OPV is capable of higher efficiency. First, we investigate in a semi-empirical way the influence of bandgap(s) and band offsets on the power conversion efficiency. Second, we also include the influence of the reorganization energy of the charge generation process. Using a slightly different approach, we then consider the influence of the exciton binding energy on the maximum power conversion efficiency. Finally, we introduce the dielectric constant as a parameter in the analysis.

Our analysis suggests that there is no fundamental thermodynamic reason for OPV to have a theoretical efficiency limit lower than the Shockley-Queisser one. It simply shows that there is much work to do on improving molecular materials to overcome present limitations. The trivial conclusion is that in the limit of assuming a donor/acceptor combination of ideal organic materials the same result is obtained as when taking an ideal inorganic p-n junction.

8116-38, Session 8

Recombination dynamics as a key determinant of open-circuit voltage in organic bulk-heterojunction solar cells

A. Maurano, Imperial College London (United Kingdom) and Merck Chemicals Ltd. (United Kingdom); D. Credgington, B. O'Regan, I. McCulloch, Imperial College London (United Kingdom); M. Carrasco-Orozco, S. Tierney, Merck Chemicals Ltd. (United Kingdom); M. Morana, Konarka Austria Forschungs und Entwicklungs GmbH (United Kingdom); J. R. Durrant, Imperial College London (United Kingdom)

Polymer photovoltaic devices based on bulk heterojunction blends of semiconducting polymers and soluble fullerene derivatives have shown impressive advances in power conversion efficiency. However, their efficiencies are still too low to make them commercially attractive. One of the key factors limiting the efficiency is the relatively modest voltage outputs, with open circuit voltage (VOC) typically being less than half of the optical bandgap. In this work, we compare the VOC of BHJ cells fabricated from four polymer donors and we show that VOC is limited not only by material energetic[1] but also by the dynamics of non-geminate charge recombination within the blend.[2]

Transient photovoltage[3] and charge extraction[4] were used to calculate, under realistic working conditions for solar cells, the non-geminate recombination flux J_{rec} that affects VOC according to the formula: $VOC = (IP - EA) / e + \ln(J_{SC} / J_{rec}) / \gamma(\alpha + 1)$, where IP is the ionisation potential of the donor polymer, EA the electron affinity of the acceptor and α , γ are experimentally determined parameters. This formula encompasses three different influences upon VOC. IP - EA represents the ultimate limit to VOC. The charge photogeneration flux (proportional to JSC) creates electron and hole Fermi level splitting, and the charge recombination flux (proportional to J_{rec}) acts at open circuit conditions to limit this splitting. The values of VOC determined by this methodology are compared to measured values and show very close correspondence.

1. Scharber, M.C., et al., *Advanced Materials*, 2006. 18(6): p. 789-+.
2. Maurano A., et al., *Advanced Materials*, 2010, 22, 4987-4992.
3. Shuttle, C.G., et al., *Applied Physics Letters*, 2008. 92(9): p. 3.
4. Shuttle, C.G., et al., *Applied Physics Letters*, 2008. 93(18): p. 3.

8116-39, Session 9

Oxide/organic interfaces: their role in controlling OPV device efficiency

N. R. Armstrong, J. Gantz, G. Macdonald, B. Zacher, The Univ. of Arizona (United States)

The composition and energetics of oxide/organic interfaces play a critical role in the efficiency of organic solar cells. These interfaces arise in cases where the donor or acceptor components are in direct contact with a transparent conductive oxide (TCO), or where an oxide "interlayer" is inserted between the TCO and the donor or acceptor layer. This talk will focus on the modeling and characterization of interfaces formed between ITO and various small molecule donors, where the polarity of the donor is quite low (e.g. pentacene) or where a strong internal dipole is present in the donor (e.g. TiOPc) leading to specific interactions between the donor layer and the oxide. Significant changes to local vacuum levels are seen during deposition of either type of donor layer, however, for the polar donors there is a clear indication that orientation of the donor matters, and affects charge harvesting, and OPV performance. For the less polar donor layers OPV performance is not strongly coupled to ITO surface composition, whereas for the polar donors even sub-monolayer changes in oxide surface composition can strongly affect OPV performance. We will also review recent conductive tip AFM studies of these interfaces, and modeling studies at small length scales which show the importance of electrode composition, and the mitigating role that interlayer films can play in improving OPV performance.

8116-40, Session 9

Beyond energy-level engineering: the effects of the solid-state environment on the ionisation energies and electron affinities of organic molecular semiconductors for organic photovoltaics

B. J. Powell, P. E. Schwenn, P. L. Burn, The Univ. of Queensland (Australia)

Energy level engineering has become one of the central ideas in organic optoelectronics; particularly in the field of organic photovoltaics. However, this paradigm has led to significant ambiguities and errors in the literature. To investigate and address these issues we calculate solid-state ionisation energies and electron affinities of a range of organic molecular semiconductors from density functional theory and the polarizable continuum model. We show that the differences between these results and measurements from (inverse) photoemission are on the same scale as the differences between the measured values reported by different groups. We compare our results with *in vacuo* calculations and estimates of the ionisation energies and electron affinities from the eigenvalues of the Kohn-Sham equations. *In vacuo* calculations overestimate the ionisation energies measured in the solid state, but underestimate solid state electron affinities. However, the Kohn-Sham eigenvalues predict the measured ionisation energies nearly as well as the full calculation. However, we show that the apparent accuracy of the Kohn-Sham eigenvalues is fortuitous and arises from the cancellation of the errors due to the use of Kohn-Sham molecular orbital energies as predictions of ionisation energies and electron affinities and the neglect of the polarizable solid state environment. These results stress the importance of descriptions based on molecular states rather than molecular orbitals when designing and characterising materials for organic electronic and optoelectronic devices.

8116-41, Session 9

Small molecules and polymers in organic photovoltaic devices: interfaces and energy levels

S. E. Watkins, F. H. Scholes, K. N. Winzenberg, J. Jasieniak, T. Ehlig, B. Singh, R. A. Evans, A. Gupta, M. Gao, G. J. Wilson, P. Kempainen, Commonwealth Scientific and Industrial Research Organisation (Australia)

In this paper we describe several of our approaches to materials characterisation that aim to accelerate the assay of new materials for use in organic photovoltaics. We describe results for blends based on both small molecules and polymers. For the system based on dibenzochrysenes, differences between the energy transfer processes in blends with either fullerenes or conjugated polymers are described. For the former, efficient solar cells can be made in both bulk heterojunction and bilayer configurations. For the latter, incomplete fluorescence quenching shows unfavourable energy transfer pathways that differ with changes to the blend ratio. The assay of materials and material blends by Photo Electron Spectroscopy in Air is described. We also present results from our high-throughput approach to the fabrication of bilayer devices - a device structure with a simplified interface that reduces the complexities of the bulk heterojunction assembly. We demonstrate that the use of bilayer devices enables a large material and device parameter space to be effectively spanned to rapidly assay the viability of new materials in organic solar cells.

8116-42, Session 9

The impact of interfaces on the performance of organic photovoltaic cells

R. Steim, F. R. Kogler, J. Hauch, Konarka Technologies GmbH (Germany)

Organic photovoltaics (OPV) is a promising technology to solve future energy supply scenarios. The ongoing improvement of the absorber materials resulted recently in certified efficiencies of up to 8.3 % making it more and more interesting for large scale applications like Building Integrated Photovoltaics (BIPV). For BIPV applications performance under non-optimal conditions, like low light, is equally important as the efficiency at 1sun illumination. Optimal performance of OPV requires more than just an optimized absorber layer. While the interplay of the absorber layer with interface materials [1] is always a prerequisite for high performance, it is paramount for low light performance. Unadjusted interface materials can lead to the S-shape current voltage characteristics which drastically reduce the performance of OPV cells in all conditions. For low light applications however, interface materials have to provide highly selective, homogeneous and pinhole free contacts, eliminating hot spots that can be tolerated under 1sun illumination. [2, 3] In the end, the performance of the full OPV module is of importance which is determined by the interplay of all included materials.

[1] R. Steim et al., Interface materials of organic solar cells, *Journal of Materials Chemistry* 20, 2499 (2010).

[2] R. Steim, *The Impact of Interfaces on the Performance of Organic Photovoltaic Cells*, KIT Scientific Publishing 2010, ISBN: 978-3-86644-526-0.

[3] R. Steim et al., Formation and impact of hot spots on the performance of organic photovoltaics, *APL* 94, 043304 (2009).

8116-43, Session 9

Charge separation dynamics at inorganic/organic nanostructured hybrid photovoltaic interfaces

R. Eichberger, C. Strothkaemper, I. Thomas, T. Hannappel, K. Schwarzburg, Helmholtz-Zentrum Berlin für Materialien und Energie GmbH (Germany); C. Fasting, Freie Univ. Berlin (Germany); A. Bartelt, R. Schuetz, Helmholtz-Zentrum Berlin für Materialien und Energie GmbH (Germany)

In nanostructured hybrid photovoltaic devices containing thin organic interfacial absorber layers photo-induced charge separation can be divided into three basic sequences: Light harvesting, charge separation across the heterogeneous interface and charge transport through electron and hole conducting media. Depending on the chemical nature and thickness of the absorber layer, electronic alignment and density of acceptor or trap states at the interface, and finally the conductivity of the transport electrodes, the time scales of the charge separation sequences can be very diverse. For efficient light harvesting - especially in all solid state dye sensitized solar cells (DSSCs) - the hybrid interface is a major limiting part because the generated electrons and holes can recombine on a very fast time scale. We used femtosecond broadband transient absorption spectroscopy in ultrahigh vacuum and terahertz (THz) photoconductivity to study the initial injection dynamics and the early back reaction in competition with carrier escape into the bulk material. The dynamics of different absorber concepts ranging from organic model chromophores to simple antenna FRET systems adsorbed on TiO₂ nanoparticle and ZnO nanorod films were measured in our complementary experimental setup. Differences in the encountered interfacial dynamics arising from properties of the two electrodes will be discussed.

8116-44, Session 10

Semi-transparent polymer photovoltaic devices with good transparency color-perception and color-rendering properties

A. Colsmann, A. Puetz, U. Lemmer, Karlsruhe Institut für Technologie (Germany)

Window integrated photovoltaics for automotive and building applications are a promising market segment for organic solar modules. Besides semi-transparency, window integrated applications require a reasonable transparency perception. However, a reasonable transparency perception does not necessarily imply good color rendering. The color rendering of items under illumination of transmitted light is of utmost importance when integrating semi-transparent photovoltaic devices in windows or overhead glazings. For example, (transmitted) white light that mainly contains blue and yellow parts of the visible spectrum will render white surfaces acceptably but is incapable of rendering reddish objects.

Therefore, in this work we present efficient ($\eta \approx 3\%$) semi-transparent organic solar cells incorporating a polymer/fullerene blend poly[(4,4'-bis(2-ethylhexyl)dithieno[3,2-b:2',3'-d]silole)-2,6-diyl-alt-(2,1,3-benzothiazole)-4,7-diyl] : [6,6]-phenyl C71-butric acid methyl ester (PSBTBT:PC70BM) with an extended absorption to the infrared. In order to account for different illumination situations such as bright sunlight or cloudy skies we investigated different light sources shining through the semi-transparent device. The transmitted light exhibits remarkable color rendering properties making this polymer/fullerene combination and the respective solar cells suitable for real-life window applications. These properties are moreover tunable by the incorporation of suitable dyes and organic absorbers into the device architecture.

8116-45, Session 10

Scrutinizing molecular stacking of polymeric, fibrous scaffold fabricated with freeze-dry method: messages to making of polymer heterojunction solar cells

C. Cheng, Institute of Atomic and Molecular Sciences (Taiwan); Y. Huang, Academia Sinica (Taiwan); Y. Lan, Institute of Atomic and Molecular Sciences (Taiwan); P. Huang, Fu-Jen Catholic Univ. (Taiwan); C. Chen, Academia Sinica (Taiwan); P. Huang, Fu-Jen Catholic Univ. (Taiwan); J. Wang, Institute of Atomic and Molecular Sciences (Taiwan) and National Taiwan Univ. (Taiwan)

The efficiency of polymer solar cells has been greatly improved with bulk heterojunction (BHJ) concept that introduces increased donor-acceptor interface for charge separation. Physical blending with ensuing annealing, though eliciting ordered nano-domains for exciton diffusion, would inflict breaking of long-range order that impairs charge transport and, additionally, might not be generally applied to new molecular systems, owing to intricate inter-molecular interaction. We demonstrate a means to fabricate P3HT/PCBM BHJ solar cell based on freeze-dry method. Its power conversion efficiency (3.6%) is comparable to that of conventional BHJ cells. A 3-D fibrous P3HT scaffold, being first concocted with the simultaneously grouted PCBM in solution, sustains while the solvent sublimates at a low temperature. The following thermal annealing then actuates local ordering of molecular aggregates. Its Raman-spectroscopy characterization shows that three contiguous peaks with disparate intensities, together corresponding to the C=C stretching of the thiophene ring in P3HT, connote distinct conjugated lengths and/or molecular stacking configurations. The dominated peak confers a higher occupation than that from the mixed spin-coating layer (77% vs. 60%), implying that more propitious P3HT agglomerates develop in such fibrous scaffold. Additionally, the analogous absorption strength at the lowest two vibronic transitions of the freeze-dry sample is indicative of its larger concordant domains according to H-aggregate model of P3HT aggregates. This study bestows material scientists a common

platform to create and preserve charge-transport pathway that is crucial to realize BHJ solar cells with their specially designed molecules, without undergoing extensive try-and-errors.

8116-46, Session 10

Harvesting additional solar inventory through low-power photon upconversion

F. N. Castellano, Bowling Green State Univ. (United States)

One focus of our research program involves the study of sensitized triplet-triplet annihilation (TTA) in solution using highly photostable metal-organic chromophores in conjunction with energetically appropriate organic molecules with large singlet-triplet gaps. Selective visible light excitation of the long-wavelength absorbing sensitizer efficiently generates long-lived triplet states which serve as energy transfer donors. In the presence of appropriate molecular acceptors, diffusion controlled triplet-triplet transfer takes place, producing the excited triplet state of the acceptor while regenerating the ground state of the sensitizer. When sufficient numbers of the sensitized triplets are produced, TTA takes place which results in either frequency upconverted light or the formation of desired chemical products. Various combinations of donor and acceptor have been explored and data will be presented on a number of these systems spanning the near-visible to the near-IR. This presentation will also feature many examples of upconversion phenomena realized in solid-state materials along with emerging classes of acceptor/annihilator chromophores. Finally, attempts to integrate upconversion-based photoaction into operational photovoltaics will be discussed.

8116-47, Session 10

Nanolaminate architectures for flexible encapsulation

S. Graham, H. Kim, A. Bulusu, Georgia Institute of Technology (United States)

The development of high performance barrier films for organic solar cells is seen as a critical step in packaging and reliability of these devices. While organic/inorganic multilayers have been developed for these technologies, some concerns exist in the long term durability of the organic layers when exposed to solar environments. Thus, inorganic multilayers which provide similar barrier performance are under development as an alternative barrier film for use in solar cells.

In this work, we investigate the development and performance of inorganic nanolaminate films for high performance flexible barriers. Nanolaminates were made using PECVD as well as atomic layer deposition. Results show that ultra high barriers can be made using combinations of Al₂O₃/ZnO and Al₂O₃/Zr₂O with dyads on the order of 4nm. A combination of xray diffraction and XPS were used to analyze and understand the changes in morphology at the interfaces of the dyads and link them to the improvement in barrier performance. Exposure to humid environments is also performed to understand their susceptibility to corrosion by water vapor as seen in the case of pure Al₂O₃. Finally, the stresses and mechanical flexibility of these barrier films will be discussed.

8116-48, Session 10

Blade coating for single- and multi-layer polymer solar cell

H. Meng, National Chiao Tung Univ. (Taiwan); E. Chen, National Tsing Hua Univ. (Taiwan); H. Zan, National Chiao Tung Univ. (Taiwan); S. Horng, National Tsing Hua Univ. (Taiwan); Z. Chen, A*STAR Institute of Materials Research and Engineering (Singapore)

Organic semiconductors can be deposited in large area with nearly no material waste by blade coating method. First a blade with 60 micron gap to the substrate moves rapidly to form a wet layer, which is then immediately dried by heating to avoid dissolution of underneath organic layer and uniformity problem due to liquid flow. The variation less than 10 nm around mean thickness of 150 nm can be achieved for a range of 10 cm for the solid film. This method is applied to solar cell as well as OLED. For single layer solar cell with P3HT electron donor and PCBM acceptor power conversion efficiency of 3.6 % is achieved by rapid dried toluene solution, in contrast to the slow solvent evaporation process in dichlorobenzene solution required for spin coating. In addition to lower toxicity, rapid blade coating and drying in toluene enhance the throughput. The PEDOT:PSS layer can also be deposited by blade coating. Tri-layer structure with pure P3HT as the electron blocking and pure PCBM as hole blocking layer made by blade coating shows efficiency of 4.1 %. When low band-gap polymer is used in place of P3HT the efficiency is raised to 5 %. The cathode evaporation can be replaced with a simple vacuum-free metal transfer from a rubber mold proven for OLED. In order to further reduce the cost, ITO electrode is replaced by modified Al with semitransparent Ag top electrode for inverted solar cell with top illumination. Efficiency of 3 % is achieved.

8116-49, Session 11

Modelling charge transport and recombination in organic photovoltaic materials

J. Nelson, J. M. Frost, T. Kirchartz, R. MacKenzie, Imperial College London (United Kingdom); J. Kirkpatrick, Univ. of Oxford (United Kingdom)

The behaviour of organic donor-acceptor heterojunction solar cells is not readily described by conventional semiconductor device models. In particular, the competition between charge collection and charge recombination is influenced by the disordered nature of charge transport and the heterogeneous nature of the microstructure. In order to select and design materials with potential for higher performance, methods are needed to help understand first, how charge dynamics are related to the chemical and physical structure of the component materials and second, how the dispersive nature of the charge dynamics influences the current-voltage response of a photovoltaic device. We use a multi-scale modelling approach to simulate charge dynamics in organic electronic materials, incorporating molecular modelling of the microstructure of organic films, quantum chemical calculation of intermolecular charge transfer rates and simulation of current transport and recombination. We have adapted continuum models of device behaviour to incorporate energetic disorder via a density of states function based on the microscopic studies. We will show how such an approach can be used to help explain the optoelectrical behaviour of organic photovoltaic materials and devices.

8116-50, Session 11

Design rules for fullerene/polymer composites used in organic bulk-heterojunction solar cells

P. A. Troshin, D. K. Susarova, E. A. Khakina, O. Mukhacheva, A. Goryachev, Institute of Problems of Chemical Physics (Russian Federation); C. Kaestner, Technische Univ. Ilmenau (Germany); S. A. Ponomarenko, Institute of Synthetic Polymeric Materials (Russian Federation); H. Hoppe, Technische Univ. Ilmenau (Germany); V. F. Razumov, Institute of Problems of Chemical Physics (Russian Federation); D. A. M. Egbe, S. Sariciftci, Johannes Kepler Univ. Linz (Austria)

We present here a comprehensive set of the results on photovoltaic

performance of approximately 300 different photoactive systems based on combinations of 25 fullerene derivatives and 12 conjugated polymers. A thorough analysis of the obtained data allowed us to reveal some important correlations between the molecular structures of the polymer and fullerene counterparts, their physical properties (solubility), the morphology of their photoactive blends and their photovoltaic performance. The observed relationships might be used as guidelines for rational design of novel material combinations for fullerene/polymer organic solar cells.

It will be demonstrated that many fullerene/polymer composite systems have rather predictable behavior. Considering molecular structures of both polymer and fullerene derivative it becomes possible to approximately predict the morphology of their composites. In turn, the nanomorphology of the fullerene/polymer blends was shown to have a direct quantitative correlation with their photovoltaic performance. Therefore, a clear relationship between the molecular structures of the materials and their photovoltaic performance has been established for the first time. These results create a solid background for the development of computational approaches (similar to QSAR) for rational design of novel photoactive materials for organic photovoltaics.

8116-51, Session 11

Investigating the loss-mechanisms of photocurrent in low bandgap donor-acceptor copolymer based solar cells: photo-carriers recombination

S. Chen, K. R. Choudhury, F. Steffy, J. Subbiah, C. M. Amb, J. R. Reynolds, F. So, Univ. of Florida (United States)

Bulk-heterojunction (BHJ) photovoltaic devices based on the semiconducting polymer poly(3-hexylthiophene-2,5-diyl) (P3HT) and fullerenes have been extensively investigated and optimized, with power conversion efficiencies (PCEs) approaching 5 % and fill factor (FF) close to 70%. However, further improvement in this material system is constrained by the limited absorption in the solar spectrum. The bottleneck of limited absorption can be overcome using low bandgap donor-acceptor conjugated copolymers with absorption edge extended to the near IR range. High short-circuit current has been achieved in a quite a few low bandgap polymer: PCBM systems with PCEs reaching ~7%. However, the FFs in these cells are low (< 0.60), impeding further enhancement in efficiency. PCEs beyond 7% can be achieved if the fill factor values approach to those in the P3HT:PCBM system.

In this study we investigate the physical processes that limit the extraction of photocurrent and the FF in a low bandgap polymer: fullerene system. We studied the transport and recombination of photo-carriers in the poly[(4,4'-bis(2-ethylhexyl)dithieno[3,2-b:2',3'-d]silole)-2,6-diyl-alt-(2,1,3-benzothiadiazole)-4,7-diyl] (DTS-BTD): PCBM BHJ system and compare the results with the highly optimized blend of P3HT:PCBM. Mobility measurements shows well balanced transport of electrons and holes in DTS-BTD: PCBM cells; this rules out the possibility that photocurrent loss is due to unbalanced transport. Two different techniques are used to study the photo-carrier recombination mechanisms under different extraction fields. Long photo-carrier lifetimes obtained at low extraction fields by photo-CELIV measurements indicate that the photocurrent is not limited by recombination in this regime. In comparison, carrier recombination rates under open-circuit condition obtained from transient photo-voltage measurements are significantly higher. Finally, the energetic disorder of the system was determined by the photo-CELIV measurements and the results suggest that the carrier recombination rate is related to the energetic disorder present in the material which might be related to the morphology of the bulk heterojunction.

8116-53, Session 11

Measurement and characterization of the mobility-lifetime product and recombination mechanisms in bulk-heterojunction organic photovoltaic materials

C. Lombardo, E. Danielson, A. Dodabalapur, The Univ. of Texas at Austin (United States)

The mobility-lifetime product, in bulk heterojunction (BHJ) organic photovoltaic cells, is an important parameter for understanding charge transport within these materials. Hecht's original derivation for charge collection was for a vertical photodetector and discrete photon sensing events. In order to measure the mobility-lifetime product BHJ organic photovoltaic cells, Hecht's equation has been adapted to a lateral geometry, steady-state illumination, and to the measurement of electrical current flowing in lateral solar cell devices. By fitting experimental data from devices with carrier transit lengths ranging from 100 nm to 20 μm to the reformed equations, we have been able to measure the drift length of charge carriers within the BHJ material. Using this information, we have determined the mobility-lifetime product as a function of the electric field. In addition to the mobility-lifetime product, the charge carrier generation rate from the disassociation of photogenerated excitons can also be independently determined from these measurements. Additional electrical current measurements as a function of light intensity, ranging from 1 mW/cm² to 1000 mW/cm², have been used to characterize mechanisms of charge carrier recombination within these materials. Recombination rates as a function of electric field and device length have been determined as well as the functional form of the recombination rate as it relates to carrier concentration ($U \propto n^x$). For this study, P3HT:PCBM and P3HT:C71-PCBM has been employed due their wide use among researchers as well as their potential for commercialization.

8116-90, Session 11

Nanoscale-resolved optoelectronic properties as a probe to the internal morphology of working OPV cells

F. A. Castro, National Physical Lab. (United Kingdom); W. C. Tsoi, Imperial College London (United Kingdom); P. Nicholson, National Physical Lab. (United Kingdom); J. Kim, Imperial College London (United Kingdom); C. Murphy, D. Roy, National Physical Lab. (United Kingdom); J. Kim, Imperial College London (United Kingdom)

Organic photovoltaic device efficiency has had a remarkable increase from 5% to over 8% in the last three years alongside an increase in industrial investment. Yet, a clear prototype material combination has not emerged and it is likely that different companies will proceed development with their own proprietary organic semiconductor materials rather than all using a common system as is the case with Si solar cells. To increase competitiveness and reduce product development time, detailed understanding and characterisation of the nanomorphology and surface distribution of donor/acceptor phases is therefore crucial. Nowadays surface information can be readily obtained, although high resolution and reliable quantitative information is still challenging. On the other hand, probing bulk morphology and optoelectrical properties with nanometre resolution in real working devices remains an unachieved Holy Grail.

In this work we demonstrate how Photocurrent Atomic Force Microscopy (PC-AFM) can be used to obtain key nanometre scale morphological and optoelectronic insight relating to donor and acceptor phases within the bulk of a working bulk-heterojunction solar cell. By combining it with surface-only sensitive techniques we can separate the effects of the bulk from those of the surface and clarify how the local internal film morphology affects bulk device efficiency. We also identify signatures of donor (or acceptor) rich areas on the surface and obtain direct proof for the need to use selective electrode interlayers, which provides important information into how devices should be optimised.

Conference 8117: Organic Field-Effect Transistors X

Monday-Tuesday 22-23 August 2011 • Part of Proceedings of SPIE Vol. 8117 Organic Field-Effect Transistors X

8117-01, Session 1

Synthesis and characterizations of linear- and angular-shaped naphthodithiophenes for organic semiconductors

K. Takimiya, Hiroshima Univ. (Japan)

A straightforward synthetic approach that exploits linear- and angular-shaped naphthodithiophenes (NDTs) being potential as new core structures for organic semiconductors is described. The newly established synthetic procedure involves two important steps; one is the chemoselective Sonogashira coupling reaction on the trifluoromethanesulfonyloxy site over the bromine site enabling selective formation of *o*-bromoethynylbenzene substructures on the naphthalene core, and the other is a facile ring closing reaction of fused-thiophene rings from the *o*-bromoethynylbenzene substructures. As a result, three isomeric NDTs, naphtho[2,3-*b*:6,7-*b'*]dithiophene, naphtho[2,3-*b*:7,6-*b'*]dithiophenes, and naphtho[2,1-*b*:6,5-*b'*]dithiophene are selectively synthesized. Electrochemical and optical measurements of the parent NDTs indicated that the shape of the molecules plays important role to determine the electronic structure of the compounds; the linear-shaped NDTs formally isoelectronic with naphthalene have lower oxidation potentials and more red-shifted absorption bands than those of the angular-shaped NDTs isoelectronic with chrysene. On the contrary, the performance of the thin-film-based field-effect transistors (FETs) using the dioctyl- or diphenyl- derivatives were much influenced by the symmetry of the molecules; centrosymmetric derivatives tend to give higher mobility (up to 1.5 cm² V⁻¹ s⁻¹) than axisymmetric one (~ 0.06 cm² V⁻¹ s⁻¹), implying that the intermolecular orbital overlap in the solid state is influenced by the symmetry of the molecules. These results indicate that the present NDT cores, in particular the linear-shaped, centrosymmetric naphtho[2,3-*b*:6,7-*b'*]dithiophene, are promising building blocks for the development of organic semiconducting materials.

8117-02, Session 1

Stable and high-performance fused thiophene polymer semiconductors

M. He, J. Li, W. Niu, M. Sorensen, J. Matthews, J. Hu, A. Wallace, D. Schissel, Corning Incorporated (United States); Z. Bao, D. Kaefer, Stanford Univ. (United States)

A family of fused-ring thiophene copolymers has recently been reported as semiconducting materials with high performance for thin film transistor applications. Initially, a comparison of the properties of different fused thiophene copolymers showed that polymers with even-numbered fused thiophene cores exhibited much higher field-effect mobility than the others with odd-numbered cores due to the much smaller lamellar spacing in the packing structure.

To get further insight into the structure-property relationship in these novel fused thiophene polymer semiconductors, additional, newly synthesized polymers were investigated. Device characterization demonstrated that polymer performance strongly depends upon side chain length, film deposition solvents and repeat unit symmetries.

8117-03, Session 1

Charge transport properties of carbazole dendrimers in organic field-effect transistors

K. E. Mutkins, S. Chen, E. B. Namdas, P. Meredith, B. J. Powell, P. L. Burn, The Univ. of Queensland (Australia)

The majority of organic semiconductors used in Organic Field-Effect transistors (OFETs) display spatially anisotropic charge transport. As

such, specific treatments and processing conditions are required in order to achieve optimal molecular alignment within the conducting channel to maximise device efficiency and speed. In our paper we describe how molecular shape affects the transport of charge in conducting organic field effect transistor channels by looking at dimension-rich, planar and pseudo-planar materials that potentially display isotropic charge transport. We report carbazole-based dendrimers of up to the third generation in OFETs and demonstrate how altering the number of dendrons, the dendrimer generation, and dimensionality affects their overall charge transport properties and device performance. We will also report computational studies that help elucidate the charge transport properties of the materials. To this end we demonstrate a maximum field effect mobility of 2.8×10⁻⁴ cm²/Vs for a 3-dimensional dendrimer used as an active layer in an OFET. Finally, we show that the dendrimers form stable OFETs with no change in mobility for at least 4 months after fabrication.

8117-04, Session 1

Crystal engineering of heteroacenes for thin film transistor applications

M. A. Loth, R. Hallani, Univ. of Kentucky (United States); J. Sherman, Univ. of California, Santa Barbara (United States); S. R. Parkin, Univ. of Kentucky (United States); T. Nguyen, Univ. of California, Santa Barbara (United States); J. E. Anthony, Univ. of Kentucky (United States)

Our group has made progress using small molecule acenes as organic semiconductors for thin film and single crystal transistors. Substitution of acenes and heteroacenes with silylethylene groups directly influences crystal packing, which in turn impacts device performance. The location and type of heteroatom also affects crystal packing and thin film formation. For the linear heteroacenes anthradithiophene (ADT) and anthradifuran (ADF), similar packing was observed for the same silylethylene groups, but ADF derivatives were stable five times longer in light and air. The highest mobilities were observed when two-dimensional π stacking was achieved. The nonlinear benzo-bis[b]benzothiophene (BTBTB) derivatives did not follow the same trend and fewer derivatives showed high mobility performance.

Single crystal transistors were obtained from fluorine functionalization on the heteroacene backbone. These devices provided mobility maxima without rigorous optimization for film growth and device structure. Thin film transistor and single crystal data for several of these new semiconductors will be presented.

8117-05, Session 1

Lamello-columnar mesophase formation in a side-chain liquid-crystal pi-conjugated polymer architecture

A. Attias, I. Tahar-Djebbar, F. Mathevet, D. Kreher, Univ. Pierre et Marie Curie (France); B. Heinrich, B. Donnio, D. Guillon, Univ. de Strasbourg (France)

The self-organization of π -conjugated organic materials forming highly ordered supramolecular architectures has been extensively investigated in the last two decades in view of optoelectronic applications. Indeed, the control of both the mesoscopic and nanoscale organization within thin semiconducting films is the key issue for the improvement of charge transport properties and achievement of high charge carrier mobilities. The self-organization of a side-chain liquid crystal semiconducting polymer where (i) the backbone is a π -conjugated polymer and (ii) the side groups are π -conjugated discotic mesogens was investigated. The synthetic route is based on Grignard methathesis (GRIM) and the thermotropic polymorphism is studied by polarized optical

microscopy, differential enthalpy and temperature-dependence X-ray diffraction experiments. The main result is that this strategy leads to the supramolecular self-assembly of this side-chain liquid crystal semiconducting polymer in a peculiar lamello-columnar mesophase where a 2D oblique columnar lattice perforates a lamellar structure. Transport properties will be also investigated.

8117-06, Session 1

Physicochemically stable polymer-coupled oxide dielectrics for multipurpose organic electronic applications

H. Yang, Inha Univ. (Korea, Republic of); S. H. Kim, Pohang Univ. of Science and Technology (Korea, Republic of); M. Jang, Inha Univ. (Korea, Republic of); C. Park, Pohang Univ. of Science and Technology (Korea, Republic of)

We have introduced a chemically coupled polymer layer onto inorganic oxide dielectrics from a dilute chlorosilane-terminated polystyrene (PS) solution. As a result of this surface modification, hydrophilic oxide dielectrics gained hydrophobic and physicochemically stable properties. On such PS-coupled SiO₂ or AlO_x dielectrics, various vacuum- and solution-processable organic semiconductors could develop highly ordered crystalline structures that provided higher field-effect mobilities (FETs) than other surface-modified systems and negligible hysteresis in organic field-effect transistors (OFETs). In particular, the use of PS-coupled AlO_x nano-dielectrics was found to enable a solution-processable triethylsilylethynyl anthradithiophene OFET to operate with $\mu\text{FET} \sim 1.26 \text{ cm}^2\text{V}^{-1}\text{s}^{-1}$ at a gate voltage below -1 V. In addition, a complementary metal-oxide semiconductor-like organic inverter with a high voltage gain of approximately 32 was successfully fabricated on a PS-coupled SiO₂ dielectric.

8117-07, Session 2

Diketopyrrolopyrrole based solution processable organic semiconductors for high performance organic electronics

P. M. Sonar, S. P. Singh, A*STAR Institute of Materials Research and Engineering (Singapore); Y. Li, Univ. of Ottawa (Canada); Z. Ooi, A*STAR Institute of Materials Research and Engineering (Singapore); T. Ha, The Univ. of Texas at Austin (United States); Z. Chen, A*STAR Institute of Materials Research and Engineering (Singapore); A. Dodabalapur, The Univ. of Texas at Austin (United States)

Low band gap organic semiconductors based on diketopyrrolopyrrole (DPP) (polymers and small molecules) are gaining attention in the organic electronics community due to their promising performance in organic thin-film transistors (OTFTs) and organic photovoltaic (OPVs). These materials are emerging as an interesting category for these applications due to their tunable HOMO-LUMO energies, wide light absorption and interesting charge transport properties. The photo physical, electrochemical, morphological and electrical properties of DPP based semiconductors are primarily controlled by the modulation in chemical structures by selecting suitable conjugated blocks (either donor or acceptor) adjacent to DPP in a backbone which is either strong or weak by nature. Solid-state packing, π - π and intermolecular interactions are dependent on the nature of the conjugated blocks in the backbone. Using a versatile building block with straightforward and inexpensive synthesis, one can make a library of promising low band gap functional materials.

Design and synthesis of the novel DPP based push-pull organic semiconductor comprised of interesting donor/acceptor moieties in conjugated backbone will be presented. These materials are synthesized via Stille and Suzuki coupling routes. Using some of the novel materials,

we have achieved high hole carrier mobility close to $1 \text{ cm}^2/\text{V}\cdot\text{s}$ in p-channel OTFTs. Additionally, our rationally designed donor-acceptor copolymer also showed highest hole ($0.35 \text{ cm}^2/\text{V}\cdot\text{s}$) and electron ($0.40 \text{ cm}^2/\text{V}\cdot\text{s}$) mobility in ambipolar OTFTs. The balanced hole and the electron mobility values observed in this polymer are highest among known ambipolar organic semiconductors. These materials are also used as an active component for the fabrication of organic solar cells and we could achieve high efficiencies $> 4.5\%$ under simulated AM 1.5 solar irradiation of $100 \text{ mW}/\text{cm}^2$. Our first report about low band gap DPP based acceptors also showed promising performance in OPV devices.

8117-08, Session 2

Conductors and semiconductors for advanced organic electronics

T. Meyer-Friedrichsen, Heraeus Clevis GmbH (Germany); R. Lubianez, Heraeus Materials Technology LLC (United States)

As the performance of organic electronics usually is minor to the classical inorganic electronics world, the breakthrough of organic electronic technologies will largely depend on cost effectiveness. This implies either the use of inexpensive materials and processing technologies or very effective utilization of the materials. The latter can be achieved by self-assembling processes in which only monolayers of the active materials are necessary to build fully functional electronic devices. The production process can also be very simplified by the self-assembly of the material on the substrate surface.

We have previously designed SAM-semiconductors which self-assemble on a dielectric SiO_x-surface to dense monolayers creating self-assembled monolayer field effect transistors (SAM-FETs) [1]. We will present new results broadening this concept to SAM-materials combining semiconductor and dielectric layer for low voltage TFTs. The use of the air and water insensitive phosphonic acid group as a linker for SAM-semiconductors simplifies the processing to SAM-FETs. The phosphonic acid group shows effective and reliable binding on AlO_x surfaces. This concept has recently been proven by using an Al-gate electrode with a 3.6 nm thick AlO_x surface and an oligothiophene semiconductor functionalized with an undecenyl phosphonic acid linker which self-assembled on the surface of TFTs with low operation voltages [2].

[1] Smits et al., Nature 2008, 455, 956.

[2] Novak et al., Nano Letters 2011, 11, 156.

8117-09, Session 2

Phthalocyanine derivatives for solution-processed organic thin-film transistors

Y. Geng, Changchun Institute of Applied Chemistry (China)

Phthalocyanines (Pcs) are 18 π -electron disc-like aromatic macrocycles with 2D π -electron delocalization over the whole molecules. In fact, various metal phthalocyanines (MPcs) have been used in the fabrication of organic thin film transistors (OTFTs) by vacuum deposition. OTFTs with the mobility beyond $1.0 \text{ cm}^2/\text{V}\cdot\text{s}$ have been demonstrated with vanadyl phthalocyanine (OVPC) and titanyl phthalocyanine (OTiPC). However, solution processed OTFTs based on soluble Pcs usually display inferior device performance. We think two aspects have to be considered for the poor device performance: (1) the introduction of substituents may alter the packing motif of Pc rings, leading to the large intermolecular distance and the small the π -electron orbital overlap; (2) the difficult edge-on alignment of disc-like Pcs molecules for the formation of charge transport channels along the source-drain direction.

We postulate that using less substituents may reduce the effect of substituents on the π -stacking of Pc molecules. Therefore, two series of tetraalkyl substituted OVPCs have been synthesized and fully characterized. It was found that solution processed OTFTs exhibited mobilities in the range of 10^{-4} to $10^{-1} \text{ cm}^2/\text{V}\cdot\text{s}$ depending on the location of the four alkyls. In particular cases, neat isomers can be separated by common lab column chromatography in gram scale. The molecules

adopt 1D or 2D slipped cofacial π - π stacking motif with inter-planar distance less than 3.7 Å. The best device showed mobility up to 0.13 cm²/V s with threshold voltage lower than 5 V.

8117-10, Session 2

Thieno[3,2-b]thiophene diketopyrrolopyrrole containing polymers for high-performance OFETs

H. Bronstein, Imperial College London (United Kingdom)

We report the synthesis and polymerization of a novel thieno[3,2-b]thiophene-diketopyrrolopyrrole based monomer. Copolymerization with thiophene affords a polymer with a maximum hole mobility of 1.95 cm² V⁻¹ s⁻¹, which is, to date, the highest reported mobility from a polymer based OFET. Bulk heterojunction solar cells comprising this polymer and PC71BM give a power conversion efficiency of 5.4%.

8117-11, Session 2

High-k/fluoro-polymer bi-layer as a gate dielectric for pentacene TFTs: toward balance among low operating voltage, high performance, high electrical stability

H. Moon, W. Shin, M. Kim, B. Cho, S. Yoo, KAIST (Korea, Republic of)

Here we propose a bi-layer consisting of high-k material (HfO₂ : k~17) and fluoro-polymer (Cytop) as a gate dielectric layer that ensures high performance, low operating-voltage, and high electrical stability in organic thin-film transistors (OTFTs). Both mobility and electrical stability were shown to exhibit a significant improvement upon addition of a Cytop layer on HfO₂. It is noted that a thinner Cytop layer is preferred for a lower operating-voltage due to its relatively low dielectric constant (k~2.1). Our study shows, however, that there is a critical thickness for the Cytop layer below which the performance and stability of OTFTs made thereof start to degrade. The reasons for these limitations are discussed based on the morphological studies on both Cytop and pentacene layers. We then present our systematic way to select the optimal HfO₂/Cytop dielectric structure through a parametric study considering the balance among performance, operating-voltage, and electrical stability.

8117-12, Session 3

Structural and energetic disorder and their effect on charge transport in semiconducting polymers

A. Salleo, J. Rivnay, R. J. Noriega, Stanford Univ. (United States); M. F. Toney, SLAC National Accelerator Lab. (United States)

From the materials standpoint, semiconducting polymers are interesting as they are neither crystalline nor amorphous and their microstructure plays a central role in governing charge transport. Using advanced synchrotron-based X-ray characterization techniques we are able to define and measure structural order at different length-scales. Understanding disorder is the key to determining charge transport mechanisms. For instance, static cumulative disorder (e.g. paracrystallinity) -which I will show how to measure quantitatively- provides a fundamental justification to using a mobility edge model with a distribution of tail states in the gap. Coherence lengths in all relevant directions (lamellar stacking, pi-pi stacking and backbone) can also be defined and measured. Furthermore, a structural interpretation of these trap states will be provided. Near band-edge traps are important in devices as they manifest themselves as a broad sub-threshold region in

transistor characteristics or as recombination sites in solar cells. A better understanding of the relationship between disorder, microstructure and transport is of fundamental importance for the rational design of new synthetic semiconductors.

8117-13, Session 3

Microstructure evidence for dominance of on-chain charge transport in polymer semiconductors

D. M. DeLongchamp, National Institute of Standards and Technology (United States)

Organic electronics enables solution-based manufacturing for displays, photovoltaics, and sensors. NIST has established a program in organic electronics to develop measurement methods to characterize the electronic and interfacial structure of organic electronics materials with respect to processing methods, processing variables, and materials characteristics. We use a combination of polarized absorption spectroscopies (IR, vis, and X ray), scanning probe techniques, scattering techniques, and transmission electron microscopy to reveal details of semiconductor microstructure at organic thin film transistor (OTFT) interfaces. These measurements establish clear correlations between primary chemical structure, processing, film microstructure, and OTFT performance. Establishing these fundamental relationships can reveal practical guidelines for synthesis and processing.

We demonstrate this strategy through investigations of solution-processable polymer semiconductors with hole mobility comparable to that of amorphous silicon. The packing motifs of these materials run the gamut from well-ordered crystals with edge-on conjugated planes and vertically interdigitated linear side chains to less-ordered crystals with face-on conjugated planes and laterally interdigitated, branched side chains. The polymer crystal packing behaviors can be explained in terms of molecular geometry and the reconciliation of side chain packing constraints with those of the conjugated backbone. Additional packing structure details can be discerned using anisotropic films prepared using directional casting or strain-based techniques. The emergence of polymer semiconductors that exhibit high lateral hole mobility without having significant edge-on conjugated plane packing, together with mobility anisotropy measurements in strained polymer semiconductors, suggest that on-chain charge transport is more dominant than chain-to-chain charge transport via cofacial pi-stacking in polymer-based OTFTs.

8117-14, Session 3

Soft x-ray spectro-microscopy and transmission electron microscopy of high-performance polymer-small molecule blend organic field-effect transistors

K. W. Chou, Z. Kui, R. Li, King Abdullah Univ. of Science and Technology (Saudi Arabia); J. Smith, T. D. Anthopoulos, Imperial College London (United Kingdom); A. Hexemer, Lawrence Berkeley National Lab. (United States); R. Sougrat, King Abdullah Univ. of Science and Technology (Saudi Arabia); J. E. Anthony, M. A. Loth, Univ. of Kentucky (United States); M. J. Heeney, I. McCulloch, Imperial College London (United Kingdom); A. Amassian, King Abdullah Univ. of Science and Technology (Saudi Arabia)

The fluorinated acene 2,8-difluoro-5,11-bis(triethylsilyl)ethynyl) anthradithiophene (diF-TES-ADT) blended with amorphous poly(triarylamine)s (PTAA) has shown great promise for organic field-effect transistor (OFET) electronics due to its surprisingly high charge carrier mobility, ease of solution processing and device performance uniformity. The microstructure and morphology of the diF-TES-ADT:PTAA

blend film are believed to be the key factors in achieving these high mobility values. The small-molecule provides efficient charge transport pathways, while the amorphous polymer PTAA acts as a matrix and aids uniformity and ease of processing.

A critical concentration of the small-molecule is required for the blend system to obtain high performance OFETs. For diF-TES-ADT concentrations greater than 20 wt.%, the small-molecule-rich phase starts to form but percolation - which is critical for in-plane carrier transport - occurs when a significant fraction of the molecular crystallites form conduction pathways. A mobility threshold is observed at about 39 wt.% diF-TES-ADT. Above this value uniform, polycrystalline films can be fabricated yielding OFETs with hole mobilities approaching $2 \text{ cm}^2/\text{Vs}$. However, high concentrations of diF-TES-ADT lead to the formation of non-uniform films and significantly reduced hole mobility.

We report on the spectro-microscopic investigation of the diF-TES-ADT:PTAA blend film using scanning transmission x-ray microscopy (STXM) and transmission electron microscopy (TEM). The STXM is equipped with an elliptically polarizing undulator, allowing us to image the degree of in-plane orientation between different molecular crystallites. The percolation pathways, domain misorientations, and grain boundary formation were studied for different concentrations of the small-molecule with both techniques.

8117-15, Session 3

Analysis of the molecular packing at the dielectric interfaces in organic field-effect transistors by synchrotron x-ray diffraction

S. C. Mannsfeld, SLAC National Accelerator Lab. (United States)

In the saturated "on"-state of an organic thin film transistor (OTFT) device, the electrical current predominantly flows in the first few molecular layers,[1] and consequently the packing and exact molecular arrangement in these layers determine the material's intrinsic electrical resistance. Triisopropylsilyl(TIPS)-functionalized pentacene/thiotetracene[2] exhibit very high OFET device performance in vacuum-deposited and solution-cast films (field effect mobility $\mu > 1 \text{ cm}^2/\text{Vs}$). Despite a large number of studies investigating the relationship between film morphology and transistor performance, especially for TIPS-pentacene, the actual molecular packing has not been precisely determined.

The combination of Grazing incidence X-ray diffraction (GIXD) using synchrotron radiation and advanced crystallographic refinement calculations can provide detailed information about the molecular packing in thin films as thin as a fraction of a monolayer.[3] Here we employ this combination of methods and present a detailed analysis of the molecular packing at the semiconductor/dielectric interface in TIPS-functionalized pentacene/thiotetracene thin film transistors,[4] including self-assembled monolayer (SAM) dielectric surface modifications of the silicon oxide surface.

References

[1] A. Dodabalapur, L. Torsi, H.E. Katz, *Organic Transistors*, Science 268, 270-271 (1995).

[2] M.-L. Tang, A.D. Reichardt, T. Siegrist, S.C.B. Mannsfeld, Z. Bao, *Chem. Mater.* 20, 4669 (2008).

[3] S.C.B. Mannsfeld, A. Virkar, C. Reese, M.F. Toney, Z.Bao, *Adv. Mater.* 21, 2294 (2009).

[4] S.C.B. Mannsfeld, M.L. Tang, Z. Bao *Adv. Mater.* 23, 127 (2011).

8117-16, Session 3

Microstructural origin of high field-effect mobility in diketo pyrrolo-pyrrole polymer semiconductors with branched alkyl side chains

X. Zhang, L. J. Richter, D. M. DeLongchamp, R. J. Kline, National Institute of Standards and Technology (United States); I. McCulloch, M. J. Heeney, R. S. Ashraf, J. Smith, T. D. Anthopoulos, Imperial College London (United Kingdom); B. C. Schroeder, Y. H. Geerts, Univ. Libre de Bruxelles (Belgium); D. A. Fischer, National Institute of Standards and Technology (United States); M. F. Toney, SLAC National Accelerator Lab. (United States)

Field effect mobilities of $\sim 0.4 \text{ cm}^2 \text{ V}^{-1} \text{ s}^{-1}$ or even higher were exhibited by a series of highly soluble diketo pyrrolo-pyrrole (DPP)-bithiophene copolymers with disordered, bulky 2-octyldodecyl side groups. In this work, we systematically characterized the thin film microstructure of these DPP polymers with a suite of spectroscopic and microscopic techniques including: grazing incidence X-ray diffraction (GIXD), near edge X-ray absorption fine structure (NEXAFS) spectroscopy, variable angle spectroscopic ellipsometry (VASE), Fourier transform infrared spectroscopy (FTIR), atomic force microscopy (AFM), and dark-field transmission electron microscopy (DF-TEM). We revealed a transition from a preferentially edge-on orientation of the conjugated plane to a preferentially plane-on orientation/bimodal orientation distribution upon increasing attachment density of the branched alkyl side chains. Although the highest mobilities were obtained from thin films with edge-on conjugated plane orientation and in-plane liquid-crystalline textures, those with plane-on orientation/bimodal orientation distribution and no discernable in-plane texture still exhibited mobilities higher than $0.3 \text{ cm}^2 \text{ V}^{-1} \text{ s}^{-1}$. Based on the fact that the backbones of all these DPP polymers are strongly oriented within the film plane, we argue that the strong preference of the backbone to lie in the substrate plane is the primary cause for excellent field-effect mobilities, while other factors, such as in-plane liquid-crystalline texture, are secondary and can further enhance charge transport.

8117-17, Session 4

Oligo- and polymer-single-crystalline thin-film transistors

A. L. Briseno, Univ. of Massachusetts Amherst (United States)

In this presentation I will discuss a crystallization protocol by employing low molecular weight polymers, or "oligomers". We have developed a structure-property relationship from these materials and determined the electronic and molecular properties of this class of oligomers. Our approach to this project was to synthesize a series of oligomers from the benchmark building block, didodecylquaterthiophene (DDQT) and employ standard cross-coupling chemistry to produce low-molecular weight oligomers with well-controlled conjugation lengths and narrow polydispersities. We fabricated oligomer single-crystalline films as test structures for measuring carrier mobilities in field-effect transistors.

8117-18, Session 4

Organic single-crystal transistors: development of solution processes and charge transport mechanisms

T. Uemura, J. Takeya, Osaka Univ. (Japan)

Organic single crystal transistors were first introduced mainly to study fundamental charge transport in organic semiconductors without

complication from grain boundaries which polycrystalline devices always suffer. Then, rubrene single crystals exhibited mobility of more than 20 cm²/Vs, indicating that the intrinsic performance of organic transistors is higher than believed before.

In this presentation, we report our recent progress in the study of organic single-crystal transistors, incorporating devices from several newly synthesized organic semiconductor materials. In order to promote development of solution-processed organic transistors, we have investigated techniques of crystallization in fabricating semiconductor films from solution. Regulating direction of the crystal growth, we successfully formed crystalline films with the mobility as high as 5-10 cm²/Vs from new compounds of C_n-BTBT and C_n-DNNT. Using a newly developed printing technique, these high-mobility solution-crystallized transistors are fabricated into 5 X 5 matrix arrays during the film growth, demonstrating that the method can be suitable for mass-producing the devices on large-area plastic substrates.

Comprehensive measurements of Hall effect and temperature dependent mobility are also performed for various single-crystal transistors. As the result, one can tell their fundamental electronic states in terms of their electronic coherence, i.e. to what extent the electronic charge is delocalized over molecules. In most of the high-mobility systems such as rubrene, C_n-BTBT and C_n-DNNT, band-like carriers are accumulated with their full coherence, whereas large molecular fluctuation at room temperature partially destroys electronic coherence in pentacene and C60. The observation can give a prescription to design molecules which realize high-mobility band transport.

8117-19, Session 4

Drastic control of texture in high-performance n-type polymeric semiconductor and implications for charge transport

J. Rivnay, Stanford Univ. (United States); M. F. Toney, SLAC National Accelerator Lab. (United States); A. F. Facchetti, Polyera Corp. (United States); A. Salleo, Stanford Univ. (United States)

The achievement of a printable, highly stable, and high performance (up to 0.85cm²/Vs) n-type polymer, poly{[N,N'-bis(2-octyldodecyl)-naphthalene-1,4,5,8-bis(dicarboximide)-2,6,-diy]-alt-5,5'-(2,2'-bithiophene)}, P(NDI2OD-T2), has renewed interest in low cost complementary circuit and logic applications. The origins of P(NDI2OD-T2)'s high electron mobility, including the morphological chain packing in the bulk, as well as the specifics of backbone proximity and orientation with respect to the interface, are of great interest for further improving materials and device performance. Furthermore, the ability to tune microstructure and texture allows for a better understanding of performance limitations for this particular material, and facilitates the development of general structure-property design rules. Control of film texture from face-on to mostly edge-on is observed for the bulk P(NDI2OD-T2) morphology when annealing to the melting point of the polymer followed by a slow cooling back to ambient temperature. We use a variety of diffraction techniques including complete pole figures and Fourier transform peak shape analysis to quantify the texture change, relative degree of crystallinity, and crystalline order. We find a shift from 77.5% face-on to 94.6% edge-on lamellar texture, as well as a two fold increase in degree of crystallinity. The textural change causes a significant drop in the electron only diode current density upon melt annealing, while little change is observed in the in-plane transport of bottom gated thin film transistors, suggesting the texture change is most evident in the bulk, and that the (bottom) surface structure is either different from the bulk, or crystalline order and texture play less of a role in transistor transport for this material.

8117-20, Session 4

Small crystals of organic semiconductors for transistors

W. Hu, Institute of Chemistry (China)

Comparing with large organic crystals (millimeter to centimeter size or larger), micro- and nanometer sized small organic crystals have their potential merits. First, it is both material- and time-saving to grow small crystals. Second, devices based on the "small" crystals could keep all the advantages of organic single crystals, to provide a way not only for high performance devices, but also for the characterization of organic semiconductors more efficiently. Third, the effective use of the small crystals will be helpful for the integration of organic single crystals to micro and nanoelectronic devices from the "bottom-up" approach. Finally, crystals at micro and nanometer scale will appear some new properties, new phenomena and new applications. Here, organic micro- and nanocrystals, including the design of new materials, the controllable growth of crystals, structure-property studies, and the fabrication of devices and circuits based on crystals, are introduced.

8117-21, Session 4

Nanowire crystals of conjugated polymers and their field-effect transistors

H. Dong, W. Hu, Institute of Chemistry (China)

Single crystals are the optimal candidates for revealing the intrinsic properties of materials and investigating the structure-property relationship due to their attracting characteristics of long-ranged molecular order, low charge trap density and no grain boundaries. However, to date, compared with inorganic and organic small molecular crystals, conjugated polymer crystals possess great challenges to control growth, device fabrication and the exploration of their properties. Herein, with a derivative of poly(para-phenylene ethynylene)s (PPE) as target, we obtained large-area, high quality PPE nanowire crystals through self-assembly technique. Moreover, high performance organic field-effect transistors based on PPE crystal nanowires have been fabricated, exhibiting the highest mobility approaching 0.1 cm² V⁻¹s⁻¹, opening the door of applications of polymer crystals in organic electronics.

8117-43, Poster Session

Simple fabrication of high-mobility transistor arrays using highly aligned printed organic nanowires

S. Min, T. S. Kim, Pohang Univ. of Science and Technology (Korea, Republic of); B. J. Kim, J. H. Cho, Soongsil Univ. (Korea, Republic of); T. Lee, Pohang Univ. of Science and Technology (Korea, Republic of)

According to the information technology trend toward highly-integrated and high-performance electronic devices, needs for nano-structured devices are increasing. Semiconducting nanowires, the most representative 1-D nano-structure, possess many attractive properties for application to the electronic devices. There are published several methods for preparing organic nanowires (ONWs). However, they have some problems to be solved; alignment, positioning, etc. We realized the highly aligned polymer nanowire arrays by using an electrohydrodynamic (EHD) nozzle printer which contains the precision linear motor stage-collector. We applied the EHD-nozzle printing to fabricate the highly aligned nanowire field-effect transistors (FETs) based on poly(3-hexylthiophene): poly(ethyleneoxide) (P3HT:PEO) blend (80:20, w/w) which showed a high mobility of 0.0148 cm²/V s. On the other hand, we also demonstrated the organic nanowire lithography to make nano-patterns. By using organic nanowire lithography, we have successfully fabricated the P3HT:PEO blend nanowire FETs which has channel length

(~340 nm) and width (~300 nm) in nanometer regime, which showed a field-effect mobility of $0.009 \text{ cm}^2/\text{V s}$. Furthermore, we used the solid polymer electrolytes consisting of an ionic liquid and triblock copolymer for the gate dielectric material of nanowire transistor. Finally, we have fabricated the low-voltage operating organic nanowire FETs with nanochannel length, resulting in high on/off ratio and high field-effect mobility.

8117-44, Poster Session

The charge transport and morphology of organic semiconductor nanowires fabricated by soft lithography

T. S. Kim, S. H. Kim, C. Park, T. Lee, Pohang Univ. of Science and Technology (Korea, Republic of)

Although one-dimensional nanostructures of inorganic semiconductors have been developed very actively for future nano-electronic applications, inorganic nanowires have critical drawbacks of difficulties to make aligned and patterned large-area structures for real applications. Organic semiconductor nanowires will attract much attention due to their easy patterning and alignment. The transport and morphology of macroscopic organic transistors have been explained thoroughly to date. However, the relationship between the charge transport and morphology of organic semiconductor nanowires is not well understood, which is required to design the high performance nano electronics. We have successfully fabricated the aligned organic nanowires using discontinuous dewetting of organic semiconductor solutions on nano relief patterns defined by phase shift lithographic method. We have compared the performance charge transport properties of the organic semiconductor wires with that of the standard organic semiconductor films formed by using solution process. And we have analyzed the effect of the morphology of the organic semiconductor wires on the charge transport.

8117-45, Poster Session

Bottom-contact electrodes based on metal/metal oxide bilayers coated with self-assembled monolayers (SAMs) for low-cost, high-performance organic thin-film transistors

S. Lee, H. Moon, S. Yoo, KAIST (Korea, Republic of)

We present our study on high performance bottom contact organic thin film transistors (OTFTs) that are based on (i) metal / transition metal oxide (TMO) bilayer; and on (ii) additional self-assembled monolayers (SAMs) treatment. Typical OTFTs rely on gold (Au) as source(S) and drain(D) electrodes owing to its high work-function. Instead of such precious metals, we have used aluminum (Al), and solved the high hole-injection barrier issue by depositing TMO with a high work function on top of Al electrodes. With the additional treatment of the TMO surface with SAMs, the effective work function of our proposed S/D electrodes may further be tuned and the quality growth of organic materials may be achieved at the same time, enabling a relatively high mobility even in bottom contact OTFTs. For example, devices with S/D electrodes consisting of molybdenum trioxide (MoO_3) layers deposited on top of Al electrodes demonstrated mobility around $\sim 0.1 \text{ cm}^2/\text{Vs}$ with pentacene used as a active layer; those with additional SAM treatment demonstrated enhanced mobility around $\sim 0.3 \text{ cm}^2/\text{Vs}$, approaching the mobility of common top-contact pentacene TFTs. Our results indicate that the proposed Al/TMO/SAMs composite electrode is a good candidate for high-performance bottom-contact OTFTs.

8117-46, Poster Session

H-aggregation strategy in the design of molecular semiconductors for highly reliable organic thin film transistors

T. K. An, Pohang Univ. of Science and Technology (Korea, Republic of); S. Kim, Gyeongsang National Univ. (Korea, Republic of); C. Park, Pohang Univ. of Science and Technology (Korea, Republic of); S. Kwon, Gyeongsang National Univ. (Korea, Republic of)

The present study was devised based on the following three considerations: i) previously reported organic semiconductors generally have shown J-aggregation with head-to-tail molecular stacking; ii) large area π -stacking between adjacent molecules can be realized by H-aggregation, which occurs when molecules stack side-by-side; and iii) H-aggregation induces stable morphologies in thin films and reproducible transistor performances. We describe a novel synthetic strategy to induce H-aggregation between adjacent molecules in the thin film state. We designed four types of quaterthiophene derivative with end-groups composed of cyclohexyl ethyl (CE4T), cyclohexyl butyl (CB4T), dicyclohexyl ethyl (DCE4T), and dicyclohexyl butyl (DCB4T). All materials showed high solubility in common organic solvents. UV-vis absorption and grazing-incidence wide-angle X-ray scattering (GIWAXS) analyses indicated that the asymmetric derivatives, CE4T and CB4T, tended to form H-aggregation whereas the symmetric derivatives, DCE4T and DCB4T, tended to form J-aggregation.

The field-effect mobilities of devices that incorporated the asymmetrical molecules, CE4T and CB4T, were quite high, above $10^{-2} \text{ cm}^2/(\text{V s})$, due to H-aggregation, whereas the field-effect mobilities of devices that incorporated symmetrical molecules, DCE4T and DCB4T, were poor, below $10^{-4} \text{ cm}^2/(\text{V s})$, due to J-aggregation. More importantly, H-aggregation within the thin film provided stable crystalline morphologies in the spin-coated films, and, thus, thin film transistors (TFTs) using cyclohexylated quaterthiophenes yielded highly reproducible transistor performances. The distributions of measured field-effect mobilities in transistors based on cyclohexylated quaterthiophenes with H-aggregation were remarkably narrow.

8117-47, Poster Session

Poly(diketopyrrolopyrrole-benzothiadiazole) with ambipolarity approaching 100% equivalency

S. Cho, Univ. of Ulsan (Korea, Republic of); J. Lee, Ulsan National Institute of Science and Technology (Korea, Republic of); S. H. Park, Pukyong National Univ. (Korea, Republic of); C. Yang, Ulsan National Institute of Science and Technology (Korea, Republic of)

It was generally agreed that conventional conjugated polymers exhibited either high hole transport property or high electron transport property. Although ambipolarity has been demonstrated from specially designed polymers, only a few examples have exhibited ambipolar properties under limited conditions. Furthermore, there is no example with 'equivalent' ambipolar properties, yet. We describe the realization of equivalent ambipolar organic FET by using a single-component Vis-NearIR absorbing diketopyrrolopyrrole(DPP)-benzothiadiazole(BTZ) copolymer, namely PDTDPP-alt-BTZ. PDTDPP-alt-BTZ shows not only ideally balanced charge carrier mobilities for both electrons ($0.09 \text{ cm}^2\text{V}^{-1}\text{s}^{-1}$) and holes ($0.1 \text{ cm}^2\text{V}^{-1}\text{s}^{-1}$) but also its inverter constructed with the combination of two identical ambipolar FETs exhibits a gain of ~ 35 .

8117-22, Session 5

Organic and hybrid thin-film transistors with novel architectures and high stability

B. Kippelen, J. Kim, D. K. Hwang, S. P. Tiwari, W. J. Potscavage, Jr., C. Fuentes-Hernandez, Georgia Institute of Technology (United States)

Over the last decades, organic thin-film transistors (OTFTs) have made great progress. The field-effect mobility in OTFTs has improved to a level where organic semiconductors compete with amorphous silicon (a-Si). However, an advantage with organic semiconductors is that the performance levels of n-channel and p-channel devices are comparable which is important for the design of complementary circuits. Despite these advances in field-effect mobility, long-term environmental and operational stabilities are still two major issues before OTFTs can be commercialized and realize their full potential.

In the first part of this talk we will discuss the performance of OTFTs based on bi-layer gate dielectrics. In particular, we will report on devices fabricated from solution processed organic semiconductors with a top gate geometry. Such devices show an average mobility value of 0.46 ± 0.08 cm²/Vs and operate at voltages below 8 V. These devices do not show any significant degradation in mobility nor change in threshold voltage after 20,000 multiple scans, after a 24 h constant dc bias stress, or after exposure to air for over a year. We will show that the long lifetime of these devices can be attributed to a compensation mechanism of two different degradation processes due to the bi-layer architecture of the gate dielectric.

In the second part of the talk, we will report on hybrid organic-inorganic complementary inverters composed of pentacene and amorphous InGaZnO for p- and n- channel thin-film transistors (TFTs) fabricated on flexible polyethersulfone substrates. The p- and n- channel TFTs showed saturation mobility values of 0.15 and 3.8 cm²/Vs, respectively. Hybrid complementary inverters at a supply voltage of 25 V showed a high gain of 130 V/V at a switching threshold voltage of 12.5 V. Operating these inverters at the ideal supply voltage yielded high and balanced noise margins with values of 84% of their theoretical maximum. We will also present a new co-planar channel geometry for the realization of such transistors and complementary inverters wherein n- and p-type channels are horizontally distributed with different channel widths to achieve balanced operation. Using this geometry, we could demonstrate high performance ambipolar-like transistors consisting of amorphous-InGaZnO (mobility of 10 cm²/Vs) and pentacene channels (mobility of 0.3 cm²/Vs) with performance parameters comparable to those of unipolar transistors.

8117-23, Session 5

Ambipolar field-effect transistors based on conjugated polymers: structural-property relationship and charge-induced absorption

Z. Chen, Institut Matériaux Microélectronique Nanosciences de Provence (France); M. J. Lee, Univ. of Cambridge (United Kingdom); M. Bird, Brookhaven National Lab. (United States); M. M. Nielsen, Danmarks Tekniske Univ. (Denmark); H. Sirringhaus, Univ. of Cambridge (United Kingdom)

Ambipolar charge transport with balanced electron and hole mobilities has been discovered as an intrinsic property of many organic semiconductors. This has opened up exciting opportunities for the application of organic materials in new device architectures such as complementary-like voltage inverters with a single semiconducting material and light-emitting FETs. Even though conjugated polymers exhibiting balanced hole and electron field-effect mobilities (both > 0.01 cm² V⁻¹ s⁻¹) have been realized, there often exist differences between electron and hole transport behavior in aspects such as mobility-temperature dependence, threshold voltage, hysteresis and bias-stress. Scientific understanding of mechanisms limiting ambipolar transport

is therefore of both fundamental and practical interest. In this paper, we present a charge transport study based on semicrystalline polymer systems including poly(3,3"-di-n-alkyltersephenylene) (PSSS) and the recently-developed diketopyrrolopyrrole based copolymers. Compared to polythiophene, the lower band gap of polyselenophene allows more efficient electron injection from common metal electrodes (gold or aluminum). As a result, when combined with dielectrics of relatively few electron traps, balanced hole and electron mobilities both of the order of 0.01 cm² V⁻¹ s⁻¹ are realized in top-gate/bottom-contact PSSS FETs. Correlating with structural and device property characterizations, we employ charge-modulation spectroscopy to further study the polaron absorption spectra for both the hole and electron on the same FET in order to understand fundamental differences or similarities between their respective wavefunctions.

8117-24, Session 5

Controlling electric dipoles in the gate dielectric and its applications for enabling air-stable n-channel organic transistors

Y. Chung, Y. Nishi, B. Murmann, Z. Bao, Stanford Univ. (United States)

We present a novel method to control the turn-on voltage of organic field-effect transistors (OFETs) and to enable air-stable operation of n-channel OFETs. In this work self-assembled monolayers (SAMs) with different anchor groups are used in the gate dielectric. The dipole-generating SAMs vary the built-in electric potential by 0.41 ~ 0.50 V. This potential difference results in consistent shifts of the turn-on voltage in OFETs. Different from previous studies, our approach maintains an ideal interface between the dipole layers and the semiconductor while significantly changing the built-in potential. Due to this interface we effectively change the electrical characteristics of OFETs with minimum impact on the charge transport in the organic semiconductor. We further demonstrate the application of the SAM dipoles to enable air-stable operation of n-channel organic transistors, which are normally not stable in air. Our n-channel OFETs exhibit an average mobility of 1.65 (± 0.11) cm²/Vs after a 24-hour exposure to air, and they still operate with an average mobility of 0.73 (± 0.06) cm²/Vs even after one week in air.

8117-25, Session 5

Fast behavioral modeling of organic CMOS devices for digital- and analog-circuit applications

S. Jacob, A. Daami, R. Gwoziecki, R. Coppard, Commissariat à l'Énergie Atomique (France)

Organic thin film technologies have opened a new range of interest into the optoelectronics industry. Nevertheless the physics and devices modeling still present a lack of accuracy. In order to provide designers with the latest performances of our organic CMOS technology, we have chosen to use behavioral modeling of our devices. In our paper, we show that behavioral modeling has the capability of describing the performances of single devices on our CMOS technology with a very good accuracy.

Fully printed organic CMOS devices and circuits have been processed and characterized in order to validate our behavioral device models. In particular, measurements have been carried out on several digital circuits like inverters, ring oscillators, NAND gates and different types of FLIP-FLOPs. Analog circuits such as OTA amplifiers, comparators, rectifiers, current mirrors and differential pairs have also been measured. Simulations of these circuits have been performed using our device behavioral models under common EDA commercial tools. We show that our behavioral device models enable to reproduce properly the different CMOS circuits performances in static as well as dynamic modes opening the way for designing a wide range and more complex digital and analog

organic applications. Finally we show that our behavioral modeling is applicable to more complex circuits to describe their functionalities.

8117-26, Session 5

Enhancement-mode polymer vertical transistor with operation voltage of 1.5 V, on/off current ratio of 10^4 , and subthreshold swing of 96 mV/decade

Y. Chao, National Chiao Tung Univ. (Taiwan); H. Tsai, National Tsing Hua Univ. (Taiwan); H. Zan, Y. Hsu, H. Meng, National Chiao Tung Univ. (Taiwan); S. Horng, National Tsing Hua Univ. (Taiwan)

Organic vertical transistors recently attract many attentions because of their low operation voltages which are essential for low-power-consumption electronic devices. Organic static induction transistor (SIT) is a famous vertical transistor which achieves high on/off current ratio of 10^3 at low operation voltage of 3 V. Another vertical transistor is the polymer space-charged-limited transistor (SCLT), which is a three-terminal device functions similar to the vacuum tube triode. However, parameters that seriously influence the subthreshold swings were never systematically studied for any vertical transistor. Besides, normally-on characteristics of these vertical transistors were commonly observed. A non-zero voltage was required to turn off the transistor which made the power consumption inevitable. A normally-off vertical transistor is therefore needed to be realized as a power-saving device. In this work, an enhancement-mode SCLT with normally-off operation is realized. The subthreshold swing as low as 96 mV/decade is demonstrated by enhancing the base control on the magnitude of potential barrier. Simulations on the potential distribution at the central vertical channel provide a reasonable explanation and verify the experimental result. This subthreshold swing is the lowest one in various vertical transistors and close to the theoretical limit of $\ln 10 \times kT/q = 60$ mV/decade in silicon metal-oxide-semiconductor field-effect transistor at room temperature. The realization of a normally-off vertical transistor with low operation voltage of 1.5 V, low subthreshold swing of 96 mV/decade, and high on/off current ratio of 10^4 makes a high-speed and low-voltage operation circuit possible.

8117-27, Session 6

Phase-control of solution-processable, small-molecular semiconductors for fabrication of single-component, high-mobility transistors

N. Stingelin-Stutzmann, Imperial College London (United Kingdom)

Solution-processable, small-molecular semiconductors, such as 6,13-bis(triisopropylsilylethynyl) (TIPS) pentacene and 2,8-fluoro-5,11-bis(triethylsilylethynyl) anthradithiophene (FADT) have been found to display mobilities of beyond $1 \text{ cm}^2/\text{Vs}$. However solution processing of these promising small molecules is still challenging as often blends are required to realise such a performance at high yield. This requires in most cases intricate control of the phase separation process; and generally optimum device performance is limited to top-gate architectures. For practical applications, simpler materials systems and field-effect transistor (FET) architectures are, however, required to exploit the touted potential for low-cost manufacturing of this class of functional organic molecules. Here we demonstrate on the example of 5,11-bis(triethylsilylethynyl)anthradithiophene (TES ADT) and b-tetraethyl(triisopropylsilylethynyl)pentacene (BTE TIPS) that judicious phase control when depositing these materials from solution allows fabrication of high-performance, single component active layer FETs (bottom gate/bottom contact structures) at high yield.

8117-28, Session 6

Facile one-step growth of highly crystalline ordered soluble acene crystal arrays for organic transistors: mechanism of crystal growth during dip coating

C. Park, Pohang Univ. of Science and Technology (Korea, Republic of)

The preparation of uniform large-area highly crystalline organic semiconductor thin films that show outstanding carrier mobilities has yet to be fully understood and controlled in the field of organic electronics, including organic field-effect transistors. Quantitative control over the drying speed during dip-coating permits optimization of the organic semiconductor film formation, although the kinetics of crystallization at the air-solution-substrate contact line are still not well understood. Here, we report the facile one-step growth of self-aligning, highly crystalline, uniform soluble acene crystal arrays that exhibit excellent field-effect mobilities (greater than $1.5 \text{ cm}^2\text{V}^{-1}\text{s}^{-1}$) over large areas via an optimized dip-coating process. We found that optimized acene crystals grew only when solvent evaporation at the contact line matched the substrate lift rate in the presence of low boiling point solvents. Variable-temperature dip-coating experiments using various solvents and lift rates were performed to corroborate the conclusions of the crystallization behavior. This bottom-up study of soluble acene crystal growth during dip-coating provides conditions under which one may obtain uniform organic semiconductor crystal arrays with high crystallinity and mobilities over large substrate areas, regardless of the substrate geometry.

8117-29, Session 6

Organic semiconductor thin-film formation by solution processing

A. Amassian, King Abdullah Univ. of Science and Technology (Saudi Arabia)

Current state-of-the-art approaches to understand and control the microstructural and morphological evolutions of solution-processed thin film deposition for organic thin film transistors are either limited to a combinatorial experimental investigation or single scale analysis, and provide only limited data for analysis - limited to the final structure, morphology and performance. In situ analysis, while very mature in other thin film-intensive applications, is further complicated by the incompatibility of many traditional characterization techniques with the processing environments and/or speeds with which solution-based methods, including drop-, spin- and shear-casting, fabricate thin films. These challenges hinder our ability to understand the mechanisms of organic thin film growth at a meaningful and helpful level and may slow down development of future processes or the discovery of new high-performance organic semiconductors. In this talk, we show that many of these challenges can be addressed by use of a range of approaches, from simple lab-based methods, such as interferometry and quartz crystal microbalance, to more sophisticated approaches, such as fast, time-resolved video-microscopy and synchrotron X-ray scattering, to gain insight into the state of the solution, the solute, as well as nucleation and thin film formation phenomena at the solid-liquid and liquid-ambient interfaces during solution processing. These experiments have shed some light into the complex mechanisms of formation of small-molecule, polymer and blended thin films for high performance organic thin film transistors.

8117-30, Session 6

High-performance pentacene thin-film transistors fabricated by organic vapor-jet printing (OVJP)

C. Yun, S. Lee, H. Moon, M. Kim, S. Yoo, KAIST (Korea, Republic of)

We present high mobility thin-film transistors (TFTs) that are based on pentacene thin films deposited by organic vapor-jet printing (OVJP) method. Printing of organic semiconductors has been regarded as the key element in printed organic electronics, and much attention has been paid to the ink-jet printing relying on solution-processable materials. Different from the ink-jet printing, OVJP can make a fine pattern of organic thin-films without any solvent [M Shtein et al, Adv. Mater., 16, 1615 (2004)], allowing for use of well-known high-mobility small molecules such as pentacene and rubrene. In addition, the complicated well-definition process, commonly adopted in ink-jet printing method, is not needed to define the channel area of organic TFTs (OTFTs) in the OVJP method. In this work, we demonstrate pentacene TFTs with the mobility on the order of 0.5cm²/Vs, which is comparable to that of the same OTFTs fabricated by the conventional vacuum thermal evaporation. A special attention is paid to the optimization of the carrier gas temperature of the OVJP and the surface treatment below the channel. In addition, we introduce the "jet-on-demand"-type operation of our proposed OVJP system in which deposition of organic materials can be controlled point by point in a digital manner, which will be highly beneficial for the fabrication of organic integrated circuits.

8117-31, Session 6

Adapting conformation and self-assembly in pi-conjugated materials through non-covalent interactions

P. J. Skabara, Univ. of Strathclyde (United Kingdom)

Ladder or ribbon type conjugated polymers are of interest due to their ability to form highly planar and conjugated structures. This feature is advantageous if one requires a low band gap material and/or efficient p-p stacking for high levels of charge mobility. However, for reasonable solubility, ladder and ribbon structures usually require derivatization by long or branched alkyl chains, which in turn have an insulating effect on the electrical properties of the polymer. Consequently, a trade-off exists between electronic characteristics and solubility. To avoid this conflict an ideal material would need to have conformational freedom in solution to allow for good solubility (without the need of large solubilising groups), and be able to reorganise upon solidification to give a predominantly planar structure. To this end, we have been looking at heteroatomic non-covalent interactions within pi-conjugated structures to promote planar and well organised films. Electroactive units have been incorporated into these structures to manipulate the energy levels of the materials and enhance charge transport properties. Herein, we report several examples of such materials and their application in organic thin film transistors.

8117-32, Session 6

Tuning the threshold voltage in organic thin-film transistors by local channel doping using photoreactive interfacial layers

B. Stadlober, JOANNEUM RESEARCH Forschungsgesellschaft mbH (Austria); M. Marchl, Technische Univ. Graz (Austria); M. Edler, Montan Univ. Leoben (Austria); A. Haase, A. Fian, JOANNEUM RESEARCH Forschungsgesellschaft mbH (Austria); G. Trimmel, Technische Univ. Graz (Austria); T. Griesser, Montan Univ. Leoben (Austria); E. Zojer, Technische Univ. Graz (Austria)

We demonstrate an easy and reproducible way to switch OTFTs from enhancement to depletion mode by a photochemical reaction using photo-acid generators as interfacial layers, and demonstrate that this allows the fabrication of good quality depletion-load inverters with tuneable characteristics [1]. This is achieved by significant refinement of the concept of chemical channel doping by replacing the covalently bonded silane layers bearing sulfonic acid groups with photoacid generator polymers. The goal hereby is to use them as an interface-modification layer, whose properties can be patterned photochemically, as the acid group is formed only upon illumination. The suggested fabrication method enables an accurate local control of the threshold voltage through the illumination dose by a method that is fully compatible with lithographic techniques omnipresent in conventional semiconductor industry.

[1] Marco Marchl, Matthias Edler, Anja Haase, Alexander Fian, Gregor Trimmel, Thomas Griesser, Barbara Stadlober, and Egbert Zojer., Adv. Mat. 22, 5361 (2010).

8117-33, Session 7

Printed thin-film transistors: materials and applications

A. C. Arias, Univ. of California, Berkeley (United States) and Palo Alto Research Center, Inc. (United States); T. N. Ng, G. Whiting, L. Lavery, Palo Alto Research Center, Inc. (United States)

The Palo Alto Research Center (PARC) is conducting a technical program to develop and prototype disposable flexible sensor tapes to be used in several applications including the detection of the occurrence of events that cause traumatic brain injury (TBI). The sensor tape has integrated sensors, signal conditioning electronics, non-volatile memory and a thin film battery. The electronic circuits are based on jet-printed organic electronics with the emphasis on low-voltage electronics due to the limitations of the battery size. We integrate pressure, acoustic, acceleration and temperature sensors based on piezoelectric polymers such as PVDF or PVDF-TrFE copolymer. These materials were chosen because of low-power requirements, low drift and relatively simple fabrication. Polymer/polymer and polymer/small molecules blends are used in the fabrication of light sensors. In this talk I will focus on the main challenges of the program: materials performance, TFT voltage operation, and inkjet printing as a manufacturing technology. We have demonstrated all printed p-type TFTs with mobility of 1.6 cm²/Vs and n-type TFTs with mobility of 0.8 cm²/Vs. We have characterized the charge trapping rates for n- and p-channel devices and assessed the inverter gain and noise margin. All printed inverters showed a typical gain of 8 with VDD at 10V and -3dB cutoff at 150 kHz for a load of 0.02pF. We have integrated printed inverters with printed accelerometers, printed acoustic and pressure sensors and showed operation between 0-1000g, 100-140dB and 5-100 psi respectively.

8117-34, Session 7

Patterned-electrode vertical organic FET: comprehensive, theoretical, and experimental study

A. J. Ben-Sasson, N. Tessler, Technion-Israel Institute of Technology (Israel)

We present a theoretical and experimental investigation of the Patterned Electrode Vertical Organic Field Effect Transistor (PE-VOFET). This investigation demonstrates the role of the PE structural parameters in determining the potential surface shape and, in turn, the charge carrier concentration and the device I-V behavior. We show that the biased gate forms virtual contacts at the PE nano-features (i.e. perforations) which form a vertical channel that switches the device behavior from the contact-limited regime to the space-charge-limited regime. On and off channels' spatial separation, a unique device property, is presented and exploited to improve device performance.

We present optimization guidelines regarding the PE structural parameters: PE thickness, features' diameter and potential barrier. Using Block-Copolymers self-assembled layers[1] we obtain a large area PE having nano-features with distinctive structures where shape, size and material composition can be tuned and hence also modeled in relative accuracy. We fabricate PE-VOFET and show that, as predicted by the simulation, the aspect ratio of the perforations in the electrode is critical for the on/off ratio performance. For the same average perforation size, changing the electrode thickness from 10nm to 6nm results in on/off ratio varying from less than 10^2 to 10^4 .

Finally, based on the combined experimental and theoretical effort, in-situ method for extraction of device structural/ electrical parameters is presented. One such parameter of interest is the vertical mobility.

[1] A. J. Ben-Sasson, E. Avnon, E. Ploshnik, O. Globberman, R. Shenhar, G. L. Frey, and N. Tessler, Applied Physics Letters 95 (21), 3 (2009).

8117-36, Session 7

A high performance solution processable organic semiconductor material for OTFT devices

C. J. Newsome, J. C. Carter, R. J. Wilson, J. H. Burroughes, Cambridge Display Technology Ltd. (United Kingdom)

In this work we demonstrate the performance of thin film transistor devices based on a solution processable organic semiconductor with a field effect mobility of up to $2\text{cm}^2/\text{Vs}$. The performance of the material is demonstrated in a top gate, bottom contact device architecture operational in ambient conditions without the requirement of device encapsulation. From a device performance aspect, we also highlight the influence that contact resistance has on the mobility, and show how considering the interfaces of the device and selection of solvent for the semiconductor, the device mobility can be improved. The focus of our device performance is based on a spin coating deposition method for the semiconductor film. However, the material is soluble in a wide range of organic solvents compatible with alternative deposition methods.

8117-37, Session 7

Vertically stacked complementary inverters with solution-processed organic semiconductors

J. Kim, C. Fuentes-Hernandez, D. K. Hwang, S. P. Tiwari, W. J. Potscavage, Jr., B. Kippelen, Georgia Institute of Technology (United States)

We report on a vertically stacked complementary inverter geometry in which an [6,6]-phenyl C61 butyric acid methyl ester (PCBM) n-channel TFT is stacked on top of a 6,13-bis(triisopropylsilylethynyl) (TIPS) pentacene and poly(triarylamine) (PTAA) blend p-channel TFT. In this study, a 75 nm-thick Al_2O_3 was used as a bottom-gate dielectric for the n-channel TFT and a 40 and 50 nm-thick CYTOP and Al_2O_3 bi-layer was used as a top-gate dielectric for the p-channel TFT. The CYTOP layer was deposited by spin casting. The Al_2O_3 films were deposited at 110°C using atomic layer deposition. The capacitance density of the top- and bottom-gate dielectric were found to be 35 and 114 nF/cm^2 , respectively. With a shared common gate electrode positioned between two dielectric layers, bottom-contact p- and top-contact n-channel TFTs showed saturation mobility values of 0.25 and $0.0038\text{ cm}^2/\text{Vs}$ and threshold voltages of -3.9, and 0.3 V, respectively. At 8 V, the inverter yielded a gain value of -28 V/V with a switching threshold voltage value of 4 V. In contrast to horizontally distributed inverters, the use of inverters with vertically stacked p- and n-channel TFTs allows solution processable semiconductors without the need of cross-linking the semiconductor layers. They also increase the packing density, and improve the drivability of microelectronic circuits by reducing the interconnection lengths and parasitic resistances. The independent control of the gate dielectric

thicknesses is also an important design parameter that can be used to further optimize the performance of these inverters.

8117-38, Session 8

Morphology of cleaved rubrene surface and its evolution in ambient environment

R. J. Thompson, Univ. College London (United Kingdom) and London Ctr. for Nanotechnology (United Kingdom); C. Kloc, Nanyang Technological Univ. (Singapore); N. Curson, O. Mitrofanov, Univ. College London (United Kingdom) and London Ctr. for Nanotechnology (United Kingdom)

Surface charge concentration as well as charge carrier mobility in rubrene crystals can be manipulated by varying environmental conditions. A reliable method for modifying and controlling these electronic properties locally would allow designing electronic circuits on rubrene surface. Cleaved rubrene crystals offer reproducible and unoxidized surfaces required for investigation of the environmental dependence. To understand the underlying physical mechanisms of the charge transport modification, we studied the surface morphology of cleaved rubrene surface and found that the newly created surfaces exhibit molecular reorganization in the normal ambient environment. The evolution of the surface morphology and local conductivity was characterized with atomic force microscopy over a period starting from several minutes up to two years after cleaving. The cleaved surface was found to exhibit the formation of nanoscale beads ($\sim 10\text{-}40\text{ nm}$ high), regular clusters of matter aligned along molecular step edges, and fingers, narrow molecular structures, one rubrene molecule high, and in excess of 1 micron long. Conductive AFM studies show that the beads exhibit insulating behavior and a band bending effect on the surface nearby. Their formation has a strong environmental dependence, which has implications for the operation of rubrene field-effect transistors in the ambient environment. To identify the origin of these surface features we applied several surface characterization techniques, including photoluminescence spectroscopy and time of flight second ion mass spectroscopy. In this presentation we will discuss the evolution of cleaved rubrene surfaces and processes that can be key to understanding of the environmental dependence of charge transport in rubrene.

8117-39, Session 8

Impedance spectroscopy for pentacene field-effect transistor -channel formation process in transistor operation

Y. Tanaka, Y. Noguchi, Chiba Univ. (Japan); M. Kraus, W. Brütting, Univ. Augsburg (Germany); H. Ishii, Chiba Univ. (Japan)

In order to understand the operation mechanism of organic field-effect transistors (OFETs) in detail, it is important to investigate the voltage dependence of the effective capacitance in OFET. It is known that the conduction channel is formed by the injected carriers from the electrode. Therefore the channel formation processes have been extensively studied by various evaluation methods, scanning probe microscopy, electron spin resonance, second harmonic generation, displace current measurement (DCM) and impedance spectroscopy (IS). Among these methods, IS is the commonly-used method to obtain capacitance-voltage (C-V) curves, and carrier injection, accumulation processes have been studied. In principle, IS is two-terminal measurement, however, OFETs are three-terminal device. Thus, carrier behaviors in transistor operation cannot be observed by using conventional IS. In this study, we have proposed IS measurement system to investigate C-V relationship of an operating transistor by applying a voltage between a source and drain electrodes with an isolated battery, and succeeded to obtain an obvious change of the capacitance during the channel formation, suggesting the pinch-off condition. By using this method, we can investigate the carrier behaviors in more detail, which it is difficult to evaluate from the output and transfer curves. In addition to IS, DCM is also a kind of C-V method, which can

observe the channel formation and annihilation processes separately. Since these two kinds of C-V methods directly observe the carriers in channel region in transistor operation, it is expected that further quantitative understanding of operation mechanism and the improvement of the device performance.

8117-40, Session 8

High performance organic transistors based on monolayer graphene

K. Cho, Pohang Univ. of Science and Technology (Korea, Republic of)

Here, we introduced several high performance graphene-based organic transistors using a monolayer graphene. Firstly, we developed high performance bottom-contact pentacene field-effect transistors (FETs) with graphene source/drain electrodes by transferring and patterning chemical vapor deposition (CVD)-grown monolayer graphene films. We showed that polymer residues remaining on graphene surfaces induce a stand-up orientation of pentacene, thereby controlling pentacene growth such that the molecular assembly is optimal for charge transport. Secondly, transparent/flexible carbon-based pentacene FETs using monolayer graphene electrodes were successfully assembled on flexible plastic substrates and showed high performances. Thirdly, we also fabricated graphene FETs using CVD-grown monolayer graphene with controlled doping by self-assembled monolayers.

8117-41, Session 8

Low temperature processing of high mobility ZnO thin film transistors on flexible substrates

M. A. McLachlan, J. B. Franklin, R. Hewlett, S. Thomas, M. P. Ryan, T. D. Anthopoulos, Imperial College London (United Kingdom)

The development of low temperature routes for the deposition of thin oxide layers onto flexible or organic functionalised substrates is necessary in a wide range of electronic materials, including the deposition of transparent conducting layers on flexible substrates, preparing optical spacers in tandem solar cells and LEDs and creating electron accepting layers in organic photovoltaics.

Here we report the deposition of highly crystalline ZnO thin film transistors at temperatures 100 nm) and their orientation Figure 1 play an important role in determining the device characteristics. By comparing device performance of PLD prepared films on PET/ITO with a PMMA dielectric together with ZnO deposited on Si/SiO₂ substrates we have gained an insight into the defect chemistry and electronic structure of the devices prepared.

References

J. B. Franklin, B. Zou, D.W. McComb, P. Petrov, M.P. Ryan, and M.A. McLachlan, Optimised Pulsed Laser Deposition of ZnO Thin Films on Transparent Conducting Substrates. Journal of Materials Chemistry, In press.

8117-42, Session 8

Top-gate pentacene and amorphous InGaZnO channel thin-film transistors and inverters with high-operational stability

J. Kim, C. Fuentes-Hernandez, D. K. Hwang, W. J. Potscavage, Jr., H. Cheun, S. P. Tiwari, B. Kippelen, Georgia Institute of Technology (United States)

We report on highly stable hybrid complementary inverters composed of top-gate pentacene and amorphous InGaZnO TFTs. Pentacene and amorphous InGaZnO (a-IGZO) channels were fabricated on top of Ti/Au source-drain electrodes on glass substrate. The CYTOP layer was deposited by spin casting. A CYTOP/Al₂O₃ bi-layer was used as gate dielectric. The Al₂O₃ film was deposited at a temperature of 110 °C using atomic layer deposition (ALD). An Al electrode was fabricated by thermal evaporation and served as gate electrode. The p-channel pentacene and n-channel a-IGZO TFTs showed hysteresis-free current voltage characteristics with saturation mobility values of 0.10 and 4.80 cm²/Vs, respectively, and large on-off current ratios of 10⁴ and 10⁵, respectively, at a voltage of 8 V. Both TFTs showed excellent electrical stability with negligible variations under continuous multiple scans up to 500 cycles and less than 6 % variations after continuous direct current (DC) bias stress for 1 hour at gate-to-source (VGS) and drain-to-source (VDS) voltages of 8 V. The inverters yielded hysteresis-free voltage transfer characteristics for forward and reverse input biases due to the hysteresis-free current voltage characteristics with a static DC gain value of -45 V/V and a switching threshold voltage (VM) of 3.3 V at a supply voltage of 8 V. Therefore, the implementation of the complementary inverters with the use of amorphous fluoropolymer/high-k inorganic bi-layer as a top-gate dielectric for organic p-channel and inorganic n-channel TFTs is a promising way to realize complementary circuits with high operational stability. The operational stability of these inverters under various conditions of bias stress will be discussed.

Conference 8118: Organic Semiconductors in Sensors and Bioelectronics IV

Wednesday–Thursday 24–25 August 2011 • Part of Proceedings of SPIE Vol. 8118
Organic Semiconductors in Sensors and Bioelectronics IV

8118-01, Session 1

Organic photodiodes as monolithically integrated detectors in micro-optical systems

B. Lamprecht, G. Jakopic, JOANNEUM RESEARCH Forschungsgesellschaft mbH (Austria); H. Dittlbacher, Karl-Franzens-Univ. Graz (Austria)

Organic photodiodes open new possibilities concerning the integration into micro-optical systems. The ease of processing, based on layer-by-layer vacuum deposition, and the possibility to deposit these devices basically on any substrate as well as the possibility to tune the spectral response make organic photodiodes attractive for integrated systems, especially allowing facile integration with planar chip-based systems. The heart of organic photodiodes is a sequence of ultrathin (below 100 nm) photoactive layers of organic small molecules. Upon light absorption in the semiconductor layers electrical charges are generated, which provide an electrical signal at the electrodes placed in sandwich geometry above and below the organic layers.

For the application of these devices as integrated detectors two examples will be presented. We demonstrate the monolithic integration of an organic photodiode with a planar optical stripe waveguide, micro-structured by UV photolithography. The photodiode's absorbing layers, are deposited directly on the waveguide core. Along an overlap length the optical energy gradually "leaks" out of the waveguide into the photodiode, producing attenuation in the waveguide and an electrical signal at the photodiode electrodes.

Furthermore we present the utilization of the organic diodes for the direct electric detection of surface plasmon polaritons (SPP). In contrast to standard organic photodiodes the plasmon diode consists of organic layers sandwiched between two opaque metal electrodes, one of which additionally serves as a SPP waveguide. SPPs propagating along this waveguide and entering the diode area excite excitons in the organic materials which gives rise to an electric current that can be directly measured.

8118-02, Session 1

Ultrasensitive solution-processed polymer infrared photodetectors

X. Gong, The Univ. of Akron (United States)

Photodetectors sensitive to the full UV-visible to infrared spectrum are very desirable for scientific and technological applications, but conventional semiconductor detectors are limited to narrow sub-bands of the spectrum. Here we report ultrasensitive solution processed photodetectors fabricated by narrow band-gap semiconducting polymers as the electron donors and inorganic quantum dots with high electrical conductivity as the electron acceptors. Polymer photodetectors with photo-response from from 300nm to 2200nm and detectivity larger than $10^{11} \text{ cm Hz}^{1/2}/\text{W}$ were demonstrated. All these values are comparable to or even better than their inorganic counterparts.

8118-03, Session 1

An integrated organic-based sensing device: toward all-organic compact biochemical sensors

R. Liu, Ames Lab. (United States); T. Xiao, Ames Lab. (United States) and Iowa State Univ. (United States); J. Shinar, Ames Lab.

(United States); R. Shinar, Iowa State Univ. (United States)

Arising industrial demands boost the interests in searching for miniaturized, disposable biochemical sensors. The recent massive development and efficiency enhancement in both organic photovoltaics (OPVs) and organic light-emitting diodes (OLEDs) enables the possibility of an organic-based sensor which serves the above-mentioned needs. Specially focused on oxygen detection, this work puts the effort on developing the first integrated organic-based oxygen sensing device, which leads the way for more compact, low-cost and biocompatible biochemical sensors.

8118-04, Session 1

Integrated organic optical sensor arrays based on ring-shaped organic photodiodes

B. Lamprecht, E. Kraker, G. Jakopic, M. Sagmeister, S. Köstler, JOANNEUM RESEARCH Forschungsgesellschaft mbH (Austria); T. Abel, T. Mayr, Technische Univ. Graz (Austria); H. Dittlbacher, Karl-Franzens-Univ. Graz (Austria)

We present an integrated optical sensor platform suitable for the parallel detection of multiple parameters in an array format. This sensor technology combines fluorescent sensor layers with ring-shaped thin-film organic photodiodes (oPDs), serving as integrated fluorescence detectors. The sensing layers are deposited by screen printing on the upper side of a PET substrate, which is exposed to an analyte, whereas the ring-shaped photodiodes are monolithically integrated, by vapour phase deposition, on the backside of the transparent substrate, in correct alignment to the sensing layers. The monolithic integration of sensor layers and detectors on one common substrate as well as the special ring shaped form of the photodiodes guarantees that a maximum of the fluorescent light emitted from the sensor layers is collected. A key advantage of the above described sensor geometry is the straightforward potential to realise sensor arrays for the parallel detection of multiple parameters: different sensor spots are illuminated by a common homogeneous large area light source, e.g. an OLED, and are read-out by individual integrated organic photodiodes, surrounding the respective sensor layers. Three different sensing principles including absorbance, fluorescence and surface plasmon resonance can be applied in the same basic sensor platform. The functionality of the concept is demonstrated by an integrated oxygen sensor. Sensor schemes for the analytical parameters carbon dioxide, temperature and ammonia, are proposed. Efficient front end electronics enabling intensity and time domain detection of sensor signals for the testing and characterisation of the integrated sensor devices have been developed.

8118-05, Session 2

Approaches to enhance OLEDs' suitability for (bio)chemical sensing applications

J. Shinar, Iowa State Univ. (United States)

Challenges associated with the use of continuous and pulsed OLEDs as the excitation source in photoluminescence-based (bio)chemical sensors and approaches to alleviate such challenges are presented. The challenges include broad electroluminescence (EL) bands, limited light extraction from the front of the OLED due to total internal reflection & waveguiding in the organic + ITO layers and the glass substrate, and transient EL following a bias pulse, including EL decay tails. Approaches to alleviate such challenges include choosing suitable OLED materials and structures, including the use of microcavity and UV OLEDs, and the design of OLED pixels integrated with microlens arrays.

8118-06, Session 2

Integrated semiconductor optoelectronic devices for real-time and indicator-free detection of aqueous nitric oxide

Y. Chao, S. Yeh, H. Zan, G. Chang, H. Meng, National Chiao Tung Univ. (Taiwan); C. Hung, T. Meng, Academia Sinica (Taiwan)

A real-time and indicator-free sensor specific to nitric oxide (NO) is realized for the first time by integrating a sensing hydrogel film, a top-emitting polymer light-emitting diode (PLED), a silicon photodetector, and two organic filters. The top-emitting PLED is utilized to excite the sensing film specific to NO, and the photoluminescence (PL) of the sensing film is transformed into electric signal by the photodetector. Light signal is therefore transformed into electric signal for recording. The PL spectrum of the sensing hydrogel film has a peak at 675 nm. The selectivity of the sensing hydrogel film is very high; molecules such as nitrite, nitrate, hydrogen peroxide, oxygen, and carbon monoxide can not induce PL change. The influence of the excitation light on the out-put photocurrent of the photodetector is diminished by two delicately selected organic filters based on their absorption spectra. Lead phthalocyanine (PbPc) is deposited on a top-emitting PLED as a filter for generating an excitation light without overlapping the emission maximum of the sensing hydrogel film. Poly(3-hexylthiophene) (P3HT) is placed in front of the photodetector as another filter to remove the excitation light. The EL spectrum of the top-emitting PLED without PbPc ranges from 500 nm to 700 nm, but after deposition of 200 nm PbPc, its spectrum range is narrowed and almost no emission around 675 nm can be observed. This sensor demonstrated a fast photocurrent response to NO with response time within 5 min.

8118-07, Session 2

Hybrid infrared-to-visible up-conversion device

D. Y. Kim, J. W. Lee, T. Lai, D. W. Song, F. So, Univ. of Florida (United States)

Recently, we reported an organic infrared up-conversion device capable of converting 0.83 μm near infrared (NIR) light to green light by incorporating an organic NIR sensitizing layer in an organic light emitting device (OLED). Here, we demonstrated a low cost hybrid infrared-to-visible up-conversion device with infrared sensitivity up to 1.5 μm using inorganic colloidal PbSe nanocrystals as a NIR sensitizer. PbSe nanocrystals were chosen because their optical absorption can be tuned from 0.7 μm to 2.0 μm .

The hybrid devices have the following structure: indium tin oxide (ITO) as an electrode, ZnO nanocrystals as a hole blocking layer, PbSe nanocrystals as a NIR sensitizing layer, 1,1-bis[(di-4-tolylamino phenyl)cyclohexane (TAPC) as a hole transporting layer (HTL), 4,4-N,N-dicarbazole-biphenyl (CBP) doped with Irppy3 as an emitting layer, tris[3-(3-pyridyl)-mesityl]borane (3TPYBM) as a hole blocker/electron transporting layer (ETL) and LiF/aluminum as a cathode. A control OLED without the NIR sensitizing layer was also fabricated. The luminance-current-voltage (LIV) characteristics were measured in the dark and NIR illumination (0.7 μm ~ 1.7 μm). Without NIR irradiation, electroluminescence emission was not observed until the applied voltage reached 17 V. When the device was irradiated with infrared light, electroluminescence was observed at 8 V. The hybrid up-conversion device shows the photon (IR)-to-photon (Green) conversion efficiency up to 3.9 %. Also, the green emitted light in hybrid up-conversion device shows a linear dependence with the optical power density.

8118-08, Session 2

Printed hybrid systems for sensor applications and systems

E. J. W. List, Technische Univ. Graz (Austria) and NTC Weiz GmbH (Austria)

Comfortable, wearable sensors and computers will enhance every person's awareness of his or her health condition, environment, chemical pollutants, potential hazards, and information of interest. In agriculture and the food industry there is a need for to constantly monitor the condition and needs of plants, animals, and farm products. Yet many of these applications depend upon the development of novel, cheap and easy to implement and integrated devices and sensors. Organic semiconductors, inorganic materials and hybrids have proven to combine a number of intriguing optical and electronic properties with easy processing. As it will be reviewed in this contribution these materials are believed to find their application in many electronic devices and fabrication processes. Moreover, this material class will allow for the development of smart disposable devices in health-, food- and environmental monitoring, diagnostics and control, possibly integrated into arrays of sensor elements for multi-parameter detection. In this contribution we report on the design, realisation and characterization of novel active partly printed semiconductor sensor devices (oFETS, OLEDs, LECs), particular gas sensors, and IR detectors.

8118-09, Session 3

Organic electrochemical transistors: working principle and applications in sensing

F. Cicoira, Consiglio Nazionale delle Ricerche (Italy); S. Yang, Univ. of Illinois at Urbana-Champaign (United States); G. Tarabella, S. Iannotta, Consiglio Nazionale delle Ricerche (Italy); G. G. Malliaras, Ecole Nationale Supérieure des Mines de Saint-Étienne (France)

Organic electrochemical transistors (OECTs) are particularly promising for applications in chemical and biological sensing. OECTs consist of a conducting polymer film (transistor channel) in contact with an electrolyte. A gate electrode immersed in the electrolyte controls the doping level of the conducting polymer. OECTs can be operated in aqueous electrolytes, providing an interface between the worlds of biology and electronic materials. The inherent signal amplification of OECTs has the potential to yield sensors with low detection limits and high sensitivity. The vision is to build a disposable "lab on a chip", a diagnostic device consisting of multiple sensors, where one can input a drop of analyte and receive an analysis of as many indicators of health as possible.

In my talk I will present recent studies on OECTs, which highlight how the device characteristics can be tailored via the appropriate choice of the device geometry and the materials used for channel, gate electrode and electrolyte. 1-4 Experimental results are used to formulate a numerical model to establish design rules for OECT based sensors. A deeper understanding the OECT working principle is expected to push the limits of electrochemical detection and expand the range of application of OECT based sensors.

8118-10, Session 3

Ultra-thin and flexible organic electrochemical electrodes and transistors for neural interface

D. Khodagholy Araghy, T. Doublet, M. Gurfinkel, E. Ismailova, Ecole Nationale Supérieure des Mines de Saint-Étienne (France); C. Bernard, Univ. de la Méditerranée (France); G. G. Malliaras, Ecole Nationale Supérieure des Mines de Saint-Étienne (France)

Conference 8118: Organic Semiconductors in
Sensors and Bioelectronics IV

Unique properties of organic semiconductors such as biocompatibility, mechanical flexibility, and chemical sensitivity enable them to interface with living organisms. Poly(3,4-ethylenedioxythiophene) doped with poly(styrene sulfonate) (PEDOT:PSS) is an interesting material to interface with neurons. It provides a suitable surface for cell adhesion; also it is capable of ionic conduction, which enables new modes for interfacing with neurons. We report ultra thin and flexible PEDOT:PSS-based devices for interfacing with neurons. The first device is an array of 64 PEDOT:PSS based electrodes. The device is encapsulated in a 3micron thick stand-alone Parylene C film, which acts as both substrate and insulation layer. Owing to its flexibility, the device can cover the surface of a rat brain for global field potential analysis. The second device is an array of 128 electrochemical transistors based on PEDOT:PSS, with channel lengths of 30 microns. We discuss the sensitivity of these devices and their potential in neurological disorder studies.

8118-11, Session 3

Wearable electrochemical biosensor for monitoring performance athletes

K. J. Fraser, R. Byrne, Dublin City Univ. (Ireland)

Nowadays, wearable sensors such as heart rate monitors and pedometers are in common use. Several products are already on the market, such as the Lifeshirt®, the body monitoring system developed by BodyMedia® and the Nike-Apple iPod Sports kit which facilitates individualized feedback control of performance during exercise periods. The use of wearable systems such as these for personalized exercise regimes for health and rehabilitation is particularly interesting. This area is growing exponentially, as the economics of healthcare increasingly point to the need to provide remote monitoring of patient progress, rather than the current hospital focused model. In particular, the true potential of wearable chemical sensors, which for the real-time ambulatory monitoring of bodily fluids such as tears, sweat, urine and blood has not been realized. This is due to the difficulties associated with sample generation, collection and delivery, sensor calibration, wearability and safety issues.(1)

Herein, we present the fabrication, characterization and the performance of a wearable, robust, flexible and disposable electrochemical biosensor system based on novel ionic liquid polymer gels (ionogels)(2, 3) for monitoring in real time mode the concentration of glucose and lactate in sweat and saliva generated during an exercise period. Up to now glucose and lactate analysis has been carried out using awkward invasive methods followed by laboratory analysis. The approach presented here can provide immediate feedback regarding sweat and saliva composition, which is of great interest to performance athletes.

1. D. Diamond, S. Coyle, S. Scarmagnani, J. Hayes, Chemical Reviews 108, 652 (2008).
2. S. Y. Yang et al., Chemical Communications 46, 7972 (2010).
3. A. Kavanagh, R. Byrne, D. Diamond, A. Radu, Analyst 136, 348 (2011).

8118-28, Poster Session

Electrical readout of photochromic state

H. M. Edrees, X. Chen, N. K. Pervez, O. A. Winn, Columbia Univ. (United States); T. J. Cumberbatch, The Cooper Union for the Advancement of Science & Art (United States); I. Kymissis, Columbia Univ. (United States)

Photochromic materials reversibly switch between two states under optical excitation. These states are usually differentiated based on their optical properties, but they can also be differentiated using electrical probes. In our experiments we study interdigital capacitors on glass substrates with a dielectric layer made using LCR Hallcrest UP44/BL14 blue photochromic powder. By measuring shifts in capacitance under different wavelengths of illumination, we use on wafer electrical measurements to differentiate between two photochromic states of the dielectric. This allows for electrically read optically programmable devices, enabling memory devices and new kinds of integrated sensors.

8118-29, Poster Session

Electrochemical transistors with ionic liquids for enzymatic sensing

K. J. Fraser, R. Byrne, F. Benito-Lopez, D. Diamond, Dublin City Univ. (Ireland); S. Warren, E. Dempsey, Institute of Technology Tallaght (Ireland); R. M. Owens, G. G. Malliaras, Ecole Nationale Supérieure des Mines de Saint-Étienne (France)

Over the past decade conducting polymer electrodes have played an important role in bio-sensing and actuation.[1] Recent developments in the field of organic electronics have made available a variety of devices that bring unique capabilities at the interface with biology.[2,3] One example is organic electrochemical transistors (OECTs) that are being developed for a variety of bio-sensing applications, including the detection of ions,[4-6] and metabolites, such as glucose[7] and lactate[8].

Room temperature Ionic Liquids (RTILs) are organic salts, which are liquid at ambient temperature. Their non-volatile character and thermal stability makes them an attractive alternative to conventional organic solvents. [9] Here we report an enzymatic sensor based on an organic electrochemical transistor that use RTIL's as an integral part of its structure and as an immobilization medium for the enzyme and the mediator. Further investigation shows that these sensing platforms can be incorporated into flexible materials such as carbon cloth and can be utilized for bio-sensing, such as enzymatic sensing. The aim is to incorporate the overall platform in a wearable sensor to improve athlete performance with regards to training.

- 1 S. Y. Yang, F. Cicoira, R. Byrne, F. Benito-Lopez, D. Diamond, R. A. i. n. M. Owens and G. G. Malliaras, Chem. Commun., 2010, 46, 7972-7974.
- 2 M. Berggren and A. Richter-Dahlfors, Adv. Mater., 2007, 19, 3201.
- 3 R. M. Owens and G. G. Malliaras, MRS Bull., 2010, 35, 449.
- 4 J. T. Mabeck, J. A. DeFranco, D. A. Bernards, G. G. Malliaras, S. Hocde and C. J. Chase, Appl. Phys. Lett., 2005, 87, 013503.
- 5 D. A. Bernards, G. G. Malliaras, G. E. S. Toombes and S. M. Gruner, Appl. Phys. Lett., 2006, 89, 053505.
- 6 P. Lin, F. Yan and H. L. W. Chan, ACS Appl. Mater. Interfaces, 2010, 2, 1637.
- 7 Z.T.Zhu, J.T.Mabeck, C.C.Zhu, N.C.Cady, C.A.Battand G. G. Malliaras, Chem. Commun., 2004, 1556.
- 8 S. Y. Yang, J. A. DeFranco, Y. A. Sylvester, T. J. Gobert, D. J. Macaya, R. M. Owens and G. G. Malliaras, Lab Chip, 2009, 9, 704.
- 9 K. J. Fraser and D. R. MacFarlane, Aust. J. Chem., 2009, 62, 309-321.

8118-30, Poster Session

Evaluating oxygen presence in OLEDs by utilizing an oxygen-sensitive phosphorescent dye

A. Smith, R. Liu, J. Shinar, R. Shinar, Iowa State Univ. (United States)

Oxygen introduced into the active layers of OLEDs during and following fabrication can lead to device degradation. To assess the level of oxygen in OLEDs we first evaluated the response of commonly used emitting layers to varying oxygen levels. This was done by doping the organics layers (i.e., Alq3, NPD and PVK) with the phosphorescent oxygen-sensitive dye Pd octaethylporphyrin (PdOEP) and monitoring the photoluminescence (PL) decay time of PdOEP following exposure to various O2 levels. A pulsed LED was used in these reference experiments that related the PL decay time to the O2 level. We next fabricated OLEDs with the same doped emissive layers and monitored the PdOEP PL decay times. These values were compared to the reference data to assess the O2 level following device fabrication. The electroluminescence (EL) decay time of the devices following a bias pulse was also monitored to compare the decay processes that occur under EL and PL excitation.

8118-31, Poster Session

Photonic applications of nanoparticle dispersions of organic semiconductors produced using pulsed laser ablation (PLA)

M. H. Sayyad, F. Wahab, Z. Ahmad, Ghulam Ishaq Khan Institute of Engineering Sciences and Technology (Pakistan)

There is growing interest in the synthesis and characterization of nanoscaled materials because of their unique properties and applications. Most of these studies have been devoted to the nanoparticles of metals and inorganic semiconductors. A large number of organic semiconductors have been synthesized and many are being synthesized every year but little is known about the nanoparticles of organic semiconductors and their photonic applications. Very recently, we have reported the fabrication and study of organic diodes [1, 2], sensors [3-5] and an OFET [6]. We have undertaken production of the nanoparticle dispersions of organic semiconductors in liquids using pulsed laser ablation with the aims to see the (i) potential of this method, and (ii) investigate photonic applications of these dispersions. In this work, we report the production of nanoparticle dispersions of p and n-type organic semiconductors using PLD. To test the potentiality of these nano-sized materials for photonics applications, different types of photonic sensors are fabricated and investigated. Results of these studies will be reported.

References:

1. Z. Ahmad, M.H. Sayyad, Physica E 41 (2009) 631.
2. M. Shah, M. H. Sayyad, Kh. S. Karimov, M. M. Tahir, Physica B 405 (2010) 1188.
3. M. Saleem, M. H. Sayyad, Kh. S. Karimov, M. Yaseen, M. Ali, Sens. Actuat. B 137 (2009) 442.
4. M. H. Sayyad, M. Saleem, Kh. S. Karimov, M. Yaseen, M. Ali, K. Y. Cheong, A. F. Mohd Noor, Appl Phys A 98 (2010) 103.
5. F. Aziz, M. H. Sayyad, Kh. S. Karimov, M. Saleem, Z. Ahmad, S. M. Khan, Journal of Semiconductors, 31 (2010) 114002
6. M. H. Sayyad, Z. Ahmad, Kh. S. Karimov, M. Yaseen, M. Ali, J. Phys. D Appl. Phys. 42 (2009) 105112.

8118-12, Session 4

Highly tunable organic semiconductor lasers for sensing applications

U. Lemmer, S. Klinkhammer, X. Liu, C. Vannahme, T. Mappes, Karlsruher Institut für Technologie (Germany)

Organic semiconductors combine the ease of processing with advantageous optical and electronic properties. A particular interesting feature of these materials is the broad optical gain spectrum allowing for the realization of widely tunable lasers. In a combination with a nanoscopic surface relief pattern, distributed feedback lasers can be realized. Tunability can be achieved, e.g. by a wedge shaped waveguide which results in a spatial variation of the local laser wavelength. Such structures can be realized both with small molecular as well as polymeric semiconductors. Another interesting method for achieving tunability is the combination of organic semiconductors with electrically addressable liquid crystals. This approach enables a direct electrical of the laser wavelength. Organic semiconductor lasers can be pumped by inorganic laser diodes and can be used as the light source for spectroscopy systems without the need for further costly elements. An important feature of organic semiconductor lasers is the possibility to combine these active optoelectronic elements with passive waveguides for integrated biomedical sensing systems. The emission from an integrated distributed feedback laser can be efficiently coupled into a waveguide in a lab-on-chip platform fabricated by hot embossing.

8118-13, Session 4

Conjugated polymer laser sensors for explosive vapor detection

I. D. W. Samuel, Y. Wang, Y. Yang, G. Tsiminis, G. A. Turnbull, Univ. of St. Andrews (United Kingdom)

We show that conjugated polymer distributed feedback (DFB) lasers can be effective sensors of explosive vapors. Such lasers are attractive because of their low thresholds, simple fabrication and simple alignment. We use dinitrobenzene (DNB) as a model explosive vapor and report its effect on a range of organic semiconductors. For DFB lasers made from the widely available polymer polyfluorene, we find that exposure to 10 ppb of DNB increases the threshold by a factor 1.8, and decreases the slope efficiency of the laser by a factor of 3. The time-dependence of the response is studied and a 60% drop in output observed after 46 seconds. The factors influencing the response time will be discussed.

8118-14, Session 4

Fluorene-based fluorescent dendrimers for the detection of explosives

P. E. Shaw, H. Cavaye, P. L. Burn, P. Meredith, The Univ. of Queensland (Australia)

The detection of explosives is crucial for national security, military operations and the remediation of minefields. However, detection in the field is difficult because many explosives have low vapour pressures and the majority of existing sensing technologies are too bulky to be portable. The detection of nitrated compounds such as the explosive trinitrotoluene (TNT) and the plastic explosives taggant 2,3-dimethyl-2,3-dinitrobutane (DMNB) by fluorescence quenching is a significant development as it promises trace level detection in a compact device.

We report the results of an investigation of the sensing performance of two bifluorene dendrimers alongside that of the chemically related conjugated polymer poly(9,9-di-n-octylfluorene-2,7-yl) (PFO) in solution and thin films.[1] The dendrimers consist of a planar first generation bifluorene and a three dimensional variant with four bifluorene branches arranged tetrahedrally around an adamantyl centre. Stern-Volmer measurements show that the adamantyl-centred dendrimer possesses the highest quenching constant of the three sensing compounds. Fluorescence anisotropy measurements in solution show that there is rapid exciton migration between the arms on the adamantyl-centred dendrimer. This feature allows any of the four chromophores in a dendrimer to be quenched by a single analyte thus resulting in an amplification of the quenching response, an effect typically associated with conjugated polymers.[2] These results highlight the potential for using fluorescent dendrimers as chemosensors as well as a platform for understanding structure-property relationships.

[1] H. Cavaye et al, Macromolecules 2010, 43:10253.

[2] J. S. Yang and T. M. Swager, Journal of the American Chemical Society 1998, 120(46):11864.

8118-15, Session 4

Carbon nanotube hexa-peri/hexa-benzocoronene bilayers for detecting nonpolar volatile cancer biomarkers in humid atmospheres

U. Tisch, Y. Zilberman, G. Shuster, H. Haick, Technion-Israel Institute of Technology (Israel)

Specific volatile biomarkers in a person's exhaled breath are linked to the cellular biochemical processes of the body and mark the onset and progression of disease. Detecting volatile biomarkers of cancer

Conference 8118: Organic Semiconductors in Sensors and Bioelectronics IV

(e.g. C4-C11 straight or monomethylated alkanes) in exhaled breath is currently being investigated as a novel approach to cancer diagnostics. Chemiresistors composed of quasi-2D random networks of carbon nanotubes (RN-CNTs) are attractive for sensing applications but the detection of nonpolar cancer biomarkers in realistic breath samples is challenging, because they are screened by the high content of water vapor in the breath. We have demonstrated the feasibility of dense caplayers of hexa-dodecyl-hexa-peri-hexabenzocoronene (HBC-C12) as on-chip extractors of representative simulated cancer biomarkers for RN-CNT chemiresistors. We were able to detect and distinguish between different nonpolar biomarkers of cancer in the gas phase by covering 30%-90% of the surface of RN-CNT chemiresistors with HBC-C12 caplayers. Remarkably, the bilayer with the highest HBC-C12 coverage was insensitive to water, which marks a major step towards the development of sensors for breath testing. HBC-C12 /RN-CNT bilayers with different HBC-C12 surface coverage could form a sensor array with excellent discriminative abilities between polar and nonpolar analytes, between different polar analytes, as well as between different nonpolar analytes at very low concentrations, and in the presence of water. Ultimately, this could lead to the development of cost-effective, lightweight, low-power, non-invasive diagnostic tools for cancer screening via breath analysis.

8118-16, Session 5

Integrated sensors for point-of-care detection

J. C. de Mello, Imperial College London (United Kingdom)

Microfluidic devices have shown themselves to be highly effective for laboratory-based research, where their superior analytical performance has established them as efficient tools for genetic sequencing, proteomics, and drug discovery. However to date they have not been well suited to point-of-care diagnostic applications, where cost and portability are of primary concern. Although the microfluidic chips themselves are cheap and small, they must generally be used in conjunction with bulky optical detectors, which are needed to identify or quantify the analytes or reagents present.

Here we report the use of miniature on-chip light sources and photodetectors based on light-emitting polymers (LEPs). The LEPs add minimal size and weight to the microfluidic chips, allowing for the creation of low cost, quantitative, integrated diagnostic devices. We also discuss some recent developments in microfluidic technology and passive optical components that are designed to improve the sensitivity and cost-competitiveness of the integrated sensors.

8118-17, Session 5

Solid-state dendrimer sensors

P. L. Burn, H. Cavaye, P. E. Shaw, G. Tang, P. Meredith, The Univ. of Queensland (Australia)

Detection of explosives can play an important role in combating terrorism and humanitarian de-mining in war-torn countries. Many detection systems used for identifying the presence of explosives are cumbersome or not portable. Luminescent conjugated polymers have been successfully used in portable detectors where the presence of the analyte is detected by a decrease in the luminescence. We have discovered that light-emitting dendrimers can also be used for effective detection of explosive analytes [1-5]. Dendrimers are comprised of a core, dendrons (branched units), and surface groups, which are found at the distal ends of the dendrons. In this presentation we will describe our recent steps in designing dendrimers that can sense explosives, discuss the effect of the components within and the shape of the dendrimer on the sensing process. We will show that the explosive analytes can be rapidly detected. Finally, we will discuss how the solution measurements that are typically used to screen materials can be misleading in terms of real device performance.

1. H. Cavaye, et al, Proceedings of SPIE-The International Society for Optical Engineering, 2009, 7418 (Organic Semiconductors in Sensors

and Bioelectronics II), 741803.

2. S. Richardson, et al Appl. Phys. Lett., 2009, 95, 063305.

3. H. Cavaye, et al Langmuir, 2009, 25(21), 12800.

4. D. A. Olley, et al, Chem. Mater., 2011, 23, 789.

5. Hamish Cavaye, et al, Macromolecules, 2010, DOI: 10.1021/ma102369q.

8118-18, Session 5

Free base porphyrins for dual mode NO₂ optical sensors

P. A. Lane, U.S. Naval Research Lab. (United States); T. H. Richardson, The Univ. of Sheffield (United Kingdom)

The optical response of free base porphyrins to NO₂ has been measured, both in solution and in Langmuir-Blodgett (LB) films. Exposure of 5,10,15,20-tetrakis(3,4-bis[ethyl hexyloxy]phenyl)-21H,23H-porphine (EHO-TPP) in solution to NO₂ results in significant changes to the absorption spectrum. A sharp reduction in the intensity of the Soret and Q bands is accompanied by the rise of two new bands at 464 and 697 nm. The original absorption spectrum recovers within 15 seconds of removing the analyte under slightly elevated temperatures (>50°C). Porphyrins are also fluorescent materials, giving rise to the possibility of fluorescence detection. A solution of 5,10,15,20-tetrakis[4-(allyloxy)phenyl]-21H,23H-porphine (AO-TPP) was exposed to 50 ppm NO₂ and then its absorption and fluorescence spectra were measured. AO-TPP is commercially available and differs with EHO-TPP only in the alkoxy substituents. The absorption spectrum of AO-TPP responds in the same manner as EHO-TPP. The fluorescence peak at 658 nm blue-shifts and narrows, whereas the peak at 720 nm is substantially enhanced upon exposure to NO₂. The fluorescence intensity also decreases by 90%. Several other tetraphenyl porphyrins were tested, with free base porphyrins showing the strongest response and metalloporphyrins showing a weak response. Potential embodiments of porphyrin-based sensors will be discussed.

8118-19, Session 6

Correlation of charge transport and sensing behavior in organic semiconductor field-effect chemical sensors

D. A. Duarte, B. H. Cobb, A. Dodabalapur, The Univ. of Texas at Austin (United States)

The sensing response of organic and polymer semiconductor based field-effect chemical sensors is closely tied to charge transport and injection phenomena. Trapping phenomena play an important role in sensor response in large channel length devices. The partition coefficient is related to the morphology of the semiconductor material and the interface. In low-mobility devices and amorphous semiconductor based devices, trapping competes with carrier concentration enhancements for polar analytes. The role of the receptor as a mediator in the analyte-semiconductor interaction will be clarified.

8118-20, Session 6

What can we learn from the integration of biological membranes into OTFT sensors?

G. Palazzo, D. Angione, S. Cotrone, M. Magliulo, Univ. degli Studi di Bari (Italy); A. Mallardi, Consiglio Nazionale delle Ricerche (Italy); L. Torsi, Univ. degli Studi di Bari (Italy)

Innovative organic thin-film transistor (OTFT) realized through the full integration in the electronic device of either single lipid bilayer

Conference 8118: Organic Semiconductors in
Sensors and Bioelectronics IV

either stacks of membranes containing the membrane protein bacteriorhodopsin (bR) will be presented. Coupling between the organic semiconductor and biological membrane is actuated by assembling supra-molecular structures resulting in a device where the membranes is an integral part of the OTFT. The response of these OTFTs depends on the properties of the integrated biological membrane and thus opens a new way of probing the events involving biological membranes. The cell membranes are deeply involved in crucial cellular functions organelles are deeply involved in crucial cellular functions such as adhesion, trafficking, recognition, and signalling. Probably the most familiar form of cellular signaling is the synaptic transmission, the central event of the whole nerve transmission. Anaesthetics are drugs and chemicals that strongly hinder the synaptic transmission. We have found that lipid bilayer and bR integrating OTFTs tested against volatile-anesthetics (concentration 1-5%) reveal drug-induced membrane changes [1]. Such devices can act as selective anaesthetic sensors allowing label-free detection and operate at low reagent and power consumption and can be readily miniaturized and automatized in portable and disposable devices. The responses to anesthetics obtained with lipid bilayer and bR integrating OTFTs will be discussed and it will be shown how the results of the present study challenges the anesthetic mechanisms model relying on the so far provided evidence that clinically relevant doses (2.4 %) do not alter lipid bilayers overall-structure, significantly.

References

[1] L. Torsi, G. Palazzo, D. Angione, N. Cioffi, M. Magliulo, S. Cotrone, G. Scamarcio, L. Sabbatini, A. Mallardi. European Patent. EP 10425146.7 Submitted May 3rd, 2010.

8118-21, Session 6

Natural and nature-inspired semiconductors for organic electronics

M. Irimia-Vladu, E. Glowacki, Johannes Kepler Univ. Linz (Austria); P. A. Troshin, V. F. Razumov, N.N. Semenov Institute of Chemical Physics (Russian Federation); S. Bauer, S. Sariciftci, Johannes Kepler Univ. Linz (Austria)

Organic electronics provide a huge potential for the development of electronic products that are non-toxic, environmentally friendly, and biodegradable. An ideal solution for the production of such devices involves the fabrication of electronics either from natural materials, or from materials that have been proved to be at least biodegradable or biocompatible. Natural or nature-inspired small molecule semiconductors have been recently successfully implemented in organic photovoltaics and field effect transistors, and afforded performances on par with state-of-the-art synthetic organic materials. Among the materials we have exploited are naturally-occurring carotenoids, indigo, anthraquinone derivatives, nucleic bases, and various sugars, to name a few. We have demonstrated fully-biodegradable devices and circuits featuring natural substrates, dielectric and semiconducting layers.

8118-22, Session 6

An organic semiconductor platform that preserves neuronal firing and enables field-effect devices in vitro cell culture environment

V. Benfenati, S. Toffanin, G. Generali, A. Stefani, G. Turatti, R. Capelli, Istituto per lo Studio dei Materiali Nanostrutturati (Italy); F. Dinelli, Istituto per i Processi Chimico-Fisici (Italy); R. Zamboni, Istituto per la Sintesi Organica e la Fotoreattività (Italy); M. Muccini, Istituto per lo Studio dei Materiali Nanostrutturati (Italy)

The complex biomedical open issues underlining the brain function raise an increasing demand for advanced biomedical tools that enable real-time recording and manipulation of communication signals between neural cells. Microelectronic devices intended to be directly interfaced

with neural cells should satisfy two main conditions: 1) biological activity of the cell should be preserved; 2) the device should be able to operate in conditions that, at least in vitro, mimic the biological environment. Due to their chemical similarities to biological systems, softness and flexibility, organic semiconductors (molecular systems and polymers) are promising bio-interfacing materials, offering improved compatibility, as compared to traditional silicon-based electronic materials, for integration in devices intended for neuroscience fundamental investigations and applications.

Here, we assess the effects of perylene-diimide derivate (P13) thin-films on peripheral neuron growth and electrophysiological properties. Our results show that primary sensory DRG neurons remain viable for many days and displayed neurite outgrowth on P13-PDL-laminin coated surfaces. Importantly, neurons grown on P13-thin film fire and retained excitability properties. In addition, we determine the effect of typical real in vitro condition for neuronal cell culture environment on P13-n-type OFET electrical performances. P13-based OFET preserve their characteristics in terms of electron mobility and threshold voltage values after 16 days of in vitro treatment, showing the ability of this device to operate after exposure to cell plating and biological environment (5% CO₂, 95% humidity, 37°C).

Our results introduce a novel organic semiconductor platform that represent an important step towards the goal of developing a fully bio-integrated organic electronic device, for transduction and stimulation of electrical cell activity.

8118-23, Session 7

A photonic field-effect transistors platform for bio-sensing

M. Muccini, S. Toffanin, R. Capelli, G. Generali, Istituto per lo Studio dei Materiali Nanostrutturati (Italy); F. Dinelli, Istituto per i Processi Chimico-Fisici (Italy); A. Stefani, G. Turatti, V. Benfenati, Istituto per lo Studio dei Materiali Nanostrutturati (Italy)

A major challenge in lab-on-a-chip device fabrication is to develop a photonic miniaturized disposable platform for point-of care diagnostics that is capable of performing quantitative diagnostic tests that are currently limited to a hospital laboratory setting. The development of miniaturized cheap and disposable photonic devices for bio sensing, in which organic photonic field-effect transistors are used for light generation [1], would constitute a radically new generation of devices with unprecedented sensitivity and superior reliability at a markedly reduced cost. Here, we introduce the concept of using a tri-layer organic heterostructure in OLETs [2] providing a novel approach to dramatically improve OLET performance and match the required parameters for use onto point-of-care diagnostic components. In these devices the semiconductor is composed by a central emitting layer sandwiched between an electron and a hole carrying layer. The device operates as a contactless OLED with lateral ambipolar field effect charge transport. The physical separation between the charge transport and the light emission regions intrinsically eliminates exciton-charge annihilation while the location of the light emission area multi-micron away from the electrodes prevents electrode-induced photon losses. Our devices are 100X more efficient than the equivalent OLED fabricated using the same heterostructure and 10X more efficient than any other reported OLETs.

1. M. Muccini, Nature Materials, 5, (2006) 605.
2. R. Capelli, et al., Nature Materials, 9, (2010) 496.

8118-24, Session 7

Conformable organic electronics

M. M. de Kok, H. Schoo, G. T. van Heck, J. van den Brand, TNO Science and Industry (Netherlands)

Wearable, cheap electronics and photonics will open up a world of new applications such as devices for phototherapy and biomedical sensors. To realise electronic devices which are wearable there is a need for thin,

comfortable and stretchable solutions.

Holst Centre is developing foil technology for organic LEDs, photodetectors, circuitry on foil and interconnection technology that is compatible with roll to roll production. In order to achieve wearable systems, the choice of materials for performance, biocompatibility and comfort need to be combined with a system design that will allow stretchability. As foil based organic electronics are bendable and flexible in one direction but not intrinsically stretchable, tiled systems may provide a viable approach. We will show details of the system design and the production technologies leading to stretchable systems.

8118-25, Session 7

An active matrix-arrayed microphone with acoustic bandwidth response

Y. Hsu, I. Kymissis, Columbia Univ. (United States)

We have demonstrated a monolithically integrated two dimensional (8X8) active matrix microphone fabricated on a flexible polymer piezoelectric sheet (polyvinylidene difluoride) which uses thin film organic field effect transistors to both locally amplify the piezoelectric charge signal and switch individual elements, allowing for sensing site localization. The integrated design of the sensor and amplifier eliminates a previously dominant parasitic capacitance, allowing an acoustic bandwidth response, and the flexible, thin film form factor allows maximum versatility in applications. Each sensor element is controlled by an organic thin film transistor. The switch transistor is sized significantly smaller than the amplifying/sensing transistor to optimize the cell isolation, on/off characteristic, and parasitic load. The sensor element converts the charge response of the polyvinylidene difluoride (PVDF) sheet into a current signal, overcoming downstream parasitic charge sharing from both switch transistors and interconnects. The device is tested using both turbulent air current and far field acoustic excitation in this work. Our design extends the bandwidth of a locally amplified piezoelectric sheet sensor to the acoustic range, and demonstrates a monolithically integrated active matrix sensing architecture capable of sensing in the acoustic range and mapping both boundary layer and far field acoustic excitation for a variety of applications.

8118-26, Session 7

Ultra-flexible organic integrated circuits for medical sensor applications

T. Sekitani, The Univ. of Tokyo (Japan)

We report organic complementary circuits that continue to operate without degradation while being folded into a radius of less than 100 μm . Taking advantages of the organic circuits with high mechanical stability and high electrical performances, we demonstrate medical catheters with a transistor active matrix and sheet-sensors wrapped around it that enables the spatially resolved measurement of physical or chemical properties inside long, narrow tubes. This enormous flexibility and bending stability is enabled by a very thin plastic substrate (12.5 μm), an atomically smooth planarization coating, and a hybrid encapsulation stack that places the transistors in the neutral strain position.

Conference 8119: Terahertz Emitters, Receivers, and Applications II

Sunday 21 August 2011 • Part of Proceedings of SPIE Vol. 8119 Terahertz Emitters, Receivers, and Applications II

8119-01, Session 1

Reflection-geometry sub-terahertz-wave imaging for biological materials using an integrated photonic transceiver

H. Ito, H. Yamamoto, Kitasato Univ. (Japan); Y. Muramoto, T. Ishibashi, NTT Photonics Labs. (Japan)

Reflection-geometry THz imaging is a promising technique for security inspection and medical diagnosis since biological substances, such as human body, has large absorption coefficient due to containing water. To realize such measurements, a circulator operating at very high frequencies is required. However, availability of the conventional circulator consisting of a branched-waveguide and a small ferrite piece is limited for operations below 170 GHz. Thus, we developed a microstrip-line-based circulator circuit, and realized a resonant circulation function at around 270 GHz. A peak internal signal-to-background (S/B) ratio was evaluated to be as large as about 10. The fabricated circulator was integrated with a photomixer (uni-traveling-carrier photodiode) and a Schottky barrier diode to construct a compact photonic transceiver module for the reflection-geometry imaging. The RF-modulated optical signal was generated by optical heterodyning of two 1.55- μm laser diodes, and was converted into continuous sub-THz waves. Two-dimensional imaging was performed using a horn antenna, dielectric lenses, and an X-Y stage. The characteristic of the circulator was evaluated by measuring images of metal test patterns at frequencies from 240 to 310 GHz. Although the image resolution decreased with the signal frequency deviation from the resonant condition due to the S/B ratio decrease, it was confirmed that a practical contrast could be obtained for a bandwidth of about 20 GHz even with an S/B ratio below one. Based on these results, we could successfully demonstrate in-vivo imaging of a human finger at 270 GHz.

8119-02, Session 1

Experimental verification of the explosives identification model in THz range

P. Zagrajek, R. Ryniec, T. Trzcinski, N. Palka, Military Univ. of Technology (Poland)

The explosives identification is the crucial aspect of counterterrorism performance. The aim of our study is to develop the identification system based on a proper classification model. Most of the algorithms used to determine the models in the process of identification signals are based on the minimization a error rate as a sum of squares error model, usually. The numerical verification are often based on the same sets of data used in the process of a model estimation. The model verification based on the sets of data collected in similar but different conditions than that used in determining process, provides a more objective assessment of the quality of the model. Set of fourteen optimal frequencies for distinction eleven explosives in real environment, with influence the atmosphere, was obtained using statistical methods in the OptoLab Project.

The modeling process was based on measurement data obtained with FT-IR spectrometer. The algorithm use Hitran numerical model of atmosphere to include the absorption of terahertz radiation in water. In order to find the optimal set of fourteen frequencies measure data points, Monte Carlo method in conjunction with principal components analysis (PCA) was applied. A narrow band detector (theoretical) for analysis was used. The numerical analysis was carried out in the range from 0.3-1.2 THz.

The paper presents an experimental verification of the model with system based on TDS spectrometer and tunable narrow band sources and wide band detectors. These two particular methods were chosen to exclude an influence of measurement system on verification process.

8119-03, Session 1

Explosives identification model in reflection mode for THz security system

R. Ryniec, T. Trzcinski, P. Zagrajek, M. Szustakowski, Military Univ. of Technology (Poland)

Over the past few years rapid development of investigations in the THz area is observed. The research include spectral analysis of the THz signals to solve problem of materials identification as well. Results, published by various authors, concern distinction of several compounds mainly in transmission mode. An examination of the identification systems is particularly important for the security systems to detect terrorist threat early enough.

The most perspective security system to detect dangerous materials is active system works in a reflection regime.

In this paper a methodology to obtain model to identify several compounds was presented. The main purpose was to find a limit number of frequencies suitable for distinction eleven explosives. This model includes absorption of THz radiation in free air. The modeling process was based on measurement data obtained with Time Domain Spectroscopy reflectance data. The statistical algorithm were used to extract features of substances, then.

System identification refers to the problem of estimating a system that best describes the measure data. Feature extraction is a critical step in the pattern recognition process. The quality of the feature extraction methods can render the classification task either trivial or futile. Ideally features should be chosen such that there is a small intraclass variation and a large interclass variation.

The measurement was carried out in room conditions, at 1 meter path. Monte Carlo method and sum of squared difference (SAD) criteria was used to obtain 14 optimal frequencies. As a set of training model and test model measure data set by x-y scan sample was used. The Mahalanobis distance metric was used to verify the model.

8119-04, Session 1

Pulsed terahertz reflection-scattering measurements

S. A. Lo, E. J. Heilweil, National Institute of Standards and Technology (United States)

The terahertz spectral region, which is relatively uncharted, has been the focus of many research groups for its potential applications in spectroscopy, imaging and communication. Conventionally, terahertz spectroscopy and imaging systems operate through the principle of measuring the transmission of sample by applying a normally incident broadband picosecond terahertz pulse and optically gating the transmitted pulse with a gating laser pulse in either an electro-optic crystal or a photoconductive antenna. While this method is appropriate for most laboratory test samples, it is impossible to separate the contribution of absorption and scattering from samples that have spatial features that are close to the terahertz wavelength such as cardboard and cloth.

We have developed a method allowing us to measure the angular dependent pulsed scattering and reflection from samples by slightly modified an existing pulsed terahertz imaging system. The sample under test is placed at an angle to the incident terahertz wave and a rotating mirror pair periscope is used to pick up reflected/scattered terahertz wave from the sample. A separate mirror that is rotated at exactly half the angular resolution of the periscope is used to redirect the collected terahertz scattering at a fixed direction so that it is gated with the fixed ZnTe electro-optical gating arm of our terahertz setup. Using this approach, we successfully measured and report the reflection-scattering

Conference 8119:
Terahertz Emitters, Receivers, and Applications II

characteristics of a flat gold mirror, a paper index card and other samples.

8119-05, Session 1

A scanned beam THz imaging system for medical applications

Z. D. Taylor, Univ. of California, Los Angeles (United States); W. Li, J. Suen, Univ. of California, Santa Barbara (United States); P. Tewari, D. Bennett, N. Bajwa, Univ. of California, Los Angeles (United States); E. Brown, Wright State Univ. (United States); M. Culjat, W. Grundfest, R. Singh, Univ. of California, Los Angeles (United States)

Research into THz medical imaging has been a topic of increased interest over the last decade due to improvements in source and detector technology. One aspect of THz medical imaging research not often addressed is pixel acquisition phenomenology. Current THz imaging systems typically use translation stages to raster scan a sample beneath a fixed THz beam. While these techniques produce high resolution images of characterization targets and animal models they do not scale well to human imaging where clinicians are unwilling to strap patients to translation stages. This paper presents a scanned beam THz imaging system that can acquire a 1 cm² area with 1 mm² pixels and a per pixel SNR of 30 dB in less than 5 seconds. The system translates a focused THz beam across a stationary target using a spinning polygonal mirror and HDPE objective lens. The illumination is centered at 525 GHz with ~ 125 GHz of 3 dB bandwidth and the components are designed to optically co-locate the stationary source and detector ensuring normal incidence across a 50 mm x 50 mm field of view (FOV) at standoff of 190 mm. Component characterization as well as images of targets and tissue analogues are presented and medical applications discussed. These results are the first ever reported for a short standoff, high resolution, scanned beam imaging system and represent an important step forward for practical integration of THz medical imaging where fast image acquisition times and stationary targets (patients) are requisite.

8119-06, Session 1

Recent advances in molecular spectroscopy and its application to frequency stabilization of terahertz quantum-cascade lasers

H. Hübers, Deutsches Zentrum für Luft- und Raumfahrt e.V. (Germany) and Technische Univ. Berlin (Germany); R. Eichholz, S. Pavlov, H. Richter, A. Semenov, Deutsches Zentrum für Luft- und Raumfahrt e.V. (Germany); M. Wienold, L. Schrottke, M. Giehler, R. Hey, H. Grahn, Paul-Drude Institut für Festkörperelektronik (Germany)

High-resolution gas phase spectroscopy at terahertz (THz) frequencies is a powerful tool for the investigation of the structure and energy levels of molecules and atoms. Besides that, important information on the Doppler and pressure broadening can be obtained. In the low THz region, different methods have been developed, which are mostly based on fundamental microwave oscillators or harmonic generation. In contrast, spectroscopy above 2 THz is hampered by the lack of frequency tunable, continuous-wave (cw), powerful, and narrow linewidth radiation sources. THz quantum-cascade lasers (QCL) have attractive features for spectroscopy, namely, their small intrinsic linewidth, frequency agility, and high output power.

We will report on recent advances in molecular spectroscopy with THz QCLs. The spectrometer is based on several QCLs operating between 3 and 3.5 THz with a few mW output power. The QCLs have been developed for cw operation, high output powers, and low electrical pump powers. Efficient carrier injection is achieved by resonant longitudinal-optical phonon scattering. The QCLs are integrated in a compact Stirling

cooler and their emission is guided through an absorption cell to a Ge:Ga detector. The performance of the spectrometer, its sensitivity, and spectroscopic examples will be presented. In a particular application, a QCL is going to be used as a local oscillator in THz heterodyne spectrometer. This requires a sub-MHz frequency stabilization of its emission frequency. This is achieved by locking the frequency of the QCL to a molecular absorption line. Finally, we will discuss the prospects of THz QCLs in high-resolution molecular spectroscopy.

8119-07, Session 2

Limitations of THz QCLs, an experimental approach and an alternative

N. Péré-Laperne, Ctr. National de la Recherche Scientifique (France); L. de Vaultier, Y. Guldner, Ecole Normale Supérieure (France)

Terahertz quantum cascade lasers (QCLs), based on AlGaAs/GaAs heterostructures, are limited in terms of working temperature and supply. We present experimental data on one particular QCL structure under a strong magnetic field applied parallel to the growth axis. The emitted power shows strong oscillations as a function of B. The analysis of these oscillations exhibits two mechanisms of non-radiative relaxation, an elastic scattering mechanism (interface roughness) and an inelastic one (LO-phonon). Due to electron thermal distribution in Landau Levels (LLs) of the injector state, LO-phonon emission can break population inversion in a THz QCL under magnetic field. This latter scattering process is put in evidence thanks to magnetic field but is limiting operation at high temperature without B. One possible alternative is the use of another material, AlGaN/GaN heterostructures. Thanks to its high value of LO phonon energy, this material theoretically demonstrates the ability to emit in the THz range at room temperature. We are presenting two structures, one optically pumped and another one electrically pumped.

8119-08, Session 2

Tunable vertical emission in a THz quantum cascade structure

F. Jasnot, L. De Vaultier, Y. Guldner, G. Bastard, Ecole Normale Supérieure (France); A. Vasanelli, C. Manquest, C. Sirtori, Univ. Paris 7-Denis Diderot (France); M. Beck, J. Faist, ETH Zürich (Switzerland)

The application of a magnetic field parallel to the growth axis of a quantum cascade structure (QCS) breaks the two-dimensional parabolic subband $|n\rangle$ into a ladder of equidistant discrete Landau levels (LLs) $|n,p\rangle$ separated by the cyclotron energy. Inter-LL emission (cyclotron emission) has some particular features. The light is transverse electric (TE) polarized and thus is emitted through the surface of the sample contrary to intersubband transition where the light is transverse magnetic (TM) polarized and is emitted through the side of the device. Moreover, cyclotron emission fulfils the selection rule $\Delta p = \pm 1$. Here, the purpose of our device is to use an elastic scattering mechanism to transfer electrons from LL $|2,0\rangle$ to $|1,p\rangle$ and to collect cyclotron emission.

Spectra as a function of magnetic field exhibit a wide variety of peaks at different energies. In addition to cyclotron emission, other peaks appear. We assume that they are the result of activate optical transitions that are normally forbidden in ideal structures. The identification of the dominant mechanism has been demonstrated performing magnetotransport experiments. Voltage as a function of magnetic field clearly shows that electron-electron interaction is the dominant mechanism. This structure is the first step in the realization of a tunable THz VCSEL.

Conference 8119:
Terahertz Emitters, Receivers, and Applications II

8119-09, Session 2

Modeling temperature effects in terahertz step-well quantum cascade structures with diagonal optical transitions

W. Freeman, Naval Air Warfare Ctr. Weapons Div. (United States);
G. Karunasiri, Naval Postgraduate School (United States)

Temperature effects in terahertz (THz) step well quantum cascade (QC) structures are investigated. Step well QC structures with diagonal optical transitions that use fast intrawell electron-longitudinal optical (LO)-phonon scattering for depopulation are considered. A density matrix method is used to model the electron transport coherence and is incorporated into the Monte Carlo simulations of these structures. A phenomenological dephasing time is also included in these simulations. The influence of the lattice temperature on the population inversion is modeled and the effects due to the gain spectrum broadening as well as potential device performance are also considered.

8119-10, Session 2

Ultrafast Gain switching of THz quantum cascade lasers: THz pulse amplification and injection seeding

S. S. Dhillon, N. Jukam, D. Oustinov, J. Madeo, Ecole Normale Supérieure (France); S. Barbieri, C. Manquest, C. Sirtori, Univ. Paris 7-Denis Diderot (France); S. Khanna, E. Linfield, G. Davies, Univ. of Leeds (United Kingdom); J. Tignon, Ecole Normale Supérieure (France)

Terahertz (THz) time domain spectroscopy (TDS) is a powerful technique used to generate and detect ultrafast pulses of broadband THz radiation. In order to generate THz pulses, near-infrared femtosecond lasers are used to excite photoconductive antennas or nonlinear crystals. Although the peak THz electric fields generated by these sources can be relatively high, the field amplitude per unit frequency is small owing to the large spectral bandwidth of the generated THz pulse. A compact, practical and direct amplifier of THz pulses is therefore of great interest.

A promising candidate for a THz amplifier is the recently realised THz quantum cascade laser (QCL). In this semiconductor-based source laser action takes place through intersubband transitions. Recently THz TDS has been used to measure the gain spectra of QCLs. In these experiments, the QCL essentially acts as an amplifier of THz probe pulses that are transmitted through the laser. However, the amplification is limited by gain clamping, which fixes the gain to the sum of the waveguide and mirror losses during laser action. Here we circumvent gain clamping and demonstrate large amplification of THz pulses by ultrafast gain switching of a QCL. The latter is turned on at picosecond time scales before the onset of laser action using an integrated Auston switch. This unclamps the gain by placing the laser in a non-equilibrium state that allows large amplification of the electromagnetic field within the cavity. This technique offers the potential to produce high field THz pulses that approach the QCL saturation field.

8119-22, Session 2

Quantum-dot based nonlinear source of THz radiation

A. Andronico, Univ. Paris 7-Denis Diderot (France); J. Claudon, M. Munsch, CEA-CNRS (France); I. Favero, S. Ducci, Univ. Paris 7-Denis Diderot (France); J. Gérard, CEA-CNRS (France); G. Leo, Univ. Paris 7-Denis Diderot (France)

In the last few years, considerable research efforts have been put into the fabrication of THz sources. However, despite the many approaches

envisioned to satisfy the growing application demands, the current state-of-the-art THz emitters fall short of being at the same time compact, operating at room temperature, and potentially low cost. Sources based on nonlinear optical effects like difference frequency generation provide an appealing alternative route. Unfortunately, typical sources of this type rely on external pump lasers, which makes the overall systems not practical outside research laboratories. An interesting perspective is provided by highly confining semiconductor photonic structures, where the integration of pump laser and frequency converter promises major improvements in overall performance and for any potential application. Here we will introduce a novel active nonlinear source emitting THz radiation at room temperature and excited by the emission of electrically pumped InAs quantum dots. The parametric optical process takes place in a high quality factor AlGaAs microcavity where the quasi-phase-matching of whispering-gallery modes is fulfilled via the circular symmetry of the cavity and an appropriate choice of the interacting modes. Based on recent technologic achievements, we will present numerical results for the nonlinear efficiency and will compare our source to existing frequency-conversion-based THz emitters. In the last part of the talk, we will discuss the source's attractive features: room-temperature operation, electrical pumping, custom emission wavelength, and the perspectives of coherent detection and two-dimensional array schemes.

8119-11, Session 3

Recent advances of terahertz quantum cascade lasers

M. Razeghi, Northwestern Univ. (United States)

No abstract available

8119-12, Session 3

InGaAs/GaAsSb: a new material system for terahertz quantum cascade lasers

G. Strasser, C. Deutsch, H. Detz, A. Benz, M. Nobile, M. A. Andrews, P. Klang, W. Schrenk, K. Unterrainer, Technische Univ. Wien (Austria)

We present a novel material system for THz QCLs: InGaAs/GaAsSb, lattice matched to InP. This aluminium-free material system allows to combine a moderate conduction band offset (360 meV) with the lower effective InGaAs electron mass (0.043 m_0), offering a higher gain compared to GaAs based THz QCLs. The lower barrier mass (0.045 m_0 for GaAsSb) and nonparabolicity allow for thicker barrier layers in the devices, relaxing the demands on the epitaxy. In this contribution we present the second generation of InGaAs/GaAsSb THz QCLs, where the threshold current density could be reduced from 2 kA/cm² to 0.75 kA/cm² operating up to 135 K.

8119-13, Session 3

Terahertz quantum cascade lasers coupled with high efficiency to the low loss optical modes of cylindrical hollow-core waveguides

M. S. Vitiello, Consiglio Nazionale delle Ricerche (Italy)

No abstract available

8119-14, Session 3

Intersubband lasing without global inversion in diluted nitride-quantum wells

M. Fernandes Pereira, Jr., Sheffield Hallam Univ. (United Kingdom); S. Tomic, Daresbury Lab. (United Kingdom)

The first demonstration of intersubband lasing without inversion has been realized by exploiting the nonparabolicity of the conduction subbands and local population inversion near $k=0$ even though the lowest subband may have larger global occupation [1].

Later on, also exploiting bandstructure engineering, valence-band-based designs have been proposed [2,3] and more recently a mechanism combining bandnonparabolicity with a k -space filtering for hole intervalence transitions in quantum wells has been introduced [4].

In this paper we investigate the possibility of interconduction band gain without global inversion by engineering the conduction band effective masses so that the upper lasing subband has an effective mass considerably smaller than the lower lasing subband that could not be obtained in conventional III-V materials. We recover the expected dispersive gain shape for similar masses and contrasting results if the effective masses characterizing the relevant subbands are very different [5].

References

- [1] J. Faist, F. Capasso, C. Sirtori, D.L. Sivco, A.L. Hutchinson, M. S. Hybertsen and A. Y. Cho, Phys. Rev. Lett. 76, 411(1996).
- [2] G. Sun, A. Liu and J.B. Khurgin, Appl. Phys. Lett. 72, 1481 (1998).
- [3] L. Friedman, G. Sun and A. Soref, Appl. Phys. Lett. 78, 401 (2001).
- [4] M.F. Pereira Jr., Phys. Rev. 78, 245305 (2008).
- [5] M.F. Pereira and S. Tomi, Appl. Phys. Lett. 98, 061101 (2011).

8119-15, Session 4

Electric control of THz reflectivity assisted by interface phonon-polaritons

S. Vassant, F. Marquier, A. Archambault, J. Greffet, Lab. Charles Fabry (France); F. Pardo, J. Pelouard, Ctr. National de la Recherche Scientifique (France)

We present the design and fabrication of a THz modulator. We use an original approach by using interface-phonon-polaritons combined with epsilon near zero material on a AlGaAs/GaAs heterostructure.

The system is composed of a doped GaAs substrate, a spacer layer (AlAs/GaAs superlattice), a single quantum well (AlGaAs/GaAs/AlGaAs), and a metallic grating. The substrate and grating acts as two mirrors forming a Fabry-Perot cavity and also allows the coupling of an incident THz wave to an interface mode in the quantum well. This mode is composed of two coupled interface-phonon-polaritons at each of the well/barrier interface.

This mode is highly confined in the quantum well because the dielectric function of the well (GaAs) is near zero at the mode frequency. This leads to a high enhancement of the electric field perpendicular to the interfaces. Thus the interaction between this mode and intersubband transitions in the well is enhanced, and the coupling of the incident field to the mode can be controlled by applying a tension to the quantum well. When the well is depleted, the structure present a high coupling efficiency of the incident THz field with the quantum well mode and the reflectivity is low. When the well populates with electrons, intersubband transitions change the dielectric properties of the well, the coupling is less efficient and the reflectivity gets higher.

THz reflectivity measurements demonstrate a amplitude change in reflectivity of 15% at room temperature with a single quantum well at a frequency of 8.5 THz.

8119-16, Session 4

mm wave and THz imaging using very inexpensive neon-indicator lamp detector focal-plane arrays

N. S. Kopeika, Ben-Gurion Univ. of the Negev (Israel); A. Abramovich, Ariel Univ. Ctr. of Samaria (Israel); A. Levanon, D. Rozban, A. Akram, Ben-Gurion Univ. of the Negev (Israel) and Ariel Univ. Ctr. of Samaria (Israel); H. Joseph, Ben-Gurion Univ. of the Negev (Israel); O. Yadid-Pecht, Ben-Gurion Univ. of the Negev (Israel) and Univ. of Calgary (Canada); A. Belenky, S. Lineykin, Ben-Gurion Univ. of the Negev (Israel)

The chief bottleneck holding back development of inexpensive real time mm wave and terahertz imaging is the cost of detectors. One solution is the use of neon indicator lamps costing typically about 30 - 50 cents each as detectors. NEP is typically on the order of 10^{-9} W/Hz^{1/2} in direct detection. In heterodyne detection, minimum detectable signal is about 2 orders of magnitude less than in direct detection, and decreases with increasing reference power.

Focal plane arrays of 8X8 such detectors have been constructed, and good quality 32X32 pixel images obtained at 100 GHz. Presently, a new board to record 32X32 pixel images with a single snapshot each is under construction and should be available shortly. We plan to use it to obtain not only 32X32 pixel images, but also 64X64 and, hopefully, 128X128 pixel images as well.

8119-17, Session 4

About possibility to eliminate of influence of water vapour on detection and identification of substance using the THz laser pulse

V. A. Trofimov, N. V. Peskov, Lomonosov Moscow State Univ. (Russian Federation)

One of the modern problems taking place for detection and identification of substances is an influence of water vapour on THz signal reflected from sample. The vapour of water distorts the signal and its spectrum. Hence, we get the signal which contains information about water. We propose one of the possible approaches to avoid this influence on the detection and identification of substance.

This approach concludes in full elimination of spectral lines corresponding to absorption lines of water from spectrum of signal. Then we reconstruct the signal with new spectrum and make the spectral dynamic analysis for identification of substances. The efficiency of our approach is demonstrated by its application for signal reflected from explosive or for the signal which is constructed by us. It is essential that we consider the THz pulse with a few cycles. This pulse has broad spectrum.

8119-18, Session 4

Highly absorbing nano-scale metal films for terahertz bi-material sensors

F. Alves, K. Apostolos, D. Grbovic, G. Karunasiri, Naval Postgraduate School (United States)

Interest in terahertz (THz) imaging has significantly increased in recent years. This radiation is non ionizing and hence favorable to applications seeking human exposure, especially medical diagnoses and security screening. It has been demonstrated in previous work that bi-material MEMS detector arrays show a great potential to be used for THz imaging. Our work aims to identify nano-scale metal films that can be integrated with the sensor elements to enhance absorption in the THz range of interest. Finite element simulation of absorption in chromium (Cr)

Conference 8119:
Terahertz Emitters, Receivers, and Applications II

films was found to absorb close to 50% between 1 and 10 THz, when the thickness of the layer is about 5 nm. Similarly, it was found that similar thickness nickel (Ni) film can absorb close to 35% in the same THz range. The reduction of absorption in Ni is due to its higher conductivity compared to that of Cr. Different thicknesses (10 - 30 nm) of Cr and Ni layers were deposited on a Si substrate using e-beam evaporation and the wafers were characterized using a Fourier transform infrared spectrometer (FTIR) extended to THz range. The measured absorption of the films gave a good match with that of the simulations. Further analysis showed that by decreasing the surface fill-factor of Ni it is possible to increase absorption up to the values obtained for the Cr films. This result indicates that Ni films can be used in bi-material MEMS detectors with absorption comparable to that of Cr films, with the advantage of presenting much lower levels of residual stress after fabrication.

the kind and density of the gas. However, the peak radiation frequencies reported are almost independent of those parameters. From the laser-gas interaction point of view, the terahertz generation mechanism is not enough understood. We demonstrate a frequency-tuning scheme that uses the laser pulse duration to control the ultrafast-spark current timescale. We also propose a simple physical model to explain the generation of terahertz radiation with the laser propagation in an ultrafast-spark. The radiation frequency depends on the temporal waveform of its electric field, i.e., the Fourier transformation of the electric waveform gives the frequency of the radiation. The electron density in the spark plasma is almost constant for laser pulse durations 30-300 fs at a laser intensity of 5×10^{14} W/cm². The THz peak frequency scales with the reciprocal of the ionization time, i.e., the laser pulse duration, and the plasma sheath current model explains this behavior.

8119-19, Session 4

THz wave up-frequency turning by rapidly plasma creation

M. Nakata, T. Higashiguchi, N. Yugami, Utsunomiya Univ. (Japan); Y. Sentoku, Univ. of Nevada, Reno (United States); R. Kodama, Osaka Univ. (Japan)

Manipulation of the electromagnetic wave by laser-plasma interaction is one of the most attractive topics in order to realize blight radiation sources with tunable frequency. It has opened a novel research field called plasma photonics. In the last decade, not only the theoretical works but also experimental ones have been studied for plasma application of a short, tunable radiation sources. As the recent interests, the generation of terahertz radiation has been extensively investigated in experiments of the laser-plasma interaction and formation of filaments by intense laser propagating in air or gas. The THz radiation has a lot of potential applications in imaging, biological sensing, surface investigation, and condensed matter studies, and so on. High power radiation sources are required for these applications, however the power of conventional THz sources, e.g. the photo-conductive antenna or the device based on optical rectification phenomena excited by the femtosecond laser pulse, is limited still in a range of micro-watt.

We had performed the proof of principle experiment of the flash ionization, which is an important step to realize a tunable high power radiation source. We have verified the physical mechanism of upshift of radiation from rapid creation of plasma in the ZnSe crystal. The plasma creation time is much shorter than the period of the source THz wave. Radiation frequencies up to 3.3 THz were detected. The results support the potentiality of developing tunable and short pulse coherent radiation sources with a frequency THz region.

8119-20, Session 4

Tunable terahertz radiation from an ultrashort-laser-pulse-induced discharge in biased air

F. Suzuki, T. Higashiguchi, H. Anno-Kashiwazaki, N. Yugami, Utsunomiya Univ. (Japan); Y. Sentoku, Univ. of Nevada, Reno (United States); R. Kodama, Osaka Univ. (Japan); P. Muggli, The Univ. of Southern California (United States)

Strong beams of coherent radiation are essential to induce nonlinear excitation phenomena in biology and material sciences. Optical-field-induced ionization by an ultrashort laser pulse produces ultrabroadband bursts of radiation with photon energies ranging from radio-wave at the microsecond timescale to x-ray at the attosecond timescale. As the laser pulse drives an ultrafast-spark with high current it induces nonlinear spectral conversion in a few femtoseconds and generates terahertz electromagnetic waves. Broadband terahertz generation has been reported in air and rare gases. If the radiation frequency depends on the electron plasma density, it should vary with the laser pulse intensity, and

Conference 8120: Photonic Fiber and Crystal Devices: Advances in Materials and Innovations in Device Applications V

Sunday-Monday 21-22 August 2011 • Part of Proceedings of SPIE Vol. 8120

Photonic Fiber and Crystal Devices: Advances in Materials and Innovations in Device Applications V

8120-01, Session 1

Ternary and quaternary selenide crystals for nonlinear optical applications

N. B. Singh, G. Kanner, D. Knuteson, K. Green, M. Marable, R. Jones, D. Kahler, B. Wagner, A. Berghmans, M. King, S. McLaughlin, Northrop Grumman Electronic Systems (United States)

We have developed several ternary and quaternary sulfide and selenide crystals for nonlinear optical applications. We present an overview on the crystal growth and characterization of crystals for nonlinear optical (NLO) conversion efficiency. We have summarized the performance of gallium selenide (GaSe), Silver gallium selenide (AgGaSe₂), thallium arsenic selenide (Tl₃AsSe₃), and silver gallium germanium selenide (AgGaGe₃Se₈ and AgGaGe₅Se₁₂) crystals. All these crystals were grown by vertical Bridgman method in quartz ampoules by using stoichiometric compounds synthesized from constituting elements. The significant problem of cleaving of GaSe was reduced in ternary and quaternary compounds, however, second order harmonic generation (SHG) coefficient decreased significantly from 75pm/V observed for GaS crystals. Experimental results showed that binary, ternary and quaternary compounds transmit up to 16 μ m, have high value of nonlinear conversion merit (d^2/n^3 , d is the NLO coefficient, n is the refractive index) and have lowest absorption coefficient compared to arsenides, phosphides and other nonlinear optical (NLO) materials.

8120-02, Session 1

Design and experimental investigation of optical beam deflector based on LiNbO₃ crystal

A. Yan, Y. Zhi, J. Sun, Shanghai Institute of Optics and Fine Mechanics (China); R. Shu, Shanghai Institute of Technical Physics (China); Y. Zhou, W. Lu, L. Liu, Shanghai Institute of Optics and Fine Mechanics (China)

Laser beam deflectors are important optical elements with a large variety of applications in the measurement techniques, optical communications, laser imaging lidar, etc. Electro-optic beam deflector is a technique of growing importance in modern optics technology and is currently seeing considerable interest. The electro-optic deflector can provide a high-speed beam scanning due to motionless component, and the corresponding structure design may help to realize high angle scanning resolution. LiNbO₃ crystal has some distinct advantages, such as high response speed, availability of large volume materials and low cost, so it has very extensive applications in the area of optic-electro component.

In this paper, a novel high speed electrooptic N×N array laser beam deflector is proposed and experimentally investigated. In the proposed deflector, the device uses cascaded electro-optic beam splitter units and deflection prism array to produce a 2-D array of beam positions with a wide field of view. Experimental results achieved with a 3×3 array deflector based on LiNbO₃ crystal for 1.55- μ m radiation are described. The large range far-field beam array scanning can be achieved. The beam scanning and tracking can be real-time controlled by programming. The experimental and theoretical results indicate that the proposed high speed electro-optic deflector is feasible and can be fabricated using presently known technologies.

8120-03, Session 1

Application of wavelength scanning for measuring water vapour concentration by distributed laser diode

J. Chang, G. Zhou, F. Song, Y. Zhang, Q. Wang, S. Zhang, Z. Wang, Shandong Univ. (China)

A new technique which takes advantage of distributed feedback laser diode (DFB-LD) wavelength scanning to measure water vapour concentration is presented. Wavelength scanning of water vapour absorption peak at 1368.6 nm is realized by saw tooth modulation of current injected into DFB-LD. Absorption profile is gotten by intensity normalization which is used to reduce the outside affection such as power drift, fiber loss, etc. Peak absorption rate can be gotten by arithmetic processing the absorption profile. Concentration is gotten by peak absorption rate according to Beer-Lambert law and absorption coefficient of water vapour in HITRAN database. In addition, theoretical work on the pressure affection to light intensity absorption rate has been done, the results are verified by experiment data. It is found that the resolution of measurement is improved if peak absorption rate is replaced by area integral of the absorption profile to calculate the concentration; this is because of the absorption line broadening under high pressure.

8120-04, Session 1

Optical and physical properties of Er³⁺-Yb³⁺ co-doped tellurite fibers

L. C. Barbosa, E. Fernandez Chillce, Univ. Estadual de Campinas (Brazil)

The results concerning to the optical and physical properties of Er³⁺-Yb³⁺ co-doped Tellurite glasses and fibers are presented in this work. The Tellurite fibers are based on glasses with the composition: TeO₂-WO₃-Nb₂O₅-Na₂O-Al₂O₃-Er₂O₃-Yb₂O₃. The Tellurite fibers were fabricated by using the rod-in-tube method and a Heathway drawn tower. The absorption and emission spectra (ranging from 350 to 1750 nm) of the Tellurite fibers were obtained by using a white light source, a 980nm pump laser, and an Optical Spectrum Analyzer (OSA). The Amplified Spontaneous Emission (ASE) spectra around 1550 nm band were analyzed for fiber lengths from 1 to 65 cm. The Er³⁺-Yb³⁺ co-doped Tellurite fibers show be more efficient to the generation of up-conversion processes compared to that of Er³⁺-doped Tellurite fibers.

8120-05, Session 1

Localization of laser pulse and slow-light propagation in nonlinear photonic crystal

V. A. Trofimov, Lomonosov Moscow State Univ. (Russian Federation); S. Lan, South China Normal Univ. (China)

We investigate laser pulse propagation in 2D nonlinear photonic crystal or in 1D layered nonlinear structure at the conditions of soliton formation in nonlinear elements of the photonic crystal. The formation of soliton depends on input light intensity, duration of pulse and shape of elements from which the photonic crystal consists. In 2D case the soliton formation depends on focusing of laser beam and on presence of laser energy in neighbouring elements of the photonic crystal. These solitons move with slow velocity inside the elements of the photonic crystal. Under certain conditions the soliton can stop. This phenomenon can be used for data storage. The similar solitons can appear in many elements of photonic crystal.

8120-06, Session 1

Design and fabrication of single- and coupled-cavity thin-film structures for optical switching

L. Diao, Advanced Materials Analytics Consulting (United States)

All-optical switching based on optical Kerr effect is feasible in single and coupled-cavity thin film structures comprised of high-index and low-index materials. It was shown that the FOM (index change/cavity index) required for bistable operation can be reduced to the order of 10⁻² with high index contrast single cavity structure and FOM can be reduced to the order of 10⁻³ with high index contrast 3- cavity structure. In this report we will present the simulation results using novel band-pass filter structures. Fabrication of coupled-cavity dielectric thin film structures can be achieved by RF PVD and PECVD and RF PVD is a better choice for precise control of thin film properties. We will report successful fabrication of thin film coupled cavity structures made of silicon dioxide (n=1.45) and silicon nitride (n=1.90) by RF PVD. The simulated linear transmissions of such structures match those of the fabricated structures almost exactly. Measured thin film stress, uniformity and surface roughness will be presented. The Kerr-type nonlinear materials with high refractive index and high nonlinear coefficient suitable for RF PVD processing will be discussed.

8120-08, Session 1

Nano-sized lasers and single-photon emitters using coupled colloidal quantum dots to photonic crystal resonators

J. Tang, Academia Sinica (Taiwan)

We observed large Purcell effects due to exciton-photon couplings between colloidal CdSe/ZnS quantum dots (QDs) and a resonant nano-sized Si-based nano-sized disk or a photonic crystal resonant cavity. We demonstrated either operation modality as an efficient single-photon emitter or an ultralow-threshold nanolaser at visible wavelength and at room temperature. Our work provided the feasibility of using flexible QDs/nanodisk composite as a promising building block for realizing Si-based optoelectronics at room-temperature operation.

8120-09, Session 2

Preparation of BaTiO₃ thin films by pulsed laser deposition

A. M. Darwish, H. Alkhaby, S. Wilson, Dillard Univ. (United States); B. Koplitz, Tulane Univ. (United States)

BaTiO₃ films were deposited by the pulse Laser Deposition technique to prepare thin dielectric layers for multilayer ceramic chip capacitors. The BaTiO₃ films were successfully prepared by ablation of BaTiO₃ ceramic and Ti metal source using the Nd:YAG pulse laser. The films deposited at room temperature and 800°C were amorphous and crystalline phases, respectively. The intensity of (110) and (111) peaks increased as Ba/Ti ratios were close to stoichiometric composition. BaTiO₃ films. The surface morphology of the thin film was studied by optical techniques using both the RHEED and AFM. The surface morphology will be discussed at different temperatures. The dielectric constant and dissipation factor of BaTiO₃ films measured at 1 kHz were 140~190 and 3~6%, respectively. The capacitance decreased with increasing the temperature and varied only between 789pF and 741pF in the temperature range 0~135°C.

8120-10, Session 2

Photoinduced electrokinetic redistribution of metal nanoparticles during holographic grating recording in the ferroelectric crystal

N. V. Kukhtarev, T. V. Kukhtareva, E. Harris, A. K. Chilvery, J. Wang, Alabama A&M Univ. (United States)

We have investigated photoinduced redistribution of metal nanoparticles, placed on the surface of the ferroelectric photorefractive crystal during recording of dynamic holograms. Motivations for this study were improvement of sensitivity for recording of dynamic holographic gratings, for application in non-destructive testing of materials.

From the other hand, different electrokinetic processes involved in the photoinduced redistribution of nanoparticles may be important for optimization of energy conversion by advanced solar cells that use nanoparticles.

The home-made biosynthesized gold and silver colloidal solutions were spread as a thin layer on the ferroelectric photorefractive crystal surface. Holographic gratings were recorded in photorefractive crystal of Fe:LiNbO₃ (Fe:LN) by the HeNe laser (λ=633nm) to avoid direct influence of laser light on nanoparticles. Photorefractive holographic grating initially recorded in the crystal volume produce spatially modulated electric field on the crystal surface. This field led to electrophoretic redistribution of the nanoparticles on the crystal surface that result also in additional contribution to the electric field pattern and also change diffraction efficiency of hologram. In addition, we have recorded holographic grating in Fe:LN placed in 5mm cuvette with silver nanoparticles nanofluid and observed nanoparticles distribution along grating line.

Moreover, we have observed photogeneration of electrical pulses from the crystal when we used CW or pulsed lasers. We explain these electrical pulses by laser induced photogalvanic and pyroelectric effects. Both optical and electrical signals were enhanced, by applying nanoparticles to the crystal surface.

8120-11, Session 2

The spectroellipsometric adaptive identifier for ecological monitoring

F. Mkrtchyan, Institute of Radio Engineering and Electronics (Russian Federation)

The creation of multichannel polarization optical instrumentation and use of spectroellipsometric technology are very important for the real-time ecological control of aquatic environment. Spectroellipsometric devices give us high precision of measurements.

This report is aimed to describe:

- A technology of combined use of spectroellipsometry and algorithms of identification and recognition that allowed the creation of a standard integral complex of instrumental, algorithmic, modular and software tools for the collection and processing of data on the aquatic environment quality with forecasting and decision - making functions

- A compact measuring - information multichannel spectroellipsometric system (device) for monitoring the quality of aquatic environment, that is based on the combined use of spectroellipsometry and training, classification, and identification algorithms.

This spectroellipsometric system will differ from modern foreign analogues by the use of a new and very promising method of ellipsometric measurements, an original element base of polarization optics and a complex mathematical approach to estimating the quality of a water object subjected to anthropogenic influence.

Unlike foreign analogues, the system has no rotating polarization elements. This allows one to increase the signal-to-noise ratio and the long-term stability of measurements, to simplify and reduce the price of multichannel spectroellipsometers.

**Conference 8120: Photonic Fiber and Crystal Devices:
Advances in Materials and Innovations in Device Applications V**

The system will be trainable to the recognition of the pollutants of aquatic environment.

A spectroellipsometer in laboratories of V.A. Kotelnikov's Institute of Radioengineering and Electronics, Russian Academy of Sciences is designed for in-situ real time measurements of spectra of ellipsometric parameters Psi and Delta with consequent changeover to spectra of transmitted and reflected signal from water media in frames of used physical model of water environment

A compact measuring - information multichannel spectroellipsometric system (device) is applied for monitoring the quality of natural and waste water, that is based on the combined use of spectroellipsometry and training, classification, and identification algorithms.

8120-12, Session 2

Optimization of photonic crystal fibers for endlessly single mode propagation, low loss, and flattened chromatic dispersion

N. Bala, Institute of Engineering and Technology (India); R. S. Kaler, Thapar Univ. (India); R. Kaler, Rayat Bahra Group of Institutions (India)

With recent advancements in the field of photonic bandgap materials, a new class of optical waveguides known as photonic crystal fibers (PCFs) has attracted much attention for their large potential of applications. PCFs are made of a periodic arrangement of fused silica and air-holes running parallel to the axis of the fiber. With an array of air-hole surrounding the silica core region provides flexibility to design a wide range of index contrast between core and cladding which helps in tuning the transmission characteristics such as Dispersion, loss and Non-linearity. The dispersion and loss properties of the photonic crystal fiber are tailored by adjusting the design parameters such as radius of the air-hole. In this paper, index guiding photonic crystal fiber with a triangular array of circular air-holes in the cladding have been investigated by fully-vectorial mode solver. The propagation characteristics of PCFs such as effective index, chromatic dispersion and confinement loss are calculated. The effects of structural design parameters (such as the air-hole size) on the confinement loss and chromatic dispersion are analyzed. The effective V-parameter for the single mode operation is accurately calculated for different air-hole size diameter. It is found that it is possible to achieve single-mode propagation, zero-dispersion or flattened dispersion in PCF with low loss at the telecommunication wavelength 1.55 μ m. It is concluded that chromatic dispersion and confinement loss in the PCFs is more affected by the air-hole radius of the first ring. Flattened dispersion and low confinement loss in PCF is obtained by the enlarging the radius of the air-hole size in the first ring. Different fiber design models are presented for low loss and flat dispersions results.

8120-13, Session 2

The effect of stable menisci shapes on the zinc distribution in CdZnTe crystals grown by dewetted Bridgman technique

L. Braescu, Univ. de Vest din Timisoara (Romania)

The unusual thermophysical properties of the CdZnTe crystals (high melt viscosity, a large latent heat of fusion, fairly large equilibrium segregation coefficient, etc.) cause considerable difficulty in maintaining uniform zinc composition in the grown crystal. The disadvantages can be overcome by the dewetted Bridgman technique in which the crystal is grown detached from the ampoule wall by a liquid free surface at the level of the solid-liquid interface, called liquid meniscus, which creates a gap between the grown crystal and the ampoule wall that bring together low contact stress with low thermal stress. Crystal growth experiments showed that, in some conditions, chemical impurities at the liquid surface may lead to unintended contamination that can increase the wetting

angle artificially. This high sensitivity of the wetting angle changes the meniscus shape, and hence the dopant distribution in the grown crystal.

For evaluating numerically the effect of the menisci shapes on the Zn distribution in CdZnTe crystals grown by dewetted Bridgman technique, a pseudo quasi-steady state model is considered in the framework of a 2D axisymmetric geometry containing two types of stable menisci: (i) a "S" shape meniscus that correspond to the sum-of-the-angles criterion $\alpha_e + \theta_c = 180^\circ$. Numerical computations including incompressible fluid flow in the Boussinesq approximation, heat and mass transfer, and Marangoni effect, are performed using finite element technique. It is proven that a convex meniscus assures the best impurity distribution.

8120-14, Session 2

Quasi-phase matching in SOS-based parametric wavelength converters for mid-infrared application

Y. Huang, E. Tien, S. Gao, S. K. Kalyoncu, Q. Song, F. Qian, E. Adas, D. Yildirim, O. Boyraz, Univ. of California, Irvine (United States)

Mid wavelength infrared (MWIR) spectral range is the window for a wide variety of applications, including free space communication, thermal and biomedical imaging, optical sensing, chemical spectroscopy and missile guidance/countermeasures. While these applications are mostly achieved through free-space optics, their guided wave alternatives can be far more attractive in terms of compactness, portability and ease of mass production. However, conventional Silicon-on-Insulator (SOI) platform is no longer applicable to MWIR due to large loss associated with the silica substrate. Instead, Silicon-on-Sapphire (SOS) technique was proposed to support MWIR applications. Particularly, frequency band wavelength converter using SOS waveguides can convert incoming MWIR optical carriers to near-IR and utilize the well-established photonic devices in the telecommunication window. In this study, we designed quasi phase matched silicon-on-sapphire waveguides suitable for MWIR wavelength conversion to achieve higher conversion efficiency than that can be achieved in uniform waveguide geometries. Quasi phase matching utilizing alternating dispersion shifted fibers has been studied in fibers. Here we design planar waveguides with periodic change in waveguide width by $\sim 0.5\mu$ m to reset phase accumulation and provide ever-increasing gain profile. With the fabrication flexibility of large cross-section of MWIR waveguides, the possibility of using quasi-phase-matching can provide >30 dB conversion efficiency enhancement and increase the conversion bandwidth by 2x. Such improvement may facilitate the fabrication of parametric oscillators that can improve the conversion efficiency by 50dB.

8120-15, Session 2

An optical leaky wave antenna with silicon perturbations for electronic control

S. Campione, Q. Song, O. Boyraz, F. Capolino, Univ. of California, Irvine (United States)

An optical leaky wave antenna (OLWA) is a device that radiates a light wave into the surrounding space from a leaky wave (LW) guided mode or receives optical power from the surrounding space into a guided optical mode. In this work, we propose and provide a 3D analysis of a novel CMOS compatible OLWA made of a silicon nitride (Si₃N₄) waveguide comprising periodic silicon implantations which allow electronic tuning capability. The analysis presented here includes the effect of the number of semiconductor perturbations, the antenna radiation pattern and directivity. We show that the number of the silicon implantations has to be large to provide a long radiating section required to achieve radiation with high directivity. In other words, the proposed structure allows for a very narrow-beam radiation. Preliminary results are confirmed by exploiting leaky wave and antenna array factor theory, as well as verified by means of two full-wave simulators (HFSS and COMSOL). Our purpose

**Conference 8120: Photonic Fiber and Crystal Devices:
Advances in Materials and Innovations in Device Applications V**

is to ultimately use PIN junctions as building blocks for each silicon implantation for the electronic control of the radiation. In particular, the electronic tunability of the optical parameters of silicon (such as refractive index and absorption coefficient) via current injection renders itself the ideal platform for optical antennas that can facilitate electronic beam control, and boost the efficiency of optoelectronic devices such as light-emitting diodes, lasers and solar cells, and bio-chemical detection capabilities.

8120-16, Session 2

Soliton propagation in slow-light photonic crystal waveguides

S. Rawal, R. K. Sinha, Delhi Technological Univ. (India)

High refractive index contrast structures such as photonic crystal waveguides have been demonstrated to be a promising approach to the achievement of slow light behaviour. By carefully engineering the photonic dispersion relationship, one may obtain unique opportunities for the realization of devices that exploit slow light effects. As optical pulses propagate through photonic crystal waveguides; their evolution in both the time and frequency domains is governed by the interplay of linear dispersion and nonlinearity. Two photon absorption, free carrier absorption, free carrier dispersion, etc. are important nonlinear effects that influence the behaviour of short laser pulses in silicon photonic crystal waveguides. However soliton dynamics will dominate the propagation of femtosecond pulses in PhC waveguides when the group velocity dispersion is strongly anomalous because of large waveguide dispersion. In the proposed paper, we numerically investigate the impact of slow light enhanced nonlinear absorptions on the propagation of solitons in silicon-on insulator photonic crystal channel waveguides. Evolution of the solitonic pulses is quantified by the misfit parameter and it has been shown that the optimum pulses are obtained from the output at low input powers for high slow down factors. However at high input powers, slow light enhanced higher order nonlinear losses such as two photon absorption and free carrier absorption come into play.

8120-17, Session 3

Real-time holographic information processing at near infrared using ruthenium-doped sillenite crystals

K. Hsu, S. H. Lin, National Chiao Tung Univ. (Taiwan)

Real-time holographic information processing at the infrared wavelength using photorefractive crystals is reported. Crystal growth and improvements of holographic recording characteristics in Ru-doped Bi₁₂SiO₂₀ (BSO) and Ru-doped Bi₁₂TiO₂₀ (BTO) crystals at near infrared are presented. By using green light pre-exposure significant operation speed of 60 ms is achieved without necessity to apply an external electric field. Real time recording and reconstruction of images at near infrared and its applications for bio-image processing are demonstrated.

8120-18, Session 3

Optical properties of woven arrays of bi-component extruded polymer fibers

F. J. Aranda, J. Perry, D. Archambault, L. Belton, J. Carlson, D. Ziegler, B. Kimball, M. L. Hoey, U.S. Army Research, Development and Engineering Command (United States)

Directionally reflective fiber arrays were woven with polymer fibers. Fiber cross sections produced using a tri-component fiber extruder comprised standard circular as well as right angle retro-reflection features that run the entire length of the fiber. The fiber features are formed by an extrusion

process where the polymer fiber material is forced through a series of plates resulting in the cross section having the desired shape. The woven fiber arrays were evaluated for their optical properties. Results for spectral reflectivity, spatial reflectance signature and photometric reflectance properties are presented. A comparison of the results obtained for the woven fiber arrays and those obtained for bundles of similar fibers are discussed. The implementation of fiber arrays through the use of weaving techniques allows for the realization of a number of unique and useful optical effects. As evidenced by the spectral measurements, the color of the woven arrays can be controlled by a number of means: for example by the inclusion of dyes, nanoparticles, and by post-processing applications of thin films. The present work represents a logical extension of previously reported experiments with unwoven fibers with retro-reflective features (1).

(1) F. J. Aranda, J. Perry, D. Archambault, L. Belton, J. Carlson, D. Ziegler, B. Kimball, Optical properties of a retro-reflection fiber cross section formed via tri-component fiber extrusion, Proc. SPIE 7781, pp. 778107, 2010.

8120-19, Session 3

Micro-size tapered silica fibers for sensing applications

L. C. Barbosa, E. Fernandez Chillcce, Univ. Estadual de Campinas (Brazil)

In this work we show results of controlled tapered fibers using a Vytran instrument. The tapered silica fibers were produced by drawing a 50µm length by heating time. The minimum taper diameter was around 3µm and the maximum taper length was around 600µm. The evanescent field effect, in the near infra red (NIR) region, was observed on the tapers with diameter inferior to 10µm. These micro-size tapers no modify the waveguide dispersion spectra. This device could be used to splice a conventional fiber to photonic crystal fibers and also as liquid sensors.

8120-20, Session 3

The optimized PWM driving for the lighting system based on physiological characteristic of human vision

P. Wang, C. Uang, Y. Hung, Z. Ho, I-Shou Univ. (Taiwan)

Saving energy, White-light LED plays a main role in solid state lighting system. Find the best energy saving driven solution is the engineer endless hard work. Besides DC and AC driving, LED using Pulse Width Modulation (PWM) operation is also a valuable research topic. The most important issue for this work is to find the drive frequency and duty for both energy saving and better feeling on the human vision sensation. In this paper, psychophysics of human vision response to the lighting effect, including Persistence of vision, Bloch's Law, Broca-Sulzer Law, Ferry-Porter Law, Talbot-Plateau Law, Contrast Sensitivity, will be discussed and analyzed.

From the human vision system, we found out that there are three factors: the flash sensitivity, the illumination intensity and the background environment illumination, that are used to decide the frequency and duty of the PWM driving method. A set of controllable LED lamps with adjustable frequency and duty is fitted inside a non-closed box is constructed for this experiment.

When the background environment illumination intensity is high, the variation of the flash sensitivity and illumination intensity is not easy to observe. Increasing PWM frequency will eliminate flash sensitivity. When the duty is over 70%, the visual sensitivity is saturated. For warning purpose, the better frequency range is between 7Hz to 15Hz and the duty cycle can be lower down to 70%. For general lighting, the better frequency range is between 200Hz to 1000Hz and the duty cycle can also be lower down to 70%.

**Conference 8120: Photonic Fiber and Crystal Devices:
Advances in Materials and Innovations in Device Applications V**

8120-21, Session 3

Designing low cost LED display for the billboard

Y. Hong, C. Uang, P. Wang, Z. Ho, I-Shou Univ. (Taiwan)

With quickly advance of the computer, microelectronics and photonics technologies, LED display panel becomes a new electronic advertising media. It can be used to show any information whatever characters or graphics. Most LED display panels are built of many Light-Emitting Diodes arranged in a matrix form. The display has many advantages such as low power, low cost, long life and high definition. Generally the LED display panel's driving system is very complex. The design rule of LED display panel's drive becomes more and more important, because the display panel can show rich color with LED development that meets the market requirements.

Cost is always the most important issue in public market domain. In this paper, we report a design methodology of LED display panel's driver based on the microprocessor control unit (MCU) system based on HT48R10A and HT1632C to control the RGB 3 color LED display panel and the modular panel size is 24*16 in matrix form. The HT1632C is a memory mapping LED display controller, it can be used on many applications, such as digital clock, thermometer, counter, voltmeter or other instrumentation readouts. Three pieces of HT1632C are used to drive a 24*16 RGB LED display panel, in our design case. Each HT163C chip is used to control one of the R, G and B color. As the drive mode is driven in DC mode, the RGB display panel can create and totally of seven colors under the control of MCU HT48R10A. The MCU generates the control signal to drive HT1632C. In this study, the software design rule adopt with dynamic display principle. When the scan frequency is 60Hz, LED display panel will get the clear picture and be able to display seven colors.

8120-22, Session 3

Mathematical modeling of 1D binary photonic tuner and realization of temperature sensor

A. Lahiri, M. Chakraborty, Institute of Engineering and Management (India)

In recent years photonic crystals have become a favored area of research due to their diversified applications. In this paper we propose a mathematical model for analyzing the photonic band gap of a 1D binary photonic crystal (GaAs and air) which allows us to use it effectively as a photonic tuner which is an integral part of any optical amplifier. As optical parameters like reflection and refraction follows similar pattern from each plane within a photonic crystal, we can take help of characteristic matrix for a single plane and multiply (m) times where the crystal consists of (m) periods. Using the fact that the characteristic matrix comes out to be unimodular and taking help of Cayley-Hamilton theorem and Chebyshev polynomials, we expand the matrix of the entire system to derive the location and width of photonic band gaps. Higher stop bands occur at lower frequency of incoming radiation and central bandgap wavelength decreases with increasing angle of incidence. The power transmitted by the tuning crystal decreases for radiations away from normal. Using a polarizer model, the attenuation is computed to be proportional to $\log|\cos 2\theta|$, where θ is the angle of incidence. The mathematical modeling developed can also be extended for realization of n-array photonic crystal. We have also considered the refractive index modulation with respect to temperature for using it as a temperature sensor.

8120-23, Session 3

Broadband wavelength conversion based on two-pump four-wave mixing in silicon waveguides

S. Gao, Zhejiang Univ. (China); E. Tien, Y. Huang, Q. Song, Univ.

of California, Irvine (United States); S. He, Zhejiang Univ. (China); O. Boyraz, Univ. of California, Irvine (United States)

Four-wave mixing (FWM) in silicon waveguides is considered as a promising solution for high-density integrated signal processing components such as optical regenerator and wavelength converter. To achieve a viable solution for real-life applications, broad conversion bandwidth is a critical parameter. Many efforts have been made to improve the conversion bandwidth such as optimizing the waveguide geometries or designing special waveguide structures. FWM can be divided into single-pump or two-pump FWM according to one or two pumps are used. Most of previous investigations were based on the single-pump FWM. The two-pump FWM were also used to generate multiple idlers around the signal by using a multi-longitudinal-mode pump or multiple mixing sidebands by injecting two pumps and a signal into the silicon waveguide. In principle, the use of single pump in silicon waveguides comes with rigid phase matching since the dominated factors, both the pump wave number and the pump power, are hard to be tuned due to the inherent principle of single-pump FWM and the nonlinear losses. However, the two-pump FWM shows more flexibility to achieve the phase matching since it can be easily tuned by changing the setting of the pump wavelengths. As a result, the conversion bandwidth has the possibility to enhance in the two-pump regime. In this paper, we will analyze the broadband performance of the two-pump FWM by comparing it with the single-pump FWM. In addition, the schemes of pump setting for broadband wavelength conversion will also be theoretically presented and experimentally demonstrated.

8120-24, Session 3

Raman amplification characteristics of telluride glass photonic crystal fibers

B. Dabas, V. Kumar, M. Rajput, R. K. Sinha, Delhi Technological Univ. (India)

Photonic Crystal Fibers (PCF), have generated broad interest due to their unique guidance properties, such as the endlessly single mode operation, controllable dispersion, large birefringence, supercontinuum generation and soliton propagation which are not achieved in standard silica glass fiber. Non-silica glasses such as telluride, fluoride and chalcogenide glasses have excellent optical transparency in the wavelength range of 0.5-5 μm , 0.4-6 μm and 1-16 μm respectively. In contrast, the transmission window of silica is limited to < 3 μm . High-index non-silica glasses such as tellurides and chalcogenides also possess nonlinear refraction coefficients n_2 that are at least an order of magnitude higher than that of fluoride or silica. Furthermore, compared to fluoride and chalcogenide glasses, telluride is much less toxic, more chemically and thermally stable, and hence is a highly suitable fiber material for infrared nonlinear applications. In this paper, we present the dispersion and raman amplification characteristics of telluride glass photonic crystal fibers (PCFs). The variation of effective index of guided mode, dispersion and effective area with wavelength in hexagonal lattice telluride glass PCF is calculated by using finite element method (FEM). The raman gain characteristics of Telluride PCF is numerically calculated by solving Raman propagation equations for pump and single power evolution. We compare the gain characteristics with conventional silica PCF and findout that the Raman gain efficiency in Telluride PCFs can be highly improved. The proposed Telluride PCF can be designed to operate in an endlessly single-mode regime and also findout that the PCF with a small pitch constant has the highest raman gain

8120-25, Session 4

Color retrieval for fringe projection techniques

W. Su, National Sun Yat-Sen Univ. (Taiwan)

Fringe projection techniques are powerful tools to find the 3D profile of an object. However, color on the inspected object might be damaged due

**Conference 8120: Photonic Fiber and Crystal Devices:
Advances in Materials and Innovations in Device Applications V**

to the fringe projection. In this paper, an approach to recover the color distribution on the object is proposed. This makes it possible to enhance the performance of 3D image vision.

8120-26, Session 4

Read-only solid-state volume holographic optical correlator

T. Zhao, J. Li, L. Cao, Q. He, G. Jin, Tsinghua Univ. (China)

Volume holographic correlator (VHC) based on the photorefractive crystal is a promising optical processing unit (OPU) because of its parallel multi-channel correlation as well as the integration of both memory and processor. Recently, thousands of parallel channels have been realized in our laboratory. The computing speed of the VHC can be about two orders over that of the electronic micro-processor. The computing accuracy the VHC has been greatly improved by some effective methods, such as speckle modulation method and interleaving method, etc. For practical applications, the compact size and the simple structure are expected. In the reported compact correlators, both the recording system and correlation readout system are considered for miniaturization. An elaborate beam steering configuration is employed for the angular multiplexing and a laser with high power and stable modes is employed for the holographic exposure. Thus, the compact and complex recording system could limit the desired performance of the VHC. In this work, a read-only volume holographic correlator is proposed. After the recording of all of the correlation database pages by angular multiplexing, a stand-alone read-only solid-state VHC will be separated from the VHC recording facilities which include the high-power laser and the angular multiplexing system. The stand-alone VHC has its own low power readout laser and very compact and simple structure. Since there are two lasers are employed for recording and readout, respectively, the optical alignment tolerance of the laser illumination on the SLM is very sensitive. The two-dimensional angular tolerance is analyzed based the theoretical model of the volume holographic correlator. The experimental demonstration of the proposed read-only VHC is introduced and discussed. The compact and simple read-only VHC can still hold the advantages of high parallelism and high speed, which will be helpful to the realization of the VHC for practical applications as an optical processing unit.

8120-27, Session 4

Terahertz wave propagation in surface plasmon photonic crystal

S. Singh, V. Dillu, R. K. Sinha, R. Bhattacharyya, Delhi Technological Univ. (India)

Plasmonics is an exciting new device technology, as, it offers a way to beat the diffraction limit and thus opens a route to sub-wavelength optics and miniaturization of devices. Surface Plasmon Polariton (SPP) are surface bound electromagnetic waves propagating at the interface of metal and dielectric. Light waves couple with these electron oscillations resulting in propagating surface waves or localized excitations depending on the geometry used. Electromagnetic energy can be guided in structures with sub-wavelength dimension by converting optical mode into nonradiative surface plasmon mode. Since, terahertz (THz) waves may find many potential applications in the field of spectroscopy, free space sensing, environmental sensing and medical imaging, therefore SPP concept can be utilized to obtain subwavelength confined guided wave propagation at THz frequencies.

In this paper, we have proposed a One dimensional (1D) photonic crystal waveguide of 1D periodic array of air holes in Silicon (Si) bonded with Polyvinylidene fluoride (PVDF) material to support Plasmon like excitations in THz range similar to the ones found at the metal or dielectric interfaces in the visible range.

The band structure of the plasmonic photonic crystal, hence formed is investigated and also with the introduction of a defect by removing single

central hole provides a subwavelength scale plasmonic single mode localization for terahertz frequency. Also, the transmission spectrum of the cavity mode and Quality factor has been calculated for the proposed structure. We can therefore find application of this structure to develop a highly efficient single molecule detection method in terahertz frequency domain.

8120-29, Session 4

One-shot in-line digital holography by random phase mask

Y. W. Yu, C. Wu, C. Sun, National Central Univ. (Taiwan)

The in-line digital holographic system is highly desired since it could provide four times space-bandwidth product than that of off-axis configurations. To get rid of the twin images, many methods of one shot in-line digital holography have been proposed, including linear filtering, phase retrieval methods and reference beam modulation technique. These methods are either space-bandwidth wasting or time consuming for computer calculation. In this paper, we propose a novel technique for one shot digital hologram. We insert a random phase mask with known phase distribution in the signal beam, which causes the signal to distribute uniformly on the CCD. In this condition, the zero-order diffracting noise can be removed directly by subtracting a constant. The twin image cannot be reconstructed, since it does not satisfy the phase conjugating condition of the random phase mask. Therefore, only the signal is retrieved, and only one-shot is needed for the digital hologram. This technique is demonstrated by the simulation. Although the back propagating twin image diffused by the random phase mask induces noise, it can be suppressed by well selected system parameters. In some conditions, the noise is as small as the speckle noise and can be neglected.

8120-30, Session 4

General formula for one-shot in-line digital holography by quaternary reference modulation

Y. W. Yu, C. Wu, C. Sun, National Central Univ. (Taiwan)

Many methods have been proposed to remove the twin image of the in-line digital hologram, including phase shifting interferometer (PSI), linear filtering, phase retrieval methods, and reference beam modulation techniques. Phase-shifting provides precise result, but it requires multiple captures of image. It is therefore not well adapted to measure dynamic wavefront. Linear filtering and phase retrieval can work with a single capture, but they are often not as successful as PSI. Reference beam modulation method such like pixilated spatial carrier based phase shift interferometry can not only work with single capture, but also provide a precise calculation result as good as PSI. However the space-bandwidth product of the pixilated spatial carrier based phase shift interferometry is still limited to 1/4 of general PSI. Recently, it has been shown that well selected reference beam modulation can be applied to improve the spatial bandwidth. In this paper, we propose a general formula for one-shot digital holography by quaternary reference modulation, which makes the design of reference beam modulation flexible and simple.

8120-31, Session 4

Beam quality factor of supermodes emerging from a multicore photonic crystal fiber

G. Feng, Sichuan Univ. (China); L. Zhang, Carestream Co. (China)

Based on the Helmholtz equations, the full-vector finite element method was used to analyze supermodes emerging from a multicore photonic crystal fiber. The influences of fiber structural parameters on supermode

**Conference 8120: Photonic Fiber and Crystal Devices:
Advances in Materials and Innovations in Device Applications V**

field were studied. The beam quality factors of coherent and incoherent superposition of the several supermodes emerging from the multicore fiber have been calculated by using the second-order moment method. The results indicate that, in the case of incoherent superposition, the larger the fraction intensity carried by the higher-order mode, the larger the beam quality factor M^2 . However, in the case of the coherent superposition, the value of the M^2 parameter of the mixed mode may be greater than that of the higher-order constituent supermode.

8120-32, Session 4

Study on propagation of femtosecond laser pulses in photonic crystal fiber and micro/nanofiber loop

L. Zhang, Carestream Co. (China); G. Feng, Sichuan Univ. (China)

Supercontinuum generation (SCG) using a femtosecond Ti:Sapphire laser as a pump source and fiber (or fiber loop) as a nonlinear element is investigated by numerical modeling. The SCG of single-mode fiber, photonic crystal fiber, micro/nanofiber and micro/nanofiber loop is investigated experimentally. Through proper design of the photonic crystal fiber and micro/nanofiber loop, we obtain over 300-nm wavelength range with flattened dispersion characteristics. Compared with single-mode fiber, spectrum broadening of microfiber is larger. We also demonstrate that the flatness of SCG from the micro/nanofiber loop can be controlled by shifting the cross angle between two ports of the micro/nanofiber loop. According to our results, the dimension and structure of the fiber plays an important role in effecting the dispersion and then the generation of supercontinuum.

8120-57, Session 4

Experiments of electrically controlled optical choppers based on H-PDLC gratings

J. Zheng, Univ. of Shanghai for Science and Technology (China)

A novel electrically controlled optical chopper based on holographic polymer dispersed liquid crystal (H-PDLC) gratings is put forward and experimentally conducted in this paper. The H-PDLC phase type grating is fabricated first, after that a controllable electrical driving source and controlling system are specially designed for H-PDLC based chopper. Using the programmable driving circuit, the H-PDLC chopper can modulate a light beam with variable frequencies at different duty ratios, and generate the sinusoidal modulation to replace the traditional rectangular modulation. Experimental results on one-channel and two-channel H-PDLC optical choppers showed that, in comparison with mechanical chopper counterpart, this device had many advantages such as rapid response, without moving parts, easy to be operated and easy integration etc. The convenience of changing its frequencies, duty ratio and modulation curve configuration is its biggest advantage over mechanical ones, which promises the new device with a good application prospect in modern frequency modulation optical system.

8120-07, Poster Session

Waste heat: light beam converter based on light down conversion in silicon

V. K. Malyutenko, V. V. Bogatyrenko, O. Y. Malyutenko, V. Lashkaryov Institute of Semiconductor Physics (Ukraine)

We come up with new concept for waste heat conversion into beam of wideband radiation based on enhancement of below-bandgap thermal emission of semiconductor ($L_{out}=3-12 \mu m$) caused by above-bandgap optical pump ($L_{in} 100\%$ provided the Si plate is initially transparent in L_{out} band and kept at $T>500 K$). As a matter of fact we demonstrate that fundamental three-body (electron-photon-phonon) interaction in

semiconductor could give a rise to contactless extraction of waste heat the plate is bathed by.

8120-33, Poster Session

A kind of single-polarization single-mode photonic crystal fiber

J. Liang, M. Yun, M. Liu, F. Xia, Qingdao Univ. (China)

Unlike other optical fibers that support two orthogonal polarization modes, single-polarization single-mode (SPSM) fibers guide only one polarization of the fundamental mode. This kind of photonic crystal fibers (PCFs) can significantly improve the stability of optical devices and the communication system due to their high extinction ratio and no polarization mode coupling, so they can be widely used in many applications, such as fiber optic gyroscopes, current sensors and high-power fiber lasers. In order to realize wideband SPSM operation area, there should be a very large refractive index difference between the core and the cladding which may be the main reason that conventional fibers hardly realize. Two methods can be used to realize SPSM PCFs. The first one is to design a PCF structure that one polarization of the fundamental modes is unguided. The second one is to design a structure that maintain a very large differential loss between the two orthogonal polarization modes. In references, some kinds of PCFs have been proposed to realize SPSM region, and the broadest single-polarization bandwidth is about 400nm.

In this paper a kind of single-polarization and single-mode totally internal reflection photonic crystal fiber (SPSM TIR-PCF) is proposed. It is a PCF structure with elliptical air holes in the cladding and four large holes introduced in the first ring. A full-vector plane wave expansion method with anisotropic perfectly matched layers is employed to analyze this PCF structure. The numerical results show that this PCF structure can realize ultra-broad SPSM bandwidth as 540nm with the confinement loss less than 0.1dB/km, the broadest bandwidth as far as our knowledge goes. Moreover, the structure that we proposed can realize a high nonlinear coefficient.

8120-34, Poster Session

Maximum fixing efficiency of thermal fixing in LiNbO3:Fe

P. Hou, Y. Zhi, L. Liu, Shanghai Institute of Optics and Fine Mechanics (China)

Maximum fixing efficiency of thermal fixing in LiNbO3:Fe crystal is investigated. Based on Kukhtarev's band transport model and Kogenlik's theory, the mechanisms leading a high diffraction fixed hologram in LiNbO3:Fe crystal is analyzed. With the same oxidation state and dopant concentration, the developed efficiency for low light intensity depended on the recording wavelength. Holographic gratings are recorded using three typical recording wavelengths including 488nm, 514nm, and 633nm respectively. To obtain a volume grating with the maximum fixed diffraction efficiency, the optimal switching from recording step to thermal fixing is taken into consideration. The fixed holograms are developed by original recording setup. Diffraction efficiencies of recording and thermal fixing are measured by two-wave coupling technique. Both experimental results and theoretical simulation are presented. Through the theoretical and experimental results analyzed and compared, the blue beam was the optimal recording wavelength for maximum fixing efficiency of thermal fixing in LiNbO3:Fe. This work can obtain high persistent diffraction of the nonvolatile holographic storage in LiNbO3:Fe crystals.

**Conference 8120: Photonic Fiber and Crystal Devices:
Advances in Materials and Innovations in Device Applications V**

8120-35, Poster Session

Trace and profile measurements for dynamic objects

W. Su, C. Kuo, National Sun Yat-Sen Univ. (Taiwan)

A fringe projection technique for finding the absolute shape at a sequence of time for a dynamic object is proposed. This method makes it possible to simultaneously identify the trace and the speed of the dynamic object.

8120-36, Poster Session

Speckle-reduction for fringe patterns using the 1D empirical mode decomposition

W. Su, C. Lee, C. Lee, National Sun Yat-Sen Univ. (Taiwan)

We present a database system based on the empirical mode decomposition (EMD) to automatically reduce the speckle in a fringe pattern. With reference to the database, speckles on the fringe pattern can be efficiently and robotically reduced. Percentage of the removed speckles can be predicted as well.

8120-37, Poster Session

Real-time profilometry using double-fringe projection techniques: a compact design for endoscopes

W. Su, C. Hung, National Sun Yat-Sen Univ. (Taiwan); W. Su, National Changhua Univ. of Education (Taiwan)

A profile measurement approach using two diffractive elements to generate two fringe patterns is presented. Only one phase measurement needed for operation. In conjunction with the endoscope, the compact design makes it possible to inspect dynamic object inside the body cavity.

8120-38, Poster Session

Investigation of two-center recording with variable sensitizing light intensity in doubly-doped LiNbO₃ crystal

Z. Chai, East China Normal Univ. (China); Y. Zhi, Shanghai Institute of Optics and Fine Mechanics (China); Q. Zhao, East China Normal Univ. (China); L. Liu, Shanghai Institute of Optics and Fine Mechanics (China)

The two-center holographic recording method, reported by K. Buse et al in 1998, has attracted attention because of ability to record persistent holograms. Three important performance measures in holographic storage are the dynamic range, recording sensitivity and persistence. From 1998 optimizations for high recording sensitivity and dynamic range are performed by experimental and theoretical investigation, and in all investigation the sensitizing light intensity and the recording light intensity in the recording process are stable. The maximum sensitivity can be achieved with high sensitizing intensity, whereas the maximum dynamic range is obtained when the sensitizing and the recording intensities are of the same order.

In this paper we investigate two-center recording with that the sensitizing light intensity is changed with time in the recording process. Some schemes of the sensitizing light intensity variation are designed. In each scheme, the spatio-temporal dynamics of nonvolatile grating formation is investigated through jointly solving the two-center material equations and the coupled wave equations, and the performance of two-center

recording is calculated. The results show that the sensitizing light decay in the recording process can result in the higher recording sensitivity and dynamic range.

8120-39, Poster Session

Airy beam manipulation based on the metallic slit array

D. Choi, Y. Lim, I. Lee, B. Lee, Seoul National Univ. (Korea, Republic of)

Non-diffracting beam, Airy beam, has attracted a lot of interest due to its special properties. Non-spreading in the free space, freely accelerating propagation, and self-healing of Airy beam were proved by not only simulations but also experiments. To induce Airy wave packet which is the solution of normalized paraxial equation of diffraction, the phase mask generated from the spatial light modulator (SLM) is used. Gray-scale patterns of the SLM give Airy phase modulations to an incident Gaussian beam.

To utilize above-mentioned properties of Airy beam to the nanoscale optical device, the light focusing and beaming mechanism based on the metal slit array is considered. When plane wave is incident to the metal slab of subwavelength metallic slits, light is passing through the metallic slits with surface plasmon polaritons which are electromagnetic waves propagating along the interface between a metal and a dielectric material. The phase retardation of the SPP wave at the exit of the metal slit is determined by the width and height of each slit. Based on Huygens' principle, diffracted light from the slit ends can be focused or collimated in the free space due to the different phases at each slit. We adopt the metal slit array with different height which causes the Airy phase instead of the method using the phase mask from the SLM. The numerical simulation and its detection with the holographic microscopy are conducted. This result could help Airy beam manipulation with compact size.

8120-40, Poster Session

Thermal effects on spectral modulation properties of high-power light-emitting diodes

Z. Vaitonis, P. Vitta, V. Jakstas, A. Zukauskas, Vilnius Univ. (Lithuania)

Owing to simple modulation means, light-emitting diodes (LEDs) find numerous cost-efficient applications in fiber-optical and open-space communication as well as in optical measurements and sensing. However, LEDs feature a relatively broad emission spectrum, which is sensitive to both carrier injection rate and junction temperature. In particular, the oscillation of crystal-lattice and electron temperatures in LEDs driven by modulated current can have different effect on the modulation depth and phase in different parts of the spectrum. In this work we report on the effect of selfheating on spectral modulation properties of high-power LEDs. The spectral dependence of modulation depth exhibited a pronounced dip in the vicinity of the peak wavelength, especially at low frequencies. Basically, the drop in modulation depth can be attributed to thermal quenching of emission due to a decrease of the ratio of the radiative and nonradiative recombination rates and thermal excitation of the indirect valleys of the conduction band, as well as to high carrier density invoked efficiency droop. However in the long-wavelength region of the spectrum, the effect of thermal quenching is counterbalanced by the thermal modulation of peak wavelength due to the dependence of semiconductor band gap energy on temperature. Meanwhile in the short-wavelength region, the modulation depth exhibits a linear increase with photon energy due to the electron temperature governed modulation of the electron distribution function. These thermal effects also result in a nonmonotonous spectral variation of modulation phase. Our results provide improved knowledge for the application of LEDs as sources of modulated light.

**Conference 8120: Photonic Fiber and Crystal Devices:
Advances in Materials and Innovations in Device Applications V**

8120-41, Poster Session

Periodical poling of lithium niobate crystals with Li-enriched surface layer

A. R. Poghosyan, I. A. Ghambaryan, Institute for Physical Research (Armenia); R. Guo, The Univ. of Texas at San Antonio (United States); E. S. Vardanyan, Institute for Physical Research (Armenia)

Reduction of the electric field necessary for domain switching is the extremely actual problem as the field reduction not only will simplify technology of creation of periodic structures, but also will facilitate obtaining of necessary off-duty factor and obtain micro- and nanodomain structures.

We suggest two approaches for production of periodically poled lithium niobate crystals by surface modification of congruent crystals: first - by Li enrichment during annealing and second - by deposition a thin layer of stoichiometric lithium niobate film on the +Z face of a crystal. Li enrichment of crystal surface has been made by sample annealing in Li₃NbO₄ or LiNbO₃:Li₃NbO₄ (1:1) powder during 0.5 or 1 h at 800-1100oC. Stoichiometric lithium niobate film with 100-200 nm thickness was deposited by sol-gel method. Both methods have allowed to create on the surface of congruent sample a layer with composition close to stoichiometric and to reduce a poling electric field without changing of the composition of crystal volume and thereby to keep all advantages of congruent crystal. The periodically poled elements (period 7 μm, deff>14 pm/V) combining high optical quality (like congruent crystal) and a low poling field ensuring high quality PP structure (like in stoichiometric crystals) were successfully produced.

8120-42, Poster Session

Influence of structural modification on left-handed plasmonic antenna for green light: from isotropic to chiral

M. Rajput, R. K. Sinha, B. Dabas, Delhi Technological Univ. (India)

We demonstrate the effect of left-handed material structure modification on dispersion and resonance properties. We evaluate and compare dispersion and resonance properties of double nanorod structure, double nanorod ring structure, H structure and chair type structure. It is worth noticing that with some structural modification, the properties of the structure changes from isotropic to uni-axial anisotropic and further to chiral left-handed material. The Demonstration of near-field transmission spectrum reveals the production of the local-field enhancement up to 102 for the green light. It is shown that index matching to the incident medium and compensated losses due to the gain assistance lead to the light amplification in the designed structure. Radiations from the designed structures are well explained by their electrical and magnetic moments and it is also in good agreement with FDTD analysis. Designed isotropic structure gives Negative real values of both permeability (μ) and permittivity (ϵ) with extremely ultra-low imaginary values for visible light is obtained by applying coupled dipole approximation. Near-field and far-field resonance reveals light amplification and high directionality for the designed nano-antenna. 3-D FDTD method is employed to evaluate the far field spectrum with effect of the structure modification of the designed structure. The structure modification exhibits some unique dispersion and resonant properties that may govern imaging applications.

8120-43, Poster Session

Numerical demonstration of soliton dynamics in chalcogenide As₂Se₃ glass photonic crystal fiber

B. Dabas, J. Kaushal, M. Rajput, R. K. Sinha, Delhi Technological Univ. (India)

Photonic Crystal Fibers (PCF), consisting of air hole array running along the fiber length, shows unique properties which are attractive for applications that can not be realized in conventional fibers. PCF guides light via one of the two mechanisms: effective index guidance & Photonic Band Gap (PBG) effect. Recently research work is focused on non-silica compound glasses like chalcogenide and soft glasses etc, have been effectively used in formation of PCFs for investigation of non-linear propagation in PCFs. Chalcogenide glasses are based on sulphur, selenium, tellurium and the addition of other elements such as arsenic, germanium, antimony, gallium, etc. Chalcogenide glasses are promising nonlinear materials especially in the longer wavelength infrared (IR) region. The large refractive index of chalcogenide glasses (compared to other glasses) of 2.4 to 3.0 opens up the possibility of achieving compact nonlinear devices. In this paper, soliton pulse generation and collision in chalcogenide As₂Se₃ glass Photonic Crystal Fiber (PCF) is numerically studied using our own algorithm developed for Fourth-Order Runge-Kutta in the Interaction Picture (RK4IP) method. The numerically obtained value of soliton collision length is found to be in good agreement with the theoretical value obtained by the inverse scattering transform, thus providing a verification of the accuracy of the method in solving Generalized Nonlinear Schrödinger Equation (GNLSE). We also calculate the value of wavelength for least distortion for soliton optical pulses, and study its variation with the pitch for chalcogenide As₂Se₃ glass PCF. We also calculate the value of wavelength for least distortion for soliton optical pulses.

8120-44, Poster Session

Kerr nonlinear wideband optical filters of the basis of 2D photonic crystal

I. V. Guryev, I. A. Sukhoivanov, A. O. Alvarez, J. A. Andrade-Lucio, M. Trejo-Durán, E. Alvarado Mendez, E. Vargas-Rodriguez, Univ. de Guanajuato (Mexico)

Today, a lot of scientific investigation resources are directed to create integrated all-optical data processing system which may become replacement for electronic processors.

In our work, we investigate the temporal properties of the wideband optical filter on the basis of 2D nonlinear photonic crystal (PhC) which presents great interest as a basis for all-optical logic in the data processing and storage.

Particularly, assuming immediate response of the nonlinear material, we concentrate our attention at the investigation of theoretical limits of the optical reaction of the PhC required to provide the bistability effect.

As a result of the work, we present the theoretical model of the bistable wideband filter on the basis of 2D PhC and the parameters of the ultra-short pulses which provide maximum contrast of the bistability. The devices with the parameters found in the work, provide the possibility to create the all-optical flip-flop devices as well as optical memory modules.

There have been determined minimum duration of the ultra-short pulse at which the bistability is possible in the investigated filters.

8120-45, Poster Session

Interfacial state density and terahertz radiation on oxide-GaAs interface

C. Chang, M. Hsu, Chinese Military Academy (Taiwan); W. Chen, National Cheng Kung Univ. (Taiwan); J. Huang, Chinese Military Academy (Taiwan); Y. Wang, Nan Jeon Institute of Technology (Taiwan)

The amplitude of terahertz radiation (THz) from a series of oxide films on GaAs was measured by time resolved THz emission system. The barrier heights and the densities of the interfacial states are determined from the PR intensity as a function of the pump power density. The oxide-GaAs structures fabricated by in situ molecular beam epitaxy exhibit low interfacial state densities in the range of 10^{11} cm⁻². It is

**Conference 8120: Photonic Fiber and Crystal Devices:
Advances in Materials and Innovations in Device Applications V**

found that the amplitude of THz radiation from Al₂O₃-, Ga₂O₃-, and Ga₂O₃(Gd₂O₃)-GaAs structures are increases with interfacial electric field. The reason is that the electric field is lower than the “critical electric field”, the amplitude is proportional to the product of the electric field and the number of photo-excited carriers. However, as the field higher than the critical electric field, sample of air-GaAs structure, the lower THz amplitude was obtained due to the maximum drift velocity declines slightly as the field increases.

8120-46, Poster Session

Contactless electroreflectance study of the PTCDI thin film structure

W. Chen, W. Chou, National Cheng Kung Univ. (Taiwan); C. Chang, Chinese Military Academy (Taiwan)

Contactless electroreflectance (CER) has been applied to provide information on the optical properties occurring in thin films of N,N'-dialkyl-3,4,9,10-perylene tetracarboxylic diimide (PTCDI-C_nH_{2n+1}, n = 2-13) compounds sandwiched between ITO and aluminum electrodes (Al/PTCDI-C_nH_{2n+1}/ITO/glass substrate) under ambient conditions. Electromodulated optical responses of the Al/PTCDI/ITO thin film structures were characterized at various modulation voltage and temperatures. The optical transitions were perturbed by the energy shifts of the electronic states due to Stark effect induced by the modulation electric field. The feature of spectrum increases with the increasing modulation voltage. The energy transitions of the Al/PTCDI/ITO system can be obtained from the peak positions in the electroreflectance spectrum. As the temperature increasing from 30 K, the modulated transmission signal is also increased, and becomes complex as the temperature is further increased. The energy transitions involving the PTCDI molecular states remain almost constant as the temperature varies.

8120-47, Poster Session

Study on deflection characteristics of electro-optic scanners with special geometrical shapes

L. Wan, B. Shi, Z. Lu, L. Chao, Guangxi Univ. (China)

The electro-optic scanners based on ferroelectric domain prisms have the advantages of small-size, high-speed and absence of moving parts and are of interest in many applications including advanced laser radar, fiber-optic switching networks, optical sensors and laser printers. For traditional rectangular scanners, they have an important drawback of small deflection angle. Some non-rectangular scanners such as the trapezoidal, horn, half-horn and parabola shape have been developed to improve the scanning performances in near ten years. The deflection characteristics of all non-rectangular scanners relate to their variable width along propagation direction. They are dependent on both the change of index gradient and the width of the device. In this paper, three types of scanners which their width are varied with parabolic, hyperbolic and exponential functions are studied. The equations of deflection angle and ray trajectory of three types of electro-optic scanners are given and their deflection properties are investigated by numerical analysis. The deflection characteristics and sensitivities are compared to each other. It is helpful for the design of electro-optic scanners with fine performance.

8120-48, Poster Session

Optical properties of PTCDI thin films studied by contactless electroreflectance

W. Chen, W. Chou, National Cheng Kung Univ. (Taiwan); C. Chang, Chinese Military Academy (Taiwan); M. Tsai, National Cheng Kung Univ. (Taiwan)

Contactless electroreflectance (CER) is used to investigated the optical properties of N,N'-dialkyl-3,4,9,10-perylene tetracarboxylic diimide (PTCDI-C_nH_{2n+1}, n: 2-13) thin films sandwiched between ITO and aluminum electrodes (Al/PTCDI-C_nH_{2n+1}/ITO/glass substrate) under ambient conditions. Electromodulated optical responses of the Al/PTCDI/ITO thin-film structures were characterized at various biases and temperatures. The optical transitions of PTCDI were perturbed by the energy shifts of the electronic states due to Stark effect induced by the modulation electric field. The modulated spectrum of PTCDI is strongly enhanced by performing the first derivatives on the absorption spectrum of the PTCDI that involves the fundamental transitions, doping states, and Davydov splitting. Moreover, the intensity of field-induced transition peak of PTCDI increases with the increasing modulation voltage of CER. The transition energies between the lowest unoccupied molecular orbital and highest occupied molecular orbital of the Al/PTCDI/ITO system can be obtained from the peak positions of the electroreflectance spectrum. As the temperature is increased from 30 K, the modulated signal intensity of PTCDI is increased; however, the transition energies of the PTCDI molecular states remain almost constant.

8120-49, Poster Session

Infiltrated plasmonic photonic crystal cavity for sensing

S. Singh, V. Dillu, R. K. Sinha, R. Bhattacharyya, Delhi Technological Univ. (India)

Plasmonics by confining electromagnetic waves on metallic surfaces in the form of localized and propagating surface plasmon polariton (SPP) have completely reshaped the field of photonics and provided it with an unprecedented tool to handle the demands of smaller, faster and better devices as compared to what we use today. Nanocavity efficiently traps light in the cavity volume thereby increasing light matter interaction.

Sensors based upon surface plasmon resonance offer simple design, show extremely high sensitivity to refractive index changes, respond to minute amounts of analytes and therefore have applications in chemical sensors and biosensors.

We have proposed surface plasmonic photonic crystal (SPPC) nanostructured cavity based infiltrated sensor for the sub-wavelength confinement of light by placing a low loss silver substrate (permittivity: ϵ_m) below the 1D photonic crystal waveguide of silicon slab with air holes ($\epsilon_d = 11.56$), with an optimized lattice constant and radius of holes. The cavity is introduced by removing central air hole of the plasmonic crystal waveguide.

Plasmonic TM mode with vertical electric field along Y direction (E_y) is obtained for the proposed structure and the mode profile of the SPPC structure is calculated using 3D FDTD method. The side air holes of the cavity are engineered to obtain single mode localization of resonating wavelength and the sensitivity of the resonating cavity mode is calculated by varying refractive index of the content of air holes. Plasmonic bandgap, transmission spectra, Quality factor and sensitivity are calculated and possible application in the area of sensing is assessed

8120-50, Poster Session

The thermal dissipation of LED under the influence of ceramic porous film

M. Hsu, C. Chang, F. Shyu, Chinese Military Academy (Taiwan); Y. Wang, Nan-Jeon Institute of Technology (Taiwan)

The temperature had an important influence in the life time of light emitting diodes (LED). In this study, we fabricated the ceramic porous films, by vacuum sputtering, soldered the LED lamps to enhance both of the heat transfer and heat dissipation. In our samples, the ceramic enables transfer the heat from electric device to the aluminum plate quickly and the porous increase the quality of the thermal dissipation between the PCB and aluminum plate, as compared to the industrial processing. The ceramic films were characterized by several subsequent

**Conference 8120: Photonic Fiber and Crystal Devices:
Advances in Materials and Innovations in Device Applications V**

analyses, especially the measurement of real work temperature. The X-Ray diffraction (XRD) diagram analysis reveals those ceramic phases were successfully grown onto the individual substrate. The morphology of ceramic films was investigated by the atomic force microscopy (AFM). The results show porous film fabricated by vacuum sputtering has low sheet resistivity, high critical load, and thermal conduction to the purpose. At the same time, it had transferred heat and limited work temperature, under 80, of LED successfully.

8120-51, Poster Session

Characterization of channel waveguides fabricated by high-dose proton implantation in Nd:YAG

M. A. Lopez-Urquieta, Ctr. de Investigaciones en Óptica, A.C. (Mexico) and Univ. Nacional Autónoma de México (Mexico); E. Flores-Romero, Univ. Nacional Autónoma de México (Mexico); G. V. A. Vazquez, Ctr. de Investigaciones en Óptica, A.C. (Mexico); H. A. Marquez, Ctr. de Investigación Científica y de Educación Superior de Ensenada (Mexico); J. A. Rickhards, R. A. Trejo-Luna, Univ. Nacional Autónoma de México (Mexico)

In this work we present the laser performance of channel waveguides which operate at 1064nm at room temperature. These 30 channel were made on Nd: YAG crystal by proton implantation with different widths (10, 15 and 20µm) forming sets of 10 waveguides which are separated by a distance of 215 µm. The results shown are the luminescence spectra and laser emission characteristics such as pump power threshold and slope efficiency. The spectroscopic characterization indicates that the optical properties of the waveguide in comparison with the bulk material are preserved after the implantation process and that this is a potential technique to develop compact and efficient lasers.

8120-52, Poster Session

Nano-antenna-based optical fiber probe

J. Park, Seoul National Univ. (Korea, Republic of); J. Kim, Korea Univ. (Korea, Republic of); S. Roh, Seoul National Univ. (Korea, Republic of); K. Kim, Sejong Univ. (Korea, Republic of); H. Shin, Korea Institute of Science and Technology (Korea, Republic of); B. Lee, Seoul National Univ. (Korea, Republic of)

We propose a resonant optical Yagi-Uda nano-antenna fabricated at the end of the optical fiber probe for the sake of extracting the information of the angular directivity by absorption of directional emission as a subwavelength optical microscopy. A Yagi-Uda nano-antenna consists of a feed element surrounded by a reflector and three directors. The reflector and directors are optimized in length with regards to resonance of the antenna elements, and the gap between elements is identified numerically using a finite-element method. We used an electron beam lithography process to mount the metal nano-antenna structure on the surface of the optical fiber probe, followed by e-beam evaporation of a 30 nm thickness of gold. To verify the characteristics of the probe based nano-antenna, directional emission from the metal slit with asymmetric dielectric surface gratings is probed and detected using the photomultiplier tube. Our approach of the nano-antenna based fiber probe is promising for various applications such as detection of directional emission.

8120-53, Poster Session

Growth, characterization, and applications of ZnO/MgZnO multilayer structures

S. Yin, Q. Li, T. Li, Y. Gao, J. Yao, The Pennsylvania State Univ.

(United States)

In this paper, the growth of ZnO/MgZnO multiple layer structure is presented. The properties of the growth structure are quantitatively characterized by XRD, photoilluminance, and electronic microscopy. The applications of this unique ZnO/MgZnO structure is also discussed.

8120-54, Poster Session

Enhance Raman signal with tunable and controllable photonic nanostructures

S. Yin, C. Wang, Y. Chang, The Pennsylvania State Univ. (United States); P. Ruffin, U.S. Army Armament Research, Development and Engineering Ctr. (United States); C. Brantley, E. Edwards, U.S. Army Research, Development and Engineering Command (United States); C. Luo, General Opto Solutions, LLC (United States)

In this paper, we present a new method for enhancing the Raman signal by using tunable and controllable photonic nanostructures. This new approach not only offers the capability of adjusting the enhancing factor but also improve the signal-to-noise ratio of the standoff Raman signal detection.

8120-55, Poster Session

Terahertz wave generation with multi-physics mechanisms

S. Yin, Y. Gao, J. Yao, The Pennsylvania State Univ. (United States)

In this paper, we present a new method of terahertz wave generation by employing multiple physics mechanism, which can improve the overall efficiency of terahertz wave generation.

8120-56, Poster Session

Electrically and mechanically tunable photonic metamaterials

S. Yin, Y. Chang, C. Wang, The Pennsylvania State Univ. (United States); C. Luo, General Opto Solutions, LLC (United States)

In this paper, a unique electrically and mechanically tunable photonic metamaterial is presented, which has the advantages of fast tuning speed and wide tuning range. The potential applications of this unique tunable photonic metamaterial is also discussed.

8120-58, Poster Session

Influence of structural parameters of tunable triangular lattice photonic crystal on photonic band gap

A. Huang, J. Zheng, Univ. of Shanghai for Science and Technology (China)

Tunable photonic crystal (PC) can control photonic band gap through changing the refractive index of liquid crystal (LC) by adding an electric field, optical field or changing its temperature, which can change the orientation of LC's direction vector. Plane wave expansion method (PWE) is used to simulate the band gap of 2D tunable triangular lattice PC with structure of cylinder, square column and regular hexahedron column. The influence of changing rods shape, rotation angle and filling ratio on 2D

**Conference 8120: Photonic Fiber and Crystal Devices:
Advances in Materials and Innovations in Device Applications V**

Phenylacetylene LC photonic band gap(PBG) are discussed when the substrate material is Ge and Si respectively. It is found that there isn't absolute PBG in any condition, but big tuning range of TE polarized wave can be achieved by changing the index of liquid crystal. The tuning range of PBG reaches to maximum (≈ 0.0830) when the substrate material is Ge, rotation angle is 0° , and $d/a = 0.85$, this is much better than the result of C. Y. Liu (≈ 0.0299). This structural parameter can provide theoretical instruction for field sensitive polarizer with great tuning range, and foundation of tritulating waveguide optical switch, tunable filter and optical attenuator.

8120-59, Poster Session

High-frequency holographic polymer dispersed liquid crystal optical chopper array for frequency division multiplexed fluorescence confocal microscope system

Y. Jiang, J. Zheng, P. Tang, A. Huang, Z. Zhou, Univ. of Shanghai for Science and Technology (China)

High-frequency two-channel optical chopper array based on Holographic Polymer Dispersed Liquid Crystal (H-PDLC) material is reported in this article. It is an innovative application of H-PDLC material making use of its prominent optoelectronic characteristics, which has drawn much attention in recent years. Photopolymerization Induce Phase Separation (PIPS) method is adopted in fabrication of H-PDLC material. The proposed H-PDLC optical chopper array is more competitive than traditional mechanical ones because it not only avoids mechanical movements and frequency shift but also has shorter switch-on and switch-off time, higher integrated level and ability to operate various waveform modulations. When the proposed H-PDLC optical chopper array is used as beam modulator in Frequency Division Multiplexed Fluorescence Confocal Microscope (FDMFCM) system, it helps the system to obtain better Signal-Noise Ratio (SNR), smaller volume, more independent channels and more efficient scanning. The FDMFCM system conducts successful parallel detection of rat neural cells. Colored images with a spatial resolution at micrometer scale are obtained. And fluorescence intensity signals from two different points on the sample cells which represent concentration of certain kind of proteins in the cells are achieved as well. The experimental results show that the proposed H-PDLC optical chopper array is practical when working at a high modulation frequency. It improves temporal resolution of FDMFCM system and it also provides a possibility to develop the FDMFCM system into a multi-channel system.

8120-60, Poster Session

A novel photonic magnetometer for detection of low-frequency magnetic fields

J. Matthews, L. Bukshpun, R. Pradhan, Physical Optics Corp. (United States)

A novel photonic magnetometer for a variety of applications is being developed. The detection mechanism is similar to existing fiber-optic magnetometers, in which a magnetostrictive element transduces magnetic field variations into changes in optical path length, subsequently detected through optical interferometry. Single-axis and three-axis vector magnetometers have been designed, and other application-specific configurations have also been investigated. The sensor noise floor is estimated at 20 pT/rtHz for frequencies of 0.1 Hz and above, with a dynamic range of over 100,000 nT. The sensor can be compact (down to 1 cm³) and can consume less than 100 milliwatts of power. These features, combined with its low 1/f noise, and wide dynamic range, make POC's photonic magnetometer an easily deployable detector of low frequency magnetic fields. Potential applications of the photonic magnetometer, including space-based measurement of geomagnetic fields, medical biomagnetic imaging, vehicle detection, mine detection, heading sensors, low-frequency

communications, and deep eddy current nondestructive evaluation, have been explored as well.

8120-61, Poster Session

Quality factor of silicon-on-insulator integrated optical ring resonator

C. Xue, Y. Jin, D. Cui, X. Tong, Y. Shubin, W. Zhang, North Univ. of China (China)

MOEMS (micro optical electronic mechanical system) and inertia device based on nano optical waveguide and micro-processing technology have been the research focuses which attract many scholars in recent years. IORR is the major sensing and communication element among them. It has an irreplaceable position in the production of micro-electro mechanical device because its ultra-high quality factor and small mode volume. Light transmission in micro-ring resonator, coupling and various physical phenomena due to interaction with the external field are the foundation of integration optical design and manufacture. SOI material is the most promising material for IORR due to the high effective index contrast between Silicon and its typical buried insulator material (SiO₂). The high effective index contrast leads to natural vertical optical confinement and implies very small Silicon waveguide dimensions. In this paper, we designed waveguide and micro ring resonator on SOI platform. At the same time we designed grating coupler on waveguide for efficiently coupling with a single mode optical fiber. We fabricated the waveguide and ring resonator with micro processing technology and experimentally observed obvious coupling phenomenon. Without any optimization craft we got a high quality factor of ring resonator. Our devices were fabricated on a SOI wafer with a top silicon layer thickness of 340 nm and a buried oxide thickness of 1 μm. The optical waveguides and optical ring resonator were fabricated by two steps. Firstly, the positive resist PMMA was spun on the pattern with electron-beam lithography (EBL) system at 100kV electron beam for exposure. Residual photo resist in exposure area was removed and the developed graphic as a mask for dry etching. Secondly, Inductively-coupled-plasma (ICP) reactive-ion etch (RIE) was then applied to transfer the pattern and etch through the 340 nm silicon layer. At last the grating is determined on the waveguide and etched by focused ion beam (FIB). The quality factor of ring resonator is demonstrated as high as $8.96 \times 10^3 - 1.33 \times 10^4$.

8120-62, Poster Session

Recent advances of IR supercontinuum with single crystal fibers and waveguides

S. Yin, The Pennsylvania State Univ. (United States); P. Ruffin, U.S. Army Armament Research, Development and Engineering Ctr. (United States); C. Brantley, E. Edwards, U.S. Army Research, Development and Engineering Command (United States); J. Cheng, J. Yao, The Pennsylvania State Univ. (United States); C. Luo, General Opto Solutions, LLC (United States)

In this paper, the recent advances of broadband visible-IR supercontinuum generation by single crystal fibers and waveguides and its applications are presented.

8120-63, Poster Session

Optical and electro-optic properties of potassium lithium tantalate niobate single crystals

Y. Li, J. Li, Harbin Institute of Technology (China) and The Univ. of Texas at San Antonio (United States); Z. Zhou, Harbin Institute of Technology (China); A. S. Bhalla, R. Guo, The Univ. of Texas at

**Conference 8120: Photonic Fiber and Crystal Devices:
Advances in Materials and Innovations in Device Applications V**

San Antonio (United States)

Potassium lithium tantalate niobate single crystals with the composition of $K_{0.95}Li_{0.05}Ta_{1-x}Nb_xO_3$ ($x=0.15, 0.20, 0.25, \text{ and } 0.30$) have been grown using the top seeded solution growth method. In addition to the determination of their dielectric, pyroelectric, and piezoelectric properties, the crystals have been systematically investigated for their optical and electrooptic properties. Using minimum deviation measurement the index of refraction as a function of temperature at given wavelength is obtained. A modified Mach-Zehnder interferometer coupled with a computer interfaced dynamic scanning scheme was adapted to measure the electrooptic coefficients. Longitudinal and transverse EO coefficients are reported in this paper as function of frequency of the modulating electric field. The selected KLTN crystals have been found to have good piezoelectric properties and high electromechanical coupling factors among the lead free ferroelectric crystals of high Curie transition temperatures. Their high EO coefficients, high figure of merit as EO modulator, and high laser damage threshold also forecast their outstanding potential in various electro-mechanical-optical coupled applications.

8120-64, Poster Session

**Pyrooptic evaluation of ferroelectric crystals
for radiated heat energy conversions**

S. Zhu, T. Patel, R. McIntosh, A. S. Bhalla, R. Guo, The Univ. of Texas at San Antonio (United States)

Pyrooptic effects of selected ferroelectric materials were studied using dynamic (Chynoweth) pyroelectric measurements as a function of modulating frequency and the wavelength of the electromagnetic wave radiation. A comparison with the results obtained on $LiTaO_3$ and PMN-PT [Ref. 1] single crystals is presented. Pyrooptic responses under both mechanically clamped (approximately constant strain) and mechanically free boundary (approximately constant stress) conditions were studied in order to optimize the pyroelectric output. Numerical simulations based on finite element analysis were adopted to evaluate temperature gradient distribution and the effective time constant of the given testing configuration. Circuit analysis was also attempted to simulate the performance of the material under test. The combined experimental and numerical simulation results are used to guide the design of the potential device for radiated heat energy harvesting suitable for self-sustained sensors. Pyroelectric crystals are of unique potential for certain energy conversion applications complementary of photovoltaic cells. The dynamic pyrooptic measurement is shown to be an effective testing method for evaluating the performance of a family of pyroelectric materials.

[Ref. 1]. Elric Von Eden, NSF EE REU Penn State Annual Research Journal Vol. I (2003) p. 211

Conference 8155B: Single-Photon Imaging II

Wednesday 24 August 2011 • Part of Proceedings of SPIE Vol. 8155B Single-Photon Imaging II

8155B-101, Session 7

Future use of silicon photomultipliers for the fluorescence detection of ultra-high-energy cosmic rays

M. Stephan, T. Hebbeker, M. Lauscher, C. Meurer, T. Niggemann, J. Schumacher, RWTH Aachen (Germany)

A sophisticated technique to measure extensive air showers initiated by ultra-high-energy cosmic rays is by means of fluorescence telescopes. Secondary particles of the air shower excite nitrogen molecules of the atmosphere, which emit fluorescence light when they de-excite. Due to their high photon detection efficiency (PDE) silicon photomultipliers (SiPMs) promise to increase the sensitivity of today's fluorescence telescopes which use photomultiplier tubes - for example the fluorescence detector of the Pierre Auger Observatory. On the other hand drawbacks like a small sensitive area, a strong temperature dependency and a high noise rate have to be managed.

We present plans for a prototype fluorescence telescope using SiPMs and a special light collecting optical system of Winston cones to increase the sensitive area. In this context we made measurements of the relative PDE of SiPMs depending on the incident angle of light. The results agree with calculations based on the Fresnel equations. Furthermore, measurements of the brightness of the night sky are presented since this photon flux is the main background to the fluorescence signals of the extensive air showers. To compensate the temperature dependency of the SiPM, frontend electronics make use of temperature sensors and microcontrollers to directly adjust the bias voltage according to the thermal conditions. To reduce the noise rate we study the coincidence of several SiPM signals triggered by cosmic ray events. By summing up these signals the SiPMs will constitute a single pixel of the fluorescence telescope.

8155B-102, Session 7

Silicon single photon imaging detectors

D. F. Figer, Rochester Institute of Technology (United States); B. F. Aull, MIT Lincoln Lab. (United States)

Single photon imaging detectors promise the ultimate in sensitivity by eliminating read noise. This could provide extraordinary benefits for photon-starved applications, e.g. imaging exoplanets, fast wavefront sensing, and probing the human body through transluminescence. Recent implementations are often in the form of sparse arrays that have less than unity fill factor. For imaging, their fill factor is typically enhanced through the use of microlenses, at the expense of photometric and spatial information loss near the edges and corners of the pixels. Other challenges include afterpulsing and the potential for photon self-retriggering. Both effects produce spurious signal that can degrade the signal to noise ratio. This talk will review development and potential application of single photon counting detectors, including highlights of initiatives in the Center for Detectors at the Rochester Institute of Technology and MIT/Lincoln Laboratories. Current projects include megapixel single photon counting imaging detectors for the Thirty Meter Telescope and a future NASA terrestrial exoplanet mission and imaging LIDAR detectors for planetary and Earth science space missions.

8155B-103, Session 7

Design and evaluation of a one-dimensional high-resolution CMOS position-sensitive detector using skewed pixel arrays

X. Song, M. Sasaki, K. Asada, The Univ. of Tokyo (Japan)

The position sensing system consists of the incident light source, the

target object and the position sensor. The incident light from the laser hits the target object and then reflects to the sensor which detects the peak position of the reflected profile. However, when the incident profile is broad unexpected errors will be caused due to the incident profile not perfectly Gaussian and the roughness of the target surface that leads to the distortion of the reflected profile, at the same time it is very difficult to generate a normal incident profile narrower than pixel-pitch, thus we propose to detect the extremely sharp dark print from an alternating Phase Shift Mask (PSM) to solve these problems. In this thesis, we describe a one-dimensional(1-D) high resolution optical Position Sensitive Detector (PSD) based on a novel architecture using Skewed Pixel Arrays (SPA). The proposed position sensor has been designed, implemented on a chip using standard 0.18 μ m CMOS process and has been successfully tested.

8155B-104, Session 8

Reduced afterpulsing using rapid quenching techniques

J. C. Campbell, A. Holmes, Univ. of Virginia (United States)

Afterpulsing in InGaAs/InP single photon avalanche photodiode (SPAD) is one of the primary performance limitations, particularly for those applications that require high-speed information collection or transmission. One approach that has proved effective in reducing the negative impact of afterpulsing is rapid quenching. Techniques to accomplish this include short-pulse gated quenching, sinusoidal gating, self-differencing, and passive quenching with active reset. This talk will review these methods and present current state-of-the-art performance with respect to single photon detection efficiency, dark count rate, and afterpulse probability.

8155B-105, Session 8

Single-photon FPAs based on 32 x 128 Geiger-mode APD arrays

M. A. Itzler, M. Entwistle, X. Jiang, K. Patel, M. Owens, K. Slomkowski, S. Rangwala, Princeton Lightwave, Inc. (United States); P. Zalud, T. Senko, J. Tower, J. Ferraro, SRI International Sarnoff (United States)

We describe the design, fabrication, and performance of focal plane arrays (FPAs) with a 32 x 128 pixel format for use in 3 D LADAR imaging applications requiring single photon sensitivity. These FPAs incorporate InP/InGaAsP Geiger-mode avalanche photodiodes (GmAPDs) on a 50 μ m pitch to detect single photons at 1064 nm with high efficiency and low dark count rates. We present results for key performance parameters and provide an overview of the operational features of these FPAs.

8155B-106, Session 8

Photon counting arrays for deep space optical beacon acquisition and tracking

W. H. Farr, Jet Propulsion Lab. (United States)

No abstract available

8155B-107, Session 9

Physics of self-recovering single photon avalanche detectors

Y. Lo, J. Cheng, S. You, S. Rahman, Univ. of California, San

Diego (United States)

InGAs single-photon avalanche photodetectors with self-quenching and self-recovering capabilities are particularly attractive to focal plane array architecture since the quenching circuit for each pixel is not needed. We present physical models to show that bandgap engineering can control the self-recovering time by more than 3 orders of magnitude, so is a highly efficient way to design the device characteristics for specific applications.

Our model includes two mechanisms for carrier escape over the barrier to achieve self-recovery: thermionic emission and field-assisted tunneling. The model predicts that the carrier escape time, which is directly related to the self-recovering time, can be controlled over a range from 1 ns to > 1 μ s. On the other hand, the quenching time of the device (i.e. time to stop the current pulse triggered by a single photon) can be as short as 50 ps. The physical models show good agreement with the experimental results.

The analysis produces insight about the intrinsic device characteristics and a clear guideline towards device design and optimization. It also helps explain some experimentally observed phenomenon such as strong dependence of self-recovering time on bias voltage.

8155B-108, Session 9

Kilometer range depth imaging using time-correlated single-photon counting

G. S. Buller, N. J. Krichel, A. McCarthy, R. H. Hadfield, Heriot-Watt Univ. (United Kingdom)

Active depth imaging approaches have numerous potential applications in a number of disciplines, including environmental sensing, manufacturing and defence. The high sensitivity and picosecond timing resolution of the single-photon counting technique can provide distinct advantages in the trade-offs between required illumination power, range, depth resolution and data acquisition durations. These considerations must also address requirements for eye-safety, especially in applications requiring outdoor, kilometer range sensing. We present a scanning time-of-flight imager based on high repetition-rate (>MHz) pulsed illumination and a silicon single-photon detector. In advanced photon-counting experiments, we have employed the system for unambiguous range resolution at several kilometers target distances, multiple-surface resolution based on adaptive algorithms, and a cumulative data acquisition method that facilitates detector characterisation and evaluation. We consider a range of optical design configurations and discuss the performance trade-offs in more detail. Much of this work has been performed at wavelengths around 850nm for convenient use with Si-based single photon avalanche diode detectors, however we will also discuss the performance at wavelengths around 1500nm, which provide more relaxed eye safety requirements, reduced solar background levels and improvements in atmospheric transmission.

8155B-109, Session 10

Time-correlated single-photon counting with superconducting single-photon detectors

R. H. Hadfield, M. G. Tanner, C. M. Natarajan, J. A. O'Connor, N. J. Krichel, G. S. Buller, Heriot-Watt Univ. (United Kingdom)

Superconducting single-photon detectors (SSPDs) based on niobium nitride nanowires [1] have emerged over the past decade as a highly promising technology for time-correlated single-photon counting applications. These devices offer free-running infrared photon counting with low dark counts, nanosecond recovery times and timing jitter below 100 ps FWHM. SSPDs have been successfully integrated into practical detector systems and have played a prominent role in pushing back the frontiers of optical quantum information science [2]. In this presentation we discuss how SSPDs can be used in a wide range of other TCSPC applications. Studies of single-photon emitters [3] open the pathway

to new biophotonics applications. Single-photon laser ranging studies [4] have opened the route to depth imaging and atmospheric sensing applications. Recent studies of position dependent timing delay across a large area meander SSPD [5] indicate that there is also potential to use these devices as single-photon cameras.

[1] Gol'tsman et al Applied Physics Letters 79 (6) 705 (2001)

[2] Hadfield RH et al Nature Photonics (3) 696 (2009)

[3] Stevens MJ et al Applied Physics Letters 89 031109 (2006)

[4] Warburton RJ et al Optics Letters 32 (15) 2266 (2007)

[5] O'Connor et al submitted to Applied Physics Letters 2011

Acknowledgements:

This work is supported by the UK Engineering and Physical Sciences Research Council and the Royal Society of London. We thank colleagues at NICT Japan and TU Delft the Netherlands for providing detectors used in this work, and at NIST USA for support in building practical detector systems

8155B-110, Session 10

Polar-azimuthal angle-dependent efficiency of different infrared superconducting nanowire single-photon detector designs

M. Csete, A. Sipos, Univ. of Szeged (Hungary); F. Najafi, K. K. Berggren, Massachusetts Institute of Technology (United States)

The illumination-angle-dependent absorptance was determined for three types of superconducting-nanowire single-photon detector (SNSPD) designs: 1. bare periodic niobium-nitride (NbN) stripes with dimensions of conventional SNSPDs, 2. same NbN patterns integrated with ~ quarter-wavelength hydrogensilsesquioxane-filled nano-optical cavities, 3. similar cavity-integrated structures covered by a thin gold film acting as a reflector. A three-dimensional finite-element method based on the RF module of the COMSOL software package was applied to determine the optical response and near-field distribution as a function of p-polarized light illumination orientations specified by polar- and azimuthal-angles. The numerical results proved that the absorptance of NbN in these SNSPD devices might be maximized via simultaneous optimization of the polar and azimuthal illumination angles. Complementary transfer-matrix-method calculations were performed on artificial composite layers of analogous film-stacks to uncover the phenomena contributing to the appearance of extrema on the optical response of NbN-patterns acting as P-structures. This comparative study showed that the absorption in bare NbN patterns is zero at the angle corresponding to total internal reflection (TIR). The NbN absorptance curve indicates a maximum at TIR in cavity-integrated structures due to the phase shift introduced by the quarter-wavelength HSQ layer. The reflector promotes the NbN absorptance at small and very large polar angles, but the available absorptance is limited by attenuated TIR in polar angle-intervals, where surface modes are excited on the gold film.

8155B-112, Session 11

Single photon counting linear mode avalanche photodiode technologies

G. M. Williams, Jr., Voxel, Inc. (United States)

The need for high-speed single photon counting detectors and detector arrays, which are sensitive throughout the near-infrared (NIR) spectrum, is unmet by existing technologies. Geiger mode (Gm) avalanche photodiodes (APDs) have limited sensitivity and high afterpulse event rates. Attempts to improve Gm APD technology through active and passive quenching of the avalanche pulse, negative feedback pulse suppression, gated biasing, and dynamic biasing, although implemented differently, all attempt to reduce the magnitude of the Geiger mode pulse to reduce the trap filling in the junction. At these low gain values, Gm APD technology becomes susceptible to a variety of noise sources.

In contrast to Gm APDs, low noise linear mode (lm) APD technology can accomplish this objective, allowing single photon counting to be achieved with low afterpulse rates. The lm APD technology also readily provided single amplitude information.

A high gain linear mode APD technology will be presented, which has low excess noise characteristics at high gain values. It will be shown how the linear mode APD technology can simultaneously achieve high detection efficiency, low dark count rates, and high count rates. It will also be shown how linear mode APDs can statistically discriminate dark counts from photon events. The statistics of the avalanche buildup process will also be discussed.

8155B-114, Session 11

High performance SPAD array detectors for parallel photon timing applications

I. Rech, C. Cammi, A. Gulinatti, Politecnico di Milano (Italy); P. Maccagnani, Istituto per la Microelettronica e Microsistemi, CNR (Italy); M. Ghioni, S. Cova, Politecnico di Milano (Italy)

Over the past few years there has been a growing interest in monolithic arrays of single photon avalanche diodes (SPAD) for spatially resolved detection of faint ultrafast optical signals. SPADs implemented in planar technologies offer the typical advantages of microelectronic devices (small size, ruggedness, low voltage, low power, etc.). Furthermore, they have inherently higher photon detection efficiency than PMTs and are able to provide, beside sensitivities down to single-photons, very high acquisition speeds.

In order to make SPAD array more and more competitive in time-resolved application it is necessary to face problems like electrical crosstalk between adjacent pixel, high detection efficiency in the red spectral range, large area, low dark counting rate. Moreover to develop array with high number of pixel became more and more important to develop all the TCSPC electronics with picosecond resolution to create a new family of detection system for TCSPC applications. Recent advances in our research on single photon time resolved array is here presented.

8155B-115, Session 11

Deep ultraviolet (254 nm) focal plane arrays

E. Cicek, Z. Vashaei, R. P. McClintock, M. Razeghi, Northwestern Univ. (United States)

Below 290 nm the ozone layer absorbs nearly 100 percent of the solar energy reaching the earth. This creates a natural low background that is ideally suited for detection of man-made UV emission. In this study we report the development of the world's first high quantum efficiency back-illuminated 254 nm deep ultraviolet (UV) photodetectors and focal plane arrays (FPAs). We initially studied the novel pulse atomic layer deposition (PALE) technique to grow high quality crack free thick AlGaIn with high Al content, and we successfully realized the growth of a 600 nm thick Al_{0.6}Ga_{0.4}N:Si-In low-resistance UV-transparent lateral conduction layer on high quality AlN template layer. On top of this conduction layer a p-i-n active region consisting of 100nm n-Al_{0.58}Ga_{0.42}N followed by 200nm unintentionally doped Al_{0.55}Ga_{0.45}N and 50nm p-Al_{0.55}Ga_{0.45}N was grown. In order to form ohmic contacts, a thin highly doped p-GaN layer was deposited on the top of the device. Then the material was processed into single element detectors, and a 320 x 256 array of 25 μm x 25 μm pixels, with a unit cell size of 30 μm x 30 μm, by applying standard lithography techniques. Subsequently the back-illuminated FPAs are hybridized to a matching ISC 9809 silicon readout integrated circuit (ROIC). The device performance and the major technical issues associated with the realization of high-quality solar-blind FPAs are discussed in details and solutions to the major problems are outlined where available.

8155B-116, Session 11

Comparison of 16-channel laser photoreceivers for topographic mapping

M. A. Krainak, G. Yang, X. Sun, W. Lu, NASA Goddard Space Flight Ctr. (United States); X. Bai, P. Yuan, P. A. McDonald, J. C. Boisvert, R. L. Woo, K. Wan, R. Sudharsanan, Spectrolab, Inc. (United States); V. W. Aebi, D. F. Sykora, K. A. Costello, Intevac Photonics, Inc. (United States)

Topographic mapping lidar instruments must be able to detect extremely weak laser return signals from high altitudes including orbital distance. The signals have a wide dynamic range caused by the variability in atmospheric transmission and surface reflectance under a fast moving spacecraft. Ideally, lidar detectors should be able to detect laser signal return pulses at the single photon level and produce linear output for multiple photon events. Silicon avalanche photodiode (APD) detectors have been used in most space lidar receivers to date. Their sensitivity is typically hundreds of photons per pulse, and is limited by the quantum efficiency, APD gain noise, dark current, and preamplifier noise. NASA is pursuing three approaches for a 16-channel laser photoreceiver for use on the next generation direct-detection airborne and spaceborne lidars. We present our measurement results and a comparison of their performance.

8155B-111, Session 12

Superconducting single-photon detectors: devices and applications

B. Calkins, B. Baek, M. J. Stevens, N. A. Tomlin, A. E. Lita, A. Lamas-Linares, S. D. Dyer, V. B. Verma, S. Bradley, T. Gerrits, A. L. Migdall, R. P. Mirin, S. W. Nam, National Institute of Standards and Technology (United States)

In recent years, superconducting single-photon detectors have become an enabling technology for advanced experiments and applications in quantum optics and quantum information. In the years to come, they hold the promise of redefining optical power metrology and allowing ultra-sensitive imaging. In this talk, I will present work that our group at NIST has done with two types of cryogenic single-pixel single-photon detectors, coupled to optical fiber at room temperature. The Transition-Edge Sensor (TES) is a micro-calorimeter device operating at a temperature of ~0.1K, which converts the heat pulse of individual photons into a measurable signal. We fabricate these devices embedded in an optical cavity to maximize absorption at a design wavelength and have achieved > 95% end-to-end system detection efficiency at several target wavelengths in the near-IR, including 850 nm and 1550 nm. This efficiency makes possible multi-photon quantum correlation experiments which are nearly impossible with conventional single-photon detectors. In addition, the calorimeter design is inherently photon-number resolving, which enables certain photon-number heralding schemes and allows for super-resolved imaging with a single-pixel scan. The Superconducting Nanowire Single-Photon Detector (SNSPD) is an ultranarrow wire superconducting meander detector operating at a temperature of ~4K, which snaps into a resistive state with the impact of a single photon. The incredible speed and timing jitter (~30 ps FWHM) that these devices are capable of enables source-emission correlation and time-of-flight measurements at much higher resolution than traditional devices. Finally, I will discuss ongoing improvements that we are making to these devices and potential future applications.

8155B-113, Session 12

Increased detection efficiency with superconducting single photon detectors

R. Heeres, S. N. Dorenbos, V. Zwiller, Technische Univ. Delft (Netherlands)

We present several schemes that we have implemented to boost the detection efficiency of superconducting nanowire single photon detectors. The integration with plasmonics waveguides is particularly interesting as it enables the integration of complex quantum optics experiments all on a chip.

2011 Optics + Photonics

Optical Engineering + Applications

Technical Summaries

spie.org/op

Conference Dates: 21–25 August 2011

Exhibition Dates: 23–25 August 2011

San Diego Marriott Marquis and Marina, San Diego Convention Center
San Diego, California, USA

Connecting minds for global solutions

Contents

8121:	The Nature of Light: What are Photons? IV	2
8122:	Tribute to Joseph W. Goodman	15
8123:	Eleventh International Conference on Solid State Lighting	20
8124:	Nonimaging Optics: Efficient Design for Illumination and Solar Concentration VIII	33
8125:	Optomechanics 2011: Innovations and Solutions	39
8126:	Optical Manufacturing and Testing IX	47
8127:	Optical Modeling and Performance Predictions V	58
8128:	Current Developments in Lens Design and Optical Engineering XII; and Advances in Thin Film Coatings VII	63
8129:	Novel Optical Systems Design and Optimization XIV	68
8130:	Laser Beam Shaping XII	74
8131:	Optical System Alignment, Tolerancing, and Verification V	81
8132:	Time and Frequency Metrology III	87
8133:	Dimensional Optical Metrology and Inspection for Practical Applications	91
8134:	Optics and Photonics for Information Processing V	100
8135:	Applications of Digital Image Processing XXXIV	107
8136:	Mathematics of Data/Image Pattern Coding, Compression, and Encryption with Applications XIV	121
8137:	Signal and Data Processing of Small Targets 2011	126
8138:	Wavelets and Sparsity XIV	136
8139:	Advances in X-Ray/EUV Optics and Components VI	148
8140:	X-Ray Lasers and Coherent X-Ray Sources: Development and Applications	157
8141:	Advances in Computational Methods for X-Ray Optics II	169
8142:	Hard X-Ray, Gamma-Ray, and Neutron Detector Physics XIII	178
8143:	Medical Applications of Radiation Detectors	193
8144:	Penetrating Radiation Systems and Applications XII	199
8145:	UV, X-Ray, and Gamma-Ray Space Instrumentation for Astronomy XVII	204
8146:	UV/Optical/IR Space Telescopes and Instruments: Innovative Technologies and Concepts V	210
8147:	Optics for EUV, X-Ray, and Gamma-Ray Astronomy V	219
8148:	Solar Physics and Space Weather Instrumentation IV	233
8149:	Astronomical Adaptive Optics Systems and Applications V	241
8150:	Cryogenic Optical Systems and Instruments XIV	245
8151:	Techniques and Instrumentation for Detection of Exoplanets V	250
8152:	Instruments, Methods, and Missions for Astrobiology XIV	262
8153:	Earth Observing Systems XVI	272
8154:	Infrared Remote Sensing and Instrumentation XIX	290
8155A:	Infrared Sensors, Devices, and Applications	301
8156:	Remote Sensing and Modeling of Ecosystems for Sustainability VIII	311
8157:	Satellite Data Compression, Communications, and Processing VII	319
8158:	Imaging Spectrometry XVI	327
8159:	Lidar Remote Sensing for Environmental Monitoring XII	332
8160:	Polarization Science and Remote Sensing V	339
8161:	Atmospheric Optics: Turbulence and Propagation	349
8162:	Free-Space and Atmospheric Laser Communications XI	354
8163:	Quantum Communications and Quantum Imaging IX	362
8164:	Nanophotonics and Macrophotonics for Space Environments V	371
8165A:	Unconventional Imaging and Wavefront Sensing VII	377
8165B:	Adaptive Coded Aperture Imaging and Non-Imaging Sensors V	385

Conference 8121: The Nature of Light: What are Photons? IV

Monday-Thursday 22-25 August 2011 • Part of Proceedings of SPIE Vol. 8121
The Nature of Light: What are Photons? IV

8121-01, Session 1

A loophole in correlated photon statistics

A. F. Kracklauer, Private Consultant (Germany)

Experiments on correlated photon pairs, e.g., tests of Bell inequalities, are encumbered with the challenge of identifying valid pairs. Noise in the form of accidental coincidences between photons not produced as a correlated pair, must be excluded. Usually, this is thought to be achieved by both reducing the intensity of the pair-generation-stimulus so as to isolate genuine pairs with larger time buffer intervals, and then by selecting only pairs within as narrow a time window as is feasible (while retaining instrumental stability). Herein we present results of a study of a contravening phenomena, based on physically feasible models of photo detection, which surprisingly lead to enhanced corruption of the data using these two tactics. It will shown that to date taken data is compatible with the existence of this phenomena, so that done experiments must be considered inconclusive.

8121-02, Session 1

Toward an event-based corpuscular model for optical phenomena

H. De Raedt, F. Jin, Univ. of Groningen (Netherlands); K. F. L. Michielsen, Forschungszentrum Jülich GmbH (Germany)

We present an event-based corpuscular model (EBCM) of optical phenomena that does not require the knowledge of the solution of a wave equation of the whole system and reproduces the results of Maxwell's theory by generating detection events one-by-one. The EBCM gives a cause-and-effect description for every step of the process, starting with the emission and ending with the detection of the photon. By construction, the EBCM satisfies Einstein's criterion of local causality and allows for a realistic interpretation of the variables that appear in the simulation model. The EBCM is entirely classical in the sense that it uses concepts of the macroscopic world and makes no reference to quantum theory but is nonclassical in the sense that it does not rely on the rules of classical Newtonian dynamics. The key feature of our approach is that it uses adaptive processes to mimic the interaction of the particles with the optical components such as detectors, beam splitters etc. We demonstrate that one universal EBCM for the interaction of photons with matter suffices to explain the interference and correlation phenomena that are observed when individual photons are detected one by one. This EBCM gives a unified description of multiple-beam fringes of a plane parallel plate and single-photon Mach-Zehnder interferometer, Wheeler's delayed choice, photon tunneling, quantum eraser, two-beam interference, double-slit, Einstein-Podolsky-Rosen-Bohm and Hanbury Brown-Twiss experiments. Of course, this model produces the frequency distributions for observing many photons that are in full agreement with the predictions of Maxwell's theory and quantum theory.

8121-03, Session 1

Proposal for an interference experiment to test the applicability of quantum theory to event-based processes

K. F. L. Michielsen, M. Richter, T. Lippert, Forschungszentrum Jülich GmbH (Germany); B. Barbara, Institut NÉEL (France); S. Miyashita, The Univ. of Tokyo (Japan); H. De Raedt, Univ. of Groningen (Netherlands)

We propose a realizable single-particle Mach-Zehnder interferometer

experiment in which the path length of one arm can change before each passage of a particle through the interferometer. We demonstrate that the analysis of the time-series produced by this experiment can be used to determine to which extent quantum theory provides a description of the observed detection events that goes beyond statistical averages. This is important because quantum theory postulates that it is fundamentally impossible to give an explanation that goes beyond the description in terms of frequency distributions to observe events. Although in practice, it may be impossible to give such an explanation, the present state of knowledge does not support the premise that it impossible in principle. Moreover, as there exist event-based, locally causal corpuscular models that reproduce the statistical results of quantum theory for this experiment if the path lengths are fixed during experiment (the simplest one being given in De Raedt H., De Raedt K. and Michielsen K., Europhys. Lett., 69 (2005) 861), this premise is untenable. We also show that the proposed experiment may be used to refute whole classes of event-based, locally causal corpuscular models for optical phenomena.

8121-05, Session 1

Controversy among giants and a simple test regarding the "photon" nature of light

W. T. Rhodes, Florida Atlantic Univ. (United States)

On reading Ulf Leonhardt's book *Measuring the Quantum State of Light* shortly after its publication, I became interested in a conceptual tool described by Leonhardt designed to aid one in the understanding of the action of beam splitters in photon-starved systems. What intrigued me most about the model is that it suggested differences in the results of a low-light-level demonstration of the photon-by-photon development of Young's fringes, depending on whether a lossless beam-splitter attenuator is placed directly after the source point or is placed directly before the two pinholes. At a meeting on quantum optics soon thereafter, I brought my observation to the attention of two giants in the area of the quantum state of light. One, without hesitation, said to me concerning my conjecture, "You are absolutely right." The other, with equal absence of hesitation, declared me "Wrong." The presence of controversy on this issue is interesting in itself. The availability of a simple experiment-which I shall describe in this talk-for testing the concept is potentially important.

8121-06, Session 2

Gauss's Law for gravity and observational evidence reveal no solar lensing in empty vacuum space

E. H. Dowdye, Jr., Pure Classical Physics Research (United States)

An application of the Mathematical Physics of Gauss's Law for gravity along with intense observational evidence, reveal that solar lensing does not occur in the empty vacuum space slightly above the plasma rim of the sun. The thin plasma atmosphere of the sun represents a clear example of an indirect interaction involving an interfering plasma medium between the gravitational field of the sun and the rays of light from the stars. There is convincing observational evidence that a direct interaction between light and gravitation in the empty vacuum space above the solar rim simply does not occur. Historically, all evidence of light bending has been observed predominantly near the thin plasma rim of the sun; not in the empty vacuum space far above the thin plasma rim. An application of Gauss' law clearly shows that, if the light bending rule of General Relativity were valid, then a light bending effect due to the gravitational field of the sun should be easily detectable with current technical mean in Astrophysics at various analytical Gaussian spherical surfaces of

**Conference 8121:
The Nature of Light: What are Photons? IV**

solar radii, namely, 2R, 3R, 4R, 5R, ..., respectively, where R is one solar radius. An effect of at least one half, one third, one fourth, one fifth, etc., respectively, of the observed light bending noted at the solar rim within currently technical means should be easily observable effects. We note that a gravitational bending effect on the rays of starlight is yet to be observed by modern astronomical means at these distances just slightly above the plasma rim of the sun; a clear violation of the light bending rule of General Relativity. Moreover, the events taking place at the center of our galaxy under intense observations by the astrophysicists since 1992, present convincing evidence that a direct interaction between light and gravitation simply does not take place. The highly studied region, known as Sagittarius A*, is thought to contain a super massive object or a black hole, a most likely candidate for gravitational lensing. The past two decades of intense observation in this region have revealed not a shred of evidence for gravitational lensing. The evidence is clearly revealed in the time resolved images of the rapidly moving stellar objects orbiting about Sagittarius A*.

8121-07, Session 2

The high-velocity version of classical mechanics

R. T. Dorn, Independent Researcher (United States)

A good understanding of the actual mechanism for the attraction between an electron and positron is necessary for the study of electron - positron phenomenon such as annihilation and pair production. This "action at a distance" force has mathematical descriptions, but the underlying phenomenon is really not well understood. Our intuitive understanding of how force is delivered through the action of an impulse comes from our everyday experience and is described by Newton's Laws. If we extend this classical mechanical line of reasoning to these more mysterious forces, it leads to the derivation of a high velocity version of $F = ma$. The basis of this model is Newton's notion that gravity could be attributed to multiple impacts of invisible bodies. In this model it is assumed that such an acceleration field is made up of tiny bodies that travel at the speed of light and that these bodies deliver energy to accelerated particles by elastic collisions. The result is a model that is similar to relativistic equations and predicts a maximum velocity for the accelerated particle.

8121-08, Session 2

Alternative realization for the composition of relativistic velocities

M. Fernández-Guasti, Univ. Autónoma Metropolitana-Iztapalapa (Mexico)

The reciprocity principle requests that if an observer, say in the laboratory, sees an event with a given velocity, another observer at rest with the event must see the laboratory observer with minus the same velocity. The composition of velocities in the Lorentz-Einstein scheme does not fulfil the reciprocity principle because the composition rule is neither commutative nor associative. In other words, the composition of two non-collinear Lorentz boosts cannot be expressed as a single Lorentz boost but requires in addition a rotation. The Thomas precession is a consequence of this composition procedure. Different proposals such as gyro-groups have been made to fulfil the reciprocity principle.

An alternative velocity addition scheme is proposed consistent with the invariance of the speed of light and the relativity of inertial frames. An important feature of the present proposal is that the addition of velocities is commutative and associative. The velocity reciprocity principle is then immediately fulfilled. This representation is based on a transformation of a hyperbolic scator algebra. The proposed rules become identical with the special relativity addition of velocities in one dimension. They also reduce to the Galilean transformations in the low velocity limit. The Thomas gyration needs to be revised in this nonlinear realization of the special relativity postulates. The deformed Minkowski metric presented here is compared with other deformed relativity representations.

8121-59, Session 2

Relativity: a pillar of modern physics or a stumbling block

G. S. Sandhu, Independent Researcher (India)

Currently, the theory of Relativity is being regarded as one of the main pillars of Modern Physics, essentially due to its perceived role in high energy physics, particle accelerators, relativistic quantum mechanics, and cosmology. Since the founding assumptions or postulates of Relativity and some of the resulting consequences confound the logic and common sense, a growing number of scientists are now questioning the validity of Relativity. The advent of Relativity has also ruled out the existence of the 19th century notion of aether medium or physical space as the container of physical reality. Thereby, the Newtonian notions of absolute motion, absolute time, and absolute reference frame have been replaced with the Einsteinian notions of relative motion, relative time, and inertial reference frames in relative motion. This relativity dominated viewpoint has effectively abandoned any critical study or advanced research in the detailed properties and processes of physical space for advancement of Fundamental Physics. In this paper both special theory of relativity (SR) and general relativity (GR) have been critically examined for their current relevance and future potential. We find that even though Relativity appears to be a major stumbling block in the progress of Modern Physics, the issue needs to be finally settled by a viable experiment [Phys. Essays 23, 442 (2010)] that can detect absolute motion and establish a universal reference frame.

8121-10, Session 3

Planck's constant h not only governs atomic shell energies, moreover, is also responsible for the neutrons and protons internal structure (charge and size)

E. H. Berloff, Leopold-Franzens-Univ. Innsbruck (Austria)

The discrepancy between the neutron's inherent magnetic flux and the flux quantum lead to a new model for the internal structure of neutrons and protons. A highly charged core Mass X is surrounded by 4 tetrahedral arranged π^0 mesons. Nuclear forces are of repelling character. Coulomb forces keep the system in balance and attempts due to collisions enlarging the system are compensated by bubbling out electrons from the core mass X. The neutrons decay is core charge dependent. A core charge asymmetry gives the proton its macroscopic charge; it shrinks until the core charge reaches 47.e.

8121-11, Session 3

The physical origin of the uncertainty theorem

A. Giese, Consultant (Germany)

Elementary particles can be explained by an interpretation of quantum mechanics that is based upon that of Louis de Broglie, the discoverer of the wave properties of a particle.

According to this, elementary particles can be described using a predominantly classical model. This model is derived from the presence of relativity in all matter, and furthermore from properties such as mass, spin and magnetic moment. According to this model an elementary particle is made up of a pair of sub-particles which orbit each other. The internal field which binds the sub-particles extends outward from the particle. It causes the particle to appear from the outside like a wave, and to undergo interference, for example when passing through a double slit. This understanding conforms to the approach of Louis de Broglie, who characterized the external part of the alternating field as a "pilot wave".

The problem with measuring the dynamic parameters of an elementary particle is that those parameters are determined by the reaction of its surrounding wave. This surrounding wave on the one hand extends

Conference 8121:
The Nature of Light: What are Photons? IV

outward from the particle, but on the other hand it is locally concentrated around the position of the particle. This fact, the spatial delimitation, limits the determination of the wave parameters using the rules of the Fourier transform. Hence it reduces the information that can be obtained about the parameters to a degree described by the uncertainty relation. The properties of the particle itself, however, are not at all uncertain in this view.

This derivation of uncertainty does not support the very general consequences drawn from the uncertainty principle as used by contemporary QM.

To apply this understanding to the photon, we have to assume that the photon has a kind of core, like leptons and quarks. This gives rise to further questions which need to be discussed.

8121-12, Session 3

Microscope and spectroscopy results are not limited by Heisenberg's Uncertainty Principle!

N. S. Prasad, NASA Langley Research Ctr. (United States)

A reviewing of many published experimental and theoretical papers demonstrate that the resolving powers of microscopes, spectroscopes and telescopes can be enhanced by orders of magnitude better than old classical limits by various advanced techniques including de-convolution of the CW-response function of these instruments. Heisenberg's original analogy of limited resolution of a microscope, to support his mathematical uncertainty relation, is no longer justifiable today. Modern techniques of detecting single isolated atoms through fluorescence also over-ride this generalized uncertainty principle. Various nano-technology techniques are also making atoms observable and location precisely measurable. Even the traditional time-frequency uncertainty relation or bandwidth limit can be circumvented while doing spectrometry with short pulses by deriving and de-convolving the pulse-response function of the spectrometer just as we do for CW input.

8121-13, Session 3

Arising of the entangled photon in the one-dimensional high finesse nanocavity

V. F. Cheltsov, Moscow State Mining Univ. (Russian Federation);
A. Cheltsov, Q-MOL LLC (United States)

This work is a continuation of papers presented by the author at the Optics and Photonics Symposium (2009) and is devoted to the case of the high finesse nanocavity with the average photon escaping rate $\Gamma = \eta c/R \ll g$ -coupling constant. The case is of special interest as possible pretender for a qubit in quantum computers. The probability distribution to find photon in the (ω, t) -space, investigated in the interval $0 \leq \Gamma/4g \ll 1$ has triplet structure with very low central peak and satellites at frequencies $\approx (\omega \pm g)$. The latter emerge as result of emission from two upper atomic split sublevels. The peak is produced by ensuing reabsorptions of satellites by atom through its upper sublevels. Oscillating as $t^2 \cos(gt)$ and decaying fast, the peak is accompanied with the simultaneously arising satellites. When the peak disappears the satellites become stationary. The steady state is quenched with continuum of final states. The profile of structure consisting of two identical components has the time-dependence $t \exp(-t/4)$ and the spectral width of satellites is by order less than the distance between them. These components with frequencies $(g \pm \omega)$ have the average photon energies equal to $1/2(g \pm \omega)$ where factor "1/2" accounts for normalization condition. The satellites amplitudes reach maximum at $\Gamma/4g = 0.05$. The profile of this structure has been found to have the form $t \exp(-t/4)$ with maximum attained for $\Gamma/4g = 0.05$ and average photon cavity life-time proportional to $4 \ln 2$. We named the structure "entangled photon".

8121-14, Session 4

Interplay between theories of quantum classical signals: classical representation of entanglement

A. Y. Khrennikov, Linnaeus Univ. (Sweden)

We present a model, prequantum classical statistical field theory (PCSFT), which provides a classical random signal representation of quantum correlations, including correlations for entangled quantum systems. This talk is dedicated to Einstein's vision of physics and specifically his hope for what quantum theory could and, in his view, should be. In particular, two of Einstein's dreams about the future of quantum theory are realized in this book: reduction of quantum randomness to classical ensemble randomness and total elimination of particles from quantum mechanics (QM) — creation of a field model of quantum phenomena (cf., e.g., Einstein and Infeld). Thus, contrary to a number of the so-called "no-go" arguments and theorems advanced throughout the history of quantum theory (such as those of von Neumann, Kochen-Specker, and Bell), quantum probabilities and correlations can be described in a classical manner. There is, however, a crucial proviso. While this I argue that QM can be interpreted as a form of classical statistical mechanics (CSM), this classical statistical theory is not that of particles, but that of fields.

8121-15, Session 4

Understanding the masses of elementary particles: a step towards understanding the massless photon

K. O. Greulich, Fritz Lipmann Institute (Germany)

A so far unnoticed simple explanation of elementary particle masses is given by $m = Z \cdot m_{\text{electron}}/\alpha$, where $\alpha (= 1/137)$ is the fine structure constant or coupling constant of quantum electrodynamics.

$Z = 3(M - L/2) + S$, where $M = 1, \dots, 12, 24, 26$ and $S = 1, 2, 3$ depending on the strangeness of the particle and $S = 0, L = 1$ for leptons and the nucleon. The mass at rest is identical to the gravitational potential of two Planck masses at a distance of the deBroglie wavelength of the particle. Photons can be described similarly when the Planck masses are replaced by hypothetical massless objects.

Literature:

Greulich, K.O. Calculation of the masses of all fundamental elementary particles with an accuracy of approximately 1% J Mod Phys 1, 300 - 302 (2010)

http://www.fli-leibniz.de/www_kog/ Then click "Physics"

8121-17, Session 4

Quantum points/patterns, part 1: from geometrical points to quantum points in sheaf framework

M. G. Zeitlin, A. N. Fedorova, Institute of Problems of Mechanical Engineering (Russian Federation)

We consider some generalization of the theory of quantum states, which is based on the analysis of long standing problems and unsatisfactory situation with possible interpretations of quantum mechanics. We demonstrate that the consideration of quantum states as sheaves can provide, in principle, more deep understanding of some phenomena. The key ingredients of the proposed construction are the families of sections of sheaves with values in the category of the functional realizations of infinite-dimensional Hilbert spaces with special (multiscale) filtration.

The questions we hope to answer are:

Conference 8121:
The Nature of Light: What are Photons? IV

- i) How may we enlarge the amount of (physical) information stored in one (quantum) physical point?
- ii) Relation between structureless geometrical points and physical points (or point objects like (point) (particles) with rich (possible hidden) structure.
- iii) How we may resolve (physical) point/quantum state to provide such a structure.
- iv) A new look in new framework for localization, entanglement, measurement, and all that.
- v) How we may explain/re-interpret a standard zoo of standard interpretations/phenomena (multiverse, wave functions collapse, hidden parameters, Dirac self-interference, ensemble interpretation, etc) of Quantum Mechanics in the new framework.

The goal of the first part (of two) is to compare the following key objects which are basic for any type of the exposition of Quantum Mechanics (and other related areas): Geometrical points vs. Physical Points (or Point Objects, or One-Point-Patterns); Point functions vs. Sheaves; Partial Differential Equations (and proper orthodox approaches) vs. Pseudodifferential Equations (via Microlocal analysis and all that). We will continue heuristic Part 1 by more technical Part 2 where we compare: Fourier/Gaussian modes vs. (pretty much) Localized (but non-gaussian) Physical Modes; Fourier Analysis vs. Local Nonlinear Harmonic Multiscale Analysis (including wave- and other -lets and multiresolution); Standard Quantum Images vs. Quantum Patterns generated by Multiresolution and as a final point, Categorification Procedure(s) for Quantum Mechanics.

8121-18, Session 4

Quantum points/patterns, part 2: from quantum points to quantum patterns via multiresolution

A. N. Fedorova, M. G. Zeitlin, Institute of Problems of Mechanical Engineering (Russian Federation)

It is obvious that we haven't any unified framework covering a zoo of (mostly) discrepant interpretations of QM, as well as satisfactory explanation/understanding of main ingredients of a phenomena like entanglement, etc.

The starting point is an idea to describe the key object of the area, namely point objects (physical points). Usually, for the modeling of real physical point objects, one can consider equivalence between them and standard geometrical points.

As direct consequence, our dynamical variables (wave function or density matrix or the Wigner function) are described by means of point functions. It seems reasonable to have the rich structure for a model of the (quantum) physical point (particle) in comparison with the structureless geometrical point.

All above looks like Physical Hypothesis but it is more or less well known from the mathematical point of view if we accept the right (Wigner-Moyal) picture. In that framework, Strict Deformation Quantization approach, all equations are pseudodifferential and as immediate consequence we need to change point functions by sheaves what provides the clear resolution of the (Physical) Point: as a result it is no more structureless but acquires the rich (possible hidden at first glance) structure. In such an approach Quantum States are (roughly speaking) sections of the coherent sheaves or contravariant functors from the proper category describing space-time to other one properly describing the complex dynamics of Quantum States/Patterns. The objects of this category are some filtrations on the Hilbert space of States.

Definitely, we need a proper analytical/numerical machinery to realise such approach. We present a family of methods which can describe the creation of nontrivial states (patterns), localized, chaotic, entangled or decoherent, from the basic localized (nonlinear) eigenmodes which are more realistic for the modeling of quantum dynamical process than the orthodox linear gaussian-like coherent states.

8121-61, Poster Session

Shapiro Delay: a frequency dependent transit time effect; not a 4D space-time effect

S. Ghazanshahi, California State Univ., Fullerton (United States); E. H. Dowdye, Jr., Pure Classical Physics Research (United States)

First noticed by Irvin L. Shapiro in 1964, the transit time required for a microwave signal to propagate through space, arrive at a satellite orbiting Venus or Mercury, required a measurable time delay for the reply signal to propagate back to the earth to be received at the antenna of the observatory. The time delay was noticeably affected by the relative position of the sun. Controlled measurements conducted by Shapiro determined that the time-tagged microwave signals had measurable effects that varied as a function of the impact parameter of the microwave beam relative to the sun. The delays were observed to be in the 100's of microseconds when the impact parameter of the microwave beam was at a minimum. After repeated measurements, varying time delays were recorded and were referred to as the Shapiro delay. These measurements permitted a precise determination of the electron density profile of the solar wind as a function of the radial distance r from the sun. Significant findings reveal that, for all microwave signals propagating in the solar wind atmosphere of the solar system, the waves are subjected to a frequency dependent plasma index of refraction n that exceeds unity, i.e., $n > 1.0000000000$. For optical, IR and UV wavelengths, the plasma index of refraction is practically $n = 1.0000000000$ and these wavelengths are virtually unaffected by the widespread atmosphere of the expanding solar wind described by the electron density profile. Thus, the Shapiro delay is a frequency dependent transit-time effect and cannot be a space-time effect of General Relativity since it is independent of frequency.

8121-62, Poster Session

Explanation of relativistic phenomena on the basis of interactions of particle energy, applied energy, and field energy

V. P. Fernando, Natural Philosophy Alliance (Canada)

The present dynamic theory identifies that in parallel with position related, gravitational energy finding expression in terms of the universal constant G , the energy of motion finds expression in terms of the universal constant c . Constant c , primarily is the determinant of structural configurations of energy of motion, internal energy of particles, and of photons, in a multiplicity of ways. The value c , enters into expression of relativistic phenomena as the ratio of energy of motion Mvc and particle energy Mc^2 . This ratio is $(v/c)/(1-v^2/c^2)^{1/2}$. Gamma-factor arises because, energy of motion pc (applied to overcome the inertia M of the particle), itself has inertia $m = pc/c^2$, which classical mechanics has omitted to simplify physics of slow motion. By rectifying such omissions and defects in the classical conceptual framework, and discerning that interactions of gravitation as well as motion are regulated by two specific algorithms, all principal relativistic phenomena are explained dynamically. These algorithms show that the stability of configuration of a system is attained by induction of energy from the universal field. These algorithms also provide the insight that phenomena related to motions of photons, such as aberration, and physical basis Fresnel's formula too are regulated by similar algorithms.

8121-63, Poster Session

Diffraction described by virtual particle momentum exchange: the "diffraction force"

M. J. Mobley, Arizona State Univ. (United States)

Particle diffraction can be described by an ensemble of particle paths

**Conference 8121:
The Nature of Light: What are Photons? IV**

determined through a Fourier analysis of a scattering lattice where the momentum exchange probabilities are defined at the location of scattering, not the point of detection. This description is compatible with optical wave theories and quantum particle models and provides deeper insights to the nature of quantum uncertainty. In this paper the Rayleigh-Sommerfeld and Fresnel-Kirchoff theories are analyzed for diffraction by a narrow slit and a straight edge to demonstrate the dependence of particle scattering on the distance of virtual particle exchange. The quantized momentum exchange is defined by the Heisenberg uncertainty principle and is consistent with the formalism of QED. This exchange of momentum manifests the “diffraction force” that appears to be a universal construct as it applies to neutral and charged particles. This analysis indicates virtual particles might form an exchange channel that bridges the space of momentum exchange.

8121-19, Session 5

Wave-particle duality: not in optical computing

H. J. Caulfield, Fisk Univ. (United States)

The much-discussed wave-particle duality permits operations that are pure wave or pure particle, with no ambiguity. As wave operations with passive components do not require energy, it is possible to make a number of zero energy devices. The most recent of these is Boolean logic. Like most opticians, I have never encountered a situation in which I am genuinely puzzled about whether any particular operation is done in the wave domain or in the particle domain (photons). Only recently did I figure out the types of computations that can be done in the wave domain - saving time, energy, speed, and so on. One approach that can be done in the wave domain is to find computations that do what nature does (Unitary Transformations). For two years now, I have known how to do logic in the wave domain, and was somewhat puzzled. After all, everyone knows that Boolean logic requires a nonlinear operation that, to my knowledge, requires a nonlinearity. As is often the case, what everybody knows is not true. So I have sought and will report here the solution. We can do Boolean logic in the wave domain, but not the way everyone has thought it should be done. Once again, we must formulate the question carefully if we seek to have nature provide us the answer. The solution is one of the many three-step processes found in technology. In this case it is of the form:

Particle (Input) → Wave (Lookup Table) → Particle (Detection)

As should be clear, the particle operations require energy dissipation, but the wave operation can be done at zero energy but only in optics.

8121-20, Session 5

On information transmitted using a photon

S. C. Kak, Oklahoma State Univ. (United States); P. Verma, G. MacDonald, The Univ. of Oklahoma - Tulsa (United States)

We present new research providing the basis of transmission of information using polarization states of photons and its application in cryptography. Current quantum cryptography applications are based on the BB84 protocol which is not secure against photon siphoning attacks. Recent research has established that the information that can be obtained from a pure state in repeated experiments is potentially infinite. This can be harnessed by sending a burst of photons confined to a very narrow time window and whereas conventional view would be that such a narrow burst would carry a single bit of information. The proposed method represents an entirely new way of transmitting secret information, with potentially significant applications to cryptography and communications. While polarization shift-keying methods have been proposed earlier, our method is somewhat different in that it proposes to discover the polarization state of identical photons in a burst from a laser which codes binary information.

8121-21, Session 6

The extraterrestrial casimir effect

R. C. Storti, Delta Group Engineering, P/L (Australia)

Application of the Electro-Gravi-Magnetic (EGM) Photon radiation method to the Casimir Effect (CE), suggests that the experimentally verified (terrestrially) neutrally charged parallel-plate configuration force, may differ within extraterrestrial gravitational environments from the gravitationally independent formulation by Casimir. Consequently, the derivation presented herein implies that a gravitationally dependent CE may become an important design factor in nanotechnology for extraterrestrial applications (ignoring finite conductivity + temperature effects and evading the requirement for Casimir Force corrections due to surface roughness).

8121-22, Session 6

Doppler phenomena determined by photon-cosmic field interactions

V. P. Fernando, Natural Philosophy Alliance (Canada)

The principle of conservation of energy in all interactions of matter or photons in motion, can be accounted for, only if an inflow or outflow of energy from the cosmic field is assumed. This paper by discerning the algorithm of gravitation, first traces out how energy from the cosmic field alters the frequency, hence time of an atomic clock in a GPS satellite orbit. Then by discerning an analogous algorithm, it demonstrates how inflow of energy from the cosmic field underlies Fresnel's result when a photon passes through a moving medium. Michelson-Morley experiment was warranted by the mathematical finding based on kinematic concepts, of the second order difference in the frequency, between the two cases - observer at rest and the source of light moving, and vice-versa. The dynamic reality is that momentum mc of a photon cleaves into two parts (active and passive). When the observer is moving towards the source, the active part acquires the value $m(c-v)$ and the other $+mv$, and when the observer moves away, the active part acquires the value $m(c+v)$ and the other $-mv$. This renders the second order difference sought in the Michelson experiment to be redundant. Further, in the final result the velocity of light remains constant at c , instead the frequency changes, in conformity to Planck's law $E = hf$, and confirms that there is an inflow and an outflow of energy respectively in the two cases, from the Cosmic Energy Field. An integral explanation of Doppler shift and Aberration is offered.

8121-23, Session 6

The constancy of c everywhere requires space to be a stationary and complex tension field

C. Roychoudhuri, Univ. of Connecticut (United States); A. M. Barootkoob, Independent Consultant (United States)

If photons are perpetually propagating classical wave packets moving with the extreme velocity “ c ”, then it requires a sustaining complex cosmic tension field (C2TF), which is stationary everywhere. Then Michelson-Morley experiment should naturally produce null results except for minute Fresnel drags being within the Earth's atmosphere. Further, if C2TF has a built-in weak dissipative property towards electromagnetic waves, its frequency should decrease slowly with the distance of propagation through the C2TF, which would eliminate the need for the hypothesis of “expanding universe”. We will present appropriate mathematical relations along with a suitable wave equation whose solution incorporates the Hubble constant that does not require Doppler shift. The success of this hypothesis would imply that stable particles are complex 3D resonant oscillations of the C2TF, eliminating the need to have the hypothesis of “wave-particle duality”.

Conference 8121:
The Nature of Light: What are Photons? IV

8121-24, Session 6

About luminiferous world ether

P. O. Demyanenko, National Technical Univ. of Ukraine (Ukraine)

In the physics of electromagnetic (EM), and specifically, light waves, uncertain situation takes place: the waves actually exist, but medium of their occurrence is not determined.

Persistent experimental investigations of demonstration of luminiferous ether physical properties were always ineffective. Taking it into account as well as an absence of any privileged coordinate system in the Universe to link ether, Einstein proposed generally to reject this concept and exclude it from science usage. EM waves herewith should be considered as definite self-contained physical objects.

With the lapse of time this situation became usual one, however it could not be satisfactory in world view context. Thus "waves" are the changes in medium's state (its disturbance), which propagate within the medium and carry the energy. This entire means that existence of waves beyond the medium is nonsense.

Analyzing the problems as to EM ether and waves, we propose the hypothesis, which can consistently associate all set of problems. In accordance with our hypothesis the concept of structure of our world (OW) should be revised. If we accept the structure of OW in accordance with our hypothesis, we do not need in certain "ether-medium" for providing the condition for exiting of EM waves. There these waves exist due to existence of properly arranged OW. Traditional concept of ether is not a "medium", which can fill by itself usual 3D space (volume) in OW, but a separate entity, which could be considered as a constituent part of OW, but not a filling part. This concept allows determining OW with the time elapsed over it as a certain 3D-frontier between other changeless in time worlds.

8121-25, Session 6

The necessity of two fields in wave phenomena

M. Fernández-Guasti, Univ. Autónoma Metropolitana-Iztapalapa (Mexico)

Wave phenomena involve perturbations whose behaviour is equivalent in space and time. The perturbations may be of very different nature but they all have to conform with the notion of a field, that is, a scalar or vector quantity defined for all points in space. Some wave phenomena are described in terms of only one field. For example water waves where the perturbation is the level above or below from the equilibrium position. Nonetheless, electromagnetic waves require the existence of two fields. I shall argue that in fact, all wave phenomena involve two fields although we sometimes perform the description in terms of only one field.

To this end, the concept of cyclic or dynamical equilibrium will be put forward where the system continuously moves between two states where it exchanges two forms of energy. In a mechanical system it may be, for example, kinetic and potential energy. Differential equations that form an Ermakov pair require the existence of two linearly independent fields. These equations possess an invariant. For the time dependent harmonic oscillator, such an invariant exists only for time dependent potentials that are physically attainable.

According to this view, two fields must be present in any physical system that exhibits wave behaviour. In the case of gravity, if it exhibits wave behaviour, there must be a complementary field that also carries energy. It is also interesting that the complex cosmic tension field proposed by Chandrasekar involves a complex field because complex functions formally describe two complementary fields.

8121-26, Session 7

The nature of the photon in the view of a generalized particle model

A. Giese, Consultant (Germany)

The particles on which particle physics generally focuses are leptons and quarks. In accelerators, leptons, quarks, and those particles which are composed of quarks (e.g. mesons) are investigated.

Using the properties of particles, such as their mass, spin and magnetic moment, and from the relativistic behaviour of matter - which can be derived from the 'zitterbewegung' of the electron - we can draw up a model in which a particle is composed of a pair of sub-particles which orbit each other. This model conforms to the quantum mechanical concepts of Louis de Broglie. It replaces the idea of particle-wave duality, based upon Heisenberg's interpretation of QM, by the so-called pilot wave. The particle model allows the properties of particles to be described using concepts derived to a considerable extent from classical physics. This includes the precise determination of the mass and the magnetic moment of the particle without resorting to a Higgs field, vacuum polarization, or similar QM devices.

If we apply this particle model, which has been developed for leptons and quarks, to the photon, then this has some specific implications. A logical consequence of it is that the photon, too, must be composed of sub-particles orbiting each other. - The talk will discuss the aspects of the photon for which this model can help our understanding of it and those for which our understanding may be complicated.

8121-27, Session 7

The birth of a photon

K. O. Greulich, Fritz Lipmann Institute (Germany)

A step towards better understanding the physics of the photon is to consider how it is emitted from a single atom or molecule. Quantum mechanics describes this by a photon generation operator which is blind for details of this process. Before emission, the photon energy is concentrated in a sub - Angstrom³ volume. Since even a beam of single optical photons is diffracted by a micrometer slit, some time later it must "fill" a micrometer³ volume. This statement is independent on whether one regards the photon as point like with a spatial uncertainty given by the Heisenberg relationship or as a wavepacket with micrometer dimension. In any case, the energy density decreases by 12 orders of magnitude. The process resembles rather a vigorous explosion than typical textbook representations. What may be the time course of this expansion? Is it instantaneous as quantum mechanics may suggest or does it proceed with the speed of light? Why does it stop, i.e why is the energy not diluted to infinity? What experiments could answer such questions? What consequences has this for a model of the photon?

Literature:

Greulich KO The emission of a single photon from a single atom or molecule - An experimenter's view Single Mol 2002 3.1, 19-23
http://www.fli-leibniz.de/www_kog/ Then click "Physics"

8121-28, Session 7

Non-equilibrium mechanisms of light in the microwave region

J. H. J. Mortenson, General Resonance, LLC (United States)

A significant advance in quantum mechanics - the discovery of Einstein's hidden variables - was presented at the previous meeting. These discoveries are providing a richer and more classical understanding of interactions between light and matter. This New Physics has revealed that what was described in the past as the "photon", is not really an elementary particle of light. Previous definitions inadvertently limited various degrees of freedom and attributed the property of indivisibility

**Conference 8121:
The Nature of Light: What are Photons? IV**

to what is actually a collection of elementary light particles. The true elementary “particle” of light is the single wave of light, i.e., a single oscillation of electromagnetic energy.

Quantum chemists however, relying on prior incomplete photon concepts, hypothesized that photon energies equal to or greater than bond energies were necessary to produce chemical or material reactions. Light in the microwave region was therefore theorized to exert only thermal effects in such reactions. Numerous experiments with microwaves suggested otherwise, however, but no quantum mechanical framework existed to explain any non-thermal or non-equilibrium mechanisms. In the absence of a mechanistic explanation, the clear and reproducible experimental evidence was simply disregarded by many scientists.

The recent advances in quantum mechanics have now provided a firm mechanistic framework for the explanation of non-equilibrium and non-thermal effects by microwaves. These non-equilibrium mechanisms include resonant absorption, resonant electron stimulation, and resonant acoustic transduction, thereby providing rational frameworks for many previously unexplained experimental results. This New Physics dramatically expands the reach of practical engineering applications beyond the previous limitations of photochemistry and into lower frequency regions of the electromagnetic spectrum.

8121-29, Session 8

Creation and fusion of photons

A. Meulenberg, Jr., S. Ramadass, Univ. Sains Malaysia (Malaysia)

Light, from a star, begins as a photon. Fusing with uncountable others, it forms a minuscule component of a spherical wave that eventually is better represented as a plane wave. Moving further through the universe, its energy density drops until it begins to recombine into photons. This paper seeks to learn about the interaction of light with light (and with matter) during this process. The Hanbury Brown Twist (HBT) Effect gives a model for the observed nature of stellar light that has traveled across the universe. What are the physical mechanisms underlying this model? Comparison is made with both laser light and that from atomic radiation.

Keys to the ‘coherence’ length observed and measured in non-solar stellar light is the low convergence angle from the source and perhaps the distance from the source. How much interaction does light have with matter during its cross-universe transit? If it is not insignificant, then the thought that the HBT effect could be light interacting with light must be reexamined.

Maxwell did not believe in photons. Therefore his equations, based on the wave nature of light, did not include any nonlinearities, or boundary conditions, that could lead to photonic structures. His equations are complete, relativistically correct, and unchallenged after nearly 150 years. However, even though his far-field solution has been considered as the basis for photons, it is probable that radiation from atomic electrons are not quite what many ‘classical’ models try to represent as the source of photons.

8121-30, Session 8

Birth of a two-body photon

R. T. Dorn, Independent Researcher (United States)

The two body photon model assumes that an electron and a positron have been accelerated to the speed of light. The tenets of relativity theory would lead one to believe this to be impossible. It has long been thought that a body cannot be accelerated to the speed of light because the relativistic mass would become infinite. This conceptual problem is addressed with the realization that it is not necessary to resort to the concept of a velocity dependent mass. Instead, the force could be considered to be velocity dependent. The relativistic equations of motion can be rearranged and interpreted such that the force varies with velocity instead of the mass. When the velocity reaches the speed of light, instead of dividing by zero and interpreting the equations as implying a nonphysical infinite mass, the equations show a finite mass with an

applied force of zero. The equations can still take on the indeterminate form of 0/0, but standard mathematical analysis of this situation will show that the equations predict that a body can reach the speed of light. Furthermore, under the influence of an inverse square force, a body can be accelerated to the speed of light over very short distances and provide the initial conditions necessary for the birth of a two body photon.

8121-31, Session 8

A wave theory of the photoelectric effect

H. H. Lindner, Consultant (United States)

The author will demonstrate that the photoelectric and Compton effects are best explained by a wave theory of light and electrons. Light is a spreading wave in electromagnetic (EM) space. Electrons are not particles but are extended EM wave-structures. Electrons absorb and emit light in discrete wave-packets. Once emitted, the wave-packet begins to spread by diffraction like all radiation. The wave-packet that an electron absorbs is the product of superpositioning of the source waves and background EM radiation of all frequencies (vacuum fluctuations). This quantization is electronic, not luminal. Planck’s constant, h , is an electron-structure constant and does not refer to freely propagating light itself.

8121-32, Session 8

The conservation of light’s energy, mass, and momentum

J. H. J. Mortenson, General Resonance, LLC (United States)

The discovery of Einstein’s hidden variables was presented at the previous “Nature of Light” meeting, and revealed that Max Planck’s famous quantum formula, “ $E = h\nu$ ”, was incomplete (“ E ” is energy, “ h ” Planck’s action constant, and “ ν ” frequency). Planck assumed the formula as a given to derive the black body radiation function. A minor mathematical irregularity led Planck to use an abbreviated quantum formula, rather than his original quantum relationship, “ $E = h \nu t$ ” (“ h ” is the energy constant for light, and “ t ” the measurement time variable).

Unaware of the mathematical issue, many struggled with interpretation of the action constant in regards to energy, mass and momentum. Although Einstein described the conservation of energy and mass, his framework was necessarily incomplete because of the hidden energy constant. De Broglie attempted to provide a complete picture for the conservation of energy, mass and momentum, however he encountered the same difficulties, bemoaning that it was “impossible to consider an isolated quantity of energy”.

With the newly discovered energy constant such consideration is now possible. The paradox of light’s rest mass yields to simple calculation - 7.372×10^{-51} kg/oscillation - within the same order of magnitude as Luo’s calculated upper limits for photon mass. Bending of light by massive gravitational objects becomes a natural, mechanical consequence of the gravitational attraction between light’s mass and matter. Momentum of light (2.21×10^{-42} kg m/sec oscillation) is readily determined, and the conservation of energy, mass and momentum for both matter and light emerges in a mechanical framework.

8121-33, Session 8

Analysis of spectrometric data and detection processes corroborate photons as diffractively evolving wave packets

N. Tirfessa, Manchester Community College (United States); C. Roychoudhuri, Univ. of Connecticut (United States)

In a previous paper [Proc. SPIE Vol.6372-29 (2006), “Do we count

Conference 8121:
The Nature of Light: What are Photons? IV

indivisible photons or discrete quantum events experienced by detectors?], we have proposed that photons are diffractively evolving classical wave packet as a propagating undulation of the Complex Cosmic Tension Field (C2TF) after the excess energies are released by atomic or molecular dipoles as perturbations of the C2TF. The carrier frequency of the pulse exactly matches the quantum condition $\Delta E = h\nu$ and the temporal envelope function creates the Lorentzian broadening of the measured spectral lines. In this paper we compare and contrast the QM prescribed natural line width of emitted spectra and the Doppler free laser absorption spectra to further validate our photon model. Since a diffractively spread out wave packet cannot deliver all of its energy to an angstrom size detector, the stimulation of a detecting molecule by multiple wave packets are required to deliver the required quantum of energy and influence the emission of a photo electron. QM does not bar level- (or, band-) transition in a quantum device achieved through energy exchange delivered simultaneously by multiple classical or quantum entities. Case examples will be cited to validate the assertions in this paper.

8121-34, Session 9

Beyond the paraxial approximation for OAM light waves

A. M. Guzman, C. Beetle, Florida Atlantic Univ. (United States)

We explore the limits of the paraxial approximation for OAM waves and possible consequences of the use of L as a good quantum number instead of the total angular momentum J of the radiation. Generalized Stokes parameters for the OAM of a light wave can be measured by the phase space tomographic reconstruction of its Wigner distribution. We propose simultaneous measurements of the Stokes parameters for polarization and the generalized Stokes parameters for OAM waves for Laguerre-Gauss modes as a function of the propagation distance, in order to measure deviations from the field quantization in the paraxial approximation.

8121-35, Session 9

Studies on reaction kinetics under coherent microwave irradiations

M. Sato, National Institute for Fusion Science (Japan)

A richer and more classical understanding of interactions between light and matter(1) were investigated at the microwave frequency. As the microwave processing uses monochromatic frequency and single phases electromagnetic oscillations, it remained us the word of "coherency". The wave gets spatial modulation by the non-uniformity in the materials and decreases phase velocities to the order of electron thermal velocities. The energy transmits back and forth between the waves and electrons during each cycle of oscillation and a part of energy is left in collective motions of the electron "clouds" via Landau damping mechanism. When the build up time of collective motions is shorter than the relaxation time to thermal motion, a collective kinetic motions can give the thermodynamic work to the material that generates various thermally non-equilibrium reactions. It is the origin of so called non-thermal effects of microwave.

The reduction speeds of metal oxide powders ($\text{CuO} \rightarrow \text{Cu}_2\text{O}$), irradiating by 2.45GHz H-field, were measured to investigate an amount of kinetic work and the thermal energy. The Arrhenius plots showed that the apparent activation energy was $E^* = 80 \text{ kJ/mol}$. On the other hand, an identical samples was heated by infrared light showing $G = 320 \text{ kJ/mole}$. It is clear that the work energy $W = G - E^* = 210 \text{ kJ/mol}$ was supplied by kinetic works to the redox reactions.

According to the literature(1), the periods of time getting the work energy was estimated to $\tau_w = h\nu / dq/dt = 4.4 \times 10^{-6} \text{ (sec)}$, and the numbers of cycles to accumulate work energy = $4.4 \times 10^{-6} \times 2.45 \text{ GHz} = 104$ cycles.

(1) Juliana H. J. Mortenson, "The elementary quantum of Light" Proc. of SPIE (2009) Vol. 7421 74210T-1

8121-36, Session 9

Light's infinitely variable energy speed in view of the constant speed of light

J. H. J. Mortenson, General Resonance, LLC (United States)

The discovery of Einstein's hidden variables was presented at the previous "Nature of Light" meeting, and revealed that Max Planck's famous quantum formula was incomplete. His complete quantum formula revealed a previously hidden energy constant, time variable, and a sub-photonic elementary particle of light (the single oscillation). Einstein embraced Planck's work, yet struggled with the conflict between Galilean relativity and Lorentzian constant light speed, prompting Einstein's Special Theory of Relativity. Later, with the energy constant still hidden, De Broglie could not model a fundamental quantity of energy and resorted to phase and group velocities.

The energy constant now allows one to consider a sub-photonic light particle and its fundamental quantity of energy in regard to time, space, speed and velocity. What emerges is a remarkably fresh and yet classical perspective. Einstein envisioned light energy as being confined in space in volumetric packets. Einstein's 3-D quantum model suggests that those discrete and localized packets are single oscillations of light. The length of one quantum packet is equal to the wavelength, along which its $6.626 \times 10^{-34} \text{ J}$ of energy is distributed. The entire energy packet travels at the constant speed of light, according to Lorentz. The speed with which an entire packet of energy can be absorbed by matter varies, however, relative to the length of the packet, pursuant to Galileo's relativity principle, and can be much faster than the constant speed of light. This is consistent with supraluminal information and sub-photonic transmission experiments, and provides realistic mechanisms for new optical and photonic engineering applications.

8121-37, Session 9

Investigation of the irradiance (optical field) originated from an elementary atomic dipole transition

E. H. Berloff, Leopold-Franzens-Univ. Innsbruck (Austria)

The irradiance of an atomic dipole transition -screened at microscopic distances from its origin - reveals interesting details not always evident when dealing with light phenomena. The basis of this investigations are pure classical. The HERTZ vector- formalism was used (BORN & WOLF). The special features of the electrodynamic radiation behaviour of such an atomic transition solely became evident when generally made disregards were suspended. However, the complexity of the originating equations forced one to treat the problem numerically. All computations were done due to a dipole elongation of $0,1 \text{ \AA}$ with an oscillation frequency corresponding to the YAG-laser wavelength, $\lambda_Y = 1,064 \text{ \mu m}$.

Strikingly a Fourier analysis of the irradiance (Poynting vector) doesn't replicate this frequency, moreover, it reveals harmonics. Up to $\sim 0,1 \text{ \mu m}$ the fourth harmonic dominates, second harmonic is also appearing albeit at a minor amount. Beyond $0,1 \text{ \mu m}$ fourth and second harmonic exchange their appearance. Up to 100 nm from the dipole centre sixth and eighth harmonics are also present but at minor strengths.

Outside the source centre the optical field is perceived as light wave and practically, instead of the presumed YAG wavelength, we measure double this frequency, namely green light.

At distances below $0,1 \text{ \mu m}$ the fourth harmonic prevails being capable of performing a two photon absorption.

8121-38, Session 9

Virtual and real photons

A. Meulenber, Jr., Univ. Sains Malaysia (Malaysia); P. G. Vaidya, Indian Institute of Science (India); S. Ramadass, Univ. Sains

**Conference 8121:
The Nature of Light: What are Photons? IV**

Malaysia (Malaysia)

Maxwell did not believe in photons. However, his equations lead to electro-magnetic field structures that are considered to be photonic by Quantum Electro Dynamics. They are complete, relativistically correct, and unchallenged after nearly 150 years. However, even though his far-field solution has been considered as the basis for photons, as they stand and are interpreted, they are better fitted to the concept of virtual rather than to real photons. Comparison between static-charge fields, near-field coupling, and photonic radiation will be made and the distinctions identified. The questions about similarities in, and differences between, the two will be addressed.

It is probable that radiation from atomic electrons is not quite what many so-called 'classical' models try to represent as the source of photons. The functional difference in Coulomb vs harmonic potentials makes for a major difference in the radiation field from the low angular-momentum electron orbitals (not so for the more circular orbits). Therefore, a third form of EM radiation (non-photonic) is suggested. It is possible that this is a portion of the evanescent wave phenomenon about all charged matter. As such it would be equivalent to virtual photons and yet still "fill the universe." Feynman's and Jackson's failure to identify the differences can be partially forgiven for the excellence in their respective classic texts. We will try to rectify that situation and thereby establish a grounds for better understanding both kinds of photons and their physical (as distinct from just their mathematical) interaction with charged particles and each other.

8121-39, Session 10

Possible evidence for unmediated momentum transfer between light waves

W. R. Hudgins, Science for Humanity Trust, Inc. (United States); A. Meulenberg, Jr., Univ. Sains Malaysia (Malaysia) and Science for Humanity Trust, Inc. (United States); S. Ramadass, Univ. Sains Malaysia (Malaysia)

Dowling and Gea-Benacloche proved mathematically that "...under certain circumstances, it is possible to consistently interpret interference as the specular reflection of two electromagnetic waves off each other..." Combining experiment, model, and logic, we confirm this statement. Contrary to the supposition that electromagnetic waves/photons cannot interact, it is possible to interpret the results to indicate that out-of-phase waves and opposite polarity photons repel or, at least, cannot pass through each other. No energy is detected in the dark/null zones of wave interference. Because energy is absent, the exchange of momentum through the null zone must redirect/repel light waves into bright zones.

Our Zero-Slit Experiment (ZSX) provides diffraction free interference in air between two portions of a divided laser beam. This experiment was initiated in the attempt to completely cancel a section of these two beams by recombining them in air when they are 180 degrees out-of-phase. We have been able to reduce the interference pattern to a double bright zone (with 3 null zones), but no further. This pattern is qualitatively identical to a pattern of interference for a beam and its reflection from a front-surface mirror plus its mirror image. Thus, visually and mathematically, it is impossible to distinguish the two images. It is not surprising that a photon can create its mirror image in a conductive surface in the same manner that a charge creates its mirror image. The fact that the second beam can accurately represent the radiation from moving charges has interesting implications.

8121-40, Session 10

Why does the wave particle dualism become evident, particularly at optical wavelengths?

K. O. Greulich, Fritz Lipmann Institute (Germany)

At radio wavelengths "photons" are not really needed. The description of this part of the electromagnetic spectrum as waves is completely

satisfying. In turn, in the range of cosmic radiation, the description of photons as "particles" is sufficient. However, this may not be intrinsic basic physics but caused by the choice of detectors. Radio detectors are solid metal rods - antennae. The energy density and the wavelength of a radio photon are much smaller than those of the antenna. In the range of cosmic radiation, the detectors are essentially single atoms. The energy density of such a photon is much higher, the wavelength much smaller. The primary process of photon detection at optical wavelengths usually occurs at a single atom, a limited group of atoms or a band in a solid state detector. There, the energy density is comparable to the energy density of the detected photon. Depending on the detailed conditions, a wave or a beam of particles is perceived.

Literature:

Karl Otto Greulich Single photons cannot be extracted from the light of multi - atomlight sources In: The Nature of Light: What Are Photons?, edited by Chandrasekhar Roychoudhuri, Al F. Kracklauer, Katherine Creath, Proceedings of SPIE Vol. 6664, 66640B, (2007)

Greulich K.O. Single molecule experiments challenge the strict wave particle dualism of light Int. J. Mol Sci 11 304-311 (2010)

http://www.fli-leibniz.de/www_kog/ Then click "Physics"

8121-41, Session 10

Nature of EM waves as observed and reported by detectors for radio, visible, and gamma frequencies

M. Ambroselli, P. Poulos, C. Roychoudhuri, Univ. of Connecticut (United States)

Characteristic transformations measured by detectors dictate what conclusions we can draw about the signal we study. This paper will review the models behind the interaction processes experienced by detectors sensing radio, visible and gamma-ray signals and analyze why the conclusions about the nature of EM-waves should necessarily appear to be different and contradictory. The physical interaction processes between the EM-waves and the materials in the different detectors, the LCR circuit, photo and gamma detectors, are distinctly different. So drawing a definitive conclusion regarding the nature of EM-waves is fraught with pitfalls. We discuss how to bring conceptual continuity among these different interpretations of the interaction processes by imposing some logical congruence upon them.

8121-42, Session 10

Physical processes behind a Ti:Sa femtosecond oscillator

M. Fernández-Guasti, E. Nava-Palomares, F. Acosta, Univ. Autónoma Metropolitana-Iztapalapa (Mexico); C. Roychoudhuri, Univ. of Connecticut (United States)

The sharply peaked comb structure that arises from a mode-locked cavity is usually explained in terms of the superposition of monochromatic waves with integer wavelength multiples of the round trip of the cavity. However, the non interference of waves implies that these wave-fields cannot sum themselves without matter interaction [1,2]. The summation has to be carried out either by a nonlinear medium whose output involves the wave-mixing and/or it is performed by the detector. The output of a femtosecond Titanium Sapphire oscillator is analyzed with the above mentioned framework in mind. The spectrum is obtained in mode-locked and non mode-locked operation via a grating spectrometer for different cavity detunings. The time dependence is measured via a fast photodiode to record the repetition rate. A frequency resolved optical gating (FROG) device is used to resolve the temporal shape of the femtosecond pulses. The data is examined from three viewpoints: a) the superposition takes place within the cavity, b) the superposition occurs at the detector, c) the superposition takes place with no medium. [1] C. Roychoudhuri, "Principle of non-interaction of

**Conference 8121:
The Nature of Light: What are Photons? IV**

of Waves (NIW) principle in this conference series. The NIW-principle implies that even the diffracted secondary wavelets propagate conjointly but without re-arranging their spatial energy distribution unless one inserts some interacting material medium within the diffracting beam. Accordingly, we anticipate that the evolution of the measurable energy distribution in the diffraction pattern will be different in the presence of gain medium whose gain profile varies in the direction orthogonal to the cavity axis. We also anticipate that a cavity with high gain profile will generate the stable spatial eigen-mode with a fewer number of passes through the cavity than with lower gain, or no gain. We will also present the mode evolution process when the seed signal is a pulse of length that is shorter than that of the cavity. We believe this paper will provide useful insights to the students who are introduced to the concept of spatially well defined Gaussian laser modes for the first time.

8121-48, Session 11

Coherence and frequency spectrum of a Nd:YAG laser: generation and observation devices

M. Fernández-Guasti, H. Palafox, Univ. Autónoma Metropolitana-Iztapalapa (Mexico); C. Roychoudhuri, Univ. of Connecticut (United States)

The coherence of a Nd:YAG CW laser is analyzed using a Michelson interferometer. Fringe contrast is measured as the path difference is varied by changing the length of one arm. The fringe contrast, as expected, is maximum when there is no path difference between arms. However, the fringe contrast does not decrease monotonically. It decreases and then increases several times before fading away. This behaviour is reminiscent of the fringe contrast depending on aperture and the uncovering of the Fresnel zones. In order to evaluate the mode structure it is necessary to consider the geometric parameters and Q factor of the cavity, the medium gain curve and the type of broadening.

The non interference of waves principle requires that two (or more) modes competition or their interference can only take place through matter non linear interaction. Therefore, and in addition, it is important to consider the setup and type of detectors employed to monitor the frequency and/or time dependence. In as much as speckle is recognized as an interference phenomenon taking place at the detector plane, say the retina, the role of the sensing element in the detection of mode beats should also be decisive.

8121-49, Session 11

Visualizing superposition process and appreciating the principle of non-interaction of waves

M. Ambroselli, C. Roychoudhuri, Univ. of Connecticut (United States)

We demonstrate the dynamic evolution of superposition effects to underscore the importance of visualizing interaction processes. The model recognizes the principle of Non-Interaction of Waves. Recordable linear fringes, bisecting the Poynting vectors of the two crossing beams, have time evolving amplitude patterns in the bright fringes because the two superposed E-vectors oscillate through zero values while staying locked in phase. If a detector registers steady stable bright fringes, it must do so by time integration. The QM recipe to model energy exchange by taking the square modulus of the sum of the complex amplitudes has this time integration built into it. So, we will underscore the importance of assigning proper physical processes to the mathematical relationships: the algebraic symbols should represent physical parameters of the interactants and the mathematical operators connecting the symbols should represent allowed physical interaction processes and the guiding force.

This presentation will be based on a series of papers published in the

last three proceedings of this conference, "The nature of light: What are photons?", by Prof. C. Roychoudhuri, besides the following publications:

- [1] Roychoudhuri, J. of Nanophotonics, "Principle of non-interaction of waves", J. Nanophoton. Vol. 4, 043512 (2010). doi:10.1117/1.3467504.
- [2] Lee et al, Opt. Express, 11(8), 944-51 (2003); "Measuring properties of superposed light beams carrying different frequencies"; [<http://www.opticsexpress.org/abstract.cfm?URI=OPEX-11-8-944>].
- [3] Roychoudhuri, Phys. Essays 19 (3), September (2006); "Locality of superposition principle is dictated by detection processes".

8121-50, Session 12

The nature of light in Indian epistemology

S. C. Kak, Oklahoma State Univ. (United States)

Light was taken as a kind of a wind (collection of particles) within the Indian atomic theory of Vaisheshika which is ascribed to Kanada of 600 BC. According to Vaisheshika, the atom (anu) is the fundamental unit and it is indivisible because it is a state for which direct measurement cannot be defined. Since it cannot be described completely, it can neither be further divided nor can be spoken of as having parts. Further the motion it possesses is non-observable directly which makes the atom abstract in a conventional sense. Space and time are like two mediums through which all matter is observed and they form the matrix of reality. Kanada's framework defies the usual categories of realist versus idealist, since for him matter in itself is a result of motion. Kanada's emphasis on analysis of categories is also found in the complementary tradition of logic. The idea of tanmatra in the cosmology of Sankhya, which is viewed as a kind of potential out of which materiality emerges, has features similar to that of anu in the Vai eshika system. Kanada's distinction between intrinsic and extrinsic motions and his claim that the atom, which has only intrinsic motion, is unobservable leads to the remarkable conclusions that intrinsic motion is different from the usual material motion because it is uniform in all directions.

8121-51, Session 12

Two-slit interference and wave-particle duality for single photons from Observer's Mathematics point of view

D. Knots, B. Khots, Compressor Controls Corp. (United States)

When we consider and analyze physical events with the purpose of creating corresponding mathematical models we often assume that the mathematical apparatus used in modeling, at least the simplest mathematical apparatus, is infallible. In particular, this relates to the use of "infinitely small" and "infinitely large" quantities in arithmetic and the use of Newton - Cauchy definitions of a limit and derivative in analysis. We believe that is where the main problem lies in contemporary study of nature. We have introduced a new concept of Observer's Mathematics (see www.mathrelativity.com). Observer's Mathematics creates new arithmetic, algebra, geometry, topology, analysis and logic which do not contain the concept of continuum, but locally coincide with the standard fields.

We proved the following theorems:

Theorem 1 (Two-slit interference). Let Ψ_1 be a wave from slit 1, Ψ_2 - from slit 2, and $\Psi = \Psi_1 + \Psi_2$. Then the probability of Ψ is a wave equals to 0.5.

Theorem 2 (Wave-particle duality for single photons). If v is small enough, then λ is a random variable.

Conference 8121:
The Nature of Light: What are Photons? IV

8121-52, Session 12

Two types of arguing in physics: a critical discussion

A. I. Vistnes, B. Jagielski, Univ. of Oslo (Norway)

In quantum optics one kind of arguing is as follows: "Interference is a manifestation of the intrinsic indistinguishability of the photon paths." (quotation from Zou, Wang and Mandel, Phys.Rev.Lett. 67 (1991) 318-321). Arguments like this were used by Bohr and Einstein in the 1930s and has been in use ever since. The double slit experiment where the slits are located in a movable screen, is a classical example. Heisenberg's uncertainty relation was then used in a coarse manner, and was based on very abstract thoughts. The alternative argument is based on diffraction, and offers a far more detailed picture where the interaction of light and matter is considered in detail instead of in a superficial way. We claim that the principle of "indistinguishability of the photon paths" may lead to explanations being in direct conflict with a more detailed interaction-based description. Two examples will be given: the Bohr-Einstein model of the double slit, and the Zou, Wang, Mandel coherence experiment from 1991 (reference given above). We conclude that detailed interaction-based arguments should be preferred instead of very abstract, nonspecific arguing in physics, and point out that some conclusions drawn so far in quantum optics may not be the full story.

8121-53, Session 12

Simple alternative model of the dual nature of light and its Gedanken experiment

F. Hénault, Univ. de Nice Sophia Antipolis (France)

In this paper is presented a simple alternative model of the dual nature of light, based on the deliberate inversion of the original statement from P. A. M. Dirac: "Each photon interferes only with itself. Interference between different photons can never occur." Such an inversion stays apparently compatible with the experimental results reported from different recent experiments. A Gedanken experiment having the capacity to test the proposed model in single photon regime is described, and its possible outcomes are discussed. The proposed setup could also be utilized to assess the modern interpretation of the principle of complementarity.

8121-54, Session 13

Beyond relativity and quantum mechanics: space physics

H. H. Lindner, Consultant (United States)

Relativity and Quantum Mechanics are the products of an esoteric metaphysics and epistemology imposed upon physics by Albert Einstein. Subjective idealism holds that the observers' conscious experiences are the only reality and that science should only describe the observers' experiences and measurements, not attempt to explain the nature and causes of things. Einstein eliminated ether theory from physics by reducing physics to mere description; eliminating the need for any physical explanation of fundamental phenomena. This program is the source of unreality, paradoxes and schisms in physics. Albert Einstein did not fully comprehend the nature of his own program nor adhere to it consistently; resulting in confusion. In order to understand the physical Cosmos, we need a revolution similar to the Copernican Revolution. We must again remove the observer from the center of physics and hypothesize about the nature and causes of Cosmic phenomena. When we do so, it becomes apparent that space itself is the causal nexus of all physical phenomena. Space physics requires the reinterpretation of all known phenomena, concepts, and mathematical models.

8121-55, Session 13

Did Michelson and Morley test the wrong phenomenon?

G. N. Mardari, The Johns Hopkins Univ. (United States)

Light is a combination of two types of phenomena. It propagates as an electromagnetic field (expressing the wave aspect), but also as a stream of photons (expressing the particle aspect). When we measure the speed of light, do we measure the speed of the waves, or the speed of the particles? Michelson and Morley tested the speed of light for invariance. According to their results, the speed of light does not exhibit the relativistic properties of a wave. Therefore, it must correspond to the speed of a particle (the photon). By implication, the nature of fundamental waves has not been tested yet. In classical physics, the electron is also described as a dual entity: a particle with an associated field. The speed of the electron is the speed of the particle. The speed of the waves must correspond to the rate of propagation of changes in the associated field. This conclusion implies that the speed of magnetic pulses cannot be identical to the speed of light. It must also violate the principle of invariance. Both of these predictions are verifiable.

8121-56, Session 14

Experiment versus theory: do physicists still know the difference?

C. Rangacharyulu, Univ. of Saskatchewan (Canada)

Physics is an experimental science, quite distinct from mathematics or philosophy. Almost all physical laws are simple generalizations of experimental observations with, perhaps, the exception of Newton's laws. Newton's laws were likely the first attempt to offer operational definitions to physical parameters and provide a mathematical basis to quantify experimental observations. At least for some time, there was a clear distinction between the experimental observations from the corresponding theoretical formulations to interpret the meanings of data. In modern times, the theoretical assumptions are very much part of the preparation of experiments and interpretation of results of measurements, which makes us question the very meaning of test of experiment against theoretical predictions.

In this talk, I would provide a brief survey of the modern experiments where the interpretation of experimental data so heavily relies on the theoretical arguments, it becomes clear that we are begging the question rather than answering the question.

8121-57, Session 14

The coming revolution in physics

T. Silverman, IIAS (United States)

The foundations of Relativity and Quantum theory are compromised by profound conceptual difficulties that have blocked unification of these "twin pillars" of physical science and thus a fundamental understanding of gravity, light and physical phenomena generally. Current efforts to supersede these difficulties without directly addressing them, as exemplified by the approaches that go by the name of String Theory, are unlikely to lead to long term success. Moreover, it is found that quantization-of-action and Lorentz invariance are general, emergent properties of dynamical systems comprising periodic fluctuations in the underlying degrees of freedom. Therefore, mathematical models that "wire in" these attributes - instead of deriving them from the underlying model - do not furnish a theoretical foundation for their interpretation. With these considerations in view, a framework for a quantum theory of gravity and a new understanding of light is presented and discussed.

8121-58, Session 14

Appreciation of the nature of light demands enhancement over the prevailing scientific epistemology

C. Roychoudhuri, Univ. of Connecticut (United States)

The principle of Non-Interaction of Waves (NIW-principle) in the linear domain has been known in physics. But the prevailing Measurable Data Modeling Epistemology (MDM-E), achieving success over the last few centuries, obscured the identification of the NIW-principle. Measured data and the theory always matched except for a detector constant. So, we propose the Interaction Process Mapping Epistemology (IPM-E). IPM-E builds upon MDM-E and goes deeper by demanding the visualization of the interaction processes that give rise to the measurable data. IPM-E helps clarify the roots behind the famous QM "Measurement Problem" as an inherent limit in nature and hence cannot be solved by any mathematical theorems. All of our theories, irrespective of their magnitude of successes, are necessarily incomplete as they are founded on hypotheses containing incomplete information about the nature. IPM-E guides us to iteratively review and reconstruct successful theories to inch towards cosmic reality.

8121-60, Session 14

Quantum epistemology: the Växjö viewpoint

A. Y. Khrennikov, Linnaeus Univ. (Sweden)

This paper is about a series of meetings in Växjö and debates on foundations of quantum mechanics and its epistemology which took place during these meetings. The Växjö series of conferences played an important role in elaboration of epistemology of modern quantum mechanics, the epistemology of quantum physics enlightened by quantum information theory. One of the main lessons of this remarkable series is huge diversity of opinions on foundations. After all we can firmly declare that the common viewpoint that the community of people interested in quantum foundations can be split into orthodox Copenhagen School and a small group of outsiders who dream of the comeback of determinism does not match the real situation. It became completely clear that the group of orthodox Copenhagen School is very diverse. The degrees of their beliefs in completeness of quantum mechanics vary substantially. Many of the brightest followers of Copenhagen School have proposed original ideas on possibilities to go beyond current quantum. On the other hand, majority of people who does not believe in Bohr's claim about completeness of quantum mechanics do not at all dream of recovery of Laplacian determinism of particles. A variety of novel approaches to go beyond current quantum have been proposed, including various classical field-type models. In conclusion, we can say that the meetings in Växjö clearly demonstrated that nowadays limits and validity of boundaries of quantum mechanics is a hot topic attracting the attention of the whole quantum community and characterized by diversity of opinions. The Växjö interpretation of quantum mechanics, the realistic interpretation based on coupling of quantum probability to classical (Kolmogorovian or von Mises) probability, attracts a lot of attention.

Conference 8122: Tribute to Joseph W. Goodman

Sunday 21 August 2011 • Part of Proceedings of SPIE Vol. 8122 Tribute to Joseph W. Goodman

8122-01, Session 1

High-resolution imaging through horizontal path turbulence

W. T. Rhodes, D. F. Pava, S. R. Malinda Silva, F. R. Dagleish, G. Nootz, Florida Atlantic Univ. (United States)

Imaging through long-path turbulence, as in the case of horizontal-path imaging, has long presented special problems for the optical imaging community because the isoplanatic patch is diminishingly small. In this paper we describe a method based on Fourier telescoping concepts that appears to provide a means of achieving diffraction-limited resolution with a large-aperture system. The scheme requires active illumination of the object. The basic concept will be presented along with preliminary experimental results.

8122-02, Session 1

Gigapixel synthetic-aperture digital holography

J. R. Fienup, A. E. Tippie, Univ. of Rochester (United States)

Building on the work of Goodman and Lawrence (1967), we have extended digital holographic imaging to gigapixel scales with 2-D aperture synthesis. Sub-pixel registration algorithms were required to mosaic together hundreds of arrays of data and phase-error correction algorithms were required to correct for system instabilities.

8122-03, Session 1

Illustrative EDOF topics in Fourier optics

N. George, X. Chen, W. Chi, Univ. of Rochester (United States)

No abstract available

8122-04, Session 1

Linear systems formulation of non-paraxial scalar diffraction theory

J. E. Harvey, CREOL, The College of Optics and Photonics, Univ. of Central Florida (United States)

Goodman's popular linear systems formulation of scalar diffraction theory includes a paraxial (small angle) approximation that severely limits the conditions under which this elegant Fourier treatment can be applied. In this paper a generalized linear systems formulation of non-paraxial scalar diffraction theory will be discussed. Diffracted radiance (not intensity or irradiance) is shown to be shift-invariant with respect to changes in incident angle only when modeled as a function of the direction cosines of the propagation vectors of the usual angular spectrum of plane waves. This revelation greatly extends the range of parameters over which simple Fourier techniques can be used to make accurate diffraction calculations. Non-paraxial diffraction grating behavior (including the Woods anomaly phenomenon) and wide-angle surface scattering effects for moderately rough surfaces at large incident and scattered angles are two diffraction phenomena that are not limited to the paraxial region and benefit greatly from this extension to Goodman's Fourier optics analysis. The resulting generalized surface scatter theory has been shown to be valid for rougher surfaces than the Rayleigh-Rice theory and for larger incident and scattered angles than the classical Beckman-Kirchhoff theory. This has enabled the development of a complete linear systems formulation of image quality, including not only diffraction effects and geometrical aberrations from residual optical design errors, but surface scatter effects from residual optical fabrication errors as well. Surface scatter effects can

thus be balanced against optical design errors, allowing the derivation of optical fabrication tolerances during the design phase of a project.

8122-05, Session 1

Fourier transforms by white-light interferometry: Michelson stellar interferometer fringes

J. B. Breckinridge, California Institute of Technology (United States)

The white-light compensated rotational shear interferometer (coherence interferometer) was developed in an effort to study the spatial frequency content of white-light scenes in real-time and to image sources of astronomical interest at high spatial frequencies through atmospheric turbulence. This work was inspired by Professor Goodman's studies of the image formation properties of coherent (laser) illuminated transparencies. The need for a coherent laser source to illuminate a transparency does not enable real-time processing. Real-time processing is possible using white-light interferometry. This paper reviews the image formation properties of the coherence interferometer its development and its applications to physical optics, optical processing and astrophysics (imaging of the surfaces of stars and search for exoplanets).

8122-06, Session 1

Coherence holography and photon-correlation holography: marriage between holography and statistical optics

M. Takeda, The Univ. of Electro-Communications (Japan); W. Wang, Heriot-Watt Univ. (United Kingdom); D. N. Naik, The Univ. of Electro-Communications (Japan)

Traditionally, holography and statistical optics have been regarded as mutually separated fields of optics. For a long time, this seems to have restricted synergy of knowledge in holography and coherence theory. Recently we proposed two new techniques of unconventional holography, called coherence holography and photon-correlation holography, which bridge the gap between the two fields.

The principle of coherence holography is based on the fact that a coherence function obeys the same wave equation as the optical field. In coherence holography, a hologram is illuminated by spatially incoherent light, and a 3-D object is reconstructed as the 3-D distribution of a spatial coherence function rather than the field itself. Just as a computer-generated hologram can create a 3-D image of a non-existing object, a computer-generated coherence hologram can create an optical field with a desired 3-D distribution of spatial coherence function. Thus coherence holography opens up a new possibility of optical tomography and profilometry based on a synthesized spatial coherence function, and a coherence hologram also serves as a generator of coherence vortices.

The principle of photon-correlation holography is based on the combination of the concept of coherence holography with that of Hanbury Brown and Twiss intensity interferometry.

The principle and applications of coherence holography will be reviewed with particular emphasis on the space-time analogy in coherence theory, as well as the formal analogy between an optical field and its coherence function, which gives an insight into the methodology for coherence holography and the new concept of spatial frequency comb for dispersion-free optical coherence tomography and profilometry.

8122-07, Session 1

Optical information processing

D. Psaltis, Ecole Polytechnique Fédérale de Lausanne (Switzerland)

No abstract available

8122-08, Session 1

Fourier filtering grows much better with age

H. J. Caulfield, Alabama A&M Univ. (United States)

Professor Goodman's best known publication is certainly his book on Fourier Optics. That is still valid, but the use of Fourier transform filtering for pattern recognition has been limited. After almost 50 years of effort, it still led to an unfortunate dilemma. Fourier filtering applies a linear discriminant in parallel to each pixel in the input. Were it not for that linearity, it could not do the space-invariant (I am thinking images, but this applies to 1D and 3D signals as well). So unless we restrict applications to simple linearly discriminable target sets, The discrimination ability of Fourier filtering will be very poor.

All of that changed with the invention of what I call Margin Setting. It is not a new pattern recognition algorithm. Instead, it is a method that uses any pattern recognition algorithm to achieve much better discrimination with that discriminant type. Margin Setting itself will not be explained in this abstract.. But I can describe some of what it does.

Here are its uses that I will show in my talk: Margin Setting accomplishes

- Wonderful preprocessing for or against texture, spectral content, polarization, and the like
- Unchanged target locating ability
- Dramatically improved discrimination
- The evaluation of target parameters such as scale and pose
- Massive bandwidth reduction

I will suggest that these operations amount to a kind of Artificial Visual Perception. I will argue that Artificial Perception is key to future conscious machines and key to understanding

8122-09, Session 2

Volume holographic spectral-spatial imaging of biological tissue

R. K. Kostuk, The Univ. of Arizona (United States)

A volume holographic imaging system is described that is capable of both spatial and spectral imaging of biological tissue samples. The primary component of this system is a multiplexed volume holographic element. The holograms are highly Bragg selective (0.0180 in angle) and all wavefronts to be selected from multiple depths within the tissue sample. The high selectivity also allows for high lateral spatial resolution ($<4\mu\text{m}$). Two modes of operation of the system have been investigated. The first uses an LED with 20-40 nm spectral bandwidth. The spectral bandwidth determines the field of view of the system. The second mode of operation uses laser excited dyes deposited on the tissue sample. The dyes react with cancerous cells and act as markers to identify suspicious tissue areas. Several illumination systems have been implemented and a prototype endoscope version has also been demonstrated.

8122-10, Session 2

Retinal imaging using curved detectors

L. Hesselink, Y. Takashima, E. Perederey, Stanford Univ. (United States)

For almost a century ray optics programs have been used to trace rays through optical systems to optimize their performance. Images were either recorded on film or other suitable recording medium, or the optics were used by a human to enhance visual quality and resolution, with little room for post image processing to improve performance and quality. Design tradeoffs were typically made between performance, physical characteristics such as size and weight, and cost. With the advent of digital recording media, a new dimension is added to this tradeoff space: computation. Since only the final image is of interest to a human, an intermediate recorded image does not necessarily have to be esthetically pleasing or sharp. We can tradeoff optical imaging performance against post detection digital processing.

In this invited talk we describe how curved detectors can significantly reduce cost, size and weight at the expenses of additional post-recording processing. Examples of very large FOV simple lens systems will be presented.

8122-11, Session 2

Modern scalar diffraction theory

H. H. Arsenault, Univ. Laval (Canada); P. García-Martínez, Univ. de València (Spain)

Classical scalar diffraction theory used the Green Function approach to solve the wave equation, as described in Goodman's classical Fourier Optics book. Arsac proposed a new approach based on Distribution Theory. More recently we attempted to derive the equations directly from relativistic Quantum Mechanics, based on the fact that the wave equation is equivalent to the expression for the invariance of the modulus of the light Energy-momentum four-vector.

8122-13, Session 2

Fourier optics in the mirror of digital computers

L. P. Yaroslavsky, Tel Aviv Univ. (Israel)

The paper by J. Goodman of 1967 on numerical reconstruction of holograms was, along with papers by A. Lohmann on computer generated holograms, was one of the first signs heralded the advent of new era in the evolution of imaging optics that nowadays culminated in a new imaging technology, computational imaging. Computers have become an integral part of optical imaging systems and even sometimes completely replace such optical devices as lenses and diffractive gratings. To do optics in computers, one needs discrete representation of optical signals and transforms. Optical transforms are represented in computers by their discrete versions. Particularly, Fourier optics is represented through different versions of Discrete Fourier Transform (DFT). Being discrete representation of the optical Fourier transform, DFT features a number of peculiarities that cast a new light on such fundamental properties of the Fourier Transform as sampling theorem and the uncertainty principle. In the paper, we formulate the Discrete Sampling Theorem, prove that signals with N samples with bounded DFT spectrum with $K \text{ Ksgnl Kspctr} > N$ and present examples of such "band-limited/space-limited" signals that remain to be so for whatever large N .

8122-14, Session 2

Reflections on speckle: old and new results

C. Dainty, National Univ. of Ireland, Galway (Ireland)

One of the first descriptions of speckle was by Karl Exner in 1877 and in the early 1900s Lord Rayleigh derived many of the statistics of speckle. But it was the invention of the laser in 1960 that triggered many publications re-discovering the phenomenon: the very high spatial coherence of the laser meant that speckle was visible in any situation involving an optically rough surface or random medium. In this early

period, unpublished reports by Joe Goodman in 1963 provided the authoritative analysis of the statistics of speckle patterns, and these were particularly valuable because they were written so logically and clearly. Since the early sixties, there have been over 5000 peer-reviewed publications involved with speckle in one way or another, so this subject has fascinated many scientists and engineers. In this talk, I will review some of the basic statistical properties of speckle, starting with the first order probability density function of intensity and the second order correlation function and power spectrum. I will then discuss the dual role of speckle as both a source of unwanted noise and a carrier of essential information, as in optical coherence tomography. I will with two more recent developments. The first is the use of adaptive optics to modify speckle fields, something that might ultimately find application to the scattering of light in tissue. The second is the phenomenon of optical vortices, which dominate speckle fields: a technique for completely eliminating these vortices using cascaded adaptive optics systems will be presented.

8122-24, Session 2

Solar sails, optical tweezers, and other light-driven machines

M. Mansuripur, College of Optical Sciences, The Univ. of Arizona (United States)

Electromagnetic waves carry energy, linear momentum, and angular momentum. When light (or other electromagnetic radiation) interacts with material media, both energy and momentum are usually exchanged. The force and torque experienced by material bodies in their interactions with the electromagnetic field are such that the energy as well as the linear and angular momenta of the overall system (i.e., the system of field plus matter) are conserved. Radiation forces are now used routinely to trap and manipulate small objects such as glass or plastic micro-beads and biological cells, to drive micro- and nano-machines, and to contemplate interstellar travel with the aid of solar sails. In this presentation I will discuss those properties of the electromagnetic field that enable such wide-ranging applications.

8122-15, Session 3

Exploring light-matter interaction processes to appreciate various successes behind the Fourier theorem

C. Roychoudhuri, Univ. of Connecticut (United States)

Goodman's contribution to the theory & applications of Fourier optics is simply outstanding. When a scientific field becomes extremely matured in the world of application, it is obvious that it must have captured some of the real operational cosmic logics since working instruments must emulate (conform to) interaction processes in nature. Broad engineering successes also imply that it is time to ponder if the mathematical theory and the hypotheses behind it, have captured and reached the unchangeable final form, or the theory should be re-evaluated from its very foundation once again. I believe in perpetual iteration of all successful theories since they are always incomplete since they are all formulated based on incomplete knowledge of the universe. And engineers are best prepared to stimulate such iterations since they always emulate nature's interaction processes from many different angles for many different purposes.

This talk is derived from:

- [1] C. Roychoudhuri, "Principle of non-interaction of waves", *J. Nanophoton.*, Vol. 4, 043512 (2010); doi:10.1117/1.3467504.
- [2] C. Roychoudhuri, "Why we need to continue the 'What is a Photon?' conference: to re-vitalize classical and quantum optics." SPIE Conf. Proc. Vol. 7421-28 (2009). Keynote presentation.
- [3] C. Roychoudhuri, "Bi-centenary of successes of Fourier theorem! Its power and limitations in optical system designs"; SPIE Conf. Proc. Vol. 6667, paper #18 (2007). Invited paper.

8122-16, Session 3

Singular beams in metrology and nanotechnology

J. Shamir, Technion-Israel Institute of Technology (Israel)

Optical singularities are localized regions in a light field where one or more of the field parameters, such as phase or polarization, become singular with associated zero intensity. Focused to a small spot, the electromagnetic field around the singularity has interesting characteristics, in particular when it interacts with matter. The light scattered by a material object within the strongly varying optical field around the singularity is extremely sensitive to changes and can be exploited for metrology with high sensitivity and the study of physical processes on a nanometer scale. Metrological applications to be discussed include object positioning with an accuracy of at least 20 nm and nano-particle analysis. It is shown that sub-wavelength particles can be easily detected and characterized. On the physical side, aspects of a strong longitudinal field component are discussed. The excitation of plasmonic resonance in nano sized objects will be also addressed indicating the possibility of anomalous absorption effects.

8122-17, Session 3

Optical coherent processors in phase-space representations

J. Ojeda-Castaneda, Univ. de Guanajuato (Mexico)

In applied optics, often one is faced with a trade-off between two functions that are a Fourier transform pair. For an insightful analysis of the limitations, as well as for analyzing the proposals for overcoming this trade-off, it is convenient to use a phase-space representation. However, phase-space representations appear to be mathematically demanding /1/.

We recognize that coherent optical processors are useful for visualizing simultaneously the two domains of a Fourier transform pair. And hence, coherent optical processors are indeed helpful for understanding and for displaying Phase-Space representations.

Here, we explore the use of coherent optical processors for overcoming some classical optics trade-offs, which are associated to a Fourier transform pair. We show that certain complex amplitude masks are able to reduce the impact of focus errors on the modulation transfer function (MTF) /2/. Furthermore, based on the space- time analogy, we show that a similar procedure is useful for correcting residual time aberrations, which are present when electro-optic sinusoidal phase modulators generate temporal lenses /3/.

References

1. Markus Testorf, Bryan Hennelly and Jorge Ojeda-Castaneda, "Phase-Space Optics Fundamentals and Applications", (McGraw-Hill Professional, 2010)
2. J. Ojeda-Castañeda, E. Yépez-Vidal and E. García-Almanza, "Complex Amplitude Filters for Extended Depth of Field", *Photonics Letters of Poland*, Vol. 2, No. 4, 162-164 (2010)
3. L. E. Munioz-Camuniez, V. Torres-Company, J. Lancis, J. Ojeda-Castañeda, and Pedro Andrés, "Electro-optic time lens with an extended time aperture", *J. Opt. Soc. Am. B*, Vol. 27, No. 10, 2110-2115 (2010)

8122-18, Session 3

On propagation of optical coherence

B. E. A. Saleh, CREOL, The College of Optics and Photonics, Univ. of Central Florida (United States)

Joseph W. Goodman pioneered the use of linear systems to describe light propagation through optical components. In the 1980s this has motivated me to describe propagation of partially coherent light using

bilinear systems (second-term in a Volterra series description of a nonlinear system). More recently, I considered the propagation of the second-order optical coherence function through a linear optical system. Normally, this involves linear operations in a space of two positions (and/or two times). However, with one point fixed, the dependence on the other point can always be thought of as propagation through the linear system twice (forward and backward). This is described as a cascade of linear operations in a space of a single position (and/or single time). The familiar operations that describe propagation of the optical field through linear systems, such as diffraction and imaging (or dispersion of optical pulses), may therefore be directly applicable to the propagation of the coherence function, and can readily explain well-known phenomena such as the Van Cittert-Zernike theorem. This approach, which reduces the dimensionality of the space by a factor of two while requiring double passage through the system, is also applicable to linear systems with random components, such as phase screen. It can be used to interpret effects such as Anderson localization for optical beams traveling through a parallel array of waveguides with random coupling.

8122-19, Session 3

Fourier optics and near-field superlens

Y. Sheng, G. Tremblay, Y. Gravel, Univ. Laval (Canada)

Superlens of negative index material can collect the evanescent waves for ideal imaging with nano-metric resolution. Metallic near-field superlens of a sole negative permittivity, but a positive permeability at optical frequency is more realizable. The fundamental Fourier optics is applied to the near-field superlens with the transfer function defined as the transmission coefficient of the superlens for spatial components, which is computed with the transfer matrix of multilayer system, the surface plasmon polariton (SPP) resonance within the superlens layer, or with the SPP waveguide theory. The total transfer function is a product of that of the superlens with the free space propagation filters in the object and image layers. The impulse response of this linear system is the Fourier transform of the transfer function. However, when the nano-object structures as slits, holes, grooves and bumps are modeled as oscillating dipole sources, the space invariance condition can be not respected within the dimension of the dipoles, so that the superlens is usually characterized by imaging of two nano-slits. The scattered field over the surface of lossy earth has been studied by Sommerfeld in 1909 involving the Zenneck surface wave. In the 2D cases we find the close-form rigorous solution of the Sommerfeld integral by introducing two parameterizations of the integral spaces and choosing appropriate branch-cut integral paths. The results is in agreement with the recent experiment on the transient SPP and is useful not only for near field imaging, but also beam collimating, focusing and enhancement by nano-plasmonic structures

8122-20, Session 3

From Fourier optics to integrative engineering

T. Jansson, A. A. Kostrzewski, Physical Optics Corp. (United States)

This paper describes evolution of technical directions at Physical Optics Corporation (POC), from physical optics, in general, and Fourier Optics, in particular, to: integrative optics, integrating: optics, electronics, mechanics, and even further to: Integrative Engineering, integrating the above disciplines with QA and IA. This specific type of interdisciplinary system integration is a kind of Integrative, Interactive, Interdisciplinary, and Intelligence (I4) approach, leading to Small System Integration (SSI) at POC. This presentation describes the I4 transformation, including such examples as: Crush-Survivable Video Recorder and Data Transfer/Storage Avionics systems, (a kind of black box), 360o FOV telescopic camera with Electronic Zooming, Self-sustainable C4ISR sensor, conformable e-wearables and other devices representing defense and Homeland Security.

8122-21, Session 3

Phase-sensitive coherence and the classical-quantum boundary in ghost imaging

B. I. Erkmen, Jet Propulsion Lab. (United States); N. D. Hardy, D. Venkatraman, F. N. C. Wong, J. H. Shapiro, Massachusetts Institute of Technology (United States)

The theory of partial coherence has a long and storied history in classical statistical optics. The vast majority of this work addresses fields that are statistically stationary in time, hence their complex envelopes only have phase-insensitive correlations. The quantum optics of squeezed-state generation depends on nonlinear interactions producing baseband field operators with phase-insensitive and phase-sensitive correlations. Utilizing quantum light to enhance imaging has been a topic of considerable current interest, much of it involving biphotons, i.e., streams of entangled-photon pairs. Biphotons have been employed for quantum versions of optical coherence tomography, ghost imaging, holography, and lithography. However, their seemingly quantum features have been mimicked with classical-state light, questioning wherein lies the classical-quantum boundary. We have shown, for the case of Gaussian-state light, that this boundary is intimately connected to the theory of phase-sensitive partial coherence. Here we present that theory, contrasting it with the familiar case of phase-insensitive partial coherence, and use it to elucidate the classical-quantum boundary of ghost imaging.

An object's ghost image results from correlating the output from a high-spatial-resolution detector, whose illumination has not interacted with that object, with the output from a single-pixel (bucket) detector, whose illumination has undergone such an interaction. Ghost imaging has been done with pseudothermal (classical) and biphoton (quantum) light. We show, both theoretically and experimentally, that classical phase-sensitive light produces ghost images most closely mimicking those obtained with biphotons, and we derive the resolution, field-of-view, and signal-to-noise ratio of a standoff-sensing ghost imager, taking into account target-induced speckle.

8122-22, Session 3

Digital holography and tissue dynamics spectroscopy: on the road to high-content drug discovery

D. D. Nolte, Purdue Univ. (United States)

Tissue dynamics spectroscopy (TDS) uses short-coherence-gated dynamic speckle from living tissue to detect sub-cellular motion as a novel imaging contrast agent. Tissue dynamics spectroscopy is a digital holographic imaging technique that uses wide-field illumination to extract sub-cellular motion as deep as 1 mm inside tissue as a function of three-dimensional location. Motility contrast presents an unexpected imaging approach that is well-matched to the problem of imaging the effects of broad classes of drugs, and allows us to explore how function defines cellular motion, and how altered function is detected as changes in motion.

Speckle images of tumor tissues shimmer due to cellular motility, and statistical properties of the dynamic speckle are obtained by capturing temporally fluctuating images at successive depths. Different perturbations on the cellular biochemistry show significantly different responses in the three frequency bands. These different responses represent distinct signatures that relate to the mode of action of the various perturbations. Differential changes in the fluctuation spectra (measured through the dynamic speckle) as a function of time show distinct signatures that are specific to the modes of drug action. These signatures can be used to construct high-content screens of drug candidates. The label-free character of motion as a contrast agent, the sensitivity and specificity of motion to cellular function, and the three-dimensional access to tissue properties far from surface effects, make tissue dynamics spectroscopy an attractive new approach for high throughput label-free screening of drug candidates.

8122-23, Poster Session

Computational photography: advances and challenges

E. Y. Lam, The Univ. of Hong Kong (Hong Kong, China)

In the mid-1990s when digital photography began to enter the consumer market, Dr. Goodman and I embarked on an exploration on how computation would affect the imaging system design. The field has since grown to be known as computational photography. In this paper I'll describe some of its recent advances and challenges, and discuss what the future holds.

Conference 8123: Eleventh International Conference on Solid State Lighting

Monday-Wednesday 22-24 August 2011 • Part of Proceedings of SPIE Vol. 8123
Eleventh International Conference on Solid State Lighting

8123-01, Session 1

Optical design and lighting application of an LED-based sports lighting system

L. H. Boxler, Musco Sports Lighting, LLC (United States)

This paper describes both the optical development of an LED based sports lighting system and the results of the application of the system to an actual sport field. A traditional sports lighting fixture is generally composed of a single 1500 watt HID light source with faceted metal reflectors used to control the light distribution. The efficacy of the HID light source is equivalent or nearly equivalent to most LED light sources, putting LEDs at a large cost disadvantage in a high light output application such as sports lighting. To assess the feasibility and applicability of LEDs in a sports lighting application, an LED based sport light has been developed and installed on a small soccer field specified to have an average maintained illuminance level of 30 footcandles. An existing HID sport lighting system was also installed on the same size soccer field adjacent to the LED field with the same average footcandle level for comparison. Results indicate that LEDs can provide equivalent average illumination, however the LED system component and structural cost is substantially higher. Despite the high cost, it was found that improved optical control afforded by the optical design used in the system provides a significant improvement in spill light control and on field uniformity. The significant improvement in on field uniformity provides the opportunity to re-evaluate specifications with the possibility of specifying minimum light levels rather than average light levels while maintaining playability. This could provide an advantage for LED systems.

8123-02, Session 1

Design, simulation, and measurement of LED reading lamp with non-axisymmetrical reflector and freeform lens

W. Chao, Y. Chen, J. A. Whang, National Taiwan Univ. of Science and Technology (Taiwan)

With the rapid development of various types of digi-readers, such as i-Pad, Kindle, and so on, non-self-luminous type has an advantage, low power consumption. This type of digi-reader reflects the surrounding light to display so it is no good at all to read under dim environment. In this paper, we design a LED lamp for a square lighted range with low power consumption. The e-book is about 12cm x 9cm, the total flux of LED is 3 Lm, and the LED lamp is put on the upper brink of the panel with 6cm height and 45 degree tilted angle. For redistributing the energy, the LED lamp has a freeform lens to control the light of small view angle and a non-axisymmetrical reflector to control the light of large view angle and create a rectangular-like spot. In accordance with the measurement data, the proposed optical structure achieves that the power consumption of LED light source is only 90mW, the average illumination is about 200 Lux, the uniformity of illumination is over 0.7, and the spot is rectangular-like with precise light/dark cutting-off line. Our designed optical structure significantly increases the efficiency of light using and meets the environmental goal of low energy consumption.

8123-03, Session 1

Investigation of tunable LED lighting for general illumination employing preliminary activity recognition sensor network

M. Thompson, OSRAM SYLVANIA Inc. (United States)

Digitally controlled lighting systems equipped with colored LEDs can produce a range of different qualities of white light, adjustable to users' requirements. Sensor networks allow lighting changes to be actuated in response to the location, activities, and paths of the occupants. We explore strategic control of RYGB LEDs forming white light, in response to an preliminary activity recognition sensor system, as well as the associated human factors. This paper reports and discusses the results of an ongoing research project applying the principles of tunable lighting, encompassing three main domains:

- (a) Tunable LED light system with controls;
- (b) Sensor network;
- (c) Human factors studies

The main goal is to understand best practices in tunable lighting for general illumination, especially based on potential for energy savings and improved visual comfort.

We are interested on one hand in the integration of LED system, controls and sensor network (hardware and software domains) and on the other hand on how the visual system perceives changes in the spectral components of white illuminants. An experimental tunable LED system and sensor network was installed in an occupied office environment, where a series of human factors experiments were conducted to assess realistic visual performance under changing lighting conditions.

8123-05, Session 1

Optical system design for a reflector-based LED food lighting module

A. Bäuerle, Fraunhofer-Institut für Lasertechnik (Germany) and RWTH Aachen (Germany); C. Schnitzler, RWTH Aachen (Germany); R. Wester, Fraunhofer-Institut für Lasertechnik (Germany); M. Kirsten, BARO GmbH & Co. KG (Germany); H. Schlüter, Alux-Luxar GmbH & Co. KG (Germany); P. Loosen, RWTH Aachen (Germany) and Fraunhofer-Institut für Lasertechnik (Germany)

We report on the development and experimental analysis of an LED lighting module for use in a high-end food lighting environment. Goods that are advertised in these lighting situations put high demands on color homogeneity and the rendering of certain color components. At the same time, energy regulations require the overall lighting fixture to be efficient. One possible approach is to use PVD coated metal reflectors that show up to 98% reflectivity across the visible spectrum but whose optical properties degrade if the surface curvature gets too high.

We present an adapted optical design that allows for homogeneous illumination in terms of both illuminance and colour by combining reflective elements. Within the optical setup, multiple elements of a low degree of deformation are combined to yield the desired illumination result, combining aspects of imaging and non-imaging optics. The selective texturing of reflector surfaces introduces scattering that enables the use of RGBW LEDs without any visible colour fringes. Using electronic controls, the spectrum of the light can be adjusted to yield optimum colour rendering without significant losses in efficiency. From a prototypical lighting module, energy efficiency and perceived quality of light are assessed in comparison with conventional light sources for various lighting situations.

Possible further applications for this setup include architectural and general lighting as well as process illumination.

8123-06, Session 1

Non-axisymmetrical freeform design for short LED street lamp

C. Jen, Y. Chen, J. A. Whang, National Taiwan Univ. of Science and Technology (Taiwan)

Based on energy savings trend, LED has been developing as the main force of the future lighting, especially the road lighting. For controlling the intensity distribution of LED, the concept of freeform design has been proposed in many articles with transmission or reflection components but mainly focus on axial symmetrical types or dual axial symmetrical types. We, in this paper, design a non-axisymmetrical freeform system applying in a short LED street lamp whose dimension is 10cm (W) x 10cm (L) x 7cm (H) that has an advantage, easy maintaining. For coordinate transformation and simplifying the non-axisymmetrical system, we create two virtual surfaces and design the slope of each discrete point on the freeform surface to control the light path between the two virtual surfaces and avoid the total internal reflection. The short street lamp has four LEDs to light 3m square and each LED light a triangle area. According to the simulation results, the uniformity of illumination is 1:3 and the optical efficiency is more than 80% that meet the legal requirements of street lamp. In short, to reduce manufacturing and maintenance costs, the proposed design is appropriate to use in the actual lighting on the road and to replace the traditional street lamps.

8123-07, Session 2

Phosphor-free white: the prospects for green direct emitters

C. Wetzel, Rensselaer Polytechnic Institute (United States)

No abstract available

8123-08, Session 2

Material properties of MOCVD-grown AlGaIn layers influenced by the in-incorporation

T. Y. Lin, L. Li, Y. L. Chung, J. R. Jiang, National Taiwan Univ. (Taiwan); Y. Lee, Tung Nan Institute of Technology (Taiwan); S. Yao, Z. C. Feng, National Taiwan Univ. (Taiwan); D. Wu, National Chung Hsing Univ. (Taiwan); I. T. Ferguson, The Univ. of North Carolina at Charlotte (United States)

AlGaIn epilayers were grown on sapphire (0001) by MOCVD, with intermediate growths of low/high temperature AlN nucleation layers. Variable flow rates of TMIn, 0, 50 and 500 sccm were introduced. Three AlGaIn samples were originally designed with similar Al composition of ~20%. Rutherford backscattering determined accurately Al content which decreased with increasing In-flow. Main photoluminescence bands spread over 310-350 nm with peaks in 320-335 nm. PL (10-300K) exhibited anomalous temperature dependent emission behavior of S-shaped shift, red-blue-red shifts. Carriers transfer between different luminescent centers. Abnormally high activation energy was obtained, indicating that excitons are not in the free states. Raman Scattering and spectral line shape analysis led to an optical determination of the electrical property free carrier concentration of AlGaIn. Our results on In-doped AlGaIn provide useful information for designing UV-LEDs.

8123-09, Session 2

Highly efficient InGaIn/GaN blue LED on large-sized Si (111) substrate comparable to those on sapphire

J. Kim, Samsung Advanced Institute of Technology (Korea, Republic of)

Based on the high crystalline quality of n-GaN on Si template, highly efficient InGaIn/GaN LEDs grown on 4 and 8 inch silicon substrates comparable to those on sapphire substrates have been successfully demonstrated. The n-GaN on Si template consists of AlN nucleation layer, transition layer and over 3 μm -thick Si doped n-GaN layer with $4.5 \times 10^{18} \text{ cm}^{-3}$ doping concentration. The transition layer which consists of AlGaIn layers and the unique epitaxial structure which consists of the dislocation reduction layer and stress compensation layers were grown to control the stress and reduce the dislocation, simultaneously. The full width at half maximum (FWHM) values of GaN (0002) and (10-12) ω -rocking curves were 260 and 360 arcsec, respectively. On top of n-GaN layer, 7 pairs of AlGaIn/GaN/InGaIn layers for the effective current spreading, a five-period multi-quantum-well active region consisting of 4 nm-thick InGaIn wells and 5 nm-thick GaN barriers, AlGaIn layer for blocking electron overflow and p-GaN cap layers were grown. The measured relative internal quantum efficiency of 8 inch InGaIn/GaN LED on Si, which was compared with 4 inch commercial InGaIn/GaN LED on sapphires, was measured about 90% based on the intensity dependent photo-luminescence method. At driving current of 350 mA, the overall output power of 1X1 mm² LED chips exceeded 420 mW and forward voltage was 3.2 V under un-encapsulated condition, which is the best value among the reported values of blue LED grown on Si substrates. The internal quantum efficiency of 76% at injection current of 350 mA was measured.

8123-10, Session 2

Digital precursor injection approach for improved indium-rich InGaIn epilayers grown by HPCVD

N. Dietz, R. Atalay, S. Gamage, H. Koralay, I. Senevirathna, U. Perera, Georgia State Univ. (United States)

Ternary In_{1-x}Ga_xN alloys have great potential in high-efficient spectral agile light sources, detectors, advanced high speed optoelectronics and optical communication devices. However, the presently encountered processing gaps between group III-nitride binaries limits the formation of high-quality ternary In_{1-x}Ga_xN over the whole composition range. The most visible encountered processing gap is the difference in the optimum growth temperatures for InN and GaN, which can be more than 300°C under low-pressure organometallic chemical vapor deposition growth. As a potential pathway to overcome the temperature gap, we explored in the recent year years the pressure dependency of surface chemical reactions and growth surface stabilization, utilizing a high-pressure chemical vapor deposition (HPCVD) reactor system. In this contribution will we extend the studies to encountered differences in the surface reaction chemistry during the deposition of InN and GaN epilayers. To address the different surface reactions in the growth of ternary In_{1-x}Ga_xN alloys, a combined digital ternary precursor injection scheme has been explored, which takes in account the optimum precursor injection sequences for the binary alloys. In this contribution we discuss the influence of pulse separations on the phase purity and stability of indium-rich In_{1-x}Ga_xN epilayer and resulting structural and optical properties.

8123-11, Session 2

Structural and optical properties of InGaN/GaN multiple quantum well light-emitting diodes prepared by metalorganic chemical vapor deposition

J. R. Jiang, M. H. Wang, Z. C. Feng, National Taiwan Univ. (Taiwan); B. Zhang, Huazhong Univ. of Science and Technology (China); Z. Zhou, Peking Univ. (China); A. G. Li, RAINBOW Optoelectronics Material Shanghai Co. Ltd. (China); X. Y. Li, B. L. Liu, Xiamen Univ. (China); D. Wu, National Chung Hsing Univ. (Taiwan)

We have performed a comparative structural and optical investigation on typical industry-manufactured blue emission InGaN/GaN MQW LED wafers with different indium composition and structural parameters, grown by MOCVD. Structural and optical properties were studied by various advanced analytical techniques. The effects of indium compositions and QW parameters, determined by HRXRD and HRTEM, were studied. HRTEM also revealed the dislocation distribution and the so-called V-shape defects. PL, PLE and TRPL in 10-300K and under different excitation and detection wavelength, were employed to study comprehensively the MQW luminescence mechanism, localization effect, carrier recombination and transferring dynamics, corresponding to the HRTEM observations and correlating to the lighting efficiency and LED device performance, which are significant to find the key to design high efficiency LEDs.

8123-42, Poster Session

Effects of voltage modulation of individual RGYB LEDs on the high power phosphor LED for color temperature and luminous efficiency

H. Chen, G. Wu, C. Yang, Y. Lo, J. Zhou, S. Li, National Yunlin Univ. of Science and Technology (Taiwan)

This study investigated the variations of color temperature and luminous efficiency for the high power phosphor Light-Emitting Diodes (LEDs) with the single LED of red, green, yellow and blue, respectively. First, the base voltages of white LEDs will be set up for the color temperature of 7500K (D75 cool white). Then we tuned individual voltages of RYGB LEDs to investigate the variations of color temperature and luminous efficiency. These results exhibited that changing the voltage of red LED had the broadening range of color temperature from 7500 K to 1500 K and variation of luminous efficiency from 68 to 44 lm/W. Then the green LED only could tune the high color temperature from 7500K to 8200K and have the small variation of luminous efficiency from 68 decreasing to 51 lm/W. Simultaneously, though the yellow LED could tune the middle range color temperature from 7500K to 4700K, but need the large variation of luminous efficiency from 68 to 40 lm/W. The luminous efficiency had rapid variation from 68 to 27 lm/W and out of the color temperature of 20000K for the voltage tuning of blue LED. When we used low power blue LED, it could fine-tune color temperature from 7500K to 8500K resulting of the power of blue LED(0.2W) was too small to phosphor white LED(1W). Therefore, the regulation tuning voltage of the red LED could show the warm color temperature and low variant of luminous efficiency. The color shifts (uv) of red and yellow LEDs always be under the Planck's curve with the increasing of color temperature but not for green LED.

8123-43, Poster Session

Encapsulation structure with reflective slop to improve light extraction for OLED lighting

C. Lee, J. Lee, Korea Electronics Technology Institute (Korea,

Republic of); D. Choi, Hanyang Univ. (Korea, Republic of); M. Kwak, Korea Electronics Technology Institute (Korea, Republic of)

Recently, organic light emitting diodes (OLEDs) have attracted to solid-state lighting due to self emitting property, high brightness at low current density, high efficiency and slim shape. To use illumination, properties of OLED are required to improve for efficiency and long life time. So we developed new encapsulation structure to improve light extraction for OLEDs and life time. Emitted light in OLEDs propagates all directions and materials have each other refractive index, so its external efficiency is low about 20% by total ref. To reduce this light loss, we designed new encapsulation structure. New encapsulation glass cap was excavated by wet etching in order to insert glass substrate. And it was worked to have two steps of reflective slope edges. A glass substrate that OLED was deposited was inserted in this cap and attach on first step of encapsulation glass cap. On the reflective slope, the reflective layer, aluminum was coated to improve reflectivity. Two reflective slope edges reflected the waveguided light from a glass substrate and an OLED. Also, to reduce reflective index by air between OLED and encapsulation glass, we filled up this gap with the suitable refractive index material. Also this material performed a role to improve lifetime. As adopted this cap, brightness and lifetime was increased about 20% and 15% than the cap of general structure.

8123-44, Poster Session

Light-extraction improvement of GaN LEDs using nano-scale top transmission gratings

A. Ellaboudy, G. Chavoor, X. Jin, S. Trieu, California Polytechnic State Univ., San Luis Obispo (United States) and Peking Univ. (China); C. Xiong, X. Kang, B. Zhang, G. Zhang, Peking Univ. (China)

Gallium Nitride (GaN) light emitting diodes (LEDs) embody a large field of research that aims to replace inefficient, conventional light sources with LEDs that have lower power, high luminosity, and longer lifetime. The conventional GaN LEDs have only a few percent light extraction efficiency. A common way to solve this light trapping issue is to etch a periodic structure at the light extraction surface and/or at the bottom reflective layer of the LED. In this paper, we present a Finite-Difference Time-Domain GaN LED model. The LED structures are: 200nm p-GaN, 50nm MQWs, 400nm n-GaN, 200nm n-GaN 2PhC grating. The CW light source is placed in the center of MQWs. The time monitor is above the LED to collect output power. Three design parameters define the grating layer: grating height, grating width, and grating period. First, we fix the grating height at 200nm, select the 50% filling factor, and sweep the grating period from 100 to 1000 nm. We find that the n-GaN grating layer has the highest light extraction output at a period around 700nm. Compared to the non-grating case, it has 27% light extraction improvement, which is agree with published experimental data of Peking University. Then, we sweep the above three parameters and all their possible permutations. And the light extraction improvement design optimization charts are developed. Some nano-grating structure improve light extraction of the LED devices, but some gratings actually lower the light extraction rate compared to the non-grating case.

8123-45, Poster Session

Multi-functional colorimeter designed for color analyses

F. Sametoglu, O. Celikel, TÜBİTAK National Metrology Institute (Turkey)

A multifunctional colorimeter is designed for measuring colorimetric properties of reflective and transparent materials. In order to illuminate samples, a special light source based on mixtures of a high power cool-white (CW) and a near-ultraviolet (n-UV) light emitting diodes (LEDs) via a fiber optic combiner is constructed. Insufficient spectral

Conference 8123:
Eleventh International Conference on Solid State Lighting

power distribution of CW LED over 380 nm - 410 nm are improved by using the mixture of light. A barium-sulphate coated integrating sphere capable of meeting standard measurement conditions of $d/8^\circ$ and $0^\circ/45^\circ$ for colorimetric analysis is designed. The integrating sphere has a sample port (18 mm in diameter) and three illumination/measurement ports (each of which has 9 mm in diameter). The mixture of light is transferred from the light source to the illumination port of the sphere by using a fiber optic cable having core diameter of 1 mm. Collimators are used at the illumination port for illuminating samples. Light reflected or transmitted from the sample is measured by means of a designed detector composed of a RGB-photodiode and stray light reduction tube. Photocurrents generated at outputs of RGB-photodiode are converted to voltages by using a three-channel transimpedance amplifiers having gain selection switches from 1×10^6 to 5×10^9 .

A special detector composed of RGB-photodiode and diffuser is also designed for measuring colorimetric and photometric properties of emissive surfaces like television or computer monitors. Design details and optical characterization of the colorimeter are presented herein.

8123-46, Poster Session

Improving reliability of LED package by inorganic gas barrier thin film

Y. Lu, Y. Lee, C. Sung, Lextar Electronics Corp. (Taiwan)

Research on inorganic thin film developed as gas-barrier protection for LED package is reviewed. The Si_3N_4 , SiO_2 , Al_2O_3 and $\text{SiO}_2+\text{TiO}_2$ inorganic thin film gas barrier coated on the surface of LED packages were prepared by sputter method, their structure characterization and luminescent properties were also investigated. These kinds of compounds show different water/vapor permeation in different thickness vary from 20nm to 100nm. One of the interesting results of this work is that the inorganic thin film could prevent water react with phosphor or silver layer from air, which provides the potential as a long life package in LED packing technology. Performance of gas barrier had been checked by different reliability tests. The reliability tests include (i) High temperatures and high humidity life test ($T_A=60^\circ\text{C}$, $\text{RH}=90\%$), (ii) Resistance to soldering heat ($T_{\text{sol}}=260^\circ\text{C}$, 10 sec, Pretreatment: $85\% \text{RH}, 24\text{hrs}$). It was demonstrated that samples with inorganic gas barrier show better optical performance than uncoated sample. The life decay analyses showed that the uncoated sample has cut down over 25% after 2000hrs. However, Si_3N_4 thin film coated sample could successfully suppressed optical intensity decay less than 10% after 2000hrs. Furthermore, the deviation of CIE distribution also could be improved from 0.011 to 0.003. This result shows that Si_3N_4 is an attractive candidate as a potential gas barrier in LED packing technology. The present results provide important information on the optimization of LED package reliability by coating inorganic thin film on the surface of package.

8123-47, Poster Session

Efficiency droop improvement in GaN-based light-emitting diodes by graded-composition electron blocking layer

C. Wang, National Chiao Tung Univ. (Taiwan); S. Chang, National Chiao Tung Univ. (Taiwan) and Epistar Corp. (Taiwan); W. Chang, J. Li, H. Kuo, T. Lu, S. Wang, National Chiao Tung Univ. (Taiwan)

Carrier overflow out of the active region as well as inefficient injection and transportation of holes have been identified to be the major reasons of efficiency droop. To reduce the carrier overflow, an $\text{Al}_x\text{Ga}_{1-x}\text{N}$ electron blocking layer (EBL) was adopted in common LED structures. However, the polarization-field induced band bending and the valance band offset (E_v) at the interfaces of GaN and EBL are considered to retard the injection of holes. We have designed a graded-composition electron blocking layer for InGaN/GaN LED. The simulation results showed that the triangular barrier of conventional EBL at valance band could be balanced, while the slope of conduction band could be increased by

increasing the band gap of $\text{Al}_x\text{Ga}_{1-x}\text{N}$ along [0001] direction. As a result, the hole concentration in MQWs was significantly increased, while the electron distribution within the GEBL region and p-GaN was enormously decreased over 2 orders, indicating the GEBL can effectively improve the capability of hole transportation across the EBL as well as the electron confinement. Furthermore, the LED structure with GEBL was realized by MOCVD. The L-I-V characteristics of GEBL LED showed better electrical characteristics due to the improvement in hole injection and the higher-efficiency p-type doping in GEBL, as compared to the conventional LED. More importantly, the efficiency droop was reduced from 34% in conventional LED to only 4% in GEBL LED at 200 A/cm².

8123-48, Poster Session

InGaN-GaN MQW LEDs with current blocking layer formed by Mg-H bonds

C. Chen, L. Hsia, J. Chao, J. D. Guo, Lextar Electronics Corp. (Taiwan)

For most of the Sapphire-based LEDs, both n- and p-type electrodes are formed on the same side because sapphire substrate is an insulating material. The p-type electrode area consists of a thick wire-bonding pad and extended finger electrode on the top side. In such a structure, the thick p-pad metal inevitably blocks part of the light output and reduces the light extraction efficiency. In addition, due to the not-so-good conductivity of the thin transparent layer, there often exists current crowding effect around the p-pad. This may further reduce the quantum efficiency and device reliability as well. To increase LED external quantum efficiency is one of the important topic in LED technology.

In this work, we demonstrate an enhancement of the light output power of GaN light emitting diodes (LEDs) by using Mg-H bonds as current blocking layer (CBL). The formation of Mg-H bonds is achieved by annealing the SiN_x film on the p-GaN surface and then removing it. Through annealing process, the region that deposited with SiN_x film will increase in the resistivity of the metal-semiconductor contacts and the p-type neutral regions. The forward voltage of Mg-H CBL-LED slightly increased 0.03V and the light output power improved 2.54% enhancement than the without CBL reference. The formation of Mg-H will form a current-blocking layer that improve the current horizontal spreading in the transparent layer, is applied to InGaN-GaN LEDs to enhance the external quantum efficiency.

8123-49, Poster Session

Optical and electrical properties of GaN-based light emitting diodes grown on micro and nano-scale patterned Si substrate

C. Chiu, C. Lin, National Chiao Tung Univ. (Taiwan); D. Deng, Hong Kong Univ. of Science and Technology (Hong Kong, China); H. Kuo, National Chiao Tung Univ. (Taiwan); K. Lau, Hong Kong Univ. of Science and Technology (Hong Kong, China)

We investigate the optical and electrical characteristics of the GaN-based light emitting diodes (LEDs) grown on Micro and Nano-scale Patterned silicon substrate (MPLDs and NPLEDs). The transmission electron microscopy (TEM) images reveal the suppression of threading dislocation density in InGaN/GaN structure on nano-pattern substrate due to nanoscale epitaxial lateral overgrowth (NELOG). The plan-view and cross-section cathodoluminescence (CL) mappings show less defective and more homogeneous active quantum well region growth on nano-porous substrates. From temperature dependent photoluminescence (PL) and low temperature time-resolved photoluminescence (TRPL) measurement, NPLEDs has better carrier confinement and higher radiative recombination rate than MPLDs. In terms of device performance, NPLEDs exhibits smaller electroluminescence (EL) peak wavelength blue shift, lower reverse leakage current and decreases efficiency droop compared with the MPLDs. These results suggest the feasibility of using NPSi for the growth of high quality and power LEDs on Si substrates.

8123-50, Poster Session

The study of measurement method for the junction temperature and thermal resistance in LED lightings

J. Park, H. Lim, LED-IT Fusion Technology Research Ctr. (Korea, Republic of); J. Jang, Yeungnam Univ. (Korea, Republic of)

The forward voltage, light emission and lifetime of LED lightings are closely related with the junction temperature. Recently, the alternative techniques for measuring junction temperature of LED packages have been reported, which include optical and electrical test method. Based on electrical test method, we propose how to evaluate the LED junction temperature of LED lightings by examining relation between the forward voltage variation and the junction temperature. In case of LED lighting, it is very difficult to measure junction temperature because of high voltage, high current and too many variables as compared with single LED package. In this study, LED lighting is placed in a temperature chamber and connected to precise current source (or LED drive) and measurement equipment to be able to measure a voltage and current simultaneously. K factor was experimented in condition of typical driving current at different temperatures ranging between 298 and 368 K. At room temperature, the corresponding forward voltage value was measured. And after the LED lighting continuously operated over one hour, the unchangeable forward voltage was measured. From these results, the junction temperature can be easily calculated by using formula based on EIA/JESD51-2 standard. The measured junction temperature in this method is expected to provide useful information to predict adequate lifetime of LED lighting.

8123-51, Poster Session

Energy-saving approaches to solid state street lighting

A. Zukauskas, P. Vitta, R. Stanikunas, A. Tuzikas, I. Reklaitis, A. Stonkus, H. P. Vaikevicius, Vilnius Univ. (Lithuania)

Commercial high-power light-emitting diodes (LEDs) have already attained luminous efficacy comparable to that of high pressure sodium (HPS) lamps, which are widely used in street lighting. However in comparison with slowly and inefficiently dimmed yellowish HPS lamps, LEDs offer efficient dynamic dimming and more appropriate color. We consider a solid-state street lighting concept based on three energy saving aspects, namely, savings due to improved visual performance under white solid-state light sources, weather sensitive luminance regulation, and intelligent lighting tracking of pedestrians and vehicles at low traffic density. Potential energy savings due to improved visual performance were estimated from the psychophysical investigation of human reaction time measured using an off-axis visual stimuli placed under various light sources (HPS lamp, warm white and daylight phosphor converted LEDs, and RGB LED cluster). Measurements of road luminance under different road surface conditions were collated with the statistical data for night time in Lithuania (60% dry, 10% wet, and 30% snowy). The intelligent vehicle/pedestrian tracking was tested using a 300 m long test ground consisting of 12 solid-state street luminaires controlled by a microwave motion sensor network. Rough estimations have shown that improved visual performance, weather sensitive three-level (dry-wet-snowy) luminance regulation, and intelligent tracking offered by solid-state street lighting can reduce the consumed luminous energy to about 90%, 80%, and up to 75% of that generated by uncontrolled HPS lamps, respectively, with the total energy saving effect in the Northern countries of about 50% for equal luminous efficacy of the LED and HPS light sources.

8123-52, Poster Session

LEDs on curved ceramic substrate with primary optics for modification of luminous intensity

A. Wei, Power Lens Technology Inc. (Taiwan); J. Sze, Instrument Technology Research Ctr. (Taiwan); J. Chern, Power Lens Technology Inc. (Taiwan)

A conventional LED chip is mounted on a flat substrate, leading to mere the forward emission (luminous intensity distribution with the angular spread 180°). To realize a LED bulb with the backward emission, a common method is exploiting diffuse surfaces. However, the out-coupling luminous flux is reduced around 10%. In this study, a curved substrate is used to efficiently achieve the forward and the backward emission. Meanwhile, the required curved substrate is realized by a ceramic printed circuit board (PCB), resulting in a cost-efficient chip-on-board (COB) structure. Further, such a COB LED luminaire can be packaged with primary optics. With proper design of the primary optics, the luminous intensity can be adjusted to fit the applications of streetlights. One example has been designed, fabricated and measured. The fabricated single unit is mounted on a heat-sink, while the measured luminous intensity distribution is shown as a bat-wing with the beam-angle of 132.6°. To realize a streetlight, 21 units have been assembled with related electronics and mechanics recently. The measurement of the designed streetlight is on-going and the reports of the results will be provided soon.

8123-53, Poster Session

Effects of pitch and shape for diffraction grating in LED fog lamp

H. Chen, J. Lin, National Yunlin Univ. of Science and Technology (Taiwan); J. Wu, Ming Chuan Univ. (Taiwan); S. Ma, Feng Chia Univ. (Taiwan); C. Yang, National Yunlin Univ. of Science and Technology (Taiwan)

The characteristics of light-emitting diodes (LEDs) that make them energy-efficient and long-lasting light source for general illumination have attracted a great attention from the lighting industry and commercial market. As everyone know LEDs have the advantages of environmental protection, long lifetime, fast response time (μs), low voltage and good mechanical properties. Their high luminance and the wide region of the dominant wavelengths within the entire visible spectrum mean that people have high anticipations for the applications of LEDs. People also found wide application in solid state lighting, like as street lighting, back lighting, sign lighting, lamp lighting and so on. A high brightness LEDs would like to used for the illumination on both street and automobile. The output lighting from reflector in the traditional fog lamp was required to fit the standard of the ECE regulation. Therefore, this study investigated the effects of pitch and angle for a diffraction grating in LED fog lamp. The light pattern of fog lamp must be satisfied ECE automobile technical regulations, so a design of diffraction grating to shift the lighting was required. We used two 1W LEDs (Cree XLamp XPE LEDs) as the light source in the fog lamp for the illumination efficiency. Then, an optimal simulation of diffraction grating was done for the pitch and angle of the diffraction grating at the test plane of 25 meters. The best pitch and angle was 2mm and 60 degree for the grating shape of triangle type.

8123-54, Poster Session

Investigation of GaN-based light emitting diodes on thermal stress

Y. Cho, H. Lim, M. Park, J. Jang, LED-IT Fusion Technology Research Ctr. (Korea, Republic of)

Conference 8123:
Eleventh International Conference on Solid State Lighting

We have investigated the degradation of the optical power and the I-V characteristics of

InGaN/GaN light-emitting diodes(LEDs) during the thermal stress on golden hot plate. We have analyzed the effect of high temperatures on the degradation of high brightness LEDs: a set of thermal stress tests have been carried out on LEDs produced by different manufacturers. At each step of the ageing tests, LEDs have been set on golden hot plate for a complete electro-thermal analysis of their properties. Thermal treatment has been found to induce output power decrease, modification of the spectral properties of the devices and operating voltage increase. The degradation of the optical properties has been found to be thermally activated: ageing tests carried out at different temperature levels; 25 to 250 at a constant current, the optical power was significantly reduced. The experimental results showed that the power loss, wavelength peak shift, and spectrum intensity reduction increase as the temperature increase.

In this paper, we have proposed a new concept of LED by which we can estimate the lifetime of blue LEDs with high accuracy. Two kinds of LEDs from different manufacturers were analyzed in this study using proposed LEDs. Optical and electrical characteristics such as light-output degradation and reverse leakage current of high-power blue LED were investigated and analyzed.

8123-55, Poster Session

Atomic distribution of transition metals in III-nitrides

R. W. Nicholas, M. H. Kane, The Univ. of Oklahoma (United States)

Understanding atomic distributions on the order of nanometers is becoming increasingly essential to solid-state electronic device design. The local composition of any singular constituent can have a great effect on a host of materials properties. Atom probe tomography is currently the only characterization technique that can provide direct physical detection of ionic species of atoms. This work presents the first case of GaMnN thin films that are characterized utilizing the state of the art local electrode atom probe (LEAP) to determine the atomic ordering of Mn in an effort to help understand room-temperature ferromagnetic exchange mechanisms in wide bandgap dilute magnetic semiconductors.

The distribution of Mn on the atomic scale was found to be random in nature with no evidence for the predisposition of Mn to form dimers, trimers or clusters that may lead to room-temperature ferromagnetism that has been observed in the samples. This is attributed to surface segregation of Mn during the growth process, leading to a concentration of Mn well below the solubility limit near the buffer layer where data was collected.

This work proves consistent with previous magnetic analysis in that most isolated Mn atoms will result in paramagnetic behavior. This behavior, coupled with the effects of ferromagnetic clusters yields previously observed superparamagnetic behavior. Atom probe tomography corroborates where in the sample these clusters lie, aiding in the ultimate goal of understanding the structure-property-growth condition relationships for the tailoring of specific MOCVD processes that will lead to the ability to selectively control spintronic device functionalities.

8123-56, Poster Session

Growth of novel buffer layers for III-nitride LEDs by pulsed electron deposition

N. Arefin, R. W. Nicholas, R. Dooly, M. H. Kane, The Univ. of Oklahoma (United States)

Pulsed electron beam deposition (PED) allows for the growth of high crystalline quality films at much lower growth temperatures than metal organic chemical vapor deposition and molecular beam epitaxy. PED also represents a potential replacement to pulsed laser deposition

especially for very high bandgap materials, as PLD has higher setup costs due to the requirement of excimer lasers. The low temperature growth of PED also allows for the integration of dissimilar materials, which inhibits interdiffusion, backetching, and chemical reactions during the growth process. This approach may allow for the implementation of III-nitrides with lattice-matched oxide substrates, or for the integration of chemically soluble buffer layers which can be removed to improve thermal management or light extraction. In this work, we have explored the epitaxial deposition of GaN films on chemically soluble buffer layers (ZnO, CrN) using PED. The as-grown films were characterized using X-ray diffraction, atomic force microscopy, and transmission electron microscopy. The results show that this technique may provide a new avenue for integration of III-nitrides on lattice matched but chemically reactive substrates.

8123-57, Poster Session

Self-assembled microlens on LED using hydrophilic effect

G. J. Su, H. Wei, National Taiwan Univ. (Taiwan)

In this paper, we propose a self-assembled microlens arrays (MLAs) on top of light emitting diodes (LED) based on hydrophilic effect by UV Ozone treatment. A SU-8 mask with opening is used to obstruct the UV Ozone treatment and produce zones which are more hydrophilic on LEDs with SU-8 base layer on it. After hydrophilic zones are produced and the SU-8 mask is removed, the substrate with hydrophilic zones is dipped in and out of diluted SU-8 solution with slow and constant velocity. Finally, MLA is formed after UV curing and baking. There are several influence parameters, including diameter of hydrophilic zone, contact angle, and viscosity of diluted SU-8. Larger diameter, longer UV Ozone time, and more concentrated of diluted SU-8 induce longer focal length. Optical measurement revealed a good optical performance from the fabricated MLAs. By this approach, the fabrication is low cost and low time-consuming.

8123-58, Poster Session

Study on colony image acquisition and analysis system

W. Wang, Henan Polytechnic Univ. (China)

In this paper, colony image acquisition system design and construction are discussed and presented. To make colony image of stable and good quality, camera chosen, lightning design and colony plate should be considered. Recently, many researchers and developers have made efforts for this kind of systems. By investigation, some existing systems have some problems since they belong to a new technology product. One of the main problems is image acquisition. In order to acquire colony images with good quality, an illumination box was constructed as: the box includes front lightning and back lightning, which can be selected by users based on properties of colony dishes. With the illumination box, lightning can be uniform; colony dish can be put in the same place every time, which make image processing easy. A digital camera in the top of the box connected to a PC computer with a USB cable, all the camera functions are controlled by the computer.

8123-59, Poster Session

Optimal design of light distribution of LED luminaries for road lighting

W. Lai, W. Chen, X. Liu, Chongqing Univ. (China)

No abstract available

8123-12, Session 3

Photo-recycling effects in LED lighting

C. Sun, National Central Univ. (Taiwan)

No abstract available

8123-13, Session 3

From dark to bright: novel daylighting applications in solid state lighting

H. G. Adler, OSRAM SYLVANIA Inc. (United States)

The term "daylighting" is used in various ways, on one hand in a more architectural sense, i.e. using existing daylight to illuminate spaces, and on the other, more recently, for using light sources to replicate daylight. The emergence of solid state lighting (SSL) opens up a large number of new avenues for daylighting. SSL allows innovative controllability of intensity and color for artificial light sources that can be advantageously applied to daylighting. With the assistance of these new technologies the combination of natural and artificial lighting could lead to improvements in energy savings and comfort of living beings. Thus it is imperative to revisit or even improve daylighting research so that lighting and building networks of the future with their sensor, energy (e.g. HVAC) and lighting requirements can benefit from the new emerging capabilities. The current talk will review existing daylighting concepts and technology and discuss new ideas. An example of a tunable multi-color SSL system will be shown.

8123-48, Session 3

Intensity shaping and the application efficiency of indoor OLED lighting

P. Y. Ngai, J. Fisher, M. M. Lu, Acuity Brands Lighting, Inc. (United States)

Most indoor lighting is uniform, targeted for the most demanding visual tasks, a practice driven by limitations of conventional lighting systems, resulting in waste. It has been shown that discrete low-luminance tiles of OLED lighting can achieve a practical overhead lighting system that precisely tunes illumination for user requirements, resulting in energy savings, increased comfort, and enhanced flexibility. In this paper, the application efficiency of OLED lighting is further explored by evaluating how intensity shaping can vary photometric performance, create more targeted lighting effects, and increase the types of lighting applications for which OLED can be considered. Several non-Lambertian distributions are considered, along with multiple configurations of OLED panels.

8123-49, Session 3

Toward mass production of OLED lighting

C. Lee, C. Chen, C. Yang, C. Fang, T. Chang, AU Optronics Corp. (Taiwan)

Toward mass production of OLED lighting, differential application field, satisfying performance and competitive cost structure are all very important. In this article, from manufacture point of view, challenges and potential approaches to achieve such performance and cost structure will be discussed. Besides, comparison of OLED lighting with other light sources in some specific application field will be also described.

8123-14, Session 4

Degradation of lumen and chromaticity of high-power glass-doped phosphor-converted white-light-emitting diodes under thermal and humid tests: lighting phosphor technology (YAG, etc.)

W. H. Cheng, C. Tsai, J. Wang, National Sun Yat-Sen Univ. (Taiwan)

Intensity degradation of high-power LEDs is a well-known issue, which has been until recently mainly attributed to the degradation of the chip material. With the introduction of new improved chip materials the problem has shifted to the LED packaging and association with reliability. However, the high-power LED packaging and association with reliability have been less investigated. In this study, the reliability study of thermal and humid tests for high-power white-light-emitting diode modules (WLEDMs) incorporating Ce:YAG doped glass, instead of conventional Ce:YAG doped silicone, as a phosphor layer is presented. An exploring comparison study of lumen loss, chromaticity shift, and transmittance loss of high-power WLEDWs with Ce:YAG doped glass and Ce:YAG doped silicone under thermal aging, thermal shock, and damp heat tests was performed. The thermal aging results showed that the WLEDs with the doped glass at 4 wt% concentration exhibited two times less lumen loss, chromaticity shift, and transmittance loss than with the doped silicone. The damp heat results showed that the WLEDWs with doped glass at 2~8 wt% doping concentrations exhibited 67~69%, 49~65%, and 35~67% better improvements than doped silicone for the lumen loss, chromaticity shift, and transmittance loss, respectively. However, the performance of the WLEDMs did not significantly show difference between doped glass and silicone under thermal shock tests. The glass as Ce:YAG doped layer is used for WLEDMs due to the glass having five times higher glass transition temperature (T_g) of 750° compared to conventional silicone of 150° that can exhibit high thermal stability and humidity resistance.

8123-15, Session 4

Optical performances degradation of InGaN/GaN MQW LEDs related to fluorescence shift of copolymer-based silicone coating

R. Baillet, L. Bechou, C. Belin, T. Buffeteau, I. Pianet, C. Absalon, Y. Deshayes, Y. Ousten, Univ. Bordeaux 1 (France)

GaN-based LEDs are currently used in a wide range of applications as solid-state lightning, backlighting or full-color displays. Up to date, the polymer degradation mechanisms are not fully understood. Moreover, polymer-based packaging degradation impacts operational reliability of InGaN/GaN MQW LEDs thus limiting their performances. Accelerated ageing tests (30mA/358K/1500h) performed on packaged InGaN/GaN MQW LEDs have reported a fluorescence shift of silicone oil responsible for optical losses. Physics of failure methodology mixing electro-optical failure signatures and physico-chemical analyses is proposed. Electrical and optical characteristics highlight a 65% drop of optical power and an increase of one decade of leakage current spreading at the silicone oil/chip interfaces. Through measurements of the copolymer silicone coating fluorescence emission spectra, we demonstrate that the polymer degradation enlarges the LED emission spectrum (7%) and shifts central wavelength (5 to 7 nm). To understand such fluorescence shift, Attenuated Total Reflection, Nuclear Magnetic Resonance (NMR) and mass spectrometry have been performed. The copolymer molecular structure has not been affected after ageing regarding phenyl, methyl and siloxane patterns (neither chain fracture nor mass decay) while NMR and mass spectrometry evidence the presence of unidentified low molecular weight molecules disappearing after ageing. A first hypothesis results in the polymerization of other unidentified molecules as NMR demonstrates the diffusion of high molecular weight molecules (mass ratio of 100) after ageing. Both temperature and photodegradation of the silicone oil are

Conference 8123:
Eleventh International Conference on Solid State Lighting

assumed to be responsible for the polymerization of the unidentified molecules. Further investigations are in progress to determine the unidentified molecules.

8123-16, Session 4

The analysis of thermal effect on color performance for white LEDs

C. Chen, H. Wu, C. Sun, National Central Univ. (Taiwan)

For general phosphor converted LED packaging, the chromatic performance of an LED changes with the increasing temperature. In this paper, we try to analyze and predict the thermal effect on the phosphor and the blue die. Our experimental results show that the output power, correlated color temperature, and color coordinate of white LEDs will vary as the temperature rises. The output power of the blue and yellow light will decay with rising temperature. In addition, the spectrum of the blue die is red-shift and the phosphor is blue-shift with the rising temperature. According to the various emission spectra of the bare chip, the ability of blue light absorbed by YAG phosphor will change. In the study, we introduce a concept "absorbability" to analyze properties in white LEDs, which are combined with the excitation spectrum of YAG phosphor and the emission spectrum of blue bare chip. Then, we combine the thermal effect with the absorbability to minimize the deviation of correlated color temperature and color coordinate of white LEDs with the rising temperature. Finally, we can predict the variance of color performance with various operation temperatures in the white LED packaging combined with different bare chips.

8123-60, Session 4

Methods for estimating junction temperature of AC LEDs

A. Jayawardena, Y. Liu, N. Narendran, Rensselaer Polytechnic Institute (United States)

Light-emitting diodes operating on alternating current (AC) are gaining popularity in lighting applications. The junction temperature of an LED has significant influence on its performance, including light output, luminous efficacy, service life, and reliability. Since junction temperature cannot be measured directly, most methods presently used with DC LEDs are indirect and provide estimations of junction temperature. Although there are many proven methods for estimating the junction temperature of DC LEDs, only a few methods have been proposed for AC LEDs. In the study presented in this paper, three different methods were investigated and analyzed to understand their accuracies in estimating AC LED junction temperature. In one method, a low reference current pulse was used to measure the voltage across the AC LED junction that estimated the junction temperature. In the second method, an active cooling system was used to recover the initial current (rms) and estimate the junction temperature. In the third method, the peak wavelength value of the spectrum was used to estimate the junction temperature. Results from all three methods were compared and analyzed to determine their accuracies. The details of the methods and the associated results will be presented and discussed.

8123-18, Session 5

Compact collimators for high-brightness LEDs using dielectric multilayers

H. J. Cornelissen, Philips Research Nederland B.V. (Netherlands);
H. Ma, C. Ho, M. Li, Technische Univ. Delft (Netherlands)

A novel method is presented to inject the light of millimeter-sized high-brightness LEDs into light guides of sub-millimeter thickness. Use is made of an interference filter that is designed to pass only those modes that will propagate in the light guide by total internal reflection. Other

modes are reflected back to the LED cavity and recycled, leading to an increased brightness.

A collimator has been designed and made that is only 1mm thick, with a diameter of 6.5mm. It creates a beam of 26deg Full Width at Half Maximum. Presently, collimators with these characteristics have a thickness of 10-20mm and a diameter of 20-30mm and require careful mounting and alignment. The new collimator contains a 4.5micron thick interference filter made of 54 layers of Nb₂O₅ and SiO₂ layers. The filter is optically coupled to the LED with Silicone adhesive which makes the configuration very robust. A cylindrical lightguide, tapered from 6.5mm to 2.5mm diameter and 1mm thick captures the light that passes the filter, folds the light path and redirects the beam. Measurements on collimator prototypes show good agreement with the designed characteristics.

This promising approach enables much more compact collimators optics that offer material cost savings and design freedom.

8123-19, Session 5

Freeform lens design for LED illumination with high uniformity and efficiency

W. C. Chen, H. Y. Lin, National Taiwan Univ. (Taiwan)

In this paper, design examples related to LED illumination are presented. We design a freeform lens according to the initial LED light source intensity distribution so that the light rays emitted from a LED through the lens can achieve high uniformity and efficiency on the prescribed target plane. Because the model is of rotational symmetry, we consider just a 2-D lens shape and then sweep to get the 3-D result. Here a procedure based on the Snell's law and "edge-ray principle" for designing the freeform lens is proposed. First of all, we analyze the LED intensity distribution and subdivide it into parts. Then we calculate the zones on the target plane where the subdivided light rays should be distributed to. Finally we use an analytic approximate method to construct the freeform lens. After constructing the freeform lens, we simulate for the optical model by using the ray-tracing software LightTools®. The simulation results are very close to our expectation, that is, most light rays are distributed to the zones as designed. And it also shows that the Cree XLamp XR-E LED light source through the freeform lens can achieve up to 93% uniformity and 90% efficiency including Fresnel losses for a 1 m distance away and 1 m radius of circular illumination plane. This method utilizes simple processes and the model can be easily constructed; so they can be very useful for designing LED illumination. As long as variables such as the distance and range of the illumination plane are prescribed, the lens of secondary optics can be designed to achieve high uniformity and efficiency for LED illumination.

8123-20, Session 5

Sapphire side wall shaping by laser scribing

Y. Chen, F. Wenffy, L. Hsia, J. Chao, J. D. Guo, Lextar Electronics Corp. (Taiwan)

To increase LED light extraction efficiency is the one of the important topic in LED technology. Due to the difference of reflective index between GaN, sapphire and air, most of emitting light will be trapped in substrate materials. Therefore, there are many solutions that used to solve the problem such as surface texture, and pattern sapphire substrate. In this paper, we will discover a method to increase the light extraction efficiency in sapphire base LED. In this method, the laser scribing was used to shape sapphire side wall to form the regular trapezoid and pour trapezoid shape. We found that the regular trapezoid can make more light escape from sapphire side wall when the angle from side wall to the bottom side of sapphire substrate is about 131°. On TO-can, the regular trapezoid and pour trapezoid can improve ~5% and ~10% light output enhancement individually compared with straight sapphire side wall on p-GaN roughness LED structure. But interestingly, the efficiency of blue light transfer to white of the regular trapezoid sapphire shaping is better than pour trapezoid shaping in white light on L/F type. The detail mechanism will be reported in this talk.

8123-21, Session 5

Using Taguchi method to design LED lamp for zonal lumen density requirement of ENERGY STAR

J. Yu, Y. Chen, J. A. Whang, National Taiwan Univ. of Science and Technology (Taiwan)

In recent trend, LED begins to replace traditional light sources since it has many advantages, such as long lifespan, low power consumption, environmentally mercury-free, broad color gamut, and so on. According to the zonal lumen density requirement of ENERGY STAR, we design a triangular-prism structure for LED light tube. The optical structure of the current LED light tubes consists of the array of LED and the semi-cylindrical diffuser in which the intensity distribution of LED is based on Lambertian and the characteristics of diffuser are BTDF: 63%, transmission: 27%, and absorption: 10%. We design the triangular-prism structure at the both sides of the semi-circular diffuser to control the wide-angle light and use the Taguchi method to optimize the parameters of the structure that will control the 15% of total flux to light the area between 90 degree and 135 degree and to avoid the total internal reflection. According to the optical simulation results, the 85% of total flux is within 90 degree and the 15% of total flux is between 90 degree and 135 degree that match completely with the Solid-State Lighting (SSL) Criteria V. 1.1 of ENERGY STAR.

8123-22, Session 5

Profiling the optical distribution of a white organic light emitting diode as a lighting source

H. Yang, National Taipei Univ. of Technology (Taiwan); J. Su, National Taiwan Univ. of Science and Technology (Taiwan); L. Chen, National Taipei Univ. of Technology (Taiwan); Y. Lien, National Taipei Univ. of Technology (Taiwan); S. Peng, National Taiwan Univ. of Science and Technology (Taiwan); Y. Chen, National Taipei Univ. of Technology (Taiwan)

The optical distribution of a white organic light-emitting diode (WOLED) was experimentally investigated and profiled by using a microscopic goniometer equipped with optical power meter. WOLED has become a potential planar lighting source due to its unique planar device structure consisted of multiple organic layers sandwiched by cathode and anode electrodes on glass substrate. The optical field distribution of a WOLED planar lighting source is expected to be different from that of conventional LED as a point lighting source. It is crucial for understanding its optical distribution of a planar lighting source to design lighting source system by WOLED. The optical distribution of a WOLED with 1cm x 1cm lighting area was profiled by a microscopic goniometer in which we are able to pinpoint any spot in lighting area and measure its microscopic optical power independently. The profile of its optical distribution can be established by combining individual microscopic optical power from measured spots across the lighting area. The optical distribution of a WOLED is generally observed as uniform distribution by naked eyes. Our experimental result revealed that the optical distribution of a planar WOLED lighting area behaves like Gaussian distribution rather than uniform distribution as observed by naked eyes. It is also indicated that the optical profile of a WOLED planar lighting source is analogous to a point lighting source in microscopic point of view.

8123-23, Session 5

Freeform reflector design for LED street lighting

C. Li, P. Schreiber, Fraunhofer-Institut für Angewandte Optik und

Feinmechanik (Germany); A. Walkling, C. Schierz, Technische Univ. Ilmenau (Germany); M. Schwede, V. Guehne, JENOPTIK Polymer Systems GmbH (Germany)

Faceted freeform reflectors were designed for intelligent street lighting with LED cluster arrays for main traffic roads. Special attention was paid to achieve highly efficient illumination on both wet and dry road surfaces. CIE reflection tables W4 and C2 were applied in the simulation for these two conditions, respectively. The design started with plane facets, then - to avoid artifacts from the images of the individual LEDs - plane facets were replaced with cylindrical facets. To get further more flexibility for the design and optimization, freeform facets were employed, modeled by extruding two different conic curves together. Besides of achieving well-proportioned road luminance distribution, the basic shapes of the reflectors were also formed to control stray light caused by multiple reflections within the reflector and by reflecting the light from neighbor clusters within the cluster array. The merit functions useful transmission of light to the road as well as overall and lengthwise uniformity according to road illumination standards. Due to the large amount of variables, the optimization was carried out sequentially facet by facet. The design loops included compromising with manufacturing limitations for plastics molding and thorough analysis of conformity with DIN EN 13201 standards for ME road lighting classes. The calculated reflector profiles are realized by plastic injection molding.

8123-24, Session 6

High-reflectance and low-resistance nano-patterned Pt alloy contact to p-type GaN

C. Chang, C. Liu, National Central Univ. (Taiwan)

A self-formed nano-network meshed Pt layer formed on the epitaxial (0001) GaN substrate upon thermal annealing. EBSD analysis shows that, while the meshed Pt layer was forming on the GaN surface, Pt atoms rearranged themselves in (111)-preferred orientation on (0001) GaN. The (111) Pt/(0001) GaN interface represents the most energy-favored stacking configuration.

In this talk, we will report a high transmittance (in visible range) and low-resistance p-GaN contact for high-power LEDs by using this unique meshed Pt layer. Besides using the meshed Pt layer as the transparent conducting layer for the horizontal LED chips, we also combine the meshed Pt layer with the Ag reflector as the high reflective and low resistance p-GaN contact scheme for the vertical LED chips (thin-GaN LED). In addition, we found that by alloying the Pt layer with Au or Ag, the de-wetting of the Pt alloy thin film can be more controllable on the GaN surface. The de-wetted Pt alloy layers were found to have good ohmic-contact with p-GaN. All the optical and electrical characterizations of LEDs with the meshed Pt (Pt alloys) layer would be present in this talk.

8123-25, Session 6

Improvement of GaN-based light emitting diodes using p-type AlGaIn/GaN superlattices with a graded Al composition

S. J. Lee, S. Han, C. Cho, Gwangju Institute of Science and Technology (Korea, Republic of); H. Shim, Y. Kim, Samsung Electro-Mechanics (Korea, Republic of); S. Park, Gwangju Institute of Science and Technology (Korea, Republic of)

We investigated the effect of graded Al composition in the p-type AlGaIn/GaN superlattices (SLs) of InGaIn/GaN multiple quantum well (MQW) light-emitting diodes (LEDs) to improve their performance. The InGaIn/GaN MQW LEDs with p-type AlGaIn/GaN SLs were grown on a c-plane (0001) sapphire substrate by metalorganic chemical vapor deposition (MOCVD). The LEDs with grading I and grading II consisted of Al compositions in p-type AlGaIn barriers that varied from 0 to 16% and from 16 to 0%, respectively. The integrated electroluminescence (EL)

Conference 8123:
Eleventh International Conference on Solid State Lighting

intensity of LEDs with grading I and grading II was higher by 10% and 7.6% than that of LEDs without grading at 350 mA, respectively. The external quantum efficiency (EQE) of LEDs with grading I and grading II was increased by 9.5% and 6.5% at a current density of 30 A/cm², respectively, compared to that of LEDs without grading. The improvement of output power and EQE of LEDs with Al composition grading can be attributed to the increased hole injection by the reduced AlGaIn barrier heights and the suppression of the potential spikes between AlGaIn and GaIn in SLs. These results indicate that a graded AlGaIn layers in p-type AlGaIn/GaN SLs alleviate the efficiency droop mostly at low current density.

8123-26, Session 6

High-quality vertical light emitting diodes fabrication by mechanical lift-off technique

S. Hsu, Tamkang Univ. (Taiwan)

For the past decade, wide band gap GaN-based semiconductors have attracted much attention due to the important applications of high brightness light emitting diodes in solid state lighting. These devices were grown heteroepitaxially onto foreign substrates like sapphire and SiC and led to the shortage of high quality GaN substrates. The sapphire is the most commonly used substrate because of its relatively low cost, but also has the limitation of high-power performance due to its poor electrical and thermal conductivity. In the last decade, a laser lift-off (LLO) and chemical lift-off (CLO) technique have been used to fabricate the freestanding GaN membrane for high performance optoelectrical devices. However, the LLO and MLO may induce some damages at elevated temperature in GaN epilayer, i.e., decrease the lighting performance during lift-off process. Here, we demonstrate the fabrication of mechanical lift-off (MLO) high quality thin-GaN with hexagonal inverted pyramid (HIP) structure for vertical light emitting diodes (V-LEDs).

In this experiment, the high quality thin-GaN LED devices are fabricated by Au-Si wafer bonding and MLO process. Si material is chosen due to its high thermal conductivity which helps to quickly dissipate heat generated by LEDs. The density of threading dislocations was supposed to be efficiently reduced by re-growth GaN epilayer on HIP structure. The stress relaxation of the transferred GaN films is studied by varying the bonding thickness in the range from 5 μm to 50 μm. The residual stress states of the transferred GaN thin films are characterized by Raman spectroscopy measurement. Finally, the PL and EL spectrum of MLO V-LEDs are also measured to prove the improvement of lighting performance.

8123-27, Session 6

Single-chip phosphor-free white LEDs

X. Guo, B. L. Guan, Beijing Univ. of Technology (China)

With the realization and rapid development of GaN light-emitting-diodes (LEDs), white LEDs using GaN-based materials have attracted a lot of attentions and interests both in research and in industrial applications, such as for indicators, backlights, and especially in general illumination. To date, there are two leading approaches to achieve white LEDs. One is to put red, green and blue LEDs (RGB-LEDs) together in space and mix these three primary colors to produce white light. The other approach is to use blue or UV LEDs to excite one or more phosphors covered on them to give white light. LEDs using this approach are called phosphor-converted LEDs (pc-LEDs). Although RGB-LEDs have high efficacy, instantaneous color and intensity controllability, the practical implementation has numerous challenges, including the spatial light mixing and complicated feedback control system. For the pc-LEDs, their lifetime is limited by the phosphors covered on them. The power or the efficacy of pc-LEDs usually decreases due to the wavelength conversion occurred in the phosphor from the blue region to the yellow region, degrading the efficacy of LED itself. Moreover, some phosphors result in some environmental problems both in preparation and in use of this kind of white LEDs, such as the use of chlorine and cadmium.

In this study, the single-chip phosphor-free white light source made of two different LEDs was investigated. An InGaIn/GaN LED and an AlGaInP LED are integrated together by wafer-bonding technology. By choosing two complementary wavelengths with a certain power ratio, the combination of EL lights from the two LEDs yields white light located on the chromaticity diagram near to the standardized Illuminant C.

8123-28, Session 6

Low-temperature electroluminescent behaviors of InGaIn/GaN-based nanorod light emitting diode arrays

L. Chen, National Taiwan Univ. (Taiwan)

For InGaIn/GaN based nanorod devices using top-down etching process, the optical output power is affected by non-radiative recombination due to sidewall defects (which decrease light output efficiency) and mitigated quantum confined Stark effect (QCSE) due to strain relaxation (which increases internal quantum efficiency). Therefore, the exploration of low-temperature optical behaviors of nanorod light emitting diodes (LEDs) will help identify the correlation between those two factors. In this work, low-temperature EL spectra of InGaIn/GaN nanorod arrays was explored and compared with those of planar LEDs. The nanorod LED exhibits a much higher optical output percentage increase when the temperature decreases. The increase is mainly attributed to the increased carriers and a better spatial overlap of electrons and holes in the quantum wells for radiative recombination. Next, while the nanorod array shows nearly constant peak energy with increasing injection currents at the temperature of 300K, the blue shift has been observed at 190K. The results suggest that with more carriers in the quantum wells, carrier screening and band filling still prevail in the partially strain relaxed nanorods. Moreover, when the temperature drops to 77K, the blue shift of both nanorod and planar devices disappears and the optical output power decreases since there are few carriers in the quantum wells for radiative recombination

8123-29, Session 7

LED lighting standardization overview

J. Jiao, OSRAM Opto Semiconductors Inc. (United States)

This presentation provides comprehensive overview of standardization process and new standards for LED general lighting applications. In particular it focuses on the standards that are developed or under developing by ANSI, NEMA, IESNA, UL, IEEE and other organizations. The detailed LED lighting terminologies, testing, and requirements including system or component level specifications in terms of luminous efficacy, photometry and chromaticity, lumen maintenance, electrical, thermal and other environmental conditions, etc. will be discussed. The government specifications for Solid-State Lighting programs such as Energy Star will also be introduced.

8123-30, Session 7

Methods for measuring work surface illuminance in adaptive solid state lighting networks

B. Lee, M. H. Aldrich, J. Paradiso, Massachusetts Institute of Technology (United States)

Lighting control is in the midst of radical change. Present-day state-of-the-art lighting systems tend to be overly complex, designed with many degrees of freedom to address any user's lighting needs. Yet, the user interfaces of these systems are woefully lacking, frequently denigrated to a panel of buttons with select presets that are often cryptically defined, poorly labeled, and seldom desirable. While some higher-end systems

Conference 8123:
Eleventh International Conference on Solid State Lighting

offer a touch screen to select graphically-illustrated presets, these rigid assumptions lead to user frustration. Most attempts to integrate sensor feedback into commercial systems exploit simple motion sensors to activate all lighting in a space when one occupant moves. This is generally an energy-wasteful choice and, is not much better than the converse: turning off all the lights when the occupant doesn't move for a while.

The inherent control flexibility implied by solid-state lighting - united with the rich details offered by sensor networks - prompts us to rethink lighting control. In this research, we focus on both modulated photonic and geometric methods of measuring the work surface illuminance and ambient light, as detected by our sensor network, for controlling solid-state lighting networks. We discuss these techniques, including the lessons learned from our prior research. We present a new method for measuring the illuminance of an arbitrary luminaire at the work surface, without user disruption, by decomposing the modulated light into its fundamental and harmonic components. We fully derive and provide the results of this method, including its performance in our latest adaptive lighting testbed.

8123-31, Session 7

Addressing the variables in LED product design to ensure product reliability

P. F. Keebler, F. D. Sharp, Electric Power Research Institute, Inc. (United States)

Continuing developments in LED lighting are leading to more lighting products for illumination in LED fixtures for the residential, commercial, and industrial facilities. Most of the research in the past ten years has been aimed at developing LEDs with higher brightness, higher efficacies, good color performance and longer life. Many efforts have been accomplished to develop LED driver circuits to drive LED arrays, even drivers that are dimmable. Manufacturers are increasing their level of concern with the performance and life of the whole LED product with a renewed emphasis on reliability. Reliability for LED products not only involves thermal management, fixture design, and driver loading but also how products respond to electrical disturbances that occur in the building electrical environments where the products must function. EPRI research has demonstrated that the immunity of LED lighting systems to common everyday electrical disturbances is critical to establishing the reliability needed to ensure expected performance and for their survival during product life. Test results showing the application of voltage surges, transients, and sags among other disturbances will be presented. This paper will discuss the application of the results of EPRI research in this area, the test protocol associated with EPRI system compatibility concept, examples of how applying the concept has identified reliability problems in LED products, and how the reliability of these LED systems can be easily improved.

8123-32, Session 7

Statistical approach to color rendition properties of solid state light sources

A. Zukauskas, R. Vaicekauskas, A. Tuzikas, P. Vitta, Vilnius Univ. (Lithuania); M. S. Shur, Rensselaer Polytechnic Institute (United States)

Versatility in composing the spectral power distribution of solid-state light sources offers vast possibilities in color rendition engineering. In particular, the use of narrow-band spectral components allow for controlling two principle color rendition properties of illumination, color fidelity and chromatic contrasting. We present the results on the assessing and optimization of color rendition properties of solid-state light sources using on a recently introduced statistical approach to color quality of illumination. The method relies on the computational grouping of a large number of test color samples (e.g., the Munsell palette of 1269 samples) depending on the color shifts in respect of the experimentally

established just perceived differences of chromaticity and luminance. The method allows for introducing single-format and easy-to-understand color rendition indices, such as Color Fidelity Index (percentage of the test samples having the color shifts smaller than the perceived color differences) and Color Saturation/Dulling Indices (percentage of the test samples having the color shift vectors with a perceivable increase/decrease in chromatic saturation). Within this approach, practical solid-state lamps, such as phosphor converted light-emitting diodes (LEDs) and polychromatic LED clusters were attributed to several distinct types, such as high-fidelity, color saturating, or color dulling light sources. Optimization of spectral power distributions of solid-state lamps in respect of different color rendition properties was performed and light sources with dynamically tailored color rendition properties were developed. The statistically assessed color rendition properties were validated using a psychophysical investigation.

8123-33, Session 8

Thermal analysis of mid-UV LEDs light sources

S. Graham, Georgia Institute of Technology (United States); A. M. Khan, Univ. of South Carolina (United States); V. Adivarahan, Nitek, Inc. (United States)

The development of mid-UV solid state light sources hold promise for applications such as biological sensors and water purification. Due to their wavelength of emission, these devices are often grown on sapphire or AlN substrates and then flip chip bonded to a submount and then a power electronics or optoelectronics package to dissipate the heat. Maximizing the thermal dissipation is critical to improving the efficiency and reliability of these devices. However, very little has been done to elucidate the thermal response of mid UV-LED emitters.

In this work, a combination of forward voltage thermometry, Raman spectroscopy, and IR thermography are used to analyze the thermal response of mid-UV LED light sources made using micro-pixel LEDs. Transient thermal analysis using structure function modeling and transient forward voltage temperature measurements provide insight into the packaging thermal resistance. Corresponding light out put was measured using an ocean optics spectrometer. Combined with finite element analysis, a detailed description of the parameters impacting heat dissipation from these devices is presented along with methods to reduce thermal resistance.

8123-34, Session 8

Study of transient thermal measurement for high-power LED package

W. Liu, C. Liu, T. Yang, National Central Univ. (Taiwan)

A transient thermal measurement system is developed to measure the transient behavior of the junction temperature of LED in the very early operation stage. For the typical LED package, heat would be generated from the LED chip and conducting to the first-level Cu substrate via the Ag-epoxy TIM (Thermal Interface Material) interface, then, dissipated into the heat sink via the thermal paste. Using the current-developed transient thermal measurement system, we can study the thermal-dissipation characteristics of every heat-transferring path or interfaces in the LED package.

In this research, we investigated the transient behavior of the junction temperature of the studied LED package using the Cu substrates with various dimensions. The Cu substrate varies with the diameter (1.0 to 2.5 cm) and thickness (0.4 to 3.0 mm). From preliminary results on the transient behavior of the junction temperature of the studied LED package, we found that the heat transferring rate highly depends on the dimension of the Cu substrate. Also, in the steady-state condition (after 100-seconds current driving), the junction temperature decreases with the thickness of Cu substrates with a constant diameter. Yet, the junction temperature does not have a linear proportional relation with the diameter

Conference 8123:
Eleventh International Conference on Solid State Lighting

of the Cu substrate. The lowest junction temperature occurred at the middle range of diameter of the Cu substrates (about 1.5 cm in diameter). In this talk, we will report the established transient thermal measurement system and the analytic results to understand the detail characteristics of every heat-transferring path or interfaces in the LED package.

8123-35, Session 8

Evaluating the junction temperature of AC LEDs by DC and AC methods

H. Fu, K. Tai, C. Wang, P. Chou, Industrial Technology Research Institute (Taiwan); Y. Zong, Y. Ohno, National Institute of Standards and Technology (United States)

Alternating-current (AC) driven light-emitting diodes (LEDs) have become the trend of solid-state lighting (SSL) products. The junction temperature is an important index of LEDs reliability and efficiency. In other words, with proper thermal management of AC LEDs lighting products, the high performance of SSL products will be achieved. In order to obtain the junction temperature, we study and compare two published evaluating methods differentiating between the measurements of DC and AC in this paper. The first method is in which a low reference current having a pulse width was applied and the corresponding voltage across the device was measured and correlated to the junction temperature. The second method is using an active heat sink for recovering the root mean square (RMS) current of the first half cycle to estimate the junction temperature. The experimental evidence showed different aspects and variations of evaluating the AC LEDs junction temperature. The variations of evaluating junction temperature were caused by the switch time and phase of different source measurements in the first method and the capture time of the first half cycle in the second method. With proper capture time, the rising junction temperature in the second method might be negligible.

8123-36, Session 8

Measuring the junction-to-ambient thermal resistance of a LED lamp directly and accurately

K. Shih, K. Hua, Lawrence Technological Univ. (United States)

The junction temperature of a LED determines its life expectancy and light conversion efficiency. It is critically important to measure the junction to ambient thermal resistance of a LED lamp directly and accurately. With this information we can easily predict the thermal behavior of a LED lamp at any drive current and ambient temperature. However, it is difficult to measure LEDs that are packaged into an enclosure without taking the system apart. Some lamp makers use time consuming, expensive computer based modeling program to calculate the junction temperature of a LED inside a LED lamp. Other lamp manufacturers use indirectly measurement methods to estimate the junction temperature. Because these methods are NOT direct measurement of the LED junction temperature under the real working condition; their results are not verifiable. This paper describes a method that measures the junction to ambient thermal resistance of an assembled LED lamp directly and accurately while under its real working condition. This measurement method not only reduces the time and cost to characterize the thermal behavior of a lamp, but also drastically improves the accuracy of the measurement.

8123-37, Session 8

Measurement of thermal resistance of first-level Cu substrate used in high-power multi-chips LED package

C. Yang, C. Liu, National Central Univ. (Taiwan)

Thermal dissipation is the one of key issues for the application of high-power LEDs package. To achieve an excellent thermal system for high-power LED, an effective thermal substrate is required. Currently, high thermally conductive Cu substrate is used as the first-level dissipation substrate. However, there is no systematical study on investigating the effect of the dimensions on the thermal performance of first-level Cu substrate.

Thermal resistance of the first-level Cu dissipation substrate (RCu) with different Cu thickness is investigated in this work. Using the "constant-forward-voltage" method, the thermal resistances of the first-level Cu dissipation substrates (RCu) were measured against different Cu thickness. In the initial increase in the Cu thickness (up to 0.6 mm), RCu decreases with the Cu thickness. As the Cu thickness over 0.6 mm, RCu starts to slightly increase with the Cu thickness. The thermal resistance (RCu) of the Cu substrate is composed of the z-direction thermal resistance (Rz) and the two-dimensional horizontal spreading resistance (Rs). The initial increase in RCu should attribute to the decrease in both Rs and Rz with the Cu thickness. After the initial increase in RCu, the RCu would increase and be dominated by the Rz increase with the Cu thickness. Intriguingly, a minimum RCu value occurs at the Cu thickness of about 0.6 mm. Also, in this study, we discuss the possible inaccuracy factors of the "constant-forward-voltage" method.

8123-38, Session 9

Electroluminescence emission from hybrid light emitting diode of p-ZnO/(InGaN/GaN) multiquantum wells/n-GaN

Y. Choi, T. Park, S. Kim, G. Jung, S. Park, Gwangju Institute of Science and Technology (Korea, Republic of)

We report on the fabrication and characteristics of hybrid light-emitting diodes (LEDs) which consist of antimony (Sb) doped p-ZnO, (InGaN/GaN) multiquantum wells (MQWs), and n-GaN. The Sb-doped p-ZnO films with a hole concentration of $1.18 \times 10^{18}/\text{cm}^3$ and mobility of $0.71 \text{ cm}^2/\text{V s}$ were deposited on InGaN/GaN MQWs to fabricate hybrid LEDs by metalorganic chemical vapor deposition (MOCVD). After the growth of hybrid LEDs structure, a rapid thermal annealing (RTA) was carried out in an N₂ ambient gas for 1 min to activate Sb-doped p-ZnO. The forward voltage and series resistance of hybrid LEDs were measured as 3.0 V and 11.8 Ω , respectively. An electroluminescence (EL) emission at a wavelength of 468 nm is observed from the hybrid LEDs. The EL intensity of hybrid LEDs increases as injection current increases, showing that the Sb-doped p-ZnO layer acts as a hole injection layer in the hybrid LEDs. Furthermore, the EL peaks are red-shifted as the injection current is increased, indicating that the compressive strain in MQWs is relaxed due to Sb-doped p-ZnO layer. Micro-Raman spectra show that the tensile strain of ZnO nanorods in p-ZnO:Sb layer is expected to compensate the compressive strain in MQWs, reducing the strain induced piezoelectric field in MQWs.

8123-39, Session 9

Growth and characteristics of titanium oxide nanoparticles-coated nonpolar a-plane GaN by spin coating method

J. Kim, Korea Univ. (Korea, Republic of) and Korea Electronics Technology Institute (Korea, Republic of); J. Son, K. Baik, Korea Electronics Technology Institute (Korea, Republic of); J. H. Park, Korea Univ. (Korea, Republic of); S. Hwang, Korea Electronics Technology Institute (Korea, Republic of)

Non polar a-plane (11-20) GaN structure which was coated TiO₂ nanoparticles by spin coating method has been successfully grown on r-plane (1-102) sapphire substrates to improve light extraction efficiency and crystal quality. It was found that average size of titanium oxide nanoparticles is approximately 500 nm from scanning electron

microscopy (SEM). From photoluminescence (PL) results at 13 K of Si-doped GaN samples, basal plane stacking faults (BSFs) and near band edge (NBE) emission peaks were observed at 3.434 eV and 3.484 eV, respectively. We also found the temperature-induced band-gap shrinkage from temperature dependence PL, which was fitted well with empirical Varshni's equation. The room temperature PL intensity of TiO₂ coated multiple quantum wells (MQWs) sample was 20 % higher than that of reference sample. High-resolution x-ray diffraction analysis of films showed an anisotropy of strain with in-plane orientation. The full width at half maximum (FWHM) along the GaN [0001] and [1-100] directions were 564 arcsec and 490.8 arcsec, respectively. A small deviation of FWHM values compared with reference sample at in-plane crystal direction is attributed to relatively uniform in-plane strain. An improvement of crystal quality was also demonstrated by calculation of lattice constants, strain and PL results.

8123-40, Session 9

Tridoping and fabrication of ZnO homojunction by RF magnetron sputtering

B. Lakshmi Narayanan, G. Subramaniam, T. Balasubramanian, G. Nammalvar, National Institute of Technology, Tiruchirappalli (India)

The present study deals the novel approach of tridoping into ZnO to realize low resistive p-ZnO thin film and hence to fabricate the ZnO homojunction by RF magnetron sputtering. The tridoping i.e. simultaneous doping of two potential acceptors (As & N) and a donor (Al) has been achieved by As back diffusion from GaAs substrate and different AlN doped ZnO targets (0.5, 1 & 2 mol%). The diffused arsenic from GaAs substrate into ZnO film has been confirmed by Rutherford backscattering depth profile analysis. The grown films have been characterized by Hall measurement, X-ray diffraction (XRD), room temperature and low temperature Photoluminescence (PL). The Hall measurement showed that the low resistivity of $8.6 \times 10^{-2} \Omega \text{cm}$ and high hole concentration of $4.7 \times 10^{20} \text{cm}^{-3}$ for the 1% AlN concentration. The obtained resistivity is much lower than that of monodoped and codoped ZnO films. The Hall measurement results have been well justified by XRD and PL analysis. The presence of dopants in the film has been confirmed by Energy dispersive spectroscopy. The fabricated homojunction with the low resistive film (i.e. best tridoped film) has been characterized to determine the junction parameters.

8123-41, Session 9

Intense white luminescence from amorphous silicon oxycarbide (a-SiC_xO_y) thin films

S. Gallis, Univ. at Albany (United States) and IBM Corp. (United States); V. Nikas, H. Suhag, M. Huang, A. E. Kaloyeros, Univ. at Albany (United States)

Strong room-temperature white luminescence emitted from amorphous silicon oxycarbide (a-SiC_xO_y) films grown by thermal chemical vapor deposition (TCVD) is reported in this study. The emission spectra from the films cover a broad spectral range, from blue-violet to near infrared, depending on excitation energy. Furthermore, the effects of carbon concentration ($8.4 \text{ at.} \% < C < 25 \text{ at.} \%$) in the material and post-deposition annealing treatments (O₂ and forming gas 5% of H₂ ambient up to 1100°C) on the white luminescence are studied. It was found that photoluminescence (PL) intensity was well correlated with Si-O-C/Si-C-O bond density, determined from the Fourier transform infrared spectroscopy (FTIR) analysis. For samples with very low C concentration (<5at%), PL was shown to quench to close to zero values after annealing in O₂ ambient in atmospheric pressure, even at 500 °C, while it remained unaffected in the films with higher C content. Interestingly, it was found that white PL could be significantly enhanced when the samples were excited at higher pump energy, under ultraviolet laser light (325nm) and the emitted light was visible with naked light even in a bright room environment. The findings suggest that C- and Si-related oxygen defect centers may play the role of luminescence sources in the strong white light emission observed from amorphous silicon oxycarbide films and they may be responsible for the thermal stability of a-SiC_xO_y against oxidation.

Conference 8124: Nonimaging Optics: Efficient Design for Illumination and Solar Concentration VIII

Sunday-Monday 21-22 August 2011 • Part of Proceedings of SPIE Vol. 8124
Nonimaging Optics: Efficient Design for Illumination and Solar Concentration VIII

8124-01, Session 1

Illumination devices for uniform delivery of light to the oral cavity for photodynamic therapy

C. Canavesi, Univ. of Rochester (United States); W. J. Cassarly, Synopsys, Inc. (United States); T. H. Foster, Univ. of Rochester Medical Ctr. (United States); J. P. Rolland, Univ. of Rochester (United States)

To date, the lack of delivery mechanisms for light to the oral cavity remains a barrier to the treatment of oral cancer with photodynamic therapy (PDT). The greatest impediment to medical practitioners is the current need to shield the normal tissues of the oral cavity, a costly and time-consuming procedure. In this research, we present the design of illumination devices to deliver light to the oral cavity for PDT, which will facilitate administration of PDT in the clinic. The goal for such an illumination device, as indicated by our clinical collaborators at Roswell Park Cancer Institute in Buffalo, NY, is to limit exposure of healthy tissue and produce an average irradiance of 100 mW/cm² over the treatment field, with spatial non-uniformities below 10%. Furthermore, the size of the device must be compact to allow use in the oral cavity. Our research led to the design and fabrication of two devices producing spatial non-uniformities below 6% over a treatment area of 0.25 cm² by design. One device consisted of an appropriately-sized reflector, inspired by solar concentrators, illuminated by a cylindrical diffusing fiber optimally located within the reflector; another was a solid lightpipe with a combination of optimized tapered and straight components.

8124-02, Session 1

Construction of freeforms in illumination systems via Cartesian oval representation

D. Michaelis, P. Schreiber, C. Li, A. Bräuer, Fraunhofer-Institut für Angewandte Optik und Feinmechanik (Germany)

Freeforms in illumination systems are directly constructed by adapting some ideas of Oliker and co-workers [1]. The freeform is created by a set of primitive surface elements which are generalized Cartesian ovals including the optical response of the residual system. Hamiltonian theory of ray optics can be used to determine the family of primitives, which is in particular a simple task if the freeform is the exit or the entrance surface of the illumination system. For simple optical systems an analytical description of the primitives is possible. Contrarily, for more complex optics a conventional ray-tracer is additionally utilized to determine the required system's information, like the optical path lengths or mixed characteristics. To this end, a discrete set of rays is traced through the residual systems and the required relations are interpolated to obtain a quasi-analytic representation of the primitives.

For sources with a pronounced extension as well as ray divergence the inevitable "smearing out" effect [2] can be reduced by anticipating the corresponding blurring in the illumination task. To this end, the freeform construction method for point or collimated sources is combined with a linear chi-square algorithm.

The potential of this approach is demonstrated by some examples, e.g. freeform optics including collimating or deflection elements.

[1] V.I. Oliker, in "Trends in Nonlinear Analysis", 193-224 (Springer, 2003).

[2] F. R. Fournier, W. J. Cassarly, J. P. Rollanda, Proc. of SPIE 7103, 71030I (2008).

8124-03, Session 1

Design, manufacturing and measurements of a metal-less V-groove RXI collimator

D. Grabovickic, Univ. Politécnica de Madrid (Spain); J. C. Miñano, P. Benítez, Univ. Politécnica de Madrid (Spain) and Light Prescriptions Innovators, LLC (United States)

A metal-less RXI collimator has been designed. Unlike to the convectional RXI collimators, whose back surface and central part of the front surface have to be metalized, this collimator does not include any mirrored surface. The back surface is designed as a grooved surface providing two TIR reflections for all rays impinging on it. The main advantage of the presented design is lower manufacturing cost since there is no need for the expensive process of metalization. Also, unlike to the conventional RXI collimators this design performs good colour mixing. The first prototypes of V-groove RXI collimator have been made of PMMA by direct cutting using a five axis diamond turning machine. The experimental measurements of the RXI collimator are presented.

8124-04, Session 1

Uniform light distribution by using microlenses with various focal lengths

I. Hsu, G. J. Su, National Taiwan Univ. (Taiwan)

The increasing demands for non-self-emissive portable display devices jointly stimulate the needs for additional front light units to provide extra illumination to compensate for the ambient light in dim environment. The advantages of light emitting diodes (LED), such as high efficiency and small size, make it an ideal source for the compact unit, but direct LED lighting is impractical. Secondary optics is commonly adopted in illumination occasions to ensure the output from the LED dies meet the overall specification. Considering an oblique incidence situation, light mapping redistribution is inevitable. In this paper, we propose a beam shaping method adopting microlens array with various focal length to achieve uniform light distribution. The design is based on edge ray principle, which considers each microlens individually. Microlenses with various focus were made by photoresist thermal reflow process to verify the novel design.

8124-05, Session 2

The hybrid SMS-DSF method of nonimaging optical design

J. C. Bortz, N. E. Shatz, SAIC (United States)

The recently developed hybrid simultaneous-multiple-surface, dual-surface-functional (SMS-DSF) method of nonimaging optical design combines the discrete SMS method with the DSF method to obtain improved optical performance relative to the discrete SMS method alone. We review the hybrid SMS-DSF method and present a new variation that uses differential ray tracing to further enhance optical performance.

8124-06, Session 2

Fundamental bounds for antenna harvesting of sunlight

H. Mashaal, J. M. Gordon, Ben-Gurion Univ. of the Negev (Israel)

**Conference 8124: Nonimaging Optics:
Efficient Design for Illumination and Solar Concentration VIII**

The tantalizing prospect of using antennae for solar power conversion received preliminary consideration, but was not pursued in earnest due to the daunting challenges in suitable materials, fabrication procedures, and the rectification (conversion to DC power) of frequencies approaching 1 PHz (10^{15} s^{-1}). Recent advances in nanomaterials and nano-fabrication technologies have prompted revisiting the solar antenna strategy. Coherence theory informs us that even ostensibly incoherent radiation is partially coherent on a sufficiently small scale. Based on a generalized broadband analysis, it will be shown how the partial coherence of sunlight, exhibiting transverse partial coherence on a scale of two orders of magnitude larger than its characteristic wavelengths, impacts the potential of harvesting solar energy with an aperture antenna (a coherent detector), and a fundamental bound will be established. These results quantify the tradeoff between intercepted power and averaged intensity with which the effect of increasing antenna size (and hence greater system simplicity) can be evaluated.

8124-07, Session 2

On the challenge of flux concentration at grazing incidence for neutrons and x-rays

B. Khaykovich, D. E. Moncton, Massachusetts Institute of Technology (United States); N. Ostroumov, Ben-Gurion Univ. of the Negev (Israel); M. V. Gubarev, NASA Marshall Space Flight Ctr. (United States); D. Feuermann, J. M. Gordon, Ben-Gurion Univ. of the Negev (Israel)

Concentrator designs for thermal neutrons and x-rays are severely constrained by the requirement of grazing incidence, i.e., the exceedingly small angles for total external reflection at mirror surfaces. The étendue limit for flux concentration must be tempered by this extreme limitation, and the design principles of nonimaging optics must be reconsidered. We establish fundamental limits to flux concentration for certain classes of neutron and x-ray optics, and thereby provide perspective for the performance of established designs. Examples of tailoring mirror contours for progressively higher concentration are presented. A basic bound for the potential of nesting mirror designs to improve flux concentration is also derived, against which the performance of published corresponding systems can be compared. Based on these observations, we present concepts for improving the attainable target flux density from neutron and x-ray sources.

8124-08, Session 3

Principles of thermodynamically efficient concentrators

R. Winston, W. Zhang, L. Jiang, Univ. of California, Merced (United States)

No abstract available

8124-09, Session 3

New vistas in solar concentration with gradient-index optics

P. Kotsidas, V. Modi, Columbia Univ. (United States); J. M. Gordon, Ben-Gurion Univ. of the Negev (Israel)

Certain classes of gradient-index lenses can achieve both perfect imaging and flux concentration at the étendue limit. Although useful in microwave technology, eponymous Luneburg lenses have been viewed as esoteric idealizations for visible and near-infrared radiation due to the paucity of suitable materials and fabrication methods. We show that the classic Luneburg problem was constrained in subtle, implicit ways that can be relaxed. With the extra degrees of freedom,

we demonstrate new gradient-index profiles that can accommodate both realistic, readily-available materials and existing manufacturing technologies, while compromising neither perfect imaging nor maximum concentration (confirmed by raytrace simulation) - thereby opening new vistas for solar concentration and other visible and near-infrared applications. Specifically, the broader genres of solutions identified here permit a far smaller range of refractive indices than previously believed, with minimum required refractive index values well above unity, at arbitrary lens f-number, with remarkable insensitivity to dispersion losses when compared to conventional lenses. A variety of lens shapes are considered, from fully spherical, to hemispherical and truncated versions thereof.

8124-10, Session 3

Solar thermal system for lunar ISRU applications: development and field operation at Mauna Kea, HI

T. Nakamura, Physical Sciences Inc. (United States)

Physical Sciences Inc. (PSI) has been developing the optical waveguide (OW) solar power system. Figure 1 shows a schematic representation of the system. In this system solar radiation is collected by the concentrator array which transfers the concentrated solar radiation to the optical waveguide (OW) transmission line made of low loss optical fibers. The OW transmission line directs the solar radiation to the thermal receiver for thermochemical processing of lunar regolith for oxygen production on the lunar surface. Key features of the proposed system are:

1. Highly concentrated solar radiation ($\sim 4 \times 10^3$) can be transmitted via the flexible OW transmission line directly to the thermal receiver for oxygen production from lunar regolith;
2. Power scale-up of the system can be achieved by incremental increase of the number of concentrator units;
3. The system can be autonomous, stationary or mobile, and easily transported and deployed on the lunar surface; and
4. The system can be applied to a variety of ISRU processes.

This paper discusses development of the ground-based solar thermal power system and its application to (i) surface stabilization of the native soil and (ii) carbothermal oxygen production. Both experiments were conducted at the ISRU analog test, Mauna Kea, HI during January - February, 2010. The experiment for surface stabilization of the native soil was conducted in collaboration with Northern Center for Advanced Technology (NORCAT), Ontario, Canada, and experiment for carbothermal oxygen production was conducted in collaboration with Orbital Technologies Corporation (ORBITEC), Madison, WI.

8124-11, Session 3

Spiral nonimaging optical designs

P. Zamora, P. Benitez, J. C. Miñano, Univ. Politécnica de Madrid (Spain); J. F. Vilaplana, Light Prescriptions Innovators Europe, S. L. (Spain)

Faceted optical elements such as Fresnel or TIR lenses usually have manufacturing constraints that limit their geometry. Manufacturing technologies as injection molding or embossing specify their production limits for minimum radii of the vertices or draft angle for demolding, for instance. In some demanding nonimaging applications, these restrictions may limit the optical efficiency of the system or affect the generation of undesired artifacts on the illumination pattern.

We present a novel concept, in which the surfaces are not obtained from the usual revolution symmetry with respect to a central axis (z axis), but they are calculated as free-form surfaces in such a way that they describe a spiral trajectory around z axis (each facet converting into the adjacent one after each turn). The main advantage of this new concept lies in the manufacturing process: a molded piece can be easily separated from its mold just by applying a combination of rotational

**Conference 8124: Nonimaging Optics:
Efficient Design for Illumination and Solar Concentration VIII**

movement around axis z and linear movement along axis z. By applying this “spiral” movement, demolding is possible even for designs whose cross section shows negative draft angles, allowing for maximum efficiency and avoiding the light incidence on the corner radii by design.

This family of spiral designs may have many different applications. Nevertheless we will focus on non-imaging optics, especially on illumination and photovoltaic concentration. Several new spiral designs, which rotational-symmetric equivalent cannot be manufactured with conventional techniques will be presented, demonstrating its ease of manufacturing and its optimum optical properties with computer ray-trace simulated results.

8124-12, Session 4**Angular dependence of surface relief gratings for solar and lighting applications**

T. M. de Jong, Technische Univ. Eindhoven (Netherlands); D. K. G. de Boer, Philips Research Nederland B.V. (Netherlands); C. W. M. Bastiaansen, Technische Univ. Eindhoven (Netherlands) and Queen Mary Univ. of London (United Kingdom)

Inexpensive and compact solar concentrators can be designed using transmission gratings that diffract sunlight into total internal reflection when applied on top of a light guide. In order to couple the incoming light efficiently into the light guide, the gratings should combine a large diffraction angle with a high diffraction efficiency and low angular and wavelength dispersion. Similarly, such gratings can be useful for out-coupling from light guides and in solid state lighting applications. We study the design and fabrication of gratings that fulfill these requirements. Rigorous Coupled Wave Analysis is used for a numerical study of the influence of various parameters on the diffraction efficiency and the angular dependence of the grating. We show that for sub-wavelength grating periods highest diffraction efficiencies will be achieved when the grating is produced as a surface relief structure. For such surface relief gratings we demonstrate the presence of specific regions in the full space of conical angles of incidence where highly efficient in-coupling occurs. The distribution of the diffraction efficiency over angular space can be varied by adjusting the grating geometry. For slanted gratings the efficiency regions corresponding to positive orders are promoted at the cost of those corresponding to negative orders or vice versa. Two-dimensional, crossed gratings result in a distribution of the diffraction efficiency over a wider angular range. Our theoretical results are supported by experiments. We used the photoresist SU-8 to show that gratings with the desired dimensions can be fabricated by interference holography and demonstrated the desired properties.

8124-13, Session 4**Evaluation and comparison of different designs and materials for Fresnel lens-based solar concentrators**

L. Fu, R. Leutz, H. P. Annen, Concentrator Optics GmbH (Germany)

Optics with high optical efficiency and reliability are the key components for CPV modules as well as high efficiency solar cells and a high accuracy tracker. The present paper describes the optical design, simulation and materials, including a direct comparison of geometrically identical lens designs for three materials.

As primary optical element (POE), a rotationally symmetric nonimaging Fresnel lens with centerline prisms of variable height and constant step size was chosen. The lens area of 150 x 150 mm² results in a geometrical concentration ratio of 790X. The lenses are assembled in a 5x4 parquet. Concentrator Optics designed and fabricated parquets of identical focal length and lens size in three materials: PMMA, SOG, and thermoformable silicone on glass. These parquets are called the Triple Primaries, and serve as test samples and off-the-shelf products. Tests are under way

for accelerated aging and optical performance. All primaries are hot embossed or cast.

The Fresnel lenses focus impinging sunlight onto secondary optical elements (SOE). The challenge in designing SOE lies in the combination of requirements on maximum light homogenization, additional concentration and acceptance half-angle, manufacturing complexity and mounting effort. Two SOE designs were developed. The first design is a domed kaleidoscope providing very homogeneous distribution of the sun light on the cell surface even in case of tracking errors. The second design uses an aspherical half-egg shape and has significant advantages in terms of manufacturing effort and costs. Both SOEs are blank-molded in glass.

POE and SOE are designed as optical train. Therefore, optical tests are run to determine manufacturing quality and optical efficiency of the primary lenses and secondaries. The laboratory tests are compared with the simulation results.

Acknowledgment: This study is part of the Triple Primaries project, initiated as research project for various primary and secondary optics in combination with cells, by Concentrator Optics, Azur Space Solar and Isuzu Glass.

8124-14, Session 4**Limiting acceptance angle to maximize efficiency in solar cells**

E. D. Kosten, H. A. Atwater, California Institute of Technology (United States)

Within a detailed balance formalism, the open circuit voltage of a solar cell can be found by taking the band gap energy and accounting for the losses associated with various sources of entropy increase. Often, the largest of these energy losses is due to the entropy associated with spontaneous emission. This entropy increase occurs because non-concentrating solar cells generally emit into 2 pi steradian, while the solid angle subtended by the sun is only 6.85x10⁻⁵ steradian. Thus, for direct normal irradiance, non-concentrating solar cells with emission and acceptance angle limited to a narrow range around the sun could see significant enhancements in open circuit voltage and efficiency. With the high degree of light trapping we expect given the narrow acceptance angle and the ray optics brightness theorem, the optimal cell thickness will result in a discrete modal structure for most materials. Thus, limiting the acceptance and emission angle can be thought of as coupling to only a subset of radiating modes, or, alternatively, as altering the modal structure such that some radiating modes become bound modes. We have shown the correspondence between the ray optics picture and the modal picture, by deriving the ray optics results for light trapping under angular restrictions using a modal formulation. Using this modal formulation we can predict the light trapping and efficiencies for various thin structures under angular restriction. We will discuss these predicted efficiencies and various options for implementing broadband and angle-specific concentrators.

8124-15, Session 4**Investigation of scattering profiles for passive solar light collectors**

A. N. Bharathwaj, B. Srinivasan, Indian Institute of Technology Madras (India)

We explore the use of light scattering off diffuser elements to enhance the collection efficiency in a passive solar collection system. A passive solar collection system is an optical alternative for the existing systems which use mechanical components for sun tracking in turn leading to uniformity in the light output. It consumes no power, is rugged, portable and a cost efficient solution for solar light collection systems and is based on manipulating the angular distribution of the incident solar radiation.

One major drawback of the passive solar systems is the poor collection

Conference 8124: Nonimaging Optics:
Efficient Design for Illumination and Solar Concentration VIII

efficiency at off-axis illumination. The off axis rays don't contribute to the collection efficiency and hence the poor performance. To counter this, we investigated the use of scatterers to enhance the performance at off-axis case. It was observed through simulations using ASAP that the Light uniformity improved by 50% when incorporating an arbitrary profiled scattering surface. The scattering surface scattered off the off-axis rays such that it was suitable for light collection.

We also tried out different shapes for the scattering surface and simulation results showed a curved scattering medium offered a 11% increased performance and was much more suited to the collection needs as the off-axis rays are always normally incident on it. This led to the trial of exploring other possible surface profiles for the scattering mediums commercially available in ASAP environment. Preliminary experiments are underway to establish the link between the scattering profile and the angular distribution of the scatter radiation and also on the development of a passive solar light collection system.

8124-16, Session 5

Free-form Fresnel RXI-RR Köhler design for high-concentration photovoltaics with spectrum-splitting

M. Buljan, Univ. Politécnica de Madrid (Spain); P. Benitez, Light Prescriptions Innovators, LLC (United States); R. Mohedano, Light Prescriptions Innovators Europe, S. L. (Spain); J. C. Miñano, Light Prescriptions Innovators, LLC (United States)

Development of a novel, practical, high-concentration PV optics using four-junctions (4J) of existing high-efficiency solar cells via spectrum splitting is presented. The novel HCPV Fresnel RXI-RR Köhler concentrator concept uses the combination of a commercial concentration GaInP/GaInAs/Ge 3J cell and a Back-Point-Contact (BPC) concentration silicon cell for efficient spectral utilization, and external confinement techniques for recovering the multijunction cell's reflection. The design targets an equivalent cell efficiency greater than 45%, and CPV module efficiency greater than 38%, achieved at a concentration level larger than 500X and wide acceptance angle ($\pm 1^\circ$).

The primary optical element (POE) is a flat Fresnel-Köhler lens, and the secondary optical element (SOE), a monolithic free-form Köhler RXI-RR concentrator, with an embedded cost-effective high-performance band-pass filter that reflects or refracts the light rays while crossing the device. In the RXI-RR SOE concentrator, the RR illuminates the BPC silicon cell, while the RXI illuminates the 3J cell. This last illumination is asymmetric from one hemisphere, allowing the use of a confining cavity in the other hemisphere to efficiently collect the light reflected by the grid lines and the semiconductor surface of the triple junction cell. RXI-RR free-form surfaces are calculated using an iterative process in three dimensions. The Köhler integration guarantees a uniform illumination of the two cells, free from spatial chromatic aberration.

A first proof-of concept prototype has been manufactured, and preliminary measurements show an efficiency increase over the 3J cell greater 10% under real sun operation, results that will be shown at the conference.

8124-17, Session 5

Static high-irradiance solar concentration by gradient-index optics

P. Kotsidas, V. Modi, Columbia Univ. (United States); J. M. Gordon, Ben-Gurion Univ. of the Negev (Israel)

Novel solutions for realistic gradient-index (GRIN) lenses are presented, that create the possibility of nominally stationary photovoltaic concentrators capable of daylong averaged flux concentration levels of order 10^3 . One transfers the burden of precision solar tracking FROM massive units on which numerous solar modules are mounted, TO miniaturized mechanical components inside modules that are

completely stationary. The best optical properties for this aim would appear to be perfect imaging - a case where imaging and nonimaging objectives coalesce because perfect imaging is non-trivially synonymous with attaining the fundamental limit to concentration. Our GRIN profiles surmount limitations of classical Luneburg solutions that resulted in GRIN lenses being deemed physically unattainable idealizations for sunlight. To wit, while preserving perfect imaging, our GRIN profiles eliminate the need for refractive indices near unity, markedly reduce the range of refractive indices required, and permit arbitrary focal length. They are also amenable to realistic materials and fabrication technologies. Raytrace simulations confirm that they offer an unprecedented solution to this problem - even accounting for chromatic aberration and misalignment. Eliminating massive precision tracking of large photovoltaic arrays in favor of precision cm-scale lens tracking inside the modules opens the possibility of rooftop CPV. The perception that high solar concentration is inseparably linked to massive trackers is supplanted here by a different paradigm.

8124-18, Session 5

High-efficiency Köhler photovoltaic concentrators with external light confinement

P. Zamora, P. Benitez, J. C. Miñano, M. Buljan, Univ. Politécnica de Madrid (Spain)

We present a novel and advanced optical design for a CPV concentrator in order to increase module electrical efficiency by means of lowering reflected light on the solar cell surface, based on a confinement cavity. If we are able to minimize this reflection on the cell surface, the amount of light absorbed by the device will thus be greater. This reduction in light reflection is achieved by designing an external confinement cavity ad hoc for the system.

External confinement cavities have been proposed in the past, but they had always had difficulties of integration with classical secondary optical elements, generally presenting kaleidoscopic homogenization. However, the recent invention of high-performance Köhler concentrators (as it is the case of Fresnel-Köhler (FK) and Fresnel-RXI Köhler (FRXI) concentrators), fully compatible with the use of external cavities, will allow for this practical integration. The external cavity is added to the concentrator secondary element (SOE).

We will be able to achieve very high single-module electrical efficiencies if we apply this external confinement cavity to high optical efficiency CPV modules. For example, for a FK concentrator module (presenting a proved measured peak electrical efficiency over 30%, close to 33% @ $T_{cell}=25^\circ C$), the addition of an external cavity leads to a total peak electrical efficiency of around 35% (@ $T_{cell}=25^\circ C$).

8124-19, Session 5

Linear Fresnel lens Concentrators, revisited

W. Zhang, R. Winston, Univ. of California, Merced (United States)

No abstract available

8124-20, Session 6

Nested aplanatic optics

A. Goldstein, D. Feuermann, Ben-Gurion Univ. of the Negev (Israel); G. D. Conley, H2Go, Inc. (United States); J. M. Gordon, Ben-Gurion Univ. of the Negev (Israel)

Dual-mirror aplanatic optics can provide efficient, ultra-compact, high-irradiance solar concentration, recently developed for concentrator photovoltaics. However, inherent limitations place the focus inside the optic and therefore mandate a terminal dielectric concentrator to extract the concentrated sunlight to the solar cell outside the optic, with the

**Conference 8124: Nonimaging Optics:
Efficient Design for Illumination and Solar Concentration VIII**

affiliated need for an optical bond to the cell. Can a modified design strategy site the focus outside the optic - and hence eliminate the need for a terminal concentrator and optical bond - without compromising concentrator compactness, low shading losses, or even the pragmatic advantage of the primary and secondary mirrors being coplanar toward facilitating the alignment of optical components? We show how judiciously nested dual-mirror aplanats can satisfy all these objectives, with sample performance evaluations based on raytrace simulation.

8124-21, Session 6

Integrating tracking in concentrating photovoltaics using laterally moving optics

F. Duerr, Y. Meuret, H. Thienpont, Vrije Univ. Brussel (Belgium)

In this work the concept of tracking-integrated concentrating photovoltaics (CPV) is studied and its capabilities are quantitatively analyzed. In contrast to the clear separation between static CPV modules and external solar trackers, the here introduced general concept of a tracking-integrated concentrating photovoltaic system is to transfer part of this external solar tracking functionality to the concentrating optics within the module. This tracking integration can only be achieved through the introduction of additional degrees of freedom, such as relative movement between the optics and solar cells. This design strategy desists from ideal concentration performance to reduce the external mechanical solar tracking effort in favor of a compact installation, possibly resulting in lower overall cost.

The proposed optical system relies on the use of two laterally moving plano-convex lenses to achieve high concentration over a wide angular range. Its optical design is based on an extended Simultaneous Multiple Surface (SMS) algorithm. This extended design algorithm is presented and used to design tracking-integrated optical systems comprising two movable plano-convex lenses and thus two curved optical surfaces. In comparison to a single meniscus lens, also consisting of two curved optical surfaces comprising a laterally moving receiver, the additional moving optics helped to raise the concentration performance considerably.

This design approach enables a strong reduction of the external solar tracking effort along with high concentration ratios for both, line and point concentration systems. Ray tracing simulations show that this novel system design outperforms its conventional concentrating photovoltaic counterparts.

8124-22, Session 6

Optical characterization of nonimaging focusing heliostat

K. Chong, Univ. Tunku Abdul Rahman (Malaysia)

The greatest challenge in designing a heliostat capable of focusing the sunlight onto a small receiver throughout a year is to optimize astigmatism. A novel nonimaging focusing heliostat consisted of many small movable element mirrors that can be dynamically maneuvered in a line-tilting manner has been proposed for the astigmatic correction in a wide range of incident angle ranging from 0 deg to 70 deg. In this article, a comprehensive analysis of the new heliostat with total reflective area of 25 m² and slant range of 25 m using ray-tracing method has been carried to analyze the optical performance including solar concentration ratio, spacious uniformity of solar flux distribution, spillage loss, and variation in flux distribution with time and day. The optical analysis of the heliostat in the application of solar power tower system has embraced the cases of 1×1, 9×9, 11×11, 13×13, 15×15, 17×17 and 19×19 arrays of concave mirrors attached to the heliostat frame provided that the total reflective area remains the same. To achieve a smooth simulated result of solar flux distribution, a total number of 8.11 × 10⁹ rays per heliostat are traced in the simulation. The simulated result has shown that the maximum solar concentration ratio at a high incident angle of 65 deg can be improved from 1.76 suns (single mirror) to 104.99 suns (9×9 mirrors),

to 155.93 suns (11×11 mirrors), to 210.44 suns (13×13 mirrors), to 246.21 suns (15×15 mirrors), to 259.80 suns (17×17 mirrors) and to 264.73 suns (19×19 mirrors).

8124-23, Session 6

Optimum design and efficiency improvement for organic luminescent solar concentrators

C. Wang, L. S. Hirst, R. Winston, Univ. of California, Merced (United States)

No abstract available

8124-24, Poster Session

Optical characterization of solar furnace system using fixed geometry nonimaging focusing heliostat and secondary parabolic concentrator

K. Chong, C. Lim, W. Keh, J. Fan, F. A. Rahman, Univ. Tunku Abdul Rahman (Malaysia)

A novel solar furnace system has been proposed to be consisted of a Nonimaging Focusing Heliostat (NIFH) and a smaller parabolic concentrator. In this design, the primary NIFH heliostat consists of 11×11 array of concave mirrors with focal length equal to target distance and dimension 1×1 m² each to form a total reflective area of 121 m² while the secondary parabolic concentrator has a focal length of 30 cm. To simplify the design and reduce the cost, fixed geometry of the primary heliostat is adopted to omit the requirement of continuous astigmatic correction throughout a year. The overall performance of the novel solar furnace configuration can be optimized if the heliostat's spinning-axis is fixed in the orientation dependent on the latitude angle so that the annual variation of incidence angle is the least, which ranges from 33 deg to 57 deg. A comprehensive optical analysis of the novel solar furnace system has been carried using ray-tracing method for different target distances such as 50 m and 100 m, where the target distance is defined as the distance between the central point of heliostat and the vertex of parabolic reflector. To obtain a smooth flux distribution plot, a total number of 2.41 × 10¹⁰ rays per heliostat are traced in the simulation. The simulated results have shown that the maximum solar concentration ratio ranges from 20,529 suns to 26,074 suns for the target distance of 50 m, and ranges from 40,366 suns to 43,297 suns for the target distance of 100 m.

8124-25, Poster Session

A hemispherical static concentrator with double-aspheric compensated lens array for continued collecting sunlight

W. Chen, Y. Chen, J. A. Whang, National Taiwan Univ. of Science and Technology (Taiwan)

Natural light is an inexhaustible and environmentally friendly energy. The solar energy exposed to the earth everyday is about three thousand times to the global energy consumption. Therefore, it would be a considerably large energy saving if we collect and guide the sunlight for lighting. Currently, there are two types of solar concentrators for collecting sunlight purpose, namely, active and static. The former is more efficient, but needs costly active sun-tracking system for supplement; the latter is cheaper, but is limited for certain time slots. In static systems, a hemispherical concentrator can gather the sunlight with longer time, but the collected flux is not stable and the energy density of optical fiber is lower than the illuminance of sunlight. We, in this paper, propose a hemispherical static concentrator that consists of double aspheric

Conference 8124: Nonimaging Optics:
Efficient Design for Illumination and Solar Concentration VIII

compensated lens array. The double layers of lenses are designed with large tolerance for continued collecting sunlight and the apertures of lenses are larger than optical fiber for increasing the energy density. According to the simulation results, we get uniform distribution of collected flux from 10 a.m. to 4 p.m. that is less than 10% change. Moreover, the energy density of optical fiber is about 50 Lm/cm² in summer when the illuminance of sunlight is about 120,000 Lux.

8124-26, Poster Session

Effect of scattering of cover glass for silicon and dye-sensitized solar cells

H. Chen, W. Lu, Y. Lo, S. You, National Yunlin Univ. of Science and Technology (Taiwan)

The study would investigate the effect of the scattering model on the photoelectric conversion efficiency for the silicon solar cell and dye-sensitized solar cell (DSSC). We will examine the accuracy of optical simulation of these solar cells by the A class standard measurement of AM1.5G at the light source of 1000 W/m². The scattering lighting of DSSC always is occurred by the particle size of the titanium dioxide (TiO₂) and the distribution of the layer. Anyway, the silicon solar cell would absorb the lighting by the energy band of the silicon. Therefore, Mie scattering theory is a useable model to describe the scattering mechanism and then bidirectional scattering distribution function (BSDF) could describe the scattering status for the silicon solar cell and DSSC. The regular pattern of the cover glass including the type, size, deep and smooth would effected the scattering model of the silicon solar cell and DSSC for the absorption efficiency. We found the absorption efficiency would be enhanced at the scatter pattern of big deep and smooth round. The scattering pattern at the front always was better than at the back for the cover glass at the efficiency of lighting absorption. The absorption efficiency of DSSC would be higher than the silicon solar cells at the same scattering pattern. The optical simulation and measurement data showed the scattering pattern would improve the absorption efficiency of 2% to 5% for silicon solar cell and 5% to 8% for DSSC.

Conference 8125: Optomechanics 2011: Innovations and Solutions

Monday-Thursday 22-25 August 2011 • Part of Proceedings of SPIE Vol. 8125
Optomechanics 2011: Innovations and Solutions

8125-32, Poster Session

Automated semi-spherical irradiance meter

M. Tecpoyotl-Torres, G. Vera-Dimas, J. J. Escobedo-Alatorre, Univ. Autónoma del Estado de Morelos (Mexico); J. Varona-Salazar, Univ. Bonaterra (Mexico); R. Cabello-Ruiz, A. Zamudio-Lara, Univ. Autónoma del Estado de Morelos (Mexico)

In previous work, we have developed a semi-spherical irradiance meter, based on a mobile arm, where the detector was located, that showed an acceptable performance. However, the number of the discrete points under analysis was limited by the mechanical arrangement.

In this work, a new approximation is developed based on the obtained experience, the suggestions given by a manufacturer of illumination sources interested in our work, and based on the recent advances in other areas related to measurement prototypes.

In this new approximation the mechanical stage has been improved. The detector is located on a rectangular ring (which is assumed as joined two mobile branches in order to compensate the weights), who described trajectories of 170°. The illumination source is located at the center of the mobile support, which rotates 360°. The movement of the system is determined by two step motors. The mechanical arrangement has the enough rigidity, in order to support the precision required for the acquisition stage, based on a DSPIC. Measurements of illumination sources with different sizes can be possible by using adjustable lengths of the base and the ring.

The advantages of the new meter are: Its low costs (as it is built with recyclable materials), a reliable detection based on a single photo-detector, which has demonstrated its effectiveness. The received power by the detector is useful to obtain the irradiance profile of the lighting source under test.

8125-33, Poster Session

Alignment protocol for effective use of hard x-ray quad collimator for micro-crystallography

S. Xu, N. Venugopalan, R. Sanishvili, R. F. Fischetti, Argonne National Lab. (United States)

In October 2009, a quad, mini-beam collimator was implemented at GM/CA CAT that allowed users to select between a 5, 10, or 20 micron mini-beam or a 300 micron scatter guard for macromolecular crystallography. Initial alignment of each pinhole to the optical axis of each path through the mini-beam collimator is preformed under an optical microscope using an alignment jig. Next, the pre-aligned collimator and its kinematic mount are moved to the beamline and attached to a pair of high precision translation stages attached to an on-axis-visualization system for viewing the protein crystal under investigation. The collimator is aligned to the beam axis by two angular and two translational motions. The pitch and yaw adjustments are typically only done during initial installation, and therefore are not motorized. The horizontal and vertical positions are adjusted remotely with high precision translational stages. Final alignment of the collimator is achieved using several endstation components, namely, a YAG crystal at the sample position to visualize the mini-beam, a CCD detector to record an X-ray background image, and a PIN diode to record the mini-beam intensity. The alignment protocol and its opto-mechanical instrumentation design will be discussed in detail.

*GM/CA CAT is funded with Federal funds from the National Cancer Institute (Y1-CO-1020) and the National Institute of General Medical Science (Y1-GM-1104). Use of the Advanced Photon Source was supported by the U.S. Department of Energy, Basic Energy Sciences, Office of Science, under contract Number DE-AC02-06CH11357.

8125-34, Poster Session

Stably joint optical tables

R. J. Medina Lopez, S. C. Corzo-Garcia, S. M. Anderson, R. M. Carriles, A. J. Ruiz-Marquez, E. Castro-Camus, Ctr. de Investigaciones en Óptica, A.C. (Mexico)

We present a simple and practical method for joining pneumatically floated optical tables. To demonstrate our method we joined two optical tables in an uncentered T-shape. We then used a Michelson interferometer to compare the stability of the entire T-structure versus a single unconnected table. The measurements demonstrate that the rigidity of the joint and unjoint tables are comparable. We also found the optimal master-slave leg configuration by calculating the stress on the joint and confirmed the calculations by Michelson interferometry. The vibration damping for the T-structure against the unjoined tables was measured finding comparable results. This method can significantly reduce costs of large optical tables and will be useful to extend existing optical tables without manufacturer modification.

8125-35, Poster Session

Compact dynamic microfluidic iris array

C. Kimmle, U. Schmittat, C. Döring, H. Fouckhardt, Technische Univ. Kaiserslautern (Germany)

In a first step a variable iris based on microfluidics has been realized. Light attenuation is achieved by the absorption of an opaque liquid (f.e. black ink). The modulation can be achieved by fluid displacement via a transparent elastomer (silicone) half-sphere. The silicone calotte is hydraulically pressed against a polymethylmethacrylate (PMMA) substrate, such that the opaque liquid is squeezed away, this way opening the iris. With this approach we can reach a dynamic range of more than 60 dB. The system has response times in the ms to s regime.

Depending on the design of the silicone structure either a single iris or an iris array can be realized. So far the master for the silicone structure has been fabricated by precision mechanics. In experiments the aperture diameter has been changed continuously from 0 to 8 mm for a single iris and 0 to 4 mm in case of a 3 x 3 iris array.

In a second step we have combined such an iris array with a PMMA lens array to a compact module, the distance of both arrays equaling the focal length of the lenses. This way even spatial frequency filter arrays could be realized.

We also show the possibility to extend the iris array concept to an array with many elements (f.e. 100 x 100), using lithographic techniques for the master. Such arrays could be used e.g. in light field cameras.

8125-36, Poster Session

Thermo-opto-mechanical analysis of a cubesat lens mount

J. Champagne, College of Optical Sciences, The Univ. of Arizona (United States) and Space Dynamics Lab. (United States)

Small satellites called cubesats have given students at universities and high schools the opportunity to conduct experiments in space in the past decade. This has mostly been possible due to low cost and quick development times. A popular cubesat payload has been optical imaging systems for the study of planet Earth from space. Due to budget, space, and time constraints, commercial photographic lenses of the double-Gauss type are prime candidates for cubesat optics. However, photographic objectives are not designed to operate in a space

Conference 8125:
Optomechanics 2011: Innovations and Solutions

environment and modifications are usually necessary. One method of improving optical performance of the objective over large temperature variations is by replacing the stock lens mount with a different material. This paper describes the thermo-opto-mechanical analysis of several lens mount materials for a double-Gauss imaging system suitable for a cubesat.

8125-37, Poster Session

The design and verification of a robust secondary mirror adjustment mechanism for airborne optical remote sensing instruments

P. Huang, Y. Cheng, Instrument Technology Research Ctr. (Taiwan)

Optical system architecture of Cassegrain telescope is usually applied for spaceborne and airborne optical remote sensing instruments. The optical system has to overcome the intense shock and vibration during launch process, and successfully survive and keep the optical performance for mission operations. Therefore, it's adopted for most design to fix the primary mirror and adjust the orientation and position of the secondary mirror to meet the optical performance specification.

In order to achieve the required optical performance, the adjustable support mechanism for secondary mirror shall be designed with five degrees of freedom for secondary mirror adjustment. And the precision of adjustable mechanism has to achieve the level of micrometer and arc-second. In addition to the adjustment function, the mechanism shall be robust enough to survive under the vibration condition of 15G without deformation and damage.

This work presents a developing design of adjustable support mechanism of secondary mirror for airborne optical remote sensing instruments. And several reference planes and shims have been designed in this mechanism. The shims and one of the structural parts can be released and are properly grinded to the desired thickness.

The proposed mechanism has been verified by an experimental model. The reassembled accuracy is 5 arc-second and 2 μm . Furthermore, the adjustable orientation and position accuracy can achieve 5 arc-second and 2 μm respectively, depending on the grinding and measurement precision. The accuracy can drive the optical system performance to diffraction limit. After verification, we confirm the proposed design of adjustable support mechanism can be applied to airborne optical systems, and has the good potential in spaceborne applications.

8125-38, Poster Session

On the accuracy of framing-rate measurements in ultra-high-speed rotating mirror cameras

M. Conneely, H. O. Rolfnes, C. Main, D. McGloin, P. A. Campbell, Univ. of Dundee (United Kingdom)

Rotating mirror systems based on the Miller Principle are a mainstay modality for ultra-high speed imaging within the range 1-25 million frames per second. Importantly, the temporal accuracy of measurements made with such systems is sensitive to the frame rate reported during data acquisition. The purpose for the present investigation was to examine the validity of reported frame rates in a widely used commercial system (a Cordin 550-62 model) by independently measuring the framing rate at the instant of triggering. In the event, we found a small but significant difference between such measurements: the average discrepancy (over the entire spectrum of frame rates used) was found to be $1.15 \pm 0.95\%$, with a maximum difference of 2.33%. The principal reason for this discrepancy was traced to non-optimized sampling of the mirror rotation rate within the system software. This paper thus serves three purposes: (i) we highlight a straightforward diagnostic approach to facilitate scrutiny of rotating-mirror system integrity; (ii) we raise awareness of the intrinsic errors associated with data previously acquired

with this particular system and model; and (iii), we recommend that future control routines address the sampling issue by implementing real-time measurement and reporting at the instant of triggering.

8125-01, Session 1

Optomechanical design for cost-effective DEMVAL systems

A. Ison, Sandia National Labs. (United States)

Sticker shock for opto-mechanical hardware designed for advanced optical DEMVAL systems can lead to program loss. In opto-mech design it is important to manage this risk through easily manufacturable and inexpensive hardware for lower budget programs. The optical and opto-mech design teams must work closely to optimize the system design for manufacture, and assembly. This often results in unique/creative design solutions. Outlined are some novel optomechanical structure concepts, with 5 degrees of freedom, used to design a low cost optical system. The concepts discussed include inexpensive magnetic kinematic mounts, flexure rings for lens preloading, simplistic drop-in lens housing designs, and adjustable tooling ball metering rods which accommodate alignment in 5 degrees of freedom.

8125-02, Session 1

A tip/tilt mirror with large dynamic range for the ESO VLT Four Laser Guide Star Facility

N. Rijnveld, R. Henselmans, TNO Science and Industry (Netherlands)

A critical element in the Four Laser Guide Star Facility (LGSF) for the ESO Very Large Telescope (VLT) is the Optical Tube Assembly (OTA), consisting of a stable 20x laser beam expander and a tip/tilt mirror, the Field Selector Mechanism (FSM). This paper describes the design and performance testing of the FSM. The driving requirement for the FSM is its dynamic range: a stroke of ± 6.1 mrad with less than 1.5 μrad RMS absolute accuracy.

The FSM design consists of a Zerodur mirror, bonded to a plate spring and strut combination to allow only tip / tilt motion. Two spindle drives actuate the mirror, using a stiffness based transmission to dramatically increase resolution. Absolute accuracy is achieved with two differential inductive sensor pairs.

A complete prototype of the FSM is realized to optimize the control configuration and measure its performance. Friction in the spindle drive is overcome by creating a local velocity control loop between the spindle drives and the shaft encoders. Absolute accuracy and low pointing jitter is achieved by using a cascaded low bandwidth control loop with feedback from the inductive sensors.

The absolute accuracy is measured with an autocollimator. The results show good agreement between the measured and predicted performance. The FSM complies to the dynamic range requirement, while being realized with mostly low cost off-the-shelf products.

8125-03, Session 1

Design and development of the fibre cable and fore optics of the HERMES Spectrograph for the AAT

S. Case, L. Gers, J. Brzeski, Australian Astronomical Observatory (Australia)

We report on the development of the fibre slit of the High Efficiency and Resolution Multi Element Spectrograph (HERMES). Discussed is the fibre positioning and mounting techniques of 400 fibres, the mounting and alignment of the slit relay optics and coupling between the fibres and

Conference 8125:
Optomechanics 2011: Innovations and Solutions

the relay optics using an index matching gel solution.

An investigation into stress sources was undertaken in the development of the fibre v-groove subassembly to ensure the focal ratio degradation (FRD) of the fibre was minimised, by employing low-shrinkage adhesives. Thermal effects on FRD due to changing the temperature of the slitlet component were also investigated, and it was concluded that there are negligible effects with this change in temperature (~1% change in output numerical aperture).

The relay optics magnify the group of ten fibres by a factor of two. This is mounted in high precision v-groove mounts. These optics are also mounted to high precision and each of the systems is aligned to each individual fibre v-groove assembly. There are 40 of these subassemblies, which are located in a what can be described by a spherical surface in space.

8125-04, Session 1

Design and development of a fast-steering secondary mirror for the Giant Magellan Telescope

M. K. Cho, National Optical Astronomy Observatory (United States); A. Corredor, C. Dribusch, The Univ. of Arizona (United States); K. Park, Y. Kim, Korea Astronomy and Space Science Institute (Korea, Republic of); I. Moon, Korea Research Institute of Standards and Science (Korea, Republic of)

The Giant Magellan Telescope (GMT) will be a 25m class telescope which is one of the extremely large telescope projects in the design and development phase. The GMT will have two Gregorian secondary mirrors, an adaptive secondary mirror (ASM) and a fast-steering secondary mirror (FSM). Both secondary mirrors are 3.2 m in diameter and built as seven 1.1 m diameter circular segments conjugated 1:1 to the seven 8.4m segments of the primary. The FSM has a tip-tilt feature to compensate image motions from the telescope structure jitters and the wind buffeting. The support system of the lightweight mirror consists of three axial actuators, one lateral support at the center, and a vacuum system. A parametric study and optimization of the FSM mirror blank and central lateral flexure design were performed. This paper reports the results of the trade study. The optical image qualities and structure functions for the axial and lateral gravity print-through cases, thermal gradient effects, and dynamic performances will be discussed for the case of a light-weighted segment with a center thickness of 140 mm weighing approximately 105 kg.

8125-05, Session 2

Training of optomechanical engineers at the University of Rochester

V. L. Genberg, Sigmadyne, Inc. (United States)

The University of Rochester is well known for the Institute of Optics as well as a strong mechanical engineering program. In recent years, there has been collaboration between the two departments on a variety of topics. This summer, a new faculty member will further the collaboration with a joint appointment in both departments. There is a new cross-listed course in Optomechanics, which is described in this paper. An additional course in Precision Engineering and Testing will soon be offered. As yet, there is no formal specialization in Optomechanics, but many students create their own program from available courses. Students have the opportunity to participate in the several research areas which cross discipline boundaries. A design team of students is building a 16" telescope which they hope can become the basis of an intercollegiate design contest. In addition to full semester courses, there is a summer program of short courses available to working engineers.

8125-06, Session 3

Optomechanical design of an ultrahigh-resolution inelastic x-ray scattering spectrometer at the Advanced Photon Source

D. Shu, S. Stoupin, R. Khachatryan, K. Goetze, T. Roberts, Y. Shvyd'ko, Argonne National Lab. (United States)

A prototype of a novel ultrahigh-resolution inelastic x-ray scattering spectrometer has been designed and tested at undulator-based beamline 30-ID, at the Advanced Photon Source (APS), Argonne National Laboratory. This state-of-the-art instrument is designed to meet challenging mechanical and optical specifications for producing ultrahigh-resolution inelastic x-ray scattering spectroscopy data for various scientific applications.

The optomechanical design of the ultrahigh-resolution inelastic x-ray scattering spectrometer as well as the preliminary test results of its precision positioning performance are presented in this paper.

Work supported by the U.S. Department of Energy, Office of science, Office of Basic Energy Sciences under Contract No. DE-AC02-06CH11357.

8125-07, Session 3

Design and development of an optical system with SiC support structure

I. K. Moon, H. Yang, H. Rhee, J. Song, Y. Lee, Korea Research Institute of Standards and Science (Korea, Republic of)

A support structure of the optical system comprises a series of substructures which are interconnected to support the optical components and their mechanisms. The main structure employing lightweight cylindrical shape of SiC main frame is optimized for high image quality and low weight constraint. To fulfill the optical and mechanical performance requirements extensive finite element analyses using I-DEAS and optical analyses with PCFRINGE has been conducted for the structure of optical system. Analyses include static deformation (gravity and thermal), frequency, dynamic and response analysis, and optical performance evaluations for minimum optical deformation. Image motion is also calculated based on line of sight sensitivity equations integrated in finite element models. A parametric process was performed for the design optimization to produce highest fundamental frequency for a given weight, as well as to deal with the normal concerns about global performance. Alignment and test plan for an optical system will be discussed as well.

8125-08, Session 3

High-precision optical systems with inexpensive hardware: a unified alignment and structural design approach

E. G. Winrow, Sandia National Labs. (United States)

High precision optomechanical structures have historically been plagued by high costs for both hardware and the associated alignment and assembly process. This problem is especially true for space applications where only a few production units are produced. A methodology for optical alignment and optical structure design is presented which shifts the mechanism of maintaining precision from tightly toleranced, machined flight hardware to reusable tooling. Using the proposed methodology, optical alignment error sources are reduced by the direct alignment of optics through their surface retroreflections (pips) as seen through a theodolite. Optical alignment adjustments are actualized through motorized, sub-micron precision actuators in 5 degrees of freedom. Optical structure hardware costs are reduced through the use of simple shapes (tubes, plates) and repeated components. This approach

Conference 8125:
Optomechanics 2011: Innovations and Solutions

produces significantly cheaper hardware and more efficient assembly without sacrificing alignment precision or optical structure stability. The design, alignment plan and assembly of a 4" aperture, carbon fiber composite, Schmidt-Cassegrain concept telescope is presented.

8125-09, Session 3

RF-mechanical performance of the Haystack radio telescope

K. B. Doyle, MIT Lincoln Lab. (United States)

The Haystack radio telescope is being upgraded to support imaging radar applications at 96 GHz requiring diffraction-limited performance over an elevation range of 10 - 40 degrees. The Cassegrain antenna includes a 120-foot diameter primary reflector that is comprised of 432 reflector panels and a 10-foot diameter monolithic subreflector that is mounted on a hexapod assembly. Mechanical performance requirements of the antenna are based on meeting an RF wavefront error requirement of 210 μm rms that account for fabrication, alignment, and environmental errors. Fabrication errors include the manufacturing of the primary reflector panels and the machining of the subreflector. Alignment errors include mounting the panels to the subframes, and the mounting of the subframes to the antenna backstructure. Environmental contributions include the effects from gravity, thermal gradients, and diurnal thermal variations. Details of the reflector fabrication and alignment along with the environmental performance modeling are discussed to meet overall system mechanical requirements.

8125-10, Session 3

Optomechanical tolerancing with Monte Carlo analysis

V. L. Genberg, G. J. Michels, Sigmadyne, Inc. (United States)

Mechanical tolerances within an optical system can consist of a wide array of variables including machining tolerances, variability in material properties, uncertainty in applied loads, and discrete resolution of actuation hardware. This paper discusses methods to use integrated modeling and Monte Carlo techniques to determine the effect of such tolerances on optical performance so that the allocation of such tolerances is based upon optical performance metrics. With many random variables involved, statistical approaches provide a useful means to study performance metrics. Examples include the effect of mount flatness on surface RMS and Zernike coefficients and the effect of actuator resolution on the performance of an adaptively corrected deformable mirror. Tolerances impacting line-of-sight errors are also addressed.

8125-12, Session 4

Deformation analysis of tilted primary mirror for an off-axis beam compressor

J. H. Clark III, U.S. Naval Observatory (United States); F. E. Penado, Northern Arizona Univ. (United States); J. Dugdale, U.S. Naval Observatory (United States)

The Navy Prototype Optical Interferometer (NPOI) array, located near Flagstaff, Arizona, collects and transports stellar radiation from six primary flat collectors (siderostats) through a common vacuum relay system to a beam combiner station where the beams are combined, fringes obtained and modulated, and data recorded for further analysis. The siderostats are capable of redirecting a 38 cm diameter stellar beam to the vacuum relay system, which has the capacity of redirecting only a smaller 12.5 cm diameter beam. We have determined the number of observable stellar objects for the current system configuration in which any portion of the beam greater than 12.5 cm is wasted to be

approximately 6,000. The original design of the array, however, includes space for a beam compressor, tilted up at 20 degrees relative to the horizon, and positioned between each siderostat and the vacuum relay system. The effect from the addition of beam compressors is to increase the number of potential stellar observables to 65,000. This is due to the 9-times increase in collection area. A set of off-axis beam compressors were procured in 2004; however, they were found to have unacceptably high mechanical vibratory characteristics. These compressors were investigated and mitigation techniques discussed in a previous paper. The present paper addresses the analysis of the actual primary mirror, which is almost 2-1/2 times thicker than originally requested. The deflection due to gravity effects on its surface figure versus tilt angle is analyzed and compared with allowable deformations, and the results presented and discussed.

8125-13, Session 4

Vibration analysis using digital image processing for in vitro imaging systems

Z. Wang, S. Wang, C. Gonzalez, Abbott Point of Care Inc. (United States)

In this paper, we propose a novel method for an optical microscope imaging system in-plane rigid-body vibration self measurement by processing digital images taken from a dot patterned calibration target. The method utilizes the system's own imaging system without additional sensors. This paper presents a method for analyzing vibrations within a biological sample imaging system is provided. By imaging a target having one or more identifiable features in fixed positions while the target is stationary using an imaging system, the in-plane coherent spacing of the identifiable features can be determined. By imaging the target a plurality of times during operation of the imaging system and comparing the stationary images to the operational images, the incoherent displacements of the identifiable features of the target can be identified. By evaluating the incoherent displacements of the identifiable features, one or more vibration frequencies associated with those incoherent displacements can be found. In some embodiments, the method may further include the step of determining which component in the imaging system is a source of one or more of the vibration frequencies. Then power spectrum density (PSD) analysis is performed for both intra and inter frame incoherent movements. From the PSD plots, the vibration sources can be identified. It also gives a descriptive statistics of the vibration displacement distribution of the random vibration contents. This study helps microscope imaging system design retrofit, vibration source identification and vibration geometric moments measure. An example for analyzing a biological sample is provided.

8125-14, Session 4

Strength of glass from hertzian line contact

W. Cai, B. Cuerden, R. E. Parks, J. H. Burge, College of Optical Sciences, The Univ. of Arizona (United States)

Glass optics are frequently mounted using line contact interfaces with cylindrical or toroidal metal interfaces. The Hertzian line contact that results can create a large stresses in the glass, including a tensile stress that occurs at the surface near the interface. For contacts with short radii, analysis shows this tensile stress can easily be greater than the strength of the glass, providing reason for concern. However, we show by finite element modeling and by sample testing that for most cases, the effects of this stress are benign. Cracks caused by this stress concentration will propagate only as deep as the stress field, which is typically only a few microns. At this level, such cracks do not have any effect on the optical element, and have an insignificant effect on the strength of the element. This leads to a prediction, which we have verified, that sharp-edged metal interfaces can be used for many applications without risk of fracturing the glass elements due to the resulting stress concentration.

8125-15, Session 5

Analysis of lens mount interfaces

K. A. Chase, J. H. Burge, College of Optical Sciences, The Univ. of Arizona (United States)

Lenses are typically mounted into precision machined barrels, and constrained with spacers and retaining rings. The details of the interfaces between the metal and the glass are chosen to balance the accuracy of centration and axial position, stress in the glass, and the cost for production. This paper presents a systematic study of sharp edge, torroidal, and conical interfaces and shows how to control accuracy, estimate stress, and limit production costs.

Results are presented from computer models, finite element simulations, and experimental testing.

8125-16, Session 5

Analytic results for high-precision and cryogenic lens holders

A. Boesz, Kayser-Threde GmbH (Germany); F. U. Grupp, Univ.-Sternwarte München (Germany); N. Geis, Max-Planck-Institut für extraterrestrische Physik (Germany); R. Bender, Univ.-Sternwarte München (Germany)

The optical system of EUCLID Near Infrared Spectrometer & Photometer (NISF) is composed of 4 lenses, bandpass filters and grisms. The lenses are made of different materials: the corrector lens (fused silica) directly behind the dichroic and the lenses L1 (CaF₂), L2 (LF5G15), and L3 (LF5G15) that are mounted in a separate lens barrel design. Each lens has its separate mechanical interface to the lens barrel, the so called adaption ring.

The adaption ring shall provide the necessary elasticity caused by the different CTE of the lens and ring materials, as well as shall allow the high position accuracy of the lenses relative to the lens barrel and the optical axis.

The design drivers for the adaption ring are high precision, cryogenic operation temperature (120 -150K) and the large dimension of the lenses (170 mm). The design concept of the adaption ring is based on solid state springs which shall both provide sufficient protection against vibration loads at ambient temperature as well as high precision (< ±10µm) and stability at cryogenic temperatures.

Criteria for the solid state spring design shall be low radial forces at cryogenic conditions to avoid any refractive index and polarization variations. The design shall be compliant to the large temperature differences between assembly and operation, the high precision and non-deformation requirements of the lenses as well as to the deviating CTEs of the selected lens materials.

The paper describes the selected development approach including justification, thermal and structural analysis as well as preliminary test results.

8125-17, Session 5

A parametric finite-element model for evaluating segmented mirrors with discrete, edgewise connectivity

J. A. Gersh-Range, Cornell Univ. (United States); W. R. Arnold, Jacobs Engineering Group Inc. (United States); M. A. Peck, Cornell Univ. (United States); H. P. Stahl, NASA Marshall Space Flight Ctr. (United States)

Since future astrophysics missions require space telescopes with apertures of at least 10 meters, there is a need for on-orbit assembly methods that decouple the size of the primary mirror from the choice of

launch vehicle. One option is to connect the segments edgewise using mechanisms analogous to damped springs. To evaluate the feasibility of this approach, a parametric ANSYS model has been developed. This model constructs a mirror using rings of hexagonal segments and a set of geometric parameters that includes the mirror diameter, the size of the gap between segments, the number of rings, the mirror curvature, and the aspect ratio. The connectivity determines whether the mirror is monolithic or segmented: for a monolithic mirror, the edges of adjacent segments are connected continuously, while for a segmented mirror, the edges of adjacent segments are connected at discrete locations corresponding to the mechanism locations. The mechanism properties and placement are additional parameters.

To compare the performance of the segmented mirror to that of the equivalent monolith, the model determines the mode shapes, natural frequencies, and disturbance response of each mirror. As an example, this paper presents the case of a mechanism that is analogous to a set of four collocated single-degree-of-freedom damped springs. The results of these parameter studies suggest that such mechanisms can be used to create a 15-m mirror that behaves similarly to a monolith, although fully predicting the segmented mirror performance would require incorporating measured mechanism properties into the model.

8125-18, Session 5

A tool for bonded optical element thermal stability analysis

G. L. Klotz, Klotz Optical and Mechanical Engineering and Technologies (United States)

An analytical tool is presented which supports the opto-mechanical design of bonded optical elements. Given the mounting requirements from the optical engineer, the alignment stability and optical stresses in bonded optical elements can be optimized for the adhesive and housing material properties. While a perfectly athermalized mount is desirable, it is not realistic. The tool permits evaluation of element stability and stress over the expected thermal range at nominal, or worst case, achievable assembly and manufacturing tolerances. Selection of the most appropriate mount configuration and materials, which maintain the optical engineer's design, is then possible.

The tool is based on a simple stress-strain analysis using Hooke's Law in the worst case plane through the optical element centerline. The optimal bondline is determined for the selected adhesive, housing and given optical element materials using the basic athermalization equation. Since a mounting solution is expected to be driven close to an athermalized design, the stress variations are considered linearly related to strain. A review of these basic equations, the tool input and output capabilities and formats and a simple example will be discussed.

The tool was originally developed to analyze the pointing stability of a circumferentially bonded fiber optic ferrule. It is, however, equally useful for evaluating any thick, or thin, optical element. Edge bonded windows, filters, mirrors and prisms, whether circular, or rectangular, can be easily evaluated for alignment stability and maximum stress. The tool is currently designed to run in Microsoft Excel. Future versions of the tool will include an extended adhesive, housing and optical element material properties library and run in MATLAB.

8125-19, Session 6

Application of modal testing to characterize ground based telescope elastic motion and its effect on image quality

J. Lukens, B. C. Steele, Quartus Engineering Inc. (United States); G. Gates, N. Kaiser, J. S. Morgan, Univ. of Hawai'i (United States)

No abstract available

8125-20, Session 6

Thermal stress failure criteria for a structural epoxy

P. Côté, N. Desnoyers, INO (Canada)

Representative failure data for structural epoxies can be very difficult to find for the optomechanical engineer. Usually, test data is only available for shear configuration at room temperature and fast pull rate. On the other hand, the slowly induced stress at extreme temperature is for many optical systems the worse-case scenario. Since one of the most referenced epoxy for optical assembly is the 3M Scotch-weld EC-2216 B/A Gray, better understanding its behavior can benefit a broad range of applications.

The objective of this paper is two-fold. First, review data for critical parameters such as Young's modulus and coefficient of thermal expansion. Secondly, derive failure criteria from correlation between a thermal stress experiment and finite element model.

Instead of pulling out a standard tensile specimen, it is proposed to test thin bondline geometry to replicate the optical device usage. Four test plates are assembled at the Institut National d'Optique (INO) in Quebec City, Canada with bondlines of 75µm and 150µm. To detect the failure of the epoxy, the low level vibration signature of a cantilever Invar plate is monitored as temperature changes. Following the finite element analysis, a failure criterion is found to better match the experimental results than generic lap shear data.

8125-21, Session 6

Acquisition, simulation, and test replication of weapon firing shocks applied to optical sights

K. D. Ball, D. A. L. Gardner, Qioptiq Ltd. (United Kingdom)

As part of a capability improvement programme, a requirement was placed to develop a comprehensive understanding of the transient inertial shock loads exerted on visible and IR weapon systems through standard field operation. The knowledge was intended to aid in the development of new techniques for mechanical analysis simulations and representative 'in house' testing.

Weapon integrated sight systems have experienced huge technological advancement in recent years current systems give the user thermal and image intensified capabilities combined with high recognition and detection range. To satisfy customer requirements system designs must incorporate complex electronics, innovative optical materials and advanced mounting techniques, all of which are susceptible to failure under operational loads. Failures can be direct mechanical breakdown, permanent deformation, or interference / momentary non-conformance resulting from amplification of load through excitation of a components natural frequency.

This paper describes the non-intrusive mechanical field data acquisition and subsequent analysis and test integration techniques, performed on complex opto-mechanical weapon mounted systems. These systems when mounted in tactical configuration with a wide range of military equipment are subjected to variable random vibration and shock loading; consistent with standard operational requirements. As a result of the multi-directional field data acquisition, innovative techniques have been developed enabling the synthesis of the transient recordings for the purpose of finite element analysis. Further investigations have revealed new possibilities in applying accurately controlled 'in-house' loading for low cost representative test purposes.

8125-22, Session 6

Novel optical refraction index sensor

E. S. Arroyo-Rivera, H. S. De los Reyes-Cruz, M. S. Lopez-Cueva, A. A. Castillo-Guzman, R. Selvas, Univ. Autonoma de

Nuevo Leon (Mexico)

The optical industry is increasing rapidly in recent years. The refraction parameter is a feature of any material and therefore there is a lot of research to development an instrument capable of measuring it. Among the techniques in the state of the art, we can find the Fresnel method, the Christianson method, and some interferometric methods. However, these methods have demonstrated to be confident when the analyzed material is monolayer. The complexity of the measuring increases as long as the numbers of layers are presented in the material. The setup consisted of a diode laser, a focusing lens, a z-axis-scanner, a photo-detector, an electronic and software system to interpret the signals.

This work describes a novel optical refraction index sensor which is based on the analysis of double reflection lecture detection. This process initially identifies the thickness of a semitransparent solid or liquid material by the retro-reflection of a laser diode at 633nm, 800nm, 915nm and 980nm as a function of distance along the device under test. For the index detection, a lens is attached in a Z-axis-scanner to find the focusing point. This feedback signal brings how depth is penetrated the beam and also how far traveled the beam path. As we know, the refractive index is indirectly related to the traveled beam path at different materials, the data of the thickness at each layer is treating with a geometrical analysis of the beam velocity and all data can provides us of the refractive index at each material. The system is compact, robust and reliable.

8125-23, Session 6

Adhesive bond cryogenic lens cell margin of safety test

D. M. Stubbs, C. L. Hom, H. C. Holmes, J. C. Cannon-Morret, O. F. Lindstrom, J. W. Irwin, L. A. Ryder, T. T. Hix, J. A. Bonvallet, H. S. Hu, I. V. Chapman, C. Lomax, E. T. Kvamme, G. S. Feller, Lockheed Martin Space Systems Co. (United States); M. M. Haynes, Composite Technology Development, Inc. (United States)

The Near Infrared Camera (NIRCam) instrument for NASA's James Webb Space Telescope (JWST) has an optical prescription which employs four triplet lens cells. The instrument will operate at 37K after experiencing launch loads at ~293K and the optic mounts must accommodate all associated thermal and mechanical stresses, plus maintain an exceptional wavefront during operation.

Lockheed Martin Space Systems Company (LMSSC) was tasked to design and qualify the bonded cryogenic lens assemblies for room temperature launch, cryogenic operation, and thermal survival (25K) environments. The triplet lens cell designs incorporated coefficient of thermal expansion (CTE) matched bond pad-to-optic interfaces, in concert with flexures to minimize bondline stress and induced optical distortion. A companion finite element study determined the bonded system's sensitivity to bondline thickness, adhesive modulus and adhesive CTE. The design team used those results to tailor the bondline parameters to minimize stress transmitted into the optic.

The challenge for the Margin of Safety (MOS) team was to design and execute a test that verified all bond pad/adhesive/optic substrate combinations had the required safety factor to generate confidence in a very low probability of optic/bond failure during the warm launch and cryogenic survival conditions. Because the survival temperature was specified to be 25K, merely dropping the test temperature to verify margin was not possible. A shear/moment loading device was conceived that simultaneously loaded the test coupons at 25K to verify margin.

This paper covers the design/fab/SEM measurement/thermal conditioning of the MOS test articles, the thermal/structural analysis, the test apparatus, and the test execution/results.

8125-24, Session 7

A few observations about mounting moderately sized mirrors

M. I. Kaufman, National Security Technologies, LLC (United States)

Most of the mirror mounting literature has focused on small (less than 0.1 meters) or large (greater than 1 meter) mirrors. We will examine the theory and practice of mounting moderately sized mirrors (between 0.1 and 1 meter). Two examples will be taken from optical diagnostic systems designed for the National Ignition Facility (NIF). One of the examples will be for a mirror with a poor aspect ratio (i.e. diameter to thickness ratio greater than 15:1).

8125-25, Session 7

Lens mount with ring-flexures for athermalization

H. Kihm, H. Yang, Y. Lee, Korea Research Institute of Standards and Science (Korea, Republic of); J. Lee, Cheongju Univ. (Korea, Republic of)

We present a new athermal lens mounting scheme made of cascaded ring flexures. Two circular grooves are concentric at the adhesive injection hole and fabricated monolithically on a lens cell or a barrel itself. The ring flexure can accommodate six degree-of-freedom motions by controlling dimensional parameters. We evaluate thermo-elastic deformations by interferometric measurements and verify the results with finite element analyses. Also we compare the athermal performances from a simple elastomeric mount and a ring-flexured mount. This lens mounting scheme would be a promising candidate for environmentally challenged optical systems like space and military applications.

8125-26, Session 7

Mounting small optics for cryogenic space missions

P. V. Mammini, C. L. Hom, H. C. Holmes, M. S. Jacoby, E. T. Kvamme, Lockheed Martin Space Systems Co. (United States)

The Near Infrared Camera (NIRCam) instrument for NASA's James Webb Space Telescope (JWST) includes numerous optical assemblies. The instrument will operate at 37K after experiencing launch loads at ~293K and the optic mounts must accommodate all associated thermal and mechanical stresses, plus maintain an exceptional wavefront during operation.

Lockheed Martin Space Systems Company (LMSSC) conceived, designed, assembled, tested, and integrated the mirror and lens assemblies for the NIRCam instrument.

This paper covers the design, analysis, and test of the instruments key optical assemblies.

8125-27, Session 7

Design considerations of a slit diaphragm flexure used in a precision mirror gimbal

B. C. Cox, National Security Technologies, LLC (United States)

Two precision mirror gimbals were designed using slit diaphragm flexures to provide two-axis precision mirror alignment in space-limited applications. Both gimbals are currently in use in diagnostics at the National Ignition Facility: one design in the Gamma Reaction History (GRH) diagnostic and the other in the Neutron Imaging System (NIS)

diagnostic. The GRH gimbal has an adjustment sensitivity of 0.1 mrad about both axes and a total adjustment capability of +/- 6 degrees; the NIS gimbal has an adjustment sensitivity of 0.8 μ rad about both axes and a total adjustment range of +/- 3 degrees. Both slit diaphragm flexures were electro-discharge machined out of high-strength titanium and utilize stainless steel stiffeners. The stiffener-flexure design results in adjustment axes with excellent orthogonality and centering with respect to the mirror in a single stage; a typical two-axis gimbal flexure requires two stages. Finite element analyses are presented for both flexure designs and a design optimization of the GRH flexure is discussed.

8125-28, Session 8

Backlighting for alignment of optics in first diffraction order path

A. Amphawan, Univ. of Oxford (United Kingdom)

In a typical Fourier transform by a convex lens, the first diffraction order deviates from the axis of the zeroth diffraction order. When the angle of deviation of the first diffraction order with respect to the zeroth diffraction order is very small, launching a laser beam into an optical fiber located in the axis of the first diffraction order presents a challenge. To facilitate this, a backlighting technique is proposed. The step-by-step alignment procedure for this is described. It is evident that the backlighting technique improves the power coupling efficiency into the optical fiber.

8125-29, Session 8

Large stable aluminum optics for aerospace applications

D. Vukobratovich, Raytheon Missile Systems (United States); J. Schaefer, Raytheon ELCAN Optical Technologies (United States)

Aluminum mirrors offer the advantages of lower cost, shorter fabrication time, more rugged mounting, and same material athermalization when compared to classical glass mirrors. In the past these advantages were offset by controversial dimensional stability and high surface scatter, limiting applications to IR systems. Raytheon developed processes to improve long term stability, and reduce surface scatter. Six 380 mm aperture aluminum mirrors made using these processes showed excellent stability, with figure changes of less than 0.01 wave RMS (1 wave = 633 nm) when cycled 10 times between -51 and +71 deg. C. The VQ process developed at ELCAN reduces surface scatter in bare aluminum mirrors to below 20 angstroms RMS, and has been used in hundreds of production mirrors up to 300 mm aperture. These processes were employed in the fabrication of two lightweight single arch 600 mm aluminum mirrors. The two mirrors were produced in four months, with a mounted surface figure of 0.22 waves RMS and surface roughness of 20 angstroms. Mounted fundamental frequency was 218 Hz, and no figure distortion was observed at preload levels four times higher than design. Subsequently the mirrors performed well when subjected to severe environmental loadings in a Raytheon test system. This technology is being extended to ultra-lightweight sandwich mirrors, which are competitive with other technologies in many aerospace applications such as UAV surveillance systems and satellite optics.

8125-30, Session 8

Comparative analysis of the efficiency of several open-back mirror lightweighting approaches using machining parameters now available for a Zerodur blank of 1.2m aperture

T. B. Hull, L-3 Communications Tinsley Labs. Inc. (United States); A. R. Clarkson, G. Gardopee, L-3 IOS Brashear (United States); R. Jedamzik, A. Leys, SCHOTT North America, Inc.

Conference 8125:
Optomechanics 2011: Innovations and Solutions

(United States); J. Pepi, L-3 Communications SSG-Tinsley
(United States); M. Schäfer, V. Seibert, A. Thomas, T. Werner, T.
Westerhoff, SCHOTT North America, Inc. (United States)

We evaluate several open-back mirror lightweighting approaches now offered in Schott Zerodur® realizing more aggressive figures-of-merit than in the past. A f/1.3 mirror 1.2 meters in diameter has been selected, since significant lightweighting often is required of a mirrors around this size for both spaceborne and terrestrial telescope applications, and methods applied are well illustrated for this size. Each lightweighting approach will be taken to its current limit and is required to meet a common free-free natural frequency, and to be compatible with machining parameters now available. We will also recognize optical processes, and constrain the results for the same expected magnitude of residual substructure print-through, as well as considering optical testing. Other mirror parameters, including facesheet and core thickness, cell size and cell wall thickness, and even partially closing the back are adjusted to achieve this stiffness and other constraints. The resulting relative mass and thickness then become figures-of-merit. We will also evaluate the relative machining time as an index of relative cost and duration of the lightweighting process. We expect that these figures-of-merit can be extrapolated to somewhat smaller or larger mirror diameters, and that the more aggressive machining parameters now available will extend the use of open-backed mirrors into the domain where expensive closed-back sandwich-mirrors were previously required.

8125-31, Session 8

Optimal window engineering

A. E. Hatheway, Alson E. Hatheway Inc. (United States)

Mechanical engineers are sometimes called upon to come up with specifications for a minimum price and minimum mass (weight) window. Usually the shape of the window is known, the spectral pass-band is known and the allowable contributions to image blur is known. This paper presents an engineering method for quantifying the trade-off between price and mass in a window.

Conference 8126: Optical Manufacturing and Testing IX

Monday-Wednesday 22-24 August 2011 • Part of Proceedings of SPIE Vol. 8126 Optical Manufacturing and Testing IX

8126-01, Session 1

Optical manufacturing and testing requirements identified by the NASA Science Instruments, Observatories and Sensor Systems Technology Assessment

H. P. Stahl, NASA Marshall Space Flight Ctr. (United States)

In August 2010, the NASA Office of Chief Technologist (OCT) commissioned an assessment of 15 different technology areas of importance to the future of NASA. Technology assessment #8 (TA8) was Science Instruments, Observatories and Sensor Systems (SIOSS). SIOSS assess the needs for optical technology ranging from detectors to lasers, x-ray mirrors to microwave antenna, in-situ spectrographs for on-surface planetary sample characterization to large space telescopes. The needs assessment looked across the entirety of NASA and not just the Science Mission Directorate. This paper reviews the optical manufacturing and testing technologies identified by SIOSS which require development in order to enable future NASA high priority missions.

8126-02, Session 1

Technologies for producing segments for extremely large telescopes

D. D. Walker, Zeeko Ltd. (United Kingdom); R. Evans, S. Hamidi, P. Harris, H. Li, M. Parry-Jones, OpTIC Glyndwr Ltd. (United Kingdom); G. Yu, Glyndwr Univ. (United Kingdom)

We describe a new process-chain being used to produce eight 1.4m hexagonal mirror segments for the European Extremely Large Telescope project. The first is a reference sphere for metrology, and the others are prototypes of a cluster of aspheric segments near the edge of the 42m telescope pupil. OpTIC Glyndwr has created a new pilot plant in North Wales, based around the integration of a highly bespoke full-aperture test-tower designed and built in-house, with a Zeeko 1.6m polishing machine, and supported by independent profilometry. The existing 1.2m and 600mm Zeeko machines are being used for process development and optimization, which is continuing through the segment programme. The process chain starts with direct aspherising of the hexagonal segments on the Cranfield BoX ultra-precision grinder, and continues through smoothing, polishing, form-correction and edge-rectification using the Zeeko CNC platform. The paper describes the development of the technology and progress to date, and anticipates how the process-chain is expected to evolve through the seven segments to increase both process speed and surface quality.

8126-04, Session 1

ZERODUR for stress mirror polishing

R. Jedamzik, T. Westerhoff, C. Kunisch, SCHOTT AG (Germany)

Stress mirror polishing is considered for the generation of the aspherical shaped primary mirror segments of the thirty meter telescope (TMT). For stress mirror polishing it is essential to precisely know the elastic response of glass ceramic substrate materials under a given deformation load. In the past it was experimentally shown that glass ceramics do not respond instantaneously to loading and unloading conditions, this effect was called "delayed elasticity".

Recently it was shown that it is possible to use a model to predict the characteristic thermal expansion behaviour of individual ZERODUR batches for a given temperature profile. A similar approach will be used to predict the elastic behaviour of ZERODUR under time dependent loads.

In this presentation the delayed elasticity effect of ZERODUR® is reviewed. The elastic response of the material to load conditions is shown and discussed. First results of a model approach based on experimental results and tools that have been built up for the modelling of the thermal structural relaxation effect of ZERODUR® will be presented.

8126-05, Session 1

Design and fabrication of a 3m class light weighted mirror blank for the E-ELT M5

R. Jedamzik, V. Seibert, A. Thomas, T. Westerhoff, SCHOTT AG (Germany); M. Müller, M. Cayrel, European Southern Observatory (Germany)

In the recent past SCHOTT has proven its capability for the manufacturing of large light weighted ZERODUR® mirror blanks for telescope projects like for example the GREGOR solar-telescope. In 2010 SCHOTT was awarded with a study to develop a design for the M5 mirror blank of the ESO E-ELT.

The tip and tilt M5 mirror of the European Extremely Large Telescope (E-ELT) requires a demanding approach in light weighting. The approximately 3 m x 2.5 m elliptical plano mirror is specified to a weight of less than 500 kg with high Eigenfrequencies and low deformation under different inclination angles.

The study was divided into two parts. The first part targeted on an optimized lightweighted design with respect to performance and processability with the help of finite element modelling. In the second part of the study a concept for the processing sequence including melting, cold-processing, acid etching and handling of the M5 blank was developed. With the fabrication of a prototype section SCHOTT demonstrated its capability to manufacture the demanding features including pockets with 350 mm depth, thin walls and sloped pocket bottoms.

This presentation shows the results of the design work, processing concept and demonstrator fabrication.

8126-06, Session 1

Optical finishing properties of silicon-infiltrated silicon carbide

E. J. Gratrix, M Cubed Technologies, Inc. (United States); F. Tinker, Aperture Optical Sciences, Inc. (United States); P. B. Mumola, P. B. Mumola, LLC (United States)

Silicon Carbide (SiC) has been considered to be a leading candidate material for future lightweight telescopes and opto-mechanical structures based on its high specific stiffness and thermal stability. A number of companies have successfully demonstrated processes to manufacture complex, net-shape, lightweight mirror substrates with apertures exceeding one meter. The cost of optical finishing such mirrors has nonetheless continued to be an obstacle to the widespread adoption of SiC as a mirror material with the exception of niche cryogenic applications. Nearly all current processes for producing SiC mirror substrates yield surfaces that are unsuitable for optical polishing unless they are first coated with CVD-Silicon or CVD-SiC. The cost of CVD coating and the non-uniformity of this relatively thick layer of material unfortunately add to the optical finishing cost. This paper addresses the material removal and polishing characteristics of Si-infiltrated SiC and compares these properties to those of CVD-SiC. The results indicate that high quality optical surfaces, with micro-roughness on the order of 1.0 nm rms, can be obtained without the need for CVD cladding while preserving the thermal and structural advantages typical of SiC.

8126-52, Session 1

European ELT mirrors development

E. Ruch, J. Carel, H. Leplan, F. Poutriquet, Sagem Défense Sécurité (France)

Sagem - Reosc has been awarded by ESO several contracts for the manufacturing and testing of seven prototype segments of the E-ELT primary mirror, the design of the 6 meters convex secondary mirror and the active support system, the large thin shell for the adaptive M4 mirror and the design of the extremely lightweighted tip tilt M5 mirror.

The main purpose of the development efforts are to assess the segment feasibility and define a baseline process for the serial production of more than one thousand of these segments. The paper will present the results obtained so far on the different prototypes segments and compared them to the requirement of the future E-ELT segments.

The presentation will also address the manufacturing and the testing of the prototype thin shells of 2,5 meter diameter and 2 mm thin that have been recently delivered to ESO. We will present the technical results that have been achieved.

8126-07, Session 2

Piezoelectric deformable mirror based on monolithic PVDF membranes

G. A. Finney, Kratos Defense & Security Solutions, Inc. (United States); K. D. Spradley, Advanced Optical Systems, Inc. (United States); B. S. Farmer, NeXolve Corp. (United States)

Deformable mirrors using polyvinylidene fluoride (PVDF) membranes in a bimorph configuration have been previously studied by numerous investigators. Kratos Defense and Security Solutions, in partnership with Advanced Optical Systems, Inc. and Mantech NeXolve Corporation, have been evaluating the utility of unimorph PVDF films for fabrication of deformable mirrors. Actuation using a unimorph film is based upon creating a gradient in the piezoelectric response of the film through a proprietary process. This property eliminates the requirement to bond multiple films to generate curvature and improves the optical quality of the films. Analytical approximations to describe the behavior of the film under applied loads and voltages have been developed. To assist in the development and design of the films, a multiphysics design tool has been developed by tightly integrating several commercial software packages. This tool has then been used to model the performance of the films and extract significant material parameters from experimental results. This paper reports on these initial results and characterization of this novel material.

8126-08, Session 2

Progress on 4m class ZERODUR mirror production

T. Westerhoff, R. Jedamzik, A. Klein, C. Klein, SCHOTT North America, Inc. (United States)

The first monolithic ZERODUR 4 m class mirror was ordered by the German Max Planck Institute for Astronomical Physics in 1968. The technological ability to actively compensate the bending of the mirror substrate under gravity initiated the development from heavy non active thick mirror substrates to ever thinner thicknesses starting with the NTT, the New Technology Telescope of ESO.

The thinner the mirror substrates are becoming the more demanding are the requests on homogeneity of material properties to ensure best performance over the clear aperture at every spot.

In this paper we present results on material properties achieved for the 4 m class mirror substrates recently delivered by SCHOTT. The CTE homogeneity, the internal quality regarding striae, bubbles and inclusions

as well as stress birefringence data are reported. Improvements in CNC processing and overall manufacturing process for the very thin 4 m class blanks are discussed.

8126-09, Session 2

Open-source data analysis and visualization software platform

D. W. Kim, B. Lewis, J. H. Burge, College of Optical Sciences, The Univ. of Arizona (United States)

Optical engineering projects often require massive data processing with many steps in the course of design, simulation, fabrication, metrology, and evaluation. A Matlab-based data processing platform has been developed to provide a standard way to manipulate and visualize various types of data that are created from optical measurement equipment. The operation of the software platform via the graphical user interface is easy and powerful. Data processing is performed by running modules that use a proscribed format for sharing data. Complex operations are performed by stringing modules together using macros. While numerous modules have been developed to allow data processing without the need to write software, the greatest power of the platform is provided by its flexibility. A developer's toolkit is provided to allow development and customization of modules, and the program allows a real-time interface with the standard Matlab environment. This software, developed by the Large Optics Fabrication and Testing group at the University of Arizona, is now publicly available. We present the capabilities of the software and provide some demonstrations of its use for data analysis and visualization. Furthermore, we demonstrate the flexibility of the platform for solving new problems.

8126-10, Session 2

Measuring the residual stress of transparent conductive oxide films on PET by the double-beam shadow Moiré interferometer

H. Chen, K. Huang, Y. Lo, H. Chiu, G. Chen, National Yunlin Univ. of Science and Technology (Taiwan)

The purpose of this research was to construct a measurement system which can fast and accurately analyze the residual stress of the flexible electronics. In which, representative transparent conductive oxide (TCO) films, such as tin-doped indium oxide (ITO), gallium-doped zinc oxide (GZO) films and aluminum-doped zinc oxide (AZO) films, were deposited by RF magnetron sputtering using corresponding oxide targets on PET substrate. As we know that the shadow moiré interferometry is a useable way to measure the large deformation. So we set up a double beam shadow moiré interferometer to measure and analyze the residual stress of TCO films on PET. In this measurement system, a beam splitter splits one beam into two beams to pass through a reference grating with the identical incident angle and create a deformation shadow grating on the object surface. Then we used CCD to retrieve moiré pattern which is created by shadow grating and reference grating. The feature was to develop a mathematical model and combine the image processing software. By the LabVIEW graphical software, we could measure the distance which is between the left and right fringe on the pattern to solve the curvature of deformed surface. Hence, the residual stress could calculate by the Stoney correction formula for the flexible electronics. We also had done the error analysis for the system whose relative error could be under 2%. Therefore, shadow moiré interferometer is an accurate, fast, and simple system for the residual stress on TCO/PET films.

8126-11, Session 3

MicroFinish Topographer: surface finish metrology for large and small optics

R. E. Parks, Optical Perspectives Group, LLC (United States)

Conference 8126:
Optical Manufacturing and Testing IX

The MicroFinish Topographer (MFT) is a temporal phase measuring interferometer attachment to the Point Source Microscope that uses 4D Technology 4Sight software for data analysis. The MFT is designed to set directly on a large optic to measure the surface roughness. Tip, tilt and focus adjustments allow breaking out the fringes and finding maximum contrast with the help of the software. Tests have shown the MFT gives the same roughness values even on non-isolated samples as do traditional surface roughness profilers. Results of these tests will be given.

The convenience of making in situ roughness measurements led to the obvious question of whether the same device could measure roughness on small samples, something smaller in diameter than the 120 mm diameter support ring for the large optics version. This is easily done by turning the unit over and placing smaller samples on a support plate that kinematically holds the sample above the 10x Mirau objective. The close coupling of the sample to the objective eliminates the need for vibration isolation in all but the worse environments. Again, results of measurements made on the MFT will be shown alongside those from other profilers.

The suite of well designed and coordinated hardware and software make surface roughness measurement quick and easy on the widest possible range of sample sizes without the need for replicas or vibration isolation hardware.

8126-12, Session 3

Infrared reflection deflectometry system for optical surface measurement in grinding stage: the IR SCOTS

T. Su, W. Park, R. E. Parks, P. Su, J. H. Burge, College of Optical Sciences, The Univ. of Arizona (United States)

A rapid, robust and accurate system for measurement of specular surface has been adopted at the Steward Observatory Mirror Lab in University of Arizona. This system, called SCOTS (software configurable optical test system), is based on reflection deflectometry and is similar to a reversed traditional Hartmann test. It uses an LCD screen to illuminate the surface under test; a camera captures reflected light for surface slope analysis. In comparison to interferometry, SCOTS provides similar results with a simpler optical system and a larger dynamic range. By using an infrared source (in this case an electrically heated alloy wire), the same idea can be applied to make measurements of ground surfaces which are diffuse reflectors in visible wavelength. A linear stage is used to scan the alloy wire through the field, while an infrared camera is used to collect data. This IR system could be applied early in the grinding stage of fabrication of the large telescope mirrors to minimize the surface shape error imparted during processing. This advantage combined with the simplicity of the optical system (no null optics, no high power carbon dioxide laser) would improve the efficiency and shorten processing time.

8126-13, Session 3

Phase-shifting Zernike interferometer wavefront sensor

S. Rao, J. K. Wallace, E. Serabyn, Jet Propulsion Lab. (United States)

A phase-shifting Zernike interferometer measures the electric field in the pupil plane of an optical instrument, with advantages over a traditional Shack-Hartmann sensor. When operated as a long-stroke interferometer, it measures the absolute phase across the pupil as a function of wavelength. A common-path, all-reflective design makes it minimally sensitive to vibration, polarization, and wavelength. We describe the optical system, review the theory of operation, and review results from a laboratory demonstration of this novel instrument.

8126-14, Session 3

Flexible null interferometry of the aspherical surface

H. Chang, C. Liang, C. Liang, National Central Univ. (Taiwan)

A novel optical testing method is developed to test the surface deformation of the asphere without using any additional holograms or null optics. The principle optical testing method is based on the geometrical null utilizing merely 4 axes of geometrical motions. The optical null of the tested aspherical surface is achieved at the partial surface of an axial symmetrical surface. By adapting the vibration insensitive phase shifting algorithm, we are able to extract the phase of the interferogram reflected from an asphere during the rotational scanning motion in the presence of mechanical vibration induced from the stages. The azimuthal phase stitching method is used to stitch the tangential phase after interferogram measurement to form a complete asphere surface profile. The four motions geometrical null principle is illustrated and the preliminary measurement results are shown.

8126-15, Session 3

Dynamic surface roughness profiler

B. T. Kimbrough, N. Brock, 4D Technology Corp. (United States)

A dynamic profiler is presented that is capable of measuring surface roughness while mounted directly to optical polishing equipment or while resting directly on large optics. Utilizing a special CCD camera incorporating a micro-polarizer array and a proprietary 460nm LED source, quantitative measurements were obtained with exposure times of <100 usec. The polarization-based interferometer utilizes an adjustable polarizer to optimize fringe contrast and signal to noise for measurement of optical surfaces ranging in reflectivity from 1 to 100%. A new phase calculation algorithm is presented that nearly eliminates phase-dependent errors resulting in shot noise limited performance. In addition to its vibration immunity, the systems light weight, <5 kg, compact envelope, 24 x 24 x 8 cm, integrated alignment system, and multiple mounting options facilitate use both directly resting on large optical surfaces and directly mounted to polishing equipment, stands, gantries and robots. In this paper we present measurement results for both on-optic and stand-mounted configurations. A fully automated tripod mounting system for on-optic measurements is demonstrated. Measurement results presented show an RMS repeatability <0.005 nm and an RMS precision < 0.1nm which are achieved without active vibration isolation.

8126-16, Session 4

Cryo stability of HB-Cesic optics

M. R. Kroedel, ECM GmbH (Germany)

For large future space optics the requirements are more and more challenging with respect to mass, size and stability. In the past two years ECM tested together with his partners extensively the cryo stability of HB-Cesic material under various conditions.

In this paper we will report the test configuration and results from sample testing up to two large measurement and qualification campaigns of HB-Cesic optics.

The first mirror was a 600 mm mirror, which was polished directly without any overcoatings and the second mirror was an 800 mm mirror with a silicon layer on the optical surface. Both mirrors were tested to cryogenic temperatures of 10 to 100 K.

8126-17, Session 4

Analysis of fine-grinding techniques in terms of achievable surface qualities

O. W. Föhnle, K. Hauser-Bergen, FISBA OPTIK AG (Switzerland)

In Optical Fabrication of e.g. glass lenses or tungsten carbide tools for hot glass molding processes, two goals have to be achieved: the desired surface shape and the required surface quality (level of surface roughness and sub-surface damage (ssd)) have to be generated. To that aim, abrasive processes, e.g. grinding and polishing, are applied subsequently. In particular, the fine grinding has to leave a minimum level of ssd since this determines the time needed for the subsequent costly polishing process. In this paper we report on an analysis of three different fine grinding techniques in terms of achievable surface qualities: fixed abrasive cnc grinding, traditional loose abrasive grinding and fluid jet grinding, where a fine grinding slurry is accelerated by a nozzle and guided onto the surface to be machined (a similar approach to Fluid Jet Polishing). To detect the level of ssd, two non destructive methods were applied. A traditional one where the sample under test consists of two optically contacted parts and intensity-detecting Total Internal Reflective Microscopy (iTIRM). Experimental studies have been carried out. A.o. the generated surface qualities have been analyzed if these techniques are set up with the same abrasive grain sizes. In addition, the level of ssd is detected if they are set up to generate the same level of surface roughness. While in FJP wear is caused by the kinetic energy of the impinging particles, in cnc and traditional grinding, there is a macroscopic contact between tool and surface causing a higher level of ssd.

8126-18, Session 4

Fabricating and testing of complex optical elements with high precision

H. Wang, V. Giggel, G. Derst, T. Koch, Carl Zeiss Jena GmbH (Germany)

The very strong requirement for the super precision optics for the microlithography has been driving the development of optical fabrication and testing technologies since last twenty years. These technologies are basis for manufacturing high-end optics. In addition to the requirements on reasonable costs for manufacturing arbitrary surface shapes, the optics with $\lambda/100$ quality, aspheric and freeform optics mean always challenges with both fabrication and test, because experienced optical technicians should know exactly what they measure at first and then decide how to achieve the required quality using different iterative processes. These iterative processes are based on the commercial available figuring and polishing machines and Zeiss CCP (computer controlled polishing) technology. The testing has been performed using both commercial available interferometers and Zeiss self developed metrologies. The materials used cover all types of typical optical materials, in particular the CaF₂ and fused silica.

8126-19, Session 4

Analytical process design for chemo-mechanical polishing of aspheres

F. Klocke, O. Dambon, D. Waechter, Fraunhofer-Institut für Produktionstechnologie (Germany)

This work deals with the chemo-mechanical sub-aperture polishing using spiral tool path and pressure inflated membrane tools. The choice of machining parameters is often based on empirical try-outs and iterative corrections. However, an economic manufacturing of glass aspheres in small lot sizes requires first part right strategies. To get there, an analytical process design, which chooses the best process parameters in regard to the geometry, material and initial quality of samples, based on

knowledge instead of experiments is essential.

This work contributes to gain efficiency in polishing aspheres from ground to polished quality by a systematical investigation of process parameters and by presenting a method for calculating the effect of major input parameters on the local distribution of material removal. It is based on Preston's equation and takes into account the influence of the input parameters on the spot size, local relative velocity, pressure and dwell-time. The analytical methods enable the prediction of the effect of changing parameters on the edge and center effects as well as general deviations in the radius of curvature, when polishing aspheres. In the second place, they enable the control of shape deviations by varying process parameters dynamically. The necessary experimental investigations, the mathematical model and application examples for controlling the radius of curvature and the edge effect will be presented. In conclusion, the analytical methods for choosing appropriate process parameters will help increasing significantly the efficiency in chemo-mechanical polishing of glass aspheres and can be even applied to free-forms.

8126-28, Poster Session

The slow tool servo diamond turning of optical freeform surface for astigmatic contact lens

C. Chen, Instrument Technology Research Ctr. (Taiwan); Y. Cheng, Instrument Technology Research Ctr. (Taiwan) and National Tsing Hua Univ. (Taiwan); W. Hsu, H. Chou, Instrument Technology Research Ctr. (Taiwan); P. Wang, National Tsing Hua Univ. (Taiwan); D. P. Tsai, Instrument Technology Research Ctr. (Taiwan) and National Taiwan Univ. (Taiwan)

Three ultra-precision machining processes namely fast tool servo, slow tool servo and diamond milling, are frequently used to produce optical freeform surface. Though slow tool servo has the advantages of no extra attachment and fast setting-up, the complicated three dimensional tool shape compensation and tool-path generation are major reasons for resulting in poor form accuracy, pre-matured tool failure and poor surface finish. This research aimed to develop a model of three dimensional tool shape compensation for generating 3D tool path in slow tool servo diamond turning of asymmetrically toric surface such as in astigmatic contact lens.

The toric surface can be used to correct the astigmatism. The disposable contact lens can't make with toric surface in the past. Because of the progress of the freeform optics machining technology, the astigmatic contact lens has been manufactured by casting method recently. For the casting method, the plastic optical mould made by plastic injection method was used to generate the contact lens. The nickel plating steel mould with toric surface of plastic injection will be manufactured by slow tool servo diamond turning in this research. The form accuracy of freeform surface was measured by UA3P with user define function and the form error has also been corrected. Finally, the form error of both x and y direction and fully surface are less than 0.3 μ m and 0.5 μ m, respectively. The surface roughness is less than 5nm.

8126-29, Poster Session

The fabrication of high filling factor double side micro lens array with high alignment accuracy

Y. Cheng, Instrument Technology Research Ctr. (Taiwan) and National Tsing Hua Univ. (Taiwan); C. Chen, W. Hsu, Instrument Technology Research Ctr. (Taiwan); P. Wang, National Tsing Hua Univ. (Taiwan); D. P. Tsai, Instrument Technology Research Ctr. (Taiwan) and National Taiwan Univ. (Taiwan)

Laser has the advantage of monochromaticity, coherence, divergence

Conference 8126:
Optical Manufacturing and Testing IX

and directionality. The micro lens array has been widely used for laser beam shaping in order to approach the good uniformity of lighting area. For the application of illumination system, the double side micro lens array should be with high filling factor, high form accuracy, good surface roughness, and great alignment accuracy of two side surfaces.

Recently, a variety of processes for the fabrication of micro lens array have been developed, for instance, the photolithography process, E-beam lithography on sol-gel materials, gray-tone and Focus Ion Beam. But these methods have drawbacks of low form accuracy, poor surface roughness, bad alignment accuracy of double side micro lens array and not easily to get high filling factor.

In this research, the ultra-precision slow tool servo diamond shaping and plastic injection method for micro lens array fabrication had been studied. The high form accuracy and good surface roughness of ultra precision diamond cutting is well known. The complexity micro structure of high filling factor micro lens array via the planning of cutting tool path had been used in this research. The high alignment accuracy of both sides micro lens array has been aligned by fixture design. The form accuracy and surface roughness were less than 0.1 μ m and 10nm, respectively. The alignment error of both sides micro lens array was less than 10 μ m.

8126-42, Poster Session

Mirror segments for large mirror systems of weak optical signals detectors for UV spectral range

P. Schovaneck, M. Hrabovsky, M. Palatka, M. Pech, D. Mandat, L. Nozka, A. Dejneka, Institute of Physics of the ASCR, v.v.i. (Czech Republic); J. Jankuj, Meopta - optika, s.r.o. (Czech Republic); M. Vujtek, Palacký Univ. Olomouc (Czech Republic)

Authors introduce some results of high quality segments testing for the construction of the large-area light-weight mirror systems for UV detectors of weak optical signals. For this category of the optical components an increase of demands on technology production is typical. This is caused by various reasons.

1. Width to diameter ratio is 1:100 for this type of segments. For astronomical mirrors this ratio is about 1:10. This is the reason why the manufacturing technology of the light-weight segment surfaces was changed. Similarly, usually used testing methods of the shape of the optical surfaces are changed. The shapes of the surfaces are evaluated by the minimal spot diameter of the reflected beam which contains 95% of the incident signal energy.

2. Processing technology of working surfaces was enhanced because of the UV light wavelength. The technology must respect the fact that the amount of diffused light in the short UV wavelength region is increasing in the dependence on the surface roughness of the mirror.

3. Surface reflectivity is not the only important parameter of the optical reflecting thin film systems in this kind of applications. Surface roughness and homogeneity of thin films are taken into account of testing methods also.

8126-43, Poster Session

Manufacturing process optimization of phase plates for depth extension microscope systems

C. Hsu, H. Sung, Y. Chen, W. Cheng, C. Liang, C. Chang, Industrial Technology Research Institute (Taiwan)

Extended depth of focus (EDoF) technology can be used for imaging systems by merging phase coding design and digital signal processing. This paper presents an application of EDoF in the microscope platform, comparing the phase plate component fabrication in different conditions by ultra-precision diamond machining and the performance of the EDoF. A cubic phase plate component is an illustration of diamond

machining about the peak-to-valley (PV) error of the cubic surface and the performance of the EDoF. In addition to cubic phase plate, we also design other phase plates such as axial symmetric and non-symmetric plates to evaluate the feasibility by the process and experiment on the microscope platform. Because the sag variation of the component is very small for this phase plate, how to determine the optimal cutting conditions which can stabilize the quality of the fabricated phase plate is very important. So the SPDT (single point diamond turning) was applied to the manufacture of a variety of optical components for its high precision. In the paper, the effect of cutting conditions such as feed rate, pitch and depth of cut are investigated. And the results are as following, the average roughness height of the surface without subsequent polishing was found below 20 nm. The accuracy of the symmetric and non-symmetric phase plate was found between 0.2 μ m and 1 μ m. Therein the symmetric plate was suited to commercialization. The purpose of this study is to compare the relationship between PV error of cubic surface and imaging restoration quality, which maybe a good benchmark in this field.

8126-44, Poster Session

An intuitive concept for manufacturing and inspecting of aspherical components

H. Chou, Instrument Technology Research Ctr. (Taiwan)

In this paper we propose an intuitive concept for manufacturing and inspecting of aspherical components. Two types, parabolic and cylinder, of plano-convex and plano-concave aspherical lenses were made by LOH 120S form generation machine. Three form error measurement methods were used known as coordinate measuring machine (CMM), interferometer with CGH null lens and inspection with combined pair lenses. Ultra high accuracy CMM from Brown & Sharpe Co., CGH cylinder null and CGH aspheric null from Diffraction International and OWI 150 ASPH CGH interferometer from OptoTech GmbH play the roll for measurement. CMM was used as a surface profiler to inspect the surface shape, and the software GRAPHER was also used as analysis tool to exam asphere numerical datum. The difference between theoretical and practical is as a surface polishing revised reference. The finished plano-convex and plano-concave aspherical lenses can be combined to be a plane lens. The individual and combined lenses were inspected on OPTOTECH OWI 150 ASPH CGH interferometer. The compared interference patterns has shown with the Diffraction International CGH Aspheric Null "ASPHERIC 1" and CGH Cylinder Null "H80F2C". Through the procedure, the combined plano-convex and plano-concave aspherical lenses should be a perfect match plane lens and the individual lens might be an aspherical test standard element for quick inspection.

8126-45, Poster Session

Verification program for a high-precision large cryogenic lens holder

A. Boesz, Kayser-Threde GmbH (Germany); N. Geis, Max-Planck-Institut für extraterrestrische Physik (Germany); F. U. Grupp, R. Bender, Univ.-Sternwarte München (Germany)

The Near Infrared Spectrometer and Photometer (NISF) of EUCLID requires high precision large lens holders (170 mm) at cryogenic temperatures (120K - 150K). The four lenses of the optical system are made of different materials: fused silica, CaF₂, and LF5G15 that are mounted in a separate lens barrel design. Each lens has its separate mechanical interface to the lens barrel, the so called adaption ring.

The performance of the lens holder design shall be verified by an adapted test facility including an optical metrology system. The characterization of the lens deformation and displacement (decenter, tilt) due to thermally induced loads are driven by the require submicron precision range and at the operational thermal condition.

The surface deformation of the lens and its holder is verified by interferometric measurements, while tilt and position accuracy are

Conference 8126:
Optical Manufacturing and Testing IX

measured by fibre based distance sensors. The pre-selected distance measurement sensors have the capability to measure in a few mm range with submicron resolution at ultra high vacuum, in vibration environments and at liquid nitrogen temperatures and below.

The calibration of the measurement system is of crucial importance; therefore the sensors shall be mounted on a stiff well characterized reference structure made of Zerodur.

The verification program is currently under development at KT under an MPE contract. The paper presents the vacuum chamber design, the metrology system, the used Ground Support Equipment and the attained performance of the high precision lens holder design.

8126-46, Poster Session

Flexible manufacturing of large aspheres for VLT's Optical Tube Assemblies

G. P. Gubbels, R. Henselmans, C. van Druenen, TNO Science and Industry (Netherlands)

For the ESO Very Large Telescope TNO is making four Optical Tube Assemblies for the Four Laser Guide Star system. Each OTA is a large Galilean beam expander, which expands a 15 mm diameter, 25W CW 589 nm input laser beam to a 300 mm diameter output beam. The L2 lens is a 380 mm conical convex lens with a radius of curvature of 637 mm and conic constant $k = -0.4776$.

The paper describes the deterministic polishing and flexible metrology tool (NANOMEFOS) that are used in TNO's value chain for high-accuracy asphere and freeform production. NANOMEFOS enables the universal non-contact measurement of aspheres and freeforms up to 500 mm diameter with a high accuracy, equivalent to normal interferometers and with interferometric axial and lateral resolution (or better!). Besides flexibility NANOMEFOS is also an absolute measurement system giving it the advantages of coordinate measuring machines combined with interferometric accuracy.

In this paper we describe e.g. the research that was needed for good spiral polishing in order to prevent mid-spatial generation on our (size limited) Zeeko FJP600 polishing robot.

The initial error after grinding and pre-polishing was almost 6 μm . This data was obtained by measuring more than 2 million data points in about 15 minutes (data spacing 0.4 mm). Such high point density and absolute measurement data cannot be achieved in such short time with any other state of the art 3D metrology instruments. This high point density is especially useful to reveal mid-spentials that are inherent to corrective (local) machining processes. The final result after 5 polishing runs was about 300 nm PV and 27 nm rms. Principally the amount of polishing runs could have been less, but that was not possible because of the used polishing cloth that had a lifetime of about 5 hours.

8126-47, Poster Session

New approach for pre-polish grinding with low subsurface damage

J. B. Johnson, D. W. Kim, College of Optical Sciences, The Univ. of Arizona (United States); R. E. Parks, College of Optical Sciences, The Univ. of Arizona (United States) and Optical Perspectives Group, LLC (United States); J. H. Burge, College of Optical Sciences, The Univ. of Arizona (United States)

For an optical surface to be properly prepared, the amount of material removed during polishing must be greater than the volume of grinding damage. An intermediate stage grind between loose abrasive figuring and polishing can reduce the total volume of subsurface damage. This results in less time and expense needed during the polishing phase. We investigated the grinding rate and subsurface damage depth for Trizact diamond tile pads. Trizact shows a sizeable reduction in the overall subsurface damage compared to loose abrasives. This understanding of

the abrasive behavior allows us to create a better grinding schedule that more efficiently removes material and finishing with less overall damage than traditional loose abrasives.

8126-48, Poster Session

Optical contacting of low-expansion materials

G. Kalkowski, M. Rohde, C. Rothhardt, S. Risse, R. Eberhardt, Fraunhofer-Institut für Angewandte Optik und Feinmechanik (Germany)

We report on direct bonding of glass to glass for optical and precision engineering applications. Fused silica (SiO_2) and ultra-low-expansion (ULE) glass materials with coefficients of thermal expansion of about $5 \cdot 10^{-7}/\text{K}$ and $1 \cdot 10^{-8}/\text{K}$ at room temperature, respectively, were investigated. Large glass wafers of up to 150 mm diameter and about 1.5 mm thickness were bonded to massive glass substrates of up to 20 mm thickness.

Successful bonding was achieved after extensive chemical cleaning and low pressure plasma surface activation, using a commercial wafer bonding equipment. High quality (optically transparent) bonds with a very low fraction of aerial defects were obtained at relatively low temperatures under compressive forces of several tens of kN in a high vacuum environment. Typically, only small unbound locations occurred at the rim, where insufficient pressure had been applied in the bonding process.

Bonding strengths were estimated from destructive "razor-blade" testing of bonded wafer pairs /1/ and resulted in bond energies up to about 2 J/m² for bonding temperatures of only 250° Celsius. For surface activation, N₂-plasma was tested in comparison to O₂-Plasma. Under nominally identical bonding conditions with respect to temperature and pressure, N₂ plasma was found to give slightly stronger bonds than O₂ plasma. Although influences of surface roughness cannot be fully excluded, ULE materials also appear to bond slightly stronger than fused silica, in general.

This work was supported by BMBF/DLR (Germany) under contract No. 50YB0814.

8126-49, Poster Session

A novel packaging method for stable microsphere coupling system

S. Yan, W. Zhang, North Univ. of China (China)

A novel method to enhance the robustness of the microcavity coupling system (MCS) is presented by encapsulating and solidifying the MCS with a low refractive index (RI) curable UV polymer. The process is illustrated in detail for a typical microsphere with a radius R about 240 μm . Three differences of the resonant characteristics before and after the package are observed and analyzed. The first two differences refer to the enhancement of the coupling strength and the shift of the resonant spectrum to the longer wavelength, which are both mainly because of the microsphere surrounding RI variation. Another difference is the quality factor (Q-factor) which decreases after the package due to the polymer absorption. Moreover, Experimental results demonstrate that the packaged MCR has much better robust performance than the unpackage sample.

The enhancement of the robustness greatly promotes the microcavity research from fundamental investigations to application fields.

8126-50, Poster Session

The photoanisotropy in the holographic media on the basis of silver halide emulsion

V. G. Shaverdova, S. S. Petrova, A. L. Purtseladze, V. I.

Conference 8126:
Optical Manufacturing and Testing IX

Tarasashvili, Institute of Cybernetics (Georgia)

The experimental results of the induced photoanisotropy in the media on the basis of small and super small grained color-sensitive silver halide emulsions are presented. It was shown that in the given layers after the irradiation of the polarized light with wave-length actinic for the given sensitizers and of the following specific development the photo-induced anisotropy was visualized. It turns out that weakly expressed anisotropy of the latent image multiplied more than on the two order of magnitude. The high stability, the possibility of working in the red region and with low power energy sources, with wide controlled characteristics are represented the main advantage of such media. As it was shown in this investigation, value of the photo anisotropic parameters can be changed in wide-ranging after the specific physicochemical treatment: hypersensitizing, specific worked out developers, thermal treatment, fixing (in case of need). Each of the procedure has such essential value, that the separated examination was needed. Some technological regimes which reduced to the optimization of the parameters of the photo anisotropy are presented. Quantitative measurements have been spent on the spectrosensitometer, by the polarized radiation of a photometric lamp spread out in a spectrum. The measurements energy of the wavelength were spent in the focus of the device by means of the thermoelectric receiver having possibility to move smoothly on a scale of wavelength. Complex birefringence was measured on modernized spectrophotometer. The exposure and spectral characteristics of photoanisotropy was given. It was shown the possibility of carry out polarization-holographic diffraction elements on this material.

8126-51, Poster Session

Development of high-performance, stable, and moisture-resistant polarization-sensitive materials

I. Chaganava, G. A. Kakauridze, B. N. Kilosanidze, G. Datukishvili, Institute of Cybernetics (Georgia)

Existing high-performance stable polarization sensitive materials based on bisazodyes introduced into water-soluble polymer matrices (particularly, on the basis of modified azodye Mordant Pure Yellow M) require a protection against external moisture. By-turn this decreases the advantage of such materials and limits the field of their application. There are developed new stable polarization sensitive media on the basis of the hydrophobic components which does not require an additional protection from moisture. The lipophilic bisazodye toolidine derived orthotolidinebisazophenol chromophoric component is specially synthesized which is liposoluble analogue of water-soluble Mordant Pure Yellow M. Materials was obtained on the basis of this bisazodye introduced in different polymers. These moisture resistant materials at the same time can be applied as a protective layer that improves the efficiency of the materials. The difference between the natures of the solubility of media effectively isolates the recording layers from each other. To increase the thermal stability of the material we have synthesized media by the introduction bisazodye into the chemical composition of macromolecules main chain of thermally stable, transparent, hydrophobic and amorphous polymer with a linear structure. The kinetic of inducing photoanisotropy of the obtained materials was investigated. The study of photoanisotropic properties of the obtained main chain materials showed the possibility of their work both in a stable and dynamic regime. The different types of polarization holographic gratings with high diffraction efficiency of 30-50% were recorded on the obtained materials by laser beams in the wavelength range of 441 - 488 nm.

8126-21, Session 5

Non-contact profilometry of E-ELT segments at OptIC Glyndwr

C. Atkins, Univ. College London (United Kingdom); J. Mitchell, Cranfield Univ. (United Kingdom); P. Rees, OptIC Glyndwr Ltd.

(United Kingdom)

Following a 'Call for Tenders' by the European Southern Observatory (ESO) a collaboration headed by OptIC Glyndwr Ltd is producing seven prototype segments for the European Extremely Large Telescope (E-ELT). Each hexagonal segment is 1.4 m in diameter with a radius of curvature of 84 m and the combination of 984 segments will lead to a primary mirror with a diameter of 42 m. The polishing of the prototype segments occurs in-house at OptIC Glyndwr using a Zeeko polishing machine, while in-situ interferometry is undertaken using a specifically designed optical test tower, built above the polishing machine. To validate the radius of curvature of the final prototype segments an on-machine non-contact profiler has been developed in collaboration with the Diamond Light Source (DLS). The profiler attaches to the bridge of the polishing machine and is removed during a polishing cycle. The design of the profiler is based upon a nanometre optical measuring machine (NOM) system which determines the height at a series of points across the surface through the integration of measured slope data.

This paper will present results from on-machine profilometry taken during the fabrication of the ESO prototype segments. Both individual profiles and stitched 2D surface maps will be presented in conjunction with interferometric data. In addition, the measurement accuracy of the NOM system and the effect of random and systematic errors will be discussed.

8126-22, Session 5

Electronic speckle pattern interferometric testing of JWST primary mirror segment assembly

K. Z. Smith, D. M. Chaney, Ball Aerospace & Technologies Corp. (United States); B. N. Saif, NASA Goddard Space Flight Ctr. (United States)

The James Webb Space Telescope (JWST) Primary Mirror Segment Assembly (PMSA) was required to meet NASA Technology Readiness Level (TRL) 06 requirements in the summer of 2006. These TRL06 requirements included verifying all mirror technology systems level readiness in simulated end-to-end operating conditions. In order to support the aggressive development and technology readiness schedule for the JWST Primary Mirror Segment Assembly (PMSA), a novel approach was implemented to verify the nanometer surface figure distortion effects on an in-process non-polished beryllium mirror surface. At the time that the TRL06 requirements needed to be met, a polished mirror segment had not yet been produced that could have utilized the baselined interferometric optical test station. The only JWST mirror segment available was a finished machined segment with an acid-etched optical surface. Therefore an Electronic Speckle Pattern Interferometer (ESPI) was used in coordination with additional metrology techniques to perform interferometric level optical testing on a non-optical surface. An accelerated, rigorous certification program was quickly developed for the ESPI to be used with the unfinished optical surface of the primary mirror segment. The ESPI was quickly implemented into the PMSA test program and optical testing was very successful in quantifying the nanometer level surface figure deformation changes in the PMSA due to assembly, thermal cycling, vibration, and acoustic testing. As a result of the successful testing, the PMSA passed all NASA TRL06 readiness requirements.

8126-23, Session 5

Cryogenic optical testing results of JWST aspheric test plate lens

K. Z. Smith, T. C. Towell, Ball Aerospace & Technologies Corp. (United States)

The James Webb Space Telescope (JWST) Secondary Mirror Assembly (SMA) is a circular 740mm diameter beryllium convex hyperboloid that has a 23.5nm-RMS ($\sqrt{27}$ RMS) on-orbit surface figure error requirement.

**Conference 8126:
Optical Manufacturing and Testing IX**

The radius of curvature of the SMA is $1778.9113\text{mm} \pm 0.45\text{mm}$ and has a conic constant of -1.6598 ± 0.0005 . The on-orbit operating temperature of the JWST SMA is 22.5K. Ball Aerospace & Technologies Corp. (BATC) is under contract to Northrop Grumman Aerospace Systems (NGAS) to fabricate, assemble, and test the JWST SMA to its on-orbit requirements including the optical testing of the SMA at its cryogenic operating temperature. BATC has fabricated and tested an Aspheric Test Plate Lens (ATPL) that is an 800mm diameter fused silica lens used as the Fizeau optical reference in the ambient and cryogenic optical testing of the JWST Secondary Mirror Assembly (SMA). As the optical reference for the SMA optical test, the concave optical surface of the ATPL is required to be verified at the same 20K temperature range required for the SMA. In order to meet this objective, a state-of-the-art helium cryogenic testing facility was developed to support the optical testing requirements of a number of the JWST optical testing needs, including the ATPL and SMA. With the implementation of this cryogenic testing facility, the ATPL was successfully cryogenically tested and performed to less than 10nm-RMS (≈ 63 RMS) surface figure error levels for proper reference backout during the SMA optical testing program.

8126-24, Session 5

The design of MTF test system based on point light source

R. Fu, Nanjing Univ. of Science & Technology (China)

The MTF test system consists of point light source, off-axis parabolic mirror, image acquisition system, stepping motor control system and the computer.

The white light passes through a group of high-precision microscope and forms a point light source which is located in the focus point of an off-axis parabolic reflector modules, the light is reflected by the off-axis parabolic reflector and becomes parallel light beam. The focus length of the off-axis parabolic mirror is 1000mm. A sample lens is merged in the light beam, it can converge the light on its focus point and form the Airy circle.

The Airy circle was enlarged by the high-precision microscope and is obtained by the CCD camera through delay lens. The stepper motor controls the position of the high-precision microscope and CCD through a two-dimensional mobile platform, so as to insure the Airy circle is in the focus of the high-precision microscope. The image acquired by the CCD is transferred to the computer through image capture devices card. After image preprocessing, the data passed to the calculation module of MTF information processing, and finally get the MTF of the lens.

The results of this test system in the middle-frequency part show more consistent, but a moderate low-frequency part of the curve down, high-frequency part, they fall very quickly.

The following factors are response on possible deviation, the deviation caused by optical imaging system, the deviation caused by CCD, the deviation caused by Stepping Motor.

8126-25, Session 5

The optical metrology system for cryogenic testing of the JWST primary mirror segments

J. B. Hadaway, The Univ. of Alabama in Huntsville (United States); D. M. Chaney, L. B. Carey, Ball Aerospace & Technologies Corp. (United States)

The James Webb Space Telescope (JWST) primary mirror is 6.6 m in diameter and consists of 18 hexagonal mirror segments each approximately 1.5 m point-to-point. Each primary mirror segment assembly (PMSA) is constructed from a lightweight beryllium substrate with both a radius-of-curvature actuation system and a six degree-of-freedom hexapod actuation system. With the JWST being a near to mid-infrared observatory, the nominal operational temperature of a PMSA is 45 K. Each PMSA must be optically tested at 45 K twice, first to

measure the change in the surface figure & radius-of-curvature between ambient & cryogenic temperatures and then to verify performance at cryo following final polishing. This testing is conducted at Marshall Space Flight Center's (MSFC's) X-Ray & Cryogenic Facility (XRCF). The chamber & metrology system can accommodate up to six PMSAs per cryo test. This paper will describe the optical metrology system used during PMSA cryogenic testing. This system evolved from systems used during the JWST mirror technology development program. The main components include a high-speed interferometer, a computer-generated holographic null, an absolute distance meter, a tiltable window, and an imaging system for alignment. The optical metrology system is used to measure surface figure error, radius-of-curvature, conic constant, prescription alignment, clear aperture, and the range & resolution of the PMSA actuation systems.

8126-26, Session 5

Nanometer profile measurement of large aspheric optical surface by scanning deflectometry with rotatable devices

M. Xiao, S. Jujo, S. Takahashi, K. Takamasu, The Univ. of Tokyo (Japan)

High accuracy mirrors and lenses with large dimension are widely used in the huge telescopes and other industry field. For measuring near flat surface and spherical optical surfaces, interferometers are widely used because of their high accuracy and high efficiency. Scanning deflectometry is also used for measuring optical near flat surface with uncertainty of sub-nanometer. However, for measuring aspheric surface with large departure from perfect spherical surface both of these methods are difficult to use. The key problem for scanning deflectometry is that high accuracy autocollimators usually have limited measuring range which is less than 1000 arc-second, so it cannot be used for measuring surface with large slope. We have proposed a new method for measuring large aspheric surface with large slope based on scanning deflectometry method. Rotatable devices are used to enlarge the measuring range of autocollimator. We proposed a method to connect the angle data which are cut by the rotation of the rotatable devices. The error caused by the rotation is propagated. The uncertainty propagation analysis of our proposed method is done. The simulation result shows that when measuring a large aspheric surface with a diameter over 300 mm and with a slope of 10 arc-degrees the uncertainty is less than 30 nanometers. Numerical simulation is also done to show that the analysis match the analysis well. For the verification of our proposed method, experimental devices are set up. A spherical optical surface with diameter of 35 mm and curvature radius of 5000 mm is measured. Measuring range of autocollimator is successfully enlarged by our proposed method. Experimental result shows that the standard deviation of 10 times measurement is less than 20 nm which is larger than the theoretical value. Random drift and systematic error is found in the experiment result. Temperature drift is considered to be the main reason for the systematic error.

8126-20, Session 6

A complete qualification methodology for coatings of precision glass molding tools

K. Georgiadis, O. Dambon, F. Klocke, Fraunhofer-Institut für Produktionstechnologie (Germany)

The demand for complex-shaped optical components is rapidly rising, driven by their significant advantages over traditional optics. Precision glass molding, a replicative process where a glass blank is heated and isothermally pressed between high precision molds, is the technology of choice for the production of complex-shaped optical components. However, significant thermal, mechanical and chemical loads during the process limit the lifetime of the molds. Protective coatings can significantly extend their lifetime and are therefore necessary in order

Conference 8126:
Optical Manufacturing and Testing IX

to make the technology economically viable. However, the coating properties have to be exactly customized to the individual application conditions, or else an improvement in the tool performance cannot be guaranteed.

Currently, the biggest challenge is to ensure the reliability of newly developed coatings without resorting to extensive and expensive practical testing. Due to the special materials and properties (e.g. brittle substrates, very thin metallic coatings, operation under high temperatures), the usual testing methods like scratch test, nanoindentation, Rockwell test etc. either cannot be used or don't provide useful results. In this work, a new application-specific methodology for the qualification of such coatings is presented, which uses a three-tier approach. First, the basic mechanical and structural characteristics of the coatings are determined. Then application-specific tests at elevated temperatures that focus on the contact behavior between glass and coating are performed. Finally, the wear behavior of the coating is evaluated using a new testing setup that models the conditions during molding. Thus, a meaningful estimation of the coating lifetime in combination with a particular glass can be made with confidence.

8126-27, Session 6

Commercialising corrective polishing technology to maintain a global competitive edge in the first 10 years of Zeeko

R. R. Freeman, Zeeko Ltd. (United Kingdom)

Zeeko launched its first aspheric polishing machine in 2001 4 years after the MRF machine had been introduced and so well received by the global optics industry. Having entered the market second, in order to succeed the Zeeko solution had to offer functionality and performance that the market leader was unable to provide. Initially product sales were slow but this paper tells the story of the way that the early launch of a genuine free-form software solution coupled with the combining of multiple ablation solutions (Bonnet "Classic" polishing, ZeekoJet polishing, pitch polishing and Grolishing) on one platform helped Zeeko establish a competitive offering. Having successfully positioned its more universal technology in the market place, machines, software and metrology began to evolve in a most interesting way. The paper describes this evolution in detail examining the innovation and technological developments that real life applications drove into the product offering. It describes developments on the software side, with the creation of a "Metrology Toolkit" that provided multiple and universal import/ export interfaces for metrology data and CAD data for a wide array of different metrology and CAD packages. The introduction of various stitching solutions is described to provide pseudo 3-D surface data maps for use by the corrective polisher as well as the handling of difficulties such as interferometer image distortion that had to be accommodated as optical metrology stepped from the analogue to the digital domain. The paper finally concludes with evolution and the introduction of on-machine metrology solutions for large optics fabrication that have been seamlessly integrated with the controls system of the polisher itself.

8126-30, Session 6

From Herschel to Gaia: 3-meter class SiC space optics

M. Bougoin, J. Lavenac, BOOSTEC S.A. (France)

Herschel and Gaia are two cornerstone missions of ESA which embark 3 - meter class optics. These instruments require so high thermal and mechanical stability that the SiC technology turned out to be indispensable.

The Boostec SiC material has been selected first for its high specific stiffness and thermal stability. But it also shows a perfect isotropy of all its physical properties and it is remarkably more stable than the glass-ceramics in time and also against space radiations. This SiC material has

furthermore been fully qualified for application at cryogenic temperature (Herschel and also JWST NIRSPEC).

The Boostec manufacturing technology of very large size SiC components includes i) manufacturing 1.5 - meter class monolithic sintered parts and then ii) assembly based on a brazing process. The former one is a near net shaping process which allows manufacturing at reasonable costs and also within short time.

Herschel is one of the six telescopes made of Boostec SiC which are successfully operating in space. It includes a 3.5 m primary mirror, a secondary mirror and an hexapod. It weighs only 315 kg and its WFE is kept below 6 μm rms despite an operating temperature of 70 K.

Gaia is made of more than 280 SiC parts of 80 different types. The most challenging of them is undoubtedly its highly stable structure, the 3 meters torus. This quasi octagonal and hollow shaped ring is made of 19 SiC elements brazed together. It weighs only 200 kg. All the Gaia hardware has been successfully manufactured and it is now being integrated and tested at Astrium facilities.

8126-53, Session 6

Fluid jet and bonnet polishing of optical moulds for applications from visible to x-ray

A. T. H. Beaucamp, Zeeko Ltd. (United Kingdom) and Chubu Univ. (Japan); R. R. Freeman, Zeeko Ltd. (United Kingdom); A. Matsumoto, Y. Namba, Chubu Univ. (Japan)

Electroless Nickel (ENI) and binderless Tungsten Carbide (WC) are widely used to make replication moulds for optics ranging from consumer camera lenses to highaccuracy X-ray mirrors. Aspheric shape generation is generally performed by diamond turning in the case of Nickel, and micro-grinding in the case of Tungsten Carbide. Both machining methods fail in general to meet the ultra-precision criteria required by an increasing number of applications. A 7-axis CNC machine equipped with sub-aperture fluid jet and processed bonnet polishing technology was used to develop deterministic finishing processes on both Electroless Nickel and Tungsten Carbide. Corrective polishing to less than $\lambda/20$ (<31nm PV) form error can be achieved, as well as the ability to smooth surface texture down to 1nm Ra or less.

8126-31, Session 7

Recent developments on swing arm optical CMM: self-calibration and measuring optical surfaces in grinding stage

P. Su, Y. Wang, C. J. Oh, R. E. Parks, J. H. Burge, College of Optical Sciences, The Univ. of Arizona (United States)

The Swing arm Optical CMM (SOC) is an important metrology technique for highly aspheric surface testing because of its versatility. It is configurable for measuring concave, convex and plano surfaces, it can make in situ measurements, and it has high precision performance rivaling full aperture interferometric tests.

Errors in the SOC bearing that have odd symmetry are self-calibrated due to the test geometry. In the past, even bearing errors were calibrated against a full aperture interferometric test. Recently, we developed a dual probe self calibration mode for the SOC. Data from the dual probes can be used to calibrate the swing-arm air bearing errors since both probes see the same bearing errors while measuring different portions of the test surface. With the dual probe model, the SOC can be fully self-calibrated without requiring any external reference.

Until recently, the SOC has only been used for measuring polished surfaces due to limitations imposed using the interferometric probes. To enlarge the measurement range of the SOC, we have developed a systematic data reduction model and calibration procedure for a laser triangulation (LT) probe. The calibrated probe is insensitive to the surface angle variation during the measurement. With the LT probe, the SOC

has been used to measure highly aspheric optical surfaces during their grinding stage. Initial measurement results from a ground surface with an aspheric departure of 1.8mm and angular variation of the normals of more than 1 degree show that the SOC with the LT probe can make measurements with an accuracy better than 0.25micron rms and is limited by the calibration of the probe scaling effect.

8126-32, Session 7

Total integrated scatter from moderately rough surfaces with arbitrary correlation widths and incident angles

J. E. Harvey, N. Choi, CREOL, The College of Optics and Photonics, Univ. of Central Florida (United States); S. Shroeder, A. Duparre, Fraunhofer-Institut für Angewandte Optik und Feinmechanik (Germany)

Surface scatter effects from residual optical fabrication errors can severely degrade optical performance. The total integrated scatter (TIS) from a given mirror surface is determined by the ratio of the spatial frequency banded-limited or "relevant" rms surface roughness to the wavelength of light. For short-wavelength (EUV/X-ray) applications, even state-of-the-art optical surfaces can scatter a significant fraction for the total reflected light. In this paper we present parametric plots of the TIS for optical surfaces with arbitrary roughness, surface correlation widths and incident angles. Surfaces with both Gaussian and ABC or K-correlation power spectral density (PSD) functions have been modeled. These parametric TIS predictions provide insight necessary to determine realistic optical fabrication tolerances necessary to satisfy specific optical performance requirements.

8126-33, Session 7

Extended range roughness measurements in non-ideal environments

K. Creath, 4D Technology Corp. (United States) and College of Optical Sciences, The Univ. of Arizona (United States)

This paper describes recent research into developing extended range dynamic interferometry where the range can be extended to enhance surface roughness measurements made in non-ideal environments. These techniques do not require expensive vibration isolation systems. Since this is ongoing research, we will be providing an up-to-date review of the techniques and experiments showing recent results.

8126-34, Session 7

High-speed and -accuracy measurement of optical rotation by liquid crystal modulators

M. Tanaka, Y. Nakashima, H. Amamiya, Atago Co., Ltd. (Japan); Y. Otani, Utsunomiya Univ. (Japan)

Optical characteristics of material that has optical activity have been used for the concentration measurement of the saccharide and amino acid for a long time. Some principal of optical rotation measurement techniques have been proposed by a rotating polarizer method, a Faraday cell method. A high-speed and high-accuracy measurement of optical rotation is proposed by dual liquid crystal polarized modulators which are specialized multi-stacked cells with over-drive method for high speed drive.

8126-35, Session 7

Instantaneous measurement Fizeau interferometer with high-spatial resolution

D. Sykora, Zygo Corporation (United States)

Surface and wavefront metrology in vibration prone and turbulent environments often require that multiple phase shifts be encoded onto the interference signal within a single shuttered camera frame, typically of 100 μ sec integration time, to adequately freeze the environmental disturbance and acquire quality signal data. The use of full-sensor single camera architectures mitigates critical alignment and signal balancing required of alternative simultaneous multi-image detection. Localized spatial phase shifting has been implemented in this full-sensor technique to extract the phase at each pixel through introduction of a carrier fringe. We report here on a new instantaneous Fizeau-type interferometer optimized for light-efficient single-frame carrier fringe acquisition that avoids the troublesome phase sensitivity to birefringence of polarization-based approaches. Fully coherent optics designed to perform with large slope differentials between interfering wavefronts provide maximized spatial resolution and instrument transfer function (ITF) beyond 250 cycles/aperture at all zoom settings. Results are documented for measurement of an etched phase step and custom periodic artifact. ITF beyond 500 cycles/aperture is also reported for an optional configuration where temporal phase shifting interferometry is enabled.

8126-36, Session 8

Air-driving fluid jet polishing

Z. Yu, C. Kuo, C. Chen, W. Hsu, Instrument Technology Research Ctr. (Taiwan); D. P. Tsai, Instrument Technology Research Ctr. (Taiwan) and National Taiwan Univ. (Taiwan)

The fluid jet polishing (FJP) is widely used for modern optical fabrication in recent years. FJP was originated from the demand for steep concave or complex aspherical elements and the inability of the conventional polishing for those elements. However, FJP method has to pump the slurry in a high pressure, in order to have the energy for material removal.

In this study, we proposed an air-driving FJP system which draws slurry utilizing an air/water mixer. The air-driving FJP system is mainly composed by an air/water mixer, compressed air, pressure and flow rate regulators, and a nozzle. The high speed air flow in the air/water mixer draws out the slurry from the slurry tank, and the slurry is guided to mix with air flow inside the nozzle cavity. Then, the combined fluid slurry is emitted from the nozzle. The air-driving FJP system was preliminarily tested on N-BK7 and ZERODUR® plates with different air pressure and dwell time.

The test results show that the air-driving system could get a Gaussian-like removal shape with 3 kg/cm² compressed air source and the depth of removal is about 100 nm within 5 seconds dwell time. The compressed air improves the kinetic energy of each abrasive, and makes it more efficient in material removal. Furthermore, the Gaussian-like removal shape is more convenient for tool path planning and surface waviness control of corrective polishing.

8126-37, Session 8

Optical bonding reinforced by femtosecond laser welding

F. Lacroix, Institut Franco-Allemand de Recherches de Saint-Louis (France); D. Hélie, R. Vallée, Univ. Laval (Canada)

Since a few years micro-welding by femtosecond (fs) laser pulses of dielectrics has demonstrated a great potential for micro-optical manufacturing. However, fs laser micro-welding of dielectrics created some variation of the refractive index which can be considered as optical defects for an optical component. We have demonstrated the capability

**Conference 8126:
Optical Manufacturing and Testing IX**

to realize bonding of large optical components with or without optical coating by direct bonding reinforced by fs laser micro-welding.

The first step consists in creating a direct optical bonding free of any impurity between the two pieces to join. In a second step the contact field is sealed by fs laser welding. This technique creates a sealed direct bonding surface free of any adhesive between the two substrates which can be as different as silicon and fused silica or BK7 and fused silica windows. Even though direct bonding is mechanically strong, it does not resist well to elastic or plastic deformation. Different thermal dilatation of the assembled pieces might be catastrophic for direct contact bonding. By fs laser sealing of the direct contact bonding surface, we reinforce the effective bond of the two pieces, which now can support thermal choc. This bond is free of any impurity, any adhesive, any organic vapour and there is no risk of coloration by ageing of an organic adhesive.

This technique may be used to create a sandwich of doped and un-doped materials to realize laser active media which can be pumped by wave guide effect in the un-doped material and which is reinforced against thermal lens effect.

8126-38, Session 8**Incorporating VIBE into the precision optics manufacturing process**

J. DeGroot Nelson, A. Gould, C. Klinger, R. A. Wiederhold, M. Mandina, Optimax Systems, Inc. (United States)

The VIBE process is a full-aperture, conformal polishing process incorporating high frequency and random motion designed to rapidly remove sub-surface damage in a VIBE pre-polish step and eliminate mid-spatial frequency (MSF) errors in a VIBE finishing step. The VIBE process has potential to be introduced in two areas of today's modern optics manufacturing process. The first instance is replacing the conventional pre-polishing step with the rapid VIBE pre-polish step. Results will be discussed in this paper that show 10 - 50x higher removal rates compared to conventional polishing for a variety of optical materials. High removal rates combined with the compliant lap results in damage-free surfaces that have the same form that was generated by the CNC generation process for spherical and non-spherical surfaces. The second potential area to incorporate VIBE into today's modern optics manufacturing process is as a finishing step after deterministic sub-aperture polishing to remove mid-spatial frequency errors. By selectively altering the compliant properties of the VIBE pad, and adjusting the frequency of the VIBE motion, VIBE finishing can reduce the mid-spatial frequencies caused from sub-aperture polishing processes while maintaining the desired corrected surface form. This paper will serve as an in-depth review of the VIBE process and how it complements other modern CNC optics manufacturing technologies, as well as highlighting recent VIBE advances specifically in the area of conformal optic fabrication.

8126-39, Session 8**Computer-aided manufacturing for freeform optical elements by ultraprecision micromilling**

S. Stoebenau, R. M. Kleindienst, M. Hofmann, S. Sinzinger, Technische Univ. Ilmenau (Germany)

The successful application of computer-aided manufacturing (CAM) is a key issue for the fabrication of freeform optical elements. Different classes of freeform surfaces demand for specific CNC-code programming techniques. Two strategies have been exploited and will be presented in our contribution. The first strategy is adopted to handle freeform surfaces that can be described analytically by polynomial equations. As a versatile example used e.g. in integrated optical microsystems, the fabrication of an astigmatic biconic lens by ultraprecision micromilling is investigated. We took advantage of the direct programming capabilities arising from state-of-the-art machine

controls. The tooling trajectories are calculated by the control unit during the machining process. The calculations comprise the solution of the polynomial equations that define the shape and the local slope necessary for a tool cutting edge radius compensation. The second strategy is a more classical implementation of the CAM process. Herein, the preliminary results from the optical designing process are transferred into a CAD/CAM software module by means of a solid model. As this procedure doesn't necessarily need a closed analytical description of the surface it is the most general solution. The solid model in combination with a very precise knowledge about the cutting edge geometry allows for a pre-machining calculation of the tooling trajectories. As an example for this strategy, a freeform element integrating different optical functionalities (laser beam deflection and shaping) has been fabricated. We present the design strategies, the fabrication process and finally the characterization concerning surface quality, shape accuracy and optical performance.

8126-40, Session 8**Calibration and optimization of computer-controlled optical surfacing for large optics**

D. W. Kim, College of Optical Sciences, The Univ. of Arizona (United States); H. M. Martin, The Univ. of Arizona (United States); J. H. Burge, College of Optical Sciences, The Univ. of Arizona (United States)

Precision optical surfaces can be efficiently manufactured using a computer controlled optical surfacing (CCOS) process. Most of the CCOS processes are based on the dwell time control of a fabrication tool on the workpiece according to the desired removal and the tool influence function (TIF), which is the material wear function by the tool. Some major topics to improve current CCOS processes were investigated to provide new solutions for the next generation CCOS processes. A rigid conformal (RC) lap using a visco-elastic non-Newtonian medium was newly invented. It conforms to the aspheric surface shape, yet maintains stability to provide natural smoothing. The smoothing removes mid-to-high frequency errors while a large tool runs over the workpiece to remove low frequency errors. A parametric smoothing model was also introduced to predict the smoothing effects. A parametric edge TIF model to represent measured edge TIFs was developed and demonstrated. This model covers the non-linear removal behavior as the tool overhangs the workpiece edge. These new tools and models were applied to a new process optimization technique called non-sequential optimization. The non-sequential approach performs a comprehensive dwell time optimization using multiple TIFs for the entire CCOS runs simultaneously. An overview of these newly implemented CCOS features will be presented with some actual CCOS run results.

8126-41, Session 8**Centration of optical elements**

E. Milby, J. H. Burge, College of Optical Sciences, The Univ. of Arizona (United States)

Axissymmetric optical components such as lenses are frequently centered with the use of rotary air bearings, guided by optical instrumentation that uses reflected or transmitted light. When the position of the element is adjusted to null the error from the optical test, the element is potted in place using an adhesive. This paper systematically explores methods of adjusting the elements and potting them in place with a goal of defining the accuracy that can be expected. Analysis of the performance is supported with experimental data.

Conference 8127: Optical Modeling and Performance Predictions V

Thursday 25 August 2011 • Part of Proceedings of SPIE Vol. 8127 Optical Modeling and Performance Predictions V

8127-01, Session 1

Design of nonparaxial optical systems with refractive and diffractive elements on a base of the local thin optics model

M. A. Golub, Tel Aviv Univ. (Israel)

Whereas quality optical systems demand essentially nonparaxial geometrical optics, diffraction calculations are often restricted to paraxial approximation and thin lens model of Fourier optics. However main and ghost nonparaxial diffraction orders must be considered in the frame of polychromatic interference and diffraction of physical optics. Straightforward calculation of numerically approximated diffraction integrals between each pair of sequential optical surfaces suffers from accumulated sampling and aliasing errors, and seems not practical for complex and diffraction limited optical systems. The problem is not only in limited capabilities of modern computers and high space-bandwidth product but in optimizing a solution before deep understanding of a model.

We built and implemented a model of cascaded optical systems combining modern optical design with ideas of photonic structures, by exploiting geometrical optics at large number of smooth optical surfaces and diffraction on a single diffractive surface. Non-paraxial estimations for an impact of wavelength change, mismatch of diffractive groove depths, phase nonlinearity, and staircase approximation were derived. Finally, we developed (a) generalized ray tracing method for diffractive, refractive and reflective surfaces based on finding a local focus position by direct calculation of local wavefront curvatures; (b) separated ray-tracing for several diffractions orders with subsequent superposition of their complex amplitudes with complex weight coefficients derived from diffraction efficiencies and phases; (c) equivalent lens method for multi-lens systems; (d) closed form analytical solutions for diffraction efficiency at resonance domain surface relief photonic structures with period slightly exceeding the wavelength. Applied optical systems were successfully modeled.

8127-02, Session 1

Reverse optimization in physical optics modeling

G. N. Lawrence, Applied Optics Research (United States); A. W. Yu, NASA Goddard Space Flight Ctr. (United States)

In reverse optimization, one begins with a nominal design assuming that is perfectly manufactured and perfectly aligned. The parameters of the design are then adjusted so that the performance matches experimentally determined performance. Reverse optimization is a means of determining the internal details of the system. Reverse optimization can identify the internal root causes of the effects and provide the exact prescription ready for immediate implementation in system improvement.

In the late 80's reverse optimization using geometrical ray tracing was applied to the alignment of complex, highly asymmetric mirror systems using a Hartmann sensor and a lens design optimization program that employed ray tracing and damped least squares (DLS) optimization. All modes of misalignment were found by misaligning the ideal system to find the best fit to the experimental data. A full prescription of all misalignments could be found and all corrections applied simultaneously.

With the great advances in computer speed, we can now apply the reverse optimization method to full physical optics systems including full diffraction at all steps, laser gain, nonlinear optics, resonant oscillations, etc. The targets for DLS optimization may consist of specific performance measures and wavefront or irradiance maps that may consist of many millions of points. Wavefront and irradiance maps are often available from widely available beam diagnostic instruments.

With many millions of targets, some reformulation of the DLS

mathematics is in order to skip explicit intermediate steps, speed the calculations, and remove memory redundancy with on-the-fly calculation. Some simple examples will serve to illustrate the capability of the reverse optimization method.

8127-03, Session 1

Optical modeling of the NASA high output maximum efficiency resonator (HOMER) laser

G. N. Lawrence, Applied Optics Research (United States); D. B. Coyle, D. Poullos, A. W. Yu, NASA Goddard Space Flight Ctr. (United States)

The NASA High Output Maximum Efficiency Resonator (HOMER) laser is intended for the DESDynI mission (Deformation, Ecosystems Structure and Dynamics of Ice), under design by the NASA-GSFC. This device employs a zigzag amplifier, complex diode side pumping, a graded reflectivity mirror (GRM), and an unstable resonator configuration. For modeling the zigzag amplifier, a 3D exact pixel matching algorithm has been developed that can model all folding and overlap interactions in full complexity in the 3D volume. In spite of the many millions of points in the volume, the exact pixel matching algorithm facilitates rapid calculation. We report progress to incorporate thermal modeling, detailed diode side pumping, GRM, and unstable resonator convergence into the model.

Central issues in the modeling include methods of streamlining the calculations and efficient handling of the gigabyte data that require 64 bit code and a high degree of multithreading. The system is studied for pitch and yaw stability of the end mirrors, detailed defects and failures of individual diode pumps, and other real-world errors in the system that could affect long term performance.

8127-04, Session 1

New phase retrieval for single-shot x-ray Talbot imaging using windowed Fourier transform method

K. Nagai, H. Itoh, G. Sato, T. Nakamura, K. Yamaguchi, T. Kondoh, S. Handa, T. Den, Canon Inc. (Japan)

We propose a new phase retrieval technique using a Windowed Fourier Transform (WFT) method for single-shot X-ray Talbot imaging. The WFT method has been studied to improve the noise robustness of the Fourier Transform (FT) method. In the WFT method, the phase map is retrieved from the spectrum corresponding to the carrier fringe, and the spatial resolution increases as the window function narrows. However, the spatial resolution is limited because an undesired pattern is superposed on the retrieved phase map when the width of window function is narrower than a certain size.

In our proposed method, we introduce an additional step to remove the undesired pattern from the phase map. In the case of the narrow window function, the WFT spectrum including the phase information is overlapped by other extended spectra. This overlap interferes with the retrieved phase and causes the undesired pattern. The additional step removes the overlaps from the desired spectrum analytically. By using the additional step, the high-resolution phase map can be obtained because the window function can be narrower than that of the original WFT method.

In this presentation, we demonstrate phase retrieval of a fringe pattern obtained by the two-dimensional X-ray Talbot interferometer using the proposed WFT method. The differential phase maps of a complex-shaped object along both x- and y- axes were retrieved from a single fringe pattern. Compared to the previous FT method, differential phase maps were obtained in high resolution with an effective noise reduction.

Conference 8127:
Optical Modeling and Performance Predictions V

8127-05, Session 1

Lambert's multiple reflection model revisited

C. F. Hahlweg, Helmut-Schmidt Univ. (Germany)

In last years paper on the idea of Lambertian reflection we gave a partial translation of an almost lost chapter by Johann Heinrich Lambert on multiple reflection in dioptric systems as a gimmick. The problem of multiple reflections in optical systems and appropriate counteractive measures is of special interest in scatterometric devices, but also in high dynamic range imaging. The present paper is dedicated to a deeper discussion of the model proposed by Lambert. This leads - besides the use of ray tracing methods for direct simulation - to a system theoretical approach including the Fourier optical consequences. Further a revision and completion of the translation will be given in the appendix.

8127-06, Session 1

Fourier planes vs. Scheimpflug principle in microscopic and scatterometric devices

C. F. Hahlweg, Helmut-Schmidt Univ. (Germany)

Scatterometric methods usually concentrate on gathering and analyzing scatter distributions in power domain. The analysis is mainly based on the relation between scatter distribution and Fourier transform of the reflection function of the surface under consideration. Imaging scatterometers in principle gather the Fourier image of the illuminated spot, which in microscopy would be the primary diffraction image. Therefore imaging scatterometers can be used as microscopes as well, which requires an additional positive lens or equivalent mirror. It is obvious that combined designs are interesting in surface inspection: because of the loss of phase information in both direct and scatter image, there is still non-redundant information besides the intersection set of both images. For the design and adjustment of such combined devices it is of high interest to identify the Fourier images. While a more or less paraxial dioptric device in orthogonal view has well defined Fourier planes, in an off-axis device with paraboloid or elliptical mirrors the Fourier image is concerned by the Scheimpflug relations, further by a significant vignetting effect, which have to be considered in design and alignment. In the present paper we discuss theory and practical applications and design and adjustment strategies.

8127-23, Session 1

System gain optimization in direction detection lidar system

L. Wu, Y. Zhao, Y. Zhang, Y. Zhang, J. Wu, Harbin Institute of Technology (China)

This paper presents an equivalent direct detection receiver model by statistical method which simplifies the random impulse responses of electrons counting of returned signal, background radiation and dark current as a Gaussian random process with high enough gain. An investigation based on Gaussian distribution of system output in ICCD scannerless range-gated Lidar system is conducted with the calculations of error probability, absolute error and relative error. As the unique manipulated variable, optimized system gains are calculated separately based on the Gaussian model of the random process to achieve the lowest error probability, the lowest absolute error and relative error. The simulations show that the values of optimized gains tend to increase along with the target distance, although the increasing speeds are different. To meet multiple requests, an evaluation model based on cost function is constructed with different weights. The simulation shows that the evaluation model is capable of setting optimized gains for different circumstances and the settings of the weights are vital to the performance of Lidar system.

8127-07, Session 2

A convenient telescope performance metric for imaging through turbulence

G. Z. Angeli, Thirty Meter Telescope (United States)

This paper will provide an overview of the various image quality metrics used in astronomical imaging and explain in details a new metric, the Normalized Point Source Sensitivity. It is based on the Equivalent Noise Area concept, an extension of the EE80% metric and is intuitively linked to the required science integration time. As it was proved in recent studies, the PSSN metric properly accounts for image degradation due to the spatial frequency content of a given telescope aberration and the effects of various errors can be multiplicatively combined, like those expressed in Central Intensity Ratio. Extensions of the metric for off-axis imaging and throughput degradation will be presented. Wavelength and spatial frequency dependence of PSSN will be discussed. While the proper calculation of the PSSN metric requires the precise knowledge of the PSF of both the optics and atmosphere, there are useful approximations capable of linking PSSN to the Zernike decomposition as well as the PSD of the aberrations. Besides the summary of various aspects of the Point Source Sensitivity, the paper will provide many numerical examples derived for the Thirty Meter Telescope.

8127-09, Session 2

Extending Comet's workspace for STOP analysis through the integration of the WaveTrain Wave Optics software

M. Panthaki, CoMeT Solutions Inc. (United States); S. C. Coy, MZA Associates Corp. (United States)

The Comet Performance Engineering Workspace is an environment that enables integrated, multi-disciplinary modeling and design/simulation process automation. One of the many multi-disciplinary applications of the Comet Workspace is for the integrated Structural, Thermal, Optical Performance (STOP) analysis of complex, multi-disciplinary space systems containing Electro-Optical (EO) sensors such as those which are designed and developed by and for NASA and the Department of Defense. The CometTM software is currently able to integrate performance simulation data and processes from a wide range of 3-D CAD and analysis software programs including CODE VTM from Optical Research Associates and SigFitTM from Sigmadyne Inc. which are used to simulate the optics performance of EO sensor systems in space-borne applications.

Over the past year, Comet Solutions has been working with MZA Associates of Albuquerque, NM under a contract with the Air Force Research Laboratories to extend the use of the Comet commercial software by creating a custom adaptor for the WaveTrainTM wave optics software developed and maintained by MZA Associates and used by the Air Force Research Laboratory to enable them to perform STOP analysis of optics systems deployed on air-borne platforms.

The presentation will review the current status of this code integration effort for AFRL and the projected areas of application in directed energy programs conducted for the U.S. government and aerospace/defense industry organizations.

8127-10, Session 3

The correct lens mount lightweight design of thermal cycle stress in Cassegrain telescope

M. Hsu, Instrument Technology Research Ctr. (Taiwan)

The Cassegrain telescope system was design for space environment. The correct lens mount assembly was including as correct lens, lens mount, spacer, mount barrel and retainer. The system mass budget allocated to correct lens assembly was 5 Kg. Meanwhile, according

Conference 8127:
Optical Modeling and Performance Predictions V

with optical design the correct lens was made by Fused Silica, the lens diameter was 130mm, the mass was 2.3 Kg. Therefore, remain mass budget was 2.7 Kg, include the lens mount, spacer, mount barrel and retainer. The telescope system main deformation was caused by thermal deformation on space orbit. The correct lens mount initial design was made by invar material. The invar material properties CTE (Coefficient of Thermal Expansion) was only $1 \times 10^{-6}/^{\circ}\text{C}$, low CTE would be resistance to thermal deformation, but invar density was $8 \times 10^{-6} \text{ kg/mm}^3$. If all components were made by invar, the total mass was over 2.7 kg. Thus, the components material would consider with titanium alloy (CTE was $8.6 \times 10^{-6}/^{\circ}\text{C}$, density was $4.43 \times 10^{-6} \text{ kg/mm}^3$) or aluminum alloy (CTE was $23.6 \times 10^{-6}/^{\circ}\text{C}$, density was $2.81 \times 10^{-6} \text{ kg/mm}^3$). The titanium alloy density was lighter than invar 1.83 times, but CTE was higher than invar 8.6 times. The aluminum alloy density was lighter than invar 2.84 times, but CTE was higher than invar 23.6 times. The lens mount thermal deformation would effect correct lens surface wavefront error and introduce optical aberration. This article was analysis the correct lens assembly thermal deformation and optical performance in different lens mount material. From above conditions, using FEM (Finite Element Method) and optical software, simulation and optimization the lens mount to achieve system mass requirement.

8127-11, Session 3

A compliant static deformable mirror for wavefront error cancellation

F. E. Penado, Northern Arizona Univ. (United States); J. H. Clark III, U.S. Naval Observatory (United States); J. Dugdale, Lowell Observatory (United States)

The Navy Prototype Optical Interferometer (NPOI) array, located near Flagstaff, Arizona, transports the stellar radiation from six primary collectors through a 9-reflection vacuum relay system, resulting in six separate combinable wavefronts. A total of 54 reflection mirrors (6 collectors x 9 reflections each) is required for all six primary collectors. Ground-based optical interferometry requires very high quality, ideally flat, relay mirrors. In practice, the manufacturing methods available will not produce flat mirrors, so for fabrication purposes the surface error of each of the 54 mirrors is specified to be no greater than 32 nm peak-to-valley. However, once mounted in the 9-element optical train, the errors from each mirror do not necessarily cancel one another, but can actually add and increase the resultant wavefront distortion for that path. This leads to fringe contrast reduction, reduced ability to fringe track, and a reduction in the limiting magnitude of observable objects. In a previous paper, it was shown that it is possible to mitigate the resultant wavefront distortion by using a phase-shifting interferometer combined with a single compliant static deformable mirror and control system. In that work, the mirrors tested showed a fairly uniform, concentric concavity deformation, which a single, centrally located actuator may significantly improve. In this paper, we extend the previous analysis to consider an off-center actuator acting on a mirror having an equivalently deformed surface resulting from the superposition of manufacturing errors of several flat relay mirrors. This initial shape applied to a single mirror was determined from the resultant wavefront distortion of a 7-reflection optical relay system using phase-shifting interferometer data. Finite element analysis results indicating how resultant wavefront error in the initially deformed mirrors can be collectively cancelled are presented and discussed.

8127-12, Session 3

BigBoss Telescope

M. J. Sholl, Univ. of California, Berkeley (United States)

BigBOSS is a proposed DOE-NSF Stage IV ground-based dark energy experiment designed to study baryon acoustic oscillations (BAO) and the growth of large-scale structure with an all-sky galaxy redshift survey. The project involves modification of existing facilities operated by the National Optical Astronomy Observatory (NOAO). Design and systems engineering of a 3 degree field of view transmissive corrector, atmospheric dispersion

corrector, and 5000 actuator fiber positioning system are presented. Areas discussed include overall systems engineering budgets, survey plan, optical performance, throughput, thermal design and stray light.

8127-13, Session 3

Method for integration strain analysis as applied to the James Webb Space Telescope integration process

K. Dziak, K. M. Patterson, ITT Corp. Geospatial Systems (United States); C. L. Buttaccio, MSC.Software Corp. (United States)

When assembling a telescope structure for optimal performance in a zero gravity environment, it is desirable to assemble the structure in such a manner as to minimize residual stress and strain in the structure in its final zero gravity operating environment. Since satellite telescopes are assembled in a gravity field, it is impossible to eliminate all residual strain because the structures are deformed in the gravity field during assembly. The release of deformation that occurs during launch to zero gravity imparts residual strain in the telescope structure that can cause stress and optical misalignments. This paper describes a finite element method for predicting the impacts of these residual strains for low stiffness systems that undergo significant deformations during the 1g integration process.

8127-14, Session 4

Effects of accelerations and surface conditions on a pre-designed lightweight primary mirror

C. Chan, Instrument Technology Research Ctr. (Taiwan)

The effects of self-weight on the ground and acceleration force during launch process on the primary mirror of a Cassegrain telescope have both been studied in the paper. Finite element method and Zernike polynomial fitting are applied to the ZERODUR® primary mirror with a pre-designed lightweight configuration on the back. The relation between several selected surface treatment conditions and the mirror characteristic strength as well as the safety factors under various launch accelerations have been investigated. It is found that the surface treatment on the mirror surface needs to be at least ground using a D251 or finer tool to keep the load safety factor of the primary mirror structure of the telescope higher than 1.5 aerially.

8127-15, Session 4

Line-of-sight jitter analysis for the LLCD space terminal telescope

K. E. Nevin, K. B. Doyle, MIT Lincoln Lab. (United States)

An earth-based ground terminal and a lunar orbiting space terminal are being developed as part of NASA's Lunar Laser Communications Demonstration program. The space terminal is designed to minimize mass and power requirements while delivering high bandwidth data rates using a four-inch aperture telescope and a 0.5 watt beam. Design challenges for the space terminal include meeting pointing stability requirements of 5 urad and diffraction-limited wavefront error requirements. The use of efficient optomechanical analysis simulations were used to drive the material selection and mounting methods for the space terminal cassegrain telescope. This included the analysis of the primary mirror that was designed to meet system LOS jitter, thermal and assembly distortion, and stress requirements subject to operational vibration and thermal disturbances while surviving the non-operational launch load environment.

Conference 8127:
Optical Modeling and Performance Predictions V

8127-16, Session 4

Integrated modeling of jitter MTF due to random loads

V. L. Genberg, Sigmadyne, Inc. (United States); K. B. Doyle, MIT Lincoln Lab. (United States); G. J. Michels, Sigmadyne, Inc. (United States)

Space borne astronomical telescopes are subjected to random dynamic disturbances from the host spacecraft that create line-of-sight (LoS) jitter errors, which decrease image quality. Special software tools and techniques have been developed to determine the degradation in image quality as measured by the modulation transfer function (MTF) and to identify regions of the telescope to be redesigned in order to minimize the LoS jitter response. A general purpose finite element program is used to find the natural frequencies and mode shapes of the telescope. Each of the optical surfaces for each mode shape is then decomposed into average rigid body motion and elastic deformation. Automated calculation of the LoS equations based on the optical prescription of the telescope provides the LoS response due to expected random loads. The percent contribution of each mode shape to the total LoS jitter is reported. This identifies regions of the telescope structure to redesign to minimize the response of the telescope. The LoS error due to the random input is then decomposed into drift and jitter components based on a specified sensor integration time. The random jitter is converted to a jitter MTF response function which may be used to modify the MTF function of the nominal optical system yielding the resulting optical system MTF in the operational random environment.

8127-17, Session 4

Dynamic suppression design of metering structure for James Webb Space Telescope optical testing

K. M. Patterson, D. A. Hostetler, C. L. Buttaccio, ITT Corp. Geospatial Systems (United States)

In precision optical testing, it is desirable to provide a unified metering structure between the optical test source and the test article to limit the effects of incoming vibration sources. In this manner, the entire optical test structure may be vibration isolated as a single unit. Cryogenic temperature requirements and the size requirements for testing the James Webb Space Telescope make it cost prohibitive to develop a single rigid optical metering structure. This paper demonstrates the advantages and challenges of supporting the James Webb Space Telescope on a flexible, support from above, metering structure.

8127-18, Session 5

20 years of Hubble Space Telescope optical modeling using Tiny Tim

J. E. Krist, Jet Propulsion Lab. (United States); R. N. Hook, European Southern Observatory (Germany)

Optical modeling is typically done during the design phase by experienced engineers, but for astronomers using the Hubble Space Telescope (HST), knowledge of the point spread function (PSF) is often critical to analyzing their data obtained from orbit. Astronomers unfamiliar with optical simulation techniques need access to PSF models that properly match the conditions of their observations (i.e., instrument, filter, stellar color, field position), so any HST modeling software needs to be both easy-to-use and have detailed information on the telescope and instruments. The Tiny Tim PSF simulation software package has been the standard HST modeling software since its release in early 1992. A stand-alone, freely-available program written in C, Tiny Tim can compute PSFs for all of the HST imaging instruments. The user simply answers a few basic questions (PSF size, field position, filter, object spectrum,

subsampling) and Tiny Tim will compute the PSF using simple far-field propagation. We discuss the evolution of Tiny Tim over the years as new instruments and optical properties have been incorporated (optical surface error maps derived from phase retrieval, field dependent CCD charge diffusion, optical distortions, etc.). We also demonstrate how Tiny Tim PSF models have been used for HST data analysis.

8127-19, Session 5

Improved integrated modeling of thermo-optic effects

G. J. Michels, V. L. Genberg, Sigmadyne, Inc. (United States)

Accurate optical analysis of the thermo-optic effects in transmissive media requires representation of complex distributions of refractive indices that relate to the thermal profile within the optical media. Such complex refractive index representations must be available to the ray tracing calculations while such calculations are performed along the ray path. The process begins with a thermal analysis to determine the temperatures throughout each optic in the system. Once the temperature profile is known, the refractive index profiles can be determined and supplied to the optical analysis. This paper describes an interface between Sigmadyne/SigFit and a user defined gradient index lens commonly available in commercially available optical analysis software. The interface consists of a dynamic link library (DLL) which supplies indices of refraction to a user defined gradient index lens as ray tracing calculations are being performed. The DLL obtains its refractive index description from a database derived from the thermal analysis of the optics. This process allows optical analysis software to perform accurate ray tracing analysis for an arbitrary refractive index profile induced by the change in the index of refraction due to temperature changes (dn/dT). The process is demonstrated with ORA/CODEV as the optical analysis software and MD Nastran as the finite element thermal analysis software. The DLL will provide more accurate results than current approaches involving the application of an integrated OPD map to the lens entrance surface.

8127-20, Session 5

Concurrent engineering of an infrared telescope system

D. A. Thomas, J. Geis, J. Lang, L. Peterson, F. Roybal, J. Tanzillo, The Aerospace Corp. (United States)

Complex products are best developed in a collaborative design environment where engineering data and CAD/CAE results can be shared across engineering discipline boundaries within a common software interface. This paper provides an example of an infrared telescope and spectrometer system designed in a Simulation Driven Engineering (SDE) software environment by an integrated team consisting of mechanical, structures, thermal, optics, and controls engineers.

8127-21, Session 5

High precision thermal, structural, and optical analysis of an external occulter using a common model and the general purpose multi-physics analysis tool Cielo

E. J. Cady, M. Chainyk, A. Kissil, M. B. Levine, G. J. Moore, Jet Propulsion Lab. (United States); C. C. Hoff, Cielo Software Engineering (United States)

The design and analysis of external occulters has relied on numerous feature rich commercial toolsets which do not share the same finite element basis, level of mesh discretization, data formats and compute

Conference 8127:
Optical Modeling and Performance Predictions V

platforms. Accuracy requirements, design change turnaround time and design space investigations are challenges in the current process.

Cielo is an open, object-based, multidisciplinary, high-performance compute environment that addresses these major shortcomings. Funded through the Jet Propulsion Laboratory's internal Research and Technology Development program, Cielo combines state-of-the art best practices from industry and academia and offers high-performance computing and third-party software development to create an extensible framework. Cielo is MATLAB-hosted, can run on serial and massively parallel architectures, includes native high-performance modules for thermal, structural, and optical aberration analyses, and offers plug-in technologies for finite element methods development and utilization of external numerical libraries. Cielo works from a common model with multi-physics attributes. The ASCII data input format is based on Nastran which is the industry standard.

We outline the optical performance requirements of the occulter with special attention to in plane deformations of the occulter petal edges. We present steady state and transient thermal analyses on a detailed finite element model resulting in high precision temperature fields which are directly used for subsequent structural deformation analyses without interpolation or data transfer. We compare the results of Cielo with results from commercial off the shelf tools and demonstrate the need of a detailed model for both thermal and structural analysis to predict quality edge deformations which can be used to demonstrate how the design meets stringent accuracy requirements.

8127-22, Session 5

Uncertainty quantification in high-fidelity integrated structural-thermal-optical models for simulation-based verification and validation

L. D. Peterson, S. C. Bradford, J. E. Schiermeier, G. S. Agnes, S. A. Basinger, D. C. Redding, Jet Propulsion Lab. (United States); D. E. Womble, Sandia National Labs. (United States)

Flight system certification using an integrated system model would challenge conventional tools, because of the necessary realism, credibility and speed. When a simulation is provided to a decision maker, it is important that errors in the prediction be minimized and quantified to the extent practical and necessary for the application. But these requirements conflict: high fidelity models can be too slow and computationally expensive for uncertainty quantification.

This paper will present the use of the high performance Sierra mechanics tools for overcoming this limitation. For this study, the Sandia-developed Sierra thermal tool Aria and the solid mechanics tool Adagio are coupled to the JPL MACOS optics analysis tool. Unlike conventional tools, where results would be passed from a separate thermal to structural to optical code, this toolset creates a truly coupled multiphysics simulation. The thermal-structural-optical mapping is done automatically within the simulation. This allows iterators such as DAKOTA to apply efficient, directed search algorithms for uncertainty quantification. Moreover, the thermal, structural and optical meshes can be different, allowing independent convergence of the meshes. These simulations can be scaled from desktop workstations to very large clusters with many thousands of processors, so that many model iterations can be computed in a timely fashion.

We will demonstrate these tools on an especially designed benchmark problem. We will examine the relative convergence rates of thermal, structural and optical discretization meshes for this problem, assess the use of adaptive meshing and mesh error estimation, and compare various methods for uncertainty quantification.

Conference 8128: Current Developments in Lens Design and Optical Engineering XII; and Advances in Thin Film Coatings VII

Monday-Tuesday 22-23 August 2011 • Part of Proceedings of SPIE Vol. 8128

Current Developments in Lens Design and Optical Engineering XII; and Advances in Thin Film Coatings VII

8128-17, Poster Session

Testing and design of a low-cost large scale solar simulator

Q. Meng, Sr., Chang'an Univ. (China) and Xi'an Jiaotong Univ. (China); W. Yuan, Xi'an Jiaotong Univ. (China)

To simulate solar radiation at the earth's surface, a new economical multiple-lamp solar simulator was designed. The solar simulator is comprised of 188 reflector sunlight dysprosium lamps whose light spectrum is very similar to air mass 1.5 (AM1.5) solar spectrum terrestrial standards. Lamps are configured in a hexagonal pattern with 15 columns of 12 or 13 lamps at a lamp-to-lamp spacing and column-to-column spacing of 295mm. Without altering the radiation spectral distribution, the average irradiance on target irradiated area can be adjusted over a wide range between 150 and 1100W/m² by means of the variation of lamps number or/and lamp-to-irradiated area distance. At the height of 2.0m the solar simulator provides 2m×1.5m irradiated area with over 1000 W/m². Measurement of irradiance indicates that the multiple-lamp simulator conforms to Class B of ASTM (American Society for Testing and Materials) Standard (ASTM E927-2005) in regard to spectrum match, irradiance uniformity and stability. To enlarge the effective irradiated area, two large mirror-like stainless steel plates was mounted on both of the long sides of the solar simulator. The radiation characteristics of simulator are improved and the optimized effectively irradiation surface is expanded up to 81.6%.

8128-18, Poster Session

The influence of thermal effects on the optical and electric properties of Alumina-doped zinc-oxide films prepared by DC Magnetron Sputtering

C. Tang, J. Wang, C. Lin, Y. Li, C. Jaing, Minghsin Univ. of Science and Technology (Taiwan)

Al-doped ZnO (AZO) films have wide range of applications in optical and optoelectronic devices. AZO films have advantage in highly transparent, stability to hydrogen plasma and low cost to alternative ITO film. AZO film was prepared by direct-current (DC) magnetron sputtering from ceramic ZnO:Al₂O₃ target. The AZO films were compared in two different conditions. The first is substrate heating process, in which AZO film was deposited by different substrate temperature with room temperature, 150° and 250°. The second is vacuum annealing process, in which AZO film with deposited at room temperature have been annealed at 250 and 450 in vacuum. The optical, electrical, grain size and surface structure properties of the films were studied by UV-VIS-NIR spectrophotometer, Hall effect measurement equipment, x-ray diffraction, and scanning electron microscopy. The resistivity, carrier mobility, carrier concentration, and grain size of AZO films were 1.92×10⁻³ Ω-cm, 6.38 cm²/Vs, 5.08×10²⁰ #/cm³, and 31.48 nm respectively, in vacuum annealing of 450 . The resistivity, carrier mobility, carrier concentration, and Grain Size of AZO films were 8.72×10⁻⁴ Ω-cm, 6.32 cm²/Vs, 1.13×10²¹ #/cm³, and 31.56 nm respectively, when substrate temperature was at 250 . Substrate heating process is better than vacuum annealed process for AZO film deposited by DC Magnetron Sputtering.

8128-19, Poster Session

The research of relationships between residual stress and columnar angles in oblique deposition of magnesium fluoride thin films

C. Jaing, Minghsin Univ. of Science and Technology (Taiwan); M. Liu, W. Cho, National Central Univ. (Taiwan); C. Tang, Minghsin Univ. of Science and Technology (Taiwan); Y. Liou, Chienkuo Technology Univ. (Taiwan); J. Wang, Minghsin Univ. of Science and Technology (Taiwan); C. Lee, National Central Univ. (Taiwan)

A report on the relationships between residual stress and columnar angles in oblique deposition of magnesium fluoride thin films is presented. MgF₂ films were prepared on fused quartz and BK7 glass substrates using a resistive heating Mo boat at both substrate temperatures of room temperature and 220 °C. The various deposition angles with respect to the substrate normal were acquired by rotating the substrate holder. The morphology of the cross section and the columnar angles with respect to the substrate normal in columnar microstructures of the MgF₂ films were investigated using a JEOL JSM-6700 SEM. A phase-shifting Twyman-Green interferometer along with the phase-reduction algorithm was applied to measure the variations of substrate curvatures before and after the MgF₂ films were deposited on BK7 glass substrates, which had a 25.4 mm diameter and a thickness of 1.5 mm. Therefore the residual stress in the MgF₂ films was calculated by utilizing Stoney's expression and the variations of substrate curvatures. The MgF₂ films have obviously columnar microstructures from SEM pictures without respect to substrate temperatures. The columnar angles of the MgF₂ films increase with the deposition angles. However, the columnar angle of the MgF₂ film, deposited at a substrate temperature of room temperature, is not equal to that at 220 °C when the MgF₂ films are prepared at the same deposition angle. Also, the trend of stress behavior of the MgF₂ films, deposited at a substrate temperature of room temperature, is different from that at 220 °C due to the generation of thermal stress.

8128-20, Poster Session

The design of beam shaping focusing lens applied in solar energy concentration

S. Ma, C. Lee, Feng Chia Univ. (Taiwan); Y. Lee, J. Wu, Ming Chuan Univ. (Taiwan); C. Tseng, Feng Chia Univ. (Taiwan)

In this paper, we proposed a new configuration of concentrator in solar PV system. A special optical system in the concentrator used in focusing sun light to solar cell is composed of an aspherical surface and a specific diffusing surface. The uniform-squared light pattern is obtained on the solar cell, the shape and size of light pattern can be modulated by the parameters of the diffusing surface. In order to decrease the weight of the lens, the concentrator in fresnel lens type is built at last. Besides, the optical efficiencies formed by the aspherical concentrator and Fresnel concentrator are about 92% and 77%, the concentrations are about 720mW/mm² and 640mW/mm², and the acceptance angles are about 0.35° and 0.30°, respectively. The tolerance in assembling the component of the concentrator is also discussed in detail.

8128-21, Poster Session

Opto-mechanical design of one binocular with tunable lens

A. Santiago-Alvarado, F. Iturbide Jimenez, Univ. Tecnológica de la Mixteca (Mexico); S. Vázquez-Montiel, J. Muñoz Lopez, Instituto Nacional de Astrofísica, Óptica y Electrónica (Mexico); M. Campos Garcia, Univ. Nacional Autónoma de México (Mexico)

The optical systems of multiple focusing are traditionally designed and manufactured with rigid lenses and frames that can be moved such as zoom systems used in cameras, binoculars, video camera, etc. Moreover tunable lenses are more suitable because they are compact, lightweight and allow a wide range of focusing by changing its shape. In this paper, we propose the design and development of opto-mechanical system of a binocular, using tunable lens; to perform the mechanical design of the mount is require an esthetic and ergonomic studies coupled with stress-strain analysis. In this paper, we proposed the opto-mechanical design of one binocular with tunable lens as eyepiece. The tunable liquid lens is composed of a cylindrical metallic mount with a compartment for two transparent elastic surfaces filled with water. Finally, the opto-mechanical behavior of the proposed binoculars is presented.

8128-01, Session 1

Cryogenic lens design case study: Gemini Planet Imager spectrograph

S. Thibault, Univ. Laval (Canada)

Making a lens design working at cryogenic temperature is a real challenge. Both optical and mechanical designer must work together to prevent problems during operation. The Gemini Planet Imager (GPI), currently under construction will be a facility instrument for the 8-m Gemini South telescope. The science instrument is a cryogenic integral field spectrograph based on a lenslet array. The integral field nature of the instrument allows for a full mapping of the focal plane at coarse spectral resolution. With such a data cube, artifacts within the PSF such as residual speckles can be suppressed. Additionally, the initial detection of any candidate planet will include spectral information that can be used to distinguish it from a background object: candidates can be followed up with detailed spectroscopic observations. The optics between the lenslet array and the detector are essentially a standard spectrograph with a collimating set of lenses, a dispersive prism and a camera set of lenses in a folded assembly. This paper describes by a step by step process from the first preliminary design to the final cryogenic system for both optical and mechanical design. We also discussed the assembly procedure (room temperature vs cryogenic compensation), the test support equipments and finally the laboratory optical performances over the field of view.

8128-02, Session 1

Eliminating dewar Narcissus artifacts induced by moving optics in infrared staring focal plane sensors

P. M. McCulloch, C. Olson, T. D. Goodman, L-3 Communications Sonoma EO (United States)

Lens designers must consider Narcissus artifacts during the design and optimization of lenses for staring infrared imagers. The traditional Narcissus effect occurs when the focal plane sees its own reflection from an optical surface, and many design metrics such as YNI or marginal ray angle-of-incidence have been proposed to control self-reflections.

However, staring infrared imagers have multiple cold surfaces within the dewar assembly. The cold stop, cold filter, dewar window, and coating features all contribute to Narcissus-like artifacts on the focal plane.

Although non-uniformity correction (NUC) can remove static artifacts, lenses with focus or zoom groups create a dynamic Narcissus artifact that cannot be eliminated by such correction alone. Dynamic Narcissus artifacts often manifest as bright or dark rings apparent to the human eye, although they may lie near the noise floor of the imager. Additionally, strong field curvature of an imaged Narcissus artifact can further complicate the identification of its source and obscure its predicted contribution to the final image.

We present a detailed experimental case study showing how a simple pupil ghost metric compares to traditional Narcissus metrics in a lens exhibiting dewar Narcissus and how the metric can be used for optimization to eliminate the artifact.

8128-03, Session 1

Development of multi-spectral lenses for thermal imaging technique

S. N. Bezdidko, Open Joint-Stock Co. (Russian Federation); E. I. Morozova, The Freelancers, Moscow (Russian Federation); Y. A. Roy, Open Joint-Stock Co. (Russian Federation)

The modern level of development of optoelectronic devices requires the creation of devices, providing maximum information content in different weather conditions, day and night. The solution to this problem is possible only through the creation of optoelectronic devices operating in various ranges of the optical spectrum simultaneously (multi-spectral optoelectronic devices).

One of the problems in the development of multi-spectral optoelectronic devices is the creation of a common optical system that provides for the integration of information of optical channels in a single integrated optical scheme.

The report presents the results of work on the creation of thermal lenses, working simultaneously in two regions of the spectrum of 3-5 microns and 8-12 microns, shows the results of the specific development of such lenses and their aberration characteristics.

8128-04, Session 2

Optical transmittance of high-efficiency cavity with photon recycling

C. Lin, X. Lee, W. Chien, C. Sun, National Central Univ. (Taiwan)

In this paper, a high-efficiency cavity providing extreme high energy transmittance with photon recycling is reported and demonstrated. The cavity contains a diffuser and the high reflectivity surfaces. The optical efficiency of the cavity is calculated by a formula with considering photon recycling. Furthermore, various kinds of diffusers are applied to change the optical transmittance as well as the light pattern. When the reflectivity of the inner wall of the lighting cavity was about 96 %, the optical efficiency of the cavity is higher than 90 % with use of several diffusers. The lighting patterns are formulated and discussed incorporated with the cavity efficiency. The experimental measurement as well as the calculation is demonstrated in the paper.

8128-05, Session 2

Optical design of the adjustable flashlight based on a power white-LED

J. Cai, Y. Lo, C. Sun, National Central Univ. (Taiwan)

In the paper, we design an adjustable flashlight, which can provide the spotlight and the floodlight in different modes. For most users, there two illumination modes are requested mostly. In such two modes, one is high density energy of the light pattern and the other is the uniform light pattern in a wide view field. In designing the adjustable flashlight, we first

**Conference 8128: Current Developments in Lens Design and
Optical Engineering XII; and Advances in Thin Film Coatings VII**

build a precise optical model for the high-power LED produced by CREE in mid-field verification to make sure the accuracy of our simulation. Typically, the lens is useful to be the key component of the adjustable flashlight, but the optical efficiency is low. Here, we apply a so-called total internal refraction (TIR) lens to the flashlight. By defocusing the TIR lens, the flashlight can be quickly changed into the beam size and energy density to various applications. We design two segments of the side of the TIR lens so that they can be applied to the two modes, and the flashlight provides a high optical efficiency for each mode. The illuminance of the center of light pattern at 2 m away from the lamp is also higher than using the lens in the spotlight and the floodlight. It provides good lighting functions for users.

8128-06, Session 2**High energy-efficiency B+R LED beam shaping with micro-lens diffuser for agricultural lighting**

Y. Chang, X. Lee, C. Sun, National Central Univ. (Taiwan)

Fluorescent lamps and incandescent lamps are common lighting sources for an agricultural lighting. However, the spectral characteristics and the property of arbitrary radiation of the traditional light source make the lighting not effective in energy consumption. In the application of agricultural lighting with high energy efficiency, a beam shaping technology to condense most of lights onto the planted areas is desired. In this paper, a beam shaping of a LED luminaire with a reflector and a micro-lens array is proposed and demonstrated. The LED luminaire can not only effectively shape the lighting pattern into a rectangle of the planted areas but also can mix blue and red light uniformly for complete photosynthesis. In the paper, the design and corresponding experimental results will be presented and discussed. The parameters including illumination uniformity, optical utilization factor and optical efficacy of the luminaire will be presented.

8128-07, Session 3**Range-balancing the large binocular telescope**

A. Rakich, Large Binocular Telescope Observatory (United States)

The Large Binocular Telescope (LBT) consists of two 8.4 m telescopes mounted on a common alt-az gimbal. The telescope has various modes of operation, including prime-focus, bent- and direct-Gregorian modes. The telescopes can feed independent instruments or their light can be combined in one of two interferometric instruments, giving an interferometric baseline of over 22 m.

With all large telescopes, including the LBT, collimation models or modeled values for hexapod positions, are required to maintain reasonable optical alignment over the working range of temperatures and telescope elevations. Unlike other telescopes, the LBT has a highly asymmetric mechanical structure, and as a result the collimation models are required to do a lot more "work", than on an equivalent aperture monocular telescope that are usually designed to incorporate a Serurier truss arrangement.

LBT has been phasing in science operations over the last 5 years, with first light on the prime-focus cameras in 2006, and first light in Gregorian mode in 2008. In this time the generation of collimation models for LBT has proven to be problematic, with large departures from a given model, and large changes in pointing, being the norm. A refined approach to generating collimation models, "range balancing", has greatly improved this situation. The range-balancing approach to generating collimation models has delivered reliable collimation and pointing in both prime focus and Gregorian modes which has led to greatly increased operational efficiency. The details of the range-balancing approach, involving the separation of pointing and coma rotations, are given in this paper.

8128-08, Session 3**Advanced optical design for DNA sequencing systems**

K. Sobolev, A. Joobeur, ASML (United States); C. Uhrich, Complete Genomics, Inc. (United States); D. Aziz, Midbar West, Inc. (United States)

Latest advances in DNA sequencing techniques require development of high NA immersion microscope systems with large field of view, increased resolution and very tight distortion correction.

This paper discusses optical design and tolerance analysis of NA 1.0 immersion microscope system with field of view size over 1 mm to be used for four color fluorescence spectroscopy. Described microscope system includes immersion objective lens and four tube lens setup corrected for wide wavelength range from 490 nm to 712 nm. We will discuss critical aspects of designing this kind of optical system including special glass selection required for chromatic correction.

The first part of the paper describes overall system configuration, its differences from conventional microscope system, and how these differences affect image quality requirements.

In the second part we describe optical design difficulties associated with large field of view, wide spectral range and tight distortion correction. The most important aspects optical design is choosing design form and glass selection to successfully correct chromatic aberrations including axial and lateral colors, spherochromatic aberration and other field varying chromatic aberrations. Since application requirements limit glass selection to low fluorescence glass types the glass optimization is especially difficult.

8128-10, Session 3**Development and experimental verification of an intraocular scattering model**

C. Jiang, T. Jhong, Y. Chen, C. Sun, National Central Univ. (Taiwan)

It is well-known that the scattering behavior in human eyes causes the disability glare effect. The main contributions of ray scatter in human eyes are composed of volumetric scatter in cornea, volumetric scatter in crystalline lens, and surface diffusion at retina fundus. In order to simulate the disability glare effect, a rigorous intraocular scattering model was built into a biometry-based human eye model. The eye model employed empirical anatomic and optical data of ocular parameters and had the functionality of age and accommodation. The resulting visual acuity and chromatic dispersion matched the behavior in real human eyes.

The first part of the scattering model was to add scattering particles in the crystalline lens, where the particle parameters such as the refractive index, size, and obstruction area were calculated from the data in the literature. The second part was the construction of the retina diffusing surface. The retina fundus was considered as a Lambertian surface and had the corresponding reflectance at visible wavelengths. The volumetric scattering in cornea was also simulated by adding scattering particles. The particle parameters were varied until the veiling luminance of the eye model matched the values calculated from the CIE disability glare general formula with age 40 and zero p-value for black iris. By replacing the transparent lens with a cataractous lens, the disability glare formula of cataracts was generated. The MTF of the intraocular scattering model showed nice correspondence with the data measured by a double-pass experiment.

8128-11, Session 4**Novel plasma-enhanced sputter process for new applications**

P. Biedermann, Evatec Ltd. (Switzerland)

Conference 8128: Current Developments in Lens Design and Optical Engineering XII; and Advances in Thin Film Coatings VII

Emerging applications in 3D and laser optics necessitate increasingly complex optical thin film stacks. Typical designs include multiple band pass filters or thick multilayers where conventional coating techniques cannot satisfy yield requirements for economical volume production whilst still maintaining the highest environmental and optical tolerances. A novel plasma enhanced sputtering process controlled by a combination of Plasma Emission Monitoring (PEM) and in situ Broadband Optical Monitoring has been investigated with the goal of achieving the coating stability and surface roughness associated with coating flux energy levels of around 20eV reported for Ion Beam Sputter (IBS) whilst still maintaining the advantageous high coating rates for conventional sputter processes. Coating set up and results will be presented for spectral and mechanical stability, run to run repeatability, and surface scatter and compared with those achieved by conventional sputter techniques.

8128-12, Session 4**Unexpected absorption in anti-reflection coatings used in infrared systems**

C. Panetta, P. Fuqua, C. Chu, J. Barrie, The Aerospace Corp. (United States)

Infrared (IR) optical systems require a range of exotic materials, many with fairly large indices of refraction. The mismatch in the index between the optical element and the surrounding medium can result in reflection losses that approach 50%. Anti-reflection (AR) coatings are applied to these elements in order to improve the optical transmission and minimize artifacts through a system. There have been several instances of significant, unexpected, transmission loss in IR systems, with that loss being attributed to either initial AR coating problems or subsequent degradation of the coatings. Likely candidates for the loss mechanism are water trapped into the optical coatings during deposition and water being incorporated into coating voids or grain boundaries during exposure to ambient humidity. Five different AR coatings have been procured from four different manufacturers to study the cause of the observed losses, with this paper reporting on the preliminary results of lab tests to characterize the different samples.

8128-13, Session 5**Design of a free-form lens system for short distance projection**

B. Yang, Univ. of Shanghai for Science and Technology (China)

As a digital image display device, projectors have been widely used in conference rooms and classrooms. With the development of high resolution image source devices and longer life-time light sources such as LED, projector becomes a good solution for home theatre applications now. Projector has many advantages compared with large screen LCD TV. It is compact, cheaper and consumes less power. Traditional projector lens has a very small projection angle so a long working distance is needed to form a big screen display. Such long working distance limits the application of projectors at home. In this paper we present a free-form lens system design for short distance projection. The difficulties of the optical design of such short distance projector lens lies in the distortion control and high order aberration correction. Free-form surface shape and non-rotational symmetrical structure provide us more freedoms for optimization. The catadioptric structure is also used to reduce the overall length of the whole system. The designed projector lens system consists of two parts. The first part is a rotationally symmetrical lens system which corrects the basic aberrations. The second part contains 2 free-form lenses and a reflector which eliminate the distortion and further corrects the basic aberrations. We achieve 40~60inch projected image size at a display screen which is 150~250mm away from the lens system. The object NA is 0.15 and the image source used is a 0.45inch WXGA DMD. The maximum distortion for all fields at all distances is less than 2%.

8128-14, Session 5**Progress in the SMS design method for imaging optics**

L. Wang, Univ. Politécnica de Madrid (Spain); P. Benitez, J. C. Miñano, Univ. Politécnica de Madrid (Spain) and Light Prescriptions Innovators, LLC (United States); J. Infante Herrero, G. Biot, Univ. Politécnica de Madrid (Spain)

The Simultaneous Multiple Surfaces (SMS) was developed as a design method in Nonimaging Optics during the 90s. Later, the method was extended for designing Imaging Optics. The application of the SMS method for imaging optics was first introduced for the design of an ultra-high numerical aperture RX lens composed by two aspheric surfaces. More recently the extension to up to four aspherics was developed. Different from traditional optical design methods based on multi-parametric optimization techniques, SMS method is a direct construction method for selected ray-bundles, meridian or skew ray-bundles. This gives the SMS method an additional interest since it can be used for exploring solutions far from the paraxial approximation where the multi-parametric techniques can get lost because of the multiple local minima.

Different SMS algorithms can be utilized, depending on the ray-bundles selected for the design. For instance, in three-surface designs, three meridian ray-bundles (3M) or one meridian and two skew ray bundles (1M-2S) can be selected for the calculation, the latter proving a better sampling of the phase space. In this work, we will compare different SMS algorithms for a new lens structure that combines 2 reflecting surfaces and 2 refracting surfaces in one solid piece, for a design of 720mm focal length, f/6 and 0.650 diagonal field of view. With this catadioptric lens structure we have achieved designs with excellent performance (RMS spot size <12 μm), with total system length less than 35 mm, and the results obtained with the different algorithms will be presented.

8128-15, Session 5**Distributed wavefront coding for wide angle imaging system**

H. Zhang, M. Larivière Bastien, S. Thibault, Univ. Laval (Canada)

The emerging paradigm of imaging systems, known as wavefront coding, which employs joint optimization of both the optical system and the digital post-processing system, has not only increased the degrees of design freedom but also brought several significant system-level benefits. The effectiveness of wavefront coding has been demonstrated by several proof-of-concept systems in the reduction of focus-related aberrations and extension of depth of focus. While the previous research of wavefront coding has been mainly focused on the imaging system with small or modest field of view (FOV), we present a preliminary study of the wavefront coded applied to panoramic optical systems. Unlike the traditional wavefront coded systems which only require the constancy of modulation transfer function over an extended focal range, the wavefront coded panoramic systems emphasize particularly on the mitigation of significant off-axis aberrations such as field curvature, coma, and astigmatism. We first analyze the limits of using a traditional generalized cubic polynomial pupil phase mask for wide angle system. The results show that a traditional approach can work when the variation of the off-axis aberration is modest. Consequently we proposed to study how a distributed wavefront coding approach where the phase mask is not in the pupil plane can be used for wide angle lens. Some cases are discussed theoretically, designed with Zemax, and illustrated graphically.

8128-16, Session 5

Progressive addition lens design by optimizing NURBS surface

Y. Liu, National Taiwan Univ. (Taiwan); W. Hsu, Y. Cheng, Instrument Technology Research Ctr. (Taiwan); G. J. Su, National Taiwan Univ. (Taiwan)

Progressive addition lenses (PAL) are used to compensate presbyopia, which is induced by losing accommodation of elder eyes.

These eyes need different optical power provided by eye glasses while watching objects at different distance. A smaller optical power is required in further distance and a larger one in nearer zone. A progressive addition lens can provides different power requirements in one piece of lens.

This paper introduces a whole process of PAL production, from design, fabrication, to measurement. The PAL is designed by optimizing NURBS (Non-uniform rational B-spline) surface. Parameters of merit function are adjusted to design lenses with different specifications. The simulation results confirm that the power distributes as expected and cylinders are controlled under its adding power. The effect for presbyopic eyes has also been examined.

Imaging analysis for an eye model wearing designed PALs shows the feasibility of our design. Besides, sample lenses have been fabricated and measured. We used precise-machining to produce the molds for plastic injection. Then, the samples were produced by injecting polycarbonate to the molds. Finally, Ultra Accuracy 3D Profilemeter was used to measure the sample PALs. Examinations shows that our designs are achievable and feasible in practice use.

Conference 8129: Novel Optical Systems Design and Optimization XIV

Monday 22 August 2011 • Part of Proceedings of SPIE Vol. 8129 Novel Optical Systems Design and Optimization XIV

8129-01, Session 1

3D image capture through the use of an astigmatic projected pattern

G. C. Birch, J. S. Tyo, J. Schwiegerling, College of Optical Sciences, The Univ. of Arizona (United States)

Three-dimensional displays have become increasingly present in consumer markets. However, the ability to capture three-dimensional images cheaply and without major modifications to current cameras is uncommon in commercial systems. Our goal is to create a modification to a common commercial camera that allows a three dimensional reconstruction. We desire such an imaging system to be inexpensive and easy to use. Furthermore, we require that any three-dimensional modification to a camera does not reduce its resolution. The purpose of this project is to enable inexpensive three-dimensional image capturing devices, and in doing so close the loop between consumer three-dimensional display and capture.

We present a possible solution to this problem. A commercial digital camera is used with an astigmatic projector system to capture images of a scene. By using an astigmatic projected pattern we are capable of creating two different focus depths for horizontal and vertical features of the projected pattern, thereby encoding depth into the projected pattern. By carefully choosing a pattern we are able to exploit this differential focus in image processing. Wavelet transforms are performed on the image that pick out the projected pattern. By taking ratios of certain wavelet transforms we are able to correlate the distance an object at a particular transverse position is from the camera to the wavelet transform ratios.

We will present information regarding construction, calibration, and images produced by this system. The nature of linking a projected pattern design and image processing algorithms will be discussed.

8129-02, Session 1

3D imaging with a single-aperture 3-mm objective lens: concept, fabrication, and test

S. Bae, R. Korniski, Jet Propulsion Lab. (United States); H. Shahinian, Skull Base Institute (United States); H. Manohara, Jet Propulsion Lab. (United States)

A technique for achieving a full-color 3D image using a single camera is presented. Unlike a typical 3D-imaging system comprised of two independent cameras each contributing one full-color viewpoint, here two full-color viewpoints in a single-lens camera are created utilizing a form of spectral multiplexing from a series of different scene illuminations. The spectral multiplexing works with a bipartite-filter composed of a complementary pair of multiple bandpass filters, coupled with a series of spectral illumination bands (SIBs) each matched to the bandpasses of one or the other filter. When the bipartite-filter is mounted at the pupil of the objective, it divides the single pupil into two, and makes the openings of the pupils depend on the SIBs. A color image is then realized by mixing the series of SIBs that contain a combination of red, green, and blue (RGB) colors collected from each of the viewpoint. We believed that the technique was advantageous in miniaturizing a 3D camera. We applied this technique to fabricating a 3D camera composed of 3-mm lenses. In this paper, we will present the details of the concept, materials, and method used for building the camera and the results validating the concept.

8129-03, Session 1

Wide and narrow dual image guidance system for ground vehicle on fast focusing and stereo matching operation

A. Akiyama, Kanazawa Technical College (Japan); N. Kobayashi, Kanazawa Institute of Technology (Japan); E. Mutoh, Kawasaki Heavy Industries Ltd. (Japan); H. Kumagai, Tamagawa Seiki Co., Ltd. (Japan); H. Ishii, Nihon Univ. (Japan)

We have developed the wide and narrow dual image guidance system for ground vehicle on fast focusing and stereo matching operation. The wide focusing catches the averaged distance information of the outside world. The wide image stereo matching operation extracts the feature image area of objects from the focused wide images. The next narrow focusing on the extracted feature image area finds its fine distance information. Further finer distance information comes from the narrow focused image stereo matching operation.

The fast focus image is derived from the calculating the developed wavelet focus measure value of the horizontal high pass image and the vertical high pass image of the Daubechies wavelet transformed image. The highest wavelet focus measure value among them gives the best focus image directly. This focusing operation works finely similar to the other differential image techniques.

We used the stereo matching operation to find the direction of the local points on the wide focused image to make the further narrow focusing. The narrow focusing makes the clear distance image realizing the object edge or the good contrast of the object surface. Further narrow image stereo matching gives us the volume information of the focused image area.

For this operation we equipped the view control and focus control function each color video camera and mounted them on the 2 axis space direction set equipment system. Further the developed wide and narrow dual image guidance system is placed on the ground vehicle to find the appropriate direction and surface to move

8129-04, Session 1

Reflective autofocus image system with MEMS deformable mirrors and freeform design

W. Chang, G. J. Su, National Taiwan Univ. (Taiwan)

In this paper we proposed an miniature auto-focus image system without moving parts. We had presented a 2-Mega-Pixel auto-focus module by combining reflective optics and MEMS deformable mirror. This design can be further improved. We expanded 2-Mega-Pixel image plane to 8-Mega-Pixel image plane and corrected the aberration by adding one more lens as a stop. For the concern of the cost, we distributed the optical power of the adding lens to the fixed mirror and the deformable mirror, and we designed them as freeform surfaces to compensate aberrations. Finally, a 8M pixel auto-focus image system whose FOV is $\pm 26^\circ$ can be achieved. The MTF at full spatial frequency is above 25%.

8129-05, Session 1

Continuous optical zoom module based on two deformable mirrors for mobile device applications

Y. H. Lin, G. J. Su, National Taiwan Univ. (Taiwan)

Conference 8129:
Novel Optical Systems Design and Optimization XIV

In recent years, optical zoom function of the mobile camera phones has been studied. However, traditional systems use motors to change separation of lenses to achieve zoom function, suffering from long total length and high power consumption, which is not suitable for mobile phones use. Adopting MEMS polymer deformable mirrors in zoom systems have the potential to reduce thickness and have the advantage of low chromatic aberration. In this paper, we proposed a 2X continuous optical zoom systems for mobile phones, using two deformable mirrors, suitable for 2-Mega-Pixel image sensors. In our design, the thickness of the zoom system is about 10 mm. The smallest EFL (effective focal length) is 4.5mm at field angle of 52° and the f/# is 3.5. The longest EFL of the module is 9mm and the f/# is 5.

8129-06, Session 2

Development of low-coherence light sheet illumination microscope for fluorescence-free bioimaging

Z. Xu, T. E. Holy, Washington Univ. School of Medicine in St. Louis (United States)

Light Sheet Illumination Microscopy is an imaging modality featuring the novel arrangement with the illumination axis perpendicular to the detection axis. In this technology a well defined light sheet is generated and aligned precisely to the focal plane of the microscope objective and thus only the thin in-focus layer of the sample is illuminated and imaged, thereby avoiding out-of-focus light. Besides the inherent optical sectioning function, other advantages include fast imaging speed, high longitudinal resolution and decreased light-induced heating or toxicity. Though promising, this microscopy is currently restricted in imaging fluorescently labeled tissue; in inspection of intact tissue using scattered light the acquired images suffers from intense speckles because of the severe coherence in the illumination. This work aims to build a microscope capable of achieving the intrinsic images of the fluorescence-free sample with reduced or eliminated speckles, by developing a low coherence light sheet illumination. To diminish the spatial coherence the sample is illuminated with tens of independent sub-beams (without inter-coherence) illuminating the field of view of the microscope with diverse incident angles. The temporal coherence is dramatically reduced by employing a supercontinuum laser with a broad spectrum as the original light source. The new microscopy significantly extends the functionality of Light Sheet Illumination Microscopy and will enable many new bioimaging applications.

8129-07, Session 2

Design considerations for biomedical optical imaging systems

R. Liang, Carestream Health, Inc. (United States)

Designing an efficient system for biomedical imaging requires a solid understanding of special requirements of optical systems for biomedical imaging and optical components used in the systems. This presentation will discuss some special considerations when designing optical systems for biomedical imaging.

8129-08, Session 2

Retinal tracking system for jumping spiders

C. Canavesi, Univ. of Rochester (United States); S. Long, Univ. of Massachusetts Amherst (United States); D. Fantone, Univ. of Rochester (United States); E. Jakob, Univ. of Massachusetts Amherst (United States); R. Jackson, Univ. of Canterbury (New Zealand); D. P. Harland, AgResearch Ltd. (New Zealand); J. P. Rolland, Univ. of Rochester (United States)

We present an optical system for tracking the retinal movement of a jumping spider as a stimulus is presented to it. The system, designed using only off-the-shelf optical components and one custom aspheric plate, consists of three sub-systems that share a common path: a visible stimuli presentation sub-system, a NIR illumination sub-system and a NIR retinal imaging sub-system. A 25 mm clearance was maintained between the last element and the spider to ensure a more stable positioning of the spider in the system. The stimuli presentation system relays an image from a display to the spider eye, matching the 15 arcmin resolution of the two principal eyes of the spider and producing a virtual image at a distance of 250 mm from the spider, with a visual full field of view of 55 degrees. When viewing a stimulus, the jumping spider moves its retinas, which cover a field of only 0.6 degrees, and directs them to view different places in the visual field. The retinal imaging system was designed to use a NIR camera to track changes of 0.5 degrees in the field of view seen by the spider. By tracking retinal movement across the images that are presented to spiders, we will learn how they search for visual cues to identify prey, rivals, and potential mates.

8129-09, Session 2

SOI strip waveguide microring resonator for homogeneous biosensing

S. Malathi, N. Mangal, Indian Institute of Science (India); S. S. Cochin Univ. of Science & Technology (India); R. V. Honnunar, S. Talabattula, Indian Institute of Science (India)

We report the simulation cum analytical results obtained for homogenous or bulk sensing of protein on Silicon-on-insulator(SOI) strip waveguide based microring resonator. The strip waveguides provide higher optical mode confinement. The radii of the rings are 5µm and 20µm; the waveguide dimensions are 300x300 nm and a gap of 200 nm exists between the ring and bus waveguide.

The protein analyte is uniformly distributed over a thickness which exceeds the evanescent field penetration depth of 100nm. The SOI platform was considered following the analysis of the penetration depth of evanescent field which was found to be the least compared to polymer and silicon rich nitride (SRN) based waveguides. A lesser penetration depth of the evanescent field allows it to interact more with the bio-layer in comparison to its surroundings which ultimately results in better sensitivity. Moreover, the difference in the effective index and propagation constant of the ring and bus waveguide are taken into consideration by including a detuning parameter = $(1 - 2)/2$.

The Q-factor for the devices is ~ 9500 and ~18000 while the finesse is ~180 and ~90 for 5µm and 20µm respectively. The sensitivities of the resonators are 27.5 nm/RIU and 5nm/RIU respectively. The analytical and simulated results corresponding to the effective index Neff of the fundamental mode for our device were found to be comparable.

8129-10, Session 3

Scalability of a cross-platform multi-threaded non-sequential optical ray tracer

A. W. Greynolds, Ruda-Cardinal, Inc. (United States)

Design optimization increases the computational workload of engineering calculations by orders-of-magnitude. Multiple-core computers are now the norm so that all computationally intensive algorithms should be transparently multi-threaded if possible. Ray tracing is still the work-horse of optical engineering where it's usually sequential for image analysis and non-sequential for illumination or stray light calculations. The question is how well do various implementations scale with the number of threads/cores/processors. The GeOIE optical engineering software implements multi-threaded ray tracing with just a few simple cross-platform OpenMP directives. Timings as a function of the number of threads are presented for two quite different ZEMAX non-sequential sample problems running on a dual-boot 12-core Apple computer and compared to not only ZEMAX but also FRED (plus single-threaded ASAP and CodeV). Also

Conference 8129:
Novel Optical Systems Design and Optimization XIV

discussed are the relative merits of using Mac OS X or Windows 7, 32-bit or 64-bit mode, single or double precision floats, and the Intel or GCC compilers. It is found that simple cross-platform multi-threading can be more efficient than the Windows-specific kind used in the commercial codes and who's the fastest ray tracer depends on the specific problem. It should be noted that besides ray trace speed, overall productivity also depends on other things like visualization, ease-of-use, documentation, and technical support which are not rated here.

8129-11, Session 3

Modeling the role of phosphor grain packing in compact fluorescent lamps

N. Pannier, M. Filoche, B. Sapoval, Ecole Polytechnique (France); T. Le Mercier, V. Buissette, Rhodia (France)

A ray-tracing method is performed to study the optical properties of phosphor powder coating in fluorescent. The phosphor particles are represented as micron-size spheres. These are substantially larger than the wavelengths of the visible and the ultraviolet light to be modelled as rays.

The mercury discharge is represented by a UV source, sending a large number of rays in randomly chosen direction at a wavelength of 254 nm. Each ray interacting with a phosphor particle can be reflected, refracted, absorbed and transmitted. The direction of refracted rays is calculated using Snell's law. The ratio of reflected to incident intensity of non polarized light is computed employing Fresnel's equation. Ideal absorption spectrum and excitation spectrum for three rare-earth phosphors are used.

We investigate the role of grain size, of the distribution of sizes, of the thickness of the phosphor layers and of their packing density. This last parameter seems to play a crucial role in the system efficiency. Reducing the density of the phosphor layer decreases accordingly the probability for an ultraviolet ray to be absorbed, and consequently the emission of visible light. On the other hand, increasing the density dramatically raises the number of obstacles in the output path of a visible ray. This behaviour suggests that there might be an optimal density for which the power of visible light received on the top side is maximal. Our results are in good agreement with previous simulations and experiments.

8129-12, Session 3

Simulation and optimization of a sub-micron beam for macromolecular crystallography using SHADOW and XOP at GM/CA CAT at the APS

Z. Liu, S. Xu, D. W. Yoder, R. F. Fischetti, Argonne National Lab. (United States)

The small, high intensity and low convergence beams available on beamlines at 3rd generation synchrotron sources have been a boon to macromolecular crystallography. It is now becoming routine to solve structures using a beam in the 5 - 20 micron (FWHM) range. However, many problems in structural biology suffer from poor S/N due to small (a few microns) crystals or larger inhomogeneous crystals. In addition, theoretical calculations and experimental results have demonstrated that radiation damage may be reduced by using a micron-sized X-ray beam. At GM/CA CAT we are developing a sub-micron, low convergence beam to address these issues. The sub-micron beam capability will be developed on the existing beamline 23ID-D where the minimum beam size available to users is currently 5 microns in diameter. The target goals are a beam size of ~0.8 micron (FWHM) in diameter, with a beam convergence of less 0.6 milli-rads, a flux greater than 5x10¹⁰ photons/sec, and an energy range from 5 to 35 keV. Four optical systems will be compared: 1) a single set of highly demagnifying Kirkpatrick-Baez (K-B) mirrors, 2) multiple Fresnel Zone Plates (FZP), 3) a set of K-B mirrors focusing to a secondary source that is imaged by another set of K-B

mirrors, and 4) a set of K-B mirrors focusing to a secondary source that is imaged by a FZP. Here we will present the results of a design optimization based on ray trace simulations (SHADOW), flux calculations (XOP), and experimental results on 23ID.

8129-14, Session 3

Hearing at the speed of light: using interferometry to detect sound

M. G. Heyns, V. L. Hamilton, J. A. Hart, J. A. McKay, Franklin W. Olin College of Engineering (United States); V. Doherty, Eidolon Optical, LLC (United States)

In this study, a unique dual beam laser interferometer capable of detecting sound through solid resonant media has been developed. The system detects the vibrations of a specular surface induced by acoustic frequencies in the spoken register by using laser interferometry for real-time reproduction of the audio signal over large ranges. The system utilizes a unique optical configuration and conventional signal processing techniques to increase the signal to noise ratio, sensitivity, and range of the interferometer. The configuration allows for a clear and distinctive interference fringe pattern at greater than normal range. Numerical calculations, simulations, and experimental results verify the feasibility and applicability of this novel interferometer.

8129-15, Session 3

Innovating spectrometry studies at undergraduate level using a linear CCD array

A. Garg, R. Sharma, V. Dhingra, Acharya Narendra Dev College (India)

Students are less enthused in performing various spectrometry experiments in a conventional optics laboratory at the undergraduate level. In order to motivate students towards spectrometry, the present development focuses on innovating spectrometry experiments in undergraduate optics laboratory by integrating a linear CCD (Charge Coupled Device) for optical intensity capture using LabVIEW programme and a Digital Storage Oscilloscope with NI LabVIEW Signal Express. In the first step, students can calibrate wavelength in terms of pixels position using a standard light source. Then this calibration can be used to display and measure the colour spectrum, emission spectrum of various light sources. Various experiments performed include characterizing various LEDs in terms of wavelengths emitted for use in measurement of Planck's constant experiment, measuring characteristics wavelengths in emission spectra of hydrogen lamp (for calculating Rydberg's constant) and sodium lamp.

8129-27, Session 3

Determination of off-axis aberrations of imaging systems using on-axis measurements

J. H. Burge, College of Optical Sciences, The Univ. of Arizona (United States)

No abstract available

8129-16, Session 4

Ultra-compact telephoto lens design with SMS method

L. Wang, Univ. Politécnic de Madrid (Spain); P. Benitez, J.

Conference 8129:
Novel Optical Systems Design and Optimization XIV

C. Miñano, Univ. Politécnica de Madrid (Spain) and Light Prescriptions Innovators, LLC (United States); J. Infante Herrero, Univ. Politécnica de Madrid (Spain); M. de la Fuente, Indra Sistemas, S.A. (Spain); G. Biot, Univ. Politécnica de Madrid (Spain)

The Simultaneous Multiple Surfaces (SMS) was developed as a design method in Nonimaging Optics during the 90s. Later, the method was extended for designing Imaging Optics. The application of the SMS method for imaging optics was first introduced for the design of an ultra-high numerical aperture RX lens composed by two aspheric surfaces. More recently the extension to up to four aspherics was developed. Different from traditional optical design methods based on multi-parametric optimization techniques, SMS method is a direct construction method for selected ray-bundles, meridian or skew ray-bundles. This gives the SMS method an additional interest since it can be used for exploring solutions far from the paraxial approximation where the multi-parametric techniques can get lost because of the multiple local minima.

In this work, we propose a new lens structure that combines 2 reflecting surfaces and 2 refracting surfaces in one solid piece, for a design of 720mm focal length, f/6 (aperture diameter 120 mm) and 0.650 diagonal field of view. The difficulty in these Catadioptric-type designs is to maintain high performance with small overall system length, which is very important in some space-limited applications like UAV (Unmanned Aerial Vehicle). The lens surfaces are rotational symmetric and calculated with SMS method to have good control of non-paraxial rays. We have achieved designs with excellent performance (RMS spot size <12 μm), with total system length less than 35 mm. Compared to traditional designs, the solid lens designs are much more compact, easy to assemble and thus cost-saving.

8129-17, Session 4

Fresnel lens solar concentrator simulation cache

A. J. Davis, Reflexite Energy Solutions (United States)

Plano polymeric Fresnel lens solar concentrators continue to fulfill a market requirement as a system component in high volume cost effective Concentrating Photovoltaic (CPV) electricity generation. Design and optimization is preferably performed using comprehensive system simulation tools, but before investing in the effort to build a complete virtual model framework, much insight can be gathered beforehand by generating a parameterized simulation cache and referencing those results.

To investigate the performance space of the Fresnel lens, a fast simulation method which is a hybrid between raytracing and analytical computation is employed to generate a cache of simulation data. This data is post-processed to yield results that are not readily achieved via derivation. Example plots that can be used for look-up purposes will be included.

Lens parameters that will be interrogated include focal length, index of refraction, prism fidelity, aperture, transmission and concentration ratio. In order to compactly represent a large variety of lens configurations, some variables that define the Fresnel lens will be parameterized.

Analysis will be limited to Fresnel lens prisms oriented toward the photovoltaic (PV) cell and the plano surface directed toward the sun. The reverse of this configuration is rarely encountered in solar concentration applications and is omitted.

8129-18, Session 4

Novel free-form optical surface design with spiral symmetry

P. Zamora, P. Benitez, J. C. Miñano, Univ. Politécnica de Madrid (Spain); J. F. Vilaplana, Light Prescriptions Innovators Europe, S.

L. (Spain)

Many optical designs present several manufacturing constraints that limit their geometry. Manufacturing technologies as injection molding or embossing specify their production limits. These restrictions may affect several important properties of these designs.

We present a novel concept, in which optical surfaces are not obtained from the usual revolution symmetry with respect to a central axis (z axis), but they are calculated as free-form surfaces in such a way that they describe a spiral trajectory around z axis. The main advantage of this new concept lies in the manufacturing process: a molded piece can be easily separated from its mold just by applying a combination of rotational movement around axis z and linear movement along axis z. By applying this "spiral" movement, demolding process renders very easy.

To prove this new manufacturing concept, we will present a new spiral design, whose rotational-symmetric equivalent cannot be manufactured with conventional techniques. Thus we will demonstrate its ease of manufacturing and its optimum optical properties with computer ray-trace simulated results. Our design transforms a flat input wavefront into an output wavefront describing a ray trajectory such that generates a ring-shape spot on the receiving plane.

8129-19, Session 4

Optical design of automotive headlight system incorporating digital micromirror device

Y. Fang, National Kaohsiung First Univ. of Science and Technology (Taiwan)

In this research we propose a new integral optical design for an automotive headlight system with an advanced light-emitting diode and digital micromirror device (DMD). In recent years, the popular adaptive front-lighting automobile headlight system has become a main emphasis of research that manufactures will continue to focus great efforts on in the future. Traditionally, automobile headlights have all been designed as a low beam light module, whereas the high beam light module still requires using accessory lamps. In anticipation of this new concept of integral optical design, we have researched and designed a single optical system with high and low beam capabilities. To switch on and off the beams, a DMD is typically used. Because DMDs have the capability of redirecting incident light into a specific angle, they also determine the shape of the high or low light beam in order to match the standard of headlight illumination. With collocation of the multicurvature reflection lens design, a DMD can control the light energy distribution and thereby reinforce the resolution of the light beam.

8129-20, Poster Session

Blocking probability analysis with and without wavelength convertors in all-optical WDM networks

A. Wason, Rayat & Bahra Institute of Engineering & Bio-Technology (India); R. S. Kaler, Thapar Univ. (India); R. Kaler, Bahra Group of Institutes, Patiala Campus (India)

The blocking probability of a lightpath request (or a call) is an important performance measures of a wavelength-routed all optical networks. This blocking probability can be affected by many factors such as network topology, traffic load, number of links, algorithms employed and whether wavelength conversion is available or not. In this paper we have proposed mathematical models to reduce the blocking probability of the WDM optical network. This blocking probability calculation was based on the availability and non-availability of wavelength convertors. The model can also be used to evaluate the blocking performance of realistic networks such as NSFNet topology and hence used to improve its performance of those network topologies. Results show that these

Conference 8129:
Novel Optical Systems Design and Optimization XIV

models work better without wavelength convertors than with wavelength convertors. Also, when the load applied to the network is increased the blocking probability of that network is decreased, both with and without wavelength conversion. Hence, these models can be applied for the better performance of those networks where the load applied is higher. The results have proved that blocking probability also decreases with the increase in the number of wavelengths. The comparison of both the models (with wavelength convertors and without wavelength convertors) have also been made and analysis can be made on the basis of results that the performance of the model without wavelength convertors gives better output than the model with wavelength convertors.

8129-21, Poster Session

Laser-based study of geometrical optics at school level

A. Garg, V. Dhingra, R. Sharma, A. K. Singh, D. Joshi, K. Sandhu, P. Wadhawan, P. Chakravarty, V. Sharma, Z. Khan, Acharya Narendra Dev College (India)

Students at the school level from grade 7 to 12 are taught various concepts of geometrical optics but with little hands-on activities. Light propagation through different media, image formation using lenses and mirrors under different conditions and application of basic principles to characterization of lenses, mirrors and other instruments has been a subject which although fascinates students but due to lack of suitable demonstrating setups, students find difficulty in understanding these concepts and hence unable to appreciate the importance of such concepts in various useful scientific apparatus, instruments and devices. Therefore, students tend to cram various concepts related to geometrical optics instead of understanding them. As part of the extension activity in the University Grants Commission major research project "Investigating science hands-on to promote innovation and research at undergraduate level" and University of Delhi at Acharya Narendra Dev College SPIE student chapter, students working under this optics outreach programme have demonstrated various experiments on geometrical optics using a five beam laser ray box and various optical components like different types of mirrors, lenses, prisms, optical fibers etc. The various hands-on activities includes demonstrations on laws of reflection, image formation using plane, concave and convex mirrors, mirror formula, total internal reflection, light propagation in an optical fiber, laws of refraction, image formation using concave and convex lenses and combination of these lenses, lens formula, light propagation through prisms, dispersion in prism, defects in eye- Myopia and hypermetropia and basic working of some optical instruments like camera and telescope. Students have been evaluated through pre and post tests in order to measure the improvement in their level of understanding.

8129-22, Poster Session

Optical sensor for the determination of adulteration in petrol: design and development

K. Kishor, R. K. Sinha, A. D. Varshney, V. Kumar, Delhi Technological Univ. (India)

In this paper, we report design and development of optical sensor for the determination of adulteration in petrol using optical time-domain reflectometer (OTDR). OTDR is generally used to find out faults in optical fibers but we effectively use this technique for the determination of the percentage of adulteration in petrol. This OTDR method enables detection of adulteration in petrol very accurately. The OTDR measurement method reported in this paper is easy to carry out and also a cost effective tool for the determination of adulteration in petrol.

In this experiment, we transmit several pulses of different wavelengths in optical fiber at the one end and measured the back reflection from other end of the optical fiber which is dipped in the given sample of the petrol. On the basis of back reflection recorded, we determine the

percentage of adulteration in petrol comparing reflections from pure petrol. These measurements have been repeated several times with different percentage of adulteration in petrol. We found that the result obtained is very accurate, and method is highly sensitive even for the very low percentage of adulteration in petrol. It is reported that this optical-fiber based sensors for determination of adulteration in petrol is very economical, user friendly and most important eco-friendly.

8129-23, Poster Session

Variation of optical polarization in reflected light by redistribution of electric charge in metals

J. G. Suárez-Romero, E. Hernandez-Gomez, Instituto Tecnológico de Querétaro (Mexico)

We report in this work the observation of changes in the difference of the phase delay of the parallel and perpendicular components of an optical beam when it is reflected by a metal surface which is altered with electric charge. A quasimonochromatic linearly polarized beam is directed to a piece of steel where it is reflected, the polarization of the reflected beam is in general elliptical. The module of each polarization component and their difference of phase are measured with an ellipsometer. The piece of metal is grounded for first measurements, when static charge is induced on the metal the phase delay of the components changes obtaining a rotation of the elliptical polarization.

The metallic surface is polished to obtain specular reflection only. The incidence angle is 75 grad approximately; this angle is the principal angle of incidence. The azimuthal angle of the incident beam is set such that a circularly polarized reflected beam is obtained. When the piece of steel is altered with static charge the circular polarization gets elliptical. Given that the module of the reflectance components of the material does not change the only way is a change in the phase of the reflectance components. An interesting application of this effect is the rotation of the polarization of a beam without a reduction of its intensity.

8129-24, Poster Session

Optical design for LED dental lighting with imaging optic technique

Y. Kwon, H. Lim, S. Bae, LED-IT Fusion Technology Research Ctr. (Korea, Republic of); J. Jang, Yeungnam Univ. (Korea, Republic of)

Because of a lot of merit, LED is started to replace halogen lamp in many illumination applications like as indoor lighting, outdoor lighting, automotive lighting and so on. Especially, LED has no heat radiation, more comfortable than halogen lamp as medical luminaire. There are some products to replace conventional halogen lamp in market already. But have issues of low efficiency and dim pattern boundary. For solve the problem, we developed LED dental lighting as this research.

We did a research as follows.

First of all, selected optimum LEDs and mixed it for higher CRI, target CCT and illuminance.

The following step is optical module design. Light directional characteristics of dental lighting must be concentrated to illuminate a part. Because This part is oral cavity, The feature of illumination pattern is rectangular. For uniformity of illuminance and clearer pattern boundary at reference distance, we designed it as direct type (no use reflector) by imaging optic technique. First, Image is rectangular feature, so object must be the same feature with magnification in general imaging optics. But the emitting surface feature of LED (1W grade) is square or circular generally. For that reason, made object as rectangular source with rectangular lightguide. This optical component was designed for higher efficiency by illumination optic technique. Next, we designed optical lenses based on imaging optic technique for image object feature using Code V. set to high NA for light efficiency in this design.. Fundamentally,

Conference 8129:
Novel Optical Systems Design and Optimization XIV

Finally, This product is luminaire so illumination simulation and result analysis were executed by LightTools as illumination design software.

8129-25, Poster Session

Broadband optical antenna with a disk structure

I. Wang, The Hong Kong Polytechnic Univ. (Hong Kong, China)

Broadband optical antennas are of interest as they can transmit more information like traditional microwave UWB antennas. This paper presents a design of broadband optical antennas with a concentric disk structure. An equivalent circuit for the optical antenna with a disk structure is introduced. The broadband radiation at optical frequencies was demonstrated via the computer simulation.

8129-28, Poster Session

Design and evaluation of wide field-of-view optical antenna

P. Deng, X. Yuan, Y. Zeng, M. Zhao, Huazhong Univ. of Science and Technology (China)

The free space optical communication systems should utilize optical antennas with beam tracking mechanisms. However, the narrow field of view and optical aberration of antennas degrade the tracking performance of the system. To overcome the problems, we investigate the wide field of view optical antenna technology. The optical antenna consists of fish eye lens, compensating lens and a 125 mm diameter catadioptrics telescope with off-axis aspheric surface mirrors. The structures and performances of the optical device elements are numerically analyzed so that their design can make positive contribution in enlarging the field of view and reducing the optical aberration. The optical antenna of free space optical communication has been optimum designed. The proposed optical antenna could not only provide a wide field of view with approximately 60 degree and expand the rang for tracking mechanism, but also mitigate the optical aberration and improve tracking accuracy for free space optical communication systems in turbulent atmosphere.

Conference 8130: Laser Beam Shaping XII

Sunday-Monday 21-22 August 2011 • Part of Proceedings of SPIE Vol. 8130 Laser Beam Shaping XII

8130-01, Session 1

Beam shaping in the MegaJoule laser project

J. Luce, Commissariat à l'Énergie Atomique (France)

The LMJ (Laser Mega-Joule) is dedicated to inertial confinement fusion. To perform this type of experiment, 160 square beams are frequency converted and focused into a target filled with a deuterium tritium mixture. This means to achieve 10^{15} W/cm² laser intensity at 351 nm per bundle of 4 beams. The laser architecture can be divided into 4 blocs: a fiber source featuring gaussian beam, E: 1nJ, λ : 1053nm, τ : 5ns; a pre-amplifier module (square beam, E: 1J); a four pass main amplifier boosters (E: 15kJ/beam) and then converting, focusing final optics (λ : 351nm, E: 8kJ/beam).

We propose to review the technics used to shape these beams along their propagation through the LMJ. Going upstream from the target to the laser source, specific optics are designed to meet the beam shaping requirement. A focusing grating and a pseudo-random phase concentrate the energy into the target. A deformable mirror controls and compensates the spatial phase defect occurring during the propagation through the main slab amplifiers. A liquid crystal cell shapes the beam in order to compensate the gain profile of the main amplifiers. It also protects the growth of damages that take place in the final chain optics. At last, a phase mirror shapes a square flat top mode from a gaussian beam within a regenerative amplifier.

All these optical components have one common principle: they control the phase of the laser field.

8130-02, Session 1

High peak power laser beam control with adaptive optics

A. V. Kudryashov, Active Optics NightN Ltd. (Russian Federation)

Some peculiarities of the use of adaptive optical elements and the whole system to correct for the aberrations of high power lasers are discussed in this paper. The examples of the use of adaptive system to correct for the aberrations of some high peak power TiS and glass lasers are presented. As a corrector we used bimorph multi electrode deformable mirror while as a sensor - Shack-Hartmann wavefront sensor.

8130-03, Session 1

Advances in MEMS deformable mirror technology for laser beam shaping applications

S. Cornelissen, P. Bierden, Boston Micromachines Corp. (United States)

Adaptive optics has made advances in the past years to move the technology into a broader range of applications and uses. This includes the extension of the technology from traditional astronomical and biological imaging systems to the fields of beam control for laser communication, laser machining and pulse shaping. In this talk I will describe ongoing work at Boston Micromachines and our collaborators in the field of micromachined deformable mirrors (DMs) for these applications. A MEMS mirror has been designed and fabricated for the use as a spatial and temporal shape controller for pulsed lasers. The design of the device, specifications, and potential applications of this device will be discussed. Also discussed will be the implementation of metric based control of wavefronts and the characteristics of MEMS devices required for high speed, high precision control.

8130-04, Session 1

Improve temporal contrast by cross-polarized wave generation at a sub-petawatt laser facility

N. Xie, W. Huang, X. Wang, L. Sun, Y. Guo, Q. Li, China Academy of Engineering Physics (China)

Temporal contrast is a key factor affecting the application of ultraintense and ultrashort pulse laser facilities. In this study, we attempt to improve temporal contrast for ultraintense and ultrashort pulses in a 300 TW laser facility by cross-polarized wave (XPW) generation, which is a new technique developed recently to improve temporal contrast for ultrashort pulses effectively. Preliminary experiments were carried out to study the XPW generation efficiency and the enhancement of temporal contrast in the front end system of the ultraintense and ultrashort laser facility, i.e. the super intense laser for experiment on the extremes (SILEX-I), with a wavelength of 800 nm. The results show that the relationships between the efficiency of cross-polarized wave generation and crystal orientation/input intensity are in good agreement with theoretical predictions. Prepulses and the amplified spontaneous emission (ASE) pedestal are suppressed significantly and the temporal contrast is improved by two orders of magnitude. Higher and stabler contrast should be obtained if the extinction ratio of the polarizer-analyzer pair and energy stability of input pulses are improved. To amplify the temporally cleaner pulses, a double chirped-pulse amplification (CPA) system is designed and output energy of 300 mJ will be achieved for the front end system.

8130-05, Session 2

Generation of pure TEM₀₀ modes using a friendly intra-cavity laser beam shaping technique

T. Godin, E. Cagniot, M. Fromager, Ecole Nationale Supérieure d'Ingenieurs de Caen et Ctr. de Recherche (France); N. Passilly, FEMTO-ST (France); M. Brunel, Univ. de Rouen (France); K. Ait-Ameur, Ecole Nationale Supérieure d'Ingenieurs de Caen et Ctr. de Recherche (France)

The authors present a variant of the Fox & Li method [1] performing intra-cavity laser beam shaping for resonators containing an arbitrary number of amplitude and phase diffractive optics. This one consists in modeling just a single round-trip as a cavity equivalent sequence, and then propagating the desired resonant field through it. Consequently, this new approach, which preserves the ease of implementation of the original method (equivalent sequence of lenses) while removing its main drawbacks (random starting field distribution and hundreds of round-trips), is workable within an optimization process (Adaptive Simulated Annealing) iterating upon the features of the cavity until the input and the output fields match as much as possible. As an illustration, the problem of forcing a laser to oscillate on a single high-order transverse mode, which is a challenge in today's research world [2], has been considered. In particular, from numerical simulation, we deduce a simple model for generating such modes with a pi-phase plate inserted into a plano-concave cavity. This model has been tested experimentally within an active cavity with a diode-pumped Nd:YVO₄ laser and an excellent agreement with numerical predictions has been found: a phase aperture located quite close to the concave mirror, and whose normalized radius κ is so that $2\kappa^2$ corresponds to a zero of a p-order Laguerre polynomial, was sufficient to generate single cylindrical TEM₀₀ modes ($p = 1, 2, 3$) as long as its radius is correctly chosen. The laser based the optimized features was perfectly stable, whatever the order of the generated mode [3].

[1] A. G. Fox and T. Li, Bell Syst.Tech. J. 40, 453-458 (1961).

[2] A. Hasnaoui et al., Opt. Commun., 284, 1331-1334 (2011).

[3] E. Cagniot et al., J. Opt. Soc. Am. A., to be published (2011).

8130-06, Session 2

Laser guide star elongation and distributed launch optics

K. J. Jones, WBAO Consultant Group (United States)

Laser beam shaping is particularly challenging with Laser Guide Stars (LGS) and large telescopes. In Adaptive Optics (AO), LGS elongation becomes significant with TMT (30 m) and E-ELT (42). It significantly reduces performance of Shack-Hartmann and curvature wavefront sensors. To determine the dimension of the laser source, we need to know: Na layer column abundance, centroid height, Na concentration and Na layer thickness. The LGS spot elongation is a function of the vertical sodium layer thickness and the orthogonal offset of the observer of the laser beam. R. Ragazzoni (2004) suggested that LGS elongation might be reduced by distribution of launch optics around the telescope primary or secondary, all beams focusing and combining at the required elevation of 93 km.

Although TMT and E-ELT deal with the same parameters with respect to AO LGS, they apply them differently. For TMT (B. Ellerbroek, 2010), there will be 6 laser guide star wavefront sensors. Both center and side launch configurations have been considered, but the former is preferred due to cost and current progress.

For E-ELT, LGS spot elongation was analyzed for over a year with nocturnal as well as seasonal NA variation. The orthogonal offset is 21 m. Assuming a laser of sufficient power, a telescope could observe at low latitudes for more than 250 days per year. Six laser guide stars and three natural guide stars are foreseen with the launch position at the edge of the aperture preferred. Elongation then depends on the sodium density profile.

Performance of the two telescopes will be compared for system complexity as well as anticipated performance.

8130-07, Session 2

Gaussian Content as a beam profile figure of merit of coherent beams

S. Ruschin, Tel Aviv Univ. (Israel); E. Yaakobi, E. Shekel, Civan Advanced Technologies Ltd. (Israel)

We report first experimental results demonstrating the conservation of the Gaussian Content (GC) [1] upon propagation, and its implementation as beam quality FOM. Basically the GC is defined by means of the closest approximation of a measured laser profile to a standard spherical-Gaussian beam, and explicitly is defined by the overlap integral between the measured beam profile and the optimal or "best fit" (BF) Gaussian. The GC appears to be of great relevance for applications where coherence is the main concern. Examples of such applications are coherent beam combing and coupling of a laser output to a single-mode optical fiber. The GC is limited to the range $0 \leq GC \leq 1$, and well-defined for any square-integrable function. One of the main properties of the GC is its preservation upon propagation in free-space or transmission through first-order (ABCD-type) optical elements. In this presentation we confirm experimentally that property: it is shown that a non-Gaussian laser beam, originating from a semiconductor source changes its shape significantly while propagating through the focal region yet the value of its GC remains almost unchanged. The determination of the GC requires as data acquisition 2-3 intensity profile scans around the focusing plane and an extra calculation step in order to retrieve the phase of measured beam. This was accomplished by means of a standard routine. Analysis, application cases and further experimental results will be presented.

[1] S. Ruschin and E. Shekel, "Proposal of Gaussian Content as a Laser Beam Quality Parameter" Submitted to Applied Optics.

8130-10, Session 2

Spatial and temporal shaping for large mode area fiber laser system

Y. Deng, China Academy of Engineering Physics (China)

With the development of high power laser technology, a focus density about 1022W/cm² can be achieved in laboratory, and scientists are aiming for much higher level. As fiber lasers have many advantages over the traditional solid state lasers, for example high efficiency, high reliable, high stability, low thermo effect and etc, high energy Peta Watt (PW) laser facilities will adopt fiber laser front end. In order to scale output energy of fiber laser system, it maybe comprise much amplification stage. Also the nonlinear effect such as SBS, SRS etc. will happened when the power is very high. For the purpose of reducing nonlinear effect still with high power and high energy, they adopt large mode area fiber amplifier. An increase of the core size and decrease of the NA in large mode area (LMA) double cladding fibers can substantially reduce the power density still with single transverse mode, which is beneficial to high power fiber laser systems. But when a seeded laser pulse was coupling into a large mode area fiber amplifier, the model noise will be found, which mostly caused by large mode area fiber's fabrication. And as there are much stage fiber amplification, the amplified spontaneous emission (ASE) will greatly depress laser pulses' signal to noise ratio (SNR). The low signal and noise ratio level of the fiber laser front end system has many disadvantages for PW laser facilities.

In order to suppress mode noise and to enhance pulses' SNR, we study the spatial and temporal shaping for large mode area fiber laser system. For spatial pulse shaping, we used method of mode area adapting to suppress mode noise. For purpose of temporal pulse shaping, a method of nonlinear polarization rotation caused by Optical Kerr effect in fiber was used. By spatial and temporal pulse shaping methods, cleared pulses with a strictly single mode in spatial and a cleaned pulse without ASE pedestal were obtained.

With the development of high power laser technology, a focus density about 1022W/cm² can be achieved in laboratory, and scientists are aiming for much higher level. As fiber lasers have many advantages over the traditional solid state lasers, for example high efficiency, high reliable, high stability, low thermo effect and etc, high energy Peta Watt (PW) laser facilities will adopt fiber laser front end. In order to scale output energy of fiber laser system, it maybe comprise much amplification stage. Also the nonlinear effect such as SBS, SRS etc. will happened when the power is very high. For the purpose to reducing nonlinear effect still with high power and high energy, they adopt large mode area fiber amplifier. An increase of the core size and decrease of the NA in large mode area (LMA) double cladding fibers can substantially reduce the power density still with single transverse mode, which is beneficial to high power fiber laser systems. But when a seeded laser pulse was coupling into a large mode area fiber amplifier, the model noise will be found, which mostly caused by large mode area fiber's fabrication. And as there are much stage fiber amplification, the amplified spontaneous emission (ASE) will greatly depress laser pulses' signal to noise ratio (SNR). The low signal and noise ratio level of the fiber laser front end system has many disadvantages for PW laser facilities.

In order to suppress mode noise and to enhance pulses' SNR, we study the spatial and temporal shaping for large mode area fiber laser system. For spatial pulse shaping, we used method of mode area adapting to suppress mode noise. For purpose of temporal pulse shaping, a method of nonlinear polarization rotation caused by Optical Kerr effect in fiber was used. By spatial and temporal pulse shaping methods, cleared pulses with a strictly single mode in spatial and a cleaned pulse without ASE pedestal were obtained.

8130-38, Session 2

Intra-cavity vortex beam generation

A. Forbes, CSIR National Laser Ctr. (South Africa) and Univ. of KwaZulu-Natal (South Africa); D. Naidoo, CSIR National Laser Ctr. (South Africa); K. Ait-Ameur, Ecole Nationale Supérieure d'Ingenieurs de Caen et Ctr. de Recherche (France)

No abstract available

8130-11, Session 3

Annular ring zoom system using two positive axicons

F. M. Dickey, FMD Consulting LLC (United States); J. D. Conner, U.S. Photonics Inc. (United States)

The production of an annular ring of light with a variable diameter has applications in laser material processing and machining, particle manipulation, and corneal surgery. This can readily be accomplished using a positive and negative axicon pair. However, negative axicons are very expensive and difficult to obtain with small diameters. In this paper, we present a design of an annular ring zoom system using two positive axicons. One axicon is placed a distance before a primary lens that is greater than some prescribed minimum, and the second axicon is placed after the primary lens. The position of the second axicon determines the ring diameter. The ring diameter can be zoomed from some maximum design size to a zero diameter ring (spot). Experimental results from a developmental system will be presented.

8130-12, Session 3

Evaluation of DMD-based high-precision beam shaping using sinusoidal-flat-top beam profile generation

J. Liang, R. N. Kohn, Jr., M. F. Becker, D. J. Heinzen, The Univ. of Texas at Austin (United States)

We evaluated system performance of a high-precision beam shaper using a digital micromirror device (DMD) as a binary-amplitude spatial light modulator followed by a telescope with an adjustable pinhole low-pass filter. Beam shaping quality was measured by comparing intensity and wave-front conformity to the target function, and by energy conversion efficiency. We demonstrated various flattop beam profiles with narrow spatial frequency content. For a raw camera image, we achieved 0.81-1.12% intensity root-mean-square (RMS) error and a nearly uniform wave front for both coherent and incoherent light sources of different visible and infrared wavelengths. Diffraction efficiency analysis determined optimized operation wavelength ranges for different orders. Experiments achieved 19.8% Gaussian-flattop power conversion efficiency using a 781 nm laser diode.

This paper extends beam-shaping experiments to target functions with arbitrary spatial frequency content. Analyses of intensity errors were conducted for output beam profiles consisting of pure sinusoids on a flattop beam. Pattern design errors were predicted by the spectral content of binary DMD patterns produced by an error diffusion algorithm. We also investigated the impact of input profile and pixel location on digitization error and estimated the best possible performance of iterative pattern refinement by numerical simulation.

In addition, sinusoidal-flattop profiles with different frequencies were chosen for system evaluation. As an example, experiments demonstrated 1.5-2% RMS error over a 1.23x1.23 mm² square region for a 0.66 mm period sinusoidal-flattop beam. We expect that the error of any target profile with band-limited spatial frequency content can be estimated by superposition of the single-frequency results.

8130-13, Session 3

Generation of flat top focusing with second order full Poincaré beams

W. Cheng, W. Han, Q. Zhan, Univ. of Dayton (United States)

Two-dimensional flattop beam shaping with spatially variant polarization can be obtained using Full Poincaré (FP) beams under low numerical aperture focusing condition. FP beams are a new class of beams that span the entire surface of Poincaré sphere. In this work, we report the flattop focusing with second order FP beams generated through linear combination of orthogonally polarized fundamental Gaussian (LG00) and second order Laguerre Gaussian (LG02) beams. The fundamental Gaussian produces a solid spot and the LG02 produces with a donut distribution around the x-polarized solid spot. One problem of using higher order LG beam is the larger dark center area of LG02 mode that causes ripples in the resultant profile of combination with fundamental Gaussian. This is solved by slightly defocusing the y-polarized LG02 beam with respect to the x-polarized component to axially separate the focal points of the two orthogonally polarized components. A preferred flat-top profile can be found at a position between the two focal points where the intensity and size of the two components are comparable. Due to the use of the second order FP beam, the edge roll-off is much steeper compared with the case of first order FP beam. The theoretical beta-value is calculated to be 5.88 and experimentally it is found to be 6.65 for an incident beam diameter of 7.0 mm. Another significant advantage is that this beam shaping technique is insensitive to the input beam size, which has been confirmed experimentally.

8130-14, Session 3

Synthetic design and integrated fabrication of multi-functional hybrid beam shapers

R. M. Kleindienst, R. Kampmann, S. Stoebenau, S. Sinzinger, Technische Univ. Ilmenau (Germany)

Novel applications in the fields of optical beam shaping, imaging and sensing require the implementation of more and more complex optical functions. In general for this purpose optical systems are modularly extended by adding conventional optical components. This approach automatically comes along with an increasing system size and weight as well as potentially higher assembly and maintenance costs. Hybrid optical freeform components can help to overcome this tradeoff. They merge several optical functions within fewer but more complex optical surfaces, e.g. elements comprising shallow refractive/reflective and high frequency diffractive structures. However, providing the flexibility and precision essential for their realization is one of the major challenges for both optical components design and fabrication.

In our contribution we present a reflective hybrid beam shaper offering beam deflection, transformation and splitting capabilities. Dividing our work into three main parts, we first report on the applied design, simulation and optimization methods. To synthesize the reflective basic shape, composed of a 90°-beam deflection, a Gaussian-to-tophat beam shaping function and an aberration controlled Fourier lens function, we used wave optical and ray tracing calculations respectively. Furthermore additional diffractive structures, realizing the beam splitting function, were optimized by rigorous computations. In the second part we present an integrated machining technique suitable for rapid prototyping as well as the fabrication of molding tools for low cost mass replication of this hybrid beam shaper. To produce the different feature sizes with an optical surface quality we successively combine mechanical machining modes with precisely aligned ps-laser ablation. In the concluding part the shape accuracy and surface quality are demonstrated with profilometric measurements and experimental investigations of the optical performance proving the applied fabrication methods and design-synthesis.

8130-15, Session 3

Experimental realization of high-efficiency switchable optical OAM state generator and transformer

Y. Li, J. Kim, M. J. Escuti, North Carolina State Univ. (United States)

We introduce a high efficiency method to control orbital angular momentum (OAM) state of light by using switchable q-plates and switchable forked polarization gratings (FPGs). We successfully fabricated both elements and realized fast electric-optical switchable controlling on OAM state, whereas the methods by previous works offered either fixed or slow modification. We recently introduced FPG with special photo-aligned liquid crystal architecture that modify Pancharatnam-Berry phase, as an highly efficient OAM state controller. Q-plate is another well known OAM state generator, which converts circularly polarized light into a fixed OAM state associated with its q charge. We now report on our experimental implementation of electrically switchable FPGs and switchable q-plates based on liquid crystal cell. The special designed anisotropy is obtained by photo-alignment and liquid crystal technology. For FPGs, high-quality patterning is achieved by polarization holography. In both elements, external electric field applied on the cell can fast switch the element between OAM generating (on) mode and transmissive (off) mode. The electric-optical behavior is characterized. Converting efficiency and switching time of both elements are measured. As compact optical elements, switchable q-plates and switchable FPGs are highly efficient and flexible. They are the ideal units to compose multistage OAM state controlling system, which could benefit a lot to the realization of extreme high capacity information applications, among many others.

8130-16, Session 4

Comparing flat top and Gaussian focal beam shapes when micromachining steel

T. E. Lizotte, O. P. Ohar, Hitachi Via Mechanics (USA), Inc. (United States)

Laser micromachining, drilling and marking is extensively used within the aerospace, automotive and firearms industries. The unique properties of lasers make them ideal tools for micromachining a wide diversity of materials, including steel alloys [1]. We describe the results of micromachining of low carbon steel and stainless steel alloys, using a high powered diode pumped solid state (DPSS) laser operating at a wavelength of 355nm. The laser was configured with beam conditioning optics to produce either a flat top beam or a Gaussian output which was then sent through a galvanometer scanner and telecentric lens beam delivery system. This paper outlines the interrelationship of process variables of both a flat top beam shape and Gaussian beam shape. Process variables measured included the optimum laser focus plane, energy density, pulse frequency, galvanometer scan rate, and number of pulses, pulse overlap and focal spot diameter. Optimum process performance was evaluated based on a statistical dimensional comparison of the micromachined features from each test coupon, including uniformity and surface roughness of the micromachined surface, the minimization of surface irregularities (stalagmite type slag / debris / corn row patterns) and taper angle of the micromachined feature side walls.

8130-17, Session 4

Laser beam shaping for studying thermally induced damage in diamond

B. N. Masina, Council for Scientific and Industrial Research (South Africa); A. Forbes, Council for Scientific and Industrial

Research (South Africa) and Univ. of KwaZulu-Natal (South Africa)

We outline the generation of shaped laser beams for the laser heating of industrial diamond. By shaping the pump light, we may customise the source term of the heat equation, and thereby generate custom thermal gradients across the diamond. In this paper we will present theoretical and experimental results on this subject, with the aim of controlled study of the thermal properties of diamond.

8130-18, Session 4

Reducing beam shaper alignment complexity: diagnostic techniques for alignment and tuning

T. E. Lizotte, Hitachi Via Mechanics (USA), Inc. (United States)

Safe and efficient optical alignment is a critical requirement for industrial laser systems used in a high volume manufacturing environment. Of specific interest is the development of techniques to align beam shaping optics within a beam line; having the ability to instantly verify by a qualitative means that each element is in its proper position as the beam shaper module is being aligned. There is a need to reduce these types of alignment techniques down to a level where even a newbie to optical alignment will be able to complete the task. Couple this alignment need with the fact that most laser system manufacturers ship their products worldwide and the introduction of a new set of variables including cultural and language barriers, makes this a top priority for manufacturers. Tools and methodologies for alignment of complex optical systems need to be able to cross these barriers to ensure the highest degree of up time and reduce the cost of maintenance on the production floor. Customers worldwide, who purchase production laser equipment, understand that the majority of costs to a manufacturing facility is spent on system maintenance and is typically the largest single controllable expenditure in a production plant. This desire to reduce costs is driving the trend these days towards predictive and proactive, not reactive maintenance of laser based optical beam delivery systems [1]. With proper diagnostic tools, laser system developers can develop proactive approaches to reduce system down time, safe guard operational performance and reduce premature or catastrophic optics failures. Obviously analytical data will provide quantifiable performance standards which are more precise than qualitative standards, but each have a role in determining overall optical system performance [1]. This paper will discuss the use of film and fluorescent mirror devices as diagnostic tools for beam shaper module alignment off line or in-situ. The paper will also provide an overview methodology showing how it is possible to reduce complex alignment directions into a simplified set of instructions. Two examples will be used including a UV DPSS laser and UV Excimer laser beam shaper alignment process.

8130-19, Session 4

Efficient laser ablation using beam shaping and beam splitting

R. S. Patel, J. Bovatsek, A. Tamhankar, Spectra-Physics®, a Newport Corp. Brand (United States)

Efficient use of the available energy from a laser source is important to achieve maximum material removal for the laser material processing applications. Especially, with availability of short pulse width high energy per pulse pulsed lasers it is necessary to deposit optimal amount of energy to achieve most efficient ablation and removal of material with minimal heat affected zone. While there are various ways one can deliver optimal amount of energy to the target material we have chosen beam shaping and beam splitting technique. We have shown that using beam shaping and beam splitting material removal efficiency can be improved. Experimental data for scribing Silicon and Sapphire in most efficient way is presented.

8130-21, Session 5

Diamond turning considerations for the manufacture of beam shaping optics

G. E. Davis, G. L. Herrit, A. R. Hedges, II-VI Infrared (United States)

Advances in diamond turning technology have offered optical engineers new degrees of freedom in the design of beam shaping optics. While designers have these new manufacturing methods at their disposal, they may not be aware of special process limitations that impact the cost and quality of components. The purpose of this paper is to present some of these critical manufacturing issues in the context of various beam shaping applications. We will discuss four key diamond turning technologies and the types of beam shaping optics that they are best-suited to produce. These technologies include the standard 2-axis diamond turning lathe, slow tool servo (STS) which introduces a programmable spindle position to the lathe, fast tool servo (FTS) which is a separate fast-acting limited-stroke axis, and diamond micromilling which incorporates an additional spindle that rotates a diamond end mill at very high speed. Within the discussion we will present various beam shaping applications, the associated optical surface shapes, and the process limitations involved with their production. In summary we will present this data in a matrix that will help the optical engineer design solutions that balance performance with manufacturability.

8130-22, Session 5

Diffraction beam shapers used for optical testing

K. J. Kanzler, JENOPTIK Optical Systems, Inc. (United States)

Diffraction beam shapers can be used to gather information about input laser beams. This paper will describe some techniques for using DOE beam shapers to characterize important parameters for TEM₀₀ mode laser beams. Parameters like beam diameter, ellipticity and M-squared will be reviewed. These beam shapers along with other DOEs can be used in real time to adjust input beam parameters for precision laser applications. Optical modeling simulations and real test data will be presented to demonstrate these techniques.

8130-37, Session 5

Spatial beam shaping for lowering the threshold energy for femtosecond laser pulse photodisruption

A. Hansen, T. Ripken, A. Heisterkamp, Laser Zentrum Hannover e.V. (Germany)

High precision femtosecond laser surgery is achieved by focusing femtosecond (fs) laser pulses in transparent tissues to create an optical breakdown and therefore a tissue dissection through photodisruption. For moving applications in ophthalmology from corneal or lenticular applications in the anterior eye to vitreal or retinal surgery in the posterior eye the applied pulse energy needs to be minimized in order to not harm the retina. However, the aberrations of the anterior eye elements cause a distortion of the wave front and consequently an increase in size of the irradiated area and a decrease in photon density in the focal volume. Therefore, higher pulse energy is required to still surpass the threshold irradiance. In this work, aberrations in an eye model consisting of a planoconvex lens for focusing and HEMA (2-hydroxyethyl-methacrylate) in a water cuvette as eye tissue were corrected with a deformable mirror in combination with a Hartmann-Shack-sensor. The influence of an adaptive optics aberration correction on the pulse energy required for photodisruption was investigated. A reduction of the threshold energy was shown in the aberration-corrected case and the spatial confinement

raises the irradiance at constant pulse energy. As less energy is required for photodisruption when correcting for wave front aberrations the potential risk of peripheral damage is reduced, especially for the retina during laser surgery in the posterior eye segment. This offers new possibilities for high precision fs-laser surgery in the treatment of several vitreal and retinal pathologies.

8130-20, Session 6

Imaging micro lens array beam integrator system design for fiber injection

T. E. Lizotte, Hitachi Via Mechanics (USA), Inc. (United States); F. M. Dickey, FMD Consulting LLC (United States)

This paper documents the design, analysis and testing of beam integrator systems for the investigation of the injection of a single mode laser into square and round fibers (two sizes each), and a rectangular fiber. This research focused on methods that could enhance the development of a uniform speckle pattern at the output end of the fiber, the injection systems are designed to fill the modes of the fiber (as much as practicable) and match the NA of the fiber. The designs for the square and rectangular fibers are based on lenslet array components available from off-the-shelf fabricators. It can be argued that the number of modes injected into the fiber is proportional to the number of lenslets in the input beam. Evaluation at the design phase leaned towards lenslet arrays with small lenslet sizes. However, diffraction limits how small the lenslet arrays can be. For this reason the final designs were configured using a micro lens array based imaging integrator approach. An overview and test results will be presented to evaluate the benefits and limitations of such fiber injection techniques.

8130-23, Session 6

Combination of a micro lens multi-spot generator with a galvanometer scanner for flexible parallel micromachining of silicon

M. Zimmermann, BLZ Bayerisches Laserzentrum GmbH (Germany) and Erlangen Graduate School in Advanced Optical Technologies (Germany); M. Schmidt, Friedrich-Alexander- Univ. Erlangen-Nürnberg (Germany) and BLZ Bayerisches Laserzentrum GmbH (Germany) and Erlangen Graduate School in Advanced Optical Technologies (Germany)

Multi focus optics are used for parallelizing production and for large-scale material processing. These elements split the beam into a periodic spot pattern with a defined grid and spot size. The challenge lies in the generation of a homogeneous envelope. Additionally the demand for flexible systems for an in-process changing of optical properties increases. Different components for multi spot generation like diffractive optical elements or micro lens arrays were investigated. Diffractive optical elements offer a lot of freedom in the generation of arbitrary intensity distributions. The disadvantage is the complex design of these elements, the limits regarding flexibility and the relatively cost-intensive production.

Within the paper we present the investigation of a micro lens array in a fly's eye condenser setup for the generation of homogeneous spot patterns. The multi spot generator is combined with a galvanometer scanner for forming an arbitrary shaped laser beam into a spot-, ring or arbitrary array pattern. We show the principal functionality of the multi-spot generator by using wave optical simulation and principles of Fourier optics. Furthermore constraints of this setup are demonstrated. The multi spot scanner is used for micro structuring of silicon on a polyimide with a nanosecond diode pumped solid state laser. The ablation rate and structure quality are compared to single spot processing.

8130-24, Session 6

Applying of refractive beam shapers in combination with laser scanning optics

A. V. Laskin, MolTech GmbH (Germany); V. V. Laskin, AdIOptica Optical Systems GmbH (Germany)

Combining the refractive beam shapers with laser scanning optics is often considered to realize various industrial laser technologies as well as techniques used in scientific and medical applications. Today the 2- and 3-axis galvo mirror scanners with F-theta, telecentric or other lenses as well as gantry systems are widely used in different applications like micromachining, solar cell manufacturing, welding, drilling holes and others which performance can be improved by applying of beam shaping optics. And due to their unique features, such as low output divergence, high transmittance as well as extended depth of field, the refractive field mappers provide a freedom in building an optimum optical system. There will be considered several optical layouts based on various refractive beam shapers piShaper to generate laser spots of uniform intensity which sizes span from several tens of microns to millimetres. Examples of real implementations will be presented as well.

8130-25, Poster Session

Strong reducing of the laser focal volume

T. Godin, Ecole Nationale Supérieure d'Ingenieurs de Caen et Ctr. de Recherche (France); S. S. Ngcobo, Council for Scientific and Industrial Research (South Africa); E. Cagniot, M. Fromager, Ecole Nationale Supérieure d'Ingenieurs de Caen et Ctr. de Recherche (France); A. Forbes, Council for Scientific and Industrial Research (South Africa)

Many applications of lasers seek nowadays for focal spots whose corresponding volume is getting smaller and smaller in order to ensure high spatial resolution. The latter is usually limited by the Rayleigh criterion. To go beyond the diffraction limit, is nowadays a subject under strong investigations, and this property is called as super-resolution which usually relates to the focusing of light into a spot having dimensions smaller than the diffraction limit. Our objective has been to develop a new method for obtaining super-resolution that we believe to be more efficient than existing methods. Indeed, we are able to decrease the focal volume by a factor of several hundred, when existing methods do not exceed few tenths. Another interesting feature of our method is the decoupling between transversal and longitudinal resolutions within the focal volume, contrary to Gaussian beams whose depth of field is proportional to the square of its beam-waist. The method that has been developed theoretically and experimentally is based on two steps: First, the laser is forced to oscillate on a high-order but single transversal mode TEM₀, which is secondly spatially beam-shaped thanks to a proper Diffractive Optical Element (DOE) that allocates the super-resolution feature. These results will provide a technological leap in the improvement of spatial resolution of many laser applications such as: 3-D laser prototyping, non-linear microscopy, micro and nano-processing of materials, optical tweezers, etc.

8130-26, Poster Session

Laser beam shaping and mode conversion using vortex phase structures

R. Soskind, West Windsor - Plainsboro High School South (United States); Y. G. Soskind, DHPC Technologies (United States)

In this paper, we present a novel technique for beam shaping and mode conversion of elliptical laser beams employing vortex phase elements. We show that a vortex phase element with topological charge $m=1$ can effectively transfer an elliptically shaped fundamental TEM₀₀ mode into

a TEM₀₁ mode. When used with a spatial light modulator, the proposed technique allows beam shape adjustments by applying electrical control signals. Compared to existing static mode conversion techniques, the presented technique may perform dynamic switching between the different laser modes. The developed technique may have several practical applications in the fields of photonics and laser optics, including beam splitters and interferometers, fiber lasers, high speed optical modulators, and optical tweezers.

8130-28, Poster Session

Properties of propagation-independent laser beams in the presence of obstructions

M. Soskind, West Windsor - Plainsboro High School South (United States); Y. G. Soskind, DHPC Technologies (United States)

In this paper, we discuss the properties of propagation-independent structured laser beams. We show the influence of different beam obstructions on the resulting structure of the beams. We present a reconstruction technique that, in spite of the remarkable self-healing properties of propagation-independent beams, allows us to define the size and shape of the obstructions encountered by the structured beam during propagation. The presented technique may have several practical applications in the fields of photonics and laser optics, including high resolution microscopy, optical information processing, and optical cryptography.

8130-30, Poster Session

Pulse stretcher based on multilayer volume holographic gratings

L. Guo, Shandong Univ. of Technology (China); A. Yan, Shanghai Institute of Optics and Fine Mechanics (China); S. Fu, Shandong Univ. of Technology (China); X. Liu, Shanghai Institute of Optics and Fine Mechanics (China); X. Ge, Shandong Univ. of Technology (China)

A system of multilayer volume holographic gratings (MVHG) is composed of multiple layers of volume holographic gratings separated by intermediate layers. As a novel diffraction elements, because of more free parameters, multilayer volume holographic gratings have become an ideal candidate for various promising technological applications such as optical interconnects, pulse shaping and optical filters

In this paper, a pulse stretcher system based on MVHGs is shown. The diffraction properties of the pulse stretcher under ultrashort pulse are investigated using the modified multilayer coupled wave theory. The spectral intensity distributions of the diffracted beam are calculated. The diffraction bandwidth, diffraction pulse duration and the total diffraction efficiency of the pulse stretcher are also analyzed. The pulse broadening is accomplished by adjusting the width of the intermediate layer of a system of MVHGs. The calculation results show that using this new pulse stretcher system to broaden pulse has many advantages: the efficiency of diffraction is high, the structure of stretcher is adjustable to vary the amount of temporal broadening of the light pulse, and the structure is also more compact than alternative approaches.

8130-31, Poster Session

Improvement of combining efficiency of coherent beam combination from phase-locked laser array by optimizing design of Dammann grating

B. Li, A. Yan, X. Lv, J. Sun, L. Liu, Shanghai Institute of Optics

and Fine Mechanics (China)

The output power from a single laser is typically limited by effects such as gain saturation, nonlinearities and optical facet damage. In recent years, much attention has been paid to coherent beam combination of laser arrays that can produce a laser with higher output power and brightness than that of individual lasers. With recent advances in beam combining technology, laser arrays are becoming a viable alternative for high power, high beam quality laser systems. Many researchers have studied beam combination in laser arrays using various techniques such as the Talbot cavity, structured mirrors, self-imaging resonator, active phase correction and phase gratings. However, there still exists the limitation that a significant percentage of energy resides in undesired sidelobes of the far field of phase-locked laser arrays. This unavoidably leads to a reduction of beam quality. Recently, Yan propose an efficient beam combining technique for coherent laser arrays that uses a phase plate and a conjugate Dammann grating (CDG) in the front and back focal plane of a Fourier lens, respectively. But the combining efficiency and the beam quality are not high in their experiment because of the design and fabricated errors of the phase grating.

In this paper, we demonstrated an efficient technique for optimizing design of Dammann gratings and highly improved combining efficiency of a coherent beam combination system from phase-locked laser array. The system uses a conjugate Dammann grating and a phase plate in the back and front focal plane of a Fourier lens. Using genetic algorithm, we optimized the Dammann grating and the corresponding phase plate. The combining efficiency and beam quality of the combined beam can be improved evidently. This will be valuable for obtaining high power and high beam quality laser beams.

8130-32, Poster Session

Comparison of the diffraction characteristics of continuous wave, ultrashort laser pulse and chirped ultrashort pulse diffracted by multi-layer reflection volume holographic gratings

A. Yan, J. Sun, Y. Zhou, Y. Zhi, L. Liu, Shanghai Institute of Optics and Fine Mechanics (China)

Volume holographic gratings (VHG) are of wide interest in many applications because of their properties of high diffraction efficiency, excellent wavelength selectivity and angular selectivity. Recently, because of more free parameters, multi-layer volume holographic gratings (MVHG) have become an ideal candidate for various promising technological applications such as optical interconnects, pulse shaping and optical filters. Therefore, a knowledge of the diffraction behaviors of such system would be very valuable for characterizing and optimizing such volume diffractive optical elements.

In this paper, we extend the coupled wave theory of multi-layer gratings to study the Bragg diffraction properties of continuous wave, ultrashort laser pulse and chirped ultrashort pulse, and present a systematically theoretical analysis on the spectrum distribution of the diffracted intensities, the diffraction bandwidth, and the total diffraction efficiency of a system of MRVHG. The system of MRVHG is composed of multiple layers of reflection VHG separated by intermediate layers. The comparisons of the diffraction characteristics for these beams are investigated. The analysis and observations of this paper will be valuable for the accurate analysis of the interaction of ultrashort optical pulses and a variety of periodic structures, facilitating the design and the investigation of novel optical devices based on multiple layers of MVHG.

8130-34, Poster Session

Optical design and modern optical device applied to laser beam shaping lens module

C. Tsai, Kun Shan Univ. (Taiwan); Y. Fang, Z. Chen, G. Huang, J. Huang, C. Lin, W. Li, National Kaohsiung First Univ. of Science and Technology (Taiwan)

The aim of this research is to analyze the difference size of laser spot diameter when the GRIN lens and the aspheric lens are employed in laser reshaping system, respectively. Two kinds of lens designs based on genetic algorithm (GA) optimization are presented in this research. One is composed of one spherical lens and one Grin lens, the other is composed of one spherical lens and one aspheric lens. Two proposal designs are analyzed to find out one the best result in laser shaping system. Traditionally optical optimization softwares which employ least damping square (LDS) method have their difficulties in dealing with flat top beam shaping process because it is neither well-defined as image optics nor non-image optics. The GA will help us find the fit coefficients of aspheric lens and the well GRIN profile to achieve the laser shaping requirement. In this research, two kinds of designs with the GA which has been comprehensively employed in many applications before, for symmetry system, are demonstrated to get the optimum laser shaping in the uniformity of flat top. The GA program will be written in macro language of Light Tool. The simulation results show that the GA is very useful for laser shaping optimization.

8130-35, Poster Session

The investigation of optical vortices and hexagonal patterns in three plane wave interference

L. Kreminska, C. L. Corder, J. Teten, The Univ. of Nebraska at Kearney (United States)

We demonstrated that optical vortices can be created by means of interference of three waves from a common laser source. Different intensity patterns can be generated starting from common two wave interference fringes up to regular hexagonal structures. The created vortices exist throughout the transition from two wave to complete three wave interference and have been shown to move along predictable lines in space under contrast perturbations. The law of conservation of topological charge was fulfilled for the interference of three waves.

8130-36, Poster Session

Dynamic parabolic optical lattice

A. Ruelas, S. López-Aguayo, J. C. Gutiérrez-Vega, Instituto Tecnológico y de Estudios Superiores de Monterrey (Mexico)

We introduce and discuss the shaping properties of a novel optical lattice that we call dynamic parabolic optical lattice (DPOL). While the transverse structure of the DPOL is characterized by a suitable superposition of parabolic nondiffracting beams with different transverse wave numbers, its longitudinal structure exhibits a controlled periodic modulation. We address the existence and the controlled stability of two-dimensional solitons in DPOLs and characterize its propagation. An efficient numerical method for constructing nondiffracting parabolic beams and DPOLs is presented as well.

Conference 8131: Optical System Alignment, Tolerancing, and Verification V

Sunday-Monday 21-22 August 2011 • Part of Proceedings of SPIE Vol. 8131
Optical System Alignment, Tolerancing, and Verification V

8131-01, Session 1

Reducing asymmetric imaging errors through selective assembly and tolerance desensitization

M. C. Funck, RWTH Aachen (Germany); P. Loosen, RWTH Aachen (Germany) and Fraunhofer-Institut für Lasertechnik (Germany)

Asymmetric imaging errors are frequently the main cause for tight tolerances and high demands on manufacture and assembly of optical systems. In order to increase robustness and reduce manufacturing cost a designer can include tolerance sensitivities in the optimization function in order to find insensitive designs. This procedure is commonly referred to as desensitization and a number of means to achieve this have been developed in the past using both global and local optimization methods. It can be frequently observed that desensitization redistributes sensitivities thereby reducing the sensitivity of very sensitive parameters but slightly increasing the sensitivity of formerly insensitive parameters. While using compensation to reduce some of the most sensitive parameters can have a positive impact on tolerance desensitization lateral compensation is often expensive to realize. Some of the complexity of alignment procedures and mechanical mounts can be alleviated by using selective assembly during series production. Selective assembly is based on measurements of components and subassemblies aiming at finding best matches prior to the assembly.

We investigate the potential of using tolerance desensitization in conjunction with selective assembly to reduce asymmetric errors in imaging optical systems. The investigations concentrate on strategies to find tolerance insensitive design forms under the presence of selective assembly compensators and the selection of suitable parameters for desensitization and measurement. Tolerancing for selective assembly and effects of production volume will be discussed.

8131-02, Session 1

Impact of tolerance accuracy to design desensitization

R. M. Bates, A. D. Greengard, FiveFocal LLC (United States)

Several methods have been demonstrated for desensitization of a lens design to manufacturing errors with the result of increased as-built performance at the expense of a slightly reduced nominal performance. A recent study demonstrated a targeted desensitization method tuned for the most sensitive lens parameters can greatly increase yield for a known set of manufacturing tolerances. The effectiveness of such a targeted desensitization relies on two key pieces of information; lens sensitivities - easily obtained through modeling software - and manufacturing tolerance distributions gleaned from accurate metrology over many samples. Targeted desensitization to known and unknown manufacturing tolerances is examined with case studies for a typical camera objective, LWIR imager, and miniature camera lens demonstrating the yield impact of using known tolerance distributions in design.

8131-03, Session 1

Tolerancing molded plastic optics

M. P. Schaub, Raytheon Missile Systems (United States)

Compared to glass optics, differences in the materials, configurations and manufacturing processes of molded plastic optics lead to differences in the approach to their design and analysis. This paper discusses

differences in tolerance analysis between molded plastic optic and conventional glass optic systems.

8131-04, Session 2

The sine condition as an alignment tool

M. B. Dubin, J. H. Burge, College of Optical Sciences, The Univ. of Arizona (United States)

The sine condition is typically thought of as a design tool. It can, however, be used to test the alignment of a system or used as a tool during alignment. The primary method for doing this is to look for linearly field dependant astigmatism. This aberration is a key indicator of the state of alignment. This test can be used as a final acceptance test, or in some cases, it can be used to determine the misalignment in the system. This paper presents the basic concept, an alternate way to think about how it works and some experimental results that demonstrate how it functions.

8131-05, Session 2

Laser system tolerancing and alignment techniques at the National Ignition Facility

S. C. Burkhart, Lawrence Livermore National Lab. (United States)

The National Ignition Facility (NIF) is the world's largest optical system, with over 14,000 large and small optics, positioned and aligned during commissioning, with a substantial fraction actively aligned each laser shot. The laser system was completed, with the first 192 beam participation shot on March 10, 2009. Designed for stockpile stewardship, inertial confinement fusion research, and basic high energy density science, the NIF is in full operation and conducting laser shots using 1.3MJ, 351nm, 20ns pulses to <1cm targets. A brief overview of the facility and it's status will be presented.

The beam-to-target alignment requirement is 50µm RMS for the 192 beam ensemble. In addition there are internal pointing and centering requirements in the laser to ensure beams stay within their allowed apertures. These top level requirements were distributed to design teams in a tolerance stack-up for installation, active alignment, vibration, and drift. To first order, these teams and their respective project phases comprise the mechanical design staff, precision survey and component placement, optical systems alignment commissioning, and active alignment systems. We will describe these phases, the tolerancing tools used, and the alignment methods employed to achieve the operational success achieved by NIF to date.

Target Diagnostic positioning and pointing has received intense attention by the NIF project in the past 2 years of operation. We will review the methods used to position and point X-ray and neutron imaging diagnostic fields of view to within 100µm of laser target, and plans for improved diagnostic alignment systems based upon precision survey and photogrammetry.

This work performed under the auspices of the U.S. Department of Energy by Lawrence Livermore National Laboratory under Contract DE-AC52-07NA27344.

8131-06, Session 2

Design, assembly, and testing of a photon Doppler velocimetry probe

R. M. Malone, National Security Technologies, LLC (United States)

Conference 8131:
Optical System Alignment, Tolerancing, and Verification V

States); M. E. Briggs, Los Alamos National Lab. (United States); B. Cata, E. P. Daykin, D. O. DeVore, D. L. Esquibel, D. K. Frayer, B. C. Frogget, National Security Technologies, LLC (United States); M. R. Furlanetto, Los Alamos National Lab. (United States); C. H. Gallegos, National Security Technologies, LLC (United States); D. B. Holtkamp, Los Alamos National Lab. (United States); M. I. Kaufman, K. D. McGillivray, National Security Technologies, LLC (United States); L. E. Primas, M. A. Shinas, Los Alamos National Lab. (United States)

A novel fiber-optic probe measures the velocity distribution of an imploding surface along many lines of sight. Reflected light from each spot on the surface is Doppler shifted with a small portion of this light propagating backwards through the launching fiber. The reflected light is mixed with a reference laser in a technique called Photon Doppler Velocimetry, providing continuous time records.

A matrix array of 56 single-mode fibers sends their light through a relay system consisting of three types of lenses. Seven sets of these relay lenses are grouped into a close-packed array allowing the interrogation of seven regions of interest. A six-faceted prism with a hole drilled into its center was used to direct the light beams into different regions. Several types of relay lens systems have been evaluated, including doublets and molded aspheric singlets. The optical design minimizes beam diameters and also provides excellent imaging capabilities. One of the fiber matrix arrays can be replaced by a coherent bundle. To minimize back reflections, this special bundle will have alternating rows of fibers to transmit or receive light.

The close-packed array of seven relay systems provides 392 beam trajectories. The pyramid prism has its six facets polished at two different angles varying the density of surface point coverage. The fiber matrix arrays are angle polished at 8° to minimize back reflections. This causes the minimum beam waist to vary along different trajectories. Precision metrology on the direction cosines trajectories is measured to satisfy environmental requirements for vibration and temperature.

8131-07, Session 2

Using point source microscope (PSM) to find conjugates and assist in alignment of elliptical and parabolic off-axis mirrors

M. B. Borden, R. E. Parks, College of Optical Sciences, The Univ. of Arizona (United States)

Though the Point Source Microscope (PSM) is primarily an alignment instrument, it can also be used to determine the conjugates of elliptical and parabolic off-axis mirrors. With the PSM mounted to an XYZ stage and the mirror placed approximately at either the sagittal or tangential focus, the PSM can be adjusted to the exact focus of the mirror. To minimize spot size as well as coma, the aperture of the mirror is reduced by using a mirror covering with a hole in it. Determining the appropriate hole sizing is discussed in further detail in this publication. With the PSM positioned at optimal focus, a laser range finder is then used to determine the exact conjugate distance of the mirror. This is accomplished by positioning the back surface of the range finder at the cat's eye location (focus of the PSM's objective lens) of the PSM. As the range finder measures distances from its back surface, the distance acquired is the conjugate of the mirror. The same procedure is then repeated for the other conjugate. Using the foci of these two conjugates, the sagittal and tangential radii of curvature (R_s and R_t) can be calculated. These values can then be used to find the distance from the mirror vertex to the optical axis (h) as well as the vertex radius (R_v). This information is to be used to aid in the positioning of the mirror in an optical system.

8131-08, Session 3

Achieving tolerances in an intolerant world: telephoto contact lenses and other unconventional imaging systems

J. Ford, E. J. Tremblay, Univ. of California, San Diego (United States)

Optical system design is always constrained by achievable fabrication tolerances, and there is a constant balance between design performance and the cost or yield of the fabrication process. However, many of the best designs are achieved by starting from the manufacturing platform, and modifying the basic structure of the system to take maximum advantage of symmetries in the system. We will describe several optical systems whose symmetries have allowed us to bypass some of the more problematic tolerances. The first is a multi-reflection imaging system using concentric aspheric mirrors, diamond turned into a single optical element, which allowed us to create a 3x magnification Galilean telescope just 1 mm thick, designed to be incorporated into a contact lens as a vision aid. The second system is a multi-scale lens design which explores a different type of symmetry: a bilateral moncentric primary lens, followed by over 200 identical secondary optics, which together form an aggregate 2000 megapixel imager. And the third system is a non-imaging solar concentrator using micro-optic lenslets and micro-reflectors which couple incident sunlight into a slab waveguide, where the problem of aligning the lenslets to the micro-reflectors has been bypassed by using the focal spot from each lenslet to form (or reveal) its corresponding injection feature.

8131-09, Session 3

Tolerancing considerations for visual systems

J. Schwiegerling, The Univ. of Arizona (United States)

The eye is often the final detector in imaging systems. Here we examine some of the aspects of the eye and the human visual system and see how they relate to the overall performance of the optical system. Tolerances on MTF and chromatic aberration are explored.

8131-10, Session 3

Orthogonal polynomials and tolerancing

J. R. Rogers, Synopsys, Inc. (United States)

Previous papers have established the inadvisability of applying tolerances directly to power-series aspheric coefficients. The problem is a low correlation between any one coefficient and optical quality. The reason is that the individual terms are not orthogonal, so an error in one coefficient can be almost completely balanced by appropriate changes in the other coefficients. If only one coefficient differs from its nominal target, then the difference may be regarded as an error, and one can consider applying a tolerance to it. However, when multiple coefficients depart from their nominal values, then it is no longer known that the departures of the coefficients from nominal are actually "errors"; in fact, the departures might be what is necessary to optimally balance the departures of other coefficients. In such a case it is not appropriate to restrict the departure of each individual term from its nominal value.

Zernike surfaces and the new Forbes surface types have certain orthogonality properties over the circle described by the "normalization radius." This suggests that one could apply tolerances directly to the coefficients of such surface types, at least for surfaces close to the aperture stop. However, at surfaces away from the stop, the optical beam is smaller than the surface, and the aspheric terms are not orthogonal over the area sampled by the beam. It is unclear what problems this causes.

In this paper, we investigate the breakdown of orthogonality as the surface moves away from the aperture stop, and the implications of this to tolerancing.

Conference 8131:
Optical System Alignment, Tolerancing, and Verification V

8131-11, Session 3

Systems modeling and optical verification of a proposed infrared telescope

R. S. Upton, M. W. Noble, National Solar Observatory (United States)

A multi-level optical systems modeling and verification strategy for a space-based infra-red telescope is presented. The level of optical systems modeling is directly related to the number and complexity of the model inputs, and the type of wavefront sensing and focus control simulated during telescope testing and operations. The modeling inputs include residual surface polishing error, thermal print through, mirror rigid body misalignments, and secondary mirror actuator step error. The outputs of the model include coherent PSF effects such as those arising from manufacturing errors, and incoherent effects, such as those arising from the jitter errors of the telescope and space-craft pointing. The optical modeling strategy is encapsulated in MATLAB and ZEMAX as stand-alone applications at the least complex optical model, and then as DDE actively connected packages for the most complex model. The optical modeling is used at the Applied Physics Laboratory to directly support optical systems development, engineering information quality, and system validation guidance.

8131-12, Session 4

Maintaining hexapod range while co-pointing the Large Binocular Telescope

A. Rakich, Large Binocular Telescope Observatory (United States)

The Large Binocular Telescope on Mt Graham in Arizona consists of two 8.4 m telescopes mounted on a common gimbal. Each independent telescope has hexapods controlling the position of individual optical elements. These can be used to drive each telescope to point to a common target (or known offsets to these) as is required for many of the observational modes of the telescope. The hexapods have a limited range of travel, particularly the primary mirror hexapods. This paper discusses the approach that has been taken to achieve optical co-pointing while maintaining the maximum possible range of travel in the hexapods.

The approach described here is, starting with collimated but not co-pointed telescopes, to first calculate a coma-free rotation of the optical elements that will equalize the percentage consumption of range on pairs of hexapod elements that effect (X,Y) pointing; i.e. (X,ry) and (Y,rx) respectively. On a collimated telescope this results in a state which maximizes the available range of travel of the hexapods for a given set of initial hexapod values. Next a further calculation step is taken which achieves optical co-pointing. This step takes into account what range of travel is available for each hexapod for the given "range-balanced" starting point, then allocates a percentage of the required optical co-pointing to each telescope so as to minimize the maximum departure from range-balance on each side.

This technique has been applied successfully to both the prime-focus and "bent-Gregorian" modes of the telescope.

8131-13, Session 4

LIDAR metrology for prescription characterization and alignment of large mirrors

B. H. Eegholm, Sigma Space Corp. (United States); W. L. Eichhorn, NASA Goddard Space Flight Ctr. (United States); R. J. von Handorf, Ball Aerospace & Technologies Corp. (United States); J. E. Hayden, Sigma Space Corp. (United States); R. G. Ohl, NASA Goddard Space Flight Ctr. (United States); G. W.

Wenzel, QinetiQ North America (United States)

We describe the use of LIDAR, or "laser radar," as a fast, accurate, and non-contact tool for the measurement of the radius of curvature (RoC) of large mirrors. We report the results of a demonstration of this concept using a commercial laser radar system. We measured the RoC of a 1.4m x 1m aperture, spherical mirror with a nominal RoC of 4600 mm with a manufacturing tolerance of +/- 6mm. The rectangular aperture of the mirror is related to its role as ground support equipment used in the test of part of the James Webb Space Telescope (JWST). The RoC of such a large mirror is not easily measured without contacting the surface. From a position near the center of curvature of the mirror, the LIDAR scanned the mirror surface, sampling it with 1 point per 3.5 cm². The measurement consisted of 3983 points and lasted only a few minutes. The laser radar uses the LIDAR signal to provide range, and encoder information from angular azimuth and elevation rotation stages to provide the spherical coordinates of a given point. A best fit to a sphere of the measured points was performed. The resulting RoC was within 20 ppm of the nominal RoC, also showing good agreement with the results of a laser tracker-based, contact metrology. This paper also discusses parameters such as test set alignment, scan density, and optical surface type, as well as future possible application for full prescription characterization of aspherical mirrors, including radius, conic, off-axis distance, and aperture.

8131-14, Session 4

Pupil alignment considerations for large deployable space telescopes

B. J. Bos, R. G. Ohl, NASA Goddard Space Flight Ctr. (United States)

For many optical systems the properties and alignment of the internal apertures and pupils are not critical or controlled with high precision during optical system design, fabrication or assembly. In wide angle imaging systems, for instance, the entrance pupil position and orientation is typically unconstrained and varies over the system's field of view in order to optimize image quality. Aperture and pupil tolerances typically do not receive the same amount of scrutiny as optical surface aberrations or throughput characteristics because performance degradation is typically graceful with misalignment, generally only causing a slight reduction in system sensitivity near the edges of an instrument's field of view due to vignetting. But for a large deployable space-based observatory like the James Webb Space Telescope (JWST), we have found that pupil alignment is a key parameter. For in addition to vignetting, JWST pupil errors cause uncertainty in the wavefront sensing process that is used to construct the observatory on-orbit. Furthermore they also open stray light paths that degrade the science return from some of the telescope's instrument channels. In response to these consequences, we have developed several pupil measurement techniques for the cryogenic vacuum test where JWST science instrument pupil alignment is verified. These approaches use pupil alignment references within the JWST science instruments; pupil imaging lenses in three science instrument channels; and a unique pupil characterization mechanism in the optical test equipment. This allows us to verify the lateral pupil alignment of the JWST science instruments to approximately 1-2% of their pupil diameters.

8131-15, Session 4

Stray light in PICARD SODISM instrument: design, check, flight results, and alignment issues

P. Etcheto, Ctr. National d'Études Spatiales (France); M. Mireille, M. M. Meftah, G. Thuillier, Lab. Atmosphères, Milieux, Observations Spatiales (France); P. Assus, Observatoire de la Côte d'Azur (France)

Conference 8131:
Optical System Alignment, Tolerancing, and Verification V

The PICARD satellite, dedicated to the monitoring of solar activity, includes several imaging and radiometric instruments. One of them, SODISM, is a high resolution radio-imaging telescope measuring the Sun diameter and total flux in near UV and visible wavelengths. Besides its mirrors, it includes highly reflective components which generate ghost images, disturbing both the Sun edge area and the aiming channel. The Sun aiming sensor is also disturbed by stray light. These effects are compound by tilt tolerances, which shift the ghosts from the nominal image.

The stray light study was performed through ASAP modelling, based on measured components, broad source incoherent ray tracing and multiple splits, since some high order ghosts were significant while the primary ghosts were blocked. Each path was studied separately, checking its effect on instrument performance and the possible effect of tilts. The most critical ones could be reduced by design improvements, while some relatively intense ghosts proved tolerable due to their location and shape.

These improvements were implemented on the flight model. Ground tests and flight results show some residual ghosts, which could not be fully suppressed due to mechanical tolerances. They shall be taken into account by image processing.

8131-25, Session 4

Alignment and testing of the NIRSpec filter and grating wheel assembly

T. Leikert, Carl Zeiss Optronics GmbH (Germany)

In order to perform spectrometric measurements, the Near Infrared Spectrometer (NIRSpec) aboard the James Webb Space Telescope (JWST) needs the ability to select various spectral band widths and split these up into its comprised wavelengths. These functions are achieved by the Filter Wheel Assembly (FWA) and the Grating Wheel Assembly (GWA). The filters of the FWA select a different bandwidth of the spectrum each while the gratings on the GWA yield specific diffractive characteristic for spectral segmentation. A high spectral sensitivity as well as the ability to detect the spectra of various objects at the same time result in high requirements regarding the positioning accuracy of the optics of both mechanisms in order to link the detected spectra to the 2-dimensional images of the observed objects.

The NIRSpec mechanism including FWA and GWA will operate at temperature levels below 42K which are established during testing inside of a cryostat. However the alignment and testing of these mechanisms requires a lot of thought since there is very limited access to the item under test within such a device. Alignment needs to be preloaded based on simulations and testing is reduced to optical methods and evaluation of electrical signals.

This paper describes the methods used for the various alignment steps, the corresponding tests and their precision of measurement as well as the achieved accuracies in the mechanism performance.

8131-16, Poster Session

Alignment estimation performances of merit function regression with differential wavefront sampling in multiple design configuration optimization

E. Oh, Yonsei Univ. (Korea, Republic of) and Korea Ocean Research & Development Institute (Korea, Republic of); S. Kim, Yonsei Univ. (Korea, Republic of)

In our earlier study, we suggested a new method called Multiple Design Configuration Optimization ('MDCO' hereafter) method that combines the merit function regression (MFR) computation with the differential wavefront sampling method. In this study, we report alignment state estimation performances of the method while applying it to three target optical systems. They are i) a two-mirror Cassegrain telescope of

58mm in diameter for deep space earth observation, ii) a three-mirror anastigmat of 210mm in aperture for ocean monitoring from the geostationary orbit, and iii) on-axis/off-axis pairs of a extremely large telescope of 27.4m in aperture. First we introduced known amounts of alignment state disturbances to the target optical system elements. Example alignment parameter ranges may include, but not limited to, from 800microns to 10mm in decenter, and from 0.1 to 1.0 degree in tilt. We then ran alignment state estimation simulation using MDCO, MFR and DWS. The simulation results show that MDCO yields much better estimation performance than MFR and DWS over the alignment disturbance level of up to 150 times larger than the required tolerances. In particular, with its requirement of single field measurement, MDCO exhibits greater practicality and application potentials in shop floor optical testing environment.

8131-17, Poster Session

A multi-objective approach in the optimization of optical systems taking into account tolerancing

B. Fonseca Carneiro de Albuquerque, Instituto Nacional de Pesquisas Espaciais (Brazil); L. Liao, J. Sasián, College of Optical Sciences, The Univ. of Arizona (United States)

In this paper we propose the use of a Multi-Objective approach for the lens design optimization problem. In this novel way of treating the problem, we will look and optimize at the same time the image quality and the system tolerancing, but different from the published methods we don't combine both criteria in a single merit function. As a result we get a set of non-dominated solutions that generates the Pareto Front. This method gives better insights about the available trade off solutions for the problem. The Multi-objective optimization can be easily implemented with evolutionary methods of optimization, which has been applied in the problem of lens design with good results.

8131-18, Poster Session

A case study for cost-effective lens barrel design

M. Saayman, Denel Dynamics (South Africa); J. H. Burge, College of Optical Sciences, The Univ. of Arizona (United States)

A case study is presented to illustrate some of the cost-driving trade-offs involved in optomechanical systems design, where simple lens barrels are concerned. We examine two different lens barrel designs for a double Gauss lens, and compare them in terms of cost, manufacturability, and performance. We show that the cost and turnaround time can differ significantly between the two approaches. We also show how the optomechanical tolerances (axial spacing, element decenter, and element tilt) are realized in each design, in order to satisfy the optical performance requirements.

8131-19, Poster Session

Statistical truths of tolerance assignment in optical design

R. N. Youngworth, Light Capture, Inc. (United States)

The process of assigning tolerances to optical designs is intrinsically statistical, regardless of volume. Papers covering the statistics of tolerancing, however, have been infrequent. This paper will discuss a number of probabilistic nature of tolerancing that all optical designers and engineers should understand.

Conference 8131:
Optical System Alignment, Tolerancing, and Verification V

8131-20, Poster Session

Use of geometric dimensioning and tolerancing for precision optical assemblies

C. L. Hopkins, J. H. Burge, College of Optical Sciences, The Univ. of Arizona (United States)

Design metrics such as wavefront error and RMS spot size can be of great importance in evaluating an optical system. However, they don't mean much at the component level especially in the fabrication of hardware for mounting optics. Machinists and inspectors rely on the proper application of Geometric Dimensioning & Tolerancing (GD&T) to evaluate the quality of their work. This paper will examine techniques for selecting component level tolerances and geometric controls which can be communicated to the parts fabricator by analyzing their impact on system performance.

The process presented is based on a generic optical system with a given set of image quality metrics. First, raytrace software is used to determine position and orientation requirements for each optical component. Next, solid models of several approaches are generated for mounting the optics and various methods of geometric control are applied to each approach. Tolerances are chosen based on a statistical 3-D tolerance analysis of the solid model configuration such that position or orientation requirements are met. Each mounting approach and GD&T scheme is then evaluated based on manufacturability.

Using this technique, the optomechanical design engineer will be able to associate individual part manufacturing tolerances to over-all system performance. Geometric Dimensioning & Tolerancing will be in accordance with ASME Y14.5M.

8131-21, Poster Session

Low uncertainty alignment using computer generated holograms

M. B. Dubin, L. Coyle, College of Optical Sciences, The Univ. of Arizona (United States)

The Wide Field Corrector for the Hobby Eberly Telescope is a four mirror corrector that is designed to work with a spherical primary. Because of the required performance, the alignment tolerances on the mirrors are tight. In addition, the amount of aberration in the corrector makes it very difficult to align the mirrors optically. To accomplish this alignment task, a new approach has been developed to sense the misalignment of the mirrors. Computer generated holograms are aligned to the axis of the mirrors and then these holograms are aligned to each other. This paper presents the basic concept, how it will be implemented in the Wide Field Corrector and experimental results showing what the level of uncertainty is.

8131-22, Poster Session

Thin profile solar concentrators with high angular tolerance using wedge prism and diffractive gratings

T. Waritanant, National Central Univ. (Taiwan); S. Boonruang, National Science and Technology Development Agency (Thailand); T. Chung, National Central Univ. (Taiwan)

A novel design of thin profile solar concentrators with large angular tolerance is proposed comprising of a wedge prism and diffractive gratings which concentrate a broad solar spectrum up to 500 nm (from 400 to 900 nm). The design utilizes two different diffractive gratings. Transmission grating fabricated on top of the wedge prism operates on shorter wavelengths of the solar spectrum while reflection grating fabricated under the wedge prism operates on longer wavelengths. The diffracted light rays from each grating that satisfy total internal

reflection (TIR) condition within the wedge prism are then guided through to the collection surface of the wedge prism. Both gratings are blazed with different angles to ensure that the power of the diffracted light is concentrated in one direction. The simulation model of this design is constructed using Coupled Wave Analysis (RCWA) for the calculation of each grating's diffraction efficiency and geometrical optics calculation for the tracing of each ray produced by grating diffractions and surface refractions. The results from simulation model show maximum collection efficiency of more than 53% and maximum concentration ratio of 3.7. Large angular tolerance is achieved with full width at half maximum of collection efficiency for different incident angles being 106 degrees and 19 degrees on each plane of incident. This characteristic of the design reduces the need of precise alignment and tracking system requires by most commercially available solar concentrators.

8131-23, Poster Session

Mercury Imaging X-ray Spectrometer (MIXS) in BepiColombo mission: environmental tests

M. Pajas, Instituto Nacional de Técnica Aeroespacial (Spain)

The Mercury Imaging X-ray Spectrometer (MIXS) onboard ESA's mission BepiColombo to Mercury will measure X-rays emitted from the surface and the magnetosphere.

BepiColombo will journey to Mercury during a 6 years long cruise. It will enter in orbit around Mercury in 2020, starting an observational programme planned for at least 2 years, with 2 dedicated spacecraft:

Mercury Planetary Orbiter (MPO), built by ESA,

Mercury Magnetospheric Orbiter (MMO), provided by JAXA in collaboration with ESA.

One of the main instruments of the BepiColombo mission will be the "Mercury Imaging X-ray Spectrometer" (MIXS), with its complementary instrument "Solar Intensity X-ray and particle Spectrometer" (SIXS). MIXS+SIXS will allow to map the chemical composition of the Mercury surface with a large spatial resolution (few tens of km).

MIXS is being developed by a European Consortium led by University of Leicester (UL).

INTA-CAB is responsible for the Spanish contribution to MIXS.

The INTA facilities are being used to perform the complete qualification of MIXS at instrument level. The qualification will be very critical, due to the harsh environment around Mercury, the lack of redundancy and the long cruise phase (6 years) required to arrive to the final orbit around Mercury.

The testing activities at INTA are performed following the requirements indicated in the ESA EID-A, and include:

- Mechanical vibration.
- Thermal vacuum cycling.
- Electromagnetic Compatibility.

Functional tests of the FM and FS models will be performed before, during and after each of the tests, by using a radioactive source illuminating the detectors.

8131-24, Poster Session

The alignment of the Cassegrain telescope primary mirror and iso-static mount by using CMM

W. C. Lin, S. Chang, Instrument Technology Research Ctr. (Taiwan)

In order to meet both optical performance and structural stiffness requirements of the Cassegrain telescope, the primary mirror shall be mounted with the main plate by iso-static mount and the secondary mirror shall be hold and fixed by the truss structure. This article describes of the alignment of the Cassegrain telescope primary mirror and iso-

Conference 8131:
Optical System Alignment, Tolerancing, and Verification V

static mount by using coordinate-measuring machine(CMM), and the design and assembly of mechanical ground support equipment(MGSE). The primary mirror adjusting MGSE consists of three X,Y,Z linear stages and point contact platforms, which hold the mirror while avoid the rotated movement when adjusting the stage. This MGSE provide the adjustment of tilt and height for the mirror. After the CMM measurement, the coordinates of measured point on the mirror will be analyzed by the software based on least square fitting to find the radius of curvature, conic constant, decenter and tilt, etc. According to these results, the mirror posture will be adjusted to reduce the decenter and tilt by the designed MGSE. The tilt in X and Y direction are reduced within 0.02 degrees and the distance deviation from the best fitted profile of the mirror to the main plate shall be less than 0.015mm .

Conference 8132: Time and Frequency Metrology III

Wednesday–Thursday 24–25 August 2011 • Part of Proceedings of SPIE Vol. 8132 Time and Frequency Metrology III

8132-01, Session 1

Precision spectroscopy on atomic hydrogen and its influence on fundamental constants

C. G. Parthey, A. N. Matveev, J. Alnis, A. Beyer, R. Pohl, K. Predehl, N. N. Kolachevsky, T. Udem, T. W. Hänsch, Max-Planck-Institut für Quantenoptik (Germany)

For the last five decades precision spectroscopy on atomic hydrogen along with hydrogen's calculable atomic structure have been fueling the development and testing of quantum electro-dynamics (QED) and have led to the precise determination of the Rydberg constant and the proton charge radius. Furthermore, the outstanding precision in measuring the 1S-2S transition has been used to set limits on a possible variation of fundamental constants and violation of Lorentz boost invariance. It promises a stringent test of the charge conjugation/parity/time reversal (CPT) theorem by comparison with the same transition in antihydrogen.

Two recent measurements of the 1S-2S transition in atomic hydrogen have pushed the accuracy below the $1e-14$ level for the first time. For one of these measurements we have used the world's longest dedicated optical fiber link (900 km) to phase-coherently connect the hydrogen frequency to a remote cesium fountain clock. The results can be used to set new limits on a possible Lorentz boost invariance violation.

A recent measurement of the Lamb shift in muonic hydrogen by R. Pohl et al. has allowed to determine the proton charge radius with ten times higher accuracy as before. However, the obtained value differs by five standard deviations from the proton charge radius obtained from ordinary hydrogen. The discrepancy hints to a problem in either theory or experiment. We hope to contribute to the resolution by providing additional experimental input to the adjustment calculations which are used to determine the proton charge radius and the Rydberg constant.

8132-02, Session 1

Fiber-based frequency combs with relative frequency stability of 10⁻²⁰-level

H. Inaba, Y. Nakajima, K. Iwakuni, K. Hosaka, A. Onae, M. Yasuda, D. Akamatsu, F. Hong, National Institute of Advanced Industrial Science and Technology (Japan)

Fiber-based frequency comb (fiber-comb) is an indispensable tool in the field of optical frequency standard and metrology. Broad control bandwidth of the carrier-envelope offset frequency (fCEO) and the repetition rate (frep) are required if we are to reduce the comb mode linewidth. High-speed control of the fCEO can be achieved by varying the pump power in the mode-locked fiber laser. High-speed control of the cavity length (frep) control has also been achieved by varying the effective optical length of the laser cavity using an intra-cavity electro-optic modulator (EOM). We have reported fiber-combs with relative frequency stability of 10^{-19} level and relative linewidth of 10 mHz level. Although the relative stability and linewidth of the fiber comb exceed the uncertainty of present optical clocks, the margin of the stability and the linewidth is not sufficiently large. Therefore, in this study, we have tried to improve the relative frequency stability of the combs. Especially, we employ a mode-locked erbium-doped fiber laser with an intra-cavity wave-guide EOM as a comb source in order to improve the robustness. We also reduce the number of the optical amplifier branches in the comb system to diminish the fiber noise. We were able to obtain the servo bandwidth of approximately 1.4 MHz (for cavity length control) and 400 kHz (for fCEO control). Beat frequencies between two independent combs locked to a common 1064 nm reference laser (out-of-loop beat) were measured at several wavelengths. Consequently, relative frequency stability of 10^{-20} -level has been observed at 10 000-s averaging time.

8132-03, Session 1

High harmonic generation in VUV via passive enhancement of near infrared femto-second pulses

K. Wakui, K. Hayasaka, T. Ido, National Institute of Information and Communications Technology (Japan)

VUV with a high repetition rate is obtained via the high harmonic generation method using a passive enhancement cavity for NIR femto-second pulses. An interesting application of such quasi-cw VUV would be directly probing VUV transitions for optical clocks.

Our Ti:S oscillator generates NIR pulses whose repetition rate, bandwidth, and averaging intensity are 112MHz, 20nm, and 850mW, respectively. The passive enhancement cavity is made of six mirrors and a high NIR reflector with grating structure for VUV. Xenon gas was used as the nonlinear media. The average intensity of the outcoupled 5th harmonic (159nm) was measured to be 1.5uW.

8132-04, Session 1

VUV frequency combs and limitations of intracavity high-harmonic generation due to plasma dynamics

R. J. Jones, D. R. Carlson, J. Mongelli, E. M. Wright, College of Optical Sciences, The Univ. of Arizona (United States)

The dynamic intracavity ionization of a dilute gas target can substantially alter the pulse formation inside resonant fs enhancement cavities. We numerically and experimentally study these effects and how they affect intracavity high harmonic generation.

8132-05, Session 2

Precision measurements and advanced laser systems for applications on Earth and in space

A. Peters, Humboldt-Univ. zu Berlin (Germany) and Ferdinand-Braun-Institut (Germany)

This talk will present an overview of the activities of the Optical Metrology group at the Humboldt University Berlin. These include optical tests of the foundations of special relativity and matter wave experiments in gravitational physics, which are performed in terrestrial laboratories as well as in microgravity environments (drop tower, upcoming space missions). A special focus will be on novel, hybrid integrated laser systems which have been developed at the Ferdinand-Braun-Institut specifically for such precision measurement applications.

8132-07, Session 2

Overcoming the quantum projection noise (QPN) limit without preparation of the spin-squeezed state

N. Shiga, National Institute of Information and Communications Technology (Japan); M. Takeuchi, The Univ. of Tokyo (Japan)

Atomic clocks have reached the Quantum Projection Noise (QPN) limit of stability and it has been proposed to use the entangled atomic ensemble in order to overcome the QPN limit. Here, we propose a noble method

that could possibly overcome the QPN limit without need of preparing the entangled atomic ensemble, and we call it “Coherence-Maintained (CM) Ramsey method.”

Traditional Ramsey method measures a phase difference between atom and the Local Oscillator (LO), so in principle it is capable of suppressing the LO noise down to white phase noise level. However, destruction of the coherence of the atomic spin accompanied with projection measurement introduces the additional noise and therefore limited to white frequency noise, which is called QPN limit.

The proposed CM Ramsey method employs dispersion measurements, i.e. Faraday rotation, in order to measure the phase difference without destroying the atomic phase. By repeating the CM Ramsey method with sufficiently small dead time, one could suppress the LO noise down to white phase noise level, achieving the $1/\tau$ dependence of the Allan variance that can overcome the QPN limit. For the best stability, we need a proper feedback mechanism, and that is still under progress.

We are preparing a proof-of-principle experiment using the ensemble of trapped Yb ions with hyperfine splitting (12.6 GHz) as a clock transition and report the current status of the experiment as well.

8132-08, Session 3

Frequency of the $^{40}\text{Ca}^+$ Optical Clock transition and evaluation of systematic shifts

Y. Huang, Q. Liu, J. Cao, B. Ou, P. Liu, H. Guan, X. Huang, K. Gao, Wuhan Institute of Physics and Mathematics (China)

The trapping and laser cooling $^{40}\text{Ca}^+$ ion on the way towards optical frequency standards has been developed on our group.

A single $^{40}\text{Ca}^+$ ion is trapped in a miniature Paul trap. A commercial Ti: Sapphire laser and one home-build diode laser at 729 nm are locked to two high-finesse ULE cavities separately by the PDH method.

The single ion fluorescence line shape signal is optimized by minimizing the excess micromotion

The three magnet coil pairs aligned along three perpendicular directions are set to generate an arbitrary magnetic field. The full Zeeman profile components of the clock transition are achieved by counting the number of the quantum jumps observed in a fixed time period at different frequency.

The systematic frequency shifts are evaluated with a “clock” transition at 729 nm. The total systematic uncertainty of the clock resonance has been characterized to about 10^{-15} . The center frequency of $^{40}\text{Ca}^+$ $4s2S1/2 - 3d2D5/2$ optical clock transition were measured by an fs comb system referenced to a standard hydrogen maser. And we lock the 729 nm laser system to atomic transition is made by the four points locking method. A standard Allan deviation of less than 10^{-14} at 2000 s is obtained for the comparison between the $^{40}\text{Ca}^+$ optical frequency standard and a H-Maser using a femtosecond laser frequency comb.

8132-09, Session 3

Resolved atomic interaction sidebands in an optical clock transition

A. M. Rey, M. Bishof, Y. Lin, M. Swallows, M. Martin, JILA (United States); A. Gorshkov, California Institute of Technology (United States); J. Ye, JILA (United States)

We report the observation of resolved atomic interaction sidebands (ISB) in the ^{87}Sr optical clock transition when atoms at microkelvin temperatures are confined in a two-dimensional (2D) optical lattice. The ISB are a manifestation of the strong interactions that occur between atoms confined in a quasi-one-dimensional geometry and disappear when the confinement is relaxed along one dimension. The emergence of ISB is linked to the recently observed suppression of collisional frequency shifts in [1]. At the current temperatures, the ISB can be resolved but are broad. At lower temperatures, ISB are predicted to be substantially

narrower and usable as powerful spectroscopic tools in strongly interacting alkaline-earth gases.

[1] M. D. Swallows et al., Science, 3 February 2011 (10.1126/science.1196442).

8132-10, Session 3

Frequency shifts of colliding fermions in optical lattice clocks

K. Gibble, The Pennsylvania State Univ. (United States)

Decoherence of trapped gases makes the otherwise identical particles distinguishable. The distinguishability of particles has been controversial because several experiments have observed that particles appear spectroscopically identical in the presence of decoherence. This has led to an argument that even distinguishable fermions could not produce a collision shift, but recently a shift was observed in a fermion lattice clock. We offer an explanation of these experiments based on singlet and triplet states of colliding particles. We discuss the shifts for clocks, the relevance of mean field energies, the relation to other recent treatments, and eliminating shifts with strong interactions.

8132-11, Session 4

Optical direct comparison of ^{87}Sr optical lattice clocks using a >50 km telecommunication fiber link

H. Hachisu, A. Yamaguchi, M. Fujieda, M. Kumagai, S. Nagano, T. Ido, National Institute of Information and Communications Technology (Japan); T. Takano, The Univ. of Tokyo (Japan); M. Takamoto, H. Katori, The Univ. of Tokyo (Japan) and Japan Science and Technology Agency (Japan)

The stability of state-of-the-art optical clocks has recently reached 10^{-18} level. The remarkable development requires an improvement in frequency comparison technique in order to certify the same level of identical frequencies. Frequency transfer using optical fiber network is one of the most promising scheme. In this aspect, an ^{87}Sr -based-optical lattice clock in NICT is compared to that of the University of Tokyo using a >50 km fiber link. The comparison has resulted in the 10^{-15} level of fractional frequency difference. Further improvement is on the way to attain the 10^{-16} level, which has not been demonstrated by using the conventional satellite link.

8132-12, Session 4

Frequency comparison of optical lattice clocks

M. Takamoto, T. Takano, H. Katori, The Univ. of Tokyo (Japan)

Optical lattice clocks are expected to be highly stable by taking advantage of a large number $N \gg 1$ of atoms, which improves the quantum projection noise (QPN) limit as $1/\sqrt{N}$. However, their actual stability is severely limited by the instability of probe laser. We demonstrated the frequency comparison of two optical lattice clocks synchronously interrogated by a common probe laser to cancel out the probe laser's frequency noise. The Allan standard deviation of 1×10^{-17} was achieved for an averaging time of 2,000 s, which is close to the QPN limit for about 1,000 atoms.

8132-13, Session 4

Progress toward an optical lattice clock with 1e-17 fractional inaccuracy

M. Swallows, M. Bishof, Y. Lin, S. Blatt, M. Martin, C. Benko, A. M. Rey, J. Ye, JILA (United States)

Optical atomic clocks based on ensembles of neutral alkaline earth atoms trapped in a magic wavelength optical lattice are promising candidates for the next generation of frequency standards. These clocks can in principle equal the impressive accuracy achieved by single-ion clocks, while surpassing them in terms of stability. One obstacle that must first be overcome is an atomic density-dependent collisional shift of the clock transition, which can occur even if the clock is based on an ensemble of spin-polarized ultracold fermions. We have greatly reduced this shift in the JILA Sr optical lattice clock by trapping atoms in a two-dimensional optical lattice. By doing so, we exploit a novel quantum many-body effect to suppress collisional shifts in lattice sites containing $N > 1$ atoms. We have made a high precision measurement of these effects, and find that the collisional shift in our 2D lattice clock is $0.5 \pm 1.7 \times 10^{-17}$ at normal operating densities. Shifts of the clock transition due to room-temperature blackbody radiation are another limiting source of systematic inaccuracy for the JILA Sr standard. We are currently upgrading our apparatus to allow interrogation of the clock transition inside a cryogenically shielded region. Finally, we are constructing a new ultrastable laser system which will exhibit a fractional frequency stability at the 10^{-16} level for short time scales. With this new laser system, the JILA Sr standard should exhibit quantum projection noise-limited stability.

8132-14, Session 5

Atomic frequency standards at NICT

T. Ido, National Institute of Information and Communications Technology (Japan)

Three atomic frequency standards including a strontium lattice clock, a single calcium ion clock, and cesium fountain clock are in operation in National Institute of Information and Communications Technology (NICT), Japan. The relative stability between two optical clocks, Sr and Ca⁺, has been recently measured to be in 10^{-16} level. Evaluation of the systematic shifts, on the other hand, is underway for both clocks. In addition after reviewing the characteristics of these atomic standards, our effort to obtain a stable local oscillator using an optical cavity of 30cm length is also presented.

8132-15, Session 5

Recent progress of time and frequency research in NIM

Z. Fang, T. Li, X. Gao, Y. Lin, National Institute of Metrology (China)

Recent progresses in the field of time and frequency metrology in NIM mainly include: the accomplishment of NIM5 cesium fountain clock with an uncertainty of 2.5×10^{-15} ; progress of a strontium optical lattice clock; progress of self-developed erbium fiber optical frequency comb and its intended application for ultra-low phase noise microwave generation, etc.

8132-16, Session 6

Current status of the 171Yb optical lattice clock at NMIJ, AIST

M. Yasuda, T. Kohno, K. Hosaka, H. Inaba, Y. Nakajima, D. Akamatsu, F. Hong, National Institute of Advanced Industrial Science and Technology (Japan)

An optical lattice clock plays an important role in the field of optical frequency standard and metrology. Although the single Al⁺ ion based optical clock is presently demonstrating an outstanding performance, optical lattice clocks are being actively studied worldwide to realize their potential. Recently we have succeeded in developing an optical lattice clock using a fermionic 171Yb atoms contained in a one-dimensional optical lattice. Since then, we have been working to improve our clock. Our error budget indicates that the major source of the uncertainty is the poor signal to noise ratio of the observed spectrum coming from the shot-to-shot atom number fluctuation. Therefore, we implemented an atom-number normalization scheme at the final stage of the lattice spectroscopy. The principle of the atom-number normalization scheme is two sequential measurement of the unexcited / excited atom number. Then the excitation rate of the clock transition can be calculated with the initial atom-number fluctuation cancelled out. We could easily observe Zeeman components of the carrier spectrum by the calculated excitation rate using atom-number normalization, with a single scan of the clock laser frequency. We have also developed a new clock laser system using a narrow-linewidth optical frequency comb, which is phase-locked to a narrow-linewidth Nd:YAG laser (1064 nm). We will lock the clock laser frequency using the observed atomic spectrum. Thus we can measure the stability and update the uncertainty evaluation of our Yb optical lattice clock.

8132-17, Session 6

Time and frequency activities at NRC

P. Dubé, A. A. Madej, J. E. Bernard, L. Marmet, M. Gertszvolf, National Research Council Canada (Canada)

I will report on the current activities and latest results from the Time and Frequency group at the National Research Council of Canada (NRC). The NRC cesium fountain, FCs1, is undergoing an evaluation of its systematic shifts for an eventual contribution to International Atomic Time (TAI) and also for a re-measurement of the absolute frequency of the strontium ion. The design goal for FCs1 is a total relative uncertainty of 10^{-15} . The main contributions to the error budget of FCs1 are from the C-field inhomogeneity and the spin exchange. The uncertainty associated with recent measurements of these shifts will be presented. The optical frequency activities at NRC are primarily concerned with the trapped and laser-cooled single ion of 88Sr⁺. A new ion trap of the endcap design was successfully loaded in May 2010. This new trap provides optical access along three orthogonal directions for minimization of the micromotion. It is expected that the fractional frequency uncertainty on the systematic shifts of the ion clock transition will be reduced below 10^{-16} once micromotion is minimized. This will offer an opportunity for a re-measurement of the ion clock frequency at the accuracy limit set by the time standards. The latest developments on these activities will be presented at the conference.

8132-18, Session 6

Time and frequency metrology at PTB: recent results

V. Gerginov, Physikalisch-Technische Bundesanstalt (Germany)

The status of time realization and optical frequency measurements at PTB will be discussed. Two caesium fountain primary frequency standards are used for International Atomic Time (TAI) contributions, for the realization of the time scale UTC(PTB), and for frequency measurements of the 171Yb⁺ single-ion and the 87Sr lattice optical clocks. With the help of optically-stabilized microwaves as a reference for the caesium fountain primary standards, a quantum projection noise limited operation of the fountain CSF1 was demonstrated. Atom loading using a slow atomic beam source was implemented in CSF2, which improves the fountain stability. The uncertainty of both fountains is reduced due to a new estimation of the distributed cavity phase shifts.

The 171Yb⁺ ion offers two narrow optical transitions, both of which can be used as a frequency reference. This allows for an independent

stabilization of two clock lasers to transitions in the same atomic system. The two transitions show different sensitivities to external perturbations, which can be used to control frequency shifts, and to search for temporal variations of the fine structure constant.

Frequency measurements of the ^{87}Sr optical lattice clock were performed against the caesium fountain CSF1. They are in agreement with the values reported by other groups. Investigations of the blackbody radiation shift are in progress.

Conference 8133: Dimensional Optical Metrology and Inspection for Practical Applications

Monday-Tuesday 22-23 August 2011 • Part of Proceedings of SPIE Vol. 8133
Dimensional Optical Metrology and Inspection for Practical Applications

8133-01, Session 1

Measurement technology based on laser internal/external cavity tuning

S. Zhang, Tsinghua Univ. (China)

For an ordinary cavity laser with two cavity mirrors, if the length of lasers cavity changes half wavelength the laser frequency changes one longitudinal mode separation. For a three cavity laser, in which a feedback mirror is used to feed the laser output beam back into the laser cavity, the external cavity changes half wavelength the laser intensity changes one time. This presentation gives some research results in measurement based on changing (tuning) the length of laser internal/external cavity. HeNe laser cavity tuning nanometer displacement measurement instruments (laser nanometer rulers), HeNe laser feedback effect displacement measurement, Nd:YAG laser feedback effect nanometer displacement measurement, benchmark of phase retardation measurement instruments of a wave-plate based on laser frequency splitting, in-site phase retardation measurement instruments of a wave-plate based on laser feedback and polarization hopping, Quasi-common-path Micro-chip Nd:YAG laser feedback interferometers, non-contact surface profile measurement. Some of these instruments are in applications and behave some advantages without replacers.

8133-02, Session 1

Micron-feature surface mapping interferometer for hard-to-access locations

G. Abramovich, K. G. Harding, GE Global Research (United States)

This paper describes a compact imaging Twyman-Green interferometer to measure small features such as corrosion pits, scratches and digs on hard to access objects such as mounted turbine blades. The shoebox size interferometer was designed to guarantee proper orientation and working distance relative to the inspected section. The system also provides an extended acceptance angle to permit the collection at selected view points on a subject. We will also describe the various image shifting techniques investigated as part of the prototype. In operation, a reference flat is driven by a piezoelectric actuator and the interference image is relayed to the camera using a 10X objective. All the components including the camera and the laser source were integrated into the compact enclosure with the exception of power supplies. The interferometer has shown to provide sub-micron depth resolution and diffraction limited spatial resolution (a few microns). This paper will present the final performance achieved with the system and provide examples of applications.

8133-03, Session 1

Study on three-dimensional shape measurement of partially diffuse and specular reflective surfaces with fringe projection technique and fringe reflection technique

L. Huang, A. K. Asundi, Nanyang Technological Univ. (Singapore)

Three-dimensional shape metrology using fringe projection technique and fringe reflection technique are effective ways to reconstruct three-dimensional shape with different reflectance properties. Fringe projection technique is used for measuring objects with diffuse surfaces and relies on the principle of triangulation, while fringe reflectometry is used for specular reflective specimens based on principle of reflection.

While fringe projection technique directly provides the profile, fringe reflectometry measures the slope of the surface from which the profile is integrated. Actually, certain surfaces with reflectance, which is partially diffuse and partially specular, can be measured with both techniques mentioned above. For both methods, projected patterns are computer generated and phase shifting methods are applied. For fringe projection profilometry the sensitivity of three-dimensional measurement directly depends on system calibration and geometric configuration. Furthermore, the precision of dimensional measurement directly relies on the system sensitivity and the precision of phase measurement. For the fringe reflection technique, the sensitivity of dimensional measurement does not directly depend on geometry, which actually only directly determines the slope measuring sensitivity. Hence, phase measuring precision only directly yields the precision of slope measurement, which will influence the accuracy and precision of three-dimensional dataset through the following integration process. In this paper, the performance of these two fringe based techniques when measuring partially diffuse and specular reflective targets are analyzed with respect to their sensitivity and accuracy. The measuring sensitivity and precision of both techniques are compared and discussed theoretically in mathematical models and experimentally with actual measurement of some partially diffuse and specular surfaces.

8133-04, Session 1

Auto-exposure for 3D shape measurement using a DLP projector

S. Zhang, L. Ekstrand, Iowa State Univ. (United States)

Automatically adapting the camera exposure time based on the optical property of the measured object is crucial for industrial applications where a minimum human intervention is usually desirable, and 3D shape measurement with digital fringe projection techniques is not an exception. However, it is very challenging to realize such a capability for a conventional fringe projection system where only a finite increment of camera exposure time is allowed due to the digital fringe generation nature. We recently proposed a new technique for 3D shape measurement that only requires binary structured patterns to realize conventional phase-shifting algorithms. Specifically, the sinusoidal fringe patterns are realized by properly defocusing the projector. Because this technique coincides with the operation mechanism of the digital-light-processing (DLP) projector, it permits the use of an arbitrary exposure time for 3D shape measurement. And because an arbitrary exposure can be used, this new technique provides the opportunity to develop a strategy camera exposure time control automatically. This paper will present a 3D shape measurement system that could change its exposure time automatically according to the optical property of the measured object. This technique optimize the exposure time analyzing the percentage of saturated pixels when a uniform pure white is shining onto the object. We have found that by controlling the exposure time automatically, the high-quality 3D shape measurement can always be achieved for any type of diffuse objects. This paper will present the principle of the technique and show some experimental results.

8133-05, Session 1

A novel phase reconstruction method using frequency shifting

C. Zhang, X. Liu, H. Chen, X. Peng, Shenzhen Univ. (China)

Phase reconstruction is the key technology of PMP (Phase Measuring Profilometry) widely used in three dimensional (3-D) shape measurements for scientific and industrial purposes. Phase reconstruction is a two-step process: phase evaluation and phase unwrapping. Mostly, there

are two methods used for phase evaluation: one is the FTP (Fourier Transform Profilometry) and the other is the phase-shifting technique. FTP could evaluate the phase with a single-shot fashion so it can be used in dynamic measurement while the phase-shifting technique has a better performance in precision and reliability so it is widely used in the measurement required high precision. In this paper, we propose a novel method using the frequency-shifting technique for the phase evaluation rather than using the FTP or the phase-shifting technique. This paper will describe the proposed algorithm in detail and perform error analysis. The computer simulation and the experimental results will also be presented. The comparison of the proposed algorithm with the phase-shifting technique is also discussed. According to the formulation of proposed algorithm, we find out that the error sources are determined. To reduce the error of this method, we suggest an error-compensating method, which is initially used in the phase-shifting technique, and apply it to our method. Some preliminary experimental results demonstrate the validity of proposed approach.

8133-06, Session 2

Profilometry based on wavelength-spacing tunable multi-wavelength fiber laser source

S. Park, M. Jeong, C. Kim, Pusan National Univ. (Korea, Republic of)

Various interferometer technologies have been developed for profilometry and tomography. Recently, the optical frequency comb has been developed to induce an interferometric signal of the interferometer. The optical frequency comb light source can be implemented by using a fiber ring laser scheme with optical gain and wavelength selecting filter in the cavity.

In this work, we present a novel multi-wavelength fiber laser source, which shows an optical frequency comb spectrum with wavelength-spacing tunability. The tunable wavelength-spacing is implemented by the motorized polarization differential delay line in the Sagnac loop interferometer. The polarization differential delay line is an optical device that splits the light into orthogonal polarization and varies the time that one polarization travel compared to the other before combining them together. It is possible to change easily the comb interval with simple control electronics.

By using of this novel interferometric scheme, we can achieve the interferometric signal depending on the optical path difference between the sample and reference. As combining the peak positions from the signal information, the surface profile can be obtained successfully.

8133-07, Session 2

Surface profile measurement using broadband dual SOA wavelength-swept laser

H. S. Lee, M. Jeong, C. Kim, Pusan National Univ. (Korea, Republic of)

We demonstrate a broadband wavelength-swept laser using two gain medium for the surface profile imaging with higher resolution. The configuration of wavelength-swept fiber ring laser consists of two semiconductor optical amplifiers (SOA's) around 800 nm, two isolators, two 3 dB fiber couplers, two polarization controllers, a fiber Fabry-Perot tunable filter and an output fiber coupler. Since two laser cavities are built with two SOA's of the center wavelength of 800 nm and 830 nm, respectively, the wavelength swept laser has a capability of a broadband sweeping range of more than 60 nm. The measured axial resolution is less than 5 μm and the average output power of this laser is measured to 5 mW. We also demonstrate a 3 dimensional surface profile using a Fourier-domain optical coherence tomography image technique based on the proposed wavelength-swept laser.

8133-08, Session 2

Non-phosphor white LED light source for interferometry

V. Heikkinen, B. Wälchli, J. Aaltonen, H. Rääkkönen, I. Kassamakov, E. Hægström, Univ. of Helsinki (Finland)

Solid state light sources are replacing a tungsten filament based bulbs in Scanning White Light Interferometric (SWLI) measurement systems. Sources such as white LEDs generate less heat, have shorter switching times, allow stable spectrum and have longer lifetimes than traditional lamps. Phosphor based white LEDs produce a wide spectrum but have two separate peaks which causes interferogram ringing. This makes measuring multi layered structures difficult and may degrade measurement precision also when measuring a single reflecting surface. The LEDs spectral stability and switching time are also degraded due to the phosphor. Most non phosphor white LEDs have non gaussian spectra, but multi LED based white LEDs can achieve switching times and stability similar to single color LEDs. By combining several LEDs and by controlling their input current independently it is possible to create almost an arbitrary spectrum.

We designed a new light source based on non phosphor white LED (American Opto Plus LED, L-513NPWC-15D) combined with single color LEDs to fill the spectral gap between the blue and yellow peaks of the non phosphor white LED. By controlling the LEDs individually a wide nearly gaussian shaped spectrum was achieved. This wide continuous spectrum creates short interferograms (FWHM $\sim 1 \mu\text{m}$) with low side peaks. To demonstrate the properties of this source we measured through a 5 μm thick polymer film. The measured interferograms show how the well localized interference created by the source allows measurement of both surfaces of thin films simultaneously.

8133-09, Session 2

Color pattern projection method for three-dimensional measurement

T. Wakayama, T. Yoshizawa, Saitama Medical Univ. (Japan)

There is a special requirement for measuring and evaluating various parts inside a car in the fields of automobile industry. In regards to a strong requirement from car manufacturers, there were no appropriate measuring instruments available inside a car. To meet this requirement, we have proposed to incorporate a recent digital device such as a single MEMS mirror into projection optics. These key devices in our projection technique brought the mechanism of the projection from time domain to spatial domain. Due to this revision, first of all, such a small size system like a palm-top camera became attainable, and low cost measurement system has been potentially realized. Moreover, we adopted phase-shifting technique which is most popular technique applicable to industrial dimensional measurement and inspection in automobile industry and others. The camera will be potentially as small as a photographic digital camera in dimensional size. In this system, we control a single MEMS mirror and a laser diode to produce the projection pattern with appropriate period and arbitrarily structured intensity distributions like a sinusoidal and a binary pattern. In this paper, we propose recent improvement of the principle and its applications. We have developed three-dimensional measurement method based on a single MEMS mirror using three-color laser diodes and 3-CCD camera. The measurement method has combined the merits of pattern projection method using two colors with the merits of optical sectioning method, simultaneously.

8133-10, Session 2

High-speed triangulation-based point sensing using phase detection

K. G. Harding, GE Global Research (United States)

**Conference 8133: Dimensional Optical Metrology
and Inspection for Practical Applications**

Triangulation sensors have been in wide use for many years. Most point sensors use a laser spot, which is detected using either a lateral effect photodiode or a linear detector array. The centroid of the spot is used to determine the range using triangulation. On many engineered surfaces, this spot image may suffer from speckle, surface texture, or other issues that limit the ability to repeatedly measure the centroid. Many analysis means, such as fitting of the spot, zero crossing, and averaging methods have been tried to make the sensor more robust to surface influenced noise. This paper will present a system using a split image and phase detection to obtain the range. The speed of the sensor is gained by using simple point photodiodes and a moire effect to obtain the phase measurement. The paper will discuss the pros and cons of this approach, and show results on untreated metal parts.

8133-11, Session 2**Improving the resolution and accuracy of a compact 3-D shape measurement system**

K. Deng, P. S. Huang, Univ. of Michigan-Shanghai Jiao Tong Univ. Joint Institute (China)

We have recently developed a compact 3-D shape measurement system based on the combined stereovision and phase shifting method. This system consists of a miniature projector (Pico Projector from Texas Instruments) and two small cameras arranged as a stereo pair. The projector projects phase shifted fringe patterns, which are captured by both cameras simultaneously. The two phase maps calculated are used for stereo matching. The 3-D shape of the object is then reconstructed by the triangulation method. This research focuses on improving the resolution and accuracy of the measurement system. First, we use a 2-D Hermite interpolation method to achieve accurate stereo matching at the sub-pixel level. Then we use the averaging of multiple fringe images to reduce random noise of the system. Finally, we use an error compensation method to reduce the measurement error within the measurement volume, which is mainly caused by lens distortion. Experimental results show that after the above measures, a resolution of better than 10 μm and an accuracy of better than 100 μm within a measurement range of 100 x 67 mm can be achieved. This paper will describe the methods used and presents the experimental results obtained.

8133-12, Session 3**Development of a probe for inner profile measurement and flaw detection**

T. Yoshizawa, T. Wakayama, Saitama Medical Univ. (Japan); Y. Kamakura, NPO 3D Associates (Japan)

There are various requirements for measuring the inner diameter and/or inner profile of pipes, tubes and other objects similar in shape. Especially in mechanical engineering field, serious problems come from automobile industry because the inner surface of engine blocks or other die casts are strongly requested to be inspected and measured by non-contact methods (not by the naked eyes inspection using a borescope). If the inner diameter is large enough like water pipes or drain pipes, complicated and large equipment may be applicable. However, small pipes with a diameter ranging from 10mm to 100mm are difficult to be inspected by such a large instrument as is used for sewers inspection. And we propose an instrument which has no moving elements such as a rotating mirror for scanning a beam. This measurement method is based on optical sectioning using triangulation. This optically sectioned profile of an inner wall of pipe-like objects is analyzed to produce numerical data of inner diameter or profile. Here, we report recent development of the principle and applications of the optical instrument with a simple and compact configuration. In addition to profile measurement, we found flaws and defects on the inner wall were also detected by using the same probe. Up to now, we have developed probes with the diameter of 8mm to 25mm for small size objects (12mm to 100mm in diameter) and the 80mm probe for larger samples such as 600mm size container.

8133-13, Session 3**Surface profile measurement using a modified stereomicroscope**

P. S. Huang, J. Gao, D. Wu, Univ. of Michigan-Shanghai Jiao Tong Univ. Joint Institute (China)

Stereomicroscopes are widely used in scientific research as well as medical and industrial applications. Traditional stereomicroscopes provide visual depth perception but not quantitative measurement. In this research, we propose to modify a traditional stereomicroscope so that it can be used to provide quantitative 3-D surface profile measurement. The method we use is the combined stereovision and phase shifting method, which was proposed recently for high-accuracy 3-D surface shape measurement. A miniature projector (Pico Projector from Texas Instruments) is used to project phase-shifted fringe patterns to the object surface through one of the two optical channels. Two identical black-and-white cameras are used to capture the images of the object surface, one for each channel of the stereomicroscope. The calculated phase maps are used for stereo matching at the sub-pixel level. The 3-D surface profile is reconstructed using the triangulation method. With a zoom ratio of 1~6.3x, we can achieve a field of view of 2~12.6 mm with a resolution of 0.2~1.26 μm respectively (0.01% of the field of view). Experimental results will be presented to demonstrate the performance of the developed instrument.

8133-14, Session 3**Automated 3D imaging system for CZT wafer inspection and characterization**

Y. Liao, E. Heidari, G. Abramovich, C. Nafis, GE Global Research (United States); A. Butt, GE Global Research (United States); J. Czechowski, K. Andreini, K. G. Harding, J. E. Tkaczyk, GE Global Research (United States)

We describe the design and evaluation of the 3D stereo, near infrared, imaging system for CZT inspection system. The system provides rapid acquisition and data analysis that results in detailed mapping of crystal defects across the area of wafers up to 100mm diameter and through thicknesses of up to 15mm. In addition, through 3D cluster analysis, it identifies the classes of the global defects. In order to determine the actual detection limit, we used a Scanning Electron Microscope (for surface impurities) and a micron resolution confocal microscope (for embedded impurities) and compared the data to corresponding small impurities detected by our system. Finally, we analyzed the functional relationship between the electrical characteristics of the CZT wafers to their physical impurities.

8133-15, Session 3**Low noise surface mapping of transparent plane-parallel parts with a low coherence interferometer**

L. L. Deck, P. J. de Groot, Zygo Corporation (United States)

Highly polished plane parallel optics are found in many industries, but are particularly important in the data storage and photo-lithography industries. In those applications, the glass surface characteristics have become especially demanding, requiring extremely low noise measurements of the surface profile to control the fabrication process and minimize the adverse affects of surface irregularities on performance associated with these glass components. We describe the capabilities of a low-noise phase-shifting equal-path interferometer especially designed for high-precision surface mapping of transparent plane-parallel parts. The interferometer applies spatially and temporally incoherent illumination to minimize noise and isolate the surface of interest. With a 100mm aperture, less than 0.1% distortion, 50pm surface height precision

and 50 μ m lateral sampling, the interferometer is designed to capture the spatial frequencies with the fidelity required for current and next generation disks and other thin glass structures.

8133-16, Session 4

Challenges faced in applying 3D non-contact metrology to turbine engine blade inspection

J. Ross, GE Aviation (United States); K. G. Harding, GE Global Research (United States); E. Hogarth, GE Aviation (United States)

Turbine airfoils are key components used in several important industries: jet engines for commercial and military aircraft propulsion, steam turbine generators, and automatic transmissions. Of these applications, aircraft engines have the most critical requirements for control of airfoil geometry. Today, aircraft airfoil shapes are typically measured by three methods: dedicated hard gauges, coordinate measurement machines (CMMs), and in a small, but growing number of shops, 3D non-contact inspection systems. Optical 3D systems offer the potential to collect many more points than have been practical in the past at speeds usable in production. But there are many challenges to be addressed, such as surface reflectivity, data alignment, and the wide range of shapes to be inspected without taking a long time to do so. This paper will discuss the lessons learned from the application of 3D non-contact metrology systems as applied to the measurement of critical aircraft engine parts.

8133-17, Session 4

Evaluating a hybrid 3-dimensional metrology system: merging data from optical and touch probe devices

J. R. Gerde, U.S. Customs and Border Protection (United States); W. A. Christens-Barry, Equipose Imaging, LLC (United States)

In a project to meet requirements for CBP Laboratory analysis of footwear under the Harmonized Tariff Schedule of the United States (HTSUS), a hybrid metrology system comprising both optical and touch probe devices has been assembled. A unique requirement must be met: To identify the interface-typically obscured in samples of concern-of the "external surface area upper" (ESAU) and the sole without physically destroying the sample. The sample outer surface is determined by discrete pointcloud coordinates obtained using laser scanner optical measurements. Measurements from the optically inaccessible insole region are obtained using a coordinate measuring machine (CMM). That surface similarly is defined by pointcloud data.

Mathematically, individual command scanner data sets are transformed into a single, common reference frame. Custom software then fits a polynomial surface to the insole data and extends it to intersect the mesh fitted to the outer surface pointcloud. This line of intersection defines the required ESAU boundary, thus permitting further fractional area calculations to determine the percentage of materials present.

With a draft method in place, and first-level method validation underway, we examine the transformation of the two dissimilar data sets into the single, common reference frame. We also will consider the six previously-identified potential error factors versus the method process. This paper reports our on-going work and discusses our findings to date.

8133-18, Session 4

In vitro interferometric characterization of dynamic fluid layers on contact lenses

B. C. Primeau, The Univ. of Arizona (United States); J. E. Greivenkamp, College of Optical Sciences, The Univ. of Arizona (United States); J. J. Sullivan, 3M Co. (United States)

The anterior refracting surface of the eye when wearing a contact lens is actually the thin fluid layer that forms on the surface of the contact lens. Under normal conditions, this fluid layer is less than 10 microns thick. The fluid layer thickness and topography change over time and are affected by the material properties of the contact lens, and may affect vision quality and comfort. An in vitro method of characterizing dynamic fluid layers applied to contact lenses mounted on mechanical substrates has been developed using a phase-shifting Twyman-Green interferometer. This interferometer continuously measures light reflected from the surface of the fluid layer, allowing precision analysis of the dynamic fluid layer. Movies showing this fluid layer behavior can be generated. The fluid behavior on the contact lens surface is measured, allowing analysis beyond what typical contact angle or visual inspection methods provide.

The interferometer system has measured the formation and break up of fluid layers. Different fluid and contact lens material combinations have been used, and significant fluid layer properties have been observed in some cases. The interferometer is capable of identifying features in the fluid layer less than a micron in depth with a spatial resolution of about ten microns. An area on the contact lens approximately 6 mm wide can be measured with the system.

This paper will discuss the interferometer design and analysis methods used. Measurement results of different material and fluid combinations are presented.

8133-19, Session 4

Profile measurement of thin films by linear wavenumber-scanning interferometry

O. Sasaki, S. Hirakubo, S. Choi, T. Suzuki, Niigata Univ. (Japan)

A halogen lamp and an acousto-optic tunable filter are used to create a light source whose wavenumber is scanned exactly and linearly with time through detection of a phase change of an interference signal produced by the wavenumber scanning. When the linearly wavenumber-scanned light is incident into a film and there is no reference light, the interference signal becomes a sinusoidal wave whose frequency is an integral multiple p of a fundamental frequency. First the length of the detected interference signal is determined to be one period of the fundamental frequency and the wavenumber-scanning width for one period of the fundamental frequency is also determined. Next when a reference light is used, the interference signal consists of three sinusoidal waveforms with different frequencies. The optical path difference of the front surface of the film is adjusted so that three sinusoidal frequencies are integral multiples of the fundamental frequency. The positions of the front and rear surfaces of the film can be obtained from the wavenumber-scanning width and phases of the two sinusoidal waveforms related to the two surfaces. The film thickness was about 4 microns and $p=4$, and the wavenumber-scanning width was about 0.00033 1/nm. The measurement error was less than 10 nm.

8133-29, Poster Session

A novel laser tracking testbed for robot trajectory errors

A. Li, X. Jiang, Z. Li, Y. Bian, Tongji Univ. (China)

A novel measurement of laser coarse-fine coupling tracking is proposed for robot trajectory errors, which can not only meet the requirements of the large range, rapid response and dynamic tracking, but also achieve the high accuracy of submicroradian magnitude due to the ingenious system setup.

As the key components of the laser testbed, the tracking range of coarse tracking mechanism is no less than $\pm 15^\circ$ in pitch angle and $\pm 180^\circ$ in azimuth angle with the tracking accuracy better than 50 μ rad. While the fine tracking range is no less than 1400 μ rad both in level and vertical field angle with the tracking accuracy better than 0.5 μ rad. The mating relations among the prism deviation angle, step motor stepping angle

**Conference 8133: Dimensional Optical Metrology
and Inspection for Practical Applications**

and encoder resolution are studied to meet the test requirements of robot trajectory.

The mathematic model of robot errors is studied according to the motion definition of circular and linear trajectory. The optimization algorithm to remove system error and improve the position accuracy of robot motion is deduced. After building a robot experiment platform together with the laser tracking test system, the optical alignment is performed before the robot test. The relations between the laser tracking test system and the robot pose, especially the harmonious motion parameters, are studied. The calibration method of robot errors, as well as some error factors affecting the test uncertainty, is given to be considered according to the test experiment results.

8133-30, Poster Session**Three-dimensional optical microscopy based on angle deviation method for submicron structure measurements**

M. Chiu, C. A. Chen, C. Ten, National Formosa Univ. (Taiwan)

An optical microscope with high magnification can measure the three-dimensional profile of a submicron structure by use of the angle-deviation method in one shot. The expanded laser beam with a wavelength of 632.8nm reflected from the test surface and then passing through an optical microscope involves the surface profile information. From geometrical principle, the ray reflected and deflected a small angle from the surface normal causes by the slope of the surface. This angle can be transformed to the intensity or reflectance by use of an angular sensor. The angle-to-reflectance transform is done by a parallelogram prism near at the critical angle. Thus, the contrast of one point on the image pattern after the angular sensor is proportional to its surface height. The image recorded by CCD displays the two-dimensional image and its contrast pattern represents its surface height profile. In addition, the two- and three-dimensional surface profiles are obtained in real-time. The lateral and axial resolutions are within 1 μ m and several nanometers, respectively.

8133-31, Poster Session**Multi-probe system comprising three laser interferometers and one autocollimator for measuring flat bar mirror profile with nanometer accuracy on a high-precision micro-coordinate measuring machine**

P. Yang, The Univ. of Tokyo (Japan)

With the development of super-precision machining technology, it has also become increasingly important to evaluate surface geometry (straightness, flatness) with nanometer accuracy. Therefore, we described a multi-probe system comprising three laser interferometers and one autocollimator to measure a flat bar mirror profile with nanometer accuracy. The laser interferometers probe the surface of the flat bar mirror that is fixed on top of a scanning stage, while the autocollimator simultaneously measures the yaw error of the scanning stage. The flat bar mirror profile and horizontal straightness motion error are reconstructed by an application of simultaneous linear equation and least-squares methods. The average measurement uncertainty of the flat bar mirror profile was simulated to be only 10 nm with installation distances of 10 and 21 mm between the first and second, and first and third interferometers, respectively. To validate the simulation results, a pre-experiment was built using an X-Y linear stage driven by a stepper motor with steps of 1 mm along the X direction. Experiments were conducted with fixed interferometers distances as the same in the simulation, on a flat bar mirror. The two standard deviation of the flat bar mirror profile is mainly fitting the range of simulation results. Comparison of our measured data with the results measured by ZYGO's interferometer system showed agreement to within approximately 10 nm. The results

from the pre-experiment verify the performance of multi-probe method. Moreover, we have designed and built the multi-probe system on a high-precision micro-coordinate measuring machine to eliminate the systematic error of the moving stage.

8133-32, Poster Session**Bending measurement technique based on single-mode optical fiber with low-normalized frequency**

S. O. Gurbatov, O. B. Vitrik, Y. N. Kulchin, Institute for Automation and Control Processes (Russian Federation)

One of the urgent tasks of natural and man-made objects monitoring is the registration of bending deformations, including distributed bends with large radius of curvature appearing at the construction stage or during the operation of the facilities. This problem arises, for example, in monitoring construction and hydraulic engineering objects, pipelines, as well as, aircraft, rocket and shipbuilding objects.

In this paper, the task of the registration of bending deformation in large-scale objects is proposed to solve on the basis of guided radiation losses measurement arising from the bending of single-mode optical fiber. However, significant losses occur in standard optical fibers used in fiber-optic communications systems at the radii of curvature less than a centimeter, which does not allow them to measure the bending deformation with small curvature. Another problem arises when registering the bending deformation by the proposed method is the oscillatory dependence of optical power attenuation coefficient on bending radius in the single-mode fiber waveguide.

As a result, fiber optic method for measuring bending deformation using optical fiber waveguide with low normalized frequency has developed. It was shown that an optical fiber waveguide working in a single mode regime with low normalized frequency is appropriate to use for registration of bending deformation with large curvature radiuses. Experimentally demonstrated is a 140-fold increase in sensitivity of optical fiber to bending. Zero refraction index contrast on the optical cladding/air boundary is shown to be necessary for suppression of oscillations in the dependence of fundamental mode attenuation coefficient on bending radius.

8133-33, Poster Session**An improved arterial pulsation measurement system based on optical triangulation and its application in the traditional Chinese medicine**

J. Wu, W. Lee, Y. Lee, Ming Chuan Univ. (Taiwan); C. Lin, National Yunlin Univ. of Science and Technology (Taiwan); J. Chiou, Ming Chuan Univ. (Taiwan); C. Tai, National Yunlin Univ. of Science and Technology (Taiwan); J. Jiang, National Taiwan Univ. (Taiwan)

An improved arterial pulsation measurement (APM) system that uses three LED light sources and a CCD image sensor to measure pulse waveforms of artery is presented. The relative variations of the pulses at three measurement points near wrist joints can be determined by the APM system simultaneously. These pulsations contain useful information that can be used as diagnostic references in the traditional Chinese medicine (TCM). The height of arterial pulsations measured by the APM system achieves a resolution of better than 2 μ m. In addition, the designed APM system is well suited for evaluating and pre-diagnosing the health of a human being in the TCM clinical practice. Two measurement results are presented in this study.

8133-34, Poster Session

The application of laser triangulation method on the blind guidance

J. Wu, Ming Chuan Univ. (Taiwan); J. Wang, St. John's Univ. (Taiwan); W. Fang, Y. Shan, National Taiwan Univ. (Taiwan); S. Ma, Feng Chia Univ. (Taiwan); H. Kao, St. John's Univ. (Taiwan); J. Jiang, National Taiwan Univ. (Taiwan); Y. Lee, Ming Chuan Univ. (Taiwan)

A new apparatus for blind-guidance is proposed in this paper. The optical triangulation method is used to realize the system we proposed. The main components comprise a laptop, a camera and two laser modules. One laser module emits a light line beam vertically. Another laser module emits a light line beam horizontally. The track of the light line beam on the ground or on the object is captured by the camera, and the image is sent to the laptop for computation. The system can calculate the object width and the distance between the object and the blind in terms of the light line positions on the image. Based on the experiment, the distance could be measured with an accuracy of better than 3% within the range of 60 to 150 cm. And the object width could be estimated with an accuracy of better than 3% within the range of 60 to 150 cm.

8133-35, Poster Session

Multichannel adaptive interferometer based on dynamic photorefractive holograms for nanometrology

M. N. Bezruk, R. V. Romashko, Institute for Automation and Control Processes (Russian Federation)

Multichannel adaptive measuring interferometry system is developed. Key element of the system is dynamic hologram written in photorefractive crystal (PRC). Due to ability of dynamic hologram to be rewritten, an adaptive interferometer is capable to work in unstable environment. Multichannel system operated at single wavelength. Interchannel cross-talk free operation of the system is achieved by holograms spatial multiplexing in PRC without application external electric fields to crystal. It is shown that increase of channels number does not lead to sensitivity diminishing. We used CdTe:V as a photorefractive crystal.

It was founded that sensitivity of single channel when all other channels are turned off is 16.2. Turning on all channels does not affect on RDL in channel. Average value of RDL for all channel was amounted (17.1 ± 1.1).

Consequently, if number of multiplexing channels is increased, sensitivity of interferometer does not decrease in case if an optical beams from different channels does not overlapped in crystal. Therefore using of orthogonal geometry of wave mixing makes possible to create adaptive measuring system with very great number of channels. Thus if we have PRC of 6×6 mm² and object beams with lateral diameter 0.7 mm it is possible to create 70 channel interferometer.

It was experimentally founded that using fast semiconductor CdTe:V recording time of holograms was 3ms at light intensity 140 mW/mm². It allows to provide cut frequency of adaptive interferometer of 700 Hz. It make possible to provide steady work of multichannel interferometer in unstable conditions which characterized by noise impact with typical frequency of 50÷100 Hz.

8133-36, Poster Session

Measuring hairiness in carpets by using surface metrology

R. A. Quinones, Sr., B. Ortiz-Jaramillo, S. A. Orjuela Vargas, S. De Meulemeester, L. Van Langenhove, W. Philips, Univ. Gent (Belgium)

Recently a new carpet scanner using structured light triangulation was designed. The scanning consists in capturing with a camera the reflection of a laser line progressively projected along the carpet surface. The performance of classical scanners was improved by placing the carpets in a drum, to better capture the structure given by the piles. Range images were built by detecting per frame the dominant edges at different scales using wavelet space representation. This method excludes information given by hairs, which is a relevant characteristic in the evaluation. We recently present an automatic grading system already generic for carpets with low pile construction and without color patterns. The grades are computed using linear models with texture features extracted from the range images. Appearance changes in carpets with high pile construction were still not well detected, because those changes are also related to other characteristics such as thickness and hairiness. Therefore, algorithms measuring such characteristics in the carpet structure were still required. We present in this paper an approach based on surface metrology that directly measures the hairiness of the carpet from the frames. We measure the distances between the maximum intensity of the laser line reflection and the reflection given by the hairs. We found that these features are complementary to the previous texture features explored. The use of the automatic grading has been expanded including some carpets types with high pile construction by combining features based on both features. The full method can be used to evaluate other material surfaces.

8133-37, Poster Session

Phase shifting interferometry for measurement of transparent samples

D. I. Serrano-García, N. Toto-Arellano, A. Martínez-García, J. A. Rayas-Álvarez, Ctr. de Investigaciones en Óptica, A.C. (Mexico)

A Michelson interferometer was implemented to analyze a phase object by using polarization phase-shifting interferometry.

The Michelson interferometer produces two beams with circular polarization of opposite rotations one respect to the other obtained by a combination of a quarter-wave plate Q and a linear polarizing filter P₀ that generates linearly polarized light at an appropriate azimuth angle entering the Michelson interferometer. Using two retardation plates (QL and QR) with mutually orthogonal fast axes placed in front of the two beams (A, B) to generate left and right nearly-circular polarized light.

The system is coupled to a 4-f system with bi-Ronchi gratings in the Fourier plane. Diffraction orders appear in the image plane, forming a rectangular array were around each order, an interference pattern appears due to the optical fields associated to each beam when proper matching conditions are met. The interference of the fields associated with replicated beams centered on the diffraction orders is achieved by a proper choice of the beams spacing with respect to the gratings period.

In this paper we propose an optical system using single-shot phase shifting interferometry modulated by polarization, presenting insensitivity against external vibration allowing measuring dynamics events with high accuracy because the optical configuration allows obtaining n-interferograms in one shot.

Experimental results are presented to the study of a thin phase object.

8133-38, Poster Session

Remote ultra sensible microphone laser

G. E. Sanchez Guerrero, C. Guajardo González, P. M. Viera González, R. Selvas Aguilar, L. G. Ramos Traslósheros, Univ. Autonoma de Nuevo Leon (Mexico)

This paper presents an optical fiber Mach-Zehnder interferometer which is arranged in a configuration of an ultra-sensible sound detector. This consists in a U-bench mount, a 3dB beam splitter, a few meters of telecom fiber, a 633nm He-Ne laser, a sound acquisition system, and a remote reflective detach surface. The optomechatronic device also enables to capture sound vibration in free air at remote reflective

**Conference 8133: Dimensional Optical Metrology
and Inspection for Practical Applications**

vibrate surface at a distance as long as 5 meters. In our case, light is launched into the fiber interferometer and one path arm is broken by a U-bench mount. The other arm is the reference arm which path remains unchanged. A beam-splitter in the U-bench extracts the beam out of the fiber components and deviates the beam somewhere. This beam bounced off this vibration surface and is caught back through a beam splitter located in between the U-bench mount. Then, the fiber interferometer processes this signal back and a photo-detector acquires this modulated optical signal and by help of a system is demodulated and pre-amplifies the incoming signal into a digital sound signal. The high sensibility of the device is enough to catch sound vibration at a distance as long as 5 meters and process in a sound recorded file. The system is compact, robust, reliable and cost effective and is suggested as an instrument that can find application where is required a surveillance non-detectable device or a perimeter building protection.

8133-39, Poster Session**Design and characterization of image acquisition system and its optomechanical module for chip defects inspection on chip sorter**

M. Chen, P. Huang, Y. Chen, Y. Cheng, Instrument Technology Research Ctr. (Taiwan)

Chip sorter is one of packaging facilities in chip manufacture. The defects will occur for a few of chips during manufacturing processes. If the size of chip defects is larger than a criterion of impacting chip product quality, these flawed chips have to be detected and removed. Defects inspection system is then developed with frame CCD imagers. There're some drawbacks for this system, such as image acquisition of pause type, complicated acquisition control, easy damage for moving components, etc. And acquired images per chip have to be processed in radiometry and geometry and then pieced together before inspection. They impact the accuracy and efficiency of inspection. So the approaches of image acquisition system and its opto-mechanical module will be critical for system improvement.

In this article, design and characterization of a new image acquisition system and its opto-mechanical module are presented. Defects with size of greater than 15 μ m have to be inspected. Inspection performance shall be greater than 0.6 m/sec. Thus image acquisition system shall have the characteristics of having (1) the resolution of 5 μ m and 10 μ m for optical lens and linear CCD imager respectively; (2) the lens magnification of 2; (3) the line rate of greater than 120 kHz for CCD output. The design of structure and outlines for new system and module are also described in this work.

Proposed system has advantages of such as transporting chips in constant speed to acquire images, using one image only per chip for inspection, no image-mosaic process, simplifying the control of image acquisition. And the inspection efficiency and accuracy will be substantially improved.

8133-40, Poster Session**Experimental exploration on the correlation coefficient of static speckles in Fresnel configuration**

D. Li, Univ. College Dublin (Ireland); D. Kelly, Technische Univ. Ilmenau (Germany); J. T. Sheridan, Univ. College Dublin (Ireland)

The correlation coefficients of static speckles in three dimensions are derived and the results verified using computer simulations and experimental measurements. The investigation shows that longitudinal correlation coefficients of speckle patterns decrease monotonically along the radial direction, based on which an alignment algorithm to align the optical axis with the centre of the detector is proposed. Position shift of the peak coefficient appears when off-axis speckle pattern correlated

with its longitudinally displaced counterpart, from which the out-of-plane displacement of the diffuser can be measured at the recording plane. Two applications indicated by the results are explored.

8133-41, Poster Session**High-resolution diameter estimation of micro-thin wires by a novel 3-D diffraction model**

K. K. Vyas, Indian Institute of Science (India)

Micro-thin wires are of significant importance to academia, research laboratories as well as industries engaged in micro-fabrication of products related to diverse fields like micromechanics, bio-instrumentation, optoelectronics etc. Critical dimension metrology of such wires often demands diameter estimation with tight tolerances. Amongst other measurement techniques, Optical Diffractometry under Fraunhofer approximation has emerged over years as a non-destructive, robust and precise technique for on-line diameter estimation of thin wires. However, it is observed that existing Fraunhofer models invariably result in experimental overestimation of wire diameter, leading to unacceptable error performances particularly for diameters below 50 μ m. In this paper, a novel diffraction model based on Geometric theory is proposed and demonstrated to theoretically quantify this diameter overestimation. The proposed model utilizes hitherto unused paths-ways for the two lateral rays that contribute to the first diffraction minimum. Based on the 3-D geometry of the suggested model, a new 'correction function' is defined. The theoretical analysis reveals that the actual diameter of the diffracting wire is a product of two factors: overestimated diameter by the existing models and the newly proposed correction function. The analysis reveals further that the said correction function varies non-linearly with diameter and presents a dependence only on the experimentally measured diffraction angle. Based on the proposed model, the communication reports for the first time, a novel diameter-inversion procedure which not only corrects for the overestimated diameter by existing models but also facilitates wire diameter-inversion with high resolution. Micro-thin metallic wires having diameters spanning the range 1-50 μ m are examined. Simulations and experimental results are obtained that corroborate the theoretical approach.

8133-42, Poster Session**Absolute thickness measurement of silicon wafer using wavelength scanning interferometer**

Y. Ghim, Korea Research Institute of Standards and Science (Korea, Republic of); A. Suratkar, Intel Corp. (United States); A. Davies, The Univ. of North Carolina at Charlotte (United States); Y. Lee, Korea Research Institute of Standards and Science (Korea, Republic of)

Silicon wafers are widely used in various applications of semiconductor and solar cell. One of interesting issues for mass production for silicon wafers is quality control, especially for thickness uniformity. In this paper, we describe wavelength scanning interferometry based on spectroscopic reflectometry using infrared light (4 nm tuning range at 1550 nm) for three-dimensional thickness measurements of thin wafers less than 100 μ m with fine lateral and depth resolution. Other optical methods that are based on Fourier techniques are limited to thicker wafers when using such a short tuning range source. For example, the minimum thickness measurable with the conventional Fourier-based technique using a 4 nm-tunable (500 GHz) 1550 nm laser is approximately 170 μ m. Thus our proposed method enables a significant extension of thickness measurements and represents a significant advance. It is also interesting that the so-called 'ripple-error' or 'fringe-bleed through' is much reduced with a reflectometry-based analysis compared to a Fourier-based analysis. Our proposed method was verified by measuring and testing several wafers with various thicknesses.

8133-20, Session 5

Error analysis and compensation in phase-shifting surface profiler

Q. Hu, QUEST Integrated, Inc. (United States)

This paper analyzes the error sources in phase-shifting surface profiler, including phase-shifting generation, color imbalance, phase-shifting algorithms, surface contour extraction, and data analysis, etc. Some methods to improve the measurement accuracy and resolution are also proposed including transfer functions and look-up tables for various error sources. The limitations in accuracy are also discussed. Some initial test results will be given to verify the feasibility.

8133-21, Session 5

Uniaxial 3D shape measurement with a binary phase-shifting technique using projector defocusing

S. Zhang, L. Ekstrand, Y. Xu, Iowa State Univ. (United States)

In an attempt to compensating the phase errors induced by improperly defocused binary structured patterns, we found that: (1) the phase error can be described as a function of depth z ; and (2) the error function is monotonic on either side (positive or negative) of the perfectly focal plane (0). These findings provide not only the opportunity to compensate for this type of phase errors through software, but also the potential to retrieve the depth z by analyzing phase errors. The former has been proven successful previously. Moreover, our further analysis indicates that the phase error is intrinsic to the depth z and is independent of viewing perspective. In other words, the phase error is theoretically invariant to the viewing direction of a camera. This indicates that (1) the 3D information can be retrieved by analyzing the phase errors, and (2) the 3D information can be obtained even if the camera captures images from the same angle as the projector projection. In other words, it does not require triangulation for depth retrieval, which is fundamentally different from most 3D shape measurement techniques where triangulation is mandatory. This paper will present this uniaxial 3D shape measurement technique based on the analysis of defocused binary structured patterns. Comparing with a conventional triangulation-based method, this technique has the advantage of measuring deep holes, and has the merit of developing more compact 3D systems. This paper will present the principle of the proposed technique and will show some preliminary experimental results.

8133-22, Session 5

Completely localized and parallel iterative algorithms for shift-variant image deblurring

S. B. Sastry, M. Subbarao, Stony Brook Univ. (United States)

Two completely localized algorithms for deblurring shift-variant defocused images are presented. The algorithms exploit limited support domain of 2D shift-variant point spread functions (PSFs) to localize the deblurring process. Focused image at each pixel is modeled by a truncated Taylor-series polynomial and a localized equation is obtained which expresses the blurred image as a function of the focused image and its derivatives. This localized equation forms the basis of the two algorithms. The first algorithm iteratively improves the estimated focused image by directly evaluating the localized equation for a given blurred image. The second algorithm uses the localized equation in a gradient descent method to improve the focused image estimate. The algorithms use spatial derivatives of the estimate and hence exploit smoothness to reduce computation. However, no assumptions about the blurring PSFs such as circular symmetry or separability are required for computational efficiency. Due to complete localization, the algorithms are fully parallel, that is, the focused image estimates at each pixel is

computed independently. Performance of the algorithms is compared quantitatively with other shift-variant image restoration techniques, both for computational efficiency and for robustness against noise. The new algorithms are found to be faster and do not produce any blocking artifacts that are present in sectioning methods for image restoration. Further, the algorithms are stable and work satisfactorily even in the presence of large blur. Simulation results of the algorithms are presented for both Cylindrical and Gaussian PSFs. The performance of the algorithms on real data is discussed.

8133-23, Session 5

Surface sensitivity reduction in laser triangulation sensors

M. Daneshpanah, K. G. Harding, GE Global Research (United States)

Distance measurements based on laser triangulation sensors is in widespread use in various sectors of industry. These sensors offer a simple, non-contact and fast solution to measure displacement, position, vibration and thickness. However, as the measurement accuracy requirements increase, such sensors become prone to part surface sensitivity since they heavily rely on a uniform back-scatter of the laser spot - which is not always achievable on micro-textured, non-lambertian surfaces. The non-uniform backscattered light results in a spot with non-uniform intensity distribution imaged on the position sensitive device (PSD) such as a linear detector array or a lateral effect photo diode. Although very sensitive, almost all commercial sensors only measure centroid rather than geometrical centers of the imaged spot. Any non-uniform spot intensity will trigger erroneous measurements. The most common solution for surface sensitivity reduction includes signal processing and statistical averaging which is combined with moving the part and making multiple measurements to achieve a better accuracy. Some systems using CCD/CMOS based sensors have attempted advanced fitting methods and even phase shift analysis that have shown some success in minimizing surface sensitivity but adding to system complexity, cost and measurement time. In this paper we discuss sources of measurement noise including surface texture, speckle, beam deflection and asymmetry. We also explore a few solutions using dithering as well as the use of volumetric speckle fields to reduce surface sensitivity. We show that a simple ditherer would induce additional error and suggest a solution to compensate for it. Our main focus is on fast measurements of a stationary target where the surface texture and roughness can vary randomly during the operation.

8133-24, Session 5

Method for the evaluation 3D non-contact inspection systems

K. G. Harding, GE Global Research (United States)

Three dimensional, optical measurement systems are becoming more widely used in applications ranging from aerospace to automotive. These systems offer the potential for high speed, good accuracy, and more complete information than older contact based technology. However, the primary standards employed by many to evaluate these systems were specifically designed around touch probe based coordinate measurement machines (CMMs). These standards were designed to work with the limitations of touch probes, and in many cases can not measure the types of features and errors associated with non-contact systems. This paper will discuss the deficiencies of employing contact based characterization tests to non-contact systems, and suggest a new set of tests specifically to cover the many aspects pertinent to non-contact, optical 3D measurement systems. Some of the performance aspects addressed in this characterization method includes: sensitivity to surface reflectivity and roughness, the effect of angle of incidence of measurements, means to characterize volumetric variations that may fit complex functions, and considerations of both spatial and depth resolutions. Specific application areas will be discussed as well as the

use of artifacts to provide practical functional data that can predict system performance on real world parts.

8133-25, Session 6

Surface resistivity/conductivity of different organic-thin films by shearography

K. J. Habib, Kuwait Institute for Scientific Research (Kuwait)

Optical shearography techniques were used for the first time to measure the surface resistivity/conductivity of different organic-thin films, without any physical contact. Different organic coatings, ACE Premium-grey Enamel, a yellow Acrylic Lacquer, and a gold Nail Polish, on a metallic alloy, i.e., a carbon steel, was investigated at a temperature range simulating the severe weather temperatures in Kuwait, especially between the daylight and the night time temperatures, 20-60 oC. The investigation focused on determining the in-plane displacement of the coatings, which amounts to the thermal deformation (strain) with respect to the applied temperature range. Then, the alternating current (AC) impedance (resistance) of the coated samples was determined by the technique of electrochemical impedance spectroscopy (EIS) in 3.5 % NaCl solution at room temperature. In addition, a mathematical model was derived in order to correlate between the AC impedance (resistance) and to the surface (in-plane) displacement of the samples in solutions. In other words, a proportionality constant (surface resistivity or conductivity=1/ surface resistivity) between the determined AC impedance (by EIS technique) and the in-plane displacement (by the optical interferometry techniques) was obtained. Consequently the surface resistivity () and conductivity () of the coated samples in solutions were obtained. Also, electrical resistivity values () from other source were used for comparison with the calculated values of this investigation. This study revealed that the measured value of the resistivity for the anodized coated samples were in a good agreement with the one found in literature for the same coatings.

8133-26, Session 6

High-resolution electric speckle pattern interferometry by using only two speckle patterns

Y. Arai, Kansai Univ. (Japan)

Electric speckle pattern interferometry (ESPI) with using fringe scanning methods is a useful method for the out of plane and in-plane deformation displacement measurement of an object with some rough-surfaces. Now, the temporal carrier technology by using a high speed camera is also employed for a large deformation measurement. However, in the measurement which should treat with a much faster deformation phenomenon, the higher speed camera than an ordinary camera is required in order to grab images smoothly. As the results, it is getting to be difficult to set up the optical system physically and financially. In order to solve the problems, the development of new analyzing methods that can measure the deformation distribution of the object by the limited information without using a much higher speed camera has been required. In this paper, a new measurement method is developed by using basic characteristics of speckle phenomena. In the new method, the special optical system that can record some spatial information in each speckle is constructed. The high resolution deformation analysis by using only two speckle patterns before and after deformation process can be realized by using the new optical system. In experimental results, it can be confirmed that the resolution-power of the new method is more precise than 1/100 wavelength of the light source in optical system, and is also equivalent to the resolution-power of ordinary method which is required to at least 3 sheets of speckle patterns in the deformation analysis.

8133-27, Session 6

Optical low coherence for thin plate's non-destructive testing

Y. Zhu, R. Pan, Nanjing Univ. of Aeronautics and Astronautics (China); Z. Wang, Hebei Univ. of Science and Technology (China); S. Chen, Nanjing Univ. of Aeronautics and Astronautics (China)

It is more urgent to provide new methods of thin plate's non-destructive in industrial applications, such as wind turbine blades, aircraft skin. The method of this paper based on optical low coherence and acoustics is introduced to thin plate's non-destructive detection. A high-resolution and rapidly coherence testing system are designed with broadband light source and Lamb wave piezoelectric. An optical-fiber Michelson interferometer is set up, which used to detect the signal of thin plate's vibration. An acoustic source is applied to produce excitation signal. Acoustic excitation signal which can change optical signal is affected by damage location. Therefore the damage of thin plate can be detected. Signal is processed by wavelet transform algorithm in order to improve accuracy and reduce noise. A verification experiment which consists of many wave with different damage is applied to prove the accurate location result. This method is characterized by such advantages as non-contact, non-destructive, high-resolution, and rapidly.

8133-28, Session 6

Developing the color full-scale Schlieren technique for flow visualization

C. Chen, Y. Hung, C. Ting, National Taipei Univ. of Technology (Taiwan)

The full-scale schlieren technique was famous and especially developed for flow visualization with large area of test section. This article further presents the color full-scale schlieren technique which captures more colorful images and also promotes the resolution of images. In this work, the developed color full-scale schlieren technique used the light source which penetrates through the linear grating color mask with alternated red, green, and blue colors. The applied light source is made as flat plate module structure which is convenient for varying area of the light source. The width of the grating color lines is 5 mm and the applied area of light source as well as its test section in this article are 2x2 and 1x1 m² respectively. In future, this developed color full-scale schlieren technique will be further used for e.g. CO flow visualization during incomplete combustion process of fuel gas. The results in this work show beautiful images and also with expected high sensitivity.

Conference 8134: Optics and Photonics for Information Processing V

Wednesday–Thursday 24–25 August 2011 • Part of Proceedings of SPIE Vol. 8134
Optics and Photonics for Information Processing V

8134-01, Session 1

Optical hybrid analog-digital signal processing based on spike processing in neurons

M. P. Fok, P. R. Prucnal, Princeton Univ. (United States)

Technologies for real-time signal processing have received considerable attention due to their processing power for numerous applications. Neuromorphic engineering provides the capability of performing practical computing and signal processing based on the biophysical model of neuronal computation. Spike processing in neurons is of particular interest due to its efficiency and cascability that benefits from hybrid analog-digital processing. We propose and demonstrate an optical hybrid analog-digital signal processing primitive that implements the functionality of an integrate-and-fire neuron. This optical primitive has a processing speed that is nine-orders of magnitude faster than a biological neuron and is capable of performing high-capacity signal processing. It employs a Ge-doped nonlinear optical fiber and off-the-shelf semiconductor devices. Utilizing this hybrid analog-digital processing primitive, we can implement processing algorithms that are too complex for existing optical technologies and have a much higher bandwidth compared with existing electronic technologies. The spiking neuron comprises a small set of basic operations (delay, weighting, spatial summation, temporal integration, and thresholding), and is capable of performing a variety of processing functions, depending on how it is configured. It opens up a range of optical processing applications for which electronic processing is too slow. In this paper, an overview of optical hybrid analog-digital signal processing will be presented. Several simple photonic neuromorphic circuits, including the auditory localization algorithm of the barn owl and the crayfish tail-flip escape response will also be introduced.

8134-02, Session 1

Autonomous wireless radar sensor mote for target material classification

K. M. Iftekharruddin, M. Khan, E. McCracken, L. Wang, R. Kozma, The Univ. of Memphis (United States)

An autonomous wireless sensor network consisting of different types of sensor modalities is a topic of intense research due to its versatility and portability. These types of autonomous sensor networks commonly include passive sensor nodes such as infrared, acoustic, seismic, and magnetic. However, fusion of another active sensor such as Doppler radar in the integrated sensor network may offer powerful capabilities for many different sensing and classification tasks. In this work, we demonstrate the design and implementation of an autonomous wireless sensor network integrating a Doppler sensor into wireless sensor node with commercial off the shelf components. We also investigate the effect of different types of target materials on the return radar signal as one of the applications of the newly designed radar-mote network. Different types of materials can usually affect the amount of energy reflected back to the source of an electromagnetic wave. We obtain mathematical and simulation models for the reflectivity of different homogeneous non-conducting materials and study the effect of such reflectivity on different types of targets. We validate our simulation results on effect of reflectivity on different types of targets using real experimental data collected through our autonomous radar-mote sensor network.

8134-03, Session 1

Multi-objective adaptive composite filters for object recognition

J. L. Armenta, V. H. Diaz-Ramirez, J. J. Tapia-Armenta, Ctr. de Investigación y Desarrollo de Tecnología Digital (Mexico)

A new algorithm to design optimal trade-off correlation filters for pattern recognition is presented. The algorithm is based on a heuristic optimization of several conflicting quality metrics simultaneously. By the use of the heuristic algorithm the impulse response of a conventional composite filter is iteratively synthesized until an optimal trade-off of the considered quality metrics is obtained. Computer simulation results obtained with the proposed filters are provided and compared with those of existing trade-off correlation filters in terms of recognition quality measures in cluttered, noisy, and geometrically distorted input scenes.

8134-04, Session 1

Distortion-invariant face recognition using multiple phase-shifted reference-based joint transform correlation technique

M. N. Islam, Farmingdale State College (United States); V. K. Asari, Univ. of Dayton (United States); M. A. Karim, Old Dominion Univ. (United States)

We have developed a novel face recognition technique utilizing optical joint transform correlation (JTC) technique which provides with a number of salient features as compared to similar other digital techniques, including fast operation, simple architecture and capability of updating the reference image in real time. The proposed technique incorporates a synthetic discriminant function (SDF) of the target face estimated from a set of different training faces to make the face recognition performance invariant to noise and distortion. The technique then involves four different phase-shifted versions of the same SDF reference face, which are individually joint transform correlated with the given input scene with unknown faces and other objects. Appropriate combination of correlation signals yields a single cross-correlation peak corresponding to each potential face image. The technique also involves a fringe-adjusted filter to generate a delta-like correlation peak with high discrimination between the target face and the non-target face and background objects. Performance of the proposed face recognition technique is investigated through computer simulation where it is observed to be efficient and successful in different complex environments.

8134-05, Session 1

Acceleration of radial basis functions for visual robot calibration using GPGPUs

T. M. Taha, Univ. of Dayton (United States)

In this paper we present the acceleration of Radial Basis Functions on GPGPUs for visual calibration of industrial robots.

8134-06, Session 1

Margin setting: the early years

H. J. Caulfield, Alabama A&M Univ. (United States)

Pattern recognition in terms of algorithms (there are many of them) and

Conference 8134:
Optics and Photonics for Information Processing V

performance figures of merit, and problems each algorithm has. Linear discriminants are simple but not work at all well in problems not that simple. Advanced algorithms such as the Support Vector Machine are much more complex, but they allow solutions to much harder problems. Moreover, most pattern recognition algorithms allow little if any user controls. Margin Setting removes those and other major problems that occur in almost every hard pattern recognition algorithms - problems like

- Too few members in the training set (Those samples are sometimes expensive to obtain). We have shown that fewer than 10 samples of many difficult-to-classify problems often suffice.
- Too many members of the training set (This is sometimes called the overtraining problem). We have demonstrated that it is absent in Margin Setting.
- The VC dimension problem. (The VC or Vapnik-Chervonenkis dimension tells us how many regions can be discriminated in a hyperspace of N dimensions using a specific kind of discriminant. If we use a discriminant that can be viewed ahead of time as incapable, we cannot expect a good result) With Margin Setting problem complexity and discriminant complexity are decoupled.
- The complexity problem (This is a close relative of the VC dimension problem. The discriminant must be at least as complex as the problem. This is a theorem proved by Yasser Abu Mostafa.) In Margin Setting that problem no longer exists.

8134-07, Session 2

Analyzing the OFDMA capacity in SISO and MIMO for wireless communication systems

S. Mohseni, M. A. Matin, Univ. of Denver (United States)

Orthogonal Frequency Division Multiple Access (OFDMA) is a technique that it uses several narrow bands for transmitting the large amounts of digital data over a radio wave simultaneously. The Multiple Access (MA) is part of the abbreviation which refers to this fact that the data which are sent in downlink can be received and used by many users at the same time. In OFDM, the OFDM symbols in time are sequentially allocated to the different users, but in the OFDMA the system directly allocates them to the different users.

In another word, The OFDMA is a multi-user version of Orthogonal Frequency Division Multiplexing (OFDM). OFDMA by spacing the channels much closer to each other can use the spectrum more efficient. Even though there are different ways for partitioning the radio resource for multiuser communication system, because of the advantages that OFDMA has, it has always been considered as the first choice for broadband wireless network.

In this paper, the structure of the OFDMA, the channel capacity for Single Input single output (SISO) and Multi Input Multi Output (MIMO) for OFDMA discuss and study, and then the conditions that make OFDMA optimal or suboptimal discuss. When the OFDMA is not optimal we show what the performance gap is; then finally we propose an algorithm for computing the OFDM and OFDMA capacity. All the simulations have been done in MATLAB.

8134-08, Session 2

Performance analysis of coded OFDM fiber-optics communications

K. J. Bhatia, R. S. Kaler, Thapar Univ. (India); T. S. kamal, Sant Longowal Institute of Engineering and Technology (India); R. Kaler, Thapar Univ. (India)

A novel high spectral efficiency all-optical sampling orthogonal frequency-division multiplexing scheme is proposed using space frequency Block coding (SFBC) techniques and nonlinear behavior of vertical-cavity surface-emitting laser diodes is exploited by relative intensity to noise (RIN). We show that in long-haul fiber optics communications, SFBC-coded OFDM increases spectral efficiency

and reduces the influence of chromatic dispersion in optical-OFDM system if RIN is adjusted to -155 dB/Hz. We investigated the optimal values for linewidth and RIN for a coded optical-OFDM system for its better performance. The limiting value of linewidth should be 6.5 MHz up to which optical power remains almost constant and RIN value corresponding to this linewidth is measured to be -155 dB/Hz. and the average value of RIN is measured to be -125 dB/Hz. The results of PMD simulations for Optical-OFDM and thermal noise-dominated scenario are observed for different DGDs and the worst-case scenario ($k = 1/2$), assuming that the channel state information is known on a receiver side. The OFDM signal bandwidth is set to $BW = 0.25 B$ (where B is the aggregate bit rate set to 10 Gb/s), the number of subchannels is set to $NQAM = 64$, FFT/IFFT is calculated in $NFFT = 128$ points, the RF carrier frequency is set to $0.75 B$, the bandwidth of optical filter for SSB transmission is set to $2 B$, and the total averaged launched power is set to 0 dBm. The guard interval is obtained by cyclic extension of $NG = 2 * 16$ samples. The Blackman-Harris windowing function is applied. The 16-QAM OFDM with and without channel estimation is observed in simulations. The effect of PMD is reduced by (1) using a sufficient number of subcarriers so that the OFDM symbol rate is significantly lower than the aggregate bit rate and (2) using the training sequence to estimate the PMD distortion. For DGD of $1/BW$, the RZ-OOK threshold receiver is not able to operate properly because it enters the BER error floor. Note that 16-QAM OFDM without channel estimation enters the BER floor, and even advanced FEC cannot help much in reducing the BER.

8134-09, Session 2

A new technique for compensating the effects of carrier frequency offset (CFO) for orthogonal frequency division multiplexing

S. Mohseni, M. A. Matin, Univ. of Denver (United States)

Orthogonal frequency division multiplexing (OFDM) has been selected for broadband wireless communication system. OFDM can provide large data rates with sufficient robustness to radio channel impairments. One of the major drawbacks for OFDM system is Carrier frequency offset (CFO). Frequency offset has been recognized as a major disadvantage of OFDM. The OFDM systems are sensitive to the frequency synchronization errors in form of Carrier Frequency Offset (CFO), because it can cause the Inter Carrier Interference (ICI) which can lead to the frequency mismatched in transmitter and receiver oscillator. Lack of the synchronization of the local oscillator signal (L.OSC); for down conversion in the receiver with the carrier signal contained in the received signal can cause to degrade the performance of OFDM. On the other hand the orthogonality of the OFDM relies on the condition that transmitter and receiver operate with exactly the same frequency reference. To compensate the effect of CFO the researchers have proposed various CFO estimation and compensation techniques and algorithms by now.

In this paper, the reason of creating CFO and the effects of the CFO on the performance of the OFDM system will study. The major CFO estimation algorithm and techniques will be reviewed and discussed in literature briefly and then our proposed algorithm and technique for estimating and compensation of the effect of CFO will be offered.

8134-10, Session 2

Computational reacquisition of a real three-dimensional object for integral imaging without matching of pickup and display lens array

J. Jung, J. Hong, G. Park, K. Hong, B. Lee, Seoul National Univ. (Korea, Republic of)

The research field of three-dimensional (3D) technologies is considerably widened from 3D display to various applications. Among them, integral imaging and its applications are remarkable methods to acquire and

Conference 8134:
Optics and Photonics for Information Processing V

display a volumetric 3D object with full parallax. However, integral imaging has fundamental issues between acquisition and display phase, which are the pseudoscopic problem and matching of lens specification in pickup and display phase. The depth information of real object is reversed between pickup and display phase because of the direction of rays in acquisition and display phase. It is called the pseudoscopic problem. In addition, the lens array used in display phase has to be matched with pickup lens array for reconstructing 3D object without flipping.

In this paper, we propose the computational reacquisition method to overcome the pseudoscopic and matching problem between acquisition and display phase. First, the depth information of real object is extracted with high precision using optical flows of sub-images. To reconstruct the volumetric 3D object with reversal of depth information, we adopt the triangular mesh reconstruction between point clouds in virtual space. After reconstruction, the real 3D object can be captured in orthoscopic geometry using OpenGL, which can be rotated and translated in reacquisition process. Furthermore, the reacquisition process can generate the elemental image without matching of pickup lens array.

In this paper, we present the experimental results of pickup, reconstruction, reacquisition, and display with various specification of lens array. The proposed method can help to broadcast 3D contents using integral imaging.

8134-11, Session 2

Spectrum analysis of optical signals is based on the resonance phenomenon

M. A. Vaganov, O. D. Moskaletz, St. Petersburg State Univ. of Aerospace Instrumentation (Russian Federation)

Receiving of spectroscopic information by the known modern spectral devices is based on the spatial processing of analyzed optical radiation. This method of receiving spectroscopic information requires a precise alignment and a rigid construction that considerably increases mass and sizes of device.

The spectral device considered in this paper carries out spectral decomposition based on the resonance phenomenon, i.e. the spectral decomposition is implemented by the principle of the narrow-band optical filtration in n parallel channels. Each channel contains the narrow-band optical filter (resonator) which has been set on the certain wave length.

In contrast to the traditional spectral devices, this device can make parallel analysis of optical radiation spectrum, excepting a direct contact with the field of radiation sources. The group of optical fibers realizes the function of transmitting analyzed optical radiation on the given distance.

The results of experimental research are given. These results prove functionality of this spectrum analyzer of optical signals. Furthermore the results of experimental research of white light radiation source are given. The metal halogen lamp was used as a source of white light radiation. This lamp is a part of the spectrum analyzer and is used as the standard source for adjustment of spectral device.

This device realizes ideas of patent 86734 of the Russian Federation.

8134-12, Session 3

High-resolution imaging of retinal neural function

X. Yao, The Univ. of Alabama at Birmingham (United States)

Stimulus-evoked fast intrinsic optical signals (IOSs) in the retina may provide a new method to evaluate the functional connectivity of photoreceptors and inner neurons. In this experiment, we demonstrate the feasibility of IOS imaging of a frog retina slice preparation that allows simultaneous observation of stimulus-evoked responses from the photoreceptors to inner neurons. Robust IOSs were consistently detected from stimulus activated photoreceptor outer segments, inner

plexiform layer (IPL), and ganglion cells; and weak IOSs could be occasionally identified in the outer nuclear layer, outer plexiform layer, and inner nuclear layer between the PR and IPL. At the photoreceptor layer, high magnitude IOSs were mainly confined to the area covered by the visible light stimulus. In comparison, IOSs of the IPL and ganglion layer could spread beyond the image area. High resolution IOS images showed complex spatial distributions of positive and negative IOSs at different retinal layers. At the photoreceptor and ganglion layers, positive and negative optical responses were mixed at a sub-cellular scale. We speculate that the positive and negative signal complexity might result from different types of localized light scattering and transmission changes associated with single activated photoreceptor or ganglion cells. We consistently observed that the IPL was dominated by positive-going optical responses. We hypothesize that the positive signal that dominated the IOS response in the IPL might be related to light scattering changes due to light-regulated release of synaptic vesicles at nerve terminals.

8134-13, Session 3

Development of strain visualization system for microstructures using single fluorescent molecule tracking on three dimensional orientation microscope

S. Yoshida, K. Yoshiki, Univ. of Hyogo (Japan); M. Hashimoto, Osaka Univ. (Japan); T. Namazu, S. Inoue, Univ. of Hyogo (Japan)

We developed a high-spatial-resolution observation system for stress-strain distribution.

In micro/nanostructures, heterogeneous mechanical properties due to preexisting defects cause unpredictable deformations. Non-contact assessment without damage of this heterogeneity is important for industrial and scientific applications such as MEMS (microelectromechanical system)/NEMS (nanoelectromechanical system), polymers, and biological tissue. We suggest a scheme to visualize the heterogeneous distribution of strain in micro/nanostructures by tracing the geometric arrangement of fluorescent single-molecule markers (tracers) sprayed onto the surface of the structures. Deformation between the two tracers is calculated from variations in their physical relationship. Because the density of the distributed tracers limits the spatial resolution of visualization, we traced both the 3D position and 3D molecular orientation of each tracer, which indicate the displacement and surface normal direction of local points on the surface, respectively, to suppress the reduction of spatial resolution due to aliasing.

We sprayed single molecules on a MEMS scanning mirror by ultrasonic atomization to trace the 3D position and 3D orientation-simultaneously. We determined the 3D position by SMD (single-molecule detection), widely used in bioscience research, and 3D orientation by 3D-orientation microscopy, developed previously by us. The 3D orientation microscope detected the molecular orientation from the angular polarization distribution of fluorescence emitted by the tracers. We estimated the spatial resolution as <500 nm in the observation plane and <5000 nm in the depth direction, and the angular resolution was $<3.95^\circ$.

We visualized the strain distribution at the joining area between a supporting beam and the frame of the MEMS mirror.

8134-14, Session 3

Accurate colour control by means of liquid crystal spatial light modulators

I. Moreno, J. L. Martínez, Univ. Miguel Hernández de Elche (Spain); P. García-Martínez, Univ. de València (Spain); M. Sánchez-López, Univ. Miguel Hernández de Elche (Spain)

We present the application of a simple physical model to accurately predict the broadband spectral transmittance and colorimetric properties of a twisted-nematic liquid crystal display (TNLCD). We spectroscopically calibrate the retardance parameters to evaluate the spectrum of the

Conference 8134:
Optics and Photonics for Information Processing V

light transmitted by a TNLCD sandwiched between two linear polarizers. When the TNLCD is illuminated with a broadband light source, the full spectrum can be predicted as a function of the addressed grey level for any arbitrary orientation of the polarizers. When the TNLCD is illuminated with spectrally separated components onto different pixels, and then recombined, a full colour and luminance control is achieved. Experimental results confirming the validity of the proposed systems are presented, both on the measured spectral responses as well as on the trajectories at different chromatic diagrams. The presented results can be useful for optoelectronic systems requiring an accurate control of the spectral characteristics of the light.

8134-15, Session 3

Two-dimensional phase imaging based on closed-loop feedback control

E. Watanabe, The Univ. of Electro-Communications (Japan); M. Toshima, Japan Women's Univ. (Japan); C. Fujikawa, Tokai Univ. (Japan)

Recently, in the biomedical measurement field, to advance the clarification of cell's function, the quantitative measurement with non-invasive diagnosis for a transparent object has become needed.

To observe the shape of transparent biological cell, in the present day, the fluorescence microscope is used to convert phase information into intensity information using a fluorescent substance. Also, the phase contrast microscope is used to convert relative phase information into intensity information. If absolute phase information can be acquired noninvasively, it becomes possible to obtain the quantitative three-dimensional shape on the biological cell.

In addition, the refractive index modulation type optical elements with microstructure, including the optical waveguide devices and the high dispersion Volume Phase Holographic (VPH) grating, are developed with the advancement of optical communications technology. Since optical devices are often manufactured using optical sensitization resin, they do not have mechanical structure. So, stylus method and a scanning electron microscope (SEM) cannot be used for evaluation. The structure is estimated by comparing the characteristic with simulation results. Therefore, a simple method to directly measure the refractive index distribution is desired.

We are developing the scanning Mach-Zehnder type interferometer that detects refractive index distribution as phase change, assuming transparent object with a constant thickness and smooth change in refractive index. We have been able to measure and confirm phase variations less than a wavelength from a small fraction of a wavelength to several wavelengths in linear scale by introducing the feedback control technique. In this paper, we describe the high accuracy vertical phase measurement system we have constructed, and the two-dimensional scanner for the biological cell in the fluid medium, followed by the report of fundamental evaluation result as applications in tissue engineering.

8134-16, Session 3

Converting a 3D surface into a set of points with directional scattering properties for high-resolution radar response simulation

H. Perälä, M. Väilä, J. Jylhä, I. Venäläinen, A. J. E. Visa, Tampere Univ. of Technology (Finland)

It is practical and efficient to simplify targets to point scatterers in radar simulations. With low-resolution radars, the radar cross section (RCS) is a sufficient feature to characterize a target. However, RCS is dependent only on the aspect angle and totals the target scattering properties to a scalar value for each angle. Thus, a more detailed representation of the target is required with high-resolution radar techniques, such as Inverse Synthetic-Aperture Radar (ISAR). Traditionally, high-resolution targets have been modeled placing identical point scatterers in the shape of

the target, or with a few dominant point scatterers. As extremely simple arrangements, these do not take the self-shadowing into account and are not realistic enough for high demands.

Our radar response simulation studies required a target characterization akin to RCS, which would also function in high-resolution cases and take the self-shadowing and multiple reflections into account. Thus, we propose an approach to converting a 3-dimensional surface into a set of scatterers with locations, orientations, and directional scattering properties. The method is intended for far field operation, but could be used in the near field with alterations. It is based on ray tracing which provides the self-shadowing and reflections naturally. In this paper, we present ISAR simulation results employing the proposed method. Being invariant to the used radar wavelength, the extracted scatterer set enables the fast production of realistic simulations including authentic RCS scattering center formation. This paper contributes to enhancing the reality of the simulations, yet keeping them manageable and computationally reasonable.

8134-17, Session 3

Improving spatial coherence in high power lasers

A. D. McAulay, Lehigh Univ. (United States)

Two ways to improve spatial coherence in high power beams are considered and compared, spatial filter and adaptive optics. High-power in lasers is usually produced by using a succession of optical amplifiers. As intensity increases in optical amplifiers or lasers, spatial coherence decreases because of uneven heating and other nonlinearities. It is common to use a spatial filter in the form of a pinhole after each stage that will block the parts of the beam that are spatially incoherent and would scatter sideways out of the beam. The loss of light blocked by the pinhole lowers amplification so that more amplifiers are required. An alternative approach to improving spatial coherence uses adaptive optics. In this case the wavefront is measured using a wavefront sensor such as a Hartman wavefront sensor or with a photonic crystal, (A. D. McAulay and H. Tong, SPIE 5435-13 April 2004). The measurements are used to compute settings for a deformable mirror (A. D. McAulay, Optical computer architectures, Wiley 1991), (A. D. McAulay, Optical Engineering, 25(18), Jan. 1986). This involves a complicated feedback loop and discretization of the wavefront sensor and deformable mirror that limits the accuracy depending on the application. We discuss the pros and cons for each approach to determine which approach is more suitable for what application. For example adaptive optics is used for improving spatial coherence in the Airborne laser program (ABL). On the other hand spatial filters are used in some inertial confinement experiments for nuclear fusion.

8134-22, Poster Session

High-quality edge-enhancement imaging in optical microscopy

S. Wei, Nankai Univ. (China); S. Zhu, Nankai Univ. Affiliated Hospital (China); X. Yuan, Nankai Univ. (China)

Since biological cells are weak-phase objects, their images formed in bright-field optical microscopes are usually displayed with small contrast. A famous technology to solve this problem is coherent spatial image filtering with a spiral phase structure which has been used as a spatial filter to implement a radial Hilbert transform for optical filtering in image processing, leading to a strong and isotropic edge contrast enhancement of both amplitude and phase objects. We report a Bessel-like amplitude modulated spiral phase filtering system for real-time spatial image edge enhancement in optical microscopy. The method is based on a Fourier 4-f spatial filtering system. And this method can transform phase gradient to intensity distribution. We compare the PSF of Bessel-like amplitude modulated spiral phase filter, conventional spiral phase filter, dark field spiral phase filter and the Laguerre-Gaussian modulated spiral phase filter. And the proposed technique further reduces the imaging diffraction

Conference 8134:
Optics and Photonics for Information Processing V

noise with the new filter. Experimental verifications in edge enhancement are implemented by a phase-only spatial light modulator for realizing the amplitude modulated spiral phase. It is shown that the proposed technique is able to achieve high contrast cells edge enhancement with high resolution.

8134-23, Poster Session

Characteristic values of Mueller-matrix images of biological tissues during the diagnostics of physiological changes

A. V. Dubolazov, Yuriy Fedkovych Chernivtsi National Univ. (Ukraine)

In this work, we have theoretically grounded conceptions of characteristics points observed in coordinate distributions of Mueller matrix elements for a network of human tissue biological crystals. The interrelation between polarization singularities of laser images inherent to these biological crystals and characteristic values of above matrix elements is found. We have determined the criteria for statistical diagnostics of pathological changes in the birefringent structure of biological crystal network by using myometrium tissue as an example. The paper deals with investigating the processes of laser radiation transformation by biological crystals networks using the singular optics techniques. The results obtained showed a distinct correlation between the points of "characteristic" values of coordinate distributions of Mueller matrix ($M=0$; $+1$) elements and polarization singularities (L- and C-points) of laser scattering field.

8134-24, Poster Session

Complex degree of mutual anisotropy in diagnostics of biological tissues physiological changes

A. V. Dubolazov, Yuriy Fedkovych Chernivtsi National Univ. (Ukraine)

To characterize the degree of consistency of parameters of the optically uniaxial birefringent liquid crystals (protein fibrils) nets of biological tissues (BT) a new parameter - complex degree of mutual anisotropy is suggested. The technique of polarization measuring the coordinate distributions of the complex degree of mutual anisotropy of biological tissues is developed. It is shown that statistic approach to the analysis of complex degree of mutual anisotropy distributions of biological tissues of various morphological and physiological states and optical thicknesses appears to be more sensitive and efficient in differentiation of physiological state in comparison with investigations of complex degree of mutual polarization of the corresponding laser images.

8134-25, Poster Session

A fractal and statistic analysis of Mueller-matrix images of phase inhomogeneous layers

A. V. Dubolazov, Yuriy Fedkovych Chernivtsi National Univ. (Ukraine)

The features of polarization tomography of optically anisotropic architectonic nets of biological tissues of different morphological structure have been investigated. The criteria of early diagnostics of the appearance of degenerative-dystrophic and pathological changes of the structure of biological tissues optically anisotropic architectonics have been determined. Specific features of the formation of local and statistical polarization structures of laser radiation scattered in phase-inhomogeneous layers of biological tissue were studied. The distribution

of azimuth and ellipticity of boundary field polarization was found to correlate with the orientation-phase structure of multifractal phase-inhomogeneous layers. A method of polarization phase reconstruction of BT architectonics was suggested. Polarization fractalometry of two-dimensional parameters of Mueller matrixes of biological tissue images is effective in diagnostics of changes of coordinate distributions of orientations and optical anisotropy of their architectonic nets, formed by the collagen bundles. The set of diagnostically urgent properties, determining the interconnection between statistic, correlation and fractal characteristics of 2D Mueller matrixes parameters of biological tissue images and their physiological state has been determined.

8134-26, Poster Session

Study the effect of the symbol time offset (STO) for OFDM in wireless communication systems

S. Mohseni, M. A. Matin, Univ. of Denver (United States)

Orthogonal Frequency Division Multiplexing (OFDM) which is a digital multi-carrier modulation scheme has been accepted by most of the wireless communication systems and has a wide range of applications, i.e. WLAN IEEE 802.11a, Ultra-wideband (UWB), Digital Video Broadcasting (DVB) and so on.

In OFDM systems three significant synchronization errors can occur, Symbol Time Offset (STO), Sampling Clock Frequency Offset (SCFO), and Carrier Frequency Offset (CFO).

STO can create two problems; phase shift (phase distortion), and Inter Symbol Interference (ISI) which can reduce the performance of OFDM system. By using the STO estimation techniques with using of the synchronizing technique in receiver, the effect of phase shift can be compensated and we can overcome the effect of STO.

In this paper we discuss and investigate the cause of creating STO and its effect for OFDM communication systems. We also talk about a few proposed algorithms for STO estimation technique in literature, and then we propose our STO Estimation algorithm for removing and canceling this phenomenon with showing the simulation result. All the simulations have been done in MATLAB.

8134-27, Poster Session

Extended focal depth and lateral super resolution in optical coherent tomography system

W. Liang, Univ. of Jinan (China); M. Yun, M. Liu, F. Xia, Qingdao Univ. (China)

The resolution of the Optical Coherence Tomography (OCT) system is defined the depth resolution and the lateral resolution of the system. The depth resolution is dependent on the coherence length and the lateral resolution depends on the beam waist on the sample. In OCT, the depth (axial) and the lateral resolutions are independent of one another. Optical axial resolution can thus be increased by selecting a broad band source since the coherence length of the light source is inversely proportional to the bandwidth. The numerical aperture (NA) of the lens that focuses the beam on the sample determines the lateral resolution. Large NA results in a high lateral resolution. However, the depth of focus which is defined by two times of Raleigh range of the focused beam will be decreased. This is a trade-off between lateral resolution and depth of focus.

In this paper, a new kind of polarization pupil mask, which consists of a three-portion half-wave plate between two parallel quarter-wave plates, is introduced into the OCT systems. has the ability to realize the focal shift and extend the focal depth in a small range when used as an apodizer in the optical imaging system. The results show that high focal depth which is two times of the original optical system and the lateral superresolution can be realized at the same time. Furthermore, it is shown that the focal shift strongly depends on the phase of the half-wave plate, and there is a linear relation between of them.

8134-28, Poster Session

A new method for acquiring the complex hologram in optical scanning holography

M. Zhu, E. Dai, L. Liu, A. Yan, J. Sun, Y. Wu, Y. Zhou, Y. Zhi, Shanghai Institute of Optics and Fine Mechanics (China)

In this paper, we propose a new method that can acquire the complex hologram of a 3D object for optical scanning holography (OSH) by using polarized optical elements and a 90 degree 2x4 optical hybrid. The 3D object is scanned by two coaxial beams with orthogonal polarization and the transmitted/or reflected signal light is divided into two beams by a polarized beamsplitter (PBS). Then these two separated beams pass through a quarter and a half wave plates, respectively, and heterodyne detected by a 90 degree 2x4 optical hybrid with two balanced detectors. The complex hologram, which contains the 3D information of the object, can be constructed from the outputs of the balanced detectors of the optical hybrid. Compared with the conventional OSH, the acousto-optic modulator and complex electronic system are not needed in this method. Another advantage of this method lies in its high efficiency since there is no energy loss in the generation of the scanning beam by using the polarized optical elements. This method should be used for 3D holographic microscopy and 3D holographic television.

8134-29, Poster Session

Study on resampling interpolation algorithms for Fresnel telescope imaging system

X. Lv, L. Liu, A. Yan, J. Sun, B. Li, Shanghai Institute of Optics and Fine Mechanics (China)

Fresnel telescope full-aperture synthesized imaging lidar is a new high resolution active laser imaging technique. It is based on the optoelectronic data collection from the relative scanning between target and two co-centric coaxial beams of orthogonal polarization quadratic wavefronts. Optical receiving system of low quality is allowed to be used to increase optical receiving aperture and decrease laser transmitting power due to the use of an optical hybrid. In the operational mode with moving target by beam scanning, because of the movement of the target, space distribution of the complex data is not regular or uniform. What's more, if the target is a mesh target or moves in oblique line, the space distribution and the numerical value of sampling data will be more complex.

In order to use FFT in signal processing, the sampling data should be uniform in quadrature space distribution. As a result, algorithms for fresnel telescope imaging system should include resampling interpolation process. We test several resampling interpolation algorithms for Fresnel telescope. Mathematical analysis and computer simulation are also given. The work is found to have substantial practical value and offers significant practical benefit for high resolution imaging of Fresnel telescope laser imaging lidar.

8134-30, Poster Session

The location of laser beam cutting based on the computer vision

Y. Wu, Shanghai Institute of Optics and Fine Mechanics (China); S. Zhu, Shanghai Kasu Intelligent Technology Co., Ltd. (China); Y. Zhi, W. Lu, J. Sun, E. Dai, A. Yan, L. Liu, Shanghai Institute of Optics and Fine Mechanics (China)

Based on the computer vision theory, this article researched the algorithm for the location of laser beam cutting. This article combines Canny operator and thresholding image. It overcomes the inaccuracy of edge detection and clutter jamming problem which are caused by the poor quality of acquired images. Collecting the key points of target edge,

making B-spline curves fitting, it solved the problem that target edge is jagged. And it uses interpolation algorithm to locate the point for laser beam cutting. At last, we developed corresponding and professional software system which is based on Visual Studio2003 C#.

8134-31, Poster Session

Sample spectra of optical signals

A. Zhdanov, O. D. Moskaletz, St. Petersburg State Univ. of Aerospace Instrumentation (Russian Federation)

New kind of optical signals spectral processing is considered. This processing is performed as optical radiation sample spectrum analysis. The sample spectrum means analysis on discrete sequence of finite time intervals. These spectra are variable in time and introduced into optical spectral measurements theory for the first time. Presently optical spectral devices operate with the power spectrum. At the same time a detailed examination of optical spectrum analyzing procedures requires the non-traditional theory introduction for optical spectral measurements of complex time-variable spectra. Complex instantaneous and moving optical spectra are known.

Optical range spectral devices that can measure sample spectra are considered as linear systems. That totally corresponds to Fourier integral theory. Comprehensive description of any linear system is its response to a delta effect. Complex spectrum spread function of an optical spectral device that performs sample spectrum analysis is introduced as a response to the delta function. This spectrum spread function allows determining the most important in spectrum measurement theory spectral device input-output ratio and in measurement of complex sample spectra. This ratio is a linear integral operator. The complex spectrum spread function is integral operator kernel.

Complex sample spectrum in optical range can be obtained by using a dispersive system. Examination the single optical pulse distribution in a dispersive medium is the theoretical basis of measurement the complex sample spectrum. Dispersive system is considered to be an optical four-pole network. Transfer function is its comprehensive description. The dispersive system parameters are defined to allow the optical signals complex spectrum measurement. The transition to traditional optical spectroscopy power spectra is considered. These spectra are the time quadratic averaging complex sample spectra result. Transition to the power spectrum includes quadratic photodetection and partial quadratic effects summation.

8134-32, Poster Session

Development of the visual encryption device using higher-order birefringence

H. Kowa, T. Murana, K. Iwami, N. Umeda, Tokyo Univ. of Agriculture and Technology (Japan); M. Tsukiji, Uniop Co. Ltd. (Japan); A. Takayanagi, Tokyo Univ. of Agriculture and Technology (Japan)

We propose and demonstrate a novel visual encryption device composed of higher-order birefringence elements. When a material which has higher-order birefringence is placed between a pair of polarizers and illuminated with white light to observe it, it appears just white. In contrast, when it is illuminated with monochromatic light, the transmitted intensity varies depending sinusoidally on the wavelength. Array of such material can express information (e.g. letters and/or images) by controlling birefringence of each pixel. If the birefringence phase difference is adjusted for a certain wavelength, the information will be clearly displayed with a certain wavelength. We call this wavelength a key wavelength. The encryption device was fabricated by controlling the amount of higher-order birefringence so as to give a high contrast only at the key wavelength under polarized illumination. Thus, the information stored in the device can be decoded only by illuminating it with the key wavelength.

To confirm the validity of the encryption principle, we constructed a 3 x

Conference 8134:
Optics and Photonics for Information Processing V

3 pixel device in which commercial retarder films were laminated. The fabricated device was observed by the illumination of monochromatic light. The readout was performed with the monochromatic light of key wavelength, and the stored letter could be clearly observed. On the other hand, the brightness of pixel was random distribution in the readout experiment with the illumination that was not the key wavelength, and the letter could not be recognized.

Furthermore, stored information can be easily distributed to multiple physical keys which show arbitrary images. In this case, the birefringence phase difference is obtained by summing the values of retardation of each pixel of physical keys. The decoded result is obtained by superimposing them and taking the exclusive-OR (XOR) using the encoded values. It was shown that the observed image with the experimental device was decoded by superimposing (XORing) the two images with different physical key.

8134-33, Poster Session

A common-path white-light shearing interferometer with adjustable spatial carrier

G. Chen, China Academy of Engineering Physics (China)

No abstract available

8134-19, Session 4

Effects on beam alignment due to neutron-irradiated CCD images at the National Ignition Facility

A. A. S. Awwal, A. M. Manuel, P. S. Datte, S. C. Burkhart, Lawrence Livermore National Lab. (United States)

The 192 laser beams in the National Ignition Facility (NIF) are automatically aligned to the target-chamber center using images obtained through charged coupled device (CCD) cameras. Several of these cameras are in and around the target chamber during an experiment. Current experiments for the National Ignition Campaign are attempting to achieve nuclear fusion. Neutron yields from these high energy fusion shots expose the alignment cameras to neutron radiation. The present work explores modeling and predicting laser alignment performance degradation due to neutron radiation effects, and demonstrates techniques to mitigate performance degradation. Camera performance models have been created based on the measured camera noise from the cumulative single-shot fluence at the camera location. We have found that the effect of the neutron-generated noise for all shots to date have been well within the alignment tolerance of half a pixel, and image processing techniques can be utilized to reduce the effect even further on the beam alignment.

8134-20, Session 4

Automated segmentation of the dynamic heart tube in OCT images with Snake based on noise model

S. Sun, Clemson Univ. (United States)

To segment the dynamic heart tube in optical coherence tomography (OCT) images is essential for studying heart development. However, it is a great challenge to process the very large 2D, 3D and 4D (3D volumes + time) OCT slices manually. So, segmentation with computer automatically is critical. Due to its noisy feature, as well as the deformable aspect of the object, the heart tube, it is difficult to carry out the segmentation with conventional approach. An active contour model (Snake), in which objects are detected in a given image using techniques of curve evolution, is thought as a good solution to this issue. In this paper, a segmentation algorithm of the dynamic heart tube in OCT images with

Snake is explored. Firstly, the noise of the OCT image is analyzed in detail and the mathematic model of the noise is established and tested. Secondly, the image is denoised, the coarse contour of the image is detected and a new convolution kernel for the Snake is proposed, considering the noise characteristic of the OCT image. The performance of the proposed system is compared with the existing ones and the pros and cons are discussed. Finally, a fast algorithm is discussed.

8134-21, Session 4

Research on testing instrument and method for correction of the uniformity of image intensifier fluorescence screen brightness

Y. Qiu, Nanjing Univ. of Science & Technology (China)

To test the parameters of image intensifier screen is the precondition for researching and developing the third generation image intensifier. The picture of brightness uniformity of tested fluorescence screen shows bright in middle and dark at edge. It is not so direct to evaluate the performance of fluorescence screen. We analyze the energy and density distribution of the electrons, After correction, the image in computer is very uniform. So the uniformity of fluorescence screen brightness can be judged directly. It also shows the correction method is reasonable and close to ideal image. When the uniformity of image intensifier fluorescence screen brightness is corrected, the testing instrument is developed. In a vacuum environment of better than 1×10^{-4} Pa, area source electron gun emits electrons. Going through the electric field to be accelerated, the high speed electrons bombard the screen and the screen luminize. By using testing equipment such as imaging luminance meter, fast storage photometer, optical power meter, current meter and photosensitive detectors, the screen brightness, the uniformity, light-emitting efficiency and afterglow can be tested respectively. System performance are explained. Testing method is established; Test results are given. Photocathode, microchannel board and fluorescence screen are the three important photoelectrical components that determine the imaging performance of dim light and UV image intensifier. In the production of screen, due to lack of equipment to evaluate the production quality of the fluorescence screen, the result is that the related products has low quality pass rates and at the same time the price stays high. Testing Instrument of Image Intensifier Fluorescence Screen is urgently needed. With the developing of the research work of Third generation Image Intensifier, the performance of Photocathode, microchannel board has been significantly improved, so to test of screen performance is particularly important. Then Multi-Parameter testing instrument of image intensifier fluorescence screen is developed and the research findings and developed product are introduced in this paper.

8134-34, Session 4

Nonlinear fringe-adjusted JTC-based face tracking using an adaptive decision criterion

I. Leonard, Institut Supérieur d'Electronique du Nord (France); A. Alfalou, Institut Supérieur de l'Electronique et du Numerique (France); M. S. Alam, Univ. of South Alabama (United States)

In this paper, we propose a new technique for rotation invariant recognition and tracking of the face of a target person in a given scene. We propose an optimized method for face tracking based on the Fringe-adjusted JTC architecture. To validate our approach, we used the PHPID data base containing faces with various in-plane rotations. To enhance the robustness of the proposed method, we used a three-step optimization technique by: (1) utilizing the fringe-adjusted filter (HFAF) in the Fourier plane, (2) adding nonlinearity in the Fourier plane after applying the HFAF filter, and (3) using a new decision criterion in the correlation plane by considering the correlation peak energy and five largest peaks outside the highest correlation peak. Several tests were made to reduce the number of reference images needed for fast tracking while ensuring robust discrimination and efficient of the desired target.

Conference 8135: Applications of Digital Image Processing XXXIV

Monday-Wednesday 22-24 August 2011 • Part of Proceedings of SPIE Vol. 8135
Applications of Digital Image Processing XXXIV

8135-01, Session 1

Statistical segmentation and porosity quantification of 3D x-ray micro-tomography

D. M. Ushizima, J. B. Ajo-Franklin, P. Nico, A. A. MacDowell, E. W. Bethel, Lawrence Berkeley National Lab. (United States)

Synchrotron particle accelerators enable the acquisition of high-resolution micro-tomography, allowing imaging of solid materials at micrometer level. Consequently, there is generation of large data files, which undermines the performance of several image processing and segmentation algorithms. We propose a methodology to filter, segment and extract features from stacks of image slices of porous media, using efficient algorithms. A first step is responsible for reducing the image noise through signal-to-noise ratio analysis, so that one can tune scale parameters to the filtering algorithm. Next, a fast anisotropic filter removes ring artifacts from each slice, smoothing homogeneous regions while preserving borders. Later, the image is partitioned using statistical region merging, exploiting the intensity similarities of each segment. At last, we calculate the porosity of the material based on the solid-void ratio. Our contribution is to design a pipeline tailored to deal with large data-files, to use free libraries and to run on high performance computers. We illustrate our methodology using more than 2,000 micro-tomography images from 4 different porous materials imaged using high-resolution x-ray. Also, we compare our results with common, yet fast algorithms often used for image segmentation, which includes median filtering and thresholding. This paper is part of an effort to implement nondestructive techniques to quantify properties in the interior of solid objects, including information on their 3D geometries, which supports modeling of the fluid dynamics into the pore space of the host object.

8135-02, Session 1

Evaluation of the paper surface roughness on real-time using image processing

A. O. Pino, Univ. Politècnica de Catalunya (Spain)

Surface roughness measurement is one of the central measurement problems in paper industry. Measurements require laboratory conditions, but there is a need for measuring the roughness during the production process. At the moment, air leak methods (Bendtsen, Bekk, Sheffield and Parker Print Surf) are standardized and employed as roughness rating methods. We present an experimental approach to measure of the roughness of the paper online based in the analysis of speckle pattern on the surface. The image formed by speckle in the paper surface is considered as a texture, and therefore texture analysis methods are suitable for the characterization of paper surface. The properties of this speckle pattern are used for estimation and quantification of roughness parameter. We applied digital image processing using statistics of second order, specifically the gray level co-occurrence matrix (GLCM), so this method can be considered as non-contact surface profiling method. The results are contrasted to air leak methods (Bendtsen and Bekk).

8135-03, Session 1

Methodology for approximating and implementing fixed-point approximations of cosines for order-16 DCT

A. T. Hinds, InfoPrint Solutions Co. (United States)

No abstract available

8135-04, Session 1

Contactless cardiac pulse measurements during exercise using imaging PPG with motion-artifacts reduction

Y. Sun, S. Hu, V. Azorin-Peris, Loughborough Univ. (United Kingdom); S. E. Greenwald, Barts and The London School of Medicine and Dentistry (United Kingdom); J. Chambers, Loughborough Univ. (United Kingdom); Y. Zhu, Shanghai Jiao Tong Univ. (China)

Compared to the contact photoplethysmographic (PPG) sensor, imaging PPG (iPPG) could provide comfortable physiological assessment over a wide range of anatomical locations. However, the characteristic of susceptible to motion artifacts limits the application range of iPPG systems. In this paper, continuous monitoring of the respiratory and pulsatile variation during cycling exercise was taken via an experimental iPPG system with motion artifacts reduction techniques. To evaluate the reliability and sensitivity of the iPPG system and also motion cancellation techniques, two levels of the physical exercise were introduced. A 12 minutes continuous recording was taken from each of 10 volunteers. The time-frequency-representation (TFR) method was used to visualize the time-dependent behavior of the signal frequency. The results show that heart and respiration rates could be successfully traced even under a high-intensity physical exercise. This feasibility study therefore lead to a new insight in accurate clinical assessment and remote sensing of vital signs for sports purpose.

8135-05, Session 1

Page layout analysis and classification in complex scanned documents

M. S. Erkilinc, M. Jaber, E. Saber, Rochester Institute of Technology (United States); P. Bauer, Hewlett-Packard Co. (United States)

In this paper, a classification algorithm is proposed to locate and extract text, image, line and strong-edge regions in color-scanned documents. The algorithm is developed to handle simple to complex page layout structure and content (text only vs. book cover that includes text, lines, graphics and/or photos). Text and image recognition in scanned document is an essential application for document retrieval from digital archives and web sites. The proposed algorithm can also be used for object-oriented rendering in a printing pipeline.

The methodology consists of four modules. The first module employs wavelet analysis to generate a text-region candidate map which is enhanced by applying a Run Length Encoding technique for verification purposes. The image extraction module is based on block-wise segmentation where basis vector projections are used. The basis vectors give an initial map for image/pictorial regions. Moreover, Hough transform is utilized to locate lines in the scanned document. Techniques for edge detection, edge linkages, and line-segment fitting are utilized to detect strong-edges in the last module. After those four region maps are obtained, using a Markov Random Field model in an Iterative Computational Mode framework is employed to generate a final page layout map.

8135-06, Session 1

Gas plume detection algorithms for thermal hyperspectral imagery

E. M. Burdette, L. L. West, S. E. Lane, J. M. Cathcart, Georgia Tech Research Institute (United States)

Remote detection and identification of gaseous plumes is of interest in many areas, including pollution detection, geothermal emissions monitoring, and military target analysis. Spectral gas plume analysis has been enabled by hyperspectral imaging radiometers, leading to the development of numerous plume detection algorithms and data processing techniques. To date such processes have largely been applied to datasets collected during controlled gas releases, where the gas temperature, concentration, and background radiance are known. Using a novel dataset showing gaseous plumes emitted continuously by underground thermal features at Yellowstone National Park, we apply known material identification algorithms to detect the presence of individual gas species in a mixed gas cloud. Prior to applying detection algorithms, we explore data pre-processing variations on image irregularity and off-angle correction. Because the sensor transforms the spectral features of the materials it observes depending on material geometry and location within the scene, among other factors, developing an accurate spectral radiance signature of the gas or gases of interest is a challenging aspect of gas plume identification. We therefore present results from different target modeling and discrimination efforts preceding the intra-scene search for target matches. We demonstrate the successful detection and identification of carbon dioxide gas from a mixture of water vapor, hydrogen sulfide, and carbon dioxide. Thoughts on generalizing our detection methods for application to other uncontrolled gas release scenarios are also presented.

8135-07, Session 1

Estimation of camera matrix in lunar surface using N-views

P. Duraisamy, Univ. of North Texas (United States)

This paper focuses 2D-3D camera pose estimation in lunar surface using craters as features by N-views. The estimation of 2D-3D camera pose in lunar surface is a challenging problem due to lack of conventional features like points, lines and corners. We used craters as our feature using generalized Hough transform. The pose estimation is implemented by determining extrinsic camera parameters using crater matching between images. We also shown the validity of the approach by experimenting on N-views using crater as features.

8135-08, Session 1

A method of improving structured light scanning point cloud using stereo image processing

R. Shi, L. Zhu, Y. Yu, Beijing Univ. of Civil Engineering and Architecture (China)

Main defect of the structured light scanning is that the edge part is lost in the point clouds of scanned object. This study is to present a method that can remedy the flaw.

Many scholars try to combine laser scanning data with digital images. Because there are more detailed textures in the images, and many kinds of algorithms can be used to extract the image edge to improve the laser scanning point cloud. Thereby, the structured light scanning should be more feasible since its images are the original data accessed. This research tried to combine the image processing method to a structured light system in order to improve the quality of the point cloud and the TIN derived. The approach is followed as below: Firstly, a high-precision edge extraction algorithm is used to extract the edge from each image

of a pair of stereo image respectively. Exactly, a Positioning Operator is adopted to position the point and edge of the image feature by sub-pixel accuracy. Secondly, based on an Epipolar Constraint, the corresponding image features (point and edge) are determined only from the results of the feature extraction. The 3D coordinates of every pair of points are calculated with the functions of photogrammetry and then, the 3D edge model is built. Thirdly, the 3D edge model is transformed to the unified structured light coordinate system by a coordinate transformation algorithm. After overlying the edge part of the 3D model to the original point cloud from structured light system, their hiatus can be restored and the resolution of the original point cloud can be improved.

8135-09, Session 1

Pattern recognition with composite correlation filters designed from noisy training images

P. M. Aguilar-Gonzalez, V. I. Kober, Ctr. de Investigación Científica y de Educación Superior de Ensenada (Mexico)

Correlation filters for target detection are usually designed under the assumption that the appearance of a target is explicitly known. Because the shape and intensity values of a target are used, correlation filters are highly sensitive to changes in the target appearance in the input scene, such as those of due to rotation or scaling. Composite filter design was introduced to address this problem by accounting for different possibilities for the appearance of the target within the input scene. However, explicit knowledge for each possible appearance is still required. In this work, we propose composite filter design when an object to be recognized is given in noisy training images and its exact shape and intensity values are not explicitly known. Optimal filters with respect to the peak-to-output energy criterion are derived and used to synthesize a single composite filter that can be used for distortion invariant target detection. Parameters required for filter design are estimated with suggested techniques. Computer simulation results obtained with the proposed filters are presented and compared with those of common composite filters.

8135-10, Session 1

Multi-classification of objects in cloudy environments

O. G. Campos Trujillo, V. H. Diaz-Ramirez, F. J. Ramirez Arias, Ctr. de Investigación y Desarrollo de Tecnología Digital (Mexico)

A two-step procedure for the reliable recognition and multiclassification of objects in cloudy environments is presented. The input scene is preprocessed with the help of an iterative algorithm to remove the effects of the cloudy environment followed by a complex correlation filtering for the multiclassification of target objects. The iterative algorithm is based on a local heuristic search inside a moving window using a nonlinear signal model for the input scene that relates the scene-depth and the intrinsic parameters of the environment such as the scattering coefficient, ambient light, and objects reflectance. A main objective of the local search is to estimate the scene-depth inside the moving window that maximizes the local contrast of the restored image inside the window. The preprocessed scene is therefore correlated with a multiclass correlation filter based in complex synthetic discriminant functions. The correlation filter is constrained to yield prespecified magnitude and phase values at the central locations of the training images. The magnitude information in the output complex correlation plane is used for recognition of objects whereas the phase information is employed for the classification of the recognized targets. Computer simulation results obtained with the proposed approach in synthetic and real cloudy images are presented, discussed, and compared with existing similar methods in terms of different performance metrics.

8135-11, Session 1

3D object recognition with integral imaging using neural networks

C. M. Do, Univ. of Connecticut (United States)

An overview of three-dimensional (3D) object recognition using neural networks is presented. Three dimensional sensing and imaging of 3D objects is performed using an integral imaging optical set up. Neural network technique is applied to recognize 3D objects. Experimental results are presented together with computational results for performance assessment.

8135-12, Session 1

LADAR range image interpolation exploiting pulse width expansion

J. W. Motes, R. K. Martin, K. Mathews, Air Force Institute of Technology (United States)

Laser radar (LADAR) systems produce both a range image and an intensity image. When the transmitted LADAR pulse strikes a sloped surface, the returned pulse is expanded temporally. This makes it possible to estimate the gradient of a surface, pixel by pixel. This paper seeks to find the gradient of the surface of an object from a realistic LADAR return pulse that includes probabilistic noise models and atmospheric effects. Interpolation techniques applied to the embedded information in the gradient will allow the sampling density to be taken at below the Nyquist criterion while still facilitating an effective 3D reconstruction of an image.

8135-73, Session 1

Fast computing of discrete cosine and sine transforms of types VI and VII

R. Chivukula, Y. A. Reznik, Qualcomm Inc. (United States)

Discrete Sine Transform (DST) of type VII has recently been shown to be useful for image and video coding.

At the same time, type VII as well as type VI transforms seem escaped attention of researchers working on fast algorithms, and to the best of our knowledge no such algorithms have been published yet. In this paper we derive a family of fast algorithms for discrete cosine and sine transforms (DCT and DST) of types VI and VII by establishing a mapping between these transforms and Discrete Fourier Transform of length $2N+1$, where N is the length of the original DCT/DST transforms.

We use this mapping to derive complete designs of DST and DCT transforms of lengths $N=4, 8, \text{ and } 16$.

8135-13, Session 2

Seam carving for semantic video coding

M. Décombas, Thales Communications S.A. (France) and Telecom ParisTech (France); F. Capman, E. Renan, Thales Communications S.A. (France); F. Dufaux, B. Pesquet-Popescu, Telecom ParisTech (France)

No abstract available

8135-14, Session 2

Mosaic-guided video retargeting for video adaptation

C. Tsai, T. Yen, C. Lin, National Tsing Hua Univ. (Taiwan)

Video retargeting from a full-resolution video to a lower-resolution display will inevitably cause information loss. Content-aware video retargeting techniques have been studied to avoid critical visual information loss while resizing a video. Maintaining the spatio-temporal coherence of a retargeted video is very critical on visual quality. In this paper, we propose the use of a panoramic mosaic to guide the scaling of corresponding regions of video frames in a video shot to ensure good spatio-temporal coherence. In the proposed method, after aligning video frames in a shot to a panoramic mosaic constructed for the shot, a global scaling map for these frames is derived from the panoramic mosaic based on a rate-distortion optimization framework. Subsequently, the local scaling maps of individual frames are derived from the global map and is further refined according to spatial coherence constraints. Our experimental results show that the proposed method can minimize the information loss due to retargeting while maintaining spatio-temporal coherence.

8135-15, Session 2

Dependent video coding using a tree representation of pixel dependencies

G. Valenzise, L. Amati, Politecnico di Milano (Italy); A. Ortega, The Univ. of Southern California (United States); S. Tubaro, Politecnico di Milano (Italy)

Motion-compensated prediction induces a chain of coding dependencies between pixels in video. In principle, an optimal selection of encoding parameters (motion vectors, quantization parameters, coding modes) should take into account the whole temporal horizon of a GOP. However, in practical coding schemes, these choices are made on a frame-by-frame basis, thus with a possible loss of performance. In this paper we describe a tree-based model for pixelwise coding dependencies: each pixel in a frame is the child of a pixel in a previous reference frame. We show that some tree structures are more favorable than others from a rate-distortion perspective, e.g., because they entail a large descendance of pixels which are well predicted from a common ancestor. We favor such structures by adding a special "discount" term to the conventional Lagrangian cost adopted at the encoder. The proposed method has a global impact on the encoder performance, since it affects the choice of: motion vectors; quantization parameters; and coding modes. We modified a state-of-the-art H.264/AVC codec to embed our tree model. Our experiments demonstrate that taking into account the temporal dependencies between pixels can lead to substantial coding gains for sequences with little motion, whereas there is still large room for improvement in sequences with medium-to-high motion.

8135-16, Session 2

Perceived quality of DIBR-based synthesized views

E. Bosc, Institut National des Sciences Appliquées de Rennes (France); R. Pepion, P. Le Callet, Univ. de Nantes (France); M. Koppel, P. Ndjiki-Nya, Fraunhofer-Institut für Nachrichtentechnik Heinrich-Hertz-Institut (Germany); L. Morin, M. Pressigout, Institut National des Sciences Appliquées de Rennes (France)

This paper considers the reliability of usual assessment methods when evaluating virtual view synthesized images in the multi-view video context. Virtual views are generated from Depth Image Based Rendering (DIBR) algorithms. Because DIBR algorithms involve geometric transformations, new types of artifacts come up. The question regards the ability of commonly used methods to deal with such artifacts. This

Conference 8135:
Applications of Digital Image Processing XXXIV

paper investigates how correlated usual metrics are to human judgment, and in which way they can be used to assess perceived quality of synthesized views. The experiments consist in assessing seven different view synthesis algorithms by subjective and objective methods. Three different 3D video sequences are used in the tests. Resulting virtual synthesized sequences are assessed through objective metrics and subjective protocols. Results show that usual objective metrics can fail assessing synthesized views, in the sense of human judgment.

8135-17, Session 2

Centralized and interactive compression of multiview images

A. Gelman, P. L. Dragotti, Imperial College London (United Kingdom); V. Velisavljevic, Deutsche Telekom AG (Germany)

In this paper, we propose two multiview image compression methods. The basic concept of both schemes is the layer-based representation, in which the captured three-dimensional (3D) scene is approximated by planar depth layers characterized by a constant depth value. The first algorithm is centralized scheme where each layer is de-correlated using a separable multidimensional wavelet transform applied across the viewpoint and spatial dimensions. The transform is modified to efficiently deal with occlusions and disparity variations for different depths. Although the method achieves a high compression rate, the joint encoding approach infers transmission of all data to the users. By contrast, in an interactive setting, the users request only a subset of the captured images, but in an unknown order a priori. We address this scenario in the second algorithm by substituting the viewpoint transform with Distributed Source Coding (DSC) principles so that we exploit the redundant structure of multiview data and still maintain random access capabilities at the image level. We also demonstrate that both proposed compression schemes outperform H.264/MVC and JPEG 2000.

8135-18, Session 2

Intra prediction based on image inpainting methods and perceptual encoder control

P. Ndjiki-Nya, D. Doshkov, H. Kaprykowsky, T. Wiegand, Fraunhofer-Institut für Nachrichtentechnik Heinrich-Hertz-Institut (Germany)

Recent investigations have shown that one of the most beneficial elements for higher compression performance, especially in high-resolution video, is the incorporation of larger block partitioning of slices. In this work, we will address the question of how to integrate perceptual aspects into new video coding schemes based on large block structures. This is rooted in the fact that high frequency texture regions yield high coding costs when using classical prediction modes as well as encoder control based on the mean squared error criterion. To handle this problem, we will investigate the incorporation of novel intra predictors based on image completion methods. Furthermore, the integration of a perceptual-based encoder control using the well-known structural similarity index will be analyzed. A major aspect of this work is the evaluation of the coding results in a quantitative (i.e. statistical analysis of changes in mode decisions) as well as qualitative (i.e. coding efficiency) manner.

8135-19, Session 2

On the use of directional transforms for still image coding

T. Bruylants, A. Munteanu, J. Cornelis, P. Schelkens, Vrije Univ. Brussel (Belgium)

In the recent years, a lot of research was performed on the use of

directional transforms for the compression of still imagery, with the main focus on the application of block-based directional adaptive discrete wavelet transforms (B-DA-DWT). Although similar to that of the classic discrete wavelet transforms, this class of transforms provides the extra ability to adapt to the geometric features in an image. Other work proposes a segmentation driven (SD-DA-DWT) approach in order to minimize various artifacts caused by the B-DA-DWT and to improve the overall coding performance. However, as a significant drawback, all of the proposed methodologies suffer from the fact that extra side-information needs to be coded, depending on the type of applied transform. The generated overhead is not negligible and often seems to compensate the original targeted performance gains, while at the same time significantly increasing the complexity of the transform algorithm. Moreover, in combination with rate-distortion driven entropy coding, several types of artifacts appear at lower bit-rates, causing severe degradation of visual performance. This paper describes various considerations and trade-offs that were made during the search towards a practical solution that improves compression performance and visual quality when using directional adaptive transforms in still image coding. Next to a general introduction and overview of technology on directional transforms, it also presents various objective and subjective performance results and comparisons of the respective methodologies.

8135-20, Session 2

Performance analysis of WebP and VP8 based on subjective evaluations

F. De Simone, J. Lee, L. Goldmann, T. Ebrahimi, Ecole Polytechnique Fédérale de Lausanne (Switzerland)

Today, several alternatives for compression of digital pictures and video sequences exist to choose from. Beside standard solutions, like JPEG, JPEG 2000, JPEG XR, H.264/AVC-MPEG 4, to mention some examples, open access options like the WebP image compression and the VP8 video compression are currently gaining popularity. In this paper, we present the methodology and the results of the rate-distortion performance analysis of WebP and VP8. The analysis is based on the results of subjective quality assessment experiments, which have been carried out to compare the two algorithms to a set of state of the art image and video compression standards.

8135-21, Session 2

Advances in region-based texture modeling for video compression

F. Zhang, D. R. Bull, Univ. of Bristol (United Kingdom)

This paper will present a region-based video compression algorithm which uses texture segmentation and classification as a basis for efficient coding. Within the framework of a conventional block based codec, our approach exploits both texture warping and dynamic texture synthesis. A perspective motion model is employed to warp static textures and a texture model based approach is used to synthesise dynamic textures. Spatial and temporal artefacts are prevented by a new in-loop video quality metric. The proposed method has been integrated into an H.264 video coding framework with results offering significant bitrate savings (up to 50%) for similar visual quality, across a range of formats and content.

8135-22, Session 3

Predictive video decoding using GME and motion reliability

Y. M. Chen, I. V. Bajic, Simon Fraser Univ. (Canada)

In this paper, we present an improved approach to predictive video decoding based on global and local motion reliability. Global motion

Conference 8135:
Applications of Digital Image Processing XXXIV

estimation and region segmentation are the fundamentals in our method to extract global and local reliability information from received motion vector (MV) field. This reliability analysis is then utilized to refine MV field and determine the ordinal depth of all moving regions. A temporal interpolator is finally applied to compose a future frame. Our results indicate the proposed method achieves better visual quality compare to other state-of-the-art frame prediction approaches, particularly in the sequences involving moving camera and objects

8135-23, Session 3

Effective packetization algorithm of LT codes for stable video streaming over wireless network

D. Lee, W. Kim, H. Song, Pohang Univ. of Science and Technology (Korea, Republic of)

In this work, we propose an effective And-Or tree based packetization algorithm of Luby Transform (LT) codes to provide stable video streaming services by minimizing the deterioration of video streaming service quality caused by lost packets over error-prone wireless network. To accomplish our goal, the proposed packetization algorithm considers the relationships among encoded symbols of LT codes based on an And-Or tree analysis tool, and then puts the these encoded symbols into packets to minimize the packet loss effect during packet transmission and improve the decoding success rate of LT codes by reducing the correlations among packets. We conduct a mathematical analysis to prove performance of our packetization algorithm of LT codes compared with conventional packetization algorithm. Finally, the proposed system is fully implemented in Java and C/C++, and widely tested to show that the proposed packetization algorithm works reasonably well. The experimental results are provided to demonstrate that the proposed packetization algorithm supports more stable video streaming services with higher peak signal-to-noise ratio (PSNR) than the conventional packetization algorithm with various packet loss patterns, including random and burst packet loss patterns.

8135-24, Session 3

An improved approximate decoding with correlated sources

M. Kwon, H. Park, Ewha Womans Univ. (Korea, Republic of)

We consider ad hoc sensor network topologies that aim for distributed delivery of correlated multimedia data. In order for efficient data delivery, we deploy network coding technique in conjunction with approximate decoding algorithm. The algorithm can utilize the additional information of correlated source data in the decoding process, thereby leading to significantly improved decoding performance and enhanced robustness for delay-sensitive applications. One of main advantages of the algorithm is to enable receivers to decode the original source data even when the number of received data packets is not sufficient for perfect decoding. Hence, this is the key for delay-sensitive applications such as multimedia delivery. We further enhance the approximate decoding algorithm, such that it can consider the case where the source data have a linearly changing correlation over time. We study the several properties of the proposed algorithm and show what impacts of the source correlation are on the decoding performance. This study is fundamental research with straightforward idea, but essential step to extend the former study and extract properties which enable the theory to have wide application. Our experimental results confirm that the proposed algorithm improves the performance of the approximate decoding.

8135-26, Session 3

Reinventing multimedia delivery with MPEG's DASH

I. Sodagar, H. Pyle, Microsoft Corp. (United States)

A technical overview of MPEG's DASH standard and examples of how to use standard in applications.

8135-70, Session 3

The need for an Internet video compression standard

L. M. Bivolarski, Skype, Inc. (United States); M. Raad, RAAADTECH Consulting (Australia)

This paper presents the argument for the development of an Internet video compression standard. The history and science of video compression is reviewed with a focus on identifying how network technology has influenced video compression technology. It is argued that the use of the Internet to deliver video content, an application it was not designed for, and the fact that the Internet is here to stay, calls for a critical look at existing video compression standards. An analysis of the performance of these standards in delivering content over the Internet is provided with an explanation of why these standards have shortcomings in this application domain. Because of this, it is argued, video compression technology for the Internet will need to be different to what is used in other application domains. The paper further presents a discussion on what the technical characteristics of video compression technology would need to be for it to deliver high quality video over the Internet in an interoperable manner, thereby concluding that a new video compression standard is needed.

8135-27, Session 4

Optimized adaptive HTTP streaming for mobile devices

H. Kalva, B. Furht, V. Adzic, Florida Atlantic Univ. (United States)

No abstract available

8135-28, Session 4

Dynamically configurable software architecture for multi-media streaming

M. Biswas, R. Pinnamaraju, Marvell Semiconductor, Inc. (United States)

No abstract available

8135-29, Session 4

Color enhancement for portable LCD displays in low-power mode

H. H. Chen, K. Shih, National Taiwan Univ. (Taiwan)

No abstract available

8135-30, Session 4

A novel autostereoscopic display system to provide seamless stereoscopic view changes

C. Kim, Korea Advanced Institute of Science and Technology (Korea, Republic of); H. Lee, W. Cheong, N. Hur, Electronics and Telecommunications Research Institute (Korea, Republic of)

No abstract available

8135-32, Session 4

A distributed multi-channel demand-adaptive p2p VoD system with optimized caching and neighbor-selection

H. Zhang, Univ. of California, Berkeley (United States); M. Chen, The Chinese Univ. of Hong Kong (Hong Kong, China); A. Parekh, K. Ramchandran, Univ. of California, Berkeley (United States)

We design an optimized distributed P2P Video-on-Demand (VoD) caching system. The caching nodes are heterogeneous "micro-servers", e.g., idle PC users, set-top boxes and infrastructure nodes. Given limited storage, bandwidth and number of users they can connect to and serve simultaneously, we aim to optimize video caching on these distributed nodes. Our caching scheme has the following salient features: (1) it optimizes network topology; (2) it achieves provably optimal throughput, and is adaptable to varying supply and demand patterns across multiple video channels irrespective of video popularity; and (3) it is fully distributed and requires little or no maintenance overhead. The combinatorial nature of the network topology building and the system demand for distributed algorithms makes the problem uniquely challenging. By utilizing Lagrangian decomposition and Markov chain approximation based arguments, we address this challenge by designing two distributed algorithms running in tandem: a primal-dual storage and bandwidth allocation algorithm and a "soft-worst-neighborchoking" topology-building algorithm. Our scheme provably converges to a near-optimal solution, and is easy to implement in practice. Packet-level simulation results show that the proposed scheme achieves minimum server load under highly heterogeneous combinations of supply and demand patterns, and is robust to system dynamics of nodes churn, nodes asynchrony, and random delays in the network.

8135-71, Session 4

Perceptual compressive sensing scalability in mobile video

L. M. Bivolarski, Skype, Inc. (United States)

Scalability features embedded within the video sequences allows for streaming over heterogeneous networks to a variety of end devices. Compressive sensing techniques that will allow for lowering the complexity increase the robustness of the video scalability are reviewed. Human visual system models are often used in establishing perceptual metrics that would evaluate quality of video. Combining of perceptual and compressive sensing approach outlined from recent investigations. The performance and the complexity of different scalability techniques are evaluated. Application of perceptual models to evaluation of the quality of compressive sensing scalability is considered in near perceptual y lossless coding scheme.

8135-33, Session 5

On the visual quality enhancement of super-resolution images

A. H. Yousef, Old Dominion Univ. (United States); Z. Rahman, NASA Langley Research Ctr. (United States); M. A. Karim, Old Dominion Univ. (United States)

Super-resolution (SR) is the process of obtaining a higher resolution image from a set of lower resolution (LR) blurred and noisy images. One may, then, envision a scenario where a set of LR images is acquired with a sensor on a moving platform. In such a case, an SR image can be reconstructed in an area of sufficient overlap between the LR images which generally have a relative shift with respect to each other by subpixel amounts. The visual quality of the SR image is affected by many factors such as the optics blur, the inherent signal-to-noise ratio of the system, quantization artifacts, etc. In addition to these factors, for the system described above, the number of scenels (scene elements) i.e., the number of overlapped images used for SR reconstruction within the SR grid and their relative arrangement is a key factor in determining the quality of the SR image. In most cases of microscanning techniques, the subpixel shifts between the LR images are pre-determined: hence the number of the scenels within the SR grid and their relative positions with respect to each other are known and, as a result, can be used in obtaining the reconstructed SR image with high quality. However, in the scenario described in this research, the LR images have relative shifts that are unknown. Even when the correct shifts have been obtained, the arrangement of the LR scene elements does not form a pre-determined grid as required by most micro-scanning algorithms. This random pattern of subpixel shifts can lead to unpleasant visual quality, especially at the edges of the reconstructed SR image. Also, depending on the available number of the LR images and their relative positions, it may be only be possible to produce SR along a single dimension— diagonal, horizontal or vertical, and use interpolation in the orthogonal dimension because there isn't sufficient information to produce a full 2D image. Thus, in this paper we investigate the impact of the number of overlapped regions and their relative arrangement on the quality of the SR images, and propose a technique that optimally allocates the available LR scenels to the SR grid in order to minimize the expected unpleasant visual artifacts

8135-34, Session 5

An image-set for identifying multiple regions/ levels of interest in digital images

M. Jaber, M. S. Bailly, Y. Wang, E. Saber, Rochester Institute of Technology (United States)

In the field of identifying regions of interest (ROI) in digital images, several image-sets are referenced in the literature; the open-source ones mostly present a single main object (usually located at or near the image center as a pop-out). In this paper, we present a comprehensive image-set (with its ground-truth) which will be eventually made publically available. The database includes images that signify multiple-regions-of-interest or multiple-levels-of-interest. The former terminology signifies that the scene has a group of subjects/objects (not necessarily spatially-connected regions) that share the same level of perceptual priority to the human observer while the latter indicates that the scene is complex enough to have primary, secondary, and background objects. Our methodology for developing and conducting a psychophysical experiment employed to generate the proposed image-set is described. The image-set is developed to be used in training and evaluation of ROI detection algorithms. Applications include image compression, thumbnailing, summarization, and mobile phone imagery.

8135-35, Session 5

A channel-based color fusion technique using multispectral images for night vision enhancement

Y. Zheng, Alcorn State Univ. (United States)

A fused image using multispectral images can increase the reliability of interpretation because it combines the complimentary information apparent in multispectral images. While a color image can be easily interpreted by human users (for visual analysis), and thus improves observer performance and reaction times. We propose a fast color fusion method, termed as channel-based color fusion, which is efficient for real time applications. Notice that the term of "color fusion" means combing multispectral images into a color-version image with the purpose of resembling natural scenes. On the other hand, false coloring technique usually has no intention of resembling natural scenery. The framework of channel-based color fusion is as follows, (1) prepare for color fusion, preprocessing (denoising, normalization and enhancement) and image registration; (2) form a color fusion image by properly assigning multispectral images to red, green, and blue channels; (3) fuse multispectral images (gray fusion) using a wavelet-based fusion algorithm; and (4) replace the value component of color fusion in HSV color space with the gray-fusion image, and finally transform back to RGB space. In night vision imaging, there may be two or several bands of images available, for example, visible (RGB), image intensified (II), near infrared (NIR), medium wave infrared (MWIR), long wave infrared (LWIR). In the full paper, we will present the channel-wise color fusions with two-band (e.g., NIR + LWIR, II + LWIR, RGB + LWIR) or three-band (e.g., RGB + NIR + LWIR) multispectral images.

8135-36, Session 5

From index to metric: using differential geometry to define a global visual quality metric

T. Richter, Univ. Stuttgart (Germany)

While traditional image quality metrics like MSE are mathematically well understood and tractable, they are known to correlate weakly to image distortion as observed by human observers. To address this situation, many full reference quality indices have been suggested over the years that correlate better to human perception, one of them being the well-known Structural Similarity Index by Wang and Bovik. However, while these expressions show higher correlations, they are often not very tractable mathematically, and in specific are rarely metrics in the strict mathematical sense. Specifically, the triangle inequality is often not satisfied, which could either be seen as an effect of the human visual system being unable to compare images that are visually too different, or as a defect of the index capturing the global situation correctly. In this article, the latter position is taken, and it is shown how the SSIM can be understood as a local approximation of a global metric, namely the geodesic distance on a manifold. While the metric cannot be computed explicitly in most cases, it is nevertheless shown that in specific cases its expression is identical to Weber's Law of luminance sensitivity of the human eye.

8135-37, Session 5

EEM quantization revisited: asymptotic optimality for variable rate coding

T. Richter, Univ. Stuttgart (Germany)

Equal-Expectation Magnitude Quantization (EEM) aims at minimizing the distortion of a quantizer with defined reconstruction points by shifting the deadzone parameter such that the expectation value of the signal equals the reconstructed value. While intuitively clear, this argument is

not sufficient to prove rate-distortion optimality.

In this work, it is shown that the EEM quantizer is rate-distortion optimal up to third order in an expansion in powers of the quantization bucket size in the high-bitrate approximation, and the approximating series for the optimal quantizer is computed.

This result is compared to an even simpler quantization strategy based on the Lloyd-Max quantizer which selectively sets coefficients to zero. It is shown that both strategies lead to the same asymptotic expansion for the threshold parameter, but zeroing coefficients provides optimality in one additional order in the quantization bucket size.

8135-38, Session 5

Wavefront aberration function from hard contact lenses obtained with two different techniques

A. S. Cruz Felix, E. Lopez-Olazagasti, J. D. Sánchez-de-la-Llave, G. Ramírez-Zavaleta, E. Tepichín, Instituto Nacional de Astrofísica, Óptica y Electrónica (Mexico)

The analysis and measurement of the wavefront aberration function are very important tools in the field of visual optics; they are used to understand the performance of the human eye in terms of its optical aberrations. In recent years, we have compared, through two different methods, the wavefront aberration function of a reference refractive surface of 5 mm in diameter and we have demonstrated its equivalence[1]. Now, we want to extend these results to hard contact lenses. These hard contact lenses have been subjected to different laser ablation techniques which are typically used in refractive surgery. Our goal is to characterize the resultant ablation profile. We show our preliminary results obtained for both, a non-ablated hard contact lens and the corresponding ablated samples.

[1] Cruz Félix, A. S., Ibarra, J., López, E., Rosales, M., Tepichín, E., "Comparison between two different methods to obtain the wavefront aberration function." Proc. of SPIE Vol. 7798, 77981U- 77981U-8 (2010).

8135-39, Session 5

Improve the image discontinuous problem by using color temperature mapping method

W. Jeng, O. Mang, C. Lai, National Chiao Tung Univ. (Taiwan)

This article mainly focuses on image processing of ring field capsule endoscope. First, it used the ring field capsule endoscope (RFCE) to take the images, the sample is a paramecium geometric picture, but the images captured by RFCE were blurred due to the RFCE has aberration problems in the image center and lower light uniformity affect the image quality. To solve the problems, image processing can use to improve it. Therefore, the images captured by different time can use Person correlation coefficient algorithm to connect all the images, and using the color temperature mapping way to improve the discontinuous problem in the connection region. After the image processing the Person correlation coefficient is 0.72 higher than the original 0.69 which is without using color temperature mapping.

8135-42, Session 6

On MPEG work towards a standard for visual search

Y. A. Reznik, Qualcomm Inc. (United States)

This paper reviews recent work by MPEG standards committee (ISO/IEC JTC1 SC29 WG11) towards a standard enabling efficient and interoperable design of Visual Search applications. We will explain the scope and requirements for the standard, details of the evaluation framework, and timeline envisioned by the Call for Proposals.

8135-43, Session 6

Compressing a set of CHoG features

V. R. Chandrasekhar, Stanford Univ. (United States); Y. A. Reznik, Qualcomm Inc. (United States); G. Takacs, D. M. Chen, S. S. Tsai, B. Girod, Stanford Univ. (United States)

This paper offers a novel compression scheme based on Digital Search Trees (DST) for compressing an unordered set of CHoG features. The order in which a set of features is transmitted does not matter for computer vision applications as they are typically based on “bag-of-words” matching. Hence, by ordering features, one can potentially gain an additional $\log_2(m!)$ bits compared to when features are transmitted in the original order. The proposed scheme first builds a DST from a set of features and uses the structure of the DST to define a canonical ordering on the feature set. The subsequent coding scheme results in close to $\sim \log_2(m!)$ bits savings as predicted by theory.

8135-44, Session 6

3D face reconstruction from limited images based on differential evolution

Q. Wang, J. Li, Old Dominion Univ. (United States); V. K. Asari, Univ. of Dayton (United States); M. A. Karim, Old Dominion Univ. (United States)

3D face modeling has been one of the greatest challenges for researchers in computer graphics for many years. Various methods have been used to model the shape and texture of faces under desired illumination and pose conditions from a given image. In this paper, we propose a novel method for the 3D face synthesis and reconstruction by using a simple and efficient global optimizer. A 3D-2D matching algorithm which employs the integration of 3D Morphable model (3DMM) and Differential Evolution (DE) is addressed. In 3DMM, the estimation process of fitting shape and texture to 2D images is considered as the problem of approximating global minima in a high dimensional feature space, in which optimization is apt to local convergence. Unlike the traditional scheme used in 3DMM, DE appears to be robust against stagnation in local minimum and sensitivity to initial value in face reconstruction. Benefiting from DE's successful performance, 3D face models are created based on single 2D image with respect to various illumination and pose context. The preliminary experiment results demonstrate that we are able to automatically create virtual 3D faces from single 2D images with high performance. The validation process showed that there is a small difference between the input images and 2D faces generated by synthesized 3D model.

8135-45, Session 6

Automated crystal detection from microscopic protein crystal images

J. Gubbi, S. Marusic, The Univ. of Melbourne (Australia); M. Parker, St. Vincent's Institute of Medical Research (Australia); M. Palaniswami, The Univ. of Melbourne (Australia)

Synthesis of protein crystals is a critical step in rational drug discovery. Due to advancement in application of robotics in crystal development, there is an urgent need to build systems which can identify protein crystals as they crystallize. Presently, this procedure is performed manually where the user has to go through large number of images in identifying protein crystals. The proposed method is aimed at detecting crystal formation and classifying them to known crystal types from a large dataset of microscopic images. Conventional spatial domain techniques, such as edge detection or morphological operators fail due the significant high spatial frequency noise or texture information, which although largely imperceptible when viewing the original images, poses significant challenges in segmenting only the crystals. The other issue is the

presence of non-crystal artifacts and other features (such as water drop edges) which render a number of techniques reported in the literature inconclusive in the correct classification of crystals. A combination of Dual Tree - Complex Wavelet Transform, Hough transform and Support Vector Machines is used in the proposed method. The edge detection is performed within this framework is the Laplacian of Gaussian method. It achieves far better results than edge detection on raw images alone. This has been applied to individual subbands, where the most promising results are obtained from low resolution subbands. The results are shown to out-perform the most promising systems reported in literature in terms of detecting crystal formation and in accurate classification of crystals.

8135-46, Session 6

Early forest fire detection using principal component analysis of infrared video

J. A. Saghri, R. F. Radjabi, California Polytechnic State Univ., San Luis Obispo (United States); J. T. Jacobs, Raytheon Co. (United States)

Early detection and mitigation of forest fires can reduce state/national budget deficits, property damage, pollution, and save lives. A novel and promising land-based early forest fire detection scheme is proposed which relies on exploitation of fire plume temporal signature (temporal reflectance variation, or thermal scintillation/frequency). The presence of fire plume signature is detected via application of principal component analysis continuously to stream of IR video images of a fire prone region. Unlike common techniques which rely on measurement and discrimination of fire plume directly from its infrared and/or visible reflectance imagery, this scheme is based on exploitation of fire plume temporal signature, i.e., its reflectance variation/temporal frequency. The method is simple and relatively inexpensive to implement. Land-based infrared (IR) cameras are strategically located in potential fire-prone areas. The sequence of IR video feed from each camera is digitally processed via principal component analysis (PCA) to detect the presence of fire plume temporal signature. Since plume temporal and spatial reflectance values are random and uncorrelated, PCA conveniently captures the plume footprint in the resulting lower-order principal component (PC) images. Preliminary results are promising.

8135-47, Session 6

Semi-automatic ground truth generation for license plate recognition

S. Wang, Industrial Technology Research Institute (Taiwan); H. Lee, Tzu Chi Univ. (Taiwan)

The purpose of ground truth data is to provide an absolute reference to be compared with algorithms' results. However, collecting ground truth data for real-life applications is an important but very disturbing task. This is particularly true for license plate recognition applications because of time-consuming manual. In this paper, we present a method of semi-automatic ground truth generation for license plate recognition in video sequences. The method started from detection of repeated character-line regions to eliminate non-interesting regions followed by a general license plate recognition system to recognize the numbers. Then, we proposed a vehicle leaving detection mechanism to predict vehicle leaving by a license-plate-centric tracking method. The leaving event would be used to reset the voting numbers of the tracked vehicle and to restrict the searching areas of the next input frame. Once the vehicle is out of the camera field of view, the license-plate-centric tracking mechanism is used to detect the timestamp of the vehicle entering. Finally, the ground truth data of the passing vehicle is collected with the three attributes, i.e., the timestamps of entering and leaving and the identity numbers of the vehicle. In our experiments, all frames with the license plate heights ranging from 12 to 40 pixels were captured from an entrance at the North gateway of National Chiao-Tung University, Taiwan. The result shows that the proposed method can achieve low false alarms rate and miss rate.

8135-40, Poster Session

A study on portable fluorescence imaging system

H. C. Chang, National Applied Research Labs. (Taiwan)

The fluorescent reaction is that an organism or dye, excited by UV light (200-405 nm), emits a specific frequency of light; the light is usually a visible or near infrared light (405-900 nm). During the UV light irradiation, the photosensitive agent will be induced to start the photochemical reaction. In addition, the fluorescence image can be used for fluorescence diagnosis and photodynamic therapy of skin diseases, which has become a useful tool to provide scientific evidence in many biomedical researches. However, most of the methods on acquiring fluorescence traces are still stay in primitive stage, catching by naked eyes and researcher's subjective judgment. This article presents a portable camera to obtain the fluorescence image and to make up a deficit from observer competence and subjective judgment. Furthermore, the portable camera offers the different exciting light sources (375nm and 395 nm) for user to record fluorescence image and makes the recorded image become persuasive scientific evidence. In addition, when the raising the rate between signal and noise, the signal processing module will not only amplify the fluorescence signal up to 70 %, but also decrease the noise to 50% from environmental light.

8135-41, Poster Session

Full-field white-light optical coherence tomography of red blood cells

I. V. Smirnov, E. V. Bogolyubova, A. L. Kalyanov, V. V. Lychagov, V. P. Ryabukho, N.G. Chernyshevsky Saratov State Univ. (Russian Federation); L. I. Malinova, Saratov State Medical Univ. (Russian Federation)

Full-field scanning white light OCT used to human red blood cells investigation. A software package was developed to data visualization and interpretation. An algorithms of computer vision was used.

The Full-field white light OCT is based on optical scheme of Linnik interferometer. Stepper motor was used to object movements along the optical axis. We used an incandescent lamp as a light source and a CCD camera without IR filter for interferograms registration. This combination of a source and a detector allowed us to obtain a spatial resolution of about 1 micron.

Developed algorithm of signal processing combines the principles of low-coherence interferometry and full-field tomography, providing a high speed scanning and great accuracy. It is also possible to visualize a profile of the sample surface in three-dimensional mode, as the most intuitive way of presenting the data.

The investigation of blood slides from patients with various pathologies was conducted using the developed software. The blood glucose concentration effect on a shape of red blood cells was ascertained. In the paper the radius and shape of the surface of red blood cells of patients with various pathologies were compared. Findings are in good agreement with the results obtained by other methods including cytometry.

8135-48, Poster Session

Simulations of optical autofocus algorithms based on PGA in SAIL

N. Xu, L. Liu, Q. Xu, Y. Zhou, J. Sun, Shanghai Institute of Optics and Fine Mechanics (China)

The phase perturbations due to propagation effects can destroy the high resolution imagery of Synthetic Aperture Imaging Ladar (SAIL). Some autofocus algorithms for Synthetic Aperture Radar (SAR) were developed and implemented. Phase Gradient Algorithm (PGA) is a well-known one

for its robustness and wide application, and Phase Curvature Algorithm (PCA) as a similar algorithm expands its applied field to strip map mode. In this paper the autofocus algorithms utilized in optical frequency domain are proposed, including optical PGA and PCA respectively implemented in spotlight and strip map mode. Firstly, the mathematical flows of optical PGA and PCA in SAIL are derived. The simulations model of the airborne SAIL is established, and the compensation simulations of the synthetic aperture laser images corrupted by the random errors, linear phase errors and quadratic phase errors are executed. The compensation effect and the cycle index of the simulation are discussed. The simulation results show that both the two optical autofocus algorithms are effective while the optical PGA outperforms the optical PCA, which keeps consistency with the theory.

8135-49, Poster Session

A hardware implementation of nonlinear correlation filters

S. Martinez-Diaz, H. Castañeda Giron, Instituto Tecnológico de La Paz (Mexico)

Correlation methods have been used extensively the last few decades for pattern recognition, in images. With the purpose of design robust correlation filters several approaches have been proposed. Recently, nonlinear correlation filters for distortion-invariant pattern recognition were introduced. The filters are designed as a logical combination of binary objects. In this case, pattern recognition is carried out with a space-variant nonlinear operation, called morphological correlation, which is applied among images. In order to obtain invariance to geometrical distortions, the filters are designed including distorted versions of a reference object. These kinds of filters are robust to non Gaussian noise and non-homogeneous illumination. A drawback of nonlinear filters is the high computational cost of the correlation process. On the other hand, the calculation of nonlinear correlation can be parallelized by using specialized hardware. With the intention of reduce processing time, in this paper we propose a parallel coprocessor, implemented on a Field Programmable Gate Array (FPGA). FPGA's have been used in several applications as an auxiliary processor, which executes the more time consuming tasks. Simulation results of proposed system are provided and discussed.

8135-50, Poster Session

An image processing method for reducing the impact of external vibration on MEMS IR imaging system

C. Gong, L. Dong, M. Hui, Y. Zhao, Beijing Institute of Technology (China)

Nowadays, the research of IR imaging system based on a micro-electro-mechanical-system (MEMS) micro-cantilever is becoming a hot field of infrared imaging. However, it is generally acknowledged that the MEMS IR imaging system cannot resist various external vibrations. The paper describes a real-time digital image processing method for reducing the impact of the vibrations and improving the quality of IR images. The method includes two steps which are motion detection and morphological denoising. We have applied it to the MEMS IR imaging system successfully. The method and its processing results are presented in the paper.

8135-51, Poster Session

Accuracy of image restoration using microscanning image system

J. L. Lopez-Martinez, V. I. Kober, Ctr. de Investigación Científica y

Conference 8135:
Applications of Digital Image Processing XXXIV

de Educación Superior de Ensenada (Mexico)

Various techniques for image recovery from degraded observed images using microscanning image system were proposed. The methods deal with additive, multiplicative interferences, and sensor's noise. Basically, they use several observed images captured with small spatial shifts. In this paper, we analyze the tolerance of restoration methods to small shift errors (subpixel spatial errors) during camera microscanning. Computer simulation results of obtained with the restoration methods using degraded images from an imperfect microscanning system are compared with those of ideal microscanning system in terms of signal restoration criteria.

8135-52, Poster Session

Dense and accurate motion and strain estimation in high-resolution speckle images using an image-adaptive approach

C. Cofaru, W. Philips, W. Van Paepegem, Univ. Gent (Belgium)

Digital image processing methods represent a viable and well acknowledged alternative to strain gauges and interferometric techniques for determining full-field displacements and strains in materials under stress. This paper presents an image adaptive technique for dense motion and strain estimation using high-resolution speckle images that show the analyzed material in its original and deformed states. The algorithm starts by dividing the speckle image showing the original state into irregular cells taking into consideration both spatial and gradient image information present. Subsequently the Newton-Raphson digital image correlation technique is applied to calculate the corresponding motion for each cell. Adaptive spatial regularization in the form of the Geman-McClure robust spatial estimator is employed to increase the spatial consistency of the motion components of a cell with respect to the components of neighbouring cells. To obtain the final strain information, local least-squares fitting using a linear displacement model is performed on the horizontal and vertical displacement fields. To evaluate and validate the presented image partitioning and motion estimation techniques two numerical and two real experiments are employed. The numerical experiments simulate the deformation of a specimen with constant strain across the surface as well as small rigid-body rotations present while real experiments consist specimens that are subjected to uniaxial load. The results indicate very good accuracy of the recovered strains as well as better rotation insensitivity compared to classical techniques.

8135-53, Poster Session

A new planar pattern for camera calibration

X. Liu, D. He, Shenzhen Univ. (China); Y. Yin, Tianjin Univ. (China); C. Zhang, X. Peng, Shenzhen Univ. (China)

In this paper, we proposed a new planar pattern as the calibration target for camera calibration. The pattern consists of ninety-nine circular markers with almost uniform distance but not. In order to calibrate the camera by this planar pattern, we have to know the accurate coordinates of these ninety-nine markers, for which the image process and close-range photogrammetry techniques were employed. Firstly, we took multiple photos of the inaccurate planar pattern from different multi-poses. Then all circular markers in the photos could be detected automatically and the image-coordinates of markers would also be located using image process techniques. Secondly, we detected the homonymous markers from different photos due to the markers' special topology relation in the pattern. Thirdly, the 3D coordinate of markers with a scale-constraint would be constructed accurately based on close-range photogrammetry technique. And the scale could be achieved from an accurate actual distance between two markers. Finally we multiplied the 3D coordinates of markers computed by photogrammetry by this scale, and obtained the actual 3D coordinates of these markers. With these markers, whose coordinates were corrected, we calibrated a

CCD camera and achieved valid results with low re-projection error. The experimental results validated the advantage of this pattern as calibration target, high-precision, low-cost and easy-implementation, which can be widely applied in vision measurement and camera calibration.

8135-54, Poster Session

In vivo full depth of eye-imaging spectral-domain optical coherence tomography

C. Dai, Shanghai Institute of Technology (China)

It is necessary to apply the spectral-domain optical coherence tomography (OCT) to image the whole eye segment for practically iatrical use, but the imaging depth of spectral-domain OCT technique is limited by CCD resolving power. By now, no result about this research has been reported. In our study, a new dual channel dual focus OCT system is adopted to detect the whole eye. The cornea and the crystalline lens are simultaneously imaged by using full range complex spectral-domain OCT in one channel, the retina is detected by the other. The new system was successfully tested in imaging of the volunteer' eye. The preliminary results presented in this paper demonstrated the feasibility of this approach.

8135-55, Poster Session

An efficient lane marker detection algorithm using Log-polar transform and RANSAC

J. Kim, H. Lim, LED-IT Fusion Technology Research Ctr. (Korea, Republic of); C. Lee, J. Jang, Yeungnam Univ. (Korea, Republic of)

Recently lane detection algorithm is an essential part of the intelligent vehicle systems and has many applications such as driver assistance system (DAS), lane departure warning system (LDWS), lane keeping system (LKS) and so on. This lane detection algorithm has received considerable attention since the 1990's. However, the lane detection algorithm has especially the hard problems, for examples, parked and moving vehicles, bad quality lines, shadows cast from trees, buildings and irregular/strange lane shape, emerging and merging lanes, sun glare, writings and other markings on the road (e.g. pedestrian crosswalks).

We develop an efficient lane markers detection algorithm based on the log-polar transform and the random sample consensus (RANSAC) algorithm. To extract the optimal lane marker points, we set firstly the regions of interest (ROIs) with variable block size and perform the preprocessing steps which are smoothing filtering and the adaptive thresholding within ROIs. Then the lane markers are extracted by using a Canny edge operator. From the extracted lane markers, the end points of lane marker are selected to fit a segment of straight or curve lane for each ROI. To fit the lane model, we adopt the general road model which is the parabola model, these points are transformed to the log-polar space. The straight lane and curve lane can be classified at the log-polar space easily. Finally, we use the RANSAC to detect the exact lane markers of road. The experiments are performed on our database that has many different conditions including various weather and road.

8135-56, Poster Session

Segmentation and classifying of synapses in microscopic images

S. Yona, A. Katsman, D. Gitler, Y. Yitzhaky, Ben-Gurion Univ. of the Negev (Israel)

One of the parameters which determine the characteristics of synapses is the number of vesicles and their spatial spread. These vesicles can be marked fluorescently and be identified through optical instruments.

Conference 8135:
Applications of Digital Image Processing XXXIV

The purpose of this work is to classify and quantify synapses and their properties in the cultures of a mouse's hippocampus, from images acquired by a microscope. Quantification features include the number of synapses, their intensity and their size characteristics.

The images obtained by the microscope contain hundreds to several thousands of synapses with various elliptic-like shape features and intensities. These images also include other features such as glia cells and other biological objects beyond the focus plane. Those features reduce the visibility of the synapses and interrupt the segmentation process.

The proposed method performs first a background subtraction. Then, suspected centers of synapses are identified as local maxima points, and the tendency of identified bell-like objects to be synapses is evaluated according to their intensity properties. Next bulks of synapses are distinguished from single synapses and finally, the borders of each identified synapse and bulk are detected.

Delimiting the borders of the synapses is important in order to determine the amount of vesicles in the whole synapse and not just in its center. As for the detection of the centers of the synapses, results indicate a better performance of the proposed algorithm over previous iterative methods, when measuring rates of true positive (centers of synapse that were identified) and false positive (objects that were falsely identified as centers).

8135-57, Poster Session

A method for improved localization of edges in multi/hyperspectral imagery

S. R. Vantaram, E. Saber, Rochester Institute of Technology (United States)

Detection of edges has been a long standing low-level visual processing problem especially in the image understanding and analysis realm. Gradient (scalar or vector) computation finds an important place in various image processing and computer vision tasks such as object detection, recognition and feature extraction, to name a few. Acquisition of functional/useful gradient maps from remotely sensed data for applications such as segmentation, classification, anomaly and change detection etc., to name a few, has often proven to be an extremely challenging task. In this paper, we propose an enhanced vector field gradient estimation approach for remote sensing imagery. Our work based on the principle that adjusting the partial derivatives of individual channels of a multi-band image to only comprise of contributions towards their associated local scalar gradient maxima using a non-maximal suppression scheme, before being employed in a vector field approach for gradient computation, can yield highly localized responses in the eventual gradient map. More specifically, the novelty of the proposed algorithm lies in the fact that it leverages the advantages of non-maximal suppression to enhance the results arising from a vector field gradient approach, as opposed to its conventional use for enhancing the outcomes obtained from a gradient calculation of a scalar field (single band image). The proposed algorithm was tested on several multispectral and hyperspectral image datasets with favorable results.

8135-58, Poster Session

Enhancement of the accuracy of the astronomical measurements carried on the wide-field astronomical image data

M. Rerábek, P. Páta, Czech Technical Univ. in Prague (Czech Republic)

Accuracy of the astronomical measurements is more than important with respect to astronomical image data evaluation. This measurement precision decreases due to optical aberrations which are present in each real optical system. Especially the wide-field systems contain a lot of different kinds of high order optical aberrations which have

negative impact to the image quality and imaging system transfer characteristics. Therefore, for precise astronomical measurement (astrometry, photometry) over the entire field of view, it is very important to comprehend how the optical aberrations affect the transfer characteristics of optical system. There are the relations between amount of high order optical aberrations and astrometry measurement precision discussed in this paper. This contribution also describes two experiments used to improve the accuracy of the astrometry. First one focuses on the using of point spread function (PSF) model in known deconvolution algorithms. The principal difficulty is that these systems are space variant and it means that Fourier approaches can no longer be used for restorations of original image. Deconvolution algorithm and partially invariant model of optical system, which allows us to use Fourier appliance will be presented. The second approach how to improve the astronomical measurements is to use novel detection algorithm using PSF model which is based on the aberrations modelling.

8135-59, Poster Session

A novel dimming algorithm using local boosting algorithm for LED backlight system in LCD TVs

J. Lee, J. Kim, H. Lim, LED-IT Fusion Technology Research Ctr. (Korea, Republic of); K. Seong, J. Jang, Yeungnam Univ. (Korea, Republic of)

Since the conventional LCD TVs have the high light leakage of liquid crystals, it is difficult to realize the real black color. And it brings about a low contrast ratio. To reduce the light leakage and increase the contrast ratio, the backlight dimming technology has been developed.

We decide the brightness of input image using classification method which uses the max level and the average level. And then we apply the proposed local dimming boost algorithm for the optimal local dimming method. We make accurately the local dimming data, the original image has need to classify whether a dark image or a bright image. The proposed dimming algorithm divided into two methods that the max level and the average level. And then we increased contrast ratio of gray image by 30% for classify gray level of image correct. In an experiment increases about 30% of the contrast ratio makes optimal image of dimming data generation. After aforementioned process, we make use of average level data or max level data and generated first dimming data. Since the aforementioned backlight-dimming algorithm totally reduces image brightness, the following local dimming boosting algorithm is proposed to improve image contrast ratio and reduce power consumption. To solve the drawbacks of above-mentioned conventional dimming methods, we propose the boosting algorithm for the optimal local dimming method

The experimental results show that the proposed algorithm has higher contrast ratio and lower power consumption than the conventional methods.

8135-60, Poster Session

Photoacoustic laser Doppler velocimetry using the self-mixing effect of RF-excited CO₂ laser

J. Choi, Honam Univ. (Korea, Republic of)

A LDV with simple structure, in which the feedback of scattered light was used, was constituted and evaluated in order to measure the rotation speed of a body of revolution by using the CO₂ laser. Some part of the scattered light occurring when laser light was projected on a moving object was projected into a laser resonator, so that it may create a self-mixing with eigen optical frequency. The self-mixing of the light was altered into the doppler-shifted frequency due to the subtle pressure change in the resonator caused by the photoacoustic effect. The altered frequency is in proportion to the rotation speed of the rotating body,

Conference 8135:
Applications of Digital Image Processing XXXIV

it was possible to measure the speed of the object by observing the frequency caused by the pressure occurring inside the laser resonator. And it was found out that the measured value of doppler-shifted frequency, which was carried out changing the speed of the object and the incident angle of laser light to the object, was in accordance with the established theory. There was 5% of error between the established theoretical values and the actually measured values when the wavelength of the laser was 10.59 .

8135-61, Poster Session

Uniformly spaced 3D modeling of human face from two images using parallel particle swarm optimization

Y. Chang, Y. Tsao, Chang Gung Univ. (Taiwan); S. Lee, Chang Gung Memorial Hospital (Taiwan)

Three dimensional numerical modeling of human face has many potential applications, such as virtual reality, animation, visual surveillance, and face recognition. While many commercial optical systems are available for 3D human face surface data reconstruction, the systems normally use more than two cameras. This requirement is due to the difficulty of searching corresponding locations on images captured from different viewpoints, especially when the cameras are located far apart from each other. This work proposes a scheme for finding the correspondence between uniformly spaced locations on one of the images using only two cameras. The approach utilizes structured light to enhance patterns on the images and is initialized with the scale-invariant feature transform (SIFT). Successive locations are found in order by searching for the best match of transformed patches using a parallel version of the particle swarm optimization (PSO) algorithm. The algorithm is modified such that consistent results are obtained in a restricted period of time. In the algorithm, each swarm is assigned with different parameters realizing diverse search behaviors. Parallelism is achieved by sharing a pre-determined number of particles with higher cost values between the swarms through a buffer, called the common pool. Furthermore, false locations of the resultant 3D data are singled out for correction by searching for outliers from fitted curves. Case studies show that the scheme is able to correctly generate 456 evenly spaced 3D coordinate points in 23 seconds from a single shot of projected human face using a PC with 2.66GHz Intel Q9400 CPU and 4GB RAM.

8135-62, Poster Session

Face recognition using spectral and spatial information

S. A. Robila, M. Chang-Reyna, Montclair State Univ. (United States); N. D'Amico, Univ. of Maryland, College Park (United States)

Accurate individual identification is an essential part of any authentication protocol. Often, such identification is done using biometrics. Among biometrics, face recognition provides an unobtrusive and if needed discrete method of classifying individuals, a task that has become increasingly important in many fields swamped by deluge of data available (but lack of human analysts) such as surveillance, law enforcement, and access control. Spectral imaging, i.e. images collected over hundreds of narrow contiguous light spectrum intervals constitute a natural choice for expanding face recognition image fusion, especially since it may provide information beyond the normal visible range, thus exceeding the normal human sensing. While face recognition from grayscale or color images has seen a considerable research effort, little was done to investigate the use of spectral imaging for this problem.

Our work is geared at designing an efficient method for facial recognition by using hyperspectral imaging. In previous work we have separately investigated the use of spectra matching and image based matching. In spectra matching, individual face spectra are being classified based on spectral similarities. In image based matching, we investigated various

approaches based on orthogonal subspaces (such as PCA and OSP). In the current work we provide an automated unsupervised method for face recognition that starts by detecting the face in the image and then proceeds to perform both spectral and image based matching. The results are then fused in a single classification decision. The algorithm is tested on an experimental hyperspectral image database of 17 subjects each with four different facial expressions and viewing angles. Our results show that the decision fusion leads to improvement of recognition accuracy when compared to the individual approaches as well as to recognition based on regular imaging.

The work expands on previous band extraction results and has the distinct advantage of being one of the first that combines spatial information (i.e. face characteristics) with spectral information. In addition, the techniques are general enough to accommodate differences in skin spectra.

8135-63, Poster Session

Optimized retinal nerve fiber layer segmentation based on optical reflectivity and phase retardation for polarization-sensitive optical coherence tomography

B. Wang, A. S. Paranjape, T. E. Milner, H. G. Rylander III, The Univ. of Texas at Austin (United States)

Segmentation of retinal nerve fiber layer (RNFL) from swept source polarization-sensitive optical coherence tomography (SS-PSOCT) images is fundamental to determine RNFL thickness and calculate birefringence. Traditional RNFL segmentation methods based on image processing and boundary detection algorithms utilize only optical reflectivity contrast information, which is strongly affected by speckle noise. We propose a fully automated RNFL segmentation method based on both optical reflectivity and phase retardation in RNFL to achieve optimized RNFL segmentation. The upper boundary of the RNFL is relatively easy to detect since the transition from the vitreous to the inner limiting membrane is abrupt and is characterized by high contrast due to the difference in refractive index. The lower boundary of the RNFL is a transition zone from the birefringent axons of the retinal ganglion cells to the cell bodies themselves. This transition is best detected anatomically by the change in birefringence at the lower boundary of the RNFL. Simple filtering followed by edge detection techniques is applied to SS-PSOCT clustered scan images to estimate preliminary RNFL segmentation. Three incident polarization states and Levenberg-Marquardt nonlinear fitting of normalized Stokes vectors on Poincaré sphere allow determination of phase retardation from the preliminary segmentation based solely on optical reflectivity contrast. Optimized RNFL segmentation is then achieved by moving the lower boundary of preliminary RNFL segmentation and searching for the local minimum of Levenberg-Marquardt fitting uncertainty. This method finds optimized RNFL segmentation with lowest achievable fitting uncertainty and optimizes the phase retardation measurement. Clinical results from a healthy volunteer illustrate that the proposed segmentation method estimates phase retardation in RNFL with lower uncertainty than traditional approaches.

8135-64, Poster Session

Meteor automatic imager and analyzer: current status and preprocessing of image data

K. Fliegel, P. Páta, S. Vitek, Czech Technical Univ. in Prague (Czech Republic); P. Koten, Astronomical Institute of the ASCR, v.v.i. (Czech Republic)

In this paper we present current progress in development of new observational instruments for the double station video experiment called MAIA (Meteor Automatic Imager and Analyzer). The main goal of the MAIA project is to monitor activity of the meteor showers and sporadic

Conference 8135:
Applications of Digital Image Processing XXXIV

meteor each night for the period of at least 3 years. The system is based on the two stations with the gigabyte Ethernet cameras, sensitive image intensifiers and automatic processing of the recorded data. Electro-optical characteristics of the system were previously measured in the laboratory and the result confirmed our expectations according to image quality and resolution. Recently first night sky observation was carried. This paper presents further analysis of imaging parameters based on acquisition of testing video sequences in real environment at different light conditions. Among the most important characteristics belong to the noise model, PSF, conversion function, flat-field and dark frame. Based on these results, preprocessing algorithms are developed and tested to get the best possible image data for astronomical analysis from the double station system.

8135-65, Poster Session

Open source database of images DEIMOS: stereoscopic images

K. Fliegel, S. Vitek, M. Klíma, P. Páta, Czech Technical Univ. in Prague (Czech Republic)

In this paper we present current progress in the project DEIMOS (Database of Images: Open Source). The DEIMOS database is created as an open-source database of images and videos for testing, verification and comparing of various image and/or video processing techniques. This paper is focused on description of new stereoscopic content available in the database. This database of stereoscopic images with various parameters in acquisition and image processing is intended for testing and optimization of metrics for objective image quality assessment. There are many similar databases for 2D content but the number of available databases is still very limited in the case of stereoscopy. Our database is annotated with mean opinion scores of perceived image quality from human observers for each testing condition and also contains eye tracking data captured in subjective experiment. Dependence of perceived image quality on particular testing condition is quantified and discussed.

8135-66, Poster Session

Roadmap for biometric facial recognition with correlation filters

S. Pinto-Fernandez, V. H. Diaz-Ramirez, Ctr. de Investigación y Desarrollo de Tecnología Digital (Mexico)

Facial recognition has become a very important tool for authentication of individuals in many critical applications such as security surveillance in airports and border crossing. Pattern recognition with correlation filter has been very popular in last decades because it has a good mathematical basis, and can be implemented in digital programmable systems and in hybrid opto-digital processors at high rate. In this paper we present a comparison performance between different facial recognition algorithms considering principally correlation based methods. We present several computer simulations results obtained with the considered algorithms and we compare their performance in terms of recognition and classification ability, tolerance to input scene distortions, and computational complexity.

8135-67, Poster Session

A mathematical morphology-based approach for vehicle detection in road tunnels

A. Frías-Velázquez, J. O. Niño-Castaneda, V. Jelača, A. P?urica, W. Philips, Univ. Gent (Belgium)

A novel approach to automatically detect vehicles in road tunnels is presented in this paper. Non-uniform and poor illumination conditions

prevail in road tunnels making difficult to achieve robust vehicle detection with either standard object or motion detectors. Apart of the tunnel lighting, other important sources of illumination are the head and rear lights of the vehicles, which may drastically change the scene conditions, and thus the appearance of the vehicles. Also, shadows and reflections are an issue, since they cause a considerable number of false detections.

The proposed vehicle identification approach consists of the following steps: Image pre-processing, morphological background subtraction, clustering, and object validation. In order to cope with the illumination issues, we propose a local higher-order statistic filter to make the detection invariant to illumination changes and pass the image into a high-pass domain. A background model of the tunnel is generated in this new domain, and a morphological-based background subtraction is then applied. The outcome of this last step are parts of vehicles detected, which are clustered by using information like centroid coordinates, area, and lane position. The vehicle's boundaries are approximated by getting the convex hull of the clustered segments. Finally, a vehicle validation test is run to discard false detections.

An evaluation test comparing our approach with a benchmark object detector has been conducted. The results show that our approach outperforms the benchmark object detector in terms of false detection rate and the overlapping area between convex hull and the ground truth segmentation of the vehicles.

8135-68, Poster Session

Swimming behavior detection for nitocra spinipes in water quality evaluation

Z. Jia, Henan Polytechnic Univ. (China)

The Environmental Protection Agency has over the years suggested a number of biological tests for characterization of industrial waste water, among which a test with the brackish water crustacean Nitocra spinipes can be found. It is of substantial interest to design a low-cost early warning test apparatus for brackish water. The principle of a test is to monitor the swimming behaviour of Nitocra spinipes by the use of digitized video films in daylight or indoor illumination. In our study, grown animals are of a size between 0.6 to 0.8 mm, and it is empirically known that their swimming behaviour is affected by the amount of toxic substances in the water. The first processing step is to manually mark the position of each animal on a starting image, then find out the image difference between starting image and the image in the sequence, finally find out locations of animals on the new image. The processing result is satisfactory.

8135-69, Poster Session

Combining C_Mean clustering and LBP for outdoor face images

Z. Jia, W. Wang, Henan Polytechnic Univ. (China)

For facial recognition, a number of algorithms have been tested on standard databases in internet (e.g. ORL and YALe: indoor images), the facial recognition accuracy (rate) is over 90%. In the same way, the algorithms are tested on OculuAI database or Celebrity database (outdoor images), the recognition rate drastically decreases. Comparing Celebrity database with standard database such as ORL and YALe, it is distinctly manifest that the Celebrity database is more variable in facial rotating angle as well as ornaments such as hat, ring, and earrings etc., which make the images more complicated. To increase the accuracy of facial recognition, a new algorithm is studied by combining C_Mean clustering algorithm and LBP algorithm, the developed new algorithm can increase facial recognition accuracy greatly in OculuAI database, and the testing results are satisfactory.

8135-72, Poster Session

**Tree structure matching pursuit based on
Gaussian scale mixtures model**P. Liu, D. Liu, Z. Liu, J. Wei, Ctr. for Earth Observation and Digital
Earth (China)

Compressed Sensing (CS) theory has gained so much attention recently in the areas of signal processing. In Compressed Sensing (CS) theory, the most important prior is the sparsity of the transform coefficients. The sparsity and the sample measurements decide how well the signal can be accurately reconstructed. However, except for the sparsity, there are other important priors about transform coefficients such as the tree structure and the statistical dependencies that could be employed in CS reconstruction. The tree structure of the coefficients has been employed in such method as model based CS and the statistical dependency of the coefficients is employed in such method as Bayesian based CS. In fact, the two priors about the transform coefficients can be combined into Matching Pursuit method to acquire better result in CS image construction.

In this paper, we propose to introduce the Gaussian Scale Mixtures (GSM) model into the tree structure based Orthogonal Matching Pursuit (TSOMP) reconstruction algorithm. The tree structure based Orthogonal Matching Pursuit method selects a group of tree nodes in the greedy algorithm based reconstruction. But the tree structure is often badly influence by the noise in the iteration and the errors produced by the greedy search algorithm. Then the statistical dependencies of the coefficients are used to increase the stability in searching the tree structure subspace. This enhances the clustering feature of the transform coefficients. In every iteration, firstly, the tree structure is searched by greedy algorithm and the intra-scale dependences of the coefficients is made use of; secondly, the GSM smoothing is employed to regularize the tree structure of the transform coefficients, this GSM model is the priors of the inter-scale dependences of the coefficients, and it will reduce the noise corrupting to image details; then thirdly, a image reconstruction is preformed by solving of a linear equation; at last, instead of directly using the magnitudes of the wavelet coefficients obtained in the previous searching, the estimated wavelet coefficients by the GSM model are used to construct the new tree structure subspace for the next iteration. In the proposed method, the statistical feature priors form the inter-scale dependences of the coefficients and the tree structure priors from intra-scale dependences of the coefficients are combined to improve the accuracy of the Orthogonal Matching Pursuit algorithm, and then the noise and instability in compressed sensing reconstruction are well reduced.

Experiments were performed to compare the proposed method with some existing state-of-the-art CS recovery algorithms such as Orthogonal Matching Pursuit, Bayesian Compressive Sensing and the Tree-Structured Wavelet Compressive Sensing. We also compare these methods under the different level of noise situation. Experimental results show that the proposed method improves reconstruction accuracy for a given number of measurements and more image details are recovered.

Conference 8136: Mathematics of Data/Image Pattern Coding, Compression, and Encryption with Applications XIV

Sunday-Wednesday 21-24 August 2011 • Part of Proceedings of SPIE Vol. 8136
Mathematics of Data/Image Pattern Coding, Compression, and Encryption with Applications XIII

8136-01, Session 1

Noise tolerant dendritic lattice associative memories

G. X. Ritter, M. S. Schmalz, E. T. Hayden, Univ. of Florida (United States)

Linear classifiers based on the real numbers with addition and multiplication feature prominently in the literature pattern recognition. Another approach to the construction of pattern classification operators involves the use of the extended real numbers (the reals with positive and negative infinity) together with addition, maximum, and minimum operations. These lattice-algebra based pattern classifiers have been shown to exhibit superior information storage capacity, fast training and convergence, high pattern classification accuracy, and low computational cost. Such attributes are not generally found, for example, in classical neural nets based on the linear inner product. In a special type of lattice associative memory (LAM), called a dendritic LAM or DLAM, by varying the design of noise or error acceptance bounds, it is possible to achieve noise-tolerant pattern classification.

This paper presents theory and algorithmic approaches for the computation of noise-tolerant lattice associative memories (LAMs) under a variety of input constraints. Of particular interest are the classification of nonergodic data in noise regimes with time-varying statistics. DLAMs have successfully been applied to pattern classification from hyperspectral remote sensing data, as well as spatial object recognition from digital imagery. The authors' recent research in the development of DLAMs is overviewed, with experimental results that show utility for a wide variety of pattern classification applications. Performance results are presented in terms of measured computational cost, noise tolerance, classification accuracy, and throughput for a variety of input data statistics and noise levels.

8136-02, Session 1

Algorithms for adaptive nonlinear pattern recognition

M. S. Schmalz, G. X. Ritter, E. T. Hayden, Univ. of Florida (United States); G. Key, Frontier Technology, Inc. (United States)

In Bayesian pattern recognition research, static classifiers have featured prominently in the literature. A static classifier is essentially based on a static model of input statistics, thereby assuming input ergodicity that is not realistic in practice. Classical Bayesian approaches attempt to circumvent the limitations of static classifiers, which can include brittleness and narrow coverage, by training extensively on a data set that is assumed to cover more than the subtense of expected input. Such assumptions are not realistic for more complex pattern classification tasks, for example, object detection using pattern classification applied to the output of computer vision filters. In contrast, with a two-step process, it is possible to render the majority of static classifiers adaptive such that the tracking of input nonergodicities is supported. Firstly, one develops operations that dynamically insert (or resp. delete) training patterns into (resp. from) the classifier's pattern database, without requiring that the classifier's internal representation of its training database be recomputed. Secondly, one develops and applies a pattern replacement algorithm designed to optimize the pattern database for a given set of performance measures.

This paper presents theory and algorithmic approaches for the efficient computation of adaptive linear and nonlinear pattern recognition operators, in particular, tabular nearest-neighbor encoding (TNE), classical neural nets and lattice associative memories (LAMs). Of

particular interest are the classification of highly nonergodic data in noise regimes with time-varying statistics. The TNE paradigm, as well as lattice neural networks (LNNs) and dendritic LAMs discussed herein, have been successfully applied to the computation of object classification in hyperspectral remote sensing and target recognition applications. The authors' recent research in the development of adaptive LAMs, LNNs, and DLAMs is overviewed, with experimental results that show utility for a wide variety of pattern classification applications. Performance results are presented in terms of measured computational cost, noise tolerance, classification accuracy, and throughput for a variety of input data statistics and noise levels.

8136-03, Session 1

Massively parallel computation of lattice associative memory classifiers

M. S. Schmalz, G. X. Ritter, E. T. Hayden, W. H. Chapman, Univ. of Florida (United States)

Over the past 25 years, concepts and theory derived from neural networks (NNs) have featured prominently in the literature of pattern recognition. Classical NNs based on the linear inner product offer challenges based on the use of multiplication and addition operations. In contrast, NNs having nonlinear kernels based on Lattice Associative Memories (LAM) theory tend to concentrate their work primarily in addition and maximum/minimum operations. The emergence of LAM-based NNs, with their superior information storage capacity, fast convergence and training due to relatively lower computational cost, as well as noise-tolerant classification has extended the capabilities of neural networks far beyond the limited applications potential of classical NNs.

This paper explores theory and algorithmic approaches for the efficient computation of LAM-based neural networks, in particular lattice neural nets and dendritic lattice associative memories. Of particular interest are massively parallel architectures such as graphics processing units (GPUs). Originally developed for video gaming applications, GPUs hold the promise of very high computational throughput (e.g., over a teraflop peak throughput for an Nvidia Fermi processor) without compromising numerical accuracy (e.g., the Fermi GPU supports double precision arithmetic). Unfortunately, currently-available GPU architectures feature a limited memory hierarchy that can produce unacceptably high data movement latencies for relatively simple operations, unless careful design of theory and algorithms is employed. Advantageously, the Fermi GPU is optimized for efficient computation of joint multiply and add operations. As a result, the linear or nonlinear inner product structures of NNs are inherently suitable to the Fermi's (and other GPU's) computational capabilities. The authors' recent research in quantification of GPU performance for inner-product operations is overviewed, with experimental results that show utility for a wide variety of pattern classification applications using classical NNs or lattice-based NNs. Performance results are presented in terms of measured throughput for a variety of data burdens and partitioning approaches.

8136-04, Session 1

Fractal based watermarking of color images

L. McLauchlan, Texas A&M Univ.-Kingsville (United States); M. Mehrübeoglu, Texas A&M Univ. Corpus Christi (United States)

Digital watermarking continues to be an open area of research. In this work, fractals are employed to spatially embed the watermark(s) in the RGB domain. The watermarks are tested separately in each of the three

planes R, G, and B. A blind detection scheme is utilized in which the only information required for detection are the fractal(s) used for the embedding. Next, combinations of embedding in the RG, RB, GB, and RGB planes are used. The efficacy of the embedding combinations in the various planes are studied to determine the best combinations for the tested fractals, images and attacks. The results are compared with previously published methods by the authors.

8136-05, Session 2

The optimum discrete scan-type approximation of low-pass type signals bounded by a measure like Kullback-Leibler divergence

Y. Kida, Ohu Univ. (Japan); T. Kida, Tokyo Institute of Technology (Japan)

We present a running approximation of discrete signals by a FIR filter bank that minimizes various worst-case measures of error, simultaneously.

We assume that the discrete signal is a sampled version of unknown original band-limited signal that has a main lobe and small side-lobes.

The output signal of the filter bank is a final approximation signal.

To restrict frequency characteristics of signals in this discussion, we impose two restrictions to a set of signals.

One is a restriction to a weighted-energy of the Fourier transform of the discrete signal treated actually in the approximation and another is a restriction to a measure like Kullback-Leibler divergence between the initial analog signal and the final discrete approximation signal.

Firstly, we show interpolation functions that have an extended bandwidth and satisfy condition called discrete orthogonality.

Secondly, we present a set of signals and a running approximation satisfying all of these conditions of the optimum approximation.

8136-06, Session 2

Extension of the concept of multi-legged-type signals to the optimum multi-dimensional running approximation of multi-dimensional band-limited signals

Y. Kida, Ohu Univ. (Japan); T. Kida, Tokyo Institute of Technology (Japan)

The original multi-dimensional band-limited signal can be reconstructed from its discrete sample values based on the Shannon sampling theorem. But, it uses an infinite number of sample values.

Hence, if we use a finite number of sample values, we cannot avoid error of approximation.

On the other hand, the running approximation by a multi-dimensional FIR filter bank using shift-invariant interpolation filters is increasing its importance in modern multi-dimensional signal processing.

Hence, the minimization of running approximation errors in a FIR multi-dimensional filter bank for multi-dimensional band-limited signals is the important problem of multi-dimensional signal processing.

In this discussion, we explain briefly a new concept of multi-legged-type signals that are combined signals of many one-dimensional band-limited signals, each body segment of which constitutes a set of small separable domains made by scan-type approximation.

Then, we extend this concept to multi-dimensional hyper signal space and, based on this concept, we propose an approximation method of the extended multi-dimensional multi-legged-type signals and we prove that the presented approximation is the optimum.

Then, introducing a measure of error that becomes quite large for errors

caused by the running approximation and becomes small otherwise, we present extended optimum approximation that minimizes various worst-case measures of approximation error at the same time.

Application of multiple-input multiple-output/space division multiplexing system is discussed. Some examples are given.

8136-11, Session 2

Limited-photon 3D image recognition using photon-counting integral imaging

C. M. Do, Univ. of Connecticut (United States)

An overview of three-dimensional (3D) image recognition using photon-counting integral imaging is presented. A Poisson distribution model is used to generate photon-counting elemental images and reconstruct 3D images. Slices of 3D reconstructed images are the image source for recognition purpose. Experimental and computational results are shown to evaluate the performance of the method.

8136-08, Session 3

Aligning images with CAD models via quaternion optimization

P. F. Stiller, Texas A&M Univ (United States)

This paper introduces an algorithm for “mapping” information in a 2D image onto a 3D CAD model of an object. For example, imagine an image of an object taken at a remote location. The object has some surface damage requiring the fabrication of a patch. The photo of the damaged area is transmitted back to the facility that will design and fabricate the patch. The goal is to align the image with a CAD model of the original object, so that the exact location of the damage can be determined and precisely the correct patch manufactured. We assume that the user is able to identify a minimum of 4 feature points in the image and the corresponding feature points on the CAD model. Beyond that, we assume no information other than knowledge of the size of the camera’s CCD and the location of the center of projection in the image. Our algorithm, known as the quaternion optimization algorithm, optimally positions the camera in CAD space so as to align the matched features appropriately, and permits the mapping of other image pixels (the damaged area) to the CAD model. Surprisingly the solution for the camera position comes down to minimizing the value of a homogeneous quartic polynomial over the unit 3-sphere in 4 space (unit quaternions). The algorithm has been tested in conjunction with researchers and engineers at Etegent Technologies, Ltd. in Cincinnati, Ohio using photos of a damaged surface on an aircraft and a CAD model of the airplane.

8136-09, Session 3

The optimum approximation of multi-dimensional vector signals by multi-input multi-output matrix filter banks

Y. Kida, Ohu Univ. (Japan); T. Kida, Tokyo Institute of Technology (Japan)

We consider multi-dimensional multi-input multi-output systems composed of multi-dimensional analysis-filter matrices, multi-dimensional interpolation-filter matrices and middle sampler matrices of multi-dimensional signals.

Under the condition that the multi-dimensional analysis-filter matrices and the middle sampler matrices are given, we consider a problem of approximating the multi-dimensional input-signal vector by the multi-dimensional output-signal vector of the above system.

We assume that the set of input-signal vectors of this system is contained in a certain given set of input-signal vectors.

The output vector of the system is equal to the sum of products between impulse responses of the interpolation-filter matrices and the discrete sample values that are identical to the output of the middle sampler matrices.

We prove that the proposed approximation minimizes any upper-limit measure of approximation error compared to any other approximation using the same set of sample values.

If the ordinary Fourier transform is adopted in the formulation, we show a fast calculation method of the optimum interpolation-filter matrices.

An example is given that clarify the effectiveness of the proposed method.

8136-10, Session 3

The optimum running approximation of band-limited signals based on new concept of multi-legged-type signals in a hyper domain

Y. Kida, Ohu Univ. (Japan); T. Kida, Tokyo Institute of Technology (Japan)

Sampling theorem of one-dimensional band-limited signals proved that the original signal can be reconstructed from its discrete sample values.

But, it uses an infinite number of sample values.

Hence, if we use a finite number of sample values, we cannot avoid error of approximation.

On the other hand, an approximation by a filter bank using shift-invariant interpolation filters is increasing its importance in modern signal processing.

Hence, the minimization of approximation errors in a filter bank for band-limited signals is the important problem of signal processing.

Specially, the minimization of the error associated with running approximation by the FIR filter bank is one of the most difficult problems of the signal processing.

In this discussion, we introduce a new concept of multi-legged-type signals in a hyper-space, each body segment of which constitutes a set of small separable domains made by scan-type approximation.

Based on this concept, we propose an approximation method of the multi-legged-type signals and we prove that the presented approximation is the optimum.

Then, introducing a measure of error that becomes quite large for errors caused by the running approximation and becomes small otherwise, we present extended optimum approximation that minimizes various worst-case measures of the running approximation error at the same time.

Moreover, an application of multiple-input multiple-output/space division multiplexing system is discussed. Some examples are given.

8136-23, Session 3

3D model-based still image object categorization

R. Petre, T. B. Zaharia, TELECOM & Management SudParis (France)

This paper proposes a novel recognition scheme algorithm for semantic labeling of 2D object present in still images. The principle consists of matching unknown 2D objects with categorized 3D models in order to infer the semantics of the 3D object to the image. We tested our new recognition framework by using the MPEG-7 and Princeton 3D model databases in order to label unknown images randomly selected from the web. Results obtained show promising performances, with recognition rate up to 84%, which opens interesting perspectives in terms of semantic metadata extraction from still images/videos.

8136-12, Session 4

Theory and experiments of remote tracking and measurements of moving objects

C. J. Hu, Southern Illinois Univ. at Carbondale (United States) and Sunnyfuture, Boulder (United States)

As the author published and will publish in several SPIE conferences (4 papers in the period of January 2009 to April 2011), we can use a novel image processing method, the LPED or Local Polar Edge Detection Method, developed by the author in the last 2 years, to recognize and to track remotely any moving object on the ground by an IR camera used in conjunction with a signal processing chip installed on-board in a communication satellite. Live experiments using simulated satellite IR snapshots of a moving ground vehicle, sampled at periodical times, showed that the VB6 software designed by the author can automatically track this moving vehicle in consecutive snapshots and automatically measure its distance of movement, speed of movement, and angular change of object orientation between any two adjacent snap-shots. It can also numerically predict the vehicle's immediate future movement at the latest snap-shot. All these can be done in real-time. The automatic, real-time print-outs of numerical measurements are seen to be quite accurate compared to the ones we can measure manually by using protractor and ruler on the snapshots. Single vehicle tracking and measurements are to be presented in live in this coming April, D&S Conference, Orlando.

Design and experiments to generalize this single-vehicle measurements to multiple-vehicle automatic tracking and measurements are 90% completed at the present time. Both theory and experiments of the multiple vehicle measurements will be explained and demonstrated in live in this conference.

8136-13, Session 4

Optimizing feature extraction in image analysis using experimented designs, a case study evaluating texture algorithms for describing appearance retention in carpets

S. A. Orjuela Vargas, R. A. Quinones, Sr., B. Ortiz-Jaramillo, F. Rooms, R. De Keyser, W. Philips, Univ. Gent (Belgium)

The variety of techniques available for extracting characteristics from images may result in a high amount of data to be analyzed. In many image processing investigations the relevant features of interest are visually chosen, implying human subjectivity. With this method dependences between the processes involved in image analysis are not evaluated, decreasing reliability of the results.

Conducting a planning phase in advance using the experimental design theory ensures reliability of the results. The main advantage is the identification of dependences between processes, optimally detecting process combinations while both the development time and overall costs are reduced. Only few investigations applying experimental design theory in image analysis exist, most of them focusing in applications rather than in the method.

We present a case study, evaluating texture algorithms for describing appearance retention in carpets, which is evaluated by assigning numbers to different degrees of changes in appearance. Recently, we found that Local Binary Pattern (LBP) techniques are appropriate for quantifying such changes. Therefore, we consider in this experiment, texture algorithm based on the latest extensions of the LBP technique. We first quantify monotonicity and discriminance from the description of texture features vs the numbers. Then, we evaluate the performance of the techniques using probability values obtained from statistical tests. We evaluate dependences between techniques, types of carpets and different image resolutions. Finally, inferences and results are clearly stated and communicated by interpreting the probability results. The main concepts of the theory are presented in detail for using it in other image applications.

8136-14, Session 4

Edge pattern analysis for edge detection and localization

B. Jiang, National Institute of Aerospace (United States)

Edge detection processing plays an important role in image processing, and at its most basic level classifies image pixels into edges and non-edge pixels. The accuracy of edge detection methods determines the eventual success or failure of computerized analysis procedures which follow the initial edge detection determinations. In view of this downstream impact, considerable care should be taken to improve the accuracy of the front-end edge detection. In general, edges would be considered as abrupt changes or discontinuity in intensity of an image. Therefore, most of edge detection algorithms are designed to capture signal discontinuities but the spatial character of especially complex edge patterns has not received enough attention. The edge detection operation generally has two main steps: filtering, and localization. I temporarily neglect the effect of filtering process, and assume the selective filter is ideal in the first step. The focus of this paper is on the second step whose aim is accurately detecting and localizing sharp, local intensity changes. Edges can be divided into basic patterns such as pulse, step and ramp: different types have different shapes and consequent mathematical properties. In this paper, the behavior of various edge patterns, under first, second, even higher, derivatives are examined and analyzed to determine how to accurately detect and localize these edge types, especially reducing "double edge" effect that is one important drawback to the derivative method. General rules about the depiction of edge patterns are proposed to reduce localization error in the discrete domain of the digital image. Besides from the ideal patterns, other patterns representing basic edge categories, such as stair, are examined to broaden the initial analysis. Experiments conducted to test my propositions support the idea that edge patterns are instructive in enhancing the accuracy of edge localization.

8136-21, Session 4

Multi-dimensional feature extraction from 3D hyperspectral images

M. Mehrùbeoglu, Texas A&M Univ. Corpus Christi (United States)

A hyperspectral imaging system has been set up and used to capture hyperspectral image cubes from various samples in the 400-1000 nm spectral region. The system consists of an imaging spectrometer attached to a CCD camera with fiber optics light source as the illuminator. The significance of this system is its capability to capture 3D spectral and spatial data that can then be analyzed to extract information about the underlying samples, monitor the variations in their response to perturbation or changing environmental conditions, and compare optical properties. In this paper preliminary results are presented that analyze the 3D spatial and spectral data in reflection mode to extract features to differentiate among different classes of interest using biological and metallic samples. Studied biological samples possess homogenous as well as non-homogenous properties. Metals are analyzed for their response to different surface treatments, including polishing. Similarities and differences in the feature extraction process and results are presented. The mathematical approach taken is discussed. The hyperspectral imaging system offers a unique imaging modality that captures both spatial and spectral information that can then be correlated for future sample predictions.

8136-22, Session 4

Interactive region-based retrieval

A. Bursuc, T. B. Zaharia, TELECOM & Management SudParis (France); F. Prêteux, Mines ParisTech (France)

This paper presents a novel method for retrieving different instances of a

region or object of interest in a video database. We propose a dynamic region construction and matching algorithm aiming at obtaining the most similar instance of the query model from each candidate image. An interactive selection mechanism allows the user to select an object directly from the video and to start a query using as input this information in order to access visually similar content.

8136-07, Poster Session

A novel calibration method of CCD camera for LAMOST

Y. Gu, Y. Jin, Z. Chao, Univ. of Science and Technology of China (China)

Large Sky Area Mult-object Fiber Spectroscopic Telescope - LAMOST, with a 1.75m-diameter focal plane on which 4000 optical fibers are arranged, is one of major scientific projects in China. During the surveying process of LAMOST, the optical imaging system makes the astrometric objects be imaged in the focal plane, and the optical fiber positioning system controls the 4000 fibers to be aligned with these objects and obtain their spectrum. In order to correct the positioning error of these optical fibers, the CCD camera is used to detect these fibers' position in the way of close-range photogrammetry.

As we all know, the calibration quality of the CCD camera is one of the most important factors for detection precision. However, the camera calibration has two following problems in the field work of LAMOST. First, the camera parameters are not stable due to the changes of on-site work environment and the vibration during movement. So, the CCD camera must be on-line calibrated. Second, a large-size high-precision calibration target is needed to calibrate the camera, for the focal plane is very big. Making such a calibration target, it is very difficult and costly. Meanwhile, the large calibration target is hard to be fixed on LAMOST because of the space constraint.

In this paper, an improved bundle adjustment self-calibration method is proposed to solve the two problems above. The results of experiment indicate that this novel calibration method needs only a few control points while the traditional calibration methods need much more control points to get the same precision. So the method could realize the on-line high-precision calibration of CCD camera for LAMOST.

8136-15, Poster Session

Experimental test of turbulence prediction algorithms

D. Del Moro, M. Stangalini, R. Piazzesi, F. Berrilli, Univ. degli Studi di Roma Tor Vergata (Italy)

Short time-scale prediction of the evolution of turbulent processes is of interest in many applications, among these Adaptive Optics (AO). Three possible approaches to this problem are the attempts to predict its evolution through Auto Regressive Moving Average (ARMA) modelling, Neural Networks or linear approximations. Each of these approaches involves an algorithm which forecasts a future turbulence state using as input the knowledge of past measured states.

An experimental test to compare these different approaches has been set up at the Tor Vergata University Solar Physics Laboratory: a Kolmogorov spectrum turbulence introduces aberrations in the optical path of an AO system and the data from a Shack-Hartmann sensor is used to predict the successive state of the wavefront.

The results, advantages and drawbacks of the three different methods are compared.

8136-16, Poster Session

A comparative test of different compression methods applied to solar high resolution images

D. Del Moro, Univ. degli Studi di Roma Tor Vergata (Italy); E. Pietropaolo, Univ. degli Studi dell'Aquila (Italy); F. Giannattasio, F. Berrilli, Univ. degli Studi di Roma Tor Vergata (Italy)

In this work we conduct a comparative study on different data compression methods applied to high resolution images of the solar surface acquired at the Solar Dunn Telescope in Sacramento Peak with the IBIS (Interferometric Bidimensional Spectrometer) instrument.

Our aim is to perform an estimation of the quality, efficiency and workload of the considered computing techniques both in the so-called lossless modality, where in the reconstruction phase there is no loss of information, and in lossy mode, where it should be possible to reach a high compression ratio at the expense of image information. In the latter case we quantify the quality with image analysis conventional methods and more specifically with the reconstruction of physical parameters through standard procedures used in this kind of observations. The considered methods constitute the most frequently adopted image compression procedures in a variety of fields of application; they exploit in different ways the properties of the Discrete Wavelet Transforms often coupled with standard entropy coders or similar coding procedures applied to the different bit planes in order to allow a progressive handling of the original image.

In the lossless approach we found that all methods give a compression ratio around 2. For a lossy compression we reached a compression ratio of 16 (equivalent to a 1 bit per pixel) without any perceptual difference between original and reconstructed images.

The degree of accuracy of such an approach will be shown in the final presentation.

8136-20, Poster Session

N-order phase unwrapping system tolerant to noise

M. A. Navarro Rodriguez, J. C. Estrada, M. Servin, Ctr. de Investigaciones en Óptica, A.C. (Mexico)

The present work shows preliminary results of a phase unwrapping technique used in interferometry. Wrapped phase maps are the result of the modulus 2π ambiguities caused for the phase recovery function \arctan . Here we present a recursive n-order phase unwrapping system that removes the ambiguities, it's robust to noise and fast.

The system is able to recover the unwrapping phase in presence of high noise, according to stability of the system that can be controlled. This high noise causes line sequential integrations of phase differences to fail. The system is not numerically-heavy in comparison with other methods that tolerate the noise. The application areas of the system can be: optical metrology, magnetic resonance, and those imaging systems where information is obtained as a demodulated wrapped phase map.

8136-18, Poster Session

The research on pattern recognition in distributed fiber sensor system

H. Wu, D. Zhao, Fudan Univ. (China)

Distributed Fiber Sensor System is a new type of system, which could be used in long-distance condition for monitoring and inspection. Position determination analysis toward this system is popular in previous papers, but pattern recognition of the output signals of the sensor has been missed for a long time. This function turns to critical especially when it is used for real security project in which quick response to intrusion is a must. This paper provides a MFCC-based approach to extract features of the sensing signals and does the recognition experiments using neural network, which could be used for pattern recognition in real project, and the approach is proved by large practical experiments and projects.

8136-19, Poster Session

Image analysis and pattern recognition for the localisation of medical devices in the operational field

P. L. Chirco, M. Zanarini, SOFTEC Technology & Research (Italy)

Localisation of devices can be of paramount importance during surgery, in particular when probes are used.

A simple but effective system has been developed based on the geometric matching analysis of the image of the operational field as acquired by an over-viewing visual camera. Indeed, a target object containing known patterns is placed around the head of the probe; an accurate system for imaging identifies and locates the patterns.

The instrumentation needed for the localisation is simple and work in the visual light environment.

Conference 8137: Signal and Data Processing of Small Targets 2011

Tuesday-Thursday 23-25 August 2011 • Part of Proceedings of SPIE Vol. 8137
Signal and Data Processing of Small Targets 2011

8137-01, Session 1

2D-3D image registration using Lidar and aerial image in lunar surface

P. Duraisamy, Univ. of North Texas (United States)

In this paper we discuss about registration between 2D image -3D data in lunar surface. It is challenging problem to register between two different modalities in lunar surface due to lack of conventional features. We used craters as features to register between two different modalities. We also used extrinsic camera parameters for estimating camera pose estimation without any apriori knowledge. We validated our approach on two different views of data sets using craters as feature.

8137-02, Session 1

Algorithm development for outlier detection and background noise reduction during NIR spectroscopic data processing

D. Abookasis, Ariel Univ. Ctr. of Samaria (Israel); J. J. Workman, Biotechnology Business Associates (United States) and Liberty Univ. (United States)

This study describes a hybrid processing algorithm for use during calibration/validation of near-infrared spectroscopic signals based on spectra cross-correlation and pre-processing filtering combined with a partial-least square regression (PLS) analysis. In the first step of the algorithm, exceptional signals (outliers) are detected and removed based on spectra correlation criteria we have developed. Then, signal filtering based on orthogonal signal correction (OSC) was applied, before being used in the PLS model, to filter out background variations. After outlier screening and OSC treatment, a PLS calibration model matrix is formed. Common statistics such as standard error of cross-validation mean relative error, coefficient of determination, etc. were computed to assess the fitting ability of the algorithm. Once a model has been built, it is used to predict the concentration of the unknown (blind) samples. Algorithm performance was tested on several hundred blood samples prepared at different hematocrit and glucose levels using blood materials from thirteen healthy human volunteers. During measurements samples were subjected to extreme variations in temperature, flow rate, and sample pathlength. Experimental results which show a significant decrease in standard error of prediction in comparison to the factorial approach highlight the potential, applicability, and effectiveness of the proposed method.

8137-03, Session 1

A data-driven approach for processing heterogeneous categorical sensor signals

C. P. Calderon, A. Jones, S. Lundberg, R. C. Paffenroth, Numerica Corp. (United States)

False alarms generated by sensors pose a substantial problem to a variety of fusion applications.

We focus on situations where the frequency of a genuine alarm is "rare" but the false alarm rate is high.

The goal is to mitigate the false alarms while retaining power to detect true events.

We propose to utilize data streams contaminated by false alarms (generated in the field) to compute statistics on a single sensor's misclassification rate.

The nominal misclassification rate of a deployed sensor is often suspect because it is unlikely that these estimates were tuned to the specific environmental conditions in which the sensor was deployed.

Recent categorical measurement error methods will be applied to the collection of data streams to "train" the sensors and provide point estimates along with confidence intervals for the misclassification and estimated prevalence. By pooling a relatively small collection of misclassified random variables arising from a single sensor and using data-driven misclassification rate estimates along with estimated confidence bands, we show how one can transform the stream of categorical random variables into a test statistic with a known distribution. The procedure shows promise for normalizing sequences of misclassified random variables coming from different sensors (with a priori unknown population parameters) to comparable test statistics; this facilitates "fusion" through various downstream processing mechanisms. We envision using such output to feed false discovery methods that exploit the comparable test statistics in a chemical sensor fusion context where reducing false alarms and maintaining substantial power is important.

8137-04, Session 1

Backscatter behaviour and tracking of ogive shaped objects in optical range

C. F. Hahlweg, Helmut-Schmidt Univ. (Germany)

In recent years session we presented devices and methods for laser based trajectory measurement of hand gun bullets, which also included the estimation of light scatter from such bodies in free flight. While our first approach for gathering the scatter qualities of arbitrary projectiles using metrological image processing resulted in a polar fourier series of the outer contour of the projectile, which could be used to calculate the scatter behavior, the question of determining the contour as an parameterized ogive came up, which then could also be used to determine the type of projectile literally on the fly - assumed high enough image resolution. The present paper is understood as a continuation of last years papers with focus on the scatter characteristics of ogive shaped bodies and the metrological identification of the ogives of projectiles.

8137-05, Session 1

A combined target spectral-spatial dense descriptor feature for improved tracking performance

J. J. Weinheimer, S. G. Beaven, P. V. Villeneuve, Space Computer Corp. (United States)

In EO tracking, target features can be used to improve performance since they help distinguish the targets from each other when confusion occurs during normal kinematic tracking. In this paper we introduce a method to encode target spatial information into a signature, allowing us to convert the problem of spatial template matching into one of signature matching. This allows us to apply multivariate algorithms commonly used to process Hyperspectral data to panchromatic imagery. In addition, we also show how the spatial signature can be naturally extended with spectral information to produce a signature that contains both spectral and spatial information to provide a more unique target feature.

To this end, we introduce a new descriptor called Spectral DAISY for encoding spatial information into a signature, based on the concept of the DAISY1 dense descriptor. We demonstrate the process on real data and show how the combined spatial/spectral feature can be used to improve target/track association over spectral or spatial features alone.

8137-06, Session 1

Design and analysis of an FMCW radar system for vehicle tracking

N. Gale, A. Roy, L. Hong, Wright State Univ. (United States)

The ability to accurately detect and track ground vehicles is an essential component in many applications from traffic monitoring and enforcement to automatic cruise control and automated collision avoidance. Over the last few decades frequency modulated continuous wave (FMCW) radar have become the industry standard for these applications due to their compact size, low power, and high data rate. There are several companies that provide these sensors at low cost, but the sensors can require expensive test equipment to calibrate. The ability to use these sensors right out of the box without expensive calibration practices is a key to deploying these sensors rapidly and at low cost. An uncalibrated commercial-off-the-shelf (COTS) FMCW radar system was used to collect data along the roadside with vehicles moving within the sensor's field of view. A moving target indication (MTI) technique is used to suppress stationary background clutter, while magnitude thresholding and CFAR approaches are applied for signal detection. These detections are fed into an extended Kalman filter framework using both nearest neighbor and probabilistic approaches for data association. Results from the tracking scenarios are compared to ground truth in the form of GPS data that was collected from onboard the moving vehicles.

8137-07, Session 1

Game theoretic approach to similarity based image segmentation

D. Shen, G. Chen, Consultant Professional (United States); Y. Zheng, Alcorn State Univ. (United States)

Image segmentation problem is to decompose a given image into segments, i.e. regions containing "similar" pixels. This problem can be straightforwardly cast into a clustering problem, where pixels represent the objects to cluster. In this way a cluster corresponds to a segment of the image. There exist different more or less complicated ways of defining a similarity measure between two pixels. In particular standard approaches take into account brightness, color, texture or boundary informations, or combinations of them in order to build a good similarity measure. In this paper, we offer a similarity based image segmentation approach based on game theory. The basic idea behind our approach is that the similarity based clustering problem can be considered as a multi-player non-cooperative "clustering game". Within this context, the notion of a cluster turns out to be equivalent to a classical equilibrium concept from game theory, as the latter reflects both the internal and external cluster conditions alluded to before. We also show that there exists a correspondence between these equilibria and the local solutions of a polynomial, linearly-constrained, optimization problem, and provide an algorithm for finding them. Experiments on image segmentation problems show the superiority of the proposed approach.

8137-08, Session 2

Optimal filters with heuristic 1-norm sparsity constraints

M. Yazdani, R. Hecht-Nielsen, Univ. of California, San Diego (United States)

We present a design method for sparse optimal Finite Impulse Response (FIR) filters that improve the visibility of a desired stochastic signal corrupted with white Gaussian noise. We emphasize that the filters we seek are of high-order but sparse, thus significantly reducing computational complexity. An optimal FIR filter for the estimation of a desired signal corrupted with white noise can be designed by maximizing the signal-to-noise ratio (SNR) of the filter output with the constraint that

the magnitude (in 2-norm) of the FIR filter coefficients are set to unity [Makhoul 1981]. This optimization problem is in essence maximizing the Rayleigh quotient and is thus equivalent to finding the eigenvector with the largest eigenvalue. While such filters are optimal, they are rarely sparse. To ensure sparsity, one must introduce a cardinality constraint in the optimization procedure. For high-order filters such constraints are computationally burdensome due to the combinatorial search space. We relax the cardinality constraint by using the 1-norm approximation of the cardinality function. This is a relaxation heuristic similar to the recent sparse filter design work of Baran, Wei, and Oppenheim [Baran et al 2010]. The advantage of this relaxation heuristic is that the solutions tend to be sparse and the optimization procedure reduces to a convex program, thus ensuring global optimality. In addition to our proposed optimization procedure for deriving sparse FIR filters, we show examples where sparse high-order filters significantly perform better than low-order filters, whereas complexity is reduced by a factor of 10.

8137-09, Session 2

Passive ranging: optimal maneuvers and performance bounds

P. F. Singer, Raytheon Space & Airborne Systems (United States)

The passive ranging equations and conditions on the ownship dynamics, necessary for solution, are inferred. Solutions for range and range rate are then obtained for constant velocity and constant acceleration targets. Expressions for the bias and variance of these estimators of range and range rate are then developed. The resulting set of coupled, nonlinear, ordinary differential equations are solved for the ownship maneuvers which minimize the range variance for a given range bias. The optimal ownship maneuver in terms of the range and range rate variances is then determined. The Cramer-Rao and Bhattacharyya lower bounds on the range and range rate variances are evaluated.

8137-10, Session 2

A physics-based approach to particle flow for nonlinear filters

F. E. Daum, J. Huang, A. Noushin, Raytheon Co. (United States)

We have solved the well known and important problem of "particle degeneracy" using a new theory, called particle flow. Our filter is four orders of magnitude faster than standard particle filters for any given number of particles, and we required many orders of magnitude fewer particles to achieve the same filter accuracy. Our filter beats the EKF accuracy by several orders of magnitude for difficult nonlinear problems. Our theory uses exact particle flow to compute Bayes' rule, rather than a pointwise multiply. We do not use resampling or proposal densities or importance sampling or any other MCMC method. But rather, we design the particle flow with the solution of a linear first order highly underdetermined PDE, like the Gauss divergence law in electromagnetics. We study over a dozen methods to solve this PDE, including: (1) irrotational flow (i.e., the gradient of the solution of Poisson's equation); (2) incompressible flow (like subsonic flow in air); (3) compressible flow (like supersonic flow in air); (4) variational methods (e.g. optimal control); (5) Gauss' and Hertz' variational method; (6) direct integration in terms of d-1 arbitrary functions; (7) complete integrals (i.e., in terms of d-1 arbitrary constants); (8) Fourier transform of the divergence form of our PDE; (9) Gromov's h-principle; (10) generalized inverse of linear differential operator; (11) generalized inverse of a certain matrix that integrates basis functions; (12) generalized method of characteristics (due to Bellman); (13) differential quadrature (also due to Bellman); (14) Jacobi's method, and hybrids of the above. We show numerical results for many examples.

Our basic methodology is the same as in physics: (a) derive a PDE; (b) solve the PDE; and (c) test the solution with experiments. In our work, the last step corresponds to numerical experiments rather than physical experiments. This three step methodology in physics has been

Conference 8137:
Signal and Data Processing of Small Targets 2011

remarkably successful (e.g., Euler's continuity eq. for fluid flow, Poisson's eq., Fourier's heat equation, Maxwell's equations, Schroedinger equation, Dirac equation, Yang-Mills equations, Einstein's field equation for general relativity, Fokker-Planck eq., Boltzmann transport eq., Navier-Stokes eq., Euler-Lagrange eqs., Hamilton-Jacobi eq., Klein-Gordon eq., Seiberg-Witten eqs., etc.). More specifically, our theory benefits from many notions developed in physics and especially fluid dynamics (irrotational flow, incompressible flow, Hamiltonian dynamics, Poisson's eq., etc.). That is, we have used a physics based approach to nonlinear filters.

8137-11, Session 2

A survey of maneuvering target tracking Part VId: sampling-based nonlinear filtering

X. Li, V. P. Jilkov, The Univ. of New Orleans (United States)

This paper is Part VId of a comprehensive survey of maneuvering target tracking without addressing the so-called measurement-origin uncertainty. It provides an in-depth coverage of sampling-based nonlinear filters, commonly referred to as particle filters, developed particularly for handling the uncertainties induced by potential target maneuverers as well as nonlinearities in the dynamical systems commonly encountered in target tracking. Various implementations and tracking applications are reviewed. Also addressed are computational issues, such as different schemes for resampling and parallel processing.

8137-12, Session 2

Tracking with biased measurements

S. V. Bordonaro, Naval Undersea Warfare Ctr. (United States); P. Willett, Y. Bar-Shalom, Univ. of Connecticut (United States)

In many target tracking applications, estimation of target position and velocity is performed in Cartesian coordinates. Use of Cartesian coordinates for estimation stands in contrast to the measurements, which are traditionally the range, azimuth and elevation measurements of the spherical coordinate system. It has been shown in previous works that the classical nonlinear transformation from spherical to Cartesian coordinates introduces a bias in the position measurement. Various means to negate this bias have been proposed. In many active SONAR and RADAR applications, the sensor also provides a Doppler, or range rate, measurement. Use of Doppler in the estimation process has also been proposed by various authors. The goals of this paper are two-fold. The first goal is to show that a bias, similar to the bias shown by previous authors for conversion of position measurements, exists when measuring Doppler from a moving platform. The second is to examine the effects of biased measurements on estimation performance and the effectiveness of proposed compensation approaches.

8137-13, Session 2

Breaking the Bayesian bottleneck

F. E. Daum, J. Huang, Raytheon Co. (United States)

We show numerical results for many examples of nonlinear filtering problems, including: diverse nonlinearities, various levels of stability of the plant (as gauged by the eigenvalues of the Jacobian of the plant) including both stable and unstable plants, process noise, measurement noise, initial uncertainty in the state vector, dimension of the plant, number of particles, multimodal densities, etc. It turns out that the accuracy of the filter varies by many orders of magnitude depending on the values of these parameters.

We have solved the well known and important problem of "particle degeneracy" using a new theory, called particle flow. Our filter is four orders of magnitude faster than standard particle filters for any given number of particles, and we required many orders of magnitude fewer particles to achieve the same filter accuracy. Our filter beats the

EKF accuracy by several orders of magnitude for difficult nonlinear problems. Our theory uses exact particle flow to compute Bayes' rule, rather than a pointwise multiply. We do not use resampling or proposal densities or importance sampling or any other MCMC method. But rather, we design the particle flow with the solution of a linear first order highly underdetermined PDE, like the Gauss divergence law in electromagnetics.

8137-14, Session 2

Improving multi-sensor tracking with the addition of lesser quality radar data

C. A. Rea, M. E. Silbert, Naval Air Systems Command (United States)

The ability to track multiple maneuvering targets, such as boats or even people, in using multiple sensors is a difficult and important problem. However, often the sensors used are different, with different accuracies and different detection capabilities. It becomes problematic to determine how best to combine the data from these sensors. Since each sensor provides information, and information is additive, then theoretically the best estimate should be obtained by combining the information from all sensors. In previous work it was shown that multiple disparate sensors do not improve the state estimations of a tracker when compared to using only the single best sensor. This paper will look at how to best use all data available to a data fusion engine, regardless of source, and aims to answer the questions "Does the best tracking performance truly result from throwing away data? Can the performance of the single high quality sensor be surpassed utilizing all data?" Current fielded systems use a "best of breed" approach when selecting which data to integrate into a track. We will investigate using a modified IMM and compare it to existing algorithms to find if "best of breed" is really the best of breed.

8137-15, Session 3

Multiple-hypothesis tracking for the cyber domain

S. Schwoegler, S. S. Blackman, Raytheon Space & Airborne Systems (United States); J. Holsopple, CUBRC (United States); M. Hirsch, Raytheon Co. (United States)

This paper discusses how methods used for conventional multiple hypothesis tracking (MHT) can be extended to domain-agnostic tracking of entities from non-kinematic constraints such as those imposed by cyber attacks in a potentially dense false alarm background. MHT is widely recognized as the premier method to avoid corrupting tracks with spurious data in the kinematic domain but it has not been extensively applied to other problem domains. The traditional approach is to tightly couple track maintenance (prediction, gating, filtering, probabilistic pruning, and target confirmation) with hypothesis management (clustering, incompatibility maintenance, hypothesis formation, and N-association pruning). However, by separating the domain specific track maintenance portion from the domain agnostic hypothesis management piece, we can begin to apply the wealth of knowledge gained from ground and air tracking solutions to the cyber (and other) domains. These realizations led to the creation of Raytheon's Multiple Hypothesis Extensible Tracking Architecture (MHETA).

In this research, we showcase MHETA for the cyber domain, plugging in a well established method, CUBRC's INformation Engine for Real-time Decision making, (INFERD), for the association portion of the MHT. The result is a CyberMHT. We demonstrate the power of MHETA-INFERD using both simulated and real-world data. Using metrics from both the tracking and cyber domains, we show that while no tracker is perfect, by applying MHETA-INFERD, advanced non-kinematic tracks can be captured in an automated way, perform better than non-MHT approaches, and decrease analyst response time to cyber threats.

8137-16, Session 3

Discrimination and tracking of dismounts using low-resolution aerial video sequences

R. Narayanaswami, A. Tyurina, D. Diel, R. K. Mehra, Scientific Systems Co., Inc. (United States); J. M. Chinn, Air Force Research Lab. (United States)

In this paper we investigate the detection and tracking of dismounts using low resolution aerial video sequences (IR and EO). This process consists of (1) alignment, (2) detection of moving objects and (3) extraction of features of moving objects and (4) tracking. The resolution of the data in our algorithm testing and implementation was in the range of 10-50 pixels on target. We start with frame to frame registration of the video signal to identify background versus moving foreground for identification of potential dismounts with the further aim of classification. Moving objects are defined as areas of significantly different pixels in a current frame and an average of several previous frames. The identified moving objects are classified by size to obtain sub images containing potential dismounts. Tracking starts with chip construction and feature extraction and consists of the following steps (1) Track the object of interest through the video stream, discard if spurious, (2) Construct a chip of sub images and (3) Compute features: static from frames and kinematic from the entire chip. Kinematic features include frequency of intensity variation of pixels relative to the center of area of the dismount. The tracking mechanism should be robust to changes of viewing angle, lighting and partial occlusions. The method we have presently implemented is based on known inter-frame alignment parameters, estimated speed of tracked objects, and their static features, such as size, color etc. The temporal frequencies of pixel intensities can distinguish moving objects such as cars from dismounts.

8137-17, Session 3

Application of a joint tracking and identification method to dismount targets

S. S. Blackman, R. A. Rosen, K. V. Krikorian, C. G. Durand, S. Schwoegler, Raytheon Space & Airborne Systems (United States)

This paper presents a method for tracking dismounts/humans in a potentially dense clutter background. The proposed approach uses Multiple Hypothesis Tracking (MHT) for data association and Interacting Multiple Model (IMM) filtering. The problem is made difficult by the presence of random and persistent clutter, such as produced by moving tree branches. There may also be moving targets, such as vehicles and animals, that are not of interest to the user of the tracking system but that must be tracked in order to separate these targets from the targets of interest. Thus, a joint tracking and identification method has been developed to utilize the features that are associated with dismount targets. This method uses a Dempster-Shafer approach to combine feature data to determine the target type (dismount versus other) and feature matching is also used in the track score used for MHT data association.

The paper begins by giving an overview of the features that have been proposed in the literature for distinguishing humans from other types of targets. These features include radar cross section, target dynamics, and spectral and gait characteristics. For example, the spread of the Doppler/velocity spectrum is a feature that is sent to the tracker and a large width will be an indication that the observation is from an animal, rather than a vehicle. Then, a distinct periodic pattern, such as a peak at about 2 Hz, can be used to identify the target as a human and, along with the target speed, may even be used as a target signature. The manner in which these features are estimated during signal processing and how these data are included in the track score is described.

A test program that was conducted in order to produce data for analysis and development is described. Typical results derived from real data, collected during this test program, are presented to show how feature data are used to enhance the tracking solution. These results show that the proposed methods are very effective in separating the tracks on dismounts from those formed on clutter and other objects.

8137-18, Session 3

Comparison of a grid-based filter to a Kalman filter for the state estimation of a maneuvering target

M. E. Silbert, The George Washington Univ. (United States) and NAVAIR (United States); T. Mazzuchi, S. Sarkani, The George Washington Univ. (United States)

Providing accurate state estimations of a maneuvering target is an important, but difficult problem. This problem occurs when needing to track maneuvering boats or even people wandering around. In an earlier paper, a specialized grid-based filter was introduced as an effective method to produce accurate state estimates of a target moving in two dimensions, while requiring only a two-dimensional grid. As was shown, this grid-based filter produces accurate state estimates because the filter can capture the kinematic constraints of the target directly, and thus account for them in the estimation process. In this paper, the relative performance between a grid-based filter and a Kalman filter is investigated. In particular, the state estimations (position and velocity) from a grid-based filter are compared to those from a Kalman filter, against a maneuvering target. This comparison will incrementally increase the maneuverability of the target to determine how maneuverable the target must be to gain the benefit from a grid-based filter. The paper will discuss the target motion model, the corresponding implementation of the grid-based filter, and the tailoring of the Kalman filter used for the study. The results will show that the grid-based filter typically performs at least as good as the Kalman filter, but often performs better. A key disadvantage of the grid-based filter is that it is much more computational than a Kalman filter. The paper will discuss the straightforward parallelization of the computations, making the processing time for the grid-based filter closer to those needed for a Kalman filter.

8137-19, Session 3

A Gaussian sum filter framework for space surveillance

J. T. Horwood, N. D. Aragon, A. B. Poore, Numerica Corp. (United States)

While standard Kalman-based filters, Gaussian assumptions, and covariance-weighted metrics work remarkably well in data-rich tracking environments such as air and ground, their use in the data-sparse environment of space surveillance is more limited. In order to properly characterize non-Gaussian density functions arising in the problem of long term propagation of state uncertainties, a framework for a Gaussian sum filter is described which achieves uncertainty (covariance) consistency and an accurate approximation to the Fokker-Planck equation up to a prescribed accuracy. The filter is made efficient and practical by (i) using coordinate systems adapted to the physics (i.e., orbital elements), (ii) only requiring a Gaussian sum to be defined along one of the six state space dimensions, and (iii) the ability to initially select the component means, covariances, and weights by way of a lookup table generated by solving an offline nonlinear optimization problem. The efficacy of the Gaussian sum filter and the improvements over the traditional unscented Kalman filter are demonstrated within the problems of data association and maneuver detection.

8137-20, Session 3

Multiple model cardinalized probability hypothesis density filter

R. Georgescu, P. Willett, Univ. of Connecticut (United States)

Mahler introduced a new approach to tracking in which target states and measurements are modeled as random finite sets. The resulting

Conference 8137:
Signal and Data Processing of Small Targets 2011

Probability Hypothesis Density (PHD) filter propagates the first-moment approximation to the multi-target Bayesian posterior distribution.

The follow up Cardinalized PHD (CPHD) filter is a recursive filter that propagates both the posterior likelihood of (an unlabeled) target state and the posterior cardinality density (probability mass function of the number of targets).

Extensions of the PHD filter to the multiple model (MM) framework have been published and were implemented either as a particle filter or a Gaussian Mixture (GM), for the case of linear and later nonlinear target dynamics and/or measurement models.

In this work, we introduce the multiple model version of the more elaborate CPHD filter. We present a detailed derivation of the prediction and update steps of the MMCPHD in the case of two nearly constant velocity models and proceed to a GM implementation. The new filter is accompanied by a track management scheme dealing with events such as track initiation, update, merging, spawning and deletion.

We tested the new tracker on the challenging Metron multistatic sonar dataset. Metrics of performance are reported, such as track probability of detection, track fragmentation, number of false tracks and RMSE, and the improvements made possible by the multiple model version of the CPHD over the single filter are highlighted.

8137-21, Session 3

Group targets tracking using hypergraph matching for data association

S. Wu, SRI International Sarnoff (United States)

Group moving targets are number of targets independently moving in a physical space but keeping their relative order or pattern invariant. The up to date state-of-art multi-target tracking (MTT) data association methods (GNN, JPDA, MHT) are easily fail on group targets tracking problems, since the tracker-to-observation ambiguity cannot be resolved if only using the track to observation information.

A hypergraph G is represented by $G = \{V; E\}$, where V is a set of elements called nodes or vertices, E is a set of non-empty subsets containing d -tuple of vertices called hyperedges. It can be used as a new mathematic tool to represent a group of moving targets if we let each target be a vertex and a d -target subset be an hyperedge. Under this representation, this paper reformulates the traditional MTT data association problem as an hypergraph matching one between the hypergraphs formed from tracks and observations, and shows that the traditional approach (only uses the vertex-to-vertex information) which is a special case under the proposed framework. In addition to the vertex-to-vertex information, since the hyperedge-to-hyperedge information is also used in building the assignment matrix, the hypergraph matching based algorithms give better performance than that from the traditional methods in group target tracking problems. We demonstrate the declaration from simulations as well as video based geotracking examples.

8137-39, Poster Session

A cost-effective and open mobile sensor platform for networked surveillance

W. Sheng, G. Li, J. Du, C. Zhu, Oklahoma State Univ. (United States)

In this paper, a compact, low-cost and open multi-agent mobile sensor platform for networked surveillance is presented. A compact sensor design is realized by off-the-shelf components: an iRobot Create, an Atom processor-based computer, a Hokuyo laser range finder, and a Q24 fisheye camera. The software system consists of three main modules: a control module for iRobot movement, a data acquiring module for sensor reading, and a data processing module for navigation and target tracking. All modules are built on the open source Robot Operation System (ROS).

This platform is used to form a mobile sensor network for military

surveillance research. Compared to traditional stationary surveillance systems, our platform is capable of higher mobility and therefore, achieving better surveillance performance in terms of confidence of target tracking and adaptability. We develop novel algorithms for target tracking, which is realized by fusing the data from the omnidirectional camera and the laser range finder. Due to the distributed computing nature of the platform, we also conduct cooperative target-tracking through the fusion of multiple mobile sensors.

The performance of the proposed mobile surveillance system is evaluated through experiments. The results from the experiments prove that the proposed platform is a promising tool for networked surveillance research and practice. Future research problems that could be investigated using this platform are also discussed in this paper. This work results from a project supported by a DURIP program through the DoD Army Research Office.

8137-38, Poster Session

A survey of maneuvering target tracking Part VIc: approximate nonlinear density filtering in discrete time

X. Li, V. P. Jilkov, The Univ. of New Orleans (United States)

This paper is Part VIc of a comprehensive survey of maneuvering target tracking without addressing the so-called measurement-origin uncertainty. It provides an in-depth coverage of various approximate density-based nonlinear filters in discrete time developed particularly for handling the uncertainties induced by potential target maneuvers as well as nonlinearities in the dynamical systems commonly encountered in target tracking. An emphasis is given to more recent results, especially those with good potential for tracking applications. Approximate techniques for density-based nonlinear filtering in mixed time have been covered in a previous part. Sampling-based nonlinear filtering will be surveyed in a forthcoming part.

8137-40, Poster Session

Performance evaluations of multipath, multitarget tracking using PCRLB

M. Subramaniam, McMaster Univ. (Canada); K. Punithakumar, GE Healthcare (Canada); M. McDonald, Defence Research and Development Canada (Canada); T. Kirubarajan, R. Tharmarasa, McMaster Univ. (Canada)

In this paper, we study the performance of the multipath-assisted multitarget tracking using multiframe assignment for initiating and tracking multiple targets by employing one or more transmitters and receivers. The basis of the technique is to use the posterior Cramer-Rao lower bound (PCRLB) to quantify the optimal achievable accuracy of target state estimation. In real scenarios, it is more appropriate to assume that the locations of the reflection points/surfaces are not accurately known to the receiver. This leads to a challenging problem of fusing the direct and multipath measurements from the same target where the multipath-reflection mode is unknown. The problem becomes more complex due to missed target detections and when non-target originated measurement returns are present due to false alarms and clutter. We used different topological configurations in our evaluations and showed that incorporating multipath information improves the performance of the algorithm significantly in terms of estimation error. This work is motivated by tracking ground targets using bearing and time difference of arrival (TDOA) measurements. Simulation results are presented to show the effectiveness of the proposed method.

8137-41, Poster Session

Bayesian approach to joint super-resolution and trajectory estimation for closely spaced objects via infrared focal plane data

L. Lin, H. Xu, W. An, National Univ. of Defense Technology (China)

This paper addresses the problem of super-resolution for midcourse closely spaced objects (CSO) using infrared focal plane data. Within a short time window, the midcourse CSO trajectories on the focal plane can be model as following a straight line with a constant velocity. Thus, the object's initial state(initial projection positions and velocities on the focal plane)exclusively corresponds to its trajectory on the infrared focal plane. The objects initial state and radiant intensities, as well as the objects number and the sensor noise variance, are considered random variables, and a Bayesian model is proposed which is utilized to define a posterior distribution on the parameter space. To maximize this posterior distribution, we use a reversible jump Markov chain Monte Carlo (RJMCMC)method to perform the Bayesian computation. The proposed approach uses the multiple time-consecutive frames to estimate the model parameters directly, thus not only avoiding data association in multi-target tracking but also gaining a higher performance of super-resolution. Simulation results show that the proposed approach is effective and feasible.

8137-42, Poster Session

Evaluation of automated algorithms for small target detection and non-natural terrain characterization using remote multi-band imagery

E. Hallenborg, Space and Naval Warfare Systems Ctr. Pacific (United States)

Experimental remote sensing data from the 8 to 12 micron wavelength NASA Thermal Infrared Multispectral Scanner (TIMS) have been a valuable resource for multispectral algorithm proof-of-concept, a prime example being a spectral small target detector founded on maximum likelihood theory, termed the Generalized Linear Feature Detector (GLFD) (Yu et al., 1993; Yu et al., 1997); GLFD tests on low signal-to-clutter ratio rural Australian TIMS imagery yielded a detection rate of 5 out of 7 (71%) for small extended targets, e.g. buildings up to 10 meters in extent, at a 1 part per million false alarm rate. Separately, techniques such as Independent Component Analysis (ICA) have since shown good promise for small target detection as well as terrain feature extraction (e.g., Kuan & Healey, 2004; Winter, 2008). In this study, we first provide higher-confidence GLFD performance estimates by incorporating a larger set of TIMS imagery and ground truth. Secondly, alongside GLFD we perform ICA, which effectively separates many non-natural features from the highly cluttered natural terrain background; in particular, our TIMS results show that a surprisingly small subset of ICA components contain the majority of non-natural "signal" such as paved roads amid the clutter of soil, rock, and vegetation.

8137-43, Poster Session

Tracking a large number of CSO using the particle PHD filter via optical sensor

L. Lin, H. Xu, W. An, W. Sheng, D. Xu, National Univ. of Defense Technology (China)

We propose a filtering framework for tracking a large number of closely spaced objects (CSO) that is based on the particle probability hypothesis density (PHD) filter and multiassignment data association. The original particle PHD filter suffers from drawbacks of slow track initiation and unstable multi-target state estimation performance when being applied to

tracking large numbers of CSO. In order to cope with these drawbacks, a novel birth particle sampling scheme is present first to quicken track initiation, which samples birth particles around measurements, and carry out this sampling process after the particle PHD filter update process not only avoiding invalid birth particles update but also holding uninformative weights for birth particles, and then a non-iterative multi-target estimation technique is proposed, which partitions each particle to the specific measurement using maximum likelihood test and selects the resulting particle clusters with highest cluster-weights for estimating multi-target state. Furthermore, the unresolved measurements from CSO make it necessary to relax traditional one-to-one association restriction, thus a multiassignment track-to-estimation approach is present here to allow for the multiple-to-one track-to-estimation association. Meanwhile, an M/N rule for track initiation and multiple consecutive misses for track deletion are used to account for the sensitivity of the PHD filter to missed detections and false alarms. Simulation of tracking target complex on the infrared focal plane, and experiment of tracking flying bird swarm with real video data, are performed, and the results show that the proposed filtering framework is effective and efficient

8137-44, Poster Session

Nonlinear dynamic stochastic filtering of signal phase in interferometric systems

M. A. Volynsky, I. P. Gurov, A. E. Veisel, Saint-Petersburg State Univ. of Information Technologies, Mechanics and Optics (Russian Federation)

Interferometric methods are widely used in measurement of geometric quantities, optical metrology and non-contact testing. High accuracy, noise-immunity and fringe processing speed play an important role in practical use of interferometric systems.

In last decade, the new approach to interference fringe processing was proposed based on fringe recurrence dynamic evaluating interference fringe parameters like fringe amplitude, frequency and phase [1,2]. This approach is based on using recurrence algorithms, in which fringe signal value is predicted to a following discretization step using full information available before this step, and fringe signal prediction error is used for step-by-step dynamic correcting the fringe parameters. A few versions of the recurrence fringe processing algorithm, in particular, in the form of extended Kalman filtering were successfully applied to interference fringe parameters evaluating in rough surface profilometry, multilayer tissue evaluating, and optical coherence tomography, in analyzing 2-D fringe patterns.

New results were recently obtained using Markov model of interference fringes with random initial conditions and stochastic filtering that confirmed advantage in accuracy and possibility to recover unwrapped fringe phase with respect to well-known extended Kalman filtering method. Comparison in accuracy and stability of the both approaches was conducted and discussed in detail.

REFERENCES

1. I. Gurov and D. Sheynihovich, "Interferometric data analysis based on Markov nonlinear filtering methodology", J. Opt. Soc. Am. A 17, 21-27, 2000.
2. I. Gurov, E. Ermolaeva, and A. Zakharov, "Analysis of low-coherence interference fringes by the Kalman filtering method", J. Opt. Soc. Am. A. 21, No. 2, 2004.

8137-45, Poster Session

Noise-induced outpulsing technique for energy efficiency improvement of laser radar systems

M. G. Serikova, E. G. Lebedko, Saint-Petersburg State Univ. of Information Technologies, Mechanics and Optics (Russian Federation)

Conference 8137:
Signal and Data Processing of Small Targets 2011

Laser radar systems are widely used as space orientation systems by military, geodetic surveying, and in space applications. There are stringent requirements for a false alarm probability (of the order of 0.0001) for the systems. The complex target environment and a receiver noises cause the attenuation of the signal-to-noise ratio (down to 15 or lower).

New signal processing technique for laser radar systems is suggested. The technique provides the signal detection during an interval between a receiver noise bursts. As a result of the given technique the system is more energy efficient. The principle is that a pulse shoot is matched with a trailing edge of a noise burst and the signal presence decision is made according to a leading edge of the next burst. There is a contradiction between requirements for the impulse frequency (some MHz) and false alarm probability, that's why double-threshold processing is offered. The lower level induces outpulsing while the higher one determines target detection performance.

Since duration of such time intervals is random, statistic analysis was made via modulation testbed. The latter is based on a low-lighted electron-multiplier phototube as a noise source. Eventually distribution laws of two-level crossing interval were defined. As a result the optimal threshold configuration, filter parameters and mean outpulsing frequency were found. Mentioned results provide low false alarm probability (about 0.0001 or less) with improvement of the system energy efficiency (~30%) at the same time.

8137-22, Session 4

3D ISAR image reconstruction of targets through 2D rotations

Z. Qiao, J. Lopez, G. Garza, The Univ. of Texas-Pan American (United States)

In our paper, we study three dimensional Inverse Synthetic Aperture Radar (ISAR) imaging of objects through two dimensional rotations. We consider a second axis of rotation so that the target is undergoing rotational motion in two dimensions. Two algorithms for forming a 3D image of such a target scene are presented in detail. Our imaging algorithms are derived from a scalar wave equation model. The first of which is based on a far-field Fourier Transform inversion scheme, whereas the second algorithm is based off a filtered back projection inversion scheme, which does not require the use of a far-field approximation. Finally, we will show the 3D simulations for the two algorithms.

8137-23, Session 4

Improved multiframe data association using smoothing for multiple maneuvering target tracking

R. Tharmarasa, McMaster Univ. (Canada); N. Nandakumaran, Curtin Univ. of Technology (Australia); M. McDonald, Defence Research and Development Canada (Canada); T. Kirubarajan, McMaster Univ. (Canada)

Data association is the crucial part of any multitarget tracking algorithm in a scenario with multiple closely spaced targets, low probability of detection and high false alarm rate. Multiframe assignment, which solves the data association problem as a constrained optimization, is one of the well-known methods to handle the measurement origin uncertainty. If the targets do not maneuver, then multiframe assignment with one or two frames will be enough to find the correct data association. However, more frames must be used to decide the data association for maneuvering targets. Smoothing, which uses measurements beyond the estimation time, provides better estimates of the target states. The cost of assigning a target to a measurement can be calculated more accurately if better estimates of the targets states are available. In this paper, we propose an improved multiframe data association with better cost calculation using multiple model smoothing. The effectiveness of the proposed algorithm is demonstrated on simulated data.

8137-25, Session 4

Automatic track initialization and maintenance in heavy clutter using integrated JPDA and ML-PDA algorithms

K. Harishan, R. Tharmarasa, T. Kirubarajan, McMaster Univ. (Canada); T. Thayaparan, Defence Research and Development Canada (Canada)

Target tracking in high clutter or low signal-to-noise environments presents many challenges to tracking systems. Joint Maximum Likelihood estimator combined with Probabilistic Data Association (JMLPDA) is a well known parameter estimation solution for the initialization of tracks of very low observable, low signal-to-noise-ratio targets in higher clutter environments. On the other hand, the Joint Probabilistic Data Association (JPDA) algorithm, which is commonly used for track maintenance, lacks automatic track initialization capability. This paper presents an algorithm to automatically initialize and maintain tracks using an integrated JPDA and JMLPDA approach that seamlessly shares information on existing tracks between the JMLPDA (used for initialization) and JPDA (used for maintenance) components. The motivation is to share information between the maintenance and initialization stages of the tracker, that are always on-going, so as to enable the tracking of an unknown number of targets using the JPDA approach in heavy clutter. The effectiveness of the new algorithm is demonstrated on a heavy clutter scenario and its performance is compared against that of the standard JPDA tracker.

8137-27, Session 4

Labeled labelless multitarget tracking with features

D. Crouse, P. Willett, Univ. of Connecticut (United States)

Past work has shown the benefits of using Minimum Mean Optimal Sub-Assignment (MMOSPA) estimates for multitarget tracking. Namely, that one can get the "smoothness" of the estimates associated with Minimum Mean Squared Error (MMSE) estimation coupled with the resistance to track coalescence associated with Maximum Likelihood (ML) estimation. Though MMOSPA estimates are typically "labelless", that is, one does not know which estimate corresponds to which target, recent work has established a probabilistic framework for maintaining track identity probabilities.

In this paper, we extend such work to allow for the use of classification information derived from features or attributes to improve the performance of the tracker. We also note the difference between a target's "identity" and the nature of the target as determined by classification information.

8137-28, Session 4

Adaptive multi-target-tracker

C. Sung, Fraunhofer-Institut für Optronik, Systemtechnik und Bildauswertung (Germany)

On successive images, objects are either imaged in small size or in large size. Thus, in a long sequence, such as a highway scene or an airspace scene, images of cars or planes may range from small blob-like image structures to extended-dimensional image structures (and vice versa). In this case, the development of a process chain for automatic object tracking is a great challenge, since it requires the use of different approaches in combination, regarding both the extraction of image features and the grouping of characteristics.

An adaptive multi-target tracker combines various methods for object detection and tracking such as feature-based methods and trajectories-based tracking, thus providing meaningful results with variable shape, brightness and size of the target images.

Conference 8137:
Signal and Data Processing of Small Targets 2011

An adaptive multi-target tracker is generic, since it offers a choice of alternative methods for the individual tasks, depending on the tasks, the used image sensors and the type of motion of the target objects. In the case of a high dynamic scene, dynamically varying parameter values must be used for the detection of object images and object tracking. This requires an automatic generation of parameter values by adaptive adjustment.

In this paper, the selected process chains for the automatic and seamless tracking of multiple object images and for the interpretation of target objects in image sequences are presented. Detailed descriptions of objects are extracted from the images for the interpretation of target objects. The comparison with existing object descriptions in the search system permits to decide what the object represents.

8137-36, Session 4

Parallel processing for particle filters: or what could I do with a billion particles?

F. E. Daum, J. Huang, A. Noushin, Raytheon Co. (United States)

Modern computer technology allows us to use hundreds or thousands of processors for particle filtering. For example, GPUs are now very inexpensive and easy to use, and in many applications they yield several orders of magnitude speedup, but not for particle filters, which suffer from the bottleneck due to resampling. In particular, one thousand processors applied to standard particle filters typically results in only a factor of ten speedup, and the root cause of this large discrepancy is the resampling of particles that is required by standard particle filters. It would be much better to avoid resampling in particle filters. It turns out that we have invented a new theory of particle filters that never resamples particles, and hence avoids this well known bottleneck to parallelization, and hence our new particle flow filter is embarrassingly parallelizable.

The usual naive expectation is that if we use 1,000 processors then we can speedup an algorithm by roughly a factor of 1,000. Reality has taught us otherwise. Moreover, the theory and practice of parallel processing developed many decades ago teaches us that such an expectation is naive for particle filters. We review the somewhat sparse literature on parallelization of particle filters, and we show (using simple block diagrams) that our new theory does not suffer from such bottlenecks.

It is easy to run particle filters with billions of particles today, both on PCs and GPUs, and we have done so for a number of interesting applications.

The best paper on the subject of parallel processing for standard particle filters is: "A GRAPHICS PROCESSING UNIT IMPLEMENTATION OF THE PARTICLE FILTER," Gustaf Hendeby, Jeroen D. Hol, Rickard Karlsson, Fredrik Gustafsson; 15th European Signal Processing Conference (EUSIPCO 2007), Poznan, Poland, September 3-7, 2007. In particular, figures 5 & 6 in this excellent paper make it crystal clear that resampling is the big problem, and that hundreds or thousands of processors only speeds up the runtime by less than a factor of ten. To understand these issues better, one should scrutinize this most excellent paper by Hendeby et al.

8137-37, Session 4

Analogies between physical particles and particles in filters

F. E. Daum, Raytheon Co. (United States)

Physical particles share many characteristics with particles as currently used in particle filters, as listed in the following table (items 1 to 6):

item	physical particles	particles in filters
1. mass	yes	yes
2. probability density		yes (Schrödinger-Born) yes
3. gradient dynamics		yes yes
4. fluid flow	yes	yes (e.g., irrotational, incompressible)
5. birth & death	yes	yes (resampling)

6. wave-particle duality	yes	yes (ODEs for particles to solve PDEs)
7. charge, spin, etc.	yes	no
8. quantization of mass, charge, spin, etc.		yes no
9. symmetries (time, space, rotation, CPT, gauge invariance)	yes	no
10. anti-particles	yes	no but adjoint method is analogous (backwards time)
11. principle of least action	yes	no but it has been suggested for log-h by Mahendra Mallick
12. Heisenberg uncertainty principle	yes	not really, but Cramér-Rao bound is roughly analogous
13. super strings	yes	sort of (regularized LeGland)
14. quantum cohomology	yes	sort of for log-h (1st order linear underdetermined PDE)

We will elaborate on the analogies listed in this table for both standard particle filters as well as log-homotopy filters. For example, the fundamental equation for log-homotopy is a first order linear underdetermined PDE, and the task is to find a unique solution efficiently using a system of ODEs (i.e., particles). Thus, the wave-particle duality is clearly evident for log-homotopy particle filters. In physics wave-particle duality is manifested in simple optical experiments and theories going back to Newton & Huygens. Second, wave-particle duality is famous in quantum experiments and theory. Third, wave-particle duality is one way to describe the solution of the Hamilton-Jacobi equation (a PDE) using particles that obey the Euler-Lagrange equations (ODEs); this duality is evident in both classical physics (optics and mechanics) and quantum mechanics and quantum field theory. Quantum cohomology is a relatively new string theory that attempts to solve a first order linear overdetermined PDE system, to compute Gromov-Witten invariants for quantum gravity, analogous to log-homotopy filters, which must solve a first order linear underdetermined PDE. It is not surprising that we can use the same tricks invented for physics to compute a unique solution of this PDE; for example, assume that the velocity field is the gradient of a potential (see Daum & Huang, "Exact particle flow" April 2010). In fact, essentially all of the ten methods that we have used so far for our exact particle flow were borrowed from physics.

Moreover, there are other properties of physical particles that could be used in more advanced particle filters using log-homotopy (items 10 to 14). But perhaps the most interesting and useful question is why the particles in filters do not have charge & spin and other quantum numbers, and furthermore, why mass is not quantized in particle filters (items 7 to 9). One way to explain this difference is that physical particles are quantized owing to symmetries, whereas there are no such symmetries for particle filters. In particular, the usual story in physics is that elementary particles are quantized due to the compactness of the non-Abelian group of symmetries (e.g., gauge invariance of various types). Although this story is coherent and compelling and in amazingly good agreement with today's low energy experiments, it is not really a fundamental explanation, or at least not for some physicists (e.g., John Wheeler, Stephen Wolfram, Seth Lloyd, Murray Gell-Mann, Jacobson, Erik Verlinde, et al.).

Hence, in search of a more fundamental explanation, one can speculate that this is because the technology used by filters is floating point arithmetic in general purpose computers, whereas physical particles at the Planck scale actually are roughly analogous to bits in our modern computers. This line of speculation reminds us of John Wheeler's famous essay, "It from bit," which speculates that physics could be explained using something like Shannon information (i.e., bits and entropy and limits of propagation of information) as the fundamental stuff. For example, Erik Verlinde recently derived Newton's & Einstein's gravity equations using Shannon information theory ("On the origin of gravity and the laws of Newton" January 2010). Similarly, this reminds us of Norbert Wiener's analysis that shows that bits are essentially optimal to encode Shannon information when cost is linear in quantization scale; all modern computers use bits, and hence engineers and the market in the 20th and early 21st centuries seems to concur with Wiener's analysis. We can further speculate that God awarded the contract for making and maintaining particles to the lowest bidder, who naturally followed Wiener's optimal design for quantizing mass, charge, spin, etc. If we limit our perspective to electrons vs. protons and neutrons,

**Conference 8137:
Signal and Data Processing of Small Targets 2011**

Wiener's analysis holds very accurately (i.e., two levels of mass to a very good approximation). Actually, Wiener showed that the optimal number of levels of quantization was slightly greater than 2, and this matches physical particles very well. In physics, it is remarkable how often Wiener's magic number 2 appears in this context; for example: future vs. past in time, fermions vs. bosons, particles vs. forces, matter vs. anti-matter, positive vs. negative unit charge on electrons & protons, left vs. right, up vs. down, quadratic Lagrangians, strong vs. weak fields, stable vs. unstable particles & theories, E vs. M in Maxwell's theory, even vs. odd parity, etc. etc.

It would be extremely presumptuous to think that we could know why God made the World that we see; however, it is somewhat less presumptuous to speculate on why humans in the 21st century on Earth see the World as the assortment of quantized particles evident in our experiments. This is a subtle but crucial distinction. The latter focuses on the limitations of human perception with 21st century technology, whereas the former attempts to understand God's intentions.

There are three reasons for such speculations: (1) invent better particle filters using ideas from physics; (2) understand fundamental issues in physics better using ideas from particle filters; and (3) it is fun. In particular, we will explore the benefits of exploiting symmetries for particle filters, analogous to Sanjoy Mitter's use of gauge invariance to understand exact finite dimensional filters thirty years ago.

8137-29, Session 5**Dynamic sector processing using 2D assignment for rotating radars**

B. K. Habtemariam, R. Tharmarasa, T. Kirubarajan, McMaster Univ. (Canada); M. Pelletier, ICx Radar Systems (Canada)

Electronically scanned array radars as well as mechanically steered rotating antennas return measurements with different time stamps during the same scan while sweeping from one region to another. Typically, data association algorithms wait till the end of a whole scan to process the returns in that scan in order to satisfy the common "one measurement per track" assumption. For example, multitarget tracking algorithms like the Multiple Hypothesis Tracker (MHT) and the Multiframe Assignment Tracker (MFA) wait to receive the full scan of measurements before data association, which is a crucial step before updating tracks. Data processing at the end of a full scan results in delayed state updates. This issue is more apparent while tracking fast moving targets with low scan rate sensors.

In this paper we present new dynamic sector processing algorithm using 2-D assignment for continuously scanning radars. A complete scan can be divided into sectors, which could be as small as a single detection, depending on the scanning rate and scarcity of targets. Data association followed by filtering and target state update can be done dynamically while sweeping from one end to another. Along with the benefit of immediate track updates, continuous tracking results in challenges such as multiple targets spanning multiple sectors and targets crossing consecutive sectors. Also, associations after receiving a sector may require changes in association in previous sectors. Such difficulties are resolved by the proposed recursive generalized 2-D assignment algorithm that uses a dynamic Hungarian assignment technique. The algorithm offers flexibility with respect to changing cost and size for fusing of measurements received in consecutive sectors. Furthermore the proposed technique can be extended to multiframe assignment for jointly processing data from multiple scanning radars. Experimental results based on rotating radars are presented.

8137-30, Session 5**Benchmarks for target tracking**

D. T. Dunham, Vectrass, Inc. (United States); P. D. West, Georgia Tech Research Institute (United States)

The term benchmark originates from the chiseled horizontal marks that

surveyors made, into which an angle-iron could be placed to bracket ("bench") a leveling rod, thus ensuring that the leveling rod can be repositioned in exactly the same place in the future. A benchmark in computer terms is the result of running a computer program, or a set of programs, in order to assess the relative performance of an object by running a number of standard tests and trials against it. This paper will discuss the history of simulation benchmarks that are being used by multiple branches of the military and agencies of the US government. These benchmarks range from missile defense applications to chemical biological situations. Typically, a benchmark is used with Monte Carlo runs in order to tease out how algorithms deal with variability and the range of possible inputs. We will also describe problems that can be solved by a benchmark.

8137-31, Session 5**Information exchanged between fusion tracker and other fusion functions**

O. E. Drummond, CyberRnD, Inc. (United States)

Multiple-sensor data fusion offers the opportunity for substantial improvement in functional performance compared to single sensor processing. Data fusion processing, however, could be substantially more complex than processing with data from a single sensor. Consequently, data fusion processing typically involves more processing functions than processing with data from a single sensor. Accordingly, the fusion tracker function may be required to provide more and better information to the other fusion-level/network-level functions. The fusion track function may also be required to receive and act on more information from the other fusion functions than the information typically received by a single sensor tracker. The types of information that might be required by the fusion tracker function to be provided to the other fusion functions plus the types of information provided by the other fusion functions that the fusion tracking function might have to utilize are the subject of this presentation.

A data-fusion processing system could be fairly simple or sophisticated and complex or anywhere in between these two extremes depending on the specifics of application. The fusion processing design depends on the requirements; the characteristics, limitations, and locations of the sensors, processors, threat, communications, and operating conditions; the location of the users; and the state of the art of fusion processing. Thus the type and functional decomposition of a data fusion processing system for one applications could be very different from another application and thus, the exchange of information between the fusion tracker function and other fusion functions could be different. These issues are summarized as background for the discussion of the specifics of the type of information provided by the fusion tracker function to the other fusion functions. The introduction also provides background for the discussion of the specifics of the type of information provided by the other fusion functions to the fusion tracker function and the type of special processing needed to act on that information. Note also that the fusion tracker function could be simply a single tracker if the fusion processing is centralized and would involve multiple trackers if fusion processing is distributed.

8137-32, Session 5**Regression data classification with data reduction techniques and support vector machines**

D. Zhao, Univ. of Connecticut (United States)

The recent advances in data collection and storage capacities have led to information overload in many applications, e.g., on-line monitoring of spacecraft operations with time series data. It is therefore desirable to perform data reduction before storage or transmission of the data. For the Turbofan engine degradation simulation data sets, the failure of the system is determined by the combination of five key components. The datasets consist of three input parameters and twenty one sensor

Conference 8137:
Signal and Data Processing of Small Targets 2011

outputs. The dimensionality of the acquired data is lower than the space that is measured in. Therefore, data reduction techniques are expected to help reduce run time while maintaining an acceptable level of performance of the classifier.

We apply several data reduction techniques to the data sets with the goal of determining the remaining useful life (RUL) of each engine component using Support Vector Machines and PSVM classifiers. We investigated 2-class and 4-class situations. The correct rate of the classifiers was in the range of 70%.

Based on our tests, data reduction techniques coupled with SVM-type classifiers provided a significant reduction in processing load with an acceptable loss in performance.

8137-33, Session 5

Cooperative sensing in mobile sensor networks based on distributed consensus

W. Sheng, H. M. La, Oklahoma State Univ. (United States)

Mobile sensor networks (MSNs) have wide applications such as military target detection and tracking, detection of toxic chemicals in contaminated environments, and search and rescues in disasters, etc. In many applications, a core problem is to conduct cooperative scalar field mapping (or searching) over a large area of interest.

Centralized solutions to the scalar field mapping may not fit for large mobile sensor network due to the single-point-of-failure problem and the limited scalability. In this paper, autonomous mobile sensor networks are deployed to map scalar fields in a cooperative and distributed fashion. We develop a cooperative sensor fusion algorithm based on distributed consensus filters. In this algorithm, each agent receives measurements from its neighboring agents within its communication range, and iteratively updates the estimate of the unknown scalar field and an associated confidence map. A motion planning algorithm is used to obtain a path for complete coverage of the field of interest. A distributed flocking control algorithm is adopted to drive the center of the mobile sensor network to track the desired paths. Computer simulations are conducted to validate the proposed algorithms. We evaluate the mapping performance by comparing it with a centralized mapping algorithm. Such a cooperative sensing approach can be used in many military surveillance applications where targets may be small and elusive.

This work results from a project supported by a DURIP program through the DoD Army Research Office.

8137-34, Session 5

Spectrally assisted target tracking

L. E. Hoff, Hoff Engineering (United States); E. M. Winter, Technical Research Associates, Inc. (United States)

Tracking of multiple vehicles can be accomplished with a single band high-resolution sensor as long as the vehicles are continuously in view. However, in many cases the vehicles pass through or behind blackouts, such as through tunnels or behind tall buildings. In these cases, the vehicles of interest must be re-acquired and recognized from the collection of vehicles present after the blackout. The approach considered here is to add an additional sensor to assist a single band high-resolution tracking sensor, where the adjunct sensor measures the vehicle signatures for recognition and re-acquisition. The subject of this paper is the recognition of targets of interest amongst the observed objects and the re-acquisition after a blackout. A GLRT algorithm is compared with the Spectral Angle Mapper (SAM) and Euclidian distance algorithms. All three algorithms were evaluated on a simulated database of signatures created by measuring samples from old automobile gas doors. The GLRT was the most successful in recognizing the target after a blackout and could achieve a 95% correct reacquisition rate. The results show the feasibility of using a hyper spectral sensor to assist a multi target tracking sensor by providing target recognition for reacquisition.

8137-35, Session 5

Maneuvering small target defeat with distributed sensor concept: DISCO vehicles

M. K. Rafailov, RICHER International LLC (United States)

DISCO sensors create a grid of weapons that may act as an Agile Kill Vehicle by addressing non-ballistic- maneuvering target threat. Distributed Sensor Concept - DISCO was proposed to enhance probability of ballistic target engagement with multiple space-distributed sensor weapons forming closed network of sensors interchanging frame and GNC data. DISCO does not need a standoff sensor(s) coordinating weapon flight while target acquisition capability is equal or exceeding those weapons operating with stand-off sensors. In the same time distributed in space DISCO sensors create a grid of weapons that may act as Agile Kill Vehicle by addressing non-ballistic- maneuvering target threat. In this presentation we will discuss ability of DISCO sensors to form such a grid with individual weapon sensors having limited divert and attitude control as well as sensing capabilities and to address the issue of maneuvering target defeat.

Conference 8138: Wavelets and Sparsity XIV

Sunday-Wednesday 21-24 August 2011 • Part of Proceedings of SPIE Vol. 8138 Wavelets and Sparsity XIV

8138-01, Session 1

SAR moving target imaging in a sparsity-driven framework

O. Onhon, M. Cetin, Sabanci Univ. (Turkey)

In synthetic aperture radar (SAR) imaging, sparsity-driven imaging techniques have been shown to provide high resolution images with reduced sidelobes and reduced speckle, by allowing the incorporation of prior information about the scene into the problem. Just like many common SAR imaging methods, these techniques also assume the targets in the scene are stationary over the data collection interval. Here, we consider the problem of imaging in the presence of targets with unknown motion in the scene. Moving targets impose phase errors in the SAR data and these errors cause defocusing in the corresponding spatial region in the reconstructed image. We view phase errors resulting from target motion as errors on the observation model of a static scene. Based on these observations we propose a method which not only benefits from the advantages of regularization-based imaging but also compensates the errors arising due to the moving targets. Considering that in SAR imaging the underlying scene usually admits a sparse representation, a nonquadratic regularization based framework is used. The proposed method is based on minimization of a cost function which involves regularization terms imposing sparsity on the reflectivity field to be imaged, as well as on the spatial structure of the motion-related phase errors, reflecting the assumption that only a small percentage of the entire scene contains moving targets. Experimental results demonstrate the effectiveness of the proposed approach in reconstructing focused images of scenes containing multiple targets with unknown motion.

8138-03, Session 1

Refractive index map reconstruction in optical deflectometry using total-variation regularization

L. Jacques, A. Gonzalez Gonzalez, E. Fournouo, P. Antoine, Univ. Catholique de Louvain (Belgium)

We study the resolution of an inverse problem arising in Optical Deflectometry: the reconstruction of refractive index map of transparent materials from laser deflection measurements under multiple orientations. This problem is solved from a standard convex optimization procedure aiming at minimizing the Total Variation of the map (as a prior information) while matching the observed data (fidelity constraint). In this process, the forward measurement operator, mapping any index map to its deflectometric observation, is simplified in the Fourier domain according to a modified Projection-Slice theorem. Our method is also applicable to other imaging techniques such as differential phase-contrast X-ray tomography.

8138-04, Session 1

Compressively sampling the plenacoustic function

R. Mignot, G. Chardon, L. Daudet, Ecole Supérieure de Physique et de Chimie Industrielles (France) and Univ. Pierre et Marie Curie (France)

This study deals with the sampling of the sound field in a room, more precisely the evolution of the "Room Impulse Response" (RIR) as a function of the spatial positions of the source and the receiver, the so-called plenacoustic function.

With standard Shannon sampling, the measurement of a time-varying 3-D image requires a number of measurement points / microphones

that is unreasonably large for practical use. However, informed by the physical nature of the signal, the « Compressed Sensing » (CS) principle can reduce the number of sensors if the signal is approximately sparse in some dictionaries. Here, we apply CS to the acquisition and interpolation of the plenacoustic function in a spatial domain, based on the sparsity of the soundfield on a dictionary of plane waves. Unfortunately, because of space dimensionality and size of atoms, even the simplest standard sparse decomposition algorithms are too expensive in terms of CPU and memory requirements.

Two new algorithms are presented. The first one exploits the structured sparsity of the sound field, with orthogonal projections of the estimated modal deformations onto a basis of plane waves sharing the same wavenumber. The second algorithm computes a sparse decomposition on a dictionary of independent plane waves, with a time / space variable separation to reduce the memory usage.

Both methods are compared to the regular sampling on synthetic signals. Their performance is evaluated according to the size and configuration of the sensor array, the size of the reconstruction domain and the time / frequency limit.

8138-05, Session 2

An iterative weighted one-norm minimization algorithm for sparse signal recovery

O. Yilmaz, H. M. Mansour, M. P. Friedlander, The Univ. of British Columbia (Canada)

We propose an iterative algorithm that solves a sequence of weighted one-norm minimization problems to recover sparse signals from incomplete linear measurements. The algorithm utilizes the ability to extract partial support information from the solutions to standard and weighted one-norm minimization. The weights are adjusted to promote non-zero coefficients in subsets of the support estimates that remain invariant between iterations. We provide extensive experiments to show that our algorithm outperforms state of the art sparse recovery techniques.

8138-06, Session 2

Deterministic matrices with the restricted isometry property

D. G. Mixon, Princeton Univ. (United States)

The state of the art in compressed sensing uses sensing matrices which satisfy the Restricted Isometry Property (RIP). Unfortunately, the known deterministic RIP constructions fall short of the random constructions, which are only valid with high probability. In this paper, we propose different constructions and compare with the literature.

8138-07, Session 2

Application of frames in digital fingerprinting

N. Kiyavash, Univ. of Illinois at Urbana-Champaign (United States); D. G. Mixon, Princeton Univ. (United States); C. Quinn, Univ. of Illinois at Urbana-Champaign (United States); M. Fickus, Air Force Institute of Technology (United States)

We show case a novel application for frames in digital rights management. Specifically, we consider the problem of digital fingerprinting as a game between the fingerprint embedder aiming to protect the digital content and a coalition of attackers working to defeat the scheme. We demonstrate that frames are particularly well suited as additive fingerprint designs against Gaussian averaging collusion attacks from the fingerprint embedder's viewpoint. On the other hand, we

characterize the coalition's best strategies in terms of having the highest chance of evading detection.

8138-08, Session 2

Non-orthogonal fusion frames

P. G. Casazza, Univ. of Missouri-Columbia (United States)

Fusion frames have found broad application to problems in sensor networks, distributed processing and much more. We will show that by using non-orthogonal projections, we can find significantly larger classes of tight and sparse fusion frames.

8138-09, Session 2

Grassmannians in frame theory

J. Cahill, Univ. of Missouri-Columbia (United States)

The grassmannian is the set of k dimensional subspace of an n dimensional vector space. This set naturally parametrizes isomorphism classes of frames. We will present several results which exploit this fact.

8138-10, Session 3

Higher degree total variation (HDTV) algorithms for biomedical inverse problems

M. Jacob, Y. Hu, Univ. of Rochester (United States)

We introduce generalized regularization functionals to overcome the practical problems associated with current total variation (TV) schemes such as poor approximation properties, poor contour regularity, and staircase artifacts. Based on a reinterpretation of the classical TV penalty, we derive a novel isotropic TV scheme involving higher order derivatives. This approach considerably minimizes the staircase artifacts and patchy reconstructions that are commonly observed in TV reconstructions. In addition, we introduce a novel rotation invariant anisotropic HDTV penalty to improve the regularity of the edge contours. We apply the algorithm to several biomedical inverse problems, which demonstrates the improved performance.

8138-11, Session 3

Smooth sampling trajectories for sparse recovery in MRI

R. M. Willett, Duke Univ. (United States)

Recent attempts to apply compressed sensing to MRI have resulted in pseudo-random k -space sampling trajectories which, if applied naively, may do little to decrease data acquisition time. This paper shows how an important indicator of CS performance guarantees, the Restricted Isometry Property, holds for deterministic sampling trajectories corresponding to radial and spiral sampling patterns in common use. These theoretical results support several empirical studies in the literature on compressed sensing in MRI. A combination of Gersgorin's Disc Theory and Weyl's sums lead to performance bounds on sparse recovery algorithms applied to MRI data collected along short and smooth sampling trajectories.

8138-12, Session 3

Non-iterative and exact inverse scattering solution using compressive MUSIC

J. Ye, O. Lee, K. Jin, KAIST (Korea, Republic of)

Inverse scattering problem is to recover the unknown targets from the measurements of scattered fields, and has various bioimaging applications such as microwave imaging, ultrasound imaging, T-ray tomography and etc. Recently, we showed that the problem can be exactly solved non-iteratively using compressive sensing approach by exploiting the joint sparsity. The main contribution of this paper is to extend the idea and demonstrate that near optimal solution can be obtained for any number of snapshots using so-called compressive MUSIC algorithm, where parts of unknown support is found by compressive sensing and the remaining support can be found deterministically using a generalized MUSIC criterion. Numerical results verify that this method outperforms the conventional algorithms.

8138-13, Session 3

Numerical evaluation of subsampling effects on image reconstruction in compressed sensing microscopy

Y. Le Montagner, Institut Pasteur (France) and Telecom ParisTech (France); M. de Moraes Marim, Institut Pasteur (France); E. Angelini, Telecom ParisTech (France); J. Olivo-Marin, Institut Pasteur (France)

When undergoing a reconstruction through a compressed sensing scheme, real microscopic images are affected by various artifacts that lead to detail loss. Here, we discuss how the sampling strategy and the sub-sampling rate affect the CS reconstruction, and how they should be determined according to a targeted accuracy level of the reconstruction. We investigate the relevance and limits of theoretical results through several numerical reconstructions of test images. We discuss the quantitative and qualitative artifacts that affect the reconstructed signal when reducing the number of measurements in the Fourier domain. We conclude by extending our results to real microscopic images.

8138-14, Session 3

Fresnelab: sparse representations of digital holograms

M. Liebling, Univ. of California, Santa Barbara (United States)

Digital holography plays an increasingly important role for biomedical imaging; it has particularly low invasiveness and allows quantitatively characterizing both amplitude and phase of propagating wave fronts. Fresnelets have been introduced as both a conceptual and practical tool to reconstruct digital holograms, simulate the propagation of monochromatic waves, or compress digital holograms. Propagating wave fronts that have, in their originating plane, a sparse representation in a traditional wavelet basis have a similarly sparse representation in propagation-distance-dependent Fresnelet bases. Although several Fresnelet applications have been reported in the past, no implementation has been made widely available. Here we describe a Matlab-based Fresnelet toolbox that provides a set of user-friendly functions to implement several, previously described algorithms, including a multi-scale Fresnel transform and a sparsity-based autofocusing tool for digital holography.

8138-15, Session 4

Phase retrieval via matrix completion

T. Strohmer, Univ. of California, Davis (United States)

The problem of reconstructing a signal from the magnitude of its Fourier transform plays a key role in numerous applications. This problem, also known as phase retrieval, has challenged engineers, physicists, and mathematicians for decades. We present a theoretical and numerical framework to phase retrieval via matrix recovery. Among others, our

approach allows us to recover the phase of a signal or image via convex optimization.

8138-16, Session 4

Block sparsity models for broadband array processing

P. T. Boufounos, Mitsubishi Electric Research Labs. (United States); B. Raj, Carnegie Mellon Univ. (United States); P. Smaragdis, Univ. of Illinois at Urbana-Champaign (United States) and Adobe Systems Inc. (United States)

Recent work has demonstrated the power of sparse models and representations in signal processing applications and has provided the community with computational tools to use it. In this paper we explore the use of sparsity in localization and beamforming when capturing multiple broadband sources using a sensor array. Specifically, we reformulate the wideband signal acquisition as a block sparsity problem, in a combined frequency-space domain. In this domain the signal is sparse in the spatial domain but has support in all frequencies. Using techniques from the model-based compressive sensing literature we demonstrate that it is possible to robustly capture, reconstruct and localize multiple signals present in the scene.

8138-17, Session 4

Deterministic compressed sensing

S. Jafarpour, Princeton Univ. (United States)

The central goal of compressed sensing is to capture attributes of a signal using very few measurements.

The limitations of the random sensing framework include performance guarantees, storage requirements, and computational cost. This talk will describe two deterministic alternatives.

The first is based on expander graphs. We show that by reformulating signal reconstruction as a zero-sum game we can efficiently recover any sparse vector. We also demonstrate resilience to Poisson noise.

The second is based on error correcting codes. We show that order Reed Muller codes optimize average case performance. We also describe a very simple algorithm, one-step thresholding, that succeeds where more sophisticated algorithms, developed in the context of random sensing, fail completely.

8138-18, Session 4

Compressed sensing with coherent and redundant dictionaries

D. Needell, E. J. Candes, Stanford Univ. (United States); Y. C. Eldar, Technion-Israel Institute of Technology (Israel); P. Randall, Princeton Univ. (United States)

This talk will present new results on signal recovery from undersampled data for which the signal is not sparse in an orthonormal basis, but rather in some arbitrary dictionary. The dictionary need not even be incoherent, and thus this work bridges a gap in the literature by showing that signal recovery is feasible for truly redundant dictionaries. We show that the recovery can be accomplished by solving an L1-analysis optimization problem. The condition on the measurement matrix required for recovery is a natural generalization of the well-known restricted isometry property (RIP), and we show that many classes of matrices satisfy this property. This condition does not impose any incoherence requirement on the dictionary, so our results hold for dictionaries which may be highly overcomplete and coherent. We will also show numerical results which highlight the potential of the L1-analysis problem.

8138-19, Session 5

Sparse signal recovery using a hybrid L0-L1 minimization algorithm

D. Liang, L. Ying, Univ. of Wisconsin-Milwaukee (United States)

In compressed sensing, the commonly used L1 minimization is known to shrink the magnitude of recovered signal when the number of measurements is not sufficient. Homotopic L0 minimization requires fewer measurements, but may not be as robust to noisy measurements or compressible signals that are not strictly sparse. The objective of this work is to develop a compressed sensing algorithm that has the benefit of both L1 and homotopic L0 minimizations and requires fewer measurements than either of them. We propose a hybrid L0-L1 quasi-norm minimization algorithm. The hybrid L0-L1 quasi-norm is defined to be a piecewise function which is the L0 quasi-norm if the element of the signal is greater than a threshold, and the L1 norm if the element is below the threshold. The threshold to discriminate large and small elements is updated iteratively, where the value is initialized using the "first jump role" with the signal recovered by L1 minimization. In order to guarantee convergence, a cost function that is strictly concave, continuous and differentiable is designed to approach the desired hybrid L0-L1 quasi-norm as a sequence limit. The proposed algorithm then solves a sequence of minimization problems where the cost function is updated iteratively. Simulations are carried out for both strictly sparse and compressible signals. Recovery from noisy measurements is also tested. We also discuss the choice of threshold τ . Results of success-rate curves demonstrate that the proposed algorithm improves the reconstruction accuracy of homotopic L0 or L1 minimization when the same number of measurements is used.

8138-20, Session 5

Diffuse imaging: replacing lenses and mirrors with omnitemporal cameras

A. Kirmani, V. K. Goyal, Massachusetts Institute of Technology (United States)

Conventional imaging is steady-state light sensing using focused optics. The variations of the light field with time are not exploited. We develop a novel signal processing framework for imaging that uses omnidirectional, time-varying illumination and unfocused, time-resolved sensing to replace traditional optical elements such as mirrors and lenses. We demonstrate that with these omnitemporal cameras, it is possible to accomplish tasks that are impossible with traditional cameras. In particular, we generalize the existing work on non-line of sight imaging for looking around corners. We show that using our proposed algorithms and image acquisition architecture, it is possible to image complex occluded scenes at high signal-to-noise ratio and high resolution. We accomplish this without the use of mirrors or specialized ultra-fast optics, by acquiring time-resolved measurement of the light reflected off diffuse surfaces in response to multiplexed spatio-temporal illumination. We also discuss another application of our framework for 3D mapping of large-scale scenes, such as outdoor environments, using a network of omnitemporal cameras. Our proposed imaging applications may be realized with commercially-available, low-bandwidth hardware used in standard optical communication systems. Imaging using single-pixel omnitemporal cameras will allow us to create application-specific, cheap, and robust solutions for acquiring structure and intensity information about natural scenes.

8138-21, Session 5

Analytic sensing for systems governed by the wave equation

V. Tsiminaki, I. Jovanovic, D. Kandaswamy, Ecole Polytechnique Fédérale de Lausanne (Switzerland); T. Blu, The Chinese Univ.

of Hong Kong (Hong Kong, China); D. Van De Ville, Ecole Polytechnique Fédérale de Lausanne (Switzerland)

No abstract available

8138-22, Session 6

Frame completions for optimally robust reconstruction

M. Fickus, M. J. Poteet, Air Force Institute of Technology (United States)

We find what vectors one should add to a frame so that the resulting new frame is optimally robust with respect to noise. Here, we measure the quality of a given frame by the average reconstruction error induced by noisy measurements; this mean square error is the trace of the inverse of the frame operator. We discuss which new vectors one should add to a given frame in order to reduce this mean square error as much as possible.

8138-23, Session 6

Geometry and optimization on spaces of finite frames

N. Strawn, Duke Univ. (United States)

A finite (μ, S) -frame variety consists of the real or complex matrices $F = [f_1 \dots f_N]$ with frame operator $FF^* = S$, and satisfying $\|f_i\| = \mu_i$ for all $i = 1, \dots, N$. Here, S is a fixed Hermitian positive definite matrix and $\mu = [\mu_1 \dots \mu_N]$ is a fixed list of lengths. These spaces generalize the well-known spaces of finite unit norm tight frames. We explore the local geometry of these spaces and develop geometric optimization algorithms based on the resulting insights.

We study the local geometric structure of the (μ, S) -frame varieties by viewing them as intersections of generalized tori (the length constraints) with distorted Stiefel manifolds (the frame operator constraint). Exploiting this perspective, we characterize the nonsingular points of these varieties by determining where this intersection is transversal in a Hilbert-Schmidt sphere. A corollary of this characterization is a characterization of the tangent spaces of (μ, S) -frame varieties, which is leveraged to validate explicit local coordinate systems. Explicit bases for the tangent spaces are also constructed.

Geometric optimization over a (μ, S) -frame variety is performed by combining knowledge of the tangent spaces with geometric optimization of the frame operator distance over a product of spheres. Given a differentiable objective function, we project the full gradient onto the tangent space and then minimize the frame operator distance to obtain an approximate gradient descent algorithm. Finally, we apply the approximate gradient descent procedure to numerically construct equiangular tight frames, Grassmannian frames, and Welch bound equality sequences with low mutual coherence.

8138-24, Session 6

Sparse dual frames

S. Li, San Francisco State Univ. (United States); T. Mi, Y. Liu, Renmin Univ. of China (China)

In applications a frame is oftentimes prescribed by the physics of the system. Succinct representations of functions/signals in such applications will depend on good choices of dual frames. Sparse dual frames have values in such concise function/signal representations. We present a study on sparse dual frames using the popular ℓ_1 -minimization formulation. Duals of substantial sparsity are obtained. Given a Gabor frame, studies on dual Gabor wave functions give rise to, in most case, the most compact dual Gabor function. There are still open problems

about the analysis of the bound for the most sparse dual frames from either deterministic or probabilistic senses. Current results and open problems will be discussed.

8138-25, Session 6

Spectral graph wavelet frames with compact supports

Y. M. Lu, Harvard School of Engineering and Applied Sciences (United States)

In this paper, we construct a new family of wavelet frames for functions defined on graphs. The proposed wavelet frames are near-tight and have compact supports in the graph domain. Furthermore, the analysis and synthesis operators of the frames can be implemented as a sequence of local "averaging" operations. This desirable feature makes it practical to implement the proposed graph wavelet transform in distributed sensor network applications.

8138-26, Session 6

A domain-knowledge-inspired mathematical framework for the description and classification of H&E stained histopathology images

R. Bhagavatula, Carnegie Mellon Univ. (United States); M. L. Massar, Air Force Institute of Technology (United States); J. A. Ozolek, Children's Hospital of Pittsburgh (United States); C. A. Castro, Magee-Womens Research Institute and Foundation (United States); M. Fickus, Air Force Institute of Technology (United States); J. Kovacevic, Carnegie Mellon Univ. (United States)

We present the current state of our work on a mathematical framework for identification and delineation of histopathology images---local histograms and occlusion models. Local histograms are histograms computed over defined spatial neighborhoods whose purpose is to characterize an image locally. This unit of description is augmented by our occlusion models that describe a methodology for image formation. In the context of this image formation model, the power of local histograms with respect to appropriate families of images will be shown through various proved statements about expected performance. We conclude by presenting a preliminary study to demonstrate the power of the framework in the context of two histopathology image classification tasks that, while differing greatly in application, both originate from what is considered an appropriate class of images for this framework.

8138-27, Session 7

Sparsity-promoting seismic inversion with incoherent wavefields

F. J. Herrmann, S. Aravkin, T. van Leeuwen, The Univ. of British Columbia (Canada)

During this presentation, we will give an overview on how dimensionality-reduction approaches from compressive sensing and stochastic optimization can be used to make seismic inversion more efficient. We show that recently popularized source-phase encoding techniques correspond to instances of compressive sensing. When combined with stochastic optimization these techniques lead to a new generation of efficient seismic-data processing, imaging, and inversion techniques designed to work on dimensionality-reduced incoherent wavefields.

8138-28, Session 7

Sparse data representation for the reconstruction of N-dimensional seismic wavefields

M. D. Sacchi, Univ. of Alberta (Canada)

Seismic wavefields depend of 4 spatial dimensions and time. The 4 spatial coordinates are defined by the x-y position of sources and receivers. Exploration seismology utilizes a large areal distribution of sources and receivers to image the earth interior. Logistic and economical constraints often lead to irregularly sampled seismic volumes. This talk concentrates on efforts to reconstruct these multidimensional wavefields prior to imaging. At the core of the problem is the sparse representation assumption in an auxiliary domain which leads to algorithms that permit to estimate unrecorded observations.

8138-29, Session 7

Wavelets and wavelet-like transforms on the sphere and their application to geophysical data inversion

F. J. Simons, Princeton Univ. (United States); I. Loris, Univ. Libre de Bruxelles (Belgium); E. Brevdo, Princeton Univ. (United States); I. C. Daubechies, Duke Univ. (United States)

There are now a whole series of flexible parameterizations to represent data on the sphere. Starting with the venerable spherical harmonics, we have the so-called Slepian basis, harmonic splines, wavelets and wavelet-like Slepian frames. In this presentation we focus on the latter two: spherical wavelets developed for geophysical applications on the cubed sphere, and the Slepian "tree", a new construction that shares aspects of Slepian-like concentration and wavelet-like multiresolution. We discuss the basic features of these new mathematical tools, and focus in particular on their usage as model parameterizations for large-scale global geophysical problems that benefit from sparsity-promoting "inversion" algorithms.

8138-30, Session 7

Compressive near-field imaging of subwavelength topography

A. Fannjiang, Univ. of California, Davis (United States)

We study the near-field imaging of surface topography (the object) by compressed sensing techniques. The standard approach in the literature typically requires the full measurement of the scattered field along a plane above the object. In our approach we assume that the object has a sparse (or compressible) Fourier or wavelet expansion and reconstruct the object by using comparably sparse measurement. In particular we apply our scheme to image subwavelength topographies.

Employing the angular spectrum representation of the scattered field, we decompose the problem into two stages: the first stage being a linear inversion for a modified object and the second a nonlinear fitting of the boundary conditions. The modified object arises as a result of intrinsic nonlinearity of the imaging problem. We apply the compressed sensing techniques to the first stage to identify the significant Fourier/wavelet modes present in the modified object. We also develop a theoretical estimate for these significant modes within a reasonable error bound.

For the fitting of the boundary conditions, we consider two different approaches: the first is a local, point-by-point fitting and the second a global, nonlinear least square fitting in the Fourier/wavelet domain.

We show that the compressed sensing techniques combined with the Fourier/wavelet fitting provide the best performance especially when the Rayleigh hypothesis becomes invalid.

8138-31, Session 8

Compactly supported shearlets: theory and applications

G. Kutyniok, J. Lemvig, W. Lim, Univ. Osnabrück (Germany)

Many important problem classes in applied sciences are governed by anisotropic features. Shearlet analysis might by now be considered the most versatile and successful methodology to efficiently represent such features, in particular, because it allows a unified treatment of the continuum and digital realm. However, although compact support is often required for applications, most research has so far focussed on band-limited shearlets.

In this talk, we will discuss the construction of compactly supported shearlet frames for 2D and 3D data, which will be also shown to optimal sparsely approximate anisotropic features. Finally, we will present some numerical results.

8138-32, Session 8

Sparse image representations using discrete shearlet transform

W. Lim, G. Kutyniok, Univ. Osnabrück (Germany)

In this talk, we will talk about a new multiscale directional representation scheme called the discrete shearlet transform and its various applications in image processing.

We then briefly discuss our ongoing work to construct a compactly supported directional system which is not only a tight frame but also provides optimally sparse approximation of cartoon-like images.

8138-34, Session 9

Algebraic pursuits for sparse recovery in redundant frames

V. Cevher, Ecole Polytechnique Fédérale de Lausanne (Switzerland)

We propose and analyze acceleration schemes for hard thresholding methods with applications to sparse approximation in linear inverse systems. Our acceleration schemes fuse combinatorial, sparse projection algorithms with convex optimization algebra to provide computationally efficient and robust sparse recovery methods. We compare and contrast the (dis)advantages of the proposed schemes with the state-of-the-art, not only within hard thresholding methods, but also within convex sparse recovery algorithms.

8138-36, Session 9

Sparse modeling with BM3D-frames in inverse imaging

A. Danielyan, V. Katkovnik, K. O. Egiazarian, Tampere Univ. of Technology (Finland)

Following the idea of BM3D filtering, we recently proposed a novel type of frames based on the non-local similarity and collaborative 3-D transform domain representation: the BM3D-frames. In this paper we review the construction and properties of BM3D-frames and demonstrate that they provide a sparse image model, which can be efficiently utilized as regularization in various inverse problems. In particular, we consider image deblurring from Gaussian and Poissonian data and super-resolution. The solution is obtained by iterative procedure which minimizes a variational functional where a maximum likelihood fidelity term is combined with a penalty on complexity of the BM3D-frame

representation of the estimate. Simulation experiments demonstrate numerical and visual superiority of the proposed algorithms over current state-of-the-art methods confirming the advantage of the BM3D-frames as a sparse image modeling tool.

8138-40, Session 10

Root-exponential accuracy for coarse quantization of finite frame expansions

R. A. Ward, New York Univ. (United States); F. Krahmer, Univ. of Bonn (Germany); R. Saab, Duke Univ. (United States)

Signal quantization is a fundamental problem in the digital age. Viewing a signal as a real-valued vector, quantization involves replacing the vector with coefficients that are each chosen from a finite alphabet. A particularly robust quantization method using redundant finite-frame representation entails approximating a d -dimensional vector, say x , with an N -dimensional vector q , where $N > d$, taking values in a finite alphabet. The quantity N/d is referred to as the oversampling ratio.

In this talk, we show that by quantizing appropriate frame coefficients of signals using sigma-delta quantization schemes, it is possible to achieve root-exponential error accuracy in the oversampling rate. Previously only polynomial accuracy was shown.

8138-41, Session 10

Mask design for high-resolution optical imaging

A. Pezeshki, W. Dang, R. Bartels, Colorado State Univ. (United States)

We study the design of optical masks and the viability of single pixel imaging and compressive sampling for high resolution fluorescence microscopy. This paper is invited to the Frame Theory and Sparse Approximations session.

8138-42, Session 10

Suboptimality of nonlocal means algorithm on images with sharp edges

A. Maleki, Rice Univ. (United States)

This is based on a joint work with Richard Baraniuk and Manjari Naraya.

The long history of image denoising is testimony to its central importance in image processing. A wide range of denoising have been developed, ranging from simple convolutional smoothing and Wiener filtering to total variation methods and sparsity-exploiting wavelet shrinkage.

One of the successful denoising approaches proposed to date is the nonlocal means algorithm. Despite the success of the nonlocal means in applications, the theoretical aspects of this algorithm have been unexplored. In this talk we explain the asymptotic risk analysis of the nonlocal means image denoising algorithm for Horizon class images that are piecewise constant with a sharp edge discontinuity. We prove that the mean-square risk of nonlocal means is suboptimal and in fact is within a $\$log\$$ factor of the mean square risk of wavelet thresholding.

8138-43, Session 10

Spectral tetris fusion frame constructions

A. Heinecke, Univ. of Missouri-Columbia (United States)

Spectral tetris is a flexible and elementary method to derive unit norm frames with a given frame operator. One important application is the

construction of fusion frames, a natural framework for performing hierarchical data processing. Fusion frames constructed by spectral tetris are desirable from a computational viewpoint as they are optimally sparse, i.e. have the maximal number of zero entries for their fusion frame operators when represented in the standard orthonormal basis. We talk about the construction of fusion frames by spectral tetris that not only have a prescribed fusion frame operator but moreover have a prescribed sequence of dimensions for their subspaces.

8138-44, Session 10

Signal recovery from notches of the spectrogram

B. G. Bodmann, C. L. Liner, Univ. of Houston (United States)

We review the effect of quasi-periodization on the short-time Fourier transform when the window function is a Gaussian. The notches, also known as zero-crossings, of an appropriately periodized short-time Fourier transform determine a signal up to an overall constant factor if the signal is band-limited and has finitely many non-zero sample values. More generally, at least approximate recovery is possible if the signal is sufficiently concentrated in time and frequency. We investigate a strategy for deconvolution based on zero-crossings, assuming that the signal has an integrable short-time Fourier transform, and additional sparseness properties.

8138-45, Session 10

Separation of data using sparse approximations

G. Kutyniok, Univ. Osnabrück (Germany); D. L. Donoho, Stanford Univ. (United States)

Modern data is customarily of multimodal nature, and analysis tasks typically require separation into the single components. Although a highly ill-posed problem, the morphological difference of these components often allows a precise separation. A novel methodology consists in applying l_1 minimization to a composed dictionary consisting of tight frames each sparsifying one of the components.

In this talk, we will first discuss a very general approach to derive estimates on the accuracy of separation using cluster coherence and clustered/geometric sparsity. Then we will use these results to analyze performance of this methodology for images consisting of cartoons and texture.

8138-46, Session 11

Sparse methods and deformable models for improved signal and disease diagnosis

J. Huang, The Univ. of Texas at Arlington (United States); D. N. Metaxas, Rutgers, The State Univ. of New Jersey (United States)

No abstract available

8138-47, Session 11

TrackLab: ensemble of online visual trackers

M. Yang, University of California at Merced (United States)

We present an ensemble of online object tracking algorithms that we develop and provide an in-depth critical evaluation against other state-of-the-art methods. We demonstrate that the strength of weakness of these algorithms and propose mechanisms to exploit these methods for different situations.

8138-48, Session 11

Sparse representations for facial recognition

I. A. Kakadiaris, M. Papadakis, S. Shah, Univ. of Houston (United States)

In this talk, we review work at the UH Computational Biomedicine Lab in the area of sparse representations for Face Recognition. First, we will focus on the robust detection of facial component-landmarks (e.g., eyes, nose) in the presence of pose-illumination variations and partial occlusions. Our method utilizes a variety of adaptive descriptors combined into a cascade of boosted classifiers. These descriptors come from an ensemble of sparse representations aimed at identifying singularities whose relative joint spatial configuration characterizes each of the sought component-landmarks. Second, we will provide an overview of a method for the selection of compact and robust features for 3D face recognition. This method is based on a Markov Random Field model for the analysis of lattices and provides a measure field that estimates the probability of each vertex being “discriminative” or “non-discriminative” for a given classification task. The resulting biometric signature consists of 360 coefficients, based on which we are able to build a classifier yielding recognition rates than surpass those currently reported in the literature.

8138-49, Session 12

Dictionary learning and tomography

V. Etter, I. Jovanovic, M. Vetterli, Ecole Polytechnique Fédérale de Lausanne (Switzerland)

No abstract available

8138-50, Session 12

On structured sparsity and selected applications in tomographic imaging

A. Pžurica, F. Bai, J. Aelterman, S. Vanlooche, H. A. Luong, Univ. Gent (Belgium); B. Goossens, Univ. Gent (United States); W. Philips, Univ. Gent (Belgium)

Signal recovery from partial information making use of sparsity priors demonstrated great potentials in signal/image processing. Recent research shows importance of encoding structured sparsity, admitting that in most but purely random signals/images not all the sparse patterns are equally likely. In this paper, we review some formulations of structured sparsity (including block sparsity and graph sparsity) and analyze their application in selected tomographic imaging modalities. In some of these modalities, like magnetic resonance imaging, “standard” compressive sensing is highly popular, but the potentials of more general structured sparsity models are yet to be explored. In others, like microwave tomography, reconstruction from highly incomplete data is typically done using heuristic regularization and we demonstrate potentials of prior models enforcing structured sparsity.

8138-51, Session 12

A general framework for transmission and emission tomography based on the XPAD3 hybrid pixels camera

S. Anthoine, J. Aujol, Y. Boursier, M. Clothilde, Aix-Marseille Univ. (France)

Cone Beam Computerized Tomography (CBCT) and Positron Emission Tomography (PET) Scans are medical imaging devices that require solving ill-posed inverse problems.

The models considered come directly from the physics of the acquisition devices, and take into account the specificity of the (Poisson) noise.

We propose various fast numerical schemes to compute the solution and consider non differentiable regularizations (total variation, wavelet l1-regularization).

Results obtained on simulations and real data acquired by the ClearPET/XPAD PET/CT demonstrator developed at CPPM indicate that the proposed algorithms compare favorably with respect to well-established methods and provide a first estimate of the dose reduction that can be considered.

8138-52, Session 12

Accelerated parallel MR imaging with spread spectrum encoding

M. H. Izadi, G. Puy, J. R. F. Marquès, Ecole Polytechnique Fédérale de Lausanne (Switzerland); R. Gruetter, Ecole Polytechnique Fédérale de Lausanne (Switzerland) and Univ. of Geneva (Switzerland) and Univ. de Lausanne (Switzerland); J. Thiran, Ecole Polytechnique Fédérale de Lausanne (Switzerland); D. Van De Ville, Ecole Polytechnique Fédérale de Lausanne (Switzerland) and Univ. of Geneva (Switzerland); P. Vanderheynt, Ecole Polytechnique Fédérale de Lausanne (Switzerland); Y. Wiaux, Ecole Polytechnique Fédérale de Lausanne (Switzerland) and Univ. of Geneva (Switzerland)

Magnetic resonance imaging probes signals in Fourier space. Accelerating the image acquisition while preserving resolution is currently of utmost importance. Firstly, parallel imaging reduces the acquisition time by a multiple coil acquisition. Secondly, other approaches seek to reconstruct the image from incomplete Fourier coverage. In particular, the recent spread spectrum technique underpinned by the theory of compressed sensing resides in encoding the image by pre-modulation with a linear chirp before uniform random Fourier under-sampling. In the present work we advocate the combination of parallel imaging and spread spectrum in order to achieve enhanced accelerations, through simulations and real data reconstructions.

8138-53, Session 12

Compressed sensing in k-space: from magnetic resonance imaging and synthetic aperture radar

M. E. Davies, C. Du, S. Kelly, G. Rilling, I. W. Marshall, Y. Tao, The Univ. of Edinburgh (United Kingdom)

We will consider two imaging applications of compressed sensing where the acquired data corresponds to samples in the Fourier domain (aka k-space). The first one is magnetic resonance imaging (MRI), which has been one of the most standard examples in the compressed sensing literature. The second one is synthetic aperture radar (SAR). While the physical processes involved in these two situations are very different, in both cases in idealized conditions the raw data can be viewed as a set of lines in k-space. We will consider the similarities and differences between the two imaging modalities including: dealing with complex valued images, appropriate image models and sampling patterns and the nature and treatment of noise.

8138-55, Session 13

Compressive sensing in MRI with complex sparsification

J. Ji, Y. Dong, Texas A&M Univ. (United States)

MRI signals are inherently complex. Applications of sparsity-constrained imaging methods such as compressive sensing MRI can be enhanced by considering this fact. Specifically, complex transforms such as dual tree complex wavelet transforms can sparsify MR images better than the generic total variation operator or the real wavelet transforms. Therefore, a new method using complex sparsifications can achieve improved image reconstructions. Computer simulations and results from practical MRI applications show and characterize the advantages and limitations of the new method.

8138-56, Session 13

A novel parametric model-driven compressed sensing regularization approach for quantitative MRI from incomplete data

A. A. Samsonov, J. V. Velikina, Univ. of Wisconsin-Madison (United States)

In quantitative MRI, several source images are reconstructed from k-space data and then fit by a modeling equation to yield parametric maps. Several papers have proposed to use model to directly estimate parameters from data, or to design overcomplete dictionary for compressed sensing image estimation. Both approaches suffer from long reconstruction times and pitfalls associated with multidimensional nonlinear estimation. We propose a method incorporating model equation into iteratively-reweighted least squares for fast and robust source image estimation from incomplete data. Our method interleaves estimation with updating the sparsifying transform to conform to the physical model. The method was validated for variable flip angle T1 mapping up to 20x acceleration.

8138-68, Session 13

Sparse feature and image reconstruction from sparse measurements

W. Guo, Case Western Reserve Univ. (United States); W. Yin, Rice Univ. (United States)

We present new schemes to recover sparse features of interest and images of higher qualities from fewer measurements than the current state-of-the-art methods. When the sampling rate is very low, classical image reconstruction methods lead to results full of artifacts, and edges detected from which involve a lot of false positives. Observing that edges in an image are much sparser than the image itself, we cast the edge detection in a sparse optimization scheme. The detected edges can be used to define a weighted anisotropic total variation model to reconstruct images with fine features and high contrast.

8138-57, Session 14

Blind-multichannel image reconstruction for parallel MRI using compressive sensing

H. She, R. Chen, The Univ. of Utah (United States); D. Liang, Univ. of Wisconsin-Milwaukee (United States); E. V. DiBella, H. Wan, The Univ. of Utah (United States); L. Ying, Univ. of Wisconsin-Milwaukee (United States)

In this paper we consider image reconstruction from undersampled

multichannel MRI data without the prior knowledge of the coil sensitivity functions. A new technique integrating multichannel blind deconvolution (MBD) and compressive sensing (CS) is developed for joint estimation of the image function and the sensitivity functions. The method is different from the conventional MBD in that the data are undersampled and different from CS in that the sensing matrix is unknown. The method formulates the reconstruction problem as minimizing a cost function, which consists of a data consistent term and two regularization terms exploiting the sparsity of the image and coil sensitivities in the finite-difference domain respectively. Random sampling pattern was used to satisfy the incoherence requirement of CS. The cost function is a nonlinear, nonconvex function of the unknowns. Alternate minimization is used to reduce the computational complexity, where the coil sensitivities are fixed in reconstruction of the image and the image is fixed in reconstruction of the sensitivities. The process is repeated iteratively until the value of the cost function is below a certain constant. The method was evaluated using a number of datasets acquired from 3 Tesla MRI systems. Phantom and in vivo experimental results demonstrate that the proposed method can improve the reconstruction quality over the existing GRAPPA method.

8138-58, Session 14

Morphological paradigm-free mapping: getting most out of fMRI data

C. Caballero Gaudes, Univ. Hospital of Geneva (Switzerland); D. Van De Ville, Univ. Hospital of Geneva (Switzerland) and Ecole Polytechnique Fédérale de Lausanne (Switzerland); N. Petridou, Univ. Medical Ctr. Utrecht (Netherlands); F. Lazeyras, Univ. Hospital of Geneva (Switzerland); P. Gowland, The Univ. of Nottingham (United Kingdom)

Paradigm Free Mapping of the blood oxygenated-level dependent responses observed in functional magnetic resonance imaging (fMRI) studies can provide supplementary information about cortical activations in experimental scenarios where the precise timing of the responses cannot be hypothesized in advance. The presence of non-neuronal physiological and instrumental confounds makes it a challenging task. In this work, we propose a novel approach for fMRI data analysis that decomposes the voxel time series into its morphological components: movement-related signals, low-frequency instrumental drifts, physiological fluctuations, neuronal-related haemodynamic signal and thermal random noise. Our algorithm is based on an overcomplete representation of the time series with an additive linear model. Specifically, each component can be represented with a distinctive morphological dictionary, and the signal's representation is recovered by means of a least-squares estimator, which is regularized by the L1-norm of the coefficients in the activity-related dictionary. Similar to morphological component analysis, an adapted block coordinate relaxation procedure is used to automatically separate these additive components. We first show results using simulated data as a proof-of-concept, showing promising results in terms of the estimation of the components and robustness against mismatches in the assumed haemodynamic response model, and next we illustrate the feasibility for experimental data acquired on a 7T MR scanner. We envision that this decomposition approach will become more useful with the widespread use of ultrahigh-field MR systems and adds an exciting new possibility for exploratory analysis of fMRI data situated between conventional general-linear-model fitting and relatively unconstrained approaches such as independent component analysis.

8138-59, Session 14

Regularizing GRAPPA using simultaneous sparsity to recover de-noised images

D. S. Weller, Massachusetts Institute of Technology (United States); J. R. Polimeni, Athinoula A. Martinos Ctr. for Biomedical

Imaging (United States); L. Grady, Siemens Corporate Research (United States); L. L. Wald, Athinoula A. Martinos Ctr. for Biomedical Imaging (United States); E. Adalsteinsson, V. K. Goyal, Massachusetts Institute of Technology (United States)

To accelerate magnetic resonance (MR) imaging, the frequency domain (k-space) is undersampled in the phase encoding directions; however, uniform undersampling in the frequency domain results in aliasing in the spatial (image) domain. To mitigate aliasing, multiple receiver coils measure k-space in parallel, each with different spatial weightings, and the missing k-space data is recovered using GRAPPA, a parallel imaging method that utilizes linear combinations (a convolution kernel) of those different spatial weightings to approximate the necessary frequency shifts. However, the combination of undersampling and parallel imaging produces images with significantly reduced SNR; this SNR loss needs to be mitigated to accommodate further acceleration. Compressed sensing (CS) is one approach to de-noising sparse images. Because MR images are known to be approximately sparse in transform domains like the DWT, and incoherent sampling is easily accomplished in k-space, CS can be applied to the problem of de-noising images produced from undersampled MR data. In this work, the GRAPPA method is modified to choose the linear combination weights to produce sparse full k-space images. The optimization problem regularizes the least-squares fit of ACS lines using a nonconvex simultaneous sparsity penalty function of the coil images resulting from the GRAPPA reconstruction using the kernel. Relative to GRAPPA alone, this approach improves the RMSE of images reconstructed from highly undersampled data.

8138-35, Session 15

Learned dictionaries for sparse image representation: properties and results

K. Skretting, K. Engan, Univ. of Stavanger (Norway)

Sparse representation of images using learned dictionaries have been shown to work well for applications like image denoising, inpainting, image compression, etc. In this paper dictionary properties are reviewed from a theoretical approach, and experimental results for learned dictionaries are presented. The main dictionary properties are the upper and lower frame (dictionary) bounds, and (mutual) coherence properties based on the angle between dictionary atoms. Both L0 sparsity and L1 sparsity are considered by using a matching pursuit method, order recursive matching Pursuit (ORMP), and a basis pursuit method, i.e. LARS or Lasso. For dictionary learning the following methods are considered: Iterative least squares (ILS-DLA or MOD), recursive least squares (RLS-DLA), K-SVD and online dictionary learning (ODL). Finally, it is shown how these properties relate to an image compression example.

8138-60, Session 15

Blind compressed sensing over a union of subspaces

J. Silva, Duke Univ. (United States)

We address simultaneous signal recovery and dictionary learning based on compressive measurements. Multiple signals are analyzed jointly, with multiple sensing matrices, under a union-of-subspaces assumption. This problem is important, e.g., in image inpainting applications.

One of our main contributions is that we consider compressive measurements; previous work on Blind Compressed Sensing is also extended by considering multiple sensing matrices and relaxing restrictions on the dictionary. Conditions are given for recovery of the dictionary and signals with high probability. Additionally, a practical algorithm is presented, and convergence conditions are defined. Experimental results for image inpainting demonstrate the capabilities of the algorithm.

8138-61, Session 15

Topographic dictionary learning with structured sparsity

J. Mairal, Univ. of California, Berkeley (United States); R. Jenatton, G. Obozinski, F. Bach, Institut National de Recherche en Informatique et en Automatique (France)

We consider the problem of dictionary learning for data admitting sparse representation, and exploit structured sparsity for modeling dependencies between dictionary elements. To achieve this goal, we regularize the decomposition coefficients of input signals with a group-sparsity penalty where the groups overlap, and present several algorithmic tools to solve the corresponding challenging optimization problems. Our method is flexible enough to efficiently handle any group structure. In particular, when learned on natural image patches and with groups organized on a 2D-grid, the dictionary elements naturally organize themselves on a topographic map, producing similar results as topographic ICA.

8138-62, Session 15

Design of a tight frame of 2D shearlets-based on a fast non-iterative analysis and synthesis algorithm

B. Goossens, J. Aelterman, H. A. Luong, A. Pžurica, W. Philips, Univ. Gent (Belgium)

The shearlet transform is a recent sibling in the family of geometric image representations that provides a traditional multiresolution analysis combined with a multidirectional analysis. In this paper, we present a fast DFT-based analysis and synthesis scheme for the 2D discrete shearlet transform. Our scheme conforms to the continuous shearlet theory to high extent, provides numerical perfect reconstruction (up to floating point rounding errors) in a non-iterative scheme and is highly suitable for parallel implementation (e.g. FPGA, GPU). We show that our discrete shearlet representation also is a tight frame and the redundancy factor of the transform is around 2.6, independent of the number of analysis directions. Experimental denoising results indicate that the transform performs the same or even better than several related multiresolution transforms, while having a significantly lower redundancy factor.

8138-63, Session 15

A diagonally-oriented DCT-like 2D block transform

I. W. Selesnick, Polytechnic Institute of NYU (United States); O. G. Guleryuz, DoCoMo Communications Labs. USA, Inc. (United States)

Due to the prevalence of edge content in images, various directional transforms have been proposed for the efficient representation of images. Such transforms are useful for coding, denoising, and image restoration using sparse signal representation techniques. This paper describes a new non-separable 2D DCT-like orthonormal block transform that is oriented along block diagonals (45 degrees). The approach taken in this paper is to extend to two-dimensions one approach (of several) for constructing the standard 1D DCT. The proposed transform is obtained as the eigenvectors of particular matrices, as is the standard 1D DCT.

8138-64, Session 16

RF transient classification using sparse representations over learned dictionaries

D. I. Moody, Los Alamos National Lab. (United States) and Univ. of Maryland (United States); S. P. Brumby, K. L. Myers, N. H. Pawley, Los Alamos National Lab. (United States)

Automatic classification of transient radio frequency (RF) signals is of particular interest in persistent surveillance applications. Because such transients are often acquired in noisy, cluttered environments, and are characterized by complex or unknown analytical models, feature extraction and classification can be difficult. We propose a fast, adaptive classification approach based on non-analytical dictionaries learned from data. Conventional representations using fixed (or analytical) orthogonal dictionaries, e.g., Short Time Fourier and Wavelet Transforms, can be suboptimal for classification of transients, as they provide a rigid tiling of the time-frequency space, and are not specifically designed for a particular signal class. They do not usually lead to sparse decompositions, and require separate feature selection algorithms, creating additional computational overhead. Pursuit-type decompositions over analytical, redundant dictionaries yield sparse representations by design, and work well for target signals in the same function class as the dictionary atoms. The pursuit search however has a high computational cost, and the method can perform poorly in the presence of realistic noise and clutter. Our approach builds on the image analysis work of Mairal et al. (2008) to learn a discriminative dictionary for RF transients directly from data without relying on analytical constraints or additional knowledge about the signal characteristics. We then use a pursuit search over this dictionary to generate sparse classification features. We demonstrate that our learned dictionary is robust to unexpected changes in background content and noise levels. The target classification decision is obtained in almost real-time via a parallel, vectorized implementation.

8138-65, Session 16

Tight frame 6-band symmetric wavelets with limited redundancy

F. Abdelnour, Univ. of Pittsburgh Medical Ctr. (United States)

We consider the design of 6-channel tight frame (TF) symmetric wavelet with scaling factor $M=4$. While orthogonal symmetric filterbanks with $M=4$ exist, the additional degrees of freedom resulting from relaxing the orthogonality condition lead to smoother limit functions with improved frequency resolution. Moreover, frames have been shown to perform better than the critically sampled counterparts for such applications as noise removal. There has been interest in frame-based wavelets. While a majority of published work on wavelet frames design has focused on the case $M = 2$, it is possible to design frames with other scaling factors. For example, in earlier work wavelets based on 6-channel tight frame with $M = 4$ nonsymmetric filterbanks are designed using Groebner basis. In addition to improved frequency resolution, frames with $M = 4$ offer a reduced redundancy for the same number of filters. Such filterbanks offer design flexibility, allowing additional degrees of freedom and desirable properties such as smoothness of underlying limit functions when compared with their orthogonal counterparts, symmetry, and dense time-frequency plane.

In this paper we design a 6-channel tight-frame symmetric filterbank $\{h_0, h_1, h_2, h_3, h_4, h_5\}$ using Groebner basis methods. The resulting filters have linear phase, limited redundancy, and smooth limit functions. It was possible to obtain filterbanks with K_0 (zeros at $z = -1$ and $z = \pm j$ for the lowpass filter) up to 5 and K_{min} (zeros at $z = 1$ for bandpass/highpass filters) of 1 or greater. The paper elaborates on the theory of the wavelets based on tight frame with scaling factor of 4, describes the design process, and discusses filterbank design examples.

8138-66, Session 16

Sparse signal representations using the tunable Q-factor wavelet transform

I. W. Selesnick, Polytechnic Institute of NYU (United States)

The tunable Q-factor wavelet transform (TQWT) is a fully-discrete wavelet frame for which the Q-factor, Q , of the underlying wavelet and the redundancy, R , of the transform are easily and independently specified. In particular, the specified parameters Q and R can be real-valued. Therefore, by tuning Q , the oscillatory behavior of the wavelet can be chosen to match the oscillatory behavior of the signal of interest, so as to enhance the sparsity of a sparse signal representation. We demonstrate the sparse representation of several oscillatory signals using the TQWT. The TQWT is well suited to fast algorithms for sparsity-based inverse problems because it is a Parseval frame, easily invertible, and can be efficiently implemented using radix-2 FFTs. The TQWT can also be used as an easily-invertible discrete approximation of the continuous wavelet transform.

8138-54, Session 17

Parallel magnetic resonance imaging using multichannel sampling theory and beyond

L. Ying, Univ. of Wisconsin-Milwaukee (United States); Z. Liang, Univ. of Illinois at Urbana-Champaign (United States)

Parallel imaging using phased array coils has emerged as a technique to significantly speed up the magnetic resonance imaging process. In this talk, we describe parallel MRI from a signal processing perspective, invoking the multichannel sampling theory (and filter bank theory). We discuss some outstanding practical issues and present our recent development in sampling schemes and reconstruction algorithms to address these issues. .

8138-67, Session 17

Blind linear models for the recovery of dynamic MRI data

M. Jacob, S. Goud, Univ. of Rochester (United States)

Classical accelerated dynamic MRI schemes rely on the sparsity or banded structure of the data in specified transform domains (eg. Fourier space). Clearly, the utility of these schemes depend on the specific data and the transform. For example, these methods only provide modest accelerations in free-breathing myo-cardial perfusion MRI. We introduce a novel blind linear model to recover the data when the optimal transform is not known apriori. Specifically, we pose the simultaneous recovery of the optimal linear model /transform and its coefficients from the measurements as a non-convex optimization problem. We also introduce an efficient majorize maximize algorithm to minimize the cost function. We demonstrate the utility of the algorithm in considerably accelerating free breathing myocardial perfusion MRI.

8138-69, Session 17

Sparse dictionary learning for resting-state fMRI analysis

J. Ye, P. K. Han, K. Lee, KAIST (Korea, Republic of)

Recently, there has been increased interest in the usage of neuroimaging techniques to investigate what happens in the brain at rest. Functional imaging studies have revealed that the default-mode network activity is disrupted in AD. However, there is no consensus, as yet, on the choice of analysis method for the application of resting-state analysis for disease

classification. This paper proposes a novel compressed sensing based resting-state fMRI analysis tool called Sparse-SPM. Sparse-SPM is a new spatially adaptive data-driven fMRI analysis method that implements sparse dictionary learning based on sparsity of the signal instead of independence. From individual and group analysis, the proposed approach shows better performance compared to other conventional methods, such as ICA and seed-based approach, in classifying the AD patients from normal using resting-state analysis.

8138-70, Session 18

3D discrete shearlet transform and video denoising

D. Labate, P. Negi, Univ. of Houston (United States)

The shearlet representation, a multiscale pyramid of well-localized waveforms defined at various locations and orientations, was recently proved to provide optimally sparse representations for a large class of 3D data. In this paper, we present the first discrete numerical implementation of the 3D shearlet transform. The algorithm combines a cascade of multiscale decomposition with a stage of directional filtering, based on the use of Pseudopolar FFT. The filters resulting from this decomposition can be implemented as finite-length filters, which ensures that the numerical implementation is highly efficient. To demonstrate the capability of the 3D Discrete Shearlet Transform, we consider a number of problems from video denoising. The performance of the algorithm is successfully compared against other state-of-the-art multiscale denoising techniques, including curvelets and surfacelets.

8138-71, Session 18

Efficient multiscale and multidirectional representation of 3D data using the 3D discrete shearlet transform

B. Goossens, H. A. Luong, J. Aelterman, A. P?urica, W. Philips, Univ. Gent (Belgium)

In recent years, there has been a lot of interest in multiresolution representations that also perform a multidirectional analysis. These representations often yield very sparse representation for multidimensional data. The shearlet representation, which has been derived within the framework of composite wavelets, can be extended quite trivially from 2D to 3D. However, the extension to 3D is not unique and consequently there are different implementations possible for the discrete transform. In this paper, we investigate the properties of two relevant designs having different 3D frequency tilings. We show that the first design has a redundancy factor of around 7, while in the second design the transform can attain a redundancy factor around 3.5, independent of the number of analysis directions. Due to the low redundancy, the 3D shearlet transform becomes a viable alternative to the 3D curvelet transform. Experimental results are provided to support these findings.

8138-72, Session 18

Multi-composite wavelet estimation

G. R. Easley, System Planning Corp. (United States); D. Labate, Univ. of Houston (United States); V. M. Patel, Univ. of Maryland, College Park (United States)

In this work, we present a new approach to image denoising derived from a general representation known as wavelets with composite dilations. These representations extend the traditional wavelet framework by allowing for waveforms to be defined not only at various scales and locations but also at various orientations. The shearlet representation is, perhaps, the most widely known example of composite wavelets.

However, many other representations are obtained within this framework, where directionality properties are controlled by different types of orthogonal matrices, such as the newly defined hyperbolets. For this talk, we show how to take advantage of different wavelets with composite dilations to sparsely represent important features in an image, and then use a hybrid thresholding method to obtain improved estimates from noisy observations.

8138-73, Session 18

3D-rigid motion invariant texture discrimination

M. Papadakis, R. Azencott, Univ. of Houston (United States); S. Jain, The Johns Hopkins Univ. (United States); S. Upadhyay, Univ. of Houston (United States)

This paper studies the problem of invariant 3D-rigid motion texture discrimination for discrete 3D-textures that are spatially homogeneous by modeling them as stationary Gaussian random fields. The latter property and our formulation of a 3D-rigid motion of a texture reduce the problem to the study of 3D-rotations of discrete textures. We formally develop the concept of 3D-texture rotations in the 3D-digital domain. We use this novel concept to define a 'distance' between 3D-textures that remains invariant under all 3D-rotations of the texture. This concept of 'distance' can be used for a monoscale or a multiscale 3D-rotation invariant testing of the statistical similarity of the 3D-textures.

Conference 8139: Advances in X-Ray/EUV Optics and Components VI

Monday-Wednesday 22-24 August 2011 • Part of Proceedings of SPIE Vol. 8139
Advances in X-Ray/EUV Optics and Components VI

8139-01, Session 1

Micro- and nano-focusing system at Japanese XFEL

H. Mimura, The Univ. of Tokyo (Japan); M. Yabashi, RIKEN (Japan); H. Ohashi, Japan Synchrotron Radiation Research Institute (Japan) and RIKEN (Japan); H. Yumoto, Japan Synchrotron Radiation Research Institute (Japan); H. Yokoyama, S. Imai, T. Kimura, S. Matsuyama, Osaka Univ. (Japan); Y. Hachisu, H. Ohmori, RIKEN (Japan); K. Yamauchi, Osaka Univ. (Japan); T. Ishikawa, RIKEN (Japan)

Focusing system is very important for various applications at X-ray free electron laser facilities, because extremely intensive X-ray laser beam is realized. In Japan, the XFEL facility will be completed at SPring-8 site this year. We are now developing focusing system specialized for Japanese XFEL. In this presentation, we will introduce the overview of the design and performances of the focusing optical system.

This presentation includes optical simulation for design of optical system, fabrication of focusing mirrors and development of focusing units.

8139-02, Session 1

Nested KB mirror fabrication for synchrotron hard x-ray nanofocusing

B. Shi, W. Liu, C. Liu, J. Qian, K. Ruben, A. M. Khounsary, P. Zachack, Argonne National Lab. (United States); J. Z. Tischler, G. E. Ice, Oak Ridge National Lab. (United States); L. Assoufid, Argonne National Lab. (United States)

A pair of traditional KB mirrors consists two concave mirrors arranged perpendicular to each other at separate positions. A pair of nested (or Montel [1]) KB mirrors also consists two concave mirrors perpendicular to each other, but standing side by side. Compared to traditional KB mirrors, nested KB mirrors can give more working space, collect larger divergence [2], and give a higher demagnification [3]. Although nested KB mirrors collected less x-ray flux than traditional KB mirrors, nested KB mirrors are capable of deliver a higher x-ray flux by enabling more efficient collecting of x-rays and wide energy range x-ray beam compared with other micro/nano focusing x-ray mirrors.

We report the fabrication method of our nested platinum KB mirrors for synchrotron hard x-ray micro/nanofocusing system. The first set of nested KB mirrors includes two 40 mm mirrors fabricated by depositing Pt on the Si substrate using the magnetron sputtering technique. The beamline tests have been performed and an about 150 nm x 150 nm focus spot was achieved [3]. Due to the gap between the nested KB mirrors, which caused the less efficiency, a second pair of KB mirrors was fabricated and one side of the horizontal focusing mirror was cut and polished to reduce the gap. This pair of nested KB mirrors have been tested and results the gap has been narrowed from 10 microns to 3 microns.

References

1. M. Montel, X-ray microscopy with catamegonic roof mirrors, X-ray microscopy and microradiography, Academic Press, New York, pp. 177-185, 1957.
2. G.E. Ice, et al., J. Appl. Crystallogr., 42, 1004, 2009.
3. W. Liu, et al. Nucl. Instr. and Meth. A (2010), doi: 10.1016/2010.11.080.

* This work is supported by the U. S. Department of Energy, Office of Science, Office of Basic Energy Sciences, under Contract No. DE-AC02-06CH11357.

8139-03, Session 1

A dynamically-figured mirror system for high-energy nanofocusing at the ESRF

R. Barrett, R. Baker, P. Cloetens, Y. Dabin, C. Morawe, H. Suhonen, R. Tucoulou, A. Vivo, L. Zhang, European Synchrotron Radiation Facility (France)

The design, manufacture and characterisation of a Kirkpatrick-Baez (KB) configuration mirror system for high-throughput nanofocusing down to 50 nm beam sizes are described. To maximize the system aperture whilst retaining energy tunability, multilayer coated optics are used in conjunction with 2 dynamically figured mirror benders. This approach, which has been developed at the ESRF for many years, allows the focusing performance to be optimized when operating the system in the 13-25 keV photon energy range.

Developments in the key technologies necessary for the production of mirror bending systems with dynamic figuring behaviour close to the diffraction limit requirements are discussed. These include system optimisation via finite element analysis (FEA) modelling of the mechanical behaviour of the bender-mirror combination, manufacturing techniques for precisely-shaped multilayer substrates, multilayer deposition with steep lateral gradients and the stitching metrology techniques developed for the characterisation and figure optimisation of the strongly aspherical surfaces. The mirror benders have been integrated into a compact and stable assembly designed for routine beamline operation and results of the initial performance of the system at photon energies up to 29keV at the ESRF ID22NI endstation will be presented.

8139-04, Session 1

Development of hard x-ray imaging optics with four aspherical mirrors

S. Matsuyama, N. Kidani, Osaka Univ. (Japan); H. Mimura, The Univ. of Tokyo (Japan); Y. Sano, Osaka Univ. (Japan); K. Tamasaku, Y. Kohmura, M. Yabashi, T. Ishikawa, RIKEN (Japan); K. Yamauchi, Osaka Univ. (Japan)

To realize achromatic full-field X-ray microscopy with a spatial resolution less than 50 nm, we have developed a total reflection mirror system with two pairs of an elliptical mirror and a hyperbolic mirror, which is called "an Advanced Kirkpatrick-Baez system". A designed optical system has 200x and 300x magnifications in vertical and horizontal directions. The four mirrors with a figure accuracy of 2 nm were fabricated using elastic emission machining (EEM), microstitching interferometry (MSI) and relative-angle-determinable stitching interferometry (RADSI). One-dimensional tests for forming a demagnified image of a slit were carried out at an X-ray energy of 11.5 keV at BL29XUL (EH2) of SPring-8. As a result, a sharp beam with a FWHM of 43 nm was observed. Also, an obtained width of a field of view was 12 micron in the region of a resolution better than 50 nm. For two-dimensional (2D) imaging, we have developed a mirror manipulator with autocollimators and laser displacement meters. As a preliminary 2D test, an approximately 300-nm resolution in 2D was obtained. The poor result was caused by misalignments. We'll perform a 2D imaging test, in which we use the improved mirror manipulator, in this April. We'll present the results of 2D imaging in the meeting.

8139-05, Session 1

Automated in-situ optimisation of bimorph mirrors at Diamond Light Source

J. P. Sutter, S. G. Alcock, K. J. S. Sawhney, Diamond Light Source Ltd. (United Kingdom)

Bimorph mirrors are used on synchrotron beamlines throughout the world to focus or collimate light. They minimise wavefront distortion by permitting not only the overall figure, but also the local slope errors, to be corrected using varying voltages on the individual electrodes. However, the optimisation procedure is complex, requiring both accurate in-situ measurement of the slope errors and quick calculation of the voltage corrections. The first has been achieved using a simple custom-built "X-ray eye" to gather data by the pencil beam method already used on ex-situ slope measuring profilers. The second has been achieved using Jython scripts that calculate the voltages by the well-known interaction matrix method. In-situ data are highly repeatable and in good agreement with ex-situ data collected at the Diamond NOM. These procedures may be applied to any type of active mirror and to static optics as well. Diffraction from the incident slits is shown to limit the spatial resolution of the pencil beam method in the hard X-ray case.

8139-06, Session 1

At-wavelength metrology and diffraction-limited focusing of bendable soft x-ray KB mirrors

D. J. Merthe, K. A. Goldberg, V. V. Yashchuk, S. Yuan, R. Celestre, J. Macdougall, W. R. McKinney, I. Mochi, G. Y. Morrison, T. Warwick, H. A. Padmore, Lawrence Berkeley National Lab. (United States)

Realizing the full experimental potential of high-brightness, next generation synchrotron and free-electron laser light sources requires the development of reflecting x-ray optics capable of brightness preservation, and high-resolution nano-focusing. At the Advanced Light Source (ALS) beamline 5.3.1, we are developing broadly applicable, high-accuracy, in situ, at-wavelength wavefront measurement techniques to surpass 100-nrad slope measurement accuracy for diffraction-limited Kirkpatrick-Baez (KB) mirrors.

The at-wavelength methodology we are developing relies on a series of wavefront-sensing tests with increasing accuracy and sensitivity, including scanning-slit Hartmann tests, grating-based lateral shearing interferometry, and quantitative knife-edge testing. We will describe the original experimental techniques and alignment methodology that have enabled us to optimally set a bendable KB mirror to achieve a focused, FWHM spot size of less than 150 nm, with 1 nm (1.24 keV) photons at 3.3 mrad numerical aperture. The predictions of wavefront measurement are confirmed by the knife-edge testing.

The side-profiled elliptically bent mirror used in these one-dimensional focusing experiments was originally designed for a much different glancing angle and conjugate distances. Visible-light long-trace profilometry was used to pre-align the mirror before installation at the beamline. This work demonstrates that high-accuracy, at-wavelength wavefront-slope feedback can be used to optimize the pitch, roll, and mirror-bender forces in situ, using procedures that are both deterministic and repeatable. Supported by the U.S. Department of Energy under Contract No. DE-AC02-05CH11231.

8139-07, Session 2

A double multilayer monochromator for the B16 Test beamline at the Diamond Light Source

K. J. S. Sawhney, I. P. Dolbnya, S. M. Scott, Diamond Light Source Ltd. (United Kingdom); M. K. Tiwari, Raja Ramanna Ctr. for Advanced Technology (India); G. M. Preece, S. G. Alcock, A. W. Malandain, Diamond Light Source Ltd. (United Kingdom)

The B16 Test beamline has been built at the 3-GeV Diamond Light Source, and it is in user operation since January 2008. It has been recently upgraded with the addition of a double multilayer monochromator (DMM), which provides further functionality and versatility to the beamline. The multilayer monochromator is equipped with two pairs of multilayer optics (Ni/B4C and Ru/B4C) to cover the wide photon energy range of 2 - 20 keV, with good efficiency. The DMM provides a broad bandpass / high flux operational mode for the beamline and, when used in tandem with the Si 111 double crystal monochromator, it gives a very high higher-order harmonics suppression. The design details of the DMM and the first commissioning results obtained using the DMM will be presented.

8139-08, Session 2

Spatial coherence studies on x-ray multilayers

C. Morawe, R. Barrett, K. Friedrich, R. Klünder, European Synchrotron Radiation Facility (France)

The degree of coherence preservation of x-ray multilayers was investigated using Talbot imaging on the ESRF undulator beamline ID06. Several W/B4C multilayer mirrors with variable d-spacings were studied with monochromatic light at different photon energies. To understand the respective influence of the underlying substrate and the multilayer coatings, measurements were made under total reflection, at different Bragg peaks, and on the bare substrates. In addition, samples with different substrate quality were compared. The relation between spatial coherence preservation and the visibility of characteristic line structures in the x-ray beam will be discussed.

8139-09, Session 2

Interface diffusion kinetics and lifetime scaling in multilayer Bragg optics

R. W. E. van de Kruijs, S. Bruijn, A. E. Yakshin, FOM-Institute for Plasma Physics Rijnhuizen (Netherlands); F. Bijkerk, FOM-Institute for Plasma Physics Rijnhuizen (Netherlands) and Univ. Twente (Netherlands)

Multilayer reflective coatings play an enabling role in the development of optics for the EUV wavelength range. This holds in particular for applications in solar telescopes, x-ray free electron lasers, and EUV photolithography. In general, these applications all demand stable optics performance over long lifetimes and therefore allow no changes to occur in the internal multilayer structure. In reality, internal changes in the multilayer structure will occur by means of radiation absorption, or more in general, by thermal load of the optical system.

We show that for Mo/Si multilayers, the internal structure changes under thermal load due to thermal diffusion induced dense interface layer growth, reducing the optical contrast and changing the reflected wavelength. We focus on early-stage diffusion behavior at relatively low temperatures, where MoSi₂ silicide interface growth clearly follows a scaling law from which diffusion constants for the system can be obtained. Arrhenius plots show temperature scaling with a single activation energy, with activation energy depending on the exact nature

Conference 8139:
Advances in X-Ray/EUV Optics and Components VI

of the interface being formed. Using Arrhenius analysis, the diffusion constants in a multilayer system can be predicted at specific application temperatures, which allows for accurate optics thermal lifetime prediction.

Using the methods developed, we compared Mo/Si based multilayer coatings with different diffusion barriers, aimed at improving thermal stability, and discuss their relevance to optics performance and optics lifetime. The method described here is of general interest for any multilayer application that is subjected to enhanced thermal loads and represents the enormous technology gain that this type of optics has experienced the last decade.

8139-10, Session 2

Ultra-dense multilayer-coated diffraction gratings for EUV and soft x-rays

D. L. Voronov, E. H. Anderson, R. Cambie, S. Cabrini, S. D. Dhuey, Lawrence Berkeley National Lab. (United States); L. I. Goray, Russian Academy of Sciences for Research and Education (Russian Federation); E. M. Gullikson, F. Salmassi, T. Warwick, V. V. Yashchuk, H. A. Padmore, Lawrence Berkeley National Lab. (United States)

Diffraction gratings with high efficiency and high groove density are required for EUV and soft x-ray spectroscopy techniques (such as Resonant Inelastic X-ray Scattering, RIXS) designed for state-of-the-art spectral resolution and throughput. We report on recent progress achieved at the Advanced Light Source (ALS) in development of ultra-dense multilayer coated blazed (MBG) gratings.

In order to fabricate a high quality MBG grating, one should address two main challenges. The first one is to fabricate nano-period saw-tooth substrates with perfect groove profile and atomically smooth surface of the blazed facets. The second challenge relates to uniform deposition of a multilayer on a highly corrugated surface of the substrates. We show that the required saw-tooth substrates with groove density up to 10,000 lines/mm can be fabricated using high resolution interference and e-beam lithography techniques followed by wet anisotropic etching of silicon. Peculiarities of growth on the saw-tooth substrates of a variety of multilayers, optimized to provide high diffraction efficiency in EUV wavelength range, are also under investigation. With cross-sectional TEM we reveal a transformation of the structure of the multilayer stack, consisting in smoothing of the groove profile of a coated grating. The multilayer profiles measured with the TEM are used for diffraction efficiency simulations and investigation of the impact of the smoothing on grating performance. Thus, we show that a strong smoothing of the grating grooves results in deterioration of the blazing ability of the gratings. This work was supported by the US Department of Energy under contract number DE-AC02-05CH11231.

8139-11, Session 2

Development of super mirrors for high-resolution x-ray LMJ microscopes

P. Troussel, D. Denetiere, R. Rosch, C. Reverdin, L. Hartmann, Commissariat à l'Énergie Atomique (France); F. Bridou, E. Meltchakov, F. Delmotte, Lab. Charles Fabry de l'Institut d'Optique (France)

With regards of Laser Mégajoule (LMJ) facility, our laboratory is developing advanced High Resolution X-ray Imaging (HRXI) microscopes. Shrapnel and X-ray loading on this laser imposed to place any HRXI as far away from the source as possible. Grazing incidence X-ray microscopes are the best solution to overpass this limitation. We have designed imaging diagnostics, with a long working distance (> 50 cm) and high resolution. All of them are composed of multi-toroidal mirrors. The microscopes reflect x-rays up to 10 keV using non-periodic multilayer coatings (Super mirrors).

We present these W/SiC Super mirrors, developed in collaboration with the LCFIO. The mirrors were designed and optimized with home made calculation code. Super mirrors are dedicated to work at 0.7° grazing incidence using a reflectivity above 35 %. Metrology for x-ray reflectance in the all range on the synchrotron radiation facility BESSY II is presented.

We have also implemented this coating on a Wolter-like microscope working at a different grazing incidence (0.6°) in order to increase the band pass of reflectivity until 20 keV. We display a reflectivity better than 35 %. Potentialities of this HRXI microscope are presented.

8139-12, Session 3

Total-reflection zone plate as a new device for x-ray nanofocusing

H. Takano, Univ. of Hyogo (Japan); T. Tsuji, Univ. of Hyogo (Japan) and Japan Synchrotron Radiation Research Institute (Japan); Y. Kagoshima, Univ. of Hyogo (Japan)

X-ray focusing beam has important potential to give most of conventional x-ray analytical procedures a high spatial resolution with a high flux density. The x-ray focusing techniques have been dramatically improved according to development of synchrotron radiation sources and focusing optics. Focusing mirrors with graded multilayer reflector and multilayer Laue lenses are the typical focusing devices to lead the best performances of focusing in the x-ray region. These devices, however, require ultra-high precision techniques for their fabrication.

When x-rays are incident to a zone pattern on a flat substrate with a glancing angle satisfying total reflection condition to zone material, and when the x-rays reflected and diffracted by the zones make focus as well as Fresnel zone plate, the focal size is determined not by the smallest fabricated size of zone on substrate but by that of effective zone size reduced by the glancing view effect. Therefore, high focusing performance can be expected although fabrication of the focusing device is relatively easy to the other x-ray devices. We have developed the focusing device as a total-reflection zone plate (TRZP) for hard x-ray nanofocusing. The TRZP with the finest zone width of 700 nm, fabricated by conventional electron beam lithography, could focus 10 keV x-rays to 14.4-nm size.

In the presentation, theoretical and practical focusing limit of TRZP will be discussed. And advanced types for high efficiency using laminar grating structure and for point focusing using a conical substrate will be suggested as further approaches.

8139-13, Session 3

Characterization of a 20-nm hard x-ray focus by ptychographic coherent diffractive imaging

J. Vila Comamala, A. Diaz, M. Guizar-Sicairos, Paul Scherrer Institut (Switzerland); A. Manton, Bundesanstalt für Materialforschung und -prüfung (Germany); C. M. Kewish, Synchrotron SOLEIL (France); V. A. Guzenko, O. Bunk, C. David, Paul Scherrer Institut (Switzerland)

Recent advances in the fabrication of diffractive X-ray optics have demonstrated the focusing of hard X-rays to focal spots below 30 nm. However, the characterization of these novel devices is not straightforward using conventional methods such as knife edge scans or by using test objects that are previously known. Here, we have used ptychographic scanning coherent diffractive imaging to characterize a 20 nm-wide X-ray focus produced by Fresnel zone plate at a photon energy of 6.2 keV. An ordinary scanning transmission X-ray microscope was modified to perform the ptychographic scans on a test object. The ptychographic algorithms allowed the reconstruction of the image of the test object as well as the 3D reconstruction of a focused hard X-ray beam waist, with high spatial resolution and dynamic range. The technique was used to characterize state-of-the-art zone-doubled Fresnel zone plates that were expected to concentrate the X-ray beams into focal

Conference 8139:
Advances in X-Ray/EUV Optics and Components VI

spots below 25 nm in size. The reconstructed wavefields confirm that the zone-doubled diffractive lenses were focusing the incoming radiation into spots as small as 20 nm. This method yields a full description of the focusing field at any propagation distance, including wavefront aberrations at the plane of the lens, and demonstrates its usefulness for metrology and alignment of nanofocusing X-ray optics. It is very robust against the longitudinal position of the sample, and requires no previous knowledge of the test object.

8139-14, Session 3

Coherent high-resolution x-ray microscopy for mesoscopic photonic crystals

I. I. Snigireva, A. A. Snigirev, European Synchrotron Radiation Facility (France)

We developed a high-resolution transmission X-ray microscopy (HRTXM) technique, based on the use of parabolic refractive lenses. The immediate benefit of a lens-based approach is the possibility to retrieve the Fraunhofer diffraction pattern and real-space images in the same experimental setup. This approach is methodologically similar to the traditional method of studying crystalline samples with high-resolution transmission electron microscopy.

The HRTXM experiment was carried out at the micro-optics test bench of beamline ID06. X-rays from 10 to 20 keV were used. The setup consists of condenser - used for sample illumination in imaging mode and as Fourier transformer in diffraction mode, the tunable objective lens and two (large area and high resolution) CCD detectors. At maximum magnification, a resolution of ~100 nm was achieved. We demonstrate the applicability of the HRTXM approach to volume-specific studies of periodic mesoscopic structures, such as natural and artificial opals and inverted photonic crystals.

Short acquisition times with modern area detectors allow the method to be extended to time-resolved studies and combined 3-D real/reciprocal space mapping. Characterization of the real crystal structure during photonic crystal growth is an example of a practical application of this new technique.

8139-15, Session 3

Revisiting the “forgotten” first zoomable refractive x-ray lens

W. H. Jark, Sincrotrone Trieste S.C.p.A. (Italy)

Did anybody ever ask the question: Will I get an x-ray focus, when I operate a Kirkpatrick-Baez mirror pair beyond the critical angle for total reflection?

The first, who could do so, P.Kirkpatrick, already gave an affirmative answer. Infact such a system of two crossed concave lenses can produce an x-ray focus as well. The result was published (P. Kirkpatrick, JOSA 39, 796 (1949)), patented (US 2,559,972) and then it was mostly forgotten. This latter fate is understandable as the system has a rather small effective aperture, limited by significant absorption. This contribution would like to discuss whether the device can today provide more interesting properties in combination with more recent developments in the field of x-ray research. First it will be shown, that the object properties can now be predicted more easily in the framework of the theory for refractive x-ray lenses. Related experimental data will be presented. And finally possible applications will be discussed.

8139-16, Session 4

Commissioning status of XFEL facility at SPring-8

M. Yabashi, K. Tono, RIKEN (Japan); T. Togashi, RIKEN (Japan)

and Japan Synchrotron Radiation Research Institute (Japan); T. Sato, Y. Inubushi, RIKEN (Japan); K. Takeshita, S. Takahashi, H. Kimura, H. Ohashi, S. Goto, RIKEN (Japan) and Japan Synchrotron Radiation Research Institute (Japan); T. Hatsui, T. Tanaka, H. Tanaka, T. Ishikawa, RIKEN (Japan)

An XFEL facility in Japan has been constructed from FY2006 to FY2010 at the SPring-8 campus by a joint project team of RIKEN and JASRI. The facility will provide high-quality XFEL radiation above 10 keV with a moderate acceleration energy of 8 GeV. After successful construction of the facility, we have observed the first electron beam in February 21th of 2011. We will start full commissioning towards stable lasing in April. I will introduce the commissioning status and perspective on development of XFEL applications and instrumentations.

8139-17, Session 4

Upgrade status of hard x-ray 100-nm probe beamlines BL37XU and BL39XU at SPring-8

T. Koyama, H. Yumoto, Y. Terada, M. Suzuki, N. Kawamura, M. Mizumaki, N. Nariyama, T. Matsushita, Y. Ishizawa, Y. Furukawa, T. Ohata, H. Yamazaki, T. Takeuchi, Y. Senba, Y. Matsuzaki, M. Tanaka, Y. Shimizu, H. Kishimoto, T. Miura, K. Takeshita, Japan Synchrotron Radiation Research Institute (Japan); H. Ohashi, Japan Synchrotron Radiation Research Institute (Japan) and RIKEN (Japan); M. Yamamoto, RIKEN (Japan); S. Goto, M. Takata, Japan Synchrotron Radiation Research Institute (Japan) and RIKEN (Japan); T. Ishikawa, RIKEN (Japan)

Under the government project aimed at creating a low-carbon society, a trace element analysis beamline BL37XU and a magnetic materials beamline BL39XU at SPring-8 have been upgraded to provide nano-probe analysis to their users and scheduled to start operation in May 2011.

In order to realize nanobeam analysis, we constructed new experimental hutches which are located about 80 m from the light source, and designed and will install Kirkpatrick-Baez (KB) mirrors and corresponding manipulators. By taking advantage of extended beamline, high demagnification optical design is available. Therefore nanofocusing beam with relatively long working distance and high photon flux density is feasible. Furthermore, liquid-nitrogen cooled Si double crystal monochromators, which were improved to low vibration, were employed in place of existing monochromators.

Designed KB mirror parameters are shown as follows. A targeted focusing beam size and a photon flux density were designed to be 100 nm and over 1×10^{10} (photons/sec/100×100nm²). Mirror lengths were designed to be 300 mm (vertical focusing mirror) and 200 mm (horizontal focusing mirror). Focal lengths were designed to be 460 mm (V) and 200 mm (H). A working distance was designed to be 100 mm. Aperture acceptance areas of mirrors were designed to be about 1 mm (V) × 0.7 mm (H). A coating material was adopted to be Rh for a high X-ray reflectivity up to 15 keV. In order to reduce the mechanical vibration and the thermal drift, mirror manipulators are set up onto a granite table with a thickness of 700 mm and a weight of over 2800 kg, and a temperature of new experimental hutches are planned to control precisely within ±0.05 degree.

In this paper, we report current status of these beamlines.

8139-18, Session 5

Characterization of the FERMI@Elettra's on-line energy spectrometer

C. Svetina, A. Abrami, I. Cudin, C. Fava, S. Gerusina, R. Gobessi, L. Rumiz, G. Sostero, M. Zangrando, D. Cocco, Sincrotrone Trieste S.C.p.A. (Italy)

Conference 8139:
Advances in X-Ray/EUV Optics and Components VI

FERMI@Elettra is a the Free Electron Laser (FEL) under commissioning at Sincrotrone Trieste. It will provide a fully coherent and transform limited radiation with a very high brilliance in the VUV/Soft X-ray range. The first part of the photon transport system, aimed to deliver the radiation into the experimental chambers, is dedicated to the beam diagnostic.

This section, called PADReS (Photon Analysis, Delivery and Reduction System) includes the Beam Defining Apertures, Beam Position Monitors, Intensity Monitors, Photon Energy Spectrometer and the transversal coherence measurement system. All the diagnostic will be not invasive and shot to shot with the only exclusion of the transversal coherence measurement. Among these, the photon energy spectrometer is an essential instrument to aid the machine physicist to properly set up the insertion devices as well as to characterize the photon pulses energy distribution during the experiments with sub-meV resolution. In this article we describe the working principles of the Variable Line Spacing (VLS) diffraction gratings applied to the spectrometer as well as the design concept and ray tracing and efficiency simulations. Metrological results of the optics involved and the first characterization results with FEL radiation will be shown. A comparison between the simulated performances and the first data obtained with real radiation will be presented too.

8139-19, Session 5

Heydemann interpolation correction for energy linearisation of soft x-ray monochromators

J. Krempasky, U. Flechsig, P. Oberta, Paul Scherrer Institut (Switzerland); R. Follath, Helmholtz-Zentrum Berlin für Materialien und Energie GmbH (Germany)

Material science research in the soft-X ray regime at the Swiss Light source accommodates five beam lines where the monochromators rely on in-vacuum angular encoders for positioning mirror and gratings. Despite the factory-calibration of the quadrature signals from these rotary encoders, the energy linearization for spectroscopic data requires accurate calibration of the encoder quadrature signals. We discuss the application of the Heydemann correction algorithm for the quadrature signals and compare the linearized angular readout with autocollimator data. Without this calibration the positioning errors go beyond the slope errors of the optical elements which in turn may produce errors up to 100 meV in the soft-X ray spectroscopy. We show some examples where such errors produce sizeable effects in soft-X ray spectroscopy

8139-20, Session 5

Johansson crystals for x-ray diffractometry and demanding spectroscopy applications

B. Ehlers, B. Verman, L. Jiang, B. Kim, D. Wilcox, Rigaku Innovative Technologies, Inc. (United States)

Johansson crystals are known for many decades as x-ray optical elements with a high resolving power and small foci. However, in the past their use in applications requiring a small focus and a narrow bandpass were limited due to imperfections that were caused by the applied manufacturing technologies. In particular, while high performing Johansson crystals were manufactured in small quantities in research facilities, they were not available commercially. RIT has developed a technological process of Johansson crystals fabrication that allows the preservation of crystals structure. The angular precision of the bending process of atomic planes and the final crystal surface is better than 4 arcseconds. Results for Silicon and Germanium crystals will be shown.

Several technological processes were developed to achieve the high performance of the crystal optic. This includes a crystal topography system to measure the lattice imperfections of the crystal blank. The system uses a 20 mm wide, collimated x-ray beam with a divergence of approximately 7 arcseconds to measure the rocking curve of the crystals

over a wide area. Results of the crystal pre-selection process of several different Germanium crystals from different manufacturers are shown.

Crystals manufactured with this technology are being coupled with a laboratory x-ray microfocusing source and focus dimensions of less than 10 micrometers are achieved while rejecting K alpha 2 radiation. Examples of the crystals design and results of the performances of the assembled crystal optic will be presented.

8139-21, Poster Session

Application of focusing X-ray spectrograph with spatial resolution and uniform dispersion in Z-pinch plasmas measurement

Q. Yang, Y. Ye, G. Chen, Z. Li, Q. Peng, China Academy of Engineering Physics (China)

A new focusing X-ray spectrograph with spatial resolution and uniform dispersion (FSSRUD) is described. Uniform dispersion (i.e., the linear dispersion is a constance, or in other words, the X-rays are dispersed on the detector with uniform spacing for every wavelength) is realized by bending the crystal of a spectrograph into a special shape. Since the spatial coordinate of the spectrum obtained by the FSSRUD varies linearly with X-ray wavelength, it is very convenient for identification and processing of the experimental data. In addition, an optimized spectrograph capability can be achieved by customizing the bent shape of the crystal and other spectrograph parameters to satisfy the given requirements of routine measurement. The spectrograph capability is first analyzed using a ray tracing method, the principle to design the shape of the crystal for the FSSRUD is then presented and the spectrograph is constructed for measuring the spectrum of Z-pinch plasmas.

8139-22, Poster Session

The influence of working gas pressure on interlayer mixing in magnetron-deposited Mo/Si multilayers

Y. P. Pershin, E. N. Zubarev, V. V. Kondratenko, V. A. Sevryukova, Kharkov Polytechnical Institute (Ukraine); D. L. Voronov, E. M. Gullikson, Lawrence Berkeley National Lab. (United States); I. A. Artioukov, A. V. Vinogradov, P.N. Lebedev Physical Institute (Russian Federation)

The influence of Ar gas pressure (1-4 mTorr) on the growth of amorphous interfaces in Mo/Si multilayers deposited by magnetron sputtering was investigated by the methods of cross-sectional transmission electron microscopy and small-angle x-ray scattering ($\lambda = 0.154$ nm). An increase of the Ar pressure was found to result in reduction of the thicknesses of amorphous inter-layers, with composition of the layers being enriched with molybdenum. The indicated interface modification improves the EUV reflectance of Mo/Si multilayer mirrors.

This work was supported by the US Department of Energy under contract number DE-AC02-05CH11231.

8139-23, Poster Session

Flush imaging of fine structures of cellular organelles by contact x-ray microscopy with a high intensity laser plasma x-ray source

M. Kado, M. Kishimoto, M. Ishino, Japan Atomic Energy Agency (Japan); S. Tamotsu, K. Yasuda, Nara Women's Univ. (Japan); Y. Kinjo, Tokyo Metropolitan Industrial Technology Research Institute (Japan); K. Shinohara, Waseda Univ. (Japan)

Conference 8139:
Advances in X-Ray/EUV Optics and Components VI

Laser plasma x-ray sources have high intensity and short pulse duration, and are suitable for x-ray microscopy in biology. They make wet live biological specimens possible to be imaged with a single shot x-ray exposure and several works have been done to image them. However there were no reports on the imaging of fine structures of cellular organelles in a live biological cell since higher x-ray intensity is needed for it. We have developed a high intensity laser plasma x-ray source, cooperating it with contact x-ray microscopy, and observed fine structures of cellular organelles in a wet biological cells.

It is also important to identify obtained features in the x-ray images since the x-ray microscopy is a novel technology and no references have been provided yet to help identify cell organelles. We have proposed to observe the same biological cells with an optical fluorescence microscope and an x-ray microscope for direct comparison to identify cell organelles in the x-ray images. For this purpose, we have developed PMMA photoresist onto transparent glass plate and cultivated biological cells directly on the PMMA photoresist. X-ray images were obtained right after obtaining fluorescence images of them. Comparing the x-ray images and the fluorescence ones of cellular organelles such as actin filaments and mitochondria we have been clearly able to identify those organelles in the x-ray images and to observe fine structures of them.

8139-24, Poster Session

Scaling of laser produced plasma UTA emission down to 3 nm for next generation lithography and short wavelength imaging

A. Endo, Waseda Univ. (Japan); T. Higashiguchi, T. Otsuka, N. Yugami, Utsunomiya Univ. (Japan); P. Dunne, B. Li, T. Cummins, C. O'Gorman, T. Donnelly, G. D. O'Sullivan, Univ. College Dublin (Ireland)

An engineering prototype high average power 13.5-nm source has been shipped to semiconductor facilities to permit the commencement of high volume production at a 100W power level in 2011. In this source, UTA (unresolved transition array) emission of highly ionized Sn is optimized for high conversion efficiency and full recovery of the injected fuel is realized through ion deflection in a magnetic field. By use of a low density target, satellite emission is suppressed and full ionization attained with short pulse CO₂ laser irradiation. The UTA is scalable to shorter wavelengths, and Gd is shown to have similar conversion efficiency to Sn (13.5nm) at a higher plasma temperature, with a narrow spectrum centered at 6.7nm, where a 70% reflectivity mirror is anticipated. Optimization of short pulse CO₂ laser irradiation is studied, and further extension of the same method is discussed, to realize 100W average power down to a wavelength of 3 nm.

8139-25, Poster Session

Improved resolution for soft-x-ray monochromatization using lamellar multilayer gratings

R. van der Meer, B. Krishnan, Univ. Twente (Netherlands); I. V. Kozhevnikov, A.V. Shubnikov Institute of Crystallography (Russian Federation); M. J. de Boer, Univ. Twente (Netherlands); B. Vratzov, NT&D - Nanotechnology and Devices (Germany) and Univ Twente (Netherlands); B. M. Bastiaens, J. Huskens, W. van der Wiel, K. J. Boller, Univ. Twente (Netherlands); F. Bijkerk, FOM-Institute for Plasma Physics Rijnhuizen (Netherlands)

Lamellar Multilayer Gratings (LMG) offer improved resolution for soft-x-ray (SXR) monochromatization, while maintaining a high reflection efficiency in comparison to conventional multilayer mirrors (MM). A Coupled-Waves Approach (CWA) was used to calculate SXR diffraction by LMGs. From this CWA, a single-order regime was identified in which the incident wave only excites a single diffraction order. It was shown that

in this regime the angular width of the zeroth-order diffraction peak, and thus the resolution, simply scales with Γ (lamel-to-period ratio) without loss of peak reflectivity. To obtain maximal peak reflectivity the number of bi-layers must be increased by a factor of $1/\Gamma$. Optimal LMG resolution and reflectivity is obtained in this single-order regime, requiring grating periods of only a few hundred nm, lamel widths $1\mu\text{m}$ [1].

For the fabrication of LMGs with these dimensions, a novel process based on UV-Nanolithography (UV-NIL) and modified Bosch etching is used. Successful fabrication of LMGs with periods down to 200nm, line widths of 60nm and multilayer stack heights of $1\mu\text{m}$ is demonstrated. SXR reflectivity measurements have been performed on these LMGs at the PTB beamline at the BESSYII synchrotron facility. The resolution is demonstrated to be improved by a factor of 4 compared to conventional MM. Further analysis of these SXR reflectivity measurements is currently being performed.

[1] I.V. Kozhevnikov, R. van der Meer, H.M.J. Bastiaens, K.-J. Boller and F. Bijkerk, Opt. Exp. 18, 16234 (2010)

8139-27, Poster Session

Development of a specimen holder combined with ultra thin film laser plasma x-ray source for compact contact-type soft x-ray microscope to observe hydrated living biological cells

M. Ishino, M. Kado, Japan Atomic Energy Agency (Japan); K. Shinohara, Waseda Univ. (Japan); Y. Yamamoto, I. Hirai, Osaka Univ. (Japan); M. Kishimoto, M. Nishikino, N. Hasegawa, Japan Atomic Energy Agency (Japan); S. Tamotsu, K. Yasuda, Nara Women's Univ. (Japan); T. Kawachi, Japan Atomic Energy Agency (Japan)

Ultra thin gold films having a thickness of few ten nano-meter are favorable laser plasma source targets for a soft x-ray microscope, because ultra thin films emit intense soft x-rays of water window region from the rear side with respect to the surface of short pulse laser irradiation. Using rear side emissions, the distance between the x-ray source and the specimens can be reduced and the short distance increases the x-ray flux on specimens. In addition, the microscope system is designed to be compact, when the specimen holder and x-ray source are combined in one piece.

The biological specimen holder combined with a gold ultra thin film plasma target has been developed for a contact-type soft x-ray microscope. This x-ray microscope system does not need any x-ray optics such as a condensed and/or an objective optics causing a degreasing of x-ray photons. Specimen holder equipped with the plasma target keeps biological specimens in wet condition from vacuum. X-ray images of hydrated living macrophages have been obtained successfully by use of the newly developed specimen holder. These experimental results reveal that the soft x-ray image can be taken safely before the debris from plasma target reaching to specimen. Specimen holder combined with plasma x-ray source will be a key component of a compact soft x-ray microscope using in a laboratory.

8139-28, Poster Session

Fabrication of micro accelerator platform for x-ray applications

J. Zhou, J. McNeur, G. Travish, Univ. of California, Los Angeles (United States); R. Yoder, Manhattanville College (United States)

With recent advances in nanotechnology, traditionally bulky systems such as particle accelerators can be scaled down to portable sizes. Here we present a prototype micro accelerator platform which is a laser powered optical structure made of dielectric materials on a small chip. As the drive

**Conference 8139:
Advances in X-Ray/EUV Optics and Components VI**

laser comes in and oscillates in the vacuum gap between the dielectrics, the electric field can build up to as high as 1GV/m and electrons travelling through the gap can get an energy boost.

Fabrication of the device involves advanced lithography, various thin film depositions, as well as fine surface finishing. Details of each of the processes will be discussed, and preliminary beam test results will be presented. The reflection and transmission measurements of the prototype device on the drive laser will be presented, and the resonance frequency and strength will be evaluated. This micro-sized structure can be used for electron acceleration to produce radiations such as X-ray in a compact device.

8139-29, Poster Session**Shorter wavelength EUV source around 6.X nm by rare-earth plasma**

T. Otsuka, Utsunomiya Univ. (Japan); D. Kilbane, T. Cummins, C. O’Gorman, T. Donnelly, P. Dunne, G. D. O’Sullivan, Univ. College Dublin (Ireland); W. Jiang, Nagaoka Univ. of Technology (Japan); A. Endo, Waseda Univ. (Japan); T. Higashiguchi, N. Yugami, Utsunomiya Univ. (Japan)

In recent years, dense plasmas have been focused on as high efficiency and high power sources of EUV radiation. The development of sources of EUV emission with a wavelength less than 10 nm is a subject of considerable interest. Wavelengths shorter than 10 nm are especially useful for next generation semiconductor lithography toward the final stage beyond the 13.5-nm EUV source and for other applications, such as material science and biological imaging near the water window. In particular, in our setup, EUV emission at the relevant wavelength is coupled with a Mo/B4C and/or La/B4C multilayer mirror with a reflective coefficient of 40% at 6.5-6.7 nm.

We have demonstrated a laser-produced plasma extreme ultraviolet source around 6.5-6.7 nm using rare-earth targets of Gd and Tb coupled with a Mo/B4C multilayer mirror, attributed to hundreds of thousands of near-degenerate resonance lines in unresolved transition array resonance lines. We have observed the variation of spectral behavior of resonance line emission in Gd plasmas in the 6.7 nm region when different laser wavelengths are used to change the critical electron densities. As the effects of self-absorption on the resonance lines in the Gd plasmas are large, it is important to produce low density plasma using long laser wavelength and/or low-initial target concentration of Gd. The spectrum based on the low initial density target was narrower and more intense than that of the pure solid target. As a result, the maximum CE was observed to be 1.3% and the spectral purity was also improved.

8139-30, Poster Session**Characterization of broadband emission around 40 nm from potassium plasma**

H. Terauchi, M. Yamaguchi, T. Otsuka, Utsunomiya Univ. (Japan); T. Higashiguchi, N. Yugami, Utsunomiya Univ. (Japan) and Japan Science and Technology Agency (Japan); T. Yatagai, Utsunomiya Univ. (Japan); R. M. D’Arcy, P. Dunne, G. D. O’Sullivan, Univ. College Dublin (Ireland)

In recent years, the desorption spectrometer employing a compact, efficient discharge-produced microplasma XUV source in 20-100 nm broadband spectral region has been proposed, which has advantage of not damage or melting the surface even after irradiation. Photon energies of XUV source in 20-100 nm are high enough to induce photochemical reactions in most materials including hydrogen, carbon, and oxygen. We have already demonstrated a 40-nm XUV source which based on discharge-produced potassium plasma at a time-averaged electron temperature of about 12 eV and a current of about 200 A. However, the spectrum of the capillary discharge-produced plasma has the contamination due to a capillary material ablation. So, It is difficult to

understanding the pure potassium plasma emission behavior.

We characterize the emission spectra of a potassium plasma and its temporal behavior at 39 nm. To understanding the potassium spectral behavior without contamination effect, we use a laser-produced plasma to control the plasma parameters by changing the laser intensity and wavelength. Potassium ions produced strong broadband emission around 40 nm ranging from K²⁺ to K⁴⁺ ions at a time-averaged electron temperature of about 12 eV. Emission at 39 nm is caused during the recombining phase and it was reproduced by hydrodynamic simulation which accounted for atomic processes. As the emission spectral behavior of the laser-produced potassium plasma XUV source is similar to that of the hollow cathode-mode discharge-produced plasma spectrum, it indicates that the emission from the discharge-produced plasma occurs in a region of high electron density close to 10²⁰ cm⁻³.

8139-31, Poster Session**Diffraction efficiencies of holographic laminar and blazed types gratings for use in a flat-field spectrometer in an energy range of 50-200 eV for transmission electron microscopes**

T. Imazono, T. Kawachi, M. Koike, Japan Atomic Energy Agency (Japan); M. Koeda, T. Nagano, H. Sasai, Y. Oue, Z. Yonezawa, S. Kuramoto, Shimadzu Corp. (Japan); K. Sano, Shimadzu Emit Co., Ltd. (Japan)

We have been developing a compact wavelength-dispersive soft x-ray spectrometer to be attached to transmission electron microscopes. This spectrometer places emphasis on the low energy region for the demanding analysis of the lithium K emission spectrum (~54.3 eV) in the development of lithium-ion batteries. For this purpose, a flat-field holographic spherical grating of a 1200-lines/mm groove density was designed employing aspheric wavefront recording system. Laminar and blazed master (LM and BM) gratings and their respective replica (LR and BR) gratings were fabricated by holographic exposure and ion-beam etching methods. Absolute diffraction efficiencies in an energy range of 50-200 eV at the angle of incidence of 86 degree were measured by the reflectometer installed in the soft x-ray beamline (BL-11) at SR Center of Ritsumeikan University, Japan. The first order diffraction efficiencies of the LM gratings were 5-20% in the measured energy range and 6-9% at 54.3 eV. Those of the BM gratings strongly depended on the blaze angles but they were 5-27% and ~11%, respectively. The replica gratings of both the laminar and blazed types showed the comparable first-order diffraction efficiencies with their respective master gratings.

8139-33, Poster Session**High spatial resolution with zoomable sawtooth refractive lenses?**

W. H. Jark, Sincrotrone Trieste S.C.p.A. (Italy)

Sawtooth refractive lenses for x-ray focusing can easily be visualised as opened alligators mouths. The mouth closure provides zooming as it changes the amount of prism to traverse for off-axis rays. Optically speaking the material distribution in such a device follows stepwise a parabola. As such it would focus x-rays as long as one can consider it to be a “thin lens”. This approximation is only valid for rather long focal lengths. In fact high spatial resolution will require shorter focal length for which the lens structure is “thick”. It will be shown that this limits the obtainable spatial resolution to just submicrometer dimensions. This limitation can be overcome with some systematic modifications on the structure. Then Fermat’s principle of constant optical paths can be respected even in thick lenses and consequently the lens could finally provide diffraction limited focusing. The lens remains partly zoomable and the spatial resolution can be identical to the ultimate resolution obtainable with stacks of identical refractive lenses.

Conference 8139:
Advances in X-Ray/EUV Optics and Components VI

8139-34, Poster Session

The effect of surface residual stress on the performance of high quality x-ray mirrors

J. A. Maj, Argonne National Lab. (United States)

The use of high quality X-ray mirrors on synchrotron beamlines as low-pass, harmonic rejection and even high heat load optical elements has become routine. Nearly perfect optical surfaces generated on substrates held in strain-free fixtures are of paramount importance to their success. Production of these mirrors requires extensive care, yet the effect of residual fabrication stresses has not been closely studied. This paper examines the effect of surface and near-surface residual stress on the performance of hard X-ray mirrors using topography, surface diffraction and X-ray reflectivity techniques. The present approach complements the information provided by standard optical metrology, giving a more comprehensive understanding of polishing induced mirror deformation on X-ray reflectivity. This information is invaluable for the characterization of future, coherence preserving optics where scattering and evanescent sub-surface X-ray penetration may impact beam quality.

* The submitted manuscript has been created by UChicago Argonne, LLC, Operator of Argonne National Laboratory ("Argonne"). Argonne, a U.S. Department of Energy Office of Science laboratory, is operated under Contract No. DE-AC02-06CH11357. The U.S. Government retains for itself, and others acting on its behalf, a paid-up nonexclusive, irrevocable worldwide license in said article to reproduce, prepare derivative works, distribute copies to the public, and perform publicly and display publicly, by or on behalf of the Government.

8139-35, Poster Session

Metrology of a Pt-coated nested x-ray focusing KB mirror system

J. Qian, B. Shi, W. Liu, L. Assoufid, Argonne National Lab. (United States)

This poster describes surface metrology of a nested KB mirror system designed to focus polychromatic hard x-rays from the 34-ID beamline at the Advanced Photon Source (APS). The two mirrors were fabricated at the APS using profile coating [1]. One of the mirrors, horizontal mirror, exhibits a height-error-accuracy of 0.76 nm rms and the vertical mirror is 3 nm rms. The mirror system produced a 2-D focal spot size of 150 nm x 150 nm with the focal length of 60 mm.

Reference:

1. Bing Shi, Chian Liu, Jun Qian, Wenjun Liu, Lahsen Assoufid, Ali Khounsary, Raymond Conley, Jr., and Albert T. Macrander, "Platinum Kirkpatrick-Baez mirrors for a hard x-ray microfocusing system made by profile coating," Proc. SPIE 7802, 780200 (2010)

* This work is supported by the U. S. Department of Energy, Office of Science, Office of Basic Energy Sciences, under Contract No. DE-AC02-06CH11357.

8139-36, Poster Session

X-ray topography study of sapphire and quartz single crystals for high-resolution x-ray spectroscopic analyzers

R. Khachatryan, X. Huang, M. Wiczorek, J. Maj, Argonne National Lab. (United States)

Single crystals of silicon and are most preferred conventional crystals for fabricating X-ray spectroscopic analyzers. While silicon and germanium have a highly symmetric, mono-atomic diamond crystal structure, sapphire [1] and quartz have more complex unit cells of lower symmetry with two different types of atoms. The reduced symmetry leads to more than one order of magnitude of more possible backscattering planes

to match unique photon energies to be studied. The larger unit cells of sapphire or quartz with reduced symmetry also means that most of the reflections tend to have weaker scattering contributions per reflecting lattice plane, so more planes contribute to a Bragg reflection, resulting in a narrower bandwidth and better resolution. Therefore, sapphire and quartz are promising crystals for making next-generation spectroscopic analyzers, particularly for resonant inelastic X-ray scattering (RIXS) analyzers with high energy resolution in the range from of 1-20 meV. Compared with silicon and germanium crystals which are generally defect free, however, commercial sapphire and quartz crystals may contain various crystalline defects, such as dislocations, inclusions, voids, and growth sector boundaries, that can significantly affect the bandpass, efficiency, and focusing properties of the analyzers [2]. In order to evaluate the general crystalline quality and to choose the best available crystals as substrates for analyzers, we have used synchrotron white beam X-ray topography to study sapphire crystals (as well as quartz) acquired from different vendors. In this presentation we will present the detailed results of X-ray topography and double-crystal rocking curve measurements from these crystals. In particular, we will demonstrate how the defects affect the X-ray reflection efficiency and bandpass of the analyzers from comparison of different samples with different qualities.

1. H. Yavas, E.E. Alp, Harald Sinn, A. Alatas, A.H. Said, Y. Shvid'ko, T. Toellner, R. Khachatryan, S.J.L. Billinge, M. Zahid Hasan, W. Sturham. Nuclear Instruments and Methods in Physics Research 582,149(2007)
2. J.P. Sutter, A.Q.R. Baron, D. Miwa, Y. Nishino, K.Tamasaku, T. Ishikawa. J. Synchrotron Rad.13,278(2006)

8139-37, Poster Session

Characterization of beryllium foils for coherent x-ray applications of synchrotron radiation and XFEL beamlines

S. Goto, S. Takahashi, Japan Synchrotron Radiation Research Institute (Japan); Y. Inubushi, K. Tono, T. Sato, M. Yabashi, RIKEN (Japan)

We characterized beryllium foils for synchrotron radiation beamline windows especially in coherent x-ray applications and reported that physical-vapor-deposited (PVD) beryllium shows the best performance compared with the conventional powder and ingot beryllium foils. In 2009, however, supplier of PVD foil, Brush Wellman, discontinued the fabrication due to loss of reproducibility by the old PVD machine. We sought an alternative PVD foil and tried to characterize the foils fabricated by NGK Insulators, Ltd. in Japan. Experiments were performed using spatially coherent x-rays at 1-km beamline BL29XU in SPring-8. We observed transmission x-ray images using Hamamatsu zooming tube with spatial resolution of 0.5 microns. X-ray wavelength was 0.1 nm and sample to detector distances were set to be 125 mm and 1580 mm to obtain direct near and diffraction-enhanced far images, respectively. We found that non-uniformity in the 300 microns x 300 microns field is 3% (rms) for the polished 60-micron-thick PVD foil which is almost similar value to that of Brush Wellman. We are reopening the way toward better beryllium window. New foils of NGK will be installed at the first beamline BL3 of XFEL in SPring-8 and will be characterized using fully coherent x-rays of XFEL.

8139-38, Poster Session

Thermal-contact-conductance measurement for high-heat-load optics components at SPring-8

T. Takeuchi, Y. Senba, H. Ohashi, S. Goto, Japan Synchrotron Radiation Research Institute (Japan)

Thermal contact in water or cryogenic cooling is used for high-heat-load component at the synchrotron radiation beamline. Reliable data of the

Conference 8139:
Advances in X-Ray/EUV Optics and Components VI

thermal contact conductance (TCC) are crucial for the design of high-heat-load components in term of insertion material, contact pressure, temperature range, and surface condition. In SPring-8, for example, cryogenic cooling is used for silicon monochromator crystal with indium insertion metal at interface between copper block and silicon crystal. To reduce strain on the silicon crystal with lower contact pressure and higher thermal conductivity, we are seeking the condition of the silicon-indium-copper system and alternative insertion material such as graphite foil. To measure the TCC in quick measurement cycle to obtain under various TCC conditions, we are improving the TCC measurement system regarding setup facilitation, precise temperature measurement, and thermal insulation around sample. Several TCC results in the low-contact-pressure region of 0.1-0.5 MPa will be presented for silicon-indium-copper and silicon-graphite-copper systems.

8139-39, Poster Session

ESRF multilayer white beam test bench

K. Friedrich, C. Morawe, J. Peffen, M. Osterhoff, European Synchrotron Radiation Facility (France)

The ESRF optics group has developed a versatile vacuum chamber to study the impact of the white synchrotron beam on multilayer coatings. The device is equipped with a cooling system for the multilayer samples to distinguish thermal effects from pure radiation induced ones. Various long term irradiation tests were performed on W/B4C, Ru/B4C, and Pd/B4C systems using a high power undulator source with an incoming load up to 200 W. This test bench allows for an in-situ observation of the reflectivity spectrum, complemented by ex-situ measurements before and after the exposure. In the future, the system can be equipped with a Shack Hartmann wave front analyzer to perform in-situ metrology of the multilayer surface.

The work will describe the concept of the white beam test bench and present first experimental results.

8139-40, Poster Session

Experimental test of refractive lenses made from shape memory polymers

G. Pavlov, Institute of Problems of Chemical Physics (Russian Federation); I. I. Snigireva, A. A. Snigirev, European Synchrotron Radiation Facility (France); T. Sagdullin, Institute of Microelectronics Technology and High Purity Materials (Russian Federation)

We present the first experimental study of the focusing properties of two-dimensional parabolic refractive lenses made from shape memory polymers. The lenses were manufacturing using a new technology combining polymer synthesis and product forming at the same stage under the UV radiation. Light activated shape memory polymers allow to produce refractive lenses with high degree of accuracy. The tested lenses have 0.05 mm radius of curvature at the apex of parabola and 2 mm aperture. The experiment was carried out at the Micro Optics Test Bench of the ID06 beamline at the ESRF. The lenses were tested using monochromatic X-rays of 10 keV. Two sets of lenses with focal distances of 6 m and 4 m were used. The lens optical properties in terms of resolution, efficiency and gain were measured. The radiation stability test was performed.

8139-41, Poster Session

Progress on single crystal beryllium windows

A. M. Khounsary, B. P. Lai, J. Ilavsky, Argonne National Lab. (United States); A. Rack, European Synchrotron Radiation Facility (France); S. Goto, Japan Synchrotron Radiation Research Institute (Japan); O. Chubar, Brookhaven National Lab. (United States)

Previously, we reported on the development of highly polished single crystal beryllium windows for X-ray applications. Windows made of single crystal beryllium, unlike the common windows, are essentially free from granular boundaries, voids, impurities, and inclusions in the bulk, thus we have been able to polish them (on both sides) to a few angstrom rms roughness. With a uniform internal structure and smooth surfaces, polished single crystal beryllium windows were expected to transmit an incident X-ray beam without any significant phase perturbation.

In this paper, we report on our X-ray characterization of the single crystal X-ray windows. We show that in comparison with the commercially available windows, single crystal beryllium X-ray windows show significantly less small angle scattering and all but preserve the beam wave front. The cause of sporadic faint features in the transmitted images is discussed and quantified using wave front simulation. Results of brazing and pressure testing of the single crystal windows are presented and discussed.

8139-42, Poster Session

Slumping monitoring of glass and silicone foils for x-ray space telescopes

M. Miika, Institute of Chemical Technology (Czech Republic); L. Pina, Czech Technical Univ. in Prague (Czech Republic); M. Landova, Institute of Chemical Technology (Czech Republic); L. Sveda, Czech Technical Univ. in Prague (Czech Republic); V. Semencova, Rigaku Innovative Technologies Europe (Czech Republic); R. Havlikova, Czech Technical Univ. in Prague (Czech Republic); R. Hudec, Astronomical Institute, ASCR (Czech Republic); A. J. Inneman, Rigaku Innovative Technologies Europe (Czech Republic)

We focused on time monitoring of the thermal slumping of glass and silicone foils. Our goal is the development of optimal technology for producing high quality reflectors for the mirrors of large aperture x-ray space telescopes. Observations delivered by these telescopes could solve many puzzles of current astrophysics. The telescope's crucial part will be a high throughput heavily nested mirror array with the angular resolution not bigger than 5 arcsec. Its construction requires precise and light-weight segmented optics with surface micro-roughness of only few 0.1 nm. Promising materials are glass or silicon foils shaped by thermal forming. In our approach we formed the foils without a mandrel supporting them only at their edges. The desired parameters can be achieved only through optimizing the forming process. To reduce the number of slumping experiments, we can supply some data by modeling. For our model development, we recorded the changing shape of the foils. For 3 hours, we were taking snapshots of the shape every five minutes at constant temperature above the glass transition point. The final shape was measured with the Taylor-Hobson mechanical profilometry. Observed plastic deformation of the foils was controlled by viscous flow. The deflection of the middle part increased practically linearly with time and its speed strongly increased with temperature. We determined the heat-treatment temperature and time for the manufacture of the foils with the radius between 1 and 2 m. These data we utilize in the development of the mathematical model for the optimization of the slumping process.

Conference 8140: X-Ray Lasers and Coherent X-Ray Sources: Development and Applications

Tuesday-Thursday 23-25 August 2011 • Part of Proceedings of SPIE Vol. 8140
X-Ray Lasers and Coherent X-Ray Sources: Development and Applications

8140-01, Session 1

FEL-pumped inner-shell photoionized x-ray laser

N. Rohringer, Lawrence Livermore National Lab. (United States) and Max Planck Advanced Study Group at CFEL (Germany); R. A. London, Lawrence Livermore National Lab. (United States); D. P. Ryan, Colorado State Univ. (United States); J. Dunn, Lawrence Livermore National Lab. (United States); J. J. Rocca, M. A. Purvis, Colorado State Univ. (United States); F. Albert, R. Hill, Lawrence Livermore National Lab. (United States); J. D. Bozek, SLAC National Accelerator Lab. (United States)

Since the invention of the laser fifty years ago, laser amplification of atomic transitions have been extended to increasingly high power and shorter wavelength. We report on the first successful realization of an atomic x-ray lasing scheme based on photoionization of inner-shell electrons in Neon by the Linac Coherent Light Source (LCLS). By focusing LCLS pulses of 960 eV photon energy into a dense Neon gas sample to a micrometer sized spot, a long narrow plasma column is created on a fs time scale by photoionization of a K-shell electron. Thereby, a population inversion of the 2p-1s transition in singly ionized Neon is established, lasting for only 2.7 fs due to the subsequent Auger decay of the created core hole. Fluorescence photons emitted at the front end of the plasma column get amplified by stimulated emission, resulting in ultra bright, high-intensity x-ray pulses at 850 eV photon energy of fs duration at the exit of the plasma column. The experimental results will be discussed in conjunction with theory and self-consistent gain calculations.

8140-04, Session 1

Using the X-FEL to photo-pump x-ray laser transitions in He-like Ne

J. Nilsen, N. Rohringer, Lawrence Livermore National Lab. (United States)

Nearly four decades ago H-like and He-like resonantly photo-pumped laser schemes were proposed for producing X-ray lasers. However, demonstrating these schemes in the laboratory has proved to be elusive because of the difficulty of finding a strong resonant pump line. With the advent of the X-ray free electron laser (X-FEL) at the SLAC Linac Coherent Light Source (LCLS) we now have a tunable X-ray laser source that can be used to replace the pump line in previously proposed laser schemes and allow researchers to study the physics and feasibility of photo-pumped laser schemes. In this talk we use the X-FEL at 1174 eV to photo-pump the singly excited 1s2p state of He-like Ne to the doubly excited 2p3p state and model gain on the 2p3p-2p2s transition at 174 eV and the 2p3p-1s3p transition at 1018 eV. We explore possible quenching of the gain due to strong non-linear coupling effects from the intense X-FEL beam. We compare this with photo-pumping the He-like Ne ground state to the 1s3p singly excited state followed by lasing on the 3p-2s and 3d-2p transitions at 158 and 151 eV. Experiments are being planned at LCLS to study these laser processes and coherent quantum effects.

8140-05, Session 1

Energetics, saturation, and scaling of atomic x-ray lasers pumped by photo ionization from a free electron laser

R. A. London, N. Rohringer, J. Dunn, F. Albert, Lawrence Livermore National Lab. (United States); J. J. Rocca, D. P. Ryan, M. A. Purvis, Colorado State Univ. (United States); J. D. Bozek, SLAC National Accelerator Lab. (United States)

We describe the output characteristics of a Ne K-alpha x-ray laser pumped by a free electron laser. Models are discussed for the geometry, output energy, and gainlength of the atomic laser as related to the density of the gain medium and basic characteristics of the pump, such as the wavelength, energy and focus. The gainlength and power at saturation are estimated. The wavelength scaling of this scheme is discussed.

8140-06, Session 2

Advances in OFI soft x-ray lasers at LOA

S. Sebban, Ecole Nationale Supérieure de Techniques Avancées (France)

Thanks to the most recent works on x-ray laser and on high order harmonics (HHG), it is now possible to produce a 10 Hz soft x-ray energetic laser beam having very high optical qualities. The solution consists in seeding the XRL amplifier medium by a HHG beam. This concept was successfully realized in LOA and an extensive investigation of the source have been performed. Here we present experimental and numerical results on the spatial and spectral characterization of a Ni-like krypton laser seeded by a harmonic beam.

8140-07, Session 2

Spectral width of seeded and ASE XUV lasers: experiment and numerical simulations

A. Klisnick, L. Meng, Univ. Paris-Sud 11 (France); D. Alessi, Colorado State Univ. (United States); O. A. Guilbaud, Univ. Paris-Sud 11 (France); Y. Wang, M. Berrill, B. M. Luther, S. Domingue, L. Urbanski, Colorado State Univ. (United States); D. Benredjem, Univ. Paris-Sud 11 (France); A. Calisti, Univ. de Provence (France); S. M. de Rossi, D. Joyeux, Institut d'Optique Graduate School (France); M. C. Marconi, J. J. Rocca, Colorado State Univ. (United States)

In this paper we will describe our recent progress in the investigation of the spectral properties of collisional XUV lasers, including both experimental measurements and numerical calculations.

Using a wavefront-division, variable path-difference interferometer [1, 2], we have characterized the temporal coherence and the spectral width of an injection-seeded transient XUV laser emitted at 18.9 nm from a Mo plasma, developed at CSU (USA) [3]. Our results show that the temporal coherence of the beam is significantly increased by the injection-seeded operation, compared to the standard ASE mode, while the spectral linewidth is in both cases as small as ~ 3 mÅ. We show that our measurements are supported confirmed by detailed numerical simulations.

Using the PPP code [4] we have calculated the linewidth of the 4d-4p

**Conference 8140: X-Ray Lasers and Coherent X-Ray Sources:
Development and Applications**

(J 0-1) lasing line in Ni-like Mo and Ag over a range of electron density and temperature which are relevant to collisional excitation pumping of XUV lasers. We discuss the relative contribution of homogeneous and inhomogeneous broadening to the overall profile. The variation of the calculated linewidth over with Ne and Te provides an estimate of the ultimate shortest duration that can be reached in the injection-seeded mode, depending on the conditions of density and temperature in the amplification zone.

References

- [1] A. Klisnick et al, J.Q.S.R.T. 99 (2006) 366
- [2] O. Guilbaud et al, Opt. Lett. 35 (2010) 1326
- [3] Y. Wang et al, Phys. Rev. A 79 (2009) 023810
- [4] A. Calisti et al, Phys. Rev. E 81 (2010) 016406

8140-08, Session 2

Fully-coherent wake and ASE-suppressed 20-uJ 150-fs amplified high-order harmonic pulse demonstrated with 1D time-dependent Bloch-Maxwell code

E. Oliva, P. Zeitoun, Ecole Nationale Supérieure de Techniques Avancées (France); M. Fajardo, Univ. Técnica de Lisboa (Portugal); D. Ros, Univ. Paris-Sud 11 (France); S. Sebban, Ecole Nationale Supérieure de Techniques Avancées (France); P. Velarde, Univ. Politécnica de Madrid (Spain)

Seeding plasma-based soft-x-ray lasers (PBSXR) with high order harmonics (HOH) is a promising way to obtain fully coherent, short (hundreds of femtoseconds), tens of microJoules pulses. Nevertheless, up to date only 1 μJ , 1 ps pulses have been demonstrated seeding plasmas created from gas targets [1] and solid targets [2]. As the amplification process couples plasma hydrodynamics, atomic processes and the propagation of electromagnetic fields, a careful optimization of seed and amplifier properties is essential to reach multi-microJoule, hundreds of fs regime. Recent papers [3,4,5] showed that short and wide (up to 1 mm) plasmas present an optimal gain zone and up to 20 μJ could be extracted when seeding. Nevertheless, the temporal duration and profile of the output beam is still not optimal. Simulations show that the HOH is weakly amplified whereas most of the energy is within a long (several picoseconds) wake induced by the HOH [6,7].

In addition to this, these simulation pointed out the presence of deleterious Amplified Spontaneous Emission (ASE). In order to obtain intense pulses useful for practical applications is crucial to reduce the duration to hundreds of fs and obtain ASE-suppressed, structure-free (ideally only an amplified HOH) pulses. Using the 1D Bloch-Maxwell code DeepOne we will show that fully coherent, wake and ASE-suppressed, 20 μJ , 150 fs pulse can be obtained when optimizing at the same time both the seed and the plasma conditions.

8140-09, Session 2

Signal build-up from noise and seeding in plasma based x-ray lasers

C. M. Kim, K. A. Janulewicz, Gwangju Institute of Science and Technology (Korea, Republic of); H. Stiel, Max-Born-Institut für Nichtlineare Optik und Kurzzeitspektroskopie (Germany); M. Nishikino, N. Hasegawa, T. Kawachi, Japan Atomic Energy Agency (Japan); J. Lee, Gwangju Institute of Science and Technology (Korea, Republic of)

In the spectral region of extreme ultraviolet (XUV) or soft x-rays, very successful and reasonably efficient CPA technique cannot be easily employed due to the lack of efficient optical components and sufficiently broadband (in absolute values) gain medium (X-ray laser shows at 10 nm

$\Delta\lambda=0.001$ nm). The typical situation in the current practice is as follows: the weak ultra-short pulse in the form of high harmonic signal has pulse width of few fs ($\Delta\lambda=0.2$ nm) and is amplified in a spectrally much narrower gain medium (plasma) [1]. The relaxation time of the medium macroscopic polarization is longer than the width of the input pulse, and one faces the situation that amplification occurs in the coherent regime. This is a very unique experimental situation. The gain of the medium is very high, reaching 70 cm^{-1} , and the random character of strong spontaneous emission can significantly affect the amplification process. As a consequence, the proper description of the medium kinetics and the interaction process should reflect all these elements which usually are not observed in the optical region.

To take into account all of these elements in the most comprehensive way, we used the model based on Maxwell-Bloch equations without adiabaticity assumption. The model incorporates the random character of spontaneous emission [2,3], time-dependent gain by using the pump function obtained from laser-plasma simulation, and level degeneracy by treating the degenerate states separately. With this model, the complete information on the radiation field, i.e. both amplitude and phase can be obtained. This analysis provides a new perspective on the amplified spontaneous emission and coherent amplification of ultra-short pulses in a high-gain medium.

The typical pulse shape and polarization history of the injected amplified pulse can be traced using this model. Additionally, the same model is able to picture the pulse build-up from the spontaneous noise in an amplified spontaneous emission (ASE)-based x-ray laser (XRL). The experimental results on the XRL pulse shape give us a very useful bench-mark for the validity of the formulated model and its mathematical description. It was found that amplification of the spontaneous noise is accompanied by clear changes in the radiation polarization, however in a limited space (laser mode). These effects will be discussed in detail.

- [1] C. M. Kim, K. A. Janulewicz, H. T. Kim, and J. Lee, Phys. Rev. A 80, 053811 (2009)
- [2] O. Larroche, D. Ros, A. Klisnick, A. Sureau, C. Möller, and H. Guennou, Phys. Rev. A 62, 043815 (2000)
- [3] C. M. Kim, J. Lee, and K. A. Janulewicz, Phys. Rev. Lett. 104, 053901 (2010).

8140-10, Session 2

Strong field amplification of XUV: phase matching aspects

J. Seres, E. Seres, Friedrich-Schiller-Univ. Jena (Germany); B. Ecker, GSI Helmholtzzentrum für Schwerionenforschung GmbH (Germany); B. Landgraf, Friedrich-Schiller-Univ. Jena (Germany); D. C. Hochhaus, D. Zimmer, V. Bagnoud, B. Aurand, B. Zielbauer, T. Kuehl, GSI Helmholtzzentrum für Schwerionenforschung GmbH (Germany); C. Spielmann, Friedrich-Schiller-Univ. Jena (Germany)

The dependence of the yield of high-order harmonic generation (HHG) on several important experimental parameters has been successfully modelled [1]. We extended this description by adding a stimulated emission process and named it self-seeded x-ray parametric amplification (XPA) [2,3]. Beyond the super-quadratic increase of the XUV signal, which can be explained by HHG theory in a limited pressure range, other observed characteristics (exponential growth, gain narrowing, strong blue shift etc.) and their scaling with intensity and pressure [2,3] can only be explained accurately by the new XPA model.

For an experimental verification, we used the femtosecond front-end of the PHELIX laser system delivering 350-fs-long 7 mJ pulses and the JETI laser system delivering 30-fs-long, 1 J pulses, both at a repetition rate of 10 Hz. We focused the laser beam to a diameter, which suitable to reach the necessary peak intensity of about $1\text{-}2\times 10^{14}\text{ W/cm}^2$ for realization of XPA in Argon gas in the spectral range of 40-50 eV. Aside atomic and free electron dispersion we included in our improved model also Gaussian beam, atomic and Gouy phase shifts, and the effect of the group velocity mismatch. This extended XPA theory fully describes the observed scaling

**Conference 8140: X-Ray Lasers and Coherent X-Ray Sources:
Development and Applications**

of the XUV yield with pressure, intensity, jet position, etc. Further steps towards the development of bright x-ray source will be discussed.

- [1] He, X. et al. Phys. Rev. A 79, 063829 (2009)
- [2] J. Seres, et al. Nature Phys. 6, 455 (2010)
- [3] J. Seres, et al. Nature Phys. 6, 927-929 (2010)

8140-11, Session 3**Coherent x-ray generation in relativistic laser - gas jet interactions**

A. S. Pirozhkov, M. Kando, T. Z. Esirkepov, Japan Atomic Energy Agency (Japan); P. Gallegos, Rutherford Appleton Lab. (United Kingdom); E. N. Ragozin, P.N. Lebedev Physical Institute (Russian Federation); A. Y. Faenov, T. A. Pikuz, J. K. Koga, H. Kiriya, Japan Atomic Energy Agency (Japan); P. McKenna, Univ. of Strathclyde (United Kingdom); M. Borghesi, Queen's Univ. Belfast (United Kingdom); K. Kondo, H. Daido, Japan Atomic Energy Agency (Japan); Y. Kato, The Graduate School for the Creation of New Photonics Industries (Japan); D. Neely, Rutherford Appleton Lab. (United Kingdom); S. V. Bulanov, Japan Atomic Energy Agency (Japan)

We present experimental results, theory, and simulations concerning two novel sources of coherent x-ray radiation generated in the relativistic laser-plasma interactions ($>10^{18}$ W/cm²) employing gas jet targets.

The first source is based on a relativistic mirror reflecting a counter-propagating laser pulse. A strongly nonlinear breaking wake wave driven by an intense laser pulse can act as a partially reflecting relativistic mirror (the Flying Mirror). Such a mirror directly converts a laser pulse into a high-frequency (XUV or x-ray) ultrashort pulse due to the double Doppler effect. In the experimental demonstration with a 9TW J-KAREN laser, the Flying Mirror generated in a He gas jet partly reflected a 1TW pulse, providing up to $\sim 10^{10}$ photons, 60nJ ($\sim 10^{12}$ photons/sr) in the XUV (12.8-22 nm).

The second source, demonstrated experimentally with the 9TW J-KAREN and 120TW Astra Gemini lasers, is based on a novel harmonic generation mechanism. Odd and even order harmonics are emitted forward out of the gas jet; such harmonics are generated by linearly as well as circularly polarized pulses. For example, the 120TW laser pulses produced harmonics with $\sim 2 \times 10^{13}$ photons/sr (~ 300 uJ/sr) in the spectral range from 115 to 125eV. The experimentally demonstrated harmonics cannot be explained by previously known mechanisms (atomic harmonics, betatron radiation, nonlinear Thomson scattering, etc). We introduce a novel harmonic generation mechanism based on the relativistic laser-plasma phenomena (self-focusing, cavity evacuation, bow wave generation), mathematical catastrophe theory which explains the formation of electron density singularities (cusps), and collective radiation of a compact charge driven by a relativistic laser.

8140-12, Session 3**Ultrafast nanoscale imaging using high order harmonic generation**

H. Merdji, Commissariat à l'Énergie Atomique (France)

Ultrafast coherent diffraction using soft and hard X-rays is actually revolutionizing imaging science thanks to new sources recently available. This powerful technique extends standard X-ray diffraction towards imaging of non-crystalline objects and leads actually to a strong impact in physics, chemistry and biology. New ultrashort pulses recently available hold the promise of watching matter evolving with unprecedented space and time resolution. Femtosecond coherent and intense radiation in the soft X-ray ($\lambda = 10$ -40 nm) is currently produced in our laboratory, from highly non linear frequency conversion (high harmonic generation). A high intensity UV-X coherent beam is obtained using a loose focusing

geometry, which allows coupling a very high amount of Ti:Sapphire laser system energy in the HHG process. Using a long gas cell and a long focal length lens, the emitting volume can be increased by orders of magnitude compared to standard HHG set-ups. This approach, allows reaching up to 1×10^{11} photons per shot for the 25th harmonic ($\lambda = 32$ nm).

We have recently taken up the challenge of ultrafast coherent imaging of nanometric objects, such as nano-particles using our table-top soft X-ray source. We have very recently demonstrated nanoscale imaging in a single shot mode reaching 70 nm spatial resolution and 20 femtoseconds snapshot [1]. We then implemented a recently proposed holographic technique using extended references. This technique, easy to implement, allows a direct non iterative image reconstruction. In the single shot regime, we demonstrated a spatial resolution of 110nm.

This opens fascinating perspectives in imaging dynamical phenomena to be spread over a large scientific community. We will briefly present perspectives in the investigation of femtosecond phase spin-reversals of magnetic nano-domains or ultrafast molecular rearrangements.

- [1] A. Ravasio et al., Physical Review Letters 103, 028104 (2009).
- [2] D. Gauthier et al., Physical Review Letters 105, 093901 (2010).

8140-13, Session 3**Application of XUV high harmonics to attosecond nonlinear spectroscopy**

K. Midorikawa, RIKEN (Japan)

There has been growing interest in applying high-order harmonic fields to atomic/molecular physics in the XUV region. However, the application of ultra-broadband nature of high harmonic spectra has not been explored yet. We have proposed and demonstrated Attosecond Nonlinear Fourier Transform Spectroscopy for investigating the ionization/dissociation pathway induced by a two or more photon process with high-order harmonics [1, 2]. The unique feature of this method is the use of the autocorrelation technique for measuring the pulse shape of an attosecond pulse train and relies on the extremely broad harmonic spectra of the attosecond pulse train ranging from visible to extreme ultraviolet region.

This spectroscopy would be also beneficial for other intense extreme ultraviolet-soft X-ray light sources, such as X-ray free electron lasers, which are utilized for exploring the nonlinear interaction of high-energy photon with matter, because we can eliminate the strong background signals due to ions or electrons produced by one-photon absorption if we apply this spectroscopy.

References

- [1] T. Okino, K. Yamanouchi, T. Shimuzu, R. Ma, Y. Nabekawa, and K. Midorikawa, J. Chem. Phys. 2008, 129, 161103.
- [2] Y. Furukawa, Y. Nabekawa, T. Okino, S. Saugout, K. Yamanouchi, and K. Midorikawa, Phys. Rev. A 2010, 82, 013421

8140-14, Session 3**Polarization control of high order harmonics in the EUV photon energy range**

B. Vodungbo, Ecole Nationale Supérieure de Techniques Avancées (France)

Several attempts have been made to obtain circularly polarized harmonics. For example, already in the 1990's, it has been shown that using an elliptically polarized driving laser, elliptically polarized harmonics could be obtained. The generation efficiency, however, drops dramatically with increasing ellipticity of the driving laser. More recently, elliptically polarized harmonics have been obtained in molecular gases, but the degree of circular polarization is low (< 40 %). We also note that all these previous studies have focused on rather low order harmonics and only sparse data are available for wavelengths lower than 25 nm.

In contrast to these previous reports, we chose a two-step procedure to

**Conference 8140: X-Ray Lasers and Coherent X-Ray Sources:
Development and Applications**

obtain circularly polarized harmonics. First, linearly polarized harmonics are generated as efficiently as possible by focusing a linearly polarized infrared laser (40 fs, 0.25 TW) into a neon filled gas cell. Second, these harmonics are circularly polarized by a four-reflector phase-shifter. By this method we obtained fully circularly polarized high harmonics in the extreme ultraviolet range (18 - 27 nm). The efficiency of the polarizer has been measured and is of the order of a few percents thus being significantly more efficient than currently demonstrated direct generation of elliptically polarized harmonics. This demonstration opens up new experimental capabilities based on high order harmonics, for example, to observe chiral molecules in biology or magnetic structures in materials science.

8140-15, Session 4

Stable and fully controlled long-time operation of a soft X-ray laser for user applications experiments

D. Ros, Univ. Paris-Sud 11 (France)

LASERIX is a high power laser facility intended to realize and use for applications transient collisional X-ray lasers at various wave-lengths. In addition new types of XRL schemes giving rise to emission at short wavelengths will be developed using the high energy LASERIX driver. Thus, this laser facility will both offer Soft X-ray lasers in the 30-7 nm range and auxiliary IR beam that could be also used to produce XUV sources. This experimental configuration highly enhances the scientific opportunities of the facility. In-deed it will be possible to realize both X-ray laser experiments and more generally pump/probe experiments, mixing IR and XUV sources.

8140-16, Session 4

Probing of high energy density plasmas using EUV and x-ray lasers

G. J. Tallents, L. Wilson, D. S. Whittaker, E. Wagenaars, The Univ. of York (United Kingdom)

Probing of high energy density plasmas using extreme ultra-violet (EUV) and x-ray lasers is shown to be a useful technique to deduce plasma parameters such as opacity. We will discuss potential pump-probe experiments which will be possible with plasma based EUV lasers and x-ray free electron lasers (XFELs). Our modelling studies show that solid carbon and iron can be heated by focused XFEL pulses of irradiance 10^{17} Wcm⁻² so that after a picosecond or so equilibrium plasmas of temperatures up to 400 eV are produced in a uniform solid density of micron thickness. A low intensity probe pulse can then be used to measure the opacity or other parameters of such plasmas before expansion (on timescale > ps) causes departures from solid density. Similar experiments can be carried out with laboratory based EUV lasers and we will report an investigation being undertaken at the LASERIX facility in France.

8140-17, Session 4

Observation of the laser-induced surface dynamics by the single-shot x-ray laser interferometer

N. Hasegawa, Japan Atomic Energy Agency (Japan)

The dynamical processes of the laser-induced surface modifications such as laser ablation come to attract much attention for the micro processing by the ultra-short laser pulse. It is difficult to observe these phenomena directly, because they are non-repetitive, unrepeatable, and occur very rapidly (pico-second) in a very small (micron) area. We have developed a soft x-ray laser (SXRL) interferometer capable of the single-shot imaging

of the nano-scale structure dynamics. The SXRL is suitable for probing the initial process of the surface morphological changes, because it has a short wavelength (Ni-like Ag, 13.9 nm) and short duration (< 10ps). It can precisely probe the surface, because the penetration depth for the material is very small (<10 nm). The interferometer consists of the reflection optics (Mo/Si multi-layer or Pt-plated mirrors) and the interference fringes are produced on the detector surface by a pair of mirrors having a relative incline angle (double Lloyd's mirrors). The depth and lateral resolutions of the interferometer were around 1 nm and 1.8 μ m, respectively. By using this interferometer, the very early stage of the ablation process was observed for the Pt surface irradiated with the 70 fs Ti:sapphire laser pulse.

In addition, we have developed a method of precise temporal synchronization between the SXRL and the pump laser (Ti:sapphire laser) by using the temporal fiducial light produced from the pump laser. The SXRL and the fiducial light were measured by the x-ray streak camera. The precision was better than a few pico-seconds, which is comparable with the SXRL pulse width.

8140-18, Session 4

Coherent XUV sources for applications

O. A. Guilbaud, S. Kazamias, K. Cassou, M. Pitmann, S. Daboussi, B. Cros, J. Lagron, G. Maynard, Univ. Paris-Sud 11 (France); S. Bastiani, Ecole Polytechnique (France); L. Meng, A. Klisnick, D. Ros, Univ. Paris-Sud 11 (France)

During the last session of SPIE conference important progress in compact coherent XUV sources were presented. The practical adaptation of sources schemes to applications is now becoming an important issue for facilities proposing beam lines based on this kind of sources.

In this paper we will describe recent work performed with the LASERIX facility in order to develop sources for applications. During the last SPIE conference, we presented a setup enabling the generation of soft x-ray laser with only one beam (D. Zimmer et al. Optics letters 2010) enabling a more stable operation. Comparison with the classical GRIP scheme will be discussed in terms of output energy, source size and reproducibility. The possibility of generating high order harmonic in parallel (i.e with the presence of an important long pulse before the main pulse) will also be discussed.

The presence of a small prepulse arriving prior to the two main pulses led to a longer target lifetime enabling real 10Hz soft x-ray laser operation on an hour timescale. Preliminary interpretation of this phenomenon will be presented.

We will also describe an hosted experiment dedicated to the temporal characterisation of a GRIP x-ray laser using a picosecond resolution streak camera.

Because the driving laser of LASERIX is a high energy Ti-Sa laser, it is possible to generate high order laser harmonic in parallel of soft x-ray laser. We will conclude this paper by a presentation of theoretical and experimental work performed on this subject. We will emphasize the experimental efforts undertaken to achieve high order harmonic generation in capillary waveguide and to obtain quasi-phase matching in multimode regime.

8140-19, Session 5

Advances in high repetition rate table-top soft x-ray lasers

J. J. Rocca, Y. Wang, D. Alessi, B. M. Luther, B. A. Reagan, D. H. Martz, A. H. Curtis, K. Wernsing, M. Berrill, V. N. Shlyaptsev, F. J. A. Furch, Colorado State Univ. (United States)

We will discuss recent advances in the development of ASE-based and injection-seeded high repetition rate table-top soft x-ray lasers resulting from research conducted at Colorado State University. We have recently reported gain-saturated operation of a table-top 10.9 nm wavelength

**Conference 8140: X-Ray Lasers and Coherent X-Ray Sources:
Development and Applications**

laser operating at 1 Hz repetition in the 4d1S0→4p1P1 transition of nickel-like Te in a plasma excited by a newly developed high energy Ti:sapphire pump laser. Utilizing the same pump laser we obtained laser pulse energies of up to 10 μJ and an average power of 20 μW in the 13.9 nm line of Ni-like Ag. Efforts conducted to extend these result to shorter wavelengths will be discussed. We will also report results of studies conducted to characterize the properties of the beams resulting from injection-seeding solid-target plasma amplifiers with high harmonic pulses.

We will also discuss the development of all-diode-pumped soft x-ray lasers. Efficient pumping of the driver laser with diode lasers opens the possibility to develop a new generation of higher repetition rate, more compact, soft x-ray lasers for applications. In the first demonstration of a diode pumped soft x-ray laser we achieved lasing at 10 Hz repetition rate lasing in 18.9 nm wavelength line of Ni-like Mo ions using a cryo-cooled Yb:YAG chirped-pulse-amplification pump laser system. The status of the development of this new soft x-ray laser will be reviewed.

8140-20, Session 5**Towards high photon-number soft x-ray lasers**

B. Ecker, Gesellschaft für Schwerionenforschung GmbH (Germany) and Johannes Gutenberg Univ. Mainz (Germany) and Helmholtz-Institut Jena (Germany); B. Aurand, Gesellschaft für Schwerionenforschung GmbH (Germany) and Johannes Gutenberg Univ. Mainz (Germany) and ExtreMe Matter Institute (Germany); D. C. Hochhaus, Gesellschaft für Schwerionenforschung GmbH (Germany) and ExtreMe Matter Institute (Germany) and Frankfurt Institute for Advanced Studies (Germany); T. Kuehl, Gesellschaft für Schwerionenforschung GmbH (Germany) and Johannes Gutenberg Univ. Mainz (Germany) and Helmholtz-Institut Jena (Germany); P. Neumayer, Gesellschaft für Schwerionenforschung GmbH (Germany) and ExtreMe Matter Institute (Germany) and Frankfurt Institute for Advanced Studies (Germany); H. Zhao, B. Zielbauer, Gesellschaft für Schwerionenforschung GmbH (Germany) and Helmholtz-Institut Jena (Germany); D. Zimmer, Gesellschaft für Schwerionenforschung GmbH (Germany) and Johannes Gutenberg Univ. Mainz (Germany); K. Cassou, S. Daboussi, O. A. Guilbaud, S. Kazamias, D. Ros, Univ. Paris-Sud 11 (France); P. Zeitoun, Ecole Nationale Supérieure de Techniques Avancées (France)

A novel route of soft x-ray laser (SXRL) development at GSI is aiming at an increase in photon numbers, pursuing the ambition of providing a high-brilliance XUV light source that can be used for plasma diagnostics like Thomson scattering [1], radiography or interferometry. In order to achieve this goal we designed a new pumping geometry called Butterfly configuration, which allows for simultaneously pumping two SXRL targets. The setup utilizes both the new double-beam option of the PHELIX laser and a Mach-Zehnder interferometer to provide two individual double-pulse pump beams. We will report on two recent experimental campaigns investigating a single- and double-target configuration. The first will be dedicated to the study of the influence of the line focus width [5], with special interest in the losses due to transverse lasing. The second will concentrate on using the optimized output of the first SXRL target as a seed source for the second SXRL target. Former double-stage SXRL experiments have successfully proven an amelioration in the SXRL beam quality [2-4], however a gain in photon number by seeding is still to be demonstrated. We will present our newly developed pumping scheme and compare the results obtained from the experimental campaigns with ARWEN simulations.

[1] G. Gregori, Experiment Proposal at PHELIX (2009)

[2] S. Sebban, Physical Review A, Vol. 61, Issue 4 (2000)

[3] M. Tanaka, Opt. Lett. 28, 1680-1682 (2003)

[4] M. Nishikino, Appl. Opt. 47, 1129-1134 (2008)

[5] E. Oliva, Opt. Lett. 34, 2640-2642 (2009)

8140-21, Session 5**Bloch-Maxwell modelling of multi-mJ 100-fs fully-coherent amplified high-harmonic pulse**

P. Zeitoun, E. Oliva, Ecole Nationale Supérieure de Techniques Avancées (France)

With their unmatched yield up to 10¹⁵ photons (12 mJ) per pulse [1], i.e. about 1,000 times the typical energy/pulse of soft X-ray free-electron lasers, laser-created plasma remained the most promising soft X-ray amplifier. However, such high energy is achieved so far only in the regime of Amplification of Spontaneous Emission (ASE) coupled with the so-called Quasi-steady-state (QSS) pumping scheme. Such conditions are known for producing weakly coherent and very long, 100 ps, pulses, limiting their attractiveness to some specific applications. Attempt in seeding with high harmonics such plasma led to weakly amplified seed overwhelmed by the ASE [2]. Using our 1D time-dependant Bloch-Maxwell code, DeepOne, we clarified the bottlenecks in seeding QSS amplifiers. We thus proposed and numerically tested a new seeding regime demonstrating unprecedented fully coherent pulse with multi-mJ energy and 100 fs duration [3].

1- Rus B. et al, Phys. Rev A 66, 063806 (2002)

2- Ditmire T. et al, Phys. Rev. A, 51, 6 (1995)

3- Zeitoun P. et al, submitted for publication.

8140-22, Session 5**Coherent x-ray mirage**

N. M. Nagorskiy, S. A. Magnitskii, Lomonosov Moscow State Univ. (Russian Federation); A. J. Faenov, T. A. Pikuz, Joint Institute for High Temperatures (Russian Federation); M. Tanaka, M. Kishimoto, M. Ishino, M. Nishikino, Y. Fukuda, M. Kando, T. Kawachi, Japan Atomic Energy Agency (Japan); Y. Kato, The Graduate School for the Creation of New Photonics Industries (Japan)

Mirage in the X-ray spectral range has been detected for the first time. Experimentally interference rings in spatial profile of output radiation of the transient oscillator-amplifier X-ray laser were observed. The rings are consistently recorded both in a single laser shot and at averaging over many laser flashes. It is shown that a virtual X-ray point source emerges in the vicinity of the second plasma when amplification takes place. This virtual source is phased with the initial radiation of generator and is formed as optical mirages emerge in the earth atmosphere.

The experiment with the soft X-ray laser (SXRL) facility has been performed at Kansai Photon Science Institute (KPSI) of Japan Atomic Energy Agency (JAEA). The spatially coherent SXRL pulse was generated from the silver plasma mediums using an oscillator-amplifier configuration with Ag foil double targets. The generated SXRL beam from Ag double targets had a wavelength of 13.9 nm, bandwidth of less than 10⁻⁴, pulse duration time of 7 ps, and a beam divergence of 1.2 mrad (H) x 0.4 mrad (V). The SXRL system worked in 0.1 Hz regime with the output energy of the order of 300 nJ.

The registered effect can be used as a principle method of X-Ray lithography in the manufacture of large-scale integrated circuits.

8140-23, Session 6

Applications of the LCLS x-ray free electron laser for high-energy density science

R. W. Lee, Lawrence Livermore National Lab. (United States); P. Audebert, M. Gauthier, A. Levy, Ecole Polytechnique (France); M. Cammarata, D. M. Fritz, H. J. Lee, B. Nagler, SLAC National Accelerator Lab. (United States); F. Deneuille, C. Fourment, Univ. Bordeaux 1 (France); J. Gaudin, European XFEL GmbH (Germany); B. I. Cho, P. A. Heimann, Lawrence Berkeley National Lab. (United States); J. Dunn, A. Graf, S. J. Moon, R. L. Shepherd, A. Steel, Lawrence Livermore National Lab. (United States); H. Chung, International Atomic Energy Agency (Austria); M. Fajardo, G. Williams, Univ. Técnica de Lisboa (Portugal); O. Ciricosta, S. M. Vinko, J. S. Wark, Univ. of Oxford (United Kingdom)

LCLS, the first x-ray FEL has been operational since late 2009. The facility provides x-ray from 600 eV to 10 keV in the fundamental. The LCLS operates at 120 Hz, with pulses from ≤ 10 fs to 300fs containing up to 3mJ of energy. We will discuss the implementation of early High Energy density Science experiments that have been performed. These experiments cover LCLS-solid interaction which measured the spectral response, high pressure warm dense matter creation, self-Thomson scattering from solid and liquid jet samples, scattering from shocks, and x-ray generated cluster explosions. These experiment were performed in the extant end station, while the MEC (Matter in Extreme Conditions) end station is being constructed. A brief discussion of the MEC, which will be ready for users in January 2012, will be presented

8140-24, Session 6

Coherent x-ray imaging at the Linac Coherent Light Source

M. M. Seibert, G. J. Williams, S. Boutet, SLAC National Accelerator Lab. (United States)

Cohernet X-ray imaging at the LCLS is supported by a dedicated instrument on the hard X-ray line in the far experimental hall. The CXI instrument combines X-ray focusing optics and diagnostics, a sample environment and a pixel array detector, i.e. all components necessary for coherent diffraction experiments. The optics provide 100nm, 1 μ m and 10 μ m focal spots at the sample interaction region though the use of Beryllium lenses and KB mirrors. The sample chamber houses a five degree of freedom holder for fixed targets, holds a gas-phase injector designed around an aerodynamic lens and provides various ports for integration of user supplied hardware, such as custom sample delivery systems and diagnostics. Diffraction patterns are recorded on the Cornell SLAC - Pixel Array Detector (CS-PAD). This modular detector consists of 32 silicon direct-detection chips bump bonded to Application Specific Integrated Circuits (ASICs) and arranged in four quadrants around a central hole. Each of the 2M pixels is 110 x 110 μ m in size and the dynamic range is greater than 10^3 . The detector can be positioned at various distances from the interaction region. The distance available in the forward scattering geometry, with the detector downstream of the sample chamber ranges from 2.5m. Of this travel range, 0.5m is provided by an in-vacuum translation stage that allows moving the detector during the experiment. Additionally, the detector chamber can be mounted upstream of the sample to record backscattering.

First nanocrystallography experiments with the CXI instrument have shown diffraction from protein crystals to a resolution of better than 2 Å .

8140-25, Session 6

Spectroscopic studies of hard x-ray free-electron laser-heated foils at 1016 Wcm-2 irradiances

J. Dunn, R. L. Shepherd, A. Graf, A. Steel, J. Park, R. W. Lee, Lawrence Livermore National Lab. (United States); P. Audebert, A. Levy, M. Gauthier, J. Fuchs, Ecole Polytechnique (France); D. M. Fritz, M. Cammarata, D. Milathianaki, H. J. Lee, B. Nagler, SLAC National Accelerator Lab. (United States); C. Fourment, F. Deneuille, Univ. Bordeaux 1 (France); G. Williams, M. Fajardo, Univ. Técnica de Lisboa (Portugal); J. Gaudin, European XFEL GmbH (Germany); S. M. Vinko, O. Ciricosta, J. S. Wark, Univ. of Oxford (United Kingdom)

We report a recent experiment where the first hard x-ray beam line, X-ray Pump Probe (XPP) instrument at the Stanford Linac Coherent Light Source (LCLS) free electron laser, was used to heat thin foils to high energy densities ~ 107 J/cm³. An intense 9 keV, 60 fs duration beam with energy of 2 - 4 mJ at the XPP beam line was focused using beryllium lenses to an irradiance approaching 1016 Wcm⁻². Targets of 0.5 - 4 μ m thick foils of Ag and Cu were studied using a suite of diagnostics including Fourier Domain Interferometry, energy calorimetry and grating and crystal spectrometers. The experimental details and spectroscopic results from the campaign will be described.

This work performed under the auspices of the U.S. Department of Energy by Lawrence Livermore National Laboratory under Contract DE-AC52-07NA27344. The experiment was carried out at the Linac Coherent Light Source, a National User Facility operated by Stanford University for the US Department of Energy

8140-26, Session 6

Hard X-FEL source diagnostics and beamline optics metrology at LCLS using a grating interferometer

S. Rutishauser, O. Bunk, Paul Scherrer Institut (Switzerland); J. Grünert, H. Sinn, L. Samoylova, European XFEL GmbH (Germany); J. Krzywinski, M. Cammarata, D. M. Fritz, SLAC National Accelerator Lab. (United States); C. David, Paul Scherrer Institut (Switzerland)

X-ray grating interferometry is a method for differential X-ray phase measurements that has been deployed at several synchrotron sources.

It is based on a phase shifting beam splitter and an absorbing analyzer grating. Due to its high sensitivity in the order of 10 nrad and the option to analyze single shots independently, it is highly interesting for XFEL optics diagnostics.

We have implemented a grating interferometer at the XPP endstation of LCLS at a photon energy of 9 keV.

It has been used to measure XFEL source properties, such as induced longitudinal (accuracy < 5 m) and transverse source point displacements (accuracy < 5 μ m) and shot-to-shot source point fluctuations. Shot-to-shot fluctuations are analyzed using a moiré technique. Using one-dimensional grating structures, this analysis can be carried out with high spatial resolution in one direction of interest, whereas the use of two-dimensional gratings allows a simultaneous measurement in two perpendicular directions.

Furthermore, the wavefront distortions induced by beamline optics such as mirrors, monochromators or focusing lenses have been analyzed. Using a specifically adapted interferometer configuration, the wavefront downstream of focusing elements has been recorded and propagated to the focus in order to determine the focal spot size.

For stationary phenomena, such as the influence of optical elements, high spatial resolution wavefront data has been recorded by averaging

**Conference 8140: X-Ray Lasers and Coherent X-Ray Sources:
Development and Applications**

over multiples shots and using a phase stepping technique.

The technique is expected to develop into a useful diagnostics tool both for LCLS and future hard XFEL sources.

8140-27, Session 6**Single-shot intensity/position monitor for hard x-ray FEL sources**

Y. Feng, H. Lemke, D. M. Fritz, M. Cammarata, R. Aymeric, J. B. Hastings, SLAC National Accelerator Lab. (United States)

A non-destructive diagnostics device was developed to measure the intrinsic pulse-to-pulse intensity and position fluctuations of the SASE-based LCLS hard X-ray FEL, and was based on the detection of back-scattered X-rays from a partially-transmissive thin target using a quadrant X-ray diode array. This intensity/position monitor was tested on the X-ray Pump-Probe instrument of the LCLS and shown to be capable of achieving a relative intensity precision of 0.1% and position sensitivity of 5 μm limited only by the Poisson statistics of the X-rays collected in the diodes.

8140-37, Poster Session**Ne-like Ti x-ray laser driven by a single femtosecond laser**

Y. Li, China Univ. of Mining and Technology (China); A. Teng, Y. Sun, China Univ. of Mining and Technology (United States)

The new scheme is presented for Ne-like Ti X-ray laser driven by a single laser pulse. According to the self-similarity method, we analyze the properties of Ne-like Ti slab plasma generated by irradiation of the femtosecond laser with various front edges. Scaling laws for the temperature, scale length, and electron density are obtained. The characteristics of scaling laws at different input parameters are analyzed. The results show that X-ray laser can be generated by a single femtosecond laser. During the period of pulse front edge, the characteristics of temperature, scale length, and electron density are affected by the growth tendency of light intensity. The femtosecond laser with a gentle front edge is profitable to drive X-ray laser. Our results provide a new program for experiments using a single laser pulse to drive X-ray laser.

8140-38, Poster Session**Dynamics of the ultrashort laser pulse in a capillary discharge-preformed argon plasma channel**

S. Sakai, J. Miyazawa, T. Higashiguchi, N. Yugami, Utsunomiya Univ. (Japan)

The interaction of an ultrashort, intense laser pulse with a wide variety of optical waveguides has been demonstrated in various applications, including electron acceleration, nonlinear wavelength conversion, short wavelength laser, and high-order harmonic generation. In the high-order harmonics generation experiments, the blue-shifted spectra have been reported in the pinched plasma channel in the kA discharge current and the non-pinched plasma channel in the ampere region. The numerical simulation and the analyzed spectra of the spectral behavior of the ultrashort laser pulse in the preformed rare-gas discharge channel, however, have not been reported. In order to understand the propagation dynamics of the ultrashort laser pulse, it is important to analyze of spectral behavior of the laser pulse in the capillary discharge-produced plasma channel in the stable propagation point of view.

We observed the spectra of the transmitted laser pulse without and with the plasma channel. The blue-shifted spectrum in the gas-filled capillary

without plasma was shifted to be about 8 nm at the peak spectral intensity with the bandwidth of 15 nm (FWHM). In this case, the change of the refractive index is large, because the ionization was induced from the neutral gas phase to the multi-charged state ions of Ar^{10+} . In the plasma channel the slight blue-shifted frequency component was also observed due to the more ionization by the laser field in the preformed argon plasma channel. A one-dimensional (1D) particle-in-cell (PIC) simulation is reproduced the experimental results of the spectral behavior propagating the ultrashort laser pulse.

8140-39, Poster Session**Observation of water window soft x-ray radiation in elongated low-inductive capillary discharges**

V. A. Burtsev, D.V. Efremov Scientific Research Institute of Electrophysical Apparatus (Russian Federation) and A.F. Ioffe Physical Technical Institute (Russian Federation)

In this report, results of observation and experimental research of EUV and soft x-ray radiation, generated in elongated low-inductive capillary discharges with close spacing of electrode system and energy supply by the double forming line through the long transmitting line are presented. In carried out experiments, running waves of sliding avalanche discharge were used for preionization of working gas (Ar). After such wave achieves the outer tubular electrode, the transformation of electrical field occurs and the component of radial field comes to longitudinal ones. In this moment longitudinal electrical field strength reaches maximum value, and then quickly falls because of high current low impedance discharge developing.

This maximal transient electrical field courses in discrete steps running away of a part of plasma electrons in a very narrow range of initial gas pressure (0.1-0.25 Torr) and for shot time interval (< 5 ns). These fast electrons in the process of inelastic collisions ionize and excite multiply charged ions, quantum transitions of which gave the generation not only EUV, but also SXR (2-4 nm) ranges. This is conformed by semiconductor filtered Si-diode measurements. We used the method of absorbing foils with different thickness for evaluation of photons energy.

Discovered phenomenon allows looking otherwise on the problem of creation of discharge pumped short wave soft x-ray lasers and initiated further researches, namely spectroscopic measurements.

This work was supported by the grants 06-08-00828 and 09-08-00160 of Russian Foundation for Basic Research.

8140-40, Poster Session**Strategies for EUV microscopy using a lab-scale top x-ray laser source**

D. Bleiner, F. Staub, J. E. Balmer, Univ. Bern (Switzerland)

High-brightness Extreme-Ultraviolet (EUV) sources for laboratory operation are needed in nano-fabrication and actinic ("at-wavelength") inspection of the EUV masks for high-volume manufacturing in next generation lithography. Laser-plasma sources have the required compactness and power scalability to achieve the demanding requirements. The generation of coherent photons across a line plasma can dramatically improve the imaging quality. We evaluated the capabilities of a lab-scale amplified spontaneous emission (ASE) EUV laser source combined with different optical designs, namely an all-reflective design using multilayer optics and a diffractive design using Fresnel zone plates (FZP). The multilayer optics is characterized by a higher throughput and handiness of system alignment. However, high magnification demands high NA, which can lead to spherical aberration. Off-axis tilt of the condenser/objective pair has caused a distortion in the horizontal illumination profile. These drawbacks are potentially addressed using a Schwarzschild design. The spectral purity of the EUV laser overcomes limitations of FZP's chromatic aberration. The high photon

flux of 1011 ph/shot mitigates throughput limitations of the FZP. The performance is benchmarked using a peculiar sample, i.e. a Siemens star, that allows determining the contrast at various spatial frequencies (modulation transfer function) in single-shot images.

8140-41, Poster Session

Repetitive XUV laser based on the fast capillary discharge

J. Schmidt, K. Kolacek, O. Frolov, V. Prukner, J. Straus, Institute of Plasma Physics of the ASCR, v.v.i. (Czech Republic)

XUV lasers are new sources whose applicability to technological and scientific research appeared just only about twenty years ago. Our laboratory has been studying high-current capillary discharge as a potential XUV/soft X-ray laser source over the past 12 years. We have designed, assembled and built two experimental apparatuses CAPEX and CAPEX-U fed from one source (Marx generator). On both these devices we have observed a very strong amplification of Ne-like argon line at 46.9 nm. The experimental device CAPEX-U is more powerful and has laser-triggered spark gap in comparison with the older apparatus CAPEX. The both devices CAPEX and CAPEX-U are fully operational.

Recently, for possible testing and application purposes we have built a new small Marx generator capable to run in a repetitive regime. Its repeating frequency is currently up to 1 Hz. The generator is covered by metal sheets and feeds CAPEX facility and ensures its full independence on CAPEX-U machine.

This paper reports on the first experimental results of the new experimental set-up of CAPEX apparatus (repetitive lasing at 46.9 nm), mainly set-up description, electrical parameters, laser pulse stability, etc.

This research has been supported by the MEYS (contract LC528 and LA08024), and GA AS CR (contract KAN300100702).

8140-42, Poster Session

Time-resolved XUV radiation diagnostics from nitrogen discharge Z-pinching plasma

M. Nevrlka, A. Jancarek, J. Hubner, Czech Technical Univ. in Prague (Czech Republic); D. Sheftman, Technion-Israel Institute of Technology (Israel); L. Pina, Czech Technical Univ. in Prague (Czech Republic); P. Vrba, Institute of Plasma Physics of the ASCR, v.v.i. (Czech Republic); M. Vrbova, Czech Technical Univ. in Prague (Czech Republic)

XUV radiation from nitrogen filled capillary discharge plasma was diagnosed using a 10^4 grooves/mm SiNx free-standing transmission grating. The resolution bandwidth 0.3 nm was achieved. Time dependence of 13.4 nm line emitted power was recorded by photomultiplier in order to verify inherence of resonant radiation emission corresponding to NVII 2-3 laser transition. An increase of the emitted power is expected during the pinch decay caused by recombination processes. We report here the results obtained with 90 mm long capillary discharge supplied by a current pulse with maximum amplitude of 50kA and quarter-period of 80 ns. This high-current pulse was generated by a 2.5 ohm water line high-voltage generator which is used for underwater wire explosion experiments and which was adjusted into capillary discharge design using results of PSPICE simulations. Initial nitrogen pressures were varied in the range of (20 - 500) Pa. According to MHD and kinetic simulations of the discharge plasma a feeble pumping is expected in this case. Results of our measurements proved the highest rate of upper laser recombination pumping of $4.5 \cdot 10^8 \text{ sec}^{-1}$ for the initial pressure 180 Pa, which is not high enough for efficient amplification of spontaneous emission. Observations of time integrated spectra proved high electrode erosion and capillary wall ablation. Technological problems connected with high-current capillary discharges are pointed out and analyzed.

8140-43, Poster Session

Formation mechanism of non-uniform structure in the gain distribution and its effect to the plasma x-ray lasers

A. Sasaki, Japan Atomic Energy Agency (Japan)

Plasma x-ray lasers have been studied toward shorter wavelengths and higher output power. Using transient collisional excitation (TCE) scheme with grazing incidence pumping (GRIP), lasing has been obtained by small pumping energies, but the output power is still very limited. In the plasma, considerable non-uniformity of the gain distribution is sometimes seen, which limits the output power and coherence of the x-ray laser beam. In this presentation, formation of the spatial structure in the plasma is investigated on the basis of the detailed atomic and radiative processes. Firstly, the atomic energy levels and rate coefficients are calculated, and secondly the pressure of the plasma is calculated by coupled CR-model and radiation transport as a function of the temperature and density. The emissivity and opacity of the plasma decrease significantly when the ionization exceeds Ni-like state as the bound electrons in $n=4$ shell are lost; one may see the plasma changes from an opac low-ionized state to a transparent highly-ionized state at their characteristic radiation energy. This may cause the decrease in the radiation pressure in the plasma, resulting in a non-monotonic behavior of the isotherm in the PV plane. In this presentation, the pressure and free energy of the plasma are investigated, to find the possibility to have phase-transition like behavior in the plasma, and to identify the critical temperature to cause the structure formation, and then whether it has an effect on the gain distribution of the x-ray lasers is discussed. Segregation of the plasma is also investigated.

8140-44, Poster Session

Soft x-ray laser-ablation mass spectrometry depth profiling of compound semiconductor heterostructures

I. Kuznetsov, F. Dong, J. Filevich, E. R. Bernstein, D. C. Crick, M. McNeil, Colorado State Univ. (United States); W. Chao, E. H. Anderson, A. Sakdinawat, Y. Liu, D. T. Attwood, Univ. of California, Berkeley (United States); J. J. Rocca, C. S. Menoni, Colorado State Univ. (United States)

We exploit the unique interaction properties of 26.5 eV photons from intense focused soft x-ray laser pulses² with materials¹ to analyze the chemical composition of nanofilms. We have investigated Si, GaAs, and InSnO semiconducting films; HfO₂ and SiO₂ dielectrics, Au and Cr, and others with depth profiling resolution of 20-50 nm. The experiments were carried out by using a mass spectrometry nanoprobe that uses a capillary discharge Ne-like Ar laser¹ for ablation. The focused output from the soft x-ray laser creates a plasma mostly through single photon ionization. The short absorption length of most materials at 46.9 nm wavelength results in a depth resolution in the range 20 to 50 nm. Consecutive single shot absorption events are used to construct the depth profile.

1 M. Berrill, F. Brizuela, B. Langdon, H. Bravo, C.S. Menoni, and J.J. Rocca, J. Opt. Soc. Am. B, 2008. 25(7): p. B32-B38.

2 S. Heinbuch, M. Grisham, D. Martz, and J.J. Rocca, Optics Express, 2005. 13(11): p. 4050-4055.

8140-45, Poster Session

Complex numerical research and optimization of EUV laser on hydrogen-like ions of nitrogen in low-inductive discharges

N. V. Kalinin, V. A. Burtsev, D.V. Efremov Scientific Research Institute of Electrophysical Apparatus (Russian Federation)

**Conference 8140: X-Ray Lasers and Coherent X-Ray Sources:
Development and Applications**

New results of complex numerical research of possibilities for creation of an effective recombination type 13.4 nm laser on hydrogen-like ions of nitrogen, obtained in plasma of low-inductive high-current pinching discharges, are presented. The attention mainly is focused on problems of obtaining plasma with needed non-equilibrium recombination ion composition and effective electron cooling. In carried out researches the 1D 2T RMHD code with account of dynamics, non-equilibrium ionization of plasma with complex composition, radiation transport in continuous and linear spectra and energy transmission from a generator of high voltage pulses to plasma load through a long line. The coefficient of amplification of a weak signal was defined by means of non-stationary model of all-level kinetics.

One and two-stage compression of plasma column in pinching discharges was studied. The second regime allows to obtain more dense and high ionized plasma column. This regime consists from small expanding of a plasma column after the first compression and its subsequent compression with using of the discharge current exceeding on amplitude the first wave. The similar behavior of discharge current is caused by changing of the condition matching plasma column with the transporting line.

One considered different mechanisms of electron cooling and forming recombination nonequilibrium many-component plasma of multi-charge ions. Namely, by radial expansion of the plasma column and radiative heat efflux by proper radiation of plasma, and linear radiation of hard impurity ions. In the first case, typical for regimes with low initial gas pressure ($< 10^{-10}$ Torr) one observed more quick falling of plasma density than electron temperature. In the second case, realizing at high gas pressure ($\geq 10^{-10}$ Torr), when the proper radiation of plasma sufficiently influences on dynamics of column and characteristics of plasma, current-carried radiative collapsing shock waves are used for plasma compression and then electron cooling. Namely, such waves give possibilities to realize deep cooling in super dense plasma for nanosecond time.

Results of calculation of amplification coefficient for the line of the transition 3-2 in hydrogen-like ions of nitrogen at two-step compression of plasma column and radiative heat efflux by linear radiation of argon ions showed, that it is possible to have $g_m \sim 3^{-1}$.

8140-46, Poster Session**Characterization of the temporal duration of the XUV laser pulse at the LASERIX facility**

L. Meng, Univ. Paris-Sud 11 (France); S. Bastiani, Ecole Polytechnique (France); O. A. Guilbaud, M. Pittman, S. Kazamias, K. Cassou, S. Daboussi, D. Ros, A. Klisnick, Univ. Paris-Sud 11 (France)

We report recent experimental measurements of the duration of a Ni-like Mo transient XUV laser emitted at 18.9 nm and generated under GRIP geometry at the LASERIX facility. We have used an ultra-fast X-ray streak camera (AXIS Photonique), able to reach a resolution better than 1 ps. A new trigger line was implemented, yielding a shot-to-shot jitter of less than 50 ps. The KBr photocathode was positioned close to the plane of the magnified near-field image of the XUV laser emitting aperture. The focusing of the image, by translating the imaging mirror, was used to carefully adjust the signal level in order to avoid saturation induced by charge-space effects. The sweep speed was calibrated in-situ by generating a double-pulse XUV laser.

Durations as short as 3 ps were measured for a 23° GRIP angle and a 750 fs short pulse laser duration. We will also present and discuss our study of the effect of these two parameters on the measured pulse duration.

8140-47, Poster Session**Spectroscopic measurements of photo-excited highly charged ions of Fe and F**

A. Graf, G. Brown, Lawrence Livermore National Lab. (United States); J. Crespo Lopez-Urrutia, S. Bernitt, Max-Planck-Institut für Kernphysik (Germany); P. Beiersdorfer, Lawrence Livermore National Lab. (United States); C. Beilmann, Max-Planck-Institut für Kernphysik (Germany); J. Clementson, Lawrence Livermore National Lab. (United States); S. Eberle, Max-Planck-Institut für Kernphysik (Germany); S. Epp, L. Foucar, Deutsches Elektronen-Synchrotron (Germany); M. Leutenegger, NASA Goddard Space Flight Ctr. (United States); S. Kahn, SLAC National Accelerator Lab. (United States); K. Kubicek, V. Maeckel, Max-Planck-Institut für Kernphysik (Germany); F. S. Porter, NASA Goddard Space Flight Ctr. (United States); A. Rasmussen, SLAC National Accelerator Lab. (United States); J. Rudolph, M. Simon, R. Steinbrugge, Max-Planck-Institut für Kernphysik (Germany); E. Trabert, Lawrence Livermore National Lab. (United States)

We report on recent spectroscopic measurements of line emission from photo-excited highly charged ions. The FLASH portable EBIT ion cloud was used as a target for the LCLS free electron laser at the soft x-ray (SXR) end station. Numerous instruments were used to diagnose the plasma including an Iplet calorimeter, a variable line spacing grating spectrometer and a Wien filter based ion extraction system. This work focuses mostly on data obtained with the grating spectrometer. Attention is given to line emission from highly charged Fe and F. Some details of the experiment and preliminary results will be given.

This work performed under the auspices of the U.S. Department of Energy by Lawrence Livermore National Laboratory under Contract DE-AC52-07NA27344. The experiment was carried out at the Linac Coherent Light Source, a National User Facility operated by Stanford University for the US Department of Energy. Portions of this research were carried out at the Linac Coherent Light Source (LCLS) at the SLAC National Accelerator Laboratory. LCLS is an Office of Science User Facility operated for the United States Department of Energy by Stanford University.

8140-48, Poster Session**Spectral modeling of Fe XVII pumped by a free-electron x-ray laser**

J. Clementson, Lawrence Livermore National Lab. (United States)

The combination of electron beam ion traps (EBITs) with accelerator-based light sources allows for new regimes of atomic physics to be explored, such as line-formation processes in photo-ionized plasmas. Measurements where intense x-ray emission has been directed into an EBIT with trapped ions have previously been performed at the BESSY-II synchrotron and the FLASH free-electron laser in Germany [1, 2]. The novel Linac Coherent Light Source (LCLS) at the Stanford SLAC laboratory is the worlds brightest source of coherent x rays. The very high spectral density of the LCLS beam may pump atomic resonances from ground or excited levels in highly charged ions that are created and trapped in an EBIT.

The atomic structure and x-ray pumping of neonlike Fe XVII have been calculated and modeled under LCLS conditions using the Flexible Atomic Code (FAC) [3]. Fe XVII is one of the most frequently observed spectra from astrophysical sources and therefore of interest for plasma diagnostics. The calculations include oscillator strengths, radiative transition probability rates, autoionization rates, photo-ionization cross sections, and line emissivities.

This work was performed under the auspices of the US DOE by LLNL under Contract No. DE-AC52-07NA-27344.

[1] M. C. Simon et al., Phys. Rev. Lett. 105(18), 183001 (2010)

[2] S. W. Epp et al., J. Phys. B 43(19), 194008 (2010)

[3] M. F. Gu, Can. J. Phys. 86(5), 675 (2008)

8140-49, Poster Session

Alternative analysis of experimental results on x-ray parametric amplification

S. Kazamias, S. Daboussi, O. Guilbaud, K. Cassou, D. Ros, B. Cros, G. Maynard, Univ. Paris-Sud 11 (France)

We present a comprehensive theoretical analysis of the conditions that lead to absorption limited generation of high order harmonics in the case of low energy, long pulse duration infrared pump laser beams. With these pump laser beam parameters, tight focussing is necessary to reach the high laser intensity required for high non linear response at the atomic level. A limitation of phase-matching is then induced through the so-called Gouy phase shift. We explain how the positive atomic dispersion can compensate for that effect and derive the conditions for perfect phase matching. The influence of gas pressure, harmonic order, maximum laser intensity and focussing conditions are analysed. We claim that our theory comprehensively explains recently published experimental results [1], [2] contrary to the « XPA » analysis proposed by the authors.

Reference :

[1] J.Seres, E.Seres, D.Hochhaus, B.Ecker, D.Zimmer, V.Bagnoud, T.Kuehl et C.Spielmann, Nature Physics 6, 455 (2010)

[2] S. Kazamias, S. Daboussi, O. Guilbaud, K. Cassou, C. Montet, O. Neveu, D. Ros, B. Cros et G. Maynard, Nature Physics 6, 926 (2010)

8140-02, Session 7

Identification of Auger electron heating and excited states coupling effects irradiating solids with XUV Free Electron Laser Radiation at intensities larger than 1016 W/cm²

F. B. Rosmej, F. Petitdemange, E. Galtier, Univ. Pierre et Marie Curie (France)

In the past few years, the development of light sources of the 4th generation, namely XUV/X-ray Free Electron Lasers provides to the scientific community outstanding tools to investigate matter under extreme conditions never obtained in laboratories so far. We have studied a solid-to-plasma transition by irradiating Al foils with the FLASH XUV free electron laser (Hamburg, Germany) under exceptional conditions: photon energy of 92 eV, pulse duration of 20 fs, micro-focusing and intensities larger than 10¹⁶ W/cm². Intense XUV self-emission has been observed showing spectral features that are consistent with emission from regions of very high density, but that go beyond single inner-shell photo-ionization of solid.

Auger heating of the electrons in the conduction band that occurs immediately after the absorption of the XUV laser energy by the crystal has been identified as the dominant heating mechanism via characteristic features of intra-shell transitions [1].

We present simulations that allow studying Auger heating and the subsequent evolution of the radiation emission of near solid density matter. Particular emphasize is paid to the multi-charge state inverse Auger-effect in dense environments which is proposed to explain the target emission when the conduction band at solid density becomes more atomic like as energy is transferred from the electrons to the ions. Finally we discuss the simulations along with the first available experimental data [1].

[1] E. Galtier, F.B. Rosmej, D Riley et al: "Decay of cristaline order and equilibration during solid-to-plasma transition induced by 20-fs microfocused 92 eV Free Electron Laser Pulses", Physical Review Letters 2011.

8140-28, Session 7

Nano-scale imaging mass spectrometry of biological materials with soft x-ray lasers

C. S. Menoni, J. Filevich, I. Kuznetsov, F. Dong, E. R. Bernstein, D. C. Crick, M. McNeil, Colorado State Univ. (United States); A. Sakdinawat, Y. Liu, Univ. of California, Berkeley (United States); W. Chao, E. H. Anderson, Lawrence Berkeley National Lab. (United States); D. T. Attwood, Univ. of California, Berkeley (United States); J. J. Rocca, Colorado State Univ. (United States)

We describe a novel application of soft x-ray lasers that allows to identify the molecular composition of a single bio-organism at the sub-cell level. Our method uses a capillary discharge soft x-ray laser (SXRL) [1] whose pulsed output is focused onto a sample by means of a free standing Fresnel zone plate lens. The SXRL can efficiently ionize atoms and molecules via single photon ionization. The ions generated by SXRL ablation are accelerated through the opened central zone of the ZP towards a time of flight mass analyzer. The use of 46.9 nm SXRL light allows to achieve a lateral spatial resolution of < 200 nm and a depth resolution of ~ 20 nm, due to the small absorption depth of carbon-containing materials at this wavelength. Single shot mass spectra from uniform samples consisting of alanine, glycine, and lysine have been obtained. The spectra show signatures of the molecular ion and several fragment ions. The high spatial and lateral resolution and single shot ablation capabilities will enable to construct three dimensional mass images of cells and micro-organisms.

8140-29, Session 7

Table top nanopatterning by de-magnified Talbot Effect

L. Urbanski, Colorado State Univ. (United States) and NSF Engineering Research Ctr. for Extreme Ultraviolet Science & Technology (United States); P. W. Wachulak, Military Univ. of Technology (Poland); A. Isoyan, Synopsys, Inc. (United States); A. G. Stein, Brookhaven National Lab. (United States); C. S. Menoni, J. J. Rocca, M. C. Marconi, Colorado State Univ. (United States) and NSF Engineering Research Ctr. for Extreme Ultraviolet Science & Technology (United States)

We describe the extension of the coherent imaging by Talbot effect as an alternative to nanofabrication of periodic arrays of unit cells, each one with an arbitrary design. A periodic object composed of a two dimensional array of tiles, forms highly accurate real images of itself at distances that are integer multiples of the Talbot distance without the necessity of any optics. Illuminating the periodic transmission mask with a convergent coherent soft X-ray (SXR) beam, we demonstrated the possibility to print de-magnified replicas of the mask.

The Talbot mask was fabricated on a 25 nm thick membrane of Si₃N₄ using standard electron-beam lithography. The pattern was created in a 65 nm thick hydrogen silsesquioxane (HSQ) photoresist layer. A SXR =46.9 nm capillary discharge laser was used to replicate the Talbot mask. The laser beam was reflected in a spherical multilayer mirror close to normal incidence which spectrally filters the beam and simultaneously produces a convergent wavefront illumination.

A photoresist coated Si wafer was placed in the calculated working distance of the first Talbot plane, approximately 1mm, where the self-image of the Talbot mask was generated. The clear replica of the mask produced by the Talbot effect was recorded in the photoresist using typically 100 laser shots. The convergent beam illumination produced a reduced replica of the mask as compared with the collimated beam illumination. The de-magnification can be controlled by changing the distance between the mask and the mirror

Results showing different de-magnifications will be presented. This experiment opens the possibility to control the size of the printing with a very simple optical setup.

8140-30, Session 7

Movies of nanoscale dynamics using soft x-ray laser illumination

S. Carbajo, I. D. Howlett, F. Brizuela, M. C. Marconi, J. J. Rocca, C. S. Menoni, Colorado State Univ. (United States); W. Chao, E. H. Anderson, Lawrence Berkeley National Lab. (United States); A. Sakdinawat, Y. Liu, D. T. Attwood, Univ. of California, Berkeley (United States); A. V. Vinogradov, I. A. Artioukov, P.N. Lebedev Physical Institute (Russian Federation)

We report the first demonstration of stop-motion imaging with nanoscale spatial resolution using a compact soft x-ray laser. A Ne-like Ar capillary discharge laser operating at 46.9 nm wavelength was used in combination with a full field soft x-ray microscope to capture sequences of images of a rapidly oscillating atomic force microscope tip with a spatial resolution of ~ 50 nm. The microscope is arranged in transmission configuration and employs reflective and diffractive optics to obtain full-field images with a single laser shot of ~ 1 ns duration. Snapshots of a magnetic force microscopy (MFM) tip oscillating at 82 kHz were acquired and used to make a movie that depicts the motion of the tip. This novel technique allows to make movies of nanoscale dynamic phenomena with high temporal resolution.

8140-31, Session 7

Recent results on x-ray imaging at Lebedev Physical Institute

I. A. Artioukov, A. N. Mitrofanov, N. L. Popov, A. V. Vinogradov, O. F. Yakushev, P.N. Lebedev Physical Institute (Russian Federation); A. V. Popov, Institute of Terrestrial Magnetism, Ionosphere and Radiowave Propagation (Russian Federation); Y. A. Bugayev, O. Y. Devizenko, V. V. Kondratenko, Kharkov Polytechnic Institute (Ukraine)

The talk presents a number of recent results related to incoherent and coherent imaging in hard and soft X-ray regions. Special attention is paid to the development of theoretical framework of grazing reflection imaging with the coherent X-rays. Basically similar to coherent transmission, the grazing reflection mode proves to enable a quantitative X-ray microscopy including phase retrieval. In addition, the reflection X-ray microscopy can work with a wider class of samples (not necessarily thin) and produce images of the objects in natural environment. The developed theoretical approaches and computer codes are based on the parabolic wave equation and generalization of the Fresnel integral to obliquely illuminated objects. The results of simulation of coherent reflection imaging are given for the optical schemes with and without lenses.

The second part of the presentation deals with soft X-ray microscopy based on multilayer mirrors operating at the wavelength near 4.8 nm ("carbon window" spectral region). Problems and findings related to construction of a compact microscope based on discharge X-ray source are discussed.

8140-32, Session 7

Assessment of illumination characteristics of soft x-ray laser-based full-field microscopes

I. D. Howlett, F. Brizuela, S. Carbajo, D. Peterson, M. C. Marconi, J. J. Rocca, C. S. Menoni, Colorado State Univ. (United States); A. Sakdinawat, Y. Lui, D. T. Attwood, Univ. of California, Berkeley (United States)

We present a method for analyzing the illumination of soft x-ray full-field microscopes. The method consists of imaging a set of periodic gratings and obtaining the Fourier spectra from these images in two

perpendicular directions. Analysis of the cutoff frequency of the imaging system provides information on angular conditions of the illumination. Furthermore, the analysis allows the optical transfer function of the imaging system to be obtained when the object is well characterized, for example, from a scanning electron image. The results of the analyses compare well with independent measurements of the modulation contrast function from which half-pitch grating resolution values of ~ 55 nm and ~ 38 nm were obtained for microscopes that use 46.9 nm and 13.2 nm laser illumination respectively [1,2]. The ability to characterize the illumination conditions in the EUV/SXR microscopes with a fast and simple analysis is critical to adjust the illumination to achieve the best spatial resolution and obtain the highest quality images.

Work supported by the Engineering Research Centers Program of the National Science Foundation under NSF Award Number EEC-0310717

[1] C.A. Brewer, et al., "Single-shot extreme ultraviolet laser imaging of nanostructures with wavelength resolution," *Optics Letters*, 2008. 33(5): p. 518-520.

[2] G. Vaschenko, et al., "Sub-38 nm resolution tabletop microscopy with 13 nm wavelength laser light," *Optics Letters*, 2006. 31(9): p. 1214-1216.

8140-33, Session 8

Sub-10-nm wavelength Ni-like-ion collisional x-ray lasers

J. E. Balmer, F. Staub, C. Imesch, D. Bleiner, Univ. Bern (Switzerland)

We report on recent progress achieved in x-ray laser research at the University of Bern. Using the existing 10-TW Nd:glass CPA (chirped-pulse amplification) laser system in the grazing-incidence pumping (GRIP) scheme, saturated x-ray lasing is demonstrated on the 4d - 4p, $J = 0-1$ line of Ba at a wavelength of 9.2 nm, using a main pumping pulse energy of 9 J. A small-signal gain coefficient of ~30 cm⁻¹ and a gain-length product of ~16 at saturation have been measured. Intense lasing was also observed on the 8.9-nm line of La at a main pulse energy of 12 J. Crucial to these results was the introduction of a second, relatively intense (~10%) prepulse less than ~100 ps before the 1.2-ps duration main pulse, in addition to the 2.8% prepulse that irradiated the target 2.4 ns earlier. Travelling-wave excitation was used throughout. For handling convenience, compound targets (BaF₂, LaF₃) were used, either in the form of windows or coated onto glass slides. Lasing on multiple lines (9.6 and 10.4 nm) was observed for CsI targets with lasing on the 10.4-nm I line being very weak.

8140-34, Session 8

Line width measurement of a capillary discharge soft x-ray laser

M. C. Marconi, L. Urbanski, Colorado State Univ. (United States) and NSF Engineering Research Ctr. for Extreme Ultraviolet Science & Technology (United States); L. Meng, Univ. Paris-Sud 11 (France); M. Berril, Colorado State Univ. (United States) and NSF Engineering Research Ctr. for Extreme Ultraviolet Science & Technology (United States); O. Guilbaud, Univ. Paris-Sud 11 (France); J. J. Rocca, Colorado State Univ. (United States) and NSF Engineering Research Ctr. for Extreme Ultraviolet Science & Technology (United States); A. Klisnick, Univ. Paris-Sud 11 (France)

Compact capillary discharge soft x-ray lasers have become a true work horse for experiments with intense coherent short wavelength light on a table-top. They have enabled experiments in high resolution imaging, nano-scale patterning, nano-scale plasma diagnostics, and photophysics and photochemistry. Practically every output beam parameter of these lasers has been characterized with one exception: the linewidth and temporal coherence.

**Conference 8140: X-Ray Lasers and Coherent X-Ray Sources:
Development and Applications**

We report the first measurements of the line width emission of a capillary discharge Ne-like argon soft x-ray laser operating at a wavelength of 46.9 nm. The measurements were conducted using a wavefront-division bi-mirror interferometer specifically designed to measure the temporal coherence of soft x-ray sources. The line profile was inferred from the measurements of the fringe visibility as a function of the optical path difference. The evolution of the linewidth was studied as a function of length of the amplifier plasma column.

The bi-mirror interferometer produced clear interference patterns which are recorded in a CCD camera. The interference is observed in a rectangular region where the reflections from the two bi-mirrors superpose. The relative alignment of the two beams determines the orientation and period of the interference fringes. Changing the optical path difference (OPD) between the two beams it is possible to obtain curves of the fringe visibility vs OPD. After fitting these data points with a Gaussian curve a typical bandwidth of $4 \cdot 10^{-5}$ was obtained.

The preliminary analysis of the experimental results shows a almost constant value of the linewidth for all capillaries lengths. The lack of inhomogeneous saturation re-broadening indicates that even in this relatively low density plasma the contributions of homogenous broadening and collisional redistribution effects are significant in determining the laser line profile.

8140-35, Session 8

**Polarization measurements of plasma excited
x-ray lasers**

A. L. Aquila, Deutsches Elektronen-Synchrotron (Germany); D. Bleiner, Univ. Bern (Switzerland); S. Bajt, Deutsches Elektronen-Synchrotron (Germany); J. E. Balmer, Univ. Bern (Switzerland)

Plasma excited X-ray lasers are a developing technology for many scientific applications. The photon energies, and peak brilliance of these lasers sources are well suited for probing atomic, molecular and solid state systems. The development and improvement in these laser systems also drives a need for metrologies of the properties of these lasers. Our research implements X-ray optics, designed to operate at the Brewster's angle, to measure the polarization state of a Ni-like Sm laser. The device determines the polarization state on a shot to shot basis and opens the possibility for polarization control of plasma excited X-ray lasers and thus probing spin polarized electronic states.

8140-36, Session 8

High energy density plasmas and x-ray lasers

V. N. Shlyaptsev, J. J. Rocca, Colorado State Univ. (United States); A. Pukhov, Heinrich-Heine-Univ. Düsseldorf (Germany); A. Noy, Univ. of California, Merced (United States)

We will be discussing the modeling of two novel regimes in laser produced plasma and electrical discharges which may allow to deposit very high energy densities (HED) into the plasma. Utilizing relatively small university-scale facilities these methods could reach HED up to 1 Gigajoule per cc - which so far was typically reachable only by spherical compressions in large installations. For the reference, by convention HED corresponds to energy densities exceeding 0.1 MJ per cubic centimeter, and, for example, laser produced plasma can be considered HED at the temperature 1 keV and electron density equal to critical density for 1 micron laser radiation.

We will also describe parameters of x-ray lasers which benefit from increased plasma energy density. Modeling results will be compared with our current experiments.

Conference 8141:

Advances in Computational Methods for X-Ray Optics II

Sunday-Wednesday 21-24 August 2011 • Part of Proceedings of SPIE Vol. 8141
Advances in Computational Methods for X-Ray Optics II

8141-01, Session 1

X-ray refractive optics: goals, challenges, and research opportunities

A. A. Snigirev, European Synchrotron Radiation Facility (France)

The latest advances in X-ray refractive optics developments bring new possibilities to the design of next generation beamlines. This paper outlines the main goals faced and the challenges to be addressed by researchers in this area. The main emphasis will be given to the growing needs for developing wave-optical modeling of coherent hard X-ray optics in multi-lens arrangements. In this way, the requirements for computational tools for new coherent microscopy and interferometry techniques will be discussed.

8141-02, Session 1

Hard x-ray nanobeam characterization by ptychographic imaging

C. G. Schroer, S. Hönig, A. Goldschmidt, R. Hoppe, J. Patommel, D. Samberg, A. Schropp, S. Stephan, Technische Univ. Dresden (Germany); M. Burghammer, European Synchrotron Radiation Facility (France)

Modern hard x-ray scanning microscopes at synchrotron radiation sources generate x-ray beams with lateral sizes well below 100 nm. Characterizing these beams in terms of shape and size by conventional techniques, such as knife-edge scans, is tedious, requires highly accurate test objects and stages, and yields only incomplete information. Since recently, we use a ptychographic scanning coherent diffraction imaging technique in order to characterize hard x-ray nanobeams in scanning x-ray microscopes. In addition to a high resolution image of the test object used in the scan, a detailed quantitative picture of the complex wave field in the nanofocus is obtained with high spatial resolution and dynamic range. Both are the result of high statistics due to the large number of diffraction patterns. The method yields a complete description of the focus, is robust against inaccuracies in sample positioning, and requires no particular shape or prior knowledge of the test object. With this information, the exit wave field behind the nanofocusing optic can be reconstructed, giving detailed insight into its aberrations.

8141-26, Session 1

Next generation optics for high-resolution inelastic x-ray scattering: theory and experiment

Y. Shvyd'ko, Argonne National Lab. (United States)

Principles and optical schemes of the angular-dispersive backscattering monochromators and analyzers, will be presented, supported by numerical simulations based on dynamical theory of multiple-crystal x-ray Bragg diffraction. The novel x-ray optics has a potential of achieving sub-meV energy resolution, spectral functions with sharper tails, and better momentum transfer resolution in inelastic x-ray scattering (IXS) experiments, as compared to the state of the art IXS optics. Results of the first tests, at the APS, of the in-line angular-dispersive backscattering monochromators/analyzers, termed CDDW, will be presented, in which a 0.4 meV resolution have been demonstrated. Experimental results will be compared with theoretical predictions.

8141-04, Session 2

Theoretical modelling of coherence properties of hard x-ray synchrotron sources and free-electron lasers based on statistical optics approach

I. Vartaniants, A. Singer, Deutsches Elektronen-Synchrotron (Germany)

A general theoretical approach based on the results of statistical optics is used for the analysis of the transverse coherence properties of third generation hard x-ray synchrotron sources and x-ray free-electron lasers (XFEL). Correlation properties of the wavefields are calculated at different distances from an equivalent Gaussian Schell-model source. This model is used to describe coherence properties of the 5 m undulator source at the synchrotron storage ring PETRA III. In the case of XFEL sources the decomposition of the statistical fields into a sum of independently propagating transverse modes is used for the analysis of the coherence properties of these new sources. A detailed calculation is performed for the parameters of the SASE1 undulator at the European XFEL. It is demonstrated that only a few modes contribute significantly to the total radiation field of that source.

8141-05, Session 2

Modeling of coherence properties of the 3rd harmonic radiation (2.7 nm) at FLASH based on the wavefront propagation

A. Singer, I. Vartaniants, Deutsches Elektronen-Synchrotron (Germany)

With the advent of the free-electron lasers (FEL) highly coherent x-ray radiation has become available. New areas of research utilizing the high coherence properties of these sources emerged. The understanding of the coherence properties of the radiation and their dependence upon propagation through various optical elements is of vital importance for scientific community, including experimentalists planning experiments and beamline scientist designing the optical systems. Nowadays, most propagation codes used for propagation of FEL radiation are based on the Fourier optics approach, which is valid for the fully coherent radiation. This approach is, however, not well suited to describe the coherence properties of partially coherent sources, like FELs. Here we present a method for the propagation of partially coherent radiation using coherent mode decomposition and wavefront propagation. In our work the partially coherent radiation is decomposed into a sum of independent coherent modes. Each mode is propagated separately using conventional wavefront propagation techniques. In the end the summation of the modes gives the coherence properties of the propagated radiation. As an example, the 3rd harmonic radiation at the wavelength of 2.7 nm from FLASH was analyzed. In particular, the coherence properties of the plane grating monochromator (PG2) beamline at FLASH, which includes a set of focusing mirrors, were determined by this approach. The results of these simulations are compared with the transverse coherence and intensity measurements carried out at this beamline.

Conference 8141:
Advances in Computational Methods for X-Ray Optics II

8141-06, Session 2

Development of partially-coherent wavefront propagation simulation methods for 3rd and 4th generation synchrotron radiation Sources

O. Chubar, Brookhaven National Lab. (United States); J. Baltser, Univ. of Copenhagen (Denmark); L. Berman, Y. S. Chu, K. Evans-Lutterodt, A. Fluerasu, S. Hulbert, K. Kaznatcheev, M. Idir, R. Y. Reininger, D. A. Shapiro, Q. Shen, L. Wiegart, H. Yan, Brookhaven National Lab. (United States)

Partially-coherent wavefront propagation calculations have proven to be feasible and very beneficial for 3rd and 4th generation synchrotron radiation (SR) sources. This type of calculations uses the framework of classical electrodynamics for the description, on the same accuracy level, of emission by relativistic electrons moving in magnetic fields of accelerators, and propagation of the emitted radiation wavefronts through beamline optical elements. This enables accurate prediction of performance characteristics for beamlines exploiting high SR brightness (including the beamlines targeting operation at or close to the diffraction limit) and/or high spectral flux. Detailed analysis of radiation degree of coherence, offered by the partially-coherent wavefront propagation method, is of paramount importance for modern storage-ring based SR sources, which, thanks to extremely small sub-nanometer-level electron beam emittances, produce substantial portions of coherent flux in X-ray spectral range. We will present examples of partially coherent wavefront propagation simulations using SRW code and the resulting optimization of the design parameters of beamlines at National Synchrotron Light Source II. We will also discuss directions of further related developments such as extension of libraries of physical-optics based propagators for beamline optical elements, applications for optical metrology, data processing for coherence experiments, parallelization of CPU-intensive calculations, combination of different complementary simulations techniques, and interfacing with other popular simulations packages such as SHADOW.

8141-07, Session 2

A Monte Carlo approach for simulating the propagation of partially coherent x-ray beams

A. Prodi, Univ. of Copenhagen (Denmark); E. Knudsen, P. Willendrup, Risø National Lab. (Denmark); C. Ferrero, European Synchrotron Radiation Facility (France); R. Feidenhans'l, K. Lefmann, Copenhagen Univ. (Denmark)

Advances at SR sources in the generation of nanofocused beams with a high degree of transverse coherence call for effective techniques to simulate the propagation of partially coherent X-ray beams through complex optical systems in order to characterize how coherence properties such as the mutual coherence function (MCF) are propagated to the exit plane [1].

Here we present an approach based on Monte Carlo sampling of the Green function. A Gauss-Shell Stochastic Source with arbitrary spatial coherence is synthesized by means of the "Gaussian copula" statistical tool [2]. The Green's function is obtained by sampling Huygens-Fresnel waves with Monte Carlo methods and is used to propagate each source realization to the detector plane. The sampling is implemented with a modified Monte Carlo ray tracing scheme where the optical path of each generated ray is stored. Such information is then used in the summation of the generated rays at the detector to account for coherence properties.

This approach is used to simulate the cases of propagation in free space and with reflective optics and compared with Physical Optics and theoretical results [3].

References

- [1] I. A. Vartanyants and A. Singer, New J. Phys. 12 035004 (2010).
- [2] D. D. Duncan et al., J. Opt. Soc. Am. A 25, 231 (2008).

[3] S. K. Sinha et al., PRB 57, 2740 (1998).

8141-09, Session 3

Cross-platform wave optics software for XFEL applications

L. Samoylova, European XFEL GmbH (Germany); A. Buzmakov, A.V. Shubnikov Institute of Crystallography (Russian Federation); O. Chubar, Brookhaven National Lab. (United States); G. Geloni, H. Sinn, European XFEL GmbH (Germany)

We present a project aimed at development of a novel and unique software environment, suited and capable of solving a wide set of problems of X-ray FEL optics. The new software package will deliver a set of tools designed for: (1) calculation of spontaneous radiation from XFEL undulators and seamless tailoring of the output of XFEL radiation simulation codes (GENESIS, FAST) with wave front propagation code; (2) calculation of coherent and partially-coherent X-ray beam propagation through basic elements of XFEL beamlines, in particular through long grazing incidence mirrors, and monochromator crystals; (3) a choice and composition of optical elements for experimental stations, e.g. KB mirrors, CRLs, zone plates, apertures, etc; (4) application examples for modeling of whole beamlines.

The complex of programs will be based upon SRW libraries [1] plus a set of Matlab scripts or Python binding to provide access to these libraries. A user-friendly graphical interface, GUI, will be developed on the basis of the existing script interface. The software can be used by the XFEL experimental groups and groups responsible for scientific instruments for planning experiments and processing the experimental data. It will be further developed and supported by the European XFEL and provided as such free of charge to the scientific community. Several application examples, specific for XFEL will be presented. Possible ways for parallelization of calculations will be also discussed.

[1] O.Chubar, P.Elleaume, Proceedings of EPAC-98 (1998), 1177

8141-10, Session 3

Toolbox for advanced x-ray image processing

T. E. Gureyev, Y. Nesterets, D. Thompson, S. W. Wilkins, A. W. Stevenson, J. A. Taylor, Commonwealth Scientific and Industrial Research Organisation (Australia)

A software system has been developed for high-performance Computed Tomography (CT) reconstruction, simulation and other X-ray image processing tasks utilising remote computer clusters optionally equipped with multiple Graphics Processing Units (GPUs). The system has a streamlined Graphical User Interface for user interaction with the cluster. This differentiates it from most software available on today's compute clusters, which typically require some familiarity with parallel computing environment from the user. Apart from extensive functionality related to X-ray CT in plane-wave and cone-beam forms, the software includes multiple functions for X-ray phase retrieval and simulation of phase-contrast imaging (propagation-based, analyser crystal based and Talbot interferometry). Other facilities include several methods for image deconvolution, simulation of various phase-contrast microscopy modes (Zernike, Schlieren, Nomarski, dark-field, interferometry, etc.) and a large number of conventional image processing operations (such as FFT, algebraic and geometrical transformations, pixel value manipulations, simulated image noise, various filters, etc.). All operations can be applied to batches of images in a variety of standard image formats. Some scripting capabilities are also included. The architectural design of the system is briefly described, as well as the two-level parallelization of the most computationally-intensive modules utilising both the multiple CPU cores and multiple GPUs available in a local PC or a remote computer cluster. Finally, some results about the current system performance are presented. This system can potentially serve as a basis for a comprehensive toolbox for X-ray image analysis and simulation, that can efficiently utilise modern multi-processor hardware for advanced scientific computations.

Conference 8141:
Advances in Computational Methods for X-Ray Optics II

8141-11, Session 3

Partially coherent x-ray beam simulations: mirrors and more

M. Osterhoff, Georg-August-Univ. Göttingen (Germany) and European Synchrotron Radiation Facility (France); C. Morawe, C. Ferrero, European Synchrotron Radiation Facility (France); T. Salditt, Georg-August-Univ. Göttingen (Germany)

Partially coherent x-ray beam simulations: mirrors and more

Penetration, micro-resolution, and scattering were the keywords of x-ray analyses in the 20th century. But in the last 15 years, a great class of coherent imaging techniques has emerged as new tools, allowing for low-dose imaging of biological specimen on the nanoscale.

Apart from experimental and technical challenges, a better understanding of partially coherent beam propagation is the key for exploiting the new methods' full performance. We present a simulation framework to calculate the mutual intensity and the degree of spatial coherence of typical x-ray focusing and filtering devices used at 3rd generation synchrotron radiation sources.

We propose the following modeling scheme: A set of independent point-sources yield independent basic fields, which are superposed in a stochastic manner; by taking the ensemble average, both partially coherent intensity and degree of coherence can be obtained from the mutual intensity. By including real structure effects, like height deviations of focusing mirrors, and vibration of optical components, advanced predictions of x-ray beams can be made. This knowledge is expected to improve reconstruction results from coherent imaging experiments.

Coherence simulations of focusing mirrors are presented and validated with analytical results; experimental tests are shown, too. Coherence filtering by use of x-ray waveguides is shown both numerically as well as analytically. We also present first simulations for partially coherent focusing by compound refractive lenses. The influence of vibrations on the degree of coherence is discussed within our model.

8141-12, Session 3

Polycapillary optics: comparison of computational modeling and experimental results

C. A. MacDonald, R. Schmitz, Univ. at Albany (United States)

Polycapillary optics are commonly used for x-ray fluorescence and have been designed as focusing collectors for x-ray astronomy, to produce large area collimated beams for wafer analysis, and to provide small focused beams for protein crystallography with low power x-ray sources. They are also being developed for a number of medical applications, including mammography, scintigraphy and orthovoltage therapy. Additional applications are extensions of measurements normally performed at synchrotrons into laboratory or clinical settings because of the increased efficiency of source utilization. The realization of these applications has been advanced by the recent marked improvement in available optic quality and reproducibility. Manufacturing progress has been assisted by the development of simulation analyses which allow for increasingly accurate assessment of optics defects. Three dimensional Monte Carlo models are based on interactions between photons and the walls of the optic, represented as surface normals. Extensive modeling is made of defects including profile error, roughness, and waviness (midrange spatial frequency slope errors). Comparison of focal spot size, angular divergence, and transmission from collimating and focusing lenses are compared with measured results.

8141-13, Session 4

PHASE: a universal software package for the propagation of time dependent coherent light pulses along grazing incidence optics

J. Bahrdt, Helmholtz-Zentrum Berlin für Materialien und Energie GmbH (Germany)

The software package PHASE includes routines for the propagation of coherent light within the stationary phase approximation (SPA). The code is based on nonlinear analytic transformations of electric field arrays across longitudinally extended optical elements. Recently, the representation of the optical elements (OEs) has been extended to 8th in the OE-coordinates. Each element is represented by an individual matrix and the combination of several elements is done by simple matrix multiplications. This method can be interpreted as a thick lens approach whereas the usual method which is based on Fourier optics is a thin lens approximation. Both methods have advantages and disadvantages. Recently, the package has been extended to Fourier optics algorithms. Now, the appropriate propagator can be selected from the same interface which is running under IDL. Furthermore, a direct comparison of both methods from the same interface is possible which helps to evaluate the advantages and limitations of both methods.

8141-14, Session 4

Modeling the coherence properties of polycapillary optics

A. M. Zysk, Illinois Institute of Technology (United States); R. W. Schoonover, M. A. Anastasio, Washington Univ. in St. Louis (United States)

Polycapillary x-ray optical devices may potentially be useful for coherence-based imaging techniques such as in-line phase-contrast imaging, but to date their analysis has been limited to output intensity alone. To assess the coherence properties of these devices, new simulation techniques have been developed to capture the phase information of propagating wavefields and allow for investigation of coherence properties from extended sources. These techniques employ the coherent mode decomposition and geometric propagation of individual modes through the optic. The result is a quantification of capillary-to-capillary coherence properties and correlation of output wavefield coherence to parameters of the optic and source.

8141-15, Session 4

McXtrace: a modern ray-tracing package for x-ray instrumentation

E. Knudsen, Risø National Lab. (Denmark); J. Baltser, A. Prodi, Univ. of Copenhagen (Denmark); P. Willendrup, Risø National Lab. (Denmark); M. Sanchez del Rio, C. Ferrero, European Synchrotron Radiation Facility (France); R. Feidenhans'l, K. Lefmann, Copenhagen Univ. (Denmark)

Ray-tracing is a well established simulation method to characterize the propagation of x-ray beams through optical elements within the geometrical approximation.

Here we present the developments of the McXtrace project [1], a free, open source software package for simulations and optimization of complete instruments, designed to bring Monte Carlo ray tracing to a new level of performance.

The package adopts the principles and code structure of McStas [2], a software designed for neutron beams for the same purpose, now a de facto standard tool in the neutron scattering community.

In particular, McXtrace presents the following advantages over existing

Conference 8141:
Advances in Computational Methods for X-Ray Optics II

codes:

1. Modular. Users can easily build an instrument model by simply choosing its building blocks from existing library of tested components.
2. Powerful. New components are constantly being developed by the user community to respond to the needs of state of the art development in synchrotron radiation devices, i.e. in multilayer mirrors, partially coherent sources, compound refractive lenses, etc. No knowledge of the low-level code implementation is required to develop a McXtrace component.
3. Fast. At each run the meta-language describing the simulation is automatically translated into ANSI-C code, allowing to exploit the machine-dependent optimization options of the C-compiler.

We will illustrate the above points by simulating selected instances of the ID11 beamline at ESRF.

References:

- [1] McXtrace project website at <http://www.mcxtrace.org>
- [2] K.Lefmann and K.Nielsen, McStas, a General Software package for Neutron Ray-tracing Simulations, Neutron News 10 (20), (1999).

8141-16, Session 5

Undulator emission analysis: comparison between measurements and simulations

T. Moreno, P. Ohresser, Synchrotron SOLEIL (France)

Optics like crystals and multilayers are efficient elements to analyse the emission of undulators in soft and hard X-ray domain. Equipments containing such optics are used at SOLEIL for 6 years in order to align front end beamlines (diaphragms and primary slits) with the axis of emission of the undulator. From the HU52 undulator of DEIMOS beamline, we compare DIAGON measurements with simulations in order to evaluate undulator magnetic fields versus the gap in linear 0° polarisation

8141-17, Session 5

Optimization of a coherent soft x-ray beamline for coherent scattering experiments at NSLS-II

D. A. Shapiro, O. Chubar, R. Y. Reiningger, C. Sanchez-Hanke, Brookhaven National Lab. (United States)

The coherent soft x-ray beamline at the NSLS-II will deliver 1013 coherent photons per second in the energy range of 0.2-2 keV. The source, a dual-inline EPU, and beamline optics should be optimized in such a way as to deliver the highest possible coherent flux in a 10-30 μm spot for use in coherent scattering experiments. Using the computer code SRW, we simulate the photon source and focusing optics in order to investigate the conditions which provide the highest usable coherent intensity on the sample. In particular, we find that a magnetic chicane is needed to correct for the relative phase between the two EPUs and that the optimum phase setting produces a spectrum in which the desired wavelength is slightly red-shifted thus requiring a larger aperture than originally anticipated. This setting is distinct from that which produces an on-axis spectrum similar to a single long undulator. Furthermore, partial coherence calculations, utilizing a multiple electron approach, indicate that a high degree of spatial coherence is still obtained over such an aperture. The aperture sizes which maximize the signal-to-noise ratio of a double-slit experiment are calculated. This combination of high coherence and intensity is ideally suited for x-ray ptychography experiments which reconstruct the scattering density from micro-diffraction patterns. This technique is briefly reviewed and a novel illumination scheme utilizing a gaussian spatial filter is presented.

8141-18, Session 5

Optical design of the NSLS-II CHX beamline

K. Kaznatcheev, O. Chubar, L. Wiegart, M. Carlucci-Dayton, K. Evans-Lutterodt, L. Berman, A. Fluerasu, Brookhaven National Lab. (United States)

Ultra-low emittance third-generation synchrotron radiation sources, such as NSLS-II offer excellent opportunities for a development of experimental techniques exploiting x-ray coherence. Among the first six beamlines to be constructed by 2014, the coherent hard x-ray (CHX) beamline is dedicated to measuring the time- evolution of nanometer-sized objects via x-ray photon correlation spectroscopy. For the optical design of such beamline, there is a trade-off between the light coherence needed to distinguish individual speckles and phase acceptance (high intensity) required to measure fast dynamics. In the past, phase-space filtering with pinholes placed in- front of the sample was used to filter a single diffraction-mode, but such approach entangles the x-ray spot size with the required degree of coherence and imposes a severe penalty at non- optimum geometry. We proposed new design with an intermediate aperture placed after focusing optics. The size of intermediate horizontal aperture is defined by the highest mutual coherence required, and, for the current design, is restricted to 1.5Lcoh (transverse coherence length) leading a fringe visibility of 0.6. Wave-front preserved optics (compound refractive lens (CRL)) projects the aperture image onto the sample. By employing the focusing in horizontally direction more light can be passed through the slit trading the visibility of the speckles for higher flux. Consequently, the proposed optical design will accommodate equally well the requirements of different techniques; from the high coherence needed for coherent- diffraction imaging to full flux approaching $\sim 10^{13}$ ph/s for Si DCM energy window, as demanded by incoherent small-angle scattering. The beamline performance as validated by wave-propagation analysis will be discussed with an emphasis on realistic SR source and optics simulation.

8141-19, Session 5

Design optimization of bendable x-ray mirrors

W. R. McKinney, K. A. Goldberg, M. R. Howells, D. J. Merthe, Lawrence Berkeley National Lab. (United States); S. Yuan, OmniVision Technologies, Inc. (United States); V. V. Yashchuk, Lawrence Berkeley National Lab. (United States)

Convenience and cost often lead to synchrotron beamlines where the final Kirkpatrick-Baez (KB) focusing pair must relay the final image to different samples at different image distances [Proc. FEL2009, 246-249 (2009)], either for different experimental chambers, or diagnostics. We present an initial analytical approach, starting from, and extending the work of Howells et al. [OE 39(10), 2748-62 (2000)] to analyze the trade-offs between choice of mirror, bending couples and the given, shaped sagittal width of the optic. Both experimentally and in simulation, we have found that sagittally shaped optics can perform with high quality at significantly different incidence angles and conjugate distances. We present one successful demonstration from the ALS Optical Metrology Beamline 5.3.1.

8141-20, Session 5

Simulation with ray-tracing and wave front propagation of the NSLS-II SRX beamline

V. de Andrade, J. Thieme, O. Chubar, Y. Yao, Brookhaven National Lab. (United States)

The sub-micron resolution X-ray spectroscopy beamline (SRX) is one of the six project beamlines of NSLS-II at Brookhaven National Laboratory. SRX will benefit from the ultra low emittance of this new synchrotron radiation source and address a wide variety of scientific applications

Conference 8141:
Advances in Computational Methods for X-Ray Optics II

studying complex systems heterogeneous at the sub-micrometer scale. This presentation focuses on the KB branch (ΔE : 4.65-23 keV). Its main optical components consist of a horizontally focusing mirror creating a secondary source whose size is adjustable with slits, a horizontally deflecting monochromator and two sets of Kirkpatrick-Baez mirrors as focusing optics for operations requiring either high flux or high resolution. In a first approach, the beamline layout was optimized with ray-tracing calculations using ShadowGUI. As a result, the shape, location and quality parameters of the optics were specified for achieving either the most intense or the smallest monochromatic beam possible on the target (1013 and 1012 ph/s respectively in a sub-micron and a sub-100 nanometer spot). In the high-resolution mode, the final spot size is diffraction limited and the optics are coherently or partially coherently illuminated. Hence, ray-tracing calculations are not solely sufficient and a wave front propagation study was performed using SRW. This provides a more realistic estimate for the focal spot size when the KB mirrors are partially coherently illuminated, especially at higher energies. SRW results show a diffraction limited spot size of 55 nm, achieved with the previously optimized beamline layout with realistic mirror quality parameters.

8141-21, Session 5

Cost-effective ray-tracing optimization of the design of a prototype x-ray optical unit

M. M. Civitani, P. Conconi, G. Pareschi, INAF - Osservatorio Astronomico di Brera (Italy)

The ray-tracing is power-full technique for the design and the prediction of the performances of an X-Ray optics. When working with traditional monolithic shells, the possible design is quite constrained once fixed the focal length, the dimensions of the module and the field of view: simulations are used to determine the effective area and optical performances of realized mandrels and shells, taking into account for example profile errors or roundness measurements. Instead, when the optics are segmented into two separate reflective surface, integration errors with respect to position and rotation of the plates play an important role and may be also used to recover intrinsic plate errors. Moreover when the mirror segments are produced by replica, it is possible to optimize the design of a module to be cost effective. In this paper we present the design of a prototype module for the International X-ray Observatory (IXO) resulting from a proprietary ray tracing code. The module will be composed by 20 plate pairs all made with the same integration forming mandrel. The degradation of optical performances of the prototype are expected to be limited to few arc seconds.

8141-22, Session 6

Reliable before-fabrication forecasting of expected surface slope distributions for x-ray optics

V. V. Yashchuk, Y. V. Yashchuk, Lawrence Berkeley National Lab. (United States)

Numerical simulation of the performance of new beamlines and those under upgrade requires sophisticated and reliable information about the expected surface slope and height distributions of planned x-ray optics before they are fabricated. Obtaining such information should be based on the metrology data measured from existing mirrors that are made by the same vendor and technology, but, generally, with different sizes and slope and height rms variations. In this work, we demonstrate a method for highly reliable forecasting of the expected surface slope distributions of the prospective x-ray optics. The method is based on an autoregressive moving average (ARMA) modeling of the slope measurements with a limited number of parameters. With the found parameters of the ARMA model, the surface slope profile of an optic with the newly desired specification could reliably be forecast. We demonstrate the high accuracy of this type of forecasting by comparing the power spectral density distributions of the measured and forecast

slope profiles. Supported by the U.S. Department of Energy under Contract No. DE-AC02-05CH11231.

8141-23, Session 6

Automated suppression of errors in LTP-II slope measurements with x-ray optics

Z. Ali, C. L. Cummings, E. E. Domning, N. Kelez, W. R. McKinney, D. J. Merthe, G. Y. Morrison, B. V. Smith, V. V. Yashchuk, Lawrence Berkeley National Lab. (United States)

Systematic error and instrumental drift are the major limiting factors of sub-microradian slope metrology with state-of-the-art x-ray optics. Significant suppression of the errors can be achieved by using an optimal measurement strategy suggested in [V. V. Yashchuk, Rev. Sci. Instrum. 80, 115101/1-10 (2009)]. Here, we report on development of an automated kinematic, rotational system that provides fully controlled flipping, tilting, and shifting of a surface under test. The system is integrated into the Advanced Light Source long trace profiler, LTP-II, allowing for complete realization of the advantages of the optimal measurement strategy method. We provide details of the system's design, operational control and data acquisition. The high performance of the system is demonstrated via the results of high precision measurements with a spherical test mirror. This work is supported by the U.S. Department of Energy under Contract No. DE-AC02-05CH11231.

8141-24, Session 6

X-ray optics shape error evaluation coupling innovative shape metrology and 3D ray-tracing

G. Sironi, INAF - Osservatorio Astronomico di Brera (Italy) and Media Lario Technologies (Italy)

We present the advances we achieved in simulating optical performance degradation due to shape errors. This study has been carried on in the context of the New Hard X-ray Mission optical module prototype developing. We reached an accuracy of 1 arcsec on the simulation of the geometrical angular resolution at the focal plane associating shape error measurements acquired by means of an innovative 3D profilometer expressly designed to a 3D ray-tracing developed for double reflection telescopes.

8141-25, Session 6

Using MapleSim to model a six-strut kinematic mount for aligning optical components

A. M. Duffy, B. W. Yates, Y. Hu, Canadian Light Source Inc. (Canada)

The performance of a synchrotron beamline depends on the accurate positioning of its optical components and often ray tracing simulations are done for an ideal situation of perfect alignment. During construction a lot of effort is put into precisely locating components and making necessary adjustments. After the initial survey it is still necessary to move optical components for various reasons - usually to improve focusing or change photon energy. The mounts that hold these components can be quite complicated and modeling their motion is vital to understanding how they affect the performance of the beamline. In this paper we examine the behavior of a six-strut kinematic mount using MapleSim (a drag-and-drop physical modeling tool that uses advanced symbolic computation techniques to produce simulation models and generates equations describing the system of interest). This software creates a dynamic simulation of the system with 3-D visualization and has a point-

**Conference 8141:
Advances in Computational Methods for X-Ray Optics II**

probe feature that allows us to investigate and understand precisely how a mirror pole moves with its mount and quantify any cross-coupled motion that may occur during actuator adjustments. This positional information can be used to mitigate so called cosine errors and used in an x-ray tracing program such as Shadow.

8141-27, Session 7

Theory and numerical simulations of x-ray nanofocusing by bent crystal in back diffraction geometry

A. Suvorov, Brookhaven National Lab. (United States); H. Ohashi, S. Goto, T. Ishikawa, RIKEN (Japan)

A point-to-point x-ray focusing of a spherical wave by means of cylindrically bent crystal in symmetric Bragg back diffraction geometry was investigated theoretically and simulated numerically. To separate the focal plane from an incident x-ray beam, a thin flat crystal was introduced into the setup. The effect of flat crystal diffraction on the focusing performance of the double crystal setup is discussed. It is shown that the aberration free focusing can be achieved with aspherical surface shape of the strongly bent crystal. A correction term for the surface displacement function free from spherical aberrations is derived. Thorough numerical simulations demonstrated agreement with the theoretical analysis and excellent focusing performance of 2.4 nm.

8141-28, Session 7

Temporal and coherence properties of hard x-ray FEL radiation following Bragg diffraction by crystals or multilayers

V. A. Bushuev, Lomonosov Moscow State Univ. (Russian Federation); L. Samoylova, H. Sinn, T. Tschentscher, European XFEL GmbH (Germany)

Undulator systems of the novel X-ray Free Electron Laser (XFEL) facilities, based on Self-Amplified Spontaneous Emission (SASE) principle, will provide hard X-ray radiation from 5-24 keV. Preservation, transport and tailoring of such X-ray pulses are a big challenge for X-ray optics systems. In this work, we explore the transformation of XFEL pulse radiation and its statistical properties in the process of diffraction on crystals in Bragg and Laue geometry and free-space propagation of incident and diffracted radiation. We present a statistical diffraction theory for limited in space SASE X-ray pulses, which allows to calculate spatial-temporal coherence function of the reflected and transmitted radiation.

The SASE XFEL radiation consists of pulses limited in three dimensions with irregular multi-spike structure [1]. Coherent and time-resolved experiments will strongly depend on the properties of the incoming radiation passed through beamline optical elements to experimental stations. The evolution of SASE XFEL pulses and its statistical properties during propagation through a double crystal monochromator in Bragg and Laue diffraction geometry [2] as well as through a double multilayer structure [3] are investigated analytically and by numerical modelling.

[1] G. Geloni, E. Saldin, L. Samoylova, E. Schneidmiller, H. Sinn, Th. Tschentscher, M. Yurkov, *New J. Phys.* 12 (2010) 035021

[2] V. Bushuev, *J. Synchrotron Rad.* 15 (2008) 495

[3] V. Bushuev, L. Samoylova, *Nucl. Instr. and Meth. A* (doi:10.1016/j.nima.2010.10.036)

8141-36, Session 7

Dynamical modeling of high-energy-resolution x-ray optics

Y. P. Stetsko, J. W. Keister, D. S. Coburn, C. N. Kodituwakku, A. Cunsolo, Y. Cai, Brookhaven National Lab. (United States)

Detailed theoretical analysis of ultrahigh-energy-resolution x-ray optics, such as backscattering CDW [1], inline CDDW [2] and 4-bounce [3] monochromators and analyzers, has been carried out based on computer modeling within the framework of the dynamical theory of x-ray diffraction [4]. This analysis identifies several important techniques which can be used to align precisely and efficiently the optical elements, including elements in exact back reflection, of the monochromator, and for the precise determination of the energy and energy bandwidth of the monochromator.

Comparative theoretical analysis of the CDW/CDDW monochromators with the 4-bounce ones has also been performed. We show that, given the same energy resolution and angular acceptance, the former schemes are more advantageous as they produce higher luminosity and smaller beam footprint on the diffraction surface of the crystals, and therefore require shorter crystal length.

Optical schemes involving the use of exact back reflections from crystals having a high degree of structural perfection and high crystallographic symmetry are always accompanied with multiple-wave diffraction that introduces destructive contributions to the scattering intensity of x-ray optics. Theoretical analysis of such contributions has been performed in details. An important method to avoid the destructive contribution of the multiple-wave diffraction without loss of luminosity and energy resolution of x-ray backscattering optics has been identified and tested. The computer modeling also shows good agreement with experimental results.

[1] Yu. Shvyd'ko et al., *Phys. Rev. Lett.* 97, 235502 (2006).

[2] Yu. V. Shvyd'ko. *Advanced Designs of Angular Dispersive X-ray Monochromators*, (to be published). See also Conceptual Design Report for NSLS-II (<http://www.bnl.gov/nsls2/project/CDR/>), Section 11.5.2.

[3] M. Yabashi et al., *Rev. Sci. Instrum.* 72, 4080 (2001).

[4] Yu. P. Stetsko and S.-L. Chang, *Acta Crystallogr.*, 53, 28 (1997).

8141-29, Session 8

X-ray imaging diagnostics for magnetically confined and laser-produced fusion plasmas

N. A. Pablant, M. Bitter, L. F. Delgado-Aparicio, K. Hill, Princeton Plasma Phys. Lab. (United States); M. Sanchez del Rio, European Synchrotron Radiation Facility (France)

The use of x-ray emission from magnetic confinement and laser-produced fusion research plasmas has long been an essential non-perturbative diagnostic technique. Recent advances in x-ray detection technology have dramatically improved the ability of x-ray imaging and spectroscopic diagnostics to accurately measure plasma parameters. With these advancements, detailed characterization of the diagnostic system properties has become ever more important. We present an overview of current and future x-ray diagnostic requirements for fusion plasmas and describe, in particular, diagnostic systems employing spherically bent crystals and viewing characteristic x-ray lines from trace impurities with energies in the range 2-20keV. These include imaging x-ray crystal spectrometers which employ a single crystal in a 1D spectroscopic imaging configuration to measure profiles of the plasma ion and electron temperatures and plasma rotation velocities in devices such as the C-Mod and EAST tokamaks and on the LHD stellarator. Design and simulation requirements for planned diagnostic installations on ITER will also be discussed. In addition, we present proposed diagnostics based on monochromatic 2D imaging using matched pairs of spherically bent crystals. Diagnostics utilizing both the 1D and 2D configurations have been proposed for use with laser-produced fusion plasmas at the National Ignition Facility (NIF). These proposed

Conference 8141:
Advances in Computational Methods for X-Ray Optics II

diagnostics present unique design challenges due to the high spatial and temporal resolutions required. Finally we describe current applications of computational x-ray optical techniques to these diagnostic systems and discuss desired simulation capabilities.

8141-30, Session 8

X-ray wavefront modeling of Bragg diffraction from crystals

J. P. Sutter, Diamond Light Source Ltd. (United Kingdom)

The diffraction of an X-ray wavefront from a slightly distorted crystal can be modelled by the Takagi-Taupin theory, an extension of the well-known dynamical diffraction theory for perfect crystals. Maxwell's equations applied to a perturbed periodic medium yield two coupled differential equations in the incident and diffracted amplitude. These equations are discretized for numerical calculation into the determination of the two amplitudes on the points of an integration mesh, beginning with the incident amplitudes at the crystal's top surface. The result is a set of diffracted amplitudes on the top surface (in the Bragg geometry) or the bottom surface (in the Laue geometry), forming a wavefront that in turn can be propagated through free space using the Fresnel-Kirchhoff integral. The performance of the Diamond Light Source I20 bent-crystal dispersive spectrometer has here been simulated using this method. Methods are shown for transforming displacements calculated by finite element analysis into local lattice distortions, and for efficiently performing 3-D linear interpolations from these onto the Takagi-Taupin integration mesh, allowing this method to be extended to crystals under thermal load or novel mechanical bender designs.

8141-31, Session 8

Simulation of diffraction profiles for sagittally bent Laue crystals

X. Shi, Brookhaven National Lab. (United States)

Sagittally bent Laue crystal monochromators have been developed and are being extensively used at the National Synchrotron Light Source, USA. The rocking curves of such crystals are known to be significantly wider than those of perfect crystals as a result of the lattice distortion introduced by the sagittal bending. The existing analytical model explains the rocking curve broadening as well as the reflectivity observed.

Many theoretical methods were developed for calculating diffraction profiles of meridionally (in the diffraction plane) bent crystals. In this work, we extend these methods to accommodate sagittally bent crystals. The total lattice distortion angle for anisotropic crystals under sagittal bending is adapted into the multi-lamellar approximation using the rotating crystal method, in which the incident angle changes through each lamella. In addition, the Penning-Polder theory is examined for sagittally bent crystals with the uniform strain gradient. Finally, examples of these simulation results are presented and the merit of each method is discussed.

8141-32, Poster Session

Optimization software for the collimator of the Mars-XRD diffractometer: an update

C. Pellicciari, L. Marinangeli, International Research School of Planetary Sciences (Italy)

Mars-XRD is an X-ray diffractometer developed for the in situ mineralogical analysis of the Martian soil and it is a part of the payload of the ESA ExoMars mission. The main components of the Mars-XRD experiment are a Fe55 radioactive source, a collimator and a CCD-based detector system. For spectroscopic requirements, the beam section should not be larger than 0.5 x 10 mm² at sample distance.

To improve the X-ray flux, we are studying a collimator with converging blades which permits to use the entire source emission and tune the beam section.

In order to better estimate the efficiency of this new collimator and because of the high number of variables, a C++ program has been written that look for the best blades configuration among billion of combinations. In addition to the collimator configuration, this software simulator gives the sample photons distribution for different angles of the tilt of the source and for each couple of blades.

The optimized collimator transmits a flux 30% higher than a system with converging blades with the same aperture each and 5 times higher than a two windows collimator. Tilting the source of 40 degrees the flux became 10% weaker but the angular resolution increase of 20%.

This software simulator could be used also for the optimization of collimator system for the other wavelength and applications (e.g. radiotherapy).

8141-33, Poster Session

Combined charged-particle and x-ray simulations using Bmad

D. Sagan, J. Y. Chee, K. D. Finkelstein, G. H. Hoffstaetter, D. H. Bilderback, Cornell Univ. (United States)

The Bmad software library, developed at Cornell University, has proved to be a useful tool for accelerator simulations owing to its modular, object-oriented design. Bmad has been used to simulate the CESR storage ring for many years, and now, to design and analyze the proposed x-ray Energy Recovery Linac (ERL) at Cornell. One goal of recent Bmad development is to be able to do combined simulations of charged-particle beams and the x-ray beams that they create.

Ultimately a complete framework to simulate an ERL from gun cathode (including space-charge) to photon generation & tracking through x-ray experimental stations will be developed. We are now developing photon tracking through crystal and focusing capillary optics. A further long-term goal is to integrate Bmad with the forthcoming revision of the Shadow tracking code. Discussed will be present status and future plans.

8141-34, Poster Session

Monte Carlo simulations on the scattered power from irradiated mirrors and crystals

E. Secco, M. Sanchez del Rio, European Synchrotron Radiation Facility (France)

We developed a computer tool for accurate evaluation of the absorbed and re-scattered power from optical elements (mirrors, crystals and attenuators) in a synchrotron beamline. The results of these calculations are used for further heat load calculations using Finite Elements Methods. The radiation re-scattered from a mirror or a crystal receiving high power load can damage the opto-mechanical components placed in the chamber. A precise estimation of this power and its energy spectrum is necessary to assist in the design of the shielding inside the new optical chambers for the Upgrade Programme at the ESRF.

The Monte Carlo simulation package PENELOPE [1] was used to build a user code that uses the synchrotron spectrum or a monochromatic beam as input and calculates the spectrum and the amount of energy absorbed, transmitted, or back-scattered. The program output was tested against the NIST tabulated values of the mass energy absorption coefficient [2]. Some results for the heat load calculation will be presented for three cases i) a Glidcop mirror for the SESAME Synchrotron [3], ii) a silicon crystal in use at the ESRF beamline ID06, and iii) a Laue crystal for the new monochromator of the ESRF ID17 beamline.

1) Salvat, F., Fernandez-Varea, J.M., and Sempau, J.: PENELOPE-2008, A Code System for Monte Carlo Simulation of Electron and Photon Transport, OECD ISBN 978-92-64-99066-1 <http://www.oecd-nea.org/tools/abstract/detail/nea-1525>

Conference 8141:
Advances in Computational Methods for X-Ray Optics II

[2] Hubbell, J.H. and Seltzer, S.M. (2004), Tables of X-Ray Mass Attenuation Coefficients and Mass Energy-Absorption Coefficients (version 1.4). [Online] Available: <http://physics.nist.gov/xaamdi> [2011, Feb. 2]. National Institute of Standards and Technology, Gaithersburg, MD.

[3] Salah, W and Sanchez del Rio, M. Geometrical layout and optics modeling of the surface science beamline station at the SESAME synchrotron radiation facility J. Synchrotron Radiation 2011 (in press)

8141-35, Poster Session

The xraylib library for x-ray-matter interaction cross sections: new developments and applications

T. Schoonjans, Univ. Gent (Belgium); M. Sanchez del Rio, European Synchrotron Radiation Facility (France); A. Brunetti, Univ. degli Studi di Sassari (Italy); C. Ferrero, European Synchrotron Radiation Facility (France); L. Vincze, Univ. Gent (Belgium)

X-ray based analytical techniques have seen a surge in popularity over the last decades. This had led to an increased interest in cross sections and atomic parameters, which are of fundamental importance in both quantitative and qualitative analysis. In X-ray fluorescence (XRF), for example, quantification using either the fundamental parameter method or Monte-Carlo simulations is only possible if accurate data of X-ray interactions with matter are available. Such data can be obtained in two ways: experimental and computational through quantummechanical calculations. Several authors have published databases and tabulations in the literature, but none of them are presented in the form of freely available library functions which can be easily included in software applications for X-ray techniques.

In an effort to solve the problem of interfacing the data to the user, Brunetti et al. designed a software package called xraylib based on a shared ANSI C language library. The physical data included in the package is a compilation of several popular datasets including for example photoionization-, Rayleigh-, and Compton cross sections as well as absorption edge energies, fluorescence line energies and fluorescence yields. In this work we will present not only the features of the original xraylib package, but also introduce some novelties that were recently added such as partial photoelectric effect cross sections, refractive indices, Compton broadening profiles and bindings with popular programming languages.

The xraylib package can be downloaded from <http://github.com/tschoonj/xraylib>

8141-37, Poster Session

Advanced simulations of x-ray beam propagation through CRL “transfocators” using ray-tracing and wavefront propagation methods

J. Baltser, Univ. of Copenhagen (Denmark); E. Knudsen, Risø National Lab. (Denmark); O. Chubar, Brookhaven National Lab. (United States); K. Lefmann, R. Feidenhans'l, Copenhagen Univ. (Denmark); A. A. Snigirev, European Synchrotron Radiation Facility (France)

Applying two complementary simulation methods -- geometrical ray-tracing and partially-coherent wavefront propagation -- guarantees solid results and provides complete description of X-ray beam propagation through the CRL and other optical elements present in a beamline. The ray-tracing offers high CPU efficiency and simplicity of the simulations and provides good accuracy in cases of low X-ray coherence. On the other hand, the partially-coherent wavefront propagation method

allows for accurate description of X-ray beams at conditions of both low and high coherence, and enables for keeping track of the degree of coherence at the propagation through individual optical elements, for the expense of higher overall complexity and CPU-intensity of calculations.

In this work we used the newly developed McXtrace ray-tracing package [1] and the SRW wave-optics code [2] to simulate X-ray undulator radiation beam propagation through an in-vacuum transfocator (IVT) as it is implemented at ID-11 at ESRF [3]. The results of the simulations are in good agreement with the experimental data.

8141-38, Poster Session

SHADOW3-API: the application program interface for the ray tracing code SHADOW

N. Canestrari, D. Karkoulis, M. Sanchez del Rio, European Synchrotron Radiation Facility (France)

A new version (3.0) of SHADOW [1] has been developed. SHADOW3 is written in Fortran 2003 and follows the new computer engineering standards. The users can always execute the program in the traditional file oriented approach of the precedent version. Moreover, advanced users can create personalized scripts, macros and executables using the new Application Programming Interface (SHADOW3-API). It also allows binding of SHADOW3 with several popular programming languages such C, C++, python and IDL. We describe the SHADOW3 API structure, and illustrate its use with some examples.

SHADOW3 can be run in parallel machines under different environments. We implemented a version using the Open Message Parsing Interface (OpenMPI), to take full advantage of modern multi-core processors. The next plan is to accelerate SHADOW3 with the use of Graphics Processing Units (GPUs). This will open the door to extending the already very popular ray tracing tool to applications simulating 2D and 3D experiments (like imaging, tomography) and to integrating the optics calculations into a consistent synchrotron data analysis framework.

[1] F. Cerrina and M. Sanchez del Rio “Ray tracing of X-Ray Optical Systems” Ch. 35 in Handbook of Optics (Vol V, 3rd Edition), M. Bass ed. Mc Graw Hill, New York (2009)

8141-39, Poster Session

Ray tracing application in hard x-ray optical characterization and alignment: Soleil first wiggler beamline case

X. Dong, T. Moreno, Synchrotron SOLEIL (France)

Characterization of hard x-ray beamlines can be accurately performed through ray tracing simulation methods, and ray-tracing based optical mis-alignment adjustment technique is practically useful for the beamline initial alignment and commissioning. We describe here the way and the tools we use at SOLEIL to develop hard x-ray beamlines such as Psiché, which is a high pressure diffraction beamline using a wiggler source in the range from 15keV to 50 keV. Ray tracing simulations are performed with SpotX, taking into account the thermal surface deformations (from FEA calculations) and the surface defects due to the polishing and the bending (from the profilometer measurements) of the optics, to study carefully the defect effects on beam properties, to optimize the optical alignment process and to eliminate these defect effects by re-adjusting the optics, try to pursue the best performance of the beamline.

8141-40, Poster Session

A toolkit for the x-ray optics simulation software package XOP/ShadowVui

B. C. Meyer, Lab. Nacional de Luz Sincrotron (Brazil)

Conference 8141:
Advances in Computational Methods for X-Ray Optics II

The design of a synchrotron beamline is supported by various software simulation packages containing source simulation, characterization of X-ray optics, ray-tracing simulation and others separately. Beamline designers and operators often require instantly data of the beam parameter, which is only feasible with an unified and more user-friendly software package. The new developed toolkit is a first step in that direction.

Photon flux, bandwidth, beam size and beam divergence are the chosen parameters used for the beamline design and optimization. A tool was developed, which allows to scan these parameters by changing any input parameter, for example the photon energy, the vertical mirror position or the horizontal slit size. A tabular input allows scanning with arbitrary parameters or even different file names (e.g. filter material, surface profile).

We present two methods of calculating power density profiles on the optical components, one by ray-tracing and the other by transmission calculation using the DABAX library. The second method only considers flat optics, but is a good approximation and faster than the method based on ray-tracing.

The validation of the developed tools is shown by a comparison of the simulated beam parameters and the measured ones, which was performed at the Superconducting Wiggler Beamline (SCW) and the Undulator Beamline (PGM) recently turned into operation at the Brazilian Synchrotron Light Source (LNLS). We report also the capability of the parameterized scanning method for the alignment of the optics during the commissioning phase of the beamlines.

8141-41, Poster Session

XOP v2.4: recent developments of the x-ray optics software toolkit

R. J. Dejus, Argonne National Lab. (United States); M. Sanchez del Rio, European Synchrotron Radiation Facility (France)

XOP v2.4 consists of a collection of computer programs for calculation of radiation characteristics of x-ray sources and their interaction with matter. Many of the programs calculate radiation from undulators and wigglers, but others, such as x-ray tube codes, are also available. The computation of the index of refraction and attenuation coefficients of optical elements using user-selectable databases containing optical constants is an important part of the package for calculation of beam propagation. Coupled computations are thus feasible where the output from one program serves as the input to another program. Recent developments, including enhancements to existing programs, are described in detail.

* Work supported by the U.S. Department of Energy, Office of Science, Office of Basic Energy Sciences, under Contract No. DE-AC02-06CH11357.

8141-42, Poster Session

Conceptual design for a dispersive XAFS beamline in the compact storage ring MIRRORCLE

N. Canestrari, European Synchrotron Radiation Facility (France); V. Roger, P. Jeantet, O. Leynaud, L. Ortega, Institut NÉEL (France); H. Yamada, T. Hanashima, Ritsumeikan Univ. (Japan); J. Lorenzo, Institut NÉEL (France); M. Sanchez del Rio, European Synchrotron Radiation Facility (France)

We present the conceptual design of a XAFS beamline for MIRRORCLE [1], a new compact laboratory X-Ray source. This machine accelerates electrons to 20 MeV in a ring and produces x-rays when the electrons collide onto a thin target. The radiation emitted has a white spectrum due to both synchrotron and bremsstrahlung emission. The electrons are recovered after collisions, and the emitted light has high flux, large energy spectrum and an important angular dispersion.

We opted for a simple design using a collimator, slits, a curved crystal, the sample environment and a CCD. The beamline parameters have been optimized by defining and optimizing a figure of merit. It includes parameter like position of the mirror, ray of curvature, slit aperture, reflecting angle, etc. to optimize the flux into the sample, energy bandwidth and energy resolution. This optimization includes room constraints (distances among elements), mechanical constraints (minimum curvature radii available) and optical constraints. Further ray tracing simulations using SHADOW3 have been performed to check all the theoretical results, refine the final parameters, quantitative flux calculations and for simulating the image on the CCD.

[1] <http://www.photon-production.co.jp/e/PPL-HomePage.html>

The LABSYNC project (Laboratory compact light sources) has been funded by the European Commission under the Seventh Framework Programme (Grant No. 213126) "FP7-INFRASTRUCTURES."

Conference 8142:

Hard X-Ray, Gamma-Ray, and Neutron Detector Physics XIII

Monday-Wednesday 22-24 August 2011 • Part of Proceedings of SPIE Vol. 8142
Hard X-Ray, Gamma-Ray, and Neutron Detector Physics XIII

8142-01, Session 1

Recent progresses in THM CZT detector for medical imaging and security applications

S. A. Awadalla, J. Mackenzie, P. Marthandam, S. Taherion, J. Kumar, H. Chen, Redlen Technologies (Canada)

Recent works in the post growth annealing processes of CdZnTe using Traveling Heater Method (THM) for crystals of 10 and 15 mm thickness used for homeland security, has reduced the size and density of Te inclusions, which in turn resulted in improved crystal uniformity and performance of both ^{241}Am and ^{137}Cs spectra. In addition, more progress has been made on optimizing device metallization and geometry using extended cathode design which led to a perfect ohmic contact and improved device efficiency for thinner devices used in high flux x-ray and medical imaging applications respectively. Examples of the progress in the above mentioned areas will be presented.

8142-03, Session 1

Manipulation of charge transport and the internal electric field distribution in CdZnTe crystals using light

L. C. Teague, A. L. Washington II, M. C. Duff, Savannah River National Lab. (United States); M. Groza, V. Buliga, A. Burger, Fisk Univ. (United States)

CdZnTe (CZT) semiconducting crystals are of interest for use as room temperature X- and γ -ray spectrometers. Several studies have focused on understanding the various electronic properties of these materials, such as the surface and bulk resistivities and the distribution of the electric field within the crystal. Specifically of interest are how these properties are influenced by a variety of factors including structural heterogeneities, such as secondary phases (SPs) and line defects as well as temperature effects. We have used a variety of techniques to probe and manipulate the electrical properties of two CZT crystals that were grown using two types of methods and had substantially different defect densities and compositional volumes. We will describe and compare the variations observed in surface and bulk resistivities of these crystals as a function of light illumination at various wavelengths. Furthermore, we will correlate these results to changes in the internal electric field distribution that we observed through transmission images based on the Pockels effect. The specific responses of the two crystals and the observed changes in their electrical properties provide further insight into the detailed relationships between charge transport and material characteristics in CZT.

8142-04, Session 1

Characterizations of extended defects in CdZnTe detectors

A. E. Bolotnikov, G. Camarda, Y. Cui, R. Gul, A. M. Hossain, K. H. Kim, G. Yang, R. B. James, Brookhaven National Lab. (United States)

New results from testing of CdZnTe (CZT) detectors using IR transmission microscopy, white X-ray beam diffraction topography and chemical etching will be presented. Correlations with micron-scale X-ray mapping and gamma-ray spectral responses will also be provided. The particular roles of sub-grain boundaries and dislocations on charge transport in CZT material and CZT device performance will be emphasized.

8142-12, Session 1

The influence of steering electrodes on CZT pixellated x-ray detectors

D. Kitou, Univ. of Surrey (United Kingdom) and Science and Technology Facilities Council (United Kingdom); M. C. Veale, Science and Technology Facilities Council (United Kingdom); C. G. Allwork, P. J. Sellin, Univ. of Surrey (United Kingdom); P. Seller, Science and Technology Facilities Council (United Kingdom); A. Lohstroh, V. Perumal, Univ. of Surrey (United Kingdom); M. Wilson, Science and Technology Facilities Council (United Kingdom)

The use of steering, or inter-pixel, electrodes has been reported by various authors to improve the spectroscopic performance of both CZT single element [1, 2] and pixel detectors [3] by reducing inter-pixel charge sharing. Steering electrodes are used to influence the local weighting field close to the collecting electrode, which strongly improves the charge collection behaviour and spectroscopic performance of the device.

In this paper we use a dedicated ASIC, the PIXIE ASIC, to study charge sharing and the effect of steering electrodes on device performance. The PIXIE ASIC has been developed at RAL, as part of the HEXITEC collaboration [4], and contains 3 arrays of 9 pixels on a 250 μm pitch and a single array on a 500 μm pitch; each pixel contains a low noise charge amplifier and output buffer [5].

The ASIC has been developed to directly investigate the effect of electrode geometry on charge induction, charge sharing and the spectroscopic performance of CZT small pixel detectors; specifically the influence of steering electrodes on device performance.

The device simulation software Silvaco ATLAS has been used to model the electric field distribution in the CZT devices and how steering electrodes locally modify the field in the near-pixel region. These simulations will be compared to experimental measurements to fully understand the effects of steering electrode geometries on CZT detector performance.

8142-05, Session 2

Results of CdTe pixel detectors using Medipix2 and Medipix3 read-out electronics

M. Fiederle, A. Fauler, S. Procz, A. Zwerger, Albert-Ludwigs-Univ. Freiburg (Germany)

Pixel detectors have been processed using 1 mm thick CdTe wafers. The detectors have two different pixel pitches of 55 and 110 μm and an active area of 14x14 sqmm. The detectors have been selected from THM grown CdTe wafers. The wafers have been characterized by infrared microscopy and Contactless Resistivity Mappings to obtain the material properties.

The detectors have been flip-chip bonded to Medipix2 and the new Medipix3 read-out electronic chips. The correlation of the material properties with the performance of the pixel detectors is the focus of this work. The detectors have been characterized by x-ray tubes and gamma radiation. The performance of the pixel detectors will be discussed regarding spatial resolution by MTF, the efficiency and the possibility of energy resolving methods.

The possibility of high spatial resolution of 55 μm will be evaluated regarding the thickness of 1 mm of the detector samples.

The feature of the Medipix3 with five energy threshold will be used for spectroscopic images. The performance of a CdTe detector with the Medipix3 read-out will be discussed for the application in Colored X-ray Imaging.

8142-06, Session 2

Mapping the x-ray response of a CdTe sensor with small pixels using an x-ray microbeam and a single photon processing readout chip

E. Fröjdh, C. Fröjdh, B. Norlin, G. Thungström, Mid Sweden Univ. (Sweden)

CdTe is a promising material for X-ray imaging since it has high stopping power for X-ray photons. However defects in the material, non ideal charge transport properties and long range X-ray fluorescence can deteriorate the image quality, especially for applications of spectral imaging. In this project we have investigated the response of 1 mm thick CdTe sensors bonded to Timepix readout chips. The pixel pitch is 55 and 110 μm . The measurements have been done using an X-ray microbeam entering the sensor at a small incident angle. The width of the beam was around 10 μm . Due to the small size of the beam and the pixelation of the sensor the response around defects can be investigated by scanning. Also depth of interaction can be measured by the same method. The readout chip has been operating in Time over threshold mode thus measuring the energy of each X-ray interaction, also separating scattered and fluorescent photons interacting in different pixels. Measurements have been done in both electron and hole collection mode. The results give evidence of distorted electrical field around certain defects in the material and also show the small pixel effect.

8142-07, Session 2

Evaluation of characteristics of CdTe detector by laser pulses

Y. Suzuki, T. Ito, A. Koike, T. Okunoyama II, A. Miyake, Y. Neo, H. Mimura, T. Aoki, Shizuoka Univ. (Japan)

Measurements concerning the internal electric field, carrier generations, and transportation of electron are required to clarify the dynamic properties of CdTe gamma / X-ray detector. In addition, the position and the timing of the carrier generation should be controlled to obtain more accurate inner properties.

Therefore, the focused pulse laser irradiated to side of CdTe detector was used for control the incident position and timing accurately. This amount of photon correspond to γ -ray energy and pulse frequency correspond to γ -ray dose.

In this study, we use Schottky diode type CdTe of 0.5 mm thickness and pulse laser with wavelength of 633 nm. As a result, the change of output pulse height is observed corresponding to distribution in depletion layer at the Schottky interface.

8142-08, Session 2

Energy discriminated x-ray CT using high count rate photon counting CdTe detector

T. Aoki, A. Koike, Shizuoka Univ. (Japan) and ANSeeN Inc. (Japan); T. Okunoyama II, Shizuoka Univ. (Japan) and Shizuoka Univ. (Japan); H. Morii, Shizuoka Univ. (Japan) and ANSeeN Inc. (Japan); S. Singh, M. Kimura, T. Yamakawa, H. Mimura, Shizuoka Univ. (Japan)

The high count rate photon counting type CdTe detector, which can take full spectrum (2048ch) at 500kcps with X-ray tube source, was developed. The detector is small and stable for long time operation with very small polarization. The detector was mounted in CT system with micro-focused X-ray tube and XYZ-liner and rotation stages. We could obtain clear image with less beam hardening effect. We can change the energy -threshold or energy-band on software after imaging because each pixel has full energy spectrum. We could easily find optimized

threshold by changing the threshold energy while watching the screen on computer. This result shows new energy discriminated X-ray CT performance.

8142-09, Session 2

High resolution CdTe X- and gamma-ray detectors with a laser-formed p-n junction

V. A. Gnatyuk, V. Lashkaryov Institute of Semiconductor Physics (Ukraine) and Shizuoka Univ. (Japan); T. Aoki, Shizuoka Univ. (Japan); E. V. Grushko, L. A. Kosyachenko, Yuriy Fedkovych Chernivtsi National Univ. (Ukraine); O. I. Vlasenko, V. Lashkaryov Institute of Semiconductor Physics (Ukraine)

Room temperature X- and gamma-ray detectors, fabricated on the basis of CdTe diodes, have been usually suffered from an increase in leakage current with rising reverse bias voltage that was applied to extend the depletion region and thus improve energy resolution and efficiency. The dominant charge transport mechanism in the In/CdTe/Au diodes, formed by laser-induced doping of the surface region of high resistivity p-like CdTe crystals, is generation process in the space-charge region of the reverse-biased p-n junction near the In/CdTe contact. At higher bias voltages, an additional increase in leakage current is attributed to electron injection from the opposite Au/CdTe contact to the bulk of CdTe and hence into the p-n junction. In order to limit leakage current and improve the charge collection at the junction, a very steep high rectification barrier has been formed by extremely heavy n-type doping of a thin surface layer of crystals. This was achieved by carrying out laser-induced doping in liquid medium (water or methanol) to provide a high intensity of laser-induced stress and shock waves which had been considered as the main mechanism of solid phase doping. Moreover, the special processing was developed, including chemical and thermal procedures, to modify the surface state of the CdTe crystals before deposition of an In dopant film and electrodes. Finally, the room temperature In/CdTe/Au diode detectors have been obtained with record high energy resolution (0.7% at 662 keV peak of a Cs-137). The electrical and detection properties of the detectors have been investigated.

8142-02, Session 3

Characterization of CdTe and Cd(0.9)Zn(0.1)Te crystals grown from a low temperature solution process for radiation detector applications

K. C. Mandal, R. M. Krishna, T. C. Hayes, P. G. Muzykov, Univ. of South Carolina (United States); A. E. Mendez Torres, Savannah River National Lab. (United States)

Spectrometer grade CdTe and Cd(0.9)Zn(0.1)Te (CZT) crystals, grown at low temperature, have been characterized. The single crystals were grown from high purity Cd and zone refined Zn and Te in three zone furnaces installed in our laboratory. The furnaces feature custom pulling and rotation, using in-house electronics and software. The semi-insulating (SI) CdTe and CZT crystals exhibited high resistivity ($5\text{--}8 \times 10^{10} \Omega\text{-cm}$) and low Te-inclusions. The crystals also showed good electron mobility-lifetime product (electron $\mu\tau = 6 \times 10^{-3} \text{ cm}^2/\text{V}$). Optical absorption/transmission, x-ray photoelectron spectroscopy (XPS), electrical characterization including deep level transient spectroscopy (DLTS) measurements, and nuclear radiation detection testing was performed on the surface modified and unmodified CdTe and CZT crystals. Nuclear detection measurements were performed with Am-241 (60 keV) and Cs-137 (662 keV) radiation sources, showing a 2.4% and 1.4% energy resolution (FWHM), respectively, for surface modified CZT detectors.

Conference 8142:
Hard X-Ray, Gamma-Ray, and Neutron Detector Physics XIII

8142-10, Session 3

Performance evaluation on the first Polaris 3-D CdZnTe detector system

Z. He, F. Zhang, W. R. Kaye, Y. A. Boucher, W. Y. Wang, C. Wahl, J. M. Jaworski, S. J. Kaye, J. Berry, Univ. of Michigan (United States)

Each Polaris system consists of eighteen $2 \times 2 \times 1.5 \text{ cm}^3$ CdZnTe detectors, has a total detection volume of 108 cm^3 and is capable of real-time gamma-ray imaging in the energy range of about 40 keV up to 3 MeV. The first Polaris system was delivered to DOD DTRA in the middle of October 2010. Since then, this system has been tested by independent operators in Nevada during October to December of 2010, in Oak Ridge National Laboratory during January to March of 2011, and has been extensively tested by our research group at the University of Michigan. Test results on the first Polaris system will be summarized, including its energy resolution, detection efficiency, gamma-ray imaging angular resolution and gamma-ray imaging efficiency. Some new capabilities of the Polaris system will also be introduced.

8142-11, Session 3

Development of large-volume CZT cross-strip detectors

K. Lee, J. W. Martin, A. Garson, M. Beilicke, Q. Guo, Washington Univ. in St. Louis (United States); M. Groza, A. Burger, Fisk Univ. (United States); H. S. Krawczynski, Washington Univ. in St. Louis (United States)

Cadmium Zinc Telluride (CZT) is the detector material of choice for the detection of hard X-rays with excellent spatial and energy resolutions without cryogenic cooling. We are developing large-volume ($0.5 \times 3.9 \times 3.9 \text{ cm}^3$) cross-strip CZT detectors with the objective to combine the excellent performance achieved so far only with pixelated CZT detectors with a reduced number of readout channels. In this contribution, we present a detailed study of such large-volume CZT substrates from the company Orbotech contacted as cross-strip detectors. As readout contact dimensions can contribute to noise and affect the overall capabilities of a detector, we compare the detection efficiency and spectroscopic performance achieved with four different strip widths deposited simultaneously on the same substrate. In addition, we investigate the effects of a steering grid on the detection efficiency and energy resolution of the detector. Finally, we compare the experimental results with those from detailed detector simulations. Our results show that CZT cross-strip detectors combine excellent energy resolutions with high detection efficiencies and are a promising alternative to pixelated CZT detectors.

8142-13, Session 3

Performance characteristics of pixelated CZT crystals used on the GammaTracker project

E. M. Becker, C. E. Seifert, M. J. Myjak, L. E. Erikson, D. R. Balvage, R. P. Lundy, Pacific Northwest National Lab. (United States)

The GammaTracker project at Pacific Northwest National Laboratory is a handheld radioisotope identification device which uses eighteen pixelated Cadmium-Zinc Telluride (CZT) crystals to provide energy resolution approaching that of high-purity germanium without cryogenic cooling. Additionally, these crystals can be used to provide directional and imaging capabilities that cannot be found in other handheld detectors. A significant number of CZT crystals have been procured during the development of the GammaTracker system. These crystals undergo a two-stage testing procedure in order to assure the crystal quality

and meet project requirements. Key parameters that determine the quality of the crystals include the breakdown characteristics, pixel-by-pixel resolution, and mobility-lifetime product ($\mu\tau$). This presentation will provide and discuss the results of the testing procedure and their implications.

The Information Release (IR) request entitled, "CZT Abstract" has been approved by all the reviewers.

The IR number assigned to this product is: PNNL-SA-77708

8142-14, Session 3

Direct measurement of structural defects and their influence on CdZnTe detectors

A. M. Hossain, A. E. Bolotnikov, G. Camarda, Y. Cui, R. Gul, K. Kim, K. Kisslinger, D. Su, G. Yang, L. Zhang, R. B. James, Brookhaven National Lab. (United States)

Cadmium Zinc Telluride (CdZnTe) radiation detectors currently encounter a number of problems related to material uniformity and charge transport properties, which deteriorate the overall device performance and hence restrict their widespread deployment for potential applications in national security and medical imaging. Such deterioration in the detector's performance results from various point- and extended-crystalline defects, like vacancies, impurities, dislocations, precipitates, etc., which are primarily generated during crystal growth and post-growth treatment. We are systematically investigating various extended crystalline defects, like dislocations, micro-twins, and precipitates, in CdZnTe crystals grown under various conditions. In this study, we employed high-resolution electron microscopy (TEM and STEM), along with energy/wavelength dispersive X-ray spectroscopy (EDS/WDS). Their combination facilitated our acquisition of comprehensive information on structural defects in detector-grade CdZnTe crystals. In addition, we probed the electron-beam-induced current (EBIC) across specific defects by introducing, for the first time, a high-precision tungsten probe that allowed us to differentiate those defects directly. We correlated our findings from these different characterization methods to assess the crystalline defects, and to identify their origin and their influence on the performance of the fabricated devices. Our endeavor demonstrated distinct structural defects in the crystals, such as stacking faults, dislocation loops, and precipitates that likely are major causes in degrading the electrical properties of the devices, and eventually limiting the detector's performance.

8142-15, Session 4

Surface and defect correlation studies on high resistivity 4H-SiC bulk crystals and epitaxial layers for radiation detectors

K. C. Mandal, P. G. Muzykov, R. M. Krishna, T. C. Hayes, T. S. Sudarshan, Univ. of South Carolina (United States)

High resistivity silicon carbide (SiC) has potential applications for room temperature radiation detectors because of its wide band gap, good charge transport properties and high radiation hardness. Crystallographic defects and impurities in this material are the two major factors limiting the performance of SiC based radiation detectors. Therefore their study is highly demanded for the development of high resolution radiation detectors from this material. In this work, we present electrical and defect characterization studies of semi-insulating bulk 4H SiC crystals and epitaxial layers. Study of the extended defects was accomplished using electron beam induced current (EBIC) measurements and chemical etching in molten KOH in conjunction with optical microscopy, scanning electron microscopy (SEM), and atomic force microscopy (AFM) for defect identification and detailed study of the etch pit structure. Results of the investigation correlating SEM contrast with the etch pit structure for different types of threading dislocations will be presented. Study of the electrically active defects and impurities, and carrier transport

**Conference 8142:
Hard X-Ray, Gamma-Ray, and Neutron Detector Physics XIII**

properties, were conducted using glow discharge mass spectroscopy (GDMS), thermally stimulated current (TSC) measurements, high temperature resistivity (HTR) studies and Hall effect measurements. The TSC and HTR measurements revealed deep level centers at 1.1-1.2 eV and 1.56 eV in bulk 4H SiC samples, which we associate with intrinsic defects. The obtained results are correlated with the capability of bulk crystals and epitaxial layers for the detection of low energy x-rays, gamma rays, α -radiation, and tritium detection.

8142-16, Session 4**Efficiency and decay time measurement of phosphors for x-ray framing cameras usable in harsh radiation background**

N. Izumi, J. A. Emig, J. D. Moody, C. Middleton, J. P. Holder, K. Piston, V. Smalyuk, C. A. Hagmann, J. Ayers, J. R. Celeste, C. J. Cerjan, B. Felker, K. Krauter, C. Sorce, S. M. Glenn, D. K. Bradley, P. M. Bell, Lawrence Livermore National Lab. (United States); J. L. Bourgade, S. Darbon, Commissariat à l'Énergie Atomique (France); J. D. Kilkenny, General Atomics (United States)

Phosphors are key components of x-ray framing camera and x-ray/optical streak cameras. In these cameras, incoming x-rays or optical signals are converted to electrons that are multiplied, gated, or deflected, then converted back to optical signals again using phosphors. On implosion experiments at the National Ignition Facility, these instruments must operate in a harsh ionizing radiation background environment (mostly neutrons and gamma-rays produced by inelastic scattering of neutrons). In this environment, a significant improvement in signal-to-background ratio can be obtained by utilizing a phosphor with a high optical output and fast decay time. We present measurements of conversion efficiency and decay times for various phosphor materials, enabling optimal design of framing cameras and streak cameras for implosion experiments. Prepared by LLNL under Contract DE-AC52-07NA27344.

8142-17, Session 4**Long-term room temperature stability of TlBr gamma detectors**

A. Conway, L. F. Voss, A. J. Nelson, P. R. Beck, R. J. Nikolic, S. A. Payne, Lawrence Livermore National Lab. (United States); H. Kim, L. J. Cirignano, K. S. Shah, Radiation Monitoring Devices, Inc. (United States)

TlBr is a material of interest for use in room temperature gamma detector applications due to its wide bandgap 2.7 eV and high average atomic number (TI 81, Br 35). Researchers have achieved energy resolutions of 1.2 % at 662 keV, demonstrating the potential of this material system. However, these detectors are known to polarize using conventional configurations, limiting their use. Continued improvement of room temperature, high resolution gamma ray detectors based on TlBr requires further understanding of the degradation mechanisms. While high quality material is a critical starting point for excellent detector performance, we have found that the long term stability of these detectors is greatly dependent on the processes used in detector fabrication and can be improved with a "field annealing" step. Characterization and analysis of the effects of the fabrication process on long term stability of TlBr detectors using conventional electrodes at room temperature will be presented.

This work was performed under the auspices of the U.S. Department of Energy by Lawrence Livermore National Laboratory under Contract DE-AC52-07NA27344. This work was supported by The Domestic Nuclear Detection Office in the Department of Homeland Security.

8142-18, Session 4**comparison of SEM and optical analysis of DT neutron tracks in CR-39 detectors**

P. A. Boss, SPAWARSYSCEN Pacific: San Diego (United States); L. Forsley, JWK International Corp. (United States); P. Carbonnelle, Univ. Catholique de Louvain (Belgium); M. S. Morey, J. R. Tinsley, J. P. Hurley, National Security Technologies, LLC (United States)

Columbia Resin 39 (CR-39), a polyallyldiglycol carbonate polymer, has been used as a solid state nuclear track detector (SSNTD) to detect energetic nuclear particles. As an energetic, charged particle traverses through CR-39, it creates along its path an ionization trail that is more sensitive to chemical etching than the bulk material. After etching, the tracks due to energetic particles have the appearance of holes or pits. The most common method employed to analyze these tracks is optical microscopy. However, atomic force microscopy (AFM) and scanning electron microscopy (SEM) have also been used by others to analyze tracks in CR-39 resulting from exposure to either alpha or proton sources. In this communication, tracks resulting from exposure to a DT neutron source were examined both optically and by SEM. The purpose of the analysis was to compare the two techniques and to determine whether additional information on track geometry could be obtained by SEM analysis. The use of these techniques to examine triple tracks, diagnostic of ≥ 9.6 MeV neutrons, observed in CR-39 used in Pd/D co-deposition experiments will also be discussed.

8142-19, Session 4**Position sensitive gamma ray measurements using mercuric iodide strip detectors**

S. K. Chaudhuri, A. Lohstroh, Univ. of Surrey (United Kingdom); A. Hardie, L. L. Jones, P. Seler, Rutherford Appleton Lab. (United Kingdom); P. J. Sellin, Univ. of Surrey (United Kingdom)

Mercuric iodide, because of its high Z components and high resistivity, has presented itself as a suitable x- and gamma-ray detector material for spectroscopic purposes. Because of excellent absorption coefficients for hard x-rays even for small volume detectors, HgI₂ detectors can be suitably used as very compact position sensitive devices. In addition, recent availability of superior detector grade material has renewed the interest of application of HgI₂ crystals for imaging.

In the present work we report the performance of two HgI₂ strip detectors, designed at University of Surrey, as one dimensional position sensitive devices. The two devices were designed so as to sit side by side to form a prototype array. Each device consists of 13 palladium strips and a planar Pd back contact deposited on a 27 x 13 x 1.4 mm HgI₂ crystal, fabricated by Constellation Technologies, USA. The strips were pitched at 2 mm and are 1.7 mm wide and 10 mm long. Gamma spectroscopy has been performed on all strips separately at various energies up to 662 keV. It was found that the detectors have a moderate energy resolution and all the strips have more or less similar characteristics. For position sensitive measurements, an analog readout system has been designed in collaboration with Rutherford Appleton Laboratory. The read-out system consists of an ASIC which collects and processes the signal from all the strips of the two-detector array simultaneously. We will present a comprehensive summary of the spatial resolution and spectroscopic performance of the system.

8142-20, Session 5**CMOS solid-state photomultipliers for high energy resolution calorimeters**

E. B. Johnson, C. J. Stapels, X. Chen, C. Whitney, E. C. Chapman, G. Alberghini, R. Rines, Radiation Monitoring Devices,

Conference 8142:
Hard X-Ray, Gamma-Ray, and Neutron Detector Physics XIII

Inc. (United States); F. Augustine, Augustine Engineering (United States); R. Miskimen, Univ. of Massachusetts Amherst (United States); J. F. Christian, Radiation Monitoring Devices, Inc. (United States)

High-energy, gamma-ray calorimetry typically employs large scintillation crystals coupled to photomultiplier tubes. To achieve valued physics measurements, these calorimeters are segmented to the limits associated with the costs of the crystals, photomultiplier tubes, and support electronics. A cost-effective means for construction of a calorimeter system is to use solid-state photomultipliers (SSPM) with front-end electronics, which has roughly half the cost, but the SSPM must provide the necessary energy resolution defined by the physics goals. We have developed a large-area SSPM (1 cm × 1 cm) for readout of large scintillation crystals, and one particular application of reading out PbWO₄ crystals in a gamma-ray calorimeter pushes the limits of the solid-state photomultiplier. The nature of PbWO₄ requires high-energy (> 1 GeV) gamma-rays for device evaluation, as the light yields are low, and a high energy deposition also requires a large volume to completely absorb the gamma-ray energy characterized by the Molière radius. These two constraints restrict device evaluation with test sources, such as ²²Na. The SSPM and readout electronics have been developed for the calorimeter with supporting front-end electronics for readout of four scintillation crystals for complete instrument evaluation with a high-energy gamma ray, but initial tests with test sources and bright scintillation materials (LYSO, CLLB) indicate that the detector will provide sufficient energy resolution. We will review each signal and noise contribution from the large-area SSPM and provide predicted device performance as a function of light intensity and operating conditions, providing the baseline information on expected detector performance.

8142-21, Session 5

A hybrid reflective/refractive/diffractive achromatic fiber-coupled radiation resistant imaging system for use in the spallation neutron source (SNS)

L. C. Maxey, Oak Ridge National Lab. (United States); J. Kumler, JENOPTIK Optical Systems, Inc. (United States); T. R. Ally, A. M. Brunson, F. D. Garcia, K. C. Goetz, K. E. Hasse, M. A. Mitchell, M. L. Simpson, T. J. Shea, Oak Ridge National Lab. (United States); T. Lindsey, D. Brown, T. Victorio, JENOPTIK Optical Systems, Inc. (United States)

A fiber-coupled imaging system for monitoring the proton beam profile on the target of the Spallation Neutron Source was developed using reflective, refractive and diffractive optics to focus an image onto a fiber optic imaging bundle. The imaging system monitors the light output from a chromium-doped aluminum oxide (Al₂O₃:Cr) scintillator on the nose of the target. Metal optics are used to relay the image to the lenses that focus the image onto the fiber. The material choices for the lenses and fiber were limited to high-purity fused silica, due to the anticipated radiation dose of 108 R. In the 1st generation system (which had no diffractive elements), radiation damage to the scintillator on the nose of the target significantly broadened the normally monochromatic (694 nm) spectrum. This created the need for an achromatic design in the 2nd generation system. This was achieved through the addition of a diffractive optic for chromatic correction. An overview of the target imaging system and its performance, with particular emphasis on the design and testing of a hybrid refractive/diffractive high-purity fused silica imaging triplet, is presented.

8142-22, Session 5

Cryogenic CMOS avalanche diodes for nuclear physics research

X. Chen, E. B. Johnson, C. J. Stapels, C. Whitney, R. Rines, E. C. Chapman, G. Alberghini, J. F. Christian, Radiation Monitoring Devices, Inc. (United States)

Exploration in nuclear physics may require extreme conditions, such as temperatures down to a few Kelvin, high magnetic fields of several Tesla, or the small physical dimensions of a few centimeters. As a standard for radiation detection uses scintillation materials, it is desirable to develop photodetectors that can operate under these harsh conditions. Though photomultiplier tubes (PMTs) have been used for most applications for readout of scintillation materials, they are bulky, highly susceptible to magnetic fields, and present a large heat load in cryogenic environments. Avalanche photodiodes are a reasonable alternative to PMTs in that they are extremely compact and less susceptible to magnetic fields. Photodiodes have been developed in a commercial CMOS process for operation at temperatures below 100 Kelvin. We present the overall operation of the photodiodes approaching 5 Kelvin. The diodes show an overall decrease in quantum efficiency with respect to room temperature operation with a wave length dependence, the decrease from room temperature to 5 Kelvin is no more than roughly 50%. A gain of 100 is achieved at reasonably low biases rough 30 V. At about 30 Kelvin, the diodes exhibit an internal resistive term, which generates a second breakdown point. Though these characteristics are not ideal, the prototype diode shows a proportional response to the intensity of light pulses down to 150 detected photons. The properties of the photodiodes and the readout electronics will be discussed for general photon detection below 100 K.

8142-23, Session 5

A prototype high detective quantum efficiency imaging panel based on fiber-optic scintillation glass array (FOSGA) for megavoltage imaging

S. S. Samant, A. Gopal, Univ. of Florida (United States); J. E. Bacia, Jr., Pacific Northwest National Lab. (United States)

Megavoltage imaging has applications in nondestructive imaging for homeland security, radiotherapy, and industrial manufacturing. Current commercial systems are limited by low image quality as measured by detective quantum efficiency (DQE). These systems yield measured DQE=0.01-0.02, limiting efficacy for detection based on automated signal processing. Past efforts to improve DQE have included novel scintillators and manufacturing of large crystal structures. An alternative novel design for a 2D x-ray imager, based on a modification of existing amorphous silicon (a:Si) or flat-panel imagers, is presented. The panel utilizes a fiber-optic scintillation glass array (FOSGA) consisting of scintillation fibers bundled within a pixilated thick sintered tungsten housing. The tungsten housing is constructed using a lithographic manufacturing technique for high fabrication accuracy. The Tb-doped fibers emit light in the 555-565nm range (matched to the sensitive region of current a:Si photodiodes), with a decay time of 2ms (100-to-40%). Monte Carlo simulations, linear cascaded systems analyses, and film studies have been carried out to validate and optimize image quality for radiation beams in the 1-6MV range. An 8cmx8cm prototype array was fabricated using Tb-doped fibers (9mm length, 0.9mm diameter) loaded into a tungsten matrix (1.1mm pixel pitch, 0.1mm septa), yielding measured DQE=0.05 (vs theoretical DQE=0.07) for 6MV imaging, an order of magnitude improvement in image quality over current commercial imagers. Design parameters of a large field-of-view FOSGA imager for cargo container security imaging are presented: 5cm thick FOSGA array, 0.4-1mm pixel pitch, 50-70% fill factor, DQE>0.2 for 1-6MV range.

8142-25, Session 6

Covariance spectroscopy applied to nuclear radiation detection

R. Trainham, National Security Technologies, LLC (United States)

Covariance spectroscopy is a method of processing second order moments of data to obtain information that is usually absent from average spectra. In nuclear radiation detection the techniques of covariance spectroscopy represent a generalization of nuclear coincidence techniques. Correlations and fluctuations in data streams encode valuable information about radiation sources, transport media, and detection systems, and gaining access to the extra information can aid many problems in radiation detection and source identification. Covariances can be used to de-noise data, untangle complicated spectra, uncover overlapping peaks, accelerate source identification, and sense directionality.

Correlations existing at the source level are particularly valuable since many radioactive isotopes emit correlated gammas and neutrons. Correlations also arise from interactions within detector systems, as well as in the environment. In particular, correlations from Compton scattering and pair production within a detector array can be usefully exploited even in detection scenarios where direct measurement of source correlations would be unfeasible. We present a covariance analysis formalism, with particular emphasis on its connection to traditional coincidence techniques, and we present experimental results to illustrate the utility of the concepts.

8142-27, Session 6

Recognition of 235U enrichment based on autocorrelation function of source-driven neutron pulse signal

J. Jin, W. Biao, F. Peng, Chongqing Univ. (China)

This paper describes a recognition mechanism of 235U enrichment based on the relationship between the autocorrelation function of neutron pulse signal and the 235U enrichment in source-driven nuclear material identification system(NMIS). The mechanism includes two steps: First, obtains the curve distance between autocorrelation functions of the signal to be measured and the reference signal. Meanwhile, the wavelet de-noising on autocorrelation functions is introduced into this step to get more accurate curve distance. Second, derives the relationship between the curve distance and the 235U enrichment by linear fitting or artificial neural network(ANN) to accomplish the recognition of 235U enrichment. The experimental results show that the wavelet de-noising can reduce the negative influence of the fluctuation in neutron pulse signal, and ensures the ability of autocorrelation functions to reflect the varying 235U enrichment. The linear fitting and the ANN can both determine the distance-enrichment relation curve to identify the 235U enrichment in different conditions. The experimental results have proved the reliability and validity of the recognition mechanism which provides guarantee for the recognition of 235U enrichment by NMIS.

8142-28, Session 6

Prompt neutron multiplicity measurements with portable detectors

S. Mukhopadhyay, R. S. Wolff, R. J. Maurer, S. E. Mitchell, P. Guss, National Security Technologies, LLC (United States)

Rapid detection of kilogram quantities of SNM during maritime transportation is a challenging problem for the U.S. Department of Homeland Security. Counting neutrons emitted by the SNM and partitioning them from the background neutrons of various origins is the most effective passive means of detecting the SNM. Unfortunately, neutron detection, counting, and partitioning in a maritime environment

is complex due to the presence of spallation neutrons and to the complicated nature of the neutron scattering in that environment.

A prototype fission meter is being designed by National Security Technologies, LLC, using a thin uniform coating of 10B as a neutron converter inside a large array of thin (4 mm diameter) copper tubes. The copper tubes are only 2 mil thick, and each holds the stretched anode wire under tension and high voltage. The tubes are filled with proportional counter gas (a mixture of 90%/10% of Ar/CO₂). The tubes operate in proportional counter mode and attract mobile charged particles () created in the nuclear interaction 10B(n,)7Li.

Several MCNPX calculations covering substantial design parameter space of neutron multiplicity detectors have been performed and are presented here. The efficiency of thermal neutron detection of this proposed detector will be compared to that of the commercially available Fission Meter (manufactured by ORTEC). Pulse height spectra originating from the charged particles created in the nuclear reaction

10B(n,) 7Li* + 2.310 MeV (94%) - excited state

10B(n,) 7Li + 2.792 MeV (6%) - ground state

will be examined, and the response to incident gamma rays will be demonstrated.

Acknowledgment

This work was done by National Security Technologies, LLC, under Contract No. DE-AC52-06NA25946 with the U.S. Department of Energy.

8142-61, Session 6

Transparent oxyhalide glass and glass ceramics for gamma-ray detection

C. Han, M. Barta, M. Dorn, J. Nadler, R. Rosson, B. Wagner, B. Kahn, Georgia Tech Research Institute (United States); Z. Kang, Georgia Tech Research Institute (United States) and Georgia Institute of Technology (United States)

Nuclear radiation detection is a popularly-discussed topic with increasing importance in today's society. Conventional scintillator based gamma ray detectors use single-crystal materials such as NaI:TI, LaBr₃:Ce, which provide excellent radiation detection properties, but suffer from their environment-related fluctuation, high cost and size limitation. The incorporation of nano-phosphors or Quantum Dots (QD) into a transparent host matrix has been studied recently as a cost-saving alternative that may solve the scalability and stability problems while still providing considerable optical performance. In this work, a new glass based detecting material with promising gamma ray detection performance will be reported. Transparent oxyhalide aluminosilicate glasses containing cerium doped gadolinium halide nanocrystal were prepared by a melt-quenching method followed by anneal at different temperatures to control the density of nano-crystals precipitate. Samples were then casted and polished for optical characteristic tests. The preliminary results indicated a similar gamma ray detection efficiency compared to a conventional NaI:TI detector and a gamma-ray peak resolution of ~27% at 662 KeV from some of these samples. By controlling element composition and ratio/size of the in-situ precipitated nano-particles, radiation detection performance is expected to be further optimized and will be studied by X-ray diffraction (XRD), Energy dispersive X-ray Spectroscopy (EDS), Differential Thermal Analysis (DTA), photoluminescence (PL), photo-luminescent excitation (PLE) and scintillation spectral measurements.

8142-29, Session 7

Optical properties of halide and oxide scintillators

D. J. Singh, Oak Ridge National Lab. (United States)

Knowledge of optical properties of scintillators is important both for the optimization of scintillator systems and development of new materials

Conference 8142:
Hard X-Ray, Gamma-Ray, and Neutron Detector Physics XIII

particular ceramic scintillators. Recent developments, including new density functionals that accurately predict band gaps, have made it possible to perform quantitative calculations of optical properties of scintillator materials. We used these techniques to obtain optical properties of a large number of high light output halide and oxide scintillators. These calculations showed that many halide scintillators have remarkably little optical anisotropy and may be good candidates for development as ceramic scintillators. These include materials such as $\text{CaI}_2:\text{Eu}$ that have very high light output and other favorable properties but are difficult to develop due to crystal growth issues.

8142-30, Session 7

Proportionality studies of multivalent metal halide scintillators

K. S. Shah, Radiation Monitoring Devices, Inc. (United States)

In this paper, experimental results of proportionality of various multivalent metal halide scintillators are presented. These proportionality measurements have been conducted using isotopic sources with gamma-ray energy varying from 14 keV to 1275 keV. Proportionality results are presented for various sub-groups within the multivalent metal halides (with Ce^{3+} , Eu^{2+} and in some instances, Pr^{3+} activators) to illustrate clear trends that have been observed for these sub-groups. Some proportionality results for selected compositions with varying activators are also presented. For example, Ce^{3+} and Pr^{3+} activators have been studied in LaBr_3 with little change in proportionality. Effect of microstructure of a given scintillator on its proportionality has also been explored by comparing results for single crystals with those for ceramics.

8142-31, Session 7

Performance of $\text{SrI}_2(\text{Eu})$ Gd-based transparent ceramics and bismuth-loaded polymer scintillators

N. J. Cherepy, S. A. Payne, Z. M. Seeley, B. L. Rupert, B. W. Sturm, R. D. Sanner, T. A. Hurst, S. E. Fisher, O. B. Drury, P. Thelin, Lawrence Livermore National Lab. (United States); A. Burger, Fisk Univ. (United States); K. S. Shah, Radiation Monitoring Devices, Inc. (United States); L. A. Boatner, Oak Ridge National Lab. (United States)

For gamma ray spectroscopy, we have discovered a new single crystal scintillator, Strontium Iodide doped with Europium, $\text{SrI}_2(\text{Eu})$, that offers energy resolution for gamma spectroscopy comparable to that of Lanthanum Bromide doped with Cerium, and considerably better than Thallium-doped Sodium Iodide, $\text{NaI}(\text{Tl})$. Encapsulated 1 in 3 $\text{SrI}_2(\text{Eu})$ crystals routinely provide energy resolution at 662 keV of <3%.

Transparent ceramics are fully dense monoliths of micron-scale crystallites, formed by sintering high purity ceramic nanopowders, generally of a single pure phase cubic crystal structure. While the best energy resolution is obtained with single crystal scintillators, such as $\text{SrI}_2(\text{Eu})$, transparent ceramics offer the possibility of low-cost, net-shape fabrication of oxide scintillators, with benefits of mechanical ruggedness, stability in air and radiation hardness. Transparent ceramic Cerium-doped Gadolinium Garnet, $\text{GYGAG}(\text{Ce})$, fabricated at LLNL, offers 4.8% resolution at 662 keV with PMT readout, and with low-noise silicon photodetector readout, <4% can be obtained. For radiographic imaging applications, we are developing transparent ceramic Europium-doped Gadolinium Lutetium Oxide, $(\text{Gd},\text{Lu})_2\text{O}_3(\text{Eu})$, which offers high density of 8-9 g/cm³ and a high light yield of 70,000 Photons/MeV. Key to its performance for imaging applications is attaining extremely low optical scatter by optimizing fabrication conditions.

Due to their availability in large sizes at low cost, plastic scintillators, generally based on Polyvinyltoluene, are used in many applications where a higher density material exhibiting a photopeak would be preferred. Recently, we demonstrated that a cm-scale Bismuth-loaded polymer scintillator can provide energy resolution of <7% at 662 keV.

8142-32, Session 8

Towards an understanding of nonlinearity in scintillator detector materials

G. A. Bizarri, Lawrence Berkeley National Lab. (United States)

It has been known for more than 50 years that the light emitted by a scintillator under high-energy excitation (gamma, alpha, proton...) is not always proportional to the amount of absorbed energy. The deviation from the linearity of luminosity versus absorbed energy is known as non-proportionality. In addition to its academic interest, this phenomenon has been considered central for scintillator development due to its implication in the limitation of achievable detectors performance. Although non-proportional response was studied intensively during the second part of the 20th century, understanding of its origin and implications on scintillator performance were mainly qualitative. Research in the 1960's uncovered a correlation between proportional response and ionization density, while in the 1980's non-proportionality was proposed as the main reason of energy resolution deviation from the counting statistics limit. It is only recently that the bridge between qualitative and quantitative understanding has been crossed, mainly driven by the large effort undertaken to discover new high-resolution scintillators. Developing such detector materials prompted efforts to gain a deeper understanding of the microscopic processes involved in scintillation mechanisms and so in non-proportionality. In this talk, the phenomenology of past and present understanding of non-proportional response will be reviewed. Based on recent experimental, computational and theoretical works, the relation between nonlinear response and energy resolution degradation will be addressed. Finally, the relation between material parameters and proportionality will be evaluated. These recent works are leading towards a deeper understanding of nonlinearity in scintillator detector materials and should result in the development of new high performance scintillator materials.

8142-33, Session 8

Dependence of nonproportionality in scintillators on diffusion of excitons and charge carriers

R. T. Williams, J. Q. Grim, Q. Li, K. B. Ucer, Wake Forest Univ. (United States)

Dipole-dipole and Auger quenching processes that are generally regarded to be at the root of nonproportionality depend respectively on the 4th or 6th power of the electron track radius, which in turn expands as the square root of Dt , where D is the effective diffusion coefficient for the mixture of excitons and charge carriers comprising the track. The range of D across semiconductor and scintillator radiation detectors is large, e.g. 8 decades from holes in HPGe to self-trapped holes in CsI:Tl . Thus the diffusive dilution rate of excitation density subject to nonlinear quenching depends on the 2nd or 3rd power of a parameter (D) that spans 8 decades! We present the functional form of nonlinear quenching predicted by diffusive track dilution and show that it provides an excellent fit of empirical nonproportionality across a wide range of semiconductor and oxide radiation detectors. We also show that diffusion drives nonlinear branching between excitons and free carriers in the track when electron and hole mobilities are unequal, and that this nonlinear branching coupled with linear trapping on defects produces the "halide hump" seen in electron yield data for activated halide scintillators. The conventional Onsager radius for carrier pairing is shown to be replaced by a much smaller decision radius in the electrochemical potential landscape of the track, and different e/h diffusion rates dominate the decision on branching to excitons or free carriers. Nonproportionality is shown to be largely independent of activator concentration in this transport-based model. Picosecond time-resolved measurements and K-dip spectroscopy provide good experimental checks on the model.

8142-34, Session 8

Electron cascades and stopping power in scintillator materials

F. Gao, Y. Xie, Z. Wang, S. N. Kerist, L. W. Campbell, R. M. Van Ginhoven, Pacific Northwest National Lab. (United States)

The development of new and improved materials for radiation detection is driven by unmet detector requirements for nuclear non-proliferation, homeland security, imaging for medical diagnosis and treatment, and fundamental science. An advanced Monte Carlo code (NWEGRIM - Northwest Electron and Gamma Ray Interactions in Matter) has been further developed and applied to study electron cascades and energy transfer efficiencies and to calculate stopping power and its fluctuation in NaI and LaBr₃, and the results are compared to those published by our group for CsI. These simulations provide information on the creation and spatial distribution of electron-hole pairs, allowing some important intrinsic properties and energy resolution to be evaluated. Also, the stopping power (dE/dx) in a number of scintillator materials has been calculated for energies ranging from 50 eV to 1 MeV, and the results have been compared with those obtained by the Bethe-Block theory, which is an important component for phenomenological model of scintillation processes. The calculated stopping powers are in good agreement with the Bethe-Block theoretical values at high energies, but show some deviations in the low energy regions. The simulations also yield the fluctuations of dE/dx, which have been compared with the Landau fluctuations. Furthermore, the spatial and energy distributions of electrons at the end of the electron cascade determined by NWEGRIM are used as inputs to study the spatial distribution of thermalized electrons in CsI as a function of incident γ -ray energy using a semi-classical theory of electron thermalization model, as implemented in a Monte Carlo transport code of electron-hole pairs. The possible implications of the present results to the study of nonlinearity have been discussed.

8142-35, Session 8

Physics of scintillator nonproportionality

S. A. Payne, S. Sheets, B. W. Sturm, N. J. Cherepy, L. Ahle, S. Dazeley, Lawrence Livermore National Lab. (United States); W. W. Moses, G. A. Bizarri, Lawrence Berkeley National Lab. (United States)

We have developed a phenomenological model of scintillator nonproportionality that requires only two parameters be adjusted to fit the nonproportionality curves of over 30 scintillators, for which experimental data was obtained on our facility known as the Scintillator Light Yield Nonproportionality Instrument (SLYNLI). The two parameters entail accounting for the: (1) fraction of mobile electrons and/or holes produced following the cascade, and (2) exciton-exciton annihilation loss mechanism (based on the classical Birks model). We find that the materials naturally group according to the composition of the host medium, as alkali halides, multivalent halides, fluorides, silicates, simple oxides, and organics. In other words, the nonproportionality curves for each of these material groups are quite similar, although there is a significantly smaller, yet measurable, impact by the identity and concentration of the activator. We also briefly review the work of other researchers on the possible mechanistic under-pinning of this model. Lastly, we deduce the predicted degradation in the resolution from nonproportionality by incorporating the influence of Landau fluctuations, or the instantaneous variance in stopping power as the electron is losing energy and coming to rest.

This work was supported by the Department of Energy, NA-22 and the Department of Homeland Security (DNDO), and was performed by Lawrence Livermore National Laboratory under contract DE-AC52-07NA27344 and by Lawrence Berkeley National Laboratory under contract DE-AC02-05CH11231.

8142-36, Session 8

Bond order potential-based molecular dynamics model for CZT melt-growth simulations

X. Zhou, D. K. Ward, B. M. Wong, F. P. Doty, Sandia National Labs. (United States)

CdTe-based Cd_{1-x}Zn_xTe (CZT) alloy compound is the leading semiconductor for γ -ray detection. The wide-spread deployment of the CZT detectors, however, is currently limited by the high costs of detector-grade materials due to their low manufacturing yields. The formation of defects such as grain boundaries, tellurium inclusions / precipitates, and dislocations during crystal growth has been the limiting factor for the property non-uniformity and the resulting low manufacturing yields. The problem is that while these defects can easily form and are prevalent in the material, their formation mechanisms are not well understood and hence they are difficult to remove. To enable the study of correlation between growth conditions and defect generation on a fine scale using high fidelity molecular dynamics simulations, we have been developing an analytical bond-order potential for the CZT system. The functional forms of the potential were directly derived from the tight-binding theory under the condition that the first two levels of the expanded Green function for the $[\sigma]$ - and $[\pi]$ - bond orders are retained. The potential incorporates primary ($[\sigma]$) and secondary ($[\pi]$) bonding and the valence-dependence of the heteroatom interactions. The potential parameters are parameterized considering properties of a variety of elemental and compound configurations (with coordination varying from 1 to 12) including small clusters, bulk lattices, defects, and surfaces. As a first stage for modeling CZT, preliminary parameterization has been completed for the CdTe system. It is demonstrated that this CdTe bond-order potential not only predicts a structural and binding energy trend close to that seen in experiments and ab initio calculations, but also reasonable melting temperatures for equilibrium Cd, Te, and CdTe phases and various CdTe (001) surface reconstructions. Most importantly, we have validated this potential by demonstrating its ability to predict the liquid phase growth of zinc-blende CdTe crystals. The emergence of such a BOP-based method begins to enable defect formation mechanisms in CZT crystals to be studied at a fidelity level comparable to ab initio methods and a scale level comparable to empirical molecular dynamics simulation methods.

This work is supported by the NNSA/DOE Office of Nonproliferation Research and Development, Proliferation Detection Program, Advanced Materials Portfolio. Sandia National Laboratories is a multi-program laboratory managed and operated by Sandia Corporation, a wholly owned subsidiary of Lockheed Martin Corporation, for the U.S. Department of Energy's National Nuclear Security Administration under contract DE-AC04-94AL85000.

8142-37, Session 9

New approach for high quality CZT crystals

D. J. Knuteson, N. B. Singh, A. Berghmans, D. Kahler, B. Wagner, M. King, S. McLaughlin, Northrop Grumman Electronic Systems (United States); A. E. Bolotnikov, R. B. James, Brookhaven National Lab. (United States)

Results will be presented for the growth of CdZnTe by the low pressure Bridgman growth technique utilizing novel choked seeding. CZT detectors are the current state of the art for high resolution, portable room temperature gamma-ray detectors, but widespread use has been slowed due to low yields and limited availability and the resulting high prices. We expect to reduce grain boundaries with choked seeding, which will increase yield and lower prices. In addition, the high purity commercial raw materials will be further refined to reduce impurities and deep level traps. The crystals will be grown in the programmable multi-zone furnace (PMZF), which was designed and built at Northrop Grumman's Bethpage facility to grow CZT on Space Shuttle missions. Results of the purification and crystal growth will be presented as well as characterization of crystal quality and detector performance.

Conference 8142:
Hard X-Ray, Gamma-Ray, and Neutron Detector Physics XIII

8142-38, Session 9

Residual stress determination in CZT and CMT ingots using synchrotron white beam x-ray diffraction topography

K. Kim, A. E. Bolotnikov, G. Camarda, A. M. Hossain, G. Yang, Y. Cui, R. Gul, R. B. James, Brookhaven National Lab. (United States)

CdTe-based CZT (CdZnTe) and CMT (CdMnTe) material show excellent X-ray and gamma-ray detector performance at room temperature. Residual stress generated during crystal growth by extended defects and thermal gradients play an important role in the micro-structural details and associated detector-performance properties. SWBXT (synchrotron white beam X-ray diffraction topography) is a non-destructive technique capable of providing information on the nature and distribution of structural defects such as dislocations, inclusions/precipitates, stacking faults, growth sector boundaries, twins, and low-angle grain boundaries in crystals. CZT and CMT ingots were grown by the Bridgman method using facilities at Brookhaven National Laboratory. We will present data on the evolution and distribution of residual stress in CZT and CMT slabs taken from the tip to heel of the ingots.

8142-39, Session 9

A traveling magnetic field (TMF) for active control of the Bridgman growth of CZT crystals

G. Samanta, A. Yeckel, J. J. Derby, Univ. of Minnesota, Twin Cities (United States)

Large, single crystals of cadmium zinc telluride (CZT) are needed for portable, low-cost, and sensitive devices to monitor radioactive materials. However, while CZT improvements are needed, the growth of these crystals is not well understood. We aim to advance the practice of crystal growth by applying physics-based, computational process models along with modern process control theory. Specifically, we are developing model-based control for the growth of cadmium zinc telluride crystals via the Bridgman method.

In this presentation, we describe a novel approach that may be employed to actively control features of CZT growth in Bridgman systems, namely the application of a traveling magnetic field (TMF). The application of TMF produces Lorentz forces through the molten phase, and these forces can be tuned in magnitude and spatial orientation to profoundly impact melt flows. In turn, these flows modify heat and mass transfer, influencing the shape of the melt-solid interface and segregation along the interface. Since the applied TMF can be instantaneously changed, it provides for a potentially ideal control action, if its complicated effects can be predicted and understood. This is the immediate goal of our work; we discuss the mathematical formulation of our TMF analysis and, more importantly, our initial results on the effects of TMF applied to a prototypical CZT growth system.

Supported in part by DOE/NNSA, DE-FG52-08NA28768, the content of which does not necessarily reflect the position or policy of the United States Government, and no official endorsement should be inferred.

8142-40, Session 9

Growth, characterization, and fabrication of thick detectors from As-grown Cd_{0.9}Zn_{0.1}Te:In by traveling heater method

U. N. Roy, S. Weiler, J. Stein, ICx Technologies Inc. (United States); M. Groza, V. Buliga, A. Burger, Fisk Univ. (United States)

CdZnTe, commonly known as CZT is the material of paramount

importance for hard X-ray and gamma ray spectroscopy and imaging applications at room temperature. Over the years, the quality of CZT crystals and its charge transport properties has improved significantly making it an attractive detector material especially for homeland security applications. The applications for homeland security demand large and thick detectors to provide a sufficient stopping power for fast detection of high energy gamma photons. The availability of large (μr^2) CZT (greater than $10^{-2} \text{ cm}^2/\text{V}$) material makes it possible to fabricate long-drift (larger thickness) detectors with high resolution. Traveling heater method (THM) has proven to be the best technique for mass production of CZT with good compositional uniformity. However, THM grown CZT has mainly been reported to require post growth annealing to achieve detector grade material. Elimination of the post growth annealing process is a challenge, which will reduce the production cost and increase the availability of material for large detectors. In order to meet this challenge, we are continuously putting our effort to improve our THM growth technique in order to achieve as-grown detectors with reasonable resolution. In this paper, we will report the characterization of as-grown CZT by our variant of THM and fabrication of thick detectors in order to evaluate the as-grown CZT crystals. Performance of the devices with different device geometry will also be discussed.

8142-41, Session 9

Segregation and interface shape control during EDG growth of CZT crystals

N. Zhang, A. Yeckel, J. J. Derby, Univ. of Minnesota, Twin Cities (United States)

The availability of large, single crystals of cadmium zinc telluride (CZT) with uniform properties is key to improving the performance of gamma radiation detectors fabricated from them. Toward this goal, crystal growth modeling is a powerful tool to complement experiments and characterization.

In this presentation, we discuss the validation of our computational models by comparison with experimental zinc distributions via photoluminescence measurements of Burger (Fisk University) and Lynn (Washington State University) for a CZT crystal grown using the electrodynamic gradient-freeze (EDG) method. Furthermore, we predict non-classical zinc distributions for crystals grown in larger-scale EDG systems using classical thermal growth profiles. This surprising result is consistent with many prior growth outcomes where "anomalous" zinc distributions have been observed, quite different from the segregation behavior exhibited by traditional Bridgman growth systems.

We follow with a novel analysis to optimize EDG growth profiles to promote the growth of CZT crystals with a uniformly convex interface shape. Such interface shapes may be very beneficial toward reducing the probability of new grain formation, thus improving the single-crystal yield for a growth run. We also demonstrate that growth under these optimized thermal profiles results in zinc composition that is much more uniform than achieved using classical profiles. We make the case that these results can be put directly into practice using existing EDG growth systems.

Supported in part by DOE/NNSA, DE-FG52-08NA28768, the content of which does not necessarily reflect the position or policy of the United States Government, and no official endorsement should be inferred.

8142-42, Session 9

Effects of thermal annealing on the structural- and opto-electronic properties of CdZnTe crystals

G. Yang, A. E. Bolotnikov, Brookhaven National Lab. (United States); P. M. Fochuk, Yuriy Fedkovych Chernivtsi National Univ. (Ukraine); G. Camarda, Y. Cui, A. M. Hossain, K. Kim, R. Gul, R. B. James, Brookhaven National Lab. (United States)

Conference 8142:
Hard X-Ray, Gamma-Ray, and Neutron Detector Physics XIII

Thermal annealing is a promising approach to improve the property of CdZnTe (CZT) crystals. We will report on the structural- and opto-electronic properties of as-grown and annealed CZT crystals using white X-ray beam diffraction topography, IR transmission microscopy, current-voltage measurements, and low-temperature photoluminescence spectroscopy. New results from recent multi-step and long-term annealing experiments will be presented and discussed.

8142-43, Session 10

Testing hybrid contacts for CZT Frisch ring detectors

G. Camarda, A. E. Bolotnikov, Y. Cui, R. Gul, A. M. Hossain, K. H. Kim, G. Yang, R. B. James, Brookhaven National Lab. (United States)

The edge effects and the electron trapping still represent two limitations in the current design of virtual Frisch ring CZT detectors and need to be solved before they can be successfully commercialized. We proposed a novel design of the anode contact which helps to reduce the edge effects by focusing the electric field towards the central axes of the detector. The measurements techniques and the new results are presented.

8142-44, Session 10

Deep-level transient spectroscopy measurements of traps in CdZnTe crystals due to extended defects

R. Gul, A. E. Bolotnikov, K. Kim, G. Camarda, Y. Cui, A. M. Hossain, G. Yang, R. B. James, Brookhaven National Lab. (United States)

In the present research highly resistive CdZnTe detectors are investigated for defects by means of I-DLTS (current deep level transient spectroscopy). Various experiments are performed in different crystals by changing the applied bias voltage and filling time. The study is focused on traps in the temperature range of 300-400 K, previously related to defects associated with Te-rich phases. The energies of the traps found in the range 10-300 K are almost constant among different samples and vary within the experimental and systematic error of the measurement, except for the deep trap at high temperature. This behavior is different than the other traps present in the crystals. Based on the experimental results and theoretical predictions, this particular trap is identified as an extended-defect-induced trap.

8142-45, Session 10

Evaluation of CdZnTe material for the NuSTAR flight detectors using x-ray diffraction topography

P. H. Mao, V. Bhalerao, B. W. Grefenstette, F. A. Harrison, H. Miyasaka, V. R. Rana, California Institute of Technology (United States)

The {em Nuclear Spectroscopic Telescope Array (NuSTAR)} mission will carry the first hard X-ray (5 - 80 keV) focusing telescopes to orbit.

Each of the two NuSTAR focal planes contains a \$2 times 2\$ array of four CdZnTe hybrid pixel detectors. Each hybrid consists of a CdZnTe detector procured from Endicott Interconnects Detection & Imaging Systems (formerly eV Products) with the anode patterned in a 32 x 32 array of 0.6-mm pixels, bonded to Caltech's custom low-noise {em NuCIT} ASIC readout. {em NuSTAR's} requirements for sub-arcminute imaging and spectral resolution better than 1.5 ~keV FWHM (from 60 - 80 keV) over the entire field of view place tight constraints on the uniformity

and quality of acceptable CdZnTe material. During the {em NuSTAR} program, we found white beam x-ray diffraction topography (WXDT) to be the most efficient and reliable means of selecting candidate CdZnTe crystals for hybridization. Gamma-ray source scanning of crystals with a monolithic readout proved to be time-consuming and insufficient given the poor spectral resolution possible in such a setup, and IR imaging alone proved to be an insufficient tool for selection of high-quality material. During the {em NuSTAR} program, we fabricated and tested a total of 41 hybrids. In this paper we present performance results, including spectral resolution, leakage current, and uniformity of spatial response of both flight and flight-reject detectors, and we correlate these with features evident in the WXDT images.

8142-46, Session 10

Etch pit density in single crystal CdZnTe and CdTe correlated with growth parameters

C. J. Havrilak, Washington State Univ. (United States); K. A. Jones, Raytheon Co. (United States); K. G. Lynn, Washington State Univ. (United States)

Surface dislocations were revealed in single crystal CdZnTe and CdTe using chemical etching by the Everson etch (W.J. Everson et al.). Dislocation etch pits on the (111)B face were studied and photographed under both optical and scanning electron microscopes. The crystal ingots were grown using the modified vertical Bridgman (MVB) technique with different chemical compositions and growth parameters. For these ingots, etch pit density, shape and distribution were examined and compared with the varying growth techniques. Charge transport properties of the detectors were measured by current-voltage measurements and mobility-lifetime products, $\mu\tau$, were also correlated and included in the conclusive analysis. A combination of detector grade and non-detector grade ingots were tested. Near infra-red microscopy was used to compare the amount of secondary phases present in the bulk of the crystals with dislocation etch pits on their surface. The average etch pit density (EPD) for the samples in this study was found to be $5.0 \times 10^4 \text{ cm}^{-2}$. It was concluded that a low EPD is required for an ingot to have quality detector properties. Location of a sample inside of an ingot also played an important role in the EPD, the farther away from the crucible wall and the heel of the ingot - the lower the EPD and the better the detector properties. It was also shown that the rate of the ingot cool down following growth affected the EPD, quenched ingots had a lower EPD than non-quenched. Statistical data and analysis on all the above mentioned results will be provided.

8142-47, Session 10

Fabrication and characterization of Cd(0.9)Zn(0.1)Te Schottky diodes for nuclear radiation detectors

K. C. Mandal, P. G. Muzykov, R. M. Krishna, T. C. Hayes, T. S. Sudarshan, Univ. of South Carolina (United States)

Semi-insulating cadmium zinc telluride (CZT) has been the primary semiconductor material used in room-temperature high resolution x-ray and γ -ray detectors for Homeland security, infrared focal plane array, space astronomy, medical imaging, and environmental monitoring applications. In spite of the high performance of radiation detectors based on CZT, the CZT crystal quality has not been fully optimized adversely affecting the detector performance. Therefore further studies of electrically active defects and correlations with the crystal structure and device performance are highly demanded for improved CZT radiation detectors.

The fabricated Schottky diodes showed very good rectification properties with low reverse bias leakage current. The diodes were also characterized using electron beam induced current (EBIC) measurements to investigate crystallographic defects. The EBIC images, obtained for the first time, were correlated with transmission infra-red images of CZT

Conference 8142:
Hard X-Ray, Gamma-Ray, and Neutron Detector Physics XIII

crystals and the EBIC contrast was attributed to the nonuniformities in spatial distribution of Te inclusions. Further characterization included current-voltage (I-V), capacitance-voltage (C-V), Hall effect measurements, and thermally stimulated current (TSC) measurements. The TSC measurements revealed shallow and deep level centers with activation energies 0.25- 0.4 eV and 0.65 - 0.8 eV respectively, which we attribute to intrinsic defects mostly associated with excess of Te (Te anisite and its complexes). In this work, we will present crystal growth process, structural, electrical, optical and defect characterization, fabrication of CZT Schottky diodes, and testing using Am-241 (60 keV) and Cs-137 (662 keV) radiation sources.

8142-24, Poster Session

Detector array with improved spatial resolution for digital radiographic system

O. D. Opolonin, V. D. Ryzhikov, Sr., S. A. Galkin, V. G. Volkov, O. K. Lysetska, Sr., Institute for Scintillation Materials (Ukraine); S. A. Kostioukevitch, V. Lashkaryov Institute of Semiconductor Physics (Ukraine)

A detector array of "scintillator-photodiode" type with improved spatial resolution has been developed.

For obtaining shadow X-ray images, a receiving-detecting circuit (RDC) with a detector array was developed for 200 mm scanning field. The circuit was integrated into two digital radiographic system models.

The first model consisted of RDC, linear motor (minimum movement step less than 1 micron) and X-ray source (Ua max=160 kV, Ia max=45 mA).

The second model consisted of RDC, mechanism for movement and rotation of the inspected object, and X-ray source (Ua max=140 kV, Ia max=1 mA). The presence of the rotation mechanism allowed realization of multi-view scanning mode (60 views), resulting in substantially higher informativity of non-destructive testing and technical diagnostics.

Using these model digital radiographic systems and standard testing objects - EN 462-5 (set of wire pairs), grooving sensitivity reference No.2 (GOST 7512-82), set of iron wires DIN 62 Fe (10 ISO 16), we have evaluated spatial resolution (not worse than 1.25 line pairs/mm) and detecting ability (better than 0.2 mm steel wire behind 6 mm steel).

The use of a 16-channel analog to digit converter as part of RDC allowed broadening the dynamic range and improving, as compared with previous results, resolution of the model system over thickness from 0,9% to 0,4% (behind 6 mm steel).

Thus, our studies have shown that the developed detector array for obtaining shadow X-ray images with high spatial resolution can be successfully used with X-ray sources of up to 160 kV anode voltage.

8142-48, Poster Session

Carrier transportation properties in M-p-n and Schottky CdTe diode detector

M. Kimura, Shizuoka Univ. (Japan); A. Koike, Shizuoka Univ. (Japan) and ANSeeN Inc. (Japan); T. Okunoayama, ANSeeN Inc. (Japan) and Shizuoka Univ. (Japan); H. Morii, Shizuoka Univ. (Japan) and ANSeeN Inc. (Japan); S. Singh, T. Yamakawa, H. Mimura, Shizuoka Univ. (Japan); T. Aoki, Shizuoka Univ. (Japan) and ANSeeN Inc. (Japan)

The photon counting CdTe detector by using pulse rise height for high count rate detection was developed. The detector can measure not only pulse rise height for energy estimation but also pulse rise time. The energy spectrum after polarization in high bias voltage and before polarization in low bias voltage was so similar, but the pulse rise time was difference. In this paper, we have compared polarization properties of M-p-n type CdTe diode and Schottky one. We will estimate changing internal electric field by using this measurement.

8142-49, Poster Session

Structure distortions and scintillation properties of elpasolite halide scintillators

P. Yang, Sandia National Labs. (United States); F. P. Doty, X. Zhou, Sandia National Labs., California (United States); M. A. Rodriguez, C. B. DiAntonio, Sandia National Labs. (United States); T. Chavez, Sandia National Labs., California (United States); J. V. Branson, Sandia National Labs. (United States); E. Von Loef, W. M. Higgins, U. Shirwadkar, K. S. Shah, Radiation Monitoring Devices, Inc. (United States)

The crystal structure, thermal properties, and scintillation properties of several new elpasolite halide compounds (A₂BCX₆) and their solid solutions are studied. These materials, based on a cubic, double perovskite structure, are particularly attractive for advanced gamma-ray spectroscopy applications due to a unique combination of high energy resolution and excellent proportionality recently discovered in the elpasolite halide family. These cubic compounds are relatively easy to grow in large sizes and have the potential to be made in polycrystalline forms for radiation detectors. When substituting ions with different sizes, a small lattice distortion can be introduced. The distortion changes the crystal symmetry, and affects the optical, thermal and elastic properties. These changes can have profound implications on material manufacturability and costs. Therefore, it is advantageous to develop a material model that can effectively predict the crystal structure of favorable new compounds that are highly manufacturable for practical applications. In this study, we will compare the structural change predicted by a classic Goldschmidt tolerance factor, SPuDs calculation¹, and our own embedded ion method (EIM), using the structural information of these new materials and literature data for validation purposes. Correlations of these structural changes with respect to their scintillation properties will be explored.

1. M. W. Lufaso and P. M. Woodward, "Prediction of the Crystal Structures of Perovskites using the Software Program SPuDs," Acta Cryst. B57, 735-738 (2001).

This work is supported by the NNSA/DOE Office of Nonproliferation Research and Development, Proliferation Detection Program, Advanced Material Portfolio. Sandia is a multiprogram laboratory operated by Sandia Corporation, a Lockheed Martin company, for the United States Department of Energy's National Nuclear Security Administration under contract DE-AC04-94AL85000.

8142-50, Poster Session

Growth of GaGdN by MOVPE for semiconductor neutron detector

H. Kaneko, T. Nishioka, A. Miyake, T. Aoki, T. Nakano, Shizuoka Univ. (Japan)

We have aimed at the achievement of the new neutron imaging device by compound semiconductor with Gd converter. We have suggested a neutron detector by using internal conversion electrons, which are generated by Gd atom. The wide bandgap semiconductor GaN, which has less gamma-ray sensitivity, is selected to distinguish neutron from background gamma-ray.

GaN has been widely researched for optoelectronic devices. Therefore, basically growth and processing techniques about GaN have already been developed.

We could estimate that GaGdN for neutron detectors is possible to be fabricated by mixing Gd to GaN, because the GaGdN multiple quantum wells have been achieved in the field of spin electronics. In this work, GaGdN has been grown by metal organic vapor phase epitaxy (MOVPE) using the precursors; trimethylgallium (TMG), tris-cyclopentacenyldgadolinium (Cp₃Gd) and NH₃ for the Ga, Gd and N, respectively. The epitaxial structure of films consisted of a 450nm-thick GaN buffer layer, a 300nm-thick GaGdN layer, and a 150nm-thick GaN

**Conference 8142:
Hard X-Ray, Gamma-Ray, and Neutron Detector Physics XIII**

cap layer on c-plane Al₂O₃ substrate. The GaGdN were structurally characterized by XRD, and the GaGdN (0002) peak was observed as the lower angle peak than the GaN (0002) peak from buffer and cap layers. This result indicated that Gd-doping makes lattice constant enlarge and we can estimate the composition of Gd is about 1% from the GaGdN (0002) peak in XRD.

8142-51, Poster Session

E-beam electron mobility study on CZT and Csl

S. A. Baker, National Security Technologies, LLC (United States); A. Burger, Fisk Univ. (United States); L. A. Franks, Consultant (United States); M. Groza, Fisk Univ. (United States); D. Schwellenbach, J. A. Young, National Security Technologies, LLC (United States)

DOE/NV/25946--1152 Cadmium zinc telluride (CZT) semiconductor material is at the forefront of much research on room-temperature radiation detection. This poster presents a study of electron beam charge induced mobility in the solid-state crystal CZT. The intent is to correlate conductivity characteristics with crystal CZT mix ratio in the compound of cadmium, zinc and tellurium. We examine electrical charge (pulse) propagation in room-temperature CZT versus bias voltage. Tests are conducted on monolithic CZT 15 × 15 × 10 mm³. Initial tests induce charge excitation with a pulsed laser source. Further tests utilize pulsed, nanosecond range, electron beam excitation in the tens of keV. Experimental results will be discussed. Follow on tests will study thallium-doped cesium iodide, Csl(Tl), scintillator material. Optical emission to electron beam excitation is observed for scintillators in correlation with bias voltage and electron beam energy.

8142-52, Poster Session

Synthesis of a potential semiconductor neutron detector crystal LiGa(Se/Te)₂: materials purity and compatibility effects

A. C. Stowe, K. Joyce, J. Morrell, Y-12 National Security Complex (United States); P. Battacharya, E. Tupisyn, A. Burger, Fisk Univ. (United States)

Recent years have seen an increase in need for radiation detection materials for scientific and security applications. The standard technology is ³He gas tube detectors; however, the increased usage has resulted in a pending global shortage of ³He gas. Many alternative radiation detector materials are being considered, including semiconductor-based detectors. For neutron detection, a ⁶Li or ¹⁰B-based neutron absorber layer is added to the semiconductor crystal in order to efficiently detect the neutrons. The efficiency is limited by the thickness of the absorber layer which must remain small to allow the alpha particle created during the reaction of a neutron with the absorber to reach the semiconductor. If, however, the semiconductor crystal contains the neutron absorber directly within its crystal lattice, the number of absorber atoms can be larger thus increasing the theoretical neutron detection efficiency. Lithium containing chalcopyrite crystals (I-III-VI₂) such as LiGaSe₂ and LiGaTe₂ have electronic band gaps appropriate for detection of thermal neutrons. One of the primary challenges in growing a high quality crystal of such a material is the reactivity of lithium metal. The presence of nitrides, oxides, and a variety of alkali and alkaline earth metal impurities prevent pure synthesis and truncate crystal growth by introducing multiple nucleation centers during growth. Multiple lithium metal purification methods have been investigated which ultimately raised the metal purity to 99.996%. Multi-cycle vacuum distillation removed all but 40 ppm of metal impurities in lithium metal. LiGa(Se/Te)₂ were then synthesized with the high purity lithium metal by a variety of conditions. Lithium metal reacts violently with many standard crucible materials. Thermodynamic studies were undertaken to insure that an appropriate crucible choice was made,

with high purity iron and boron nitride crucibles being the least reactive practical materials. Once conditions were optimized for synthesis of the chalcopyrite, vertical Bridgman crystal growth resulted in red crystals. The optical, electronic, and thermodynamic properties were collected.

8142-54, Poster Session

Gamma ray nonvolatile sensor comparison between SONOS and SNOS capacity device

W. Hsieh, Minghsin Univ. of Science and Technology (Taiwan); H. D. Lee, ETOMS Electronics Corp. (Taiwan); S. Wu, National Nano Device Labs. (Taiwan); F. Jong, Southern Taiwan Univ. of Technology (Taiwan)

The typical Silicon-Oxide-Nitride-Oxide-Silicon (SONOS) and Silicon-Nitride-Oxide-Silicon (SNOS) capacity devices can be candidate for nonvolatile Gamma radiation sensors. In case of SONOS and SNOS Gamma Radiation sensors, the Gamma ray radiation induces significant decrease of threshold voltage. The changes of threshold voltage for SONOS and SNOS after Gamma ray expose can be correlated to the dose of Gamma ray exposure as well. In this paper, the change of threshold voltage for SONOS and SNOS after Gamma ray expose were compared. This capacity device with ONO gate dielectric in this study has demonstrated the better feasibility of using SONOS capacity device for Gamma Ray dosimeter.

1. INTRODUCTION

When a MOS structure is irradiated by gamma rays, the positive charges build-up at Si-SiO₂ interface and the interface state creation occur [1]. The irradiation effects of a Metal-Nitride-Oxide- Silicon (MNOS) device with stacked insulation layers composed silicon nitride and silicon dioxide has been reported [2]-[5]. However the detailed mechanism of the charged trappings has not been understood yet. In this study, the radiation-induced trapped charges in the insulation layer of SONOS and SNOS capacity structure are investigated. This Gamma ray radiation induces significant decrease of threshold voltage for SONOS and SNOS. It is considered that these changes are due to significant increase of positive trapped charges in the gate dielectric ONO and NO after Gamma ray irradiation. In this paper, the changes of threshold voltage for SONOS and SNOS after Gamma ray expose were compared. The change of threshold voltage for SONOS is more than the one for SNOS. This capacity device with ONO gate dielectric in this study has demonstrated the better feasibility of using SONOS capacity device for Gamma Ray dosimeter.

2. PROPOSED MECHANISM

In case of MOS structure, a MOS structure is irradiated by gamma rays, the positive charges build-up at S-O interface and the interface state creation occur. It is considered that the amount of trapped holes due to irradiation is greater than the amount of trapped electron near the S-O interface. For writing data in the SONOS and SNOS capacity, Gamma ray radiation and fixed gate voltage was applied on these SONOS and SNOS capacity devices simultaneously. When these SONOS and SNOS capacity structure are irradiated by gamma rays, the electron-hole pairs are generated throughout the gate insulation layers. These free carriers are swept by electric field, and some of them are captured by the charge trap centers, especially at the Oxide-Nitride (O-N) interface and Silicon- Oxide (S-O) interface. The amounts of captured charge depend on the local density and capture cross section of the trap centers. When a positive gate voltage was applied on these SONOS and SNOS capacity devices, the holes generated by radiation in the insulation layers are swept toward Silicon base side by electric field and some of the holes are captured by the charge trap centers at the O-N interface and S-O interface; however the electrons generated by radiation in the insulation layers are swept toward poly silicon gate side by electric field and some of electrons are captured by the charge trap centers at the O-N interface. As shown in experiment data, the Gamma ray radiation induces significant decrease of threshold voltage for SONOS and SNOS capacity. It is considered that the amount of trapped holes due to irradiation in gate insulator is greater than the amount trapped electron. It is suggested that the amount of hole traps at O-N interface and S-O

**Conference 8142:
Hard X-Ray, Gamma-Ray, and Neutron Detector Physics XIII**

interface is higher than the electron traps at O-N interface. The trapped charges change the electrical characteristic of these SONOS and SNOS capacity devices in terms of gate diode capacity, gate threshold voltage, and drain current. For the data read, the change of gate threshold voltage in this case can be correlated to the amount of trapped charges and the exposure dosage of Gamma radiation as well. These trapped charges can be always accumulated in gate dielectric layer, so dose record can't be destroyed by data write and read. For the dosage data erase, data in these SONOS and SNOS capacity devices can be erased to original null state by charges injection. In this paper, the change of threshold voltage for SONOS and SNOS after Gamma ray expose were compared. As shown in experiment data, the change of threshold voltage for SONOS is more than the one for SNOS. It is suggested that the amount of positive trapped charges in the ONO gate dielectric layer is greater than the one in the NO gate dielectric layer; so the decrease of threshold voltage for SONOS is more than the one for SNOS. This capacity device with ONO gate dielectric in this study has demonstrated the better feasibility of using SONOS capacity device for Gamma Ray dosimeter.

3. EXPERIMENTAL

In this study, the N type SIS capacity structures were fabricated on P-type Si substrate. Two kind of SIS capacity with gate dielectric SiO₂-Si₃N₄-SiO₂ (ONO) & Si₃N₄-SiO₂ (NO) were compared. The thickness of gate dielectric for the capacity with N-O gate dielectric is 200Å-50Å. The thickness of gate dielectric for the device with O-N-O gate dielectric is 50Å-200Å-50Å. In this paper, the changes of threshold voltage between SONOS & SNOS after Gamma ray expose were compared. To write data on these SONOS and SNOS capacity devices, Gamma radiation was exposed and a positive six volts gate voltage was applied on these SONOS and SNOS capacity devices simultaneously. For the data read, the change of gate threshold voltage in this case can be correlated to the exposure dosage of Gamma radiation as well. These trapped charges can be always accumulated in gate dielectric layer, so dose record can't be destroyed by data write and read. For the dosage data erase, data in these SONOS and SNOS capacity devices can be erased to original null state by opposite charges injection.

4. RESULTS AND DISCUSSIONS

As illustrated in figure 1 it can be seen that the capacity to voltage curves (C-V curve) of SNOS shifted to the left after 5 Mrad Gamma ray irradiation. This implies that Gamma ray radiation induces a decrease of threshold voltage for SNOS. The amount of decrease of threshold voltage is about 0.6 volts. It is considered that the change is due to increase of positive trapped charges in the gate dielectric NO layer after Gamma ray irradiation. From figure 2, it also can be seen that the capacity to voltage curves (C-V curve) of SONOS shifted far to the left after 5 Mrad Gamma ray irradiation. This implies that Gamma ray radiation induces a significant decrease of threshold voltage for SONOS. The amount of decrease of threshold voltage is up to about 0.9 volts. It is considered that the change is due to significant increase of positive trapped charges in the gate dielectric ONO layer after Gamma ray irradiation. The electron-hole pairs are generated throughout the insulation layers, when these SONOS and SNOS capacity devices structure are irradiated by gamma rays. These free carriers are swept by electric field, and some of them are captured by the charge trap centers, especially at the Oxide-Nitride (O-N) interface and Silicon- Oxide (S-O) interface. As shown in experiment data, the change of threshold voltage for SONOS is more than the one for SNOS. The dependencies of threshold voltage shifts on radiation dose in ONO gate dielectric is more than the one in NO gate dielectric. It can be explained that the amount of positive trapped charges in the ONO gate dielectric layer is greater than the one in the NO gate dielectric layer; so the decrease of threshold voltage for SONOS is more than the one for SNOS. It is suggested that the amount of hole traps at O-N interface in ONO gate dielectric layer is more than the one in the NO gate dielectric layer. This capacity device with ONO gate dielectric in this study has demonstrated the better feasibility of using SONOS capacity device for Gamma Ray dosimeter. As illustrated in Figure 3, the decrease of threshold voltage for SONOS are plotted against the total Gamma ray radiation dose received. When Gamma ray radiation dose increase, the change amount of threshold voltage for SONOS also increase. The dependencies of the threshold voltage on radiation dose can be explained in the following manner. When Gamma ray radiation dose increase, the amount of positive trapped charges in the gate dielectric ONO layer also increase. The decrease of gate

threshold voltage in this case can be correlated to the increase of positive trapped charges in the insulator and the increase of exposure dosage for Gamma radiation as well.

5. CONCLUSION

As shown in experiment data, the change of threshold voltage for SONOS is more than the one for SNOS. The dependencies of threshold voltage shift on radiation dose in ONO gate dielectric is more than the one in NO gate dielectric. It can be explained that the amount of positive trapped charges in the ONO gate dielectric layer is greater than the one in the NO gate dielectric layer; so the decrease of threshold voltage for SONOS is more than the one for SNOS. It is suggested that the amount of hole traps at O-N interface in ONO gate dielectric layer is more than the one in the NO gate dielectric layer. This capacity device with ONO gate dielectric in this study has demonstrated the better feasibility of using SONOS capacity device for Gamma Ray dosimeter.

8142-55, Poster Session

Synchrotron radiation studies of spectral features caused by Te inclusions in CdZnTe

C. C. T. Hansson, A. Owens, European Space Research and Technology Ctr. (Netherlands); F. Quaranti, Technische Univ. Delft (Netherlands); V. Gostilo, Baltic Scientific Instruments (Latvia); D. Lumb, European Space Research and Technology Ctr. (Netherlands); A. Kozorezov, Lancaster Univ. (United Kingdom); A. Webb, DESY (Germany)

The use of CdZnTe (CZT) as a high energy X-ray and γ -ray detection medium has been recognised for a long time due to its high stopping power and wide band gap, potentially allowing for fano-limited spectroscopy and room temperature operation [1].

Fano-limited spectroscopy for CZT crystals is currently limited by defects in the crystal structure, including twins and sub-grain boundaries; Te inclusions and dislocations, introduced during growth of the material [2]. For mined crystals the most detrimental defects affecting the spectroscopic performance in thick detectors has been shown to be Te inclusions [3].

While the effects of small inclusions, <3 μ m, can be compensated for by depth sensing techniques (assuming concentrations below 10¹⁶ cm⁻³) [3] larger inclusions introduce a variation in the collected charge carrier number that can not be corrected for. The lower band gap and increased impurity solubility of Te [3][4] is believed to introduce trapping levels, and possibly affecting the electric field profile inside the detector [2], leading to a varied trapping probability in the area of inclusions.

In this experiment a 10mm CZT coplanar grid detector having large Te inclusions [5] were exposed to pencil beam synchrotron radiation in order to study spectroscopic features introduced by the defect structure of Te inclusions at different X-ray energies.

The analysis of the detector spectral response and the potential use of the technique to investigate inclusions in wide band gap semiconductors will be discussed.

References:

- [1] D.S. McGregor and H. Hermon, "Room-temperature compound semiconductors radiation detectors", Nucl. Instr. And Meth. A 395, 101-124, 1997.
- [2] A.E. Bolotnikov et al. "Extended defects in CdZnTe radiation detectors", IEEE Trans. Nucl. Sci. 56, 4, 1775-1783, 2009.
- [3] A.E. Bolotnikov et al. "Performance-limiting defects in CdZnTe detectors", IEEE Trans. Nucl. Sci. 54, 4, 821-827, 2007.
- [4] G. Yang et al., "Impurity gettering effect of Te inclusions in CdZnTe single crystals", J. Cryst. Growth. 311, 99-102, 2008.
- [5] A. Owens et al, "Hard X- and γ -ray measurements with large volume coplanar grid CdZnTe detector", Nucl. Instr. And Meth. A 563, 242-248, 2006.

8142-56, Poster Session

Computational assessment of the impact of gamma-ray detector material properties on spectroscopic performance

D. V. Jordan, B. S. McDonald, J. E. Baciak, Jr., E. A. Miller, W. Hensley, E. Siciliano, Pacific Northwest National Lab. (United States)

Pacific Northwest National Laboratory (PNNL) is performing a computational assessment of the impact of several important gamma-ray detector material properties (e.g. energy resolution and intrinsic detection efficiency) on the scenario-specific spectroscopic performance of these materials. The research approach combines 3D radiation transport calculations, detector response modeling, and spectroscopic analysis of simulated energy deposition spectra to map the functional dependence of detection performance on the underlying material properties. This assessment is intended to help guide formulation of performance goals for new detector materials within the context of materials discovery programs, with an emphasis on applications in the threat reduction, nonproliferation, and safeguards/ verification user communities. The research results will also provide guidance to the gamma-ray sensor design community in estimating relative spectroscopic performance merits of candidate materials for novel or notional detectors.

The research design comprises a parameter study in the composition, size, and effective response characteristics of a set of notional, homogenous detector materials. We model the energy deposition spectrum registered in a cylindrical gamma-ray spectrometer deployed in a variety of application scenarios relevant to wide-area radioisotope anomaly detection and identification, safeguards (material holdup in a uranium-processing facility; UF₆ cylinder enrichment assay), and active interrogation (delayed-gamma emission from neutron or photon-induced fission). We subject ensembles of Poisson-blurred spectra to peak location and peak-area analysis, and map appropriate statistical metrics (e.g. detection probability or assay precision) of spectroscopic performance as functions of the underlying material parameters. The paper describes the computational methods and discusses representative results for each deployment scenario.

8142-57, Poster Session

Peculiarities of the melting and cooling processes in the CdTe-ZnTe system near CdTe side

L. P. Shcherbak, O. V. Kopach, P. M. Fochuk, I. Nakonechnyj, Yuriy Fedkovych Chernivtsi National Univ. (Ukraine); A. E. Bolotnikov, R. B. James, Brookhaven National Lab. (United States)

The investigations of peculiarities of the melting and cooling processes in the CdTe-ZnTe system with ZnTe content up to 10 mol. % by the Differential Thermal Analysis (DTA) was carried out. The influence of heating and cooling conditions (heating/cooling rate, melt maximum temperature, melt holding duration at maximum temperature) on melting and crystallization processes parameters was investigated. Using the Kissinger equation $\ln(V_h/T_m^2) = A + E_a/(RT_m)$, which shows interrelation between heating rate (V_h) and maximal temperature of the melting process endothermic effect (T_m) the melting process activation energy (E_a) is estimated. Based on the obtained data the liquidus and solidus lines of the CdTe - ZnTe system with ZnTe content up to 10 mol. % are constructed.

8142-58, Poster Session

High-temperature study of the detector-grade CZT under the zinc overpressure

P. M. Fochuk, I. Nakonechnyj, O. V. Kopach, O. E. Panchuk, Yuriy Fedkovych Chernivtsi National Univ. (Ukraine); A. E. Bolotnikov, R. B. James, Brookhaven National Lab. (United States)

Many publications appeared in recent years on CZT properties as material for γ -detector application. But still, there is a gap in understanding of its point defects structure. The high-temperature treatment of CZT samples under Cd and Te overpressure had been described in several papers. However its properties under Zn overpressure has not been studied yet. We measured the Hall effect of several Cd_{1-x}Zn_xTe:In samples under the zinc overpressure at 500-1100 K. It was shown that long-term annealing results in obtaining of high-resistive material that can be used in producing of inclusion-free detector-grade material.

8142-59, Poster Session

Characterization of the surfaces of CdTe(111) single crystals after laser processing

D. Gnatyuk, L. V. Poperenko, I. V. Yurglevych, National Taras Shevchenko Univ. of Kyiv (Ukraine); T. Aoki, Shizuoka Univ. (Japan)

Chemical etching and laser irradiation have been widely used for surface processing of CdTe and such treatments modify the structure and state of the crystal surface. The optical properties of opposite sides of CdTe(111) single crystals subjected to irradiation with nanosecond single pulses of the second harmonic of a YAG:Nd laser with energy density below and above the melting threshold have been studied by multiple-angle-of-incidence single-wavelength ellipsometry. The ellipsometric parameters Δ and Ψ were obtained at several light incidence angles and the principal angle and minimum value of the azimuth of the restored linear polarization were calculated. The data were interpreted by the semi-infinite medium model and it is assumed that there were no films or layers on the crystal surface. Also the one-layer model was applied and the relief of the crystal was considered as a top layer. The refraction n and absorption k indexes of the surface layer were calculated using the fundamental ellipsometric equation and method of thickness curves. The obtained effective thickness d (~10-20 nm) in the chemically etched samples was in agreement with the root mean square height of the roughness obtained by AFM technique. The applicability of the both models is an evidence of an increase in the refractive index of the CdTe surface layer due to laser-induced effects and it is associated to enriching of the modified surface with tellurium which has larger refraction ($n \sim 6$ at 632.8 nm). The laser irradiation effects on polar sides of CdTe(111) crystals are analyzed.

8142-60, Poster Session

Correlations of secondary phases (SPs/ inclusions) with mobility lifetime ($\mu\tau_e$) of the electrons in CZT crystals using IR microscopy

S. Bhaladhare, W. G. Munge, K. G. Lynn, Washington State Univ. (United States)

Cadmium Zinc Telluride (CdZnTe/CZT) crystals were grown using a modified vertical Bridgman growth technique with 10 % Zn concentration at Washington State University (WSU). Analyses of the effects of volume (vol. %) %, number density (cm⁻³), mean diameter (μ m) of secondary phases (SPs) and thickness (mm) of the CZT crystals on single crystal properties such as carrier mobility lifetime ($\mu\tau_e$) and resistivity (ρ) were performed. Correlations were observed between $\mu\tau_e$ (cm² V⁻¹) of

Conference 8142:
Hard X-Ray, Gamma-Ray, and Neutron Detector Physics XIII

different CZT crystals and vol. %, number density, mean diameter of secondary phases and thickness of the crystals. High μ_{re} and lower SP vol. % values were obtained for the ingots grown with rapid cool down times and with no intentional amounts of excess Te/Cd. The effects of the SPs on the μ_{re} values were established for the SPs whose mean diameters were $\leq 4 \mu\text{m}$ and $> 4 \mu\text{m}$. These studies indicate vol. % and mean diameter of SPs are the important parameters for CZT crystal performance as a radiation detector.

8142-62, Poster Session

Lithium and boron based semiconductor detectors for thermal neutron counting

A. Kargar, H. Kim, L. J. Cirignano, J. P. Tower, H. Hong, W. M. Higgins, K. S. Shah, Radiation Monitoring Devices, Inc. (United States)

Thermal neutron detectors in planar configuration were fabricated from LiInSe₂ and B₂Se₃ crystals grown at RMD Inc. All fabricated semiconductor devices were characterized for the current-voltage (I-V) characteristic and neutron counting measurement. Pulse height spectra were collected from ²⁴¹AmBe (neutron source on all samples), ¹³⁷Cs and ⁶⁰Co. In this study, the resistivity of all crystals is reported and the collected pulse height spectra are presented for all fabricated devices. The current-voltage (I-V) characteristic curves obtained for planar devices fabricated from the LiInSe₂ crystals showed resistivity around $1.1 \times 10^{11} \Omega \text{ cm}$ to $5.8 \times 10^{11} \Omega \text{ cm}$. The resistivities of B₂Se₃ samples were estimated to be around $2.3 \times 10^{13} \Omega \text{ cm}$ to $3.8 \times 10^{13} \Omega \text{ cm}$. The discrimination of the neutrons and gamma rays was performed by shielding the device from the ²⁴¹AmBe with two 1/4-inch layers of boron shielding materials. As a result of shielding the detector from ²⁴¹AmBe source with neutron absorbing materials, the counting curve was suppressed significantly. This proves the neutron counting through ⁶Li(n, α)³H reaction for LiInSe₂ crystals and neutron counting through ¹⁰B(n, α)⁷Li reaction for B₂Se₃ crystals. Note that, the ²⁴¹AmBe neutron source was custom designed with polyethylene around the source as the neutron moderator, mainly to thermalize the fast neutrons before reaching the detectors. In summary, both LiInSe₂ and B₂Se₃ crystals showed reasonable response to thermal neutron of ²⁴¹AmBe source.

8142-63, Poster Session

A large area x-ray imager with online linearization and noise suppression

R. Durst, B. L. Becker, J. Kaercher, T. He, G. Wachter, Bruker AXS, Inc. (United States)

A new large area imager for X-ray crystallography is described based on active pixel sensor technology. In order to meet the demanding requirements for crystallography the detector is designed with real time correction for reset noise, nonlinearity, spatial uniformity and bad pixels. The design of the detector is described along with its operating characteristics including noise, DQE and quantum gain. We describe new techniques to rapidly calibrate and characterize the X-ray imager.

8142-64, Poster Session

Electric field in Au/CdTe/In under x-ray and laser radiation

V. Dedic, J. Franc, Charles Univ. in Prague (Czech Republic); P. J. Sellin, Univ. of Surrey (United Kingdom); R. Grill, Charles Univ. in Prague (Czech Republic); P. Veeramani, Univ. of Surrey (United Kingdom)

Accumulation of space charge at deep levels resulting in deformation of internal electric field represents one of the main factors affecting the charge collection efficiency in CdTe and CdZnTe X-ray and gamma ray semiconductor detectors.

In this contribution we present the dependence of electric field profiles acquired by Pockels effect on the wavelength of the laser used for generation of free carriers. The result are compared to profiles acquired with the continuous spectrum of X-rays from X-ray tube. We demonstrate both experimentally and theoretically the possibility to control the profile of the internal electric field by compensation of the space charge formed by carriers trapped at deep levels QT with space charge QM present due to band bending at the Au/CdTe and In/CdTe interfaces.

The electric field decreases from the cathode forming a dead layer below the anode, when no X-ray radiation was applied. This situation corresponds to a prevailing positive space charge QT. The profile of the electric field approaches a constant value with an increasing X-ray flux. Further increase of radiation flux results finally in the formation of a dead layer below the cathode. The results can be explained by accumulation of negative space charge trapped at deep levels that compensates the positive QM.

The demonstrated mechanism represents a way to address the problems associated with electric field modification and reduced charge collection efficiency in CdTe X-ray detectors operated at high fluxes of X-ray photons.

Conference 8143: Medical Applications of Radiation Detectors

Wednesday–Thursday 24–25 August 2011 • Part of Proceedings of SPIE Vol. 8143
Medical Applications of Radiation Detectors

8143-22, Poster Session

Test apparatus to monitor time-domain signals from semiconductor-detector pixel arrays

K. Haston, H. B. Barber, L. R. Furenid, E. Salcin, The Univ. of Arizona (United States)

No abstract available

8143-23, Poster Session

Design considerations for MAPMT-based monolithic scintillation camera

L. R. Furenid, H. B. Barber, E. Salcin, Ctr. for Gamma-Ray Imaging, The Univ. of Arizona (United States)

No abstract available

8143-01, Session 1

Performance tests of CdZnTe-based compact gamma camera

Y. Cui, Brookhaven National Lab. (United States); T. Lall, Hybridyne Imaging Technology, Inc. (Canada); B. Tsui, The Johns Hopkins Outpatient Ctr. (United States); J. Yu, The Johns Hopkins Univ. (United States); G. Mahler, A. Bolotnikov, P. Vaska, G. De Geronimo, P. O'Connor, G. Meinken, Brookhaven National Lab. (United States); J. Joyal, J. Barrett, Molecular Insight Pharmaceuticals (United States); G. Camarda, A. Hossain, K. H. Kim, G. Yang, R. B. James, Brookhaven National Lab. (United States); M. Pomper, S. Cho, The Johns Hopkins Outpatient Ctr. (United States); K. Weisman, Midstate Medical Ctr. (United States); Y. Seo, Univ. of California, San Francisco (United States); J. Babich, N. LaFrance, Molecular Insight Pharmaceuticals (United States)

In this presentation, we will introduce a compact gamma camera for high-resolution prostate cancer imaging using Cadmium Zinc Telluride (CdZnTe or CZT) radiation detectors. CZT is a semiconductive material with wide band-gap and relatively high electron mobility thus can operate at room-temperature without cooling. CZT detector is a photon-electron direct conversion device, thus it potentially can offer high energy resolution in gamma-ray detection, enables energy-resolved imaging, and reduces the background of Compton scattering events. In addition, CZT material has high stopping power for gamma-ray; in medical imaging applications, a few mm thick CZT material can provide sufficient detection efficiency for 100-200-keV gamma rays. Because of these advantages, CZT detectors are becoming popular for several SPECT medical imaging applications. Most recently, we designed a compact gamma camera using CZT detectors coupled to an application-specific-integrated-circuit (ASIC). This camera works as an inter-rectal probe to image the prostate gland at a short distance of 1-5 cm, offering high detection efficiency and high spatial resolution, and potentially can detect prostate cancers at an early stage. In this presentation, we will report the performance tests results of this gamma camera.

8143-02, Session 1

A novel SPECT camera for molecular imaging of the prostate

A. Cebula, D. Gilland, Univ. of Florida (United States); D. Wagenaar, Gamma Medica, Inc. (United States); A. Bahadori, Univ. of Florida (United States)

The objective of this work is to develop an improved SPECT camera for dedicated prostate imaging. Complementing the recent advancements in molecular imaging agents for prostate cancer, this device has the potential to assist in distinguishing benign from aggressive cancers, to guide biopsy, and to aid in focal therapy procedures. The camera is designed to achieve better spatial resolution, photon detection sensitivity, energy resolution and overall signal-to-noise ratio relative to conventional SPECT cameras. This is achieved using a multi-pinhole collimator that has a saddle-shaped contour upon which the patient sits, thus greatly reducing the source-to-detector distance. The prostate gland and surrounding pelvic region project through 16 tungsten pinholes into the saddle surface and onto the detector comprised of cadmium zinc telluride modules (1" x 1") that are tiled in a 2D matrix. In addition to improving collimator spatial resolution, the small source-to-detector distance allows image magnification, which improves the effective intrinsic spatial resolution.

Theoretical calculations show that the spatial resolution/detection sensitivity of the proposed SPECT camera can rival or exceed high resolution, 3D PET, and further signal-to-noise advantage is attained with the better energy resolution of the CZT modules. Photon transport simulation studies have been performed to evaluate the system design of the dedicated prostate camera. Realistic source distributions are created using virtual human models, which are combined with attenuating objects representing the multi-pinhole collimator and detector array. Further work will focus on developing multi-pinhole iterative reconstruction and optimizing system design parameters based on reconstructed image quality.

8143-03, Session 1

Stereo-viewing collimator system for breast cancer lesion localization

B. L. Welch, Dilon Technologies (United States); C. Lorino, D. Chiarella, T. Hodge, Montgomery Cancer Ctr. (United States)

A number of dedicated gamma camera systems are being used in the diagnostic workup of breast cancer patients and have demonstrated the ability to detect cancers missed by mammography and ultrasound. To become a standard of care, these systems need a mechanism to localize suspected tumors for biopsy. A stereotactic lesion localization system has been developed to allow gamma guided needle biopsy. The purpose of this work is to present the results of the clinical performance of this system on a group of patients. Twenty three patients who were indicated for needle biopsy based on clinical findings of an abnormality on a diagnostic gamma image as part of their clinical workup were imaged with the stereotactic system. The area of concern was then localized with the stereotactic lesion localization system. The lesion was located in each stereo image and the X, Y and Z coordinates were calculated. The resulting location was correlated to a specific (X, Y) location within a grid in the paddle and to a specific depth (Z) using a needle guide. The resulting pathology was compared to the clinical evidence to determine concordance. This work presents several case examples including clinical imaging and the results of pathology. This stereotactic lesion localization system provides a clinically viable method for localizing lesions seen in gamma imaging and addresses an important limitation to the broad acceptance of this imaging technique by allowing accurate

**Conference 8143:
Medical Applications of Radiation Detectors**

lesion localization and biopsy under the guidance of a set of gamma camera images of the breast.

8143-04, Session 1**Dose reduction in molecular breast imaging**

D. J. Wagenaar, S. Chowdhury, J. W. Hugg, Gamma Medica, Inc. (United States); R. A. Moats, Children's Hospital of Los Angeles (United States) and The Univ. of Southern California (United States); B. E. Patt, Gamma Medica, Inc. (United States)

No abstract available

8143-05, Session 1**Ultrahigh resolution CZT/CdTe detectors with a hybrid pixel-waveform readout system**

L. Meng, L. Cai, Univ. of Illinois at Urbana-Champaign (United States); F. K. Tang, The Univ. of Chicago (United States)

In this paper, we will report on the development of a hybrid pixel-waveform (HPWF) readout system for highly pixelated (with a few hundred μm pitch size) CZT and CdTe gamma ray detectors. This readout system is based on an energy-resolved photon counting (ERPC) ASIC for reading out the anode pixels, working in coincidence with a high-speed circuitry for sampling the cathode waveform. This approach could provide an ultrahigh spatial resolution, an excellent timing resolution and a reasonable spectroscopic performance at the same time. The rationale behind the HPWF readout system are the following. First, the cathode waveform could provide precise energy information using digital processing techniques that takes into account the effect of charge trapping. This helps to alleviate the difficulties in extracting energy information from the tiny anode pixels, with the presence of severe charge sharing and charge loss. Second, the cathode waveform could provide a timing information at a precision well beyond that available with anode pixel readout. The latter is limited by the intrinsic uncertainties in charge collection process. Finally, it could also provide reliable DOI information, by measuring the electron drifting time in sampled waveforms. In contrast, deriving DOI information from the cathode-to-anode ratio is unreliable for detectors having pixel sizes similar to or smaller than the anticipated signal electron cloud size in the detector. In summary, the proposed readout system provides a relatively practical solution for extracting precise energy, timing and spatial information from CZT or CdTe detectors, which could offer a promising candidate for future high-performance multi-modality gamma ray imaging systems.

8143-06, Session 2**Computer simulations to demonstrate new inversion methods for Compton camera data**

B. D. Smith, The Univ. of Texas at San Antonio (United States)

New inversion methods for image reconstruction from Compton camera data are presented here. These methods depend upon which of two models is assumed for the data. Both of these models have been proposed previously by other researchers. Using these methods require measuring new sets of data that have not been measured before. Measuring these sets of data require using a new camera design. Intriguingly, this new design has the potential of having more sensitivity than the conventional camera design. To illustrate these inversion methods computer simulations are used to reconstruct a mathematical phantom.

One set of reconstructed images demonstrates that a parallel projection of the distribution of the radioactivity can be produced from one positioning of the camera. A second set illustrates that a three-dimensional reconstruction of the distribution can be obtained by moving

the camera 180 degrees around the distribution. In addition, possible improvements in these inversion methods to make them more practical are discussed. In particular, the quality of the images could be improved by incorporating more than the minimum amount of data required by the inversion methods into the reconstruction process. Undoubtedly, incorporating the imaging physics (e.g., Doppler broadening and Klein-Nishina distribution) and the instrumentation issues (e.g., finite spatial, energy, and temporal resolution) that are known to degrade the performance of Compton cameras into the reconstruction process will additionally improve the quality of the resulting images.

8143-07, Session 2**Application of 3-D CdZnTe detectors on proton cancer therapy**

Z. He, Univ. of Michigan (United States); J. T. Polf, F. Zhang, The Univ. of Texas M.D. Anderson Cancer Ctr. (United States); W. R. Kaye, Y. A. Boucher, W. Y. Wang, J. M. Jaworski, Univ. of Michigan (United States); D. Maklin, The Univ. of Texas M.D. Anderson Cancer Ctr. (United States)

Three-dimensional position-sensitive CdZnTe detectors can perform excellent gamma-ray spectroscopy, achieving energy resolutions better than 1% FWHM at 662 keV, and real-time gamma-ray imaging. This work describes our exploratory research to extend the dynamic range of current 3-D CdZnTe detectors from 3 MeV to 9 MeV, and initial measurements on positron annihilation and characteristic prompt gamma-ray emissions in a clinical proton therapy environment. These measurements will shape design considerations on future systems for treatment verification and assessment based on the measurement of secondary gamma emissions during proton treatment delivery.

8143-08, Session 2**Spect imaging onboard radiation therapy systems**

J. E. Bowsher, Duke Univ. Medical Ctr. (United States) and Duke Univ. (United States); S. Yan, Duke Univ. (United States); J. R. Roper, Duke Univ. Medical Ctr. (United States); W. M. Giles, Duke Univ. (United States); F. Yin, Duke Univ. Medical Ctr. (United States) and Duke Univ. (United States)

Radiation therapy machines now frequently include onboard x-ray transmission imaging systems which can image patients as they are in position for radiation therapy. These onboard systems have advanced radiation therapy, fostering techniques such as stereotactic body radiation therapy, and more generally improving targeting of treatment regions and sparing of healthy tissue. However, these onboard x-ray transmission systems primarily image physical characteristics such as electron density. Herein we consider SPECT as a method for onboard imaging. Such technology could enable accurate and precise radiation therapy targeting, as well as real-time modulation of radiation therapy, based on molecular and functional properties. It is molecular and functional properties that primarily distinguish tumor from surrounding healthy tissue and that relate directly to appropriate radiation dose. However, onboard SPECT is challenged by clinical time frames of about 4 minutes. To address this, we consider a multi-pinhole system for SPECT imaging of the target vicinity. A robotic arm is proposed to navigate the detector through the tight onboard geometry and to optimize detector trajectory about the target region. Computer-simulation studies suggest that effective imaging can be achieved with 4-minute scan times. This imaging approach also has applications beyond radiation therapy.

Conference 8143:
Medical Applications of Radiation Detectors

8143-09, Session 2

Fast regional readout CMOS active pixel sensor for radiotherapy treatment verification

H. Zin, E. J. Harris, J. P. F. Osmond, P. M. Evans, Institute of Cancer Research (United Kingdom) and Royal Marsden NHS Trust (United Kingdom)

Advanced radiotherapy techniques such as intensity modulated radiation therapy (IMRT) and velocity modulated arc therapy (VMAT) requires verification of complex treatments and tracking of multileaf collimators (MLC). Current techniques using electronic portal imaging devices (EPID) or fluoroscopic based imaging have several limitations such as low image contrast and slow imaging speed or unnecessary skin dose. Novel complementary metal oxide semiconductor active pixel sensor (CMOS APS) have the potential to overcome these limitations by utilising fast, region of interest (ROI) readout functionality of up to 400 frames per second. Performance of the sensor region of interest readout was examined and sensor dead time was measured using a novel technique via an in-house fast moving light source. Characterisation of the sensor provides further understanding of the sensor characteristics, and allows corrections for sensor non-linearity, non-uniformities and dead time to be applied in radiotherapy treatment verification and tracking. Application of the sensor in radiotherapy imaging to verify and track the multileaf collimator (MLC) was made in camera configuration coupled to a gadolinium oxide (Gadox) scintillator screen. The sensor was first calibrated using open field beam of various dose rates and later used to verify complex Volumetric Modulated Arc Radiotherapy Treatment (VMAT). Automatic leaf tracking algorithm has demonstrated CMOS APS ability to track complex VMAT delivery beyond 50 sampling per second.

8143-10, Session 3

Promising new drug delivery architectures enabled by precise silicon micro- and nanofabrication

D. Fine, Methodist Hospital Research Institute (United States); C. Chiappini, The Univ. of Texas at Austin (United States); T. Hu, B. Godin-Vilentchouk, R. Serda, E. Tasciotti, P. Decuzzi, A. Grattoni, X. Liu, Methodist Hospital Research Institute (United States); M. Ferrari, Methodist Hospital Research Institute (United States) and Rice Univ. (United States)

The application of nanotechnology towards the diagnosis and treatment of disease seeks to exploit the unique properties of nanoscale and nanopatterned materials and devices, including enhanced energy conversion, increased permeability, and the modulation of diffusive transport. In the context of drug delivery, nanotechnology approaches can provide sustained targeted release of therapeutic agents while improving the circumvention of biological barriers and protecting the payload from the immune system. Two promising drug delivery platforms will be presented: the nanochannel drug delivery system (nDS) and the multi-stage drug delivery vector (MSV). The nDS is an implantable drug reservoir interfaced to a silicon-based nanofluidic membrane capable of modifying diffusive transport from a classical concentration dependent regime described by Fick's law to a concentration independent zero-order release. Such a zero-order release profile stems from nanoconfinement where surface effects at the solution/channel wall interface dominate over bulk fluid properties. MSVs are systemically delivered and loaded with multiple delivery stages (i.e. drug loaded liposomes) for the sequential circumvention of biobarriers. Porous silicon particles comprise stage 1 with controlled size, shape, porosity, and pore size whose surface is biochemically functionalized to control particle degradation rates, improve immune system evasion, and enable specific targeting of the vasculature. Silicon micro- and nanofabrication, a mature technology developed for over 40 years for the semiconductor industry, provides the platform to manufacture these devices with precision and accuracy.

8143-11, Session 3

Depth of interaction compensation for high resolution SPECT imaging using crystalline microcolumnar films

V. V. Nagarkar, H. Bhandari, S. R. Miller, H. Kudrolli, Radiation Monitoring Devices, Inc. (United States); B. Miller, H. B. Barber, The Univ. of Arizona (United States)

No abstract available

8143-12, Session 3

High-performance imaging of stem cells using single-photon emissions

D. J. Wagenaar, Gamma Medica, Inc. (United States); R. A. Moats, Children's Hospital of Los Angeles (United States) and The Univ. of Southern California (United States); N. E. Hartsough, DxRay, Inc. (United States); D. Meier, J. W. Hugg, Gamma Medica, Inc. (United States); D. Gazit, G. Pelled, Cedars-Sinai Medical Ctr. (United States); B. E. Patt, Gamma Medica, Inc. (United States)

No abstract available

8143-13, Session 3

High-resolution, anamorphic, adaptive small-animal SPECT imaging with silicon double-sided strip detectors

H. L. Durko, College of Optical Sciences, The Univ. of Arizona (United States); T. E. Peterson, Vanderbilt Univ. (United States); H. H. Barrett, L. R. Furenlid, College of Optical Sciences, The Univ. of Arizona (United States)

Recent advances in radiotracers for amyloid plaques, coupled with the development of suitable mouse models for Alzheimer's disease motivate the need for high-resolution small-animal brain imagers capable of monitoring disease progress and/or response to therapy. Silicon-based devices are ideal for the detection of the low-energy photons from iodinated radiotracers, and photolithographic fabrication techniques allow for the production of high-resolution double-sided strip detectors, in which the measurements of very large numbers of virtual pixels are read out by separate x and y position-sensitive electrodes.

We are developing a prototype imaging system that consists of two sets of movable, keel-edged copper-tungsten blades configured as crossed slits. These apertures can be positioned independently between the object and detector, producing an anamorphic image in which the axial and transaxial magnifications are not equal. The detector is a 60 × 60 mm², millimeter-thick megapixel silicon double-sided strip detector. The flexible nature of this system allows the application of adaptive imaging techniques. For example, a series of low-magnification projections could be used to determine and define a region of interest. For each high-resolution projection, the system could then calculate the optimal axial and transaxial magnifications to project the object in such a way that an anamorphic image fills the detector area. We will discuss system details, calibration and acquisition methods, and our progress towards biological imaging applications.

Conference 8143:
Medical Applications of Radiation Detectors

8143-14, Session 3

TlBr gamma-ray spectrometers for SPECT

H. Kim, A. Kargar, L. J. Cirignano, A. V. Churilov, G. Ciampi, W. M. Higgins, S. Kim, Radiation Monitoring Devices, Inc. (United States); F. Olschner, Cremat, Inc. (United States); K. S. Shah, Radiation Monitoring Devices, Inc. (United States)

Thallium bromide appears to be a very promising semiconductor material for gamma-ray detectors in small animal SPECT imaging. It has the potential to provide very high detection efficiency, low noise and high energy as well as spatial resolution. TlBr has high atomic number constituents and high density, wide semiconducting band gap, and based on recent measurements, good charge transport parameters. Furthermore, the material melts congruently at a modest temperature (460 degC), which allows use of melt-based crystal growth approaches such as Bridgman and Czochralski to produce large volume TlBr crystals. The cubic crystal structure of TlBr also simplifies crystal growth.

8143-15, Session 3

Grazing angle Mach-Zehnder interferometer using reflective gratings and a polychromatic uncollimated light source

C. K. Kemble, J. Auxier, S. Lynch, E. E. Bennett, N. Y. Morgan, H. H. Wen, National Institutes of Health (United States)

Grating-interferometer based phase-contrast x-ray imaging promises improved sensitivity over absorption radiography. For greater phase sensitivity, however, interferometer gratings need periods below 2 microns. Two challenges inhibit using x-ray transmission gratings with periods below 2 microns: difficult fabrication, and low interference-fringe visibility. The latter challenge occurs when ultra-dense gratings are used with a polychromatic source. To solve both problems, we propose a symmetric Mach-Zehnder interferometer that utilizes grazing-angle reflective gratings.

First, our interferometer setup has a grazing x-ray incidence angle on the reflective gratings, making the gratings' effective periods significantly smaller than their physical periods. We are therefore able to realize effective periods below 2 microns using standard photolithography techniques (N.P.L. Gratings for X-ray Spectroscopy, L. A. Sayce and A. Franks, Proc. Royal Society, Series A, 282(1390), pp. 353-357(1964)).

Second, current polychromatic-source Talbot-interferometer designs operate in the near field range. Near-field operation limits phase sensitivity because decreasing the grating's period quadratically decreases the Talbot distance. We instead use a far-field interferometer, a grazing-angle symmetric Mach-Zehnder interferometer, which provides near ideal fringe contrast with polychromatic and un-collimated sources in the far field.

After presenting this idea's visible light analog (Grazing angle Mach-Zehnder interferometer using reflective phase gratings and a polychromatic, un-collimated light source, C. K. Kemble et al., Optics Express, 18(26), pp. 27481-27492 (2010)), we now present the first x-ray interferometry results using a bench top tungsten-target x-ray source of 0.15 mm spot size. We also address the limitation of small vertical field of view from the grazing angle geometry.

8143-16, Session 4

Optimizing CdTe detectors and ASIC readouts for high-flux x-ray imaging

W. C. Barber, DxRay, Inc. (United States); E. Nygard, Interon AS (Norway) and DxRay, Inc. (United States); J. C. Wessel, N. Malakhov, Interon AS (Norway); N. E. Hartsough, T. Ghandi, DxRay, Inc. (United States); G. Wawrzyniak, Interon AS (Norway);

J. S. Iwanczyk, DxRay, Inc. (United States)

Developments in room temperature cadmium telluride (CdTe) based solid state imaging arrays for energy-resolved single photon counting in medical x-ray imaging are discussed. A number of x-ray imaging applications can benefit from these developments including mammography, radiography, and computed tomography (CT). Energy resolved photon counting can provide reduced dose through optimal energy weighting, compositional analysis through multiple basis function material decomposition, and contrast enhancement through spectroscopic x-ray imaging of metal nanoparticles. Extremely high flux can occur in x-ray imaging and energy integrating detectors with a large dynamic range and good detection efficiency have been conventionally used. To achieve the benefits of energy resolved photon counting, imaging arrays with a large count rate range and good detection efficiency are required. Compound semiconductor radiation detectors with pixellated anode arrays electrically connected to application specific integrated circuits (ASICs) can provide fast, efficient, low-noise performance with adequate energy resolution however this can only be achieved with a careful optimization of the CdTe sensors and ASICs together. We have designed and constructed a CdTe imaging array, 3 mm thick with a 16 x 16 grid of electrical contacts inter-connected to a 256 channel ASIC, with a counting range up to 2×10^7 counts per second per mm². Result description of the from this device as well as a description of the optimization methods used in the design are presented and discussed.

8143-17, Session 4

Mcps-range photon-counting x-ray computed tomography system

E. Sato, Y. Oda, Iwate Medical Univ. (Japan); A. Abudurexiti, Toreck, Inc. (Japan); O. Hagiwara, T. Enomoto, The Toho Univ. (Japan); S. Sugimura, Tokyo Denpa Co. Ltd. (Japan); H. Endo, Iwate Industrial Research Institute (Japan); S. Sato, A. Ogawa, Iwate Medical Univ. (Japan); J. Onagawa, Tohoku Gakuin Univ. (Japan)

Although the count rate has been increased to sub-Mcps using a CdTe detector system, the rate can be increased to approximately 20 Mcps using a short-decay-time scintillator in conjunction with a high-speed photoelectric detector. Therefore, we performed fundamental study on high-speed photon counting and energy discrimination. We also constructed a first-generation photon-counting X-ray CT system to confirm the energy-discrimination effect using a comparator in a multipixel-photon-counter (MPPC) module.

A photon-counting X-ray CT system consists of an X-ray generator, a turntable, a translation stage, a two-stage controller, a multipixel-photon-counter (MPPC) module, a 1.0-mm-thick Lu₂(SiO₄)O (LSO) single crystal (scintillator), a counter card (CC), and a personal computer (PC). Tomography is accomplished by repeating the linear scan and the rotation of an object, and projection curves of the object are obtained by the linear scan using the detector consisting of an MPPC module and an LSO scintillator. The pulses of the event signal from the module are counted by the CC in conjunction with the PC. The lower level of the photon energy is roughly determined by a comparator circuit in the module, and the unit of the level is the photon equivalent (pe). Thus, the average photon energy of the X-ray spectra for imaging increases with increasing the pe value. The maximum count rate was approximately 10 Mcps, and energy-discrimination CT was roughly carried out.

8143-18, Session 4

Cancer diagnosis using a conventional x-ray fluorescence camera with a cadmium-telluride detector

E. Sato, Iwate Medical Univ. (Japan); T. Enomoto, O. Hagiwara, The Toho Univ. (Japan); A. Abudurexiti, K. Sato, Toreck, Inc.

Conference 8143:
Medical Applications of Radiation Detectors

(Japan); S. Sato, A. Ogawa, Iwate Medical Univ. (Japan); J. Onagawa, Tohoku Gakuin Univ. (Japan)

Narrow-energy-width bremsstrahlung X-rays produced from the tungsten tube are very useful for exciting various elements. In particular, we are very interested in cancer diagnosis using iodine- and gadolinium-based contrast media for medical imaging and several nanoparticle suspensions. Therefore, we have developed a reflection-type XRF camera utilizing a conventional X-ray generator and performed mapping for iodine and gadolinium molecules.

X-ray fluorescence (XRF) analysis is useful for mapping various molecules in objects. Bremsstrahlung X-rays are selected using a 3.0-mm-thick aluminum filter, and these rays are absorbed by iodine, cerium, and gadolinium molecules in objects. Next, XRF is produced from the objects, and photons are detected by a cadmium-telluride detector. The K photons are discriminated using a multichannel analyzer, and the number of photons is counted by a counter card. The objects are moved and scanned by an x-y stage in conjunction with a two-stage controller, and X-ray images obtained by molecular mapping are shown on a personal computer monitor. We carried out molecular mapping using the X-ray camera, and K photons from cerium and gadolinium molecules were produced from cancerous regions in nude mice.

8143-19, Session 4

Color management and calibration techniques at the University of Arizona

S. F. Hashmi, H. Roehrig, E. A. Krupinski, The Univ. of Arizona (United States)

Purpose: The purpose of a research project at the Radiology Research Lab at the University of Arizona is to address consistent color and grayscale presentation for digital color displays used in medical image interpretation.

Currently color monitors are quickly entering the market for displaying grayscale and color information as they are ubiquitous and also less costly. Color displays are being used in a lot of disciplines in medicine, such as Pathology Ophthalmology, dermatology, etc because of the inherent color associated with these fields. The absence of any validated methods available to reliably calibrate these color displays prompted us to build a laboratory with equipment capable of developing and implementing such a color calibration protocol.

The expectation is that once such a protocol is developed, it can be standardized and is easy to implement across the board. This standardization will help in diagnosing a disease in an early and correct manner.

Methods: The proposed method starts with the calibration of the display under test. Calibration parameters are defined and all the necessary measurements are done with the help of a PR670 Spectroradiometer. This ensures that the calibration is well controlled and conforms to our specifications.

The next steps are 'Characterization and Profiling' as well as 'Verification' of the profile. This is done using some known color samples and comparing the measurements with PR670 Spectroradiometer.

The next step is to calculate color accuracy and delta-E values and we are still on course to do it and hopefully the results will be available very soon.

Our laboratory setup includes a computer using an AMD Phenom-II processor and a Windows XP operating system with SP3 update on it. In addition the computer's CPU has a 4 GB Ram. There is a state of the art NVIDIA Quadro FX3700 graphics card. The CPU handles two displays at the same time.

The primary display is a Samsung display, which is usually our display number-1 and the secondary display is our Display under Test. A variety of programs related to our Research Project are installed in the CPU; the most important one of them is MatLab.

At this time three medical image displays are available and have been used already for our work: NEC-2690 WUXI2, NDS -DOME E3cHB and

EIZO- RX320. Software for their operation and associated Pucks for their calibration are installed in the computer. The native resolution, response time and Luminance values of these displays is shown in the table below:

	Luminance	Resolution	Response time
EIZO	300 cd/m2	1536X2048	20 ms
NDS-DOME300	300 cd/m2	1536X2048	24ms
NEC	150 cd/m2	1920X1200	16ms

The Spectro-Radiometer, PR-670, we have is used to make corrections for the errors of the Pucks. The spectral region of the Spectroradiometer ranges from 380 nm to 780 nm. It provides spectra in steps of 1.56 nm. It is basically a very sensitive and accurate detector array. The Spectroradiometer is connected to the computer through a USB connection and is controlled through MatLab.

Results: At this moment, we are testing our profiles for their accuracy and the next step is to go towards color difference calculation.

Conclusions: A calibration facility for Color LCDs has been developed at the University of Arizona and is operating. Preliminary results are encouraging.

The issue of calibration and profiling that can simultaneously achieve DICOM and L* tone reproduction curve and good color rendition must be addressed. Particularly for low-cost color sensors, the issue of accurate calibration must be addressed as well as the reliability with low cost color sensors (Pucks).

8143-20, Session 4

Calibration and verification of DICOM software at the University of Arizona

S. F. Hashmi, H. Roehrig, The Univ. of Arizona (United States)

At the University of Arizona a research project is underway which addresses consistent color and consistent grayscale presentation for digital color displays used in medical image interpretation, specifically for Pathology. Since there were no validated methods available to reliably calibrate color displays we decided to build a laboratory with equipment capable to develop and implement a color calibration protocol. One of the most important items is a spectro-radiometer PR-670.

For our first experiment we concentrated on verification of the QUBYX Perfectum Calibration Software. The specific objectives were:

1. Verify if the "PerfectLum" software from "Qubyx Ltd." would calibrate an LCD Display to DICOM GSDF part 14 standards. FIT and LUM tests were performed to verify the conformance and the deviation was quantified.
2. On the calibrated display, quantitative evaluation of Luminance response done and deviation quantified. Also the deviation was checked for class A or class B threshold, 10% and 20% deviation respectively.
3. Verify if the "Display Conformance" function in "PerfectLum" software returns the correct values for FIT, LUM and AAPM luminance response test.

All three objectives were met and PerfectLum calibrated display confirmed to the AAPM TG18 standards.

8143-21, Session 4

An x-ray tube based room-temperature Compton spectrometer with application to material characterization

S. Olesinski, G. Harding, Morpho Detection Germany GmbH (Germany)

A description is given of the principle of operation, design and technical realization of a Compton spectrometer. In contrast to many other devices that have been discussed in the literature, the Compton spectrometer

**Conference 8143:
Medical Applications of Radiation Detectors**

described here combines an electron-impact x-ray source with a room-temperature semiconductor detector.

It is shown that the momentum resolution (0.6 au) of the Compton spectrometer for the K characteristic lines emitted by the tube anode is adequate to resolve the Doppler broadening originating in electron momentum distributions of low atomic number elements, such as carbon, nitrogen and oxygen. Experimental Compton-broadened spectra from a range of common materials are presented. Methods to extract Compton profiles from the experimental spectra, by accounting for the continuous component of the x-ray tube emission and the multiplet nature of the characteristic lines, are illustrated. The application of this Compton spectrometer to material characterization is briefly discussed.

Conference 8144: Penetrating Radiation Systems and Applications XII

Sunday-Wednesday 21-24 August 2011 • Part of Proceedings of SPIE Vol. 8144
Penetrating Radiation Systems and Applications XII

8144-01, Session 1

Preliminary investigation of lanthanum-cerium bromide self-activity removal

D. Yuan, P. Guss, National Security Technologies, LLC (United States)

It has been reported that detectors made of lanthanum-cerium halides [LaBr₃:Ce and CeBr₃] have superior energy resolution for gamma-radiation detection compared to what is offered by conventional sodium iodide [NaI:Tl] detectors. Although superior energy resolution may be observed, one major barrier that has hindered the rapid adaptation of lanthanum halides is their self-activity, due primarily to the presence of isotope ¹³⁸La, and the α contamination, due to the trace amount of actinides. It has also been observed that the lanthanum-cerium halides contain a substantial amount of self-activity caused by the radioactive isotope. Additionally, LaBr₃:Ce spectra are also affected by β contaminations in the low-energy region. To use either LaBr₃:Ce or CeBr₃ for high-sensitivity gamma detection, it may be necessary to have the self-activity as well as α and β contaminations removed or reduced. This paper describes a novel algorithmic approach for self-activity and contamination reduction for LaBr₃:Ce and CeBr₃ detectors using a third reference NaI:Tl detector. We present a computational procedure for separating self-activity from the gamma spectra obtained by LaBr₃:Ce detectors. With the self-activity spectra pre-calculated, it is possible to perform real-time self-activity removal. This procedure can be implemented as an automatic self-activity subtraction module for gamma radiation detectors made of LaBr₃:Ce and/or CeBr₃ crystals. With this approach, it is possible to develop a new generation of LaBr₃:Ce detectors capable of producing spectra as clean as those obtained by conventional NaI(Tl) detectors, but with much improved energy resolutions.

8144-02, Session 1

A fissionable scintillator for neutron flux monitoring

S. Stange, E. I. Esch, Los Alamos National Lab. (United States); E. Burgett, Idaho State Univ. (United States); R. Del Sesto, R. Muenchausen, F. Taw, F. K. Tovesson, Los Alamos National Lab. (United States)

Neutron flux from linear accelerators is conventionally monitored using ionization chambers containing one or more foils thinly coated with a fissionable or fissile material. Due to the long pulse rise times resulting from the ionization mechanism, fission chambers are prone to pulse pile-up in high-neutron-flux environments. In addition, their relatively low efficiencies result in extremely long counting times in low-flux environments. To ameliorate these effects, a novel type of neutron flux monitor, consisting of fissionable material loaded in a liquid scintillator, has been developed, characterized, and tested in the beam line at the Los Alamos Neutron Science Center. This is a rugged, cost-efficient detector with high efficiency, a short signal rise time, and the ability to be used in low neutron-flux environments. Compared with a conventional fission chamber, the fissionable scintillator displays a significantly higher event rate. Related research on nanocomposite scintillators for gamma-ray detection suggests the possibility of extending this approach by synthesizing fissionable material nanoparticles and loading them into an organic scintillator. We will present results of the design and characterization process and an analysis of the results of the beam line experiments.

8144-03, Session 1

Light yield measurement method for milled nanosized inorganic crystals

A. Li, North Carolina State Univ. (United States) and Los Alamos National Lab. (United States); E. A. McKigney, Los Alamos National Lab. (United States); R. P. Gardner, North Carolina State Univ. (United States); N. A. Smith, M. P. Hehlen, Los Alamos National Lab. (United States)

In an effort to improve currently available scintillators, composite scintillators consisting of nanosized inorganic crystals embedded in a matrix have been explored by McKigney et al (2007). In the process of producing such a detector, several steps are involved: the preparation of the nanosized inorganic crystals, the characterization of the inorganic crystals, and the dispersion of the crystals in a permanent matrix. In this work, the preparation of nanosized inorganic crystals involves milling the inorganic crystals in powder form to the appropriate size. However, since milling is known to introduce defects in the milled material, the performance of the milled material must be characterized. One of the most important quantities of the milled inorganic crystals is their light yield, and it may be measured by the radioluminescence technique. However, the common radioluminescence light yield measurement technique does not take into account the concentration of the inorganic crystals in individual samples, which may vary during processing. In this work, a new method of characterizing the light yield of the processed inorganic crystals will be explored and discussed; this method will take into account explicitly the concentration of the inorganic crystals.

8144-04, Session 1

Investigation into nanostructured lanthanum halides and CeBr₃ for nuclear radiation detection

P. Guss, R. E. Guise, S. Mukhopadhyay, D. Yuan, National Security Technologies, LLC (United States)

Nanocomposites may enable the use of scintillator materials such as cerium-doped lanthanum fluoride and cerium bromide (CeBr₃) without requiring the growth of large crystals [1]. Nanostructured detectors may allow us to engineer immensely sized detectors of flexible form factors that will have a broad energy range and an energy resolution sufficient to perform isotopic identification. Furthermore, nanocomposites are easy to prepare and very low in cost. It is much less costly to use nanocomposites rather than grow large whole crystals of scintillator materials; with nanocomposites fabricated on an industrial scale, costs are even less. Nanostructured radiation scintillator detectors may improve quantum efficiency and provide vastly improved detector form factors. Quantum efficiencies up to 60% have been seen in photoluminescence from silicon nanocrystals in a densely packed ensemble [2]. We have fabricated nanoparticles with sizes <10 nm and characterized their nanocomposite radiation detector properties. This work also attempted to extend the gamma energy response on both low- and high-energy regimes by demonstrating the ability to detect low-energy x-rays and relatively high-energy activation prompt gamma rays simultaneously using nanostructured lanthanum bromide, lanthanum fluoride, or CeBr₃. Nanoscale properties of lanthanum halides and CeBr₃ promise to extend the gamma energy response on both low- and high-energy regimes. Nanostructured lanthanum halides and CeBr₃ may be able to detect low-energy x-rays and relatively high-energy activation prompt gamma rays simultaneously. Preliminary results of this investigation are consistent with a significant response of these materials to nuclear radiation.

Index Terms-CeBr₃, LaBr₃:Ce, LaCl₃:Ce, Nanoparticle Detector, Resolution.

Conference 8144:
Penetrating Radiation Systems and Applications XII

ACKNOWLEDGEMENT

This work was done by National Security Technologies, LLC, under Contract No. DE-AC52-06NA25946 with the U.S. Department of Energy.

REFERENCES

- [1] P. Guss, ANS Nevada Chapter 2010 Joint Topical Meeting; Las Vegas, Nevada; April 18-23, 2010.
- [2] R. E. Del Sesto, "Development of nanocomposite scintillators", LALP-07-030 Spring 2007.

8144-05, Session 1

Defect creation by swift heavy ion induced secondary electrons

N. C. Mishra, R. Biswal, Utkal Univ. (India); D. Kanjilal, D. K. Avasthi, Inter Univ. Accelerator Ctr. (India)

Evolution of 150 nm thick c-axis oriented YBa₂Cu₃O_{7-y} (YBCO) thin films under 200 MeV Ag ion irradiation is studied by in situ temperature dependent resistivity, and in situ low temperature x-ray diffraction. Irradiation at extremely low ion fluences (108 to 109 ions cm⁻²) and at low temperature (79 K) revealed a new mode of materials modification by these swift heavy ions (SHI). In addition to amorphized latent tracks directly induced by the SHI and a strained region around each ion track, point defects in the form of oxygen disorder were found to be created selectively in the CuO basal planes of YBCO structure by secondary electrons emanating from the ion paths. The radius of this newly found oxygen disordered region is 97 nm, which is much larger than the radius (1.9 nm) of the amorphized ion tracks determined from the fluence dependence of the intensity of XRD peaks. The secondary electrons could thus induce global change in the structure and superconducting transition of YBCO, and provided a way of creating oxygen disorder in YBCO matrix even with oxygen content close to 7, which was not possible earlier. Conventional low energy electron irradiation permits the penetration of the electrons only up to a few nanometers from the surface of a target material, thus precluding its efficacy in modifying the bulk. SHI induced secondary electrons however are created all along the ion path up to a depth of few tens of microns and hence can create defects well inside the bulk region.

8144-06, Session 2

Investigation of the possibility of gamma-ray diagnostic imaging of target compression at NIF

D. Lemieux, College of Optical Sciences, The Univ. of Arizona (United States); G. P. Grim, Los Alamos National Lab. (United States); H. B. Barber, The Univ. of Arizona (United States)

At the National Ignition Facility (LLNL), 14.1 MeV neutrons produced by the fusion burn can interact with carbon nuclei in the polymer ablator via $^{12}\text{C}(n, n^{\prime}\gamma)^{12}\text{C}$ to make 4.44 MeV gamma-rays. The number of gamma-rays produced by this process is expected to be of order 10⁻³ of the neutrons produced. High-resolution gamma-ray imaging of the ¹²C distribution should provide useful diagnostic imaging of the remaining ablator material during compression and hence its spatial distribution. The multiple-pinhole optics and detector technologies required for such a gamma-ray imaging system appear to be quite similar to LANL's existing neutron imaging system at NIF. Over the ~ 30 m flight path, the gamma rays precede the fusion neutrons by ≥ 400 ns, so the detector signals are separable. We will describe the results of simulations of three candidate imaging detectors using GEANT4. The three configurations include a scintillator slab with focusing optics, a pixelated scintillator with fiber optics and a pixelated Cherenkov radiator with fiber optics. We will discuss simulation results, criteria for choosing the best system and further prospects.

8144-07, Session 2

Radiation induced noise in x-ray imagers for high-yield inertial confinement fusion experiments

C. A. Hagmann, J. Ayers, P. M. Bell, D. K. Bradley, J. R. Celeste, C. J. Cerjan, J. A. Emig, B. Felker, J. P. Holder, N. Izumi, K. Krauter, J. D. Moody, K. Piston, C. Sorce, V. Smalyuk, Lawrence Livermore National Lab. (United States); J. Bourgade, S. Darbon, Commissariat à l'Énergie Atomique (France); J. D. Kilkenny, General Atomics (United States)

The large fluence of energetic neutrons produced in high-yield inertial confinement fusion (ICF) experiments creates a variety of backgrounds in x-ray imagers viewing the implosion. Electrons scattered by secondary gammas produce Cherenkov and possibly scintillation in the fiberoptic of the imager as well as excitation of the phosphor screen. Noise is also produced in the image recorder itself (film or CCD) via energy deposition by electrons and heavy charged particles such as protons and alphas. We will present results from background measurements performed at the OMEGA facility in Rochester, NY and compare them to Monte Carlo calculations. This work performed under the auspices of the U.S. Department of Energy by Lawrence Livermore National Laboratory under Contract DE-AC52-07NA27344

8144-08, Session 2

Advanced gated x-ray imagers for experiments at the National Ignition Facility

S. M. Glenn, P. M. Bell, R. Benedetti, D. K. Bradley, J. R. Celeste, R. F. Heeter, C. A. Hagmann, J. P. Holder, N. Izumi, Lawrence Livermore National Lab. (United States); J. D. Kilkenny, General Atomics (United States); J. R. Kimbrough, G. A. Kyrala, N. Simanovskaia, R. Tommasini, Lawrence Livermore National Lab. (United States)

X-ray imaging is integral to the measurement of the properties of hot plasmas. To this end, a suite of gated x-ray imagers have been developed for use in a wide range of experiments at the National Ignition Facility (NIF). These instruments are sensitive to x-rays over the range of 0.7-90keV and can acquire images at 20ps intervals for source intensities ranging over several orders of magnitude. We review the design, technology, and construction of these instruments and present recent results obtained from NIF experiments in which gated x-ray imagers have played a key role.

The radiation environment associated with Inertial Confinement Fusion (ICF) experiments presents unique challenges for x-ray imaging. We report on the performance of gated imagers that have been optimized for this harsh environment and describe diagnostics to be deployed in the near future that will provide x-ray images of imploding ICF capsules in the presence of backgrounds associated with neutron yields above 10¹⁶. Such images will provide crucial data that will enable even higher neutron yields and successful ignition.

This work was performed under the auspices of the U.S. Department of Energy by Lawrence Livermore National Laboratory under Contract DE-AC52-07NA27344.

8144-09, Session 2

Prompt radiochemical diagnostics for inertial confinement fusion experiments

G. P. Grim, R. Rundberg, M. Fowler, J. Wilhelmy, Y. Wang, T. Archuleta, R. Aragonéz, Los Alamos National Lab. (United States)

Conference 8144:
Penetrating Radiation Systems and Applications XII

At the recently completed National Ignition Facility (NIF), Lawrence Livermore National Laboratory, Livermore California, current ignition are based on the $d(t,n)\alpha$ reaction. This abbreviated set of diagnostics provides an incomplete picture of implosions. Prompt radiochemical techniques, based on neutron and charged particle, provide a novel perspective on experimental performance. These additional diagnostics allow for measurement of hydrodynamic mix both within the burning plasma, and at the boundary with the ablator, as well as ablator implosion velocity and neutron spectral information. We present the status of prompt radiochemical techniques being developed at Los Alamos National Laboratory, with emphasis on the progress being made to collect and count target debris in ICF experiments.

Supported under the auspices of DOE Contract DE-AC-52-06-NA25396. LA-UR-09-01840 TSPA

contract DE-AC-52-06-NA25396. LA-UR-09-01840 TSPA

8144-10, Session 3

Compact pyroelectric-driven gamma generator

A. J. Antolak, K. Leung, D. H. Morse, T. N. Raber, Sandia National Labs., California (United States)

No abstract available

8144-13, Session 3

Compact coaxial microwave neutron generator

W. C. Johnson, A. J. Antolak, K. Leung, T. N. Raber, Sandia National Labs., California (United States)

No abstract available

8144-14, Session 3

Burst-mode 4 MHz CMOS-hybrid imaging system for multi-frame proton radiography

K. Kwiatkowski, P. Nedrow, C. Morris, F. Merrill, A. Saunders, Los Alamos National Lab. (United States)

The performance of a 4-Mframe/s burst-mode imager with 3-frame in-pixel storage will be discussed. The 720×726 px ultra-fast hybrid FPA and camera were fabricated by Rockwell Scientific (now Teledyne Imaging Sensors). Six cameras have been in operation for several years, in a variety of static and dynamic experiments at the 800MeV proton radiography (pRAD) facility at the LANSCE accelerator. The cameras can operate with per-pulse adjustable inter-frame time of 250ns to 2s, with an exposure/integration-time as short as 180ns. With a 70 ms readout time, the camera can be externally synchronized to 0.1-to-5Hz, 50-ns wide proton beam pulses, and record 1000-frame radiographic movies of 5-to-30 minute duration. The effectiveness and dependence of the global electronic shutter on the pixilated Si-sensor bias voltage and other parameters will be discussed. The spatial resolution dependence of the imaging system on various monolithic and "structured" scintillators and phosphor screens will be presented.

We will also describe features of a new-generation 10-frame 1024×1024 pixel, 50-ns shutter, 12-bit dynamic range imager, which is now in a final design stage.

8144-15, Session 3

Current trends in gamma radiation detection for radiological emergency response

S. Mukhopadhyay, National Security Technologies, LLC (United States)

Passive and active detection of gamma rays from shielded radioactive materials including special nuclear materials is an important task for any radiological emergency response organization. This article reports on the current trends and status of gamma radiation detection objectives and measurement techniques as applied to nonproliferation and radiological emergencies. In recent years, since the establishment of the Domestic Nuclear Detection Office (DNDO) by the Department of Homeland Security (DHS), a tremendous amount of progress has been made in the areas of detection materials (scintillators, semiconductors), imaging techniques (Compton imaging, use of active masking and hybrid imaging), data acquisition systems with digital signal processing (DSP), Field Programmable Gate Arrays (FPGA) and embedded isotopic analysis software (viz. Gamma detector response and analysis software (GADRAS), fast template matching) and data fusion (merging radiological data with geo-referenced maps, digital imagery to provide better situational awareness). In this stride to progress, a significant amount of interdisciplinary research and development has taken place - techniques and spin-offs from medical science (like x-ray radiography, tomography), materials engineering (systematic planned studies on scintillators to optimize each of the several qualities of a good scintillator, nano-particle applications, quantum dots, and photonic crystals, just to name a few). No trend analysis of radiation detection systems would be complete without mentioning the unprecedented strategic position taken by the National Nuclear Security Administration (NNSA) to deter, detect, and interdict illicit trafficking in nuclear and other radioactive materials across international borders and through the global maritime transportation - the so-called Second Line of Defense.

Acknowledgment:

This work was done by National Security Technologies, LLC, under Contract No. DE-AC52-06NA25946 with the U.S. Department of Energy.

8144-22, Session 3

Self-occluding quad NaI directional gamma radiation detector for stand-off radiation detection

D. A. Portnoy, J. Mattson, R. Feuerbach, J. Heimberg, The Johns Hopkins Univ. Applied Physics Lab. (United States)

Currently there is a significant amount of interest in stand-off radiation detection (a common test case is 1 mCi of Cs137 at 100 meters). The challenge is to separate small radiation signals from large varying background radiation. Many systems developed to address this problem rely on coded-aperture and/or Compton imaging. These imaging systems tend to be large, heavy, complex, and therefore expensive, in addition to being for the most part operationally untested. The self-occluding directional gamma radiation sensor is relatively small (<40 kg), inexpensive, and simple in design. Laboratory and field measurements suggest that these sensors will work as well as the gamma imaging systems for many radiation detection applications at a fraction of the cost, weight, and complexity. An azimuth can be resolved with a standard deviation of 7° in 10 seconds for a source yielding 45 CPS at the detector in a 300 CPS background radiation field. This paper describes the Self-Occluding Quad NaI Directional Gamma Radiation Detector, the impact of gamma energy and distance on angular precision and accuracy, and potential applications.

8144-16, Session 4

Compton imaging tomography technique for NDE of large nonuniform structuresV. Grubsky, V. Romanov, T. Jansson, Physical Optics Corp.
(United States)

We describe a new NDE technique called Compton Imaging Tomography (CIT) for reconstructing the complete three-dimensional (3D) internal structure of an object, based on the registration of multiple two-dimensional Compton-scattered x-ray images of the object. A CIT NDE system is typically based on a 200-kV x-ray source and a sensitive x-ray camera. Unlike the traditional Computed Tomography (CT), CIT does not rely on Radon transform for 3D data reconstruction. Instead, other specific image processing approaches are required for optimum 3D data interpolation and beam attenuation artifact removal. Currently, CIT provides high resolution (<1 mm) and sensitivity (<5% of material density difference) with virtually any materials, including lightweight structures and organics, which normally pose problems to conventional x-ray computed tomography due to low contrast. CIT technique requires only one-sided access to the object, has no limitation on the object's size, and can be applied to high-resolution real-time in-situ NDE of large structures, for example aircraft/spacecraft components. Theoretical and experimental results will be presented.

8144-18, Session 4

Shipping container interrogation using a dense plasma focus device

R. P. Keegan, F. Tsang, E. C. Hagen, National Security Technologies, LLC (United States); R. O'Brien, D. Lowe, Univ. of Nevada, Las Vegas (United States)

Work is underway at National Security Technologies, LLC (NSTec), to test the feasibility of using a 2.45 MeV Dense Plasma Focus Device (DPF) to interrogate full-scale ISO shipping containers to identify smuggled fissionable material. The DPF produces a single pulse of 5×10^{11} neutrons within a time window that is about 100 ns wide, so that the effective yield is 5×10^{18} neutrons per second. This pulse generates fission in any fissionable material present, and then delayed gamma rays and neutrons are gross counted for up to 60 seconds starting at 1-3 seconds after the pulse. These delayed radiations are counted using large area (109 cm \times 68.6 cm \times 5.1 cm) EJ-200 polyvinyl toluene (PVT) detectors placed around the outside of the shipping container. The concept for operations involves placing the shipping container in the interrogation system and then gross counting background for five minutes. The DPF is then pulsed once and the delayed radiations are gross counted. The five-minute background is then subtracted from each raw delayed measurement to give the decay profile of the radiation from the shipping container. The concept has been modeled using MCNPX and the ideas will be experimentally tested at the DPF laboratory in early 2011. At the time of presentation of this paper a comparison will be made between the model and the experimental data. Issues related to induced radioactivity in the laboratory after the DPF pulse will be known and addressed. MCNPX simulations already performed indicate that the technique has significant potential.

8144-19, Session 4

FTIR and UV-VIS spectroscopic studies of high gamma irradiated Poly(vinylidene fluoride-hexafluoropropene) (PVdF-HFP)

O. S. Liz, Sr., A. Medeiros, L. O. Faria, Univ. Federal de Minas Gerais (Brazil)

Poly(vinylidene fluoride) [PVdF] is a semicrystalline linear homopolymer composed by the repetition of CH₂-CF₂ monomers. The Poly(vinylidene

fluoride-co-hexafluoropropene) [P(VdF-HFP)] is a copolymer which is obtained with the random introduction of fluorinated [-CF₂-CF-CF₃-] monomers, with 6 fluorine atoms, in the PVdF main chain. Gamma radio-induced changes in the physical and chemical properties were investigated using Fourier Transform Infrared Spectroscopy (FTIR) and Ultraviolet / Visible Spectroscopy (UV-VIS). In a first investigation, for doses ranging from 1 to 100kGy, the FTIR spectra revealed the radio-induction of an absorption band at 1852 cm⁻¹. This peak, generally attributed to stretching of the C=O bonds in carbonyl compounds, is probably originated by the oxidation of the polymer chains, as it is irradiated free in the air. We believe that the irradiation causes breaking of C-F bonds, thus leaving holes to be filled by oxygen atoms. A systematic investigation has shown that the band intensities increase as the gamma dose increases, presenting a linear relation between the gamma delivered dose and the absorption peak intensities, which can be used for detecting gamma doses ranging from 10 to 100kGy. The signal fading was also measured and it is 5% in a period of 60 days.

The UV-VIS Spectroscopy has been also used in this investigation in order to verify the appearing of C=C conjugated bonds, once some fluorinated PVdF copolymers have been reported to show linear behavior of UV absorption intensities with the exposed gamma dose. However, the spectra showed no unambiguous correlation with dose. The FTIR studies have showed that the P(VdF-HFP) copolymers are a great promise for the use in high dose radiation dosimetry.

8144-20, Session 4

6 MeV electron beam induced diffusion of iodine in isotactic polypropylene

N. L. Mathakari, V. N. Bhoraskar, S. D. Dhole, Univ. of Pune (India)

Thin films of polypropylene having size 15 mm X 15 mm X 350 μ m immersed in 1 N iodine solution were irradiated with 6 MeV electron beam from the Microtron accelerator at the fluences varying from 0.5×10^{15} to 2.5×10^{15} electrons/cm². A few samples were also directly irradiated with the 6 MeV electron beam in the same fluence range. The electron irradiated and electron-beam-iodinated samples were characterized by using several techniques such as weight gain, weight loss, Energy Dispersive Spectroscopy (EDS), SEM, FTIR, UV-Visible spectroscopy and XRD. The analysis based on weight gain and EDS indicates that the electron beam increases the iodine intake in the samples increases with the electron fluence. The SEM analysis also indicates that the iodine clusters decrease in size and increase in number with electron fluence. The weight loss analysis carried over the period up to 159 hours at various intervals indicates that the weight loss due to volatile nature of iodine decreases with the fluence. The increase in iodine intake and prevention in its reverse diffusion is attributed to the electron beam induced free volume, defects and increases chemical activity in the polypropylene. The UV-Visible analysis reveals that, the band gap of directly irradiated polypropylene decreases from 4.96 to 4.13 eV. This is attributed to radiation induced carbonization process. On the contrary, the band gap of radiation-iodinated polypropylene decreases from 4.96 to 3.38 eV. This indicates that iodine supports the radiation induced band gap reduction process. FTIR indicates that presence of iodine during irradiation prevents the oxidation of polypropylene which usually takes place after irradiation. XRD analysis shows that direct electron irradiation does not affect the crystallinity to a notable extent. But the intensity of XRD peaks significantly decreases in case of electron-beam-iodinated samples. This indicates that the iodine causes the distortion in the crystalline structure of polypropylene due to its electronegative properties.

8144-21, Poster Session

The melting latent heat of semicrystalline PVDF: an efficient tool for evaluating high gamma doses

A. Medeiros, O. S. Liz, Sr., L. O. Faria, Univ. Federal de Minas Gerais (Brazil)

**Conference 8144:
Penetrating Radiation Systems and Applications XII**

The use of dosimetric systems based on polymers has several advantages such as atomic composition, which can be closer to the material of interest for radiation processing industry, among others. One of the main drawbacks is related to signal loss over time (Fading). This limitation is not unique to polymeric dosimeters and it is present in all chemical dosimeters. In this paper we shall describe the results of our investigation of a new proposed polymeric dosimeter for high gamma dose dosimetry. Now the dosimetry is based on the measurement of the heat of fusion (H_{melt}) of the crystalline part of the homopolymer Poly(vinylidene fluoride) [PVDF]. We have found that H_{melt}, measured by DSC scan, is unambiguously related to the delivered doses ranging from 100 to 3,000 kGy. On the other hand, further systematic fading analysis have proved that the H_{melt} of PVDF has no significant change up to eight months after irradiation, maintaining a linear relationship with the absorbed dose. In order to explain the results of this investigation in terms of the formation of new chemical bonds and the decrease in the crystalline order we have simultaneously taken FTIR and XRD spectrograms together with the DSC scans. Both the very large range of dose measurement (1 to 3,000 kGy) and also the possibility of evaluating high gamma doses until eight months after irradiation make PVDF homopolymer a very good candidate to be investigated as commercial high gamma dose dosimeters.

8144-23, Poster Session**Apodized aperture imaging optics for Compton-scattered x-ray and gamma-ray imaging systems**

V. Romanov, V. Grubsky, T. Jansson, Physical Optics Corp. (United States)

To improve the resolution and field of view of high-energy Compton-scattered x-ray and gamma-ray imaging systems, we have developed and tested apodized imaging optics, based on apertures with depth-dependent cross sections fabricated in an x-ray absorbing material (typically, lead or tungsten). By ray-tracing modeling, we determined the optimum aperture shapes (apodizations) that maximize the field of view and/or resolution of the system. Such optimized apodized apertures can increase the field of view by a factor of 4-5, compared to cylindrical-pinhole optics having the same resolution. Although such apodized apertures can be used in single-aperture x-ray optics, they are particularly suitable in high-resolution, high-energy coded-aperture arrays, where they help to achieve the optimum imaging performance due to the negligible variation of their point spread function with the angle of incidence. Potential applications of this technology include non-destructive evaluation (NDE) of materials and structures, in particular Compton imaging tomography (CIT), x-ray and gamma-ray astronomy, and medical imaging. We will demonstrate our modeling and experimental results for both single-aperture and coded-aperture apodized optics.

8144-24, Poster Session**X-ray imaging in an environment with high-neutron background on National Ignition Facility**

V. Smalyuk, J. Ayers, P. M. Bell, D. K. Bradley, J. R. Celeste, C. J. Cerjan, J. A. Emig, B. Felker, C. A. Hagmann, J. P. Holder, N. Izumi, K. Krauter, J. D. Moody, K. Piston, C. Sorce, J. L. Bourgade, S. Darbone, J. L. Kilkenny, Lawrence Livermore National Lab. (United States)

X-ray imaging diagnostics instruments will operate in a harsh ionizing radiation background environment on implosion experiments at the National Ignition Facility. These backgrounds consist of mostly neutrons and gamma rays produced by inelastic scattering of neutrons. Imaging systems based on x-ray framing cameras with film and CCD's have been designed to operate in such harsh neutron-induced background

environments. Some imaging components were placed inside a shielded enclosure that reduced exposures to neutrons and gamma rays. Modeling of the signal and noise of the x-ray imaging system will be presented and compared with experimental data.

This work performed under the auspices of the U.S. Department of Energy by Lawrence Livermore National Laboratory under Contract DE-AC52-07NA27344.

8144-26, Poster Session**SSPM scintillator readout for gamma radiation detection**

S. A. Baker, National Security Technologies, LLC (United States); C. J. Stapels, Radiation Monitoring Devices, Inc. (United States); J. A. Young, J. A. Green, R. E. Guise, National Security Technologies, LLC (United States); L. A. Franks, Consultant (United States)

Silicon-based photodetectors offer several benefits relative to photomultiplier tube based scintillator systems. Solid-state photomultipliers (SSPM) can realize the gain of a photomultiplier tube (PMT) with the quantum efficiency of silicon. The advantages of the solid-state approach must be balanced with adverse trade-offs, for example from increased dark current, to optimize radiation detection sensitivity. We are designing a custom SSPM that will be optimized for green emission of CsI(Tl). A typical field gamma radiation detector incorporates NaI(Tl) and a radiation converter with a PMT. A PMT's sensitivity peaks in the blue wavelengths and is well matched to NaI(Tl). We present results of photomultiplier sensitivity relative to conventional SSPMs and have modeled design improvements. Prototype fabrications are in progress.

This work was done by National Security Technologies, LLC, under Contract No. DE-AC52-06NA25946 with the U.S. Department of Energy.

Conference 8145: UV, X-Ray, and Gamma-Ray Space Instrumentation for Astronomy XVII

Sunday-Wednesday 21-24 August 2011 • Part of Proceedings of SPIE Vol. 8145
UV, X-Ray, and Gamma-Ray Space Instrumentation for Astronomy XVII

8145-01, Session 1

Status of the CCD camera for the eROSITA space telescope

N. Meidinger, Max-Planck-Institut Halbleiterlabor (Germany)

The approved German X-ray telescope eROSITA will be accommodated on the Russian satellite SRG. The general scientific goal is the exploration of the X-ray Universe in the energy band from 0.3 keV up to 10 keV with excellent energy, time and spatial resolution and large effective telescope areas. After launch to Lagrange point L2, the observational program divides into an all-sky survey and pointed observations.

We present the design of the seven flight cameras and describe the detector configuration. Focus is set on important recent amendments concerning the camera. A 3cmx3cm large, back-illuminated, 450µm thick and fully depleted PNCCD is the main item of the camera. The eROSITA flight CCD chips have been developed and produced in the MPI semiconductor laboratory in the course of further development of the XMM-Newton PNCCD. Their performance was at first tested on chip-level by means of a so-called 'cold chuck probe station' permitting even spectroscopic measurements. Based on these results, we select the flight-CCDs for integration into the seven eROSITA detector modules.

For a detailed characterization of the CCD and its dedicated analog readout ASIC, various tests were carried out. Another aim of the tests was to evaluate the optimum detector operating conditions in terms of operating sequence, supply voltages and operating temperature.

Furthermore, substantial part of testing were radiation hardness tests of the eROSITA CCD and its readout ASIC with protons. This is essential to evaluate the long-term stability of the detectors.

8145-02, Session 1

Development of the data acquisition system for the X-ray CCD camera (SXI) on board ASTRO-H

T. Fujinaga, Japan Aerospace Exploration Agency (Japan); N. Anabuki, Osaka Univ. (Japan); S. Aoyama, Univ. of Miyazaki (Japan); H. Kawano, Yokohama National Univ. (Japan); K. Matsuta, M. Ozaki, T. Dotani, C. Natsukari, K. Shimizu, Japan Aerospace Exploration Agency (Japan); H. Nakajima, K. Hayashida, H. Tsunemi, H. Uchida, S. Ueda, S. Komatsu, Osaka Univ. (Japan); T. Murayoshi, K. Mori, Univ. of Miyazaki (Japan); J. S. Hiraga, The Univ. of Tokyo (Japan); S. Ikeda, T. Watanabe, Kogakuin Univ. (Japan)

Development of the X-ray CCD (SXI) on board ASTRO-H is presented focusing on the data acquisition system. Basic functions of the system were verified with the BBM, and we are currently developing the EM. The functions implemented in the BBM are generation of the timing clocks, delta-sigma-ADC, and SpaceWire communication. The ADC was realized combining ASIC and FPGA. The verification test of the digital part showed that the SpaceWire communication was stable over 24 hours, and the data transfer speed was 4.4 Mbps. We performed the ⁵⁵Fe irradiation test using a prototype CCD cooled down to -30 degrees Celsius. After tuning the sampling timing and installing low-pass filters, we obtained the energy resolution of 164 eV at 5.9 keV (FWHM). This resolution is slightly worse than the requirement to SXI. The final-version BBM, which is under verification, was designed to have the digital and analog architecture identical to the flight model except for the FPGA and parts specification.

8145-03, Session 1

Development of the X-ray CCD for SXI on board ASTRO-H

S. Ueda, K. Hayashida, H. Nakajima, N. Anabuki, H. Uchida, H. Tsunemi, M. Fujikawa, H. Mori, Osaka Univ. (Japan); T. Kohmura, T. Watanabe, K. Kawai, S. Ikeda, K. Kaneko, Kogakuin Univ. (Japan); K. Sakata, S. Todoroki, H. Mizuno, N. Yagihashi, Rikkyo Univ. (Japan); T. Dotani, M. Ozaki, Japan Aerospace Exploration Agency (Japan); T. G. Tsuru, Kyoto Univ. (Japan)

We have been developing X-ray CCD for the Soft X-ray Imager (SXI) on board ASTRO-H, an X-ray astronomy mission to be launched in FY2013. The SXI employs P-channel BI CCDs with a thick depletion layer of 200µm. Each CCD has an imaging area of 31 mm square, and 4 chips covers a wide FOV of 38 arcmin. Basic performance of the prototype P-channel BI CCD was verified to meet or close to the SXI requirements, including the fact that the device was fully-depleted with depletion thickness over 200 µm. Nevertheless, its soft X-ray (below 1 keV) response showed significant low energy tail with comparable or larger magnitude than the main peak component. The tail was more enhanced for the lower energy X-rays, indicating its origin is charge loss in the surface layers of the CCD. We have made several test CCD chips with different treatment or structures of the layers beneath the entrance window. At least one of the test chip show reduced low energy tail. We confirmed this by irradiating fluorescent X-rays, first. We also irradiated monochromatic X-rays of various energies from 0.25keV to 1.8keV at the KEK-PF Synchrotron Facility, and confirmed the low energy tail of this test CCD was reduced by about one order of magnitude. In addition, we will report the basic performance of the SXI EM CCD, and a charge injection technique for it.

8145-04, Session 1

Development of the soft x-ray imager (SXI) for ASTRO-H

H. Tsunemi, K. Hayashida, Osaka Univ. (Japan); T. G. Tsuru, Kyoto Univ. (Japan); T. Dotani, Japan Aerospace Exploration Agency (Japan); J. S. Hiraga, The Univ. of Tokyo (Japan); N. Anabuki, Osaka Univ. (Japan); A. Bamba, Japan Aerospace Exploration Agency (Japan); I. Hatsukade, Univ. of Miyazaki (Japan); T. Kohmura, Kogakuin Univ. (Japan); K. Mori, Univ. of Miyazaki (Japan); H. Murakami, Rikkyo Univ. (Japan); H. Nakajima, Osaka Univ. (Japan); M. Ozaki, Japan Aerospace Exploration Agency (Japan); H. Uchida, Osaka Univ. (Japan); M. Yamauchi, Univ. of Miyazaki (Japan)

ASTRO-H will be launched in FY2013, carrying X-ray mirrors for the X-ray calorimeter (SXS), the hard X-ray imager (HXI) and the soft X-ray imager (SXI). We are developing an X-ray CCD camera (SXI). The biggest advantage of the SXI is that it has a large field of view (38' square). We have developed the CCD, CCD-NeXT4, that is a P-channel type CCD. It has a thick depletion layer of 200µm with an imaging area of 30.72mm square. Since it is back-illuminated, it has a good low energy response and is robust against the impact of micro-meteorites. We will employ 4 chips to cover the area more than 60mm square. We will employ a mechanical cooler so that we can cool the CCD to -120C. The basic design of the cooler is identical employed for previous satellites (SUZAKU and Akari) while we will add a balancer to reduce the vibration environment. The cold part of the SXI is completely isolated from the interior of the satellite to avoid the contamination. We will also introduce an analog ASIC that is placed very close to the CCD. It performs well,

**Conference 8145: UV, X-Ray, and Gamma-Ray
Space Instrumentation for Astronomy XVII**

having a similar noise level to that assembled by using individual parts used on SUZAKU. We decided to employ a radio-active source rather than a modulated X-ray source for onboard calibration. The SXI passed the CDR and will get into the FM production phase.

8145-05, Session 2

Design and tests of the hard X-ray polarimeter X-Calibur

M. Beilicke, P. Dowkontt, A. Garson, Q. Guo, K. Lee, Washington Univ. in St. Louis (United States); J. Tueller, NASA Goddard Space Flight Ctr. (United States); H. S. Krawczynski, Washington Univ. in St. Louis (United States)

X-ray polarimetry promises to give qualitatively new information about high-energy sources, such as binary black hole systems, rotation and accretion powered neutron stars, Microquasars, Active Galactic Nuclei and Gamma-Ray Bursts. Furthermore, hard X-ray polarimetric observations of galactic sources can place uniquely sensitive constraints on Lorentz Invariance violations. We designed, built and tested a hard X-ray polarimeter X-Calibur to be used in the focal plane of the InFOCuS grazing incidence hard X-ray telescope. The polarimeter combines a low-Z Compton scatterer with a high-Z Cadmium Zinc Telluride (CZT) detector assembly to measure the polarization of 10-80 keV X-rays. X-Calibur makes use of the fact that polarized photons Compton scatter preferentially perpendicular to the electric field orientation. In contrast to competing designs, which use only a small fraction of the incoming X-rays, X-Calibur achieves a high detection efficiency of order unity. We report on the technical design of X-Calibur, the X-Calibur and InFOCuS sensitivity on short and long duration balloon flights, and present detailed laboratory calibration measurements.

8145-06, Session 2

Balloon test flight of a fast scintillator Compton telescope

P. Bloser, M. Julien, J. Ryan, J. Legere, M. McConnell, The Univ. of New Hampshire (United States); R. M. Kippen, S. Tornga, Los Alamos National Lab. (United States)

The field of medium-energy gamma-ray astronomy urgently needs a new mission to build on the success of the COMPTEL instrument. This mission must achieve a sensitivity significantly greater than that of COMPTEL in order to advance the science of relativistic particle accelerators, nuclear astrophysics, and diffuse backgrounds and bridge the gap between current and future hard X-ray missions and the high-energy Fermi mission. Such an increase in sensitivity can only come about via a dramatic decrease in the instrumental background. We are currently developing a concept for a low-background Compton telescope that employs modern scintillator technology to achieve this increase in sensitivity. Specifically, by employing LaBr₃ scintillators for the calorimeter, one can take advantage of the unique speed and resolving power of this material to improve the instrument sensitivity and simultaneously enhance its spectroscopic performance and thus its imaging performance. We have constructed a small scientific balloon payload consisting of a prototype of such an instrument. We present the preliminary results from the first flight of this prototype in Summer 2011.

8145-07, Session 2

Spectral calibration and modeling of the NuSTAR CdZnTe pixel detectors

T. Kitaguchi, H. Miyasaka, V. Bhalerao, R. W. Cook, B. W. Grefenstette, F. A. Harrison, P. H. Mao, V. R. Rana, California Institute of Technology (United States); S. Boggs, A. Zoglauer,

Univ. of California, Berkeley (United States)

The Nuclear Spectroscopic Telescope Array (NuSTAR) mission will carry the first focusing hard X-ray telescopes to orbit. The NuSTAR focal plane consists of four CdZnTe hybrid pixel detectors, each with an active collecting area of 2cm x 2cm on a side, 2mm thick. Each hybrid consists of a 32 x 32 array of 600 micron pixels, read out with the Caltech custom low-noise NuCIT ASIC. In order to characterize the spectral response of each pixel to the degree required to meet the science calibration requirements, we have developed a model based on Geant4 together with the Shockley-Ramo theorem customized to the NuSTAR hybrid design. This model combines a Monte Carlo of the X-ray interactions with subsequent charge transport within the detector. The combination of this model and calibration data taken using radioactive sources of ⁵⁷Co, ¹⁵⁵Eu and ²⁴¹Am enables us to determine electron and hole mobility-lifetime products for each pixel, and compare actual to ideal performance expected for defect-free material. In this paper we describe the NuSTAR spectral calibration program, the charge transport model, and we present results obtained by fitting data from NuSTAR flight and engineering model detectors.

8145-08, Session 3

Development micro-satellite TSUBAME for polarimetry of gamma-ray bursts

Y. Yatsu, T. Enomoto, K. Kawakami, K. Tokoyoda, T. Toizumi, N. Kawai, K. Ishizaka, S. Matsunaga, Tokyo Institute of Technology (Japan); T. Nakamori, J. Kataoka, Waseda Univ. (Japan)

We are developing an university class micro-satellite "TSUBAME" to measure polarizations of gamma-ray bursts in hard X-ray energy band.

For this mission we designed and optimized a compact and high sensitive hard X-ray polarimeter utilizing anisotropy of the Compton scattering. Unsurprisingly, any micro-satellites have critical limitations on size, mass, and power consumption, that constrain the effective area of detectors. However high luminosities of GRBs allow us to measure their polarizations only if we start observations just after the ignitions. TSUBAME overcomes this problem by using compact and high-torque actuators of Control Moment Gyros, that enables high speed attitude control faster than 6 deg/s. For real-time detection and localization of GRBs, we also developed wide field burst monitor, that consists of scintillation gamma-ray counters mounted on five different surfaces of the satellite. Cooperating with the attitude control system, TSUBAME can start a pointing observation within 15 s since the detection for any GRBs that explode in the burst monitor's half-sky field of view. In this presentation the status of development and feasibility study of this satellite program are reported.

8145-09, Session 3

The Cosmic Vision M3 mission studies: status and overview of the astrophysics candidates

M. Gehler, L. Puig, A. Stankov, N. Rando, European Space Research and Technology Ctr. (Netherlands)

Within the framework of the European Space Agency's Cosmic Vision 2015-2025 programme, a third call for mission proposals (M3) was released to identify candidate missions for a launch slot in 2020-2022 that are to be studied in detail. The progress on the M3 astrophysics mission candidate studies is presented in this paper.

The third medium-sized launch opportunity of the Cosmic Vision programme limits the candidates to VEGA or Soyuz-compatible spacecraft to be launched from Kourou with a cost ceiling of 470 M €. Following the first down-selection by the advisory structure, the selected proposals are undergoing internal studies in the Concurrent Design Facility. The mission concepts of the proposals are developed, the requirements refined, and the feasibility of the missions is assessed. The paper provides a summary of the status of these studies and

**Conference 8145: UV, X-Ray, and Gamma-Ray
Space Instrumentation for Astronomy XVII**

describes the different spacecraft designs. A thorough description of the model payloads is given with special emphasis on their characteristics, requirements, design, and technical implementation.

8145-10, Session 3**First results from the Far-ultraviolet Imaging Rocket Experiment (FIRE)**

B. L. Gantner, J. Green, M. Beasley, R. Kane, Univ. of Colorado at Boulder (United States); T. Schultz, The Univ. of Iowa (United States)

The Far-ultraviolet Imaging Rocket Experiment (FIRE) is a sounding rocket payload that is designed to search for young, hot stars at 900-1000 Å. FIRE is a prime-focus system where the mirror is parabolic and coated with silicon carbide. It also uses 5 multi-channel plates in a charge amplification detector with the top plate coated with rubidium bromide (RbBr) to give the highest response over the desired wavelengths. Since the noise from Lyman-alpha photons would swamp the signal, a 2000 Å pure indium filter sits in front of the detector. To ensure that the filter would survive the acoustic vibrations of launch, a small vacuum canister was built around the filter and detector that opened during ascent to allow the collection of data. Imaging at 900-1000 Å allows us to study the star formation rate within different regions of target galaxies. FIRE was also designed to compliment the GALAX mission with similar resolution and field-of-view. Combined with GALEX data, FIRE can create three-color images of the FUV.

FIRE launched for the first time on January 28th, 2011 from the Poker Flat Research Range in northern Alaska. The first flight targeted the Whirlpool galaxy (M51) and used G191B2B as a calibration target. I will present the scientific motivation, design, calibration and initial results of the FIRE instrument and its first flight.

8145-11, Session 3**Fabrication and calibration of FORTIS**

B. T. Fleming, S. R. McCandliss, M. E. Kaiser, P. D. Feldman, The Johns Hopkins Univ. (United States); J. Kruk, A. S. Kutyrev, M. J. Li, D. A. Rapchun, S. H. Moseley, NASA Goddard Space Flight Ctr. (United States); O. H. Siegmund, A. Martin, J. V. Vallerga, Univ. of California, Berkeley (United States)

The Johns Hopkins University sounding rocket group is nearing completion of the Far-ultraviolet Off Rowland-circle Telescope for Imaging and Spectroscopy (FORTIS); a sounding rocket borne multi-object spectro-telescope designed to provide spectral coverage of 43 separate targets in the 900 - 1800 Angstrom bandpass over a 30' x 30' field-of-view. Using "on-the-fly" target acquisition and spectral multiplexing enabled by a GSFC microshutter array, FORTIS will be capable of observing the brightest regions in the far-UV of nearby low redshift ($z \sim 0.002 - 0.02$) star forming galaxies to search for Lyman alpha escape, and to measure the local gas-to-dust ratio. A large area ($\sim 45 \text{ mm} \times 170 \text{ mm}$) microchannel plate detector from Sensor Sciences provides an imaging channel for targeting flanked by two redundant spectral outrigger channels. The grating is ruled directly onto the secondary mirror to increase efficiency. In this paper, we discuss the recent progress made in the development and fabrication of FORTIS, as well as the results of early calibration and characterization of our hardware, including mirror/grating measurements, detector performance, and early operational tests of the microshutter arrays.

8145-12, Session 4**The Warm-Hot Intergalactic Medium Explorer (WHIMex) Mission**

C. F. Lillie, Northrop Grumman Aerospace Systems (United States); W. C. Cash, Univ. of Colorado at Boulder (United States); R. L. McEntaffer, The Univ. of Iowa (United States); W. W. Zhang, NASA Goddard Space Flight Ctr. (United States); S. L. O'Dell, NASA Marshall Space Flight Ctr. (United States); M. S. Elvis, Harvard-Smithsonian Ctr. for Astrophysics (United States); M. Bautz, Massachusetts Institute of Technology (United States)

This baryonic matter is thought to result from gravitational collapse of moderately over-dense, dark-matter filaments of the Cosmic Web. The chemical enrichment of the Cosmic Web appears to arise from galactic super winds and early generations of massive stars.

WHIMex will test these theories, distinguish between competing models, and provide new insights into galaxy evolution and the structure of the universe. At a resolution of $R = \lambda/\delta\lambda = 4000$, absorption lines in the spectra of distant X-ray sources are resolved down to their thermal width, providing the temperature and velocity information needed to attack astrophysical problems. WHIMex will measure absorption lines from species such as O VII and O VIII, the primary tracers of 400,000 to 3,000,000 K gas. These lines, which are too weak and narrow to confidently study with existing instruments, become accessible with the high sensitivity of WHIMex.

High-resolution X-ray spectroscopy has been identified by the ASTRO2010 decadal panel as a high-priority capability in the coming decade for a wide variety of science goals. Unfortunately, no other planned mission can address this science until the International X-ray Observatory flies, no earlier than the late 2020s. WHIMex achieves its high level of performance in a single-instrument, affordable package using X-ray optical technologies developed for flight on IXO and NuSTAR by academic, industrial and government research centers. The technology readiness levels of all the components are high. We plan to build an optical test module and raise the optical system readiness level to TRL 6 during Phase A.

8145-14, Session 4**eROSITA**

P. Predehl, Max-Planck-Institut für extraterrestrische Physik (Germany)

eROSITA (extended ROentgen Survey with an Imaging Telescope Array) will be the core instrument on the Russian Spektrum-Roentgen-Gamma (SRG) mission. The mission will consist of an all-sky survey lasting for four years plus a phase of pointed observations on selected objects. eROSITA consists of seven Wolter-I telescope modules, each equipped with 54 Wolter-I shells having an outer diameter of 360 mm. In the focus of each mirror module, a framestore pn-CCD provides a field of view of 1° in diameter.

eROSITA is fully approved and funded by the German Space Agency DLR and Max-Planck-Society. The instrument is now in phase C/D: The flight mirror production is ongoing, the telescope structure is built and ready for the integration of subsystems. In parallel, the work in house (cameras, electronics etc.) is running, many components are already qualified.

8145-29, Session 4**The DUAL mission concept**

P. von Ballmoos, Institut de Recherche en Astrophysique et Planétologie (France)

During a 3-year exposure of every γ -ray source in the sky, DUAL's All-Sky Compton Imager (ASCI) performs sensitive γ -ray spectroscopy and

**Conference 8145: UV, X-Ray, and Gamma-Ray
Space Instrumentation for Astronomy XVII**

polarimetry in the energy band 100 keV-10 MeV. The ASCI measures polarization in a large number of γ -ray bursts; it unveils the distribution and ultimately the origin of galactic positrons; it performs a detailed all-sky survey of the radioactive Milky Way, clarifying long-lived activities from supernovae and novae; and it studies excitation lines from as yet unknown MeV cosmic-rays interacting with the interstellar medium. The deep all-sky survey naturally monitors galactic black holes, neutron stars, pulsars, magnetars, and simultaneously, a full sky of Active Galactic Nuclei. DUAL's capability of measuring polarization provides a powerful new diagnostic of magnetic fields - for studying acceleration in neutron star magnetospheres and for their role in the origin of γ -ray emission and jets from accreting BHs, both galactic and extragalactic.

Simultaneous with its all-sky survey, the ASCI serves as a low-background focal plane detector for two optical modules, the Laue-Lens Optic (LLO) and the Coded-Mask Optic (CMO). DUAL will, for the first time ever, make use of focusing optics to concentrate high-energy photons onto a small focal spot. With its Laue-Lens Optic (LLO), during dedicated pointings, DUAL will observe radioactive ^{56}Ni and ^{56}Co in a sizable sample of SNIa at distances of up to 30-40 Mpc. Focusing will bring the long awaited sensitivity leap needed to answer pressing astrophysical questions of our age: What are Type Ia Supernova progenitors? How do their nuclear flames burn in degenerate matter? Are the ancient ones from which we infer an accelerating Universe well calibrated using a local sample?

The Coded-Mask Optic (CMO) dramatically enhances ASCI's imaging capabilities in the Galactic Center and Bulge. During deep, dedicated, observations high angular resolution ($10''$ - $40''$) will be achieved in this single region. DUAL's CMO will be able to disentangle the emission of compact objects in the Galactic Center, and most importantly, map out the, as yet, unresolved bulge of e^+e^- annihilation radiation in order to identify the sources of positrons that have puzzled high-energy astronomers for over 30 years

8145-15, Session 5**Progress in new ultraviolet reflective coating techniques**

M. Beasley, Univ. of Colorado at Boulder (United States); S. Nikzad, F. Greer, Jet Propulsion Lab. (United States)

Our project investigates the capabilities of Atomic Layer Deposition (ALD) to create very thin, high-efficiency coatings of MgF_2 over aluminum. Significant improvement over existing coatings is predicted by theory. Our work will create several coated small samples to verify that technique reliably prevents the oxidation of aluminum, and will subsequently be expanded to larger substrates to prove our technique's scalability to larger optical components. An improved coating therefore would enable the production of vastly more sensitive instruments in the 90 - 200 nm range. The durability of these coatings will also be verified by accelerated lifetime testing that exposes the samples to extremes of temperature, humidity, and reactive oxygen environments.

8145-16, Session 5**Atomically precise surface and interface engineering via atomic layer deposition to enable high-performance materials, detectors, and instruments**

F. Greer, M. Hoenk, B. Jacquot, T. J. Jones, S. Monacos, Jet Propulsion Lab. (United States); E. Hamden, Columbia Univ. (United States); M. Beasley, B. L. Gantner, Univ. of Colorado at Boulder (United States); S. Nikzad, Jet Propulsion Lab. (United States)

Future UV instruments have the potential to revolutionize our understanding of the formation and habitability of the modern universe.

Unfortunately, harnessing their full potential for UV astronomy is difficult, and there are significant materials challenges that constrain their performance. Most materials are highly absorbing in the UV making optical elements such as filters and anti-reflection coatings very complex to manufacture. Those few materials that are transparent must be high quality and made extremely precisely as thickness variations of as little as 2nm can dramatically shift performance. However, recent advances employing unique surface engineering approaches such as atomic layer deposition (ALD) have made significant strides in improving the throughput and photon detection capabilities of UV instruments. ALD is a thin film deposition technique similar to CVD where a desired film is grown using sequential surface reactions, one monolayer at a time. The properties inherent to the ALD method enable growth of smooth, dense, pin-hole free films with angstrom level thickness control over arbitrarily large surface areas. ALD is well-suited for the growth of multilayer stacks of films with sharp interfaces and is sufficiently gentle as to allow it to be applied directly onto silicon detectors themselves. This presentation will discuss how we have used atomic layer deposition and other surface engineering approaches to tailor materials and their interface properties in the fabrication of filters and anti-reflection coatings, demonstrating the robustness in performance that is obtained by achieving atomic level precision at all steps in the fabrication process.

8145-17, Session 5**Semitransparent GaN-based photocathode structures for high-sensitivity UV imaging**

A. M. Dabiran, A. M. Wowchak, P. P. Chow, SVT Associates, Inc. (United States); J. Hull, A. S. Tremsin, O. H. Siegmund, Univ. of California, Berkeley (United States)

Negative electron affinity (NEA) semiconductor photocathodes are commonly used in combination with electron multipliers, such as microchannel plates (MCPs), to fabricate sensitive phototubes. In recent years, there have been significant improvements in the performance of these detectors by enhancing photocathode quantum efficiency (QE), and by advances in MCPs and readout techniques. We have previously fabricated high efficiency GaN-based UV photocathodes, grown by RF plasma-assisted molecular beam epitaxy (MBE), with QE as high as 80% at 120 nm for operation in the opaque mode. However, these devices generally show much lower QE in semitransparent mode (i.e., backside illumination) which is most suitable for integration with MCPs. To improve the QE, both the photoelectron generation by light absorption and electron emission processes need to be optimized. The latter requires thinner photocathode films for semitransparent mode to allow efficient extraction of photoelectrons generated at the back of the film. The common wisdom is that the thinner films also mean less light absorption hence the measured QE values of 20% for very thin films (<50 nm). In this presentation, we will discuss new photocathode structures that take advantage of thinner p-GaN films without suffering from charging effects due to the low in plane conductivity. We will also present other GaN-based photocathode structures that show NEA photoemission, without the need for surface activation by Cs evaporation, for stable and long-life operation in harsh environments.

8145-18, Session 5**FUV quantum efficiency degradation of cesium iodide photocathodes caused by exposure to thermal atomic oxygen**

J. B. McPhate, Univ. of California, Berkeley (United States); J. Anne, Lockheed Martin Space Systems Co. (United States); J. Bacinski, Lockheed Martin Corp. (United States); B. A. Banks, NASA Glenn Research Ctr. (United States); C. Cates, P. Christensen, Lockheed Martin Space Systems Co. (United States); B. A. Cruden, NASA Ames Research Ctr. (United States); L. Dunham, PPI (United States); E. Graham, Lockheed Martin

**Conference 8145: UV, X-Ray, and Gamma-Ray
Space Instrumentation for Astronomy XVII**

Corp. (United States); D. W. Hughes, R. A. Kimble, O. L. Lupie, M. B. Niedner, NASA Goddard Space Flight Ctr. (United States); S. N. Osterman, S. V. Penton, Univ. of Colorado at Boulder (United States); C. Proffitt, Space Telescope Science Institute (United States); D. E. Pugel, NASA Goddard Space Flight Ctr. (United States); O. H. Siegmund, Univ. of California, Berkeley (United States); T. Wheeler, Space Telescope Science Institute (United States)

The color dependence of the measured decline of the on-orbit sensitivity of the FUV channel of the HST Cosmic Origins Spectrograph (HST-COS) indicated the principal loss mechanism to be degradation of the cesium iodide (CsI) photocathode of the open-faced FUV detector. A leading contender for this degradation is contamination by atomic oxygen (AO), prompting an investigation of the interaction of AO with CsI. To address this question, opaque CsI photocathodes were deposited on stainless steel substrates employing the same deposition techniques and parameters used for the photocathodes of the HST-COS FUV detector. The as-deposited FUV quantum efficiency of these photocathodes was measured in the 117-174 nm range. Several of these photocathodes were exposed to varying levels of thermalized, atomic oxygen (AO) fluence (produced via an RF plasma). The post AO exposure QE's were measured and the degradation of sensitivity versus wavelength and AO fluence are presented.

8145-19, Session 5**Advances in microchannel plates and photocathodes for ultraviolet photon counting detectors**

O. H. Siegmund, Univ. of California, Berkeley (United States)

Microchannel plate imaging detectors with photon counting capability have been employed for numerous NASA missions dedicated to spectroscopy and imaging in the ultraviolet. Recent advances in microchannel plate and photocathode materials and processes have begun to enhance the performance and scope of these tools. We will discuss the potential of these advances and their application to large format devices up to 20 x 20 cm, improvements in secondary emission coefficient and its effect on quantum detection efficiency, and the results for new materials providing longer lifetimes.

8145-20, Session 6**UV/optical/NIR detectors for photon counting and high-efficiency applications in astronomy and other fields**

S. Nikzad, Jet Propulsion Lab. (United States)

Discoveries beyond the current UV/optical NASA missions require new instrument capabilities. Such missions under planning and review will search for Earth like exo-planets, search for life in planets far from our own, perform spectroscopic studies of intergalactic medium, and perform planetary atmospheric studies. These new instruments place exacting requirements on detectors. One such requirement is the ability to detect single photons. Until now, the combination of high signal to noise ratio requirement, requirement of gain, coupled with large format, uniformity, and linearity has made these requirements out of reach for solid-state detectors. We report on our latest results on detectors with high QE response in far UV and near UV for photon counting applications. We will also discuss our end-to-end back illumination processes at JPL's Microdevices Laboratory and the various applications of the detectors under development.

8145-21, Session 6**The use of CCDs and EM-CCDs on the off-plane x-ray grating spectrometer readout camera system on the International X-ray Observatory**

J. H. Tutt, A. D. Holland, R. D. Harriss, D. J. Hall, N. J. Murray, S. J. Barber, The Open Univ. (United Kingdom); J. Endicott, M. Robbins, e2v technologies plc (United Kingdom); R. L. McEntaffer, The Univ. of Iowa (United States)

The OP-XGS on the International X-ray Observatory is designed to produce spectroscopic data in the soft X-ray energy range of 300 eV to 1,000 eV with a resolution $\Delta E/E > 3,000$. As well as using conventional CCDs for the XGS grating readout camera system, the possibility of extending the range of the proposed band-pass, through the use of EM-CCDs, down to 200 eV has been considered. Amplifying the signal before the readout register effectively suppresses the devices readout noise allowing lower energy X-ray photons, which produce low numbers of e-h pairs per interaction, to be detected allowing the band-pass to be extended. In order for the instrument to achieve the necessary resolution across the band-pass, multiple orders of dispersed light from the XGS are used. As different orders will fall onto the same part of the CCD array, the energy resolution of the device is used in order to differentiate between these orders. However, due to the stochastic nature of the gain amplification process in an EM-CCD, this energy resolution (FWHM) is degraded and so an investigation into whether or not the necessary energy resolution can be achieved was conducted at BESSY II with the results presented. The degradation of the X-ray peak FWHM is described by the spectral resolution factor which is analogous to the Excess noise factor, but for Fano adjusted regimes. The technology development achieved in this study may also have an outlet in the recently proposed WHIM-EX mission at NASA.

8145-23, Session 6**Radiation testing of mini-orthogonal transfer array CCDs**

B. J. LaMarr, M. Bautz, S. Kissel, G. Prigozhin, Massachusetts Institute of Technology (United States); B. E. Burke, V. Suntharalingam, M. J. Cooper, MIT Lincoln Lab. (United States)

Orthogonal transfer array CCDs were originally developed by the University of Hawaii and MIT Lincoln Laboratory for use in the focal planes of the ground-based Panoramic Survey Telescope and Rapid Response System (Pan-STARRS).

These devices may also be useful in space-based applications in X-ray astronomy, so we have conducted a series of tests to determine their sensitivity to proton radiation encountered on-orbit. We report effects of typical on-orbit proton exposure on charge transfer efficiency, dark current, noise and spectral resolution as a function of device operating temperature and readout parameters.

8145-24, Session 6**High-sensitivity and high-stability silicon photodiode for the DUV, VUV, and EUV spectral ranges**

S. Nihtianov, L. Shi, Technische Univ. Delft (Netherlands); F. Scholze, A. Gottwald, Physikalisch-Technische Bundesanstalt (Germany)

In the paper, the optical and electrical performances of a newly developed silicon photodiode, with delta-doped boron surface, are introduced. Due to its extremely shallow p-n junction, with depletion

**Conference 8145: UV, X-Ray, and Gamma-Ray
Space Instrumentation for Astronomy XVII**

zone starting only a few nanometers below the top surface, the photodiode demonstrates very high responsivity in all sub-visible ultraviolet (UV) ranges: DUV (deep ultraviolet), VUV (vacuum ultraviolet) and EUV (extreme ultraviolet), covering a spectrum from 220 nm down to 1 nm wavelength and below. To our best knowledge, it is the only solid state photo-detector (based on silicon, III-V materials or diamond), which performs well in all UV ranges. Particularly, the B-photodiode demonstrates simultaneously high responsivity in all UV ranges, approaching the theoretical maximum at 13.5 nm wavelength (EUV) of ~0.27A/W, in combination with high radiation hardness. The B-photodiode has excellent electrical characteristics, with saturation current values typical for high-quality silicon diodes, and a high breakdown voltage. Experimental results prove the extremely high radiation hardness of the B-photodiode, when exposed to high EUV dose in the order of a few hundred kJ/cm². No change of the responsivity is noticed within the measurement uncertainty. In the DUV and especially VUV ranges, which are more challenging with respect to radiation hardness, the B-photodiode demonstrates an initial slight drop of responsivity (<1%), after which it stabilizes its performance. The drop of responsivity recovers with time. The recovery process can be accelerated by a short thermal treatment (1-2 hours) at 100-200°C. The homogeneity of responsivity over the active diode area is very high and without additional top capping layers, it is within the measurement uncertainty.

8145-25, Poster Session**An EUV spectrometer on earth-orbiting satellite for planetary science**

I. Yoshikawa, K. Sakai, G. Murakami, H. Ishii, K. Yoshioka, The Univ. of Tokyo (Japan)

An earth-orbiting Extreme Ultraviolet spectroscopic mission, EXtreme ultraviolet spectroSCOPE for EXospheric Dynamics explore (EXCEED) that will be launched in 2012 is now under development. The EXCEED mission will carry out observations of Extreme Ultraviolet (EUV: 60 -145 nm) emissions from tenuous plasmas around the planets (Mercury, Mars, Venus, and Jupiter). It is necessary for planetary EUV spectroscopy to avoid the Earth's atmospheric absorption, therefore we have to observe above the Earth's atmosphere. In this paper, we will introduce the general mission overview, the instrument, and the scientific targets.

8145-26, Poster Session**The opto-mechanical design of the Colorado High-resolution Echelle Stellar Spectrograph**

R. Kane, M. Beasley, K. France, E. Burgh, J. Green, Univ. of Colorado at Boulder (United States)

We present the Colorado High-resolution Echelle Stellar Spectrograph. The design uses a mechanical collimator made from a grid of square tubing, an objective echelle grating, a holographically ruled cross-disperser, with a new 40 mm MCP with a cross strip anode. The optics are suspended using carbon fiber rods epoxied to titanium inserts to create a space frame structure. A preliminary design is presented.

8145-27, Poster Session**Gain sag in the FUV detector of the Cosmic Origins Spectrograph**

D. J. Sahnou, The Johns Hopkins Univ. (United States); A. Aloisi, P. E. Hodge, D. Massa, C. Oliveira, R. Osten, C. Proffitt, A. Bostroem, Space Telescope Science Institute (United States); J. B. McPhate, Univ. of California, Berkeley (United States); S. Beland, S. N. Osterman, S. V. Penton, Univ. of Colorado at Boulder (United States)

The Cosmic Origins Spectrograph (COS) on the Hubble Space Telescope (HST) uses a large-format cross delay line (XDL) detector in its Far Ultraviolet (FUV) channel. While obtaining spectra, light falls non-uniformly on the detector due to the optical design and the spectral properties of the object being observed; in particular, bright emission lines from geocoronal Lyman-alpha can fall on the detector in more than 20 locations. As a result, some areas of the detector have received a much greater exposure than others. This non-uniform illumination has led to a time- and position-dependent change in the gain of the microchannel plates, which causes variations in the overall detector performance. We will discuss the effects of this gain sag on the science data, and discuss mitigation strategies which are being implemented in order to maximize the detector lifetime.

Conference 8146: UV/Optical/IR Space Telescopes and Instruments: Innovative Technologies and Concepts V

Sunday-Wednesday 21-24 August 2011 • Part of Proceedings of SPIE Vol. 8146
UV/Optical/IR Space Telescopes and Instruments: Innovative Technologies and Concepts V

8146-01, Session 1

Commissioning and in-flight calibration results of the lunar reconnaissance orbiter's Lyman alpha mapping project (LRO/LAMP) UV imaging spectrograph

M. W. Davis, R. Gladstone, M. H. Versteeg, T. K. Greathouse, A. Stern, J. W. Parker, A. Steffl, K. D. Retherford, D. C. Slater, Southwest Research Institute (United States)

The Lunar Reconnaissance Orbiter's Lyman Alpha Mapping Project (LAMP) is a lightweight (6.1 kg), low-power (4.5 W), ultraviolet spectrograph based on the Alice instruments now in flight aboard the European Space Agency's Rosetta spacecraft and NASA's New Horizons spacecraft. Its primary job is to identify and localize exposed water frost in permanently shadowed regions (PSRs) near the Moon's poles, and to characterize landforms and albedos in PSRs. We describe the in-flight radiometric performance and commissioning results and compare them to the ground calibration measurements.

Lunar Reconnaissance Orbiter (LRO) launched on June 18, 2009 and reached lunar orbit four days later. LAMP commissioning activities began on July 27, 2009 and were completed on September 9, 2009. LAMP has since been routinely observing the lunar surface from LRO's 50-km altitude polar orbit. The commissioning measurements described herein, along with monthly stellar observations, serve to calibrate the LAMP science results throughout the mission.

8146-02, Session 1

Radiometric performance results of the Juno ultraviolet spectrograph (Juno-UVS)

M. W. Davis, R. Gladstone, T. K. Greathouse, D. C. Slater, M. H. Versteeg, K. B. Persson, G. Winters, S. C. Persyn, J. S. Eterno, Southwest Research Institute (United States)

We describe the radiometric performance and ground calibration results of the Juno mission's Ultraviolet Spectrograph (Juno-UVS) flight model. Juno-UVS is a modest power (9.0 W) ultraviolet spectrograph based on the Alice instruments now in flight aboard the European Space Agency's Rosetta spacecraft, NASA's New Horizons spacecraft, and the LAMP instrument aboard NASA's Lunar Reconnaissance Orbiter. Its primary job will be to characterize Jupiter's UV auroral emissions and relate them to in situ particle measurements.

8146-03, Session 1

Real scale ray tracing simulation of space earthshine measurement with improved BRDF model of lunar surface

J. Yu, D. Ryu, S. Kim, Yonsei Univ. (Korea, Republic of)

The discrepancy in annual changes of Earth albedo anomaly among the Had3CM prediction, ground and low earth orbit measurements attracts great academic attention world-wide. As a part of our on-going study for better understanding of such discrepancy, we report a new Earthshine measurement simulation technique. It combines the light source (the Sun), targets (the Earth and the Moon) and a hypothetical detector in a real scale integrated Monte-Carlo ray tracing (IRT) computation environment. The Sun is expressed as a Lambertian scattering sphere, emitting 1.626×10^{26} W over 400nm-700nm in wavelength range. Whilst

we are in the process of developing a complex Earth model consisting of land, sea and atmosphere with appropriate BRDF models, a simplified Lambertian Earth surface with 0.3 in uniform albedo was used in this study. For the moon surface, Hapke's BRDF model is used with double Henry-Green phase function. These elements were then imported into the IRT computation of radiative transfer between their surfaces. First, the irradiance levels of Earthshine and Moonshine lights were computed and then confirmed that they agree well with the measurement data from Big Bear Solar Observatory. They were subsequently used in determination of the Earth bond albedo of about 0.3 that is almost identical to the input Earth albedo of 0.3. These computations prove that, for the first time, the real scale IRT model was successfully deployed for the Earthshine measurement simulation and, therefore, it can be applicable for other ground and space based measurement simulation of reflected lights from the Earth and the Moon.

8146-04, Session 2

JWST science and system overview

M. C. Clampin, NASA Goddard Space Flight Ctr. (United States)

The James Webb Space Telescope (JWST) is a large aperture (6.5 meter), cryogenic space telescope with a suite of near and mid-infrared instruments covering the wavelength range of 0.6 μ m to 28 μ m. JWST's primary science goal is to detect and characterize the first galaxies. It will also study the assembly of galaxies, star formation, and the formation of evolution of planetary systems. JWST is a segmented mirror telescope operating at \sim 40K, a temperature achieved by passive cooling of the observatory, via a large, 5-layer membrane-based sunshield. We present an overview of the observatory design, the mission science objectives, the integration and test program and review the concept for science operations of JWST. With construction of the observatory progressing rapidly across all elements of the observatory, we will report on recent highlights such as the completion of the first JWST primary mirror segment. We will also review the predicted performance of the JWST observatory, based on initial measurements of the telescope optics and instrumentation.

8146-05, Session 2

Status of the James Webb space telescope integrated science instrument module system

M. A. Greenhouse, NASA Goddard Space Flight Ctr. (United States); V. A. Balzano, Space Telescope Science Institute (United States); P. S. Davila, M. P. Drury, J. L. Dunn, S. D. Glazer, G. I. Henegar, E. L. Johnson, R. A. Lundquist, J. C. McCloskey, R. G. Ohl IV, R. A. Rashford, B. J. Savadkin, M. F. Voyton, NASA Goddard Space Flight Ctr. (United States)

The Integrated Science Instrument Module (ISIM) of the James Webb Space Telescope (JWST) is discussed from a systems perspective with emphasis on development status and advanced technology aspects. The ISIM is one of three elements that comprise the JWST space vehicle and is the science instrument payload of the JWST. The major subsystems of this flight element and their build status are described.

8146-06, Session 2

JWST mirror production status

L. D. Feinberg, NASA Goddard Space Flight Ctr. (United States); B. B. Gallagher, Ball Aerospace & Technologies Corp. (United States)

**Conference 8146: UV/Optical/IR Space Telescopes
and Instruments: Innovative Technologies and Concepts V**

The James Webb Space Telescope is a three mirror anastigmat (TMA) telescope with a primary mirror, a secondary mirror, and a tertiary mirror. The JWST mirrors are constructed from lightweight beryllium substrates and the primary mirror consists of 18 hexagonal mirror segments each approximately 1.5 meters point to point. Ball Aerospace and Technologies Corporation leads the mirror manufacturing team and the team utilizes facilities at 6 locations across the U.S. The manufacturing process for each individual mirror assembly takes approximately six years due to limitations dealing with the number of segments and manufacturing & test facilities. The 18 flight primary mirrors, the secondary mirror, and the tertiary mirror are all advanced in the mirror production process with many segments through the final polishing process, coating process, assembly, vibration, and acceptance testing. Presented here is a status of where all the flight mirrors are in the manufacturing process.

8146-07, Session 2

James Webb space telescope primary mirror integration: testing the multiwavelength interferometer on the test-bed telescope

G. Olczak, D. J. Fischer, ITT Corp. Geospatial Systems (United States)

The James Webb Space Telescope (JWST) integration includes a center of curvature test on its 18 primary mirror segment assemblies (PMSAs). This necessary test is the only ground test that will demonstrate the ability to align all 18 PMSAs. Using a multi-wavelength interferometer (MWIF) integrated to the test bed telescope (TBT), a one-sixth scale model of the JWST, we verify our ability to align and phase the 18 PMSAs. In this paper we will discuss data analysis and test results when using the MWIF to align the segments of the TBT in preparation for alignment of the JWST.

The data flow is unique because of the necessity to determine the relative piston between segments over a large range and with high precision. We will show that using the two wavelengths per measurement provided by the MWIF it is possible to reduce the piston error from over a millimeter to less than a micron, while simultaneously controlling all other degrees of freedom. This data flow includes built-in diagnostics such as the ability report the uncertainty in the current pose estimation.

8146-08, Session 2

Measuring the cryogenic optical alignment between the telescope element and the instruments module of the James Webb space telescope

T. L. Whitman, G. Olczak, ITT Corp. Geospatial Systems (United States)

The alignment between the Aft Optical Subsystem (AOS) and the Integrated Science Instruments Module (ISIM) is non-adjustable in orbit, so the alignment must be carefully verified in a cryogenic vacuum environment prior to launch. Optical point source locations calibrated by optical metrology instruments are imaged through the AOS onto the Science Instruments to determine focal, lateral, and clock angle alignment. The pupil image of the AOS is overlaid onto the pupil image of the NIRCcam to determine the tip and tilt alignment. In addition, an image from fiducial lights at the Primary Mirror checks the pupil alignment between the telescope entrance pupil, the telescope pupil mask, and the NIRCcam aperture stop. The image positions are combined to determine the relative alignment between the Optical Telescope Element (OTE) and the ISIM in all six degrees of freedom with corresponding alignment uncertainties. Uncertainties in the position of focused images of the test sources and images from the pupils are derived from sensitivities of an optical model of the system and the Science Instrument sensing capability. Additional uncertainty in the pupil alignment measurement is

due to uncertainty in the analytical removal of gravity effects that simulate the on-orbit alignment environment.

8146-09, Session 2

In-process testing for cryo-figuring 1.5 meter diameter auto-collimating flats

D. J. Fischer, ITT Corp. Geospatial Systems (United States)

Three auto-collimating flats (ACFs) of 1.5 meter clear aperture are being manufactured for use in the JSC Cryo-Optical Metrology test of the James Webb Space Telescope. In-process interferometric testing of the ACFs is used to guide their surface-figure processing. The surface measurement is performed in a vacuum chamber at both room (+20 °C) and cryogenic (-240 °C) temperatures. With a 12-inch beam diameter FizCam interferometer, sub-aperture measurements are taken across the ACF diameter at multiple rotations. These measurements are stitched together to compute the surface figure. The figure change between room-temperature and cryogenic temperature is measured and used to enable cryo-figuring based on room-temperature measurements. The data analysis is calibrated to account for gravity sag on test-set optics and surface aberrations caused by vacuum pressure and temperature gradients on vacuum-chamber windows. The first ACF is complete and meets specification with surface error of less than 75 nm RMS.

8146-10, Session 2

JWST-NIRSpec optics polishing and integration

R. Geyl, Sagem SA (France)

In the beginning of 2010, SAGEM-REOSC delivered to Astrium GmbH the last model of the optics for Near InfraRed SPECtrograph (NIRSPEC) instrument to be installed on-board the James Webb Space Telescope (JWST) and constituting a key European contribution to this challenging project. We will report the various steps of polishing, coating, integration and cryo test of this rather unusual all-SiC optics for such a high performance space spectrographic instrument.

8146-11, Session 3

Summary of the NASA science instrument, observatories, and sensor systems (SIOSS) technology assessment roadmap

H. P. Stahl, NASA Marshall Space Flight Ctr. (United States)

In August 2010, the NASA Office of Chief Technologist (OCT) commissioned an assessment of 15 different technology areas of importance to the future of NASA. Technology Assessment #8 (TA8) was Science Instruments, Observatories and Sensor Systems (SIOSS). SIOSS assessed the needs for optical technology ranging from detectors to lasers, x-ray mirrors to microwave antenna, in-situ spectrographs for on-surface planetary sample characterization to large space telescopes. This needs assessment looked across the entirety of NASA and not just the Science Mission Directorate. This paper summarizes the SIOSS findings and recommendations.

8146-12, Session 3

Key enabling technologies for future space telescopes

C. F. Lillie, R. S. Polidan, Northrop Grumman Aerospace Systems (United States)

**Conference 8146: UV/Optical/IR Space Telescopes
and Instruments: Innovative Technologies and Concepts V**

Future Space Telescope missions need new technologies to meet their requirements for increasingly higher performance at an affordable cost. With the constrained budgets that are forecast for NASA and the DoD for the next several years, this decade is the time to develop the key technologies that will enable the orders of magnitude in performance that will be required by missions in the 2020's. Among these technologies are large, deployable space structures; low-cost, lightweight optics; more sensitive, large area detectors; and wave front sensing and control methods.

In this paper we review the requirements for future missions, discuss the current state of the art, and outline a roadmap for future technology developments.

8146-13, Session 3**Metamaterials for optical and photonic applications for space: preliminary results**

L. M. G. Venancio, European Space Research and Technology Ctr. (Netherlands); S. Hannemann, cosine Research B.V. (Netherlands); G. Lubkowski, M. Suhrke, Fraunhofer-Institut für Naturwissenschaftlich-Technische Trendanalysen (Germany); H. C. Schweizer, L. Fu, P. Schau, H. W. Giessen, K. Frenner, Univ. Stuttgart (Germany)

A new domain of optical effects is nowadays within reach thanks to structured metallo-dielectric materials (metamaterials) demonstrating optical properties unknown in nature.

The European Space Agency (ESA) in the frame of its General Study Program (GSP) has started to investigate the opportunity of using metamaterials in space applications. In that context, ESA has initiated two GSP activities which main objectives are 1) to identify the metamaterials and associated optical properties which could be used to improve in the future the performances of optical payloads in space missions, 2) to design metamaterial based devices addressing specific needs in space applications.

The range of optical functions for metamaterials to be investigated is wide (spectral dispersion, polarisation control, light absorption, straylight control ...) and so is the required spectral range, from 0.4 μ m to 15 μ m.

In the frame of these activities several applications have been selected and the designs of metamaterial based devices are proposed.

8146-14, Session 3**Update on parametric cost models for space telescopes**

H. P. Stahl, NASA Marshall Space Flight Ctr. (United States)

Since the June 2010 Astronomy Conference, an independent review of our cost data base discovered some inaccuracies and inconsistencies which can modify our previously reported results. This paper will review changes to the data base, our confidence in those changes and their effect on various parametric cost models.

8146-15, Session 4**Optical performance of the 100 sq deg FOV telescope for NASA's Kepler exoplanet mission**

D. C. Ebbets, P. D. Atcheson, C. K. Stewart, P. T. Spuhler, Ball Aerospace & Technologies Corp. (United States)

Kepler is NASA's first space mission dedicated to the study of exoplanets. The primary scientific goal is statistical - to estimate the frequency of planetary systems associated with sun-like stars, with

particular interest in the detection of earth-size planets in the habitable zone. The approach is to monitor a large number of stars, approximately 150000, continuously for 3 ½ years with a 30 minute cadence to detect the faint photometric signals of transiting planets across the stellar disks of those systems in Kepler's line of sight. An Earth-Sun analog is expected to produce a transit depth of about 80 parts per million, lasting for at most a few tens of hours, and repeating once per "year". The instrumentation for Kepler was designed to provide photometric data with a precision of 20 ppm in 6.5 hours for 12th magnitude stars, resulting in an SNR of 4 for an Earth-Sun analog transit. This paper summarizes how these scientific requirements led to the choice of a Schmidt design form for the telescope, and engineering requirements on the field of view, throughput, spectral bandpass, image quality, scattered light, thermal and opto-mechanical stability and in-flight adjustment authority. We review the ground-based integration, alignment and test program that preceded launch readiness, and we describe the in-flight commissioning that optimized the optical performance of the Kepler observatory.

8146-16, Session 4**In-flight photometric performance of the 96Mpx focal plane for NASA's Kepler exoplanet mission**

D. C. Ebbets, V. S. Argabright, J. Stober, J. Van Cleve, Ball Aerospace & Technologies Corp. (United States); D. A. Caldwell, NASA Ames Research Ctr. (United States)

Kepler is NASA's first space mission dedicated to the study of exoplanets. The primary scientific goal is statistical - to estimate the frequency of planetary systems associated with sun-like stars, with particular interest in the detection of earth-size planets in the habitable zone. The approach is to monitor a large number of stars, approximately 150000, continuously for 3 ½ years with a 30 minute cadence to detect the faint photometric signals of transiting planets across the stellar disks of those systems in Kepler's line of sight. An Earth-Sun analog is expected to produce a transit depth of about 80 parts per million, lasting for at most a few tens of hours, and repeating once per "year". The instrumentation for Kepler was designed to provide photometric data with a precision of 20 ppm in 6.5 hours for 12th magnitude stars, resulting in an SNR of 4 for an Earth-Sun analog transit. This paper reviews the considerations that were included in the overall architecture, detailed design, fabrication and testing of the instrument that led to the expected performance at the time of launch. The exquisite precision of the flight data has revealed additional effects, both instrumental and astrophysical, that have provided a deeper understanding of the performance of the flight hardware, to enhanced operational procedures, and to novel post-processing of the data stream. The current state-of-the-art is providing data approaching the sensitivity needed to detect transits of terrestrial planets orbiting 12th magnitude stars and fainter.

8146-17, Session 5**Fiber-based imaging and interferometry**

E. Serabyn, A. Ksendzov, K. M. Liewer, S. R. Martin, D. P. Mawet, Jet Propulsion Lab. (United States)

The phased array coronagraph is based on combining the light from an array of small collecting telescopes with an array of single mode fibers, thus potentially eliminating the need for a large monolithic or segmented telescope. However, the use of a fiber bundle enables a range of architectures, from interferometric beam combination to direct imaging, and from the use with monolithic or segmented telescopes to telescope arrays. Here we describe several potential configurations and uses, both on the ground and in space, and delineate the resultant requirements imposed on the fiber array.

8146-18, Session 5

An optical fiber-based high contrast imager

S. R. Martin, K. M. Liewer, A. Ksendzov, E. Serabyn, Jet Propulsion Lab. (United States)

Arrays of single mode fibers can be used to form segmented pupils of almost arbitrary geometry. Such pupil arrays can be used both for interferometric imaging, for example by non-redundant aperture masking or in direct imaging systems such as the phased array coronagraph. Achieving control over the optical coupling, phase and dispersion for fiber arrays of reasonable size is a technological challenge. Progress has been made using a monolithic block of single mode fibers, lens arrays and masks, and mirror arrays. On one testbed, arrays of up to 37 beamlets are being combined to form a single image. On a second testbed, control of dispersion between fibers of slightly different length is being evaluated. The combination of the techniques being demonstrated has a range of potential uses in astronomy. In this paper we discuss the results from the testbeds.

8146-19, Session 5

Improving images from an adaptive optics system

D. Mozurkewich, Seabrook Engineering (United States)

This Fourier camera is an optical interferometer but lacks the complexity usually associated with one. It uses a micro-lens array to divide the aperture into segments. Optical fibers followed by another micro-lens array rearrange the pupil. A beam combiner takes the rearranged pupil and forms spectrally-dispersed fringes. Even though it can handle a large number of apertures, the beam combiner is simple, consisting of three lenses and a prism. The beam combiner has been built and tested; it works as advertised. I am still assembling the micro-lens/optical fiber array.

The prototype divides the input aperture into 90 sub-apertures. No light is thrown away except from coupling efficiency issues. I combine those sub-apertures to measure just over 600 spatial frequencies (not all independent), each in about 200 spectral channels. All data fits onto a single, 1500x2000 pixel CCD.

As long as the wavefront output of the AO system is better than about a quarter wave, I can take long exposures, limited only by the well depth of the detector and changes in the shape of the target. Detector quantum efficiency and number of pixels are not issues. Wavefront errors from the AO system reduce my fringe contrast, but that can easily be calibrated. This calibration removes the systematics that were in the image formed by the AO system. Wavefront errors do reduce the signal to noise of the fringe measurement but that noise is essentially white and can be reduced by combining multiple images.

8146-20, Session 5

Recent progress in vector vortex coronagraphy

E. Serabyn, D. P. Mawet, J. K. Wallace, Jet Propulsion Lab. (United States)

The vortex coronagraph has great potential for enabling high-contrast observations very close to bright stars, and so for reducing the size of space telescopes needed for exoplanet characterization missions. Here we discuss recent developments in vortex coronagraphy, including the production of vector vortex masks, their measured performance, and unique wave front sensing architectures that vortex phase masks enable. In particular, we describe optical techniques that allow the effective use of vortex phase masks with on-axis telescopes, and the direct measurement of speckle phase.

8146-22, Session 5

Six-fold spectral resolution boosting using TEDI at the Mt. Palomar near-infrared Triplespec spectrograph

D. J. Erskine, Lawrence Livermore National Lab. (United States); J. Edelstein, Univ. of California, Berkeley (United States); P. S. Muirhead, Cornell Univ. (United States); M. W. Muterspaugh, Tennessee State Univ. (United States); K. R. Covey, Cornell Univ. (United States); D. Mondo, A. Vanderburg, P. M. Anderson, D. Kimber, M. M. Sirk, Univ. of California, Berkeley (United States); J. P. Lloyd, Cornell Univ. (United States)

An interferometric optical technique called 'spectral reconstruction' is capable of increasing a spectrograph's resolution performance by large factors, well beyond its classical limits. We have demonstrated a 6-fold increase in the Triplespec effective spectral resolution, from $R=2,700$ to $R=16,000$ by applying special Fourier processing to a delay series of exposures taken with the near-infrared TEDI interferometer and the Triplespec spectrograph at the Mt. Palomar Observatory 200 inch telescope. The performance improvement is observed in both stellar and telluric features simultaneously over the entire spectrograph bandwidth (0.9-2.45 micron). By expanding the delay series, we anticipate achieving resolutions of $R=30,000$. The technique, processing and results are described.

8146-23, Session 6

A low-cost, high-performance 1.2m off-axis telescope built with NG-Xinetics silicon carbide

J. J. Rey, J. A. Wellman, R. J. Wollensak, R. G. Egan, Northrop Grumman Xinetics (United States)

The search for extrasolar habitable planets is one of three major astrophysics priorities identified for the next decade. These missions demand very high performance visible-wavelength optical imaging systems. Such high performance space telescopes are typically extremely expensive and can be difficult for government agencies to afford in today's economic climate, and most lower cost systems offer little benefit because they fall short on at least one of the following three key performance parameters: imaging wavelength, total system-level wavefront error, and aperture diameter. Northrop Grumman Xinetics has developed a simple, lightweight, low-cost telescope that will address the near-term science objectives of this astrophysics theme with the required optical performance, while reducing the telescope cost by an order of magnitude. Breakthroughs in SiC mirror manufacturing, integrated wavefront sensing, and high TRL deformable mirror technology have finally been combined within the same organization to offer a complete end-to-end telescope system in the lower end of the Class D cost range. This paper presents the latest results of real OAP polishing and metrology data, an optimized optical design, and finite element derived WFE estimates to describe the predicted optical performance of the Zodiac II mission proposed to NASA Goddard in February 2011.

8146-24, Session 6

Polarization compensation of Fresnel aberrations in telescopes

N. Clark, NASA Langley Research Ctr. (United States); J. B. Breckinridge, California Institute of Technology (United States)

Large aperture space telescopes are built with low F#s to accommodate the mechanical constraints of launch vehicles and to reduce resonance frequencies of the on-orbit system. Inherent with these low F# is Fresnel

**Conference 8146: UV/Optical/IR Space Telescopes
and Instruments: Innovative Technologies and Concepts V**

polarization which effects image quality. We present the design and modeling of a nano-structure consisting of birefringent layers. Analysis shows a device that functions across a 400nm bandwidth tunable from 300nm to 1200nm. This Fresnel compensator device has a cross leakage of less than 0.001 retardance.

8146-25, Session 6

ZERODUR: new results on bending strength and stress corrosion

P. Hartmann, SCHOTT AG (Germany)

ZERODUR® strength data and information are required for the design of structures, which will be subject to mechanical loads throughout their lifetime or at least during some periods thereof such as lightweight mirrors for space telescopes. Comparison of data acquired twenty years ago with recent ones show astonishing reproducibility. An influence of the specimen preparation process on the width of the breakage stress distribution generally leading to higher values has been observed.

New data are available for diamond grain D25 fine ground surface condition.

The stress corrosion coefficient, an important parameter needed to calculate the long time behavior of structures subject to tensile stress in their surface has been determined from breakage data sets obtained with different stress load increase rates.

Conditioning of Zerodur specimen with stress free storage under varying humidity and humidity exposure times has shown no influence on strength.

8146-26, Session 7

The SPICA Coronagraph Instrument (SCI) and its use for the study of exoplanets

K. Enya, Japan Aerospace Exploration Agency (Japan)

We present an introduction to the Space Infrared Telescope for Cosmology and Astrophysics (SPICA) mission, emphasizing the SPICA Coronagraphic Instrument (SCI) and its use for the study of exoplanets. SPICA is a JAXA-ESA mission with a 3m class telescope cooled to 6K, with launch planned for 2018. The SPICA mission provides us with a unique opportunity to make high contrast observations because of its large telescope aperture, simple pupil shape, and the capability for making infrared observations from space. The SCI is one of the proposed focal plane instruments for SPICA: it is designed especially for a concentrated study of exoplanets.

The primary objectives for the SCI are the direct coronagraphic detection and spectroscopy of Jovian exoplanets in the infrared, while monitoring transiting planets is another important target.

The specifications and an overview of the design of the instrument are shown. In the SCI, coronagraphic and non-coronagraphic modes are applicable both to imaging and spectroscopy.

We include a report on current progress in the development of key technologies for the SCI in the infrared.

8146-27, Session 7

The Euclid-NISP instrument optics and tolerancing approach

F. U. Grupp, Max-Planck-Institut für extraterrestrische Physik (Germany) and Univ. Sternwarte München (Germany); E. Prieto, Observatoire Astronomique de Marseille-Provence (France); P. Spano, F. M. Zerbi, INAF - Osservatorio Astronomico di Brera (Italy); N. Geis, Max-Planck-Institut für extraterrestrische Physik

(Germany); R. Bender, Max-Planck-Institut für extraterrestrische Physik (Germany) and Univ. Sternwarte München (Germany)

The Euclid satellite as a potential part of the ESA cosmic vision programme will carry the Near Infrared Spectrometer and Photometer as one of its two instruments. NISP is fed by a 1.2m Korsch type telescope and covers a field of 0.5 square degrees. This makes Euclid-NISP one of the largest scientific space optical systems ever flown with respect to FoV and optics size.

With this paper we present the instruments optical concept and a tolerancing approach that takes into account the separation in responsibilities between telescope and instrument. A practice-oriented way of incorporating the surface irregularities of the 4 aspheric surfaces in the lens system of NISP is shown.

8146-28, Session 7

Enhancing undergraduate education in engineering and science at MIT through the development of a CubeSat space telescope

M. W. Smith, D. W. Miller, S. Seager, Massachusetts Institute of Technology (United States)

CubeSats are a class of extremely small satellites that conform to a standardized 10 cm x 10 cm x 10 cm, 1 kg form factor. This miniaturization, along with a standardized deployment device for launch vehicles, allows CubeSats to be launched at low cost by sharing the trip to orbit with other spacecraft. Part of the original motivation for the CubeSat platform was also to allow university students to participate more easily in space technology development and to gain hands-on experience with flight hardware. The Department of Aeronautics and Astronautics along with the Department of Earth, Atmospheric, and Planetary Studies (EAPS) at the Massachusetts Institute of Technology (MIT) recently initiated a three semester-long course that uses the development of a CubeSat-based science mission as its core teaching method. Serving as the capstone academic experience for undergraduates, the goal of this class is to design and build a CubeSat spacecraft that serves a relevant science function, such as the detection of exoplanets transiting nearby stars. This project-based approach gives students essential first hand insights into the challenges of balancing science requirements and engineering design. Students are organized into subsystem-specific teams that refine and negotiate requirements, explore the design trade space, perform modeling and simulation, manage interfaces, test subsystems, and finally integrate prototypes and flight hardware. In this work we outline the heritage of capstone design/build classes at MIT, describe the class format in greater detail, and give first semester results on the ability to meet learning objectives using this pedagogical approach.

8146-29, Session 7

The primordial inflation explorer (PIXIE)

A. J. Kogut, D. T. Chuss, NASA Goddard Space Flight Ctr. (United States); J. L. Dotson, NASA Ames Research Ctr. (United States); D. J. Fixsen, Univ. of Maryland (United States); M. Halpern, G. F. Hinshaw, The Univ. of British Columbia (Canada); S. S. Meyer, The Univ. of Chicago (United States); S. H. Moseley, NASA Goddard Space Flight Ctr. (United States); M. D. Seiffert, Jet Propulsion Lab. (United States); D. N. Spergel, Princeton Univ. (United States); E. J. Wollack, NASA Goddard Space Flight Ctr. (United States)

The Primordial Inflation Explorer is an Explorer-class mission to measure the gravity-wave signature of primordial inflation through its distinctive imprint on the linear polarization of the cosmic microwave background. PIXIE uses an innovative optical design to achieve background-limited sensitivity in 400 spectral channels spanning 2.5 decades in frequency

**Conference 8146: UV/Optical/IR Space Telescopes
and Instruments: Innovative Technologies and Concepts V**

from 30 GHz to 6 THz (1 cm to 50 micron wavelength). Multi-moded non-imaging optics feed a polarizing Fourier Transform Spectrometer to produce a set of interference fringes, proportional to the difference spectrum between orthogonal linear polarizations from the two input beams. The differential design and multiple signal modulations spanning 11 orders of magnitude in time combine to reduce the instrumental signature and confusion from unpolarized sources to negligible levels. PIXIE will map the full sky in Stokes I, Q, and U parameters with angular resolution 2.6 deg and sensitivity 0.2 μ K per 1 deg square pixel. The principal science goal is the detection and characterization of linear polarization from an inflationary epoch in the early universe, with tensor-to-scalar ratio $r < 10^{-3}$ at 5 standard deviations. In addition, the rich PIXIE data will constrain physical processes ranging from Big Bang cosmology to the nature of the first stars to the physical conditions within the interstellar medium of the Galaxy. We describe the PIXIE instrument and mission architecture needed to detect the signature of an inflationary epoch in the early universe using only 4 semiconductor bolometers.

8146-30, Session 7

**C3D (compact CMOS camera demonstrator)
for UKube-1**R. D. Harriss, A. D. Holland, S. J. Barber, S. Karout, B. J. Dryer,
N. J. Murray, The Open Univ. (United Kingdom)

The Open University, in collaboration with e2v technologies PLC and XCAM Ltd, have been selected to fly an EO (earth observation) technology demonstrator and in-orbit radiation damage characterisation instrument on board the UK Space Agency's UKube-1 pilot Cubesat programme. Cubesat payloads offer a unique opportunity to rapidly build and fly space hardware for minimal cost providing easy access to the space environment. Based around the e2v 1.3 MPixel 0.18 micron process eye-on-Si CMOS devices, the instrument consists of a radiation characterisation imager as well as a narrow field imager (NFI) and a wide field imager (WFI). The narrow and wide field imagers are expected to achieve resolutions of 25 m and 350 m respectively from a 650 km orbit, providing sufficient swathe width to view the southern UK with the WFI and London with the NFI. The radiation characterisation experiment has been designed to verify and reinforce ground based testing that has been conducted on the e2v eye-on-Si family of devices and includes TEC temperature control circuitry as well as RADFET in-orbit dosimetry. Of particular interest are SEU and SEL effects. The novel instrument design allows for a wide range of capabilities within highly constrained mass, power and space budgets providing a model for future use on similarly constrained missions, such as planetary rovers. Scheduled for launch in December 2011, this 1 year low cost programme should not only provide valuable data and outreach opportunities but also help to prove flight heritage for future missions.

8146-31, Session 7

ESA M3 mission candidate ECHOL. Puig, K. Isaak, I. Escudero-Sanz, D. Martin, P. Cruzet,
N. Rando, European Space Research and Technology Ctr.
(Netherlands)

The Exoplanet Characterisation Observatory is an M-class mission candidate within the science program Cosmic Vision 2015-2025 of the European Space Agency. It was selected in February 2011 as one of 4 missions to enter an assessment phase (phase 0/A). This process involves the definition of science and mission requirements as well as a preliminary model payload, followed by an internal Concurrent Design Facility study planned for July 2011. Parallel industrial studies will follow in 2012, after which the 4 missions will be reviewed to identify candidates entering Phase A/B1 studies in 2013.

The ECHO mission aims at characterising the atmospheric content of known transiting exoplanets, potentially from giant Hot Jupiters down to Super-Earths orbiting in the habitable zone of M-dwarf stars. For this purpose, it will use a 1 m class telescope, feeding a Vis-NIR spectrometer

and covering the wave lengths from 0.4 micron to 9 microns, with a potential extension up to 16 microns. While spatial differentiation of the exoplanet and its host star is not necessary, spectral differentiation will be achieved by making differential measurements of in- and out-of transit frames to cancel the star signal.

This paper describes critical science and mission requirements, and gives an overview of the model payload design. It also reports on the results of a Concurrent Design Facility (CDF) study, providing a description of the spacecraft design, including critical subsystems such as AOCS and thermal/cryogenics.

8146-32, Session 7

**Optical design trade study for the Wide Field
Infrared Space Telescope [WFIRST]**D. Content, J. M. Howard, J. E. Mentzell, J. P. Lehan, NASA
Goddard Space Flight Ctr. (United States)

The WFIRST mission concept was created by the Astro2010 Decadal Survey from multiple science white papers and the JDEM Omega payload concept; the Astro2010 report "New Worlds, New Horizons" [NWNH] was released in August 2010. This mission will be a flagship space telescope at L2 studying exoplanets [via gravitational microlensing], probing Dark energy, and surveying the near infrared sky. Since the release of NWNH the WFIRST project has been working with the newly formed WFIRST science definition team (SDT) to refine mission and payload concepts. We present the driving requirements as currently understood for the WFIRST payload optical design. Examples of designs potentially consistent with the requirements are given, and the trade space is discussed.

8146-43, Session 7

**The JWST near-infrared spectrograph
NIRSpec: results from the first set of
instrument-level cryogenic testing**

P. Ferruit, G. Bagnasco, S. M. Birkmann, T. Böker, European Space Research and Technology Ctr. (Netherlands); G. Cresci, INAF - Osservatorio Astrofisico di Arcetri (Italy); G. de Marchi, European Space Research and Technology Ctr. (Netherlands); B. Dorner, Observatoire de Lyon (France) and Ctr. de Recherche Astrophysique de Lyon (France); R. Ehrenwinkler, EADS Astrium GmbH (Germany); M. Falcolini, G. Giardino, European Space Research and Technology Ctr. (Netherlands); X. Gnata, EADS Astrium GmbH (Germany); P. Jakobsen, P. L. Jensen, European Space Research and Technology Ctr. (Netherlands); M. Kolm, H. Maier, M. Maschmann, P. Mosner, A. Rödel, EADS Astrium GmbH (Germany); F. Rosales-Ortega, Univ. Autónoma de Madrid (Spain); P. Rumler, J. Salvignol, P. Strada, European Space Research and Technology Ctr. (Netherlands); M. Stuhlinger, European Space Astronomy Ctr. (Spain); M. B. J. te Plate, European Space Research and Technology Ctr. (Netherlands); T. Wettemann, EADS Astrium GmbH (Germany)

The Near-Infrared Spectrograph NIRSpec is one of the four instruments of the James Webb Space Telescope (JWST). NIRSpec will cover the 0.6-5.0 micron range and will be capable of obtaining spectra of more than 100 objects simultaneously in its multi-object spectroscopy (MOS) mode. It also features a set of slits for high contrast spectroscopy of individual sources, as well as an integral-field unit (IFU) for 3D spectroscopy. Manufactured in Europe by EADS Astrium for the European Space Agency (ESA), it is scheduled for delivery to NASA at the end of 2011.

In the first months of 2011, the flight model has undergone its first set of instrument-level cryogenic testing. After providing an update on the

**Conference 8146: UV/Optical/IR Space Telescopes
and Instruments: Innovative Technologies and Concepts V**

instrument status, we will present the results of this test campaign. As the MOS mode could not be tested during this first calibration period, we will focus on the fixed-slit and integral field modes of the instrument.

NIRSpec is a core instrument of the James Webb Space Telescope. Covering the 0.6-5.0 micron range, it features a multi-object spectroscopy mode, a set of slits for high-contrast spectroscopy and an integral-field unit for 3D spectroscopy. Manufactured in Europe by EADS Astrium for ESA, it is scheduled for delivery to NASA at the end of 2011.

The instrument has recently undergone its first set of instrument-level cryogenic testing. After providing an update on the instrument status, we will present the results of this test campaign with a particular emphasis on the fixed-slit and integral field modes of the instrument.

8146-33, Poster Session**The space instrument SODISM, a telescope to measure the solar diameter**

M. M. Meftah, Ctr. National de la Recherche Scientifique (France)

PICARD is a satellite dedicated to the simultaneous measurement of the absolute total and spectral solar irradiance, the diameter and solar shape, and to the Sun's interior probing by the helioseismology method. These measurements obtained throughout the mission will allow study of their variations as a function of solar activity. The objectives of the PICARD mission are to improve our knowledge of the functioning of our star through new observations and the influence of the solar activity on the climate of the Earth.

PICARD was launched on June 15, 2010 on a Dnepr-1 launcher from Dombrovskiy Cosmodrome, near Yasny, Russia.

The satellite was placed into the heliosynchronous orbit of 730 km with inclination of 98.28 degrees.

SODISM (SOLAR Diameter Imager and Surface Mapper), an instrument of the PICARD payload, is an 11-cm Cassegrain imaging telescope developed at CNRS (Centre National de la Recherche Scientifique) by LATMOS (Laboratoire, ATMosphere, Milieux, Observations Spatiales) associated with a 2Kx2K CCD (Charge-Coupled Device), taking solar images at five wavelengths. It carries a four-prism system to ensure a metrological control of the optics magnification.

The first image of the Sun was taken by SODISM instrument on July 22, 2010. It is a raw image, level L0, thus obtained before processing, at 607 nm wavelength in a very narrow band of 0.7 nm width.

SODISM allows us to measure the solar diameter and shape with an accuracy of a few milliarcsseconds, and to perform helioseismologic observations to probe the solar interior. SODISM is an innovative technology.

The helioseismology program consists in two observing modes at a wavelength of 535 nm in the continuum. The first one generates images of the whole solar disc at low resolution and is aimed at studying the properties of the medium degree eigenmodes of oscillations. The second one is focusing on a narrow corona centered around the limb. In this region where the granulation signal is weak and where the modes of oscillation are expected to be amplified, helioseismic measurements in intensity should bring new information on the deep internal structure of the Sun.

In this article, we describe the instrument concept and design and give an overview of the thermal stability of the telescope.

8146-34, Poster Session**Measured aspheric surface irregularities as input to the Euclid-NISP tolerancing**

U. Fuchs, asphericon GmbH (Germany); F. U. Grupp, Univ.-Sternwarte München (Germany); S. Kiontke, asphericon GmbH (Germany); R. Bender, Max-Planck-Institut für extraterrestrische Physik (Germany) and Univ.-Sternwarte München (Germany)

e present the approach of using measured surface irregularities and departures from design parameters of already manufactured lenses as input to the Euclid-NISP instrument tolerancing.

Representative lenses have been precisely characterized and their deviations from initial design parameters have been measured and then modelled by ZEMAX optical design software. In a second step these simulations are taken as a realistic input to a future system performance evaluation and system tolerancing approach.

8146-36, Poster Session**A filter mount for the Euclid dark-energy mission**

R. Holmes, U. Grözinger, P. Bizenberger, O. Krause, Max-Planck-Institut für Astronomie (Germany)

The Euclid dark energy mission is competing in the European Space Agency's Cosmic Vision Program. The satellite survey mission will image the entire extragalactic sky in the visible and near infrared. The Near-Infrared Imaging Photometer (NIP) requires large transmissible optics, including three NIR filters (Y: 920-1146 J: 1146-1372 and H: 1372-2000nm) with a diameter of ~130 mm and a thickness of 12 mm. The mounting of these massive, 330 g per element, fused silica filters into the filter wheel mechanism is challenging.

In this paper we present work undertaken at the Max-Planck-Institut für Astronomie, Germany during the Euclid Phase A Study, ending in the summer of 2010. We present two designs of the filter mounting structure. In both designs, the filters are mounted in an Invar element, which is fixed into a recess in the titanium filter wheel. Kapton foil is included between the fused silica and the metal elements to prevent small protrusions in these hard materials causing high localized stresses in the optical glass. These two designs differ at their interface between the Invar element and the filter wheel. In one design we implement a rigid interface and in the other we create flexible elements in the Invar to accommodate the different thermal contraction between the components.

The design considerations, finite element analysis and prototyping results, both cool down and vibration tests, are detailed. The down-selection between the two designs, based on the results from the prototyping campaign, is also discussed. We conclude with recommendations on future developments of mounts of this type.

8146-37, Poster Session**Laboratory prototype camera for the Whipple mission: a mission to detect and categorize small objects in our solar system**

A. T. Kenter, R. Kraft, Harvard-Smithsonian Ctr. for Astrophysics (United States); S. S. Murray, The Johns Hopkins Univ. (United States); C. Alcock, Harvard-Smithsonian Ctr. for Astrophysics (United States)

The proposed Whipple mission will detect and categorize the size and distance of small objects in the outer Solar system by detecting the characteristic diffraction pattern created when they pass between the observatory and a distant star. Since such a transit is a rare occurrence, the light curves of several tens of thousands of stars will be monitored simultaneously at video rates to look for these "occultations".

The time signature of such a diffraction event has a total duration of ~.1 -10 seconds, and depends on the size and distance of the object.

The Whipple focal plane consists of nine Teledyne H2RG HyVISI detectors and nine dedicated Teledyne SIDECAR ASICs. The time signature of a and event is detected by a simple algorithm implemented in an on-board FPGA signal processor.

As part of a proposal preparation effort, we have made a prototype working engineering model of one facet of the Whipple focal plane. This facet consists of a HyVISI H2RG and a SIDECAR laboratory cryo-

**Conference 8146: UV/Optical/IR Space Telescopes
and Instruments: Innovative Technologies and Concepts V**

development kit.

To test the entire detection process we constructed a light curve simulator that projects a field of stars on the detector. The projected stars have representative size to reflect the quality of the expected telescope. The "projected" stars are temporally modulated to mimic the light curve of an occultation/diffraction event.

We present details of system construction, performance, and light curve simulations.

8146-38, Poster Session**The space instrument SOVAP of the PICARD mission**

M. M. Meftah, Ctr. National de la Recherche Scientifique (France);
C. Conscience, A. Chevalier, Royal Meteorological Institute of Belgium (Belgium)

PICARD is a Satellite dedicated to the simultaneous measurement of the absolute total and spectral solar irradiance, the diameter and solar shape, and the Sun's interior probed by helioseismology method. Its objectives are the study of the origin of the solar variability and the study of the relations between the Sun and the Earth's climate. PICARD was launched on June 15, 2010. The Satellite was placed into the heliosynchronous orbit of 730 km with inclination of 98.28 degrees. The payload consists in two absolute radiometers measuring the TSI (Total Solar Irradiance) and an imaging telescope to determine the solar diameter, the limb shape and asphericity.

SOVAP (Solar VARIability Picard) is an experiment developed by the Belgian STCE (Solar Terrestrial Center of Excellence) with a contribution of the CNRS (Centre National de Recherche Scientifique) composed of an absolute radiometer provided by the RMIB (Royal Meteorological Institute of Belgium) to measure the TSI and a bolometer provided by the ROB (Royal Observatory of Belgium) used to increase the TSI sampling. The continuous observation of the solar irradiance at the highest possible precision and accuracy is an important objective of the earth climate change. This requires: high quality metrology in the space environment. In this article, we describe the SOVAP instrument, its performances and uncertainties.

8146-39, Poster Session**Ray tracing based on finite element model and geometry of Ha and white light telescope**

Z. Chen, M. Wu, S. Yang, X. Gu, S. Wang, F. Zhao, National Astronomical Observatories (China)

The Ha and White Light Telescope(HWT)is one of the payloads of the Chinese Space Solar Telescope(SST). To evaluate the optical performance of the telescope system under complex environment, ray tracing based on finite element model and geometry were introduced. The principles and processes of ray tracing algorithm combining FEM and GEM(Geometry model) are presented, which based on the traditional ray tracing algorithm and the shape function interpolation concept of Finite Element Model (FEM). The surface normal vector transformation relation between the deformed surface and the un-deformed surface is given, which is a pre-requisite for ray tracing combining FEM and GEM. The principles and processes make possible and practicable a new way to perform Structural Thermal Optical Performance(STOP) Analysis of diffraction limited opt-mechanical systems, which are easily influenced by elastic deformation. Application of the method to Ha solar telescope shows an MTF degradation when the system experiences an overall temperature rise of 5 and 10 .

8146-40, Poster Session**Astronomical telescope with holographic primary objective**

T. D. Ditto, 3DeWitt LLC (United States)

A dual dispersion telescope with a plane grating primary objective was previously disclosed that can overcome intrinsic chromatic aberration of dispersive optics while allowing for unprecedented features such as million object spectroscopy, extraordinary étendue, flat primary objective with a relaxed figure tolerance, gossamer membrane substrate stowable as an unsegmented roll inside a delivery vehicle, and extensibility past 100 meter aperture at optical wavelengths. The novel design meets many criteria for space deployment. Other embodiments are suitable for airborne platforms as well as terrestrial and lunar sites. One problem with this novel telescope is that the grazing exodus configuration necessary to achieve a large aperture is traded for throughput efficiency. Now we show how the hologram of a point source used in place of the primary objective plane grating can improve efficiency by lowering the diffraction angle below grazing exodus. An intermediate refractive element is used to compensate for wavelength dependent focal lengths of the holographic primary objective.

8146-41, Poster Session**NIRAM: a near-infrared spectrometer project design for the Brazilian Aster mission**

A. Hetem, Univ. Federal do ABC (Brazil)

The Aster mission consists in a spacecraft to rendezvous with a near-earth asteroid, 2001 SN263, in 2018. In this work, we present the first outlines of our project which uses the expertise of space engineers together with astrophysicists, working on solar systems small bodies, who are proposing the Near-Infrared Spectrometer for the Aster mission, the first Brazilian mission to deep space. The results from this instrument will help to characterize the surface composition and its relations to the mineralogical properties within the surface morphology. Analysis of these spectra, in combination with other parameters, shall provide diagnosis of the presence and species composition of minerals and several other molecules that may be present. The most interesting minerals have absorption characteristics due to electron vibration in their reflection infrared spectral bands. The chosen spectral band, from 1 to 3.5 microns, allows recognizing the presence of water, carbon dioxide, olivines and other important elements. An important achievement will be the involvement of Brazilian industry and universities in the conception, design and construction of this instrument. The technologies to be developed involves the areas of infrared optics, electronic sensors, automation and control of space systems, structures and new materials, thermal devices and data and image processing.

8146-42, Poster Session**A second generation tunable spatial heterodyne spectrometer for observing diffuse emission line targets**

S. S. Hosseini, W. M. Harris, Univ. of California, Davis (United States)

We report on progress toward development of a second-generation tunable spatial heterodyne spectrometer (TSHS) at the fixed focus of the Coudé Auxiliary Telescope (CAT) in the Shane observatory at Lick Observatory. SHS instruments are a class of interferometric sensor capable of providing a combination of large étendue, high resolving power ($R = \lambda/d\lambda \sim 10^5$) and wide field of view (FOV~0.5 degree) at Optical and UV wavelengths in a compact format. The TSHS implementation addresses the bandpass limitation of the basic SHS through controlled rotation of pilot mirrors in the interferometer. The use

**Conference 8146: UV/Optical/IR Space Telescopes
and Instruments: Innovative Technologies and Concepts V**

of a single grating as both a dispersing and beam-splitting element in the all-reflective SHS greatly relaxes the precision required in the alignment of the other optical elements relative to a more typical scanning Fourier Transform Spectrometer and allows the TSHS implementation to be accomplished with low-cost commercial rotation stages. The new design builds on a previous design originally tested in 2007, and will address several issues identified with the input beam, output imaging, and grating efficiency (Dawson and Harris, 2009). Here we will discuss the design considerations going into this new system and the initial results of the installation and testing of the TSHS and the future plans.

Conference 8147: Optics for EUV, X-Ray, and Gamma-Ray Astronomy V

Tuesday-Thursday 23-25 August 2011 • Part of Proceedings of SPIE Vol. 8147
Optics for EUV, X-Ray, and Gamma-Ray Astronomy V

8147-01, Session 1

ASTRO-H soft x-ray telescope (SXT)

Y. Soong, The Ctr. for Research and Exploration in Space Science (United States) and Universities Space Research Association (United States); T. Okajima, P. J. Serlemitsos, NASA Goddard Space Flight Ctr. (United States)

ASTRO-H is an X-ray astrophysics satellite that will be built with US-Japanese collaborative effort. On board are four Wolter-type X-ray mirrors, among which two of them are soft X-ray mirrors, energy range from a few hundred eV to 15 keV, currently being fabricated in the X-ray Optics Lab at Goddard Space Flight Center, NASA. The focal point instruments will be a calorimeter (GSFC) and a CCD camera (Osaka U.), respectively. The reflectors of the mirror are made of aluminum substrate, of which the thickness gauged at 152 μm , 229 μm , and 305 μm of the alloy 5052, with epoxy replication on smooth Pyrex cylindrical mandrels to acquire the X-ray reflective surface. The epoxy layer is 10 μm nominal and surface gold layer of 0.2 μm . Improvements on angular response over the Astro-E/Suzaku mirrors come from reducing the figure, the roundness, and the grazing angle/radius mismatching errors of the reflectors, and tighter specs on supporting structure to reduce the reflector positioning and the assembly errors. In this paper, we report the results of calibration of the engineering module of soft X-ray Telescope, and project the quality of the flight mirrors.

8147-02, Session 1

Development of ultra-thin thermal shield for ASTRO-H x-ray telescopes

Y. Tawara, S. Sugita, A. Furuzawa, Nagoya Univ. (Japan)

Thermal environment of ASTRO-H X-ray telescopes will be controlled by using both a metal-coated thin plastic film called a thermal shield(TS) placed in front of each telescope and a heater installed in the telescope housing.

In order to keep high X-ray transmission, plastic film should be very thin. Thickness of the film for HXT(Hard X-ray Telescope)-TS is 2.5 micron and that for SXT(Soft X-ray Telescope)-TS is 0.2 micron.

This paper discusses engineering difficulties related to using very thin film and properties related to thermal control. Discussions are designing the TS assembly to survive launch environment such as acoustic oscillation and vibration, deal with issues related to surviving direct solar, space debris, and atomic oxygen irradiation in orbit, and testing the TS integrity.

8147-03, Session 2

The Focusing Optics X-ray Solar Imager (FOXSI)

S. Christe, NASA Goddard Space Flight Ctr. (United States); S. Krucker, L. Glesener, Univ. of California, Berkeley (United States); M. V. Gubarev, B. Ramsey, NASA Marshall Space Flight Ctr. (United States); S. Ishikawa, S. Saito, T. Takahashi, Univ. of Tokyo (Japan)

The Focusing Optics X-ray Solar Imager (FOXSI) is a sounding rocket payload (NASA LCAS) to test hard x-ray focusing optics and position-sensitive solid state detectors for solar observations. Today's leading solar hard x-ray instrument, RHESSI, provides excellent spatial and spectral resolution. Yet, due to its use of indirect imaging, the derived images have a low dynamic range (<30) and sensitivity. This makes it

difficult to study faint x-ray sources in the solar corona which are crucial for understanding particle acceleration at the Sun. Grazing-incidence x-ray focusing optics combined with position-sensitive solid state detectors can overcome both of these limitations and will enable the next breakthrough in understanding impulsive solar energy release. FOXSI is a collaboration between the Space Science Laboratory at the University of California, Berkeley, the NASA GSFC, the NASA MSFC, which is providing the grazing-incidence optics, and JAXA/ISAS, which is providing double-sided silicon strip detectors. Scheduled for its first launch in October 2011, FOXSI will be a pathfinder for the next generation of solar hard x-ray observatories.

8147-04, Session 2

SRG/ART-XC

M. N. Pavlinsky, V. V. Akimov, V. A. Levin, I. Y. Lapshov, A. Tkachenko, N. Semena, V. Arefev, A. Glushenko, A. Yaskovich, R. Burenin, S. Sazonov, M. Revnitsev, M. Buntov, S. Grebenev, A. Lutovinov, M. Kudelin, Space Research Institute (Russian Federation); S. V. Grigorovich, D. N. Litvin, V. P. Lazarchuk, I. Roiz, M. Garin, Russian Federal Nuclear Ctr. - All-Russian Research Institute of Experimental Physics (Russian Federation); M. V. Gubarev, B. D. Ramsey, R. F. Elsner, S. L. O'Dell, NASA Marshall Space Flight Ctr. (United States)

Spectrum Roentgen Gamma (SRG) is an X-ray astrophysical observatory, developed by Russia in collaboration with Germany. The mission will be launched in 2013 from Baikonur, by a Zenit rocket with a Fregat upper stage. SRG will be placed in a 6 months period halo orbit around L2. The scientific payload is made of two independent telescopes. The former, a soft-x-ray survey instrument eROSITA, is being provided by Germany, while the latter, is a medium-x-ray-energy survey instrument ART-XC whose development by Russia.

ART-XC will consist of seven independent, but co-aligned, telescope modules with seven corresponding cadmium-telluride focal plane detectors. Each will operate over the approximate energy range of 6-30 keV (pointing mode), with an angular resolution of 1 arcmin, field of view of 30 arcmin and energy resolution about 10% on 14 keV. The NASA Marshall Space Flight Center (MSFC) will fabricate part of the mirror modules, to complement mirror modules which will be fabricated in Russia.

8147-05, Session 2

Performance of mirror shell replicated from new flight quality mandrel for eROSITA mission

D. Vernani, Media Lario Technologies (Italy)

Focusing mirrors manufactured via galvanic replication process from negative shape mandrels is the chosen solution for eROSITA X-ray mission. Media Lario Technologies (MLT) is the industrial enabler manufacturing, in collaboration with Max Planck Institute (MPE) and German Space Agency (DLR), the Optical Payload for eROSITA including the flight quality mandrels. The mandrel manufacturing holds a crucial role in the process of fabrication of the optics. In fact, the shape accuracy and the roughness of the replicated mirrors are strongly affected by the mandrel starting quality. For the mandrels production an evolution of the approach used for the manufacturing of past mission mandrels (JET-X, XMM) has been developed. The low energy angular resolution of the eROSITA mirror payload needs to be 15 arcsec HEW or better and HEW of 20 arcsec at 8.05keV. Replicated mirrors with performance in this

Conference 8147:
Optics for EUV, X-Ray, and Gamma-Ray Astronomy V

range for low energy have been obtained in the past by using mandrels that have superior geometrical shape accuracy (i.e. typically a factor of two or more better). A proprietary multistep surface finishing process has now been developed for reaching the aggressive performance requirements demanded by the mission. The status and the metrology of the eROSITA series mandrels manufactured so far, by using the advanced polishing process, are presented. In the paper, the x-ray performance of mirror shells (as measured at MPE PANTER facility) replicated from a flight quality eROSITA mandrel, are reported.

8147-06, Session 2

Development and testing of the eROSITA mirror modules

V. Burwitz, P. Friedrich, H. W. Bräuninger, B. Budau, W. Burkert, J. Eder, M. Freyberg, G. D. Hartner, E. Pfeffermann, P. Predehl, Max-Planck-Institut für extraterrestrische Physik (Germany); L. Arcangeli, G. Borghi, A. Borroni, O. Citerio, I. Ferrario, G. Grisoni, F. Marioni, A. Ritucci, M. Rossi, G. Valsecchi, D. Vernani, Media Lario Technologies (Italy)

MPE will provide the X-ray Survey Telescope eROSITA for the Russian Spektrum-Roentgen-Gamma Mission to be launched in 2012.

It consists of a compact bundle of 7 co-aligned mirror modules with a focal length of 1600 mm and 54 nested mirror shells each. Therefore, its sensitivity in terms of effective area, field-of-view (61'), and angular resolution (15" HEW on-axis) will yield a high grasp of about 1000 cm² deg² around 1 keV with an average angular resolution of ~26" HEW over the field-of-view (30" including optical and spacecraft error contributions).

After an extended test program on single mirror shells, assembled test modules (6 shells) and a qualification model we have now started integration of flight mirror modules. We will give a résumé on the development and test program including key improvements to the shell integration method. Moreover, we will report on the integration progress and present first results on the X-ray performance of partially integrated mirror modules.

8147-07, Session 2

The optics system of the New Hard X-ray Mission: status report

S. Basso, G. Pareschi, O. Citterio, G. Tagliaferri, D. Spiga, L. Raimondi, B. Salmaso, V. Cotroneo, INAF - Osservatorio Astronomico di Brera (Italy); G. Borghi, G. Valsecchi, A. Orlandi, D. Vernani, R. Binda, F. Marioni, S. Moretti, Media Lario Technologies (Italy); G. Sironi, INAF - Osservatorio Astronomico di Brera (Italy); P. Attinà, Thales Alenia Space (Italy); B. M. Negri, Agenzia Spaziale Italiana (Italy)

The New Hard X-ray Mission (NHXM) is a mission focussed on a broad energy band, from 0.2 to 80 keV, coupled with a sensitive polarimeter. The mission is currently undergoing the Phase B study and it has been proposed to ESA as a small-size mission to be further studied in the context of the M3 call. The performance is reached with a focal length of 10m and with 4 modules, each composed by 70 mirror shells obtained with the electroforming process. The substrate of the mirror shells is NiCo and they are multilayer coated. The focal plane is mounted on an extensible bench. Three of the four modules are equipped with a couple of detectors, a low energy detector covering a range from 0.2 to 15 keV and a high energy detector efficient until 80 keV. The fourth module is dedicated to the polarimetry with imaging capabilities. In this article the latest development in the design and manufacturing of the optics is presented. The design has been optimizing in order to increase as more as possible the effective area in the high energy band and the manufacturing of the mirror shells benefits from the latest development

in the mandrel production (figuring and polishing), in the multilayer deposition and in the integration improvements.

8147-08, Session 2

Angular resolution measurements of a hard x-ray optic for the New Hard X-ray Mission at SPring-8

D. Spiga, INAF - Osservatorio Astronomico di Brera (Italy); L. Raimondi, INAF - Osservatorio Astronomico di Brera (Italy) and Università degli Studi dell' Insubria (Italy); A. Furuzawa, Nagoya Univ. (Japan); S. Basso, INAF - Osservatorio Astronomico di Brera (Italy); R. Binda, G. Borghi, Media Lario Technologies (Italy); V. Cotroneo, Smithsonian Ctr. for Astrophysics (United States); G. Grisoni, Media Lario Technologies (Italy); H. Kunieda, H. Matsumoto, H. Mori, T. Miyazawa, Nagoya Univ. (Japan); B. M. Negri, Agenzia Spaziale Italiana (Italy); A. Orlandi, Media Lario Technologies (Italy); G. Pareschi, B. Salmaso, G. Tagliaferri, INAF - Osservatorio Astronomico di Brera (Italy); K. Uesugi, Japan Synchrotron Radiation Research Institute (Japan); G. Valsecchi, D. Vernani, Media Lario Technologies (Italy)

The realization of X-ray telescopes with imaging capabilities in the hard (> 10 keV) X-ray band requires the adoption of optics with shallow (< 0.25 deg) grazing angles to enhance the reflectivity of reflective coatings. On the other hand, to obtain large collecting area large mirror diameters (< 350 mm) are necessary. This implies that mirrors with focal lengths ≥ 10 m shall be produced and tested. Full-illumination tests of such mirrors are usually performed with on-ground X-ray facilities, aimed at measuring their effective area and the angular resolution; however, they in general suffer from effects of the finite distance of the X-ray source, e.g. a loss of effective area for double reflection. These effects increase with the focal length of the mirror under test; hence a "partial" full-illumination measurement might not be fully representative of the in-flight performances. Indeed, a pencil beam test can be adopted to overcome this shortcoming, because a mirror at a time is exposed to the X-ray flux, and the beam divergence can be compensated by tilting the optic. In this work we present the result of a hard X-ray test campaign performed at BL20B2 beamline of the SPring-8 synchrotron radiation facility, aimed at characterizing the Point Spread Function (PSF) of a multilayer-coated Wolter-I mirror shell manufactured by Nickel electroforming. The mirror shell is a demonstrator for the NHXM hard X-ray imaging telescope (0.3 - 80 keV), with a predicted HEW (Half Energy Width) close to 20 arcsec. We also show the results of the reconstruction of the PSF at monochromatic X-ray energies of 15 to 63 keV.

8147-09, Session 2

From x-ray telescopes to neutron focusing

M. V. Gubarev, NASA Marshall Space Flight Ctr. (United States); B. Khaykovich, Massachusetts Institute of Technology (United States)

In the case of neutrons the refractive index is slightly less than unity for most elements and their isotopes. Consequently, thermal and cold neutrons can be reflected from smooth surfaces at grazing-incidence angles. Hence, the optical technologies developed for x-ray astronomy can be applied for neutron focusing. The focusing capabilities of grazing incidence neutron imaging optics have been successfully demonstrated using nickel mirrors. The mirrors were fabricated using an electroformed nickel replication process at Marshall Space Flight Center. Results of the neutron optics experiments will be presented. Challenges of the neutron imaging optics as well as possible applications of the optics will be discussed.

Conference 8147:
Optics for EUV, X-Ray, and Gamma-Ray Astronomy V

8147-10, Session 3

ESA led IXO optics development status

M. Bavdaz, E. Wille, K. Wallace, B. Shortt, N. Rando, ESTEC (Netherlands); M. J. Collon, cosine Research B.V. (Netherlands); G. Pareschi, Osservatorio Astronomico di Brera (Italy); F. Christensen, DTU-space (Denmark); M. Krumrey, Physikalisch-Technische Bundesanstalt (Germany); M. Freyberg, Max-Planck-Institut für extraterrestrische Physik (Germany)

The International X-ray Observatory (IXO) is a candidate mission in the ESA Space Science Programme Cosmic Visions 1525, and is being studied as a joint mission with NASA and JAXA.

The mission is building on novel optics technologies to achieve the required performance for this demanding astrophysics observatory. The Silicon Pore Optics (SPO) is the baseline technology and is being developed by an industrial consortium. As a back-up technology, slumped glass optics is being developed in Europe and the USA, and work is progressing on improved reflective coatings.

This paper will present the status of the developments led by ESA, which are being implemented in a phased approach, addressing the performance, environmental compatibility and industrial production.

Further, the progress with the X-ray test facilities and associated beam-lines will be reported.

8147-11, Session 3

Design, fabrication, and characterization of silicon pore optics for IXO

M. J. Collon, R. Günther, M. D. Ackermann, R. Partapsing, G. Vacanti, M. W. Beijersbergen, cosine Research B.V. (Netherlands); M. Bavdaz, K. Wallace, E. Wille, European Space Research and Technology Ctr. (Netherlands); M. Olde Riekerink, J. Haneveld, A. Koelewijn, Micronit Microfluidics BV (Netherlands); C. van Baren, SRON Nationaal Instituut voor Ruimteonderzoek (Netherlands); M. Krumrey, Physikalisch-Technische Bundesanstalt (Germany); M. Freyberg, Max-Planck-Institut für extraterrestrische Physik (Germany)

Silicon pore optics is a technology developed to enable future large area X-ray telescopes, such as the International X-ray Observatory (IXO), a candidate mission in the ESA Space Science Programme 'Cosmic Visions 2015-2025'. IXO uses nested mirrors in Wolter-I configuration to focus grazing incidence X-ray photons on a detector plane. The IXO optics will have to meet stringent performance requirements including an effective area of $>2.5 \text{ m}^2$ at 1.25 keV and $>0.65 \text{ m}^2$ at 6 keV and angular resolution better than 5 arc seconds. To achieve the collecting area requires a total polished mirror surface area of $\sim 1300 \text{ m}^2$ with a surface roughness better than 0.5 nm rms. By using commercial high-quality 12" silicon wafers which are diced, structured, wedged, coated, bent and stacked, the stringent performance requirements of IXO can be attained without any costly polishing steps. Two of these stacks are then assembled into a co-aligned mirror module, which is a complete X-ray imaging system. Included in the mirror module are the isostatic mounting points, providing a reliable interface to the telescope. Hundreds of such mirror modules are finally integrated into petals, and mounted onto the spacecraft to form an X-ray optic of approximately 4 m in diameter.

In this paper we will present the silicon pore optics mass manufacturing process and latest X-ray test results of mirror modules mounted and tested in flight configuration.

8147-12, Session 3

Mass production of silicon pore optics for the International X-ray Observatory

E. Wille, K. Wallace, M. Bavdaz, European Space Research and Technology Ctr. (Netherlands)

Silicon Pore Optics (SPO) provide a high angular resolution with a low areal density as required for the International X-ray Observatory (IXO). The present baseline consists of populating the IXO mirror assembly with about 2000 SPO mirror modules. During the development of the process steps of the SPO technology, the specific requirements of a future mass production have been considered right from the beginning. The manufacturing methods heavily utilise off-the-shelf equipment from the semiconductor industry, robotic automation and parallel processing. This allows to upscale the present production flow in a very cost effective way, to produce hundreds of mirror modules per year.

Considering manufacturing predictions based on the current status of the SPO technology, we present an analysis of the time and resources that will be required for the IXO mirror mass production within a future flight programme. This includes the full production process starting with 300 mm Si wafers up to the integration of the mirror modules. We present the times required for the individual process steps and deduce the number of machines that will be required to produce 4 mirror modules per day. A preliminary timeline for building and commissioning the infrastructure, and for the production of the mirror modules required for a flight project, is presented.

8147-13, Session 3

Silicon pore optics for astrophysical missions

G. Vacanti, M. J. Collon, R. Günther, M. D. Ackermann, R. Partapsing, M. W. Beijersbergen, cosine Research B.V. (Netherlands); M. Olde Riekerink, Micronit Microfluidics BV (Netherlands); J. Haneveld, Micronit Microfluidics BV (United States); A. Koelewijn, Micronit Microfluidics BV (Netherlands); C. van Baren, SRON Nationaal Instituut voor Ruimteonderzoek (Netherlands); P. Müller, M. Krumrey, Physikalisch-Technische Bundesanstalt (Germany); M. Freyberg, Max-Planck-Institut für extraterrestrische Physik (Germany)

The establishment of Silicon Pore Optics (SPO) as the technology of choice for the implementation of future large X-ray space optics has opened up the road to its use in all classes of X-ray missions with varying scientific goals. This interest has given us the possibility to broaden the design parameter space which is normally considered for SPO optics. In doing so a number of classical space X-ray optics design issues (e.g., field of view, stray light, baffling, aberrations) have been tackled. In this paper we report on recent results achieved in this effort. Particular attention will be given to the issues of stray light and baffling, a topic upon which a combination of analytical, simulation, and data analysis means can be effectively brought to bear. Missions considering the use of SPO optics have requirements spanning more than 2 orders of magnitude in energy, and a factor 20 in focal length. The possibilities that can be considered and the trade offs that must be made when applying SPO to such a wide range of optical designs will be illustrated, and some of the possible solutions discussed.

8147-14, Session 3

Compatibility of silicon pore optics with launchers and operation conditions

M. D. Ackermann, M. J. Collon, cosine Research B.V. (Netherlands); C. van Baren, SRON Nationaal Instituut voor Ruimteonderzoek (Netherlands); R. Günther, R. Partapsing,

**Conference 8147:
Optics for EUV, X-Ray, and Gamma-Ray Astronomy V**

cosine Research B.V. (Netherlands); D. Kampf, K. Zuknik, Kayser-Threde GmbH (Germany); E. Wille, M. Bavdaz, European Space Research and Technology Ctr. (Netherlands)

In this paper, we present the first results of vibration and thermal testing of Silicon Pore Optics (SPO). Silicon pore optics are one of the main candidates for forming the optics of a number of future spaced based X-ray observatories, the largest of which is the International X-ray Observatory (IXO). The main requirement for the optics is to combine a low weight with a very high optical resolution (5"). In order to guarantee this resolution once the optics are launched into space, one needs a very good understanding of the thermal and mechanical behavior under the expected conditions, such as in-orbit operation, or the (non-operational) conditions of a rocket launch. To gain confidence in the behavior of SPO under these harsh mechanical and thermal conditions, a series of finite element (FE) models have been developed. These models are used to predict the mechanical and optical response of the optics to the applied stresses. In parallel to the development of the FE models, a series of vibration and thermal test have been carried out. The results of these first series of environmental tests have been compared to the predicted behavior, and the models have been refined to correctly mimic the results found during the real life tests. With these models, we can now confidently predict the behavior of the optics under different conditions, and show that the optics are capable surviving a rocket launch, and resolve 5" in orbit.

8147-15, Session 4**Fabrication and metrology of the NuSTAR flight optics**

W. W. Craig, Univ. of California, Berkeley (United States) and Lawrence Livermore National Lab. (United States); H. An, K. L. Blaedel, Columbia Univ. (United States); F. E. Christensen, Technical Univ. of Denmark (Denmark); T. A. Decker, Columbia Univ. (United States); J. Gum, NASA Goddard Space Flight Ctr. (United States); C. J. Hailey, L. C. Hale, Columbia Univ. (United States); C. P. Jensen, Technical Univ. of Denmark (Denmark); J. Koglin, K. Mori, M. Nynka, Columbia Univ. (United States); M. V. Sharpe, NASA Goddard Space Flight Ctr. (United States); M. Stern, G. Tajiri, Columbia Univ. (United States); W. W. Zhang, NASA Goddard Space Flight Ctr. (United States)

We describe the fabrication of the NuSTAR flight optics. The NuSTAR optics are a glass-graphite-epoxy composite structure previously utilized on the HEFT balloon experiment but employed for the first time in space-based X-ray optics by NuSTAR. The optics are produced with custom designed assembly machines. The fabrication employs a novel approach - error correcting monolithic assembly and alignment - to ensure that there is no stack up error in the optics fabrication. The normal, tedious optical alignment of shells is replaced with precision mechanical assembly confirmed with in situ metrology of mounted glass pieces. Other details crucial to the performance of the optics such as epoxy application, outgassing, thermal creep, strength testing of various optics components and environmental testing will also be discussed. Figure measurements obtained with back surface mechanical metrology of mounted glass shells will be compared with X-ray measurements and with predictions based on initial glass figure and other factors contributing to the optics point spread response.

8147-16, Session 4**NuSTAR ground calibration: the Rainwater Memorial Calibration Facility (RaMCAf)**

N. F. Brejnholt, F. E. Christensen, DTU Space (Denmark); C. J. Hailey, J. Koglin, Columbia Univ. (United States)

The Nuclear Spectroscopic Telescope Array (NuSTAR) is a NASA Small Explorer mission that will carry the first focusing hard X-ray (5-80keV) telescope to orbit. The ground calibration of the three flight optics was carried out at the Rainwater Memorial Calibration Facility (RaMCAf) built for this purpose.

In this article we present the facility and its use for the ground calibration of the three optics.

8147-17, Session 4**First results from the ground calibration of the NuSTAR flight optics**

J. Koglin, H. An, Columbia Univ. (United States); D. Barret, Institut de Recherche en Astrophysique et Planétologie (France); N. M. Barrière, Univ. of California, Berkeley (United States); K. L. Blaedel, Columbia Univ. (United States); N. F. Brejnholt, F. E. Christensen, DTU Space (Denmark); T. A. Decker, Columbia Univ. (United States); W. W. Craig, Univ. of California, Berkeley (United States) and Lawrence Livermore National Lab. (United States); B. W. Grefenstette, California Institute of Technology (United States); C. J. Hailey, Columbia Univ. (United States); F. A. Harrison, California Institute of Technology (United States); A. C. Jakobsen, C. P. Jensen, DTU Space (Denmark); K. K. Madsen, California Institute of Technology (United States); K. Mori, M. Nynka, Columbia Univ. (United States); M. J. Pivovarov, Lawrence Livermore National Lab. (United States); A. Ptak, NASA Goddard Space Flight Ctr. (United States); C. Sleator, Columbia Univ. (United States); J. K. Vogel, Lawrence Livermore National Lab. (United States); P. von Ballmoos, Centre d'Etude Spatiale des Rayonnements (France); N. J. S. Westergaard, DTU Space (Denmark); D. R. Wik, NASA Goddard Space Flight Ctr. (United States); D. L. Windt, Columbia Univ. (United States); W. W. Zhang, NASA Goddard Space Flight Ctr. (United States)

We describe initial results from the ground calibration of the NuSTAR flight optics. NuSTAR is a hard X-ray satellite experiment to be launched in 2012. Two optics with 10.15 m focal length focus X-rays with energies between 6 and 79 keV onto CdZnTe detectors located at the end of an extendible mast.

Analysis will be presented on the angular resolution and effective area of the flight optics. The X-ray data was acquired at the Rainwater Memorial Calibration Facility (RaMCAf) at Columbia University. RaMCAf has an X-ray source located approximately 150 meters from the NuSTAR optics, and provides X-rays up to nearly 100 keV. A variety of detectors including a Silicon Drift detector, a Germanium spectrometer and a phosphor-imaging CCD camera are available for diagnostics. Results for the angular resolution will be compared with ray trace predictions of performance based on mechanical stylus metrology of the glass obtained during construction of the optics, and laser interferometry of the glass pieces obtained prior to mounting. The effective area of the optics will be compared with predictions based on a detailed optics and detector response model, augmented by reflectivity measurements on witness samples.

8147-18, Session 4**X-ray optics for the IXO mission and beyond**

W. W. Zhang, NASA Goddard Space Flight Ctr. (United States)

X-ray optics is essential to the advancement of x-ray astronomy. Currently operating missions and upcoming missions have set the optics technology bar for future missions like IXO. In this paper we report technical progress that has been achieved in recent years toward meeting IXO requirements, with emphasis on fabrication of mirror

Conference 8147:
Optics for EUV, X-Ray, and Gamma-Ray Astronomy V

segments. We will also report on a plan and strategy on how to meet IXO requirements in the next few years so that a rigorous implementation schedule and cost estimate can be made in time for IXO to enter the next decadal survey. Toward the end of this presentation we will attempt to go beyond IXO requirements to look into the possibility of making x-ray optics with angular resolutions better than 1" and effective areas well above 1 m².

8147-19, Session 4

IXO glass mirrors development in Europe

G. Pareschi, M. Ghigo, O. Citterio, M. M. Civitani, L. Proserpio, P. Conconi, G. Tagliaferri, A. Zambra, S. Basso, D. Spiga, INAF - Osservatorio Astronomico di Brera (Italy); G. Parodi, F. Martelli, BCV Progetti S.r.l. (Italy); D. Gallieni, M. Tintori, A.D.S. International S.r.l. (Italy); M. Bavdaz, E. Wille, European Space Research and Technology Ctr. (Netherlands)

The mirrors of the International X-ray Observatory (IXO) consist of a large number of high quality segments delivering a spatial resolution better than 5 arcsec. A study concerning the slumping of thin glass foils for the IXO mirrors is under development in Europe, funded by ESA and led by the Brera Observatory. After a preliminary trade-off study, we have focused the effort on the "Direct" slumping approach, based on the use of convex moulds. In this case during the thermal cycle the optical surface of the glass is in direct contact with the mould surface. The thin plates are made of thin glass sheets (0.4 mm thick), with a reflecting area of 200 mm x 200 mm. The adopted integration process foresees the use of reinforcing ribs for bonding together the plates and forming in that way a rigid and stiff stack of segmented mirror shells; the stack is supported by a thick backplane. During the bonding process the plates are constrained to stay in close contact with the surface of the master (i.e. the same mould used for the hot slumping process) by the application of a vacuum pump suction. In this way the spring-back deformations and low frequency errors still present on the foil profile after slumping can be corrected. In this paper we will give an overview and a status report of the project.

8147-20, Session 4

Production of the IXO glass segmented mirrors by hot slumping with pressure assistance: tests and results

M. Ghigo, INAF - Osservatorio Astronomico di Brera (Italy); L. Proserpio, INAF - Osservatorio Astronomico di Brera (Italy) and Univ. Degli Studi dell'Insubria (Italy); S. Basso, INAF - Osservatorio Astronomico di Brera (Italy); M. Bavdaz, European Space Research and Technology Ctr. (Netherlands); O. Citterio, INAF - Osservatorio Astronomico di Brera (Italy); M. M. Civitani, INAF - Osservatorio Astronomico di Brera (Italy) and Univ. Degli Studi dell'Insubria (Italy); P. Conconi, INAF - Osservatorio Astronomico di Brera (Italy); F. Martelli, BCV Progetti S.r.l. (Italy); R. Negri, G. Pagano, INAF - Osservatorio Astronomico di Brera (Italy) and Politecnico di Milano (Italy); G. Pareschi, INAF - Osservatorio Astronomico di Brera (Italy); G. Parodi, BCV Progetti S.r.l. (Italy); D. Spiga, L. Raimondi, INAF - Osservatorio Astronomico di Brera (Italy); L. Terzi, INAF - Osservatorio Astronomico di Brera (Italy) and Politecnico di Milano (Italy); E. Wille, European Space Research and Technology Ctr. (Netherlands); A. Zambra, INAF - Osservatorio Astronomico di Brera (Italy)

The Astronomical Observatory of Brera (INAF-OAB), with the support of ESA, is involved in the study of a glass shaping technology for the

production of the IXO grazing incidence segmented optics. This paper reports on the production by means of hot slumping technology with pressure of the mirror plates that are produced for the realization of prototypes. In particular, a new experimental set-up is described. In order to optimize the slumping process, in addition to Fused Silica (already investigated in the past) two new materials are considered for making the convex slumping mould: Zerodur K20 and Silicon. We will report on the latest performed slumping tests and results.

8147-21, Session 4

Fabrication update on non-contact mirror slumping technology for the International X-ray Observatory mirrors

A. M. Al Hussein, M. L. Schattensburg, R. K. Heilmann, Massachusetts Institute of Technology (United States)

Glass sheets with high surface quality and angular resolution of 5 arcsec are in demand for the International X-Ray Observatory. A method of thermally shaping individual sheets of glass using porous mandrels as air bearings has been developed which eliminates the problems of sticking and dust particle-induced distortion which plague traditional slumping methods. Initial experiments have focused on the shaping of flat sheets. A detailed mathematical model of the process has been developed, allowing prediction of final surface quality based on process parameters including air pressure, glass thickness variations and orientation of the gravity vector during the process. Improvements over earlier surface quality results are reported through achieving feedback control of process pressure, and issues with the repeatability of these results are investigated and addressed through the next generation of our slumping platform.

The design process and fabrication of our new slumping facility will be presented. In addition to scaling the design to accommodate larger flats, slumps are horizontally to float the glass and minimize contact during the process. New capabilities also include active gap control and air-flow temperature control. Preliminary results of slumped glass with the new platform will be presented for different process parameters.

8147-22, Session 5

Design and analysis of mirror modules for IXO and beyond

R. S. McClelland, Stinger Ghaffarian Technologies, Inc. (United States); C. Powell, NASA Goddard Space Flight Ctr. (United States)

Advancements in X-ray astronomy demand thin, light, and closely packed optical elements which lend themselves to segmentation of the annular mirrors and, in turn, a modular approach to the mirror design. A baseline modular concept for the International X-Ray Observatory (IXO) Soft X-Ray Telescope (SXT) consisting of 14,000 segmented glass mirrors divided into 60 modules was developed and extensively analyzed. Through this development, our understanding of module loads, mirror stress, shock sensitivity, thermal performance, and gravity distortion have greatly progressed. The latest progress in each of these areas is discussed herein. Gravity distortion during horizontal X-ray testing, on-orbit thermal performance, and accommodation of large mirror spans have proved especially difficult design challenges. In light of these challenges, fundamental trades in modular X-ray mirror design have been performed. Based on the driving requirements of minimal distortion during horizontal X-ray testing and launch mass, an alternate FMA design utilizing smaller modules was developed and analyzed. This alternate design better accommodates horizontal X-ray testing, improves thermal performance, and allows for the use of smaller mirror segments while maintaining the required FMA mass. The cost and production schedule implications of fabricating a larger number of smaller modules were explored. Smaller modules have significant advantages in mass production but increase the effort required to align modules into the FMA structure.

8147-23, Session 5

Alignment and integration of lightweight mirror segments

T. C. Evans, Stinger Ghaffarian Technologies, Inc. (United States); K. C. Chan, Univ. of Maryland, Baltimore County (United States); J. Mazzarella, Stinger Ghaffarian Technologies, Inc. (United States); T. T. Saha, NASA Goddard Space Flight Ctr. (United States)

The International X-Ray Observatory (IXO) observatory has requirements of effective area of 2.5 square meters combined with an angular resolution of five arc-seconds. To accomplish both of these goals, thin glass optics must be used to minimize weight and observatory size. The challenge of constraining thin optics without distortion is being investigated. Two separate approaches are being studied, using actuators to form the mirror into a desired shape at the Smithsonian Astrophysical Observatory (SAO), and preserving the fabricated mirror without distortion at NASA's Goddard Space Flight Center (GSFC). The latter approach focuses on minimizing distortion added during alignment and bonding of the mirror segment to the permanent housing. Within GSFC, two separate strategies are being pursued simultaneously with one focusing on bonding flat tabs on the back surface of the optic and the other focusing on bonding small pins to the side edges of the optic. Both technologies are proving to show promise going through many test cycles culminating in x-ray test results. Based on current error budget allocation and future goals, technology development will continue paving the way towards demonstrating thin glass optics capabilities.

8147-24, Session 5

Design of the IXO optics based on thin glass plates connected by reinforcing ribs

M. Ghigo, S. Basso, INAF - Osservatorio Astronomico di Brera (Italy); M. Bavdaz, European Space Research and Technology Ctr. (Netherlands); O. Citterio, INAF - Osservatorio Astronomico di Brera (Italy); M. M. Civitani, INAF - Osservatorio Astronomico di Brera (Italy) and Univ. degli Studi dell'Insubria (Italy); P. Conconi, INAF - Osservatorio Astronomico di Brera (Italy); F. Martelli, BCV Progetti S.r.l. (Italy); G. Pareschi, INAF - Osservatorio Astronomico di Brera (Italy); G. Parodi, BCV Progetti S.r.l. (Italy); L. Proserpio, INAF - Osservatorio Astronomico di Brera (Italy) and Univ. degli Studi dell'Insubria (Italy); D. Spiga, INAF - Osservatorio Astronomico di Brera (Italy); E. Wille, European Space Research and Technology Ctr. (Netherlands); A. Zambra, INAF - Osservatorio Astronomico di Brera (Italy)

Effective area requirements for the large X-ray mirror of the International X-ray Observatory (IXO) are about 3 m² at 1keV, 0.65 m² at 6 keV and 150 cm² at 30 keV. Because of its large dimension, the telescope cannot be realized as a monolithic structure but rather it requires the integration and assembly in the telescope optical bench of a number of basic module units, called X-ray Optical Unit (XOU). We are currently studying a method for the production of these basic units that is based on the slumping technology for the production of thin glass segmented mirrors. It foresees the implementation of a stacking integration concept based on the use of reinforcing ribs connecting the glass segments in order to create very stiff structures. This paper reports on the last design of the single optical module and describe the results of FEM analyses that show how it is possible to use an innovative approach to the integration of the slumped glass foils.

8147-25, Session 5

The integration machine: design, development and validation of an alternative process for the integration of slumped-glass segments into an x-ray module

M. M. Civitani, S. Basso, O. Citterio, P. Conconi, M. Ghigo, G. Pareschi, L. Proserpio, D. Spiga, G. Tagliaferri, A. Zambra, INAF - Osservatorio Astronomico di Brera (Italy); D. Gallieni, M. Tintori, A.D.S. International S.r.l. (Italy); F. Martelli, G. Parodi, BCV Progetti S.r.l. (Italy); M. Bavdaz, E. Wille, European Space Research and Technology Ctr. (Netherlands)

The International X-ray Observatory (IXO) is being studied as a joint mission by the NASA, ESA and JAXA space agencies. The main goals of the mission are large effective area (>3m² at 1 keV) and a good angular resolution (<5 arcsec HEW at 1 keV). The Brera Astronomical Observatory (Italy), under the support of ESA, is developing an alternative method for the realization of the X-Ray Optical Units, based on the use of slumped thin glass segments to form densely packed modules in a Wolter type I optical design, so that each plate pair focus x-ray onto the focal plane in two reflections. In order to reach the very challenge integration requirements, it has been developed an innovative assembly approach for aligning and mounting the IXO mirror segments, making use of glass reinforcing ribs that connect the facets to each-other and guarantee an active correction for major existing figure errors. The Integration Machine (IMA) that has been developed to allow the integration of the Plate Pairs into prototype XOU stacks. In this paper we present the design, the development and the validation status of the system. Moreover are presented the results obtained with the first integrated stack prototype, called Proof of Concept (POC) and consisting in two integrated Plate Pairs.

8147-26, Session 5

Evaluation of the epoxy for the integration of slumped-glass segments into an x-rays module

M. M. Civitani, M. Riva, G. Pagano, B. Salmaso, S. Basso, G. Pareschi, INAF - Osservatorio Astronomico di Brera (Italy); G. Parodi, F. Martelli, BCV Progetti S.r.l. (Italy)

The International X-ray Observatory (IXO) is under study as a joint mission by the NASA, ESA and JAXA space agencies. The main goals of the mission are to obtain a large effective area (>3m² at 1 keV) and a good angular resolution (<5 arcsec HEW at 1 keV). The Brera Astronomical Observatory (Italy), under the support of ESA, is developing an alternative method for the realization of the X-Ray Optical Units. Each module is assembled as a stack of thin mirror shells and spacers made of glass and glued together. Therefore the epoxy is a crucial component in determining the structural and optical performance of the X-Ray module. In this paper we describe the characterization process that has been followed to evaluate the epoxy selected for the IXO module prototype assemblies.

8147-27, Session 6

Coating design and developments for the International X-ray Observatory

A. C. Jakobsen, D. Della-Monica Ferreira, F. E. Christensen, DTU Space (Denmark); M. Krumrey, Physikalisch-Technische Bundesanstalt (Germany); B. Shortt, European Space Research and Technology Ctr. (Netherlands); M. Collon, M. D. Ackermann, cosine Research B.V. (Netherlands)

Conference 8147:
Optics for EUV, X-Ray, and Gamma-Ray Astronomy V

We present a novel coating design for the International X-ray Observatory - IXO. The design makes use of both simple bilayer coatings of Ir and B4C, more complex constant period multilayer coatings and finally graded period multilayer coatings to enhance the effective area and cover the energy range from 0.1 to 40 keV. We also present the coating technology used for these designs and present test results from coatings deposited on realistic IXO wafers and show compatibility with masking technologies on flat and bent substrates.

8147-29, Session 6

NuSTAR flight coatings: what did we really do

F. E. Christensen, A. C. Jakobsen, DTU Space (Denmark); K. K. Madsen, California Institute of Technology (United States); N. F. Brejnholt, A. Hornstrup, DTU Space (United States); A. Fabricant, Columbia Univ. (United States); N. J. S. Westergaard, DTU Space (Denmark); J. Koglin, Columbia Univ. (United States); J. Momberg, DTU Space (Denmark); W. W. Craig, M. J. Pivovarov, Lawrence Livermore National Lab. (United States); D. L. Windt, Reflective X-Ray Optics LLC (United States)

The NuSTAR mission will be the first satellite mission to carry focusing telescopes reaching into the hard X-ray band above 10 keV. This is accomplished by using depth graded multilayer coatings on thin slumped glass segments precision aligned in a double cone approximation to a Wolter I geometry. Three flight optics have been completed. Each flight optic carries 2340 mirror segments. The first flight optic was coated with W/Si and Pt/SiC multilayers, while the two subsequent flight optics were coated with W/Si and Pt/C coatings. In this paper we give the updated multilayer recipes we used in each case, describe lessons learned relating to the preparation and cleaning of the slumped glass substrates before coating, describe details of the planar magnetron sputtering technique used for the coating including uniformity and show representative data and modeling from witness samples taken at 8 keV at DTU-Space and at higher energies at the Rainwater Memorial Calibration facility (RaMCaf) at Columbia and the NSLS at Brookhaven

8147-30, Session 6

Release coatings for replication of x-ray optics

S. E. Romaine, Harvard-Smithsonian Ctr. for Astrophysics (United States); J. L. Boike, Jacobs Technology (United States); R. Bruni, Harvard-Smithsonian Ctr. for Astrophysics (United States); D. Engelhaupt, The Univ. of Alabama in Huntsville (United States); P. Gorenstein, Harvard-Smithsonian Ctr. for Astrophysics (United States); B. D. Ramsey, NASA Marshall Space Flight Ctr. (United States)

X-ray astronomy grazing incidence telescopes use the principle of nested shells to maximize the collecting area. Some of the more recent missions, such as XMM-Newton, have used an electroformed nickel replication process to fabricate the mirror shells. We have been developing coatings to simplify and improve this electroforming process.

We have reported previously on our results using flat mandrels. This paper presents our recent results on using this same process to separate uncoated replicas and replicas with multilayer coatings from Wolter-1 mandrels. We present AFM and X-ray reflectivity data on mandrels and replicas.

8147-31, Session 6

Differential deposition to correct surface figure deviations in astronomical grazing-incidence x-ray optics

K. Kilaru, B. D. Ramsey, M. V. Gubarev, NASA Marshall Space Flight Ctr. (United States)

A coating technique is being developed to correct the surface figure deviations in reflective-grazing-incidence X-ray optics. These optics are typically designed to have precise conic profiles, and any deviation in this profile, as a result of fabrication, results in a degradation of the imaging performance. To correct the mirror profiles, physical vapor deposition has been utilized to selectively deposit a filler material inside the mirror shell. The technique, termed differential deposition, has been implemented as a proof of concept on miniature X-ray optics developed at MSFC for medical-imaging applications. The technique is now being transferred to larger grazing-incidence optics suitable for astronomy and progress to date is reported.

8147-32, Session 7

A user-friendly web interface for x-ray telescopes design and simulation

V. Cotroneo, Harvard-Smithsonian Ctr. for Astrophysics (United States); D. O. Di Pasquale, CNR Istituto per le Tecnologie della Costruzione (Italy)

The design of a Wolter X-ray telescope takes into account the geometrical dimensioning of the shells and the choice of the coatings for each of them. In this work we present a user-friendly web interface aimed to the design of multi-shell Wolter telescopes and the calculation of their effective area. Some example of use cases are presented.

8147-33, Session 7

Point spread function computation of Wolter-I x-ray mirrors from surface profile and roughness

L. Raimondi, Univ. degli Studi dell'Insubria (Italy) and INAF - Osservatorio Astronomico di Brera (Italy); D. Spiga, INAF - Osservatorio Astronomico di Brera (Italy)

The mirror Point Spread Function (PSF) degradation in the X-ray band is determined by the optical quality of its focusing optics. When the surface profile is analyzed in terms of Fourier components, figure errors comprise the spectral regime of long spatial wavelengths, whilst microroughness falls in the regime of short spatial wavelengths. Usually, the first effect is simulated by means of geometrical optics, while the second contribution - strongly dependent on the energy of X-rays - is derived from the first order scattering theory. This classical approach, however, suffers from some uncertainties in the determination of the boundary of the two regimes.

The aim of this work is to overcome this limitation and compute the PSF of an X-ray mirror shell in a typical Wolter-I configuration at any energy, given the complete surface topography. The adopted method applies the Huygens-Fresnel principle to the measured/simulated profiles and fully accounts for the surface roughness PSD (Power-Spectral-Density). We already applied this method to single reflection mirrors. In this work, we extend it to the case of Wolter-I mirror shells.

We present the PSF simulations at several energies, from the UV band (dominated by aperture diffraction) to hard X-rays (dominated by scattering). In particular, we analyze the impact of different spatial regimes on the PSF degradation as a function of energy in the X-ray and UV bands. Our results are in full agreement with ray-tracing simulations and with analytical results based on scattering theory (where these

Conference 8147:
Optics for EUV, X-Ray, and Gamma-Ray Astronomy V

approaches are applicable). Moreover, we analyze the aperture diffraction contribution in the UV band and study how different spatial regimes contribute to the Half Energy Width of the PSF. Finally we compare our predictions with the PSF of a real mirror shell.

8147-34, Session 7

Right-sizing the mirror segment for x-ray optics

M. Biskach, NASA Goddard Space Flight Ctr. (United States)

The flight mirror assembly (FMA) for the International X-Ray Observatory (IXO) consists of 14,000 mirrors that reflect incoming X-Rays at a small grazing angle to the onboard instruments and detectors. The 0.4 mm thick mirror segments require precise alignment and secure final placement with a low amount of distortion to meet IXO requirements. Mirror size affects how the mirrors are supported throughout the metrology, alignment, and bonding stages. Larger size mirrors are more susceptible to distortions caused by gravity and other factors which in part ultimately determine the final performance characteristics of the IXO FMA. This paper outlines a comprehensive study using Finite Element Analysis (FEA) on the size of the X-Ray optics currently used for IXO to determine the optimal size of mirrors that balances the amount of distortion introduced in the handling and bonding processes with outside factors such as module size, equipment / facility factors, and mirror fabrication. A broad list of considerations is also presented for optics sizing related to future X-Ray missions that will have increasingly stringent optical requirements.

8147-35, Session 8

Forming mandrels for x-ray mirror substrates

P. N. Blake, T. T. Saha, W. W. Zhang, NASA Goddard Space Flight Ctr. (United States); S. L. O'Dell, T. J. Kester, W. D. Jones, Marshall Space Flight Ctr. (United States)

Future x-ray astronomical missions, like the International X-ray Observatory (IXO), will likely require replicated mirrors to reduce both mass and production costs. Accurately figured and measured mandrels - upon which the mirror substrates are thermally formed - are essential to enable these missions. The challenge of making these mandrels within reasonable costs and schedule has led the Goddard and Marshall Space Flight Centers to develop in-house processes and to encourage small businesses to attack parts of the problem. Both Goddard and Marshall have developed full-aperture polishing processes and metrologies that yield high-precision axial traces of the finished mandrels. Outside technologists have been addressing challenges presented by subaperture CNC machining processes: particularly difficult is the challenge of reducing mid-spatial frequency errors below 2 nm rms. The end-product of this approach is a realistic plan for the economically feasible production of mandrels that meet program requirements in both figure and quantity.

8147-36, Session 8

Progress on precise grinding and polishing of thin-glass monolithic shell

O. Citterio, G. Motta, V. Cotroneo, M. M. Civitani, L. Proserpio, G. Pareschi, INAF - Osservatorio Astronomico di Brera (Italy); E. Mattaini, INAF - IASF Milano (Italy); P. Conconi, INAF - Osservatorio Astronomico di Brera (Italy); J. Arnold, LT Ultra Precision Technology GmbH (Germany); G. Parodi, BCV Progetti S.r.l. (Italy)

The production of lightweight, thin monolithic shells for high angular resolution X-ray telescopes requires the use of a material with good

mechanical and thermal properties, easy to sustain optical grinding and polishing and available on the market. Fused Silica satisfies these requirements and it has been selected for the present investigation. The challenge manufacturing process of thin (<2 mm for 500 mm diameter) glass Wolter-I like shells is to reach a precise profile (<1 micron shape error) with a very low surface microroughness (<0,1 nm) and avoiding the presence of subsurface damages which could increase the brittleness of the glass. Starting from a double cone profile quartz glass tube a sequence of grinding, fine grinding and polishing processes is performed in order to progressively reach the desired quality of the shell. This process needs a very stiff and precise CNC machine and a good metrology system. On the other hand the shape and the thinness of the concerned shell introduce a series of bending related problems. This paper reports on the development activities on going at OAB to set this kind of process.

8147-37, Session 8

Progress on the magnetic field-assisted finishing of MEMS micropore x-ray optics

R. E. Riveros, M. A. Tan, H. Yamaguchi, Univ. of Florida (United States); I. Mitsuishi, Japan Aerospace Exploration Agency (Japan); K. Ishizu, T. Moriyama, T. Ogawa, Y. Ezoe, Tokyo Metropolitan Univ. (Japan); M. Horade, S. Sugiyama, Ritsumeikan Univ. (Japan); Y. Kanamori, Tohoku Univ. (Japan); N. Yamasaki, K. Mitsuda, Japan Aerospace Exploration Agency (Japan)

Microelectromechanical systems (MEMS) micropore X-ray optics were proposed as an ultralightweight, high-resolution, and low cost X-ray focusing optic alternative to the large, heavy and expensive optic systems in use today. Their monolithic design which includes high-aspect ratio curvilinear micropores with minimal sidewall roughness has proved difficult to realize. When made by either deep reactive ion etching or X-ray LIGA, the micropore sidewalls (reflecting surfaces) exhibit unacceptably high surface roughness. A magnetic field-assisted finishing (MAF) process was proposed to reduce the micropore sidewall roughness of MEMS micropore optics and improvements in roughness have been reported. At this point, the best surface roughness achieved is ~3 nm Rq on nickel optics and ~0.2 nm Rq on silicon optics. These improvements bring MEMS micropore optics closer to their realization as functional X-ray optics. This paper details the manufacturing and post-processing of MEMS micropore X-ray optics including results of recent polishing experiments with MAF.

8147-38, Session 9

Metrology of IXO mirror segments

K. C. Chan, NASA Goddard Space Flight Ctr. (United States)

The high angular resolution of 5" (half-power diameter) for the International X-ray Observatory (IXO) is to be achieved with lightweight modular optics compactly populated with thin mirror segments. The resolution requirement posts unique challenges for fabrication, mounting and metrology of these segments. In this paper, we shall discuss the metrology of a single pair of these segments. We shall present our current metrological methods, prediction of the performance, and measurements of the state-of-the-art segments of which the performance of single bonded pairs approaches 5". We also address our approach in metrology for future optics beyond 5".

8147-39, Session 9

Grazing incidence wavefront sensing and verification of x-ray optics performance

T. T. Saha, S. Rohrbach, W. W. Zhang, NASA Goddard Space Flight Ctr. (United States)

Conference 8147:
Optics for EUV, X-Ray, and Gamma-Ray Astronomy V

Evaluation of interferometrically measured mirror metrology data and characterization of a telescope wavefront can be powerful tools in understanding of image characteristics of an x-ray optical system. In the development of soft x-ray telescope for the International X-Ray Observatory (IXO), we have developed new approaches to support the telescope development process.

Interferometrically measuring the optical components over all relevant spatial frequencies can be used to evaluate and predict the performance of an x-ray telescope. Typically, the mirrors are measured in a mount that minimizes the mount and gravity induced errors. In the assembly and mounting process the shape of the mirror segments can dramatically change. We have developed wavefront sensing techniques suitable for the x-ray optical components to aid us in the characterization and evaluation process of these changes.

Hartmann sensing of a telescope and its components is a simple method that can be used to evaluate low order mirror surface errors and alignment errors. Phase retrieval techniques can also be used to assess and estimate the low order axial errors of the primary and secondary mirror segments.

In this paper we describe the mathematical foundation of our Hartmann sensing technique and phase retrieval technique. We show how these techniques can be used in the evaluation and performance prediction process of x-ray telescopes.

8147-40, Session 9

MPR: innovative 3D free-form optics profilometer

G. Sironi, O. Citterio, INAF - Osservatorio Astronomico di Brera (Italy) and Media Lario Technologies (Italy); A. Ritucci, R. Subranni, Media Lario Technologies (Italy); M. Stroebel, LT Ultra Precision Technology GmbH (Germany); G. Borghi, A. Orlandi, Media Lario Technologies (Italy); R. Widemann, LT Ultra Precision Technology GmbH (Germany); G. Pareschi, INAF - Osservatorio Astronomico di Brera (Italy); B. M. Negri, Agenzia Spaziale Italiana (Italy)

This paper presents the huge advance in metrology represented by a new free-form profilometer/rotodimeter (MPR). This metrological machine was developed by Media Lario Technologies and LT-Ultra Precision Technology in the frame of the Italian Space Agency (ASI) contract for the manufacturing of a New Hard X-ray Mission (NHXM) optical module prototype. The need of a new high performances metrological machine is a direct consequence of the tightening of the tolerance on hard X-ray optics shape errors. In the case of NHXM the aim to maintain an angular resolution of 15 arcsec up to 30 keV implies a requirement for the optics shape error of maximum 100 nm on dynamical range of the whole optics, up to 600 mm.

The realized MPR is a non-contact versatile machine respecting these specifications, with the capability to measure a large variety of optics with free-form profile, from the cylindrical-like shapes for grazing incidence optics to normal incidence geometries.

A solid mechanical design based on the use of stable X-Y hydrostatic bearings combined with a high resolution optical detection unit, i.e. a chromatic optical sensor and laser interferometers, allows the achievement of low noise level and high profile measurement repeatability.

These characteristics make the MPR extremely precise and accurate, inasmuch as measurements can be acquired in flight at relatively high speed maintaining the shape error below 100 nm.

The paper is organized as follows: firstly, a brief description of the hard X-ray astronomy context and the requirements settled for the related optics is given (Section 1). Secondly, a description of the MPR design and operation is shown (Section 2). Finally, the experimental results are presented (Section 3). In conclusion, a synthesis of the achieved metrological innovation is shown (Section 4).

8147-41, Session 9

Development of multi-beam long trace profiler

K. Kilaru, NASA Marshall Space Flight Ctr. (United States); D. J. Merthe, Z. Ali, Lawrence Berkeley National Lab. (United States); M. V. Gubarev, T. J. Kester, NASA Marshall Space Flight Ctr. (United States); W. R. McKinney, Lawrence Berkeley National Lab. (United States); P. Z. Takacs, Brookhaven National Lab. (United States); V. V. Yashchuk, Lawrence Berkeley National Lab. (United States)

In order to fulfill the angular resolution requirements and make the performance goals for future NASA missions feasible, it is crucial to develop instruments capable of fast and precise figure metrology of x-ray optical elements for further correction of the surface errors. The Long Trace Profilometer (LTP) is an instrument widely used for measuring the surface figure of grazing incidence X-ray mirrors. In the case of replicated optics designed for x-ray astronomy applications, such as mirrors and the corresponding mandrels have a cylindrical shape and their tangential profile is parabolic or hyperbolic. Modern LTPs have sub-microradian accuracy, but the measuring speed is very low, because the profilometer measures surface figure point by point using a single laser beam. The measurement rate can be significantly improved by replacing the single optical beam with multiple beams. The goal of this study is to demonstrate the viability of multi-beam metrology as a way of significantly improving the quality and affordability of replicated x-ray optics. The multi-beam LTP would allow one- and two-dimensional scanning with sub-microradian resolution and a measurement rate of about ten times faster compared to the current LTP. The design details of the instrument's optical layout and the status of optical tests will be presented.

8147-61, Poster Session

The current status of reflector production and hard x-ray characterization for ASTRO-H/HXT

T. Miyazawa, A. Furuzawa, Y. Kanou, K. Matsuda, M. Sakai, N. Yamane, H. Kato, Y. Miyata, K. Sakanobe, M. Sasaki, T. Yamagishi, Y. Haba, K. Ishibashi, H. Matsumoto, Y. Tawara, H. Kunieda, Nagoya Univ. (Japan); N. Ishida, A. Suzuki, Tamagawa Engineering Co., Ltd. (Japan); N. Ohtsu, Tamagawa Engineering Co., Ltd. (Japan); H. Mori, K. Tamura, Y. Maeda, M. Ishida, Japan Aerospace Exploration Agency (Japan); H. Awaki, Ehime Univ. (Japan); T. Okajima, NASA Goddard Space Flight Ctr. (United States); K. Uesugi, Y. Suzuki, Japan Synchrotron Radiation Research Institute (Japan)

Japan's sixth X-ray satellite mission ASTRO-H, which is planned to be launched in 2014, is designed to carry four science payloads to cover the wide energy range between 0.3 keV to 600 keV. One of the key instruments is Hard X-ray Telescope (HXT) to cover hard X-rays up to 80 keV. The HXT is thin-foil, multi-nested conical optics as well as Suzaku XRT. To reflect hard X-rays efficiently, reflector surfaces are coated with depth-graded Pt/C multilayer. The diameter and focal length are 450 mm and 12000 mm, respectively. We need to fabricate more than 5000 foil reflectors for the two flight telescopes in consideration of yield ratio of 50 %. The mass production of the reflectors for the flight model has been going on since August 2010. The screening of replication mandrels with profilometer is ongoing. In addition, we have introduced new screening method with optical image reflected from mandrel surface. We have adopted new type replication mandrel, we called "glass coated mandrel", which consists of glass tube coated with thin glass sheet for large size mandrels. The selected 74 pairs of multilayer mirrors which consist of six bands (13 pairs at 65 mm and 90 mm, 15 pairs at 100 mm and 120 mm, 10 pairs at 135 mm, 8 pairs at 160 mm in radius, respectively) have been characterized at a large synchrotron radiation facility, SPring-8 beamline

**Conference 8147:
Optics for EUV, X-Ray, and Gamma-Ray Astronomy V**

BL20B2. We present the current status of reflector production and hard x-ray characterization for HXT.

8147-62, Poster Session**New multilayer design for ASTRO-H/hard x-ray telescope and missions beyond**

Y. Miyata, H. Kunieda, Nagoya Univ. (Japan); K. Tamura, Japan Aerospace Exploration Agency (Japan)

Japan's sixth X-ray satellite missions, ASTRO-H, features two hard X-ray telescopes with depth-graded, multilayer reflectors. Our laboratory has advanced the technology for multilayer reflectors through development of a balloon-borne experiment, InFOCuS. While its base model for the multilayer design (with the minimum incident angle of 0.11 degrees and 8m focal length) is adequate for the ASTRO-H mission, we opt to improve it further so that better performance can be derived with the minimum incident angle of 0.07 degrees and 12m focal length. The improved design has resulted in the reduction of layers from 28 to 10-21 layers per reflector while gaining higher reflectivity by 3-5% at 40-70 keV.

A multilayer optics will be used in IXO, a joint project by NASA, ESA and JAXA. IXO's principal design requires its energy bandpass of 0.1-40 keV with the minimum incident angle of 0.18 degrees and 20m focal length. With the narrower bandpass and the larger incident angles, it necessitates following changes in the multilayer design: adjustment of top Pt layer thickness and a total number of top layers to boost reflectivity (especially in the lower energy band), and refinement of Pt/C-layer spacing and depth-graded period below the third layer to bunch up the Bragg peaks tightly in the required hard X-ray band. In this presentation, we discuss the key parameters for IXO's multilayers to achieve a larger effective area at 30-40 keV.

8147-63, Poster Session**Mathematical formalism for designing wide-field x-ray telescopes: mirror nodal positions and detector tilts**

R. F. Elsner, S. L. O'Dell, B. D. Ramsey, M. C. Weisskopf, NASA Marshall Space Flight Ctr. (United States)

We report on the present status of our continuing efforts to develop a method for optimizing wide-field nested x-ray telescope mirror prescriptions. Utilizing extensive Monte-Carlo ray trace simulations, we find an analytic form for the root-mean-square dispersion of rays from a Wolter I optic on the surface of a flatfocal plane detector as a function of detector tilt away from the nominal focal plane and detector displacement along the optical axis. The configuration minimizing the ray dispersion from a nested array of Wolter I telescopes is found by solving a linear system of equations for tilt and individual mirror pair displacement. Finally we outline our initial efforts at expanding this method to include higher order polynomial terms in the mirror prescriptions.

8147-64, Poster Session**MT_RAYOR: a versatile raytracing tool for x-ray telescopes**

N. J. S. Westergaard, Technical Univ. of Denmark (Denmark)

A raytracing tool, MT_RAYOR, for the analysis of X-ray telescopes based on the Wolter-1 design and approximations has been developed in the Yorick interpreted language. The optical properties of the reflecting surfaces are modelled by coefficients of reflection and tables for the micro-roughness scattering so that there is no model dependency involved. Mirror deformations on a length scale larger than 1 mm may be included. The photon source can be a celestial point source with

a given spectrum and additional functions make the simulation of extended sources rather straightforward. The detector properties such as pixellation, RMF, and quantum efficiency can be added to simulate a complete observation. An X-ray source of any shape at a finite distance for the simulation of calibration experiments can also be modelled. Results from preliminary analyses of the Indian SXT on Astrosat, NuSTAR, and IXO are presented.

8147-65, Poster Session**Accurate modeling of the x-ray multilayer scattering from surface microroughness characterization**

B. Salmaso, D. Spiga, R. Canestrari, L. Raimondi, INAF - Osservatorio Astronomico di Brera (Italy)

Several hard X-ray imaging telescopes of the next future will be characterized by a high angular resolution. To this end, it is necessary to produce optics with a very low surface microroughness, as this is responsible of X-ray scattering, which results in image quality degradation especially at the higher energies. To the smooth surface approximation, it is possible to compute the X-Ray Scattering (XRS) from the Power Spectral Density (PSD) of the surface roughness. Indeed, multilayers coatings will be used to reflect X-rays beyond 10 keV; in this case the scattering pattern is more complicated but it can still be computed from the PSDs of each interface and the cross-correlation functions of the rough profiles. A growth model able to describe the roughness evolution of the surfaces enables us to compute the XRS of the multilayer, which can be directly compared to the experimental data. With this approach we aim to validate the roughening model assumed and to accurately predict the scattering pattern we expect on the focal plane. In this work we show the application of this formalism: direct measurements of the PSDs for substrates and the outermost layer of several multilayers samples are used as input for the code to model the PSD growth. XRS measurements of these samples, performed at the energy of 8.05 keV, are presented to validate the modeling achieved.

8147-66, Poster Session**The Marshall grazing incidence x-ray spectrograph (MaGIXS)**

K. Kobayashi, The Univ. of Alabama in Huntsville (United States); J. Cirtain, NASA Marshall Space Flight Ctr. (United States); L. Golub, E. Hertz, P. Cheimets, D. Caldwell, K. Korreck, Harvard-Smithsonian Ctr. for Astrophysics (United States); B. M. Robinson, P. Reardon, The Univ. of Alabama in Huntsville (United States); T. J. Kester, C. Griffith, M. R. Young, NASA Marshall Space Flight Ctr. (United States)

The Marshall Grazing Incidence X-ray Spectrograph (MaGIXS) is a stigmatic grazing-incidence spectrograph experiment designed to observe spatially resolved soft X-ray spectra of the solar corona for the first time. The instrument consists of a Wolter Type-1 sector telescope and a slit spectrograph. The telescope mirror pair is a monolithic Zerodur mirror with both the parabolic and hyperbolic surfaces. The spectrograph comprises a pair of paraboloid mirrors acting as a collimator and re-imaging mirror, and a planar varied-line-space grating, with reflective surfaces operate at a graze angle of 2 degrees. This produces a flat spectrum on a detector covering a wavelength range of 0.6 to 2.4 nm (0.5 to 2.0 keV). The design achieves 1.5 pm spectral resolution and 5 arcsec spatial resolution (2.5 arcsec / pixel) over an 8 arcminute long slit. The spectrograph is currently being fabricated as a laboratory prototype. A flight candidate telescope mirror is also under development. The entire experiment is designed to fit a NASA sounding rocket payload, and is being proposed for flight.

Conference 8147:
Optics for EUV, X-Ray, and Gamma-Ray Astronomy V

8147-68, Poster Session

Development of a EUV test facility at the Marshall Space Flight Center

E. A. West, S. Pavelitz, NASA Marshall Space Flight Ctr. (United States); K. Kobayashi, B. M. Robinson, The Univ. of Alabama in Huntsville (United States); J. Cirtain, J. A. Gaskin, A. Winebarger, NASA Marshall Space Flight Ctr. (United States)

This paper will describe a new EUV test facility that is being developed at the Marshall Space Flight Center (MSFC) to test EUV telescopes. Two flight programs, HiC - high resolution coronal imager (sounding rocket) and SUVI - Solar Ultraviolet Imager (GOES-R), set the requirements for this new facility. This paper will discuss those requirements, the EUV source characteristics, the wavelength resolution that is expected and the vacuum chambers (Stray Light Facility, Xray Calibration Facility and the EUV test chamber) where this facility will be used.

8147-43, Session 10

Laue lenses for hard x- and gamma-ray: new prototype results

F. Frontera, Univ. degli Studi di Ferrara (Italy); V. Liccardo, Univ. degli Studi di Ferrara (Italy) and Univ. de Nice Sophia Antipolis (France); G. Loffredo, Univ. degli Studi di Ferrara (Italy); V. Valsan, Univ. degli Studi di Ferrara (Italy) and Univ. de Nice Sophia Antipolis (France); E. Virgilli, V. Carassiti, F. Evangelisti, Univ. degli Studi di Ferrara (Italy); S. Squerzanti, A. Cotta Ramusino, Istituto Nazionale di Fisica Nucleare (Italy); E. Caroli, J. B. Stephen, INAF - IASF Bologna (Italy)

Laue lenses are the most efficient technique to focus hard X-rays above 70-100 keV. We report on new results on the development activity of broad band Laue lenses for hard X-/gamma-ray astronomy (70/100-600 keV).

After the development of first prototype, whose building method and performance was presented at the SPIE conference on Astronomical Telescopes (Frontera et al. 2008), we have improved the lens assembling technology. We present the results obtained from the new prototype and we will also show results obtained in terms of focal spot with respect to the theoretical expectations.

8147-44, Session 10

The LAUE project for broadband gamma-ray focusing lenses

E. Virgilli, F. Frontera, C. Guidorzi, Univ. degli Studi di Ferrara (Italy); V. Liccardo, Univ. degli Studi di Ferrara (Italy) and Universite' de Nice - Sophia Antipolis (France); G. Loffredo, Univ. degli Studi di Ferrara (Italy); V. Valsan, Univ. degli Studi di Ferrara (Italy) and Universite' de Nice - Sophia Antipolis (France); V. Carassiti, F. Evangelisti, Univ. degli Studi di Ferrara (Italy); S. Squerzanti, M. Statera, Istituto Nazionale di Fisica Nucleare (Italy)

We overview the Laue project, supported by the Italian Space Agency, for developing advanced technologies for crystal production and assembling of broad band (70-600 keV) gamma-ray lenses. In particular we will discuss the apparatus set up to assemble single crystal tiles in the lens and how we face the divergence of the source employed.

We will report results of simulations devoted to the optimization of the lens petal and the expected performance of an entire lens for space applications will also be presented.

8147-45, Session 10

Proposal for a high-reflectivity Laue lens tuned on the 511-keV emission line

I. Neri, R. Camattari, V. Bellucci, Univ. degli Studi di Ferrara (Italy); V. Guidi, Istituto Nazionale di Fisica Nucleare (Italy)

Study of the 511-keV line resulting from the electron-positron annihilation would be precious to search for the location of positron sources in our Galaxy. For this aim, a Laue lens as space-borne telescope would provide a higher-efficiency concentration of photons if the lens is made of curved instead of mosaic crystals. It has been shown that superficial indentations are an efficient method for bending crystals. Measurements carried out at ESRF on a Si crystal bent by indentations exhibited record diffraction efficiency of 95% at 150 keV, which corresponds to a reflectivity of nearly 42% if the absorption through its 25.5 mm-thickness is included. However, in the harder x-ray domain, crystals with higher atomic number would be more suitable because for such materials reflectivity is larger than for Si. An interesting candidate for extension of the indentation technique is Ge, because of its crystalline similarity to Si. Hence, in the framework of the "Laue project", we propose to use Ge crystals bent by indentations to concentrate the 511-keV photons with very high reflectivity. By including the absorption through the crystal, reflectivity has been calculated to be 85% for 3 mm-thick Ge crystal. The energy passband would be a water-bag distribution, as determined by the curvature of crystal. If such a distribution is tuned across the 511-keV line, very high signal-to-noise detection of such radiation is foreseen.

8147-67, Session 10

Developing a second generation Laue lens prototype: high-reflectivity crystals and accurate assembly

N. M. Barrière, J. A. Tomsick, S. Boggs, A. Lowell, Univ. of California, Berkeley (United States); P. von Ballmoos, Institut de Recherche en Astrophysique et Planétologie (France)

Laue lenses are an emerging technology that will enhance gamma-ray telescope sensitivity by one to two orders of magnitude in selected energy bands of the 100 keV - 1.5 MeV range. This optic would be particularly well adapted to the observation of faint gamma ray lines, as required for the study of Supernovae, Novae and Galactic positron annihilation. It could also prove very useful for the study of hard X-ray tails from a variety of compact objects, especially making a difference by providing sufficient sensitivity for polarization to be measured by the focal plane detector. Our group has been addressing the two key issues relevant to improve performance with respect to the first generation of Laue lens prototypes: obtaining large numbers of efficient crystals and developing a method to fix them with accurate orientation and dense packing factor onto a substrate. We will present preliminary results of an on-going study aiming to enable large number of crystals suitable for diffraction at energies above 500 keV. In addition, we will show the first results of the Laue lens prototype assembled using our beamline at SSL/UC Berkeley, which demonstrates our ability to orient and glue crystals with accuracy of a few arcsec, as required for an efficient Laue lens telescope.

8147-47, Session 11

High-resolution x-ray characterization of mosaic crystals for hard x- and gamma-ray astronomy

C. Ferrari, E. Buffagni, L. Marchini, A. Zappettini, Consiglio Nazionale delle Ricerche (Italy)

For hard x-ray astronomy in the 100-1000 keV energy range Laue lenses

Conference 8147:
Optics for EUV, X-Ray, and Gamma-Ray Astronomy V

have been proposed, where the focusing elements are made of single mosaic crystals in order to increase the diffraction efficiency with respect to perfect crystals.

Suitable crystals to be used for such application to increase the diffraction efficiency should have a sufficient density and a mosaicity ranging between 30 arcsec and 1-2 arcmin, depending on the lens focusing distance and resolution. In the past germanium and copper crystals, often employed as monochromators for neutrons, have been considered.

We have analyzed several crystalline materials of different degree of crystal perfection such as GaAs, Cu, CdTe, and CdZnTe as possible mosaic crystals for hard x-ray astronomy. They were measured by high resolution x-ray diffraction at 8 keV and diffraction at energies up to 700 keV at synchrotron. A surprising agreement was found between the mosaicity evaluated in Bragg diffraction geometry with x-ray penetration of the order of few tens micrometers and in Laue transmission geometry at synchrotron.

It was found that:

-CdTe and CdZnTe crystals exhibit low angle grain boundaries preventing the formation of a single diffracted x-ray beam;

-Cu crystals exhibit mosaicity of the order of several arcmin, however a very deep etching is needed to remove the cutting damage;

-GaAs crystals grown by LEC method show mosaicity between 15 and 30 arcsec and good diffraction efficiency up to energies of 700 keV.

Annealing and surface damage were considered as possible methods to increase the GaAs crystal mosaicity.

8147-48, Session 11

Quasi-mosaic crystals for high-resolution focusing of hard x-rays through a Laue lens

R. Camattari, V. Bellucci, V. Guidi, I. Neri, Univ. degli Studi di Ferrara (Italy)

Observation of the sky within hard x-ray domain would enable the study of many sources and violent events occurring in the Universe. However, to take full advantage of this potential, the next generation of instruments working in this energy domain will have to achieve an improvement in sensitivity by at least an order of magnitude with respect to existing telescopes. Bragg diffraction in Laue geometry is being proposed to efficiently concentrate x-ray photons. Mosaic crystals can be used, but their mosaicity (FWHM of the angular distribution of the diffraction planes) may not be adequately controlled during the growth, and diffraction efficiency is ultimately limited to 50%. On the other hand, bent crystals have no intrinsic efficiency limitation and feature a very well controlled energy bandpass, this latter being proportional to the curvature. In the framework of the "Laue project", we propose the usage of bent crystals exploiting the Quasi-Mosaicity. This latter is an effect of mechanical anisotropy in crystals that manifests itself along selected crystallographic directions. Thus, as a result of primary curvature imparted to the crystal, a secondary curvature (Quasi-Mosaic curvature) occurs. We demonstrated that a proper combination of primary and Quasi-Mosaic curvatures allows high-efficiency diffraction and high-resolution focusing of diffracted photons. As compared to traditional mosaic crystals with same size and energy passband, a Laue lens based on Quasi-Mosaic crystals would increase the signal-to-noise ratio up to two orders of magnitude. Moreover, for this latter, no mosaic defocusing would occur, making it possible measurements at very high resolution.

8147-49, Session 11

Bent crystals as high-efficiency optical elements for hard x-ray astronomy

E. Buffagni, C. Ferrari, F. Rossi, L. Marchini, A. Zappettini, Consiglio Nazionale delle Ricerche (Italy)

The focusing of hard x-rays (with energies in the 70 keV - 1 MeV range) is a crucial point for astronomy in the x- and gamma-ray energy range. The use of a Laue lens made of single crystals in the Laue diffraction configuration has been proposed to efficiently collect rays of these energies.

In order to increase the diffraction efficiency bent crystals based on SiGe alloy with composition gradients can be used as optical elements showing excellent performances. For bent crystals the diffraction range is given by the total curvature of the crystal lattice planes and the diffraction efficiency can reach values close to 100%. Unfortunately a large production of such crystals seems prevented by the difficulty in the crystal growth and the yield rate.

In this work we propose a different strategy to obtain bent crystals. The bending can be achieved by a controlled surface damaging, which introduces defects in a superficial layer of few tens nanometers in thickness undergoing a highly compressive strain.

Several silicon and mosaic gallium arsenide crystals were afterwards treated to obtain bent crystals. High resolution x-ray diffraction measurements in Bragg condition at low energy x-rays allowed to determine the local and mean curvature radius of each sample. Curvature radii between 2 and 30 m were easily obtained in wafers of different thicknesses.

Preliminary results of measurements performed at high gamma energies at synchrotron and showing high diffraction efficiency are also reported.

8147-50, Session 11

Bent crystals by superficial indentations for high-efficiency concentration of hard x-ray photons by a Laue lens

V. Guidi, R. Camattari, V. Bellucci, I. Neri, Univ. degli Studi di Ferrara (Italy); N. M. Barrière, Univ. of California, Berkeley (United States)

Curved crystals for broad-band Laue lens are very promising since they allow concentrating hard x-rays with higher diffraction efficiency than for mosaic crystals, showing a uniform distribution of the energy passband. With this regard, there has been proposed several methods, e.g., external mechanical forces, thermal or composition gradient. However, most of these methods have severe limitations for a space-borne telescope such as excessive weight and fabrication reproducibility. In the framework of the "Laue project", we propose a technique to fabricate self-standing curved crystals by generating a permanent curvature within the crystal. This technique relies on superficial indentations on a mono-crystal by a diamond saw. Irreversible compression of the crystal beneath and beside the indentations causes deformation, resulting in a uniform curvature within the crystal. Indented Si crystals were characterized at ESRF and efficiently diffracted up to 500 keV, peaking 95% at 150 keV. Extension of the method to materials with higher atomic number, e.g., Ge, has been undertaken to provide high-efficiency diffraction up to 800 keV, this energy range being significantly wide for many applications in astrophysics. With respect to other techniques, the method of indentations is cheap, simple and reproducible, being based on mass production tools. Another important feature is that it is possible to control the energy passband of crystals by simply measuring the morphological curvature.

8147-51, Session 12

X-ray Optics for WHIMex, the Warm Hot Intergalactic Medium Explorer

W. C. Cash, Univ. of Colorado at Boulder (United States); R. L. McEntaffer, Univ. of Iowa (United States); W. W. Zhang, NASA Goddard Space Flight Ctr. (United States); S. Casement, C. F. Lillie, Northrop Grumman Aerospace Systems (United States); M. L. Schattenburg, M. Bautz, Massachusetts Institute of

Conference 8147:
Optics for EUV, X-Ray, and Gamma-Ray Astronomy V

Technology (United States); A. D. Holland, Open Univ. (United Kingdom); H. Tsunemi, Osaka Univ. (Japan); S. L. O'Dell, NASA Marshall Space Flight Ctr. (United States)

The soft x-ray band is loaded with diagnostics that allow absorption line spectroscopy of hot, thin gas from the ground state. Of particular interest is the WHIM, which contains the bulk of our Universe's baryons, mostly ionized and at high temperatures. In this paper we describe the optical design of WHIMex, an Explorer concept designed to extend Ultraviolet observations, like those from Copernicus, FUSE and HST, up into the X-ray. It features a compact array of slumped thin glass paraboloid-hyperboloids with 15" quality, feeding off-plane diffraction gratings. The spectrum is dispersed onto an array of CCD's which is placed at the 7m focus by an extendable bench. With spectral resolution of 4000 in the 0.15 to 2.0keV band, and collecting area as high as 500 square centimeters, WHIMex can open the the high temperature intergalactic medium to direct observation and explore the physics of a wide array of other high energy phenomena.

8147-53, Session 12

Development of off-plane gratings for WHIMex and IXO

R. L. McEntaffer, The Univ. of Iowa (United States); W. C. Cash, Univ. of Colorado at Boulder (United States); W. W. Zhang, NASA Goddard Space Flight Ctr. (United States); S. Casement, C. F. Lillie, Northrop Grumman Aerospace Systems (United States); M. L. Schattenburg, MIT Kavli Institute for Astrophysics and Space Research (United States); A. D. Holland, Open Univ. (United Kingdom); H. Tsunemi, Osaka Univ. (Japan); M. Bautz, MIT Kavli Institute for Astrophysics and Space Research (United States); S. L. O'Dell, NASA Marshall Space Flight Ctr. (United States)

Future X-ray astronomical missions will need to address a number of important goals such as studying the dynamics of clusters of galaxies, determining how elements are created in the explosions of massive stars, and revealing most of the "normal" matter in the universe which is currently thought to be hidden in hot filaments of gas stretching between galaxies. In order to achieve these goals, spectrometers capable of high resolution and high throughput are necessary for the lowest X-ray energies, 0.3-1.0 keV. We present recent progress in the development of off-plane reflection grating technology for use on upcoming missions. Off-plane grating spectrometers consist of an array of gratings capable of reaching resolutions above 3000 ($\lambda/\Delta\lambda$). Concept designs have been made for the International X-ray Observatory X-ray Grating Spectrometer. More recently however, we have designed an Optics Module Assembly for WHIMex, an Explorer mission concept that incorporates a Wolter telescope, steering flats, and an array of gratings. This paper will discuss these designs and the application of off-plane arrays for the future.

8147-54, Session 12

Fabrication update on critical-angle transmission gratings for soft x-ray grating spectrometers

R. K. Heilmann, A. Bruccoleri, P. Mukherjee, M. L. Schattenburg, M. Bautz, J. Davis, D. Dewey, R. Foster, D. Huenemoerder, H. Marshall, N. Schulz, MIT Kavli Institute for Astrophysics and Space Research (United States)

The critical-angle x-ray transmission (CAT) grating spectrometer (CATXGS) on board the International X-Ray Observatory is an example of a design that provides high-resolution spectroscopy (FWHM $E/\Delta E = 3000 - 5000$) with greater than 1,000 cm² effective area over the 0.3 - 1.0 keV photon energy band for studies of the Warm-Hot Intergalactic Medium, the Interstellar Medium, warm absorption and outflows in Active Galactic

Nuclei, coronal emission from stars, and other areas of strong interest to the astrophysics community. The CATXGS instrument concept consists of a lightweight grating array at maximum distance from focus, and a single linear CCD readout array. As a blazed transmission grating design it easily exceeds performance requirements with relaxed tolerances and significant resolution margins. The CAT gratings that comprise a grating array combine the traditional advantages of transmission (low mass, relaxed figure and alignment tolerances) and blazed reflection gratings (high broad-band diffraction efficiency). We have fabricated the required freestanding, ultra-high aspect-ratio grating bars from silicon-on-insulator wafers using both wet and dry etch processes. The grating bars are supported by an integrated Level 1 support mesh, and a coarser external Level 2 support mesh. We will present fabrication results on the integration of CAT gratings and the different high-throughput support mesh levels, as well as recent x-ray data analysis of 3 and 6 micron deep wet-etched prototypes.

8147-55, Session 13

The Extreme Physics Explorer and micro-channel plate optics

M. R. Garcia, M. S. Elvis, S. E. Romaine, J. Chappell, D. Patnaude, L. Brenneman, I. Evans, Harvard-Smithsonian Ctr. for Astrophysics (United States); G. Fraser, R. Willingale, Leicester Univ. (United Kingdom); E. Silver, Harvard-Smithsonian Ctr. for Astrophysics (United States)

The Extreme Physics Explorer (EPE) is a concept for a large area, moderate angular resolution X-ray timing/spectroscopy mission designed to observed bright sources to test QED and General Relativity.

EPE would use ultra-lightweight microchannel plate optics (MCPO) with a long, ~30m, focal length, to provide 5m² effective area focused to ~1 arcmin at an Explorer class mass. These optics provide a factor of 10 improvement in area to mass ratio over current state of the art. The X-rays would be focused onto an X-ray calorimeter array. By spreading the signal over the array the count-rate limitations of X-ray calorimeters are largely overcome.

We describe science drivers for such a mission, and discuss the design trade space for the large area MCPO, and the challenges of the large area MCPO design. The possibilities for including a polarimeter, which would expand the science case, are also discussed.

8147-56, Session 13

Large-angle observatory with energy resolution for synoptic x-ray studies (LOBSTER-SXS)

P. Gorenstein, Harvard-Smithsonian Ctr. for Astrophysics (United States)

The soft X-ray band hosts the largest and most diverse range of variable sources than any other region of the electromagnetic spectrum. They are stars, compact binaries, SMBH's, as well as the X-ray components of Gamma-Ray Bursts, their soft X-ray afterglows, and recently discovered very high redshift gamma-ray bursts and soft X-ray flares from supernova. We describe a concept for a very wide field (~ 4 ster) modular focusing X-ray telescope system with high sensitivity that can measure positions with arc second accuracy, the precision required to identify fainter and increasingly more distant events. The dimensions and the materials of all the telescope modules are identical or nearly so. All but two modules are part of a cylindrical lobster-eye telescope made with flat mirrors that focus in one dimension and utilize a coded mask for angular resolution in the other. Their positioning accuracy is the order of an arc minute. The two remaining modules are orthogonal and in series along a radius of the cylinder. They are configured as a Kirkpatrick-Baez telescope that focuses in two dimensions. It refines the arc minute positions of the lobster-eye modules to an arc second and provides

**Conference 8147:
Optics for EUV, X-Ray, and Gamma-Ray Astronomy V**

larger effective area for spectral and temporal measurements. This telescope system is more powerful and versatile than either a 2D coded mask or a 2D lobster-eye telescope of similar size. Very wide field X-ray telescopes have become feasible as the ability to fabricate large area arrays of position sensitive CCD and CMOS detectors has improved. An instrument with considerably more sensitivity than current all-sky or wide field X-ray detectors would be compatible with a modest NASA Explorer mission.

8147-57, Session 13

A new x-ray interferometer

S. Kitamoto, H. Murakami, D. Takei, K. Sakata, Y. Yoshida, Rikkyo Univ. (Japan)

We report a proposal of a new X-ray interferometer for future celestial observations. An X-ray interferometer is a possible optics in order to get a diffraction limited resolution for X-rays. If the interferometer is constructed from flat mirrors, the technology might be easier than that for a "so-called" telescope with an aspheric- polished mirror, but still difficult. Especially, a very long optics-length is generally required to get a reasonable size of a fringe pattern.

We propose a new idea for an X-ray interferometer using beam splitters. By using beam splitters, we can completely align two beams, which will be superposed, with each other. Consequently its optics-length can be short and the size of the fringe pattern is determined by the alignment precision. We studied a design of an interferometer optic with the beam splitter and propose a modified type of a Mach-Zehnder interferometer.

We have started a study of this type of a simple X-ray interferometer with beam splitters. For a laboratory model, we are designing a "grazing incident" Mach-Zehnder interferometer with multi-layer flat mirrors and beam splitters. The beam splitter is designed and fabricated with Mo/Si multi-layers tuning the layer thickness to reflect O-K or C-K X-rays. We will report the design and study of the new type X-ray interferometer and the status of the laboratory experiment.

8147-58, Session 13

Toward adaptive x-ray telescopes

S. L. O'Dell, NASA Marshall Space Flight Ctr. (United States); T. W. Button, The Univ. of Birmingham (United Kingdom); V. Cotroneo, W. N. Davis, Harvard-Smithsonian Ctr. for Astrophysics (United States); P. Doel, Univ. College London (United Kingdom); C. H. Feldman, Univ. of Leicester (United Kingdom); M. D. Freeman, Harvard-Smithsonian Ctr. for Astrophysics (United States); M. V. Gubarev, J. J. Kolodziejczak, NASA Marshall Space Flight Ctr. (United States); A. G. Michette, King's College London (United Kingdom); B. D. Ramsey, NASA Marshall Space Flight Ctr. (United States); P. B. Reid, Harvard-Smithsonian Ctr. for Astrophysics (United States); D. Rodriguez Sanmartin, The Univ. of Birmingham (United Kingdom); T. T. Saha, NASA Goddard Space Flight Ctr. (United States); D. A. Schwartz, Harvard-Smithsonian Ctr. for Astrophysics (United States); S. Trolier-McKinstry, R. H. T. Wilke, The Pennsylvania State Univ. (United States); R. Willingale, Univ. of Leicester (United Kingdom); W. W. Zhang, NASA Goddard Space Flight Ctr. (United States)

Future x-ray observatories will require high-resolution (25 m^2) apertures. Even with the next generation of heavy-lift launch vehicles, launch-mass constraints and aperture-area requirements will limit the areal density of the grazing-incidence mirrors to about 1 kg/m^2 or less. Achieving sub-arcsecond x-ray imaging with such lightweight mirrors will require excellent mirror surfaces, precise and stable alignment, and exceptional stiffness or deformation compensation. Attaining and maintaining alignment and figure control will likely involve adaptive (in-space adjustable) x-ray optics. In contrast with infrared and visible

astronomy, adaptive optics for x-ray astronomy is in its infancy. In the middle of the previous decade, two efforts began to advance technologies for adaptive x-ray telescopes: The Generation-X (Gen-X) concept studies in the United States, and the Smart X-ray Optics (SXO) Basic Technology project in the United Kingdom. This paper discusses relevant technological issues and summarizes progress toward adaptive x-ray telescopes.

8147-59, Session 13

Adjustable grazing incidence x-ray optics: measurement of actuator influence functions and comparison with modeling

V. Cotroneo, W. N. Davis, P. B. Reid, D. A. Schwartz, Harvard-Smithsonian Ctr. for Astrophysics (United States)

The present generation of X-ray telescopes is focused either on a high image quality (e.g. Chandra with sub-arc second resolution) or a large effective area (e.g. XMM), while future planned observatories (e.g. IXO) point to greatly enhance the effective area, maintaining moderate (~ 5 arc second) image quality. To go beyond the limits of present and planned missions, the use of thin adjustable optics for the control of low-order figure error is needed to obtain the high image quality performance of precisely figured mirrors along with the large effective area of thin mirrors.

The adjustable mirror prototypes under study at CfA are based on two different principles and designs: 1) thin film lead-zirconate-titanate (PZT) piezo actuators directly deposited on the mirror back surface, with the strain direction parallel to the glass surface (for tenth arc second angular resolution and large effective area), and 2) conventional lead-magnesium-niobate (PME) electrostrictive actuators with their strain direction perpendicular to the mirror surface (for 3 - 5 arc second resolution and moderate effective area).

Flat test mirrors of these adjustable optics have been built and operated. We present the comparison between theoretical influence functions as obtained by finite element analysis and the measured influence functions obtained from the two test configurations.

8147-60, Session 13

Adjustable x-ray optics: correction for gravity-induced figure errors

D. A. Schwartz, V. Cotroneo, W. N. Davis, M. D. Freeman, P. B. Reid, Harvard-Smithsonian Ctr. for Astrophysics (United States)

To extend the effective collecting area for future X-ray astronomy observatories, it is necessary to use highly nested, very thin glass shells. The capability to adjust the figure of these shells on-orbit is essential in order to achieve present state-of-the-art imaging capability of order $1/2$ arcsec resolution. We are pursuing concepts to carry out this adjustment using piezo-electric crystals deposited directly on the back sides of the reflectors, and divided into a pattern of discrete actuators by individually controlled electrodes. In this paper we carry out a simulation of how well gravity induced errors might be corrected by this process. We perform a finite element analysis of a conical glass piece 205mm axially by 410mm azimuthally, and with 1m radius of curvature. This gives the individual influence functions. Then we apply a 1g force axially, using various constraint conditions, and calculate the coefficients of the set of influence functions such that the adjusted shape minimizes the slope errors.

Conference 8148: Solar Physics and Space Weather Instrumentation IV

Sunday-Wednesday 21-24 August 2011 • Part of Proceedings of SPIE Vol. 8148
Solar Physics and Space Weather Instrumentation IV

8148-01, Session 1

A collimator for measurements of the loss cone flux of energetic electrons

J. D. Sullivan, Air Force Research Lab. (United States) and Boston College (United States); C. Parker, Air Force Research Lab. (United States)

An energetic electron collimator for the measurement of loss cone fluxes in the Earth's radiation belts is presented. This design addresses the problem of measuring low intensity fluxes in the presence of a large omni-directional background flux. This disc loaded collimator comprises stainless steel baffles and tungsten vanes. Electron rejection is accomplished via logarithmic baffle spacing with vanes placed more closely deep within the collimator. The collimator was fabricated. Its response was validated at the Goddard Spaceflight Center's Radiation Effects Facility. The baffled design shows an angular cutoff greater than three orders of magnitude at the geometric cutoff angle for electron energies less than 500 keV.

8148-02, Session 1

The energetic particle telescope (EPT) performances

M. Cyamukungu, G. Grégoire, Ctr. for Space Radiations (Belgium)

Forecasting of energetic particle fluxes on time scales of hours to weeks, at a given position in space can be achieved, based on experimentally determined particle lifetimes and real-time measurements of contamination-free spectra. These kinds of direct measurements that do not need post-processing can be provided by the Energetic Particle Telescope (EPT) developed at the Center for Space Radiations (UCL-Belgium) and which can directly acquire energy spectra of electrons (0.2 - 10 MeV), protons (4 - 300 MeV), α -particles (16 - 1000 MeV) and heavier ions (up to 300 MeV/nucleon).

This paper contains a brief description of the EPT setup and channel definition along with the calibration and validation methodology. The performances of the EPT are presented, including the particle discrimination capability, the maximum flux rate along with results of the Flight Model qualification for PROBA-V satellite.

8148-03, Session 1

Characterization of sensitivity degradation seen from the UV to NIR by RAIDS on the International Space Station

A. W. Stephan, U.S. Naval Research Lab. (United States); A. B. Christensen, The Aerospace Corp. (United States); S. A. Budzien, U.S. Naval Research Lab. (United States); R. L. Bishop, J. H. Hecht, The Aerospace Corp. (United States); K. R. Minschwaner, New Mexico Institute of Mining and Technology (United States)

This paper presents an analysis of the sensitivity changes experienced by four of the eight sensors that comprise the Remote Atmospheric and Ionospheric Detection System (RAIDS) after more than a year operating on board the International Space Station (ISS). These sensors include the Extreme Ultraviolet Spectrograph (EUVS) that covers 55-110 nm, the Middle Ultraviolet (MUV) and Near Ultraviolet (NUV) sensors that combine to cover 190-400 nm, and the Near Infrared Spectrometer

(NIRS) that covers 722-874 nm. The scientific goal for RAIDS is comprehensive remote sensing of the temperature, composition, and structure of the lower thermosphere and ionosphere from 85-300 km. RAIDS was installed on the ISS Japanese Expansion Module External Facility (JEM-EF) in September of 2009. After initial checkout the sensors began routine operations that are only interrupted for sensor safety by occasional ISS maneuvers as well as a few days per month when the orbit imparts a risk from exposure to the Sun. This history of measurements has been used to evaluate the rate of degradation of the RAIDS sensors exposed to an environment with significant sources of particulate and molecular contamination. The RAIDS EUVS, including both contamination and detector gain sag, has shown an overall signal loss rate of 0.2% per day since the start of the mission. The MUV has shown a 30% loss with an exponential folding time of about 45 days. The NIRS has shown stability to within 1% over the first year of operations.

8148-04, Session 1

The RAIDS experiment on the ISS: on-orbit performance

S. A. Budzien, A. W. Stephan, U.S. Naval Research Lab. (United States); R. L. Bishop, A. B. Christensen, J. H. Hecht, The Aerospace Corp. (United States); K. R. Minschwaner, New Mexico Institute of Mining and Technology (United States)

The Remote Atmospheric and Ionospheric Detection System (RAIDS) is new NASA experiment studying the Earth's thermosphere and ionosphere from a vantage point on the International Space Station (ISS). RAIDS along with a companion hyperspectral imaging experiment were launched in September 2009 to operate as the first US payload on the Japanese Experiment Module-Exposed Facility. The scientific objectives of the RAIDS experiment are to study the temperature of the lower thermosphere (100-200 km), to measure composition and chemistry of the lower thermosphere and ionosphere, and to measure the initial source of OII 83.4 nm emission.

The RAIDS sensor complement includes three photometers, three spectrometers, and two spectrographs which span the wavelength range 50-874 nm and scan or image the atmospheric limb 90-300 km. After installation aboard the ISS, RAIDS underwent a 30-day check-out period before entering science operations. RAIDS is serving as a pathfinder for atmospheric remote sensing from the ISS, and the experiment team gained valuable operational insights throughout the first year of the mission. We present on-orbit sensor performance and discuss the ISS as a platform for atmospheric limb measurements.

8148-05, Session 1

Characterization of Teledyne microdosimeters for space weather applications

C. D. Lindstrom, Air Force Research Lab. (United States); J. D. Sullivan, Boston College (United States); B. K. Dichter, F. A. Hanser, Assurance Technology Corp. (United States); D. Carsow, Air Force Research Lab. (United States) and National Research Council (United States); G. E. Galica, Assurance Technology Corp. (United States)

Ideally, a space weather nowcasting system would rely on ubiquitous coverage of the near earth space environment. However, such an approach is difficult if not impossible to achieve in practice because of the extreme cost of space access as well as the large region that needs to be covered. In recent years, this has been recognized by those working on forecasting the space particle environment. Approaches

Conference 8148:
Solar Physics and Space Weather Instrumentation IV

relying on data assimilation using results of high-grade scientific instruments/missions or physics based models combined with data-limited miniature instruments have been proposed to address this. One possible limited-data sensor that has been recently developed is a single (hybrid) chip dosimeter that uses a conventional silicon detector to measure the total radiation dose. This microdosimeter (as named by the manufacturer Teledyne) offers the potential advantage of small size, low cost, and well-calibrated response (compared to radfets) that may enable easy piggybacking onto existing missions. It is, however, important that the response of this device be carefully characterized in order to use it for space particle measurements. Here the linearity with dose, angular response, and energy response of the microdosimeter for both protons and electrons will be characterized through both Monte Carlo simulations and laboratory measurements. In addition, its potential usefulness for space particle measurements as well as total dose will be briefly addressed.

8148-06, Session 2

The Fabry-Perot interferometer prototype for ADAHELI solar small mission

F. Berrilli, M. Cocciolo, R. Piazzesi, D. Del Moro, L. Giovannelli, Univ. degli Studi di Roma Tor Vergata (Italy); S. Selci, Consiglio Nazionale delle Ricerche (Italy); A. Egidi, Univ. degli Studi di Roma Tor Vergata (Italy)

The spectrometric element of the narrow band unit of the Interferometer for SOLAR DYNAMICS (ISODY) focal plane suite, on board of the ADAHELI satellite is formed by two Fabry-Perot interferometers (FPI) used in classic mount and in axial-mode, and in series with a set of narrow-band interference filters. The filters are mounted on a filter-wheel placed between the two etalons to reduce the ghosts produced by the inter-reflections.

Because no large interferometers for the imager are required (50 mm in diameter) space-qualified Fabry-Perot interferometers, with a capacity servo-control for both spacing and parallelism, have been adopted.

Although some industries produce space-qualified FPIs we started in optics laboratories of Physics Department of University of Rome Tor Vergata (UTOV) the design and realization of a Fabry-Perot Interferometer prototype in order to investigate low-cost solutions suitable for small missions. The proposed FPI design is discussed, giving details on the prototype realization.

8148-07, Session 2

Liquid crystals Lyot filter for solar coronagraphy

S. Fineschi, G. Capobianco, G. Massone, L. Zangrilli, INAF - Osservatorio Astronomico di Torino (Italy); T. Baur, Meadowlark Optics, Inc. (United States)

This work describes a liquid crystal Lyot tunable-filter and polarimeter (LCTP) designed to achieve high spatial resolution imaging and two-dimensional spectrophotometry of the Fe XIV, 530.3 nm, solar coronal emission-line. The LCTP is a bandpass filter with a full width at half maximum of 0.15 nm at a wavelength of 530.3 nm. The center wavelength of the bandpass is tunable in 0.01 nm steps from 528.64 nm to 533.38 nm. It is a four stage Lyot filter with all four stages wide-field. The free spectral range between neighboring transmission bands of the filter is more than 2.7 nm. The wavelength tuning is non-mechanical using nematic liquid crystal variable retarders (LCVR's). A separate LCVR, in tandem with the filter, is used for the polarization measurements. A prototype of the LCTP has been built and used for coronagraphic observations during the 2010 solar eclipse. Its measured performances and potential applications for space-based coronagraphy are presented here.

8148-08, Session 2

Ground-based synoptic instrumentation for the solar observations

K. S. Balasubramaniam, Air Force Research Lab. (United States); A. Pevtsov, National Solar Observatory (United States)

We will describe the status of current ground-based solar spectroscopic and imaging instruments used in solar observations. We will describe the advantages and disadvantages of using these two classes of instruments with examples drawn from the Improved Solar Optical Observing Network (ISOON) and Synoptic Long Term Investigations of the Sun (SOLIS) Network. Besides instrumental requirements and lessons learned from existing ground-based instruments, this talk will also focus on the future needs and requirements of ground-based solar optical observations.

8148-09, Session 2

Figure testing and calibration of the ISOON Fabry-Perot etalons

B. M. Robinson, The Univ. of Alabama in Huntsville (United States); K. S. Balasubramaniam, National Solar Observatory (United States); F. Pitts, J. Justice, ARINC, Inc. (United States)

We present the methods and results for the figure testing and spectral calibration of the narrow- and wide-band etalons for the Improved Solar Optical Observing Network's dual-etalon tunable imaging filters. The ISOON system comprises a distributed network of ground-based patrol telescopes that gather full-disk data for the monitoring of solar activity and for the development of more reliable space weather models. The etalon figure testing consists mainly of testing the cavity flatness and coating uniformity of each etalon. For this testing a series of exposures is taken as the etalon is tuned through a stable spectral line and a full-aperture line profile correlation method is employed to map the variations in the effective cavity thickness. Calibration of the etalons includes absolute calibration of the cavity mean spacing change corresponding to a controller step and calibration of plate parallelism and spacing settings for each spectral region of interest. Both acceptance testing and calibration were performed in a laboratory environment using spectral sources. A calibration method that uses illumination in the telluric lines is also described. This latter method can be used to conduct calibration in the field without the use of an artificial light source.

8148-10, Session 3

The SOLAR-C mission: current status

T. Shimizu, Japan Aerospace Exploration Agency (Japan); S. Tsuneta, H. Hara, National Astronomical Observatory of Japan (Japan); K. Ichimoto, Kyoto Univ. (Japan); K. Kusano, Nagoya Univ. (Japan); T. Sekii, National Astronomical Observatory of Japan (Japan); T. Sakao, Japan Aerospace Exploration Agency (Japan); Y. Suematsu, T. Watanabe, National Astronomical Observatory of Japan (Japan)

Two mission concepts (plan A: out-of-ecliptic mission and plan B: high resolution spectroscopic mission) have been studied for the next Japanese solar mission Solar-C, which will follow the scientific success of the Hinode mission. For studies, the Solar-C working group is organized in ISAS/JAXA with participation of scientists in Japanese solar physics community and with participation of US and European scientists in sub-working group activities. The plan A mission has a focused suite of instruments designed to study the solar interior flows by helioseismology, surface magnetic fields, transition region, and extended corona from an orbit inclined at least 40 degrees to the ecliptic plane. The plan B mission has three large state-of-art advanced telescopes to

**Conference 8148:
Solar Physics and Space Weather Instrumentation IV**

study energy flows and fundamental physical processes governing the dynamic solar atmosphere through elementary magnetic structures with high spatial resolution, high throughput, high cadence spectroscopic and polarimetric observations seamlessly covering the entire atmosphere from photosphere and chromosphere to transition region and corona. We are in the final phase of the selection and will soon give priority to one of the mission concepts to proceed for realizing Solar-C in 2019. The evaluation of the two concepts is being done from various points of view including science, technical and programmatic issues. Solar-C will only be realized with the enthusiastic participation of the space agencies and US and European scientists in all phases. This paper will present the current state of development for both the mission concepts and discuss more details of the Solar-C mission concept in higher priority.

8148-11, Session 3

Photon-counting soft x-ray telescope for the Solar-C mission

T. Sakao, Japan Aerospace Exploration Agency (Japan); N. Narukage, M. Shimojo, S. Miyazaki, National Astronomical Observatory of Japan (Japan); K. Watanabe, S. Imada, T. Dotani, Japan Aerospace Exploration Agency (Japan); E. E. DeLuca, Harvard-Smithsonian Ctr. for Astrophysics (United States)

We report instrument outline as well as science of the photon-counting soft X-ray telescope that we have been studying as a possible scientific payload for the Japanese Solar-C mission whose projected launch around 2019.

Soft X-rays (~1-10 keV) from the solar corona include rich information on (1) possible mechanism(s) for heating the bright core of active regions seen in soft X-rays (namely, the hottest portion in the non-flaring corona), (2) dynamics and magneto-hydrodynamic structures associated with magnetic reconnection processes ongoing in flares, and even (3) generation of supra-thermal distributions of coronal plasmas associated with flares.

Nevertheless, imaging-spectroscopic investigation of the soft X-ray corona has so far remained unexplored due to difficulty in the instrumentation for achieving this aim. With the advent of recent remarkable progress in CMOS-APS detector technology, the photon-counting X-ray telescope will be capable of, in addition to conventional photon-integration type exposures, performing imaging-spectroscopic investigation on active regions and flares, thus providing, for example, detailed temperature information (beyond the so-far-utilized filter-ratio temperature) at each spatial point of the observing target.

The photon-counting X-ray telescope will employ a Walter type I optics with a piece of a segmented mirror whose focal length 4 meters, combined with a focal-plane CMOS-APS detector (0.4-0.5"/pixel) whose frame read-out rate required to be as high as 1000 fps.

Expected scientific performance of the photon-counting X-ray telescope will also be discussed together with prospects for the technology development for realizing the telescope.

8148-12, Session 3

Short telescope design of 1.5-m aperture solar UV visible and IR telescope aboard Solar-C

Y. Suematsu, Y. Katsukawa, National Astronomical Observatory of Japan (Japan); T. Shimizu, Japan Aerospace Exploration Agency (Japan); K. Ichimoto, Kyoto Univ. (Japan); T. Horiuchi, Y. Matsumoto, PLANET Inc. (Japan); N. Takeyama, Genesis Corp. (Japan)

We present a basic design of one of major planned instrumental payload for SOLAR-C/Plan-B: the Solar Ultra-violet Visible and near IR observing Telescope (SUVIT). We studied a short telescope design for 1.5 m

aperture solar Gregorian telescope with the compact design of off-axis three-mirror collimator unit to accommodate a launcher's nosecone size, a wide observing wavelength coverage from UV (down to 250 nm) through near IR (up to 1100 nm), and an 0.1 arcsec resolution in the field of 200 arcsec diameter. The large aperture is essentially important to attain scientific goals of Solar-C/Plan-B, especially for accurate diagnostics of the dynamic solar chromosphere as revealed by HINODE, but make it difficult to design the telescope because of solar heat load ten times more than Hinode introduced into the telescope. Detailed study of optical and thermal design of the telescope assembly of SUVIT for diffraction-limited performance at visible wavelength is presented, which consists of an aplanatic Gregorian telescope of 2.8 m primary-secondary mirror separation, heat rejection optics at the primary focus, afocal and achromatic optics between the telescope and focal plane instruments, and an envelope shield tube which ensures the thermal control of the entire telescope.

8148-13, Session 3

Focal plane instruments for the solar UV-Vis-IR telescope aboard SOLAR-C

Y. Katsukawa, Y. Suematsu, National Astronomical Observatory of Japan (Japan); T. Shimizu, Japan Aerospace Exploration Agency (Japan); K. Ichimoto, Kyoto Univ. (Japan); N. Takeyama, Genesis Corp. (Japan)

We present a conceptual design of a focal plane instrument for the Solar UV-Vis-IR Telescope (SUVIT) aboard the next Japanese solar mission SOLAR-C. A primary purpose of the telescope is to achieve precise as well as high resolutional spectroscopic and polarimetric measurements of the solar chromosphere with a big aperture of 1 - 1.5 m, which is expected to make a significant progress in understanding basic MHD processes in the solar atmosphere. The focal plane instrument consists of two packages: A filtergraph package is to get not only monochromatic images but also Dopplergrams and magnetograms using a tunable narrow-band filter and interference filters. A spectrograph package is to perform accurate spectro-polarimetric observations for measuring chromospheric magnetic fields, and is employing a Littrow type spectrograph. The most challenging aspect in the instrument design is wide wavelength coverage from 280 nm to 1.1 μ m to observe multiple chromospheric lines, which is to be realized with a lens unit consisting of fluoride glasses. A high-speed camera for correlation tracking of granular motion is also implemented in one of the packages for an image stabilization system, which is essential to achieve high spatial resolution.

8148-14, Session 4

MgII observations using the MSFC solar ultraviolet magnetograph

E. A. West, J. Cirtain, NASA Marshall Space Flight Ctr. (United States); K. Kobayashi, G. A. Gary, J. M. Davis, The Univ. of Alabama in Huntsville (United States)

This paper will describe the scientific goals of our sounding rocket program, the Solar Ultraviolet Magnetograph Investigation (SUMI). This paper will present a brief description of the optics that were developed to meet SUMI's scientific goals, discuss the spectral, spatial and polarization characteristics of SUMI's optics, describe SUMI's flight which was launched 7/30/2010, and discuss what we have learned from that flight.

8148-15, Session 4

SOHO/CELIAS solar EUV monitor absolute solar EUV irradiance measurements and how they are affected by choice of reference spectrum

D. L. Judge, S. R. Wieman, L. Didkovsky, The Univ. of Southern California (United States)

The SOHO/CELIAS Solar EUV Monitor (SEM) has measured absolute EUV solar irradiance nearly continuously over a 15 year period that includes both the cycle 22/23 (1996) and cycle 23/24 (2008) solar minima. Calibration of the SEM flight instrument and verification of the data have been maintained through measurements from a series of sounding rocket calibration underflights that have included a NIST calibrated SEM clone instrument as well as a Rare Gas Ionization Cell (RGIC) absolute detector. The SOLERS 22 fixed reference solar spectrum is used to calculate absolute EUV flux values from SEM raw data. Specifically, the reference spectrum provides a set of weighting factors for determining a weighted average for the wavelength dependent SEM efficiency, and is used in the correction for second order contamination in the first order channels, and in the comparison between SEM flux measurements with broader-band absolute RGIC measurements. SOHO/SEM EUV flux measurements for different levels of solar activity will be presented to show how the choice of reference spectrum affects these SEM data. Both fixed (i.e. SOLERS 22) and non-fixed (Solar Irradiance Platform/Solar 2000 and SDO/EVE/MEGS spectra) reference spectra have been included in this analysis.

8148-16, Session 4

Overview of chromospheric Lyman-Alpha spectropolarimeter (CLASP)

N. Narukage, S. Tsuneta, T. Bando, R. Kano, M. Kubo, H. Hara, Y. Suematsu, Y. Katsukawa, R. Ishikawa, K. Ueda, National Astronomical Observatory of Japan (Japan); H. Watanabe, K. Ichimoto, Kyoto Univ. (Japan); T. Sakao, Japan Aerospace Exploration Agency (Japan); K. Kobayashi, The Univ. of Alabama in Huntsville (United States); J. Trujillo Bueno, Instituto de Astrofísica de Canarias (Spain)

The solar chromosphere is an important boundary, through which all of the plasma, magnetic fields and energy in the corona and solar wind are supplied. Since the Zeeman splitting is typically smaller than the Doppler line broadening in the chromosphere and transition region, it is not effective to explore weak magnetic fields. However, this is not the case for the Hanle effect, when we have an instrument with high polarization sensitivity ($\sim 0.1\%$).

We are planning a sounding rocket experiment to be launched in 2014 summer, "Chromospheric Lyman-Alpha SpectroPolarimeter (CLASP)", to detect linear polarization produced by the Hanle effect in Lyman-alpha line (121.6 nm) and to make the first direct measurement of magnetic fields in the upper chromosphere and lower transition region. To achieve the high sensitivity of $\sim 0.1\%$ within a rocket flight (5 minutes) in Lyman-alpha line, which is easily absorbed by materials, we design the optical system mainly with reflections. The CLASP consists of a classical Cassegrain telescope, a polarimeter and a spectrometer: i) The primary mirror is coated by the "cold mirror coating", which has high reflectivity in Lyman-alpha and low reflectivity in other wavelengths to minimize the heat load and the visible light contamination. ii) The polarimeter consists of a rotating 1/2-wave plate and two reflecting polarization analyzers. One of the analyzer also works as a beam splitter to give us two orthogonal linear polarizations simultaneously. iii) Two Spherical Varied-Line-Space (SVLS) gratings for each polarization component disperse and focus spectral images on two CCD cameras separately.

8148-17, Session 4

LEMUR (large European module for solar ultraviolet research): the VUV imaging spectrograph for the JAXA's Solar-C mission

L. Teriaca, Max-Planck-Institut für Sonnensystemforschung (Germany); G. A. Doschek, U.S. Naval Research Lab. (United States); L. K. Harra, Univ. College London (United Kingdom); C. M. Korendyke, U.S. Naval Research Lab. (United States); U. H. Schuehle, Max-Planck-Institut für Sonnensystemforschung (Germany); T. Shimizu, Japan Aerospace Exploration Agency (Japan)

LEMUR is a VUV imaging spectrograph with a resolution and effective area an order of magnitude higher than currently available for solar studies. It is currently proposed as ESA's participation in the Solar-C mission. Spectroscopic observations with sufficient resolution to observe the flow and dissipation of energy from the chromosphere into the transition region and corona as well as multi-million-degree flare plasmas, are essential for understanding the physical processes heating the corona and accelerating the solar wind. The LEMUR observations directly address these questions and are critical to the scientific success of the Solar-C mission and to the advance of solar physics.

LEMUR consists of a 30-cm steerable mirror illuminating a slit assembly located 3.6 m away. The slit is imaged and dispersed by a TVLS grating that focuses the solar spectrum over the detectors. The simple two-element design provides the high throughput necessary for high spatial and temporal resolution observations. The system has no entrance filter. The mirror is coated with a suitable multilayer with B4C top-coating, providing a reflectance peak around 18.5 nm besides the usual B4C range above 50 nm. This remarkable wavelength coverage allows the simultaneous recording of spectral lines formed at all temperatures between 0.02 MK and 20 MK. The grating is divided into two channels. One operates around 18.5 nm and the other at wavelengths above 50 nm. The system is designed to provide resolved spectra with a spatial resolution corresponding to 200 km x 200 km (0.28") projected area. A large format CCD array with an aluminum filter is foreseen for the short wavelength channel. Three intensified CCD cameras will record spectra above 50 nm.

8148-18, Session 5

The coronal suprathermal particle explorer (C-SPEX)

J. D. Moses, C. M. Brown, G. A. Doschek, Y. Ko, C. M. Korendyke, J. M. Laming, C. E. Rakowski, D. G. Socker, A. Tylka, U.S. Naval Research Lab. (United States); D. R. McMullin, Space Systems Research Corp. (United States); C. K. Ng, U.S. Naval Research Lab (United States) and George Mason Univ. (United States); S. R. Wassom, Utah State Univ. (United States); M. A. Lee, The Univ. of New Hampshire (United States); F. Auchère, Institut d'Astrophysique Spatiale (France); S. Fineschi, INAF - Osservatorio Astronomico di Torino (Italy)

The primary science objective of the Coronal Suprathermal Particle Explorer (C-SPEX) is to investigate the spatial and temporal variations of coronal suprathermal particle populations that are seeds for acceleration to solar energetic particles (SEPs). It is understood that such seed particle populations vary with coronal structures and can change responding to solar flare and coronal mass ejection (CME) events. Models have shown that higher densities of suprathermal protons can result in higher rates of acceleration to high energies. Understanding the variations in the suprathermal seed particle population is thus crucial for understanding the variations in SEPs. However, direct measurements are still lacking.

C-SPEX will measure the variation in the suprathermal protons across

Conference 8148:
Solar Physics and Space Weather Instrumentation IV

various coronal magnetic structures, before/after the passage of CME shocks, in the post-CME current sheets, and before/after major solar flares. The measurements will not only constrain models of SEP acceleration but also constrain models of the production of suprathermal particles from processes such as magnetic reconnection at the Sun. Understanding the causes for variation in the suprathermal seed particle population and its effect on the variation in SEPs will also help build the predictive capability of SEPs that reach Earth which constitutes an important factor of space weather.

The C-SPEX measurements will be obtained from instrumentation on the International Space Station (ISS) employing well-established UV coronal spectroscopy techniques. The unique aspect of C-SPEX is a >100-fold increase of light gathering power over any previous or currently planned UV coronal spectrometer. It is demonstrated C-SPEX will thus overcome the limitations in signal to noise that have thwarted prior attempts to observe suprathermals in the corona. The ISS is an excellent platform from which to conduct these observations, contrary to popular expectations. The issues of pointing stability and contamination of UV optics are demonstrated to be manageable in the proposed program.

The present lack of a means to predict the variability of SEP intensities and the likelihood C-SPEX will help develop such predictions makes the proposed investigation directly relevant to each of the three strategic objectives of the NASA Heliophysics Research Strategic Objectives.

8148-19, Session 5

The Lyman-alpha telescope of the extreme ultraviolet imager on solar orbiter

U. H. Schuehle, Max-Planck-Institut für Sonnensystemforschung (Germany); J. Halain, Univ. de Liège (Belgium); S. Meining, L. Teriaca, Max-Planck-Institut für Sonnensystemforschung (Germany)

On the Solar Orbiter mission, the Extreme Ultraviolet Imager (EUI) set of filtergraph-telescopes consists of two high-resolution imagers (HRI) and one dual-band full Sun imager (FSI) that will provide extreme ultraviolet and Lyman- α images of the solar atmosphere. The Lyman- α HRI is one channel of the EUI suite of telescopes that will provide imaging of the solar atmosphere at the hydrogen Lyman- α line at unprecedented high cadence at a spatial resolution of one arcsecond.

For vacuum-ultraviolet imaging of the Sun the main requirements for the instrumentation are high resolution, high cadence, and large dynamic range. We present here the novel solutions of the instrument design and show in detail the predicted performance of this telescope. We describe in detail how the high throughput and spectral purity at 121.6 nm is achieved. The technical solutions include multilayer coatings of the telescope mirrors for high reflectance at 121.6 nm, combined with interference filters and a multichannel-plate intensified CMOS active pixel camera. We make use of the design flexibilities of this camera to optimize the dynamic range in the focal plane.

8148-20, Session 5

SCORE (sounding-rocket coronagraphic experiment): pre and post-flight calibrations

S. Fineschi, INAF - Osservatorio Astronomico di Torino (Italy); M. Romoli, Univ. degli Studi di Firenze (Italy); E. Antonucci, INAF - Osservatorio Astronomico di Torino (Italy); J. D. Moses, J. S. Newmark, U.S. Naval Research Lab. (United States); G. Massone, G. Capobianco, D. Telloni, L. Zangrilli, INAF - Osservatorio Astronomico di Torino (Italy); F. Landini, M. Pancrazzi, M. Focardi, Univ. degli Studi di Firenze (Italy); M. G. Pelizzo, Univ. di Padova (Italy); F. Auchère, Institute d'Astrophysique Spatiale (France)

SCORE, the Sounding-rocket Coronagraphic Experiment, is part of

the sub-orbital payload HERSCHEL. On September 14, 2009, SCORE successfully flew its first sub-orbital mission with HERSCHEL. SCORE is a coronagraph with an all-reflective telescope designed to obtain images of the solar coronal emission in the visible, ultraviolet and extreme ultraviolet (EUV) wavelengths. The telescope optics are coated with an innovative multilayer optimized for the EUV line HeII, 30.4 nm, and with a cap-layer that extends the optics reflectivity to the UV (100 nm) and visible (500 nm) wavelengths. Filters select the HI Lyman-alpha, 121.6 nm, line and the polarized broadband visible-light emission from the solar corona.

This presentation will describe the pre- and post-flight calibrations carried out at the US. Naval Research Laboratory, US White Sands Missile Range and the Turin Astronomical Observatory, Italy. The calibration activities included measurements of the stray-light rejection level, vignetting function, radiometric and polarimetric response.

8148-21, Session 6

SiC/Mg multilayer coatings for SCORE coronagraph: long term stability analysis

M. G. Pelizzo, Lab. for Ultraviolet and X-ray Optical Research (Italy); S. Fineschi, INAF - Osservatorio Astronomico di Torino (Italy); A. J. Corso, P. Zuppella, Lab. for Ultraviolet and X-ray Optical Research (Italy); D. L. Windt, Reflective X-Ray Optics LLC (United States); P. Nicolosi, Lab. for Ultraviolet and X-ray Optical Research (Italy)

SiC/Mg multilayers have been used as coatings of the Sounding-rocket CORonagraphic Experiment (SCORE) telescope mirrors launched during the NASA HERSCHEL program. This coating couple has been largely studied by researchers since it provides higher performances than a standard Mo/Si multilayer; the SCORE mirrors show in fact a peak reflectance of around 40% at HeII 30.4 nm. Nevertheless, long term stability of this coating is an open problem. A study on the aging and stability of this multilayer has been carried on. SiC/Mg multilayer samples characterized by different structural parameters have been deposited. They have been measured just after deposition and three years later to verify degradation based on natural aging. Experimental results and analysis are presented.

8148-22, Session 6

Development of multilayer thin film filters for the full sun imager on solar orbiter

F. Auchère, X. Zhang, Institut d'Astrophysique Spatiale (France); F. Delmotte, E. Meltchakov, Lab. Charles Fabry de l'Institut d'Optique (France)

Membranes a few hundred nanometers thick are used in EUV optics to make, for example, beams splitters or bandpass filters. Despite their necessity in numerous applications these components are, because of their thinness, extremely fragile and their implementation in space instruments is always difficult. In the frame of the Solar Orbiter mission of ESA, the authors are developing for the EUI instrument suite thin film filters of high optical efficiency (transmittance, spectral selectivity) that are more robust than traditional components. We present the optical and mechanical properties of the prototype components.

8148-23, Session 6

High-resolution solar imaging with a photon sieve

J. M. Davila, NASA Goddard Space Flight Ctr. (United States)

Dissipation in the solar corona is expected to occur in extremely thin

**Conference 8148:
Solar Physics and Space Weather Instrumentation IV**

current sheets of order 1-100 km. Emission from these current sheets should be visible in coronal EUV emission lines. However, this spatial scale is far below the resolution of existing imaging instruments, because conventional optics cannot be easily manufactured with sufficient surface figure accuracy to obtain the required < 0.1 arcsec resolution. A photon sieve, a diffractive imaging element, can be manufactured to provide a few 10-3 arcsec resolution, with much more relaxed tolerances than conventional imaging technology.

A simple design for a sounding rocket payload is presented that obtain 80 mArcsec imaging with a 100 mm diameter photon sieve to image Fe XIV 334 and Fe XVI 335. These images will not only show the structure of the corona at a resolution never before obtained, they will also allow a study of the temperature structure.

8148-24, Session 6**Effect of varying heat load on lightweighted solar telescope mirror**

R. K. Banyal, B. Ravindra, Indian Institute of Astrophysics (India)

The next generation large aperture telescopes will probe the solar atmosphere at unprecedented detail. From the point of thermal management alone, the lightweighted mirrors offer significant advantages over heavy monolithic mirrors. Apart from significant reduction in weight, a lightweighted mirror reaches the thermal equilibrium with surroundings rapidly, thus reducing the detrimental effect of 'mirror seeing' on image quality. The lightweighting structure is created by removing pockets of material from the mirror blank in the form of triangular, hexagonal or circular cores without significantly affecting the rigidity and stiffness of the mirror. The resulting structure has side walls and ribs of certain thickness that supports the reflecting face plate of the mirror. Unlike solid mirror, the core structure created by the lightweighting process leads to material inhomogeneities within the mirror blank. The most conspicuous fallout of the different cell geometries and side wall structure is the appearance of thermal footprints on the reflecting surface. In this paper, we present our finite element method studies of surface deformations arising from thermally induced stress and temperature inhomogeneities inside a 2-m class lightweighted mirror. A simple physics-based model is used as an input to account for the existing thermal conditions at the observatory site. A comparative study is also made for two commonly used mirror substrate materials for optical telescopes, namely silicon carbide and Zerodur. The insight gained from these simulations will provide a valuable input for estimating the error budget and designing an efficient and stable thermal control system for the primary mirror.

8148-25, Session 6**Fabrication and metrology of the high-resolution coronal imager (Hi-C) primary and secondary mirrors**

B. M. Robinson, The Univ. of Alabama in Huntsville (United States); C. Griffith, T. J. Kester, M. R. Young, NASA Marshall Space Flight Ctr. (United States); W. Podgorski, Harvard-Smithsonian Ctr. for Astrophysics (United States); K. Kobayashi, The Univ. of Alabama in Huntsville (United States); J. Cirtain, NASA Marshall Space Flight Ctr. (United States)

The High Resolution Coronal Imager (Hi-C) is a high-resolution EUV solar imaging telescope designed to achieve ~ 0.2 arcsec resolution (0.1 arcsec pixel size). It is currently under development for a 2012

sounding rocket flight. Its primary and secondary mirrors are being fabricated and tested by the NASA Marshall Space Flight Center ES31 Optics Team. The figure specification for each mirror is given as a slope requirement extended to spatial periods of 4 mm, while higher spatial frequencies fall in the range of the roughness and microroughness specifications. These normal incidence, EUV mirrors serve as very high optical quality substrates for a ~ 50 layer-pair EUV coating. We present

the results of the mirror fabrication effort and detail some of the methods, implemented in Matlab code, to analyze the metrology data obtained for each mirror element during the fabrication process.

8148-26, Session 6**Spectral features: an overview**

H. H. Van Brug, TNO Science and Industry (Netherlands)

Most earth observation satellites use an on board diffuser to perform solar calibration measurements. The diffuser leads to, due to the narrow bandwidth of the spectrometer, speckle effects. Since the speckle patterns changes with about everything it is virtually impossible to calibrate out the speckle effects and they therefore limit the achievable accuracy.

In this presentation an overview of all our findings and insights in spectral features and ways to reduce them will be given. The specially designed SanDiff will be presented and the ideas behind it will be discussed. The modeling of the spectral features amplitude will be an important part of the presentation since this leads to the possibility to predict the achievable accuracy of the instruments before they are launched.

Special emphasis will be on the wavelength band where the largest problems are, the infra red band about $2.3\mu\text{m}$.

8148-27, Session 6**Atmospheric turbulence and high-precision ground-based solar polarimetry**

N. Krishnappa, A. J. Feller, Max-Planck-Institut für Sonnensystemforschung (Germany); S. Ihle, H. Soltau, PNSensor GmbH (Germany)

High-precision full-Stokes polarimetry at near diffraction limited spatial resolution is important to understand numerous physical processes on the Sun. In view of the next generation of ground based solar telescopes, we have explored, through numerical simulation, how polarimetric accuracy is affected by atmospheric seeing, especially in the case of large aperture telescopes with increasing ratio between mirror diameter and Fried parameter. In this work we focus on higher-order wavefront aberrations while suppressing tip/tilt terms. The numerical generation of time-dependent turbulence phase screens is based on the well-known power spectral method and on the assumption that the temporal evolution is mainly caused by wind driven propagation of frozen-in turbulence across the telescope. To analyze the seeing induced crosstalks between the Stokes parameters we consider different polarization modulation schemes, driven at frequencies between 1 Hz and several 100 Hz.

Further, we have started the development of a new fast solar imaging polarimeter, based on pnCCD detector technology from PNSensor. The first detector will have a size of 264×264 pixels and will work at frame rates of up to 1kHz, combined with a very low readout noise of 2-3 e-. The camera readout electronics will allow for buffering and accumulation of images corresponding to the different phases of the fast polarization modulation. A high write-out rate (~ 30 frames/s) will allow for post-facto image reconstruction. We will present the concept and the expected performance of the new polarimeter, based on the above-mentioned simulations of atmospheric seeing.

8148-28, Poster Session**Ly-alpha Polarimeter design for CLASP rocket experiment**

H. Watanabe, Kyoto Univ. (Japan); N. Narukage, M. Kubo, R. Ishikawa, T. Bando, R. Kano, S. Tsuneta, National Astronomical Observatory of Japan (Japan); K. Kobayashi, The Univ. of

**Conference 8148:
Solar Physics and Space Weather Instrumentation IV**

Alabama in Huntsville (United States); K. Ichimoto, Kyoto Univ. (Japan)

A sounding-rocket program called the Chromospheric Lyman-Alpha Spectro-Polarimeter (CLASP) is planned to be launched in 2014 summer. CLASP will observe the solar chromosphere in Ly-alpha (121.6 nm), aiming to detect the linear polarization signal produced by the Hanle effect for the first time. The polarimeter of CLASP consists of a half-waveplate, a beam splitter, and a polarization analyzer.

We use Magnesium Fluoride (MgF₂) as a material of these optical components, because MgF₂ exhibits birefringent property and high transparency at UV wavelength. We performed two experiment to know the optical constants of MgF₂ at Ly-alpha wavelength.

The first one is the retardation measurement of a stacking waveplate made of MgF₂ to derive the difference between ordinary and extraordinary refractive index. The retardation of a waveplate is determined by observing the modulated intensity come out of a rotating waveplate and a polarization analyzer. The thickness difference of a stacking waveplate needed for 180-degree retardation is 14.60 μm. The second experiment is the reflectance-and-transmittance measurement against oblique incident angles for the electric vector parallel and the electric vector perpendicular light. The ordinary refractive index and extinction coefficient along ordinary and extraordinary axis are derived with a least-square fitting in such a way that the reflectance and transmittance satisfy the Kramers-Kronig relation. The reflection at the Brewster's Angle of MgF₂ plate works as a good polarization analyzer.

We developed an engineering model of CLASP polarimeter using the MgF₂ half-waveplate, and polarization analyzers, and discuss the performance of this polarimeter.

8148-29, Poster Session**DIMMI-2h a MOF-based instrument for ADAHELI solar small mission**

F. Berrilli, Univ. degli Studi di Roma Tor Vergata (Italy); P. F. Moretti, Consiglio Nazionale delle Ricerche (Italy); D. Del Moro, M. Stangalini, Univ. degli Studi di Roma Tor Vergata (Italy); S. M. Jefferies, Univ. of Hawai'i (United States); G. Severino, M. Oliviero, INAF - Osservatorio Astronomico di Capodimonte (Italy)

The Doppler-Intensity-Magnetograms with a Magneto-optical filter Instrument at two heights (DIMMI-2h) is a double channel imager, using Magneto Optical Filters (MOF) in the potassium 770 nm and sodium 589 nm lines, proposed for solar small mission Advanced Astronomy for HELIophysics (ADAHELI). The instrument will provide simultaneous dopplergrams (velocity fields), intensity and longitudinal magnetic flux images at two heights in the solar atmosphere corresponding to low and high photosphere.

The spatial resolution (approximately 4 arcsec) and the high temporal cadence (15 s) will permit investigation of low and medium oscillating modes (from 0 to below 1000) up to approximately 32 mHz in the frequency spectrum. The acquisition of long-term simultaneous velocity, intensity and magnetic information up to these high frequencies will also permit the study of the propagation and excitation of waves with a frequency resolution never obtained before.

8148-30, Poster Session**The intensity effect in magneto-optical filters**

F. Berrilli, Univ. degli Studi di Roma Tor Vergata (Italy); M. Oliviero, G. Severino, INAF - Osservatorio Astronomico di Capodimonte (Italy); P. F. Moretti, Consiglio Nazionale delle Ricerche (Italy); S. M. Jefferies, Univ. of Hawai'i (United States)

Magneto-Optical Filters (MOF) are low-cost, low-weight instruments largely used on ground and particularly suitable for space applications. Therefore, any effort useful to improve the setup and calibration of MOFs

is worthwhile.

We used a laser system for determining the bandpasses of the two vapour cells, the Magneto-Optical Filter and the Wing Selector (WS), which are the core of solar narrow-band filters based on the MOF technology. A new result, which we called the Intensity Effect, was found: the MOF and WS bandpasses depend not only on the temperature at which the cell is heated and the external magnetic field in which the cell is embedded,

but also on the radiation intensity entering the cell. A theoretical interpretation of the Intensity Effect is proposed in terms of the kinetic equilibrium of the potassium atomic populations inside the vapour cell.

The Intensity Effect must be taken into account in setting-up MOF based instruments for solar and stellar observations as well as for modelling the MOF and WS spectral transmissions.

8148-31, Poster Session**OPSys: an optical payload systems facility for testing space coronagraphs**

S. Fineschi, G. Massone, G. Crescenzo, G. Capobianco, INAF - Osservatorio Astronomico di Torino (Italy); F. Anselmi, Alca Technology srl (Italy)

The Turin Astronomical Observatory recently completed construction in Altec, Turin, of a new Optical Payload System (OPSys) facility for tests of contamination sensitive optical space flight instruments. The facility is specially tailored for tests on solar instruments like coronagraphs. The solar simulator is an off-axis parabolic mirror collimating the light from the source with the solar angular divergence.

This presentation will describe the SPOCC's vacuum system and optical design, and the post-flight stray-light tests to be carried out on the Sounding-rocket Experiment (SCORE). This sub-orbital coronagraph is the prototype of the METIS coronagraph for the ESA Solar Orbiter mission. Solar Orbiter closest perihelion is one-third the Sun-Earth distances. The plans will be illustrated for testing METIS simulating in SPOCC the coronagraph observing conditions from the Solar Orbiter perihelion.

8148-32, Poster Session**Long term stability of optical coatings in close solar environment**

M. G. Pelizzo, A. J. Corso, P. Zuppella, Lab. for Ultraviolet and X-ray Optical Research (Italy); P. Nicolosi, Univ. degli Studi di Padova (Italy)

Observations of the solar atmosphere and surface are required in order to understand the solar activity and its influence on Earth. The ESA Solar Orbiter mission is conceived to be carried on such observations at the closest distance ever reached from the Sun, being the minimum perihelion at only 0.28 AU. At these distance, the spacecraft and instruments are immersed in a very harsh environment, characterized by high temperature and high density of ions carried on by the solar wind components. The stability of the optical components in these working conditions are a crucial point for the proper instruments functioning. In this work we present a series of experiment conceived for validating the optical coatings through the investigation of the environment effects. Experimental results that show the effects of solar wind low energy particles bombardment on coatings and multilayers are presented.

8148-33, Poster Session**Slitless solar spectroscopy**

J. M. Davila, NASA Goddard Space Flight Ctr. (United States); S. Jones, The Catholic Univ. of America (United States)

Conference 8148:
Solar Physics and Space Weather Instrumentation IV

Spectrographs have traditionally suffered from the inability to obtain line intensities, widths, and Doppler shifts over large spatial regions of the Sun quickly because of the narrow instantaneous field of view. This has limited the spectroscopic analysis of rapidly varying solar features like, flares, CME eruptions, coronal jets, and reconnection regions. Imagers have provided high time resolution images of the full Sun with limited spectral resolution.

In this paper we present recent advances in deconvolving spectrally dispersed images obtained through broad slits. We use this new theoretical formulation to examine the effectiveness of various potential observing scenarios, spatial and spectral resolutions, signal to noise ratio, and other instrument characteristics.

This information will lay the foundation for a new generation of spectral imagers optimized for slitless spectral operation, while retaining the ability to obtain spectral information in transient solar events.

8148-34, Poster Session

Earth-Affecting Solar Causes Observatory (EASCO): a mission at the Sun-Earth L5

N. Gopalswamy, NASA Goddard Space Flight Ctr. (United States); F. Auchère, Institut d'Astrophysique Spatiale (France)

Coronal mass ejections (CMEs) corotating interaction regions (CIRs) originate from the closed and open magnetic regions on the Sun, respectively. Imaging these source regions is important because CMEs and CIRs have important space weather consequences. The current understanding of CMEs primarily comes from the SOHO and STEREO missions, but these missions lacked some key measurements: STEREO did not have a magnetograph; SOHO did not have in-situ magnetometer). From the Sun-Earth line, SOHO was not well-suited for observing Earth-directed CMEs because of the occulting disk. STEREO's angle with the Sun-Earth line is changing constantly, so only a limited number of Earth-directed CMEs were observed in profile. In order to overcome these difficulties, we proposed a new L5 mission concept known as the Earth-Affecting Solar Causes Observatory (EASCO). The mission concept was recently studied at the Mission Design Laboratory (MDL), NASA Goddard Space Flight Center. The aim of the MDL study was to see how the scientific payload consisting of ten instruments can be accommodated in the spacecraft bus, what propulsion system can transfer the payload to the Sun-Earth L5, and what launch vehicles are appropriate. The study found that all the ten instruments can be readily accommodated and can be launched using an intermediate size vehicle such as Taurus II with enhanced faring. The study also found that a hybrid propulsion system consisting of an ion thruster (using ~55 kg of Xenon) and hydrazine (~10 kg) is adequate to place the payload at L5. The transfer will take about 2 years and the science mission will last for 4 years around the next solar maximum in 2025. The mission can be readily extended for another solar cycle to get a solar-cycle worth of data on Earth-affecting CMEs and CIRs. This paper describes the EASCO mission, the scientific payload, and the results of the MDL study.

8148-35, Poster Session

Space-qualified liquid-crystal variable retarders for wide FOV coronagraphs

N. Uribe-Patarroyo, A. Alvarez-Herrero, P. García Parejo, J. Vargas, R. L. Heredero, R. Restrepo, Instituto Nacional de Técnica Aeroespacial (Spain); V. Martínez-Pillet, Instituto de Astrofísica de Canarias (Spain); J. C. del Toro Iniesta, A. Lopez, Instituto de Astrofísica de Andalucía (Spain); S. Fineschi, G. Capobianco, INAF - Osservatorio Astronomico di Torino (Italy); M. Georges, Centre Spatial de Liège-CSL (Belgium); M. López, Visual Display S.L.L. (Spain); G. Boer, ARCOptix S.A. (Switzerland); I. G. Manolis, European Space Research and Technology Ctr. (Netherlands)

Liquid-crystal variable retarders (LCVRs) are an emergent technology for space-based polarimeters, following its success as polarization modulators in ground-based polarimeters and ellipsometers. Although they provide many advantages to both ground- and space-based instrumentation with respect to more traditional modulators, they have some characteristics that should be taken into account and, if necessary, addressed during the instrument design. One of the more important properties of any polarization modulator is its angular acceptance. In the case of nematic LCVRs, due to the very principle in which they provide variable retardance, the angular sensitivity is variable, and is a function of the retardance state (given by applied voltage) of the LCVR. At some retardance regimes, this dependence can be large and might not be affordable by the polarimetric signal-to-noise ratio requirements.

Wide-field double nematic LCVRs were proposed to address this shortcoming (Y. Itoh et al., Jpn. J. Appl. Phys. Lett. 30, L1296 -L1299 (1991)) and used in a tunable filter (G. A. Kopp et al., Appl. Opt. 36, 291 (1997)). In the framework of the project "Validation of LCVRs for the Solar Orbiter Polarization Modulation Package" (A. Alvarez-Herrero et al., Polarization Science and Remote Sensing V, SPIE 2011), we designed and built wide-field LCVRs, modelled their angular acceptance and validated this technology for space environmental conditions, including a campaign studying the effects of gamma, proton irradiation, vibration and shock, thermo-vacuum and ultraviolet radiation. Additionally, we propose some improvements that could improve even further the performance of this technology in space applications.

Liquid-crystal variable retarders (LCVRs) are an emergent technology for space-based polarimeters, following its success as polarization modulators in ground-based polarimeters and ellipsometers. Wide-field double nematic LCVRs address the high angular sensitivity of nematic LCVRs at some voltage regimes. We present a work in which wide-field LCVRs were designed and built. A detailed model of their angular acceptance was made, and we validated this technology for space environmental conditions, including a campaign studying the effects of gamma, proton irradiation, vibration and shock, thermo-vacuum and ultraviolet radiation.

Conference 8149:

Astronomical Adaptive Optics Systems and Applications V

Sunday-Wednesday 21-24 August 2011 • Part of Proceedings of SPIE Vol. 8149
Astronomical Adaptive Optics Systems and Applications IV

8149-01, Session 1

Integration and test of the Gemini Planet Imager

S. Thomas, B. A. Macintosh, D. T. Gavel, D. Dillon, J. R. Graham, Univ. of California, Santa Cruz (United States); D. W. Palmer, Lawrence Livermore National Lab. (United States); R. Doyon, Univ. de Montréal (Canada); J. Dunn, L. Saddlemyer, National Research Council Canada (Canada); J. E. Larkin, Univ. of California, Los Angeles (United States); B. R. Oppenheimer, American Museum of Natural History (United States); A. Sivaramakrishnan, Space Telescope Science Institute (United States); J. K. Wallace, Jet Propulsion Lab. (United States); R. Soummer, Space Telescope Science Institute (United States); B. J. Bauman, L. A. Poyneer, Lawrence Livermore National Lab. (United States); C. Marois, National Research Council Canada (Canada); J. Chilcote, Univ. of California, Los Angeles (United States)

The race to higher contrast imaging is an ongoing theme in exoplanet imaging, both from earth and from space. Next-generation instruments such as the Gemini Planet Imager (GPI) and SPHERE are designed to achieve contrast ratios of 10^6 - 10^7 ; this requires very good wavefront correction and coronagraphic control of diffraction. GPI is a facility instrument, now in integration and test, with first light on the 8-m Gemini South telescope expected by the beginning of 2012. It combines a 1700 subaperture AO system using a MEMS deformable mirror, an apodized-pupil Lyot coronagraph, a high-accuracy IR interferometer calibration system, and a near-infrared integral field spectrograph to allow detection and characterization of self-luminous extrasolar planets at planet/star contrast ratios of 10^6 . In this paper we will discuss the status of the integration and test happening at the University of Santa Cruz California.

8149-03, Session 1

The TMTracer: a modeling tool for the TMT alignment and phasing system

P. K. Piatrou, G. A. Chanan, Univ. of California, Irvine (United States)

The Alignment and Phasing System (APS) is one of the key parts of the Thirty Meter Telescope (TMT) active optics system, with the responsibility for evaluating and correcting the pre-adaptive optics wavefront delivered by the telescope. APS is a high complexity system comprising a multi-channel wavefront-sensing instrument that produces as many as 250,000 discrete measurements and control software that delivers commands to about 12,000 active optics system actuators. The APS software is designed to guide the instrument development and predict its performance via simulation and also ultimately to serve the physical instrument itself.

The software is built around a modeling tool we have developed called TMTracer, which is tailored to the optical alignment of extremely large segmented telescopes. We will present the underlying philosophy of TMTracer, as well as its architecture and sample simulation results that demonstrate its capabilities.

8149-04, Session 1

Athermal design of the optical tube assemblies for the ESO VLT Four Laser Guide Star Facility

R. Henselmans, D. Nijkerk, M. Lemmen, F. Kamphues, TNO Science and Industry (Netherlands)

TNO is developing the Optical Tube Assemblies (OTAs) for the ESO VLT Four Laser Guide Star Facility. The OTAs are Galilean 20x beam expanders, expanding a 15 mm diameter input beam to a steerable 300 mm diameter output beam with a wavefront quality requirement of 50 nm rms. The allowed defocus under the influence of the changing environmental air temperature (0 - 15°C , -0.7°C/hr gradient) is only 0.2 fringes. It is a refractive design, consisting of a small negative entrance lens (L1), a 45° tip-tilt field selector mirror (FSM) and a positive 380 mm diameter aspherical exit lens (L2). The FSM can point the beam over a 6 arcmin field of view radius with 0.1 arcsec rms accuracy. Main subject of this paper is the thermal stability.

The thermal behaviour of the system has been analyzed by combining optical, lumped mass and FE analyses. The refractive index of glass and air changes with temperature, from the environmental influences and laser absorption. The defocus of the system therefore depends on the temperature of L1, L2, the air, and the structure between the lenses, with an error budget of only a few micrometers. A design that is passively athermalized over a large temperature range as well as under the influence of thermal gradients has hereto been developed. Realization is currently underway, and thermal performance tests will be shown.

8149-05, Session 1

Overview of the control strategies for the TMT alignment and phasing system

P. K. Piatrou, G. A. Chanan, Univ. of California, Irvine (United States)

In this paper we present the current status of control algorithm development for the Thirty Meter Telescope (TMT) Alignment and Phasing System (APS). We discuss ways to address the main challenges inherent in the active control of extremely large segmented telescopes: high complexity of the control problem, disentangling the aberrations on the primary, secondary and tertiary mirrors, and the tight requirements for residual errors. We also present preliminary APS performance estimates derived from simulations.

8149-07, Session 2

Advancements in laser tomography implementation at the 6.5m MMT telescope

E. A. Bendek, College of Optical Sciences, The Univ. of Arizona (United States); M. Hart, The Univ. of Arizona (United States)

Laser tomography capability using the Multi Laser Guide Star system is being implemented at the 6.5 m MMT telescope at Mt. Hopkins AZ. The system uses five range gated and dynamically refocused Rayleigh laser beacons to perform the tomographic sampling of the atmosphere. The correction is then applied to the wavefront using the 336-actuator adaptive secondary mirror of the telescope. Laser tomography will be attempted by means of a least squares reconstructor, which is obtained using an additional infinite conjugated natural guide star. This paper also discuss methods to find the pupil misregistration of each laser and

information about the turbulence intensity distribution C_n^2 , which are important to optimize the system for least square tomography approach but are critical to build analytic tomographic reconstructors.

8149-08, Session 2

Wavefront control with SCEAO: concepts and first on-sky results

O. Guyon, F. Martinache, C. Clergeon, R. Russell, Subaru Telescope, National Astronomical Observatory of Japan (United States); T. Groff, Princeton Univ. (United States); V. Garrel, Subaru Telescope, National Astronomical Observatory of Japan (United States)

The Subaru Coronagraphic Extreme Adaptive Optics (SCEAO) system uses advanced coronagraphic technique for high contrast imaging of exoplanets and disks as close as $1 \lambda/D$ from the host star. In addition to unusual optics, achieving high contrast at this small angular separation requires a wavefront sensing and control architecture which is optimized for exquisite control and calibration of low order aberrations. The SCEAO system was thus designed to include the wavefront sensors required for bias-free high sensitivity and high speed wavefront measurements. Information is combined from two infrared wavefront sensors and a fast visible wavefront sensors to drive a single MEMS type deformable mirror mounted on a tip-tilt mount. The wavefront sensing and control architecture is highly integrated with the coronagraph system. We describe the architecture and show recent results obtained on sky during our recent engineering observations.

8149-09, Session 2

A sensitivity comparison between the non-linear curvature wavefront sensor and the Shack-Hartmann wavefront sensor in broadband

M. Mateen, Air Force Research Lab. (United States); O. Guyon, Subaru Telescope, National Astronomical Observatory of Japan (United States); M. Hart, The Univ. of Arizona (United States)

In this paper we present results from a side-by-side comparison of the non-linear curvature wavefront sensor (nCWFS) with the Shack-Hartmann wavefront sensor (SHWFS). The non-linear curvature technique is derived from the successful curvature wavefront sensing concept, but uses a non-linear wavefront reconstruction scheme. The nCWFS approaches the theoretical sensitivity limit imposed by fundamental physics by taking advantage of wavefront spatial coherence in the pupil plane. Interference speckles formed by natural starlight encode wavefront aberrations with the sensitivity set by the telescope's diffraction limit (λ/D) rather than the seeing limit of more conventional linear WFSs. The nCWFS offers high sensitivity on reasonably bright targets $m_V < 15$.

In our last paper we showed verification of the nCWFS technique and an initial comparison of the nCWFS with the SHWFS at monochromatic light. In this paper we extend the analysis to polychromatic light. We have designed an experiment that allows for polychromatic compensation by use of refractive optics and minimizes chromatic aberration of the diffraction-limited speckles. The current design is ready to be implemented on a telescope. We show results of a comparison of the wavefront correction performed by the nCWFS and the SHWFS for broadband imaging. Phase Wheels are used to generate atmospheric turbulence in the lab. Our results show that the exquisite control of low order aberrations by the nCWFS delivers significant gain in sensitivity over the SHWFS.

8149-10, Session 2

Image plane phase-shifting wavefront sensor for giant telescope active and adaptive optics

F. Hénault, Univ. de Nice Sophia Antipolis (France)

Since the realization of the twin Keck telescopes of 10-meter diameter built atop the Mauna Kea in Hawaii, the technology of segmented mirrors has become a cornerstone for on-going projects of Extremely Large Telescopes (ELT). Here the individual mirror segments should actually be phased (i.e. reconstruct the surface of an ideal giant mirror) within an accuracy typically better than one tenth of the operating wavelength. This could be done using existing Wavefront Sensors (WFS), but may also involve the development of alternative methods: herein is described a new generation WFS operating in the image plane and able to sense differential piston errors of the segments with residual errors around 10 nm by means of a phase-shifting technique. We describe the principle of the method in both monochromatic and polychromatic light and present its achievable performance in terms of limiting magnitude of the guide star in presence of various noise sources. It is emphasized that the technique is also applicable for co-phasing sparse aperture interferometers, or more generally to any Adaptive Optics (AO) system making use of image plane WFS.

8149-12, Session 3

Demonstration of 17 cm robust carbon fiber deformable mirror for adaptive optics

S. M. Ammons, Lawrence Livermore National Lab. (United States); M. Hart, The Univ. of Arizona (United States); B. Coughenour, College of Optical Sciences, The Univ. of Arizona (United States); R. Romeo, R. Martin, Composite Mirror Applications, Inc. (United States)

CFRP composites provide several advantages as a substrate for thin-shell adaptive secondary mirrors, including high stiffness to-weight ratio, robustness, and zero coefficient of thermal expansion (CTE). We use 8 and 17 cm prototype CFRP thin-shell deformable mirrors to show that residual CTE variation may be addressed with mounted actuators for a variety of mirror sizes. We present measurements of surface quality at a range of temperatures characteristic of mountaintop observatories. For the 8 cm piece, the figure error of the Al-coated reflective surface under best actuator correction is ~ 43 nm RMS, placing it into consideration for use in near-IR astronomy. The low surface error internal to the outer ring of actuators (17 nm RMS at 15 C and 33 nm RMS at -5 C) suggests that larger mirrors will have a similar figure quality under actuator correction on ground-based Adaptive Optics systems. Surface roughness is low (< 3 nm P-V) at a variety of temperatures. We present new figure quality measurements of the larger 17 cm piece, showing that the figure error does not scale sharply with mirror diameter. These experiments demonstrate CFRP's potential as a lightweight, robust substrate for large, 1-m thin-shell deformable secondary mirrors.

8149-13, Session 3

Bending modes for active optics

B. W. Smith, Lowell Observatory (United States); B. Cuerden, The Univ. of Arizona (United States)

While the concept of wavefront decomposition is a foundation of active optics systems, the choice of basis functions for mirror figure control is divided. The common functions are Zernike polynomials, ubiquitously used for wavefront descriptions, and bending (also called minimum energy or vibration) modes which offer optimal performance. We present a look at the comparative performance between the two approaches, and discuss an implementation approach which seeks to combine much of the analytic and interface simplicity of Zernike polynomials with the improved performance of bending modes.

8149-20, Session 3

Linear estimation of the Giant Magellan Telescope inter-segment piston error from wave-front sensor data

M. Hart, Ctr. for Astronomical Adaptive Optics, Steward Observatory (United States)

The Giant Magellan Telescope (GMT) will place seven 8.4 m diameter primary mirror segments on a common mount to form a single co-phased aperture of 25 m. High order adaptive optics based around an adaptive secondary mirror will be used to operate the telescope at the diffraction limit in the near infrared. Critical to the performance of the telescope will be real-time correction of atmospherically-induced phase errors between the primary mirror segments. The gaps between the segments, where the aberrated wavefront is not explicitly measured by the sensors of the adaptive optics, are approximately 30 cm at their narrowest points.

In an idealized case where the atmospheric phase aberration is characterized by layers of frozen turbulence moving over the telescope pupil with their respective wind velocities, the instantaneous piston differences between the mirror segments could, despite the missing wavefront information, be well estimated by examining the immediate history of the aberration. Aberration in the gaps at any given time would be visible to the sensors in earlier data. The real value of the approach is hard to assess from simulations, which almost always model the atmosphere as layers of frozen flow and therefore can be expected to yield overly optimistic results. These considerations have led to a study of data from the first-light AO system now running on the Large Binocular Telescope (LBT), which closely mimics one of the GMT segments. The data are of very high quality and realistically capture the temporal behavior of the wavefront. I use data from two nights to show that the GMT segment piston errors may be estimated to <30 nm accuracy with a simple linear estimator, but that in fact looking back in time, at least over a period of about 10 ms, is not helpful.

8149-14, Poster Session

Na variability and LGS elongation: impact on wavefront error

K. J. Jones, WBAO Consultant Group (United States)

Variation in density structure and altitude of mesospheric sodium impact the performance of Adaptive Optics using the sodium laser guide stars. A column through a 15-20 km thick layer is illuminated and backscattered photons are created in the direction of the science target. With larger entrance apertures, LGS are seen as cylinders with an intensity structure that reflects the density structure of the sodium layers. Such elongation spreads the sodium light over more WFS pixels and reduces signal-to-noise ratios. Sodium layer structures change due to wind shear, gravity wave overturning and turbulence, course variation in the centroid altitude of the sodium layer, so the AO system is degraded. This effect is proportional to the square of the telescope diameter: 30 m for TMT and 42 m for E-ELT.

Na variation and consequent elongation is generally determined by means of lidar. For TMT, the Large Zenith Telescope (LZT) lidar employs a Nd:YAG-pumped dye laser. Backscattered photons are collected with a 6 m mercury primary mirror of the LZT. This allows meter-scale spatial resolution and sub-second temporal resolution. The lidar system serving the ESO Paranal observatory is based on a 589.0 laser generated by mixing the 1064 and 1319 nm outputs from seeded neodymium YAG lasers.

Na variability will be examined and the resulting LGS elongation analyzed for its impact on Adaptive Optics systems. TMT and E-ELT will be compared for mitigation of LGS elongation and wavefront error.

8149-15, Poster Session

On numerical simulation of high-speed CCD/CMOS-based wavefront sensors in adaptive optics

M. V. Konnik, J. S. Welsh, The Univ. of Newcastle (Australia)

Wavefront sensors, which use solid-state CCD or CMOS photosensors, are sources of errors in adaptive optics systems. Inaccuracy in the detection of wavefront distortions introduce considerable errors into wavefront reconstruction and leads to overall performance degradation of adaptive optics system. The accuracy of wavefront sensors is significantly affected by photosensor noise. Thus it is crucial to formulate a high-level image sensor system model that enable adaptive optics engineers to simulate realistic effects of noise from wavefront sensors. However, the complexity of solid-state photosensors and multiple noise sources makes it difficult to formulate an adequate model of the photosensors. Moreover, the characterisation of the simulated sensor and comparison with real hardware is often incomplete due to lack of comprehensive standards and guidelines. Such circumstances lead to oversimplified models of wavefront sensors and consequently imprecise numerical simulation results.

The paper presents an approach for the modelling of noise sources for CCD and CMOS sensors that are used for wavefront sensing in adaptive optics. Both dark and light noises such as fixed pattern noise, photon shot noise, and a read noise, as well as, charge-to-voltage noises are described. Procedures for characterisation of both light and dark noises of the simulated photosensors are provided. Numerical simulation results of a photosensor for high-frame rate Shack-Hartmann wavefront sensor are presented.

8149-16, Poster Session

Influence of photosensor noise on accuracy of cost-effective Shack-Hartmann wavefront sensors

M. V. Konnik, J. S. Welsh, The Univ. of Newcastle (Australia)

A Shack-Hartmann (SH) wavefront sensor (WFS) is used in most modern adaptive optics systems where precision and robustness of centroiding are important issues. The accuracy of the SH WFS depends not only on lenslet quality but also on the measurement accuracy of centroids, especially in low-light conditions. In turn, accuracy depends on light and dark noises that are inevitably present in solid-state photosensors. Using a comprehensive mathematical model of the CMOS photosensor, the accuracy of the Shack-Hartmann wavefront sensor is assessed and analysed for each type of noise.

In this paper, new results regarding the influence of different noise sources from a CMOS photosensor on centroiding in Shack-Hartmann wavefront sensors are presented. For the numerical simulations, a comprehensive mathematical model of photosensor's noise was formulated. The influence of light and dark noises as well as pixelisation factor have been assessed. Analysis of the wavefront sensor's accuracy is provided. Results should be of interest for further development of high-speed wavefront sensors.

8149-17, Poster Session

Research on calibration method of LAMOST fiber robot

Z. Liu, Z. Chao, H. Hu, J. Wang, J. Chu, Univ. of Science and Technology of China (China)

Large sky area multi-object fiber spectroscopy telescope (LAMOST) is an innovative reflecting schmidt telescope. One of its key technology is 4000 dual rotational fiber robot located in the focal plane.

Conference 8149:
Astronomical Adaptive Optics Systems and Applications V

In accordance with the requirements of the star-observations and the positioning mode of the fiber robot, we confirm seven necessary precise positioning parameters and a calibration curve for each fiber robot. It is difficult to obtain these parameters rapidly in the complex field environment. We attempt to discuss the calibration problem based on CCD, due to the camera aberration, the spherical focal plane and the high-precision positioning requirement.

We propose a fast calibration method, include of CCD camera calibration using the installation location of the fiber robot in the focal plane, spherical coordinate rotation algorithm, multi-subregion calibration and coordinate splicing based on installation location. Finally, we describe the calibration process of the LAMOST fiber robot.

8149-18, Poster Session

An automated aircraft detection system to prevent aircraft illumination from the laser guide star beacons at the MMT and LBT

K. Newman, M. Hart, The Univ. of Arizona (United States)

High powered guide star laser beams are a potential hazard for aircraft. Currently at the MMT telescope located on Mt. Hopkins in Southern Arizona, five Rayleigh guide stars create a total of 25 W of power at 532nm wavelength. The ARGOS laser guide star for the LBT located on Mt. Graham in Southern Arizona will generate six Rayleigh guide stars with a total of 108 W at 532nm. We present an automated system for use at the MMT and the LBT designed to detect aircraft and shutter the lasers when aircraft illumination is pending. The detection system at the MMT uses a single wide-angle CCD camera mounted to the optical support structure of the telescope. The LBT system employs two wide-field CCDs, and an additional bore-sighted infrared camera. The CCDs integrate frames for 2 seconds to produce streaks from anti-collision beacons required for all aircraft. Successive frames are compared using image processing software to detect streaks and movement in the field. If an aircraft is detected, the position and projected trajectory are calculated and compared to the position of the laser beams. If an aircraft illumination is suspected, the laser safety shutter is closed and a message is sent to the laser operator. As a safety precaution, a "heartbeat" signal is required to keep the laser shutter open.

8149-19, Poster Session

Status report on the large binocular telescope's ARGOS ground-layer AO system

M. Hart, The Univ. of Arizona (United States); S. Rabien, Max-Planck-Institut für extraterrestrische Physik (Germany); L. Busoni, INAF - Osservatorio Astrofisico di Arcetri (Italy)

ARGOS, the laser-guided adaptive optics system for the Large Binocular Telescope (LBT), is now under construction at the telescope. By correcting atmospheric turbulence close to the telescope, the system is designed to deliver high resolution near infrared image quality over a field of 4 arc minute diameter. Each side of the LBT is being equipped with three Rayleigh laser guide stars derived from six 18 W pulsed green lasers and projected into two triangular constellations matching the size of the corrected field. The returning light is to be detected by wavefront sensors that are range gated within the seeing-limited depth of focus of the telescope. Wavefront correction will be introduced by the telescope's deformable secondary mirrors driven on the basis of the average wavefront errors computed from the respective guide star constellation. Measured atmospheric turbulence profiles from the site lead us to expect that by compensating the ground-layer turbulence, ARGOS will deliver median image quality of about 0.2 arc sec across the JHK bands. This will be exploited by a pair of multi-object near-IR spectrographs, LUCIFER1 and LUCIFER2, with 4 arc minute field already operating on the telescope.

Conference 8150: Cryogenic Optical Systems and Instruments XIV

Wednesday–Thursday 24–25 August 2011 • Part of Proceedings of SPIE Vol. 8150
Cryogenic Optical Systems and Instruments XIII

8150-23, Poster Session

Testing and calibration of phase plates for JWST optical simulator

Q. Gong, NASA Goddard Space Flight Ctr. (United States); J. Chu, Orbital Sciences Corp. (United States); S. C. Tournois, Sigma Space Corp. (United States); W. L. Eichhorn, D. A. Kubalak, NASA Goddard Space Flight Ctr. (United States)

Three phase plates were designed to simulate the JWST segmented primary mirror wavefront at three on-orbit alignment stages: coarse phasing, intermediate phasing, and fine phasing. The purpose is to verify JWST's on-orbit wavefront sensing capability. Amongst the three stages, coarse alignment is defined to have piston error between adjacent segments being 30 μm to 300 μm , intermediate being 0.4 μm to 10 μm , and fine is below 0.4 μm . The phase plates were made of fused silica, and were assembled in JWST Optical Simulator (OSIM). The piston difference was realized by the thickness difference of two adjacent segments. This paper emphasizes the testing and calibration of the phase plates at ambient and at cryo. The parameters to be calibrated are piston and wavefront errors. Dispersed Fringe Sensor (DFS) method was used for coarse and intermediate piston measurement. Point Diffraction Interferometer (PDI) was used for fine piston and wavefront error. In order to remove piston's 2 π uncertainty with PDI, three laser wavelengths, 640nm, 660nm, and 780nm, were used for the measurement. The same tests were performed at ambient and at cryo. The test setup, analysis algorithm and the results at ambient and cryo are presented. The phase plate design concept and its application (i.e. verifying the JWST on-orbit alignment algorithm) are described. The layout of JWST OSIM and the function of phase plates in OSIM are also addressed briefly.

8150-24, Poster Session

Development of four-color simultaneous imager for efficient and reliable color measurements in the era of large-scale surveys

D. Kinoshita, C. Wu, T. Chen, R. Huang, P. Shen, National Central Univ. (Taiwan)

A four-color simultaneous imager is now being developed as a first generation astronomical instrument for 2-m telescope which is being built at Lulin observatory in Taiwan. The aim of this instrument is to conduct immediate and intensive follow-up observations of newly identified objects detected by Pan-STARRS PS1 sky surveys. A set of dichroic mirrors split the light from the telescope, and the images are recorded by four CCD imagers. A fully depleted CCD is used for y-band camera to enhance the sensitivity, and three deep depleted CCDs are used for r', i', and z'-band cameras. A simultaneous imager is useful to provide reliable color measurements of transient objects and moving objects even under relatively poor sky conditions. It also improves the observing efficiency. We report the scientific objectives, overall design, development strategy, current status of the development, and characterization of unit cameras under the CCD temperature of -100 deg C.

8150-25, Poster Session

A panchromatic imaging Fourier transform spectrometer for the NASA Geostationary Coastal and Air Pollution Events Mission

J. Wu, R. W. Key, J. Blavier, S. P. Sander, Jet Propulsion Lab. (United States)

This paper summarizes the design and development of the Panchromatic Imaging Fourier Transform Spectrometer (PanFTS) for the NASA Geostationary Coastal and Air Pollution Events (GEO-CAPE) Mission. The PanFTS instrument will advance the understanding of the global climate and atmospheric chemistry by measuring spectrally resolved outgoing thermal and reflected solar radiation. With continuous spectral coverage from the near-ultraviolet through the thermal infrared, this instrument is designed to measure pollutants, greenhouse gases, and aerosols as called for by the NASA GEO-CAPE mission. The PanFTS instrument is a hybrid based on spectrometers like the Tropospheric Emissions Spectrometer (TES) that measures thermal emission, and those like the Orbiting Carbon Observatory (OCO), and the Ozone Monitoring Instrument (OMI) that measure scattered solar radiation. Simultaneous measurements over the broad spectral range from UV to IR are accomplished by a two sided interferometer with separate optical trains and detectors for the UV-visible and IR spectral domains. This allows the instrument design to be independently optimized for both spectral domains. The overall design is compact because the two sides share a single common interferometer optical path difference mechanism (OPDM) and metrology laser as well as a number of other instrument systems including the line-of-sight pointing mirror, the data management system, thermal control system, electrical system, and the mechanical structure. The PanFTS breadboard instrument has been tested in the laboratory and demonstrated the basic functionality for simultaneous measurements in the visible and IR. It is now operating in the field measuring the atmospheric chemistry across the Los Angeles basin.

8150-01, Session 1

Emittance properties of multiwalled carbon nanotubes coatings in the infrared spectral region

M. A. Quijada, J. G. Hagopian, S. A. Getty, E. J. Wollack, NASA Goddard Space Flight Ctr. (United States)

Recent visible wavelength observations of Multiwalled Carbon Nanotubes (MWCNT) coatings have revealed that they represent the blackest materials known in nature with a Total Hemispherical Reflectance (THR) less than 0.25%. This makes them as exceptionally good absorbers, with the potential to provide order-of-magnitude improvement in stray-light suppression over current black surface treatments when used in an optical system. Here we extend the characterization of this class of materials into the infrared spectral region to further evaluate their potential for use on instrument baffles for stray-light suppression and to manage spacecraft thermal properties to dissipate heat through radiant heat transfer process. These characterizations will include the wavelength-dependent Total Hemispherical Reflectance properties in the mid-IR and far-infrared spectral regions (2-to-100 μm). Determination of the temperature-dependent emittance will be investigated in the temperature range of 20-to-300 K. These results will be compared against other more conventional black coatings such as Z-306 or Acktar black coatings among others. We will also provide numerical electromagnetic model calculations for tuning the MWCNT growth geometry to further enhance performance in the infrared spectral region.

Conference 8150:
Cryogenic Optical Systems and Instruments XIV

8150-02, Session 1

A novel approach to tribological measurements at harsh conditions

E. Weltevreden, E. van der Heide, TNO Science and Industry (Netherlands)

When dealing with high-tech equipment, accurate positioning is of the utmost importance to ensure durability and a productive lifetime. Unexpected high friction or wear of positioning mechanisms can lead to unnecessary down-time or products that are not up to specification.

To ensure a sufficient lifetime, it is necessary to know beforehand how the sliding and rolling contacts will behave over time. This demand becomes more stringent when the machine operates at extreme conditions, e.g. vacuum or extremely low temperatures. Traditional greases and mineral oil based lubricants do not perform adequately in such extreme environments, since they either contaminate the vacuum or do not provide sufficient film thickness. TNO recently developed an unique measuring application, the TNO cryotribometer, in order to measure friction and wear of position mechanisms at harsh conditions. The centre of the tribometer consists of a rotating disk, which can be actuated by means of a stepper motor using a feedthrough. Because of the temperature (120 K to 420 K) and the pressure (1 bar to 10⁻⁶ mbar) in the vacuum chamber, the feedthrough had to be isolated to ensure a proper measurement. Measurements were conducted using a spherical shaped surface which was placed against the test disk by means of dead-weight. The results show that the contact pressure and the sliding velocity influenced the friction level greatly. This set-up is currently used to find and analyse different material combinations, which demonstrate a constant friction level under cryogenic vacuum conditions. Only when the friction level is constant accurate positioning can be guaranteed.

8150-03, Session 1

Cryogenic half-wave plate polarimeter using a superconducting magnetic bearing

J. M. Klein, Univ. of Minnesota, Twin Cities (United States)

We present an implementation of a superconducting magnetic bearing (SMB) for use as a rotation mechanism for half-wave plate (HWP) polarimetry and discuss the integration of this system into a millimeter-wave balloon-borne polarimeter. In this implementation the 24 cm diameter HWP is enclosed by NdFeB ring magnet, which forms the rotor of the SMB. The stator is made of YBCO high temperature superconductor and is heat sunk to a liquid helium bath. At temperatures above the superconducting transition of YBCO, a warm support mechanism suspends the rotor relative to the stator and provides sufficient thermal conductance to cool the 5.6 kg rotor to 77 K in less than 20 hours. The rotor is belt-driven by a pulley that is connected to a motor outside the cryostat. A rotor-mounted chopper wheel, in combination with a cryogenic laser and diode detector, provide angular encoding for the HWP. We demonstrate robust, remote operation of this system with the EBEX balloon-borne payload. Rotation speed was 2 Hz, RMS angular encoding accuracy during the flight was 0.01 degrees and RMS rotation speed variation was 0.2%. We discuss sources of power dissipation and rotation speed variations. We characterize the resonant frequencies and time constants of the system. We find that the radial resonance frequency is $r(2)$ that of the axial one, consistent with predictions for an SMB. The implementation is a candidate for low noise space applications because of the absence of stick-slip friction and low wear.

8150-04, Session 1

A flux-pinning mechanism for segment assembly and alignment

J. A. Gersh-Range, M. A. Peck, Cornell Univ. (United States); H. P. Stahl, Marshall Space Flight Ctr. (United States)

Currently, the most compelling astrophysics questions include how planets and the first stars formed and whether there are protostellar disks that contain large organic molecules. Although answering these questions will require space telescopes with apertures of at least 10 meters, it is challenging to construct such large space telescopes by scaling up previous designs; the limited capacity of a launch vehicle places an upper bound on the diameter of a monolithic primary, and beyond a certain size, deployable telescopes cannot fit in any current launch vehicle fairing. One potential solution is to connect the primary mirror segments edgewise using flux-pinning mechanisms. A type of interaction between a magnet and a type II superconductor, flux pinning is analogous to a damped spring force.

In the baseline design, a flux-pinning mechanism consists of a magnet and a superconductor separated by a predetermined gap, with the amount of damping adjusted by placing aluminum near the interface. Since flux pinning is possible only when the superconductor is cooled below a critical temperature, flux-pinning mechanisms are uniquely suited for cryogenic space telescopes. These non-contact mechanisms operate best at low temperatures, unlike mechanical mechanisms, which can have problems with lubrication, CTE matching, and thermal snap. By placing these mechanisms along the edges of the mirror segments, a primary can be built up over time. Since flux pinning requires no mechanical deployments, the assembly process can be robotic or use some other non-contacting scheme. Advantages of this approach include scalability and passive stability.

8150-05, Session 1

Space and air-borne sensor testing in a cryogenic test environment at Arnold Engineering Development Center

H. Lowry, S. L. Steely, R. Nicholson, J. Gastineau, M. L. Fedde, J. M. Labello, Aerospace Testing Alliance (United States)

Performance testing of space imaging systems is crucial to meeting the requirements of such systems for all types of space applications. The use of infrared scene projection systems in the cryo-vacuum ground test environment is essential to this testing and is a challenging task. Experiences from the space test facilities at Arnold Engineering Development Center (AEDC) can offer lessons learned from its experience in projection technologies, optical system design, optical material characteristics and measurement (including cryodeposition), positioning systems, and pertinent analytical tools involved in performing ground testing of a sensor system under flight conditions. For over 30 years, the space chambers at AEDC have performed space sensor characterization, calibration, and mission simulation testing on space-based, interceptor, and air-borne sensors. This paper describes recent work at AEDC in the utilization and proposed enhancement of this cryo-vacuum test capability.

8150-06, Session 2

James Webb space telescope system cryogenic optical test plans

L. D. Feinberg, NASA Goddard Space Flight Ctr. (United States); M. Waldman, Sigma Space Corp. (United States); A. A. Barto, Ball Aerospace & Technologies Corp. (United States); T. L. Whitman, ITT Corp. Geospatial Systems (United States)

The James Webb Space Telescope Optical Telescope Element (OTE) and Optical Telescope Element/Integrated Science Instrument Module (OTIS) will be tested at the same time in the final and only cryogenic optical test of the full observatory. Due to the size and temperature of JWST, this is a complex test which has undergone changes in the last year aimed at reducing test execution risk. We will summarize the test plan changes, architecture changes, and predicted timeline changes for this test. We will also explain the checkout plans for assuring the test will go smoothly.

Conference 8150:
Cryogenic Optical Systems and Instruments XIV

8150-07, Session 2

Cryogenic performance of the JWST primary mirror segment engineering development unit

D. M. Chaney, Ball Aerospace & Technologies Corp. (United States); J. B. Hadaway, The Univ. of Alabama in Huntsville (United States); J. A. Lewis, B. B. Gallagher, R. J. Brown, Ball Aerospace & Technologies Corp. (United States)

The JWST (James Webb Space Telescope) primary mirror consists of 18 hexagonal mirror segments each approximately 1.5 meters point to point. The mirror segments are constructed from a lightweight beryllium substrate with both a radius-of-curvature actuation system and a six degree-of-freedom hexapod actuation system. The manufacturing process for each individual mirror assembly takes approximately six years due to limitations dealing with the number of segments and manufacturing & test facilities. In order to catch any manufacturing or technology roadblocks, as well as to streamline specific processes, an Engineering Development Unit (EDU) was built to lead the mirror manufacturing flow. This development unit has all of the same requirements as the flight units and is actually considered to be one of the flight spare mirrors. The EDU was manufactured with a lead time of approximately six months over the other mirrors to assure adequate time to optimize each step in the manufacturing process. Manufacturing and test occurred at six locations across the U.S. with multiple trips between each. The EDU recently completed this arduous process with the final cryogenic performance test of the mirror assembly taking place at Marshall Space Flight Center's (MSFC) X-Ray & Cryogenic Facility (XRCF). Testing included survivability tests to 25 Kelvin, hexapod & radius-of-curvature actuation systems testing, and cryogenic figure & prescription testing. Presented here is a summary of the tests performed along with the results of that testing.

8150-08, Session 2

Cryogenic thermal distortion performance characterization for the JWST ISIM structure

J. D. Johnston, E. Cofie, J. E. Hylan, E. L. Johnson, J. T. Pontius, D. B. McGuffey, M. D. Nowak, R. G. Ohl, NASA Goddard Space Flight Ctr. (United States)

The James Webb Space Telescope (JWST) Integrated Science Instrument Module (ISIM) Structure is a precision optical metering structure for the JWST science instruments. The ISIM Structure consists of a bonded composite frame supported by kinematic mounts. Optomechanical performance requirements place stringent limits on the allowable thermal distortion of the metering structure between ambient and cryogenic operating temperature (~35 K). The project made a significant investment to develop capabilities to predict and metrologize cryogenic thermal distortion of the ISIM Structure. This paper focuses on thermal distortion testing and successful verification of performance requirements for the flight ISIM Structure. The ISIM Structure Cryo-Set Test was completed in Spring 2010 at NASA Goddard Space Flight Center in the Space Environment Simulator Chamber. During the test, the ISIM Structure was thermal cycled twice between ambient and cryogenic (~35 K) temperatures. Photogrammetry was used to metrologize the Structure in the ambient and cryogenic states for each cycle to assess both cooldown thermal distortion and repeatability. The metrology system developed for this test has been discussed in past SPIE papers. This paper will provide new details on the post-processing of the metrology datasets completed to compare measurements with performance requirements. The full paper will provide an overview of the ISIM Structure, summarize relevant optomechanical performance requirements, provide an overview of the ISIM Structure Cryo-Set Test, discuss the post-processing of the metrology data for comparison with performance requirements, and demonstrate compliance of the measured performance with requirements.

8150-09, Session 2

Cryogenic thermal distortion model validation for the JWST ISIM structure

J. D. Johnston, E. Cofie, NASA Goddard Space Flight Ctr. (United States)

The James Webb Space Telescope (JWST) Integrated Science Instrument Module (ISIM) Structure is a precision optical metering structure for the JWST science instruments. Optomechanical performance requirements place stringent limits on the allowable thermal distortion of the metering structure.

A significant effort was completed to develop capabilities to predict and metrologize cryogenic thermal distortion of the ISIM Structure. This paper focuses on thermal distortion finite element modeling, analysis, and model validation for the flight structure. Extensive thermal distortion analysis was completed during the design phase for the ISIM Structure to demonstrate that thermal distortion requirements were achieved. Recently completed cryogenic performance testing has verified that the ISIM Structure meets optomechanical performance requirements related to cooldown from ambient to cryogenic operating temperatures (~35 K). The extensive metrology dataset generated during performance testing has been used to validate predictions from the thermal distortion model. Comparison of test measurements and model predictions demonstrate the adequacy of thermal distortion modeling uncertainty factors adopted during the design phase, and provide a bound on the accuracy of the model predictions. This paper will provide an overview of the test configuration and results, describe the thermal distortion model of the test, and provide a comparison of test results and analytical predictions from the model.

8150-11, Session 3

The wavelength calibration of the JWST near infrared spectrograph (NIRSpec)

S. M. Birkmann, T. Böker, P. Ferruit, G. Giardino, P. Jakobsen, G. de Marchi, M. Sirianni, M. B. J. te Plate, J. Savignol, European Space Research and Technology Ctr. (Netherlands); X. Gnata, T. Wettemann, EADS Astrium GmbH (Germany); B. Dorner, Observatoire de Lyon (France); G. Cresci, INAF - Osservatorio Astrofisico di Arcetri (Italy); F. Rosales-Ortega, Univ. Autónoma de Madrid (Spain); M. Stuhlinger, European Space Astronomy Ctr. (Spain); R. E. Cole, J. A. Tandy, C. Brockley-Blatt, Univ. College London (United Kingdom)

The Near Infrared Spectrograph (NIRSpec) is one of four science instruments aboard the James Webb Space Telescope (JWST) that is to be launched later this decade. NIRSpec is sensitive in the wavelength range from ~0.6 to 5.0 micron and operates at temperatures ≤ 40 K. It offers multi-object, fixed slit, and integral field spectroscopy with seven selectable dispersers. The on-ground spectrophotometric calibration of the instrument is performed by means of continuum and line emission lamps. NIRSpec also contains an internal calibration assembly (CAA) that will provide the wavelength and radiometric calibration in orbit. Due to thermal constraints, the CAA features low power tungsten filament lamps in combination with long-pass and Fabry-Perot like interference filters, which need to be calibrated at instrument level. We will report on the wavelength calibration of the NIRSpec flight model and the CAA, carried out during the first cryogenic performance testing. Emphasis will be put on the challenges that can be expected when using temperature dependent, resolved lines with asymmetrical profiles for wavelength calibration.

**Conference 8150:
Cryogenic Optical Systems and Instruments XIV**

8150-12, Session 3

Calibrating the position of images and spectra in the NIRSpec instrument

G. de Marchi, S. M. Birkmann, T. Böker, P. Ferruit, G. Giardino, P. Jakobsen, M. Sirianni, M. B. J. te Plate, J. Savignol, European Space Research and Technology Ctr. (Netherlands); X. Gnata, R. Barho, M. Kosse, P. Mosner, EADS Astrium GmbH (Germany); B. Dorner, Observatoire de Lyon (France); G. Cresci, INAF - Osservatorio Astrofisico di Arcetri (Italy); F. Rosales-Ortega, Univ. Autónoma de Madrid (Spain); M. Stuhlinger, European Space Astronomy Ctr. (Spain); T. Gross, T. Leikert, Carl Zeiss Optronics GmbH (Germany)

The Near Infrared Spectrograph (NIRSpec) is one of four science instruments aboard the James Webb Space Telescope (JWST). NIRSpec offers multi-object, fixed slit, and integral field spectroscopy in the wavelength range from ~0.6 to 5.0 micron. There are eight user selectable optical elements in NIRSpec, six gratings, a double-pass prism, and a mirror. All these elements are mounted on the grating wheel assembly (GWA). The precise knowledge of the position and tilt of the mirror is critical for target acquisition, and that of the dispersers essential for an accurate extraction of science data. Therefore, the GWA is equipped with magneto-resistive position/tilt sensors. We will present the first results concerning the stability and repeatability of the GWA, obtained during the NIRSpec flight model ground test campaign, and the performance of the sensors and their calibration.

8150-13, Session 4

JWST NIRCам flight mirror assemblies

P. V. Mammini, H. C. Holmes, L. W. Huff, F. P. Lopez, M. S. Jacoby, Lockheed Martin Space Systems Co. (United States)

The Near Infrared Camera (NIRCам) instrument for NASA's James Webb Space Telescope (JWST) has an optical prescription which includes numerous fold mirror assemblies. The instrument will operate at 37K after experiencing launch loads at ~293K and the optic mounts must accommodate all associated thermal and mechanical stresses, plus maintain an exceptional wavefront during operation.

Lockheed Martin Space Systems Company (LMSSC) conceived, designed, assembled, tested, and integrated the mirror assemblies for the NIRCам instrument.

This paper covers the design, assembly, and test of two of the instruments key fold mirrors; First Fold Mirror Assembly and Shortwave Fold Mirror Assembly.

8150-14, Session 4

NIRCам coronagraphic Lyot stop: design, fabrication, and testing

Y. Mao, T. S. Kubo, T. B. Andersen, M. Virgen, H. M. Chan, G. S. Feller, L. W. Huff, S. F. Somerstein, E. H. Smith, Lockheed Martin Space Systems Co. (United States); S. D. Horner, NASA Ames Research Ctr. (United States); J. E. Krist, C. A. Beichman, Jet Propulsion Lab. (United States); C. Barone, R. Schmidt, D. Levin, S. Seymour, Max Levy Autograph, Inc. (United States); D. M. Kelly, M. J. Rieke, The Univ. of Arizona (United States)

The NIRCам instrument on the James Webb Space Telescope (JWST) will provide coronagraphic image capability to search for extrasolar planets in the wavelength range 2 - 5 microns. This capability is realized by a set of Lyot pupil stops with patterns matching the occulting mask located in the JWST intermediate focus plane in the NIRCам optical

system. The complex patterns with transparent apertures are made by photolithographic process with metal coating in the opaque region. The optical density needs to be high for the opaque region, and transmission needs to be high at the aperture. The Lyot stop needs to be operated at cryogenic conditions. We will report the Lyot stop design, fabrication and testing in this paper. This work was performed and funded by NASA Goddard Space Flight Center under Prime Contract NAS5-02105.

8150-15, Session 4

Flight build of the collimator and shortwave camera optics for the NIRCам instrument

E. T. Kvamme, H. C. Holmes, Lockheed Martin Space Systems Co. (United States)

The Near Infrared Camera (NIRCам) instrument for NASA's James Webb Space Telescope (JWST) has an optical prescription which employs six triplet lens cells. The instrument will operate at 37K after experiencing launch loads at ~293K and the optic mounts must accommodate all associated thermal and mechanical stresses, plus maintain an exceptional wavefront during operation.

The Lockheed Martin Advanced Technology Center (LMATC) has built and tested the collimator and camera optics for use on the NIRCам flight instrument. This paper presents an overview of the driving requirements, a brief overview of the changes in the opto-mechanical design since our last presentation, a discussion of the collimator and shortwave camera triplet assembly processes, and finally the mechanical and optical test results as they relate to mechanical and optical performance.

8150-16, Session 4

Design, build, and test of the NIRCам focal plane array housing

D. R. Little, M. S. Jacoby, E. R. Casco, Lockheed Martin Space Systems Co. (United States)

The Near Infrared Camera (NIRCам) instrument for NASA's James Webb Space Telescope (JWST) has an optical prescription which terminates at two focal plane arrays for each module. The instrument will operate at 37K after experiencing launch loads at ~293K and the focal plane array housings must accommodate all associated thermal and mechanical stresses, while keeping the FPAs aligned. The main purpose of the FPAH is to provide a stray light, contamination, and radiation shield to the Focal Planes. The design includes a fold mirror used to direct incoming light up to the detectors and mechanical support for the Application Specific Integrated Circuits (ASIC). A six degree of freedom shim is used to align the Focal Plane Assembly at the operating temperature of 37 Kelvin. This paper will provide an overview of the FPAH design including an update to the Fold Mirror design described in previous papers. Analysis and test results of the ambient temperature optical and vibration testing will be presented.

8150-17, Session 5

Tracking the surface figure error of the pick off mirror throughout build and environmental testing of the focus and alignment mechanism qualification unit of the near infrared camera of JWST

B. Witherspoon, Lockheed Martin Space Systems Co. (United States)

The Pick Off Mirror (POM) sits at the end of the Focus and Alignment Mechanism (FAM) of NIRCам. The POM takes the light delivered by the

**Conference 8150:
Cryogenic Optical Systems and Instruments XIV**

telescope and steers it into the NIRCcam instrument. At strategic points during the build and test of the Pick Off Mirror and its mechanism (the FAM) the surface figure error (SFE) of the mirror was monitored. This metric was used to track the health of the mirror throughout this testing regime. For example, the team ran an SFE test before and after Vibration testing the FAM. In this paper, we will provide an overview of the testing regime and the results of these periodic SFE tests. These results lead to the qualification of the POM and FAM designs for flight on the James Webb Space Telescope.

8150-18, Session 5

Qualifying the flight design of the focus and alignment mechanism of the near infrared camera on the James Webb space telescope

B. Witherspoon, Lockheed Martin Space Systems Co. (United States)

The Focus and Alignment Mechanism (FAM) is the opto-mechanical, cryogenic mechanism that positions the Pick Off Mirror (POM) for the Near Infrared Camera of the James Webb Space Telescope. The POM is used to direct the light collected by the telescope into the Near Infrared Camera. This paper is a follow on to SPIE Paper 7439C-49. In this paper, we will summarize the design and role of this opto-mechanical mechanism and present the results of the environmental testing of the Qualification Unit. The testing consisted of 7 thermal cycles from ambient temperature to 26 Kelvin, as well as a 2 X Mechanism Life test at this cryogenic temperature plateau. These results lead to the qualification of the POM and FAM designs for flight on the James Webb Space Telescope.

8150-19, Session 5

Redesign and test of cryogenic mechanism for improved stiffnessC. S. Clark, M. S. Jacoby, P. V. Mammini, H. C. Holmes,
Lockheed Martin Space Systems Co. (United States)

The Near Infrared Camera (NIRCcam) instrument for NASA is one of the four science instruments installed into the Integrated Science Instrument Module (ISIM) of the James Webb Space Telescope (JWST) intended to conduct scientific observations over a five year mission lifetime. The NIRCcam instrument will have a Pupil Imaging Lens actuator assembly (PIL) to provide a means of imaging the primary mirror for ground testing, instrument commissioning, and diagnostics which must operate at from 293K to 37K and be in support of the usual launch environments.

More refined optic prescriptions and initial PIL vibration test data lead to the re-design of the PIL. This paper discusses the re-design of the lens mounts to accommodate a new optic prescription. This paper also details the analysis of vibration test data that lead to the re-design of a stiffer bearing mount for the PIL flight mechanism that would ultimately be tested to show appropriate margins for meeting program vibration test requirements.

8150-20, Session 5

Fret wear mediation of NIRCcam filter wheel assembly

B. I. Privari, Lockheed Martin Space Systems Co. (United States)

We will discuss a fret wear solution developed for the James Webb Space Telescope NIRCcam filter wheel assembly by implementation of a hard coating. With mechanisms and structures designed for space flight application, titanium is often selected as the choice material of construction. Titanium offers a low-density high strength material that is good for use with many optical instruments due to its' favorable thermal

properties. An important factor to consider with titanium mechanisms and structures are component fits and the vibration environment that must be survived during launch. In many instances, small (slip) fits between titanium components can cause fret wear during launch induced vibration. Titanium is particularly susceptible to fret wear, although other materials also demonstrate the fret wear. A discussion of several coating alternatives and associated wear testing will be presented along with the selection of an optimal solution.

8150-22, Session 5

Top lessons learned during the development of components for NIRCcam

A. A. Nordt, Lockheed Martin Space Systems Co. (United States)

No abstract available

Conference 8151: Techniques and Instrumentation for Detection of Exoplanets V

Tuesday-Wednesday 23-24 August 2011 • Part of Proceedings of SPIE Vol. 8151
Techniques and Instrumentation for Detection of Exoplanets V

8151-01, Session 1

Laboratory demonstration of high-contrast imaging at inner working angles better than 2 I/D

R. Belikov, E. Pluzhnik, F. C. Witteborn, D. H. Lynch, T. P. Greene, P. T. Zell, NASA Ames Research Ctr. (United States); O. Guyon, The Univ. of Arizona (United States)

Coronagraph technology is advancing and promises to directly image and spectrally characterize extrasolar Earth-like planets in the foreseeable future (such as the 2020 decade) with a telescope as small as 1.5m. A small Explorer-sized telescope can also be launched in the 2010 decade capable of seeing debris disks as dim as tens of zodis and potentially a few large planets. The Phase Induced Amplitude Apodization (PIAA) coronagraph makes such aggressive performance possible, providing high throughput and high contrast close to the diffraction limit. We report on the latest results from a testbed at NASA Ames that is focused on developing and testing the PIAA coronagraph. This laboratory facility was built in 2008 and is designed to be flexible, operated in an actively thermally stabilized air environment, and to complement collaborative efforts at NASA JPL's High Contrast Imaging Testbed. For our wavefront control we are using small Micro-Electro-Mechanical-System deformable mirrors (MEMS DMs), which promise to reduce the size of the beam and overall instrument, a consideration that becomes very important for small telescopes. We describe our lab progress and results, which include (as of February 2010): the demonstration of 5.4e-8 average raw contrast in a dark zone from 2.0 - 5.2 I/D and of 3.6e-6 contrast from 1.5-2.5 I/D (in monochromatic light); the testing of the next-generation reflective PIAA mirror set built by Tinsley and designed for broadband; and finally, the testing of a slightly modified PIAA coronagraph that is capable of achieving 1e-6 contrasts at 1 I/D.

8151-02, Session 1

Influence of surface errors on the design of PIAA mirrors using numerical and semi-analytical propagation models.

A. Carlotti, Princeton Univ. (United States); L. Pueyo, The Johns Hopkins Univ. (United States)

A ray-optics designed PIAA pair of mirrors cannot provide the contrast levels necessary to the direct detection of exo-earth. Apodizing the edges of the incoming beam before it reaches the first mirror can increase this contrast. Since the pre-apodizer only attenuates the diffraction effects due to the propagation from the first mirror to the second one, its benefits can be cancelled if the surface quality of the mirrors is too low. As the pre-apodizer limits the throughput of the system, estimating its actual ability to increase the contrast is crucial. In order to estimate the influence of the surface errors on the usefulness of the pre-apodizer, we compute the propagated electric field using two different tools: the semi-analytical model developed by Pueyo and a purely numerical model based on the Huygens integral. Random cosines aberrations are introduced through the mapping function in the first case and directly on the mirrors surfaces in the second. A statistical analysis is then made and the results are compared and discussed. It appears that there is a limit to the maximum contrast that PIAA mirrors can provide. This limit is set by the surface quality and cannot be reached by increasing the strength of the pre-apodizer but with a higher deformation of the mirrors and a smaller distance between them. Finally, as an adaptive optics system must be used to attenuate the optical aberrations created outside of the PIAA, it can also be used to increase the final contrast.

8151-03, Session 1

Laboratory testing of a phase-induced amplitude apodization (PIAA) coronagraph

B. D. Kern, Jet Propulsion Lab. (United States); O. Guyon, The Univ. of Arizona (United States); A. Give'on, A. C. Kuhnert, A. F. Niessner, Jet Propulsion Lab. (United States)

We present high-contrast images from laboratory testing of a Phase-Induced Amplitude Apodization (PIAA) coronagraph at NASA's High Contrast Imaging Testbed (HCIT). Using a deformable mirror (stopped down to a 30-actuator diameter circle) and wavefront estimation and control algorithms, we create a "dark hole" in the monochromatic point-spread function suitable for exoplanet imaging. This dark hole has an average intensity of 3×10^{-8} relative to the unocculted peak intensity, extending from $2.2 \lambda/D$ to $4 \lambda/D$ on one side of the star image. We discuss techniques used to perform wavefront estimation and control, limitations to improving contrast, and plans for future testing.

8151-04, Session 1

Low-cost diamond turned high-precision PIAA optics: laboratory results and novel high-throughput designs

K. Balasubramanian, E. J. Cady, Jet Propulsion Lab. (United States); L. Pueyo, The Johns Hopkins Univ. (United States); S. B. Shaklan, X. An, Jet Propulsion Lab. (United States); R. Belikov, NASA Ames Research Ctr. (United States); O. Guyon, The Univ. of Arizona (United States)

Off-axis, high-sag PIAA optics for high contrast imaging present challenges in manufacturing and testing. With smaller form factors and consequently smaller surface deformations (<80 microns), diamond turned fabrication of these mirrors becomes feasible. Though such a design reduces the system throughput, it still provides 2 I/D inner working angle. We report on the design, fabrication, measurements, and initial assessment of the novel PIAA optics in a coronagraph testbed. We also describe a four mirror PIAA coronagraph that relaxes apodizer requirements and significantly improves throughput while preserving the low-cost benefits.

8151-05, Session 1

Studies of the effects of optical system errors on the HCIT contrast performance

E. Sidick, S. B. Shaklan, A. Give'on, B. D. Kern, Jet Propulsion Lab. (United States)

The High Contrast Imaging Testbed (HCIT) at the Jet Propulsion Laboratory employs a broadband wavefront correction algorithm called Electric Field Conjugation (EFC) to obtain the required 10⁻¹⁰ contrast. This algorithm works with one or multiple deformable mirrors (DM's) to create a "dark-hole" in a predefined region of the image plane where terrestrial planets would be found. It achieves the desired high contrast level in two stages. The first is the reconstruction stage. In this stage, the algorithm provides an estimate of the aberrated complex electric field in the image plane based on pairs of images taken at the final image plane using different DM configurations. The second is the correction or the electric field conjugation stage. In this stage the algorithm generates a correction based on the electric field estimated in the first stage. The correction is then applied to the DM actuators to null the image electric

field in the predefined dark-hole region.

We have investigated the effects of DM actuator errors and the optic position errors on the efficiency of the EFC algorithm in a Lyot coronagraph configuration. Considered cases include dead actuators, lateral and longitudinal movement of the occulting mask, and the lateral movement of a flat optical surface. The structural design of the optical system as well as the parameters of various optical elements used in the analysis are drawn from those of the HCIT system that have been implemented with one DM. The simulation takes into account the surface errors of various optics. The optical simulation algorithm uses MACOS (Modeling and Analysis for Controlled Optical Systems) as its analytic tool. Hence it is capable of performing full three-dimensional near-field diffraction analysis on HCIT's optical model. Results of some of these studies have been verified by actual measurements.

8151-06, Session 1

Exosystem modeling with multiple data sources

D. Savransky, N. J. Kasdin, Princeton Univ. (United States)

We present a unified description of exosystem data gathered by various means (including astrometry, doppler spectroscopy, transit photometry and imaging) as partial observations of a Markov process defined by a single parameter set. Using dynamic filtering and sequential parameter estimation, this description allows us to systematically update existing exosystem models with new observations and derive estimates of the fit parameter errors. We present multiple examples of potential applications for various combinations of detection methods and discuss the utility of known distributions of exosystem parameters to initialization of all forms of orbit fitting.

8151-07, Session 1

Taking the vector vortex coronagraph to the next level for ground- and space-based exoplanet imaging instruments: review of technology developments in the USA, Japan, and Europe

D. P. Mawet, European Southern Observatory (ESO) (Chile) and Jet Propulsion Lab. (United States); N. Murakami, Hokkaido Univ. (Japan); C. Delacroix, O. Absil, Univ. de Liège (Belgium); N. Baba, Hokkaido Univ. (Japan); J. Baudrand, A. Boccaletti, Observatoire de Paris à Meudon (France); R. Burruss, Jet Propulsion Lab. (United States); R. A. Chipman, College of Optical Sciences, The Univ. of Arizona (United States); S. Habraken, Univ. de Liège (Belgium); S. Hamaguchi, Hokkaido Univ. (Japan); C. Hanot, Univ. de Liège (Belgium); A. Ise, Hokkaido Univ. (Japan); M. Karlsson, Uppsala Univ. (Sweden); B. D. Kern, J. E. Krist, A. C. Kuhnert, M. B. Levine, K. M. Liewer, B. P. Mennesson, D. Moody, Jet Propulsion Lab. (United States); H. Murakami, Japan Aerospace Exploration Agency (Japan); A. F. Niessner, Jet Propulsion Lab. (United States); J. Nishikawa, National Astronomical Observatory of Japan (Japan); N. O'Brien, JDSU (United States); K. Oka, Hokkaido Univ. (Japan); P. Park, Jet Propulsion Lab. (United States); P. Piron, Univ. de Liège (Belgium); L. Pueyo, The Johns Hopkins Univ. (United States); P. Riaud, Univ. de Liège (Belgium); M. Sakamoto, Hokkaido Univ. (Japan); E. Serabyn, Jet Propulsion Lab. (United States); M. Tamura, National Astronomical Observatory of Japan (Japan); J. T. Trauger, Jet Propulsion Lab. (United States); D. Shemo, JDSU (United States); J. Surdej, Univ. de Liège (Belgium); N. Tabirian, BEAM Engineering for Advanced

Measurements Co. (United States); W. Traub, J. K. Wallace, Jet Propulsion Lab. (United States); K. Yokochi, Tokyo Univ. of Agriculture and Technology (Japan)

The Vector Vortex Coronagraph (VVC) is one of the most promising next generation coronagraphs for future ground- and space-based exoplanet imaging/characterization instruments, as recently demonstrated on sky and in the lab. It provides small inner working angle, high throughput, simplicity of implementation. It has recently demonstrated high contrasts (these proceedings).

Manufacturing technologies for devices covering wavelength ranges from the optical to the mid-IR, are maturing quickly. We will review the current status of technology developments supported by NASA in the USA (Jet Propulsion Laboratory, University of Arizona, JDSU and Beam Co), Europe (University of Liege, Observatoire de Paris-Meudon, University of Uppsala) and Japan (Hokkaido University, and Photonic lattice), using liquid crystal polymers, subwavelength gratings, and photonic crystals, respectively.

We will then focus on concrete perspectives for the use of the VVC on upcoming extreme adaptive optics facilities, extremely large ground-based telescopes, and space-based internal coronagraphs.

8151-08, Session 1

Stability error budget for an aggressive coronagraph on a 3.8-m telescope

S. B. Shaklan, L. F. Marchen, J. E. Krist, M. Rud, Jet Propulsion Lab. (United States)

We evaluate in detail the stability requirements for a band-limited coronagraph with an inner working angle as small as $2 \lambda/D$ coupled to an off-axis, 3.8-m diameter telescope. We have updated our methodologies since presenting similar work for the Terrestrial Planet Finder Coronagraph mission that worked at $4 \lambda/D$ and employed an 8th-order mask to reduce aberration sensitivities. In the previous work, we determine the tolerances relative to the total light leaking through the coronagraph. Now, we separate the light into a radial component, which is readily separable from a planet signal, and an azimuthal component, which is easily confused with a planet signal. In the current study, throughput consideration require a 4th-order coronagraph. This, combined with the more aggressive working angle, places extraordinarily tight requirements on wavefront and opto-mechanical stability. We find that the stability requirements are driven mainly by coma that leaks around the coronagraph mask and mimics the localized signal of a planet, and focus that scatters light into the background, decreasing SNR. We also show how the requirements would be relaxed if a low-order aberration detection system could be employed.

8151-09, Session 1

Imaging power of fibered nulling telescopes for extra-solar planets characterization

F. Hénault, Univ. de Nice Sophia Antipolis (France)

We discuss the imaging properties of monolithic pupil, nulling telescopes equipped with a focal plane waveguide array, which could be envisaged as a precursor space mission for future nulling interferometer arrays searching for habitable planets outside of our solar system. Three different concepts of nulling telescopes are reviewed, namely the unmasked Sheared-Pupil Telescope (SPT), a variant of the SPT where the exit pupil is limited by a Lyot stop, and a Super-Resolving Telescope (SRT) having multiple, non-overlapping exit sub-apertures. For each case simple theoretical relationships allowing to estimate the nulling rate, Signal-to-Noise Ratio (SNR) and Inner Working Angle (IWA) of the telescopes are established or recalled, and numerical simulations are conducted. The results of this preliminary study show that the most promising designs should either be the masked SPT having reduced entrance sub-pupils, or a SRT associated with an adequate

Techniques and Instrumentation for Detection of Exoplanets V

leakage calibration procedure, depending whether deep nulling or high radiometric efficiency are preferred.

8151-10, Session 1

Current results of the PERSEE testbench: the cophasing control and the polychromatic null rate

J. Lozi, ONERA (France) and Ctr. National d'Études Spatiales (France) and Partenariat Haute resolution Angulaire Sol Espace (France); F. Cassaing, ONERA (France) and Partenariat Haute resolution Angulaire Sol Espace (France); J. Le Duigou, Ctr. National d'Études Spatiales (France); B. Sorrente, J. Montri, ONERA (France) and Partenariat Haute resolution Angulaire Sol Espace (France); J. Reess, E. Lhome, J. M. Buey, Observatoire de Paris à Meudon (France) and Partenariat Haute resolution Angulaire Sol Espace (France); F. Hénault, A. Marcotto, P. Girard, Observatoire de la Côte d'Azur (France); M. Barillot, Thales Alenia Space (France); M. Ollivier, Univ. Paris-Sud 11 (France); V. Coudé du Foresto, Observatoire de Paris à Meudon (France) and Partenariat Haute resolution Angulaire Sol Espace (France)

Stabilizing a nulling interferometer at a nanometric level is the key issue to obtain deep null depths. The PERSEE breadboard has been design to study both cophasing and typical null rate, in the most realistic disturbing environment of a space mission. This presentation focuses on the current results of the PERSEE bench. In terms of metrology, we cophased at 0.33 nm rms for the piston and 60 mas rms for the tip/tilt. A Linear Quadratic Gaussian (LQG) control coupled with an unsupervised vibration identification allows us to maintain that level of correction, even with characteristic vibrations of nulling interferometry space missions. Those performance, with an accurate design and alignment of the bench, currently lead to a polychromatic unpolarised null depth of $1.6e-5$ stabilized at $2e-7$ on the $[1.65-2.4]$ μm spectral band (38% bandwidth). This recent null depth can be improve by optimizing the calibration scheme. With those significant results, we give the first more general lessons we have already learned from this experiment, both at system and component levels for a future space mission.

8151-11, Session 1

The possibility of application of polarization-holographic elements for the discovery and characterization of exoplanets

G. A. Kakauridze, B. N. Kilosanidze, Institute of Cybernetics (Georgia)

The information on the state and degree of polarization of light scattered by the atmosphere of the exoplanets and reflected from their surface can give the possibility of their detection and characterization. A polarimetric method provides an additional channel of information by finding polarization signal against a background of an unpolarized starlight. Polarization- olographic element with complex distribution of anisotropy and gyrotropy in the band is suggested for detection and characterization of exoplanets by means of real time analysis of the state and degree of polarization of light that went into the entrance pupil of the telescope and also determination of the dispersion of this state. The main advantage of such an element is its extraordinary simplicity and compactness, which is especially important for its installation on the space telescopes. Unlike currently used astropolarimeters the polarimeter on the basis of such an element will not contain any mechanically moving or electronically tunable components, and will not introduce any distortion in the polarization state of light, as there will be no reflections from any internal surfaces which causes its accuracy. The element decomposes the light incident on it into the orthogonal circular and linear

bases, forming diffraction orders. The element has an angular dispersion and decomposes each diffraction order in the spectrum. Simultaneous measurement of the intensities of the diffracted beams allows all four Stokes parameters to be determined and the dispersion of this state. The possibility of the creation of suitable higheffective element and its application for main goal is discussed.

8151-12, Session 2

TPF-Interferometer: a decade of development in exoplanet detection technology

S. R. Martin, A. Ksendzov, O. P. Lay, R. D. Peters, D. P. Scharf, Jet Propulsion Lab. (United States)

The last decade has seen great advances in interferometric nulling technology, propelled at first by the SIM and KECK nulling programs and then by the Terrestrial Planet Finder Interferometer. In the infrared at N-band (using a CO₂ laser at 10.6 micron wavelength) the first million to one nulls were reported on a KECK testbed in 2003. For TPF-I, nulls needed to be both deep and broadband, and a suite of testbeds was designed and built to study all aspects of achromatic nulling and system implementation, including formation flying technology. Also, observatory designs were drawn up and studied against performance models. Modeling revealed that natural variations in the alignment and control of the optical system produced an "instability noise" signal and this realization led to a redesign of the preferred layout (at least on this side of the Atlantic) to a rectangular formation. The complexity of the early TPF-I spacecraft design was mitigated by the infusion of ideas from Europe and produced the current X-Array design which utilizes simple reflectors to form the apertures together with a stretched three dimensional formation geometry. This paper summarizes the main achievements of the infrared nulling technology program including the development of adaptive nulling for broadband performance and the demonstration of starlight suppression by 100 million to one.

8151-13, Session 2

Assessing the performance limits of internal coronagraphs through end-to-end modeling: a NASA TDEM study

J. E. Krist, D. P. Mawet, Jet Propulsion Lab. (United States); R. Belikov, NASA Ames Research Ctr. (United States); L. Pueyo, The Johns Hopkins Univ. (United States); D. Moody, J. T. Trauger, S. B. Shaklan, Jet Propulsion Lab. (United States)

We are conducting a study of three internal coronagraphs (PIAA, vector vortex, hybrid bandlimited) to understand their behaviors in realistically-aberrated systems with wavefront control (deformable mirrors). This study consists of two milestones: (1) develop wavefront propagation codes appropriate for each coronagraph that are accurate to 1% or better (compared to a reference algorithm) but are also time and memory efficient, and (2) use these codes to determine the wavefront control limits of each architecture. We discuss the results from the study so far, with emphasis on representing the PIAA and vector vortex coronagraphs and the wavefront control behaviors of those systems. This study is funded by the NASA ROSES Technology Demonstrations for Exoplanet Missions (TDEM) program.

8151-14, Session 2

Vacuum nuller testbed performance, characterization and null control

R. G. Lyon, M. C. Clampin, P. Petrone, P. Thompson, M. Bolcar, T. Madison, U. Mallik, NASA Goddard Space Flight Ctr. (United States); M. C. Noecker, S. E. Kendrick, Ball Aerospace &

Techniques and Instrumentation for Detection of Exoplanets V

Technologies Corp. (United States); M. A. Helmbrecht, Iris AO, Inc. (United States)

The Visible Nulling Coronagraph (VNC) can detect and characterize exoplanets with filled, segmented and sparse aperture telescopes, thereby spanning the choice of future internal coronagraph exoplanet missions. NASA/Goddard Space Flight Center (GSFC) has developed a Vacuum Nuller Testbed (VNT) to advance this approach, and assess and advance technologies needed to realize a VNC as a flight instrument.

The VNT is an ultra-stable testbed operating at 15 Hz in vacuum. It consists of a Mach-Zehnder nulling interferometer; modified with a "W" configuration to accommodate a hex-packed MEMS based deformable mirror (DM), coherent fiber bundle and achromatic phase shifters. The 2-output channels are imaged with a vacuum photon counting camera and conventional CCD. Error-sensing and feedback to DM and delay line with control algorithms are implemented in a real-time architecture.

The inherent advantage of the VNC is that it is its own interferometer and directly control its errors by exploiting images from bright and dark channels simultaneously. Conservation of energy requires the sum total of the photon counts be conserved independent of the VNC state. Thus sensing and control bandwidth is limited by the target stars throughput, with the net effect that the higher bandwidth offloads stressing stability tolerances within the telescope.

We report our recent progress with the VNT towards achieving an incremental sequence of contrast milestones of 10^8 , 10^9 and 10^{10} respectively at inner working angles approaching $2\lambda/D$. Discussed will be the optics, lab results, technologies, and null control. Shown will be evidence that the milestones have been achieved.

8151-15, Session 2**A hybrid Lyot coronagraph for the direct imaging and spectroscopy of exoplanet systems**

J. T. Trauger, D. Moody, B. Gordon, J. E. Krist, D. P. Mawet, P. Park, Jet Propulsion Lab. (United States)

We report the design, fabrication, and performance of a hybrid focal-plane occulter for Lyot coronagraphy. It is composed of thickness-profiled metallic and dielectric thin films, vacuum deposited on a fused silica substrate. Band-limited in both the real and imaginary parts of the complex attenuation pattern, it provides the theoretical basis for mathematically perfect starlight suppression. Together with a deformable mirror for control of wavefront phase, the hybrid Lyot coronagraph potentially exceeds billion-to-one contrast over dark fields extending to within $3\lambda/D$ of the central star, over spectral bandwidths of 20% or more, and with throughput efficiencies up to 60%.

The science capabilities of the hybrid Lyot coronagraph are described in the context of the ACCESS mission, a representative exoplanet space telescope concept study for the direct imaging and spectroscopy of exoplanet systems. This work has been supported by NASA's Technology Demonstration for Exoplanet Missions (TDEM) program.

8151-16, Session 2**Phase-induced amplitude apodization (PIAA) coronagraphy: recent results and future prospects**

O. Guyon, The Univ. of Arizona (United States) and Subaru Telescope, National Astronomical Observatory of Japan (United States); R. Belikov, NASA Ames Research Ctr. (United States); B. D. Kern, A. C. Kuhnert, A. Give'on, S. B. Shaklan, Jet Propulsion Lab. (United States)

The Phase Induced Amplitude Apodization (PIAA) concept uses aspheric optics to apodize a telescope beam for high contrast imaging. The

lossless apodization, achieved through geometrical redistribution of the light (beam shaping) allows designs of high performance coronagraphs, ideally suited for direct imaging of exoplanets similar to Earth around nearby stars. The PIAA coronagraph concept has evolved since its original formulation to mitigate manufacturing challenges and improve performance. Our group is currently aiming at demonstrating PIAA coronagraphy in the laboratory to $1e-9$ raw contrast at $2\lambda/D$ separation. Recent results from the High Contrast Imaging Testbed (HCIT) at NASA JPL demonstrate contrasts about one order of magnitude from this goal at $2\lambda/D$.

In parallel with our high contrast demonstration at $2\lambda/D$, we are developing and testing new designs at a complementary testbed at NASA Ames, and solving associated technical challenges. Some of these new PIAA designs have been tested that can further mitigate PIAA manufacturing challenges while providing theoretically total starlight extinction and offering 50% throughput at less than $1\lambda/D$. Recent tests demonstrated on the order of $1e-6$ contrast close to $1\lambda/D$ (while maintaining $5e-8$ contrast at $2\lambda/D$).

8151-17, Session 2**Advanced speckle sensing for internal coronagraphs**

M. C. Noecker, Ball Aerospace & Technologies Corp. (United States); S. B. Shaklan, J. K. Wallace, Jet Propulsion Lab. (United States); R. Belikov, NASA Ames Research Ctr. (United States); N. J. Kasdin, Princeton Univ. (United States)

A 4-8m telescope carrying a coronagraph instrument is a leading candidate for an anticipated flagship mission to detect and characterize Earth-size exoplanets in the 2020s. The telescope and instrument will need exquisite stability and precise control of the incoming wavefront to enable detection of faint companions ($1e-10$ of the star) at an angular separation of 2-4 Airy radii. In particular, wavefront errors cause speckles in the image, and variations in those speckles can confound the exoplanet detection. This challenge is compounded by the background light from zodiacal dust around our Sun and the target star, which limits the speed with which we can estimate and correct the speckles. We are working on developing coherent speckle detection techniques that will allow rapid calibration of speckles on the science detector, allowing subtraction in post-processing or correction with deformable mirrors. The expected speed improvement allows a much quicker timeline for measurement & calibration, which reduces the required telescope stability requirement and eases both the flight system design and the challenge of ground testing. We will describe the experiments and summarize progress to date.

8151-18, Session 2**Design, tolerancing, and prototyping of starshades for exoplanet detection and characterization**

N. J. Kasdin, D. N. Spergel, Princeton Univ. (United States); D. Lisman, S. B. Shaklan, M. W. Thomson, L. F. Marchen, P. J. Dumont, Jet Propulsion Lab. (United States); D. J. Tenerelli, Lockheed Martin Space Systems Co. (United States); B. A. Macintosh, R. E. Rudd III, Lawrence Livermore National Lab. (United States); J. Mikula, NASA Ames Research Ctr. (United States)

Starshades provide the starlight suppression needed for detecting and characterizing exoplanets with a much simpler telescope and instrument than is required for the equivalent performing coronagraph. In this paper we describe progress on our Technology Development for Exoplanet Missions project to design, manufacture, and measure a prototype occulter petal. We focus on the key requirement of manufacturing a

precision petal while controlling its shape within precise tolerances. The required tolerances are established by modeling the effect that various mechanical and thermal errors have on scatter in the telescope image plane and by suballocating the allowable contrast degradation among these error sources. We discuss the deployable starshade design, representative error budget, thermal analysis, and prototype manufacturing. We also present our metrology system and methodology for verifying that the petal shape meets the contrast requirement.

8151-19, Session 2

A photon-counting detector for exoplanet missions

D. F. Figer, J. Y. Lee, D. J. Stauffer, B. J. Hanold, Rochester Institute of Technology (United States)

This paper summarizes progress of a project to develop photon-counting detectors for NASA exoplanet missions through a radiation testing program. The project, funded by NASA ROSES TDEM, uses a 256x256 pixel silicon Geiger-Mode Avalanche Photodiode (GM-APD) per pixel, each individually bump-bonded to a silicon readout circuit. Each pixel independently registers the arrival of a photon and can be reset and ready for another photon within 100 ns. The pixel has built-in circuitry for independently counting photo-generated events. The readout circuit is multiplexed to read out the photon arrival events. The signal chain is inherently digital, allowing for noiseless transmission over long distances. The detector always operates in photon counting mode and is thus not susceptible to excess noise factor that afflicts other technologies. It continues operating with shot-noise limited performance up to extremely high flux levels, $>10^6$ photons/second/pixel, and delivers signal-to-noise ratios on the order of thousands for higher fluxes. Its performance is expected to be maintained at a high level throughout mission lifetime in the presence of the expected radiation dose.

8151-20, Session 3

The exoplanet microlensing survey by the proposed WFIRST Observatory

J. Kruk, D. Bennett, E. Cheng, S. Gaudi, N. A. Gehrels, NASA Goddard Space Flight Ctr. (United States); A. M. Tanner, Georgia State Univ. (United States); T. Sumi, Osaka Univ. (Japan); R. K. Barry, NASA Goddard Space Flight Ctr. (United States); W. Traub, J. H. Catanzarite, Jet Propulsion Lab. (United States); S. Kane, California Institute of Technology (United States); J. Anderson, Space Telescope Science Institute (United States); J. Beaulieu, Institut d'Astrophysique (France)

The New Worlds, New Horizons report released by the Astronomy and Astrophysics Decadal Survey Board in 2010 listed the Wide Field Infrared Survey Telescope (WFIRST) as the highest-priority large space mission for the coming decade. This observatory provides wide-field imaging and slitless spectroscopy at near infrared wavelengths. The scientific goals are to obtain a statistical census of exoplanets using gravitational microlensing, measure cosmic acceleration by multiple methods, and perform other astronomical surveys to be selected through a guest observer program.

A Science Definition Team has been established to assist NASA in the development of a Design Reference Mission that accomplishes this diverse array of science programs with a single observatory. In this paper we will present the current WFIRST payload concept and the expected capabilities for planet detection.

8151-21, Session 4

The performance of SPHERE in the integration lab

F. P. Wildi, Observatoire de Genève (Switzerland); K. Dohlen, D. Le Mignant, Observatoire Astronomique de Marseille-Provence (France); J. Charton, A. Costille, S. Rochat, D. Mouillet, J. L. Beuzit, Lab. d'Astrophysique de l'Observatoire de Grenoble (France); M. Feldt, Max-Planck-Institut für Astronomie (Germany); P. Puget, Lab. d'Astrophysique de l'Observatoire de Grenoble (France); A. Baruffolo, INAF - Osservatorio Astronomico di Padova (Italy); A. Boccaletti, Observatoire de Paris à Meudon (France); R. U. Claudi, INAF - Osservatorio Astronomico di Padova (Italy); P. Feautrier, Lab. d'Astrophysique de l'Observatoire de Grenoble (France); T. Fusco, ONERA (France); R. G. Gratton, INAF - Osservatorio Astronomico di Padova (Italy); M. Kasper, European Southern Observatory (Germany); M. P. Langlois, Ctr. de Recherche Astronomique de Lyon (France); A. Pavlov, Max-Planck-Institut für Astronomie (Germany); C. Petit, ONERA (France); J. H. Pragt, ASTRON (Netherlands); P. Rabou, Lab. d'Astrophysique de l'Observatoire de Grenoble (France); R. Roelfsema, ASTRON (Netherlands); J. Sauvage, ONERA (France); H. M. Schmid, ETH Zurich (Switzerland)

SPHERE, the extra-solar planet imager for the Very Large Telescope is a program that has been running since 2006. The instrument is now nearing completion and it is in the final integration stage in 2011.

The 3 science instruments of SPHERE have now been completed and have passed the internal acceptance, while the complex common path with the extreme Adaptive optics system, the coronagraphs and the calibration module is aggressively progressing.

This presentation will review the performance of the three focal instruments of SPHERE at the time of their internal acceptance (The dual band imager, the integral field spectrograph and the imaging polarimeter) as they were measured in their integration facilities, using an entrance optical beam simulating a perfect AO system.

In addition, we will present the performance of the AO system which is integrated separately from the rest of the system.

Last but not least, we will also disclose the very first results obtained on the fully integrated system.

8151-22, Session 4

The ZIMPOL high-contrast imaging polarimeter for SPHERE: sub-system test results

R. Roelfsema, ASTRON (Netherlands); D. Gisler, ETH Zurich (Switzerland); J. H. Pragt, ASTRON (Netherlands); H. M. Schmid, A. Bazzon, ETH Zurich (Switzerland); C. Dominik, Univ. van Amsterdam (Netherlands); A. Baruffolo, INAF - Osservatorio Astronomico di Padova (Italy); J. Beuzit, J. Charton, Lab. d'Astrophysique de l'Observatoire de Grenoble (France); K. Dohlen, Observatoire Astronomique de Marseille-Provence (France); M. Downing, European Southern Observatory (Germany); E. Elswijk, ASTRON (Netherlands); M. Feldt, Max-Planck-Institut für Astronomie (Germany); M. de Haan, ASTRON (Netherlands); N. Hubin, M. Kasper, European Southern Observatory (Germany); C. U. Keller, Utrecht Univ. (Netherlands); J. Lizon, European Southern Observatory (Germany); D. Mouillet, Lab. d'Astrophysique de l'Observatoire de Grenoble (France); A. Pavlov, Max-Planck-Institut für Astronomie (Germany); P. Puget,

Techniques and Instrumentation for Detection of Exoplanets V

S. Rochat, Lab. d'Astrophysique de l'Observatoire de Grenoble (France); B. Salasnich, INAF - Osservatorio Astronomico di Padova (Italy); P. Steiner, ETH Zurich (Switzerland); C. Thalmann, R. Waters, Univ. van Amsterdam (Netherlands); F. P. Wildi, Observatoire de Genève (Switzerland)

SPHERE (Spectro-Polarimetric High Contrast Exoplanet Research) is one of the first instruments which aim for the direct detection from extra-solar planets. The instrument will search for direct light from old planets with orbital periods of several months to several years as we know them from our solar system. These are planets which are in or close to the habitable zone. ZIMPOL (Zurich Imaging Polarimeter) is the high contrast imaging polarimeter subsystem of the ESO SPHERE instrument. ZIMPOL is dedicated to detect the very faint reflected and hence polarized visible light from extrasolar planets. The search for reflected light from extra-solar planets is very demanding because the signal decreases rapidly with the orbital separation. For a Jupiter-sized object and a separation of 1 AU the planet/star contrast to be achieved is on the order of 10^{-8} for a successful detection. This is much more demanding than the direct imaging of young self-luminous planets. ZIMPOL is located behind an extreme AO system (SAXO) and a stellar coronagraph. SPHERE is foreseen to have first light at the VLT at the end of 2011. ZIMPOL is currently in the subsystem testing phase. We describe the results of verification and performance testing done at the NOVA-ASTRON lab. We will give an overview of the system noise performance, the polarimetric accuracy and the high contrast testing. For the high contrast testing we will describe the impact of crucial system parameters (like detector modes, integration time, instrument polarization, HWP switching, instrument modes, coronagraph choice) on the contrast performance. We also describe the results of the first static optics test of ZIMPOL together with the complete SPHERE system. SPHERE is an instrument designed and built by a consortium consisting of LAOG, MPIA, LAM, LESIA, Fizeau, INAF, Observatoire de Genève, ETH, NOVA, ONERA and ASTRON in collaboration with ESO.

8151-23, Session 4**Near infrared interferometric spectroscopy with TEDI**

J. Edelstein, Univ. of California, Berkeley (United States); D. J. Erskine, Lawrence Berkeley National Lab. (United States); P. S. Muirhead, K. R. Covey, Cornell Univ. (United States); M. W. Mutterspaugh, Tennessee State Univ. (United States); P. M. Andelson, D. Kimber, D. Mondo, A. Vanderburg, M. M. Sirk, Univ. of California, Berkeley (United States); J. P. Lloyd, Cornell Univ. (United States)

The TripleSpec - Exoplanet Discovery Instrument (TEDI) interferometric spectrometer, a hybrid of an interferometer and a moderate resolution echelle spectrograph (TripleSpec, $R=2,700$), performs radial velocimetry and spectral synthesis at infrared wavelengths (0.9 - 2.4 μm) from the Cassegrain focus of the Palomar 200" telescope. Here we present results from on-sky observations of standard and science targets following an instrumental upgrade development. Velocity precision stability of < 30 m/s and six-fold spectral resolution boosting has been achieved.

8151-24, Session 4**First light results for the fibered imager for single telescope (FIRST) on the Lick 3m-Shane telescope**

E. Huby, G. S. Perrin, Observatoire de Paris à Meudon (France); F. Marchis, Univ. of California, Berkeley (United States); S. Lacour, Observatoire de Paris à Meudon (France); T. Kotani, Japan Aerospace Exploration Agency (Japan); E. L. Gates, Lick

Observatory (United States); E. Choquet, Observatoire de Paris à Meudon (France); G. Duchene, Univ. of California, Berkeley (United States); J. M. Woillez, W. M. Keck Observatory (United States)

We present the first on-sky results obtained with the Fibered Imager for Single Telescope (FIRST). Observations have been made in July (7 nights) and October (5 nights) 2010 at Lick Observatory with the 3m-Shane Telescope and using its Adaptive Optics system optimized in the near-infrared.

The FIRST instrument combines both techniques of single mode fibers interferometry and pupil remapping. The pupil of the telescope is divided into several sub-pupils. The flux corresponding to each sub-pupil is injected into single mode fibers such that the spatial phase fluctuations are removed (only atmospheric piston terms remain). The fiber outputs are rearranged according to a non redundant configuration in order to measure the visibilities and phases for each baseline independently. The principle is the same as for the technique of aperture masking but in our case we can use the entire pupil and thus increase the sensibility.

Simulations predict a dynamic range up to 10^6 close to the central star ($\sim 1/D$) at visible to near-infrared wavelengths (corresponding to a few tens of milliarcseconds at 600nm with an 8m-telescope). Laboratory experiments successfully demonstrated the cogency of the concept. We have recently set up a 9fibers-prototype on the 3m-Shane telescope and the first on-sky observations confirmed it as well : the first measured closure phases on a non resolved star (Vega) are biased (11°) but stable (4° rms).

8151-25, Session 4**The Subaru coronagraphic extreme AO project**

F. Martinache, O. Guyon, V. Garrel, C. Clergeon, Subaru Telescope, National Astronomical Observatory of Japan (United States); T. D. Groff, Princeton Univ. (United States); P. Stewart, The Univ. of Sydney (Australia); R. Russell, Subaru Telescope, National Astronomical Observatory of Japan (United States); C. Blain, Univ. of Victoria (Canada)

In 2009 our group started the integration of the SCExAO project, a highly flexible, open platform for high contrast imaging at the highest angular resolution, inserted between the coronagraphic imaging camera HiCIAO and the 188-actuator AO system of Subaru. In its first version, SCExAO combines a MEMS-based wavefront control system feeding a high performance PIAA-based coronagraph, that apodizes the telescope pupil while preserving throughput and angular resolution. It also includes a coronagraphic low-order wavefront sensor, a non-redundant aperture mask and a visible imaging mode with fast low readout detector, all of them designed to take full advantage of the angular resolution (40 mas in the H-band) that an 8-meter telescope has to offer. We present the first on-sky results acquired during SCExAO's spring 2011 engineering campaign and discuss the lessons learned from them.

8151-26, Session 4**The Subaru coronagraphic extreme AO (SCExAO) system: fast visible imager**

V. Garrel, O. Guyon, Subaru Telescope, National Astronomical Observatory of Japan (United States); P. Baudoz, Observatoire de Paris à Meudon (France); F. Martinache, Subaru Telescope, National Astronomical Observatory of Japan (United States); P. Stewart, The Univ. of Sydney (Australia); J. Lozi, ONERA (France); T. D. Groff, Princeton Univ. (United States)

The Subaru Coronagraphic Extreme Adaptive Optics (SCExAO) system is an instrument designed to be inserted between the Subaru AO188

Conference 8151:
Techniques and Instrumentation for Detection of Exoplanets V

system and the infrared HiCIAO camera in order to greatly improve image contrast in the very close (less than 0.5") neighbourhood of stars. Next to its infrared coronagraphic path, a visible path has been implemented, composed of an high-order wavefront sensor and a visible scientific imager. Both rely on the ability of EMCCD cameras to provide fast frame rate at the photon noise limit. Benefiting from both adaptive optics correction and new data processing techniques, the visible imager is a powerful tool for high angular resolution imaging and opens numerous new science opportunities. We propose here a new image processing algorithm, based on the selection of the best signal for each spatial frequency. A factor 2 to 3 gain in Strehl ratio is obtained compared to the AO long exposure time depending on the image processing algorithm used and the seeing conditions. The system is able to deliver diffraction limited images at 650 nm (17 mas FWHM). Based on first on-sky results, we also demonstrate that this approach requires up to 10 times less exposure time than classic Lucky Imaging.

8151-27, Session 5

Diffraction pupil telescope for high-precision space astrometry

O. Guyon, The Univ. of Arizona (United States) and Subaru Telescope (United States); E. A. Bendek, College of Optical Sciences, The Univ. of Arizona (United States); S. M. Ammons, Lawrence Livermore National Lab. (United States); T. D. Milster, College of Optical Sciences, The Univ. of Arizona (United States); R. Belikov, NASA Ames Research Ctr. (United States); S. B. Shaklan, M. Shao, Jet Propulsion Lab. (United States); R. A. Woodruff, Lockheed Martin Space Systems Co. (United States)

A concept for high precision astrometry with a conventional wide field telescope is presented, enabling a space telescope to perform simultaneously coronagraphic imaging of exoplanets, astrometric measurement of their orbits and masses, and deep wide field imaging for a wide range of astrophysical investigations.

Our concept uses a diffractive telescope pupil (primary mirror), obtained by placing a regular grid of small submillimeter spots on the primary mirror coating. When the telescope is pointed at a bright star, the wide field image contains both a large number of background stars used for astrometric referencing, and faint diffraction spikes created by the grid of dots on the primary mirror. The diffraction spikes encode instrumental astrometric distortions due to optics or the detector, allowing precise measurement of the central star against a large number of faint background stars.

With up to a few percent of the primary mirror area covered by the dots, the fraction of the central starlight located in the diffraction spikes is kept sufficiently small to allow full sensitivity deep imaging over the telescope's field of view. Since the dots are regularly spaced, they do not diffract light at small angular separations, and therefore allow full coronagraphic imaging capability. We show that combining simultaneous astrometric and coronagraphic measurements allows improved detection and characterization of exoplanets by constraining the planet(s) characteristics with both measurements. Our preliminary astrometric accuracy error budget shows that sub-micro arcsecond astrometry can be achieved with a ~1.5 m diameter telescope, and that astrometric accuracy improves rapidly with telescope diameter.

8151-28, Session 5

Micro-arcsecond relative astrometry from the ground with a diffractive pupil

S. M. Ammons, Lawrence Livermore National Lab. (United States); E. A. Bendek, O. Guyon, The Univ. of Arizona (United States)

We are developing a diffractive pupil concept for space-based

simultaneous astrometric/coronagraphic detection of exo-earths. Extended diffraction spikes generated by a dotted primary mirror are referenced against a wide-field grid of background stars to calibrate changing optical distortion and achieve sub-microarcsecond astrometric precision on bright targets. Also critical is the use of controlled telescope rolling to average detector noise perpendicular to the diffraction spikes. We intend to validate 0.14 microarcsecond single-axis astrometric precision on a scaled-down testbed of a 1.4-m space telescope at the University of Arizona.

We describe applications of this concept to ground-based uncrowded astrometry using a transmissive pupil mask and a wide-field camera to image ~100 background reference stars (30"x30"). Final relative astrometric precision is limited by differential tip/tilt jitter caused by high altitude layers of turbulence. A small telescope (< 2 m) equipped with a transmissive pupil mask would achieve single-axis precision of 70 microarcseconds per epoch in 1 hour on bright stars ($V < 12$) and a large telescope (6-10 m) could achieve as low as 10 microarcseconds, an order of magnitude better than space-based facilities available today. Permitting the sky to naturally roll and averaging signals over many thousands of pixels helps to mitigate the effects of detector imperfections. We present a proposed design to test the concept with a 20" diffractive pupil mask on a small telescope in Arizona.

8151-29, Session 5

Dynamic distortion calibration using a diffracting pupil: high-precision astrometry laboratory demonstration for exoplanet detection

E. A. Bendek, College of Optical Sciences, The Univ. of Arizona (United States); S. M. Ammons, Lawrence Livermore National Lab. (United States); T. D. Milster, College of Optical Sciences, The Univ. of Arizona (United States); O. Guyon, The Univ. of Arizona (United States)

Detection of earth-size exoplanets using the astrometric signal of the host star requires sub microarcsecond measurement precision. One major challenge in achieving this precision using a medium-size (<2-m) space telescope is the calibration of dynamic distortions. We propose a diffractive pupil technique, which uses an array of approximately 50um dots on the primary mirror that generate polychromatic diffraction spikes in the focal plane. The diffraction spikes encode optical distortions in the optical system and may be used to calibrate astrometric measurements. This concept can be used simultaneously with coronagraphy for exhaustive characterization of exoplanets (mass, spectra, orbit). At University of Arizona a high precision astrometry laboratory is being developed to demonstrate the capabilities of this diffractive pupil concept. We aim to achieve 10 μ s single-axis precision in the laboratory, simulating 0.14 μ s precision on a 1.4 m space telescope. Here we describe this laboratory and present the data and results obtained so far. We consider a plan to test a diffractive pupil with a high contrast PIAA coronagraph to demonstrate that the diffraction spikes do not affect the coronagraph performance, as they diffract light only at large angular separations, well outside the coronagraph field of view

8151-30, Session 5

NEAT: a microarcsec astrometric telescope

M. Shao, B. Nemati, C. Zhai, Jet Propulsion Lab. (United States)

NEAT, Nearby Earths Astrometric Telescope is a concept for a 1m space telescope with sub 1 microarcsec precision in 1 hr. The concept is based on a very simple optical design that has only one optic and hence no beam walk related systematic errors that could produce milliarcsec sized systematic biases in normal telescopes. The second aspect of the concept is a laser metrology system to calibrate the focal plane. Microarcsec astrometry with a small telescope requires centroiding of

**Conference 8151:
Techniques and Instrumentation for Detection of Exoplanets V**

stellar images to 1e-5 pixels, and for this to happen we have to know where the pixels are at 1e-5 pixels as well as the QE(x,y) within each pixel. This paper describes the mission concept as proposed to ESA as an M class mission.

The mission could search 75~100 nearby stars for planets as small as the Earth in a 1 AU orbit.

The telescope is a single long focus off axis parabola.

8151-31, Session 5**Micropixel-level image position sensing testbed**

B. Nemati, M. Shao, C. Zhai, H. Erlig, R. Goullioud, X. Wang, Jet Propulsion Lab. (United States)

Image position sensing at the few micro-pixels level would enable technology for a wide range of astronomical goals, from search for exoplanets to dark energy. Monitoring the position of an image to this level of accuracy requires metrology of the pixel positions, knowledge of the intra-pixel quantum efficiency variation, as well as a linearized image position algorithm. JPL's Micropixel Centroiding Testbed (MCT) uses a low-expansion bench to stabilize the locations of fiber tips which illuminate a CCD with a set of 'stars' as well as heterodyne metrology fringes. In this paper we describe the test and present the first results.

8151-32, Session 6**Designing an optimal estimator for more efficient wavefront correction**

T. D. Groff, N. J. Kasdin, Princeton Univ. (United States)

Space-based coronagraphs for future earth-like planet detection will require focal plane wavefront control techniques to achieve the necessary contrast levels. These correction algorithms are iterative and the control methods require an estimate of the electric field at the science camera, which requires nearly all of the images taken for the correction. In order to maximize science time the amount of time required for correction must be minimized which means reducing the number of exposures required for correction. This drives reducing both the number of iterations and the number of exposures per iteration required to achieve a targeted contrast. Given the large number of images required for estimation, the ideal choice is to use fewer exposures to estimate the electric field. Here we demonstrate an optimal estimator that uses prior knowledge to create the estimate of the electric field. In this way we can optimally estimate the electric field by minimizing the number of exposures required to estimate under an error constraint. The performance of this method is compared to a pairwise estimator which is designed to give the least-squares minimal error. This allows us to evaluate the number of images necessary to achieve a contrast target and is the first step towards generating an adaptive algorithm which combines estimation and control to optimize the entire correction problem.

8151-33, Session 6**Unified coronagraph and wavefront control design**

N. J. Kasdin, A. Carlotti, T. Groff, R. J. Vanderbei, Princeton Univ. (United States)

Numerous coronagraph designs for high-contrast have been proposed over the last decade with a number of them in advanced stages of technology development. These coronagraph designs are differentiated by various performance metrics, such as throughput, inner working angle, bandwidth, ease of implementation (a surrogate for cost), sensitivity, and robustness. Some are being considered for very high-contrast (greater than 10^{11}) and small inner working angles to enable

imaging of terrestrial planets in the habitable zone of nearby stars. In this paper we show that every coronagraph works on the same principal---it must modify the amplitude of the electric field across the exit pupil in order to create a final high-contrast image. This may be done through apodization, phase plates, remapping, or phase and amplitude adjustment at intermediate image planes. Unfortunately, phase and amplitude errors in the telescope limit the achievable contrast. All practical systems must include the capability for both amplitude and phase control of the wavefront. We demonstrate that whatever coronagraph is chosen, it need only be designed to achieve contrast to the level at which amplitude errors dominate. The remaining contrast will be achieved via the wavefront control system; the final inner working angle is determined by the deformable mirrors. We present a number of designs using shaped pupils and multiple deformable mirrors and discuss the design tradeoffs. We also show that the same algorithms can be used to design aspheric mirrors rather than deformable mirrors similar to pupil mapping systems.

8151-34, Session 6**Optimizing broadband wavefront control to correct amplitude and phase aberrations**

T. D. Groff, N. J. Kasdin, A. Carlotti, Princeton Univ. (United States)

The Stroke Minimization algorithm developed at the Princeton High Contrast Imaging Laboratory has proven symmetric dark hole generation using minimal stroke on two deformable mirrors (DM) in series. We extend the concept of minimizing DM actuation to achieve symmetric dark holes in broadband light. This requires simultaneously correcting both amplitude and phase aberrations over the bandwidth. Here we address the relationship of amplitude and phase aberrations with wavelength and the implication for wavefront control and design tolerances. This drives the number of deformable mirrors, their locations in the optical path, and design constraints on the deformable mirrors. Broadband suppression is achieved experimentally by using three wavelengths to define the bandwidth of correction in the optimization problem. This windowed approach to Stroke Minimization makes the optimization in wavelength tractable and allows for estimation only at a single wavelength which reduces the number of exposures required for correction. The output of the estimation algorithm is extended to the higher and lower wavelengths by establishing a functional relationship of the image plane electric field in wavelength. The accuracy of the functional relationship will ultimately bound the achievable bandwidth, therefore as a metric these results are also compared to estimating each wavelength separately.

8151-35, Session 6**Pair-wise, image plane-based electric field estimation for high-contrast coronagraphy**

A. Give'on, B. D. Kern, S. B. Shaklan, Jet Propulsion Lab. (United States)

In this paper we describe the estimation methodology for image plane-based electric field measurements for high contrast coronagraphic imaging. A deformable mirror (DM) shape is modified to create diversity in the image plane of the science camera where the intensity of the light is measured. The DM is adjusted to create complementary pairs of intensity patterns from which the complex field is estimated. Along with the Electric Field Conjugation correction algorithm, this estimation method has been used in various high contrast imaging testbeds to achieve the best contrasts to date. We demonstrate the effectiveness of this method through laboratory experiments for both narrow-band light (2%) and broadband light (10%).

Conference 8151:
Techniques and Instrumentation for Detection of Exoplanets V

8151-36, Session 6

Kernel-phases for high-contrast detection beyond the resolution limit

F. Martinache, Subaru Telescope, National Astronomical Observatory of Japan (United States)

The detection of high contrast companions at small angular separation appears feasible in conventional direct images using the self-calibration properties of interferometric observable quantities. In the high-Strehl regime, soon to be available thanks to the coming generation of extreme Adaptive Optics systems on ground based telescopes, and already available from space, quantities comparable to the closure-phase that are used with great success in non-redundant masking interferometry, can be extracted from direct images, even taken with a redundant aperture. These new phase-noise immune observable quantities, called kernel-phases, are determined a-priori from the knowledge of the geometry of the pupil only. Analysis of HST/NICMOS archive and other ground based AO images, using this new kernel-phase algorithm, demonstrates the power of the method, and its ability to detect companions at the resolution limit and beyond.

8151-37, Session 7

Nondimensional representations for occulter design and performance evaluation

E. J. Cady, S. B. Shaklan, Jet Propulsion Lab. (United States)

An occulter is a spacecraft with a precisely-shaped optical edges which flies in formation with a telescope, blocking light from a star while leaving light from nearby planets unaffected. Using linear optimization, occulters can be designed for use with telescopes over a wide range of telescope aperture sizes, science bands, and starlight suppression levels. It can be shown that this optimization depends primarily on a small number of independent nondimensional parameters, which correspond to Fresnel numbers and physical scales and enter the optimization only as constraints. We show how these can be used to span the parameter space of possible optimized occulters; this data set can then be mined to determine occulter sizes for various mission scenarios and sets of engineering constraints. This also may be used to compare performance for missions of different scales and bandpasses, and we use this to discuss some point designs applicable to future telescopes.

8151-38, Session 7

A starshade petal error budget for exo-earth detection and characterization

S. B. Shaklan, L. F. Marchen, D. Lisman, E. J. Cady, S. R. Martin, Jet Propulsion Lab. (United States); N. J. Kasdin, Princeton Univ. (United States); P. J. Dumont, Jet Propulsion Lab. (United States)

We have looked in detail at the shape requirements on starshade petals and have found several factors that significantly relax the requirements compared to our earlier work. First, by adopting an observational scenario where the occulter spins about its axis on timescales short relative to the zodi-limited integration time, typically several hours, scatter from localized petal errors is smoothed into annuli around the center of the image plane. This results in a large reduction in the background flux variation. It also reduces thermal gradients. Second, after completing development of a prototype petal and planning a second one, several manufacturing errors were found to be negligible, allowing us to allocate a larger fraction of the error budget to the more challenging aspects. Finally, a more thorough Monte-Carlo analysis of random errors allowed us to relax requirements compared to several 'worst case' scenarios reported earlier. We compare the requirements for four cases: we assume telescope of 1.5 and 4 m diameter, and inner working angles of 75 and 90 mas.

8151-39, Session 7

Position sensing and control at the Princeton occulter testbed

D. Sirbu, Princeton Univ. (United States); E. J. Cady, Jet Propulsion Lab. (United States); N. J. Kasdin, R. J. Vanderbei, M. Carr, M. Galvin, E. Kao, M. McElwain, J. A. Spechler, Princeton Univ. (United States)

Direct imaging of planets around other solar systems requires starlight suppression. One space-based mission concept involves the usage of an external occulter, a second spacecraft specially shaped to create a deep shadow on the space telescope. At the Princeton Occulter Testbed, a subscale experiment was designed to test long-distance beam propagation and verify the numerical diffraction propagation. We present a scheme for inferring relative position of the occulter and telescope from diffraction leakage outside of the suppression passband. In this experiment, the optical mask consists of an inner portion which represents the scaled occulter mask and an outer ring that minimizes diffraction effects at the dark hole. A new optical mask was designed with the inner mask operating over a suppression band covering the visible wavelengths and an outer ring that minimizes diffraction effects over the camera's sensitivity wavelengths. The testbed was also outfitted with two-degrees of freedom control at the observation plane that allows a position sensing experiment to determine sensitivity localization sensitivity.

8151-40, Poster Session

Higher-precision radial velocity measurements with the SOPHIE spectrograph using octagonal-section fibers

S. Perruchot, Observatoire de Haute-Provence (France); F. Bouchy, Institut d'Astrophysique de Paris (France) and Observatoire de Haute-Provence (France); I. Boisse, Institut d'Astrophysique de Paris (France); R. F. Diaz, G. Hébrard, Institut d'Astrophysique de Paris (France) and Observatoire de Haute-Provence (France); A. Santerne, Observatoire Astronomique de Marseille-Provence (France); B. Chazelas, F. A. Pepe, Observatoire de Genève (Switzerland); G. Moreaux, Observatoire Astronomique de Marseille-Provence (France); K. Arnaud, D. Tézier, Ctr. de Physique des Particules de Marseille (France); G. Avila, European Southern Observatory (Germany)

High-precision spectrographs play a key role in exoplanet searches using the radial velocity techniques. But at the accuracy level of 1 m/s, required for super-Earth characterization, stability of spectrograph performance is crucial considering variable observing conditions such as seeing, guiding errors, telescope vignetting and ambient temperature.

In fiber-fed spectrographs such as HARPS or SOPHIE, the fiber link scrambling properties are one of the main issues. Both the stability of the fiber near-field uniformity at the spectrograph entrance and of the far-field illumination on the echelle grating (pupil) are critical for high-precision radial velocity measurements because of the spectrograph geometrical field and aperture aberrations. We conducted tests on the SOPHIE spectrograph at the 1.93-m OHP telescope to measure the instrument sensitivity to the fiber link light feeding conditions: star decentering, telescope vignetting by the dome, defocussing.

To significantly improve on current precision, we studied a fiber link modification considering the spectrograph operational constraints. We have thus developed a new link which includes a piece of octagonal-section fiber, having good scrambling properties, lying inside the former circular-section one, and we tested the concept on a bench to characterize near-field and far-field scrambling properties.

This modification has been implemented in Spring 2011 on all four links of the SOPHIE spectrograph and tested for the first time directly on

the sky to demonstrate the gain compared to the previous fiber link. Scientific validation for exoplanet search and characterization has been achieved by observing standard stars and known low-mass exoplanets.

8151-41, Poster Session

Design of a star, planet and exo-zodiacal cloud simulator for the nulling testbench PERSEE

F. Hénault, P. Girard, A. Marcotto, N. Mauclert, Univ. de Nice Sophia Antipolis (France); J. Le Duigou, Ctr. National d'Études Spatiales (France)

On-going developments on the PERSEE nulling testbench include the realization of a focal plane simulator featuring one central star, an extra-solar planet orbiting around it, and Exo-Zodiacal Clouds (EzC) surrounding the observed stellar systems. PERSEE (Pégase Experiment for Research and Stabilization of Extreme Extinction) is a laboratory testbench jointly developed by a Consortium of six French institutes and companies, incorporating Observatoire de la Côte d'Azur (OCA) who is in charge of the manufacturing and procurement of the future Star and Planet Simulator (SPS). In this communication is presented a complete description of the SPS, including general requirements, techniques employed for simulating the observed planet and EzC, opto-mechanical design and expected performance. Current status of the activities is summarized in the conclusion.

8151-42, Poster Session

Debris sightings in the Kepler field

F. C. Witteborn, J. Van Cleve, W. J. Borucki, NASA Ames Research Ctr. (United States); V. S. Argabright, Ball Aerospace & Technologies Corp. (United States); P. Hascall, Orbital Network Engineering Inc. (United States)

A small fraction of Kepler telescope exposures are rejected because of transient, excess background in the field. The patterns of illumination vary from broad streaks to diffuse patches, sometimes filling the focal plane. Examination of such images and their temporal variation shows that they can be attributed to nearby particles crossing the field-of-view of the telescope. Most of the particles appear to be receding. The visual appearance and frequency are consistent with the "debris storms" reported by STEREO SECCHI observers and which they found to be coincident with meteoroid impacts. In addition, a few events, lasting several hours each, appear to be caused by more distant, extended sources. The tracking cameras, located at the opposite end from the telescope's entrance, and pointed at roughly right angles to its line-of-sight, also detected moving light sources. Their behavior was consistent with the main telescope sightings. Future missions requiring precise, uninterrupted photometry and pointing may benefit from understanding this phenomenon and mitigating it by design and data analysis.

8151-44, Poster Session

Relaxing the sensitivity of nuller coronagraphs to finite stellar diameters using apodization

A. Carlotti, Princeton Univ. (United States); C. J. Aime, Univ. de Nice Sophia Antipolis (France); Y. Rabbia, Observatoire de la Côte d'Azur (France)

Nuller coronagraphs such as the Achromatic-Interfero-Coronagraph can perfectly cancel the starlight by destructively interfering it with itself, if the star is unresolved and exactly on-axis. Small pointing errors as well as the finite stellar diameter of the targeted star can however ruin the

performances of this type of coronagraph. Observed at 600nm with an AIC behind a 10m telescope, the Sun at 10pc would present an apparent angular diameter of 1 mas that would induce a star-leakage of $10^{(-6)}$ at 0.1". The expected flux ratio between a Sun-like star and an Earth-like planet is however much higher (10^{10} in the visible). We show through an analytical formalism that an apodized nuller coronagraph (ANC) can achieve planet detections with much higher contrasts. We use for demonstrative purposes specific apodization profiles such as Sonine profiles, concentric ring profiles or cosine profiles. Expressions of the local contrast ratio and of the signal-to-noise ratio are derived. The possibility to estimate the performances of other types of apodizations such as spheroidal prolate apodizations through numerical simulations is considered, although the additional integration over the stellar disk is computationally challenging.

8151-45, Poster Session

Pressure and temperature stabilisation of an existing Échelle spectrograph II

F. U. Grupp, Max-Planck-Institut für extraterrestrische Physik (Germany) and Univ.-Sternwarte München (Germany); A. Brucalassi, Max-Planck-Institut für extraterrestrische Physik (Germany); F. Lang, Univ.-Sternwarte München (Germany); S. M. Hu, Shandong Univ. (China); R. Holzwarth, Max-Planck-Institut für Quantenoptik (Germany) and Menlo Systems GmbH (Germany); T. Udem, Max-Planck-Institut für Quantenoptik (Germany); U. Hopp, Univ.-Sternwarte München (Germany); R. Bender, Max-Planck-Institut für extraterrestrische Physik (Germany)

First results from the pressure stabilization and extended temperature stabilisation of the existing FOCES high resolution Échelle spectrograph are presented with this paper.

A pressure stabilize environment slightly above the environmental weather dependant pressure is created for FOCES. In addition a two layer onion shell like temperature stabilization is applied to keep the instrument stable with respect to environmental conditions.

Detailed analysis of the level of stability for both temperature and pressure are performed. First results of the instrument stability are being evaluated in this stabilized environment.

8151-46, Poster Session

Speckle identification to assist the direct detection of exoplanets

E. Young, N. J. Kasdin, A. Carlotti, M. G. Littman, Princeton Univ. (United States); M. C. Noecker, Ball Aerospace & Technologies Corp. (United States)

One of the major limitations to detecting exoplanets in high-contrast images is confusion with residual quasi-static speckles, formed due to aberrations in the optical system. Speckles look like the image of a planet, therefore threatening the planet detection. However, we can take advantage of their different behavior and optical coherence by using interference to distinguish speckles from the image of a planet. Princeton is designing and building a testbed suitable for coherent speckle detection studies. Our technique adds deliberate perturbations to a deformable mirror (DM) to create a reference field from the starlight on the image plane detector. Large variations in intensity on the detector are therefore caused due to the interference between the prior residual speckle field and the reference field. We study specific functions on the DM to see the new reference field created and to capture an image. We then analyze the series of images (as we change the known function placed on the DM) to estimate the amplitude and phase of the speckles. The interference term allows us to distinguish speckles from the incoherent planet signals. This generic technique works with any type of

coronagraph, ground or space-based. However, we illustrate the results with simulations and lab data designed for a shaped pupil coronagraph.

8151-47, Poster Session

Wide-field telescope design for the KMTNet project

S. Kim, B. Park, C. Lee, Korea Astronomy and Space Science Institute (Korea, Republic of); L. G. Kappler, N. Kappler, TBR Construction & Engineering (United States); W. M. Poteet, H. Cauthen, D. R. Blanco, CP Systems, Inc. (United States); J. U. Lee, Cheongju Univ. (Korea, Republic of); M. K. Cho, National Optical Astronomy Observatory (United States); I. Yuk, M. Chun, Korea Astronomy and Space Science Institute (Korea, Republic of); H. Jin, Kyung Hee Univ. (Korea, Republic of); J. U. Teran, S. Freestone, M3 Engineering & Technology Corp. (United States); S. Cha, Korea Astronomy and Space Science Institute (Korea, Republic of)

The Korea Astronomy and Space Science Institute (KASI) will develop three 1.6m optical telescopes for the Korea Micro-lensing Telescope Network (KMTNet) project.

These will be installed at three southern observatories with different time zones by early 2014 to monitor dense star fields like the Galactic bulge and Large Magellanic Cloud. The primary scientific goal of the project is to discover numerous extra-solar planets using the gravitational micro-lensing technique.

We have completed the final design of the telescope. The most critical design issue was wide-field optics. The project science requires the Delivered Image Quality (DIQ) of less than 1.0 arcsec FWHM within 1.2 degree radius FOV, under atmospheric seeing of 0.75 arcsec.

We chose the prime-focus configuration and realized the DIQ requirement by using four corrector lenses with all spherical surfaces.

We will also present the design details such as the optical alignment, focus system with three linear actuators on the top ring, and friction drive system.

8151-48, Poster Session

Achieving high-precision ground-based photometry for transiting exoplanets

O. Guyon, Subaru Telescope, National Astronomical Observatory of Japan (United States)

An analysis of the sources of error affecting ground-based transit photometric accuracy is presented. The terms other than photon noise can be dramatically reduced by hardware choices and data processing algorithms. In particular, the effect of scintillation can be reduced by apodization of the pupil, proper time weighting of the measurements, and simultaneous multi-color photometry. Differential extinction can be calibrated by a combination of PSF modeling, multi-color photometry, and analysis of spatial and temporal correlations in a wide field image. Conventional imaging systems are thus usually poorly suited for high precision photometry.

A low cost camera system was recently deployed on the Mauna Loa observatory to increase our understanding of the effects limiting photometric precision and test some of the improvements achieved by hardware and data reduction techniques optimized for transit photometry. The system offers a 150 sq deg field with a 70mm entrance aperture, and 3-band simultaneous photometry at a 0.01 Hz sampling. The detector is a low-cost commercial 3-color CMOS array, and is an attractive cost-effective choice for high precision transit photometry. The design of the system and early results are presented.

8151-49, Poster Session

Recent results of the second generation of vector vortex coronagraphs on the high-contrast imaging testbed at JPL

D. P. Mawet, D. Moody, B. D. Kern, E. Serabyn, A. F. Niessner, A. C. Kuhnert, J. T. Trauger, Jet Propulsion Lab. (United States)

Coronagraphy is necessary to image and characterize extra-solar planets. The vortex coronagraph is one solution amongst many others. It presents many advantages (simplicity, small inner working angle, high throughput) and so it has been developed by NASA for the past 3 years. Here we report on the results of an experiment conducted on the high contrast imaging testbed at JPL. New contrast records have been established, which make this coronagraph more attractive than ever.

8151-50, Poster Session

Zodiac II: debris disk science from a balloon

G. Bryden, W. Traub, L. C. Roberts, Jr., R. Bruno, Jet Propulsion Lab. (United States); S. Chakrabarti, Boston Univ. (United States); P. Chen, Jet Propulsion Lab. (United States); L. Hillenbrand, California Institute of Technology (United States); J. Krist, Jet Propulsion Lab. (United States); C. F. Lillie, Northrop Grumman Aerospace Systems (United States); B. A. Macintosh, Lawrence Livermore National Lab. (United States); D. P. Mawet, B. P. Mennesson, D. Moody, K. R. Stapelfeldt, Jet Propulsion Lab. (United States); D. Stuchlik, NASA Goddard Space Flight Ctr. (United States); J. T. Trauger, G. Vaischt, S. C. Unwin, Jet Propulsion Lab. (United States)

Zodiac II is a proposed balloon-borne science investigation of debris disks around nearby stars. Debris disks are analogs of the Asteroid Belt (mainly rocky) and Kuiper Belt (mainly icy) in our Solar System.

We will measure the size, shape, brightness, and color of each disk.

These measurements will enable us to answer these fundamental questions: what do debris disks tell us about the evolution of planetary systems; how are debris disks produced; how are debris disks shaped by planets; what materials are debris disks made of; how much dust do debris disks make as they grind down; and how long do debris disks live?

In addition, Zodiac II will observe hot, young exoplanets, as targets of opportunity.

The Zodiac II instrument is a 1.1-m diameter SiC telescope and an imaging coronagraph on a gondola carried by a stratospheric balloon. Four mid-latitude flights will be operated: two overnight flights in the US, and two half-global flights in the Southern Hemisphere, totaling about 123 hours of observing time.

The data from Zodiac II is a set of four-color images of each debris disk, in broad bands, at visible wavelengths. Zodiac II will answer its science questions by making accurate, multi-wavelength images of the debris disks around about 25 of the available 104 known targets.

On these targets, it will be 100 times more sensitive than HST with ACS; no existing telescope can match the Zodiac II contrast and resolution performance. A second objective of Zodiac II is to use the near-space environment to raise the Technology Readiness Level (TRL) of SiC mirrors, internal coronagraphs, deformable mirrors, and wavefront sensing and control, all potentially needed for a future space-based telescope for high-contrast exoplanet imaging.

8151-51, Poster Session

The performance of the new Fabry-Perot calibration system of HARPSF. A. Pepe, F. P. Wildi, B. Chazelas, Observatoire de Genève
(Switzerland)

ESO's radial velocity spectrograph HARPS is arguably the most successful ground based extra-solar planet hunting instrument today. It has been shown recently that one of the largest contributor of this instrument's error budget is the wavelength calibration error. Three years ago we have started a program to upgrade HARPS with a new calibrator system in the form of a Fabry-Perot etalon. In the mean time, this system has been installed, tested and improved on-site. It has now passed the science commissioning phase and is offered to the community as an observation mode of HARPS. It's performance is essentially photon limited, which in the present configuration means that a calibration noise of 0.1m/s is achieved. Our presentation will review the system design, the lessons learned and show the details of the performance.

8151-52, Poster Session

Deep UV to NIR Space Telescopes and Exoplanet Coronagraphs: a trade study on throughput, polarization, mirror coating options and requirementsK. Balasubramanian, S. B. Shaklan, A. Give'on, L. F. Marchen,
Jet Propulsion Lab. (United States)

The NASA Exoplanet program and the Cosmic Origins program are exploring technical options to combine the visible to NIR performance requirements of a space coronagraph with the general astrophysics requirements of a space telescope covering the deep UV spectrum. Are there compatible options in terms of mirror coatings and telescope architecture to satisfy both goals? In this paper, we address some of the main concerns, particularly relating to polarization in the visible and throughput in the UV. On-axis and off-axis telescope architectures employing coating options compatible with current technology are considered in this trade study.

Conference 8152: Instruments, Methods, and Missions for Astrobiology XIV

Tuesday-Thursday 23-25 August 2011 • Part of Proceedings of SPIE Vol. 8152
Instruments, Methods, and Missions for Astrobiology XIV

8152-01, Session 1

Searching for a second sample of life on Earth: the lesson of arsenic

P. C. W. Davies, Arizona State Univ. (United States)

In the absence of a known mechanism for life to emerge from non-living precursors, it is impossible to meaningfully assign a probability to the emergence of life on an earthlike planet. Life on Earth may be a freak phenomenon, unique in the observable universe, or alternatively just one example of an almost inevitable progression from matter to life in a universe teeming with biology. Since the biogenesis mechanism is unlikely to be definitively identified in the foreseeable future, it makes sense to focus instead on empirical methods. If life is probable on earthlike planets then it should have arisen many times on Earth. If that were the case, then there may be extant terrestrial micro-organisms belonging to a separate tree from standard life, and intermingled with it. I shall describe a program of research aimed at discovering a "shadow biosphere" of weird life, using the recent excitement concerning arsenic life as a proof of concept.

8152-02, Session 2

Investigations of microfossils in carbonaceous meteorites and ancient terrestrial rocks at the A. A. Borisyak Paleontological Institute (RAS)

A. Y. Rozanov, Paleontological Institute (Russian Federation)

Bacterial Paleontology studies carried out at the A. A. Borisyak Paleontological Institute of the Russian Academy of Sciences have shown that pseudomorphoses of filamentous and coccoidal bacteria are present in many carbonaceous meteorites, although they are absent in other meteorites studied. In this paper we review the studies of the forms detected in various carbonaceous meteorites and compare them with microfossils found in phosphorites and other ancient terrestrial rocks.

8152-03, Session 2

Filamentous trichomic prokaryotes in carbonaceous meteorites: indigenous microfossils, minerals, or modern bio-contaminants?

R. B. Hoover, NASA Marshall Space Flight Ctr. (United States); A. Y. Rozanov, Paleontological Institute (Russian Federation)

Large complex filaments have been detected in freshly fractured interior surfaces of a variety of carbonaceous meteorites. Many exhibit the detailed morphological and morphometric characteristics of known filamentous trichomic prokaryotic microorganisms. In this paper we review prior studies of filamentous microstructures encountered in the meteorites along with the elemental compositions and characteristics of the, fibrous evaporite minerals and filamentous cyanobacteria and homologous trichomic sulfur bacteria. The meteorite images and elemental compositions will be compared with data obtained with the same instruments for abiotic microstructures and living and fossil microorganisms in order to evaluate the relative merits of the alternate hypotheses that have been advanced to explain the nature and characteristics of the meteorite filaments. The possibility that the filaments found in the meteorites may be comprise modern bio-contaminants will be evaluated in light of their observed elemental

compositions and data by other researchers on the detection of indigenous complex organic biosignatures, and extraterrestrial amino acids and nucleobases found in the Murchison CM2 and the Orgueil CI1 carbonaceous meteorites.

8152-04, Session 2

Multicellular algae from lower proterozoic (2.45 Ga) weathering crusts of Kola Peninsular

M. M. Astafieva, Paleontological Institute (Russian Federation); A. Y. Rozanov, Paleontological Institute (United States); R. B. Hoover, NASA Marshall Space Flight Ctr. (United States)

New interesting data were received from the ancient weathering crusts aged ca. 2.45 Ga from the hole bored under the direction of our Norwegian colleagues V. Melezchik and A. Lepland while working on the International Continental Drilling Program (ICDP). The hole is situated in the Monchegorsk Region of Kola Peninsular.

Weathering crusts are indicators of continental sedimentation conditions. The question of bacterial colonization of land is interesting by itself. Investigations in this field are rather fruitful. Active role of bacteria in the formation of the most ancient weathering crusts has been already proven and supposition concerning bacterial colonization of land from the very beginning of sedimentary rocks formation, i.e. from the very beginning of geological annals, has been made.

What is the principle interest of the last find? Fossil remains of the highly organized for that time forms were found. These forms here and there merge with the rock matrix, here and there they submerge or penetrate into the rock. That is why it is possible to suggest that these forms were buried in situ, but not a later contamination. Judging by morphology, the found structures probably refer to green or red algae. However the exact systematic position of these finds is not very important. The main thing is that they referred to eucaryotes, and moreover - to multicellular eucariots. So high level of organization of forms with the age more than 2.4 Ga is the evidence of the fact that the level of atmosphere oxygenation was much higher than it was earlier considered to be (the latest reconstruction needs modification) and that middle surface temperatures could not differ from recent temperatures more than 15-20o.

The study was executed within the framework of the complex program of basic research of the Presidium of the Russian Academy of Sciences "Origin of Biosphere and Evolution of Geo-biological Systems" (subprogram II) and was supported by the Russian Foundation for Basic Research, projects 08-04-00484 and SS-65493.2010.4. The samples were received due to International Continental Drilling Program (ICDP).

8152-05, Session 3

Nonbiogenic amino acids in natural bitumens and problem of genetic identification of geo- and astro-problematics

N. P. Yushkin, A. Lysiuk, Institute of Geology (Russian Federation)

Nucleotides, proteins and their components - amino acids, often referred to as biogenic, have long been known to be present in various geological objects of both biogenic and non-biogenic origin. Amino acids were also found in the organic matter of many cosmic bodies and various geological objects of different genetic nature.

Our studies of mechanisms of crystallization and supermolecular ordering in natural solid hydrocarbons aimed to analyze peculiarities of amino acids contents in bitumens of various types and in highly carbonaceous

**Conference 8152:
Instruments, Methods, and Missions for Astrobiology XIV**

substances (shungite), to reveal their relation to the structural genetic nature of the hydrocarbons and to obtain the information to gain an insight into amino acids genesis.

Amino acids from natural solid hydrocarbons, like other organic compounds, have essentially abiogenic origin. This fact suggests polymerization and self-organization of monomers bringing about multi-functional structures, homologous to biopolymeric ones.

Experiments on the thermal and radiation influence on natural bitumens testified about abiogenic intensive synthesis of amino acids, including also His, Lys, Arg, Phe, considered to be reliable biomarkers by many researchers. The radiosynthesis resulted in the increasing concentration of predominantly left modifications Gly, β -Ala, L-Ala, L-Ile, L-Val, L-Leu, L-Pro, L-Ser, L-Ala. The same phenomenon was observed in phitofulgurites resulted from lightning impacts into accumulations of dry vegetation.

Hence, the reliable identification of biomorphic structures requires additional criteria apart from biochemical ones.

Thus, our investigations showed the presence of amino acids in all genetic and structural types of natural solid carbonaceous substances, revealed the typomorphism of amino acids content in their different types, presented regular increasing amino acids content with increasing temperature of formation and ordering of the substances, revealed possibility of abiogenic synthesis of amino acids and established its optimal conditions.

8152-06, Session 3

Biomineral microstructures in ferromanganese nodules: evidence of the biological and abiogenous origin

G. Lysyuk, Institute of Geology (Russian Federation)

Manganous oxide is one of the most widespread and practically important objects, in formation and transformation of which microorganisms play an active role. Manganous oxide is characterized by the joint presence of both well crystallized modifications, and fine phases with the lowest order strength (with the contents of reehtgenoamorphous component till 50 - 60% at significant concentration of ore component). This fact will now has no enough strict scientific explanation. We examined formation of reehtgenoamorphous nano-dimensional manganous oxide from positions of biogenic mineral formation. Objects of our researches were nano-dimensional phases of the iron-manganous nodules and manganous residual soil.

Electronic-microscopic investigations showed a great expansion of mineralized biofilms on the studied samples. The content of the bacterial mass make (%): MnO - 28.34; Fe₂O₃ - 17.14; SiO₂ - 7.11; CaO - 2.41; TiO₂ - 1.90; Na₂O - 1.74; Al₂O₃ - 1.73; MgO - 1.30; P₂O₅ - 1.25; SO₃ - 1.25; CoO - 0.68; CuO - 0.54; NiO - 0.53; K₂O - 0.50.

Another development of a bacteria factor during formation of manganous oxide is occurrence of fossilized cyanobacterial mat with the content (%): MnO - 48.35; Fe₂O₃ - 6.23; MgO - 8.76; Al₂O₃ - 5.05; SiO₂ - 4.45; NiO - 3.63; Na₂O - 2.30; CuO - 2.19; CaO - 1.31; K₂O - 0.68. The use atomic-force microscopy method allows determining size of some cells of cyanobacteria with the 200nm at length and about 70nm across diameter. Electronic- microscopic investigations showed that the phase data is a mineralized glycocalix, composed of nanodimensional flakes of todorokite.

8152-07, Session 4

Pre-biotic organic synthesis: laboratory simulation experiments and their significance for the origin of life in the solar system

M. H. Engel, D. H. Engel, The Univ. of Oklahoma (United States)

It is commonly assumed that the origin of life on Earth and perhaps

elsewhere in the solar system was preceded by the synthesis and accumulation of organic compounds essential for life as we know it (e.g. amino acids, sugars, purines, pyrimidines, etc.) by non-biological processes. Over the past century, laboratory simulation experiments using a variety of inorganic precursors and energy sources have resulted in the synthesis of some, but not all of the compounds required for life. More importantly, the mechanisms by which these simple organic compounds initially combined to form the more complex structures (proteins, nucleic acids, etc.) upon which all life is based remain elusive. Here we report a summary of the progress to date concerning pathways for the pre-biotic synthesis of organic matter and their significance for the origin of life in the solar system.

8152-08, Session 4

Potential exoplanet pseudo-biosignatures

G. A. Konesky, K-Plasma Ltd. (United States)

Current exoplanet detection techniques are biased toward large, massive planets in very close orbits to their host star, so-called "hot Jupiters." Since they are far from the habitable zone around that host star, any potential biosignature, such as methane, would likely have an abiotic origin. Similarly, other biogenic gases, including oxygen (and resulting ozone), nitrogen, carbon dioxide, carbon monoxide, methane, nitrogen dioxide, ammonia, nitrous oxide, sulfur dioxide, hydrogen sulfide, carbonyl sulfide, dimethyl sulfide, and various non-methane hydrocarbons, have alternate abiotic sources. We consider both biotic and abiotic sources for these gases.

Given the great distances these potential exoplanet biosignature gases would need to be spectroscopically detected, we primarily concentrate on potential biogenic gases that would be abundant, especially oxygen and ozone. In general, there are few abiotic geochemical processes that would produce free oxygen in any significant quantity, although volcanic hydrogen has been considered as a reducing agent to "soak up" oxygen on the early Earth. The history of the rise of oxygen on Earth, and the "Great Oxidation Event" might then be taken as the archetype of exoplanet biosignatures.

There is evidence that water was once abundant on Venus, as indicated by high deuterium/hydrogen atmospheric ratios, and on Mars, by its observed water-based surface mineralogy. While some water remains on Mars on its poles and likely underground, both planets lost considerable quantities through photodissociation, with the liberation of hydrogen to space, and the retention of oxygen. If similarly observed on distant exoplanets, it could be mistaken as a pseudo-biosignature.

8152-09, Session 4

Developing an astrobiological search protocol through the Taphonomic window

R. S. Shapiro, California State Univ., Chico (United States)

It is generally agreed by the astrobiological community that any fossil or extant life forms to be found outside of Earth would likely be archaea or bacteria or their near analogue. Paleontologists and geochemists are developing a library of evidence from ancient Earth sediments as well as active extreme environments. Yet, while there has been much research addressing the challenges in modeling the processes to create an extraterrestrial fossil record, less attention has been focused on establishing the taphonomic parameters in preserving the record.

Taphonomy encompasses the study of the processes involved in creating and later modifying the fossil record. Specific to astrobiologic missions is an understanding of how near-surface weathering and rock alteration might change the mineralogical and morphological character of any fossil structures. The most likely causes of alteration would come from: heat and pressure due to bolide impact, igneous intrusion, and chemical changes due to interaction with reducing or oxidizing fluids.

Modeling these alteration pathways and the resulting deposits is extremely challenging. As of yet, there is little agreement on what the

Conference 8152:
Instruments, Methods, and Missions for Astrobiology XIV

original conditions might encompass on another planet or satellite. Tectonic activity is quite diverse in our solar system and the resulting deformation structures would have very different consequences for any fossil-bearing strata. Most critically, the ancient gas and fluid compositions of the various planets and satellites—specifically the timing of potential liquid water—is still being unraveled. Generic models can be developed from Earth-analogues as a starting point for delineating key questions for future missions.

8152-10, Session 4

The changes of spectroscopic characteristics of sulfur-reducing bacteria: *Desulfuromonas acetoxidans* under the influence of different metal ions

O. M. Vasylyiv, O. I. Bilyy, V. B. Getman, I. V. Kushkevych, S. O. Hnatysh, Ivan Franko National Univ. of L'viv (Ukraine)

The Earth was settled only by the microorganisms during more than 80% of organic evolution. They prevailed in the biosphere more than 0.5 billion years ago. There were methanogens, sulfate-, iron- and sulfur-reducing bacteria which belonged to such genera as *Methanobacterium*, *Desulfuovibrio*, *Rhuminococcus*, *Desulfuromonas* and others that made an overwhelming contribution into the formation of different minerals of the Earth's crust. *Desulfuromonas acetoxidans*, which is regarded to the oldest microorganisms, are uncoloured gram-negative obligatory anaerobic bacteria that have an ability to reduce sulfur to hydrogen sulfide. Sulfur bacteria have a great effect on the biogeochemistry of the aquatic environments because of their ability to reduce and precipitate of toxic metal ions. Using strains of these bacteria, which have a high heavy metals' resistance, allow to neutralize the toxicity of hydrogen sulfide, which is the final product of dissimilation sulfur reduction, and these metals as the result of their particular binding and forming the insoluble precipitations. In this study the interaction between bacteria *Desulfuromonas acetoxidans* and such heavy metal ions as copper, lead, zinc and cadmium has been investigated. The light scattering properties' changes of bacterial cells *D. acetoxidans* on the base of their size distribution and relative content under the influence of investigated metal ions have been observed by the new method of measurement. It includes sounding of flow suspended bacterial cells by monochromatic coherent light, registration of signals of co-operation of sounding radiation with the explored microbiological objects by detects amplitudes and durations of scattered light impulses.

8152-11, Session 5

Ramifications of a sterile Mars

G. V. Levin, Arizona State Univ. (United States)

The seldom considered ramifications of a sterile Mars are explored. The Martian environment has been extensively defined by analyses performed by 22 successful missions, composed of eight landers and 14 flybys and orbiters, and by countless Earth-based observations, plus the detailed examination of Martian meteorites. The individual and collective parameters that could preclude life are examined. No single or combination of these measurements precludes the ability of Mars to support even a wide number of terrestrial microbial species, let alone possible alien life forms. Some yet unknown factor or combination of factors would have to be responsible for Mars' failure to generate life or to successfully harbor viable forms received from space. Since Mars is so Earth-like, the red planet's sterility would constitute a severe blow to the concept of a cosmic biologic imperative, and would raise the daunting prospect that Earth is a unique or very rare habitat.

8152-12, Session 5

Io and its role in the Jupiter system

R. Lopes, Jet Propulsion Lab. (United States)

Jupiter's moon Io is the solar system's most volcanically active body and the only place other than Earth where large-scale silicate volcanism has been observed. Io's volcanic activity significantly affects the Jovian system, including causing aurorae on Jupiter, forming the Io torus and neutral cloud, and causing sulfur to be transported by Jupiter's magnetosphere and implanted into Europa's ice. Although Io is not considered a target of interest from an astrobiology point of view due to its lack of water, it is important in this context for several reasons. (1) Io's high heat flow and prodigious rate of volcanism make it unique among the silicate bodies, providing insight into processes that operated very early in the histories of the terrestrial planets, including Earth. (2) Io's geologic activity is the result of heat transfer from the tidally-flexed interior to the surface. Io is the best target for the study of tidal heating, a process of fundamental importance to the evolution of planetary satellite systems, and one that may greatly expand the habitability zone for extra-terrestrial life. (3) Io's exotic chemistry is unique in the solar system. Io's surface is dominated by SO₂ frost, sulfur allotropes, and silicates, but unidentified materials remain. Unlike its neighbors Europa, Ganymede, and Callisto, Io has no water, though a 3.15 micron feature in its spectra could arise from the OH stretch transition in a hydroxide (Carlson et al., 1997, *Geophys. Res. Lett.* 24). (4) Io's volcanic plumes transport volatiles into space, and from Io to Europa. Understanding Io's sources and sinks of volatiles is therefore key to understanding the Jupiter system as a whole, including the icy satellites where conditions may exist suitable for life. Our knowledge of Io has been substantially expanded by planetary missions such as Galileo and New Horizons, but many questions remain. The study of Io is considered a major objective in future missions to the Jovian system.

8152-13, Session 5

Does Saturn's Titan have an active surface: could indications of surface activity be consistent with a pre-biotic environment?

R. M. Nelson, Jet Propulsion Lab. (United States)

The surface of Saturn's moon Titan has been reported to change over time. During the Cassini spacecraft's seven year orbital tour of the Saturnian system the Visual and Infrared Mapping Spectrometer (VIMS) reported spectrophotometric changes at a region called Hotei Reggio (a.k.a. Hotei Arcus) near 26S,78W [1,2]. This variation is consistent with the deposition, followed by coverage or dissipation, of ammonia frost. Cassini RADAR images found that Hotei Reggio, has lobate "flow" forms, suggesting a volcanic terrain there [3] and at other locations on Titan including Sotra Facula, a 60 km subcircular feature near 40W 15S [4].

It has not escaped our attention that ammonia, in association with methane and nitrogen, the principal species of Titan's atmosphere, may replicate the environment at the time that life first emerged on earth. If Titan is currently active then these results raise the following questions: What is the full extent of current geologic activity? What are the ongoing processes? Are Titan's chemical processes today supporting a prebiotic chemistry similar to that under which life evolved on Earth?

1. Nelson et al. LPSC abs. 2158 2007
2. Nelson et al. *Icarus*, 199, 429-441, 2009.
3. Wall et al. *GRL* VOL. 36, L04203, 2009
4. Kirk, R. L. et al AGU Fall Meeting 2010, abstract #P22A-03.

8152-14, Session 5

High-sensitivity biomarker imaging using surface enhanced Raman spectroscopy (SERS)

Z. Tanaka, NASA Ames Research Ctr. (United States) and Univ. of California, Santa Cruz (United States); B. Chen, NASA Ames Research Ctr. (United States)

The detection of various biological agents, in general, and bacterial pathogens, in particular, has garnered much recent attention in the field of diagnostic microbiology and astrobiology studies. Surface Enhanced Raman Spectroscopy (SERS) has been successfully applied to the detection of field samples in various environments. Emergent to SERS is the possibility for imaging. In particular, our SERS imaging technique is capable of simultaneously demonstrating high spatial resolution as well as composition sensitivity for biomolecules and bacteria/viruses due to its potential advantage of molecular specificity. Raman or SERS imaging can provide high throughput chemical information with, spatial distributions of analytes with resolution in the micrometer range.

Facile and reproducible SERS signals from *Shewanella oneidensis* were obtained utilizing silver nanoparticles (AgNPs) and silver nanowires (AgNWs). Additionally, SERS images identify the distribution of SERS hot-spots. One important observation is the synergistically enhanced SERS signal when AgNPs and AgNWs are used in conjunction, due to constructively enhanced electromagnetic field. The talk will further this technique for future field deployment in the context of fiber optical instrument development in our lab. For an example, a custom-built, 1064nm near-infrared (NIR) fiber-Raman spectrometer that has been lab tested to characterize organic carbon content in 1.7Byr old stromatolite mineral samples obtained from Mars-analog environments. Compared to visible excitations, the NIR Raman has profoundly less background fluorescence and is suited to be deployed autonomously on Mars "test" rovers.

8152-15, Session 5

The brines of the Phoenix landing site, the potential for life to adapt to them, and the implications for life elsewhere

N. O. Rennó, H. Elliott, G. Martinez Martinez, D. Halleaux, B. Block, G. Dick, J. Hoffman, Univ. of Michigan (United States); S. B. Joye, The Univ. of Georgia (United States); C. P. McKay, NASA Ames Research Ctr. (United States); O. Prieto-Ballesteros, F. Gomez Gomez, E. Mateo-Marti, M. Paz Zorzano, Ctr. de Astrobiología (Spain)

Renno et al. [2009] presented physical and thermodynamical evidence that liquid brines were observed at the Phoenix landing site on Mars' Arctic. Then, Zorzano et al. [2009] showed experimentally that liquid brines could form by deliquescence at the Phoenix landing site. Renno et al. [2009] shows that the thermodynamics of freeze-thaw cycles could produce brine pockets almost anywhere on Mars, where ground ice is present near the surface. The presence of liquid brines on Mars has important implications for its habitability because many terrestrial microbes thrive in brines [Boetius and Joye, 2009].

We are analyzing the Phoenix mass spectrometer and atmospheric science data with focus on the understanding of the formation and stability of liquid brines on Mars' Arctic. In parallel, we are conducting laboratory experiments to study the range of environmental conditions that can support the presence of liquid brines on Mars. The 'Centro de Astrobiología' group is conducting studies of the habitability of liquid brines to give insights on "Planetary Conditions for Life." Our study has the potential to shed light on the capability of microbial life to adapt to the environmental conditions of the Phoenix landing site, and its implications for life elsewhere. Here we describe our laboratory experiments and present preliminary results.

8152-16, Session 6

Microscopy instrumentation in the search for extraterrestrial microbes

J. Davis, Delaware State Univ. (United States); E. V. Pikuta, R. B. Hoover, National Space Science and Technology Ctr. (United States); C. R. Sabanayagam, Delaware State Univ. (United States)

A space microscope that is capable of imaging and collecting spectral information on microbial life forms could potentially be used to explore extraterrestrial environments for extant or extinct life. In our previous studies we demonstrated that the laser-induced autofluorescence spectra, or intrinsic fluorescence, of microbial extremophiles are unique and thus can be used to identify and distinguish different species. Microbial extremophiles were examined under 1000x magnification, and the fluorescence was passed through dispersion optics and projected onto a high quantum efficiency camera. Autofluorescence studies are favored over those that involve the use of external fluorescent labels mainly because the former can perform in situ analysis with little sample preparation (e.g., label mixing). We discuss another imaging modality, dark-field microscopy that is a complementary label-free imaging technique. The optical scattering spectra of a variety of extremophiles are presented, and the utility of a dark-field space microscope is discussed.

8152-17, Session 6

L.I.F.E. (Laser Induced Fluorescence Emission) as non-invasive tool to assess photosynthetic pigments in ice ecosystems

M. Tilg, B. I. Sattler, Univ. Innsbruck (Austria); M. C. Storrie-Lombardi, Kinohi Institute (United States); R. Psenner, Univ. Innsbruck (Austria)

Ecosystems of the cryosphere harbour active microbial communities which contribute significantly to the global carbon budget. The sensitivity of many psychrophiles to even moderate changes in temperature, and the logistical difficulties associated with either in situ analysis or sampling makes it difficult to study microbial metabolism in ice ecosystems in a high resolution. Since surface communities are mainly autotrophic, an in-situ non-invasive technique to assess the photosynthetic potential is required which can be provided by laser-induced fluorescence emission (L.I.F.E.). L.I.F.E. is an in situ laser scanning technique to detect photoautotrophic pigments such as phycoerythrin without contamination of the system. 532nm green lasers excite photopigments in cyanobacteria and produce multiple fluorescence signatures between 550nm and 750nm including carotenoids, phycobiliproteins which would enable a non-invasive in-situ detection.

L.I.F.E has already been tested in remote ecosystems like Antarctica (Lake Untersee, Lake Fryxell), but until now no calibration was set to convert the L.I.F.E. signal into pigment concentration. Here we describe the standardization for detection of Phycobiliproteins (Phycoerythrine) which are found in red algae, cyanobacteria, and cryptomonads. Similar methods are already used for detection of phytoplankton in liquid systems like oceans and lakes by NASA's Airborne Oceanographic LIDAR since 1979. The possibility to use L.I.F.E. in ice ecosystems though is a novelty. Due to the new technique of photoautotrophic pigment detection in ice L.I.F.E can be used for search for life on Mars or other icy exoplanets.

8152-18, Session 6

ExoMars Raman Laser Spectrometer breadboard overview

A. G. Moral, E. Díaz, G. Ramos, O. Barcos, Instituto Nacional de Técnica Aeroespacial (Spain); C. P. Canora, Ingeniería y Servicios

Conference 8152:
Instruments, Methods, and Missions for Astrobiology XIV

Aeroespaciales (Spain); F. Rull, Univ. de Valladolid (Spain); I. Hutchinson, R. Ingley, Univ. of Leicester (United Kingdom); C. Tato, SENER Ingeniería y Sistemas S.A. (Spain)

The Raman Laser Spectrometer (RLS) is one of the Pasteur Payload instruments, within the ESA's Aurora Exploration Programme, ExoMars mission.

The RLS Instrument will perform Raman spectroscopy on crushed powered samples deposited on a small container after crushing the cores obtained by the Rover's drill system.

The RLS Instrument is composed by the following units:

SPU (Spectrometer Unit): a combined spectrometer unit with a thermally controlled CCD detection.

iOH: (Internal Optical Head): an optical unit which focus the laser excitation light over the sample, and filters the scattered Raman signal for its processing at the SPU. The iOH also provides an autofocus mechanism.

ICEU (Instrument Control and Excitation Unit): within this unit it is housed the laser source and the FEE for signal processing; it also contains the power and processor modules.

Other instrument units are EH (Electrical Harness), OH (Optical Harness) and SW.

During last 2010 and beginning of 2011, an instrument BB programme has been developed, by RLS AIV Team to achieve the Technology Readiness level 5 (TRL5) for delta PDR in response to ESA requirements.

RLS BB concept has been designed as modular as possible in order to be able to upgrade the breadboard in a step by step process. In this way the complete RLS chain can be validated as a whole, but component by component if necessary. As far as possible, RLS baseline optical critical parameters, interfaces and functionalities has been kept (but for the nominal environment).

It is planned to have a fully operative breadboard, conformed from different unit and sub-units breadboards that would demonstrate the end-to-end performance of the flight representative units by 2011 Q3.

8152-19, Session 6

Raman Laser Spectrometer for ExoMars

C. Pérez Canora, Instituto Nacional de Técnica Aeroespacial (Spain)

The Raman Laser Spectrometer (RLS) is one of the Pasteur Payload instruments, within the ESA's Aurora Exploration Programme, ExoMars mission.

ExoMars 2018 main Scientific objective is "Searching for evidence of past and present life on Mars". Particularly, the RLS scientific objectives within ExoMars Mission are as follows:

- identify organic compound and search for life
- identify the mineral products and indicators of biologic activities
- characterize mineral phases produced by water-related processes
- characterize igneous minerals and their alteration products
- characterise water/geochemical environment as a function of depth in the shallow subsurface

Raman Spectroscopy is used to analyse the vibrational modes of a substance either in the solid, liquid or gas state. It relies on the inelastic scattering (Raman Scattering) of monochromatic light produced by atoms and molecules. The radiation-matter interaction results in the energy of the exciting photons to be shifted up or down. The shift in energy appears as a spectral distribution and therefore provides an unique fingerprint by which the substances can be identified and structurally analyzed.

RLS expected main characteristics are as follows:

- Laser excitation wavelength: 533 nm
- Irradiance on sample: 0.6 - 1.2 kW/cm²
- Spectral range: 150-3800cm⁻¹

- Spectral resolution: 6 cm⁻¹ lower spectral wavenumbers; 8 cm⁻¹ long spectral wavenumbers
- Spectral accuracy: < 1 cm⁻¹
- Spot size: 50 microns

Instrument performances are being evaluated by means of simulation tools and development of a BB campaign currently on going.

8152-20, Session 6

A new spectrometer concept for Mars exploration

M. Colombo, T. Belenguer, M. Fernández, Instituto Nacional de Técnica Aeroespacial (Spain)

The Raman Laser Spectrometer (RLS) instrument is included in the ExoMars program Pasteur payload and it is focused on the analytical analysis of the geochemistry content and elemental composition of the observed crushed samples obtained by the Rover.

One of the most critical Units of the RLS instrument is the Spectrometer unit (SPU) that performs Raman spectroscopy technique and operates in a very demanding environment (radiation, temperature, dust, etc.) with very restrictive design constraints (mass, power, schedule). It is a very small optical instrument capable to cope with 0.09 nm/pixel of resolution and withstand with the Martian environment (operative temperature conditions: from -40 oC to 6 oC). The selected solution is based on a single transmissive holographic grating especially designed to actuate as the dispersion element.

At this stage of the project SPU Team is improving and optimizing the SPU FM design and Delta

RLS PDR will take place on July 2011. SPU PDR is expected on Autumn 2011.

In parallel, a set of activities have been already started by RLS SPU Team in order to achieve the TRL 5 for RLS Delta PDR:

- Grating validation test campaign: first results have been very successful.
- SPU breadboard which main AIT objectives are to:
 - Determine concepts feasibility and demonstrate the technical principles of immediate interest.
 - Ensure manufacturing tolerance and optical compensators.
 - Verification of the optical analytical models.
 - Validate RLS SPU radiometric model.
 - Verification of the susceptibility to thermal gradient in axis and some critical tolerances.

8152-21, Session 7

Biosignatures for detecting unicellular and multicellular organisms in extreme environments

J. Seckbach, The Hebrew Univ. of Jerusalem (Israel); J. Chela-Flores, The Abdus Salam International Ctr. for Theoretical Physics (Italy)

With respect of our anthropocentric point of view most organisms dwell in what we consider to be "normal" environments, while others, which are called extremophiles, may thrive in harsher conditions. These living organisms are mainly of unicellular (both prokaryotes and, to a lesser extent, there are some eukaryotes). But the extremophiles also include multicellular organisms, including protozoa, algae, worms, insects and crustaceans. In their evolution both unicellulars and multicellulars have adapted to their corresponding niches. In this presentation we will survey specific extremophiles in some detail. We have selected one example of a unicellular red alga *Cyanidium caldarium* (with its cohorts), and

Conference 8152:
Instruments, Methods, and Missions for Astrobiology XIV

discuss also a minute animal, the water bear Tardigrade. The harsher conditions referred above for the habitats of the extremophiles include various temperature ranges [thermophiles vs. cryophiles]. Others prefer the lower pH ranges (acidophiles) or higher level of pH (alkaliphiles). The organisms living in high salt solutions are the halophiles that could survive even in saturated salinity medium. In the depths of the oceans and in subterrenean environments we may find the barophiles, or pressure bearing organisms. Several microbes can live under anoxia and utilize anaerobic metabolism, or even thrive under various gaseous atmospheres (such as CO₂, ammonia, or methane). It is well known that some bacteria had already lived for millions of years in a dormant desiccated status before being revived in the laboratory.

Astrobiology is concerned with all of these extremophiles, as they may be models for surviving in similar environments elsewhere in the universe. One major question concerns the more restricted search for life exclusively through the exploration of the Solar System. In this case, the main focus is on the preparation of suites of experiments that may attempt to discover the habitability of planets and their satellites. In this context we ask ourselves: What biosignatures can facilitate life detection, both unicellular and multicellular, in extreme environments? The environments that are within reach of present and future space missions are firstly, Mars in the inner Solar System. Secondly, the moons of the giant planets of the outer Solar System are also within reach. Significant examples are Europa, the Jupiter satellite—a leading candidate—and two moons of Saturn: Titan and Enceladus.

8152-22, Session 7

Review of Archaea

E. V. Pikuta, National Space Science and Technology Ctr. (United States); J. Tang, Noblis Falls Church (United States)

Archaea were separated from Eubacteria after discovery of their specific of cell outer membrane that usually not affected by common antibiotics. Phylogenetic analyses introduced by Karl Wöese supported this separation. Presently, only two phyla Crenarchaeota and Euryarchaeota include the valid representatives. Another three phyla that were proposed based on sequence analyses of environmental samples, do not contain validly published species, and for this reason could not be included in the subject consideration.

In this article, we are providing the update and comparative analyses for this domain, discussing unique features of this group and Evolution, estimating their physiology in the matrix of physic-chemical factors, and outlining future perspectives in their study.

8152-23, Session 7

Archaeal surface appendages: their function and the critical role of N-linked glycosylation in their assembly

K. F. Jarrell, D. B. Nair, G. M. Jones, Queen's Univ. (Canada); S. M. Logan, E. Vinogradov, J. F. Kelly, National Research Council Canada (Canada)

Many cultivated archaea are extremophiles and as such various archaea inhabit some of the most inhospitable niches on the planet in terms of temperatures, pH, salinity and anaerobiosis. Different archaeal species have been shown to produce a number of unusual and sometimes unique surface structures. The best studied of these are flagella which are fundamentally different from bacterial flagella and instead bear numerous similarities to bacterial type IV pili in their structure and likely assembly. The major structural proteins, flagellins, are made as preproteins with type IV pilin-like signal peptides processed by a specific signal peptidase. In addition, the flagellins are glycoproteins with attached N-linked glycans. These posttranslational modifications have been studied in the archaeon, *Methanococcus marisalpinis*, which also possesses another surface appendage, an unusual version of type IV pili, of which the major constituent is also a glycoprotein. Analysis of mutants unable to make

either or both flagella and pili demonstrated that both structures are essential for attachment to surfaces. Mutants defective in the assembly and biosynthesis of the tetrasaccharide N-linked to the flagellins have been isolated. Investigations of these mutants by electron microscopy, mass spectrometry and motility assays have demonstrated that flagellins possessing no attached glycan or a glycan truncated to a single sugar cannot assemble flagella on their surface. Mutants which can attach a glycan of 2 or 3 sugars to flagellins assemble flagella but they are impaired in their swimming compared with wildtype cells which attach the tetrasaccharide to their flagellins.

8152-24, Session 8

Deep subsurface biodiversity: remarkable novelty and flexibility despite proposed geochemical constraints

E. Van Heerden, Univ. of the Free State (South Africa); G. Borgonie, Univ. Gent (Belgium); A. Jugdave, Univ. of the Free State (South Africa); A. Garcia-Moyano, Univ. of Bergen (Norway); D. Lithauer, Univ. of the Free State (South Africa); T. Onstott, Univ. of Bergen (Norway)

Microbial populations in the deep subsurface extend to depths below where nutritional and environmental parameters limit the ability of microbes to survive. Highly diverse microorganisms occur in expanses where carbon sources are not evident. The studies of the deep subsurface exposed valuable information of the ecology of microbes, the chemical and geological factors associated with these thriving and diverse microbial populations and more insight were gained into their metabolism using genomic and proteomic tools.

Low cell mass samples were concentrated by either massive or tangential flow filtration systems. Complete biodiversity studies were done using 16S and 18S rRNA gene clone libraries, operational taxonomic units (OTU) were calculated using distance based and richness parameters (DOTUR). Microbial isolations were attempted using selective media followed by pyrosequencing and annotation analyses. Proteome analyses, including expression and kinetic, were completed on various proteins from subsurface microbes. Each geological setting provides new insight into its particular associated geochemistry and how it influences the biodiversity. With increasing depth and temperature lower diversity is recovered, however several sites reveal surprisingly high interspecies diversity, even for eukarya.

Here we even report species of the phylum Nematoda that have been detected in or recovered from fracture water at 0.9-3.6 km depth in South Africa, and includes a new species *Halicephalobus mephisto* that tolerates high temperature, reproduces asexually and preferentially feeds upon subsurface bacteria. Twenty-two water samples were collected from 6 boreholes ranging in depth from 0.5 to 3.6 km in 5 different South African mines. Beatrix Au Mine borehole water yielded a new species, *Halicephalobus mephisto* sp. n., 18x500 μm in size.

We extend the current knowledge on subsurface cycling by comparing of anaerobic and chemolithotrophic metabolic reactions to indicate that SO₄²⁻-reduction is the dominant metabolic process at high and low salinities and that matrix diffusion can sustain planktonic fracture microbial concentrations of ~10⁸ cells mL⁻¹. Methanogenesis becomes more dominant with declining salinities. Neither acetogenesis nor syntrophic degradation of abiogenic hydrocarbons appears to be the source of the observed carboxylic acids, but regardless respiration leads to direct in situ carbonation within the fractures.

8152-25, Session 8

High-density 16S microarray and clone library-based bacterial and archeal diversity of Icelandic hot springs

P. A. Vaishampayan, Jet Propulsion Lab. (United States); A.

Conference 8152:
Instruments, Methods, and Missions for Astrobiology XIV

Probst, Univ. Regensburg (Germany); K. Venkateswaran, Jet Propulsion Lab. (United States)

It is beyond any doubt that the search for life on other planets should be microbial in nature. As the extraordinary ability of microorganisms to overcome the challenges posed by these "extreme" environments prove testament to life's resolve, and compelled us to believe that life could persist almost anywhere on Earth, and possibly beyond.

We present here a comprehensive microbial diversity study of samples from Icelandic hot springs. Sampling was performed in a vegetated hot springs system of Hveragerdi area (Iceland), that was about 20 m long and could be divided into three interconnected hot spring pools (P1, P2 and P3) and one opening or mud hot spring at the beginning of the system with no surface connection with others. The temperature was at the range of 57° to 100°C and the pH from 2.9 to 3.8. Additionally, samples were collected from two geographically distinct hot springs of Leirgerdur (L1) with high acidic pH (2.0) and Hrifla spring (HS1) with neutral pH (7.0).

Though numerous studies have described the microbial populations of hot springs using cloning based and other molecular approaches, this is the first investigation to study a comprehensive microbial diversity using High-Density 16S Microarray. We have observed diverse bacterial and archaeal OTUs in samples for which cloning approach fail to detect any OTUs. Effect of abiotic forces in shaping microbial community structure and comparative diversity was also studied in detail.

8152-26, Session 8

The Dry Valley Lakes, Antarctica: a key to evolutionary biomarkers on Europa and elsewhere

J. Chela-Flores, The Abdus Salam International Ctr. for Theoretical Physics (Italy) and Instituto de Estudios Avanzados, Caracas (Venezuela); J. Seckbach, The Hebrew Univ. of Jerusalem (Israel)

In a new approach to the search for biomarkers on Europa we first discuss the main geochemical motivations and concepts. We continue with the specifications of the relevant instrumental techniques. In doing so, we have kept the molecular and evolutionary background to a minimum. We must underline that so far there is a surprising lack of literature on the search with available instrumentation of biomarkers for eukaryotes, or for simple metazoans in likely environments of the Solar System. We discuss whether sulfur traces on Jupiter's moon Europa could be of microbial origin and whether further stages of evolution can be identified. The chemical elements and compounds detected by the Galileo Mission have been conjectured to be endogenic, most likely of cryovolcanic origin, due to their non-uniform distribution in patches. The Galileo space probe first detected the sulfur compounds, as well as revealing that this moon almost certainly has a volcanically heated and potentially habitable ocean hiding beneath a surface layer of ice. There are options for sorting out the source of the surficial sulfur in future exploration of Europa. Returning to Europa is being planned with the Europa Jupiter System Mission, EJSM (Grassett et al., 2009). What is most relevant, oceans may be present on other Galilean moons, but so far we are only aware of a single Jovian moon- Europa- that has its ocean in direct contact with its silicate mantle, unlike the case of Ganymede. However, if terrestrial microbes can thrive in extreme environments, similar microorganisms might also be extant on some of the icy Galilean satellites. Furthermore, since extremophiles have not only succeeded in establishing themselves in the most unlikely ecosystems, but also they have thrived by chemosynthesis of a stunning suite of elements, why would they not thrive as well on some of the oceans of the Galilean satellites? (Seckbach and Chela-Flores, 2011). The question of habitability by the identification of reliable bioindicators is a major priority for astrobiology. We discuss the present objectives of the future mission to Europa, the EJSM. We consider especially the options for approaching the challenge of selecting the right instrumentation for the identification of a potential biota on Europa. In other words, we raise the following question: What are the challenges facing current technology

with miniaturised instruments compatible with realistic payload budgets for identifying prokaryotic microorganisms? This is a question in biogeochemistry. More importantly, we ask what are the challenges yet to overcome with only minor alterations in the payload mass constraints for deciding whether the same available instrumentation can be used for the identification of eukaryotes and simple metazoans? This is a question to be answered in the context of molecular biology.

8152-27, Session 8

Diverse nucleotide compositions and sequence fluctuation in rubisco protein genes

T. Holden, S. Dehipawala, E. Cheung, R. Bienaime, G. Tremberger, Jr., P. Schneider, D. Lieberman, T. D. Cheung, Queensborough Community College (United States)

The rubisco protein is arguably the most abundance protein on Earth and it is notoriously inefficient in its enzyme action in the Calvin cycle. X-ray studies show that the tertiary structure is necessary for the required conformational folding while circular dichroism studies on its associated unfolding rates demonstrate the necessary secondary structure for its enzyme function. The biology dogma of transcription and translation necessitates the study of the rubisco gene in various species. Genome studies via BLAST reveal diverse composition in the associated nucleotide sequences among species. Pre-plant rubisco-like protein study shows similar results. The threshold requirement for functional photosynthesis could be satisfied by selection of diverse nucleotide sequences indicative of multiple evolutionary pathways. Whether the pathways contain an extra-terrestrial source could be speculative but interesting. Shannon entropy of the nucleotide composition and fractal dimension of the nucleotide sequence in terms of its atomic number fluctuation suggest relatively less experienced evolutionary pressure as compared to radiation resistant sequences. The nucleotide interaction would appear to pose very little additional constraints on rubisco production. Similar photosynthesis process that could utilize host star radiation would not compete with radiation resistant process from the biology dogma perspective in environments such as Mars and exoplanets just off the habitable zone.

8152-28, Session 8

Technologically important extremophile 16S rRNA sequence Shannon entropy and fractal property comparison with long term dormant microbes

T. Holden, N. Gadura, S. Dehipawala, E. Cheung, M. Tuffour, P. Schneider, G. Tremberger, Jr., D. Lieberman, T. D. Cheung, Queensborough Community College (United States)

Technologically important extremophiles including oil eating microbes, uranium and rocket fuel perchlorate reduction microbes, electron producing microbes and electrode electrons feeding microbes were studied in terms of their 16S rRNA sequences, a standard practice in comparative phylogeny studies. Microbes that were reported to have survived a prolonged dormant duration were also studied. Examples included the recently discovered microbe that survives after 34,000 years in a salty environment while feeding off organic compounds from other trapped dead microbes. Shannon entropy of the 16S rRNA nucleotide composition and fractal dimension of the nucleotide sequence in terms of its atomic number fluctuation analyses suggest a selected range for these extremophiles as compared to other microbes; consistent with the experience of relatively mild evolutionary pressure. However, most of the microbes that have been reported to survive in prolonged dormant duration carry sequences with fractal dimension between 2 and 2.01 (N = 10 out of 12). Similar results are observed for halophiles, red-shifted chlorophyll and high radiation resistant microbes. The results suggest that prolonged dormant duration, in analogous to high salty or radiation

**Conference 8152:
Instruments, Methods, and Missions for Astrobiology XIV**

environment, would select high fractal 16S rRNA sequences. Candidate choices for high fractal 16S rRNA microbes could offer protection for prolonged spaceflights. BioBrick gene network manipulation could include extremophile 16S rRNA sequences in synthetic biology and shed more light on exobiology and future colonization in shielded spaceflights. Whether the high fractal 16S rRNA sequences contain an asteroid-like extra-terrestrial source could be speculative but interesting.

8152-29, Session 8**Anaerobic cultures from preserved tissues of baby mammoth**

E. V. Pikuta, National Space Science and Technology Ctr. (United States); D. Fisher, Univ. of Michigan (United States); R. B. Hoover, NASA Marshall Space Flight Ctr. (United States)

Microbiological analysis of several cold-preserved tissue samples from the Siberian baby mammoth known as Lyuba revealed a number of culturable bacterial strains that were grown on anaerobic media at 4 °C. Lactic acid produced by LAB (lactic acid bacteria) group, usually by members of the genera *Carnobacterium* and *Lactosphaera*, appears to be a wonderful preservative that prevents other bacteria from overdominating a system. Permafrost and lactic acid preserved the body of this one-month old baby mammoth and kept it in exceptionally good condition, resulting in this mammoth being the most complete such specimen ever recovered.

The diversity of novel anaerobic isolates was expressed on morphological, physiological and phylogenetic levels. Here we discuss the specifics of the isolation of new strains, differentiation from trivial contamination, and preliminary results for the characterization of cultures.

8152-30, Session 8**The nature of water within bacterial spores: protecting life in extreme environments**

C. V. Rice, The Univ. of Oklahoma (United States)

The bacterial spore is a formidable container of life, protecting the vital contents from chemical attack, antimicrobial agents, heat damage, UV light degradation, and water dehydration. The exact role of the spore components remains in dispute. Nevertheless, water molecules are important in each of these processes. The physical state of water within the bacterial spore has been investigated since the early 1930's. The water is found two states, free or bound, in two different areas, core and non-core. It is established that free water is accessible to diffuse and exchange with deuterated water and that the diffusible water can access all areas of the spore. The presence of bound water has come under recent scrutiny and has been suggested the water within the core is mobile, rather than bound, based on the analysis of deuterium relaxation rates. Using an alternate method, deuterium quadrupole-echo spectroscopy, we are able to distinguish between mobile and immobile water molecules. In the absence of rapid motion, the deuterium spectrum of D₂O is dominated by a broad line, whose line shape is used as a characteristic descriptor of molecular motion. The deuterium spectrum of bacterial spores reveals three distinct features: the broad peak of immobilized water, a narrow line of water in rapid motion, and a signal of intermediate width. This third signal is assigned this peak from partially deuterated proteins with the spore in which N-H groups have undergone exchange with water deuterons to form N-D species. Likewise, desiccation changes intensity of the rapid water signal while the signals for immobilized water and deuterated proteins remain unchanged. As a result of these observations, the nature of water within the spore requires additional explanation to understand how the spore and its water preserve life.

8152-31, Session 8**Future outlook for SETI**

S. Bowyer, Univ. of California, Berkeley (United States)

Initially, the Search for Extra-Terrestrial Intelligence emphasized the radio band, but soon searches were carried out in other bands. No signals have yet been detected. New searches and research efforts will dominate the future SETI landscape. The detection of planetary systems suggests there will be far more planets than expected, but many with unstable orbits. Unfortunately, water, a necessity for the development of life, may be the result of an odd set of unlikely circumstances. On the positive side, recent laboratory work on the origin of life suggest that life forms may be easily produced. Interesting times for SETI!

The idea that a credible search for Extra-Terrestrial Intelligence could be carried out evolved beginning in the middle of the last century. Initial work emphasized searches in the radio band but soon searches were developed investigating other bands of the electromagnetic spectrum. No signals have been detected. However, by 2010 several radio searches were close to starting that would have provided a huge increase in detection capabilities. In addition, a major discovery was the detection of a surprising number of planetary systems. This increases the potential locations for extraterrestrial intelligence. However, the systems that have been discovered show that the formation of planetary systems results in many systems that are unstable. In a worst case scenario, there will be far more stars with planetary systems but few planets with stable orbits. An additional complexity is the requirement, based on very general grounds, that water is a necessity for the development of life. But the origin of water on Earth appears to be the result of an odd set of circumstances which might be unlikely. Despite these uncertainties most workers in the field continue to be optimistic regarding the likelihood of eventually detecting an alien signal. Tragically, the extremely sensitive search with the Allen Telescope at Hat Creek has been cancelled for funding reasons. Nonetheless, work continues on developing even more sensitive searches. A brief summary of work carried out to date, and a description of some of the innovative new ideas now being developed, will be provided.

8152-32, Session 9**The origins of the translation machinery may provide insight to the emergence of the last universal common ancestor**

G. E. Fox, Q. Tran, M. R. Tirumalai, Univ. of Houston (United States)

Efforts to understand the last universal common ancestor, LUCA, have largely focused on the nature of that ancestor, whether genote or progenote, and the genes that were likely present. Also of interest is the issue of why LUCA emerged when it did, rather than at an earlier or later stage. In order to gain insight to early events in the emergence of living systems, we are studying the evolutionary history of the translation machinery. Many ribosome components are universal in all Domains of life, and hence likely were present before LUCA while other aspects differ and hence were likely added after LUCA. Using timing events such as the order of addition of components during ribosome assembly, it is possible to infer the relative age of various components. The ribosome is thought to fundamentally be a Brownian motor, the modern version is a dynamic machine with key coordinated movements occurring during each synthesis cycle. These include ratcheting of the 30S subunit, opening and closing of the L1 stalk and movement of the tRNAs through the decoding center as a result of GTP cleavage by elongation factor G. These movements are associated with ribosomal components that appear to have been incorporated at approximately the time of LUCA. For example, 5S ribosomal RNA, which is thought to play a role in coordinating the various movements by transmitting signals between the peptidyl transferase center and the decoding site, exhibits modest structure differences in the three Domains of life. This suggests that it was present in almost final form at the time of LUCA. It is hypothesized here that dramatic improvements in the efficiency of protein synthesis

had a global impact on emerging biological systems resulting in the emergence of LUCA.

8152-33, Session 9

Ribosomal paleontology and resurrection: molecular fossils from before coded protein

L. D. Williams, C. Hsiao, J. C. Bowman, C. R. Bernier, J. Peters, D. M. Schneider, E. O'Neill, Georgia Institute of Technology (United States)

The translational machinery is life's most ancient assembly. The origins and early development of the translation machinery remain imprinted in the extant ribosome, in sequences, folding, and function. To mine the information contained within the ribosome, we are developing new methods of molecular paleontology. We will recapitulate fundamental steps in the origin and evolution of the ribosome, and will determine the relative ages of ribosomal components. We are biochemically resurrecting working models of ancestral ribosomes. We are developing timelines for critical steps in the evolutionary history of the ribosome. The results of these studies will help provide keys to understanding the origin of proteins and RNA, and the origin of life. We use structure- and sequence-based comparisons of the Large Subunits (LSUs) of *Haloarcula marismortui* and *Thermus thermophilus*. Using an onion analogy, we have sectioned the superimposed bacterial and archaeal LSUs into concentric shells, using the sites of peptidyl transfer as the centers. This spherical approximation allows shell-by-shell dissections and comparisons that clearly capture significant information along the evolutionary timeline. The results support the notion that ever-older molecular fossils are revealed as one bores toward the center of the LSU onion. The conformations and interactions of both RNA and proteins change over time. The frequency with which macromolecules assume regular secondary structural elements, such as A-form helices containing Watson-Crick base pairs (RNA) and α -helices and β -sheets (protein), increases with time. The conformations of the oldest ribosomal protein components suggest they are molecular fossils of the non-coded peptide ancestors of ribosomal proteins.

8152-36, Session 9

Comets as parent bodies of CI1 carbonaceous meteorites and possible habitats of ice-microbiota

N. C. Wickramasinghe, Cardiff Univ. (United Kingdom); R. B. Hoover, NASA Marshall Space Flight Ctr. (United States); A. Y. Rozanov, Paleontological Institute (Russian Federation); J. Wallis, Cardiff Univ. (United Kingdom)

Recent studies of comets and cometary dust have confirmed the presence of biologically relevant organic molecules along with clay minerals and water ice. It is also now well established by deuterium/hydrogen ratios that the CI1 carbonaceous meteorites contain indigenous extraterrestrial water. The evidence of extensive aqueous alteration of the minerals in these meteorites led to the hypothesis that water-bearing asteroids or comets represent the parent bodies of the CI1 (and perhaps CM2) carbonaceous meteorites. These meteorites have also been shown to possess a diverse array of complex organics and chiral and morphological biomarkers. Stable isotope studies by numerous independent investigators have conclusively established that the complex organics found in these meteorites are both indigenous and extraterrestrial in nature. Although the origin of these organics is still unknown, some researchers have suggested that they originated by unknown abiotic mechanisms and may have played a role in the delivery of chiral biomolecules and the origin of life on Early Earth.

In this paper we review these results and investigate the thermal history of comets. We show that permanent as well as transient domains of liquid water can be maintained on a comet under a plausible set of assumptions. With each perihelion passage of a comet volatiles are

preferentially released, and during millions of such passages the comet could shed crustal debris that may survive transit through the Earth's atmosphere as a carbonaceous meteorite. We review the current state of knowledge of comets and carbonaceous meteorites. We also present the results of recent studies on the long-term viability of terrestrial ice-microbiota encased in ancient glacial ice and permafrost. We suggest that the conditions which have been observed to prevail on many comets do not preclude either survivability (or even the active metabolism and growth) of many types of eukaryotic and prokaryotic microbial extremophiles—including algae, cyanobacteria, bacteria and archaea. It is argued that the chemical and morphological biomarkers detected on comets and carbonaceous meteorites can be explained by ancient microbial activity without the need to invoke unknown abiotic production mechanisms.

8152-37, Session 9

The biological big bang: the first oceans of primordial planets at 2-8 million years explain Hoyle/Wickramasinghe cometary panspermia

C. H. Gibson, Univ. of California, San Diego (United States)

Hydrogravitational dynamics cosmology of Gibson/Schild 1996 predicts all of the primordial hydrogen-helium gas produced by the big bang fragments into proto-globular-star-cluster clumps of a trillion earth-mass planets at 300 Kyr. The first stars formed promptly from these hot gas planets. The first chemicals created by supernovae seeded the planets so oceans of water at critical temperature 647 K could host organic chemistry and the first life, distributed to the 10^{80} planets of the big bang by comets produced in star formation. The biological big bang time is between 2 Myr when oceans first condensed and 8 Myr when they froze. A flood of new information from new space telescopes supports the HGD cosmology scenario, which predicts thirty million planets per star in million solar mass clumps comprise the dark matter of galaxies. The biological big bang scenario explains the Hoyle/Wickramasinghe concept of cometary panspermia by providing a hot, nourishing, cosmological primordial soup and the means for transmitting the resulting life forms widely throughout the big bang universe. A solid astrophysical basis is provided for astrobiology.

8152-38, Session 9

Genesis of oil and hydrocarbon gases within Mars, other planets and moons within our solar system: organic origin (source rocks or direct biogenic sink?)

P. K. Mukhopadhyay, Global Geoenergy Research Ltd. (Canada)

No abstract available

8152-39, Session 10

Status of the UC-Berkeley SETI efforts

E. J. Korpela, Univ. of California, Berkeley (United States)

For nearly three decades, a group of researchers at the University of California have been involved in progressively more sophisticated searches for signals due to extraterrestrial civilizations. The initial searches were in the radio portion of the spectrum and looked for narrow band signals. Recent searches have expanded the parameter space to include signals that are narrow band in accelerated reference frames and short duration pulsed signals that have been dispersed by interstellar matter. Similarly the searches have expanded to the visible and, soon, infrared portions of the spectrum. These searches include searches for both nanosecond scale pulses, and narrow emission lines from lasers. We report the status of these ongoing searches.

8152-41, Session 10

Threshold effects in assembling the genome of a primitive cell in a young planet

D. J. Mullan, Univ. of Delaware (United States)

The pre-biotic era of a planet's development extends over a time interval which may be as long as gigayears or may be much shorter, possibly a few Myr. During this time interval, molecules in the oceans of a planet in the habitable zone undergo a finite number of collisions N_c . The value of N_c is well constrained in regards to velocity and cross-section, and it depends on the total number N_m of relevant monomers. When expressed in terms of the nucleotides which can be generated abiotically (such as demonstrated by Powner et. al. 2009), the occurrence of N_c collisions allows for a certain sampling of genomic phase space for an organism with RNA genetic material. From considerations of the large degree of "neutrality" which accompanies the replacement of monomers in many biomolecules, there can be a vast reduction (factor $Q \gg 1$) in the size of the relevant phase space compared to cases where all monomers are invariant. Given the size of the reduced RNA phase space for a grouping of p genes, we ask: how densely could this phase space have been sampled by reactions in aqueous solution on a young planet during the pre-biotic era? Formally, if Q is large enough ($Q \geq Q_{ra}$), the RNA phase space can in principle be sampled densely during the prebiotic era. However, the formal solution $Q \geq Q_{ra}$ is of no practical interest if Q_{ra} exceeds a well-defined upper limit Q_{max} which is controlled by the need to retain some specificity in the operations of biomolecules. For genetics based on doublet codons, Q_{ra} can be less than Q_{max} in the pre-biotic Earth as long as $p \leq 10-15$. Such an RNA phase space could have been sampled densely in the pre-biotic era provided that N_m is larger than a critical value. This sets a threshold for the assembly of the genome of a primitive cell: if the monomers can reach a concentration of 10⁻⁷ molar, we estimate that the presence of a few tons of monomers would suffice to allow emergence of a primitive genome in ≈ 10 Myr.

8152-42, Session 10

The cometary biosphere and the origin of life

R. B. Sheldon, Consultant (United States)

It is commonly asserted that panspermia merely dislocates the origin of life (OOL) from a place we know a lot about (Earth) to a place we know very little about (extra-terrestrial), so that it is more of an excuse for not being able to solve OOL than for courageously facing the Earth-based challenge. We argue that panzooia--the theory that the biosphere is mostly on comets rather than on rocky planets--is a superior theory to panspermia, moving the OOL problem from warm ponds to cold comets. This changes the nature of the OOL problem from a focus on change (evolution) to a focus on transport. Physically, we use the trivial example of horizontal gene transport from comets versus the warm pond evolution to illustrate the difference between addition and multiplication of information. If we convert the OOL problem into an information theoretic problem, this refocus on transport makes OOL a question of distributed information, where the network contains as much or more information as the nodes. We model this as a conservation of Shannon information in spacetime + its Fourier transform, where we calculate the way in which panzooia can approach the information densities of life--i.e. OOL. While this doesn't provide a detailed mechanism for OOL, it does make tremendous progress increasing the probability of OOL due to distributed information.

8152-44, Session 10

ExoMars Raman laser spectrometer breadboard: detector design and performance

I. Hutchinson, R. Ingley, Univ. of Leicester (United Kingdom); H. G. M. Edwards, Univ. of Leicester (United Kingdom) and Univ. of Bradford (United Kingdom); A. G. Moral, E. Diaz, G. Ramos, O. Barcos, C. Pérez Canora, Instituto Nacional de Técnica Aeroespacial (Spain); F. Rull, Unidad Asociada CSIC-CAB (Spain); C. Tato, SENER Ingeniería y Sistemas S.A. (Spain); P. Pool, e2v technologies plc (United Kingdom)

The Raman Laser Spectrometer is scheduled for launch on board the ESA Exomars mission in 2018. Its purpose is to perform analysis of the Raman signal scattered from crushed core samples retrieved from up to 2m below the Martian surface. In support of this activity an RLS breadboard instrument has been assembled at INTA (Instituto Nacional de Técnica Aeroespacial, Madrid) whose focal plane incorporates an inverted mode CCD cooled to between -10°C and -40°C. The thermal, mechanical and detector design of this elegant breadboard instrument focal plane is described, and the system performance is evaluated in terms of the noise performance, signal to noise ratios and dynamic range for key detector operating modes. The predicted performance of the flight model focal plane is also described, which includes an analysis of the effects caused by the radiation environment.

8152-45, Session 10

The design and development of a detector assembly for a portable Raman/LIBS spectrometer

I. Hutchinson, R. Ingley, Univ. of Leicester (United Kingdom); H. G. M. Edwards, Univ. of Leicester (United Kingdom) and Univ. of Bradford (United Kingdom); B. Ahlers, TNO Science and Industry (Netherlands); F. Rull, Unidad Asociada CSIC-CAB (Spain); M. Sovago, TNO Science and Industry (Netherlands); G. R. Davies, R. Motamedi, Vrije Univ. Amsterdam (Netherlands); P. Pool, e2v technologies plc (United Kingdom)

This paper describes the design, operation and performance of a detector assembly specifically developed for a combined Raman/LIBS (Laser Induced Breakdown Spectroscopy) spectrometer. The portable (low mass, low power, small volume), analytical instrument was built by TNO Space (under contract to ESA) for the ExoMars programme and was designed to be used for the in-situ analysis of samples from planetary surfaces or the moon. The trade-offs associated with selecting a detector that is appropriate for performing both Raman and LIBS spectroscopy are identified and the operating modes adopted for optimum instrument performance are described. Data obtained with the detector assembly (from both the Raman & LIBS channels of the instrument) are presented for a variety of sample types (selected based on their relevance to planetary surface studies). The performance levels of the instrument are assessed in terms of the signal to noise achieved for each sample type across a range of detector operating temperatures.

Conference 8153: Earth Observing Systems XVI

Tuesday-Thursday 23-25 August 2011 • Part of Proceedings of SPIE Vol. 8153 Earth Observing Systems XVI

8153-01, Session 1

Science highlights and lessons learned from the Atmospheric Infrared Sounder (AIRS)

T. S. Pagano, Jet Propulsion Lab. (United States)

The Atmospheric Infrared Sounder (AIRS) on the Aqua spacecraft measures the hyperspectral infrared spectrum (3.7-15.4 microns) of the atmosphere with nearly twice global daily coverage. National Weather Prediction (NWP) centers worldwide assimilate the AIRS spectra at its native resolution of 13.5 km, however the majority of the data are rejected due to cloud "contamination". The spectra are also used to retrieve cloud cleared radiances and atmospheric temperature and water vapor profiles with high accuracy and product resolutions approaching 50km per retrieval. Assimilation of these products into the forecast models has shown considerably higher impact, however, this methodology has not yet become operational at the NWP centers. Additional products including cloud properties and trace gases including carbon monoxide, methane, carbon dioxide, and sulfur dioxide are also retrieved from AIRS and used in a wide variety of scientific investigations. These investigations include atmospheric transport and global circulation, atmospheric chemistry, climate processes and anthropogenic impacts to Earth's atmosphere. While the AIRS has been very successful in its meeting the mission objectives, there is much we have learned over the years that would need to fold into the requirements of future systems. These lessons include requirements on the instrument measurement itself, such as coregistration and higher spatial and spectral resolution. Results from the NASA Science Community Workshop in IR and MW Sounders relating to AIRS requirements and concerns are covered. Also lessons related to the instrument design and calibration are identified and put into context of how to reduce instrument artifacts when attempting to meet a new and more challenging set of requirements. This paper looks back at what was achieved and forwards towards what needs to be done in the future to meet the growing needs of the scientific community.

8153-02, Session 1

Sensitivity of AIRS and IASI radiometric calibration to scene temperature

D. A. Elliott, H. H. Aumann, Jet Propulsion Lab. (United States)

High radiometric accuracy under all conditions (such as scene temperature and scan angle) is critical for establishing a climate-quality data record. In this study we compare radiances of both AIRS and IASI using the difference each instrument sees between the brightness temperature at 1231 cm⁻¹ and that at 961 cm⁻¹. We collected spectra at 17 different sites distributed around the world in tropical, temperate, desert, and arctic climates. For perfectly calibrated instruments, the brightness temperature differences should closely agree, since diurnal differences caused by the differing orbits cancel to first order. We examine observed differences (indicative of calibration artifacts) as functions of scene temperature, time of day, and scan angle. AIRS is a cooled grating array spectrometer with 2378 spectral channels in the wavelength range from 3.7 to 15.4 microns. AIRS began routine operations in September 2002. IASI is a Fourier Transform spectrometer covering the range 3.6 to 15.5 microns in three bands. The spectral resolutions of AIRS and IASI are similar. IASI data have been available since July 2007.

8153-03, Session 1

Evaluation of deep convective clouds as stable references for climate research using AIRS data

H. H. Aumann, Y. Jiang, D. A. Elliott, Jet Propulsion Lab. (United States)

Changes due to global warming are expected to be the order of 100 mK/decade in temperatures and 1%/decade in cloud amounts. The detection of such small changes are facilitated by observations covering many decades. They also require a very accurate absolute calibration. We use Deep Convective Clouds (DCC) in the tropical zone as a reference for the evaluation of the absolute calibration accuracy and stability of infrared radiometers. Since DCC cover about 1% of the tropical zone, thousands of DCC can be seen every day. We illustrate the method with Atmospheric Infrared Sounder (AIRS) data and apply it to data from the Infrared Interferometric Spectrometer (IRIS). The method is general and can be applied retrospectively to any infrared radiometer like HIRS, AVHRR and GOES. AIRS is on the EOS Aqua satellite, which was launched into a 1:30 PM ascending node polar sun-synchronous orbit in May 2002 and is expected to continue to produce high quality data until 2015 or longer. Two copies of the IRIS flew on Nimbus satellites between April 1970 and January 1971.

8153-04, Session 1

Performance and operations impact of the spaceborne environment on the Atmospheric Infrared Sounder

S. E. Broberg, H. H. Aumann, D. A. Elliott, Jet Propulsion Lab. (United States); K. R. Overoye, BAE Systems (United States); M. H. Weiler, ATK Space Systems (United States)

NASA is increasingly considering instrumentation in space with longer and longer lifetimes, 5 years or more. The validity of the ground based calibration is potentially compromised by exposure of the instrument to ultraviolet radiation, water/ice, molecular (polymer) contamination, the space radiation environment, as well as mechanical relaxation/fatigue effects. We use 9 years of on-orbit data from the Atmospheric InfraRed Sounder (AIRS) to examine the impact of such environments, both expected and unexpected.

8153-05, Session 1

Improved surface and tropospheric temperatures determined using only shortwave channels: The AIRS Science Team Version-6 retrieval algorithm

J. Susskind, NASA Goddard Space Flight Ctr. (United States); J. M. Blaisdell, L. Iredell, SAIC (United States)

The Goddard DISC has been analyzed AIRS/AMSU data from September 2002 to the present using the AIRS Science Team Version 5 retrieval algorithm. This talk will describe, and show results using, the AIRS Science Team Version-6 retrieval algorithm which contains significant improvements in retrieval methodology compared to Version-5. The most significant improvement in retrieval methodology compared to Version-5 is the use of only shortwave channels in the physical retrieval of land and ocean surface skin temperatures, which are determined simultaneously with shortwave surface spectral emissivity and bi-directional reflectance. As in Version-5, the physical retrieval uses only shortwave CO₂ channels in the determination of tropospheric temperatures, with longwave CO₂ channels being used primarily to determine cloud cleared radiances for all channels. Significant improvements have also been made in QC methodology, allowing for high quality retrievals under most cloud conditions which are optimized separately for data assimilation purposes and for climate monitoring. This approach, which also allows for the generation of very accurate "AIRS Only" retrievals under most cloud cover conditions that make no use of AMSU observations, is possible using AIRS observations because AIRS has very low noise channels extending to 2660 cm⁻¹. These findings imply that accurate soundings can be generated from geostationary orbit with a high spectral resolution

Conference 8153:
Earth Observing Systems XVI

IR sounder, without being accompanied by a microwave sounder, as long as the IR sounder has very low noise in the shortwave spectral region.

8153-06, Session 2

The improved MODIS solar diffuser screen vignetting function calculation and its implementation in RSB calibration

Z. Wang, Sigma Space Corp. (United States); X. Xiong, NASA Goddard Space Flight Ctr. (United States); W. L. Barnes, Univ. of Maryland, Baltimore County (United States)

The MODIS high-gain ocean color bands (B8-B16) are calibrated with its solar diffuser screen (SDS) closed so that the vignetting function (VF) of SDS is necessary for the calculation of their calibration coefficients. Since there was no pre-launch system level characterization of the SDS VF, a series of yaw maneuvers were carried out at the mission beginning for each MODIS to enable its on-orbit characterization. Current VF was derived from the low-gain bands (B1-B7 & B17-B19) data and applied to high-gain ocean color bands, with the assumption that all bands and detectors should share the same VF. As expected, errors in VF characterization will be carried over into the calibration coefficients for the bands that use the SDS for their on-orbit calibration. In this paper, an improved VF calculation method, still using the yaw data as input, is presented. The new method considers the frame-level mismatch of the detector footprint on the solar diffuser (SD) so that a proper SD image frame adjustment is needed when the VF of the low-gain bands is transferred to high-gain bands. A set of band-and-detector dependent VFs can be derived using this approach. The implementation of the new VFs has effectively reduced seasonal oscillations from up to 1.0% to 0.2% in Aqua MODIS high gain band calibration coefficients.

8153-07, Session 2

Adjustments to the MODIS Terra radiometric calibration and polarization sensitivity in the 2010 reprocessing

G. Meister, B. A. Franz, NASA Goddard Space Flight Ctr. (United States)

There are two units of the Moderate Resolution Imaging Spectroradiometer (MODIS) orbiting the earth. The first was launched in December 1999 on NASA's Earth Observing System (EOS) Terra satellite, the second on the Aqua satellite in May 2002. Both MODIS instruments are calibrated using on-board calibrators and lunar irradiances. For MODIS Aqua, these calibration sources have been sufficient to produce high quality ocean color products up to 2007. For MODIS Terra, this has not been the case. The Ocean Biology Production Group at NASA has derived radiometric corrections using SeaWiFS ocean color products as truth fields. The assumption was made that the NIR bands (bands 15 and 16) do not require any adjustments. In the 2010 reprocessing of MODIS Terra ocean color data, these corrections have been applied to the whole mission life span of 10 years. This paper presents the corrections to the radiometric gains and to the instrument polarization sensitivity, demonstrates the improvement to the Terra ocean color products, and discusses issues that need further improvement.

The largest corrections are needed for the short wavelength bands (bands 8 and 9). In addition to significant radiometric gain corrections as a function of scan angle (up to 10% for large incidence angles on the scan mirror), the polarization sensitivity at the end of scan has increased dramatically for large incidence angles on the MODIS scan mirror, up to about 50%. The magnitude of the corrections decreases strongly with wavelength, to the extent that the corrections needed for the red bands (bands 13 and 14) is on the order of only 1% or less. The small magnitude of the corrections required for the longer wavelengths gives support to the assumption that the NIR bands do not require any modifications. Applying the corrections to the MODIS Terra data leads to

ocean color products with similar global trends as for MODIS Aqua, but with greater radiometric uncertainty due to the additional corrections.

8153-08, Session 2

MODIS on-orbit calibration uncertainty assessment

X. Xiong, NASA Goddard Space Flight Ctr. (United States); K. Chiang, J. Sun, A. Wu, Sigma Space Corp. (United States)

MODIS has 20 reflective solar bands (RSB) and 16 thermal emissive bands (TEB). Compared to its heritage sensors, MODIS was developed with very stringent calibration uncertainty requirements. As a result, MODIS was designed and built with a set of on-board calibrators (OBC), which allow key sensor performance parameters and on-orbit calibration coefficients to be monitored and updated. In terms of its calibration traceability, MODIS RSB calibration is reflectance based using an on-board solar diffuser (SD) and the TEB calibration is radiance based using an on-board blackbody (BB). In addition to on-orbit calibration coefficients derived from its OBC, calibration parameters determined from sensor pre-launch calibration and characterization are used in both the RSB and TEB calibration and retrieval algorithms. This paper provides a brief description of MODIS calibration methodologies and an in-depth analysis of its on-orbit calibration uncertainties. Also discussed in this paper are uncertainty contributions from individual components and differences due to Terra and Aqua MODIS instrument characteristics and on-orbit performance.

8153-09, Session 2

MODIS cloud optical property retrieval uncertainties derived from pixel-level VNIR/SWIR radiometric uncertainties

S. E. Platnick, NASA Goddard Space Flight Ctr. (United States); G. Wind, Science Systems and Applications, Inc. (United States); X. Xiong, NASA Goddard Space Flight Ctr. (United States)

Moderate Resolution Imaging Spectroradiometer (MODIS) retrievals of optical thickness and effective particle radius for liquid water and ice phase clouds employ a well-known VNIR/SWIR solar reflectance technique. For this type of algorithm, we evaluate the quantitative uncertainty in simultaneous retrievals of these two cloud parameters to pixel-level radiometric calibration estimates and other fundamental (and tractable) error sources.

The technique, first implemented in MOD06 Collection 5 processing, uses sensitivity calculations derived from pre-computed cloud reflectance look-up tables coupled with estimates for the effect of various error sources on cloud-top reflectance. An important error source is instrument radiometric calibration (other tractable sources included in Collection 5 are surface spectral albedo and atmospheric corrections). We will show cloud retrieval uncertainties derived from new MODIS L1B VNIR and SWIR band pixel-level uncertainty estimates that will be used in Collection 6 processing. Because of the nature of the approach, results will deal exclusively with pixel-level uncertainties associated with plane-parallel clouds; real-world radiative departures from a plane-parallel model are an additional consideration. While we demonstrate the uncertainty technique with operational 1 km MODIS retrievals from the Terra and Aqua satellite platforms, the technique is applicable to any reflectance-based satellite or air-borne sensor retrieval using similar spectral channels.

8153-10, Session 2

Uncertainty assessment of the SeaWiFS on-orbit calibration

R. E. Eplee, Jr., SAIC (United States); G. Meister, NASA Goddard Space Flight Ctr. (United States); F. S. Patt, SAIC (United States); B. A. Franz, C. R. McClain, NASA Goddard Space Flight Ctr. (United States)

Ocean color climate data records require water-leaving radiances with 5% absolute and 1% relative accuracies as input. Because of the amplification of any sensor calibration errors by the atmospheric correction, the 1% relative accuracy requirement translates into a 0.1% long-term radiometric stability requirement for top-of-the-atmosphere radiances. Monthly observations of the Moon provide the primary monitor of the on-orbit instrument response for SeaWiFS. The rigorous on-orbit calibration program developed and implemented for SeaWiFS by the NASA Ocean Biology Processing Group (OBPG) Calibration and Validation Team (CVT) has allowed the CVT to maintain the stability of the radiometric calibration of SeaWiFS at 0.13% or better over the mission. The uncertainties in the resulting calibrated top-of-the-atmosphere (TOA) radiances can be addressed in terms of accuracy (biases in the measurements), precision (scatter in the measurements), and stability (repeatability of the measurements). Comparison of the residuals of the lunar observations from the USGS RObotic Lunar Observatory (ROLO) photometric model of the Moon with gains derived from the vicarious calibration of SeaWiFS against the Marine Optical Buoy (MOBY) show that the calibration biases for SeaWiFS are 2-3%. The solar diffuser-derived on-orbit signal-to-noise analysis and the lunar residual analysis show that the precision of the SeaWiFS TOA radiances is 0.12%. The combined uncertainties for the SeaWiFS TOA radiances are 2-3%, with a long-term stability of 0.13%. These results allow the OBPG to produce climate data records from the SeaWiFS ocean color data.

8153-11, Session 3

Landsat Data Continuity Mission (LDCM) overview and status

P. A. Sabelhaus, NASA Goddard Space Flight Ctr. (United States)

The Landsat Data Continuity Mission (LDCM) is the follow-on mission to Landsat 7 and will be the eighth mission in the Landsat series. The mission is in development via an interagency partnership between the National Aeronautics and Space Administration (NASA) and the Department of Interior (DOI) / United States Geological Survey (USGS). The LDCM satellite will carry two earth-observing sensors, the Operational Land Imager (OLI) to collect image data for nine spectral bands in the reflective portion of the spectrum and the Thermal Infrared Sensor (TIRS) to collect coincident image data for two thermal spectral bands. The LDCM ground segment will control the satellite and will receive, process, archive, and distribute the science data collected by the OLI and TIRS instruments. The USGS Earth Resources Observation & Science Center (EROS) will distribute LDCM data products at no cost to requestors. The mission objective is to continue the Landsat program's collection, archive, and distribution of multispectral imagery affording global, synoptic, and repetitive coverage of the Earth's land surfaces at a scale where natural and human-induced changes can be detected, differentiated, characterized, and monitored over time. The LDCM launch readiness date is currently December 2012. This paper will provide an overview and the latest status of the LDCM mission.

8153-12, Session 3

LDCM OLI and TIRS sensor performance

B. L. Markham, NASA Goddard Space Flight Ctr. (United States)

The LDCM will have two pushbroom Earth-imaging sensors: Operational Land Imager (OLI) and Thermal InfraRed Sensor (TIRS). The OLI has

the reflective 30-meter and panchromatic 15-meter ETM+ bands plus bands at 443 nm and 1375 nm. The TIRS has two 100-meter bands that spectrally split the ETM+ thermal band. OLI has completed performance testing, though analysis is still in progress. Radiometric analyses completed to date indicate: Polarization sensitivity: 1-2%; Signal-to-Noise Ratio: at signal levels about 5-10% of full scale, between 6-12 times better than ETM+, e.g., 250 versus 30; radiometric stability over 16 days: better than 0.5% (2-sigma); coherent noise: not visible; detector operability: 100% (no dead or inoperable detectors). Linearity, uniformity, absolute calibration, spatial response, spectral response and other analyses are continuing. TIRS commenced performance testing in February 2011 with initial focus testing to confirm that the focus is within requirements. Radiometric tests will be upcoming in March 2011.

8153-13, Session 3

Landsat 8 on-orbit characterization and calibration system

E. Micijevic, R. Morfitt, M. Choate, U.S. Geological Survey (United States)

The Landsat Data Continuity Mission (LDCM) is planning to launch the Landsat 8 satellite in December 2012, which continues an uninterrupted record of consistently calibrated globally acquired multispectral images of the Earth started in 1972. The satellite will carry two imaging sensors: the Operational Land Imager (OLI) and the Thermal Infrared Sensor (TIRS). The OLI will provide visible, near-infrared and short-wave infrared data in nine spectral bands while the TIRS will acquire thermal infrared data in two bands. Both sensors have a pushbroom design and consequently, each has a very large number of detectors to be characterized.

Image and calibration data downlinked from the satellite will be processed by the U.S. Geological Survey (USGS) Earth Resources Observation and Science (EROS) Center using the Landsat 8 Image Assessment System (IAS), a component of the Ground System. In addition to extracting statistics from all normal Earth images acquired, the IAS will process and trend results from analysis of special calibration acquisitions, such as solar diffuser, lunar, shutter, night, lamp and blackbody data, and preselected calibration sites. The trended data will be systematically processed and analyzed, and calibration and characterization parameters will be updated using both automatic and customized manual tools. This paper describes the analysis tools and the system developed to monitor and characterize on-orbit performance and calibrate the Landsat 8 sensors and image data products.

8153-14, Session 3

Modeling the image performance of the Landsat Data Continuity Mission sensors

J. R. Schott, S. D. Brown, M. G. Gartley, A. D. Gerace, Rochester Institute of Technology (United States)

The LDCM will carry two new pushbroom imagers. The nine band Operational Land Imager (OLI) and the two band Thermal Infrared Sensor (TIRS) represent significant changes in Landsat Sensor Technology, as does the plan to generate a common data product from two sensors (registered 11 band data). This effort is designed to generate synthetic images that will predict the LDCM performance pre-launch, will support trouble shooting of instrument behavior during initialization and operation, and perhaps most importantly, can support Landsat remote sensing science activities throughout the mission. This paper reports on the initial results, which focused on geometric issues associated with; orbital dynamics, sensor focal plane design specifics, scene geometry, and the impact of jitter on image quality and radiometric issues which included; the impact of TIRS spectral response variation on banding and approaches to simulate detector-to-detector and array-to-array non-uniformities (gain and bias) and non-linearities. The approach involves modifying the DIRSIG image simulation model to allow detailed modeling of the Landsat orbit and LDCM sensors parameters and generation of

a test scene to allow full end-to-end image simulations incorporating illumination, atmospheric, sensor geometry, and radiometry effects as a function of time, meteorology, and spectral range from the visible through the long wave infrared and spatial effects. The results reported here will include evaluation of band-to-band regeneration impacts on spectral purity, jitter impacts on OLI image quality, and simulation of sources of image non-uniformity.

8153-15, Session 3

The Operational Land Imager: prelaunch spectral characterization and performance

J. A. Barsi, B. L. Markham, J. A. Pedelty, NASA Goddard Space Flight Ctr. (United States)

The Landsat Data Continuity Mission (LDCM) will carry the Operational Land Imager (OLI) as one of its payloads. This instrument is a derivative of the Advanced Land Imager (ALI), flown on Earth Observing-1 (EO1) though it's mission is to continue the operational land imaging of the Landsat program. The OLI follows the highly successful Landsat-5 and Landsat-7 in continuing to populate an archive of earth images that dates back to 1972.

The OLI has significant changes from the Landsat Thematic Mapper instruments, given that is the first pushbroom instrument in the program. However, it is intended to be a continuity mission, so the spatial coverage and spectral bands are similar. The suite of OLI's multispectral bands cover the same bandpasses but the panchromatic band is narrower than that of the ETM+. The OLI also has a shorter wavelength blue band for better resolution of coastal waters and a new band to aid in the detection of Cirrus clouds in the atmosphere. The thermal bands traditionally carried on the TM instruments have been moved to a separate instrument, also onboard the LDCM spacecraft.

Given the pushbroom design of the instrument, each OLI multi-spectral band consists of nearly 7000 detectors. Among other requirements, the specifications require that the uniformity within a band be better than 0.5% across the whole field of view. To this end, Ball Aerospace performed extensive testing at the component and instrument level. This paper will cover the results of the tests that attempt to validate the uniformity requirements, including in-band response, out-of-band response, and spectral smile across the focal plane.

8153-16, Session 3

Bias estimation for the Landsat 8 Operational Land Imager

K. J. Vanderwerff, R. Morfitt, USGS Ctr. for Earth Resources and Observation and Science (United States)

The Operational Land Imager (OLI) is a pushbroom sensor that will be a part of the Landsat Data Continuity Mission (LDCM). This instrument is the latest in the line of Landsat imagers, and will continue to expand the archive of calibrated earth imagery. One important step in producing a calibrated image from instrument data is accurately accounting for the bias of the imaging detectors. Several factors make estimating the bias difficult for OLI including bias variability and the quantization of the downlinked data. Typically, the bias is simply estimated by averaging dark data on a per-detector basis. However, dark images taken during OLI pre-launch testing exhibited variation that correlated with the variation in concurrently collected data from a special set of detectors on the focal plane. These detectors are sensitive to certain electronic effects but not to incoming electromagnetic radiation. Data collected from these special detectors may be used to compensate for this per-frame bias variation. In addition to bias variability, a systematic bias error is introduced by the truncation of the 14-bit instrument data to 12-bit integers by the spacecraft. This systematic error can be removed, but the larger quantization error remains. This paper describes the variability of the bias, the effectiveness of an approach to estimate and compensate for it, as well as the errors due to truncation and how they are reduced.

8153-17, Session 4

Results from solar reflective band end-to-end testing for VIIRS F1 sensor using T-SIRCUS

J. McIntire, Sigma Space Corp. (United States); D. I. Moyer, The Aerospace Corp. (United States); J. K. McCarthy, Northrop Grumman Aerospace Systems (United States); F. DeLuccia, The Aerospace Corp. (United States); X. Xiong, J. J. Butler, NASA Goddard Space Flight Ctr. (United States); B. W. Guenther, National Oceanic and Atmospheric Administration (United States)

Verification of the Visible Infrared Imager Radiometer Suite (VIIRS) End-to-End (E2E) sensor calibration is highly recommended before launch, to identify any anomalies and to improve our understanding of the sensor on-orbit calibration performance. E2E testing of the Reflective Solar Bands (RSB) calibration cycle was performed pre-launch for the VIIRS Flight 1 (F1) sensor at the Ball Aerospace facility in Boulder CO in March 2010. VIIRS reflective band calibration cycle is very similar to heritage sensor MODIS in that solar illumination, via a diffuser, is used to correct for temporal variations in the instrument responsivity. Monochromatic light from the NIST T-SIRCUS was used to illuminate both the Earth View (EV), via an integrating sphere, and the Solar Diffuser (SD) view, through a collimator. The collimator illumination was cycled through a series of angles intended to simulate the range of possible angles for which solar radiation will be incident on-orbit. Ideally, the measured instrument responsivity should be the same whether the EV or SD view is illuminated. Monitors were present on both the integrating sphere and collimator, allowing for real-time tracking of the responsivities over data collections roughly equivalent to an on-orbit calibration cycle. The ratio of the measured responsivities was determined at each collimator angle and wavelength. In addition, the Solar Diffuser Stability Monitor (SDSM), a ratioing radiometer designed to track the temporal variation in the SD BRF by direct comparison to solar radiation, was illuminated by the collimator. The measured SDSM ratio was compared to the predicted ratio.

8153-18, Session 4

A maximum likelihood approach to determine sensor radiometric response coefficients

N. Lei, Sigma Space Corp. (United States)

Optical sensors aboard Earth orbiting satellites such as the Moderate Resolution Imaging Spectroradiometer (MODIS) and the next generation Visible/Infrared Imager Radiometer Suite (VIIRS) assume that the sensors' radiometric response in the Reflective Solar Bands (RSB) may be described by a quadratic polynomial, in relating the spectral radiance to the digital number readout. For the case of VIIRS, the coefficients are to be determined before launch through an attenuation method, although the linear coefficient will be further determined on-orbit through observing the Solar Diffuser. In determining the quadratic polynomial coefficients through the attenuation method, a Maximum Likelihood (ML) approach is applied in carrying out the least-square procedure. Crucial to the ML least-square procedure is the computation of the weight. The weight not only has a contribution from the noise of the sensor's digital count, but also has an important contribution from the error in digitization of the count. In addition, the mathematical expression used in the least-square procedure has a crucial role in the weight calculation due to the fact that both the independent and the dependent variables contain random noises. We shall show the details in calculating the weight. Furthermore, we shall show the impact of the fitting residuals in the attenuator's transmittance on the coefficients' uncertainties (for VIIRS). We compute the values as well as the uncertainties for the coefficients and compare the results obtained from the traditional method.

8153-19, Session 4

VIIRS F1 “best estimate” relative spectral response characterization by the government team

C. C. Moeller, Univ. of Wisconsin-Madison (United States); J. McIntire, T. Schwarting, Sigma Space Corp. (United States); D. I. Moyer, The Aerospace Corp. (United States)

The VIIRS Flight 1 (F1) instrument completed sensor level testing at the Raytheon El Segundo, CA facility in 2009 and is moving forward towards a launch on the NPP platform late in 2011. The sensor level testing, consisting of ambient and thermal vacuum (TVAC) phases, was designed to provide characterization for all elements of sensor performance, populating the Sensor Data Record (SDR) algorithm lookup tables (LUTS) and establishing compliance on performance metrics. As part of its oversight on this project, the VIIRS government team, consisting of NASA, Aerospace Corp., and MIT/Lincoln Lab participation has been tasked to perform an independent (from industry) data analysis and review of the VIIRS F1 sensor level test data, producing estimates of key performance and LUT essentials.

One of the key factors of the VIIRS sensor performance is the relative spectral response (RSR) characterization. Test data to derive RSR for all VIIRS spectral bands was collected in the TVAC environment using the Spectral Measurement Assembly (SpMA), a dual monochromator system with tungsten bulb and ceramic glow bar sources. Spectrally contiguous measurements were made, including the inband (IB) and out-of-band (OOB) spectral regions of each band. These measurements were analyzed by the government team to produce a complete (IB+OOB) RSR for 22 of the 23 VIIRS bands (exception of the Day-Night Band, DNB). This paper will provide insight on key aspects and findings of the RSR data analysis, including detector to detector variation and OOB features, as well as present the government team “best estimate” RSR (released into the public domain in fall, 2010) to the community. A review of RSR performance metric results (center wavelength, bandpass, extended bandpass, integrated out-of-band) will also be presented.

8153-20, Session 4

Comparison of VIIRS prelaunch RVS among independent studies

A. Wu, J. McIntire, Sigma Space Corp. (United States); X. Xiong, NASA Goddard Space Flight Ctr. (United States); F. J. De Luccia, The Aerospace Corp. (United States); J. A. Cronkhite, Sigma Space Corp. (United States)

VIIRS is a key sensor carried on the NPOESS, developed recently from predecessor instruments including AVHRR, OLS, MODIS, and SeaWiFS. The VIIRS response versus scan angle (RVS) was characterized prelaunch in lab ambient conditions and will be used on-orbit to characterize the response for scan angles. This document provides three RVS results obtained from NICST, Raytheon and Aerospace. A comparison of the RVS results is conducted for each band, detector and half angle mirror (HAM) side. The associated RVS uncertainties are examined and compared with the relative differences found between independent studies. Results show that the agreement is within 0.1% for all bands except for RSB band M9, where a difference of 0.2% results from the application of the atmospheric water vapor correction for laboratory conditions during the test by Raytheon. NICST has slightly larger RSB RVS uncertainties but still well within the 0.3% total uncertainty allowed for the RVS characterization.

8153-21, Session 4

NASA/GSFC assessment of NPP VIIRS ocean color data products: hope and risk

K. R. Turpie, NASA Goddard Space Flight Ctr. (United States) and Science Applications International Corp. (United States); C. R. McClain, G. Meister, NASA Goddard Space Flight Ctr. (United States); G. Eplee, R. A. Barnes, F. S. Patt, W. D. Robinson, NASA Goddard Space Flight Ctr. (United States) and Science Applications International Corp. (United States)

For several years, the NASA/Goddard Space Flight Center (GSFC) NPP VIIRS Ocean Science Team (VOST) has provided substantial scientific input to the NPP project regarding the use of Visible Infrared Imaging Radiometer Suite (VIIRS) data to create science quality ocean color data products. This work produced an assessment of the NPP project and the VIIRS instruments capability to produce science quality ocean color data products. This assessment found that the operational algorithms were years behind those developed by NASA/GSFC and would not be adequate to either produce science quality data or provide the consistency needed to continue the current NASA climate data record (CDR).

Furthermore, inadequacies in the program also undermined that objective, such as [lack of] support for a research processing stream or mission-level reprocessing. The group also evaluated the sensor design, performance attributes, and satellite operational issues and how these influence the Ocean Color data product quality. In particular, several sensor characteristics [were] evaluated, such as crosstalk, out-of-band (OOB) response, stray light, and polarization sensitivity. The conclusion was that most characteristics were similar to earlier instruments, including SeaWiFS and MODIS Aqua. OOB is significant for VIIRS, but not larger than the largest effects with SeaWiFS.

The polarization sensitivity was found to be less overall than MODIS and much better characterized prelaunch. Crosstalk effects are worse than earlier instruments, however, the characterization tests showed smaller impact than originally thought. Though instrument performance and calibration risks exist, it was concluded that programmatic and algorithm issues dominate concerns.

8153-22, Session 5

The NASA Enhanced MODIS Airborne Simulator

J. Myers, Univ. of California, Santa Cruz (United States); S. E. Platnick, NASA Goddard Space Flight Ctr. (United States); T. A. Ellis, Univ. of California, Santa Cruz (United States)

The new NASA Enhanced MODIS Airborne Simulator (eMAS) is based on the legacy MAS system, which has been used extensively in support of the NASA Earth Observing System program since 1995. eMAS consists of two separate instruments designed to fly together on the NASA ER-2 and Global Hawk high altitude aircraft.

The eMAS-IR instrument is an upgraded version of the legacy MAS line-scanning spectrometer, with 38 spectral bands in the wavelength range from 0.47 to 14.1 μm . The original LN₂-cooled MAS MWIR and LWIR spectrometers are replaced with a single vacuum-sealed, Stirling-cooled assembly, having a single MWIR and twelve LWIR bands. This spectrometer module contains a cold optical bench where both dispersive optics and detector arrays are maintained at cryogenic temperatures to reduce infrared background noise, and ensure spectral stability during high altitude airborne operations.

The EMAS-HSI instrument is a stand-alone push-broom imaging spectrometer, with 202 contiguous spectral bands in the wavelength range from 0.38 to 2.40 μm . It consists of two Offner spectrometers, mated to a 4-mirror anastigmat telescope. The system has a single slit, and uses a dichroic beam-splitter to divide the incoming energy between VNIR and SWIR focal plane arrays. It will be synchronized and

Conference 8153:
Earth Observing Systems XVI

bore-sighted with the IR line-scanner, and includes an active source for monitoring calibration stability.

eMAS is intended to support future satellite missions including the Hyperspectral Infrared Imager (HyspIRI), the National Polar-orbiting Operational Environmental Satellite System (NPOESS) Preparatory Project (NPP), and the follow-on Joint Polar Satellite System (JPSS).

8153-23, Session 5

Development of a low-cost student-built multispectral sensor for the International Space Station

D. R. Olsen, H. J. Kim, J. Ranganathan, S. Laguette, The Univ. of North Dakota (United States)

Built by students and faculty at the University of North Dakota (UND), the International Space Station (ISS) Agricultural Camera (ISSAC) is a multi-spectral Earth-imaging sensor currently onboard the ISS. Capabilities include three spectral bands (green, red, near-infrared), moderate (20-30 m) spatial resolution, and off-nadir pointing (+/-30 degrees) for episodic rapid-response imaging. We describe the low-cost electro-optical design approach, which relies on modified commercial components operating within a passive vibration isolation mounting, installed inside the Window Observational Research Facility and viewing the Earth through the US Laboratory Science Window. Interfaces, safety, and other factors unique to the human-rated operational environment of the ISS are outlined. Limitations of the student-centric development environment and constraints of operating from the ISS are addressed, as well as the benefits and opportunities of such. Pre-launch sensor characterization results, including spatial distortion and radiometric measurements, indicate Earth remote sensing using such a sensor is a viable approach for demonstrative operational missions. An element of the ISS National Laboratory, ISSAC was launched on HTV-2 in January 2011. Plans are presented for sensor operations, now set to commence in summer 2011. Student operators at UND will receive sensor tasking requests from public end users, upload commands, process telemetry, and deliver imagery; all as part of a broader applied research initiative known as the Upper Midwest Aerospace Consortium (UMAC). The mission of UMAC is to develop, support, and enable adoption of innovative Earth science applications, such that informed decision making can improve both environmental sustainability and societal economics.

8153-24, Session 5

SENTINEL-2 level 1 image processing and performances

S. J. Baillarin, A. Meygret, Ctr. National d'Études Spatiales (France); P. Martimort, European Space Research and Technology Ctr. (Netherlands); C. Dechoz, B. Petrucci, Ctr. National d'Études Spatiales (France); F. Spoto, European Space Research and Technology Ctr. (Netherlands); P. J. Henry, Ctr. National d'Études Spatiales (France); O. Colin, ESRIN (Italy); C. Isola, European Space Research and Technology Ctr. (Netherlands)

In partnership with the European Commission and in the frame of the Global Monitoring for Environment and Security (GMES) program, the European Space Agency (ESA) is developing the Sentinel-2 optical imaging mission devoted to the operational monitoring of land and coastal areas.

The Sentinel-2 mission is based on a satellites constellation deployed in polar sun-synchronous orbit. While ensuring data continuity of former SPOT and LANDSAT multi-spectral missions, Sentinel-2 will also offer a wide range of improvements such as a global coverage, a large field of view (290km), a high revisit capability (5 days with two satellites), a high resolution (10m, 20m and 60m) and multi-spectral imagery (13 spectral

bands).

In this context, the Centre National d'Études Spatiales (CNES) supports ESA to define the system image products and to prototype the relevant image processing techniques.

First, this paper presents the Sentinel-2 system and the image products that will be delivered: starting from raw decompressed images up to accurate ortho-images in Top of Atmosphere reflectances. The stringent image quality requirements are also described, in particular the very accurate target geo-location.

Then, the prototyped image processing techniques will be addressed. Both radiometric and geometric processing will be described with a special focus on the automatic enhancement of the geometric physical model involving a global set of reference data.

Finally, the very promising results obtained by the prototype will be presented and discussed. The radiometric and geometric performances will be provided as well as the associated computing time spent on the target platform.

8153-25, Session 5

SPnPS: a Space Plug-n-Play Spectrometer for constellation CubeSat applications

S. R. Watchorn, Scientific Solutions, Inc. (United States); R. Doe, K. Leveque, SRI International (United States); J. Noto, Scientific Solutions, Inc. (United States)

The CubeSat initiative envisions inexpensive, easily reproducible satellite packages for Earth-viewing remote sensing applications, such as space weather modeling (including winds and temperatures) and spectral probes of vegetation canopies, among other applications. A constellation of CubeSat payloads could provide worldwide coverage for measuring these and similar phenomena. Such payloads require lightweight, robust, standardized components. For remote sensing payloads, one of the most difficult components to standardize and make robust for high-resolution applications (such as wind measurements in space weather) is the spectrometer itself.

The Space Plug-and-Play Spectrometer (SPnPS) is an answer to that problem. Using a monolithic Spatial Heterodyne Spectrometer (requiring no moving parts for high resolution sensing) at its heart, the SPnPS system allows for standardized spectrometer insertion into an optical train. Coupled with standard avionics developed according to the Space Plug-and-Play Avionics (SPA) initiative, SPnPS allows for easily reproducible and re-taskable spectrometer packages for CubeSat-based applications.

This presentation will talk about the very early stages of SPnPS development, including modeling its "tradespace:" the resolution, sensitivity, and field of view attainable within the CubeSat size, weight, and power constraints; the preliminary optical design of the system; and a breadboard (brassboard) avionics mock-up to simulate the final-version SPnPS payload.

8153-26, Session 5

Preliminary error budget for the reflected solar instrument for the Climate Absolute Radiance and Refractivity Observatory

K. J. Thome, NASA Goddard Space Flight Ctr. (United States); T. Gubbels, Sigma Space Corp. (United States); R. A. Barnes, Science Applications International Corp. (United States)

The Climate Absolute Radiance and Refractivity Observatory (CLARREO) mission addresses the need to observe high-accuracy, long-term climate change trends and to use decadal change observations as the most critical method to determine the accuracy of climate change. The CLARREO Project will implement a spaceborne earth observation mission designed to provide rigorous SI-traceable observations (i.e.,

Conference 8153:
Earth Observing Systems XVI

radiance, reflectance, and refractivity) that are sensitive to a wide range of key decadal change variables. The instrument suite includes emitted infrared spectrometers, global navigation receivers for radio occultation, and reflected solar spectrometers. The measurements will be acquired for a period of five years and will enable follow-on missions to extend the climate record over the decades needed to understand climate change. This work describes a preliminary error budget for the RS sensor. The RS sensor will retrieve at-sensor reflectance over the spectral range from 320 to 2300 nm with 500-m GIFOV and a 100-km swath width. The current design is based on an Offner spectrometer with two separate focal planes each with its own entrance aperture and grating covering spectral ranges of 320-640, 600-2300 nm. Reflectance is obtained from the ratio of measurements of radiance while viewing the earth's surface to measurements of irradiance while viewing the sun. The requirement for the RS instrument is that the reflectance must be traceable to SI standards at an absolute uncertainty <0.3%. The calibration approach to achieve the ambitious 0.3% absolute calibration uncertainty is predicated on a reliance on heritage hardware, reduction of sensor complexity, and adherence to detector-based calibration standards. The design above has been used to develop a preliminary error budget that meets the 0.3% absolute requirement. Key components in the error budget are geometry differences between the solar and earth views, knowledge of attenuator behavior when viewing the sun, and sensor behavior such as detector linearity and noise behavior. Methods for demonstrating this error budget are also presented.

8153-27, Session 5

Optical design of the Ocean Radiometer for Carbon Assessment

M. E. Wilson, M. A. Quijada, E. Waluschka, C. R. McClain, NASA Goddard Space Flight Ctr. (United States)

The ORCA instrument is designed to be an ocean color radiometer with a large number of spectral bands and high SNR values, with moderate spatial resolution. The bandpass ranges from the near UV to the SWIR. The approach taken is to use conventional optics and detectors with a nonstandard approach of using time delay integration in the cross track direction to boost the SNR. A wedged depolarizer, similar to SeaWiFS, is used to minimize the variation in instrument response to changes in polarization of the incoming beam. Diffraction gratings are used to disperse the light into many different wavelength bands. A rotating telescope, similar to SeaWiFS, is used to provide a large field of regard.

8153-28, Session 6

Optical testing performance for the Ocean Radiometer for Carbon Assessment

M. A. Quijada, M. E. Wilson, E. Waluschka, C. R. McClain, NASA Goddard Space Flight Ctr. (United States)

The Ocean Radiometer for Carbon Assessment (ORCA) is a new design for the next generation remote sensing of ocean biology and biogeochemistry. ORCA is configured to meet all the measurement requirements of the Decadal Survey recommend Aerosol, Cloud, and Ecology (ACE), the Ocean Ecosystem (OES) radiometer and the Pre-ACE climate data continuity mission (PACE). Under the auspices of a 2007 grant from NASA Research Opportunity in Space and Earth Science (ROSES) and the Instrument Incubator Program (IIP), a team at the Goddard Space Flight Center (GSFC) has been working on a functional prototype with flightlike fore and aft optics and scan mechanisms. As part of the development efforts to bring ORCA closer to a flight configuration and in order to reduce cost, we have conducted component-level optical testing using standard spectrophotometers and system-level characterizations using nonflight commercial off-the-shelf (COTS) focal plane array detectors. Although these arrays would not be able to handle flight data rates, they are adequate for optical alignment and performance testing. The purpose of this presentation is to describe the results of this testing performed at GSFC and the National Institute

of Standards and Technology (NIST) at the component and system level. Specifically, results for ORCA's spectral calibration ranging from the near UV, visible, and near-infrared spectral regions and polarization results will be discussed for the blue and red channels.

8153-29, Session 6

ORCA's depolarizer

E. Waluschka, M. E. Wilson, M. A. Quijada, B. McAndrew, L. Ding, NASA Goddard Space Flight Ctr. (United States)

The Ocean Radiometer for Carbon Assessment (ORCA), currently being developed at Goddard, is a hyper spectral instrument with a spectral range extending from 350nm to 880nm. Its radiometric measurement accuracy will depend, in part, on the extent to which it is insensitive to linearly polarized light. A wedge type depolarizer is used to reduce ORCA's polarization sensitivity over its entire spectral range. The choice for this approach is driven by the large spectral range and to a certain extent is also influenced by the currently orbiting SeaWiFS instrument's use of a wedge depolarizer and its low polarization sensitivity. The wedge depolarizer's design, its modeled and measured depolarization characteristics are presented.

8153-30, Session 6

Characteristics of a new type of Mie scattering volume diffuser and its use as a spectral albedo calibration standard for the solar reflective wavelength region

D. F. Heath, Ball Aerospace & Technologies Corp. (United States)

Emerging instrumental requirements for remotely sensing tropospheric trace species have led to a rethinking by some of the paradigm for SI traceability of the spectral irradiance and radiance radiometric calibrations to spectral albedo which has units of sr^{-1} which is not a SI unit. In the solar reflective wavelength region the spectral albedo calibrations of space instruments are tied often to either the spectral albedo of a solar diffuser or the Moon.

This new type of Mie scattering diffuser (MSD) is non-porous, capable of withstanding high temperatures, and is more Lambertian than PTFE a.k.a Spectralon. It has the potential of covering the solar reflective wavelength region from the UV through the SWIR. Laboratory measurements have shown that the specular reflectance component is negligible from 200 nm through 3000 nm. A 3.0 mm-thick MSD has a typical diffuse reflectance ~ 70 % and a diffuse transmittance ~20% from 250 nm to 2500 nm. The sum of the diffuse reflectance and the diffuse transmittance is ~ 90 % which indicates that internal absorption by multiple scattering is small. This MSD, a true volume diffuser, exhibits a high degree of radiometric stability which suggests that measurements of its spectral albedo at the NIST STAR II facility could provide a NIST traceable spectral albedo standard. Measurements are currently in progress on its radiometric stability under a simulated space environment of high energy ionizing and UV solar radiation for its eventual use in space as a solar diffuser.

8153-31, Session 6

RF-excited plasma lamps for use as sources in OGSE integrating spheres

A. V. Arcchi, G. A. McKee, C. N. Durell, Labsphere, Inc. (United States)

Integrating spheres for optical calibration of remote sensing cameras have traditionally been made with Quartz Tungsten Halogen (QTH) lamps because of their stability. However, QTH lamps have the spectrum of a blackbody at approximately 3000K, while remote sensing cameras

Conference 8153:
Earth Observing Systems XVI

are designed to view a sun-illuminated scene. This presents a severe significant mismatch in the blue end of the spectrum. Attempts to compensate for this spectral mismatch have primarily used Xenon lamps to augment the QTH lamps. However, Xenon lamps suffer from temporal instability that is not desirable in many applications. This paper investigates the possibility of using RF-excited plasma lamps to augment QTH lamps. These plasma lamps promise to be more stable than Xenon and have a smoother spectrum. The paper presents measurements of spectra and stability. The spectrum is measured from 320 nm to 2500 nm and the temporal stability from DC to 10 MHz. The RF-excited plasma lamps are quite small, less than 10mm in diameter and about 15 mm in length. This makes them quite suitable for designing reasonably sized reflective optics for directing their light into a small port on an integrating sphere. The paper reports on the design and testing of such an optic.

8153-32, Session 6

Using a hyperspectral image projector to test remote sensing instruments

J. P. Rice, National Institute of Standards and Technology (United States)

NIST is developing, along with several collaborators, a Hyperspectral Image Projector (HIP) for system-level performance testing of multispectral sensors. The HIP is capable of projecting realistic spatial scenes with high-fidelity spectral content into sensors. The current HIP prototype has a spatial resolution of 1024 x 768 pixels and a spectral range of 450 nm to 2400 nm, with spectral resolution from 2 nm in the visible to 5 nm in the short-wave infrared. The HIP can simulate top-of-the-atmosphere spectral radiance over a 10 mm x 14 mm, f/3 image, and this can be collimated to stimulate remote sensing instruments. Also, the spectral radiance of the projected scenes can be measured with a NIST-calibrated spectroradiometer, such that the spectral radiance projected into each pixel of the sensor under test can be accurately known. We describe the experimental characterization of the HIP, and the use of the HIP in testing remote sensing instruments.

8153-33, Session 6

Thermal stability of a 4 meter primary reflector for the Scanning Microwave Limb Sounder

R. E. Cofield IV, Jet Propulsion Lab. (United States); E. P. Kasl, DR Technologies Inc. (United States)

We describe the fabrication and thermal-stability analysis and test of a composite demonstration model of the Scanning Microwave Limb Sounder (SMLS) primary reflector, having full 4m height and 1/3 the width planned for flight. SMLS is a space-borne heterodyne radiometer which will measure pressure, temperature and atmospheric constituents from thermal emission between 180 and 660 GHz. Current MLS instruments in low Earth orbit scan pencil-beam antennas (sized to resolve about one scale height) vertically over the atmospheric limb. SMLS, planned for the Global Atmospheric Composition Mission of the NRC Decadal Survey, adds azimuthal scanning for better horizontal and temporal resolution and coverage than typical orbit spacing provides. SMLS combines the wide scan range of the parabolic torus with unblocked offset Cassegrain optics. The resulting system is diffraction-limited in the vertical plane but highly astigmatic in the horizontal, having a beam aspect ratio ~1:20. Symmetry about the nadir axis ensures that beam shape is nearly invariant over +/-65 degrees of azimuth. The antenna feeds a low-noise SIS receiver whose FOV is swept over the reflector system by a small scanning mirror. Using finite-element models of antenna reflectors and structure, we evaluate thermal deformations and the resulting optical performance for 4 orbital environments and isothermal soak. We compare deformations with photogrammetric measurements made during wide-range (ambient+[-97,+75]degrees C) thermal soak tests of the primary in a chamber. This range exceeds predicted orbital soak ranges by large

factors, implying in-orbit thermal stability of 0.21 micron rms/degree C, which meets SMLS requirements.

8153-34, Session 7

NEON ground validation capabilities for airborne and space-based imagers

J. T. McCorkel, M. A. Kuester, T. U. Kampe, National Ecological Observatory Network, Inc. (United States)

Airborne remote sensing measurements provide the capability to quantitatively measure biochemical and biophysical properties of vegetation at regional scales, therefore complementing surface and satellite measurements. The National Ecological Observatory Network (NEON) will build three airborne systems to allow for routine coverage of NEON sites (60 sites nationally) and the capacity to respond to investigator requests for specific projects. Each airborne system will consist of an imaging spectrometer, waveform lidar and high-resolution digital camera. Remote sensing data gathered with this instrumentation needs to be quantitative and accurate in order to derive meaningful information about ecosystem properties and processes. Also, comprehensive and long-term ecological studies require these data need to be comparable over time, between coexisting sensors and between generations of follow-on sensors. NEON's calibration plan for the airborne instrument suite relies on intensive laboratory, on-board, ground-based characterization as well as inter-sensor comparisons. As part of these efforts, NEON organized a pathfinder mission in September 2010 to test prototype techniques and procedures for field sampling and sensor validation. Imaging spectroscopy data from AVIRIS and waveform lidar data were acquired in addition to ecological field sampling at the Ordway-Swisher Biological Station near Gainesville, Florida. This paper presents NEON's capabilities for validation of at-sensor radiance of airborne and space-based sensors and shows results from the September 2010 pathfinder mission.

8153-35, Session 7

Comparison of diffuse sky irradiance calculation methods and effect on surface reflectance retrieval from an automated radiometric calibration test site

N. P. Leisso, J. S. Czaplak-Myers, College of Optical Sciences, The Univ. of Arizona (United States)

The Remote Sensing Group at the University of Arizona is currently refining an automated system for the absolute radiometric calibration of earth-observing sensors. The Radiometric Calibration Test Site (RadCaTS) relies on semi-permanent instrumentation at the Railroad Valley test site to collect data from which surface reflectance and an atmospheric characterization is determined. Multispectral surface reflectance is determined from calibrated ground viewing radiometers and assimilated to determine the hyperspectral reflectance used in radiative transfer calculations. The reflectance retrieval algorithm relies on an accurate determination of the diffuse sky irradiance for the time of interest. Currently, diffuse sky irradiance is modeled using the atmospheric characterization as input into MODTRAN5. This work investigates the accuracy of the diffuse sky modeling by comparing modeled results to measurements made at the test site. Diffuse sky irradiance from several alternative methods are also presented. Surface reflectance is computed for each method and compared to in-situ measurements taken with a portable spectroradiometer. Top-of-atmosphere spectral radiance results are computed for MODIS using modeled and in-situ measurements and a comparison of results is presented.

8153-36, Session 7

ROSAS: a RObotic Station for Atmosphere and Surface characterization dedicated to on-orbit calibration

A. Meygret, Ctr. National d'Études Spatiales (France); R. P. Santer, Univ. du Littoral Côte d'Opale (France); B. Berthelot, VEGA Technologies SAS (France)

La Crau test site is used by CNES since 1987 for vicarious calibration of SPOT cameras. The former calibration activities were conducted during field campaigns devoted to the characterization of the atmosphere and the site reflectances. Since 1997, an automatic photometric station (ROSAS) was set up on the site on a 10m height pole. This station measures at different wavelengths, the solar extinction and the sky radiances to fully characterize the optical properties of the atmosphere. It also measures the upwelling radiance over the ground to fully characterize the surface reflectance properties. The photometer samples the spectrum from 380nm to 1600nm with 9 narrow bands. Every non cloudy days the photometer automatically and sequentially performs its measurements. Data are transmitted by GSM (Global System for Mobile communications) to CNES and processed. The photometer is calibrated in situ over the sun for irradiance and cross-band calibration, and over the Rayleigh scattering for the short wavelengths radiance calibration. The data are processed by an operational software which calibrates the photometer, estimates the atmosphere properties, computes the bidirectional reflectance distribution function of the site, then simulates the top of atmosphere radiance seen by any sensor over-passing the site and calibrates it.

This paper describes the instrument, its measurement protocol and its calibration principle. Calibration results are discussed and an error budget is presented. It details the surface reflectance characterisation and presents SPOT4 and SPOT5 calibration results deduced from the estimated TOA radiance. The results are compared to these sensors official calibration

8153-59, Poster Session

Radiometric quality of the MODIS bands at 667 and 678nm

G. Meister, B. A. Franz, NASA Goddard Space Flight Ctr. (United States)

The MODIS instruments on Terra and Aqua were designed to allow the retrieval of fluorescence effects over ocean. The high radiometric accuracy needed to retrieve the small fluorescence signal lead to a dual gain design for the 667 and 678nm bands. This paper discusses the benefit obtained from this design choice and provides justification for the use of only one set of gains for global processing. Furthermore, other radiometric artifacts and algorithm issues impacting the fluorescence products are evaluated as well, especially instrument straylight contamination. The straylight contamination is evaluated in case studies at ocean/cloud boundaries. The performance of the two units on Terra and Aqua is compared. Since the radiometric trending of the MODIS Terra red bands has been tied to the MODIS Aqua red bands by NASA's Ocean Biology Processing Group, the focus of this paper is on the MODIS Aqua products.

8153-60, Poster Session

Using the moon for Terra MODIS MTF characterization

Z. Wang, T. J. Choi, Sigma Space Corp. (United States); X. Xiong, NASA Goddard Space Flight Ctr. (United States)

The on-orbit MTF of MODIS instrument can be accurately measured by

its on-board SpectroRadiometric Calibration Assembly (SRCA). For other earth-observing instruments without calibrators similar to SRCA, the sharp edge of the moon can provide a reasonable high-contrast target for their on-orbit MTF characterization. In this paper, we propose a method to characterize MODIS MTF using its lunar observations and present the results for Terra MODIS over its entire mission. For each lunar calibration event, the images of the moon from multiple scans are taken and traced across the right edge to form an edge spread function (ESF). The ESF is used to calculate the line spread function (LSF) through differentiation. The MTF in along-scan direction is then derived through the Fourier Transform of LSF. We will show that the long-term trending of lunar MTF generally agrees with that derived from the SRCA. As expected, lunar MTF results show relatively large variations. This is mainly because of the lunar surface non-uniformity and the sensor's low spatial resolution, making it difficult to accurately locate the lunar edge in a sub-pixel level. Improvements to the current method are also discussed in this paper.

8153-61, Poster Session

Characterization of MODIS mirror-side dependent response in the reflective solar spectral region

X. Geng, Sigma Space Corp. (United States); A. Angal, Science Systems and Applications, Inc. (United States); J. Sun, A. Wu, T. J. Choi, Sigma Space Corp. (United States); X. Xiong, NASA Goddard Space Flight Ctr. (United States)

The MODIS instruments onboard the Terra and Aqua spacecrafts, launched in December 1999 and May 2002, respectively, have successfully operated through the present time. MODIS collects the earth view (EV) data via a two-sided paddle wheel scan mirror at angles of incidence (AOI) from 10.5 to 65.5 degrees. This paper describes the methodologies used to characterize MODIS reflective solar bands (RSB) EV mirror-side dependent responses and calculate on-orbit changes in their relative responses versus scan angle (RVS). It evaluates the long-term trends of response differences between two mirror sides using different EV targets. Results show that the on-orbit changes in the properties of the scan mirror are wavelength and AOI dependent with large changes seen at shorter wavelengths and larger AOI. Starting from 2005, the mirror-side dependent responses have gradually exhibited some seasonal dependent features in a few Terra MODIS visible spectral bands, which are mainly due to changes in the scan mirror's polarization properties. In addition to fully characterizing on-orbit changes of MODIS scan mirror properties, results and discussions provided in this paper will help understand their impact on the Level 1B data products and support our future effort to maintain MODIS data quality.

8153-63, Poster Session

The VIIRS ocean data simulator enhancements and results

W. D. Robinson, F. S. Patt, SAIC (United States) and NASA Goddard Space Flight Ctr. (United States); B. A. Franz, NASA Goddard Space Flight Ctr. (United States); K. R. Turpie, SAIC (United States) and NASA Goddard Space Flight Ctr. (United States); C. R. McClain, NASA Goddard Space Flight Ctr. (United States)

The VIIRS Ocean Science Team (VOST) has been developing a VIIRS Ocean Data Simulator to create realistic VIIRS SDR datasets based on MODIS water-leaving radiances. The simulator is helping to assess instrument performance and scientific processing algorithms. Several changes were made in the last two years to complete the simulator and broaden its usefulness.

The simulator is now fully functional and includes all sensor characteristics measured during prelaunch testing including electronic and optical crosstalk influences, polarization sensitivity, and relative

Conference 8153:
Earth Observing Systems XVI

spectral response. Also included is the simulation of cloud and land radiances to make more realistic data sets and to understand their important influence on ocean color data when combined with instrument artifacts. The tables used in the processing including aerosol and Rayleigh radiances have been modeled using VIIRS relative spectral responses.

The capabilities of the simulator were expanded to work in an unaggregated sample mode and to produce scans with additional samples beyond the standard scan. Both these features improve the capability to realistically simulate artifacts which act on individual instrument samples and which may originate from beyond the actual scan boundaries. The simulator was expanded to simulate all 16 M bands and the EDR processing was improved to use these bands to make an SST product.

The simulator is being used to generate global VIIRS data from and in parallel with the MODIS Aqua data stream. Instrument artifact impact studies have also been conducted using the simulator. This paper discusses the simulator improvements and results from the global processing and artifact impact studies.

8153-64, Poster Session

Remote monitoring systems

F. Mkrtchyan, Institute of Radio Engineering and Electronics (Russian Federation)

Now wide development in the world is received by multichannel monitoring systems of remote basing. Such systems allow to receive the operative information on an environment condition in different scales.

These systems the important place is occupied with the systems focused on studying of water systems. The technique of detection offered in given work and identification of the abnormal phenomena in the water environment (microwave and optical) combines presence with application of possibilities of remote measurements algorithmic and the software, allowing to solve measurement and detection problems in real time.

The effective decision of these problems is impossible without wide introduction in practice of researches of the automated systems of gathering, storage and data processing on the basis of modern computer systems with application of technology of open systems.

Already created methods and algorithms possess ability to overcome such difficulties, as scantiness and not stationarity information, presence small statistically non-uniform samples.

It is obvious that complex research of the given land and remote measurements can raise reliability of estimations of parameters of natural systems and solve a problem of planning of these measurements. Application of means of remote monitoring in many cases is connected with acceptance of the statistical decision on presence on a surveyed part of studied space of this or that phenomenon. One of features of conditions of gathering of the information for such decision is the impossibility of reception statistical samples great volumes. Therefore working out and research of optimum algorithms of distinction of the casual signals characterized by samples of the limited volume, in the conditions of parametrical aprioristic indefinite are necessary.

8153-65, Poster Session

Results of MODIS band-to-band registration characterization using on-orbit lunar observations

X. Xiong, NASA Goddard Space Flight Ctr. (United States); J. Sun, Sigma Space Corp. (United States); A. Angal, Science Systems and Applications, Inc. (United States)

Since launch, lunar observations have been made regularly by both Terra and Aqua MODIS and used for a number of sensor calibration and characterization related applications, including radiometric stability

monitoring, spatial characterization, optical leak and electronic cross-talk characterization, and calibration inter-comparison. MODIS has 36 spectral bands with a total of 490 individual detectors. They are located on four focal plane assemblies (FPA). This paper focuses on the use of MODIS lunar observations to characterize its band-to-band registration (BBR). In addition to BBR, the approach developed by the MODIS Characterization Support Team (MCST) can be used to characterize MODIS detector-to-detector registration (DDR). Long-term BBR results developed from this approach are presented and compared with that derived from a unique on-board calibrator (OBC). Results show that on-orbit changes of BBR have been very small for both Terra and Aqua MODIS and this approach can be applied to other remote sensing instruments.

8153-66, Poster Session

Enabling radiometric validation and on-orbit calibration: flight software of the CERES scanning radiometer

K. K. Teague, G. L. Smith, Science Systems and Applications, Inc. (United States); K. J. Priestley, NASA Langley Research Ctr. (United States)

Five CERES scanning radiometers have been flown to date. The Proto-Flight Model flew aboard the Tropical Rainfall Measuring Mission spacecraft in November 1997. Two CERES instruments, Flight Models (FM) 1 and 2, are aboard the Terra spacecraft, which was launched in December 1999. Two more CERES instruments, FM-3 and FM-4, are on the Aqua spacecraft, which was placed in orbit in May 2002. These instruments continue to operate after providing over a decade of Earth Radiation Budget data. FM-5 has been integrated to the NPP spacecraft, scheduled for launch this year. Another CERES instrument, FM-6, is being built for use on the JPPS C-1 spacecraft and a successor to these CERES instruments is presently in the definition stage. This paper describes the evolving role of flight software in the operation of these instruments to accomplish the Science objectives of the mission and also to enable execution of supplemental tasks. The CERES software interface was designed to allow for on-orbit modification, and as such, constantly evolves to meet changing needs.

The CERES flight software was originally written in the early 1990's by Walter Mallory of the Space Division of TRW, now Northrop-Grumman, using C code. There are two sets of software in each CERES instrument, each running on an Intel 80C186 processor. The Data Acquisition Processor (DAP) controls the elevation scanning mechanism, the contamination covers, internal calibrations, and the thermal control subsystem. The Instrument Control Processor controls the azimuth scanning assembly, internal sequences, and is responsible for the spacecraft and DAP interfaces.

8153-67, Poster Session

The measured point response functions of the CERES Flight Model 5 instrument

J. L. Daniels, G. L. Smith, Science Systems and Applications, Inc. (United States); K. J. Priestley, NASA Langley Research Ctr. (United States); H. Biting, Northrop Grumman Corp. (United States)

The Clouds and Earth Radiant Energy System (CERES) Flight Model 5 instrument is scheduled to be placed in orbit aboard the NPP spacecraft in order to continue the Climate Data Record for Earth radiation budget. The CERES instrument is a three channel radiometer and measures solar radiation reflected by the Earth, radiation emitted by the Earth and radiation in the 8 to 12 micron window of the atmosphere. CERES data will be used together with measurements from the VIIRS (Visible Infra-red Imager Radiometer Suite), also on the NPP, to compute cloud information for each CERES pixel. The VIIRS pixels are an order of magnitude

Conference 8153:
Earth Observing Systems XVI

smaller than those of CERES, so it is necessary to know the response of the instrument to a point within the CERES field of view as it scans. This effect is denoted the point response function (PRF). Knowledge of the PRF is also needed to validate accurately the geo-location of the CERES measurements. The Radiative Calibration Facility of the Space Division of Northrup-Grumman, the designer and builder of the CERES instruments, includes the PRF Source, which is an optical device for measuring the PRF. The PRF Source provides a suitable light beam which is measured by the CERES instrument as it scans in vacuum. This paper presents the analysis of these tests and the resulting PRF for each of the three channels and compares the measured PRFs to that predicted theoretically.

8153-69, Poster Session

Initial operation results of in-orbit radiometric calibration for geostationary ocean color imager

S. Cho, S. Lee, E. Oh, H. Han, Y. Ahn, J. Ryu, Korea Ocean Research & Development Institute (Korea, Republic of)

As the world's 1st ocean color observation satellite in geostationary orbit, Geostationary Ocean Color Imager(GOCI) was successfully co-developed by Korea Aerospace Research Institute (KARI) and EADS Astrium in France by the request and supervision of the Korea Ocean Research & Development Institute (KORDI).

GOCI was successfully launched at Kourou Space Center in French Guiana by Ariane 5 ECA Launch Vehicle in 27 June 2010(KST). After the successful launch, GOCI in-orbit test campaign was operated for sensor validation during six months. From the first half of 2011, nominal operation and data distribution service of GOCI is planned under the responsibility of the Korea Ocean Satellite Center(KOSC) in KORDI. During the in-orbit test campaign, GOCI functional test for the performance check of GOCI sub-systems. GOCI radiometric tests was followed after the success of GOCI functional test. GOCI radiometric model, the reference internal radiative transfer function of GOCI H/W, was characterized by the GOCI Solar calibration image acquisition. GOCI radiometric linear gains calculated from initial in-orbit solar calibration varies about 5% comparing with the ground test results. For the GOCI in-orbit radiometric calibration, Solar Diffuser and Diffuser Aging Monitoring Device(DAMD) are implemented into shutter wheel of GOCI. Diffuser aging monitoring is operated from GOCI in-orbit radiometric test. In-orbit measured GOCI diffuser aging factor for six months during GOCI in-orbit tests is about 3%. In this paper, we present the initial operation results of preliminary characterization result of GOCI in-orbit solar calibration operated at in-orbit test period.

8153-70, Poster Session

NPP VIIRS geometric performance status

G. Lin, INNOVIM (United States); R. E. Wolfe, NASA Goddard Space Flight Ctr. (United States); M. Nishihama, Sigma Space Corp. (United States)

Visible Infrared Imager Radiometer Suite (VIIRS) instrument on-board the National Polar-orbiting Operational Environmental Satellite System (NPOESS) Preparatory Project (NPP) satellite is scheduled for launch in October, 2011. The instrument geometric performance includes sensor (detector) spatial response, band-to-band co-registration (BBR) and pointing stability. They have been calibrated and characterized through ground testing under ambient and thermal vacuum conditions, numerical modeling and analysis. This paper summarizes the results, along with anomaly investigations, and describes paths forward for characterizing on-orbit BBR and spatial response, and for improving instrument on-orbit performance in pointing and geolocation.

VIIRS sensor spatial response is measured by line spread functions (LSFs) in the scan and track directions for every detector. We parameterize the LSFs by: 1) dynamic field of view (DFOV) in the

scan direction and instantaneous FOV (IFOV) in the track direction; 2) modulation transfer function (MTF) for the 17 moderate resolution bands (M-bands); and 3) horizontal spatial resolution (HSR) for the five imagery bands (I-bands). We define VIIRS BBR for M-bands and I-bands as the overlapped fractional area of angular pixel sizes from the corresponding detectors in a band pair, including nested I-bands with M-bands. The ground tests result in static BBR matrices. VIIRS pointing stability includes scan plane tilt, scan rate and scan start position variations, and thermally induced pointing variations with respect to orbital position. These will be tracked or corrected.

8153-71, Poster Session

High-temperature fixed points for pre-launch calibration of Earth observing sensors

Y. Yamada, J. Ishii, National Institute of Advanced Industrial Science and Technology (Japan)

Radiometric pre-launch calibration of earth observing multispectral sensors such as ASTER was performed traceable to defining fixed-point blackbodies of the International Temperature Scale of 1990. The highest temperature of these is the copper point at 1357.77 K, which was sufficient for the calibration of the shortest band at around 560 nm. However, with the next generation hyperspectral sensors with the spectral band extending down to 400 nm, the copper point blackbody radiance drops rapidly and decreases by two orders of magnitude from that at 560 nm. Therefore, a fixed-point of higher temperature, possibly around 2000 K, is desired.

The authors have proposed high-temperature fixed points of metal-carbon systems for temperature standards use, which have now become a part of the high-temperature traceability system in Japan as well as in other countries. Application of these fixed points to hyperspectral sensor calibration is of high interest.

In this presentation, a fixed-point cell of Co-C eutectic (1597 K) for remote sensor calibration application is described. To enable alignment of the radiance comparator utilizing a grating monochromator, an enlarged aperture design is employed for the fixed-point cell while at the same time retaining the outer dimension to fit in existing fixed-point furnaces. Extension of the technique to Pt-C eutectic (2011 K) or Cr₃C₂-C peritectic (2100 K) systems is envisaged.

8153-73, Poster Session

Effects of geometric misregistration on cross-calibration of sensors

G. Chander, R. Rengarajan, U.S. Geological Survey (United States); A. Shrestha, Science Systems and Applications, Inc. (United States); D. L. Helder, South Dakota State Univ. (United States)

The appearance of the ground areas in images captured by sensors may vary due to differences in sensor type, sensor altitudes, imaging, and viewing geometry. This can make image registration extremely difficult for data acquired even on the same-day within a few minutes apart. The effect of viewing geometry on the appearance of images is even more pronounced in sensors with a large view angle. Image registration plays a significant role in providing accurate cross-calibration results and can be a major source of error when cross-calibration is performed using the region of interest (ROI) from image pairs. In general, to minimize the effect of misregistration and spatial non-uniformity, large homogenous regions are preferred for cross-calibration. However, the uncertainty caused by image misregistration needs to be investigated for better understanding of cross-calibration uncertainty among various imaging platforms. This paper presents the results of the sensitivity study to determine the effect of misregistration of the ROI in several images. Five representative land cover types (desert, rangeland, grassland, deciduous forest, and coniferous forest) were selected for the study. Several cloud-free images acquired over the lifetime of the Landsat 5 Thematic Mapper (TM) sensor

Conference 8153:
Earth Observing Systems XVI

were selected from each site, and a moving window technique was used to model potential misregistration within standard image products.

8153-74, Poster Session

Calibration of the AVHRR near-infrared (0.86 μm) channel at the Dome C site

S. Uprety, C. Cao, National Oceanic and Atmospheric Administration (United States)

AVHRR is a heritage polar instrument with more than 30 years of global earth observation. Due to absence of onboard calibrator for VNIR channels, AVHRR sensors relies on desert sites for relative calibration with uncertainties primarily due to lack of rigorous site characterization and atmospheric effects. This study aims at quantifying the long term degradation of near-infrared channel (0.86 μm) of AVHRR using Antarctic Dome C site which has very small atmospheric effects. All afternoon-orbit NOAA series AVHRR instruments are considered for this study. Though the TOA reflectance data exists only during austral summer for Dome C, the degradation estimated using TOA reflectance time series for the respective instruments is comparable to those from the previous studies. The degradation estimated suggests that NOAA-7 and -9 have largest drift (more than -3% per year) compared to the other instruments which have less than -1.5% drift per year. The AVHRR channel 2 (0.86 μm) calibration using desert sites has always been challenging due to high uncertainty mainly introduced by the presence of water vapor absorption wavelength. The study shows that, due to extremely cold and dry climate of Dome C, the water vapor absorption effect is negligible and thus it is possible to calibrate near-infrared (0.86 μm) channel with calibration uncertainty less than 1%.

8153-76, Poster Session

Evaluation of climate change in 40 years by using AIRS and IRIS hyperspectral infrared measurements

Y. Jiang, H. H. Aumann, Jet Propulsion Lab. (United States); M. Lau, Y. Yung, California Institute of Technology (United States)

Outgoing longwave radiation (OLR) measurements over a long period from satellites provide valuable information for the climate change research. Due to the different coverage, spectral resolution and instrument sensitivities, the data comparisons between different satellites could be problematic and possible artifacts could be easily introduced. We have analyzed the data taken by IRIS in 1970 and by AIRS from 2002 to 2010. We used the spectra between 650 cm^{-1} and 1350 cm^{-1} for nadir view footprints in order to match the IRIS's measurements. Most of the possible sources of error or biases have been carefully handled, these include the errors from the data editing, spatial coverage, missing data (spatial gap), and spectral resolution, spectra frequency shift due to the fields of view, sea surface temperature fluctuations, clear sky determination, and spectra response function symmetry. It is extremely important when comparing spectra in the high slope spectra regions where possible large artifacts could be introduced.

8153-77, Poster Session

A comparison of ice cloud and dust aerosol physical characteristics in Taklimakan desert

Y. Ma, W. Gong, Wuhan Univ. (China)

Classification is an indispensable step in spaceborne lidar data processing. The depolarization signal is achieved from the perpendicular channel divided by the parallel channel at 532 nm. It is a very helpful parameter; and makes a description of the particle's shape. In general, common aerosol is spherical and dust aerosol is crystalline and non-

spherical, but the relationship also exists between ice cloud and water cloud. If we directly add the depolarization ratio to classifier as a higher dimension scheme, this just makes the ice cloud and dust aerosol more confusable, and it becomes more difficult to discriminate the ice cloud and dust aerosol, the precision of aerosol retrieval cannot be further improved.

We try to improve the performance of classifier, so the physical characteristics of cloud/dust layer are the important reference for future study. In this paper, the Aqua-MODIS remote sensing image is introduced, though these data the dust and cloud is easy classified by eyes. Then select the synchronous observations from CALIPSO, after finding the layers altitude and calculating their physical characteristics (depolarization ratio, attenuated backscattering and so on). By choosing a dust storm happened in Taklimakan deserts, 2007, we can find some different exist between them. For example, the cloud exist at N: 40°-41° and N: 44°-44.5° is altocumulus, and the clouds top exceed 10km and 5km respectively, the depolarization ratio of clouds is higher than aerosol, the average value are 0.436 and 0.384 respectively. Compared with dust aerosol, the non-spherical characteristic of ice cloud expressed more obviously. Clouds and aerosol yielded large color ratio value, but compare these two clouds, the color ratio are 1.03999 and 1.16094 respectively. This means the size of ice particles in the higher altitude are smaller than the lower altitude.

8153-78, Poster Session

Angular variation of GOES imager scan mirror reflectance

X. Wu, National Oceanic and Atmospheric Administration (United States); D. Ryan-Howard, Massachusetts Institute of Technology (United States); T. C. Stone, U.S. Geological Survey (United States); G. Sindic-Rancic, F. Yu, National Oceanic and Atmospheric Administration (United States); M. Weinreb, Riverside Technology Inc. (United States); M. Grotenhuis, National Oceanic and Atmospheric Administration (United States)

As the GOES Imager scans along the east-west direction, the angle of light incident upon the Imager's scan mirror varies from approximately 40° to 50°. The scan mirror emissivity in the infrared spectrum varies slightly with incidence angle. This variation has been quantified before launch with measurements on witness samples in the laboratory and after launch with measurements of space scans, and the observations have been properly corrected on orbit to ensure data quality (Weinreb et al. 1997). It has long been hypothesized that the Imager scan mirror reflectance in the visible spectrum may also vary with incidence angle. Recent advances in laboratory measurement and vicarious calibration using the Moon make it possible to examine this hypothesis, both in laboratory and on orbit, in a similar way as for the infrared channels. The research is on-going and will be reported at the conference.

8153-79, Poster Session

Topographic mapping experiment with Chinese airborne SARMapper

J. Zhang, Chinese Academy of Surveying and Mapping (China); Z. Zhao, Wuhan Univ. (China); G. Huang, Chinese Academy of Surveying and Mapping (China)

Aiming for steep terrain relief and complex geomorphic types, the practical airborne SAR mapping system of China developed by a group led by CASM was constructed. Some factors limit the application of airborne SAR mapping such as geometric and radiometric distortion, shadow, difficult field work etc. In order to cope with these shortcomings, some new methods and mapping technical flow were proposed according to difficult terrain area covered by cloud, fog, ice, and snow perennially, lush vegetation and diverse species, steep terrain etc. Face to challenges how to get precise DEM, Digital Orthophoto Map

Conference 8153:
Earth Observing Systems XVI

(DOM), and Digital Line Graphic map (DLG), several key technologies and solutions were studied, such as DEM extraction through refined interferometry, stereogrammetry, and DEM fusion, DOM generation with single/multi-polarization or single/quad-polarization SAR images acquired from multi-direction, DLG generation under stereo-environment. Based on these technologies, SAR mapping workstation is used to map in such a large area of difficult terrains. It can be used to process airborne and spaceborne SAR images to produce DOM, DEM and DLG. And then the comprehensive experiment in Qinling Mountain Area was carried on. Firstly, interferometric parameters were calibration by angle reflector. Secondly, different resolution of X band interferometric SAR and P band polarimetric SAR data were acquired by the integrated airborne SAR data acquisition system. Finally, mapping experiments in scale of 1:10000 and 1:50000 were carried on these areas, and mapping production was generated by the SAR mapping workstation. Experimental results have proved that the system works well. The production could satisfy the mapping accuracy of 1:10000 and 1:50000.

8153-80, Poster Session

A ground-based hyperspectral sensor system: field imaging spectrometer system (FISS)

J. Wang, Institute of Remote Sensing Applications (China); L. Zhang, J. Yan, Institute of Remote sensing Applications (China); Q. Tong, Institute of Remote Sensing Applications (China)

Recently, to stimulate the development of the field imaging spectrometry in China, we have developed a new ground-based hyperspectral sensor system: Field Imaging Spectrometer System (FISS). This paper describes the main performance and preliminary applications of the China's first field imaging spectrometer system, including its imaging principle, structural design, main technology parameters, and its latest field applications. Before the specific applications, the FISS was accurately spectrally, radiometrically and spatially calibrated in the laboratory, which largely ensured its afterwards quantitative applications reliable. Laboratory calibration results provided a profound understanding of the FISS system. The FISS covers a VIS/NIR spectral range of 437-902 nm, which is split into 344 spectral channels. The spectral resolution of each channel was precisely calibrated better than 5 nm; meanwhile absolute radiometric calibration of the FISS with less than 5% calibration error for each band was achieved using a well calibrated integrating sphere. There are 215 channels with signal to noise ratios (SNRs) greater than 500 (62.5% of the bands). In addition, through spatial calibration in the laboratory, the spatial resolution of the FISS nearly reaches its theoretical level with the instantaneous field of view (IFOV) of 1mrad. The high performance levels in spectral, radiometric and spatial responses achieved by the FISS implicated its potential applications in various fields, including geology, food science, agriculture, forestry, and urban research. Fortunately our recent applications in crop-weed discrimination, offshore marine environment monitoring, milk discrimination, and estimation of vegetation biochemical information using the FISS have Preliminary confirmed the perfect ability in its field measurements and applications.

8153-81, Poster Session

Atmospheric correction of HJ-1 A/B CCD over land

Q. Fu, Institute of Remote Sensing Applications (China) and China Ctr. for Resource Satellite Data and Applications (China); X. Min, China Ctr. for Resource Satellite Data and Applications (China); L. Sun, Shandong Univ. of Science and Technology (China)

Atmosphere is a large uncertainty factor in the surface reflectance measurement, when examining the Earth's surface from a satellite

platform. Atmospheric correction is one of the key elements to obtain accurate Geographical and biophysical products for earth observation purposes. The algorithms of atmospheric correction continue to be refined and improved in these years.

HJ-1 A/B CCD is one of the key instruments operating on HJ-1 A/B satellites, launched on September 6, 2008 by China, with a spatial resolution of 30 meters. HJ-1 A/B CCD has three visible bands and one near-IR band. The combination of two CCD cameras can get a swath width of 700 km and revisit per 48-hour. However, for lacking of shortwave infrared band, especially bands near 2.1 μ m, atmospheric correction of HJ-1 A/B CCD over land is very hard. To facilitate the operational atmospheric correction of HJ-1 A/B CCD datasets, a new algorithm of HJ-1 A/B CCD AOD retrieval is developed by introducing MODIS surface reflectance products (MOD09) as base-knowledge. HJ-1/ CCD blue band surface reflectance was retrieved through MOD09 blue band surface reflectance by band matching of the two sensors, and aerosol optical thickness was retrieved based on it.

In this paper, On the basis of sensitivity analysis on atmospheric condition and the geometry, the look-up table (LUT) of atmospheric correction coefficient is created using 6S. The calculated reflectance of HJ-1 A/B CCD was compared with the in-situ measurement reflectance and the MODIS surface reflectance outputs (MOD09), results indicated that this proposed atmospheric correction method has a preferable precision.

8153-37, Session 8

CERES FM-5 on the NPP Observatory: predicted performance and early orbit validation plans

K. J. Priestley, NASA Langley Research Ctr. (United States); G. L. Smith, S. Thomas, Science Systems and Applications, Inc. (United States)

To understand our climate, it's necessary to understand energy flows which govern movements and temperatures of the atmosphere and oceans. Solar radiation absorbed by the Earth and its emission as outgoing longwave radiation (OLR) are the heat source and heat sink for this heat engine. The Clouds and Earth Radiant Energy System (CERES) Flight Model FM-1 and FM-2 sensors aboard Terra and the FM-3 and FM-4 sensors aboard the Aqua spacecraft have provided the first CERES observed decadal Earth Radiation Climate Data Record (CDR). To assure continuity of this CDR the CERES FM-5 sensor will fly on the NPP spacecraft, scheduled for launch in October 2011.

In late 2006, FM-5 was removed from storage and completed abbreviated radiometric characterization tests to verify performance. In 2008, the sensor was re-manifested on the NPP mission, removed from storage, the interfaces modified, and again subjected to the full pre-launch radiometric characterization campaign. Integration on the NPP spacecraft occurred in 2008 with environmental and performance testing executed at the observatory level.

NPP's orbit will have the same inclination but higher altitude than Aqua. The Early Orbit Validation & Calibration campaign will consist of exercising all operational modes of the sensor, characterizing scan angle dependent offsets, observing the onboard calibration sources to establish traceability to the pre-launch radiometric scale, as well as initiate the intercalibration opportunities with other CERES sensors which are operating on NASA's Terra and Aqua missions.

8153-38, Session 8

Pre-launch sensor characterization of the CERES Flight Model 5 (FM5) instrument on NPP mission

S. Thomas, Science Systems and Applications, Inc. (United States); K. J. Priestley, NASA Langley Research Ctr. (United States)

Conference 8153:
Earth Observing Systems XVI

States); M. Shankar, N. P. Smith, M. G. Timcoe, Science Systems and Applications, Inc. (United States)

Clouds and the Earth's Radiant Energy System (CERES) instrument was designed to measure broadband radiances in reflected shortwave and emitted outgoing longwave energy. The 3-sensor CERES instrument measure radiances in 0.3 to 5.0 micron region with Shortwave sensor, 0.3 to >100 microns with Total sensor and 8 to 12 micron region with Window sensor. Flight Model 5, the sixth of the CERES instruments is scheduled to launch aboard the NPP spacecraft on October 2011. An accurate determination of the radiometric gains and spectral responsivity of CERES FM5 sensors was accomplished through rigorous calibrations at Northrop Grumman Aerospace Systems' (NGAS) Radiometric Calibration Facility (RCF). The longwave calibration of the total and window sensors are achieved using the Narrow Field-of-View Blackbody (NFBB) source which is tied to International Scale of 1990 (ITS '90). A Shortwave Reference Source (SWRS) along with the Transfer Active Cavity radiometer (TACR) which acts as the transfer standard of NFBB source, is used to determine the radiometric responsivity and spectral response estimates of the SW sensor and shortwave portion of the Total sensor. The spectral responsivity in longwave region is determined using a Fourier Transform Spectrometer (FTS) system. CERES instrument also perform calibrations using on-board sources during pre-launch testing which serve as a traceability standard to carry the ground determined sensor radiometric gains to orbit. This paper covers the calibration philosophy and the results from ground calibration testing of FM5 sensors conducted in 2008. The sensor radiometric gain responses calculated using primary sources and performance of the sensors using on-board sources will be discussed.

8153-39, Session 8

**On-orbit solar calibration contamination/
degradation effects on the Clouds and Earth's
Radiant Energy System (CERES) in-flight
calibration system**

R. S. Wilson, Science Systems and Applications, Inc. (United States); K. J. Priestley, NASA Langley Research Ctr. (United States); S. Thomas, P. C. Hess, Science Systems and Applications, Inc. (United States)

The Clouds and Earth's Radiant Energy System (CERES) scanning thermistor bolometers measure earth-reflected solar and earth-emitted long-wave radiances. The bolometers measure the earth radiances in the (0.3-5.0 microns), (0.3->100 microns) (8->12) microns spectral bands. December 1999, the second and third set of CERES sensors were launched on the Terra Spacecraft. May 2003, the fourth and fifth set of bolometers was launched on the Aqua Spacecraft. The mirror attenuator mosaic (MAM), a solar diffuser plate, was built into the CERES instrument package calibration system in order to define in-orbit shifts or drifts in the sensor responses. The MAM diffuser reflecting type surface consists of an array of spherical aluminum mirror segments, which are separated by a Merck Black A absorbing surface. In their first year of operation the Terra and Aqua MAMs showed shifts in their calibrations larger than expected. Shifts of this nature have been seen in other Solar viewing instruments in the past. A possible explanation has attributed change to pre-orbit or on-orbit contamination/degradation combined with solar ultraviolet/atomic oxygen induced chemical changes to the diffuser plate or contaminant during solar exposure. The synergistic effect of these elements can affect the optical properties of the spherical mirror segments and the black absorbing mask. In this paper, the results of a literature search and lab experiments to zero in on possible physical and chemical mechanisms which can explain the observed elements of the CERES solar calibration time-series will be presented. Comparisons are also made between the TRMM, Terra and the Aqua CERES instruments during their MAM solar calibrations.

8153-40, Session 8

**Infrared sensitivity study of the Clouds and
Earth's Radiant Energy System (CERES)
Instrument Sensors**

M. Shankar, S. Thomas, Science Systems and Applications, Inc. (United States); K. J. Priestley, NASA Langley Research Ctr. (United States); D. R. Walikainen, Science Systems and Applications, Inc. (United States)

The Clouds and Earth's Radiant Energy System (CERES) mission currently employs four instruments onboard two spacecraft to measure the earth's reflected shortwave energy and the earth emitted thermal energy that represent the two components of the earth's energy budget. These measurements are made through three sensors that measure different spectral regions- a Shortwave channel that measures the 0.3 to 5 microns wavelength band, a Total channel that measures all the incident energy (0.3 to 200 microns) and a Window channel that measures the 8 to 12 micron wavelength band. The radiances measured in each channel (filtered radiances) are used to estimate the incident (unfiltered) shortwave and longwave radiances using knowledge of the response functions of each of the measurement channels as well as theoretical knowledge of the energy spectrum of the particular earth scene being measured. For longer wavelengths particularly in the far infrared, both the earth scene spectra as well as the instrument spectral response functions are not very well characterized because of the difficulties in obtaining models for the earth scene spectra as well as the limitations in the capabilities to measure the spectral responses over a very large spectral range. This results in errors in obtaining estimates of the unfiltered radiances. This paper will focus on studying the sensitivity of the CERES sensors to these inaccuracies and its impact on the errors in estimation. In addition, those spectral regions in the longwave infrared where the CERES instruments are most sensitive will be identified.

8153-41, Session 8

**The CERES calibration strategy of the
geostationary visible channels for CERES
cloud and flux products**

D. Morstad, Science Systems and Applications, Inc. (United States); D. R. Doelling, NASA Langley Research Ctr. (United States); B. R. Scarino, R. Bhatt, Science Systems and Applications, Inc. (United States)

The Clouds and Earth's Radiant Energy System (CERES) project has greatly improved the understanding of the role of clouds and energy cycles in global climate studies. CERES flux and cloud properties rely on not only CERES broadband fluxes and MODIS cloud properties but also relies on operational geostationary (GOES, METEOSAT, MTSAT) derived fluxes and clouds in between CERES measurements to properly account for the diurnal cycle. The high quality of the CERES products relies on a consistent radiometric calibration of the un-calibrated geostationary visible sensors and MODIS. To achieve this consistency, the calibration of a reference sensor must be transferred to the other instruments.

Historically, Terra-MODIS and Aqua-MODIS, both of which employ solar diffusers, have been regarded as having a well-calibrated visible channel (650 nm). Recent analysis has revealed that the Aqua-MODIS instrument to be more stable than the MODIS instrument onboard the Terra satellite. For this reason, Aqua-MODIS has been chosen as the reference sensor while Terra-MODIS adjustments can be used to put it on the same radiometric scale as Aqua-MODIS. The ray-matching technique can be used to transfer the calibration of the well-calibrated MODIS instrument to the un-calibrated GEO sensors. Additionally, empirically derived BRDF models for pseudo-invariant test sites and deep convective clouds (DCC) have been developed and applied for monitoring and validating the GEO calibration.

Latest results include GEO calibration updates for the 2000-2010

Conference 8153:
Earth Observing Systems XVI

time period where Aqua/Terra-MODIS cross calibration trends are in agreement with calibration trends obtained from pseudo-invariant test sites and DCC. These results are in preparation for CERES Edition4 products, which will include updated geostationary calibration coefficients and cloud retrieval improvements.

8153-42, Session 9

Using MODIS to calibrate NOAA series AVHRR reflective solar channels

A. Wu, Sigma Space Corp. (United States); A. Angal, Science Systems and Applications, Inc. (United States); X. Xiong, NASA Goddard Space Flight Ctr. (United States)

Nearly 30 years of continuous observations made by a series of AVHRR sensors have offered a great potential for studies of global environment and climate change. In order to achieve this objective, each sensor must be accurately and consistently calibrated. This is not an easy task as there is no onboard calibrator for AVHRR solar reflective channels and vicarious calibration often needs to accumulate enough observations to derive useful trends. In this study, we select CEOS (the Committee on Earth Observation Satellites) endorsed Cal/VaI desert sites to track the long-term stability of reflective solar channels of NOAA-17 AVHRR (launched on June 24, 2002) and re-calibrate them using well-calibrated MODIS as reference. A site-specific Bi-directional Reflectance Distribution Function (BRDF) developed based on observations made by MODIS is used to normalize AVHRR observed reflectances. Impacts of atmospheric water vapor on AVHRR to MODIS reflectance ratios are corrected with the total water vapor content derived from the split-window temperature difference technique. Finally, MODIS-based AVHRR calibration coefficients on top of its prelaunch values are provided in time-dependent look-up tables (LUT). A further validation is performed using MODIS and AVHRR observations obtained over Antarctic Dome C site where impact due to atmospheric water vapor is negligibly small.

8153-43, Session 9

Long-term cross-calibration of the Terra ASTER and MODIS over the CEOS calibration sites

H. Yamamoto, A. Kamei, R. Nakamura, S. Tsuchida, National Institute of Advanced Industrial Science and Technology (Japan)

Remotely sensed optical satellite data can provide spatial and temporal information for various research field on global monitoring. Many recent researches have used this technology as an attractive tool, and recent studies have provided information for the integration of various satellite data and products. The accuracy of higher-level satellite products depend on the radiometric accuracy.

The Advanced Spaceborne Thermal Emission and Reflection Radiometer (ASTER) and the Moderate Resolution Imaging Spectroradiometer (MODIS), which are onboard the Terra platform, have contributed to the global researches with both fine and coarse spatial resolution. Both of ASTER and MODIS sensor have been operated more than 10 years, and it is very useful for cross-calibration because of their simultaneous observations mostly without BRDF effect. This cross-calibration will contribute to the understanding of relative accuracy each other. Although this kind of research needs the homogeneous, large, and flat test site(s), the CEOS IVOS subgroup arranges the pseudo-invariant standard test sites for cross calibration, which are able to evaluate the long-term stability among multiple sensors. This paper shows the TOA reflectance comparison between ASTER and MODIS sensor over the CEOS pseudo-invariant standard test sites.

8153-45, Session 9

Verification of GSICS GEO-LEO correction products using GEO-GEO inter-calibration

F. Yu, Earth Resources Technology, Inc. (United States); X. Wu, National Oceanic and Atmospheric Administration (United States); G. Sincic-Rancic, Joint Ctr. for Satellite Data Assimilation (United States)

The Global Space-based Inter-Calibration System (GSICS) was developed aiming to improve the calibration accuracy of operational satellite instruments through inter-calibration between different instruments. Over the past few years, NOAA has been routinely providing the GSICS correction products for the Geostationary Operational Environmental Satellite (GOES) Imager and Sounder radiance by inter-calibrating GEO radiometers to the well-calibrated hyper-spectral instruments on-board Low Earth orbit (LEO) satellites. The inter-calibration between instruments on two GEO satellites over the overlapped area, developed to monitor instrument performance and to detect potential calibration anomaly, can also be used to verify the GSICS GEO-LEO correction products when the difference of spectral response functions (SRF) and viewing condition can be compensated for. In this study, the collocated pixel pairs between GOES-11 and -12/13 are identified when two GEO instruments coincidentally view the same pixel at similar viewing zenith angle. The double difference between GSICS corrected observation and simulated radiance with Community Radiative Simulation Model (CRTM) at the collocated pixels is then used to evaluate the correction accuracy. To compensate for the bias introduced from different SRFs, the observed and calculated spectra of each instrument are convolved with SRF of the other. Results of this study will be presented in the coming meeting.

8153-46, Session 9

Cross-calibration of HIRS aboard NOAA satellites using MetOp IASI

R. Chen, I. M. Systems Group, Inc. (United States); C. Cao, National Oceanic and Atmospheric Administration (United States)

The 30 years of observations from High-Resolution Infrared Radiation Sounder (HIRS) aboard NOAA series of satellites have been widely used in numerical weather prediction and climate studies. However, there are significant discrepancies in the HIRS measurements between different satellites. The HIRS data from NOAA satellites series need to be recalibrated to establish an accurate and consistent temporal series before it can be used for climate changing detection. In this study, the HIRS radiance measurements from NOAA satellites (NOAA-6-19) are recalibrated using the hyper-spectral IASI radiance measurements from MetOp satellite as reference. For the satellites after NOAA 15, the HIRS measurements from the NOAA satellites are compared with the matched IASI measurements at Simultaneous-Nadir-Overpass (SNO) locations. For the satellites before NOAA 15, the HIRS measurements are compared with the recalibrated HIRS measurements from the successive NOAA satellite at SNO locations. A detailed analysis of the biases is performed to quantify the root causes of the biases, including both spectral and radiometric causes. By removing these biases, our analysis shows that the HIRS measurements from the NOAA series of satellites can be recalibrated and made traceable to IASI measurements with improved radiometric and spectral calibration.

8153-56, Session 9

Impact of near-cloud boundaries on radiometric performance of imaging sounders: an examination of FTS and dispersive spectrometer error sources

T. Ramond, Ball Aerospace & Technologies Corp. (United States); A. B. Newbury, DigitalGlobe, Inc. (United States); M. Stephens, Ball Aerospace & Technologies Corp. (United States)

Meteorological sounding data provided by atmospheric imaging sounders have applications in weather forecasting, atmospheric chemistry, and climate monitoring. Realistic scenes for these instruments vary in both spatial and spectral content and such variations can impact their radiometric performance. As sounders are developed to provide climate records with demanding long-term radiometric accuracy requirements, it becomes increasingly important to understand the effect of scene variations on the performance of these instruments. We have examined the noise performance and radiometric accuracy of two geostationary sounder architectures in cloudy scenes: a Fourier Transform Spectrometer (FTS) and a dispersive spectrometer. Factors such as stray light, ghosting, scattering, and line-of-sight jitter in the presence of scene inhomogeneities are considered. Quantitative estimates of the radiometric errors associated with sounding in cloudy scenes are made for each architecture. We find that in a dispersive system the dominant error in a cloudy scene originates from ghosting within the instrument, while in an FTS the dominant error originates from scene modulation created by line-of-sight jitter in a partially cloudy scene coupling into signal modulation over the scale of the changing optical path length of the interferometer. In this paper we describe the assumptions made and the modeling performed. We also describe how each factor influences the radiometric performance for that architecture.

8153-47, Session 10

Virtual green band for GOES-R

I. Gladkova, M. D. Grossberg, F. Shahriar, The City College of New York (United States)

The ABI on GOES-R will provide imagery in two narrow visible bands (red, cyan), which is not sufficient to directly produce color (RGB) images. In this paper we present a method to estimate a 550 nm green band from a simulated ABI multi-spectral image. To address this problem we propose to use statistical learning methods to train and update functions that implement an estimator, using data from MODIS imager. The need to combine many parameters from multiple bands rules out the straightforward use of traditional look-up tables because the number of entries in look-up tables grows exponentially with the number of parameters. Other basic approaches such as simple linear regression will not produce satisfactory results due to the underlying non-linearity of the data. The relationship among different spectra for cloud footprints will be radically different from that of desert or forest. The approach we propose is to use piecewise polynomial regressions on the multi-spectral input. Our predictor consists of a classifier, which assigns an ABI pixel to a class based on the array of values from all the simulated ABI bands at that pixel. To each class is associated a set of coefficients for a multi-variable polynomial predictor for the 550 nm green band to be predicted. Thus the parameters of the predictor consist of parameters of the classifier, as well as coefficients of the multi-variable polynomial for each class. To determine these classifiers we will use methods based on K-means clustering, as well as standard multi-variable polynomial regression.

8153-48, Session 10

WEB recourse to perform the atmospheric correction of satellite data

M. V. Engel, V.E. Zuev Institute of Atmospheric Optics (Russian Federation); S. V. Afonin, V. V. Belov, V.E. Zuev Institute of Atmospheric Optics (Russian Federation) and Tomsk State Univ. (Russian Federation)

At present, the importance of the atmospheric correction (AC) of data of remote surface temperature measurements is well recognized. The AC capabilities are provided practically by all most widespread software products (such as ERDAS and ENVI). Nevertheless, in some cases the AC is totally ignored or performed with accuracy insufficient to solve a particular thematic problem. AC tasks, in particular, necessitate the use of large volume of accurate a priori information on the optical-meteorological state of the atmosphere.

The current development level of information and telecommunication networks allows research to be performed on the basis of the spatially distributed information and calculation resources. Such an approach is used as a basis for a WEB resource to perform the atmospheric correction of remote measurement data, which is currently being developed at Institute of Atmospheric Optics SB RAS (IAO SB RAS). The AC algorithm is based on the optical models of the atmosphere and data of satellite measurements (such as thematic products of MODIS spectroradiometer), stored both in remote databases and in databases inside the WEB resource. The use of the data from the distributed sources provides the necessary a priori optical-meteorological information.

The calculational capabilities of the WEB resource are implemented on the basis of well-known programs for simulating the optical radiative transfer through the atmosphere (e.g., MODTRAN, 6S). This work is also based on the algorithms and methods of AC of remote measurement data, developed at IAO SB RAS, and on local software tools, developed on the basis of these methods.

8153-49, Session 10

South Atlantic anomaly filter for satellite UV observation

J. Niu, L. E. Flynn, National Oceanic and Atmospheric Administration (United States)

A South Atlantic Anomaly (SAA) filter has been developed to filter out large amounts of noise caused by high energy protons hitting onto the optical instrument focal plane when the satellite passes through the SAA region. The filter is based on the Empirical Orthogonal Function (EOF) analysis. The EOF vectors derived from an orbit outside of the SAA region were used to represent the observations coming from the noisy SAA region. Then using the clear EOF vectors, the observations within SAA region are rebuilt with just the first five to ten principle components. The filter works well for wavelength shorter than 310 nm. In this region signals are contributed primarily from the upper atmosphere where the cloud effects are small. Tests on L1B data from Ozone Monitoring Instrument (OMI) and Global Ozone Monitoring Experiment-2 (GOME2) have been conducted. It is expected that this filter can help to improve the measurements and retrievals for the OMPS nadir profiler in the SAA region.

8153-50, Session 10

Graphyte software for integrated remote sensing research using HPCC

M. D. Grossberg, I. Gladkova, J. K. Gabaldon, P. K. Alabi, J. K. Neiman, The City College of New York (United States)

Conference 8153:
Earth Observing Systems XVI

Graphyte is software for distributed research collaboration and prototyping.

Rather than impose a new system structure, our goal is to integrate tools, interfaces, and data that scientists are already using. In addition, we incorporate some of the best practices from modern software engineering: distributed version control, grid and cloud computation, data management, and advanced analysis and visualization tools with multiple clients---including a web based interface. The first prototype of Graphyte provided a web interface for editing python scripts to read, statistically analyze, and visualize NOAA's remote sensing data. Based on user feedback, we have completely restructured the system to better accommodate NOAA's current workflow. The system now handles other coding languages, including Fortran, IDL, and C/C++, besides python. Execution is managed by a sophisticated job system that is able to use grid and cloud HPCC resources.

Another important aspect of the next generation version of Graphyte is that it provides fine-grained user and group permissions. This allows researchers to select with whom they want to share code, data, and results. This is a critical pre-requisite for any practical adoption in a research context. In addition to the wide, and deep functionality provided through installed open-source libraries---such as for GIS, economic analysis, machine learning, statistics, image processing, physics, and visualization of data,---we provide wrappers for data readers to provide convenient access to NOAA and NASA remote sensing data.

8153-51, Session 11

Latest decade's spatial-temporal properties of aerosols over China

X. Gu, T. Yu, T. Cheng, J. Guo, H. Chen, D. Xie, Institute of Remote Sensing Applications (China)

Aerosols are one of the most important parameters affecting the Earth's energy balance and hydrological cycle[1]. They can arouse uncertainties effects on climates. With the development of economic activities, the cities of China are unfortunately exposed to high concentrations of aerosol particles, which often are immediately evident as a dense haze over the city. To narrow the uncertainties associated with the direct and indirect aerosol effects on climates, the spatial-temporal properties of aerosol is investigated over China. The study use the Aerosol Optical Depth (AOD) derived from the radiance measurements performed by the Moderate Resolution Imaging Spectroradiometer (MODIS) instrument on board the Terra and Aqua satellites from 2002 to 2010.

The most prominent changed regions are the North China and East China. The high AOD values occur in 2004, 2006 and 2007 year, respectively. The tendencies of AOD are in good agreement with corresponding AOD tendencies based on data from Aerobot Robotic Network (AERONET) stations in the study region[2]. Seasonal AOD maxima are obtained in spring (March to May) and summer (June to August) seasons, due to large humidity and biomass burning, respectively. Dust activities in spring are frequent occurrences that also lead to high aerosol loading. AOD minima are obtained in winter (December to February) seasons. The result of our analysis reveal significant trend of seasonal AOD in the North China. The obvious ascending tendency of AOD occur in summer and autumn (September to November) seasons. Conversely, the decreasing tendency appear in spring and winter seasons.

REFERENCES

[1] Remer, L.A., Kaufman, Y.J., Tanré, D., Mattoo, S., Chu, D.A., Martins, J.V., Li, R.R., Ichoku, C., Levy, R.C., Kleidman, R.G., Eck, T.F., Vermote, E., Holben, B.N. "The MODIS aerosol algorithm, products and validation". *Journal of Atmospheric Sciences*, 62, 947-973, 2005

[2] C. D. Papadimas, N. Hatzianastassiou, N. Mihalopoulos, X. Querol, and I. Vardavas. "Spatial and temporal variability in aerosol properties over the Mediterranean basin based on 6-year (2000-2006) MODIS data". *JOURNAL OF GEOPHYSICAL RESEARCH*, VOL. 113, D11205, 2008

8153-52, Session 11

Satellite observation of air pollutants over northern China

P. Wang, H. Yu, G. Wang, X. Zong, Institute of Atmospheric Physics (China)

Much attention has been paid to northern China region because of the fast economic growth and also fast developing air pollution. Satellite observation could be most efficient to monitor the regional air quality, including suspended particles and concentrations of trace gases such as NO₂, SO₂, O₃. During the Beijing Olympic Games, in order to ensure good air quality for Beijing Olympic Games, a series of measures for improving air quality were carried out in Beijing and its surrounding areas. 300,000 high emission vehicles were prohibited on roads, 2,000,000 cars were restricted on roads by the policy "odd days for odd number cars, even days for even number cars". A large number of plants and factories were temporarily closed or limited in producing capability, or works after meeting the emission standard. Satellite observational data were used to monitoring the air quality over northern China during this period. The Aura-OMI data was used to monitor O₃ and tropospheric NO₂ column amount. The Terra- and Aqua- MODIS data was used to monitor aerosol loading. During the Beijing Olympic Games, due to the strict ensuring measures for good air quality, more than 40% reduction in NO₂ column was found from satellite observation. On the same time, the ground-based standard CE-318 sunphotometer data was used to validate the retrieval data of MODIS, and the MAXDOAS measurement to validate the retrieval data of Aura-OMI. Also the lidar monitoring for aerosol vertical distribution and tower measurements for gas pollutants and their layer distribution were conducted.

8153-53, Session 11

MclIDAS-V: a tool for developing and evaluating science applications for weather and climate data

T. H. Achtor, T. D. Rink, Univ. of Wisconsin-Madison (United States)

The fifth generation of the Man-computer Interactive Data Access System (MclIDAS-V) is a java-based, open-source, freely available system that provides powerful data manipulation and visualization capabilities. The unique capabilities of the MclIDAS-V software support development of innovative techniques for creating and evaluating algorithms, visualizing data and products in 4 dimensions, and validating results. The GEO/ GEOSS program seeks to make the global network of weather monitoring observations, databases and forecasting model output available to the international user community. Thus, MclIDAS-V can be a very valuable tool for researchers and operational users within the GEO/ GEOSS domain. As MclIDAS-V has moved from the development stage to a mature software package, new development is focusing on adding functionality and expanding access to new data types. This paper will present results from several research projects involving current and future environmental satellites, demonstrating how the MclIDAS-V software can be used to acquire satellite and ancillary data, create imagery and products using both scripting and interactive data manipulation tools, and evaluate output through on-board validation techniques.

8153-54, Session 11

MclIDAS-V: a data analysis and visualization application for GEOSS

T. D. Rink, Univ. of Wisconsin-Madison (United States)

MclIDAS-V, the next-generation MclIDAS, is entirely new code-base being built on top a modern, cross-platform software framework which supports development of 4-D interactive displays and integration of

wide-array of geophysical data. As the replacement of McIDAS, the development emphasis is on future satellite observation platforms such as JPSS and GOES-R. Data interrogation, analysis and visualization capabilities have been developed for multi- and hyper-spectral instruments like MODIS, AIRS and IASI, and are being extended for application to VIIRS and CrIS. Compatibility with current geostationary platforms, and GOES-R ABI baseline and AWG Framework products has been demonstrated. The abstract data model, which can internalize most any geophysical data, and Python based user defined computation tools, opens up new possibilities for data fusion techniques, for example, polar and geostationary, (LEO/GEO), synergy, cross-instrument product synthesis and inter-calibration and validation. Data access is local, or remote via OpenDAP/THREDDS, and ADDE. McIDAS-V follows an object-oriented design model, using the Java programming language, allowing specialized extensions for new sources of data, novel displays and interactive behavior. The distributed reference application, can be customized, and the system has a persistence mechanism allowing sharing of the application state across the internet. McIDAS-V is open-source, and free to the public.

8153-55, Session 12

Geometric/radiometric calibration from ordinary images for high-resolution satellite systems

C. Latry, Ctr. National d'Études Spatiales (France)

For high resolution systems, radiometric and geometric calibration and performance assessment are very important matters. They are usually based upon dedicated acquisitions : uniform landscapes for noise performance, knife edge target for Modulation Transfer Function assessment, specific landscapes with well known Ground Control Points for geometric characterization....

This induces heavy programming constraints when adding the cloudiness contingency.

However, thanks to image processing techniques, both radiometric and geometric accurate information may be retrieved from a standard image.

This paper aims to present two techniques respectively devoted to noise and geometric characteristics assessment from standard images.

The noise computation technique is based upon the assumption that high spatial frequencies are sufficiently weakened by MTF so that only noise remains near Nyquist frequency. The mathematical tool may be Fourier Transform or wavelet packet decomposition. The output is a noise assessment over the full radiance range, while the classical method using a uniform landscape only gives noise information for one radiance value. It is particularly well suited to high resolution systems with low MTF values at Nyquist.

The second technique is based upon matching processing between spectral bands assuming the imaging system focal plane has staggered arrays. Averaging the disparity images issued from the dense matching process yields very accurate information on focal plane layout as well as high frequency attitude perturbances.

Results obtained on simulated images as well as Worldview-2 real products are detailed.

8153-58, Session 12

SAR data for subsurface saline lacustrine deposit detection and primary interpretation on the evolution of the vanished Lop Nur Lake

Y. Shao, H. Gong, Institute of Remote Sensing Applications (China)

Lop Nur is a huge vanished lake located at the east end of Tarim Basin, northwest of China and finally dried up before 70's. With the advantage of penetration capability and sensitivity to moist saline materials, SAR revealed the subsurface lacustrine deposits and delineated partially the buried shorelines and made a complete picture of Lop Nur Lake that leads to three important scientific findings in this study. Based on scattering mechanism interpretation of polarimetric and multiple frequency SAR data, field investigation and sample analysis it is found the total area of the vanished Lop Nur lake is more than 10,000 km² which is much larger than 5335 km² as reported. The relative younger West Lake is superposed on the top of the lacustrine deposit of East Lake so the west part of the shoreline was buried and not visible in optical remote sensing images, which made the well known "Ear" feature of Lop Nur; Therefore the Lop Nur Lake actually has nearly circular, closed shoreline. The drying-up process of East Lop Nur Lake went through six phases according to the shorelines interpreted from multiple SAR data. The shrinking phases of Lop Nur Lake indicate the climate changes between dry and wet environment conditions.

Conference 8154: Infrared Remote Sensing and Instrumentation XIX

Sunday-Monday 21-22 August 2011 • Part of Proceedings of SPIE Vol. 8154
Infrared Remote Sensing and Instrumentation XIX

8154-01, Session 1

A field-widened spectrometer-interferometer: back from the past to measure ionospheric- thermospheric energetics

S. J. Wellard, Space Dynamics Lab. (United States)

Recent broadband observations by the SABER sensor aboard the TIMED satellite hint at intriguing new vibration-rotation excitation and loss processes that occur in the energy dissipation of the ionosphere-thermosphere as it responds to solar storms. To address the questions exposed by the SABER data, SDL's field-widened interferometer has been brought back after three decades to again fly into or above aurorally disturbed atmosphere to gain the data needed to better understand the different processes of ionosphere-thermosphere energetics. The paper discusses the evaluation and design phases (laboratory evaluation, a rocket flight, and a satellite flight) needed to prepare this elegant and unique interferometer to reach its goal of making high resolution (0.5 cm⁻¹) and wide bandwidth (1300-8000 cm⁻¹) measurements of the ionosphere-thermosphere world-wide. Design details of interferometer will be presented along with comparisons between a standard Michelson interferometer and the field-widened sensor to illustrate just how the Bouchareine and Connes field-widened form provides the enhanced performance needed for the new missions. The paper also describes how the improved Interferometer design will leverage advances in modern electronics, detectors, bearing design and software to gain significant improvements in the performance of the upgraded field-widened interferometer-spectrometer when compared with the heritage instrument.

8154-02, Session 1

Testing of highly accurate blackbodies

H. Latvakoski, M. Watson, S. Topham, D. K. Scott, Space Dynamics Lab. (United States)

Many organizations, including Space Dynamics Laboratory, have built blackbodies with calculated emissivities of 0.995 to 0.9999 and estimated radiance temperature uncertainties of a few hundred mK or less. However, the calculated performance has generally not been demonstrated through testing or comparison with other high-performance blackbodies. Intercomparison is valuable; historically, when equipment or experimental results have been intercompared they are often found to disagree by more than the claimed uncertainties. Blackbody testing has been limited because testing at the required accuracy (0.1% or better in radiance) is a significant expense. Such testing becomes essential when proven, SI-traceable, absolute accuracy is required, such as for the CLARREO mission which has an absolute accuracy requirement of 0.1 K (3 sigma) at 220 K over most of the thermal infrared and needs high-performance blackbodies to support this requirement. Properly testing blackbodies requires direct measurement of emissivity and accurate measurement of radiance or comparison of radiance from two blackbodies. This presentation will discuss these testing needs, currently available test equipment, and testing and test results for a CLARREO prototype blackbody.

8154-03, Session 1

Advancements in understanding auroral ionosphere-thermosphere coupling from infrared remote sensing

C. J. Mertens, NASA Langley Research Ctr. (United States); X.

Xu, Science Systems and Applications, Inc. (United States); S. J. Wellard, Space Dynamics Lab. (United States)

Recent discoveries from analysis of measurements made by the Sounding of the Atmosphere using Broadband Emission Radiometry (SABER) instrument on the Thermosphere-Ionosphere-Mesosphere Energetics and Dynamics (TIMED) satellite have shown that NO(v) 5.3 um emission is the primary mechanism of dissipating solar-geomagnetic storm energy in the thermosphere. Further insight into the ionosphere-thermosphere (IT) storm-time response emerged from observations and analysis of the SABER 4.3 um channel radiances, which showed that nighttime 4.3 um emission is dominated by NO+(v) during geomagnetically disturbed conditions. Analysis of SABER NO+(v) 4.3 um emission led to major advances in the understanding of E-region ion-neutral chemistry and kinetics, such as the identification of a new source of auroral 4.3 um emission, which also provides a new context for understanding auroral infrared emission from O2(1-Delta). Surprisingly, NO+(v) 4.3 um emission is the second largest contribution to solar-geomagnetic infrared radiative response and provides a non-negligible contribution to the "natural thermostat" thought to be solely due to NO(v) 5.3 um emission. Despite these major advances, a fully physics-based understanding of the two largest sources of storm-time energy dissipation in the IT system from NO(v) and NO+(v) is lacking because of the limited information content contained in SABER's broadband infrared channel measurements. On the other hand, detailed information on the chemical-radiative excitation and loss processes for NO(v), NO+(v), and O2(1-Delta) emission is encoded in the infrared spectrum, of which SABER only provides an integral constraint. Consequently, a prototype infrared field-wide Michelson interferometer (FWMI) is currently under development to advance our understanding of IT storm-time energetics beyond the current state of knowledge. In the near term, the prototype FWMI will be transitioned to a rocket-borne payload for a science campaign dedicated to the study of auroral ion-neutral coupling within in the IT system. It is anticipated that progress in the developments of the FWMI technology, along with advancements in a physics-based understanding of the fundamental chemical-radiative mechanisms responsible for IT infrared emission, will play an integral role in the future planning of a satellite-based E-region science mission. In this presentation, a survey of recent SABER discoveries in IT ion-neutral coupling will be given, open questions in a physics-based understanding of chemical-radiative vibration-rotation excitation and loss from important IT infrared emitters will be identified, and the FWMI and other instrument requirements necessary to address these open science questions will be presented.

8154-04, Session 1

Laser technology development for future NASA spaceborne laser missions

M. A. Stephen, A. W. Yu, M. A. Krainak, S. X. Li, NASA Goddard Space Flight Ctr. (United States)

At NASA's Goddard Space Flight Center, we have been doing in-house research and working with several industry partners to develop laser technology for the 2nd Ice Cloud and Land Elevation Satellite (ICESat-2) mission, scheduled to launch in 2016. ICESat-2 will fly a single instrument, the Advanced Technology Laser Altimeter System (ATLAS), which will use the time-of-flight of laser pulses to make topographic measurements of the Earth's surface. The ATLAS laser will be a 1064 nm MOPA (master oscillator power amplifier) system that is frequency-doubled to the green. We have been focusing on advancing the technology readiness of these technologies for a space environment. The 1064 nm MOPA technology developed is quite versatile and can be used for several future infrared NASA laser missions including LIST and ASCENDS. In this paper, we will discuss the laser technology developed thus far for ICESat-2 and how this technology can be

**Conference 8154:
Infrared Remote Sensing and Instrumentation XIX**

applied to meet future needs. The ATLAS laser technology that is being advanced differs from conventional laser altimeter systems in which high repetition rate of tens of kHz, pulse energies of hundreds of microjoules and sub-nanosecond pulses are used for the science measurements. This represents a new era in space-based instrumentation for the space agency. We will discuss scientific goals and likely instrument requirements for these missions.

8154-05, Session 1**Latest developments for low-power infrared laser-based trace gas sensors for sensor networks**

S. So, Sentinel Photonics (United States) and Princeton Univ. (United States); D. Thomazy, Sentinel Photonics (United States); W. Wang, Princeton Univ. (United States); O. Marchat, Princeton Univ. (United States) and ETH Zurich (Switzerland); G. Wysocki, Princeton Univ. (United States)

Scientific and industrial researchers are beginning to require ultra-low power, compact laser based sensor systems for the most demanding environmental and space-borne applications. The latest in developments for such sensors have demonstrated proof-of-concept sensors which can provide near-IR to mid-IR based semiconductor laser sensors which dissipate between 0.3-5 W and fit in the palm of a hand. Three novel innovations have greatly improved the potential size, compactness, and cost of these sensors: 1) a novel quasi-Lissajous multipass cell, 2) more efficient mid-IR quantum cascade laser based sources which operate at around room temperature, and 3) power efficient, fully integrated, and compact laser controllers, detector electronics, and data acquisition systems. Additionally, for paramagnetic molecules, Faraday rotation spectroscopy also provides extremely compact, robust sensor systems which consume minimal power. Such FRS based sensor architectures can eventually enable high precision NO₂ wireless sensor networks, a critical technology for future air quality assessments.

The latest results from 4 projects will be described: 1) an ultra compact CO₂ sensor using QCLs which consumes less than 5W, 2) a high dynamic range Faraday rotation spectrometer for O₂ using a multipass cell and balanced detection, 3) a fully ruggedized compact laser spectrometer at 2.7 microns for outdoor wireless sensor networks, and 4) a novel multipass cell using spherical mirrors which provide high number of passes similar to an astigmatic Lissajous beam spot pattern.

These results will be described in detail, with a projection for performance of future sensors based on this technology.

8154-06, Session 1**Temperature sensor for scanning thermal microscopy based on photoluminescence of microcrystal**

A. Sayoud, N. Tranny, J. Jouart, P. Grossel, Univ. de Reims Champagne-Ardenne (France); M. Diaf, Univ. Badji Mokhtar (Algeria); T. Duvaut, Univ. de Reims Champagne-Ardenne (France)

A new sensor is developed for measurement of local temperature and its imagery at sub-micrometric scale. This sensor is based on a thermal-resistive probe and on photoluminescence of crystal. The final purpose is to develop a new device calibrated in temperature and capable of acquiring images of local temperature. Indeed, the temperature of the sensor can be obtained from two distinct ways: one from the parameters of thermal probe and the other from the green photoluminescence generated in the anti-Stokes mode by the Er ions directly excited by a red laser.

The thermal probe is a thermal-resistive probe in Wollaston wire whose thermal-resistive element is in Platinum/Rhodium. This probe is usually

used in scanning thermal microscopy. An electrical current is used to induce a Joule effect heating. Its temperature is estimated from the probe electrical characteristics and a modelling. A transparent microcrystal of Cd_{0.7}Sr_{0.3}F₂: Er³⁺(4%)-Yb³⁺(6%) of 5µm in diameter is glued at the end of the probe. This luminescent material has the particularity to give an emission spectrum with intensities sensitive to small temperature variations.

A first temperature calibration using a heater allows the evaluation of the crystal temperature from the intensity measurements at 522, 540 and 549 nm by taking advantage of particular optical properties due to the crystalline nature of Cd_{0.7}Sr_{0.3}F₂: Er³⁺-Yb³⁺. The temperature of probe microcrystal is then assessed as a function of electric current by applying the Boltzmann's equations linking the intensities of emission lines to the temperature. The first results will be presented and discussed.

8154-08, Session 2**Mid-infrared chirped laser dispersion spectrometer for remote detection of trace chemicals**

G. Wysocki, M. Nikodem, Princeton Univ. (United States); D. Weidmann, Rutherford Appleton Lab. (United Kingdom)

Remote trace gas detection plays an important role in numerous applications including environmental sensing, industrial monitoring and security. Sensitive chemical detection by means of optical absorption requires measurements of small optical power changes in presence of a large background (the total photodetected light intensity). Detection of refractive index change, which is inherent to molecular absorption, provides theoretically baseline-free measurement. Recently a chirped laser dispersion spectroscopy (CLaDS) was introduced (Wysocki and Weidmann OE18, p26123, 2010). CLaDS enables fast and quantitative trace-gas detection with large immunity to optical power fluctuations. This feature makes the CLaDS technique well suited for remote sensing.

In this paper we will present performance of a CLaDS system designed specifically for long-range remote sensing applications. The system is based on a mid-infrared quantum cascade laser operating at 4.52µm (2210cm⁻¹) and targets the most intense, fundamental vibrational band of nitrous oxide (N₂O). CLaDS is based on two-color dynamic interferometric heterodyne detection. The optical signal collected by a telescope is focused onto a fast room-temperature photodetector. A RF spectrum analyzer acquires and demodulates the photodetected RF heterodyne beatnote. As the laser is chirped across a molecular transition, the dispersion produces a frequency modulation of the heterodyne beatnote. The RF analyzer performs frequency demodulation to recover information of the refractive index change. Based on preliminary experiments we estimate the detection limit for N₂O to be of <1ppbv for path-lengths of ~100m and 1s integration time. In this paper a detailed system configuration, performance tests and future directions will be discussed.

8154-09, Session 2**Precision spectroscopy with frequency combs at 3.4 µm**

E. Baumann, F. R. Giorgetta, I. Coddington, W. C. Swann, N. R. Newbury, National Institute of Standards and Technology (United States)

We discuss precision spectroscopy with a fiber comb-based spectrometer at 3.4 µm. Our goal is to explore comb-based spectroscopy as an alternative to high-resolution FTS or swept laser systems for rapid, high-resolution, high-accuracy measurements of gas line shapes. The spectrometer uses dual femtosecond fiber laser combs at 1.5 µm with slightly different repetition rates. The output of each femtosecond fiber laser comb is down converted via difference frequency generation (DFG) against a cw 1-µm fiber laser in a PPLN crystal to create two frequency

**Conference 8154:
Infrared Remote Sensing and Instrumentation XIX**

comb sources at 3.4 μm . Both the cw 1- μm fiber laser and fiber laser combs are referenced back to a Hydrogen maser through a third self-referenced frequency comb. Therefore, the absolute frequency axis for the 3.4- μm combs is known. One 3.4- μm comb is transmitted through methane and heterodyned against the second, offset comb to measure the gas absorption and dispersion. Doppler-broadened methane spectral lines are measured to below 1-MHz uncertainty. This frequency accuracy is significantly higher than for FTS systems. Unlike saturated absorption techniques, the dual comb spectrometer allows for simultaneous measurement of multiple groups of lines and without the need of a strong saturating laser beam. We will also discuss an alternative configuration of a comb-assisted DFG spectrometer. A rapidly tunable cw 1.5- μm laser is referenced to the dual fiber laser combs at 1.5 μm and then down-converted by DFG to 3.4 μm to provide a rapidly tunable 3.4 μm source with a known absolute frequency that can be used in a tunable laser spectrometer.

8154-49, Session 2**A pulsed quantum cascade laser-based wavelength modulation spectroscopy for open-path gas sensing**

J. Manne, A. Lim, W. Jäger, J. Tulip, Univ. of Alberta (Canada)

Quantum cascade (QC) lasers have been extensively used in closed path configurations for gas sensing applications.[1-3] The biggest challenge in utilizing these lasers (either pulsed or cw) for open-path spectroscopy lies in obtaining a proper background subtraction to retrieve absorption information. Open path spectroscopy is important since it can provide integrated absorption measurements over long distance and consequently can be used for atmospheric monitoring of different molecules. Here, we report the results of wavelength modulation spectroscopy (WMS) with a pulsed QC laser which can open new avenues for sensitive open -path gas sensing. Pulsed WMS has many advantages over its continuous wave (cw) counterpart. The pulsed QC laser is much easier to fabricate than the cw QC laser. Pulsed QC lasers are typically used with 1-2% duty cycle so the power consumed is a small fraction of that in a cw device. Moreover, high frequency pulses of light with relatively higher intensity are much easier to detect than modulated cw light.[4] Additionally, this technique is independent of laser characteristics. The implementation of such new mid-infrared laser technologies into industrial trace gas analyzers holds great promise.

A pulsed QC laser operating at 957 cm^{-1} was used which provides an output power of $\sim 5\text{mW}$ at 2% duty cycle. The laser is excited with short current pulses at a repetition rate of 500 kHz. First, the QCL was characterized and operating parameters were optimized for gas sensing applications. CO_2 or water vapour spectral lines were used for all these measurements. A linear sub-threshold current ramp at 20Hz was added to the excitation pulse train which resulted in a $\sim 2.5\text{ cm}^{-1}$ frequency scan. We utilized demodulation approach to catch the envelop of the pulses and thus avoiding high speed electronics. We then combine the ramp with a sine modulation at 10kHz, and detect the second harmonic signal using a in-house designed and built phase locked loop (PLL) detection circuit.

8154-10, Session 3**The TROPOMI instrument performance and their impact**

M. Esposito, cosine Research B.V. (Netherlands)

TROPOMI is an advanced non-scanning imaging absorption spectrometer operating in the UV, VIS, NIR and SWIR wavelength ranges. TROPOMI is being developed by a joint venture of Dutch parties and builds on the success of the SCHIAMACHY, GOME and OMI instruments. It will be launched as part of the ESA's Sentinel-5 precursor mission now planned for 2014.

In order to guarantee the continuity in atmospheric trace gases retrieval

and the consequent understanding of climate change, TROPOMI will fill the gap between the current SCHIAMACHY instrument, onboard the ESA's ENVISAT satellite, and OMI instrument, onboard the NASA's AURA mission both coming to an end, and the Sentinel-5 satellite now planned for launch around 2020.

Simulations of the instrument's channels are taking place to evaluate the impact of instrument performance on retrieved data products. They will be shown and discussed.

8154-11, Session 3**The calibration of the multispectral imager on board the EarthCARE spacecraft**

A. Perez-Albinana, R. V. Gelsthorpe, A. Lefebvre, European Space Research and Technology Ctr. (Netherlands); M. Sauer, K. Kruse, R. Münzenmayer, EADS Astrium GmbH (Germany); G. C. Baister, M. Chang, Surrey Satellite Technology Ltd. (United Kingdom)

The European Space Agency (ESA) is currently developing, in co-operation with the Japan Aerospace Exploration Agency (JAXA) the EarthCARE satellite mission with the basic objective of improving the understanding of the cloud-aerosols-radiation interactions within the Earth's atmosphere.

As part of the EarthCARE payload, the MSI instrument will provide images of the earth in 7 spectral bands in the visible and infrared parts of the spectrum, with a spatial ground resolution of 500 m and an image width on the ground of 150 km.

The radiometric accuracy of the MSI instrument is of paramount importance to accurately retrieve the physical properties of clouds and aerosols from the radiometric measurements in the different MSI spectral channels. The pre-launch calibration campaign together with the in-flight calibration facilities that the MSI instrument incorporates, ensure the fulfillment of the radiometric requirements of the mission.

The overall calibration approach for the MSI instrument is described in this paper, including the pre-launch and in-flight calibration activities.

8154-12, Session 3**Development of tunable polarimetric optical scattering instrument from 4.3-9.7 microns**

J. C. Vap, S. E. Nauyoks, T. M. Fitzgerald, M. A. Marciniak, Air Force Institute of Technology (United States)

To examine the polarimetric Bidirectional Scatter Distribution Function (BSDF) of samples in the mid-wave infrared (MWIR) and long-wave infrared (LWIR), a full Stokes polarimetric optical scatter instrument has been developed which is tunable from 4.3-9.7 microns. Six tunable external-cavity quantum-cascade lasers (EC-QCL, 4.3-4.6, 4.8-5.2, 5.2-5.7, 5.6-6.5, 7.4-8.2 and 8.1-9.7 microns) were introduced into the instrument, taking it from four discrete wavelengths (544 and 632 nm, and 3.39 and 10.6 microns) to a nearly continuous waveband of 4.3-9.7 microns. The polarimeter is realized through a dual-rotating-retarder configuration, which allows full Mueller-matrix extraction over the tunable wavelengths since the retarders are much less than one-half-wave at any wavelength in the band. Optical characterization of the polarimeter components was conducted to establish performance baselines for the system. While the dynamic range of the system at the previous discrete wavelengths ranged from 15 orders of magnitude at 544 nm to 12 at 3.39 microns, the dynamic range with the tunable QCL's is 9 orders of magnitude. Polarimetric BSDF measurements on IR standard samples are underway and being analyzed using existing BSDF models. Measurements on novel optical materials, such as nanostructured materials, are also underway, but may require the development of new BSDF models to fully interpret the results.

8154-13, Session 4

Quantum electro-optical interface in nanowire devices

M. E. Reimer, G. Bulgarini, M. Hocevar, Technische Univ. Delft (Netherlands); E. Bakkers, Technische Univ. Delft (Netherlands) and Technische Univ. Eindhoven (Netherlands); L. P. Kouwenhoven, V. Zwiller, Technische Univ. Delft (Netherlands)

The unique electronic and optical properties of one-dimensional nanowires are advantageous in the combination of both transport and optics. The merging of these two research fields promises an electro-optical interface between 'stationary' qubits [1] and 'flying' qubits [2]. The ultimate aim of this interface is to coherently convert an electron spin into a photon and vice-versa for the long-distance transfer of quantum information.

In this work, we study the electro-optical interface consisting of individual InAsP quantum dots embedded in one-dimensional InP nanowire devices. We first demonstrate a high emission count rate, exhibiting single photon emission from the exciton ground state by exploiting the nanowire geometry to achieve a wave-guide effect. Next, we show charge control and that we can isolate a single electron in the quantum dot either by depleting the nanowire with an electrostatic back-gate or through tunneling with an applied electric field along the nanowire growth axis [3]. Utilizing an on-chip micro-prism, we extract the spin information of a lying nanowire device. Promising for entangled photon generation in the presence of an asymmetric dot shape, we show that the binding energy of the biexciton can be removed in a lateral electric field [4]. Finally, by embedding the quantum dot within the depletion region of a nanowire p-n junction, remarkably, we observe an efficient conversion of light into an electrical signal that is more than two orders of magnitude more efficient than the current state-of-the-art quantum dot photo-detector [5].

References:

- [1] S. Nadj-Perge, S. M. Frolov, E. P. A. M. Bakkers, and L. P. Kouwenhoven. *Nature* (London) 468, 1084-1087 (2010);
- [2] M.H.M. van Weert et al., *Nano Lett.* 9 (5), 1989-1993 (2009);
- [3] M.P. van Kouwen et al., *Nano Lett.* 10, 1817-1822 (2010);
- [4] M.E. Reimer et al., *Nano Lett.* 11 (2), 645-650 (2011);
- [5] M. P. van Kouwen et al., *Appl. Phys. Lett.* 97, 113108 (2010).

8154-14, Session 4

Near-infrared semiconductor-nanostructured light detectors

S. Höfling, S. Goepfert, F. Hartmann, C. Schneider, D. Bisping, Julius-Maximilians-Univ. Würzburg (Germany); D. L. Press, Stanford Univ. (United States); M. Kamp, L. Worschech, A. W. B. Forchel, Julius-Maximilians-Univ. Würzburg (Germany)

Novel nanostructured III-V semiconductor devices are investigated for light detection in the near infrared spectral region. Single-electron memories based on site-controlled InAs quantum dots embedded in a GaAs/AlGaAs quantum-wire transistor were fabricated and studied. By using a nanohole structure template on a modulation-doped GaAs/AlGaAs heterostructure, two single InAs quantum dots were centrally positioned in a quantum-wire transistor so that pronounced shifts of the transistor threshold occur by charging of the QDs with single electrons. Single-electron read and write functionalities up to room temperature were observed and the memory function can be also controlled by light with a wavelength in the telecommunication range. Furthermore, AlGaAs/GaAs/AlGaAs double barrier resonant tunneling diodes (RTD) with an embedded GaInNAs absorption layer have been fabricated for telecom wavelength light detection at room temperature. The absorption layer was lattice matched grown within the GaAs system of the RTD. We demonstrate that the devices exhibit typical RTDs characteristic and they are light sensitive at the telecom wavelength 1.3 μm in the order of

just a few nW. Routes to further reduce the detection limit are discussed whereas the envisaged devices have prospects to deliver sensitivities approaching the quantum limit.

The authors thank M. Emmerling and A. Wolf for technical assistance. Financial support by the German Ministry of Education and Research (BMBF) within the projects "Eiphrik" and "nanoQUIT" is gratefully acknowledged.

8154-15, Session 4

Self-recovered InGaAs single photon avalanche detector with patterned Zn-diffused structure

Y. Lo, J. Cheng, S. Rahman, Univ. of California, San Diego (United States)

A novel InGaAs single-photon avalanche detector is presented. The detector has a built-in mechanism to quench the multiplication process triggered by the absorption of a single photon without any external quenching circuit. This self-quenching and self-recovering function is obtained via bandgap engineering. An InP/InAlAs heterojunction is formed to tentatively stop the electron transport. The accumulation of electrons at the heterojunction forms a charge layer that partially shields the electric field in the multiplication region, thus quenching the current response to a single photon. The design eliminates the need for external quenching circuits and is particularly attractive to array device.

However, one technological challenge for such SPAD is the large number of surface states at the mesa edge. These surface states create early breakdown, after-pulsing and dark counts that can severely limit the single photon detection efficiency. In conventional InGaAs APDs, the effect of surface states at the mesa edge can be minimized by using the Zn-diffusion process to define the multiplication region. However, the field crowding effect associated with the Zn-diffusion profile introduces new problems. Although various guard ring structures may alleviate the problem of field crowding, the process is extremely critical. A slight deviation from the designed profile could cause significant performance penalty due to the extremely high gain in Geiger-mode operation. Here we invented a patterned Zn-diffusion structure that utilizes instead of avoiding the field crowding effect to define the avalanche areas. Using this concept, we have demonstrated 20% single-photon detection efficiency at 1550nm wavelength, with plenty of room for further performance improvement.

8154-16, Session 4

New interface control of type II superlattice photo detectors for high performance infrared applications

A. Moy, SVT Associates, Inc. (United States)

IR photo detectors are in high demand for various military and civilian applications, such as airborne surveillance, remote sensing, environmental monitoring, and spectrometry. Since the type II InAs/GaSb superlattice (T2SL) was first proposed for IR detection in 1987, the performance of T2SL photo detectors has improved considerably and is currently comparable to that of state-of-the-art HgCdTe photo diodes. Here we report the advancement of T2SL photo diodes through a novel design with enhanced interface control. A modified T2SL structure with thick InSb interlayer and GaAs layer was introduced to extend the cutoff wavelength and enhance quantum efficiency (QE). Besides forming the boundary at the InAs-GaSb interface our theoretical analysis shows that InSb plays another more important role in T2SL structure, especially for LWIR T2SLs. Namely, the cutoff wavelength of the T2SL device can be adjusted more effectively by intentionally changing the InSb thickness. Additionally, the thicker InSb layer and GaAs layer will improve the overlap of the wave functions of electrons and holes in the T2SL, which will lead to higher QE. Applying this new design, resistance-area product

Conference 8154:
Infrared Remote Sensing and Instrumentation XIX

(R0A) is measured as high as 5.5 Ohm-cm^2 at 85K for photo diodes with 12.8 micron cutoff. The fabricated photo diode with 2.4-micron-thick absorber shows responsivity of 3.7 A/W at 10.6 micron and Johnson noise limited peak detectivity of $1.0 \times 10^{11} \text{ cmHz}^{1/2}/\text{W}$ at zero bias at 83 K under 300 K background radiation with a 2π field-of-view.

8154-17, Session 4

The role of InAs thickness on the material properties of InAs/GaSb superlattices

H. J. Haugan, G. J. Brown, F. Szmulowicz, Air Force Research Lab. (United States); S. Elhamri, Univ. of Dayton (United States); B. Olson, T. F. Boggess, The Univ. of Iowa (United States)

The epitaxial growth parameters optimized for mid wavelength infrared (MWIR) InAs/GaSb superlattices (SL) growth are not directly applicable for long wavelength infrared (LWIR) SL growth. We have observed a two orders of magnitude spectral intensity drop in photoconductivity as the InAs layer thickness increases from 7 monolayers (MLs) to 16 MLs with a fixed GaSb layer thickness of 7 MLs, while the theoretical absorption strength indicates only a decrease of about a factor of three. Since the measured Hall properties of MWIR and LWIR SLs were very different- majority carriers in MWIR (LWIR) SLs were holes (electrons), material factors likely account for the discrepancy between measured signal and predicted optical strength. Since a key factor in infrared detector performance is dark-current related noise, especially in active region of photodiodes, we studied the number of charge carriers and the mobility and their recombination dynamics in this series of samples. We adjusted several growth parameters to keep low background carrier concentrations and improve carrier lifetimes in LWIR SLs using temperature dependent Hall effect and pump-probe measurements.

8154-18, Session 4

Growth and performance of superlattice-based detectors

A. Khoshakhlagh, D. Z. Y. Ting, A. Soibel, L. Høglund, J. Nguyen, S. A. Keo, A. Liao, J. M. Mumolo, S. D. Gunapala, Jet Propulsion Lab. (United States)

The type-II InAs/GaSb strained layer superlattice (SLS) system has been investigated as a promising system for infrared (IR) detection ever since it was proposed by Smith and Mailhot [1] over three decades ago. The advantages of this system lie in the fact that the effective band gap of the SLS can be tailored over a wide range ($3 \mu\text{m} < \lambda < 30 \mu\text{m}$) by varying the thickness of two "mid bandgap" constituent materials, namely GaSb and InAs. Tunneling currents are also reduced due to a larger electron effective mass. Large splitting between heavy-hole and light-hole valence subbands due to strain in the SLS contributes to the suppression of Auger recombination.

The flexibility of the SLS materials system as well as the elegant design of barrier infrared detectors (BIRDs) offer great potential both for higher-operating temperature and low background applications. This technology is further enhanced by the availability of GaSb substrates in diameters of up to 100mm. Our team has focused on the manufacturability of BIRD and superlattice-based focal plane arrays (FPAs) by leveraging off of an existing knowledge base for producing FPAs with III-V materials as well as the dedicated antimonide growth program at JPL.

In this paper, we will discuss molecular beam epitaxy (MBE) growth techniques for producing large area device wafers in the antimonide material system, as well as the status of superlattice diodes grown and characterized at the Jet Propulsion Laboratory designed for infrared absorption in the in both the MWIR and LWIR.

[1] D.L.Smith and C.Mailhot, J. Appl. Phys. 62, 2545 (1987).

8154-19, Session 4

Type II superlattice barrier infrared detector

D. Z. Y. Ting, A. Soibel, A. Khoshakhlagh, J. Nguyen, L. Høglund, S. D. B. Rafol, S. A. Keo, A. Liao, J. M. Mumolo, J. K. Liu, S. D. Gunapala, Jet Propulsion Lab. (United States)

Remarkable progress has been achieved in the antimonide-based superlattices since the analysis by Smith and Mailhot (1987) first pointed out their advantages for infrared detection. In the LWIR, type-II InAs/Ga(In)Sb superlattices have been shown theoretically to have reduced Auger recombination and suppressed band-to-band tunneling. Suppressed tunneling in turn allows for higher doping in the absorber, which has led to reduced diffusion dark current. The versatility of the antimonide material system, with the availability of three different types of band offsets, provides great flexibility in device design. Heterostructure designs that make effective use of unipolar barriers have demonstrated strong reduction of G-R dark current. As a result, the dark current performance of antimonide superlattice based single element LWIR detectors is now approaching that of the state-of-the-art MCT detector. To date, the antimonide superlattices still have relatively short carrier lifetimes; this issue needs to be resolved before type-II superlattice infrared detectors can achieve their true potential. The antimonide material system has relatively good mechanical robustness when compared to II-VI materials; therefore FPAs based on type-II superlattices have potential advantages in manufacturability. Improvements in substrate quality and size, and reliable surface leakage current suppression methods, such as those based on robust surface passivation or effective use of unipolar barriers, could lead to high-performance large-format LWIR focal plane arrays.

8154-20, Session 5

Performance optimization and first astronomical observations of the Stratospheric Observatory for Infrared Astronomy (SOFIA)

J. Wolf, NASA Ames Research Ctr. (United States); D. Backman, SOFIA / USRA (United States); U. Lampater, Univ. Stuttgart (Germany); P. M. Marcum, NASA Ames Research Ctr. (United States); E. Pfueller, A. Reinacher, H. Roeser, M. Wiedemann, Univ. Stuttgart (Germany); E. T. Young, SOFIA / USRA (United States)

The Stratospheric Observatory for Infrared Astronomy, SOFIA, is a modified Boeing 747SP aircraft that carries a 2.7 meter infrared telescope to flight altitudes of up to 13.7 km (45,000ft) to conduct astrophysical measurements in the wavelength range of 0.3 to 1600 μm . Observations at infrared wavelengths, where SOFIA's performance is optimized, target objects in the universe that are too cold to radiate at visible wavelengths, regions of the universe that are hidden at shorter wavelengths by the absorption of interstellar dust, and astrophysically significant spectral features that provide unique characterization of interstellar gas conditions and composition.

The observatory has accomplished significant milestones in 2010/2011. Test flights with the open telescope port have established the safety and reliability of the modified aircraft. The in-flight pointing stability of the telescope and its chopping secondary mirror have been measured and fine tuned using images of one of SOFIA's science instruments (FORCAST) and of a dedicated Fast Diagnostic Camera (FDC). The first science targets observed include the star forming region M42 in Orion and the starburst galaxy M82. Images were taken at wavelengths out to 37 μm , a wavelength that cannot be accessed by any telescope on the ground due to absorption in the Earth's atmosphere. In the summer of 2011, guest investigators who were selected through an open and competed call for proposals will use SOFIA to acquire their proposed data.

Conference 8154:
Infrared Remote Sensing and Instrumentation XIX

8154-22, Session 5

The evolution of the performance of the AVHRR, HIRS and AMSU-A instruments on board MetOp-A after over four years in orbit

D. R. Battles, Raytheon Co. (Germany); R. W. Lambeck, Perot Systems Government Service (United States); A. Perez-Albinana, European Space Research and Technology Ctr. (Netherlands); R. V. R. Mundakkara Kovilakom, I. M. Systems Group, Inc. (United States); X. Wu, C. Cao, National Oceanic and Atmospheric Administration (United States); H. Bauch, VEGA Deutschland GmbH (Germany); F. Montagner, European Organisation for the Exploitation of Meteorological Satellites (Germany)

The MetOp series of satellites constitute the space segment for the EUMETSAT Polar System (EPS), the European contribution to the Initial Joint Polar System, being developed in co-operation with the National Oceanic and Atmospheric Administration (NOAA) of the USA, to provide meteorological data from the polar orbit.

The first MetOp satellite was launched on 19 October 2006 on a Soyuz launcher from the Baikonur Cosmodrome in Kazakhstan. Following the successful completion of the commissioning campaign, the MetOp-A satellite and its ground segment were declared operational by both agencies, NOAA and EUMETSAT, during the summer of 2007. Now approaching its mission lifetime goal of five years in service, the performance trends presented in this paper take on special significance.

The Advanced Very High Resolution Radiometer (AVHRR), the High-resolution Infrared Radiation Sounder (HIRS) and the Advanced Microwave Sounding Unit-A (AMSU-A) instruments constitute the operational meteorological payload provided by NOAA that, in addition to the EUMETSAT provided Microwave Humidity Sounder (MHS), is flown on both the NOAA Polar Orbiting Satellites (POES) and the EUMETSAT MetOp satellites.

It is well known that the varying geometrical relationships between the Sun and the Earth throughout the year affect to some degree the performance of the instruments onboard Earth orbiting satellites. Following the commissioning of MetOp-A, EUMETSAT and NOAA have continued monitoring the long term trends in in-orbit performance of AVHRR, HIRS and AMSU-A. The data acquired since the launch of the satellite has allowed studying how the yearly seasonal variations, as well as aging, have affected the instrument performance. This paper presents the evolution of the performance of the AVHRR, HIRS and AMSU-A for more than four years since the launch of the MetOp-A satellite.

8154-23, Session 5

HIRDLS radiance corrections and improved atmospheric products

M. Belmonte Rivas, J. C. Gille, National Ctr. for Atmospheric Research (United States)

This paper details the updated radiance correction algorithms for the HIRDLS infrared limb-scanning radiometer on board the EOS Aqua satellite. The need for radiance corrections arise from the partial blocking of the radiometer field of view, both into the target atmosphere and the calibration loads, by an object whose emission appears to be driven by the thermal environment of the host platform and mechanically coupled to the motion of the scan mirror - most likely a detached sheet of insulating Kapton. This work provides a description of the steps involved in the radiance correction algorithms, from the characterization of the blockage emission (including mechanically coupled oscillations) for later subtraction, to radiance recalibration using selected atmospheric standards. Improving our understanding and effective removal of the systematic errors brought along by the blocking radiance has allowed for ever weaker trace gas signals to emerge from the instrumental noise floor. Sample new and improved HIRDLS atmospheric products will be shown.

8154-24, Session 5

Significant contributions to weather and climate research using AIRS Science Team Version 5 products

J. Susskind, O. Reale, G. I. Molnar, NASA Goddard Space Flight Ctr. (United States); L. Iredell, Science Systems and Applications, Inc. (United States)

This is an overview paper briefly describing the AIRS instrument and the AIRS Science Team retrieval methodology as well as highlighting very significant recent results we have obtained utilizing AIRS Science Team Version-5 products with regard to both improving forecasting skill as well as explaining climate phenomena. We have conducted a number of forecast impact experiments assimilating AIRS Version-5 Quality Controlled temperature profiles into the GSFC GEOS-5 Data Assimilation System (DAS) and showed that a significant improvement in the accuracy of global 7 day forecast skill, as well as in the forecasted intensity and track of severe storms, compared to that obtained using the NCEP operational DAS procedure of assimilating observed AIRS radiances rather than retrieved temperature profiles. We have also shown that spatial anomaly time-series of Outgoing Longwave Radiation (OLR) computed using AIRS Version 5 products match those of OLR observed by CERES very closely for the 8 1/2 year overlap period September 2002 through February 2010, and furthermore that use of AIRS products explain the source of recent global and tropical mean decreases in OLR observed by CERES in terms of the effect of El Nino/La Nina oscillations on the spatial anomaly time series of mid-tropospheric water vapor and cloud cover, especially in the tropics. A brief description of the AIRS Science Team Version 6 retrieval algorithm will also be given, which has a number of theoretical improvements compared to Version-5.

8154-25, Session 6

Digital scanner infrared focal plane technology

N. R. Malone, Raytheon Co. (United States)

Advancements in finer geometry and technology advancements in circuit design now allow placement of digital architecture on cryogenic focal planes while using less power than heritage analog designs. These advances in technology reduce the size weight and power of modern focal planes. In addition the interface to the focal plane is significantly simplified and is more immune to EMI. The cost of the sensor has been significantly reduced by placing the Analog to digital converters on the Read Out Integrated Circuits.

8154-26, Session 6

Evolution of large-format impurity band conductor focal plane arrays for astronomy applications

R. E. Mills, Raytheon Co. (United States)

Raytheon Vision Systems (RVS) has developed a family of high performance large format infrared detector arrays whose detectors are most effective for the detection of long and very long wavelength infrared energy. This paper describes the evolution of the present state of the art one mega-pixel Si: As Impurity Band Conduction (IBC) arrays toward a four mega-pixel array that is desired by the astronomy community. Raytheon's Aquarius-1k, developed in collaboration with ESO, is a 1024 × 1024 pixel high performance array with a 30µm pitch that features high quantum efficiency IBC detectors, low noise, low dark current, and on-chip clocking for ease of operation. This large format array was designed and delivered primarily for ground-based astronomy applications and the latest data from ESO will be presented. Raytheon, in collaboration with NASA, is also designing a 2048 × 2048 pixel high performance array with

**Conference 8154:
Infrared Remote Sensing and Instrumentation XIX**

a 25 μ m pitch that will feature high quantum efficiency IBC detectors, low noise, low dark current, and on-chip clocking for ease of operation and have sensitivity out to 27 μ m wavelength. This version will also incorporate flight qualified packaging to support space-based astronomy applications. The 2k x 2k readout circuit will be based on the successful design used for the on the Mid-Infrared Instrument (MIRI) aboard the James Webb Space Telescope (JWST). Previous generations of RVS IBC detectors have flown on several platforms, including NASA's Spitzer Space Telescope and Japan's Akari Space Telescope.

8154-27, Session 6

Large-format high-operability low-cost infrared focal plane array performance and capabilities

J. W. Bangs, D. Lindsay, J. L. Vampola, F. B. Jaworski, C. L. Mears, R. Wyles, J. F. Asbrock, E. Norton, M. Reddy, K. Rybnicek, A. Levy, Raytheon Co. (United States)

Large format detector arrays responsive uniformly over spectral 1-5 μ m wavelength range are available with RVS' high quality HgCdTe detector epitaxial layers on large area 15 cm diameter wafers. Large wafers enable both low cost HD staring FPAs such as 30cm silicon wafers are helping competitiveness of commercial IC foundries, as well as ability to approach giga-pixel format detector arrays with a seamless 10cm x 10cm continuous image plane size possible. Onto this substrate it is straightforward growth path to an 5kx5k μ m pitch 25 Mega-pixel infrared focal plane array (FPA) with smaller pitches allowing even greater format along the 10cm die length. This paper describes arrays 1.5 to 4 Mega-pixel infrared HgCdTe developed by RVS for demanding higher performance applications. Performance data for both the detector and ROIC for typical SWIR and MWIR FPAs operating at 85K will be presented. This paper will provide FPA performance capability for small pitch large format HgCdTe/Si detector arrays fabricated at RVS and manufacturing readiness low cost Mega-pixel infrared FPAs for current and future wide FOV high-resolution systems.

8154-28, Session 6

Staring MWIR, LWIR and 2-color and scanning LWIR polarimetry technology

N. R. Malone, Raytheon Co. (United States)

Polarimetry sensor development has been in work for some time to determine the best use of polarimetry to differentiate between manmade objects and objects made by nature. Both MWIR and LWIR and 2-color staring Focal Plane Arrays (FPAs) and LWIR scanning FPAs have been built at Raytheon Vision Systems each with exceedingly higher performance. This paper presents polarimetric performance comparisons between staring 2562 MWIR, 2562 LWIR, 5122 LWIR/LWIR staring FPAs and scanning LWIR FPAs.

LWIR polarimetry has the largest polarimetric signal level and a larger emissive polarimetric signature than MWIR which makes LWIR less dependent on sun angles. Polished angled glass and metal objects are easily detected using LWIR polarimetry.

While single band 9-11 μ m LWIR polarimetry has advantages adding another band between 3 and 7 μ m improves the capability of the sensor for polarization and spectral phenomenology. In addition the 3-7 μ m band has improved NEDT over the 9-11 μ m band due to the shorter detector cutoff reducing the Noise Equivalent Degree of Linear Polarization. (NEDOLP).

To gain acceptance polarimetric sensors must provide intelligence signatures that are better than existing non-polarimetric Infrared sensors. This paper shows analysis indicating the importance of NEDOLP and Extinction ratios.

8154-29, Session 6

Historical advancements in UV/Vis/NIR SiPIN focal plane technology

N. R. Malone, Raytheon Co. (United States)

Landsat, MODIS, NPOESS VIIRS and Bepi Columbo are a few of the well know space programs that have been part of the evolution of SiPIN focal plane technology. Pixels have become smaller, power has been reduced, Quantum efficiency has increased beyond 400-900 nm. The ability to tune the FPA to the customer's desired wavelength is available. The ability to hybridize large format FPAs with operability exceeding 99.9% is now routine. Focal planes are now digital allowing the elimination of the size weight and power required to support external Analog to Digital Convertors.

8154-30, Session 6

Advancements in large-format SiPIN hybrid focal plane technology

N. R. Malone, Raytheon Co. (United States)

Silicon PIN (P-type, Intrinsic, N-type) hybrid focal planes can be produced in significantly larger sizes, use significantly lower power and eliminate the need for a mechanical shutter significantly reducing cost and weight of a similar CCD (Charge-Coupled Device) design. Programmable gain and simultaneous broad dynamic range capability have also been recently incorporated into Silicon PIN hybrid focal-planes. Operability of > 99.996 has been achieved on a 26 Mega-pixel array. A read noise floor of less than 10 electrons and dark current less than 1 e-/s have also been achieved. Broadband quantum efficiency (QE) greater than 90% between 450-900 nm is typical. In addition MTF approaches theoretical performance and bias levels have been reduced from greater than 100V to as little as 5 Volts.

8154-31, Session 7

Venus atmospheric and surface studies from VIRTIS on Venus Express

G. E. Arnold, Deutsches Zentrum für Luft- und Raumfahrt e.V. (Germany); P. Drossart, Observatoire de Paris à Meudon (France); G. Piccioni, INAF - IASF Roma (Italy)

The Visible and Infrared Thermal Imaging Spectrometer (VIRTIS) on Venus Express, after more than five years in Venusians' orbit, provided an enormous amount of new data including a three-dimensional view of Venus atmosphere and global surface properties of the planet. VIRTIS is a complex imaging spectrometer that combines three unique data channels in one compact instrument. Two of the channels are committed to spectral mapping (VIRTIS-M) and a third one to high spectral resolution studies (VIRTIS-H). The paper gives an overview about the experiment goals, the instrument performance, and discusses some selected scientific results achieved by VIRTIS on board Venus Express. These include studies of the surface from night emission in the NIR atmospheric window of Venus, results of the structure and proprieties of the lower, middle and upper atmosphere, including dynamics, polar vortex, nightglows, and NLT effects.

8154-32, Session 7

A new perspective on Mercury's surface composition and temperatures: Mercury Radiometer and Thermal infrared Imaging Spectrometer (MERTIS)

G. E. Arnold, Deutsches Zentrum für Luft- und Raumfahrt e.V. (Germany); H. Hiesinger, Westfälische Wilhelms Univ. (Germany); J. Helbert, G. Peter, Deutsches Zentrum für Luft- und Raumfahrt e.V. (Germany)

MERTIS (MERcury Radiometer and Thermal Infrared Spectrometer), scheduled for launch on board the BepiColombo Mercury Orbiter, will be the first mid-infrared imaging spectrometer to explore the innermost planet of the Solar System from orbit. The instrument is an advanced IR technology designed to study the surface composition, and surface temperature variations of planet Mercury. High resolution and global mid-IR spectral and temperature data obtained by MERTIS will contribute to a better understanding of Mercury's genesis and evolution. MERTIS uses an uncooled microbolometer detector array. It combines a push-broom IR grating spectrometer (TIS) with a radiometer (TIR) sharing the same optics, instrument electronics, and in-flight calibration components for a wavelength range of 7-14 and 7-40 μm , respectively. The paper summarizes the scientific objectives, observational goals, and introduces the technical overview and actual instrument development status of the experiment.

8154-33, Session 7

Deep space instrument design for thermal infrared imaging with MERTIS

I. Walter, Deutsches Zentrum für Luft- und Raumfahrt e.V. (Germany); T. Zeh, Kayser-Threde GmbH (Germany); J. Helbert, Deutsches Zentrum für Luft- und Raumfahrt e.V. (Germany); H. Hiesinger, Westfälische Wilhelms Univ. (Germany); A. Gebhardt, Fraunhofer-Institut für Angewandte Optik und Feinmechanik (Germany); H. Hirsch, Astro- und Feinwerktechnik Adlershof GmbH (Germany); J. Knollenberg, Deutsches Zentrum für Luft- und Raumfahrt e.V. (Germany); E. Kessler, Institut für Photonische Technologien e.V. (Germany); M. Rataj, Space Research Ctr. (Poland); J. Habermeier, ECM GmbH (Germany); G. Peter, Deutsches Zentrum für Luft- und Raumfahrt e.V. (Germany)

MERTIS is a miniaturized thermal infrared imaging spectrometer onboard of ESA's cornerstone mission BepiColombo to Mercury. It shall provide measurements in the spectral range from 7-14 μm with a spatial resolution of maximal 300 m and 80 spectral channels in combination with radiometric measurements in the spectral range from 7-40 μm .

The instrument concept therefore integrates two detector systems sharing a common optical path consisting of mirror entrance optics and reflective Offner spectrometer. Uncooled micro-bolometer and thermopile radiometer technology are implemented for lowest power consumption. Subsequent viewing of different targets including on-board calibration sources will provide the desired performance. Special attention is spent on the fully passive thermal design in the harsh environment around Mercury.

The article will provide an overview of the 3 kg - instrument design and highlight the concept of the subsystems and technologies used. The status of the development process will be reported.

8154-34, Session 7

Laboratory activity in support for MERTIS on BepiColombo

A. Maturilli, Deutsches Zentrum für Luft- und Raumfahrt e.V. (Germany)

MERTIS onboard the ESA BepiColombo mission will measure thermal infrared spectra emitted from the surface of Mercury. To analyze this unique and new dataset, an appropriate spectral library of analogue materials, measured in conditions as close as possible to Mercurian, is strongly needed. In the Planetary Emissivity Laboratory (PEL) at the German Aerospace Center (DLR) in Berlin we can perform emissivity measurements at high temperatures and under vacuum conditions. The PEL is equipped with a Bruker Vertex 80V FT-IR spectrometer, coupled to an evacuable high temperatures emissivity chamber, and can acquire spectra in the entire 1 to 100 μm spectral range. The innovative heating system, based on induction properties, allows heating the samples to temperatures of up to 700K permitting measurements under realistic conditions for the surface of Mercury. As a complementary tool, the same instrument can measure bi-directional reflectance spectra of samples, with variable incoming and outgoing angles between 13° and 85°, or even transmission spectra of thin slabs of material, optical filters, optical window materials, etc, in the complete 1 to 100 μm spectral range. With a similar but older purged Bruker IFS 88 instrument we can measure bi-directional reflectance spectra of samples, with variable incoming and outgoing angles between 5° and 85° in the extended spectral range from 0.4 to 16 μm , providing us the opportunity to support the MASCS camera on NASA MESSENGER mission.

8154-35, Session 7

Observing the surface of Venus after VIRTIS on VEX: new concepts and laboratory work

J. Helbert, A. Maturilli, M. D'Amore, Deutsches Zentrum für Luft- und Raumfahrt e.V. (Germany); N. T. Müller, Deutsches Zentrum für Luft- und Raumfahrt e.V. (Germany) and Westfälische Wilhelms Univ. (Germany); R. Nadalin, Active Space Technologies GmbH (Germany)

The VIRTIS on the ESA mission VenusExpress (VEX) was the first instrument to routinely map the surface of Venus using the near infrared windows from orbit. The instrument is the flight spare of the VIRTIS instrument on the ESA Rosetta comet encounter mission. Originally designed to observe a very cold target far from the Sun, it was adapted to work in the Venus environment. The instruments main purpose on VEX was to study the structure, dynamics and composition of the atmosphere in 3 dimensions. The idea of surface studies were introduced very late in the mission planning and VIRTIS was never specifically adapted for this purpose. For example the wavelength coverage was not optimal and only the long wavelength flank of the main atmospheric window at 1.02 μm could be imaged. Despite these issues VIRTIS was an excellent proof-of-concept and far exceeded our expectations. It provided significant new scientific results and could show for example that Venus had volcanic activity in the very recent geological past.

After the very successful proof-of-concept it is now time to assess in more details what can be done with NIR observations of Venus. To support this we have been setting up the Planetary Emissivity Laboratory in Berlin which allows taking emissivity measurements in the spectral range of the atmospheric windows at sample temperatures of 500°C. This would provide a baseline for considering new instrument designs for future Venus missions, which we will outline.

Conference 8154:
Infrared Remote Sensing and Instrumentation XIX

8154-36, Session 7

MERTIS: configuration of measurement sequences for a maximized image SNR

T. Säuberlich, C. Paproth, M. Bauer, H. Jörn, Deutsches Zentrum für Luft- und Raumfahrt e.V. (Germany)

MERTIS (MERcury Thermal infrared Imaging Spectrometer) is an advanced thermal infrared remote sensing instrument that is part of the ESA mission BepiColombo to planet Mercury. Since the instrument is designed to work in the thermal infrared range detecting radiation using an uncooled micro-bolometer matrix it is necessary to pay special attention on the development of proper scene signal extraction methods, which eliminate undesired signal portions from the measurement data. In order to evaluate the signal data proper measures for the signal and noise strengths have to be defined being compatible with the different measurement sequences the instrument can be driven with.

Shown here is a theoretical model reflecting the periodic measurements of MERTIS during orbit operation using a shutter device. The model includes the noisy characteristics of the instrument's analog channel which is used for the image acquisition. Although the analog channel itself is not explicitly modeled in detail, a precise noise strength prediction can be achieved. The prediction results depend both on the specific shutter open/close measurement sequence used and a system specific temporal autocovariance function which can be easily estimated from simple image data cubes. The predictions become very precise if a proper pre-processing of the image datasets removing the most strong disturbing signal portions is done before. Being able to predict the noise strength for arbitrary measurement sequences and giving respect to the system's physical limits - e.g. shutter speed - an optimal measurement sequence can be found giving a maximized SNR of the images of MERTIS.

8154-37, Session 7

MERTIS: identifiability of spectral mineralogical features in dependence of the signal to noise ratio

C. Paproth, T. Säuberlich, J. Helbert, Deutsches Zentrum für Luft- und Raumfahrt e.V. (Germany)

The ESA deep-space mission BepiColombo to planet Mercury will contain the advanced infrared remote sensing instrument MERTIS (MERcury Radiometer and Thermal infrared Imaging Spectrometer). The mission has the goal to explore the planets inner and surface structure and its environment. With MERTIS investigations of Mercury's surface layer within a spectral range of 7-14 μ m shall be conducted to specify and map Mercury's mineralogical composition with a spatial resolution of 500m. Due to the limited mass and power budget the used micro-bolometer detector array will only have a temperature-stabilization and will not be cooled.

The performance of the instrument is estimated by the theoretical description of the signal to noise ratio and the optics including the Offner spectrometer. The expected signal to noise ratio will be in the order of 100 and is mainly dependent of the surface temperature and the wavelength. The derived theoretical models are used to execute simulations to compute the passage of the infrared radiation of a hypothetical mineralogical surface composition and surface temperature through the optical system of MERTIS. The resulting noisy spectra are used to determine spectral features of the minerals. So it is possible to evaluate the conditions which are necessary to achieve the scientific goals of MERTIS. The intent is to estimate the spectral positions of mineralogical features like the Christiansen feature which will be difficult because of the low signal to noise ratio and the low contrast of real mineral spectra.

8154-38, Session 7

MERTIS: geometrical calibration of thermal infrared optical system by applying diffractive optical elements

M. Bauer, Deutsches Zentrum für Luft- und Raumfahrt e.V. (Germany)

Geometrical sensor calibration is essential for space applications based on high accuracy optical measurements, in this case for the thermal infrared push-broom imaging spectrometer MERTIS. The goal is the determination of the interior sensor orientation. A conventional method is to measure the line of sight for a subset of pixels by single pixel illumination with collimated light. To adjust angles which define the line of sight of a pixel a manipulator construction is used. A new method for geometrical sensor calibration is using diffractive optical elements (DOE) in connection with laser beam equipment. Diffractive optical elements (DOE) are optical microstructures which are used to split an incoming laser beam with a dedicated wavelength into a number of beams with well-known propagation directions. As the virtual sources of the diffracted beams are points at infinity which gives an image invariant against translation. This particular feature allows a complete geometrical sensor calibration with one image avoiding complex adjustment procedures which means a significant reduction of calibration effort.

A new thermal infrared (TIR) suited DOE calibration facility is designed and implemented with customized TIR-DOE for geometrical TIR optical system calibration. We present a new method for geometrical calibration of thermal infrared optical systems. The fundamentals of this new technology and results of a TIR infrared optical system calibration by applying the new thermal infrared (TIR) calibration facility are shown.

8154-39, Poster Session

Self-compensating Faraday current sensor

J. L. Flores-Nuñez, H. C. Beltrán, Univ. de Guadalajara (Mexico); J. A. Ferrari, Univ. de la República (Uruguay); G. Garcia-Torales, J. Cabrera, Univ. de Guadalajara (Mexico)

In recent decades, considerable effort has been devoted to develop new transducers for monitoring current on electric power systems. Optical current devices have many advantages with respect to conventional current transducers e.g., Rogowski coils; they have simple insulation structure, immunity to electromagnetic interference, wide dynamic range and bandwidth, accurate transient response, and show no saturation or hysteresis effects. Therefore, these optical devices are considered to be an optimum interface between high-voltage lines and electronic equipment expected to monitor on power systems.

We present a optical current sensor architecture, which is based on a polarimetric configuration and utilizes a control system for self-compensating the Faraday effect. In the proposed setup, the sensing element -a TGG crystal- is placed near the conductor carrying the current to be measured. Linearly polarized light passes through the sensor head, which rotates the polarization plane an angle proportional to the electrical current in the conductor. Afterwards the light travels in the free space, reaching a Faraday modulator placed some distance away from the conductor carrying the current. This device is used to compensate the rotation of the plane of polarization induced by electrical current at sensor head. The control system is operated in a closed-loop mode using a magneto-optical feedback through a simple current-driven solenoid to maintain constant optical output from the polarimeter. Considering that some of the optical and electrical parameters of the sensor head and the Faraday modulator are known, the electrical current carried by the conductor can be measured. Validation experiments are presented.

Conference 8154:
Infrared Remote Sensing and Instrumentation XIX

8154-40, Poster Session

Vectorial shearing interferometer applied in the faint sources detection

J. Sanchez Preciado, G. Garcia-Torales, J. L. Flores-Nuñez, Univ. de Guadalajara (Mexico)

Into space, stars are the most common source of light. Planets, comets and other types of rocks reflect the incoming light from near stars. It's said that a planet is hidden when the light from the star is brighter than the reflected light from the planet. Vectorial Shearing Interferometer (VSI) is able to distinguish between the light coming from the planet and the light coming from the star, obtaining information about size and form of the planet. We present a method to detect faint sources in the way of bright sources using a VSI. We implement an algorithm based into the estimation of the wavefront from multiple directional derivatives in order to detect the presence of an object. Experimental results are shown.

8154-42, Poster Session

Designing of an intelligent flight instrumentation unit using embedded RTOS

R. Estrada-Marmolejo, G. Garcia-Torales, J. L. Flores-Nuñez, H. H. Torres-Ortega, Univ. de Guadalajara (Mexico)

Micro Unmanned Aerial Vehicles (MUAV) must know its spatial position in order to control its flight control, which is done by Inertial Measurement Units (IMUs). Some inertial sensors like MEMS have made it possible to reduce the size and power consumption of such units. Commonly the flight instrumentation operates independently of the main processor. This work presents a design which is able of reducing size and power consumption of the complete system of a MUAV. This is done by coupling the inertial sensors to the main processor leaving any intermediate level of processing aside. Using Real Time Operating Systems reduces the number of intermediate components, increasing MUAV reliability. One advantage is the possibility to control several different sensors with a single communication bus. This feature of the MEMS sensors makes a smaller and a less complex MUAV design possible.

8154-43, Poster Session

Characterization of narrow-band near-IR diodes arranged in array patterns

A. Ortega, G. Paez, M. Strojnik, Ctr. de Investigaciones en Óptica, A.C. (Mexico)

We examined old, not-well documented paintings before the process of restoration for presence of any invisible signatures and dates, as well as original line drawings and possible painted-over or hidden images. With the availability of the LEDs in the IR, emitting only in the invisible portion of the EM spectrum, we connected them in various two-dimensional array distribution to allow us to sample the surface of the art work with approximately uniform illumination, but different peak wavelength. We describe the extended area infrared LED illumination sources as to their geometrical arrangement, and their resulting spectral, spatial, and power output characteristics. With the especially designed LED based light sources, we were able to make visible the history of the painting and we observed the back-up material in detail.

8154-44, Poster Session

MetOp/HIRS pre-launch characterization data reanalysis

T. Chang, I. M. Systems Group, Inc. (United States); C. Cao,

National Oceanic and Atmospheric Administration (United States)

Instrument self-emission and nonlinear response play important roles in analyzing satellite thermal infrared radiometers, and can affect the accuracy of Earth scene radiance retrieval if uncorrected. This paper presents a simplified self-emission model for infrared radiometers and analyzes the interrelationships between the instrument self-emission, detector nonlinearity, and calibration intercept and slope variations using MetOp/HIRS prelaunch characterization data. HIRS is a traditional cross-track line scanning radiometer in the infrared and visible spectrum, including 12 long wave infrared channels (669-1529cm⁻¹), 7 short wave infrared channels (2188-2657cm⁻¹), and 1 visible channel, with beamsplitters and a rotating filter wheel assembly consisting of 20 spectral filters separates individual channels. The warm filters and other in-path components generate self-emission which becomes the majority of the total radiance falling on the detector. The pre-launch TV data allow us to evaluate the self-emission using the simplified model. It was found that the self-emission contributions at the detectors are in the range of 95% to 97%. The self-emission fluctuates with the instrument temperature and causes the variation in instrument response, including the variations of intercept and the instrument gain. The quantification of these variations provides guideline for on-orbit calibration algorithm improvement. The self-emission model is improved and its impact on MetOp/HIRS on-orbit calibration and Earth scene retrieval are also assessed. Potential applications of this model to other infrared radiometers and sounders are also discussed.

8154-45, Poster Session

Precise uniform light source based on optically connected integration spheres for optical instrument calibration

L. A. Mikheenko, V. N. Borovytsky, A. Timofeev, National Technical Univ. of Ukraine (Ukraine)

The paper proposes the light sources in form of several optically connected integration spheres. The principal advantages of these light sources are high photometric and metrological characteristics. The principal field of their application is calibration of remote sensing instruments and sensitive megapixel cameras. The light source contains several primary integration spheres of small diameters which are installed on a secondary integration sphere of bigger diameters. The initial light sources - halogen lamps or light emitted diodes are installed in the primary integration spheres. These spheres are mounted on the secondary integration sphere. The radiation comes from the primary integration spheres to the secondary one through a diaphragm which diameter can be varied. The secondary integration sphere has an output aperture. It has been investigated a light source with output aperture diameter 0.2 m and 3 primary integration spheres. It guarantees output radiance from 0.01 to 1000 W/(st m²), radiance nonuniformity in output aperture smaller 0.5%, non-linearity of output radiance control - smaller 0.1 %. The paper presents the results of theoretical and experimental research including techniques for radiance calculation and design recommendations. There are discussed the metrological accuracy and selection of optimal parameters. It is proved that the proposed light sources make possible minimization of total metrological error down to 0.5 % even when non expensive components are used for assembling them. The proposed light sources can be considered as one of the best candidates for calibration of remote sensing instruments working in optical range 0.4 - 2.2 mkm.

8154-46, Poster Session

Updated level-1 processing after two-years operation of TANSO-FTS

H. Suto, A. Kuze, K. Shiomi, M. Nakajima, Japan Aerospace Exploration Agency (Japan)

Conference 8154:
Infrared Remote Sensing and Instrumentation XIX

To monitor the global column concentration of carbon dioxide (CO₂) and methane (CH₄) from space, the Greenhouse gases Observing SATellite (GOSAT) was launched on January 23, 2009, and has started the operational observation. Thermal and Near Infrared Sensor for Carbon Observation- Fourier Transform Spectrometer (TANSO-FTS) has been continuously measuring CO₂ and CH₄ distributions globally every three days, and data distribution to the public started from Feb. 16, 2010. During two years operational periods, the radiometric, geometric and spectroscopic characterizations of TANSO have been continuously conducted with updating the Level-1 processing algorithm. To make a precise spectroscopic observation, correction algorithms were newly developed, demonstrated and installed on operational processing. Two major corrections are discussed. One is correction of the scan-speed instability caused by micro-vibration from satellite. Through the on-orbit data analysis, degrading spectroscopic accuracy caused by periodically micro-vibrations was found, and these distortion effects were compensated with applying the re-sampling technique for interferogram. The other is non-linearity correction in the electronics. In this presentation, the detail of on-orbit characteristics and the current status of TANSO will be discussed.

8154-47, Poster Session

Characterization and measurements collected from Infrared Grazing Angle Reflectometer

M. R. Benson, M. A. Marciniak, Air Force Institute of Technology (United States); J. Burks, Air Force Research Lab. (United States)

Recently, the Air Force Institute of Technology acquired a piece of equipment known as the Infrared Grazing Angle Reflectometer, or IGAR. IGAR is used for measuring the Directional Hemispherical Reflectance, or DHR, of samples at infrared wavelengths and incidence angles close to grazing. DHR is a ratio of power reflected into the entire hemisphere above a planar surface to incident power, and is of great interest to the photonic community and the Air Force. IGAR's DHR data can be compared with the Bidirectional Reflectance Distribution Function, or BRDF, measurements taken by our scatterometer. While other devices typically measure DHR at or near normal incidence, IGAR is novel as it allows us to make measurements with the angle of incidence ranging from 30 to 85 degrees, giving us a very unique data set. In addition, IGAR is equipped with a tunable laser source, allowing us to measure DHR at wavelengths ranging from 9.2 to 10.7 microns. Additional lasers can be easily added, and future plans include integrating our tunable quantum cascade lasers, extending our wavelength range from 4.3 to 9.7 microns. IGAR utilizes a hemi-elliptical mirror and a five-sided pyroelectric detector to measure DHR. By using this setup, IGAR can make low noise measurements while still capturing all of the reflected light. Our future sample set includes infrared material standards such as infragold, carbon nanotubes, nanostructured devices, and various layered media.

8154-48, Poster Session

Cost effective method to measure strain independent of temperature using a half etched fiber Bragg grating

M. Kondiparthi, Indian Institute of Science (India)

A novel approach for the measurement of strain independent of temperature is proposed. This approach is based on the fact that an applied strain on a half etched fiber Bragg grating leads to a change in spectral area of FBG reflection. Previously, relative shift in the two peaks of the FBG reflection of half-etched FBG is used as a signature to measure strain, which demands costly Optical spectrum analyzer. An FBG written in a fiber optic cable, which has two different clad diameters over its length, is considered for analysis. The clad diameter changes at half the FBG length. When such FBG is illuminated with a broadband source, strain applied on the same can be estimated by measuring the reflected radiation using an optical power meter (photodiode), hence, replacing the necessity of an optical spectrum analyzer. Temperature changes leads to a shift in the entire reflection, keeping the spectral area unaltered, hence allowing one to measure strain independent of temperature.

For an applied strain on an initially uniform half etched FBG, along with a peak split in the reflection spectrum, there will be an increase in the spectral area, which can be detected by measuring the optical power reflected back from the FBG. These variations are predominant for specific length strength combinations. For different length strength combinations, plots between the spectral area and applied strain were obtained using Transfer matrix approach. As an eg, from simulated plots, a 'spectral area-strain' monotonic range of 5nm can be obtained for a 1cm long grating.

Conference 8155A: Infrared Sensors, Devices, and Applications

Monday-Thursday 22-25 August 2011 • Part of Proceedings of SPIE Vol. 8155A
Infrared Sensors, Devices, and Applications

8155A-47, Poster Session

Simultaneous 1310/1550 dual-band optical frequency domain imaging for spectroscopic investigations

Y. Mao, S. Chang, E. Murdock, C. Fluerau, National Research Council Canada (Canada)

High-speed swept-source has received much attention in recent years for applications in optical frequency domain imaging (OFDI). The swept sources published so far produce sweeping in only one single wavelength band for both polygonal mirror filter based and piezo-tunable Fabry-Perot (FP) filter based swept source, based on our knowledge. We report a novel simultaneous high-speed 1310/1550 swept laser source for spectroscopic OFDI with low computation cost. Synchronized dual-wavelength tuning is performed by using two cavities and narrow-band wavelength-filters with a single dual-window polygonal scanner. Measured average output powers of 60 mW and 27 mW have been achieved for 1310 and 1550 nm bands, respectively, while the two wavelengths were swept simultaneously from 1227 nm to 1387 nm for 1310 nm band and from 1519 nm to 1581 nm for 1550 nm band at an A-scan rate of 65 kHz. A broadband wavelength-division multiplexing is used for coupling two wavelengths into a common-path single-mode GRIN-lensed fiber probe to form a dual-band common-path OFDI. Simultaneous imaging at 1310 and 1550 nm is achieved. This technique allows potentially for in vivo endoscopic high-speed functional OFDI with high quality spectroscopic contrast.

8155A-01, Session 1

DARPA perspective for imaging technology

N. K. Dhar, Defense Advanced Research Projects Agency (United States)

No abstract available

8155A-02, Session 1

Planar integrated plasmonic infrared spectral sensor

R. E. Peale, Univ. of Central Florida (United States); C. J. Fredricksen, LRC Engineering Inc. (United States); P. Figuierdo, Univ. of Central Florida (United States); J. W. Cleary, Solid State Scientific Corp. (United States); W. R. Buchwald, Air Force Research Lab. (United States)

A planar integrated spectral sensor consisting of quasi-broad band infrared source, waveguides, surface-plasmon molecular interaction region, and an array of dispersion elements and detectors is described. The source is a multi-mode quantum cascade laser whose center frequency is chosen to coincide with a characteristic absorption line of chemical or biological analyte of interest. The waveguides consist of thin semiconductor tapers that float ~10 microns above a conductor surface and adiabatically convert the ordinary photonic waveguide modes into surface plasmon polaritons (SPP). An interaction region between ingoing and outgoing taper waveguides is activated with chemical recognition elements that selectively bind and concentrate the analyte of interest. In this interaction region, the bound molecules remove certain infrared frequency components at their characteristic vibrational frequencies. The specific conductor used to host surface plasmons is chosen to have infrared plasma frequency to enhance confinement of infrared

surface plasmons and their overlap with the analyte. The infrared surface plasmons are then converted back to a photonic waveguide mode in the outgoing taper, and this mode is sampled by a series of different ring resonators, each with its own detector.

8155A-03, Session 1

Electrical passivation of anti-reflective microstructures in mercury cadmium telluride

J. Pattison, P. S. Wijewarnasuriya, U.S. Army Research Lab. (United States); N. K. Dhar, Defense Advanced Research Projects Agency (United States)

Inductively coupled plasma etching was applied to create anti-reflective structures in HgCdTe. Conformal deposition of passivating materials was accomplished through atomic layer deposition of Al₂O₃ and SiO₂ layers. Scanning electron microscopy was used to characterize the microstructures after ICP etch and again after ALD. Infrared reflectance and transmission measurements were performed on as grown, ICP etched, and ALD passivated samples to demonstrate an increase in absorbance due to the AR structures. Planar sister samples of MCT were exposed to similar ICP etch conditions and passivated by ALD. The electrical passivation of the planar samples was studied through photoconductive decay measurements in order to compare the minority carrier lifetime of as-grown, etched, and passivated material. Planar sample served as proxies for the etched material, as the required electric field of the PCD experiment does not pass through the anti-reflective microstructure layer.

8155A-04, Session 1

Design of readout integrated circuit with enhanced capacitance mechanism for dual-band infrared detector

Y. Lu, T. Sun, Y. Liu, S. Shiu, H. Shieh, National Chi Nan Univ. (Taiwan); S. Tang, W. Lin, Chung Shan Institute of Science and Technology (Taiwan)

This thesis will propose a solution to solve over dark current by sharing capacitor, avoiding output signal distortion because of integration voltage saturation. The integration capacitance can change by adding switch in pixel circuit; it will increase two times than original capacitance. This circuit also provide the function of output either single-band or dual-band by switching different sensor. This readout integrated circuit design has adopted TSMC 0.35um 2P4M CMOS 5V process, worked by 5V power supply and operated at 3MHz clock rate. The dual-band pixel circuit uses interlace structure, the pixel circuit area of two wavelengths are both 30um x 30um. The mid-wave and long-wave sense current are from 1nA to 2nA and 6nA to 8nA, respectively. The output swing is 2.8V.

There are four major contributions in this paper. First, we introduce the design of dual-band infrared focal plane array, and provide analog and digital control circuit blocks. Then we introduce inner circuit design, including pixel circuit column select circuit and output buffer stage circuit. Second, we explain the sharing capacitor module in pixel circuit, and then we design the interlace readout integrated circuit by 40x16 array size. Third, we provide the simulation result. Finally, we discuss the trend of circuit application.

Conference 8155A:
Infrared Sensors, Devices, and Applications

8155A-05, Session 1

Enabling NIR imaging at room temperature based on quantum dots

S. Le Calvez, H. Bourvon, C. Philippot, H. Kanaan, S. Meunier-Della-Gatta, P. Reiss, Commissariat à l'Énergie Atomique (France)

If imaging in visible light is now a well-mastered technology, imaging in near infrared at room temperature remains a challenge. In our everyday life, many applications appeared for imaging in near infra-red like sensing, night vision and biological diagnostics. However, if silicon based detectors are very performing in visible, they become inefficient over 1000nm. Other solutions as microbolometers or InGaAs detectors are not mature enough or too expensive to be efficient in this wavelength range. That's why colloidal quantum dots materials are interesting as they have the appealing property to absorb at a tunable wavelength determined by their nature and diameter and also because their processability in solution make them a key solution for low cost applications on either solid or flexible substrates. Then, we can assume that imagers may be made from processing near infra-red quantum dots solutions on top of active matrix backplane.

We will present, a way to synthesize PbS quantum dots with a stabilizing CdSe/ZnS double-shell. The nanocrystal core presents a 6nm core that makes it absorb around 1450nm. This quantum dot was then incorporated in a stack to prepare a device. Pixels smaller than 50µm were obtained with a detectivity higher than 10^9 Jones. We will report at the conference a comparison of the different wet deposition process used like non patternable coating as spin coating or patternable ones as inkjet printing or stamping. We will focus on the optimized parameters and the successful performances of our devices.

8155A-07, Session 1

Long-wave infrared InAs/GaSb strain layered superlattice barrier heterostructure detectors

S. A. Myers, N. Gautam, E. Plis, M. N. Kutty, B. Klein, T. Schuler-Sandy, S. Krishna, Ctr. for High Technology Materials (United States)

Long-wave infrared (LWIR) detector technologies with the ability to operate at or near room temperature are very important for many civil and military applications including chemical identification, surveillance, defense and medical diagnostics. Eliminating the need for cryogenics in a detector system can reduce cost, weight and power consumption; simplify the detection system design and allow for widespread usage. In recent years, infrared (IR) detectors based on uni-polar barrier designs have gained interest for their ability to lower dark current and increase a detector's operating temperature.

Our group is currently investigating nBn and pBp detectors with InAs/GaSb strain layer superlattice (SLS) absorbers (n) and contacts (n), and AlGaSb and InAs/AlSb superlattice electron and hole barriers (B) respectively. For the case of the nBn structure, the wide-band-gap barrier material (AlGaSb) exhibits a large conduction band offset and a small valence band offset with the narrow-band-gap absorber material. For the pBp structure (InAs/AlSb superlattice barrier), the converse is true with a large valence band offset between the barrier and absorber and a small or zero conduction band offset. Like the built-in barrier in a p-n junction, the heterojunction barrier blocks the majority carriers allowing free movement of photogenerated minority carriers. However, the barrier in an nBn or pBp detector, in contrast with a p-n junction depletion layer, does not contribute to generation-recombination (G-R) current.

In this report we aim to investigate and contrast the performance characteristics of an SLS nBn detector with that of and SLS pBp detector.

8155A-08, Session 1

Addressing surface leakage in type-II InAs/GaSb superlattice materials using novel approaches to surface passivation

E. A. DeCuir, Jr., J. W. Little, U.S. Army Research Lab. (United States); N. Baril, U.S. Army Night Vision & Electronic Sensors Directorate (United States); P. Ye, Purdue Univ. (United States)

Poor surface stability of InAs/GaSb SL photodetectors continues to be a major hurdle to the realization of high performance devices in this material system. While there has been continual improvement in material quality over the years, surface instability is still a major limiting factor in long-wavelength infrared detectors which ultimately hampers detector performance. This study focuses on a two step approach towards the successful passivation of long-wavelength InAs/GaSb superlattice structures. This entails various initial chemical passivation of the surface to remove surface oxides and satisfy dangling bonds followed by a robust dielectric treatment via plasma-enhanced chemical vapor deposition of SiO₂ on the mesa sidewalls. Alternatively, an atomic layer deposition process of Al₂O₃ or HfO₂ was also used to treat the mesa sidewalls in an effort to mitigate the effects of rapidly formed native oxides during device processing. The variable area diode analysis technique employing diodes of variable diameter (20-400µm) enabled the investigation of surface resistivity as a result of different passivation treatments. Temperature dependent studies of the dark current enabled an understanding of the dominating current mechanism, while temperature dependent capacitance-transient measurements were used on select diodes to gauge the presence and activation energy of defects that may be contributing to excessive dark currents in these diodes.

8155A-09, Session 1

Avalanche photodiodes for high-resolution UV imaging applications

A. K. Sood, Magnolia Optical Technologies, Inc. (United States); R. D. Dupuis, Georgia Institute of Technology (United States); N. K. Dhar, Defense Advanced Research Projects Agency (United States); R. S. Balcerak, System Planning Corp. (United States)

High resolution imaging in UV band has a lot of applications in Defense and commercial applications. The shortest wavelength is desired for spatial resolution which allows for small pixels and large formats. UVAPD's have been demonstrated as discrete devices demonstrating gain. The next frontier is to develop UV APD arrays with high gain to demonstrate high resolution imaging.

We will discuss model that can predict sensor performance in the UV band using APD's with various gain and other parameters for a desired UV band of interest. SNR's can be modeled from illuminated targets at various distances with high resolution under standard atmospheres in the UV band and the solar blind region using detector arrays with unity gain and with high gain APD's.

We will present recent data on the GaN based APD's for their gain, detector response, dark current noise and the 1/f noise. We will present various approaches and device designs that are being evaluated for developing APD's in wide band gap semiconductors. The paper will also discuss state of the art in UV APD and the future directions for small unit cell size and gain in the APD's.

8155A-10, Session 1

Visible-blind ultraviolet photodetector fabricated on double heterojunction of n-ZnO/LAO/p-Si

D. Tsai, H. Wang, C. Kang, J. He, National Taiwan Univ. (Taiwan)

**Conference 8155A:
Infrared Sensors, Devices, and Applications**

A visible-blind UV photodetector (PD) based on a double heterojunction of n-ZnO/insulating LaAlO₃ (LAO)/p-Si grown by pulsed laser deposition has been fabricated. The photodetector shows a rectification ratio of similar to 10⁴ at ±2 V and a dark current of 9 nA at a reverse bias of -2V. The photoresponse spectrum indicates a visible-blind UV detectivity of our devices with a high UV/visible rejection ratio. The LAO layer, acting as a barrier layer, prevents minority carrier to transport from p-Si base under visible light illumination due to the high potential barrier between p-Si and LAO. These results clearly demonstrate that n-ZnO/LAO/p-Si PDs hold high potential in the next-generation visible-blind UV PDs.

8155A-11, Session 2

Reducing the read noise of H2RG detector arrays by more efficient use of reference signals

B. J. Rauscher, NASA Goddard Space Flight Ctr. (United States)

We present a process for characterizing the correlation properties of the noise in large two-dimensional detector arrays, and describe an efficient process for its removal. In the case of the 2k × 2k HAWAII-2RG detectors (H2RG) detectors from Teledyne which are being used on the Near Infrared Spectrograph (NIRSpec) on the James Webb Space Telescope (JWST), we find that we can reduce the read noise by about half. Noise on large spatial scales is dramatically reduced. With this relatively simple process, we provide a performance improvement that is equivalent to a significant increase in telescope collecting area for high resolution spectroscopy with NIRSpec.

The method is based on Principal Components Analysis (PCA) of the NIRSpec detector subsystem (DS). The DS includes two H2RG detector arrays and a pair of cryogenic SIDECAR ASICs. The PCA showed that the covariance matrix's eigenvectors are sines and cosines, and that the noise is temporally stationary in consequence. Building on this, we studied the correlation properties between the regular outputs, the reference output, the reference pixels, and blanked off pixels used as references in Fourier space. A significant finding is that a set of frequency dependent weights must be applied to the reference output before it is used differentially. The correct weights reject noise at frequencies >~3 kHz, and correct for non-unity gain at lower frequencies. When the correct frequency dependent weights are used with the other references in a similar manner, we find that we can significantly reduce the noise and greatly reduce the degree of noise correlation.

8155A-12, Session 2

A 260 megapixel visible/NIR mixed technology focal plane for space

R. W. Besuner, Univ. of California, Berkeley (United States); C. J. Bebek, Lawrence Berkeley National Lab. (United States); G. M. Haller, SLAC National Accelerator Lab. (United States); S. E. Harris, Univ. of California, Berkeley (United States); P. A. Hart, SLAC National Accelerator Lab. (United States); H. D. Heetderks, P. N. Jelinsky, M. L. Lampton, Univ. of California, Berkeley (United States); M. E. Levi, Lawrence Berkeley National Lab. (United States); S. E. Maldonado, SLAC National Accelerator Lab. (United States); N. A. Roe, Lawrence Berkeley National Lab. (United States); A. J. Roodman, L. Sapozhnikov, SLAC National Accelerator Lab. (United States)

Mission concepts for NASA's Wide Field Infrared Survey Telescope (WFIRST), ESA's Euclid mission, as well as next-generation ground-based surveys, require large mosaic focal planes to image visible and near infrared (NIR) wavelengths. We have developed space-qualified detectors, readout electronics and focal plane design techniques that can be used to intermingle CCDs and NIR detectors on a single, silicon carbide (SiC) cold plate. This enables optimized, wideband observing

strategies. The CCDs, developed at Lawrence Berkeley National Laboratory, are fully-depleted, p-channel devices that are backside illuminated and capable of operating at temperatures down to 110K. The NIR detectors are 1.7µm and 2.0µm wavelength cutoff H2RG@ HgCdTe, manufactured by Teledyne Imaging Sensors under contract to LBNL. Both the CCDs and NIR detectors are packaged on 4-side abutable SiC pedestals with a common mounting footprint supporting a 44mm mosaic pitch. Both types of detectors have direct-attached, readout electronics that convert the detector signal directly to serial, digital data streams and allow a flexible, low cost data acquisition strategy to enable large data rates. A mosaic of these detectors can be operated at a common temperature that achieves the required dark current and read noise performance necessary for dark energy observations. We report here the qualification testing and performance verification for a focal plane that accommodates a 4x8 array of CCDs and HgCdTe detectors.

8155A-46, Session 2

Nondestructive moisture sensing in in-shell nuts using near infrared (NIR) reflectance spectroscopy

C. V. Kandala, J. Sundaram, Agricultural Research Service (United States)

Ability to determine the moisture content (MC) of certain nuts such as peanuts and pecans, while they are in their shells, rapidly and nondestructively is useful in their harvest, sale and processing. It was found earlier that, with commercially available NIR spectrometers the moisture contents of Valencia type in-shell peanuts could be estimated within permissible accuracies. In this work a custom made NIR instrument was used to predict MC of two varieties of peanuts, while they are in their shells, and the results were compared with those obtained by standard methods. Spectral data from 1000 nm to 2500 nm was collected for Valencia and Virginia types of in-shell peanuts in the moisture range of 6% to 26%. Partial least squares (PLS) analysis was performed on calibration groups in each type, certain pretreatments were applied, and models were developed for prediction. Models with low standard error of calibration and best R² values were selected for MC predictions. Predicted values were compared with reference values obtained by standard methods and goodness of the fit was judged from the standard error of prediction (SEP) and the R² values. Results obtained for both types were good, and suggest the possibility of designing a low-cost NIR instrument useful for the peanut industry.

8155A-48, Session 2

Novel EO/IR sensor technologies

K. L. Lewis, Electro Magnetic Remote Sensing Defence Technology Ctr. (United Kingdom)

The Electro-Magnetic Remote Sensing (EMRS DTC) was established in 2003 to provide a centre of excellence in sensor research and development, supporting new capabilities in key military areas such as precision attack, battlespace manoeuvre and information superiority. The DTC was set up as a partnership between UK Industry, the academic science base and the UK Ministry of Defence, to develop advanced and affordable technology in support of mission-oriented defence capabilities. In the area of advanced electro-optic technology, the DTC has supported work on discriminative imaging, advanced detectors, laser components/ technologies, and novel optical techniques. This paper will summarise some of the results achieved in the DTC's programme, using examples drawn from each of the key theme areas, supported by the results of field trials in realistic military environments.

Conference 8155A:
Infrared Sensors, Devices, and Applications

8155A-14, Session 3

Quantum well and quantum dot device research at the Army Research Lab.

P. N. Uppal, U.S. Army Research Lab. (United States)

No abstract available

8155A-15, Session 3

The performance improvement calculation of C-QWIP with a high T_c superconducting electron filter

J. Sun, K. Choi, U.S. Army Research Lab. (United States)

The Corrugated Quantum Well Infrared Photodetector (C-QWIP) holds significant performance and other advantages over other infrared detectors. However, one disadvantage of the detector is the relatively low operating temperature needed to suppress the dark current. By coating two additional layers (thin insulator and high critical temperature (T_c) superconductor) on the top contact layer of a C-QWIP wafer, the top three layers of the detector form a high-T_c superconducting single electron tunneling junction. It could act as an electron filter because of the presence of an energy gap in superconductors. Since the photo electrons and dark electrons of a C-QWIP are well separated in energy, most dark current is conducting below the quantum well (QW) barrier height and most photo current is conducting above the barrier height. Most dark electrons thus could be blocked by the junction while most photo electrons pass the junction by applying an appropriate voltage. Our calculation shows that the filter could provide 40% or 70% improvement in Noise Equivalent Temperature Difference (NETD) of detector focal plane arrays (FPAs) at normal operating temperature depends on the detector emitter photocurrent to dark current ratio is = 1 (emitter is BLIP) or = 0.1 (emitter is far from BLIP). For both cases, the filter could increase the detector FPAs operating temperatures up to 90K (30K improvement) with 10% to 20% NETD improvement respectively.

8155A-16, Session 3

A frequency domain model for the spatial fixed-pattern noise in infrared focal plane arrays

O. J. Medina, J. E. Pezoa, S. N. Torres, Univ. de Concepción (Chile)

The multiplicative and additive components of the Fixed-pattern Noise (FPN) in Infrared (IR) Focal Plane Arrays (FPAs) are typically modeled as time-stationary, spatially unstructured random processes. Even though the latter assumption is convenient, it is also inaccurate due to FPN is indeed observed as a spatial pattern, with random intensity values, superimposed over the true images. In this paper, the spatial structure in both the multiplicative and the additive components of the FPN has been modeled in the frequency domain. The key observation in the proposed models is that regular spatial patterns manifest themselves as narrowband components in the magnitude spectrum of an image. Thus, the spatial structure of FPN can be abstracted in a straightforward manner by approximating the spectral response of the FPN. Moreover, the random intensity of FPN has been also modeled by matching the empirically estimated distributions of the intensity values of both multiplicative and additive components of the FPN. Experimental characterization of FPN has been conducted using black-body radiator sources, and the theoretical as well as practical applicability of the proposed models has been illustrated by both synthesizing FPN from three different IR cameras and by proposing a simple yet effective metric to assess the amount of FPN in FPA-based cameras.

8155A-17, Session 3

A multidimensional approach for stripping noise compensation in hyperspectral imaging devices

P. F. Meza, F. I. Parra, S. N. Torres, J. E. Pezoa, P. Coelho, Univ. de Concepción (Chile)

Stripping noise compensation (SNC) algorithms for push-broom hyperspectral cameras (PBHCs) are primarily based on image processing techniques. These algorithms rely on the spatial and temporal information available at the readout data; however, they disregard the large amount of spectral information also available at the data. In this paper such flaw has been tackled and a multidimensional approach for SNC is proposed. The main assumption of the proposed approach is the short-term stationary behaviour of the spatial, spectral, and temporal input information. This assumption is justified after analyzing the optoelectronic sampling mechanism carried out by PBHCs. Namely, when the wavelength-resolution of hyperspectral cameras is high enough with respect to the target application, the spectral information at neighbouring photodetectors in adjacent spectral bands can be regarded as a stationary input. Moreover, when the temporal scanning of hyperspectral information is fast enough, consecutive temporal and spectral data samples can also be regarded as a stationary input at a single photodetector. The strength and applicability of the multidimensional approach presented here is illustrated by compensating for stripping noise real hyperspectral images. To this end, a laboratory prototype, based on a Photonfocus Hurricane hyperspectral camera, has been implemented to acquire data in the range of 400-1000 [nm], at a wavelength resolution of 1.04 [nm]. A mobile platform has been also constructed to simulate and synchronize the scanning procedure of the camera. Finally, an image-processing--based SNC algorithm has been extended yielding an approach that employs all the multidimensional information collected by the camera.

8155A-18, Session 3

Study of unipolar HgCdTe nBn and Auger-suppressed hybrid structure photodetectors

A. M. Itsuno, J. D. Phillips, Univ. of Michigan (United States); S. Velicu, EPIR Technologies, Inc. (United States)

Conventional state-of-the-art HgCdTe p-n heterojunction infrared devices face performance limitations due to thermal generation-recombination mechanisms and challenges related to processing technology, particularly with achieving low, controllable in-situ p-type doping using molecular beam epitaxy (MBE) growth techniques. These issues motivate the need for improved device performance at higher operating temperatures and/or device structures requiring simplified fabrication processes. To address these challenges, two proposed alternative HgCdTe detector structures are investigated in further detail: 1) a unipolar HgCdTe implementation of the nBn structure and 2) a novel Auger-suppressed unipolar hybrid nBv_n structure. Both structures rely on bandgap engineered barrier layers to suppress SRH and Auger processes, respectively, contributing to the dark current density and performance limitations. The unipolar devices provide the benefit of a simplified fabrication process, where p-type doping requirements are eliminated. Numerical physics-based device simulations utilizing established HgCdTe material parameters and incorporating tunneling contributions and generation-recombination mechanisms will be used to study the performance characteristics of both devices, with more emphasis placed on the proposed nBv_n architecture. Past work has predicted near equivalent performance characteristics of nBn devices to those achieved by ideal p-n heterojunction devices. Alternatively, the nBv_n device is expected to exhibit both SRH and Auger suppression due to the nature of the structure, thus, achieving a lower dark current density than that observed in current detector technology for the same temperatures. This demonstration would have significant implications for high temperature detector operation regarding reduction in power and cooling requirements without sacrificing device performance.

8155A-19, Session 3

New approach to noise factor measurement on microchannel plate of optoelectronic detector

L. Liu, Y. Qiu, Y. Qian, Nanjing Univ. of Science & Technology (China)

The micro-channel plate (MCP) is an important part to imaging quality of image intensifier. To do research and analysis work on the MCP parameter have practical significance to the understanding of the performance and then can help to know where improvement should be made and then achieve a best performance entire tube. In most of parameters of MCP, the inspection of noise characteristics is a key point.

In this paper, a new method for noise factor determination in MCP is described, which allows one to carry out the measurement on the MCP instead of overall image intensifier.

Firstly a math model to noise power factor of MCP is established. The noise factor is defined as the ratio of the square of input signal to noise ratio to the square of output signal to noise ratio.

Then a measurement system is developed, which consists of vacuum chamber, electron gun, high voltage supply, imaging luminance meter, control units, signal processing circuit, A/D converter, D/A converter, communication unit, industrial computer and measurement software.

Based on this system, we carry out the testing of the noise power factor of MCP. The noise power factor results are obtained. Through the comparison to the sample MCP's noise characteristics, it can be concluded that this new approach and testing device to noise power factor measurement of MCP are reliable.

8155A-20, Session 3

Study of recombination mechanisms limiting the performance of Sb-based III-V type II superlattices for infrared detectors

B. C. Connelly, G. D. Metcalfe, P. H. Shen, M. Wraback, U.S. Army Research Lab. (United States)

Type II strained layer superlattice (T2-SLS) technology is currently being developed as an alternative to existing HgCdTe photodetectors and quantum well infrared photodetectors for use as large format focal plane arrays in the 8-12 μm long-wave infrared (LWIR) and 3-5 μm mid-wave infrared (MWIR) wavelength ranges. T2-SLSs are expected to possess lower Auger recombination rates than HgCdTe detectors due to the ability to engineer the bandgap. However, T2-SLS material is currently limited by non-radiative Shockley-Read-Hall (SRH) recombination, resulting in short minority carrier lifetimes (10's of nanoseconds at 77 K) that do not approach the theoretical limit of the Auger recombination rate. It is important to investigate the minority carrier lifetime, since it is a primary limiting factor in the performance of these devices. We use time-resolved photoluminescence (TRPL) measurements to study the minority carrier lifetime as a function of temperature and excitation density for a series of SLS absorber samples. Experimental results on sets of samples that vary the SLS absorber width, the doping level of the SLS and the hole-well and SLS period will be presented along with modeling results. Time-domain measurements of the photoluminescence signal demonstrate multiple exponential decay, which provide information on background carriers, acceptor states and trap states. The temperature dependence of the TRPL signal shows that the carrier lifetime is dominated by SRH recombination. Limits to the radiative and Auger recombination coefficients are determined from high-injection measurements.

8155A-21, Session 3

Photoluminescence study of long-wavelength infrared superlattice detectors

L. Hoglund, A. Soibel, D. Z. Y. Ting, A. Khoshakhlagh, C. J. Hill, J. Nguyen, A. Liao, S. A. Keo, S. D. Gunapala, Jet Propulsion Lab. (United States)

Photoluminescence (PL) is a non-destructive characterization method that reveals information about the optical properties and the material quality of the material studied. Information about the material quality is obtained from the PL intensity and the width of the PL peak. By measuring the variation of PL amplitude and the peak position with temperature and excitation power, the physical properties of the superlattice such as the carrier recombination processes and the variation of the band gap with temperature can be studied. In this work, we investigated the temperature and wavelength dependence of the PL intensity for type II InAs/GaSb long wavelength complementary barrier infrared detector (CBIRD) superlattices in the temperature range 10 - 298 K. The influence of Shockley Read Hall and Auger recombination processes on the minority carrier lifetime was determined from the temperature and excitation power dependence of the PL intensity. These studies show full suppression of the Auger recombination processes for CBIRD detectors with 10 micrometer cut-off wavelength. Furthermore, we observed a linear decrease of the PL intensity with increasing cut-off wavelength of LWIR CBIRDs and found this trend unchanged in the temperature range 10 - 77 K. The observed dependence originates from the decreasing overlap between the electron and hole wave functions as the superlattice period increases.

8155A-22, Session 3

Cryogenic focal plane flatness measurement with optical zone slope tracking

J. Edelstein, M. M. Sirk, Univ. of California, Berkeley (United States); M. Hoff, Lawrence Berkeley National Lab. (United States); P. N. Jelinsky, R. W. Besuner, Univ. of California, Berkeley (United States); P. E. Perry, M. E. Levi, C. J. Bebek, Lawrence Berkeley National Lab. (United States); H. D. Heetderks, Univ. of California, Berkeley (United States)

Large-area cryogenic focal planes for visible to near infra-red astronomical imaging and spectroscopic space-based observatories, on missions such as WFIRST or EUCLID, must be planar in order to match the sensor plane to the focal surface of their fast optical telescope feeds. The plane flatness requirements are demanding, as focal planes of half-meter scales must be held flat to within a few 10's of microns while cooled to 140K. Verifying cryogenic focal plane flatness is challenging as micron level excursions need to be measured within and across a dozen 5-cm sensors inside a high-vacuum chamber and without using physical contact. We report an optical flatness measurement scheme applied to the LBL 35 x 18 cm, 32-sensor, CCD / HgCdTe focal plane developed for the JDEM. The scheme uses a telescope-fed micro-lens array that samples the focal plane to measure changes in the slope of local sensor zones.

8155A-23, Session 3

Temperature dependence of electron transport in GaN/AlGaIn quantum cascade detectors

S. V. Gryshchenko, M. V. Klymenko, O. V. Shuliika, Kharkov National Univ. of Radio Electronics (Ukraine); I. A. Sukhoivanov, Univ. de Guanajuato (Mexico)

**Conference 8155A:
Infrared Sensors, Devices, and Applications**

Quantum cascade detectors are promising structures for high-efficiency detection of infrared radiation. The quantum efficiency and response in these structures are strongly dependent on phonon mediated electron transport in the extractor region. In this work we investigate the influence of extractor design and temperature on transport properties of quantum cascade detector. For this purpose we realize numerical calculation of electron lifetimes considering electron-phonon and electron impurities scattering. Electron-phonon interactions are treated using Harrison's formula (Harrison P., Quantum wells, wires and dots, John Wiley & Sons, 2010, 564 p.) which allows to calculate lifetime of carriers with temperature and structure design taking into account. Transport characteristics of quantum cascade detectors have been computed using density matrix theory. As a result, we have obtained the system of ordinary differential equations describing dynamics of electron distribution functions and intersubband correlations. The theory has been developed using Hartree-Fock approximation for Coloumb interactions of electrons. Managing carrier lifetime in quantum wells gives us possibility to increase quantum efficiency and response. Obtained results are evidence that there exists optimal temperature range for high efficiency detecting. This range is dependent on structure design parameters including widths and materials of semiconductor layers. Also we have provided band engineering intended for minimization of electron lifetimes in the extractor.

8155A-24, Session 4**AlGaAn-based III-nitride tunnel barrier hyperspectral detector**

F. Shahedipour-Sandvik, Univ. at Albany (United States); N. Tripathi, College of Nanoscale Science & Engineering (United States); L. D. Bell, Jet Propulsion Lab. (United States)

We report on the recent progress made toward development of a III-nitride based tunable hyperspectral detector pixel with the potential advantages of reduced system complexity and increased dynamic control on the detection parameters in the context of existing hyperspectral detection systems. We discuss the concept, experiments and simulation of devices along with the different obstacles to be overcome before this technology can mature into a commercial application. Currently available hyperspectral detectors, apart from being bulky, have limited detection range for visible and IR regions of the spectrum. The proposed device has the potential to provide a wider range of detection wavelengths extending to the UV, visible and IR region, and real-time wavelength tunability without the use of filters and gratings.

This provides a great advantage over the existing hyperspectral detectors. The small size along with other important properties offered by the III-nitride material system, including the possibility of growth of the device structure on silicon substrate, enables integration with Si CMOS for system-on-chip realization.

8155A-25, Session 4**Earth limb infrared clutter model from measurements**

M. Kendra, K. Kraemer, Air Force Research Lab. (United States); D. Mizuno, R. R. O'Neil, Boston College (United States)

Mid-Course Space Experiment (MSX) infrared (IR) observations in the earth limb were used to obtain spatial power spectral densities (PSD's) for five sensor bands over a wide range of earth limb background clutter conditions. These backgrounds include daytime, nighttime, terminator, aurora, polar mesospheric cloud, atmospheric gravity wave, stratospheric warming, airglow, and other observations collected over approximately 100 episodic data collection events. Using a subset of detectors and restricting detector tangent altitude variations, a total of more than 33,000 high-quality PSD's were generated. For infrared detection of unresolved objects where the solid angle of the object is much smaller than the instantaneous field-of-view of a sensor element, the spectral component at high spatial frequencies is a critical metric. PSD's were

therefore constructed in the spatial domain using one minute data segments, which allowed spatial scale assessment from 0.01-10 cycles/km. PSD's that met the clutter model selection criteria were identified, accumulated, and processed to obtain a small set of empirical, altitude-based model parameters. We describe the MSX sensor bands, data and data processing employed for PSD generation and final reduction to obtain model parameters. Key model features are discussed with emphasis on object detection against stressing limb backgrounds. The model was constructed in a way that facilitates optical design and system engineering application. In particular, it may be used to address important space situational awareness (SSA) questions concerning detection thresholds, loss of track, false positive detections, and object identification, discrimination, and object state determination.

8155A-26, Session 4**Heat bearing device "Wärmepeilgerät 60"**

M. Krake, Helmut-Schmidt-Univ. (Germany); H. Rothe, Helmut-Schmidt Univ. (Germany)

The "Wärmepeilgerät 60" was a passive infrared device, meaning in this case it collected the infrared emissions radiated by ships. The advantage of passive devices versus active devices was, (i) that the enemy could not detect a passive device because it was not using a spotlight or something like this, (ii) and a much bigger detection range. Being developed in the beginning of the 40s by Zeiss the "Wärmepeilgerät 60" was used e.g. for coastal defense in Denmark. A squadron consisted of a pilot unit and four heat bearing devices. When a ship was detected by one of the heat bearing devices, the other ones were also directed to that target. Because of the distance of the devices always different target angles were measured. This gave the possibility for the pilot unit to transform the measured angles into fire control data for the coastal defense artillery. The devices were able to detect battleships up to 25 kilometers away and smaller ships, like torpedo boats, could be detected up to 15 kilometers away. This is more than current devices can achieve. Optical layouts and circuit diagrams will be presented and discussed in the paper.

8155A-27, Session 4**Evaluation of H2RG stability for infrared Earth-observing systems**

P. W. Sullivan, W. K. Edens, E. H. Darlington, The Johns Hopkins Univ. Applied Physics Lab. (United States); D. O. Neil, NASA Langley Research Ctr. (United States)

Although originally developed for low-flux astronomical applications, the space qualification and availability of the Teledyne HAWAII H2RG detector makes it appealing for high-precision Earth-observing systems. We have evaluated the performance of a science-grade H2RG detector for the GEO-CAPE gas correlation radiometer instrument concept in which North America would be imaged from geosynchronous orbit alternately through gas species cells (carbon monoxide and methane) and reference cells to measure the column density of these trace gases. In this shot noise-limited measurement, the signal-to-noise ratio is determined by the co-adding time afforded by the detector's stability and the required temporal resolution.

To assess temporal stability, the detector was operated in a cryogenic dewar with monitored blackbody illumination. Parallel 32-channel, 16-bit digitization of the detector output is accomplished by the Teledyne SIDECAR ASIC which clocks the detector to achieve subframe integration times of 10 milliseconds. We will present findings on the temporal instabilities of the detector system, including burst noise and bias drifts. With proper use of available reference signals, the instability can be reduced well below 0.1%. The read noise and power consumption of this operational mode have also been measured against increased clock speed. These findings are relevant to many applications requiring high relative sensitivity in a limited co-adding time, from Earth and planetary science to transiting exoplanet detection.

Conference 8155A:
Infrared Sensors, Devices, and Applications

8155A-28, Session 4

IR detector for hydrocarbons concentration measurement in emissions during petroleum and oil products storage and transportation

A. Vasilyev, Kuban State Technological Univ. (Russian Federation)

Oil storage in reservoirs and its transportation in tanks of liquefied cargo carrier accompany with loss of hydrocarbons, which leads to economic damage and environmental pollution.

Oil contains about 99,2% of saturated hydrocarbons. We offer to measure its concentration by method of infrared spectra absorption on the wave length 3.4 micron. Offering device is to be set on the pressure-and-vacuum valve of tanks and reservoirs.

This method based on spectral transparency with reference channel and synchronous detection. Introduced infrared detector will allow to carry on automatic and continuous monitoring of saturated hydrocarbons evaporation which will help to choose correct methods of prevention such losses and to control its faultless operation.

8155A-29, Session 4

eSNR improvement in indirect detection of mid-IR signals by wavelength conversion in SOS waveguides

Y. Huang, S. K. Kalyoncu, E. Tien, S. Gao, Q. Song, F. Qian, E. Adas, D. Yildirim, O. Boyraz, Univ. of California, Irvine (United States)

With a transparency window up to 6 μm , sapphire can serve as a platform to support silicon photonic integrated circuit in MWIR. Planar waveguide devices based on silicon-on-sapphire (SOS) are emerging as a bridge between MWIR and SWIR through frequency band conversion process. While these devices are widely proposed to amplify MWIR signals and generate MWIR source, it can also be inversely utilized to achieve MWIR light detection. Here MWIR signals are down-converted to telecommunication wavelength (1.55 μm) through SOS waveguides and indirectly detected by SWIR detectors. Since detectors at telecommunication wavelengths exhibit superior performances in terms of speed, noise and sensitivity, the indirect detection scheme can be a promising candidate to improve the detection performance.

In this report, we analyze performance of the indirect detection of MWIR signals by wavelength conversion in SOS waveguides. Particularly we modeled and compared the noise performance of the indirect detection with direct detection using state-of-the-art MWIR detectors. We show that, in addition to advantages of room temperature and high speed operation, the proposed indirect detection can improve the electrical signal-to-noise ratio up to 50dB, 23dB and 4dB compared to direct detection by PbSe, HgCdTe and InSb detectors respectively. The improvement is more pronounced in detection of weak MWIR signals.

8155A-30, Session 4

Compact LC-tuned Fourier transform imaging spectrometer

X. Xia, A. V. Parfenov, E. A. DeHoog, A. Shapoury, T. M. Aye, M. Shih, Physical Optics Corp. (United States)

Multispectral and hyperspectral imaging devices have numerous military and industrial applications, including reconnaissance, targeting, guidance, remote sensing, biomedical imaging, environmental and agricultural monitoring, pollution monitoring, navigation, and law enforcement. Grating-based hyperspectral imaging remote sensor systems such as the Compact Airborne Spectral Sensor (COMPASS) hyperspectral imager (HSI), have been developed by the Army Night

Vision and Electronic Sensors Directorate (NVESD), which operates from 400 nm to 2350 nm, and represents a major step in the practical implementation of visible and infrared (IR) sensors. State-of-the-art airborne hyperspectral imagers with two-dimensional (2D) focal plane arrays (FPA) for midwave infrared (MWIR) and longwave infrared (LWIR) have been built and deployed. Examples include the ARES and SEBASS that use prism dispersive imaging spectrometers covering the MWIR (3-5 μm) or LWIR (7.6-13.4 μm). GIFTS for NASA is an example of imaging Michelson Fourier transform spectrometers (FTS) operating in the MWIR/LWIR bands. However, the potential applications of all these hyperspectral systems are limited by their large size, high power consumption, heavy weight, and significant cost. In this paper, we demonstrate the novel hyperspectral imaging using a LC-based electro-optic (EO) tuning imaging Fourier-Transform spectrometer (FTS) which could result in a compact, lightweight, low-cost, low-power, spectral imaging sensor, that can be integrated with small airship platforms for reconnaissance, surveillance, and target acquisition missions. Details of fabrication and experimental results will be presented.

8155A-31, Session 4

Real-time 4D subsurface corrosion inspection using ultrahigh-speed, Fourier-domain optical coherence tomography (OCT)

A. Rodriguez, Naval Sea Systems Command (United States); J. U. Kang, The Johns Hopkins Univ. (United States)

Optically-gated reflectometry based on low coherence interferometry has found important applications in surface and sub-surface imaging. This is because of the high spatial resolution, the relative simplicity, and the superior signal discrimination of the technique when used in highly scattering materials.

When this type of optically gated reflectometry is used in a scanning mode it is termed optical coherence tomography (OCT). Until recently, the vast majority of applications for OCT have been in biology.

In our work we will demonstrate the application of high speed, common path optical coherence tomography system techniques to detect and study defects and subsurface structures in a variety of non-biological coated metallic materials. This is particularly useful for inspection of corrosion under coated surfaces. We have also imaged through plastic and composite materials. In most cases, the material under study was highly scattering, which rendered non-gated imaging impossible. In each case the spatial positions of internal defects were determined, both qualitatively and quantitatively.

Our OCT apparatus utilizes a design that allows rapid scans in a plane perpendicular (X-Z) or parallel (X-Y) to the sample surface while also maximizing the spatial resolution over the entire scan area. The system uses a GPU (general processing unit found on many video cards) multi-processor algorithm to create a 3D rendering of the scanned area in real time at more than 30 frames per second and a resolution of 2 to 5 μm (10-6 meters).

8155A-32, Session 4

High-speed, multispectral, thermal instrument development in support of HypsIRI-TIR

W. R. Johnson, S. J. Hook, M. C. Foote, B. T. Eng, B. M. Jau, Jet Propulsion Lab. (United States)

The Jet Propulsion Laboratory is currently developing a prototype multispectral thermal instrument in support of the Hyperspectral Infrared Imager (HypsIRI) - Thermal Infrared (TIR) space mission. HypsIRI mission was recommended by the National Research Council Decadal Survey (DS) and includes a visible shortwave infrared (SWIR) pushboom spectrometer and a multispectral whiskbroom thermal infrared (TIR) imager. Data from the HypsIRI mission will be used to address key science questions related to the Solid Earth and Carbon Cycle and

**Conference 8155A:
Infrared Sensors, Devices, and Applications**

Ecosystems focus areas of the NASA Science Mission Directorate. The prototype instrument addresses the technology readiness level (TRL) of a few key subsystems of the TIR. Current designs for the HypsIRI-TIR space borne imager utilize eight spectral bands delineated with filters. The system will have 60m ground resolution, better than 200mK noise equivalent delta temperature (NEDT), 0.5C absolute temperature resolution with a 5-day repeat from LEO orbit. The prototype instrument will use mercury cadmium telluride (MCT) technology at the focal plane and operate in time delay integration mode. A custom read out integrated circuit (ROIC) will provide the high speed readout hence allowing the high data rates needed for the 5 day repeat. The current HypsIRI requirements dictate a ground knowledge measurement of 30m (3sigma), so the prototype instrument will tackle this problem with a newly developed interferometric metrology system. This system will provide an absolute measurement of the scanning mirror to an order of magnitude better than conventional optical encoders. This will minimize the reliance on ground control points hence minimizing post-processing (e.g. geo-rectification computations).

8155A-33, Session 4**Summary of the Operational Land Imager Focal Plane Array for the Landsat Data Continuity Mission**

K. A. Lindahl, W. L. Burmester, K. Malone, R. J. Schrein, R. Irwin, Ball Aerospace & Technologies Corp. (United States)

The Landsat missions are the longest continuous record of changes in the Earth's surface as seen from space. The next follow-on activity is the Landsat Data Continuity Mission (LDCM). The LDCM objective is to extend the ability to detect and quantitatively characterize changes on the global land surface at a scale where natural and man-made causes of change can be detected and differentiated. The Operational Land Imager (OLI) is one of two instruments on the LDCM spacecraft. OLI will produce science data for the reflective bands, which include 6 visible and near-infrared (VNIR) and 3 short-wave infrared (SWIR) bands. The OLI instrument utilizes a pushbroom design with 15.5 deg field of view. As a result, the OLI Focal Plane Array (FPA) cross track dimension is large, and the FPA is a critical technology for the success of the mission. The FPA contains 14 critically aligned Focal Plane Modules (FPM) and consists of 6916 imaging pixels in each of the 8 multi-spectral bands, and 13,832 imaging pixels in the panchromatic band. Prior to integration into the FPA, the FPMs were characterized for radiometric, spectral, and spatial performance. The Flight FPA has been built and its performance has also been characterized. In this paper, the critical attributes of the FPMs and FPA are highlighted. A detailed description of the FPM and FPA test sets is provided. The performance results that demonstrate compliance to the science mission requirements are presented.

8155A-34, Session 5**Nanoengineered optics using carbon nanotubes and graphene**

S. Kar, S. Sridhar, Northeastern Univ. (United States)

No abstract available

8155A-35, Session 5**Low-cost solution processed quantum dots for SWIR imaging**

E. J. Klem, J. S. Lewis, C. Gregory, D. Temple, RTI International (United States)

While InGaAs-based focal plane arrays (FPAs) provide excellent detectivity and low noise for SWIR imaging applications, wider scale

adoption of systems capable of working in this spectral range are limited by high costs, limited spectral response, and costly integration with Si ROIC devices. RTI has demonstrated a novel photodiode technology based on IR-absorbing solution-processed PbS colloidal quantum dots (CQD) that can overcome these limitations of InGaAs FPAs. We have fabricated devices with quantum efficiencies exceeding 50%, and detectivities that are competitive with that of InGaAs. Dark currents of ~ 2 nA/cm² were measured at temperatures compatible with solid state coolers. Additionally, by processing these devices entirely at room temperature we find them to be compatible with monolithic integration onto readout ICs, thereby removing any limitation on device size. We will show early efforts towards demonstrating a direct integration of this sensor technology onto a Si ROIC IC and describe a path towards fabricating sensors sensitive from the visible to 1700 nm at a cost comparable to that of CMOS based devices. This combination of high performance, dramatic cost reduction, and multispectral sensitivity is ideally suited to expand the use of SWIR imaging in current applications, as well as to address applications which require a multispectral sensitivity not met by existing technologies.

8155A-36, Session 5**MBE growth of ZnTe and HgCdSe on Si: a new IR material**

Y. Chen, G. N. Brill, U.S. Army Research Lab. (United States); D. J. Benson, U.S. Army Night Vision & Electronic Sensors Directorate (United States); P. S. Wijewarnasuriya, U.S. Army Research Lab. (United States); N. K. Dhar, Defense Advanced Research Projects Agency (United States) and U.S. Army Research Lab. (United States)

Recently we have explored the potential of a new class of IR materials based on HgCdSe grown by molecular beam epitaxy (MBE). Since scalable large area and high quality bulk substrate, such as GaSb, is commercial available and is closely lattice matched to HgCdSe and exact lattice matched to HgCdSeTe, one will expect to obtain scalable large area, high quality HgCdSeTe with low dislocation density, once the optimized growth conditions are established. This new IR material system, if proved successful, will mitigate the problems associated with lack of scalable large area and low cost substrates for HgCdTe/CdZnTe and relatively high dislocation density for scalable large area HgCdTe/Si IR materials. However, direct growth of HgCdSe on GaSb appears to be very challenging due to lack of dual III-V and II-VI chambers needed to properly prepare GaSb for the growth. As an alternate approach we use MBE grown ZnTe/Si as substrate, which is also closely lattice matched to HgCdSe.

In this paper we will discuss our effort to utilize our expertise and extensive experience in the growth of CdTe on Si and HgCdTe on CdTe/Si to optimize the growth of high quality ZnTe on Si and the growth of HgCdSe on ZnTe/Si, with emphases on growth temperature, material fluxes, growth rate and alloy composition. X-ray full-width at half-maximum (FWHM), chemical decorating etch for dislocation density and IR transmission measurement were used to evaluate the quality of the epilayers and calibrate the growth conditions.

8155A-37, Session 5**Material characteristics of HgCdSe grown on GaSb and ZnTe/Si substrates by MBE**

G. N. Brill, Y. Chen, P. S. Wijewarnasuriya, U.S. Army Research Lab. (United States)

The Army Research Laboratory has recently initiated research on the growth and characterization of HgCdSe material by molecular beam epitaxy (MBE). HgCdSe is an infrared material that can be engineered to detect any wavelength of infrared (IR) light by controlling the Cd composition within the alloy. This compound is completely analogous to

**Conference 8155A:
Infrared Sensors, Devices, and Applications**

the much more common II-VI IR material HgCdTe, except that large area, scalable, and lattice matched substrates are commercially available for HgCdSe, specifically, GaSb. In addition, ZnTe/Si composite substrates are nearly lattice matched to HgCdSe making this a viable, and potentially cheaper, substrate for HgCdSe growth.

In this work, we will report on the first ever growth of HgCdSe on GaSb substrates by MBE and compare/contrast results to HgCdSe grown on ZnTe/Si. A systematic study of MBE growth temperature and material flux ratios were varied to ascertain the best growth conditions. HgCdSe defect structures were examined as a function of growth temperature with smooth, defect-free HgCdSe surface morphologies obtained using a growth temperature much lower than HgCdTe for comparable material fluxes. X-ray rocking curve measurements were also made to ascertain the overall crystalline quality of the material. To date, the best HgCdSe/GaSb material as measured by x-ray double crystal rocking curve resulted in a full width at half maximum (FWHM) of 160 arcsec whereas the best HgCdSe/ZnTe/Si material resulted in a FWHM of 200 arcsec. Transmission electron microscopy (TEM) was used to investigate the epilayer - substrate interface with electron diffraction showing aligned crystal structures between the HgCdSe epilayer and the substrate, as expected. FTIR data shows a linear relationship between the Se/Cd flux ratio and cut-off wavelength and indicates the easily tunable nature of the alloy. Additionally, Hall Effect measurements were taken on as-grown material as well as material annealed under varying Hg saturation conditions.

8155A-38, Session 5**Carbon nanotube-based microbolometer development for IR imager and sensor applications**

A. K. Sood, Magnolia Optical Technologies, Inc. (United States); N. K. Dhar, Defense Advanced Research Projects Agency (United States); P. S. Wijewarnasuriya, U.S. Army Research Lab. (United States)

EO/IR Sensors and imagers using nanostructure based materials are being developed for a variety of Defense Applications. In this paper, we will discuss recent modeling effort and the experimental work under way for development of next generation carbon nanostructure based infrared detectors and arrays. We will discuss detector concepts that will provide next generation high performance, high frame rate, and uncooled nano-bolometer for MWIR and LWIR bands. The critical technologies being developed include carbon nanostructure growth, characterization, optical and electronic properties that show the feasibility for IR detection. Experimental results on CNT nanostructures will be presented. We will discuss the path forward to demonstrate enhanced IR sensitivity and larger arrays.

8155A-39, Session 5**A review of growth and characterization of ZnO nanostructures for optoelectronic sensor and energy harvesting applications**

A. K. Sood, Magnolia Optical Technologies, Inc. (United States); N. K. Dhar, D. L. Polla, Defense Advanced Research Projects Agency (United States); T. Manzur, Naval Undersea Warfare Ctr. (United States); A. F. M. Anwar, Univ. of Connecticut (United States); Z. L. Wang, Georgia Institute of Technology (United States)

Next generation EO/IR integrated sensors using nanostructures are under development. Several materials are being investigated for these applications include ZnO nanostructures that have the potential applications in the UV part of the spectrum. ZnO is a unique material that exhibits both Semi conducting and piezoelectric properties and has

applications in optical sensors and energy harvesting. We will discuss current status of the effort and the path forward.

E-O Sensors are being developed for a variety of Military Systems Applications. These include UV, Visible, SWIR, MWIR and LWIR Nano Sensors. In this paper, we will discuss growth and characterization of ZnO Nanowires on a variety of substrates that include Si, ZnO, GaN, SiC and flexible substrates.

8155A-40, Session 6**DRS on multicolor bolometers**

C. C. Li, DRS Technologies, Inc. (United States)

No abstract available

8155A-41, Session 6**Driving experience and special skills reflected in eye movements**

R. Paeglis, K. Bluss, A. Atvars, Biomechanics and Physical Research Institute (Latvia)

When driving a vehicle, people use the central vision both to plan ahead and to monitor their performance feedback (research by Donges, 1978, and after). Discussion is ongoing if making eye movements do more than gathering information. Moving eyes may also prepare the following body movements like steering.

Different paradigms exist to explore vision in driving. Our perspective was to quantify eye movements and fixation patterns of different proficiency individuals, a driving learner, a novice, an experienced driver and a European level car racer. Thus for safety reasons we started by asking them to follow a video tour through a known city, remote from an infrared eye tracker sampling at 250 Hz.

The learner and novice had mean fixations shorter than the experienced driver, 0.62 sec, but longer than the racer, 0.20 sec. Both less experienced drivers often shifted their central vision away from the lane center. On the contrary, decades of driving experience enabled a person to follow the situation to the left by peripheral vision. Any eye shifts to the right were made by longer single saccades.

Experience in a motor action provides skills different from sports training. We are aiming at testing this finding in real world driving.

8155A-42, Session 6**A parametric analysis of microbolometer pixel designs**

M. J. Dumas, B. A. Lail, Florida Institute of Technology (United States)

As microbolometer pixel dimensions for infrared imagers continue to decrease the need for full-wave analysis in the design process is enhanced. Using reflectance as the validation point, an electromagnetic model of a dual layer microbolometer pixel design was created for a 25 μm pixel design, and an in-depth study of the design was performed. With this model validated, further explorations were completed with a reduced size pixel. While simulating multiple variations of specific parameters, such as bridge thickness, upper and lower cavity heights, and different absorber configurations, a new evaluation metric of dissipated power in the structure was studied. This metric, provided by finite element analysis, provides great insight into absorption properties within the microbolometer structure, properties that cannot be directly measured but that are critical to the functionality of the pixel design. In this paper parametric analysis of microbolometer pixel designs are presented via both reflectance and dissipated power full-wave analysis.

8155A-43, Session 6

Cytochrome c thin film with high temperature of coefficient resistance for infrared detection

C. H. Chu, G. J. Su, National Taiwan Univ. (Taiwan)

The cytochrome c (protein) thin film on the oxide surface has been reported high temperature coefficient of resistance (TCR). The protein thin film resistance acts as exponential grow under the constant voltage bias. It presented the TCR exceeding 20% 1/K, which is 5times better than popular VOx. We also found the protein thin film can be attached on to the SU8 photoresist surface by changing the SU8 surface more hydrophilic and simple spinning coat technique. The cytochrome c thin film on SU8 showed the high TCR. With easy fabrication methods and lower thermal conductivity of SU8 and protein, we believe that it is possible to fabricate new generation microbolometer based on cytochrome c protein and SU-8 photoresist.

8155A-44, Session 6

Simulation and fabrication of poly(methyl methacrylate) infrared rays lenses

C. Tsui, G. J. Su, National Taiwan Univ. (Taiwan)

Infrared thermography is a promising solution that can help improve our lives. However, most of the common materials used to fabricate lenses, such as glass, are opaque in the infrared range. Silicon and germanium are better solutions. But shaping these two materials are truly complicated and time-consuming. Many research works have been devoted to develop cost-effective infrared lenses. Due to material restriction, traditional lenses to focus infrared rays are expensive. On the other hand, we found that PMMA (Poly methyl methacrylate) is an ubiquitous polymer material. It is cheap and transparent in mid-IR range. More importantly, liquid PMMA can be shaped and solidified easily. Therefore, we chose PMMA as the material to design and make our IR lenses. In this paper, we choose PMMA and discuss its optical properties in mid-IR ange. We believe PMMA is a highly potential material for low-cost infrared lenses. Also, we show simulation results of a f/2.47, diameter = 11mm and focal length = 27.2mm Fresnel lens made by PMMA to emonstrate its feasibility. We made a PMMA Fresnel lenses, by using MEMS processes and embossing. The experimental results agree well with simulation data.

Conference 8156: Remote Sensing and Modeling of Ecosystems for Sustainability VIII

Monday-Tuesday 22-23 August 2011 • Part of Proceedings of SPIE Vol. 8156
Remote Sensing and Modeling of Ecosystems for Sustainability VIII

8156-09, Poster Session

Statistical normalization of 1981 - 2010 brightness temperature records from the NOAA/AVHRR

M. Vargas, National Oceanic and Atmospheric Administration (United States)

Time series of Brightness Temperature (BT) derived from the National Oceanic and Atmospheric Administration (NOAA) Advanced Very High Resolution Radiometer (AVHRR) sensors are affected by atmospheric effects, satellite orbital drift and differences between satellite missions which in turn introduce spurious trends in the data stream. Brightness temperatures from the NOAA-GVI dataset are currently used to produce the Temperature Condition Index (TCI) and the Vegetation Health Index (VH); therefore, satellite derived BTs need to be corrected with sufficient accuracy before being input into any algorithm to generate remotely sensed products to prevent biases in global long-term monitoring studies. In this research we have applied a statistical technique based on Empirical Distribution Functions (EDF) to normalize the NOAA BT records from the GVI-x dataset for the combined effect of the sources of uncertainty mentioned above, avoiding the need for physics based corrections. Results across most latitudes show that the normalized time series have no spurious trends, the estimated slope (trend) for normalized time series is close to zero at low and mid-latitudes, and the time series show improved stability. The results are tested to verify that the normalization improves the data.

8156-10, Poster Session

The extraction of multiple cropping index of China based on NDVI time-series

H. Huang, Z. Gao, Institute of Geographical Sciences and Natural Resources Research (China)

Multiple cropping index reflects the intensity of arable land been used by a certain planting system. The bond between multiple cropping index and NDVI time-series is the crop cycle rule, which determines the crop process of seeding, jointing, tasseling, and harvesting and so on. The cycle rule can be retrieved by NDVI time-series for that peaks and valleys on the time-series curve correspond to different periods of crop growth. In this paper, we aim to extract the multiple cropping index of China from NDVI time-series.

Because of cloud contamination, some NDVI values are depressed. MVC (Maximum Value Composite) synthesis is used to SPOT-VGT data to remove the noise, but this method doesn't work sufficiently. In order to accurately extract the multiple cropping index, the algorithm HANTS (Harmonic Analysis of Time Series) is employed to remove the cloud contamination. The reconstructed NDVI time-series can explicitly characterize the biophysical process of planting, seedling, elongating, heading, harvesting of crops. Based on the reconstructed curve, we calculate the multiple cropping index of arable land by extracting the number of peaks of the curve for that one peak represents one season crop.

This paper presents a method for extracting the multiple cropping index from remote sensing image and then the multiple cropping index of China is extracted from VEGETATION decadal composites NDVI time series of year 2000 and 2010. From the processed data, we can get the spatial distribution of cropping system of China, and then further discussion about cropping index change between the 10 years is conducted.

8156-18, Poster Session

Aerosol optical depth and angstrom exponent of aerosols observed using ground-based measurements in China

C. Liu, East China Normal Univ. (China)

MFRSR (multi-filter rotating shadow-band radiometer) is a ground-based instrument and used to make measures of irradiance and aerosol. This paper introduces the instrument of MFRSR, the method of calibration and data processing, and then analyses statistical properties of aerosol using observation of MFRSR during 2004-2005 in Xianghe. In order to illuminate the reliability of observing aerosol optical depth with MFRSR, we compare the results of MFRSR with AERONET data. It shows the mean differences of the two results respectively are -0.021, -0.009, -0.004 at the wavelengths of 500nm, 670nm, 870nm, and the standard deviations are 0.067, 0.051, 0.050. We also discuss the reasons for deviation of the two.

8156-19, Poster Session

Integrating satellite for drought impact assessment in a developed coastal region

Z. Gao, Institute of Geographical Sciences and Natural Resources Research (China)

This paper presents a new drought assessment method by spatially and temporally integrating the regional water stress index (RWSI) with the temperature vegetation dryness index (TVDI). With the aid of LANDSAT TM/ETM data, we were able to retrieve the land-use and land-cover (LULC), vegetation indices (VIs), and land surface temperature (LST), and derive three types of TVDI, including TVDI_SAVI, TVDI_ANDVI and TVDI_MSAVI, for the drought impact assessment in a well-developed coastal region, northern China. The classification of four drought impact categories associated with the RWSI values enables us to refine the spatiotemporal relationship between the LST and the VIs in a greater detail. Holistic drought impact assessment between 1987 and 2000 in our study area was carried out by linking RWSI with TVDIs group wise.

8156-21, Poster Session

Spatiotemporal characteristics of drought in southwest China using MODIS-based normalized difference drought index

K. Bai, C. Liu, R. Shi, East China Normal Univ. (China)

Abstract: Recently, drought has brought huge damage to local agricultural production and ecological environment in China because of its high frequency. In order to catch the large-scale land surface water information used to assess land surface drought severity quickly and accurately, normalized difference drought index (NDDI) was proposed which based on visible and near infrared band reflectance. In this thesis, drought happened in southwest China in 2010 was taken for instance, and Yunnan, Guangxi and Guizhou provinces were taken as the study area. The drought severity was evaluated with NDDI index and then the drought spatial-temporal distribution was displayed in different drought severity. Moreover, land area in different drought severity in Guizhou province was calculated.

In the paper, MODIS images and meteorological data were used. Firstly, MODIS images were preprocessed and NDDI was calculated with different index derived from MODIS images. During this process, pixel reliability data acquired from MODIS product was introduced. The main

**Conference 8156: Remote Sensing and
Modeling of Ecosystems for Sustainability VIII**

purpose of it was to eliminate noise such as clouds and ice or snow. Then, the relation between NDDI and ground-based soil moisture was validated. The result showed that NDDI demonstrated even quicker response to shallow surface drought severity than VCI. Finally, the drought spatial-temporal distribution was reoccurred with NDDI index, and also land area in different drought severity was derived.

The result showed that periods of time suffered from most severe drought conditions lasted from January to April in 2010 in Guizhou province. The maximum drought-stricken area was 132257 square kilometer and it occupied more than 75 percent of the total area of Guizhou province. Meanwhile, the maximum area suffered from most severe drought was 88246 square kilometer and it occupied more than 50 percent of the total area of Guizhou province.

8156-23, Poster Session**Research on spatial interpolation of meteorological elements in Anhui Province based on ANUSPLIN**

S. Shu, C. Liu, R. Shi, W. Gao, East China Normal Univ. (China)

High precision data fields of meteorological element is essential inputs for most kinds of large-scale regional and global models. Improvements on data accuracy can make models running more effectively and exactly. We often use IDW, Kriging and Splines as common interpolation tools, but for meteorological data the accuracy is not enough and the result has not essential smoothness. This paper attempts to use ANUSPLIN, a spatial interpolation software based on the theory of thin plate smoothing spline, to interpolate average temperature and precipitation data in different time scales. We obtained daily, monthly and annual data from 71 meteorological stations in Anhui Province as sample data. Before interpolation, we have experiments on different tactics in using ANUSPLIN models with the combination of three variants (Longitude, Latitude and Elevation) to ensure the best one corresponding every time scale source data and we find that CO2 (elevation as a covariate and the order of spline is 2) model fits daily and monthly temperature data most, CO3 model is effective for monthly and annual precipitation data. Then a comparison between the interpolated surfaces using ordinary kriging method and ANUSPLIN showed the latter one performs more accuracy and smoothness in all the time scales of temperature and precipitation: daily mean temperature interpolation's mean error can be reduced by 0.103, monthly one's by 0.091, annual one's by 0.078, monthly precipitation interpolation's mean error can be reduced by 4.649mm, annual one's by 22.194mm. Furthermore, we refer to other researches about quantitative effects on temperature with land cover changes and set a method adding land cover type as second covariate in former ANUSPLIN model. Interpolation errors show us a ideal result.

8156-24, Poster Session**The evaluation of the applicability of MODIS aerosol optical depth product in the lower and middle reaches of Yangtze River**

Y. Chen, R. Shi, C. Liu, East China Normal Univ. (China); W. Gao, Colorado State Univ. (United States) and East China Normal Univ. (China)

As an index to estimate regional air quality, aerosol plays an important role in air pollution. MODIS has a fast access to a wide range of aerosol data, however, there is no guarantee for the accuracy of its AOD product in China. This paper is an attempt to evaluate the applicability of MODIS AOD product in the lower and middle reaches of Yangtze River supported by a large amount of AERONET ground-based data from Lin'an, Taihu and Hefei sites, which, in turn, provides the dependability for monitoring aerosol by using MODIS AOD product in the future. In this research, the author used MODIS AOD value for the 10km×10km central pixel-closest to the site to match the average of AERONET data within the 1-hour

period centered on the MODIS overpass times, then made an analysis and evaluation of the fitting results. The results indicated that MODIS AOD product is not well correlated with AERONET data in 2007-2010, especially the correlation coefficient is only about 0.55 in 0.55μm band at Taihu site. MODIS AOD product is underestimated at Lin'an site, while overestimated at the others. Similarity exists in the quality of MODIS AOD product between Terra and Aqua, and the estimation of aerosol value by Terra was lower than that by Aqua. MODIS AOD product in 0.47μm band has an advantage over that in 0.66μm band as far as product accuracy is concerned. All the year around, MODIS AOD product at Taihu site is the best in quality in spring.

8156-25, Poster Session**Ten-day response of vegetation to temperature and precipitation in Xinjiang, China during the period of 1998-2009**

X. Cao, Graduate Univ. of the Chinese Academy of Sciences (China); X. Chen, A. Bao, Xinjiang Institute of Ecology and Geography (China)

In this paper, 10-day (ten-day) spatio-temporal response of vegetation to the change of temperature and precipitation was analyzed in spring, summer, autumn and whole year in Xinjiang, China during the period of 1998-2009 based on the SPOT VEGETATION-NDVI data and 10-day average temperature or precipitation data observed by 54 meteorological stations in Xinjiang through correlation analysis. The results show that the response of 10-day NDVI to temperature was more significant than that to precipitation, and the maximal response of vegetation to temperature and precipitation lagged for two 10-day periods. Seasonally, the effect of temperature and precipitation on vegetation NDVI was the highest in autumn, then in spring, and it was the lowest in summer. The response of vegetation to 10-day change of meteorological factors was positive in spring, the affecting duration was long, and it was relatively short in autumn and summer. Spatially, the 10-day maximal response of NDVI to temperature in northern Xinjiang was higher than that in southern Xinjiang. The results indicated that interannual change of temperature was not the dominant factor affecting the change of vegetation NDVI in Xinjiang, but the decrease of annual precipitation was the main factor resulting in the fluctuation of vegetation coverage. 10-day average temperature was an important factor to promote vegetation growth in Xinjiang within a year, but the effect of precipitation on vegetation growth within a year was not strong.

8156-26, Poster Session**An analysis of the relations between underlying surfaces and air temperature around city meteorological stations**

K. Liu, T. Yu, Institute of Remote Sensing Applications (China); W. Gao, East China Normal Univ. (China); Z. Gao, Institute of Geographical Sciences and Natural Resources Research (China); X. Gu, Institute of Remote Sensing Applications (China)

Based on Landsat TM remote sensing images obtained on May 28, 2007, and With 20 Beijing meteorological stations as research object, this study aims at finding the correlation between different types of underlying surfaces and Urban Heat Island (UHI) by analyzing various underlying surface types intercepted from the different-radius (1km,2km,3km,4km,5km) circular buffer zones (with 20 Meteorological Station as their center) and their corresponding air temperatures (annual average, maximum/minimums). It finds a strong positive correlation between land for construction and UHI; a negative correlation between land/grassland and UHI; but the correlation between water bodies and UHI could not be found. As far as distance of influence is concerned, land for construction is within 4 km; woodland/grassland is within 3 km. As the distance influence of land surfaces, there is also impairment

**Conference 8156: Remote Sensing and
Modeling of Ecosystems for Sustainability VIII**

conclusion on the relation between the UHI intensity and the percentage of land surface type; this study gives the initial conclusion about the critical percentage of the effect of land surface types on air temperature. Based on the effect of distance and intensity, the definition of urban meteorological stations and country meteorological stations becomes easy, this paper also provides elementary scientific basis for site selection of the meteorological station. At last, it mainly discusses the possible reasons for how the correlation between different underlying surfaces and UHI can be formed.

8156-27, Poster Session

The carbon dioxide monitoring from remote sensing based on fusion algorithm

W. Chao, East China Normal Univ. (China)

The IPCC fourth scientific assessment report suggested that the global average temperature increased by 0.74 in the past 100 years from 1906 to 2005 which will cause a tremendous impact on climate, Ecosystem and energy cycle of the earth. The IPCC hold that the increasing of the greenhouse gas is the primary reason. The carbon dioxide is the second highest concentration of greenhouse gases other than water vapor and it will be very conducive to studying global climate change if we study it first. In terms of monitoring of carbon dioxide on a global scale, it costs more time and money but not a better effect by traditional methods. The greenhouse gas can be monitored by several satellites with the development of the remote sensing, such as METOP-A/IASI, ENVISAT/SCIAMACHY, GOSAT, AIRS. However, the comprehensive utilization is the difficulty caused by the difference between spatial and temporal coverage, resolution and digital format among the datasets from different sensors. In this paper we try to find an appropriate fusion algorithm from numbers and assessed from scientific views, such as information content, integration of information, spectral fidelity. A complete fusion system will be constructed to provide data base for research in the related fields.

8156-28, Poster Session

Remote sensing of LAI-FPAR fluctuations and Synchrotron EXAFS investigation of metal absorption under stress

T. M. Holden, S. Dehipawala, E. Cheung, R. Regan, G. Tremberger, Jr., U. Golebiewska, P. J. Marchese, T. D. Cheung, Queensborough Community College (United States)

The fluctuations of leaf area index (LAI) and Fraction of Photosynthetically Active Radiation (FPAR) as reported by the MODIS 8-day product MOD15A2 over a section of Harriman State Park, New York were studied with reference to another nearby local park. The area selected for study, a seven km square grid with one km resolution, is known for its biodiversity. Time series datapoints were generated using the sums of the grid's 49 pixel measurements for each of the 46 entries that make up the annual time series. A quadratic relation has been observed that suggests that LAI/FPAR is proportional to FPAR if FPAR is considered as the forcing parameter via chlorophyll (a, b, c, d and f), in an application model for the study of biodiversity. The LAI annual time series from 2000 to 2009 follows the corresponding FPAR annual time series as expected, but with different proportionality ratios in different seasons. The fractal analysis results of the time series data suggest that the LAI sequences have a lower fractal dimension (~1.35) than those of the FPAR sequences (~1.55), consistent with the idea that biological systems are capable of regulating fluctuation. The regression of LAI sequence fractal dimension versus FPAR sequence fractal dimension exhibits an R-square of about 0.7 (N=10). The observed regression outlier for the year 2009 could be indicative of the presence of additional factors. Synchrotron EXAFS investigation of leaf samples reveals data consistent with metal absorption under stress. Further study is warranted.

8156-30, Poster Session

The theory of shortwave infrared perpendicular water stress index and its application in soil moisture retrieval under full covered vegetation condition

H. Zhang, H. Chen, Henan Institute of Meteorological Science (China)

With the analysis of SWIR and NIR spectral space, and based on the Short Wave Perpendicular Water Stress Index (SPSI) of which was constructed by Abduwasit Ghulam. The SPSI was applied in the soil moisture retrieval during the growing period of wheat in April with full cover condition. The result showed there is a high correlation coefficient between SPSI and soil moisture in 0-30 cm, and has been tested that the SPSI has a potential in the soil moisture retrieval under full cover condition.

8156-31, Poster Session

Fusing ASTER data and MODIS LAI product to generate high spatial and temporal resolution LAI data in Heihe River Basin

J. Song, Beijing Normal Univ. (China)

LAI (Leaf Area Index) is a biographic parameter determining vegetation photosynthesis, transpiration, and the energy balance of canopies. In this paper, the main object is to study on the generation of the high spatial temporal resolution LAI product by fusing Aster data and MODIS LAI product in Heihe river basin.

In this study, the field experiment sites is Heihe river basin in Gansu province, China. And the dates of Aster images imaging are 16 March, 08; 14 May, 06 and 17 June, 06 respectively. In order to get the time serial LAI variation, MODIS products are used: MODIS LAI and MODIS landcover data. We use the field measured data in Yike and Linze, Heihe river basin in Gansu province, China.

Based on the Aster LAI estimation, the main object of this paper is to generate the high spatial and high temporal resolution LAI product. One method is proposed to get high spatial and temporal resolution LAI product by fusing MODIS LAI product and Aster LAI. In this method, the LULC data is used to register with MODIS data, then the percentage of classes of PFT classification in the MODIS pixel can be calculated. And the multi-year mean MODIS LAI values are the background data, the Aster LAI is used to adjust this curve of multi-year mean MODIS LAI. And we validate LAI with high spatial and high temporal resolution using the measured data that is not to be used as the training data. The results is good and can meet our study needs.

8156-32, Poster Session

Remote sensing image variation detection on multiscale MRF fusion

W. Wang, Henan Polytechnic Univ. (China)

The paper studied a change detection method that uses the multi-scale Markov random field fusion to process different scale change detection results and take full account of the correlation between the adjacent pixels and the links of the different scale change detection results, so the fusion results are more accurate and practical. The Mahalanobis distance is applied to the change detection for the different scale images. The Mahalanobis distance decision function is a hyper-ellipsoidal decision surface in a high dimensional feature space, so it is more effective to decide the change and the non-change pixels. It needs to be proposed that the different scale change detection results are influential to the final Markov random field fusion result. The Markov random field is not only suitable to the fusion of the multi-scale change detection results, but also

**Conference 8156: Remote Sensing and
Modeling of Ecosystems for Sustainability VIII**

the fusion of the change detection results through the other methods, the studied method in this paper can be further improved.

8156-33, Poster Session

**Seepport object recognition on level-set with
shape prior clustering**

W. Wang, Z. Jia, Henan Polytechnic Univ. (China)

In this paper, in order to get a desirable image segmentation result of the interested buildings (round oil-can and square-roof buildings) in a seepport, a level-set based segmentation algorithm with shape priors is proposed. Since the algorithm inherits the advantages of the classic level-set segmentation algorithm, the contour topological changes can be automatically handled. In addition, by introducing the shape priors in the algorithm, the non-interested targets are filtered, therefore the object detection procedure is simplified. The corrupted boundary of a target is reconstructed in the segmentation process. Experiments show the algorithm studied in this paper is robust to anti-noise, compared to the other algorithms.

8156-34, Poster Session

**Research on the hydrographic net change
of Jing-Hang Great Canal in Nanwang part
during 300 years**

X. Wang, Ctr. for Earth Observation and Digital Earth (China)

Jing-Hang Great Canal is the earliest canal in the world, it has an important role in the transportation between south and north China during almost 2,000 years. But with the development new technologies, the Great Canal has lost its role from 19th century. Especially in Nanwang part of canal, it has disappeared as a dry drain now. In order to find the reason of Nanwang canal disappeared from 1700 gradually, we put forward a new method to find the change of it. In this paper, we first use an old map which draw in 300 years ago to obtain the old time environment status and correct it into nowadays remote sensing data to reveal the old sub-rivers which has run into canal in the old time. We also use some history materials to get the social information such as population data, county and village data. Second we using present remote sensing data to extract river, farmland data, we also collect the population data now in this area. In the end we compared this two period data to find the different hydrographic net in 300 years. The result will give us the answer for the canal change and give us a hint for reconstruction the Great Canal in the future.

8156-35, Poster Session

**Soil moisture spatial heterogeneity and its
remote sensing scale analysis in arid area**

Q. Zhang, Ctr. for Earth Observation and Digital Earth (China); K. Zhou, Xinjiang Institute of Ecology and Geography (China) and Peking Univ. (China); W. Gao, Colorado State Univ. (United States)

For one typical characteristic of soil moisture in arid areas is the heterogeneity in space, what scales should the soil moisture remote sensing retrieval be based on so as to not only meet the application requirements but also be provided with operability? To think over this issue, the scale features of surface water heat energy parameters was analyzed, and a scale curve was introduced in this paper. Then after analyzing the relationship of spatial scale between spatial heterogeneity of surface parameters and remote sensing observational ability, it was believed that the point of intersection in these two curves is helpful to determine the remote sensing observation scale of regional soil moisture. Therefore, to study the spatial scale characteristics of surface

parameters, in particular to test the critical point of key parameters which exists possibly is very important. From a case study, the spatial scale was quantitatively tested from four aspects: Polygon scale analysis of land cover, pixel scale analysis of land cover, spatial semi-variance analysis of land attributes, multi-Scale consistency index. As a result, the suitable spatial scale is less than 1 km, 250 m, 1 km and 240-480 m respectively. In sum, the optimum soil moisture remote sensing research scale is between 300-1000m in arid areas.

8156-36, Poster Session

**Research on the method of extracting
alteration information and metallogenic
prediction based on multi-information**

K. Zhou, Xinjiang Institute of Ecology and Geography (China) and Peking Univ. (China); Q. Zhang, Ctr. for Earth Observation and Digital Earth (China)

With the leaping of geologica data, the demand to application of geological data is increasing and complex. how better to extract the excrescent information of geochemical anomalies and models of extracting altered information have been the important problem of geologists concerned. We analyzed the spectral characteristics of typical altered minerals, summarized the spectral response characteristics of typical altered minerals on ETM+. We contrasted three kinds of models of extracting altered information, the threshold model which was basis on PCA and the SAM model which was basis on spectrum vectors, and we firstly built the MPS model on the base of analysis the method of eliminating familiar interference information. The research discovered the result of MPS model tallied with the location of the known gold spots, and avoided the obviously false abnormality information. And we made use of this model to extracting the altered information in whole study area.

8156-37, Poster Session

**A modified NDSI for the forest area for the
snow cover mapping**

S. Chen, Jilin Univ. (China); P. Lu, J. Wang, Institute of Remote Sensing Applications (China)

The snow cover plays an important role in the Earth's climate system and it is also the main source of water use and an important input to the snowmelt model. The Normalized Difference Snow Index (NDSI) is proposed to distinguish the snow cover from other land covers. However, it is challenge to identify the snow under the forest by the optical NDSI. In other words, there are big errors for the snow cover products in the forest. In the study, a model is applied to simulate the mixed spectrum of the snow and vegetation. The canopy of the vegetation is assumed as a sphere and the leaf area of the canopy quantity per volume is constant with the stochastic distribution function of the leaf area. The snow and crown surface are all thought as Lamberts and the multiple scattering between crown and ground are neglected. The gap between the vegetation canopies was calculated by the geometry optical model. Within a pixel, the vegetation and snow coverage fraction are taken into consideration for the mixed albedo model. Three situations, the snow is above and under the vegetation canopy, no snow above the canopy but the snow is under the vegetation, the snow is above the canopy but no snow under the canopy, are simulated separately. The simulated BRDF values is near to the pure snow spectrum when the snow is above the canopy, and the BRDF are similar to the pure vegetation pixel when the snow is just exist under the vegetation. In the principal plane, the simulated BRDF is owe to the hot spot effect and there is a peak value in the hot spot. The sensitive analysis indicated the BRDF is sensitive to the density and fraction of the vegetation. With the increase of the density and fraction, the BRDF is decreased. However, the BRDF is not sensitive to the LAI. By the results, the NDSI is proposed for different density and fraction of the vegetation. And the snow cover is also identified and compared to the snow cover products of EOS MODIS.

Conference 8156: Remote Sensing and
Modeling of Ecosystems for Sustainability VIII

8156-38, Poster Session

Spectral significance to investigate the distribution of metal elements under dense vegetation cover

S. Chen, Jilin Univ. (China); J. Wang, Institute of Remote Sensing Applications (China); C. Zhou, Jilin Univ. (China)

About two thirds of land surface are covered by vegetation. It is challenge to identify the rocks by spectral analysis under the dense vegetation cover. But it is necessary to take the distribution of the metal mines under the large area of vegetation for the state need with the economy developing. In the study, the leaf spectra have been field-measured for four main vegetation types in Daxin'an Mountains, Northeast China. The nodes of spectral abrupt variations are located in the wavelength 718nm for two known metal mine areas, but they are located in the wavelength 720nm for the other areas. Meanwhile, the metal elements are analyzed chemically in the laboratory for the samples of soil and vegetation (root, trunk, and leaf). It is discovered that there are high contents of metal elements for the vegetation in the known mines compared to the other area. All the pixels with the nodes in the wavelength 718nm are then calculated using Hypersion Data. Thus, the distributions of metal elements in the study area are outlined by the vegetation spectrum. The results are comparable to the geo-chemical analysis of the soil samples and it is significant to investigation the metal mine. Obviously, the method is much efficient and economic to the metal mine investigation under the dense vegetation cover.

8156-01, Session 1

MODIS-based spatiotemporal patterns of soil moisture and evapotranspiration interactions in Tampa Bay urban watershed due to the hurricane impact

N. Chang, Univ. of Central Florida (United States)

The advent of urban hydrology and remote sensing technologies opens new and innovative means to undertake event-based assessment of ecohydrological effects in urban regions. In the these landfalls, the multispectral MODIS remote sensing images can be used for the estimation of such soil moisture change in connection with the Enhanced Vegetation Index (EVI), Land Surface Temperature (LST). Supervised classification based on these patterns was performed fro Tampa Bay area on the 2 kmx2km grid with MODIS images. Machine learning with genetic programming model for soil moisture estimation shows advances in image processing, feature extraction, and change detection of soil moisture. ET data that were derived by GOES data and hydrologic models can be retrieved from the USGS web site directly. Overall, the derived soil moisture in comparison with ET time series changes on a seasonal basis shows that spatial and temporal variations of soil moisture and ET that are confined within a defined region for each type of surfaces, showing clustered patterns and featuring space scatter plot in association with the land use and cover map. These concomitant soil moisture patterns and ET fluctuations vary among patches, plant species, and, especially, location on the urban gradient. Such ecohydrological assessment can be applied for supporting the urban landscape management in hurricane-stricken regions.

8156-02, Session 1

A MODIS-based vegetation index climatology

R. Bindlish, Science Systems and Applications, Inc. (United States); T. J. Jackson, T. Zhao, U.S. Dept. of Agriculture (United States)

Our motivation here is to provide information for the NASA Soil Moisture

Active Passive (SMAP) satellite soil moisture retrieval algorithms (launch in 2014). Vegetation attenuates the signal and the algorithms must correct for this effect. One approach is to use data that describes the canopy water content or biomass, which can be estimated using vegetation indices such as the Normalized Difference Vegetation Index (NDVI) and Enhanced Vegetation Index (EVI). Vegetation parameters need to be included from ancillary sources since SMAP does not include any sensor that can provide them. This presents challenges to data processing and integration and concerns about data availability. As an alternative or back-up to routine updating of the NDVI, we are suggesting the development of a global NDVI and EVI annual cycle. This is based on the most recent long term set of observations from the MODIS instrument (10 years). A technique was developed to process the NASA MODLAND NDVI and EVI data base to produce a 10-day annual cycle for each 1 km pixel covering the Earth's land surface. Since our focus was on soil moisture, the classification rules and flags took this into consideration.

8156-03, Session 1

In-season crop inventory using RADARSAT-2 SAR and simulated Sentinel-1 data over the Canadian prairies

J. Shang, H. McNairn, B. Deschamps, X. Jiao, Agriculture and Agri-Food Canada (Canada)

Annual crop inventory provides useful information for many clients. Previous research conducted by Agriculture and Agri-Food Canada (AAFC) reveals that end-of-season crop inventories can be delivered using multi-temporal optical satellite data or a combination of radar and late-season optical images. While post-harvest crop inventory is useful, in-season information on crop acreage is desirable to assist with crop growth modeling and yield forecasting. In particular, an approach without having to rely on optical data will be even more attractive to operational crop inventory. Building on existing AAFC research, this paper will present the results of in-season crop identification and acreage estimates based on a random forest classifier using SAR data alone.

During the 2009 growing season, frequent RADARSAT-2 polarimetric data were programmed over Indian Head, Saskatchewan, Canada during the ESA-led AgriSAR campaign. A total of 57 fine-quad images were acquired in both ascending and descending passes cover a wide range of beam modes (from FQ2 to FQ20). Sentinel-1 multi-polarization data were simulated using the RADARSAT-2 data to test Sentinel-1 capabilities to support agricultural applications. More than 400 fields were surveyed covering 14 types of crops and hay-pasture land. Results indicate that data acquired with shallower incidence angles gave better overall classification accuracy. For single date, data acquired later in the growing season, near peak biomass, had the heist accuracies. Among the four linear polarizations, VV and VH provide most of the information needed for classification. Polarimetric data provide added information. In particular, it shows pronounced improvements over minor crops.

8156-04, Session 1

Remote detection of water stress in orchard canopies using MODIS/ASTER airborne simulator (MASTER) data

T. Cheng, D. Riano, A. Koltunov, M. L. Whiting, S. L. Ustin, Univ. of California, Davis (United States)

Vegetation canopy water content (CWC) is one of the key factors in successful monitoring of natural and agricultural ecosystems. In particular, accurate estimation of water content in orchard canopies could provide valuable information on water stress and help make informative decisions on irrigation strategies.

As part of a Terrestrial Hydrology NASA funded project on validating algorithms and models for estimating multi-temporal vegetation CWC from satellite imagery, an experiment was initiated in summer 2010

**Conference 8156: Remote Sensing and
Modeling of Ecosystems for Sustainability VIII**

to conduct a few field campaigns in the Central Valley of California. Concurrent with CWC sampling on the ground, MASTER (MODIS/ASTER airborne simulator) mounted on DC-8 aircraft was flown on June 29 and July 1 of 2010 to acquire morning and afternoon airborne imagery at a spatial resolution of 5.8 meters.

The aim of this experimental study was to evaluate the diurnal differences in remote estimates of CWC over Almond and Pistachio orchards to which different predefined irrigation strategies were applied. Our preliminary analysis indicates a statistical significant difference in CWC between morning and afternoon field measurements. This study will contribute to assessing the performance of MASTER data in capturing water stress signals and provide spatial and temporal patterns of CWC for further validation of estimates from ASTER and MODIS imagery.

8156-05, Session 1

Comparison of hyperspectral retrievals with vegetation water indices for leaf and canopy water content

E. R. Hunt, Jr., C. S. T. Daughtry, Agricultural Research Service (United States); J. J. Qu, L. Wang, X. Hao, George Mason Univ. (United States)

Leaf and canopy water contents provide information for leaf area index, vegetation biomass, and wildfire fuel moisture content. Hyperspectral retrievals of leaf and canopy water content are determined from the relationship of spectral reflectance and the specific absorption coefficient of water over the wavelength range of a water absorption feature. Vegetation water indices such as the Normalized Difference Water Index [$NDWI = (R_{850} - R_{1240}) / (R_{850} + R_{1240})$] and Normalized Difference Infrared Index [$NDII = (R_{850} - R_{1650}) / (R_{850} + R_{1650})$] may be calculated from multispectral sensors such as Landsat Thematic Mapper, SPOT HRG, or MODIS. Predicted water contents from hyperspectral data were much greater than measured water contents for both leaves and canopies. Furthermore, simulated spectral reflectances from the PROSPECT and SAIL models also had greater retrieved leaf and canopy water contents compared to the inputs. Used simply as an index correlated to leaf and canopy water contents, hyperspectral retrievals had better predictive capability than NDII or NDWI. Atmospheric correction algorithms estimate canopy water content in order to estimate the amount of water vapor. These results indicate that estimated canopy water contents should have a systematic bias, even though this bias does not affect retrieved surface reflectances from hyperspectral data. Field campaigns in a variety of vegetation functional types are needed to calibrate both hyperspectral retrievals and vegetation water indices.

8156-06, Session 1

Spectral bio-indicator simulations for tracking photosynthetic activities in a corn field

Y. Cheng, Earth Resources Technology, Inc. (United States); E. M. Middleton, NASA Goddard Space Flight Ctr. (United States); K. F. Huemmrich, Q. Zhang, Univ. of Maryland, Baltimore County (United States); L. A. Corp, Sigma Space Corp. (United States); P. K. E. Campbell, Univ. of Maryland, Baltimore County (United States); W. P. Kustas, U.S. Dept. of Agriculture (United States)

Accurate assessment of vegetation canopy optical properties plays a critical role in monitoring natural and managed ecosystems under environmental changes. In this context, radiative transfer (RT) models simulating vegetation canopy reflectance have been demonstrated to be a powerful tool for understanding and estimating spectral bio-indicators. In this study, two narrow band spectroradiometers were utilized to acquire observations over corn canopies for two summers. These in situ spectral data were then used to validate a two-layer Markov chain based canopy reflectance model for simulating the Photochemical Reflectance Index (PRI), which has been widely used in recent vegetation

photosynthesis and light use efficiency (LUE) studies. The PRI derived from in situ narrow band hyperspectral reflectance exhibited clear response to 1) viewing geometry corresponding to the light environment and 2) seasonal variation corresponding to the growth stage. The RT model utilized (ACRM; Kuusk, 2001) successfully simulated the response to the viewing geometry. The best simulations were obtained when the model was set to run in the two layer mode using the sunlit leaves as the upper layer and shaded leaves as the lower layer. Simulated PRI values yield much better correlations with in situ observations during the early growth, vegetative and reproductive stage ($r=0.78$ to 0.86) than in the senescence stage ($r=0.65$). Further sensitivity analysis was conducted to show the importance of leaf area index (LAI) and the sunlit/shaded ratio for the PRI simulations.

8156-07, Session 2

Evaluations of scattering-order and vegetation structure on modeling microwave vegetation signals and their impacts on applications

J. Shi, Institute for Remote Sensing Applications (China)

Passive microwave satellite measurements have been widely used in monitoring geophysical properties of the land surfaces, including surface temperature, snow depth or snow water equivalence, soil moisture, and vegetation properties. The techniques for above applications are mainly derived from the 0-order radiative transfer model, commonly called as the ω - τ model. This basic supporting theory assumes that scattering magnitude in vegetation canopy is not significant and considers the vegetation as an absorption material. In this study, we evaluate the effects in modeling microwave vegetation signals due to

The scattering-order: we compared the 0-th, 1-th, and multi-scattering radiative transfer model simulations with the experimental measurements (ground radiometer) for the short vegetations (Soybean and Cotton). It was found that 1) the 0-th and 1-th radiative transfer model were under-estimating the emissivity at C-band or higher frequencies due to a great impact of scattering effects in vegetation canopy. 2) At L-band, no significant differences between all 3 different scattering radiative transfer models in predicting the emissivities.

The vegetation structure: to simulate the vegetation structure effects in forests, we used the dynamic vegetation growth models (L-System) to simulating the different type of vegetation's geometric and structural in a statistical characteristics that including the sizes and number densities for trunks, different level of branches, and leaves. We compared the simulated results between the emissivities with the vegetation structure consideration and with that assumed the random orientation. It was found that there is a significant difference between above two considerations at L-band. It indicated that the vegetation effects might differ at the different polarizations and need to be considered in the algorithms for soil moisture and vegetation monitoring.

8156-08, Session 2

Estimations of deciduous forest biomass by analyzing vegetation microwave emission

Z. Zhang, Beijing Normal Univ. (China); J. Shi, Institute of Remote Sensing Applications (China); L. Zhang, Beijing Normal Univ. (China)

Forest biomass is an important factor in global carbon cycle and has potential impact on global climatic change. With the advantage of being independent of weather and day time, and the penetration ability, microwave techniques of active or passive are used in remote sensing. The radiometers carried in SMOS, Chinese FY-3B, or future SMAP would measure over fully or partially forested sites. The relationship between forest biomass and its microwave emissivity is of interest to be studied.

The microwave emission contribution received by the radiometer above

**Conference 8156: Remote Sensing and
Modeling of Ecosystems for Sustainability VIII**

the forest canopy comes from both the soil surface and vegetation layer. In this study, a high-order emission model, Matrix-Doubling, is employed to obtain the emissivity of a deciduous forest. A field experiment on deciduous canopy is scheduled to be carried in April, 2011 to measure the transmissivity of forest by plating metalized Aluminium foil on the forest ground to mask soil emission. The measured transmissivity as well as the forest emissivity are used to verify the Matrix-Doubling model. Assuming the forest as a nonscattering medium, with the known transmissivity, the effective single-scattering albedo is obtained for zero-order model by fitting the same emissivity with Matrix-Doubling model, finally the emission contribution of forest layer can be obtained, which is associated with forest biomass.

By analyzing the microwave emission of vegetation layer at L, C and X bands, the relationship between forest biomass with effective single-scattering albedo and transmissivity is studied, and some preliminary results will be presented in this paper.

8156-11, Session 3

**Progress in the development of airborne
remote sensing instrumentation for the
National Ecological Observatory Network
(NEON)**

T. U. Kampe, B. R. Johnson, M. A. Kuester, J. T. McCorkel, K. S. Krause, NEON, Inc. (United States)

The National Ecological Observatory Network (NEON) is a planned facility of the National Science Foundation. NEON's mission is to enable understanding and forecasting of the impacts of climate change, land use change and invasive species on continental-scale ecology. Airborne remote sensing plays a critical role by providing measurements at the scale of individual shrubs and larger plants over hundreds of square kilometers. The NEON Airborne Observation Platform is designed to bridge scales from organism and stand scales, as captured by plot and tower observations, to the scale of satellite based remote sensing. Fused airborne spectroscopy and waveform LiDAR will quantify vegetation composition and structure. Panchromatic photography at better than 30 cm resolution will retrieve fine-scale information regarding land use, roads, impervious surfaces, and built structures. NEON will build three airborne systems to allow for routine coverage of NEON sites and the capacity to respond to investigator requests for specific projects. The system design achieves a balance between performance, and development cost and risk, taking full advantage of existing commercial airborne LiDAR and camera components. To reduce risk during NEON construction, an imaging spectrometer design verification unit is under development by the Jet Propulsion Laboratory to demonstrate that operational and performance requirements can be met. As part of this effort, NEON is also focusing on science algorithm development, computing hardware prototyping and early airborne test flights with similar technologies. This paper presents an overview of system design, key requirements and development status of the NEON airborne instrumentation.

8156-12, Session 3

**Land-based infrared imagery for marine
mammal detection**

J. L. Graber, J. Thomson, B. Polagye, A. T. Jessup, Univ. of Washington (United States)

A land-based infrared (IR) camera is used to detect endangered Southern Resident Killer Whales in Puget Sound, Washington, USA. The observations are motivated by a proposed tidal energy pilot project, which will be required to monitor for environmental effects. Potential monitoring methods also include visual observation, passive acoustics, and active acoustics. The effectiveness of observations in the infrared spectrum is compared to observations in the visible spectrum to assess

the viability of infrared imagery for cetacean detection and classification.

Imagery was obtained at Lime Kiln Park, Washington from 7/6/10-7/9/10 using a FLIR Thermovision A40 camera (7.5-14 μ m, 37°HFOV, 320x240 pixels) under ideal atmospheric conditions (clear skies, calm seas, and wind speed 0-3 m/s). Whales were detected during both day (9 detections) and night (75 detections) at distances ranging from 42 to 160 m. The temperature contrast between dorsal fins and the sea surface ranged from 0.5 to 4.6 °C. Differences in emissivity from sea surface to dorsal fin are shown to aid detection at high incidence angles (near grazing). A comparison to theory is presented, and observed deviations from theory are investigated. A guide for infrared camera selection based on site geometry and desired target size is presented, with specific considerations regarding marine mammal detection. Atmospheric conditions required to use visible and infrared cameras for marine mammal detection are established and compared with 2008 meteorological data for the proposed tidal energy site. Using conservative assumptions, infrared observations are predicted to provide a 74% increase in hours of possible detection compared with visual observations.

8156-13, Session 3

**Exploring the nutrient inputs and cycles in
Tampa Bay and coastal watersheds using
MODIS images and data mining**

N. Chang, Univ. of Central Florida (United States)

A magnitude of dominant phytoplankton in estuary and bay systems may be related to water quality parameters such as dissolved oxygen, salinity, nutrient concentration, water temperature, and turbidity. Phytoplankton, nutrient level, and MODIS images of Tampa Bay in Florida were studied to explore the possibility of estimating nutrient levels (i.e., Total Nitrogen (TN) and Total Phosphorus (TP)) in the water using MODIS images. However, the dominant phytoplankton species vary spatially and temporally throughout the bay, especially near river mouths. Salinity level and river inflows may alter the abundance of phytoplankton species. There is no clue in regard to how these spatial correlations and associative links between the five sub-bay areas and the four coastal watersheds around the Tampa Bay could be in terms of nutrient inputs and cycles on a seasonal basis. The modeling effort is thus designed to retrieve the associative links by using fuzzy K-mean models and association rules that may aid in examining the nutrient inputs and cycles in Tampa Bay, Florida. It will lead to the improvement of nutrient control in terrestrial watersheds for both anthropogenic and natural sources and ultimate amelioration of the eutrophication impacts in the bay.

8156-15, Session 3

**Standoff Raman measurement of nitrates in
water**

S. Sadate, A. Kassu, C. Farley III, A. Sharma, Alabama A&M Univ. (United States); P. Ruffin, C. Brantley, E. Edwards, U.S. Army Research, Development and Engineering Command (United States)

The identification and real time detection of explosives and hazardous materials are of great interest to the Army and environmental monitoring/protection agencies. The application and efficiency of the remote Raman spectroscopy system for real time detection and identification of explosives and other hazardous chemicals of interest, air pollution monitoring, planetary and geological mineral analysis at various standoff distances have been demonstrated. In this paper, we report the adequacy of stand-off Raman system for remote detection and identification of chemicals in water using dissolved sodium nitrate and ammonium nitrate in water for concentrations between 200ppm and 5000ppm. Nitrates are used in explosives and are also necessary nutrients required for effective fertilizers. The nitrates in fertilizers are considered as potential sources of atmospheric and water pollution. The standoff Raman system used in this

**Conference 8156: Remote Sensing and
Modeling of Ecosystems for Sustainability VIII**

work consists of a 2-inch refracting telescope for collecting the scattered Raman light and a 785nm laser operating at 400mw coupled with a small portable spectrometer.

8156-16, Session 3

Design and package of a $^{14}\text{CO}_2$ field analyzer, the Global Monitor Platform (GMP)

M. R. Bright, G. Gronniger, Honeywell Federal Manufacturing & Technologies, LLC (United States)

Carbon Capture and Sequestration (CCS) is widely accepted as a means to reduce and eliminate the fossil fuel CO_2 (ff- CO_2) emissions from coal fired power plants. The success of CCS depends on near zero leakage rates over decadal time scales. Currently no commercial methods to determine leakage of ff- CO_2 are available. The Global Monitor Platform (GMP) field analyzer provides high precision analysis of CO_2 isotopes [^{12}C (99%), ^{13}C (<1%), ^{14}C ($1.2 \times 10^{-10}\%$)] that can differentiate between fossil and biogenic CO_2 emissions. Since fossil fuels contain no ^{14}C ; their combustion should lower atmospheric amounts. There is a clear mandate for monitoring, verification and accounting (MVA) of carbon capture and storage systems nationally and globally to verify CCS integrity, treaty verification (Kyoto Protocol) and to characterize the nuclear fuel cycle. Planetary Emissions Management (PEM), working with the National Secure Manufacturing Center (NSMC), has the goal of designing, ruggedizing and packaging the GMP for field deployment. The system will conduct atmosphere monitoring then adapt to water and soil evaluations. Measuring $^{14}\text{CO}_2$ will provide quantitative data for fossil fuel related CO_2 in the atmosphere and for CCS leakage. The initial design and packaging of the gas laser-optical system with custom and commercial off the shelf (COTS) optics and gas lasers was fielded in October 2010. The design consists of a ^{12}C , ^{13}C and ^{14}C laser along with two sample cells and reference cells. The data gathered and results of the packaged system will be discussed along with design changes for manufacturability, environment and cost reduction.

8156-17, Session 3

Estimation of suspended sediment concentrations in the Yellow River (China) by network monitoring records and satellite data

L. Qu, X. H. Yang, Univ. of Connecticut (United States); T. Lei, China Agricultural Univ. (China)

The sediment concentration in river flow is very important in monitoring of water quality, operation of the hydraulic facilities, and management of water resources. Commonly used sampling method is time consuming, labor intensive, and providing only point data at gauging station. The study focuses on presenting a remote sensing approach to quantify suspended sediment concentration (SSC) of the high turbid flow in the Yellow River in China, where the high sediment transportation from severe soil erosion is a big environmental concern. The new approach is based on public accessible satellite images and surface networking monitoring data. With the longest time series records, the Landsat MT and Landsat EMT+ images are chosen to establish the remote sensing approach. A large number of daily sediment records from 125 hydrological stations from 1990 to 2005 across the entire Yellow River are associated with available satellite imagery. The water reflectance is retrieved from the Landsat images by using an effective easy-to-use atmospheric correction method. Sensitivity analysis is conducted to water reflectance from Bands 2 to 5 to establish the SSC indices. According to the significance of SSC indices from the water reflectance, a correlation model between SSC and water reflectance is developed. The model is calibrated and validated by the daily sediment records from surface observation. With the result from this study, it is not only possible to map out the dynamic SSC distribution along the river, but also has the potential to recall the SSC when the historical surface observation is absent.

Conference 8157: Satellite Data Compression, Communications, and Processing VII

Tuesday-Wednesday 23-24 August 2011 • Part of Proceedings of SPIE Vol. 8157
Satellite Data Compression, Communications, and Processing VII

8157-01, Session 1

Improving a DWT-based compression algorithm for high image-quality requirement of satellite images

C. Thiebaut, C. Latry, R. Camarero, Ctr. National d'Études Spatiales (France); G. Cazanave, Magellium (France)

Past and current optical Earth observation systems designed by CNES are using a fixed-rate data compression processing performed at a high-rate in a pushbroom mode (also called scan-based mode). This process generates fixed-length data to the mass memory and data downlink is performed at a fixed rate too. Because of on-board memory limitations and high data rate processing need, the rate allocation procedure is performed over a small image area called a "segment". For both PLEIADES compression algorithm and CCSDS Image Data Compression recommendation, this rate allocation is realised by truncating to the desired rate a hierarchical bitstream of coded and quantized wavelet coefficients for each segment. Because the quantisation induced by truncation of the bit planes description is the same for the whole segment, some parts of the segment have a poor image quality. These artefacts generally occur in low energy areas within a segment of higher level of energy. In order to locally correct these areas, CNES has studied "exceptional processing" targeted for DWT-based compression algorithms. According to a criteria computed for each part of the segment (called block), the wavelet coefficients can be amplified before bit-plane encoding. As usual Region of Interest handling, these multiplied coefficients will be processed earlier by the encoder than in the nominal case (without exceptional processing). The image quality improvement brought by the exceptional processing has been confirmed by visual image analysis and fidelity criteria. The complexity of the proposed improvement for on-board application has been analysed too.

8157-02, Session 1

Adaptive compressed sensing with joint-sparsity reconstruction for hyperspectral images

H. Liu, Y. Li, Xidian Univ. (China); P. Lv, Xi'an Institute of Optics and Precision Mechanics (China); J. Song, J. Zhang, Xidian Univ. (China)

Hyperspectral imaging is an effective tool for detecting the nature of materials being imaged. However, the traditional hyperspectral image acquisition uniformly samples a large volume of data at or above the Nyquist rate and discards most of them during the compression stage to facilitate efficient storage and transmission. Obviously, this process of massive data acquisition followed by compression is extremely wasteful. Compressed sensing (CS) is a novel technology to acquire and reconstruct signals below the Nyquist rate, which explores the data redundancy to significantly reduce the number of sampled data and has great potential in hyperspectral imaging applications.

Considering that hyperspectral images have strong spectral correlation, it is not efficient enough to individually apply CS to acquire and reconstruct each band. To exploit the spectral correlation for achieving higher reconstruction performance, an efficient joint-sparsity reconstruction scheme for compressed hyperspectral image measurements is proposed in this paper. It classifies hyperspectral images into several different groups depending on their spectral correlation, and adaptively allocates the number of measurements collected for each band accordingly. In addition, the hyperspectral image similarity is introduced as a regularization term into the CS recovery problem to jointly explore the sparsity in the intra-band and inter-band domain. The experimental

results show that the proposed method achieves much better performance than many state-of-the-art algorithms in terms of both PSNR and computational complexity.

8157-03, Session 1

Further GPU acceleration of predictive partitioned vector quantization for ultraspectral sounder data compression

S. Wei, Tamkang Univ. (Taiwan); B. Huang, Univ. of Wisconsin-Madison (United States)

Large-volume ultraspectral sounder data requires compression for data storage and transfer. Predictive partitioned vector quantization (PPVQ) has been proven to be an effective lossless compression scheme for ultraspectral sounder data. It consists of linear prediction, bit depth partitioning, vector quantization, and entropy coding. In previous work, the two most time consuming stages of linear prediction and vector quantization were identified for GPU implementation. By exploiting the data parallel characteristics of these two stages, a new spatial division design will be tested in this work for further speedup compared to previous spectral division design.

8157-04, Session 1

Design of JPEG-LS encoder on GPUs

Y. Fang, Northwest A&F Univ. (China); B. Huang, Univ. of Wisconsin-Madison (United States)

Lossless JPEG (JPEG-LS) is a lossless/near-lossless image compression standard with low complexity, which consists of three independent and distinct stages called prediction, residual modeling, and context-based coding of the residuals. To parallelize the prediction and modeling stages, each thread processes each row of pixels. Then parallelized AC is run to do entropy coding of the residuals, which can be modeled as a discrete Laplace process.

8157-05, Session 1

Opportunistic network coding retransmission algorithm based on packet loss pattern

S. Xiao, Xidian Univ. (China)

Broadcast and multicast schemes are very popular for the satellite data transmission applications such as the file distribution of images that used for remote sensing, forecasting, geographic information system etc. since they are effective in bandwidth consumption in a spectrum-limited wireless space. However, providing reliable broadcast and multicast transmission over wireless networks is still a challenging problem, due to the erratic and time-varying nature of a wireless channel.

Usually, the transmission reliability is achieved through Automatic Repeat Request (ARQ) or/and Forward Error Correction (FEC) schemes. For traditional ARQ schemes, the lost packets will be sent one by one from the source node to the receiver, which is called retransmission. An efficient retransmission strategy is very important to the reliability of transmission and the bandwidth utility of the wireless network.

In this paper, an opportunistic network coding retransmission algorithm based on packet loss pattern was proposed to improve the transmission efficiency of broadcast and multicast over wireless networks. At first, a loss pattern matrix of the received packets in multiple terminals

was set up. Then a coding strategy was designed which generate retransmission packets by employing the opportunistic network coding according to the packet loss pattern. Finally, the coding packets were transmitted to different terminals from which the lost packets can be retrieved respectively. The theoretical analysis reveals the feasibility and effectiveness of proposed algorithm.

To verify the efficiency of the proposed algorithm, different criterions are defined and used in the performance comparison with previous methods. The simulation results show that the algorithm can effectively reduce the retransmission times and increase the transmission efficiency over wireless networks. It leads to better performance compared with other approaches for all pre-defined criterions under various channel conditions.

8157-06, Session 2

Fast endmember extraction method using the geometry of the hyperspectral datacube

R. Rashidi Far, S. Qian, Canadian Space Agency (Canada)

This paper proposes a new method to extract the endmembers of a hyperspectral datacube using the geometry of the datacube. The criterion used to find the endmembers in this method is the volume of the simplex. Unlike to the widely used endmember extraction method "N-FINDR", which calculates the volume of a simplex as many times as the number of the vertices of the simplex for each pixel of the datacube in searching for the replacers for the vertices, the proposed method calculates the volume only once for each pixel of the datacube by taking into account of the geometry of the hyperspectral datacube that is tackled. For each pixel, the method finds the closest vertex of the simplex to that pixel. Then the closest vertex is replaced with the pixel in calculating the volume of the potential new simplex. Computational complexity of the proposed method is one order of magnitude less than the N-FINDR. As the proposed method is using the same criterion as N-FINDR we refer it to as fast N-FINDR (FN-FINDR). The performance of the proposed method was compared with N-FINDR using an AVIRIS datacube and a HYDICE datacube. The performance of the proposed method was evaluated using three different distance measures. The comparison was also made using two different dimensionality reduction methods. It is observed that the FN-FINDR with a modified Euclidean distance works as well as the N-FINDR.

8157-07, Session 2

A new morphological anomaly detection algorithm for hyperspectral images and its GPU implementation

A. Paz, A. J. Plaza, Univ. de Extremadura (Spain)

Automatic target and anomaly detection are considered very important tasks for hyperspectral data exploitation. These techniques are now routinely applied in many application domains, including defence and intelligence, public safety, precision agriculture, geology, or forestry. Many of these applications require timely responses for swift decisions which depend upon high computing performance of algorithm analysis. However, with the recent explosion in the amount and dimensionality of hyperspectral imagery, this problem calls for the incorporation of parallel computing techniques. In the past, clusters of computers have offered an attractive solution for fast anomaly and target detection in hyperspectral data sets already transmitted to Earth. However, these systems are expensive and difficult to adapt to on-board data processing scenarios, in which low-weight and low-power integrated components are essential to reduce mission payload and obtain analysis results in (near) real-time, i.e., at the same time as the data is collected by the sensor. An exciting new development in the field of commodity computing is the emergence of commodity graphics processing units (GPUs), which can bridge the gap towards on-board processing of remotely sensed hyperspectral data. In this paper, we develop a new morphological algorithm for

anomaly detection in hyperspectral images along with its efficient GPU implementation. The parallel is implemented on latest-generation GPU architectures, and evaluated using hyperspectral data collected by the NASA's Airborne Visible Infra-Red Imaging Spectrometer (AVIRIS) over the World Trade Center (WTC) in New York, five days after September 11th, 2001.

8157-08, Session 2

Color/mono classification of scanned images

S. Youn, Yonsei Univ. (Korea, Republic of); S. W. Han, Samsung Electronics Co., Ltd. (Korea, Republic of); C. Lee, Yonsei Univ. (Korea, Republic of)

We propose a new algorithm for color/mono classification of scanned images. During scanning process, various artifacts are generated by scanner sensors. These artifacts make it difficult to design a classifier for color and mono classification. The proposed algorithm utilizes a color index that reflects pixel colorfulness. The scanned image is divided into a number of sub-blocks, a color index is computed for each sub-block. Half-tone regions are removed by low-pass filtering and clustering in the RGB space is performed to analyze neighbor pixels. All the pixels within a block are projected into RGB space and the Euclidean distances between the block center and pixels within the block are computed. If the number of pixels which are located within a certain distance from the center and are connected to the block center is larger than a threshold, we determine that the pixel has homogeneous neighbors. In this case, the achromatic distance, which is the Euclidean distance from the pixel to the gray line ($R=G=B$), is calculated. If the average of achromatic distances is bigger than a threshold, the center pixel is classified as a color pixel. To enhance reliability, the color pixel percentile can be used to classify the entire document.

8157-09, Session 2

Accelerating the Hilbert-Huang Transform on GPUs

J. Wang, B. Huang, Univ. of Wisconsin-Madison (United States)

The Hilbert-Huang Transform (HHT) is an empirical algorithm for analysis of nonlinear and nonstationary data. It consists of the empirical mode decomposition (EMD) and the Hilbert spectral analysis (HSA). The EMD method is to decompose a signal into a collection of the intrinsic mode functions (IMFs), while the HSA method is to obtain the instantaneous frequencies. The HHT has been widely used in various science and engineering applications, including remote sensing data processing. The process of extracting an IMF is to connect all the local maxima by a cubic spline line as the upper envelope and all the local minima as the lower envelope. This sifting procedure is suitable for parallel implementation. In recent years graphics processing units (GPUs) with hundreds of compute cores have become an affordable alternative to a CPU cluster for high performance computing. In this study we exploit the GPU massively parallel capabilities to accelerate the HHT with an expected significant speedup.

8157-10, Session 3

Field programmable gate array design of implementing simplex growing algorithm for hyperspectral endmember extraction

W. Xiong, Univ. of Maryland, Baltimore County (United States); C. Wu, National Taipei Univ. of Technology (Taiwan); C. Chang, Univ. of Maryland, Baltimore County (United States)

N-FINDR has been widely used for endmember extraction in hyperspectral imagery. Due to its high computational complexity

developing fast computing N-FINDR has become interest. One approach is to design field programmable gate array (FPGA) architecture for N-FINDR to reduce computing time. However, two major issues still need to be addressed. One is that the number of endmembers must be fixed regardless of applications. The other is computation of simplex volumes. This paper investigates a progressive version of N-FINDR, previously known as simplex growing algorithm (SGA) for its FPGA implementation which basically resolves these two issues.

8157-11, Session 3

GPU implementation of the maximum likelihood solution to the inverse problem for retrieval of geophysical parameters from high-resolution sounder data

S. Wei, Tamkang Univ. (Taiwan); B. Huang, Univ. of Wisconsin-Madison (United States)

The radiative transfer equation (RTE) describes the observed radiance as a result of contributions from surface properties, atmospheric temperature and absorbing gas profiles. Retrieval of these geophysical parameters from the sounder data requires an inverse solution to the RTE. In the presence of noise in observation data, the maximum likelihood estimator is often used to find the most probable solution from an ensemble described by a probability density function. In recent years graphics processing units (GPUs) with hundreds of computing cores have become affordable for scientific computation. This work explores the GPU massively parallel capabilities in accelerating the maximum likelihood solution to the remote sensing retrieval problem.

8157-12, Session 3

Visual analytics of terrestrial lidar data for cliff erosion assessment on large displays

T. Hsieh, Y. Chang, National Taipei Univ. of Technology (Taiwan)

Heavy development on cliffs places a heavy emphasis on maintaining a healthy natural environment. The ability to explore, conceptualize and correlate spatial and temporal changes of topographical records is required for the development of new analytical models that capture the mechanisms contributing towards cliff erosion. This paper presents a visualization based approach using large displays in a digital immersive environment. Visual analytics are performed for cliff erosion assessment from a terrestrial LIDAR (Light Detection And Ranging) data, including visualization techniques for the delineation, segmentation, and classification of features, change detection and annotation. Research findings are described in the context of a cliff failure observed in Solana Beach in California. The visualization system presented in this paper demonstrates the insights that can be gained by observing the temporal change of a failure mass using frequent site monitoring.

8157-13, Session 3

GPU implementation of orthogonal matching pursuit for compressive sensing

Y. Fang, Northwest A&F Univ. (China)

Compressive sensing (CS) is useful in image compression. Recovery algorithms play an important role in CS. Among those CS recovery algorithms, the orthogonal matching pursuit (OMP) algorithm achieves good performance at low complexity. The complexity of OMP comes mainly from matrix operations, e.g. matrix multiplication, matrix inverse, etc., which makes it very suited to parallelized implementation. This paper considers the GPU implementation of OMP algorithm for the CS application.

8157-14, Session 3

Real-time implementation of a full hyperspectral unmixing chain on graphics processing units

S. Sanchez, A. J. Plaza, Univ. de Extremadura (Spain)

Hyperspectral unmixing is a very important task for remotely sensed hyperspectral data exploitation. It amounts at estimating the abundance of pure spectral signatures (called endmembers) in each mixed pixel of the original hyperspectral image, where mixed pixels arise due to insufficient spatial resolution and other phenomena. The full spectral unmixing chain comprises three main steps: 1) dimensionality reduction, in which the original hyperspectral data is brought to an adequate subspace; 2) endmember extraction, in which endmembers are automatically identified from the image data; and 3) abundance estimation, in which the fractional coverage of each endmember is estimated for each pixel of the hyperspectral scene. The hyperspectral unmixing process can be time-consuming, particularly for high-dimensional hyperspectral images. Parallel computing architectures have offered an attractive solution for fast unmixing of hyperspectral data sets, but these systems are expensive and difficult to adapt to on-board data processing scenarios, in which low-weight and low-power integrated components are essential to reduce mission payload and obtain analysis results in (near) real-time. In this paper, we develop a real-time implementation of a full unmixing chain for hyperspectral data on graphics processing units (GPUs). These hardware accelerators can bridge the gap towards on-board processing of this kind of data. The considered chain comprises principal component analysis (PCA) for dimensionality estimation, extraction of endmembers using the N-FINDR algorithm, and unconstrained linear spectral unmixing. The proposed GPU implementation is shown to perform strictly in real-time for hyperspectral data sets collected by the NASA's Airborne Visible Infra-Red Imaging Spectrometer (AVIRIS).

8157-15, Session 3

GPU-accelerated CIMSS radiative transfer model

J. S. Mielikainen, Yonsei Univ. (Korea, Republic of); B. Huang, A. H. L. Huang, Univ. of Wisconsin-Madison (United States)

Radiative transfer equation (RTE) computes radiance as a nonlinear functional of surface properties and atmospheric temperature and absorbing gas profiles.

Currently, operational numerical weather prediction systems are still limited by the radiative transfer model (RTM) performance. Thus, only a few hundred of channels out of 8461 channel Infrared Atmospheric Sounding Interferometer (IASI) measurements are utilized. In this paper, we develop a Graphics Processing Unit (GPU)-based high-performance RTM for the IASI launched in 2006 onboard the first European meteorological polar-orbiting satellites, METOP-A.

In recent years the programmable commodity graphics processing unit (GPU) has evolved into a highly parallel, multi-threaded, many-core processor with tremendous computational speed and very high memory bandwidth. The radiative transfer model is very suitable for the GPU implementation to take advantage of the hardware's efficiency and parallelism where radiances of many channels can be calculated in parallel in GPUs.

Our GPU-based IASI radiative transfer model is developed to run on a low-cost personal supercomputer with 4 NVIDIA Tesla C1060 GPUs with total 960 cores, delivering near 4 TFlops theoretical peak performance.

We propose two different types of GPU RTMs. The first one, processes one profile at a time.

The second proposed GPU RTM processes more than one profile at a time in order to gain a significant speedup compared to the case of processing just one profile at a time.

The IASI radiative transfer model consists of three modules. The first

module for computing the regression predictors takes less than 0.004% of CPU time, while the second module for transmittance computation and the third module for radiance computation take approximately 92.5% and 7.5%, respectively. By massively parallelizing the second and third modules, we reached 364x speedup for 1 GPU on single-profile processing and 1455x speedup for all 4 GPUs. Both with respect to the original CPU-based single-threaded Fortran code. Similarly, using multi-profile processing, to compute 10 IASI radiance spectra simultaneously on a GPU, we reached 763x speedup for 1 GPU and 3024x speedup for all 4 GPUs, both with respect to the original single-threaded Fortran CPU code. The significant 3024x speedup means that the proposed GPU-based high-performance forward model is able to compute one day's amount of 1,296,000 IASI spectra within 6 minutes.

8157-16, Session 4

An efficient feedback-channel-based distributed video coding system

X. Wu, Y. Li, J. Song, J. Lei, Xidian Univ. (China)

Distributed Video Coding (DVC) shifts the complexity from encoder to decoder. In syndrome based DVC systems, Feedback-Channel (FC) is used to determine the required bits at the decoder, which is difficult to realize in practice. If the decoding fails, the decoder sends a request to encoder for more syndrome bits. To decrease the encoder computation complexity, the side information is only constructed at the decoder so the rate estimated at the encoder is not exact. Although better rate distortion performance could be achieved by FC rate control, the time delay of the DVC is increased. In this paper, we use an efficient correlation model to detect the correlation between source frame and simply constructed side information at the encoder. The encoder determines the initial rate for the decoder to decrease the request times for decoder efficiently. At the decoder, side information refinement algorithm is adopted to increase system efficiency while decrease the final rate. The previous decoded information is used to improve the side information quality which effects the LDPC decoding efficiency significantly. Compared with other methods, better RD performance is achieved by our proposed algorithm compared with other encoder rate control algorithms and the time delay is decreased compared with traditional FC based algorithms.

8157-17, Session 4

FAPEC in an FPGA: a simple low-power solution for data compression in space

A. G. Villafranca, Institut Cartogràfic de Catalunya (Spain) and Institut d'Estudis Espacials de Catalunya (Spain); S. B. Mignot, Observatoire de Paris à Meudon (France); J. Portell de Mora, Univ. de Barcelona (Spain) and Institut d'Estudis Espacials de Catalunya (Spain); E. García-Berro, Univ. Politècnica de Catalunya (Spain)

Future space missions are based on a new generation of instruments. These missions find a serious constraint in the telemetry system, which cannot download the large volumes of data generated to the ground. Hence, data compression algorithms are often mandatory in space, despite the modest processing power usually available on-board. We present here a compact solution implemented in hardware for such missions. FAPEC is a lossless compressor which typically outperforms the CCSDS 121.0 recommendation on realistic data sets. With efficiencies higher than 90% of the Shannon limit in most cases - even in presence of noise or outliers - FAPEC has been successfully validated in software as a robust low-complexity alternative to the recommendation. This work describes the FAPEC implementation on an FPGA, targeting the space-qualified Actel RTAX family. We have proved that FAPEC is hardware-friendly and that it does not require external memory. We have assessed the correct operation of the prototype for an initial throughput of 32 Mbits/s with very low power consumption (<50 mW). Finally, we discuss further potential applications of FAPEC, and we set the basis for

the improvements that will boost FAPEC performance beyond the 100 Mbit/s barrier.

8157-18, Session 4

Lossless compression of 3D Aurora images using adaptive-context-based prediction model in China's Arctic Yellow River Station

J. Wu, T. Teng, Xidian Univ. (China)

It is well-known that a proper prediction model and method can obviously improve the performance of prediction. But, the state-of-art compression algorithms can not effectively capture the characteristics of 3-D aurora images and can not achieve optimal compression performance. This paper proposes a lossless compression algorithm using adaptive-context-based prediction model. Prediction models used in traditional algorithms are either too small or not accuracy enough to capture the variances of aurora edges. So, we adopt a larger context prediction model according to the correlation characteristics of aurora images. Unlike conventional prediction algorithms which always use intra-prediction or inter-prediction, we choose intra-prediction or inter-prediction adaptively by testing the correlation strength among pixels in the prediction model. For intra-prediction, we adopt the prediction method used in JPEG-LS. In order to reduce the complexity and achieve high accuracy, we proposed a new algorithm for inter-prediction. Through bubble sort, we can get the eight pixels which have stronger correlations with current pixel instead of using all the pixels in the prediction model to predict current pixel. However, it does not always hold true that the eight chosen pixels all have higher inter-frame correlations. So we use a criterion to further select the pixels which are used as the final pixels for prediction. Experimental results show that the proposed adaptive-context-based prediction model can significantly reduces the complexity and guarantees the accuracy. The prediction algorithm with proposed adaptive-context-based prediction model performs better than wavelet-based lossless algorithms such as 3D-SPECK and JPEG-2000, and still outperforms JPEG-LS with a slight degradation in coding time.

8157-19, Session 4

Three-dimensional error correcting with matched interleaving for holographic data storage

H. Gu, L. Cao, Q. He, G. Jin, Tsinghua Univ. (China)

This paper presents a three-dimensional error correcting with matched interleaving (3DEC-MI) scheme for holographic data storage (HDS). For applying to various error patterns, including random errors, burst errors, and inhomogeneously distributed errors, in the HDS channel, the 3DEC-MI scheme combines the advantages of the three-dimensional error correcting scheme and the matched interleaving scheme, makes full use of the priori knowledge of the error patterns in the HDS channel, distributes errors more uniformly, and decodes data iteratively in three dimensions. It is able to eliminate the influences of non-uniform distribution of errors within a page and across pages, overcome the effects of burst errors, and correct random errors. Simulation results show that the bit-error rate (BER) of the HDS channel can be effectively reduced after correcting with the proposed scheme, the performance of which is validated in a terabyte optical disc HDS system.

8157-20, Session 4

Development of GPU-based CCSDS Rice coding

X. Wu, Y. Li, Xidian Univ. (China); B. Huang, Univ. of Wisconsin-Madison (United States)

**Conference 8157: Satellite Data Compression,
Communications, and Processing VII**

The Rice coding is the Consultative Committee for Space Data Systems (CCSDS) recommendation for lossless data compression on several different types of data. The CCSDS Rice coding is an adaptive entropy coder with a preprocessor, applied to each block of J samples. The default preprocessor uses a unit-delay predictor with positive mapping. The adaptive entropy coder concurrently applies a set of variable-length codes to a block of J consecutive preprocessed samples. The code option that yields the shortest codeword sequence for the current block of samples is selected for transmission. A unique identifier bit sequence is attached to the code block to indicate to the decoder which decoding option to use. The CCSDS Rice decoding is suitable for parallel implementation where all codeword blocks can be decoded independently and simultaneously. In order to perform high-performance Rice decoding on satellite images compressed by the CCSDS Rice coding, we propose to accelerate the Rice decoding on the Graphics Processing Units (GPUs) using Compute Unified Device Architecture (CUDA). The GPU-based Rice decoder will process many codeword blocks in a massively parallel fashion by different GPU multiprocessors. It is expected to achieve a remarkable speedup over its single-threaded CPU counterpart.

8157-21, Session 5

Unsupervised clustering and spectral unmixing for feature extraction prior to supervised classification of hyperspectral images

I. Dopido, A. Villa, A. J. Plaza, Univ. de Extremadura (Spain)

Classification and spectral unmixing are two very important tasks for hyperspectral data exploitation. Although many studies exist in both areas, the combined use of both approaches has not been widely explored in the literature. Since hyperspectral images are generally dominated by mixed pixels, spectral unmixing can particularly provide a useful source of information for classification purposes. In previous work, we have demonstrated that spectral unmixing can be used as an effective approach for feature extraction prior to supervised classification of hyperspectral data using support vector machines (SVMs). Unmixing-based features do not dramatically improve classification accuracies with regards to features provided by classic techniques such as the minimum noise fraction (MNF), but they can provide a better characterization of small classes. Also, these features are potentially easier to interpret due to their physical meaning (in spectral unmixing, the features represent the abundances of real materials present in the scene). In this paper, we develop a new strategy for feature extraction prior to supervised classification of hyperspectral images. The proposed method first performs unsupervised multidimensional clustering on the original hyperspectral image. The cluster centres are then used as representative spectral signatures for a subsequent unmixing process, and the resulting features are used as inputs to a standard (supervised) classification process. The proposed strategy is compared to other classic and unmixing feature extraction methods presented in the literature. Our experiments, conducted with several reference hyperspectral images widely used for classification purposes, reveal the effectiveness of the proposed approach.

8157-22, Session 5

Low-complexity pixel-based halftone detection

J. Ok, Yonsei Univ. (Korea, Republic of); S. W. Han, Samsung Electronics Co., Ltd. (Korea, Republic of); J. Mielikainen, C. Lee, Yonsei Univ. (Korea, Republic of)

With the advances of the internet and multimedia technologies, the digital document market grows steadily. Since most digital documents use halftone technologies, quality degradation occurs when one tries to scan and reprint such halftone images. Typically, halftone areas occupy

a portion of documents. For improved picture quality, low pass filtering is applied to the halftone areas before reprinting the scanned images. Therefore, it is necessary to extract halftone areas to produce high quality printing.

In this paper, we propose a low complexity pixel-based halftone detection algorithm. For each pixel, we consider a surrounding sub-block. If the sub-block contains any flat background, text, thin line, continuous and non-homogeneous regions, the pixel is classified as a non-halftone pixel. To reduce the complexity, we first detect flat background. Then, text and thin lines are detected. Finally, continuous and non-homogeneous regions are located. After excluding non-halftone pixels, the remaining pixels are considered as halftone pixels. Classifying a document as halftone printing or Silver-halide photo is performed by calculating the halftone pixel ratio. The proposed algorithm is memory-efficient and requires low computation cost. The proposed algorithm can easily be implemented using GPU.

8157-23, Session 5

2D orthogonal matching pursuit

Y. Fang, Northwest A&F Univ. (China); B. Huang, Univ. of Wisconsin-Madison (United States)

The problem of 2D sparse signal recovery plays an important role in practice, e.g. compressive imaging, image/video compression, etc. To exploit the correlation of 2D signals along two directions, 2D separable measuring (along row and column directions) has been proposed, which can convert the problem of 2D sparse signal recovery into a standard 1D sparse signal recovery problem with the complexity of $O(m^2 \times n^2)$.

Different from 1D sparse signal recovery, we have developed the 2D orthogonal matching pursuit (2D-OMP) algorithm for separable measurements of 2D sparse signals, which reduces the complexity from $O(m^2 \times n^2)$ to $O(m \times n^2)$. The 2D-OMP is a natural extension of the 1D-OMP. In the 2D-OMP, the dictionary contains $(n \times n)$ atoms and each atom is an $(m \times m)$ matrix. The decoder projects the $(m \times m)$ sample matrix onto the atoms and records the most significant atom. Then the decoder updates the weights of all the already selected atoms by least squares. Such procedure iterates until the Frobenius norm of the residue matrix is less than the given threshold.

8157-24, Session 5

GPU acceleration of the solution to a polarized atmospheric radiative transfer model with multiple scattering

C. Song, Y. Li, Xidian Univ. (China); B. Huang, Univ. of Wisconsin-Madison (United States)

The plane-parallel polarized radiative transfer model developed in a seminal paper by Evans and Stephens (1991) has been widely used for passive atmospheric remote sensing of the planets in the solar system. The model considers both solar and thermal energy sources and computes the monochromatic polarized radiance emerging from a vertically inhomogeneous atmosphere with multiple scattering and randomly-oriented particles of arbitrary shapes. The diffuse radiance field is expressed as a four-vector of Stokes parameters. The solution method converts the single-scattering information into a form suitable for applying the doubling and adding method to compute the optical properties of the whole atmosphere from the local properties of each infinitesimal layer. The computation for a more accurate solution could be time-consuming in many applications involving Rayleigh or Mie atmospheres in sunlight or microwave transfer through a precipitating atmosphere. In recent years the NVIDIA GPUs provide affordable supercomputing power with Compute Unified Device Architecture (CUDA) as the GPU programming tool. In this paper we take advantage of GPU massively parallel capabilities to speed up the computation of the solution to the polarized radiative transfer problem.

8157-25, Session 6

Early detection of RFI in SMOS radiometric measurements

É. Anterrieu, Observatoire Midi-Pyrénées (France) and Univ. de Toulouse (France)

The SMOS mission is a European Space Agency project devoted to the global monitoring of surface Soil Moisture and Ocean Salinity from spaceborne radiometric observations. The single payload of the mission is MIRAS, the very first Microwave Imaging Radiometer using Aperture Synthesis ever launched into space. Cross-correlating the signals collected by each pair of antennas provides samples of the so-called visibility function of the brightness temperature distribution of the scene under observation. Although MIRAS is operating in the protected L-band, the contamination of such interferometric measurements by man-made sources of radio-frequency interferences (RFI) operating very close to this band has been evidenced during the commissioning phase. Owing to the software and hardware architectures of MIRAS, the standard approaches found in the literature for detecting RFI in such signals do not solve the problem for SMOS because the sampling rate of the signals downloaded to the ground segment is too low for this purpose. A specific method should be implemented for the SMOS mission by taking into account the specificities of MIRAS with regards to the sensitivity to RFI. Contamination by RFI is an important issue for the success of the mission since it propagates from measurements to reconstructed brightness temperature maps and then to higher level products. RFI should be detected as soon as possible in the processing pipeline, namely at the L1a level of the measurements provided by MIRAS. A detection and quantification approach tailored to these measurements is presented and illustrated with data acquired during the commissioning phase.

8157-26, Session 6

Scanning pattern simulation for the meteorological payload of polar communication and weather satellites

R. Ksantini, S. Qian, Canadian Space Agency (Canada)

The Canadian Space Agency is developing a polar communication and weather (PCW) mission to provide high quality radiometric data, high spatial resolution temporal image calibration, and comprehensive ongoing ground validation of generated data and products. To improve the meteorological images (geometrically, spatially, and radiometrically) and to overcome the challenges of the meteorological payload with scan mirrors and multiple Focal Plane Arrays in a Molinya orbit imposed on the images, we carried out study to simulate and analyze the scan mirror geometry and error sources to better model the scan mirror and errors for providing guide to the system design, to overcome the problems of multiple freedom rotations and distortions of the imaging mechanism. In fact, a scanning device will not always generate a perfect orthogonal and regular grid pattern. This is because of the effects of the view zenith angle and the Earth curvature. The grid pattern is originally represented by a Field of Regard (FOR) which is sampled into identical and rectangular Fields of View (FOVs). We transform these FOVs using mirror scanner and combined rotation transformations, with least distortions and FOV slanting comparatively to the initial FOR. Then, a semi-analytical error function of the mirror rotation angles is developed to model the parametric and non-parametric errors of the meteorological images. This error function will allow better simulation and analysis of the meteorological payload scanning pattern and then improvement of the meteorological image. Experimental results of the scanning pattern analysis and simulation are provided with interpretations and conclusions.

8157-27, Session 6

Hyperspectral image spatial resolution improvement using wavelet-based Bayesian framework

Y. Zhang, M. He, Northwestern Polytechnical Univ. (China)

Hyperspectral (HS) images employ hundreds of contiguous spectral bands to capture and process spectral information over a range of wavelengths, compared to the tens of discrete spectral bands used in multispectral (MS) images. This increase in spectral accuracy is delivering more information, allowing a whole range of new and more precise applications. However, usually a trade-off exists in remote sensors, between spatial and spectral resolutions due to physical limitations, data-transfer requirements and some other practical reasons. Therefore, in most cases, high spatial and spectral resolutions are not available in a single image. Normally, the spatial resolution of HS images is still lower than that of MS images. In many applications, there is need for high accuracy both spectrally and spatially, which inspires the research on spatial resolution enhancement of HS images. In this work, a spatial resolution improvement approach for HS image is proposed, which is developed on a Bayesian estimation framework. The technique works in the wavelet domain, assuming a joint statistical model for the observed images, and a blurring and additive noise imaging model for the HS image. To keep the calculation feasible, an appropriate and applicable estimation strategy is also proposed. In the simulated experiment, the technique is validated and also compared to the state-of-the-art techniques. The experimental results illustrate that the newly proposed approach is capable of effectively improving spatial resolution of HS image and robust to noise in the observed image.

8157-28, Session 6

Parallel implementation of GPU-accelerated Kalman filter

Y. Chang, T. Hsieh, M. Huang, National Taipei Univ. of Technology (Taiwan)

The Kalman filter has been widely used in many science and engineering applications, including remote sensing, to estimate the states of a linear system that can only be observed indirectly or inaccurately in a sense of minimizing the variance of the estimation errors. The Kalman filter equations involve matrix manipulations such as matrix inversion and transpose. Modern satellite and airborne sensors with higher temporal, spectral and spatial resolutions often result in significant usage of large-scale data matrices for Earth remote sensing observations. Consequently, this poses a challenge to these computationally intensive tasks and the usage of a cost-effective high-performance computing device is desired. In this paper we propose to accelerate the Kalman filter on graphic-processing-units (GPUs). The GPU code to run on NVIDIA GPUs uses the compute unified device architecture (CUDA) language. The GPU-based Kalman filter is expected to achieve a significant speedup over its CPU-based single-threaded counterpart.

8157-29, Session 6

Joint spectral and spatial preprocessing prior to endmember extraction from hyperspectral images

G. Martin, A. J. Plaza, Univ. de Extremadura (Spain)

Hyperspectral unmixing is a very important task for remotely sensed hyperspectral data exploitation. It amounts at estimating the abundance of pure spectral signatures (called endmembers) in each mixed pixel of the original hyperspectral image, where mixed pixels arise due to insufficient spatial resolution and other phenomena. A challenging problem in spectral unmixing is how to automatically derive endmembers

from hyperspectral images, particularly due to the presence of mixed pixels which generally prevents the localization of pure spectral signatures in transition areas between different land-cover classes. A possible strategy to address this problem is to guide the endmember extraction process to spatially homogeneous areas. For this purpose, several preprocessing methods (intended to be applied prior to the endmember extraction stage) have been developed in the literature. However, most of these methods only include spatial information during the preprocessing and disregard spectral information until the subsequent endmember extraction stage. In this paper, we develop a new joint spatial and spectral preprocessing method which can be combined with any endmember extraction algorithm from hyperspectral images. The proposed method is intended to retain spectrally pure pixels which belong to spatially homogeneous areas. Our assumption is that spectrally pure signatures are more likely to be found in spatially homogeneous areas rather than in transition areas between different land-cover classes, which are expected to be dominated by mixed pixels. Our experimental results, conducted with a variety of hyperspectral images, reveal the robustness of the proposed method when compared to other similar preprocessing strategies.

8157-30, Session 7

Classified coset coding-based lossless compression of hyperspectral images

J. Song, Y. Li, H. Liu, X. Wu, K. Wang, Xidian Univ. (China)

Due to the restrained resources on board, compression methods with low complexity are desirable for hyperspectral images. Distributed source coding (DSC) based on Slepian-Wolf theorem is applied to hyperspectral image compression owing to its low complexity and high performance.

E. Magli et al proposed a scalar coset based distributed compression method (s-DSC). In their proposed scheme, each block is compressed by just retaining least significant bits (LSB) that can be viewed as index of coset while discarding the most significant bits (MSB). The decoder recovers the MSBs with the help of predicted value by choosing the MSBs that minimize the distance between the reconstructed value and predicted one. However there still exists much redundancy since the bitrate of the whole block is determined by its maximum prediction error. In fact, much fewer LSBs are enough to recover the most pixels in the block. In order to further reduce the bitrate, a classified coset coding based lossless compression method is proposed in this paper. Since the current band has similar spectral correlation with the previous band and the number of LSB to be transmitted is determined by the spectral correlation, the current block is classified using the corresponding prediction errors in the previous band to make the pixels with similar inter-band correlation cluster together. Then each class of pixels is coset coded respectively according to its own maximum prediction error.

The experimental results show that the classification could reduce the bitrate efficiently. Compared to s-DSC method without classification, the lossless compression bitrate of the proposed method is reduced by about 0.4bpp.

8157-31, Session 7

On-board compression of hyperspectral satellite data using band reordering

J. Gaucel, Thales Alenia Space (France); C. Thiebaut, R. Camarero, Ctr. National d'Études Spatiales (France)

Hyperspectral remote sensing has been widely utilized notably in high-resolution climate observation, environment monitoring, resource mapping. However, it brings undesirable difficulties for transmission and storage due to the huge amount of the data. The compression of the cube has been demonstrated to be an efficient strategy to solve these problems. Moreover, the data features have strong similarity in disjoint spectral regions due to the same type of absorbing gases. That is why a pre-processing scheme based on a similarity measurement and a re-

ordering strategy permits to enhance the compression ratio.

In this work, we first propose a review of similarity measurements and re-ordering strategies, and we give the field of application of each of them. In particular, we propose a pre-selection of these measurements and re-ordering strategies wrt the expected performance, the complexity and the robustness to an on-board implementation. In a second part, we give the performance gap between a high performance / complex approach and a spatializing approach for two compression schemes: a 3D transform (SPIHT3D) and a 3D predictive algorithm. Finally, we present the capability to implement the re-ordering in a semi-optimal, semi-fixed or fixed manner, and thereby characterize the performances in a space borne system.

8157-32, Session 7

Accelerating arithmetic encoder on GPUs

Y. Fang, Northwest A&F Univ. (China)

Arithmetic Coding (AC) is widely used in lossless data compression. However, compared to Huffman coding, its computational complexity is much more high due to multiplication and branching operations. Though any non-binary AC can be converted into binary AC of multiple bit-planes, binarization usually causes performance degradation. This paper researches the implementation of AC encoder on GPUs. The main idea is to use block AC. Each thread processes one block, so that data blocks can be encoded in parallel.

8157-33, Session 7

A novel video delivery algorithm based on 802.11e EDCA mechanism

J. Du, S. Xiao, Xidian Univ. (China)

Currently, there are still many challenges for video delivery over WLAN due to the contention of channel among four access categories (ACs) in EDCA and requirement of quality of service (QoS) for video packet delivery. In this paper, we propose a Cyclic Enqueueing Algorithm (CEA) which schedules video packets cyclically into all four AC queues based on the queue analysis of average service rate (ASR) and average arrival rate (AAR). Since each AC queue is able to transmit packets without queue delay if AAR is less than ASR, the proposed algorithm makes full use of the available capacity of each AC queue, which could obtain better delivery performance than the default configure in EDCA.

The main contributions of our work can be summarized as follows.

- i. By enqueueing video packets cyclically into all four AC queues rather than only the queue of AC_VI, the proposed CEA method can balance the load of different AC queues and reduce the queue delay of video packets so as to obtain better video delivery quality.
- ii. By using a simplified calculation of error propagation estimation within a GOP, we introduce a video packet ordering algorithm which helps obtain quality gains in the case of traffic congestion.

To verify the efficiency of the proposed algorithm, the video packets are generated from the JM reference software and the EDCA wireless network simulations are performed on NS-3 platform. Several similar algorithms are compared. The results show that the proposed algorithm offer better performance than existing methods in preserving video quality in the case of heavy load of video packets over 802.11e wireless networks.

8157-34, Session 7

Real-time lossless compression for HDTV video using GPGPU

G. Seo, J. Mielikainen, C. Lee, Yonsei Univ. (Korea, Republic of)

HD video services have been widely available in recent years. To transmit

**Conference 8157: Satellite Data Compression,
Communications, and Processing VII**

or store these HD video programs, compression is required. For example, HD video signals require about 1 Gbps and UHD (Ultra High Definition) video signals require about 4 Gbps (4k) or 15 Gbps (8k). Various lossy compression schemes have been developed, which include H.264/AVC and HEVC (high efficiency video coding). On the other hand, there are some applications which require lossless compression. For example, lossless or near lossless compression is required in studio programs. Also, video quality assessment and coding areas need efficient lossless video compression algorithm. Most conventional lossless coding methods have high complexity and require long processing time for encoding and decoding.

GPGPU (General purpose graphics processing unit) is widely used to assist CPU (Central processing unit) in computing massive data sets. Modern GPUs have programmable processors with a large amount of memory cells and processing cores.

In this paper, a parallel lossless compression algorithm with low complexity is proposed. The algorithm can encode and decode HD video sequences in real-time. The proposed algorithm compresses HD video sequences in half. Furthermore, the encoding and decoding time can be significantly reduced using GPU. The average encoding time per frame is about 17ms and decoding time is about 11ms. The algorithm can be implemented in real time for HD video sequences.

8157-35, Session 7

GPU-accelerated IDWT with SPIHT and Reed-Solomon decoding for satellite images

C. Song, Y. Li, Xidian Univ. (China); B. Huang, Univ. of Wisconsin-Madison (United States)

The discrete wavelet transform (DWT)-based Set Partitioning in Hierarchical Trees (SPIHT) algorithm is widely used in many image compression systems. In order to perform real-time Reed-Solomon channel decoding and SPIHT+DWT source decoding on a massive bit stream of compressed images continuously down-linked from the satellite, we propose a novel graphic processing unit (GPU)-accelerated decoding system. In this system the GPU is used to compute the time-consuming inverse DWT, while multiple CPU threads are run in parallel for the remaining part of the system. Both CPU and GPU parts were carefully designed to have approximately the same processing speed to obtain the maximum throughput via a novel pipeline structure for processing continuous satellite images. Through the pipelined CPU and GPU heterogeneous computing, the entire decoding system approaches a speedup of 84x as compared to its single-threaded CPU counterpart.

Conference 8158: Imaging Spectrometry XVI

Monday-Tuesday 22-23 August 2011 • Part of Proceedings of SPIE Vol. 8158 Imaging Spectrometry XVI

8158-01, Session 1

Large format imaging spectrometers for future hyperspectral Landsat mission

J. F. Silny, Raytheon Space & Airborne Systems (United States);
T. G. Chrien, The Aerospace Corp. (United States)

This paper describes a design concept for a Landsat-class imaging spectrometer. The challenge is to match the Landsat data parameters, including a 185 km swath and a 30 meter ground sample distance (GSD) from a 705 km sun-synchronous orbit with a sensor that has contiguous spectral coverage of the solar reflected spectrum (400 to 2500 nm). The result is a remote sensing satellite that provides global access imaging spectrometer data at moderate spatial resolution. Key design trades exist for the spectrometer, focal plane array, dispersive element, and calibrator. Recent developments in wide field-of-view imaging spectrometers at Raytheon are presented in support of a monolithic spectrometer approach. Features of the design include (1) high signal-to-noise ratio, (2) well-corrected spectral fidelity across a 6,000 pixel pushbroom field-of-view, (3) straightforward calibration of the data to units of absolute spectral radiance, and (4) real-time simulation of Thematic Mapper bands, vegetation indices, and water vapor maps for direct continuous downlink.

8158-02, Session 1

Optically fast, wide field-of-view five-mirror anastigmat imager for remote sensing applications

J. F. Silny, E. D. Kim, L. G. Cook, E. M. Moskun, R. L. Patterson,
Raytheon Space & Airborne Systems (United States)

Recent trends in focal plane array (FPA) technology have led naturally to the development of very large format remote sensors that require optically fast, wide field of view imaging optics. Systems that cover broad spectral ranges, such as multispectral imagers (MSI) and hyperspectral imagers (HSI), require reflective optics to provide aberration and distortion control without the complication of wavelength dependent errors induced by refractive elements. These large format systems require even wider fields of view than offered by the conventional three-mirror anastigmat (TMA) and four-mirror anastigmat (4MA) designs. Recently, Raytheon has demonstrated in hardware the first-ever aligned and tested five-mirror anastigmat (5MA) imager. The 5MA was designed with an F/3.0 optical speed and a 36 degree cross-scan FOV for use with a pushbroom imaging spectrometer. The 5MA imager has useful features such as: (1) a real entrance pupil to support full-aperture calibration or a small scan mirror, (2) an intermediate image for stray light control, and (3) a real exit pupil for optimal cold-shielding in infrared applications. A computer-aided alignment method was used to align the 5MA imager with a final target of balanced wavefront error (WFE) across the full 36 deg FOV. This paper discusses the design and development of the first-ever 5MA imager and some potential space and airborne remote sensing applications.

8158-03, Session 1

Hyperspectral microscopic imaging by multiplex coherent anti-Stokes Raman scattering (CARS)

A. T. Khmaladze, J. Jasensky, C. Zhang, X. Han, Z. Chen, Univ. of Michigan (United States)

Coherent anti-Stokes Raman Scattering (CARS) microscopy is a powerful technique to image the chemical composition of complex samples in

biophysics, biology and material science. CARS is a four-wave mixing process. The application of a narrow pump and spectrally wide Stokes pulses excites multiple Raman transitions, which are probed by a probe pulse, generating a coherent directional CARS signal with several orders of magnitude higher intensity relative to spontaneous Raman scattering. Recent advances in the development of ultrafast lasers, as well as Photonic Crystal Fibers (PCF) enables multiplex CARS. In this study, we used two scanning imaging methods. In one, the detection is performed by a photo-multiplier tube (PMT) attached to the spectrometer. The acquisition of series of images, while tuning the wavelengths allows for subsequent reconstruction of spectra at each image point. The second method executes a simultaneous detection of multiple wavelengths by a cooled CCD camera. Coupled with point-by-point scanning, it allows for a hyperspectral microscopic imaging. In particular, since the intensity of CARS signal is proportional to the product of intensities of pump, probe and Stokes scanning beams, the intensity of out of focus CARS signal drops rapidly. Thus, it is possible to use a laser scanning microscope without a confocal pinhole. In the focal plane, CARS signal is only generated where both pump/probe and Stokes beams are overlapped. Therefore, if the beams are slightly spatially shifted against one another, the spatial resolution of the CARS signal is better than the resolution achievable by a single scanning beam.

8158-04, Session 1

Novel dispersing element for a computed tomographic imaging spectrometer

C. J. Vandervlugt, M. W. Kudenov, E. L. Dereniak, College of Optical Sciences, The Univ. of Arizona (United States); G. Cord, Missile Defense Agency (United States)

A Computed Tomographic Imaging Spectrometer (CTIS) is an imaging spectrometer which can acquire a hyper-spectral data set in a single snapshot (one focal plane array integration time) with no moving parts. A specially designed dispersing element which separates light from the object cube into a grid of prismatic diffraction orders is the key element in the instrument. The capabilities of the CTIS instrument can be improved by employing a more optimized grating design. In this paper, we discuss the design of a new CTIS disperser incorporating a novel radial design pattern. Initial test results with the CTIS instrument are also presented.

8158-05, Session 1

A self-reliant RSI payload development in Taiwan

S. Weng, Y. Lian, National Space Organization (Taiwan)

Instead of outsourcing the whole FORMOSAT-2 satellite to a foreign prime contractor, the National Space Organization in Taiwan is stepping ahead to take the full responsibility of consolidating self-reliant space technology capabilities. A newly initiated program FORMOSAT-5 satellite, not only to build a heritage design of a spacecraft bus but also, self-reliantly, to leap a big step toward Remote Sensing Instrument payload development, is sailing on its voyage. Among the payload development effort, an integrated circuit of the kind Complementary Metal Oxide Semiconductor instead of Charge-coupled Device is chosen as the image sensor playing the lead role for the instrument. A Time Delay Integration scheme is applied to ideally achieve high Signal to Noise Ratio. With the advanced CMOS Image Sensor, FORMOSAT-5 is anticipated potentially to be one of the first spacecraft flying in the space. And how a supporting structure, the so-called Iso-static Mount, bearing the optical has to be implemented cautiously to eliminate the microscopic displacements ought not to be overwhelmed by its seemingly simple appearance. A simulated ISM modal analysis had been conducted and the method of bonding between the mirror and ISM had also been tested on an experimental model. Despite the foreseen technical concerns, management issues over scheduling and documentation are constantly

Conference 8158:
Imaging Spectrometry XVI

emerging owing to the payload development underwent is collaborated by several domestic industries and research centers. Regardless of challenges we may confront with, a carefully planned strategy emphasizing on the product realization processes is discussed.

8158-06, Session 2

Hyperspectral target detection and discrimination using the ACE algorithm

M. L. Pieper, D. Manolakis, R. Lockwood, MIT Lincoln Lab. (United States); T. Cooley, P. S. Armstrong, J. Jacobson, Air Force Research Lab. (United States)

One of the fundamental challenges for a hyperspectral imaging system is the detection and discrimination of subpixel objects in background clutter. The background surrounding the object, which acts as interference, provides the major obstacle to successful detection and discrimination. In many applications we look for a single signature and discrimination among different signatures is not required. However, there are important applications where we are interested for multiple signatures. In these cases, the use of spectral discrimination algorithms is both necessary and valuable. In this paper, we develop an approach to spectral discrimination based on the adaptive cosine estimation (ACE) algorithm. The basic idea is to jointly exploit the detection statistics from the various signatures and set a common threshold that ensures larger separation between signatures of interest and background. The operation of the proposed detection-discrimination approach is illustrated using real hyperspectral imaging data.

8158-08, Session 2

Effective use of sample spectral statistics to design hyperspectral imaging algorithms via unsupervised training samples

R. M. Patterson, D. Paylor, K. Liu, E. Wong, C. Chang, Univ. of Maryland, Baltimore County (United States)

Sample spectral correlation statistics (SSCS) have been used to characterize spectral targets of interest in hyperspectral data exploitation. A key issue is to how to effectively use SSCS to design and develop many hyperspectral imaging algorithms. This paper develops an approach which produces an appropriate set of training samples to generate SSCS that can be used to design various algorithms. In order for the proposed approach to work effectively two main issues need to be addressed. One is the number of training samples required to generate. The other is to design an unsupervised algorithm for finding a set of desirable training samples. Regarding the first issue a recently developed concept, virtual dimensionality (VD), OSP-based method, maximum orthogonal complement algorithm (MOCA) can be used for this purpose. As for the second issue several candidate unsupervised algorithms such as automatic target generation process (ATGP), unsupervised least squares-based algorithms can be considered. One immediate benefit from our proposed approach is to reduce computational complexity, specifically for many kernel-based algorithms such as kernel-based RX detector, kernel-based constrained minimum energy (CEM) which requires entire image pixels to produce SSCS.

8158-09, Session 2

Quantifying the co-registration of bands in spectral imaging

T. Skauli, Norwegian Defence Research Establishment (Norway); A. Fridman, Norsk Elektro Optikk AS (Norway)

In multi- and hyperspectral imaging, it is well recognized that the spatial

co-registration of different spectral bands is an important performance characteristic. It has been pointed out that both the position and shape of the point spread function must be matched between spectral bands to produce a good spectral fidelity. A hyperspectral camera with imperfect co-registration may produce spectra with severe artifacts when imaging an inhomogeneous scene. Thus the co-registration is a crucial performance parameter for a hyperspectral imager, and is often specified as “percent of a pixel”. It appears, however, that there is no universally accepted definition of this measure of co-registration. This paper discusses a specific definition of a co-registration metric based on the integrated difference between normalized point spread functions. This metric accounts for differences in both position and shape of the point spread function. The metric can be reasonably interpreted as “percent of a pixel” in a well defined sense, and it produces reasonable results in several limiting cases. The metric is illustrated by simulated and experimental data.

8158-22, Session 3

Production of imagery-derived maps to aid the Japanese earthquake/tsunami relief effort

D. Messinger, D. M. McKeown, N. G. Raqueno, S. A. Cavilia, C. R. DeAngelis, S. Maitra, W. Sun, Rochester Institute of Technology (United States)

On March 11, 2011, the magnitude 9 Tohoku earthquake and resulting tsunami struck off the coast of Japan. An estimated over 400,000 persons were displaced from their homes and the damage to the coastline and nearby urban areas was extensive. Additionally, the combined effects of the earthquake and tsunami caused damage to the Fukushima Dai'ichi Nuclear Power Station. As part of the International Charter “Space and Major Disasters”, the US Geological Survey coordinated a volunteer effort to aid in the response to the disaster. The goal of the project was to produce maps derived from civilian (NASA Landsat and ASTER) and commercially available (DigitalGlobe and GeoEye), high resolution satellite imagery to be delivered to the Japanese authorities. RIT was one of the organizations involved in this effort. This presentation will describe the timeline of the response, the challenges faced in this effort, the workflow developed, and the products that were distributed. Lessons learned from the response will also be described to aid the remote sensing community in preparing for responses to future natural disasters.

8158-10, Session 4

A hyperspectral imager for high radiometric accuracy Earth climate studies

J. Espejo, G. A. Kopp, P. Smith, G. A. Drake, K. F. Heurman, A. Lieber, B. Vermeer, Univ. of Colorado at Boulder (United States)

We demonstrate a visible and near-infrared prototype pushbroom hyperspectral imager for Earth climate studies that is capable of using direct solar viewing for on-orbit cross calibration and degradation tracking. Direct calibration to solar spectral irradiances allow the Earth-viewing instrument to achieve required climate-driven absolute radiometric accuracies of 0.2% (1 σ).

A solar calibration requires viewing scenes having radiances 10⁵ higher than typical Earth scenes. To facilitate this calibration, the instrument features an attenuation system that uses an optimized combination of different precision aperture sizes, neutral density filters, and variable integration timing for Earth and solar viewing. The optical system consists of a three-mirror anastigmat telescope and an Offner spectrometer. The as-built system has a 12.4° cross track field of view with 2.5 arcminute spatial resolution and covers a 350-1050 nm spectral range with 10 nm resolution. A polarization compensated configuration using the Offner in an out of plane alignment is demonstrated as a viable approach to minimizing polarization sensitivity.

The mechanical design takes advantage of relaxed tolerances in the

Conference 8158:
Imaging Spectrometry XVI

optical design by using rigid, non-adjustable diamond-turned tabs for optical mount locating surfaces. We show that this approach achieves the required optical performance. A prototype spaceflight unit is also demonstrated to prove the applicability of these solar cross calibration methods to on-orbit environments. This unit is evaluated for optical performance prior to and after GEVS shake, thermal vacuum, and lifecycle tests.

8158-11, Session 4

A climatology of mid-tropospheric carbon dioxide from the Atmospheric Infrared Sounder

T. S. Pagano, M. T. Chahine, E. T. Olsen, Jet Propulsion Lab. (United States)

The Atmospheric Infrared Sounder (AIRS) is a hyperspectral infrared instrument on the EOS Aqua Spacecraft, launched on May 4, 2002. AIRS has 2378 infrared channels ranging from 3.7 μm to 15.4 μm and a 13.5 km footprint at nadir. The AIRS is a "facility" instrument developed by NASA as an experimental demonstration of advanced technology for remote sensing and the benefits of high resolution infrared spectra to science investigations. AIRS, in conjunction with the Advanced Microwave Sounding Unit (AMSU), produces temperature profiles with 1K/km accuracy on a global scale, as well as water vapor profiles and trace gas amounts for CO₂, CO, SO₂, O₃ and CH₄. AIRS data are used for weather forecasting, climate process studies and validating climate models.

With over eight years of data now available, we have developed a climatology of AIRS Mid-Tropospheric Carbon Dioxide. The climatology is a fit to the observations and shows the regular seasonal structure of the horizontal distribution of CO₂ in the mid-troposphere. The climatology also allows one to study anomalies on the distribution and relate these to known global circulation patterns including El Nino Southern Oscillation (ENSO), and the Madden Julian Oscillation (MJO). The climatology is also useful for regional modeling of CO₂ fluxes by providing a nominal background field. Studies have demonstrated assimilation of AIRS mid-tropospheric observations improve prediction of near surface concentrations. Early results from the AIRS stratospheric and lower-tropospheric retrievals is discussed.

8158-13, Session 4

Early algorithm development efforts for the National Ecological Observatory Network Airborne Observation Platform imaging spectrometer and waveform lidar instruments

K. S. Krause, M. A. Kuester, J. T. McCorkel, T. U. Kampe, B. R. Johnson, NEON, Inc. (United States)

The National Ecological Observatory Network (NEON) will be the first observatory network of its kind designed to detect and enable forecasting of ecological change at continental scales over multiple decades. NEON will collect data at sites distributed at 20 ecoclimatic domains across the United States on the impacts of climate change, land use change, and invasive species on natural resources and biodiversity. The Airborne Observation Platform (AOP) is an aircraft platform carrying remote sensing instrumentation designed to achieve sub-meter to meter scale ground resolution, bridging the scales from organisms and individual stands to satellite-based remote sensing. AOP instrumentation consists of a VIS/SWIR imaging spectrometer, a scanning small-footprint waveform LiDAR, and a high resolution airborne digital camera. AOP data will provide quantitative information on land use change and changes in ecological structure and chemistry including the presence and effects of invasive species. A Pathfinder Flight Campaign was conducted over a two week period during late August to early September 2010 in order to collect representative AOP data over one NEON domain site. NASA

JPL flew the AVIRIS imaging spectrometer and NCALM flew an Optech Gemini waveform LiDAR over the University of Florida Ordway-Swisher Biological Station and Donaldson tree plantation near Gainesville Florida. The pathfinder data are discussed in detail along with how the data are being used for early algorithm and product development prototyping activities. The data collected during the campaign and prototype products are openly available to scientists to become more familiar with representative NEON AOP data.

8158-14, Session 4

Overview of the Cooperative Atmospheric Measurement Program (CAMP)

P. E. Lewis, National Geospatial-Intelligence Agency (United States)

No abstract available

8158-15, Session 5

Enhanced DIRSIG scene simulation by incorporating process models

J. Sun, D. Messinger, M. G. Gartley, Rochester Institute of Technology (United States)

The Digital Imaging and Remote Sensing Image Generation (DIRSIG) tool is a first principles-based synthetic image generation model, developed at the Rochester Institute of Technology. By calculating the sensor reaching radiance between the bandpass 0.2 to 20 μm , it produces multi/hyper-spectral images. By integrating independent first principles based sub-models, DIRSIG generates a representation of what a sensor would see with high radiometric fidelity. Currently, DIRSIG only models spatial-spectral synthetic images. In order to detect temporal changes in a process within the scene, a 'process model', which links the observable signatures of interest temporally, should be developed and incorporated into DIRSIG. This 'process model' could be external time-dependent sub-models or pre-defined by the users to predict the specific state of the objects in the scene at a specific time. In this paper, a notional system of two tanks connected by a pipe is built, with hot water coming into tank A through a second pipe and with cooled water released from tank B through a third pipe. This is a simple hydrodynamic & thermodynamic model, controlled by the state of valves in the scenario. The initial temperature and height of the water in the two tanks are pre-defined by users. Surface temperatures as a function of time are then predicted and captured as characterization maps. Users could also further define the resolution of the maps to better characterize the temporal changing information. These are then mapped onto DIRSIG geometry using uv mapping technique. Finally, a spatial-spectral-temporal synthetic image is produced.

8158-16, Session 5

PICASSO: an end-to-end image simulation tool for space and airborne imaging systems II: extension to the thermal infrared

S. A. Cota, C. J. Florio, R. A. Keller, T. S. Lomheim, B. M. Muto, The Aerospace Corp. (United States)

No abstract available

Conference 8158:
Imaging Spectrometry XVI

8158-17, Session 5

PICASSO: an end-to-end image simulation tool for space and airborne imaging systems III: extension to the thermal infrared: a worked example

P. B. Cameron, S. A. Cota, C. J. Florio, G. A. Franz, B. A. Jacoby, L. S. Kalman, M. G. Martino, The Aerospace Corp. (United States)

No abstract available

8158-18, Session 6

Alignment and characterization of high uniformity imaging spectrometers

H. A. Bender, P. Mouroulis, M. L. Eastwood, R. O. Green, S. Geier, E. B. Hochberg, Jet Propulsion Lab. (United States)

Imaging spectrometers require precise adjustments, in some cases at the sub-micrometer level, in order to achieve a uniform response over both the spectral and spatial dimensions. We describe a set of measurement techniques and their corresponding alignment adjustments to achieve the 95% uniformity specifications required for the Next-Generation airborne Imaging Spectrometer (NGIS) under development at The California Institute of Technology's Jet Propulsion Laboratory. The instrument, consisting of an Offner-type spectrometer and a two-mirror anastigmat telescope, covers the range 380-2500 nm with 5 nm sampling. A discussion will be given on each of the various measurements used to inform these adjustments, including experimental setup and preliminary test results.

8158-19, Session 6

Hyperspectral thermal emission spectrometer: alignment and preliminary results

W. R. Johnson, S. J. Hook, P. Mouroulis, S. D. Gunapala, D. W. Wilson, B. T. Eng, Jet Propulsion Lab. (United States)

The Hyperspectral thermal emission spectrometer will be the premiere airborne imaging spectrometer system used for the long wave infrared (LWIR). The pushbroom design has 512 spatial pixels over a 50-degree field of view and 256 spectral channels between 7.5 m to 12 m. Development is being undertaken end-to-end at the Jet Propulsion Laboratory and offers a complete system for understanding science concerns related to earth and water skin surface measurements. At its core are many key enabling state-of-the-art technologies including a high performance convex diffraction grating, a quantum well infrared photodetector focal plane array, and a compact Dyson-inspired optical design. The Dyson optical design allows for a very compact and optically fast system (F/1.6). It also minimizes cooling requirements due to the fact it has a single monolithic prism-like grating design which allows baffling for stray light suppression. The monolithic configuration eases mechanical tolerancing requirements which are a viable concern since the complete optical assembly is operated at cryogenic temperatures (~100K). The QWIP allows for optimum spatial and spectral uniformity and provides adequate responsivity or D-star to allow 200mK noise equivalent temperature difference (NEDT) operation across the LWIR passband. Assembly of the system is nearly complete. Alignment results are presented which show low keystone and smile distortion. This is required to minimize spatial-spectral mixing between adjacent spectral channels and spatial positions. Preliminary results show the system has adequate signal to noise for laboratory calibration targets.

8158-20, Session 6

Optical design and performance of the Ultra-Compact Imaging Spectrometer

B. Van Gorp, P. Mouroulis, D. W. Wilson, J. I. Rodriguez, H. R. Sobel, R. G. Sellar, D. L. Blaney, R. O. Green, Jet Propulsion Lab. (United States)

We present the optical design and performance of the Ultra-Compact Imaging Spectrometer (UCIS) currently under development at Caltech's Jet Propulsion Laboratory. The new instrument demonstrates a low optical bench mass of 0.5kg and compact size that enables Mars Rover or other in situ planetary applications. UCIS is a (F/4), wide field (32 \circ) design, covering the spectral range 600-2600 nm and is enabled by a simple all aluminum two-mirror telescope and Offner spectrometer. We discuss here the optical design and alignment method that enables this compact and low mass imaging spectrometer.

8158-21, Session 6

Performance of a new airborne thermal-infrared imaging spectrometer with broad area coverage and high spatio-radiometric resolution

J. L. Hall, R. H. Boucher, D. J. Gutierrez, S. J. Hansel, B. P. Kasper, E. R. Keim, N. M. Moreno, M. L. Polak, M. G. Sivjee, D. M. Tratt, D. W. Warren, The Aerospace Corp. (United States)

Results from the inaugural flight series of a new high-performance airborne thermal-infrared imaging spectrometer are described. The sensor incorporates a novel spectrometer design employing a concave diffraction grating in conjunction with a Dyson lens and acquires data in 128 spectral channels over the spectral range 7.5 - 13.5 microns. The high optical throughput (f/1.25) of this design coupled with a fast-framing focal plane array permits large whiskbroom scans while maintaining low noise performance (<0.1K NEDT), allowing swath widths up to +/-45 degrees at pixel resolutions of ~0.5 mrad. The nominal flight altitude of the instrument was designed to be 12,000 ft, resulting in a 2-m pixel on the ground at nadir. The sensor is carried on a commercial gyro-stabilized platform, which provides for considerable flexibility in collection strategy. For example, by controlling the pitch of the sensor gimbal mirror it is possible to either stare at targets or execute multiple looks. Following successful engineering trials, flights were conducted over selected science targets with known sources of gaseous emission and thermal inhomogeneity. One such location was the southern extent of California's San Joaquin Valley, where ammonia emissions from intensive dairy farming and agriculture reach notable levels. A second flight measured the active hydrothermal vent fields in the Salton Sea locale (also in Southern California). Data from these flights (the first being during daytime and the second being at night) demonstrate the radiometric sensitivity, high spatial resolution, and broad area coverage afforded by this new sensor and attest to its emission measurement capabilities.

8158-23, Session 7

Feature-based and statistical methods for analyzing the Deep Water Horizon oil spill with AVIRIS imagery

R. S. Rand, National Geospatial-Intelligence Agency (United States); R. N. Clark, E. Livo, U.S. Geological Survey (United States)

The Deep Water Horizon oil spill covered a very large geographical area in the Gulf of Mexico creating potentially serious environmental impacts on both marine life and the coastal shorelines. Knowing the oil's areal extent and thickness as well as denoting different categories of the oil's physical

Conference 8158:
Imaging Spectrometry XVI

state is important for assessing these impacts. High spectral resolution data in hyperspectral imagery (HSI) sensors such as Airborne Visible and Infrared Imaging Spectrometer (AVIRIS) provide a valuable source of information that can be used for analysis by semi-automatic approaches for tracking an oil spill's areal extent, oil thickness, and oil categories. However, the spectral behavior of oil in water is inherently a highly non-linear and variable phenomenon that changes depending on oil thickness and oil/water ratios. For certain oil thicknesses there are well-defined absorption features, whereas for very thin thicknesses sometimes there are almost no observable features. Feature-based imaging spectroscopy methods are particularly effective at classifying materials that exhibit specific well-defined spectral absorption features. Statistical methods are effective at classifying materials with spectra that exhibit a considerable amount of variability and that do not necessarily exhibit well-defined spectral absorption features. This study investigates feature-based and statistical methods for analyzing oil spills using hyperspectral imagery. It investigates the appropriate use of each approach and the possible combined use of both.

8158-24, Session 7

Detection of aircraft exhaust in hyperspectral image data

L. L. West, S. E. Lane, G. G. Gimmetstad, Georgia Tech Research Institute (United States); W. L. Smith, Hampton Univ. (United States); E. M. Burdette, Georgia Tech Research Institute (United States)

The use of hyperspectral imaging systems for detection of gases has been investigated and algorithms have been developed previously; these algorithms depend on proper modeling of the target gas and background in order for successful detection to occur. A dataset in which a LWIR Telops FIRST Hyper-Cam is utilized for the measurement of hyperspectral datacubes of aircraft plumes is investigated. The dataset itself was created at Hartsfield Jackson International Airport in Atlanta, Georgia. The Telops Hyper-Cam was oriented to allow oncoming landing aircraft to pass through the field of view of the instrument; each set of data collected consists of several datacubes of sky background pre-flight, aircraft passage, and sky background post-flight. This analysis focuses on different methods for the detection of aircraft exhaust in these hyperspectral image cubes. Gases that are known to exist in aircraft exhaust, such as water vapor and CO₂, are modeled by different methods. The modeling of these target gases is limited due to lack of specific data regarding chemical constituents or concentration. The target gases are searched for in the hyperspectral image cubes by utilizing different hyperspectral gas detection algorithms; the results shown here demonstrate the ability to detect the aircraft exhaust in hyperspectral data using multiple methods. These detections are of interest due to the fact that these exhaust gases are entrained in wake vortices; the possibility of a hyperspectral means of wake vortex detection is of great interest due to its applicability to aviation safety. This work is supported through funding from NASA.

8158-25, Session 7

IFTS measurements of laboratory-scale smokestack and flare plumes

J. L. Harley, M. Rhoby, K. C. Gross, Air Force Institute of Technology (United States)

A laboratory is being stood up for testing the capability of optical remote sensing techniques in the quantification of smokestack effluents and flare combustion efficiencies. A Telops Hyper-Cam midwave infrared (1.5-5.5 μm) imaging Fourier-transform spectrometer (IFTS) will be used to measure plumes from these laboratory-scale smokestack and flare sources. The turbulent nature of these flow fields produce instantaneous fluctuations in scene radiance. Methods have been devised to minimize scene-change artifacts in the spectra and also make use of the radiance fluctuations for velocity estimation and turbulence characterization.

Total effluent mass flow rates (kg/s) will be estimated by combining spectrally-determined species concentrations with flow rates estimated via analysis of sequential images in the raw interferogram cube. Effects of a cross-wind will be studied as it may be an important parameter in understanding flare combustion efficiencies.

8158-26, Session 7

Hyperspectral face recognition after expression changes

G. E. Healey, Univ. of California, Irvine (United States)

The performance of face recognition degrades with expression changes. In this work, we propose an algorithm that combines spectral and spatial information for face recognition. 3D Gabor filters are used for the extraction of spatial features. A principal components approach is used to predict how the spatial features change with expression changes. We demonstrate the effectiveness of the algorithm using a database of hyperspectral face images.

8158-27, Session 7

RGB imaging system for mapping and monitoring of hemoglobin distribution in skin

D. Jakovels, J. Spigulis, Univ. of Latvia (Latvia)

Multi-spectral imaging has found applications for non-contact skin chromophore mapping, providing information about concentration distribution of chromophores, e.g. oxy-/deoxy-hemoglobin and melanin. However, commercial multi-spectral imaging cameras are bulky and expensive, so limiting their clinical implementation.

Color digital camera can be regarded as an alternative, since it acquires three spectral (red (R), green (G) and blue (B)) images simultaneously. In combination with specific narrow-band spectral light sources, R-G-B imaging could become competitive for some specific applications, including the mapping of skin chromophores.

A prototype R-G-B imaging system for mapping of skin hemoglobin distribution has been designed and tested. Device basically consists of a commercial RGB sensor (CMOS, max. frame rate 87 fps for VGA resolution), RGB LED ring-light illuminator and orthogonally orientated polarizers for reducing specular reflectance. The system was examined for monitoring of hemoglobin concentration changes during specific provocations - arterial/venous occlusions and heat test. Besides, hemoglobin distribution maps of several skin malformations were obtained.

8158-28, Session 7

Hyperspectral mapping of mineral using Chang'e-1 hyperspectral data

J. Chen, X. Wang, China Univ. of Geosciences (China)

In this paper, We use the chinese-made is interference image spectrometer (IIM) to map the lunar mineral distribution for the first time. According to the discrepancy between the spectrum characteristic of IIM and end-members mineral spectrum, and the influence to the spectrum in rocks which is caused by the different proportion mineral Combination, we adapt gaussian model of correction (mixtural discriminant analysis) which is based on class pixel to map spectrogram diagram of lunar nearside. This paper analyzed the spectrum of regions which has known, obtained gaussian model parameter and residual, and made quantitative analysis on the distribution of clinopyroxene, orthorhombic pyroxene, olivine and other major lunar mafic minerals, and even the plagioclase. In terms of the Mineral distribution, We extract information of the lunar surface structure and topography and so on. Compared with the mineral map of the lunar surface of mature areas, the results are reliable.

Conference 8159: Lidar Remote Sensing for Environmental Monitoring XII

Sunday-Monday 21-22 August 2011 • Part of Proceedings of SPIE Vol. 8159
Lidar Remote Sensing for Environmental Monitoring XII

8159-01, Session 1

Active optical technology: recent developments and lessons learned

G. Komar, NASA Goddard Space Flight Ctr. (United States)

This paper provides an overview of the active optical technology developments underway for the Earth Science Division at NASA. It summarizes key results from a multiyear NASA investment program aimed at enabling new Earth science measurement capabilities, developing new techniques in the 1- and 2-micron wavelengths, and improving reliability and longevity of future NASA active sensing instruments. Examples for Earth Science measurements such as aerosols, altimetry, winds, ozone levels, and vegetation change are discussed.

8159-02, Session 2

High-efficiency laser designs for airborne and space-based lidar remote sensing systems

F. E. Hovis, R. L. Burnham, M. E. Storm, R. E. Edwards, P. Burns, E. Sullivan, J. Edelman, K. Andes, J. Rudd, B. Walters, K. Li, C. Culpepper, T. Chuang, X. Dang, J. Hwang, T. Wysocki, Fibertek, Inc. (United States)

The increasing use of lidar remote sensing systems in the limited power environments of unmanned aerial vehicles and satellites is motivating laser engineers and designers to put a high premium on the overall efficiency of the laser transmitters needed for these systems. Two particular examples upon which we have been focused are the lasers for the ICESat-2 mission and for the Laser Vegetation Imaging System-Global Hawk (LVIS-GH) system. We have recently developed an environmentally hardened candidate laser for ICESat-2 that has achieved over 11 W of 532 nm output at 10 kHz with a true wall plug efficiency to 532 nm of over 6%. For the LVIS-GH lidar we recently delivered a 4.2 W, 2.5 kHz, 1064 nm laser transmitter that achieved a true wall plug efficiency of over 10%. In our presentation we discuss the design approaches used to achieve these results.

8159-03, Session 2

Critical laser technology developments and ESA space qualification approach in support of ESA's Earth observation missions

M. Zahir, Y. Durand, European Space Research and Technology Ctr. (Netherlands)

In this paper, ESA's approach to lasers and detectors space evaluation and qualification will be explored. ESA has its own international qualification system, the ESCC system. This system guarantees reliability, assurance and quality of components, and hence a successful space mission. An overview of the ESCC (European Space Component Coordination) system, as well as the relevant ECSS (European Cooperation for Space Standards) related standards addressing components and hybrid qualification will be given. These standards are being constantly updated, through well structured working groups, constantly coming up with new ways of qualifying space components. These components are themselves constantly changing in terms of material, technology, and manufacturing processes.

The development of advanced Lidar systems for space applications and their evaluation by airborne or ground based test campaigns is an

important strategic element of the ESA Earth Observation Programme. These systems depend on robust and reliable lasers and detector at their core function. Since the early eighties, ESA has been supporting the development of the critical subsystems of any Lidar, i.e. lasers and detectors. Several missions, involving different kinds of lidars, provide the requirements to be addressed in the Lidar risk mitigation activities. They also present a challenge concerning their space qualification and reliability assurance. These missions are: ADM-Aeolus flying ALADIN a Doppler Wind Lidar; EarthCARE embarking ATLID an Atmospheric Backscatter Lidar; three missions studied for their feasibilities: WALES, A-SCOPE and ACCURATE, all using Differential Absorption Lidar in different ways to measure respectively profiles of water vapour, total column of CO₂ and greenhouse gases in an occultation geometry.

8159-04, Session 2

Conductively cooled 2 μm laser for space-based wind lidar

T. Shuman, F. E. Hovis, J. Edelman, K. Andes, J. Rudd, T. Schum, T. Chuang, Fibertek, Inc. (United States); J. Yu, U. N. Singh, M. J. Kavaya, M. Petros, NASA Langley Research Ctr. (United States)

NASA, NOAA and the DOD have been pursuing global wind measurements since the 1970s. Recently, it was determined that a hybrid system utilizing both coherent and direct detection wind lidar systems would provide the maximum science content for a space-based wind lidar. A key component of the coherent system is a conductively cooled 2 μm laser source capable of 250 mJ at 5-10 Hz. Researchers at Fibertek and NASA Langley have undertaken a jointly funded program to develop the required transmitter. The technical basis for the diode pumped head is a conductively cooled coherent design that was previously developed at NASA Langley. Working with NASA Langley, Fibertek has further refined this design approach and incorporated it into an injection-seeded, single-frequency, master oscillator/power amplifier (MOPA) that can meet the requirements of the space-based coherent wind lidar. Packaging of the transmitter that can be transitioned to a space-based system has also been developed. In our presentation we will discuss the design details, performance, and testing of the laser.

8159-05, Session 2

Qualification testing of the laser transmitter for ESA's BepiColombo Laser Altimeter (BELA)

K. Weidlich, M. Rech, Carl Zeiss Optronics GmbH (Germany); R. Kallenbach, Max-Planck-Institut für Sonnensystemforschung (Germany)

The BepiColombo Laser Altimeter (BELA) is one of 11 instruments aboard ESA's Mercury Planetary Orbiter scheduled for launch in 2014. BELA will record the surface profile of the planet while orbiting around it at a distance of about 1.000 km. The altimetry data constitute an important prerequisite for a number of remote sensing and observation techniques residing on the same orbiter. The BELA instrument comprises a laser transmitter and a receiver part, the design of the former is being presented and discussed in this paper. The laser transmitter encompasses a pair of diode-pumped, actively q-switched Nd:YAG rod oscillators which have been miniaturized, light-weighted and dimensioned for high electrical to optical efficiency. The key performance parameters of the laser will be presented. Laser design trades which are relevant for a space mission to Mercury and the BELA instrument in particular are discussed. Selection criteria for critical optical and optoelectronics components are presented.

Conference 8159:
Lidar Remote Sensing for Environmental Monitoring XII

An overview is given to the laser qualification programme which includes performance and environmental tests on several hardware models. Test results are presented which have been recorded during the qualification test campaign currently in progress at Carl Zeiss Optronics. The paper concludes with an outlook covering the remaining work until completion of the BELA laser qualification test programme and towards later space missions encompassing laser altimetry.

8159-06, Session 2

Adaptive lidar for Earth imaging from space

C. S. Weimer, T. Ramond, Ball Aerospace & Technologies Corp. (United States)

Laser remote sensing of the Earth from space offers many unique capabilities stemming from the unique properties of lasers. Lidars make possible three-dimensional characterizations that help to enable new scientific understanding of the natural processes that shape the planet's oceans, surface, and atmosphere. The recent successes of GLAS (on ICESat) and CALIOP (on CALIPSO) have begun to explore the possibilities. However, the challenges to further expand on these successes remain complex. Operation of lidars from space is limited in part by the relatively low power available to the lasers, the low signal scattered back to the instrument because of the large distance to the surface, and the need for reliable and autonomous operation because of the large investment required for satellites. The instrument complexities are compounded by the large diversity in the Earth scenes; the large variability in albedo from cloud, ice, vegetation, desert, or ocean, combined with the highly variable transmission of the laser beam through clouds, forest canopy, or ocean surface and near-surface. This paper will discuss the development of a new approach to space-based lidars that illustrates one method to dramatically expand on the capability of space-based lidars. By combining the new imaging and ranging technology of flash focal plane arrays, with the multi-beam electronic steering capability of acousto-optic beam deflectors, an adaptive lidar can be created. The lidar can adapt to ensure adequate signal-to-noise plus reduce sources of systematic errors in measurements. In addition, by using inputs from secondary sensors, or a prior knowledge of the Earth scene below, it can vary the spatial sampling to maximize science return from its measurements. Demonstration of some of the possibilities is shown from laboratory and aircraft-based testing.

8159-07, Session 3

The MERLIN mission: a space-based methane monitor

C. Stephan, M. Alpers, Deutsches Zentrum für Luft- und Raumfahrt e.V. (Germany); B. Millet, Ctr. National d'Études Spatiales (France); G. Ehret, Deutsches Zentrum für Luft- und Raumfahrt e.V. (Germany); P. H. Flamant, Lab. de Météorologie Dynamique (France); C. Deniel, Ctr. National d'Études Spatiales (France)

Methane is a powerful greenhouse gas, which has a Greenhouse Warming Potential of 23 years relative to carbon dioxide time scale of about 100 years. Thus, the radiative forcing caused by methane contributes significantly to the warming of the atmosphere. To better understand the complex global methane cycle, it is necessary to apply space-based measurements techniques in order to obtain global coverage at high precision.

The Methane Remote Sensing Lidar Mission (MERLIN) is a joint French-German cooperation on a small satellite mission for space-based measurement of spatial and temporal gradients of atmospheric methane columns on a global scale. MERLIN will be the first Integrated Path Differential Absorption (IPDA) LIDAR for methane monitoring from space. In contrast to passive methane missions like GOSAT, the lidar instrument allows to monitor methane fluxes at all-latitudes, all-seasons and during night as it is not relying on sunlight. Range-gated signal

detection ensures that possible measurement biases from unknown aerosol scattering or scattering from thin cirrus clouds are avoided. First scientific studies show a substantial reduction of the prior methane flux uncertainties in key observational regions when using synthetic MERLIN observations in the flux inversion experiments. Furthermore, MERLIN observations can be used to quantify and verify in a scientific credible way the national emission reductions of the Kyoto protocol.

The presentation gives an overview on the joint DLR and CNES mission concept with the German IPDA LIDAR on the French small satellite platform MYRIADE, its present status and briefly reports on results from scientific impact studies.

8159-08, Session 3

Airborne lidar measurements of atmospheric pressure made using the oxygen A-band

H. Riris, M. D. Rodriguez, G. R. Allan, W. E. Hasselbrack, M. A. Stephen, J. B. Abshire, NASA Goddard Space Flight Ctr. (United States)

We report on airborne measurements of atmospheric pressure using a fiber-laser based lidar operating in the oxygen A-band near 765 nm and the integrated path differential absorption measurement technique. Remote measurements of the column atmospheric mixing ratio is required for the planned Active Sensing of CO₂ Emissions Over Nights, Days, and Seasons (ASCENDS) mission. The goal of ASCENDS is to estimate the CO₂ concentration in the atmosphere in terms of mole fraction in unit of parts-per-million (ppmv) with regard to dry air. Therefore the number of both CO₂ molecules and the dry air molecules in the atmosphere column are needed. Measuring the O₂ column absorption can be used to estimate surface pressure, and knowledge of column water vapor can be used to compute the dry air column.

Our lidar uses fiber optic technology and non-linear optics to generate tunable laser radiation at 765 nm, which overlaps an absorption line pair in the Oxygen A-band. We use a pulsed time resolved technique, which rapidly steps the laser wavelength across the absorption line pair, a 20 cm telescope and photon counting detector. Our retrieval algorithm fits the O₂ lineshapes and derives the surface pressure. We will describe the approach, show O₂ absorption measurements made across horizontal paths, and those from the NASA DC-8 aircraft made on two flights in July 2010.

8159-09, Session 3

Pulsed 2-micron laser transmitters for CO₂ sensing

U. N. Singh, J. Yu, NASA Langley Research Ctr. (United States); Y. Bai, Science Systems and Applications, Inc. (United States); M. Petros, S. Chen, NASA Langley Research Ctr. (United States)

Carbon dioxide (CO₂) has been recognized as one of the most important greenhouse gases. It is essential for the study of global warming to accurately measure the CO₂ concentration in the atmosphere and continuously record its variation. Passive remote sensors under development to measure CO₂ column content cannot make measurements at night or through intervening clouds. There exists a critical need to develop energetic pulsed transmitter at a suitable wavelength to make an accurate measurement of CO₂ in the boundary layer.

An injection seeded, high repetition rate, Q-switched Ho:YLF laser has been developed at NASA Langley Research Center for a coherent/direct CO₂ differential absorption lidar. This master-slave laser system has high optical-to-optical efficiency and seeding success rate. It can potentially meet the requirements of the coherent/direct detection of CO₂ concentration by a differential absorption lidar technique from ground, air and space-based platform.

8159-10, Session 3

Pulsed airborne lidar measurements of atmospheric CO₂ column absorption to 13 km altitude

G. R. Allan, Sigma Space Corp. (United States) and NASA Goddard Space Flight Ctr. (United States)

We have developed a LIDAR technique for remotely measuring atmospheric CO₂ concentrations as a candidate for NASA's ASCENDS mission. Using a step-tuned pulsed laser transmitters, receiver scope and photon counting detectors we simultaneously measure a CO₂ absorption line in the 1570 nm band, O₂ extinction in the Oxygen A-band, surface height and backscatter. Signal processing isolates the surface echo, measures the range, and rejects laser photons scattered in the atmosphere. The gas extinction and column densities for the CO₂ and O₂ gases are estimated via the Integrated Path Differential Absorption technique. During Summer of 2009 we made 5 flights on the NASA Glenn Learjet-25 measuring atmospheric CO₂ absorption line shapes using the 1572.335 nm line at stepped altitudes from 3 to 13 km over a variety of surfaces. For 2010 measurements, we have increased the number of wavelength samples increased the receiver sensitivity and dynamic range. Incorporated an oxygen LIDAR channel measuring the doublet near 764.7 nm. We integrated the twin channel LIDAR onto the NASA DC-8 and in July participated in the NASA ASCENDS field campaign flying 5 science flights over the central valley of California, desert areas, the Pacific Ocean, and the DOE SGP ARM site. Clear CO₂ and O₂ line shapes, which changed as expected with range and altitude, were observed on all flights to 13 km altitude. The data is currently being analyzed and compared to readings from radiosondes and on board gas sensors. Details of the CO₂ measurements analysis and comparisons will be described in the presentation.

8159-11, Session 3

Carbon Dioxide Laser Absorption Spectrometer (CO₂LAS) aircraft measurements of CO₂

G. D. Spiers, R. T. Menzies, L. E. Christensen, J. C. Jacob, J. J. Hyon, Jet Propulsion Lab. (United States)

The Jet Propulsion Laboratory Carbon Dioxide Laser Absorption Spectrometer (CO₂LAS) utilizes Integrated Path Differential Absorption (IPDA) at 2.05 μm to obtain CO₂ column mixing ratios weighted heavily in the boundary layer. CO₂LAS employs a coherent detection receiver and continuous-wave Th:Ho:YLF laser transmitters with output powers around 100 milliwatts. An offset frequency-locking scheme coupled to an absolute frequency reference enables the frequencies of the online and offline lasers to be held to within 200 kHz of desired values. We describe results from 2009 and 2010 field campaigns when CO₂LAS flew on the Twin Otter and DC-8 performing measurements over varying terrains at altitudes up to 5 km. We also describe spectroscopic studies aimed at uncovering potential biases in lidar CO₂ retrievals at 2.05 μm .

8159-12, Session 3

Construction of a high-power OPO laser system for differential absorption lidar

K. O. Douglass, S. E. Maxwell, D. F. Plusquellic, J. T. Hodges, R. D. van Zee, D. V. Samarov, J. R. Whetstone, National Institute of Standards and Technology (United States)

Our goal is to develop optical measurement technology to enable accurate quantification of greenhouse-gas emissions to meet the needs of industry and regulators. A 1.064 μm high power optical parametric oscillator (OPO) operating from 1585 nm to 1646 nm was constructed

for performing differential absorption LIDAR measurements of carbon dioxide, methane, and potentially nitrous oxide. The OPO uses a Rotated Image Singly-Resonant Twisted RectAngle (RISTRA) design. The commercially available RISTRA cavity is machined from a solid block of aluminum and measures only a few inches. The compact single piece cavity design requires no mirror adjustments and image rotation provides efficient conversion and excellent beam quality. The injection seeded OPO is designed to have 70 mJ/p of signal and 30 mJ/p of idler output energy when pumped with 200 mJ/p Nd:YAG laser. The pump laser has a repetition rate of 100 Hz and a temporal pulse width of 3.5 ns. The OPO signal wave is frequency stabilized to a few MHz and operates near the transform limit which provides the high resolution needed for wind speed measurements using a Doppler shift technique. The performance of the OPO and the enhancements implemented in the DIAL system for improving retrievals are discussed.

8159-13, Session 3

Development of optical parametric amplifier for lidar measurements of trace gases on Earth and Mars

K. Numata, NASA Goddard Space Flight Ctr. (United States) and Univ. of Maryland, College Park (United States); H. Riris, S. X. Li, S. T. Wu, M. A. Krainak, J. B. Abshire, NASA Goddard Space Flight Ctr. (United States)

Trace gases in planetary atmosphere offer important clues as to the origins of the planet's hydrology, geology, atmosphere, and potential for biology. Remote measurements of methane (CH₄), water (H₂O), and other biogenic molecules (such as ethane and formaldehyde) on Mars have important connections to questions related to the existence of life on Mars. Carbon dioxide (CO₂) and CH₄ are the most important anthropogenically produced greenhouse gases. We report on the development effort of a nanosecond-pulsed optical parametric amplifier (OPA) for remote measurements of these trace gases on Mars and Earth. The OPA is pumped by a passive Q-switch NPRO (non-planar ring oscillator) at 1064nm and seeded by a continuous-wave DFB laser at 1550-1650nm. A 50-mm, MgO-doped PPLN was used as a nonlinear crystal. The OPA output light is single frequency with high spectral purity and is widely tunable both at 1600nm and 3300nm with an optical-optical conversion efficiency of ~40%. We demonstrated open-path atmospheric measurements of CH₄ (3291nm and 1651nm), CO₂ (1573nm), and H₂O (1652nm) with this laser source. The results agreed well with calibrated in-situ measurements, demonstrating the suitability of space implementation of this system.

8159-14, Session 4

An investigation of high spectral resolution lidar measurements over the ocean

E. Saiki, C. S. Weimer, M. Stephens, Ball Aerospace & Technologies Corp. (United States)

Analysis of data measured by the NASA Langley airborne High Spectral Resolution Lidar is presented focusing on measurements over the ocean. The HSRL is a dual polarized system (1064 and 532 nm) with the inclusion of a molecular backscatter channel at 532 nm. Data from aircraft flights over the Pamlico Sound out to the Atlantic Ocean, over the Caribbean west of Barbados, and off the coast of Barrow Alaska are evaluated. Analysis of the data demonstrates that the molecular channel detects the presence of water due to its ability to separate the Brillouin-Mandelshtam spectrum, i.e. the scattering spectrum of water, from the Rayleigh/Mie spectrum. The characteristics of the lidar measurements over water, land, ice, and mixed ice/water surfaces are examined. Correlations of the molecular channel lidar signals with bathymetry (ocean depth) and extraction of attenuation from the HSRL lidar measurements are presented and contrasted with ocean color data.

Conference 8159:
Lidar Remote Sensing for Environmental Monitoring XII

8159-15, Session 4

High precision long range laser altimeter for avionics and space applications

D. F. Pierrottet, Coherent Applications, Inc. (United States); F. Amzajerjian, B. W. Barnes, NASA Langley Research Ctr. (United States); T. D. Jones, G. E. Lockard, Coherent Applications, Inc. (United States); L. B. Petway, NASA Langley Research Ctr. (United States); B. D. Taylor, ATK Space Systems (United States)

A compact, high precision, long range, laser altimeter implemented for space and avionics applications is described. It was developed under the Autonomous Landing and Hazard Avoidance Technology (ALHAT) project for terrain relative navigation during the approach phase to a lunar or planetary landing.

8159-16, Session 4

Development of wide-bandwidth and low-noise HgCdTe avalanche photodiode detectors

J. Wang, M. D. Jack, Raytheon Co. (United States); X. Sun, A. W. Yu, NASA Goddard Space Flight Ctr. (United States); D. N. Hall, Univ. of Hawai'i (United States)

There are strong needs for wide bandwidth and low noise avalanche photodiode detectors (APDs) for astronomy and lidar remote sensing. Wide bandwidth requirements are driven by the use of very narrow pulse lasers, about 1 ns, for future space-based laser altimetry and the use of APDs in adaptive optics in astronomy. Low noise is driven by the extremely small number of photons bouncing back from distant objects. High sensitivity and low noise APDs can meet signal-to-noise requirements with reduced telescope aperture size and less laser power, and thereby reducing overall instrument size and cost. Investment in the development of more sensitive APDs often results in the biggest savings in overall instrument and mission cost. Traditional silicon and InGaAs APDs suffer from high excess noises. Excess noises increase rapidly at high gain, thereby reducing the advantages of high gain APDs based on silicon or InGaAs. HgCdTe APDs, with its more deterministic electron avalanche mechanism, lead to very low excess noise, very close to the theoretical limit of excess noise factor of 1. Raytheon Vision Systems (RVS), with support from NASA through NASA Goddard Space Flight Center (GSFC) and the University of Hawaii, has made breakthrough advancement in wide bandwidth and low noise HgCdTe APDs for the near infrared (NIR) region that is much more challenging than mid-wave infrared (MWIR) APDs. In this paper we will discuss RVS HgCdTe APD design, fabrication, and characterization results at RVS, NASA GSFC, and the University of Hawaii

8159-17, Session 4

Interactive aerosol lidar monitor for multiple users via network multicast

J. P. Herron, Utah State Univ. (United States); J. T. Pearson, U.S. Army Dugway Proving Ground (United States)

Dugway Proving Ground is a major range test facility charged with testing chemical and biological defense systems and materials. The facilities at DPG include state-of-the-art laboratories and extensive field test grids. A suite of mobile elastic backscatter lidar systems are used as referee systems to track and quantify biological and interferent aerosol releases on the test range. While each lidar has its own display software, it typically is only intended for and available to the system operator. The display is typically not adequate for every test scenario and requires the data to be post-processed into an acceptable format for presentation to a test client. The lidar systems are typically positioned

several kilometers from any release point or the command post. This geographic separation caused major limitations in certain test scenarios, as the data output from the lidar system was only available to other test personnel via verbal comments from the lidar operator until post test. To increase the utility and impact of the lidar systems on field testing, a real-time data visualization software package was developed for the DPG lidar systems. Multiple display types are included in the software to accommodate various testing and calibration scenarios. Data from a fielded system is uploaded to the local test network via either a direct or wireless connection. The data is sent via a UDP multicast which allows for multiple end users to receive the data without increasing the load on the server or network as there is minimal error checking, and duplication of the data is done at the router level. The software is designed for test personnel and clients of DPG to operate without significant training and only a passing familiarity with lidar systems. In addition to providing a real-time display the software can capture the data locally making a test event available for immediate review. A software description and the display philosophy for various field test scenarios are included in this presentation.

8159-18, Session 4

Lidar as a tool for fisheries management

J. H. Churnside, National Oceanic and Atmospheric Administration (United States); D. A. Hanan, Z. D. Hanan, Hanan & Associates, Inc. (United States); R. D. Marchbanks, Univ. of Colorado (United States) and National Oceanic and Atmospheric Administration (United States)

Effective management of fisheries resources requires accurate information on the population of the species under consideration. This information can be very difficult to obtain in many cases, because the fish have a wide distribution and are very mobile. Traditional ship-based techniques are limited in the area that can be covered by the speed of the vessel, which is typically less than 5 m/s. A much larger area can be surveyed in a shorter time by aircraft, and this becomes a very attractive technique for those species close enough to the surface to be observed by airborne remote sensors.

This paper describes the results of a series of airborne observations of sardine schools off the coast of California in the fall of 2010. The lidar system used a linearly-polarized transmitter and a single receiver that was sensitive to the backscattered light in the orthogonal polarization. The aircraft was also equipped with a camera to photograph schools. The camera had a broader swath than the lidar, so was able to see more of the schools at the surface. However, the lidar detected schools much deeper in the water, was not hampered by waves and sun glare, and could survey at night. The combination of lidar and photographs proved to be a very powerful survey tool for sardines, since the latter was able to identify surface targets that appear very similar to fish schools in the lidar return. Examples of these include floating mats of kelp and ship wakes.

8159-19, Session 4

Numerical simulation of the Doppler lidar measurements with high spatial resolution

E. A. Shelekhova, A. P. Shelekhov, V.E. Zuev Institute of Atmospheric Optics (Russian Federation)

To study and predict local atmospheric processes, scientists widely use mesoscale meteorological models WRF and MM5. For domain they introduce a uniform grid, the horizontal spatial resolution is defined by a cell size of this grid. Initial and boundary conditions for models are set using data of wind, which were taken from meteorological stations. It is necessary to obtain information about wind velocity with higher spatial resolution to improve a weather prediction in future. We can get this information from the Doppler lidar measurements. For VAD technique the Doppler lidar measurements are performed along arc of VAD sector scan. The arc size defines the horizontal spatial resolution of measurements.

The necessary condition of correct measurements is the sizes of arc and cell are equal for uniform grid. In this paper the numerical simulation results of measurement error profiles of wind velocity components depending on range and direction sensing for different horizontal spatial resolutions are presented.

It shows that when calculating wind velocity components by least-squares method the measurement error depends on angle of VAD sector scan and direction sensing. Since size of the arc must be constant for every grid cell, therefore angle of VAD sector scan decreases inversely proportional to the range. So measurement precision decreases essentially with increasing range for high horizontal spatial resolution, even for a fixed SNR. The results of numerical simulation show that projections of wind velocity to directions North and East (U and V respectively) are measured with different precision. For example, measurement precision of the component U is a maximum in the direction sensing of North and South and at the same time the component V is measured with large error. The components U and V are measured with the same errors in the direction sensing of north-east, north-west, south-east, south-west.

8159-20, Poster Session

Supercontinuum under the filamentation of the femtosecond laser pulse in the fused silica

E. Smetanina, V. P. Kandidov, A. E. Dormidonov, Lomonosov Moscow State Univ. (Russian Federation); V. O. Kompanets, S. V. Chekalin, Institute of Spectroscopy (Russian Federation)

Supercontinuum generation under filamentation is a result of strong non-linear interaction of high-power femtosecond pulses with Kerr media. [1,2]. The spectral broadening of light ranges from the ultraviolet to the infrared. It has been observed in transparent solids, liquids and gases. An important property of such white light is a coherence of its spectral components.

The white light continuum generated by a filament in air can be exploited for remote sensing of atmospheric gases and aerosols, lightning control, laser induced spectroscopy [1]. Supercontinuum source formed under filamentation in silica used in Cavity Ring-Down Absorption Spectroscopy (CRDS), which is a spectroscopic tool, that permits the detection of trace absorbers in gaseous, liquid, as well as solid phase [3].

In this work the supercontinuum under filamentation of the spectrally limited collimated femtosecond laser pulses in the fused silica at different wavelengths is investigated. An influence of media dispersion on supercontinuum (SC) spectra formation was analysed.

SC generation was analysed theoretically by using a numerical model of filamentation of femtosecond laser pulses in condensed media. The model describes the diffraction and nonlinear-optical interaction of femtosecond radiation with a medium taking into account the material dispersion in the condensed medium according to the Sellmeyer formula.

In a regime of one filament, in area of normal dispersion we worked with wavelengths $\lambda = 400\text{nm}$ and $\lambda = 800\text{nm}$. spectra broadening under filamentation of pulses with central wavelength $\lambda = 800\text{nm}$ is more than for spectra with central wavelength $\lambda = 400\text{nm}$: $\Delta\lambda_{800\text{nm}} = 760\text{nm} > \Delta\lambda_{400\text{nm}} = 160\text{nm}$. The broadening is asymmetric, anti-Stokes wing is more than Stokes. This results are in agreement with the statement that there is a bandgap threshold for continuum generation: $E_{\text{gap}}/h\nu = 2$, where E_{gap} is a width of bandgap of media, and $h\nu$ is an energy of quantum on the central wavelength. Above that threshold the continuum's width increases with increasing the wavelength [4]. So, broadening for $\lambda=1300\text{nm}$, in area of zero dispersion in silica, is $\Delta\lambda_{1300\text{nm}} = 1600\text{nm}$. In area of anomalous dispersion the broadening for wavelength $\lambda=1900\text{nm}$ is $\Delta\lambda_{1900\text{nm}} = 2400\text{nm}$. It was found for this wavelength, that the decreasing of spectra intense in anti-Stokes wing is nonmonotonic. There are a local minimum in spectra from 800 nm to 1200 nm, and then there are a local peak in visible range of spectra from 400 nm to 700 nm. Such spectra was observed experimentally for $\lambda = 1540\text{nm}$ in fused silica [5]. This nonmonotonic superbroadening can't be explained by 3-rd harmonic generation, because our numeric model do

not takes into account a process of 3-rd harmonic generation in fused silica. Nonmonotonic spectra behaviour we explained by interference effects of SC generated under filamentation in media with anomalous dispersion [6].

$\Delta\lambda$ was found for level: $\lg(S(\lambda)/S(\lambda_0)) = -7$, where $S(\lambda)$ is an intense of spectral component, λ_0 - central wavelength.

References

1. Couairon A., Mysyrowicz A. Femtosecond filamentation in transparent media. // Physics Reports, 2007, 441, p 47-189.
2. Kandidov V.P., Shlenov S.A., Kosareva O.G.: Filamentation of power femtosecond laser pulses. // Quantum Electronic, 2009,39,3, p 205.
3. Stelmaszczyk K., Rohwetter P., Fechner M., et al Cavity Ring-Down Absorption Spectrography based on filament-generated supercontinuum light.// Optics Express, 2009, 17, 5, p 3673.
4. Brodeur A., Chin S. L. Band-gap dependence of the ultrafast white-light continuum. // Physical Review Letters, 1998, 80, 20, p 4406.
5. Naudeau M.L. et al Observation of nonlinear optical phenomena in air and fused silica using a 100 GW , 1.54 μm source. // Optics Express, 1998, 14, 13.
6. Dormidonov A. E., Kandidov V. P. Interference Model of Femtosecond Laser Pulse Conical Emission in Dispersive Medium. // Laser Physics, 2009, 19, 10, p 1993.

8159-21, Poster Session

UVB, NOX's and Volatile Organic Compounds (VOC's) effects on DIAL-monitored urban ozone

T. Gasmí, Saint Louis Univ.- Madrid Campus (Spain)

P(14) and the P(24) lines of the (0001-1000) CO₂ band were used because they overlap the 9.6 mm of ozone and also to avoid the interference of other gases such as NH₃, H₂O and C₂H₄. The area monitored by the DIAL is a residential area situated north-west of the city of Madrid (400 27' N, 3044' W, 680m above sea level). The main source of pollution can therefore be attributed to vehicle exhaust and to a very low extent to wind transport of ozone from the industrial southern region of Madrid.

This present campaign helped in deciding on the effectiveness of such type of measures of controlling vehicle traffic to alleviate the damage caused by ozone gas to the human beings and plants. The experimental results reveal some additional evidence of the much more direct dependence of ozone concentration on both the vehicle traffic and the photochemical solar activity even during a one-day scale monitoring. The ozone concentration dependence clearly shows up during a "vehicle-free" day in Madrid City. An average decrease of 12.0 - 1.2 % of the intensity of vehicle traffic during the "free-vehicle" day resulted in lowering the ozone burden by almost 14.0 - 1.4 %. This new type of information can both stimulate the development of local models, the definition of their boundary conditions, and shed light on the dynamics and chemistry of the tropospheric ozone. Understanding these issues is key to the development of reliable risk assessments.

8159-22, Poster Session

Analysis of the dust and urban aerosol by space-borne lidar, in China

W. Gong, Y. Ma, Wuhan Univ. (China)

Many studies have been carried out to study the dust aerosol, including the use of ground-based lidar and the sun-photometer observing networks as well as spaceborne passive observations. These include the European Aerosol Research Lidar Network to Establish an Aerosol Climatology (EARLINET), the AErosol RObotic NETwork (AERONET), and the Moderate Resolution Imaging Spectroradiometer (MODIS). However, most of the ground-based observations are restricted to a limited

area, and the satellite data cannot describe the vertical distribution, concentration level, and diffusion. The satellite named CALIPSO solves this problem; it uses the spaceborne lidar to observe the atmospheric aerosol and gives precise information on the cloud tops. Using the laser beam, we can obtain the vertical profiles of the elastic backscatter of the particles.

In this paper, we put attenuated backscatter, color ratio (the ratio of attenuated backscatter in two channels), and the top of layers into the classifier, and retrieve the aerosol atmospheric coefficient in Shanghai and northern Tibet. Because the transportation of Taklimakan desert storm, the non-spherical shape and big size is expressed in Tibet, on the contrary, the regional anthropogenic factor cause the urban aerosol in Shanghai, and the urban aerosol is spherical particles. Color ratio (the ratio of attenuated backscatter in two channels) and depolarization ratio (the ratio of perpendicular channel and parallel channel of attenuated backscatter coefficients) are used to describe the particle shape and size. The biggest depolarization ratio is 0.476 in Tibet and occurred in summer, the lowest depolarization ratio is 0.065 in Shanghai and occurred in autumn.

8159-23, Poster Session

Frequency stepped pulsed wind sensing lidar

A. S. Olesen, A. T. Pedersen, K. T. Rottwitt, Technical Univ. of Denmark (Denmark)

A wind sensing lidar utilizing a Frequency Stepped pulse Train (FSPT) is demonstrated for the first time. A proof of concept is performed and wind measurements are shown. One of the advantages in the FSPT lidar is that it enables direct measurement of wind speed as a function of distance from the lidar. We show measurements in a range from 20 meters to 350 meters.

Theoretically the FSPT lidar continuously produces measurements as is the case with a CW lidar, but at the same time with a spatial resolution, and without the range ambiguity originating from e.g. clouds.

The FSPT lidar utilizes a frequency sweeping source for generation of the FSPT. The source generates a pulse train where each pulse has an optical carrier frequency shifted Δf relative to the carrier frequency of the previous pulse. In the scheme presented here, the measured frequency is dependent on which distance the signal originates from. The measured frequency is related to the Doppler frequency shift induced by the wind plus an integer number of Δf corresponding to a specific distance. The special resolution depends on the repetition rate of the pulses in the pulse train.

In this work we discuss the influence of different parameters including pulse duration, pulse power and pulse shape on the signal to noise ratio as well as spatial resolution. Proof of accuracy of the wind speed measurement will likewise be presented in the form of a comparison between measurements from the FSPT lidar to anemometers.

8159-24, Poster Session

Feature extraction from lidar point clouds using image processing methods

L. Zhu, Beijing Univ. of Civil Engineering and Architecture (China) and Michigan State Univ. (United States); A. Shortridge, D. Lusch, Michigan State Univ. (United States); R. Shi, Beijing Univ. of Civil Engineering and Architecture (China)

Airborne Lidar data have become cost-effective to collect, and data are being collected at the local and regional scales across the United States and internationally. These data are typically collected and processed into surface data products by contractors for state and local communities. Current algorithms for advanced processing of Lidar point cloud data are normally implemented in specialized, expensive software that is not available for many users, and these users are therefore unable to experiment with the Lidar point cloud data directly for extracting

customized features. The objective of this research is to identify automated, readily implementable GIS procedures to extract features like buildings, vegetated areas, parking lots and roads from Lidar data using standard image processing tools. Image processing is a relatively mature set of techniques with many effective classification methods. We explore its potential to process Lidar data in conjunction with high-resolution aerial imagery. The final procedure adopted runs as follows. First, interpolation is used to transfer the 3D points to a high-resolution raster. Raster grids of both height and intensity are generated. Second, a raster of relative height above the ground is created by subtracting bare ground height from the first return Lidar data. Third, the relative height map, a collocated high resolution aerial image, and the Lidar intensity map are conformed to generate a multi-channel image. A feature space of this image is created. Finally, supervised classification on the feature space is implemented. The approach is demonstrated and its strengths and limitations are compared to existing techniques.

8159-25, Poster Session

Modeling of a field-widened Michelson interferometric spectral filter for application in a high spectral resolution lidar

D. Liu, C. A. Hostetler, NASA Langley Research Ctr. (United States); I. J. Miller, LightMachinery Inc. (Canada); A. L. Cook, J. W. Hair, NASA Langley Research Ctr. (United States)

High spectral resolution lidars (HSRLs) are becoming increasingly important in current aircraft and future space-based aerosol remote sensing applications. The HSRL technique relies on spectral discrimination between scattering from molecules and aerosol or cloud particles, and the spectral filter can be one of the most challenging problems in HSRL system. Atomic and molecular absorption filters have been used very successfully in HSRL instruments. These filters are robust, stable, and can achieve complete separation of Mie from Cabannes backscatter; however, absorption filters are lossy and gaseous absorption lines do not exist at many convenient laser wavelengths. Fabry-Perot interferometers are another option. They are simple and can be tuned to any wavelength, but are limited by acceptance angle. Field-widened Michelson interferometers overcome the deficiencies of the aforementioned filters: they perform well at relatively large off-axis angles, are nearly lossless, and can be built to any wavelength. A compact, monolithic field-widened Michelson interferometer is being developed as the spectral discrimination filter for an HSRL system at NASA Langley Research Center. The Michelson interferometer consists of a cubic beam splitter, a solid glass arm, and an air arm. The spacer that connects the beam splitter to the air arm mirror is designed to optimize thermal compensation such that the frequency of maximum interference can be tuned with great precision to the transmitted laser wavelength. In this paper, a comprehensive radiometric model for the field-widened Michelson interferometric spectral filter is presented. The model incorporates the angular distribution and finite cross sectional area of the light source, reflectivity of all surfaces, losses by absorption, effects of scattering on surfaces, and lack of parallelism between the air-arm and solid arm, etc. The model is used to assess the performance of the interferometer in terms optical specifications, including etendue, wavefront error, beam splitter coating ratio, absorption losses, uniformity of the glass in the solid arm, etc. As such, the model is also a useful tool to evaluate performance budgets and set optical specifications for new designs of the same basic interferometer type. In this paper, the performance predicted by the model for the prototype field-widened Michelson interferometer is compared with measured results.

8159-26, Poster Session

Scannerless gain-modulated three-dimensional laser imaging radar

C. Jin, Y. Zhao, X. Sun, L. Wu, Y. Zhang, Harbin Institute of Technology (China)

Conference 8159:
Lidar Remote Sensing for Environmental Monitoring XII

Scannerless laser imaging radar will be the trend of laser imaging radar in future because it has several advantages of high frame rate, wide field of view, small size and high reliability owing to giving up mechanical scanner. A scannerless gain-modulated three-dimensional laser imaging radar is developed: Our system consists of a pulsed laser which is capable of generating 100mJ pulses with a pulse width of 10ns and a center wavelength of 532 nm, and a receiver which is a digital CCD sensor coupled to a GEN II intensifier with a 10nm bandwidth optical filter. The homogenized light beam passes through a diverging lens to flood illuminate the targets. The return light is collected by a Nikon camera lens and amplified by the image intensifier which is electronically driven and can be set to exponentially modulated gain or constant gain. The CCD sensor can record a 12 bit gray-level image with a resolution of 780×582 pixels at a 50 Hz frame rate. For a range image of the target can be extracted by processing an intensity image with exponentially modulated gain and an intensity image with constant gain, the range image is acquired at a 25 Hz frame rate. During our outdoor experiment, the range image of the targets at 500m is acquired with 2m range accuracy and the range image of the targets at about 1 kilometer is acquired with 5m range accuracy in daytime.

Conference 8160: Polarization Science and Remote Sensing V

Sunday-Monday 21-22 August 2011 • Part of Proceedings of SPIE Vol. 8160
Polarization Science and Remote Sensing V

8160-01, Session 1

Detection and tracking of RC model aircraft in LWIR microgrid polarimeter data

B. M. Ratliff, Space Computer Corp. (United States); D. A. LeMaster, R. T. Mack, Air Force Research Lab. (United States); P. V. Villeneuve, J. J. Weinheimer, Space Computer Corp. (United States); J. Middendorf, Air Force Research Lab. (United States)

The LWIR microgrid Polarized InfraRed Advanced Tactical Experiment (PIRATE) sensor was used to image several types of RC model aircraft at varying ranges and speeds under different background conditions. The data were calibrated and preprocessed using recently developed scene-based microgrid processing algorithms prior to estimation of the thermal (s_0) and polarimetric Stokes vector images (s_1 and s_2). The data were then analyzed to assess the utility of polarimetric information when the thermal s_0 data is augmented with s_1 and s_2 information for several model aircraft detection and tracking scenarios. Multi-variate analysis tools are applied in conjunction with multi-hypothesis detection schemes to assess detection performance of the aircraft under difficult background clutter conditions. In most cases we find that polarization is able to improve detection performance when compared with the corresponding thermal data. Tracking algorithms were applied to s_0 and the corresponding full polarimetric images for several model aircraft datasets. An initial assessment is performed to determine whether the added polarimetric information provides utility over s_0 alone in these model aircraft tracking scenarios.

8160-02, Session 1

Frequency-domain scene-based non-uniformity correction and application to microgrid polarimeters

W. T. Black, J. S. Tyo, College of Optical Sciences, The Univ. of Arizona (United States)

Non-Uniformity Noise is common in infrared imagers, and is usually corrected through calibration. In some classes of imagers, an initial calibration is often updated during operation by momentarily blocking the optical system with a relatively uniform temperature shutter. This periodic correction is necessary because the non-uniformity patterns (also called fixed-pattern noise) will drift in time as the sensor or scene temperatures change, and requires periodic recalibration. During these recalibration episodes, there is temporary loss of imaging functionality. A microgrid polarimeter is a special focal plane array in which pixels have different polarizing filters, permitting simultaneous measurement of polarization images with minimal loss of the original signal. Microgrid polarimeters are especially sensitive to fixed-pattern noise because the polarization signal is acquired by differentiation (or demodulation) of different pixels. Scene-based algorithms attempt to alleviate the need for recalibration of the imager through image processing techniques.

We introduce a new frequency-domain scene-based non-uniformity estimation and correction technique potentially suitable for real-time implementation. We apply the technique to infrared and microgrid polarimeter imagery and examine performance. Specific application to polarization imagery is explored. The technique demonstrates promising results for shutter-assisted (recalibration) video, for microgrid polarization systems, and for most spatially modulated sensor systems.

8160-03, Session 1

On the study of low-contrast polarization between man-made objects and natural clutter for LWIR

J. M. Romano, U.S. Army Armament Research, Development and Engineering Ctr. (United States); E. Niver, New Jersey Institute of Technology (United States)

LWIR polarimetric imagery has shown the potential in detecting man-made targets in environments where target signal to clutter ratio (SCR) is low. In conventional imagery this low contrast can be found during the diurnal changes that happen during sunrise and sundown. Some studies have demonstrated the presence of a polarimetric diurnal change in S_1 where the contrast between the clutter and the polarizing signal is close to zero. In the proposed paper we will revisit and expand the study of zero polarimetric SCR by introducing an extensive analysis of target and clutter. Our study deviates from previous published work, which compares the target signal and background signal using only the mean. Instead, in order to decide if the occurrence of SCR equal or less than zero, we propose using the following decision framework: 1) Determine the area-under-the-curve metric as a first order understanding if the SCR is close to zero. 2) Threshold the selected imagery throughout all possible thresholds and retain joint pixels while removing singletons; and finally 3) Compare the target and background statistics using the ROC curves to decide if indeed SCR is less or equal to zero. By using the ARDEC-ARL SPICE data collection, we will analyze the signal variability using the proposed method and demonstrate in what conditions low SCRs occur in S_1 and S_2 .

8160-04, Session 1

Defining a process to assess the value of multiple remotely sensed polarimetric images for target detection using spectral and polarimetric data fusion

B. M. Flusche, M. G. Gartley, J. R. Schott, Rochester Institute of Technology (United States)

A process is defined to model a particular set of image acquisition scenarios, to determine which polarimetric image (from a set of many) will produce the most impact on target detection performance, to quantify the impact of incorporating polarimetric information from multiple viewing geometries and to evaluate the performance degradation introduced by a reasonable degree of registration error. Variations of the spectral polarimetric integration (SPI) decision fusion algorithm are described, adapting the decision fusion process to accept information from multiple images as inputs, with each image taken from a different viewing geometry. A metric is introduced to assess the quality of off-nadir polarimetric information-balancing the increased ability to detect polarimetric target signatures with the degradation in performance due to the increased sensor ground sample distance. After logically identifying the best two sensor zenith angles for capturing polarimetric imagery, performance improves by exploiting those angles but a minimal return on investment is observed when additional polarimetric imagery is captured from more than two sensor zenith angles. Finally, incorporating a modest amount of registration error between each of the polarimetric images and the spectral image is shown to degrade fusion performance slightly, but often still outperforms spectral information alone.

8160-06, Session 1

Modulated polarimeters and their null spaces

R. A. Chipman, J. S. Tyo, C. F. LaCasse IV, College of Optical Sciences, The Univ. of Arizona (United States)

Since optical detectors respond only to intensity, polarimeters must modify the intensity so that the polarization parameters can be reconstructed after a series of several measurements. The traditional DRM description develops a system of linear equations that can be inverted. The DRM formalism takes a dot product between the unknown incident Stokes parameters and the analyzer vector that describes the polarimeter at that location in space and time. One of the preferred methods for obtaining the N measurements is to modulate the intensity in space, time, or wavelength with a periodically varying element. When N is greater than the number of Stokes parameters that are being reconstructed, it is common to use the pseudoinverse to affect the reconstruction because it prevents elements of the null space of the set of analyzer vectors from coupling into the estimated Stokes parameters. In this talk we demonstrate that any oscillation frequencies other than the specific ones used to modulate the signal are in that null space for the DRM; conventional DRM reconstruction assumes that any variations in the signal at other frequencies are noise that should be discarded. This assumption is perfectly valid in a range of static sensing applications. In dynamic applications, or in other modulation schemes such as microgrid polarimeters, it is desirable to reconstruct varying polarization signatures. We have developed reconstruction strategies that assume that all frequencies up to some band limit are desired, and places higher frequencies in the null space. These two examples represent the extreme cases, and in this talk we discuss how to develop an intermediate reconstruction strategy that is tailored to the SNR in any particular sensing task.

8160-07, Session 1

Target discrimination of man-made objects using passive polarimetric signatures acquired in the visible and infrared spectral bands

D. A. Lavigne, Defence Research and Development Canada (Canada); M. Breton, AEREX avionique inc. (Canada); G. R. Fournier, J. Charette, M. Pichette, Defence Research and Development Canada (Canada); V. Rivet, A. Bernier, AEREX avionique inc. (Canada)

Surveillance operations and search and rescue missions regularly exploit electro-optic imaging systems to detect targets of interest in both the civilian and military communities. By incorporating the polarization of light as supplementary information to such electro-optic imaging systems, it is possible to increase their target discrimination capabilities, considering that man-made objects are known to depolarized light in different manner than natural backgrounds. As it is known that electro-magnetic radiation emitted and reflected from a smooth surface observed near a grazing angle becomes partially polarized in the visible and infrared wavelength bands, additional information about the shape, roughness, shading, and surface temperatures of difficult targets can be extracted by processing effectively such reflected/emitted polarized signatures.

This paper presents a set of polarimetric image processing algorithms devised to extract meaningful information from a broad range of man-made objects. Passive polarimetric signatures are acquired in the visible, shortwave infrared, midwave infrared, and longwave infrared bands using a fully automated imaging system developed at DRDC Valcartier. A fusion algorithm is used to enable the discrimination of some objects lying in shadowed areas. Performance metrics, derived from the computed Stokes parameters, characterize the degree of polarization of man-made objects. Field experiments conducted during winter and summer time demonstrate: 1) the utility of the imaging system to collect polarized signatures of different objects in the visible and infrared spectral bands,

and 2) the enhanced performance of target discrimination and fusion algorithms to exploit the polarized signatures of man-made objects against cluttered backgrounds.

8160-08, Session 1

The imaging equation for a microgrid linear Stokes polarimeter

I. Vaughn, College of Optical Sciences, The Univ. of Arizona (United States)

Imaging polarimeters have currently and historically been largely used for remote sensing tasks. They have also been used to evaluate the defects and calibrate the polarization of liquid crystal displays. A particular type of polarimeter that has a great deal of unrealized potential is the microgrid array linear Stokes polarimeter. This type of polarimeter is not often used because of reconstruction errors. If these errors could be minimized, or mitigated via proper algorithmic reconstruction, then they have advantages over other types of polarimeters, mainly calibration (not much is needed) and proper operation over wide wavelength bands (due to the use of wire grid linear polarizers). In the paper I analyze an ideal imaging equation of the microgrid Stokes polarimeter, using the full vectorial electric field and Maxwell's equations. This is the forward imaging operator and assumes no noise, an ideal wiregrid polarizer, and a diffraction limited optical system.

8160-09, Session 2

Polarization state generator (PSG): a polarimeter calibration standard

A. Mahler, R. A. Chipman, College of Optical Sciences, The Univ. of Arizona (United States)

A polarization state generator (PSG) was built and calibrated which outputs weakly linearly polarized light with degree of linear polarization (DoLP) varying from 0.0005 to 0.4 with uncertainty of 0.0005. Known, low DoLP light is generated by passing collimated, unpolarized light with a defined range of field angles through a tilted plane parallel plate. The PSG was intended to act as a calibration standard based on calculated DoLP, but proved difficult to model. Therefore, DoLP was instead measured to repeatability of 0.0005.

8160-10, Session 2

System characterization and analysis of the multispectral aerial passive polarimeter system (MAPPS)

B. D. Bartlett, C. Salvaggio, J. Faulring, Rochester Institute of Technology (United States)

Passive polarimetry has been used for many different remote sensing applications and can provide useful signatures for certain types of phenomenology. While broadband polarimeters have many advantages, such as high signal to noise and small ground sample distance, there has been growing interest in the development of algorithms that take advantage of both spectral and polarimetric signals. The Multispectral Aerial Passive Polarimeter System (MAPPS) aims to produce multispectral polarimetric imagery of test scenes that can be used in algorithm development efforts. Preliminary data is presented along with a calibration and processing workflow that produces registered spectral Stokes imagery.

Conference 8160:
Polarization Science and Remote Sensing V

8160-11, Session 2

Near-infrared simultaneous Stokes imaging polarimeter: integration, field testing, and estimation error analysis

J. D. Mudge, M. Virgen, Lockheed Martin Space Systems Co. (United States)

In 2009 we reported on an optimal design of a simultaneous Stokes' imaging polarimeter in the near-infrared. The optimal design is a result the polarization elements chosen to reduce sensitivity to noise, minimize differential aberrations, and reduce image registration to a simple calibration. A polarimeter was built to the specified design, field tested and shown to produce estimated polarization of a scene, e.g., Stokes' images, near real time. This system estimates the polarization of particular scene elements relevant to remote sensing applications. The details of instrument integration and an error analysis are presented in this paper. Several sets of data will also be presented showing the instruments remote detection capabilities of disparate objects from various platforms, highlighting the versatility and durability of the polarimeter and its output.

8160-12, Session 2

M&m's: an error budgeting and performance simulator code for polarimetric systems

M. de Juan Ovelar, F. Snik, C. U. Keller, Utrecht Univ. (Netherlands)

Polarimetry is a very valuable remote-sensing technique that often yields information that is unobtainable through other techniques. Because of the increasing size and complexity of current instrumentation projects, the design of these polarimeters is only now starting to demand a formal systems engineering approach, which is common practice when designing optical systems. Although different approaches to model a polarimeter's accuracy have been described before, a complete error budgeting tool has not been developed due to the complexity of the error propagation in such systems. Errors have to be expressed as vectors, and their values are often larger than the signal itself. Such a tool will allow us to identify the components in the system that significantly degrade the polarimetric performance and estimate the polarimetric accuracy of a given design. Based on the mathematical framework established by Keller & Snik (2009), we present the M&m's code that constitutes the first attempt to get a generic error budgeting tool to model the performance and accuracy of a given polarimeter including all the potential error contributions, due to, e.g., misalignment and varying material properties, and their dependencies on physical parameters, e.g., wavelength and temperature. We also present some preliminary results from validation of the code with a laboratory set-up that mimics the EPICS polarimeter for the E-ELT, which will directly image and characterize exoplanets.

8160-13, Session 2

Modeling the polarimetric scattering properties of diffuse reflectance standards

T. A. Germer, H. J. Patrick, National Institute of Standards and Technology (United States)

Sintered polytetrafluoroethylene (PTFE), marketed at Spectralon or Fluorilon-99W, is often used as a diffuse reflectance scattering standard. Near normal incidence, its behavior is relatively close to Lambertian with a reflectance close to one. At larger angles of incidence, marked deviations from Lambertian are observed and its polarization dependence becomes more pronounced. In this paper, we will present Mueller matrix bidirectional reflectance distribution function (BRDF) measurements, performed both in and out of the plane of incidence, and compare them

to a theoretical model that assumes multiple scattering occurs in the volume of the material. These simulations use a Henyey-Greenstein phase function, generalized to account for polarization, together with a full polarimetric implementation of the adding-doubling method to account for multiple scattering. The agreement between the measured behavior and the predictions of the model (requiring only a few adjustable parameters) is quite good. These measurements and calculations may pave the way to improved standards by guiding the development of newer, better materials, and by providing a means to interpolate or extrapolate limited sets of data.

Certain commercial equipment, instruments, or materials are identified in this paper in order to specify the experimental procedure adequately. Such identification is not intended to imply recommendation or endorsement by the National Institute of Standards and Technology, nor is it intended to imply that the materials or equipment identified are necessarily the best available for the purpose.

8160-14, Session 3

Estimating particles microphysics from the polarized water-leaving radiance

A. Tonizzo, A. Gilerson, T. Harmel, A. Ibrahim, The City College of New York (United States); J. Chowdhary, Columbia Univ. (United States); B. Gross, F. Moshary, S. Ahmed, The City College of New York (United States)

Polarization in the atmosphere arises primarily from single scattering, so that angular features of the phase function are mapped directly onto the polarized radiance. By contrast, in the ocean, single scattering features tend to be washed out, due to the presence of multiple scattering and to the lower relative refractive index of hydrosols. In the open ocean (Case I waters), most particles are organic particles (both living and nonliving), covarying with chlorophyll concentration. Because of their normally low concentrations and low refractive indices, these suspended particles have a weak effect on the underwater polarization. However, in Case II waters, inorganic particles, which have a relative refractive index much higher than that of chlorophyll particles, can significantly impact the underwater polarization.

We analyze the sensitivity of the polarization of the water-leaving radiance as a function of hydrosol microphysical parameters, and specifically, of the real part of the bulk refractive index and the hyperbolic slope of the Junge-type size distribution. To insure consistency, in situ measurements of the underwater polarized light, in both Case I and Case II waters, are compared with multiple scattering radiative transfer computations. Underwater polarized radiance measurements were obtained using a custom-built polarimeter. This consists of three radiance sensors mounted on a scanning system controlled by an underwater electric stepper motor. The three radiance sensors have a linear polarizer in front of each sensor window.

A comparison between measurements and simulations is then used to derive and present estimates of the real part of the refractive index and the slope of the particle size distribution.

8160-15, Session 3

Polarization analysis of scattering light using a facet model

L. Jin, T. Tsutaki, Univ. of Yamanashi (Japan); B. Gelloz, Tokyo Univ. of Agriculture and Technology (Japan)

There were several approaches to predict optical scattering from rough surface, such as the Kirchhoff diffraction theory, the Rayleigh-Rice vector perturbation theory, etc. These approaches require the surfaces to be smooth at nanometer-order. Surfaces of objects such as tissue or skin are mostly macroscopically rough, and the incident light is to be often diffusely scattered by these diffuse surfaces. To overcome the limitation of diffraction theory, we have proposed a facet model to analyze the

**Conference 8160:
Polarization Science and Remote Sensing V**

polarization states of light diffusely scattered light by rough surface.

In this paper, we present results of scatter measurements from diffuse glass surfaces with Stokes parameters and polarization degree. The Stokes parameters are analyzed as a function of a virtual scattering angle and a longitude scattering angle. Both the virtual scattering angle and the longitude scattering angle are defined for the facet model. The facet model for scattering from a diffuse surface predicts the polarization states of scattering quite well.

The method and results of this analysis have a significant impact on the application of light scattering to the inspection and process-evaluation industry, material science, etc.

In this paper, we explain advantage of the facet model as well as the limitation of it.

8160-16, Session 3**Comparison of observed full sky polarization to radiative transfer model using AERONET retrieval data**

N. J. Pust, A. Dahlberg, J. A. Shaw, Montana State Univ. (United States)

Observed polarization and radiance images from a ground-based full-sky polarimeter are compared against a Successive Order of Scattering (SOS) radiative transfer model for cloud-free days from 2009 to 2011 in Bozeman, Montana, USA. The imaging polarimeter measures radiance and polarization in 10-nm bands centered at 450, 490, 530, 630, and 700 nm. The AERONET-retrieved aerosol optical depth, size distribution, and refractive index are used as inputs to the SOS model. MISR BRDF retrievals are used for the surface reflectance. We discuss radiance and degree of polarization comparisons between observations and models.

8160-17, Session 3**Exploring the relation between polarized light fields and optical and physical characteristics of the ocean particles for remote sensing applications**

A. Ibrahim, A. Tonizzo, A. Gilerson, T. Harmel, I. Ioannou, S. Ahmed, The City College of New York (United States)

Measurements of light intensity, usually from space borne sensors, have been used to investigate the optical properties of the constituents of Earth's ecosystem. In the ocean color research, water-leaving radiance can give useful information about inherent optical properties (IOPs). Additional consideration of polarization of the water-leaving radiance can lead to a better understanding of the physical and optical characteristics of the water body. Polarization properties strongly depend on particle microphysics, such as refractive index, effective radius, size distribution, and single scattering albedo. We used a Neural Network (NN) statistical tool to examine the relations between IOPs of the water medium and their impact on light polarization and to provide a sensitivity analysis of data sets, which were simulated using a fast polarized radiative transfer code named RayXP (Zege et al.) for different water conditions. Because of the complexity of the analysis, and in order to both simulate data and apply NN techniques to it, we simulated two separate data sets. In the first data set, we varied the IOPs and kept particles microphysics constant. In the second data set, particles compositions were varied according to a uniform distribution, while keeping the IOPs of the water body fixed. The analysis of the two separate data sets allowed us to develop a comprehensive insight into the effects of oceanic physical and optical properties on the polarization of light, and set the basis for further studies on inversion techniques using polarized light. Results of simulations are compared with measurements obtained using our custom-built underwater hyperspectral multi-angular polarimeter.

8160-18, Session 3**Dual-polarization lidar identification of ice in a corona-producing wave cloud**

J. A. Shaw, N. J. Pust, Montana State Univ. (United States)

Corona and iridescence are optical phenomena that create beautifully colored patterns of scattered light in optically thin clouds. The typical explanation is that these displays are caused by sunlight or moonlight being diffracted by small liquid water droplets with diameters near 10 micrometers and relatively uniform droplet size distribution. Ice crystals are generally considered to be too large to create diffraction patterns large enough to be seen by a human observer. However, a few previous publications have shown evidence for the possible existence of unusually small ice crystals that create these displays in clouds at temperatures far too cold to contain even super-cooled liquid water. Both ground-based lidar and airborne particle sampling have been used to confirm this situation in thin cirrus clouds. This paper presents ground-based lidar data that confirms this same situation in a mountain wave cloud.

8160-19, Session 4**Overlay measurement by angle resolved Mueller polarimetry**

A. De Martino, C. Fallet, T. Novikova, Ecole Polytechnique (France); C. Vannuffel, Lab. d'Electronique de Technologie de l'Information (France); B. H. Haj Ibrahim, Ecole Polytechnique (France)

The use of optical metrology techniques for process control is now widespread. They are fast and non-destructive, allowing higher throughputs than non-optical techniques like electron microscopies or AFM.

We present here new developments using complete Mueller polarimetry in the back focal plane of a microscope objective to characterize overlay for microelectronics industry. Based on fundamental symmetries in the physics of periodic structures and polarized light and redundancies in the angle-resolved Mueller images we define estimators which vary linearly with the overlay. As a result, overlay measurement is sensitive to both the direction and sign of the overlay, and it does not require any detailed modelling of the target structures, provided two independent targets with known overlay values are available on the wafer. Realistic simulations on optimized structures suggest that accuracies in the order of 1 or 2 nm or better should be achievable. Moreover, with high NA objectives the proposed technique can be implemented with targets with lateral sizes as small as a few μm .

Experimental results of both grating line profiles and overlay determinations will be presented. The samples, elaborated at LETI, have been accurately characterized by state-of-the-art AFM or optical imaging "box-in-box" techniques.

The latest developments on the device itself as well as the advantages, possibilities and limitations of this new metrology technique will be discussed and some relevant estimators of the overlay will be proposed.

8160-20, Session 4**Spatio-temporal modulated polarimetry**

C. F. LaCasse IV, J. S. Tyo, College of Optical Sciences, The Univ. of Arizona (United States)

Recently, a polarimetric data reduction technique has been developed that in the presence of a time varying signals and noise free measurement process can achieve an error free reconstruction provided that the signal was band limited to a limit that is set by the modulation scheme employed. Error free reconstruction for such a signal is not possible using conventional data reduction methods. The new approach provides

**Conference 8160:
Polarization Science and Remote Sensing V**

insight for processing arbitrary modulation schemes in space, time, and wavelength. Theory predicts that a polarimeter that employs a spatio-temporal modulation scheme may be able to use the high temporal resolution of a spatially modulated device combined with the high spatial resolution of a temporally modulated system to attain greater combined resolution capabilities than either modulation on scheme can produce alone. A polarimeter that contains both spatial and temporal modulation can be constructed (for example) by placing a rotating retarder in front of a micropolarizer array (microgrid). This study develops theory and analysis for the rotating retarder microgrid polarimeter to show how the available bandwidth for each channel is affected by additional dimensions of modulation and demonstrates a working polarimeter with a simulation of Stokes parameters that are band limited in both space and time with a noisy measurement process.

8160-22, Session 4

Correction of temporal division polarimeter artifacts with an optical flow technique

P. Marconnet, L. Gendre, A. Foulonneau, L. Bigué, Univ. de Haute Alsace (France)

The MIPS laboratory has implemented a high-speed portable imaging polarimeter based on the temporal division scheme. As pointed out by many authors in the literature, the temporal division scheme leads to some artifacts when the acquired scene is not static.

In a previous work, we presented a first approach to solve this issue. A temporal median filtering was successfully applied to Degree of Polarization images estimated only with two cross-polarized states images. This method permits an attenuation of the artifacts at a very high rate (we implemented it at 300Hz on a 'standard' PC, with a 320x240 image resolution), but it may alter accurate values.

Since then, we have rather worked on the implementation in a polarimetric framework of general-purpose motion-compensation-based methods. We considered global registration and block matching methods, but we finally focussed on optical flow techniques such as that presented by Brox et al. Compensating the motion of each state of polarization image allows the polarimeter to estimate the real polarization information as if there was no motion.

In this paper we detail the implementation of our technique and show how it can greatly improve the estimation of the Stokes vector obtained by a division of time polarimeter.

In a first time we explain how a motion compensation technique can be adapted to such a polarimeter, then we give some details about our implementation of the optical flow technique. Finally, comparison between various implementations is provided using synthetic and experimental data in the case when full linear polarization (i.e. the first three Stokes components) is considered.

8160-23, Session 4

Stokes vector analysis of LWIR polarimetric in adverse weather

J. M. Romano, L. E. Roth, J. Michalson, U.S. Army Armament Research, Development and Engineering Ctr. (United States)

It is understood that LWIR polarimetric imagery has the potential in detecting man-made objects in natural clutter backgrounds. Unlike Spectral and conventional broadband, polarimetric imagery takes advantage of the polarized signals emitted by the smooth surfaces of man-made materials. Studying the effect of how meteorological conditions affect polarization signals is imperative in order to understand where and how polarimetric technology can be beneficial to the warfighter. In the proposed paper we intend to demonstrate the effects of weather on the performance of Stokes vector components, S1 and S2, and the degree of linear polarization (DOLP) as detectors of man-made materials. Using the SPICE data collection, we analyze over 1,000

images and correlate the performance of each of the detection metrics to individual meteorological measurements. The chosen metrics for such analysis are: AUC or area under the curve and optimum ROC point. By using such metrics we are able to correlate background and target variability in order to understand the underlying trends between target signature and background clutter to the different weather conditions parameters.

8160-43, Session 4

Vehicle tracking through the exploitation of remote sensing and LWIR polarization science

H. S. Clouse, H. Krim, North Carolina State Univ. (United States); W. A. Sakla, O. Mendoza-Schrock, Air Force Research Lab. (United States)

Vehicle tracking is an integral component in layered sensing exploitation applications. The utilization of a combination of sensing modalities and processing techniques provides better insight about a situation than can be achieved with a single sensing modality. In this work, several robust features are explored for vehicle tracking using data captured in a remote sensing setting. Particularly, a video sequence is evaluated in the layered sensing framework. The target area is surveyed by two sensors operating across two different modalities: a LWIR polarized sensor and a LWIR sensor. We here extend our previous work ([1]) to experimental analysis on several feature sets including three classic features (Stokes images, DoLP, the Degree of Linear Polarization, and AoP, the Angle of Polarization) and two experimental features (ρ , an extension of the DoLP, and δ , the phase difference between two orthogonal projections of an observed electromagnetic wave).

8160-24, Session 5

On the optimization of polarimetric imaging systems for target detection

F. Goudail, G. Anna, Institut d'Optique Graduate School (France)

Active polarimetric imaging systems consist of illuminating a scene with polarized light and analyzing the polarization state of the scattered light before forming the image. They are invaluable tools for detecting objects in biomedical or remote sensing applications since they can reveal contrasts that do not appear in classical images. However, such systems usually have higher cost and complexity than standard imagers, and their complexity grows with the number of measurements they require (e.g., 4 measurements for a Stokes imager, 16 for a Mueller imager). Important issues are thus to determine under which condition they yield better performance than simple intensity imaging, and what is their optimal number of measurements. Recent advances have made it possible to give quantitative answers to these questions, and we will illustrate these results on two examples.

First, we will compare the contrasts obtained with Mueller, Stokes and single (scalar) polarimetric measurements in the presence of additive noise. We will show that the best contrast is always obtained with a single measurement performed with optimized illumination and analysis states. Second, we will quantitatively determine the conditions in which polarimetric imaging yields better performance than classical intensity imaging, and the conditions in which polarized illumination is preferable to illumination with natural light. We will show in particular that the answers to these questions depend on the statistics of the noise that perturbs the image.

8160-25, Session 5

Observations on the Polarimetric Imagery Collection Experiment database

M. C. Woolley, J. Michalson, J. M. Romano, U.S. Army Armament Research, Development and Engineering Ctr. (United States); D. B. Chenault, Polaris Sensor Technologies, Inc. (United States)

The Spectral and Polarimetric Imagery Collection Experiment (SPICE) is an ongoing collaborative effort that commenced in February 2010 between the US Army ARDEC and ARL. SPICE is focused on the collection of mid-wave and long-wave infrared imagery using hyperspectral, polarimetric, and broadband sensors.

The overall objective of SPICE is to collect a comprehensive database of the different modalities spanning multiple years to capture sensor performance encompassing a wide variety of meteorological (MET) conditions, diurnal, and seasonal changes inherent to Picatinny's northern New Jersey location.

Utilizing the Precision Armament Laboratory (PAL) tower at Picatinny Arsenal, the sensors are autonomously collecting the desired data around the clock at multiple ranges containing surrogate 2S3 Self-Propelled Howitzer targets positioned at different orientations in an open woodland field. This database allows for: 1) Understanding of signature variability under adverse weather conditions; 2) Development of robust algorithms; 3) Development of new sensors; 4) Evaluation of polarimetric technology; and 5) Evaluation of fusing the different sensor modalities.

In this paper, we will revisit the SPICE data collection objectives and the sensors deployed. We will present, in a statistical sense, the integrity of the data in the long-wave infrared (LWIR) polarimetric database collected from February through September 2010 and issues and lessons learned associated with a fully autonomous, around the clock data collection. We will also demonstrate sample LWIR polarimetric imagery and the performance of the Stokes parameters under adverse weather conditions.

8160-26, Session 6

Polarization measurement with space-variant retarders in liquid crystal polymers

P. Piron, B. Pascal, H. Serge, Univ. de Liège (Belgium)

At this conference, we will present a polarization analysis method using a space-variant optical retarder made of liquid crystal polymers (LCP). The liquid crystals are anisotropic molecules attached to chain-polymers as a side chain. They present useful birefringent properties for optical retarders realization. The orientation of the liquid crystals defines the optical axis of the retarder. This orientation is determined by the UV recording laser beam polarization (one or more well chosen recording beams).

Our optical retarder for the polarization analysis method performs a continuous variation in the optical axis orientation. This continuous variation is obtained by the exposure to the superposition of two circularly polarized beams with opposite handedness. These beams come from the division of one linear polarized beam into two linear polarized beams with same intensity and orthogonal polarization.

Thanks to the measurement of the intensity distribution of a completely polarized beam transmitted through the retarder and a linear polarizer, we compute the Stokes parameters of the incident beam.

Our method and the mathematical model based on Stokes-Müller representation of the polarization and on Fourier analysis of the outgoing beam will be deeply explained. Then we will describe the fabrication of our retarder and the measurement process of the polarization that we developed. Finally we will comment our experimental results.

8160-27, Session 6

Study of Stokes polarimeters based on a single twisted nematic liquid crystal panel

A. Peinado, A. Lizana, Univ. Autònoma de Barcelona (Spain); J. Vidal González, Univ. Autònoma de Barcelona (Spain) and CELLS - ALBA (Spain); C. C. Lemmi, Univ. de Buenos Aires (Argentina); J. Campos, Univ. Autònoma de Barcelona (Spain)

Polarimeters are the basic instruments to perform polarization metrology. Nowadays, they are present in many scientific and industrial applications. For instance, in a burn depth assessment for injured patients, scanning living retinal tissues, in solar imaging, in the characterization of photonic structures and detecting buried landmines.

By taking advantage that Liquid Crystal Displays act as variable retarders depending on the voltage addressed, many authors have introduced them on the setups allowing to perform dynamic polarimetric measurements. Consequently, these instruments avoid experimental errors from misalignment by conducting an accurate calibration.

In this work, we present the design, optimization and implementation of dynamic Stokes polarimeters based on a single Twisted Nematic Liquid Crystal (TNLC) panel. TNLC material enables both to introduce a retardance and to rotate the polarization ellipse orientation. For this reason, a simple setup composed by a transmissive TNLC panel and a polarizer can be built leading to a complete Stokes polarimeter. Variations of the initial setup are analyzed with the aim of minimizing the noise propagation to the Stokes vector calculations. In particular, working out of normal incidence to the TNLC panel and working on TNLC reflective mode. Moreover, we carry out an optimization of the polarization analyzers used in each configuration. Finally, we implement the optimized polarimeters and some incident Stokes vectors are measured, proving their correct operation. Results are compared with those provided by the optimal polarimeter based on a two Parallel Aligned LCD panels and so, the suitability of applying a TNLC panel on polarimeters design is confirmed.

8160-28, Session 7

Channeled spectropolarimeter using a wavelength-scanning laser and a channeled spectroscopic polarization state generator

K. Oka, T. Kinoshita, A. Ise, Hokkaido Univ. (Japan)

Channeled spectropolarimetry is a method to measure polarimetric characteristics of a light or an object utilizing the strong dispersions of high order retarders. This method requires no mechanical polarization-modulation elements and it can determine plural polarimetric parameters from a single channeled spectrum. In the previous implementations of this method, a spectrometer in the receiving optics is mainly employed for the acquisition of the channeled spectrum. This presentation discuss about another implementation of the channeled spectropolarimeter that uses a wavelength-scanning laser and a channeled spectroscopic polarization state generator (CSPSG).

This implementation has a feature that it is applicable for the spatial mapping of the polarimetric parameters. For this type of measurement, the wavelength-scanned laser light emerging from the CSPSG is expanded in diameter and then illuminates the object whose polarimetric characteristics depend on the spatial coordinates. Since no spectrometer is used and both the wavelength scanning and the polarization modulation are made by the illumination optics, an imaging optics followed by a CCD camera can be easily incorporated in the receiving optics. Two-dimensional distributions of the polarimetric parameters of the object can be determined from the flickering images. This principle was experimentally demonstrated by use of a laser diode and a CSPSG made of calcite.

Another feature of the channeled spectropolarimeter using a wavelength-scanning laser is its capability for the high wavelength-resolution acquisition of the channeled spectrum. This feature is useful for the

Conference 8160:
Polarization Science and Remote Sensing V

applications such as the full Mueller matrix measurement by use of four high-order retarders.

capable of measuring a complete Stokes vector image (S_0 , S_1 , S_2 , and S_3) in white-light.

8160-29, Session 7

Preliminary results from an infrared hyperspectral imaging polarimeter

J. Craven-Jones, M. W. Kudenov, M. G. Stapelbroek, E. L. Dereniak, College of Optical Sciences, The Univ. of Arizona (United States)

We present results from a SWIR/MWIR infrared hyperspectral imaging polarimeter (IHIP). The sensor includes a pair of sapphire Wollaston prisms and several high order retarders to form an imaging Fourier transform spectropolarimeter. The Wollaston prisms serve as a birefringent interferometer with reduced sensitivity to vibration versus an unequal path interferometer, such as a Michelson. Polarimetric data are acquired through the use of channeled spectropolarimetry to modulate the spectrum with the Stokes parameter information. The collected interferogram is Fourier filtered and reconstructed to recover the spatially and spectrally varying Stokes vector data across the image. The IHIP operates over a ± 5 degree field of view and implements a dual-scan false signature reduction technique to suppress polarimetric aliasing artifacts. In this paper, we discuss the layout and operation of the IHIP sensor, in addition to the radiometric, spectral, and polarimetric calibration techniques. Lastly, spectral and spectropolarimetric results from the laboratory and outdoor tests with the instrument are presented.

8160-30, Session 7

Spectroscopic Stokes polarimeter based on dual liquid crystal modulators

M. Tanaka, Y. Nakashima, H. Amamiya, Atago Co., Ltd. (Japan); Y. Otani, Utsunomiya Univ. (Japan)

The purpose of this research is to establish a spectroscopic Stokes polarimeter based on dual liquid crystal modulators, which are consisted of two types of phase modulator by nematic liquid crystal. It is powerful tool with some superior characteristics, non-mechanical, miniature and low consumption electricity. The polarization states of light are expressed by 4 parameters called Stokes parameters. We evaluated all Stokes parameters using some samples that are used for the evaluation of Stokes parameters by birefringence of Babinet-Soleil compensator.

8160-31, Session 7

Spectrally broadband channeled imaging polarimeter using polarization gratings

M. W. Kudenov, College of Optical Sciences, The Univ. of Arizona (United States); M. J. Escuti, North Carolina State Univ. (United States); E. L. Dereniak, The Univ. of Arizona (United States); K. Oka, Hokkaido Univ. (Japan)

A snapshot channeled linear imaging (CLI) polarimeter is demonstrated by incorporating two identical polarization gratings (PGs) into a shearing polarization interferometer. Placing the PGs in series causes the shear to become linearly proportional to the wavelength, thereby generating white-light polarization fringes at the focal point of an imaging lens. These fringes amplitude modulate the incident Stokes parameters corresponding to linearly polarized light (S_0 , S_1 , and S_2). In this paper, we theoretically and experimentally demonstrate the CLI polarimeter. Additional validation of the technique is conducted through outdoor measurements of moving targets. Furthermore, extending the CLI polarimeter's measurement capacity to include circularly polarized light is overviewed with theoretical calculations. This would make the instrument

8160-32, Session 7

A pixelated micropolarizer-based camera for instantaneous interferometric measurements

N. Brock, 4D Technology Corp. (United States)

A pixel-level micropolarizer array bonded to a scientific camera has been developed for use in commercial dynamic interferometers. The pixelated array includes the 0, 45, 90, 135 degree polarizations. Micropolarizer arrays with elements as small as 7.4 microns have been fabricated for use across the visible spectrum.

8160-33, Session 7

Full Stokes polarization camera

M. Vedel, S. Breugnot, Bossa Nova Technologies (United States)

Objective and background:

We present a new version of Bossa Nova Technologies' passive polarization imaging camera. The previous version was performing live measurement of the Linear Stokes parameters (S_0 , S_1 , S_2), and its derivatives (DOLP, AOP and others). This new version presented in this paper performs live measurement of Full Stokes parameters, i.e. including the fourth parameter S_3 related to the amount of circular polarization. A dedicated software was developed to provide live images of any Stokes related parameters such as the Degree Of Linear Polarization, the Degree Of Circular Polarization, the Angle Of Polarization among others.

Results: First we give a brief description of the camera and its technology. It is a Division Of Time Polarimeter using a custom ferroelectric liquid crystal cell. A description of the method used to calculate Data Reduction Matrix (DRM) linking intensity measurements and the Stokes parameters is given. The calibration was developed in order to maximize the condition number of the DRM. It also allows very efficient post processing of the images acquired. Complete evaluation of the precision of standard polarization parameters is described. Then we present the standard features of the dedicated software that was developed to run the camera. It provides live images of the Stokes vector components and the usual associated parameters. Finally some tests already conducted are presented. It includes indoor laboratory and outdoor measurements. This new camera will be and useful tool for many application such as biomedical, remote sensing, metrology, material studies, and others.

8160-34, Session 8

Imaging polarimeters based on liquid crystal variable retarders: an emergent technology for space instrumentation

A. Alvarez-Herrero, N. Uribe-Patarroyo, P. García Parejo, J. Vargas, R. L. Heredero, R. Restrepo, Instituto Nacional de Técnica Aeroespacial (Spain); V. Martínez-Pillet, Instituto de Astrofísica de Canarias (Spain); J. C. del Toro Iniesta, A. López, Instituto de Astrofísica de Andalucía (Spain); S. Fineschi, G. Capobianco, Istituto Nazionale di Astronomia (Italy); M. Georges, Univ. de Liège (Belgium); M. López, Visual Display S.L.L. (Spain); G. Boer, Arcoptix S.A. (Switzerland); I. G. Manolis, European Space Research and Technology Ctr. (Netherlands)

Polarimetric remote sensing in the range of the radar wavelengths has demonstrated its importance in many applications; however this

Conference 8160:
Polarization Science and Remote Sensing V

technique applied in the optical range is a relative new field which interest is quickly increasing. Applications in solar physics, astronomy, even earth observation are being extensively developed.

In this context, the use of Liquid Crystal Variable Retarders (LCVRs) as polarization modulators are envisaged as a promising novel technique for space instrumentation due to the advantage of avoiding the utilization of traditional rotary polarizing optics which implies the inclusion of mechanisms. LCVRs is a mature technology for ground applications; they are well-known and during the last ten years have undergone an important development, driven by the fast expansion of commercial Liquid Crystal Displays.

In this work a review of the state of the art of imaging polarimeters based on LCVRs is presented. All of them are ground instruments, except the solar magnetograph IMAx which flew in 2009 onboard of a stratospheric balloon as part of the SUNRISE mission payload, since we have no knowledge about spaceborne polarimeters using liquid crystal up to now. Likewise, an assessment report of the possible effects of the space environmental conditions on the LCVRs is presented. Finally, the baseline of the polarisation modulation package including LCVRs of the instruments PHI (Polarimetric and Helioseismic Imager) and METIS/COR (Multi Element Telescope for Imaging and Spectroscopy, Coronagraph) for Solar Orbiter will be described briefly as well as the activity, currently in progress, to validate this technology for the mission.

8160-35, Session 8

Prototyping for the Spectropolarimeter for Planetary EXploration (SPEX): calibration and sky measurements

G. van Harten, F. Snik, Utrecht Univ. (Netherlands); J. H. H. Rietjens, J. M. Smit, D. M. Stam, SRON Nationaal Instituut voor Ruimteonderzoek (Netherlands); C. U. Keller, Utrecht Univ. (Netherlands); E. C. Laan, A. L. Verlaan, W. A. Vliegthart, TNO Science and Industry (Netherlands); R. ter Horst, R. Navarro, ASTRON (Netherlands); K. Wielinga, Mecon Engineering B.V. (Netherlands); S. Hannemann, S. G. Moon, cosine Research B.V. (Netherlands); R. Voors, Dutch Space B.V. (Netherlands)

We present the Spectropolarimeter for Planetary EXploration (SPEX), a high-accuracy linear spectropolarimeter with moderate spectral resolution throughout the visible, that is compact (~ 1 liter), robust and lightweight. This is achieved by employing the unconventional spectral polarization modulation technique, optimized for linear polarimetry. The polarization modulator consists of an achromatic quarter-wave retarder and a multiple-order retarder, followed by a polarizing beamsplitter, such that the incoming polarization state is encoded as a sinusoidal modulation in the intensity spectrum, where the amplitude scales with the degree of linear polarization, and the phase determines the angle of linear polarization. An optimized combination of birefringent crystals creates an athermal multiple-order retarder, with a stable retardance across the field of view. Based on these specifications, SPEX is an ideal, passive remote sensing instrument for characterizing planetary atmospheres from an orbiting, air-borne or ground-based platform. By measuring the intensity and polarization spectra of sunlight that is scattered in the planetary atmosphere as functions of the scattering angle, aerosol microphysical properties (size, shape, composition), vertical distribution and optical thickness can be deduced. Such information is essential to fully understand the weather and climate of a planet. A functional SPEX prototype has been developed and calibrated, showing striking agreement with end-to-end performance simulations. To test SPEX, we performed multi-angle spectropolarimetric measurements of the Earth's atmosphere from the ground in conjunction with one of AERONET's sun photometers. Several flight opportunities exist for SPEX throughout the solar system: in orbit around Mars, Venus, Jupiter and Saturn and their moons, and the Earth.

8160-36, Session 8

MgII linear polarization measurements using the MSFC Solar Ultraviolet Magnetograph

E. A. West, J. Cirtain, NASA Marshall Space Flight Ctr. (United States); K. Kobayashi, G. A. Gary, J. M. Davis, The Univ. of Alabama in Huntsville (United States)

This paper will describe the Marshall Space Flight Center's Solar Ultraviolet Magnetograph Investigation (SUMI) sounding rocket program, with emphasis on the polarization characteristics of the VUV optics and their spectral, spatial and polarization resolution. SUMI's first flight (7/30/2010) met all of its mission success criteria and this paper will describe the data that was acquired with emphasis on the MgII linear polarization measurements.

8160-37, Poster Session

Achromatic, athermalized retarder fabrication

A. Mahler, S. McClain, R. A. Chipman, College of Optical Sciences, The Univ. of Arizona (United States)

A retarder made from sapphire, MgF₂ and quartz was designed, fabricated and its performance validated for the 0.47 μ m to 0.865 μ m wavelength region. Its specifications are as follows: at wavebands centered at 0.470 μ m, 0.660 μ m, and 0.865 μ m, the band-averaged retardance should be $90^\circ \pm 10^\circ$ for all fields and retardance should change less than 0.1° for a 1° change in temperature. Analysis indicated that a design specified by thickness alone was unlikely to meet the requirements due to uncertainties in birefringence. To address this, the following fabrication method was developed that involves monitoring retardance during polishing. The first plate was polished to a target thickness. The retardance spectrum of the first plate was then measured and used to determine a retardance target for the second plate. The retardance spectrum of the combined first and second plates was then used to specify a retardance target for the third plate. The retardance spectrum of the three plates in combination was then used to determine when the final thickness of the third plate was reached.

8160-38, Poster Session

Large format HgCdTe focal plane arrays for dual-band long-wavelength infrared detection

N. R. Malone, Raytheon Co. (United States)

Polarimetry sensor development has been in work for some time to determine the best use of polarimetry to differentiate between manmade objects and objects made by nature. Both MWIR and LWIR Focal Plane Arrays (FPAs) have been built at Raytheon Vision Systems each with exceedingly higher extinction ratios.

LWIR polarimetry has the largest polarimetric signal level and an emissive polarimetric signature which allows detection at thermal crossover and is less dependent on sun angles. Polished angled glass and metal objects are easily detected using LWIR polarimetry. While LWIR polarimetry has many advantages its resolution is not as good as MWIR.

To gain acceptance polarimetric sensors must provide intelligence signatures that are better than existing non-polarimetric Infrared sensors.

8160-39, Poster Session

Broadband Mueller matrix polarimeter

P. Raman, K. A. Fuller, D. A. Gregory, The Univ. of Alabama in Huntsville (United States)

A dual rotating retarder Mueller matrix polarimeter will be described

**Conference 8160:
Polarization Science and Remote Sensing V**

that operates in the UV-VIS-NIR region. The components were selected to allow the instrument to span the 300 nm to 1100 nm region with a resolution of 2nm. Complete Mueller matrix polarimetric characterizations of a host of optical components have been performed and a select few will be presented. This instrumentation is expected to enable exploratory research into novel methods for point and standoff detection of chemical and biological threats in the atmosphere. To this end, surrogates of hazardous materials as well as background aerosols must be characterized and differentiating features in the polarization properties correlated to specific morphologies. This potential capability is currently being explored and preliminary results will be presented.

8160-40, Poster Session**A comparison of polarization image processing across different platforms**

T. York, S. Powell, R. D. Chamberlain, V. Gruev, Washington Univ. in St. Louis (United States)

Division-of-focal-plane (DoFP) polarimeters for the visible spectrum hold the promise of being able to capture both angle and degree of linear polarization in real time and at high spatial resolution. These sensors are realized by monolithic integration of CCD imaging elements with metallic nanowire polarization filter arrays at the focal plane of the sensor. These novel sensors capture large amounts of raw polarization data and present unique computational challenges as they aim to provide polarimetric information at high spatial and temporal resolution. The image processing pipeline in a typical DoFP polarimeter is: dead-pixel compensation, per-pixel gain and offset correction, interpolation of the four sub-sampled polarization pixels, Stokes parameter estimation, angle and degree of linear polarization estimation, and conversion from polarization domain to color space for display purposes. The entire image processing pipeline must operate at the same frame rate as the CCD polarization imaging sensor (40 frames per second) or higher in order to enable real-time extraction of the polarization properties from the imaged environment. To achieve the necessary frame rate, we have implemented and evaluated the image processing pipeline on four different platforms. The first two implementations of the image processing pipeline are for a general purpose CPU using single threaded and multi-threaded paradigms. The third implementation is for a general purpose graphics processor (GPU) and the fourth is for an embedded FPGA platform. The computational throughput, power consumption, precision and physical limitations of the four implementations are described in detail and experimental data is provided.

8160-41, Poster Session**Hyperspectral measurement of the scattering of polarized light by skin**

A. Alenin, College of Optical Sciences, The Univ. of Arizona (United States); L. Morrison, C. Curiel, The Univ. of Arizona (United States); J. S. Tyo, College of Optical Sciences, The Univ. of Arizona (United States)

The goal of this study is to develop a dedicated spectropolarimeter for purposes of assessing polarization signatures in skin scattering on a regional scale. Prior research has that certain skin lesions have identifiable polarization signatures; however, those studies were limited to single lesion evaluation and do not account for the task of diagnosing a patient with a significant number of lesions over a wide area. A spectropolarimeter with enough resolution to capture whole-body images would be extremely useful in identifying and monitoring the progress of lesions of interest, as well as enabling much earlier detection of cancerous and potentially life threatening lesions.

As a precursor to the future instrument, a simpler actively illuminated Stokes spectropolarimeter was constructed to ensure the viability of such a device. This spectropolarimeter consists of a rotating retarder and a hyperspectral camera, which scans through wavelengths by means of a

Liquid Crystal Tuning Filter (LCTF). Data is captured in a serial fashion, where LCTF scans through eight wavelengths at each of the four retarder orientations. With a single acquisition taking 23 seconds to complete, it makes the issue of image registration very important. After proper alignment, the acquired images reveal that polarization sensing has merit even on a regional scale. In particular, it was found that polarization factors such as Degree of Linear Polarization (DoLP) tend to suppress many uninteresting skin features like wrinkles and skin texture, while capturing information that is not necessarily apparent in the intensity image.

8160-42, Poster Session**Multispectral measurements of atmospheric aerosols over an urban area**

M. Yasumoto, Kinki Univ. (Japan)

Polarization measurements of atmospheric aerosols have been undertaken with a portable multi-spectral polarimeter (PSR-1000) since 1996 at Kinki University campus in Higashi-Osaka in Japan, where such various instruments as NASA/AERONET photometer, PM sampler (PM2.5/PM10/OBC Dichotomous Monitor), sky camera and Mie-scattering-polarization LIDAR are set up for monitoring of the atmospheric environment.

For estimation of aerosol characteristics, e.g. optical thickness of aerosols, size distribution parameters etc, PSR-1000 observes radiance of the direct sunlight and radiance/polarization of atmospheric light at wavelengths of 443, 490, 565, 670, 765 and 865nm. PSR-1000 has been calibrated once a year based on Langley plot method at Mt. Haleakala Observatory in Maui Island in Hawaii. In order to improve the derivation of aerosol optical thickness (AOT), precise correction of molecular scattering and gaseous absorption is desired. Therefore the gaseous absorption by water vapor at 565, 670, 765, and 865nm, O₂ at 670 and 765nm and NO₂ for 443 and 490nm are reexamined at present.

It is of interest to mention that PSR-1000 detects atmospheric particles over an urban area recorded among our long-term observations.

8160-44, Poster Session**Use of polarization imaging in air-to-air detection systems**

S. Bencuya, C. A. White, S. Lin, EmergentViews, Inc. (United States)

Polarization imaging can substantially enhance detection of aircraft due to the high polarization contrast of sky and manmade objects. Air-to-air detection tests using polarization cameras were conducted for the development of a Detect Sense and Avoid (DSA) system that can be used by unmanned aircraft systems (UAS) navigating in the U.S. national airspace system (NAS).

A visible spectrum polarization camera equipped with a custom pixilated wire grid polarizer was developed for this project. The flight tests were structured to compare the performance of this polarization-camera to that of a reference conventional-camera at different flight orientations, altitudes and times of day.

A number of different polarization image processing algorithms were evaluated. A precision kernel interpolation method developed specifically for pixilated polarization cameras was determined to best maintain the native resolution of the image sensor. A novel polarization algorithm combining intensity and polarization data was constructed that clearly outperformed all other methods evaluated.

Under good visibility conditions that were not expected to favor polarization, detection range or available evasion response time, was improved by an average of 2000 feet. Under the 250 knot closing rate conditions of this test, the increase in response time available is 4 seconds. Even under the 500 knot worst case closing rate scenario for airspace under 10,000 feet, the increased available response time is 2

**Conference 8160:
Polarization Science and Remote Sensing V**

seconds.

The tests also demonstrated that conditions that differentially favor polarization camera are significantly broader than anticipated. In particular, orthogonal sun-to-camera orientation yields clearly better results. Given the prevalence of this condition (the 70% of the day when the sun angle is not very low in the sky plus all headings either not directly toward or away from the sun when it is low in the sky) this implies that the polarization would provide improvement in optical DSA performance in the vast majority of flights.

Conference 8161: Atmospheric Optics: Turbulence and Propagation

Tuesday-Wednesday 23-24 August 2011 • Part of Proceedings of SPIE Vol. 8161
Atmospheric Optics IV: Turbulence and Propagation

8161-01, Session 1

Atmospheric scintillations and laser safety

A. Zilberman, E. Golbraikh, N. S. Kopeika, Ben-Gurion Univ. of the Negev (Israel)

Laser devices are currently in widespread use in particular by armed forces for different tasks. Electro-optical sensors as well as unprotected human eyes are extremely sensitive to laser radiation and can be permanently damaged from direct or reflected beams. Laser damage depends on the interaction between the laser beam and the atmosphere in which it traverses. The atmospheric conditions, including the range, terrain features, turbulence, and atmospheric particulates, may alter the laser's effect on different electro-optical devices and systems.

When a laser beam passes through the atmosphere the refractive index inhomogeneities or optical turbulence affect the beam. As a result, temporal intensity fluctuations (scintillations) or spatial variation in intensity within a beam cross-section occur, which give rise to a rapidly varying pattern of bright and dark patches or "hot spots" at the observation or target plane. The "hot spots" are the areas where the localized beam irradiance is greater than the average across the beam.

Atmospheric scintillations pose a safety problem because small turbulent eddies and associated scintillation spots can move in an unpredictable way within the laser beam, so that an observer or sensor can be subjected to the risk of a localized irradiance (local focusing effect) much greater than that which would occur in a non-turbulent medium.

In the present work, the influence of the atmospheric channel on laser safety is investigated by use of experimental data of laser beam propagation statistics for different scenarios and atmospheric conditions.

The results can be important in the area of laser remote sensing, wireless optical communications, and active imaging.

8161-03, Session 1

Arago spot and turbulent distortions

M. I. Charnotskii, Zel Technologies, LLC (United States)

Arago (Poisson) spot is a small bright spot that is formed in the shadow of the circular obscurer, and is typically observed on the image of the entrance pupil of the Cassegrain-type telescopes. The coherent nature of the Arago spot makes it susceptible to the turbulence-induced distortions of the incident wave. Since Arago spot is easily accessible in the common free-space optical communication system, it provides a convenient way to measure the turbulence effects on the propagation path without interfering with the principal function of the optical system.

We describe the formation of the Arago spot for the annular aperture using the Fresnel optics technique, and develop a simple equation for the field and irradiance distributions in the center of the shadow area behind an obscurer. We show that, consistent with the Fresnel zone theory, the presence of the larger aperture causes the axial irradiance oscillate along the optical axis, with Arago spots changing from the unimodal to the ring shape between the maxima and minima.

We calculate the effect of the atmospheric turbulence on the average intensity distribution in the Arago spots, and propose the axial contrast degradation as a potential measure of the turbulence perturbation. Random wander of the Arago spot caused by turbulence can be an alternative way to estimate the turbulence effects. We calculate the variance of the turbulent wander, and relate it to the turbulence structure constant distribution along the propagation path. Finally, we calculate the scintillation index on the Arago spot axis, and analyze the parameters determining the weak and strong scintillation conditions for the unimodal and ring-type Arago spots.

8161-04, Session 2

Adaptive optics solutions for turbulence mitigation in different scenarios

G. Marchi, C. Scheifling, Fraunhofer-Institut für Optronik, Systemtechnik und Bildauswertung (Germany)

Several studies on different adaptive optics concept are presented in the article.

Each of the adaptive optics procedures shows its peculiar advantages when considering different situations where the image distortion due to atmospheric or artificial turbulence becomes problematic.

A setup based on the usual wavefront reconstruction techniques using a Shack-Hartmann wavefront sensor in a closed loop with a deformable mirror and a computer is shown.

The reconstruction method follows the modal compensation which has been demonstrated to be more robust and suitable than the zonal one concerning the correction of the first Zernike polynomials. Some turbulence compensation results deriving from the studies are reported.

A second procedure based on the control of a deformable mirror through a fast iterative procedure is also treated and the relative results about the compensation of laser beams as well as extended images are also shown.

A third concept, based on holographic wavefront sensing, is also presented together with the main steps in the development and application of this promising technique.

A final part in the article describes the measurements and the characteristics of the atmospheric turbulence present in direct tests.

8161-05, Session 2

The effect of free parameter estimates on the reconstruction of images corrupted by horizontal turbulence using the bispectrum

J. Bos, M. C. Roggeman, Michigan Technological Univ. (United States)

In our previous work we quantified the performance improvement resulting from using the bispectrum to reconstruct extended scenes from image sets corrupted by atmospheric seeing over horizontal path. Here we expand on that work and explore claims in literature that image reconstruction quality using the bispectrum is relatively immune to poor estimates of the point spread function used for amplitude estimation. Similar claims have been made regarding the number of paths used in the bispectrum phase estimate. The performance bounds of each of these parameters are explored in terms of the MSE of the resulting reconstructions relative to a diffraction-limited reference image. We have found that as using more than six distinct phase paths in the bispectrum phase estimate does not result in improvement enough to justify the additional computation time. Similarly, estimates of the turbulence strength used in the inverse filter PSF may deviate from the optimum by 50% or more while incurring only a 10% reduction in MSE improvement for low to moderate turbulence conditions.

8161-06, Session 2

Simulation of extended scenes imaged through turbulence over horizontal paths

J. Bos, M. C. Roggeman, Michigan Technological Univ. (United States)

Conference 8161:
Atmospheric Optics: Turbulence and Propagation

We have developed an imaging simulator which accounts for the anisoplanatic effects encountered while imaging extended scenes over horizontal paths. Using a geometric optics approach, an extended scene is divided into discrete point source. For each point source a ray is traced through discrete Kolmogorov-turbulence phase screens toward each pixel in virtual detector. The resulting images express non-uniform tilt and distortion characteristics typical in horizontal surveillance imagery. Using this simulator several large data sets were created based on a known high-resolution source image. By utilizing turbulence corrupted image sets with a known reference image, the performance of image reconstruction techniques can be expressed in terms of common metrics such as Mean Squared Error (MSE). The MSE statistics of a single image corrupted using the simulator over three turbulence conditions are examined relative to a diffraction-limited version of the reference image. To fully explore the statistics of images created by the simulator, 1000 frames have been generated.

8161-07, Session 2

Anisoplanatic wavefront error estimation using coherent imaging

R. L. Kendrick, Lockheed Martin Advanced Technology Ctr. (United States)

We have developed a technique for extracting atmospheric turbulence induced wavefront error by means of digital holography. The technique enables wavefront error determination as a function of field angle. Closed form expressions for the anisoplanatic wavefront error caused by atmospheric turbulence have been developed for comparison. We show very good agreement between experimental data and the closed form solution. The comparison is made over Cn2 values from approximately 10-12 to 10-15 m-2/3.

8161-08, Session 3

The Advanced Navy Aerosol Model (ANAM): validation of small-particle modes

A. M. J. van Eijk, TNO Defence, Security and Safety (Netherlands); J. T. Kusmierczyk-Michulec, Institute of Oceanography (Poland); A. Demoisson, J. J. Piazzola, Univ. du Sud Toulon-Var (France)

The Advanced Navy Aerosol Model (ANAM) aims at providing an estimate of aerosol extinction in the maritime environment. Over the years, various upgrades have been implemented to accommodate the coastal zone, which is characterized by a mixture of maritime and land-originated aerosols. The present contribution reports on a validation experiment at Porquerolles Island in Southern France, specifically aiming at the validation of the smaller (continental) particle modes.

8161-09, Session 3

Optical propagation profiles for shipboard application: turbulence and extinction

B. Bachmann, S. M. Hammel, Space and Naval Warfare Systems Ctr. Pacific (United States)

We describe work that will enable the comparison of collected data to beam propagation models. Optical and meteorological data will be collected over various angles of geometry during an ongoing electro-optical field campaign. Turbulence and aerosol extinction play a critical role in the maritime environment of Navy vessels, and observed extinction estimates would serve to determine model fidelity in a shipboard engagement scenario.

8161-10, Session 3

Application of year-round atmospheric transmission data, collected with the MSRT multiband transmissometer during the FATMOSE trial in the False Bay area

A. N. de Jong, TNO Defence, Security and Safety (Netherlands)

The FATMOSE trial (False Bay Atmospheric Experiment) is a continuation of the cooperative work between TNO and IMT on atmospheric propagation and point target detection and identification in a maritime environment (South Africa). The atmospheric transmission, being of major importance for target detection, was measured with the MSRT multiband optical/IR transmissometer over a path of 15.7 km over sea. Simultaneously a set of instruments was installed on a mid-path lighthouse for collection of local meteorological data, including turbulence, scintillation, sea surface temperature and visibility. The multiband transmission data allow the retrieval of the size distribution (PSD) of the particles (aerosols) in the transmission path. The retrieved PSD's can be correlated with the weather data such as windspeed, wind direction, relative humidity and visibility. This knowledge will lead to better atmospheric propagation models. The measurement period covered nearly a full year, starting in November 2009 and ending in October 2010. The False Bay site is ideal for studies on propagation effects over sea because of the large variety of weather conditions, including high wind speed from the South East with maritime air masses as well as Northerly winds, bringing warm and dry air from the continent. From an operational point of view the False Bay area is interesting, being representative for the scenery around the African coast with warships in an active protecting role in the battle against piracy. The year-round transmission data are an important input for range performance calculations of electro-optical sensors against maritime targets. The data support the choice of the proper spectral band and contain statistical information about the ranges to be expected. In the paper details on the instrumentation will be explained as well as the methods of calibration and PSD retrieval. Data are presented for various weather conditions, showing correlations between different parameters and including statistical behaviour over the year. Examples will be shown of special conditions such as refractive gain, gravity waves and showers.

8161-11, Session 3

Scintillation measurements over False Bay, South Africa

M. van Iersel, A. M. J. van Eijk, TNO Defence, Security and Safety (Netherlands)

A commercial long-range scintillometer was deployed over a 2-km path in False Bay, South Africa, for a timeframe of more than 1 year. The turbulence data retrieved from the instrument is compared to turbulence parameters inferred from micrometeorological data and models, and the relation between experimental and model-data is explored.

8161-12, Session 4

Long-range beam propagation for single-photon communications

I. Capraro, A. Tomaello, A. Dall'Arche, P. Villorosi, Univ. degli Studi di Padova (Italy)

The optical propagation in atmosphere for links of over 100 km in length is affected by several transformations of the beam parameters, resulting in an increase of the link losses. The long range optical communication at the single photon limit exploiting the quantum protocols, on the other side, differs from the classical protocols in that the signal to be transmitted cannot be intensified, being a train of very weak pulses with an average about one photon per pulse. The understanding of the

**Conference 8161:
Atmospheric Optics: Turbulence and Propagation**

propagation induced effects in both the irradiance at the receiver as well as in the temporal statistics is crucial to assess the quality of the communication and eventually the feasibility of the link. Moreover, due to large wandering of the beam centroid, the induced losses due to decoupling of the beam with the receiver are severe.

We address in this work the propagation of optical beams in scale length of several tens to a few hundreds kilometres, introducing in the experiment the collection of the whole beam combined to the measure of local irradiance at the receiver side. In addition, with the aim to stabilize the centroid position at the receiver, the propagation of two beams forming a small mutual angle is studied in the framework of the isoplanatic angle spread for low and high orders of the beam spatial modes.

The experimental models were realized in different localities of Italian Alps as well as between Tenerife and La Palma Islands of the Canary archipelagos. The whole beam at the receiver was acquired and the scintillation analysis carried out and compared to models including the local meteorological conditions.

Our study aims to point out the optimal configuration for the optical setup for the long range quantum communications, as well as to predict the modifications of the photon statistics.

8161-13, Session 4**Impact of optical turbulence on sparse aperture imaging**

M. M. Bold, Lockheed Martin Space Systems Co. (United States)

Sparse aperture telescope arrays are increasingly being used for ground based imaging of stellar and resident space objects and for making astrometric measurements as they provide exquisite angular resolution without heroic efforts to construct very large monolithic telescopes. Still, sparse aperture arrays are impacted by optical turbulence yet in some ways they make mitigation of turbulence effects easier. This paper will survey the different approaches for sparse aperture imaging arrays, discuss the impacts of optical turbulence and approaches for mitigating optical turbulence effects.

8161-14, Session 4**Design of a differential image motion monitor for measurement of optical turbulence in support of dynamic range tests**

R. Dewees, Naval Air Warfare Ctr. Aircraft Div. (United States)

We report on the development, construction, and use of a Differential Image Motion Monitor (DIMM) for measuring optical atmospheric turbulence over static, semi-dynamic, and dynamic maritime ranges. The optical properties of the DIMM that make it suitable for such measurements will be presented along with a detailed overview of its software systems. Particular emphasis will be given to the numerical methods, image feature recognition, and learning filters implemented in the DIMM software. We conclude with examples of measurements we have taken over static desert ranges at China Lake and over dynamic ship-to-boat ranges at sea.

8161-15, Session 4**Measurement and modeling of beam wander**

S. M. Hammel, K. McBryde, Space and Naval Warfare Systems Command (United States)

We investigate the effects of beam wander on an uncorrected laser system. We use field experiments to investigate atmospheric propagation effects, and the variation in irradiance at the receiver or target position is measured in several different ways. We present appropriate models for

the beam fluctuations and discuss the comparison between model and experimental data.

8161-16, Session 4**Measurement and impact of inner scale of turbulence and temporal variation in turbulence strength**

T. J. Brennan, D. C. Mann, Optical Sciences Co. (United States)

Predictions of optical performance degradation due to turbulence, whether analytic predictions or detailed physical optics simulations, often neglect the impact of short term temporal variation in turbulence strength and the inner scale of turbulence. Typical techniques for measuring turbulence parameters are only able to capture average and long term trend data. Subsequent performance modeling is generally parameterized by r_0 without consideration of short time trending of r_0 or the impact of an inner scale. A technique for measuring short time r_0 trending from a high sample rate, high resolution Shack-Hartmann wavefront sensor will be described and illustrated with horizontal path field data. The Greenwood frequency can also be estimated. The field sensor has 32×32 Hartmann subapertures and can operate at frames rates up to 8639 frames per second. Data from this sensor are also processed with a multi-resolution measurement algorithm to estimate the Hill inner scale of turbulence. Data has been collected under a range of weak to strong turbulence conditions and illustrates both high turbulence variability and credible estimates of inner scale and Greenwood frequency.

8161-05, Session 5**Twelve mortal sins of the turbulence propagation science**

M. I. Charnotskii, National Oceanic and Atmospheric Administration (United States)

In this review paper we discuss a series of typical mistakes and omissions that are made by engineers and scientists involved in the theoretical research and modeling of the optical propagation through atmospheric turbulence.

We show how the use of the oversimplified Gaussian spectral model of turbulence delivers the completely erroneous results for the average irradiance distribution, beam wander and scintillation index. We discuss the meaning and potential dangers of the use of the quadratic structure function for modeling of the turbulent perturbations. We address a series of common misconceptions related to calculations of the average beam intensity: unnecessary use of the approximations when rigorous result is available, invalid application of the RMS beam size and M2 beam quality factor to the turbulence-distorted beams, overlooking the simple theoretical result - average beam intensity is a convolution with the turbulent Point Spread Function (PSF).

We discuss a series of misconceptions that very common in of the scintillation index calculations. We recall the history of the so-called Rytov's approximation, and show that for the optical propagation in turbulence it has no advantages compare to the perturbation theory. We will clarify the infamous misunderstanding of the Rytov's approximation: vanishing scintillation at the beam focus, and show the correct weak and strong scintillation solutions for the scintillation index at the beam focus.

We discuss the flaws of the Fried model of the short-term PSF, and reveal some more accurate PSF models. We will briefly review the propagation of the polarized optical waves through turbulence and discuss the inadequacy of the recently published calculations of the electromagnetic beams calculations. We will also address the issues related to the energy conservation principle and reciprocity that have some very important consequences for the turbulence propagation, but are frequently overlooked in the current literature.

**Conference 8161:
Atmospheric Optics: Turbulence and Propagation**

8161-06, Session 5

Direct observation of length scales in clear air turbulence

J. D. Harris, C. C. Davis, Univ. of Maryland, College Park (United States)

Light can scatter off turbulent vortex filaments in the air that have different densities and indices of refraction. These filaments, or eddies, are distributed through a turbulent air flow and their scale size represents the boundary between an energy cascade down size scales that ends in viscous energy dissipation. By examining the two point transmission spatial correlation function through a slug of steady flow turbulent air, we are capable of resolving turbulent scales down to the Kolmogorov microscale. This has been verified by a separate hotwire measurement on the same flow and comparison to hotwire data in the literature. We are measuring with high spatial and temporal precision spatial and temporal correlation functions that reveal the turbulence dynamics and inner scale in conditions of single scattering. These robust measurements are made over short path lengths in conditions of known Reynold's number and average temperature without disturbing or decorating the flow. By changing the characteristics of the air flow in a volume, different length scales can be associated with different conditions. This creates a "fingerprint" that characterizes the turbulence.

8161-07, Session 5

Experimental analysis of orbital angular momentum-carrying beams in turbulence

J. A. Anguita, J. Herreros, Univ. de Los Andes (Chile)

The study of optical vortices have gained interest for their potential use in laser communications, as they could significantly increase the photon efficiency of the communication system. Optical vortices carry orbital angular momentum (OAM), a property that is related to the azimuthal phase of the complex electric field. Because OAM eigenstates are orthogonal, an arbitrary number of bits per photon can be transmitted in principle. Vortex beams with different OAM states can be easily generated and analyzed using holographic methods and this fact may stimulate the achievement of FSO communication systems with very high photon efficiencies.

In a laboratory experiment we generate, propagate, and detect laser vortex beams carrying OAM by means of computer-controlled spatial light modulators (SLM). We demonstrate that beams with OAM states from -10 to +10 can be effectively generated using different types of phase gratings, and that the generated beams keep their structure as they propagate. A turbulent air flow is induced on the propagation path using a hot plate to emulate the effects of atmospheric turbulence. The fast motion of the distorted beams is recorded with a CCD camera at high-frame rates to observe the effects of optical turbulence on the beams properties, such as radius, axial displacement, and phase structure. We analyze these attributes as they change over time, as well as we evaluate their long-term features. We show that the beam's axis displacement induced by turbulence decreases as the OAM state increases. We are working towards an effective transmitter/receiver architecture to enable the use of OAM in a modulation/multi-user scheme.

8161-18, Session 5

Atmospheric channel transfer function estimation from experimental free-space optical communications data

C. N. Reinhardt, Space and Naval Warfare Systems Command (United States); Y. Kuga, J. A. Ritcey, A. Ishimaru, Univ. of Washington (United States); S. M. Hammel, D. Tsintikidis, Space

and Naval Warfare Systems Command (United States)

The performance of terrestrial free-space optical communications systems is severely impaired by atmospheric aerosol particle distributions where the particle size is on the order of the operating wavelength. For optical and near-infrared wavelengths, fog droplets cause severe multiple-scattering and absorption effects which rapidly degrade received symbol detection performance as the optical depth parameter increases (visibility decreases). Using a custom free-space optical communications system we acquired field data for the transmitted and received signals in fog for a range of optical depths within the multiple-scattering regime. We use statistical estimation theory and stochastic analysis to derive estimators for the atmospheric channel transfer function and the related coherency function, which we then compute directly from the experimental data. We discuss the characteristics of the resulting channel transfer function estimates in terms of the physics of the atmospheric propagation channel. We investigate the behavior of the transfer function estimator using both real field-test data and simulated propagation data based on field-test conditions. We then compare the channel transfer function estimates against the predictions computed using a radiative-transfer theory model-based approach which we also developed for the free-space optical atmospheric channel.

8161-21, Session 5

Experimental generation of non-Kolmogorov turbulence with a liquid crystal spatial light modulator

I. Toselli, B. N. Agrawal, Naval Postgraduate School (United States); C. C. Wilcox, S. Restaino, U.S. Naval Research Lab. (United States)

Several experiments showed that the classical Kolmogorov power spectral density of the refractive-index sometimes does not properly describe the statistics of the atmosphere. In this paper we describe an experimental testbed able to generate non-classical Kolmogorov turbulence by using a liquid crystal spatial light modulator. The testbed is used at Naval Postgraduate School for laboratory investigation of laser beam propagation in maritime environment where a power law different from classical Kolmogorov, $11/3$, could be present. Applications of this testbed are ship to-ship free space optical communication, imaging and high energy laser weapons.

8161-19, Poster Session

Computation on propagation of the femtosecond laser pulses in air by phase screen method

P. Zou, J. Zu, X. Zhou, Shanghai Institute of Optics and Fine Mechanics (China)

The propagation and split of the filamentation of femtosecond pulses in air have been paid much attention since last a few years, however, most research works are performed without considering the turbulence effects of atmosphere due to the difficulties of utilizing analytical solutions and experiment conditions. In this paper, we will attempt to introduce a kind of numerical simulation method to analyze the transmission features of femtosecond laser pulses in turbulent air, namely, it is called multi-phase screen method which use phase screen to simulate atmospheric turbulence. The laser parameters in this presentation are as follows: 85 fs and 3.5 TW operating at 800 nm. Then some simulating results are discussed by comparing with some others works, such as irregular shapes of focal spot. Finally, in order to control the propagation or split of the filaments, some different types of phase plates are applied, although the lengthening of laser pulses propagating distance is not achieved, on the contrary, a speeding split and an exchange of energy flow are firstly observed that it is potentially helpful to other works.

8161-20, Poster Session

An investigation into the Paulding Mystery Lights

J. Bos, M. C. Roggeman, W. C. Norkus, Jr., M. A. Maurer, D. A. Sims, C. T. Middlebrook, Michigan Technological Univ. (United States)

The Paulding Mystery Light is a purportedly unexplained optical phenomenon, occurring nightly, deep in the woods of Michigan's Upper Peninsula. Each evening up to a hundred spectators gather at the end of a washed out road to observe the flickering light. In local legends, the origin of the light is often attributed to the paranormal. As a student-run research project The Michigan Tech Student Chapter of the SPIE initiated a project in 2008 to understand the cause of the Paulding Lights. A team was formed pairing graduate and undergraduate researchers and under guidance from faculty. Previous investigations by paranormal skeptics attributed the lights to automobile headlights though the exact source location was not identified. These investigators also failed to address claims that the light appeared to move or dance along the horizon. Our team applied a number of techniques toward identifying and then verifying the source location of the Paulding Light. Beginning with observation through a telescope, the team moved to using tools such as detailed topographical maps and more common tools such as Google Street View to identify a candidate source location. The candidate source location was then validated by first, recreating the light using a stopped vehicle. Additional verification was achieved by recording the traffic flow at the source location and examining the correlations both heuristically and stochastically. A spectrometer was also brought to bear on the light allowing the team to compare the spectrum of the Paulding light to the spectrum of various automotive headlamps. Our findings, presented here, indicate that the source of the Paulding light is automobile traffic on a stretch of road about 7 km from the viewing location. This conclusion is supported overwhelmingly by the data we have collected. In addition to our findings, we also provide some speculation on the cause of the more spectacular claims surrounding these mystery lights and possibilities for future work.

Conference 8162: Free-Space and Atmospheric Laser Communications XI

Wednesday-Thursday 24-25 August 2011 • Part of Proceedings of SPIE Vol. 8162
Free-Space and Atmospheric Laser Communications XI

8162-01, Session 1

Lunar optical wireless communication and navigation network for robotic and human exploration

S. Arnon, Ben-Gurion Univ. of the Negev (Israel)

Robotic exploration can improve lunar missions, increase crew productivity and reduce operational risks and cost. Broadband communication, together with location & orientation acquisition are fundamental parameters in space expeditions. We propose an optical wireless laser communication (LC) system, which provides high data-rates, that is integrated with an accurate ranging and direction finding system. In addition LC will not contaminate the moon with unwanted RF signals that could interfere with scientific measurement. The project's main goal is to examine the theoretical background and the engineering feasibility of an optical wireless communication system and an optical positioning system for ground units on the moon. This project is part of Israeli collaboration with NASA lunar science institute.

8162-02, Session 1

Lightweight, mobile free-space optical communications in disaster scenarios for transmission of Earth observation data: feasibility study

O. Topcu, L. Grobe, Technische Univ. Ilmenau (Germany); H. Henniger, Deutsches Zentrum für Luft- und Raumfahrt e.V. (Germany) and Technische Univ. Ilmenau (Germany) and Codex GmbH & Co. KG (Germany); M. Haardt, Technische Univ. Ilmenau (Germany)

Free-space optical (FSO) links are an effective alternative to radio frequency (RF) links to handle high-rate data transmission in case of a general communication service failure in disaster scenarios. Establishing high data rate links under the impacts of extreme environmental conditions, like the unregulated RF spectrum, is a very challenging issue. This paper focuses on quadcopter based earth observation system designs. Its main objective is to show that FSO communication can provide a high-rate link for dumping earth observation data from a quadcopter to a ground-station, even under disaster conditions. Before analyzing the feasibility of such an optical quadcopter downlink system, the main system structure of the FSO link will be discussed in detail. Several system designs will be compared and evaluated based on link budget calculations. In this process, a novel Grating Light Valve (GLV) retro-reflector modulator technology will be introduced in this work. The study will emphasize that a reliable 100 Mbit/s FSO data transmission will be feasible to provide necessary downlink capacity for quadcopter based earth observation systems.

8162-03, Session 1

Improved climatological characterization of optical turbulence for free-space optical communications

B. D. Felton, R. J. Alliss, Northrop Grumman Corp. (United States)

Optical turbulence (OT) acts to distort light in the atmosphere, degrading the quality of service of free-space optical communications links. Some

of the degradation due to turbulence can be corrected by adaptive optics. However, the severity of OT, and thus the amount of correction required, can vary considerably from location to location. Therefore, it is vital to understand the climatology of OT at locations of interest. In many cases, it is impractical and expensive to deploy instrumentation to characterize the climatology of OT, making simulations a less expensive and convenient alternative.

The strength of OT is characterized by the refractive index structure function C_n^2 . While attempts have been made to estimate C_n^2 using empirical models, C_n^2 can be calculated more directly from Numerical Weather Prediction (NWP) simulations using pressure, temperature, thermal stability, vertical wind shear, turbulent Prandtl number, and turbulence kinetic energy (TKE). In this work, we use the Weather Research & Forecast (WRF) NWP model to generate C_n^2 climatologies in the planetary boundary layer and free atmosphere, allowing for both point-to-point and ground-to-space estimates of the Fried Coherence length (r_0) and other seeing parameters.

Nearly two years of simulations have been performed over various regions including the Desert Southwest and Haleakala and Mauna Kea on Hawaii. The results, which have shown good agreement with in situ turbulence measurements, are being used to assist engineers in free-space optical system design and site selection studies. Results of these simulations including comparisons with in situ measurements will be presented at the conference.

8162-05, Session 2

Twelve mortal sins of the turbulence propagation science

M. I. Charnotskii, National Oceanic and Atmospheric Administration (United States)

In this review paper we discuss a series of typical mistakes and omissions that are made by engineers and scientists involved in the theoretical research and modeling of the optical propagation through atmospheric turbulence.

We show how the use of the oversimplified Gaussian spectral model of turbulence delivers the completely erroneous results for the average irradiance distribution, beam wander and scintillation index. We discuss the meaning and potential dangers of the use of the quadratic structure function for modeling of the turbulent perturbations. We address a series of common misconceptions related to calculations of the average beam intensity: unnecessary use of the approximations when rigorous result is available, invalid application of the RMS beam size and M2 beam quality factor to the turbulence-distorted beams, overlooking the simple theoretical result - average beam intensity is a convolution with the turbulent Point Spread Function (PSF).

We discuss a series of misconceptions that very common in of the scintillation index calculations. We recall the history of the so-called Rytov's approximation, and show that for the optical propagation in turbulence it has no advantages compare to the perturbation theory. We will clarify the infamous misunderstanding of the Rytov's approximation: vanishing scintillation at the beam focus, and show the correct weak and strong scintillation solutions for the scintillation index at the beam focus.

We discuss the flaws of the Fried model of the short-term PSF, and reveal some more accurate PSF models. We will briefly review the propagation of the polarized optical waves through turbulence and discuss the inadequacy of the recently published calculations of the electromagnetic beams calculations. We will also address the issues related to the energy conservation principle and reciprocity that have some very important consequences for the turbulence propagation, but are frequently overlooked in the current literature.

Conference 8162:
Free-Space and Atmospheric Laser Communications XI

8162-06, Session 2

Direct observation of length scales in clear air turbulence

J. D. Harris, C. C. Davis, Univ. of Maryland, College Park (United States)

Light can scatter off turbulent vortex filaments in the air that have different densities and indices of refraction. These filaments, or eddies, are distributed through a turbulent air flow and their scale size represents the boundary between an energy cascade down size scales that ends in viscous energy dissipation. By examining the two point transmission spatial correlation function through a slug of steady flow turbulent air, we are capable of resolving turbulent scales down to the Kolmogorov microscale. This has been verified by a separate hotwire measurement on the same flow and comparison to hotwire data in the literature. We are measuring with high spatial and temporal precision spatial and temporal correlation functions that reveal the turbulence dynamics and inner scale in conditions of single scattering. These robust measurements are made over short path lengths in conditions of known Reynolds number and average temperature without disturbing or decorating the flow. By changing the characteristics of the air flow in a volume, different length scales can be associated with different conditions. This creates a "fingerprint" that characterizes the turbulence.

8162-07, Session 2

Experimental analysis of orbital angular momentum-carrying beams in turbulence

J. A. Anguita, J. Herreros, Univ. de Los Andes (Chile)

The study of optical vortices have gained interest for their potential use in laser communications, as they could significantly increase the photon efficiency of the communication system. Optical vortices carry orbital angular momentum (OAM), a property that is related to the azimuthal phase of the complex electric field. Because OAM eigenstates are orthogonal, an arbitrary number of bits per photon can be transmitted in principle. Vortex beams with different OAM states can be easily generated and analyzed using holographic methods and this fact may stimulate the achievement of FSO communication systems with very high photon efficiencies.

In a laboratory experiment we generate, propagate, and detect laser vortex beams carrying OAM by means of computer-controlled spatial light modulators (SLM). We demonstrate that beams with OAM states from -10 to +10 can be effectively generated using different types of phase gratings, and that the generated beams keep their structure as they propagate. A turbulent air flow is induced on the propagation path using a hot plate to emulate the effects of atmospheric turbulence. The fast motion of the distorted beams is recorded with a CCD camera at high-frame rates to observe the effects of optical turbulence on the beams properties, such as radius, axial displacement, and phase structure. We analyze these attributes as they change over time, as well as we evaluate their long-term features. We show that the beam's axis displacement induced by turbulence decreases as the OAM state increases. We are working towards an effective transmitter/receiver architecture to enable the use of OAM in a modulation/multi-user scheme.

8162-18, Session 2

Atmospheric channel transfer function estimation from experimental free-space optical communications data

C. N. Reinhardt, Space and Naval Warfare Systems Command (United States); Y. Kuga, J. A. Ritcey, A. Ishimaru, Univ. of Washington (United States); S. M. Hammel, D. Tsintikidis, Space

and Naval Warfare Systems Command (United States)

The performance of terrestrial free-space optical communications systems is severely impaired by atmospheric aerosol particle distributions where the particle size is on the order of the operating wavelength. For optical and near-infrared wavelengths, fog droplets cause severe multiple-scattering and absorption effects which rapidly degrade received symbol detection performance as the optical depth parameter increases (visibility decreases). Using a custom free-space optical communications system we acquired field data for the transmitted and received signals in fog for a range of optical depths within the multiple-scattering regime. We use statistical estimation theory and stochastic analysis to derive estimators for the atmospheric channel transfer function and the related coherency function, which we then compute directly from the experimental data. We discuss the characteristics of the resulting channel transfer function estimates in terms of the physics of the atmospheric propagation channel. We investigate the behavior of the transfer function estimator using both real field-test data and simulated propagation data based on field-test conditions. We then compare the channel transfer function estimates against the predictions computed using a radiative-transfer theory model-based approach which we also developed for the free-space optical atmospheric channel.

8162-21, Session 2

Experimental generation of non-Kolmogorov turbulence with a liquid crystal spatial light modulator

I. Toselli, B. N. Agrawal, Naval Postgraduate School (United States); C. C. Wilcox, S. Restaino, U.S. Naval Research Lab. (United States)

Several experiments showed that the classical Kolmogorov power spectral density of the refractive-index sometimes does not properly describe the statistics of the atmosphere. In this paper we describe an experimental testbed able to generate non-classical Kolmogorov turbulence by using a liquid crystal spatial light modulator. The testbed is used at Naval Postgraduate School for laboratory investigation of laser beam propagation in maritime environment where a power law different from classical Kolmogorov, $11/3$, could be present. Applications of this testbed are ship to-ship free space optical communication, imaging and high energy laser weapons.

8162-04, Poster Session

Control analysis of acquirement and locking in inter-satellite laser communications

W. Lu, J. Sun, Y. Zhou, Y. Wu, A. Yan, E. Dai, Y. Zhi, L. Liu, Shanghai Institute of Optics and Fine Mechanics (China)

Process of acquirement and locking-up of complex axis system in inter-satellite laser communication has been studied. The effect of different condition parameters on the process of acquirement and locking-up have also been researched and simulated. Simulation results show that when the system with appropriate bandwidth has been adopted, both fine pointing system and coarse pointing system can satisfy three requirements of step response, stability criterion and dwell time and then finish the acquirement and locking-up of beacon laser beam. The simulation results provide the suited condition parameters for both fine pointing system and coarse pointing system, which is very helpful to the subsequent point and tracking processes.

8162-24, Poster Session

An aperture-matched phase-compensated differential phase shift keying receiver with a 90° hybrid

Z. Luan, Y. Zhou, Y. Zhi, E. Dai, J. Sun, L. Liu, Shanghai Institute of Optics and Fine Mechanics (China)

Space to ground laser communication is limited by the effects of atmosphere. Differential phase shift keying (DPSK) is suited for high data rate space to ground communication links due to its immunity of the wave front of a beam passing atmospheric turbulence, which carry the information in optical phase changes between bits. The benefit of DPSK over OOK is the 3 dB lower optical signal to noise ratio to reach a given bit error rate (BER) using a balanced receiver. An aperture-matched phase-compensated DPSK receiver with a 90° hybrid is proposed here. The receive optics are based on free-space optics. A Mach-Zehnder delay interferometer is used for differential delay which is equal to the bit period. The input pupil is imaged onto the same place by two afocal systems composed of 4f imaging lenses. The optical path difference is stabilized to a fraction of the wavelength with a fine phase adjustment which is measured by a 2x4 90° optical hybrid and closed loop electric circuit. The design and experiments are given in this paper.

8162-25, Poster Session

Designing and implementation of free-space optical communication link for last mile solution

A. Sharma, R. S. Kaler, R. Kaler, Thapar Univ. (India)

A Free Space Optical (FSO) Laser Communication Link is presented. We deal with the development of a full-duplex FSO transceiver. Experimental results explain the performance of the completed system and offer methods of maximizing efficiency of such FSO-based communication systems. We have discussed and analyzed the details technical issues related to FSO deployment in context of India. Several parameters need to analyze the performance of FSO transmission. The external parameters are the non-system-specific parameters which are related to the environment and cannot be influenced by the designer, such as the climatology of the installation location, atmospheric attenuation, scintillation, window loss, and pointing loss.

We have present simplified link budgets for non tracking and automatic tracking systems. It is interesting to note the improvement in link margin that can be obtained by use of an automatic tracking system.

8162-26, Poster Session

Ghost imaging of a Gaussian Schell pulse beam propagation in a slant non-Kolmogorov turbulent channel

Y. Zhang, Jiangnan Univ. (China)

Lensless ghost imaging with Gaussian Schell-mode pulses beam through a slant non-Kolmogorov turbulent atmosphere channel has been studied, based on the optical coherent theory and the extended Huygens-Fresnel integral. The analytical ghost-imaging formulas have been derived by the approximation of the form of spatial-temporal coherence function of the laser field in the product of the spatial and temporal coherence function, and the quadratic approximation of the wave structure function. Based on these formulas, we find that the image quality is influenced by the turbulence strength, the propagation distance, the zenith angle of communication channel, the fractal constant of the non-Kolmogorov power spectrum of atmospheric turbulence, the pulse duration of source and the coherent parameters of the partially coherent light.

8162-27, Poster Session

Analysis of facular orientation deviation during tracking and pointing in the intersatellite laser communication

B. Shen, J. Sun, Y. Zhou, B. Li, L. Pu, L. Liu, Shanghai Institute of Optics and Fine Mechanics (China)

The facular orientation during tracking and pointing in the intersatellite laser communication dominates the tracking accuracy, so it is crucial to the establishment of optical communication link. While the redistribution of the facular energy, caused by atmospheric turbulence in inter-satellite laser communication, makes it difficult to orientate the barycenter of the facula detected by the charge-coupled device, influencing the pointing accuracy finally. Therefore, it is necessary to analyse the orientation deviation in advance to provide reference to practical experiment and verification.

First of all, using a charge-coupled device, the influence of the facular energy to the orientation is studied through simulation. And then a Kolmogorov phase screen generated with modified inverse fast Fourier transform is used to simulate the effect of atmospheric turbulence. Using a charge-coupled device, the influences of time-dependent atmospheric turbulence intensity to the orientation deviation and the size of the charge-coupled device to the orientation deviation are analysed respectively. The simulated results offer significant practical benefits to the intersatellite laser communication.

8162-28, Poster Session

Simple phase-shifting method in Jamin double-shearing interferometer for testing of diffraction-limited wavefront

L. Wang, L. Liu, Z. Luan, J. Sun, Y. Zhou, Shanghai Institute of Optics and Fine Mechanics (China)

In the inter-satellite laser communication, a diffraction-limit wavefront is required. To test the wavefront, we have developed a Jamin double-shearing interferometer. The interferometer is consists of two Jamin plates to form lateral shearing and four wedge plates to divide the aperture. To improve the measurement accuracy of the wavefront, phase-shifting must be introduced to reduce its detectable wave-front height. For the interferometer, simple phase-shifting methods by laterally moving four wedge plates or one Jamin plate are proposed in this paper. When the wedge plates are laterally moved, the phase difference of two interferometric beams is changed to form phase shifting. If the first Jamin plate is laterally moved, two emitted beams are laterally shifted to change the incidence position on the wedge plates. The relation between the phase-shifting amount and the lateral displacement of the wedge plates or the Jamin plate is calculated. The lateral displacement for the phase unwrapping with four-step phase-shifting algorithm can be obtained. To avoid strict phase-shifting amount of 90 degrees, four wedge plates or one Jamin plate can also be laterally moved in five steps with equal interval and the phase can be unwrapped using the five-step phase-shifting algorithm. In experiments, phase-shifting interference patterns are obtained and analyzed. The usefulness of these simple phase-shifting methods is verified.

8162-29, Poster Session

Influence of laser beam profiles on received power fluctuation

L. Dordova, O. Wilfert, Brno Univ. of Technology (Czech Republic)

In an optical wireless link the laser beam carrying the information is propagating through the atmosphere. The situation is different if the

**Conference 8162:
Free-Space and Atmospheric Laser Communications XI**

optical communication is proceeding in a horizontal direction (e.g. the transmitter and the receiver are placed on a fixed building) or when it is proceeding vertically (e.g. communication between ground station and HAP). In both cases it is necessary to know the characteristics of the atmosphere. Phenomenon of extinction, which causes optical signal attenuation, and atmospheric turbulence, generated by temperature inhomogeneities causing scintillation, are two main negative effects influencing optical signal quality.

Gaussian beam is very often used for the transmission of information in optical wireless links. The usage of this optical beam has its advantages and, of course, disadvantages. This work focuses on possibilities of using laser beams with different distribution of optical intensity (e.g. Top Hat, central and boundary beam). Creation of the optical beams with selected optical intensity profiles will be described. Geometrical parameters of particular beams will be compared with the Gaussian beam. Optical beams will propagate through the "clear" and stationary atmosphere in the experimental part of this work. These results will be compared with the data obtained after a laser beam is passed through the turbulent and attenuated atmosphere. We will use an ultrasound fog generator for laser beam attenuation testing. To create the turbulence, infra radiators will be applied. Particular results obtained from different atmospheric conditions will be compared and using different types of optical beams will be assessed.

8162-30, Poster Session**Acquisition strategy for the satellite laser communications under the laser terminal scanning errors situation**

J. Sun, L. Liu, W. Lu, A. Yan, Y. Zhou, Shanghai Institute of Optics and Fine Mechanics (China)

Acquisition strategy is very important during the inter-satellite laser communications systems. Spatial acquisition of the companion terminals using very narrow beacon laser beams is a very difficult task especially under the laser terminal scanning errors situation. Acquisition is a statistical process. In this paper, we detailed the optimized scanning overlap factor of the beacon laser beam which depends on the scanning accuracy of the laser terminals.

8162-31, Poster Session**Influence of optical elements on the laser beam profile**

O. Wilfert, Z. Kolka, J. Poliak, Brno Univ. of Technology (Czech Republic)

In an optical wireless link the optical signal is transmitted by optical beams. The resistance of signal transmission to atmospheric phenomena is possible to solve partially by means of the special optical intensity distribution at the beam spot, i.e. by means of the special beam profile. In practice the resultant beam profile can be a surprise for users of the link if only computer models of the optical beams are used and any diffraction effect at the transmitting lens is not considered. The transmitted beam is generally given by the diffraction integral which is mathematical description of Huygens-Fresnel principle.

On the basis of Huygens-Fresnel principle it's possible to calculate the waves in a point of the receiver plane as a sum (or integral) of spherical waves coming from all individual points of transmitting aperture. It is not easy to calculate the diffraction integral namely if intensity distribution on the transmitting aperture is not constant, the spot is not circular symmetrical, and the receiver is located in near field. Let us assume the circular symmetrical beam with the constant intensity distribution at the transmitting aperture. In the receiving plane we obtain intensity distribution (so called diffraction pattern) which depends on the link range, diameter of transmitting lens, and the wavelength. We can see minima and maxima in the diffraction pattern at the receiving aperture which causes difficulties when aiming the link.

Two models of diffraction of optical beam radiated from the optical transmitter are presented and two methods of beam modeling are clarified (the method based on Bessel function integrating and the method based on FFT). Confirmation of the models elaborated is a part of the contribution.

8162-32, Poster Session**Power budget model for indoor wireless optical link**

O. Wilfert, P. Hrbakova, Brno Univ. of Technology (Czech Republic)

In an indoor optical wireless link laser beam carrying the information propagates through a room and reflects on walls and various objects. Multiple reflections and multipath distortions occur when using this link. A power budget of the indoor optical wireless link includes not only the transmitted and received power but also reflection and placement losses. The directional properties of surface reflectivity are characterized by directional reflectance of surface.

The power budget of the indoor optical wireless link and a model of the surface reflectivity are presented in the contribution. The surface reflectivity includes both diffusive and specular components. Model of the surface reflectivity is a part of the power budget of the link. The directional properties of the surface reflectivity are simulated by a special mathematical function characterizing the reflectivity and directional reflectance of surface.

The model presented in the article allows us to assess the link communication quality and make a wall surface design. In the last part of the contribution an experimental work is presented and verification of the model proposed is demonstrated.

8162-33, Poster Session**Decoding nonsystematic Reed-Solomon codes using the Berlekamp-Massey algorithm**

T. Lin, T. Truong, I-Shou Univ. (Taiwan)

It is well-known that the Euclidean algorithm can be used to find the systematic errata-locator polynomial and the errata-evaluator polynomial simultaneously in Berlekamp's key equation that is needed to decode a Reed-Solomon (RS) codes. In this paper, a simplified decoding algorithm to correct both errors and erasures is used in conjunction with the Euclidean algorithm for efficiently decoding nonsystematic RS codes. In fact, this decoding algorithm is an appropriate modification to the algorithm developed by Shiozaki and Gao. Based on the ideas presented above, a fast algorithm described from Blahut's classic book is derived and proved in this paper to correct erasures as well as errors by replacing the Berlekamp-Massey (BM) algorithm with the Euclidean algorithm.

Moreover, the simple decoding algorithm proposed in this paper is based on the fact that the codeword used in Euclid's algorithm is a nonsystematic RS code so that Truong et al's algorithm can be modified to solve the key equation for the errata-locator polynomial. Then it uses the recursive extension to compute the remaining unknown syndromes. Finally, the message symbols are thus obtained by only subtracting all known syndromes from the coefficients of the corrupted information polynomial. In other words, a polynomial division used to evaluate the messaging polynomial in the Lin-Chen-Truong (LCT) algorithm [1] can be replaced by a recursive extension and a simple addition. The speed of the new Euclidean-algorithm-based decoding approach is shown to be slightly faster than that of the LCT algorithm. Actually, a further reduction in the number of arithmetic operations of the algorithm mentioned above can be achieved by using the BM algorithm [2-6] instead of Euclid's algorithm. It can also be utilized to find the errata-locator polynomial from Berlekamp's key equation provided that the message vector has the same format as the one given previously. In fact, the decoder depicted in the seconding block algorithm in Fig 9.2 of Reference 17 is of the general derivation from the frequency-domain point of view. The derivation of the

Conference 8162:
Free-Space and Atmospheric Laser Communications XI

algorithm was missing in the literature. The advantage of the proposed decoding algorithm is that the separate computation of the Forney syndrome polynomial and the error-evaluation polynomial usually needed in the RS decoder using Euclid's algorithm is completely avoided. Simulation results show that this new decoder is considerably faster in computational time than those of existing efficient algorithms including the one using Euclid's algorithm proposed in this paper for correcting both errors and erasures of nonsystematic RS codes over GF(2^m). It is expected that this fast decoding method may be adapted to the Chase algorithm [7], a soft-decision decoding, for RS codes.

8162-34, Poster Session

Two-dimensional Doppler imaging experiment for reflective tomography laser radar

X. Jin, J. Sun, Y. S. Yan, L. Liu, Shanghai Institute of Optics and Fine Mechanics (China)

Doppler-resolved reflective tomography using single-frequency continuous lasers has been shown to be an image reconstruction which can be used to recover image information about an object with a non-imaging laser radar system. This paper presents a continuous heterodyne laser radar experimental system for Doppler imaging in reflective tomography techniques. The resulting time-dependent return signal is collected by a non-imaging optical system, which provides a one dimensional signal about the target as a function of Doppler frequency after the short time FFT at each view. Then the Filtered back-projection or Radon-Fourier transform algorithm can be used to reconstruct the target from these one dimensional signals at different views. Compared with the imaging results reported by R. M. Marino in MIT Lincoln laboratory, the innovation in our experiments is that the imaging result is the whole region covering the target, not only the outline of the target. Due to the simplification in configuration and operations without involving signal phrase processing, this technique has a great potential for applications in extensive Laser radar imaging fields.

8162-35, Poster Session

Two-dimensional image construction for range-resolved reflective tomography laser radar

Y. S. Yan, J. Sun, X. Jin, L. Liu, Shanghai Institute of Optics and Fine Mechanics (China)

Range-resolved reflective tomography is one of the most effective high-resolution imaging methods for laser sensing and imaging technologies. In experiments reported earlier by MIT Lab, only the outline of the target was recovered using reflective tomography algorithm. In our experiment, we adopted a novel imaging method which can get an imaging result of the whole region covering the target. A target of letter "E" was placed on a plane with a tilt angle to the horizontal plane and rotated about the axis perpendicular to it, the target was illuminated by parallel light pulses, the range-dependent return signal is collected by a non-imaging optical system. Filtered back-projection and Radon-Fourier transform algorithm were used to reconstruct the target, then we got a image result which has clear description of the target. After that, the imaging quality and resolution of this new approach are discussed. Our experiment system reported in this paper can achieve high imaging quality in real two-dimension image construction using reflective tomography algorithm, thus it has a great practical significance for applications in extensive imaging fields.

8162-08, Session 3

Optical scintillation measurements in a desert environment I: direct links

C. I. Moore, R. Mahon, M. R. Suite, W. S. Rabinovich, M. Ferraro, H. R. Burris, Jr., L. M. Wasiczko Thomas, U.S. Naval Research Lab. (United States)

Optical scintillation is an effect that limits the performance of many optical systems including imagers and free space optical communication links. While there is a great deal of theoretical modeling of these effects, there is much less experimental data. The Naval Research Laboratory is undertaking a series of measurement campaigns of optical scintillation in a variety of environments. In December of 2010 measurements were made over a one week period in the desert at China Lake, CA. The NRL TATS system was used to measure time resolved scintillation over a variety of different ranges and terrains. Simultaneous weather data was also taken. In this paper we present an analysis of this data for direct lasercom links including scintillation index, power spectral density and probability distribution functions. Data was taken from sunrise to sunset with scintillation ranging from weak to saturated. The correlation of scintillation with weather and time of day will also be quantified.

8162-09, Session 3

Optical scintillation measurements in a desert environment II: retroreflector links

R. Mahon, C. I. Moore, W. S. Rabinovich, M. R. Suite, M. Ferraro, H. R. Burris, Jr., L. M. Wasiczko Thomas, U.S. Naval Research Lab. (United States)

Optical scintillation is an effect that limits the performance of many optical systems including imagers and free space optical communication links. The Naval Research Laboratory is undertaking a series of measurement campaigns of optical scintillation in a variety of environments. In December of 2010 measurements were made over a one week period in the desert at China Lake, CA. The NRL TATS system was used to measure time resolved scintillation over a variety of different ranges and terrains. Simultaneous weather data was also taken. In this paper present an analysis of scintillation effects on retroreflector links. Scintillation index, power spectral density and probability distribution functions were measured. The effects of weather, range and terrain are studied. Also we examine the effects of aperture averaging using multiple retroreflectors and the backscatter enhancement effect.

8162-10, Session 3

Optical scintillation measurements in a desert environment III: high-speed imaging of scintillation

R. Mahon, C. I. Moore, W. S. Rabinovich, M. R. Suite, M. Ferraro, H. R. Burris, Jr., L. M. Wasiczko Thomas, U.S. Naval Research Lab. (United States)

Optical scintillation is an effect that limits the performance of many optical systems including imagers and free space optical communication links. The Naval Research Laboratory is undertaking a series of measurement campaigns of optical scintillation in a variety of environments. In December of 2010 measurements were made over a one week period in the desert at China Lake, CA. The NRL TATS system was used to image optical scintillation at the pupil plane of a receiver. A high speed infrared camera allowed imaging at rates of several hundred Hertz enabling scintillation to be resolved both spatially and temporally. Analysis of this data allows estimation of coherence radii, aperture averaging effects and the spatial frequency of scintillation.

Conference 8162:
Free-Space and Atmospheric Laser Communications XI

8162-11, Session 3

Optical scintillation measurements in a desert environment IV: simulated effects of scintillation on communications links

M. R. Suite, W. S. Rabinovich, C. I. Moore, R. Mahon, M. Ferraro, H. R. Burris, Jr., L. M. Wasiczko Thomas, U.S. Naval Research Lab. (United States)

Optical scintillation is an effect that limits the performance of many optical systems including imagers and free space optical communication links. The Naval Research Laboratory is undertaking a series of measurement campaigns of optical scintillation in a variety of environments. In December of 2010 measurements were made over a one week period in the desert at China Lake, CA. The NRL TATS system was used to measure time resolved scintillation over a variety of different ranges and terrains. This data has been used to determine fade rate and duration as a function of weather and link margin. Temporal correlation of fades has also been calculated. This data allows simulation of a variety of communication protocols and the effects of those protocols on link throughput. In this paper we present a comparison of different protocols for both direct and retroreflector links

8162-12, Session 4

Combined optical modulating retroreflector/radio frequency Ethernet link for controlling small robots

W. S. Rabinovich, J. L. Murphy, M. R. Suite, U.S. Naval Research Lab. (United States); W. T. Freeman, Smart Logic, Inc. (United States); M. Ferraro, R. Mahon, U.S. Naval Research Lab. (United States); K. A. Hacker, S. Reese, Naval Explosive Ordnance Disposal Technology Div. (United States)

Small, tele-operated, robots often use radio frequency based Ethernet links for control and for relaying video images back to an operator. These robots must sometimes work in noisy RF environments in which these links fail. Previous work has shown that a free space optical link using modulating retroreflectors can replace the RF link and allow operation in this kind of environment. However, free space optical links are inherently line-of-sight. Many applications require the robot to be able to maneuver to positions that are not within line-of-sight. In this work we demonstrate a serially combined FSO-RF link that allows non-line-of-sight operation. In these links an optical interrogator communicates to a pod carrying modulating retroreflectors at ranges up to 1 km. The pod also carries an RF transceiver and can be dismounted from the robot. When the robot needs to move out of line-of-sight, it can dismount the pod. The Ethernet link then flows serially from the interrogator to the pod over free space optical and then, over shorter distances, from the pod to the robot over RF. Details of the design and performance of the system will be presented.

8162-13, Session 4

InGaAs avalanche photodiode arrays for simultaneous communications and tracking

M. Ferraro, W. S. Rabinovich, J. L. Murphy, R. Mahon, H. R. Burris, Jr., L. M. Wasiczko Thomas, U.S. Naval Research Lab. (United States); W. T. Freeman, Smart Logic, Inc. (United States)

Free space optical communication uses photodetectors for two purposes: as communications receivers and, in the form of a quadrant cell or a position sensitive detector, for tracking. Generally two separate detectors are used. In this work we describe combining these functions into one device through the use of heterostructure avalanche photodiode

(APD) arrays. Combined functionality more efficiently uses the available light and allows for large area communications detector arrays that maintain the bandwidth and sensitivity of smaller, single-element, arrays. In this paper we describe a prototype 2x2 arrays and associated electronics and processing. The design tradeoffs in balancing both functions are explored and future geometries that are more effective than square arrays are described.

8162-14, Session 4

Design and implementation of pan-tilt FSO transceiver gimbals for real-time compensation of platform disturbances using a secondary control network

J. Rzasa, S. D. Milner, C. C. Davis, Univ. of Maryland, College Park (United States)

FSO systems are highly directional, and a robust system is required to keep two transceivers aligned, even when both are on moving platforms. To date, most systems have used fast steering mirrors and coarse pan-tilt platforms tied to a feedback loop based on received optical power to accomplish this task. This approach can encounter problems if the alignment of one of the transceivers is severely disrupted, or is obstructed (possibly by the geometry of an airborne platform). In developing systems for air- or space-borne FSO networks, a robust way is needed to keep the entire array of FSO platforms aligned with minimal packet loss. In this paper, we present an approach to this problem using a secondary, low data-rate, omni-directional RF network that disseminates pointing commands to all the platforms in the network, so that if the main FSO channels are disrupted, the network can recover much more quickly than if a purely RSSI-based approach were used. Utilizing custom-made high precision direct drive servo pan-tilt platforms coupled with GPS and angular orientation sensors, we can construct a pointing matrix for the entire network that is calculated and disseminated in real time over the secondary channel. We present theoretical calculations about the update rate required for alignment at certain ranges and platform speeds (and beam sizes), as well the required secondary channel capacity with respect to update rate and number of nodes. Experimental results are then presented for a link where each transceiver is mounted on a coarse vibration platform to simulate disturbances in a real network.

8162-15, Session 4

Visible light communication link study for outdoor automotive use case

K. Cui, G. Chen, Z. Xu, Univ. of California, Riverside (United States); R. D. Roberts, Intel Corp. (United States)

Outdoor visible light communication (VLC) between LED traffic lights and automobiles has been proposed for Intelligent Transportation System. However, their work was mainly based on some ideal assumptions and theoretical analysis, and link study using commercial off-the-shelf LED traffic lights under a practical application scenario has not been carried out. In this paper, we characterized visible light communication links between traffic lights and a vehicle in real environments, including background interference measurement, LED traffic lights device characterization, and corresponding link budget analysis. A prototyping system was built for both real-time BER measurement and demonstration of the feasibility of outdoor VLC for the automotive use case based on COTS components.

8162-16, Session 5

On the LDPC-coded OAM modulation for communication over atmospheric turbulence channels

I. B. Djordjevic, The Univ. of Arizona (United States); J. A. Anguita, Univ. de Los Andes (Chile); B. V. Vasic, The Univ. of Arizona (United States)

Increasing free-space optical (FSO) communication link capacity can in principle be achieved by modifying any controllable physical property of the transmitted light that augments the dimensionality of the signal space. While modulation of amplitude, phase, frequency and polarization have been extensively studied, the understanding of practical ways to use momentum modulation is in its infancy. Photons can carry spin angular momentum, a well-known property associated with polarization, and orbital angular momentum (OAM), which is associated with the azimuthal phase of the electric field of an optical beam. The OAM is a property present in certain types of laser beams, called vortex beams, which can attain multiple discrete state levels. Because the OAM states are orthogonal to each other they can be used as basis for multidimensional signal constellations. The ability to generate and analyze states with different OAMs by using interferometric or holographic methods allows the realization of energy-efficient FSO communication systems. Unfortunately, FSO communications links suffer from atmospheric turbulence and their quality-of-service (QoS) depends on weather conditions. In the presence of atmospheric turbulence, the orthogonality among OAM channels is no longer maintained.

In this paper, we study the communication over atmospheric turbulence channels based on low-density parity-check (LDPC) coded, multidimensional OAM signal constellations. The multidimensional signal constellation under study is obtained as the Cartesian product of one-dimensional signal constellation $X = \{(i-1)d, i=1,2,\dots,M\}$ (where d is the Euclidean distance between neighboring signal constellation points) as $X^N = \{(x_1, x_2, \dots, x_N) | x_i \text{ is from } X, \text{ for every } i\}$. This scheme represents an energy efficient alternative, since $\log_2(M^N)$ bits/symbol can be transmitted. We evaluate the performance of this scheme by determining conditional symbol probability density functions (PDFs) from numerical propagation data, for different turbulence strengths. Two cases of interest are considered: (i) when conditional PDFs are known on the receiver side, and (ii) when conditional PDFs are not known and Gaussian approximation is used instead. We show that in case (ii) an early error floor occurs because of inaccurate PDF assumption. The error floor is caused by OAM crosstalk introduced by atmospheric turbulence. We also show that the OAM modulation is more sensitive to atmospheric turbulence as the number of dimensions increases.

8162-17, Session 5

Performance analysis of optical wireless communications on long-range links

B. Epple, Codex GmbH & Co. KG (Germany)

Optical wireless communications over long-range atmospheric links experiences strong fading that heavily influences the performance of communication systems. Most research on this topic is focused on simulation or measurement of the link performance in terms of the bit error ratio. In this work a statistical channel model derived from measurements is used for simulations of the link performance on packet layer. For analysis of a possible improvement of packet layer performance by error protection techniques like forward error correction and automatic repeat request, additional simulations are done. All simulations are done for several communication scenarios like the maritime environment, land mobile and air-to-ground links.

8162-18, Session 5

Statistical analysis of chaotic signals generated by acousto-optic or electro-optic modulators with feedback

A. K. Ghosh, P. Verma, The Univ. of Oklahoma - Tulsa (United States)

Nonlinear optical systems with feedback may produce chaotic optical signals. Generation of chaos from such bistable optical systems has been studied for several years. Chaotic optical signals can be utilized in secure encryption of free-space optical communication systems. In general, chaos encryption of data is known to provide higher levels of security than what is available by standard cryptographic techniques.

To realize a secure optical communication link using optically generated chaos we need to know how to obtain a chaotic response and the properties of the chaotic signal. We found that an understanding of the Lyapunov exponent (LE) is essential in building a chaos-encrypted optical communication system. The LE is a measure of the amount of 'uncertainty' in the chaotic signal [1].

In this paper, we calculate the LE of a one-dimensional optical system consisting of either an electro-optic (EO) or an acousto-optic (AO) modulator with feedback to characterize and understand the behavior of the optical chaos generated. Analyzing the LE we determine several conditions on optical system's parameters so that a chaotic response is obtained. We found that the chaos generated by an EO or AO system follows a beta distribution and we determine the relation between the system parameters and the statistics of the distribution.

References

[1] A. Ghosh and P. Verma, "Lyapunov exponent of chaos generated by acousto-optic modulators with feedback," *Optical Engineering*, vol. 50, p. 017005, 2011.

8162-19, Session 5

Chaotic bandgaps in hybrid acousto-optic feedback and their implications

M. R. Chatterjee, M. A. Al-Saedi, Univ. of Dayton (United States)

The nonlinear dynamics of a hybrid acousto-optic device was examined from the perspective of the Lyapunov exponent (LE). The plots for LE versus system parameters and bifurcation maps are examined in this paper against known simulation results including chaotic encryption experiments conducted recently. It is verified that the "loop gain" (feedback gain (β) times incident light amplitude (I_{in})) needs to be greater than one as a necessary, but not sufficient condition for the onset of chaos. It is found that for certain combinations of β , I_{in} , net bias voltage (α -tot), and the initial value of the first-order scattered light ($I(0)$), there are pronounced regions of chaos in the parameter field, while for others, chaos is minimal. It is also observed that in some cases, the negative "spikes" in the LE are far larger than its positive amplitudes, hence indicating a greater tendency to become non-chaotic. Additionally, we have examined the bifurcation plots versus the two most salient system parameters, α -tot and β . These maps have revealed behavior that is by no means uniformly chaotic. It is found that the system moves in and out of chaos within distinct bands along the α -tot and β axes. These results imply strong sensitivity vis-à-vis these parameters around the passbands and stopbands, and may indicate control of chaos by appropriate parameter adjustment. Such control may have applications in biological chaos, such as arresting malignant, chaotic cell multiplication. Overall, the dynamical results compare favorably with time-domain characteristics of encrypted chaotic waveforms in signal modulation and transmission applications.

8162-20, Session 6

A 280Mbit/s infrared optical wireless communications system

D. C. O'Brien, G. E. Faulkner, R. G. Turnbull, Univ. of Oxford (United Kingdom); H. Le Minh, Northumbria Univ. (United Kingdom); M. Wolf, L. Grobe, J. Li, Technische Univ. Ilmenau (Germany); O. Bouchet, France Telecom R&D (France)

In this paper we describe an angle diversity system that operates at 280Mbits/s with a wide coverage area. The system uses commercially available components, operating at a wavelength of 860nm. Three terminals, each using seven transmitter and receiver channels were implemented, and the system was operated over a wide range of different conditions. Implementation challenges, design and performance are also discussed, together with future directions for this work.

8162-21, Session 6

Broadcast of four HD videos with LED ceiling lighting: optical-wireless MAC

O. Bouchet, P. Porcon, France Telecom R&D (France); E. Gueutier, Apiside Groupe (France)

The European project "hOME Gigabit Access network" (OMEGA) targeted various wireless and wired solutions for 1-Gb/s connectivity in Home Area Networks (HANS).

One objective of this project was to evaluate the suitability of optical wireless technologies in two spectral areas: visible light (visible-light communications - VLC) and near infrared (infrared communications - IRC). Several demonstrators were built, all of them to a large extent relying on over-the-shelf commercial components. They included a "wide-area" VLC broadcast link based on LED ceiling lighting and a laser-based high-data-rate large-coverage IRC prototype.

In this paper we discuss an adapted optical-wireless media-access-control sublayer (OWMAC), which was developed and implemented during the project. It is suitable for both infrared and visible-light communications.

The VLC prototype is based on DMT signal processing and provides broadcasting at ~ 100 Mb/s over an area of approximately 10 m².

The IRC prototype provides around 300 Mbps half duplex communication over an area of approximately 30 m². This mesh network, composed by one base station and two modules, is based on OOK modulation, multi-sector transceivers, and an ultra-fast sector switch.

After a brief discussion of the design optical-wireless data link layer and the optical-wireless switch card (OWS), we address the card development and implementation. We also present application demonstrations for the VLC and IRC prototypes and measurement results on MAC layer.

8162-22, Session 6

Full duplex ultraviolet scattering channel test and simulation

G. Chen, Z. Xu, Univ. of California, Riverside (United States)

Ultraviolet (UV) atmospheric scattering includes forward and backward scattering. For a simplex link, we simulated and tested the non-line-of-sight scattering path loss and pulse broadening in coplanar geometry earlier, accounting for forward scattering. For a full duplex link, the backscattering and off-axis effects must be taken into account. In this paper, we experimentally test and also simulate the off-axis path loss, as well as backscattering interference from a transmitter to a co-located receiver. The elevation angles and off-axis angles vary from 0° to 90°. The experimental results are compared with Monte Carlo simulation results.

8162-23, Session 6

FSO and radio link attenuation: meteorological models verified by experiment

O. Fiser, Institute of Atmospheric Physics of the ASCR, v.v.i. (Czech Republic); V. Brazda, Univ. Pardubice (Czech Republic)

Institute of Atmospheric Physics of Czech Academy is performing a continuous measurement of atmospheric attenuation on 60m experimental FSO link on 850 and 1550 nm for more than three years. Experimental site is located on isolated mountain of severe weather. Two visibility sensors and two 3D sonic anemometers both on transmitting and receiving site, rain gauge and many humidity/temperature sensors enabling the refractivity index computation are spaced along the optical link. Meteorological visibility, wind turbulent energy, intensity of turbulence, structure index of atmosphere and rain rate are correlated with the observed attenuation (structure index is computed from refractivity index as well as from anemometer measurement). The regression technique is used to estimate FSO link attenuation dependence on the above mentioned parameters. The rain attenuation in Ka band is simulated due to computer and gain due to hybrid technique is estimated. The paper shows also basic statistical behavior of the long-term FSO signal level in extreme conditions.

Conference 8163:

Quantum Communications and Quantum Imaging IX

Wednesday–Thursday 24–25 August 2011 • Part of Proceedings of SPIE Vol. 8163
Quantum Communications and Quantum Imaging IX

8163-01, Session 1

Exploiting PDC spatial correlations for innovative quantum imaging protocols

M. Genovese, Istituto Nazionale di Ricerca Metrologica (Italy)

Quantum properties of the optical field represent a resource of the utmost relevance for the development of quantum technologies, allowing unprecedented results in disciplines ranging from quantum information and metrology to quantum imaging.

In particular, in the last case various protocols have been proposed ranging from ghost imaging [1] to quantum illumination [2].

In particular Ghost Imaging can have very interesting practical applications [3].

Another kind of protocols of interest for possible application is offered by the possibility of sub shot noise measurements with quantum optical states.

In particular a very interesting example is provided by the detection of weak objects by exploiting the quantum correlations of parametric down conversion (PDC) emission: a result that could have important practical applications. A little more in detail the principle of this technique is to take advantage of the correlation in the noise of two conjugated branches of PDC emission : in fact, subtracting the noise measured on one branch from the image of a weak object obtained in the other branch, the image of the object, eventually previously hidden in the noise, could be restored [4].

In this talk, after a general summary of quantum imaging techniques, firstly we will show how we have reached a sub shot noise [5] regime and then improved this result up to reach a regime where it was possible to achieve the first experimental realisation of sub shot noise imaging of a weak absorbing object [6].

Then we will present some recent experiments addressed to realise improved ghost imaging protocols in view of practical applications.

Finally, we will present some innovative interferometric scheme exploiting spatial correlation of light.

[1] T.Pittman et al., PRA 52 (1995) R3429-R3432

[2] S. Tan et al., PRL 101 (2008) 253601; S.Lloyd, Science 321 (2008) 1463.

[3] R. Meyers et al., PRA 77 (2008) 041801.

[4] Brambilla, E., Caspani, L., Jedrkiewicz, O., Lugiato, L. A. & Gatti, A. Phys. Rev. A 77, 053807 (2008).

[5] G. Brida et al., Phys. Rev. Lett. 102, 213602 (2009).

[6] G.Brida, M. Genovese, I. Ruo Berchera, Nature Photonics 4, 227 - 230 (2010).

8163-02, Session 1

Secrets of subwavelength imaging and lithography

P. R. Hemmer, Texas A&M Univ. (United States)

To understand the limits and tradeoffs of nearly all existing subwavelength imaging techniques it sufficient to understand magnetic resonance imaging (MRI) and its generalizations. In many cases, subwavelength optical lithography can be viewed as the inverse problem to imaging and so the same principles apply. I will give a simple review of MRI and show how the most popular subwavelength imaging techniques naturally arise as special cases. I will also discuss how these techniques can be used for nanoscale optical lithography.

8163-03, Session 1

Turbulence-free quantum ghost imaging experiments and results

R. E. Meyers, K. S. Deacon, A. Tunick, U.S. Army Research Lab. (United States)

Turbulence is a serious problem for long distance imaging such as from satellites or telescopes. In this paper we discuss our turbulence-free ghost imaging approach that is virtually free from the degrading effects of turbulence. We discuss motivation for the experiments, theory, experimental setup, procedures, and results. The results suggest that thermal two-photon interference may not only be used to improve imaging through turbulence but may also lead to a resource for quantum information processing.

8163-04, Session 1

Enhanced optical resolution in target detection with phase-sensitive pre-amplification

O. Lim, Northwestern Univ. (United States); Z. Dutton, BBN Technologies (United States); G. Alon, C. Chen, Northwestern Univ. (United States); M. Vasilyev, The Univ. of Texas at Arlington (United States); P. Kumar, Northwestern Univ. (United States)

The resolution of an optical imaging system depends on the signal-to-noise ratio (SNR) of the detected optical power. The amount of spatial information lost at the image plane across all spatial frequencies determines the maximum achievable resolution of the system. Some of the lost resolution can be recovered by spatially-broadband optical pre-amplification to overcome the imperfect detection efficiency of the imaging sensors. Two types of optical amplifiers can be used to boost the received signal: Phase-insensitive amplifiers (PIAs) and Phase-sensitive amplifiers (PSAs). PSAs are capable of providing noise-free signal gain that can out-perform PIAs in SNR by 3 dB at large gains. A spatially broadband signal such as that from a LADAR can also be noiselessly amplified with a PSA. Here, we demonstrate enhanced resolution in optical detection by boosting the incoming signal with a PSA. We employ the method of hypothesis testing to investigate the optical resolution of a standard imaging system in a typical one vs. two targets sensing scenario. Optical resolution is quantified in terms of the error probability of deciding one hypothesis in the presence of the other. We show that images that are otherwise unresolved can be distinguished with higher probability after phase-sensitive pre-amplification than is possible without amplification. In this work, we demonstrate 5-dB resolution enhancement in homodyne detection at 15 dB PSA gain. We will also show the superiority of a PSA over a PIA in terms of their noise figure performance.

8163-05, Session 1

Quantum enhancement of a coherent ladar receiver using phase-sensitive amplification

P. A. Wasilousky, K. H. Smith, R. Glasser, G. L. Burdge, L. Burberry, B. Deibner, M. Silver, R. C. Peach, C. Visone, Harris Corp. (United States); P. Kumar, O. Lim, G. Alon, C. Chen, A. Bhagwat, P. Manurkar, Northwestern Univ. (United States); M. Vasilyev, M. Annamalai, N. Stelmakh, The Univ. of Texas at Arlington (United States); Z. Dutton, S. Guha, C. Santivanez, J.

**Conference 8163:
Quantum Communications and Quantum Imaging IX**

Chen, M. Silva, W. Kelly, BBN Technologies (United States); J. H. Shapiro, Massachusetts Institute of Technology (United States); R. Nair, B. J. Yen, Massachusetts Institute of Technology (United States); F. N. C. Wong, Massachusetts Institute of Technology (United States)

Typical LADAR receivers suffer from losses in their optical train that routinely limit overall photon detection efficiency (PDE) to less than 50%, thus degrading SNR. These losses arise from sub-unity quantum efficiency detectors, array fill factors, signal-local oscillator (LO) mixing efficiency (in coherent receivers), and other sources. Incorporating a phase-sensitive amplifier (PSA) into a coherent receiver allows for noiseless amplification of the target return signal, which allows effective PDE to approach 100%. We demonstrate improved SNR in a balanced-homodyne LADAR receiver by employing a PSA to raise the effective PDE to nearly 100%. We also demonstrate that the PSA offers better performance than a phase-insensitive amplifier, which cannot amplify noiselessly. We show how this PSA-enhanced receiver can be extended to simultaneously amplify multiple optical modes and how it can be used in imagery and vibrometry applications.

Short pulses (~200 ps pulse width, ~20 MHz repetition rate) from a very narrow linewidth 1560 nm source laser are amplified and passed through a nonlinear crystal to generate second harmonic light which serves as the pump for the PSA. Some of the residual 1560 nm light serves as the LO and the remainder illuminates a target in the far field. The pump light and target return signal are simultaneously passed through a nonlinear crystal to provide amplification. The resultant amplified signal is then mixed with the LO in a balanced homodyne configuration. Lateral resolution is achieved by scanning a receive mirror and range discrimination is achieved by changing the pulse repetition rate.

8163-06, Session 2**Designing quantum repeaters and networks**

W. J. Munro, NTT Basic Research Labs. (Japan); S. J. Devitt, K. Nemoto, National Institute of Informatics (Japan)

The twentieth century saw the discovery of quantum mechanics, a set of principles describing physical reality at the atomic level of matter. Quantum physics allows a new paradigm for the processing of information. Over the last decade there has been a huge worldwide effort to develop and explore quantum-information based devices and technologies. Quantum repeaters are a natural candidate to consider as they can be used both to distribute and process quantum information. There has been a significant effort worldwide to investigate and demonstrate the fundamental building blocks necessary for such repeaters. The next step is to look at the overall design of a repeater network, considering both the quantum and classical components. A repeater network must be underpinned by experimental techniques for entanglement generation, it must incorporate purification or quantum error correction to achieve high-fidelity entangled links, and must be controlled by classical communication across the network. Typically, the communication time required for classical messages to be transmitted between nodes severely limits the performance of repeater networks. In this talk we show how to maintain near-determinism throughout all aspects of a repeater network allowing for an efficient, pipe-lined architecture. More importantly we know when the end-to-end entangled pairs are going to be available and also how to minimize the requirements on resources such as quantum memories.

8163-07, Session 2**Multiplexing schemes for quantum repeater networks**

L. Aparicio, The Univ. of Tokyo (Japan); R. Van Meter, Keio Univ. (Japan)

Real-world quantum repeater networks will operate in heterogeneous

conditions, including complex topologies with multiple connections competing for resources. For these scenarios, we are comparing several different classical multiplexing schemes using simulation, measuring the aggregate throughput and fairness for each case. Our engineering goal is to articulate the conditions in which classical multiplexing strategies can be applied to quantum networks.

The multiplexing schemes considered in this work are: circuit switching like that of traditional telephony service; statistical multiplexing with a best effort approach, as used in the Internet; time division multiplexing like that used in telephony trunk lines; and spatial multiplexing, in which the quantum buffer memory resources in each repeater are divided among competing requests.

For this work, we use our proposed three-layer quantum network protocol stack designed for purify-and-swap repeaters. The physical layer simulated is a Qubus mechanism in which laser pulses of many photons generate low fidelity Bell pairs with high probability.

Our results suggest that round-robin use of a congested link gives the highest aggregate throughput, improving over circuit switching by taking advantage of resources that are forced to remain idle in the simpler approach. Spatial multiplexing proved not to be very effective as the reduction of resources extends the time needed to obtain a high-fidelity Bell pair between stations.

8163-08, Session 2**Intersatellite quantum communication feasibility study**

A. Tomaello, A. Dall'Arche, G. Naletto, P. Villorosi, Univ. degli Studi di Padova (Italy)

The shift in the Communication paradigm from the bit to the qubit is increasingly exploited in terrestrial long range links and networks, with strong potentials in secure communications, quantum computing and metrology. Several studies have also studied the feasibility of the space to ground quantum key distribution with the experimental demonstration of the single photon exchange. A new different scenario for the quantum communications is that of the intersatellite link. Experiments of classical optical communications between the ESA Artemis GEO satellite and SPOT-4 LEO satellites as well as between the pairs TerraSAR and NFIRE, both in LEO orbits, that have reached multi giga-bit per second data rate while in mutual sight. Other advantages that were proven include the significant reduction of the transmitter power budget and the increasing of the carrier frequency and beam pointing with respect to radio communications.

In this study we focus on the extension of intersatellite communications into the quantum domain. The very recent demonstration of optical quantum memories as well as of effective schemes for the generation of entangled and hyperentangled photon states are providing complementary tools supporting the feasibility of a global quantum network scenario. The long distances involved in the link as well as the fast relative motion are factors that severely constraint the conception of the quantum transceiver. However, the absence of beam degradation due to the propagation in the atmosphere as well as the relatively low background noise level are positive aspects with respect to the Earth related links. In this work we address the conception of the optical terminal and the predicted performances in the case of constellations of LEO and MEO satellite including the quantum communications and quantum teleportation.

8163-09, Session 2**Randomization techniques for the intensity modulation-based quantum stream cipher and progress of experiment**

K. Kato, O. Hirota, Tamagawa Univ. (Japan)

The quantum stream cipher by Yuen 2000 protocol (Y-00) provides a

**Conference 8163:
Quantum Communications and Quantum Imaging IX**

high-speed data encryption system for optical fiber networks. While the basic model of the quantum stream cipher consists of pseudorandom number generators and signal modulator/detector, a general model includes some additional randomization schemes. Such additional randomization techniques play important role to ensure its security. Hence development of additional randomization techniques is one of basic problems in designing the quantum stream cipher. So far, several randomization techniques for the quantum stream cipher have been proposed, but most of them were developed under the assumption that the phase shift keying is employed. Therefore the purpose of this study is to develop randomization techniques specialized for the intensity modulation-based quantum stream cipher. By proposing some randomization techniques for the intensity modulation-based quantum stream cipher, it is shown that the security of the system is completely ensured against correlation and algebraic attacks. Finally we introduce the recent progress of the experiment to realize such a sophisticated Y-00 system.

8163-10, Session 3

Multiclient quantum key distribution using wavelength division multiplexing

W. P. Grice, Oak Ridge National Lab. (United States); B. Williams, The Univ. of Tennessee (United States); R. Bennink, D. Earl, P. G. Evans, T. S. Humble, R. C. Pooser, Oak Ridge National Lab. (United States); J. Schaake, The Univ. of Tennessee (United States)

Quantum Key Distribution (QKD) exploits the rules of quantum mechanics to generate and securely distribute a random sequence of bits to two spatially separated clients. Typically a QKD system can support only a single pair of clients at a time, and so a separate quantum link is required for every pair of users. We overcome this limitation with the design and characterization of a multi-client entangled-photon QKD system with the capacity for up to 100 clients simultaneously. The time-bin entangled QKD system includes a broadband down-conversion source with two unique features that enable the multi-user capability. First, the photons are emitted across a very large portion of the telecom spectrum. Second, and more importantly, the photons are strongly correlated in their energy degree of freedom. Using standard wavelength division multiplexing (WDM) hardware, the photons can be routed to different parties on a quantum communication network, while the strong spectral correlations ensure that each client is "linked" only to the client receiving the conjugate wavelength. In this way, a single down-conversion source can support dozens of channels simultaneously--and to the extent that the WDM hardware can send different spectral channels to different clients, the system can support multiple client pairings. We will describe the design and characterization of the down-conversion source, as well as the client stations, which must be tunable across the emission spectrum.

8163-11, Session 3

Towards high bit-rate quantum key distribution

I. Lucio Martinez, P. Chan, X. Mo, C. J. Healey, Univ. of Calgary (Canada); S. Hosier, Sait Polytechnic (Canada); W. Tittel, Univ. of Calgary (Canada)

We experimentally demonstrate a fiber-based QKD system that implements the BB84 protocol supplemented with decoy states. It employs polarization encoding. Our system is characterized by the use of quantum frames, which consist of alternating sequences of high-intensity laser pulses (control frames) and faint laser pulses (quantum data). The control frames are used to assess and compensate time-varying birefringence in the communication channel. Our system is highly integrated and employs Field Programmable Gate Arrays (FPGA) and homemade drivers. The optical components of the system can generate qubits at a maximum rate of 980 MHz. To create the different polarization

and decoy states we use homemade polarization and intensity modulators in a configuration that ensures passive compensation of temperature dependent birefringence and polarization mode dispersion in these components. On the receiver side we use commercially available single photon detectors, as well as high-rate, homemade detectors based on the self-differencing technique. Our system also includes classical post-processing implemented via software: error correction is performed using low-density parity check codes, and privacy amplification is implemented using information obtained from the decoy state protocol. In our current setup, the homemade electronic drivers for the modulators and detectors limit the clock rate to 100 MHz, and the memory depth of the used FPGAs limits the effective time during which qubits can be generated per quantum frame to 10%. This results in a secret key rate over a 12 km real-world fibre link exceeding 10^4 bps.

8163-12, Session 3

Mixed-metric algorithms for information reconciliation in quantum cryptography

M. Mondin, Politecnico di Torino (Italy); F. Daneshgaran, California State Univ., Los Angeles (United States); F. Mesiti, M. T. Delgado, Politecnico di Torino (Italy); M. Laddomada, Texas A&M Univ. (United States)

This paper deals with the selection of the most appropriate metric in the mixed-channel scenario typical of Quantum Key Distribution (QKD), where both the private quantum channel and the public channel are jointly considered. On a composite private-public channel model, capacity achieving sparse-graph codes are employed for information reconciliation and pre-data sifting. The metrics derived from the two channels are jointly processed with a mixed-metric iterative decoder, with the goal of performing feed-forward error correction of the received q-bits, detect the possible presence of unauthorized eavesdroppers without the need for revealing information bits, and performing pre-data sifting.

The paper initially discusses the most suitable model for a composite scenario typical of QKD applications. Secondly, it shows how to best select and weigh appropriate metrics derived from the considered channel model, and then suggests employing forward error correction (FEC) coding as opposed to two-way communication for information reconciliation, minimizing the interactions between transmitter and receiver. The paper also shows that the average number of decoding iterations of the iterative decoder for the considered FEC code is strongly correlated with the quantum channel bit error rate (QBER). Since the QBER value is a possible indicator of the presence of an eavesdropper, this observation allows deriving a reliable method for eavesdropping detection.

Systematic low density parity check (LDPC) codes have been considered in the paper, although the concepts could be applied to other iteratively decoded capacity achieving codes as well. Extensive simulations have been performed in order to derive the performance and the efficiency of the proposed algorithms as a function of the system parameters.

8163-13, Session 4

Simultaneous quadrature detection of suppressed-carrier weak-coherent-states using a homodyne optical Costas loop receiver

J. A. Lopez Leyva, Ctr. de Investigación Científica y de Educación Superior de Ensenada (Mexico); E. Garcia, Univ. Autónoma de Baja California (Mexico); F. J. Mendieta, A. Arvizu, Ctr. de Investigación Científica y de Educación Superior de Ensenada (Mexico); P. Gallion, Telecom ParisTech (France)

Weak coherent states (WCS) are being extensively employed in

Conference 8163:
Quantum Communications and Quantum Imaging IX

quantum communications and cryptography at telecommunications wavelengths. For these low-photon-number applications, simultaneous field quadrature measurements are frequently required, such as in the detection of multilevel modulations in the communications scenario or in cryptographic applications employing continuous variables. For this task multipoint balanced homodyne detection (BHD) structures are employed, based on the splitting of the received field into its (non-commuting) in-phase (I) and quadrature (Q) components and their separate beating with a local oscillator (LO) in two BHD. This allows the simultaneous measurements of the 2 quadratures at the price of an additional noise due to the vacuum fields that leak via the unused ports. These schemes require the proper optical phase synchronization between the LO and the incoming field, which constitutes a challenge for WCS reception, especially for suppressed carrier modulations that are required for power economy. For this task, a Costas loop is implemented for low photon number WCS, with the design of an optimum feedback scheme considering the phase diffusion of WCS generated by semiconductor lasers. We implemented an optical Costas loop at 1550 nm based on polarization splitting of the laser field to detect I and Q quadratures simultaneously. We present results on the performance in phase error and bit error rate and compare with corresponding quantum limit.

8163-15, Session 4

Characterization of a gradient echo memory using homodyne tomography

R. Thomas, C. M. Kupchak, A. Heinrichs, A. I. Lvovsky, Univ. of Calgary (Canada)

The fields of quantum cryptography and quantum computation offer distinct advantages over their classical counterparts, such as absolutely secure communication and an exponential increase in computational speed. Limitations in current implementations, such as loss in optical fibres or probabilistic optical quantum gates, prevent further development and application of these technologies. This issue can be addressed by developing quantum memory for light: a device that stores and retrieves arbitrary quantum optical states. Using a warm rubidium vapour, we demonstrate coherent storage of light based upon the gradient echo memory scheme. In this scheme, the Fourier components of the input light field are mapped to atomic dipoles at different spatial locations in the cell via a linearly varying frequency gradient. A reversal of the gradient causes the re-emission of the original light pulse. Gradient echo memory is an attractive technique because of potentially high retrieval efficiencies and long storage times. We characterize the storage and retrieval of coherent states of light for both high and low mean photon numbers. The action of the memory on input light fields is experimentally measured using time-domain homodyne tomography. Using homodyne tomography to characterize the retrieval of coherent states allows us to perform coherent state quantum process tomography on the memory, and therefore fully characterize it as a quantum process, so we can infer the effect of the memory on any other quantum state of light.

8163-16, Session 4

A single-atom quantum memory

E. V. Figueroa, H. Specht, C. Nölleke, A. Reiserer, M. Uphoff, S. Ritter, G. Rempe, Max-Planck-Institut für Quantenoptik (Germany)

The implementation of quantum networks requires the development of quantum interconnects, featuring the coherent and reversible mapping of quantum information between light and matter. So far, these interfaces have been based upon the engineered exchange of information between photons and collective atomic excitations. A promising alternative is the development of interfaces between single photons and single particles of matter (e.g. single atoms). This approach has fundamental advantages as it allows for the individual manipulation of the stored atomic qubit.

We have shown previously that an atom-cavity system can be used for efficient and controlled single photon production via a vacuum

stimulated adiabatic passage (vSTIRAP). Here we demonstrate the most fundamental implementation of a quantum memory based on the reverse process, by mapping arbitrary polarization states of light into and out of a single atom trapped inside an optical cavity.

By adiabatically ramping down the power of a strong control laser pulse, we cause the atom to absorb a single photon from of a weak coherent probe pulse impinging on the cavity. During this coherent process, the phase relation of the input circular polarization modes is mapped to a relative phase between Zeeman sub-states. After a variable storage time, a second control laser pulse converts the atomic qubit back onto the polarization of a produced single photon.

This experiment is a major step in the development of a universal node of a quantum network, capable of fully controlled photon generation, qubit storage and with intriguing perspectives towards the development of quantum gates.

8163-39, Session 4

Quantum information processing with light shift blockaded atomic ensembles coupled to a cavity

S. M. Shahriar, M. Kim, Y. Tu, Northwestern Univ. (United States)

Using the process of light shift blockade, it is possible to make an ensemble of atoms behave as a deterministic qubit. The vacuum Rabi frequency for such a qubit is stronger than that of a single atom by a factor equaling the square-root of the number of atoms in the ensemble. We are studying a clusters of Rb atoms held in an array of dipole force potential wells loaded from a magneto-optic trap and placed inside a meso-scale cavity as an elementary quantum computer. In this talk, we will describe how various nearest neighbor quantum gates can be realized using this system and techniques for creating a quantum link between two such arrays with an optical fiber. We will also present preliminary results from our experiment.

8163-32, Poster Session

Generation of broadband spontaneous parametric fluorescence and its application to quantum optical coherence tomography

M. Okano, R. Okamoto, A. Tanaka, S. Subashchandran, Hokkaido Univ. (Japan); S. Ishida, N. Nishizawa, Nagoya Univ. (Japan); S. Takeuchi, Hokkaido Univ. (Japan)

Optical coherence tomography (OCT) based on Michelson interferometer has widely been utilized in biology and medicine as a type of optical biopsy. Recently, quantum optical coherence tomography (QOCT) based on Hong-Ou-Mandel interferometer has experimentally been demonstrated. By use of quantum entangled photon pairs generated via spontaneous parametric down conversion (SPDC), axial resolution of QOCT can be twice better than that of OCT in principle for a source of same bandwidth. And more, the group velocity dispersion, which may reduce the resolution of OCT, can be automatically cancelled due to the frequency correlation of quantum entangled photon pairs.

To realize high resolution QOCT, we have generated broadband spontaneous parametric fluorescence via SPDC from two nonlinear crystals (BBO) pumped by the CW laser ($\lambda = 405$ nm). The bandwidth of spectrum of generated lights from two BBO crystals has been broadened up to approximately 170 nm and this bandwidth can lead to sub-micron axial resolution of QOCT. For comparison, we have demonstrated OCT using the super luminescence diode (SLD, $\lambda_c = 810$ nm), whose bandwidth of 77 nm can lead to 4 μm axial resolution, and measured axial resolution was approximately 5 μm . Next, we try to realize high resolution QOCT using broadband spontaneous parametric fluorescence generated via SPDC and will report our recent experimental progresses.

Conference 8163:
Quantum Communications and Quantum Imaging IX

8163-33, Poster Session

Turbulence measurement and characterization for quantum ghost imaging

R. E. Meyers, K. S. Deacon, A. Tunick, U.S. Army Research Lab. (United States)

The measurement and characterization of turbulence for quantum ghost imaging and free-space quantum communications is a difficult problem. In this paper we discuss how to measure and characterize turbulence in a manner suitable to apply to quantum ghost imaging and free-space quantum communications analysis.

8163-37, Poster Session

Towards interferometric quantum lithography: observation of spatial quantum interference of the three-photon NOON state

Y. Kim, O. Kwon, S. M. Lee, Pohang Univ. of Science and Technology (Korea, Republic of); H. Kim, S. Choi, Korea Research Institute of Standards and Science (Korea, Republic of); H. S. Park, Korea Institute of Standards and Science (Korea, Republic of); Y. Kim, Pohang Univ. of Science and Technology (Korea, Republic of)

Spatial interference of quantum mechanical particles exhibits a fundamental feature of quantum mechanics. A two-mode entangled state of N particles known as NOON state can give rise to non-classical interference. We report the first experimental observation of a three-photon NOON state exhibiting Young's double-slit type spatial quantum interference. Compared to a single-photon state, the three-photon entangled state generates interference fringes that are three times denser. Moreover, its interference visibility of 0.49 is well above the limit of 0.1 for spatial super-resolution of classical origin. The demonstration of spatial quantum interference by a NOON state composed of more than two photons represents an important step towards applying quantum entanglement to technologies such as lithography and imaging.

8163-38, Poster Session

Quantum memory for a photonic polarization qubit using hot atomic vapor

Y. Cho, Y. Kim, Pohang Univ. of Science and Technology (Korea, Republic of)

We report an experimental realization of an atomic vapor quantum memory for the photonic polarization qubit. The performance of the quantum memory for the polarization qubit, realized with electromagnetically-induced transparency in two spatially separated ensembles of warm Rubidium atoms in a single vapor cell, has been characterized with quantum process tomography. The process fidelity better than 0.91 for up to 16 μ s of storage time has been achieved.

8163-17, Session 5

Simulation of entangled multiphoton state with incoherent thermal light

H. Chen, T. Peng, Univ. of Maryland, Baltimore County (United States)

I would like to report an experimental study on thermal light multiphoton qubits. Taking advantage of two-photon interference, we have successfully observed Bell type correlation from mutually incoherent and

orthogonally polarized thermal fields. The visibilities of the polarization correlation as well as the temporal anti-correlation both exceed 71%, indicating the behavior of a two-photon Bell state, or a 2-digit qubit. The success of this Bell-type experiment advances our capability of simulating the behavior of high-number-photon qubits for computation purposes.

8163-18, Session 5

Parameter dependence of the decoherence of orbital angular momentum entanglement due to atmospheric turbulence

A. Hamadou Ibrahim, F. S. Roux, CSIR National Laser Ctr. (South Africa); T. Konrad, Univ. of KwaZulu-Natal (South Africa)

The orbital angular momentum (OAM) states of light can potentially be used to implement higher dimensional entangled systems for quantum communication. Unfortunately, optical fibers in use today support only modes with zero OAM values. Free-space quantum communication is an alternative to the traditional way of communicating through optical fibers. However, the refractive index fluctuation of the atmosphere gives rise to random phase aberrations on a propagating optical beam. To transmit quantum information successfully through a free-space optical channel, one needs to understand how atmospheric turbulence influences quantum entanglement. Here, we present a numerical study of the evolution of quantum entanglement between a pair of qubits. The qubits consist of photons entangled in the OAM basis. The photons propagate in a turbulent atmosphere modeled by a series of consecutive phase screens based on the Kolmogorov theory of turbulence. Maximally entangled initial states are considered, and the concurrence is used as a measure of entanglement. We show how the evolution of entanglement is influenced by various dimension parameters, such as the beam waist, the strength of the turbulence and the wavelength of the beam. We restrict our analysis to the OAM values $l = \pm 1$ and we compared our results with previous work.

8163-19, Session 5

Towards a narrow linewidth non-degenerate source of correlated photon pairs

O. T. Slattery, L. Ma, X. Tang, National Institute of Standards and Technology (United States)

A non-degenerate entangled photon pair source can actively interface between flying qubits and stationary qubits. In this presentation, we will introduce our efforts to generate narrow linewidth non-degenerate pairs with one photon at a wavelength (1310 nm) suitable for long distance transmission and the second photon (895 nm) suitable for integration with an atomic (Cesium) ensemble for quantum memory. Spontaneous parametric down conversion (SPDC) is commonly used to produce degenerate photon pairs (both are the same wavelength), broadened to hundreds of gigahertz or a terahertz. For successful interaction with atomic ensembles, the interacting photon must achieve a very narrow linewidth, in the order of megahertz. We describe our efforts to use cavity enhanced SPDC to produce non-degenerate photon pairs with linewidths suitable for photon-atom interaction as well as long distance transmission. The experiment includes a non-linear periodically poled bulk crystal (2 cm lithium niobate) pumped at 532 nm and the resulting pairs of correlated photons are at 895 nm and 1310 nm, respectively. The single pass (no cavity) linewidth is about 4 nm at 1310 nm. By introducing the crystal into a cavity tuned to resonate at 895 nm and by relying on the principle of the conservation of energy in the non-linear interaction, the effect is to limit the generation of the pairs to the linewidths matching the resonant modes of the cavity. The resulting linewidth will be significantly narrower than the single pass linewidth. Applications include quantum repeaters and the advancement of quantum computer networks.

8163-20, Session 5

Broadband waveguide quantum memory for entangled photons

E. Saglamyurek, N. Sinclair, J. Jin, J. Slater, D. Oblak, Univ. of Calgary (Canada); F. Bussieres, Univ. of Geneva (Switzerland); M. George, R. Ricken, W. Sohler, Univ. Paderborn (Germany); W. Tittel, Univ. of Calgary (Canada)

Quantum information processing and communication relies on encoding information into quantum states of physical systems such as photons [1]. Photon-encoded quantum information travels quickly- excellent for long distance quantum communication. The resulting applications of properties of quantum physics offer secure encryption through quantum key distribution without relying on unproven mathematical assumptions [2] and, by means of quantum teleportation, allow for the disembodied transfer of quantum states between distant places [1]. Actualizing a quantum interface [3] between light and matter is imperative for construction of a quantum repeater [4], which is required to extend the current hundred kilometre quantum communication distance limit, and for information synchronization in a quantum network [5]. A pivotal characteristic of a quantum interface is the ability to faithfully map quantum entanglement [1] between light and matter.

In this work we report the reversible transfer of photon-photon entanglement into entanglement between a photon and a collective atomic excitation in a solid-state thulium-doped lithium niobate waveguide [6] (this transfer was simultaneously done in [7]). We do so using a photon-echo quantum memory protocol [8], and by increasing the spectral acceptance from the current maximum [9] of 100 megahertz to 5 gigahertz. We show, within statistical error, a perfect mapping process by violating a Bell inequality and comparing the amount of entanglement contained in the detected photon pairs before and after the reversible transfer [1]. Despite the necessity to increase the storage efficiency and storage time, this study paves the way to new explorations of fundamental and applied aspects of quantum physics.

References:

- [1] J.-W. Pan, Z.-B. Chen, M. Zukowski, H. Weinfurter, & A. Zeilinger. arXiv:0805.2853, 2008.
- [2] N. Gisin, G. Ribordy, W. Tittel, & H. Zbinden. Rev. Mod. Phys., 74 (1): 145-195, 2002.
- [3] A. I. Lvovsky, B. C. Sanders, & W. Tittel. Nat Photon, 3 (12): 706-714, 2009.
- [4] N. Sangouard, C. Simon, H. de Riedmatten, & N. Gisin. arXiv:0906.2699, 2009.
- [5] H. J. Kimble. Nature, 453 (7198): 1023-1030, 2008.
- [6] E. Saglamyurek, N. Sinclair, J. Jin, J. A. Slater, D. Oblak, F. Bussieres, M. George, R. Ricken, W. Sohler, & W. Tittel. Nature, 469 (7331): 512-515, 2011.
- [7] C. Clausen, I. Usmani, F. Bussieres, N. Sangouard, M. Afzelius, H. de Riedmatten, & N. Gisin. Nature, 469 (7331): 508-511, 2011.
- [8] H. de Riedmatten, M. Afzelius, M. U. Staudt, C. Simon, & N. Gisin. Nature, 456 (7223): 773-777, 2008.
- [9] I. Usmani, M. Afzelius, H. de Riedmatten, & N. Gisin, Nat. Commun. 1, 12 (2010).

8163-21, Session 5

Quantum interference of single photons with orbital angular momentum by a triangular slit: a Born rule

E. J. S. Fonseca, A. A. J. Jesus-Silva, J. M. Hickmann, Univ. Federal de Alagoas (Brazil)

The double-slit at single photon or electron level has been the quintessential quantum interference experiment where optical path phase

plays a key role, while photon's orbital angular momentum (OAM) brings a new dimension to interference problems with the spiral phase degree of freedom. Using OAM's two-dimensional properties, we have extended the double-slit to a tripple-slit configuration in the shape of an equilateral triangle, obtaining a triangular single photon counting quantum interference pattern, whose size depends on the photon's OAM. We have shown that this pattern is a manifestation of photon's wave-particle duality, but in contrast with the parallel slit cases, the azimuthal phase plays a fundamental role, being undistinguishable from path phase. Our results confirm that only pairs, associated here to path and azimuthal phases, contribute to the photon detection probability, as established by Born rule.

Accordingly with Born's rule, in quantum mechanics only pairs of amplitude probabilities interfere.

The results presented in this paper corroborate the principle that quantum interference always comes from correlating pairs and extend experimental verification of Born's rule for systems where OAM provides an extra degree of freedom, i.e. the azimuthal phase, which enhances indistinguishability. We also extend such experimental verification from zero dimension (one point) to two dimensions (2D).

8163-22, Session 6

Pulse-pumped up-conversion single photon detectors and their applications

L. Ma, O. T. Slattery, X. Tang, National Institute of Standards and Technology (United States)

Frequency up-conversion detectors have been developed for highly efficient single photon detection in telecommunication bands at the near infrared region. While CW pumping is commonly used in this type of detector, a pulse pumping scheme can have some advantages. For example, this type of scheme can reduce the dark count rate. The dark counts in an up-conversion detector are mainly caused by the strong pump. When the pump pulse width is equal or slightly larger than the optical signal pulse, the dark count rate can be reduced while the detection efficiency remains the same. Additionally, the limitation on the temporal resolution caused by the timing jitter of the Si-APD when used in CW pumped mode can be avoided since the pulse-pumped up-conversion detector acts as an optical sampling device, increasing the temporal resolution significantly. Finally, we make use the pulse pumped scheme into a communication system to increase its data transmission rate, which is still limited by the timing jitter, since it is usually larger than the pump pulse width itself. To increase the system's data transmission rate, we developed a multi-wavelength pulse pumping technique, in which the data detected within a single time jitter period of the Si-APD can be projected into wavelength domain and then recovered back into time domain.

We will present our research on the pulse-pumped upconversion single photon detectors and their applications, including noise reduction in quantum key distribution systems, higher temporal resolution optical sampling, and better system data transmission rate with multi-wavelength pulse pumping.

8163-23, Session 6

Towards quantum computation with incoherent thermal light

V. Tamma, Y. Shih, Univ. of Maryland, Baltimore County (United States)

One of the main challenges in quantum computation is the realization of entangled states with a large numbers of particles. Although the study of such states has allowed a strong development in understanding the physics behind multi-particle superposition, the production of entangled states of more than three particles is still a critical issue.

The efficiency of the famous Shor's algorithm decreases exponentially

**Conference 8163:
Quantum Communications and Quantum Imaging IX**

with respect to the number of entangled particles. For this reason it is of fundamental importance first to understand the role played by entanglement in quantum computation and second to study alternative physical phenomena which are able to simulate such a role without necessarily using entanglement.

Inspired by the previous works on factoring using Gauss sums, we have experimentally demonstrated a novel factoring algorithm which relies only on physical interference and on the periodicity properties of Gauss sums with continuous arguments. An important advantage of this method stands in the possibility of factoring several numbers with a single experimental run. However, in its present form this algorithm still relies on an exponential number of resources.

A more recent approach to factorization aims to achieve an exponential speed-up without entanglement by exploiting multi-photon n-order interference. In this case, the basic requirement for quantum computation is interference of an exponentially large number of multi-particle amplitudes.

8163-24, Session 6**Two coupled Jaynes-Cummings systems**

P. Xue, Southeast Univ. (China)

We fully characterize the spectrum, stationary states and linear susceptibility of two Jaynes-Cummings systems coupled together by the overlap of their respective longitudinal field modes. For weak coupling, the pair of systems are similar to a single Jaynes-Cummings system undergoing an AC Stark Effect, and for strong coupling the behavior is similar to two coupled harmonic oscillators. For in-between coupling strengths, the pair of atoms and the pair of field modes are highly entangled states, and, where the spectrum exhibits avoided crossings as a function of coupling strength, the atoms and fields are very close to being four-qubit entangled states.

Coupled Jaynes-Cummings systems are relevant to studies of quantum information and of condensed matter. Cavity quantum electrodynamics provides one strategy for implementing scalable quantum computing, and coupled Jaynes-Cummings systems are required for providing scaling to an arbitrarily large qubits. Coupled Jaynes-Cummings systems are also important in condensed matter physics as a Jaynes-Cummings lattice comprises many coupled Jaynes-Cummings systems and could lead to new states of matter not seen or expected for any other system. Our analysis provides a foundation for studying multiple Jaynes-Cummings systems for these applications.

8163-25, Session 6**Perpetual quantum computation**

K. Nemoto, S. J. Devitt, A. Stephens, National Institute of Informatics (Japan); W. J. Munro, NTT Basic Research Labs. (Japan)

Optical quantum information processing has been extensively developed both theoretically and experimentally in the last decade. The advances of optical QIP are clear in some demonstrations such as high fidelity gates and quantum walk simulations, however the scalability issue which these current implementation suffer needs to be solved before serious developments of optical quantum technology. Clearly, one way to solve this problem is to extend our capability of optical QIP to generate and control optically nonlinear operations. Towards this direction, cavity-based quantum devices has been attracted much attention.

A new architecture for optical quantum computer utilizing such photon-atom coupling device, called photonic module, was introduced in 2009. This architecture illustrated the structure and operation of a fault-tolerant, fully error corrected quantum architecture. The architecture was based on components which were all theoretically deterministic. Not only deterministic photon-photon coupling by an atom/cavity system within each photonic module and also photonic sources and detectors were simply assumed to be deterministic and of high fidelity.

In this talk, we take the optical architecture and replace the sources and detectors with the photonic module and weak coherent-light source. This will lead to a network running with highly probabilistic single photon sources and entirely constructed from one quantum component, namely the photonic module. To combat the issue of probabilistic sources, we introduce a perpetual design, where the photonic module acts as non-destructive photon detector and photons in the computer are simply recycled. In this way, probabilistic sources are responsible for two tasks. (1) Providing the photons to initialize the network and (2) replacing photons which are periodically lost during computation. This talk will demonstrate how a highly probabilistic source can be integrated into a large scale architecture without sacrificing performance or the overall design and operation of the system.

8163-26, Session 7**Toward single photon optical nonlinearities for quantum information and quantum metrology**

S. Takeuchi, R. Okamoto, M. Fujiwara, H. Takashima, M. Okano, S. Subashchandran, Hokkaido Univ. (Japan); A. Tanaka, K. Toubaru, Osaka Univ. (Japan)

In this paper, we will present our two alternative efforts for the realization on single photon optical nonlinearities for quantum information and quantum metrology. The first approach is to utilize a single light emitters embedded in a high-finesse micro sphere cavity coupled with a tapered optical fiber. We will report the control of coupling between the tapered fiber and the microsphere at the cryogenic temperature[1]. We have also succeeded in obtained phase shift spectra of the fiber microsphere system using a very weak coherent light probe with the average number of photons per 10ns (typical decay time of the diamond nitrogen vacancy centers) below 1[2].

The second approach is to utilize 'monocycle entangled photons', which is the novel two-photon states with extreme time correlation down to a few femto-second level[3]. It is pointed out that the efficiency of the second harmonic generation between the two photons will be increased dramatically using such states. We will report our recent experimental progresses on the realization of monocycle entangled photon states.

[1] H. Takashima, ..., S. Takeuchi, Opt. Exp. 18, 15169 (2010).

[2] A. Tanaka, ..., S. Takeuchi, Opt. Exp. 19, 2278 (2011).

[3] S. E. Harris, Phys. Rev. Lett. 98, 063602 (2007).

8163-27, Session 7**The Dolinar receiver in an information theoretic framework**

B. I. Erkmen, K. M. Birnbaum, B. E. Moision, S. J. Dolinar, Jr., Jet Propulsion Lab. (United States)

It is well known that optical communication at the ultimate limits set by quantum mechanics requires measurement apparatuses that extract the information encoded in optical states of light with the highest efficiency. Unfortunately, it is often a difficult and elusive goal to realize measurements that achieve these quantum mechanical limits. The Dolinar receiver exemplifies a rare instance of success where the measurement meets the Helstrom lower bound with equality. In this receiver, a time-varying local oscillator is mixed with the incoming signal prior to photodetection, and the feedback for the local oscillator is chosen such that, both globally and incrementally, the probability of incorrectly distinguishing between two coherent state symbols is minimized. Inspired by this architecture, in this paper we investigate optical communication conducted with binary phase-shift keying (BPSK) modulation, and the same adaptive receiver structure, but using an information-theoretic optimization criterion. In particular, we seek the local oscillator field that will maximize the mutual information globally between the input symbols and the photon counts over the symbol duration. We show that this is

Conference 8163:
Quantum Communications and Quantum Imaging IX

equivalent to maximizing the mutual information incrementally in each instant of time, conditioned on the past observations, and we derive the objective function that is satisfied by the optimal local oscillator. For the BPSK case, we show that the Dolinar receiver's feedback function is the local oscillator function that also maximizes the mutual information. Our formalism extends to higher dimensional constellations, but, obtaining analytic expressions for the optimum local oscillator field are often not straightforward.

8163-28, Session 7

New developments in single-photon detection: superconducting nanowires and transition edge sensors

M. J. Stevens, B. Baek, B. Calkins, S. D. Dyer, T. Gerrits, A. E. Lita, S. W. Nam, National Institute of Standards and Technology (United States)

Superconducting detectors have emerged as among the highest-performing single-photon detectors at visible and infrared wavelengths. We will discuss our recent progress in developing two different single-photon sensitive superconducting detector systems. One system uses a superconducting nanowire single-photon detector (SNSPD), and the other employs a superconducting transition edge sensor (TES). This talk will cover device fabrication, packaging in cryogenic systems, and characterizing detector performance (detection efficiency, timing jitter, dark count rate, etc.). We have implemented these detector systems in a variety of quantum optics experiments, including polarization tomography of entangled photon pairs, high-order coherence measurements, and optical Schrodinger cat state generation.

8163-29, Session 8

Toward optical switches using the Zeno effect and two-photon absorption

B. C. Jacobs, The Johns Hopkins Univ. Applied Physics Lab. (United States)

All-optical switching and logic elements could be at the forefront of next generation computing and telecommunication systems, but only if a few key issues with the technology can be resolved. We have developed an approach based on the Zeno Effect that could overcome two of the biggest challenges with this technology: the need for relatively intense optical fields; and excessive power dissipation. We have previously shown that a classical version of the Quantum Zeno Effect (QZE) can be used to implement low-loss switching, logic, and memory operations. A significant feature of our basic design is that the envisioned devices could be cascaded on a single optical chip - potentially allowing scalable all-optical information processing networks. This cascading feature could also enable efficient signal regeneration and control signal energy recapture, allowing the overall system dissipation to be very low. Here we review the basic gate operation, present theoretical estimates of the switching and signal regeneration applications, and report on experimental progress toward realizing these devices.

8163-31, Session 8

Emulating a quadrature-phase-shift state-discrimination receiver with error rate below the standard quantum limit

F. E. Becerra, J. Fan, S. Polyakov, National Institute of Standards and Technology (United States); J. Goldhar, Univ. of Maryland, College Park (United States); J. T. Kosloski, The Johns Hopkins Univ. (United States); A. L. Migdall, National Institute of Standards and Technology (United States)

In optical communication information is encoded and sent in optical coherent states. The receiver measures the state and identifies the symbol that was sent. However, perfect discrimination of coherent states is impossible due to their inherent nonorthogonality. No physical measurement can unambiguously distinguish nonorthogonal states with total certainty. The minimum probability of error for conventional receivers is referred to as the homodyne limit. However this is not the lowest probability of error allowed by quantum mechanics. While the minimum error probability for the discrimination of nonorthogonal states is given by the Helstrom bound¹ for binary phase-based communication, extending beyond binary phase schemes to a larger number of symbols in the alphabet may yield lower bounds.

We have experimentally emulated a receiver discriminating among four non-orthogonal states in a quadrature-phase-shift keying (4PSK) communication scheme with a low error rate approaching the standard quantum limit. The proposed receiver-scheme works in a feed-forward manner, with the result of each phase-discrimination stage used to update the phase of the reference signal that operates as a local oscillator for the next stage. We analyze the experimental performance of our system which emulates, by post-selection, a Bayesian strategy to update the phase of the local oscillator in each subsequent stage. We observe that above a certain total-detection efficiency of the receiver a low number of stages is sufficient to surpass the homodyne limit for 4PSK signals. In our experimental setup we demonstrate that this total detection efficiency is achievable and thus this scheme can realistically be expected to lead to a communication system that surpasses the standard quantum limit.

8163-34, Session 8

Quantum enhanced lidar resolution with multi-spatial-mode phase sensitive amplification

C. Santivanez, S. Guha, Z. Dutton, BBN Technologies (United States); M. Annamalai, M. Vasilyev, The Univ. of Texas at Arlington (United States); B. J. Yen, R. Nair, Massachusetts Institute of Technology (United States); J. H. Shapiro, Massachusetts Institute of Technology (United States)

Phase-sensitive amplification (PSA) can enhance the signal-to-noise ratio (SNR) of an optical measurement suffering from detection inefficiency. Previously, we showed that this increased SNR improves LADAR-imaging spatial resolution when infinite spatial-bandwidth PSA is employed. Here, we evaluate the resolution enhancement for realistic, finite spatial-bandwidth amplification. PSA spatial bandwidth is characterized by numerically calculating the input and output spatial modes- and their associated phase-sensitive gains - under focused-beam pumping. We then compare the spatial resolution of a baseline homodyne-detection LADAR system with homodyne LADAR systems that have been augmented by pre-detection PSA with infinite or finite spatial bandwidth. The spatial resolution of each system is quantified by its ability to distinguish between the presence of 1 point target versus 2 closely-spaced point targets when minimum error-probability decisions are made from shot-noise limited measurements. At low (5-10 dB) SNR, we find that a PSA system with a 2.5 kW pump focused to 25 m x 400 m achieves the same spatial resolution as a baseline system having 5.5 dB higher SNR. This SNR gain is very close to the 6 dB SNR improvement possible with ideal (infinite bandwidth, infinite gain) PSA at our simulated system detection efficiency (0.25). At higher SNRs, we have identified a novel regime in which finite spatial-bandwidth PSA outperforms its infinite spatial-bandwidth counterpart. We show that this performance crossover is due to the focused pump system's input-to-output spatial-mode transformation converting the LADAR measurement statistics from homodyne to heterodyne performance.

8163-35, Session 8

Quantum-enhanced ladar ranging with squeezed-vacuum injection, phase-sensitive amplification, and slow photodetectors

R. Nair, B. J. Yen, Massachusetts Institute of Technology (United States); J. H. Shapiro, Massachusetts Institute of Technology (United States); J. Chen, Z. Dutton, S. Guha, M. P. da Silva, BBN Technologies (United States)

Theory has shown that the quantum enhancements afforded by squeezed-vacuum injection (SVI) and phase-sensitive amplification (PSA) can improve the spatial resolution of a soft-aperture, homodyne-detection LADAR system. Here we show they can improve the range resolution of such a LADAR system. In particular, because an experimental PSA-enhanced system is being built whose slow photodetectors imply multi-pulse integration, we develop range-measurement theory that encompasses its processing architecture. We allow the target to have an arbitrary mixture of specular and speckle components, and will present computer simulation results demonstrating the range-resolution improvement that accrues from quantum enhancement with SVI and/or PSA.

8163-36, Session 8

Physical implementation of non-physical quantum operations: realization of the universal transpose operation

H. Lim, Y. Ra, Y. Kim, Pohang Univ. of Science and Technology (Korea, Republic of); J. Bae, Korea Institute for Advanced Study (Korea, Republic of); Y. Kim, Pohang Univ. of Science and Technology (Korea, Republic of)

The universal transpose of quantum states is an anti-unitary transformation that is not allowed in quantum theory. In this work, we investigate approximating the universal transpose of quantum states of two-level systems (qubits) using the method known as structural physical approximation. We also report its experimental implementation in linear optics. The scheme is optimal in that the maximal fidelity is attained, and also practical as measurement and preparation of quantum states that are experimentally feasible within current technologies are solely applied.

8163-40, Session 8

Toward ghost imaging with cosmic ray muons

M. D'Angelo, F. Di Lena, Univ. degli Studi di Bari (Italy); M. D'Incecco, Istituto Nazionale di Fisica Nucleare (Italy); A. Garuccio, Univ. degli Studi di Bari (Italy); R. Moro, Istituto Nazionale di Fisica Nucleare (Italy); A. Regano, F. Romano, Univ. degli Studi di Bari (Italy); G. Scarcelli, Harvard Medical School (United States)

Muons generated by cosmic rays are an interesting source to study in the context of ghost imaging: As naturally available deeply penetrating particles characterized by an extremely small De Broglie wavelength, they are promising candidates for very long distance high resolution ghost imaging.

The project Extreme Energy Events (EEE) offers a platform to study the feasibility of muon ghost imaging. To detect cosmic ray muons, EEE uses "telescopes" composed by three Multigap Resistive Plate Chambers (MRPC) with lateral spatial resolution of 1cm. Coincidences between muons have been measured by MRPC telescopes installed in two neighbor schools of L'Aquila, Italy, 180 m apart. By tracing a histogram of both the temporal and the momentum distribution of muon coincidences obtained from 9 days of data accumulation, we observe a highly visible correlation peak.

From fundamental point of view, with light, ghost imaging either employs the quantum correlations exhibited by entangled photons from SPDC, or the Hanbury-Brown and Twiss effect exhibited by chaotic light sources. Interestingly, muon pairs detected from cosmic ray showers exhibit both a chaotic/thermal component (mostly due to the multitude of incoherent cosmic rays that simultaneously reach the earth atmosphere) and a strong spatio-temporal correlation. Such a correlation represents an encouraging starting point to understand the physics behind this naturally available source and to evaluate the feasibility of ghost imaging with massive particle.

Conference 8164: Nanophotonics and Macrophotonics for Space Environments V

Monday-Tuesday 22-23 August 2011 • Part of Proceedings of SPIE Vol. 8164
Nanophotonics and Macrophotonics for Space Environments V

8164-01, Session 1

Recent progress made in testing laser diode and optical materials subjected to exposure in space

N. S. Prasad, NASA Langley Research Ctr. (United States)

In this paper, progress made so far in the performance testing of high power laser diode and thermoelectric materials sent by NASA Langley Research Center on MISSE 6 mission will be discussed. The objective of the Materials International Space Station Experiment (MISSE) is to study the performance of novel materials when subjected to the synergistic effects of the harsh space environment for several months. MISSE missions provide an opportunity for developing space qualifiable materials. The results of post-testing of several optical materials that were recently returned back after more than one year of exposure on the International Space Station (ISS) will be presented. The items were part of the MISSE 6 mission that was transported to the ISS via STS 123 on March 11, 2008 and returned to the Earth via STS 128 that was launched on August 2009. The materials experienced no visible damage during lengthy exposure in space. In the case of laser diode, a comparison of elemental analysis with pre-flight conditions will be discussed. This will be followed by results of post-flight testing of thermoelectric material samples.

8164-02, Session 1

Proton radiation testing of laser optical components for NASA Jupiter Europa Orbiter Mission

W. J. Thomes, Jr., J. F. Cavanaugh, M. N. Ott, NASA Goddard Space Flight Ctr. (United States)

The Jupiter Europa Orbiter (JEO) is NASA's element of the joint Europa Jupiter System Mission (EJSM). Based on current trajectories, the spacecraft will spend a significant amount of time in the Jovian radiation belts. Therefore, research endeavors are underway to study the radiation effects on the various parts and components needed to assemble the instruments. Data from these studies will be used for component selection and system design to ensure reliable operation throughout the mission duration. The radiation environment on the way to Jupiter is nothing new for NASA designed systems, however, the long durations orbiting Jupiter and Europa present new challenges for radiation exposure. High-energy trapped electrons and protons at Jupiter dominate the expected radiation environment. Therefore, most of the initial component level radiation testing is being done using protons. In this paper we will present in-situ monitoring of the optical transmission of various laser optical components during proton irradiation. Radiation induced optical attenuation of some components is less than would be expected, based on the authors experiences, and is attributed to the interaction of the protons with the materials. Therefore, plans for follow-on testing using other radiation sources will be discussed.

8164-03, Session 1

Mesa-isolated InGaAs avalanche photodiode damage by ionizing radiation

A. S. Huntington, M. A. Compton, L. A. Sellsted, Voxel, Inc. (United States); E. W. Taylor, International Photonics Consultants, Inc. (United States)

InGaAs avalanche photodiodes (APDs) fabricated from epitaxial material by etching detector mesas and encapsulating the etched mesas under benzocyclobutene (BCB) resin were irradiated by Co-60 gamma-rays to simulate a total ionizing dose which might be experienced in a space environment. The APDs were not under bias during irradiation. Damage to the APDs was assessed by measuring the increase in dark current following irradiation.

8164-04, Session 1

Self-trapped holes in glassy silica: basic science with relevance to photonics in space

D. L. Griscom, impactGlass Research International (United States)

Development of radiation-hard silica-based fiber optics (FOs) is greatly aided by a fundamental understanding of the radiation-induced point defects in glassy SiO₂ that absorb light in the wavelength ranges where high transmissivity is required. The molecular-scale structures of those defects that are paramagnetic are determined by electron spin resonance (ESR), and their associations with specific absorption bands are established by ESR-optical correlations involving post-irradiation thermal annealing experiments. In the past half century many point defects in pure silica have been characterized in great detail. Among the best understood trapped-hole defects are several variants of E' centers, the non-bridging-oxygen hole center, the peroxy radical, and two variants of self-trapped holes (STHs).[1] Unlike the others, the STHs decay rapidly at room temperature (according to fractal kinetics)[2] and their profound effects on transmission in the range ~400 - 1000 nm (with a tail to longer wavelengths)[2] depends on dose RATE,[2] not total dose, thus thwarting accelerated testing of FO systems for satellites - and threatening to momentarily black out FO systems exposed to radiation from nuclear detonations in space. Astonishingly, the transient absorption due to STHs can be suppressed by more than an order of magnitude by preirradiation at relatively low dose rates (at least as low as 0.25 Gy/sec) for periods ~3 months.[3,4]

[1]DL Griscom, J. Non-Cryst. Solids 352 (2006) 2601. [2]DL Griscom, Phys. Rev. B 64 (2001) 174201. [3]DL Griscom, Defects in Insulating Materials ICDIM 96, Materials Sci. Forum Vols. 239-241 (1997) 19. [4]DL Griscom, Appl. Phys. Lett. 71 (1997) 175.

8164-05, Session 1

Nanonewton thrust measurement of photon pressure propulsion using semiconductor laser

K. Iwami, T. Akazawa, T. Ohtsuka, H. Nishida, N. Umeda, Tokyo Univ. of Agriculture and Technology (Japan)

To evaluate the thrust produced by photon pressure emitted from a 100 W class continuous-wave semiconductor laser, a torsion-balance precise thrust stand is designed and tested. Photon emission propulsion using semiconductor light sources attract interests as a possible candidate for deep-space propellant-less propulsion and attitude control system. However, the thrust produced by photon emission as large as several ten nanonewtons requires precise thrust stand. A resonant method is adopted to enhance the sensitivity of the bifilar torsional-spring thrust stand. The torsional spring constant and the resonant of the stand is 1.245×10^{-3} Nm/rad and 0.118 Hz, respectively. The experimental results showed good agreement with the theoretical estimation. The thrust efficiency for photon propulsion was also defined. A maximum thrust of 499 nN was produced by the laser with 208 W input power (75 W of optical output) corresponding to a thrust efficiency of 36.7%. The

**Conference 8164: Nanophotonics and
Macrophotonics for Space Environments V**

minimum detectable thrust of the stand was estimated to be 2.62 nN under oscillation at a frequency close to resonance.

8164-06, Session 2**Pulse shaping high-energy fiber laser at low repetition rate**

P. Wan, J. Liu, L. Yang, PolarOnyx, Inc. (United States); F. Amzajerdian, NASA Langley Research Ctr. (United States)

High energy pulsed fiber lasers have been considered as an enabling technology with many applications, such as Lidars, holography, free space optical communications, and material processing due to their many advantages such as compact, light-weight and high wall-plug efficiency. In eye safe wind-profiling Lidar applications, 200 ns pulse width is required at low repetition rates down to Hz level. However, due to ASE effect and the gain dynamics in Er-doped fiber lasers, the repetition rate is limited to kHz. Q-switched solid state lasers are usually applied with comparatively low pulse repetition rates.

In recent publications we demonstrated a 10 kHz repetition rate, 150 μ J pulse energy at a wavelength of 1.5 μ m with a pulse width of 200 ns. In this paper, we have demonstrated a modulated pump scheme combined with a pulse shaping technology to generate high energy pulses at a wavelength of 1.5 μ m with low repetition rates. This method is proven to be an efficient way to mitigate SBS effects, pulse narrowing effects as well as ASE in high energy fiber lasers. We successfully generated a 200 ns seed macro-pulse comprising of a series of micro-pulses each with a pulse width less than 20 ns. After power amplification, we obtained pulse energy of 120 μ J at 500 Hz repetition rate and 90 μ J at ultra low repetition rates (10 Hz). Excellent pulse shape, high extinction ratio and power stability were achieved.

8164-07, Session 2**Grating gated HEMT for tunable THz and mm-wave detection**

R. E. Peale, N. Nader, C. J. Fredricksen, H. Saxena, G. Medhi, Univ. of Central Florida (United States); J. Hendrickson, W. R. Buchwald, Air Force Research Lab. (United States); J. W. Cleary, Solid State Scientific Corp. (United States)

Gate-voltage tunable plasmon resonances in the two dimensional electron gas of high electron mobility transistors (HEMT) provide an opportunity for tunable terahertz array detectors with applications in spectral sensing and space situational awareness. Though tunable resonant absorption has been clearly observed in optical experiments, transduction to measurable electrical signal has been elusive for HEMTs made in the InP-based materials system. This is in part due to the paucity of suitable terahertz sources and the difficulties inherent in the use of those that exist. To uncover the desired electrical effects, mm-wave devices have been designed to allow use of backward wave oscillators. Such sources have advantages such as continuous frequency tuning, frequency and amplitude modulation for lock-in detection, stability, delivery and detection using standard microwave components, and the ability to control and enhance the field using suitable cavities. Calculated resonance spectra predict the expected lock-in output as functions of frequency and gate bias to enable interpretation of the observations. Detection of terahertz-to-plasmon-to-electronic transduction will inform optimization and migration to frequencies as high as 10 THz. First observations of tunable resonant changes in channel conductance are reported.

8164-08, Session 2**2 μ m fiber laser sources and their applications**

J. Geng, S. Jiang, AdValue Photonics, Inc. (United States)

Mid-infrared fiber laser sources have attracted a lot of interest in space and defense applications. We review our latest developments of various fiber laser sources operating near 2 μ m and beyond the wavelength, which include single-frequency CW sources, nanosecond pulsed sources, mode-locked sources, and supercontinuum sources. Potential applications of these mid-infrared fiber sources will also be discussed.

8164-09, Session 3**Ultrafast coherent optical signal processing technologies and applications using stabilized optical frequency combs**

P. J. Delfyett, Jr., CREOL, The College of Optics and Photonics, Univ. of Central Florida (United States)

The development of nanophotonic systems and devices for high speed communications, interconnects and signal processing are critical for next generation space borne applications. Lightwave technologies offer the promise of high bandwidth connectivity from component development that is manufacturable, cost effective, and electrically efficient. The concept of optical frequency/wavelength division multiplexing has revolutionized methods of optical communications, however the development of optical systems using 100's of wavelengths present challenges for network planners. The development of compact, efficient optical sources capable of generating a multiplicity of optical frequencies/wavelength channels from a single device could potentially simplify the operation and management of high capacity optical interconnects and links. Over the years, we have been developing mode-locked semiconductor lasers to emit ultrashort optical pulses at high pulse repetition frequencies for a wide variety of applications, but geared toward optical communications using time division multiplexed optical links. The periodic nature of optical pulse generation from mode-locked semiconductor diode lasers also make these devices ideal candidates for the generation of high quality optical frequency combs, or multiple wavelengths, in addition to the temporally stable, high peak intensity optical pulses that one is accustomed to. The optical frequency combs enables a variety of optical communication and signal processing applications that can exploit the large bandwidth and speed that femtosecond pulse generation implies, however the aggregate speed and bandwidth can be achieved by spectrally channelizing the bandwidth, and utilize lower speed electronics for control of the individual spectral components of the mode-locked laser. This presentation will highlight our recent results in the generation of stabilized frequency combs, and in developing photonic device technologies and approaches for filtering, modulating and detecting individual comb components. We then show how these technologies can be applied in signal processing applications such as arbitrary waveform generation, arbitrary waveform measurement, synthetic aperture imaging and matched filtering for pattern recognition.

8164-10, Session 3**Photonic microdevice fabrication with femtosecond fiber laser**

H. Huang, L. Yang, J. Liu, PolarOnyx, Inc. (United States)

There is a great deal of interests and efforts in the area of femtosecond (fs) laser direct writing of transparent materials, which promises to be a powerful and flexible technique for rapid fabrication of photonic micro-device, such as gratings, waveguides and optical amplifiers. Waveguide properties depend critically on the sample material properties and writing laser characteristics. In this paper, we present the results using fs fiber laser on the micro-scale design and fabrication of photonic micro-devices using fs fiber laser direct-writing technique. Single line writing of doped/undoped glasses with respect to the focused laser beam at different pulse energies, repetition rates and writing speeds has been investigated at first. Then the waveguide properties were characterized in terms of their transmission, reflection and gain data. It was found that specific consideration of the pulse energy and repetition rate, writing

**Conference 8164: Nanophotonics and
Macrophotonics for Space Environments V**

speed and number of fabrication scans should be taken into account in order to fabricate low-loss positive index guiding waveguide devices in a specific type of glass. Furthermore, three-dimensional microfluidic networks in glasses have also been demonstrated. The channel size can be changed by using different laser pulse energy or different pulse repetition rate. The modified regions in both waveguides and microfluidic networks were checked by Scan Electron Microscope to understand the spatial profile of the laser-exposed regions. These two techniques can be combined to produce micro-devices that incorporate on a single glass chip optical system with microfluidic system.

8164-11, Session 3

Design of microdisk modulators and detectors for high-speed integrated WDM systems

G. W. Taylor, Univ. of Connecticut (United States); J. Cai, B. Pile, Y. Zang, ODIS, Inc. (United States)

It is anticipated that future VLSI integrated circuits will be optoelectronic with optical and electronic I/O. It will also involve a significant level of on-chip optical interconnects to connect CPU cores with cache memory and perform routing functions between functional blocks. Thus, in conjunction with transistors, the circuits will require a significant density of lasers, detectors and modulators. To achieve these densities with future scalability, the optimum geometries for laser, detector, modulator, and switch functions are microresonators. The resonance characteristic enables a reduced form factor and, further, it enables WDM to be employed within the chip. In this paper, the microdisk will be evaluated as an absorption and phase modulator in the context of POET (Planar OptoElectronic Technology), a new technology approach for optoelectronic integrated circuits. The modulation is obtained by the blue shift of the absorption edge with the injection of channel charge. The large absorption change provides unique control over of the resonator characteristics, whereas the majority of reported microresonator modulators rely mostly on index change. It will be shown that the POET absorption modulator achieves full on-off switching with voltage inputs of 0.3V and an electrically-dominated bandwidth of 50GHz for a 10um diameter disk. Furthermore a row these disks may access the same straight waveguide to achieve WDM with wavelength separations of about 2nm. Using a similar geometry, a row of wavelength selective detectors can be implemented to provide an optimum WDM interface.

8164-12, Session 4

Resonant optoelectronic thyristor switches as elements for optical switching fabrics

G. W. Taylor, Univ. of Connecticut (United States); J. Cai, B. Pile, ODIS, Inc. (United States); Y. Zang, Univ. of Connecticut (United States)

Optical switching fabrics are networks of devices that enable input to output routing of optical packets with arbitrary connectivity, providing that two separate input channels do not require simultaneous connection to the same output port, i.e. a contention. The goal of any fabric is to establish a connection pattern through the network by using the routing code contained in the header. Thus a successful approach must allow OE conversion of the header in real time to resolve contentions. A novel approach is described to implement the fabric with arrays of 2x2 switches where the switches are resonant microdisks coupled to waveguides. The switches have the unique ability to be written with optical inputs which therefore allows the signal pattern to be set up by the first passage of the header through the fabric. Functionally, these switches are OE thyristors and have a storage function which allows the state of the fabric to be set for all subsequent packets until a reset or clear function is applied. The resonant property allows several switches with different wavelengths to share the same waveguide. Thus an N wavelength WDM fabric is enabled with a throughput that is N times the

simple fabric. A typical value for N is 5-10 based on the free spectral range of the disk. This paper will discuss the fabric design and progress towards its implementation in POET (Planar OptoElectronic Technology), a new OE technology implementation which integrates the optically resonant devices with complementary transistors for design of control circuits.

8164-13, Session 4

Small form factor optical fiber connector evaluation for harsh environments

M. N. Ott, W. J. Thomes, Jr., R. F. Chuska, R. C. Switzer, D. E. Blair, NASA Goddard Space Flight Ctr. (United States)

For the past decade NASA programs have utilized the Diamond AVIM connector for optical fiber assemblies on space flight instrumentation. These connectors have been used in communications, sensing and LIDAR systems where repeatability and high performance are required. Recently Diamond has released a smaller form factor optical fiber connector called the "Mini-AVIM" which although more compact still includes the tight tolerances and the racking feature of the heritage AVIM. NASA Goddard Space Flight Center Photonics Group in the Parts, Packaging and Assembly Technologies Office has been performing evaluations of this connector to determine how it compares to the performance of the AVIM connector and to assess its feasibility for harsh environmental applications. Vibration and thermal testing was performed on the Mini AVIM with both multimode and singlemode optical fiber using insitu optical transmission monitoring. Random vibration testing was performed using typical launch condition profiles for most NASA missions but extended to 35 Grms which is much higher than most requirements. Thermal testing was performed up to a -55°C to +125°C range. The test results include both unjacketed fiber evaluations and cabled assembly. The results are presented here. The data indicates that the Mini-AVIM provides a viable option for small form factor applications that require a high performance optical fiber connector.

8164-14, Session 4

Fiber optic cables for transmission of high-power laser pulses

W. J. Thomes, Jr., M. N. Ott, R. F. Chuska, R. C. Switzer, D. E. Blair, NASA Goddard Space Flight Ctr. (United States)

High power pulsed lasers are commonly deployed in harsh environments, like space flight and military missions, for a variety of systems such as LIDAR, optical communications over long distances, or optical firing of explosives. Fiber coupling of the laser pulse from the laser to where it is needed can often save size, reduce weight, and lead to a more robust and reliable system. Typical fiber optic termination procedures are not sufficient for injection of these high power laser pulses without catastrophic damage to the fiber endface. In the current study, we will review the causes of fiber damage during high power injection and discuss our new manufacturing procedures that overcome these issues to permit fiber use with high reliability in these applications. A brief review of the design considerations for high peak power laser pulse injection will be presented to familiarize the audience with all the areas that need to be considered during the design phase will be included as an introduction. The majority of the presentation will then focus on the proper polishing methods for high power use with an emphasis on laser polishing of the fibers. Results from recently build fibers will be shown to demonstrate the techniques.

8164-15, Session 4

OLTARIS: an efficient web-based tool for analyzing materials exposed to space radiation

T. C. Slaba, NASA Langley Research Ctr. (United States); A. M. McMullen, Rochester Institute of Technology (United States); S. A. Thibeault, C. A. Sandridge, M. S. Cloudsley, S. R. Blattnig, NASA Langley Research Ctr. (United States)

The near Earth space radiation environment includes energetic galactic cosmic rays (GCR), high intensity proton and electron belts, and the potential for solar particle events (SPE). These sources may penetrate shielding materials and deposit significant energy in sensitive electronic devices on-board spacecraft and satellites. Material optimization methods may be used to reduce the exposure and extend the operational lifetime of individual components and/or systems. Since laboratory experiments are expensive and may not cover the range of particles and energies relevant for space applications, such optimization may be done computationally with efficient algorithms that include the various constraints placed on the component, system, or mission. In the present work, the web-based tool OLTARIS (On-Line Tool for the Assessment of Radiation in Space) is presented, and the applicability of the tool for rapidly analyzing exposure levels within either complicated shielding geometries or user-defined material slabs exposed to space radiation is demonstrated. An example approach for material optimization is also presented. Slabs of various advanced multi-functional materials are defined and exposed to several space radiation environments. The materials and thicknesses defining each layer in the slab are then systematically adjusted to arrive at an optimal slab configuration.

8164-16, Session 5

Molecular photonics in space environments: a review

J. Pérez-Moreno, Katholieke Univ. Leuven (Belgium)

Although much of the early developments of organic and polymer-based materials were fueled by the research on space materials, most of the optoelectronic applications for usage in space or terrestrial adverse environments are still dominated by semiconductors. In this paper, we review past and present efforts to incorporate organic-based materials into photonic devices that are suitable for applications in space environments, and discuss what are the main challenges that materials based on organics must meet in order to become fully integrated into photonic devices that can operate in space and space-related environments.

8164-17, Session 5

Hyper-Rayleigh scattering as a screening tool for the optimization of piezoelectric polymers

J. Pérez-Moreno, K. Clays, Katholieke Univ. Leuven (Belgium)

The use of piezoelectric polymers has been proposed and investigated in different Space-related environments, for example, as ultra-light mirrors in space telescopes or as piezoelectric actuators. Even though some piezoelectric polymers have been shown to be as efficient as the more traditional piezoelectric crystals, no systematic exploration of the different molecular motives available for piezoelectricity has been performed, partly due to experimentally challenging conditions: new structures must be generated in enough quantity to be able to produce thin films, and with measurable piezoelectric response. Consequently, few structure-property relationships have been derived for the piezoelectric performance of polymer based materials. We show how, under certain conditions, the characterization of the second-order nonlinear molecular response through the Hyper-Rayleigh scattering technique, can be

used to predict the piezoelectric response of the molecules in a film. In contrast to the piezoelectric characterization, a Hyper-Rayleigh experiment can be performed with minimal amounts of chromophores (~mg) in solution, and is relatively quick. Therefore, we propose to use the Hyper-Rayleigh scattering technique as a screening tool for the search of optimized piezoelectric polymers.

8164-18, Session 5

The effect of energy spectrum on the nonlinear response of a quantum system

S. Shafei, M. G. Kuzyk, Washington State Univ. (United States)

It is well-known that the experimental values of the off-resonant first and second hyperpolarizabilities of molecules fall far below their respective fundamental limits. However, Monte Carlo simulations, in which the transition moments and state energies are chosen randomly but are constrained by the sum rules, reveal no gap between the numerically generated data and the fundamental limit. Previous studies suggest that the gap might be due to the unfavorable distribution of the eigenenergies.

In the present work we use the Monte Carlo method to study the nonlinear optical response classified by energy spacing of the system, aiming to understand some unresolved questions: (1) The results suggest an explanation for the origin of the factor of 20-30 gap between the best molecules and the fundamental limits. Increasing E , defined as the ratio of energy difference between the first excited and the ground states to the energy difference of the second excited state and the ground state, yield larger first and second order nonlinear response. (2) The results also confirm the validity of three-level ansatz, which states that when the first and second hyperpolarizabilities of a quantum system are at the limit, only three states contribute to the nonlinear response. Studying the number of states that contribute to the hyperpolarizabilities when E approaches zero reveals that at the limit, three states dominate the SOS expressions.

8164-19, Session 5

Unexpected second-order nonlinear optical effects in conjugated polymers

I. Asselberghs, K. Clays, T. Verbiest, G. Koeckelberghs, Katholieke Univ. Leuven (Belgium)

Conjugated polymers do not only attract great attention due to their suitability in organic transistors, light emitting diodes and solar cells, moreover, they possess unexpected record-high second-order nonlinear optical responses. Nonlinear optical polymers have been reported as attractive materials for space applications such as electro-optic modulation and optical power limiting. In this work, we report on a new approach for increased second-order nonlinear properties demonstrated in a series of polythiophene derivatives and polyphenantrenes.

8164-20, Session 6

Temperature effects of an all-fiber polarization maintaining ytterbium optical amplifier

A. D. Sanchez, Air Force Research Lab. (United States)

An overview of recent fiber based component developments is presented that lead to robust all-fiber lasers and optical amplifiers. Critical issues impacting the integration of high power rare earth doped optical amplifiers are presented. The optical performance of key fiber components is reported with emphasis on temperature effects of a monolithically integrated multi-Watt, single mode, Polarization Maintaining (PM), Ytterbium (Yb) doped double clad optical amplifier. Performance of an all-fiber optical amplifier design that integrates two

fiber coupled laser diode pumps and one PM Yb double clad feed through fiber directly in to a combiner is reported.

8164-21, Session 6

All fiber-based single-frequency Q-switched laser pulses at 2 um for lidar and remote sensing applications

W. Shi, NP Photonics, Inc. (United States); E. Petersen, N. Moor, NP Photonics, Inc. (United States) and Univ. of Arizona (United States); A. Chavez-Pirson, NP Photonics, Inc. (United States); N. Peyghambarian, NP Photonics, Inc. (United States) and Univ. of Arizona (United States)

In this paper, we report an all-fiber-based 2 um pulsed laser for the applications of LIDAR and laser remote sensing. This single-frequency actively Q-switched fiber laser is based on fiber birefringence induced by stress in the short fiber laser cavity. The cavity consists of our proprietary highly Tm doped germanate glass fiber. The highly Tm-doping concentration creates a high unit gain in active fiber, allowing for a short cavity, which creates large longitudinal mode spacing, helping to maintain lasing on a single longitudinal mode. The active fiber is fusion-spliced between two fiber Bragg gratings. In this method, a piezoelectric compresses a fiber creating stress birefringence, and this birefringence acts as a waveplate, changing the polarization state of the light in the fiber and switching the laser between high and low feedback states. The pulse width of this Q-switched fiber laser can be tuned from 10's ns to sub-us. The repetition rate can be tuned from 100 Hz to 100's kHz. The average power is in the mW-level, peak power can reach watt-level, and pulse energy in the range of 10-100 nJ without any amplifier. Moreover, this transform-limited fiber laser pulses in 100's ns regime has been successfully amplified by using newly developed large core single-mode highly Tm-doped germanate fiber 25/250 um in the power amplifier stage. Based on the monolithic MOPA configuration, > 100 uJ pulse energy has been achieved, which corresponds to a peak power of > 1 kW for transform-limited fiber laser pulses.

8164-22, Session 6

Low-noise laser at 2 micron wavelength with FM modulation

L. S. Watkins, B. Xu, R. Van Leeuwen, C. Ghosh, Princeton Optronics, Inc. (United States); E. W. Taylor, International Photonics Consultants, Inc. (United States)

We have developed a laser in the 1550nm wavelength band with very low intensity and phase noise, and are currently extending this technology to develop lasers with very similar characteristics in the 2 micron wavelength band. The 1550nm laser is a diode pumped solid-state laser using Yb:Er doped high phosphate glass for the gain medium. Both Tm doped YAP and Tm doped YAG are being investigated in a very similar laser configuration to produce lasers in the 2 micron wavelength band. Experiments are underway to investigate ionizing radiation and other effects on the lasers' properties.

The laser power will be in the 20-100mW range and be single frequency with linear polarization output into a PM fiber. The laser design applies frequency feedback control using an internal high finesse locker to stabilize the wavelength and reduce the phase noise. The laser uses piezo frequency tuning with which we have demonstrated up to 5GHz FM modulation depth in both sinusoidal and ramp profiles at up to 1kHz rates. This has applications in Doppler LIDAR and other sensor applications.

The talk will review the overall laser design including FM modulation approaches. Latest results including radiation tests for the 2 micron laser will be given.

8164-23, Session 6

Recent developments in polycrystalline oxide fiber laser materials

H. Lee, K. A. Keller, B. M. Sirn, UES, Inc. (United States); M. Cheng, F. K. Hopkins, Air Force Research Lab. (United States); T. A. Parthasarathy, UES, Inc. (United States)

Laser quality, polycrystalline oxide fibers are critical to the optimization of high energy and high power lasers. Advanced ceramic processing technology, along with a novel powder production process, make it possible to produce various oxide fibers with an outstanding optical quality for use in the fiber laser applications. The production of contaminant-free green fibers with a high packing density, as well as uniform packing distribution, is a key factor in obtaining laser-quality fibers. High quality green fibers are dependent on the powder quality combined with the appropriate slurry formulation. These two fundamental technologies were successfully developed at UES, and used to produce Yb-doped yttrium aluminum garnet (YAG) fibers* with high optical quality, high chemical purity, and suitable core diameters down to 20 microns. Current progress in developing polycrystalline oxide fibers for high energy laser applications will be reviewed.

8164-24, Session 7

Strategic photonic sensors: technology needs and challenges

S. Forbes, Air Force Research Lab. (United States)

No abstract available

8164-25, Session 7

Planar hybrid integration for the development of cost effective interferometric fiber optic gyroscopes (IFOG)

W. K. Bischel, M. A. Kouchnir, Gener8, Inc. (United States); M. Bitter, Gemfire Corp. (United States); R. Yahalom, Infiber Technology, Inc. (United States); E. W. Taylor, International Photonics Consultants, Inc. (United States)

The need for cost effective interferometric fiber optic gyroscopes (IFOG) for DoD and commercial applications requires that new approaches to the design and manufacturing of IFOG systems be developed. Monolithic integration has been demonstrated and commercialized for some optical integration applications (e.g. InP PIC optical chips), but this approach is unable to provide a complete solution for the integration of the discrete IFOG optical components. We have developed a new technology platform for IFOG optical systems based on the concept of hybrid integration. Hybrid integration enables the use of the best materials for the specific application and enables higher yields at low volumes due to the ability to yield at the individual chip level before integration. The most cost effective approach for optical integration is to leverage the more than 30 years of learning from the planar wafer-based semiconductor industry into the manufacturing of optical components.

A waveguide technology platform has been developed that includes several different processes and optical sub-components that effectively implement planar hybrid integration as a manufacturing strategy for advanced optical components. We will discuss the development of a practical set of device designs and processes that have been integrated into the first 4-channel IFOG optical engine planar waveguide hybrid chip. These include: (1)Passive waveguide platform for integration (PLC), (2)Out-of-plane mirrors and detector arrays, (3)Integration of light source arrays into a PLC chip, (4)Waveguide isolator array design and integration, (5)Chip-to-chip coupling techniques for fiberless interconnects, and (6)Lithium-niobate-PLC hybrid integration.

Conference 8164: Nanophotonics and
Macrophotonics for Space Environments V

We will present the test results for the IFOG optical engine hybrid chip in an IFOG test bed and compare the result to the typical published results for an IFOG system fabricated from discrete optical components. We will also present the results of radiation testing of the IFOG optical engine as a first step toward qualification for space based applications. A sample set will be irradiated by Co-60 gamma-rays at a nominal room temperature to determine if any permanent induced effects result from the ionizing radiation dose.

8164-26, Session 7

Radiation effects on multiple DOF MEMS inertial sensors

B. Dillard, V. Trent, M. Greene, Archangel Systems, Inc. (United States); E. W. Taylor, International Photonics Consultants, Inc. (United States)

A novel 5 degree-of-freedom MEMS sensor called the MEMS Annular Rotating Sensor (MARS) with navigation-grade accuracy is being developed. MARS has a spinning mass gyroscope heritage but provides triaxial accelerations and dual rate outputs. The MARS rotor is suspended electrostatic in vacuum, isolating the silicon mass from bulk material noise and fatigue effects. Program expectations are gyro bias stability of 0.01°/hr, angular random walk of 0.001°/rt-hr, gyro scale factor stability of 50 ppm and a bandwidth of 300 Hz. Evaluation prototypes are slated for Q4, 2011 release will have SWAP budgets of 3 cubic inches, 125 grams and 1 W for the MEMS sensor and all support hardware.

While the body of work in radiation effects on electronics is expansive, the same is not true for MEMS sensors. In this work, a set of MARS sensors are fully characterized, irradiated by Co-60 gamma rays under passive conditions and examined for total dose effects. Post-radiation comparative performance results will be presented at the conference.

8164-28, Session 8

Performance of long-wave infrared InAs/GaSb strained layer superlattice detectors

E. Plis, N. Gautam, M. N. Kutty, S. A. Myers, B. Klein, T. Schuler-Sandy, M. Naydenkov, S. Krishna, The Univ. of New Mexico (United States)

Photodetectors operating in the long-wave infrared (LWIR, 8-14 μm and beyond) spectral band could be potentially useful for a wide variety of applications such as meteorology, satellite based surveillance, terrestrial pollution monitoring, and space-based astronomy. The technologies currently dominating those applications in this wavelength range are based on interband Mercury-Cadmium-Telluride (MCT) and extrinsic silicon blocked impurity band (BIB) MCT detectors are characterized by low operation temperatures due to a low electron effective mass resulting in excessive leakage current. Moreover, they are sensitive to small changes in the alloy composition ratio during the epitaxial process, making the spatial non-uniformity a challenging problem for large format focal plane arrays (FPAs). BIB detectors are limited to even lower operation temperatures due to high thermal ionization rates.

The basic material properties of type-II InAs/GaSb strained layer superlattices (SLSs) provide a prospective benefit in the realization of photodetectors with cut-off wavelengths in LWIR range. Suppressed Auger recombination rates and larger effective mass in SLS leads to a reduction of tunneling currents and improved temperature limits of spectral detectivities compared with MCT detectors of the same bandgap. High degree of uniformity for III-V growth and processing over a large area also offers advantage for the InAs/GaSb SLS technology.

During the presentation, our efforts on fabrication of high-performance LWIR and VLWIR SLS single element detectors and FPAs will be presented. Implementation of novel nBn and pBiBn design concepts to SLS detectors, as well as multispectral operation of nBn detectors will be also discussed.

8164-29, Session 8

Thermoluminescence properties of Eu³⁺-doped CaSiO₃-(SO₄) nano phosphor

C. Rayappa, Vivekananda Degree College (India); K. P. Ramesh, Indian Institute of Science (India); B. M. Nagabhushana, M S Ramaiah Institute of Technology (India)

Porous materials are of significant interest due to their wide applications in catalysis, separation, light weight structural materials and biomaterials. Calciumsulphosilicate biomaterial doped with europium (Ca_{1-x}Eu_x SiO₃-(SO₄); x = 0.0 to 0.05) were synthesized by low-temperature solution combustion reaction. Solution combustion technique is a versatile process leading to synthesize single phase, composites, solid solutions as well as complex compound silicate phases in homogeneous form. Powder X-ray diffraction, scanning electron microscopy, Transmission electron microscope (TEM) and Fourier Transform Infrared spectroscopic techniques were used for the characterization of the synthesized products. The thermoluminescence (TL) and some of the dosimetric characteristics of Eu³⁺-activated (Ca_{1-x}Eu_x SiO₃-(SO₄)) were reported. The TL glow curve is composed of only one peak located at about 156 °C between room temperature and 500 °C. The optimum Eu³⁺ concentration is 0.003 mol % to obtain the highest TL intensity. The TL kinetic parameters of (Ca_{1-x}Eu_x SiO₃-(SO₄)) were studied by the peak shape method. The TL dose response is linear in the protection dose ranging from 1 to 80 Gy. The maximum temperature, the integral and the full width at half maximum of the thermoluminescence glow - peak as a function of the heating rate were studied in the range 2 to 25 °C/s.

8164-30, Session 8

Advances in nonlinear materials for space applications

E. W. Taylor, International Photonics Consultants, Inc. (United States)

No abstract available

Conference 8165A: Unconventional Imaging and Wavefront Sensing VII

Sunday-Monday 21-22 August 2011 • Part of Proceedings of SPIE Vol. 8165A
Unconventional Imaging and Wavefront Sensing VII

8165A-01, Session 1

Optimal prediction and correction of optical wavefronts in an adaptive optics experiment

J. Tesch, J. S. Gibson, Univ. of California, Los Angeles (United States)

This paper discusses the use of a linear time invariant controller based on optimal wavefront prediction in an adaptive optics experiment. The minimum variance predictor, which has state space form, is identified from a measured wavefront sequence by a subspace system identification method. Experimental results show the improved performance of the optimal predictor/controller as compared to a classical adaptive optics loop. In the experiment, a membrane deformable mirror adds wavefront disturbance to a laser beam, representing the effect of turbulence. A second membrane deformable mirror, with different geometry, is driven by the control loops to correct the wavefront error. A Shack-Hartmann sensor measures the wavefront error for feedback.

8165A-03, Session 1

Impact of branch points in adaptive optics compensation of thermal blooming and turbulence

M. F. Spencer, S. J. Cusumano, Air Force Institute of Technology (United States)

Adaptive optics (AO) can be used to mitigate turbulence; however, when a single deformable mirror is used for phase-only compensation of thermal blooming, analysis predicts the possibility of instability. This instability is appropriately termed phase compensation instability (PCI) and arises with the time-dependent development of spatial perturbations found within the high-energy laser (HEL) beam. These spatial perturbations act as local hot spots that produce negative-lens-like optical effects in the atmosphere. An AO system corrects for the hot spots by applying positive-lens-like phase compensations. In turn, this increases the strength of the thermal blooming and leads to a runaway condition, i.e., positive feedback, in the AO control loop. This study uses computational wave-optics simulations to model horizontal propagation with the effects of thermal blooming and turbulence for a focused Gaussian HEL beam. A point-source beacon and nominal AO system are used for phase compensation. Results show that a high number of branch points limit the development of PCI for phase compensation of only thermal blooming. For phase compensation of thermal blooming and turbulence, the number of branch points decreases and system performance is reduced. A series of computational wave-optics experiments are presented which explore the possibility for PCI.

8165A-04, Session 1

Characterization and closed-loop AO performance of a liquid deformable mirror

E. S. ten Have, Technische Univ. Delft (Netherlands); G. V. Vdovin, Flexible Optical B.V. (Netherlands) and Technische Univ. Delft (Netherlands)

A liquid deformable mirror based on total internal reflection (TIR) applying an electrostatically deformed liquid-air interface was used to perform closed-loop adaptive optical correction on a collimated beam of a HeNe-laser that was aberrated by a rotating phase disk.

The properties of the mirror and the AO system performance were observed. Characterization of the mirror included frequency and step-function responses depending on the properties of the liquids used (water and glycerol) and the influence of liquid surface motion in absence of external optical aberrations. The performance of the AO system was determined for static and dynamic aberrations for various sets of system parameters.

The frequency response of the glycerol-air interface shows a drop of 22 dB for the amplitude at a frequency of 350 Hz with respect to the DC value. Our investigation shows that the motion of the liquid surface due to vibrations of the building etc. primarily results in the lateral movement of the beam which can be significantly decreased by engaging the AO feedback. While using the phase disk AO system performance showed an improvement of the wavefront of a factor of 3 - 4 in terms of residual rms error for correction of dynamic aberrations and of a factor of 4 - 12 in terms of residual rms error and of 50 - 1800 in terms of Strehl number for static aberrations.

The successful application of the liquid mirror opens new ways for applying very large numbers of actuators in adaptive optics for e.g. astronomical observatories.

8165A-05, Session 1

Using of Hermite-Gaussian antisymmetric mode for intracavity fiber array beam combining

S. A. Dimakov, A. A. Mak, S.I. Vavilov State Optical Institute (Russian Federation)

The report introduces the results of experimental studies of intracavity fiber array beam combining. For the first time it was experimentally demonstrated generation of Hermite-Gaussian anti-symmetric mode TEM₃₀ in stable super resonator for coherent combination of beams of four fiber amplifiers. Behind the output mirror of a super resonator a super-mode was corrected by static phase corrector to receive quasi-plane wave. Maximum number of phasing fiber channels by means of suggested method has been discussed.

8165A-06, Session 1

Response analysis and experimental results of holography-based modal Zernike wavefront sensor

S. Dong, T. Haist, W. Osten, T. Ruppel, O. Sawodny, Univ. Stuttgart (Germany)

Holography based modal wavefront sensing (HMWS) employs diffractive optical elements to detect directly the amplitude of Zernike components of an aberrated wavefront. The sensor has a good linearity for single mode or multiple modes with small amplitudes. However, the crosstalk problem inherent in HMWS becomes more severe with increasing aberrations, that finally result in degrading the sensor accuracy. In this paper the working principle of HMWS is theoretically described and the cause of crosstalk is further revealed. It is found that the intermodal crosstalk due to the complexity of an input wavefront dominates the sensor performance. In order to extend the use of HMWS for simultaneous detection of multiple and large size Zernike modes (which is essential in atmospheric aberration correction), the response of HMWS is examined statistically with random aberrations created in accordance to the atmosphere turbulence model. The simulation results show that the behavior of sensor response changes randomly according to different incident beams. It is also demonstrated that the response curve trends to

approach the “theoretical curve” as aberration size decreases (close-loop case). Using this analysis, an optimization process with system parameters like pinhole size and encoded phase bias is implemented considering the turbulence strength. The sensitivity and accuracy of the sensor is further improved by using calibrated response curves. The final results show that the number of iterations needed for obtaining a residual wavefront error of 0.1λ in RMS is reduced from 18 to 3. First preliminary experimental results are shown for validating the method.

8165A-07, Session 2

High-resolution lens-free on-chip microscopy using holographic multiframe pixel super-resolution

W. Bishara, T. Su, A. F. Coskun, H. Zhu, Univ. of California, Los Angeles (United States); A. Ozcan, Univ. of California, Los Angeles (United States) and California NanoSystems Institute (United States)

We present lensfree holographic on-chip microscopy with $\sim 0.6\mu\text{m}$ resolution over 24mm^2 field-of-view (FOV). This is achieved by a partially-coherent in-line holographic imaging set-up that employs a Pixel Super-Resolution algorithm to effectively increase the space-bandwidth product of a sensor-array by synthesizing higher resolution images from multiple shifted low-resolution ones. Lensfree hologram shifting is implemented by mechanically shifting the source (e.g., an LED filtered by a $\sim 0.1\text{mm}$ pinhole) by relatively large distances of $\sim 0.1\text{mm}$. We have also implemented the use multiple LEDs to achieve pixel super-resolution without the use of any mechanical scanning. Furthermore, we have also demonstrated opto-fluidic implementation of the same scheme, where the fluidic-motion of the objects within a micro-fluidic channel is used to synthesize high-resolution lensfree holographic images. In all of these implementations, multiple shifted in-line holograms of the same object scene are acquired and processed to generate a single high-resolution hologram with a much smaller effective pixel size, which is then processed with an iterative phase-retrieval algorithm to recover complex-valued microscopic images of the objects.

The performance of this approach has been validated by imaging patterned substrates, blood samples, *C. elegans* and *Giardia lamblia* parasites. This lensfree holographic imaging modality could enable the design of light-weight, compact and cost-effective microscopes with sub-micron resolution over a large FOV, which would be valuable for point-of-care applications and for field-use in resource-poor settings. Toward this end, we also show a light-weight, field-portable implementation of this lensfree holographic microscope that is specifically aimed at diagnosis of infectious diseases such as malaria.

8165A-08, Session 2

Metamaterials-based 2D hyperlens imaging beyond the diffraction limit at visible frequencies

J. S. Rho, Z. Ye, Y. Xiong, Univ. of California, Berkeley (United States); X. Yin, Univ. of California, Berkeley (United States) and Lawrence Berkeley National Lab. (United States); Z. Liu, Univ. of California, San Diego (United States) and Univ. of California, Berkeley (United States); H. Choi, G. Bartal, Univ. of California, Berkeley (United States); X. Zhang, Univ. of California, Berkeley (United States) and Lawrence Berkeley National Lab. (United States)

Hyperlens has excited much interest, not only because of the intriguing physics also for its ability of real-time imaging sub-diffraction-limited objects into the far-field. The major breakthrough emerged with the concept of optical hyperlens, showing the first proof-of-principle for magnifying sub-diffractional images to the far-field as propagating waves.

Utilizing alternating dielectric and metallic multilayer in a cylindrical geometry, this metamaterial-based optical device achieves strong optical anisotropy supporting the propagation of waves with very large spatial frequency and adiabatically compresses its lateral wave vector while the wave propagating outward along the radial direction. Consequently, the sub-diffractional details of objects are magnified and eventually larger than the diffraction limit to be transmitted to the far field. Despite the first experimental demonstration of the cylindrical hyperlens and other hyperlens design, all the experimental demonstrations of hyperlens so far were limited to the one dimensional magnification and ultra-violet wavelengths, hindering any practical imaging applications. Here, we present a spherical hyperlens for two-dimensional sub-diffraction limited real-time imaging at visible frequencies without the need of optical scanning or image reconstruction. Designing a spherical hyperlens with flat hyperbolic dispersion supporting wave propagations with very large spatial frequency, and yet same phase speed, we are able to resolve sub-diffractional features down to 160nm , much smaller than the diffraction limit at visible wavelength of 410nm . Such a hyperlens can readily be integrated in conventional microscopes, critically expanding their capabilities beyond the diffraction limit and opening a new realm in real-time nanoscopic optical imaging of biological machineries in living cells.

8165A-09, Session 2

Lensless fluorescent microscopy on a chip using a tapered fiber optic faceplate and compressive decoding

A. F. Coskun, I. Sencan, T. Su, Univ. of California, Los Angeles (United States); A. Ozcan, Univ. of California, Los Angeles (United States) and California Nanosystems Institute (United States)

Lensfree on-chip microscopy is an emerging field that aims to replace bulky optical microscopes with much simpler and compact architectures that make-up for the lack of optical complexity through digital computation. Recently, we have introduced such a lensless fluorescent imaging technology that can achieve $\sim 10\mu\text{m}$ resolution over $>8\text{cm}^2$ field-of-view (FOV). Although this wide-field platform could potentially be rather useful for high-throughput screening applications such as rare-cell analysis as well as cytometry, there is still an important need to further improve its resolution.

Toward this end, here we demonstrate an on-chip fluorescent microscopy platform that can achieve 60mm^2 FOV without the use of any lenses, mechanical-scanning or thin-film based interference-filters. In this technique, micro-fluidic chips of interest are placed on a tapered fiber-optic faceplate that has $\sim 5\text{X}$ higher density of fiber-optic cables on its small facet compared to the large one. The fluorescent emission from the objects is then collected with a 2D-array of fibers having a period of $\sim 2\mu\text{m}$ to achieve $\sim 2.4\text{X}$ magnification over $>60\text{mm}^2$ imaging FOV. In this compact on-chip microscope, fluorescent excitation is achieved through a hemispherical-glass interface illuminated by an incoherent source. After interacting with the object volume, this excitation light is rejected by total-internal-reflection occurring at the bottom of the micro-fluidic chip. By using compressive sampling based decoding algorithms, the acquired lensfree images of the sample are rapidly processed to yield 60mm^2 FOV. This compact on-chip fluorescent microscopy platform, with its improved resolution and wide field-of-view, might impact high-throughput cytometry, rare-cell research and microarray-analysis.

8165A-10, Session 2

Extraordinary imaging properties of metalenses mediated by negative refraction

C. Ma, Z. Liu, Univ. of California, San Diego (United States)

Lenses are pervasive in optics. Imaging is one of the most fundamental functions of a lens, of which the imaging properties have been well established for centuries since the first elaboration by Kepler in 1611. Owing to the diffractive nature of light wave, the resolution of a lens

Conference 8165A: Unconventional Imaging and
Wavefront Sensing VII

system is limited to about half of the working wavelength $\sim\lambda/2$. Various metamaterial based superlenses that can achieve deep subwavelength scale resolution have been proposed and demonstrated within the last decade. Although these superlenses can achieve super resolution, they cannot focus a plane wave to a spot and thus behave differently from conventional lenses. By applying phase compensation mechanisms to metamaterials, we have recently demonstrated the plane wave focusing capability, i.e., the Fourier transform function, in the metamaterial immersion lens (MIL) and the metalens. In this work, we show a new imaging paradigm in negative refraction based lenses if a focal length can be defined, using the hyperbolic metalens as an example. In contrast to conventional lenses, a hyperbolic metalens works as a converging lens from one side but a diverging lens from the other. This distinctive focusing behavior leads to extraordinary imaging properties that are not available in common lenses. These extraordinary imaging properties significantly expand the horizon of imaging optics and optical system design.

8165A-11, Session 2

Ultrasound-modulated fluorescent contrast agent for optical imaging through turbid media

C. E. Schutt, M. J. Benchimol, Univ. of California, San Diego (United States); M. J. Hsu, Ziva Corp. (United States); S. C. Esener, Univ. of California, San Diego (United States)

Optical imaging in a highly scattering media is effective only at very shallow depths which limits its use as a diagnostic tool in biomedical imaging. By combining optical and acoustic modalities, high-contrast, physiologically-relevant optical information at higher spatial resolutions can be achieved. Hybrid imaging modalities such as acousto-optic and photoacoustic imaging improve resolution over conventional optical imaging, but tissue scattering results in poor signal-to-background ratios especially in deeper tissues. To overcome these challenges, we have developed a novel microbubble (MB) contrast agent surface-loaded with a self-quenching fluorophore. In response to ultrasound, the MB expands and contracts, generating changes in the fluorophore surface density. The changes in physical separation between fluorophores modulate the quenching efficiency and produce a fluorescence intensity modulation. To our knowledge, this is the first experimental demonstration of ultrasound modulation of fluorescence using a self-quenching MB scheme. The modulation is spatially localized to the ultrasound focal zone where the pressure is the greatest and the largest MB oscillations are induced. The modulating signal can be extracted from a large constant light background, increasing detection sensitivity. This technique can enable sensitive optical imaging with ultrasound-scale sub-millimeter spatial resolution, overcoming some challenges of optical imaging in turbid media. The MBs were prepared with a shell of phospholipid and lipophilic self-quenching fluorophore. MB ultrasound response was studied in a custom setup which monitored fluorescence emitted from an insonified sample. Fluorescence signals displayed clearly modulated intensity and the FFT of these signals showed a strong component at the ultrasound driving frequency.

8165A-12, Session 3

Optical Janus lens and its extraordinary imaging properties

Z. Liu, Univ. of California, San Diego (United States)

Optical lenses are pervasive in various areas of sciences and technologies. The lens imaging properties have been well established for centuries since the first elaboration by Kepler in 1611. It is also well known that the resolving power of a lens and thus optical systems is limited by the diffraction of light. Recently, various plasmonics and metamaterials based superlenses have been emerging to achieve super resolution and exotic imaging properties. In this talk I will introduce an

optical "Janus Lens" based on phase compensated negative refraction in metamaterials. The Janus lens performs as either converging lens or diverging lens depending on the illumination directions. Extraordinary imaging equations and properties that are different from those of all the existing optical lenses will also be presented. These new imaging properties, along with the super resolving power, significantly expand the horizon of imaging optics and optical system design.

8165A-13, Session 3

Compressive hyperspectral acquisition and unmixing

T. Sun, C. Li, Y. Zhang, K. F. Kelly, Rice Univ. (United States)

Hyperspectral hardware can be complex and the associated data processing typically demands enormous computational resources. In this paper, we investigate a low complexity scheme for hyperspectral data acquisition, compression and reconstruction. In this scheme, compressed hyperspectral data are acquired directly by a spectrometer variation of the single-pixel camera based on the principle of compressive sensing. To decode the compressed data, we propose a numerical procedure to directly compute the unmixed abundance fractions of given endmembers, completely bypassing high-complexity tasks involving the hyperspectral data cube itself. Experimental and computational evidences obtained from this study indicate that the proposed scheme has a high potential in real-world applications.

8165A-14, Session 3

Compressive echelle spectroscopy

L. Xu, K. F. Kelly, Rice Univ. (United States)

We have constructed an echelle spectrometer based on the principles of compressive sensing. While our current system operates in the visible part of the spectra, our CS method is especially beneficial when you move into the infrared and two-dimensional focal plane arrays where costs can skyrocket from \$50 for a 5 megapixel silicon sensor to tens of thousands of dollars for less than a megapixel. In addition, we will introduce a new design for the system that replaces the complicated and somewhat optically limited digital micromirror device with a simpler and more robust architecture.

8165A-15, Session 3

Experimental demonstration of compressive sensing-based Raman microscopy

M. A. Turner, K. F. Kelly, Rice Univ. (United States)

We demonstrate the experimental realization of compressive sensing applied to Raman microscopy. The theory of compressive sensing (CS) is now well-known among statistics, signal processing, and information theory fields. Certain applications were immediately apparent, such as in analog-to-digital conversion, but CS principles are proving useful in a wide range of other situations including imaging. CS guides one to sample natural signals at a rate closer to the information rate than the traditional Shannon sampling rate. Thus, CS measurement systems generally should be preferred for science and engineering problems wherever more efficient sampling would result in reduction of cost or acquisition time.

In our setup we expand a laser beam to fill the active area of a digital micromirror device (DMD) from Texas Instruments, which consists of 13.6 micron-pitch mirrors that can flip +/- 12 degrees to normal incidence. This structured illumination then travels to an objective lens that focuses the light down onto a roughly 10 square-micron area. Scattered light from the illuminated sections is then analyzed in a spectrometer. We reconstruct a hyperspectral data cube where the "wavelength" dimension

now contains Raman spectra from various points in the sample. This will be broadly useful in fields such as semiconductor metrology, cancer detection and imaging, and nanomaterials characterization. By example of Raman imaging of graphene on SiO₂, we demonstrate that for only ~20% of the acquisition time required by state-of-the-art micro-Raman systems we achieve identical performance.

8165A-16, Session 3

Single-molecule super-resolution imaging of surface enhancement hotspots

H. Cang, Univ. of California, Berkeley (United States) and Lawrence Berkeley National Lab. (United States); A. Labno, C. Lu, X. Yin, M. Liu, C. W. Gladden, Y. Liu, X. Zhang, Univ. of California, Berkeley (United States)

The invention of single molecule super-resolution imaging has allowed optical microscopy to reach electron microscopy-level resolution. We apply this new technique to probe surface enhancement hotspots. These hotspots appear on rough metallic surfaces under optical illumination where the local electromagnetic field is concentrated, giving rise to the famous surface enhancement effect. Current optical instruments' limited resolution has made it difficult to characterize hotspots, and their size is unknown. Using the Brownian motion of single fluorescent molecules enables us to probe the inside of single hotspots for the first time. We found that light is strongly confined with an exponential profile. A hotspots is as small as 15nm in width, less than 1/30 the wavelength of light.

8165A-17, Session 4

Power requirements for polarimetric SAR image imaging

S. C. Cain, Air Force Institute of Technology (United States)

Polarimetric SAR is a method for collecting images using non-imaged laser speckle returns. This approach allows reflected laser radiation to be captured incoherently over a large area and then used to reconstruct a facsimile of the illuminated target via an image synthesis algorithm. The use of incoherent detection combined with dual channel polarization measurements allows an image to be reconstructed with an effective aperture much larger than what could be achieved via traditional monolithic imaging systems. Although phase information is lost in the detection process, the dual polarization architecture captures the additional information needed to aid in the regularization of the image reconstruction problem from intensity measurements. It is the goal of this research to quantify the laser power and aperture size requirements as related to the achievable spatial resolution of the polarimetric SAR imaging system. The study is carried out via Monte-Carlo simulations which are used to infer simple relationships between laser power, aperture size, range to target and achievable spatial resolution.

8165A-18, Session 4

Imaging performance of long-range laser scanning through atmospheric turbulence

D. G. Voelz, M. S. Nairat, New Mexico State Univ. (United States)

Active laser scanning to form an image through atmospheric turbulence is studied in terms of the Optical Transfer Function (OTF). The concept considered is the illumination of a two-dimensional target by a focused laser beam that propagates through turbulence. As the beam scans the target, a record of the reflected flux versus expected beam centroid position is collected at the receiver and used to reconstruct an image. The distance between the illuminator and target is assumed to be in the Fresnel region. Spatial resolution and cut-off frequency are considered

as a function of turbulence strength and exposure time. Beam wander is included in the investigation and an OTF expression is developed to specifically describe this effect. Wave optics simulations are performed to illustrate emphasizes the performance of the scanning method and image results are compared with the theoretical model.

8165A-19, Session 4

Discrimination of multiple ranges per pixel in 3D flash ladar to enhance spatial resolution

B. J. Neff, S. C. Cain, Air Force Institute of Technology (United States)

Laser Radar imagers known as FLASH LADAR sensors can be designed to provide 2-D and 3-D images of a scene in a single pulse. For 3-D sensors, the benefit of having a range for every pixel in the image is obvious. Unfortunately, the added manufacturing complexity for 3-D sensors has restricted the spatial resolution to much lower values than 2-D sensors. Based on this limitation, it is possible that the field of view for an individual pixel will observe the pulse reflections from multiple surfaces. Fortunately, the narrow pulse width of 3-D FLASH LADAR allows us to accurately determine range to multiple surfaces close together with accuracy on the order of feet. However, the spatial mixing effects cause ambiguity as to the presence of these surfaces. The goal of this work is to develop an algorithm to enhance the utility of 3-D sensors using accurate ranging to multiple surfaces per image pixel.

Using an algorithm that determines the precise range to multiple surfaces per pixel, it will be possible to observe numerous enhancements. Among these enhancements, the following will be demonstrated. First, based on the statistical nature of the target being imaged, the relationship of each surface will be used to enhance the spatial resolution of an image. Second, the task of detecting obscured targets with a single pulse will be possible. Finally, edge detection will be enhanced which provides many benefits to include enhanced registration among an ensemble of images.

8165A-20, Session 4

Phase errors analysis and speckle reduction in synthetic aperture imaging ladar demonstration system

Y. Zhou, J. Sun, Y. Zhi, Y. Wu, N. Xu, A. Yan, L. Wang, Z. Luan, L. Liu, Shanghai Institute of Optics and Fine Mechanics (China)

A demonstrator of synthetic aperture imaging ladar (SAIL) is constructed to study the feasibility under random disturbance. Where the transmitting and receiving system are based on the free-space optics to give changeable wave front, and the local optical channel is based on fiber delay line having the nearly the same optical distance with signal optical channel to reduce the demands on the linewidth and the initial optical frequency synchronism of the each chirped laser pulse. By applying several reference dots and optical fiber loop, several kinds of phase errors, including nonsynchronous initial optical frequency, platform vibration, air turbulence, and the autologous phase disturbance of fiber delay line are extracted to study their effects on SAIL imaging. After mitigating all these timely phase errors, a well-focused two-dimensional SAIL image can be given, but apparent speckle effect also can be observed. The speckle effect comes from the spatial random distribution of target dots, which induce different effect on SAIL imaging from the effect by the timely phase errors. Apart from multilook processing method, sliding spotlight imaging mode is also used to try to reduce the speckle noise.

8165A-21, Session 5

Multiframe blind deconvolution for imaging in daylight and strong turbulence conditions

M. Hart, S. M. Jefferies, D. A. Hope, E. K. Hege, Hart Scientific Consulting International L.L.C. (United States)

We describe new computational techniques to extend the reach of large ground-based optical telescopes, enabling high resolution imaging of satellites under daylight conditions. Current state-of-the-art systems, even those employing adaptive optics, dramatically underperform in such conditions because of strong turbulence generated by diurnal solar heating of the atmosphere. Our approach extends previous advances in multi-frame blind deconvolution (MFBD) by exploiting a priori physical constraints on the imaging process that have hitherto not been incorporated or not fully exploited in MFBD algorithms. We describe early results with a new algorithm which may be used with seeing-limited image data or as an adjunct to partial compensation with adaptive optics to restore imaging to the diffraction limit even under the extreme observing conditions found in daylight.

8165A-22, Session 5

Experiments on speckle imaging using projection methods

M. Y. Loktev, G. V. Vdovin, O. A. Soloviev, S. Savenko, Flexible Optical B.V. (Netherlands)

Adaptive optics based on phase conjugation has been commonly used to compensate image blur due to atmospheric turbulence in astronomy. However, the adaptive optics is not directly applicable for extended scene imaging in turbulent conditions on horizontal paths due to strong anisoplanatism of the aberrated field. Besides, in many practical cases the wavefront information cannot be obtained and/or used. Therefore, a cost-effective approach, with or without the use of adaptive optics, is required to obtain high resolution with extended field in conditions of strong blur. Speckle imaging methods based on deconvolution of a series of images, each with its own point-spread function (PSF), are promising for implementation of such an approach.

In this paper we present some experimental results of speckle imaging applied to ground-based scenery and astronomical objects. The method of alternating projections onto convex sets is used for iterative PSF reconstruction, combined with Wiener filtering for deconvolution and several pre-processing techniques. Modifications of the optical system with variable aperture size and multiple apertures are considered.

The results of imaging on a horizontal path are reported and compared with time averaged, best frame and median filtered images, under different turbulence conditions. Resolution improvement is demonstrated in a field much wider than the isoplanatic patch size.

8165A-23, Session 5

Scene-based blind deconvolution in the presence of anisoplanatism

D. C. Dayton, Applied Technology Associates (United States)

Most non-conventional approaches to image restoration of objects observed over long atmospheric paths require multiple frames of short exposure images taken with low noise focal plane arrays. Multi-frame blind deconvolution is such an approach. In most cases the object is assumed to extend only over a single isoplanatic patch. However, when one is observing scenes over a near horizontal or downward looking path, and the isoplanatic patch size is small due to extended atmospheric turbulence over the entire slant path, and the scene usually extends over many isoplanatic patches. In addition base motion jitter in an airborne observing platform introduces a frame-to-frame linear shift that must be compensated for in order for the multi-frame restoration to be successful.

In this paper we describe a maximum a-posteriori parameter estimation approach to the simultaneous estimation of the frame-to-frame shifts and non-isoplanatic point spread functions. This approach can be incorporated into an iterative algorithm. We present a brief derivation of the algorithm as well as its application to actual image data collected from airborne and ground based platforms.

8165A-24, Session 5

Geometric super-resolution via log-polar FFT image registration and variable pixel linear reconstruction

P. N. Crabtree, J. Murray-Krezan, R. H. Picard, Air Force Research Lab. (United States); E. Cohen, Air Force Research Lab. (United States) and ARCON Corp. (United States)

Various image de-aliasing algorithms and techniques have been developed to improve the resolution of pixel-limited imagery acquired by an optical system having an undersampled point spread function. These techniques are sometimes referred to as geometric super-resolution, and are valuable tools because they maximize the imaging utility of current and legacy focal plane array (FPA) technology. This is especially true for infrared FPAs which tend to have larger pixels as compared to visible sensors. Geometric super-resolution relies on knowledge of sub-pixel frame-to-frame motion, which is used to assemble a set of low-resolution frames into a single high-resolution (HR) frame. Log-polar FFT image registration provides a straightforward and relatively fast approach to estimate global affine motion, including translation, rotation, and uniform scale changes. This technique is also readily extended to provide sub-pixel translation estimates, and to improve the resolution of rotation angle and scale factor estimates. Following motion estimation, a HR frame is assembled using variable pixel linear reconstruction (VPLR), also known as "Drizzle." We describe our algorithms and experiments, and demonstrate performance using laboratory data from both visible and long wave infrared cameras. Finally, we highlight the importance of deconvolution following VPLR.

8165A-25, Session 5

Seasonal hemispherical SWIR airglow imaging

D. C. Dayton, J. G. Allen, Applied Technology Associates (United States); M. M. Myers, J. D. Goglewski, Air Force Research Lab. (United States); R. V. Nolasco, Applied Technology Associates (United States)

Airglow luminescence in the SWIR region due to upper atmospheric recombination of solar excited molecules is a well accepted phenomenon. While the intensity appears broadly uniform over the whole sky hemisphere, we are interested in variations in four areas: 1) fine periodic features known as gravity waves, 2) broad patterns across the whole sky, 3) temporal variations in the hemispheric mean irradiance over the course of the night, and 4) long term seasonal variations in the mean irradiance. An experiment is described and results presented covering a full year of high resolution hemispheric SWIR irradiance images. An automated gimbal views 45 hemispheric positions, using 30 second durations, and repeats approximately every half hour through out the night. The gimbal holds co-mounted and bore-sighted visible and SWIR cameras. Accompanying those cameras are ground truth sensors including an additional SWIR camera, PVS-14 night vision system both focused at the horizon and a radiometer to measure the amount of energy being absorbed on the ground. Measuring airglow with respect to spatial, temporal, and seasonal variations will facilitate understanding its behavior and possible benefits, such as night vision and predicting upper atmosphere turbulence.

8165A-26, Session 5

Blind deconvolution of long exposure lens-based chromotomographic spectrometer data

S. V. Mantravadi, Air Force Office of Scientific Research (United States); S. C. Cain, Air Force Institute of Technology (United States)

Projection-based chromotomographic spectrometers are sensors that collect both spatial and spectral information with fairly simple optical as well as electronic hardware. Efforts to utilize them for remote sensing applications have met with obstacles primarily due to the fact that the impulse response of the imaging system as a function of wavelength must be known in order to reconstruct the spatial/spectral content of the scene under study. This paper reports a blind deconvolution algorithm specifically designed to reconstruct the spectrum of the scene under study as well as an estimate of the wavelength dependent atmospheric transfer function of the system. The approach uses a Bayesian framework for determining the spectral image of the scene. The seeing parameter of the atmosphere is estimated using algorithm convergence criteria. The iterative algorithm derived in this paper converges when the estimated noise variance is equal to the predicted value based on the assumption that the measurements are Poisson. The lowest value of the seeing parameter for which the algorithm converges is chosen as the seeing parameter estimate. The method is tested using simulated data with realistic turbulence and noise factors in order to demonstrate its effectiveness.

8165A-27, Session 6

Detailed comparison of a Michelson interferometer and intensity interferometer SNR for GEO stationary satellites imaging

S. R. Restaino, J. T. Armstrong, H. R. Schmitt, J. R. Andrews, U.S. Naval Research Lab. (United States)

Geo-stationary satellites (GEO) represent a very difficult imaging problem due to their distance from the Earth and apparent dimension from the observers. This is not that different than some of the more challenging astronomical imaging problems. In order to attain the required resolution in order to form a high fidelity image one needs fairly large telescopes with diameters ranging in the several tens of meters. Several projects are attempting to develop such telescopes but there are several problems. One solution would be to use existing long baseline optical interferometers or develop a new facility along these lines. When dealing with Long Baseline there are two main approaches, the Michelson interferometer and the Intensity interferometer. Arguments favoring either of these approaches have been made. It is the aim of this paper to present a complete comparison between these two techniques in terms of technical challenges, possible costs and overall signal-to-noise-ratio (SNR) etc. The comparison will be analytic and quantitative as much as possible.

8165A-28, Session 6

A study of image reconstruction algorithms for hybrid intensity interferometers

P. N. Crabtree, J. Murray-Krezan, R. H. Picard, P. J. McNicholl, Air Force Research Lab. (United States)

Intensity interferometry holds tremendous potential for remote sensing of space objects. Unlike traditional earth-based observatories which are typically limited by both the size of the primary mirror and atmospheric effects, Intensity Interferometers (IIs) are relatively unaffected by atmospheric distortions and their effective apertures can be substantially

larger than is practical for traditional observatories. Hybrid Intensity Interferometers (HIIs) are explored for their potential to improve the imagery produced by IIs, which historically have labored under SNR and fill factor challenges. Concepts for HIIs include the use of additional information furnished by partially resolved imagery from a traditional telescope, or use of phase and amplitude information from amplitude interferometers. As phase retrieval algorithms are typically used for image reconstruction from interferometric information, methods for incorporating additional information into an integrated phase retrieval process are explored. We investigate image reconstruction techniques with suitable image quality metrics.

8165A-29, Session 6

Simulated optical interferometric observations of geostationary satellites

H. R. Schmitt, U.S. Naval Research Lab. (United States); D. Mozurkewich, Seabrook Engineering (United States); S. R. Restaino, J. T. Armstrong, R. B. Hindsley, U.S. Naval Research Lab. (United States); A. M. Jorgensen, New Mexico Institute of Mining and Technology (United States)

We simulate observations of geostationary satellites using different optical interferometer configurations. We test several array designs, including the typical Y shaped array, similar to the Navy Prototype Optical Interferometer, an elliptical array, and telescopes mounted on a linear movable boom. We use aperture synthesis techniques to reconstruct images from the simulated observations and determine which configuration produces the most accurate images relative to the original ones. These simulations also take into consideration the number of telescopes needed to achieve the best results, and their separations.

8165A-30, Session 6

Laser testing of an Iris AO dielectric-coated, segmented MEMS DM

M. A. Helmbrecht, Iris AO, Inc. (United States); A. P. Norton, Univ. of California, Santa Cruz (United States); D. T. Gavel, Univ. of California Observatories (United States)

Iris AO has been developing dielectric-coated segmented MEMS DMs for use in laser applications. In order to produce high-quality ($\lambda/20$ rms or better) mirrors with the relatively thick and high-stress coatings, stress-compensation coatings have been deposited onto the underside of the mirror segments.

Deformable mirrors have been fabricated with compensation coatings targeted for 355 nm, 1064 nm and 1540 nm. The mirror segments for these DMs are 50 μm to better accommodate run-to-run stress variations, variations in stress as a result of humidity changes, and different target wavelengths.

Deformable mirrors were coated with 532 nm dielectric coatings. Preliminary measurements show that the coatings have survived exposure from a 2 W, 50 μm FWHM 532 nm CW beam onto a single segment for 30 minutes. This is approximately 100 kW/cm^2 . A 2W beam onto a single segment is equivalent to an average power handling of 630 W/cm^2 for the segment. At 2 W incident laser power, the segment heats up approximately 10-15°C above ambient temperature and peak-to-valley deformations of the segment are less than 15 nm. The DM segments can operate at temperatures exceeding 120°C. Thus we expect the power handling could be many kW/cm^2 . This paper will describe in detail more comprehensive laser testing.

8165A-31, Poster Session

Shack-Hartmann wavefront sensor with high sensitivity by using long focal length microlens array

V. Lin, H. Wei, G. J. Su, National Taiwan Univ. (Taiwan)

The performance of Shack-Hartmann wavefront sensor (SHWFS) is mainly described by the accuracy, spatial resolution, dynamic range, and sensitivity of the measurement. These factors are particularly affected by the design of the microlens array (MLA). In order to provide a large dynamic range of wavefront measurement, most of the conventional and commercial SHWFS implemented a short focal length lenslet array, which means that the measurement sensitivity is being sacrificed and the accuracy of the wavefront sensor will be degraded. However, it is also critical to detect very small displacement of SHWFS spot in order to reconstruct it into a fine wavefront variation. We fabricated long focal length MLA with various structure arrangement by thermal reflow process with Polydimethylsiloxane (PDMS) cover on the glass substrate and implemented them on the image system. A longer focal length will provide high sensitivity in determining the average slope across each lenslet under a given wavefront, and the spatial resolution of the wavefront sensor is increased by the number of lenslets across the detector. The experimental setup consists of the fabricated 245 μm diameter MLA which provides a 5.2 mm long focal distance and is paired with the CMOS as the detector. The observable smallest sensitivity is up better than $\lambda/20$ (635nm). Besides, by integration of few frame memories, the centroiding error of the image spot will be reduced remarkably which contributes in the improvement of measurement accuracy. The experimental result of the system is discussed and compared between the long focal length, the shorter focal length and the commercial SHWFS.

8165A-32, Poster Session

Optimal correction of low-order aberrations with piezoelectric and membrane deformable mirrors

G. V. Vdovin, O. A. Soloviev, M. Y. Loktev, S. Savenko, Flexible Optical B.V. (Netherlands)

For high quality of correction, certain formal restrictions on the geometry of actuators in the deformable mirrors should be satisfied

[1]. Application of these rules to the design of a deformable mirror lead to some interesting design solutions.

To achieve a very smooth, high quality correction of low-order aberrations, we have developed a 18-ch (38-ch as an ultra-smooth option) piezoelectric deformable mirror featuring zero actuator count under the beam footprint. We have demonstrated a very high quality correction of all 3-rd order aberrations, except spherical, addition of the 19-th central actuator allows for correction of spherical aberration. Reported configuration has certain advantages as a high-quality woofer in astronomical systems, and as a high-power laser deformable mirror that does not produce any hot spots in the beam.

To achieve a very low-cost high-quality correction of atmospheric turbulence, we have developed a low-order membrane deformable mirror with integrated tip-tilt stage, featuring 250 Hz bandwidth for the tip-tilt, and 1 kHz bandwidth for correction of all 3-rd order Zernike aberrations.

Experimental results on both configurations are reported for different real-life scenarios.

1. G. Vdovin, O. Soloviev, A. Samokhin, and M. Loktev, "Correction of low order aberrations using continuous deformable mirrors," *Opt. Express* 16, 2859-2866 (2008).

8165A-33, Poster Session

An imaging interferometer for compact sources

D. Mozurkewich, Seabrook Engineering (United States); J. T. Armstrong, R. B. Hindsley, U.S. Naval Research Lab. (United States); A. M. Jorgensen, New Mexico Institute of Mining and Technology (United States); S. R. Restaino, H. R. Schmitt, U.S. Naval Research Lab. (United States)

When a moderate to high precision image is required of an isolated, compact source, an optical interferometer should perform as well as a filled-aperture telescope with traditional AO. Cost is reduced since gaps in the spatial frequency coverage do not affect image quality. Spatial filtering with single-mode optical fibers, combined with self-calibration provides a better wavefront and hence less artifacting. Sensitivity is improved since only lower-order AO is needed on the individual apertures. We present the design of such a system along with analysis implying that its sensitivity approaches the sensitivity needed to image satellites at geosynchronous altitude.

8165A-34, Poster Session

Deformable mirror calibration using phase diversity in remote sensing adaptive optics

N. Miyamura, The Univ. of Tokyo (Japan)

In small satellites remote sensing, high spatial resolution has to be achieved by a lightweight sensor. To realize these contrary requirements, adaptive optics system (AOS) is used. In remote sensing, it is difficult to use a reference point source unless the satellite controls its attitude toward a star, so image-based wavefront estimation method, phase diversity, is used. We propose to estimate wavefront aberration and calibration parameters of deformable mirror (DM) simultaneously. In our AOS, a deformable mirror applies the phase diversity, and then corrects the wavefront aberrations. In a phase diversity wavefront sensing, the change in the wavefront caused by the DM is used as a priori information in solving the inverse problem. On the other hand, the influence function between the input voltage of the DM's actuator and the modulated wavefront depends on the composition and the alignment of the optics. The accurate calibration, therefore, is required. In conventional calibration method, a single actuator is displaced to measure the influence function. In our work, first the influence functions are formulated with unknown parameters. The unknown parameters in wavefront aberrations and influence functions are then estimated by using the input voltage as a priori information. Furthermore, the optimal input profile of the DM for phase diversity is investigated instead of displacing a single actuator for each measurement. We constructed the AOS for laboratory test, and proved that the modulated wavefront by DM almost consists with the ideal one using a Shack-Hartmann wavefront sensor as a reference.

8165A-35, Poster Session

Comparing the sensitivities of intensity interferometry and Michelson interferometry

J. T. Armstrong, U.S. Naval Research Lab. (United States); D. Mozurkewich, Seabrook Engineering (United States); H. R. Schmitt, Computational Physics, Inc. (United States); S. R. Restaino, R. B. Hindsley, U.S. Naval Research Lab. (United States)

Intensity interferometry, in which intensity fluctuations at separate apertures are measured and then correlated, is an attractive technique for high angular resolution measurements because of its simplicity. There is no need to transport light beams between the telescopes of the interferometer array, and the telescope optics need not be precise.

Michelson interferometry, in which light beams are brought together and the interference pattern is measured, is significantly more difficult, requiring precision optics and precise pathlength control, but it has a great advantage in sensitivity. To measure a magnitude 5 star with a squared correlation (squared fringe visibility) of 0.3 requires ~5 hours to reach $\text{SNR} = 5$ with an intensity interferometer (two 10 m telescopes, 100 MHz detection bandwidth), but requires a few milliseconds with a Michelson interferometer (two 1 m telescopes, 300 nm bandpass). However, for interferometry with a large number of array elements, the sensitivity of Michelson interferometry suffers from the fact that the light beams must be shared among many correlations, thereby reducing the sensitivity of each measurement. We explore these and other influences on the relative sensitivities of these techniques to determine under what circumstances, if any, their sensitivities become comparable.

8165A-36, Poster Session

Laboratory demonstration of Fresnel telescope imaging lidar

E. Dai, L. Liu, A. Yan, J. Sun, Y. Wu, Y. Zhou, Y. Zhi, Shanghai Institute of Optics and Fine Mechanics (China)

In this paper, we present a laboratory demonstration of Fresnel telescope imaging lidar system, whose name is derived from the Fourier telescope, for imaging the faraway objects with high resolution. Two concentric and coaxial quadratic wavefront laser beams with orthogonal polarization are used as scanning beams of the target. The scattered signal light from the target is split into two beams by a polarized beamsplitter (PBS). One beam acts as the reference beam and pass through a quarter waveplate to convert linear to circular polarization, the other beam acts as the signal beam and pass through a half waveplate to rotate the polarization by 45 degree. Then these two beams are heterodyne detected by a 90 degree 2x4 optical hybrid with two balanced detectors. To stable target, the image can be constructed by the digital processing of the outputs of the two balanced detectors by two dimensional scanning and only one dimensional scanning is needed for a moving target. The imaging resolution is higher than that of the diffraction limited optical system. Since both reference and signal beam pass through the same optical track, it may minimize the influence of the atmosphere.

Conference 8165B: Adaptive Coded Aperture Imaging and Non-Imaging Sensors V

Thursday 25 August 2011 • Part of Proceedings of SPIE Vol. 8165B
Adaptive Coded Aperture Imaging and Non-Imaging Sensors V

8165B-37, Session 7

An adaptive coded aperture imager: building, testing and trialling a superresolving terrestrial demonstrator

C. W. Slinger, Malvern Innovations (United Kingdom); H. Bennett, K. Gilholm, N. Gordon, D. Huckridge, M. E. McNie, R. Penney, QinetiQ Ltd. (United Kingdom); K. Rice, Goodrich Corp. (United States); K. Ridley, L. Russell, G. de Villiers, P. Watson, QinetiQ Ltd. (United Kingdom)

Adaptive coded aperture imaging (ACAI) is one of a new wave of computational imaging techniques beginning to be applied to meet a variety of challenging commercial, security and military needs. ACAI promises orders of magnitude performance improvements in some of these applications. In contrast to the conventional (classical) approach of focusing an image of a scene onto a detector array, ACAI encodes the incoming light prior to detection. The detected pattern is then decoded using a variety of algorithms and digital signal processing hardware to yield desired information from the scene. The patterns used to code the light can be changed with time to yield additional system benefits.

This paper describes the principles of ACAI, the practical considerations needed when applied to its use in the mid wave infrared (MWIR), and the design methods used for the construction of a large scale, wide cone-angle terrestrial demonstrator. The construction, calibration and results from laboratory and field trials of this demonstrator are then described. Tracking and imaging performance measurements are compared to the predictions of a multiphysics system model.”

8165B-38, Session 7

Intelligence supportability analysis and intelligence systems

J. Morrison, U.S. Air Force (United States)

No abstract available

8165B-39, Session 7

Adaptive coded aperture imaging: progress and potential future applications

S. R. Gottesman, A. Isser, G. W. Gigioli, Jr., Northrop Grumman Electronic Systems (United States)

Interest in Adaptive Coded Aperture Imaging (ACAI) continues to grow as the optical and systems engineering community becomes increasingly aware of ACAI's potential benefits in the design and performance of both imaging and non-imaging systems, such as good angular resolution (IFOV), wide distortion-free field of view (FOV), excellent image quality, and light weight construct. In this presentation we first review the accomplishments made over the past five years, then expand on previously published work to show how replacement of conventional imaging optics with coded apertures can lead to a reduction in system size, weight, and power (SWAP). We also present a trade space analysis of key design parameters of coded apertures and review potential applications as replacement to traditional imaging optics. Results will be presented, based on last year's work of our continuing investigation into the trade space of IFOV, resolution, effective focal length, and wavelength of incident radiation for coded aperture architectures. Finally we will discuss the potential application of coded apertures for replacing objective lenses of night vision goggles (NVGs).

8165B-41, Session 8

Systems for persistent surveillance

K. L. Lewis, Sciovis Ltd. (United Kingdom) and Electro-Magnetic Remote Sensing Defence Technology Ctr. (United Kingdom)

The Electro-Magnetic Remote Sensing (EMRS DTC) was established in 2003 to provide a centre of excellence in sensor research and development, supporting new capabilities in key military areas such as precision attack, battlespace manoeuvre and information superiority. The DTC was set up as a partnership between Industry, the academic science base and the UK Ministry of Defence, to develop advanced and affordable technology in support of mission-oriented defence capabilities. Its field of activity has included RF and Electro-Optic (EO) systems, as well as work on sensor exploitation, addressing solutions for enhancing situational awareness and for providing persistent surveillance for military operations. RF systems activities have explored techniques ranging from synthetic aperture radars to bistatic radars using non-cooperative transmissions from satellites. Under the EO system theme, work has explored the potential of active imaging using pulsed laser illumination, as well as various forms of discriminative imaging. Each of these sensor modalities has been supported by the development of toolsets for enhancing the intelligence of sensors and for data extraction, with a particular emphasis in supporting operations in asymmetric threat environments. Many of these techniques have been benchmarked in field trials held in collaboration with Dstl in the UK. This paper will present a summary of some of the key outcomes of the DTC's activities, emphasising the relevance to the provision of persistent surveillance.

8165B-42, Session 8

Optical imaging system which is sensitive to a degree of light polarization and coherence

M. A. Golub, E. Vexberg, Tel Aviv Univ. (Israel)

Polarization imaging has wide range of applications in imaging systems, microscopy, biology, electronics, distinguishing between laser and non-laser light sources. Identification of coherent and non-coherent light by spectral filters with narrow bandwidth suffers from significant degradation in sensitivity and typically insufficient contrast between segments with different degrees of coherence and polarization. Adding simple polarizer to an imaging systems binds its response to a specific state of polarization rather than to the degree of polarization.

In this work we developed and experimentally tested a method and an optical system which are highly sensitive to a transverse distribution of the degree of light polarization. The method is based on adding several different sets of polarizing components to an imaging system, recording several images, 2D mapping of Stokes parameters, and digital processing to restore a map of the degree of polarization (DOP) of the object. Important to note that proposed DOP mapping is applicable to all kind of polarization states, including circular and elliptical polarizations and discriminates between coherent and incoherent light.

Results of computer simulations and optical experiments with a CCD camera equipped with polarization measuring optical head reveal that the contrast between polarized and unpolarized light achieved by using DOP mapping is about 5 times higher than a contrast in regular imaging with a spectral filter. Best results were achieved when the background DOP is lower than 0.6. To conclude, mapping of the degree of polarization improves sensitivity of imaging, and ability to distinguish between polarized and non-polarized light.

8165B-43, Session 8

Multidimensional TOMBO imaging and its applications

R. Horisaki, J. Tanida, Osaka Univ. (Japan)

We present a framework of multi-dimensional compound-eye imaging with the thin observation module by bound optics (TOMBO) and its applications. In conventional multi-dimensional optical data acquisition, the object information is observed with two-dimensional detector array by sacrificing the observation time to scan along the axial direction or the spatial resolution to arrange filters on the detectors or the compactness of the hardware to increase the number of the detectors. The proposed framework can alleviate the problems. The advantages of TOMBO are the thinness of the compound-eye optics and the flexibility of the system design. In the proposed multi-dimensional TOMBO imaging system, each of the sub-optics equips optical coding elements to shear or to weight the multi-dimensional object information along the axial direction. The encoded information is integrated onto the detectors in the sub-optics. This system is ill-posed. The object is reconstructed by a compressive sensing algorithm. Compressive sensing solves ill-posed linear problems by employing a sparsity constraint. The framework can be applied to various optical information acquisitions. For example, in spectral imaging, the spectral datacube can be sheared by dispersive elements and weighted by color filters in the units. In polarization imaging, the polarized datacube can be sheared by birefringence elements and weighted by polarization plate. Those applications can be combined easily for higher-dimensional data acquisitions with compact hardware. We will show some numerical demonstrations.

8165B-44, Session 8

Control of optical aberrations with coded apertures

A. R. Harvey, Heriot-Watt Univ. (United Kingdom)

This presentation will describe the design of amplitude masking functions for the apparently disparate fields of imaging through aberrations and x-ray imaging with increased depth of field. The two modalities are quite different: shadow casting is the dominant process in formation of x-ray images, whilst conventional imaging is an interferometric process. The mathematical descriptions of the two imaging processes have significant commonality however and offer similar approaches to mitigation of optical aberrations.

There has been considerable progress in recent years in the use of phase techniques for the correction of aberrations in optical imaging. Adaptive optics phase correction enables the real-time correction of phase aberrations and high contrast imaging at the detector. Hybrid imaging techniques, using pupil-plane phase coding of the point-spread function, yields reduced-contrast imaging at the detector, but when used with digital image recovery enables high contrast imaging with reduced sensitivity to optical aberrations, but optimal mitigation of dynamic aberrations is difficult, particularly at infrared wavelengths.

We report here the design of coded aperture functions that, when combined with digital recovery, provide a route to mitigating optical aberrations using agile amplitude masks: the technique is thus applicable to a wide range of wavelengths as a low-cost alternative to phase-based adaptive optics. The optimisation process fundamentally aims to reduce destructive interference effects in the optical-transfer function. For imaging with hard x-rays, modulation of the source intensity function offers a mathematically similar technique for mitigating the image blur associated with extended sources.

8165B-45, Session 9

Image exploitation from encoded measurements

D. Bottisti, R. Muise, Lockheed Martin Corp. (United States)

We consider a coded aperture imaging system which collects far fewer measurements than the underlying resolution of the scene we wish to exploit. Our sensing model considers an imaging system which subsamples pixels intensities with an SLM device. The theory of compressive imaging has been studied in the context of rebuilding high resolution imagery from a smaller set of image measurements. Thus it is ideal for our application. We present a compressive imaging model to our proposed image measurement system and simulate image reconstruction performance. The compressive imaging sensing and reconstruction models are then modified to incorporate an exploitation tasks into the sensing and reconstruction process. The results being twofold: A more structured encoding for the measurement process, and an algorithm capable of reconstructing the processed imagery with the same computations as reconstructing the image itself. Essentially, we get exploitation for free. The equations are generated for an arbitrary linear filtering exploitation algorithm and we present some results based upon a quadratic correlation filtering target detection algorithm.

8165B-46, Session 9

Compressive light field imaging with hybrid measurement basis

A. Ashok, M. A. Neifeld, The Univ. of Arizona (United States)

Light field/Integral imaging refers to the measurement of spatio-angular information of a scene. Traditional light field imaging architectures, such as the plenoptic camera and the integral imager, map the four dimensional spatio-angular scene information directly onto a two dimensional detector array and typically suffer from spatio-angular resolution trade offs. Compressive light field imaging exploits the sparsity/compressibility of natural scenes to make fewer photon efficient compressive measurements that alleviate the spatio-angular resolution trade off. Recent work in the area of compressive light field imaging has investigated the performance of various compressive measurement bases, ranging from the purely random basis to the Karhunen-Loève (KL) basis. While the random basis relies solely on the scene sparsity prior, without assuming knowledge of a particular sparsity basis, the KL basis relies on the second-order statistics estimated from a representative set of scenes. In this work, we describe a hybrid measurement basis design that optimally combines a purely random basis with a known sparsity basis, such as the Wavelet basis, to improve the reconstruction performance of a compressive light field imager. The particular compressive imager architecture considered here makes compressive measurements only along the spatial dimensions of the four dimensional light field. We use a simulation study to quantify the performance of the spatial compressive light field imager for the random and hybrid bases. The simulation results show a significant performance improvement in terms of reconstruction error for the hybrid basis compared to the purely random basis.

8165B-47, Session 9

Comparison of frequency-based and spatial subdivision mask sets for passive detection and target tracking with a single photodetector

S. M. Klein, R. K. Ragade, R. W. Cohn, Univ. of Louisville (United States)

Detection and tracking of self-luminous point sources and small targets is implemented using a single, low noise photodetector together with

a programmable micromirror array. The scene is imaged onto the array and then through focusing, the product of the scene and mask pattern is integrated onto the detector. There are various approaches to designing the mirror array mask sets to query the scene for the location of the target. Two general approaches are compared in this report and their performance depends in different ways on the dynamics of the target motion. The first method derives target location as an n-bit binary number, where each bit corresponds to the spatial periodicity of the mask pattern (either a single checkerboard, or successive frames of vertical and horizontal stripes). In the second method, the mirror array is partitioned into multiple regions, each modulated at a different temporal frequency. This modulates different portions of the scene into different frequency bins that are continuously monitored. The frequency regions, together with a track-gate or guard band, can be adaptively shifted and scaled in extent as the target moves and grows/shrinks in apparent size. The spatial subdivision method proves more effective at tracking slow moving, point-like targets, while the frequency based method is more effective at tracking and maintaining a spatially extended target within the track gate. These two methods are combined in both experiments (with a 1400x1050 pixel TI DLP micromirror array) and simulation, and performance curves of their individual and combined performance are presented.

8165B-48, Session 9

Code aperture optimization for spectrally agile compressive imaging

G. Arce, H. Arguello, Univ. of Delaware (United States)

Coded aperture spectral imaging (CASSI) provides a mechanism to capture a 3D spectral cube with a single shot 2D measurement. In many applications, selective spectral imaging is sought since relevant information often lies within a subset of spectral bands. Capturing and reconstructing all the spectral bands in the observed image cube, to then throw away a large portion of this data is inefficient. This paper extends the concept of CASSI to a system admitting multiple shot measurements which leads not only to higher quality of reconstruction, but also to spectrally adaptive imaging when the sequence of code aperture patterns are optimized. The aperture code optimization problem is shown to be analogous to the optimization of a constrained, multichannel filter bank. The optimal code apertures allow the decomposition of the CASSI measurement into several subsets, each having information from only a few selected spectral bands. The rich theory of compressive sensing is used to effectively reconstruct selected filter bank spectral bands of interest from the measurements.

8165B-49, Session 9

Adaptive coded apertures for occlusion detection and motion estimation

R. M. Willett, Duke Univ. (United States)

No abstract available

8165B-50, Session 10

Establishing a MOEMS process to realise microshutters for coded aperture imaging applications

M. E. McNie, R. R. Davies, A. Johnson, QinetiQ Ltd. (United Kingdom); B. Hardy, G. Hames, D. Monk, MEMSCAP Inc. (United States); S. Rogers, Air Force Research Lab. (United States)

Coded aperture imaging has been used for astronomical applications for several years. Typical implementations used a fixed mask pattern and are designed to operate in the X-Ray or gamma ray bands. Recently

applications have emerged in the visible and infra red bands for low cost lens-less imaging systems and system studies have shown that considerable advantages in image resolution may accrue from the use of multiple different images of the same scene - requiring a reconfigurable mask. Previously reported work focused on realising such a mask in the mid-IR based on polysilicon micro-optoelectro-mechanical systems (MOEMS) technology and its integration with ASIC drive electronics using a tiled approach to scale to large format masks. The MOEMS chips employ interference effects to modulate incident light - achieved by tuning a large array of asymmetric Fabry-Perot optical cavities via an applied voltage using row/column addressing.

In this paper we report on establishing the manufacturing process for such MOEMS microshutter chips in a commercial MEMS foundry, MEMSCAP - including the associated challenges in moving the technology out of the development laboratory and the technical hurdles along the way.

Small scale (7.3 x 7.3mm) and full size (22 x 22mm) MOEMS chips have been produced and their performance tested. The results are compared with reference devices.

8165B-51, Session 10

A new photonics technology platform and its applicability for coded aperture techniques

S. R. Davis, S. D. Rommel, S. Johnson, S. Selewyn, G. Farca, M. Anderson, Vescent Photonics Inc. (United States)

An emergent electro-optic technology platform, liquid crystal (LC) waveguides, will be presented with a focus on performance attributes that may be relevant to coded aperture approaches. As a low cost and low SWaP alternative to more traditional approaches (e.g. galvos, MEMs, traditional EO techniques, etc.), LC-Waveguides provide a new technique for switching, phase shifting, steering, focusing, and generally controlling light. LC-waveguides provide tremendous continuous voltage control over optical phase delays (> 2mm demonstrated), with very low loss (one million pm/Volts) while circumventing their historic limitations; speeds can be in the microseconds and LC scattering losses can be reduced by orders of magnitude from conventional LC optics. This enables a new class of photonic devices: very wide analog non-mechanical beamsteerers (270o demonstrated), chip-scale widely tunable lasers (50 nm demonstrated), chip-scale Fourier transform spectrometers (< 5 nm resolution demonstrated), widely tunable micro-ring resonators, tunable lenses (fl tuning from 5 mm to infinity demonstrated), ultra-low power (< 5 microWatts) optical switches, true optical time delay devices (12 nsecs demonstrated) for phased array antennas, and many more. Both the limitations and the opportunity provided by this technology for use in coded aperture schemes will be discussed.

8165B-52, Session 10

Memristor-based imaging architecture opportunities for adaptive coded aperture imaging applications

T. M. Taha, C. Yakopcic, G. Subramanyam, Univ. of Dayton (United States); S. Rogers, Air Force Research Lab. (United States)

This paper explores memristor based computing architecture opportunities for imaging algorithms geared towards potential Adaptive Coded Aperture imaging applications. Memristors are a new class of devices that inherently have nonvolatile memory properties. Systems based on these devices can typically utilize fewer resources than traditional computing platforms. This allows a chip of a given area to have stronger information processing capabilities, thus reducing overall chip counts.

In this paper we describe novel memristor based computing components such memory arrays and their interactions with processors for high

**Conference 8165B: Adaptive Coded Aperture Imaging
and Non-Imaging Sensors V**

performance imaging computations. Additionally, we present calculations for the chip areas consumed by the components described.

to switch from the highly transmissive to the highly absorptive state in the near infrared, met the specified performance goals and agreed well with the theoretically predicted performance. This demonstration of the successful design, fabrication, and characterization of a reconfigurable phase change device represents a powerful step in the development of adaptive infrared metamaterials.

8165B-53, Session 10

Nanoparticle dispersed metamaterial sensors for adaptive coded aperture imaging applications

P. Banerjee, G. T. Nehmetallah, R. Aylo, Univ. of Dayton (United States); S. Rogers, Air Force Research Lab. (United States)

Nanoparticle dispersed metamaterials have been researched due to their flexibility in operating frequency, electronic tunability, ease of fabrication, and low cost. We propose binary/core-shell polaritonic/plasmonic nanoparticles in a suitable host as candidates for metamaterials, which can be used either in a single-layer or a multi-layer configuration for Adaptive Coded Aperture Imaging (ACAI) applications ranging from visible to terahertz. We demonstrate the use of this approach to enhance the functionality of (a) pressure and temperature sensors, (b) microbolometers in thermal infrared cameras, (c) directed energy transfer. Properties of the nanoparticle dispersed metamaterial are determined using effective medium theory. Tunability can be achieved through changing the nature, sizes and filling fractions of the nanoparticles, as well as electronically through changing the biasing of the host. In microbolometer application, a single layer structure can be designed to give zero reflection, thereby allowing maximum transmission to the detector. Using multilayer structures with alternating positive and negative index materials, one can design temperature and pressure sensors with minimal crosstalk by employing the additional zero-index bandgap, characteristic of such structures. Finally, by incorporating a defect layer in such multilayer structures one can realize tunable radiation patterns with specific directivities with possible applications to spectroscopy and free-space communications.

8165B-54, Session 10

Adaptive phase change metamaterials for infrared aperture control

D. H. Werner, T. S. Mayer, The Pennsylvania State Univ. (United States); C. Rivero-Baleine, Lockheed Martin Missile and Fire Control (United States); N. J. Podraza, The Pennsylvania State Univ. (United States); K. A. Richardson, Clemson Univ. (United States); J. P. Turpin, A. V. Pogrebnyakov, The Pennsylvania State Univ. (United States); J. D. Musgraves, Clemson Univ. (United States); J. A. Bossard, The Pennsylvania State Univ. (United States); S. Rogers, J. D. Johnson, Air Force Research Lab. (United States)

This talk will discuss the use of chalcogenide phase change materials to create tunable metamaterials that can be applied to aperture control in the infrared. Phase change materials exhibit large and reversible changes in optical properties (n , k) when switched between the amorphous and crystalline phases. Thermally-induced phase transitions from the insulating amorphous to the conductive crystalline state can be controlled through external means, facilitating the design of reconfigurable metamaterial devices that operate with ultrafast response times. In this work, robust global stochastic optimization algorithms were combined with full-wave electromagnetic simulation tools to design periodic subwavelength chalcogenide nanostructure arrays to meet the specified device performance goals in each phase. The measured optical properties of deposited chalcogenide thin films and nanofabrication constraints were incorporated into the optimization algorithm to guarantee that the designed nanostructures could be manufactured. By choosing the appropriate cost functions, adaptive metamaterials were designed to switch between transmissive and reflective, transmissive and absorptive, and reflective and absorptive states. The measured optical response of a nanofabricated metamaterial device, which was optimized